IMCET 2022

Türkiye 27. Uluslararası Madencilik Kongresi ve Sergisi

27th International Mining Congress and Exhibition of Turkey

22-25 Mart, March 2022, Antalya

Proceedings of the 27th International Mining Congress and Exhibition of Turkey

Antalya

www.imcet.org.tr

TMMOB
Maden Mühendisleri Odası

UCTEA
Chamber of Mining Engineers

ISBN: 978-605-01-1494-2

Published by
Baskı

TMMOB Maden Mühendisleri Odası
Kültür Mh. Yüksel Cd. No: 40 Çankaya/Ankara

March/Mart 2022
Ph/Tel: +90 312 425 10 80
Fax/Faks: +90 312 417 52 90

www.maden.org.tr
maden@maden.org.tr

IMCET 2022

Proceedings of the 27th International Mining Congress and Exhibition of Turkey

Türkiye 27. Uluslararası Madencilik Kongresi ve Sergisi Bildiriler Kitabı

Editors

Editörler

Dr. Okay Altun
Dr. Deniz Aydın
Dr. Namık Atakan Aydoğan
Dr. Ahmet Deniz Baş
Dr. Hakan Dündar
Dr. Ece Kundak
Dr. Mehtap Gülsün Kılıç
Dr. Emre Yılmazkaya

UCTEA Chamber of Mining Engineers

TMMOB Maden Mühendisleri Odası

Executive Committee of the Congress
Kongre Yürütme Kurulu

Chair Başkan	Yusuf AYDIN
Deputy Co-Chairs Başkan Yardımcıları	Dr. Okay ALTUN Dr. Mehtap GÜLSÜN KILIÇ Dr. Nejat TAMZOK Dr. Bülent TOKA
Secretary Yazman	Nadir AVŞAROĞLU Gülcan KOÇ
Treasurer Sayman	Veyis SIR
Members Üyeler	M. Erşat AKYAZILI Selim ALTUN Dr. Deniz AYDIN Dr. Namık Atakan AYDOĞAN Dr. Ahmet Deniz BAŞ Dr. Hakan DÜNDAR Necmi ERGİN Niyazi KARADENİZ Ümit KILIÇ Pelin KERTMEN Dr. Ece KUNDAK Fatih ÖZKAN Selçuk SARIDOĞAN Muharrem TORALIOĞLU İmge TÜMÜKLÜ Dr. Emre YILMAZKAYA

Board Members of UCTEA Chamber of Mining Engineers
Maden Mühendisleri Odası Yönetim Kurulu

President *Başkan*	Ayhan YÜKSEL
Vice president *II. Başkan*	Veyis SIR
Secretary *Yazman*	M. Erşat AKYAZILI
Treasurer *Sayman*	Mehmet ZAMAN
Members *Üyeler*	Hakan Baran KIRMAÇ Cem LAFÇI Gözde SALAR

FOREWORD

These Congress proceedings contain the papers which were submitted to 27th International Mining Congress and Exhibition of Turkey (IMCET 2022) held in Antalya, Turkey between March 22-25, 2022.

IMCET 2022 has been organized to gather the people from the academic world and the business world, in order to further explore and share ways to discuss topics in their respective research areas. The Congress was initiated in 1969 and has become one of the most prestigious congresses in Turkey. IMCET congresses have been a major driving force in the promotion of scientific and technical knowledge in areas such as mine planning, drilling and blasting, rock mechanics, comminution, mineral beneficiation, sustainability of the mining operations and their social impacts. The contributions of all the participants help to make the conference as outstanding as it has been.

These Proceedings are believed to furnish the scientists of the world with an excellent reference book to stimulate further study and research in all these areas. IMCET 2022 received over 150 abstracts from 20 different countries. Papers submitted to the congress went through a peer-review process for publication in these Congress proceedings. We would like to express our gratitude and appreciation for all of the reviewers who helped us maintain the high quality of manuscripts.

We would also like to take this opportunity to thank authors who submitted their papers to the Congress, sponsors and exhibitors for their support and members of the Organizing Committee working for the success of the Congress.

Ayhan YÜKSEL
Chamber of Mining Engineers
President

Yusuf AYDIN
IMCET 2022
Chairman

2013-2020 YILLARI ARASI TÜRKİYE MADENCİLİK SEKTÖRÜNDE MEYDANA GELEN İŞ KAZALARININ NİCELİKSEL ANALİZİ

QUANTITATIVE ANALYSIS OF OCCUPATIONAL ACCIDENTS IN THE TURKISH MINING SECTOR BETWEEN 2013-2020

E.G. Uçkaç[1]*, S. Önder[1]

[1] *Eskişehir Osmangazi Üniversitesi, Maden Mühendisliği Bölümü*
*(*Sorumlu yazar: eguckac@gmail.com)*

ÖZET

Madencilik sektörü tüm sektörlere kıyasla iş kazasının en çok yaşandığı sektörlerin başında gelmektedir. İş kazalarının önlenebilmesi için kazalara neden olan faktörlerin analiz edilmesi gerekir. Bu çalışmada, SGK tarafından kayıt altında tutulan 2013-2020 yılları arasında meydana gelmiş olan madencilik sektörüne ait 103.815 adet iş kazası niceliksel olarak incelenmiştir. Analizde kazaya sebep olan olay, yaralanma nedeni, yaralanma türü, yaralanan uzuv, yürütülen faaliyet, yaş, eğitim düzeyi, kaza saati, meslek gibi parametrelerin kazanın oluşumu üzerindeki etkileri incelenmiştir. Sonuç olarak; iş kazalarının çoğunlukla yeraltı işletmelerinde ve kömür-linyit çıkarılmasında olduğu, üretimde çalışan ve eğitim düzeyi düşük olan çalışanların iş kazası eğilimlerinin yüksek olduğu bulunmuştur. El makinaları ile çalışmalarda, 25-34 yaş aralığında, işe başlangıcın 2. ve 3. saatinde, operatör ve montaj gurubunda, malzeme taşıma sırasında, el ve kollarından yaralanmalarının yüksek olduğu da tespit edilmiştir.

Anahtar Sözcükler: İş kazası, kaza analizi, madencilik

ABSTRACT

Mining sector is one of the sectors where occupational accidents are experienced the most compared to all sectors. In order to prevent occupational accidents, the factors causing the accidents should be analyzed. In this study, 103,815 occupational accidents in the mining sector, which occurred between 2013 and 2020, which were recorded by the SGK, were quantitatively examined. In the analysis, the effects of parameters such as the event that caused the accident, the cause of the injury, the type of injury, part of body, the activity carried out, age, education level, time of the accident, and occupation on the occurrence of the accident were examined. As a result; It has been found that occupational accidents are mostly in underground mines and coal-lignite extraction, and workers with low education level and working in production have a high tendency to work accident. It has also been determined that injuries from the hands and arms are high in the 25-34 age range, at the 2nd and 3rd hours of the start of work, in the operator and assembly group, during material handling, while working with hand machines.

Keywords: Occupational accidents, accident analysis, mining

GİRİŞ

Madencilik sektörü, maddi ve manevi büyük kayıpların olduğu iş kazalarının gerçekleştiği çok tehlikeli çalışma kollarından birisidir. İş kazaları sebebiyle meydana gelen yaralanmalar, uzuv kayıpları ve ölümler konunun sosyal boyutunu, iş gücü ve iş günü kaybı, tıbbi müdahaleler ve tazminatlar, maddi kayıplar (makine, teçhizat, bina vb.), üretim ve verimin düşmesi ise ekonomik boyutunu ortaya

koymaktadır (Yıldırım, 2009).

Özellikle iş sağlığı ve güvenliği ile ilgili yasal düzenlemelerin temel amacının iş kazalarını önlemek olduğu dikkate alınacak olursa, bu bağlamda ve yasal düzenlemeler kapsamında alınan tüm önlemlere rağmen iş kazaları meydana gelmeye devam etmektedir. İş kazalarını önleyebilmek için kazaya sebep olan nedenlerin bilinmesi gerekir. Bu durumda iş kazası analizlerinin önemi ortaya çıkmaktadır. Bu yüzden kaza kayıtları doğru bir şekilde tutulmalı, devamlı güncellenmeli, kaza sebepleri doğru bir şekilde belirlenmeli ve alınacak tedbirlerin kararlaştırılması gereklidir (Önder vd., 2015).

Bilim vd. (2018), yaptıkları çalışmada SGK'nın 2012-2016 yıllarına ait istatistiklerini değerlendirdiklerinde, iş kazaları ve meslek hastalıkları oranlarında düşüş gözlenmektedir. Ancak bu düşüşün yeterli olmadığı belirtilmiştir. Kılıç vd. (2018), yaptıkları çalışmada ülkemizdeki kömür madenlerinde 2010-2017 yılları arasındaki yaşanan ölümlü iş kazalarını incelemişlerdir. Kömür üretiminde kullanılan yöntemlerin çeşitliliğinden kaynaklı, iş sağılığı ve güvenliği önlemlerinin yetersiz olduğunu belirlemişlerdir. Şensöğüt vd. (2019), yaptıkları çalışmada Garp Linyitleri İşletmesine ait 2015-2017 yılları arasındaki iş kazası verilerini üretim ile birlikte değerlendirmişlerdir. İş kazaları oranlarının yıllar içinde arttığı görülmekte olup kaza nedenlerinin çoğunlukla bireysel hatalardan kaynaklanmakta olduğu tespit edilmiştir. Oral (2021), yaptığı çalışmada SGK'nın 2013-2019 yılları arasındaki madencilikteki iş kazaları istatistikleri analiz edilmiş, iş kazasına uğramayan çalışanların, her 10000 'lik iş saatinde iş kazasına uğrama olasılığı %0,17 olarak tespit edilmiştir.

Bu çalışmada, 2013-2020 yılları arasına ait madencilik sektöründe meydana gelen tüm iş kazalarının analizi gerçekleştirilmiştir. Çalışmada, Sosyal Güvenlik Kurumu (SGK) tarafından elektronik ortamda tutulan İş Kazası Bildirim Formlarına ait iş kazası verileri kullanılmıştır (SGK, 2021). Veriler SGK ile yapılan yazışmalar sonucunda izinle alınmıştır.

İŞ KAZALARININ ANALİZİ

Bu çalışmada ülkemizde 2013 – 2020 yılları arasında tüm madencilik faaliyet sınıflamalarında meydana gelmiş olan iş kazaları ayrıntılı bir şekilde analiz edilmiştir. SGK tarafından iş kazası bildirim formları 2013 yılından itibaren Avrupa Birliği Standartlarına uygun olarak ESAW sınıflandırmasına göre tutulmaya başlanmıştır (ESAW, 2013). Bu nedenle verileri daha sağlıklı ele alabilmek adına 2013 yılı ve sonrası bildirim formları değerlendirilmiştir.

Türkiye'de 2013 – 2020 yılları arasında madencilik sektörüne ait toplam 103.815 adet iş kazaları verisi bulunmaktadır. Meydana gelen bu iş kazalarının yıllara göre dağılımları Şekil 1'de verilmiştir.

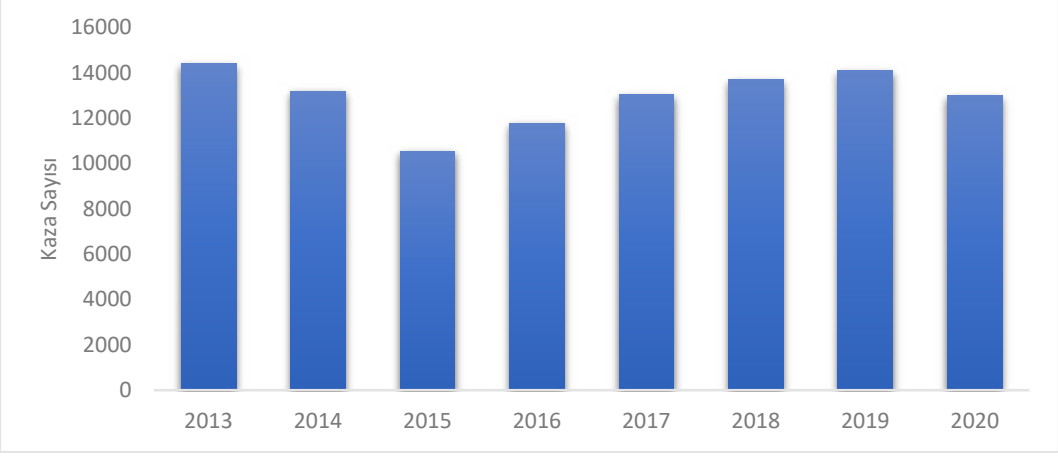

Şekil 1. Türkiye'de madencilik sektöründe meydana gelen iş kazalarının yıllara göre dağılımı

Şekil 1 incelendiğinde, iş kazalarının sayısında önce bir azalma, 2015 yılından sonra bir artış gözlenmektedir. 2015 yılındaki azalmanın, 13 Mayıs 2014' de meydana gelen Soma kazası sonrasında işletmelerde iş sağlığı ve güvenliği ile ilgili tedbirleri ve önlemlerinin etkinliğinin arttırılmış olması sonucuna ulaşılabilir. Ayrıca 2020 yılında pandemiden kaynaklı olabilecek, bir önceki yıla göre bir miktar azalma olduğu görülmektedir. Şekil 2'de iş kazası geçiren çalışanların faaliyet gruplarına dağılımları verilmiştir.

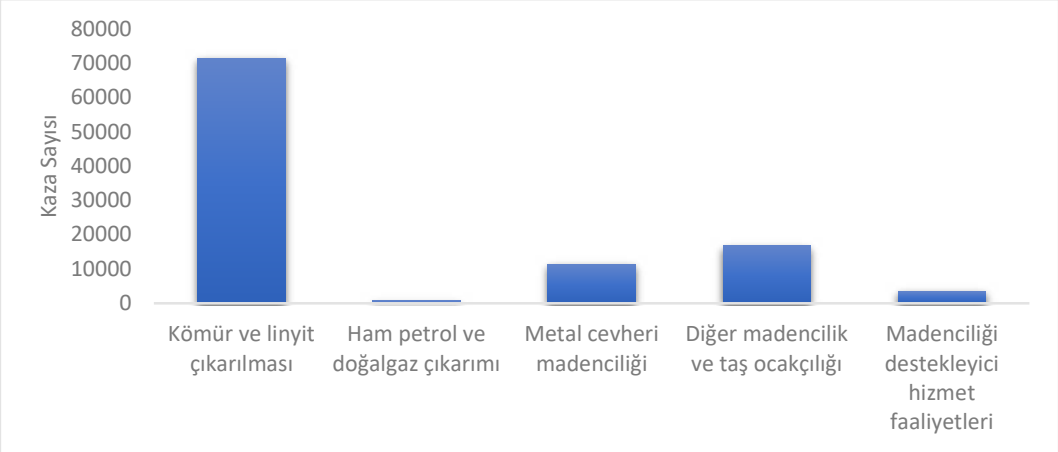

Şekil 2. 2013-2020 yılları arasında iş kazası geçiren çalışanların faaliyet gruplarına göre dağılımı

Şekil 2'deki 2013-2020 yılları arasında faaliyet gruplarına göre bakıldığında; kömür ve linyit çıkarılması faaliyet grubunda meydana gelen kazalar, madencilik sektöründeki toplam iş kazalarının %68,87' sini oluşturmaktadır. Bu durum diğer madencilik gruplarına göre kömür ve linyit grubu madencilik sektöründe çalışan sayılarının fazla olmasından da kaynaklanmaktadır. Şekil 3'te meydana gelen ölümlü, yaralanmalı ve uzuv kayıplı iş kazalarının faaliyet gruplarına göre dağılımı gösterilmektedir.

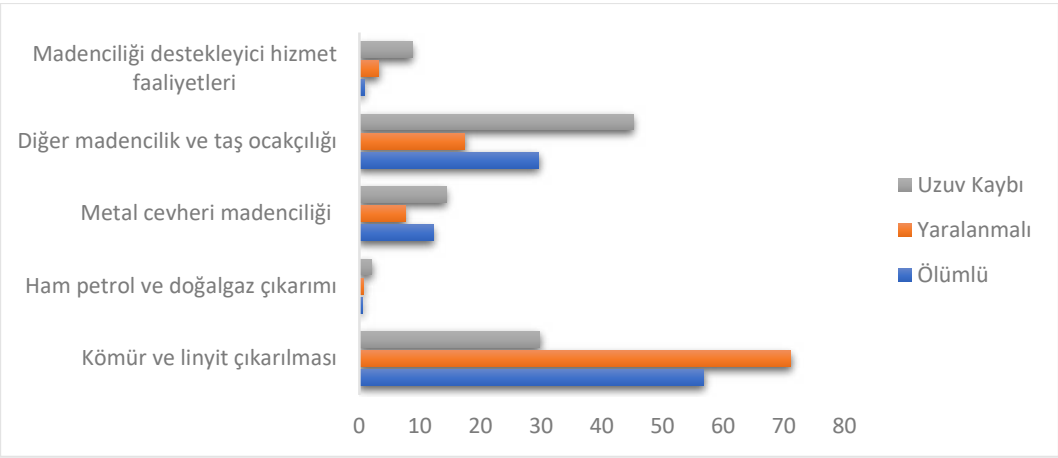

Şekil 3. 2013-2020 yılları arasında meydana gelen ölümlü, yaralanmalı ve uzuv kayıplı iş kazalarının faaliyet gruplarına göre dağılımı

Şekil 3 incelendiğinde, 2013-2020 yılları arasındaki meydana gelen ölümlü iş kazalarının %56,76'sı kömür ve linyit çıkarılması, %29,57 diğer madencilik ve taş ocakçılığı ve %12,23'ününde metal cevheri madenciliği faaliyet grubunda meydana geldiği görülmektedir. Kömür ve linyit çıkarılması faaliyet grubundaki sayısının fazla olması, 2014 yılında Soma'da meydana gelen 301 çalışanın ölümü ile sonuçlanan kazadan kaynaklanmaktadır. Bu kazanın gerçekleşmemiş olması durumunda diğer

madencilik ve taş ocakçılığı faaliyet grubundaki ölümlü iş kazası sayısının daha fazla olacağı da gözlenmektedir. Şekil 3'te 2013-2020 yılları arasında meydana gelen uzuv kayıplı kazalardan %45,12' sinin diğer madencilik ve taş ocakçılığı faaliyet grubunda olması dikkat çekmektedir. %29,74'ü kömür ve linyit çıkarılması ve %14,35'i metal cevheri madenciliği faaliyet gruplarında meydana gelmiştir. Şekil 3'te 2013-2020 yılları arasında meydana gelen yaralanmalı iş kazalarına bakıldığında; toplam yaralanmalı iş kazalarının %71,13' ünün kömür ve linyit çıkarılması faaliyet grubundan olduğu görülmektedir. %17,39'unun diğer madencilik ve taş ocakçılığı ve %7,57'sinin de metal cevheri madenciliği faaliyet gruplarında meydana gelmiştir. Şekil 4'te 2013-2020 yılları arasında meydana gelen iş kazalarının yaralanmaya neden olan olaylara göre dağılımları verilmiştir.

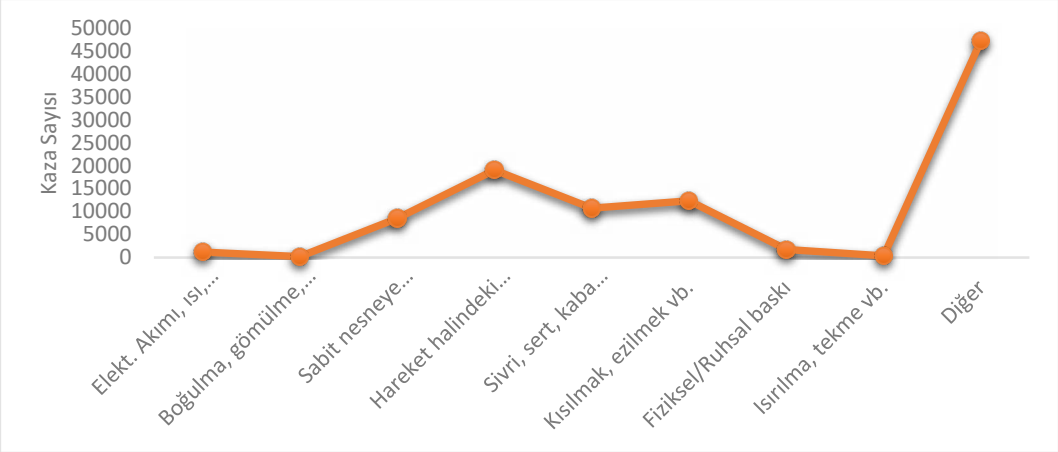

Şekil 4. 2013-2020 yılları arasında meydana gelen iş kazalarının yaralanmaya neden olan olaylara göre dağılımları

SGK tarafından iş kazalarında yaralanmaya neden olan olaylar 9 farklı grupta sınıflandırılmaktadır. Grafik incelendiğinde diğer yani "bu sınıflandırmada listelenmemiş yaralanmaya sebep olan hareket (olay)" sınıfındaki kazaların %45,52 oranında olduğu görülmektedir. Ayrıca %18,38'inin "hareket halindeki bir nesnenin çarpması, çarpışması", %11,88'inin "kısılmak, ezilmek vb." ve %10,34'ünün "sivri, uçlu, sert veya kaba bir materyal araç ile temas" yaralanmaya neden olan olayların diğerlerine göre daha fazla olduğu gözlenmektedir. 2013-2020 yılları arasında meydana gelen iş kazalarında yaralanmaya sebep olan araç/gereçlerin dağılımları Şekil 5'te verilmiştir.

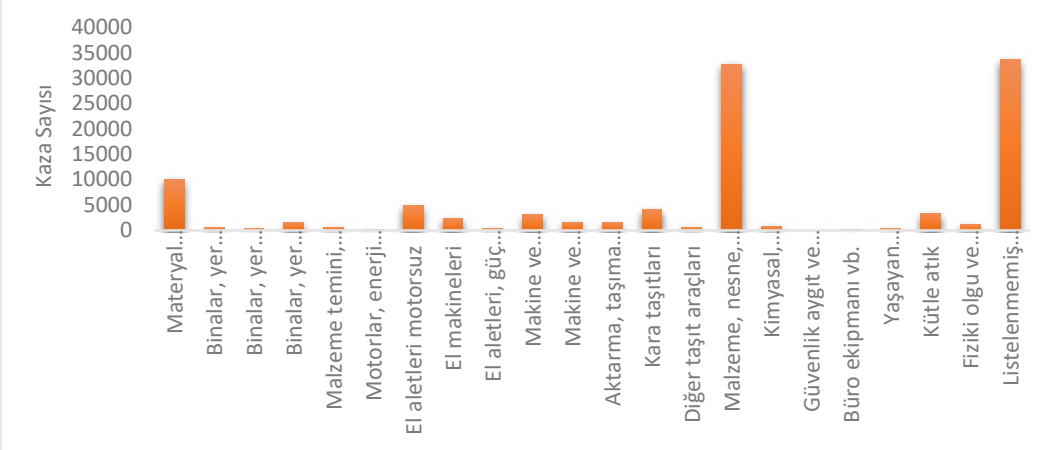

Şekil 5. Yaralanmaya neden olan araç/gereçlerin dağılımları

SGK tarafından iş kazalarında yaralanmaya neden olan araç/gereçler 22 farklı grupta

sınıflandırılmaktadır. Şekil 5 incelendiğinde, meydana gelen en fazla iş kazalarının %32,45'inin "listelenmemiş başka araçlardan", %31,50'sinin de "malzeme, nesne, ürün, makine aksamı, enkaz, tozdan" kaynaklandığı görülmektedir. Şekil 6'da 2013-2020 yılları arasında meydana gelen iş kazaları sonucunda yaralanan bölgenin vücuttaki yerlerinin dağılımları verilmiştir.

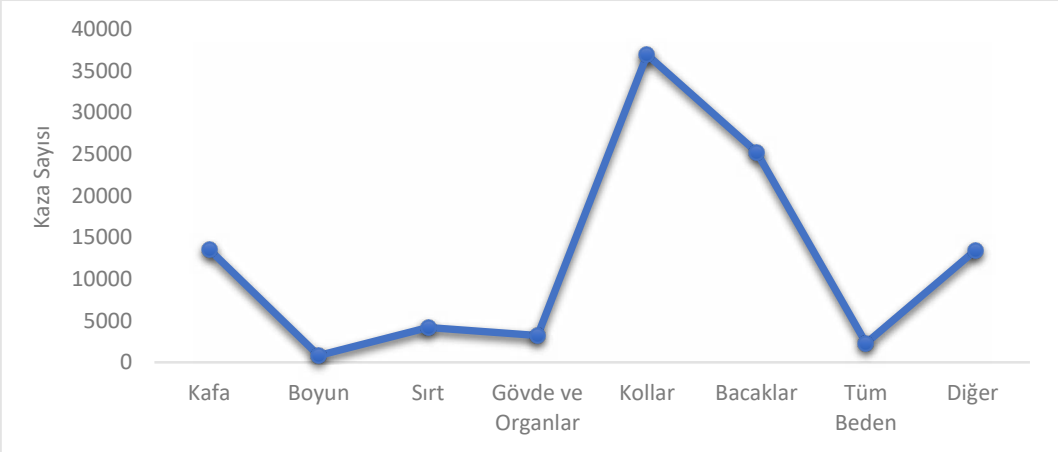

Şekil 6. Yaranın vücuttaki yerinin dağılımları

En fazla yaralanan vücut bölgelerinin, diğer vücut bölgelerine göre %35,6 oranında kollarda ve %24,3 oranında bacaklarda olduğu gözlenmektedir. Şekil 7, 2013-2020 yılları arasındaki iş kazaları sonucunda oluşan yaralanmaların türünün dağılımlarını göstermektedir.

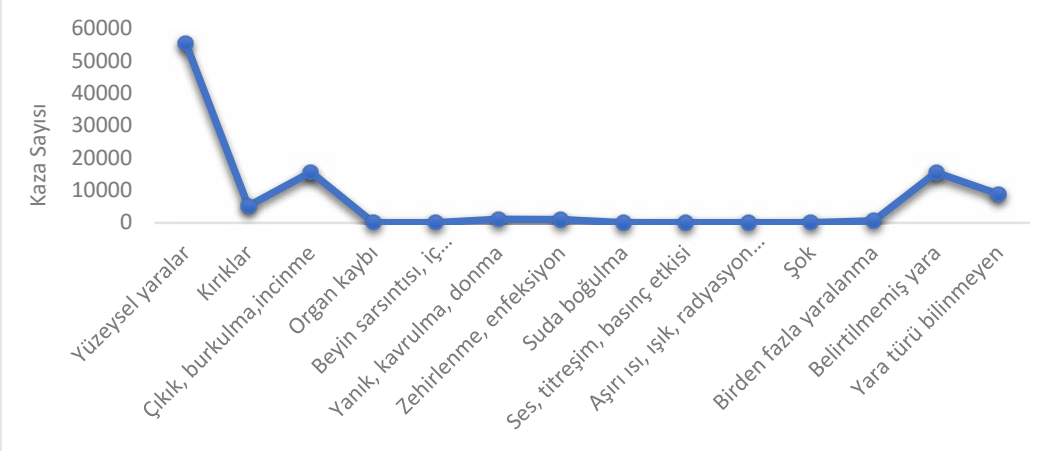

Şekil 7. Yaranın türünün dağılımları

İş kazası sonucunda meydana gelen yaranın türü 14 farklı grupta ele alınmaktadır. İş kazası geçiren çalışanlarda oluşan en fazla yaralanma türünün %53,35' inin yüzeysel yaralanmalar olduğu görülmektedir. 2013-2020 yılları arasında meydana gelen iş kazalarına sebep olan olayların dağılımı Şekil 8'de verilmiştir.

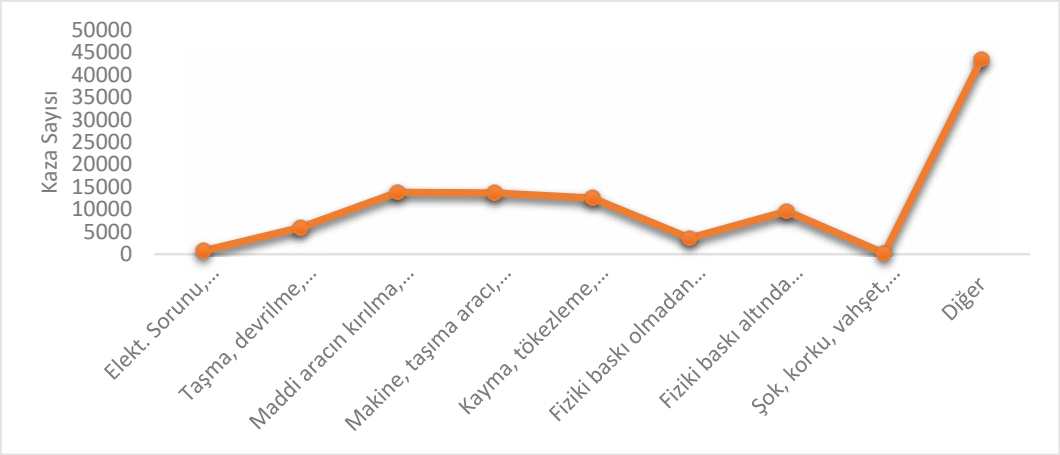

Şekil 8. Kazaya sebep olan olayların dağılımı

SGK iş kazası bildirim formunda kazaya sebep olan olayları 9 farklı grupta kayıt altına almaktadır. Şekil 8'deki grafik incelendiğinde, "diğer" yani "bu sınıflandırmada listelenmemiş başka sapma" grubunda bulunan kazalar diğer gruplara göre %41,91 oranında daha fazladır. Bunun nedeninin form doldurulurken yanlış veya dikkatsizce doldurulduğu düşünülebilir. Bunun dışında, kazaya sebep olan olaylar arasında fazla sayıda kaza bulunan gruplardan; %13,30' u "maddi aracın kırılma, patlama, ayrılma, kayma, düşme, çökmesi", %13,19' u "bir makinenin, taşıma aracının veya işleme ekipmanının, elle kullanılan alet, nesne, hayvanın denetimden çıkması (tam veya kısmi)" ve %12' si "kayma veya tökezleme, düşme, kişilerin düşmesi" dir. 2013-2020 yılları arasında meydana gelen iş kazalarının çalışılan ortama göre dağılımları Şekil 9'da gösterilmiştir.

Şekil 9. Çalışılan ortama göre dağılım

İncelendiğinde, madencilik sektöründe meydana gelen toplam iş kazalarının %56,23'ü çalışanın sürekli olarak çalıştığı sabit işyerinde, %29,75'i diğer çalışılan ortamda, %10,59'u geçici işyerinde (görevlendirme, iş seyahati vb.) ve %3,42'si belirtilmemiş ortamda meydana geldiği görülmektedir. Şekil 10'da iş kazalarının gerçekleştiği ortama göre dağılım verilmiştir.

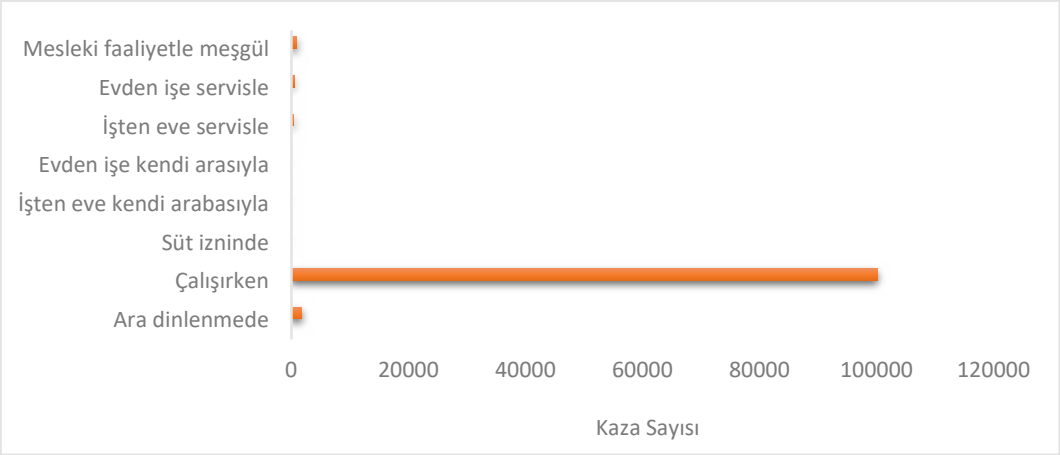

Şekil 10. 2013-2020 yılları arasında meydana gelen iş kazalarının gerçekleştiği ortama göre dağılımları

SGK iş kazası verilerinin kaydını tutarken, iş kazalarının gerçekleştiği yeri "işyeri" ve "işyeri dışında" olarak ayırmaktadır. Ara dinlenme ve çalışırken olan kazaları işyerinde, bunların dışında kalanları ise işyeri dışında olarak kabul etmektedir. Şekil 10 incelendiğinde; çalışırken ve ara dinlenmede olan kazalar sırasıyla, toplam kazaların %96,40'ını ve %1,72'sini oluşturduğu görülmektedir. Burada, "evden işe kendi arabasıyla" ve "işten eve kendi arabasıyla" grupları altında bulunan kazaların, 5510 sayılı kanunun 13. maddesine göre iş kazası kapsamına girmemesinden dolayı kayıtlarının tutulması gerekmemektedir (SSGSK, 2006). İşveren tarafından sağlanan bir taşıt ile yapılması durumunda iş kazası olarak kaydı tutulabilir. 2013-2020 yılları arasında meydana gelen iş kazalarının Şekil 11'de kazanın gerçekleştiği yer/bölüme ait dağılımları yer almaktadır.

Şekil 11. 2013-2020 yılları arasında meydana gelen iş kazalarının gerçekleştiği yer/bölüm göre dağılımları

İş kazalarının gerçekleştiği yer/bölüm, SGK tarafından 13 ayrı grup altında ele alınmaktadır. Bakıldığında, toplam kazaların %62,80'inin yeraltında ve %18,61'inin açık hava madeni grubunda meydana geldiği görülmektedir. Ayrıca "evde" yani işyeri dışında meydana gelen ve iş kazası kapsamına girmeyen kazaların kayıtlarının tutulması gerekmemektedir. Şekil 12'de 2013-2020 yılları arasında meydana gelen iş kazalarında kazazedenin kaza anında yürütmekte olduğu genel faaliyete göre dağılımları verilmiştir.

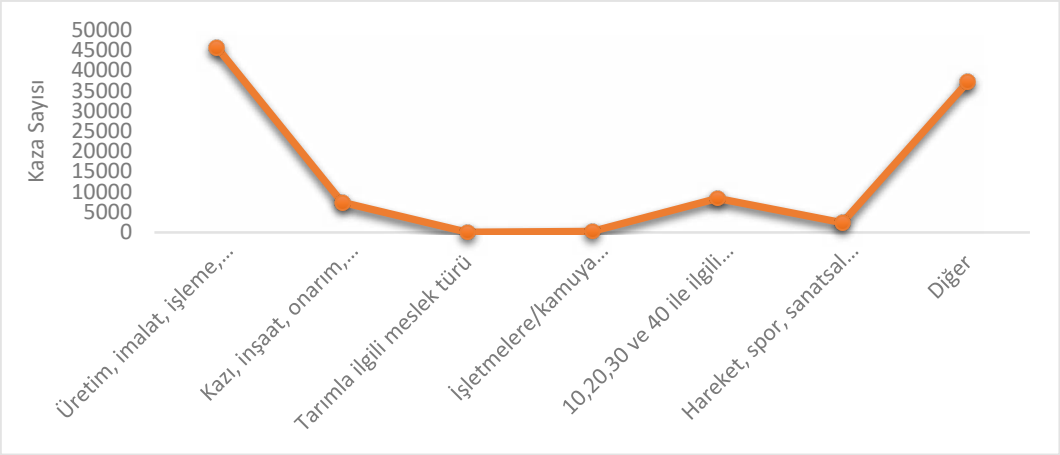

Şekil 12. Kazazedenin yürütmekte olduğu genel faaliyete göre dağılım

Yürütülmekte olan bu genel faaliyetler 7 grup altında değerlendirilmektedir. En fazla iş kazasının meydana geldiği üretim, imalat, işleme, depolama faaliyetlerinde gerçekleşen kazaların, toplam iş kazalarına göre %43,9 oranında olduğu görülmektedir. "Diğer" faaliyetler esnasında meydana gelen kazalar ise %35,80 oranındadır. Bu oranın fazla olmasından dolayı neler olduğunun ayrıntılı olarak bakılması gerekebilir. 2013-2020 yılları arasında gerçekleşen iş kazalarında, kazadan az önceki zamanda kazazedenin yürüttüğü özel faaliyetlerin dağılımları Şekil 13'te verilmektedir.

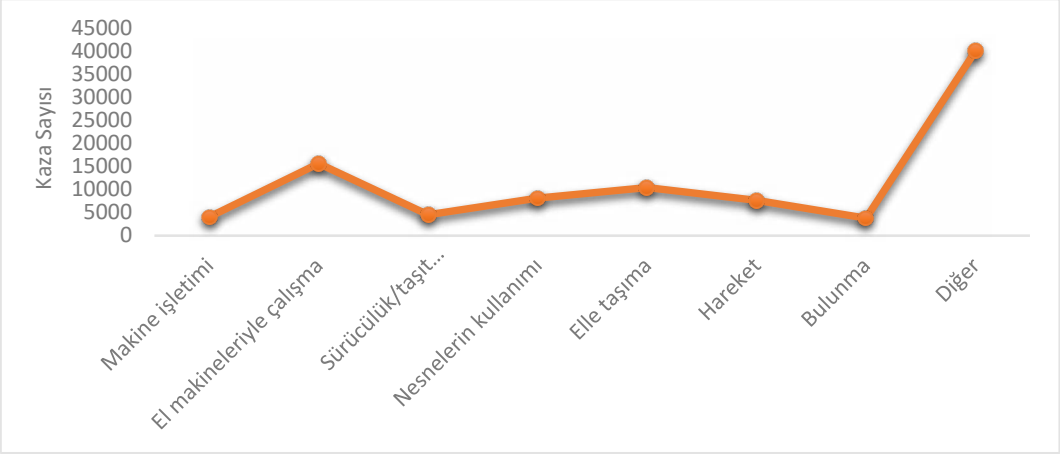

Şekil 13. Kazazedenin yürütmekte olduğu özel faaliyete göre dağılım

Bu yürütülen özel faaliyetler 8 grupta ele alınmaktadır. Şekil 13 incelendiğinde, en fazla kazanın %38,65 oranla diğer (sınıflandırmada listelenmemiş başka kaza anında kazazedenin yaptığı faaliyet) grubunda olduğu gözlenmektedir. Bunun dışında toplam kazaların, %15'i el makineleriyle çalışma, %10'u elle taşıma, %7,82'si nesnelerin kullanımı, %7,35'i hareket, %4,37'si sürücülük/taşıt aracında bulunma, %3,84'ü makine işletimi ve %3,63'ü bulunma faaliyetlerinde olduğu görülmektedir. Diğer grubunda bulunan kazaların sayısının çok daha fazla olmasından dolayı bu grup içerisinde yer alan özel faaliyetler incelenmelidir. Şekil 14, madencilik sektöründe 2013-2020 yılları arasında iş kazası geçiren çalışanların yaşlarına göre dağılımlarını göstermektedir.

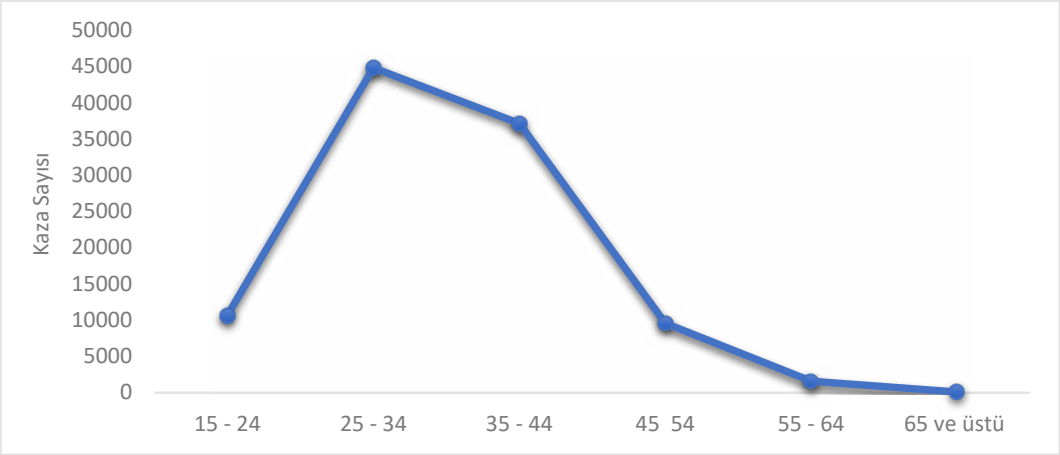

Şekil 14. Çalışanların yaşlarına göre dağılım

2013-2020 yılları arasında en fazla iş kazası geçiren çalışanların %43,15'inin 25-34 yaş aralığında ve %35,75'inin 35-44 yaş aralığında olduğu görülmektedir. 2013-2020 yılları arasında meydana gelen iş kazalarının, kazaların oluş saatlerine göre dağılımları Şekil 15'te görülmektedir.

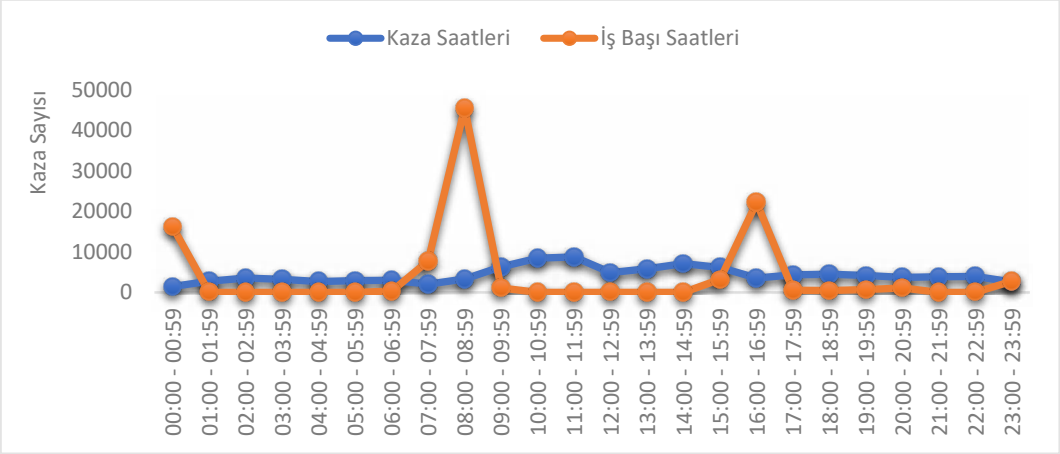

Şekil 15. İş kazalarının meydana geldiği saatler ve kaza günü iş başı saatlerinin dağılımları

Saat dilimleri ESAW Standartlarına ve SGK istatistiklerine bakılarak gruplandırılmıştır. Yukarıdaki şekilde en fazla kazanın gerçekleştiği saat dilimlerine bakıldığında, toplam iş kazalarına göre 10:00-10:59 ile 11:00-11:59 saatleri aralığında meydana gelen iş kazalarının sırası ile %8,15 ile %8,46 oranında olduğu görülmektedir. Bunun sebebi öğlen yemeği molasına yaklaştıkça çalışanların acıkmalarından kaynaklanabilecek dalgınlıklardan olduğu düşünülebilir. Şekil 17'de 2013-2020 yılları arasında gerçekleşen iş kazalarının, kazanın olduğu gün iş başı saatlerine göre dağılımları verilmiştir. Bakıldığında, %43,93'ünün 08:00-08:59 arası saatlerde, %21,45'inin 16:00-16:59 arası saatlerde ve %15,67'sinin ise 00:00-00:59 arası saatlerde iş başı yaptığı görülmektedir. Madencilik sektöründe, genellikle ikili veya üçlü vardiya sistemleri şeklinde çalışma yapılmaktadır. İlk vardiya 08:00-16:00, ikinci vardiya 16:00-24:00 ve varsa eğer üçüncü vardiya 24:00-08:00 saatleri arasında olabilir. Bu sebeple, yüzdelerin fazla olduğu saat dilimleri, bu vardiya başlangıç saatlerine denk gelmektedir. Şekil 16'da 2013-2020 yılları arasında iş kazası geçirmiş olan çalışanların, kaza günü iş başı saatleri ile kazanın meydana geldiği saat arasındaki farkların dağılımları gösterilmektedir.

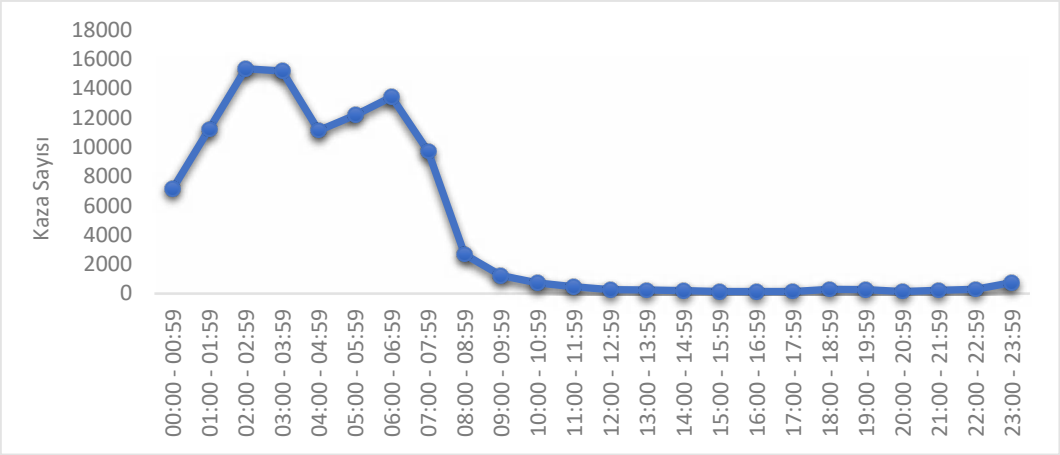

Şekil 16. İş başı saati ile kaza saati arasındaki farkın dağılımları

Meydana gelen kazalarda, en fazla %14,80'inin işe başladıktan ikinci saat diliminde (02:00-02:59) ve %14,65'inin üçüncü saat diliminde (03:00-03:59) gerçekleştiği görülmektedir. 2013-2020 yılları arasında iş kazası geçiren çalışanların öğrenim durumlarına göre dağılım Şekil 17'de verilmiştir.

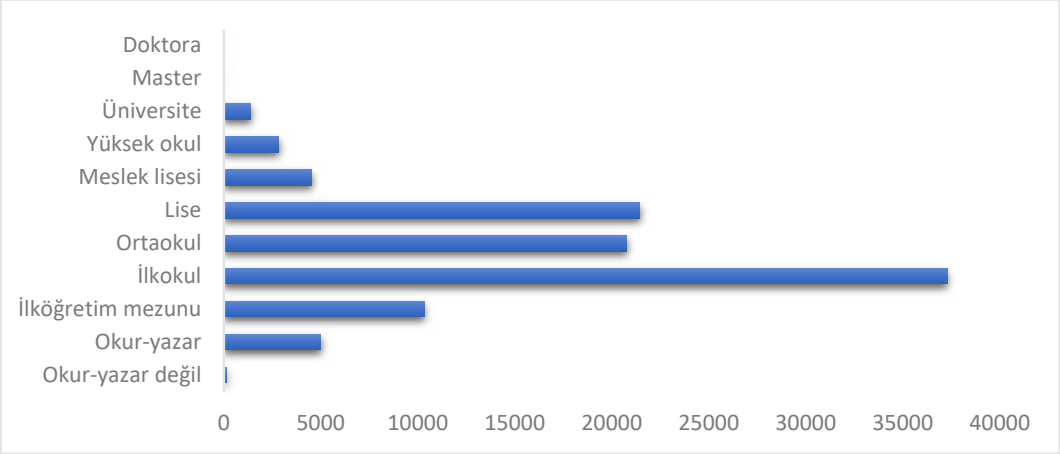

Şekil 17. Çalışanların öğrenim durumlarına göre dağılım

İş kazası geçiren çalışanlar arasından %35,9'u ilkokul, %20,6'sı lise ve %20'si de ortaokul mezunu olduğu görülmektedir. Eğitim seviyesinin artması ile kaza geçiren çalışan sayısının azaldığı gözlenmektedir. Ancak madencilik sektöründe toplam çalışan sayısının öğrenim durumu göz önüne alındığında, yüksek öğrenim mezunu çalışan sayısının da az olabileceği düşünülmelidir. Şekil 18, 2013-2020 yılları arasında iş kazası geçirmiş olan çalışanların meslek gruplarına göre dağılımlarını vermektedir.

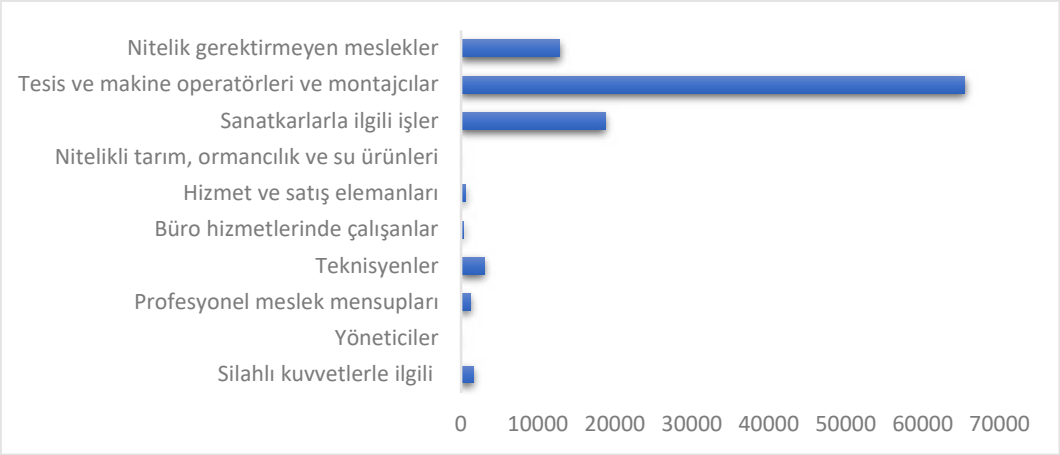

Şekil 18. Çalışanların meslek gruplarına göre dağılımları

Çalışanların mesleklerine göre yapılan incelemeler, genel bir sınıflandırma olarak ele alınmıştır. Şekil 18'e göre en fazla iş kazası geçirmiş çalışanların, %63'ünün tesis ve makine operatörleri ve montajcılar grubundan olduğu görülmektedir. Bunun sebebi ise madenci, kazmacı, iş makinesi operatörü, kamyon şoförü, mermer ocakçısı ve yeraltı maden işletmesi hazırlık elemanı gibi mesleklerin bu grup altında bulunmasıdır.

SONUÇ VE TARTIŞMA

Madencilikte ortam şartlarının sürekli olarak değişmesinden dolayı iş kazalarının meydana gelmesinin önüne geçilememektedir. Ortam şartları dışındaki iş kazalarının asıl sebeplerinin neler olduğunun tespit edilmesi durumunda kazalar önlenebilir veya azaltılabilir. Bunun içinde geçmiş kaza kayıtlarından faydalanılmalıdır. Bu çalışmada, işverenlerin SGK'ya bildirmek zorunda oldukları iş kazası bildirim formları kullanılmıştır. SGK, 2013 yılından itibaren iş kazası bildirim formlarını elektronik ortamda ve ESAW'a uygun şekilde kayıt altına almaktadır. Bu nedenle 2013 yılından 2020 yılı da dahil olmak üzere tüm madencilik faaliyet sınıflamasına giren iş kazası verileri kullanılmıştır.

Madencilik sektörlerine ait 103.815 adet iş kazası verileri incelendiğinde, kazaların %68,87'si kömür ve linyit çıkarılması faaliyet sınıfında meydana gelmiştir. Meydana gelen iş kazalarından yaralanmalı, ölümlü ve uzuv kayıplı olarak sonuçlanmış olanlar vardır. Ölümlü iş kazalarının %56,76'sı kömür ve linyit çıkarılması, uzuv kayıplı iş kazalarının %45,12'si diğer madencilik ve taş ocakçılığı ve yaralanmalı iş kazalarının %71,13'ü kömür ve linyit çıkarılması faaliyet sınıfındandır. İş kazalarının %18,38'i hareket halindeki bir nesnenin çarpması, çarpışması sonucunda yaralanmaya neden olmuştur. İş kazalarının %31,50'si malzeme, nesne, ürün, makine aksamı, enkaz, tozdan kaynaklanan yaralanmaya neden olan araç/gereçlerdendir. İş kazalarının %35,6'sı kollardan ve %24,3'ü bacaklardan yaralanma ile sonuçlanmaktadır. İş kazaları sonucunda %53,35 oranında yüzeysel yaralanmalar meydana gelmiştir. İş kazalarında kazaya sebep olan olaylara bakıldığında %13,30'u maddi aracın kırılması, patlaması, ayrılması, kayması, düşmesi, çökmesinden, %13,19'u bir makinenin taşıma aracının, işleme ekipmanı, elle kullanılan alet, nesne, hayvan gibi denetimden çıkması sonucunda meydana gelmiştir. İş kazalarının %96,40'ı çalışırken meydana gelmiştir. İş kazalarından %56,23'ü çalışanın sürekli olarak çalıştığı sabit işyerinde kaza geçirmiştir. İş kazalarının %62,80'i yeraltında ve %18,61'i açık ocak madenlerinde gerçekleşmiştir. İş kazası esnasında kaza geçirmiş çalışanların %43,9'u üretim, imalat, işleme, depolama gibi genel faaliyetleri yürütmektedir. İş kazası meydana gelmeden az önceki zamanda kaza geçirmiş çalışanların %15'i el makineleriyle ve %10'u elle taşıma özel faaliyetlerini yürütmektedir. İş kazası geçiren çalışanların %43,15'i 25 – 34 ve %35,75'i 35 – 44 yaş aralığında yer almaktadır. İş kazalarının %8,15'i 10:00 – 10:59 ve %8,46'sı 11:00 – 11:59 saat aralıklarında meydana gelmiştir. İş kazası geçirenlerin %43,93'ü 08:00 – 08:59, %21,45'i 16:00 – 16:59 ve %15,67'si 00:00 – 00:59 saat aralığında iş başı

yapmıştır. Meydana gelen kazalar iş başı yaptıktan ikinci veya üçüncü saat diliminde gerçekleştiği görülmektedir. İş kazası geçiren çalışanların %35,9'u ilkokul, %20,6'sı lise ve %20'si de ortaokul mezunu olduğu görülmektedir. İş kazası geçirmiş çalışanların %63'ünün tesis ve makine operatörleri ve montajcılar grubundan olduğu görülmektedir.

Sonuç olarak iş kazalarının sebepleri, yaralanmanın büyüklüğü, türü ve nasıl olduğu gibi etkenlerin incelenmesi, iş kazalarının tekrarlanmaması veya önlenebilmesi açısından önemlidir. Madencilik sektöründe iş kazası geçiren çalışanların çoğunun öğrenim durumlarının yüksek olmaması ve en fazla kazanın da üretim vb. faaliyetlerde gerçekleşmiş olmasından dolayı, çalışanların yapacakları işe uygun öncelikle etkin bir mesleki eğitim ve işyerinde davranış değişikliğini hedefleyen iş sağlığı ve güvenliği eğitimlerinden geçmeleri oldukça önemlidir. Çalışanlarda iş güvenliği kültürünün oluşması ile ilerleyen yıllarda iş kazalarında belirgin azalmalar kaydedilecektir.

KAYNAKLAR

Bilim, N., Dündar, S. ve Bilim, A. (2018). Ülkemizdeki Maden Sektöründe Meydana Gelen İş Kazası ve Meslek Hastalıklarının Analizi. *BEÜ Fen Bilimleri Dergisi* 7 (2), 423-432.

ESAW. (2013). European Statistics on Accidents at Work – Summary Methodology. Publications Office of the European Union, Luxembourg.

Kılıç, A. M., Kahraman, E. ve Kılıç, Ö., (2018). Türkiye Kömür Madenciliğinde Ölümlü İş Kazalarının Değerlendirilmesi. M. E. Bilir, M. Geniş, H. Duru, U. Sakız & K. Kel (Eds.), Türkiye 21. Uluslararası Kömür Kongresi Bildiriler Kitabı (s. 449-458).

Oral, T. (2021). 2012-2019 Yılları Arasında Maden Sektöründe Yaşanan İş Kazalarının Analizi ve ÇKKV Yöntemlerinin Katkısı. *Bilim, Teknoloji ve Mühendislik Araştırmaları Dergisi* 2(2): 101-109.

Önder, M., Önder S., Mutlu, M. ve Adıgüzel, E. (2015). Yerüstü Kömür Madenlerindeki Gün Kayıplı İş Kazalarının Loglineer Model ve Uyum Analizi ile İncelenmesi. Ö. Kılıç, A. M. Kılıç, M. Altıner & M. Yılmaz (Eds.), Maden İşletmelerinde İşçi Sağlığı ve İş Güvenliği Sempozyumu (s. 163-180).

Sosyal Güvenlik Kurumu Veri Yönetimi Daire Başkanlığı. (2021). Madencilik Sektörüne ait Veriler, Ankara

Sosyal Sigortalar ve Genel Sağlık Sigortası Kanunu, (2006). https://www.mevzuat.gov.tr/mevzuat?MevzuatNo=5510&MevzuatTur=1&MevzuatTertip=5

Şensöğüt, C., Ören Ö. ve Kasap Y. (2019). Garp Linyitleri İşletmesinde Son Yıllarda Meydana Gelen İş Kazalarının Analizi. *M C B Ü Soma Meslek Yüksekokulu Teknik Bilimler Dergisi* 28 (I), 13-19.

Yıldırım, H. (2009). Kapalı Devre Suni Solunum Sağlayan Cihazlar. A. M. Kılıç & Ö. Kılıç (Eds.), Maden İşletmelerinde İş Sağlığı ve Güvenliği Sempozyumu Bildiriler Kitabı (s. 273-280).

A COMPUTATIONAL ALGORITHM TO PERFORM PROBABILISTIC SAMPLING FOR MINERAL ASSAY DETERMINATION

M. Camalan

Ankara, Turkey
(camalanmahmut@gmail.com)

ABSTRACT

Mineral assay or grade of a population of particles are measured from the subsets or samples. However, sampling is prone to several sources of errors, which are impossible to determine exactly through physical surveys. A computational algorithm is presented to simulate probabilistic sampling surveys on a particle population. The use of the algorithm can lead to a true comparison between a population and its samples as the particle properties (particle size, mass, mineral grade) are known in both. The algorithm was tested on the populations with binary mineral mixtures. Although the simulated variances in sample grades are related to the fundamental sampling errors, the effect of particle size distribution on these errors may not be foreseen in Gy's equation. Some sampling methods may be susceptible to severe errors that are not related to probabilistic sampling. Also, the simulation results provide some insights for the probabilistic sampling surveys.

Keywords: Mineral, grade, probabilistic sampling, variance, simulation

INTRODUCTION

Mineral assay or grade can be broadly defined as the mass content (%) of a target mineral in a population of ore particles. The correct determination of the mineral grade is necessary not only for the mineral process design but also for the periodic monitoring of the process. The mineral grade is determined from the subsets of the particle population, which are called samples. They are collected by following sophisticated sampling protocols that aim to decrease the differences between the population and sample grade to an acceptable degree. The associated differences appear because of (i) the sampling errors by the composition heterogeneity of the population that even distribute both spatially and temporally, as well as (ii) the errors at sample preparation and analysis. These errors had been conceptually defined by Gy (1976), and later revised by the same author (Gy, 1979, 1992). Even it is impossible to avoid the fundamental sampling errors (FSE) unless (i) the samples are identical to the population or (ii) there is no composition heterogeneity (Gy, 1992; Pitard, 2019). Therefore, it is necessary to evaluate how sampling protocols and the associated errors affect the sample quality. The true evaluation, however, requires the comparison between the mineral grades of a population and its samples, which is always impossible as the former cannot be known.

This study proposes a computational algorithm that can simulate sampling surveys on any dataset of particle population containing particle properties such as particle size, shape factor, mineral composition, etc. The algorithm collects the samples by selecting and extracting the particle data from the population dataset. The particle selection in the proposed algorithm is probabilistic (equiprobable), i.e., each particle has the same probability to be selected into the sample. The algorithm can be used to simulate sampling surveys on the population. As the particle properties are known in a population and its simulated samples, they can be exactly compared without performing physical sampling surveys and rigorous statistical treatments.

The algorithm was used to simulate samples from the populations of binary mineral mixtures. Then, the mineral grades of the simulated samples were evaluated with the mineral grade of their population. As the particle selection in sampling simulations was probabilistic, the differences between a population and its simulated samples should be related to FSE, which is the error of equiprobable sampling (Gy, 1992). However, the simulated samples may not reflect the errors due to (i) spatial/temporal heterogeneity of the population and (ii) sample preparation/analysis.

METHODOLOGY

Generation of the Particle Population

The population of the ore particles consisted of binary mixtures of pyrite (density = 5 g/cm^3) and chalcopyrite (4.2 g/cm^3) minerals. The mass of the generated populations was set at 25-100 kg. The mass-weighted size distributions of the particle populations were generated by using the GGS (Eq.1) or RRB (Eq.2) distributions:

$$F_{mass}(x) = (\frac{x}{k})^n \quad (1)$$

$$F_{mass}(x) = 1 - \exp\left(-\left(\frac{x}{k}\right)^n\right) \quad (2)$$

where $F_{mass}(x)$ is the mass percent passing below the screen size of x, k and n are the size and distribution moduli, respectively. The k values for GGS and RRB were set at 25.4 and 9.53 mm, respectively. The n value of either distribution varied between 0.5 and 4. The populations generated from any GGS and RRB distribution are described as the GGS and RRB population, respectively, throughout the text.

The discrete size distributions of the populations were calculated from F_{mass}:

$$f_{mass}(i) = F_{mass}(x_i) - F_{mass}(x_{i+1}) \quad (3)$$

where $f_{mass}(i)$ is the mass percentage of the size interval i, $F_{mass}(x_i)$ and $F_{mass}(x_{i+1})$ are the mass percentages passing below the upper (x_i) and lower (x_{i+1}) screens of the size interval i, respectively. The ratio between the upper and lower screens of each size class, except the finest size fraction (pan), was nearly equal to $\sqrt{2}$. The upper and lower screens of the sink size fraction were set at 1.18 and 0 mm, respectively. The $f_{mass}(i)$ in Eq.3 was multiplied with the population mass to determine the total mass of particles in the size class i. Then, random particles were generated in the size class i:

$$x_{(i)} = (x_i - x_{i+1}) * U(0,1) * + x_{i+1} \quad (4)$$

Where $x_{(i)}$ is the diameter of a random particle in the size class i, and $U(0,1)$ is a pseudorandom real number uniformly distributed in an open interval between 0 and 1. The pseudorandom number was generated by using MATLAB's built-in RAND function based on the Mersenne-Twister algorithm (Matsumoto and Nishimura, 1998). The random particle generation was performed for each size class as long as the total mass of the generated particles was smaller than the mass of the respective size class:

$$\sum_{j_{(i)}} [\, {x^3}_{j_{(i)}} * (\rho_{py} * (100 - g_{j_{(i)}}) + \rho_c * g_{j_{(i)}}) /100] \; < \; f_{mass}(i) \quad (5)$$

where $x_{j_{(i)}}$ and $g_{j_{(i)}}$ are the diameter and chalcopyrite grade of the j^{th} random particle in the size class i, respectively, while ρ_{py} and ρ_c are the pyrite and chalcopyrite densities, respectively. No

shape factor was used to calculate particle volumes assuming that random particle generation imposed a wide distribution of the particle shape.

The chalcopyrite was distributed to the population particles, based on the rule that the chalcopyrite grades of particles followed the normal distribution. To distribute the chalcopyrite in a population, normal random grades were assigned to all particles by using MATLAB's built-in NORMRND function with a mean grade of 6 % and a standard deviation (σ) of 2. The σ was calculated from the smallest of the differences from the mean grade to grade limits (0 %, 100 %), which was further set at 3σ. The calculated σ ensured that the normal random grade could mostly fall between the grade limits due to the three-sigma rule (Pukelsheim, 1994). Nevertheless, when the random grade was lower than 0 % or higher than 100 %, the respective grade was set to the nearest grade limit.

Simulation of the Sampling Algorithm

The diameters, masses, and mineral grades of the particles in a particle population (Section 2.1) were stored in a matrix where each row included the corresponding data of a single particle. Then, a sampling survey was performed on the population matrix by selecting the data of population particles one-by-one. Each particle selection was performed by using MATLAB's built-in RANDI function based on the Mersenne-Twister algorithm (Matsumoto and Nishimura, 1998): The function generated a random integer index from the row indices of the population matrix. The particle data at the index was carried from the population to the sample matrix. Then, the same data in the population matrix was changed to zero. This ensured that when a particle was carried from the population to the sample, it could be only re-added to the sample as a dummy particle. Instead, the carried particle could have been removed from the population matrix, yet this process would reduce the computational speed severely. After the simulation had ended, the data of dummy particles were removed from the sample matrix by using logical operators and indexing.

The selection and carriage of the population particles to a sample were repeated as long as the total sample mass was smaller than the threshold sample mass (% mass of the population). Then, the sample grade was calculated from the sample matrix:

$$Sample\ Grade\ (\%) = 100 * \frac{\sum_k [x_k^3 * (\rho_c * g_k)]}{\sum_k [x_k^3 * (\rho_{py} * (100 - g_k) + \rho_c * g_k)]} \quad (6)$$

where x_k and g_k are the diameter and chalcopyrite grade (%) of the k^{th} particle in the sample, respectively. The variance in the chalcopyrite grades of the simulated samples was calculated with respect to the population grade:

$$Sample\ Variance = \frac{\sum_s^N (g_s - g_{pop})^2}{N} \quad (7)$$

where g_s is the chalcopyrite grade (%) of the s^{th} sample, g_{pop} is the chalcopyrite grade (%) of the population, N is the number of simulated samples. The sample variances were calculated by simulating and evaluating 100 samples from the populations. Also, some additional simulations were conducted to test whether changing the number of samples affected the calculated sample statistics. Figure 1, for example, showed the sample variances, which are estimated after simulating up to 10,000 samples from a GGS population (n=2, k=25.4 mm). The figure suggests that the sample variances are similar, regardless of the number of samples evaluated. Therefore, changing the number of probabilistic samples does not affect the calculated sample variance.

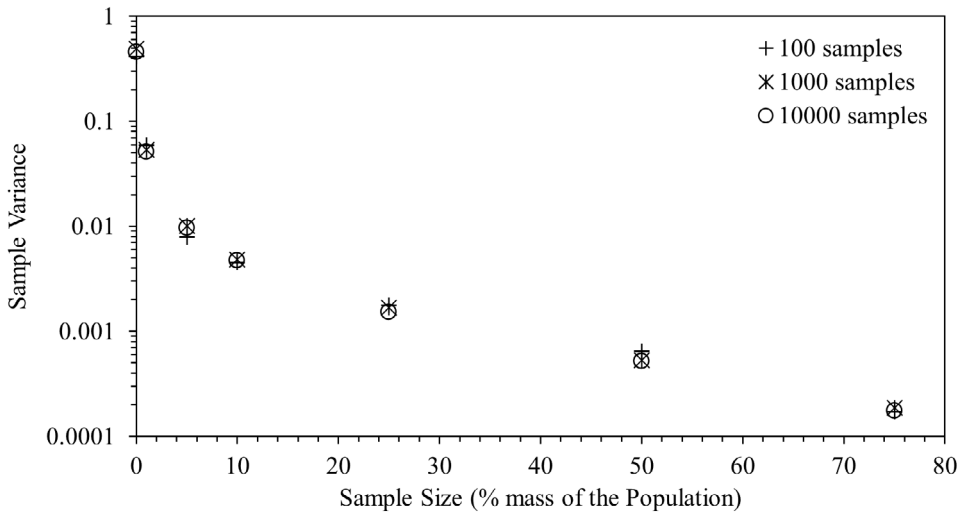

Figure 1. The simulated sample variances from a GGS population (n=2, k=25.4 mm), which are estimated from 100-10000 samples. The samples are taken from the population at unequal masses. The population mass = 100 kg.

RESULTS AND DISCUSSION

Figure 2 shows the mean, maximum and minimum grades of the samples, which are simulated from the GGS or the RRB populations with varying n. The figure suggests that the mean grades of samples are quite similar, but they are not numerically equal to their respective population grade. The result is consistent with Gy's postulation that the mean of the FSE, which is the error of equiprobable sampling, cannot be zero (Gy, 1992). Meanwhile, the distance between the maximum and minimum sample grades varies as a function of the population's size distribution: If the samples are simulated from the GGS populations with increasing n, the distance seems to expand (Figure 2a), suggesting higher variation in sample grades. If the samples are simulated from the RRB populations with increasing n, the difference will funnel (Figure 2b), showing smaller variation in the sample grades. Figure 3 also shows the sample variances, which are estimated after simulating samples from the RRB or the GGS populations with varying n. The figure suggests that the samples from the RRB populations, unlike the ones from the GGS populations, yield smaller sample variance as the n of the population increases. Gy's equation adopts the particle size range as a variable affecting the FSE variance (σ_{FSE}^2):

$$\sigma_{FSE}^2 = \left(\frac{1}{m_s} - \frac{1}{M}\right) * c * L * f * r * d^3 \quad (8)$$

where m_s is sample mass, M is the lot or population mass being sampled, d is the nominal size (95 % passing screen size) of the coarsest particle in the lot, c, L, f, r are the composition, liberation, shape, and size range factors, respectively. It is postulated that the r term in Eq.5 decreases as the ratio between d and the nominal size of the finest particle, i.e., 5 % passing screen size, increases (Gy, 1979; Wills and Finch, 2016). In other words, Eq.8 imposes that the narrower spread of particle sizes, equivalently higher n, should yield higher r and thus higher σ_{FSE}^2. However, wider GGS populations should yield higher sample variances, as discussed early, and demonstrated in Figure 3. Therefore, the sample variances can also depend on the nature of the particle size distribution, which may not be foreseen in Gy's equation.

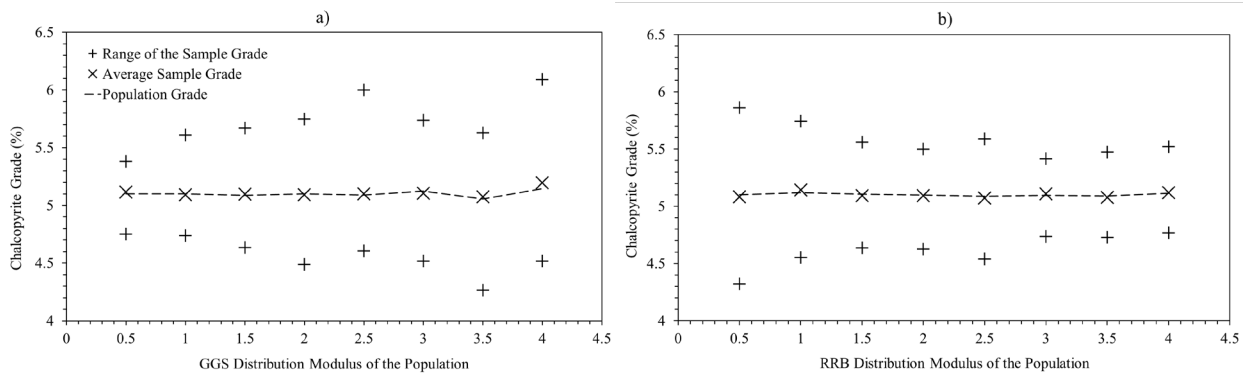

Figure 2. The mean, maximum, and minimum chalcopyrite grades of the samples, simulated from the GGS (a) or the RRB populations (b) with varying n. Population mass = 100 kg, sample size = 1 % mass of the population, number of samples = 100.

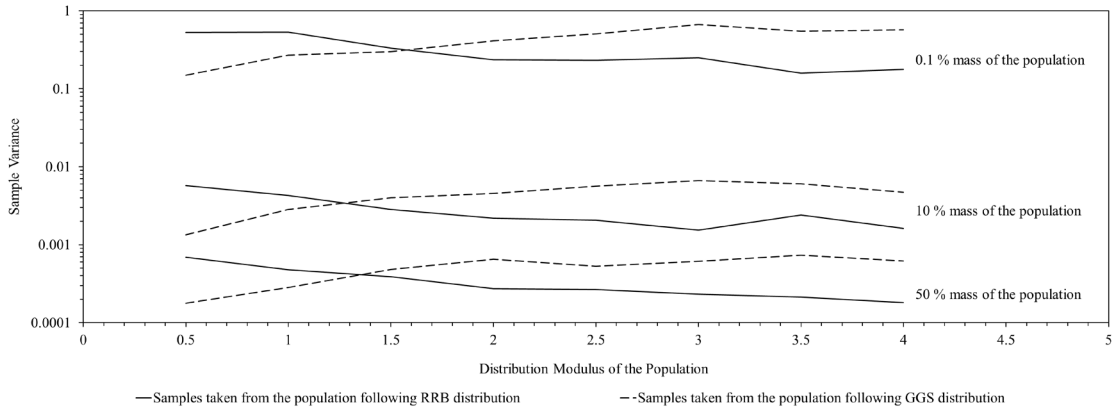

Figure 3. The sample variances that are estimated after simulating samples from the RRB or the GGS populations with varying n. The samples are taken from the populations at unequal masses. Population mass = 100 kg, number of samples = 100.

Figure 4 demonstrates the sample variances that are estimated after simulating samples of unequal masses from the GGS populations with varying n. The figure shows that taking larger samples from the GGS populations should decrease the sample variance as larger samples approach the population. Also, the sample variance can be adequately estimated by using a power function (dashed lines in Figure 4) of sample mass with an exponent of -1.16. This function is comparable with the inverse proportionality between σ_{FSE}^2 and m_s in Gy's Equation (Eq.8). Meanwhile, Figure 4 points out a rapid escalation of the sample variance when the sample size is reduced under 10-15 % mass of the population. Sampling surveys on a binary sand mixture suggested that equal-sized samples by rotary riffling yield lower sample error than the halved mixture by chute riffling or the quartered mixture by coning-quartering (Allen, 2003). These results contradict the fact that larger samples must yield less variance after probabilistic sampling, as observed in Figure 4. Therefore, the author suspects the presence of severe sampling errors on the above methods, which should not be related to probabilistic sampling.

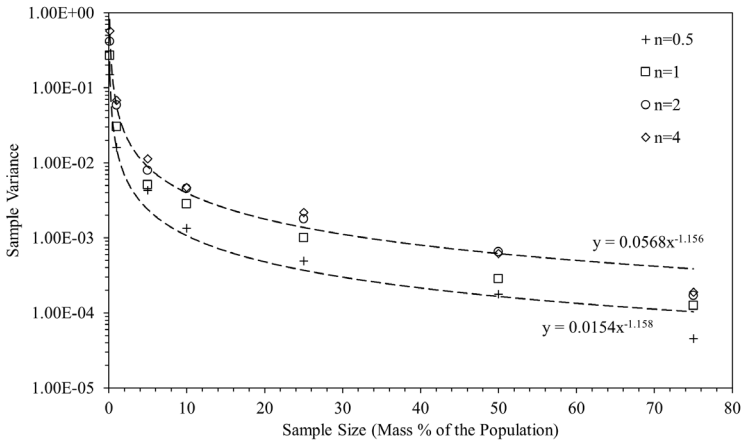

Figure 4. The sample variances that are estimated after simulating samples from the GGS populations with varying n. The samples are taken from the populations at unequal masses. Population mass = 100 kg, number of samples = 100. y = sample variance, x = sample size.

As sample variance propagates very fast under a threshold sample size (Figure 5), taking samples smaller than this threshold mass can cause large variances in the sample grades. Then, instead of collecting such samples directly, it may be beneficial to collect them after successive sampling from relatively larger samples. Figure 5, for example, shows the simulated sample variances after successive halving or quartering of the GGS populations with varying n. The results show that quartering produces smaller sample variance only if the population's n is 1.5. However, the successive halving from other populations can produce a smaller or equal variance, as compared to quartering. These results strongly suggest that successive sampling is superior to direct sampling. However, successive sampling can still suffer from the sampling errors: To demonstrate this fact, samples were simulated from the GGS populations of different masses, simply done at a constant ratio between the sample and population mass, i.e., m_s/M. Figure 6 suggests that taking samples from smaller population masses can yield larger sample variances, which will even escalate if the GGS populations have narrower particle size distribution. Such escalation can be well described by a power function (dashed lines in Figure 6) of the population mass, having a negative exponent between -0.9 and -1.2. Gy's equation (Eq. 8) imposes that the σ^2_{FSE} should be inversely proportional to M at a fixed m_s/M. Therefore, as the mass being sampled reduces at successive sampling, the reduced mass should become more susceptible to sampling errors.

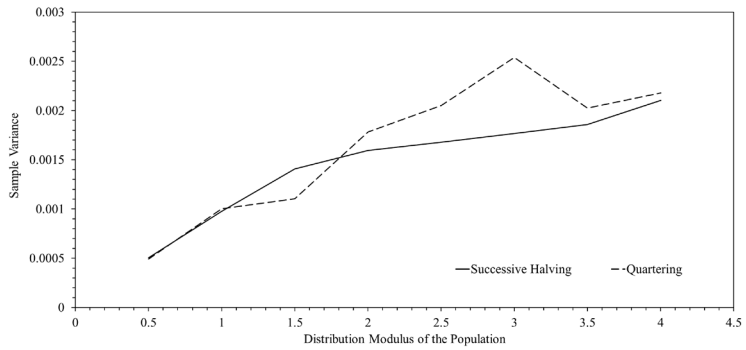

Figure 5. The simulated sample variances after successive halving or single quartering of the GGS populations with varying n. Population mass = 100 kg, sample size = 25 % of the population mass, the number of samples = 100.

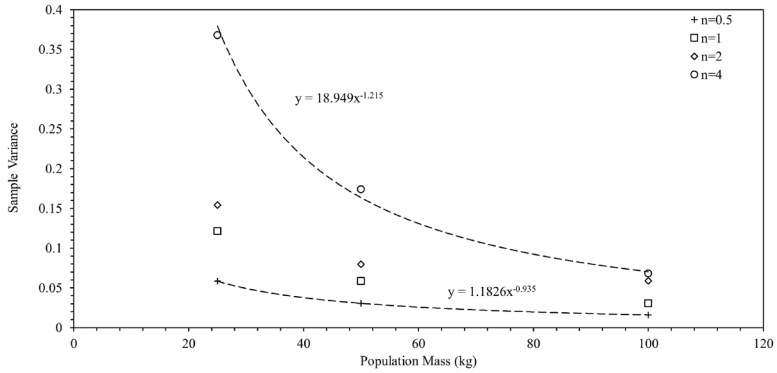

Figure 6. The sample variances that are estimated after simulating samples from the GGS populations with varying n. The populations are generated from unequal masses. Sample size = 1 % of the population mass, number of samples = 100. y = sample variance, x = population mass.

The sampling simulations were conducted on the populations in which chalcopyrite grade was normally distributed in all population particles (Section 2.1). In reality, however, the minerals may be accumulated to specific size fractions in the population, which may bring additional heterogeneity. To assess the impact of this heterogeneity, samples were simulated from a GGS population where chalcopyrite was normally distributed in the finest size fraction. Then, these samples were compared with the ones after chalcopyrite was normally distributed to all population particles. Figure 7 shows that if chalcopyrite is accumulated to the finest size fraction of the population, the sample variances will be 10 to 100 times higher, as compared to the respective variances after chalcopyrite is distributed to all population particles. Therefore, probabilistic sampling becomes inadequate if the target mineral is accumulated to a specific size fraction in the population.

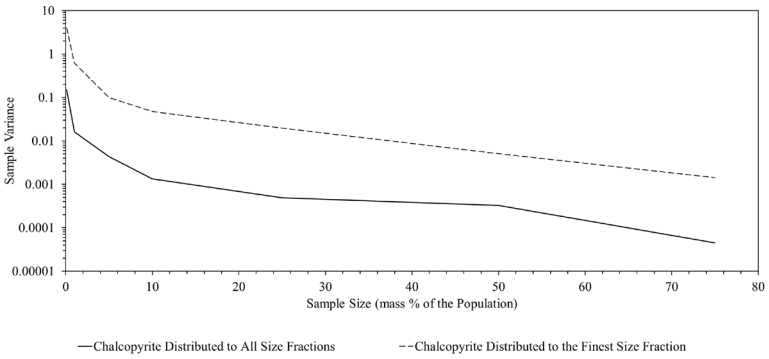

Figure 7. The sample variances that are estimated after simulating samples from the GGS population (n=0.5, k=25.4 mm, chalcopyrite grade = 5.1 %). The samples are taken from the population at unequal masses. Chalcopyrite is either distributed to all size fractions or the finest size fraction in the population. The population mass = 100 kg, the number of samples = 100.

Most of the sampling simulations were conducted on the populations in which the chalcopyrite grade of each particle was randomly generated from a normal distribution with a mean grade (Section 2.1). Also, additional simulations were conducted to assess the effect of the population's mineral grade on sample variance. For this purpose, samples were simulated from the GGS populations (n=0.5, k=25.4 mm) where the chalcopyrite grade of each particle was randomly generated from a normal distribution with varying mean grades. Then the sample variances were plotted as a function of the population grade. As shown in Figure 8, the sample variance yields a bell-shaped curve where the maximum variance is at 45-50 % population grade. It is postulated that the composition variance or σ_{FSE}^2 is

proportional to the product of the grades of the binary compositions (Wills and Finch, 2016): This proportionality causes σ_{FSE}^2 to become maximum at 50 % mineral composition, yet σ_{FSE}^2 will decay to zero as the composition approaches either to 0 or 100 %. Therefore, the bell-shaped curve of sample variance (Figure 8) is consistent with the above postulation, indicating that the probabilistic sampling errors are related to the composition variance. However, as demonstrated in Figure 9, the coefficient of sample variation ($100 * \sqrt{Sample\ Variance}/g_{pop}$) cannot reduce as the population grade reduces from 50 % to zero. Then, the sample variance should be high with respect to g_{pop} as the latter approaches to 0 %. Gy (1992) also pointed out that it would be dangerous to accept negligible FSE if the target content in a lot is concentrated below the ppb (part per billion) range. However, the algorithm could not estimate the sample variance when g_{pop} reduced below ppb level, which could be due to the number format used at the computation. Therefore, the algorithm cannot be used to assess if it is safe to accept negligible sample variances at such trace concentrations.

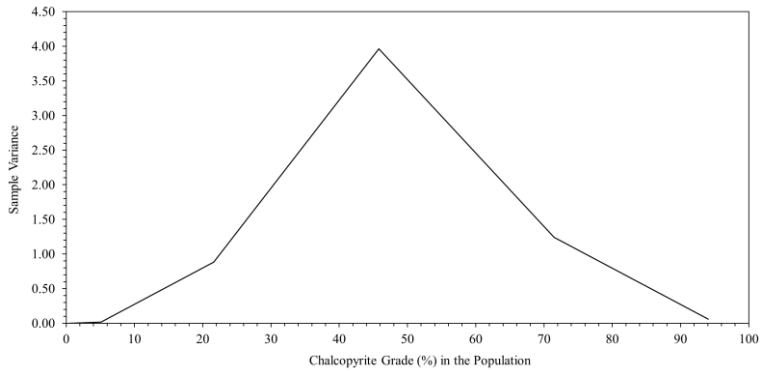

Figure 8. The sample variances from the GGS populations (n=0.5, k=25.4 mm) with varying chalcopyrite grades. The population mass = 100 kg, sample size = 1 % mass of the population, the number of samples = 100.

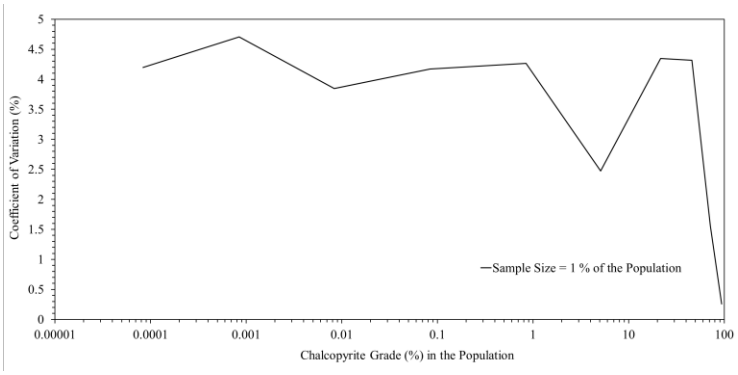

Figure 9. The coefficient of variation in sample grades that are taken from the GGS populations (n=0.5, k=25.4 mm) with varying chalcopyrite grades. The population mass = 100 kg, sample size = 1 % mass of the population, the number of samples = 100.

CONCLUSION

A computational algorithm is presented to simulate probabilistic sampling surveys on the datasets of different particle populations. The algorithm can truly assess the impact of probabilistic sampling surveys on estimating the mineral grade of particle populations. The outcomes of this study are as follows:

The variances in simulated sample grades show that the probabilistic sampling errors are related to the composition heterogeneity. However, these variances also depend on the nature of the population's particle size distribution, which may not be foreseen in Gy's equation. Also, as the mineral grade of the population approaches to 0 %, the sample variance should be very high with respect to the population. Some sampling methods may be susceptible to severe errors, which are not related to probabilistic sampling.

The results also provide some insights on probabilistic sampling surveys: Although successive sampling is susceptible to sampling errors, it may be beneficial to collect small samples by successive sampling from relatively larger samples. Probabilistic sampling surveys are inadequate if the mineral of interest is accumulated to a size fraction of the population. The number of samples taken by probabilistic sampling surveys should not affect the sample variance.

REFERENCES

Allen, T. (2003). *Powder Sampling and Particle Size Determination*. Amsterdam: Elsevier. https://doi.org/10.1016/B978-0-444-51564-3.X5000-1

Gy, P. M. (1976). The sampling of particulate materials — A general theory. *International Journal of Mineral Processing*, *3*(4), 289–312. https://doi.org/10.1016/0301-7516(76)90020-X

Gy, P. M. (1979). *Sampling of Particulate Materials Theory and Practice*. Amsterdam: Elsevier.

Gy, P. M. (1992). *Sampling of Heterogeneous and Dynamic Material Systems: Theories of Heterogeneity, Sampling and Homogenizing*. Amsterdam: Elsevier.

Matsumoto, M., and Nishimura, T. (1998). Mersenne Twister: A 623-Dimensionally Equidistributed Uniform Pseudo-Random Number Generator. *ACM Transactions on Modeling and Computer Simulation*, *8*(1), 3–30. https://doi.org/10.1145/272991.272995

Pitard, F. F. (2019). *Theory of Sampling and Sampling Practice* (Third Edit). Boca Raton: CRC Press.

Pukelsheim, F. (1994). The Three Sigma Rule. *The American Statistician*, *48*(2), 88–91.

Wills, B. A., and Finch, J. A. (2016). *Wills' Mineral Processing Technology*. Amsterdam: Elsevier.

A COMPUTER APPLICATION MODULE EVALUATING ROCK MASS QUALITY RATING

H.O. Dönmez [1, *], H. Tunçdemir [1]

[1] *Istanbul Technical University, Mining Engineering Department*
*(*Corresponding author: donmezhu@itu.edu.tr)*

ABSTRACT

The Rock Mass Quality Rating (RMQR) classification system has become one of the attractive rock classification systems today, due to its up-to-date and user-friendly nature. When the system was proposed in 2014, correlations were also provided for finding out the equivalents of the rock quality score obtained from the RMQR system in other frequently used rock classification systems like RMR and Q. This option has contributed the system easier to use for researchers and engineers. The RMQR system classifies the rock environment according to 6 basic parameters. The ranges given for these parameters and based on the scoring are the issues that should be carefully considered in determining the rock class. In this study, the ranges used to calculate the RMQR system and the relations that digitize them have been converted into MATLAB functions. Based on these converted functions, a Windows-based computer application module has been coded that basically calculates the RMQR, determines the class of the rock and gives its equivalents in the RMR and Q systems. This module, called "RMQRCalc", is an open source software by using the MATLAB graphical user interface, and is considered as a basic module that is a part of rock classification library to be made in this regard.

Keywords: Rock mass quality rating, computer application module, RMQRCalc.

INTRODUCTION

Rock Mass Quality Rating System (RMQR)

For those who will work in the rock environment, it is important to estimate the mechanical properties of the rock environment such as strength and deformation with the least cost and in the most accurate way. This is because the rock classification systems are developed that describe the characteristics of the rock environment from various parameters. One of the newly developed rock classification systems is the Rock Mass Quality Rating System (RMQR) aimed at estimating the geomechanical properties of rock masses. The RMQR System has been developed to better define the physical state of rock masses, bearing in mind the important parameters used in quantitative contemporary rock mass classification systems and avoiding parameter duplication. The system is based on input parameters such as weathering degree, the number of discontinuity sets, discontinuity range, discontinuity condition, groundwater infiltration, and water absorption conditions. The RMQR values ranging from 0 to 100 are determined from the scores assigned to them (Aydan et al., 2014). The system also defines the relationships by some practical equations that calculate the RMQR value from other commonly used rock classification systems or vice versa.

PROBLEM DEFINITION

Rock classification systems are the useful methods that the practitioners perform in the earth science engineering during the feasibility planning phase. Although many rock classification systems have been proposed until now, a few of them have been widely accepted and are actively used. Based on this phenomenon, it is essential creating an electronic library in which the most used rock

classification systems is brought and processed together. For this library, in the current study, initially, a simple computer application module, RMQRCalc, which evaluates RMQR based on Aydan (2014) is coded by the MATLAB graphical user interface. In Figure 1, the complete parameters and their relevant formulations, rock mass class information, and the code interface are given altogether.

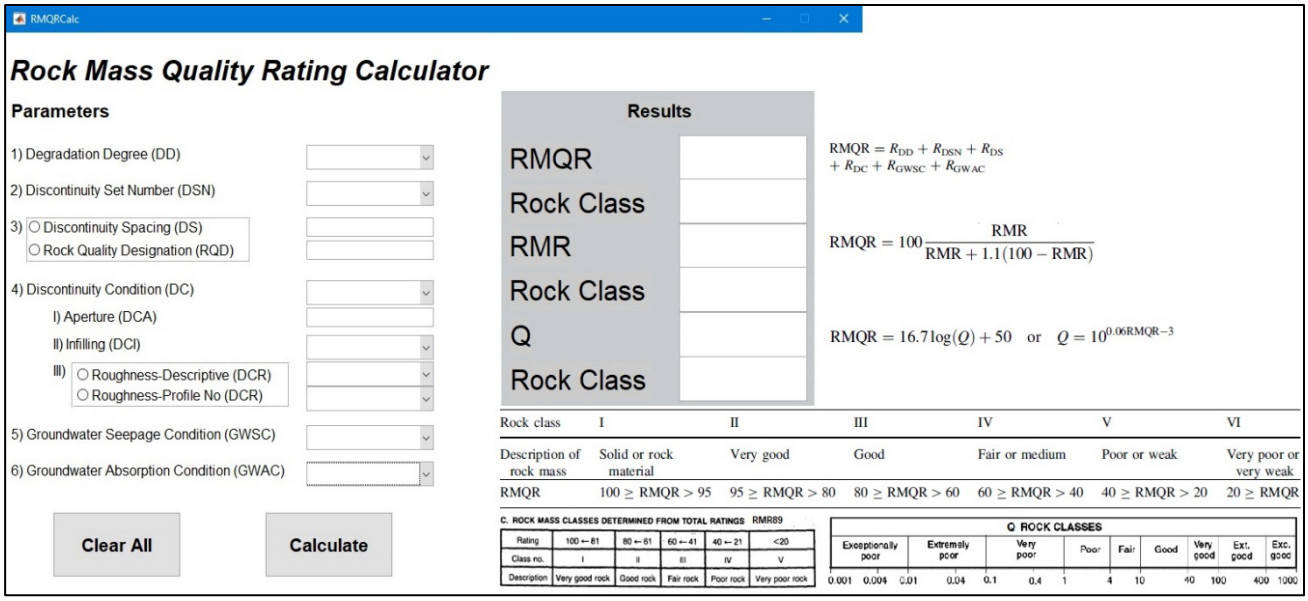

Figure 1. The code interface and parameters in the RMQR calculation based on Aydan (2014)

In RMQR, similar to other rock classification systems, the properties of most parameters are directly selected and rated. While calculating the rock quality in RMQR calculation, 6 parameters in Figure 1 and their corresponding rating values in Figure 2, 3, 4, 5, 6, 7, 8, 9, and 10 are used. These parameters are respectively degradation degree (DD) and R_{DD}, discontinuity set number (DSN) and R_{DSN}, discontinuity spacing (DS) or rock quality designation (RQD) and R_{DS}, discontinuity condition (DC) and R_{DC}, groundwater seepage condition (GWSC) and R_{GWSC}, and Groundwater absorption condition (GWAC) and R_{GWAC}.

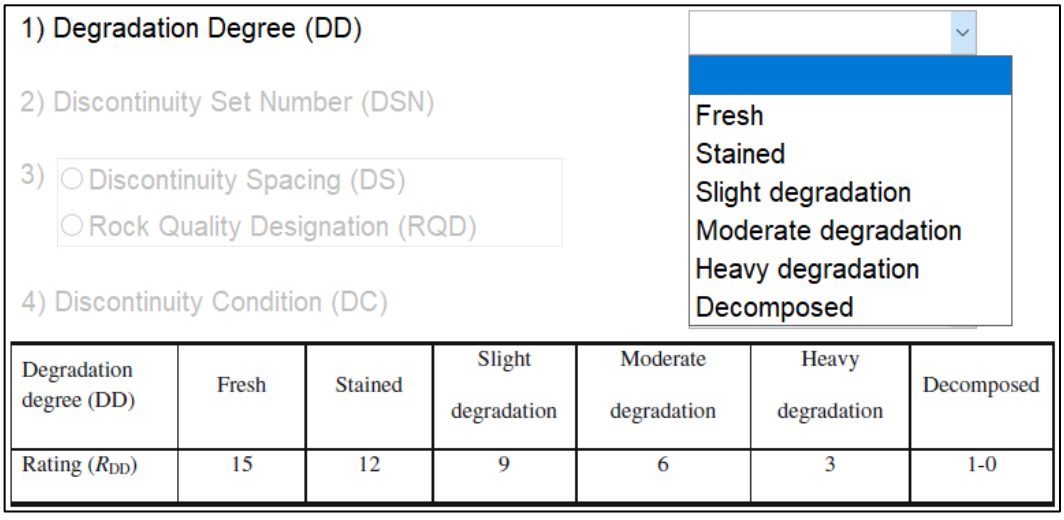

Degradation degree (DD)	Fresh	Stained	Slight degradation	Moderate degradation	Heavy degradation	Decomposed
Rating (R_{DD})	15	12	9	6	3	1-0

Figure 2. Degradation degree (DD) and rating values (R_{DD})

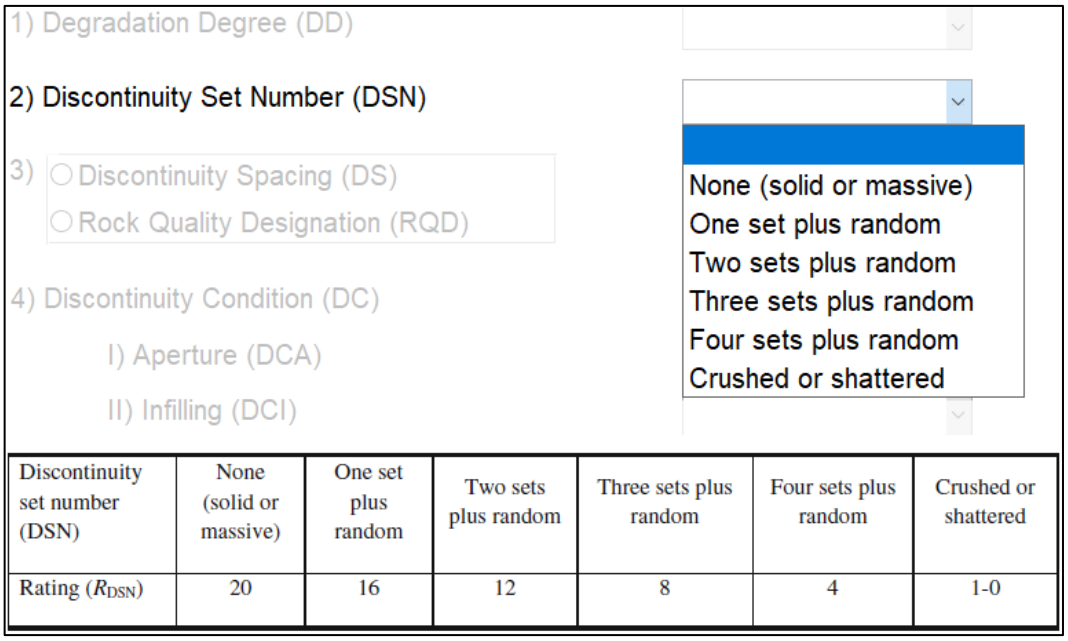

Discontinuity set number (DSN)	None (solid or massive)	One set plus random	Two sets plus random	Three sets plus random	Four sets plus random	Crushed or shattered
Rating (R_{DSN})	20	16	12	8	4	1-0

Figure 3. Discontinuity set number (DSN) and R_{DSN}

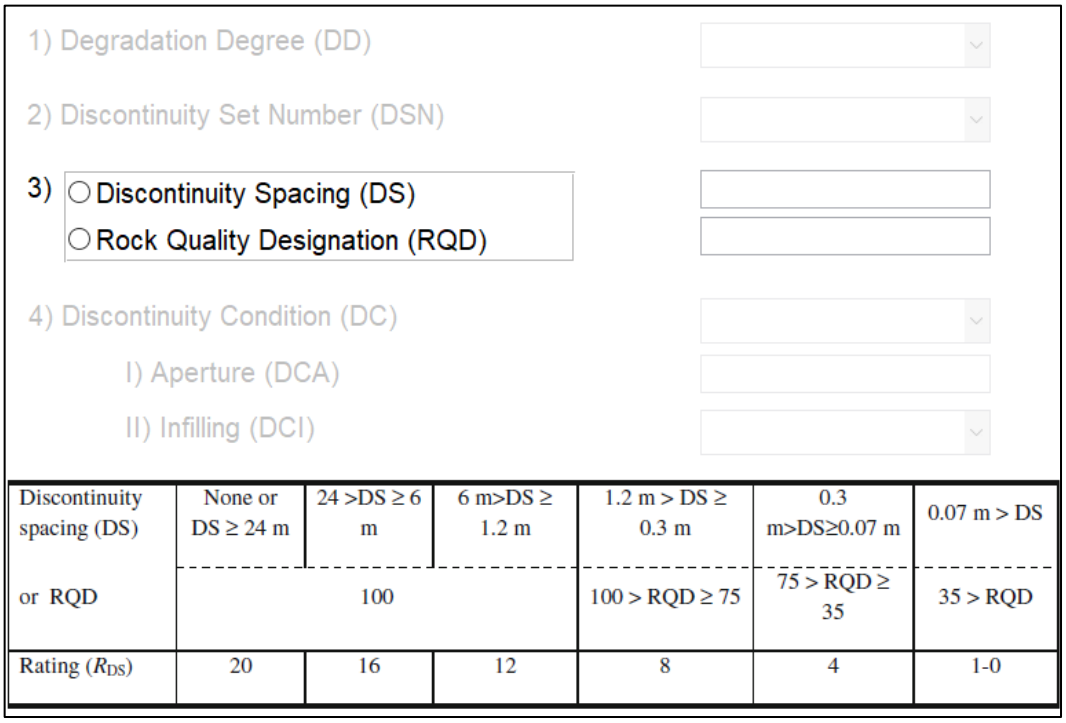

Discontinuity spacing (DS)	None or DS ≥ 24 m	24 >DS ≥ 6 m	6 m>DS ≥ 1.2 m	1.2 m > DS ≥ 0.3 m	0.3 m>DS≥0.07 m	0.07 m > DS
or RQD	100			100 > RQD ≥ 75	75 > RQD ≥ 35	35 > RQD
Rating (R_{DS})	20	16	12	8	4	1-0

Figure 4. Discontinuity spacing (DS) or rock quality designation (RQD) and R_{DS}

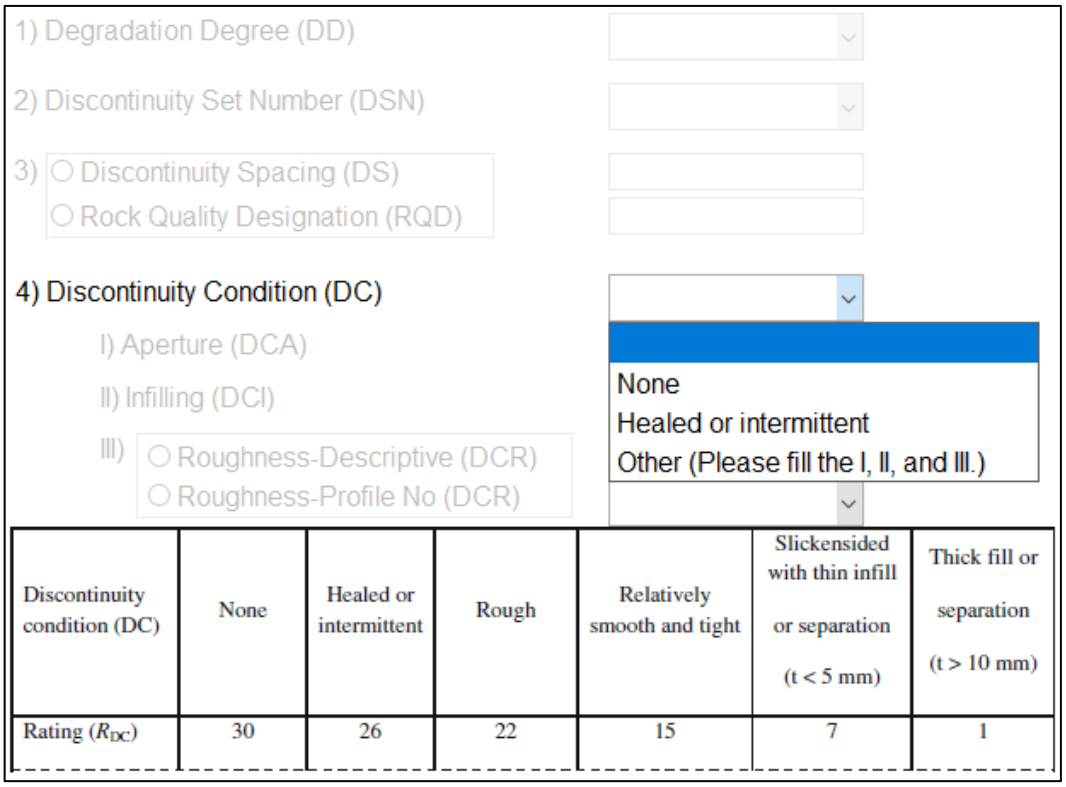

Discontinuity condition (DC)	None	Healed or intermittent	Rough	Relatively smooth and tight	Slickensided with thin infill or separation (t < 5 mm)	Thick fill or separation (t > 10 mm)
Rating (R_{DC})	30	26	22	15	7	1

Figure 5. Discontinuity condition (DC) and R_{DC}

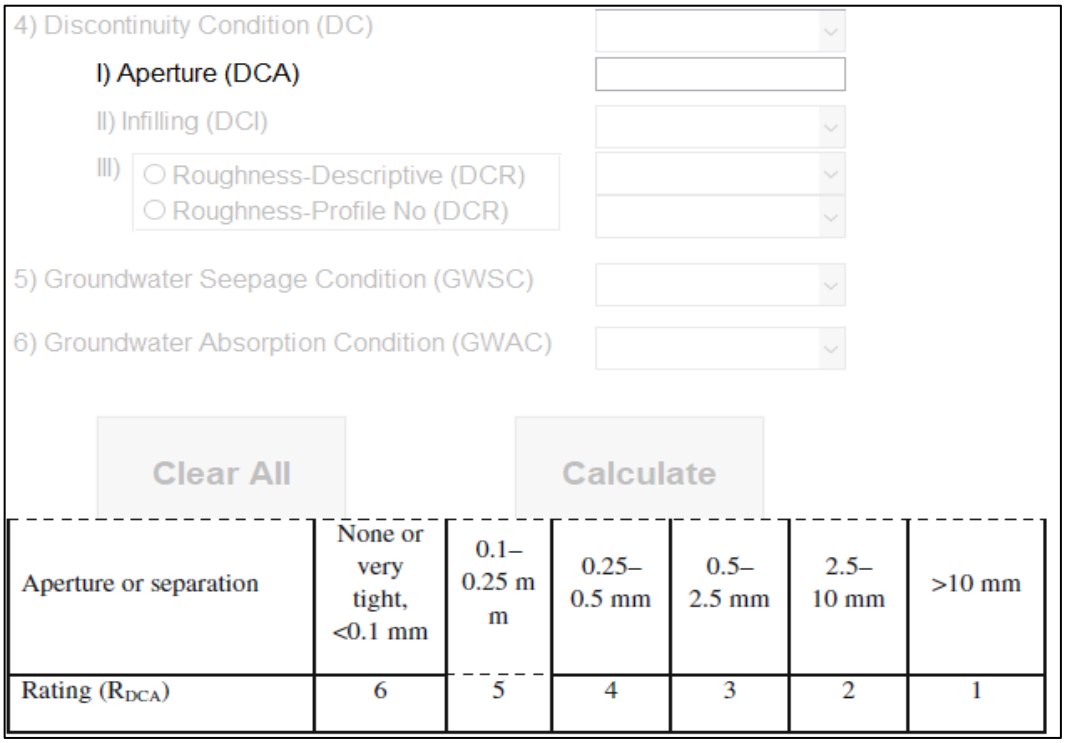

Aperture or separation	None or very tight, <0.1 mm	0.1–0.25 mm	0.25–0.5 mm	0.5–2.5 mm	2.5–10 mm	>10 mm
Rating (R_{DCA})	6	5	4	3	2	1

Figure 6. Aperture or separation (DCA) and R_{DCA}

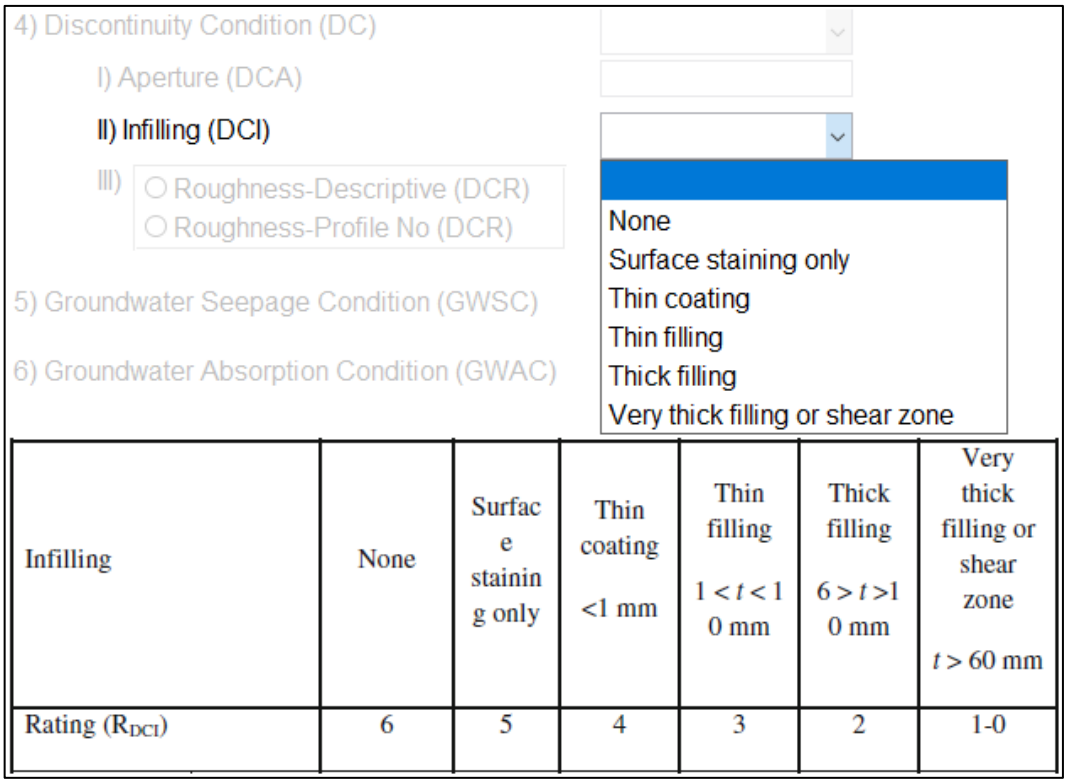

Infilling	None	Surface staining only	Thin coating <1 mm	Thin filling 1 < *t* < 10 mm	Thick filling 6 > *t* > 10 mm	Very thick filling or shear zone *t* > 60 mm
Rating (R_{DCI})	6	5	4	3	2	1-0

Figure 7. Infilling (DCI) and R_{DCI}

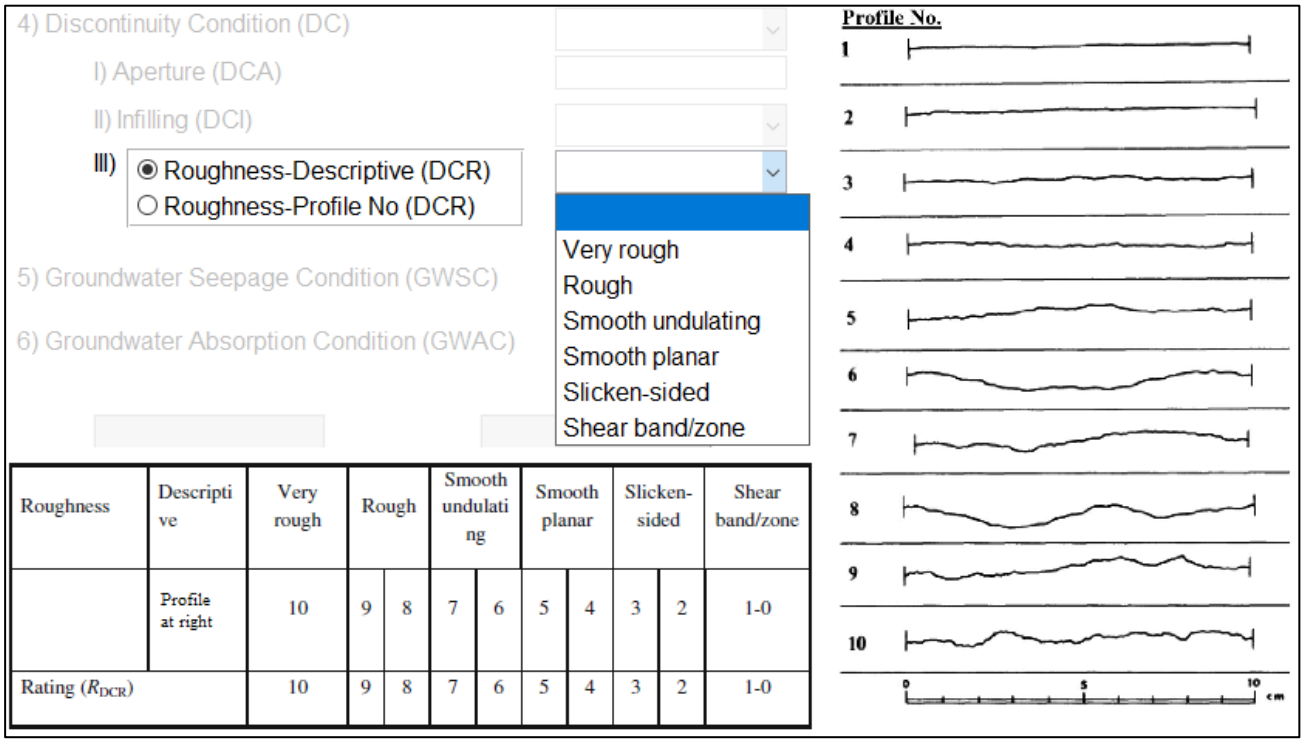

Roughness	Descriptive	Very rough	Rough		Smooth undulating		Smooth planar		Slicken-sided		Shear band/zone
	Profile at right	10	9	8	7	6	5	4	3	2	1-0
Rating (R_{DCR})		10	9	8	7	6	5	4	3	2	1-0

Figure 8. Roughness (DCR) and R_{DCR}

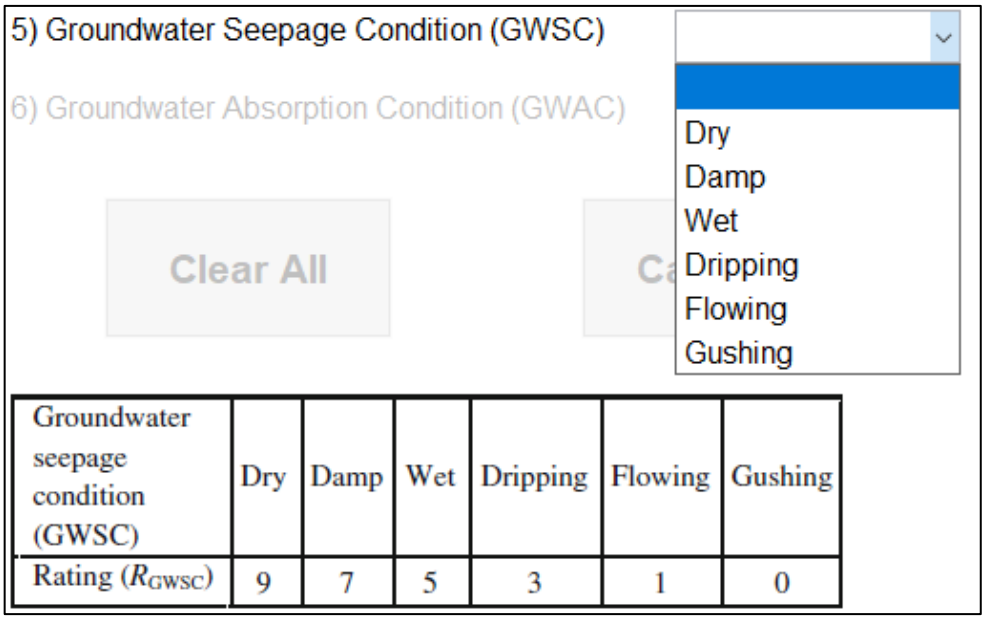

Groundwater seepage condition (GWSC)	Dry	Damp	Wet	Dripping	Flowing	Gushing
Rating (R_{GWSC})	9	7	5	3	1	0

Figure 9. Groundwater seepage condition (GWSC) and R_{GWSC}

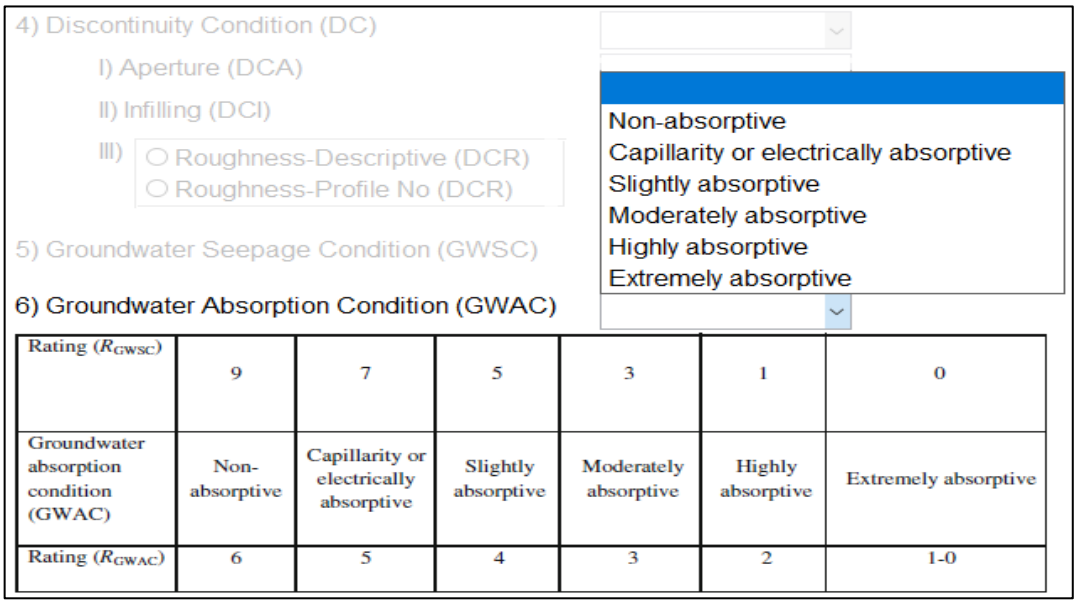

Rating (R_{GWSC})	9	7	5	3	1	0
Groundwater absorption condition (GWAC)	Non-absorptive	Capillarity or electrically absorptive	Slightly absorptive	Moderately absorptive	Highly absorptive	Extremely absorptive
Rating (R_{GWAC})	6	5	4	3	2	1-0

Figure 10. Groundwater absorption condition (GWAC) and R_{GWAC}

The discontinuity condition excluding the classes named by “None” and “Healed or intermittent” is calculated the appropriate parameters in RMQR are represented by some of the functions in the same publication. it is possible to obtain precise results in terms of 2 criteria (DS, DCA) in the system. Among these criteria, the equation proposed by the system for RDS and the equation derived within the scope of this study will be used for RDCA. Except for these two parameters, all parameters are kept constant, and it is shown in Table 1 that the rock class differs for the extreme values of each parameter. But it is not possible to detect this using only the RMQR chart.

Table 1. An example of the problem in calculating RMQR.

Parameter	Values		Ratings		RMQRCalc Ratings	
	Case 1	Case 2	Case 1	Case 2	Case 1	Case 2
1. Degradation degree (DD)	Moderate degradation	Moderate degradation	6	6	6	6
2. Discontinuity set number (DSN)	Three sets plus random	Three sets plus random	8	8	8	8
3. Discontinuity spacing (DS)	1.1	0.3	8	8	9.46	5.83
4. Discontinuity condition (DC)						
a) Aperture or separation	0.26	0.49	4	4	4.73	4.11
b) Infilling	Thin coating <1 mm	Thin coating <1 mm	4	4	4	4
c) Roughness	Smooth undulating	Smooth undulating	6	6	6	6
5. Groundwater seepage condition (GWSC)	Dripping	Dripping	3	3	3	3
6. Groundwater absorption condition (GWAC)	Moderately absorptive	Moderately absorptive	3	3	3	3
RMQR			42	42	44.19	39.94
Rock Class			Fair or medium	Fair or medium	Fair or medium	Poor or weak

METHODOLOGY

The aim of this study is to turn the RMQR system, which is a module of the electronic rock classification library to be created, into a computer program. Thus, the system will become more useful and capable of more precise classification.

In the RMQR system, scores for degradation degree (DD), discontinuity set number (DSN), infilling (DCI), roughness (DCR), groundwater seepage condition (GWSC) and groundwater absorption condition (GWAC) parameters consist of direct selections. In this section, users are directly selected without making any changes. However, it is possible to score more precisely by using the equations for Discontinuity spacing (DS), RQD and Aperture (DCA). Here, the equations given in the publication (Aydan et al., 2014) were used for DS and RQD, and the equation derived in this publication for DCA (Figure 11).

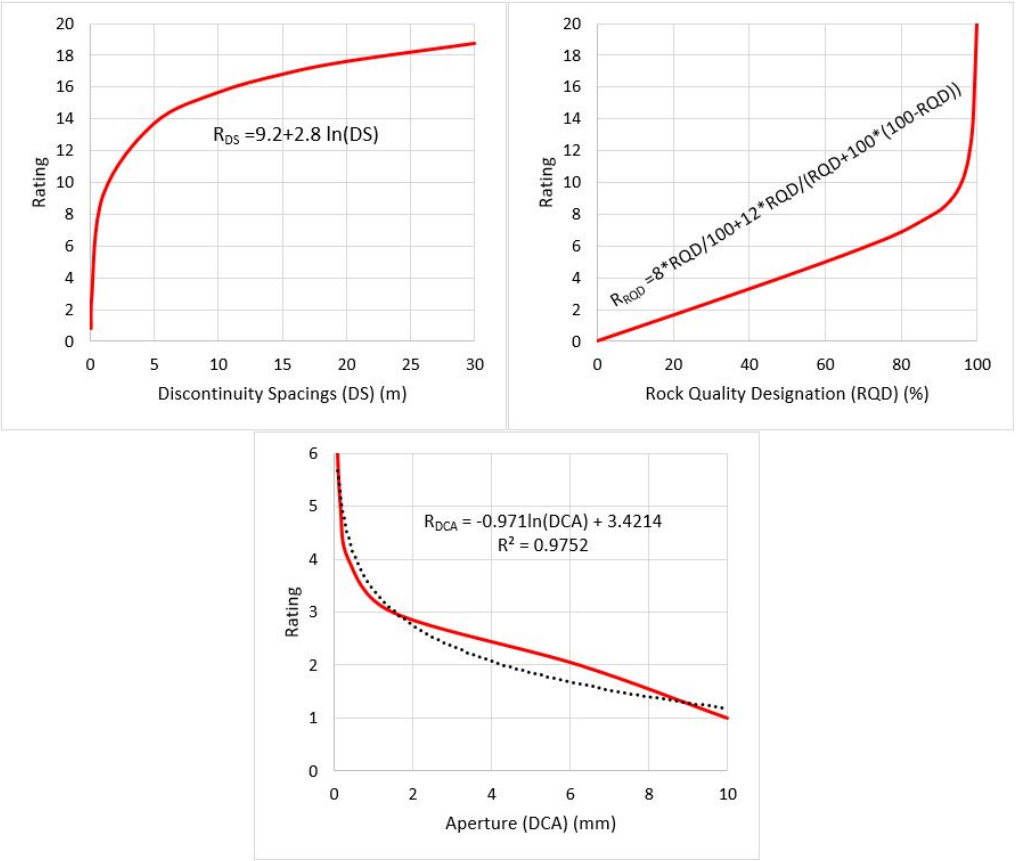

Figure 11. Curves of equations used in RMQRCalc

THE COMPUTER APPLICATION RMQRCalc

A Windows-based computer application named 'RMQRCalc' has been developed to obtain an accurate classification and an easy-to-calculate RMQR. The RMQRCalc application was designed using the MATLAB graphical user interface (GUI). The RMQRCalc obtains scores for each parameter from the values typed or selected by a user, thanks to the functions derived, and calculates the RMQR for the sum of these scores. Based on the RMQR value it has obtained, it gives its equivalents in the RMR (Bieniawski, 1989) and Q (Barton et al., 1974) systems. It determines the rock classes of each system. Screenshot of the application is given in Figure 12.

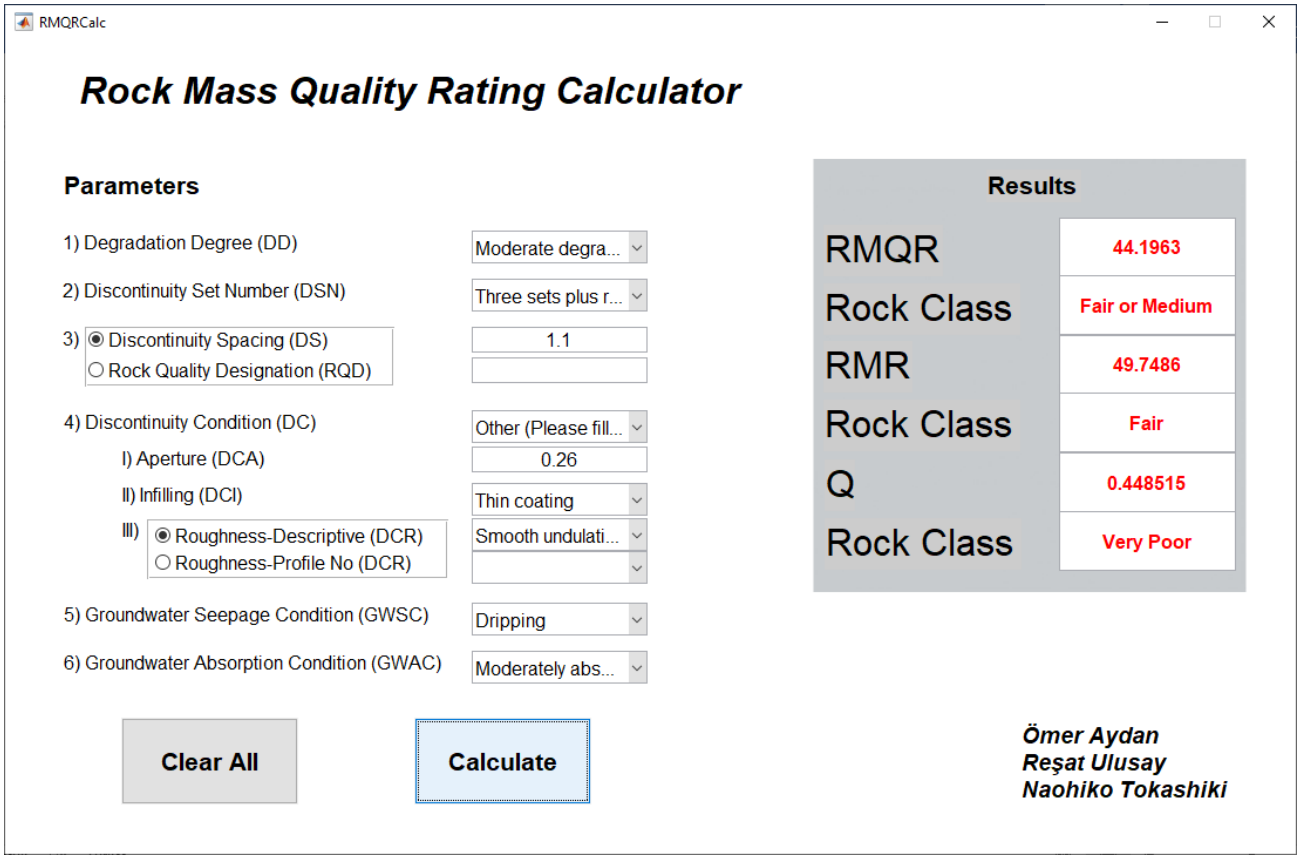

Figure 12. Screenshots from the RMQRCalc application

The program can be accessed free of charge from the link shared under this notice. The published version is 1.0 and the program will be updated with the studies and feedbacks, and access will be provided from the link.

RESULTS

The RMQR system proposed by Aydan et al. in 2014 was coded in the MATLAB graphical user interface and turned into a windows-based computer application. With the equations suggested by Aydan et al. and the equation suggested in this publication, the system has been made more precise classification. It is planned that this study will be a module of the electronic rock classification library. The program is shared with the link in this study, open to the access of all participants.

REFERENCES

Aydan, Ö., Ulusay, R., and Tokashiki, N. (2014). A New Rock Mass Quality Rating System: Rock Mass Quality Rating (RMQR) and Its Application to the Estimation of Geomechanical Characteristics of Rock Masses. *Rock Mechanics and Rock Engineering*, 47, 1255–1276.

Bieniawski, Z.T., 1989. Engineering rock mass classifications: a complete manual for engineers and geologists in mining, civil, and petroleum engineering. John Wiley & Sons.

Barton, N., Lien, R., & Lunde, J. (1974). Engineering classification of rock masses for the design of tunnelsupport (NGI Publication No. 106, p. 48). Oslo: Norwegian Geotechnical Institute.

RMQRCalc Link: https://kovan.itu.edu.tr/index.php/s/dy8DBMOLi9XCNM5

A HYBRID SEMI-QUANTITATIVE APPROACH FOR MINE CLOSURE RISK MANAGEMENT IN ANGURAN MINE, IRAN

N. Samadinia [1], M. Osanloo [1, *], S. Amirshenava [1]

[1]*Amirkabir University of Technology, Department of Mining Engineering*
([*]Corresponding author: morteza.osanloo@gmail.com)

ABSTRACT

Mining is temporary land use, and the mine life ends with the exhaustion of mineable reserve or other factors that lead mine to unplanned closure. Premature mine closure is associated with various risks. Deviation from achieving sustainable development (SD) goals is the main consequence of premature mine closure risks. The present study aimed to implement the risk management of premature mine closure and mine closure impacts. In this regard, the comprehensive approach was proposed to identify the causes that led mine to close prematurely. In addition, the impacts of mine closure risks were assessed, and the risk treatment stage was investigated to prevent or diminish the detected risks in each stage. Mine reclamation is a risk treatment option that requires the selection of suitable Post-Mining Land Use (PMLU). The suitable PMLU option is chosen based on the identified and assessed risks. To this end, a two-dimensional (2D) risk model and Multi-Criteria Decision Making (MCDM) methods were developed. The Anguran mine was selected as a case study; the results showed that the final product price reduction is the most critical reason that threatened the lead and zinc of Anguran mine to early closure. To treat this risk, by analyzing the correlation between the prices of different metals and availability factors, iron investment simultaneously was proposed to the mining company due to its adverse correlation with the price of zinc and lead. Besides, among the mine closure risks, the highest risk level is related to economic risks. To appropriate response against the recognized impacts of mine closure risks, the recreation center was recommended as the suitable PMLU.

Keywords: Premature mine closure, sustainable development, risk management, mine reclamation, multi-criteria decision making

INTRODUCTION

Mining activities promote economic growth and improve the region's social conditions, but premature mine closure will create many challenges for the area (Laurence, 2006). It is noteworthy that a significant proportion of mines are closed prematurely due to environmental, economic, and social factors (Laurence, 2006; Minaei Mobtaker and Osanloo, 2015). Premature mine closure has environmental, safety, health, social, financial, and technical risks. These occurrences can pose several challenges to achieving the region's sustainable development (SD) goals (Laurence, 2001; Kung et al., 2020). In countries with rich resources but poor government management, mine closure risks are more severe (Cui et al., 2020). Therefore, it is vital to forecast the factors that cause the mine to close prematurely and implement the risk management approach. The risk management process is a comprehensive strategy for investigating and assessing identified risks and managing high-level risks that can make an unsustainable situation (ISO 31000, 2009).

The risk management process includes three stages: risk identification, risk assessment, and risk treatment. Various researchers have considered the risk management process in the mine closure plan. (Mansouri et al., 2014; Mercer and Biggs, 2013; Sanders et al., 2019; Tones et al., 2021). However, these

cases have not developed a comprehensive approach to implement all risk management stages in mine closure. After risk identification, the most appropriate method should be considered for the risk assessment process. Numerous methods exist for assessing the risks; nevertheless, the 2D risk model is the most common method for mine closure (Gheisari et al., 2014; Laurence 2001; Kadir et al., 2017). In 2018, Amirshenava and Osanloo developed the 3D risk matrix considering the time factor in the risk management process. Implementing the mine reclamation plan and choosing the Post-Mining Land Use (PMLU) are the best procedures for the risk treatment stage. Mine reclamation can make the conditions of the mined lands safe and stable and decrease or eliminate the adverse impacts of mining activities on the site. Thus, mine reclamation based on the identified and assessed risks can be deemed a practical effort to improve the situations for Sustainable Development (SD) of the region (Amirshenava and Osanloo, 2021; Laurenece, 2011; Sloss, 2013;). Reclamation planning begins from the exploration level and is completed at the end of the mine life cycle (Lappi, 2020; Osanloo, 2017). Figure 1 shows the mine life cycle and each stage's importance based on the time and the labor force required (ICMM, 2012b).

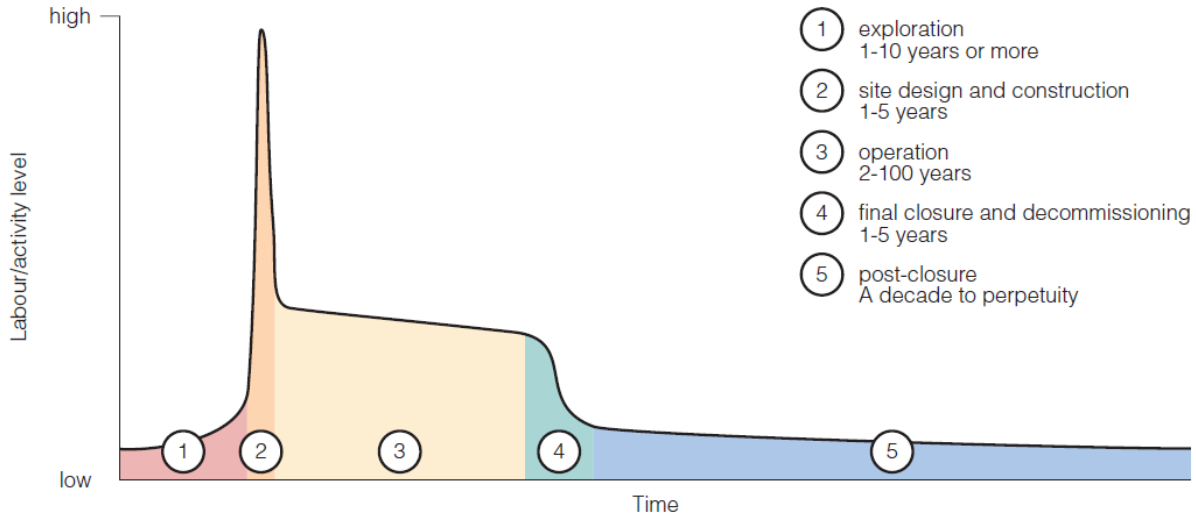

Figure 1. Mine project life cycle (ICMM, 2012b)

In choosing PMLU, the opinions of all stakeholders should be considered. Stakeholders can include local people, environmental experts, economic teams, and law authorities (Galvin, 2017; Hajkazemiha et al., 2021; Mborah et al., 2016). A reclamation plan is crucial in the mine life cycle because it covers the risks of premature mine closure and balances the consequences of mining operations in the region. According to the regions' situation, several PMLU can be selected for mined lands.

A noteworthy point in the present study is implementing the comprehensive approach for the risk management of mine closure. In this regard, as the first step, the risks that led mine to close earlier have been recognized. In the next step, the probable consequences of the mine closure were assessed. For these aims, risk levels are classified using the 2D risk assessment matrix. The most suitable PMLU has been investigated based on the determined high-level risks. To this end, the Multi-Criteria Decision Making (MCDM) method was considered the best way to figure out the most proper PMLU. Finally, the proposed comprehensive approach is verified in Iran's lead and zinc mine.

METHODOLOGY

This study seeks to provide a solution to reduce or avoid the risks of mine closure. As shown in Figure 2, a comprehensive risk management approach was developed in three stages.

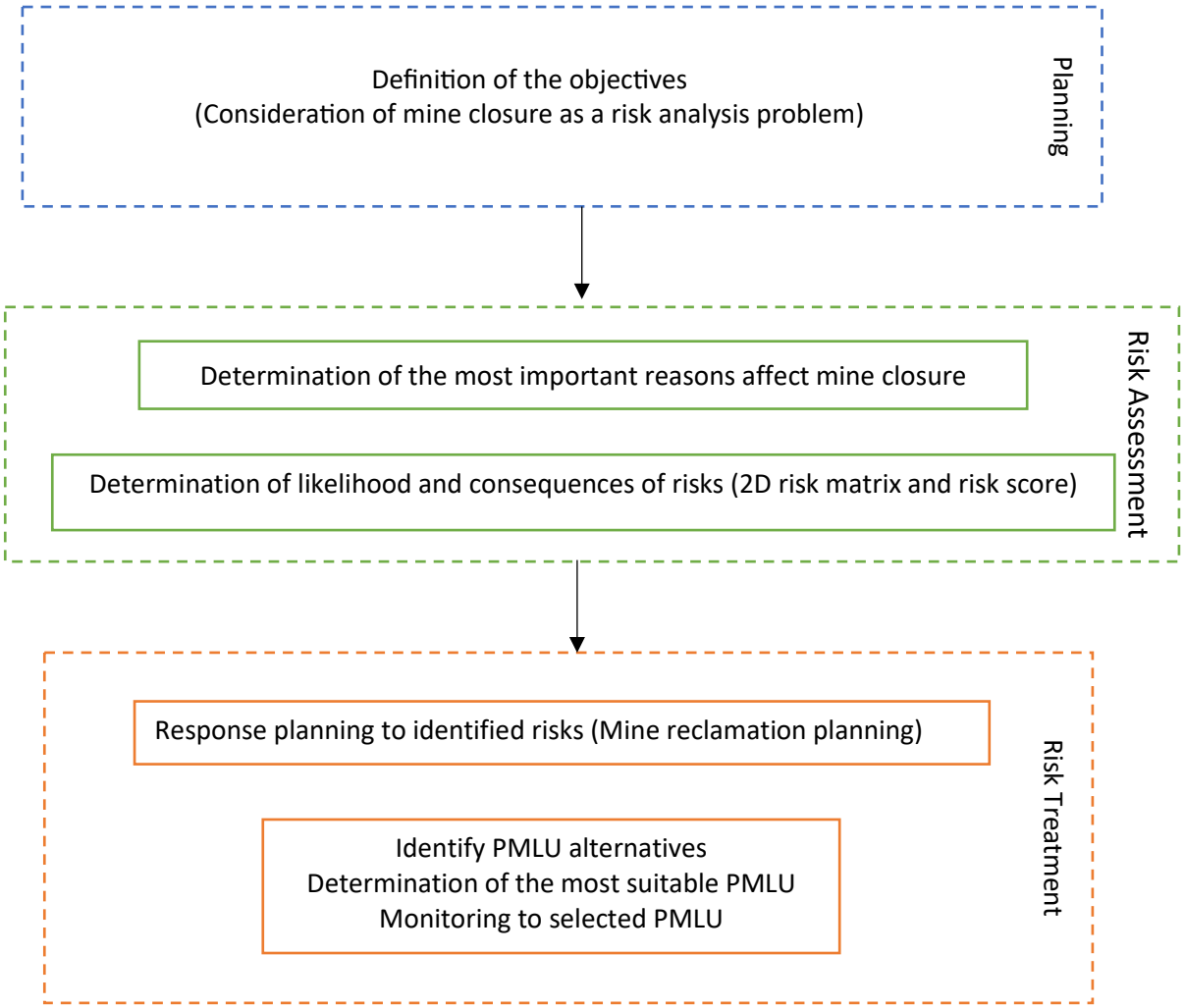

Figure 2. The framework of the mine closure risk management

Planning

The first step in the risk analysis process is problem definition and information gathering. The problem is defined as diminishing or avoiding the impacts of premature mine closure. In this regard, the Anguran mine was selected as a case study. Anguran is located 445 km northwest of Tehran in Zanjan province (Figure 3). The climate condition in this mine is cold and semi-arid. The average annual precipitation in this site is 347 mm (IMPASCO, 2021).

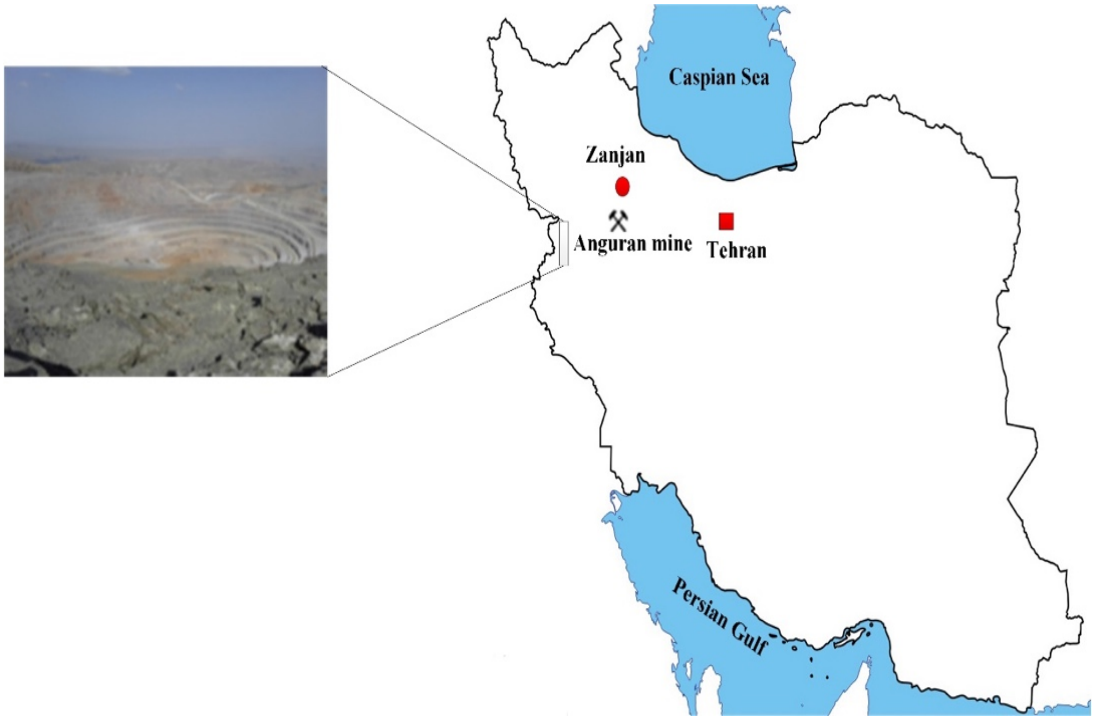

Figure 3. The Anguran mine in 445 Km of Tehran- Capital of Iran

Risk Assessment

At this risk management stage, the causes of premature mine closure risks are first identified. The probable consequences of this risk are then discussed. Semi-quantitative methods have been developed for achieving the results in this study. Qualitative methods are not accurate enough, and quantitative methods have complex calculations; Therefore, semi-quantitative methods are often used for risk analysis (Cui et al., 2020). The two-dimensional risk matrix is the basis of the research. In this risk matrix, one dimension represents the likelihood of the risk occurrence, and the other represents the risk intensity. Each matrix array converts qualitative expressions such as high, medium, and low into quantitative parameters (Amirshenava and Osanloo, 2019). Tables 1 and 2 illustrate the related causes and the possible consequences of premature mine closure.

Table 1. Causes of premature mine closure

Code	Causes of premature mine closure
R1	Increasing operating costs
R2	Reducing the price of the final product of the mine
R3	End of open-pit mining
R4	Loss of the final product sales market
R5	Overestimating of grade and tonnage
R6	Facing faults, joints, and complex geological conditions
R7	collapses of the mine pit wall
R8	Failure of tailing dam
R9	AMD generation
R10	Contamination of surface and groundwater
R11	Contamination of soil with toxic elements

R12	Excessive equipment depreciation
R13	Defect or lack of mining equipment
R14	Changing government policies under pressure from lawmakers
R15	Existence of disputes and conflicts in the ownership of the mine site
R16	The local people are against mining

A team of 10 experts was determined to answer the related questionnaires. These experts consist of engineers and managers of Anguran mine in different fields. First, after predicting the risk factors associated with premature mine closure, experts were asked about the likelihood and intensity of each risk factor occurrence. The classification of score range was formed between one and five, and the closer the score is to five, the higher the probability of occurrence and the severity of each risk factor. The Risk Score (RS) is obtained by multiplying the likelihood and intensity of risk factor occurrence. 2D risk matrix can be formed with the RS. After calculating the RS, risk levels can be categorized into three levels. Table 3 shows the relationship between the RS and risk levels.

Table 2. Consequences of premature mine closure

Code	Mine closure Risks
C1	Decreasing economic growth in the region
C2	Unexploded blast hole
C3	Decreasing skills in the region
C4	Falling into the pit
C5	Pit slop failure
C6	Unemployment
C7	Inability to pay employees' salaries
C8	Dust
C9	Changing people's lifestyles
C10	Water pollution
C11	Soil pollution
C12	AMD generation
C13	Increasing crime and violence in the region
C14	Failure to complete the reclamation plan
C15	Inability to repay debts and loans
C16	Inability to pay taxes to the government

Table 3. The relationship between the RS and risk levels

Risk Score (RS)	Risk Level	Color code
$\mathbf{RS} < 4$	Low	
$4 \leq \mathbf{RS} \leq \mathbf{14}$	Moderate	
$RS > \mathbf{14}$	High	

Risk Treatment

After the risk planning and risk assessment, an appropriate response should be considered to the identified risks. Risk response or treatment can be carried out to avoid, reduce, optimize, and transfer risks (Amirshenava and Osanloo, 2021). The best solution to risk treatment is mine reclamation. After reducing the site's pollution, mined land is prepared for PMLU implementation in the reclamation plan (Maqsoud et al., 2021). According to the mine's identified risks and general conditions, PMLU alternatives are shown in Table 4.

Table 4. Classification of PMLU alternatives

ID	PMLU	Description
P1	Agriculture	Arable land to produce the crop and earn money
P2	Forestry	Production commercial lumbers and creating a beautiful landscape
P3	Lake or Pool	Aquaculture, fishing pond, boating
P4	Construction	Construction of residential, educational, and industrial complexes
P5	Wildlife habitat	Natural parks
P6	Recreation center	Sports field, sailing, hunting, park, museum or exhibition
P7	Solar power station	Establishment of a solar power plant at the mine site

Finding the best alternatives for PMLU, related criteria were determined. Experts give a score between 1 and 10 for each option considering different criteria. A low score indicates minor positive importance, and a high score represents a high positive significance. Nevertheless, this definition is reversed in the case of capital and operating costs due to their negative nature. Table 5 illustrates the decision-making criteria for choosing the suitable PMLU.

Table 5. Decision-making criteria in PMLU selection

code	criteria
M1	Capital cost
M2	Operating and monitoring cost
M3	Increasing the income of local communities
M4	Creating job opportunities
M5	Flexibility with the local lifestyle
M6	Exposure to sunlight
M7	Precipitation
M8	Access to water resources
M9	Impact on desertification
M10	Land slope
M11	Soil quality
M12	Access

TOPSIS method is the most proper for solving this problem (Hwang and Yoon, 1981). The average and standard deviation of experts' scores to each factor are decision-making criteria. Based on the defined criteria, the most suitable PMLU can be selected.

RESULTS

Determining the Causes of Premature Mine Closure

The average and standard deviation of the experts' scores to each risk factor are shown in Table 6. Also, the risk factors are arranged by calculating the similarity index in Figure 4. According to the results, the final product's price reduction (R2) has been obtained as the most crucial reason for the early closure of the Anguran mine. The decline of minerals prices is inevitable because it is affected by many uncertainty parameters that are not easy to forecast. However, historical analysis of prices helps obtain future metals price trends, which can inform mining managers and engineers about the future conditions to take proper action.

Table 6. Result of risk causes analysis

Code	Causes of premature mine closure	Average	Standard deviation
R1	Increasing operating costs	1	0
R2	Reducing the price of the final product of the mine	2	0
R3	End of open-pit mining	2.875	0.330719
R4	Loss of the final product sales market	2.75	0.433013
R5	Overestimating of grade and tonnage	2	0
R6	Facing faults, joints, and complex geological conditions	3	0.866025
R7	collapses of the mine pit wall	2.125	0.927025
R8	Failure of tailing dam	1.875	0.330719
R9	AMD generation	2.75	0.433013
R10	Contamination of surface and groundwater	2.75	0.968246
R11	Contamination of soil with toxic elements	2.625	1.111024
R12	Excessive equipment depreciation	2.5	0.707107
R13	Defect or lack of mining equipment	2.25	0.433013
R14	Changing government policies under pressure from lawmakers	2.75	1.391941
R15	Existence of disputes and conflicts in the ownership of the mine site	1.875	0.599479
R16	The local people are against mining	1.5	0.5

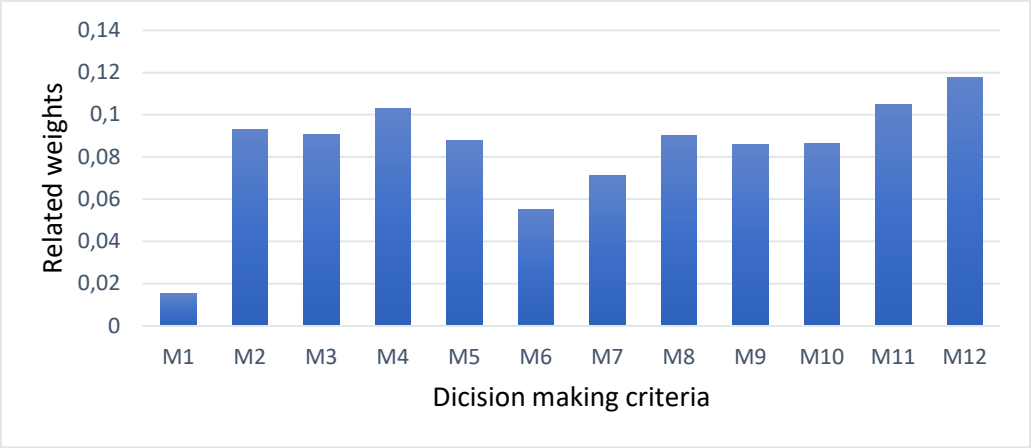

Figure 4. Comparison ranking of risk factors

Risk Matrix of Premature Mine Closure

According to Table 3, risk levels are divided into low, medium, and high-risk categories. Table 7 represents the result of the risk assessment. In addition, the 2D risk matrix is obtained by considering the likelihood in one dimension and the intensity of occurrence values in the other dimension. Figure 5 illustrates the 2D risk matrix.

Table 7. Results of risk assessment

Code	Likelihood	Consequences	RS	Color code
C1	3.25	3.5	11.375	
C2	2.5	2.25	5.625	
C3	2.75	3	8.25	
C4	3.25	3.25	10.5625	
C5	2.125	2	4.25	
C6	4	4.75	19	
C7	4.25	4.25	18.0625	
C8	1.625	1.625	2.640625	
C9	1.125	1.125	1.265625	
C10	2.25	2.25	5.0625	
C11	3	3.25	9.75	
C12	2.875	2.875	8.265625	
C13	1	1	1	
C14	2	1	2	

C15	2.25	2.125	4.78125	
C16	2.625	2.625	6.890625	

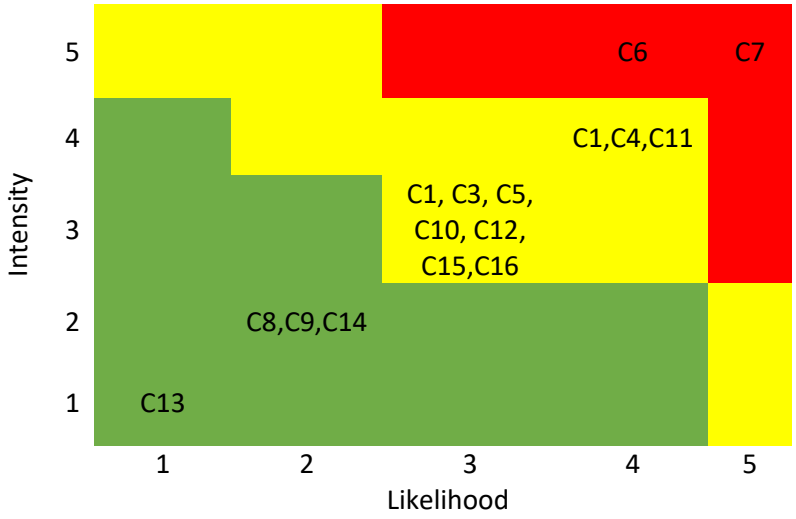

Figure 5. 2D risk matrix

Based on the results in Figure 5, many identified risks (63%) belong to the medium risk level (RS between 4 and 14). Unemployment and the inability to pay staff salaries (C6, C7) are at the highest risk of premature mine closure (RS is more than 14). Thus, making the necessary efforts to control these threats should be a priority for the mining company.

Determining of PMLU

Based on the MCDM method, a comparison between appropriate alternatives for PMLU has been developed. In Figure 6, the results of the TOPSIS method for selecting the suitable PMLU have been shown.

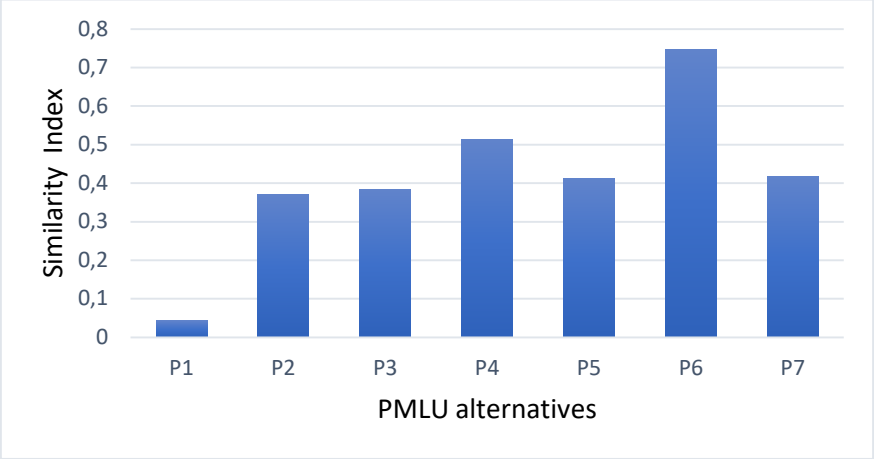

Figure 6. Results of PMLU ranking by the TOPSIS

According to Figure 6, recreation centers (P6) were obtained as the most suitable PMLU for the Anguran mine. Recreation centers can include sports complexes, boating, parks, museums, or exhibitions. Recreation centers can generate a sustainable income in the region. Therefore, by choosing this PMLU, the main risks due to the mine closure (C6, C7) are reduced or prevented.

DISCUSSION

Premature mine closure poses many risks to the mining area. These risks can be a threat to achieving the goals of SD. Therefore, in modern mining, mine closure risk management plays a vital role in maintaining mining activities in line with the principles of SD. The study evaluated premature mine closure by developing the 2D risk model and MCDM techniques. Compared to other similar studies, this research is preferred because it considers all stages of the risk management in the mine closure problem. In the planning stage, the problem was defined, and information was collected. In the risk assessment stage, recognizing possible risks that led mine to close earlier has been carried out. Finally, the most suitable PMLU was selected by MCDM analysis to treat the detected threats. For reducing the harmful impacts of mining activities, the implementation of reclamation projects has a significant role. Different reclamation methods are applied for different mines according to mineral type, mining methods, ecosystem, climate conditions, and legal requirements.

The results indicated that the final product's price reduction was known as the most crucial reason for premature mine closure. The best solution for avoiding the detected risk factor is investing in other minerals industries. In this regard, historical data of lead and zinc prices were collected and compared with other mineral prices (LME, 2021). Based on the correlation between lead and zinc prices with other minerals, correlation coefficients have been illustrated in Table 8.

Table 8. Correlation coefficients of mineral prices (January 2010 to October 2021)

	Zn	Pb	U	Pa	Al	Sn	Ag	Pt	Ni	Au	Cu	Fe
Zn	1.00	0.82	-0.49	0.44	0.79	0.37	-0.04	-0.38	-0.01	0.16	0.24	0.02
Pb	0.82	1.00	0.17	-0.13	0.69	0.64	-0.01	0.20	0.49	0.07	0.54	-0.13

Based on the results, zinc has a strong positive correlation with lead. In other words, price fluctuations are similar between zinc and lead roughly. It can be seen in Table 8 that several minerals have a negative correlation with zinc and lead. For selecting the most appropriate investment option for a mining company, in addition to the correlation coefficients, the availability factor is important too. Considering the general condition of the mining region and the possibility of investment are significant to achieve an accurate solution.

According to the results, iron investment was simultaneously proposed to the mining company due to its adverse correlation and availability factor around the mining region. Therefore, the iron market can be a reliable investment option when lead and zinc prices decline.

For risk treatment, first, the high-level risks were identified. It was observed that economic risk factors significantly impact premature mine closure consequences. By investigating seven alternatives of PMLU and twelve decision criteria, recreation centers were selected as the most suitable PMLU. Recreation centers improve the individual and social conditions in the region and play a significant role in reducing social conflicts. Suitable employment, job opportunities, local income is created by choosing

this PMLU. Thereby, this PMLU can cover the mine closure identified risks. The distance of mines from crowded cities and centers, reclamation costs, problems of polluting elements, and low probability of return on investment are among the limiting factors for choosing recreation centers as a PMLU. However, due to the lack of recreational centers in the Anguran region, selecting this option seems rational. Since the MCDM methods are compatible in this case study; Selecting these methods was the correct and most appropriate option for achieving the results.

CONCLUSION

The current study focuses on implementing the comprehensive risk management approach for premature mine closure risks. In this regard, three stages of the risk analysis were considered to manage the risks. First, identifying risks that could influence early mine closure occurrence was studied. The 2D risk matrix and MCDM techniques were developed for the risk assessment stage. Verifying this approach in the Anguran lead and zinc mine in Iran, the determination of the most critical possible reasons for the premature mine closure was on the agenda. The metal price reduction was the main risk factor that led the mine to close prematurely. By investigating the correlation of metals prices with each other and availability factors, iron investment was proposed to reduce or prevent the occurrence of this risk factor. Then, unemployment and the inability to pay staff salaries were the main consequences of premature mine closure. Also, the 2D risk matrix's results show that economic risks had significant impacts on the mining company. The seven PMLU alternatives were ranked by the TOPSIS method compared to the twelve criteria for the risk treatment stage. Finally, recreation centers were introduced as the most suitable PMLU. Different mining companies can implement the presented comprehensive approach in this study to manage the risks that threaten the SD goals in the region.

REFERENCES

Amirshenava, S., Osanloo, M., (2018). Mine closure risk management: An integration of 3D risk model and MCDM techniques. *Journal of Cleaner Production, 184,* 389-401. doi.org/10.1016/j.jclepro.2018.01.186

Amirshenava, S., Osanloo, M., (2019). A hybrid semi-quantitative approach for impact assessment of mining activities on sustainable development indexes. *Journal of Cleaner Production, 218*, 823-834. https://doi.org/10.1016/j.jclepro.2019.02.026

Amirshenava, S., Osanloo, M. (2021). Mined land suitability assessment: a semi-quantitative approach based on a new classification of post-mining land uses. *International Journal of Mining, Reclamation and Environment*, *35*(10), 743-763. https://doi.org/10.1080/17480930.2021.1949864

Cui, C., Wang, B., Zhao, Y., Zhang, Y., and Xue, L., (2020). Risk management for mine closure: A cloud model and hybrid semi-quantitative decision method. *International Journal of Minerals, Metallurgy and Materials, 27,* 1021-1035. doi.org/10.1007/s12613-020-2002-7

Galvin, J., (2017). Critical role of risk management in ground engineering and opportunities for improvement, *International Journal of Mining Science. Technology, 27*,725-731. https://doi.org/10.1016/j.ijmst.2017.07.005

Gheisari, N., Osanloo, M., Esfahanipour, A., and Mansouri, M. (2014). Closure Risk Assessment in Atashkooh Stone Quarry Using Risk Matrix. In *Mine Planning and Equipment Selection* (pp. 791-802). Springer, Cham.

Hajkazemiha, N., Shariat, M., Monavari, M., and Ataei, M. (2021). Evaluation of Mine Reclamation Criteria using Delphi-Fuzzy Approach. *Journal of Mining and Environment*, *12*(2), 367-384. http://dx.doi.org/10.22044/jme.2020.9674.1880

Hwang, C. L., Yoon, K. (1981). Methods for multiple attribute decision making. In *Multiple attribute decision making* (pp. 58-191). Springer, Berlin, Heidelberg. doi.org/10.1007/978-3-642-48318-9

ICMM (2012b), Mining's contribution to sustainable development - an overview. International Council on Mining and Metals, London, UK. Available at: www.icmm.com/library

IMPASCO, Iran Minerals Production and Supply Company, http://www.impasco.gov.ir/ (accessed 10.09.21).

ISO 31000, (2009). Risk Management - Principles and Guidelines. International Organization for Standardization.

Kodir, A., Hartono, D. M., Haeruman, H., and Mansur, I. (2017). Integrated post mining landscape for sustainable land use: A case study in South Sumatera, Indonesia. *Sustainable Environment Research*, *27*(4), 203-213.

Kung, A., Everingham, J., and Vivoda, V., (2020). Social aspects of mine closure: Governance & Regulation. Brisbane: Center for Social Responsibility in Mining. The University of Queensland.

Lappi, P., (2020). A model of optimal extraction and site reclamation. *Resource and Energy Economics, 59*. https://doi.org/10.1016/J.RESENEECO.2019.101126

Laurence, D., (2001). Classification of risk factors associated with mine closure. *Mineral Resources Engineering, 10(03)*, 315–331. doi.org/10.1142/s0950609801000683

Laurence, D., (2006). Optimization of the mine closure process. *Journal of Cleaner Production, 14,* 285-298. doi.org/10.1016/j.jclepro.2004.04.011

Laurence, D., (2011). Establishing a sustainable mining operation: an overview. *Journal of Cleaner Production, 19,* 278-284. doi.org/10.1016/j.jclepro.2010.08.019

LME, London Metal Exchange, www.lme.com (accessed 10.11.21).

Mansouri, M., Osanloo, M., and Gheisari, N. (2014). Establishing a sustainable model to reduce the risk of mine closure. In *Mine Planning and Equipment Selection* (pp. 1427-1436). Springer, Cham.

Maqsoud, A., Diaby, S., and Mbonimpa, M. (2021). Evaluation of mine site reclamation performance using physical models: Case of Ity mine (Ivory coast). *Journal of African Earth Sciences*, *176*, 104110.

Mborah, C., Bansah, K., and Boateng, K., (2016). Evaluating alternate Post-Mining land uses: A review. *Canadian Center of science and education, 5*, 14-22. 10.5539/ep.v5n1p14

Mercer, K. G., and Biggs, B. (2013, September). Managing organisational risk for mine closure. In Proceedings of the Eighth International Seminar on Mine Closure (pp. 523-535). Australian Centre for Geomechanics.

Minaei Mobtaker, M., Osanloo, M., (2015). Chaos in iron ore price prediction. In: *The Southern African Institute of Mining and Metallurgy MPES 2015* – Smart Innovation in Mining at: Sandton Convention Centre, Johannesburg, South Africa.

Osanloo, M., (2017). Mine Reclamation, third ed. Amirkabir University of Technology Publication, ISBN 964-463-090-4, p. 222 [in Persian].

Sanders, J., McLeod, H., Small, A., and Strachotta, C. (2019). Mine closure residual risk management: identifying and managing credible failure modes for tailings and mine waste. In *Proceedings of the 13th International Conference on Mine Closure* (pp. 535-552). Australian Centre for Geomechanics.

Sloss, L., (2013). Coal Mine Site Reclamation. IEA Clean Coal Centre. ISBN 978-92-9029-536-5, p. 70. doi.org/10.13140/RG.2.2.23405.13288

Tones, A., Howe, L., and du Plooy, J. (2021). Knowledge makes the work go round: Knowledge management in mine closure planning. In Mine Closure 2021: *Proceedings of the 14th International Conference on Mine Closure.* QMC Group.

Vrklijan, D., Brisevak, Z., (2016). Innovative waste management and mine closure. Minerals policy guidance for Europe.

A REVIEW OF THE NITRATE POLLUTION AND GROUNDWATER PROBLEMS DUE TO MINE BLASTS

G.G.U. Aksoy [1,*], C. Okay Aksoy [2], M. Akpınar [1]

[1]*Hacettepe University, Ankara, Turkey*
([*]Corresponding author: gulsevaksoy@hacettepe.edu.tr)
[2]*Dokuz Eylul University, İzmir, Turkey*

ABSTRACT

Underground water resources have an important place in the life of living things. The pollution and decrease of these resources cause significant problems for humanity. It is possible that blasting operations at mine sites contaminate groundwater and damage groundwater resources. One of the most important reasons for this situation is the nitrate resources found in high rates in explosives used during blasting operations. Nitrate released from explosives pollutes groundwater, making groundwater harmful to health. For this reason, nitrate pollution should be monitored and prevented as much as possible during the operations carried out at the mine sites. There are lots of nitrate sources other than explosives, these sources are used in many ways. Since the variety of nitrate sources makes it difficult to determine the cause of nitrate contamination, methods have been developed to detect it. In addition, monitoring the increase in nitrate pollution in a region is an important step to prevent this pollution. Another step to prevent nitrate pollution from mining activities is the correct use of nitrate resources in the mine site and the correct nitrate removal of these resources.

Keywords: Mining, blasting operations, groundwater, nitrate pollution

INTRODUCTION

Blasting operations performed during mining processes have huge and devastating effects on its surrounding. These operations are common for most of the mining activities. Therefore, each of these activities has adverse impacts on the environment, the health of its workers and also communities near to the mining fields. These effects can be listed mainly as follows: probability of subsidence in the mine area, groundwater pollution, sound pollution as well as air pollution at the time of drilling and blasting, and lowering of groundwater table due to excessive pumping of subsurface water. (Nowsher, 2013) In order to reduce these effects and find solutions to them, we must first be able to identify them and find their reasons. As Nowsher said, the environmental deterioration caused by mining occurs mainly as a result of inappropriate and wasteful working practices and rehabilitation measures (Nowsher, 2013).

In this article, we will review studies about the effects of blasting operations on groundwater and treatment techniques of these effects. Groundwater is one of the most valuable water sources for all living things, and affecting these sources in a bad way may result in disastrous impacts on the life of these creatures. As mentioned at the beginning, one of the effects of blasting operations on groundwater is lowering of groundwater table. Underground mining can change not only groundwater table but also groundwater flow paths and the geochemical environment (Nowsher, 2013). These changes need to be investigated carefully to diminish their effects on quality of groundwater. Mining may increase the permeability of rock units, create fresh rock surfaces, and allow water flow between previously disconnected units or between surface and groundwater. This may disturb natural geochemical systems causing dissolution/precipitation reactions and result in disturbances to groundwater quality (Nowsher, 2013). We can see the effects of these processes on the quality of

groundwater by looking at the values in Table 1 through the example of Madhyapara Granite Mine (Bangladesh).

Table 1. Water test result of sample (MGMCL-GHS-W-01) of MGM and test was conducted by BRTC, BUET (Nowsher, 2013)

SL No.	Water Quality Parameter	Unit	Concentration Present in Sample: MGMCL-GHS-W-01	Bangladesh Standard for Drinking Water (ECR, 97)	WHO Guideline Value, 2004
01	pH	-	9.54	6.5-8.5	6.5-8.5
02	Color	Pt-Co	242	15	15
03	Turbidity	NTU	115	10	10
04	Total Alkalinity (as $CaCO_3$)	mg/liter	...	...	...
05	Chloride (Cl^-)	mg/liter	46	150-600	250
06	Iron (Fe)	mg/liter	...	0.3-1.0	0.3
07	Nitrate- Nitrogen (NO_3-N)	mg/liter	4.8	10	50
08	Fluoride (F)	mg/liter	...	1	1.5
09	Total Dissolved Solids (TDS)	mg/liter	362	1000	1000
10	Fecal Coliform (FC)	CFU/100 ml	Nil	0	0
11	Total Coliform (TC)	CFU/100 ml	15	0	0
12	Total Hardness (as $CaCO_3$)	mg/liter	18	200-500	500
13	Electrical Conductivity (EC) at 25	µS/cm	510	...	...
14	Nitrite- Nitrogen (NO_3-N)	mg/liter	0.013	<1	3
15	Silica (SiO_2), Colloidal silica	mg/liter	59.9	...	...
16	Sulphate (SO_4)	mg/liter	45.4	400	250
17	Total Suspended Solids (TSS)	mg/liter	27	10	...
18	Hydrogen Sulphide (H_2S)/Odor	mg/liter	0.03	Odorless	...
19	Mercury (Hg)	mg/liter	0.002	0.001	0.001

Besides all the other effects of blasting operations, groundwater pollution related to nitrate is one of the most crucial effects. In the article, nitrate pollution is the key point of our discussion. In the following parts, we will review studies about nitrate sources, discussing how to identify nitrate sources (if it is related to blasting materials or not), making some recommendations to manage and monitor nitrate impacts, and finally suggesting treatment methods.

NITRATE

Nitrate is an anion containing nitrogen which is the main element composing the atmosphere. Chemical formula of the Nitrate is NO_3^-, and it is a component of ammonium nitrate, which is approximately 90 percent of commonly used explosives by weight (Pelham et al, 2015).

Harmful Effects of Nitrate

Nitrate is a harmful compound for water resources and also human bodies; therefore it shouldn't contaminate groundwater. Effects of nitrate on water resources may be listed as follows, eutrophication and changing oxygen concentration. In a human body, nitrate can be converted into ammonia which is a base and also very harmful for human bodies. This reaction may lead to composing N-nitroso compounds which are carcinogen for humans and also animals (Ardıç, 2013).

Sources of Nitrate

With the increasing population of humans, pollution of groundwater is scaling up and one of the reasons for this pollution is Nitrate. In addition to explosives used in mining activities, fertilizers, automobiles, animal manures and nitrogen oxides emissions from coals are also sources of nitrate pollution. With these sources, nitrate, which mixes with soil and surface waters, dissolves in groundwater after a while. As nitrate dissolves in groundwaters, pollution that will affect a wide environment may occur and adversely affect the lives of living things.

When we begin to examine nitrate pollution caused by explosives, we can observe that nitrate dissolves in the soil and then groundwater in many different ways. Degnan listed some of these ways as follows: leaching of nitrate from unexploded nitrate bearing explosive compounds such as NH_4NO_3, oxidation (nitrification) of reduced N components of explosives such as NH_4NO_3, TNT, RDX, etc. and injection of soluble NO_3^- or NO_x gases into the subsurface by blasting (Degnan et al, 2016).

Besides these processes, we can list nitrate sources in an open pit as follows (Bosman, 2009),

1. Bedrock Disturbance through Blasting, and Rock Dumps
2. Pitwater
3. Pollution Control Dam
4. Metallurgical Process Plant
5. Tailings Dam
6. Exposure Pathways

HOW TO IDENTIFY NITRATE SOURCES

The variety of nitrate sources makes it difficult to detect nitrate pollution from explosion processes. According to Patel, the largest source of nitrate in the soil is fertilizers (Patel, 2016) , and various techniques are used to separate the nitrate effect of explosives from other nitrate sources. One of the main reasons for making this distinction is to reduce the pollution that mines will create around them by observing and detecting nitrate pollution.

One of the primary ways to determine the nitrate source is to examine the ratios of nitrogen and oxygen isotopes. In order to examine these rates, water wells should be opened near the mining area and groundwater samples can be taken from them. The nitrate pollution caused by explosives can be determined by taking these samples before and after blasting and comparing them and then analyzing these samples.

When the ratio of nitrogen and oxygen isotopes was examined, it was observed that these ratios differ between the nitrate used in explosives and other nitrate sources. Blasting related nitrate peaks were characterized by low $\delta^{15}N$ and high $\delta^{18}O$ which is indicative of synthetic nitrate used in explosives (Pelham et al, 2015).

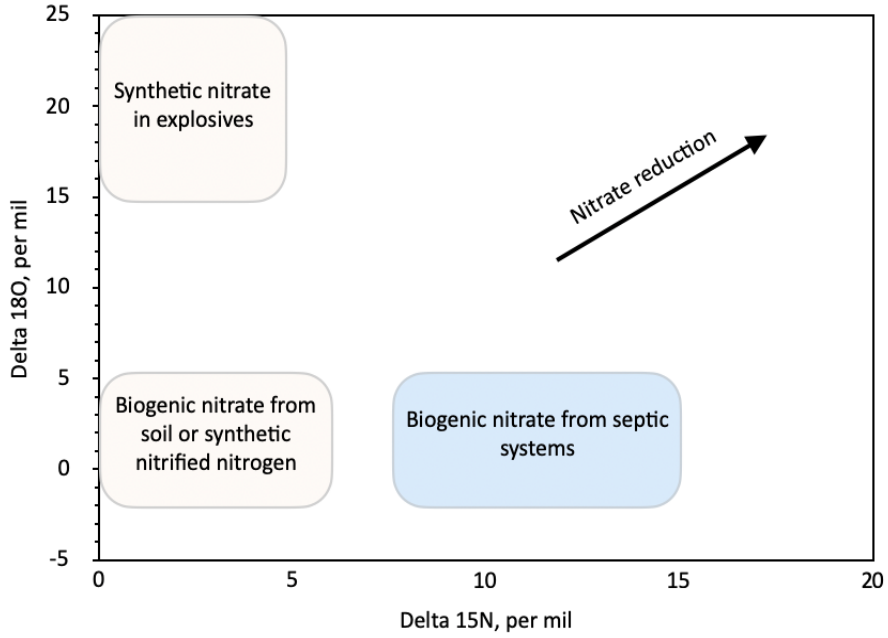

Figure 1. Graphs showing relation between δ15N and δ18O nitrate (Pelham et al, 2015)

As Pelham (2015), Degnan studied whether it is possible to find the source of nitrate in groundwater using N and O isotopes after a year. It is stated that the source of nitrate can be determined in this way, however nitrate should not be modified by the biological activities since the ratio of N and O isotopes is changed by denitrification. as mentioned before, in Degnan in 2016, they took samples from 12 wells and also 2 springs while constructing a highway in Windham, New Hampshire. By analysing elements, ions, dissolved gases and ratios of H, N and O isotopes with these samples, they concluded that the source of nitrate was synthetic. This reason is shown by low $\delta^{15}N$ and high $\delta^{18}O$ since these ratios differentiates at nitrate sourced by biogenic soil (which is constructed by nitrification) (Degnan et al, 2016).

Another interesting result which was stated by Degnan is that after eliminating effects of nitrification and computing initial grades of nitrates, it is possible to determine the source of nitrate by looking isotope graphs since these graphs show us clearly the source which can by three types: synthetic nitrate based on blasting, biogenic nitrate based on nitrification and biogenic nitrate based on septic systems (Degnan et al, 2016).

Stable isotope analysis in R environment (SIAR) is another method used in order to determine the source of nitrate. This method is used by Kazakis in 2020 with samples from groundwater at different locations after statistical analysis. The results of this study which used SIAR (a bayesian isotope mixing model) also seems promising (Kazakis et al, 2020).

RECOMMENDATIONS FOR NITRATE IMPACT MANAGEMENT AND MONITORING

Considering the negative effects of nitrate on the health of living things, some arrangements should be made in the mine fields in order to reduce these effects. By examining these regulations under two different titles as management and monitoring, we can review some suggestions for these topics.

Management Measures

The nitrate pollution that will occur can be reduced by installing some equipment at the right points in the mine site. Bosman talked about some of these equipment and the ways of using them as follows:

Implementation of appropriate stormwater management around the excavation to prevent the ingress of run-off into the excavation. This will reduce the volume of pitwater that are contaminated with nitrate, which would reduce the costs associated with the management of this water (Bosman, 2009).

Implementation of appropriate stormwater management around rock dumps through the establishment of a clean and dirty water system, which would reduce the volume of run-off contaminated with nitrate from the rock dumps (Bosman, 2009).

Implementation of appropriate containment measures for all impoundments used to store contaminated water, such as pollution control dams, return water dams and tailings dams, such as clay and plastic linings (Bosman, 2009).

In addition to these ways, we can examine the methods offered by Kemen as "Best Management Practices" under five headings.

<u>Loading Practices</u>

These practices should be done in the first phase before the blasting. Kemen listed these practices as follows (Kemen, 2010);

1. Drilling logs shall be maintained by the driller and communicated directly to the blaster.
2. Explosive products shall be managed on-site.
3. Spillage around the borehole shall either be placed in the borehole or cleaned up and returned to an appropriate vehicle.
4. Loaded explosives shall be detonated as soon as possible and shall not be left in the blast holes overnight.
5. Loading equipment shall be cleaned in an area where wastewater can be properly contained and handled in a manner that prevents release of contaminants to the environment.
6. Explosives shall be loaded to maintain good continuity in the column load to promote complete detonation.
7.

<u>Explosive Selection</u>

As Kemen stated, while selecting explosives, site conditions should be considered, especially water conditions (Kemen, 2010).

Prevention of Misfires

As Kemen stated, it is important to implement practices in order to prevent misfires (Kemen, 2010).

Muck Pile Management

As Kemen stated, muck piles should be removed from the blasting area as soon as possible and it should be prevented from contaminating groundwater (Kemen, 2010).

Spill Prevention Measures and Spill Mitigation

The fuel storage and fuel handling requirements should be paid attention. The training should be received describing what to do in the event of a spill of regulated substances (Kemen, 2010).

Monitoring Measures

We can detect the pollution caused by explosives by observing various values at various points around the mine site. Thanks to these observations, the source of the pollution that will occur later can be determined and studies can be started to reduce that pollution.

As Bosman stated, using groundwater pollution detection monitoring programs around mines, we can examine the following items: pH, electrical conductivity, sulphates, chlorides, cyanide, selected heavy metals, nitrates, ammonia, total coliforms or E. Coli, and phosphate (Bosman, 2009).

However, while making these observations, it is necessary to consider other conditions that may occur in the environment while evaluating the analyzed data. If these conditions are ignored, the results of the observations may be misinterpreted. To give an example of these inaccuracies from Bosman, in the investigation referred to above, a conclusion was made that “since no nitrate was found in samples taken from the tailings effluent, the tailings dam cannot be a source of nitrate in the community groundwater” . (Bosman, 2009) As stated, the absence of nitrate in tailings effluent does not indicate that the tailings dam is not a nitrate source. Because, as Bosman points out, in the reducing environment at the tailings dam, nitrogen is present as the ammonia species, and not as the nitrate species (Bosman, 2009).

In another study, pollutants occurred during the blasting operations at Sungun copper mine have been monitored and dissipation of these pollutants has been observed. It seems that most of these pollutants occurred because of blasting operations, have been dropped back to the mining sites and continued to mix into the atmosphere with the mining activities (Abdollahisharif et al, 2016).

An-Fo

In addition to the recommendations, it is important to know the best practices while using ANFO.

What is ANFO?

ANFO is one of the most used explosives in blasting operations during mining activities. Because of this, ANFO is one of the main nitrate resources in mining fields, which makes ANFO the biggest source of nitrate which dissolves in groundwater because of blasting operations.

4th Reduce “blow-back” if loading ANFO pneumatically.
5th Loading equipment should be cleaned in the proper area and the product shouldn’t be stored on site.

Factors contributing to the non-ideal detonation behavior of ANFO (Brochu, 2010)

1st Soil preparation
2nd Dissolution
3rd Oil wicking
4th Type of ANFO
5th Physical characteristics of AN particles
6th Storage and handling controls
7th Blast considerations
8th Loading controls

DISCUSSION

Blasting operations during mining activities cause serious environmental impacts which include groundwater pollution. These operations contaminate groundwater with nitrate. Identification of blasting operations impacts is difficult because of other nitrate sources such as fertilizers and decomposing vegetation. In order to identicate source of nitrate, isotope ratios of nitrogen and oxygen in nitrate can be used. In addition to the identification process, some best practices should be followed in mining sites. Also, nitrogen removal techniques are needed to be used in order to prevent nitrate pollution.

REFERENCES

Abdollahisharif, J., Bakhtavar, E., & Nourizadeh, H. (2016). Monitoring and assessment of pollutants resulting from bench-blasting operations. Journal of Mining and Environment, 7(1), 109-118.

Ardıç, C. (2013). İçme suyundaki nitrat konsantrasyonunun insan sağlığı üzerine oluşturduğu risklerin belirlenmesi (Master's thesis, Fen Bilimleri Enstitüsü).

Bosman, C. (2009). The Hidden Dragon: Nitrate Pollution from Open-pit Mines–A case study from the Limpopo Province, South Africa. Carin Bosman Sustainable Solutions, Pretoria, Gauteng, Republic of South Africa.

Brochu, S. (2010). Assessment of ANFO on the environment. Defence Research And Development Canada Valcartier (Quebec).

Degnan, J. R., Bohlke, J. K., Pelham, K., Langlais, D. M., & Walsh, G. J. (2016). Identification of groundwater nitrate contamination from explosives used in road construction: isotopic, chemical, and hydrologic evidence. Environmental science & technology, 50(2), 593-603.

Jermakka, J., Wendling, L., Sohlberg, E., Heinonen, H., Merta, E., Laine-Ylijoki, J., ... & Mroueh, U. M. (2015). Nitrogen compounds at mines and quarries: Sources, behaviour and removal from mine and quarry waters-Literature study.

Jermakka, J., Merta, E., Mroueh, U. M., Arkkola, H., Eskonniemi, S., Wendling, L., ... & Puhakka, J. (2015). Solutions for control of nitrogen discharges at mines and quarries: Miniman project final report.

Kazakis, Nerantzis, et al. "Origin, implications and management strategies for nitrate pollution in surface and ground waters of Anthemountas basin based on a δ15N-NO3− and δ18O-NO3− isotope approach." Science of The Total Environment 724 (2020): 138211.

Kernen, B. (2010). Rock blasting and water quality measures that can be taken to protect water quality and mitigate impacts. New Hampshire Department of Environmental Services, 1-3.

Nowsher, M. N., Ratul-Al-Istiak, H. M., Mahid, T. R., Biswas, B., Huda, S. A., Ahmed, M. T., & Hossain, H. Z. (2013). Environmental Impact Assessment of Madhyapara Granite Mine, Northwest Bangladesh. In International Conference on Mechanical, Industrial and Materials Engineering (ICMIME2013), RUET, Rajshahi, Bangladesh, Paper Id: RT-12.

Patel, R. K. (2016). Nitrates-its generation and impact on environment from mines: a review. In National conference on sustainable mining practice (pp. 2-3).

Pelham, K., Lane, D., Smerenkanicz, J. R., & Miller, W. (2009). A proactive approach to limit potential impacts from blasting to drinking water supply wells, Windham, New Hampshire. In 60th Highway Geology Symposium (p. 16).

Pelham, K., & Langlais, D. M. (2015). Sources of Nitrate in Groundwater Near Roadway Rock Blasting Sites. In 66th Highway Geology SymposiumHighway Geology Symposium.

Revey, G. F. (1996). Practical methods to control explosives losses and reduce ammonia and nitrate levels in mine water. Mining Engineering, 48(7), 61-64.

A STUDY OF EFFECTIVE PARAMETERS IN UNDERGROUND MINING METHOD SELECTION USING Z-NUMBERS THEORY

Zeinab Jahanbani[1], Majid Ataee-pour[2,] *, Ali Mortazavi[3]

[1]*Ph. D Candidate of Mining Engineering, Amirkabir University of Technology, Dept. of Mining Engineering*
[2,]**Associate Professor, Amirkabir University of Technology, Dept. of Mining Engineering,*
*(*Corresponding author: map60@aut.ac.ir)*
[3]*Professor, Amirkabir University of Technology, Dept. of Mining Engineering,*

ABSTRACT

The process of selecting an underground mining method is a critical decision-making issue with multiple criteria and depends on many important parameters such as geotechnical and geological features, technical, operational, environmental and economic parameters, political, social, and geographical factors. These factors face uncertainty, and existing uncertainties must be taken into account in the decision-making process of selecting the appropriate underground mining method. Fuzzy parameters are generally estimated through expert knowledge, but the degree of confidence in the opinion of different experts is different and the uncertainty and difference in the reliability of their opinion cannot be ignored. In this regard, Z-numbers Theory has been proposed. Each Z-number is represented by a pair of fuzzy numbers such that the first component indicates the fuzzy importance of each parameter and the second component is the reliability of the prediction of the first component. In this study, after classifying the effective factors in the selection of underground mining methods, the Z-numbers theory was used to rank and determine their importance. The results showed that in the main group of criteria technical factors and among the sub-criteria geological conditions, geometry conditions of the deposit, income per ton of ore, geomechanical conditions, and costs are the most important parameters, respectively.

Keywords: Influencing factors, underground mining method selection, uncertainty, fuzzy numbers, Z-numbers theory

INTRODUCTION

The selection of appropriate underground mining method to extract minerals from a deposit is one of the first and most important decisions in mining engineering activities from the perspective of safety, productivity, and economic issues. Different parts of an ore deposit normally vary widely in their geological, physical, chemical, and structural aspects. Depending on the dip, depth, size, and shape of the deposit, as well as the strength of the ore and host rock, several technically feasible methods may be adopted for a particular ore deposit. However, safety, financial, economic, and environmental parameters are of the most important and due attention should be paid to these parameters to select the safest and most profitable method. Therefore, selecting the most suitable method for an ore deposit, is a critical and challenging task owing to its compliance with a set of criteria (Gupta and Kumar, 2013).

To study the important and effective parameters in choosing the appropriate method for mining, many studies have been done for a long time. The first model or guide for the mining method selection is the method introduced by Peele in 1941 (Samimi Namin, 2009). Sunsequently, different

researchers have used different factors in their studies in order to decide on the mining method selection. Table 1 summarizes some of these studies.

Table 1. Criteria considered for selecting the appropriate mining method in various studies

Author	year	Criteria considered in the study
Boshkov and Wright	1973	Thickness, Shape, Dip, Strength of ore, HW, FW
Morrison	1976	Ore thickness, Strain energy accumulation
Laubscher	1981	RQD, Spacing of fractures, Joint's conditions, Underground water (hydrologic conditions)
Nicholas	1981-1992	Thickness, Shape, Dip, Overburden thickness, Grade distribution, RSS, RQD, Natural fractures and discontinuities shear strength of the ore zone, HW, FW
Hartman	1987	Depth, Strength of ore, HW, FW, Geometry conditions (Thickness, Shape, Dip)
Pakalnis et al.	1995	Thickness, Shape, Dip, Depth, Grade distribution, RMR and RSS of ore, HW, FW
Meech et al.	2002	Thickness, Shape, Dip, Depth, Grade distribution, RMR and RSS of ore, HW, FW
Alpay & Yavuz	2007	Spatial characteristics of the deposit, Geologic and hydrologic conditions, Geotechnical (soil and rock mechanics) properties, Economic considerations, Technological factors, Environmental concerns
Azadeh et al.	2010	Geometry conditions, Geomechanical conditions, Geographical conditions, Production, Mining operations, Mining aspects, Capital costs, Operating costs, Reclamation/rehabilitation costs, Income per ton of ore, Equipment worth and its usages
Gupta & Kumar	2013	Intrinsic factors, Extrinsic factors
Balusa & Singam	2017	Deposit thickness, RMR of hanging wall, Deposit dip, Deposit shape, RMR of ore, Ore grade, Ore uniformity, Recovery, Production, RMR of footwall, Technology, Depth, Dilution
FU et al.	2018	Economic benefit (Economic efficiency), Technical feasibility (physical parameters), Management complexity (the complexity of production management), Security status (safety of mining production), Environmental benefit (damage to the environment of mining methods)
Balusa & Gorai	2019	Dip, Shape, Thickness, Depth, Grade distribution, RMR of ore, RMR of hanging wall, RMR of foot wall, Productivity, Recovery, Dilution, RSS of ore, RSS of hanging wall, RSS of foot wall, Flexibility, Safety
Baji´c et al.	2020	Technical, Production, Economic

A number of these influencing criteria in the selection of underground mining methods face uncertainty and they are difficult to quantify (Gupta and Kumar, 2013). Fuzzy theories can, to some extent, fully address this uncertainty in computations. Fuzzy parameters are generally estimated through expert knowledge, but the degree of confidence in the opinion of different experts is different and the uncertainty and difference in the reliability of their opinion cannot be ignored. In this regard,

Zadeh (2011) proposed a concept called Z-numbers. Z-numbers try to do calculations based on numbers that are not completely reliable. Accordingly, each Z-number is expressed based on a pair of fuzzy numbers $(\tilde{A}, \tilde{R})$. The first component $(\tilde{A})$ is a constraint on the actual value of the given variable. The second component $(\tilde{R})$ also shows the reliability of the first component. Of course, the concept of Z-numbers was not the first attempt to show uncertainty in fuzzy numbers, but the theory of fuzzy sets of the second type, in which the degree of membership of a fuzzy set is itself fuzzy, was expressed before the theory of Z-numbers. However, this theory, unlike the theory of Z-numbers, is not able to show the degree of reliability in most sentences (Kang et al., 2012a, 2012b; Zadeh, 2011).

After Zadeh introduced the theory of Z-numbers in 2011, this theory was quickly used in various sciences such as economics, business, planning and the decision-making process (Kang et al., 2012a, 2012b). In the mining industry, due to its nature, the existence of uncertainty and variability in the influencing parameters in selection of underground mining methods play important and effective roles in the design and sustainability of underground mines (Heidarzadeh et al., 2020). Uncertainty and unreliability in these factors can be expressed as $Z = (\tilde{A}, \tilde{R})$ numbers. For example, the "deposit depth" parameter follows the fuzzy number $\tilde{A}$; While the reliability of this prediction by the expert can be indicated by another fuzzy number such as $\tilde{R}$. In the present study, due to the nature of mining and the existence of uncertainty in the factors influencing the selection of underground mining method (such as geological, operational, and geotechnical parameters, etc.), the Z-numbers theory has been used to study and classify these factors.

Z-NUMBERS

A Z-number consists of a pair of fuzzy numbers in the form of $Z = (\tilde{A}, \tilde{R})$; So that the first component $(\tilde{A})$, a restriction on the values, is a real-valued uncertain variable X and the second component $(\tilde{R})$ is a measure of the reliability for the first component. The numbers $\tilde{A}$ and $\tilde{R}$ also represent two fuzzy numbers defined by Equation (1) (Azadeh et al., 2013; Kang et al., 2012a, 2012b).

$$A = \{\langle x, \mu_A(x)\rangle | x \in X\} \tag{1}$$

Where: A: a fuzzy set on a universe X, $\mu_A: X \to [0,1]$: membership function of A and $\mu_A(x)$: membership value that describes the degree of belongingness of $x \in X$ in A.

In a graphical representation, a Z-number can be represented as Figure 1. In this example, $\tilde{A}$ is a trapezoidal fuzzy number and R̃ is a triangular fuzzy number (Azadeh et al., 2013; Kang et al., 2012a, 2012b).

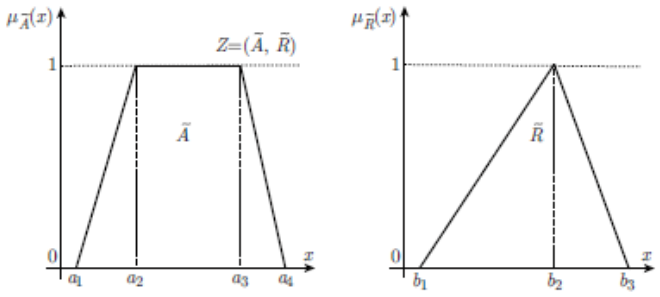

Figure 1. An example of a Z-number (Kang et al., 2012a)

Fuzzy Expectation of a Fuzzy Set

If A is a fuzzy set in which $\mu_A: X \to [0,1]$ is a membership function of A, the fuzzy Expectation of a fuzzy set is defined by Equation (2) (Kang et al., 2012a).

$$E_A(x) = \int_X x\mu_A(x)\,dx \tag{2}$$

This concept is different from the meaning of the Expectation of probability space.

Converting Z-numbers to classical fuzzy numbers

Direct calculations using Z-numbers are difficult and long calculations and have limited conditions (Zadeh, 2011). Therefore, to use these numbers, they are first converted to classical fuzzy numbers and then calculations are performed by fuzzy numbers. This process simplifies the calculations (Azadeh et al., 2013; Kang et al., 2012a).

Assume $Z = (\tilde{A}, \tilde{R})$ is a Z-number and the fuzzy numbers $\tilde{A}$ and $\tilde{R}$ are defined as $\tilde{A} = \{\langle x, u_{\tilde{A}}(x)\rangle | x \in [0,1]\}$ and $\tilde{R} = \{\langle x, u_{\tilde{R}}(x)\rangle | x \in X\}$, in which $u_{\tilde{A}}(x)$ is a trapezoidal membership function and $u_{\tilde{R}}(x)$ is a triangular membership function. In this case, the following steps are performed to convert Z-number to a classical fuzzy number:

1) First, the second component of Z-number (reliability value) is converted to a crisp number (Equation 3).

$$\alpha = \frac{\int x\mu_{\tilde{R}}(x)dx}{\int \mu_{\tilde{R}}(x)dx} \tag{3}$$

2) The weight of the second component (reliability value) is combined with the first component (restriction). The weighted Z-number can be denoted as $\widetilde{Z}^{\alpha} = \{\langle x, \mu_{\tilde{A}^{\alpha}}(x)\rangle | \mu_{\tilde{A}^{\alpha}}(x) = \alpha\mu_{\tilde{A}^{\alpha}}(x), x \in [0,1]\}$ (Equation 4 and 5).

$$E_{\tilde{A}^{\alpha}}(x) = \alpha E_{\tilde{A}}(x), \quad x \in X \tag{4}$$

$$s.t. \quad \mu_{\tilde{A}^{\alpha}}(x) = \alpha\mu_{\tilde{A}}(x), \qquad x \in X \tag{5}$$

3) Now the irregular fuzzy number (weighted restriction) becomes the regular fuzzy numbers (Equation 6 and 7). The obtained fuzzy set can be denoted as $\widetilde{Z}' = \{\langle x, \mu_{\tilde{z}'}(x)\rangle | \mu_{\tilde{z}'}(x) = \mu_{\tilde{A}}\left(\frac{x}{\sqrt{\alpha}}\right), x \in [0,1]\}$, and it is expressed through Equation (8) that ($\widetilde{Z}'$) has the same fuzzy expectation with $\widetilde{Z}^{\alpha}$.

$$E_{\tilde{Z}'}(x) = \alpha E_{\tilde{A}}(x), \qquad x \in \sqrt{\alpha}X \tag{6}$$

$$s.t. \quad \mu_{\tilde{Z}'}(x) = \mu_{\tilde{A}}\left(\frac{x}{\sqrt{\alpha}}\right), \qquad x \in \sqrt{\alpha}X \tag{7}$$

Equation (8) can be deduced from equations 4 and 6.

$$E_{\tilde{Z}'}(x) = E_{\tilde{A}^{\alpha}}(x) \tag{8}$$

By studying the equations in this section and converting a Z-number to a classical fuzzy number, it is sufficient to first determine the value of α through Equation (3) and after taking the square root of it, multiply in each parameter of the first component of Z-number, i.e. $\tilde{A}$.

INVESTIGATION AND CLASSIFICATION OF EFFECTIVE FACTORS IN THE SELECTION OF UNDERGROUND MINING METHODS

Mining method selection is one of the most important stages of mine design. Every deposit has its unique features. Numerous studies indicate that the underground mining method selection depends on the large number of factors. These factors can be classified into the following groups, i.e.: (Bogdanovic et al., 2012; Karimnia & Bagloo, 2015).

- Physical and mechanical characteristics of deposit such as local geological conditions, the strengths of the hanging and footwall, ore thickness, general shape of the deposit, slope, depth below the surface, overburden thickness, grade distribution, and quality. The main geological conditions include shear strength of the intact rock, natural fractures, shear strength of the in continuities, the orientation, length, spacing and locality of the geological structures, in situ stresses and hydrological conditions.
- Technical factors such as annual productivity, applied equipment, environmental considerations, mine recovery, flexibility of methods, machinery and mining rate
- Economic factors, such as: capital cost, operating cost, mineable ore tons, orebody grades and mineral value, and
- Exploitation factors such as annual exploitation, equipment, efficiency and environmental aspects.

In the present study, with the aim of classifying the effective parameters in the selection of underground mining methods, the available resources in this field were studied and the effective factors were investigated. Each of these studies has presented its classification to select the best mining method. In this article, by reviewing various research, a comprehensive classification of important factors in the selection of underground mining methods was performed. As shown in Table 2, the given criteria are divided into 4 main categories of technical, ambient, economic and operational/ mining factors and also 13 sub-criteria (Alpay and Yavuz, 2007, Alpay and Yavuz, 2009; Ataei et al., 2008; Ataei et al., 2013; Azadeh et al., 2010; Baji´c et al., 2020; Balusa & Gorai, 2019a, 2019b; Balusa & Singam, 2017; BOGDANOVIC et al., 2012; Dehghani et al., 2017; FU et al., 2018; Gupta & Kumar, 2013; Iphar & Alpay, 2018; Karadogan et al., 2008; Karimnia & Bagloo, 2015; MIKAEIL et al., 2009; Popović et al., 2019; Yavuz, 2015; Yazdani-Chamzini et al., 2012 Zare Naghadehi et al., 2009).

Table 2. Classification of effective factors in the selection of underground mining methods in the present study

No.	Criteria	No.	Sub-criteria
1	Technical Factors	1	Geometry Conditions of the Deposit
		2	Geomechanical Condition
		3	Geological Conditions
2	Ambient Factors	4	Geographical Conditions
		5	Static and Dynamic Loading
3	Mining & Operational Factors	6	Technological Factors
		7	Productivity Factors
		8	Environmental Concerns
		9	the complexity of production management
		10	Safety of production
4	Economic Factor	11	Costs
		12	Income
		13	Initial Investment Rate of Returns

MATERIAL AND METHODS

In this study, using the Z-numbers theory, the factors influencing the selection of underground mining methods were classified. The steps of conducting the research are presented as bellow.

Selection of Experts and Determining the Weighting Factors of Them

When sufficient information does not exist, experts´ opinions are used. In this study, 10 experts were selected to determine the weighting. It should be realized that these experts do not have the same weighting score. For this reason, in order to determine weighting scores of experts, title, experience, education time and age criteria were used. The weighting factor of each expert was obtained by dividing the sum of scores obtained from him/her divided by the total scores obtained by all experts participating in the study (Lavasani et al., 2015; Lavasani et al., 2015; Renjith et al., 2010).

Steps Used to Apply Z-Numbers

Quantification of experts' predictions about each parameter ($\tilde{A}$)

Linguistic terms have been used for quantifying expert's opinions or determining their opinion's weighting regarding each parameter. Five applied linguistic terms include very low, low, medium, high, very high which in short is VL, L, M, H, and VH. To fuzzy this section, trapezoidal fuzzy number has been used. Figure 2 represents the fuzzy domain of applied linguistic terms in this study (Chen & Hwang, 1992; Lavasani et al., 2015; Lavasani et al., 2015; Renjith et al., 2010).

Quantification of the reliability of the first component ($\tilde{R}$)

In this paper, to quantify the reliability of the first component for each parameter, the language variables Very Low (VL), Low (L), Medium (M), High (H) and Very High (VH) have been used. To fuzzy this section, a triangular fuzzy number has been used, which Figure 3 shows the fuzzy range of linguistic variables used in this research (Kang et al., 2012b).

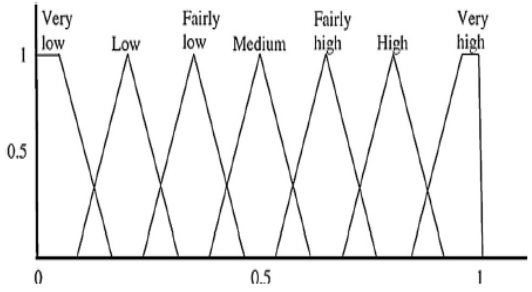

Figure 2. Linguistic terms used by experts (Mottahedi & Ataei, 2019; Renjith et al., 2010)

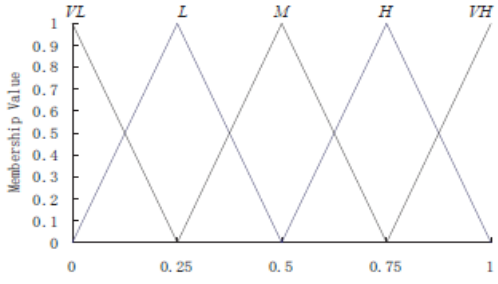

Figure 3. Linguistic variables used to quantify $\tilde{R}$ (Kang et al., 2012b)

Table 3 shows a part of the survey forms submitted. In this questionnaire, experts, based on their knowledge and experience in selecting the appropriate underground mining method, estimated the importance of each parameter ($\tilde{A}$) in the left part of that parameter. And in the right part, they considered the reliability of their predictions about each factor ($\tilde{R}$).

Table 3. A part of the survey forms used in this study

Influencing factors in underground mining method selection										
The importance of each criterion					**Criteria**	**The reliability of experts' predictions about each criterion**				
VL	L	M	H	VH		VL	L	M	H	VH
					Technical Factors					
					Ambient Factors					
					Mining & Operational Factors					
					Economic Factor					

Converting Z-Numbers to Classical Fuzzy Numbers

In this section, according to the contents of concepts section, a Z-number was converted to a classical fuzzy number (Azadeh et al., 2013; Kang et al., 2012a).

1) Determining α in each parameter using fuzzy number $\tilde{R}$: The value of α for the second component of Z-number is determined using the equation 3.

2) Multiplying $\sqrt{\alpha}$ in each parameter of the first component of Z-number ($\tilde{A}$): As mentioned, to convert Z-numbers to classical fuzzy numbers, the $\sqrt{\alpha}$ obtained from the previous step must be multiplied in each parameter of the first component of Z-number, i.e., $\tilde{A}$.

Aggregating Expert's Opinions

For aggregating experts´ opinions, the weighting factor of each expert is multiplied in his/her linguistic terms score (fuzzy number). This has been done according to equation (9) and based on a study by Clemen and Wrinkler (1999) and Renjith et al. (2010).

$$\mathrm{M_i} = \sum_{\mathrm{j=1}}^{\mathrm{n}} \mathrm{W_j A_{ij}} \qquad (\mathrm{i} = 1,2,3,\ldots,\mathrm{m}) \tag{9}$$

Where: Aij: Linguistic terms in relation to each parameter i by expert j, wj: Experts´ weighting factor j, m: the number of parameters and n: the fuzzy number of aggregating expert's opinions in relation to each parameter i.

Defuzzification And Converting Each Parameter to A Crisp Number

Defuzzification of fuzzy numbers is an important procedure for decision-making in fuzzy environment. In this study, center of area (centroid) defuzzification technique has been selected. This technique has been developed by Sugeno in 1985. This is the most used technique and is accurate. Defuzzification of trapezoidal fuzzy number $A^{\sim} = (a_1, a_2, a_3, a_4)$ is obtained using Equation 10 (Lavasani et al., 2015; Lavasani et al., 2015).

$$X^* = \frac{1}{3}\frac{(a_4 + a_3)^2 - a_4 a_3 - (a_1 + a_2)^2 + a_1 a_2}{(a_4 + a_3 - a_2 - a_1)} \tag{10}$$

Ranking of Influencing Parameters in Underground Mining Method Selection

In this section, after calculating the final weight of each parameter using Equation (10), the importance of each factor was determined and ranked based on the obtained weights. According to the results of calculations and quantify the uncertainty of parameters using Z-number theory, in the main group of criteria technical factors with a weight of 0.745, are the most important parameters. Economic factors (0.685), mining/operational factors (0.639) and ambient factors (0.594) are also in the next categories, respectively (Table 4 and Figure 4).

Among the sub-criteria influencing the selection of underground mining method, geological conditions (0.730), geometry conditions (0.717) and income per ton of ore (0.715) are the most important factors. After these parameters, geomechanical conditions, costs and initial investment rate of returns are the most important parameters, respectively (Table 5 and Figure 5).

Table 4. Final weight of criteria and their rank

Criteria	Final Weight	Ranking of Criteria
Technical Factors	0.745	1
Ambient Factors	0.594	4
Mining & Operational Factors	0.639	3
Economic Factor	0.685	2

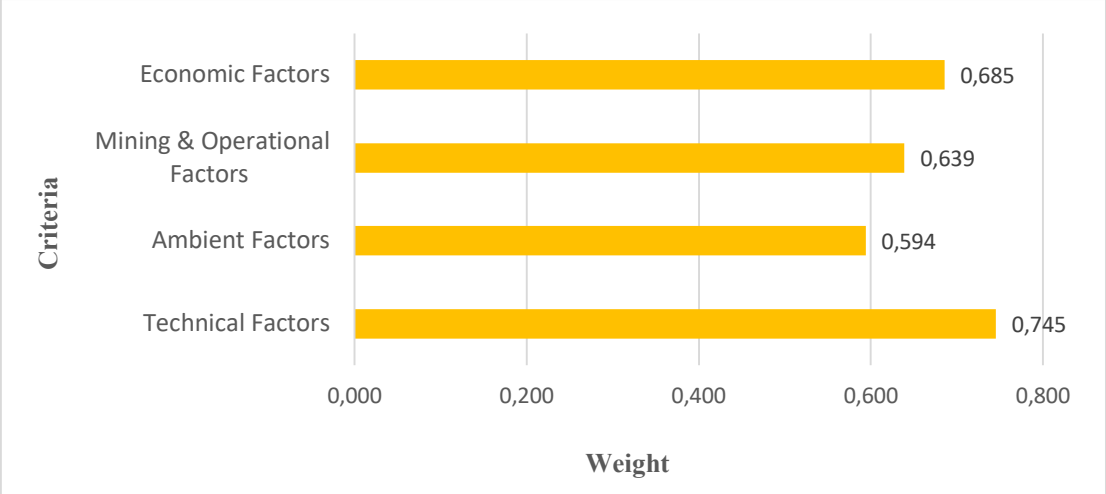

Figure 4. Final weight of criteria and their rank

Table 5. Final weight of sub-criteria and their rank

Criteria	Sub-criteria	Final Weights	Ranking of sub-criteria
Technical Factors	Geometry Conditions of the Deposit	0.717	**2**
	Geomechanical Condition	0.677	4
	Geological Conditions	0.730	**1**
Ambient Factors	Geographical Conditions	0.485	11
	Static and Dynamic Loading	0.517	9
Mining &	Technological Factors	0.493	10

Operational Factors	Productivity Factors	0.574	7
	Environmental Concerns	0.391	13
	The complexity of production management	0.466	12
	Safety of production	0.526	8
Economic Factor	Costs	0.631	5
	Income	0.715	**3**
	Initial Investment Rate of Returns	0.601	6

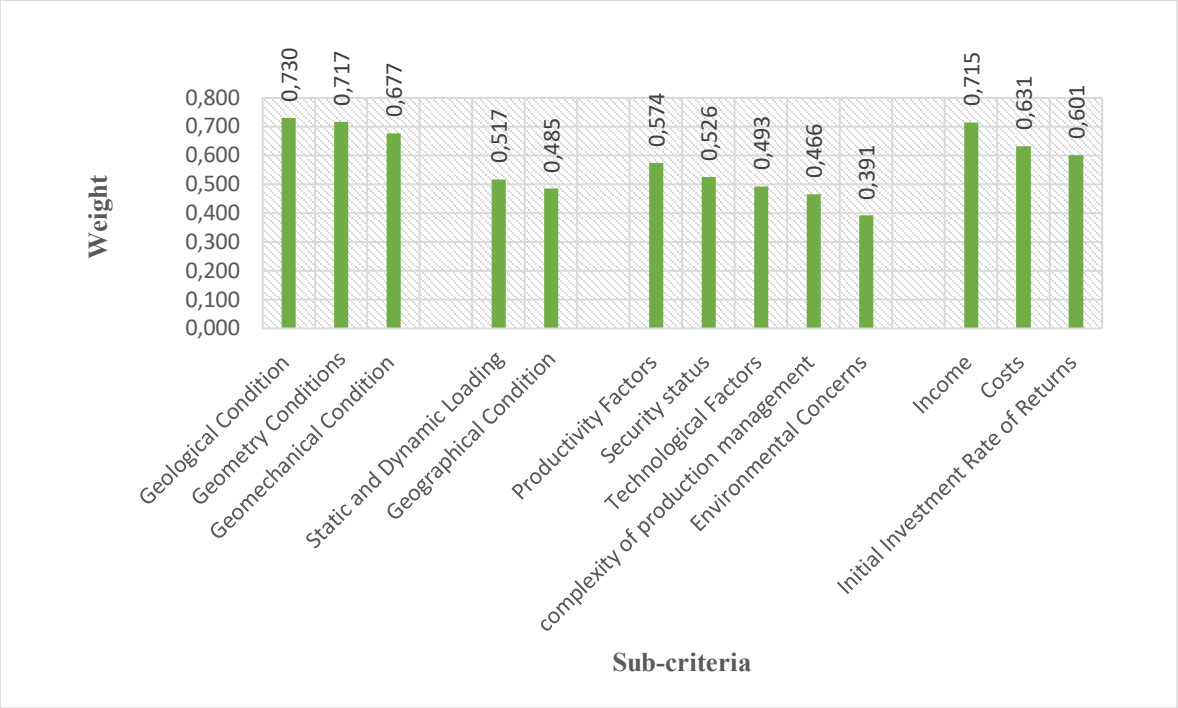

Figure 5. Final weight of sub-criteria and their rank

CONCLUSION

Selecting the best underground mining method among many alternatives is a multicriteria decision-making problem. The important factors for mining method selection include geological and mineralogical factors, geometrical features of deposit, safety, environmental parameters, economic variables, geographic characteristics, and local considerations. A number of these influencing criteria face uncertainty and they are difficult to quantify. The existing uncertainties must be considered in the decision-making process of selecting the appropriate underground mining method. Fuzzy parameters are generally estimated through expert knowledge, but the degree of confidence in the opinion of different experts is different and the uncertainty and difference in the reliability of their opinion cannot be ignored. In this regard, Z-numbers Theory has been proposed. Each Z-number is represented by a pair of fuzzy numbers such that the first component indicates the fuzzy importance of each parameter, and the second component is the reliability of the prediction of the first component. In this study, after classifying the effective factors in the selection of underground mining methods, the Z-numbers approach was used to rank and determine their importance. The results showed that in the main group of criteria technical factors and among the sub-criteria geological conditions, geometry conditions of the deposit, income per ton of ore, geomechanical conditions, and costs are the most important parameters, respectively.

REFERENCES

Alpay, S., Yavuz, M. (2007). A Decision Support System for Underground Mining Method Selection. *International Conference on Industrial, Engineering and Other Applications of Applied Intelligent Systems*, 4570, 334-343.

Alpay, S., Yavuz, M. (2009). Underground mining method selection by decision-making tools. *Tunnelling and Underground Space Technology*, 24, 137-184.

Ataei, M., Jamshidi, M., Sereshki, F., Jalali, S. M. E. (2008). Mining method selection by AHP approach. *The Journal of the Southern African Institute of Mining and Metallurgy*, 108, 741-749.

Ataei, M., Shahsavany, H., Mikaeil, R. (2013). Monte Carlo Analytic Hierarchy Process (MAHP) approach to selection of optimum mining method. *International Journal of Mining Science and Technology*, 23, 573–578.

Azadeh, A., Osanloo, M., Ataei, M. (2010). A new approach to mining method selection based on modifying the Nicholas technique. *Applied Soft Computing*, 10, 1040-1061.

Azadeh, A., Saberi, M., Zandi Atashbar, N., Chang, E., Pazhoheshfar, P. (2013). Z-AHP: A Z-number Extension of Fuzzy Analytical Hierarchy Process. *7th IEEE International Conference on Digital Ecosystems and Technologies (DEST)*, 141-147.

Baji´c, S., Baji´c, D., Glušcevi´c, B., Vakanjac, V. R. (2020). Application of Fuzzy Analytic Hierarchy Process to Underground Mining Method Selection. *Symmetry*, 12, 192.

Balusa, B. C., Gorai, A. K. (2019). Sensitivity analysis of fuzzy-analytic hierarchical process (FAHP) decision-making model in selection of underground metal mining method. *Journal of Sustainable Mining*, 18, 8–17.

Balusa, B. C., Gorai, A. K. (2019). A Comparative Study of Various Multi-criteria Decision-Making Models in Underground Mining Method Selection. *Journal of The Institution of Engineers (India): Series D*, 100, 105–121.

Balusa, B. C., Singam , J. (2017). Underground Mining Method Selection Using WPM and PROMETHEE. *Journal of The Institution of Engineers (India): Series D*, 99, 165–171.

Bogdanovic, D., Nikolic, D., Ilic, I. (2012). Mining method selection by integrated AHP and PROMETHEE method. *Annals of the Brazilian Academy of Sciences*, 84, 219-233.

Chen, S. J., Hwang, C. L. (1992). Fuzzy Multiple Attribute Decision Making", *1st Ed. Springer-Verlag Berlin. Heidelberg*, Germany, ISBN: 3-540-54998-6.

Clemen, R. T., Winkler, R. L. (1999). Combining probability distributions from experts in risk analysis. *Risk analysis*, 19, 187-203.

Dehghani, H., Siami, A., Haghi, P. (2017). A new model for mining method selection based on grey and TODIM methods. *Journal of Mining & Environment*, 8, 49-60.

Fu, Z., Wu, X., Liao, H., Herrera, F. (2018). Underground Mining Method Selection with the Hesitant Fuzzy Linguistic Gained and Lost Dominance Score Method. *IEEE Access*, 6, 66442-66458.

Gupta, S., Kumar, U. (2013). An analytical hierarchy process (AHP)-guided decision model for underground mining method selection. *International Journal of Mining, Reclamation and Environment*, 26, 324-336.

Heidarzadeh, Sh., Saeidi, A., Rouleau, A. (2020). Use of Probabilistic Numerical Modeling to Evaluate the Effect of Geomechanical Parameter Variability on the Probability of Open Stope Failure: A Case Study of the Niobec Mine, Quebec (Canada). *Rock Mechanics and Rock Engineering*, 53, 1411-1431.

Iphar, M., Alpay, S. (2018). A mobile application based on multi-criteria decision-making methods for underground mining method selection. *International Journal of Mining, Reclamation and Environment*, 33, 480-504.

Kang, B., Wei, D., Li, Y., Deng, Y. (2012). A Method of Converting Z-number to Classical Fuzzy Number. *Journal of Information & Computational Science*, 9, 703-709.

Kang, B., Wei, D., Li, Y., Deng, Y. (2012). Decision Making Using Z-numbers under Uncertain Environment. *Journal of Information & Computational Science*, 8, 2807-2814.

Karadogan, A., Kahriman, A, Ozer, U. (2008). Application of fuzzy set theory in the selection of underground mining method. *The Journal of the Southern African Institute of Mining and Metallurgy*, 108, 73-79.

Karimnia, H., Bagloo, H. (2015). Optimum mining method selection using fuzzy analytical hierarchy process–Qapiliq salt mine, Iran. *International Journal of Mining Science and Technology*, 25, 225-230.

Lavasani, M. R., Wang, J., Yang, Z., Finlay, J. (2011). Application of Fuzzy Fault Tree Analysis on Oil and Gas Offshore Pipelines. *International Journal of Marine Science and Engineering*, 1, 29-42.

Lavasani, S. M., Zendgani, A., Celik, M. (2015). An extension to Fuzzy Fault Tree Analysis (FFTA) application in petrochemical process industry. *Process Safety and Environment Protection*, 93, 75-88.

Mikaeil, R., Zare Naghadehi, M., Ataei, M., Khalokakaie, R. (2009). A Decision Support System Using Fuzzy Analytical Hierarchy Process (AHP) and TOPSIS Approaches for Selection of the Optimum Underground Mining Method. *Mining Sciences*, 54, 349-368.

Mottahedi, A., Ataei, M. (2019). Fuzzy fault tree analysis for coal burst occurrence probability in underground coal mining. *Tunnelling and Underground Space Technology*, 83, 165–174.

Popović, G., Đorđević, B., Milanović, D. (2019). Multiple Criteria Approach in the Mining Method Selection. *Industrija*, 47, 47-62.

Renjith, V. R., Madhu, G., Lakshmana Gomathi Nayagam, V., Bhasi, A. B. (2010). Two-dimensional fuzzy fault tree analysis for chlorine release from a chloralkali industry using expert elicitation. *Journal of Hazardous Materials*, 183, 103-110.

Samimi Namin, F., Shahriar, K., Bascetin, A., Ghodsypour, S. H. (2009). Practical applications from decision-making techniques for selection of suitable mining method in Iran. *Gospodarka Surowcami Mineralnymi*, 25, 57-77.

Yavuz, M. (2015). The application of the analytic hierarchy process (AHP) and Yager's method in underground mining method selection problem. *International Journal of Mining, Reclamation and Environment*, 29, 453-475.

Yazdani-Chamzini, A., Haji Yakchali, S., Zavadskas, E. K. (2012). Using an integrated mcdm model dor mining method selection in presence of uncertainty. *Economic Research*, 25, 869-904.

Zadeh, L. A. (2011). A Note on Z-numbers. *Information Sciences*, 181, 2923-2932.

Zare Naghadehi, M., Mikaeil, R., Ataei, M. (2009). The application of fuzzy analytic hierarchy process (FAHP) approach to selection of optimum underground mining method for Jajarm Bauxite Mine, Iran. *Expert Systems with Applications*, 36, 8218–8226.

AGGLO COLUMN FLOTATION OF TURKISH LIGNITE SLIME AND ŞIRNAK ASPHALTITE BY MICRO SELECTIVE COAGULATION IN MODIFIED COLUMN FLOTATION SEPARATOR

Y. I. Tosun [1,*], F. Çiçek[2]

[*1]*Şırnak University, Engineering Faculty, Mining Engineering Department, Şırnak*
*(*Sorumlu yazar: yildirimismailtosun@gmail.com)*
[2] *Azerbaijan National Science Academy, Radiation Institute, Baku*

ABSTRACT

The asphaltite reserves and current coal mining in Şırnak, were 83% of total Turkey's asphaltite reserves. This type of asphaltite should be washed with a washing plant to operate in areas where sulfur content and ash content of asphaltite were removed. Tunçbilek, Bolu Mengen and Kütahya Gediz lignite were tested in selective agglomeration by asphaltite together. The ash and sulfur contents in coal washing provided great issue due to hard washability of Şırnak asphaltite. This evaluation gave great benefits in terms of reduced costs as well as transport and environmental protection. The coal slime recovery ranged from a 20-120 mg/l fuel oil solution through with mechanical agitation of fuel oil micro coagulation followed by modified centrifuge baffle was researched. Micrographs and particle size measurements indicated that coagulates were the fine agglomerate of fuel oil micro coagulation and slime, with size ranging from 70 to 100 µm. Micro column flotation proved much as other mechanical techniques such as inclined lamella plates in column and coagulation effect was managed in agitation conditioner by fuel oil. Modified column flotation cell used to recover coagulates on the lamella bafflers temporarily. The fuel oil and surfactant adsorption was evaluated through control measurements. The influence of collector fuel oil concentration, pH and bubble size on slimes recovery was investigated. In the absence of collector, a combustible recovery of 45% was achieved, while in the presence of 20 mg/L of fuel oil it was increased to 80%, at pH 8. The slime recovery also increased with fuel oil micro coagulation increase to 30gr/l slurry and bubble size decrease, reaching 50-150 micron coagulates and bubble size around 60 µm.

Keywords: Modified flotation column, column baffling, fuel oil coagulate, selective agglomeration, slime agglo-flotation, lignite slime, agglo-flotation, slime

INTRODUCTION

In coal recovery the selective agglomeration and coagulation of solid coal slimes were tested as self coagulation with fuel oil micro coagulation and asphaltite coagulation was effective and inclined lamella baffle or flow rate and collector dosages were needed in slime coagulation and agglo-settling rates was managed at the attrition speed of 500-600 rev/min at higher speeds the agglomerated particles deteriorated and combustible yields decreased to 76% at waste management and coal recovery. The plant-based settling can be operated as mobile or integrated depending on solid content and dewatering slime and wastes evaluation methods in Şırnak. For this reason selective coagulation waste was critical on the quality of which it will be used in the oil agglomerated settling or flotation. The collection of coal slime from tailings pool and bio-waste pyrolysis was affecting the cost of waste management and recovery of coal. The application of the waste separation method was also affected the amount of solid waste to be recovered or the amount of compost to be produced. In Sırnak province, approximately 120 thousand tons of annual solid waste

and 60 thousands as coal slime at dry weight have been formed. This project has been studied in a mobile incineration plant project considering similar wastes in neighboring countries Siirt and Hakkari. In this way, it will be beneficial to recycle wastes, energy gain as well as environmental effect which can be done consciously waste classification from garbage and bio waste stream in the regions. The slime agglo-flotation and coal recovery units that integrated were also linked to the mobile system in the study and an economically sustainable economical solid waste management and combustion system in the integrated plant designed. The designed mobile coagulation and slime agglo-flotation unit ensured that the problems such as water and soil pollution and environmental waste loss, including energy production, were minimized. If the integrated mobile system is economically sustainable, it is aimed that the operating cost was low and the management was slightly economical and portable in conformity with Şırnak City Province, and an issue in Southeastern Anatolian region due to the fact of less poverty and scarcity of water resources in hard geographical conditions.

Coal Slime and Waste

The almost 211TWh total electricity in 2011, Turkey were produced primarily from imported natural gas and domestic coal [TKI, 2013]. The total amount of asphaltite resource in reserves and production in Şırnak City are over 82 million tons of available asphaltite reserve and 400 thousand tons per year, respectively [TKI 2009]. The most effective and cost-effective technologies are needed for clean coal products in today's modern technologies [EIA,2015]. Turkish coal industry needs washing technologies and high performances at lower cost with various types of local coals.

Evaluation of natural resources, in parallel with the energy needs of our country will provide economic benefits by reducing fuel imports. Basically, energy production is made from imported natural gas and has a 46% share of health. After the energy production from coal imported natural gas is located in the second row and is provided by burning coal in thermal power plants with a share of 26% (TKI, 2013). Depending on the future energy demand, the ratio is expected to increase. A total of 83 million 2ones per annum of lignite and coal in boilers and industrial furnaces production was evaluated as the need for heating and energy. The quality of coal ash minerals comprised micronized size particles (Ketkar et al., 2010,). In this study, the opening of the quarry closed in Şırnak region and the high-calorie but ash and sulfur content can be produced by washing it is considered to be the economic contribution of higher asphaltites. Şırnak asphaltites the washability studies made by developing potential flowsheets were compared accordingly wash washing plant investment and operating costs. The result of the feasibility study has identified suitable premises.

Asphaltites of Southeastern Anatolia is located in the Şırnak and Hakkari 's provinces in Turkey 120 million tons of proven reserves of Şırnak and Hakkari possible asphaltite of 0.2-1% moisture, 37-65% ash, sulfur burning 6,3-7.5% total sulfur 5.5-5.7%, 60-65% volatile matter and 2800-5600 kcal / kg has a lower temperature. Şırnak asphaltites beds are distributed or block-shaped space rock in the vein location [TTK 2009]. Avgamasya and production is done in Karatepe veins approximately 15 years. Avgamasya and Karatepe veins 15-25 and 10-20 m thick clumps form. Also Hakkari, Uludere district was spread around 1-20 m thick layer of scattered asphaltite seam and as bed layers and as veins. As well as limestone bed rock, shale, marl clay, marl and argillaceous limestone is located. Şırnak asphaltite coal is soft with shale ash and macro sized calcite, micronized minerals as pyrite and pyrrhotite inclusions are widely distributed in coal and asphaltite shale.

Washing with the Selective Agglomeration of Slime

Slime settling for washing the fine size coal (Jameson, 2001) is a method most commonly used. Some studies of coal particle size and density of mineral distribution in coal slime settling (Warner, 1985) determined that significant side kinetic and may affect efficiency. Studies particle

size increases, as can be shown that the yield decreases rapidly (Schubert, 2008). Generally yield falls in the slime settling of coarse coal, but slime settling rate is very low. Particle size is too big, not sticking on the bubbles. In contrast, a high efficiency in the fine coal slime settling and slime settling kinetics also increase (Gupta et al., 2001). In contrast, slime settling rate depends strongly on the grain size medium size coal particles. In addition, the bubble clusters formed around the coarse coal particles was determined to be effective in the coal particles floated by slime settling. Slime settling in size, the solid ratio of reagent dosage and reactive species stated that effective slime settling success (Wills and Napier-Munn, 2006, Klimpel and Hansen, 1987, Rules 1991).

Besides, the grain size on the slime settling of coal ash and mineral substances with a coupling degree of covering of the mineral ash has been determined to be in effect (Laskowski 2001, Erol et al., 2003). Washing the slime settling proper size range was found to be -500 microns. Bigger size and mechanical mixing of fine particles of coal has created different hydrodynamic effect (Jameson, 2001).

Şırnak asphaltites about coal reserves with the washability of the petrographic studies with standard slime settling pyrite and clay depending on the structure of asphaltite moved, it has been identified as hard coal washability.

Washing the Coal with Selective Agglomeration of Slime and Column Flotation

Column slime flotation of fine coal is determined could very well yield can be floated in the microbubbles (Yianatos et al., 1988). Microbubble washing water in the form of shower foam zones consisting of may be possible to obtain cleaner product coal with the addition. (Hadler et al., 2012 and Jameson, 2001) washable particularly difficult and shale and shale is a method used successfully in coal at high rates. Particle size and type of coal as the slime agglo-flotation column can easily affect efficiency. However, operating parameters, especially the foam height of the column unit, the wash water is added, and the bias ratio is flammable operating parameters affect efficiency (Finch and Dobby, 1990, Yoon, 1993, Yoon, 2000).

It was formed on an inclined foam zone to increase the effectiveness of the foam so that gravity was stated to reduce drift foam. These essential principles laid cyclonic column slime agglo-flotation cell (S-FCMC) provided a foam zone comprising inclined channels (FCMC) it proved to be effective in coal washing and widely China (Rubio, 1996) was used. The foam product has a third zone of the foam sediment are removed (Valderrama et al., 2011).

Industrial development currently demands a growing consumption of solid fuel resources in the country with the concern of environment in order to supply energy needs. This wide utilization of coals and lignite leads to a considerable amount of washing based wastes being discharged into t6ailings ponds, demanding previous treatment to avoid pollution. Additionally, waste waters or sewage sludge can be treated by washing and sludge let to the soil, providing humus carbon source and fertilizers. The environmental pollution of streams near coal fields still cause the eutrophication issue, a phenomenon characterized by algae overpopulation and the rapid growth of aquatic plants, which impair the penetration of light in the water, thus reducing photosynthesis reactions and, consequently, the amount of dissolved oxygen in the water, suffocating aquatic animals and converting the water body into an open sewer (EIA 2012). Thus, the development of carbon management was critical in strategies in the environment. There has been a considered issue for quality of energy, leading to the search for new technologies to recover the coal slimes, offering opportunities for its recovering, and contributing to energy sustainability (TTK 2009). At the present time, chemical and physicochemical processes are the most used for finer size and ultrafine size near micron sized particles and particle removal from wastewaters using sufficient conditioning (Chakner

et al., 1987, Degner 1986). Aluminum and iron salts present the disadvantage of generating coagulation of sewer sludge, which cannot be reused or reclaimed (Oats et al., 2010 a b) (Xi, 1999; Xie, 2001). Thus, there was necessary to employ solid/liquid separation for recovery of fuel oil micro coagulation and carrier techniques, such as slime agglo-flotation, which is a well-established technique for minerals separation and is also commercially used for wastewater treatment (Fuerstenau 1976, Gupta et al., 1971). This technique is based on the different hydrophobic manner of the particles to be separated. Thus, hydrophobic particles can be captured by gas bubbles and float to the liquid surface. The slime agglo-flotation requires the use of surfactants to render the particle surface more hydrophobic. The efficiency of this process depends on the probability of particle-bubble collision and attachment. For small particles there is a need for small bubbles such as those produced by column slime flotation produced finer bubbles (Nunes et al.,2011, Dai et al., 2000).

MATERIALS AND METHODS

In this study, a modified type centrifuge baffle was investigated for coagulate settling. The particle breaking and screen washing effect the agglomeration of coal. The micro coagulation conditioning with fuel oil and coagulation provided in efficient column slime agglo-flotation process, as activated sludge was considered the most versatile wave effect could be forced to move at the direction of upward bubble flow instead of settling down and was so efficient at high dense liquid medium and less efficient at less density difference. While among the many oil slime settling type of chemical processes, oil slime agglo-flotation through the use of carbon coagulation by collectors were widely employed as seen from in Figure 3.

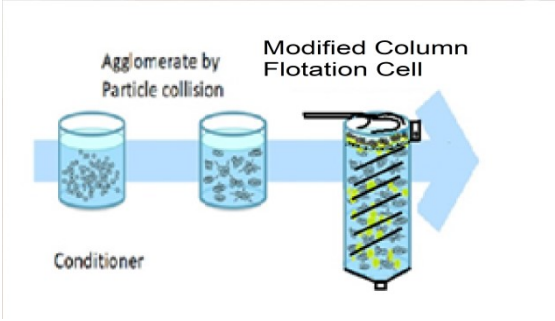

Figure 3. Schematic view of the carrier - column, slime agglo-flotation system with lamella baffle phase and air bubbling.

However, coagulates and agglomerates of carrier slime agglo-flotation by fuel oil micro coagulation fines were difficult to settle, requiring the use of bubble contact and lamella agglo-flotation separation

The particle size of the slime and the average bubble diameter were determined with a Malvern Instruments Mastersizer 2000SM capable of analyzing particles with diameters between 0.1-2000 µm. The average coagulates diameter was determined with the help of a specially designed acrylic cylindrical cell with a volume of 1 L, to fit in a Malvern Instruments Mastersizer 2000SM device. The influence of pH and current density on oil droplet diameter in a 0.1 mol/L HCl and NaCl solution was evaluated.

Column slime agglo-flotation tests were carried out in a 3L volume 110 mm diameter glass cell, with a 5 mm mesh stainless lamella at 45^{o} as shown in Figure 3. Fuel oil was used as collector conditioning and managed following separation in the lamella settling of the modified column cell.

The influence of fuel oil concentration, pH, sodium chloride concentration and flow rate on the coal yield, combustible recovery and on the carrier slime agglo-flotation and coagulation of the pH was evaluated. The coagulant sludge used in the feed of column slime agglo-flotation tests used 20 mg/L of fuel oil and 25-120 g/L fuel oil micro coagulation at 10 % solid weight rate and 0.1 mol/L NaCl as electrolyte with 0,1 mol/l HCl or NaOH as pH regulators. All reagents used were obtained from MERCK and were analytical grade.

For each test, a coal column slime agglo-flotation feed with a certain solid liquid ratio of 10% was fed into the column slime agglo-flotation cell. After 20 minutes the lamella baffle collection of the slime and lamella baffle with coagulation was determined by the micrometric method (Nikon Instruments).

RESULTS AND DISCUSSION

Coal Slime Characterization

The X-ray diffractogram of the coal clay and shale obtained from coal site selectively containing smectite and chlorite is presented in Figure 4. It can be observed that the coal slime was of a mixture of smectite clay with calcium carbonate and chlorite, which is a rate of 3,4/1,2/0,4 weight. However, the coagulation with fuel oil of clay stone particles was ion changing reactions in the sludge but chloride waters were effective in fuel oil micro coagulation site activation with coal particles instead of clay fines. Coagulation kinetics is not favored by slime and other species, such as calcium carbonate particles in the slime. It is proposed a two-step mechanism for the coagulation of coal slime was fuel oil micro coagulation activation and collector cover conditioning which is lately shown in the Figure 1 and 2.

Ionization of clay potassium and calcium carbonate

$$CaCO_3 + H_2O \rightarrow H^+ + OH^- + Ca^{2+} + CO^{3-} \quad (6)$$

Hydrolysis of clay particles

$$K_2O\ Al_2O_3\ SiO_2\ Si_2O_4\ nH_2O \rightarrow AlO_2^{3-} + K^+ + Al^{3+} + SiO_4^- + n\ H_2O + H^+OH^- \quad (7)$$

Where that iron and alkali cations was resulting in the cation exchange of Ca and Fe cations, it was found that hydrogen medium activation, hydrolysis of ions may activate clay particles for coagulation to fuel oil micro coagulation of asphaltite and carrier coagulant.

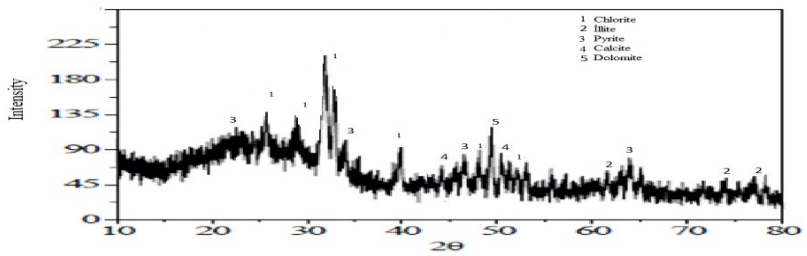

Figure 4. X-ray test result of Coal waste clay and shale

The coagulate size distribution is showed in Figure 5. Test results received by the particle size analyzer was the cumulative fractions that followed the result accumulated below a given fraction size. The frequency curve defined in the Figure 5 as the curve with peaks obtained by

Gaussian cumulative distribution. It was observed that 7% of fines in the sample have diameters below 15 µm, 70% of slimes in the coal sample had diameters below 35 µm .The average particle size of the sample was 45 micron regarded as slime but fuel oil micro coagulation was 100 micron average size and 90% of slimes in the sample have diameters below 78 µm, a size small enough to justify the use of column slime agglo-flotation to recover the coal carrier fuel oil micro coagulation agglomerates. Hence, this column centrifuge agglo-flotation method produced high agglo-flotation rates than those produced in the conventional slime settling process or even in centrifuge slime settling.

The chemical properties of Şırnak asphaltite marl and clay are given in Table 1. The proximate analysis of Şırnak asphaltite is given in Table 2.

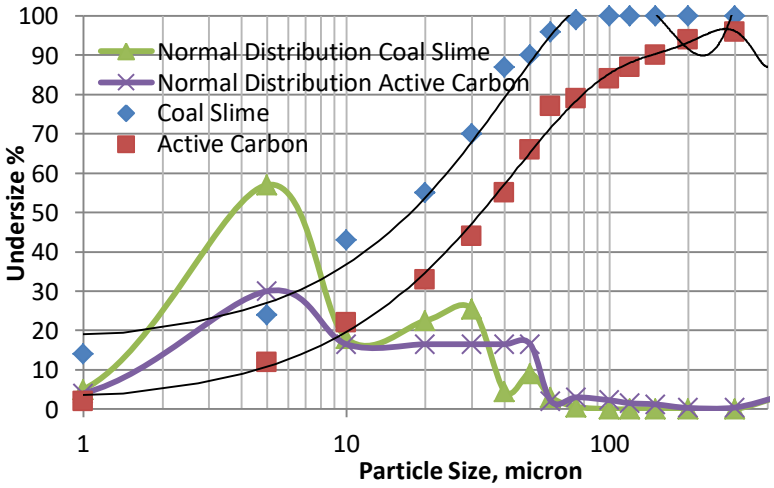

Figure 5. The size distribution and normal size distribution of Slime active carbon coagulates obtained from at pH 7,7 in Selective Coagulation

Table 1. The composition of Ash matter; Ash clay and Ash Marly shale of Şırnak Asphaltite in Selective Coagulation

%Component	ŞırnakMarl	ŞırnakŞhale
SiO_2	24.14	48.53
Al_2O_3	12.61	24.61
Fe_2O_3	7.34	7.59
CaO	29.18	9.48
MgO	4.68	3.28
K_2O	3.32	2.51
Na_2O	1.11	0.35
loss	21.43	3.09
SO_3	0.2	0.32

Table 2. The proximate analysis of Şırnak Asphaltite Slime Selective Coagulation

Coal	C%	H%	Ash%	S%	Moisture,%	Heat Value,kcal/kg
ŞırnakAsphltite Slime	17	4,5	42,1	6,6	0,5	3540

Effect Of Fuel Oil on The Coal Slime Recovery

The effect of kerosene concentration on the coal recovery by column slime flotation and on the carrier of the fuel oil micro coagulation particles is presented in Figure 4. It was observed that, in the absence of fuel oil micro coagulation, a coal recovery of 45% was achieved. The coagulated slime are randomly dissolved ions may activate shale species, hydrophilic and having average diameter around 3-5 µm depressed coal particles.

According to this research, coagulated particles caused higher entrainment and the slime agglo-flotation mechanism did not show any separation between hydrophobic and hydrophilic shale particles. This phenomenon improved higher effect on separation by ultrasonic wave forces when the particles enter the act of the wave direction to the lamella baffle column in much effect of finer clay particles occupying the spaces between the agglomerates and let remain in liquid phase. Some of the larger particles are drained back into the pulp, but the sink is carried upwards and is ultimately recovered in the concentrate. The finer the particle (<10 µm), was affected the more to remain suspended in the inter-bubble water and to be recovered by entrainment rather than by true slime agglo-flotation, a process that occurs only with hydrophobic particles (Figure 6).

In the presence of fuel oil micro coagulation, it was seen that a higher coal recovery was in the range of 68-74 % at less concentration of fuel oil (20-30 mg/ L) and a decrease of combustible recovery for concentrations above 50 mg/L.

It was shown the fuel oil adsorption on the fuel oil micro coagulation was sufficient even porous structure. According to the lamella baffle concentration was seen on fuel oil micro coagulation due to yields received by collectorless slime floating. The surface cations (Ca^{2+}or Fe^{+3}), forming apolar micelles and rendering the surface contact with shale. This kind of chemical interaction is a specific adsorption, and therefore of difficult desorption, which activated shale by sticking lamella baffle surfactant micelles and the increase of combustible recovery in the lamella baffle but ash content and yield with a recovery of 76% in the presence of 30 mg L^{-1} of fuel oil.

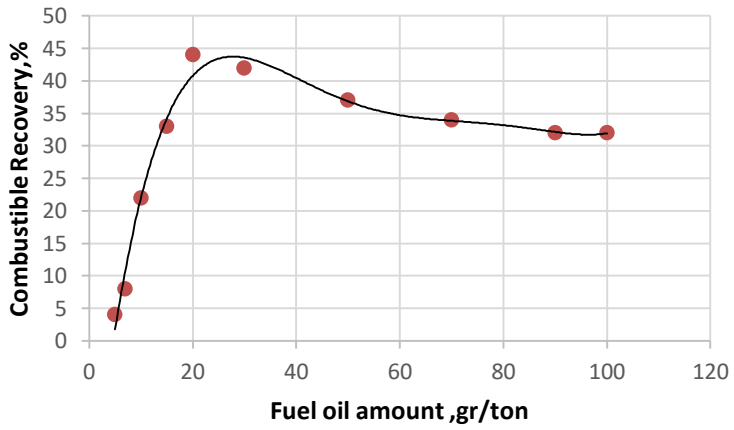

Figure 6. The coal yield of coagulate as a function of the fuel oil concentration added a 0.1mol/L HCl solution at pH 7,7 in Selective Coagulation.

Effect of pH on Coal Yield in Selective Coagulation

The effect of pH on the coal recovery and on the zeta potential of fuel oil micro coagulation and coal surfaces with fuel oil as collector is illustrated in Figure 7. It can be observed that, without fuel oil collector addition, the combustible recovery was not high at neutral pH, increased from 23% to 42% when the pH is increased from 4 to 9. Acidic pH improved the activation over coal surfaces with cleaning with the pH increase, which can contribute to the increasing clay activation by ion exchange with resulting entrainment.

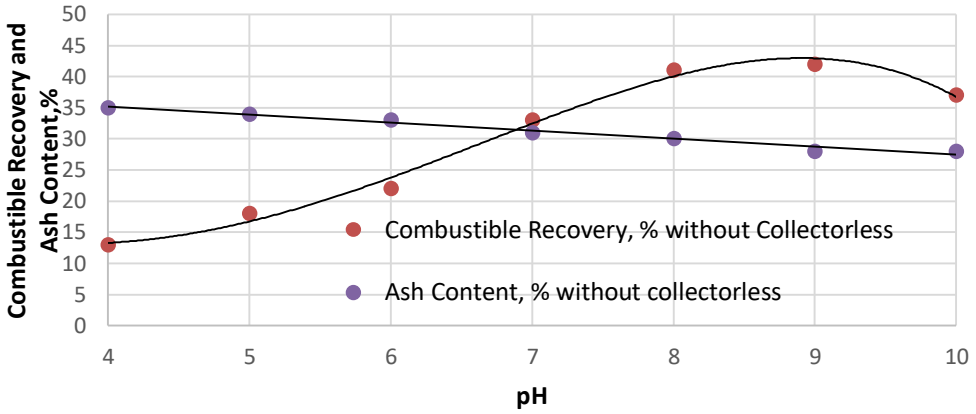

Figure 7. The asphaltite recovery in the inclined lamella column slime agglo-flotation, as change at pH changed by HCl in the presence of 50 mg/L fuel oil.

Project Design of Coal Washing Plant

The cleaning of washable hard coal needed the pre-cleaning, which was widely used heavy medium coal washing in large drums. At the fine coal in size (18-1mm) that cleaning was considered as heavy media cyclone unit (Anonymous a, b, c, 2015). Şırnak asphaltites the washing of these units Larcodems or fine coal washing unit that uses Humphrey spirals in mind it would be useful wash plant designs are made for efficiency cannot be achieved. According to the above washing test results it was analyzed in terms of investment and operating costs of the following two different designs. Implementing both A and B model design used the slime agglo-flotation column with coal slime agglo-flotation plant design also includes units shown in Figure 8. The B design that uses only coal slime agglo-flotation unit is shown in Figure 8.

Design Facility mainly heavy media cyclones, Humphrey spirals, pneumatic slime aglo-flotation unit Wemco column includes a slime agglo-flotation unit. The recently developed high-performance column slime agglo-flotation units in the slime coal washing, used with success. The conventional gravity techniques were beneficial of asphaltite washing as given plant flow diagram as shown below for the B design as shown in Figure 8.

As noted above Şırnak asphaltites 1.7 g/cm^3 can be obtained as an average of 5.25% washed clean coal ash. Şırnak asphaltites density of coal shale minerals 2.5 and has about 8% pores. That showed a washing coal density difference between 0,4-0.5 g/cm^3 which defines a close difference. That created many middlings by product in gravity separation at coaser size washing over 1 mm and nut size.

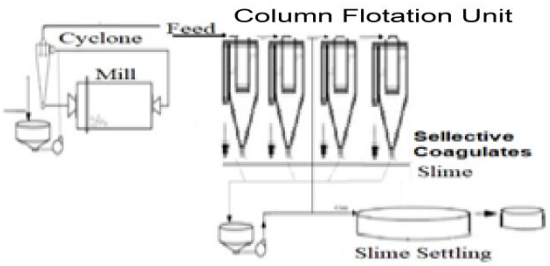

Figure 8. The proposed plant design for asphaltite cleaning with the column slime agglo-flotation.

CONCLUSIONS

The results demonstrated that coal recovery with fuel oil micro coagulation and column slime agglo-flotation can be used to recover asphaltite slime from the sludge. Slime particle sizes ranging from 30 to 76µm were obtained with 50 mg/L of fuel oil addition and 20 min conditioning was sufficient for column slime agglo-flotation. A recovery of 76% of fine slime and fuel oil micro coagulation agglomerates was managed in the control collectorless column slime aglo-flotation; however, the collector addition increased the recovery over 80% combustible matters. The addition of fuel oil micro coagulation for carrier slime agglo-flotation improved coal recovery and decreased collector reagent need at an amount one third. The combustible recovery reached a recovery of 43% without collector addition at pH 7,7 and 79 % at 120 mg/L fuel oil addition.

The test results showed that ultrasound slime agglo-flotation was an effective alternative treatment for sludge type pulps and effectively increased by decreasing pulp density in the slurry with low solid concentrations.

Due to the high ash content of Şırnak asphaltites and show that conventional slime agglo-flotation can be as low as column slime agglo-flotation The yield was also higher at certain fuel conditioning time of 20 minutes, but it was determined that the centrifuge agglo-flotation did not disturbed coagulates and not reduced combustible yield below to 56% which was sufficient, and well as clean coal product contained less sulfur. The ash content in the agglo-flotation washing plant was removed from the 42 % to 26% as waste material at high weight rate 62 %. Thus, 38% of the combustible sulfur could be disposed off.

Clean asphaltite with 25.2% ash could be produced in washing process, if carried out, and would have the 4.3% combustible sulfur, and a 6700 kcal/kg, lower heat value could be beneficial for both heating and for industrial boilers using washed clean fuel.

This washing application should be mandatory. Especially the company off-product quality, excavated shale rocks of the same color will be involved in the production by mixing will be reduced. Also washing process because there is very little difference between the density of the shale and coal will be more difficult.

The plant capacity to reduce costs researchers widely used in coal washing "modified column slime agglo-flotation" (Anonymous a, b, c, 2015). The majority needed to seek the optimal method to wash hardly washable Şırnak and Hakkari asphaltites.

Şırnak asphaltites may be washable with our technological conditions over difficult macro-economic factors that restrict the installation of washing facilities, fuel imports, environmental threats, such as economic sanctions will need to be examined.

REFERENCES

Akdemir, Ü., and I. Sönmez. (2003). Investigation Of Coal And Ash Recovery And Entrainment In Flotation. *Fuel Processing Technology 82*(1): 1–9

Anonymous a, (2015), *MultotecŞirket* web sayfası, http://www.multotec.com/category/industry/coal

Anonymous b, (2015), *MBE Şirket* web sayfası, http://www.mbe-cmt.com/en/products/pneuflot%C2%AE/pneuflot%C2%AE

Anonymous c, (2015), *CWP Şirket* web sayfası, http://cwp.com.tr/en/products.aspx?id=30

Aplan F.F., (1977), Use of the Flotation Proess Desulphurization of Coal, *Coal Desulfurization*: Wheelock T.D. (ed), ACS Symposium Series,Washington

Ata, S., and Jameson G. J. (2005), The formation of bubble clusters in flotation cells, *International Journal of Mineral Processing 76:* 123 – 139

Ata, S. (2012). Phenomena in the froth phase of flotation—A review. International Journal of Mineral Processing *102*: 1–12.

Chander S, Sharma VN. (1976), Fine Particles Processing,P. Somasundran; 525-543

Chander S., Mohal B. R., and Aplan F. F. (1987), Wetting Behavior of Coal in the Presence of Some Nonionic Surfactants, *Colloids & Surfaces* , Vol. 26 , pp. 205 – 213.

Dai, Z., Fornasiero, D. and Ralston, J., (2000), Particle-Bubble Collision Models - A Review, *Advances in Colloid and Interface Science, 85*, No. 2-3, 231-256.

Degner V.R., (1986), Flotation Machine Size Selection, *COALPREP86* Conference papers, p319-349

Despotovic, R, (1976),;Radiometric Characterization Of Precipitation Process, Fine Particles Processing ,P. Somasundran, 481-491

Erol, M., C. Colduroglu, and Z. Aktas. (2003). The Effect Of Reagents And Reagent Mixtures On Froth Flotation Of Coal Fines. *International Journal of Mineral Processing 71(1):* 131–145.

Falutsu, M., and G. S. Dobby. (1992). Froth performance in commercial sized flotation columns. Minerals Engineering *5(10*): 1207–1223

Fuerstenau M.C., (1976), *Flotation*, AIME, New York

Gupta, A. K., P. K. Banerjee, A. Mishra, and P. Satish. (2007). Effect Of Alcohol And Polyglycol Ether Frothers On Foam Stability, Bubble Size And Coal Flotation. *Fine Coal Processing*, eds. S. K. Mishra and R. R. Klimpel, 78–109. Park Ridge, NJ: Noyes Publications.

Hadler, K., M. Greyling, N. Plint, and J. J. Cilliers. (2012). The Effect Of Froth Depth On Air Recovery And Flotation Performance. *Minerals Engineering* 36: 248–253.

Hogg R,(1976), Characterization Of Mineral Surfaces, Fine Particles Processing,P. Somasundran: 482-524 IEA, 2012, World Energy Outlook

Jameson , G. J. (2001) . The Flotation Of Coarse And Ultrafine Particles. *International Journal of Mineral Processing* 72 : 12 – 15

Ketkar, D. R., Mallikarjunan, R. and Venkatachalam, S., (1991), Electroflotation Of Quartz Fines. *International Journal of Mineral Processing, 31*, No. 1-2, 127-138

Klimpel , R. R. , and R. D. Hansen . (1987). Fine *Coal Processing* . New York : Noyes Publications

Klimpel, R. R., and R. D. Hansen. (1987). Chemistry of fine coal flotation. *Fine Coal Processing* 78–109

Matis, K. A. (Ed.), (1995), Flotation Science and Engineering. Marcel Dekker, New York

Miettinen, T., Ralston, J. and Fornasiero, D., The limits of fine particle flotation, Minerals Engineering, 23, No. 5, 420-437 (2010).

Nunes, A. P. L., Peres, A. E. C., Araujo, A. C. and Valadão, G. E. S., (2011), Electrokinetic Properties Of Wavellite And Its Floatability With Cationic And Anionic Surfactants, Journal of Colloid and Interface Science, 361, 632-638

Oats, W. J., O. Ozdemir, and A. V. Nguyen. (2010). Effect Of Mechanical And Chemical Clay Removals By Hydrocyclone And Dispersants On Coal Flotation. *Minerals Engineering* 23(5): 413–419.

Rubio, J. (1996). Modified Column Flotation Of Mineral Particles. *International Journal of Mineral Processing* 48(3): 183–196

Rubio, J. (1996). Modified Column Flotation Of Mineral Particles. *International Journal of Mineral Processing* 48(3): 183–196

Schubert, H. (2008). On The Optimization Of Hydrodynamics In Fine Particle Flotation. *Minerals Engineering* 21(12): 930–936

Schubert, H. (2008). On The Optimization Of Hydrodynamics In Fine Particle Flotation. *Minerals Engineering* 21(12): 930–936.

TKI, (2009), The Turkish Ministry of Energy, Energy, Dept., Lignite Coal Report

TTK, (2009), The Turkish Ministry of Energy, Energy, Dept., Hard Coal Report

Valderrama, L., M. Santander, M. Paiva, and J. Rubio. (2011). Modified-Three-Product Column (3PC) Flotation Of Copper-Gold Particles In A Rougher Feed And Tailings. *Minerals Engineering* 24(13): 1397–1401

Warren, L. J. (1985). Determination Of The Contributions Of True Flotation And Entrainment In Batch Flotation Tests. *International Journal of Mineral Processing* 14(1): 33–44

Wills , B. A. , and Napier-Munn T. J., (2006) . *Wills' Mineral Processing Technology* . Boston : Butterworth-Heinemann

Xie , G. Y. , and Ou Z. S.. (1999) . Research on coal washing desulfurization . Journal of China University of Mining & Technology 28 (5): 502 – 505

Xie , G. Y. , and Ou Z. S.. (1999) . The study and practice of cyclonic microbial flotation column of ash and pyritic sulfur rejection from coals . Mining Science and Technology 5 : 511 – 514.

Xie , G. Y. (2001) . *Mineral Processing* . Xu Zhou, China University of Mining and Technology Press

Yianatos, J. B., J. A. Finch, and A. R. Laplante. 1988. Selectivity in column flotation froths. *International Journal of Mineral Processing* 23(3): 279–292.

Yoon, R. H. (1993). Microbubble flotation. Minerals Engineering 6(6): 619–630.

Yoon, R. H. (2000). The role of hydrodynamic and surface forces in bubble–particle interaction. *International Journal of Mineral Processing* 58(1): 129–143.

ALTIN İÇERİKLİ GALEN MİNERALİNİN YÜZEY KİMYASI VE FLOTASYON ÖZELLİKLERİNİN ARAŞTIRILMASI

INVESTIGATION OF THE SURFACE CHEMISTRY AND FLOTATION PROPERTIES OF THE GOLD-BEARING GALENA MINERAL

G. Erçelik [1], M. Terzi [1], I. Kursun Unver [1,*], O. Özdemir [1]

[1] *İstanbul Üniversitesi-Cerrahpaşa, Mühendislik Fakültesi, Maden Mühendisliği Bölümü*
(*Sorumlu yazar: ilginkur@iuc.edu.tr)

ÖZET

Bu çalışmada, İzmir ili sınırları içerisinde, Menderes bölgesinden temin edilen altın içerikli sülfürlü cevherden elde edilen saf galen minerali üzerinde yüzey kimyası incelemeleri ve flotasyon deneyleri yürütülmüştür. Bu kapsamda zeta potansiyel, kabarcık-tane yapışma süresi ölçümleri ve mikro-flotasyon deneyleri gerçekleştirilmiştir. pH'ya bağlı yapılan zeta potansiyel ölçümlerinde pH 5-11 arasındaki değerlerde galen minerali negatif yüzey yüküne sahip olduğu belirlenmiş, sıfır yük noktasının (SYN) ise pH<3 değerinde olduğu düşünülmüştür. Farklı toplayıcı türleri olan SIBX, Aero MX-505 ve Aero S-8045 ile yapılan kabarcık-tane yapışma süresi ölçümlerinde, MX-505 ile tüm dozaj ve temas sürelerinde yapışma verimi %100 olarak gerçekleşmiştir. Bu sonuç, MX-505 varlığında galen taneleri ve hava kabarcığı arasında çok kuvvetli bir etkileşim olduğunu ortaya koymuştur. Mikro-flotasyon deneylerinde ise en yüksek verim yine MX-505 varlığında sağlanmıştır. MX-505'in tüm dozajlarında, %85 üzerinde flotasyon verimi elde edilmiştir. Bununla beraber SIBX dozaj miktarındaki artışla birlikte flotasyon verimi artmış ve 2,39x10^{-8} mol/L değerinde en yüksek verim değerine ulaşılmıştır. S-8045'in tekil kullanımında ise düşük verimler elde edilmiştir.

Anahtar Sözcükler: Galen, altın, yüzey kimyası, zeta potansiyel, kabarcık-tane yapışma süresi, mikro-flotasyon

ABSTRACT

In this study, surface chemistry studies were performed on the pure galena mineral obtained from gold-containing sulfide ore of Menderes region, İzmir. In this context, the zeta potential, bubble-particle attachment time, and micro-flotation experiments were carried out. In the case of zeta potential experiments as a function of pH, the galena mineral showed a negative charge at pH 5 and 11, and no zero point of charge (ZPC) was determined, and it was thought that ZPC of galena was around at pH<3. The bubble-particle attachment experiments carried out in the presence of SIBX, Aero MX-505, and Aero S-8045 collectors indicated that the attachment efficiency was 100% in the presence of MX-505 at all dosage and contact times. This result revealed that there was a very strong interaction between the galena and the air bubble in the presence of MX-505. When the results obtained in the micro-flotation experiments were evaluated, the highest efficiency was obtained with MX-505. At all dosages of MX-505, a flotation efficiency of over 85% was obtained. Besides, with the increase in the dosage of SIBX, the flotation recovery increased and the highest recovery was obtained at 2.39x10^{-8} mol/L. On the other hand, S-8045 collector showed lower efficiency in its single-use.

Keywords: Galena, gold, surface chemistry, zeta potential, bubble-particle attachment time, micro-flotation

GİRİŞ

Metalik cevherlerin prospeksiyonu, madenciliği ve zenginleştirilmesi, kapsamlı ve emek gerektiren yoğun prosesler sonucunda gerçekleştirilmektedir. Zenginleştirilecek olan cevherin mineralojisi ve metalürjik özellikleri, üretim yöntemini ve uygulanacak zenginleştirme prosesini belirlemektedir.

Genel olarak, serbest haldeki nabit altın, tane boyutu çok küçük olmadığı sürece gravite yöntemleriyle zenginleştirilmektedir. Bununla birlikte altın birçok cevherde son derece ince boyutlarda ve genellikle katı çözelti kapanımları şeklinde bulunabilmektedir. Altın, pirit ve arsenopirit gibi bazı sülfitler içerisinde yüksek oranlarda bulunabilmektedir (Yalcin ve Kelebek, 2011). Bu minerallere ek olarak, Dünya genelindeki çeşitli sülfürlü rezervlerde altının galen ile ilişkili cevherleşmelerine de sıklıkla rastlanılmaktadır (Elliot, 1992; Ahmad vd., 2018; Khan vd., 2018). Bu tür rezervler, ince boyutlu altın tanelerinin cevher taşıyıcı mineral içerisinde kapanım halinde bulunması nedeniyle refrakter altın cevherleri olarak adlandırılırlar (Valenzuela vd., 2013). Refrakter bir cevherden altın kazanımında, siyanürleme işleminden önce altın içeren sülfit minerallerinin ve ultra ince boyutlu altın parçacıklarını konsantre edilmesi amacıyla köpük flotasyonu yöntemi kullanılabilir (Cilek ve Tuzci, 2021).

Endüstriyel ölçekli zenginleştirme yöntemlerinden biri olan köpük flotasyonunda, optimum verim ve tenör değerini yakalayabilmek için cevherin minerolojisini ve yüzey kimyasını iyi bilmek gerekmektedir. Her ne kadar literatürde galen minerali üzerine çok fazla çalışma olduğu düşünülse de, mineralin yatak özelliklerine ve oluşum şekillerine bağlı olarak, mineraller farklı özellik ve davranışlar gösterebilmektedir. Bu yüzden her bölgeye özgü farklı cevherler üzerinde detaylı test çalışmaları yapılması gerektiği düşünülmektedir. Flotasyon işleminin verimi önemli ölçüde hava kabarcıklarının hidrofobik mineral tanelerini toplama davranışına bağlıdır. Genelde ise bir mineralin flotasyon özelliği temas açısı ölçümleri ile saptanmaktadır. Bununla beraber birçok çalışmada göstermiştir ki bu yöntem her zaman bir mineralin flotasyon özelliğini tahmin edememektedir (Ye ve Miller, 1988; Yoon ve Yordan 1991).

Bir mineralin yüzebilirliğini tahmin etmede diğer bir yöntem ise bir tanenin bir hava kabarcığına yapışması için gerekli olan sürenin tespit edildiği kabarcık-tane yapışma süresi tayini ölçümleri olup bir mineralin flotasyon davranışını belirlemede temas açısına nazaran daha doğru bir yaklaşım vermektedir (Ye ve Miller, 1988; Gu vd., 2003; Su vd., 2006; Ozdemir vd. 2009; Albijanic vd., 2010). Ayrıca bir pülp içinde hemen her mineralin yüzey yükünü sıfır yapan bir pH değeri vardır. Buna Sıfır Yük Noktası (SYN) denilmektedir. Zeta potansiyel ölçümleriyle elde edilen tanelerin elektrokinetik özellikleri flotasyonla ayırma işlemini anlamada önemli bilgiler içerir (Nguyen, 1994).

Bu çalışmada İzmir ili sınırları içerisinde, Menderes bölgesinden temin eliden sülfürlü altın cevherden elde edilen saf galen minerali üzerinde, zeta potansiyeli ve kabarcık-tane yapışma süresi ölçümleri ve mikro-flotasyon deneyleri gerçekleştirilmiştir. Bu kapsamda SIBX, Aero MX-505 ve Aero S-8045 toplayıcıların altın içerikli saf galen mineralinin mikro-flotasyon kazanma verimi üzerine etkileri, dozaja bağlı olarak incelenmiştir.

MALZEME VE YÖNTEM

Malzeme

Deneylerde kullanılan altın içerikli galen cevheri; İzmir ili sınırları içerisinde, Menderes bölgesinden temin edilmiş olup, bölgede faaliyet gösteren özel bir firmanın tesis beslemesinden temsili

olarak alınmıştır. Deneylere esas numunelerin kimyasal bileşimi hakkında bilgi edinilmesi amacıyla kimyasal analize tabi tutulmuştur. Kimyasal analiz sonuçları Çizelge 1'de gösterilmiştir.

Çizelge 1. Cevherin kimyasal analiz sonuçları

Element	(%)	Element	(ppm)
S	3,23	Au	10,30
Al	1,65	Ag	15,50
Ca	3,93	Cu	661,50
Fe	5,52	Ni	68,50
K	0,96	As	1105,00
Mg	0,43	Ba	147,50
Na	0,07	Co	31,25
Ti	0,08	Cr	58,00
Mn	8,49	P	102,50
Pb	0,49	W	227,50
Zn	0,48	Mo	10,75
Si	25,82	Sr	18,60
Hafif Element	48,58		

Kimyasal analiz sonuçları değerlendirildiğinde; cevher içerisinde tespit edilen en yüksek yüzdeye sahip elementler; %48,58 oranında hafif elementler (O_2 vb.), %25,82 oranında silisyum elementidir. Bu elementler dışında %8,49 mangan, %5,52 demir, %3,93 kalsiyum, %3,23 sülfür, %1,65 alüminyum, %0,96 potasyum, %0,49 kurşun, %0,48 çinko, %0,43 magnezyum, 10,3 ppm altın, 15,5 ppm gümüş, 661 ppm bakır, 1105 ppm arsenik, 227,5 ppm volfram ve 10,75 molibden elementleri tespit edilmiştir.

Mineralojik Analiz

Deneylere esas numunelerin mineralojik özellikleri hakkında bilgi edinilmesi amacıyla her bir fraksiyonun parlak kesitleri üzerinde Nikon LV 250 optik mikroskop ve Clemex optik yazılımı kullanılarak bir dizi incelemeler yürütülmüştür. Optik mikroskop görüntüleri Şekil 1-3'te gösterilmiştir.

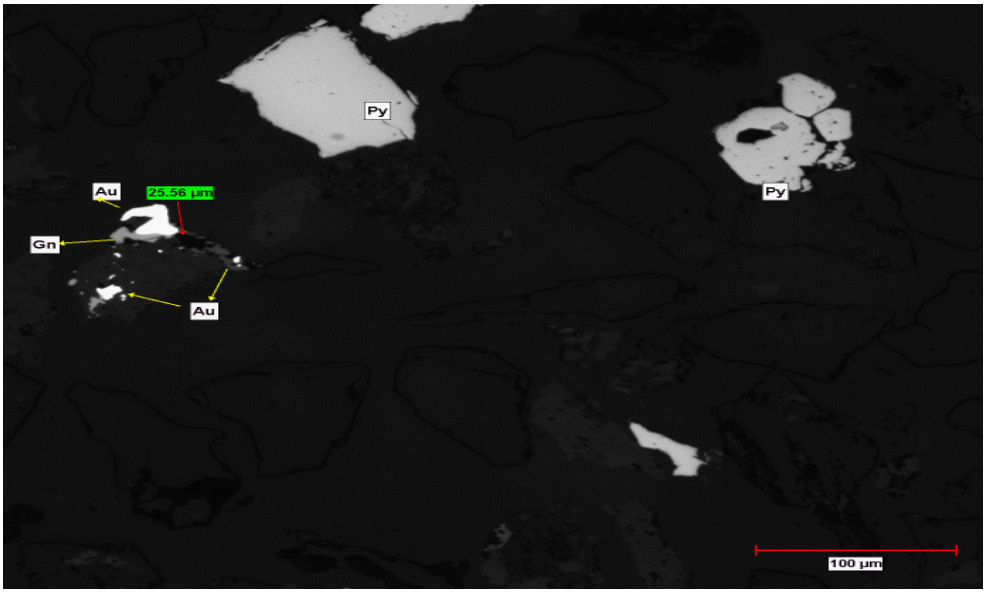

Şekil 1. + 0,106 mm fraksiyonun 50× mercek altında görüntüsü

Şekil 2. + 0,090 mm fraksiyonun 50× mercek altında görüntüsü

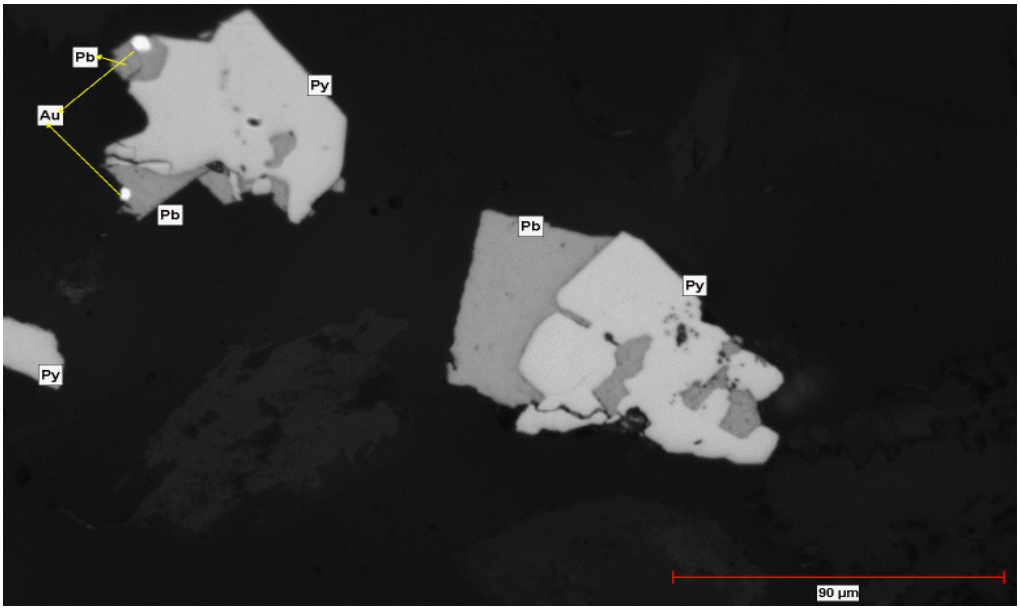

Şekil 3. + 0,038 mm fraksiyonun 50× mercek altında görüntüsü

Cevherin mineralojik bileşiminin belirlenmesi amacıyla X-Işını Kırınımı (XRD) analizi, kimyasal analiz ve mikroskop analizi gerçekleştirilmiştir. Cevher kabaca, sülfit mineralleri ile ilişkili kuvars damarları, cevherli ve hornblend kontak metamorfik kayaçlar oluşmaktadır. Cevherleşme ile ilişkili alterasyon fazı ana olarak; rodonit, rodokrozit, aksinit ve kuvars, yan kayaçta ise gang mineralleri olarak klorit, serizit, illit ve kaolinit mineralleri ihtiva ettiği tespit edilmiştir. Pirit, sfalerit, galen, kalkopirit ana mineralleridir.

Altın taneleri çok küçük boyutlarda (1-20 µm) pirit, sfalerit, galen, kalkopirit mineralleri içerisinde dağılım şeklinde bulunduğu tespit edilmiştir. Zaman zaman pirit, sfalerit ve galen minerallerinin ortak bulunduğu gözlemlenmiştir.

Numune Hazırlama

Bu kapsamda öncelikle kapalı devre olarak gerçekleştirilen kırma-eleme işlemleri sonucunda malzemenin tamamı -2 mm tane boyutuna indirilmiştir ve kuru eleme yöntemi ile üç farklı fraksiyonel boyuta (-2+1 mm, -1+0,5 mm ve -0,5 mm) sınıflandırılmıştır. Elde edilen -2+1 mm ve -0,5 mm boyutlu fraksiyonlar ise Wilfley sallantılı masa ile gravite ayrımına tabi tutulmuş ve deney sırasında konsantre bandı manuel olarak en üst noktadan kesilerek ağır mineral konsantreleri elde edilmiştir. Elde edilen konsantreler ivedi olarak 50°C'de etüvde kurutulmuş ve paketlenmiştir. Sallantılı masadan elde edilen -2+1 mm boyutlu konsantre, saf galen tanelerinin triyaj (el ile ayıklama) yöntemi ile seçilmesi ile daha ileri derecede saflaştırılmıştır. -0,5 mm boyutlu konsantrenin ise çok yüksek oranda galen içeriğine sahip olduğu gözlenmiş ve bu nedenle daha ileri bir saflaştırma işlemine tabi tutulmamıştır. El ile seçilen saf galen taneleri Şekil 4'te gösterilmiştir.

Şekil 4. Galen numunesi

Seçilen numuneler, yüzey kimyası çalışmaları için uygun tane fraksiyonuna ufalanması amacıyla el havanı ve Restch RM 200 agat öğütücü kullanılarak kademeli olarak öğütülmüştür. Öğütülen numuneler üzerinde kuru eleme işlemi uygulanarak -63+38 µm ve -38 µm tane boyutunda numuneler elde edilmiştir.

Zeta potansiyeli ölçümlerine uygun boyutta numune hazırlamak amacıyla ise kuru elemeden elde edilen -38 µm fraksiyonundaki galen ve pirit taneleri, havanlı öğütücüde 20 dk süre ile öğütülerek daha da ince (d_{80} = 10 µm) boyuta getirilmiştir.

YÖNTEM

Zeta Potansiyel Ölçümleri

Zeta potansiyel ölçümleri Brookhaven Zetaplus Zetametre ile elektroforetik yöntem kullanılarak yürütülmüştür. Bu kapsamda -38 µm boyutlu 0,3 gr galen numunesi ve 30 mL saf su (TDS<10 / pH ≈ 7) ile %1 katı oranında süspansiyon hazırlanmış ve yeterli miktarda süspansiyon 4 mL hacimli ölçüm hücresine transfer edilmiştir. Doğal pH'da gerçekleştirilen ölçümlerin ardından süspansiyona 0,1 M HCl ya da 0,1 M NaOH çözeltisi eklenmesi ile pH ayarlaması yapılmış ve farklı pH'larda (5, 7, 9, 11) ölçümler alınmıştır. Her bir pH değeri için 10 ölçüm alınmıştır. Galen mineralinin pH'ya bağlı zeta potansiyel ölçüm sonuçları Şekil 5'te gösterilmiştir.

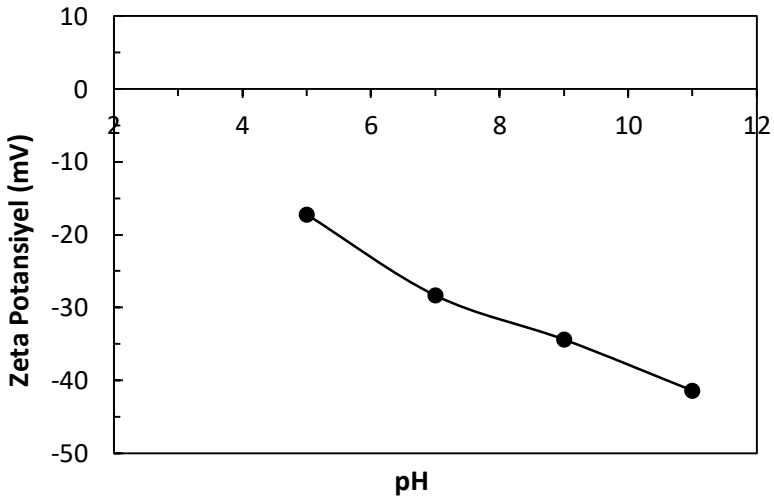

Şekil 5. Galen numunesinin zeta potansiyel-pH profili

Zeta potansiyel deneyleri kapsamında pH 5, 7, 9 ve 11 noktalarında ölçümler alınmıştır. pH ≤ 4 değerinden sonra cihazın elektrot akım değerinin artması ile sağlıklı sonuçlara ulaşılamadığı için pH 4 ve altındaki değerlerde ölçüm alınmamıştır. Zeta potansiyeli ölçümleinde galen mineralinin sıfır yük noktası (SYN) tespit edilememiştir. Literatürdeki diğer bazı çalışmalarda da bazı galen mineralinin SYN'ının bulunamadığı veya pH<3 değerinde olabileceği ortaya konulmuştur (Marek, 2009).

Mikro-Flotasyon Deneyleri

Mikro-flotasyon deneyleri tesis koşullarının simüle edilmesi amacıyla, -68+38 µm tane boyutunda galen numunesi ve saf su kullanılarak gerçekleştirilmiştir. Flotasyon deneylerinde 55 mL hacimli mikro-flotasyon hücresi kullanılmıştır ve katı oranı %1 olarak seçilmiştir. Kollektör ve köpürtücü olarak ise sırasıyla Sodyum İzoButil Ksantat (SIBX), Aero S-8045 promotor, Aerofloat MX-505 Promotor ve Frother Ore Prep F-549 kullanılmıştır. Kullanılan mikro-flotasyon hücresi Partridge and Smith hücre tasarımına sahiptir. Mikro flotasyon deney düzeneği ve SIBX kimyasalı ile örnek bir mikro-flotasyon testi Şekil 6'da, deney parametreleri ve koşulları ise Çizelge 2'de gösterilmiştir.

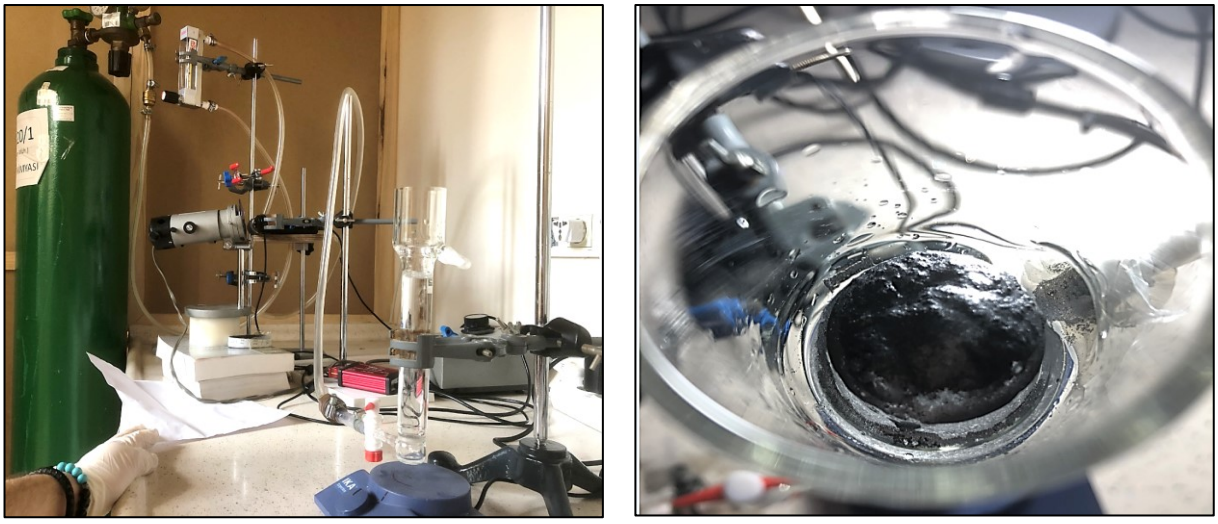

Şekil 6. Mikro-flotasyon deney düzeneği ve örnek bir deney

Çizelge 3. Mikro-flotasyon test parametreleri ve koşulları

Parametre	Koşul
Hücre Hacmi	55 mL
Su	Saf Su (TDS<10 / pH ≈ 7)
Saf Numune Miktarı	0,55 gr
Tane Boyutu	-63+38 µm
Katı Oranı	%1
Kondüsyonlama Karıştırıcı Hızı	500 dev/dk
Gaz (N2) Debisi	15 mL/dk
pH	Doğal pH (8,0-9,0)
Kollektör Türü	SIBX (Quimidroga), S-8045 (Solvay), MX-505 (Solvay)
Kollektör Kondüsyonlama Süresi	5 dk
Köpürtücü Türü	Frother Ore Prep F-549 (Solvay)
Flotasyon Süresi	1 dk

55 mL hacimde ve %1 katı oranındaki galen süspansiyonu bir manyetik karıştırıcı yardımıyla (500 dev/dk) kondüsyonlanmıştır. Kondüsyonlama süresi toplayıcı için 8 dk ve ardından köpürtücü için 2 dk süresince yapılmıştır. Kondisyonlama işlemi bittikten sonra mikro-flotasyon hücresine aktarılan süspansiyon, 15 mL/dk azot gazı ile 1 dk boyunca mikro-flotasyona tabii tutulmuştur. Yüzen ve batan kısım bir filtre kâğıdı yardımıyla susuzlandırıldıktan sonra etüvde 105°C'de kurutulmuştur. Kurutulan flotasyon ürünleri tartılarak flotasyon verimi gravimetrik olarak hesap edilmiştir.

Kabarcık-Tane Yapışma Verimi Ölçümleri

Kabarcık-tane yapışma süresi tayini için Glembotsky tasarım konsepti kullanılmış olup, ölçümler Bratton Mühendisliğin kabarcık-tane süre tayin cihazı ile gerçekleştirilmiştir. Mineral tane yatağı ve hava kabarcığı kullanılarak yapışma sürelerinin belirlendiği bu test günümüzde yaygın olarak kullanılmaktadır (Glembotsky, 1953; Ozdemir vd., 2009; Albijanic vd., 2011; Albijanic vd., 2014). Kabarcık-tane yapışma süresi ölçümlerinde -63+38 µm tane boyutundaki saf galen numuneleri kullanılmıştır. Deneyde kullanılan cihaz Şekil 7'de gösterilmiştir.

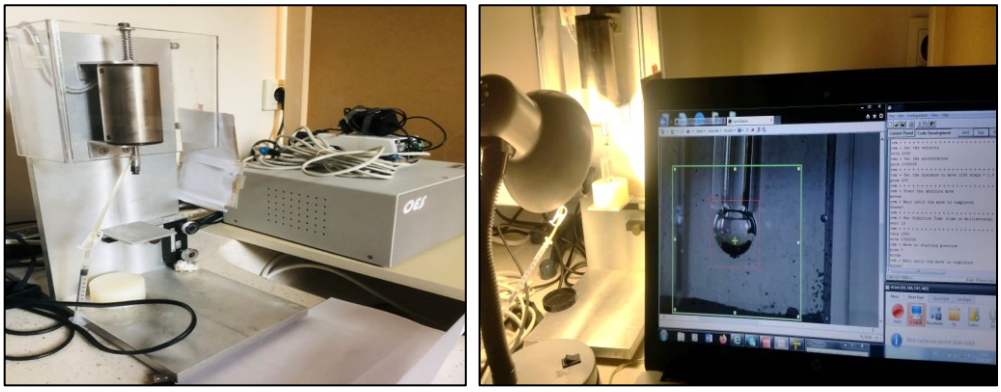

Şekil 7. Kabarcık-Tane Yapışma Süresi Tayin Cihazı – Bratton Mühendislik A.B.D.

Hassas tartı yardımıyla 0,50 g galen numunesi tartılmış ve 50 mL saf su içerisine eklenmiş böylece %1 katı oranında süspansiyon hazırlanmıştır. Hazırlanan süspansiyona istenilen dozajda toplayıcı eklenmiş ve 10 dk'lık kondüsyonlama süreci sonrasında bir damlalık yardımıyla, hücredeki yatak kalınlığı ≈1 mm olacak şekilde 4 mL'lik ölçüm hücresine transfer edilmiştir. Kabarcık-tane yapışma süresi ölçümlerinde 1 ms, 10 ms, 100 ms ve 1000 ms temas süreleri kullanılmıştır. Her bir süre için hücrede oluşturulan yatak yüzeyinin 10 farklı noktasından ölçüm alınmıştır.

BULGULAR

Mikro-Flotasyon Deneyleri

SIBX ile pH'ya bağlı (5, 7, doğal, 9 ve 11) olarak yapılan mikro-flotasyon deneyleri sonucunda elde edilen flotasyon verimleri sırasıyla %65,82; %70,73; %83,45; %79,82 ve %45,82 olmuştur. En yüksek verim, doğal pH değerinde, %83,45 olarak elde edilmiştir. Buna göre optimum pH değeri doğal pH (8,7) olarak belirlenmiştir. Akabinde farklı toplayıcıların ve bu toplayıcıların dozajlarının etkisini görebilmek amacıyla köpürtücü dozajı ve pH değeri (doğal pH) sabit tutularak bir dizi mikro-flotasyon deneyi yapılmıştır.

Köpürtücü dozajı ve pH değeri sabit tutularak yürütülen deneylerde farklı toplayıcı dozajlarında SIBX toplayıcı için en yüksek flotasyon verimi $2{,}39 \times 10^{-8}$ mol/L dozajında %89,64, S-8045 toplayıcı için $1{,}71 \times 10^{-8}$ dozajında %75,09, MX-505 toplayıcı için ise $1{,}79 \times 10^{-9}$ mol/L dozajında %99,82 olarak tespit edilmiştir. Mikro-flotasyon deney sonuçları Şekil 8'de gösterilmiştir.

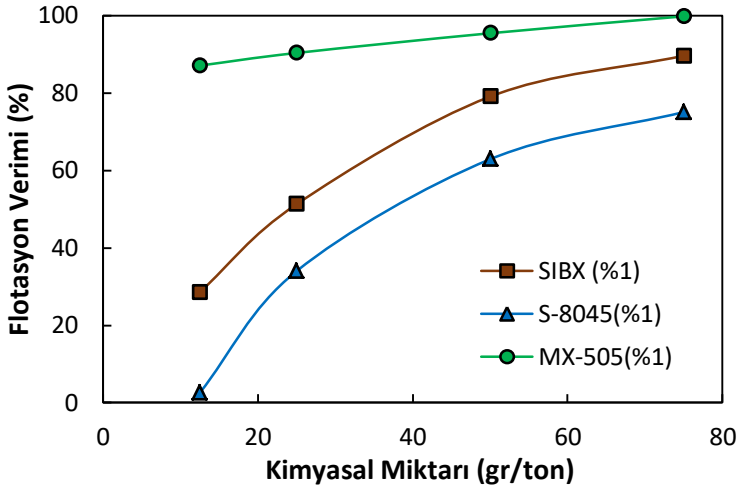

Şekil 8. Farklı toplayıcı dozajlarında mikro-flotasyon deney sonuçları

Mikro-flotasyon deneylerinde en yüksek verim MX-505 kimyasalında sağlanmıştır. MX-505'in tüm dozajlarında, %85 üzerinde flotasyon verimi elde edilmiştir. Bununla beraber SIBX kimyasalı dozaj miktarındaki artışla birlikte flotasyon verimi artış göstermiş ve $2{,}39 \times 10^{-8}$ mol/L değerinde en yüksek verim değerine ulaşılmıştır. S-8045 toplayıcısı ise tekil kullanımında diğer toplayıcılara oranla düşük verimler elde edilmiştir. S-8045 flotasyonda yardımcı toplayıcı olarak görev yapmaktadır ve elde edilen flotasyon sonuçlarına göre tekil kullanımında diğer iki toplayıcı kadar etkin olmadığı gözlemlenmiştir.

Kabarcık-Tane Yapışma Verimi Ölçümleri

Mikro-flotasyon deneyleri ile aynı toplayıcı dozajlarında, SIBX, S-8045 ve MX-505 toplayıcıları kullanılarak gerçekleştirilen kabarcık-tane yapışma süresi ölçüm sonuçları sırasıyla Şekil 9, Şekil 10 ve Şekil 11'de verilmiştir.

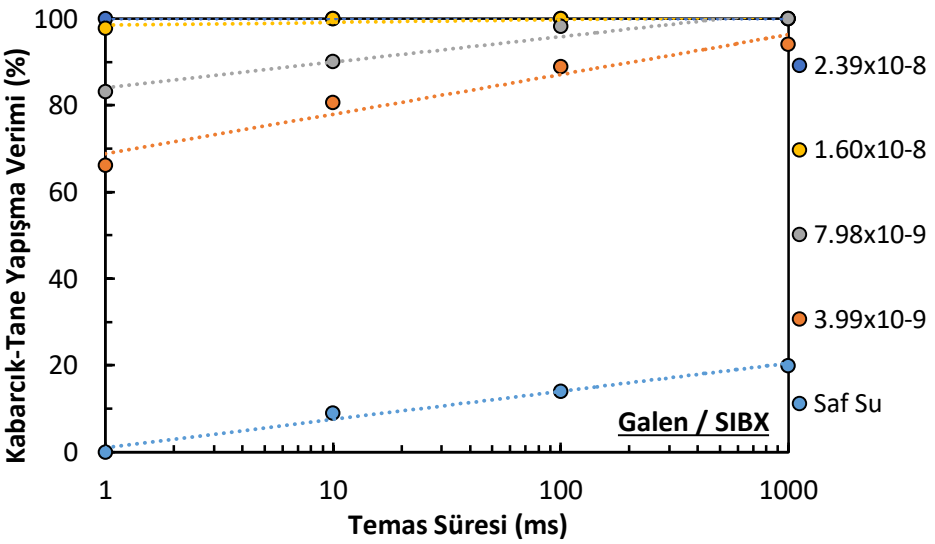

Şekil 9. SIBX varlığında kabarcık-tane yapışma süresi tayini ölçüm sonuçları

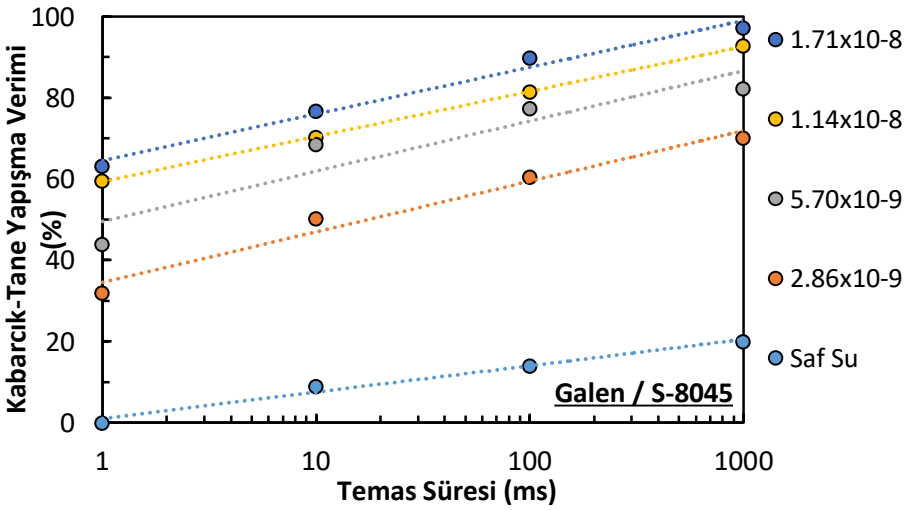

Şekil 10. S-8045 varlığında kabarcık-tane yapışma süresi tayini ölçüm sonuçları

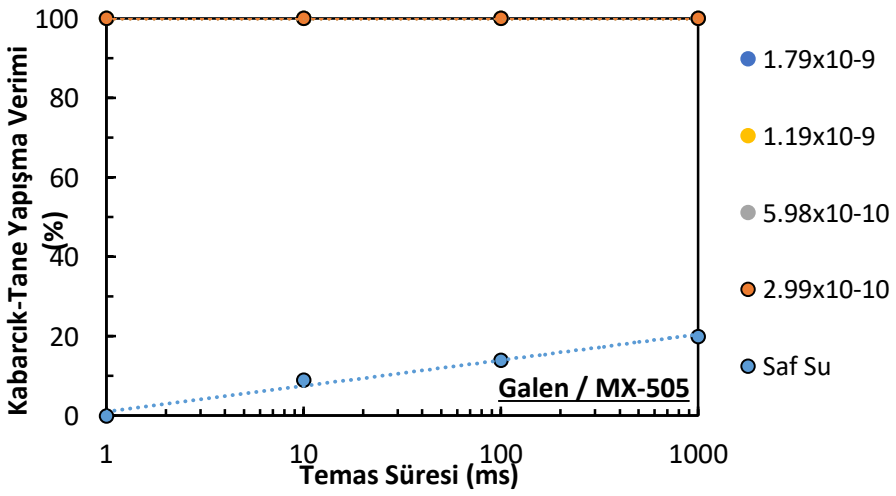

Şekil 11. MX-505 varlığında kabarcık-tane yapışma süresi tayini ölçüm sonuçları

Ölçüm sonuçlarına göre, galen tanelerinin kollektörsüz ortamda en yüksek temas süresinde bile hava kabarcığına %20 ihtimalle yapışmaktadır. Bir başka deyişle kabarcık-tane yapışma süresi ölçüm sonuçları galenin saf su içerisinde hidrofil davranış gösterdiğini teyit etmiştir. Farklı toplayıcıların farklı dozajlarında yapılan ölçümlerin sonuçlarında ise tüm dozajlarda galen taneleri ile hava kabarcığı arasında bir etkileşim olduğu ortaya konulmuştur.

Genel olarak en zayıf etkileşim S-8045 ile gözlenmiş olup, bu toplayıcının $2{,}86x10^{-9}$ mol/L ve $5{,}70x10^{-9}$ mol/L dozajlarında düşük temas sürelerinde yapışma verimi %50'nin altında kalmıştır. $1{,}14x10^{-8}$ mol/L ve $1{,}71x10^{-8}$ mol/L dozajlarında, tüm temas sürelerinde yapışma verimi %50'nin üzerinde gerçekleşmiş olup, bu noktalardaki kabarcık-tane yapışma süresinin (yapışma verimi > %50) 1 ms'nin altında olduğu söylenebilmektedir.

SIBX ile de S-8045'e benzer sonuçlar elde edilmiş olmakla birlikte, bu toplayıcının varlığında tüm dozaj ve temas sürelerinde yapışma verimi %50'nin üzerinde gerçekleşmiştir. Özellikle $1{,}60x10^{-8}$ mol/L ve $2{,}39x10^{-8}$ mol/L dozajlarında 1 ms temas süresinde bile yapışma verimi %95-100 aralığında olmuştur. Yapışma verimlerindeki bu artış, SIBX varlığında galen taneleri ve hava kabarcığı arasında S-8045'e göre daha kuvvetli bir etkileşim olduğunu ortaya koymaktadır. Sonuç olarak tüm dozaj ve temas süreleri için kabarcık-tane yapışma süresinin yine 1 ms'nin altında olduğu söylenebilmektedir.

MX-505 ile ise tüm dozaj ve temas sürelerinde yapışma verimi %100 olarak gerçekleşmiştir. Bu sonuç, MX-505 varlığında galen taneleri ve hava kabarcığı arasında çok kuvvetli bir etkileşim olduğunu ortaya koymaktadır.

Kabarcık-tane yapışma süresi ölçümlerinde 25 gr/ton dozaj miktarında yani $2{,}86x10^{-9}$ mol/L S-8045, $3{,}99x10^{-9}$ mol/L SIBX ve $2{,}99x10^{-10}$ mol/L MX-505 kimyasal dozajında çekilen görüntüler Şekil 12'de gösterilmiştir.

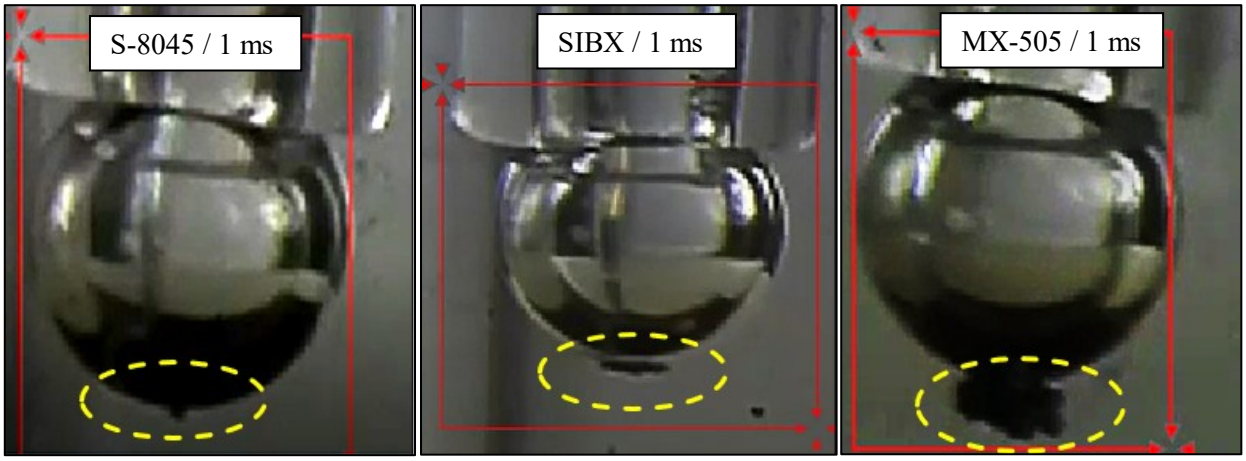

Şekil 13**.** Kabarcık-tane yapışma süresi tayini görseli

TARTIŞMA VE SONUÇ

Bu çalışmada, İzmir ili sınırları içerisinde, Menderes bölgesinden temin edilen numune; epitermal yatak özelliği göstermekte olup, cevher kuvars-rodonit içerisinde saçınım şeklinde oluştuğu tespit edilmiştir. Altın pirit ve galen mineralleri içinde ihtiva ettiği gözlemlenmiştir. Zeta potansiyel, mikro-flotasyon deneyleri ve kabarcık-tane yapışma verimi ölçümleri kullanılarak yürütülen bu çalışmada, altın içerikli galen mineralinin ksantat ve farklı iki türde ditiofosfat toplayıcıları ile flotasyonunun başarı ile yapılabileceği ortaya konmuştur. Galen mineralinin sıfır yük noktası (SYN) değeri

tespit edilememiş olup, zeta potansiyel profili incelendiğinde SYN < 3 olabileceği düşünülmektedir. Kabarcık-tane yapışma süresi açısından 1 ms sürede en etkin sonuca MX-505 kimyasalı kullanılarak ulaşılmıştır. Alkol içerikli ditiofosfat tipi bir toplayıcı olan MX-505'in galen flotasyonunda özellikle etkin olduğu tespit edilmiştir. Üç toplayıcı türü içerisinde galen flotasyon verimi açısından en iyi sonuçlara MX-505 ile ulaşılmıştır.

KAYNAKLAR

Ahmad, L., Khan, S.D., Tahir Shah, M., & Jehan, N. (2018). Gold Mineralization In Bubin Area, Gilgit-Baltistan, Northern Areas, Pakistan. *Arabian Journal of Geosciences*, 11(2), 1-12.

Albijanic, B., Amini, E., Wightman, E., Ozdemir, O., Nguyen, Bradshaw, D.J., (2011). A relationship between the bubble–particle attachment time and the mineralogy of a copper–sulphide ore. *Minerals Engineering,* 24, 1335–1339.

Albijanic, B., Ozdemir, O., Hampton, M.A., Nguyen, P.T., Nguyen, A.V., Bradshaw, D. (2014). Fundamental aspects of bubble–particle attachment mechanism in flotation separation. *Minerals Engineering*, 65, 187–195.

Albijanic, B., Ozdemir, O., Nguyen, A.V. ve Bradshaw, D. (2010). "A review of induction and attachment times of wetting thin films between air bubbles and particles and its relevance in the separation of particles by flotation", *Adv Colloid Interface Sci*, 159(1), 1-21.

Cilek, E.C., & Tuzci, G. (2021). Flotation behavior of native gold and gold-bearing sulfide minerals in a polymetallic gold ore. *Particulate Science and Technology*, 1-9.

Elliott, R.G. (1992). The geology and geochemistry of the Omai goldfield, Guyana (Doctoral dissertation, Oxford Brookes University).

Glembockij, V.A. (1953). The time of attachment of air bubbles to mineral particles in flotation and its measurement, Izv. Akad. Nauk SSSR (OTN), No. 11: 1524-1531.

Gu, G., Z. Xu, vd. (2003). Effects of physical environment on induction time of air-bitumen attachment, *Int. J. Miner. Process.*, 69(1-4): 235-250.

Khan, S.D., Okyay, Ü., Ahmad, L., & Shah, M.T. (2018). Characterization of gold mineralization in northern Pakistan using imaging spectroscopy. *Photogrammetric Engineering & Remote Sensing*, 84(7), 425-434.

Kosmulski, M. (2009). *Surface charging and points of zero charge* (Vol. 145). CRC press, 756-759

Nguyen, A.V. (1994). The collision between fine particles and single air bubbles in flotation, *J. Colloid Interface Sci.*, 162(1): 123-128.

Ozdemir, O., Karaguzel, C., Nguyen, A.V., Celik, M.S. ve Miller, J.D. (2009). Contact angle and bubble attachment studies in the flotation of trona and other soluble carbonate salts, *Miner Eng*, 22(2), 168-175.

Su, L., Z. Xu, vd. (2006). Role of oily bubbles in enhancing bitumen flotation, *Minerals Engineering* 19(6-8): 641-650.

Valenzuela, A., Valenzuela, J.L., & Parga, J.R. (2013). Effect of pretreatment of sulfide refractory concentrate with sodium hypochlorite, followed by extraction of gold by pressure cyanidation on gold removal. *Advances in Chemical Engineering and Science*, 3, 171-177

Yalcin, E., & Kelebek, S. (2011). Flotation kinetics of a pyritic gold ore. *International Journal of Mineral Processing*, 98(1-2), 48-54.

Ye, Y. ve J.D. Miller (1988). Bubble/particle contact time in the analysis of coal flotation, *Coal Prep.* (Gordon & Breach), 5(3-4): 147-166.

Yoon, R.H. ve Yordan, J.L. (1991). Induction time measurements for the quartz-amine flotation system, *Journal of Colloid and Interface Science*, 141(2): 374-383.

APPLICATION OF NANO BUBBLES IN COLUMN FLOTATION: BENEFICIATION OF IRON AND PHOSPHATE SLIMES

F. Nakhaei [1, *], M.B. Fathi [2], Z. Pourkarimi [3], F. Taghavi [4]

[1] *North West University, School of Chemical and Minerals Engineering*
*(*Corresponding Author: 36598704@nwu.ac.za)*
[2] *Urmia University, Engineering Faculty, Mining Department*
[3] *Department of Mineral Processing and Applied Research, Iran Mineral Processing Research Center*
[4] *University of Tehran, College of Engineering, School of Mining Engineering*

ABSTRACT

Fine particle flotation has been one of the main problems in many mineral processing plants. Beneficiation of iron ore and phosphate slimes is important from economic and environmental aspects. This study aimed at the purification of fine particles of iron and phosphate ores by a pilot scale flotation column (10.2 cm diameter and 400 cm height) in which Nano bubbles (NBs) were produced using a specially designed venturi hydrodynamic cavitation tube.

The iron slime sample (d_{80} equal to 45µm) was obtained from Gole-Gohar iron ore mine, one of the biggest iron concentrate producers in Iran, containing 67.5% Fe and 0.95% S. Phosphate particles with d_{80} finer than 30 µm contained 15.9% P_2O_5. This study addressed the processing of fine tailings (slimes) from phosphate and iron ore concentrators via flotation, despite the traditional view that ultrafine particles do not float. To reach this aim, an especial laboratory column flotation cell was manufactured and several comparative flotation tests were performed in presence and absence of NBs. Various parameters such as reagents dosage, air flowrate, froth depth, and NBs ratio to the cell volume were studied and optimum amounts were obtained. Results showed, flotation in presence of NBs obtained the significant increase in the phospate recovery more than 23% versus conventional flotation cell. Also, the sulfur content of iron concentrate could be reduced from 0.95% to 0.26% with iron recovery above 88% in presence of NBs.

Keywords: Iron ore, slime, phosphate, desulfurization, column flotation, nano bubbles

INTRODUCTION

In general, fine and ultrafine particles, profitable products nowadays, are disposed to the tailing dams. So, fine particles processing is important in terms of ecological and economic benefits. Flotation using nanobubbles (NBs) (<1 µm diameters) is one of the effective techniques in the recovery of fine mineral particles (Azevedo et al., 2016; Etchepare et al., 2017; Oliveira et al., 2018). In conventional processing methods such as flotation for particles less than 40 µm, because of the poor attachment (low probability of bubble-particle capture), the separation efficiency decreases and fall sharply for the ultrafine particles (< 15 µm). The results from previous studies depicted that because of NBs' large surface area, high concentration, long stability and high hydrophobic affinity, they adsorb rapidly at surfaces, and also by capillary impacts they can aggregate fine minerals, perform as nuclei for conventional bubbles, and float those aggregates (Theodorakis., 2019 ;Vaziri Hassas et al., 2018; Vaziri Hassas and Miller, 2019). So, large bubbles did not play a significant role in the process, instead the fine ones effectively adsorb the fine particles. The results of previous works showed that the purification of fine particles using NBs can improve the flotation selectivity index by more than 25% (Fan et al., 2010). Several techniques such as solvent exchange, temperature change, pressure reduction, ultrasonic method, and hydrodynamic

cavitation technique are introduced to generate nanobubbles (Hampton and Nguyen, 2010; Cho et al., 2005). Since the work of adhesion between a particle and water is always smaller than the work of cohesion of water, nanobubbles are selectively nucleated at the surface of hydrophobic particles. On the other hand, increasing solid surface hydrophobicity measured by the contact angle will lead to decrease the work of adhesion (Sobhy and Tao, 2013). On the other hand, generated nanobubbles on a particle surface also can play as a secondary collector that increase the probability of adhesion and therefore this phenomenon can reduce the need of surfactants/chemical reagents.

In this research, the capability of a column flotation assisted by hydrodynamic cavitation-generated NBs in processing of two different fine particles (phosphate and iron ores) was investigated and the results were compared with a conventional bubble generator type.

MATERIALS AND METHODS

Sampling

Flotation tests were performed on phosphate fine particles from Esfordi phosphate processing plant, located in Yazd province of Iran, and iron ore fines from Gole-Gohar iron complex located in Kerman province south of Iran.

In the Esfordi phosphate plant the main problem is that in the desliming process (the overflow of the second hydrocyclone) more than 30% of plant capacity is delivered to the tailing dam as particles with d_{80} smaller than 30 µm. These materials are similar to the feed (16% P_2O_5 content), and due to the fineness and reduction of recovery, these particles are removed from the flotation circuit. The flotation is fed from the second hydrocyclone underflow which is the final product of the grinding circuit. So, the sample of phosphate fine particles was obtained from the overflow stream of desliming hydrocyclone.

The iron sample with a relative high-grade iron was obtained from the complex waste damp which is fed by the rejected material from the main processing plant.

The analyses of sample particle-size distribution were measured by wet sieve and cyclosizer analysis for the iron ore and Laser Practice Size Analyzer (LPSA) Malvern 2000 MS, UK, for the phosphate ore. The results indicated that about 80% of the iron and phosphate samples have a particle size less than 42 µm and 29.13 µm respectively. Chemical analyses of representative samples were done to identify the amount of available compositions. The results depicted that the phosphate sample contained 15.95% P_2O_5 and 32.01% Fe_{Total} while for the iron sample about 42.2% and 1.98% were Fe and Sulphur. Based on the XRD analyses and the optical mineralogy study, the main components in the phosphate sample were apatite, hematite, quartz, calcite, talc and chlorite while for the iron sample, the gangue minerals were dickite, talk calcite, quartz, and pyrite and the main minerals were hematite, magnetite, and goethite.

Experimental Conditions and Procedures

A flotation column made of Plexiglas with a 4cm diameter and 2 m height was featured with a cavitation tube to generate NBs and a porous sparger to generate microbubbles (conventional-sized bubbles), respectively, as shown in Fig. 1.

The column was fitted with a mixing tank for the preparation and conditioning of slurry feed. The appropriate amount of reagents (collector, frother, pH regulator, and depressant) were added to the tank. The pulp feed is introduced to the upper part of the column via a peristaltic pump. Air and recirculating tailings were passed through the cavitation tube, designed for generating Nano bubbles, before being injected into the lower portion. The bottom of the flotation column was specially designed with two outlets. One of them was concentrate (for iron sample)/ tailing (for phosphate sample) stream and the other one was recycled stream that pumped through the cavitation tube for further recovery. Major process parameters such as collector dosage, gas and feed flowrates were examined individually to investigate their effects on flotation performance in the presence of nanobubbles.

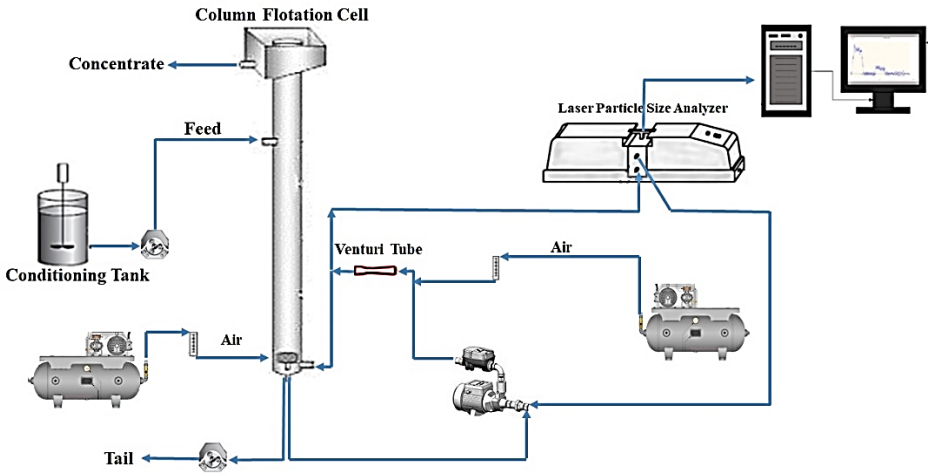

Figure 1. A schematic diagram of the applied flotation apparatus

The feed slurry was conditioned for 5 minutes with collector and frother prior to each test. All flotation tests were performed under the previous work optimum conditions that are presented in Table 1 and 2 (Nakhaei and Pourkarimi, 2020; Taghavi et al., 2022).

Table 1. Optimum conditions used in Phosphate column flotation

Parameters	**Value**
Froth depth (cm)	30
Gas flow rate (l/min-cm/s)	0.8
Flo-Y-S collector dosage (g/t)	400
Starch dosage (g/t)	500
Feed slurry flow rate (l/min-cm/s)	0.93
Wash water flow rate (l/min-cm/s)	0.13
Feed slurry solids concentration (%)	10

Table 2. Optimum conditions used in reverse column flotation of iron ores

Parameters	Value
Froth depth (cm)	20
Gas flow rate (l/min-cm/s)	0.9
Potassium Amyl Xanthate (PAX) dosage (g/t)	200
MIBC frother concentration (g/t)	100
Feed slurry flow rate (l/min-cm/s)	0.8
Feed slurry solids concentration (%)	9
Nanobubble aeration rate (l/min-cm/s)	0.15

Using venturi tubes the generation of nanobubbles was done based on the cavitation phenomenon. A Malvern mastersizer 2000 LPSA was employed for measuring the size distribution and volume of the bubbles. Before sending the solution into the venturi tubes the frother was added into the tank and mixed in appropriate time. Then the compressed air before entering the pump was added to the solution. In order to measure the bubble size, the solution containing nanobubbles was transferred to the laser particle size analyzer through pump propulsion.

RESULTS AND DISCUSSION

Bubble Size Distribution

In order to generate NBs, a venturi tube with the specified geometry, entrance diameters of 2.2 mm were used. Fig.2 shows the size characterization of bubbles generated by the optimally designed cavitation venturi tube. There are two major distribution peaks observed on the population frequency curve. As seen from the results, the average size (d_{50}) of generated nanobubbles by the cavitation tube is approximately 230 nm and for the micro size bubbles is about 100 µm. It is noteworthy that the measurement of the bubble size distribution (BSD) generated by the porous sparger, image sets with a high-speed digital camera coupled to an image analysis software (Image J) and a data acquisition system were applied. To determine the microbubble size, D_b (0.5) term at which 50% by volume of the bubbles are smaller was used as instrument output. The results showed that the diameter of the bubbles produced was in the range of 800 to 2500 µm with d_{50} 1800 µm.

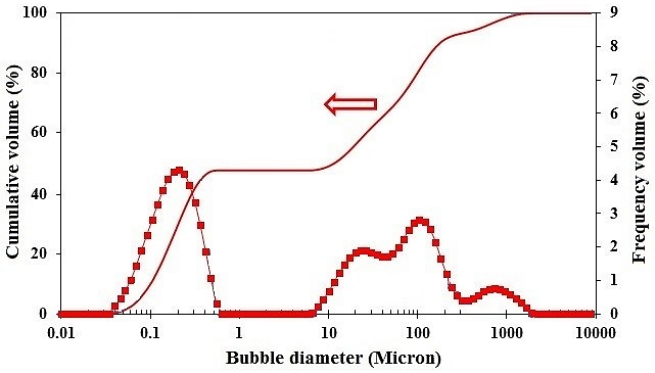

Figure 2. Bubble size distribution generated by the cavitation venturi tube (Nanobubble aeration rate = 0.11 l/min)

Column Experiments on Phosphate Minerals

The results obtained from the column tests in the presence and absence of Nano bubbles have been compared in the same conditions (Table 3). As results indicate, there are big differences in some important metallurgical performances among the flotation tests in studied settings. As the trends show in the presence of Nano bubbles, the P_2O_5 recovery has a drastic increase of 8.5% compared to the conventional conditions. On the other hand, comparison between S.E figures shows a step of 5% in increasing the values.

Table 3. Column flotation comparative results for phosphate fine particles in the presence and absence of NBs

Condition	P_2O_5 (%)	Recovery (%)	Enrichment Ratio(c/f)	S.E
NBs absence	31.66	32.74	1.99	25.60
NBs presence	30.44	41.26	1.91	30.94

Usually, the improvements of flotation S.E in presence of NBs can be attributed to the selectivity of bubbles for hydrophobic particles. In order for particles to have a successful collection with air bubbles, particles behavior in three sub-processes, including collision, adhesion, and finally detachment

occurring in flotation should go on the desired path. So, a higher collection in flotation generally leads to an improved separation efficiency (Fan et al., 2019).
In the slurry, because of NBs small ascending velocity, they will rise slowly in the slurry and have many chances to collide with and attach to fine phosphate particles (Etchepare et al., 2017, Calgaroto et al., 2015). The bubbles number density or concentration in the slurry is an important factor in flotation. Increasing the bubble number density will promote the particles collision rates and with a higher bubble number density a more efficient flotation process can take place. In contrast, the conventional-sized bubbles generated by a normal sparger due to their sizes and low collision probability cannot collect fine particles effectively. Therefore, by utilizing NBs and a such mechanism the efficiency of fine particles flotation can be effectively improved.

After clarifying the effect of NBs on the process, different flow rates in the range of 0-0.9 L/min (0-1.19 cm/s), was also investigate to determine the optimum value (Table 4).

Table 4. Effect of NBs flowrate on the column flotation performance of Phosphate ores

NBs flowrate (Cm/S)	Recovery (%)	Grade (%)
0	32.74	31.70
0.60	35.12	31.39
0.73	38.25	30.52
0.90	41.26	30.43
1.19	34.97	27.61

The results indicate that the flotation performances can be affected by NBs flow rate. As it clearly shows the ideal in the recovery can be achieved with NBs flow rate of 0.93 cm/s. As described before, in this condition the hydrophobic particles are aggregate by NBs. This aggregation can create a capillary bridging that provides more collision and connection probability. The examination on current flotation test results proves that the applied NBs are selectively attached to the surface of apatite fine particles and then the hydrophobicity of particle surfaces is improved. This phenomenon will increase the floatability rate by increasing the contact angle of particle-bubble and connectivity forces.

Column Experiments on Iron Minerals

In a specific designed laboratory-scale flotation column the effects of nanobubbles on desulfurization of iron ore was evaluated. Keeping the introduced optimum conditions, the flotation behavior of pyrite in presence of NBs was investigated. In this condition, the aeration rate of nanobubbles was adjusted to column flotation cell equal to 0.11 l/min (0.15 cm/s). The obtained results for pyrite flotation depicted that using the cavitation system noticeably results in higher flotation recovery compared in absence of NBs (Table 5). As seen from the results, variations show that in tests with optimum operational conditions, the Sulphur recovery toward the absence of nanobubbles was increased by 20% and reached around 82%. Based on the literatures, by using NBs the wettability and floatability of particles are changed through the selective adsorption of nanobubbles on the surfaces of ultra-fine pyrite and consequently improving the flotation performance and also separation efficiency are taken place.

Table 5. Column flotation comparative results for desulfurization of iron ore concentrate and sulfur recovery in the presence and absence of NBs

Condition	S grade (%)	S recovery (%)
NBs absence	1.2	61
NBs presence	0.22	81.6

The results of an optimum test were observed that in presence of nanobubbles the final concentrate with the grade of 67.7% Fe and 0.22% S can be obtained.

CONCLUSIONS

A feasibility study was carried out to evaluate the effects of nanobubbles (NBs) presence in flotation on purification of two types of fine ores (Phosphate and Iron minerals). The results for phosphate minerals showed that using NBs can significantly enhance the process efficiency with favourable grade and recovery. In the presence of NBs, the recovery of fine phosphate particles increased by 8.5%, compared to the absence of NBs. Also, in the presence of NBs a significant increase in the process separation efficiency (S.E) by 5% was observed. The results revealed that applying NBs in column flotation tests of iron ores the desulfurization efficiency of iron ore concentrate can enhance significantly. In the presence of Nano bubbles, in concentrate part (reverse flotation) the recovery of sulphur minerals increased by 20%, while the sulphur content of iron concentrate (column tailing part) reduced from 1.2% to 0.22%.

REFERENCES

A. Azevedo, R. Etchepare, S. Calgaroto, and J. Rubio, (2016), Aqueous dispersions of nanobubbles: generation, properties and features, Int. J. Miner. Eng., *94*, p. 29.

A. Sobhy, D. Tao, (2013), High-Efficiency Nanobubble coal flotation, International Journal of Coal Preparation and Utilization, *33*:242–256.

B. Vaziri Hassas, J. Jin, L.X. Dang, X. Wang, and J.D. Miller, (2018), Attachment, Coalescence, and Spreading of Carbon Dioxide Nanobubbles at Pyrite Surfaces, Int. J. Langmuir, *34,* (No. 47, p. 14317.

B. Vaziri Hassas, J.D. Miller, (2019) The effect of carbon dioxide and nitrogen on pyrite surface properties and flotation response, Int. J. Minerals Engineering, 144.

F. Nakhaei, Z. pourkarimi, (2020), "Desulphurization of Iron Ore Slime by Column Flotation with Nano-Micro Bubbles", XXX International Mineral Processing Congress in Cape Town, South Africa, 18 - 22 October.

F. Taghavi, M. Noaparast, Z. Pourkarimi, F. Nakhaei, (2022), Comparison of mechanical and column flotation performances on recovery of phosphate slimes in presence of nano-microbubbles, J. Cent. South Univ. *29*: 102—115

H. Oliveira, A. Azevedo, and J. Rubio, (2018), Nanobubbles generation in a high-rate hydrodynamic cavitation tube, *Int. J. Miner*. Eng, *116,* p. 32.

M. A. Hampton, A. V. Nguyen. (2010). Nanobubbles and the nanobubble bridging capillary force. *Advances in Colloid and Interface Science 154*(1–2): 30–55.

M. Fan, D. Tao, and Y. Tao, (2019), Effects of nanobubbles in column flotation of Chinese sub-bituminous coal, Int. J. Coal Preparation and Utilization.

M. Fan, D. Tao, R. Honaker, and Zh. Luo, (2010), Nanobubble generation and its applications in froth flotation (part III): specially designed laboratory scale column flotation of phosphate, Int. J. Mining Science and Technology (China), *20*, No. 3, p. 317.

P.E. Theodorakis, Z. Che, Surface nanobubbles (2019) Theory, simulation, and experiment: a review, Int. J. Advancesin Colloid and Interface Science.

R. Etchepare, H. Oliveira, M. Nicknig, A. Azevedo, and J. Rubio, (2017), Nanobubbles: generation using a multiphase pump, properties and features in flotation*, Int. J. Miner. Eng*, *112*, p. 19.

S. Calgaroto, A. Azevedo,and J. Rubio, (2015) Flotation of quartz particles assisted by nanobubbles, Int. J. Mineral Processing, *137*, p. 64.

S. H. Cho, J. Y. Kim, J. H. Chun, and D. J. Kim. (2005). Ultrasonic formation of nanobubbles and their zeta-potentials in aqueous electrolyte and surfactant solutions, colloids and surfaces A. *Physicochemical Engineering Aspects 269*: 28–34.

APPLICATION OF RESPONSE SURFACE METHODOLOGY IN OPTIMIZING LEACHING PARAMETERS FOR NICKEL RECOVERY FROM SPENT CATALYST

A.M. Beygian [1], M.Rezaei [1], E. K. Alamdari [1,*]

[1] *Department of Materials and Metallurgical Engineering, Amirkabir University of Technology*
*(*Corresponding Author: alamdari@aut.ac.ir)*

ABSTRACT

Reuse and recovery of nickel from different types of waste is of great environmental and economic importance. The purpose of this study was to recover nickel from steam reforming catalyst by optimizing the operating parameters using response surface methodology (RSM). To this aim, nickel oxide was converted into nickel sulfate using sulfuric acid through leaching process. The influence of three numerical independent variables, i.e., time (3-12 h), sulfuric acid concentration (1-4 molar) and liquid-to-solid ratio (3-12 mL/g), and one categorical independent variable, i.e., particle size (coarse, fine, powder) were evaluated. In order to correlate the independent variables for maximum nickel recovery, a two-factor interaction (2FI) model was suggested using central composite design (CCD) method. The results indicate that under optimum parameters of 6 h time, liquid-to-solid ratio of 9 mL/g and acid concentration of 3 M for coarse particles, maximum recovery of 94% can be attained. The characterization of nickel was examined by atomic absorption spectroscopy for confirmation of nickel recovery. The most effective parameter based on F value analysis was determined to be the liquid-to-solid ratio. Application of lower acid concentration and the fact that there is no need to crush the spent catalyst residues, decrease costs of process significantly.

Keywords: Reforming catalyst, sulfuric acid, leaching, nickel recovery, response surface methodology

INTRODUCTION

Nickel can be considered as a highly applicable metal source since it is used in various industries such as manufacture of steel and its alloys (Bassioni et al., 2015), catalyst and battery industries (Zeifert and Salmones, 2008; Goula et al., 2015; Tarabay and Karami, 2015), nickel-based alloys (Valitov, 2016), coating industries (López et al., 2012), ceramic industries (Yahia and Adel, 2014) and paint-and-varnish (Kvasnikov and Romanova, 2015). There is also a considerable demand for this metal worldwide (Apostolikas et al., 2009; Nieto et al., 2013). After stainless steel, the major use of nickel happens in manufacture of catalysts (Coulter et al., 1994). Being high-tech and expensive, these catalysts lose their catalytic properties after a specific lifetime period and become waste (Mortensen and Gardini, 2014). On the other hand, nickel is reported to have harmful properties (Duda-Chodak and Blaszczyk, 2008; Das and Reddy, 2018) and accumulation of this metal over time can have devastating effects on the environment. This is why the recovery of nickel in any way possible can prevent both additional costs and environmental damages. Several authors reported that nickel was recovered by various methods like using chelating ion exchange resin (Padh et al., 2019), ultra-sonication-assisted leaching (Oza et al., 2011), chelating agents like EDTA (Vuyyuru et al., 2010), electro-less plating and magnetic separation (Taninouchi et al., 2017).

One of the general methods used for recovery of nickel is leaching process (Wang, 2000). In this process, nickel salt is extracted from an oxide compound using an acidic medium and then joins the acid-

dependent salt composition (Kolosnitsyn et al., 2006; Nazemi and Rashchi, 2012). Nickel salts extracted in this way can be reused in industrial applications such as plating and coating, or the elemental nickel itself can be recovered through the electrowinning process. Various parameters are effective in leaching process such as time, acid concentration, particle size, temperature, liquid-to-solid ratio, etc. (Alex et al.,1993; Ghanem et al., 2008). Invascano and Roman (1975) dissolved ammonia plant's catalysts in 80% sulfuric acid solution for 50 minutes at 70 °C and reached to 99% nickel recovery in the form of nickel sulfate; this was done when catalyst particle size was about 0.09 millimeter. Loboiko et al. (1983) found that recovery of nickel in a solution of nitric acid with a purity of 60-70% at 120 °C for 2-3 h would be significant. With catalyst leaching by hydrochloric acid, Chandhary et al. (1993) found that recovery of nickel from a low-grade nickel catalyst would be up to 17.7%. Vicol et al. (1986) tried to extract a used catalyst with aqueous solution containing 15-23% ammonia at a temperature of 60 to 90 °C and in a pH range of 7.5 to 9 for retrieving nickel. Al-Mansi and Abdel Monem (2002) recycled nickel in the form of sulfate salt by direct crystallization in a concentration of 50% sulfuric acid, a solid to liquid ratio of 1:12, and a particle size smaller than 500 microns. A nickel recovery of 99% was obtained after about 5 h leaching at 800 rpm and 100 °C.

Recently, various statistical experimental design procedures have been used in different sectors for optimization of process parameters (Arshadi et al., 2016). Optimizing a system of several variables in the convectional mode requires many experiments which is time consuming and costly. Furthermore, such methods do not provide combined effect of variables and need more data for determining optimum level (Kumar et al., 2018). RSM can be a thorough approach to study a process and to figure out the best correlation among the parameters of a process, additionally This is done via developed models based on the statistical methods to configure the relation between the inputs and outputs of any process and optimizing the effect of these parameters to attain the desirable response (Mohamad Said and Mohamed Amin, 2015). To develop a model based on the statistical methods, it is necessary first to recognize the parameters that exhibit significant influence in the process. Then, experimental procedure should be designed in a way that it takes into account all the process parameters at several levels. This is followed by analyzing the experimental results using the analysis of variance (ANOVA) technique to determine which parameters show the strongest interactions and/or exhibit significant influences on the outputs of process. Based on the process response as a statistical model, the process is optimized using the variables range predicted by model. For example, Haghshenas et al. (2012) optimized physicochemical parameters in order to undertake bioleaching of sphalerite by *Acidthiobacillus ferrooxidans* using shaking bioreactors using RSM methodology.

To the best of our knowledge, there is no report on using RSM method to optimize operating parameters of leaching process to recover nickel from spent catalysts. This paper examines the combined effects of time, concentration, liquid-to-solid ratio and particle size on the leaching process. An experimental procedure was designed using central composite design (CCD) in conjunction with RSM method to optimize the leaching recovery response of nickel catalyst. Three models were presented for predicting the recovery percentages of the three different nickel catalyst particle sizes.

EXPERIMENTAL PROCEDURE

The catalyst in this study is the Rhine Catalyst, known as the steam reformer catalyst, which is used in the petrochemical industry to accelerate the production of hydrogen from methane, which is why it is also called a reformer catalyst. The overall composition of this catalyst is mainly alumina and nickel oxide, which can be called a rich source. The method for nickel extraction is generally leaching (acidification). The reaction of nickel oxide with sulfuric acid is a heterogeneous reaction. In the systems of such a reaction, the

general relationship of the rate is complicated due to the cross between physical and chemical processes. The main reaction is as follows, Where NiO is the limiting reactant.

By the means of atomic absorption spectroscopy (AAS), while dissolving 0.5 grams of this spent catalyst in an aqua containing 15 cm^3 HF, 2 cm^3 H_2SO_4 and 2cm^3 HCl, the result and therefore the composition of this solid sample is shown in table (1) Commercial grade 98% sulfuric acid was selected as the solvent for the metal oxides to produce sulfate. Distilled water was used to dilute this acid. As one of three numeric factors, acid concentrations of 1, 2, 3, and 4 molars as well as 2.5 M as the mean, were selected. This range of data was to show that the other studies used very high acid concentrations which may cause problems in deacidification and subsequent processes.

Table 1. Composition of the spent catalyst sample obtained from AAS

Substance		Co	Ni	Zn	Mg	Ca	Al	Fe	Oil	Humidity	O,C,S
Amount	(wt.%)		10.43		0.18	0.02	25.36	0.058	N.D.	N.D.	Balance
	(ppm)	76		57							

As the only categorical variable, the catalyst particle size was determined after two stages of crushing and mill grinding followed by a thorough screen breakdown. The resulting mixture was divided into three groups. The powder sample with a mean grain size of 1.2 mm, the fine sample with a mean grain size of 4 mm and finally the coarse sample which is the catalyst in its uncrushed form. To provide the required temperature for the leaching process, a simple resistive heater with a pre-heated aluminum bath as a heat transfer media was used. Contrary to other studies, the temperature of 85±3 ° C was taken as one of the constant parameters of the process. Another constant parameter, turbulence, was considered with the agitator rotation speed parameter. The reason for this, as in the case of temperature, is that it is difficult to generate turbulence in large processes. However, turbulence in this study was achieved by using a mechanical stirrer with a heavier base against vibration, and electric motor, with a polymer coated stirrer. The agitator rotational speed according to the standards of this machine was selected a constant value of 400±10 rpm.

The second numeric variable of the leach, was considered to be the ratio of liquid to solid. The L/S fraction in ml/g, with the values of 3, 6, 9, 12 and 7.5 as the mean value, were selected. According to this value and the amount of solution that was 500 milliliters, the solid catalyst content was weighed by an electronic scale of 0.01-gram accuracy and washed with distilled water in a plastic acid-resistant container. Further, the amount of water required was calculated and then measured using a graduated cylinder. Then under suitable ventilation conditions (due to the rapid release of SO_2 and H_2S) acid was slowly added to the solution. Finally, the last parameter for the leach was considered to be time, and its values were set for 3, 6, 9, 12 and 7.5 as mean. It must be noted that the alpha value for corresponding axial point for the variable parameters is set to be 3 so that axial points are in logical comparison to center points and leaching parameter ranges, as shown in table (2) The Design Expert software used in this study, offered 51 leaching experiments, Taking into account the number of replicates and central and axial points. After the completion of the leach process, a diluted solution was prepared as a final sample for atomic absorption spectroscopy to obtain the recovered nickel content.

Table 2. The variable values of leaching parameters for central composite RSM modeling

Variable Parameter	Coded Values				
	-alpha (-3)	-1	0	+1	+alpha (+3)
A: L/S ($ml.g^{-1}$)	1	2	2.5	3	4
B: Time (hour)	3	6	7.5	9	12
C: Acid Concentration (molarity)	3	6	7.5	9	12
D: Particle size (categorical)		Powder	Fine	Coarse	

RESULTS AND DISCUSSION

The results of the 51 leaching experiments after analysis via AAS, are presented in table (3). Leverage is the potential for a design point to influence the fit of the model coefficients, based on its position in the design space. Leverages near 1 should be avoided. As seen in table (3) all leverages are below 1 and the center points have the lowest of them all, it can be deduced that the model that will be fit to this data is more significant near the central points. The ratio of maximum to minimum of the responses is 2.53. A ratio greater than 10 usually indicates that a transformation is required. For ratios less than 3, transformations have little effect. No transformation was done to the response results.

As presented in table (4), sum of squares is the sum of the squared deviations from the mean for each model. The SS for the Mean is calculated first, followed by Linear model, Quadratic model, Special Cubic, Cubic, Residuals and Total. The degrees of freedom for the mean will be 1. The df for the linear, quadratic, special cubic and cubic models is the number of additional terms added to the model. The residual will contain any remaining degrees of freedom. For each source, the mean square is the sum of squares divided by the degrees of freedom. This is used to calculate the F-value for the models. The F-value is used to test the significance of adding new model terms to those terms already in the model. For instance, the significance of the linear terms is tested after removing the effect of the average and the blocks. Then, the significance of the quadratic terms is tested after removing the average, block and linear effects and so on. The P-value is the probability associated with adding these additional terms to the model. And to summarize this all, table (4) suggests a 2FI (2 factor interaction) model to be used to provide a model for the resulted responses, as the main focus is on maximizing R-Squared and to avoid lack of fits.

After furthur analysis of variance as shown in Table (5), The Model F-value of 12.06 implies the model is significant. There is only a 0.01% chance that a "Model F-Value" this large could occur due to noise. P-values less than 0.0500 indicate model terms are significant. In this case A, B, C, D and AB are significant model terms. Values greater than 0.1000 indicate the model terms are not significant. If there are many insignificant model terms, model reduction may improve model, not needed in this case. The "Lack of Fit F-value" of 1.94 implies the Lack of Fit is not significant. "Adeq Precision" measures the signal to noise ratio. A ratio greater than 4 is desirable. The model ratio of 15.808 indicates an adequate signal. Both the facts that the model F-value is significant and The "Lack of Fit F-value" is not, proves that this model can be used to navigate the design space. Finally, software presented 3 model equations, one for each of the categorical particle sizes in term of actual factors used.

Eq. (1) for Powder samples:

$$R\%_{Ni} = 287.29141 - 35.08166 \times \frac{L}{S} - 75.48491 \times C - 7.69325 \times t + 12.05388 \times \frac{L}{S} \times C + 1.19337 \times \frac{L}{S} \times t - 0.29291 \times C \times t \quad (1)$$

Eq. (2) for Fine samples:

$$R\%_{Ni} = 267.30083 - 34.17316 \times \frac{L}{S} - 77.04768 \times C - 6.47129 \times t + 12.05388 \times \frac{L}{S} \times C + 1.19337 \times \frac{L}{S} \times t - 0.29291 \times C \times t \quad (2)$$

Eq. (3) for Coarse samples:

$$R\%_{Ni} = 265.52177 - 32.51455 \times \frac{L}{S} - 80.23930 \times C - 4.70234 \times t + 12.05388 \times \frac{L}{S} \times C + 1.19337 \times \frac{L}{S} \times t - 0.29291 \times C \times t \quad (3)$$

Table 3. Central Composite design arrangement and response results

Standard Experiment Number	Variable Parameters				Response	Leverage	Point Type
	A:L/S ($ml.g^{-1}$)	B: Acid Concentration (molar)	C: Time (hour)	D: Particle Size (nominal)	Ni Recovery (%)		
1	9	3	6	Powder	85.48	0.265	Fact
2	9	3	6	Powder	92.58	0.265	Fact
3	9	2	9	Powder	64.35	0.265	Fact
4	9	2	9	Powder	57.49	0.265	Fact
5	6	3	9	Powder	66.80	0.265	Fact
6	6	3	9	Powder	57.54	0.265	Fact
7	6	2	6	Powder	76.66	0.265	Fact
8	6	2	6	Powder	67.16	0.265	Fact
9	3	2.5	7.5	Powder	43.01	0.600	Axial
10	12	2.5	7.5	Powder	85.06	0.600	Axial
11	7.5	1	7.5	Powder	39.68	0.600	Axial
12	7.5	4	7.5	Powder	75.41	0.600	Axial
13	7.5	2.5	3	Powder	59.34	0.600	Axial
14	7.5	2.5	12	Powder	67.29	0.600	Axial
15	7.5	2.5	7.5	Powder	57.64	0.094	Center
16	7.5	2.5	7.5	Powder	49.72	0.094	Center
17	7.5	2.5	7.5	Powder	66.81	0.094	Center
18	9	3	6	Fine	64.95	0.265	Fact
19	9	3	6	Fine	72.71	0.265	Fact
20	9	2	9	Fine	55.84	0.265	Fact
21	9	2	9	Fine	48.67	0.265	Fact
22	6	3	9	Fine	35.70	0.265	Fact
23	6	3	9	Fine	46.32	0.265	Fact
24	6	2	6	Fine	44.95	0.265	Fact
25	6	2	6	Fine	57.00	0.265	Fact
26	3	2.5	7.5	Fine	36.53	0.600	Axial
27	12	2.5	7.5	Fine	81.57	0.600	Axial
28	7.5	1	7.5	Fine	40.86	0.600	Axial
29	7.5	4	7.5	Fine	77.65	0.600	Axial
30	7.5	2.5	3	Fine	53.69	0.600	Axial
31	7.5	2.5	12	Fine	69.98	0.600	Axial
32	7.5	2.5	7.5	Fine	57.34	0.094	Center
33	7.5	2.5	7.5	Fine	62.15	0.094	Center
34	7.5	2.5	7.5	Fine	71.49	0.094	Center
35	9	3	6	Coarse	86.79	0.265	Fact
36	9	3	6	Coarse	94.48	0.265	Fact
37	9	2	9	Coarse	78.94	0.265	Fact
38	9	2	9	Coarse	86.45	0.265	Fact
39	6	3	9	Coarse	64.70	0.265	Fact
40	6	3	9	Coarse	56.61	0.265	Fact
41	6	2	6	Coarse	66.43	0.265	Fact
42	6	2	6	Coarse	57.75	0.265	Fact
43	3	2.5	7.5	Coarse	39.95	0.600	Axial
44	12	2.5	7.5	Coarse	92.23	0.600	Axial
45	7.5	1	7.5	Coarse	55.42	0.600	Axial
46	7.5	4	7.5	Coarse	78.46	0.600	Axial
47	7.5	2.5	3	Coarse	58.24	0.600	Axial
48	7.5	2.5	12	Coarse	86.09	0.600	Axial
49	7.5	2.5	7.5	Coarse	88.14	0.094	Center
50	7.5	2.5	7.5	Coarse	80.49	0.094	Center
51	7.5	2.5	7.5	Coarse	77.36	0.094	Center

Table 4. Sequential Model Sum of Squares

Source	Sum of Squares	Degree of Freedom	Mean Square	F-Value	p-value	
Mean vs Total	218532.54	1	218532.54			
Linear vs Mean	8488.25	5	1697.65	17.94	< 0.0001	
2FI vs Linear	**2017.81**	**9**	**224.19**	**3.6**	**0.0028**	**Suggested**
Quadratic vs 2FI	204.18	3	68.06	1.10	0.3616	
Cubic vs Quadratic	471.10	13	36.24	0.46	0.9211	Aliased
Residual	1564.23	20	78.21			
Total	231278.11	51	4533.57			

Table 5. Analysis of variance (ANOVA) for response surface

Source	Sum of Squares	Degree of Freedom	Mean Square	F- Value	p-value	
Model	**10505.97**	**14**	**750.43**	**12.06**	**< 0.0001**	**significant**
A-L/S	3237.38	1	3237.38	52.04	< 0.0001	
B-C	1521.63	1	1521.63	24.46	< 0.0001	
C-t	452.14	1	452.14	7.27	0.0106	
D-Size	2162.07	2	1080.04	17.38	< 0.0001	
AB	1357.96	1	1357.96	21.83	<0.0001	
AC	119.79	1	119.79	1.93	0.1738	
AD	198.25	2	99.12	1.59	0.2172	
BC	0.80	1	0.80	0.013	0.9102	
BD	76.34	2	38.17	0.61	0.5470	
CD	264.57	2	132.29	2.13	0.1340	
Residual	2239.52	36	62.21			
Lack of Fit	1478.64	18	82.15	1.94	0.0841	Not significant
Pure Error	760.88	18	42.27			
Total	12745.48	50				
R^2	82.43					
Adeq Precision	15.808					

Table 6. Proposed practical research values for Optimum leaching process

A: L/S ($ml.g^{-1}$)	B: C ($mol.\ L^{-1}$)	C: t (hour)	D: Size	Actual Recovery (%)	Predicted Recovery (%)
9	3	7.5	Coarse	94.36	96.32

After several repeated runs, verification was done in order to report the optimum conditions of leaching process, shown in Table (6). The value presented as the actual recovery is the average of mentioned runs. Due to F-values of 52.04 and 24.46 respectively for L/S and acid concentration, significance of the model is affected greatly by these parameters. Also, between the interaction factors in the model, AB which is the product of L/S and C, shows the highest F-value and hence the highest significance. According

to the results of this experiment in Fig. 1(a), it can be stated that from acid concentration of about 2.5 M above and simultaneously at L/S values more than about 8.5, the recovery is significant, with a concentration of 2.75 molar acid Upward and L/S of about 8.75 upwards, recovery percentages cross the 90% limit, which is desirable.

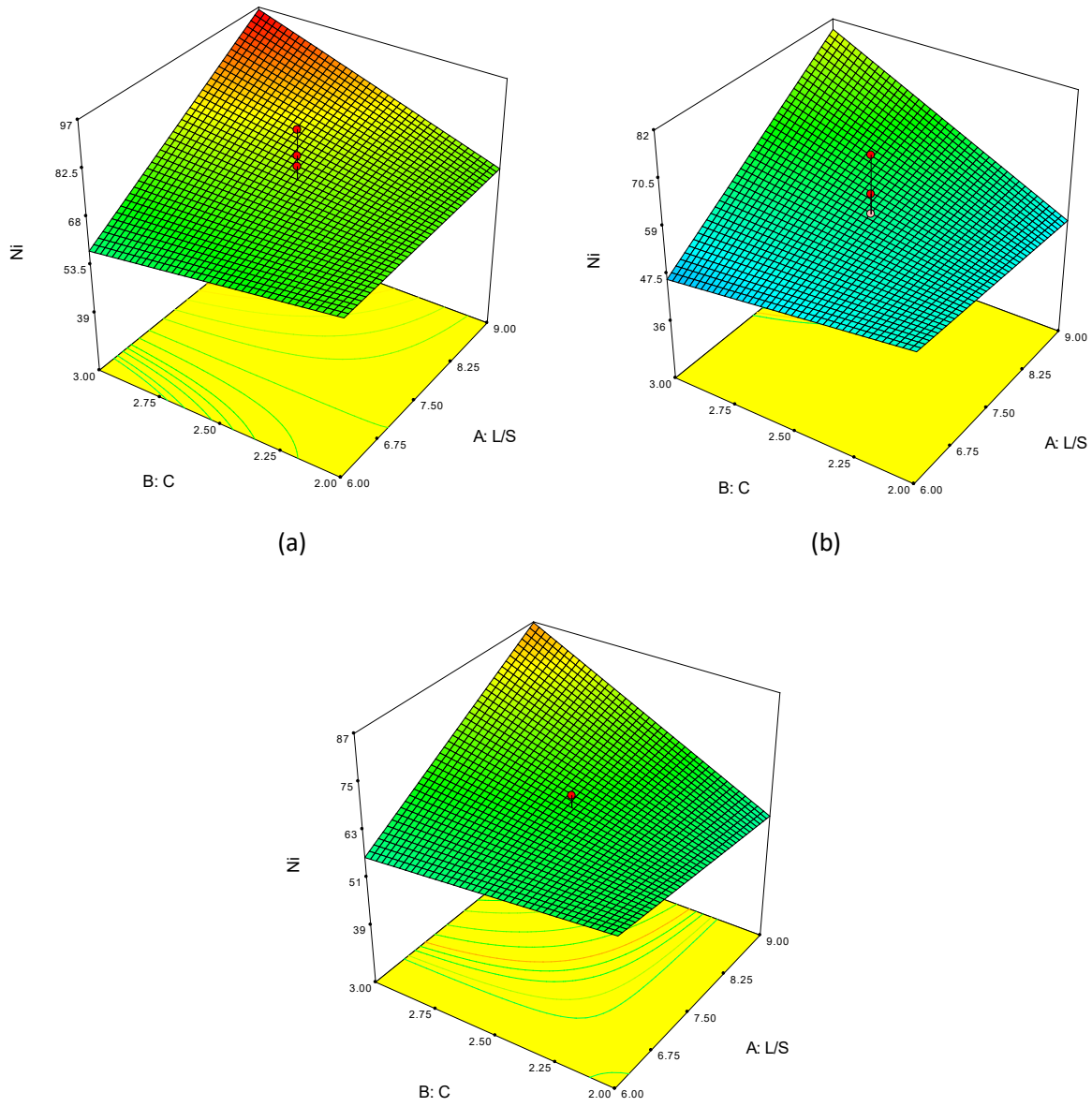

Figure 1. Surface plots of Ni recovey with respect to L/S and C for (a)Coarse, (b)Fine and (c)Powder samples at 7.5 h.

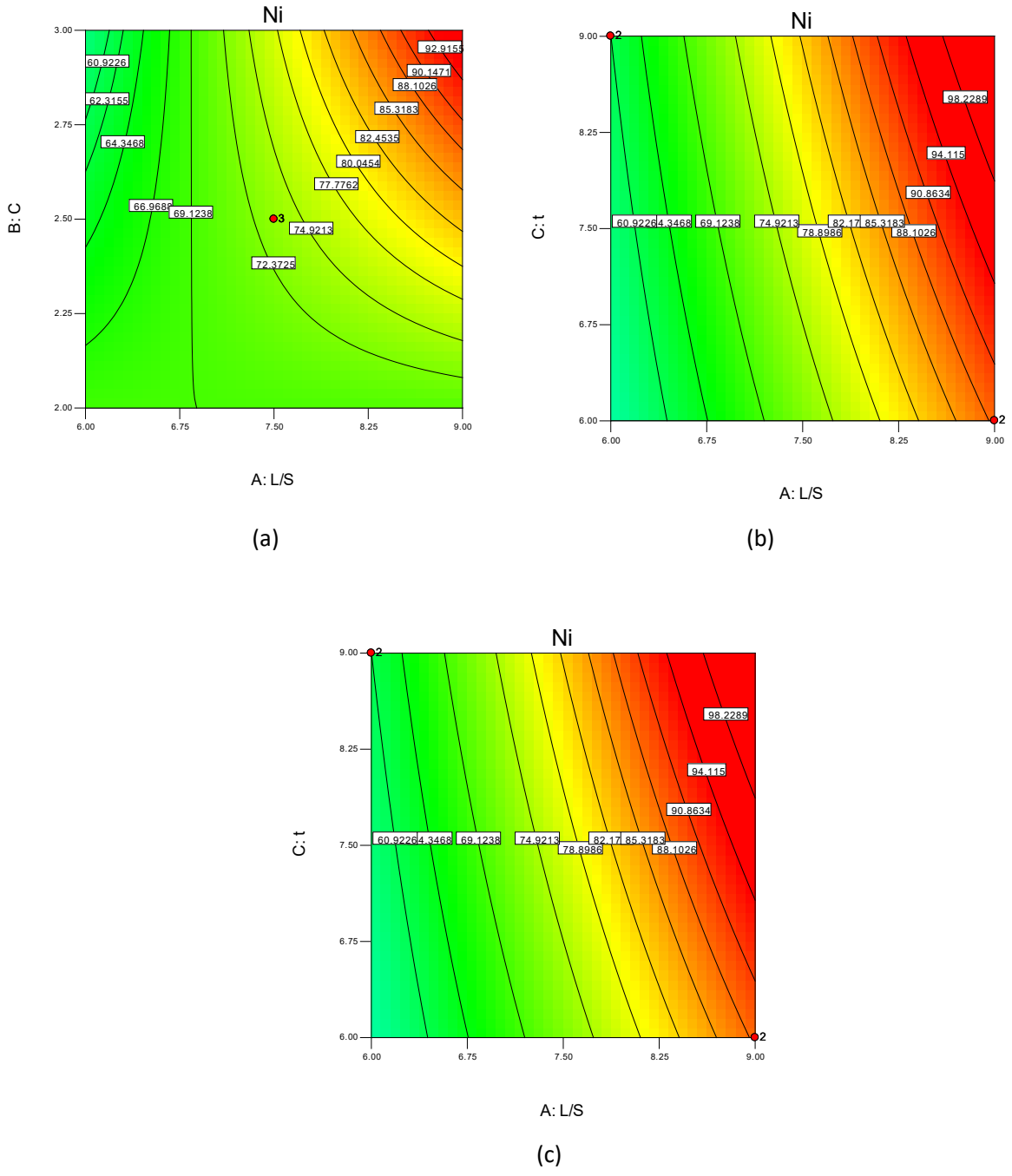

Figure 2. Countor plots of Ni recovey for coarse sample with respect to (a) L/S and C (at t=7.5), (b) L/S and t (at C=3) and (c) C and t (at L/S=9).

According to the contours drawn if Fig. 2(a), it can be seen that these two factors can be changed in opposite directions, which means that for higher recovery by adding to the L/S value, lower acid

concentration can reach the same results, and also by increasing the amount of acid concentration, it is also possible to produce the leach with the same results with lower L/S. Increasing recovery by increasing concentrations of acid and L/S values is predictable, because with increasing acid concentration, there are more sulfate ions to remove nickel from its oxide compound, which ultimately increases the reaction efficiency; by increasing L/S, the amount of solution to react with a constant ammount of solid is increased, and fresh acid is added to the reaction surface to further increase efficiency. Acording to Fig. 2(b), longer than
7.5 hour processes may show beter recovery results, but further filtration and purification, turned out to be challenging because of more impurity disolution. And ofcoarse longer times mean more amount of enery for mixer and later follow up on batch production. By extrapolating the plots of Fig2. It is obviouse in leaching that using acid concentrations of 4 molar and higher and L/S of 12 will prove recovery to be possible at shorter times, yet furthur diacidification and lower nickel content concentration (which then must be concentrated again to be used fo electrowinning) prove that such high parameters are not suitable for overall production process. Fig. 1(b), shows that in the case of fine specimens with a particle size of about 4 millimeters, given that in this size, fracture and crushing was in a way that there are particles that have been pulled and look pointy (this can be due to the particular synthesis or a particular crystalline structure of catalysts), which can be said to be sharp and heterogeneous particles, lead to a lower level for presence in the reaction And also a slight disruption of mixing. Therefore, according to the results, the range of significant recoveries has become smaller, as at acid concentrations above 3 mol/L and L/S values higher than 9, recovery can be done up to about 80%. And according to the results for these particles, at concentrations of less than 2.5 m, recovery can not be advanced forward. In these samples, to achieve recovery above 95%, the concentration of more than 4 M and L/S of more than about 12 are essential; however, energy and cost should be used for grinding.

For powder samples with a size of about 1 millimeter, as illustrated in Fig. 1(c), which have more uniform particles with a spherical shape, the results are more in common with the results of Coarse catalysts; however, the limits of significant recovery are larger in the non-crushed sample. In this sample, a recovery of about 87% can be achieved at concentrations higher than 3 mol/L and L/S values higher than 9. This range is larger than the Fine specimen range; although the cost and energy to produce these samples are double the Fine samples.

CONCLUSION

In general, increasing the amount of recovery by adding to the values of leaching parameters such as time, acid concentration and liquid to solid fraction is obvious and natural. But the point is that in some experiments under certain conditions, this natural process is not followed.

Coarse Samples

In these samples, from 7.5 hours' time up, under the same conditions, no significant change is observed in the recovery. For example, in the same conditions with an increase of time from 7.5 to 9, recovery only increased by about 3%.

The liquid to solid fraction at a constant period of time, has a significant effect on the recovery efficiency; for example, increasing this ratio from 6 to 9 restores recovery from 58% to over 96%.

In general, optimum recovery conditions for these samples can be considered as follows: the time from 6 to 7.5 hours, the concentration of acid is about 3 M and the fraction of the liquid to solid is about 9,

to recover about 96% of Ni content. it is to be noted that the parameter of the fraction of liquid to solid can be described as the most influential parameter in these samples.

Fine Samples

In these samples, recovery is generally not high; process times of 7.5 hours and longer, not only lack a positive effect, but also result in less recovery.

The effect of the liquid-to-solid fraction is very much affected by the concentration of acid in a way that it can be deduced that the recovery rate is related to the product of these two quantities.

Generally, the optimum recovery for these samples, at 7.5 h, the concentration of 3 molar acid and the liquid to solid fraction of 9, reached about 79%.

Powder Samples

In these samples, an optimal recovery time of about 9 hours can be reported. In this crushed samples, increasing time leads to more reaction of alumina. Less time is not enough to react the total amount of nickel.

In general, the simultaneous effect of the concentration of acid and the liquid to solid fraction can be expressed as a Product. The concentration of acid is better to stay in the middle and the ratio of liquid to solid should not be less than 9.

In these conditions, the optimal recovery for these samples at 9 hours' time, the acid concentration of 3 molars and the liquid to solid fraction of 9, reached about 90%.

Consequently, a non-crushed sample can be considered as the most suitable one for recovery of this nickel catalyst. This might be due to the fact that nickel is mostly accumulated on the surface on these spent catalysts. The unnecessity of grinding the specimen itself, reduces the cost of the process dramatically. The results suggest that high recovery can be attained without the use of extremely high acid concentrations, high temperatures and high liquid-to-solid ratios.

REFERENCES

Alex, Pamela, T.K. Mukherjee, and M. Sundaresan, (1993). "Leaching behaviour of nickel in aqueous chlorine solutions and its application in the recovery of nickel from a spent catalyst." *Hydrometallurgy 34*: 239-253.

Al-Mansi, N.M., and N.M. Abdel Monem. (2002). "Recovery of nickel oxide from spent catalyst." *Waste Management* 22: 85-90.

Apostolikas, A, E Frogoudakis, and J Bakallbashi. (2009). "Nickel, World Production and Demand." *3rd Balkan Mining Congress, BALKANMINE.* Izmir-TURKEY.

Arshadi. M, S.M. Mousavi, and P Rasoulnia. (2016). "Enhancement of simultaneous gold and copper recovery from discarded mobile phone PCBs using Bacillus megaterium: RSM based optimization of effective factors and evaluation of their interactions." *Waste Management.*

Bassioni, Ghada, A. Korin, and A. El-Din Salama. (2015). "Stainless Steel as a Source of Potential Hazard due to Metal Leaching into Beverages." *International Journal of Electrochemical Science* 10: 3792 - 3802.

Chandhary, AJ: Donaldson, JD, and SC: Grimes, SM Boddington. (1993). "Heavy metal in the enviroment. Part II: a hydrochloric acid leaching process process for the recovery of nickel value from a spent calalyst." 34-137.

Coulter, Kent, Xueping Xu, and D. Wayne Goodman. (1994). "Structural and Catalytic Properties of Model Supported Nickel Catalysts." *Phys. Chem* 98: 1245-1249.

Das, Kusal K., and R. Chandramouli Reddy. (2018). "Primary concept of nickel toxicity – an overview." *Journal of basic and clinical physiology and pharmacology.*

Dehghani, Kamran, Atiye Nekahi, and Mohammad Ali Mohammad Mirzaie. (2010). "Optimizing the bake hardening behavior of Al7075 using response surface methodology." *Materials and Design* 31: 1768-1775.

Duda-Chodak, Aleksandra and U. Blaszczyk. (2008). "The Impact Of Nickel On Human Health." *Hournal of Elementol* 13: 685-696.

Ghanem, R, H Farag, Y Eltaweel, and Mona E Ossman. (2008). "Recovery of nickel from spent catalyst by single- and multi-stage leaching process." *International Journal of Environment and Waste Management* 2: 540-551.

Goula, Maria A, Nikolaos D. Charisiou, Kiriakos N. Papageridis, and Andreas Delimitis. (2015). "Nickel On Alumina Catalysts For The Production Of Hydrogen Rich Mixtures Via The Biogas Dry Reforming Reaction: Influence of the synthesis method. *International Journal Of Hydrogen Energy* 40: 9183-9200.

Haghshenas, Davoud, Babak Bonakdarpour, Eskandar Keshavarz Alamdari, and Bahram Nasernejad. (2012). "Optimization Of Physicochemical Parameters For Bioleaching Of Sphalerite by Acidithiobacillus Ferrooxidans Using Shaking Bioreactors." *Hydrometallurgy* 111: 22-28.

Ivascanu, St, and O Roman. (1975). "Nickel Recovery From Spent Catalysts." *BulInst Politeh Iasi Sect* 2: 21-47.

Kolosnitsyn, V. S., S. P. Kosternova, and O. A. Yapryntseva. (2006). "Recovery of Nickel with Sulfuric Acid Solutions from Spent Catalysts for Steam Conversion of Methane." *Russian Journal of Applied Chemistry* 79: 539-543.

Kumar, Anil, Harvinder Singh Saini, and Sudhir Kumar. (2018). "Enhancement Of Gold And Silver Recovery From Discarded Computer Printed Circuit Boards by Pseudomonas Balearica SAE1 Using Response Surface Methodology (RSM)." *Biotech* 3: 8-19.

Kvasnikov, M. Yu., and O. A. Romanova. (2015). "Electrodeposited Paint-and-Varnish Nickel–Polymer Coatings." *Russian Journal of Applied Chemistry* 88: 1870-1876.

Loboiko, Aya, VI Atroshchenko, G Grin, VV Kutovoi, and NP Fedorova. (1983). "Recovering Nickel From Spent Catalyst." *Otkrytiya, Izobret, PromObraztsy,Tovarnye Zanki* 14-33.

López, JR, G Stremsdoerfer, G Trejo, R Ortega, JJ Pérez, and Y Meas. (2012). "Corrosion Resistance of Nickel Coatings Obtained by Electrodeposition in a Sulfamate Bath in the Presence of Samarium (III)." *International Journal of Electrochemical Science* 7: 12244-12253.

Mohamad Said, Khairul Anwar, and Mohamed Afizal Mohamed Amin. (2015). "Overview on the Response Surface Methodology (RSM) in Extraction Processes." *Journal of Applied Science & Process Engineering* 2: 8-16.

Mortensen, Peter M., and Diego Gardini. (2014). "Stability And Resistance Of Nickel Catalysts For Hydrodeoxygenation." *Catalysis Science & Technology* 4: 3672-3686.

Nazemi, M., and F. Rashchi. (2012). "Recovery Of Nickel From Spent Nio/Al2o3 Catalyst Through Sulfuric Acid Leaching, Precipitation And Solvent Extraction." *Waste Management & Research* 30: 492-497.

Nieto, A, V Montaruli, and M Cardu. (2013). "The Strategic Importance Of Nickel: Scenarios And Perspectives Aimed At Global Supply." *Transactions Of The Society For Mining, Metallurgy, And Exploration* 332: 510-518.

Oza, Rachit, Nikhil Shah, and Sanjay Patel. (2011). "Recovery Of Nickel From Spent Catalysts Using Ultrasonication-Assisted Leaching." *Journal of Chemical Technology & Biotechnology* 86: 1276-1281.

ASİDİK DRENAJ AÇISINDAN MADEN ATIKLARI YÖNETMELİĞİ ÜZERİNE BİR İNCELEME

AN INVESTIGATION ON THE MINING WASTE REGULATION IN TERMS OF ACIDIC DRAINAGE

M. Karadeniz *

*(*Sorumlu yazar: mhmtkaradeniz@gmail.com)*

ÖZET

"Maden Atıkları Yönetmeliği", sülfürlü madenlerde karşılaşılan asit maden drenajı (AMD) sorununa ilişkin maddeleri yönünden incelendiğinde görülmektedir ki, yönetmelik hem kavram ve hem de yöntem bakımından yanlış yönlendirebilecek bazı ifadeler içermektedir. Özellikle, yöntemler hakkındaki ifadeler çok daha önemlidir, zira sahayı temsil eden örneklerin belirlenen asit potansiyeli, gerçek değerinin altında bulunursa, alınacak önlemlerin yetersizliğine yol açması söz konusudur. Tersine, gerçek potansiyelin üzerinde bulunursa da fazladan yatırım maliyetine sebep olması olasıdır. Çünkü asit üretme potansiyelinin (AÜP) kestiriminde ön eleme amacıyla kullanılan statik testler, esas itibariyle, kimi ön kabullere dayanarak geliştirilmiştir ve bu kabuller, incelenen sahanın mineralojik özellikleriyle uyumsuz olduğunda, gerçeğe aykırı sonuçlar elde edilebilmektedir. Buradan hareketle, bu çalışmada, AMD kestiriminde kullanılan statik test yöntemlerinin, uygulandıkları maden sahasının mineralojik özelliklerine göre, karşılaşılabilecek zaafları ve üstünlükleri irdelenmiş, yönetmeliği iyileştirmek adına kimi öneriler yapılmıştır.

Anahtar Sözcükler: Yönetmelik, asit maden drenajı, statik testler, aba

ABSTRACT

When the "Mining Wastes Regulation" is examined in terms of its articles related to the acid mine drainage problem encountered in sulfide mines, it is seen that the regulation contains some statements that may mislead with regards to both concept and method. Especially, the statements about the methods are much more important because if the determined acid potential of the samples representative of the field is found below the actual value, it may lead to the inadequacy of the measures to be taken. Conversely, if it is above the actual potential, it is likely to cause additional investment costs. Because the static tests used for pre-screening in predicting the acid production potential (APP) were mainly developed based on some preliminary assumptions and when these assumptions are inconsistent with the mineralogical properties of the investigated field, unrealistic results can be obtained. From this point of view, in this study, the weaknesses and advantages of the static test methods used in the prediction of acid mine drainage, according to the mineralogical characteristics of the mine field where they are applied, were gone through and some suggestions were made in order to improve the regulation.

Keywords: Regulation, acid mine drainage, static tests, aba

GİRİŞ

"Maden Atıkları Yönetmeliği" ve onu tamamlayan mahiyetteki iki metin, "Yönetmeliğin Ekleri" ve "Maden Atıkları Yönetmeliğinin Uygulanmasına İlişkin Açıklamalar" incelendiğinde, AMD'nın (bir yerde 'asit kaya drenajı' olarak ifade edilmiş), sülfür (S^{-2}) içeren atıklarda oluşabileceği değerlendirmesinin yapıldığı anlaşılmaktadır. Bu yargı, Ek- 3 ve Ek- 4'te açık biçimde ifade edilmektedir. Ek- 4'te, "İnert Maden Atıklarının Belirlenmesi" başlığı altında, izlenecek yol için bir algoritma verilmişse de atıkların asit üretme potansiyellerinin belirlenmesinde uygulanacak yöntemler için bilgilendirme,

"Maden Atıkları Yönetmeliğinin Uygulanmasına İlişkin Açıklamalar" metninin, "Maden Atıklarının Karakterizasyonu ve Maden Atığı Bertaraf Tesislerinin Sınıflandırılması ile İlgili Açıklamalar" kısmında yapılmaktadır. Madde 3, aynen şöyle kaleme alınmıştır: "Maden atıklarının karakterizasyonunda öncelikle sülfit-sülfür (ASTM E1915, EPA 600, CEN-EN 14582) miktarına bağlı olarak asit üretme potansiyeli belirlenir. Atığın sülfit-sülfür (S^{-2}) miktarı %0,1'in üzerinde ise statik test yapılır (pr en 15875, ABA, SOBEK, Modifiye SOBEK). Bu testin sonucuna göre NP/AP<1 ise asit üreten tehlikeli maden atığı olarak sınıflandırılır ve atık karakterizasyonu sonlandırılır. NP/AP>3 ise asit üretmeyen maden atığı olarak tanımlanır."

Yönetmelik ve tamamlayıcı metinler, AMD yönünden bazı eksiklikler ve çelişkili hükümler barındırmaktadır. Kavram, algoritma ve statik test yöntemleri hakkındaki değerlendirme ve yorumlama, "Yönetmeliğin AMD Yönünden Değerlendirilmesi" bölümünde ele alınacaktır. Ancak bunun için öncelikle statik test yöntemlerini, genel hatlarıyla ele almak gerekir.

AMD KAVRAMI

Sülfürlü maden sahalarında, metal sülfürler, nemli koşullarda havayla temas ettiklerinde oksitlenirler. Ardından, bir dizi kimyasal tepkime (1, 2, 3 ve 4) meydana gelir ve açığa çıkan H^+, ortamdaki suların asitliğini yükseltir. Süreci tetikleyen mineraller demir sülfürlerdir. Genellikle, düşen pH ile birlikte, bakteriler (thiobacillus gibi) sürece dâhil olup, katalizör etkisi yaparak, tepkimelerin hızını arttırırken, tepkimeler biyo- kimyasal nitelik de kazanır.

$$FeS_2(k) + H_2O + 7/2O_2(g) \rightarrow Fe^{2+}(k) + 2SO_4^{2-}(s) + 2H^+ + \text{ısı} \quad (1)$$

$$Fe^{2+}(k) + O_2(g) + 4H^+ \rightarrow Fe^{3+}(k) + 2H_2O \quad (2)$$

$$Fe^{3+} + 3H_2O \rightarrow Fe(OH)_3(k)\downarrow + 3H^+ \quad (3)$$

$$FeS_2(k) + 14Fe^{3+} + 8H_2O \rightarrow 15Fe^{2+} + 2SO_4^{2-}(s) + 16H^+ \quad (4)$$

Oluşan asidik drenaj (AMD), potansiyel zehirli maddeleri (metaller, iyonlar, askıda katılar gibi) kimyasal, fiziksel ve biyo-kimyasal süreçle bünyesine alır. Önlem alınmadığında, kirlenmiş drenaj, karıştığı sulardaki canlıları doğrudan, ilişkideki eko-sistemi ve sonuçta insanları dolaylı biçimde etkiler. Sürekliliği, yaygınlığı, hareketliliği ve sorunu gidermenin yüksek maliyeti (Karadeniz, 2011), AMD oluşma potansiyelinin, madencilik faaliyetlerinin başlamasından önce saptanmasını elzem kılar.

Maden sahalarının asit üretebilirliğinin kestiriminde, öteden beri, çeşitli yöntemler kullanılmaktadır. Bunlar; jeokimyasal statik ve jeokimyasal dinamik (kinetik) testler, jeokimyasal ve jeoistatistiksel modellemeler, özütleme (leaching) testleri olarak sayılabilir. Saha ve laboratuvarda elde edilen verilerin, benzer başka sahalara ait verilerle karşılaştırılması ve yorumlanması da yapılabilecekler arasındadır. Belirsizlikler içermelerine karşın, jeokimyasal statik yöntemlere, basitlikleri, çabuk sonuç vermeleri, yönlendirici ve düşük maliyetli olmalarından dolayı sıklıkla başvurulmaktadır. Statik yöntemler arasında en yaygın kullanılanı, ABA (Acid- Base Accounting) testleridir. Ancak kömür madeni artıkları için önerilen standart ABA'dan başlayarak, zaman içinde, farklı ABA testleri tasarlanmıştır. Esasen, numunedeki sülfürün, kimyasal analizle bulunup hesaplama yoluyla AÜP'nin ve test ile de oluşacak asidi nötrleştirme potansiyelinin (NP- özellikle Avustralya literatüründe asit nötrleştirme kapasitesi- ANC olarak ifade edilir) ölçüldüğü testlerdir. Bunlar, B. C. Araştırma Başlangıç testi (BCAB- British Columbia Research Initial test), Alkali Üretme Potansiyeli: Sülfür Oranı testi, modifiye ABA ve NP (pH6) testidir. Ayrıca, farklı coğrafik, jeolojik ve mineralojik şartlarda, 1970'lerden itibaren devam eden araştırmalarda, adı geçen yöntemler üzerinde, geniş bir literatürü kapsayan çok sayıda değişiklik önerileri sunulmuştur.

ABA'dan ayrı olarak, temel ilkeleri farklı olan diğer bazı testler de kullanılmaktadır. Numunenin saf veya deiyonize suyla karıştırılıp doğrudan pH'ının ölçülerek asit oluşumu olup olmadığını tayine yönelik Çamur pH'ı (Sobek et al., 1978; Page et al., 1982; Price, 1997), en basit testtir. ABA testlerinin bir alt kümesi olarak nitelenen Net Asit Üretme (NAP- Net Acid Production) (Coastech Research Inc., 1989) ve Net Asit Oluşturma (NAG- Net Acid Generation) (Sobek et al., 1978; Miller et al., 1990; O'shay et al., 1990; Stewart, 2006) testleri, hidrojen peroksidin (H_2O_2) demir sülfür minerallerini hızlı oksitlemesine dayanır. ANC'ye alternatif olarak geliştirilen, Asit Tamponlama Karakteristiği Eğrisi (ABCC- Acid Buffering Characteristics Curve) (Miller ve Jeffery, 1995), numunenin yavaş titrasyonunu ve bu esnada pH değerlerinin sürekli izlenmesini içeren bir testtir.

Geliştirilen birçok yönteme ve kimi zaaflarına karşın, dünya genelinde ABA yöntemleri daha fazla kabul görmektedir.

JEOKİMYASAL STATİK TESTLER

ABA Testleri

ABA Kavramının Ortaya Çıkışı ve Gelişimi

Yerkabuğunun bileşiminin tahmin edilmesine dönük çalışmalar göstermiştir ki, yerkabuğunda, reaktif hâlde bulunan katyonik elementlerin (Ca, Mg, K ve Na gibi) oranı, anyonik veya asit üreten elementlere (S, Cl, F ve P gibi) kıyasla, daha yüksektir. Fe, Al, Si ve O dâhil, bol bulunan diğer elementlerin çözünürlükleri zayıf veya tepkime eğilimleri görece düşüktür. Asitlik veya alkalinlik üzerindeki etkileri de ikincil derecededir. Bundan dolayı, kayaç içindeki baskın elementin, o kayacın gelecekte asit üretip üretmeyeceğini tayin edeceği düşünülmüştür (Skousen et al., 1996). AMD kavramının temeli bu düşüncedir.

Başlangıçta, maden artık yığınları için sınıflama yapılmış, kayaç ve asitlik dercesine dayalı üç tür malzeme tanımlanmıştır (Skousen et al., 1996: Smith ve Tyner, 1945'den). Bu sınıflandırma, yığındaki $CaCO_3$'ın yüzdesini pozitif, SO_4'ın yüzdesini negatif altsimge sayılarla ifade ederek, bir adım ileri götürülmüştür (Knabe, 1964). Sonrasında, Knabe (1973), tüm asitlere, asit üreten minerallere (sülfitler) ve katyonların değişim kapasitesine karşı, tüm bazların toplamını dengeleyen ve "baz- asit dengesi" adını verdiği bir yöntem kullanmıştır. Kayaç rengi, sertliği, çizgi rengi, pürüzlülüğü, seyreltik HCl'de tepkimesi gibi parametrelerle her bir katmanın tanımlanmasını; pH, toplam veya piritik sülfür ve NP ölçümüyle, katmanların toksisitesinin belirlenmesini de içeren, ayrıntılı bir ABA açıklaması, ilk kez 1973'de yapılmıştır (Grube et al., 1973). Ardından ABA, Smith et al. (1974) tarafından geliştirilmiş ve kömür örtü malzemelerinin sınıflandırılmasına yönelik kullanışlı bir yöntem olarak sunulmuştur. Nihayet 1978'de, ABA yöntemi üzerinde bazı değişiklikler yapılarak (standart ABA), saha ve laboratuvar araştırmaları için işlem süreçleri yayımlanmıştır (Sobek et al.,1978).

Standart ABA

Kömür sahaları için geliştirilen, ama sonraki yıllarla beraber, metal madenlerine de uygulanan standart ABA'da, AÜP, basit bir eşitlikle (Eşitlik 5) bulunur.

$$\text{AÜP} = \%\Sigma S * 31{,}25 \text{ t } CaCO_3 \text{ eşdeğeri}/1.000 \text{ t} \quad (5)$$

Bu eşitlik, arkasında mineralojiyi, tepkime süreçlerini ve yerel koşulları içeren, bir dizi kabulü barındırır (Morin ve Hutt, 1997):

1. Numunedeki tüm sülfür, sülfit (S_2^{2-}) hâlindedir ve kaynağı pirittir.
2. Tüm sülfür oksitlenir ve sülfata (SO_4^{2-}) dönüşür.

3. Oksitleyiciler, sadece su ve oksijendir (O_2).
4. Pirit oksitlendiğinde, demir (Fe^{2+}) de Fe^{3+}'e yükseltgenir.
5. Tüm demir, $Fe(OH)_3$ hâlinde çökelir.

Kabullerin dayanağı da ortama H^+ sağlayan ve açığa çıkan H^+'i tüketen iki kimyasal tepkimedir.

$$FeS_2(k) + 7/2H_2O(s) + 15/4O_2(g) \rightarrow Fe(OH)_3(k)\downarrow + 2SO_4^{2-} + 4H^+ \quad (6)$$

$$CaCO_3(k) + 2H^+(s) \rightarrow H_2CO_3(s) + Ca^{2+}(s) \quad (7)$$

İşte, hesaplamada, üstteki eşitlikten de görülebileceği üzere, Σ sülfür dikkate alınır. Öte yandan, (6) ve (7) numaralı tepkimeler uyarınca; 2 mol $CaCO_3$(200 g), 1 mol FeS_2'nin (64 g) üreteceği asidi nötrleştirecektir. Özetle; %1 sülfür içeren 1.000 t kayayı nötrleştirmek için, 31,25 t $CaCO_3$ gerekecektir. Bu dayanaktan hareketle, Σ kükürt yüzdesi 31,25 ile çarpılarak AÜP elde edilir.

NP'nin kaynağı karbonatlar, özellikle de $CaCO_3$ ve $MgCO_3$'tır. NP'yi belirlemek için, hacmi ve derişimi fışırdama testi (fizz rating) ile (Sobek et al., 1978) saptanan HCl asit, -250 µm tane boyutundaki numuneye eklenip, tepkime duruncaya kadar kaynatıldıktan sonra, soğutulan çözelti, son pH 7 olacak şekilde NaOH ile geriye titre edilip, test tamamlandığında, tüketilen NaOH ve HCl miktarlarından, numunenin NP'i hesaplanır.

Modifiye ABA

Coastech Research Inc. (1989) tarafından geliştirilip, ayrıntılarını Lawrence'ın (1990) verdiği modifiye ABA'da, sülfatların (jips, barit gibi) asit üretmediği, o nedenle, AÜP hesabında dikkate alınmamaları gerektiği vurgulanmıştır. Sadece sülfitlerin ve ayrıca, test öncesinde numunede, sülfitlerin oksitlenmesiyle oluşmuş sülfat varlığı söz konusuysa, bunların, kolayca hidrolize olabilen oksitlenme ürünü olmaları dolayısıyla, AMD'ye katkıları olacağından, değerlendirmeye alınmaları gerektiği belirtilmiştir. NP'nin fazla tahmin edilme olasılığını azaltmak için; a) tane boyutu %80 -75 µm'ye indirilen numunenin, düşük sıcaklıkta (25- 35 ^{0}C) ve 24 saat süreyle HCl ile muamele edilmesi, b)- asidin kademeli ilâvesiyle, süreç tamamlandığında, çözelti pH'ının 1,5- 2,0 aralığında tutulması önerilmiştir. Geriye titrasyonda, son pH, 7,0 yerine, duraylılığı (stabilite) daha iyi olan pH 8,3 kullanılmıştır. pH 8,3, asitlik titrasyonlarında alışılageldik nokta olup, karbonik asidin, en baskın zayıf asit olduğu doğal sulardaki karbonat/bikarbonat için stokiyometrik denklik noktasına karşılık gelmektedir (Lawrence, 1990; Lawrence ve Wang, 1996).

Sonrasında, standart ABA yönteminde, NP değerinin, kullanılan asit miktarına bağlı olduğuna, daha yüksek fışırdama derecesinin, yüksek NP sonucunu doğuracağına, bu testin sübjektifliğine işaret edilerek, numunenin fışırdama testinde vereceği tepkiye göre, asit şiddeti ve miktarında değişiklik yapılmıştır Fazladan NP tahminini engellemek için, asidin kademeli eklenmesi, asitleme işlemi sonunda pH'ın 2,0- 2,5 arasında tutulması önerilmiştir (Wang, 1998; Lawrence ve Wang, 1997).

British Columbia Araştırma Başlangıç Testi (BCAB)

Duncan ve Bruynesteyn (1979) tarafından geliştirilen yöntem, AÜP hesaplamasında standart ABA ile bire bir aynı olmasına karşın, NP tayininde, standart ABA'dan ayrışır. Kullanılan asit, terminoloji ve nicelik birimleri farklıdır. Fışırdama testi, ısıl işlem ve bir bazla geriye titrasyon yoktur. Öğütülüp, %70 -44 µm boyutuna indirilen numune saf su eklenip karıştırılır. Sonrasında çözelti, pH, 3,5'te sabitleninceye kadar H_2SO_4 ile titre edilir. pH'ın 3,5 seçilme nedeni, bu değerin, oksitleyici biyolojik etkinlik sınırını temsil ettiği düşüncesidir. Tüketilen asit miktarından NP hesaplanır.

NP (pH6) testi

Genel olarak uygulanan su niteliği standardının pH 6,0 olduğu gerekçesiyle, BCAB testi işlem sürecinde, son pH, 6,0 olarak değiştirilmiştir ki, bu iki test arasındaki tek farktır (Lapakko, 1994). NP (pH6) testinin, asit etkinliğinin, asidik ortamdan ziyade, pH 6,0 civarında olduğu, bunun da testi diğerlerinden kayda değer ölçüde ayırdığı ifade edilmektedir (White et al., 1999).

AÜP'nin kestiriminde, Lapakko'nun (1994) önerisinden farklı olarak, maden artığının depolandığı tane boyutunda değişiklik yapmaksızın kimyasal analiz yapılması ve sülfürün, asitte çözünür sülfür üzerinden belirlenmesi gerektiği savunulmuştur (Karadeniz, 2011). NP belirlenirken, H_2SO_4 asit ilâvelerinin ardından çözeltinin karıştırılması, çözeltinin pH'ı 6,0'da sabitlendiğinde, beherin 70^0C sıcaklıktaki su banyosuna alınıp, gaz çıkışı ya da kabarcıklanma sona erene kadar bekletilmesi, bu aşama sonrasında pH yükselme eğilimi gösterirse, pH sabitleninceye değin, asit ilâvesinin sürmesi önerilmiştir. Ayrıca, NP testlerine sokulan numunelerin tane boyutunun depolama boyutu ile aynı olması gerektiği savunulmuştur (Karadeniz, 2011).

Modifiye NP (pH6) testi

Maden atığı numunesi, eser miktarda Ca ve/veya Mg karbonat içeriyorsa ya da içerdiği karbonatlar, ağırlıklı olarak siderit ($FeCO_3$), ankerit [$Ca(Fe,Mg,Mn)(CO_3)_2$] gibi demir karbonat ise, NP (pH6) yöntemi için bir değişiklik gerekir. Çünkü BCAB ve NP (pH6) yöntemlerindeki titrasyon uygulandığında, titrantın ilâve ilk damlasıyla, son pH'ın aşılması söz konusudur. Sorunu gidermek için; katı numune, 6 ilâ 8 adet beherlere alınıp deiyonize su eklenir. Birinci behere H_2SO_4 ilâvesi yapılmazken, diğerlerinin her birine, sırasıyla, artan hacimde ilâve yapılır. Tüm beherler, karıştırıcı yardımıyla çalkalanır. Belli aralıklarla çalkalamaya ara verilip, çözeltilerin pH'ları ölçülür. Ölçülen pH değerleri H^+ konsantasyonuna çevrilir. Her bir numune için, pH 6'yı temsil eden H^+ konsantasyonu ve ona karşılık gelen asit hacmi, ara kestirimle (enterpolasyon) bulunur. pH 6'da kestirilen asit hacmi, $CaCO_3$ eşdeğeri NP'ye çevrilir. Bu, "etkin" NP'dir (White et al., 1999).

Avrupa Birliği- EN 15875 Test Standardı

EN 15875, Avrupa Birliği'nde standart olarak kabul edilen bir ABA yöntemidir. Avrupa Standardizasyon Komitesi, hem AÜP, hem de NP'nin belirlenmesinde, kimi değişiklikler yapmıştır (Technical Committee, 2011). AÜP hesaplanırken, toplam sülfüre veya sülfit sülfürüne dayanılabileceği; burada, numunenin mineralojik yapısının belirleyici olduğu ifade edilmiştir.

Esas itibariyle modifiye ABA ile uyumlu EN 15875'de, NP'nin belirlendiği, işlem süreciyle ilgili olarak; testte, numune tane boyutu (%95 -125 µm) ile birlikte, asit hacim ve şiddetinin tayini gibi birincil, ortam sıcaklığının 20±5 ^{0}C olması, demineralize su kullanılması gibi ikincil değişikliklere gidilmiştir. Asitlemede kullanılacak asidin hacmini tayin için de fışırdama testi yerine, numunenin karbonat içeriği esas alınmıştır (Technical Committee CEN/TC 292, 2011).

Alkali Üretme Potansiyeli: Sülfür Oranı Testi

Yöntem, Caruccio et al. (1981) tarafından, kömür atıklarının AÜP'ni ölçmek için geliştirilmiş, Coastech Research Inc. (1989) tarafından da modifiye edilmiştir. Numunenin AÜP'i, standart ABA'da olduğu gibi, toplam sülfür dikkate alınarak belirlenir. Alkali üretme potansiyeli, numunenin -23 µm boyutuna öğütülmesinden sonra, oda sıcaklığında HCl asit ile muamele edilip belirli süre beklendikten sonra, son pH 5,0 olacak şekilde geriye titre edilerek saptanır.

ABA Haricindeki Testler

Çamur pH'ı

Ne zaman ve kim tarafından geliştirildiği tartışma konusu olan bir yöntemdir (Karadeniz, 2011). Bir numunenin hazır asitliğini- alkalinliğini tayin etmekte kullanılan, görece hızlı, basit bir testtir. Yalnızca, çözünür tuzlar ve tepkime eğilimi yüksek mineraller sürece etkiyebilir. Numune, genellikle -1 mm tane boyutuna indirildikten sonra, damıtık su ile işleme sokulur. Belirli bir süre beklenip, çamurun pH'ı ve iletkenliği ölçülür.

Net Asit Üretme (Net Acid Generation- NAG veya NAP)

NAG testi, numunedeki demir sülfürlerin güçlü bir oksitleyici olan H_2O_2 vasıtasıyla hızla oksitlenmesine dayanan bir yöntemdir (Lawrence et al., 1988). Sülfürler oksitlenince, ortam asitleşir, asidik ortam da nötrleştirici mineralleri çözer. Böylelikle, numunenin asit üretme ve nötrleştirme potansiyeli doğrudan ölçülebilir. Bu yöntemde, sülfür tayinine gerek duyulmaz. Öğütülüp -75 µm boyutuna indirilen numune, H_2O_2 ile muamele edilir ve tepkimeler bittiğinden emin olunduktan sonra belirli bir süre (gece boyu) beklenir. Ardından, pH'ı ölçülüp kaydedilen çözelti, son pH önce 4,5 sonra 7,0 olacak şekilde NaOH ile titre edilir (Stewart et al., 2006). Tüketilen NaOH hacmi ve molaritesinden, net asit üretme potansiyeli hesaplanır.

NAG testi için, oksitlemenin yetersiz olabileceği durumlar göz önüne alınarak, ardışık NAG (Sequential NAG) testi önerilmiştir. Test, tek bir H_2O_2 ilâvesi şeklinde değil, NAG pH ≥ 4,5'e ulaşıncaya kadar tekrarlanır. Hesaplamada, her tekrarda kullanılan NaOH hacmi toplanarak, hesap yapılır.

Statik Test Sonuçlarının Değerlendirilmesi- Yorumlanması

AÜP ve NP bulununca, geriye, iki değer arasındaki oranın ya da farkın hesaplanacağı, bir aritmetik işlem yapılması kalmış gibi görünür. Ancak, kömür ya da sülfürlü maden sahalarında, AMD kestirimi için sayısız çalışma yapılmış, genel yorumlara ulaşılmaya çalışılmıştır. Sonuçta, maden yataklarının ve bulundukları coğrafyanın, çoğunlukla, kendine özgü olması nedeniyle, yorumlamaların da buna göre ve karşılaştırmalı yapılmasının daha doğru olacağı görülmüştür. Bununla beraber, önerilen bazı kıstaslar Çizelge 1'de verilmiştir.

Bu kıstaslar arasında, Brodie et al. (1991) tarafından önerilen, en yaygın kabul görendir. Burada, NP/AÜP<1 ise, numune asit üretir; 1<NP/AÜP<3 ise, numune belirsizlik aralığındadır ve kinetik testlerin yapılması gerekir ve nihayet, NP/AÜP>3 ise de numune asit üretmez şeklinde değerlendirilir.

Statik Testlerde Hata Kaynakları

Aynı sahaya ait numunelerin AÜP ve NP'i farklı statik testlerle bulunması doğrultusunda yapılan çalışmalar, çoğu zaman, birbirlerini doğrulamayan, tutarsız sonuçlara ulaşıldığını göstermektedir. Kuşkusuz ilk akla gelen sebep, sahadan alınan numunelerin temsiliyeti ya da doğru bölünmemiş olma olasılığıdır. Yine, laboratuvarlarda testleri yürüten kişiye bağlı hatalarla karşılaşılması da olağandır. Bu aşamalarda bir hata yapılmamışsa bile, yine de farklı sonuçlar bulunabilmektedir. Yöntemlerin işlem süreçleri, en başında yapılan kimi kabullere dayalı olduğundan ve kabuller her sahada geçerli olamadığından, durum, doğal olarak sonuçlara yansımaktadır.

AÜP: Başta standart ABA olmak üzere, bir kısım ABA yönteminde, numunedeki sülfürün tamamının çözüneceği kabul edilir. Ancak barit ($BaSO_4$), jips ($CaSO_4.2H_2O$), anhidrit ($CaSO_4$), epsomit ($MgSO_4.7H_2O$) gibi sülfat mineralleri asit üretmez. Numune bu mineralleri içeriyorsa, bulunacak AÜP değeri gerçeğin üzerinde olacaktır. Modifiye ABA gibi, testten önce, sülfitlerin oksitlenmesiyle oluşmuş

sülfatlar dışındaki sülfatların asit üretmediğini kabul ederken, brokantit ($Cu_4SO_4(OH)_6$), alunit ($KAl_3(SO_4)_2(OH)_6$), jarosit [$KFe_3(SO_4)_2(OH)_6$)] ve melanterit ($FeSO_4 \cdot 7H_2O$) gibi sülfatlar, çözündüklerinde asit üretirler. Dolayısıyla, teste tâbi tutulan numunedeki çözünebilir sülfatlar hesaba katılmaksızın bulunacak AÜP, gerçek değerin altında olacaktır.

Ayrıca, organik S, kimyasal tepkimeye girmeye eğilimli değildir. O nedenle, organik S ya asit oluşumuna etki etmez veya etkisi ihmal edilebilecek denli düşüktür.

Çizelge 1. ABH testi yapılan numuneler için, net nötrleştirme potansiyeli (NNP) (‰ $CaCO_3$) veya NP/AÜP bazında AÜP'nin yorumlanması (White et al., 1999)

ABH	Asit	Belirsiz	Asit Değil
NNP veya (NP-AÜP)			
Appalachian Kömür-Madeni[1] Kıstası	< -5	k/b	k/b
B. C. Metal-Madeni Kıstası[2]	≤ 0	k/b	k/b
Ferguson, Morin, 1991	k/b	-20<NNP<+20	k/b
Day, 1989	<+10	k/b	k/b
NP/AÜP			
Brodie et al., 1991	< 1	1<NP/AÜP<3	> 3
Morin and Hutt, 1994	< 1	1<NP/AÜP<1,3 – 4,0	> 1.3 – 4,0

[1]Sobek et al., 1978
[2]Ferguson and Morin, 1991
* k/b kaynakta belirtilmemiş

NP: ABA testlerinde, işlem süreçlerine ilişkin değişiklik önerileri, büyük ölçüde, NP üzerine yoğunlaşmıştır. Üstelik S oranı, analizlere dayalı iken, NP değeri laboratuvarda test yapılarak belirlenir. Bu yüzden, yöntemler arasındaki asıl farklılık, NP değerinin tespitinde ortaya çıkar (Şekil 1 ve Çizelge 2).

NP'nin hesapla bulunmasına ilişkin öneriler de yapılmıştır. Maden atığında sadece kalsiyum ve magnezyum karbonatın, pH seviyesini 6,0 civarında tamponlayacağı varsayılarak, numunenin mineralojisine bağlı "MinNP" kullanılmış, bunun için aşağıdaki eşitlik (Eşitlik 8) verilmiştir (Lapakko, 1992).

$$MinNP = 10*(\%CaCO_3) + 11,9*(\%MgCO_3)\ kg / t\ CaCO_3 \quad (8)$$

Hızlı çözünen kalsiyum bazlı karbonat minerallerinin, asitliğini hızla nötrleştireceği ve tüm karbonun karbonatlardan geldiği kabulüyle, karbonat NP (KaNP) hesaplanabileceği ifade edilmiştir (Morin ve Hutt, 1997). Bunun için verilen eşitlik (Eşitlik 9);

$$KaNP = 83,3*(\%C)\ kg / t\ CaCO_3 \text{ veya } KaNP = 22,7*(\%CO_2)\ kg / t\ CaCO_3 \quad (9)$$

Paktunç (1999) da asit üreten ve tüketen bileşenler arasındaki dengenin belirlenmesinde, örneklerin mineralojik bileşimine dayalı, ayrıca diğer sülfitlerin ve birden fazla nötrleştirici mineral türünün varlığının dikkate alındığı yeni bir yaklaşım önermiştir (Eşitlik 10).

$$YNP = \sum_{x=1}^{k} \frac{W_a \times X_i \times 10}{n_{M,i} \times W_i} \quad (10)$$

Burada; YNP: yığın nötrleştirme potansiyeli, kg H_2SO_4/t, k: nötrleştirici minerallerin sayısı, W_a: H_2SO_4'ün moleküler ağırlığı, (g/mol), X_i: i mineralinin miktarı, % ağırlık, $n_{M,i}$: stokiyometrik faktör, (1 mol H_2SO_4'ü tüketmek için gereken nötrleştirici mineralin mol değeri) ve W_i: nötrleştirici i mineralinin g/mol olarak moleküler ağırlığıdır.

NP, kimyasal ve mineralojik analiz sonuçlarına dayalı hesaplama ile belirlenmesi, AÜP hesabında olduğu gibi, minerallerin tümden çözüneceği kabulüne dayanır.

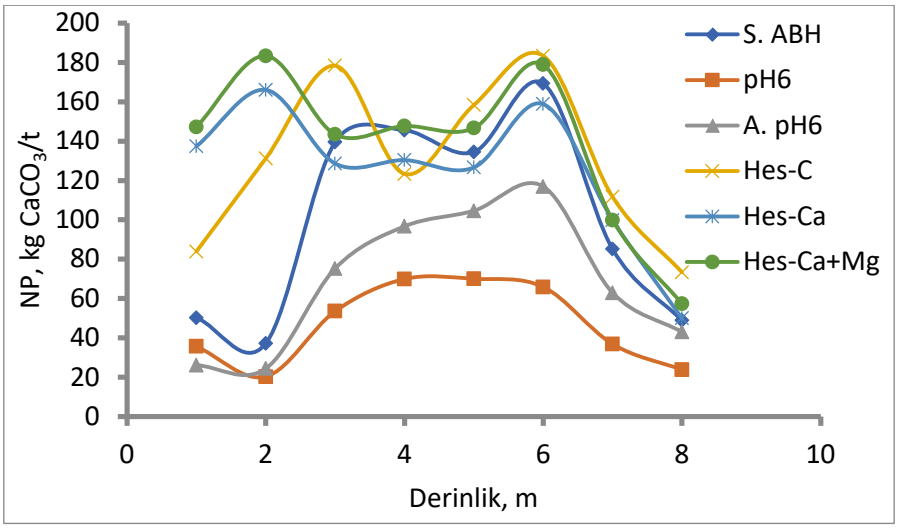

Şekil 1. Balıkesir- Balya maden sahası büyük yığın sondaj numunelerinin NP değerlerinin farklı yöntemlere göre, derinlikle değişimi (Karadeniz, 2011)

Çizelge 2. Hidrotermal kuvars- karbonat içeren altın artıklarının farklı yöntemlerle belirlenen NP değerlerinin mukayesesi- çizelge kısaltılmıştır (White et al., 1999)

	NP, kg/t $CaCO_3$		
Numune	Standart ABA	Modifiye ABA	$CaCO_3$ + $MgCO_3$
1 (T1)	230	200	207
2 (T3)	195	130	163
3 (T5)	98	92	65
4 (T7)	270	220	229
5 (T9)	18	16	14

NP testlerinde ise, kimyasal çözündürme, fiili bir durumdur. Yönteme bağlı olarak, çeşitli işlem basamaklarından oluşur, dolayısıyla fazla sayıda, hataya açık değişken (protocol variables) mevcuttur. Bunlar, maden artığının tane boyutu, kullanılan asit, asidin miktarı ve derişimi, ortam sıcaklığı, asitle muamele süresi ve eğer çözeltiye, geri-titrasyon uygulanacaksa, son pH'tır.

Tane boyutu: ABA yöntemlerine göz atıldığında, test yapılırken numunelerin tane boyutunun -250 µm ile -23 µm arasında değiştiği görülür. Tesadüfen denk gelmiyorsa, test uygulama boyutu, maden artığının depolama boyutundan farklıdır. Malzemenin tane boyutu küçüldükçe yüzey alanı artarak, kimyasal tepkimelerin hızına etki eder. Diğer yandan, artığın depolandığı tane boyutunun altına öğütülerek test edilmesi hâlinde, yığın içinde kimyasal tepkimeye girme olasılığı hiç olmayabilecekken (örneğin, çözünmeyen bir silis tanesinin içinde hapis konumu), öğütme sayesinde yeni yüzeyler açılacağından, tepkimeye de girmesi mümkün kılınmış olur. Doğru tane boyutu, o yüzden, artığın depolandığı boyuttur.

Asit türü: NP belirlenirken, karbonatları çözdüğü için, çoğunlukla, HCl asit kullanılır. BCAB ve NP(pH6) gibi az sayıda testte ise H_2SO_4 asit tercih edilir. Öte yandan, minerallerin, farklı asitler içindeki tepkime kinetikleri ve tepkime ürünleri aynı değildir. Maden sahalarında, asidik drenaj geliştiğinde, demir sülfürlerin çözünmesiyle H_2SO_4 asit oluşur. Örneğin, hidratlanmış üç değerlikli demir oksitin farklı asitlerde çözünme hızının sırasıyla HF > HCl > H_2SO_4 > $HClO_4$ olduğu, bu sıralamanın, anyonlarla Fe^{+3} iyonları arasında oluşturulan karmaşıkların azalan kararlılık sırasına uyduğu belirtilmektedir (Burkin, 1965). Pirotinin ise, H_2SO_4'e kıyasla HCl'de daha fazla çözünür olduğuna işaret edilmektedir (White et al., 1999). O nedenle, esasen testlerde H_2SO_4 asit kullanılması doğrusudur.

Asit miktarı ve derişimi: Numune, asit ile muamele edildiğinde, kullanılan asidin miktarı ve derişimi, ortam pH'ını doğrudan etkilediğinden, minerallerin çözünme hızlarına da etkisi olur. Gerekenden fazla derişimde ve miktarda asit kullanıldığında, NP değeri olması gerekenin üzerinde ya da yetersiz derişimde ve miktarda asit eklenirse de NP değeri olması gerekenden düşük bulunabilir.

Sıcaklık: Arrhenius denkleminden bilinir ki, ortam sıcaklığının artmasıyla, tepkime hızları, genelde artar. ABA testlerinde, farklı sıcaklık uygulamaları vardır. Bunun da farklı sonuçlar doğuracağı açıktır. Ayrıca, (1) numaralı tepkimeden görüleceği üzere, tepkime ekzotermiktir ve ısı açığa çıkmaktadır. Lefebvre et al. (2001), piritin oksitlenme sürecinde her mol için 1.409 kj ısı açığa çıktığı ve bu ısının, atık kaya yığınlarında sıcaklığı 70^0C'a kadar çıkardığı belirtilmiştir. Bu bakımdan, testlerin bu sıcaklığa uygun ortamda gerçekleştirilmesi gerekir.

Süre: NP belirlenirken, asitle muamele süresi genellikle sabittir, ama yöntemden yönteme değişkenlik gösterir. Oysa numunelerin mineralojik bileşim ve yapıları, tepkime süresini doğrudan etkiler. Her numuneye aynı şekilde uygulanan süre, bazıları için yeterli olabilirken, başkaları için yetersiz kalabilir. Bu durumda, belirlenen NP değeri, gerçek değerin altında bulunabilir.

Nötrleştirme tepkimelerinde başlıca mineraller, şüphesiz karbonatlardır ve karbonat mineralleri, çoğunlukla, hızlı çözünürler. NP değerini göz ardı edilemeyecek oranda etkileyebilen silikatlar arasında görece hızlı çözünebilenler varsa bile, genelde yavaş çözünürler. O nedenle, süre uygulamalarında da maden yatağının mineralojik özelliklerinin göz önünde bulundurulması, hataların azaltılması bakımından önem taşır.

Geriye- titrasyon: BCAB ve NP (pH6) testlerinde geriye- titrasyon uygulanmaz. Standart ABA, modifiye ABA ve EN 15875 yöntemlerinde, nötrleştiricilerin parçalanmasını takiben, kalan asit miktarını saptamak amacıyla geriye- titrasyon uygulanır. Bu uygulamada son pH, standart ABA'da 7,0, diğerlerinde ise, 8,3'tür. pH 7,0, nötr ortam olarak değerlendirilmesine karşın, bu çözeltilerde, hâlâ bir miktar asitlik vardır. Geriye- titrasyonda son pH 7,0'da ölçülen NP değeri, pH 8,3'e göre, 20 ilâ 30 kg/t $CaCO_3$ daha yüksektir (White et al., 1999).

YÖNETMELİĞİN AMD YÖNÜNDEN DEĞERLENDİRİLMESİ

"Maden Atıkları Yönetmeliği" ile beraber, onu tamamlayan diğer iki metin, asidik drenajı kavramları bakımından irdelendiğinde, "asit maden drenajı" ve "asit kaya drenajı" ifadelerinin aynı anlamda kullanıldığı anlaşılmaktadır. Esasen doğrudur, zira literatürde, bu ikisinin birbirleri yerine kullanıldığı bilinmektedir. Diğer taraftan, madencilik faaliyetleri dışında da asidik drenaja rastlanabilmektedir.

Demir sülfür içeren cevher oluşumları, yeryüzüne yakın seviyelerde yataklandıklarında, yüzeyleri atmosfere açıksa, oksijen ve nem etkisiyle, tamamen doğal oksitlenme tepkimeleri gelişir. Bu aşamayı çözünme, ardından da ikincil minerallerin meydana gelmesi ve çökelmeleri izler. Demir şapka (gossan) oluşur (Downing ve Mills, 2000). Yüzey suları, demir şapka ile temas ettiğinde asidik drenajlar gelişir.

Derin kazılar gerektiren büyük mühendislik yapılarının inşa faaliyetlerinde, demir sülfürlerin bulunduğu bir formasyonun yüzeyi açılırsa, yüzey akıntıları, asidik drenaja neden olabilmektedir (örnek, Halifax, Nova Scotia Airport- Kanada) (Skousen, 1996). Bu iki olgunun madencilik faaliyeti ile ilgisi olmadığından, asit maden değil, asit kaya drenajı olarak adlandırılması daha doğru olacaktır.

İkinci nokta, "Maden Atıkları Yönetmeliğinin Uygulanmasına İlişkin Açıklamalar" metninin Ç Maddesi'nin 2. Bendi'nde, "Okistli- karbonatlı cevherler dışında kalan sülfürlü cevherlerin (bakır, kurşun ve çinko madenleri ile bunları ihtiva eden pirit, pirotin, sfalerit, galen vb. ile kompleks cevherlerin) zenginleştirilmesinden kaynaklanan atıklar…" ifadesinin, kömür yataklarını kapsamadığı, hatta üç metinden hiçbirinde, "kömür ya da linyit" sözcüklerinin geçmediği görülmektedir. Oysa, geliştirilen ilk test yöntemi olan standart ABA'da çalışılan malzeme, ABD'de, Appalachia Bölgesi kömür sahalarından (coal overburden and minesoils) temin edilmiştir (Sobek et al., 1978)

Üçüncüsü, "ABA" terimi ile ilgilidir. Yine, Ç Maddesi'nin 3. Bendi'nde, "… Atığın sülfit-sülfür (S^{-2}) miktarı %0,1'in üzerinde ise statik test yapılır (pr en 15875, ABA, SOBEK, Modifiye SOBEK) …" cümlesine yer verilmiştir. Bu cümle, birden fazla yanlış içermektedir. Parantez içinde verilen statik yöntemlerin tümü ('pr en 15875', kesin standarda dönüştürülerek 'EN 15875' olmuştur), ABA yöntemleridir. Standart ABA, literatürde 'Sobek' ve 'EPA 600 ABA' adlarıyla da anılır.

Bu cümlenin, algoritma bakımdan da yanlışı vardır, çünkü başta standart ABA olmak üzere, birkaç ABA yönteminde, AÜP hesaplamasında, sadece S^{-2} değil, numunedeki (maden artığındaki) tüm sülfür, yani SO_4 da dikkate alınır. Dolayısıyla, cümle kendi içinde çelişki barındırır.

SONUÇ

AMD kestiriminde, 40 yılı aşkın bir süredir kullanılagelen statik testler, ABA ya da diğerleri, bazı kabuller üzerine kuruludur. Ancak AMD denilen olgu, oluşum ve gelişim bakımlarından, sadece maden yatağının kendi koşullarına değil, aynı zamanda, bulunduğu yerin coğrafi şartlarına, dolayısıyla, birçok paraparametreye bağlıdır (Karadeniz, 2008). Kabuller, sahaya özgü koşullarla uyuşmadığında ki, sıklıkla uyuşmaz, uygulanan yöntem yanıltıcı sonuçlar verebilir. O nedenle, yöntem tercihinde, başta maden yatağının mineralojik yapısı olmak üzere, yerel özelliklerin dikkate alınması zorunludur. Yanlış yöntem, AÜP ve NP'nin, gerçek değerlerinin üzerinde veya altında bir değer bulunmasına, bu da, alınacak tedbirlerin yetersizliğine ya da aşırı önlem dolayısıyla, gereğinden yüksek maliyete yol açabilir.

Yönetmelikte, maden artıklarının içerdiği sülfür olarak, sadece sülfidik sülfürün hesaba katılması, bazen doğru sonuç verse de bu, her zaman için geçerli olmaz.

Yönetmeliğin, birden fazla yöntemin uygulanabilmesine olanak sağlaması doğru bir yaklaşımdır, ama eksiktir. NAG gibi, diğer yöntemlerin de hâlihazırda yer verilenlere eklenmesi yerinde olur. Örneğin,

NAG yöntemi Avustralya'da kullanılmaktadır. Doğrusu, saha karakterizasyonunun başarılı yapılması ve sonrasında, yöntemin seçilmesi, gerekirse, birbirlerini doğrulamak üzere, birden fazla yöntemin uygulanmasıdır.

KAYNAKLAR

Brodie, M. J., Broughton, L. M., Robertson, A. (1991). A Conceptual Rock Classification System For Waste Management And A Laboratory Method For ARD Prediction From Rock Piles, In Proc. Second International Conference on the Abatement of Acidic Drainage. (pp. 119-135). Vol. 3., Montreal, Quebec, September 16-18, MEND Program (ed.), Quebec Mining Association, Ottawa.

Burkin, A.R. (1965). Hidrometalurjik süreçlerin kimyası, Utine, T. (Çev. 1988), TMMOB Maden Mühendisleri Odası Yayını, Net Ofset, Ankara.

Caruccio, F. T., Geidel, G., Pelletier, M. (1981). Occurrence And Prediction of Acid Drainages. *J. Energy Div. Amer. Soc. Civil Engineers*, 107, No. EYl, May.

Coastech Research Inc. (1989). Investigation Of Prediction Techniques for Acid Mine Drainage. MEND Project Report 1.16.1a, MEND, Ottawa, Ontario.

Day, S. J. (1989). Comments after presentation of: A Practical Approach To Testing For Acid Mine Drainage İn The Mine Planning And Approval Process. Presented at the Thirteenth Annual British Columbia Mine Reclamation Symposium. (pp. 7-9). June 7-8. Vernon, British Columbia.

Downing, B. W. (2014). Acid–base accounting test procedures. Acid mine drainage, rock drainage, and acid sulfate soils: causes, assessment, prediction, prevention, and remediation, Editor(s): James A. Jacobs, Jay H. Lehr, Stephen M. Testa. 229-252.

Duncan, D. W. and Bruynesteyn, A. (1979). "Determination Of Acid Production Potential of Waste Materials, *Met. Soc. AIME*, paper A79-29, 10 p.

Ferguson, K. D. and Morin, K. A. (1991). The Prediction of Acid Rock Drainage - Lessons from the Data Base. In Proceedings of the Second International Conference on the Abatement of Acidic Drainage. (pp. 83-106). September 16-18. Montreal, Canada.

Grube, W. E., Smith, R. M., Singh, R. N., Sobek, A. A. (1973). "Characterization Of Coal Overburden Materials And Minesoiles In Advance Of Surface Mining", In: Research and Applied Technology Symposium on Mined Land Reclamation. (pp. 134- 151). NCA/BCR, Pittsburg, PA.

Karadeniz, M. (2011). Balıkesir-Balya Kurşun-Çinko Madeni Flotasyon Artıklarının Asit Maden Drenajı Oluşum Potansiyelinin Derinlikle Değişiminin Araştırılması. Hacettepe Üniversitesi Fen Bilimleri Enstitüsü, Doktora Tezi, Ankara.

Knabe W. (1964). "A Visiting Scientist's Observations And Recommendations Concerning Strip-Mine Reclamation İn Ohio", *The Ohio Journal of Science*, 64(2), March, 132- 157.

Knabe, W. (1973). Development And Application of the 'Domsdorf Ameliorative Treatment` on Toxic Spoil Banks Of Lignite Opencast Mines in Germany", In: Jutnik, R. J. and Davis, G. (Eds.), Ecology and reclamation of devastated land. Vol: 2, Gordon and Breach Publishers, Inc., New York, NY. 273- 294.

Lapakko, K. A. (1992). Characterization And Static Testing Of Ten Gold Mine Tailings. In American Society for Surface Mining and Reclamation Meeting. (pp. 370- 384). Duluth- Minnesota.

Lapakko, K. A. (1994). Evaluation of Neutralization Potential Determinations for Metal Mine Waste and a Proposed Alternative. Proc. International Land Reclamation and Mine Drainage Conference, (pp. 129-137). Pittsburgh, USBM SP 06A-94.

Lawrence, R. W. and Wang, Y. (1997). Determination of Neutralization Potential in the Prediction of Acid Rock Drainage. Proceedings of Fourth International Conference on Acid Rock Drainage, (pp. 451-464). Volume I. Vancouver B. C. Canada.

Lawrence, R. W., and Wang, Y. (1996). Determination of Neutralization Potential for Acid Rock Drainage Prediction. Canadian Mend Report (89 p). Project, 1.16.3, for Hudson Bay Mining and Smelting and for Environment Canada.

Lawrence, R.W. (1990). Prediction of the Behavior of Mining and Processing Wastes in the Environment. In pro. Western Regional Symposium on Mining and Mineral Processing Wastes. (pp. 115-121). Doyle, F., (ed.), Soc. for Mining, Metallurgy and Exploration, Inc., Littleton, CO.

Lawrence, R.W., Jaffe, S. and Broughton, L.M. (1988). In-House Development of the Net Acid Production Test Method, Coastech Research.

Lefebvre, R., Hockley, D., Smolensky, J., Gélinas, P. (2001). "Multiphase transfer processes in waste rock piles producing acid mine drainage: 1: Conceptual Model And System Characterization, *Journal Of Contaminant Hydrology, 52*.1-4 137-164.

Maden Atıkları Yönetmeliği ve Ekleri, 15.07.2015 tarih ve 29717 sayılı resmî gazete (16.07.2016 tarih 29772 sayılı resmî gazete ile değişik).

Maden Atıkları Yönetmeliğinin Uygulanmasına İlişkin Açıklamalar, https://webdosya.csb.gov.tr/db/cygm/duyurular/may-ac-klama201805-20180601164229.pdf, Erişim tarihi- 25.01.2022.

Miller, S. and Jeffery, J. (1995). Advances in the Prediction of Acid Generating Mine Waste Materials. In: Proceedings of the Second Australian Acid Mine Drainage Workshop. (pp. 33-43). Charters Towers, Queensland, 28-31 March. eds. N. J. Grundon and L. C. Bell, Australian Centre for Minesite Rehabilitation Research, Brisbane.

Miller, S. D., Jeffery, J. J., and Murray, G. S. C. (1990). Identification And Management Of Acid Generating Mine Wastes - Procedures and practices in Southeast Asia and the Pacific Regions", In: Acid mine drainage designing for closure, J. W. Gadsby, J. A. Malick, S.J. Day (eds.) BiTech Publishers Ltd., Vancouver, B.C. 1-11.

Morin, K. A. and Hutt, N. M. (1994). Observed Preferential Depletion Of Neutralization Potential Over Sulfide Minerals İn Kinetic Tests: Site Specific Criteria For Safe NP/AP Ratios. In Proceedings of the International Land Reclamation and Mine Drainage Conference on the Abatement of Acidic Drainage. (pp. 148-156). April 24-29. Pittsburgh, PA.

Morin, K. A., and Hutt, N. M. (1997). Environmental Geochemistry Of Minesite Drainage: Practical Theory And Case Studies, MDAG Publishing, Vancouver, Canada.

O'Shay, T. A., Hossner, L. R., Dixon, J. B., (1990). "A Modified Hydrogen Peroxide Oxidation Method For Determination Of Potential Acidity İn Pyritic Overburden", *Journal of Environmental Quality*, 19, 778-782.

Page, A.L., Miller, R. H. and Keeney, D. R. (1982), Methods of Soil Analysis: Part 2 - Chemical and Microbiological Properties, 2nd Edn., American Society of Agronomy Inc., Soil Science Society of America Inc. 199-209.

Paktunç, A. D. (1999). Characterization Of Mine Wastes For Prediction Of Acid Mine Drainage. In: Azcue JM (ed) Environmental impacts of mining activities, Springer-Verlag, Berlin Heidelberg New York. 19- 40.

Price, W. A. (1997). DRAFT. Guidelines And Recommended Methods For The Prediction Of Metal Leaching And Acid Rock Drainage At Minesites In British Columbia. (170 p). British Columbia Ministry of Employment and Investment, Energy and Minerals Division, Smithers, BC.

Skousen, J. G., Smith, R., Sencindiver, J. (1996). The Development Of The Acid-Base Account, Acid Mine Drainage Control And Treatment (Compiled by J. G. Skousen and P. F. Ziemkiewicz), W.V.Univ., and N.M.L.R.C. 15-20.

Smith, R. M., Grube, Jr., W. E., Arkle, T., J., Sobek, A. A. (1974). Mine Spoil Potentials For Soil And Water Quality, (320 p). Environmental Protection Technology Series (EPA- 670/2- 74- 070).

Sobek, A. A., Schuller, W. A., Freeman, J. R. and Smith, R. M. (1978). Field And Laboratory Methods Applicable To Overburdens And Minesoils. (203 p). EPA-600/2-78-054. U.S. Environmental Protection Agency, Cincinnati, OH.

Stewart, W. A., Miller, S. D., Smart, R. (2006). Advances in Acid Rock Drainage (Ard) Characterisation of Mine Wastes. Paper Presented at the 7 th International Conference on Acid Rock Drainage (ICARD).

(pp. 2098 – 2119). March 26-30. St Louis MO. R.I. Barnhisel (ed.) Published by the American Society of Mining and Reclamation (ASMR), 3134 Montavesta Road, Lexington, KY 40502.

Technical Committee CEN/TC 292, 2011; “BS EN 15875- Characterization Of Waste -Static Test For Determination Of Acid Potential And Neutralization Potential Of Sulfidic Waste.

Wang, Y. (1998). Evaluation Of Np Determination By Static Tests for ARD Prediction (Doctoral Dissertation, University Of British Columbia).

White, W. W. III., Lapakko, K. A. and Cox, R. L. (1999). Static-Test Methods Most Commonly Used To Predict Acid-Mine Drainage: Practical Guidelines For Use And İnterpretation”, In: Reviews in economic geology, V. 6A, The environmental geochemistry of mineral deposits, Part A: Processes, techniques, and health issues, Plumlee, G. S. and Logsdon, M. J. (eds.), Society of Economic Geologists, Inc., Littleton, CO. 325-338.

BİR AÇIK OCAK KROM SAHASININ BİRİM MALİYETİNİN UZUN KISA-VADELİ BELLEK (LSTM) YÖNTEMİ İLE TAHMİN EDİLMESİ

PREDICTION OF UNIT COST OF AN OPEN-PIT CHROME MINE USING LONG SHORT-TERM MEMORY (LSTM) METHOD

A.C. Özdemir

Çukurova Üniversitesi, Mühendislik Fakültesi, Maden Mühendisliği Bölümü
*(*Sorumlu yazar: acozdemir@cu.edu.tr)*

ÖZET

Maden varlığı tespit edilen bir sahanın ilk olarak ekonomik yönden değerlendirilmesi gerekmektedir. Bu aşamada, toplam üretim maliyetinin toplam üretim miktarına oranı olarak bilinen birim maliyetin hesaplanması önem kazanmaktadır. Bu değer, maden sahasında üretim yapılmasının ekonomik olup olmadığının bir göstergesidir. Bu nedenle, ekonomik ve sürdürülebilir madencilik için bu parametrenin hassas bir şekilde hesaplanması ve takip edilmesi gerekmektedir. Ancak, günümüz şartlarında birim maliyetin çok fazla değişkenlik göstermesi madencilik sektörünü olumsuz etkileyen bir belirsizlik ortamı oluşturmaktadır. Bu çalışmada, birim maliyetin belirsizlik probleminin çözümünde bir derin öğrenme yöntemi olan Uzun Kısa-Vadeli Bellek (LSTM) yönteminin kullanılabilirliği araştırılmıştır. Bu yöntemin performansını değerlendirmek için örnek bir açık ocak krom madenine ait birim maliyet tahmini gerçekleştirilmiştir. Eğitim parametreleri değiştirilerek 9 farklı LSTM modeli geliştirilmiş ve bu modellerin başarısı korelasyon katsayısı (R), ortalama mutlak yüzde hata (MAPE) ve kök ortalama kare hata (RMSE) performans değerlendirme kriterleri kullanılarak ölçülmüştür. Geliştirilen modeller arasından en iyi model ile elde edilen sonuçlar (R=0.72, RMSE=2.47 ve MAPE=4.37) LSTM yönteminin başarılı bir performans gösterdiğini kanıtlamıştır. Böylece, LSTM yönteminin birim maliyetin tahmin edilmesinde kullanılabilir olduğu ve ekonomik belirsizlik problemine bir çözüm olabileceği belirlenmiştir.

Anahtar Sözcükler: Açık ocak, krom cevheri, birim maliyet, tahmin, uzun kısa-vadeli bellek (LSTM)

ABSTRACT

An area where mineral assets are detected must first be evaluated economically. At this stage, it is important to calculate the unit cost, known as the ratio of the total production cost to the total production amount. This value is an indicator of whether it is economical to produce at the mining site. Therefore, this parameter needs to be calculated and followed precisely for economical and sustainable mining. However, the high variability of unit costs in today's conditions creates an environment of uncertainty that negatively affects the mining industry. In this study, the usability of the Long Short-Term Memory (LSTM) method, which is a deep learning method, was investigated in solving the unit cost uncertainty problem. To evaluate the performance of this method, a unit cost estimation of a sample open pit chrome mine was made. By changing the training parameters, 9 different LSTM models were developed and the success of these models was measured using the correlation coefficient (R), mean absolute percent error (MAPE) and root mean square error (RMSE) performance evaluation criteria. Among the developed models, the results obtained with the best model (R=0.72, RMSE=2.47 and MAPE=4.37) proved that the LSTM method showed a successful performance. Thus, it has been determined that the LSTM method can be used in predicting the unit cost and can be a solution to the economic uncertainty problem.

Keywords: Open-pit mine, chromite ore, unit cost, prediction, long short-term memory (LSTM)

GİRİŞ

Günümüzde sürdürülebilirlik, kaynak verimliliği ve sera gazları emisyonu gibi kavramlar birçok sektörde olduğu gibi madencilik sektöründe de yaygınlaşmaktadır. Madencilik faaliyetlerinin başarılı bir şekilde yürütülebilmesi için bu kavramların iyi yorumlanması ve çalışmalara entegre edilmesi gerekmektedir. Gelişmiş ülkelerin birçoğu bu kavramların önemini benimsemiş ve Dünya genelinde insanların yaşam standartları dahil bir çok etken parametre gözden geçirilmektedir (Papetti vd., 2019). 2021 yılında yayınlanan Avrupa Yeşil Mutabakatı ve buna paralel olarak Türkiye Cumhuriyeti Ticaret Bakanlığı tarafından yayınlanan Yeşil Mutabakat Eylem Planı 2021'de Ülkelerin temiz ve döngüsel bir ekonomi politikası yürütmeleri vurgulanmıştır (European Commission, 2021; Türkiye Cumhuriyeti Ticaret Bakanlığı, 2021). Buradan da anlaşılacağı gibi herhangi bir faaliyet alanında özellikle sürdürülebilirliğin ve kaynak verimliliğinin sağlanması için ekonomik üretim modelinin geliştirilmesi zorunludur. Ülkelerin gelişimi, kalkınması ve rekabetçi olabilmesi sahip oldukları ekonomik güçle doğru orantılıdır.

Madencilik sektöründe üretime devam edilmesi veya üretimin durdurulması gibi hayati kararların alınmasında en önemli kriter o günün ekonomik koşullarıdır (Shafiee vd., 2009). Sürdürülebilir ve yüksek kaynak verimliliğine sahip bir madencilik için maliyetlerin, cevher fiyatlarının ve gelir-gider bilgilerinin eksiksiz bir şekilde kayıt altına alınması gerekmektedir. Delme-patlatma, yükleme, nakliye, akaryakıt, işçilik, bakım-onarım, yedek parça, elektrik, iş sağlığı ve güvenliği, eğitim, çevre vb. gider kalemleri üzerinde en çok durulan maliyetler arasında bulunmaktadır. Hesaplamalarda kolaylık sağlanması açısından genel olarak bu maliyetler; kazı (madencilik), konsantre (proses) ve genel-idari yönetim maliyeti olmak üzere 3 grupta değerlendirilebilir. Bir maden sahasının birim maliyet değeri bu maliyetlerin toplamının toplam üretim miktarına oranı olarak kabul edilir ve $/ton veya TL/ton cinsinden ifade edilir (Curry vd., 2014; Ahmadi ve Bazzazi, 2019; Khan ve Asad, 2019). Birim maliyet, madencilik faaliyetleri başlamadan önce hesaplanmalı ve üretim devam ederken belirli periyotlarda güncellenmelidir (Shafiee ve Topal, 2012). Burada gözlemlenecek herhangi beklenmedik veya sıra dışı bir değişimin (artış veya azalış) nedenleri mutlaka araştırılmalıdır.

Bir maden firmasının içinde bulunduğu zamanı ve geleceğini önemli derecede etkileyen birim maliyet değerinin tahmin edilmesinde ciddi belirsizlikler gözlenmektedir. 2019 yılında başlayan ve halen devam eden pandemi süreci madencilik sektöründe birim maliyetin belirlenmesini olumsuz yönde etkilemiştir. Ayrıca, pandeminin de etkisiyle son zamanlarda yaşanan ekonomik dalgalanmalar da bu belirsizlik sorunu göz ardı edilemeyecek şekilde ortaya çıkarmıştır. Birim maliyet değeri düzenli zaman aralıklarında hesaplandığından ve takip edildiğinden dolayı bir zaman serisi olarak düşünülmüştür. Özel bir yinelemeli sinir ağ türü olan uzun kısa-vadeli bellek (LSTM) yönteminin zaman serisi problemlerinin çözümünde yaygın olarak kullanıldığı bilinmektedir (Arslan ve Sekertekin, 2019). Son zamanlarda, birçok bilim alanında LSTM yöntemi ile çok değişkenli sınıflandırma ve tahmin problemleri üzerine başarılı çalışmalar gerçekleştirilmiştir (Zhang vd., 2019; Yildirim vd.,2019; Xiao vd., 2018; Zhang vd., 2018; Qin, 2019; Han vd., 2019; Tong vd., 2019; Li ve Cao, 2018). Bu nedenle, zaman serisi tahmininde yaygınlığı sürekli artan LSTM yönteminin birim maliyet tahmininde kullanılması önerilmiştir.

Bu çalışmanın amacı, LSTM yönteminin madencilik sektöründe birim maliyet değerinin tahmin edilmesinde kullanılabilirliğinin araştırılmasıdır. Bu kapsamda, LSTM yöntemi ile örnek bir açık ocak krom sahasının birim maliyet değerinin tahmini gerçekleştirilmiştir. Model eğitim parametreleri değiştirilerek 9 farklı LSTM modeli geliştirilmiş ve bu modeller performans değerlendirme kriterlerine göre karşılaştırılmıştır. Sonuç olarak, birim maliyet tahmin performansı en iyi olan LSTM modeli belirlenmiştir.

Bildirinin geri kalan kısmı şu şekilde tasarlanmıştır: çalışma sahası ve veri seti hakkında bilgilerin verildiği materyal bölümü, LSTM yönteminin açıklandığı ve performans değerlendirme kriterlerinden bahsedilen yöntem bölümü, geliştirilen modellerin örnek saha üzerinde uygulanması sonucu elde edilen çıktıların verildiği sonuçlar ve tartışma bölümü ve son olarak çalışmanın genel olarak yorumlandığı yorum bölümü yer almaktadır.

MATERYAL

Çalışma Sahası

Çalışma sahası olarak Marmara bölgesinde bulunan orta ölçekli bir açık ocak krom madeni seçilmiştir. Maden sahasında kazı ve nakliye faaliyetleri ekskavatör + kamyon sistemi ile yürütülmektedir. Sahanın ekskavatör kazısı için uygun olmayan kısımlarında delme-patlama yöntemi uygulanarak kazılacak malzemenin gevşetilmesi sağlanmaktadır. Daha sonra ekskavatör yardımı ile kamyonlara yüklenen malzeme pasa ise döküm sahasına, cevher ise stok sahasına gönderilmektedir. Stok sahasında biriktirilen malzeme cevher zenginleştirme tesisine beslenmektedir ve proses sonucunda konsantre ürün elde edilmektedir. Çalışma sahasında uygulanan iş akım şeması Şekil 1'de görülmektedir.

Krom cevherinin ortalama tenörü %10-12 cevher zenginleştirme tesisinden elde edilen konsantre ürünün tenör değeri ise %46-48 arasında değişiklik göstermektedir. Makine parkı göz önünde bulundurulduğunda aylık kazı kapasitesi ortalama 120 000 – 150 000 m^3 arasında değişmektedir. Cevher zenginleştirme tesisi ise aylık ortalama 15 000 – 20 000 ton besleme kapasitesi ile çalışmaktadır.

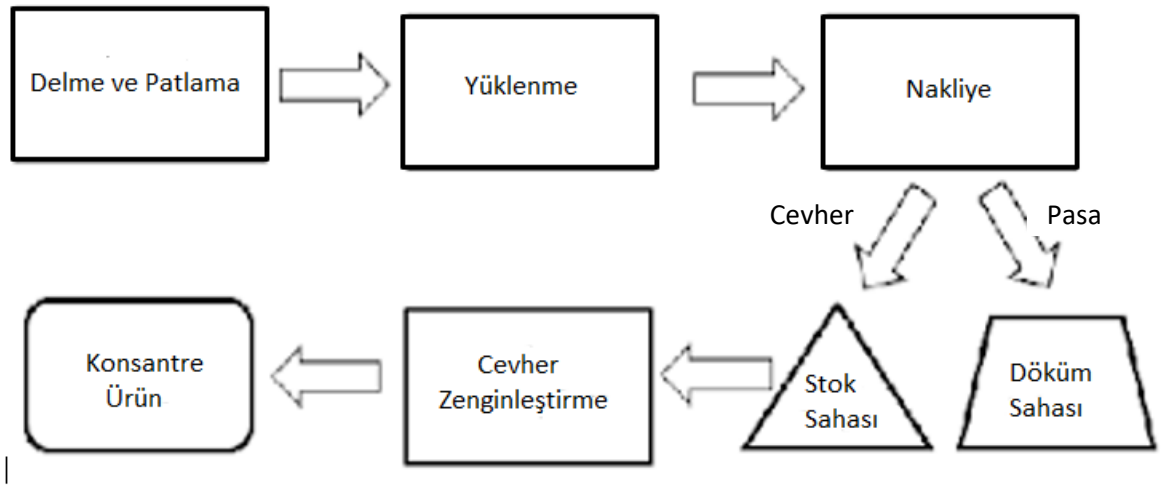

Şekil 1. Çalışma sahasında uygulanan iş akım şeması

Veri Seti

Çalışmada, 2014 Ocak-2021 Aralık dönemi arasında aylık kazı maliyeti, konsantre maliyeti, kazı miktarı ve konsantre miktarı bilgilerinin yer aldığı toplam 96 adet örnekten oluşan veri seti kullanılmıştır. Birim kazı maliyeti ve birim konsantre maliyeti sırasıyla Eşitlik 1 ve 2 kullanılarak hesaplanmıştır.

$$Birim\ Kazı\ Maliyeti\ (\$/t) = \frac{Toplam\ Kazı\ Maliyet}{Toplam\ Kazı\ Miktarı} \quad (1)$$

$$Birim\ Konsantre\ Maliyeti\ (\$/t) = \frac{Toplam\ Konsantre\ Maliyeti}{Toplam\ Konsantre\ Miktarı} \quad (2)$$

Birim maliyet değeri, birim kazı maliyeti ve birim konsantre maliyeti değerlerinin toplamı olarak belirlenmiştir. Birim maliyet hesaplanırken evrensellik sağlanması için para birimi olarak Dolar seçilmiştir. Para birimi dönüşümlerinde Türkiye Cumhuriyeti Merkez Bankasının aylık ortalama Dolar kuru değerleri esas alınmıştır (TCMB, 2022). Aylık birim kazı maliyeti ve birim konsantre maliyeti değerlerinin değişimi Şekil 2'de görülmektedir.

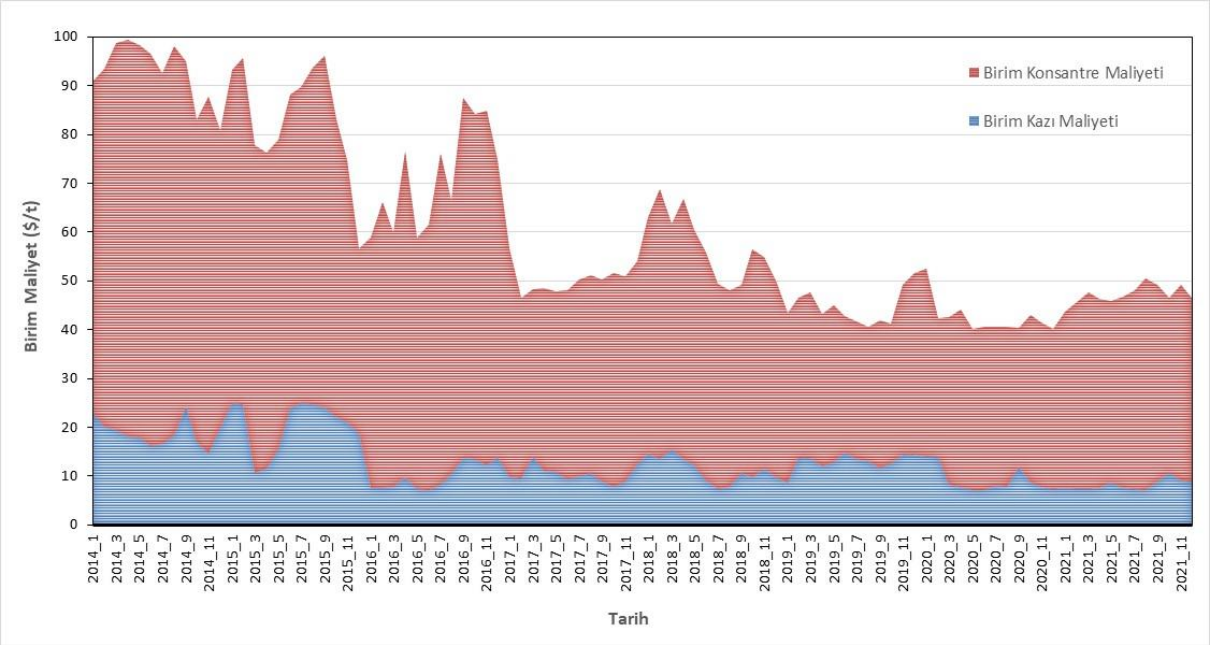

Şekil 2. Aylık birim kazı ve birim konsantre maliyet değerlerinin değişimi

Veri seti üzerinde tanımlayıcı istatistiksel analiz uygulanmış olup elde edilen sonuçlar Çizelge 1'de verilmiştir. Veri seti, geliştirilen modellerin eğitim ve test aşamalarında kullanılması için %80' i eğitim (77 veri) geri kalan %20'si (19 veri) test olmak üzere 2 gruba ayrılmıştır. Tüm çalışmalar bu veri seti üzerinden gerçekleştirilmiştir.

Çizelge 1. Tanımlayıcı özet istatistik değerleri

	Birim Kazı Maliyeti ($/t)	Birim Konsantre Maliyeti ($/t)	Birim Maliyet ($/t)
Ortalama	12.63	48.54	61.18
Ortanca	11.48	41.79	51.59
Standart Sapma	5.12	15.74	19.19
Varyans	26.21	247.66	368.21
Basıklık	0.15	-0.97	-0.94
Çarpıklık	1.01	0.61	0.74
Aralık	17.92	53.82	59.18
En Büyük	7.02	27.38	40.10
En Küçük	24.94	81.20	99.29

YÖNTEM

Uzun Kısa-Vadeli Bellek (LSTM)

LSTM ilk olarak 1997 yılında Hochreiter ve Schmidhuber tarafından ortaya çıkarılmıştır. Bu yöntem tekrarlayan sinir ağlarının özel bir türü olup zaman serilerinin tahmini için kullanılabilmektedir (Hochreiter ve Schmidhuber, 1997). LSTM yöntemi standart ileri beslemeli sinir ağlarından farklı olarak geri besleme bağlantılarına sahiptir (Siegelmann and Sontag, 1992). Geleneksel sinir ağlarının yetersiz kaldığı özellikle uzun vadeli bağımlılıkların öğrenilmesi konusunda ön plana çıkmaktadır. LSTM, çeşitli denetimli dizi öğrenme başarısı ve hafıza geçişli mimarisi sayesinde zaman serisi problemlerinde oldukça avantajlı bir yöntemdir (Ahmadi vd., 2019). LSTM ağını bir birine bağlı tekrarlayan LSTM birimleri oluşturur (Şekil 3).

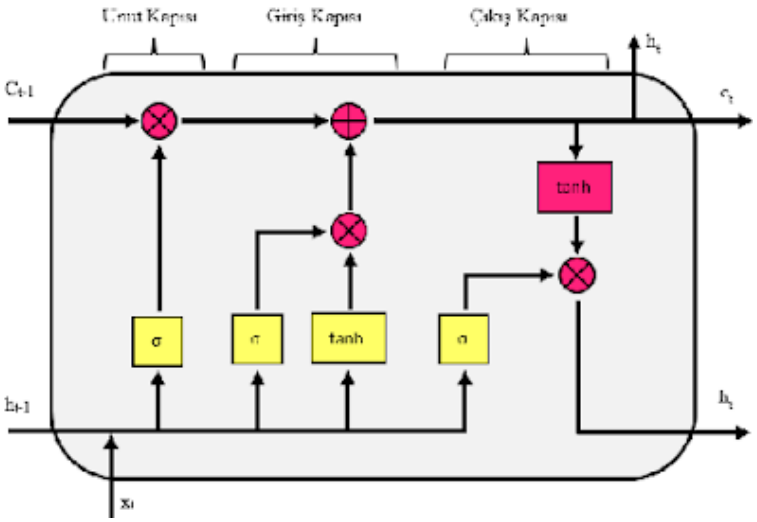

Şekil 3. Her LSTM biriminin temel mimarisi

$x = (x_1, x_2, x_3, \dots, x_t)$ dizi verisi giriş katmanı olsun, gizli (çıkış) katmanı tahmin etmek için sırasıyla $h = (h_1, h_2, h_3, \dots, h_t)$ ve hücre katmanı $c = (c_1, c_2, c_3, \dots, c_t)$ kullanılır. x dizisinin ilk değeri (x_1) ilk LSTM birimine uygulandığında gizli katmanın ilk değeri (h_1) ve güncellenmiş hücre katmanının ilk değeri (c_1).elde edilir.

t zamanında, LSTM birimi (c_{t-1}, h_{t-1}) ile beslenmesi durumunda sonuç olarak h_t ve güncellenmiş hücre katmanı c_t çıktılarına ulaşılır. t zamanında gizli katman hücre katmanı (c_t) ile şu şekilde ifade edilebilir;

$$h_t = o_t \odot tanh\, tanh\, c_t \tag{3}$$

burada $\odot$ Hadamard çarpımını (vektörlerin eleman bazında çarpımı) ve o_t ise çıkış kapısını gösterir. LSTM ağı, kapılar gibi yapılar yardımıyla hücre durumuna bilgi ekleyerek veya çıkararak yönetilir. Önceki adımlardan bilgileri içeren hücre durumu, t zaman adımı için aşağıdaki gibi verilebilir (Hochreiter ve Schmidhuber, 1997; Mathworks, 2021):

$$c_t = f_t \odot c_{t-1} + i_t \odot g_t \tag{4}$$

Eşitlik 4'te yer alan değişkenlerden giriş kapısı (i_t) Eşitlik 5'te, unut kapısı (f_t) Eşitlik 6'da, katman girişi (g_t) Eşitlik 7'de ve çıkış kapısı (o_t) Eşitlik 8'de verilmiştir (Hochreiter ve Schmidhuber, 1997; Mathworks, 2021).

$$i_t = \sigma(W_i x_t + R_i h_{t-1} + b_i) \tag{5}$$

$$f_t = \sigma\left(W_f x_t + R_f h_{t-1} + b_f\right) \tag{6}$$

$$g_t = tanh\ tanh\left(W_g x_t + R_g h_{t-1} + b_g\right) \tag{7}$$

$$o_t = \sigma(W_o x_t + R_o h_{t-1} + b_o) \tag{8}$$

burada σ sigmoid fonksiyonudur ve $\sigma(x) = (1 + e^{-x})^{-1}$ olarak ifade edilir. *W* girdi ağırlıklarını, *R* tekrarlayan ağırlıkları ve *b* bias değerini temsil etmektedir (Eşitlik 9).

$$W = \left[W_i\ W_f\ \ W_g\ W_o\ \right], R = \left[R_i\ R_f\ \ R_g\ R_o\ \right], b = \left[b_i\ b_f\ \ b_g\ b_o\ \right] \tag{9}$$

Performans Değerlendirme Kriterleri

Geliştirilen modellerin tahmin doğruluğunu belirlemek için literatürde yaygın olarak kullanılan performans değerlendirme kriterlerinden; korelasyon katsayısı (R), ortalama mutlak yüzde hata (MAPE) ve kök ortalama kare hata (RMSE) kullanılmıştır.

R bilinmeyen değerlerin bilinen değerlere göre ne kadar iyi tahmin edildiğinin istatistiksel bir ölçüsüdür. R değeri 0-1 arasında değer alır ve 1 değerine yaklaştıkça tahminin doğruluğu artar (Jamei vd., 2021). MAPE regresyon ve zaman serileri modellerinde tahminlerin doğruluğunu ölçmek için en sık kullanılan kriterlerden birisidir. Bu değer %10'dan küçük ise çok iyi tahmin; 11-20 arasında ise iyi tahmin ve 20-50 arasında ise kabul edilebilir tahmin olarak yorumlanmaktadır (Lewis, 1982). Ayrıca, hatanın büyüklüğünü ölçen RSME kriteri de makine öğrenmesi yöntemlerinde yaygın olarak kullanılmaktadır. RMSE değerinin 0'a yakın olması tahminin doğruluğu göstermektedir (Gilan vd. 2012). R, MAPE ve RMSE değerleri sırasıyla Eşitlik 10-12'de verilen formüller ile hesaplanır:

$$R = \frac{\sum_{i=1}^{n}\ \left(y_{pi} - \underline{y_p}\right)\cdot\left(y_{mi} - \underline{y_m}\right)}{\sqrt{\sum_{i=1}^{n}\ \left(y_{pi} - \underline{y_p}\right)^2 \cdot \sum_{i=1}^{n}\ \left(y_{mi} - \underline{y_m}\right)^2}} \tag{10}$$

$$MAPE = \frac{100}{n}\sum_{i=1}^{n}\ \left|\frac{y_{mi} - y_{pi}}{y_{mi}}\right| \tag{11}$$

$$RMSE = \sqrt{\frac{1}{n}\sum_{i=1}^{n}\ \left(y_{mi} - y_{pi}\right)^2} \tag{12}$$

burada y_{mi} ve y_{pi} sırasıyla *i.* örneğin gerçek ve tahmini değerlerini, $\underline{y_m}$ ve $\underline{y_p}$ sırasıyla gerçek ve tahmin değerlerin ortalamasını ve *n* ise örnek sayısını temsil etmektedir.

SONUÇLAR VE TARTIŞMA

Model parametrelerinden gizli katman sayısı 425-475, eğitim sayısı ise 125-175 değeri arasında 25 birim kadar değiştirilerek toplam 9 farklı LSTM modeli geliştirilmiştir. Eğitim aşamasında, stokastik amaç fonksiyonlarının gradyan tabanlı optimizasyonu için uyarlamalı moment tahmini (Adam) optimize edici algoritması kullanılmıştır. Bu algoritmanın seçilmesinde uygulanmasının basit, hesaplama açısından verimli, çok az bellek gereksinimine sahip ve büyük ölçekli (veri ve/veya parametre açısından)

problemler için oldukça uygun olması gibi avantajları dikkate alınmıştır (Kingma ve Ba, 2014). Geliştirilen modellerin parametre bilgileri ve elde edilen performans kriterleri Çizelge 2'de verilmiştir.

Çizelge 2. Geliştirilen modeller ve elde edilen performans kriterleri

Model	Model Parametreleri		Performans Kriterleri		
	Gizli Katman Sayısı	Eğitim Sayısı	RMSE	MAPE	R
1	425	125	5.22	9.04	0.34
2	425	150	5.07	10.21	0.80
3	425	175	4.60	8.37	0.66
4	450	125	4.01	7.26	0.36
5	450	150	2.85	5.56	0.66
6	**450**	**175**	**2.47**	**4.37**	**0.72**
7	475	125	4.01	7.75	-0.03
8	475	150	5.34	9.25	-0.12
9	475	175	5.26	8.76	0.20

Elde edilen sonuçlar değerlendirildiğinde en düşük RMSE (2.47) ve MAPE (4.37) değerlerine 6 numaralı LSTM modelinin sahip olduğu görülmektedir. Bu modeli RMSE ve MAPE kriterlerine göre sırasıyla 5, 4 ve 7 numaralı modeller takip etmektedir. R değerleri incelendiğinde en yüksek değerin 0.80 ile 2 numaralı modele ait olduğu ve bu modelden sonra 0.72 değeri ile 6 numaralı modelin geldiği anlaşılmaktadır. Sonuç olarak, birim maliyet değerinin tahmin edilmesinde 450 gizli katman ve 175 eğitim sayısına sahip 6 numaralı modelinin en başarılı LSTM modeli olduğu tespit edilmiştir.

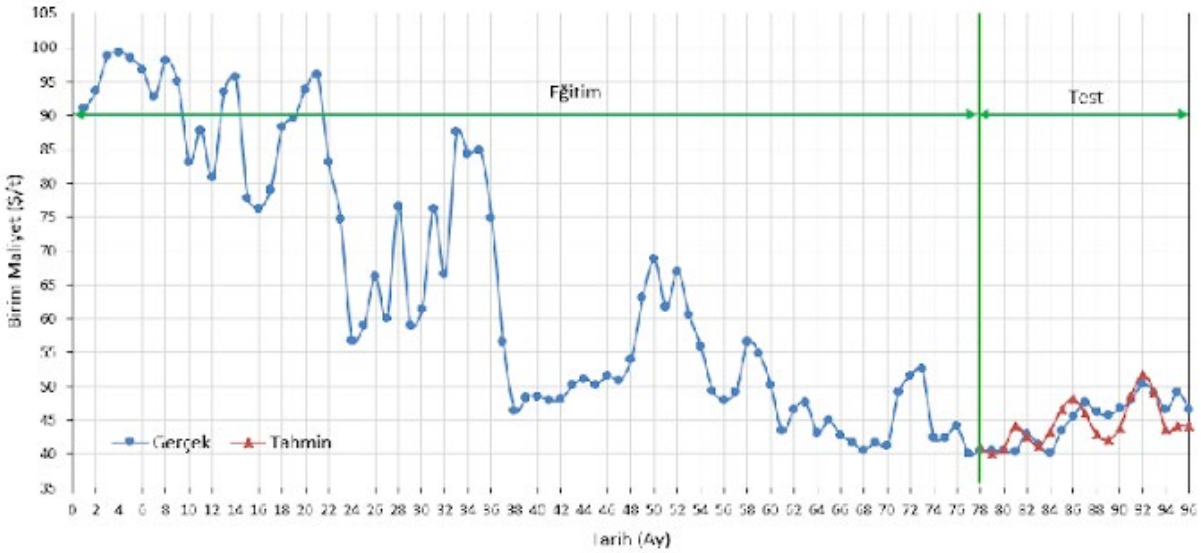

Şekil 4. Gerçek ve tahmin birim maliyet değerlerinin değişimi

LSTM modelinin tahmin performansının daha iyi anlaşılabilmesi için grafikler çizdirilmiştir. Şekil 4'te gerçek ve tahmin edilmiş birim maliyet değerlerinin değişimi görülmektedir. Test verisi üzerindeki değişimin daha iyi anlaşılabilmesi için Şekil 5'te yakınlaştırılmış görüntüsü sunulmuştur. Eğitim verilerinin

dağılımı incelendiğinde birim maliyet değerinin son aylarda bir miktar yükseliş göstermesine rağmen genel olarak bir düşüş eğiliminde olduğu fark edilmektedir. Test veri seti için elde edilen tahmin değerleri ile gerçek değerlerin benzer bir eğilim gösterdiği anlaşılmaktadır.

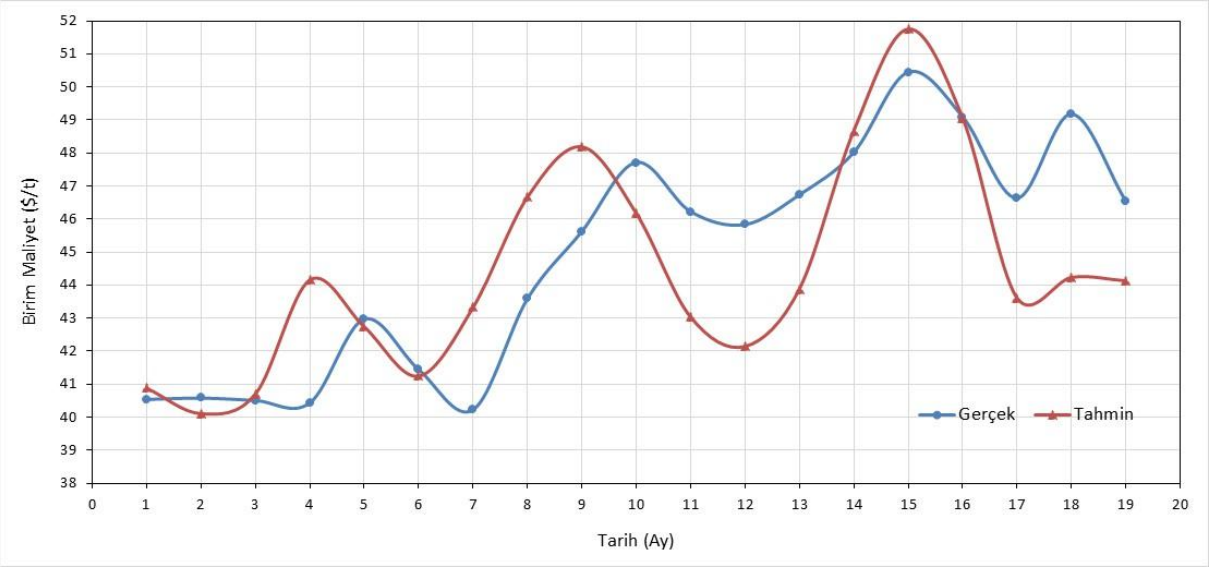

Şekil 5. Test veri seti için gerçek ve tahmin birim maliyet değerlerinin değişimi

Şekil 6'da ise tahmin değerlerinin gerçek değerlerden farkını gösteren hata grafiği verilmiştir. Hata grafiğinde verilerin bir kısmının 0 çizgisine oldukça yakın yer aldığı, geri kalanların ise kabul edilebilir uzaklıkta dağıldığı görülmektedir. Bu durum LSTM modelinin tahmin doğruluğunu desteklemektedir.

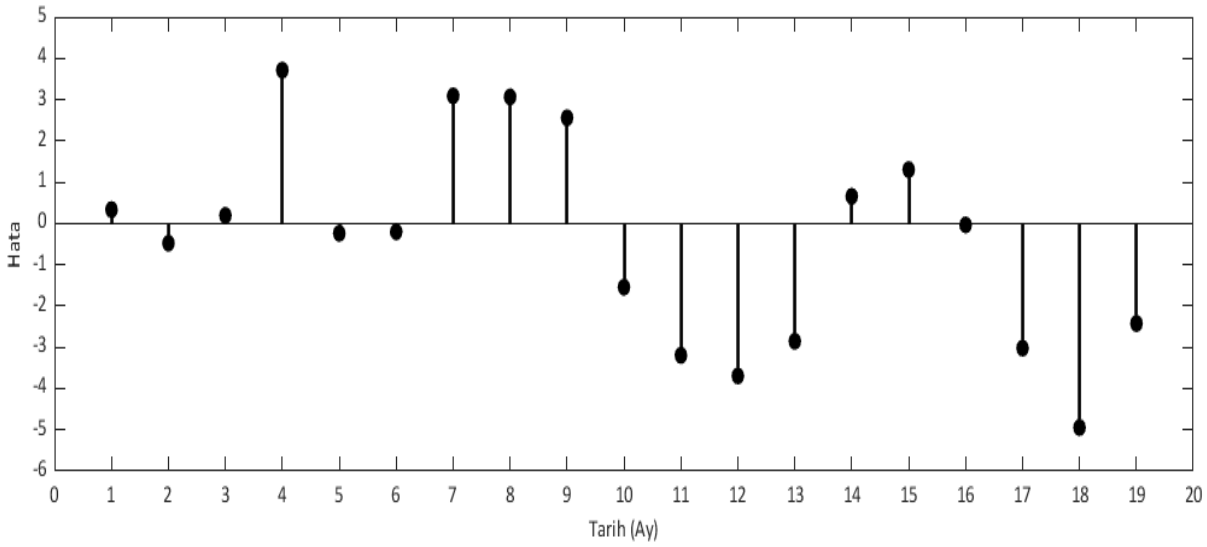

Şekil 6. Tahminin hata grafiği

Şekil 5 ve 6 beraber incelendiğinde 4. (2020-9. ay), 12. (2021-5. ay) ve 18. (2021-11.ay) aylarda gerçek ile tahmin değerleri arasındaki farkın nispeten daha fazla olduğu görülmektedir. Belirtilen tarihlerde TL-Dolar kurunda büyük hareketliliklerin olduğu gözlemlenmiştir. Bu durumun hata değerini arttırdığı ve tahmin performansını olumsuz yönde etkilediği anlaşılmaktadır.

Gerçek ve tahmin edilmiş birim maliyet değerlerinin arasındaki ilişkiyi gösteren korelasyon grafiği Şekil 7'de görülmektedir. Burada, R değerinin %70'in üzerinde olması geliştirilen LSTM modelinin güvenilir bir tahmin sonucu üretmiş olduğunu işaret etmektedir. Aynı zamanda tahminin doğruluğu belirtir ve %72 doğruluk ile tahmin yapıldığı şeklinde ifade edilebilir.

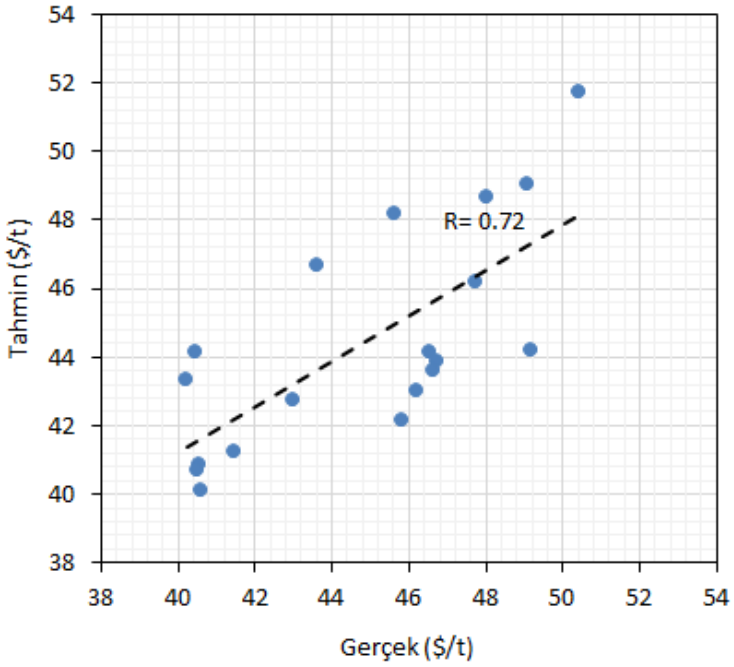

Şekil 7. Gerçek ve tahmin birim maliyet değerlerinin korelasyon grafiği

Ayrıca, gelişen bilgisayar teknolojileri ve modelleme yöntemleri sayesinde tahmin işlemlerinin oldukça kısa sürelerde tamamlandığı bilinmektedir. Bu süre kullanılan veri setinin büyüklüğüne ve bilgisayarın teknik özelliklerine göre değişmektedir. Bu çalışmada, Intel (R) Core (TM) i9-9900K CPU @ 3.60 GHz işlemci, 64 GB RAM ve Windows 64-bit işletim sistemine sahip bir bilgisayar kullanılmıştır. Geliştirilen her bir modelin sonuç üretmesi yaklaşık 2-3 dakika gibi çok kısa bir süre içerisinde gerçekleşmiştir.

YORUM

Bu çalışmada, bir açık ocak krom sahasının birim maliyet değerlerinin tahmini LSTM yöntemi kullanılarak gerçekleştirilmiştir. Model parametreleri üzerinde değişiklikler yapılarak 9 farklı LSTM modeli geliştirilmiş olup tahmin performansları karşılaştırılmıştır. Geliştirilen modellerin değerlendirilmesi sonucu RMSE= 2.47, MAPE= 4.37 ve R= 0.72 değerlerine sahip 6 numaralı modelin (450 gizli katman ve 175 eğitim sayısı ile) en başarılı LSTM modeli olduğu belirlenmiştir.

Sonuç olarak, LSTM yönteminin birim maliyet değerinin tahminindeki başarısı bir açık ocak krom madenine uygulanarak kanıtlanmıştır. Ayrıca, LSTM yöntemi benzer zaman serisi verilerinin tahmininde kullanıcılara iş gücü/zaman tasarrufu sağlayacak ve hızlı sonuç üretebilme yeteneği sayesinde kısa sürede birçok alternatif modelin karşılaştırılması imkânı sunacaktır.

Gelecek çalışmalarda, birim maliyet değerini etkileyen parametrelerin de veri setine dahil edildiği LSTM modelleri geliştirilerek bu parametrelerin tahmin performansına etkileri araştırılacaktır.

TEŞEKKÜR

Bu çalışma, Çukurova Üniversitesi Bilimsel Araştırma Fonu (Proje No: FBA-2019-11998) tarafından desteklenmiştir.

KAYNAKLAR

Ahmadi, M. R., Bazzazi, A.A. (2019). Cutoff grades optimization in open pit mines using meta-heuristic algorithms. Resources Policy, *60*, 72–82. https://doi.org/10.1016/j.resourpol.2018.12.001

Ahmadi, N., Constandinou, T., Bouganis, C. (2019). Decoding Hand Kinematics from Local Field Potentials Using Long Short-Term Memory (LSTM) Network. 9th International IEEE EMBS Conference on Neural Engineering (NER 2019), 1-5s.

Arslan, N., Sekertekin, A. (2019). Application of Long Short-Term Memory neural network model for the reconstruction of MODIS Land Surface Temperature images. *Journal of Atmospheric and Solar–Terrestrial Physics*, *194*, 105100. https://doi.org/10.1016/j.jastp.2019.105100

Curry, J.A., Ismay, M.J.L., ve Jameson, G.J. (2014). Mine operating costs and the potential impacts of energy and grinding. *Minerals Engineering, 56*, 70–80 https://doi.org/10.1016/j.mineng.2013.10.020.

European Commission, (2021). A European Green Deal, https://ec.europa.eu/info/strategy/priorities-2019-2024/european-green-deal_en (erişim tarihi: 02.11.2021)

Gilan, S.S., Jovein, H.B., Ramezanianpour, A.A. (2012). Hybrid support vector regression–particle swarm optimization for prediction of compressive strength and RCPT of concretes containing metakaolin. *Construction and Building Materials, 34*, 321–329, https://doi.org/10.1016/j.conbuildmat.2012.02.038.

Han, S., Qiao, Y.H., Yan, J., Liu, Y.Q., Li, L., ve Wang, Z. (2019). Mid-to-long term wind and photovoltaic power generation prediction based on copula function and long short term memory network. *Applied Energy*, 239, 181-191. https://doi.org/10.1016/j.apenergy.2019.01.193.

Hochreiter, S., Schmidhuber, J. (1997). Long short-term memory. *Neural Comput*. 9, 1735–1780. https://doi.org/10.1162/neco.1997.9.8.1735.

Jamei, M., Ahmadianfar, I., Olumegbon, I.A., Karbasi, M., Asadi, A. (2021). On the assessment of specific heat capacity of nanofluids for solar energy applications: Application of Gaussian process regression (GPR) approach. *Journal of Energy Storage, 33,* 102067. https://doi.org/10.1016/j.est.2020.102067.

Khan, A., Asad, M.W.A. (2019). A method for optimal cut-off grade policy in open pit mining operations under uncertain supply. *Resources Policy, 60,* 178–184. https://doi.org/10.1016/j.resourpol.2018.12.003

Kingma, D.P., Ba, J. (2014). Adam: A method for stochastic optimization. arXiv:1412.6980.

Lewis, C.D. (1982). Industrial and Business Forecasting Methods: a Practical Guide to Exponential Smoothing and Curve Fitting, London; Boston: Butterworth Scientific, 143 s.

Li, Y., ve Cao, H. (2018). Prediction for tourism flow based on LSTM Neural Network. *Procedia Computer Science*, 129, 277-283. https://doi.org/10.1016/j.procs.2018.03.076.

Mathworks, (2021). Long Short-Term Memory Networks [WWW Document]. https://www.mathworks.com/help/deeplearning/ug/long-short-term-memory-networks.html (erişim tarihi: 06.12.21).

Papettia, A., Menghia, R., Domizioa, G.D., Germania, M., ve Marconi, M. (2019). Resources value mapping: A method to assess the resource efficiency of manufacturing systems. *Applied Energy*, *249*, 326-342. https://doi.org/10.1016/j.apenergy.2019.04.158

Qin, Y., Li, K., Liang, Z., Lee, B., Zhang, F., Gu, Y., Zhang, L., Wu, F., ve Rodriguez, D. (2019). Hybrid forecasting model based on long short term memory network and deep learning neural network for wind signal. *Applied Energy*, *236*, 262-272. https://doi.org/10.1016/j.apenergy.2018.11.063.

Shafiee, S., Nehring, M., ve Topal, E. (2009). Estimating average total cost (ATC) of open pit coal mines in Australia, Proc. Australian Mining Technology Conf., Brisbane, Qld, Australia, October, CRC Mining, 134–145.

Shafiee, S., ve Topal, E. (2012). New approach for estimating total mining costs in surface coal mines, *Mining Technology*, *121(3)*, 109-116, https://doi.org/10.1179/1743286312Y.0000000011

Siegelmann, H.T., Sontag, E.D. (1992). On the computational power of neural nets. In: Proceedings of the Fifth Annual Workshop on Computational Learning Theory - COLT ’92. ACM Press, New York, New York, USA, pp. 440–449. https://doi.org/10 .1145/130385.130432.

TCMB, (2022). Döviz kurları. https://evds2.tcmb.gov.tr/index.php?/evds/serieMarket/#collapse_2 (erişim tarihi: 03.01.2022)

Tong, W., Li, L., Zhou, X., Hamilton, A., ve Zhang, K. (2019). Deep learning $PM_{2.5}$ concentrations with bidirectional LSTM RNN. *Air Quality, Atmosphere & Health*, *12(4)*, 411-423. https://doi.org/10.1007/s11869-018-0647-4.

Türkiye Cumhuriyeti Ticaret Bakanlığı, (2021). Yeşil Mutabakat Eylem Planı 2021. https://ticaret.gov.tr/data/60f1200013b876eb28421b23/MUTABAKAT%20YE%C5%9E%C4%B0L.pdf (erişim tarihi: 02.11.2021)

Xiao, L., Wang, G., Zuo, Y. (2018). Research on Patent Text Classification Based on Word2Vec and LSTM. 11th International Symposium on Computational Intelligence and Design (ISCID), Hangzhou, China, 71-74.

Yildirim, Ö., Baloğlu, U.B., Tan, R., Ciaccio, E., Acharya, R. (2019). A new approach for arrhythmia classification using deep coded features and LSTM networks. *Computer Methods and Programs in Biomedicine*, 176, 121-133.

Zhang, D., Chen, Y., ve Meng, J. (2018). Synthetic well logs generation via Recurrent Neural Networks. *Petroleum Exploration and Development*, *45(4)*, 598-607. https:// doi.org/10.11698/PED.2018.04.06.

Zhang, J., Zhu, Y., Zhang, X., Ye, M., ve Yang, J. (2018). Developing a Long Short-Term Memory (LSTM) based model for predicting water table depth in agricultural areas. *Journal of Hydrology*, 561, 918-929. https://doi.org/10.1016/j.jhydrol.2018.04.065.

Zhang, T., Song, S., Li, S., Ma, L., Pan, S., Han, L. (2019). Research on Gas Concentration Prediction Models Based on LSTM Multidimensional Time Series. *Energies*, *12(1)*, 161, doi.org/10.3390/en12010161.

BİR TAŞ OCAĞINDA YAPILAN PATLATMALARIN DARICA-2 HES YAPISINA OLAN ÇEVRESEL ETKİLERİNİN ELEKRONİK ATEŞLEME SİSTEMİ İLE EN AZA İNDİRİLMESİ: ÖRNEK UYGULAMA

MINIMIZING THE ENVIRONMENTAL EFFECTS OF EXPLOSIONS IN A QUARRY ON THE DARICA-2 HES STRUCTURE BY ELECTRONIC IGNITION SYSTEM: A CASE STUDY

G.G.U. Aksoy [1, *,] C.O. Aksoy [2], H. E. Yaman [3], A. İlhan [4]

[1] *Hacettepe Üniversitesi, Maden Mühendisliği Bölümü*
*(*Sorumlu yazar: gulsevaksoy@hacettepe.edu.tr)*
[2] *Dokuz Eylül Üniversitesi Maden Mühendisliği Bölümü*
[3] *Dokuz Eylül Üniversitesi Torbalı Meslek Yüksek Okulu*
[4] *Soner Temel İnşaat ve San. Tic. A.Ş.*

ÖZET

Bu çalışmanın amacı, kapasite artışına gidecek olan bir taş ocağında yapılacak patlatma çalışmalarının olası titreşim, hava şoku, taş savrulması risklerinin çevreye ve özellikle Darıca-2 HES proje alanına olan etkilerini incelemek ve buraya herhangi bir olumsuz etki yaratmayacak kontrollü patlatma tasarımlarını belirleyerek uygulamalı olarak sonuçlarını değerlendirmektir. Projeye konu olan faaliyet sahasını ve Darıca-2 HES lokasyonu ve projeye konu olan sahaya yakınlığını görebilmek için 10.07.2021 tarihinde yerinde gözlem, inceleme ve değerlendirmeler yapılmış; iki farklı ateşleme sistemi ile iki adet patlatma gerçekleştirilerek patlatma kaynaklı sismik ölçümler (titreşim, dalga boyu, frekans), hava şoku ölçümleri yapılmıştır. Ayrıca jeoteknik amaçlı hat etüdü gerçekleştirilmiştir. Tüm saha ölçümleri ve deneyimlerin harmanlanması ile Darıca-2 HES yapısı ve çevresine hasar vermeyecek kontrollü patlatma tasarımı yapılmış ve başarıyla uygulanmıştır.

Anahtar Sözcükler: Patlatma, titreşim, HES, hava şoku, taş savrulması, elektronik ateşleme sistemi

ABSTRACT

The aim of this study is to examine the effects of possible vibration, air shock, fly rock risks on the environment and especially on the Darıca-2 HES project area of the blasting works to be carried out in a quarry that will go to capacity increase and to determine the controlled blasting designs that will not cause any negative impact there. On-site observations, examinations and evaluations were made by us on 10.07.2021 in order to see the activity area that is the subject of the project and the Darıca-2 HES location and its proximity to the site that is the subject of the project; Two detonations were carried out with two different ignition systems, and seismic measurements (vibration, wavelength, frequency) and air shock measurements were made. In addition, a geotechnical study was carried out. With the blending of all field measurements and experiences, a controlled blasting design that will not damage the Darıca-2 HES structure and its surroundings has been made and successfully implemented.

Keywords: Blasting, vibration, HES, air shock, fly rock, electronic initiation system

GİRİŞ

Ordu ili, Mesudiye İlçesi, Darıca Mahallesindeki bir taş ocağı sınırları içerisinde "Patlatmalı Taş (Bazalt) Ocağı Kapasite Artışı" planlanan sahaya ait yer bulduru haritası Şekil 1-a'da; Taş ocağının HES'e göre konumu, aradaki yol, vadi ve derenin lokasyonu ise Şekil 1-b'de verilmiştir.

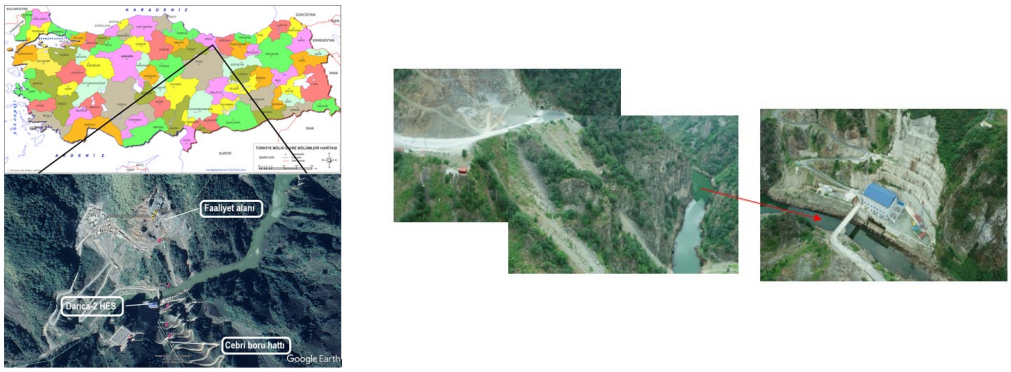

(a) (b)

Şekil 1.a) Ordu İli, Mesudiye İlçesi ruhsat sahası sınırları içerisinde faaliyet alanı, Darıca-2 HES ve Cebri boru hattının lokasyonları b) Taş ocağı, vadi, dere, Darıca-2 HES lokasyonunu gösteren drone fotoğrafı

10.07.2021 tarihinde Ordu ili, Mesudiye ilçesi Darıca mahallesinde bulunan Taş (Bazalt) Ocağında, "I-Blast " patlatma yazılımı yardımı ile kontrollü patlatma tasarımı yapılmış olup; yapılan tasarımın uygulandığı grup patlatması gerçekleştirilmiştir. Bu patlatmada, HES yapısı ve çevresinin hassasiyeti nedeniyle elektronik ateşleme yapılarak bu sistemin üstünlüğü ve güvenliğinden faydalanılmıştır.

Bu bildiride, bu sahadaki gibi etrafında kritik ve önemli yapılar olan sahalarda elektronik ateşleme sisteminin sağladığı güvenlik, hassasiyet ve duyarlılık parametrelerinin getirdiği başarılı ve kontrollü patlatma uygulamasından bahsedilmiştir.

ELEKTRONİK ATEŞLEME SİSTEMİ İLE YAPILAN UYGULAMA

Elektronik patlatıcılar bir piroteknik bileşimin yanma hızına dayanan geleneksel piroteknik patlatıcılardan daha doğru zamanlama sağlar. Elektronik patlatıcının zamanlama doğruluğu yeteneği; patlayıcı enerjisinin daha verimli uygulanmasını, parça boyutu homojenliğini, hafriyat verimliliğinde artışı, hafriyat işlemlerinde maliyet tasarrufu, patlatmanın halk tarafından daha iyi kabul görmesini, patlamanın neden olduğu titreşimlerin ve hava şokunun kontrolünü, şev stabilitesine katkıyı sağlamaktadır (Cardu vd. 2013, Cardu vd. 2015). Proje konusu patlatmaların Darıca-2 HES yapısına herhangi bir titreşim, taş savrulması, hava şoku gibi olumsuzluklar yaratmaması için tasarladığımız kontrollü patlatmada belirlediğimiz gecikmelerin zamanlama doğruluğunu tam olarak sağlayabildiği için bu uygulamada elektronik kapsüller tercih edilmiştir. Bu sebeple de hem daha güvenli hem de 0 ile 15.000 milisaniye arasında 1'er ms'lik artışlarla gecikme ataması sağlamakta olan detEX elektronik kapsüller bu uygulamada kullanılmıştır. Elektronik kapsül sisteminin ortaya koyduğu esnek gecikme atama imkânı sayesinde sahada gerçekleştirilen patlatmada delik gecikmelerinin ortaya çıkarttıkları mükerrerliğin en aza indirilmesi amaçlanmıştır.

Bu uygulama sırasında alınmış koordinatlardan anlaşıldığı üzere, Darıca-2 HES ile elektronik grup patlatma sahası arasındaki mesafe 340 metredir (Şekil 2-a). Cebri boru hattı ile elektronik grup patlatma sahası arasındaki mesafe 400 m olarak belirlenmiştir (Şekil 2-b).

(a) (b)

Şekil 2. a) Elektronik grup patlatma ve Darıca-2 HES arasındaki mesafe, b) leektronik grup patlatma ve Cebri boru hattı arasındaki mesafe 10.07.2021

Ocakta yapılan elektronik ateşleme sistemi uygulamalarındaki patlatma tasarımı Çizelge 1'de verilmiştir (Patlatma Tasarımları ve Patlatma Kaynaklı Çevresel Etkiler Kılavuzu, 2018).

Çizelge 1. 10.07.2021 Ocakta yapılan elektronik ateşleme sistemi uygulamalarındaki patlatma tasarımı

Patern Kodu	Elektronik Ateşleme Grubu	
Patlatma Kotu	*536*	Elektronik Kapsül
Patlatma Tarihi	10.07.2021	
Delik Sayısı	73 adet	
Geometri	2,6m x 3.30m	
Dip Delgi	1 m	
Delik Çapı	89 mm	
Ort. Delik Metrajı	10.5 m	
Patlayıcı Miktarı (kg)	2336kg toplam; 32kg/delik ortalama	
Yemleme Dinamiti (kg)	73 kg ; 1 kg/delik Emulsiyon bazlı kartuş dinamit	
Patlatma Saati	6:30:00 PM	
Yüzey Bağlantıları	Elektronik gecikmeler, bkz. Şekil 5	
Patern Koordinatları	X	37 T 403692.41
	Y	4508628.64
	Z	522m
Patern Litolojisi	BAZALT	

Şekil 3, patlatma deliklerinin hazırlanışını göstermektedir. Bu uygulamada KIRLIOĞLU Patlayıcı Firması tarafından üretilen, ilk yerli marka elektronik kapsüller ve ateşleme sistemi, detEX kullanılmıştır (Şekil 11).

Elektronik kapsül gecikmeleri, KIRLIOĞLU Firmasının lisanslı yazılımına sahip olduğu I-blast programı ile tarafımızca belirlenerek logger'a yüklenmiş ve sahada kapsüllere tanımlanmıştır.

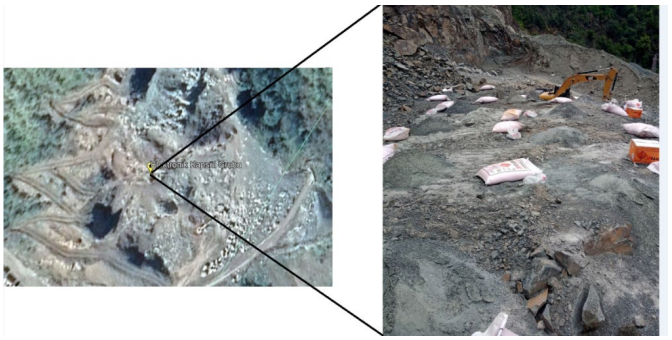

Şekil 3. Patlatma deliklerinin hazırlanışı

Şekil 4. Elektronik kapsüllerin saha uygulamasından bir görüntü

Şekil 5, deliklerin ateşleme sırası ve uygulanan elektronik gecikmeleri göstermektedir.

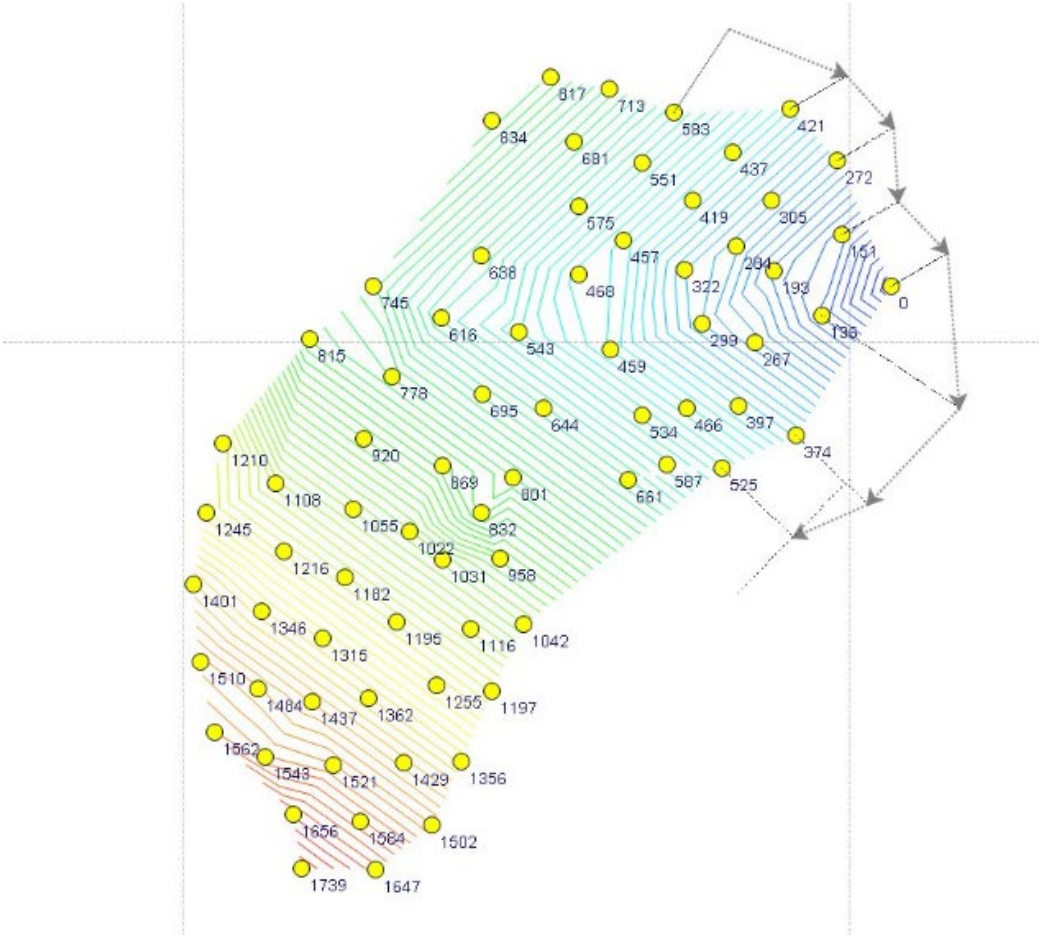

Şekil 5. Deliklere uygulanan elektronik kapsül gecikmeleri

Şekil 6'da ise sismografların ve mikrofonların yerleştirilmesini göstermektedir.

Şekil 6. Sismografların yerleşimi

Çizelge 2, elektronik ateşleme ile yapılan grup patlatmadan oluşan sismik dalgaların, sismograflarda ölçülen 3 bileşenli (T: transversal-yanal, V: Vertical-düşey, L: Longitudinal-boyuna, PVS: peak vectorel sum, vektörel toplam) parçacık hız ve frekans değerlerini göstermektedir.

Çizelge 2. Elektronik ateşlemeli grup patlatmasından oluşan sismik dalgaların, sismograflarda ölçülen parçacık hız ve frekans değerleri

Sismograf	Patlatma	Ölçüm Mesafe, m	T mm/s	V mm/s	L mm/s	PVS mm/s	Hakim Frekans Hz	Hava Şoku Pa	Hava Şoku dB
12269	**Elektronik**	86	18,16	22,48	17,65	27,76	20	25,00	121.9
14465	**Elektronik**	270	1,524	1,270	1,778	1,943	32,88	4,750	107,5
13638	**Elektronik**	365	-	-	-	-	-		
12270	**Elektronik**	447	0,127	1,397	0,254	1,408	24,00	0,750	91,48
micro	**Elektronik**	490	0,284	0,300	0,260	0,371	18,00	3,010	103,5

Bu patlatmada kullanılan toplam patlayıcı ve kapsül miktarları: 2263 kg Anfo, 73 kg kapsüle duyarlı patlayıcı (her bir adedi 1 kg) olmak üzere toplamda 2336 kg patlayıcı; 73 adet elektronik kapsüldür. Elektronik kapsüllerle yapılan patlatmanın drone görüntüsü Şekil 7'de verilmiştir. Drone videosundan anlaşıldığı üzere elektronik ateşleme sistemi ile gerçekleştirilen patlatmada hiç taş savrulması olmadığı gibi, titreşimler de planladığı gibi kontrollü patlatmaya yakışır düzeyde izin verilen limit değerlerin çok altında ölçülmüştür (Çizelge 2). Çizelge 2'deki elektronik kapsüllerle yapılan patlatmanın sismograflarda ölçülen yanal bileşen titreşim hızı değerleri ve hava şoku değerleri Şekil 8'de Google Earth de sismografların üzerine yazılarak gösterilmiş; böylece HES'e etkilerinin daha iyi anlaşılması sağlanmıştır.

Şekil 7. Elektronik ateşleme ile gerçekleştirilen patlatma görüntüsü

Şekil 8. Sismograflardan ölçülen titreşim ve hava şoku değerlerinin Google Earth üzerinde gösterimi

Her ne kadar Çizelge 2'de patlatma kaynaklı sismik dalgaların ölçüm noktasındaki titreşim hız değerleri 3 bileşende verilse de (yanal, düşey ve boyuna), Şekil 8'de sadece yanal bileşen değerleri harita üzerinde gösterilmiştir. Çünkü patlatma kaynaklı titreşimlerden yapılara ve şevlere en çok hasar veren yanal bileşenlerdir. Şekil 8'deki sismografların patlatmaya göre konumlarına ve mesafelerine dikkat edilirse, patlatmaya 86 m mesafede yol kenarına yerleştirilen sismografta 18.16 mm/s titreşim hızı ölçülmüştür. Bu sismograftan alınan sismik ve hava şoku değerlerini gösteren Şekil 9'da kırmızı ok ile gösterilen Türkiye titreşim limitleri grafiğine bakılırsa, hakim frekanslar 20 Hz civarında olduğu için 3 bileşendeki tüm titreşim hız değerlerinin (kırmızı elips ile gösterildi) hasar çizgisinin (siyah ok) altında olduğu görülebilir. Şekil 9'da verilen bir olay raporudur (event-report). Her sismograf ölçümü sonrasında bu olay raporu yazılımdan oluşturulur. Rapordan görüleceği üzere yanal (Tran), düşey (Vert), boyuna (Long) bileşende ve vektörel toplamda (PVS) titreşim hız değerleri bulunduğu gibi, sismografa eklenen mikrofonla ölçülen hava şoku değeri (micL) ve üç bileşende sismik dalga formları da raporda yer almaktadır. Patlatmaya en yakın mesafede, yol kenarına yerleştirilen sismograftan alınan 3 bileşenli dalga formları incelendiğinde, kontrollü patlatma için planlandığı gibi 2,5 saniyede sönümlenen dalga biçimleri yaratılmıştır.

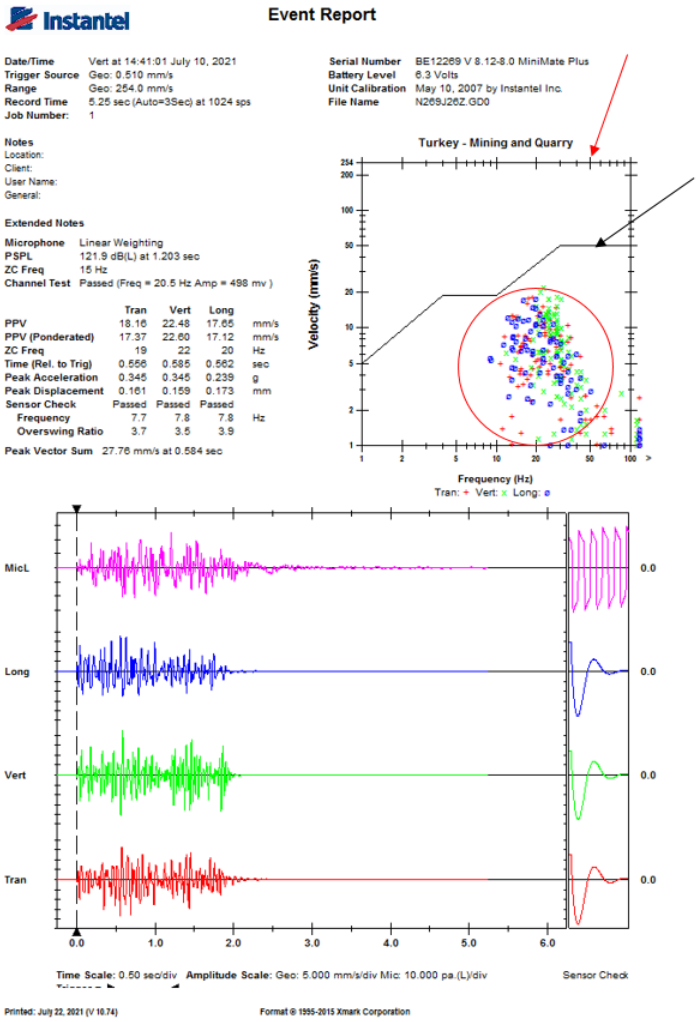

Şekil 9. Sismograf 12269'a ait olay raporu

Patlatma grubuna 270 m mesafedeki sismograf 14465'te ölçülen titreşim hızı yanal bileşende 1.524 mm/s dir ki bu değer Türk standartlarına göre olduğu gibi, en muhafazakar ve korumacı Alman standartlarına göre bile tarihi eserlere dahi hasar vermeyecek izin verilen değer olan 5 mm/s'nin altındadır (Şekil 10). Frekans açısından incelendiğinde ise, elektronik kapsülle yapılan ateşlemede, literatürde de denildiği gibi (Cardu, 2013; IME 2017; Kara vd. 2014; Mishra vd. 2017) daha yüksek frekanslı dalgalar oluşmuştur. Yüksek frekanslı dalgalar çabuk soğrulma özelliği taşıdıkları için titreşime neden olarak zarar verme özelliklerini yitirmektedirler. Bu açıdan, şevlerin duraylılığına tehdit oluşturamadan soğrulma yöneliminde olmaları istenilen bir özelliktir. Yapılar açısından değerlendirildiğinde de yüksek frekanslı dalgalar her zaman düşük frekanslı dalgalara tercih edilirler. Çünkü düşük frekanslı dalgalar yapıların doğal frekansı ile uyumlandıkları takdirde yapıları rezonansa sokarak daha büyük titreşime ve dolayısıyla hasara sebebiyet verirler. Şekil 10, sismograf 14465'e ait olay raporunu göstermektedir. Titreşim hızları bu raporda Alman DIN4150 standartına göre grafiklenmiştir. Kırmızı elips ile gösterilen üç bileşendeki titreşim hızları görüldüğü üzere tarihi yapılara dahi hasar vermeyecek limitlerin altındadır. Sismik dalgalar, vadi tabanına doğru sönümlenme eğiliminde olduğu için sismik dalgaların patlatmaya 270 m uzaklıkta sönümlenmesi bilimsel olarak şaşırtıcı değildir. S dalgalarının sudan geçemediği bilindiği için, elektronik kapsül gecikmelerini

sismik dalgaların derenin genişliğini geçemeyecek dalga boyu üretecek şekilde belirlememiz neticesinde derenin diğer tarafında bulunan HES yapılarına yakın mesafedeki sismograf 13638 hiç titreşim hızı ölçememiş; sismograf 12270 ve cebri boru yanındaki sismograf micromate ise sırasıyla 0.127 mm/s ve 0.284 mm/s titreşim hızı kaydetmiştir. Bu son iki değer aslında titreşim hız eşik değeri olan 0.5mm/s'nin altındadır yani jeofonun sismik kayıt alma eşik değerinin bile altındadır. Normalde mikrofon aparatı takılı olmasaydı ölçüm almayacak olan bu iki sismograf, Mikrofon takılı olduğu için hava şokundan tetiklenerek açılmış ve kayıt almıştır. Şekil 19, 20 ve 21 sırasıyla sismograf 13338, 12270 ve micromate'in lokasyonlarını göstermektedir.

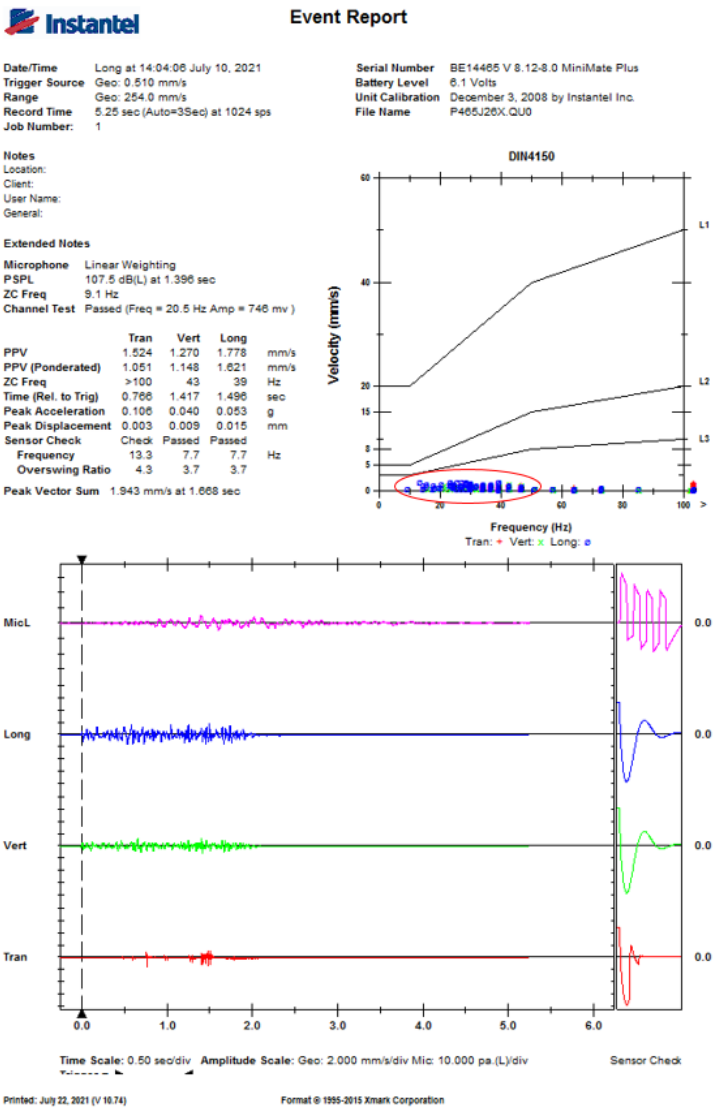

Şekil 10. Sismograf 14465'in olay rapor

JEOTEKNİK DEĞERLENDİRME

Taş ocağında farklı kaya kütlesi özelliği gösteren farklı lokasyonlarda 4 adet hat etüdü yapılmıştır. Şekil 11, bu hat etüdlerinden birine ait görseli vermektedir.

Şekil 11. Taş ocağında yapılan hat etüdü çalışmalarından bir görünüm

İncelenen bölgedeki kayaç malzemesi olan bazaltın sahada alınan numuneleri üzerinde yapılan kaya mekaniği deneyleri sonucunda ortalama porozitesi % 1.8, ortalama ağırlıkça su emme miktarı % 0.14, tek eksenli basınç dayanımı 40-80 MPa, poisson oranı 0.27, elastisite modülü 57 Gpa olarak belirlenmiş olup inceleme bölgesinde yapılan hat etüdleri neticesinde elde edilen kaya parametreleri toplu olarak Çizelge 3'te verilmiştir.

Çizelge 3. Hat etüdleri neticesinde elde edilen kaya parametreleri

Hat Etüdü No	Deformasyon Modülü (MPa)	Kohezyon (kPa)	İçsel Sürtünme Açısı (°)
1	1995,26	1130	19,39
2	1778,28	1061	18,39
3	1258,93	867	15,55
4	1122,02	806	14,64

SONUÇLAR

1. Patlatmaların çevresel etkilerinin değerlendirilmesinde kaya mekaniği deneylerine ihtiyaç duyulmamakla birlikte sahadan alınan numuneler üzerinde kaya mekaniği deneyleri yapılmış, jeoteknik hat etüdleri yapılmış ve jeomekanik açıdan saha değerlendirilmiştir. Buna göre, iyi planlandığı takdirde sahadaki kaya kütlesinin patlatmaların çevresel etkilerini (titreşim, hava şoku ve taş savrulması) kontrol edebilmeye izin verdiği belirlenmiştir.

2. İyi bir patlatma planlanması halinde, karayolu tüneline 120 m koruma mesafesi uygulanması şart değildir. Kaldı ki tarafımızca yapılan patlatmaya en yakın 86 m mesafedeki yolda herhangi bir olumsuz etki yaratacak titreşim, hava şoku, taş savrulması etkileri ölçülmemiştir. Karayolu tünelinde ölçüm alınmamıştır (yol, HES, cebri boru hattında sismik dalga yayılım mekanizmasını anlamak için). Ancak yola çok yakın olan tünel girişinde de, literatüre göre izin verilen 200 mm/s limit değer düşünülürse, yolda ölçülen 18.6 mm/s titreşimin herhangi bir zarar vermeyeceği düşünülmektedir.

3. Hava şoku değerleri izin verilen 140 dB'in çok altında ölçülmüş olduğu gibi herhangi bir taş savrulması olmamıştır.

4. Ocak sınırları içerisinde olan yola, doğru patlatma tasarımı ile 30 m mesafeye kadar patlatma yapılabilir. Çok gerekli olması durumunda burada alınabilecek önlem patlatma sırasında yolun kapatılması ve patlatma örtüsü kullanılmasıdır.

5. Çok eski yıllarda ve hangi saha ve kayada üretildiği bilinmeyen, kullanılan parametrelerin belirtilmediği formüllerle titreşim, hava şoku, taş fırlaması vb. etkilerin belirlenmesi bilimsel gerçeklikle bağdaşmamaktadır.

6. Bilinenin aksine, 1 tek delik patlatılarak alınan sismik sinyallerin modellenmesi ile çevreye zarar vermeyecek 400-500 delikli grup patlatmaları planlanabilir. Bu bilimsel gerçekle ilgili uluslararası patentler, uluslararası yayınlar tarafımızca yapıldığı gibi literatürde de bolca bulunmaktadır. Burada önemli olan delik sayısı değil doğru patlatma tasarımı yapılması ve bu tasarımın doğru patlatma elemanları ile gerçekleştirilmesidir.

7. Yapılan çalışmada olduğu gibi doğru patlatma tasarımı yapıldığında ve bu tasarımın sahada hassasiyetle uygulanması halinde sahada yapılacak patlatmaların çevre yapılara, yol, baraj tünel vb. hasar vermeyeceği; çevresel kirlenmeyi tetiklemeyeceği, yeraltu suyu akış rejimine dikkate değer etkisi olmayacağı düşünülmektedir. Çünkü bu yapılan çalışma ölçülebilir ve denetlenebilir sonuçlar içermektedir; herhangi bir formülden ya da yaklaşımdan üretilmemiştir, tamamen sahanın kendi parametrelerini içermektedir.

8. 85 delikli patlatmanın etkilerini görmek için 85 delikli patlatma yapmaya gerek yoktur. Tek delik patlatması ile de sismik dalga yayılım mekanizması öğrenilir ve 85 delikli, çevreye zarar vermeyecek kontrollü patlatmalar tasarlanabilir. 10.07.2021 tarihinde sahada 73 delikli elektronik ateşleme ile yapılan kontrollü patlatmanın titreşim, hava şoku değerlerinin, yol, HES yakını, cebri boru yakınında eser miktarda ölçülmesinden dolayı bilimsel olarak söylenebilir ki, 85 delikli grup patlatmaları, verilen paterne ve patlayıcı ve patlatma elemanlarına uyulması durumunda Darıca-2 HES yapısına, cebri borulara, tünel girişlerine herhangi bir çevresel olumsuz etki yaratmayacaktır.

TEŞEKKÜR

Bu çalışmada kendilerine ait yerli üretim Elektronik ateşleme sisteminin kullanılmasına imkan tanıyan Kırlıoğlu Patlayıcı Firmasına ve sahada patlatma operasyonunda yer alan firma mühendisi E. Taylan Edis'e teşekkür ederiz.

KAYNAKLAR

Cardu M., (2013), "A Review Of The Benefits Of Electronic Capsüls", RemRevistaEscola de Mines.

Cardu M, Muccı A., Uyar GG., (2015), "Investigating The Effects Of Benchgeometry And Delaytimes On The Blastinducedvibrations İn An Open-Pitquarry", GEAM, Vol. 144. 45-56.

DIN 4150-3. Structural vibration-effects of vibration on structures. http://webstore.ansi.org/; 1999.

IME, (2017), "EBIS Guideline, Electronic Blast Initiation System".

Kara S., Adamson W.R., Reis W.J., Trouse l R., (2014), "The Latest Generation Of The Electronic System Enhancedsafety And Productivity". *Proceda Engineering, Vol. 83*, 432- 440.

Mıshra A.K., Nigem Y.K., Singh D.R. (2017), "Controlled Blasting in a Limestone Mine Using Electronic Detonators", Journal of Geological Society of India.

Patlatma Tasarımları ve Patlatma Kaynaklı Çevresel Etkiler Kılavuzu, (2018), http://ced.csb.gov.tr/kilavuz-rehber-form- i-320

CHARACTERIZATION OF PHOSPHATE DUST FROM DJBEL-ONK, NORTHERN ALGERIA

M.I Zohir [1,*], B. Assia [1], B. Said [1], C. Abdessalam [1]

[1] *Badji-Mokhtar University Annaba, Laboratory of Mineral Processing and Environment "LAVAMINE"*
*(*Corresponding Author: mektizohir@yahoo.fr)*

ABSTRACT

Dusts are solid particles mainly due to industrial activity and especially mining activity. Their size is therefore reduced and placed on a microscopic or even nanoscopic scale. In the literature, different terms are often used indiscriminately to define this type of pollution among them: aerosols are formed of solid or liquid particles of size less than 100 micrometres. "Black smoke" are carbon particles with a diameter of less than 05 µm up to about 0.1 µm. In Algeria, the SOMIPHOS plant in Djebel El Onk is specialized in the exploitation and treatment of phosphates, dust emissions are quite high at the level of the quarry and the treatment plant, because of the use blasting and the preparation of phosphate by the dry mechanical method. The main aim of this work is to characterize the dust emitted due to the exploitation and processing of phosphate ores. The results obtained show that the dust level exceeds the international standard (1g/m^2/day), the size and size distribution of the particles is determined by the laser particle size, the FRX and the DRX are used to determine the chemical composition and mineralogical. The level of heavy metals in dust was evaluated by the analysis of Atomic Absorption Spectrometry.

Keywords: Phosphate dust, PM, airborne pollution, Algeria, Djbel –Onk plant, environment

INTRODUCTION

The Djebel El Onk SOMIPHOS plant; specializes in the exploitation and processing of phosphates, it is located in the south-east of Algeria, 100 km from the Wilaya of Tébessa and 20 km from the Algerian-Tunisian border (Fig. 01). It is implanted within in the framework of treating and producing a phosphate rich in P2O5, intended for various industries; such as the ASMIDAL plant located in the wilaya of Annaba either by rail or by road transport. The total production is in the order of a few million tonnes which is exported as raw material to several countries around the world (BEZZI N. 2005).

Due to the quality of the phosphate mining, is currently focused on Kef Essennoun. In this place ; there are two different colors of phosphate which are dark color (gray) and light color (beige).

The Djebel El Onk area consists of two parts: an open pit mine and the phosphate processing plant (Nouioua et al. 2016).

Like other human activities, the mining industry corresponding to the Djebel Onk mining complex; today poses very acute environmental problems, such as the emissions of very fine and sometimes-toxic dust, because it contains metals trace elements, which can cause pollution of air, soil and water and they can create many regional or global problems for living beings and for humans in the event of respiration.

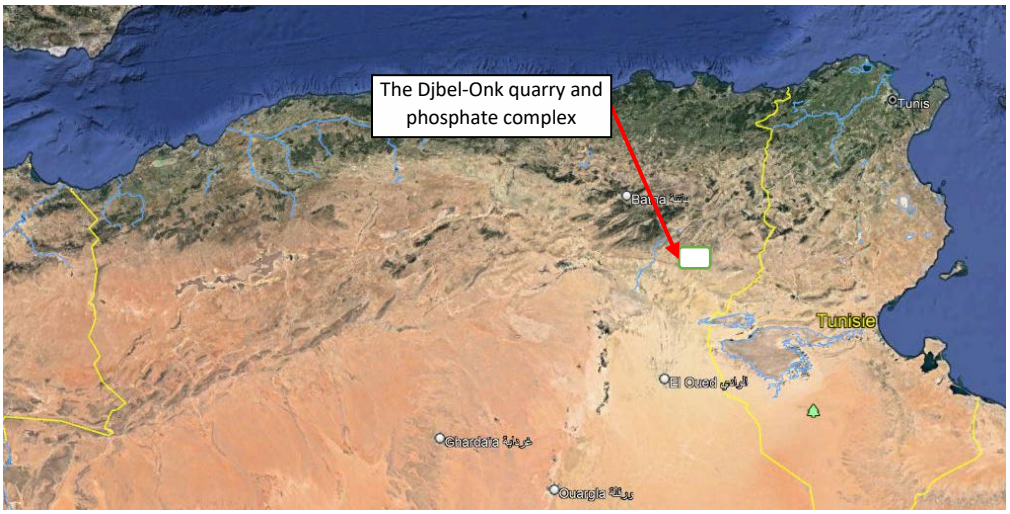

Figure 1. Location of Djbel-Onk complex

MATERIAL AND METHODS

The phosphate dust sample are obtained during collection at several points on the site, such as the waistline, the mechanical preparation workshop; the edges of the transport paths, the processing plant and finally the loading wagons and trucks silos. To achieve the objective of this work; several tests have been carried out. Beginning with the chemical composition by the FRX, the mineralogical composition carried out by XRD, the particle size distribution carried out by the laser particle size distribution, finally the shape of the particles is analyzed by the SEM imaging.

Chemical Composition

To determine the origin of the PM collected, we carried out chemical analysis of the samples by the XRF; all the samples are mixed; homogenized and analyzed. The result of the chemical composition of the dust collected, are compared with that given by the laboratory of the Djebel Onk phosphate complex (Table 1).

Table 1. Chemical composition of PM phosphate samples

Elements	P_2O_5	CO_2	SO_3	CaO	MgO	Fe_2O_3	Al_2O_3	Na_2O	K_2O	SiO_2	F	Cl (ppm)
PM of phosphate	29.31	6.93	2.80	50.8	1.67	0.32	0.33	1.27	0.071	2.16	3.56	553
Djebel-Onk phosphate	30.22	6.86	3.00	52.3	0.83	0.12	0.50	1.35	0.078	3.21	4.02	449

The comparison of the values of the composition of PM of phosphate; shows a correlation with the chemical composition of Djebel Onk phosphate. These results clearly prove that the PM collected in the installations is generated by the process of unloading, storage and unloading of phosphate.

Mineralogical Composition

X-ray diffractometer (XRD) analysis of the different particle size fractions of phosphate dust has identified the following main mineralogical phases (Figure2.):

1-) Phosphate elements of the apatitic class such as: Carbonate apatite $Ca_{10}(PO_4)_6$, Carbonate hydroxyapatite Ca_{10} $(PO_4)_3$ $(CO_3)_3(OH)_2$, Fluorapatite $(Ca_5(PO_4)3F)$, Carbonate fluorapatite $Ca_{10}(PO_4)$ $5CO_3F_{1.5}(OH)_{0.5}$, hydroxyapatite $Ca_5(PO_4)_3$ (OH) and Phosphate hydrate (NETTOUR D. 2018).

2-) Elements of gangue: Are represented mainly by carbonate and siliceous minerals such as dolomite $CaMg(CO_3)_2$, silicas in the form of Calcite $CaCO_3$, quartz SiO_2 and gypsum $CaSO_4$.

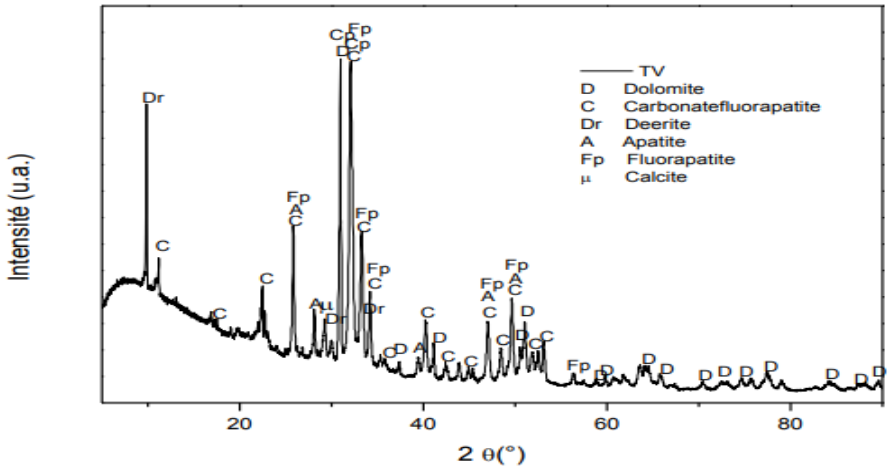

Figure 2. DRX du minerai de la poussière de phosphate

Determination of Particle Size Distributions

The particle size distribution of the phosphate dust sample; is obtained from the analysis by laser diffraction (Fig. 3). The result of the analysis showed that, more than 90% of the particles with a smaller diameter at 118µm; 50% of the particles with a diameter less than 13.3µm, and 10% of the particles have a diameter of less than 5.5µm.

These results favour deep pulmonary deposition. PM10 (particles with an aerodynamic diameter of less than 10 µm) are of major concern today, as they are small enough to penetrate deep into the lungs. Particle size can behave on the human body as follows:

Chest dust: mass fraction of inhaled particles entering the larynx (<30 µm);

Alveolar dust: mass fraction of inhaled particles, penetrating the non-ciliated airways (<15 µm). These fractions are included in the ISO 7708 standard and in the Afnor X 43-100 standard.

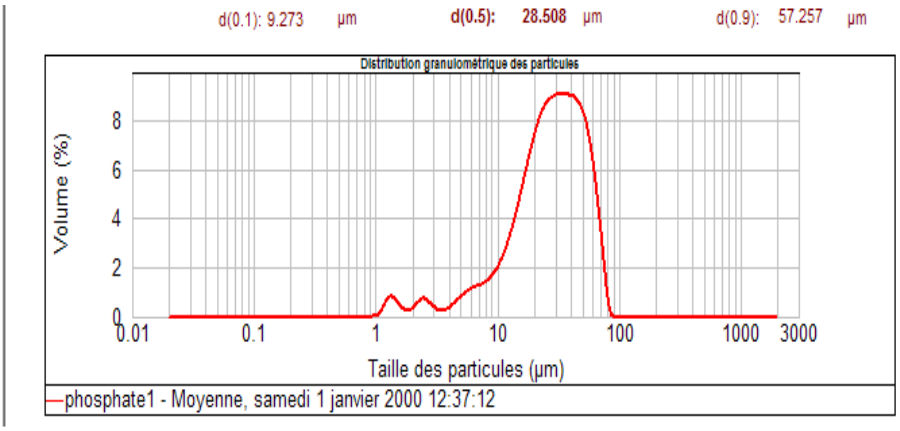

Figure.3. PM particle size by laser diffraction

Phosphate PM Morphology

The shape of PM in general can promote flight and decrease the sedimentation rate of a particle: a flat particle behaves like a leaf during its fall and will therefore settle more slowly than a spherical particle (Imen Bel Hadj 2013). The fall speed is a function of the aerodynamic diameter. PM of phosphate captured at the port of Annaba; have different morphology and irregular shape (Fig. 4).

The angular shape of the particle surface; is mainly due to the mechanical preparation of phosphates at the Djebel Onk plant, unlike natural particles where the surface is smooth and the grains are spherical in shape. For particles of irregular shape, relative movement becomes difficult due to the presence of more points of contact between them. If they are elongated and hook-shaped particles, it will be more complicated because they tend to form bridges by interlocking particles.

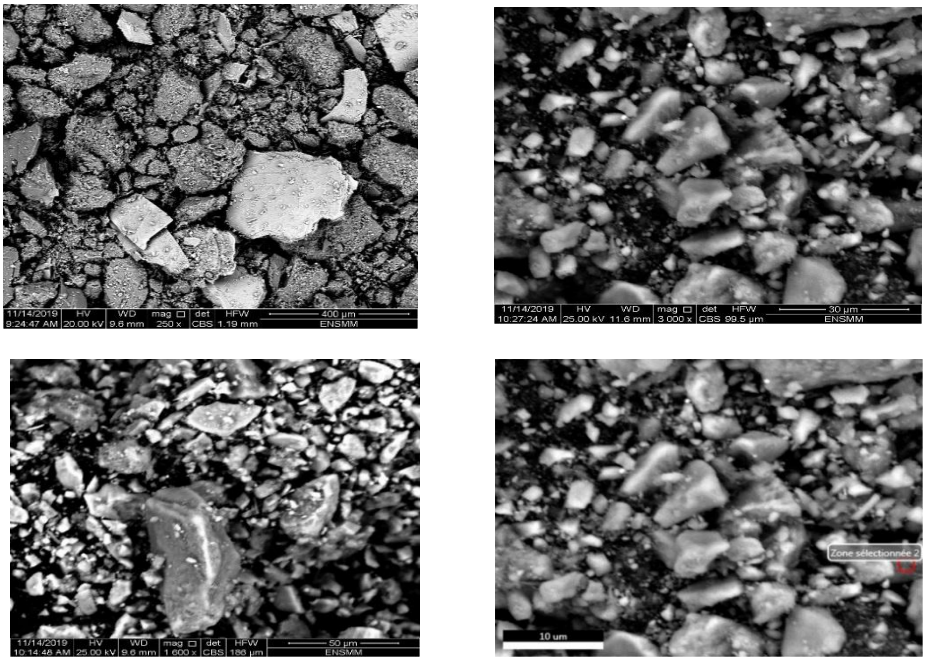

Figure 4. Phosphate dust morphology, by X-ray microanalysis coupled with a scanning electron microscope (SEM / EDX)

Heavy Metals Content in Phosphate Dust

From a purely scientific and technical point of view, heavy metals can be defined as: any metal with a density greater than 5 g/cm^3. Any metal with a high atomic number, generally higher than that of Sodium (Z = 11), presenting a danger to the environment and to humans. Any metal that can be toxic to biological systems. In environmental sciences, the heavy metals associated with the concepts of pollution and toxicity are generally: arsenic (As), cadmium (Cd), chromium (Cr), copper (Cu), mercury (Hg), manganese (Mn), nickel (Ni), lead (Pb), tin (Sn), and zinc (Zn). In our study, the composition of heavy metals and some trace metallic elements was determined by, atomic absorption spectrometry (Table 4).

Table 2. Daily and surface concentration of metals detected (µg/m^2/d), German standardization.

Element	Cd	Zn	Pb	Cu	Cr	Ni	Mn	Hg	Co	Sb
Limit µg/m^2/d	2	400	100	100	250	15	15	1	15	100
S1	8.3	113.2	15.8	23.4	122.2	13.5	11.3	3.2	2.2	12.4

The results of the metal concentrations measured for the eight stations; presents different values, those, which are higher than the German limit values, and those that are lower. We observe that the guide values for the metals of Cadmium (Cd) and mercury (Hg); have been exceeded. The limit value of Cd is 2 µg/m^2/d, on the other hand the recorded values varied between 8.7 and 1.2 µg/m^2/d.

The limit value of Hg according to the German standard, is 1 µg/m^2/d, but the results of the latter's analyzes vary between 3.2 and 0.3 µg/m^2/d in the eight measuring stations. The values of Zn, Pb, Cu, Cr, Ni, Mn, Co and Sb are below the limit of quantification. The points most exposed to fallout from the site have the highest levels of heavy metals.

Recommendation

Usually to control dust emissions, several methods can be applied. For phosphate dust, the method is special, because the product must not be touched by humidity, otherwise it will be contaminated, and therefore it is strictly forbidden to spray the dust with water especially at the unloading points of trucks and wagons. The most effective methods for reducing phosphate dust are:

1. Complete cover of the product conveyor belts
2. Unloading of trucks and wagons in well closed and airtight sheds, to prevent dust from escaping outside the installation
3. Spray the road with water Complete cover of the product conveyor belts
4. Unloading of trucks and wagons in well closed and airtight sheds, to prevent dust from escaping outside the installation.
5. Spray the road with water to prevent dust from flying away during the passage of trucks.

CONCLUSIONS

Certainly, the effects and consequences of these emissions on man and the environment are disastrous. It is probable that in the future an in-depth study will be carried out on the effects of these emissions on man, the environment, fauna and flora.

Based on the results obtained in this study, the following conclusions can be listed:

1. The chemical composition of the PM determined by the XRF, shows a correlation between the chemical composition of the PM samples from the samples and the chemical composition of the phosphate from the Djebel-Onk plant.
2. The particle size distribution of PM, determined by laser diffraction, show that more than 90% of particles with a diameter less than 118µm, 50% of particles with a diameter less than 13.3µm and 10% of particles have a diameter less than 5.5 µm. These results promote deep lung deposition upon inhalation of PM by humans.
3. PM of phosphate captured; have morphology and irregular shape of different size. The angular shape of the particle surface; is mainly due to the mechanical preparation of phosphates at the Djebel Onk phosphate plant, unlike natural particles where the surface is smooth and the grains are spherical in shape.
4. The values of Zn, Pb, Cu, Cr, Ni, Mn, Co and Sb are below the limit of quantification. The points most exposed to fallout from the site have the highest levels of heavy metals.

REFERENCES

Ben Hamla, F., Ameziane, N., & Morakchi, K. (2015). Etude physico-chimique et minéralogique d'un matériau naturel.

Benselhoub, A., Kanlı, A. I. (2020). Environmental Impacts of Air Pollution on Human Health in Annaba Region (Northeast of Algeria). In Toxic Chemical and Biological Agents (pp. 209-216). Springer, Dordrecht.

Benselhoub, A., Kharytonov, M., Bouabdallah, S., Bounouala, M., Idres, A., & Boukelloul, M. L. (2015). Bioecological assessment of soil pollution with heavy metals in Annaba (Algeria). Studia Universitatis" Vasile Goldis" Arad. *Seria Stiintele Vietii (Life Sciences Series), 25(1),* 17.

Benselhoub, A., Kharytonov, M., Bounouala, M., Chaabia, R., & Badjoudj, S. (2015). Estimation of soil's sorption capacity to heavy metals in Algerian megacities: case of Algiers and Annaba. INMATEH-Agricultural Engineering, 46(2).

Bezzi, N., Aifa, T., Hamoudi, S., & Merabet, D. (2012). Trace elements of Kef Es Sennoun natural Phosphate (Djebel Onk, Algeria) and how they affect the various Mineralurgic modes of treatment. *Procedia Engineering*, *42*, 1915-1927.

Chiazze, L., Watkins, D.K. et Fryar, C., 1992: «A case-control study of malignant and non-malignant respiratory disease among employees of a fibreglass manufacturing facility», ibid., vol. 49, pp. 326-331.

Giannadaki, D., Pozzer, A. et Lelieveld, J. (2014). Modélisation des effets mondiaux de la poussière du désert en suspension dans l'air sur la qualité de l'air et la mortalité prématurée. *Chimie et physique atmosphériques, 14 (2)*, 957-968.

Henni-Chebra, K., A. Bougara, and A. Halla (2009). "IMPACT DES RETOMBEES DE POUSSIERES CAUSEES PAR L'INDUSTRIE CIMENTIERE SUR L'ENVIRONNEMENT."

Khadidja Henni-Chebra, Abdelkader Bougara, El-Hadj Kadri (2011). Détermination du niveau d'empoussièrement engendrée par la fabrication du ciment. XXIXe Rencontres Universitaires de Génie Civil. Tlemcen, 29 au 31 Mai 2011.

Kharytonov, M., Benselhoub, A., Klimkina, I., Bouhedja, A., Idres, A., & Aissi, A. (2016). Air pollution mapping in the Wilaya of Annaba (NE of Algeria). *Mining Science, 23*.

Merlen, R. (2015). La biosurveillance: outil de surveillance de l'impact sur l'environnement des émissions atmosphériques industrielles et d'évaluation des risques sanitaires. 2268-3798.

Nordberg G, Jin T, Bernard A, Fierens S, Buchet JP, Ye T. (2002). « Low bone density and renal dysfunction following environmental cadmium exposure in China » Ambio. 31(6):478–481.

Orlowski C, Piotrowski JK, Subdys JK, Gross A. (1998). « Urinary cadmium as indicator of renal cadmium in humans: an autopsy study » Hum Exp Toxicol;17 (6):302–306.

Romdhane, S. B. (2017). Effets du climat et de la pollution de l'air sur la santé respiratoire à Tunis (Doctoral dissertation, Université Sorbonne Paris Cité ; Université des lettres, arts et sciences sociales-Tunis I. Faculté des sciences humaines et sociales).

Roy, D., & Singh, G. (2014). Source apportionment of particulate matter (PM10) in an integrated coal mining complex of Jharia coalfield, Eastern India: A review. *International Journal of Engineering Research and Applications, 4(4)*, 97-113.

COMMINUTION VS. LIBERATION: A COMPARATIVE ANALYSIS OF THEORIES AND PRACTICES ON COMMINUTION FROM INVESTMENT POINT OF VIEW, A CASE STUDY FROM URUGUAY

I.Tarjan [1, *], D. Segovia [1], H. Ferrizo [1]

[1] *Universidad de la Republica, Uruguay, Centro Universitario Region del Este*
*(*Corresponding author: ivan.tarjan@cure.edu.uy)*

ABSTRACT

Long been the discussion on different comminution techniques to achieve desired granulometry for ores and rocks for their application and/or metallurgical use with emphasis on energy saving, environmental issues and efficiency. Energy plays an important role knowing that the comminution requires the biggest part of energy supply in the processing industry, the economy (amortization) have often been left out or paid little attention when decision is made. Comminution machines use different phenomenon. From the energy side it is necessary to define working indices to establish the capacity of the machine. Sometimes, liberation is not a need, while others look for the highest liberation possible. However, much depends on the buyer's requirements of the material run out of the plant. If the "product" should be transported for further processing than the grain size will depend on logistics, price, etc. more than professional goals. The two approaches lead to some antagonistic questions and economic considerations. In general, the lower the grain size the higher the liberation, superfine is not economic to transport. Also, the higher the concentration grade the higher the price, but the grade depends on the granulometry. This paper aims to summarize recent innovations with suggestions on prioritizing operations through the case study in a magnetite ore deposit in the North-East part of Uruguay.

Keywords: Crushing, grinding, liberation, circuit improvement, energy efficiency, economy

INTRODUCTION

In the recent years a very promising iron-ore resource was found in the North-East part of Uruguay. Exploration and prospection were done in a very accurate and professional manner and probed a rich magnetite deposit, so the elaboration of a business plan and the procedure for the environmental and extraction permissions acquisition was started.

During that time the processing plant design establishment arose different issues regarding the beneficiation of the material such as concentration grade and grain size. It turned out that there are several problems to satisfy both of needs on the most economical way of separation, especially when the product price is highly volatile.

THE OBJECTIVE

According to the "buyer's specification" the product should satisfy several conditions, however, from our point of view there are two that has specific interests. Namely: the grain size cannot exceed 125 microns more than 7% (this is the condition of transportability) whereas the concentrate should reach 62% minimum (quality condition).

It worth to mention that the quality is denominated in percentage of Fe content that can lead to some misunderstanding (however it is a technical issue), simply because of the composition of hematite

itself. If we want 62% Fe content the product should be more than 100% pure hematite, clearly impossible. Therefore, the quality is meant in hematite (FeFe2O3) content. In general, the mineral is composed of magnetite (25-30%), quartz and clinopyroxenes.

The ore in general is considered to have a natural granulometry small, within 45-250 microns with exception of those collectibles that can reach of 2 cm crystals. Therefore, from the beneficiation point of view, it is very important to liberate the particles as much as possible, meanwhile the raw magnetic separation needs only an exposure of it. This is to say it is sufficient to make part of the surface of the particle free to be able to interact in the magnetic field. Consequently, during the crushing process it is possible to save considerable energy to put into it sacrifying the quality as the particles will contain big amount of additional materials and minerals that are gangue and dilute the concentration.

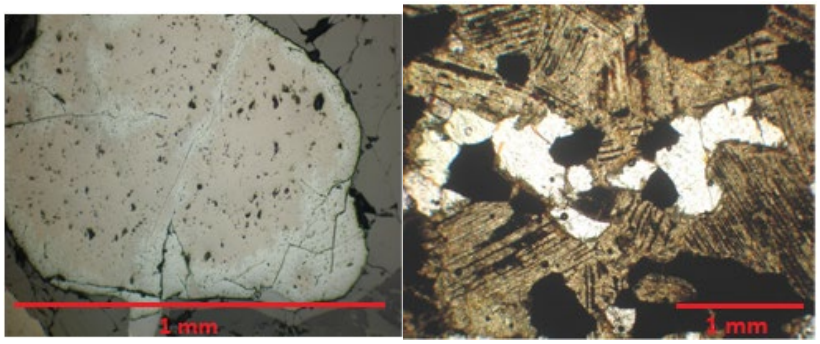

Figure 1: Show big crystals of magnetite at the size of 1-3 mm that is very favorable to all the beneficiation process.

On the other hand, with total liberation we have to consider a product size of around 75-100 microns at least, which is the common practice when the briquetting plant is located right next to the beneficiation plant. It might be an option to install a compacting machine to aggregate the powder to improve air quality and handling issues. The actual case does not require grinding to this size theoretically as the petrography shows big crystals.

However, tests made on samples do not support this idea. At the grain size range of 1-10 mm the maximum concentration reached was 41,56%, meanwhile in the range of 180 microns 63% was obtained with magnetic dry separation in our laboratory. (It is supposed that a wet separation in the lower grain size would result even better outcome, but for different reasons this method is not considered to be viable.)

Table 1. Test results at 1-10 mm grain size

Mineral separation process	Fe2O3 per-centage	Productivity percentage	Mass recovery percentage
Raw ore - Feeding material (crushed to the size of -2 mm)	27.30	100	100
Result material – Concentrate material	41.56	56.78	86.42
Tailing	8.58	43.22	13.58

Table 2. Test results at a 180-micron grain size

Mineral separation process	Fe2O3 percentage	Productivity percentage	Mass recovery percentage
Raw ore - Feeding material (crushed to the size of -2 mm)	33.61	100	100
Result material – Concentrate material	62.73	50.09	95.03
Tailing	4.38	39.3	4.09

This clearly shows that there must be an inefficient liberation during the comminution process, breakage post probably occurs within the homogeneous grain within the particle instead of through the boundaries of a heterogeneous particle. (Michaud, 2016)

It is well known that higher the quality higher the price can achieve, so it is worthwhile to look into the crushing and grinding procedures as places of expenditures in a short and a long term (capital expenditure vs. energy consumption and maintenance costs) in regards of the benefits on product price, so ROI.

THEORIES AND PRACTICES OF COMMINUTION FROM THE EFFICIENCY POINT OF VIEW

There were several attempts to establish a solid theorical background on comminution both crushing and grinding. None of them works perfectly, so we have to assume that this does not exist.

The main reason is the complexity of the process especially of grinding. The variables are numerous, there effect on the processes varies as well. Explaining grinding makes it even worth when the grinding medium is added into the consideration and has to be modelled the system entirely.

As there is no applicable solid based theory of comminution processes most of the working principles were deduced from experimental results, empirical way, most recently with the aid of statistical methods and nowadays utilizing Artificial Intelligence. Nevertheless, all of them is based on the historical results looking for different levels of approval and relationship among the “traditional” models.

Considering the three basic laws of comminution as by Rittinger, Kick and Bond all of them is widely appreciated and used in the practice, mainly for the crushing and grinding machine design and production.

Models were made in several manners that describe, measure and conclude results of different factors of fractions. For example, test and experiments of single particle breakage, particle bed formation on surfaces both on the medium and the linings and how these affect the outcome of the process and the energy consumption. An excellent summary of all of them can be found here. (Michaud, 2016)

There are promising experiments on adding extra energy before the comminution process by ultrasound handling that shows significant energy savings. (Gholami et al., 2020).

It seems like the energy density of the particle is most important factor!

In general, the energy input discussed in all theoretical scenes are supposed to use for the comminution, very little considered as waste. However, it is a very important part of recent investigations and attempts on improvements to get a better-quality product at a lower energy input with lower carbon emission.

The waste of energy is result of heat, electromechanical resistance and noise, etc. The heat mainly comes from two sources: the inner source is the release of the elastic energy accumulated in the particle at the moment of breaking apart, the outer one is the friction within the particles and/or within particles and grinding medium (these partly might contribute to the grinding process) and/or within the grinding medium only (that purely is waste if the process does not result better quality at higher temperatures). An overall 1% of energy input causes breakage (Borg et al. 2020).

Important work was done on the investigation to improve the efficiency of the comminution by experiments, using different machinery like HPGR as a highly effective solution, eliminating wet processes to improve resource savings and usage, a priori feed preparation, improving on environmental issues and sustainability (Jankovic et al., 2016; Baawuah et al.,2020; Komar Kawatra 2006; Weerasekara et al., 2013)

Something New

Because of the above one can get to a conclusion that something is missing, and process should be looked at in another way.

If all of the comminution techniques attempt to augment the energy density of the particle and it is approved working well but could not get to the level sufficiently high, it would be worth to investigate.

Conventional comminution uses compression – slow or impact – sheer forces. In primary crushing the slow compression is applied mainly (jaw crusher, roll crushers), secondary crushing applies sheering and impact, while grinding is a very complex and sophisticated way to level up the energy density. Simplifying a bit radically, the energy input comes from transfer of kinetic energy into potential energy in the case of impact crushers and cylindrical mills like ball mill or rod mill. Augmenting the energy density inside the particle a priori to crushing and grinding makes these latter more efficient and the liberation is even better. This suggests that achieving its critical level when a particle falls apart should be possible by one single step and it can happen at a considerably good liberation factor, too. As a matter of fact, there is nothing new in it, the first mention looks back around 55 years (Wiegl et al., 1967).

The potential energy is given by – simplified – the particle/grinding medium particle mass. It can be measured and/or calculated from the uniaxial, tri-axial compression tests, a drop ball test or other experiments. It cannot be found literature to test equally high force or tension resulted by the transfer of the kinetic energy that can provide the mass of the particle itself. Instead, it seems like the energy accumulation without relaxation time generates resonances that differs regarding the material composition and/or physical properties, suffering reflections and deformation on the particle contact surfaces resulting great tensions than final disintegration (Borg et al., 2020). Even further, how it can be continuously increased to maintain the comminution ratio high when a particle loses mass during the process.

The idea can be to apply the force necessary to break a particle at the force given from a uniaxial compression test and calculate the energy required. Equaling it to a kinetic energy that is a result of the mass of a particle and its velocity and find a way to achieve this in a crusher or mill and test whether it works. Other tests can be carried out with lower velocity but repeated high energy impacts as it is suggested from a “pulsing” compression test, so saving energy on this way might also be possible. (Borg et al., 2016)

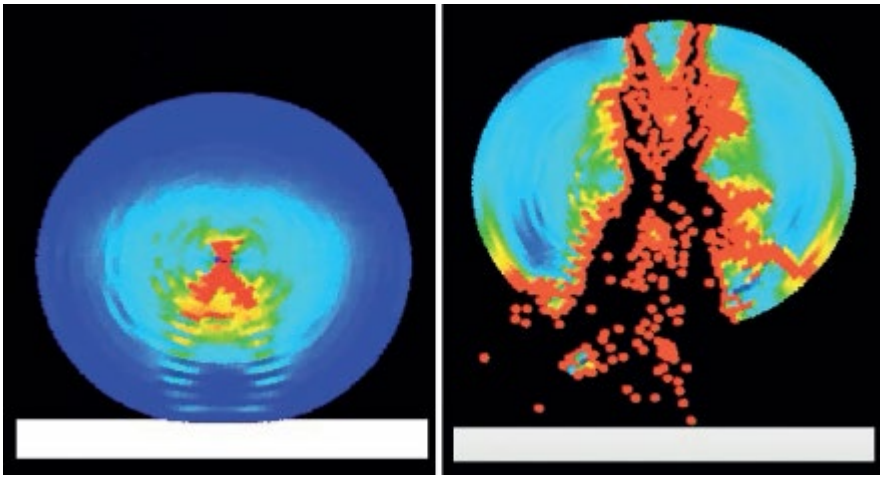

Figure 2. Numerical modelling illustration (by courtesy of Paul Cleary CSIRO) of a high velocity impact of a round particle to a solid tool at the moment of contact (left) and later disintegration (right)

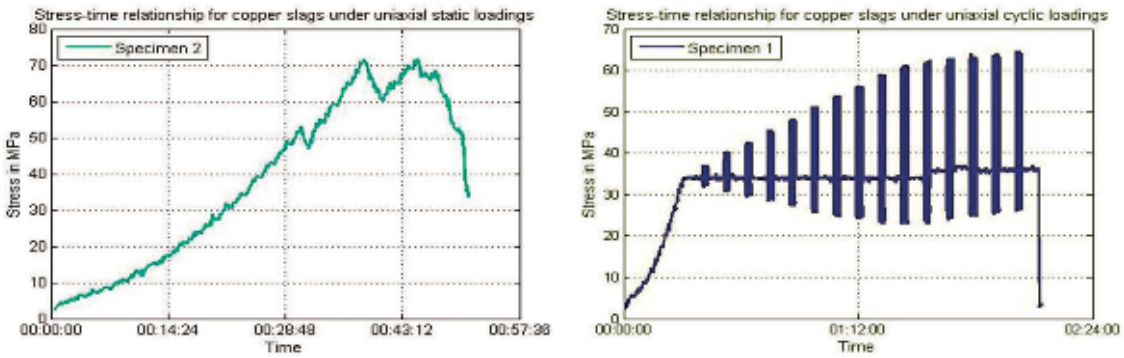

Figure 3. Results of uniaxial dynamic load test (right) and pulsated loads in several steps (left) (Borg et al.,2016)

Furthermore, in case the outcome is promising, increase the efficiency by repeat these events after constructing a model (numerical modelling, or other computational technique).

Given the above data and/or model the theoretical energy consumption can be calculated as well.

Exactly this is what happened with one of the German machine producers to be able to provide a versatile product for a versatile production.

The equipment is tested, run as pilot project in several mining sites and the efficiency is surprisingly good. The product can be graded by grain size and the liberation factor can reach to almost 100%. (Borg et al., 2020)

THE ECONOMY

Considering the above-mentioned issues and want to plan a crushing and grinding plant the capital investment comes into the discussion.

A general beneficiation plant starts with the crushing than the grinding circuit, then come all the processes to produce products running out of the plant. The energy consumption takes the highest part of the plant, as well as the capital expenditure (machine prices and installation, construction work takes considerable percentage from the entire investment.

Planning such a plant there are basic engineering practices and assumptions like i) the fines produced in every step of crushing/grinding should be taken out, ii)) the reduction ratio should be established according to the minimal loss possible (fines), iii)) energy consumption in efficiency/effectivity should be considered as priority. From the point of view energy efficiency, the first consideration is vital. The fine in the system causes most of the loss in the conversion of the energy input into effective energy to breakage.

It has to be noted, however, that in some special cases fines are a must in order to make the comminution more effective, such cases are when there must “build” a layer of material on the grinding elements (Michaud, 2016 (1)).

Aiming to improve the Return of Investment there are two ways as general: Lowering the capital expenditure and/or augmenting the incomes meanwhile saving on running costs (energy and maintenance). Might there be an equilibrium!

In our specific case the planned beneficiation plant consists of:

Option 1.	Option 2.
Jaw crusher	Jaw crusher
Cone crusher	Cone crusher
Multi-cylinder cone crusher	Multi cylinder crone crusher
Ball mill	Vertical mill
Magnetic separation	Magnetic separation

The planned CAPEX on these layouts is estimated to:	
2.000.000 USD	5.600.000 USD

Considering replacing the secondary crushing and the grinding circuit to one of the machines described it would augment the CAPEX to 6.000.000 USD

Calculating the running costs on this equipment would result:

Energy savings: 1.700 kWh in case of option 1, and 1.600 kWh in case of option 2.

The price premium for higher quality products can be considered as between 10% and 60% of standard price.

Maintenance costs should be considered as constant based on the initial expenditure, therefore the higher investment should be covered by the energy saving and the income growth.

The planned capacity is 100 t/h concentrate product in a normal yearly workload (that is 200 days, 8 hours/shift, 2 shifts/day)

Calculating with 0,40 USD/kWh energy price the savings result as 2.176.000 USD (option 1), and 2.048.000 USD (option 2), and 300.000 tons/year at a 100 USD/t price an average 15% premium should result 4.500.000 USD/year extra income. Totaling of 6.048.000 USD/year minimum result considering only the use of a different machine for size reduction, that is in the first year the investment (if it were to be considered as a change or improvement) would pay it back.

Resulting the ROI that is considerable to favor of changing the technology even in the case of short term and small-scale extraction projects.

CONCLUSIONS AND FURTHER INVESTIGATION

Improvements on comminution techniques and machinery is constantly on the steak, little has been achieved, however, as breakthrough.

Common practices help making the crushing and grinding circuits more effective like taking the fines out of the system, changing equipment to more efficient and adding and combining different phenomenon. Digital modelling helps a lot as well.

Nevertheless, for lack of well-founded theoretical bases most of this work lays on experiments and practices. It seems that investigating other types of physical characteristics of mineral particles regarding their behaviors given by homogeneity or heterogeneity, resonance frequency and its energy level, critical breakage conditions would lead us toward a more appropriate manner of comminution. Investigation must be done to measure and define these parameters and conditions as a general and – as already has been introduced – in pilot and industrial plants.

Being appropriate means sustainable, environmentally friendly, better resource management practices including energy, water, chemical usage, that finally results in better economy.

REFERENCES

Baawuah, E., Kelsey, C.,Addai-Mensah, J., Skinner, W. (2020): Economic and Socio-Environmental Benefits of Dry Beneficiation of Magnetite Ores *(Journal of Minerals, MDPI, 2020, 10, 955)*

Borg G., Scharfe, F., Kamradt, A., (2016): High velocity comminution of massive sulphide ores by VeRo Liberator technology for more energy efficient size reduction and particle liberation*. (World Mining - Surface and Underground, 68, pp. 45-52)*

Borg, G., Scharfe, F., Lempp, C., Kamradt, A., (2020): Overcoming breakage-inefficiency by high velocity impact comminution-the VeRo Liberator technology *(World of Mining-Surface and Underground-June 2020 pp 147-156)*

Gholami, H. et al. (2020): The effect of microwave's location in a comminution circuit on improving grindability of porphyry copper deposit. *(Energy sources, part A: Recovery, utilization and environmental effects, https://doi.org/10.1080/15567036.2020.1753859)*

Jankovic, A., Ozer, C., Valery, W., Duffy, K., (2016): Evaluation of HPGR and VRM for dry comminution of mineral ores *(Journal of Mining and Metallurgy, 52 A (1) (2016) pp. 11-25)*

Komar Kawatra, S. (2006): Advances in Comminution *(Society for Mining, Metallurgy and Exploration Inc. 2006, ISBN-13: 978-0-87335-246-8, ISBN-10: 0-87335-246-7)*

Michaud, D. (2016): https://www.911metallurgist.com/blog/comminution

Weerasekara, N.S., Powell, M.S., Cleary, P.W., Tavares, L.M., Evertsson, M., Morrison, R.D., (2013): The contribution of DEM to the science of comminution *(Powder Technology 248 (2013) pp. 3-24)*

Wiegl, R.L., Li, K. (1967): A random model for mineral liberation by size reduction. - *(Transact. Soc. Mining Engineers, 238: pp. 179-189*

CONCEPTUAL INVESTIGATION ON PNEUMATIC AND MECHANICAL FLOTATION REACTOR CELLS FROM DESIGNING AND METALLURGICAL PERSPECTIVES

A. Hassanzadeh [1,*], M. Safari [2], D.H. Hoang [1], M.K. Güner [3], T. Sambrook [1], P.B. Kowalczuk [2]

[1] *Maelgwyn Mineral Services Ltd.*
*(*Corresponding author: ahassanzadeh@maelgwyn.com)*
[2] *Mintek, Minerals Processing Division*
[3] *Norwegian University of Science and Technology, Department of Geoscience and Petroleum*
[4] *Helmholtz-Institute Freiberg for Resource Technology, Department of Processing*

ABSTRACT

Re-designing pneumatic flotation cells and their industrial applications have drawn mineral processors' attention over the last three decades. However, their principal privileges over the conventional mechanical and column cells have not been yet well disclosed and clearly identified in the literature. To this end, the present paper comparatively investigates the key advantages of Imhoflot™, Jameson™, and Reflux™ flotation cells over the conventionally used mechanical and column cells from different aspects. The impact of slurry means retention time, gas hold-up, bubble size distribution, and energy dissipation rate on recovery improvement of ultra-fine particles (<20 µm) were studied for all cell types. The diagnostic results showed that Reflux™, Jameson, and Imhoflot™ functionally operate similarly based on providing intensive turbulence in the downcomer and fast kinetics rate of flotation in the separation unit. Formation of sub-micron and micron-sized bubbles, effective hydrodynamic characteristics, and low capital and operating costs were found as their major advantages over the conventionally used cells on improving the recoverability of ultra-fine particles. These cells provide greater gas-hold-up values (40-60%) over the mechanical (5-20%) and column cells (5-25%) with substantially lower power inputs. It was indicated that extremely low mean slurry retention time (i.e., 1-4 min) led to a potential enhancement on their throughputs. However, the effectiveness of these cells on selective separation and improving the grade remains uncertain in the literature.

Keywords: Pneumatic flotation cell, energy dissipation rate, gas hold-up, mean particle retention time, fine particles

INTRODUCTION

Froth flotation is a physiochemically-based technique widely applied to treat thousands of million tonnes of raw materials annually. Through the years, it has been scientifically and technically proven that conventionally used mechanical flotation cells are significantly inefficient for recovering ultra-fine (<20 µm) and coarse (>200 µm) particles, time and energy-consuming (Gaudin et al., 1931; Trahar and Waren, 1976).

As known, fine and ultrafine particles cannot be easily floated using mechanical and column flotation cells (Hassanzadeh et al., 2019). One part of this poor flotation tendency lies in particle properties, including massive surface area, rapid surface oxidation, low particle inertial force, and limited particle-bubble collision probability (Gontijo et al., 2007; Safari et al., 2017; Safari et al., 2020a). The other part relates to the cell drawbacks including the inability to produce small bubbles, short retention time for such fine particles, poor and inefficient turbulence. To overcome these obstacles, one group of researchers enlarged particle size using flocculation-flotation processes (Yin et al., 2011; Li et al., 2021), another group applied micro/nano-bubble assisted flotation (Fan et al., 2012; Chipakwe et al.,

2021), while some intensified cell turbulence (Schubert, 2008; Safari et al., 2014; Testa et al., 2017; Hoseinian et al., 2019). The last group of scientists changed the cell hydrodynamics and invented reactor-separator flotation cells creating remarkable gas hold-up, small bubble sizes, and intensive turbulences (Imhof, 2006; Jameson, 2010; Cole et al., 2020). For instance, the specific advantages of Jameson cell include short residence time, small cell size, high throughput, and high concentrate production rates. It operates with no compressed air input (self-aeration system and vacuum generated in downcomer), and the vacuum developed within the downcomer produces interactions.

Since the mine cut-off grades dropped and ore mineralogy became extremely complex, the challenge of poor floatability of ultrafine and coarse particle ranges has become a serious concern for the mining and mineral processing sector. To this end, mining companies have endeavored to adapt pneumatic flotation cells into the existing circuits by replacing the column cells mainly in the cleaning and re-cleaning stages to reduce the risk (Atkinson et al., 1993). After many successful case studies for a wide variety of ore types, pioneer mining companies recently seek new technologies for effective and selective separations of ultrafine and coarse particles. For instance, Metso: Outotec Inc. presently utilizes ConcordeTM and NovaTM Cells to recover ultrafine and coarse particles, respectively. Glencore Technology applies Jameson cell mainly for ultrafine particles coupled with Isamills and also for a broad spectrum of particle ranges. FLSmidth Inc. examines RefluxTM Flotation Cell (RFC) design for initial installation in a re-cleaning stage of copper ore for upgrading recovery of a wide range of particles (Dickinson et al., 2019). Eriez testes HydrofloatTM cell and Stack flotation reactor for improving recovery of fine and ultrafine particles and coarse ones, respectively. Maelgwyn Mineral Services Ltd focuses on the Imhoflot flotation reactor using three various designs including G (gyratory), V (vertical), and H (hybrid)-cells favourable for recovering ultrafine, coarse, and wide particle ranges, respectively. Allmineral produces AllflotTM for improving the recovery of ultrafine particles. Among these technologies, ImhoflotTM flotation reactor is the oldest and widely applied for coal, base metals, and potash industries, whereas Jameson cell has more than 500 installations across the world (mainly for the coal industry) and can be considered as the most applied one. The RFC can be considered the latest technology, first tested in fine size coal flotation (Galvin et al., 2014; Galvin and Dickinson, 2014; Dickinson et al., 2015, Jiang et al., 2016). This was followed by ion flotation (Dickinson et al., 2016; Ireland et al., 2019; Baynham et al., 2020), coarse coal flotation (Sutherland et al., 2020) and pilot-scale copper flotation (Dickinson et al., 2019). Figure 1 demonstrates these advanced technologies and the corresponding suitable particle range for each one. It is worth mentioning that such graphical description (recovery vs. particle size) can be also used for flotation rate constant versus particle size qualitatively.

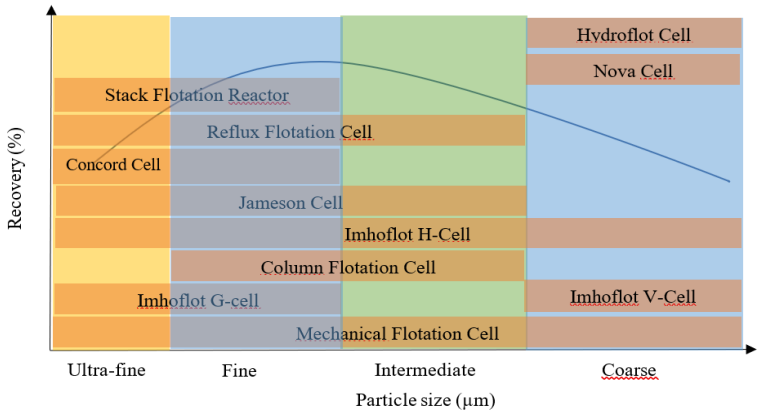

Figure 1. A schematic overview of conventionally and newly applied flotation cells

Imhoflot^{TM}, Jameson^{TM} and Reflux^{TM} are considered more complicated than the older flotation technologies i.e., mechanically agitated and column cells. It should not be forgotten that in the 1930s the Denver flotation cell was considered revolutionary and only in the 1950s using mechanical cells

became a norm. A similar story for column flotations appears from the early 1960s, however, it was only around the 1980s that a huge interest and demand started. Although pneumatic flotation machines e.g., Imhoflot™, and Jameson cell were invented in the 1980s, their application in mining industries compared to mechanical cells has still been limited for some reasons. Detailed information regarding each cell and a historical overview is given elsewhere (Moore, 2021; Mondal et al., 2021; Hassanzadeh et al., 2021a). The present work identifies some of the key characteristics of such cells and compares them with the conventional ones.

Five flotation cell types are considered in this research study: two conventional cells as mechanically agitated and column cells and three pneumatic flotation vessels i.e., Imhoflot™, Jameson Cell, and Reflux™ flotation cells. Five fundamental operating properties consist of energy dissipation rate (a.k.a turbulence kinetic energy), slurry mean residence time, gas hold-up, and bubble size distribution were conceptually and comparatively studied in detail. Since there is little information regarding the pneumatic flotation cells, the present work aims at fulfilling this gap in the literature. A conceptual description of such cells was proposed, and the crucial influential factors were analyzed in comparison with the conventionally used mechanical and column flotation cells. We believe this paper is one of the first attempts in compiling recent developments in flotation cell technologies and opens several avenues for their developments.

MATERIALS AND METHODS

Residence Time Distribution (RTD) Measurement

A laboratory Imhoflot™ V-20 flotation reactor was subjected to the RTD measurement using NaCl as a tracer. An approximate 30-50 L of water was localized in the conditioning tank before feeding the cell. Circulating water through the tank and the cell was stabilized by monitoring the feed and tailing pump speeds/flow rates to reach a steady-state condition. Noteworthy, the cell was operated in an open-circuit mode (without re-circulation) in the absence of any reagents. Afterwardes, a pre-prepared 30 mL of highly concentrated NaCL was injected into the aerator while feeding a water flow rate of 5 L/min and aeration rate of 3 L/min. A series of time-wised samples were taken from the tailing stream and their conductivity and pH were measured afterward. The obtained data were analyzed through an in-house developed software using N-Mixer and Wellller models as described elsewhere (Hassanzadeh, 2017).

Bubble Size Measurement (BSD)

A modified McGill bubble viewer was used for measuring the bubble size distribution on a pilot-scale Imhoflot™ H-16 cell. To this end, while the cell was operated by processing water, a bubble sampling tube was positioned at a specific location within the separator tank after ensuring the cell works in a steady-state condition. The measurements were performed in the absence of any frother because of having residual chemical reagents in the recirculating water. Sampled bubbles were monitored and filmed on the viewing chamber and later analyzed with the image processing toolbox of the Matlab software. The size of approximately 2000-3000 bubbles was measured and statistically analyzed. More detailed information regarding the setup can be found elsewhere (Hoang et al., 2019).

Impact Of Key Parameters

Mean Residence Time (MRT)

Slurry retention time determines the number of flotation cells and stages in a circuit required to reach a desirable grade-recovery curve. This term is typically measured by radioactive, pH, and conductivity tracers to monitor slurry/liquid discharge in open- and closed-circuits. Measuring MRT for

the mechanical and column cells in pilot and industrial scales has been broadly reported in the literature. The typical mean residence time for a mechanical cell circuit is ca. 4-20 min at the rougher stage, depending on the mineral type and the number of cells in a bank, and up to 30 min for scavengers, while for the flotation column is in the range of 18-23 min, depending on the column design (Metso, 2006). Yianatos et al. (2017) measured and modelled the residence time distribution (RTD) of industrial cells from seven flotation plants. The results showed that the RTD ranged from 9 to 41 min. The large and small tanks in series (LSTS) and two parallel perfect mixers models could reasonably represent the experimental data compared to the axial dispersion and perfect mixer (PM) models. Kennedy (2008) stated that a column cell typically requires approximately twice the residence time of a 4-cell bank of conventional cells and three times the residence time of a batch laboratory flotation cell.

It is clear that the conventional cells need long retention times to achieve an acceptable selective separation for fine and ultrafine particles. However, pneumatic-type cells show fast flotation kinetics rates due to short residence time. This is a highly critical factor for fine particles due to being oxidized through time rendering physicochemical reactions on the particle surfaces and reducing their hydrophobicities/floatabilities (Pokrajcic et al., 2020). Short residence time allows high throughput and the replacement of few cell numbers instead of several conventional cells. For instance, Harbort et al. (1997) reported the reduction in MRT of a mechanical rougher-scavenger (17.9 min) and cleaner-scavenger (30 min) circuits down to 7.5 min and 2.5 min using Jameson cells with identical flotation performances. Table 1 presents several industrial examples of Jameson flotation cell for various operating circuits reducing the number of mechanically used flotation cells (Moore, 2021). Figure 2 exhibits the liquid residence time measurement results performed on a laboratory IFR operated in a continuous mode illustrating MRT of 2.6 min. Detailed information regarding the experimental procedure and modeling will be presented in the extended version of this paper.

In the case of the RFC, one of the studies showed that residence time in the downcomer shorter than 1 s could be achieved (Jiang et al., 2019). It was considered a reasonable assumption for three reasons: i) particle collection was achieved mainly in the high shear zone within the downcomer, ii) the RFC was operated without a conventional froth zone, which was associated with particle detachment, and iii) very short cell residence times of <60 s were reported typically (Jiang et al., 2014; Dickinson et al., 2015; Jiang et al., 2019). The liquid residence time in the system ranged between 16–26 s, and the cell residence time was ranged between 23-48 sec. The cell residence time provided was calculated based on the volume of the RFC (~16 L) and all volumetric inlet flows (Cole et al., 2021). Given the system isoperated under flooding conditions, the active cell volume is the entire cell, and the cell residence time equals the cell volume divided by the volumetric feed flow, giving a cell residence time of 25.2 s (Dickinson et al., 2015)

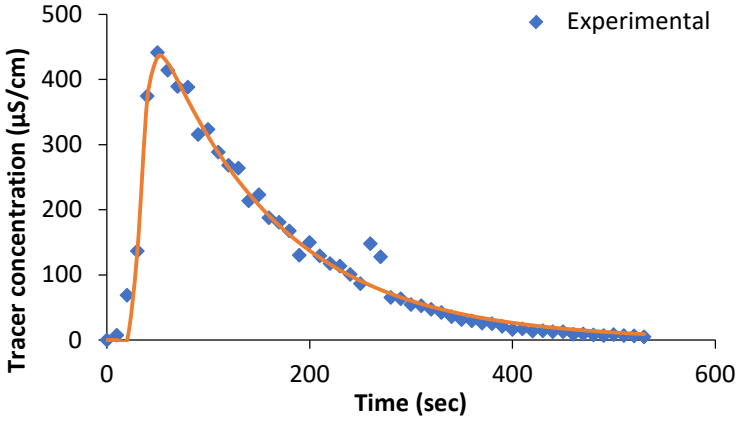

Figure 2. Presentation of RTD data experimentally measured and modeled (via the Weller model) for a V-20 (IFR cell) at feed and air flowrates of 5 L/min and 3 L/min

Table 1. Industrial installations of JFC for reducing the number of mechanical flotation cells (MFC) (Moore, 2021)

Concentration plant	Number of cells	Replacement
Hudbay's New Britannia	4	11 MFC
Philex Cu-Au mine	10	50 MFC
Ozernoye zinc mine	19	63 MFC

Bubble Size Distribution (BSD)

Bubble size distribution plays a crucial role in the particle-bubble interaction of flotation processes and significantly impacts the flotation rate and recovery of fine and ultrafine particles. As broadly reported, fine and ultrafine particles require small bubbles (micro and sub-micron-sized bubbles) to be recovered efficiently (Hassanzadeh et al., 2016; Farrokhpay et al., 2021). Figure 3 presents an approximative visualization of bubble ranges typically observed in the given cells. These ranges can vary slightly depending on the operating conditions, frother type and dosages, slurry temperature, particle properties, and mono and multivalent ions in the cell (Vazirizadeh et al., 2016; Safari et al., 2019). As seen, conventional flotation cells (i.e., MFC and column flotation cell (CFC)) cannot produce bubble diameters smaller than 0.5 mm due to their natural bubble generation mechanisms. Recently, Zahab Nazouri et al. (2021) stated that there is no unique and promising model to be used for predicting the bubble size in a column flotation cell based on the sparger orifice size and other hydrodynamic factors. Further, the Tate equation was found inapplicable for the column cells, which was in line with the results of formerly reported studies (Cho and Laskowski, 2002; Hernandez-Aguilar et al., 2006).

In contrast with MFC and CFC, reactor-separator-type cells, where the particle-bubble collision and attachment occur in a downcomer, generate a massive number of bubbles with a diameter of 0.1-0.7 mm. For example, Figure 4 demonstrates the BSD of a laboratory V-cell (one type of IFR) manifesting a 0.1-0.4 mm domain for the generated bubbles. The cavitational mechanism created by the Venturi tube and specific nuzzle designs generates such micro-bubbles. Almost the same concept is valid for JFC supplying an enormous number of small bubbles with a diameter of 0.2-0.7 mm (Harbort et al., 2002). It is worth noting that most of the methods utilized for measuring the BSD have been performed in a 2-phase (liquid-gas) system and ex-situ, while an accurate technique applicable in dynamic, in-line, and at a 3-phase (liquid-solid-gas) environment is substantially required. Broadly applied approach for measuring BSD is the photographic and optical techniques, while more detailed information regarding different approaches is given elsewhere (Khoshdast et al., 2022). Generally, there is limited practical data in the literature concerning the bubble size distributions performed in such cells, and further experimental data is required.

In the case of the Reflux flotation cell, at the highest feed-to-gas flux ratio of 9.1, the bubble diameters were remarkably small, approaching a mean value of 0.37 mm at a feed flux of 15.4 cm/s. These micro-bubbles were observed to be only a small portion of the overall population of bubbles. Hence, the reported diameters were a conservative overestimate of the mean bubble diameters, and the actual mean diameters were found slightly smaller. The bubble surface flux increased to an extraordinary 600 s^{-1}, based on a mean bubble diameter of 0.55 mm, while the underflow liquid flux was 9.5 cm/s and bubble surface flux between 178 - 600 s^{-1} (Jing et al., 2014). The bubble size at the end of the downcomer for an ion flotation process, and the top size of the bubbles for the lower two jo/jg ratios were declared around 0.74 mm (Baynham et al., 2020).

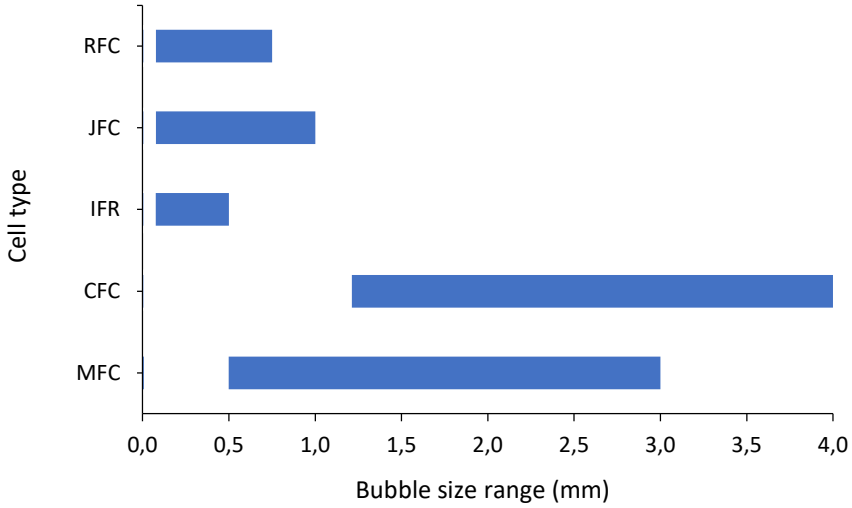

Figure 3. A demonstrative graph of the bubble size range for five types of flotation cells

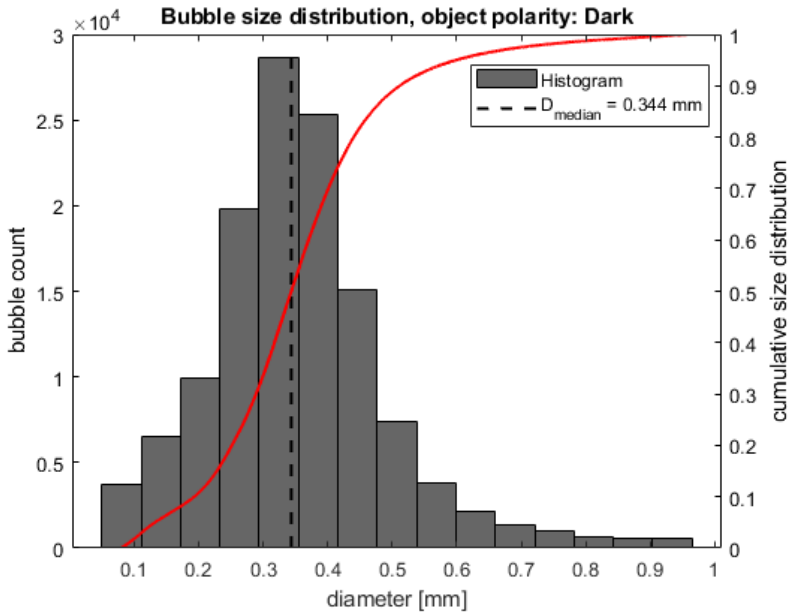

Figure 4. A typical bubble size distribution generated using Imhoflot™ H-16 cell (one type of IFR) by a modified McGill bubble size viewer (in a feldspar flotation plant, using process water without adding reagents (airflow rate=15 m^3/h, feed rate=66 m^3/h, feed pressure 2.02 bar)

Gas Hold-Up and Energy Dissipation Rate

Gas hold-up ($\varepsilon_{g,\%}$), the volume fraction of the mixture occupied by gas at any point in a flotation cell, is a critical hydrodynamic parameter in all flotation cells. This parameter is dependent on the magnitude of the gas flow rate, size and number of bubbles, frother type, and dosage (Miskovic, 2011). It has been commonly calculated by a drift-flux technique i.e., measuring the pressure difference between two tapping points and changing the measurement points through the flotation cell height to obtain the ε_g profile (Diaz-Penafiel and Dobby, 1994). This value for the mechanical and column cells is limited to 5-20% and 5-25%, respectively while exceeding these ranges leads to an undesirable turbulent and non-bobbly flow regime.

It has been widely reported that fine and ultrafine particles require intensive turbulence to reach desirable particle-bubble collision efficiency, which is predominantly controlled by the hydrodynamic properties of the cell (Schubert 2008; Kouachi et al., 2017). The typical energy input used in industrial mechanical cells (a.k.a. tank cells) ranges from 0.6-3 kW/m^3 (Deglon et al., 2000; Safari et al. 2016), although energy levels of up to 12 kW/m^3 are reported for fine particle applications. By enlarging the flotation cell volume, most of the energy is consumed for suspending the slurry than maximizing the particle-bubble interactions (Hoang et al., 2019). For example, it was shown that cells with a volume of higher than 300 m^3 reduce the specific energy input of 0.5-0.7 kW/m^3, which is 1 kW/m^3 for smaller cells. Mechanical cells have an inherently inhomogeneous distribution of energy input through the cell, with high energy input found near the impeller and much lower levels in the bulk of the cell (Koh and Schwarz, 2003). The fact that the processes of particle suspension, bubble break-up, and energy generation are all interdependent makes it difficult or impossible to optimize the conditions for flotation (Schubert, 2008). Despite these weaknesses, the robustness of the design has meant that mechanical cells overwhelmingly dominate in industrial applications, despite competition from several other cell technologies. There is little quantitative information regarding the energy consumption of reactor-separator flotation cells. Nevertheless, the energy level is significantly low due to having no moving parts (agitators) and more minor scales (in the order of ca. 5) compared to the mechanical and column flotation cells.

CONCLUSIONS

The present work demonstrates the role of four key parameters of flotation cells (i.e., slurry retention time, bubble size distribution, energy dissipation rate, and gas hold-up) in the floatability of minerals by categorizing them into two classes i.e., conventional (mechanical and column) and reactor-separator (Imhoflot™, Jameson, and Reflux™) flotation cells. The comparative outcomes are summarized in Table 2. The results showed that JFC, IFR, and RFC are principally operated similarly with slight differences. Their key advantages over the mechanical and column cells were fast flotation kinetics, low residence time, high gas hold-up, intensive turbulence in the downcomer, small bubble sizes, low capital and operating costs, small scales, and low maintenance.

Table 2. Summarized data for all studied cells considering their key parameters

Cell type	MFC	CFC	RFC	IFR	JFC
Cell residence time (MRT, min)	4-20	9-41	1-4	1-4	1-5
Superficial gas velocity (Jg, cm/sec)	0.7-2.7	2.3-4.8	1-5	0.1-0.7*	0.5-4
Gas hold-up (ε_g, %)	5-20	5-25	45-70	30-70	40-60
Bubble surface area flux (S_b, s^{-1})	50.7 (5.7-178.2)	UN**	100-200	10-90	55
Aeration pressure (psi)	3-17	22-94	90	0	0
Carrying capacity (g/min/cm^2)	1	1.27	UN	UN	2.77
First installation	1930s	1960s	2020s	1980s	1980s
BSD (mm)	0.7-3.0	1.5-3.0	0.3-0.7	0.1-0.3	0.3-0.7
Wash water	Yes (re)-cleaner	Yes	Yes	No	Yes
Energy input (kW/m^3)	1-5	UN	UN	0.5-1.5	1-2
Moving parts	Yes	No	No	No	No
Common application	Rougher-Scavenger	Cleaner	Cleaner	Cleaner	Cleaner
Throughput	High	Mid	Mid	High	High
Footprint	High	Mid	Small	Small	Small
Froth depth	Low	High	Mid	Mid	Mid

Mixing intensity	Mid	Low	High	High	High
Scale-up factor	Yes	Yes	No	No	No
Largest size (m^3)	680	110	0.1	66	40
Installed power (kW)	515	110	UN	UN	215***

* In the separator part of the cell, and the value is ca. 10-70 cm/s within the downcomer.
** UN: unknown
*** Power consumption by pumps

ACKNOWLEDGMENT

This study was performed and financially supported by The European Union's Horizon 2020 research and innovation program under grant number of 958307 (HARARE project). Authors M.K. Güner and P.B. Kowalczuk thank all partners (EIT RawMaterials, FLSmidth, KGHM, Solvay and IVL) of the project RFC-Upscaling: New Reflux Flotation Cell Technology Upscaling for Ore Flotation for our ongoing collaboration.

REFERENCES

Atkinson, B.W., Griffin, P.T., Jameson G.J., Espinosa-Gomez, R. (1993). Jameson cell Test work on copper streams in the copper concentrator of Mount Isa mines Limited, XVIII International Mineral Processing Congress, AusIMM, 23-28 May.

Baynham, S., Ireland, P., and Galvin, K.P. (2020). Enhancing ion flotation through decoupling the overflow gas and liquid fluxes, Minerals, *10(12)*, 1–17. https://doi.org/10.3390/min10121134

Chipakwe, V., R. Jolsterå, and Chelgani, S.C. (2021). Nanobubble-assisted flotation of apatite tailings: Insights on beneficiation options, ACS Omega, 6, 13888-13894. DOI: 10.1021/acsomega.1c01551

Cole M.J., Dickinson J.E., Galvin K.P. (2020). Recovery and cleaning of fine hydrophobic particles using the Reflux™ Flotation Cell, Separation and Purification Technology *240*, 116641. Doi: 10.1016/j.seppur.2020.116641.

Cole, M. J., Galvin, K.P., and Dickinson, J.E. (2021). Maximizing recovery, grade and throughput in a single stage Reflux Flotation Cell, Minerals Engineering, 163. 106761. https://doi.org/10.1016/j.mineng.2020.106761

de F. Gontijo, C., Fornasiero, D., Ralston, J. (2007). The limits of fine and coarse particle flotation, The Canadian Journal of Chemical Engineering, *85*, 739-747. https://doi.org/10.1002/cjce.5450850519

Deglon, D.A., Egya-Mensah, D., Franzidis, J.P. (2000). Review of hydrodynamics and gas dispersion in flotation cells on South African platinum concentrators, Minerals Engineering, 13(3), 235-244. https://doi.org/10.1016/S0892-6875(00)00003-0

Diaz-Penafiel, P. and Dobby, G.S. (1994). Kinetic studies in flotation columns: Bubble size effect, Minerals Engineering, *7(4)*, 465-478. https://doi.org/10.1016/0892-6875(94)90159-7

Dickinson, J., Dabrowski, B., Lelinski, D., Christodoulou, L., Galvin, K. (2019). Pilot trial of a new high rate flotation machine, Procemin Geomet, Santiago, Chile.

Dickinson, J.E., and Galvin, K.P. (2014). Fluidized bed desliming in fine particle flotation–part I. Chemical Engineering Science, *108*, 283-298. https://doi.org/10.1016/j.ces.2013.11.006

Dickinson, J.E., Jiang, K., and Galvin, K.P. (2015). Fast flotation of coal at low pulp density using the Reflux Flotation Cell, Chemical Engineering Research and Design, *101*, 74–81. https://doi.org/10.1016/j.cherd.2015.04.006

Dickinson, J.E., Neville, F., Ireland, P.M., and Galvin, K.P. (2016). Uncoupling the inherent bubble-liquid hydrodynamics of conventional Ion flotation using reflux flotation. Chemeca 2016: Chemical Engineering-Regeneration, Recovery and Reinvention, 100.

Fan, M., Zhao, Y., and Tao, D. (2012). Fundamental studies of nanobubble generation and applications in flotation. Separation Technologies for Minerals, Coal and Earth Resources, 459-469.

Farrokhpay, S., Filippov, L., Fornasiero, D. (2021). Flotation of Fine Particles: A Review, Mineral Processing and Extractive Metallurgy Review, *42(7),* 473-483. https://doi.org/10.1080/08827508.2020.1793140

Galvin, K.P., and Dickinson, J.E. (2014). Fluidized bed desliming in fine particle flotation–part II: flotation of a model feed, Chemical Engineering Science, 108, 299-309. https://doi.org/10.1016/j.ces.2013.11.027

Galvin, K.P., Harvey, N.G., and Dickinson, J.E. (2014). Fluidized bed desliming in fine particle flotation–Part III flotation of difficult to clean coal, Minerals Engineering, *66*, 94-101. https://doi.org/10.1016/j.mineng.2014.02.008

Gaudin, A.M., Groh, J.O. and Henderson, H.B. (1931). Effect of particle size on flotation, AIME Technical Publications, pp. 414, 3-23.

Harbort, G.J., Manlapig, E.V., Debono, S.K. (2002). Particle collection within the Jameson cell downcomer, Mineral Processing and Extractive Metallurgy, *111(1),* 1-10. https://doi.org/10.1179/mpm.2002.111.1.1

Hassanzadeh, A. (2017). Measurement and modeling of residence time distribution of overflow ball mill in continuous closed circuit, Geosystem Engineering, *20(5),* 251-260. https://doi.org/10.1080/12269328.2016.1275824

Hassanzadeh, A., Azizi, A., Kouachi, S., Karimi, M., Celik, M.S. (2019). Estimation of flotation rate constant and particle-bubble interactions considering key hydrodynamic parameters and their interrelations, Minerals Engineering, *141*, 105836. https://doi.org/10.1016/j.mineng.2019.105836

Hassanzadeh, A., Safari, M., Hoang, D.H. (2021). Fine, coarse and fine-coarse particle flotation in mineral processing with a particular focus on the technological assessments, In Proceedings of the 2nd International Conference on Mineral Science, Online, 1–15 March 2021. https://doi.org/10.3390/iecms2021-09383

Hassanzadeh, A., Vaziri Hassas, B., Kouachi, S., Brabcova, Z., Çelik, M.S. (2016). Effect of bubble size and velocity on collision efficiency in chalcopyrite flotation, Colloids and Surfaces A: Physicochemical and Engineering Aspects, *498*, 258-267. https://doi.org/10.1016/j.colsurfa.2016.03.035

Hernandez-Aguilar, J.R., Cunningham, R., and Finch, J.A. (2006). A test of the Tate equation to predict bubble size at an orifice in the presence of frother, International Journal of Mineral Processing, *79(2),* 89–97. https://doi.org/10.1016/j.minpro.2005.12.003

Hoang, D.H., Hassanzadeh, A., Peuker, U.A., Rudolph, M. (2019). Impact of flotation hydrodynamics on the optimization of fine-grained carbonaceous sedimentary apatite ore beneficiation, Powder Technology, *345*, 223-233. https://doi.org/10.1016/j.powtec.2019.01.014

Hoseinian, F.S., Rezai, B., Kowsari, E., Safari, M. (2019). Effect of impeller speed on the Ni(II) ion flotation, Geosystem Engineering *22(3)*, 161-168. https://doi.org/10.1080/12269328.2018.1520651

Imhof, R. US Patent No. 7,108,136 B2, Pneumatic Flotation Separation Device, application filed 19. March 2001; published 19. Sept. 2006.

Ireland, P. M., Neville, F., Dickinson, J.E., and Galvin, K.P. (2019). Enhancing extraction in ion flotation using the boycott effect, Chemical Engineering and Processing-Process Intensification, *145*, 107678. https://doi.org/10.1016/j.cep.2019.107678

Jameson, G.J., New directions in flotation machine design (2010). Minerals Engineering, *23*, 11–13, 835-841. https://doi.org/10.1016/j.mineng.2010.04.001

Jiang, K., Dickinson, J.E., and Galvin, K.P. (2019). The kinetics of fast flotation using the Reflux Flotation Cell, Chemical Engineering Science, *196*, 463–477. https://doi.org/10.1016/j.ces.2018.11.012

Jing, K., Dickinson, J. E., and Galvin, K.P. (2014). Maximizing bubble segregation at high liquid fluxes. Advanced Powder Technology, *25(4),* 1205-1211. https://doi.org/10.1016/j.apt.2014.06.003

Kennedy, D.L. (2008). Redesign of industrial column flotation circuits based on a simple residence time distribution model, MSC Thesis, Mining and Minerals Engineering, Virginia Polytechnic Institute and State University, U.S.A.

Khoshdast, H., Hassanzadeh, A., Kowalcuk, P.B., Farrokhpay, S. (2022). Characterization techniques of flotation frothers - A review, Mineral Processing and Extractive Metallurgy Review, In press.

Koh, P.T.L., Schwarz, M.P. (2003). CFD modelling of bubble–particle collision rates and efficiencies in a flotation cell, Minerals Engineering, 16, 1055–1059. https://doi.org/10.1016/j.mineng.2003.05.005

Kouachi, S., Vaziri Hassas, B., Hassanzadeh, A., Çelik, M.S., Bouhenguel, M. (2017). Effect of negative inertial forces on bubble-particle collision via implementation of Schulze collision efficiency in general flotation rate constant equation, Colloids and Surfaces A: Physicochemical and Engineering Aspects, *517*, *20*, 72-83. https://doi.org/10.1016/j.colsurfa.2017.01.002

Li, M., Xiang, Y., Chen, T., Gao, X., Liu, Q. (2021). Separation of ultra-fine hematite and quartz particles using asynchronous flocculation flotation, Minerals Engineering, *164*, 106817. https://doi.org/10.1016/j.mineng.2021.106817

Metso (2006). Basics in Minerals Processing, Section 4 – Separations. Separations. Metso Minerals.

Miskovic, S. (2011). An investigation of the gas dispersion properties of mechanical flotation cells: an in-situ approach, PhD Thesis, Mining and Minerals Engineering, Virginia Polytechnic Institute and State University, U.S.A.

Mondal, S., Acharjee, A., Mandal, U., Saha, B. (2021). Froth flotation process and its application, Vietnam Journal of Chemistry, 2021, *59(4)*, 417-425. DOI: 10.1002/vjch.202100010

Moore, P., Flotation factors, (2021). International Mining Magazine, 36.

Pokrajcic, Z., Harbort, G.J., Lawson, V., Reemeyer, L. (2020). Benefits of high intensity flotation at the head of base metal flotation circuits, Jameson Cell-2020 compendium of Technical Papers, 378-387.

Safari, M., Deglon, D. (2020). Evaluation of an attachment–detachment kinetic model for flotation. Minerals 10(11), pp. 1–12. https://doi.org/10.3390/min10110978

Safari, M., Harris, M., Deglon, D. (2014). The effect of energy input on the flotation kinetics of galena in an oscillating grid flotation cell. In: Proceedings of XXVII International Mineral Processing Congress, Santiago.

Safari, M., Harris, M., Deglon, D. (2017). The effect of energy input on the flotation of a platinum ore in a pilot-scale oscillating grid flotation cell, Minerals Engineering *110*, 69-74. https://doi.org/10.1016/j.mineng.2017.04.012

Safari, M., Harris, M., Deglon, D., Leal Filho, L., Testa, F. (2016). The effect of energy input on flotation kinetics. International Journal of Mineral Processing, *156*, 108-115. https://doi.org/10.1016/j.minpro.2016.05.008

Safari, M., Hoseinian, F.S., Deglon, D., Leal Filho, L.S., Souza Pinto, T.C. (2020b). Investigation of the reverse flotation of iron ore in three different flotation cells: Mechanical, oscillating grid and pneumatic, Minerals Engineering, *150*, 106283. https://doi.org/10.1016/j.mineng.2020.106283

Schubert, H.J. (2008). On the optimization of hydrodynamics in fine particle flotation. Minerals Engineering, 21 (12–14), 930–936. https://doi.org/10.1016/j.mineng.2008.02.012

Sutherland, J.L., Dickinson, J.E., and Galvin, K.P. (2020). Flotation of coarse coal particles in the Reflux™ Flotation Cell, Minerals Engineering, 149, 106224. https://doi.org/10.1016/j.mineng.2020.106224

Testa, F., Safari, M., Deglon, D., Filho, L.L. (2017). Influence of agitation intensity on flotation rate of apatite particles, REM - International Engineering Journal R. Esc. Minas, *70(4),* 491-495. https://doi.org/10.1590/0370-44672017700010

Trahar, W.J., Warren, L.J. (1976). The flotability of very fine particles–a review. Int. J. Miner. Process. *3(2*), 103–131. https://doi.org/10.1016/0301-7516(76)90029-6

Vazirizadeh, A., Bouchard, J., Chen, Y. (2016). Effect of particles on bubble size distribution and gas hold-up in column flotation, International Journal of Mineral Processing, 157, 163-173. https://doi.org/10.1016/j.minpro.2016.10.005

Yianatos, J., Vinnett, L., Panire, I., Alvarez-Silva, M., Díaz, F. (2017). Residence time distribution measurements and modelling in industrial flotation columns, Minerals Engineering, 110, 139-144. https://doi.org/10.1016/j.mineng.2017.04.018

Yin, W., Yang, X., Zhou, D., Li, Y., Lü, Z. (2011). Shear hydrophobic flocculation and flotation of ultrafine Anshan hematite using sodium oleate. Transactions of Nonferrous Metals Society of China, 21(3), 652-664. https://doi.org/10.1016/S1003-6326(11)60762-0

Zahab Nazouri, A., Shojaei, V., Khoshdast, H., Hassanzadeh, A. (2021). Hybrid CFD-experimental investigation into the effect of sparger orifice size on the metallurgical response of coal in a pilot-

scale flotation column, International Journal of Coal Preparation and Utilization, https://doi.org/10.1080/19392699.2021.1960318

COPPER RAFFINATE REUSE FOR INITIAL LEACHING, A BOX-BEHNKEN DESIGN

H. Movahhedi [1], A.M. Beygian [1], E.K. Alamdari [1, *]

[1] *Amirkabir University of Technology, Dept. of Materials Science and Engineering*
*(*Corresponding author: alamdari@aut.ac.ir)*

ABSTRACT

The raffinate in hydrometallurgical processes contains remarkable amounts of acid and metal ions of the target element, the release of which causes the loss of resources and environmental problems. This study proposes a method to reuse the raffinate in the extraction process cycle as a leaching agent for the copper leaching process with considerable concentrations of iron ions. Due to cementation in the process cycle and the subsequent presence of iron ions in the raffinate solution, the parameters of acid concentration, iron concentration, and liquid/solid ratio that are expected to affect leaching recovery were considered to increase copper concentration in re-leaching. The effects of leaching parameters were investigated and optimized using the Box-Behnken of response surface methodology (RSM). The concentration of copper was determined by Atomic Absorption Spectrophotometer (AAS). In addition, the comparative features of samples before and after the leaching process were analyzed using X-ray diffraction (XRD). A maximum copper concentration of 6.17 (gr/L) can be obtained under the initial acidity of 326 (gr/kg of ore), 14 (gr/L) of iron concentration, and 4 (cc/gr) of liquid/solid ratio at a leaching time of 1 hour.

Keywords: Copper leaching, raffinate, response surface methodology

INTRODUCTION

Copper is a precious and widely used element in various industries because of its high ductility, thermal and electrical conductivity (Wang, Zhang, et al. 2018). Nowadays, hydrometallurgical processes are used in copper extraction due to their high efficiency and advantages (Panda, Akcil et al. 2015). A raffinate is produced in a hydrometallurgical process which contains ions of the target element, heavy metals, and high concentrations of acid. Therefore, raffinate is an essential solution and needs to be reused (Das and Krishna 1996). Hydrometallurgical extraction processes consist of three steps: leaching, solvent extraction, and electrowinning. The leaching process is crucial and can be affected by various factors.

Generally, there are four types of leaching: heap leaching, in-situ leaching, tank leaching, and vat leaching, each of which has its advantages and disadvantages and is used under different conditions. Hip leaching requires less capital and consumes less energy than other methods (Saldaña, Toro et al. 2019). In situ leaching has the advantage of reducing drilling costs, and the resulting environmental pollution is reduced. This method is economically viable and highly effective for low-grade mines and reserves (Sinclair and Thompson 2015). In all leaching processes, the quality of the final product can be vitiated by the possible impurities entering the solution phase. The presence of iron in the electrowinning solution has destructive effects such as decreased efficiency, increased energy consumption, and altered cathodic copper morphology (Izadi, Mohebbi et al. 2017). As mentioned, solvent extraction is one of the main stages

of hydrometallurgical processes, and its purpose is to purify and increase the purity and concentration of the target element from the leaching solution (Rotuska and Chmielewski 2008).

After the extraction process is completed, the copper-free solution, if obtained from electrolysis, has a high concentration of iron (III) and, if obtained from cementation, has a higher concentration of iron but less iron (III). In this study, due to the presence of different amounts of iron with different capacities (generally resulting from cementation), experimental design with different levels of iron (II) and sulfuric acid concentrations, as well as liquid/solid ratio, was performed to optimize and increase the final copper concentration in order to eliminate solvent extraction and utilize direct electrolysis which will be discussed in future papers.

EXPERIMENTAL

Soil containing copper oxide (according to the results of XRD analysis, which will be discussed later) prepared from a copper mine was used as a raw material in leaching experiments. First, crushing and milling processes were performed on the soil. About 75% of the soil was in the particle size range of 140-320 microns. Then ICP MS analysis was performed to determine the amount of copper element. According to this analysis, the soil contains 3.9 percent of copper. XRD analysis was also performed to determine the phase of essential compounds, and the results are shown in Figure 1. Also, XRF analysis was performed to determine the values of other vital compounds in the soil, and the results are listed in Table 1.

Table 1. Soil compounds values based on XRF analysis report

Compound	SiO_2	CaO	Al_2O_3	MnO
wt%	32	19	5.7	6.5
Compound	MgO	Fe_2O_3	K_2O	SO_3
wt%	1.65	5.6	1.24	1.4

Leaching tests were performed on a 1-liter spherical glass reactor, the temperature of which was controlled by a water bath at 85°C, and equipped with a backflow cooler (glass condenser) to prevent solution evaporation. A mechanical stirrer was also used to mix the solutions at a constant stirring speed of 300 rpm during leaching. Laboratory raffinates were produced and used to optimize the copper concentration after the leaching. In each experiment, a solution with a volume of 750 cc and the required amount of sulfuric acid used as a leaching agent and soil according to the amount of liquid/solid ratio and Iron (II) sulfate heptahydrate to prepare the required amount of iron in the solution. At the end of each experiment, the vacuum filtration method was used to prepare the sample for analysis. The amount of copper in the samples was determined by AAS.

The Box-Behnken design module in the response surface methodology (RSM) was adopted using "Design-Expert" software to optimize the leaching process and the final copper concentration of the samples and analyze the interaction between the parameters. The three factors of acid and iron concentration and liquid/solid ratio were selected as variables, each with three different levels, all of which are listed in Table 2.

RESULTS AND DISCUSSION

According to the fit summary data obtained from "Design-Expert," shown in Table 3. , the linear model is a suitable model for statistical analysis and discussion of data.

Table 3. Fit summary

Source	Sequential p-value	Lack of Fit p-value	Adjusted R^2	Predicted R^2	
Linear	***< 0.0001***	***0.4804***	***0.8917***	***0.8416***	***Suggested***
2F	0.5121	0.4307	0.8869	0.7447	
Quadratic	0.1202	0.7460	0.9262	0.8369	
Cubic	0.7460		0.9021		Aliased

Table 2. lists the copper concentration values after 1 hour of leaching in each of the 17 operating surface compositions created by the RSM principles in the range of 2.798 to 7.237 (gr/L). The ANOVA results are presented in Table 2. Low p values for regression (P <0.001) and non-fit of the model were not significant (P> 0.05), indicating the suitability of the model. The final equation in terms of actual factors was proposed as follows:

Table 2. Experimental design and obtained results

RUN	Leaching Variables			Response
	Acid concentration (gr/kg of ore)	Fe concentration (gr/L)	liquid/solid ratio	Cu concentration (gr/L)
1	250	5	6	3.796
2	300	5	4	6.288
3	250	15	4	5.096
4	300	15	6	4.47
5	300	15	6	4.64
6	250	25	6	3.352
7	300	25	8	2.798
8	350	15	4	7.237
9	300	15	6	4.031
10	300	5	8	3.498
11	250	15	8	2.908
12	350	25	6	4.529
13	300	25	4	5.073
14	350	5	6	5.158
15	300	15	6	3.878
16	350	15	8	3.975
17	300	15	6	4.65

Table 2. ANOVA table

Source	Sum of Squares	Degree of Freedom	Mean Square	F-Value	P-Value

Model	***19.07***	***3***	***6.36***	***44.89***	***<0.0001***	***Significant***
A- Acid concentration	4.13	1	4.13	29.16	0.0001	
B- Fe concentration	1.12	1	1.12	7.88	0.0148	
C- Liquid/solid ratio	13.82	1	13.82	97.63	<0.0001	
Residual	1.84	13	0.1416			
Lack of Fit	1.33	9	0.1476	1.15	0.4804	Not significant
Pure Error	0.5117	4	0.1279			

$$Y = 4.62707 + 0.014367\ X_1 - 0.03735\ X_2 - 0.657188\ X_3 \quad (1)$$

Where Y is the response value of copper concentration, X_1, X_2, and X_3 represent the initial acidity, iron concentration, and liquid/solid ratio, respectively. The coefficient of determination R^2 for Equation (1) was 0.91, demonstrating the predicted copper concentration is in high accordance with the experiment results.

The composition of copper soil in optimal conditions before and after leaching was detected by the XRD and shown in Figure 1. As can be seen from it, the diffraction peak of tenorite (CuO), cuprite (Cu_2O), and copper (I) iron (III) oxide in the samples after leaching were distinctly weakened, indicating a large proportion of copper components was removed through reacting with the raffinate.

In addition to the above tables and statistical data, the 3D surface figure, the software's output, is attached in Figure 2.

CONCLUSIONS

In the present study, Box-Behnken, a module of RSM was used to discuss the interaction between factors in the process of recovering copper from copper soil using a 1-liter agitator reactor with the following results:

1. According to the developed statistical model, increasing the sulfuric acid and decreasing the initial iron concentration and liquid/solid ratio leads to an increase in the final concentration of copper.
2. According to the equation obtained from the model and the coefficients of the variables, the effect of liquid/solid ratio reduction on increasing the final copper concentration is more significant than other variables. Also, the sulfuric acid variable has a more significant effect than the initial iron concentration.

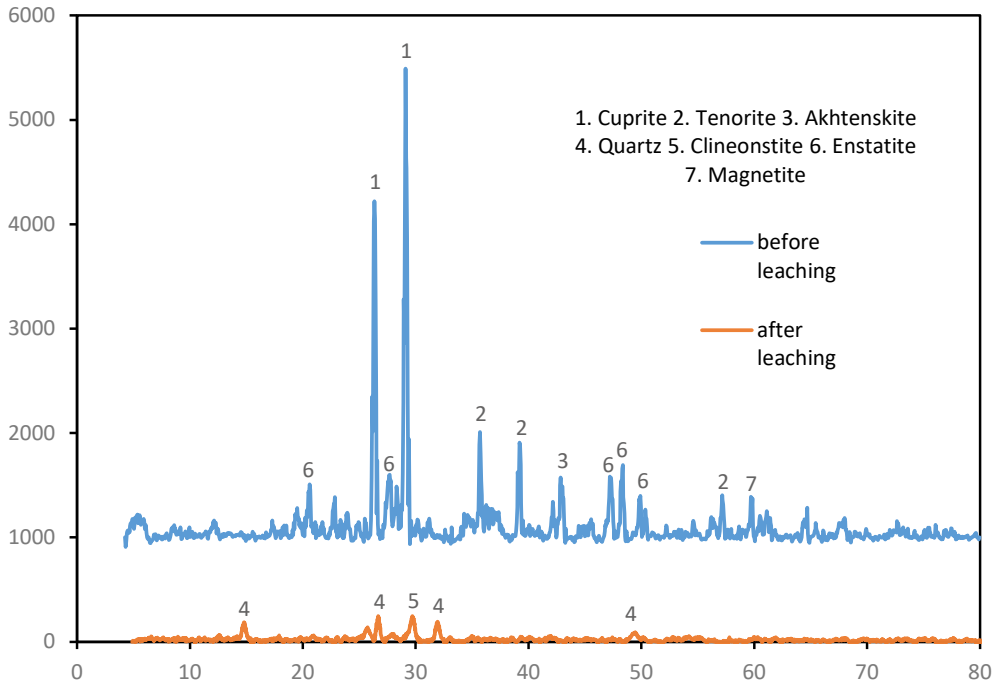

Figure 1. XRD diagram of samples before and after leaching

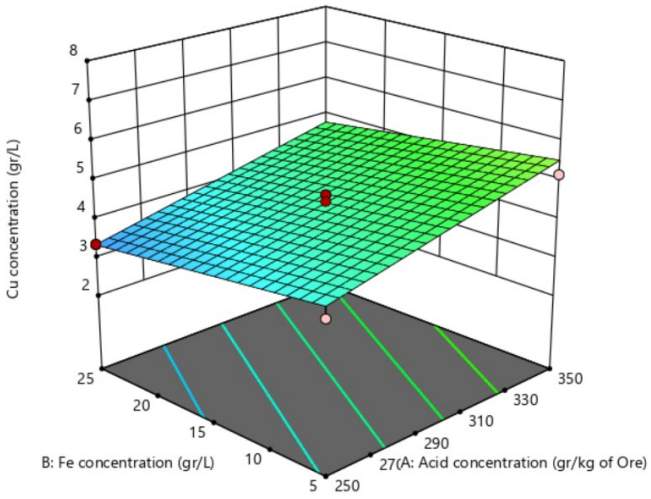

Figure 2. 3D Surface

-The effect of sulfuric acid concentration on copper recovery is more significant at low iron concentrations. Also, in a high liquid/solid ratio, the effect of acid concentration is more significant than in a low liquid/solid ratio.

-The maximum final concentration of copper that can be achieved after 60 minutes of leaching copper soil in a 1-liter reactor at a speed of 300 rpm is 7.237 (gr/L) in the following conditions: sulfuric acid: 326 (gr/kg of ore) and initial iron concentration: 14 (gr/L) and liquid/solid ratio: 4 (cc/gr).

REFERENCES

Das, S. and P. G. Krishna (1996). "Effect of Fe (III) during copper electrowinning at higher current density." *International journal of mineral processing 46***,**(1-2), 91-105.

Izadi, A., A. Mohebbi, M. Amiri and N. Izadi (2017). "Removal of iron ions from industrial copper raffinate and electrowinning electrolyte solutions by chemical precipitation and ion exchange." *Minerals Engineering 113*, 23-35.

Panda, S., A. Akcil, N. Pradhan and H. Deveci (2015). "Current scenario of chalcopyrite bioleaching: a review on the recent advances to its heap-leach technology." *Bioresource technology 196*: 694-706.

Rotuska, K. and T. Chmielewski (2008). "Growing role of solvent extraction in copper ores processing." *Physicochemical Problems of Mineral Processing 42*, 29-36.

Saldaña, M., N. Toro, J. Castillo, P. Hernández and A. Navarra (2019). "Optimization of the heap leaching process through changes in modes of operation and discrete event simulation." *Minerals 9*(7), 421.

Sinclair, L. and J. Thompson (2015). "In situ leaching of copper: Challenges and future prospects." *Hydrometallurgy 157*, 306-324.

Wang, Y., Z. Zhang, S. Kuang, G. Wu, Y. Li, Y. Li and W. Liao (2018). "Selective extraction and recovery of copper from chloride solution using Cextrant 230." *Hydrometallurgy 181*, 16-20.

CUMHURİYETİMİZİN 100. YILINDA ENERJİ HAMMADDELERİ ÜRETİMİMİZİN SPSS MODELLEMESİ İLE TAHMİNİ

PREDICTION OF OUR ENERGY RAW MATERIALS PRODUCTION IN THE 100TH ANNIVERSARY OF OUR REPUBLIC WITH SPSS MODELING

A. K. Özdoğan[1*], Y. Kinaş[2]

[1,2]Mevlana Bulvarı No:76, Beştepe/ANKARA
*(*Sorumlu Yazar: akozdogan@gmail.com)*

ÖZET

SPSS, İngilizce açılımı Statistical Package for the Social Sciences (Sosyal Bilimler İçin İstatistik Programı) olan ve Sosyal Bilimlerin yanında Fen Bilimleri vb. alanlarda, tahmin yapmak amacıyla da sıklıkla kullanılan bir bilgisayar programıdır. Program tüm yazılımlarda çalışabilmekte ve Microsoft Excel programı gibi basit ve anlaşılabilir bir görünüme sahiptir. Cumhuriyetimizin 100. Yılında Enerji Hammaddeleri Üretimimizin SPSS Modellemesi ile tahmini yapılarak geleceğe ışık tutması amacıyla toplam enerji hammaddeleri üretimi hakkında öngörüde bulunulmuştur. 2015 yılı sonrasında yaşanmış olan ölümlü kaza sayıları da değerlendirilecek olup, üretim tahmini ve yaşanabilecek ölümlü iş kazaları hakkında farkındalık oluşturmak adına değerlendirme yapılacaktır. Bu amaçla yıllara göre üretim değerleri SPSS programı ile analiz edilmiş olup değerlendirmeler yapılmıştır.

Anahtar kelimeler: Kömür, Linyit, SPSS, İSG

ABSTRACT

SPSS, which stands for Statistical Package for the Social Sciences (Statistics Program for Social Sciences) in English, and Social Sciences as well as Science and so on. It is a computer program that is frequently used in fields for making predictions. The program can work in all software and has a simple and understandable appearance like the Microsoft Excel program. In the 100th Anniversary of our Republic, our Energy Raw Materials Production was estimated with SPSS Modeling and a prediction was made about the total energy raw materials production in order to shed light on the future. The number of fatal accidents experienced after 2015 will also be evaluated, and an evaluation will be made to raise awareness about production forecasts and possible fatal occupational accidents. For this purpose, the production values according to the years were analyzed with the SPSS program and evaluations were made.

Keywords: Coal, Lignite, SPSS, OHS

GİRİŞ

Madenler hayatın her alanında kullanılmaktadır. Örneğin yaşadığımız evlerden, ulaşım için kullandığımız araçlara kadar madenlerin kullanılmadığı alan bulunmamaktadır. Türkiye dünyadaki toplam maden üretiminde 22. ve üretilen maden çeşitliliği açısından ise 8. sırada yer almaktadır.

Milyonlarca yıl önce oluşmuş bitkilerin zamanla fosile dönüşmesi ile hâkim elementi karbon olan kayaç türüne kömür denilmektedir. Kömüre dair ilk bilgiler eski Çin kaynaklarında yer almakta ve kömürü kullanan ilk toplumun Çinliler olduğu düşünülmektedir. Sömürgeleşme Döneminin sonu ve Sanayileşme Döneminin başı olan 18. Yüzyılın ikinci yarısından hemen önce insanoğlunun buhar makinesinin keşfi ile

kömür kullanımı artmıştır. Sanayileşme ile birlikte endüstri devriminin insanlığa yön vermesine sebep olmuştur. Günümüze geldiğimizde kömürün dünyada toplam görünür rezerv miktarı bir trilyon tonun üzerine çıkmıştır. Türkiye'nin toplam rezervi ise bu miktarın yaklaşık %2,1'i civarındadır. İşletilebilir rezervimiz önemli oranda linyit olup, dünya linyit üretim sıralamasında toplam üretim bakımından 1. Olan Almanya'nın ardından 2. sırada yer almaktadır. (WMD,2021) Bu bağlamda gelecek yıllardaki üretim miktarlarının tahmin edilmesi sektör paydaşlarına fikir vereceğinden önem arz etmektedir.

İşletme Ruhsat Sayıları ve Toplam Üretim Miktarlarının Genel Değerlendirmesi

Madenlerin aranması ve işletilmesi ile ilgili günümüzde yürürlükte olan 3213 sayılı Maden Kanunu gereği ruhsatlandırma süreçleri Enerji ve Tabii Kaynaklar Bakanlığı'na bağlı kuruluş olan Maden ve Petrol İşleri Genel Müdürlüğü'nce yürütülmektedir.

Maden ve Petrol İşleri Genel Müdürlüğü tarafından 31.03.2021 tarihinde yayınlanan istatistikler incelendiğinde; 3213 sayılı Maden Kanunu 2. Maddesinde alt grup olarak tanımlanmış olan arama ve işletme ruhsatlarının tamamının toplamının 14.863 olduğu, 31.03.2021 tarihi itibariyle işletme izinli olup faaliyetlerin sürdürüldüğü 7.457 ruhsat bulunmaktadır (MAPEG,2021).

Maden Kanunu 2. Maddesinde sayılan maden grupları içerisinde; "Turba, Linyit, Taşkömürü, Antrasit, Asfaltit, Bitümlü Şist, Bitümlü Şeyl, Kokolit ve Sapropel (Petrol Kanunu hükümleri mahfuz kalmak kaydıyla)" IV. Grup madenlerin (b) bendinde yer alır. Bu bent kapsamında işletme izni düzenlenmiş işletme ruhsat sayılarının toplamının 476 olup, bunların 326 tanesi linyit işletme izni düzenlenmiş işletme ruhsat sahasıdır (MAPEG,2021).

Türkiye'nin toplam kömür rezervi son yıllarda yapılan çalışmalar ile 20 milyar tonun üzerine çıkarılmış olup, rezervlerin geliştirilmesine yönelik arama faaliyetleri devam etmektedir. Üretimin yapıldığı bölgelerin genel değerlendirmesinde ise; taşkömürü üretiminde Zonguldak-Bartın bölgesi, asfaltit üretiminde Şırnak-Hakkâri bölgesi ve linyit üretiminde ise Afşin-Elbistan, Soma- Kınık, Gediz-Tavşanlı, Kale-Yatağan, Malkara- Uzunköprü, Merzifon- Osmancık, Çan-Balya, Çayırhan-Koyunağılı, Ermenek, Tufanbeyli, Orhaneli, Mengen ve Ilgın bölgeleri önemli üretim noktaları olarak öne çıkmaktadır.

Maden ve Petrol İşleri Genel Müdürlüğü tarafından 31.03.2021 tarihinde yayınlanan üretim istatistikleri incelendiğinde; Türkiye'nin son yıllardaki (2011-2020) yıllık enerji hammaddeleri üretiminde, özellikle 2018 yıllında diğer yıllara oranla daha fazla üretim yapıldığı ve yıllık ortalama üretimin 82,4 milyon bandında olduğu görülmektedir. Asfaltit özelinde üretimlerin son dört yılı incelendiğinde ise her geçen yıl üretimin arttığı görülmektedir. Taşkömürü özelinde ise üretimin son yıllarda genel olarak azalma eğiliminde olduğu gözlenmiştir. Özel sektörün linyit üretiminin ise toplam linyit üretimi içinde yaklaşık %47 ve toplam enerji hammaddeleri üretimi içinde ise %44 seviyesinde olduğu görülmektedir.

SGK tarafından yayınlanan madencilik sektöründe iş kazası sonucu hayatını kaybeden çalışan sayıları incelendiğinde; 2015 yılında 26 çalışan, 2016 yılında 11 çalışan, 2017 yılında 31 çalışan, 2018 yılında 11 çalışan, 2019 yılında 13 çalışan ve 2020 yılında 21 çalışan kömür üretim faaliyetleri sırasında hayatını kaybetmiştir (SGK,2021).

Toplam üretim miktarları esas alınarak geleceğe yönelik üretim miktarı tahmininde bulunmak enerji hammaddeleri konusunda faaliyet gösteren kamu ve özel sektör paydaşlarına fikir verecek olup, yaşanan iş kazaları sonucu hayatını kaybeden çalışanlar üzerinden değerlendirme yaparak üretim faaliyetlerinde proaktif yaklaşım için farkındalık oluşturacaktır.

YÖNTEM

Türkiye'deki linyit ve taşkömürüne ait üretim değerlerinin (bin ton) zamana göre değişimini göstermek ve ileriye dönük tahminlerde bulunabilmek amacıyla zaman serileri analiz tekniği kullanılmıştır.

Zaman Serileri Analizi

Zaman serisi analizi belirli bir zaman dilimi içerisinde gerçekleşen olayların analiz edilmesi ve ileriye yönelik bir tahminde bulunabilmek amacıyla yapılmaktadır. Zaman serileri, gözlem değerlerinin zaman içerisindeki dağılımına göre kesikli ve sürekli zaman serileri olarak ikiye ayrılmaktadır. Gözlem değerleri belirli bir zaman dilimi içerisinde sürekli elde ediliyorsa bu zaman serilerine sürekli zaman serileri denilmektedir. Kesikli zaman serilerinde ise gözlem değerleri belirli zaman aralıklarıyla elde edilmektedir.

Zaman serileri; kesikli, doğrusal ve stokastik süreç içeriyorsa Box-Jenkins modeli olarak adlandırılır. Genel doğrusal ve durağan Box-Jenkins modelleri AR, MA ve ARMA'dır. Otoregresif (AR-AutoRegressive) modeller Yule, Hareketli Ortalama (MA-MovingAverage) modeli Slutsky, AR ve MA modellerinin karışımı olan Otoregresif Hareketli Ortalama (ARMA-AutoRegressive Moving Average) modelleri ise Wold tarafından geliştirilmiştir (Ergül, 2018).

Box-Jenkins modellerinde az parametre ile zaman serisine en iyi uyan doğrusal modelin elde edilmesi amaçlanmaktadır (Hamzaçebi ve Kutay, 2004). İlk aşama modelin belirlenmesi ikinci aşama ise modelin BIC (Bayesian Bilgi Kriteri) değerine göre değerlendirmektir. En küçük BIC değerine sahip model istenen geçici model olarak belirlenir. Bu aşamalardan sonra parametrelerin ve modelin anlamlılığı test edilir. Modelin genel anlamlılığı ise Ljung-Box Q test istatistiği ile değerlendirilir. Elde edilen anlamlı model yardımıyla da ileriye yönelik tahmin yapılır (Akgül, 2003; Kadılar, 2005).

Bulgular

1973-2020 yılları arasında Türkiye'deki linyit ve taşkömürüne ait üretim değerleri (bin ton), TKİ (Türkiye Kömür İşletmeleri) ve MAPEG (Maden ve Petrol İşleri Genel Müdürlüğü) internet sayfalarından alınmıştır. Bu çalışmada linyit ve taşkömürüne ait üretim değerleri (bin ton) için zaman serileri analizi yapılarak ileriye yönelik tahmin yapılmıştır. İstatistiksel analizler için SPSS 22.0 versiyonu kullanılmıştır.

Zaman serileri analizinde kullanılan Box- Jenkins yönteminde tahmin yapılırken kullanılacak modelin belirlenebilmesi için ilk olarak zaman serisi grafiği, otokorelasyon fonksiyonu grafiği (ACF) ve kısmi otokorelasyon fonksiyonu grafikleri elde edilmiştir. Linyit ve taşkömürüne ait üretim değerleri (bin ton) grafiği Şekil 1'de verilmiştir.

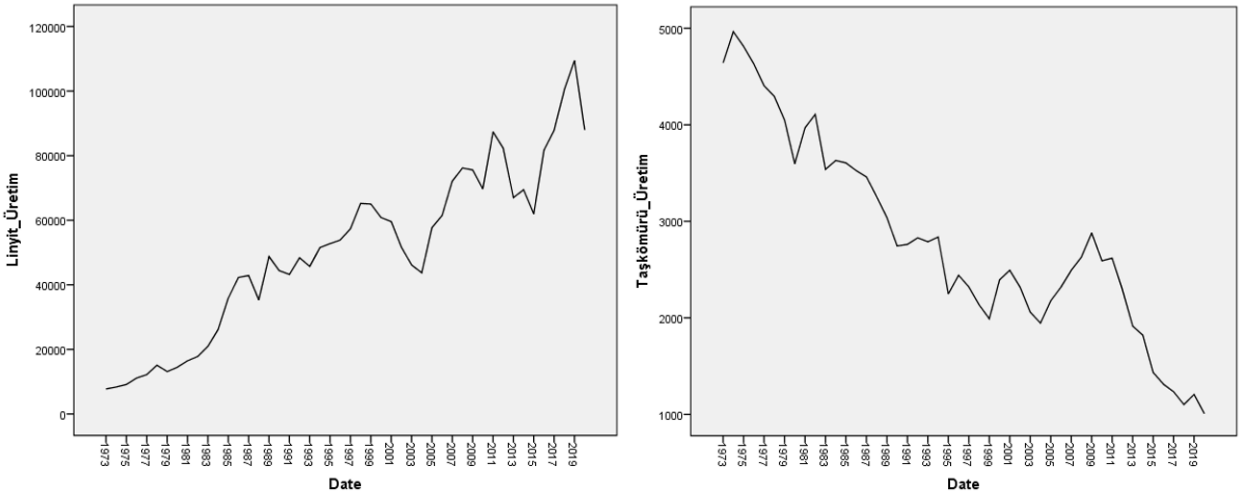

Şekil 1. Üretim değerleri (ton) grafikleri

Şekil 1'de yer alan grafik incelendiğinde grafiklerin dalgalı olduğu görülmektedir. Linyit üretim grafiği artan yönde taşkömürü üretim grafiği ise azalan yönde bir eğilim göstermiştir. Buna göre seriler durağan çıkmamıştır. Zaman serileri analizinde Box-Jenkins yönteminin kullanılabilmesi için serinin durağan olması gerekmektedir. Verilerin durağan olabilmesi için ise fark alınarak ACF ve PACF testleri yapılmıştır. Zaman serisine ait ACF ve PACF grafikleri Şekil 2 ve Şekil 3'te gösterilmiştir.

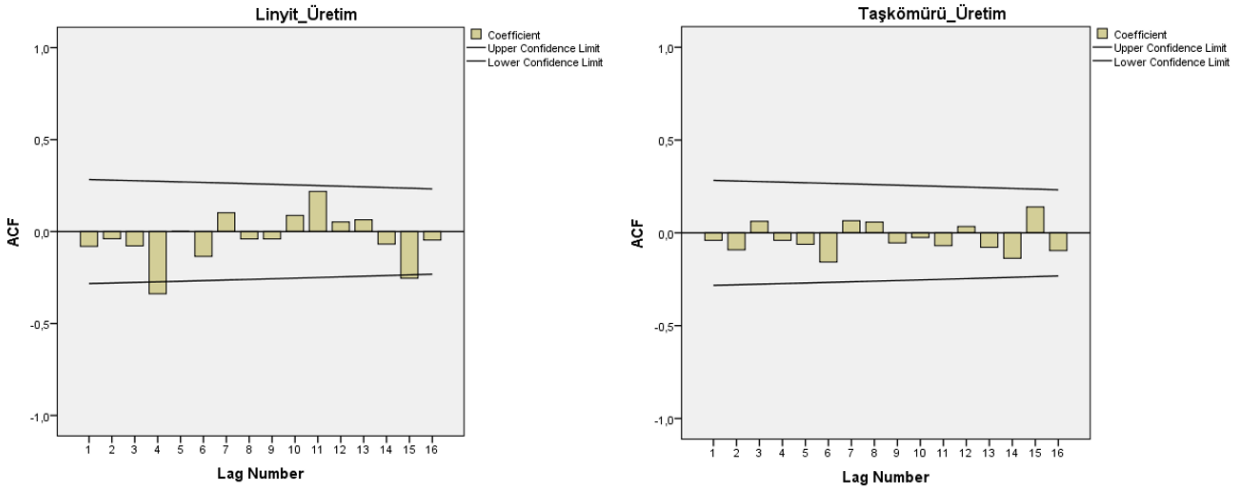

Şekil 2. Üretim değerleri (bin ton) ACF grafikleri

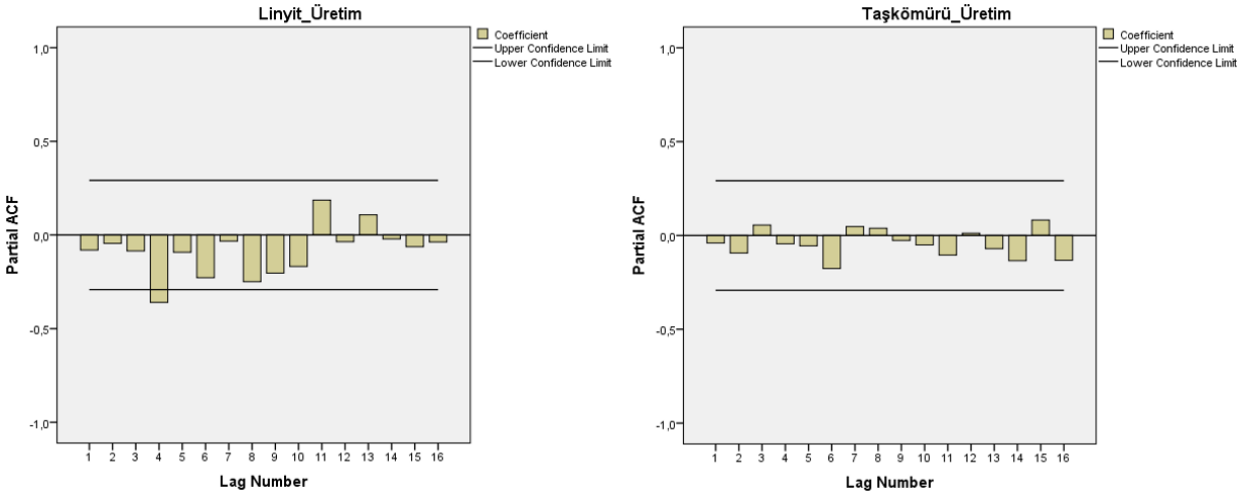

Şekil 3. Üretim değerleri (bin ton) PACF grafikleri

Şekil 2 ve Şekil 3'e göre seri durağan hale gelmiştir. Böylelikle linyit ve taşkömürü üretim değerleri (bin ton)'nin ileriye yönelik tahmin edilebilmesi için farklı ARIMA modelleri test edilmiş ve sonuçlar Çizelge 1'de yer almıştır. Çizelge 1'e göre BIC değerleri birbirine yakın çıkmıştır. Dolayısıyla bu çalışmada geçici model ARIMA (1,0,0) olarak belirlenmiştir.

Çizelge 1. Linyit ve taşkömürü üretim değerleri (bin ton) için farklı ARIMA modelleri ve BIC değerleri

Arıma Modelleri	BIC Değerleri (Linyit)	BIC Değerleri (Taşkömürü)
ARIMA (1,0,0)	18,551	11,937
ARIMA (1,0,1)	18,655	12,055
ARIMA (1,1,1)	17,997	11,103
ARIMA (0,0,1)	19,868	13,097
ARIMA (1,1,0)	18,074	11,046
ARIMA (0,1,1)	19,568	11,286

Söz konusu modelin parametre tahminlerinin anlamlılığı test edilmiştir. Bulunan değerler Çizelge 2'de gösterilmiştir.

Çizelge 2. Linyit ve taşkömürü üretim değerleri (bin ton) için ARIMA (1,0,0) parametre tahmin değerleri

	Linyit		Taşkömürü	
Parametre	**Sabit**	**AR**	**Sabit**	**AR**
Tahmin Değeri	48.480,98	0,971	2.818,24	0,988
se	29.456,67	0,038	2.279,86	0,029
t	0,646	25,393	1,236	34,655
p	0,107	0,001	0,223	0,001

Çizelge 2'ye göre hesaplanan olasılık değeri α=0,05 anlamlılık düzeyinden küçük olduğu için ARIMA(1,0,0) modelinin parametre tahminleri anlamlı çıkmıştır.

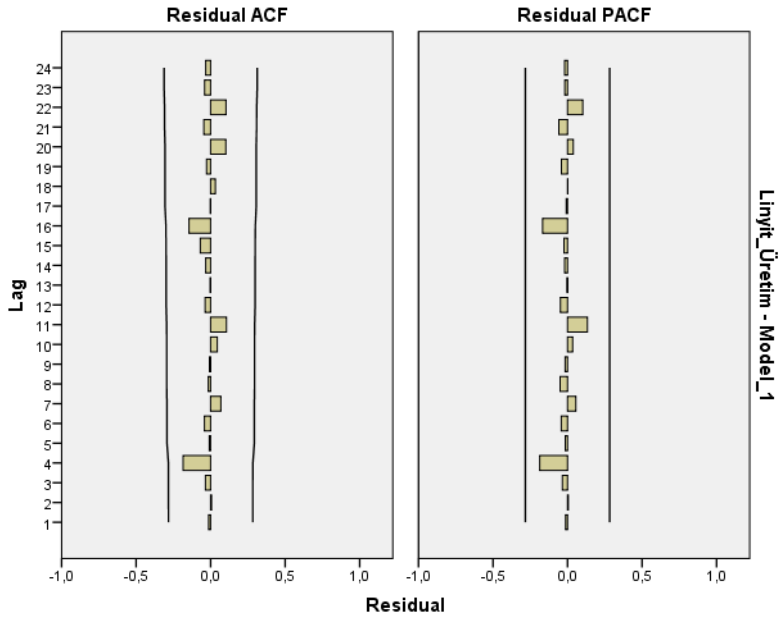

Şekil 4. Linyit ve Taşkömürü üretim değerleri (bin ton) için ARIMA(1,0,0) hata terimleri ACF grafiği

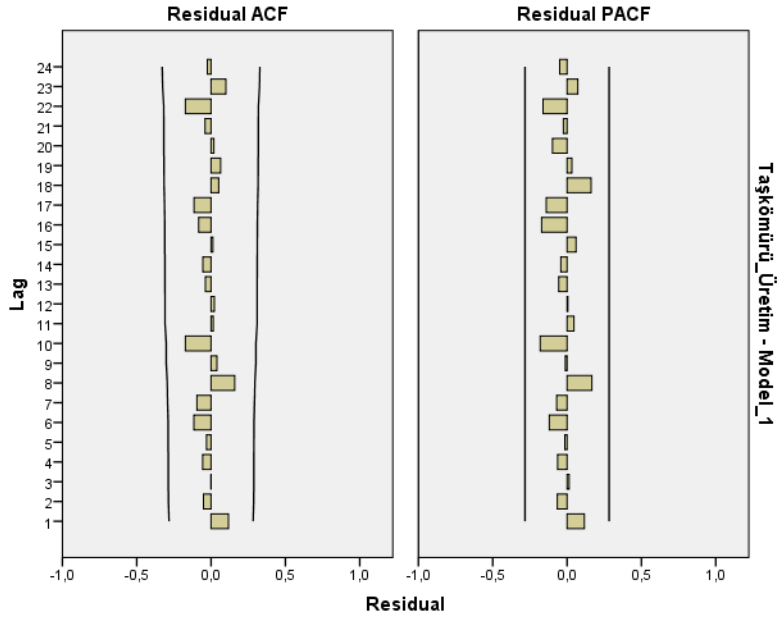

Şekil 5. Linyit ve Taşkömürü üretim değerleri (bin ton) için ARIMA(1,0,0) hata terimleri PACF grafiği

Geçici modelin uygunluğu, Ljung-Box testi ile test edilmiştir. Sonuçlar Çizelge 3'te gösterilmiştir.

Çizelge 3. Ljung-Box testi sonuçları

	Linyit	**Taşkömürü**
İstatistik Değeri	5,370	7,956
df	17	17
p	0,997	0,967

Ljung-Box testi sonucuna göre hesaplanan olasılık değerleri α=0,05 anlamlılık düzeyinden büyük olduğu için geçici model uygun bulunmuştur. Buna göre ARIMA (1,0,0) modeli kullanılarak 2021, 2022 ve 2023 yılları için tahminler yapılmış ve Çizelge 4'te gösterilmiştir.

Çizelge 4. Linyit ve taşkömürü üretim değerlerinin ARIMA(1,0,0) modeli ile tahmin değerleri

Yıl	Linyit Üretimi Tahmin Değeri (milyon ton)	Taşkömürü Üretimi Tahmin Değeri (milyon ton)
2021	110.228.000	1.050.000
2022	95.620.000	987.000
2023	102.047.000	1.102.000

SONUÇ VE ÖNERİLER

Enerji hammaddelerinin sanayi devriminde payı göz önünde bulundurulduğunda insanlığın gelişimi için geçmişte olduğu gibi günümüzde de önemi açıkça anlaşılabilmektedir. Türkiye'nin yıllık ortalama enerji hammaddeleri üretimi 82 milyon ton'un üzerinde olup son yıllarda Türkiye'de üretim miktarlarının arttığı göze çarpmaktadır.

Linyit üretim miktarlarının ARIMA ile tahmin değerleri 2021 yılında 110,22 milyon ton, 2022 yılında 95,62 milyon ton ve Cumhuriyetin 100. yılında 102,04 milyon ton olacağı tahmin edilmiştir.

Taşkömürü üretim miktarlarının ise ARIMA ile tahmin değerleri 2021 yılında 1,05 milyon ton, 2022 yılında 0,98 milyon ton ve Cumhuriyetin 100. yılında 1,1 milyon ton olacağı tahmin edilmiştir.

Toplam enerji hammaddeleri üretiminin ARIMA ile tahmin değerleri 2021 yılında 111,27 milyon ton, 2022 yılında 96,6 milyon ton ve Cumhuriyetin 100. yılında 103,14 milyon ton olacağı tahmin edilmiştir.

Son yıllarda yaşanmış olan ölümle sonuçlanmış iş kazalarının enerji hammaddeleri üretimi bakımından değerlendirilmesinde ölümlü iş kazası ortalamasının 4,6 milyon ton üretim başına 1 adet olduğu hesap edilmiştir. Üretimin 103 milyonun üzerinde olacağı tahmini göz önünde tutularak, üretimde proaktif yaklaşım ile işletmelerin geçmiş dönemde yaşanmış kazalarının oluş şekillerine göre değerlendirme yaparak tahmini üretim değerleri üzerinden oluşabilecek iş kazalarının önlenmesine ilişkin tahmin yürütmesi ve önlem alması olumlu katkı sağlayacaktır.

Bu çalışmada zaman serileri analizi yöntemi kullanılarak enerji hammaddeleri üretim miktarına ilişkin bir tahmin yapılmıştır. Dolayısıyla bu çalışmanın enerji hammaddeleri üretimine ilişkin verilerin zaman serileri analizi yöntemi ile analiz edilmesi ve buna bağlı olarak ileriye yönelik tahmin yapılması bakımından ilk çalışma olduğu söylenebilir. Çalışmada kullanılan veriler farklı madenler için araştırılarak söz konusu madenlerin geleceği hakkında geniş kapsamlı tahminlerde bulunulabilir.

KAYNAKLAR

Akgül, İ., (2003). Zaman Serileri Analizi ve ARI-MA Modelleri. Der Yayınları, İstanbul.

Ergül, B., (2018). Türkiye'deki İş Kazalarının Zaman Serisi Analiz Teknikleri ve Yapay Sinir Ağları Tekniği ile İncelenmesi*, Karaelmeas İş Sağlığı ve Güvenliği Dergisi, 2(2)*: 63-74.

Hamzaçebi, C. ve Kutay, F., (2004). Yapay Sinir Ağları ile Türkiye elektrik Enerjisi Üretiminin 2010 Yılına Kadar Tahmini. Gazi Üniversitesi Mühendislik Mimarlık Fakültesi Dergisi, 19(3).

Kadılar, C., (2005). SPSS Uygulamalı Zaman Serileri Analizine Giriş. Bizim Büro Basımevi, Ankara.

Reichl, C., Schatz, M., (2021). World Mining Data (Iron and Ferro-Alloy Metals Non-Ferrous Metals Precious Metals Industrial Minerals Mineral Fuels), Volume:36, Vienna. https://www.world-mining-data.info/wmd/downloads/PDF/WMD2021.pdf (erişim tarihi:07.12.2021)

Maden Tetkik ve Arama Genel Müdürlüğü (MTA), (2020). Kömür Arama Araştırmaları, https://www.mta.gov.tr/v3.0/arastirmalar/komur-arama-arastirmalari (erişim tarihi: 08.12.2021)

Maden ve Petrol İşleri Genel Müdürlüğü (MAPEG), (2021). Maden Üretim Değerleri, https://www.mapeg.gov.tr/maden_istatistik.aspx (erişim tarihi: 08.12.2021)

Maden ve Petrol İşleri Genel Müdürlüğü (MAPEG), 2021. Mayıs 2021 Tüm Ruhsat Listesi (yayınlanmamış).

Türkiye Kömür İşletmeleri Kurumu (TKİ), (2020). Türkiye Kömür Üretim -Tüketim İstatistikleri, https://www.tki.gov.tr/istatistikler (erişim tarihi: 08.12.2021)

Türkiye Kömür İşletmeleri Kurumu (TKİ), (2020). Dünya ve Türkiye Kömür Kaynak ve Rezerv Durumu, https://www.tki.gov.tr/istatistikler (erişim tarihi: 08.12.2021)

ÇOK OCAK İÇEREN AÇIK İŞLETMELERDE GÜVENLİK FAKTÖRÜ DEĞİŞİMİNİN İNCELENMESİ

INVESTIGATION OF THE SAFETY FACTOR CHANGE IN OPEN PIT WITH MULTI-QUARRY

C.O. Aksoy [1, *], G.G.U. Aksoy [2], H. E. Yaman [3]

[1] *Dokuz Eylül Üniversitesi Maden Mühendisliği Bölümü*

*(*Sorumlu yazar: okay.aksoy@deu.edu.tr)*

[2] *Hacettepe Üniversitesi, Maden Mühendisliği Bölümü*

[3] *Dokuz Eylül Üniversitesi Torbalı Meslek Yüksek Okulu*

ÖZET

Madencilikte her gün birçok şey değişiyor ve gelişiyor. Gelişmekte olan madencilik sektöründe, küçük madencilik alanları artık ihtiyaçları karşılayamamaktadır. Özellikle metal madenlerinde yapılan küçük ölçekli madencilik operasyonları, ekonomik çalışabilirliklerini her geçen gün kaybetmektedir. Bu nedenle günümüzde çok büyük ölçekte işletilen birçok maden sahası bulunmaktadır. Bu bildiride, birden fazla açık ocak içeren bir maden işletmesinde araştırmalar yapılmıştır. Araştırmalar, her bir açık ocağın tek başına güvenlik faktörleri ile bütün açık ocakların birlikte analiz edilmesiyle ortaya çıkan bütünleşik güvenlik faktörünün karşılaştırılması üzerine yapılmıştır. Sonuçlar incelendiğinde, bütüncül güvenlik faktörünün daha düşük olduğu görülmüştür.

Anahtar Sözcükler: Açık maden işletmesi, nümerik modelleme, şev stabilitesi, güvenlik faktörü

ABSTRACT

Many things change and develop everyday in mining. In the developing mining industry, small mining areas can no longer meet the needs. Small-scale mining operations, especially in metal mines, lose their economic operability day by day. For this reason, there are many mining sites operated on a very large scale today. In this paper, researches were conducted in a mining operation that includes more than one open pit. Research has been done on the comparison of the safety factors of each open pit alone and the integrated safety factor that is obtained by analyzing all open pits together. When the results were examined, it was seen that the overall safety factor was lower.

Keywords: Open-pit mine, numerical analysis, slope stability, Safety Factor

GİRİŞ

Açık ocak işletmelerinde şev stabilitesi ocak güvenliği için çok önemlidir. İşletme yaparken ekonomik açıdan şevleri mümkün olduğu kadar yüksek açıda tutmak, ancak güvenli sınırda olmak çok önemlidir. Bu sayede dekapaj oranı azalacak ve maden ekonomik olarak işletilebilecektir. Ama güvenlik önce gelmektedir. Bu nedenle, ocak genel şev açısı genellikle düşüktür. Ayrıca, yeraltı suyu, kaya türü, süreksizlikler vb. parametreler şev stabilitesini önemli ölçüde etkiler. Şekil 1'de şev stabilitesini etkileyen faktörler verilmiştir (Atkinson, 1977).

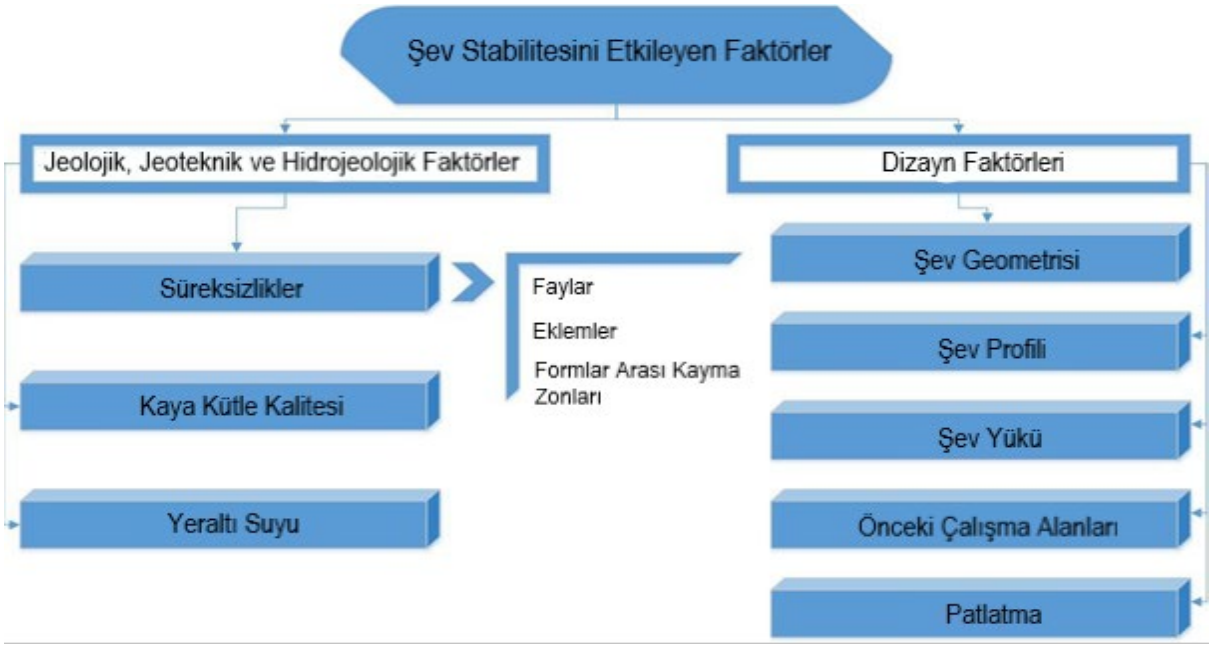

Şekil 1. Şev stabilitesini etkileyen faktörler (Atkinson, 1977)

Kaya Kütle Parametrelerinin Belirlenmesi

Kaya mühendisliğinde nihai tasarımın gerçekleştirilmesi uzun ve pahalı bir süreç gerektirir. Çalışmaların başlangıcında kaya parametrelerinin ve özelliklerinin belirlenmesi çok kritiktir. Bu amaçla bazı araştırmalar tarafından geliştirilen kaya kütle sınıflandırma sistemleri Çizelge 1'de verilmiştir (Palmström, 1995, Edelbro, 2006, Palmström ve Stille, 2007, Aksoy, 2012). Kaya kütlesinin deformasyon modülünün yerinde testlerinin, hem ekipmandan, hem test sahasının hazırlanmasından hem de test sırasında patlatma hasarından kaynaklanan ölçüm hatalarına tabi olduğu genel olarak bilinmektedir (Palmstrom ve Singh, 2001). Bu nedenle, kaya kütlesinin iyi saha karakterizasyonları ve uygun bir dolaylı yöntemin kullanılması birçok durumda pahalı yerinde ölçümlerden daha iyi sonuçlar verebilir (Palmstrom ve Singh, 2001). Mevcut deneysel veriler kullanılarak, farklı mekanik özellikler arasındaki bazı ampirik doğrudan ilişkiler ve çeşitli araştırmacılar tarafından önerilen bazı kaya kütlesi sınıflandırma parametreleri Çizelge 2'de listelenmiştir (Aydan ve diğerleri, 2014).

İnceleme alanında, mika şist, kuvars, feldspat, kalker, andezit olmak üzere 5 kaya türü hakimdir. Gerçekleştirilen analizlerde kullanılan verilerin bir kısmı tarafımıza maden sahası tarafından verilmiş olup, bir kısmı tarafımızca maden sahasından alınan sondaj numuneleri üzerinde yapılan laboratuvar analizleri ile belirlenmiştir.

Çizelge 1. Bazı kaya sınıflandırma sistemleri (Palmström, 1995, Edelbro, 2006, Palmström ve Stille, 2007, Aksoy, 2012)

İsim	**Form ve Tip***	**Ana Uygulamalar ve Açıklamalar**	**Yazar ve İlk Versiyonu**
Terzaghi kaya yükü sınıflama sistemi	Tanımlayıcı ve davranışsal form	Çelik tahkimatlı tüneller (modern tünel açma için uygun değildir)	Terzaghi (1946)
	İşlevsel tür		
Lauffer'in desteksiz durma süresi sınıflaması	Tanımlayıcı form ve Genel tür	Tünel tasarımında girdi için (muhafazakar)	Lauffer (1958)
Yeni Avustralya Tünel Açma Yööntemi (NATM)	Tanımlayıcı ve davranışsal form Tünel açma konsepti	Dayanımsız zeminlerde kazı ve tasarım için (sıkışma zemini koşullarında kullanılır)	Rabcewicz (1964, 1965)
Kaya mekaniği	Tanımlayıcı form	Kaya mekaniğine girdi için	Patching ve Coates (1968)
Zemin ve kayaların birleşik sınıflaması	Genel tür Tanımlayıcı form	Parçacıklara ve bloklara dayalı iletişim için	Deere vd. (1969)
Kaya Kalitesi Belirteci (RQD)	Genel tür Nümerik form	Karot loglamasına bağlı olarak diğer sınıflama sistemlerinde kullanılır.	Deere and Deere (1988) Deere vd. (1967)
Boyut dayanım sınıflaması	Genel tür Nümerik form	Esas olarak madencilikte kullanılan kaya dayanımı ve blok çapına göre	Franklin (1975)
Kaya Yapısı Değeri (RSR)	Fonksiyonel tür Nümerik form	Tünellerde (çelik) tahkimat tasarımı için (çelik donatılı püskürtme beton ile kullanışlı değildir)	Wickham vd. (1972)
	Fonksiyonel tür		
Jeomekanik Sınıflama Sistemi (RMR)	Nümerik form	Tünellerin, madenlerin ve temellerin tasarımı için	Bieniawski (1973)
Q Sınıflama Sistemi	Fonksiyonel tür Nümerik form	Yeraltı kazılarında tahkimat tasarımı için (tünel, geniş yeraltı açıklıkları)	Barton vd. (1974)
Madencilik RMR (MRMR)	Nümerik form	Madencilikte kaya tahkimatı	Laubscher (1975)

Tipolojik sınıflama	Fonksiyonel tür Tanımlayıcı form	İletişimde kullanım için	Laubscher (1977) Matula ve Holzer (1978)
Birleştirilmiş kaya sınıflama sistemi	Genel tür Tanımlayıcı form	İletişimde kullanım için	Wiliamson (1980)
Temel jeoteknik sınıflama (BGD)	Genel tür Tanımlayıcı form	Genel uygulamalar için	ISRM (1981)
Şev Kütle Puanlaması (SMR)	Nümerik form Fonksiyonel tür	Şevler için tahmini duraylılık problemleri ve destek teknikleri	Romana (1985)
Jeolojik Dayanım İndeksi (GSI)	Nümerik form Fonksiyonel tür	Mühendislik uygulamalarına girdi olarak kaya kütlelerinin dayanımını gösterir	Hoek (1994)
Rock Mass Index (RMI)	Nümerik form Fonksiyonel tür	Kaya mühendisliği, genel karakterizayon, tahkimat dizaynı	Palmström (1995)

*
Tanımlayıcı biçim: sisteme giriş, esas olarak açıklamalara dayalıdır;
Nümerik biçim: girdi parametrelerine karakterlerine göre nümerik değerler verilir;
Davranışsal form: girdi, bir tüneldeki kaya kütlesi davranışına dayalıdır;
Genel tip: sistem, genel bir karakterizasyon işlevi görecek şekilde tasarlanmıştır;
Fonksiyonel tip: sistem özel bir uygulama için yapılandırılmıştır (örneğin, kaya desteği için).

Çizelge 2. Kaya kütlesi sınıflandırması ile kaya kütlesinin özellikleri arasındaki doğrudan ilişkiler (Aydan vd., 2014).

Property	Empirical relation	Proposed by
Deformation modulus, E_m	$E_m = 2RMR - 100$ (GPa) (for RMR > 50)	Bieniawski (1978)
	$E_m = 10^{((RMR-10)/40)}$ (GPa)	Serafim and Pereira (1983)
	$E_m = e^{(4.407+0.081*RMR)}$ (GPa)	Jašarević and Kovačević (1996)
	$E_m = 0.0097RMR^{3.54}$ (MPa)	Aydan et al. (1997)
	$E_m = 25 \log Q$ (GPa)	Grimstad and Barton (1993)
	$E_m = \left(1 - \frac{D}{2}\right)\sqrt{\frac{\sigma_{ci}}{100}}10^{((GSI-10)/40)}$ (GPa) (for $\sigma_{ci} < 100$ MPa)	Hoek et al. (2002)
	$E_m = 100\frac{(1-0.5D)}{1+e^{((75+25D-GSI)/11)}}$ (GPa)	Hoek and Diederichs (2006)
	$E_m = 0.135\left[E_i 1 + \frac{1}{WD}\cdot\frac{RQD}{100}\right]^{1.1811}$ (GPa)	Kayabasi et al. (2003)
	$E_m = 5.6RMi^{0.3}$ (GPa) (for RMi > 0.1)	Palmström (1996)
	$E_m = 0.1(RMR/10)^3$	Mitri et al. (1994)
	$E_m = 7(\pm 3)\sqrt{10^{(RMR-44)/21}}$ (GPa)	Diederichs and Kaiser (1999)
	$E_m = 10Q^{1/3}$ (GPa)	Barton (1995)
	$E_m = 10\left(Q\frac{\sigma_{ci}}{100}\right)^{1/3}$ (GPa)	Barton (2002)
	$E_m = 10^{((GSI-10)/40)}\sqrt{\frac{\sigma_{ci}}{100}}$ (GPa)	Hoek and Brown (1997)
	$E_m = 0.0876RMR$ (GPa) (for RMR > 50)	Galera et al. (2005)
	$E_m = 0.0876RMR + 1.056(RMR - 50) + 0.015(RMR - 50)^2$ (GPa) (for RMR ≤ 50)	Galera et al. (2005)
Uniaxial compressive strength, σ_{cm} (MPa)	$\sigma_{cm} = 0.0016RMR^{2.5}$	Aydan et al. (1997)
	$\sigma_{cm} = 5\gamma\left(Q\frac{\sigma_{ci}}{100}\right)^{1/3}$	Barton(2002)
Friction angle, ϕ_m (°)	$\phi_m = 20 + 0.5RMR$	Aydan and Kawamoto (2001)
	$\phi_m = 20\sigma_{cm}^{0.25}$	Aydan et al. (1993)
	$\phi_m = \tan^{-1}\left(\frac{J_r}{J_a}\times\frac{J_w}{1}\right)$	Barton (2002)
Cohesion, c_m (MPa)	$c_m = \frac{\sigma_{cm}}{2}\frac{1-\sin\phi_m}{\cos\phi_m}$	Aydan and Kawamoto (2001)
	$c_m = \left(\frac{RQD}{J_n}\times\frac{1}{SRF}\times\frac{\sigma_{ci}}{100}\right)$	Barton (2002)
Poisson's ratio, v_m	$v_m = 0.25(1 + e^{-\sigma_{cm}/4})$	Aydan et al. (1993)
	$v_m = 0.5 - 0.2\frac{RMR}{RMR+0.2(100-RMR)}$	Tokashiki and Aydan (2010)

E_m Kaya Kütlesi Deformasyon Modülü, E_i Sağlam Kaya Young Modülü, *RMR* Kaya Kütlesi Oranı, *Q* Kaya Kütle Kalitesi, *GSI* Jeolojik Dayanım İndeksi, *D* Bozulma Faktörü, σ_{ci} Sağlam Kayanın Tek Eksenli Basınç dayanımı, σ_{cm} Kaya Kütlesinin Tek Eksenli Basınç Dayanımı, *RQD* Kaya Kalitesi Göstergesi, *RMi* Kaya Kütle İndeksi, *WD* Ayrışma Derecesi, m Kaya Kütlesinin Sürtünme Açısı, c_m Kaya Kütlesinin Kohezyonu, v_m Kaya Kütlesi Poisson'un Oranı, J_n Eklem Seti Sayısı, J_r Eklem Pürüzlülük Derecesi, J_w Eklem Suyu Derecesi, J_a Eklem Alterasyon Derecesi, *SRF* Gerilme Azaltma Faktörü, *d* Kaya Yoğunluğu (t/m^3)

Nümerik modelde kullanılan kaya parametreleri Tablo 2'deki formüllerden yararlanılarak belirlenmiş ve Çizelge 3'te verilmiştir.

Çizelge 3. Nümerik modelde kullanılan kaya parametreleri

Kaya Türleri	d (kN/m^3)	σ_c (MPa)	Ø (°)	v	c (kPa)	E_m (MPa)
MİKA ŞİST	22,80	10,67	16,71	0,25	273	405,96
FELDSPAT	22,75	20,87	22,75	0,20	414	525,87
ANDEZİT	23,61	18,53	22,62	0,22	667	553.20
KALKER	22,30	7,04	24,34	0,27	234	524.90
KUVARS	23,84	7,49	24,08	0,25	264	480.92

Nümerik Modelleme Analizi

Bu çalışmada birbirine yakın konumlanmış üç farklı açık ocağın ayrı ayrı nümerik modelleme analizi yapılmıştır. Ayrıca, tüm bu üç açık ocağı kapsayan bir nümerik modelleme analizi yapılmış ve

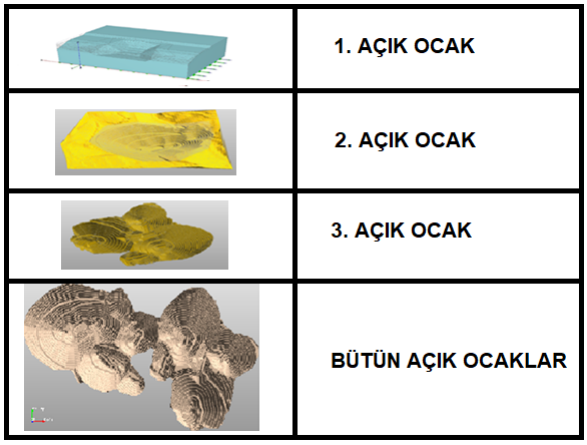

Şekil 2. Şevlerin durumu

1. Açık Ocak mikaşist, 2. Açık Ocak volkanik kaya, metamorfik kaya ve intruzif kaya, 3. Açık Ocak ise QFP ve mikaşistlerden oluşmaktadır. Şev stabilitesi analizlerinde kullanılan nümerik modelleme yazılımı "Sonlu Elemanlar Metodu" ile çalışmakta olup, 3B çözümleme yapılmıştır. Sonlu Elemanlar Yöntemi, matematiksel olarak geliştirilen ilk yöntem olduğu için diğer yöntemlerden çok daha iyi performans göstermektedir. Nümerik modelleme analizlerinde Mohr-Coulomb Yenilme Kriterleri kullanılmıştır.

Analizler genel olarak 3 aşamada gerçekleştirilmiştir, Birinci aşama, başlangıç aşaması olup, gravite yüklemesi ile başlangıç koşullarının oluşturulduğu aşamadır. İkinci aşama tüm kazı aşamalarının (her bir açık ocaktaki basamak sayısına göre alt aşamalar içermektedir) yapıldığı aşama ve , üçüncü aşama ise c-Phi yöntemi ile güvenlik faktörünün belirlendiği aşamadır. Açık Ocak 1 (Şev 1), Açık Ocak 2 (Şev 2), Açık Ocak 3 (Şev 3) ve Tüm Açık Ocaklar (Tüm Şevler) için nümerik modelleme sonuçları Şekil 3 ve Şekil 4'te verilmiştir.

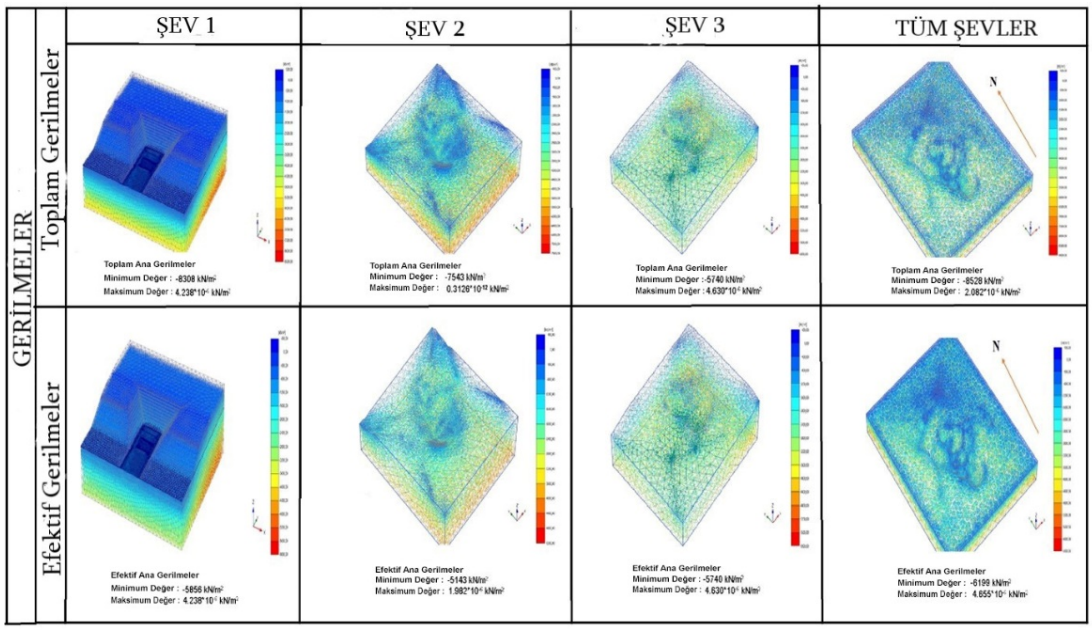

Şekil 3. Tüm nümerik model analizinin sonuçları (toplam ve efektif gerilmeler)

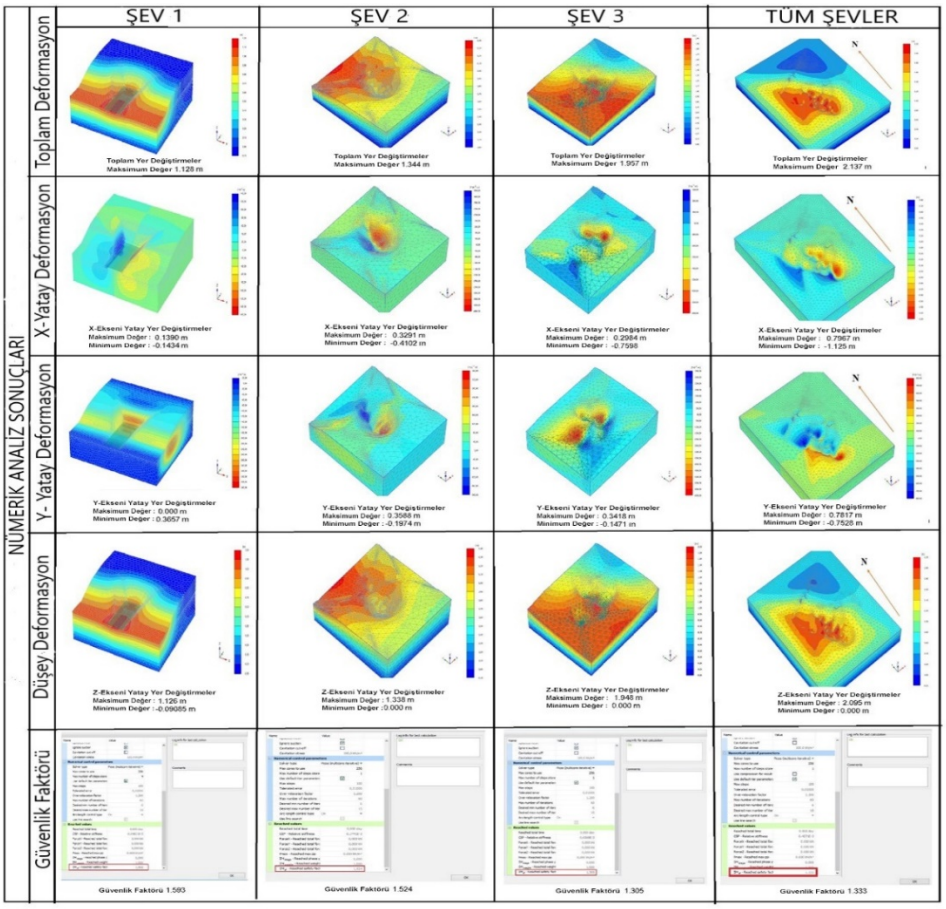

Şekil 4. Tüm nümerik modelleme analizlerinin sonuçları (deformasyonlar ve güvenlik faktörü)

NÜMERİK MODELLEME ANALİZLERİNİN SONUÇLARININ DEĞERLENDİRMESİ

Açık Ocak 1 için tüm kazılar tamamlandıktan sonra modelde meydana gelen toplam deformasyonların 1.128 m olduğu görülmektedir. Modelin yatay x-ekseninde 0.1434 m maksimum deformasyon meydana gelmiştir. Modelin yatay y-ekseninde 0.3657 m maksimum deformasyon meydana gelmiştir. Modelin düşey z-ekseninde maksimum 1.126 m deformasyon meydana gelmiştir. Model minimum $4.238*10^{-6}$ kN/m^2 ve maksimum 5856 kN/m^2 ana efektif gerilmelere sahiptir. Model minimum $4.238*10^{-6}$ kN/m^2 ve maksimum 8308 kN/m^2 ana toplam gerilmelere sahiptir. Tüm kazı aşamaları tamamlandıktan sonra c-Phi indirgeme yöntemi ile güvenlik faktörü belirlenmiştir. Modelin nihai versiyonu itibariyle oluşan güvenlik katsayısı ise 1.593 olarak belirlenmiştir.

Açık Ocak 2 için tüm kazılar tamamlandıktan sonra modelde meydana gelen toplam deformasyonların 1.344 m olduğu görülmektedir. Modelin yatay x-ekseninde maksimum 0,4102 m yatay y-ekseninde maksimum 0.3588 m, düşey y-ekseninde maksimum 1.338 m deformasyon meydana gelmiştir. Modelde maksimum 5143 kN/m^2 efektif gerilmelere ve maksimum 7543 kN/m^2 toplam gerilme oluştuğu tahmin edilmiştir. Tüm kazı aşamaları tamamlandıktan sonra c-Phi indirgeme yöntemi ile güvenlik faktörü belirlenmiştir. Modelin nihai versiyonu itibariyle oluşan güvenlik katsayısı ise 1.524 olarak belirlenmiştir.

Açık Ocak 3 için tüm kazılar tamamlandıktan sonra modelde meydana gelen toplam deformasyonların 1.957 m olduğu görülmektedir. Yatay x-ekseninde meydana gelen maksimum deformasyon miktarının 1.125 m olduğu görüşmüştür. Modelin yatay y-ekseninde maksimum 0.7817 m, düşey y-ekseninde maksimum 2.095 m deformasyon meydana geldiği tahmin edilmektedir. Model sonuçlarına göre maksimum efektif gerilmenin 5740 kN/m^2 maksimum toplam gerilmenin ise 5740 kN/m^2 olacağı değerlendirilmiştir. Bu açık ocak için tüm kazı aşamaları tamamlandıktan sonra c-Phi indirgeme yöntemi ile güvenlik faktörü hesaplaması sonrasında, güvenlik faktörünün 1.305 olduğu belirlenmiştir.

Birbirine çok yakın olan 3 açık ocağı birbiri ile etkileşiminin incelendiği modelde meydana gelen toplam deformasyonların 2.137 m olduğu görülmektedir. Modelin yatay x-ekseninde meydana gelen deformasyonlar maksimum 1.125 m, yatay y-ekseninde 0.782 m maksimum, düşey y-ekseninde 2.095 m maksimum deformasyon olduğu görülmüştür. c-Phi indirgeme yöntemi ile yapılan hesaplamada güvenlik faktörünün 1.333 olarak belirlenmiştir.

Üç açık ocağın incelendiği modele baktığımızda, Açık Ocak 1'deki toplam deformasyonun diğer ocakların etkileşimi ile yaklaşık 1.45 m'ye yükseldiği görülmektedir. Yatay deformasyonların x-ekseni ve y-eksenindeki maksimum değerlerinin sırasıyla yaklaşık 0,25 m ve 0,50 m'ye yükseldiği, z-eksenindeki düşey deformasyon değerlerinin yaklaşık 1.8 m'ye yükseldiği gözlemlenmiştir. Maksimum toplam ve efektif gerilmelerin yaklaşık 6100 kN/m^2 ve 8500 kN/m^2 'ye yükseldiği görülmektedir.

Açık Ocak 2'deki toplam deformasyonun diğer ocakların etkileşimi ile yaklaşık 2 m'ye yükseldiği görülmektedir. Yatay deformasyonların x-ekseni ve y-eksenindeki minimum değerlerinin sırasıyla yaklaşık 1.125 m ve 0.78 m'ye yükseldiği, z-eksenindeki düşey deformasyon değerlerinin yaklaşık 2.095 m'ye yükseldiği gözlemlenmiştir. Maksimum toplam ve efektif gerilmelerin yaklaşık 5800 kN/m^2 ve 7800 kN/m^2 'ye yükseldiği görülmektedir.

Son olarak, üç açık ocağın etkileşiminin incelendiği nümerik modele baktığımızda, Açık Ocak 3'deki toplam deformasyonun diğer ocaklardaki deformasyon etkilerinden etkilendiği ve 2.1 m'ye yükseldiği görülmektedir. Yatay deformasyonların x-ekseni ve y-eksenindeki minimum değerlerinin sırasıyla yaklaşık 1 m ve 0.8 m'ye yükseldiği, z-eksenindeki düşey deformasyon değerlerinin yaklaşık 2.095 m'ye yükseldiği gözlemlenmiştir. Maksimum toplam ve efektif gerilmelerin yaklaşık 6000 kN/m^2 ve 8000 kN/m^2 'ye yükseldiği görülmektedir.

SONUÇ

Görüldüğü gibi birbirinden bağımsız olarak yapılan analizler ile tüm şevlerin bir arada ele alındığı analizler arasında farklılıklar bulunmaktadır. Tüm şevler birlikte değerlendirildiğinde, toplam efektif gerilmelerin ve yatay-düşey deformasyonların her şev için bağımsız analizlerden daha yüksek olduğu görülmektedir. Bu durum özellikle güvenlik faktörünün düşük olduğu şevler için daha güvenli bir bölgede kalma gerekliliğini ortaya koymaktadır.

Tüm şevlerin analizinde, emniyet faktörü aşaması analiz edildiğinde, Şev-1 bölgesinde olası yenilme olasılığının olduğu sonucuna varılmaktadır. Bu durumda analize göre güvenlik faktörü 1.333 olarak hesaplanmıştır.

KAYNAKLAR

Aksoy C. O., Geniş M., Uyar Aldaş GG., Özacar V., Özer S.C., Yilmaz Ö., "A comparative study of the determination of rock mass deformation modulus by using different empirical approaches", Engineering Geology, 131-132, 19-28

Atkinson, T., 1977. "Surface Mining. De ingenieur", jrg 89, nr 28/29.

Aydan Ö., Ulusay A., Tokashiki N., 2014. "A New Rock Mass Quality Rating System: Rock Mass Quality Rating (RMQR) and Its Application to the Estimation of Geomechanical Characteristics of Rock Masses", Rock Mech. Rock Eng., 47, 1255-1276

Edelbro, C., Sjoberg, J., Nordlund, E., 2006. A quantitative comparison of strength cri- teria for hard rock masses. Tunnell. Undergr. Space Technol. 22, 57–68.

Palmström, A., 1995. RMi-a Rock Mass Characterization System For Rock Engineering Purposes. Ph.D. thesis. Univ. of Oslo, (www.rockmass.net).

Palmstrom, A., Stille, H., 2007. Ground behaviour and rock engineering tools for under- ground excavations. Tunnell. Undergr. Space Technol. 22, 363–376.

DATA-BASED DECISION-MAKING IN UNDERGROUND DRILLING OPERATIONS

A. Yıldız [1, *], M. Erkayaoğlu [1]

[1] *Middle East Technical University, Department of Mining Engineering*
*(*Corresponding author: artun.yildiz@metu.edu.tr)*

ABSTRACT

Natural resources are an essential part of sustainable development, and as shallow resources become depleted, the mining industry shifts intensively to underground mining. Equipment-intensive mining activities such as drilling can generate important data, particularly when consumables are examined, as they directly relate to the total production cost. The purpose of this study is to develop a data-driven approach for underground drilling activities in order to evaluate drilling efficiency using consumables. During a 1-month period, 35, 35, 30 percent of the total number of holes drilled and 35, 34, 31 percent of the total drilling were completed at night, day, and evening shifts, respectively. The distribution of failure codes in total for the night, day, and evening shifts occurred as 36, 24, and 19, respectively. The failure code 2, denoted by the bit breakout characteristic, was the most frequent failure code, with 21 pieces. The study's main purpose is to collect operational data to create a dashboard and generate online reports with consumable performance (service life and rate of penetration) outcomes. These reports can be used as supporting elements in mine management decision-making and as tools to improve the drilling efficiency of operations teams.

Keywords: Drilling, business intelligence, data analysis

INTRODUCTION

Drilling activities have downstream impacts that might cause ore dilution, the stability of underground openings, and the creation of undesired blocks in underground mining. This study aims to collect operational data for business intelligence purposes such as dashboards and online reports for rock tool performance. However, the proposed structure may also be applied for other phases of operations utilizing operational data. The developed dashboard utilizes data from an underground gold mine with a corporate data infrastructure. The increasing demand for higher production rates requires investment in mining technology. Another major factor leading operations to focus on equipment efficiency is low-grade orebodies. The potential improvements achieved through this study could generate high added value for downstream mining processes due to data utilization. Actionable processes and data visualizations can be driving forces for using data in all stages of management. Mining operations with comparably lower technology infrastructure rely on manually collected data, and it is known that the potential advantage of data is proportional to the quality and content. Data utilization and analysis have become conventional for various industries, and most modern mining operations generate vast amounts of data. The proposed data-driven dashboard and online reports provide insight into the rock tools used by different operators daily.

LITERATURE REVIEW

Increases in productivity in an equipment-intensive industry like mining may significantly influence the production capacity of raw materials. Drilling operations may be regarded as early stages of underground mining production similar to blasting, loading and hauling, development, support, and others. Various researchers utilized data analysis applications to identify mining equipment-related inefficiencies. Most of the studies are concentrated on measurement while drilling (MWD) and wear mechanisms of rock drill components. According to Teale (1965), mechanical specific energy is expressed as the proportion of work required to drill one cubic content of the rock. Kosolapov (2020) derived an equation for mechanical specific energy (MSE), a key indicator of drilling efficiency, and defined a relationship between MSE and the strength index of Protodyakonov. The association between specific explosive energy and mechanical specific energy (MSE) allows the measurement of MSE during blasthole drilling and the computation of specific explosive energy and rock strength index in the case of rotary, hydraulic, and electric drill rigs. Regotunov and Sukhov (2016) presented the results after examining the rock mass strength during roller-bit drilling. Their approach for calculating the strength properties of the local rock mass, which will be blasted, is described in detail in their paper. For determining the strength and technical features of the rocks, one of the most critical metrics was their power consumption (specific energy). Brown and Barr (1978) studied drilling parameters with a perspective of the geomechanical characteristics of rock material. It was concluded that only continuous drilling data might provide reliable mechanical information. Using rotary percussive drilling, all characteristics were divided into dependent and independent groups, as seen in Figure 1 (Isheyskiy and Sanchidrián, 2020). The rock mass properties identified were found to be independent of drill rig capacity or drilling style.

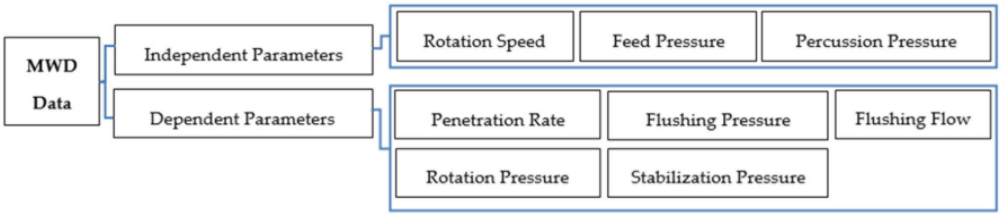

Figure 1. Brown and Barr's classification of dependent and independent measurement while drilling (MWD) features (1978)

According to Brown et al. (1984), geological variables, compressive strength, and MSE might be used to approximate mechanical and physical attributes of rocks. The rock mass's cavities and closed and open fractures were also identified using this method. Leighton (1982) identified the optimum drilling and blasting criteria for contour blasting in an open-pit copper mine. This work (Isheyskiy and Sanchidrián, 2020) was among the first to demonstrate how drilling and blasting activities may be improved by using drilling variables to calculate the rock quality index (RQI). Only two drilling metrics, thrust and penetration rate, composed the RQI and were subjected only to one kind of drilling technique. To circumvent the limitations of rock quality indicators, Lopez (1995) developed a characterization index for rocks contingent on drilling diameter, thrust, bit rotation speed, and penetration rate. It was observed that rock characterization index (Ip) was linked to rock strength since penetration rate was mainly related to geomechanical properties, so that powder factor was studied for varying Ip index values. Blastability index (BI) contingent on rock mass description (RMD) was proposed by Lilly (1986). Block structure (joint plane spacing (JPS) and joint plane orientation (JPO)) and the uniaxial compression strength of rocks (hardness), as well as specific gravity (specific gravity influence (SGI)) of rocks, were shown to be the most critical factors in blasting efficiency, according to this research. Using the given parameters, an equation for calculating BI was introduced (Isheyskiy and Sanchidrián, 2020).

$$BI = 0.5\ x\ (RMD + JPS + JPO + SGI + HD \quad (1)$$

The blastability of rock masses was also investigated by Yin and Liu (2001) using drill log data. According to Isheyskiy and Sanchidrián (2020), a novel RQI equation with two invariants has been developed, differing from previous formulations. A study by Scoble et al. (1987 and 1989) examined how drilling parameters are linked with geophysical logging. Even if it was established that the stated link was insufficient, this mainly was owing to the challenges in assessing data provided by rigs. Like Brown and Barr (1978), it was revealed that rotary drilling characteristics might be divided into two categories: driller-controlled independent variables like the speed of rotation or weight of bit and rock-dependent variables. When Schunnesson (1990) looked at different types of rocks, he found that a single criterion could be used to determine the quality of the rocks being drilled. For example, penetration rate could be used. Thus, several drilling parameters and their interactions were considered necessary (Isheyskiy and Sanchidrián, 2020). Schunnesson (1996) used revolutions per minute, torque, and penetration rate to study MWD-based rock quality concerning structural faults. The severity of rock fractures was linked to changes in rotation pressure and penetration rate. Severe fractures had been found to signify that the penetration rate and RPM were going down while the torque increased, like a jammed or stuck drill bit would. Schunnesson (1997) suggested a step-by-step normalization approach for separating interdependent drilling parameters. Only data directly dependent on differences in rock features remained after normalization, which might be used to define rock indices more correctly. It was decided to use principal component analysis (PCA) to minimize the number of measurements, such as torque and normalized penetration rate, as well as their respective variances. To eliminate depth-dependent fluctuations in the normalized parameters, Ghosh et al. (2017) utilized an expanded PCA approach that incorporated more measured and computed variables than the prior PCA approach. The authors defined five classes based on their shapes and interconnections, and the model was validated utilizing real data collected on-site. Another common research topic studied is the wear mechanisms of rock drill components.

Cement carbide rock drill inserts were tested under dry, wet, and abrasive conditions (Angseryd, From, Wallin, Jacobson, & Norgren, 2013). Difficult control circumstances and inhomogeneity resulted in poor test results. A wet and dry environment, SiO_2 and Al_2O_3 particle sizes, and load were investigated in three test series. Despite the absence of percussive impact, the top hammer inserts' surface degradation process was identical. The hardness of the insert had a considerable effect on wear. It increased the wear rate while decreasing sample hardness, and the field behavior under wet situations reflected the lab test results. A temperature gradient may also induce tensile stresses in carbide because of the cooling impact of water. Similarly, the effect of temperature was investigated via a series of experiments with findings compared across a range of conditions. As a result, contrary to common belief, the temperature had no effect on the process of wearing. It had a significant effect on the adhered rock particles. Otherwise, the areas that did not have any rock particles looked the same as the wet areas, which shows that temperature does not affect how long it takes to wear down (Angseryd et al.,2013). When working with comparably hard Al2O3 and comparatively soft SiO2 minerals, the size, and shape of the particles in the wear mechanism may be challenged. The increasing wear effect of Al_2O_3 and decreasing effect of SiO_2 was the final result of evaluating the influence of various materials on wear. However, the lower impact of SiO_2 was unknown. Furthermore, internally generated particles were sufficient to simulate SiO2 conditions, while Al2O3 did not affect the wear process. The relationship between load and wear was found to be non-existent. Pressure between the rock and the insert can cause it to break apart when it is strong enough to do so. Overall, the WC (tungsten carbide) grains break or split, which is a common side effect of the wear mechanism (Angseryd et al.,2013).

X-ray diffraction (XRD) and energy-dispersive X-ray spectroscopy (EDX) were utilized to analyze the chemical interactions between the rock and the bit, as well as the effects of the ion beam

scanning electron microscope (FIB-SEM) on these interactions (Jones, Norgren, Kritikos, Mingard, and Gee, 2017). Tribochemical calculations were also examined the impact of rock quartz content on wear. Although quartz has a harder structure than the cobalt binder phase, prior studies showed that SiO_2 presence does not considerably fracture WC crystallites, representing the predominant part of the composite. The CO combines with quartz to generate $COSi_2$, contributing to bit wear.

The chemical wear mechanism was defined as a blend of abrasion and oxidation with the assistance of water vapor in another research study (Jones et al., 2017). A rock substance embedded in the surface was monitored by Beste and Jacobsson (2009). The aim was to learn more about how quartz affects rock wear by magnifying locations where the oxide layer developed with varying elements proportions and thickness. The carbide and binder wear damage diagnosis was based on the surface oxide layer characteristics. It was explored in two situations with distinct thickness and silica/calcium-rich features, intergranular or transgranular. Jones et al. (2017) noted that the results are consistent with the findings of Beste et al. (2001, 2006, 2008) and Basse-Larssen (1985), that is, the absence of a binder phase in the outermost surface layers of the inserts. There were gaps at the boundary between the surface material and the binder phase because cobalt and carbide were split apart. There is a risk that cobalt might be released via these routes. Jones et al. (2017) stated that findings supported cobalt on the hard metal surface beneath the oxide layer (Jones et al., 2017). The conclusions of Montgomery (1968) conflicts with this study's findings; despite the assertion that the gauge and front button wear mechanisms were distinct, they were the same.

ANALYSIS OF DATA

This research’s basic concept is to implement a data-driven strategy in the mining industry. The data is the basis of this notion and requires an investment in technology to generate, collect, and analyze it. This stage also includes the management standpoint, which acknowledges the critical role of data utilization in the decision-making process. Databases allow continuous improvement to give information on operational outcomes. An underground mine provided the information from the corporate database.

As represented in Figure 2, the proposed framework describes the system that enables immediate insight for managers' decision-making processes by generating online reports through the obtained rock tools-related data. It is possible to achieve data integration by merging the data gathered at different operating stages of the drill jumbos, which are the primary data source for rock tools, with manually produced safety reports and drilling failure reports. It is possible to develop different data visualizations in the form of customized reports generated from the database established with other information from the mine, such as asset information, operational cost, and production plans.

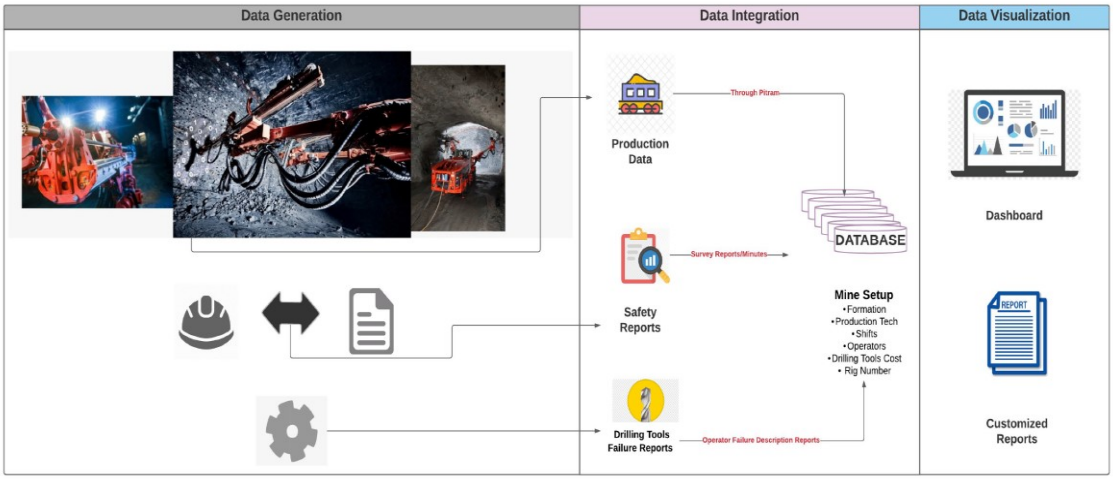

Figure 2. Framework for data visualization

Databases provide a structured environment for integration and can be considered as the essential information source for analytical tasks. Dashboards, customizable reports, and scorecards are some of the commonly used business intelligence applications that may be used to assist managers, supervisors, engineers, and operators on site. Data sources must be characterized in detail before data integration to understand the available potential. The existing data sources used in this study cover operator information, equipment data, failure codes, and type of drilling activity, as summarized in Table 1.

Table 1. Available data sources

Operators			
Operator-1	Operator-2	Operator-3	Operator-4
Operator-5	Operator-6	Operator-7	Operator-8
Operator-9	Operator-10	Operator-11	Operator-12
Operator-13	Operator-14	Operator-15	Operator-16
Equipments			
Equipment-1	Equipment-2	Equipment-3	Equipment-4
Types of Drilling			
4.2m Face	2.4m Split Set	Special Drilling	Reamed Hole
Rebar		Contour Holes	
Error Types			
Failure Code-1	Failure Code-2	Failure Code-3	Failure Code-4
Failure Code-5	Failure Code-6	Failure Code-7	Failure Code-8
Failure Code-9		Failure Code-10	
Failure Code-11			

Different dashboards were developed from the existing datasets and examined in detail. Numerous aspects of the underground drilling operation, such as drilling materials used, different kinds of drilling activities carried out in various shifts, failure codes associated with bits, and overall drilling performance, are shown in Figure 3. The visualization of the one-month duration for operational data provided an overview of the critical performance indicators of the drilling operation, which might be useful both for planning future operations and analyzing the current situation.

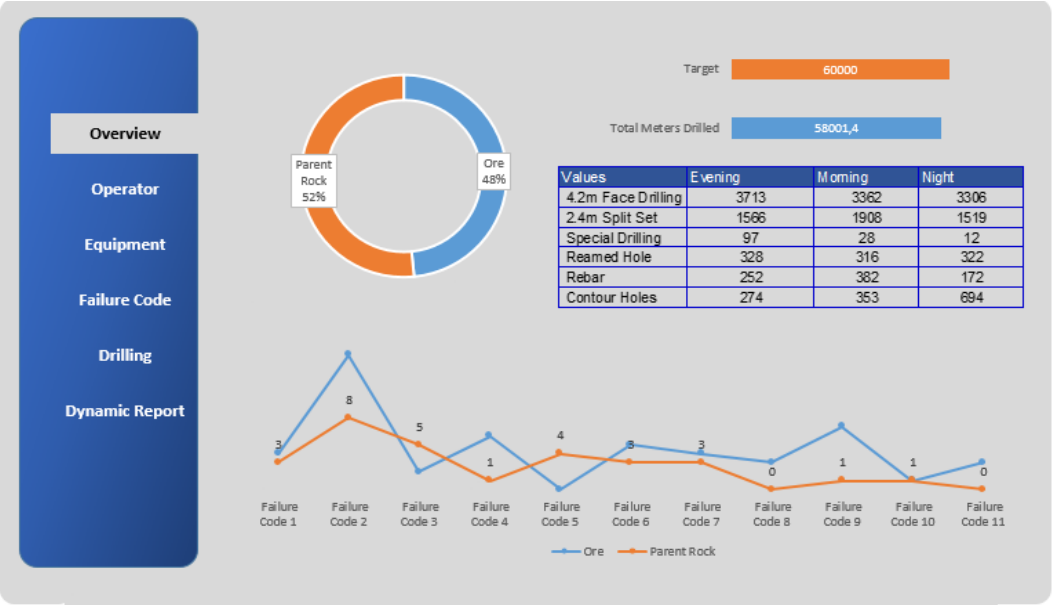

Figure 3. Overview of dashboard

Failure codes vary due to the changes in the lithological formation, operator experience, and the state of the rock bit being used. There are 11 error codes defined, and the distribution of recorded failure events throughout various shifts is shown in Figure 4. A comparison between the frequency of occurrences of the different failure codes revealed that failure code 2 defined for bit breakout is recorded 14 times during the night shift, which generates a noteworthy circumstance related to the night shift and the error code associated with it.

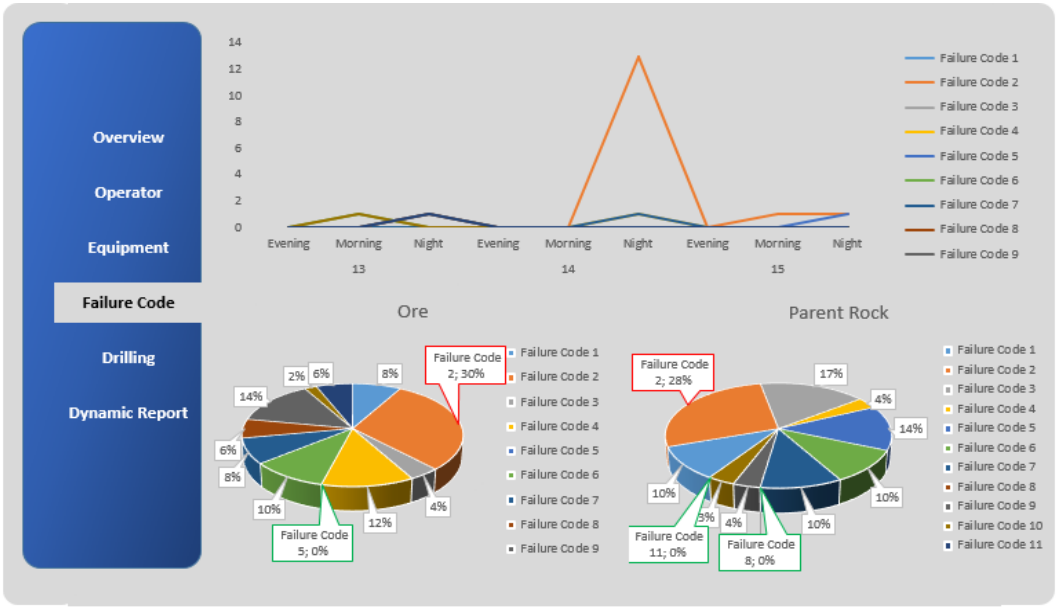

Figure 4. Distribution of failure codes based on material type

Figure 4 depicts the frequency of failure codes in relation to the kind of material being drilled. Similar to the overall frequency, failure code 2 was the most often encountered event for both material types. In contrast to failure code 5, which was the least often recorded code for ore material, failure codes 8 and 11 were the least frequently encountered codes for the material type defined as parent rock. Even though this circumstance necessitates the evaluation of other factors, it

might be a preventative measure to consider alterations in material type or equipment-related technical difficulties. Once this information is shared with the related technical staff, a maintenance event could be planned prior to an extended production loss due to this failure.

The distribution of drilling operations performed during shifts is visualized in Figure 5, together with the operators' information. The entire quantity of drilling (58,001 m) was proportioned for the evening, morning, and night shifts, and the percentage values were determined to be 35, 34, and 31, respectively. This situation demonstrates a specific operational condition of this mine as opposed to the notion that typically night shifts have comparably better performance. Production activities are more frequently interrupted in the day and evening shifts, as well as the fact that there are more factors to distract the employees supports this assumption.

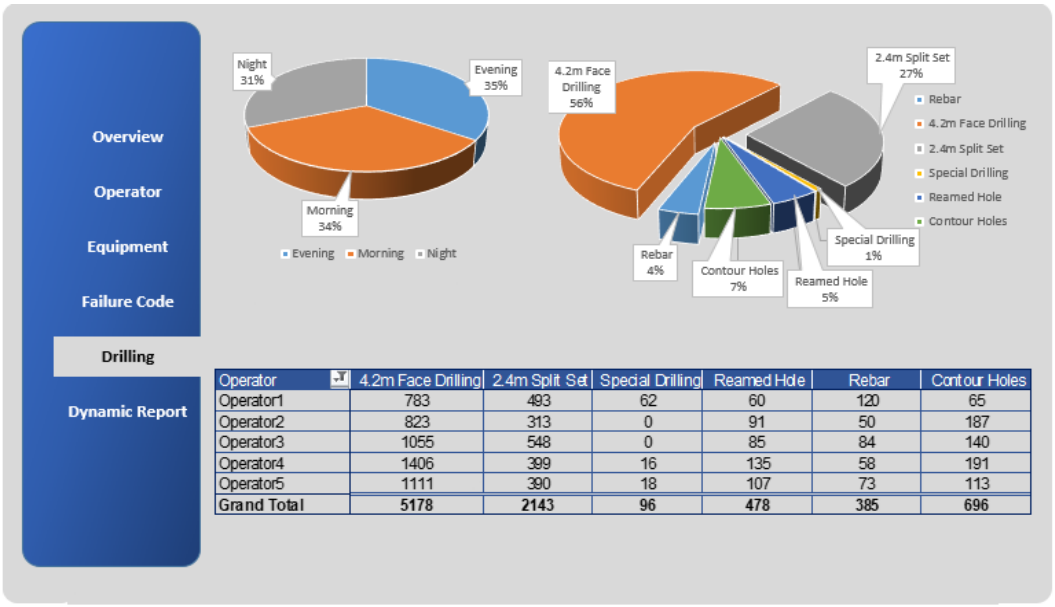

Operator	4.2m Face Drilling	2.4m Split Set	Special Drilling	Reamed Hole	Rebar	Contour Holes
Operator1	783	493	62	60	120	65
Operator2	823	313	0	91	50	187
Operator3	1055	548	0	85	84	140
Operator4	1406	399	16	135	58	191
Operator5	1111	390	18	107	73	113
Grand Total	**5178**	**2143**	**96**	**478**	**385**	**696**

Figure 5. Analysis of drill type based on shifts and operators

The data visualization for the relevant month reveals that it is necessary to investigate this case in more detail. At this point, the evaluation of shift drilling performances based on the drill types performed and the relevant operator information serves as a more representative analysis aiming to improve drilling performances per shift. The distribution of failure codes recorded for the different bits used on the jumbo drills and the distribution of different types of drilling activities performed with different equipment are shown in Figure 6.

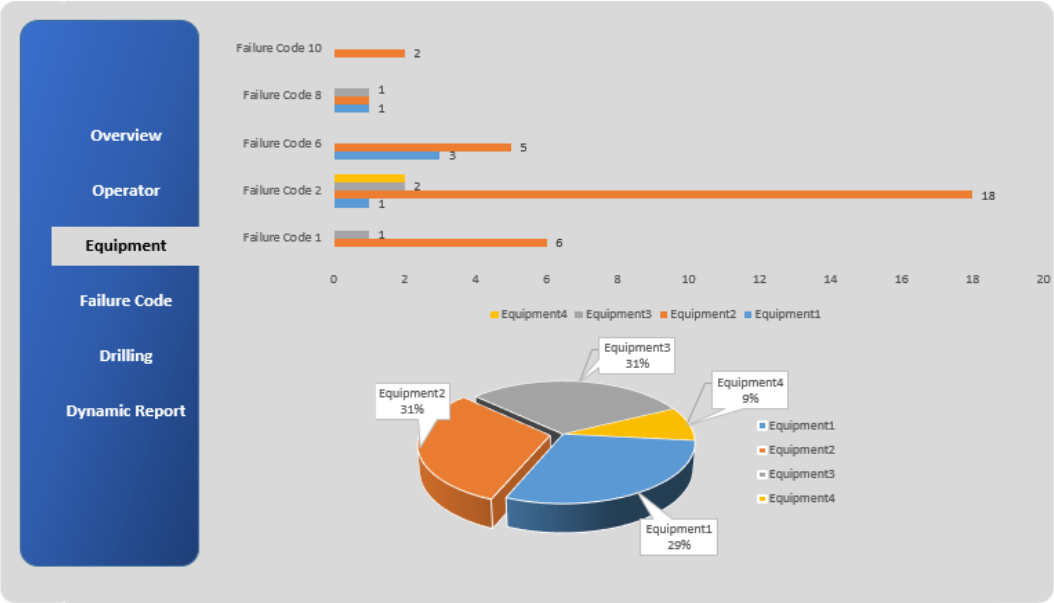

Figure 6. Type of drilling activities and failure codes based on equipment

Equipment-2 had a statistically significant increase in failure codes 2, 1, and 6 compared to other failure codes. Other operational factors that may contribute to the increased frequency of these failure codes should be explored in addition to the operator, the type of material being drilled, and the condition of the drill bit. Figure 7 depicts the monthly drilling target and achieved total drilling quantities for the operators and the monthly drilling targets together with failure code frequencies.

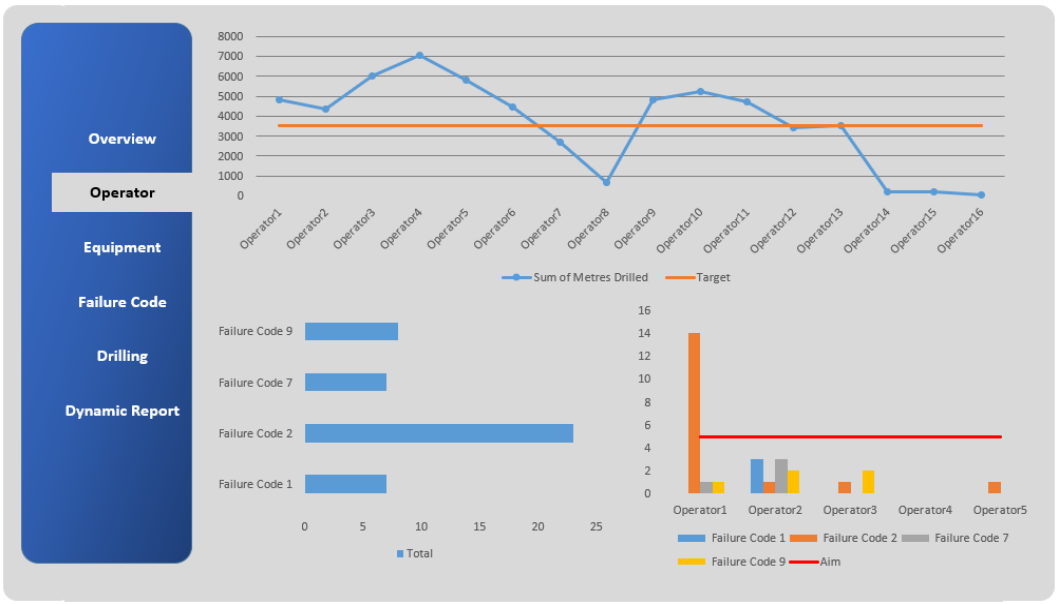

Figure 7. Operator evaluation based on targeted-actual total drilling-failure code

A dynamic report developed for the type of drilling, as seen in Figure 8, is an example of reporting that could be provided explicitly for operators, equipment, material type, and shifts over a period of time. The corporate data infrastructure available on site can be utilized to integrate extensive data. It will not only allow for comparison purposes and multi-dimensional analysis in case management perspective becomes accustomed to utilize data.

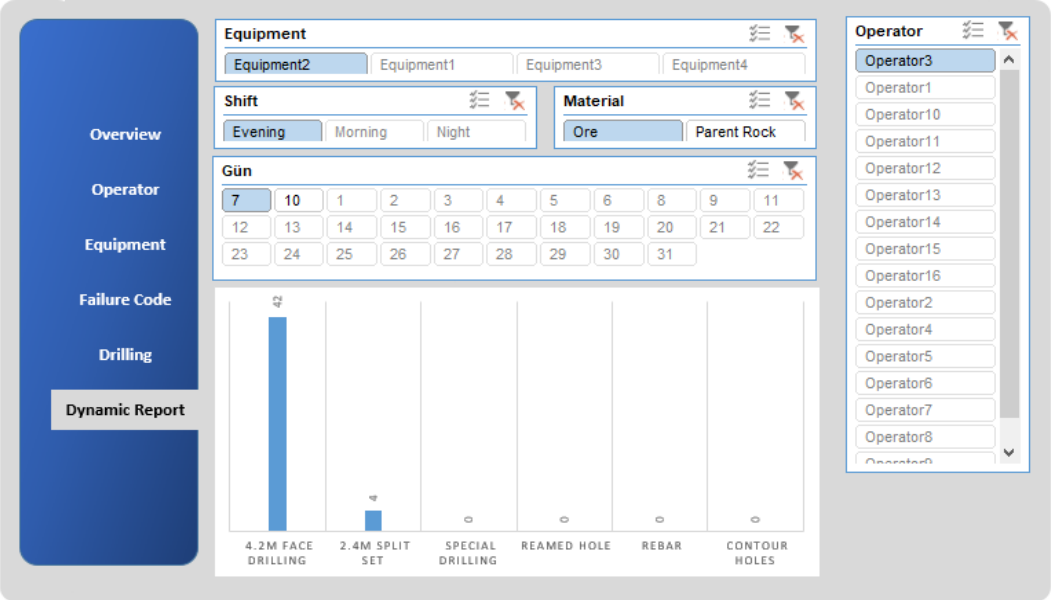

Figure 8. Operator-drill type dynamic report over a one-month period

In today's world, where the effective use of natural resources is becoming more vital, the active use of data will not only serve this goal but will also contribute positively to the corporate visibility of organizations by increasing their prominence in the field. The data that has been appropriately collected and integrated into a data warehouse can be considered the primary way of assessing performance that might be used to create a scorecard. Similarly, data usage will make it easier for the relevant operational units and managers to arrange training activities for operators, who play a critical role in the overall efficiency of the operation.

CONCLUSION AND RECOMMENDATIONS

Operational problems related to drilling operations in underground mining are evaluated by a data-based decision-making process. The main objective of the proposed processes could be to minimize the cost of drilling operations and improve productivity through the use of data. This study proves that investment in available technology to develop a data infrastructure is possible for corporate mining companies. In order to benefit from the existing data, technical expertise is required, and modern mines need the skills for data analysis and strategy development. Data analysis and data integration provide the infrastructure to build the management perspective that utilizes analytics and reporting for decision-making. Performance evaluation based on predefined targets allows for the quick assessment of operational issues and root-cause investigation using data. The widespread use of data for mining activities will become even more crucial for the efficient production of limited natural resources in the near future.

REFERENCES

Angseryd, J., From, A., Wallin, J., Jacobson, S., & Norgren, S. (2013). On a wear test for rock drill inserts. *Wear, 301(1–2*), 109–115.

Brown, E.T., Barr, M.V., (1978). Instrumented Drilling as an Aid to Site Investigations. In Proceedings of the 3rd International Congress of the International Association of Engineering Geology, Madrid, Spain, 4–8 September 1978; pp. 21–28.

Brown, E.T., Carter, P., Robertson, W., (1984). Experience with a Prototype Instrumented Drilling Rig. Geodrilling 1984, 24, 10–14.

Ghosh, R., Schunnesson, H., Gustafson., (2017). A. Monitoring of Drill System Behavior for Water-Powered In-The-Hole (ITH) Drilling. *Minerals 2017, 7,* 121.

J. Larsen-Basse, Binder extrusion in sliding wear of WC-Co alloys, *Wear 105 (1985*) 247–256.

Jones, H. G., Norgren, S. M., Kritikos, M., Mingard, K. P., & Gee, M. G. (2017). Examination of wear damage to rock-mining hardmetal drill bits. *International Journal of Refractory Metals and Hard Materials, 66*, 1–10.

Kosolapov, A.I., (2020). Modern Methods and Tools for Determining Drillability and Blastability of Rocks. Iop Conf. Ser. Earth Environ. Sci., 459, 022097.

Leighton, J.C. Development of a Correlation between Rotary Drill Performance and Controlled Blasting Powder Factors. Master's Thesis, University of British Columbia, Vancouver, BC, Canada, 1982.

Lilly, P., (1986). An Empirical Method of Assessing Rock mass blastability. In Proceedings of the Large Open Pit Mining Conference, Newman, Australia, 27–29 October 1986; pp. 89–92.

Lopez, C.; Lopez, E.; Javier, F., (1995) Drilling and Blasting of Rocks; CRC Press: Boca Raton, FL, USA, p. 408.

Navarro, J., Sanchidrian, J. A., Segarra, P., Castedo, R., Paredes, C., & Lopez, L. M. (2018). On the mutual relations of drill monitoring variables and the drill control system in tunneling operations. *Tunnelling and Underground Space Technology, 72*, 294–304.

R.S. Montgomery, (1968). The mechanism of percussive wear on tungsten carbide composites, *Wear 12*, 309–329.

Regotunov, A.S.; Sukhov, R.I., (2016) The Results of Studies of Strength Properties of Local Arrays in the Drilling Process using software and hardware complex. Subsoil Use Probl. 2016, 4, 121–129.

Schunnesson, H., (1990). Drill process monitoring in percussive drilling: A multivariate approach to data analysis. Licentiate Thesis, University of Technology, Luleå, Sweden.

Schunnesson, H., (1996). RQD Predictions Based on Drill Performance Parameters. Tunn. Undergr. Space Technol., 11, 345–351

Schunnesson, H., (1997). Drill Process Monitoring in Percussive Drilling for Location of Structural Features, Lithological Boundaries and Rock Properties, and for Drill Productivity Evaluation. Ph.D. Thesis, Luleå University of Technology, Luleå, Sweden.

Schunnesson, H., (1998). Rock Characterization using Percussive Drilling. Int. J. Rock Mech. Min. Sci., 35, 711–725.

Scoble, M.J.; Peck, J.A., (1987). Technique for ground characterization using automated production drill monitoring. Int. J. Surf. Min. Reclam. Environ. 1, 41–54.

Scoble, M.J.; Peck, J.; Hendricks, C., (1989). Correlation between rotary drill performance parameters and borehole geophysical logging. Min. Sci. Technol., 8, 301–312.

Teale, R., (1965). The Concept of Specific Energy in Rock Drilling. Int. J. Rock Mech. Min. Sci. Geomech. Abstr. 2, 57–73.

U. Beste, T. Hartzell, H. Engqvist, N. Axén, (2001). Surface damage on cemented carbide rock-drill buttons, *Wear 249*,324–329.

U. Beste, E. Coronel, S. Jacobson, (2006). Wear induced material modifications of cemented carbide rock drill buttons, Int. J. Refract. Met. Hard Mater. 24, 168–176.

U. Beste, S. Jacobson, (2008). A new view of the deterioration and wear of WC/Co cemented carbide rock drill buttons*, Wear 264 (11–12)*,1129–1141.

U. Beste, S. Jacobson, S. Hogmark, (2008). Rock penetration into cemented carbide drill buttons during rock drilling*, Wear 264 (11–12*) ,1142–1151.

DENİZLİ AVDAN VE NARLI KÖMÜR SAHALARI KAYNAK MODELİ

DENIZLI AVDAN AND NARLI COAL MINE SITES RESOURCE MODEL

C.A. Öztürk [1, *], M. Lashgari [1], Y. Türkmen [1]

[1] *İstanbul Teknik Üniversitesi, Maden Mühendisliği Bölümü*
*(*Sorumlu yazar: atilla.ozturk@itu.edu.tr)*

ÖZET

Denizli ili Tavas ilçesinde bulunan Avdan ve Narlı kömür sahaları bölgede tesis edilebilecek termik santrale hizmet edebileceği gibi aynı zamanda, Ege bölgesinde bulunan diğer termik santraller için de hammadde deposu olarak kullanılabilir özelliklerdedir. Kömür sahası Yenidere ve Sekköy olarak isimlendirilen iki farklı kömür zonunu içerir. Kömür zonları kömür damarları ve aralarına yerleşmiş bulunan ara kesmelerden oluşmaktadır. Oluşum Yenidere ve Sekköy kömürleri için benzerlik göstermedir. Sahada yapılan kaynak modelleme çalışmasında, bölgede yapılmış olan sondaj verilerini kullanarak kömür zonlarının katı modelleri ve daha sonra blok modelleri üretilmiştir. Kriging tekniğinin çalıştırılmasıyla bloklara değer atanmış ve böylece kaynağın miktar ve kalite modellemesi elde edilmiştir. Çalışmanın amacı, iki farklı ruhsat ile sınırlandırılan Avdan ve Narlı kömür sahalarının kaynak modelinin elde edilmesinin yanında, ruhsatların birleştirilmesi durumunda oluşacak yeni koşulun olası etkilerinin araştırılmasıdır.

Anahtar Sözcükler: Enerji, kaynak modelleme, kömür, ruhsat birleştirme.

ABSTRACT

Avdan and Narlı coal mine sites located in Denizli City Tavas Province is going to serve as raw material source for thermal power plant that will be constructed close to the mine site or existing Aegean region's thermal power plants. The coal mine sites consist of two different coal zones that are Yenidere and Sekkoy coal zones. Coal zones are the sum of coal seams and interburden among them. The formation are similar both for Yenidere and Sekkoy coal zones. Solid models of the coal zones were firstly determined based on the drill log database and then block models were executed. Hence, estimation of coal quality could be proceed after running kriging to determine coal resource and quality modelling. The purpose of the study is to model these two coal mine sites to understand the overall resource potential as well as the effect of merging adjacent mining area licenses sites for the optimized use of coal mine sits for energy production.

Keywords: Energy, resource modelling, coal, license merging.

GİRİŞ

Yerli kömürden enerji üretimi ülkemiz enerji politikaları açısından son yıllarda gittikçe önemi artan önemli hedeflerden biridir. Bu durum özellikle ülke ekonomisi ve gelişmişliği açısından kilit öneme sahip olan enerji üretiminin yerli kaynaklardan sağlanması ve dışa bağımlılığın azaltılması açısından son derece önemlidir. Denizli ili Tavas ilçesinde bulunan kömür sahası, bölgede tesis edilecek olan termik santrale hizmet vermeyi hedeflemenin yanında, kaynağın büyüklüğüne bağlı olarak Ege bölgesinde bulunan termik santral için de kullanılabilir bir hammadde deposuna dönüşecektir.

Bölgede kömür yapısı Sekköy ve Yenidere olarak isimlendirilen iki farklı kömür zonundan oluşmaktadır. Her iki kömür zonunda da kömür damarları ve damarların arasına yerleşmiş ara kesmeler bulunmaktadır. Kömürün mostra vermesi ve 200 m derinlere kadar ulaşmasından dolayı üretimin açık işletme faaliyetleri ile gerçekleştirilmesi planlanmaktadır. Bu durumda kömür üretim faaliyetleri sırasında dekapaj kazı miktarının yanında ara kesme miktarının da tayinine ihtiyaç duyulmaktadır. Ayrıca, kömür damarlarının sahada yapılacak madencilik faaliyetleri sırasında kısa dönem faaliyetlerine uygun olarak modellenmesi ve ara kesmelerin seleftik madencilik esaslarına göre alınmasında yarar vardır. Bu sayede kömürün üretim kaynaklı kirlenmesinin en aza indirilmesi ve termik santrale beslenecek kömürün ideal olarak temini sağlanmış olacaktır.

Kömür sahaları Avdan ve Narlı olarak isimlendirilen birbirine komşu iki farklı ruhsat ile sınırlandırılmaktadır. Kaynağın modellenmesi amacıyla oluşturulan sondaj veri tabanında Avdan sahasının kullanılabilir 103 adet sondaj verisi kullanılmıştır. Narlı bölgesindeyse modelleme 18 sondaj verisiyle gerçekleştirilmiştir. Avdan sahasındaki sondajlardan 98'i kömür damarlarını keserken, Narlı bölgesindeki tüm sondajlarda kömür kesilmiştir. Sekköy ve Yenidere kömür zonlarına ait katı modeller oluşturulduktan sonra kaynak modelleme çalışmaları yapılmıştır. Yenidere kömür zonu kendi içerisinde 3 farklı yapıdan oluşmaktadır. Ancak katı modellerde Yenidere-2 ve Yenidere-3 kömür zonları da ortaya çıkartılmıştır. Sondaj verisinin yetersiz olmasından dolayı bu kömür zonlarına ait modellerin devamı Narlı bölgesinde takip edilememiştir. Bu iki kömür zonu açık işletme faaliyetleriyle yeryüzüne çıkartılamayacak derinlikte olması ve yeterli kaynak miktarına sahip bulunmamasından dolayı kaynak olarak değerlendirilmemiştir. Bildiriye konu olan çalışmaların temel amacı, kömür sahasındaki linyitin kömür zonları özelinde kaynak ve kalite değerlendirilmesinin yapılarak, kömür sahalarının termik santralleri besleme potansiyelinin ortaya çıkartılmasıdır.

BÖLGENİN TANITIMI VE KISA JEOLOJİSİ

Kömür sahası, Denizli ili Tavas İlçesi Avdan – Narlı ve Adamharmanı köyü hudutları içerisinde yer almaktadır. Açık işletme faaliyetleri ile linyit üretiminin gerçekleştirileceği saha, Tavas ilçesinin batısında Kale ilçesinin kuzeyinde Avdan Köyü civarında bulunmaktadır. Tavas'a 37 km, Kale'ye 22 km. uzaklıktadır. Sahaya asfalt yolla ulaşılmaktadır. Kömür sahasının yer buldu haritası Şekil 1'de verilmiştir.

Ruhsat sahası değişik morfolojik özelliklere sahiptir. Derin vadilerle ayrılmış platolar üzerinde yer alan ruhsatlar olabildiği gibi tatlı meyilli ruhsat sahaları da bulunmaktadır. Bölgede İç Ege Bölgesi'nin iklimi görülmekte olup yazları serin ve kurak, kışları ılık ve yağışlıdır.

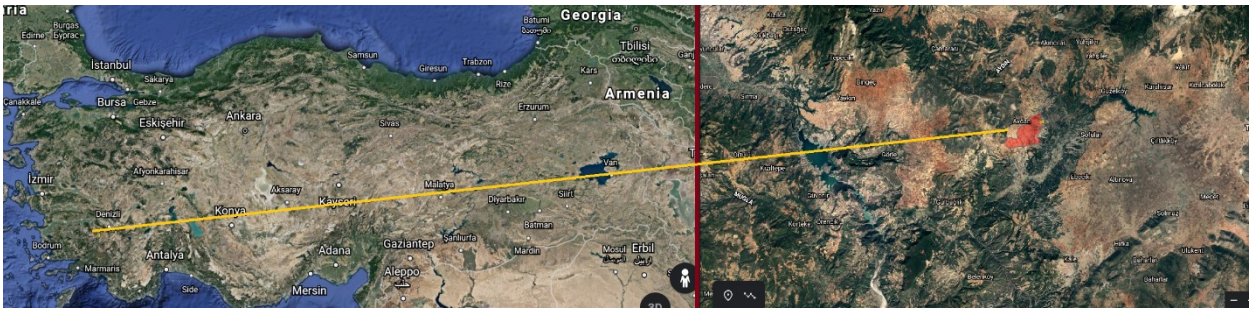

Şekil 1. Kömür sahası lokasyonu

Sahanın temelini paleozoyik- mesozoyik yaşlı kuvarsit, mermer, şist, kireçtaşı, radyolarit ve ofiyolitik kayaçlar oluşturur. Temel kayaçların üzerinde uyumsuzlukla gelen tersiyer yaşlı kayaçlar yer almaktadır. Akçay Grubu (Karadere, Mortuma, Yenidere, Kale ve bununla geçişli Künar Formasyonu) ve Muğla Grubu (Turgut, Sekköy, Yatağan ve Milet Formasyonu) olarak adlandırılan iki gruptan oluşmaktadır.

Çalışma sahası ve civarı Yenidere, Sekköy ve Yatağan formasyonları ile temsil edilmektedir. Yenidere formasyonu (Ty), oligosen yaşlı Mortuma formasyonu üzerine açısal diskordansla gelir. Kalınlığı 250- 1450 m'dir. Formasyon; Esenkaya (Tye), Ortaköy (Tyo) ve Karakaya (Tyk) Üyesi olmak üzere üçe ayrılmıştır. Esenkaya üyesi; iri çakıltaşı, çamurtaşı, kumtaşı ve silttaşlarından oluşur. 25- 550 m arasında kalınlığa sahiptir. Ortaköy üyesi; kumtaşı, silttaşı, kiltaşı ve çakıltaşından oluşmaktadır. Üyenin orta kesimlerinde kalınlıkları 2.90 m'ye kadar ulaşan linyit damarları içeren linyit horizonu bulunmaktadır. Üyenin kalınlığı 125- 600 m arasında değişmektedir. Karakaya üyesi; kiltaşı ve silttaşından oluşan üyenin kalınlığı 70- 100 m arasındadır. Yenidere Formasyonu örgülü, menderesli ırmak, kıyı ovası, lagün, delta, alüvyon ve kumsal ortamlarda çökelmişlerdir. Yaşı alt miyosendir.

Sekköy formasyonu (Tms), Avdan civarında Yenidere formasyonu üzerine uyumsuz olarak gelir. Kalınlık 50- 150 m arasındadır. Sarımsı beyaz renkli killi- mikritik- kırıntılı kireçtaşı, gri renkli silttaşı, tüf ve tüfitten oluşmaktadır. Formasyonun tabanında; kalınlıkları 0,05 – 2,20 m arasında değişen linyit damarları içeren bir zon bulunmaktadır. Sekköy Formasyonu bataklık ve göl ortamında çökelmiştir.

Yatağan formasyonu (Tmy), Sekköy üzerine uyumlu olarak gelir. Çakıltaşı, çamurtaşı, kumtaşı, tüf ve tüfitten oluşmaktadır. Kalınlığı 250 m.'ye ulaşmaktadır. Alüvyon yelpazesi çökel ortamında çökelmiştir.

Milet formasyonu (Tmm): Yatağan formasyonunun üzerine uyumlu şekilde gelir. Çalışma sahası civarında düz ve yüksek platolar oluşturmaktadır. Beyaz renkli kireçtaşı ve sarımsı bej renkli killi kireçtaşlarından oluşan birimin kalınlığı 100 – 120 m civarındadır. Göl ortamında çökelen formasyonun yaşı pliyosendir (Akgün ve Sözbilir, 2001; Alçiçek, 2010; Hakyemez, 1989; Sözbilir vd., 2000; Sözbilir, 2002).

AVDAN VE NARLI KÖMÜR SAHALARI KAYNAK MODELİ

Çalışma sahasında modellemede kullanılan sondajlara ait plan görünüm Şekil 2 ve Şekil 3'te verilmiştir. Sekköy ve Yenidere kömür zonlarının katı modelleri çıkartılmıştır. Yapılan çalışmadan üretilen katı modellerin izometrik görünümleri Şekil 4 ve Şekil 5'te görülmektedir.

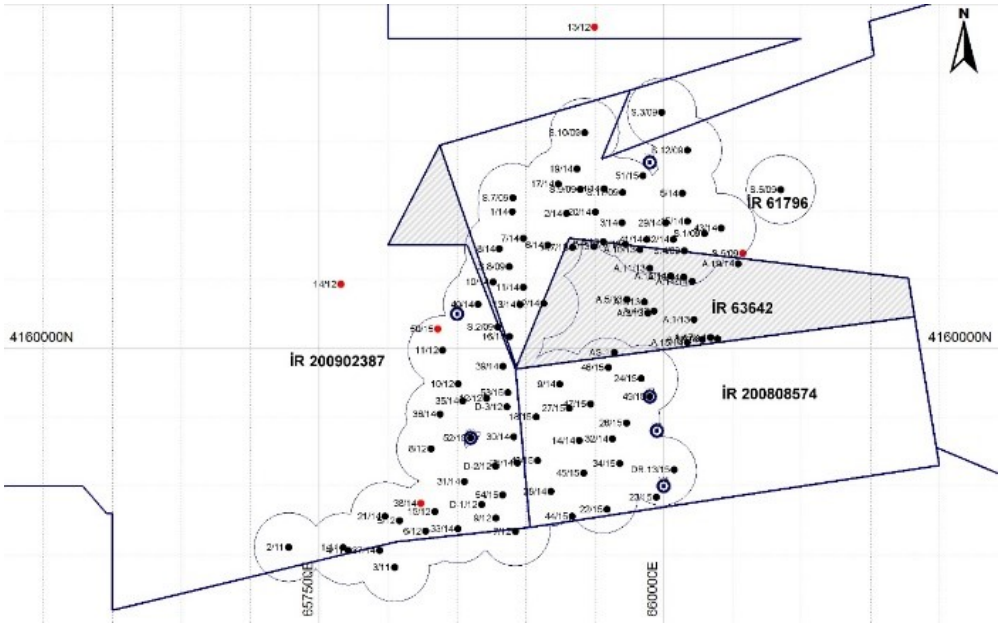

Şekil 2. Avdan sondaj lokasyonlarının plan görünümü

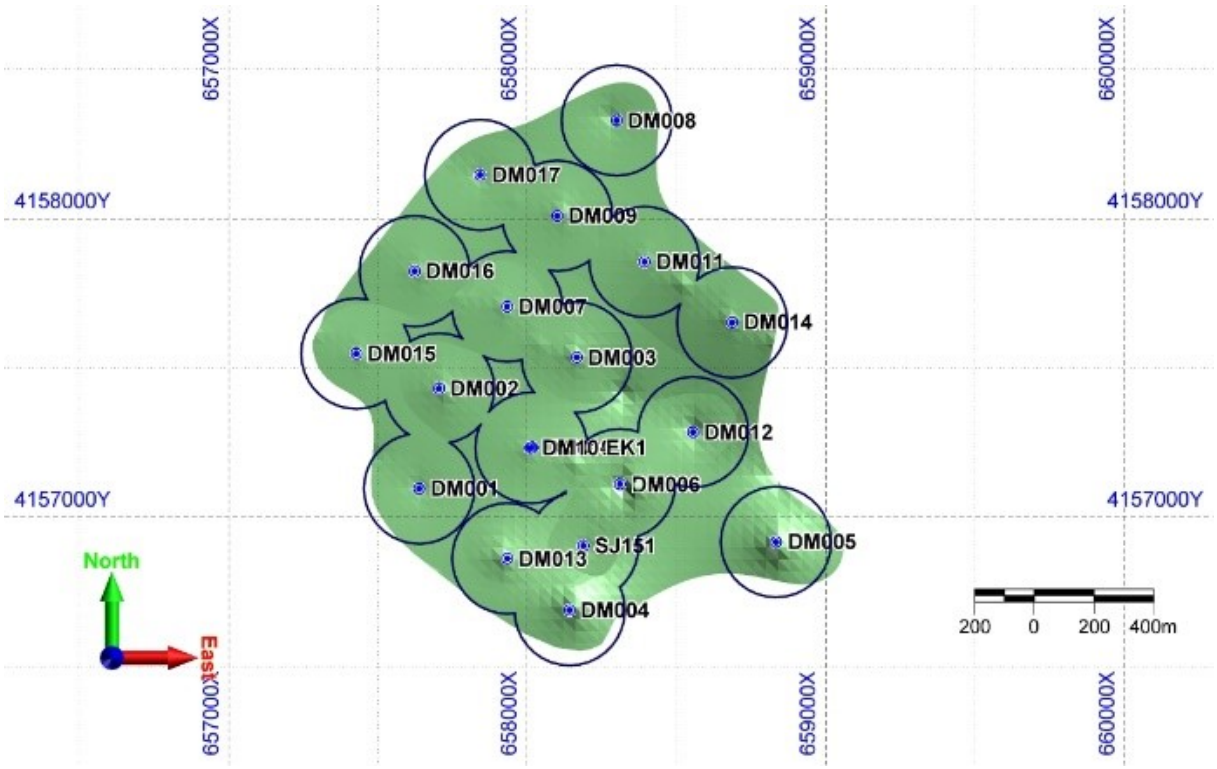

Şekil 3. Narlı sondaj lokasyonlarının plan görünümü

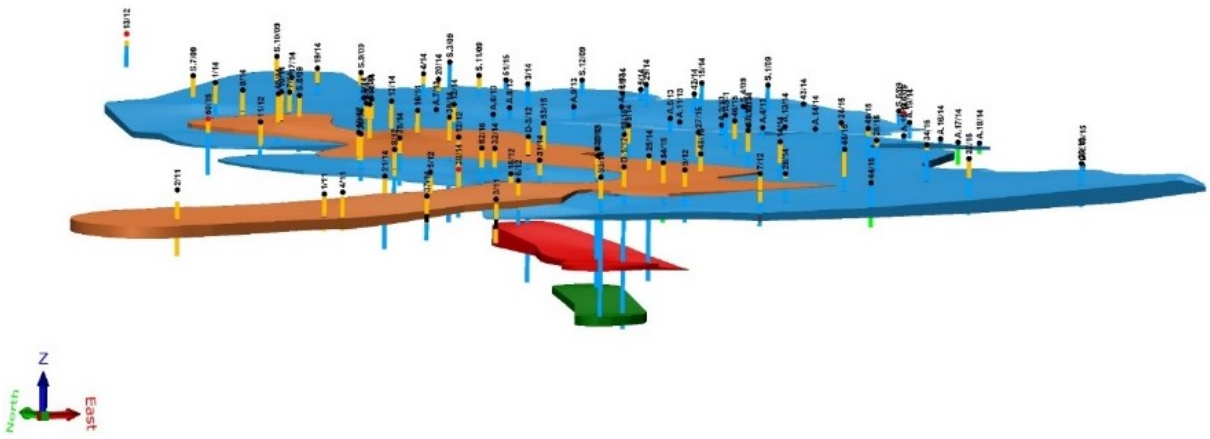

Şekil 4. Avdan kömür zonlarının katı modeli (Lashgari vd., 2016

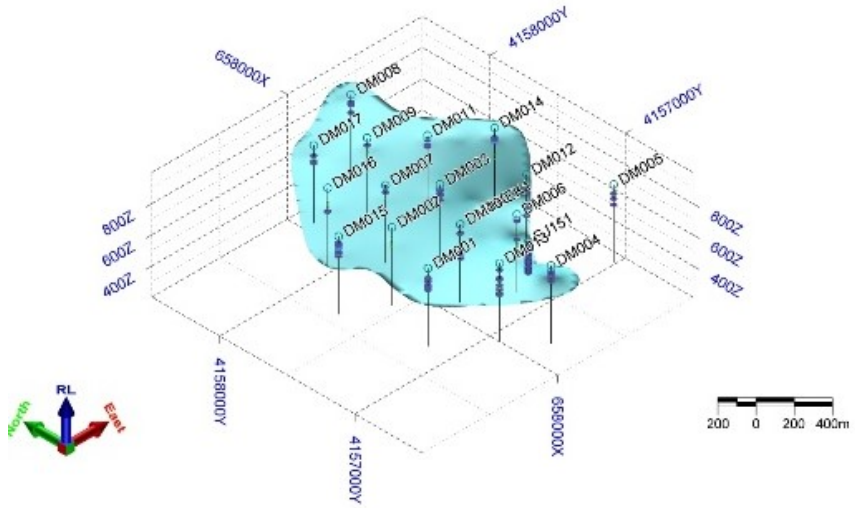

Şekil 5. Narlı kömür zonlarının katı modeli

İstatistiksel Değerlendirmeler

Kömürün kalitesinin tespit edilmesi amacıyla yaptırılan test çalışmaları sonucunda, kömürün alt ısıl değeri, toplam kükürt, nem, kül, uçucu madde ve yoğunluk değerleri tespit edilmiş ve elde edilen sonuçlara ait istatistiksel değerlendirme Çizelge 1'de ve Çizelge 2'de kömür sahaları için ayrı ayrı verilmiştir.

İki komşu saha için yapılan testlerden elde edilen kalite değişkenlerine ait basit istatistiksel çıkarımlar sahadaki kömürün kalitesinin benzerliğine işaret etmektedir. Avdan sahasındaki ortalama alt ısıl değerin 1703 kcal/kg olarak tayin edilirken bu değer Narlı sahasında 1779 kcal/kg olarak belirlenmiştir. Ortalama değerlerin bu derece birbirine yakın olması, birbirine komşu bu iki sahadaki kömürün aynı kömür zonu olduğunu desteklemektedir.

Çizelge 1. Avdan sahası kömür kalite değerlerine ait istatistiksel değerlendirmeler

Tanımlama	Alt Isıl Değeri (kcal/kg)	Toplam Kükürt (%)	Nem (%)	Kül (%)	Uçucu Madde (%)	Yoğunluk (gr/cm^3)
Ortalama	1703	2.61	41.57	25.47	24.34	1.48
Std. Sapma	410	1.18	5.50	9.56	5.15	0.11
Veri Sayısı	219	214	219	219	219	131

Çizelge 2. Narlı sahası kömür kalite değerlerine ait istatistiksel değerlendirmeler

Tanımlama	Alt Isıl Değeri (kcal/kg)	Toplam Kükürt (%)	Nem (%)	Kül (%)	Uçucu Madde (%)	Yoğunluk (gr/cm^3)
Ortalama	1779	2.24	40.09	27.25	24.75	1.42
Std. Sapma	586	1.18	7.12	11.21	5.97	0.14
Veri Sayısı	307	307	307	307	307	307

Kaynak ve Kalite Modellemesi

Avdan kömür sahasına ait ön değerlendirme sonucunda, Sekköy formasyonunda bir, Yenidere formasyonunun da ise üç farklı linyit yapısı tespit edilmiştir. Sahadaki linyit oluşum olarak delta yapısı olmasından dolayı, kömür damarlarının korelasyonundan ziyade kömür zonu olarak modellenmeleri

tercih edilmiştir. Katı modellerden de görüleceği üzere kömür zonları Sekköy, Yenidere-1, Yenidere-2 ve Yenidere-3 olarak isimlendirilmiştir. Sekköy ve Yenidere-1 olarak isimlendirilen kömür zonlarındaki linyitin açık işletmecilik faaliyetleri üretilmesi mümkündür. Yenidere-2 ve Yenidere-3 kömür zonları ise yeter ve gerek veriye sahip olmadığı için bu kömür zonlarının yeni bir dizi sondaj ile sınırlarının ve büyüklüğünün tespit edilmesine ihtiyaç vardır. Yenidere-3 kömür zonunda iki sondajda kömür kesilmiş ve kesilen kömürün kalınlığı 5.5 m'dir. Diğer sondajlarda bu derinliğe ulaşılmadığı için, Yenidere-3 kömür zonunun kaynak miktarıyla ilgili güvenilir bir bilgiye sahip olunamamaktadır. Bu iki kömür zonunu hedefleyecek bir dizi sondaj çalışmasıyla havzadaki kaynağın miktarının artması mümkün gözükmektedir.

Narlı kömür sahasında ise daha önce gerçekleştirilen çalışmadan da faydalanarak (MCS, 2015) bölgedeki kömür damarları 8 sektöre ayrılmıştır. Bu sektörler kendi içerisinde toplam 53 alt damara ayrılmıştır. Yapılan çalışmada kullanılan 19 sondajın verisinden yola çıkarak çalışma tekrar edilmiştir.

Sahadaki kömür kaynağının miktar ve kalite dağılımlarının araştırılması için jeoistatistiksel yöntemlerden faydalanılmıştır. Bu sayede, özellikle kömür kalitesinin denetlendiği değişkenlerin bölgesel olarak büyüklüklerinin en aza hata ile kestirimlerinin yapıldığı matematiksel modeller kullanılmıştır (Isaak ve Srivastava, 1989; Öztürk, 2001). Linyit zonları, jeolojik formasyonlar ve linyit kalitesinin belirlenmesinde en uygun modelleme ve interpolasyon yönteminin kullanılabilmesi için araştırmalar yapılmıştır. Modelleme çalışmalarında klasik kesit yönteminin hata payının yüksek olmasından dolayı sahadaki linyit damarları için grid model kullanılmasına karar verilmiştir. Jeolojik katmanlar ve linyit zonu damarlarının tavan ve taban yüzeyleri grid yöntemi kullanılarak modellenmiştir. Grid yönteminin kullanılması sırasında jeoistatistiksel olarak çalışmalar yapılmış ve yüzeylerin kot farklılıkları tahmin edilmeye çalışılmıştır. Yapılan çalışmalar sonucu variogram model olarak doğrusal variogram modeli ile çalışılmaya karar verilmiştir. Bu sayede elde edilen tavan ve taban yüzeyleri sayesinde hem jeolojik formasyonlar hem de linyit zonları 3B katı modele çevrilmiştir.

Avdan sahasında katı model çalışmasından sonra blok modelleme yapılmıştır. En düşük boyutu 40 cm, en büyük boyutu 4 m olan yaklaşık 3,2 milyon bloktan oluşan blok model sayesinde sahadaki kömürün kalitesi bölgesel olarak modellenmiştir. Narlı sahasında ise en düşük boyutu 25 cm en büyük boyutu 10 m olan toplam 7,04 milyon bloktan oluşan bir blok model oluşturulmuştur.

Alt Isıl Değer Dağılım Modelleri

Çalışma sahasındaki linyitin alt ısıl değerinin, kömür zonları özelinde dağılım haritaları modellenmiş ve elde edilen sonuçlar Şekil 6'da Avdan sahası için, Şekil 7'de ise Narlı sahası için verilmiştir.

Yapılan analiz sonuçlarına göre, Yeniköy kömür zonu alt ısıl değeri açısından Sekköy kömürlerine nazaran bir miktar daha zengindir. Sahanın kuzey ve güneyinde 2000 kcal/kg ve daha yüksek alt ısıl değere sahip olunurken sahanın geri kalan kısmında ise alt ısıl değeri 1500 ile 2000 kcal/kg olarak değişmektedir. Sekköy kömürlerinde ise bu oluşum tam ters olarak görülmekte sahanın ortasında daha zengin sahanın kuzey ve güneyinde ise alt ısıl değer yönünden daha fakir bölgeler yer almaktadır.

Narlı bölgesinde ise sahanın güney doğu ve kuzey batı bölgelerinde kömürün ortalama alt ısıl değeri 1800 kcal/kg ile 2300 kcal/kg değerleri arasındayken, sahanın geri kalan kısmında 1000 kcal/kg ile 1500 kcal/kg arasında değişmektedir.

Sahada kaliteyi denetleyen nem, kül, kükürt ve uçucu madde değişkenleri için de benzer dağılım haritaları elde edilerek, her bir bloğun kalite değeri tayin edilmiştir.

Bu bölümde sadece alt ısıl değerin dağılım haritaları verilerek, diğer kalite parametrelerine ait haritaların verilmesi yerine blok modellerden elde edilen değerlerin verilmesi yoluna gidilmiştir.

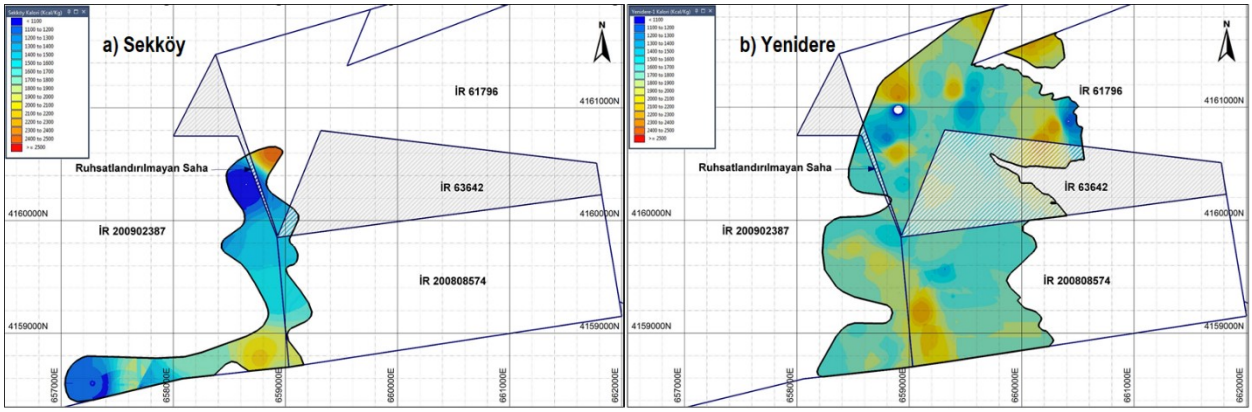

Şekil 6. Avdan bölgesi kömür zonlarının alt ısıl değer dağılım haritaları a) Sekköy b) Yenidere

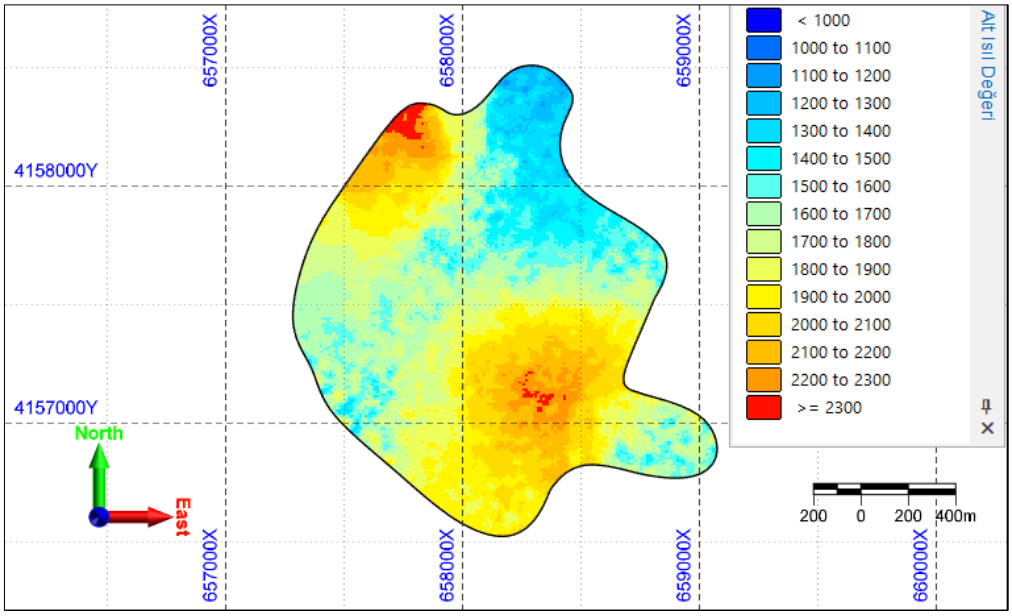

Şekil 7. Narlı bölgesi kömür zonlarının alt ısıl değer dağılım haritaları

Kaynak Kalite ve Miktar Sonuçları

Avdan bölgesinde yapılan modellemeler sonucunda, kaynağın Sekköy, Yenidere-1, Yenidere-2 ve Yenidere-3 olarak isimlendirilen dört farklı kömür zonundan oluştuğu ve bu zonlardaki linyit kaynağının miktar ve kalite değerlerine ait bilgiler elde edilmiştir. Çizelge 3'te yapılan çalışmalardan elde edilen sonuçlar verilmiştir. Yenidere-3 kömürü sadece iki sondaj ile temsil edilmesinden dolayı hesaplarda gösterilmemektedir. Yenidere-2 kömürü ise açık işletme faaliyetleriyle üretilebilir gözükmemektedir. Benzer çalışma Narlı bölgesi için de tekrar edilmiş ve elde edilen sonuçlar Çizelge 4'de verilmiştir. Narlı bölgesinde 7 farklı kömür zonu ile yapılan modellemenin çıktılarını ayrı ayrı göstermek mümkün olamadığı için blok modelin görünümü verilmiş ve Çizelge 4'de her bir kömür zonunun ve toplamda da ağırlıklı ortalamaların elde edildiği sahanın geneline ait sonuçlar verilmiştir.

Çizelge 3. Avdan sahası kaynak değerlendirme sonucunda elde edilen miktar ve kalite değerleri

Kömür Zonu	Kaynak (Ton)	Yoğunluk (gr/cm³)	Kalori (Kcal/kg)	Nem (%)	Kül (%)	Uçucu Madde (%)	Kükürt (%)
Sekköy	4 978 236	1.54	1465	39.6	28.3	26.5	2.70
Yenidere - 1	25 494 492	1.48	1768	42.5	24.0	23.6	2.34
Yenidere - 2	1 181 852	1.71	1225	30.8	43.8	18.5	4.02
Genel Toplam	31 654 580	1.50	1700	41.6	25.4	23.8	2.46

AVDAN VE NARLI KÖMÜR SAHALARININ BİRLEŞTİRİLMESİ

Kaynak modelleri hazırlanırken, kömürün devamlı olduğu sahalarda, kömür sınırları ruhsat sınırları olarak alınmakta ve kaynak miktarı ona göre hazırlanmaktadır. Ruhsat sınırları kömür sınırlarına göre tayin edilmediğinden, bu durumda sahadaki kaynağın gerçek miktarının önünde bir engel teşkil etmektedir.

Bunun yanında, birbirine komşu iki ruhsat ile sınırlandırılan kömür sahalarında, özellikle açık işletme faaliyetleri ile üretim yapılırken, işletmeler birbirlerinin dekapajını yapmak zorunda kalmamak adına kömürü topuk olarak bırakmakta bu da sahadaki kömürün zayi olmasına sebebiyet vermektedir. Şekil 6'da Avdan ve Narlı kömürlerinin ayrı iki açık ocak ile üretilmesi durumunda ortaya çıkacak muhtemel geometri verilmiştir.

Çizelge 4. Narlı sahası kaynak değerlendirme sonucunda elde edilen miktar ve kalite değerleri

Kömür zonu	Kaynak (Ton)	Birim Hacım Ağırlığı (ton/m³)	Alt Isıl Değeri (kcal/kg))	Kükürt (%)	Nem (%)	Uçucu Madde (%)	Kül (%)
A	45,596	1.30	1979	2.97	49.48	27.09	17.58
B	839,991	1.29	1939	2.84	49.77	29.48	17.86
C	1,011,775	1.35	1933	1.97	43.82	28.28	21.48
D	999,161	1.37	1820	1.98	42.39	22.86	25.58
E	6,965,540	1.38	1883	2.02	41.77	25.89	25.13
F	13,594,886	1.38	1958	2.22	41.23	26.37	23.95
G	16,155,695	1.41	1936	2.61	38.6	24.99	27.42
Toplam	39,612,644	1.39	1931	2.35	40.54	25.75	25.41

İki ocak arasında kalan bölgenin Avdan bölgesinde başlayan ve Narlı bölgesinde devam eden kömür ile dolu olma ihtimali çok yüksektir. Bu durumda, Şekil 7'de verildiği üzere, sahada yapılacak bir seri arama faaliyetiyle birlikte sahadaki kömür kaynağının artırılması mümkün olacaktır. Kömürün yüzeydeki izinden yapılan basit bir kestirimle aşağıda gösterilen bölgede 2,5 milyon ton ile 5 milyon ton arasında kömür olma ihtimali öne çıkmaktadır.

Ruhsatların birleştirilmesi kaynağın artmasını sağladığını, üretim optimizasyonu için çok daha büyük bir alanda çok farklı opsiyonlara imkân sağlamaktadır. Bunun yanında, iç döküme çok daha hızlı geçilmesine ve bağlı olarak çok daha fazla malzemenin iç dökümde depolanmasını sağlamaktadır. Bu da çevresel etkinin en aza indirilmesi anlamına gelmektedir. Ruhsat birleştirilmesi, aynı miktarda dekapaj ile

çok daha fazla kömür üretimi sağlayacağı için, madenin ekonomikliğini artıracağı gibi, komşu ruhsatların topuk bırakma mecburiyetinden kaynaklanan kömür kaybına da engel olacaktır.

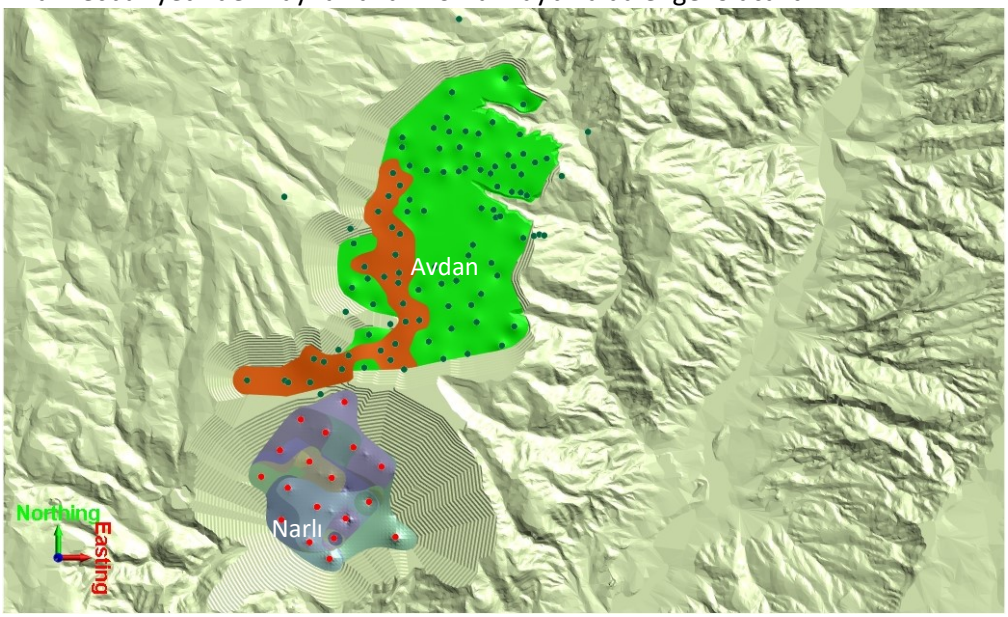

Şekil 8. Avdan ve Narlı kömürleri muhtemel açık ocak sınırları.

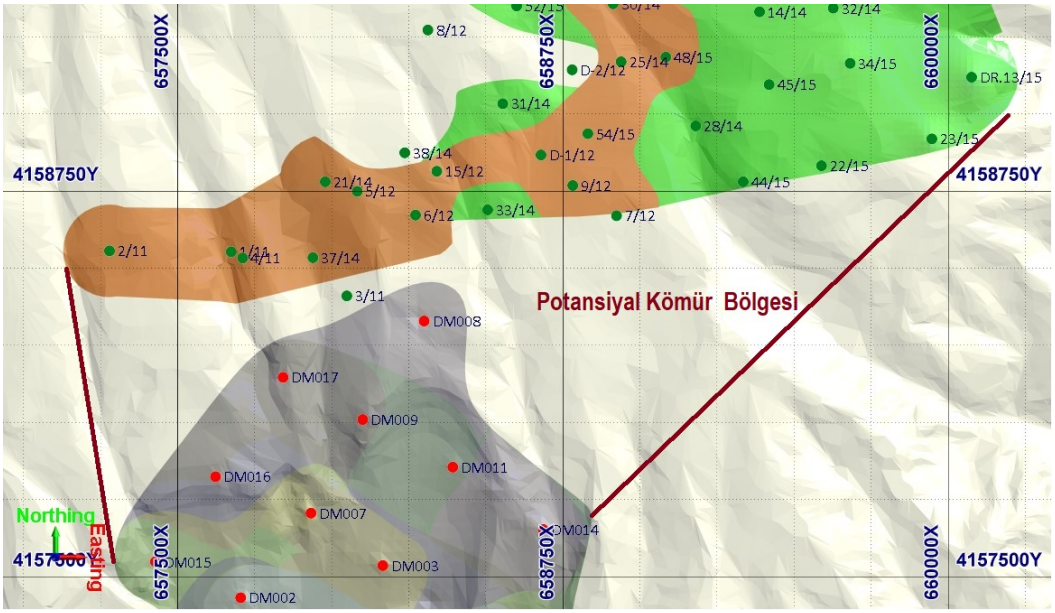

Şekil 9. İki işletme arasında kalan ve muhtemel kömür bulunan bölge.

SONUÇLAR

Bu çalışmada, Avdan ve Narlı kömür sahasındaki linyitin kaynak modellemesi için yapılan çalışmalardan elde edilen sonuçlar paylaşılmıştır. Kaynağın tespitine yönelik sondaj veri tabanı inceleme çalışmalarından sonra, Avdan ve Narlı bölgelerindeki kömür zonlarının katı ve blok modelleri üretilerek, kömür kaynağının miktar ve kalite değerleri elde edilmiştir. Elde edilen sonuçlara göre, Şekil 8'de sınırları verilen Avdan sahasında 31,6 milyon ton kaynağın ortalama alt ısıl değeri 1700 kcal/kg olarak belirlenirken, Narlı bölgesindeki kaynağın ortalama alt ısıl değeri 1936 kcal/kg olan 39,6 milyon ton kömürden oluştuğu tespit edilmiştir. Avdan bölgesinde kömür modelinde kullanılan sondaj sayının sahayı temsil etme yeteneği yeterli olduğundan kaynak görünür olarak sınıflandırılırken, Narlı

bölgesindeki sınırlı sondaj sayısından dolayı kaynak muhtemel olarak sınıflandırılmaktadır. Birbirine komşu iki ruhsat sahasının tek bir üretim projesiyle değerlendirilmesi durumunda kaynak modeli tüm kömürleri kapsayacak şekilde revize edileceğinden kaynak miktarının artması sağlanacaktır. Böylece, aynı dekapaj miktarıyla çok daha fazla kömür üretimi olacağından; üretim maliyetlerinin düşmesi, iç döküme hızlı geçilebilmesi sonucunda döküm maliyetlerinin azalmasının, dökümün çevreye olan etkilerinin en düşük seviyede tutulması ve bağlı olarak kaynağın enerji üretimde çok daha verimli bir şekilde kullanılması mümkün hale gelecektir. Bölgede üretilecek olan kömürün, 450 MWe kapasiteli bir termik santrale beslenmesiyle ilgili bir örneğin değerlendirilmesi durumunda, santralin yaklaşık 20 yıllık kömür ihtiyacının karşılanacağı ve bunun için yıllık 3,7 milyon tonluk bir üretim hedefine ihtiyaç duyulacağı sonuçları ortaya çıkmaktadır. İki ruhsatın birleştirilmesi durumunda ise, yukarıda sayılan avantajlardan dolayı, üretim kayıplarının azalması ve ruhsatlar arasındaki kömürün de üretilmesi sonucunda, termik santralin çok daha uzun yıllar bölgeden çıkartılacak kömürle beslenebileceği anlaşılmaktadır. Bu araştırma özelinde elde edilen sonuçların tüm komşu ruhsat sahalar için de geçerli olabileceği düşünülecek olunursa, ruhsat birleştirilmesi sonucunda, ülke kaynaklarının çok daha verimli kullanılacak ve ülkemiz yeraltı zenginliklerinin israf edilmesinin önüne geçilecektir.

TEŞEKKÜR

Bildiri konusu faaliyetler, Avdan Madencilik Enerji San. ve Tic. A.Ş. ve As Madencilik AŞ'ye ait Avdan ve Narlı kömür sahalarında yapılan proje faaliyetlerinin birer değerlendirilmesi olup, yazarlar, ruhsat sahibi İşletmelere vermiş oldukları destek ve izinden dolayı teşekkür ederler.

KAYNAKLAR

Akgün, F., Sözbilir, H. (2001). A palynostratigraphic approach to the SW Anatolian molasse basin: Kale-Tavas molasse and Denizli molasse. *Geodinamica Acta, 14 ,* 71-93

Alçiçek, H. (2010). Stratigraphic correlation of the Neogene basins in southwestern Anatolia: Regional palaeogeographical, palaeoclimatic and tectonic implications. *Palaeogeography, Palaeoclimatology, Palaeoecology, 291,* 297-318.

Hakyemez, H.Y. (1989). Kale-Kurbalık (GB Denizli) bölgesindeki Senozoyik yaşlı çökel kayaların jeolojisi ve stratigrafisi. *Maden Tetkik ve Arama Dergisi, 109,* 9-21.

Isaaks, E. H. ve Srivastava, R. M. (1989). An introduction to applied geostatistics. Oxford University Press, New York.

Lashgari, M. vd. (2016). Modelling a multi layer coal mine deposit a case study of Avdan lignite site in Denizli Turkey. Thirty - Third Annual Pittsburgh Coal Conference.

MCS (2015). Independent technical report to JORC (2012) Guidelines Narli coal project for As Madencilik. Proje no:30148, Teknik Rapor.

Öztürk, C.A. (2001). Maden yataklarının değerlendirilmesinde PCSV ve kriging tekniklerinin karşılaştırılması. Yüksek Lisans Tezi, İTÜ Fen Bilimleri Enstitüsü.

Sözbilir, H. (2002). Revised stratigraphy and facies analysis of the Palaeocene-Eocene supra-allochthonous sediments and their tectonic significance (Denizli, SW Turkey). *Turkish Journal of Earth Sciences, 11,* 127.

Sözbilir, H., Özer, S., Sarı, B. (2000). Stratigraphy and tectonics of the late Palaeocene-Eocene supra allochthon basin formed on the Lycian nappes, Denizli province-SW Turkey. International Earth Sciences Colloquium on the Aegean Region (pp 32). Abstracts.

DETERMINATION OF FACTORS AFFECTING METHANE EMISSION USING THE FAULT TREE ANALYSIS METHOD

METAN EMİSYONUNA ETKİ EDEN FAKTÖRLERİN HATA AĞACI ANALİZİ YÖNTEMİ İLE BELİRLENMESİ

N. Kursunoglu [1, *]

[1]*Batman University, Department of Petroleum and Natural Gas Engineering*
*(*Corresponding author: nilufer.kursunoglu@batman.edu.tr)*

ABSTRACT

The coalification process produces coal mine methane (CMM). When organic material decomposes, it creates methane gas, as well as nitrogen, carbon dioxide, and other gases. Due to the explosive nature of CMM, it is considered a hazard for underground coal mining. During mining operations, a significant amount of adsorbed methane from the coal structure is released into the mine air, posing a threat to worker safety and reducing production efficiency. Despite the use of many measures to mitigate methane leaks, methane remains a major hazard in underground coal mines. Thus, it is critical to understand the components that contribute to methane emissions to guarantee a safe work environment and effective gas control planning. The fault tree analysis (FTA) method was used in this study to determine the parameters responsible for methane emissions in coal mines. The FTA, which is a flexible and systematic approach to risk assessment that enables the identification and classification of hazards, was used to determine the effective emission factors of the study.

Keywords: Methane, emission, mine, coal, risk, fault tree analyses

ÖZET

Metan gazı kömürleşme sürecinde meydana gelir. Kömürün oluşma sürecinde, ayrışan organik materyaller metan gazının yanı sıra nitrojen, karbondioksit ve farklı gazlar üretir. Metan gazı patlayıcı özelliği nedeniyle yer altı kömür madenciliği için bir risk teşkil etmektedir. Madencilik faaliyetleri sırasında, kömür yapısındaki büyük miktarda adsorbe edilmiş metan gazı ocak havasına yayılır, bu durum iş güvenliğini tehdit eder ve üretim verimliliğini düşürür. Metan emisyonunu kontrol etmek için çeşitli yöntemler uygulanmasına rağmen, yeraltı kömür madenleri için tehdit olmaya devam etmektedir. Bu nedenle, metan emisyonunu etkileyen faktörlerin belirlenmesi, güvenli bir çalışma ortamı ve gaz kontrol planlaması sağlamak için gereklidir. Bu çalışmada, kömür madenlerinde metan emisyonuna neden olan parametreleri belirlemek amacıyla hata ağacı analizi (FTA) yöntemi kullanılmıştır. Tehlikelerin tanımlanmasına ve sınıflandırılmasına olanak tanıyan, esnek ve sistematik bir risk değerlendirme yaklaşımı olan FTA, çalışmada etkili emisyon faktörlerinin belirlenmesi için kullanılmıştır.

Anahtar Sözcükler: Metan, emisyon, maden, kömür, risk, hata ağacı analizi

INTRODUCTION

Methane is one of the most dangerous gases found in underground coal mines. It has no color, no odor, and is lighter than air. Methane that has accumulated in the roof is extremely dangerous. Because it is explosive and also results in suffocation as it depletes the oxygen content of the air. Outside of certain limits, methane is flammable. The intensity with which methane burns is dependent on the amount of oxygen and methane in the air. Between 5.5% and 15%, it is explosive. Explosions of

gas are highly hazardous for workers and mines. As a result, precautions against gas explosions in mines should be taken. These measures are intended to reduce the amount of methane in the air and to prevent explosions. Methane is a product of the gradual transformation of plant wastes accumulated during the carboniferous period. Numerous environmental factors convert these plant wastes first to peat, then to lignite, and finally to bituminous coal, whose rank increases over time. Several gases are formed at varying rates and time intervals during this process. Various gases escaped in various ways and mixed with the air or leaked between the layers. Others remained trapped within the organic matrix. A part of the free gas permeates into the pores and cracks of the coal and the adjacent layers. However, coal absorbs and adsorbs the majority of methane. The adsorbed gas is compressed onto the porous coal or stone surface. The absorbed gas is contained within the coal. During coal mining, methane gas is partially released into the atmosphere. This occurs in three distinct ways: (1) Gases are continuously emitted from extremely small pores in coal or stone, (2) Gas emissions from visible cracks and holes frequently persist for an extended period, (3) A sudden, massive gas eruption accompanied by large amounts of coal and stones. Methane emissions increase proportionally to the mine's depth. Because the methane accumulated in the depths was unable to permeate the earth.

Underground coal mining is subject to several natural hazards, the most dangerous of which is methane. It is caused by methane leakage during the hard coal extraction process. When this gas reaches a specific concentration, it turns flammable and explosive. Explosions or ignitions of methane in an underground mine heading pose a significant risk, one that has been observed to be increasing in recent years. This is due to the exploitation of methane-bearing coal beds, the depth of mining operations, and the high concentration of extraction. Fault tree analysis is one of the most effective methods for incident analysis. Accident investigations are deductive, and fault tree analysis is frequently used to determine the underlying causes of accidents. Fault tree analysis is conducted to identify the factors that contributed to the unfavorable top event. It is easier to see the relationships between the causes and to identify the root causes when the tree is constructed (McPherson, 1993; Rajput and Thakur, 2016). The purpose of this study was to investigate the root causes of methane emissions that may occur in underground coal mines using the fault tree analysis method. The study concluded by determining the probabilities of the parameters affecting methane emission.

Fault Tree Analyses

The purpose of fault tree analysis is to systematically identify the primary faults that contribute to the undesirable situation. Fault tree analysis (FTA) is a technique used for both qualitative and quantitative risk assessment. At first, qualitative analysis is used. Qualitative analysis is used to determine the top event and, as a result, the root causes by identifying the events and circumstances that prompted it. Probability theory and Boolean equations are the foundations of quantitative analysis. FTA consists primarily of two gates: And-Gate and Or-Gate. The development of these two doors essentially resulted in the development of the other doors. If all And-Gate-related events fail, the output event occurs, which is a higher-level fault tree event. According to Boolean algebra, it is represented by "+," and the probabilities of the events connected by this gate are summed. The term "Or-Gate" refers to the output event that occurs when at least one of the output events occurs. According to Boolean algebra, it is represented by "•," and the probability of the output events is determined by multiplying their probabilities (Stamatelatos and Caraballo, 2002). Table 1 contains the symbols and definitions for these gates. The FTA consists of eight main steps (Figure 1).

Table 1. Events and gates used in Fault Tree Analysis (Whitesitt, 1995).

Symbol	Description
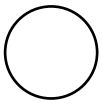 Basic event	Means an event that does not require further development or progress
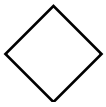 Undeveloped event	Signifies an unfinished event. This indicates that the event was unable to be developed due to a lack of data or for any other reason.
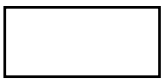 Intermediate event	Connects one or more antecedent events between logic gates.
 AND-gate	To output events occur, all events connected by the And-Gate should occur.
 OR-gate	The input event is caused by the occurrence of at least one of the output events.

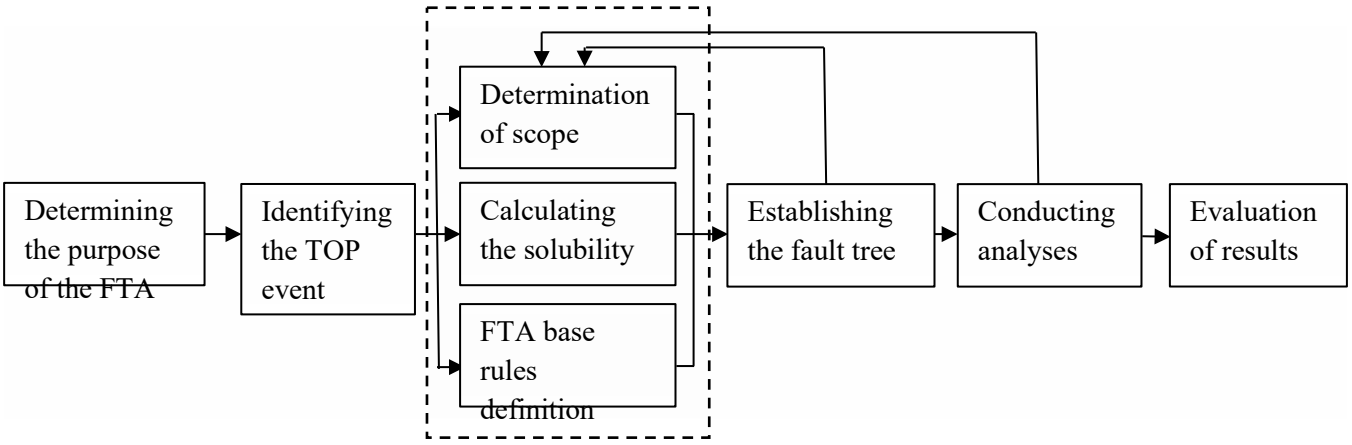

Figure 1. Fault Tree Analysis flowchart (Stamatelatos and Caraballo, 2002).

Application Of Fault Tree Analysis

The world's underground mining industry has resulted in many disasters involving methane ignition and explosions. It should be emphasized that underground coal exploitation is inevitably linked to the methane hazard and always will be. This is because methane was formed concurrently with the formation of coal beds. As a result, exploitation of these beds will naturally result in the release of this gas, which is referred to as coal-mine methane or coal-bed methane in this case. Additionally, it should be emphasized that methane, in addition to posing a safety risk in coal mines, is one of the most harmful greenhouse gases and poses a significant risk to the natural environment (Tutak and Brodny, 2019).

While the number of injuries and fatalities caused by methane emissions has decreased over time, there are still several safety concerns. As a result, a comprehensive risk assessment is a necessary component of determining the sources of methane emissions and preventing the occurrence of hazards to improve the mine environment's safety. Risk assessment is a process that enables the analysis of risk in terms of outcomes and possibilities before determining how potential risk may affect objectives and determining whether additional intervention is necessary. After hazard identification, various methods are required to comprehend the hazards' nature and mechanism of action, as well as the consequences of notable hazards. Numerous risk analysis methodologies are available. Risk assessment can be conducted qualitatively, quantitatively, or hybrid. Qualitative assessment approaches contain ‘‘what-if” analyses, checklists, task analyses, safety audits, sequentially timed event plotting (STEP) technique, and hazard and operability (HAZOP). Quantitative risk assessment approaches contain the proportional risk-assessment technique (PRAT), failure mode and effects analysis (FMEA), Fine Kinney, decision matrix risk-assessment (DMRA), and weighted risk analysis (WRA). Hybrid risk assessment approaches contain human error analysis techniques (HEAT), fault tree analysis (FTA), event tree analysis (ETA), and risk-based maintenance (RBM) (Animah and Shafiee, 2020). To analyze the events that result in methane emissions and determine their consequences in this study, the fault tree analysis method was chosen. FTA analysis was carried out using the DPL 9 Fault Tree software. The top event was determined as 'coal methane emission' as the first step of the FTA. After defining the top event, three major factors influencing the occurrence of these accidents were identified. These factors were determined as “coal properties”, “geological conditions”, and “mining parameters” (Figure 2). These factors were interconnected with the OR-gate.

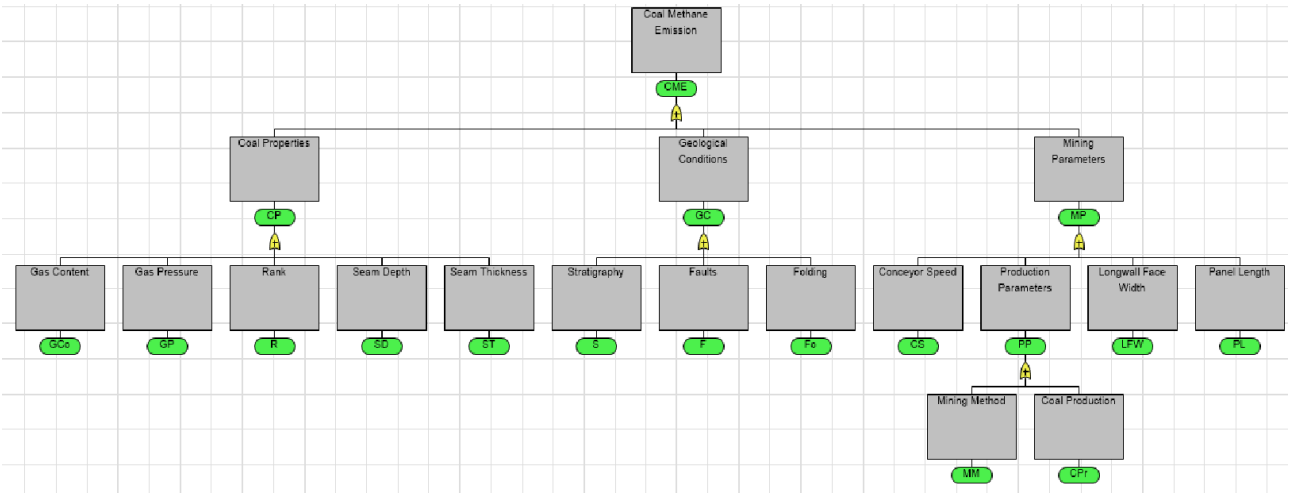

Figure 2. Fault tree of the study

The possible causes of coal properties were determined as “gas content”, “gas pressure”, “rank”, “seam depth”, and “seam thickness”. These branches could have an impact on the coal

properties. Thus, the OR-gate was used to connect them to “coal properties” (Figure 3). “Geological conditions” can be influenced by “stratigraphy”, “faults”, or “folding”. For this reason, these four parameters were connected with the OR-gate to “geological conditions” (Figure 4). “Mining parameters” can be impacted by one of four distinct basic events: “conveyor speed”, “production parameters”, “longwall face width”, or “panel length”. “Production parameters” can be affected by “mining method” or “coal production” (Figure 5).

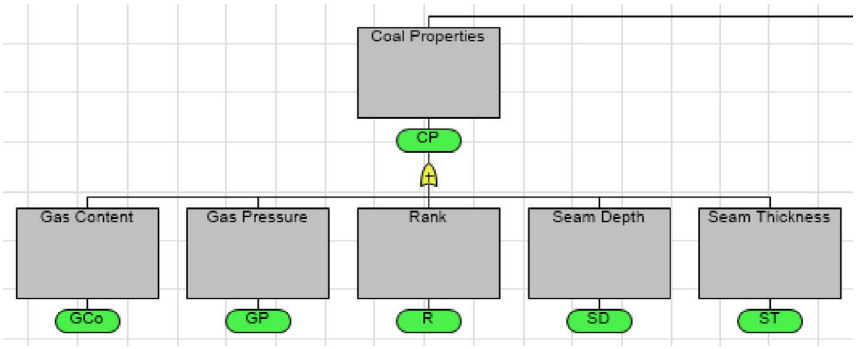

Figure 3. Fault tree of coal properties

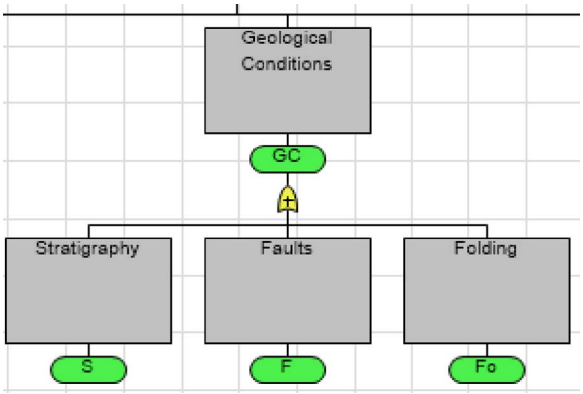

Figure 4. Fault tree of geological conditions

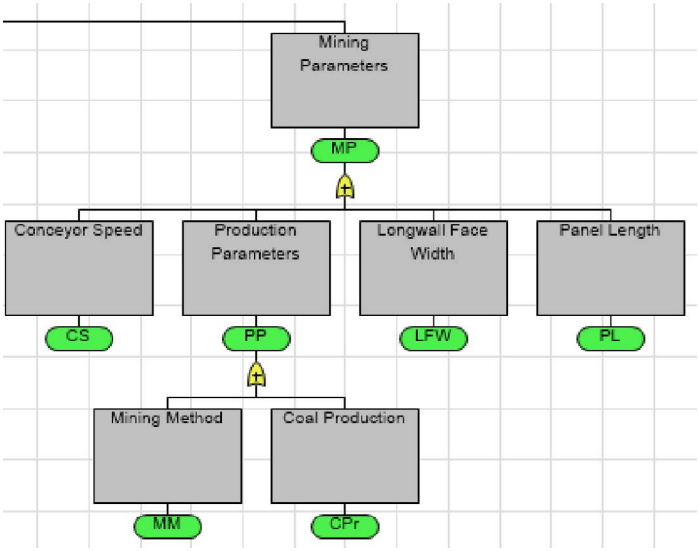

Figure 5. Fault tree of mining parameters

RESULTS

To determine the prominent emission factors, the probabilities of the basic events were assigned using the scale in Table 2. The probability of gates calculated by the software is given in Table 3. Figure 6 depicts the results graphically. The major events that resulted in methane emission were identified, including gas content, seam depth, and seam thickness.

Table 2. Probability scale (Iverson et al., 2001)

Qualitative values	Quantitative values
Certain	1
Very high	10^{-1}
High	10^{-2}
Moderate	10^{-3}
Low	10^{-4}
Very low	10^{-5}
Extremely low	10^{-6}
Practically zero	10^{-7}

Table 3. Probabilities of the basic events and gates

Gate	Basic Event	Probability
Coal Methane Emission		0.126691
Coal Properties		0.119673
	Gas content	0.100
	Gas pressure	0.001
	Rank	0.001
	Seam depth	0.010
	Seam thickness	0.010
Geological Conditions		0.002997
	Stratigraphy	0.001
	Faults	0.001
	Folding	0.001
Mining Parameters		0.004990
	Conveyor speed	0.001
	Longwall face width	0.001
	Panel length	0.001
Production Parameters		0.001999
	Mining method	0.001
	Coal production	0.010

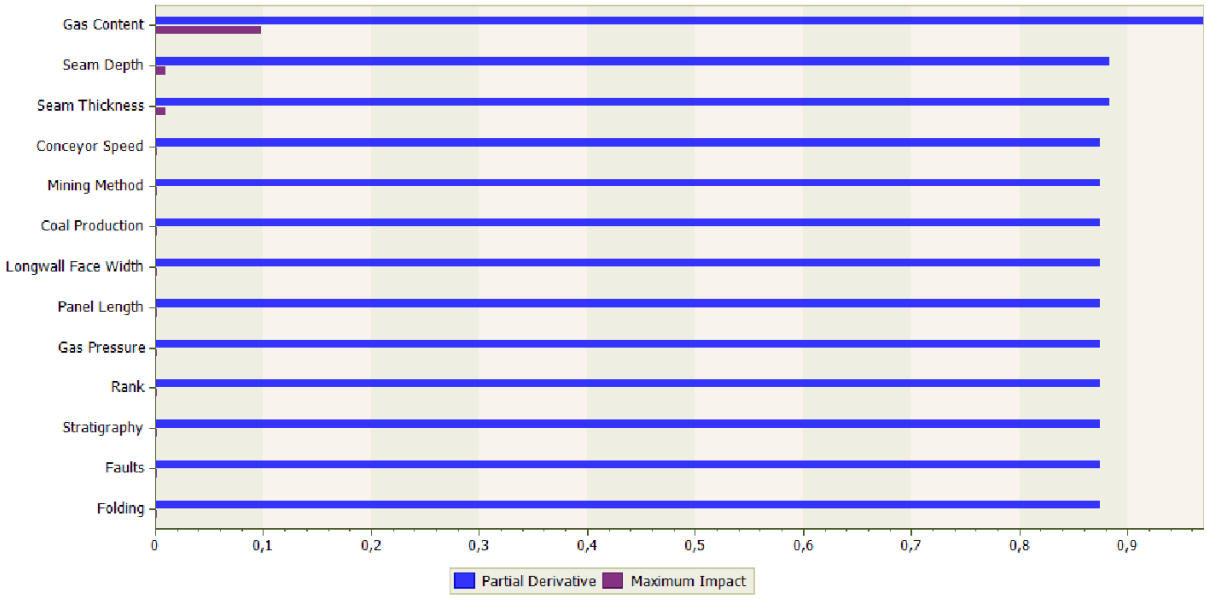

Figure 6. Graphical representation of the results

CONCLUSIONS

Several factors influence methane emissions from coal mines, including coal characteristics, geological conditions, and mining parameters. The potential methane emission causes could have a substantial effect on the incidence of emissions during mining. It is vital to identify these elements so that efficient preventive actions may be implemented, and mine ventilation air can be planned. Thus, the fault tree analysis method was chosen for analyzing the factors affecting the emission formation within the scope of the study. The fault tree analysis allows for the most effective measures to be taken to mitigate the effects of an error or failure. The prioritizing of contributors (intermediate faults and events) to unwanted occurrences is one of the most essential features of the fault tree analyses. 13 significant basic events were identified in this study. The most efficient criteria for methane emission were determined to be gas content, seam depth, and seam thickness using fault tree analyses. The probability of methane emission as a result of basic events was calculated to be 12.66%. This study enables the identification of possible causes of accidents in underground mines and the quantification of their impacts.

REFERENCES

Animah, I., Shafiee, M. (2020). Application of risk analysis in the liquefied natural gas (LNG) sector: An overview. *Journal of Loss Prevention in the Process Industries*. *63*, 103980.

Iverson, S., Kerkering, J.C., Coleman, P. (2001). Using fault tree analysis to focus mine safety research. 108th Annual Exhibit and Meeting, Society for Mining, Metallurgy, and Exploration, Denver, CO.

McPherson, M. J. (1993). Subsurface Ventilation Environmental and Engineering. Chapman & Hall.

Rajput, S., Thakur, N. K. (2016). Geological controls for gas hydrates and unconventionals (1st ed.) Elsevier.

Stamatelatos, M., Caraballo, J. (2002). Fault tree handbook with aerospace applications. Washington, DC: NASA.

Tutak, M., Brodny, J. (2019). Forecasting methane emissions from hard coal mines including the methane drainage process. *Energies*. *12*, 3840.

Whitesitt, J. E. (1995). Boolean algebra and its applications (1st ed.). Mineola, New York: Courier Dover Publications.

DETERMINATION OF STRENGTH PARAMETERS FOR SPECIMENS PREPARED BY 3D PRINTED DISCONTINUITY PLANES

A. Kırmacı[1, *], Asst.Prof.Dr. M. Erkayaoğlu[1], Asst.Prof.Dr. A.G. Yardımcı[1]

[1] *Middle East Technical University, Mining Engineering Department*
**Corresponding Author: Email: kirmaci@metu.edu.tr*

ABSTRACT

Mining activities in sustainable and safely operated underground mines depend on the design of openings using rock strength-related parameters representing site conditions as much as possible. Rock specimens must be collected and prepared for experiments to obtain intact rock properties. In particular, it is almost impossible to represent field conditions in experimental environments completely. A well-known example of this challenge is the representation of discontinuities on site. At this point, using current technologies could improve the level of representation of specimens where 3D printers could be used to manufacture existing discontinuity planes that reduce the strength of intact rock material. In this context, a 3D printed discontinuity plane is used to prepare concrete mortar specimens. Static deformability experiments of these samples were completed to determine the strength parameters. As a result, the uniaxial compressive strength value of concrete samples without discontinuity planes was obtained in addition to the samples with rough, wavy, and smooth discontinuity planes. Finally, the results were compared with stress concentration factors obtained from the numerical models.

Keywords: 3D printer, 3D printed discontinuity, concrete, numerical modeling

INTRODUCTION

Mining activities have a significant role in the sustainable development of countries. Turkey is located in a geographical region wealthy in terms of underground and surface resources. The continuously increasing demand for energy and raw materials has reinstated the critical role of mining activities. Rock mechanics experiments are of great importance in the realization of these activities. The accuracy of the rock mechanics test results and the design criteria defined according to these results ensure the continuity and reliability of mining, especially in underground operations.

In some cases, the collection and preparation of rock samples used during rock mechanics experiments can cause technical difficulties. In recent years, samples printed with 3D printers have been used worldwide by various researchers as an alternative to the samples collected and prepared in a laboratory environment. Thus, it is aimed to reduce the effort of sample preparation for the experiments and to reflect the conditions on-site more accurately by including weakness planes and different filling materials. For example, collecting core samples containing a representative discontinuity requires an expert opinion. It is expected that rock-like samples prepared by 3D printing will result in a better representation of discontinuities within the scope of the study.

As a result of the preliminary literature research in this field, 3D printer technology has been used in different areas of rock mechanics-related research (Jaber et al., 2020; Jiang et al., 2016; Ju et al., 2017; Zhou, Zhu and Xie, 2020; Wu et al., 2020). Some researchers printed rock-like samples with 3D printers, whereas others printed discontinuity planes to be placed within rock samples to carry experiments. Different researchers investigated the load displacement response for various purposes (B.

Tarasov and Potvin 2013; Verma, et al., 2021). In this study, concrete samples were prepared by using 3D-printed molds. Afterward, the individual parts of the samples were joined with plaster, which has a comparably lower strength than the laboratory samples. Static deformability tests were performed to compare mechanical properties of the different roughness profiles of discontinuities. It is foreseen that this study will contribute to rock mechanics literature and the implementation of 3D printing technology for laboratory testing of rocks.

The collection of rock samples during field studies can be considered one of the first stages of sample preparation for laboratory experiments. At this point, 3D printers might provide convenience to researchers that use complex specimen geometries for fracture mechanics or profiles that represent discontinuities. One of the research questions is whether a 3D printed sample can be used instead of a rock sample. Based on the work of Hucka and Das (1974), it has been shown that each rock type has a unique index of brittleness. This index is calculated using the formula shown below.

$$Brittleness\ Index = \frac{\sigma_c + \sigma_t}{\sigma_c - \sigma_t} \quad (1)$$

The symbols σ_c and σ_t used in the formula represent the uniaxial compressive strength value and the direct tensile strength value, respectively. The brittleness index value differs according to the rock types. While this value generally varies between 5-25 in actual rock samples, this value varies between 3.5-4 in 3D printed samples (Vrkljan, 2009). At this point, the material used in printing samples with 3D printers is creating a variance of mechanical properties. As a result of the comparison of values, it is seen that 3D printed samples might be used as artificial copies of rock samples for specific conditions.

Since the desired model can be printed easily and quickly with 3D printers, Song et al. (2018) designed four different tunnel models. The results were compared with tunneling case studies, artificial models, and numerical simulation models. PLA (polylactic acid) and powder-based materials are commonly used in 3D printers. A conventional tunnel model, single fault tunnel, double fault tunnel, and a tunnel model with rock bolt and tunnel lining were designed. Compression tests were completed with all four models, and some similarities were found in the deformation curves and failure characteristics. Likewise, these results showed similarities with the numerical simulation models developed. It has been determined that rock bolts and tunnel linings significantly reduce damage in the tunnel and increase the carrying capacity of the tunnel. The experiments were also monitored with digital image correlation systems, which captured displacement, crack initiation, and propagation.

Monitoring the failure behavior of rock samples during laboratory experiments, such as crack formation and propagation during uniaxial compressive strength testing or indirect tensile strength testing, with current technologies such as digital image correlation, high-speed cameras, thermal cameras, and acoustic emission provides researchers crucial information. Sharafisafa et al. (2019) conducted indirect tensile strength tests using disk-shaped samples taken from a 3D printer. The effect of the filling material on the failure behavior of the rock samples was investigated by opening cracks at different angles on the samples they prepared and filling the cracks in some samples with a material of different properties. Likewise, the differences between the samples with cracks not filled and samples filled with material were examined. In such analyses, it is essential to determine the exact moment of crack formation and the crack propagation behavior. The researchers were able to achieve detailed results by using a digital image correlation system. As a result of their experiments, it was determined that the samples with filling material were able to resist against higher load than the samples without filling, and shear cracks caused by shear displacement vectors during failure were observed.

Zhu et al. (2018) scanned the rock samples taken from a mine site using an X-ray computed tomography device and structurally copied them with the help of a 3D printer. Static deformability and indirect tensile strength tests were performed on the printed and actual samples recorded with a high-

speed camera. As a result, it has been observed that the uniaxial compressive strength values are very close to each other, but there is a significant difference in the unit deformation values. The reason for this is shown as the difference in the modulus of elasticity. On the other hand, crack initiation and propagation in disc samples used in direct tensile strength tests were determined with the help of the high-speed camera. As a result of the experiment, it was observed that tensile strength values were very close to each other for both samples.

Zhou and Zhu (2018) obtained five different types of samples using ceramic, gypsum, polymethyl methacrylate, SR20 (acrylic copolymer), and resin, respectively, from the materials used in 3D printers and performed static deformability experiments with them. The purpose of conducting these experiments was to determine the material that might be closest to a brittle rock. As a result of the experiments, it has been seen that the most suitable material for the brittle rock type is the resin according to the material's behavior and the maximum applied load. However, it has been mentioned that there is a problem with the brittleness properties of the resin samples. Therefore, there is still potential improvement using the testing methods such as thermal treatment or adding artificial macro and micro cracks.

Fereshtenejad and Song (2016) examined different materials in powder-based 3D printers in their study. It was observed that the materials used showed relatively lower strength values and ductile behavior. Therefore, improvement methods have been studied to enhance these properties. These methods were defined as printing direction, printing layer thickness, the saturation level of binder, uniaxial compressive strength test of samples heated to different temperatures, and examination of stress-strain deformation graphs.

By considering the printing direction, the highest strength value was observed in the samples printed with 0°, while the lowest strength value was found in the samples at 25°. Different printing layer thicknesses were tried, and it was seen that the layer thickness was not an important parameter that could affect the sample strength. Likewise, different amounts of binder saturation level were applied, and it was observed that the uniaxial compressive strength value increased by these varying amounts as an increase in the saturation level. In addition, the temperature of the materials was increased to 70℃, 100℃, 120℃, 150℃, and 170℃, respectively. The results in their initial state were compared with the samples whose temperature was increased. As a result, the value that increases the uniaxial compressive strength value the most and seems to be the ideal temperature has been found as 150 ℃.

Ban et al. (2020) scanned five concrete samples with different surfaces with 3D morphology scanner systems and completed direct shear tests on 20 samples in total by taking four different samples from each sample with the help of a 3D printer. Four different normal loads, 0.5 MPa, 1 MPa, 1.5 MPa, and 2 MPa, were applied to each surface, and shear values were obtained. As a result of the experiments, a new peak shear strength model was created.

As a result of the reviewed literature, it has been seen that the introduction of 3D printer systems into rock mechanics research in the mining industry might provide advantages during sample preparation. The convenience of preparing specimens, using a pre-designed type of material, cracks, fillings, and other structures that can be added within the samples are some of the main benefits of using 3D printers.

EXPERIMENTAL STUDY

Rock mechanics related research has been improving by integrating new technologies recently. It is possible to represent features such as discontinuities and micro-cracks in rock samples by using 3D printing technology. In this way, the effect of these conditions on the mechanical properties of the rock material can be investigated.

This study aims to examine the mechanical properties of concrete samples containing discontinuity planes by using 3D printer technology prepared for static deformability tests. The following aims will be achieved as a result of the experiments:

- Concrete samples prepared into 3D-printed molds containing different discontinuity planes were joined, and their mechanical properties were determined.
- The plaster material used to join the concrete samples was varied to represent the infilling of the printed discontinuity.
- Test results of the 3D printed concrete samples with discontinuities were compared with intact concrete samples.

The methodology of this study covers the laboratory experiments on the 3D printed concrete samples. MTS 815 test system, which provides displacement-controlled loading, was used during the experiments. The experimental setup can be seen in Figure 1.

Figure 1: MTS 815 test system and an experiment which conducted static deformability test

The 3D printer used to produce the molds is a Zortrax M300 with a single printing head, as seen in Figure 2. The maximum dimensions that can be printed are limited to 300x300x300 mm and were considered sufficient for the samples prepared for the experiments. The molds were initially designed with the help of a CAD software and then exported as STL files, as seen in Figure 2. The printer uses ABS-type filament to print the molding material due to its comparably higher strength properties. According to the technical data of the filament, the tensile strength and maximum bending stress are 30.5 MPa and 46.3 MPa, respectively.

Figure 2: Zortrax M300 Plus printer and an example of 3D printed model

Three different 3D printed molds were designed to include varying discontinuity profiles. The three types of molds have a 45° inclination plane, and for each mold sample, the roughness plane was printed as smooth, rough, and wavy, as shown in Figure 3, respectively.

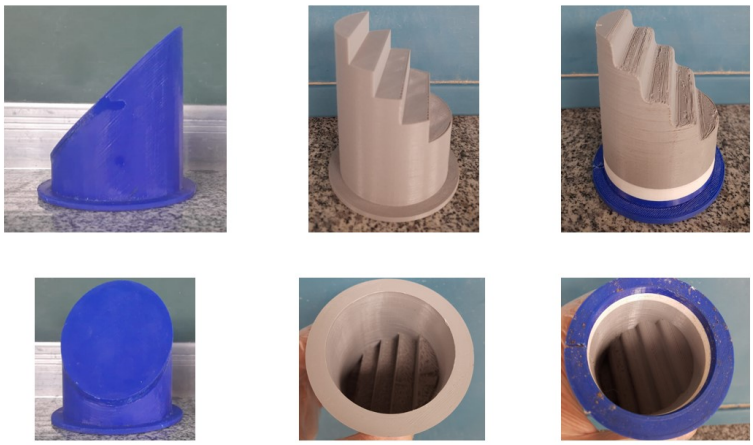

Figure 3: Different roughness planes prepared with the help of 3D printing technology

Concrete samples prepared for the laboratory tests have a mix design of cement, aggregates, and water ratio of 1:4:0.75. The prepared concrete mixture was poured into the 3D printer molds and cured for a total of seven days. Concrete samples extracted from the molds can be seen in Figure 4.

Figure 4: The concrete samples prepared with the help of 3D printed molds

Finally, the samples prepared using the 3D printed molds were joined with plaster material. The purpose of using plaster as filling material that was cured for 1 day to ensure that the discontinuity plane is represented by a material with lower strength than the rock sample. In Figure 5, the samples with smooth, rough, and wavy discontinuity planes joined with the help of plaster are seen.

Figure 5: Concrete samples with smooth, rough, and wavy discontinuity planes joined with plaster, respectively

Static deformability tests were completed on three concrete samples and four plaster samples that do not have any discontinuity planes. In this way, the mechanical properties of the concrete and plaster materials were obtained. For the concrete samples, the mix design of cement, sand, and water was kept the same. In Figure 6, the before test and after test photographs of the concrete samples can be seen.

Figure 6: Before test and after test images of concrete samples

Four different ratios were used as plaster sample designs, and the most suitable ratio was used to join the samples. In sample A1, 80% plaster and 20% aggregates, for the A2 sample, 50% plaster and 50% aggregates were used. In A3 and A4 samples, cement was substituted for aggregate, and 80% plaster, 20% cement, 50% plaster, and 50% cement ratios were used. In Figure 7, before test and after test images of 4 different plaster samples can be seen.

Figure 7: Before test and after test images of plaster samples

RESULTS AND DISCUSSION

In this section, the static deformability test results of concrete and plaster samples will be discussed. First, three concrete samples prepared with the same cement, aggregate, and water ratio were tested. Before test and after test images of concrete samples are presented in Figure 6. The experiment results for concrete samples are summarized in Table 1.

Table 1. Static Deformability Test Results for Concrete Samples with no discontinuity (Core material)

Specimen	**Dia. (mm)**	**Length (mm)**	**UCS (MPa)**	**E (GPa)**
B1	72.2	154.8	5.2	3.2
B2	72.6	152.4	2.6	7.4
B3	72.4	152.2	5.5	3.0
Average			**4.4**	**4.5**

According to the results of the experiments, an average uniaxial compressive strength value of 4.4 MPa was observed for the concrete samples, while the elastic modulus was calculated as 4.5 GPa.

After the concrete samples, static deformability tests were performed on four different plaster samples. Plaster-sand and plaster-cement ratios are mentioned in the “Experimental Study” section Table 2 shows the mechanical parameters obtained as a result of the experiments. Since plaster samples represent infilling material for the discontinuity, it was expected to have lower strength than concrete samples. Accordingly, as a result of the experiments, it was seen that the strength value of the A1 sample was lower than required, and the A4 sample was higher than required. Therefore, it was considered to use A2 (50% plaster and 50% aggregates) or A3 (80% plaster and 20% cement) samples during the experiments as the most suitable material for joining the samples. As a result, plaster samples with uniaxial compressive strength of 2.3 MPa were used to assemble the samples prepared with the 3D molds.

Table 2: Static Deformability Test Results for Plaster Samples with no discontinuity (Filling material)

Specimen	**Dia. (mm)**	**Length (mm)**	**UCS (MPa)**	**E (GPa)**
A1	71.1	154.9	1.2	1.4
A2	71.9	155.3	2.3	3.2
A3	71.9	154.9	2.9	4.6
A4*	72.1	152.2	13.1	5.2
Average			**2.2**	**3.1**
*** outlier**				

After the mechanical parameters of the concrete samples and the appropriate plaster ratio to be used to combine the samples were found, the samples taken from the 3D printers were combined, and static deformability tests were carried out. Firstly, static deformability tests of concrete samples with a 45-degree inclination and smooth discontinuity plane were carried out. Two concrete specimens with a smooth discontinuity plane were tested. In Figure 8, the before test and after test images of these experiments can be seen.

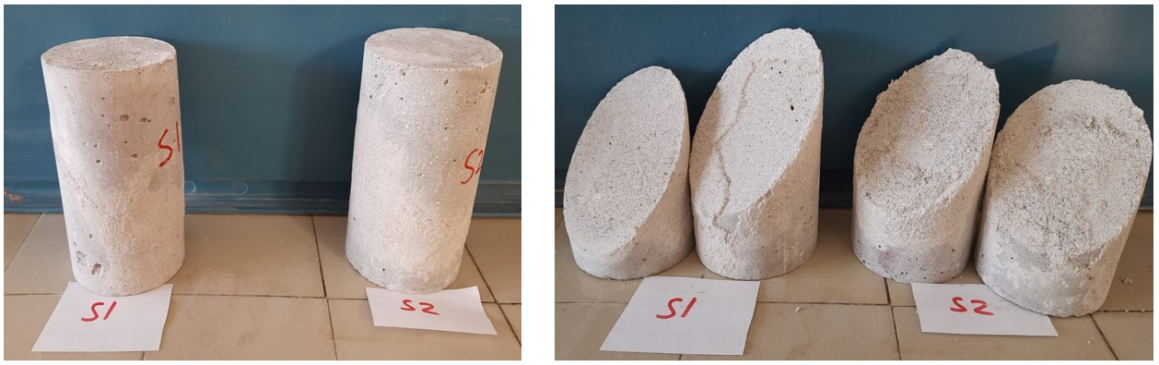

Figure 8: Before test and after test images of concrete samples with smooth discontinuity planes

As shown in Figure 8, the sample failed from the discontinuity plane, which has a lower strength value. Table 3 shows the mechanical parameters obtained as a result of these experiments.

Table 3: Static Deformability Test Results for Concrete Samples with smooth discontinuity planes

Specimen	Dia. (mm)	Length (mm)	UCS (MPa)	E (GPa)
S1	72.7	140.4	1.7	6.7
S2	72.1	145.9	3.7	3.7
Average			**2.7**	**5.2**

By considering Table 3, the average UCS value for specimens with smooth discontinuity planes is 2.7 MPa, while elastic modulus is 5.2 GPa.

Similarly, static deformability tests of concrete samples with a 45-degree inclination and rough discontinuity plane were carried out. Two concrete specimens with a rough discontinuity plane were tested. In Figure 9, the before test and after test images of these experiments can be seen.

Figure 9: Before test and after test images of concrete samples with rough discontinuity planes

As shown in Figure 9, the failure surfaces representing lower strength regions filled with plaster materials were observed. Unlike the smooth plane samples, failures occurred at the top, where the thinnest layer is located. This was explained as the stress concentration regions created by the sharp transitions of the geometry during the static deformability test. Table 4 shows the mechanical parameters obtained as a result of these experiments.

Table 4: Static Deformability Test Results for Concrete Samples with rough discontinuity planes

Specimen	**Dia. (mm)**	**Length (mm)**	**UCS (MPa)**	**E (GPa)**
R1	63.3	132.7	3.9	2.3
R2	63.1	132.1	6.5	1.7
Average			**5.2**	**2.0**

By considering Table 4, the average UCS value for specimens with rough discontinuity planes is 5.2 MPa, while elastic modulus is 2.0 GPa.

Finally, static deformability tests were carried out of concrete samples with a 45-degree inclination and wavy discontinuity plane. Two concrete specimens with a wavy discontinuity plane were tested. In Figure 10, the before test and after test images of these experiments can be seen.

Figure 10: Before test and after test images of concrete samples with wavy discontinuity planes

As shown in Figure 10, the failure properties of the wavy discontinuity planes on the concrete samples are similar to the rough discontinuity plane samples. Similarly, failure occurred in the weak plaster layer within the samples with the wavy plane, and similar stress concentration points were observed at the top of the specimen. Table 5 shows the mechanical parameters obtained as a result of these experiments.

Table 5: Static Deformability Test Results for Concrete Samples with wavy discontinuity planes

Specimen	**Dia. (mm)**	**Length (mm)**	**UCS (MPa)**	**E (GPa)**
W1	63.1	131.1	4.9	0.8
W2	63.3	131.9	4.9	2.5
Average			**4.9**	**1.7**

By considering Table 5, the average UCS value for specimens with wavy discontinuity planes is 4.9 MPa, while elastic modulus is 1.7 GPa.

Numerical modeling of each concrete sample with a different roughness plane was performed in FLAC 8.0, a time marching code based on 2D plane-strain assumption. For the input parameters of concrete and plaster, the results of the laboratory experiments were used. After generating the 2D

model, a uniaxial loading condition was defined by applying velocity from the top and bottom ends of the model. Stress analyses were carried out using an elastic material model. Interpretations considering stress concentration around discontinuity planes for the pre-failure region are presented. First, a concrete sample with a smooth discontinuity plane was modeled, as shown in Figure 11.

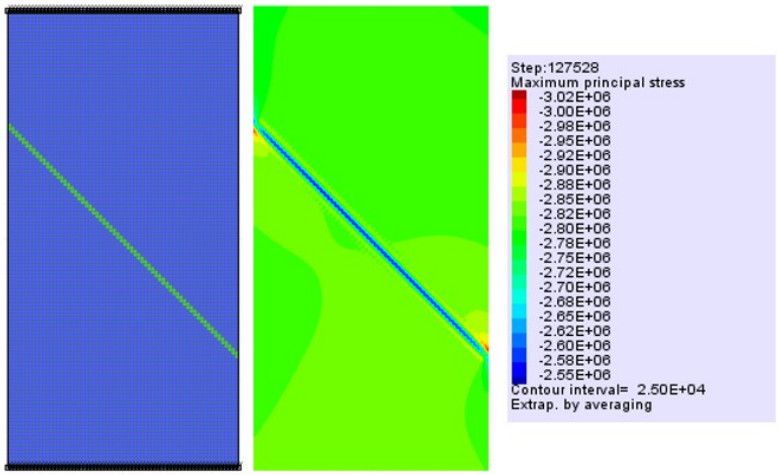

Figure 11: Numerical model and maximum principal stress for the concrete sample with smooth discontinuity plane

The numerical assessment of maximum principal stress determined from FLAC 8.0 model at 0.54 mm displacement is obtained as 3.0 MPa and it is consistent with the laboratory experiments. As shown in Figure 11, stresses observed around the plaster fill material represent a comparably lower strength than concrete. The stress distribution behavior on the numerical model is also consistent with the laboratory experiment results.

The concrete samples with a rough discontinuity plane were modeled, and the stress distribution behavior was similarly found to be conforming with the laboratory test results. Accordingly, maximum stress on the model at 0.35 mm displacement is obtained as 4.7 MPa, which is close to the laboratory testing results. Inferences related to the stress accumulation regions are also supported, as seen in Figure 12. The interpreted results indicate the stress concentration regions being closer to the sharp transition regions and lower at the thinnest layer.

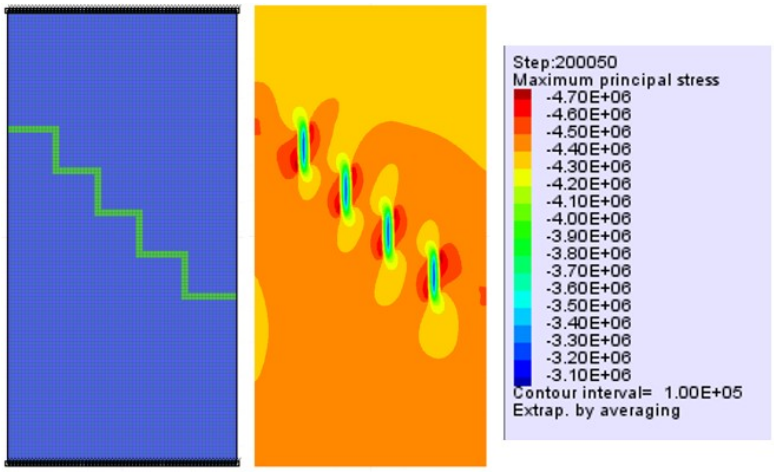

Figure 12: Numerical model and maximum principal stress for the concrete sample with smooth discontinuity plane

Finally, the 2D model of the concrete samples with a wavy profile for the discontinuity plane was modeled. According to the numerical model results, it was seen that the stress distribution behavior is similar to the rough discontinuity planes and the results are also consistent with the laboratory test results. Consequently, the stress value obtained as 3.9 MPa at a displacement of 0.54 mm, is also close to the laboratory test results. Figure 13 shows the stress distribution behavior and the maximum stress value of the concrete sample with a wavy discontinuity plane.

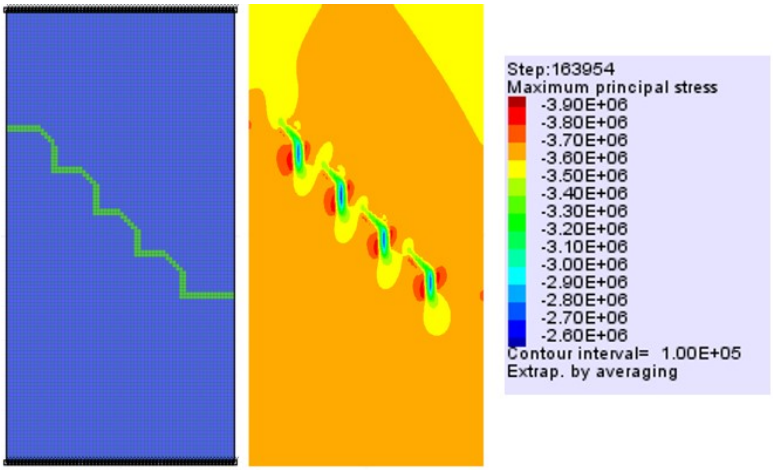

Figure 13: Numerical model and maximum principal stress for the concrete sample with wavy discontinuity plane

Stress concentration on the sample geometry was investigated by defining critical points on the models. The stress concentration values were calculated by the ratio of the stress value and the maximum stress obtained from the test results of the intact specimen. The points used for stress concentration analysis for intact specimens and specimens with different roughness planes can be seen in Figure 14.

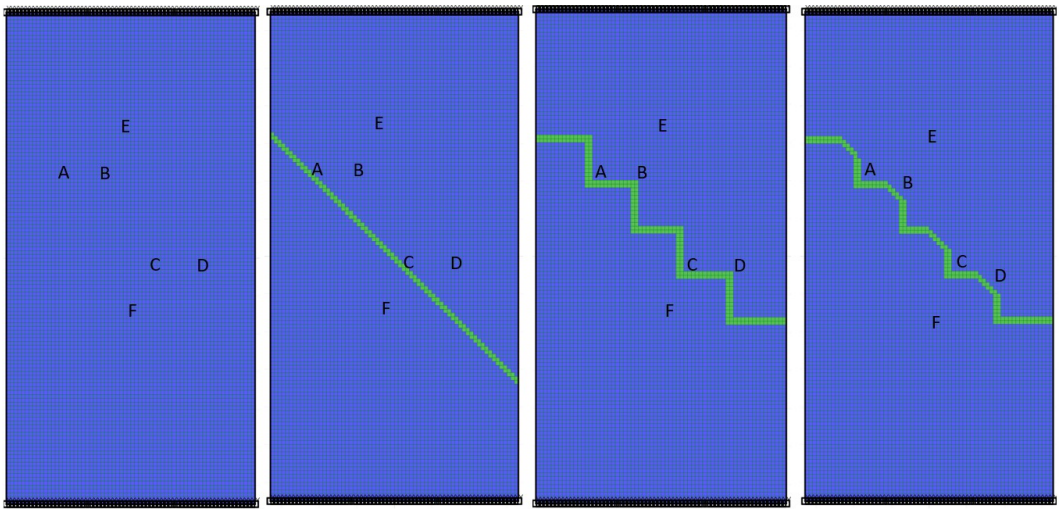

Figure 14: History points for intact specimen, smooth, rough, and wavy discontinuity planes

According to the results obtained from FLAC 8.0, the stress values were higher at the bottom part of the specimens and comparably lower at the top part. For the rough and wavy discontinuity planes, points A and C are defined to represent the region closest to the thinnest layer. In contrast, points B and D indicate the thinnest layer. As summarized in Table 6, the stress concentration values are

higher, almost more than 50%, at the close regions of the sharp transitions than the regions where the actual sharp transitions occur. These values support the inference made for the laboratory experiments results related to stress concentration regions. Stress concentration is obtained at much lower levels than the lower strength region for the smooth discontinuity plane.

Table 6: Stress Concentration Factor values for history points on the specimens

Specimen Type	Stress Concentration Factor					
	A	B	C	D	E	F
No Plane						
Smooth Plane	0.6	0.6	0.6	0.6	0.6	0.6
Rough Plane	0.9	1.1	0.9	1.1	1.0	1.0
Wavy Plane	0.8	0.9	0.8	0.9	0.8	0.8

CONCLUSION

This study covers the tests performed to obtain the mechanical properties of concrete samples with different roughness planes. First, static deformability tests were performed on concrete samples without any discontinuity plane. As a result, a uniaxial compressive strength value of 4.4 MPa, and elastic modulus of 4.5 GPa were obtained. For plaster samples representing the infilling of the discontinuity plane between the concrete specimens, it has been determined that the most suitable ratio was the mixture of 50% plaster and 50% aggregates. This mixture has a uniaxial compressive strength value of 2.3 MPa. These values are considered suitable as it was estimated that the plaster layer representing the discontinuity plane should have a lower strength value than the concrete sample itself. In the test results performed on the samples with different roughness surfaces, it was observed that the uniaxial compressive strength values in the samples with rough and wavy discontinuity planes were very close to each other. Also, these samples provided higher load values originating from the stress accumulation regions on the sharp edges. On the contrary, it was observed that the samples with smooth surface planes slipped directly from the weak plaster layer. The numerical model of the concrete samples with the different roughness discontinuity planes was also examined with the help of the 2D numerical modeling software, FLAC 8.0. Accordingly, the results are very close to the interpreted results of the 2D numerical model. It also supported the inferences from the laboratory tests about the stress concentration regions. The interpreted results indicate the stress concentration is higher at regions closer to the sharp transition and lower at the thinnest layer at the maximum displacement amount. As a result of the analysis, it was seen that the use of 3D printers for manufacturing molds could reduce the time and effort related to sample preparation. Therefore, further experimental studies will be performed with different roughness planes, infilling types, and infilling thicknesses.

REFERENCES

Ban, L., Qi, C., Chen, H., Yan, F., & Ji, C. (2020). A new criterion for peak shear strength of rock joints with a 3D roughness parameter. *Rock Mechanics and Rock Engineering, 53(4*), 1755-1775.

Fereshtenejad, S., & Song, J. J. (2016). Fundamental study on the applicability of powder-based 3D printer for physical modeling in rock mechanics. *Rock Mechanics and Rock Engineering, 49(6),* 2065-2074.

Hucka, V., & Das, B. (1974, October). Brittleness determination of rocks by different methods. In *International Journal of Rock Mechanics and Mining Sciences & Geomechanics Abstracts* (Vol. 11, No. 10, pp. 389-392). Pergamon.

Jaber, J., Marianne, C., Deck, O., Mohamed, M., Godard, O., & Samuel, K. (2020). Investigation of the mechanical behavior of 3D printed polyamide-12 joints for reduced scale models of rock mass. *Rock Mechanics and Rock Engineering, 53(6),* 2687-2705.

Jiang, C., Zhao, G. F., Zhu, J., Zhao, Y. X., & Shen, L. (2016). Investigation of dynamic crack coalescence using a gypsum-like 3D printing material. *Rock mechanics and rock engineering, 49(10*), 3983-3998.

Ju, Y., Wang, L., Xie, H., Ma, G., Zheng, Z., & Mao, L. (2017). Visualization and transparentization of the structure and stress field of aggregated geomaterials through 3D printing and photoelastic techniques*. Rock Mechanics and Rock Engineering, 50(6),* 1383-1407.

Sharafisafa, M., Shen, L., Zheng, Y., & Xiao, J. (2019). The effect of flaw filling material on the compressive behaviour of 3D printed rock-like discs. *International Journal of Rock Mechanics and Mining Sciences, 117*, 105-117.

Song, L., Jiang, Q., Shi, Y. E., Feng, X. T., Li, Y., Su, F., & Liu, C. (2018). Feasibility investigation of 3D printing technology for geotechnical physical models: study of tunnels. *Rock Mechanics and Rock Engineering, 51(8),* 2617-2637.

Tarasov, B., & Potvin, Y. (2013). Universal criteria for rock brittleness estimation under triaxial compression. *International Journal of Rock Mechanics and Mining Sciences, 59*, 57-69.

Verma, R. K., Nguyen, G. D., Karakus, M., & Taheri, A. (2021). Capturing snapback in indirect tensile testing using AUSBIT-Adelaide University Snap-Back Indirect Tensile test. I*nternational Journal of Rock Mechanics and Mining Sciences, 147*, 104897.

Vrkljan, I. (Ed.). (2009). Rock engineering in difficult ground conditions-soft rocks and karst. CRC Press.

Wu, Z., Zhang, B., Weng, L., Liu, Q., & Wong, L. N. Y. (2020). A new way to replicate the highly stressed soft rock: 3D printing exploration. Rock Mechanics and Rock Engineering, 53(1), 467-476.

Zhou, T., & Zhu, J. B. (2018). Identification of a suitable 3D printing material for mimicking brittle and hard rocks and its brittleness enhancements. *Rock Mechanics and Rock Engineering, 51(3),* 765-777.

Zhou, T., Zhu, J., & Xie, H. (2020). Mechanical and volumetric fracturing behaviour of three-dimensional printing rock-like samples under dynamic loading.

Zhu, J. B., Zhou, T., Liao, Z. Y., Sun, L., Li, X. B., & Chen, R. (2018). Replication of internal defects and investigation of mechanical and fracture behaviour of rock using 3D printing and 3D numerical methods in combination with X-ray computerized tomography. *International Journal of Rock Mechanics and Mining Sciences, 106,* 198-212.

DETERMINATION OF THE DEGREE OF RELEASE OF MINERAL PARTICLES BY IMAGE ANALYSIS SOFTWARE

T. D. Figueiredo [1, *], A. M. Braga[2], R. J. A. Fidelis[2], D. G. Magalhães[2], P. H. L. Silva[1], C. A. Pereira[1]

[1]Federal University of Ouro Preto (UFOP), Dept of Mining Engineering
*(*Corresponding author: thiagoduarte1926@hotmail.com)*
[2]Federal Center of Technological Education of Minas Gerais (CEFET/MG)

ABSTRACT

The degree of release of the mineral particles is of great importance in ore treatment operations. The incorrect interpretation of this parameter directly affects the efficiency of the mineral processing stages, and may even render projects unviable. Currently, the most usual method of determining the degree of release is the so-called Gaudin method, whose representativeness of the results depends heavily on the good practice and interpretation of the operator. This work aims to implement an image analysis software to determine the degree of freedom of minerals, reducing human participation in the process and giving greater certainty to the results. For this, the degree of release of iron ore samples from the municipality of Guanhães/MG was determined using the Gaudin method and the software developed for this study. The respective results were compared, proving the effectiveness of the computational program, concluding that, release-rate analyzes could be performed through computation, with greater speed, accuracy and accuracy.

Keywords: Release degree, computational analysis, iron ore

INTRODUCTION

Mineral concentration operations have as main objective the separation of the element of interest, called mineral-ore from gangue minerals, in order to obtain products to be used industrially. For such separation to occur, physical or physicochemical differences must exist between mineral species, and, also, that the minerals of interest are physically disaggregated to those that have no economic interest (Ferreıra, 2013).

In certain mineral deposits, the ore is naturally released, eliminating stages of fragmentation. However, in most situations, the minerals of interest are consolidated, requiring comminution steps to increase the degree of mineral release. According to Delbem (2010), the release of mineral particles is proportional to fragmentation, that is, the more fragmented the ore, the greater its degree of release. However, due to the high operational cost and the unsatisfactory performance of ultrafine particles in concentration operations, mineral fragmentation should be limited to what is necessary for operational viability.

According to Rodrigues (2016), among the variety of methods of determining the degree of release, the most used in the mineral sector is the so-called Gaudin method (1939). This method defines as a degree of freedom the percentage of a given mineral species that occurs as a free particle in relation to the total particles of a sample, and can be used for different minerals, requiring only that the mineral to be analyzed present visual difference for the other minerals. One of the main disadvantages of gaudin's method is the high dependence of the operator, since a result with greater precision needs to good practice and interpretation of it.

Taking into account this dependence of the operator, the use of computational analysis of images is increasingly justified in the study of mineral release (Ferreıra, 2013). Some techniques are already widespread, such as electron microscopy and optical image analysis, both with important limitations, whether referring to representativeness or reproducibility of results (Donskoi et al., 2014).

Delbem et al. (2015) proposes a digital analysis system capable of characterizing and determining the degree of release of different types of mineral samples semi-automatically, seeking to increase the accuracy of the procedure by reducing human influence on the results. Based on studies and methodologies such as those already mentioned, this article proposes the creation of an image analysis program that, together with mathematical software, allows obtaining quantitative results in real time, about the degree of release of ores.

MATERIALS AND METHODS

For the study, two samples of iron ore were used, made available by a mining company located in the municipality of Guanhães- MG. The first (Am1) comes from the mining front in the northern region of the mine and the second (Am2) comes from the homogenization pile.

The samples were homogenized using the canvas homogenization technique and quarted in jones type quarter. After preparation, they were submitted to the stages of washing and granulometric separation by sieving. Subsequently, the degree of release of the particles in different size ranges was determined, using the conventional method defined by Gaudin and the computational method by the aid of a software. Figure 1 summarizes the methodology used in this work, showing the procedures of this stage.

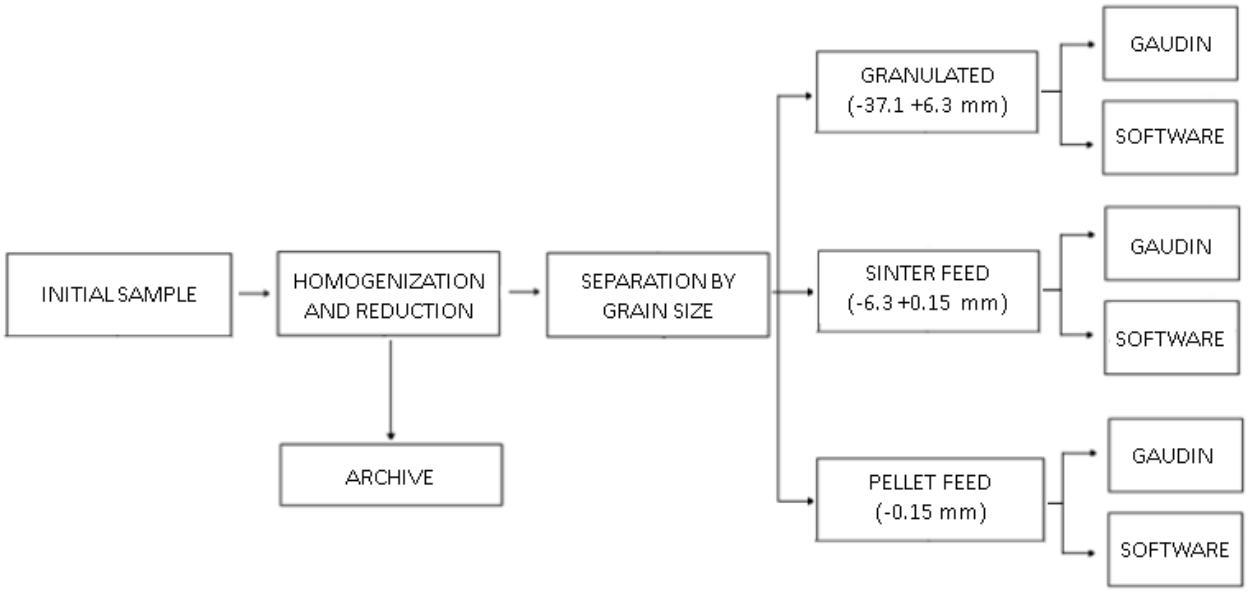

Figure 1. Methodology flowchart

Separation by Size by Sieving

This step was performed in order to separate the material into three granulometric ranges corresponding to the products of iron ore, pellet feed (<0.150 mm), sinter feed (0.150 mm to 6.3 mm) and granulated (6.3 mm to 37.1 mm). The process was performed in wet and with the use of a CDC suspended sieve, model PV-08. Figure 2 represents the three granulometric bands sampled.

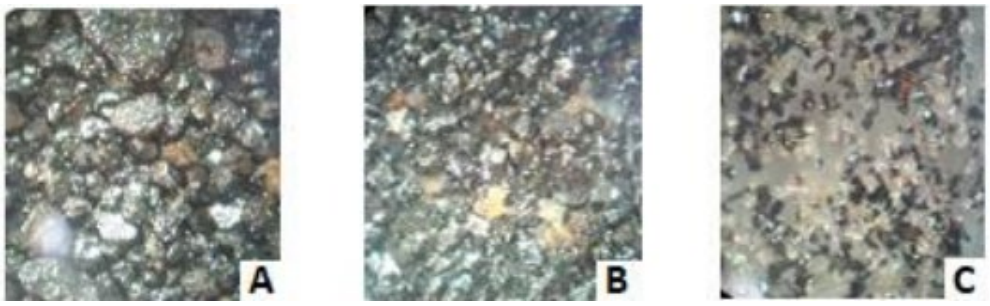

Figure 2. Granulated ore (A)- sinter feed (B) - pellet feed (C)

Determination of the Degree of Release by the Conventional Method (Gaudin)

The degree of release of the analyzed samples was determined using the Gaudin method. This method consists of counting the mineral grains of a sample in a given particle size range, evaluating the release of each particle and classifying them according to the proportion of the mineral of interest in the grain. Each particle presents a release index proportional to the percentage of the grain occupied by the mineral of interest, in the case analyzed, hematite.

For this study, 800 particles were analyzed, one by one, with the aid of a stereoscopic microscope, for each of the granulometric ranges resulting from the sieving, as shown in Figure 3. According to their respective degree of release, the particles were classified in the following ranges: (0-25%], (25%-50%], (50-75%], (75-100%).

Figure 3. Release analysis by conventional method

Particles defined in the intervals (0-25%] and (75-100%) were considered free, while the remaining particles were defined mixed particles. Thus, Eq. 1 could be applied from the formulation proposed by Gaudin (1939), providing the degree of freedom of the samples:

$$Df = \frac{\sum P_f}{\sum P_f + \sum P_m} \quad (1)$$

Being:

- Df = Degree of freedom.

- P_f = Number of free particles.
- P_mPm = Number of mixed particles.

Determination of the Degree of Release by Computational Method

The determination of the degree of particle release by the computational method was performed by means of photographs captured by a high resolution camera and analysis through self-authoring software. The developed software's function is to determine the particle release index through a color differentiation algorithm.

Figure 4 exemplifies the functioning of the computational release degree analysis program, which consists of capturing the images of particles (A), followed by binarization of them for grayscale (B). Thus, through the differentiation of shades (C), the program is able to delimit the boundaries of the particles and consequently the area of the particles by the Watershed method (D).

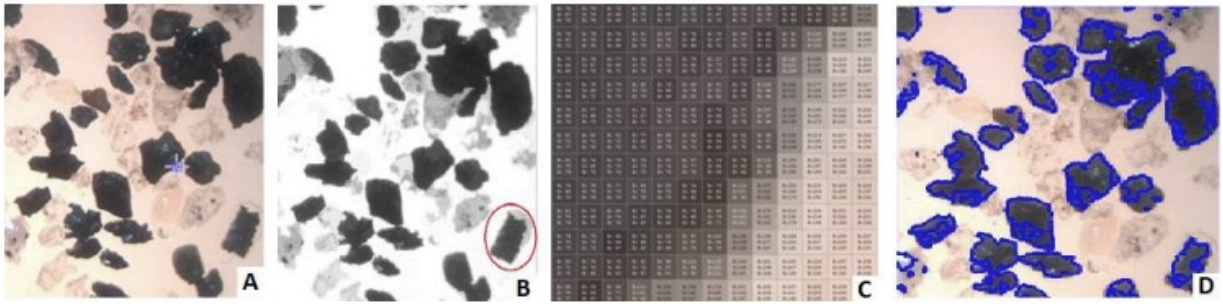

Figure 4. Principle of the software operation with a sinter feed sample.

Considering as mineral-ore darker regions and gangue the transparent or lighter areas of the grains, the software performs by identifying and counting pixels the measurement of the release of particles. The analysis performed by the program can be summarized, therefore in 5 basic steps, as described in the diagram in Figure 5.

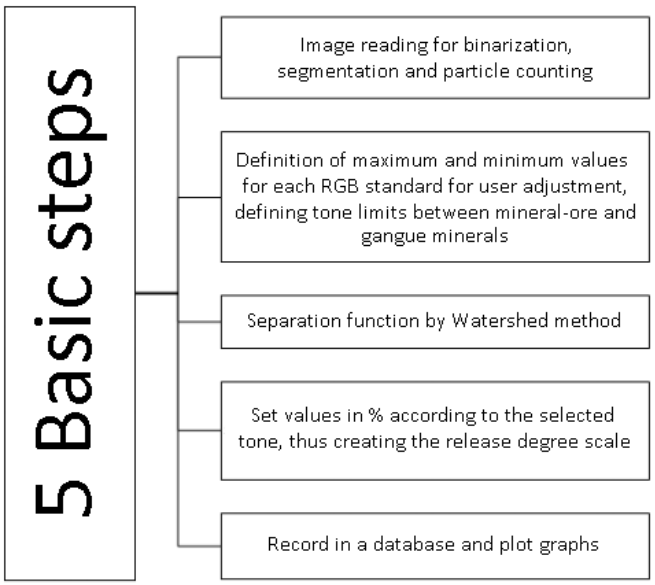

Figure 5. Basic steps to check image quality.

RESULTS AND DISCUSSION

Analysis by Conventional Method

The analysis of the degree of release of iron ore samples was initially done by the conventional method (Gaudin), with the aid of optical microscopy. The two samples (Am1 and Am2) were visually analyzed by the operator, who performed the count separately for each size fraction and, with subsequent application of Eq.1, obtained the results presented in Figure 6.

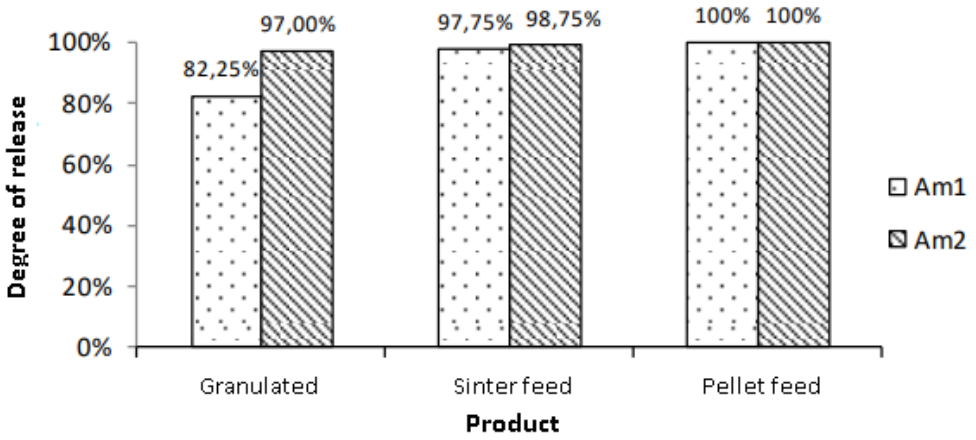

Figure 6. Degree of release of Am1 and Am2 samples by conventional method.

It is possible to observe a high release of particles from both samples, with values above 80% even in granulometry in the granulated product range. It is observed that the particles that are considered free cover a fairly extensive range of 0-25% and 75-100% and thus, a large amount of mineral grains is considered released.

Determination of the Degree of Release by Computational Method

The degree of release of am1 and am2 samples determined by the computational method could be analyzed and compared graphically. Thus, Figure 7 presents the results related to the analyses performed by software.

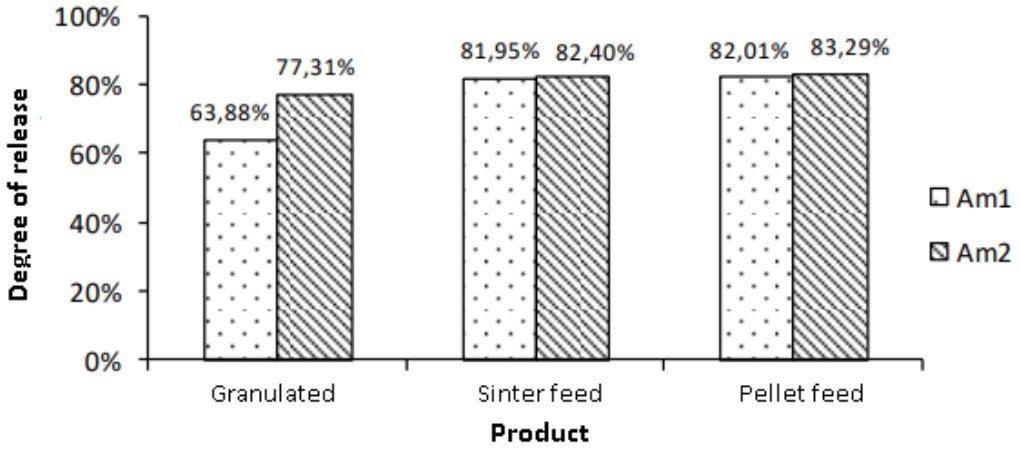

Figure 7. Degree of release of Am1 and Am2 samples by computational method.

It is possible to note that the results obtained by the computational method present a trend similar to those observed by the conventional method (Gaudin). The software demonstrated a higher degree of release referring to the particles of the Am2 sample, as well as the conventional method.

It is noticed that in granulometry in the pellet feed product range, the behavior of the samples was similar, presenting values close to particle release. This characteristic is mainly due to the fact that, as mentioned by Rodrigues and Brandão (2017), the greater the comminution of a mineral, the greater its release.

Comparison of Results by Means of Software and Conventional Method (Gaudin)

After obtaining the results of the degree of release of the samples by conventional (Gaudin) and computational methods, it was possible to compare the performance of both, determining their main peculiarities. The release of particles, when determined by the conventional method (Gaudin), presents values up to 36% higher than those obtained through the software. In addition, it is perceived that for finer granulometry, the results obtained by both methods present closer values.

This is mainly due to the fact that smaller particles have a higher degree of release and, therefore, greater ease in optical microscopy analysis. The analysis of the degree of release through the software presents values lower than those observed by the conventional method (Gaudin). Thus, it is perceived that the software provides more conservative results for the degree of particle release, thus avoiding overestimations of the data.

With this, it can be said that the software reduces the possibilities of operational problems due to errors in the definition of the degree of release of particles. Moreover, due to the fact that the computer program uses fully computerized analyses, its reliability is higher, since there is a pattern of calculation of degree of release, abandoning dependence on personal interpretations and reducing uncertainties.

CONCLUSIONS

Conventional methods of analysis of release degrees are closely related to operator expertise, which reduces the reliability and accuracy of results. With this the creation and deployment of software for this process is of great value, because it allows more accurate and faster results.

The software used has great potential for large-scale application, whether in industry or for the academic sector. Its results presented in comparison to the Gaudin method are satisfactory and promising, increasing the efficiency of mineral analysis processes.

The computational method avoids overestimations of the degree of release of the mineral, since it presents lower values and more accurately than conventional methods, because its standard of measurements is steady and uses high-tech for analysis. Thus, computational measurements of mineral release generate more stable results, so that subsequent operations of ore treatment and operational parameters defined from the degree of release of particles will not present major distortions.

ACKNOWLEDGEMENT

The authors thank CAPES, CNPq, CEFET-MG and UFOP for the support and trust deposited during the performance of this work.

REFERENCES

Delbem I. (2010). Processamento e análise digital de imagens aplicados aos estudos de liberação mineral, Msc. Thesis, Federal University of Minas Gerais, Belo Horizonte, M.G., 99 pp .

Delbem I.D., Galéry R. Brandão, P.R.G., Peres, A.E.C. (2015). Semi-automated iron ore characterisation based on optical microscope analysis: Quartz/resin classification. *Minerals Engineering* , 8, 90-96.

Donskoi E., Manuel J., Austin P., Poliakov A., Peterson M., Hapugoda S. (2014). Comparative study of iron ore characterization using a scanning electron microscope and optical image analysis. *Applied Earth Science*, 122, 217-229.

Ferreira, R.F. (2013). Estudo de liberação das fases minerais em minérios de ferro. Msc. Thesis, School of mines of Federal University of Ouro Preto, Ouro Preto, M.G., 211 pp.

Gaudin, A.M. (1939). Principles of mineral dressing. (1st. ed., Vol. 1). London, McGraw-Hill.

Rodrigues R.S. (2016). Grau de Liberação de Diferentes Tipos de Minério de Ferro das Minas de Alegria (Mariana -MG) e sua influência nas etapas de cominuição e concentração. Msc. Thesis, Engineering School of Federal University of Minas Gerais, Belo Horizonte, M.G. ,275 pp.

Rodrigues, R.S. and Brandão, P.R.G. (2017). Influência da Liberação Mineral nas Etapas de Moagem e Flotação do Minério de Ferro. *Tecnologia em Metalurgia, Materiais e Mineração*, 14, 279–287.

"DIGITAL REVOLUTION 4.0" IN THE RAW MATERIALS AND MINING INDUSTRY

MADENCİLİK VE HAMMADDELER SEKTÖRÜNDE DİJİTAL DEVRİM 4.0

H.A. Kahraman [1, *], C. Klötzer [1], M. Katapotis [1]

[1] *DMT GmbH & Co.*
([*]Corresponding Author: hakan.arden@dmt-group.com)

ABSTRACT

The concept of 'Industrial Revolution 4.0', which was first introduced in Germany and has rapidly spread to other developed countries, describes the ongoing automation of traditional production and industrial applications using modern digital technology. In this new era of Industrial Revolution 4.0, the mining industry too has inevitably started to focus on technology and digitalisation. As there are many challenges ahead in this transformation process, DMT's approach to this new era is to offer innovative and holistic Industry 4.0 solutions developed through a fastidious strategy which is expected in assisting to shape the autonomous mining vision of the future. DMT's approach to this digital transformation is to go through initially a "Digital Due Diligence Process" to assess the existing business, identify digital potentials and operating opportunities and define a digitalisation roadmap. DMT's recommendation is that this process is accompanied by independent engineering and technology advice coming from an experienced partner in process design who will establish a "Digital Transformation Office" how these identified points can deliver the expected quality, efficiency, and improvements in health and safety in line with the environmental sustainability. This approach includes three fundamental components:

"**Operations**" which cover the services used to provide companies with comprehensive guidance and support, systematic approaches to continually expand the offering of digital products and services covering the entire lifecycle of raw material extraction such as Reconnaissance, Exploration, Planning and Project Evaluation, Construction, Optimisation of Mining Operations, Environmental Aspects, Mine Closure and Site Remediation;
"**People**" which covers a corresponding digital transformation program for all employees of mining companies;
"**Processes**" which covers process optimisation for its Clients' operations.

This paper describes how a holistic approach can be implemented in this new digital era from the Consultant point of view.

Keywords: Digital revolution 4.0, mining, geology, artificial intelligence, internet of things, sensors

ÖZET

İlk olarak Almanya'da ortaya atılan ve diğer gelişmiş ülkelere de hızla yayılan "Endüstriyel Devrim 4.0" kavramı, geleneksel üretim ve endüstriyel uygulamaların modern dijital teknoloji kullanılarak süregelen otomasyonunu anlatır. Bu yeni Endüstri Devrimi 4.0 çağında, madencilik sektörü de kaçınılmaz olarak teknoloji ve dijitalleşmeye odaklanmaya başlamıştır. Bu dönüşüm sürecinde önümüze çıkacak bir yığın zorluk olduğundan, DMT'nin bu yeni döneme yaklaşımı, geleceğin otonom madencilik vizyonunu şekillendirmeye yardımcı olması amacıyla titiz bir strateji ile geliştirdiği yenilikçi ve bütünsel Endüstri 4.0 çözümleri sunmaktır. DMT'nin dijital dönüşüme

yaklaşımı, var olan işin ayrıntılı olarak değerlendirilmesi, dijital potansiyelleri ve işletme fırsatlarının belirlenmesi ve bir dijitalleşme yol haritası belirlemek için başlangıçta bir "Dijital Durum Durum Saptama Süreci"nden geçilmesidir. DMT'nin tavsiyesi, bu sürece, süreç tasarımında deneyimli bir bağımsız mühendislik ve teknoloji ortağının/danışmanın eşlik etmesi; ve bir "Dijital Dönüşüm Ofisi"nin kurularak kalite, randıman, iş sağlığı ve güvenliği ile ilgili beklentilerin çevresel sürdürülebilirlikle uyumlu tesliminin gerçekleşmesidir. Bu yaklaşım şunları içerir:

”**Operasyonlar**: Madencilik operasyonlarının optimizasyonu gibi hammadde çıkarmanın tüm yaşam döngüsünü kapsayan dijital ürün ve hizmetlerin sunumunu sürekli olarak genişletmek için sistematik yaklaşımlar, şirketlere kapsamlı rehberlik ve destek sağlamak için kullanılan hizmetler, keşif, arama, planlama ve proje değerlendirme, inşaat, çevresel unsurlar, maden kapatma ve saha iyileştirme;
“**İnsanlar**”: Madencilik şirketlerinin tüm çalışanları için ilgili bir dijital dönüşüm programı;
“**İşlemler**”: Müşteriler için süreç optimizasyonu.

Bu makale bu yeni dijital çağda bütünsel bir yaklaşımın nasıl uygulanabileceğini, Danışmanın bakışıyla yansıtmaktadır.

Anahtar Sözcükler: Dijital devrim 4.0, madencilik, jeoloji, yapay zeka, IOT, sensörler

INDUSTRIAL REVOLUTIONS

As we all are witnessing the latest period of societal transformation in human history through a revolution in industrial development currently, the previous industrial revolutions had also been the product of a similar magnitude of changes that resulted in a major structural transformation in the fabric of the societies.

The “First Industrial Revolution” is generally regarded as the transition period between 1760 and 1820 that involved a number of steam/ water-powered machine inventions that enabled and transformed limited quantity of hand production into massive production in textile manufacturing, iron industry, agriculture, and mining. This period was an inevitable culmination of the advancement made in science and technology in the late 18th Century and the beginning of the 19th Century.

The “Second Industrial Revolution”, also commonly known as the “Technological Revolution”, is the period between 1871 and 1914 that resulted in the installation of the extensive network of railways, telegraph, and electricity. A faster transfer of people and produced goods between the distant points was achieved through journeys made in railways whilst the telegrams allowed a rapid exchange of ideas and communication beyond the national boundaries at the time. Increased use of electrification also allowed factories to develop the modern production lines that resulted in a period of great economic growth at the expense of a surge in unemployment as many factory workers were replaced by machines.

The “Third Industrial Revolution”, also known as the “Digital Revolution”, started in the 1960s following the devastation of World War 2 and reached its culmination in the latter part of the 20th century. This was the period, which was catalysed by the development of semiconductors, mainframe computing (the 1960s), personal computing (1970s and 1980s), and the use of the internet (1990s). This was also the era where complex computation has started to emerge by the use of supercomputers that has enabled less human intervention in large computational process.

The concept of the “Fourth Industrial Revolution” (or “Industrial Revolution 4.0”), which was first introduced in Germany (Schwab, 2013) and has spread rapidly to other developed countries (Schwab, 2016), describes the ongoing automation of traditional production and industrial

applications using modern smart technology which was introduced in the later part of the Third Industrial Revolution. In this new system, a new production platform has been prepared by integrating large-scale machine-to-machine communication, internet of objects, rapidly increasing automation, advanced communication network, and self-monitoring and smart machines that can analyse and diagnose problems without the need for human intervention.

The common denominators observed in the previous industrial revolutions are that the fabric of the society and scale of the economics have significantly changed resulting in a new order of business and corresponding legal and administrative adjustments and changes.

The Fourth Industrial Revolution has already identified a number of structural transformation and paradigm shifts in the societies that are expected in the coming years (Schwab, 2016). These particularly include amongst many others:

The Internet of and for Things;
Automated vehicles;
Artificial Intelligence (AI) and Decision-Making;
Robotics and Services;
Cryptocurrencies and the Blockchain;
The Sharing Economy (the use of a physical good/asset, or share service or provide a service by sharing);
3D Printing in Manufacturing, Human health and Consumer Products; and
Designer beings (humans/living things) and
Neurotechnologies (first human with fully artificial memory implanted in the brain).

FOURTH INDUSTRIAL REVOLUTION AND MINING

As more of the “things” start to communicate and interact with each other in a more smart and artificial way in this Fourth Industrial Revolution particularly in the developed countries, it is inevitable that the mining segment will also benefit from this latest transformation in these economies.

Especially in countries with mining industries where wages are high, resource savings and economic extraction of raw materials can only be achieved with more automation and digitalisation.

As Schwab (2016) prophetically concluded, the winners will be those who are able to participate fully in innovation-driven ecosystems by providing new ideas, business models, products and services, rather than those who can offer only low-skilled labour or ordinary capital.

Considering the competitive nature of the business, especially the large international mining companies have already started to adjust themselves by digitising their mining operations across the value chain in line with the future generation of mines. This obviously requires a remodelling of the business for growth and sustainability while using digital technology and innovation as a catalytic enabler within an existing legacy environment that behave like individual isolated units along the route from mine to processing to transport.

The examples of this new approach have already started to populate the mines. The introduction of remotely controllable equipment and autonomous machines such as trains, trucks, drilling machines, as well as sensor driven equipment monitoring have already proven that they can significantly reduce the use of personnel in mining operations and thus the risks to human life.

In addition, the increasingly complex geological conditions encountered in the mines confront companies with the obligation to preserve and, where possible, increase the quality and quantity of raw materials by using efficient methods and equipment as well as prioritising the areas where these challenges can be met by using digital technologies.

Despite many gadgets and devices being a customary part of our daily life for many years, their widespread use in mining has just started. This includes, among other things that are taken for granted in daily life, the establishment of the "internet network" with relevant safety standards in underground mining operations. The implementation of the sensor technology currently standard in automobiles has just been started being implemented after adapting the specific requirements of mining and the associated nuisance effects of dust, mechanical stress, extreme temperatures, water or explosive gases (Clausen and others, 2020). The sensors have particularly become the driving force in efficiency and safety improvements in many mines where the digitalisation is playing a crucial role.

As Virtual Reality (VR) / Augmented Reality (AR) are commonly used in gaming industries, they also make their way into the mining industry to train and upskill the workforce used in high-risk tasks and problem solving the key operational challenges. The competency development can be reinforced better when experiential learning, gamification (adding game mechanics into nongame environments) and just-in-time reinforcement using digitally enhanced environments are used (Pagnini, 2019).

Drones are now commonly used in every aspect of the economy from delivery of goods to remote survey to entertainment. Mine industry has also started to use the drone technology both for inventory management, slope failure management of waste dumps, site surveying, traffic management, and maintenance.

It is also possible that the advancement in 3D printing may enable spare parts to be produced without sacrificing the downtime and production levels in the remote corners of the planet in near future (Pagnini, 2019).

As the satellite technology now allows shipment tracking to be monitored anywhere in the world, opportunity to create better performance in route optimisation and fleet dispatching as well as production level adjustments at the pit level that can result in an optimised integration approach from pit to port (Pagnini, 2019).

Especially in small to medium sized projects/operations in mining, it is difficult to decide where to lay the digital emphasis on and how to prioritise digitalisation and resolve many challenges which can include high capital investments in automated operations and equipment, personnel commitments, IT security, data security and protection, data processing and analysis, information quality and granularity, communication standards, legal hurdles and frameworks, concerns on quality, health, safety and environment (QHSE) and many more. The real challenge is where and how to connect the "silos" and transfer them into a digital hub.

Barnewold and Lottermoser (2021) demonstrated that 107 different digital technologies are currently pursued in mining whilst an analysis from 158 active surface and underground mines showed that the actual implementation of digital technologies is slow in general, and the uptake increases with the run-of-mine production. Large-scale mining operations appear to select and apply digital technologies suitable to their needs, whereas operations with lower production rates do not implement the currently available digital technologies to the same extent. These minor producers

may require other digital transformation solutions tailored to their capabilities and needs and applicable to their scale of operations (Barnewold and Lottermoser, 2021).

Unlike the slow-take of mining companies, the organisations which provide consultancy services to the mining operations have embraced this new digital era with open arms and started providing a number of products and services to their customers.

As an example, for these digitally equipped consultancy companies, DMT's activities, which have a history of more than two centuries in mining consultancy, also focused on technology and digitalisation in this new period of Industrial Revolution 4.0.

As part of prioritising the overall business strategy in this new era, DMT has established a digital technical group which specialised in different aspects of mining by using a range of state-of-art digital techniques to solve a number of issues.

This group can advise its clients on the upcoming challenges of digital transformation based on a broad market study and in-house technical expertise. This process generally starts with a "Digital Due Diligence" of the operations and usually continues with the establishment of a "Digital Transformation Office" (Figure 1).

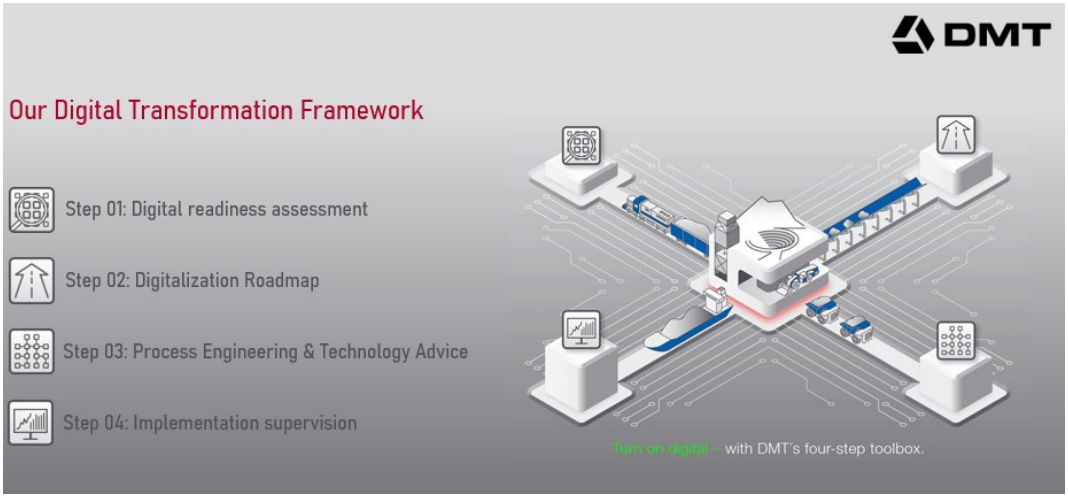

Figure 1. DMT four step toolbox approach in digital transformation for Mining 4.0

The proposed "Digital Due Diligence Process" involves assessing the existing business, identifying digital potentials and operating opportunities and defining a digitalisation roadmap and priorities (Figure 1). DMT's recommendation is that this process is accompanied by independent engineering and technology advice coming from an experienced partner in process design who will establish a "Digital Transformation Office" to deliver these identified priorities in line with the expected quality, efficiency, and improvements in health and safety and environmental sustainability (Figure 1).

As the leader of TÜV NORD GROUP's engineering division, DMT currently offers its customers innovative and holistic Industry 4.0 solutions that cover the following three main pillars (Figure 2) based on the principles of the toolbox approach explained above. These are namely Operations; People and Processes.

Figure 2. Main pillars of DMT's Mining 4.0 portfolio

OPERATIONS

In this context, the word "operations" represents the operational business that exists and DMT presents here both technologies developed in-house, and services used to provide companies with comprehensive guidance and support. Many of the in-house digital technologies in the form of advanced tools and gadgets developed by DMT are already making a significant impact for the mining operations around the world.

In addition to the development of such company-specific operational tailor-made solutions, the impact of digital transformation on the clients' employees in terms of Mining 4.0 should not be ignored. In particular, far-reaching technological changes require wide acceptance among the workforces. In addition, long-term employees, especially in the company, need to be adapted to the challenges of digitalisation. To this end, the structure and culture within the company should be further developed where DMT's corresponding transformation program for the digital world through the Digital Academy of TÜV NORD GROUP may assist all employees of its customers in great extent.

There is also a huge saving potential within mining companies, thanks to an integrated view of the technical and administrative areas. With the implementation of shared and interconnected digital systems, quality, productivity, and throughput times can be optimised from raw material extraction to product distribution. Streamlining administrative processes avoiding isolated solutions in individual areas frees up resources, which can be used to further improve operational processes. DMT has many years of experience in process optimisation, together with an extensive network of collaborators.

Core Operations

DMT is definitely at the forefront of the trend to increase productivity through digitalisation in the raw materials industry. All processes along the entire value chain are affected by this trend, with a wide range of technical solutions already available in the service portfolio. Beyond that, systematic approaches are underway to continually expand the offering of digital products and services covering the entire lifecycle of raw material extraction (Figure 3).

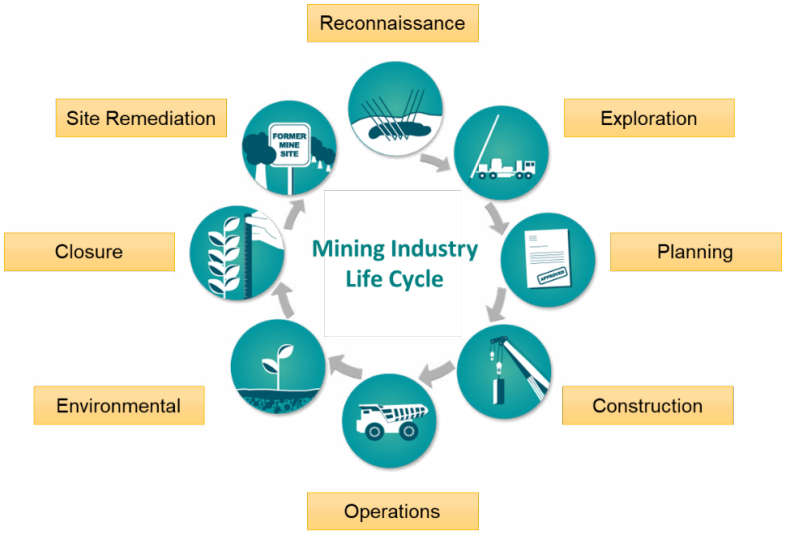

Figure 3. Life cycle of the mining industry

Reconnaissance Studies

Reconnaissance is often the first phase of mining projects, and the high degree of uncertainty at this stage is the main reason for intense efforts to minimise investment risks. The use of state-of-the-art digital technologies enables the acquisition and evaluation of high-quality data through optimum use of people and equipment. To support this work step efficiently, DMT has the power to effectively deploy adequately equipped drones, with the support of technology collaborators. Regarding integrating future developments in this sector, DMT is participating in a research project on the use of sensor-equipped drones within the framework of the European Union-funded "European Institute of Innovation and Technology Raw Materials (EIT Raw Materials)" program. DMT is developing a key technology module in the form of a software solution that, among other things, integrates the acquired data with standard software such as ArcGIS and AutoCAD, thereby greatly accelerating the creation of geological maps.

Exploration Studies

Technical progress under Industrial Revolution 4.0 also has a significant impact on exploration. That is, new advances in automation of data collection, evaluation, analysis, and model building can have a positive impact on the amount of time spent and money invested. An example of this is DMT CoreScan®3 (Figure 4), which enables the digitisation and evaluation of entire drill cores (360°) and their export to a corresponding drill core database. In addition to the analysis of the mine inventory and grain size distribution, a detailed structural evaluation can also be made in this way.

Other DMT solutions in the field of exploration, apart from active involvement in borehole drilling, borehole surveying and logging, include the application of seismic methods such as 2D and 3D seismic reflection, seismic refraction, seismic tomography, as well as their interpretation and modelling, in which large amounts of data are directed and evaluated. The results from these studies can best be used to create a "digital twin" of the mineral deposit, which is constantly updated in real time. At this point, by increasing the degree of automation, the dependence on personal experience in modelling can be reduced, thereby increasing the degree of objectivity. For this purpose, DMT uses modern proprietary software where workflow can be stored and recorded, thus ensuring better reproducibility of results.

Figure 4. DMT CoreScan®3

Planning and Project Evaluation

Within the scope of operational work, complementary short and medium-term plans are made sequentially and at regular intervals. In particular, the short-term plan should be updated daily to get the most out of machinery and other resources. Here, automation and digitisation offer a very high potential for cost savings. For example, the geological models can be updated immediately when excavating seams/ores or driving the developments in underground mines or creating blastholes in open pit mines using appropriate sensor technology. On the other hand, in the case of using transport systems, it can record in real time the motion paths of mining equipment as well as idle and downtime, resulting in significant reductions in cycle times. DMT also supports employers and investor credit institutions in feasibility studies and determination of resources and reserves in accordance with the international standards. In this process, the basis for further planning is laid by creating three- or four-dimensional models (Figure 5.) and creating initial databases. For visualisation purposes, the most advanced Virtual Reality (VR) facilities are used. With VR glasses, planning can literally be made "touchable", even for non-experts. With the use of proprietary software and a broad market study, DMT is able to offer its customers holistic solutions that integrate data from various sources. These solutions include deposit and machine data, as well as data from geotechnical monitoring systems.

In addition to providing advice to mining companies, DMT is also involved in the development of CERA, a standardised analytical and integrated certification system that guarantees the ecological, social and economic sustainability of the extraction, processing, trade and production of all mineral raw materials, including fossil fuels. This system ensures reliable traceability of certified raw materials using various technologies and proof-of-origin methods throughout the value chain. Digital technologies such as the Distributed Ledger or Blockchain play an important role, for example, as transaction databases to track trade and transport routes in a verifiable way.

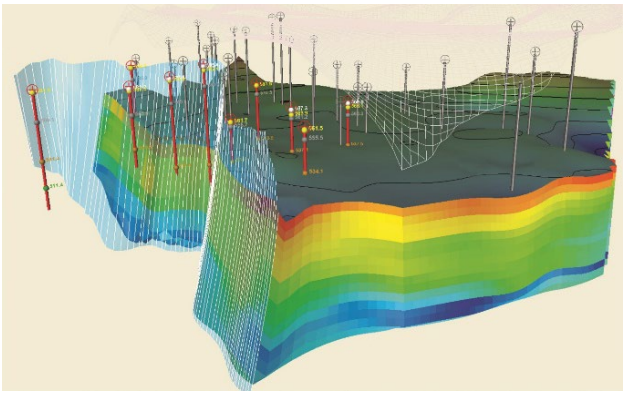

Figure 5. Utilisation of special software for the 3D visualisation of a mine

Construction

DMT's approach on this is to offer "tailor-made" engineering solutions from a single source. For example, the digitalisation used has reduced the construction times of mining-related infrastructure projects and contributed to a more efficient use of investment capital. DMT is represented at this event space by measuring instruments such as the IMAGER 5006EX (Figure 6c), the world's only high-precision, explosion-proof 3D laser scanner. The fully automatic GYROMAT can also record measurement data in real time and transmit it wirelessly (Figure 6a). With a diameter of less than 2.5 cm, the DMT SlimBoreholeScanner allows to record the number and condition of cracks in equally small boreholes and then visualise them along the entire length (Figure 6b). In contrast, geo-radar and ground radar provide high resolution searching of the ground to inspect road surfaces, power transmission lines and boreholes. Data from all devices can be combined, processed, and visualised by purpose for on-premises data platforms.

Figure 6. DMT's cutting-edge products a) GYROMAT b) SlimBoreholeScanner c) MAGER 5006EX

Optimisation of Mining Operations

In this context, DMT provides the MineSafe® platform which was developed as an in-house machine diagnostic system specifically designed for condition monitoring of machines and plants (pumps, crushers, large belt conveyors, vehicles, etc.) in the mining and processing industry. MineSafe can also be implemented as a customer-specific, controller-integrated system providing all the essential functions and components of a modern online condition monitoring system and is now available as such on Caterpillar's automation platform. The modular design allows for a wide variety of applications and a high degree of expandability thanks to the relatively simple integration of existing control systems. DMT is currently developing "MAMMA - Maintained Mine and Machine", which aims to significantly reduce the maintenance costs of machinery and systems in mining

operations by gathering, processing and clearly visualising all relevant data. This system allows for longer maintenance intervals and increased equipment availability. In the field of ventilation, systematic studies are carried out to implement adequate and adaptable practices by using "Ventilation on Demand-VOD" systems.

Whether it is the question of automating individual work steps or adapting entire process chains, DMT has positioned itself to provide tailor-made solutions and choices and support for the Clients during implementation phase.

Environmental Aspects

In addition to high productivity, Mining 4.0's objectives include security, increased efficiency, sustainability and transparency as the public's attention on the environment has significantly grown in the recent years. Negative environmental impacts due to the collapse or failure of tailings dams or similar events occurring on the mine sites impacting the environment have become immediate headlines recently. To avoid such events, continuous monitoring measures are required in addition to drilling planning. For this purpose, the DMT SAFEGUARD network platform has been developed by placing sensors in complex geo-monitoring systems with alarm functions to record ground motions, object deformations, vibrations, or geotechnical parameters. It does not matter whether the data is recorded and archived just a few times a day or more than 1000 times per second, and whether it is also temperature, water level, vibration, or video data. All information is automatically visualised according to the requirements and is accessible at any time via a decentralised and location-independent network portals. Based on SAFEGUARD, DMT is currently developing an all-in-one solution for waste monitoring under the "EIT RawMaterials" project "STINGS" and is successfully using it in a model plant in South America. This system detects ground motions using remote sensing techniques, as well as planning and installing a sensor network for geotechnical monitoring of waste. All measurement data is stored in a central database that enables complex models to be built to assess the safety of facilities and detect and warn of hazards at an early stage.

Mine Closure and Site Remediation

The life cycle of a mine is often combined with the improvement of the mine site following the end of the mining operation. Such processes are also known as "remitting funding". In many well-developed mining countries, mine operators have to allocate the monetary resources necessary during the extraction phase to ensure the regular upgrading of the mines in relation to the ultimate mine closure. The most obvious example of this is the management of water pumps in closed mines in the Ruhr and Saar region of Germany. Optimisation, automation, and digitalisation are tools used to ensure that the amount of monetary funds allocated to costs is not exceeded. As part of its water management activities, DMT compiles three-dimensional images of ground and surface waters, allowing mine operators to perform more complex analyses and calculations with "digital twins" of the groundwater. In this way, the effects of technical interventions can be predicted in different scenarios and correct measures can be taken. The SAFEGUARD system described above can also be used for continuous monitoring of indoor mining operations. By doing this, mining-induced ground motions such as slope failures can be detected and even predicted. The system is method independent and works with any data from geotechnical, surveying, geophysics, noise and vibration fields.

In addition, DMT with its global partners have developed a new system called CLOSUREMATIC which plans the closure and rehabilitation of a mine while it is still under construction. This digital product aims to eliminate the typical problems in mine closure such as loss of continuity upon changes in management and ownership, difficulties in cost estimation and

tracking, loss of closure-related data, poor coordination in closure activity and operations that compromise the goals of closure, inadequate consultation etc. The use of CLOSUREMATIC also reduces the closure related environmental and social risks. The guidance section (one of CLOSUREMATICs unique features) helps the operator to focus the actions to sectors that they are most effective and needed in a continuous manner. This has been designed in a way that the closure related actions and useful links to a knowledge base can be managed from the beginning of the mining activity even prior to mining at planning phase. Due to the precise descriptive nature of the closure process, the CLOSUREMATIC will probably be the most accurate tool in the market to estimate the costs of closure. This information can be used in determination of the financial closure related liabilities in the permitting process and also lowering the liabilities through development of a more developed and detailed closure plan.

PEOPLE

More than half of industrial companies in Germany have embedded “digital transformation” in their business strategy to simplify operations, increase sales and improve customer satisfaction. On the other hand, 30 percent of companies identify the insufficient digital qualifications of their employees as a major problem and thus a significant barrier to implementation. In addition, more than half of the companies criticise the need for a more open corporate culture in which “failure” is discussed in their companies.

These are the points where DMT, in collaboration with TÜV NORD GROUP's Digital Academy, stepped in to make employees the key to digitalisation. The core element of the employee motivation and motivation program within the company is a certified training course to become a "Digital Specialist". After all, the latest and greatest machines are only as good as the people who run them. The more digital the products, processes and machines become, the more important the education and training of employees becomes. For this reason, employees as well as managers should be prepared for a comprehensive digital transformation. The various training programs on this subject can be individually tailored to the needs and challenges of the respective companies in terms of content and duration. Due to this meticulous work, DMT’s parent company TÜV NORD was twice awarded the German Excellence Award 2020 in the "Education and Further Education" category, recognising the accuracy of the VR training of candidate experts in the fields of steam and pressure, on the one hand, and on the other hand, in the "Conversion" category. At this point, TÜV NORD and DMT can provide mining companies with tailored support solutions through courses such as using VR in the training and education of workers in both general and customer-specific mining equipment.

PROCESSES

Detailed analyses form the basis for further process optimisation. With its partners, DMT also provides consultancy services that serve to improve the performance of mining operations in terms of "Operational Excellence". The planning of equipment and materials, the control of cash flows and the management of personnel are challenging issues in terms of administrative responsibilities of mining companies. In terms of planning processes, using modern "ERP-Enterprise Resource Planning" software, accounting, shift planning, time recording, and invoicing automation are just a few examples of potential savings that can be achieved. For a company's production divisions, such systems offer advantages in material supply and storage. Through further analysis, it is also possible to timely identify materials that are required more frequently or that are particularly critical to a smooth working process. By doing this, countermeasures can be taken at the right time. As a result, there are fewer production delays, unnecessary material storage is avoided, and capacities can be lightened.

It has been pointed out before that the digital gadgets and inputs using the digital technology that have been taken for granted in our daily life for years have not yet been created or applied in mining on a large scale. In addition to the inability to provide internet signals throughout the area with relevant security standards in underground mining operations, it can be stated that even in open pit mining, communication over mobile data cannot be provided directly due to shadowing effects and dead spots. Co-synergies can be created by taking a holistic view of the existing and future necessary infrastructures. Accordingly, DMT, in collaboration with its global partners, supports and advises companies through its years of mining expertise and broad knowledge of far-reaching processes, providing one-stop solutions to help them meet the challenges of digital transformation.

CONCLUSION

In recent years, the continued digitisation of mining has brought about continuous changes in the way the raw materials industry discovers its resources, runs mining operations, processes products and ultimately delivers them to their customers. This article demonstrates DMT's Mining 4.0 concept, which is based on three pillars: "operations", "people" and "processes" and covers digital transformation holistically throughout the entire lifecycle of the raw materials industry.

Based on its long-proven ability to capture new developments and integrate them into its core competencies, DMT is passionate about the digitisation of existing products and services, but also very heavily on the development of new digital business models. DMT's aim through its stakeholders and partners inside and outside of TÜV NORD GROUP is to be at the forefront of Industrial Revolution 4.0 in the spirit of the 'Engineering-Performance' motto, to provide digitised, smart and connected solutions for the raw material sector, and thus assisting to shape the smart (autonomous) mining vision of the future. For this purpose, DMT has developed a modular four-step strategy, starting with the assessment of current processes within a company or operation (through a digital readiness assessment) and culminating in the implementation supervision of all services and solutions a customer needs for his successful digital transformation.

The mining industry like any other segments of the global economy faces new challenges in the coming years due to the introduction of many new ways and methodologies to deal with the traditional issues. The authors of this paper believe that the mining industry is in a unique position to manage the things in a completely new way as the world is rapidly moving into an era where the “artificial intelligence” and “internet of the things” will be a dominant force in decision making process. The winners will be determined by those who are able to participate fully in this innovation-driven period. One thing is definitely sure that the old and new operations will face similar challenges in implementing the ideas and innovations, but the ones who move with the time and trends will be ahead of the game. Therefore, choosing a right partner in this process is also a crucial decision in this new era.

REFERENCES

Barnewold l. and Lottermoser B.G. (2021). Identification of digital technologies and digitalisation trends in the mining industry. International Journal of Mining Science and Technology Volume 30, Issue 6, November 2020, Pages 747-757.

Clausen, E.; Nienhaus, K.; Bartnitzki, T; Baltes, R. (2020): Bergbau 4.0. In: Frenz, W. (eds.): *Handbuch Industrie 4.0: Recht, Technik, Gesellschaft*. Berlin: Springer, pp. 919-937.

Pagnini M. (2019). Data Mining for Miners from Pit to Port: Digitalization Trends in the Mining Sector. https://www.consultdss.com/digitalization-in-mining/

Schwab, Klaus (2013). "Industrie 4.0: Mit dem Internet der Dinge auf dem Weg zur 4. Industrial Revolution - vdi-nachrichten.com". 4 March 2013. Archived from the original on 4 March 2013. https://web.archive.org/web/20130304101009/http://www.vdi-nachrichten.com/artikel/Industrie-4-0-Mit-dem-Internet-der-Dinge-auf-dem-Weg-zur-4-industriellen-Revolution/52570/1

Schwab, Klaus (2016). “The Fourth Industrial Revolution”. World Economic Forum. ISBN-13: 978-1-944835-01-9. 172pp.

DÜŞÜK TENÖRLÜ LATERİTİK NİKEL CEVHERİNDEN YIĞIN LİÇİ İLE NİKEL KAZANIMININ ARAŞTIRILMASI

INVESTIGATION OF NICKEL RECOVERY FROM LOW-GRADE LATERITIC NICKEL ORE BY USING THE HEAP LEACHING

A.F. Değirmenci [1,*], Ö.Canıeren[1], O.Yılmaz[1], C.Karagüzel[1]

[1]*Dumlupınar Üniversitesi, Maden Mühendisliği Bölümü*
([*] Sorumlu yazar: ffarukddegirmenci@gmail.com)

ÖZET

Önemli bir alaşım elementi olan nikel, gelişen teknoloji ile birlikte kullanımı her geçen gün artış gösteren bir elementtir. Batarya, otomotiv, savunma sanayi başta olmak üzere birçok endüstri alanında kullanılan nikel üretimi, lateritik ve sülfitik maden yataklarından ve ikincil kaynaklardan fiziksel, kimyasal ve fizikokimyasal prosesler ile yapılmaktadır. Nikel zenginleştirmede kullanılan en yaygın proses ise basınç altında yapılan liç işlemleridir (HPAL). Bu çalışma ile Gördes Nikel-Kobalt İşletmesi'nin yüksek basınç liçi öncesi sınıflandırma ile stokladığı düşük tenörlü (%0,3 Ni içerikli) ara ürün olarak nitelendirilen cevherin yığın liçi ile kazanılması amacıyla laboratuvar ortamında kolon liçi testleri gerçekleştirilmiştir. Yığın liçini simule edecek iki farklı kolon (kare ve dairesel) ile yapılan liç testlerinde tane boyutu (-150mm, -20mm, -5mm), çözücü konsantrasyonu (-150-250gr/lt serbest asit) , liç süresi gibi çalışma parametrelerinin metal kazanma verimi üzerine etkileri araştırılmıştır. Yapılan çalışmalar sonunda düşük nikel içerikli çalışma konusu ara üründen -5mm tane boyutunda, 17 lt/ms/h besleme hızı ile verilen liç çözeltisi, 250 gr/lt serbest asitli yüksüz çözelti ile %78 verimle nikel kazanılabileceği belirlenmiştir.

Anahtar kelimeler: Yığın liçi, lateritik nikel cevheri, sülfürik asit liçi.

ABSTRACT

Nickel is an essential alloying element, which utilization is increasing day by day with the developing technology. It is used in many industrial areas, especially in the battery, automotive and defense industries. Nickel production is made from lateritic and sulphitic mineral deposits and secondary sources by physical, chemical and physicochemical processes. The most common process used in nickel beneficiation is leaching under pressure (HPAL). In this study, column leaching tests in a laboratory scale were carried out to recover the low grade (0.3% Ni content) ore by heap leaching. Two different columns (square and circular) were used to represent heap leaching. In the leaching tests, the effects of working parameters such as particle size (-150mm, -20mm, -5mm), solvent concentration (-150-250gr/lt free acid) and leaching time were investigated on metal recovery efficiency. At the end of the studies, it was observed that the nickel could be recovered from low grade ore with 78% efficiency under the optimum conditions (HL6; -5mm, 17lt/ms/h, 250 gr/lt free acid).

Keywords: Heap leach, lateritic nickel ore, sulfuric acid leaching.

GİRİŞ

Nikel, sahip olduğu fiziksel ve kimyasal özellikler sayesinde başta çelik endüstrisi olmak üzere pek çok alanda kullanılan bir metaldir. Sahip olduğu özellikler ve teknolojik gelişmeler sebebiyle nikele olan ilgi son yıllarda büyük artış göstermiş olup, mevcut veriler ışığında, nikelin 21. yüzyılda daha da fazla aranan bir metal haline geleceği beklenmektedir (Baştürkçü, 2016). Nikel-Kobalt yatakları genel olarak sülfürler, oksitler, sülfotuzlar ve arsenitler olarak sınıflandırılmaktadır. Ancak nikel ve kobalt içeriklerine göre sülfür yatakları ve laterit yataklar olarak sınıflandırılmaktadır (Çoban, 2014). Dünyadaki en büyük nikel oluşumları lateritik yataklar içerisinde bulunmaktadır. Ancak lateritik yatakların düşük tenörlü olması sebebiyle, nikel üretiminde genellikle sülfürlü yataklar tercih edilmektedir (Oxley ve Barcza, 2013). Yıllar içerisinde sülfürlü yatakların azalmasına rağmen, nikel ve nikel bileşiklerine olan talebin sürekli artışı, lateritik nikel yataklarının önemini artırmaktadır. Bunun bir sonucu olarak da lateritik nikel yataklarının ekonomik olarak değerlendirilebilirlikleri konusunda son yıllarda çok sayıda çalışma gerçekleştirilmiştir. Bu çalışmalardan bazıları aşağıda verilmiştir.

Çoban, 2014 lateritik formdaki nikel cevherini kullandığı çalışmasında, atmosferik liç ve asitle muamele-kavurma-liç aşamalarından oluşan iki ayrı hidrometalurjik proses kullanmıştır. Optimum koşullarda yapılan (150g/lt asit konsantrasyonu, 80^{o}C liç sıcaklığı ve 120 dakika liç süresi, %10 pülp yoğunluğu ve tane boyutu 0,074 mm) atmosferik liç sonucunda, lateritik cevherden nikel %69,89 verim ile kazanırken, optimum koşullarda yapılan (cevher ağırlığının 1,5 katı asit miktarı, 300°C kavurma sıcaklığı ve 60 dakika kavurma süresi, kavurma sonrası 30 dakika liç süresi ve 0,125 g/lt pülp yoğunluğunda) asitle muamele-kavurma-liç prosesi uygulanması sonucunda ise, lateritik cevherden nikel %76,8 verim ile kazanmıştır. Nasuh, 2014 çalışmasında lateritik nikel cevherinin yüksek basınç altında sülfirik asit ile kazanılabilirliğini incelemiştir. Yapılan deneysel çalışmalar sonucunda optimum çözünme koşullarını 0,3 asit/cevher oranı, 240°C liç sıcaklığı ve 60 dakikalık liç süresi olarak belirlemiş ve bu koşullarda gerçekleştirdiği yüksek basınç sülfürik asit liçi deneyi sonucunda cevherde bulunan nikelin %92,8'ini kazanmıştır. Atik, 2015 yürüttüğü çalışmasında, asidofilik bakteriler (At. ferrooxidans, At. thiooxidans, L. ferrooxidans) ve Aspergillus niger fungusu kullanılarak biyoliç yöntemiyle Çaldağ (Manisa, Türkiye) lateritik nikel cevherinden nikel kazanımını araştırmıştır. En yüksek nikel çözünme verimi, karışık bakteri kültürü ile %1 katı oranında %7 kükürt ve 2,22 g/l Fe^{+2} içeren ortamda yapılan biyoliç işleminde %97 olarak gerçekleşmiştir. Leonardou ve Dimaki, 1994 düşük tenörlü (<%1) lateritik nikel cevheri kullandığı çalışmasında, yığın liçini temsilen kolon liçi testleri gerçekleştirmiştir. Bu testlerde, sülfürik asit konsantrasyonu, kolon uzunluğu, tane boyutu ve çözeltideki katı miktarının nikel kazanımına etkisini araştırmıştır. 80 gün devam eden liç testi sonucunda, lateritik nikel cevherinden %86 verim ile nikel kazanılmıştır.

Lateritik cevherlerden nikel pirometalurjik ve hidrometalurjik olarak elde edilebilmektedir. Pirometalurjik yöntemde cevher; kurutma, kalsinasyon, kavurma, redüksiyon, ergitme gibi yüksek sıcaklıklarda gerçekleşen proseslere tabi tutulurken, hidrometalurjik yöntem atmosferik basınç veya yüksek basınç altında asit liçi yöntemlerinden oluşmaktadır (McDonald ve Whittington, 2008; Li vd., 2009). Literatürde bulunan lateritik formdaki nikel cevherinin hidrometalurjik olarak kazanıldığı çalışmalar incelendiğinde, az da olsa atmosferik şartlarda tank içinde karıştırma esasına dayanan liç tekniği, genellikle yüksek basınç liçi tekniği ve az da olsa biyolojik kazanım tekniklerinin tercih edildiği görülmektedir. Ancak lateritik nikel gibi değerli fakat cevherleşme açısından düşük tenörlü yatakların kazanımı için daha uygun olan yığın liçi tekniği üzerine sınırlı sayıda çalışmanın litearatürde bulunduğu görülmektedir.

Bu çalışmada, Manisa-Gördes'te bulunan lateritik nikel yatağından alınan cevher numunesinin yığın liçi tekniği ile çözündürülme koşullarının belirlenmesi amaçlanmıştır. Bu amaca yönelik olarak, cevher yatağından alınan temsili numunelerin ilk olarak kimyasal ve mineralojik yönden tanımlanmaları gerçekleştirilmiş, daha sonra farklı koşullarda sülfürik asit liçine tabi tutulan cevherin içerisinde bulunan esas olarak nikel (Ni), kobalt (Co), demir (Fe) ve mangan (Mn) bileşenlerinin çözünme oranları incelenmiştir. Liç deneylerinde, yığın liçini temsilen iki farklı kolon liç düzeneği kullanılmış olup, sülfürik asit konsantrasyonu, liç süresi ve tane boyutunun nikel kazanma verimine etkisi araştırılmış ve optimum şartlar belirlenmiştir.

MALZEME VE YÖNTEM

Malzeme

Çalışmaya konu olan cevher numuneleri META Nikel Kobalt AŞ.'ye ait Gördes bölgesinden temin edilmiştir. Numuneler zenginleştirme tesisinde basınç liçi öncesi yapılan eleme ile elde edilen %0.3 Ni tenörlü ön zenginleştirme ürünü olup, kimyasal analizleri ve mineralojik analizleri Tablo 1'de ve Şekil 1'de verilmiştir. Söz konusu düşük tenörlü ön zenginleştirme ürününden yaklaşık 10 ton temsili numune iş makineleri yardımıyla deneysel çalışmalarda kullanılmak üzere alınmıştır. Daha sonra alınan numuneler konileme-dörtleme yöntemi uygulanarak azaltılmış olup, bir kısmı deneysel çalışmalar için ayrılırken, diğer kısmına ise minerolojik ve kimyasal analizler yapılmıştır. Deneysel çalışmalarda kullanılacak numuneler, gerekli boyut küçültme işlemlerini takiben, -150+0,75 mm, -20mm, -5mm olacak şekilde 3 farklı tane boyutuna sınıflandırılmıştır.

Çizelge 1. Düşük tenörlü laterik nikel cevherine ait kimyasal analiz.

Al (ppm)	Ca (ppm)	Co (ppm)	Cr (ppm)	Fe (ppm)	Mg (ppm)	Mn (ppm)	Ni (ppm)	Si (ppm)
6646	118758	170	1914	91677	37409	1138	3191	201344

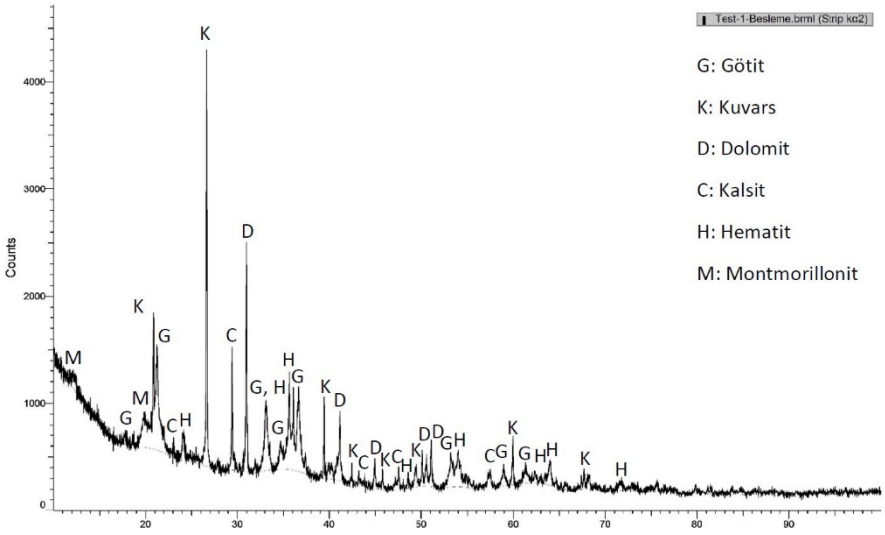

Şekil.1 Düşük tenörlü nikel cevherine ait XRD sonucu.

Şekil 1'de verilen XRD sonucu incelendiğinde; numunenin baskın olarak götit ve kuvars içerdiği gözlemlenmiştir. Bunun yanı sıra, kalsit, dolomit ve hematit mineralleri görülmüştür. Bunlara ek olarak ise, az miktarda olduğu düşünülen kil minerallerinden montmorillonite rastlanmıştır.

Yöntem

Lateritik nikel cevherinin sülfürik asit ile çözündürülmesine yönelik yapılan kolon liçi deneylerinde kullanılan düzenek Şekil 2 verilmiştir. Şekil 2'de görüldüğü gibi deney düzeneği iki farklı kolon ve sisteme boş çözücü göndermek amacıyla kullanılan peristaltik pompadan oluşmaktadır.

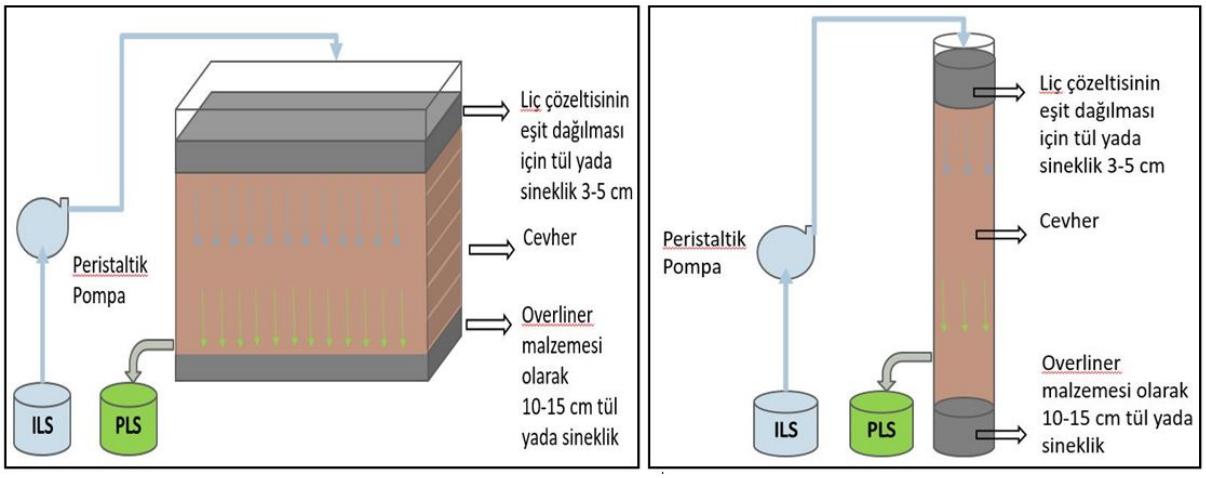

Şekil 2. Kolon liçi deney düzeneği.

Liç deneylerinde, tesiste kili uzaklaştırılmış lateritik nikel cevherleri, fleksiglas kolona (150mm çap * 2000mm yükseklik) ve kare kesitli kolona (IBC 1m*1m*1m) doldurulmuştur. Literatür verilerine göre, yığın liçi testlerinde seçilecek olan kolonun çapının, beslenecek cevherin maksimum tane boyutunun en az altı katı olacak şekilde seçilmiştir. Bu nedenle, -150+0,75 mm tane boyutlu cevhere kare kesitli kolon (IBC) ve diğer iki tane boyut grubu numuneler ise (-20mm ve -5mm) silindirik kolona doldurulmuştur. Dolum sırasında cevherin çökmesi ve mümkün olduğu kadar fazla cevher alması için hafifçe kolon duvarlarına vurularak cevherin sıkışması sağlanmıştır. Liç deneylerinde kullanılmak üzere iki farklı konsantrasyonda sülfürik çözeltisi hazırlanmıştır (düşük asit konsantrasyonu= 150 gr/lt, yüksek asit konsantrasyonu= 250 gr/lt alınmıştır). Bu çözeltiler hazırlanırken (%95-98) saflıkta sülfürik asit (H_2SO_4) ve tesis suyu kullanılmıştır. Testlerde birim cevhere liç çözeltisi debisi 17 lt/m2/h'dır. Belirli periyotlarla biriken yüklü çözelti (PLS) serbest asit konsantrasyonu ayarlandıktan sonra yüksüz çözelti (ILS) olarak geri döndürülmüştür. Stok çözeltisinde ve sıvı analizlerinden kademeli metal kazanma verimleri hesaplanmıştır. Cevherin nem tutma kapasitesinin yüksek olması nedeniyle çıkarılan metallerin kazanma verimleri hesaplamalarında aşağıdaki formüller kullanılmıştır.

Kazanım edilmiş metalin kütlesi;
Kolon Dahil;

$$g = Vp.Cp + Vf.Cf + (Vw).Ch \quad (1)$$

Kolon hariç;

$$g = Vp.Cp + Vf.Cf \quad (2)$$

Vp = Artmış PLS hacmi, lt
Cp = Artmış PLS hacmindeki metal konsantrasyonu, gr/lt
Vf = Besleme sıvısının ILS hacmi, lt
Cf = Beslemedeki ILS metal konsantrasyonu, gr/lt
Vw = Kolonda bulunan son nemi, lt
Ch = Beklemedeki ortalama sıvı konsantrasyonu, (Cp+Cf / 2)

Son metal kazanma verileri başlangıç değerlerine göre yeniden hesaplanmıştır.

$$Gerekli\ asit\ lt.= (PLS\ 'den\ ILS\ 'ye\ aktarılan\ lt)x\ (ILS\ serbest\ asit - PLS\ serbest\ asit)x\frac{1.05}{(1000x\ 1.84)} \quad (3)$$

Testler yapılırken perkolasyon (süzülme) problemi olmadıkça test devam edilmiştir. Co çözünmesini artırmak amacıyla sodyum bisülfit eklemesi yapılmıştır. Soydum bifülfit eklemesi Mn içeriğine göre ayarlanmıştır (SMBS/Mn = 1,5:1).

Liç deneyleri boyunca, kontrol altında tutulan ve nikel kazanma verimine etkisi incelenen çalışma parametreleri Tablo 2'de verilmiştir.

Çizelge 2. Kolon liçi deney parametreleri.

Test No	Tane boyutu, mm	Asit konsantrasyonu, gr/lt	Numune miktarı, kg	Kolon Tipi
T1-HL1	-150 +0,75	150	1344	Kare Kolon
T2-HL2	-150 +0,75	250	1359	
T3-HL5	-5	150	36,5	Dairesel Kolon
T4-HL6	-5	250	37,9	
T5-HL7	-20	150	37,9	
T6-HL8	-20	250	37,3	

DENEYSEL VERİLER

Yığın liçini simule etmek amacıyla laboratuvar ortamında oluşturulan kolon liçi testlerine 121 gün boyunca devam edilmiştir. Kolonlardan belirli aralıklarla numune alınmış ve numune sonuçlarına göre boş çözeltisinin (ILS) serbest asit konsantrasyonu aşağıdaki belirlenen değerlerde tutulmuştur. Yapılan kolon liçi testlerinin sonuçları Tablo 3'te verilmiştir.

Çizelge 3. Kolon liçi testlerinin sonuçları.

Test No	Tane Boyutu, mm	ILS H_2SO_4 Miktarı, gr/lt	Asit Tüketim kg/t	Ekstraksiyon, %				**Gün**
				Ni	Co	Fe	Mn	
T1-HL1	-150	150	500	48	48	25	56	121
T5-HL7	-20		800	59	50	36	62	
T3-HL5	-5		1000	63	52	46	71	
T2-HL2	-150	250	600	65	55	46	62	
T6-HL8	-20		1000	75	59	52	70	
T4-HL6	-5		1200	78	59	55	77	

Çizelge 3'te cevher tane boyutundaki değişimin metal kazanımına etkisi incelendiğinde; ince tane boyutunda tablodaki tüm metallerin (Ni-Co-Fe Mn) liç verimlerinin yükseldiği, Co metalinin ise liç verimi diğer metallere göre daha az miktarda arttığı görülmektedir. Liç besleme çözeltisinin serbest asit derişimi arttıkça, tablodaki tüm metallerin liç verimi artmıştır. Ni metalinin ise, liç veriminin tablodaki diğer metallere göre daha fazla arttığı gözlemlenmiştir. Liç besleme çözeltisindeki serbest asit konsantrasyonunun artması ile liç verimlerinin yanında asit tüketim değeri de artmaktadır. Ni-Fe metalleri için aynı tane boyutunda liç çözeltisindeki asit konsantrasyonu artırıldığında 53-121 günlerinde liç veriminin arttığı tespit edilmiştir. Co-Mn metalleri için aynı tane boyutunda liç çözeltisindeki asit konsantrasyonu artırıldığında 97-121 günlerindeki liç veriminin yükselme eğiliminin azaldığı gözlemlenmiştir.

Gerçekleştirilen kolon liçi testlerinde Ni-Co-Fe-Mn metallerinin zamana bağlı değişen metal kazanma verimleri kullanılan asit konsantrasyonu miktarına bağlı olarak gruplandırılarak Şekil 3 ve Şekil 4'te verilmiştir.

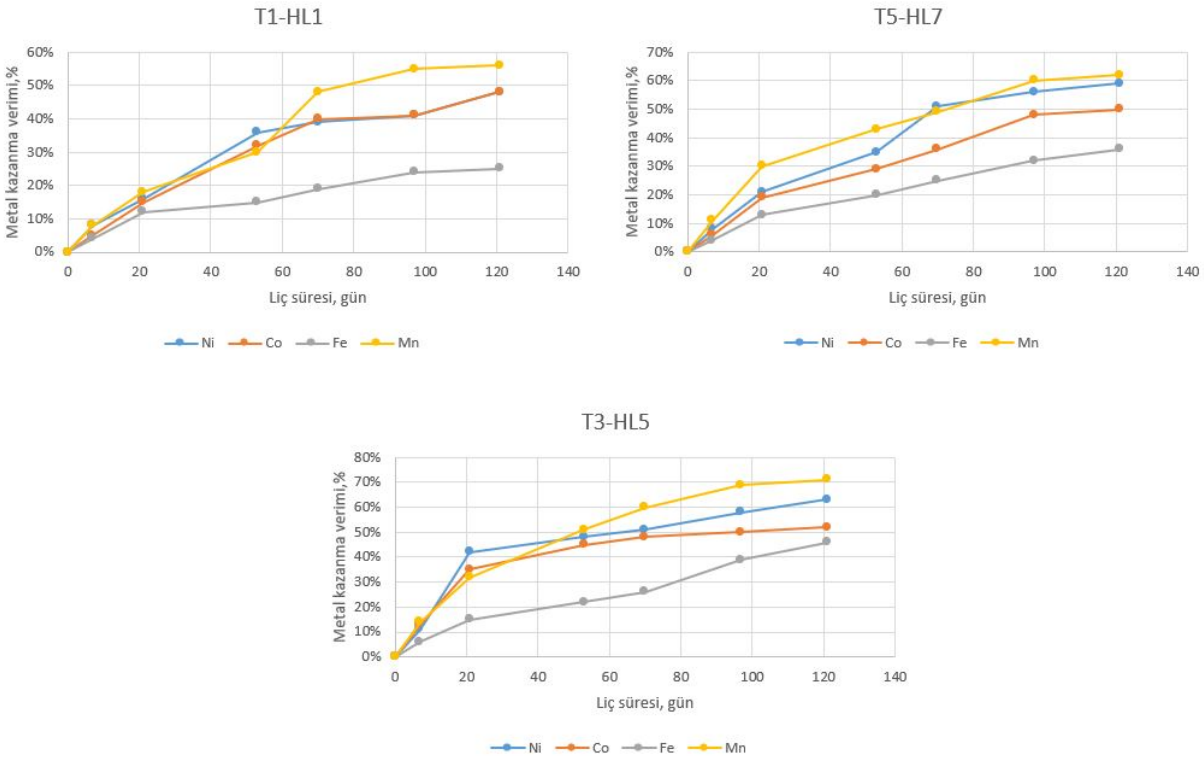

Şekil 3. Düşük konsantrasyonlu asit çözeltisi ile yapılan kolon liçi testlerinin gün-metal kazanma grafikleri (T1-HL1; T5-HL7; T3-HL5).

Düşük konsantrasyonlu asit çözeltisi ile yapılan liç testlerinin sonuçları incelendiğinde; T1-HL1, T5-HL7 nolu testlerde ilk 21 günde tüm metallerin liç verimleri birlikte hareket ederken 21-70 günleri arasında Fe metalinin liç verimi diğer metallere göre daha az miktarda artmıştır. 70-121 günleri arasında ise tüm metallerin liç verimlerindeki yükseliş hızı azalmıştır. T3-HL5 testinde ise Fe metalinin liç verimi 121 gün boyunca artmıştır. Tablodaki tüm metaller için liç süreleri incelendiğinde, tane boyutu azaldıkça liç verimi artmaktadır. Bunun yanında, ince tane boyutlarında Ni-Fe-Mn metallerinin, Co metaline göre daha verimli kazanıldığı gözlemlenmiştir. Farklı tane boyutlarında ilk 53-70 gün içerisinde Mn metalinin liç verimi artmış, takip eden günlerde ise liç veriminde daha az miktarda artışlar gözlenmiştir.

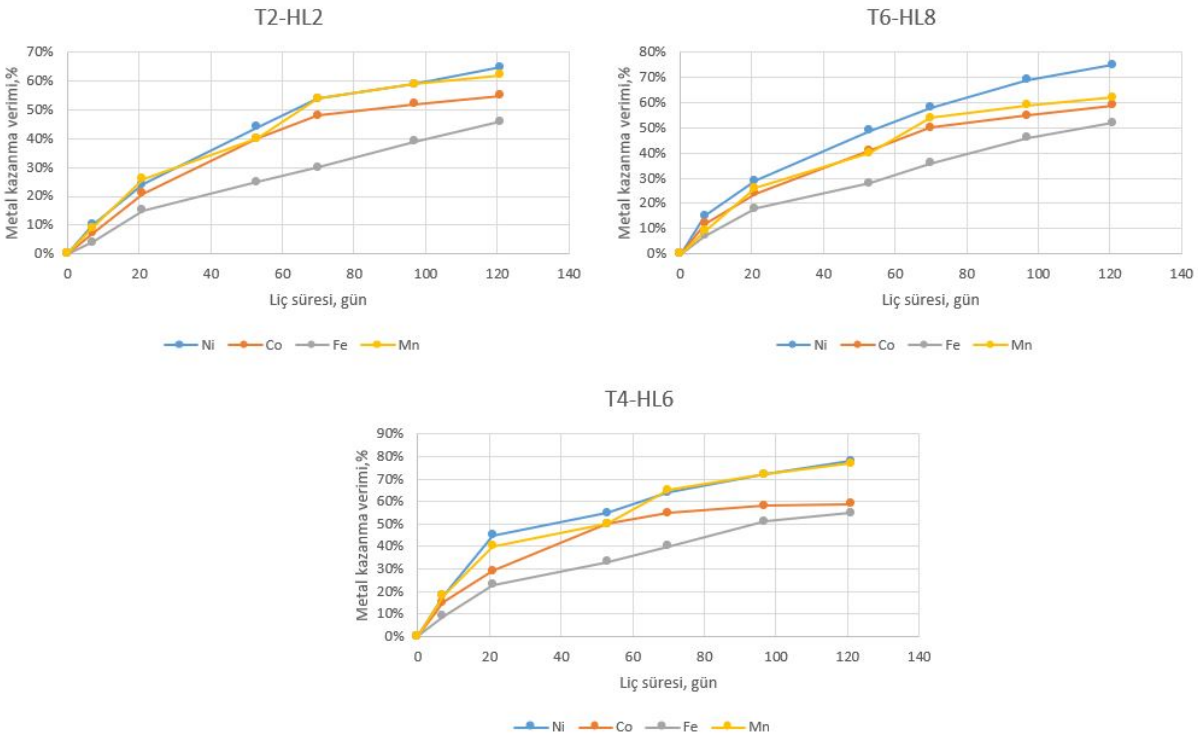

Şekil 4. Yüksek konsantrasyonlu asit çözeltisi ile yapılan kolon liçi testlerinin gün- metal kazanma grafikleri (T2-HL2; T6-HL8; T4-HL6).

Yüksek konsantrasyonlu asit çözeltisi ile yapılan liç testlerinin sonuçları incelendiğinde; 97-121 günleri arasındaki liç verimlerinde yükselme eğilimi azalmıştır.

Tüm metaller için tane boyutunun metal kazanma verimlerine etkisi incelendiğinde tane boyutu azaldıkça liç verimi arttığı görülmüştür. Tane boyunun metal kazanımına etkisinin Ni-Fe-Mn metalleri için Co metaline göre daha fazla olduğu gözlemlenmiştir. Buna bağlı olarak tane boyutu ve liç süresinin ters orantılı olduğu belirlenmiştir. Sonuç olarak, benzer yığın liçi çalışmalarında görüldüğü gibi (Rashidi, 2020), ince tane boyutu ile gerçekleştirilen liç deneyinde, iri tane boyutlarına göre maksimum liç verimlerine daha kısa sürelerde ulaşılmıştır. Bu durum ince tanelerin çözücü ile temas edeceği yüzey alanının iri taneye göre daha büyük olması ile açıklanmaktadır.

SONUÇLAR

Bu çalışmada, Gördes nikel cevherinin düşük tenörlü elek üstü ürünün değerlendirilmesi amaçlanmıştır. Düşük tenörlü ve kilinden arındırılmış (yıkanmış eleküstü) olması nedeniyle yığın liçi prosesinin uygulanabilirliği değerlendirilmiştir. Cevher hazırlama bölgesinde elek üstü olarak ayrılan düşük tenörlü cevherden temsili numune alınmıştır. Yaklaşık alınan 10 ton numuneyi dörtleme yapılarak 6 adet test numunesi elde edilmiş ve laboratuvar testleri yapılmıştır. Çalışma kapsamında; tane boyutu, sülfürik asit konsantrasyonu ve liç süresinin Ni-Co-Fe-Mn gibi elementlerin kazanımına etkileri incelenmiştir.

Elde edilen deney bulgularına göre;

Nikel metali değerli olduğu için maksimum oranda çözünmesi hedeflenmiştir. Yürütülen testler sonucunda, en yüksek liç verimi (%78) -5mm tane boyutunda ve 250gr/lt serbest asit liç çözeltisinde T3-HL5 nolu testte elde edilmiştir. Bu testteki birim asit tüketim değeri cevher tonu başına 1200kg/ton'dur.

Kobaltta nikel gibi değerli bir metaldir. Liç verimleri dikkate alındığında, aynı nikel metalinde olduğu gibi tane boyutunun azalmasına ve asit konsantrasyonunun artışına bağlı olarak, kazanma verimi de artmaktadır. Kobalt metalinin liç verimindeki artış, diğer metallere göre daha az miktarda gerçekleşmiştir. En yüksek liç verimi (%59) -5mm tane boyutunda ve 250gr/lt serbest asit liç çözeltisinde T3-HL5 testinde elde edilmiştir.

Mevcut proseste demir empürite olarak tabir edilen bir metaldir. Liç veriminin artması sonraki safsızlaştırma aşamalarında prosesin zorlaşmasına, maliyetlerinin yükselmesine ve üretim veriminin düşmesine sebep olabilmektedir. Demir metali için en düşük liç verimi (%25) -150mm tane boyutunda ve 150gr/lt serbest asit liç çözeltisinde T1-HL1 testinde elde edilmiştir. Bu testteki birim asit tüketim değeri cevher tonu başına 500kg/ton'dur.

Mangan da demir gibi empürite metalidir. Aynı demir empüritesi gibi liç veriminin artması sonraki safsızlaştırma aşamalarında prosesin zorlaşmasına, maliyetlerinin yükselmesine ve üretim veriminin düşmesine sebep olmaktadır. Mangan için en düşük liç verimi (%56) -150mm tane boyutunda ve 150gr/lt serbest asit liç çözeltisinde T1-HL1 testinde elde edilmiştir.

Testlerindeki liç verimleri dikkate alınarak 121 gün liç süresi tutulmuştur. Test süresi 121 sonrasında liç verimlerinin artışı azalmıştır.

Testler değerlendirildiğinde, değerli metaller olan nikel ve kobaltın çözünürlüğü arttıkça; empürite metallerinin çözünürlükleri ve birim asit tüketimi de artmaktadır. Bu nedenle, pH yükseltilerek empürite metallerinin ortamda azaltılması gerekmektedir. Ancak bu durumun safsızlaştırma prosesinin zorlaşmasına, üretim maliyetinin yükselmesine dolayısıyla üretim verimliliğinin düşmesine neden olacağı düşünülmektedir.

Optimum test koşullarının belirlenmesi özellikle safsızlaştırma prosesine bağlı olsa da, yığın liçini temsilen yapılan kolon liçi testleri sonucunda bazı bulgular elde edilmiştir. Elde edilen bulgulara göre, nikel kazanma verimini etkileyen en önemli iki parametre tane boyutu ve serbest asit konsantrasyonudur. Bu durum, yığın liçi tekniği ile en kısa sürede en yüksek nikel kazanma veriminin elde edilmesi için tane boyutunun minimum, ortama sağlanan asit konsantrasyonunun ise maksimum düzeyde olması gerektiğini göstermektedir.

Testlerde nikel ve kobalt çözünürlükleri göz önüne alındığında, liç verimlerinin sırasıyla %78 ve %59'a ulaştığı, bununla birlikte empürite olarak tabir ettiğimiz demir ve mangan metallerinin, mevcut HPAL prosesine göre ortamda çok daha fazla çözündüğü gözlemlenmiştir. Lateritik nikel cevherlerinin, hidrometalurjik yöntemler ile ekonomik şekilde kazanılması, birim asit tüketimi ve empürite çözünmelerine doğrudan bağlı olan bir durumdur. Elde edilen sonuçlar ve son yıllardaki nikel fiyatları dikkate alındığında, düşük tenörlü lateritik nikel cevherlerinin yığın liçi yöntemi ile kazanılmasının ekonomik olmadığını göstermektedir. Ancak ülke kaynaklarının değerlendirilmesi ve gelecek fiyatlama projeksiyonları göz önüne alındığında bu ve benzeri çalışmaların geliştirilerek devam ettirilmesi gereklilik olarak görülmektedir.

KAYNAKLAR

Atik, S. (2015). Biyoliç Yöntemiyle Lateritik Cevherden Nikel Kazanımı. Yüksek Lisans Tezi, Süleyman Demirel Üniversitesi, Fen Bilimleri Enstitüsü, Isparta.

Baştürkçü, H. (2016). Fiziksel ve Kimyasal Ön İşlemlerin Lateritik Nikel Cevherlerinin Atmosferik Liçine Etkisi. Doktora Tezi, İstanbul Teknik Üniversitesi, Fen Bilimleri Enstitüsü, İstanbul.

Çoban, O. (2014). Çaldağ Lateritik Nikel Cevherlerinden Hidrometalurjik Yöntemlerle Nikel ve Kobalt Eldesi. Yüksek Lisans Tezi, İstanbul Teknik Üniversitesi, Fen Bilimleri Enstitüsü, İstanbul.

McDonald, R.G., Whittington, B.I. (2008). Atmospheric Acid Leaching Of Nickel Laterites Review Part I. Sulphuric acid Technologies. *Hydrometallurgy*, 91, 35-55.

Nasuh, A. (2014). Eskişehir-Karaçam Lateritik Cevherinden Basınçlı Sülfürik Asit Liçi İle Nikel Kazanımı. Doktora Tezi, Hacettepe Üniversitesi, Fen Bilimleri Enstitüsü, Ankara.

Leonardou, A.S., Dimaki, D. (1994). Heap Leaching Of Poor Nickel Laterites By Sulphuric Acid At Ambient Temperature, International Symposium Hydrometallurgy '94, (pp. 193-208), Cambridge, England

Li, J., Li, X., Hu, Q., Wang, Z., Zhou, Y., Zheng, J. (2009). Effect Of Pre-Roasting On Leaching Of Laterite. *Hydrometallurgy*, 99, 84-88.

Listyarini, S. (2017). Designing Heap Leaching For Nickel Production That Environmentally And Economically Sustain, Vol.8, No:12.

Rashidi, A. (2020). Yığın Liçi İle Altın Kazanımında Yığın Özelliklerinin İyileştirilmesi. Yüksek Lisans Tezi, Zonguldak Bülent Ecevit Üniversitesi, Fen Bilimleri Enstitüsü, Zonguldak.

ECO-EFFICIENCY IN DRY COMMINUTION PRACTICES USING VERTICAL ROLLER MILL (VRM) - TECHNICAL AND ECONOMICAL ASPECTS

H.R. Manouchehri [1,*]

[1] *Northland OreTech AB,*
Mining, Mineral and Metallurgical Processing and Waste Management Consulting
(Corresponding Author: hmanouchehri@yahoo.com)

ABSTRACT

Mining industry, as the cornerstone of human civilization, is directly and indirectly responsible for up to 45% of the global economy. The industry is an energy and water consumer. It is projected that about 6-7% of total world's energy is consumed by mining activities, while about 6-8 Billion m^3 of water per annum is consumed through mining activities. The industry, facing different challenges, including resource efficiency, access to energy and water, reducing environmental foot-print, etc. Accordingly, inventing and developing machineries and processes that help to overcome these challenges are highly projected for sustainable in mining industry

Since considerable amount of energy is consumed in comminuting ores and the energy per ton of product increases as deeper and more competent reserves are brought into operations, as well as its environmental, economic and political aspects need to be considered seriously in design and operation of future mineral processing activities.

Moving towards “Green Economy” requires responsible attempts to understand and implement eco-efficient technologies. One identified technology, would be dry comminution practices by using Vertical Roller Mill (VRM). Herein the results from a collaborative scaleup project supported by European EIT-RawMats on technical, economic and environmental aspects of dry comminution process by VRM is presented and discussed.

Keywords: Eco-efficiency, dry comminution, vertical roller mil (vrm), energy, wear

INTRODUCTION

Mining industry has been the cornerstone of human civilization which is directly and indirectly contributes to 45% of the global economy. The industry is an energy and water consumer. It is projected that about 6-7% of total world's energy is consumed by mining activities from which almost half goes for size reduction for processing of the values from the rocks (Michaux, 2011; Morrison and Cleary, 2008; Batterham, 2007). The industry is responsible for 4-7% of the world’s GHG emissions as well (McKinsey, 2020). Furthermore, mining activities consume 7-9 Billion m^3 of water per annum and is partly responsible for polluting water by different processes which must be carefully understood and taking care of.

The industry faces different challenges, including resource efficiency, access to energy and water, reducing environmental foot-print, license to operate, etc. Accordingly, inventing and developing machineries and processes that help to overcome these challenges are necessities for future sustainability.

Mineral processing represents the largest consumer of energy and water and therefore mining companies are assessing mineral processing technologies and innovative approaches to improve energy and water consumption and related environmental foot print.

There is strong link between the eco-efficiency and sustainability in mining industry. The future direction for the industry is moving towards eco-efficiency. Both energy and water are critical valuables for development and must be conserved to make a balance between the environmental foot-print and economy. Minerals and metals industry contribute greatly to the global economy; however, the related environmental impact plays a critical role for future sustainability. That includes the consumption and depletion of the natural resources and producing mining wastes, emissions of GHG and pollutant to the ari, as well as water consumption and water pollutant due to releasing of different ion species and insoluble during mining and processing.

Metals and minerals production rate has been dramatically increases due to industrialization, increasing population, and technology development. Extracting of raw materials, including fuels, has dramatically increased during last 20 years, from 11.3 billion tonnes in 2000 to 17.9 billion tonnes in 2019, i.e., 58% increasing (World Mining Data, 2021).

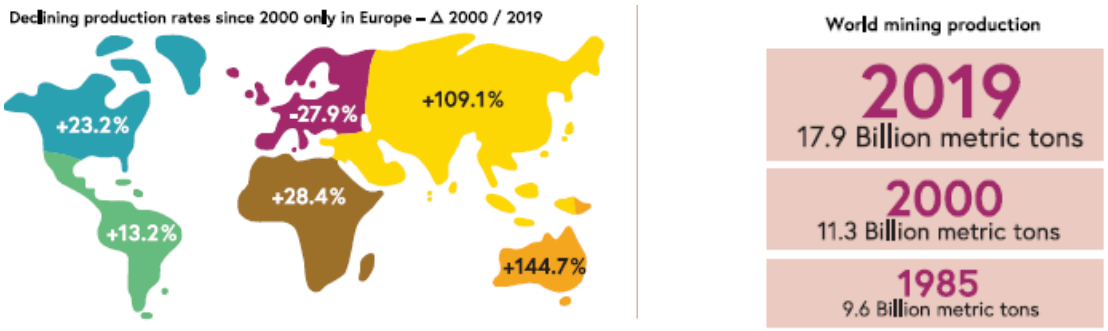

Figure 1. Mining production and declining/increasing rates of production by continents

To sustain production, mining industry requires withdrawal of freshwater. Water consumption is an important sustainability factor in particular in arid areas, such as Australia, Africa, Middle East, and South America. For example, to produce various types of metals the water consumption ranging from 2.9 m^3/t for steel production to more than 250 m^3/t for gold production.

Furthermore, water and energy consumption are directly related to the ore grade from which the metal is produced. An estimation indicated that as the grade (%) is decreasing the water consumption per ton of metal production is increasing (Norgate and Lovel, 2004).

$$Water\ Consumption(m^3/t) = 167.7 \times G^{-0.9039} \quad (1)$$

Water is strategic asset and has become a sourcex of strategic advantage and a growing source of conflict. It is an expensive asset which accounts for 10% capital expenses for infrastructures. Furthermore, mining activities impact the local water system and are responsible to contribute in an integrated water management program. Furthermore, mining is potentially a source of polluting water, therefore mining and process water must be treated before it is released to the environment. The global mining industry facing challenges due to water scarcity, global warming, lack of transparent legislations in water quality control and are seen as key partner in global sustainable development. Therefore, managing water consumption and reducing/minimizing its pollution are key in sustainability.

It is also worth to mention that the global water treatment market has reached over 260 BUS$ in 2018, from which about 4,7 BUS$ is the share of mining industry. Therefore, considering dry efficient comminution processes offer a great opportunity in reducing water consumption and minimizing its pollution (Global Water Market, 2021).

Dry Eco-Efficient Comminution for Sustainability in Mining Industry

In 2020, the world's energy consumption has reached $155*10^{12}$ kWh (558 Exa-Joule) and it is supposed to reach $265*10^{12}$ kWh by 2050 (i.e., an increasing of 1.5% per annum). Mining industry consumed about 6-7% of that energy, with the highest consumption in comminution (3-3.5%).

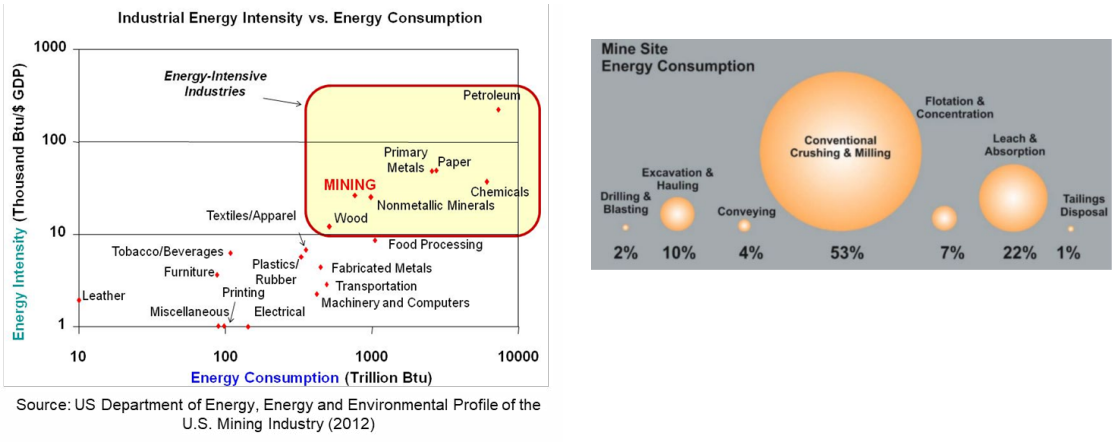

Figure 2. Industrial energy intensity (left) and distribution of mine site energy (right)

The industry is also responsible for 4-7% of the world's GHG emissions which must be reduced significantly by considering different strategies. The goals can be achieved by reducing, reusing and recycling (3Rs), reduction in energy consumption, carbon capturing and sequestration, etc.

Furthermore, the water withdrawal and its environmental impact must be reduced. In fact, grinding of the ore in wet mode to achieve the liberation for processing not only consumes water but the process water may be polluted. Therefore, moving towards dry comminution may avoid/reduce the release of different chemical species to the mine water circuit. Additionally, during milling the grinding media are consumed to size down the ore, however, the media consumption per ton of comminuted ore is defined by the ore characteristics, i.e., its hardness and abrasiveness. As the harder and more abrasive ore is ground to an specific size the media consumption is increased. It is also well understood that the media wear or media consumption is much higher in wet grinding. That means the wear is considerably less in dry grinding. Based on the type of media used for grinding, there is an embodied energy in manufacturing the media which is estimated to be at average 5-6 MW/t. consequently, the reduction in media consumption by dry grinding results in saving energy and reducing the related GHG emission.

With the decline of water resources, increasing of energy costs, and the efforts to reduce energy consumption and minimise CO_2 emission, mining companies are increasingly mindful of the value of water, energy, as well as the potential CO_2 emission and water pollutants to be reduced. Accordingly, an eco-efficient dry comminution technology, which can reduce water consumption and its polluting while reducing energy consumption would be of prime interest. The comminution stage and downstream processes should be designed and integrated through circular economy concept in which reliable grade-engineering is combined with dry comminution to improve quality of the feed and reduce tonnage in downstream wet separation process(es) to sustainably reduce water usage.

Vertical Roller Mill (VRM)

Vertical Roller Mill (VRM) is an eco-efficient dry comminution technology that can be considered for hard rock comminution and processing. A comprehensive study has been devoted to assess the potential of implementation of the technology for hard rocks and slags from metallurgical plant through the European Innovation and Technology (EIT) program on raw materials. It is a kind of roller mill that is widely used in the cement industry. Within the VRM, the interparticle comminution takes place in a material filled gap between the rotating flat grinding table and the conical grinding rollers as shown in Fig.3.

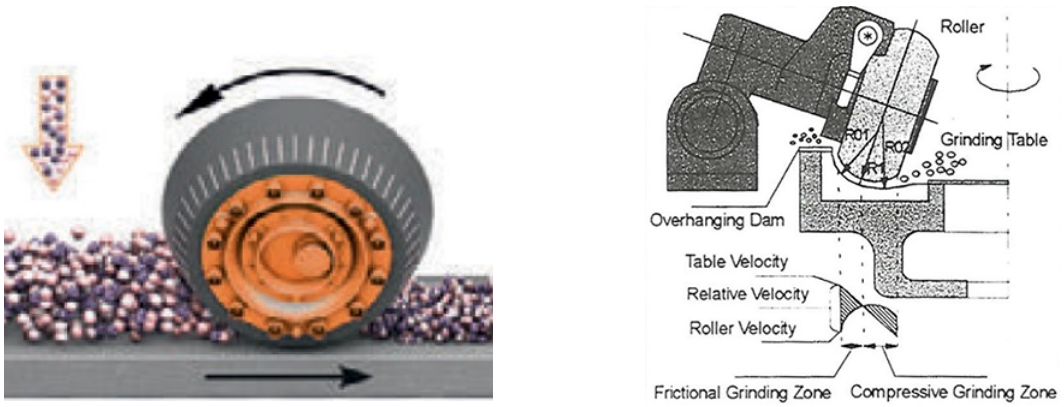

Figure 3. Interparticle comminution of the roller mill

Grinding/comminution with roller mill is done in a material filled gap between the rotating flat grinding table and the conical grinding rolls. The feed is charged to the center of the flat table and moves affected by centrifugal forces and friction towards the table's edge. Based on the mill size, the feed is nipped by conical rollers installed at the outside of the table. The grinding force is provided by rollers that are attached to the hydraulic cylinders). An efficient dynamic air classifier (air cyclone) is incorporated inside the mill to separate the ground particles (Schaefer, 2001). For optimal performance of the mill and minimizing the down-time of the mill, the rollers are equipped with wear resistant tyres made of high-Cr casting or other resistant alloys. The comminution pressure is provided by hydro-pneumatic spring system. A high pressure between 50 to 100 bar is provided to ground the ore within the gap between the rollers and the table. The low-pressure side of the hydraulic cylinder has a pressure of about 10% of the high-pressure side, therefore, the difference between high- and low-pressure sides allowing elastic movement of the roller. Within VRM comminution is done mainly by compression, however, shearing is involved as well. Furthermore, due to introducing hot air to the mill, raw materials with high moisture can be easily tolerated.

In comparison with conventional ball milling, VRM can accept larger feed size, up to 140mm. Accordingly, part of crushing might be eliminated. Furthermore, due to flexibility in adjusting grinding pressure, the fluctuations in feed properties can be easily tolerated. Overgrinding can be avoided due to possible controlling of grinding pressure and the high performance of air classifier.

MATERIALS AND METHOD

Materials

Two different raw materials/samples were received for testing, a sulfide ore from Boliden Minerals AB and a ferromanganese slag from EraMet. The samples were characterized for their comminution behaviors. Accordingly, crushing, rod milling and ball milling Bond work indexes were

determined for the materials. Furthermore, the abrasion index of the samples was defined, using standard Bond abrasion tests. The results from characteristic of the samples are shown in Table 1. The results indicates that sulfide ore can be categorized as soft to medium ore (rather low competency), however; the slag sample could be considered medium to hard ore/material (rather high competent).

Table 1. The comminution characteristics of the samples

	Crushing Work Index (Wic)	Rod Mill Work Index (Wir)	Ball Mill Work Index (Wib)	Abrasion (Ai)
Sulfide Ore	10 (kWh/t)	13 (kWh/t)	12,5 (kWh/t)	0.15 - 0.18
FeMn Slag	14 (kWh/t)	17.7 (kWh/t)	17 (kWh/t)	0.38 – 0.51

Comminution Tests

After characterization, the samples were ground to explore the potential of implementing of VRM technology for eco-efficient comminution. The comminution tests were conducted at Loesche pilot facilities in Germany. The criteria for comminution were defined on the basis of mineralogical analysis of the samples and the related processes for downstream. Accordingly, the target product sizes for comminuting were considered as d_{80}=60-65 µm for sulfide ore and d_{80}≈300 µm for the ferromanganese slag.

Comminution tests were also conducted in both wet and dry modes in ball milling in order to compare the energy consumption by different comminution technologies. Moreover, the media needed for the grinding the samples were estimated based on specific energy consumption. Accordingly, the energy needed to size down the samples to the specific target size was estimated for different comminution modes. Furthermore, the media wear for both comminution modes were calculated to estimate the related wear costs.

RESULTS AND DISCUSSIONS

Series of comminution tests were completed by using VRM and the energy needed for comminuting the samples were defined. Fig. shows the results to achieve the target sizes for the samples. For conducting grinding tests, the received samples were crushed to obtain -20 mm product. The size distribution of the crushed samples revealed that the d80 of crushed samples were at 16 mm and 8 mm for slag and sulfide ore respectively. The grinding tests were conducted, using VRM to achieve the target sizes. The results are depicted in Figs 4 and 5. Accordingly, the energy needed to gain the d_{80} = 60-65 µm is at about 7 kWh/t. However, about 4.4 kWh/t was needed to grind the slag sample to a target size of to d80 = 300 µm.

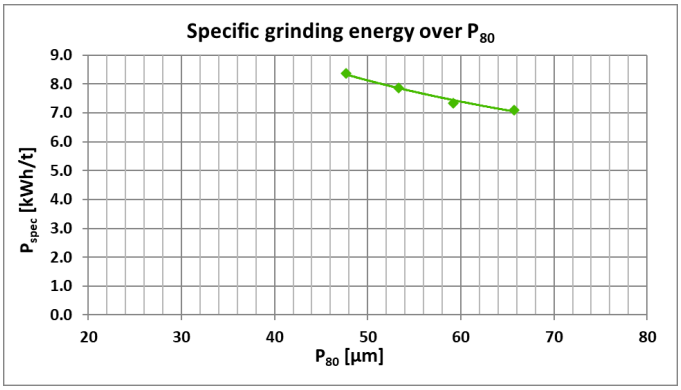

Figure 4. Energy consumption vs particle size in comminution, using VRM for sulfide ore

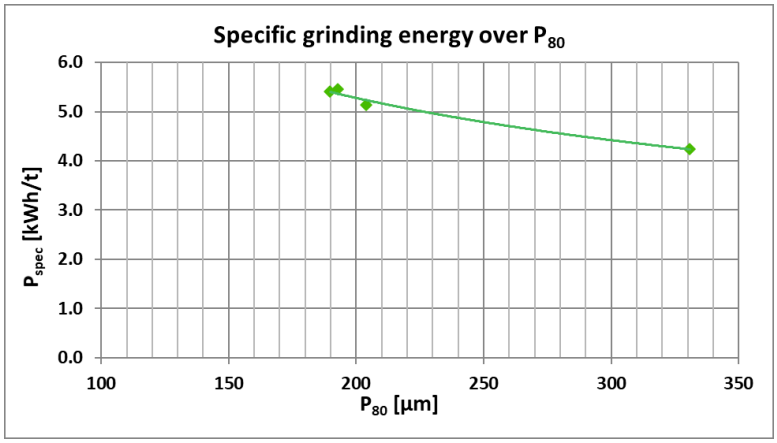

Figure 5. Energy consumption vs particle size in comminution, using VRM ferromanganese slag

Energy Estimation for Ball Milling (Based on Bond Equations)

According to the Bond theory, to comminute a material/sample to certain size, crushing followed by rod and ball millings are considered. In fact, rod milling is rather low energy consumption device, tailoring a good feed for ball mill. In theory, after crushing the feed, the rod mill accepts a feed size up to 35 mm and provide a product at d80 ~ 2mm for ball milling. However, nowadays, in practices, i.e., plant design and operation, no rod milling is considered. One reason is that high performance crushers are emerged to efficiently size down the feed to about 10 mm or even smaller and more powerful and efficient ball mill are manufactured to grind the crushed material. The energy consumption to size down the two raw materials to the target product size was estimated based on Bond equations. A rough calculation for the energy consumption are shown in Table 2.

Table 2. Estimated energy consumption for the samples in both dry and wet modes

E_{total} = EFs (10 Wi ((1/√P80)-(1/√F80))				
	F80m(µm)	P80 (µm)	Energy (kWh/t) – Wet	Energy (kWh/t) – Dry
Sulfide ore	8000	65	14.8	19.24
FeMn Slag	16000	300	9.10	11.83

According to the results, the energy consumption for grinding the samples, using VRM, is considerably lower than the conventional tumbling milling in both wet and dry modes. However, as the classification is done within the VRM, there will be additional energy consumption to separate/classified the ground products.

Except the energy calculations based on Bond equations for dry and wet comminution of the samples, a series of laboratory ball milling tests was conducted to define the energy consumption for comminuting the samples. Accordingly, the energy consumption for comminuting the sulfide ore to the target size was defined at range of 19.73 to 21,2 kWh/t in dry comminution, while for wet comminution the energy consumption was estimated at 17.9 kWh/t. Nevertheless, the calculated energy consumption are based on the finer feed size to the laboratory ball mill based on Bond ball milling tests. The same procedures were completed for FeMn slag sample and the energy needed to comminute the material to target size were at 8.75 and 10.5 kWh/t for wet and dry mode respectively.

It must be noted that, except the direct energy needed to grind the sample to specific target size, there will be an energy consumption for classification within the VRM. The energy consumption for

classification, using air cyclone, is defined on the basis of feed specifics, including feed size, its density, the product size as well as mill size, etc. Accordingly, the energy needed for classification can normally range from 50% and 100% of the energy needed for direct size reduction. However, in some cases when the coarse product is required, the energy consumption in classification may be higher than the energy needed for direct size reduction. Further calculations were done to define the total energy needed for comminuting and classifying the samples. Accordingly, the relation between the energy needed for grinding and classification were at 100% and 130% for sulfide ore and slag sample respectively. Consequently, the total energy needed for grinding and classification of sulfide ore and ferromanganese slag were estimated at 13.8 (kWh/t) and 8.9 (kWh/t) respectively.

Wear Consideration in Comminution

Grinding media wear represents a significant cost in comminution, particularly grinding. In general, the total wear process of grinding involves a number of mechanisms including abrasive and corrosive wear. More knowledge about the wear mechanisms and the relative importance of each wear component would enable one to better select grinding media for specific applications, and could lead to the development of alloys with improved resistance to wet grinding wear.

The impact of grinding media consumption on the cost of grinding. In fact, comminution accounts for an estimated 30–50% of typical mining operating costs, and of these, liner wear and media consumption account for roughly 50% of the cost. However, in some instances, media wear can constitute up to 40– 45% of the total cost of comminution. Two types of wear are common in grinding practices. i.e., abrasion and corrosive wear. However, in dry grinding, the abrasion wear plays the role that is directly related to the abrasiveness of the material to be ground and the energy needed to size down the material to the specific size. Nevertheless, in wet grinding, the corrosive wear would be predominant which is affected not only by the inherent characteristics of the ore, but by pH and Eh of the environment, type of the media used, etc. Despite the fact that the energy consumption is higher in dry grinding, the wear is higher when wet grinding is employed for sizing down any specific ore/material.

Furthermore, the filling rate and size distribution of the media play a significant role in comminution efficiency and related cost. Improper size distribution or filling level of the media charge can reduce the efficiency of grinding, causing in losing media at higher rate. Accordingly, the cost associated with grinding media is chiefly determined by two factors, i.e., the wear performance (quality) and the price of the grinding media.

Moreover, it must be noted that in comminution practices there are power consumptions related to ancillary equipment and embodied energy in media manufacturing. Steel media, e.g., rods and balls, are frequently used in tumbling to assist in ore breakage. Media consumption can cost as much as comminution power consumption (Daniel et al., 2010). Additionally, the mining, smelting, casting, and shipping of media consumes a substantial quantity of energy. Therefore, the embodied energy consumed through media wear is an important factor to be considered in evaluating eco-efficiency in comminution. Apart from the understanding of the phenomena involved in the wear of grinding media, the media consumption is typically reported as steel grams required per ore ton of treated ore. Converting the media consumption into the embodied energy consumption can help in defining more eco-efficient comminution practices. Studies have revealed that the energy consumption to produce a ton of steel an average energy of 6 MWh is required. That is without considering of recycling through life cycle assessment. The production data indicated that 2 ton of CO_2 is emitted for producing a ton of steel (Yang and Broadbent, 2017). The energy consumed by diesel trucks can be between 0.15 and 0.25 kWh/kg.km (Nylund and Erkkilä, 2005). However, the figures may change for other alloys since the metallurgy of the media and type of alloy to be used plays a role herein. For example, forged balls and low/high chrome balls require completely different manufacturing processes and feed materials (Ballantyne 2018). Accordingly, the embodied energy to manufacture both forged balls, as well as high

and low chromium balls varies from 4.8 to 6.6 kWh/kg, depending upon metallurgy type, ratio of recycled steel in the feedstock, and other parameters including transportation transport the media to site. It must be added that considerable amount of CO_2 is emitted during production of steel and other alloys, which is indirectly contribute to global warming and reducing general eco-efficiency (CO_2 emission for steel production ~$2t_{CO2}/t_{steel}$).

Furthermore, steel plants are water consumers that must be taken into account in a life cycle assessment of the comminution route. Steel is produced through two alternative routes, i.e., the integrated cycle, where steel is produced from virgin raw materials, and the electric route, which produces steel by melting scrap in an electric arc furnace (EAF). The average water intake for an modern integrated steelworks is 28.6 m^3 per ton of produced steel, with an average water discharge of 25.3 m^3 per ton of steel. For the electric route, however, the average intake is 28.1 m^3 per ton of steel, with an average discharge of 26.5 m^3 per ton of steel. Accordingly, the overall water consumption per ton of steel produced is between 1.6 m^3 and 3.3 m^3 per ton of steel (Colla et al., 2017). Steel plants use freshwater, salty and brackish ones, however, the water consumption in practices may vary and being higher base on the plant and related technology. For example, an average fresh water consumption of 7 - 8.3 m^3 per ton of steel were reported for most big steel enterprises of China in 2008, which was merely lower at range of 3 to 4.2m^3 per ton of steel (Gao, et al, 2011) in developed countries.

Accordingly, by reducing the wear/media consumption in comminution practices, possibilities offer towards reduction in embodied energy in comminution as well as conserving water per ton of reduction in steel and/or different alloy consumptions.

Wear Calculations in Comminuting Tested Samples

Although, there is no common formula/equation to determine the wear, there are different equations to estimate the wear in comminution, however, in defining the wear rate must be defined in practices by running comprehensive tests. There have been attempts in estimating wear rates in both dry and wet practices that are mainly based on collecting data from tests and plant practices. In general, as the ore abrasiveness is increasing the amount of wear is increased, however, as indicated above the wear rate is increased as the energy consumption to grind the raw material is increased. Furthermore, in wet grinding the mill electrochemistry, i.e., pulp pH and Eh, dissolved oxygen, etc., are determining factors. While, the type of media used in comminution is another determining factor. Based on the type of comminution, related energy consumption to achieve the target size, and the abrasiveness of the sample the media consumption can be calculated. Herein, the wear rates for grinding sulfide ore and ferromanganese slag were estimated considering steel media. The estimations were done based on Bond's wear equations for dry and wet grinding. Nevertheless, the wear calculations were conducted on the basis of the equation proposed by (Giblett and Seidel, 2011).

<u>Wear in Wet grinding (Bond equation)</u>

Wear Rate/Ball Consumption (kg/kWh) = $0.159*(Ai - 0.015)^{0.33}$

Wear Rate/Ball Consumption (kg/t) = Energy Consumption (kWh/t) * $(0.159*(Ai - 0.015)^{0.33}$

<u>Wear in Wet grinding (Giblett and Seidel 2011)</u>

Wear Rat /Ball Mill Media (kg/kWh) = $0.0817*(Ai)^{0.498}$

Wear Rate /Ball Mill Media (kg/t) = Energy Consumption(kWh/t) * $0.0817x(Ai)^{0.498}$

Wear in Dry grinding (Bond equation)

Wear Rate (kg/kWh) = $0.05*(Ai)^{0.5}$

Wear Rate (kg/t) = Energy Consumption (kWh/t)* $0.05*(Ai)^{0.5}$

In general, there are different factors affecting the degree of media wear in comminution practices. The media type (metallurgy), the ore/sample abrasiveness, the type of commination device rod, ball, stirred, roller, etc.), operational parameters in grinding (speed, tonnage, filling rate) and media size are the key factors defining the media wear.

Table 3 depicted the wear rate calculations for grinding the samples based on the abrasion index, Ai, and the energy consumption to grind the samples to the target size. Herein the wear was calculated based two different abrasion indexes. The calculations indicated that the wear in wet milling is considerably higher than that of dry milling. It seems that the wear calculations, based Bond equation in wet mode are rather high, however, the calculations based on Gibelett and Seidel (2011) show considerably lower values.

Table 3. Estimating the wear in milling samples

	Energy-Wet (kWh/t)	Energy-Dry (kWh/t)	Abrasion Index (Ai)	Wear* (g/t)– Wet (Bond equation)	Wear* (g/t) – Dry (Bond equation)	Wear§ (kg/t)-Wet (Gibelett & Seidel)
Sulf-Ore	9.1	11.83	0.15 - 0.18	747 - 783	229- 251	289 – 316
FeMn Slag	14,8	19.24	0.38 - 0.51	1687 - 1865	593 – 687	747- 865

Wear in Grinding by VRM

The wear measurement for grinding the samples with VRM were estimated after the pilot test. The wear for grinding rollers was measured as the bulk wear rate over the complete duration of the grinding test.

For slag sample the wear was defined as186 g/t of mild steel. In fact, the wear was measured with C45 mild steel rollers and determined as bulk average wear over the set point for the target particle size. That means the grinding media consumption is a level of medium to high based on the VRM grinding experiences. On the basis of industrial processes and the installed mill, in practice the use of different types of rollers have been experienced. Accordingly, the Metal Matrix Compound (MMC) grinding elements have considerably higher abrasive resistant, resulting is much lower specific grinding media consumption. The wear rate in industrial size Loesche VRM would, using MMC alloy, be considerably lower, i.e., about 15 times lower, than that of mild steel resulting in a specific wear rate of ~ 12 g/t.

In similar way the wear was calculated for sulfide ore. The bulk wear rate over the complete duration of the grinding test was defined as 129 g/t of mild steel. The lower wear rate for sulfide ore is due to lower abrasion index for the ore. Based on experiences in industrial processes, using Metal Matrix Compound (MMC) grinding elements, the grinding wear can be considerably reduced. Accordingly, the wear is reduced by about 15 times, resulting in a specific wear rate of ~ 8 g/t when the rollers are made from a high quality MMC material.

In fact, MMC has considerably higher abrasive wear resistant which is governed by a combination of both high hardness and toughness. MMCs are made of different hard components, including CW

(Tungsten Carbide) which significantly improves wear resistance and hardness in comparison with the composition of matrix. Due to strong metallurgical bond between the matrix and reinforced region considerably higher mechanical performances are expected, resulting in dramatically reduction in wear.

CONCLUDING REMARKS

Mining is one of the most energy intensive industries which consumes 6–7% of the world's energy. Comminution is the most energy intensive within mining processes which is responsible for almost 50% of total energy consumption in mining, from which almost 90% goes for grinding part. Accordingly, comminution processes, in particular grinding, attempts have been made to introduce grinding equipment and flowsheets to conserve energy. According to an investigation by US Department of Energy (2007), there is a potential to reduce the energy consumption in US mining industry to half by implementing the best practices scenario(s) and conducting the outcomes from research and development (R&D) activities that improve technologies. The study indicated that there are certain areas that offer tremendous opportunities in energy saving. The largest energy saving opportunities were found to be grinding and materials handling.

Moving towards "Green Economy" requires responsible attempts to implement eco-efficient technologies. One identified technology would be dry comminution practices by using Vertical Roller Mill (VRM). Within this study, an effort was made to implement VRM technology in size reduction to grind the raw material to micron sizes and evaluate its potential in reducing energy and costs in mining industry. The results indicated that the energy consumption in grinding can be considerably reduced by implementing VRM technology in comparison with conventional tumbling mills. The reduction in energy consumption is much larger when comparing VRM grinding energy with conventional milling. Considering for the sulfide ore the reduction would be more than 30% while considering the energy for classification within VRM. The reduction in energy consumption is less when comparing wet ball milling with VRM, ranging from 2.5% to 7% for comminuting slag and sulfide ore respectively. However, considering the energy needed for classification, the reduction in total energy would be higher.

Furthermore, the results from media consumption showed promising prospect in reduction in wear which is an important part of operation cost in comminution practices. Reduction in wear indirectly reduced the energy consumption as the embodied energy in manufacturing wear parts, i.e., energy needed in metallurgy and related raw materials as well as energy for the transportation, etc.

At last, but not least, moving towards energy-efficient dry comminution, could preserve the water. Water consumption is reduced and its pollutant can be avoided or minimized. Water is valuable strategic asset and has become of strategic advantages. Mining activities impact the local water system resulting in contaminating and polluting the water sources due to dissociation of different ionic species and insoluble materials. Milling operation could be a source of contaminating/polluting the water. So, dry comminution can help in reducing water consumption and its pollutants. That also reduces the costs and energy in process water treatment. However, reduction in wear/media consumption, indirectly affects the water consumption in wear materials production.

REFERENCES

Ballantyne, G. (2018). Energy Curve Enhancement Blog:7, Including grinding media consumption in the comminution energy curves.

Colla, V., Matino, I., Branca, T., Fornai, B., Romaniello, L., Rosito, F. (2017). Efficient Use of Water Resources in the Steel Industry. *Water 9, 874,* 1-15.

Daniel, M., Lane, G., McLane, E. (2010). Efficient, economics, energy and emission – emerging criteria for comminution circuit decision making. In Proceedings of XXV International Mineral Processing Congress (IMPC).

Gao, C., Wang, D., Dong, H., Cai, J., Zhu, W., Du, T., (2011). Optimization and evaluation of steel industry's water-use system. *Journal of Cleaner Production 19*, 64-69.

McKinsey, 2020. Climate risk and decarbonization: What every mining CEO needs to know. https://www.mckinsey.com/business-functions/sustainability/our-insights/climate-risk-and decarbonization-what-every-mining-ceo-needs-to-know.

Michaux, S. (2011). Sustainability in Comminution Design: Six Caveats that will change Mining Culture and Design. SMI Lecture, http://www.ceecthefuture.org/publications/sustainability-in-comminution-design-six-caveats-that-will-change-mining-culture-and-design/

Morrison, R.D., & Cleary, P.W. (2008). Towards a virtual comminution machine. *Minerals Engineering 21*, pp. 770–781.

Nylund, N-O., Erkkilä, K. (2005). Heavy-duty truck emissions and fuel consumption simulating real-world driving in laboratory conditions, DEER Conference, Chicago, Illinois.

Roland, C.A., (2002). Selecting of Rod Mills, Ball Mills and Regarding Mills, in *Mineral Processing Plant Design, Practice and Control, Vol* 1, pp. 710-754

Schaefer, H.U. (2001). Loesche vertical roller mill for the comminution of ores and minerals. *Minerals Engineering, 14(10)*, pp. 1155-1160.

U.S. Department of Energy, (2007). Mining Industry Energy Bandwidth Study. 47 pp.

World Mining Data, (2021), International Organizing Committee for the World Mining Congresses, https://www.world-mining-data.info/wmd/downloads/PDF/WMD2021.pdf

EFEMÇUKURU ALTIN MADENI ATIK DEPOLAMA TESİSİNİN EKİM 2020 EGE DENİZİ DEPREMİNDEKİ DURAYLILIK PERFORMANSI

STABILITY PERFORMANCE OF EFEMÇUKURU GOLD MINE WASTE STORAGE FACILITY IN OCTOBER 2020 AEGEAN SEA EARTHQUAKE

G. Uzunçelebi[1,*], S. Ennis[2], E. R. Castro[2], Y. S. İNCİ[1], H. Ürkmez[1]

[1] *TÜPRAG Efemçukuru Altın Madeni, İZMİR*
(Sorumlu yazar: gorkem.uzuncelebi@tuprag.com)*
[2] *Stantec, CANADA*

ÖZET

30 Ekim 2020 tarihinde merkez üssü Ege Denizi olan 7.0 (USGS) büyüklüğünde bir deprem Türkiye'nin batısında bulunan İzmir ili ve çevresini etkilemiştir. Meydana gelen deprem, yüksek nüfuslu bölgeler dahil olmak üzere geniş kapsamlı bir alanı etkileyen yer sarsıntıları ile birlikte tsunami taşkınlarına, yapıların çökmesine ve 118 kişinin ölümüne neden olmuştur. Depremin merkez üssü, İzmir şehrine yaklaşık 63 km ve Efemçukuru Altın Madeni sahasına yaklaşık 50 km uzaklıkta yer almaktadır. Efemçukuru Altın Madeni'nde yeraltı madencilik faaliyetleri süresince flotasyon atıkları ve ekonomik olmayan kayaçlar olmak üzere iki tip maden atığı ortaya çıkmaktadır. Flotasyon atıklarının bir kısmı macun dolgu olarak yeraltında kullanılmakta ve bir kısmı da susuzlaştırılarak yerüstünde inşa edilmiş kuru atık depolama tesisinde depolanmaktadır. Tüm ekonomik olmayan kayaçlar ise yerüstündeki depolama tesisinde ayrı olarak depolanmaktadır. Bu makalede söz konusu depremin karakteristik özellikleri, mevcut maden atık depolama tesislerinin deprem yükleri altındaki duraylılık performansı ve ve acil durum müdahale planının devreye alınması sunulmaktadır. Belgenin ayrıntıları görsel gözlemlere ve izleme araçlarına dayalı olarak sismik tasarımın ve ilgili performansın incelemesini içermektedir. Kuru atık depolama tesisi odak alınarak saha için hazırlanan mevcut atık yönetim sistemine ve deprem öncesi ve sonrası yapılan uygulamalara değinilmektedir. Acil durumlarda ve atık depolama tesisinin deprem yükleri altında performansını arttıracak yönetim stratejileri işletmeci ve tasarımcı işbirliği ile yıllar içinde başarılı bir şekilde geliştirilmiştir. Bu yönetim stratejisine de değinilecektir.

Anahtar Kelimeler: 2020 ege denizi depremi, efemçukuru altın madeni, sismik tasarım, acil durum planı, atık yönetim sistemi, işletme, bakım ve izleme kılavuzu (İŞBİK)

ABSTRACT

On 30 October 2020 the city of Izmir was impacted by an earthquake of magnitude 7.0 (USGS) originated in the Aegean Sea. The earthquake produced wide-ranging effects including tsunami run-up, ground shaking with local zones of high intensity that led to the collapse of structures and 118 fatalities. The epicenter was located at approximately 63 km from the city of Izmir and at approximately 50 km from the Efemçukuru mine site. The Efemçukuru mine site produces mine waste that is composed of tailings and uneconomic mine rock. A portion of the tailings and all uneconomic mine rock are stored in a surface storage facility. The remaining tailings material is stored underground. This document will describe the characteristic of the earthquake and the performance of the mine waste facilities and the emergency response plan. Details of the facilities seismic design and associated performance based on monitoring instrumentation will be presented. A focus will be placed on the current tailings management system for the site and their implementation pre and post-earthquake. Management strategies for dealing with upset condi-tions and improving the seismic performance of the structure

have also been developed successfully over time through a close operator designer cooperation. These management strategies will also be discussed.

Keywords: 2020 aegean sea earthquake, efemçukuru mine site, seismic design, emergency response plan , tailings management system, operation maintenance and surveillance (OMS)

GİRİŞ

Ege Denizi (Samos Adası) depremi 30 Ekim 2020'de sırasıyla Yunanistan ve Türkiye'de yerel saatler ile 13:51/14:51'de meydana gelmiştir. Deprem sonucunda, her iki ülkede yüksek yoğunluklu yerleşim bölgelerini kapsayan geniş bir alanda yer sarsıntıları meydana gelmiş, bazı bölgelerde tsunami oluşumları gözlenmiş ve birçok yapının hasarlanması ve yıkılması nedeni ile 118 kişi hayatını kaybetmiştir. Depremden etkilenen bölgelerde sıvılaşma, yer değiştirme ve kaya düşmeleri gibi çeşitli jeoteknik etkiler de gözlemlenmiştir.

Çalışma Alanı

Efemçukuru Altın Madeni, Türkiye'nin batısında, İzmir İli'nin yaklaşık 45 km güneyinde bulunan bir yeraltı madenidir. Maden sahası, deniz seviyesinden 550 ila 770 metre yükseklikte, yarı kurak, dağlık bir bölgede yer almaktadır. Bölgedeki genel topografya, dik tepeler ve dar vadilerle karakterizedir. Farklı yağışlı ve kurak mevsimlere yayılmış ortalama yıllık yağış yaklaşık 740 mm'dir. Madencilik faaliyetinden süresince oluşan atıklar, flotasyon atığı ve ekonomik olmayan maden kayaçlarını (pasa) kapsamaktadır. Flotasyon atıklarının bir kısmı yeraltı madenciliğin tamamlandığı alanlarda macun dolgu olarak tahkimat amaçlı olarak yeraltında kullanılmakta, kalan malzeme ise susuzlaştırılarak yerüstü kuru atık depolama tesisinde depolanmaktadır. Yeraltından çıkarılan pasa ise yerüstünde belirlenmiş ayrı bir alanda depolanmaktadır. Yerüstünde mevcutta kullanılan maden atık depolama tesisleri; Merkez Kuru Atık Depolama Alanı (M-KADT – C-TSF), Merkez Ekonomik Olmayan Kaya Depolama Alanı (M-EOKDT – C-MRSF) ve Güney Kuru Atık Depolama Alanı (G-KADT – S-TSF) olmak üzere Şekil 1.'de gösterilmektedir. Genel depolama tasarımında pasa depolama tesislerinin yerleşimi kuru atık depolama tesislerini destekleyecek şekilde entegre edilmiştir.

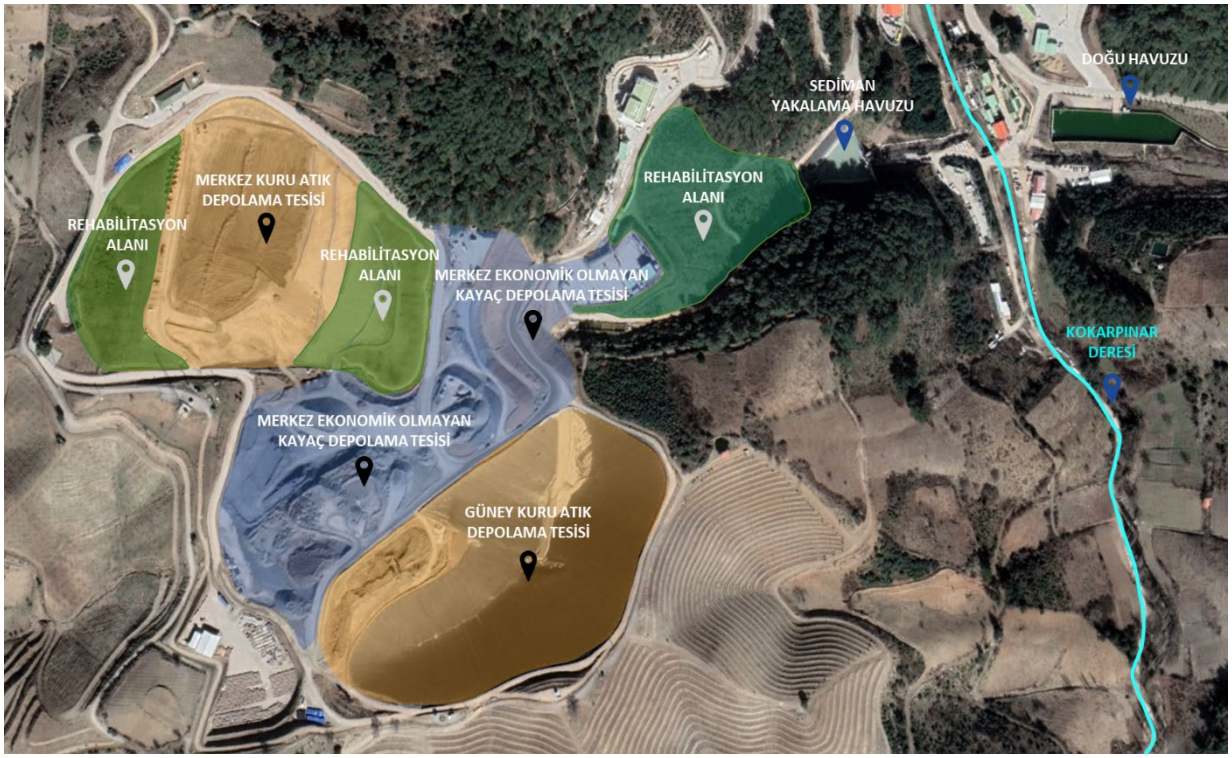

Şekil 1. Efemçukuru Altın Madeni Yerüstü Maden Atıkları Depolama Tesisleri Yerleşimi (Kasım 2020)

Flotasyon Atığı (tailings) tesiste filtrelenerek susuzlaştırılan atıklardır, ekonomik olmayan maden kaya (pasa) ise yeraltı çalışmalarından çıkarılarak taşınan ve yüzeyde depolanan malzemedir. Hem kuru atık depolama alanları hem de ekonomik olmayan kaya depolama alanları su tutucu baraj yapıları gerektirmeyen ve duraylı yapılar olarak tasarlanmış ve inşa edilmiştir (Şekil 2.). Sahanın performans hedeflerini karşılaması adına kuru atıkların ve ekonomik olmayan kayaçların yerleştirilmesi için saha atık yönetimi ekibi (yerüstü işleri birimi) tarafından sıkı yerleştirme ve sıkıştırma prosedürleri ve QA/QC uygulamaları ile yürütülmektedir. Efemçukuru Altın Madeni Kuru Atık Depolama Tesis'inde herhangi su birikimi yapılmamakta yada sıvılaşabilir malzeme tutulmamaktadır. Efemçukuru Altın Madeni'nde Kuru Atık Depolama Tesisi (KADT) ve Ekonomik Olmayan Depolama Tesisi (EOK) "Atık Dökümü ve Atık Depolama Tesisi Derecelendirme ve Tehlike Sınıflandırma Sistemi" (Waste Dump and Stockpile Rating and Hazard Classification System (WSRHC-Hawley and Cunning, 2017)) değerlendirmelerine dayalı olarak, "Orta Derecede (moderate) Riskli" tesisler olarak sınıflandırılmıştır (Stantec, 2019a ve 2019b).

KADT ve EOK tesisleri, geçirimsizlik sistemi sızıntı suyunun yer altı suyuna karışmasını önleyecek şekilde hazırlanan zemin üzerinde farklı jeosentetik geçirimsizlik malzemeleri kullanılarak inşa edilmiştir. Merkez ve Güney KADT sahalarında, birincil ve ikincil (çift astar) geçirimsizlik tabakaları ve aralarına yerleştirilen bir sızıntı tespit sistemi mevcuttur. Kuru Atık Depolama alanında jeosentetik kil astar (GCL) ve pürüzlü jeomembran kullanılmıştır. EOKDTY sahalarında ise jeomembran ile geçirimsizlik sistemi ile inşa edilmiştir. Depolama alanlarından kaynaklanan yüzey suyu akışı ve süzüntü suları, kanallar ve drenaj boruları sistemi vasıtasıyla çökeltme havuzunda toplanmakta ve atıksu arıtma tesisine gönderilmektedir. KADT ve EOKDT için tasarım depolama kapasiteleri sırasıyla yaklaşık 2,54 Mm3 kuru atık ve 1,51 Mm3 pasadır. 2011'den beri faaliyette olan madende, maden atık depolama tesislerinin hali hazırda nihai kotlarına ulaşan bazı kısımlarında yasal mevzuatlara uygun olarak kapatma (rehabilite) çalışmaları yapılmıştır (Şekil 1.). M-KADT ve M-EOKDT atık yerleşim kesitleri Şekil 2.'de gösterilmiştir.

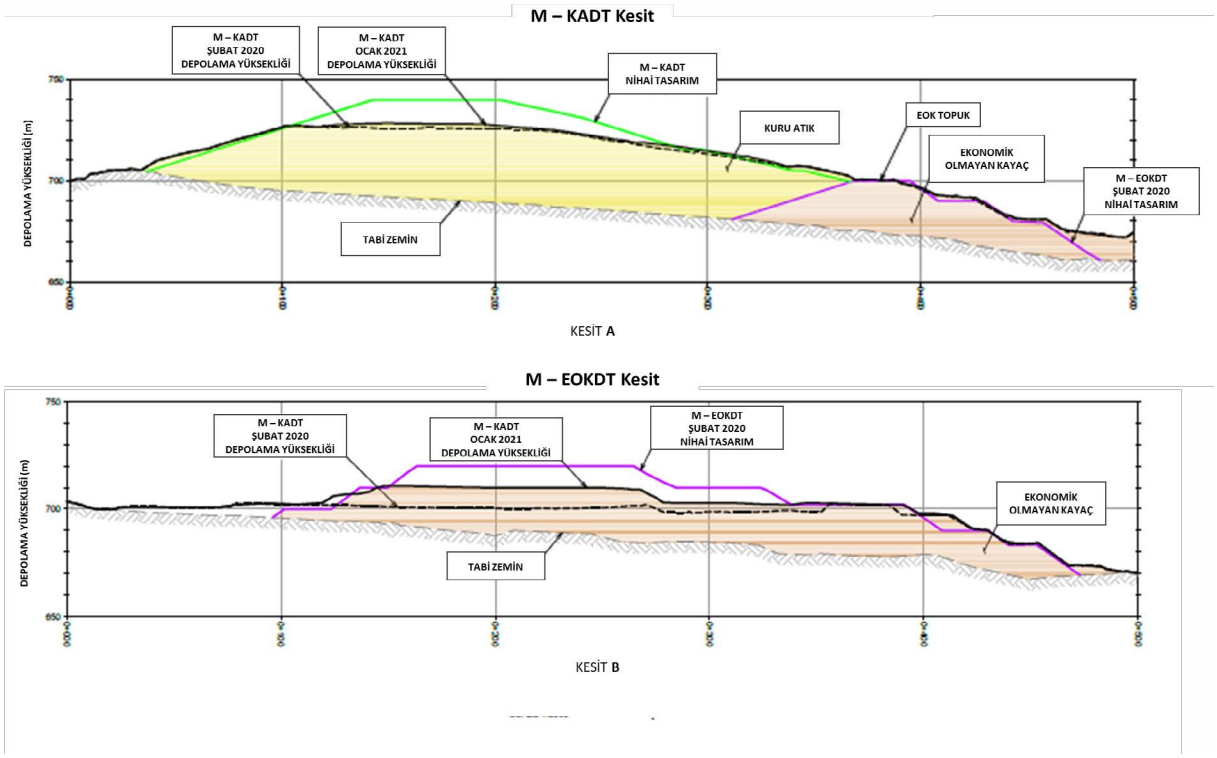

Şekil 2. Efemçukuru Altın Madeni Yerüstü Maden Atıkları Depolama Tesisleri Atık Yerleşimi (Kasım 2020)

Sismik Tektonik Hareketler

Ege Denizi bölgesinde, tarihsel olarak son 100 yılda 250 km'lik bir yarıçap içinde M6'dan daha büyük olan, orta ila büyük sismik derecede, yaklaşık 29 deprem meydana gelmiştir. Bölge etrafındaki sismotektonik ortam kompleks bir yapıya sahiptir, güneyde Afrika levhası kuzeye doğru Avrasya levhasının (Helen Yayı) altına dalar; doğuya doğru ise Anadolu levhası kuzey kenarında sağ yanal faylanma sürerek batıya doğru hareket eder. Tipik olarak, bölgedeki sismik olaylar, Helen Yayı'nın güneye doğru göçü tarafından yönlendirilen kuzey-güney uzantılarıdır. Daha yakın yıllarda bölge, 1956 yılında Yunanistan'da 20. yüzyılın en büyük sismik olayı olarak kabul edilen M 7.7 büyüklüğündeki bir depremle sarsılmıştır. (Çetin K.O.2020)

<u>30 Ekim 2020 Ege Denizi Depremi</u>

30 Ekim 2020'de Yunanistan'ın Samos Adası açıklarında Ege Denizi merkezli bir deprem (M 7.0) meydana gelmiştir. Deprem, Samos Adası'nın kuzeyinde, Avrasya levhasında sığ kabuk derinliğinde normal faylanmadan kaynaklanmış ve odak mekanizma çözümüne dayalı olarak, olay doğuya veya batıya doğru uzanan ve kuzey-güney yönlü uzantılı olarak gerçekleşmiştir. Büyüklük, bu fay için tahmin edilen maksimum büyüklüğü biraz aşmaktadır ve tarihsel arşivler, bu fay üzerinde son 19 yüzyılda bu büyüklükte bir olaya işaret etmemektedir (Çetin vd. 2020).

Yerel kuvvetli yer hareketi istasyonları fay kırılmasından sonraki 200 km içinde Yunanistan'da 11 ve Türkiye'de 66 adet olmak üzere deprem kaydetmeyi başarmış, ayrıca 200'den fazla ivmeölçer, kırılmadan 600 km'ye KADTr olan depremleri kaydetmiştir. Bu enstrümanlardan ikisi kırılma düzleminden yaklaşık 10 km uzaktadır ve en güçlü kayıtlar bu ölçümlerden sağlanmıştır (yaklaşık 0.23 g'lık pik yer ivmesi ve yaklaşık 22 cm/s'lik pik yer hızı).

USGS (ABD Jeoloji Araştırma Kurumu) tarafından geliştirilen çevrimiçi araçlar kullanılarak en yüksek yer ivmesi (PGA) konturları ve 1 saniyedeki (Sa-1s) spektral ivmenin konturları Şekil.3'te gösterildiği gibi oluşturulmuştur.

Şekil 3. Deprem konumu ve Pik Yer İvmelerinin konturları. Veriler USGS web sitesinden uyarlanmıştır.

Şekil 4. Deprem konumu ve 1 saniyedeki Spektral İvmenin konturları. Veriler USGS web sitesinden uyarlanmıştır.

Ekim 2020 Depremi sırasında sahada bir ivmeölçer olmamasına rağmen, bu projeksiyonlara dayanarak Efemçukuru Altın Madeni sahasındaki PGA'nın 0.1g ile 0.2g arasında olduğu ve Sa-1s'nin 0.2g'den yüksek olduğu tahmin edilmektedir.

Efemçukuru Altın Madeni'ne ait KADT ve EOKDT'nın Temel Sismik Tasarım Özellikleri

2016 yılında Stantec (eski adıyla Norwest Corp.), 7,2 büyüklüğündeki bir depreme dayalı olarak sismik değerlendirmeler için aşağıdaki tabloda (Tablo.1 ve 2) verilen KADT ve EOKDT tasarım temel kriterlerini geliştirmiştir. Çalışma alanında geçmişte kayıtlı sismik olayların potansiyel şiddeti göz önüne alındığında, tasarım kriterlerinde yer değiştirme membranlı alandaki potansiyel kayma yüzeyleri için20

cm'den daha az ve membranlı alanı kesmeyen kayma yüzeyleri için ise 50 cm'den daha az olacak şekilde belirlenmiştir.

Çizelge 1. KADT ve EOKDT Duraylılık Tasarım Kriterleri (Güvenlik katsayısı değerleri)

Değerlendirme	Yükleme Koşulu	Tasarım Kriteri Hedefi
Statik	İnşa sırasında veya sonunda	Güvenlik Faktörü ≥ 1.3
	Uzun Dönem	Güvenlik Faktörü ≥ 1.5
Sismik	Eşdeğer Sismik (Pseudo-static)	Güvenlik Faktörü ≥ 1.0
		Tolere Edilebilir Yer Değiştirme ≤ 20cm (Membranlı alanlar)
		Tolere Edilebilir Yer Değiştirme ≤ 50cm (Membranlı alanlar)
	Deprem sonrası (operasyon)	Güvenlik Faktörü ≥ 1.2

Çizelge 2. KADT ve EOKDT Sismik Tasarım Kriterleri

Döngü periyodu	PGA	Sa (02s)	Sa (1.0s)	Tasarım Dönemi
475 yılda 1	0.485	1.215	0.485	Operasyonel
2475 yılda 1	0.972	2.43	0.97	Kapama

KADT ve EOKDT yapıları, ulusal mevzuat gerekliliklerini ve Kanada Madencilik Birliği yönergelerini takip etmek için geliştirilmiş bir İşletme, Bakım ve İzleme (İŞBİK -OMS) kılavuzuna sahiptir. Deprem sonrası tesislerin performansı ile ilgili yapılması gereken izleme faaliyetleri yüzey prizma istasyonları, piyezometreler ve dikey su seviyesi gözlem boruları, sızıntı akışı izleme ve kapsamlı görsel denetimler olarak belirlenmiştir. Deprem sonrası izleme faaliyetlerine aşağıdaki bölümlerde yer verilmiştir.

Deprem Sonrası Yapılan Müdahaleler ve Sahanın Performansı

Acil Durum Hazırlık ve Eylem Planı

Efemçukuru Madeni için hazırlanan Kuru Atık ve Ekonomik Olmayan Kaya Depolama Tesisleri Acil Durum Eylem Planı'nda (KADT ve EOK ADEP / Emergency Response Plan - ERP), atık depolama tesislerinde meydana gelebilecek jeoteknik duraysızlık ve tehlike durumlarında veya acil durumlarda müdahalede rehberlik edecek ve yardımcı olacak bir dizi prosedür bulunmaktadır. Acil Durum Eylem Planı dökümanının, TÜPRAG'ın İŞBİK gibi mevcut yönetim sistemlerini desteklemesi ve maden genelini kapsayan Acil Durum ve Kriz Yönetim Planı (ADKYP - Emergency and Crisis Management Plan / ECMP) ile entegre edilmesi amaçlanmıştır.

Kuru Atık ve Ekonomik Olmayan Kaya Depolama Tesisleri için hazırlanan Acil Durum Eylem Planı aşağıdakileri içerir:

1. Acil Durum Eylem Planını etkinleştirmek için prosedürler ve alınacak önlemler de dahil olmak üzere, KADT ve EOKDT'de tesislerinde duraylılık ile ilgili beklenmedik acil durumlara müdahale etmek için bir plan,
2. KADT ve EOKDT tesislerini etkileyebilecek farklı olası tehlikelere karşı alınacak önlemler,
3. Potansiyel olarak etkilenen alanlar ve altyapı ile birlikte olası hasar alanlarını gösteren uygulanabilir haritalar ve tablolar,

4. Acil duruma müdahale etmek için gerekli kaynakların listesi,
5. Görev ve sorumlulukların listesi ve ilgili personelin iletişim bilgileri,
6. Acil bir durumda genel komut zinciri ve dahili bildirim protokolü,
7. ADEP'i test etmek için prosedürler ve sıklıklar; ve
8. ADEP yönetimi ve güncellenmesi için prosedürler.

Deprem Müdahalesi Planı

Depremler Kuru Atık ve Ekonomik Olmayan Kaya Depolama Tesisi şevlerinin fiziksel duraylılığını etkileyebilir, bu nedenle Efemçukuru kuru atık ve EOK depolama tesisleri için hazırlanan tasarımlarda sismik hususlar dikkate alınmıştır. Oluşabilecek hasar depremin büyüklüğüne, kaynağından olan mesafelere ve yer hareketinin özelliklerine bağlı olabilir. Acil Durum Eylem Planı yönetimi veya olay sonrası acil inceleme gerektiren durumların özeti Çizelge 4'te verilmektedir.

Çizelge 4. ADEP Yönetimi veya Olay Sonrası Acil İnceleme Gerektiren Deprem Olaylarının Özeti

Richter Deprem Büyüklüğü	**Yapıya Uzaklık (Km), ICOLD'den, 1998**
> 4.0	≤ 25 km
> 5.0	≤ 50 km
> 6.0	≤ 80 km
> 7.0	≤ 125 km
> 8.0	≤ 200 km

Deprem Müdahalesi

Ekim 2020'de meydana gelen depremin hemen ardından yaşanan sismik olayın maden atık depolama tesislerine ve ek olarak yerüstü ve yeraltı altyapısı da dahil olmak üzere madendeki bir dizi yapıyı olumsuz etkileme potansiyeli nedeniyle tüm saha çapında Acil Durum ve Kriz Yönetim Planı etkinleştirilmiştir. İlgili tesislerin derhal denetlenmesi ve ardından izleme kayıtlarının kontrol edilmesi dahil olmak üzere Kuru Atık ve Ekonomik Olmayan Kaya Depolama Tesisleri Acil Durum Eylem Planında belirtilen prosedürler takip edilmiştir. Görsel incelemeler, izleme sonuçları ve sızıntı tespit sisteminin gözden geçirilmesi sonucunda KADT ve EOKDT yapıları üzerinde gözlemlenebilir hiçbir olumsuz etki tespit edilmemiştir. İzleme lokasyonları Şekil 5.'te verilmiştir.

Deprem sonrası ADEP ve İŞBİK prosedürlerine uygun olarak Tüprag Efemçukuru Altın Madeni Atık Depolama tesisleri sorumlusu ile Kayıt Mühendisi (Engineer of Record - EoR) ve ilgili firması Stantec arasında aşağıdaki iletişim zinciri gerçekleşmiştir:

1. 30 Ekim 2020'de Tüprag Efemçukuru Altın Madeni, Kayıt Mühendisi'ne deprem olayı hakkında herhangi bir görsel hasar gözlemlenmediğini ve tüm personelin güvende olduğunu bildirmiştir.

2. 3 Kasım 2020'de Tüprag Efemçukuru Altın Madeni, Kayıt Mühedisi'ne deprem sonrası verilerin işlemesi ve incelemesi için aşağıdaki izleme noktalarının verilerini göndermiştir:

    2.1. Dikey Su Seviyesi Gözlem Boruları: C-TSF-GB-01, C-TSF-GB-02, C-TSF-GB-03, C-MRSF-GB-01, C-MRSF-GB-02, C-MRSF-GB-03, C-MRSF-GB-04, C-MRSF-GB-05 verileri,
    2.2. Sızıntı Tespit Sistemi verileri,
    2.3. Piyezometre okuma: VWP-01 ve VWP-02 (Merkez KADT tabanında yer alan piye-zometreler) verileri.

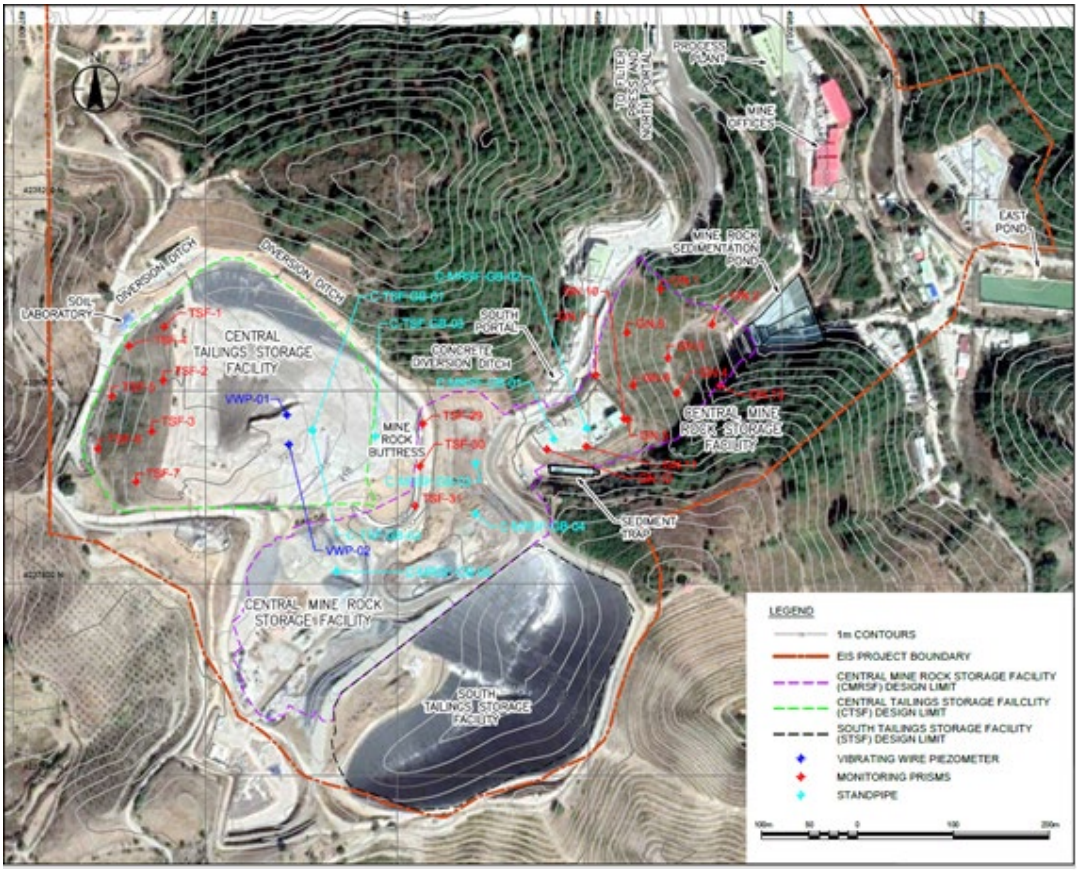

Şekil 5. Efemçukuru Altın Madeni Maden Atıkları Depolama Tesisleri İzleme Lokasyonları

İlk verilerin incelemesi sonucunda Kayıt Mühendisi, deprem olayının tesisler üzerinde olumsuz etkisi olduğuna dair bir bulgu olmadığını belirtmiştir. 5 Kasım 2020 tarihinde Kayıt Mühendisi, Efemçukuru'unda alınan önlemleri destekleyen, İŞBİK kılavuzunun ve Acil Durum Eylem Planı'nın ilgili prosedürlerini takip etmenin önemini vurgulayan bir rapor göndermiştir.

20 Kasım 2020 tarihinde Tüprag Efemçukuru Altın Madeni, Kayıt Mühendisi'ne incelenmek üzere bir deprem olayı raporu ve ayrıca aşağıdakileri içeren ek saha bilgileri göndermiştir:

1. AFAD ve Boğaziçi Üniversitesi Kandilli Rasathanesi Deprem Araştırma Enstitüsü'nden 30 Ekim 2020 tarihine ait deprem teknik raporları,
2. M-KADT ve M-EOKDT deformasyon prizmaları okuma değerleri,
3. Sızıntı tespit sistemi izleme kayıtları.

İzleme bilgilerinin gözden geçirilmesi sismik olayın ölçeği hakkında daha fazla ayrıntı sağlamıştır. Prizma okuma değerleri normal aralıklar dışında herhangi bir değişim göstermemiş ve sızıntı gözlem noktalarında herhangi bir değişiklik gözlenmemiştir.

Saha Performansı

Yukarıda belirtilen önlemleri takiben, maden atıkları depolama tesisleri sorumlusu olan Tüprag Efemçukuru Altın Madeni Yerüstü Birimi tarafından, görsel inceleme bulgularını özetleyen bir deprem raporu ve aşağıdaki Çizelge 5'te sunulan tesislerin izleme verilerinin olduğu bir ön inceleme çizelgesi hazırlamıştır.

Çizelge 5. Tüprag Efemçukuru Altın Madeni Yerüstü Birimi Deprem Sonrası İnceleme Özeti

Yapı	Kontroller	İnceleme	Sonuç
I. Kuru Atık Depolama Alanı			
a. Şevler	Çatlak, Oturma, Şişme	Görsel inceleme: tespit edilmedi.	Geçti
	Deformasyon	Deformasyon Noktaları ölçümü	Geçti
b. Membran Yüzeyleri	Hasar	Görsel inceleme: tespit edilmedi.	Geçti
c. Piezometre Ölçümleri	Piezometre Seviyesi	Piezometre ölçümleri	Geçti
d. Dikey Su Gözlem Borusu	Su Seviyesi	Aletsel Ölçüm	Geçti
e. Membran Altı Sızıntı Boruları	Sızıntı	Görsel inceleme: tespit edilmedi.	Geçti
II. EOK Depolama Alanı			Geçti
a. Şevler	Çatlaklar, Oturma	Görsel inceleme: tespit edilmedi.	Geçti
b. Membran Yüzeyleri	Hasar	Görsel inceleme: tespit edilmedi.	Geçti
c. Dikey Su Gözlem Borusu	Su Seviyesi	Aletsel Ölçüm	Geçti
III. Rehabilitasyon Alanları			Geçti
a. Şevler	Deformasyon	Deformasyon Noktaları ölçümü	Geçti
IV. Betonarme Su Yapıları			Geçti
a. KADT Ön Sediman Yaklama Havuzu	Yapısal Bozukluk	Görsel inceleme: tespit edilmedi.	Geçti
b. EOKDT Sediman Havuzu (WRSP)	Yapısal Bozukluk	Görsel inceleme: tespit edilmedi.	Geçti
c. Doğu Havuz (East Pond)	Yapısal Bozukluk	Görsel inceleme: tespit edilmedi.	Geçti
d. Kuşaklama Kanalları	Yapısal Bozukluk	Görsel inceleme: tespit edilmedi.	Geçti
e. Diğer Yönlendirme Havuzları	Yapısal Bozukluk	Görsel inceleme: tespit edilmedi.	Geçti
V. Depolama Alanları Çevreyolları	Çatlak, Döküntü	Görsel inceleme: tespit edilmedi.	Geçti
VI. Kuzey Portal	Çatlak, Oturma	Görsel inceleme: tespit edilmedi.	Geçti

Sismik olayın hemen ardından özellikle takip edilen unsurlar şev duraysızlığı ve astar hasarına yol açan iç deformasyon potansiyeli ile ilgili oluşabilecek olumsuzluklardır. Görsel incelemeler, prizmalardan elde edilen deformasyon ölçümleri ve sızıntı sisteminin izlenmesi sonucunda şev duraysızlığı ve astar hasarı sorununun olmadığını görülmüştür. Merkez Kuru Atık Depolama Tesisi'nde geçirimsizlik tabakası yakınlarına yerleştirilen piyezometre verileri incelendiğinde boşluk basınçlarında sıvılaşma ile ilişkilendirilebilecek herhangi bir sıradışı artış tespit edilmemiştir. Bu durum, atık depolama tesislerinin inşaat ve işletilme sürecinde uygulanan kalite kontrol prosedürlerinin etkinliğini açıkça ortaya koymaktadır.

SONUÇ

20 Ekim Ege depremi, İzmir bölgesinde yapısal hasar ve ölümle sonuçlanan önemli bir bölgesel sismik olay olmuştur. Deprem önemli bir büyüklükte (M 7.0) olmasına rağmen, Efemçukuru Altın Madeni sahası için yaşanan sismik ivme için tahminler 0,2 aralığında bir PGA hesaplanmıştır. Bu, 0,485'e eşit bir PGA olarak belirlenen operasyonel tasarım kriterlerinden çok daha düşüktür. Görsel inceleme ve izleme kayıtlarının sonuçları KADT ve EOKDT yapılarının performansının sismik olaydan olumsuz şekilde etkilenmediğini göstermiştir. Sahadaki tasarım, inşaat ve izleme uygulamaları göz önüne alındığında da bu beklenen bir durumdur.

Sismik olayın büyüklüğü tasarım kriterlerinin altında olsa da maden atık yönetim ekibinin verdiği yanıt, acil durum eylem planının değerini ve atık yönetimi ekibinin prosedürleri uygulamadaki etkinliğini göstermiştir. Sorumlu personelin bildirimi, olay sonrası hızlı denetimler ve izleme ve kayıt mühendisi ile iletişim, sahanın genel Acil Durum ve Kriz Yönetim Planına uygun olarak tamamlanmıştır. Efemçukuru Altın Madeni sahasındaki deneyim, atık yönetim planının geliştirilmesinde MAC-TSM standartlarının sağladığı rehberliğin önemini ve yapılan uygulamalar sonrasında ekibin çabalarının karşılığını aldığını göstermektedir.

KAYNAKLAR

Canadian Dam Association (CDA), (2014). Technical Bulletin: Application of Dam Safe-ty Guidelines to Mining Dams.

Cetin, K.O., Mylonakis, G., Sextos, A., Stewart, J., (2020). Seismological and engineering effects of the M 7.0 Samos Island (Aegean Sea) Earthquake. HAEE (Greece), EEA & EF (Turkey), EERI (USA), GEER-069. Dec. 31, 2020.

Eldorado Gold Corporation, (2017). Eldorado Gold Corporation Environmental Policy. October 2017

Hawley, P.M. and Cunning, J., 2017. Guidelines for Mine Waste Dump and Stockpile Design. 2017

Mining Association of Canada (MAC), (2019). Tailings Management Protocol.2019

Norwest Corporation, (2018). Review of Efemçukuru's Gold Mine's Tailings Manage-ment System and with MAC's Tailings Management Guidelines. January22, 2018

Norwest Corporation, (2015). Efemçukuru Mine: 2015 Central Valley Tailings Storage Facility Site Investigation and Liquefaction Assessment – Rev 0. December 18, 2015

Norwest Corporation, (2014). 2013 CPT & Drilling Investigation – Summary and Evalua-tion Rev. 0. May 8, 2014

Developing an Operation, Maintenance, and Surveillance Manual for Tailings and Water Management Facilities, Mining Association of Canada (Second Edition). February 2019.

Stantec Consulting International Ltd., (2019a). Central TSF Classification and Risk As-sessment Rev. 1. PowerPoint Presentation. December 2019

Stantec Consulting International Ltd., (2019b). Central MRSF Risk Assessment Rev. 0. PowerPoint presentation. October 2019

Stantec Consulting International Ltd., (2019c). Efemçukuru Central TSF 2019 Site Inves-tigation and Instrumentation Plan – Rev. 0. December 2019

Stantec Consulting International Ltd., (2020a). Assessment of Effectiveness of the Mine's Tailings Management System 2019 Memorandum. February 2020

Stantec Consulting International Ltd., (2020b). July 2020 Preliminary MRSF Capacity Op-timization Analysis. PPT document. July 10, 2020

Stantec Consulting International Ltd., (2020c). October 2020 Earthquake Event-EOR Re-port. December 23, 2020

Tüprag Metal Madencilik, (2014). Crisis & Emergency Management Plan. Document No EFM-5000-Pln-001T. April 2014

EFEMÇUKURU ALTIN MADENİ'NDE FİLTRELENMİŞ ATIK DEPOLAMA YÖNTEMİ UYGULAMASI

APPLICATION OF FILTERED TAILINGS STORAGE METHOD AT EFEMÇUKURU GOLD MINE

Y.S. İnci [1,*], P. Kimball [2], G. Uzunçelebi [3], H. Ürkmez [4], M.A. Erol [5]

[1] *TÜPRAG Efemçukuru Altın Madeni, İZMİR*
*(*Sorumlu Yazar: yavuz.inci@tuprag.com)*
[2] *Stantec, CANADA*
[3] *TÜPRAG Efemçukuru Altın Madeni, İZMİR*

ÖZET

Efemçuku Altın Madeni'ninde uygulanmakta olan Filtrelenmiş Atık Depolama Yöntemi madenin atık yönetim planının bir parçasıdır. Özütleme tesisinden filtre tesisine pompalanan şlam , bu tesiste pres filtreler kullanılarak susuzlaştırılır. Ardından, susuzlaştırılan filtre keki (Filtre edilmiş atık) tabanı düşük geçirgenlikli tabakalarla kaplanarak inşa edilmiş olan bir Atık Depolama Alanı'nda depolanır. Bu yöntem, sıvılaşma riskinin azalması nedeni ile depolanan yığının fiziksel duraylılığının artması, malzemenin istiflenerek yığılabilmesi nedeni ile daha küçük depolama alanı gerektirmesi, yüksek miktarlarda su depolama ihtiyacının olmaması, depolama alanı yüzeyinde yapılacak rehabilitasyon işlerinin erkenden , kademeli olarak başlanabilmesine olanak sağlayarak çevresel getirisinin yüksek olması nedenleri ile, son yıllarda, dünya madenciliğinde, giderek artan sayıdaki madende uygulanır hale gelmiştir. Bu yazıda, Filtrelenmiş Atık Depolama Yöntemi uygulamasının getirileri anlatılmakta ve sahada yapılan uygulamadan elde edilen pratik bilgiler paylaşılmaktadır.

Anahtar Sözcükler: Filtrelenmiş atık, filtrelenmiş yığın, filtrelenmiş atık yönetimi, sürdürülebilir madencilik, mevcut en iyi uygulamalar (MEU – BAP), mevcut en iyi teknikler (MET- BAT)

ABSTRACT

The Efemçukuru Gold Mine uses the filtered tailings storage method as part of its mine waste management plan. Slurry is pumped from the ore process plant to the filter plant where it is dewatered using filter presses. The dewatered filter cake (Filtered Tailings) is then stored in a tailings storage facility constructed with a low permeability base liner. This method has been increasingly applied in mining in recent years due to several benefits, including improved physical stability of stored tailings by mitigating the risk of liquefaction, reduced storage footprint due to stacking of material, not storing large volumes of water (i.e., no supernatant pond), and the environmental advantages associated with progressive reclamation. This article discusses the benefits of implementing the filtered tailings storage method and shares practical information obtained as a result of direct operational experience.

Keywords: Filtered tailings, filtered stack, filtered tailings management , sustainable mining, best available practices (BAP), best available techniques (BAT)

GİRİŞ

Efemçukuru Altın Madeni İzmir ili sınırları içindeki bir madendir. Üretim yeraltı işletmesinden yapılmakta olup günlük cevher üretimi yaklaşık 1.500 ton'dur. Cevherin zenginleştirilmesi sonucunda, su içeriği %60-70 oranında olan şlam ortaya çıkmaktadır. Bu şlam bir filtre tesisine (Şekil 1) pompalanmakta ve bu tesiste jeoteknik nem oranı %20'nin altına düşürülmektedir.

Şekil 1. Efemçukuru Madeni filtre tesisi

Madende inşaat işlerine 2008 yılında başlanmış, üretim ve de filtre tesisi 2011 yılında faaliyete başlamıştır. Filtrelenmiş atık Filtrelenmiş Atık Depolama Alanı'na Kamyonlar ile nakledilmektedir. Atık depolama alanı düşük geçirgenliğe sahip sentetik tabakalar ile kaplanmıştır.

Efemçukuru Altın Madeni'nde Filtrelenmiş Atık Depolama Yöntemi'nin Türkiye' de ilk uygulandığı madendir. Bu uygulama sırasında dikkate değer tecrübeler elde edilmiştir. Bu bildiride, Filtrelenmiş Atık Depolama Yöntemi uygulamasının sağladığı faydalar anlatılmakta ve sahada yapılan çalışmalarda elde edilen Pratik bilgiler paylaşılmaktadır.

Filtrelenmiş Atık Depolama Yönteminin Alışılagelmiş Yöntemlere Kıyasla Sağladığı Faydalar

Bu bölümde, atığın filtre edilmesi tekniğinin bir madende uygulanmasının sağlayacağı faydalardan bahsedilmektedir. Bu faydalar geleneksel atık teknolojisi ile kıyaslanarak sunulmuştur. Geleneksel atıktan kasıt su içeriği yüksek olup pompalanabilen şlamdır. Bu yöntemde şlam, atık içindeki su ve akışkan haldeki atığı emniyetli bir şekilde tutabilecek yapıların içine pompalanarak boşaltılır. Filtrelenmiş atık nedeni ile elde edilen faydalar şu şekildedir;

1. Filtrelenmiş atığın depolanma alanı geleneksel yöntem için gerekenden küçüktür. Bu durum iki nedenden dolayı böyledir; nem içeriği düşürülmüş olan atık duraylı bir yığın oluşturabilecek şekilde depolanabilir ve de sıkıştırılabilir, ikincisi filtrelenmiş atığın depolanması için bir baraj ya da su tutucu yapıya gerek duyulmaz. Geleneksel yöntemlerin uygulanabilmesi için bir atık barajı ve tutucu yapı gerekir. Baraj ve atık seviyesinin bu yapılar içinde güvenli bir yükseklikte oluşturulması gereklidir.

2. Önerilen yöntemde işletmede su geri kazanımı yüksektir. Filtre tesisinde elde edilen su sisteme, geleneksel yöntemlerdeki buharlaşma veya kaçaklar olmaksızın, doğrudan beslenebilir. Bu durum özellikle su kaynaklarının kısıtlı olduğu coğrafyalarda önemlidir. Ayrıca pompalama ve borulama işleride dikkate değer oranlarda azalacaktır.

3. Oluşturulan yapının duraylılığının yüksek olması nedeni ile bu yöntem bir su tutucu baraj yapısına gereksinim duymaz. Su tutucu atık barajlarının tasarım ve inşaatı bu yönteme kıyasla daha karmaşıktır.
4. Atıkların filtrelenerek depolanması, bir atık barajının patlayarak akış yönünde bulunabilecek insan, çevre ve altyapıya zarar vermesi riskini elimine eder. Bunun nedeni atıktaki suyun filtre tesisinde alıkonulması ve böylece oluşturulan atık yığınının sıvılaşma riskinin en aza indirilmesidir. Geleneksel yöntemde, doğal olarak, yeni gelen akışkan malzeme öncekinin üstüne yerleşir ve büyük hacimlerdeki atık potansiyel olarak sıvılaşabilir durumunu koruyarak birikir.

5. Atıkların filtrelenerek depolanması yöntemi kademeli rehabilitasyon işlemini destekler. Bu, yeni sistemin en önemli getirilerinden birisidir. Bu sistemde rehabilitasyon, maden ömrünün daha başlarında, depolama alanlarının son durumuna kavuşan kısımlarında erkenden başlayabilir. Bu durum çevresel faydalar, toplum gözünde olumlu sonuçlar doğurur, rehabilitasyon işinin, dolayısı ile de ilgili maliyetlerin zamana yayılması nedeni ile de şirkete mali faydalar sağlar.

6. Filtre edilen malzemenin taşınması kolaydır ve çalışmada esneklik sağlar. Susuzlaştırılan malzeme kolaylıkla, loder ile yüklenebilir (Şekil 2), kamyon ya da lastik bantlı konveyörler ile taşınabilir, dozer ile serilebilir ve silindir kullanılarak, tasarım gereksinimi doğrultusunda, sıkıştırılabilir.

Şekil 2.Filtrelenmiş atığın kamyona yüklenmesi

Şekil 3. Filtrelenmiş atık depolama alanı geçirimsizlik sistemi inşaatından bir görünüm

7. Fitrelenmiş atık depolama alanı inşaatına ait yatırım ve işletme maliyetleri geleneksel yönteme kıyasla yüksek olabilir. İki sistemin maliyet kıyaslaması projeye ve tesis yerine özgü olacaktır. Diger yandan ise firma yetkilileri şirketin sürdürülebilirlik performansını gözetiyor olacaklardır. Bu sistemde elde edilen yüksek duraylılık, küçük depolama alanı gereksinimi, su geri kazanımı, kademeli rehabilitasyon uygulanması ve azalan izleme gereklilikleri nedeni ile elde edilen dikkate değer getirilerin de projenin tümünün değerlendirilmesine dahil edilmesi gereklidir. Filtrelenmiş atık depolama tesisi geçirimsizlik sistemi Maden Atıkları Yönetmeliği hükümlerine uygun şekilde inşa edilir (Şekil 3).

Efemçukuru'nda Filtrelenmiş Atık Depolama Uygulaması Sırasında Elde Edilen Tecrübeler

1. Efemçukuru Altın Madeni'nde filtrelenmiş atık filtre, tesisinden atık depolama alanına, belden kırma kamyonlar ile taşınmaktadır. (Şekil 4) Malzemenin serilmesi işlemi geniş paletli bir dozer kullanılarak ince dilimler halinde yapılır. Nihai sıkıştırma işlemi ise bir silindir ile yapılır. (Şekil 5). Atığın alana yerleştirilmesi alttan üste doğru yapılır. Tabana döşeli geçirimsizlik sisteminin zarar görmemesi için ilk serim kalınlığı 50 cm. olarak uygulanır. Bu kalınlık alanda kullanılacak araç cinsine göre değişebilir. Daha sonraki tabaka kalınlıkları, serilen malzemenin uygun sıkıştırma için gereken nem içeriğine bağlı olarak en fazla 30 cm. olacak şekilde uygulanır.

Şekil 4. Filtrelenmiş atığın nakli

Şekil 5. Serme ve sıkıştırma

2. Geçirimsizlik sisteminin alana inşası hava sıcaklığının daha düşük olduğu, bu tabakaların birleştirilmesi (kaynak işlemleri) ise sıcaklığın daha yüksek olduğu zamanlarda yapılmalıdır. Alanda serim yapılırken, jeosentetik tabakalarda oluşabilecek kıvrımların kırılmamasına özen gösterilmelidir.

3. Filtre tesisindan depolama alanına gelen atığın nemi ve bu malzemenin serilip sıkıştırılmasını takiben sıkışma değerleri devamlı olarak ölçülmelidir (Şekil 6). Efemçukuru Altın Madeni filtrelenmiş atık için minimum sıkışma değeri %97 Standart Proktor olarak belirlenmiştir. Yeni projelendirme çalışmaları sırasında sahaya özel atığın kendine has sıkışma değeri tespit edilmelidir.

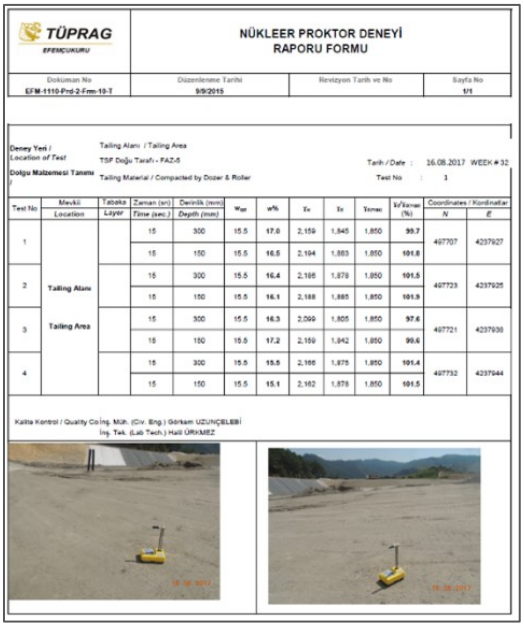

TÜPRAG EFEMÇUKURU

NÜKLEER PROKTOR DENEYİ RAPORU FORMU

Doküman No	Düzenlenme Tarihi	Revizyon Tarih ve No	Sayfa No
EFM-1110-Prd-2-Frm-10-T	9/9/2015		1/1

Deney Yeri / Location of Test: Tailing Alanı / Tailing Area; TSF Doğu Tarafı - FAZ-5
Dolgu Malzemesi Tanımı: Tailing Material / Compacted by Dozer & Roller
Tarih / Date : 16.08.2017 WEEK # 32
Test No : 1

Test No	Mevkii / Location	Tabaka / Layer	Zaman (sn) / Time (sec.)	Derinlik (mm) / Depth (mm)	W_{opt}	w%	γ_d	γ_t	γ_{max}	kr/kmax (%)	Coordinates / Kordinatlar N	E
1	Tailing Alanı / Tailing Area		15	300	15.5	17.0	2,159	1,845	1,850	99.7	497707	4237927
			15	150	15.5	16.5	2,194	1,883	1,850	101.8		
2			15	300	15.5	16.4	2,186	1,879	1,850	101.5	497729	4237935
			15	150	15.5	16.1	2,188	1,885	1,850	101.9		
3			15	300	15.5	16.3	2,099	1,805	1,850	97.6	497721	4237938
			15	150	15.5	17.2	2,159	1,842	1,850	99.6		
4			15	300	15.5	15.5	2,166	1,875	1,850	101.4	497732	4237944
			15	150	15.5	15.1	2,162	1,878	1,850	101.5		

Kalite Kontrol / Quality Cotrol: Müh. (Civ. Eng.) Görkem UZUNÇELEBİ
İnş. Tek. (Lab Tech.) Halil ÜRKMEZ

Şekil 6. Nükleer proktor test formu örneği

İstenen sıkışmanın temini için malzemenin nem içeriğinin uygun olması önemlidir. Bu nedenle istenen nem içeriği fizibilite çalışmaları sırasında tesbit edilmeli ve işletme sırasında da devamlı takip edilmelidir.Efemçukuru Altın Madeni için optimum nem içeriği (Jeoteknik nem) % 15,5 +/- 2' dir. Filtre tesisi malzemeyi her zaman optimum değerde üretemeyebilir ya da iklim koşulları nem oranını etkileyebilir. Nem oranı yüksek, çalışılan hava koşulları uygun ise, yüksek nemli malzeme daha ince kalınlıklarda serilebilir. Hava koşuluna bağlı olarak bu malzeme kısa süre tekrar serilmek üzere geçici bir yığın oluşturularak saklanabilir. Nem yüksek ve hava koşulları da uygun değilse bu malzeme, atık depolama tesisinde daha önceden tasarlanmış bir bölgede, mevsim koşullarının uygun olduğu zamanda serilmek ve sıkıştırılmak üzere saklanmalıdır. Alanda geçici olarak depolanan atıkların daha fazla neme maruz kalmaması için gerekli önlemler alınmalıdır.

Atığın alana serilmesi ve sıkıştırılmasının ardından yapılan ölçümler istenen sonucu vermez ise bu alan dozer ile riperlenerek nemini istenilen seviyeye kadar kaybetmesi sağlanmalıdır. (Şekil 7-8)

Şekil 7. Atığın nemini azaltabimesi için dozele yapılan riperleme işlemi.

Şekil 8. Nemini azaltmış olan alanın tekrar serilerek sıkıştırılması.

Geçici olarak biriktirilen nemli malzeme iklim koşullarının iyileşmesini takiben, gelecek sezonun hazırlığı kapsamında, vakit geçirmeksizin kalite iyileştirme çalışmaları kapsamında yeniden işlenerek depolama alanına, taşınmalı, serilmeli, gerekirse riperlenmeli ve kuruması sağlandıktan sonra sıkıştırma işlemi yapılmalıdır. (Şekil 9)

Şekil 9. Yüksek nem içeriğine sahip atık yığınının iyileştirilmesi çalışmaları

4. Nem, sıkıştırma değerlerinin tesbiti, değerlendirilmesi, takibi için, sadece Kuru Atık Depolama Alanı için hizmet vermek üzere, sahada bir laboratuvar kurulmalıdır. Ayrıca Akredite laboratuvarlarda malzemenin testleri (standart proktor, nem tayini, atterberg test, hidrometri, özgül ağırlık v.b.) düzenli olarak yaptırılmalıdır.

5. Sıkışma değerlerinin ölçümü için bir Nükleer Proktor Cihazı gerekecektir (Şekil 10). Cihazın temini, nakliyesi, saklanması, çalıştırılması için TAEK kurallarının gereklilikleri sağlanmalıdır. Sıkışma değerlerinin anlık takip edilebilmesi için silindirlere eklenen sistemler çalışma etkinliğini üst düzeye çıkarabilmektedir. Silindir operatörü bu sistem sayesinde anlık olarak, makina içindeki ekrandan, sıkıştırılmış alanları takip edebilmektedir. Ayrıca bu kayıtların dijital olarak depolanması sağlanabilmektedir. Hatta bu sistem sayesinde bilginin bilgisayarlardan anlık takibi de yapılabilmektedir. (Şekil 11)

Şekil 10. Nükleer proktor cihazının kuru atık depolama alanında kullanılması

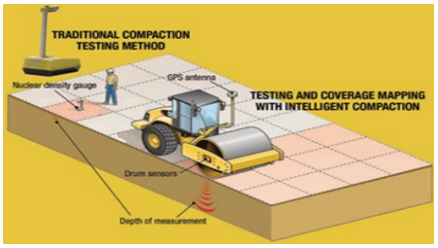

Şekil 11. Silindir kabinine yerleştirilerek zemin sıkışmasını ölçen sistem.

6. Filtre atığı nemi konusu çok boyutlu olarak ele alınmalıdır.

6.1. Atık nemi filtre tesisi performansı ve iklim koşullarına bağlı olarak her zaman uygun miktarlarda olmayabilir. Bu nedenle alanda çalışan operatörler hangi malzemeyi sereceğini, hangi malzemeyi geçici stok alanında biriktireceğini iyi bilmelidir.

6.2. Nem içeriği yağmur, kar yağışı, don, çiğ, sıcak hava nedeni ile de etkilenecektir. Bu nedenle, filtre tesisinin ürettiği malzemenin özellikle aşırı yağıştan korunabilmesi için, filtre tesisi yakınında, atık depolama alanına gönderilmeden önce içinde 1-2 gün geçici depolama yapabileceğiniz kapalı bir alan oluşturulması faydalı olacaktır. Çiğ oluşumu da alanda çalışma zorluğu yaratacaktır. Alana gelen malzemenin zamanında işlenmesi bu etkiyi azaltacaktır. Kar yağışı ya da don sonrasında da depolama alanında çalışmak zorlaşacaktır. Yağış sonrasında yüzeydeki karın ya da donan malzemenin temizlenmesi ve çalışma yüzeyinin kuruması beklenmelidir. Sonuçta, yağmur, kar, don, çiğ sonrasında yüzeyler kurumadan yeni serime geçilmemelidir. Eğer nemli koşullarda yüzeylere yeni serim yapılacak olursa, altta kalan nemli malzeme yığında jeoteknik olarak zayıf tabakalar oluşturacaktır. Ayrıca nemi yüksek, kaygan yüzeylerde çalışmak iş güvenliği sorunları yaratacaktır.

6.3. Nem içeriği yağışlar nedeni ile arttığı gibi aşırı sıcak iklim koşullarında, alana gelen atık serilip sıkıştırılmaz ise nem içeriği azalarak optimum nem değerinin altına düşebilir. Bu durumda malzemenin sıkıştırılması mümkün olmayacaktır. Bu nedenle alana gelen uygun neme sahip malzemenin vakit geçirmeksizin serilmesi ve sıkıştırılması gereklidir.

7. Meteoroji istasyonları takip edilerek yağmur, kar, don, aşırı rüzgar vb. iklim olaylarının takibi yapılarak bu bilgiler ışığında çalışmalar yönlendirilmeli, bilgiler çalışanlara iletilmeli, olası aşırı iklim olaylarının etkilerine karşı önceden hazırlıklar yapılmalıdır.

8. Su Yönetimi’ ne özel önem verilmelidir.

İşletme projesi hazırlanırken su bütçesi iyi irdelenmeli, ilgili kanallar ve boyutları, boru boyut ve sayıları olası su gelirini taşıyabilecek şekilde tasarlanmalıdır. Bölgeye ait tarihsel meteorolojik veriler toplanarak incelenmeli ve bu rakamlar su bütçesi hesaplarında yerini almalıdır. Su iletim hatları alanda, yığın içinde atık yığını tabanında su birikimine müsade etmeyecek şekilde oluşturulmalıdır. (Şekil 13), (Şekil 12-13)

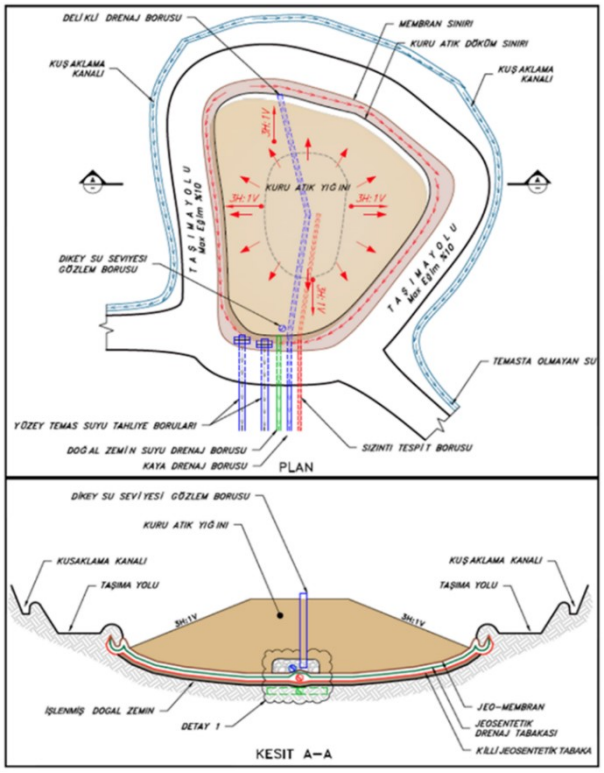

Şekil 12. Kuru atık depolama alanı su yönetim sistemi şematik örneği

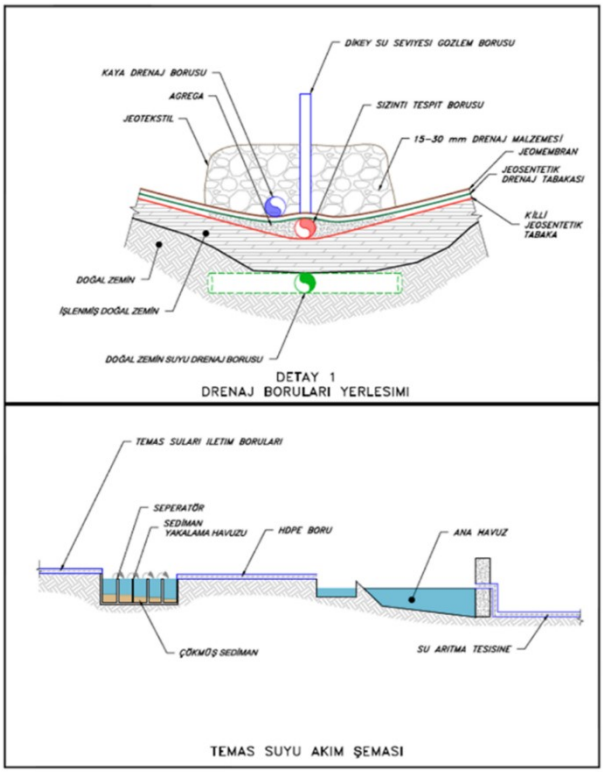

Şekil 13. Kuru atık depolama alanı su yönetim sistemi ayrıntı şematik örneği

Şekil 14. Filtrelenmiş atık depolama alanından su boşaltımı için kullanılan borular

9. Yağış sırasında atık depo yığınının yüzeyinden akacak suya karışacak sedimanı çökeltim için bir sistem oluşturulmalıdır. Atık depolama alanından toplanan temas suyunun bir ana havuzda biriktirilmesi atıksu arıtma tesisinde arıtılması gerekmektedir. Yağış sırasında yığın yüzeyindeki aşınım nedeni ile suya bir miktar malzeme karışmaktadır. (Şekil 13) Sediman içeren bu suyun direk ana havuzun kapasitesi sedimanyükünden etkilenecektir. Bu durumun önlenebilmesi için bir ön sediman yakalama havuzu inşa edilerek sedimanın bu havuzda yakalanması sonrasında temas suyunun ana havuza yönlendirilmesi faydalı olacaktır. Bu ön havuz sisteminde çökeltilen sedimanın temizlenmesi işlemi bir ekskvatör ve kamyonlar kullanılarak kolayca yapılabilir. (Şekil 14) Temizlenen sedimanın kurutulması için atık depolama alanı üzerinde belirlenen bir kısında geçici (dönemsel) kurutma havuzları hazırlanması faydalı olacaktır.

Şekil 15. Kuru atik depolama alani yüzeyinin yağişlar sonrasindaki erozyon nedeni ile aldiği şekil

Şekil 16. Sediman yakalama havuzundan çamur temizliği yapilmasi

Yağış esnasında, depolama alanı yüzeyinde, yağış nedeniyle oluşabilecek bozulmaları dolayısı ile de suya karışacak sediman miktarını azaltmak için, depo yüzeyinde sentetik malzemeler kullanarak geçici kanallar oluşturmak faydalı olacaktır. (Şekil 17)

Şekil 17. Filtrelenmiş atik depolama alaninda, erozyonun etkisini azaltmak üzere, oluşturulan geçirimsiz su atim kanallari

10. Alana döşenen su borularına ait bilgilerin kaydının tutulması gerekmektedir.

Çalışma alanına etkisi olan suların boru sistemleri (Şekil 18) ile toplanarak havuzlara iletilmesi gereklidir. Borulardan gelen suyun kalitesi, miktarı, sediman içeriği vb. konuların takibinin yapılması gereklidir. Bunun takibi için hangi borunun nereden su taşıdığının bilinmesi gerekir. Bu nedenle bu boruların döşenmesi sırasında gerekli kot, koordinat ölçümleri yapılarak bu bilgiler kayda geçirilmelidir.

Boruların su girişlerine, tıkanmaları önlemek için, yedekli su girişleri yerleştirmek ve bu girişlere uygun göz açıklığına sahip süzgeçler yerleştirmek yerinde olacaktır. (Şekil 19)

Şekil 18. Su borusu döşeme işleri

Şekil 19. Kesintisiz su akişina uygun hale getirilmiş boru ağzi

11. Depolama alanının duraylılığının takibi için izleme sistemi oluşturulmalıdır.

Bu amaç için yığının içine piezometreler (Şekil 20), yığın boyunca su seviyesi dikey gözlem boruları (Şekil 21) yerleştirilebilir, su seviyesi kontrol kuyuları tesis edilebilir, deformasyon ölçüm noktaları (Şekil 22) oluşturulabilir. Buralardan alınacak peryodik ölçüm değerleri bir arşive kaydedilerek incelenmelidir.

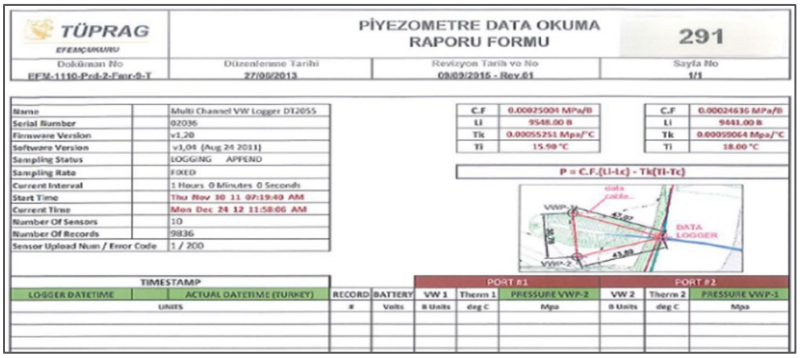

TÜPRAG EFEMÇUKURU

PİYEZOMETRE DATA OKUMA RAPORU FORMU

291

Doküman No	Düzenlenme Tarihi	Revizyon Tarih ve No	Sayfa No
EFM-1110-Prd-2-Fasr-9-T	27/09/2013	09/09/2015 - Rev.01	1/1

Name	Multi Channel VW Logger DT2055
Serial Number	92036
Firmware Version	v1.20
Software Version	v3.04 (Aug 24 2011)
Sampling Status	LOGGING APPEND
Sampling Rate	FIXED
Current Interval	1 Hours 0 Minutes 0 Seconds
Start Time	Thu Nov 30 11 07:19:40 AM
Current Time	Mon Dec 24 12 11:58:06 AM
Number Of Sensors	10
Number Of Records	9836
Sensor Upload Num / Error Code	1 / 200

C.F	0.00025004 MPa/B			C.F	0.00024636 MPa/B						
LI	9548.00 B			LI	9441.00 B						
Tk	0.00055251 Mpa/°C			Tk	0.00055064 Mpa/°C						
TI	15.50 °C			TI	18.00 °C						

P = C.F.(LI-Lc) - Tk(TI-Tc)

TIMESTAMP				PORT #1			PORT #2		
LOGGER DATETIME	ACTUAL DATETIME (TURKEY)	RECORD	BATTERY	VW 1	Therm 1	PRESSURE VWP-2	VW 2	Therm 2	PRESSURE VWP-1
UNITS		#	Volts	B Units	deg C	Mpa	B Units	deg C	Mpa

Şekil 20. Piezometre izleme formu örneği

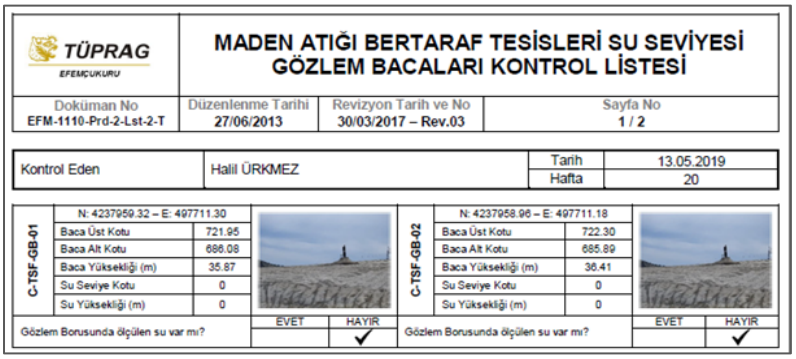

TÜPRAG EFEMÇUKURU

MADEN ATIĞI BERTARAF TESİSLERİ SU SEVİYESİ GÖZLEM BACALARI KONTROL LİSTESİ

Doküman No	Düzenlenme Tarihi	Revizyon Tarih ve No	Sayfa No
EFM-1110-Prd-2-Lst-2-T	27/06/2013	30/03/2017 – Rev.03	1 / 2

Kontrol Eden	Halil ÜRKMEZ	Tarih	13.05.2019
		Hafta	20

C-TSF-GB-01	N: 4237959.32 – E: 497711.30	C-TSF-GB-02	N: 4237958.96 – E: 497711.18
Baca Üst Kotu	721.95	Baca Üst Kotu	722.30
Baca Alt Kotu	686.08	Baca Alt Kotu	685.89
Baca Yüksekliği (m)	35.87	Baca Yüksekliği (m)	36.41
Su Seviye Kotu	0	Su Seviye Kotu	0
Su Yüksekliği (m)	0	Su Yüksekliği (m)	0

	EVET	HAYIR		EVET	HAYIR
Gözlem Borusunda ölçülen su var mı?		✓	Gözlem Borusunda ölçülen su var mı?		✓

Şekil 21. Su seviyesi dikey gözlem boruları izleme formu örneği

Şekil 22. Deformasyon ölçüm noktasi

12. Depolama alanına giriş-çıkış trafiğinin kesintisiz olabilmesi için, depolama alanında Zemin iyileştirilmesi yapılmalıdır.

Yağış sonrasında depolama alanı yüzeyi kayganlaşarak araç trafiğini olanaksız hale getirmektedir. Bu durumlarda araçların depolama alanına giriş, çıkış, manevra, boşaltma işlemlerinin aksamaması için alan içerisinde kullanılan yol yüzeyi geçici olarak inert kırmataş ile kaplanarak sorun çözülebilir. (Şekil 23)

13. Depolama alanı yüzeyinin her daim silindir ile sıkıştırılmış olmasının sağlanması gerekir. (Şekil 24)

Şekil 23. Kuru atik depolama alaninda, kesintisiz nakil sağlamak amaçli olarak, oluşturulan sağlam zemine sahip bölge.

Şekil 24. Malzemenin serim sonrasi silindir ile sikiştirilarak kabuk oluşturulmasi

Filtrelenmiş atığın alanda dozerle serilmesini takiben, gecikmeksizin silindirle sıkıştırılmasının bir çok faydası vardır. Dozerin çalışması sonucunda dozer paletlerinin yüzeyde oluşturduğu parçalı yapı nedeni ile serilen malzeme nemini hızlı bir şekilde kaybedecektir. Hava yağışlı ise bu parçalanmış yüzey yapısı daha fazla suyun tutulmasını sağlayacaktır ve yığın yüzeyi çamur ile kaplı bir alana dönüşecektir. Halbuki, serimin ardından yüzeyin silindir ile sıkıştırılması yığın yüzeyinde bir kabuk oluşturarak (Şekil 25) sıcak hava koşullarında nem kaybını, yağışlı hava koşullarında su tutulmasını ve de sıcak ve rüzgarlı havalarda toz üretilmesini önleyecektir.

Şekil 25. Dozerle yapilan serimin ardindan silindirin sikiştirma işlemi yaparak alanin yüzey pürüzlülüğünü yok ederek kabuk oluşturmasi

14. Silindir ile yüzeyde oluşturulan kabuğun korunması gerekmektedir. Yığın yüzeyinde oluşturulan kabuğun korunabilmesi için, eğer burada bir araç trafiği var ise trafiğin aynı izi takip ederek sürdürülmesi sağlanmalıdır.

15. Çalışma alanlarından ortaya çıkabilecek toz miktarının en az seviyeye indirilmesi sağlanmalıdır. Depolama alanı ciddi bir toz kaynağı olabileceği gibi örneğin nakliye yolları da ciddi toz üretimine neden olabilir. Toz bastırma işleminin etkin kılınabilmesi için şu uygulamalar faydalı olacaktır.

15.1. Depolama alanı yüzeyinde silindir ile kabuk oluşturulması ve korunması gereklidir. Yüzeylerin zaman zaman sulanması ve ardından kurumaya bırakılması bu kabuğun kalitesini artıracaktır.

15.2. Depolama alanı yüzeyi ile nakliye yollarının yıkanması/sulanması için bir arazöz kullanılmalıdır. Bu arazöz üstten su püskürtme sistemi ile donatılmış olmalıdır. (Şekil 26-27)

Şekil 26. Atık nakliye yolunda toz bastirma amaci ile arazöz kullanilmasi

Şekil 27. Filtrelenmiş atik depolama alaninin üstten püskürtme ile sulanmasi

15.3. Nakliye yollarının asfalt ile kaplanmış olması da toz üretimini azaltacak, tozla mücadeleyi kolaylaştıracaktır. (Şekil 28)

15.4. Nakliye yollarının temizliği için bir Zemin Temizleme Aracı çalıştırılmalıdır. (Şekil 29)

Şekil 28. Asfalt kaplamali nakliye yolu

Şekil 29. Zemin temizleme aracı

15.5. Nakliye yolları boyunca kurulacak fıskiye sistemi de tozun bastırılmasına yardımcı olacaktır. (Şekil 30)

15.6. Asfalt yollar dışında kalan stabilize yol kısımlarında lingo-sülfat kullanımı tozla mücadelede etkin olacaktır.

15.7. Depolama alanının nihai şekline kavuşan kısımlarının rehabilite edilmesi bu kısımlarda toz üretimini sonlandıracaktır. (Şekil 31)

Şekil 30. Nakliye yoluna yerleştirilen fiskiyeler ile yapilan sulama işlemi

Şekil 31. Nihai duruma ulaşan yüzeylerde yapilan rehabilitasyon işlemi

16. Kış aylarında olabilecek kar yağışı, don gibi durumlarda kullanılmak üzere, kesintisiz nakliyenin sağlanabilmesi için, bir Kar Kürüme ve Yol Tuzlama aracının sahada bulundurulması faydalı olacaktır.(Şekil 32)

Şekil 32. Kar kürüme ve yol tuzlama araci

17. Yapılan işlerin tümünü kapsayan bütünleşik bir yönetim sistemi oluşturulmalıdır. ‘’Sürdürülebilir Atık Yönetimi’’ ne ait uluslararası ilkeler belirlenerek gerekleri yerine getirilmelidir. Firma tutarlı duruşunu, atık yönetimi konusundaki ilkelerini firmanın politika ve taahhütlerine yerleştirerek işe başlamalıdır. Şirket bu işte çalışanlara ait hiyerarşik yapıyı kurmalı, iş tanımlarını yazılı hale getirmelidir. Şirket işle ilgili ekonomik ve yasal gereksinimleri uygulayıcıya sunmalıdır.

17.1. Uygulayıcılar atık depolama alanlarındaki işleri kapsayan bir ‘’ İşletme, Bakım, İzleme Kılavuzu’’ hazırlamalıdır. Bu kılavuzda depolama alanı sınıflaması, yasal gereklilikler,kılavuz kontrolü ve revizyonlar, yıllık gözden geçirme, roller ve sorumluluklar,yetkinlikler ve eğitimler, tesise ait tasarım ve işletme kriterleri, su yönetimi kriterleri, bitkisel toprak depolama işleri, saha ile ilgili toprak, erozyon, jeolojik, depremsellik, iklim vb. bilgiler, depolama alanı, filtre tesisi, çevresel koruma işleri, alanın bakımı ve performans izleme işleri, acil durum hazırlık planı hakkındaki bilgiler ayrıntılı olarak yer almalıdır.

17.2. Risk bazlı çalışma sistemi oluşturulmalıdır. Bu sisteme ulaşmak için; çalışma alanındaki tüm riskler tanımlanmalı, risk matrisi hazırlanmalı, risklerin yönetilebilmesi için gereken kritik kontroller belirlenmeli, acil durum başlatma eşik değerleri belirlenmelidir. Bunun sonucunda hazırlanacak ‘’Acil Durum Eylem Planları’’ nın maden genelinde geçerli olan ‘’Acil Durum Eylem Planı’’ ile uyumlu hale getirilmelidir.

18. Atık yönetim sisteminin iç ve dış denetlemeye tabi tutulması sağlanmalıdır.

19. Depolama alanı yöneticilerince her yıl için bir ‘’Yıllık Gözden Geçirme Raporu’’ hazırlanmalı ve bu rapor firma yönetimine sunulmalıdır.

20. Depolama alanı dolgusu yükseldikçe, yapılan dolgunun istenen değerlere sahip olup olmadığının test edilebilmesi için, SPT (Standart Penetration Test)(Şekil 33), CPT (Conic penetration Test)(Şekil 34) çalışmalarının yapılması gereklidir.

Şekil 33. Filtrelenmiş atık depolama alanı’nda SPT çalışması

Şekil 34. Filtrelenmiş atık depolama alanı’nda SPT çalışması

21. Depolama alanı yüzeylerinde zaman zaman 3-4 metre derinliğindeki araştırma çukurlar kazılarak yapılacak olan sıkışma kontrolleri (Şekil 35) yapılan işin test edilebilmesi için iyi bir yoldur.

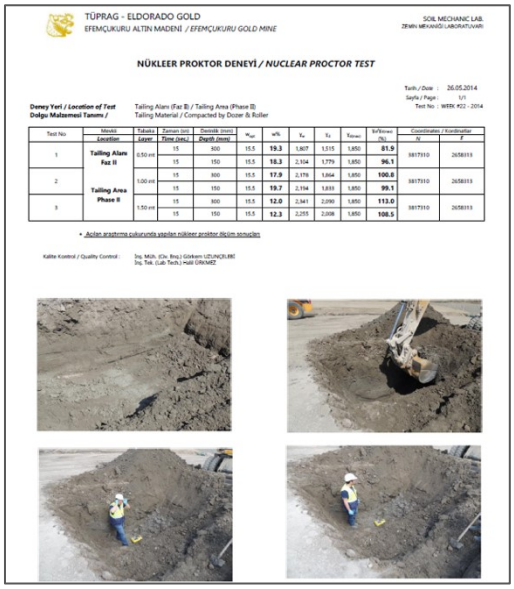
TÜPRAG - ELDORADO GOLD
EFEMÇUKURU ALTIN MADENİ / EFEMÇUKURU GOLD MINE

SOIL MECHANIC LAB.
ZEMİN MEKANİĞİ LABORATUVARI

NÜKLEER PROKTOR DENEYİ / NUCLEAR PROCTOR TEST

Tarih / Date : 26.05.2014
Sayfa / Page : 1/1
Test No : WERK #22 - 2014

Deney Yeri / Location of Test : Tailing Alanı (Faz II) / Tailing Area (Phase II)
Dolgu Malzemesi Tanımı / : Tailing Material / Compacted by Dozer & Roller

Test No.	Mevkii Location	Tabaka Layer	Zaman (sn) Time (sec.)	Derinlik (mm) Depth (mm)	w_{opt}	$w_{\%}$	γ_d	γ_1	γ_{max}	Sıkışma (%)	Coordinates / Koordinatlar N	E
1	Tailing Alanı Faz II	0.50 mt	15	300	15.5	19.3	1,607	1,515	1,850	81.9	5817310	2658113
			15	150	15.5	18.3	2,104	1,779	1,850	96.1		
2	Tailing Area Phase II	1.00 mt	15	300	15.5	17.9	2,179	1,864	1,850	100.8	5817310	2658113
			15	150	15.5	19.7	2,194	1,833	1,850	99.1		
3		1.50 mt	15	300	15.5	12.0	2,341	2,090	1,850	113.0	5817310	2658113
			15	150	15.5	12.3	2,255	2,008	1,850	108.5		

* Açılan araştırma çukurunda yapılan nükleer proktor ölçüm sonuçları

Kalite Kontrol / Quality Control : Ing. Müh. (Ch. Eng.) Görkem UZUNCILAR
Ing. Tek. (Lab Tech.) Halil ORKMEZ

Şekil 35. Test çukuru sıkışma izleme formu

22. Kuru atığın nakliyesi kamyonlar ile yapılacaksa kamyon damperinin polimer ile kaplanması dampere malzeme yapışmasını önleyecektir. Bu durum daha emniyetli ve düşük maliyetli çalışmanızı beraberinde getirecektir. (Şekil 36)

Şekil 36. Polimer ile kaplanmış kamyon damperi

SONUÇ

"Filtrelenmiş Atık Depolama Yöntemi'' uygulaması dünya madenciliğinde, terkedilmekte olan geleneksel depolama yöntemleri yerine, uygulaması hızla artan bir yöntemdir. Bu yöntem atık depolama yöntemleri içinde ''Mevcut En İyi Teknikler'' (MET - BAT) ve ''Mevcut En İyi Uygulamalar (MEU - BAP)" olarak kabul edilmiştir.

Efemçukuru Altın Madeni'nde yapılan uygulamalar , bu yöntemden beklenen faydaların fazlası ile elde edildiğini göstermiştir.

Önerilen yöntem ile oluşturulan atık yığınının mükemmel duraylılığa sahip olması nedeni ile atıkların yayılarak çevresel zararlar oluşturması olası değildir. Bu nedenle, maden yöneticilerinin işletme

projelerinin hazırlanması sırasında bu yöntemin uygulanabilmesi için özel gayret sarf etmeleri tavsiye olunur.

KAYNAKLAR

Global Tailings Review (2020). Global Industry Standard on Tailings Management. https://globaltailingsreview.org/global-industry-standard/

Mining Association of Canada (2019a). A Guide to the Management of Tailings Facilities *Version 3.1*. https://mining.ca/our-focus/tailings-management/tailings-guide/

Mining Association of Canada (2019b). Developing an Operation, Maintenance, and Surveillance Manual for Tailings and Water Management Facilities *Second Edition. https://mining.ca/our-focus/tailings-management/oms-guide/*

Norwest Corporation, (2014). 2013 CPT & Drilling Investigation – Summary and Evaluation Rev. 0. May 8, 2014

Norwest Corporation, (2018). Review of Efemçukuru's Gold Mine's Tailings Management System and with MAC's Tailings Management Guidelines. January22, 2018

Stantec Consulting International Ltd., (2019a). Central TSF Classification and Risk Assessment Rev. 1. PowerPoint Presentation. December 2019

Stantec Consulting International Ltd., (2019c). Efemçukuru Central TSF 2019 Site Investigation and Instrumentation Plan – Rev. 0. December 2019

Stantec Consulting International Ltd., (2020a). Assessment of Effectiveness of the Mine's Tailings Management System 2019 Memorandum. February 2020

TSM Tailings Review Task Force (2015). Report of the TSM Tailings Review Task Force. https://mining.ca/documents/report-tsm-tailings-review-task-force/

EFFECT OF HEMATITE MORPHOLOGY ON FLOTATION EFFICIENCY

T.D. Figueiredo [1,*], D.S. Moreira [2], F. São José [2], G.H.G. Rodrigues [1], C.A. Pereira [1]

[1] Federal University of Ouro Preto (UFOP), Dept of Mining Engineering
*(*Corresponding author: thiagoduarte1926@hotmail.com)*
[2] Federal Center of Technological Education of Minas Gerais (CEFET/MG)

ABSTRACT

Iron ore is the main mineral input in Brazilian production, being exploited in high quantities and from different minerals, among which stands out hematite (Fe2O3), mineral responsible for most of the national production of iron ore. Hematite presents different morphologies, occurring in the compact or specular form, which directly influences the efficiency of processing circuits, such as fragmentation and concentration. Knowing this, this work seeks, through microflotation tests, to evaluate the influence of morphologies of specular and compact hematite on flotation processes. The optimal operating conditions were determined by varying parameters such as pulp pH, nitrogen gas flow, reagent dosage and fragmentation mechanism. After the tests, the influence of morphology and type of hematite fragmentation for the flotation process were confirmed. The use of cationic collector allowed the mutual recovery of compact hematites and specular hematites. The ideal operating parameters were defined at: 50 cm^3/min of nitrogen flow, collector dosage of 20 mg/L and pH ≥ 8, with flotation recoveries over 85% for all minerals conditions analyzed.

Keywords: Specular hematite, compact hematite, microflotation, floatability.

INTRODUCTION

Brazil is one of the largest producers of iron ore in the world, being this the main mineral input in terms of quantity and economic representativeness in the country. Currently Brazil is the third largest producer of iron ore globally, with production estimated at approximately 430 Mt, distributed in the states of Minas Gerais (with 82.9% of the national reserves), Pará (9.9%) and Mato Grosso do Sul (2.3%) (Jesus and Joaquim, 2017).

Iron ore in Brazil is found predominantly in the form of hematite (Fe2O3), also occurring in a smaller amount in minerals such as ilmenite (FeTiO2), goethite (FeO(OH)) and magnetite (Fe3O4) (Gomes et al., 2013). Hematite, the most exploited mineral for iron production in Brazil, has varied morphologies, being found, for example, in its specular and compact form. These different morphologies for the same mineral stand out mainly in the physical and mechanical parameters, such as preferential fracture planes, mechanical resistance, shape and distribution of crystals. According to Gomes et al. (2013), compact hematite has higher mechanical strength, as well as reduced porosity and reducibility in relation to specular hematite.

For flotation to occur efficiently, several variables are taken into account, requiring to be conditioned according to optimal parameters, determined through laboratory tests. According to Aguiar (2014), in the last 40 years, the reverse cationic flotation has become one of the main methods used for hematite concentration. This process is normally performed using amine as the collector of silicate gangue minerals and starch as an iron oxide depressant.

The definition of the ideal flotation parameters of hematite therefore depends directly on its morphology. For this, one of the methods for analyzing the behavior of these minerals in processing plants is based on floatabilitytests, such as microflotation in Hallimond tubes. Through these tests, it is possible to compare different parameters for a flotation step and define the best operating conditions, whether for hematite recovery with specular or compact characteristics.

MATERIALS AND METHODS

The procedures performed during the present study are described in this topic.The characterization tests of the samples were carried out in CEFET-MG Campus II and UFMG material laboratories, while the remaining tests were carried out in chemistry laboratory of CEFET-MG Campus Araxá and UFOP Flotation laboratory. This work consisted of the analysis of representative samples of specular and compact hematite, both provided by Companhia Siderúrgica Nacional (CSN) – Casa de Pedra mine, with particle size above 150 µm.

Technological Characterization

For the technological characterization tests, a small portion of the hematite samples was reduced to less than 38 µm. The remaining material was sieved into size fraction of -150 + 106 µm for microflotation tests.

In order to analyze the influence of the fragmentation mechanism on ore characteristics, a fraction of specular hematite was fragmented by rod mill and another by disc mill. The same procedure was performed for the fraction of compact hematite, to compare the effects caused by different fragmentation mechanisms on the structure of ore grains and its behavior during the tests.

In technological characterization of the samples, their physical and morphological characteristics were determined and compared by Scanning Electron Microscopy (SEM). In addition, the specular and compact hematite samples were characterized by X-ray Diffraction analysis (XRD), seeking to determine the mineralogical composition of the samples, an important parameter for microflotation tests.

Microflotation

The microflotation tests were performed using the modified Hallimond tube, equipment coupled with a height extender, that reduces the hydrodynamic drag of fines particles during the process. This equipment allows to analyze the floatabilityof hematite using small samples of the mineral (aliquots from 1 to 2g).

To this end, a mathematical artifact is applied, capable of determining the degree of floatability of the mineral particle. Thus, the tendency of the mineral sample to be collected is represented by Eq.1.

$$Flotability\ (\%) = \frac{Flotated\ mass\ (g) x\ 100}{Sample\ mass\ (g)} \quad (1)$$

The first floatability assay of compact and specular hematites aimed to evaluate the behavior of minerals in relation to variation of nitrogen gas flow in the system without reagents addition. For this, the pH of the solution was set at 10.5, a value that, according to Viana (2006), is in the ideal pH range for iron ore flotation.

After the system adjustment, the tests for natural floatability of specular and compact hematite were performed, increasing the flow of nitrogen injected into the system by 10 cm^3/min at each assay.

The initial and final values of gas flow rate was 20 cm^3/min and 110 cm^3/min, respectively. Thus, it was possible to determine the optimal flow rate for flotation of each type of hematite.

The ideal flow rate was fixed and applied in the next tests, which evaluate the ideal dosage of reagents for hematite flotation. Collector reagent solutions (Amina Flotigam EDA 3) were prepared with 0.1% (w/v). The collector dosage had its minimum value defined at 0,5 mg/L, being gradually increased by 0.5 mg/L up to 2 mg/L. The dosage was then increased sequentially by 2 mg/L and the tests was performed until the final value of 12 mg/l.

Finally, with the optimal values of reagent dosage and gas flow defined, microflotation tests were performed to verify the optimal pH values of the system. By varying the pH values, it was possible to compare the optimal results found with the values suggested by the literature, and to determine whether the behavior of hematite during flotation follows the precepts already defined in previous studies. With the use of NaOH and HCl as pH modifiers, microflotation tests occurred at initial pH 2, ranging from 2 units to the maximum value of pH 12, in which the last test was performed. All tests performed in this stage were done in triplicate. Thus, the average values among the 3 results obtained are considered representative.

Zeta Potential

The tests for calculation of hematite Zeta potential, whose equipment used was Zeta Meter 4.0, were performed to determine the Point of Zero Charge (PZC) and the Isoelectric Point (PIE) of the mineral. For the tests, performed in duplicate, a solution of KNO3 was used as indifferent electrolyte. The pH values analyzed were 2, 4, 6 8 and 10, being adjusted by pH modulators (NaOH and HCl) at a concentration of 1% (w/v).

RESULTS AND DISCUSSION

Technological Characterization of Hematite Samples

Initially, the X-ray Diffraction assays evaluated the purity of the samples, as illustrated by Fig. 1. It is possible to observe the presence of pure hematite compact samples (a), while the presence of quartz was observed with the specular hematites (b).

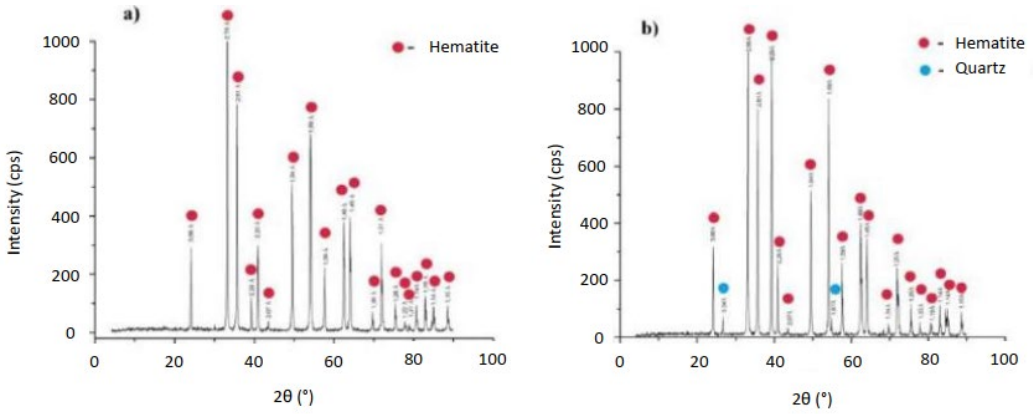

Figure 1. X-ray diffraction spectra of the hematite samples

The compact hematite samples have a high degree of purity. The specular hematite present quartz contamination promoting the reduction of the specific mass of the sample.

The analysis of the SEM results (see Fig. 2), allows us to observe that the hematites fragmented by disc mill (B and D) have greater homogeneity in relation to the samples cominuated by bar mills (A and C), presenting greater regularity in the size and shape of the grains.

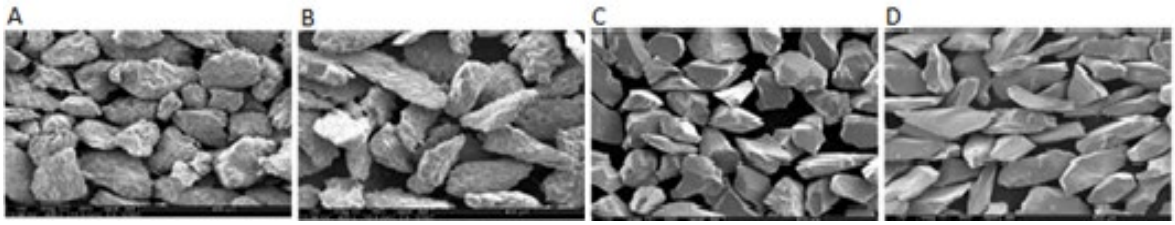

Figure 2. Specular hematite fragmented by bar mill (A) and disk mill (B). Compact hematite fragmented by bar mill (C) and disk mill (D)

There is also a difference between specular hematites (A and B) and compact hematites (C and D). The images suggest that specular hematite presents greater porosity, thus having a lower specific mass in relation to compact samples, in addition to a greater propensity to flotability.

Zeta Potential

As shown by Figure 6, the isoelectric point for compact hematite was approximately 7.2, while for specular hematite it was 6.8. It is noted that at pH above 7, the surface loads of hematites are negative, thus justifying the use of cationic collectors.

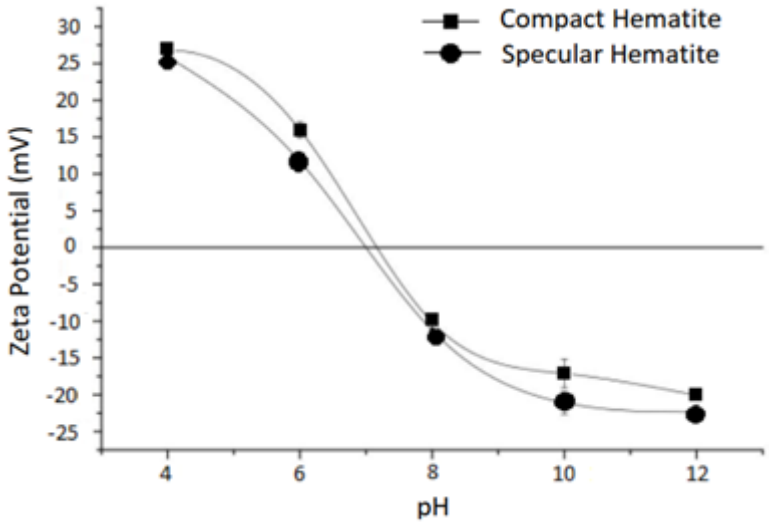

Figure 6. Zeta potential of compact and specular hematites

The zeta potential graph presents similar results to those obtained by Alexandrino (2012) and Henriques (2009). The authors performed Zeta potential tests for several iron minerals, including compact and specular hematite. As in the present article, the authors found isoeletric point values in pH range between 6 and 8.

Microflotation Tests

Flotation tests allowed the floatability of hematites in several scenarios to be evaluated. The first test sought to determine the natural floatability of hematites and optimal conditions of gas flow in the system, whose results are represented by Figure 3.

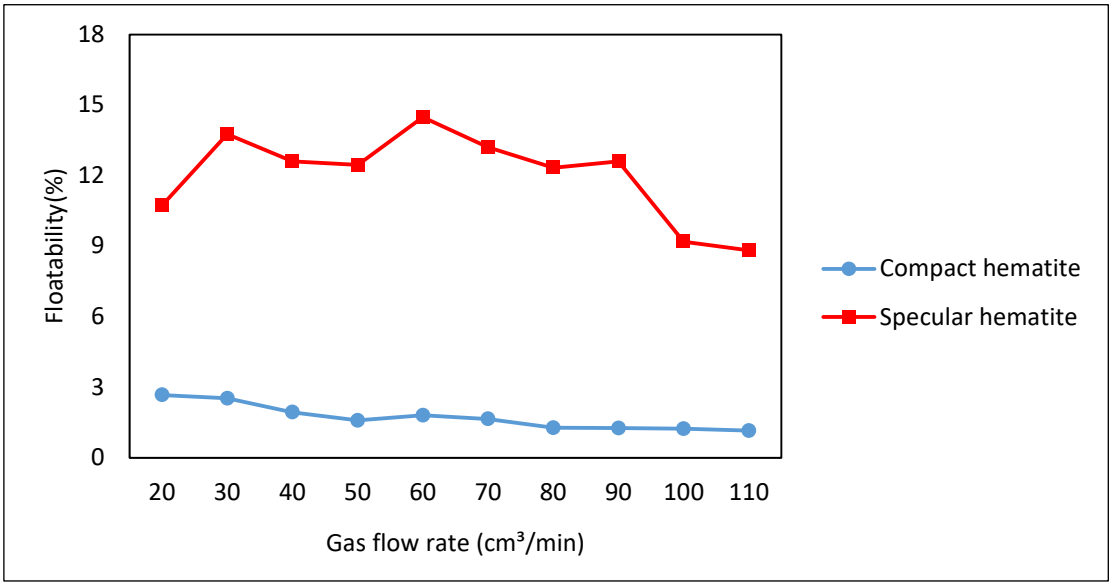

Figure 3. Natural floatability of of compact and specular hematite vs gas flow ratio in pH 10.5.

It is possible to notice that compact hematite presents natural floatabilityup to seven times lower than specular hematite. This is due to the greater porosity of specular hematite, which decreases the specific mass of particles and increases their surface area, which facilitates their loading and increases the contact area for particle-bubble interaction.

In addition, the nitrogen flows that provided a higher floatability of hematites are in the range between 50 and 60 cm^3/min, with floatability of 14.5% and 2% for specular and compact hematites, respectively. These values are supported by Baltar (2010), who defined that when gas flow is less than 50 cm^3/min, an effective interaction between mineral particles and bubbles cannot be achieved, as well as high flows promote turbulence in the system and prevent adsorption from being stable. For all this, it was concluded that the optimal flow rate for the next microflotation tests was 50 m^3/min.

Hematite floatability as a function of reagent dosage was performed with optimum gas flow (50 cm^3/min). The results in Fig. 4 show that with the addition of collector in the system, the floatability of hematite increased significantly, reaching in some scenarios values above 80% for both specular and compact hematite.

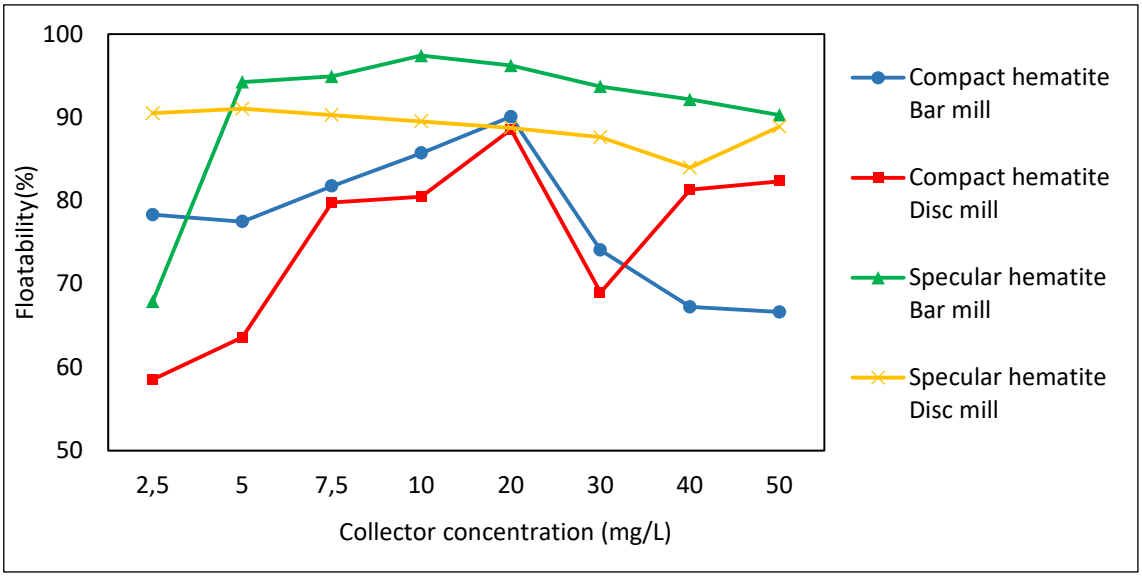

Figure 4. Effect of collector dosage on floatability of compact and specular hematite. (pH 10.5 and gas flow rate of 50cm³/min)

It is possible to observe a higher yield of specular hematites, in relation to compact hematite. The reagent dosage with the highest floatability was approximately 20 mg/L, with results between 85 and 95% of mineral recovery for all samples analized. However, it is seen that a small variation in this dosage value leads to a considerable drop in system yield, especially for compact hematite. Thus, the optimal rate of reagent dosage among those used in the assays was defined at 20 mg/L.

With the definition of optimum flow rate (50 cm³/min) and collector dosage (20 mg/L), the optimum pH for hematite flotation was determined. It is observed in Fig. 5 that the best results were obtained at pH 8, where the four samples analyzed present similar results, with floatability near of 90%. With the increase in pH, the floatability of hematites did not change significantly. Corroborating Viana (2010), at pH 10 the recovery values of hematite remained high.

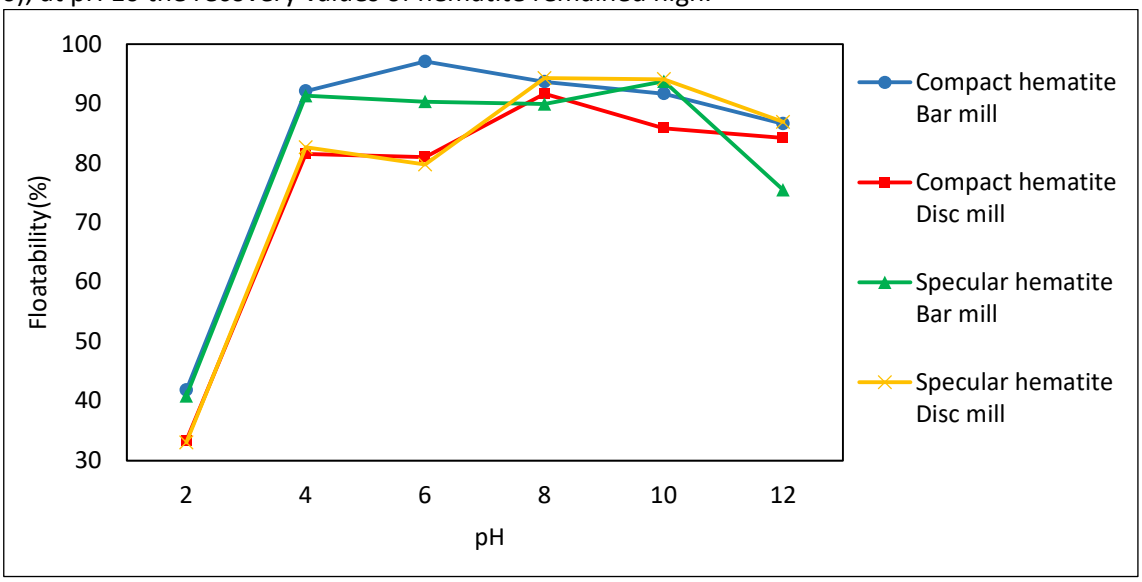

Figure 5. Effect of pulp pH on floatability of compact and specular hematite (Collector dosage of 20 mg/L and gas flow rate of 50cm³/min)

CONCLUSIONS

After analyzing the behavior of the compact and specular hematites of the Casa de Pedra Mine in flotation processes, it is perceived that the morphology of minerals has a direct and significant influence on the efficiency of their recovery. Specular hematites, because they had a lower specific mass and higher porosity in relation to compact ones, showed higher flotability.

With the addition of cationic collector, this difference was reduced, giving the mutual recovery of specular and compact hematites, with average floatabilityin the range of 85%. The optimal operational parameters for the cationic flotation of hematites were defined at: 50 cm^3/min of Gas flow rate, collector dosage of 2 mg/L and optimum pH in range equal or above 8. Finally, after the Zeta potential assays, the PIE values for the specular and compact hematites were defined, being located at pH values 6.8 and 7.2, respectively.

THANKS

The authors thanks CNPq, Gorceix Foundation, CEFET-MG and UFOP for the support and trust deposited during the performance of this work.

REFERENCES

Aguiar M. (2014). Clatratos na Flotação Catiônica Reversa de Minério de Ferro, Msc. Thesis, Engineering School of Federal University of Minas Gerais, Belo Horizonte, M.G. ,108 pp.

Alexandrino J. (2013). Correlação Entre Estado de Dispersão, Propriedades Eletrocinéticas e Flotabilidade de Hematita. Dsc.D. Thesis, Engineering School of Federal University of Minas Gerais, Belo Horizonte, MG, 125 pp.

Baltar, A. (2010). Flotação no Tratamento de Minérios.(2rd. ed., Vol. 1). Recife, Editora Pernanbuco.

Gomes, O Iglesias, J., Paciornik, S., Vieira, M., (2013). Morfometria e Classificação Automática de Hematita em Minérios de Ferro. 44th Seminário de Redução de Minério de Ferro e Matérias-Primas & 4th Simpósio Brasileiro de Minério de Ferro & 1st Simpósio Brasileiro de Aglomeração de Minério de Ferro. Belo Horizonte, Brazil.

Henriques, A. (2012). Caracterização e Estudo das Propriedades Eletrocinéticas dos Minerais de Ferro: Hematita,Goethita e Magnetita. Msc. Thesis, Federal University of Minas Gerais, Belo Horizonte, M.G., 208 pp.

Jesus, C. and Joaquim, L. (2017). Ferro. In DNPM, Sumário mineral 2016, (35nd ed., pp. 64 – 65). Brasilia: DNPM.

Martins, M., Lima, N., Filho, L., (2012). Depressão de minerais de ferro: influência da mineralogia, morfologia e pH de condicionamento, *Revista Escola de Minas*, 65, 393-399.

Viana P., (2006). Flotação de Espodumênio, Microclina, Muscovita e Quartzo com Coletores Aniônicos, Catiônicos, Anfotéricos e Mistura de Coletores. Dsc.D. Thesis, Engineering School of Federal University of Minas Gerais, Belo Horizonte, MG, 202 pp.

EFFECTS OF TEMPERATURE AND CONFINING PRESSURE ON ENERGY EVOLUTION CHARACTERISTICS AND ROCK BURST MECHANISM IN BRITTLE ROCKS

S. Akdag [1, *], M. Karakus [1], G. D. Nguyen [1], A. Taheri [1]

University of Adelaide, School of Civil, Environmental & Mining Engineering
*(*Corresponding author: selahattin.akdag@adelaide.edu.au)*

ABSTRACT

The aim of this research is to study the energy evolution characteristics of brittle rocks and understand the effects of temperature and confinement on bursting mechanism. A new method based on post-peak energy characteristics and acoustic emission response obtained from a series of uniaxial and triaxial compression tests is developed for rock burst analysis on granite samples exposed to high temperature. The axial loading is controlled using the feedback from lateral strain to obtain snap-back behaviour that is associated with energy evolution and the material response under self-sustaining failure. For each loading scenario, excess strain energies are calculated. The elastic strain energy, energy consumed by dominant cohesion weakening, and energy dissipated during mobilisation of frictional loss are quantified. The experimental results underlined that the amount of accumulated elastic strain energy increases as the confinement increases, resulting in a large potential for rock burst. It was also observed that the dominant failure pattern of granite changes from multiple longitudinal splitting to a single shear fracture and finally to multiple conjugate shear fractures as the level of temperature and confinement increases. Thermally induced damage causes less strain energy accumulation and hence the excess strain energy decreases (by ~43% compared to the room temperature conditions) with increasing temperature.

Keywords: Post-peak energy evolution, rock burst, circumferential strain control, triaxial compression test, temperature.

INTRODUCTION

As mining and civil engineering related projects such as caving mining and tunnelling operations progress to greater depths, the number of rock burst hazards has increased resulting in operational and safety challenges (Cai and Kaiser, 2018; Gao and Yang, 2021). The influence of elevated ground temperature has become remarkably significant on triggering rock burst with the increasing excavation depth (Su et al., 2017; Akdag et al., 2018). The coupling of high-stressed ground conditions and thermal damage will alter the overall mechanical behaviour of hard brittle rocks which can trigger bursting in deep engineering operations. Therefore, a deeper insight into the underlying damage mechanism of brittle rocks under high-pressure-temperature conditions is necessary to facilitate the safe construction and operation of underground excavations.

Prediction of rock burst proneness of rocks is one of the basic problems in the field of rock burst research. Various criteria and indices have been proposed to assess the rock burst proneness of rocks using, for example, strain energy storage index (W_{ET}) (Kidybiński, 1981), potential elastic strain energy (PES) (Wang and Park, 2001), peak strain energy storage index (W_{et}^{p}) (Gong et al., 2019), and residual elastic energy index (C_{EF}) (Gong et al., 2021). Despite the significant contributions of these studies for estimating and classifying the rock burst proneness of rock materials, limited work has focused on quantitatively investigating the influence of high-temperature-pressure on rock burst proneness. Therefore, further work is required to improve the understanding of rock burst proneness in highly-

stressed deep rock engineering applications. It has also been acknowledged that the manifestation of rock burst is related to the elastic stored strain energy and how this stored energy is released during unstable spontaneous failure (Tarasov and Potvin, 2013; Akdag et al., 2021). The intensity of rock burst is closely related to the energy storage capacity and dissipation of rocks. However, most, if not all, present evaluation methods do not consider the energy dissipation and excess strain energy (potential energy for rock burst) at the post-peak stage.

In the current paper, the authors investigated the rockburst proneness of thermally-treated granite under confinement. A series of circumferential strain-controlled uniaxial and triaxial compression tests were carried out on granite subjected to different temperatures under compression. The effects of high temperature and confinement on the mechanical characteristics, time-domain AE responses and energy evolution behaviour of granite were analysed. The rock burst proneness of the granite is discussed based on the energy evolution characteristics.

TEST METHODOLOGY

Circumferential Strain Controlled Uniaxial and Triaxial Compression Tests

For Uniaxial Compressive Strength (UCS) tests, rock samples were subjected to a monotonic axial loading by a closed-loop servo-controlled Instron 1282 hydraulic testing machine (Fig. 1a). The applied axial load was initially controlled using axial-strain feedback at a rate of 0.001 mm/mm/s until reaching approximately 70% of the expected peak force and then the control mode was switched to circumferential control, keeping lateral-strain rate constant by the circumferential extensometer (see Fig. 1b).

Circumferential strain controlled triaxial tests were conducted on the granite specimens exposed to temperatures up to $250\ ℃$ over confining pressures of 20, 40 and 60 MPa using the same Instron 1282 hydraulic testing machine. Circumferential strain control was utilised by means of a Hoek cell membrane fitted with four lateral strain gauges internally within the cell (Fig. 1c). The specimen was loaded axially with constant growth of a lateral strain of $1 \times 10^{-6}\mathrm{mm/mm/s}$ (Fig. 1d) and PCI-2 AE system was used to monitor the damage within the granite specimens during loading.

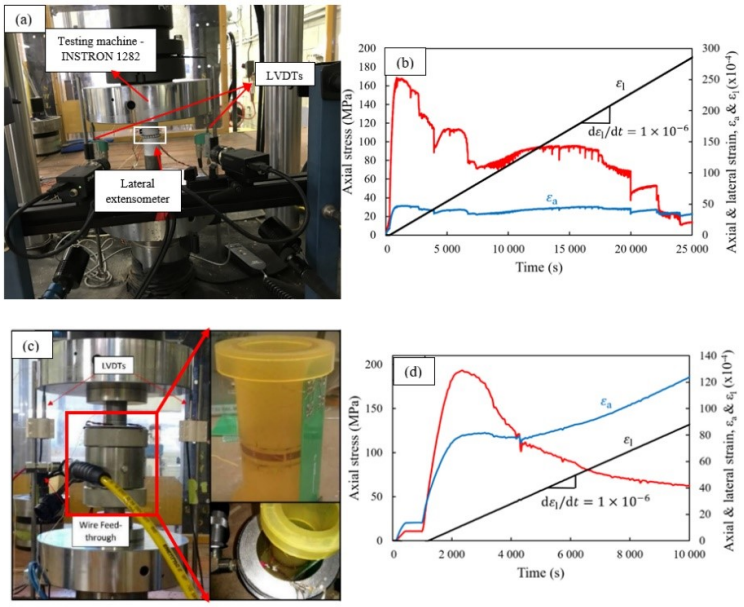

Figure 1. Testing setup and loading rates for lateral strain-controlled uniaxial (a, b) and triaxial compression tests (c, d).

TEST RESULTS

Stress-Strain Curves and Failure Modes

Fig. 2 presents the complete stress-strain curves of thermally-treated granite under different confining pressures. The failure mode of the granite changed from multiple splitting tensile fractures along the loading direction or a single shear fracture to conjugate shear failure with increasing temperature (see Fig. 2). Based on the experimental results, peak stress at 250 °C declined by ~25% when compared with the results at room temperature (25 °C) under unconfined conditions. It is the authors' interpretation that the main reason for this descending trend might have been the thermally induced micro-cracks that could cause mechanical degradation by weakening the bonding among mineral grains due to the differences in the thermal expansion properties of constituent rock minerals. This observation is consistent with the existing literature (Xu and Karakus, 2018; Yang et al., 2020), however, further investigation is needed to prove the above postulation. As confinement increased (up to 60 MPa), the peak stresses decreased by 21, 13 and 6% with increasing temperature from 25 °C to 250 °C, respectively. The confining pressure restrains the displacement and enhances the friction among grains under the condition of higher temperature.

The main failure feature of the granite was the multiple longitudinal splitting failure pattern accompanied by local shear failure when $\sigma_3 = 0$ MPa. The formation of extension cracks oriented in the direction of principal stress was the prevailing pattern of macroscopic fracturing in uniaxial compression. In moderate confining pressures, the granite specimens mainly failed by shear localisation along an inclined macroscopic shear band. Under high confinement, a conjugate shearing or ductile failure was observed in which the thermal heating could also enhance the ductility of the rock samples, as shown in Fig. 2.

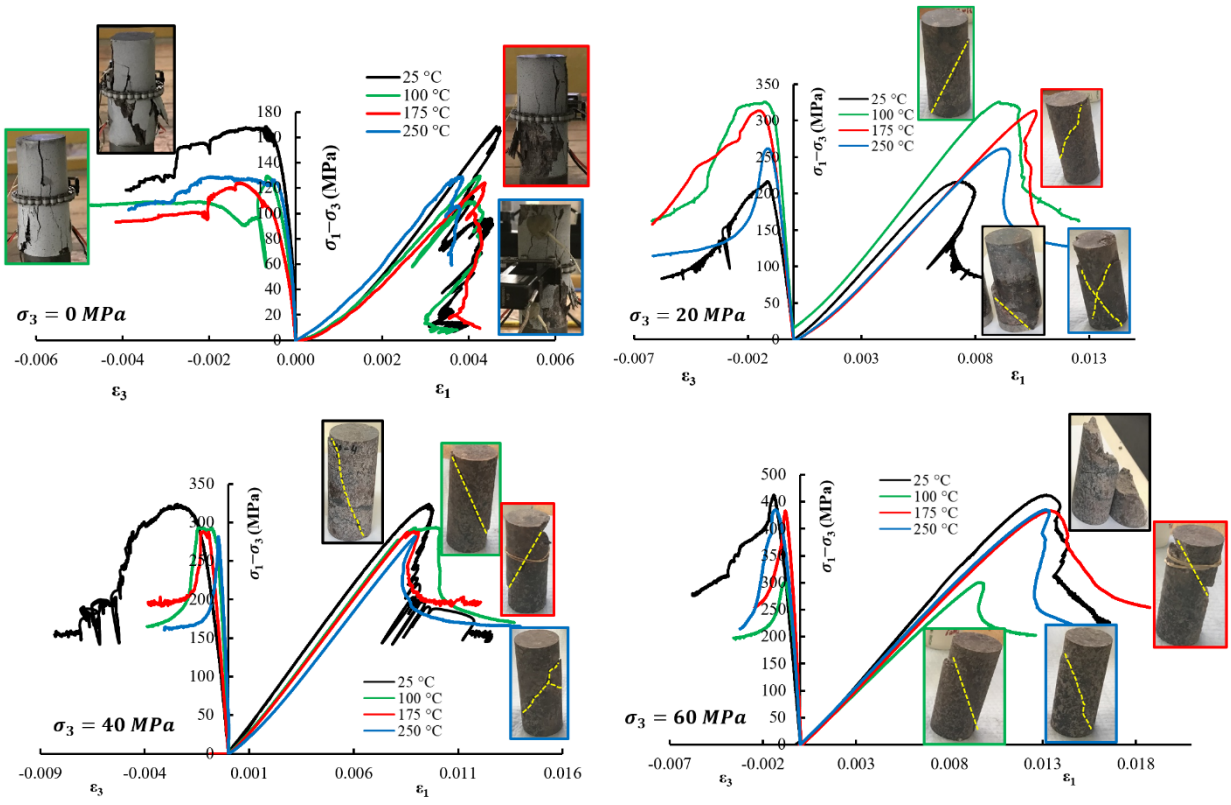

Figure 2. Complete stress-strain curves and failure modes of thermally-treated granite at various confinement

The typical AE characteristics of granite after temperature treatment under various confinement are shown in Fig.3. It can be seen that with the increase of temperature, the evolution of accumulated AE hits for granite specimens becomes slower and slower, which indicates that at higher temperatures, the granite samples undergo more ductile failure and released less elastic strain energy due to the thermally induced damage.

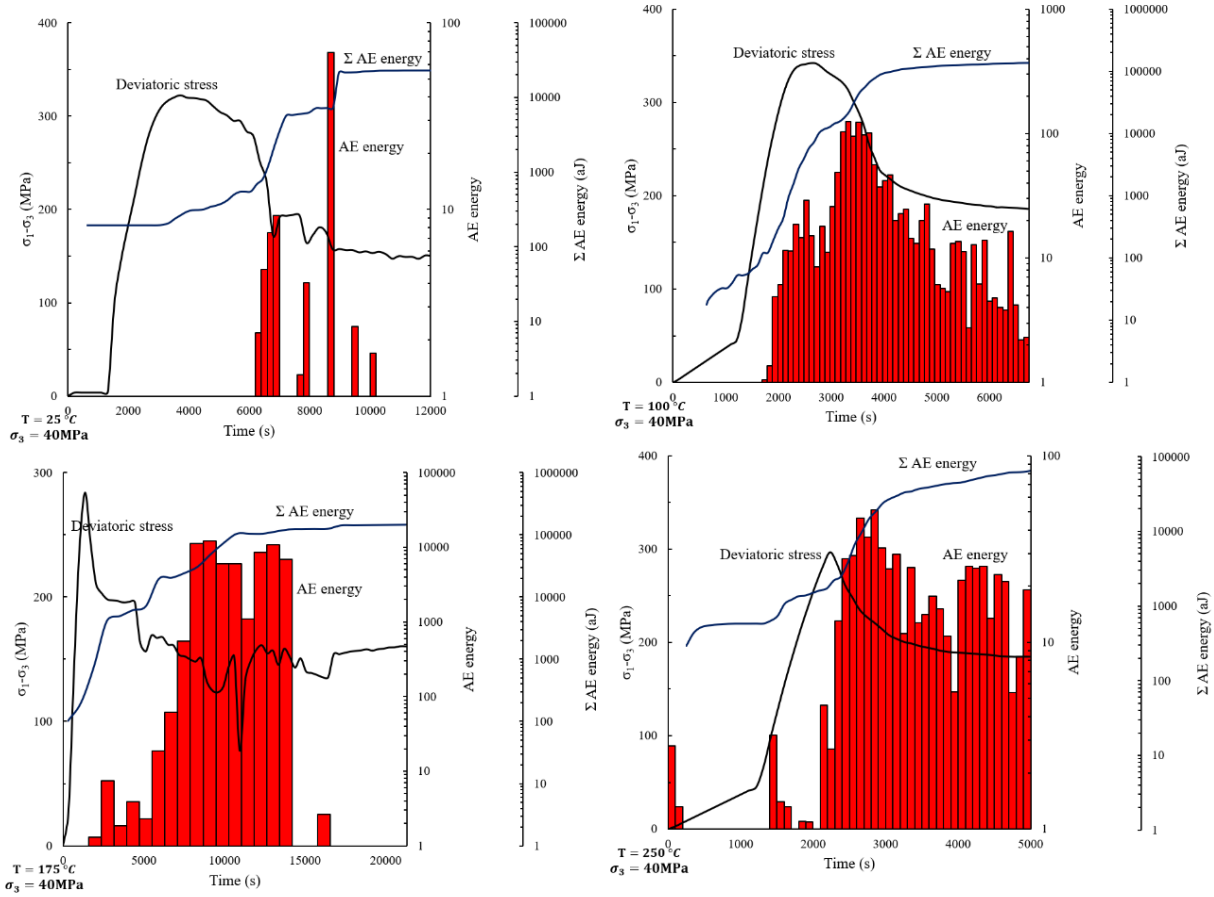

Figure 3. Evolution of AE characteristics of granite after temperature treatment ($T = 25$ ℃, 100 ℃, 175 ℃ and 250 ℃)

Post-Peak Energy Calculation Principle

Rock burst is a type of instantaneous brittle failure of rock which mainly occurs due to the stress concentration and rapid energy release at the conditions of high geo-stress. Therefore, in compression stage, enough elastic strain energy is accumulated in the rock, ensuring that it can transfer this energy into kinetic energy at the failure. The buckling of slabs or rock ejection in the sidewalls of underground excavations is a typical manifestation of rock burst damage. It is of great importance to analyse energy evolution characteristics during rock fracturing under compression condition because of the significant function of identifying the energy source of the rock burst and revealing the rock burst's vulnerability. In this study, recently proposed energy method (Akdag et al. 2021) is used to evaluate the post-peak energy balance of thermally-treated granite under different confining pressures. Fig. 4 and Eqs. 1-5 show the calculation method for the energies at the post-peak stage.

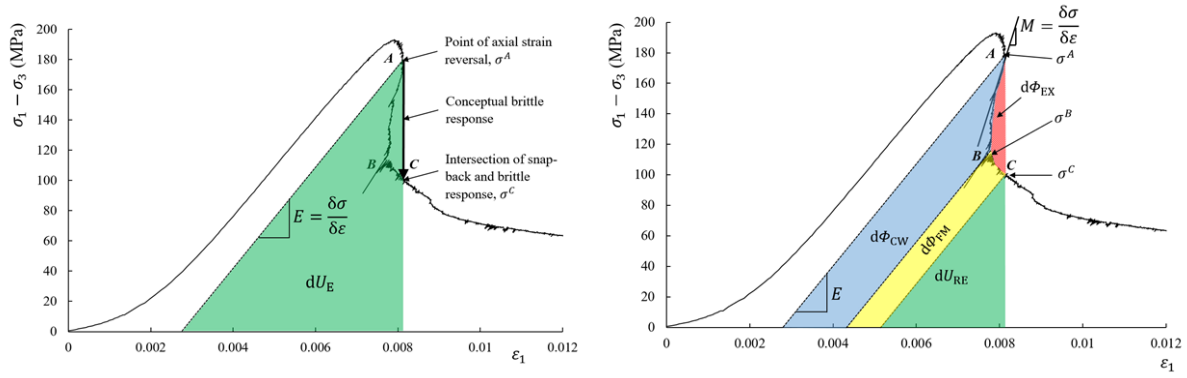

Figure 4. Energy calculation method based on the post-peak energy balance of snap-back behaviour (Akdag et al., 2021)

Here, a new energy-based rock burst proneness index Ω_{RB} is proposed:

$$\Omega_{RB} = \frac{d\Phi_{EX}}{dU_E} \tag{1}$$

where $\mathrm{d}\Phi_{\mathrm{EX}}$ and $\mathrm{dU_E}$ are the excess strain energy released during brittle failure (rock burst) and the elastic stored strain energy after Class II behaviour starts, respectively. The energy calculations are shown as follows:

$$dU_E = \frac{1}{2E}[\sigma_1^2 + 2\sigma_3^2 - 2\mu(2\sigma_1\sigma_3 + \sigma_3^2)] \tag{2}$$

$$U_1 = \int \sigma_1 d\varepsilon_1 = \sum_{i=0}^{n} \frac{1}{2}(\varepsilon_{1i+1} - \varepsilon_{1i})(\sigma_{1i} + \sigma_{1i+1}) \tag{3}$$

$$U_3 = 2\int \sigma_3 d\varepsilon_3 = \sum_{i=0}^{n} (\varepsilon_{3i+1} - \varepsilon_{3i})(\sigma_{3i} + \sigma_{3i+1}) \tag{4}$$

$$\mathrm{d}\Phi_{EX} = dU_E - \mathrm{d}\Phi_{CW} - \mathrm{d}\Phi_{FM} - dU_{RE} \tag{5}$$

where σ_{1i}, σ_{3i}, ε_{1i}, ε_{3i} are the axial and confining stresses and strains at a point i on stress-strain curve, respectively, Φ_{CW} is the energy consumption dominated by cohesion degradation during stable fracturing, Φ_{FM} is the energy dissipated during the mobilisation of frictional failure, U_{RE} is the residual stored elastic strain energy, σ_A is the point of axial strain reversal, σ_B is the point of brittle failure intersection, E is the elastic stiffness of the specimen and M ($M = \delta\sigma/\delta\varepsilon$) is the post-peak modulus between two incremental stress points, σ_i and σ_{i+1} which can vary significantly with the fracture development.

Rock Burst Proneness

The energy balance in the post-peak stage reflects the mechanism of excess strain energy which is related to the rock burst intensity. The rock burst proneness of pre-heated granite under confinement are shown in Fig.5. The results show that high-temperature-confinement have a significant influence on rock burst proneness. Based on the energy evolution analysis above, the larger the maximum dissipation energy density was, the more likely were the damage and plastic deformation occur in the granite which would result in severe rock burst. The dissipated energy can indirectly reflect the irreversible plastic deformation that occurs in the rock and the friction dissipation effect between internal fissure planes. The greater the confinement was, the larger the stored elastic strain energy and dissipated energy for cohesion weakening and friction mobilisation were. The confining pressure could restrain the

deformation within the granite and enhance the plastic deformation. In the field, however, confinement loss due to excavation is one of the major factors causing rock burst in the high-stress areas in deep mines. Therefore, assuming the accumulated elastic strain energy under confinement is released in the lab conditions, which can be considered as a free face or 'excavation' during the test, the bursting potential of the rock would be more severe at higher confining pressures.

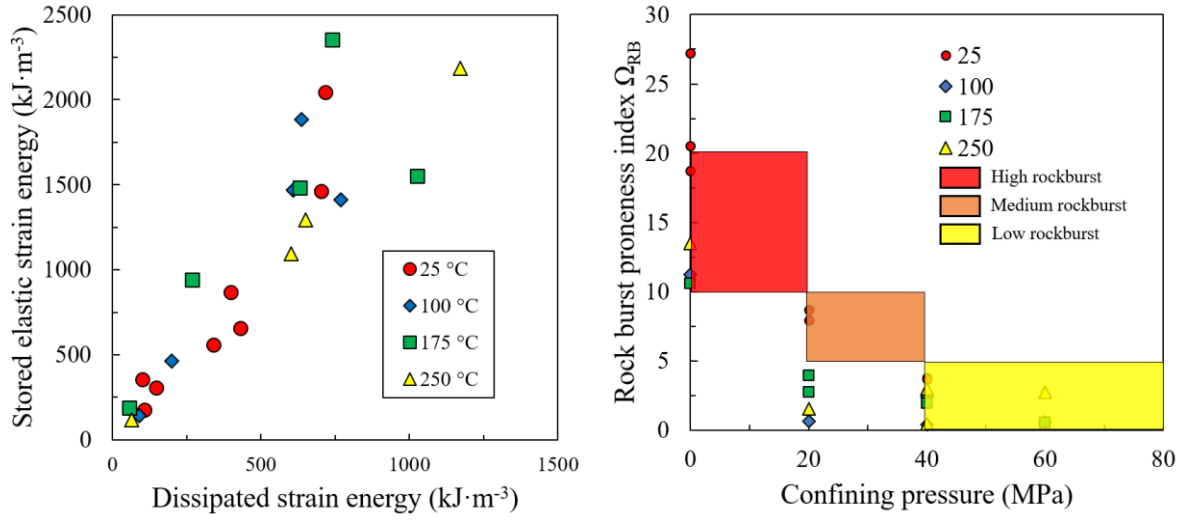

Figure 5. Rock burst proneness of thermally-treated granite under different confinement

CONCLUSION

This work proposes a simple yet effective experimental analysis for the rock burst proneness of thermally-treated granite under triaxial compression. The results show that high-temperature-confinement has a significant influence on the rock burst proneness. At the post-peak stage, higher confining pressure caused greater stored elastic strain energy and dissipated energy which would result in more severe rock burst damage in case of any confinement loss. With the increase of temperature, the strength of granite gradually weakened and the plastic failure characteristics were considerably enhanced due to the thermally-induced cracking. This approach could provide a preliminary assessment of the instability of brittle rocks in burst-prone areas to avoid potential hazards.

ACKNOWLEDGEMENTS

The authors gratefully acknowledge the financial support from the Australian Research Council and the Partner Organisation, OZ Minerals for the Linkage Project (LP150100539).

REFERENCES

Akdag, S., Karakus, M., Nguyen, G., Taheri, A., & Bruning, T. (2021). Evaluation of the propensity of strain burst in brittle granite based on post-peak energy analysis. Undergr Space, 6(1), 1-11.

Akdag, S., Karakus, M., Taheri, A., Nguyen, G., & He, M. (2018). Effects of thermal damage on strain burst mechanism for brittle rocks under true-triaxial loading conditions. Rock Mech Rock Eng, 51, 1657-1682.

Cai, M., & Kaiser, P. (2018). Rockburst support reference book, Rockburst phenomenon and support characteristics (Vol. 1). Sudbury: MIRARCO-Mining Innovation, Laurentian University.

Gao, F., & Yang, L. (2021). Experimental and numerical investigation on the role of energy. Rock Mech Rock Eng, 54, 5057-5070.

Gong, F., Wang , Y., Wang, Z., Pan, J., & Luo, S. (2021). A new criterion of coal burst proneness based on the residual elastic energy index. Int J Min Sci Technol, 31(4), 553-563.

Gong, F., Yan, J., Li, X., & Luo, S. (2019). A peak-strength strain energy storage index for rock burst proneness of rock materials. Int J Rock Mech Min Sci, 117, 76-89.

Kidybiński, A. (1981). Bursting liability indices of coal. Int J Rock Mech Min Sci, 18, 295-304.

Su, G., Chen, Z., Ju, J., & Jiang, J. (2017). Influence of temperature on the strainburst characteristics of granite under true triaxial loading conditions. Eng Geol, 222, 38-52.

Tarasov, B., & Potvin, Y. (2013). Universal criteria for rock brittleness estimation under triaxial compression. Int J Rock Mech Min Sci, 59, 57-69.

Wang, J., & Park, H. (2001). Comprehensive prediction of rockburst based on analysis of strain energy in rocks. Tunn Undergr Space Technol, 16(1), 49-57.

Xu, X., & Karakus, M. (2018). A coupled thermo-mechanical damage model for granite. Int J Rock Mech Min Sci, 103, 195-204.

Yang, S., Tian, W., Elsworth, D., Wang, J., & Fan, L. (2020). An experimental study of effect of high temperature on the permeability evolution and failure response of granite under triaxial compression. Rock Mech Rock Eng, 53, 4403-4427.

ELEKTRON TRANSFER YÖNTEMİNDE FARKLI İYONLARIN KÖMÜRDEN ORGANİK KÜKÜRT UZAKLAŞTIRILMAYA ETKİSİ

EFFECT OF DIFFERENT IONS IN ELECTRON TRANSFER METHOD ON REMOVAL OF ORGANIC SULFUR FROM COAL

U. Demir [1,*], A. Aydın [1]

[1] *Kütahya Dumlupınar Üniversitesi Mühendislik Fakültesi, Maden Mühendisliği Bölümü*
(Sorumlu yazar: ugur.demir@dpu.edu.tr)

ÖZET

Özellikle termik santrallerde kullanılan kömürde bulunan kükürt, önemli çevresel sorunlara neden olmaktadır. Bu çalışmada yüksek oranda kükürt içeren Kütahya-Gediz yöresi kömürlerinden organik kükürdün uzaklaştırılmasında Elektron Transfer Yöntemi (ETY) uygulanmıştır. Bu yöntem ile daha çok kömür bünyesinde bulunan organik kükürt bileşikleri arasındaki C-S, S-S bağlarının zayıflatılması veya kırılması amaçlanmaktadır. Direkt organik kükürdün uzaklaştırılmasına yönelik yapılan çalışmaların sayısı oldukça sınırlı seviyede, olması bu çalışmayı öne çıkarmaktadır. İki aşamada gerçekleştirilen bu çalışmada, birinci aşamada inorganik kükürdün hemen hemen tamamı uzaklaştırılmış, ikinci aşamada inorganik kükürdü uzaklaştırılmış olan kömürden, organik kükürt ETY ile uzaklaştırılmaya çalışılmıştır. Elektron transfer reaktifi olarak çeşitli metalik iyonlarının (Zn^{+2}, Ni^{+2}, Hg^{+2}) organik kükürt uzaklaştırmaya etkileri araştırılmıştır. En yüksek oranda organik kükürdün uzaklaştırılması amacıyla farklı iyon konsantrasyonları (%0,1-5), ortam sıcaklığı (22-90 ^{o}C), reaksiyon süresi (15-240 dak) ve karıştırma hızlarında (300-1300 dev/dak) deneyler gerçekleştirilmiştir. Elde edilen sonuçlardan az da olsa organik kükürdün ETY ile uzaklaştırılabildiği (yaklaşık %3) tespit edilmiştir.

Anahtar Kelimeler: Organik kükürt, elektron transfer yöntemi, kükürt uzaklaştırma

ABSTRACT

Sulfur in coal is caused several serious environmental problems especially in coal combustion and coal-fired power plants. In this study, Electron Transfer Method (ETY) was applied for removal of organic sulfur from Kütahya-Gediz coal. With this method, it is aimed to weaken or break the C-S, S-S bonds between organic sulfur compounds in coal. The reason why this study stands out is that the number of studies on the direct removal of organic sulfur is quite limited. This study was carried out in two stage, in first stage, inorganic sulfur was completely removal and in second stage organic sulfur was attempted to be removed from inorganic sulfur free coal. Different metallic ions (Zn^{2+}, Ni^{2+}, Hg^{2+}) were used as an electron transfer regents/chemicals for removal of organic sulfur. To determination of highest organic desulfurization rate, effect of experimental parameters such as ion concentration (%0,1-5), temperature (22-90 oC), reaction time (15-240 dak) and stirring speed (300-1300 rpm) were investigated. As a result, low level organic desulfurization rate (%3) has been obtained by electron transfer method.

Keywords: Organic Sulfur, Electron Transfer Method, Desulfurization

GİRİŞ

Bütün fiziksel ve kimyasal kükürt uzaklaştırma yöntemlerinde olduğu gibi, Elektron Transfer Yönteminde (ETY) de yapılması gereken ilk işlem, kömürün bünyesinde bulunan kükürt türlerinin

belirlenmesidir. Kömür bilindiği gibi, organik ve inorganik kükürt olmak üzere iki tür kükürt içermektedir. İnorganik kükürdün (pirit, markasit, jibs gibi yapılar) fiziksel kükürt uzaklaştırma yöntemleri ile tamamına yakını uzaklaştırılabilirken, organik kükürdün fiziksel yöntemler ile uzaklaştırılması mümkün değildir. Bu nedenle organik kükürt uzaklaştırmada kimyasal yöntemlerin uygulanma zorunluluğu ortaya çıkmaktadır (Mayers vd. 1972, Atar ve Corcoran 1977, Kawatra ve Eisele 2001, Sütçü 2004, Jorjani vd. 2004, Uzun ve Özdoğan 2006, Mi vd. 2007).

Kömürde bulunan organik kükürdün, aromatik ve alifatik olmak üzere iki grupta toplanması mümkündür. Aromatik ve alifatik kükürt bileşikleri farklı özellikler sergilemekte, bu özellik farklılığı uygulanan kükürt uzaklaştırma yöntemine bağlı olarak uzaklaştırılan kükürt miktarını doğrudan etkilemektedir. Alifatik kükürt bileşiklerinden bazıları arly-alkly, difenil sülfidler ve merkaptanlar sayılabilirken, aromatik kükürt bileşiklerinden bazıları tiofen, benzotiyofen ve dibenzotiyofenler olarak sayılabilir. Bu yapılar incelendiğinde, aromatik kükürt bileşiklerinin, alifatik kükürt bileşiklerine göre kimyasal işlemlere karşı daha yüksek direnç gösterdiği, bu nedenle, uzaklaştırılan kükürt bileşiklerinin içerisinde daha çok alifatik bileşiklerin olduğu görülmektedir. Ayrıca benzer durum kömüre uygulanan ısıl işlem sırasında da karşımıza çıkmaktadır. Alifatik kükürt bileşikleri düşük sıcaklıklarda (>350 ^{o}C) bozunarak deformasyona uğrarlarken, aromatik kükürt bileşikleri daha yüksek sıcaklıklara kadar yapılarını muhafaza ederek, stabil bir durum sergilemektedirler. Aromatik ve alifatik organik kükürt bileşikleri arasındaki bağların kırılması için gerekli enerji birbirinden oldukça farklıdır. C-S bağlarının kırılması için gerekli enerjiler incelendiğinde, aromatik kükürt bileşikleri arasındaki bağı kırmak için gerekli olan enerji, alifatik kükürt bileşiklerindeki bağları kırmak için gerekli olan enerjiden daha fazladır. Bu nedenle kömür bünyesinde bulunan aromatik ve alifatik organik kükürt bileşiklerinin miktarlarının ve özelliklerinin bilinmesi kükürt uzaklaştırmada büyük önem arz etmektedir (Kawatra ve Eisele 2001, Calkins 1994, Van Aelst vd. 1997, Hamamcı vd. 1997, Borah vd. 2001).

Birçok araştırmacı tarafından son zamanlarda, kömürden organik kükürt uzaklaştırma çalışmalarında Elektron Transfer Yöntemi (EYT) uygulanmaktadır. Bu yöntem ile daha çok kömür bünyesinde bulunan organik kükürt bileşikleri arasındaki C-S, S-S bağlarının zayıflatılması veya kırılması amaçlanmaktadır. Daha sonra, dışarıdan ilave edilen metal iyonları ile bağları kırılan bu kükürtlü yapıların yeni bağlar kurmaları sağlanarak, çözünebilir kükürtlü bileşiklerin oluşturulması, böylece kükürdün kömür bünyesinden uzaklaştırılması gerçekleştirilmektedir. Elektron transfer yönteminde, transfer reaktifi olarak Cu^{+}, Sn^{+2}, Ni^{+2}, Co^{+2}, Hg^{+2}, Sb^{+3} gibi iyonlar birçok araştırmacı tarafından kullanılmıştır (Prayuenyong 2002, Jagtap ve Wheelock 1995, Borah ve Baruah 1999, Borah ve Baruah 2000, Srivastava 2003, Borah 2005, Demirbaş 2006, Demir 2011, Demir ve Aydın 2016).

Yapılan kömür analizleri (kimyasal) sonucunda, kömür bünyesinde çeşitli sülfitli yapıların (FeS, PbS, ZnS vs.) varlığının tespit edilmesi, kükürdün metal iyonlarına ilgisinin olduğunu göstermektedir. Kükürt ile metal iyonları, doğal ortamda uygun şartlar oluştuğunda bağ kurmaları, elektron transfer yönteminin doğal şartlarda da oluştuğunu göstermektedir. Bu sülfitli bileşiklerin oluşması: kömür oluşumu esnasında kömürü oluşturan organik kalıntılarda bulunan kükürtlü yapılar, yeraltı sularında bulunan farklı değerliklerde ve farklı tiplerdeki eriyik haldeki metal iyonlarının (Cu^{+}, Sn^{+2}, Zn^{+2}, Ni^{+2}, Co^{+2}, Sb^{+3} gibi) kömür havzasındaki kırık ve çatlaklardan geçerken, uygun şartların oluşması sonucunda, belirtilen sülfid bileşiklerinin oluşmasına neden olduğu, şeklinde açıklanmaktadır. Doğal yollar ile elektron transferinin gerçekleşmesini sağlayan birçok reaktif madde vardır. Bu maddeler çeşitli enzimler, metaloenzimler ve bazı organik maddelerdir, bunlar doğada meydana gelen elektron transferinin sorumlularıdır. Bunların yanında birçok kükürt içeren bileşikler, özellikle amino asitler (cysteine, cystine, methiamine) de elektron transferinde önemli bir rol oynamaktadır. Elektron transferinin gerçekleşmesinde, bu reaktiflerin yanı sıra ortam pH'sı, redox potansiyeli ve metal iyonlarının konsantrasyonları da önem arz etmektedir (Borah ve Baruah 2000, Demir ve Aydın 2016).

Borah ve Baruah (2000) hem tüvenan hem de civa ile muamele edilen yüksek kükürt içerikli Hindistan Meghalaya kömürlerine, farklı sıcaklıklarda yapılan oksidasyon işleminden sonra, elektron

transfer yöntemi uygulanmıştır. En yüksek oranda kükürt uzaklaştırma tüvenan kömürde naftalin varlığında %19.17, civa ile muamele edilmiş kömürde ise %17.78 olarak gerçekleştirilmiştir. Bu yöntem uygulanarak tüvenan kömürde organik kükürdün %27.38'i uzaklaştırılabilirken, civa ile muamele edilmiş kömürde bu oran %28.45 olarak tespit edilmiştir. Yazarlar Hg ile naftalinin kullanılması, kükürt uzaklaştırma işlemi üzerinde önemli bir etkisinin olmadığını ifade etmişlerdir. Borah ve diğ. (2001) baska bir çalışmalarında aynı yöre kömürünü kullanarak civanın kükürt uzaklaştırmaya olan etkilerini araştırmışlardır. Civanın hem oksitlemeyi hızlandırdığı hem de kükürt uzaklaştırmada etkili bir madde olduğu ifade edilmektedir. Kükürde yüksek afiniteye sahip olduğu belirtilen civa, C-S arasındaki bağları zayıflattığı ve kükürt uzaklaştırma verimini arttırdığı ifade edilmiştir. Borah ve Baruah (1999) ve Borah (2005) 'de yaptıkları çalışmalarında farklı metal iyonlarının (Cu^{+}, Co^{2+}, Ni^{2+}, Sn^{2+} ve Sb^{3+}) organik kükürdün bünyeden uzaklaştırılmasındaki etkileri incelenmiştir. Srivastava (2003) farklı oranlarda kükürt ve kül içeren 12 Hindistan kömürlerinden, mineral madde ve kükürt uzaklaştırmak amacıyla demir sülfat ($Fe_2(SO_4)_3$) kullanmış, yaptığı bu çalışma ile oldukça ince boyut dağılımına sahip olan piritin %90'nından fazlasının uzaklaştırılabildiğini ifade etmiştir. $Fe_2(SO_4)_3$ kullanmasının nedeni olarak da pirite selektif olarak etki etmesi ve geri kazanılabilmesinin kolay olması gösterilmiştir.

Yapılan bu çalışmada, son zamanlarda çeşitli araştırmacılar tarafından uygulanmaya başlanan ETY ile Gediz yöresi kömürlerinde bulunan organik kükürdün Zn^{+2}, Hg^{+2} ve Ni^{+2} iyonları kullanılarak uzaklaştırılabilirliği araştırılmıştır. Organik kükürdün uzaklaştırılmasında farklı çalışma parametrelerinin (iyon konsantrasyonu, ortam sıcaklığı, işlem süresi vs.) etkilerinin belirlenmesi amacıyla sistematik deneyler gerçekleştirilmiştir.

DENEYSEL ÇALIŞMALAR

Malzeme

Deneysel çalışmalarda kullanılan kömür numuneleri, Kütahya merkeze yaklaşık 90 km ve Gediz ilçe merkezine yaklaşık 25 km mesafedeki Gökler kasabasında faaliyet gösteren özel bir şirkete ait kömür ocağından alınmıştır. Temsili olarak alınan kömür numuneleri deneysel çalışmalarda kullanılmak üzere boyut küçültme işlemine tabi tutulmuş, azaltma işlemi uygulanmış ve özelliklerinin değişmesinin engellenmesi amacıyla hava geçirmez kilitli poşetlerde depolanmıştır.

Gediz yöresi kömürleri üzerinde yapılan kısa analiz sonuçları Çizelge 1'de, elementer analiz sonuçları ise Çizelge 2'de verilmiştir. Çizelge 1 incelendiğinde yöre kömürlerinin %7,06 toplam kükürt içeriğine sahip olduğu, bu kükürdün ise yarıya yakınının (%2,89) organik kökenli olduğu görülmektedir. Ayrıca, yöre kömürlerinin yüksek oranda kül içermesine (%25,99) rağmen ısıl değerinin (5607 kcal/kg) yüksek olduğu belirlenmiş (Çizelge 1), bu hali ile yöre kömürleri yapılan petrografik incelemeler sonucu organik yapının büyük bir bölümü vitrinitten (%87) oluştuğu, vitrinit zemin üzerinde inertinit ve az miktarda eksinit olduğu belirlenmiş, ayrıca alt bitümlü kömür sınıfına (Rmax: 0,576) girdiği tespit edilmiştir. Şekil 1'de Gediz yöresi kömürlerinin taramalı elektron mikroskop (SEM) ile 20000 kez büyütülmüş görüntüsü görülmektedir. Şekil 1'den de görüldüğü üzere yöre kömürleri çok ince boyutta pirit tanecikleri içermektedir. Piritin büyük bölümü kömür parçaları içinde kenetli halde, az miktarda kükürt serbest taneler halinde bulunmaktadır. Piritler, kürecikler halinde, öz ve yarı-öz şekilli taneler halinde kendini göstermektedir. Bu pirit taneciklerinin serbestleşme boyutu ise yaklaşık 1-2 mikron civarındadır. Bu kadar ince boyutta serbestleşen piritik kükürdün fiziksel yöntemler ile uzaklaştırılabilmesi mümkün görülmemektedir. ETY reaktifi olan metalik iyonlar ($NiCl_2$, $HgCl_2$ ve $ZnCl_2$) çözelti halinde kullanılmıştır.

Çizelge 1**.** Deneysel çalışmalarda kullanılan kömür numunesinin kısa analiz sonuçları

Kısa analiz	**(%)**
Nem	3,3
Kül	25,99
Uçucu madde	32,81
Sabit Karbon	37,90
Alt Isıl Değer	5607 kcal/kg

Çizelge 2. Deneysel çalışmalarda kullanılan kömür numunesinin elementer analiz sonuçları

Elementer Analiz	**(%)**
Karbon	78,41
Hidrojen	5,12
Azot	1,61
Oksijen (farktan)	7,8
Toplam Kükürt	7,06
Organik Kükürt	2,89
Piritik Kükürt	3,55
Sülfat Kükürdü	0,62

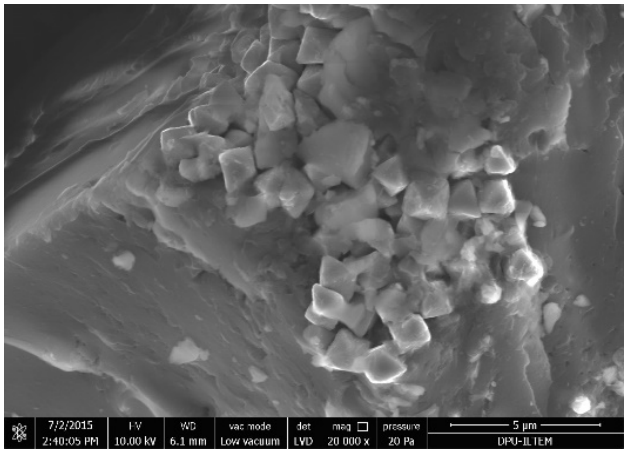

Şekil 1. Gediz yöresi kömürlerinin SEM görüntüsü (20000 kez büyütülmüş)

Yöntem

Gediz yöresi kömürlerinden organik kükürdün (%2,89) uzaklaştırılması için iki aşamalı bir çalışma gerçekleştirilmiştir. Birinci aşamada, kömür bünyesinde bulunan inorganik kükürdün (piritik ve sülfat kükürdü) hemen hemen tamamı uzaklaştırılmıştır. Bu amaçla belirlenen tane boyutuna öğütülen (-212 mikron) kömür numunesi, %30 nitrik asit (HNO_3)- %30 hidroklorik asit (HCl) karışımı ile belirlenen sürede (60 dakika) muamele edilmiş, bu işlem sonunda oluşan kömür-kimyasal karışımı süzülmüştür. Süzme işlemi sonrasında kömür numunesi içerisinde asidik çözelti bütünüyle temizleninceye kadar sıcak saf su ile defalarca yıkanmış ve etüvde kurutulmuştur. Uygulanan bu işlem ile kömür bünyesinde bulunan piritik ve sülfat kükürdünün hemen hemen tamamı (%3,55), organik kükürdün ise küçük bir bölümü uzaklaştırılmıştır. Etüvde kurutulan inorganik kükürdü uzaklaştırılmış kömür numunelerine ikinci aşama olan Elektron Transfer Yöntemi (ETY) uygulanmıştır. Bu aşamada 2 gr kömür numunesi ile metalik iyonlar ($NiCl_2$, $HgCl_2$, $ZnCl_2$ bileşikleri) çözelti halinde kullanılmıştır. 250 ml hacimli beher içerisinde karıştırılan

kömür numunesi ve iyon çözeltisi, ısıtıcılı manyetik karıştırıcı kullanılarak önceden belirlenen çalışma şartlarında (Çizelge 3) kimyasal işleme tabi tutulmuştur. Kimyasal işlem tamamlandıktan sonra karışım filtre kağıdı kullanılarak katı kısım sıvı kısımdan ayrılmıştır. Katı kısım sıcak saf su ile yıkandıktan sonra etüvde kurutulmuş (105 ^{o}C) ve gerekli analizler (kül, kükürt) standartlara uygun (ASTM D3174, ASTM D3177) olarak yapılmıştır. Çizelge 3'de deneysel çalışmalarda etkileri araştırılan çalışma parametreleri ve çalışma aralıkları verilmiştir.

Çizelge 3. Deneysel çalışmalarda uygulanan çalışma parametreleri

Çalışma Parametreleri	**Değerler**
İyon konsantrasyonu (%)	0.1, 1, 2, 3, 5
Kimyasal işlem süresi (dakika)	15, 30, 60, 90, 120, 240
Ortamın sıcaklığı (^{o}C)	22, 35, 70, 90
Karıştırılma hızı (dev/dk)	300, 500, 750, 1000, 1300
Tane boyutu (mikron)	-212

SONUÇLAR VE TARTIŞMA

İyon Konsantrasyonunun Etkisi

Gediz yöresi kömürlerinden organik kükürdün uzaklaştırılması amacıyla %0.1, 1, 2, 3 ve 5 arasında değişen konsantrasyonlarda $ZnCl_2$, $NiCl_2$ ve $HgCl_2$ çözeltileri kullanılarak çeşitli deneyler gerçekleştirilmiş ve elde edilen sonuçlar Şekil 2'de verilmiştir. %7,06 oranında toplam kükürt içeren yöre kömürlerinden, yöntem kısmında belirtilen birinci aşama işlem sonucunda %2,82 oranında organik kükürt içeren ürün (inorganik kükürt içermeyen) elde edilmiştir. Yapılan bu işlem ile inorganik kükürdün tamamı, organik kükürdün ise küçük bölümünün uzaklaştırıldığı belirlenmiştir. İkinci aşama kükürt uzaklaştırma işlemi, %2,82 oranında organik kükürt içeren kömür numunesi üzerinde yapılmıştır. Elde edilen sonuçlar incelendiğinde artan iyon konsantrasyonlarına bağlı olarak kükürt içeriğinde düşük seviyelerde de olsa sürekli bir azalmanın olduğu görülmektedir. Organik kükürt uzaklaştırma oranları incelendiğinde ise oranın oldukça düşük seviyelerde seyrettiği görülmektedir. ETY sonucunda elde edilen ürünlerin kükürt uzaklaştırma oranları $ZnCl_2$ ile % 2,77-2,82 arasında, $NiCl_2$ ile %2,71-2,78 arasında, $HgCl_2$ ile 2,85-2,88 arasında olduğu belirlenmiştir. Elde edilen ürünlerin kükürt uzaklaştırma oranlarının birbirlerine bu kadar yakın olmaları dikkate alındığında her üç iyon için %1 iyon konsantrasyonunun uygun olduğuna karar verilmiştir. Uzaklaştırılan organik kükürt oranlarındaki düşüklük, organik kükürt bileşikleri arasındaki C-S ve S-S bağların yeteri kadar zayıflatılıp, kırılamamasından kaynaklanabileceği görüşüne varılmıştır.

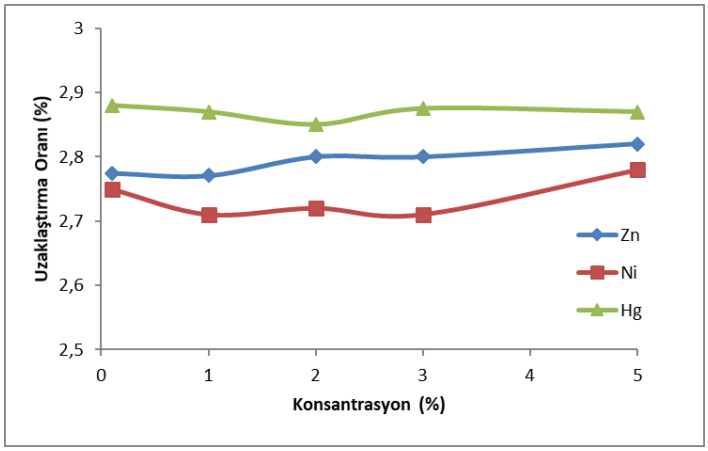

Şekil 2. İyon konsantrasyonunun kükürt uzaklaştırmaya etkisi

Kimyasal İşlem Süresinin Etkisi

Elektron transfer yönteminde, kimyasal işlem süresinin organik kükürt uzaklaştırmaya etkisini belirlemek amacıyla 15, 30, 60, 90, 120 ve 240 dakika sürelerde deneyler yapılmış ve elde edilen sonuçlar Şekil 3'de verilmiştir. Şekil 3 incelendiğinde kömür numunelerinin kükürt uzaklaştırma oranlarında çok küçük değişimler meydana gelmiştir. Kükürt uzaklaştırma oranları incelendiğinde artan süreye bağlı olarak Ni^{+2} iyonu için uzaklaştırılan kükürt oranında önce bir miktar artış gözlenmiş, devam eden işlem süresindeki artış organik kükürt uzaklaştırma oranın bir miktar azalmasına, Zn^{+2} iyonunun süreye bağlı olarak önemli bir değişimine neden olmadığına, Hg^{+2} iyonu ise süre artışına bağlı olarak önce bir miktar azalmaya, devam eden süre artışı ile uzaklaştırılan kükürt miktarında az da olsa bir artışın meydana geldiği gözlenmiştir. 240 dakikalık kimyasal işlem süresinde en yüksek oranda kükürt uzaklaştırılabilmiş fakat diğer sürelerde elde edilen kükürt uzaklaştırma oranları arasında çok bariz bir farkın olmaması nedeniyle her üç iyon içinde 30 dakikalık sürenin en uygun olduğu belirlenmiştir. Uzaklaştırılan organik kükürt oranlarındaki düşüklük daha önce de belirtildiği gibi, organik kükürt bileşikleri arasındaki C-S ve S-S bağlarının yeteri kadar deformansyona uğramamasından kaynaklanmaktadır.

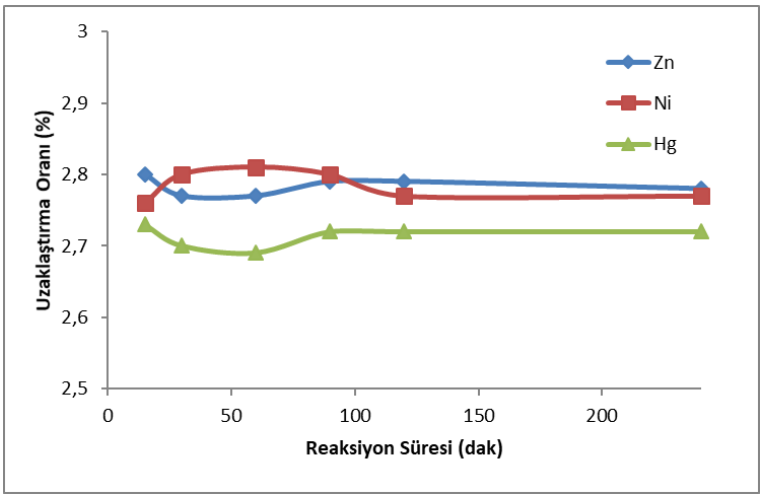

Şekil 3. Kimyasal işlem süresinin kükürt uzaklaştırmaya etkisi

Ortam Sıcaklığının Etkisi

Gediz yöresi kömürlerinden organik kükürdün uzaklaştırılmasında ortam sıcaklığının etkisinin belirlenmesi amacıyla farklı sıcaklıklarda (22, 35, 70 ve 90 ^{o}C) deneyler gerçekleştirilmiş ve elde edilen sonuçlar Şekil 4'de verilmiştir. Şekil 4 incelendiğinde, artan ortam sıcaklığı kömür numunelerinin kükürt içeriklerinde çok az bir değişimin olmasına neden olmuş, kükürt uzaklaştırma oranlarında ise yine artan ortam sıcaklığına bağlı olarak değişimin çok sınırlı seviyelerde olduğu gözlenmiş, 90 ^{o}C ortam sıcaklığında Zn+2 ile yapılan deneylerde artışın olduğu görülürken, diğer iyonlarda çok az bir değişimin olduğu belirlenmiştir (%2,7-2,9). Elde edilen sonuçların birbirlerine çok yakın olması nedeniyle oda sıcaklığının (22 ^{o}C) her üç iyon için de en uygun sıcaklık olduğuna karar verilmiştir.

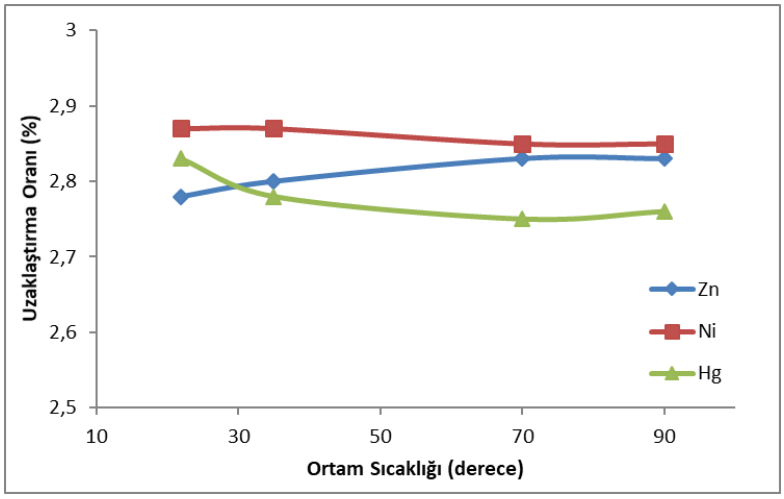

Şekil 4. Ortam sıcaklığının kükürt uzaklaştırmaya etkisi

Karıştırma Hızının Etkisi

Kimyasal işlemlerde reaksiyon hızının arttırılması ve kimyasal ile malzemenin daha fazla etkileşimini sağlamak amacıyla ortamın karıştırılması sıkça uygulanan bir durumdur. Bu nedenle yöre kömürlerinden organik kükürdün uzaklaştırılmasında karıştırma hızının etkisini belirlemek amacıyla farklı karıştırma hızlarında (250, 350, 500, 600 dev/dk) deneyler gerçekleştirilmiş ve elde edilen sonuçlar Şekil 5'de verilmiştir. Şekil 5 incelendiğinde, karıştırma hızının, kükürt uzaklaştırmada etkili bir parametre olmadığı görülmektedir. Artan karıştırma hızına bağlı olarak kömür numunelerinin kükürt içerikleri her üç kimyasal için neredeyse birbirine çok yakın seviyelerde kaldığı tespit edilmiştir. Kükürt uzaklaştırma oranları incelendiğinde ise artan karıştırma hızı ile birlikte çok küçük bir miktar artışın olduğu görülmektedir. Bu durum düşük karıştırma hızlarının kükürt uzaklaştırma için yeterli olabileceğini göstermiştir. Optimal karıştırma hızı olarak 250 dev/dk seçilmiştir.

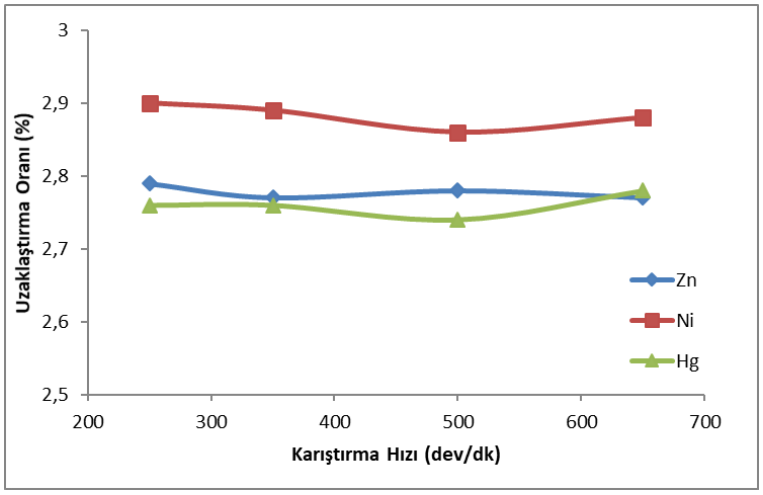

Şekil 5. Karıştırma hızının kükürt uzaklaştırmaya etkisi

SONUÇLAR

Gediz yöresi kömürlerinden organik kükürdün uzaklaştırılmasında ülkemizde fazla uygulama alanı bulamamış olan Elektron Transfer Yöntemi uygulanmış, bu amaçla $ZnCl_2$, $NiCl_2$ ve $HgCl_2$ tuzlarının çözeltileri kullanılmıştır. Her üç iyon ile yapılan deneylerde; %1 iyon konsantrasyonu, 30 dakikalık

kimyasal işlem süresi, oda sıcaklığı (22 ^{o}C) ve 250 dev/dk karıştırma hızlarında %2,8-2,95 oranları arasında organik kükürdün uzaklaştırılabileceği tespit edilmiştir. Bu sonuçlar değerlendirildiğinde $ZnCl_2$, $NiCl_2$ ve $HgCl_2$'nin organik kükürt uzaklaştırmada beklenen etkiyi gösteremediği belirlenmiştir. Bu durumun kömür bünyesindeki organik kükürt bileşiklerinin kuvvetli bağlar ile birbirine bağlı olduğu (C-S ve S-S) ve bu bağlarının yeteri kadar kırılamamasından kaynaklandığı tahmin edilmektedir. Gediz yöresi kömürlerinin içerdiği organik kükürdün, kimyasal işlemlere karşı daha fazla direnç sergilediği belirlenmiş, yöre kömürlerinin kalitesinin (alt bitümlü) linyitlere göre daha yüksek olduğunu petrografik analizlerle de ortaya koyulmaktadır.

Organik kükürdün uzaklaştırılmasında kullanılan Elektron Transfer Yönteminin düşük sıcaklık ve atmosfer basıncı altında uygulanması istenilen etkinin elde edilememesine neden olmuş, bu nedenle yüksek basınç ve sıcaklık şartlarında bu yöntemin yeniden denenmesi gerektiği düşünülmektedir.

TEŞEKKÜR

Bu çalışma, Dumlupınar Üniversitesi 2011-17 nolu Bilimsel Araştırma Projesi kapsamında desteklenmiştir.

KAYNAKLAR

Atar A., Corcoran, W., H., (1977), Sulfur compounds in coal, Ind. Eng. Cehm. Prod. Res. Dev. Vol:16 No: 2, 168-170

Aydın A., Demir U., (2013), Kütahya-Gediz kömürlerinin elektron transfer yöntemi ile kükürdünün uzaklaştirilmasi. Dumlupınar Üniversitesi, Bilimsel Araştırma Projesi, Proje No: 2011-17

Borah D., (2005), Desulphurization of organic sulphur from coal by electron transfer process with CO^{2+} ion. *Fuel Processing Technology, Vol: 86*, 509-522

Borah D., Baruah, M., K., (1999), Electron transfer process 1. removal of organic sulphur from high sulphur indian coal, *Fuel, Vol: 78*, 1083-1088

Borah D., Baruah, M.,K., Haque, I., (2001), Oxidation of high sulphur coal. Part 1. Desulphurization and evidance of the formation of oxidised organic sulphur species, *Fuel, Vol: 80*, 501-507

Borah D., Baruah, M.K. (2000), Electron transfer process. Part 2. Desulphurization of organic sulphur from feed and mercury-treated coals oxidized in air at 50, 100 and 150 ^{o}C , *Fuel, Vol:79*, 1785-1796

CalkinsW., H., (1994) ,The Chemical forms of sulfur in coal: a review, *Fuel, Vol: 73* No: 4, 475-484

Demir U., (2011), Kütahya-Gediz yöresi kömürlerinden kükürdün uzaklaştirilmasi, Doktora Tezi, Dumlupınar Üniversitesi, Fen Bilimleri Enstitüsü, Kütahya.

Demir U., Aydın A., (2016), Desulfurization of high sulfur coal by electron transfer method, XV. Mineral Processing Symposium, IMPS 2016, Istanbul, Turkey 19-21 October 2016

Demirbaş A., (2006), desulfurization of organic sulfur from lignite by an eletron transfer process, *Energy Sources Part A, Vol: 28,* 1295-1301

Hamamcı C., Kahraman,F. Düz, M. Z., (1997), Desulfurization of Southeastern Anatolian asphaltites by the meyers method, *Fuel Processing Technology, Vol: 50*, 171-177

Jagtap S.B. ,Wheelock, T.D., (1995) Coal desulfurization by ferric chloride, *Fuel Processing Technology Vol: 43* 227-242

Jorjani E,. Rezai B., Vossoughi M., Osanloo M., Abdollahi M., (2004), Oxidation pretreatment for enhancing desulfurization of coal with sodium butoxide ,*Minerals Engineering, Vol: 17*, 545-552

Kawatra S.K., ve Eisele T.C. (2001), Coal desulfurization: High-efficiency preparation methods, Printed by Edwards Brothers, Ann Arbor, Taylor & Francis Inc. 349p.

Mayers R.,A., Hamersm J. W., Land, J. S., Kraft M. L., (1972), Desulfurization of coal, *Science, Vol: 177*, 1187-1188

Mi J., Ren J,. Wang J.C,. Bao W.R,. Xie K.C,. (2007), Ultrasonic and microwave desulfurization of coal in tetrachloroethylene, *Energy Sources, Part A, Vol: 29*, 1261-1268

Prayuenyong P., (2002), coal biodesulfurization processes, *Songklanakarin J. Science Technology, Vol:24*, No: 3, 493-507

Srivastava S., K., (2003), Recovery of sulphur from very high ash fuel and fine distributed pyritic sulphur containing coal using ferric sulphate , *Fuel Processing Technology, Vol: 84*, 37-46

Sütçü H., (2004), Coal desulfurization using natural ca-based sorbents, *Coal Preparation, Vol. 24*, 249-259

Uzun D., Özdoğan S., (2006), Sulfur Removal from Original and Acid Treated Lignites by Pyrolysis , *Fuel, Vol: 85*, 315-322

Van Aelst J., Ypermanan J., Franco D. V., Mullens J., Van Poucke L., C., and Palmer S., R., (1997), Sulphur distribution in Illinois No. 6 coal subjected to different oxidation pre-treatments , *Fuel Vol: 76*, 1377-1381

EMPLOYING THE MINERALOGICAL DATA FOR SELECTING THE BEST BENEFICIATION METHOD FOR A REFRACTORY GOLD ORE

S. Gökdemir [1,*], B. Töngür [1], B. Aksanı [1], A. Harzanak [1]

[1] *Demir Export A.Ş*
*(*Corresponding author: senag@demirexport.com)*

ABSTRACT

The aim of this study is to employ the data gathered from gold deportment studies in order to select the most appropriate beneficiation method for a gold ore. Detailed core logging and mineralogical studies indicated that the resource comprised of oxidized, transition and sulfide ore zones. According to gold deportment studies, native gold grains were observed as free and/or associated with sulfides both in sulfide and transition ore zones while it is free or attached to iron oxide (mainly goethite) in the oxide zone. According to geometallurgical approach, it is important to have an insight about the recoverable metal as well as the method of the beneficiation, besides the grade and the quantity. Based on geological and mineralogical studies, experimental test plan was designed to select the most efficient beneficiation scenario. Preliminary flotation test was performed for these three ore zones separately. Based on the preliminary results, froth flotation would appear to be a proper method as pre-concentration of gold especially for sulfide and transition ore zones.

Keywords: Refractory gold, flotation, pyrite and pre-concentration

INTRODUCTION

Gold, which has attracted people attention since ancient times, is a brightly colored metal used in many industries because of its resistance to different conditions and easiness to process. The world's oldest gold producers are the Egyptians. In 5000 BC, they started to extract gold, which was alloyed with copper, from underground (Yücel M.B., 2020). Gold can be found in nature as native, electrum, tellurium, solid solution, and inclusion in other minerals. Gold deposits are classified in different ways according to the formation temperature, the rocks in which it is located, the mineralogical structure of the ore, other elements found with gold and the geodynamic environment in which the deposits are formed (Yücel M.B., 2020).

Nowadays, due to the scarcity of high-grade and easily enriched gold ore deposits, the interest on low-grade and refractory gold ore deposits are increased. According to the literature, if the gold recovery is lower than 80-90% in the standard cyanidation process, it is identified as refractory (La Brooy S., Linge H., 1994). According to La Brooy and Linge (1994), the refractoriness of gold is classified as follows:

Gold Recovery: < 50% High Refractory
Gold Recovery: 50% - 80% Medium Refractory
Gold Recovery: 80% - 90% Light Refractory
Gold Recovery: > 90% Non-Refractory

Sulfide gold bearing ores, e.g., pyrite and arsenopyrite, are becoming the most important gold sources. Typically, the gold is encapsulated or finely disseminated in these minerals and the direct cyanidation is not usually effective for gold extraction, even after the ore is ground to ultrafine size. In order to increase the gold recovery from refractory sulfide gold ores, oxidation pretreatment technologies such as pyrometallurgical, bio-metallurgical and hydrometallurgical processes were proposed. These techniques transform sulfides into oxides or sulfates thus, gold is exposed to be leached by cyanide easily.

In the case of complex ore bodies, typical assay-based block model appears to be inadequate. Because it doesn't contain information about processing method of different zones, expected recovery from the blocks and environmental issues related to whole project. Combining the various information about the resource e.g., elemental assays provided from the drill hole samples, core logging information, detailed gold deportment study, grinding test works, gravity/flotation/leach test results etc. these studies will be helpful in providing a comprehensive geometallurgical block model. This model will forecast the processing method of every zone as well as approximate gold recovery from of each block, actual cut of grade and finally the profitability of the whole project.

The Gold deportment studies are the key tools in gold processing development and its optimization (Beyuo & Agorhom, 2021). Modern gold deportment studies include physical, chemical and mineralogical assessments, combined to obtain a full understanding of the nature and variability of gold in a resource. The main aim of a gold deportment analysis is to locate and describe gold containing particles in order to determine the gold speciation, grain size and mode of occurrence (gold liberation, exposure, and mineral associations) as well as to generally characterize the mineralogical composition of the ore (Coetzee et al., 2011).

The aim of this study is to employ the data gathered from gold deportment studies in order to select the most appropriate beneficiation method. This manuscript will be started with sharing geological and mineralogical information about the ore body followed by definition and results of the metallurgical test works and finally discussion of the results.

GEOLOGICAL AND MINERALOGICAL STUDIES

According to observations and chemical studies, the gold concentration was identified in the quartz veins and, its geometry has been determined the geometry of the ore-bearing zones. Gathering information from the geochemical and the core logging studies, the oxidized zone is close to the surface and followed by transition and sulfide zones (Figures 1 and 2).

Figure 1. The Exploration Area and geological studies

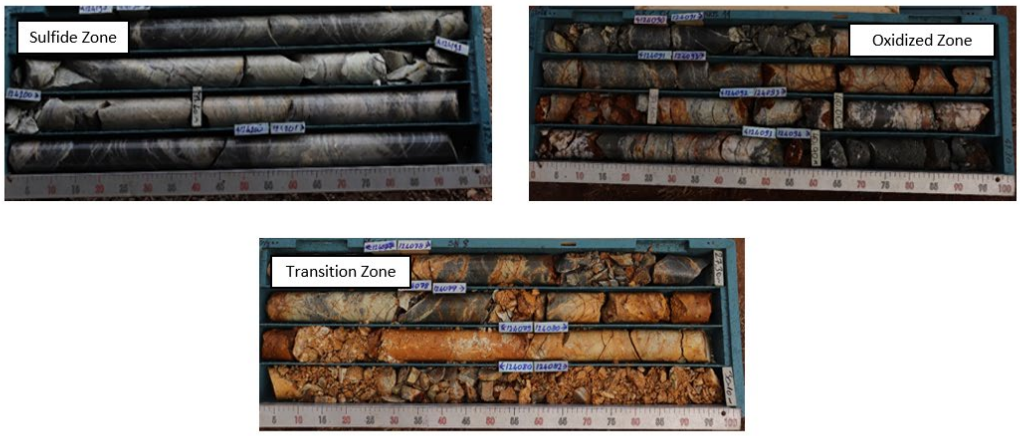

Figure 2. Drill cores taken from the zones

Based on chemical analysis of the core samples, logging studies, 3D geology-ore solid model and resource estimation studies the resource comprised of over 87% sulfide and transition zones and around 12% oxidized zone (Figure 3).

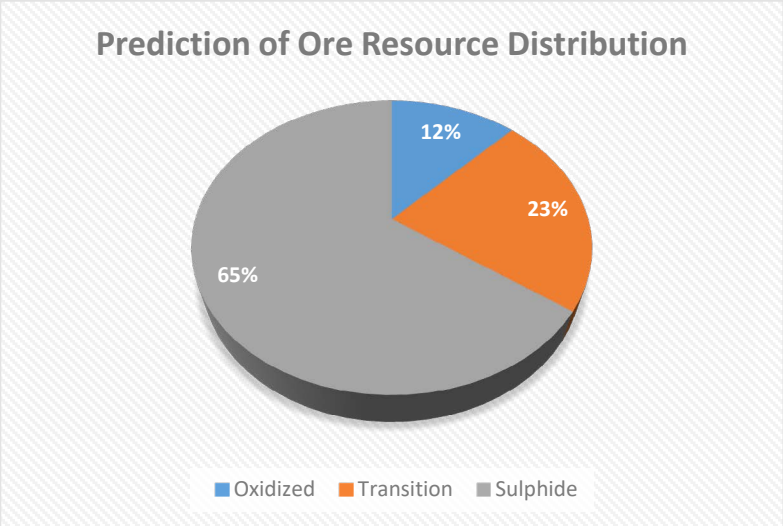

Figure 3. Prediction of ore resource distribution

In order to represent ore zones, eight samples (Table 1) were taken from different drilling holes based on their classification and depth. The gold deportment studies performed for these samples which consisted of the following steps;

1. *Assaying:* a process used to determine proportions of precious metals in ores and other industrial raw material substances.
2. *QXRD:* to determine the general mineralogy.
3. *Microscopy*: to identify & characterize gold minerals by type, grain size and association.
4. *SEM/EDX*: to determine the composition of gold grains
5. *D-SIMS:* to quantify submicroscopic gold

Table 1. The distribution of sample according to ore types

Ore Type	**Samples**
Sulfide	KT-02, KT-03, KT-06
Transition	KT-01, KT-04, KT-07
Oxidized	KT-05, KT-08

According to gold deportment, native gold grains were observed free and associated with sulfides in sulfide and transition ore zones while gold is free or attached to iron oxide ore (mainly goethite). Pyrite is the principal sulfide mineral in the sulfide ore samples whereas arsenopyrite was observed in minor quantities. Both pyrite and arsenopyrite carry gold, in the form of associated gold grains and solid solution gold. Pyrite is the most important carrier because of its greater abundance over arsenopyrite. The very large majority of the gold with sulfides is carried by particles of floatable size, >10µm free sulfides. Free sulfides <10µm carry only minor gold. In oxide and transition ores, goethite was the principal iron oxide minerals. Hematite was observed much rarer. Iron oxide minerals carry gold as associated gold grains and submicroscopic gold (colloidal-size micro-inclusions).

Figure 4 summarizes the free and attached gold distribution in various ore samples within the froth flotation perspective. Based on this information, flotation would be the preferred processing option for the

sulfide and the transitions ores. Gold recovery is promoted by the good floatability of free sulfides and free gold >10µm; and limited by the presence of difficult to float fine free gold and gold association with FeOx and rock in the transition ores.

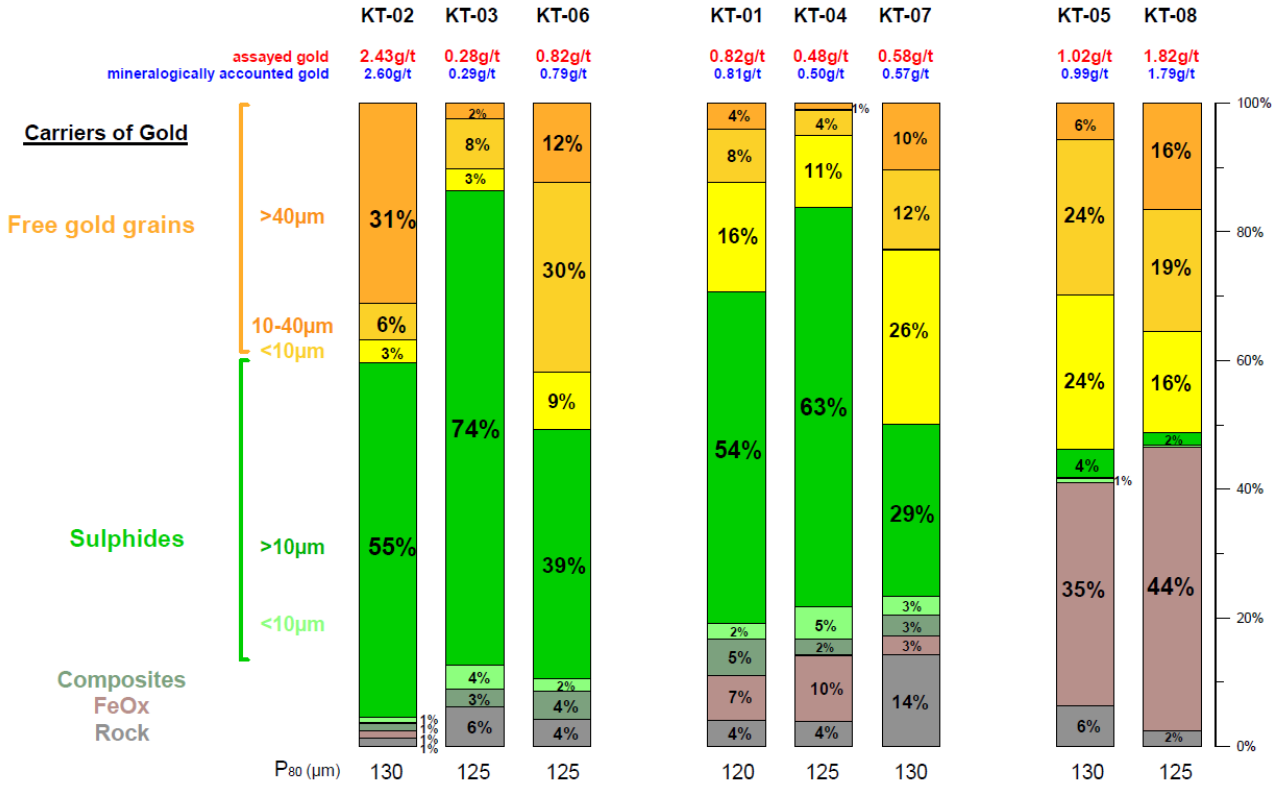

Figure 4. Deportment of gold – flotation perspective

From the leaching perspective (Figure 5), gold was divided into: exposed cyanidable (free and attached gold grains), enclosed cyanidable (gold grains cyanidable after fine grinding) and refractory (gold which cannot be recovered by direct cyanidation). Refractory gold can only be recovered by pressure and bio-oxidation.

Based on the findings and the amount of refractory gold, it seems that direct cyanidation would not be an efficient extraction method especially in the case of sulfide and transition ores. However, oxide ores seem to be appropriate for direct cyanidation especially in the fine particle size distributions. Pre-concentration methods like gravity separation and flotation can also be considered to reduce throughput and reagent efficiency.

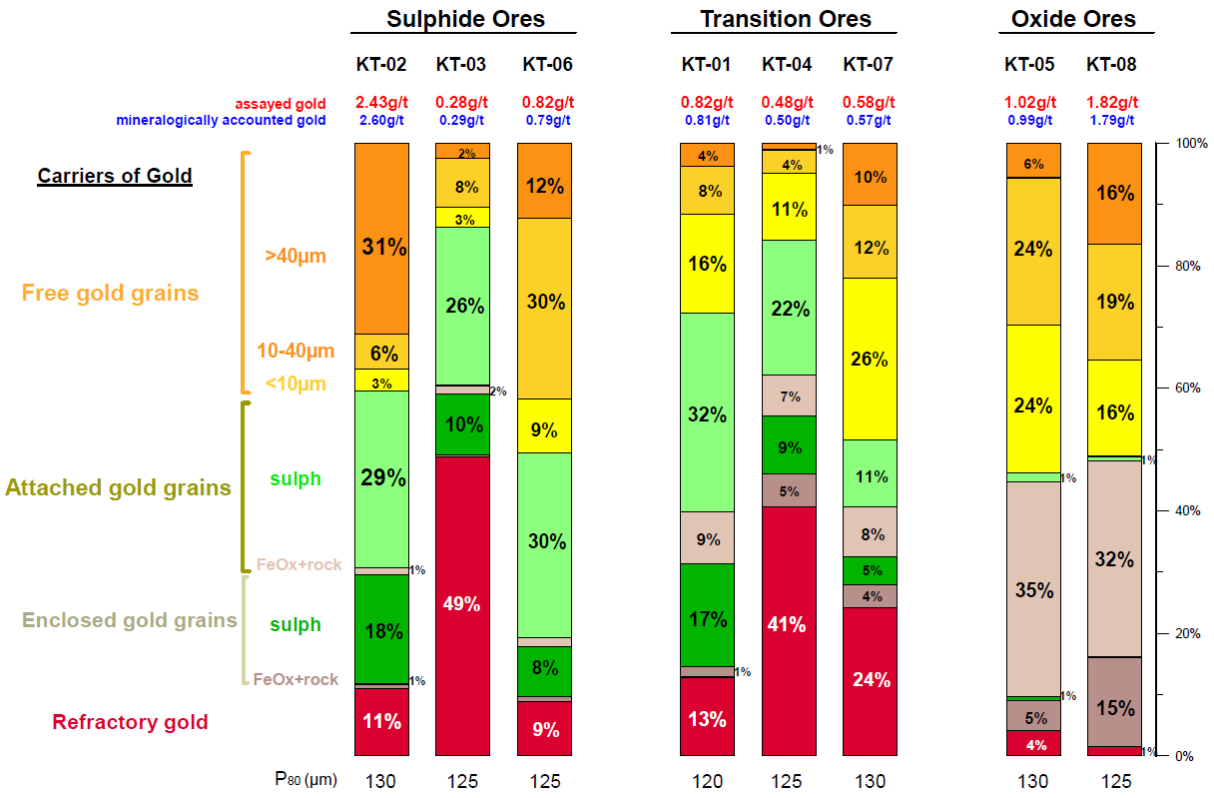

Figure 5. Deportment of gold - cyanide leach perspective

METALLURGICAL STUDIES

Based on obtained information from geological and mineralogical studies, an experimental test plan was designed in order to select the most efficient beneficiation scenario and then the samples were taken from different ore zones. The basis of the sample selection was relied on chemical analyses and macroscopic observations. The ore samples were crushed (%100 passing 2 mm) and divided into representative sub-samples for subsequent processing studies.

Sulfide Zone

Around 180 kg of core samples (equivalent to 113 m) with average 0.87 g/t Au content was taken from different six drilling holes of the sulfide zone.

To investigate the effects of grinding time on flotation performance, three tests were performed employing the lab-scale Denver type flotation machine using xanthate and MIBC as collector and frother, respectively. Based on available lab facilities, Samples were ground using the lab-scale rod mill for 15, 20 and 25 minutes. P80 (%80 passing sieve size) of the samples are 63.4, 53.8 and 44.1 µm, respectively. In the tests 2 kg/t of sodium silicate (Na_2SiO_3) were used as dispersant at the grinding stage. After 5 minutes conditioning with potassium amyl xanthate and MIBC, flotation was commenced and continued for 10 minutes. Figure 6 shows the effect of fineness of the feed on flotation recovery and concentrate grade.

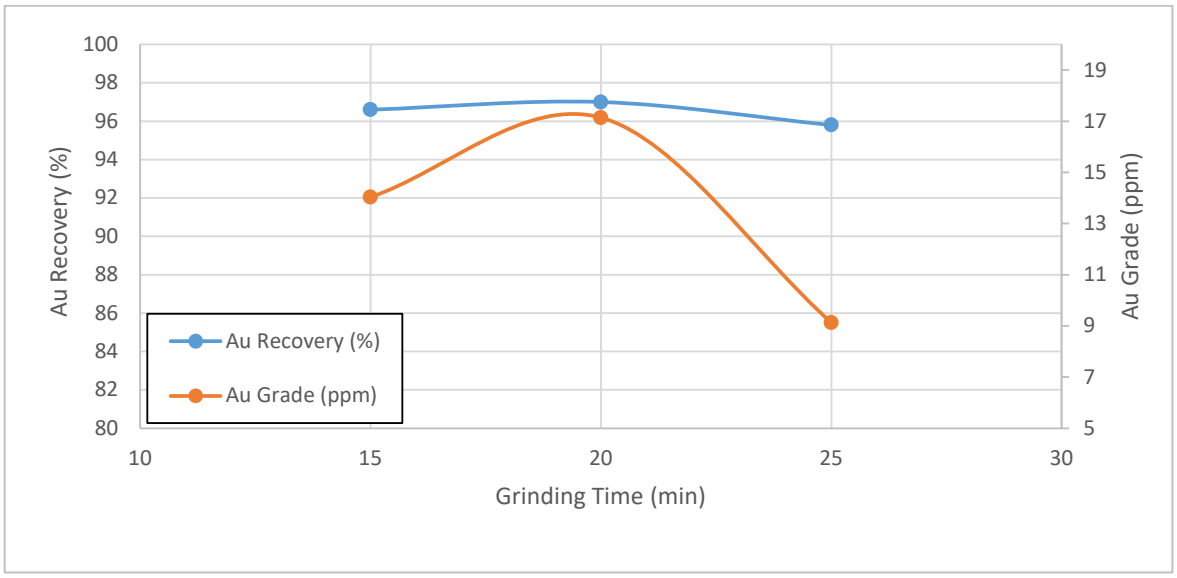

Figure 6. Flotation recovery and concentrate grade of sulfide zone

According to the results, there is not a major improvement of the gold recovery, however, increasing the grinding time reduces the concentrate grade presumably the entrainment of fine gangue particles into the concentrate.

In order to investigate the effect of copper sulfate which is widely used as activator for the sulfide minerals, two flotation tests were performed in the presence and the absence of copper sulfate. Table 2 shows the negative effects of adding $CuSO_4$ in both gold grade and recovery.

Table 2. Effects of CuSO4 addition on gold grade and recovery

%	With CuSO4	Without CuSO4
Au Grade	15.5	17.1
Au Recovery	94.5	97.0

For selecting the best collector types, five different batch flotation tests were performed adding special collectors which are well known with their positive effects on gold flotation and their combinations while keeping other variables were constant (Table 3).

Table 3. Effect of various collector type on flotation performance

%	PAX	SIPX	PAX+Aero 8055	PAX+MaxGold
Au Grade	15.5	10.8	9.4	4.3
Au Recovery	94.5	93.3	70.0	21.6

According to test results, the best flotation performance is obtainable using PAX (Potassium amyl xanthate) although SIPX is also suitable in term of recovery, but the concentrate grade is lower than the one with PAX. Combination of PAX as primary collector with other secondary collectors, did not give better results especially in the case of Maxgold 900.

Aforementioned test works were applied in the natural pH of the pulp (9-9.5) which is slightly alkaline. On the other hand, xanthate type collectors known to show better performances in the case of iron sulfides based on the surface charge of the mineral in the natural pH conditions. For examining the effect of pulp pH on the flotation performance, a comparative test work was applied using sulfuric acid for pH adjustment to the natural-slightly acidic condition (5.5-6). Unexpectedly, the results (Table 4) demonstrate a notable decline in both gold recovery and grade.

Table 4. The graph shows result of flotation recovery and grade in asidic condition

%	pH 6-6.5	pH 9-9.5
Au Grade	3.0	17.1
Au Recovery	36.6	97.0

Based on mineralogical and experimental findings, obtaining a rougher flotation concentrate with 5-6% mass pull, up to 97% gold recovery with 17 g/t Au grade is possible. Additional flotation tests would be required including cleaning stages.

Transition Zone

Around 264 kg of core samples (equivalent to 101 m) were taken from eight holes of the transition zone and crushed to minus 2mm and divided to 1 kg subsamples. The head assay of gold in prepared sample was analyzed as 1.16 g/t. For gaining information about the grindability of the ore sample, three samples were grinded using lab-scale rod mil for 15, 25 and 30 minutes. P_{80} (%80 passing sieve size) of ground samples was calculated as 62.3, 41.1 and 33.6 microns respectively.

For examining the effect of grinding time on flotation performance, four tests were performed employing the lab-scale Denver type flotation machine using potassium amyl xanthate and MIBC as collector and frother respectively. Figure 7 shows the results of these tests according to flotation recovery and concentrate grade. According to the results, although there is not a significant change in concentrates gold grade, the recovery of gold to the concentrate is slightly increased with grinding possibly improved liberation

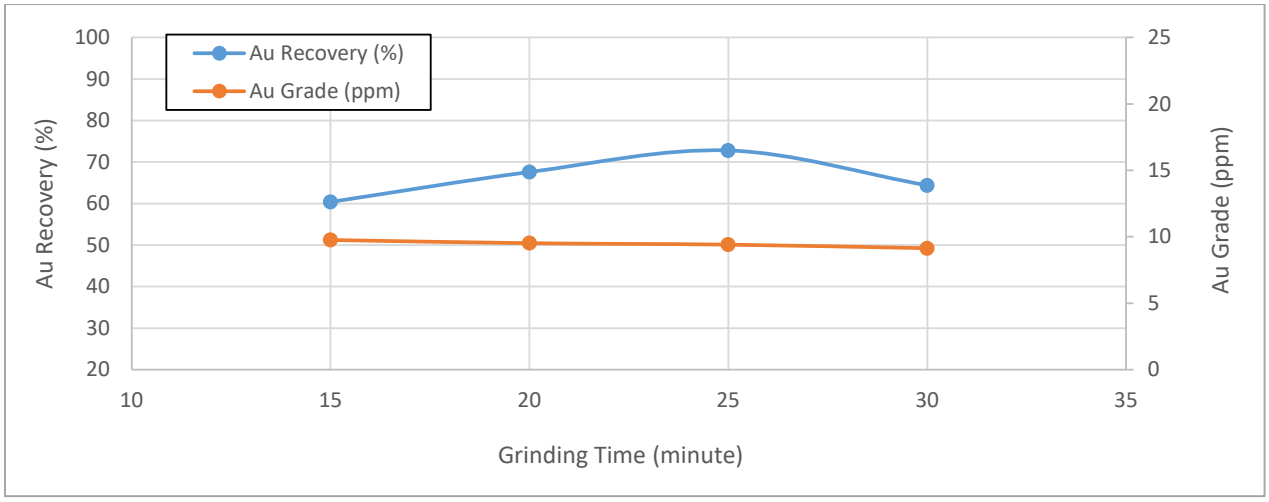

Figure 7. Flotation recovery and concentrate grade of oxide zone

It is well-known that floatability of the oxidized and secondary sulfide minerals can be restored by sulphidization (Castro & Goldfarb, 1974; Ciccu & Curreli & Ghiani, 1979; Dashti & Rashci & Abdizadeh, 2004).

Based on the mineralogical studies the transition zone is appropriate for this concept as it contains iron oxide and sulfide minerals together. In order to investigate the potential effect of sulphidization on flotation performance three test were performed with various sodium sulfide dosages while keeping other parameters constant (Table 5).

Table 5. The Effect of Sulphidization on Flotation grade and recovery

%	0.5 kg/t	1 kg/t	2 kg/t
Au Grade	5.4	6.7	10.6
Au Recovery	79.4	84.8	85.3

Based on the results, increasing the sodium sulfide dosage improves both gold grade and recovery by activation the surface of oxidized minerals. Also, sulphidization test results are showed around 25% improvement in gold recovery compared to the test result in the absence of sodium sulfide.

Similar to the sulfide zone tests, decreasing pH reduces the flotation performance in terms of both gold grade and recovery. Compared to the tests performed in natural pulp pH (8.5) and test with pH 6 adjusted by sulfuric acid, the gold recovery decreased from 84.2% with 11.9 g/t Au to 65.5% with 7.4 g/t Au.

Based on experimental results, a rougher flotation concentrates with 7-8% mass pull, 85% gold recovery with 11 g/t Au content can be obtained using sulphidization. As mentioned before, additional flotation tests would be required including cleaning stages.

Oxidized Zone

Approximately 100 kg of core samples were taken from six holes from the oxidized zone and crushed to minus 2mm and divided to 1 kg subsamples. Although gold deportment studies the gold is mainly either free or attached to the iron oxide minerals e.g., goethite, and minorly attached to sulfides and, although reasonable recovery with direct cyanidation is possible the flotation is considered in order to simplify the potential flowsheet.

For examining the effect of sulphidization on flotation performance, four tests were performed with various Na_2S dosages while keeping other parameters constant. Cyquest 4000 reagent was also added in grinding stage (15min) to improve dispersion. Pulp was conditioned with Na_2S for 15 minutes and PAX was used as collector with MIBC as frother.

Based on the results, gold recovery is increased to 79.8% with Na_2S dosage then slightly decreased to 74.6% at 2 kg/ton Na_2S (Figure 8). The concentrate grade is increased with the Na_2S dosage as well. Consequently, a rougher concentrate having almost 80% recovery with 14.5 g/t Au grade can be produced using sulphidization technique.

Detailed comminution, classification, cleaner flotation and dewatering studies would be necessary for designing and optimizing such a flowsheet. Alternatively, gravity separation techniques like shaking table and falcon separator test works is planned. The comparison of the results of flotation and gravity test works would be helpful in development of the final flowsheet.

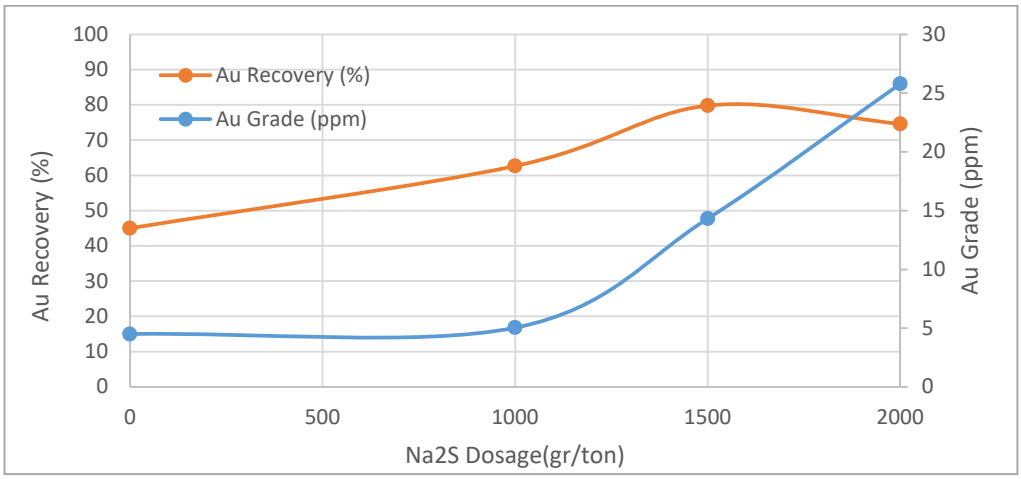

Figure 8. The Effect of Sulfidization on Flotation grade and recovery of the Oxide zone ore

RESULT AND DISCUSSION

The aim of this study is to use the gold deportment study results to select the most appropriate beneficiation method for a given ore characteristics. Based on combined geological and mineralogical information, it is possible to classify the ore into three different ore types. The gold in oxidized zone is mainly free or attached to iron oxide minerals like goethite. The gold in the sulfide zone is free or attached to sulfide minerals i.e., pyrite and arsenopyrite. The properties of transition zone are the combination of both oxidized and sulfide zones.

Based on the geological and mineralogical data, every ore zone owns different liberation, oxidation and mineralization characteristics and consequently needs distinct beneficiation method. Based on these data and in order to have a holistic beneficiation method, froth flotation studies were carried out for every ore zone samples. The results of flotation test work indicated that:

1. In the sulfide zone, obtaining a rougher concentrate with 5-6% mass pull, up to 97% gold recovery with 17 g/t gold grade is possible using a simple reagent scheme.
2. In the transition zone, a rougher concentrate, up to 85% gold recovery with 11 g/t Au content is possible using sulphidization.
3. And finally, in the oxidized zone, a rougher concentrate with gold recovery of around 80% with 14.5 g/t Au content can be obtained using sulphidization.

Further detailed flotation studies as well as alternative ore concentration methods like gravity separation would be beneficial to select the final flowsheet.

REFERENCES

Beyuo, M., Agorhom, E., Owusu C., Diaby A.L., Quaicoe I. (2016). Gold deportment and mineralogical characterization for improved recovery. 4th UMaT Biennial International Mining and Mineral Conference.

Castro S., Goldfarb J., L. J. (1974). Sulphidizing reactions in the flotation of oxidized copper minerals. International Journal of Mineral Processing, 141–161.

Ciccu, R., Curreli, L., Ghiani, M. (1979). The beneficiation of lean semi-oxidized lead–zinc ores. 13th Int. Minerals Process. Cong., Processing of Oxidized and Mixed Oxide–Sulfide Lead–Zinc Ores, 125–145.

ENERGY OPTIMIZATION OF A GRINDING CIRCUIT AT A COPPER MINE

BİR BAKIR MADENİNDE ÖĞÜTME DEVRESİNİN ENERJİ OPTİMİZASYONU

T. Sert [1, *], O. Altun [1], N.A. Toprak [1], D. Altun [1], Ö. Darılmaz [2]

[1] Hacettepe University, Mining Engineering Department
*(*Corresponding author: tolgasert@hacettepe.edu.tr)*
[2] Acacia Maden İşletmeleri A.Ş.

ABSTRACT

This study aimed to reveal the opportunities of energy improvement in the copper ore grinding circuit by optimizing the operational conditions. The circuit comprised of a ball mill and hydrocyclone, which were closed circuited to provide the desired target size for the beneficiation. The time the study started the throughput of the grinding circuit was 240 tph. The initial optimization started at the control room where the cyclone pressure was changed from 60 kPa to 100-120 kPa range and mill discharge solid was changed from 68% to 80%. As a result of the adjustment the circuit responded positively and the feed rate was able to be increased to 278 tph with the same product fineness (p80 of 102 microns). In brief 15.8% increase in throughput was obtained. The sampling campaign was performed at that level to develop the model structures to be used in the simulation studies. Within the scope of the evaluations, 8 simulations were run to predict the operational range of the circuit, the throughputs at varied product fineness, and the lower/upper limits while considering the use of 70 mm grinding balls at 32% filling. The simulations showed that the throughput could be increased to 300-320 t/h in case the proper conditions were established.

Keywords: Grinding, optimization, energy efficiency

INTRODUCTION

Grinding is an energy-intensive unit operation in mineral processing, which accounts for the majority of the operational cost in a mineral processing plant (Wills, 2016). Maintaining an optimum mill load is key to improve the efficiency energy utilization. In this study, the opportunities for energy improvement in the copper ore grinding circuit have been investigated.

The wet grinding circuit of the plant is composed of a ball mill and hydrocyclone cluster that is operated in the mode of a closed circuit. It means that the coarse product of hydrocyclone is subjected to further milling. There is a trommel screen mounted at the discharge end of the mill to discard the scats out of the circuit. The flow rate of the scats is continuously measured by the plant. There are two locations that the water is added, one is from the feed end and the other is from the discharge end prior to the wet classification. Those flow rates can be calculated after the material balancing that can be found in the following sections. The simplified flow sheet of the circuit with the sampling points indicated is illustrated in Fig.1 and the technical specifications of the machines are summarized in Table 1 and Table 2.

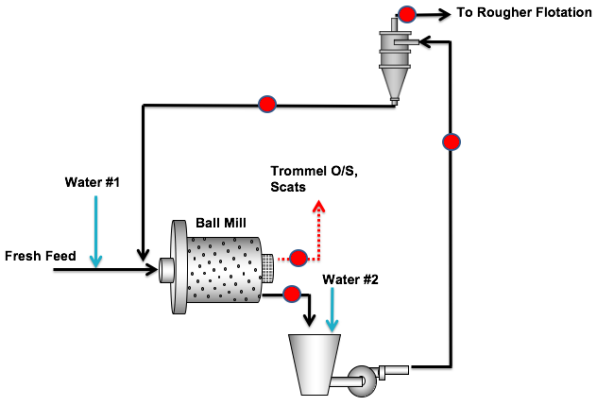

Figure. 1. Simplified flow sheet of the grinding circuit.

Table 1. Specifications of the Ball Mill

Effective Diameter (m)	Length (m)	Installed Power (kW)	Mill Speed (rpm)
5.38	8.2	4400	14

Table 2. Specifications of the Hydrocyclone.

Brand	Diameter (mm)	Feed inlet (mm)	Vortex dia. (mm)	Apex dia. (mm)	No. of available cyclones	Suggested oper. pres. (kPa)
Weir, Cavex	500	200	155	90	7	80-120

MATERIALS AND METHODS

Sampling Studies

The study has aimed to quantify the limits of the throughput. Prior to the sampling campaign, a steady state condition was reached by changing the operating conditions of the circuit at the control room. It was observed that the grinding circuit was controlled via cascade mode which allows keeping the sump level steady by increasing or reducing the speed of the pump. However, changing the pump speed disturbed the whole operation as cyclone pressure varied between 80 kPa and 110 kPa, which can also lead to change in the size distribution of the cyclone overflow stream. In order to prevent this phenomenon, the grinding circuit was controlled manually and small adjustments were made to keep the pressure and sump level at steady.

Prior to performing the sampling campaign, the plots/trends of the operating variables such as mill power, sump level, cyclone pressure, overflow %solid, were followed around 90 minutes. Table 3 tabulates the average operating conditions of the mill.

Table 3. Average operating conditions recorded during the survey.

Fresh feed (t/h)	Feed moisture (%)	Power draw of ball mill (kW)	No. of cyclone in operation	Pressure of hydrocyclone (kPa)	Speed of pump (%)	Hydrocyclone overflow solid %
278.78	1.6	2913	4	110	87.6	33.78

Material Characterization

The collected samples were characterized regarding their particle size distributions, solid percentage, work index, breakage distribution and specific gravity.
Particle size analyses were completed in two steps. Initially, the whole material was wet sieved from 26 mm to 38µm. Below that size, cyclosizer technique was applied to determine the size analysis down to 8µm. The set of data obtained from the two methods was then combined.
The experimental size distributions are depicted in Fig. 2.

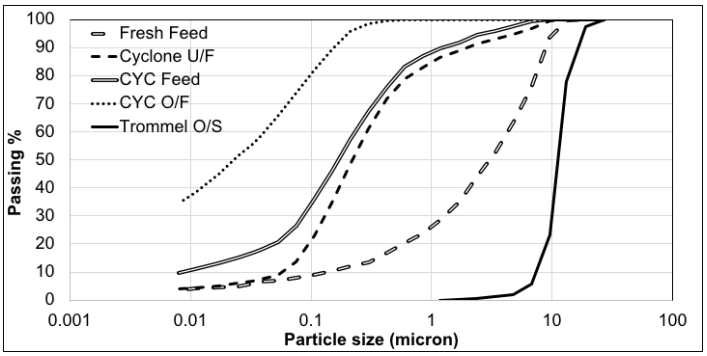

Figure 2. Experimental size distributions.

The product fineness of the grinding circuit has been followed within the control room via PSI measurement. D80 value of cyclone overflow from PSI is 102.1 µm while the size analysis result is 98 µm which are similar to each other.
Solid percentages of the streams are tabulated in Table 4.

Table 4. Measured solid percentages of the streams

Fresh Feed	Tromme l O/F	Cyc Feed	Cyc U/F	Cyc 7 U/F	Cyc O/F (Cond.)	PSI	Flot. Feed (courier)	Cyc 7 O/F	Mill Disch.
98.4	99.5	66.6	84. 7	85.1	37.1	38. 1	36.8	40.4	82.9

Bond work index test aims to determine the grindability of ore that refers to the ease with which materials can be comminuted. The data is either utilized to evaluate the grinding efficiency or to predict the product size distribution of the mill within the simulation studies. The work index of the ore was found as **13.04** kWh/t. Breakage function refers to the breakage properties of a given sample. It is determined as a result of breaking the particles at different energy levels, followed by measuring the weight distribution to subsequent size classes. It is an ore-specific property that is utilized as an input in the modelling of size reduction machines. Within the scope of the project, narrow -9.5+8 mm size fraction was prepared and then subjected to the breakage test works from three different energy levels (1.65 kWh/t, 2.01 kWh/t and 2.70 kWh/t). Following the test works, particle size distributions of broken products were determined. Three different breakage distribution functions were calculated to use in the ball mill modelling studies (Fig.3).

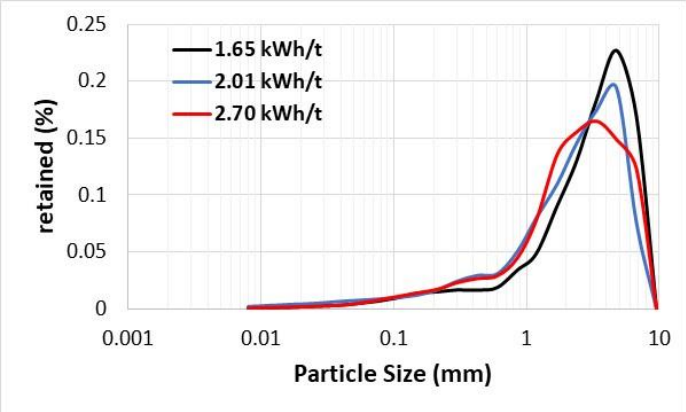

Figure 3. Calculated breakage distribution functions

Sampling Campaign, Mass Balancing and Machine Performances

Within the circuit, the flow rates of some of the streams are known and the rest is calculated statistically. In addition, the experimental data may contain errors that all should be considered during the assessments. Performing mass balancing enables calculating the unknown streams by distributing the errors arisen due to the experimental works and sampling methodologies. The study benefited from JK-SimMet software; all the missing points are calculated based on the afore-mentioned approach. The specifications of the streams regarding the flows and size characteristics are illustrated in Fig. 4. Fig. 5 depicts the plots of experimental and calculated size distributions indicating that the sampling studies were accomplished with the least sum of errors.

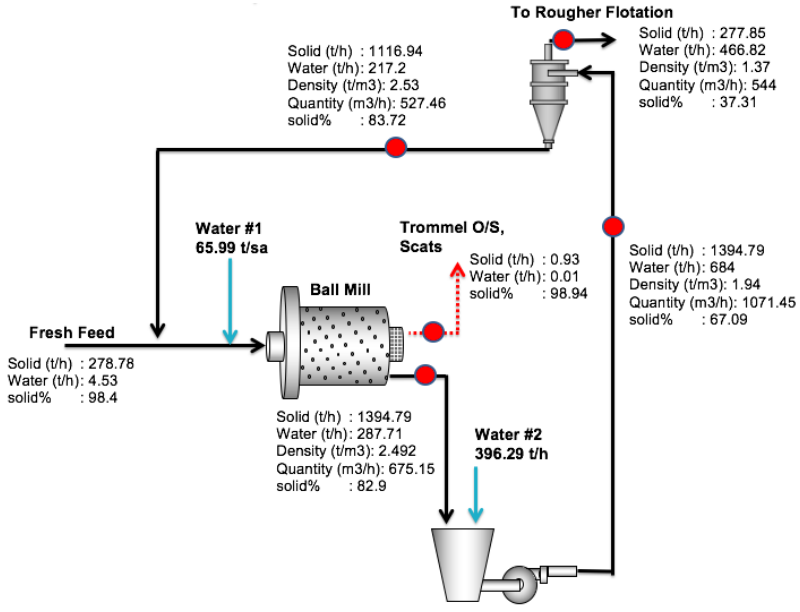

Figure 4. Results of the mass balancing.

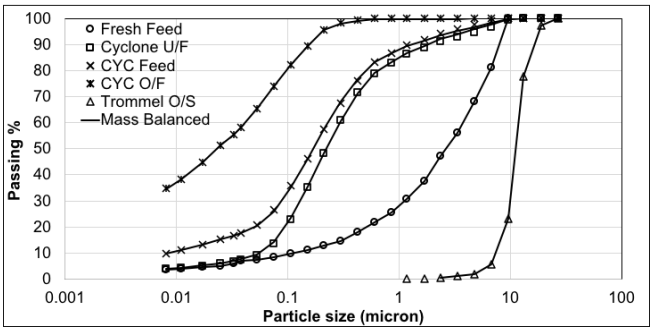

Figure 5. Comparison of the experimental and mass balanced size distributions.

The mass balanced data showed that the solid percentage of hydrocyclone overflow (37%) is different from what was indicated on the control room (33%) hence some discrepancies were observed.

RESULTS AND DISCUSSIONS

Performance Evaluation of Overall Circuit

For the overall circuit, the specific energy utilization and the size distributions of fresh feed, cyclone overflow streams were considered. Additionally, the circulating load was calculated by dividing the solid flow rate of cyclone underflow stream by cyclone overflow. Table 5 summarizes the data of the grinding circuit. It should be noted that the power consumptions of the auxiliaries were not included in the assessments.

Table 5. The data of the grinding circuit

Ball mill power (kW)	2913
Fresh feed (t/h)	278.78
Trommel oversize (t/h)	0.93
Hydrocyclone overflow to flotation feed (t/h)	277.85
Hydrocyclone underflow (t/h)	1116.94
Specific energy cons. (kWh/t)	10.48
F_{80} of Fresh feed (mm)	6.5
P_{80} of Hydrocyclone overflow (mm)	0.098
F_{50} of Fresh feed (mm)	2.7
P_{50} of Hydrocyclone overflow (mm)	0.023

The specific energy consumption of the circuit was calculated as 10.48 kWh/t for the degree of size reductions of 66.3 (RR_{d80}) and 117 (RR_{d50}). The circulating load of the milling is 401%.

Where;

RR_{d80}: reduction ratio of d_{80s}
RR_{d50}: reduction ratio of d_{50s}

The specific gravities of the streams were measured and illustrated in Fig.6. The results showed that there was an effect of centrifugal wet classification since the material of cyclone underflow was denser than that of the overflow stream. The material of the trommel oversize stream is the lightest of all.

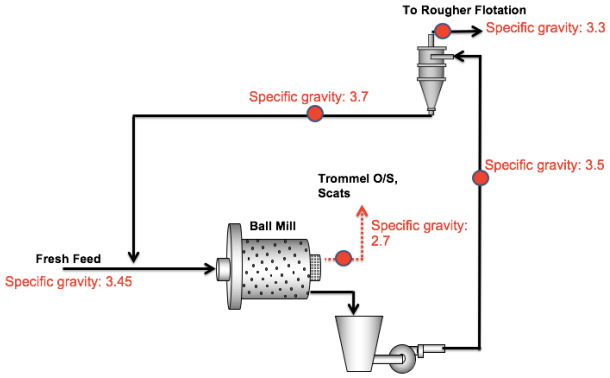

Figure 6. Specific gravities of the streams.

Within the performance analysis of the ball mill; size reduction and the trommel oversize sample, the grinding media filling and its influence on power draw and energy utilization and grinding media size were considered.

Size Reduction Performance of the Mill

Fig. 7 illustrates the size distributions of feed, product and trommel oversize samples.

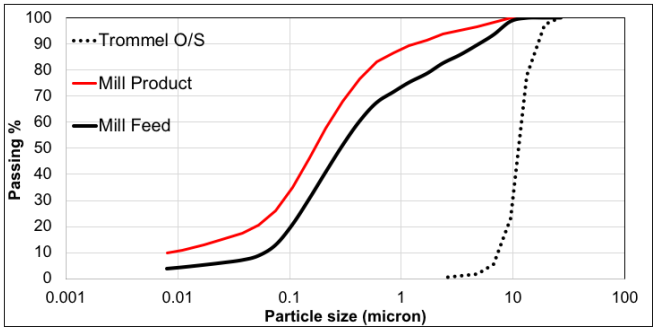

Figure 7. Size distributions around the ball mill.

The performance data of the mill is summarized in Table 6.

Table 6. Ball mill performance.

Mill power (kW)	Mill throughput (t/h)	Solid %	Feed, F_{50} (mm)	Product, P_{50} (mm)
2913	1395.72	82.9	0.288	0.17

The mass balanced data indicated that the mill was operated at 82.9% of solid content. It is a well-known fact that the higher the solid content of the mill, the finer the product up to a saturation point of 80%. Consequently, adding more water may be considered from the feed end of the mill to achieve that level. It may have impacts on the throughput. The amount of trommel oversize material was measured as 0.93 t/h. That amount may fluctuate depending on the solid content of the mill, type of ore and feed rate to the mill. The specific energy utilization of the ball mill is found as 2.09 kWh/ton for the size reduction of 1.65.

Grinding Media Filling and the Power Draw of the Mill

At the end of the sampling campaigns, ball mill was crash-stopped in order carry out mill inside measurements e.g., media filling level and media size distribution. The ball filling can be calculated from the position of the ball charge at rest. Table 7 summarizes the results of the calculations

Table 7. Media filling measurements of mill

H (cm)	Effective Diameter (cm)	Filling Ratio %
3700	5384	26.41

In another evaluation, the height from the top to the lower section of discharge grate was measured to find out the maximum available volume of the grinding media charge. The measurements showed that the level of 35-40% can be filled with the grinding media. It can be concluded that the grinding media level is well-below the optimal operating conditions. This phenomenon can also be validated from the power draw of the mill. As the installed power is 4400 kW, the mill can be operated up to 3400-3600 kW range that is the function of the media filling. During the sampling campaign, power draw was noted as 2913 kW that indicates there is a margin for adding grinding media. It is recommended to charge more grinding media into the mill by following the variation in the power draw. Such a change is expected to further increase the throughput of the mill at the same degree of fineness. The simulation studies have aimed to predict the improvements in the grinding efficiency.

Critical Speed

The speed at which the maximum power in a mill can be drawn is therefore critical and the speed at which the charge centrifuges is known as the *Critical Speed.* Wet grinding overflow discharge ball mills are usually operated at 74%-76% of critical speed. The literature also reports that it may go up to 78% that results in increased capacity. For the ball mill in operation, the number of rotations per minute was measured as between 14 rpm and 14.3 rpm. By taking the diameter and the maximum size of the grinding media into account, the critical speed is calculated as 77%. It can be concluded that the speed is at its limits.

Ball Size Evaluations

There exist different approaches in grinding media size calculations. Within the scope of this study, Rowland and Kios approach (1978) was applied, which indicates that the initial ball size is related to the characteristics of the feed (work index, particle size and size distribution, S.G. of the solids and slurry density) and the mill (diameter and critical speed). Within the calculations, 80% passing and top size of the feed size distributions were considered so as to predict the fluctuations in the performances of the crushing stages. In this regard, 6.5mm and 9.5mm sizes were inputted to Equation 5 assuming the work index and specific gravity of the ore remained constant. Table 8 gives the results of the calculations.

Table 8. Calculated ball sizes

	Grinding ball Size (mm)
Top size of feed, 9.5mm	70
80% passing, 6.5mm	58

The assessments proved that the ball size of 58 mm is sufficient for breaking the feed having d_{80} of 6.5 mm. However, 70 mm size that corresponds to feed top size can be considered as a safety issue. Above this size range can be designated as the point of start of inefficiency where the loss on the surface area of grinding media will lead to the loss of grinding efficiency. As a conclusion, 70 mm mono sized grinding ball charge has been suggested.

Performance of Hydrocyclone Cluster

The commonly preferred method of representing cyclone efficiency is by a performance or partition curve, which relates the weight fraction, or percentage, of each particle size in the feed which reports to the apex, or underflow, to the particle size. Within the study, the performances of hydrocyclone cluster (the main streams around the hydrocyclone) as well as the single unit were evaluated. In this context, cyclone no 7 was sampled and the Tromp curve of it was compared with that of the cluster. Figure 8 shows the efficiency curve of the cyclone cluster. Table 9 summarizes the process data of hydrocyclone where the water recovery was calculated. The calculations implied that the water recovery to underflow was in good agreement with the bypass value determined from the Tromp curve.

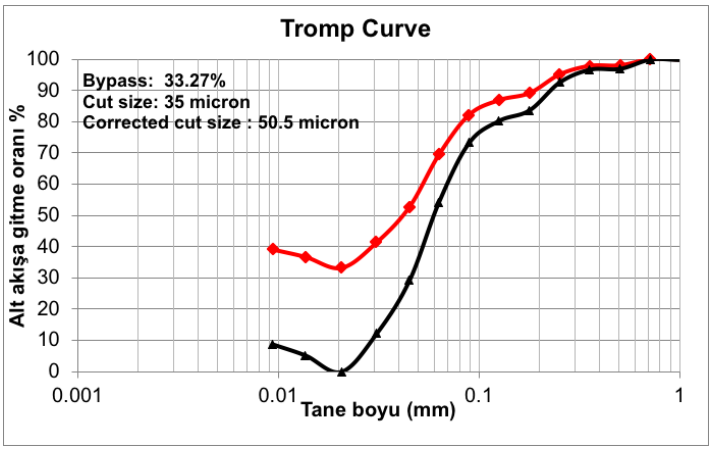

Figure 8. Actual and corrected efficiency curves.

Table 9. Process conditions of hydrocyclone

CYC O/F Solid%	37.31
Cyclone Pressure (kPa)	110
CYC Feed water (t/h)	684
CYC U/F water (t/h)	217.2
Water Rec. to underflow (%)	31.7
Bypass from Tromp curve (%)	33.2

Modelling of the Machines

Within the scope, ball mill, trommel screen and hydrocyclone units were modelled. Population balance model of Napier Munn (1996) has been used for the ball mill modelling. In modelling of the Trommel screen, the efficiency curve approach of Whiten was used. The model of Nageswararao (1978) was preferred for hydrocyclone modelling. The successes of the model fitting studies were evaluated by doing base case simulation that is expected to reflect the behavior of the sampling conditions. Fig. 9 and

Fig. 10 illustrates the circuit parameters and the agreement between the experimental and simulated size distributions.

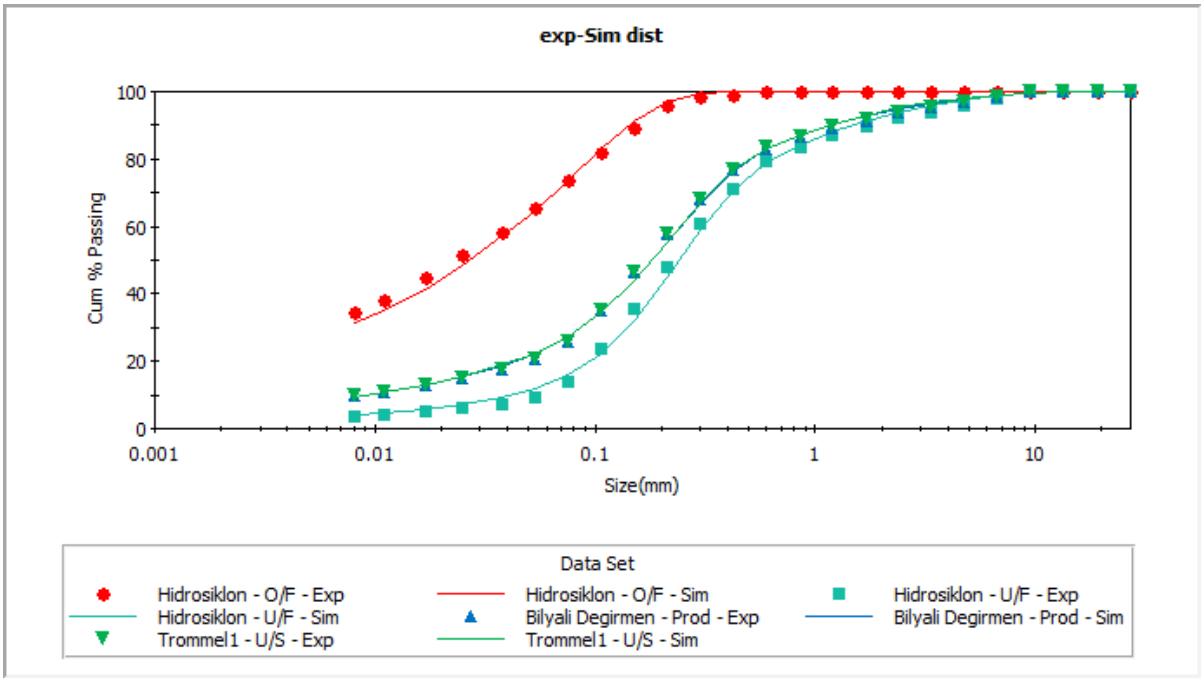

Figure 9. Experimental and simulated size distributions.

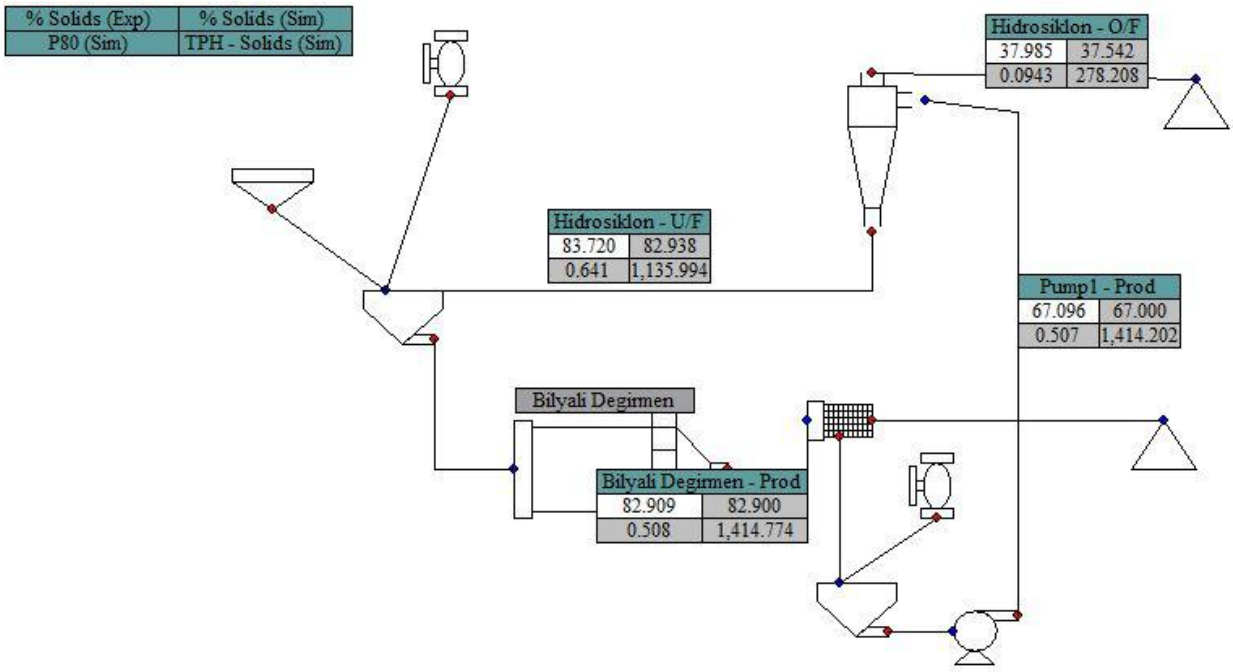

Figure 10. Base case simulation output.

Simulation Scenarios

Within the scope of the project, 8 scenarios were tested. The focus of each study is given in Table 10. The conditions of the simulation scenarios have been decided based on the previous optimization works of Altun. (Altun, 2016, 2018)

Table 10. Simulation scenarios

Simulation number	Focus
#1	350 tph for the same product fineness
#2	300 tph for the same product fineness
#3	275 tph for the same product fineness
#4	255 tph for the same product fineness
#5	Only 1 Cyclone in operation
#6	P80 of 42 microns
#7	P80 of 75 microns
#8	P80 of 117 microns

The summary of all the evaluations is presented in Table 11. It should be emphasized that all the simulations were run at 32% grinding media filling and ball size of 70 mm.

Table 11. Results of the simulations.

	Sim. #1	Sim. #2	Sim. #3	Sim. #4	Sim. #5	Sim. #6	Sim. #7	Sim. #8
Fresh feed (t/h)	350	300	275	255	130	195	265	395
Cyc O/F (t/h)	348.8	299	274	254	129.8	194	264	394
Cyc U/F (t/h)	1415	994	910	638	224	479.5	758.4	1669
Circ. load (%)	405.68	332.44	332.12	251.18	172.57	247.16	287.27	423.6
No of Cyclones	5	4	4	4	1	2	3	7
apex size (mm)	0.09	0.085	0.085	0.08	0.08	0.09	0.09	0.085
Cyc Pres. (kPa)	105-110	88	78	77	120	120	100	75
Cyc O/F Solid%	37.2	40.4	41	45	47	40.9	44.74	37.1
Cyc O/F P80 (µm)	99	98	96	92	47	42	75	117
Cyc Feed (m3/h)	1351	991	912	674	289	591.8	783.5	1566
Mill Power (kW)	3516	3516	3516	3516	3516	3516	3516	3516
S.E (kWh/t)	10.08	11.76	12.83	13.84	27.09	18.12	13.32	8.92
Mill Solid%	81	78	76	76.5	67	80	81	81

CONCLUSIONS

From Sim 1-4 it is understood that the circuit is operable at 350 t/h for the same degree of the product fineness (p_{80} of about 98 microns). With the decreasing throughput, cyclone pressure, number of cyclones in operation and the flow rates decrease significantly thus the size of apex should be changed accordingly. The power draw of the mill was predicted as 3516 kW for grinding media filling of 32% and kept constant in all through the evaluations. The down limit of the grinding circuit was questioned by the plant staff hence another simulation study was conducted when 1 cyclone is in operation (Sim #5). In that study, cyclone was tried to be operated at 120 kPa by adjusting the rest of the operating conditions such as mill solid percentage, cyclone feed solid percentage, throughput and number of cyclones. The calculations showed that the grinding circuit can be operated at 130 t/h. From Simulations 6-8 the product fineness was changed and the feed rate to the circuit was predicted. The maximum throughput (395 t/h) was achieved when p_{80} was 117 microns. For p_{80} of 42 microns the feed rate was predicted as 195 t/h.

It should be noted that in order to achieve higher throughputs, the limitations within the grinding circuit should be considered such as the design capacity of the pumps.

REFERENCES

Altun, O. (2016). Simulation aided flow sheet optimization of a cement grinding circuit by considering the quality measurements. *Powder Technology*, *301*, 1242-1251.

Altun, O. (2018). Energy and cement quality optimization of a cement grinding circuit. *Advanced Powder Technology*, *29*(7), 1713-1723.

Bond, F. C. (1952). Third theory of comminution. *Mining engineering*, *4*, 484.

Nageswararao, K. (1978). Further modelling and scale-up of hydrocyclones. *JKMRC, University of Queensland*.

Napier-Munn, T. J., Morrell, S., Morrison, R. D., & Kojovic, T. (1996). Mineral comminution circuits: their operation and optimisation.

Rowland, C. A., and D. M. Kjos. "Rod and ball mills." *Mineral Processing Plant Design (ed. AIME)* (1978): 239-278.

Wills, B. A., & Finch, J. A. (2016). Froth flotation. Wills' Mineral Processing Technology, *7*.

ENVIRONMENTAL IMPACT ASSESSMENT FOOTPRINT IN OPEN-PIT COPPER MINING

M. Heydari [1], M. Osanloo [1,*], A. Başçetin [2]

[1] *Amirkabir University of Technology, Mining Engineering Dept*
*(*Corresponding author: morteza.osanloo@gmail.com)*
[2] *Istanbul University, Engineering Faculty, Mining Engineering Dept*

ABSTRACT

With the rise of technology and the growth of population, copper consumption increases globally. However, high-grade near-surface deposits have been depleted in past years or will be depleted in the near future. Deep low-grade ore remains, creating higher environmental impacts like the greater volume of waste, higher energy consumption, and land degradation. Although the environmental impacts of copper mines have been quantified in several studies, a comprehensive environmental impact assessment (EIA) related to open-pit copper mines at the global level is missing in current literature. This study focuses on published papers from 2010 to 2021, investigating the footprint of copper mining on the environment. Most studies used quantitative approaches to assess the environmental impacts of copper mines (41% of total), among which life cycle assessment (LCA) has the highest application of 75%. The results show that the available models have shortcomings, such as excessive assumptions in LCA and expert-depended results in MCDMs. This finding indicates the need to improve the existing models and create a comprehensive EIA technique applicable in all open-pit copper mines to decrease the copper production's environmental impacts per kg and achieve a cleaner environment.

Keywords: Environmental impact assessment (EIA), open-pit mining, copper

INTRODUCTION

Mining is the first step in preparing the raw materials needed for infrastructure advance, raising human living standards, and achieving social development. Considering the world population growth rate in recent years, by 2030, the world population will be about 8.3 billion (Osanloo, 2016). On the other hand, with the growth of the urbanization rate and the desire of people to have high standards of urban life, mineral consumption increases (Kuipers et al., 2018). copper is one of the essential sources for many technologies, such as the construction industry, telecommunications, automotive, and electronics, and it is expected that its production will increase significantly in the coming decades. Between 2000 and 2018, world copper tonnage rose about 4% per year, projected to increase up to 2030 due to increasing urbanization rates (especially in developing countries such as India and China). Therefore, with increasing demand, copper exploitation in the future will be from the depths with lower grades. Copper mines are found worldwide in different climatic conditions, such as hot/cold and dry/wet, with various mineralogical and geomechanical properties. Mining higher volumes of ore from the earth's crust to achieve the consumption rate of the society's need result in more energy consumption, greenhouses gas emissions, water and soil pollution, flora and fauna destruction, and land disturbance. The average copper grades of sulfide ores have decreased from 1.18% to 0.60% over 2003-2020 in Chilean copper mines. Lower average grade results in more waste produced in the mining and

processing stages. Therefore, more water, energy, and chemical reagents are required to process low-grade copper ores efficiently. The consumption of collectors, frothers, and modifiers in flotation increases because higher amounts of low-copper grade ore are processed. These chemicals represent reagents that pose environmental risks due to their properties, classified as hazardous materials for potential health effects (Reyes-Bozo et al.,2014). As a result, assessing the environmental impacts of copper mining activities becomes more critical.

Environmental Impact Assessment (EIA) is a tool for evaluating the project's positive and negative environmental outcomes before implementing it to achieve sustainable development goals in mining projects. Today, experts and owners of the mining sector believe that society needs a green, healthy, economical, and fertile environment. The environmental impacts of copper mining have been quantified in various research (Zhang et al., 2021, Perlatti et al., 2021, Islam et al., 2019, Hong et al., 2018, Kulczycka et al., 2016, Wang et al., 2015), and some studies have examined specific aspects of the environmental impacts of copper production. However, a comprehensive model for investigating the positive and negative environmental effects of open-pit copper mines is hard to come by, which is an essential gap in the current literature. Environmental impacts are divided into temporary and permanent impacts: (1) Temporary impacts depend directly on the mining projects but disappear if the mining activity stops. (2) Structural impacts also stem directly from the mining project, but the environmental impact will continue if the mining activity stops. These impacts could be temporary (mid-term or long-term) or permanent. Concerning the potential impacts on the environment, the advancement of mining projects has certain coincidences compared to other projects. The environmental and social impacts are different, and sometimes, they remain long after the end of mining activities. Therefore, the natural impacts of mining got to be carefully evaluated within the early stage of the mining project. Also, the activities must be assessed for potential impacts after the mining operation decommission (Castilla-Gómez and Herrera-Herbert, 2015).

This study aims to survey and classify the available studies in the subject of EIA in copper mining into three groups: Qualitative, Semi-Qualitative, and Quantitative studies. Next, the most used technics are recognized, and then the shortcoming of each study is highlighted as the path toward a comprehensive EIA for copper mines modeling.

Environmental Impact Assessment in Mining

Since all mining activities cause environmental changes, identifying the mining impacts is necessary to improve the positive ones and prevent creating or controlling adverse ones. These effects can be positive (such as employment, increasing GDP and increasing government revenues, the establishment of housing estates in disadvantaged areas, and developing infrastructure such as water supply, electricity, and educational and medical centres) or negative (such as biodiversity loss, Landslide, surface and groundwater pollution, loss of vegetation and forest, and landscape disruption). All mining activities, from exploration to decommissioning, have multiple environmental effects.

Over the past few years, environmental issues have become increasingly respected and revised globally. In a comprehensive classification, the existing methods for assessing the environmental impact of mines can be divided into three groups: qualitative methods, quantitative methods, and semi-qualitative methods. In recent decades, numerous studies have been conducted to assess the environmental impact of mining activities. The following will discuss the statistical classification of the studies in the three qualitative, quantitative, and semi-qualitative groups. In general, 40 studies that evaluated the environmental impact of mines between 2010 and 2021 were reviewed in this paper.

Qualitative Studies

From 2010 to 2021, several studies have used qualitative methods for EIA of mining projects. Only the qualitative factors are assessed in this method, and the results are linguistic. Table 1 summarizes the surveyed studies that used qualitative methods in their research.

Table 1. Summary of studies of EIA in mining

Reviewed studies	EIA Methodology	Mineral type
Suopajärvi (2013)	Qualitative	**Copper**, Gold, Nickel, Iron
Morrison-Saunders et al. (2015)	Qualitative	-
Castilla-Gómez and Herrera-Herbert (2015)	Qualitative	**Copper**
Gałaś and Gałaś (2016)	Qualitative	**Copper**, Silver, Kaolin, Uranium
Mancini and Sala (2018)	Qualitative	**Copper**
Gorman and Dzombak (2018)	Qualitative	**Copper**
Hresc et al. (2018)	Qualitative	**Copper**
Ocampo-Melgar et al. (2019)	Qualitative	**Copper**, Gold
Clark (2019)	Qualitative	-
Riley et al. (2019)	Qualitative	Coal
da SilvaDias et al. (2019)	Qualitative	Iron
Lemly (2019)	Qualitative	Coal

Table 2 shows that from 2010 to 2021, 32% of studies examined the environmental impacts of open-pit mines using qualitative methods, from which 54% have examined the EIA of copper mines.

Table 2. Number of qualitative studies of EIA considering Copper mining

Total Number of Studies	Number of copper studies
12	7

Semi-Qualitative Studies

Semi-qualitative technics use multi-criteria decision-making technics to quantify the qualitative factors and assess the kind of qualitative and quantitative impacts of the project at once. Considering the nature of impacting factors in mining projects (both quantitative and qualitative), semi-quantitative methodology can be advantageous. Table 3 shows the summary of the semi-qualitative studies surveyed in this paper.

Table 3. Summary of studies of EIA in mining

Reviewed studies	EIA Methodology	Mineral type
Aryafar et al. (2012)	Semi-Qualitative	Coal
Minaei Mobtaker and Osanloo (2014)	Semi-Qualitative	-
Saini et al. (2016)	Semi-Qualitative	Coal
Ataei et al. (2016)	Semi-Qualitative	Coal
Rahmanpour and Osanloo (2017)	Semi-Qualitative	**Copper**
Heidari and Osanloo (2018)	Semi-Qualitative	Zinc and Lead
Saffari et al. (2019)	Semi-Qualitative	Cement
Sarupria et al. (2019)	Semi-Qualitative	Iron, Manganese

Amirshenava and Osanloo (2019)	Semi-Qualitative	Iron
Ataei and Masir (2020)	Semi-Qualitative	**Copper**

To summarize, from 2010 to 2021, 27% of studies examined the environmental impacts of open-pit mines using semi-qualitative methods, from which 20% have examined the EIA of copper mines (Table 4).

Table 4. Number of Semi-qualitative studies of EIA considering Copper mining

Total Number of Studies	Number of copper studies
10	2

Quantitative Studies

Quantitative studies include the ones that examined the soil, water, and air pollution or used the LCA method to investigate the emissions into the environment. Table 5 shows the summary of the surveyed studies in this group.

Table 5. Summary of studies of EIA in mining

Reviewed studies	EIA Methodology	Mineral type
Norgate and Haque (2010)	Quantitative	**Copper**, Iron, Bauxite
Northey et al. (2013)	Quantitative	**Copper**
Muñoz et al. (2014)	Quantitative	**Copper**
Reyes-Bozo et al. (2014)	Quantitative	**Copper**
Song et al. (2014)	Quantitative	**Copper**
Wang et al. (2015)	Quantitative	**Copper**
Drielsma et al. (2016)	Quantitative	**Copper**
Kulczycka et al. (2016)	Quantitative	**Copper**
Hasanipanah et al. (2018)	Quantitative	**Copper**
Hong et al. (2018)	Quantitative	**Copper**
Kuipers et al. (2018)	Quantitative	**Copper**
Islam et al. (2019)	Quantitative	**Copper**
Dong et al. (2020)	Quantitative	**Copper**
Zhang et al. (2021)	Quantitative	**Copper**
Perlatti et al. (2021)	Quantitative	**Copper**

In brief, from 2010 to 2021, 41% of studies examined the environmental impacts of open-pit mines using quantitative methods from which 100% have examined the EIA of copper mines (Table 6).

Table 6. Number of Semi-qualitative studies of EIA considering Copper mining

Total Number of Studies	Number of copper studies
15	15

RESULTS AND DISCUSSION

Reviewing the studies of copper mining EIA from 2010-2021 revealed that 41% of environmental research studies have been carried out quantitatively from 2010 to 2021, which mainly focused on

emissions measured by LCA methods or chemical analysis of soil and water samples of the surrounding areas while other environmental aspects were not investigated. 32% of the studies are qualitatively assessed from 2010-2021. This is due to the qualitative nature of the parameters studied and the lack of comprehensive quantitative methods. In 27 % of the studies, semi-quantitative methods have been used, the ineffectiveness of quantitative methods in the whole process of environmental assessment, the qualitative nature of many parameters, and the inability to quantify them by the way other than Experts, semi-quantitative methods can assess the environmental impacts of the mining project comprehensively (Table 7, Figure 1)

Table 7. Summary of reviewed studies of copper mining

	Reviewed studies	Percentage	Considering positive impacts	Copper mineral
Qualitative	12	32%	0	7
Semi-qualitative	10	27 %	1	2
Quantitative	15	41 %	1	15
Total	37	100 %	2	24

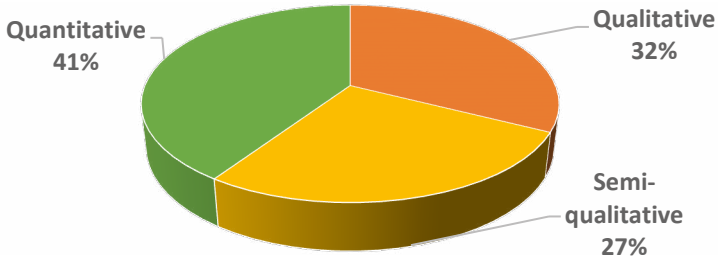

Figure 1. The rate of use of each group of assessment methods

Figure 2 shows studies surveyed regarding the mineral type. According to this picture, 63% of the surveyed studies evaluate the EIA in copper mines. Table 8 summarizes the reviewed studies, their advantages, and the shortcomings of each study.

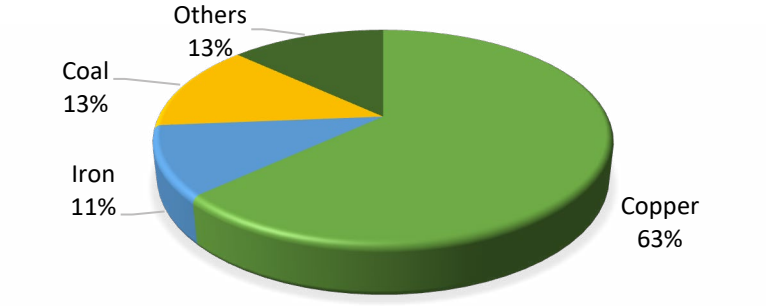

Figure 2. Percentage of studies investigated regarding the mineral type

Table 8. Summary of the studies on the environmental impact assessment of copper mines

Reviewed studies	Advantages	Shortcomings
Norgate and Haque (2010)	Evaluated the impacts of energy and greenhouse gas emissions in the life cycle of mining and mineral processing	Only energy and greenhouse gas emissions were assessed, and the other environmental impacts were ignored.
Aryafar et al. (2012)	Evaluated the environmental impacts of groundwater in mines using the fuzzy-AHP method.	A model for a particular mineral is not developed. Also, due to the use of the Folchi method, the weak points of this method are intrinsic.
Suopajärvi (2013)	Evaluation of social impacts of mining activities on environmental assessment of six mining projects in Finland.	This study did not present a model that covered the present models' defects and only stated the weaknesses of the methods.
Northey et al. (2013)	Estimated The energy, GHG emissions, and water intensity of global primary copper production.	Only three impacting factors have been estimated.
Minaei Mobtaker and Osanloo (2014)	Investigated the positive impacts of mining activities.	This research aims to use a Folchi method that has problems such as incompleteness and its dependence on personal judgment. Also, only positive effects are considered in the evaluation, and negative impacts are neglected.
Muñoz et al. (2014)	Developed a methodology to minimize social-environmental impacts in the early stages of mine design.	Only five sustainability factors were incorporated into the methodology.
Reyes-Bozo et al. (2014)	Proposed an ecology model to improve the overall environmental sustainability of copper sulphide ores flotation.	Their study assesses the soil pollution caused by the fuel and processing stage and does not consider the complete life cycle of the copper mining stages.
Song et al. (2014)	Investigation of environmental impacts of copper mining in China by LCA method .	Only greenhouse gas emissions and acidification have been investigated.
Wang et al. (2015)	Investigated the environmental effects of copper production by pyrometallurgy in China by the LCA method.	Only the metallurgical stage has been evaluated. 6 factors have been investigated in this study.
Morrison-Saunders et al. (2015)	Examined the role of environmental assessments in the design and planning of industrial and artisanal mine (ASM).	The researchers expressed their results qualitatively and did not provide a model for solving the problem.
Castilla-Gómez and Herrera-Herbert (2015)	Dynamic EIA analysis of the environment, focusing on the evolution of environmental impacts over time.	This research does not consider all the environmental impacts, such as biodiversity.

Table 8. continue: Summary of the studies on the environmental impact assessment of copper mines

Reviewed studies	Advantages	Shortcomings
Gałaś and Gałaś (2016)	Determining the importance of qualitative EIA method by comparing the quality assessment process of environmental impact.	-the assessment is qualitative -not providing a comprehensive evaluation model
Saini et al. (2016)	Establishing relationships based on earth, laboratory and satellite data analysis	Failure to provide a comprehensive model and inherent problems with the AHP method
Ataei et al. (2016)	Provide a quantitative matrix model for determining the negative effects of mining activities	Not considering the positive impacts of mining
Drielsma et al. (2016)	Investigated the current LCAs for copper mining and concluded that the existing LCA literature on mineral resource assessment is inaccurate.	Only the economic factors are applied to the previous literature on resource depletion LCA.
Kulczycka et al. (2016)	Investigated the effects of advances in metallurgical technology on the environmental impact of copper metal extraction between 2010 and 2050 using the LCA method.	The environmental impacts of the metallurgical phase have been evaluated, and only three factors have been studied.
da Silva Dias et al. (2017)	Examining the problems of existing environmental assessment methods	-the assessment is qualitative -not providing a comprehensive evaluation model
Rahmanpour and Osanloo (2017)	Evaluated the outcome of different UPL alternatives using DSS for optimal decision-making	Only the UPL selection procedure is evaluated using SD indicators, and a comprehensive model is not presented.
Mancini and Sala (2018)	Compared the different indicator sets used in the frameworks with impacts from the literature review. Working conditions and human rights are well-covered aspects in the indicator lists.	Only two of the social impacts of mining are assessed.
Gorman and Dzombak (2018)	Investigating sustainable development in the mining with resource efficiency, minimizing the damage to the land, reducing pollution.	-Qualitative and linguistic evaluation
Hresc et al. (2018)	States that EIAs do not reflect the economic impacts of mining projects on local communities health and have not been developed based on evidence that relates the economic impact of mines to health.	-the assessment is qualitative -not providing a comprehensive evaluation model
Heidari and Osanloo (2018)	Finding the interrelationship between Impacts. Considering both positive and negative impacts.	Does not develop an EIA model

Table 8. continue: Summary of the studies on the environmental impact assessment of copper mines

Reviewed studies	Advantages	Shortcomings
Hasanipanah et al. (2018)	Evaluation of ground vibration resulting from the blasting	The model is not comprehensive, only the impacts of the blasting are taken into account, and the other environmental impacts are ignored.
Hong et al. (2018)	They studied the environmental impacts of copper extraction by the LCA method.	Only the refining and recycling steps are studied, and 18 factors are evaluated in the recipe method.
Kuipers et al. (2018)	Their studies concluded that LCA is the most effective method for environmental assessment.	Five factors have been examined.
Shahhosseini et al. (2019)	Investigation of geochemical environmental conditions of arsenic and lead in dams of copper mine Middik in Kerman	The study aimed to investigate the effect of mineral activity on the concentration and stability of arsenic and lead, and other environmental impacts of mining and processing plant have been ignored.
Ocampo-Melgar et al. (2019)	Investigating public participation in increasing the environmental assessment reliability	- Use internal reports of companies that may be selective and inaccurate.
Saffari et al. (2019)	Minimizing uncertainties and personality of responses	Failure to provide a comprehensive model and inherent problems of the Folchi method
Sarupria et al. (2019)	Solving problems such as Reproducibility, Subjectivity and Non-inclusivity by stakeholders by stakeholders	Not considering the positive impacts of mining
Amirshenava and Osanloo (2019)	Determine the effect of mineral activities on sustainable development indicators	Not considering the positive impacts of mining
Clark (2019)	Introducing defects in the environmental assessment deep-sea mining	- not providing technology or applied evaluation method - not taking into account the positive impacts of mining
Riley et al. (2019)	Expression of defects in the environmental assessment in Australia on issues related to health, welfare and justice	- not taking into account other parameters related to environmental assessment - not taking into account the positive impacts of mining
da SilvaDias et al. (2019)	The results showed that EIAs have a low value for decision-makers because they do not show the actual impacts of mining activities on biodiversity.	- not taking into account the positive impacts of mining
Lemly (2019)	Prediction of possible negative impacts caused by mining activities	- not providing a functional model for solving the discussed problems

Table 8. continue: Summary of the studies on the environmental impact assessment of copper mines

Reviewed studies	Advantages	Shortcomings
Islam et al. (2019)	According to this study, LCA has been used in the metals and mining industry for decades and covers various materials, including base metal, precious metals, and fossil fuels.	Only extraction and processing steps are considered, and other measures are not considered in the evaluation. Moreover, only five factors are considered.
Ataei and Masir (2020)	Proposed a system classification using the fuzzy DEMATEL technique to study and analyze eleven impacting factor inter-relationships in open-pit mines.	Only 11 impacting factors are evaluated.
Dong et al. (2020)	Investigated the environmental impact of copper mines by LCA method.	8 Impact factors have been evaluated, and others have been ignored.
Zhang et al. (2021)	Using the LCA method, they compared the environmental impacts of copper mining with the two primary (mining) and secondary (recycling) methods.	Only the smelting and refining stages of copper tailings have been investigated. Only 14 factors are considered, and many factors are ignored.
Perlatti et al. (2021)	Investigated the impacts of an abandoned copper mine on the ecological quality of the region's ecosystem.	Only the percentage of copper remaining in abandoned copper mines' soil, water, and plant and animal species has been evaluated.

CONCLUSION

By studying the literature, it was found that 32% of environmental assessment studies used qualitative methods because many of the impacts in mines are not quantifiable. Nevertheless, qualitative researchers have personal judgment and lacks reliability. On the other hand, quantitative methods include 41% of the study, which examined the chemical content of heavy metals in water, soil, and air samples. Also, 75% of the quantitative studies used the LCA method, which evaluates the emission to the environment. Although these methods have been entirely scientific and precise to investigate mining impacts, some negative and positive effects that cannot be measured were ignored in these studies. 27% of environmental assessment studies used semi-qualitative methods in which qualitative positive and negative effects are turned into quantitative factors, and both kinds are assessed in the study. Of all the literature surveyed in this study, only two papers evaluated the positive environmental impacts of copper mines and the negative ones, which shows a critical shortcoming in the present literature.

REFERENCES

Amirshenava, S. & Osanloo, M. (2019). A hybrid semi-quantitative approach for impact assessment of mining activities on sustainable development indexes. *Journal of Cleaner Production, 218***,** 823-834.

Aryafar, A., Yousefi, S. & Doulati Ardejani, F. (2012). The weight of interaction of mining activities: groundwater in environmental impact assessment using fuzzy analytical hierarchy process (FAHP). *Environmental Earth Sciences, 68***,** 2313–2324.

Ataei, M. & MASIR, R.N. (2020). A fuzzy DEMATEL based sustainable development index (FDSDI) in open pit mining–a case study. *Rudarsko-geološk 76o-naftni zbornik,* 35.

Ataei, M., Tajvidi Asr, E., Khalokakaei, R., Ghanbari, K. & Tavakoli Mohammadi, M. (2016). Semi-quantitative environmental impact assessment and sustainability level determination of coal mining using a mathematical model. *Journal of Mining and Environment, 7***,** 185-193.

Castilla-Gómez, J. & Herrera-Herbert, J. (2015). Environmental analysis of mining operations: Dynamic tools for impact assessment. *Minerals Engineerin*g, *76*, 87-96

Clark, M. R. (2019). The Development of Environmental Impact Assessments for Deep-Sea Mining. *Environmental Issues of Deep-Sea Mining.* Springer.

Da Silva Dias, A. M., Fonseca, A. & Pereira Paglia, A. (2017). Biodiversity monitoring in the environmental impact assessment of mining projects: a (persistent) waste of time and money? *Perspectives in Ecology and Conservation, 15***,** 206-208.

Da silvadias, A. M., Fonseca, A. & Paglia, A. P. (2019). Technical quality of fauna monitoring programs in the environmental impact assessments of large mining projects in southeastern Brazil. *Science of The Total Environment, 650***,** 216-223.

Dong, D., Van Oers, L., Tukker, A. & Van Der Voet, E. (2020). Assessing the future environmental impacts of copper production in China: Implications of the energy transition. *Journal of Cleaner Production, 274***,** 122825.

Drielsma, J. A., Russell-Vaccari, A. J., Drnek, T., Brady, T., Weihed, P., Mistry, M. & Simbor, L. P. (2016). Mineral resources in life cycle impact assessment—defining the path forward. *The International Journal of Life Cycle Assessment, 21***,** 85-105.

Gałaś, S. & Gałaś, A. (2016). The qualification process of mining projects in environmental impact assessment: Criteria and thresholds. *Resources Policy, 49***,** 204-212.

Gorman, M. R. & Dzombak, D. A. (2018). A review of sustainable mining and resource management: Transitioning from the life cycle of the mine to the life cycle of the mineral. *Resources, Conservation and Recycling, 137***,** 281-291.

Hasanipanah, M., BAkhshandeh Amnieh, H., Khamesi, H., Jahed Armaghani, D., Bagheri Golzar, S. & Shahnazar, A. (2018). Prediction of an environmental issue of mine blasting: an imperialistic

competitive algorithm-based fuzzy system. *International Journal of Environmental Science and Technology,* 15**,** 551-560.

Heidari, M. & Osanloo, M. Sustainability Assessment of Angouran Lead and Zinc Mining Complex. Proceedings of the 27th International Symposium on Mine Planning and Equipment Selection-MPES (2018), (2018) Santiago, Chile. Springer, Cham, 523-534.

Hong, J., Chen, Y., Liu, J., Ma, X., Qi, C. & Ye, L. (2018). Life cycle assessment of copper production: a case study in China. *The International Journal of Life Cycle Assessment, 23***,** 1814-1824.

Hresc, J., Riley, E. & Harris, P. (2018). Mining project's economic impact on local communities, as a social determinant of health: A documentary analysis of environmental impact statements. *Environmental Impact Assessment Review, 72***,** 64-70.

Islam, K., Vilaysouk, X. & Murakami, S. (2019). Integrating remote sensing and life cycle assessment to quantify the environmental impacts of copper-silver-gold mining: A case study from Laos. *Resources Conservation and Recycling, 154***,** 104630.

Kuipers, K. J., Van Oers, L. F., Verboon, M. & Van Der Voet, E. (2018). Assessing environmental implications associated with global copper demand and supply scenarios from 2010 to 2050. *Global Environmental Change, 49***,** 106-115.

Kulczycka, J., Lelek, Ł., Lewandowska, A., Wirth, H. & Bergesen, J. D. (2016). Environmental impacts of energy-efficient pyrometallurgical copper smelting technologies: The consequences of technological changes from 2010 to 2050. *Journal of Industrial Ecology, 20***,** 304-316.

Lemly, D. A. (2019). Environmental hazard assessment of Benga Mining's proposed Grassy Mountain Coal Project. *Environmental Science & Policy, 96***,** 105-113.

Mancini, L. & Sala, S. (2018). Social impact assessment in the mining sector: Review and comparison of indicators frameworks. *Resources Policy, 57***,** 98-111.

Minaei Mobtaker, M. & Osanloo, M. Positive impacts of mining activities on environment. Conference: Beijing International Symposium on Land Reclamation and Ecological Restoration (LRER 2014), (2014) Beijing, China.

Morrison-Saunders, A., Mchenry, M. P., Wessels, J. A., Rita Sequeira, A., Mtegha, H. & Doepel, D. (2015). Planning for artisanal and small-scale mining during EIA: Exploring the potential. *The Extractive Industries and Society, 2***,** 813-819.

Muñoz, J., Guzman, R. & Botin, J. (2014). Development of a methodology that integrates environmental and social attributes in the ore resource evaluation and mine planning. *Int. J. of Mining and Mineral Engineering, 5***,** 38-58.

Norgate, T. & Haque, N. (2010). Energy and greenhouse gas impacts of mining and mineral processing operations. *Journal of Cleaner Production, 18***.** 266-27,.

Northey, S., Haque, N. & Mudd, G. (2013). Using sustainability reporting to assess the environmental footprint of copper mining. *Journal of Cleaner Production, 40***,** 118-128.

Ocampo-Melgar, A., Sagaris, L. & Gironás, J. (2019). Experiences of voluntary early participation in Environmental Impact Assessments in Chilean mining. *Environmental Impact Assessment Review,* 74**,** 43-53.

Osanloo, M. (2016). Top 10 Challenges in Mining. *6th International Conference on Computer Application in the Mineral Industries (CAMI).* Turkey.

Perlatti, F., Martins, E. P., De Oliveira, D. P., Ruiz, F., Asensio, V., Rezende, C. F., Otero, X. L. & Ferreira, T. O. (2021). Copper release from waste rocks in an abandoned mine (NE, Brazil) and its impacts on ecosystem environmental quality. *Chemosphere, 262***,** 127843.

Philips, J. (2012a.) Applying a mathematical model of sustainability to the Rapid Impact Assessment Matrix evaluation of the coal mining tailings dumps in the Jiului Valley, Romania. *Resources, Conservation and Recycling, 63***,** 17-25.

Philips, J. (2012b.) The level and nature of sustainability for clusters of abandoned limestone quarries in the southern Palestinian West Bank. *Applied Geography, 32***,** 376-392.

Philips (2013). The application of a mathematical model of sustainability to the results a semi-quantitative Environmental Impact Assessement of two iron opencast mines in iran. *Applied Mathematical Modelling*, 7839-7854.

Rahmanpour, M. & Osanloo, M. (2017). A decision support system for determination of a sustainable pit limit. *Journal of cleaner production,* 141, 1249-1258.

Reyes-Bozo, L., Godoy-Faúndez, A., Herrera-Urbina, R., Higueras, P., Salazar, J. L., Valdés-González, H., VYHMEISTER, E. & ANTIZAR-LADISLAO, B. (2014). Greening Chilean copper mining operations through industrial ecology strategies. *Journal of Cleaner Production,* 84, 671-679.

Riley, E., Sainsbury, P., Mcmanus, P., Colagiuri, R., Viliani, F., Dawson, A., Duncan, E., Stone, Y., Pham, T. & Harris, P. (2019). Including health impacts in environmental impact assessments for three Australian coal-mining projects: a documentary analysis. *Health Promotion International*, 1-9.

Saffari, A., Ataei, M., Sereshki, F. & Naderi, M. (2019). Environmental impact assessment (EIA) by using the Fuzzy Delphi Folchi (FDF) method (case study: Shahrood cement plant, Iran). *Environment, Development and Sustainability,* 21, 817-860.

Saini, V., Gupta, R. P. & Arora, M. K. (2016). Environmental impact studies in coalfields in India: A case study from Jharia coal-field. *Renewable and Sustainable Energy Reviews,* 53, 1222-1239.

Sarupria, M., manjare, S. D. & Girap, M. (2019). Environmental impact assessment studies for mining area in Goa, India, using the new approach. *Environmental Monitoring and Assessment,* 191, 1-17.

Shahhosseini, M., Doulati Ardejani, F., Amini, M., Ebrahimi, L. & MohebI Poorkani, A. (2019). Environmental geochemistry of As and Pb in a copper low-grade dump, Miduk copper mine, Kerman province, SE Iran. *Journal of Geochemical Exploration, 198*, 54-70.

Song, X., Yang, J., Lu, B., Li, B. & Zeng, G. (2014). Identification and assessment of environmental burdens of Chinese copper production from a life cycle perspective. *Frontiers of Environmental Science & Engineering,* 8, 580-588.

Suopajärvi, L. (2013). Social impact assessment in mining projects in Northern Finland: Comparing practice to theory. *Environmental Impact Assessment Review, 42*, 25-30.

Wang, H. T., Liu, Y., Gong, X. Z., Wang, Z. H., Gao, F. & Nie, Z. R. (2015). Life cycle assessment of metallic copper produced by the pyrometallurgical technology of China. Materials Science Forum. Trans Tech Publ, 559-563.

Zhang, W., Li, Z., Dong, S., Qian, P., Ye, S., Hu, S., Xia, B. & Wang, C. (2021). Analyzing the environmental impact of copper-based mixed waste recycling-a LCA case study in China. *Journal of Cleaner Production, 284*, 125256.

EVALUATION OF THE EXTRACTION OF VALUABLE MINERALS IN THE BEACH BLACK SAND IN THE COAST OF URUGUAY: SMALL SCALE MINING, ENVIRONMENT AND SOCIAL ISSUES

I.Tarjan [1, *], H. Ferrizo [1], F. Perez [1], Y. Castillo [1]

[1]*Universidad de la Republica, Uruguay, Centro Universitario Region del Este*
*(*Corresponding Author: ivan.tarjan@cure.edu.uy)*

ABSTRACT

Since the '50s it has been well known that the East Coast of Uruguay has a deposit of valuable mineral rich black beach send. It is analyzed, investigated but not exploited for economic, social, socio-economic and environmental issues. The deposit first analyzed in 1950 and defined high grade of titanium-dioxide, ferrotitanium, zircon also rare-earth minerals. For long it has not been considered an economically viable project, however several attempts were done from different investor groups to establish a reasonably profitable operation on the sites. Most of it failed because of the resistance of the local communities looking at it as a destructive and environmentally harmful activity. Nowadays, all over the world there is a great demand to find solution for the people left without jobs or income to sustain their family meanwhile governmental regulations make clear alignment on economic and environmental issues. This paper aims to describe the possibility of a small scale, low environmental impact socially and economically viable project in order to satisfy all the needs of industries and communities involved.

Keywords: Small scale mining, environment, sustainability, socio-economic impact

INTRODUCTION

The beach black sand is very well known as source of raw materials in different parts of the World. Magnetite, ilmenite and rutile are ores of iron and titan, monazite contains rare-earth minerals and normally there are zircon and garnet for other uses.The coast of Uruguay is very rich in black sand and the volume is considerable given the fact that almost all along the beaches it can be found.Prospection started in the 1950's by the initiative of the state company ANCAP to define volume and value of the material and make feasibility studies of its extraction. Several reports were made on it with different outcomes depending on the actual conditions and circumstances of publication, however all of them shown the same results in the sense of mineralogy and utility of the minerals.In 2015 started an initiative of “small scale sustainable mining” with help of the Foundation Fontaina Minelli to improve the culture of extractive industry in the country that has very interesting and rich history, anyway. To change the paradigm from looking at this activity as “the BAD” to one that can support the industry and the people with valuable prime materials without making destruction in an irresponsible manner, adding value to the society, was/is the proposal. In cooperation with the University of Republic of Uruguay that has an undergraduate course on mining in the CURE started the research and investigation of the most appropriate manner to take advantage of these resources. The situation of pandemic has an even more important effect on this project at this stage of economical restart and generate jobs and incentives to the most affected.

The Deposit and The Mineralogy

The first report was made in the area of Atlantida in 1952 by discovering and describing the minerals on the coast. Since than several other investigation and publication have been made on the subject with the same result, some of them are more detailed and shown available volumes for further works. Other detailed paper (Bossi et al. 2002) explains the geology and occurrence of the raw sand along the coastline. The signs of black sands have been observed in a large part of the Atlantic coast of Uruguay, as shown in the map (figure 1.), from the Aguas Dulces until Barra del Chuy.

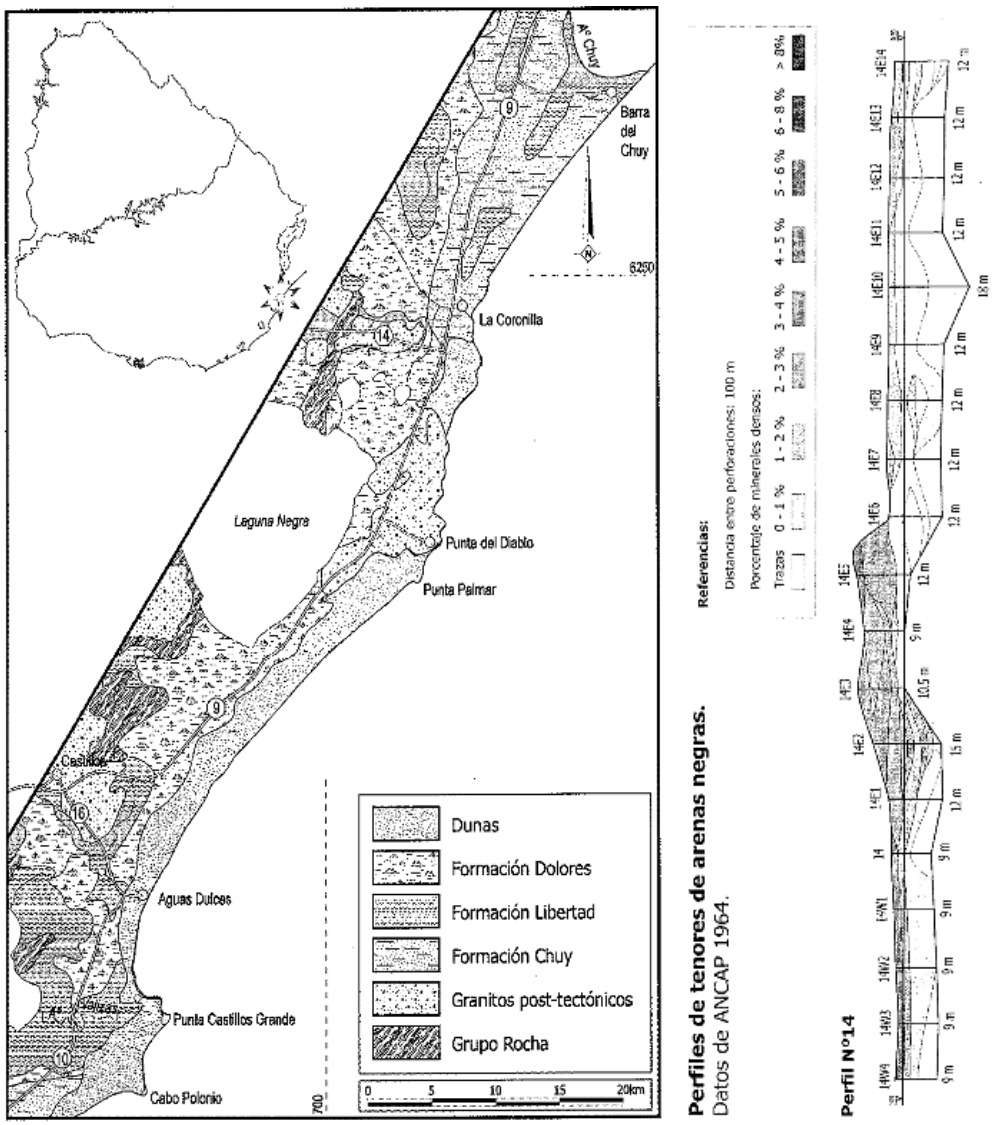

Figure 1. Geological map of one of the most studied zones with a sample profile of prospection

According to the investigations carried out, the constituent minerals of the deposit are ilmenite, monazite, rutile, zircon, garnet, epidote, tourmaline. The Aguas Dulces deposit is the one that has been investigated with the greatest emphasis, and where the preliminary results are known.

According to these tests (Soares de Lima 2002) the mineralogical association of the heavy fraction in the Aguas Dulces deposit, with the value economic is as follows: ilmenite (60%), rutile (1.2%), zircon (4.75%) and monazite (0.65%).

These documents conclude in the studied area (map) alone of approximately 22 million tons of heavy minerals that can be extracted from the surface from not more than 5 meters depth. This study covers only a small part of the coast that supposed to have the minerals from the mid-South-East beaches (Atlantida) to the very edge of the border in the South-East (Chuy). So, the prospected volume of useful material is much more than this (Soares de Lima 2002).

As per the value of the resource estimated by the referred report in 2002 was around 650 million USD in respect to the studied area. Once again, the entire resource can be considered even 3 times more.

Table 1. Updating these numbers to the current market should count as:

	ilmenite	rutil	zircon	monacite	Total
Reserve approved (ton)	5760	480	96	48	
Value (USD/t) 2002	70	354	312	1050	650 M USD
Value (USD/t) 2021	340	1200	1630	6000	6981 M USD

The composition of the material shows the following results (Bossi et al., 2002; Abre et al. 2021):

Table 2. Mineral composition of black sand

	Magnetite/ilmenite	rutil	zircon	monazit
content	60 – 80 %	0.7 - 2 %	0.5 – 15 %	2 – 11 %

Earlier studies on other sites show very similar values (Soares, C. et al. 2002)

Different samples show slightly different compositions; however, it is agreed that the genesis, formation and natural processes tend to homogenize the sand along the beaches.

A representative map in one of the other areas of interest gives details of the drilling/prospection holes and the measured content of minerals is on the Figure 2.

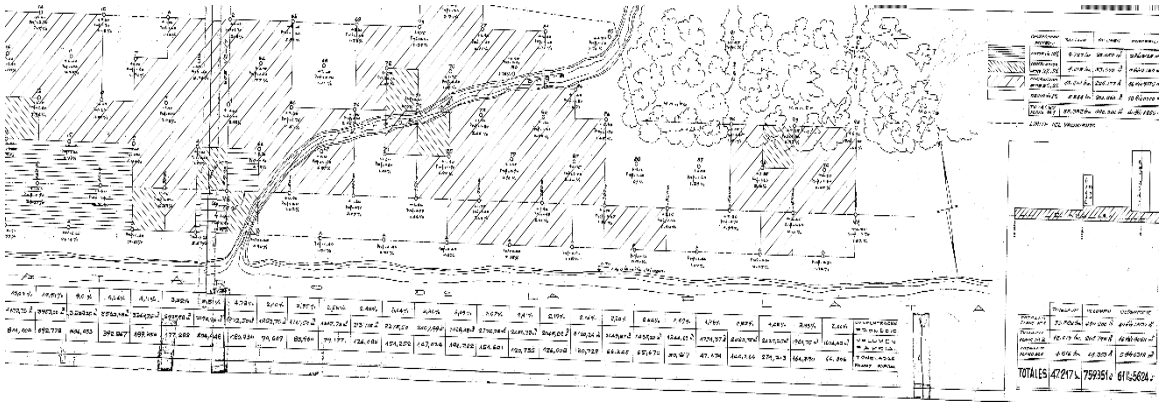

Figure 2. Exploration result map in the area of San Luis (ANCAP, 1964)

The general grain size distribution shows variation in the heavy part, which results the careful examination of the physical properties of every location in order to establish the simplest methods for

the beneficiation, like gravity separation. In the table 4. it is more likely that the finer fraction contains more heavy minerals (Soares de Lima 2002; Abre et al. 2021).

Table 3. Granulometry of the black sand

Granulometry in microns	**% weight**	**% heavy in concentrate fraction**	**Density > 2.9**	**Density < 2.9**
250 µ	0.2	50.0	0.1	0.1
250 µ a 177 µ	9.7	15.5	1.5	8.2
177 µ a 149 µ	11.3	25.7	2.9	8.4
149 µ a 105 µ	39.9	81.2	32.4	7.5
105 µ a 74 µ	30.8	89.5	27.5	3.3
Menos 74 µ	8.1	98.8	8.0	0.1

Studies on radioactive measurements of the samples also show and proves content of Polonium and/or Thorium in the heavy fraction and the monazite must bear REE as well. (Abre et al. 2021).

The above photo shows under microscope the composition of the black sand.

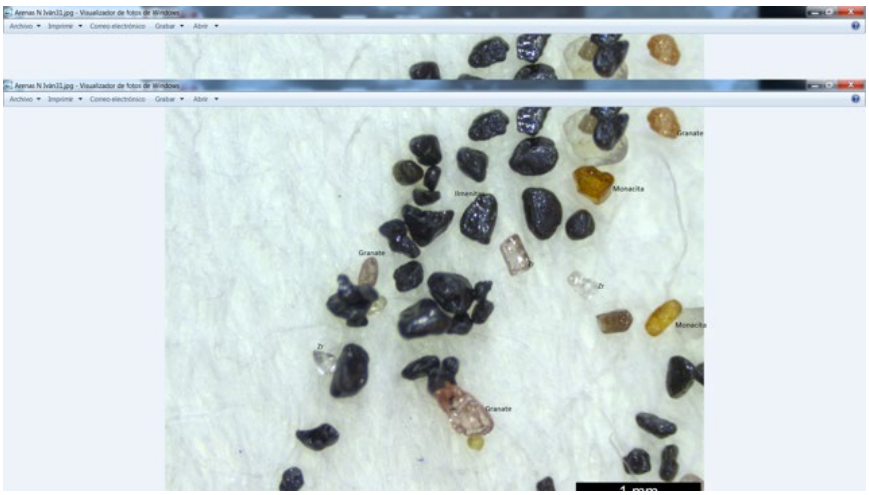

Figure 3. Microscope image of the black sand with its composition

Also, the Figure 4. above shows the distribution of the different no ferromagnetic minerals (magnetite and ilmenite were separated before the study) in the black sand. The samples are from the San Luis site.

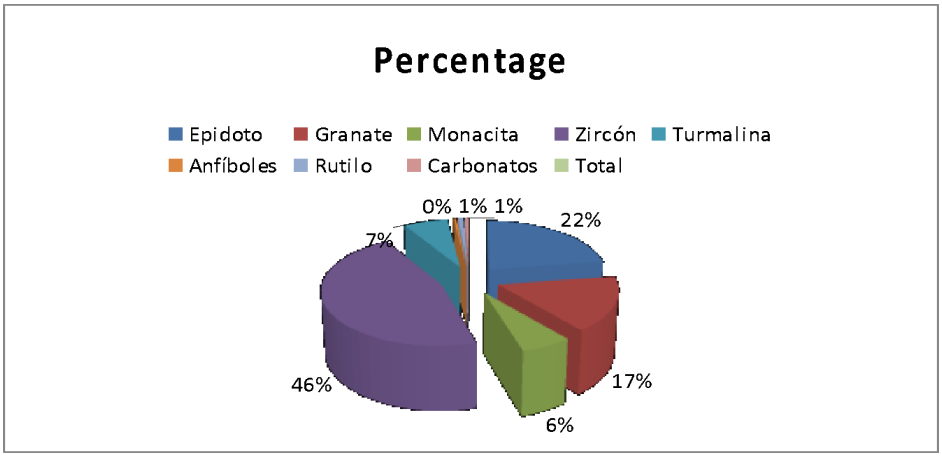

Figure 4. Distribution of the non-ferromagnetic minerals in the black sand sample of San Luis site

In summary we can be assured that this beach black sand is full of useful minerals to consider its extraction in an appropriate scale and manner.

Processing

As it is shown in table 4. the sand can be separated first by density, then magnetically to obtain semi- or intermediate products to be sold. The density difference in the minerals and the sand indicates good efficiency if concentration by simple equipment, like a concentration spiral, while the magnetic properties of the different parts allow very good and sharp separation of them. Our tests show the results below.

The most important properties of the heavy minerals are the density and magnetism. As per the first in general all of them have a density higher than 4 t/m^3.

Looking at the magnetic properties the ilmenite (with magnetite) shows ferromagnetism, there are paramagnetic minerals, and nonmagnetic ones, like zircon. Consequently, it is very viable to separate the heavy minerals with a magnetic separator to achieve concentrates or products accordingly.

Table 4. Main mineral properties and contents

Mineral	Principal product	Compositión	Density	Hardness (Mohs)	Tipical content
Ilmenite	Titan	FeTiO3	4.5/5.0	5-6	45-65% TiO2
Leucoxene	Titan	Altered Ti minerals	3.5-4.5		70-93% TiO2
Rutile	Titan	TiO2	4.23-5.50	6-6.5	95-97% TiO2
Zircon	Zircon	ZrSiO4	4.2-4.86	7.5	63-67% ZrO2 (Hf)4
Monazite	Tierras Raras	(REE) P04(Ce,La,Nd,Th)	4.6-5.4	5-5.5	50-70% REE
Xenotime	Tierras Raras	(REE) P04Y(REE)	4.40/5.10	4.5	60-68 % Y/REE

It is well known that “simple” gravity separation has good efficiency when the density ratio between different particles is more than 2:1 to 1,5:1. In our case the sand as general can be considered as a 2.3-2.6 t/m^3, while the heavy part is over 4 t/m3. These values permit us to employ equipment

simple and easy to use without important education and technical knowledge of the personnel to operate.

In the separation plant a LDMS (Low density magnetic separator) can produce high grade magnetic concentrate of iron ores, a HDMS (High density magnetic separator) would do the separation of paramagnetic materials meanwhile the rest contains the zircon and rutile with the impurities of the raw material.

Installation

As the processes are simple the extraction can be done with simple equipment, too. Install a 4x4 pick-up with a concentration spiral can process 1-4 t/h raw material with the help of a water pump to feed it and two storage dishes to receive the concentrate and the middling for further processing. Water is available from the sea or the boreholes as the water level is near the surface. There is a need for a recipient or tank for the raw material to be mixed/agitated for feeding the spiral on the top of itself.

The feed should be around 25-30% of solid content so a 30 liter/min pump can comfortably serve the equipment.

As an energy source the most convenient way would be to use a pump with a combustion motor, however there are already available good, independent/off-grid electric supplies that can serve for an installation at this size. (5) Even further, compressed air-electric power supply, or other alternatives (green hydrogen) also can be considered as they are getting more and more accessible and important from the environmental point of view.

This activity needs 2, max 3 persons on board without any prior technical knowledge or experience and processes 0,16-3,2 metric tons of black sand per 8 hours shifts.

The concentrate can be transported than to the central deposit where the magnetic separation can be taken place producing the “products”.

Environmental Impacts

The extraction of beach black send is considered as the lowest impact on the environment. Mainly because of the ore concentration is low (in our case is 2-6%), the gangue material stays in the site as washed or cleaned sand re-deposited to its original place and no need for grand installations.

In our specific case no installation of buildings or machinery is considered, only mobile equipment and temporary workplaces would be established. The capacity is low as well, but with several working groups it can reach the sufficient volume to feed the separation plant economically.

As the only additional „raw material” needed for the exploitation is water and all the activity should be done on beaches, it must not mean any inconvenience. There are no chemicals used that can contaminate the environment.

In case the energy source would not be combustible for the pump operation, but alternatives would be considered there is no air contamination, not even noise presented.

From the nature point of view the situation is a bit more shadowed. The naturally concentrated materials are on beaches, however, not inhabited ones. As well there are dunes for the vegetation and wildlife that is very important as natural barriers against the destruction of the sea and gives refuge a wild variety of flora and fauna. Nevertheless, the majority of the resource falls outside of protected

areas and a well-established administration of granting permissions can avoid any sort of environmental damage.

As per the tourism we consider that small scale, individual extraction out of season would not interfere to the interest of this industry, the job can be done with great care and attention.

Socio-Economical Impacts

At the moment of pandemic/post-pandemic condition all over the world it is a key issue to re-establish or restart economical activities. Lack of workplaces, lack of income results other type of problems to be solved: the social issues. If there were jobs, people would have an income to live on that would result resilience for the families.

To establish an appropriate business plan for this proposal not the objective of this investigation, but it should be done in case to put it on the run. But to create a very approximate balance it should be consider that:

Small scale sustainable mining can have a positive impact in this recovery. Its impact in employment, by the creation of several micro businesses, could be relevant, in particular, in areas where the lack of opportunities is the rule.

In this stage, it's possible to draw the relevant features of this business plan, prior to full development.

The first thing to notice is the presence of a resource with a certain market value, 7.000 M USD at actual prices (22 million tons)

Given the value of 7.000 M USD worth resource (22 million tons)
Capital expenditure / working group should not exceed the 2.500 USD
Capacity / working group per year can be limited to 100 tons with 20 years lifespan
Results 10.000 working group by 4 persons
Capital expenditure to a separation plant is about 500.000 USD
Profitability 30% on product sold
Costs of production in the separation plant per year (electricity+ human resources) 500.000 USD

Should result an average income of around 500-510 USD/month/person before tax and expenditures (capital payback, general costs of transport), meanwhile the „company" should receive 95 m USD/year before tax and costs.

The market for these products is located abroad, there are no national possibilities of processing.

Obviously, the above numbers depend on the actual prices, but it seems to be a good margin to propose a viable business plan that benefits all players.

CONCLUSION AND FURTHER ASSESSMENTS

The current project aims to define the way how a destructive activity - like mining – can be done with minimal environmental effect but with good social acceptance, low inversion and good return. However, it is vital to define the proper and detailed composition of the black sand regarding on the most critical metals and materials (REE, Th, Ti).

We found a very interesting and valuable source of minerals what for we are still looking for market. The results of this process are listed on different sites as semi-products or intermediate raw materials, so business plan can be assembled to look at feasibility.

The necessary investment is very low, easy to operate, clean (no need for chemicals, additives, etc.).

On the environmental side the biggest problem appears to be on the conservation sites and the opposition of ecological movements. Another caveat is the limited capacities to properly enforce any regulation of the areas of extractions. Therefore, further investigation should be done on the critical sites with unique areas of the local flora and fauna to inform the authorities for permission evaluation.

We found as well that the socio-economic impact would be huge, people could find jobs of their own account, financially viable with a very decent income for long term. However, a proper plan is necessary to put all the above on the practice, which seems to be a bit difficult in the sense of administration, distribution of information and final decisions.

REFERENCES

Abre, P., Bañobre, C., Fornaro, L., Garcia-Tenorio, R., Vioque Romero, I., 2020: Relacion entre los minerales pesados de la costa del Departamento de Rocha (Uruguay) y la emision alfa de las arenas (XXI Congreso Geologico Argentino, Sesion tecnica XX).

Abre, P., Blanco, G., Ferrizo, H., Cingolani, C., Uriz, N.,Arnol, J., 2021: Minerales pesados de la costa del departamento de Maldonado (

Ferrando, L., Bossi, J., Maldonado, S., Schipilov, A.,Campal, N., 2003:Evaluacion de arenas negras en Aguas Dulces, Departamento de Rocha, Uruguay (Revista de la Sociedad Uruguaya de Geologia, III Epoca No. 10, 2003)

Soares de Lima, C., 2002: Estudio geologico Minero del deposito de arenas negras de Aguas Dulces (Study for the Ministerio de Industria, Energia y Mineria, Direccion Nacional de Mineria y Geologia del Uruguay, 2002)

EXTRACTION DESIGN OF HIGHWALL MINING IN INDIA TO RECOVER LOCKED-UP COAL USING EMPIRICAL AND NUMERICAL SIMULATIONS

P. Pal Roy

CSIR-Central Institute of Mining & Fuel Research
(ppalroy@yahoo.com)

ABSTRACT

Many Indian opencast mines are reaching their pit limits and existence of surface dwellings mostly limits the expansion of such mines. In large number of cases, the overburden becomes so thick that coal extraction becomes uneconomical by conventional drilling and blasting. Under such circumstances, the use of highwall mining machines where a cutter is placed on the top of a system similar to a continuous miner, and taken through a conveyor into the seam almost 500-600 m deep inside, it becomes possible to extract a good proportion of such stuck-off coal which otherwise remained tapped owing to limited means and high-cost of mining. However, such mining system requires suitable scientific extraction design which is safe and productive. The CSIR-Central Institute of Mining and Fuel Research (CSIR-CIMFR) has provided the extraction design to recover 45 to 60% of locked-up coal using empirical and numerical simulations. This paper provides the scientific elucidation of the design technology adopted by CSIR-CIMFR in the first four potential opencast mines in India along with their safety and productivity aspects.

Keywords: Highwall mining, web pillar, pillar strength, roof convergence, safety factor

INTRODUCTION

Several opencut coalmines, around the globe, are reaching their pit limits. Existence of surface dwellings in many places limits the expansion of currently running opencut mines. Also, in many cases, the overburden becomes so thick that coal extraction becomes uneconomical.

Continuous highwall mining (CHM) is a relatively new technology which can extend the life of opencast mines without disturbing the surface dwellings, while maintaining economy and productivity. It is a remotely operated coal mining technology which consists of the extraction of coal from a series of parallel entries driven into the coal seam from the face of the highwall. These entries are unmanned, unsupported and unventilated. This technology uses highwall mining machines such as a continuous miner which takes through a conveyor inside the seam almost 500 to 600 m. In the present day, penetrations up to 500 m have been consistently achieved with highwall mining systems, in contrast to auger mining wherein penetrations are limited to 100–150 m. The method comprises extraction of coal from a series of parallel entries driven in the coal seam from the face of the highwall. The method can be successful only if a feasible extraction design is made considering the complex rock geology and existence of multiple coal seams especially in Indian coalfields, which is unique in many respects.

The CSIR-Central Institute of Mining and Fuel Research (CSIR-CIMFR), Dhanbad a constituent R&D laboratory under the aegis of Council of Scientific and Industrial Research (CSIR) came out with the first extraction design for the complex Indian geo-mining conditions existing at the three highwall mining sites at Ramagundem Opencast Project-II and Medapalli OCP of M/s Singareni Collieries Company Ltd (SCCL), and Quarry SEB and AB, West Bokaro of M/s Tata Steel Ltd. (TSL). CSIR-CIMFR also worked for stability of highwall slope and improvement of blasting efficiency and pre-split blasting for the formation of highwall benches at Sharda Opencast Project of M/s South-Eastern Coalfields Ltd. (SECL), which was a very challenging task offered by M/s Cuprum Bagrodia Limited, who had been operating the highwall mining system at Sharda Project very successfully (CIMFR Technical Reports: GC/MT/139/2007-2008; GC/MT/174/2008-2009; CNP/2586/2010-2011 and CNP/4012/2014-15).

In India, the first highwall mining system started operation on 10th December 2010 at Opencast Project-II (OC-II), Ramagundam Area-III (RG-III) of Singareni Collieries Company Ltd. (SCCL). The extraction design at this site was provided by CSIR-CIMFR and the same was operated by Advanced Mining Technology (AMT) of Hyderabad using ADDCAR highwall mining system of USA. The machine started extraction of locked-up coal beneath the opencut highwall under the guidance and monitoring of CSIR-CIMFR. Over two lakh ton of locked-up coal was recovered from seam-I and seam-II. Extraction in seam II had problems due to unexpected geological discontinuities and poor roof conditions. However, in seam-I, the extractions went smoothly with almost all the holes extracted to full-length as per the design opted by CSIR-CIMFR. Almost 1/5th of the total project cost of highwall mining was recovered from OC-II.

The machine was then shifted to the second nearby mine namely Medapalli Opencast Project of SCCL (Singareni Collieries Company Limited) for extraction of 6 seams. It extracted around 8 lakh tonn of trapped coal from 4 Seams and almost the complete HWM project cost was recovered from Medapalli OC Project. There had been no safety issues due to judicious guidance right through.

The Tata Steel Limited (TSL), West Bokaro Division proposed to extract the locked-up coal in the final pit slope of Quarry SEB and that lay below Banji village in Quarry AB at West Bokaro Group of Collieries using the Continuous Highwall Mining (CHM) system. In that context, CSIR-CIMFR carried out the feasibility study on the design and safety aspects of highwall mining for implementation.

At Quarry SEB seams V, VI, VII, VIII, IX, X Lower, X Upper and XI existed in ascending order and were exposed on the highwall towards the eastern side of the quarry. At Quarry AB, the coal seams left below Banji village and those considered feasible for extraction from the final highwall abutting the village boundary included seams V, VI, VII and VIII, occurring in ascending order. All the seams were gently dipping, with 3-7° inclination and occurred at a depth of 16-150 m within the proposed highwall mining sites.

At Quarry SEB, no significant surface features existed, whereas Banji village has been densely populated with residential houses, to be protected from surface subsidence on a long-term basis. The final pit slope in both the quarries had been designed by CSIR-CIMFR (CSIR-CIMFR, 2000; 2008c). Starting in April 2016, up till March 2019, the coal production from West Bokaro Collieries touched 1.5 million tonne costing nearly US $36.4 million (Indian Rupees 248 crore).

At Sharda Project, CSIR-CIMFR worked for two different assignments namely (i) Design of optimum highwall slope and (ii) Basting efficiency and pre-split blasting for formation of highwall benches. The powder factor in the production blasting was drastically improved from 1.3-1.4 m^3 of rock per kg of explosive consumption to around 2.0 m^3 of rock per kg of explosive resulting in huge savings on explosive consumption as well as environmental implications of such blasting operations.

DESIGN ASPECTS

Web pillars were designed for all the seams separately for each block. The methodology adopted for the empirical design is given below (Loui et al., 2013a, 2013b, 2013c, 2013d; Loui et al., 2014).

Estimation of Pillar Strength

The estimation of pillar strength was done using CSIR-CIMFR pillar strength formula, which reads as-

$$S = 0.27\sigma_c h^{-0.36} + \left(\frac{H}{250}+1\right)\left(\frac{W_e}{h}-1\right) \text{MPa} \quad (1)$$

Where,

S = strength of the pillar, MPa
σ_c = strength of 25 mm cube coal sample
h = working height, m
H = depth of cover, m
W_e = equivalent width of pillar, m = 2W for long pillar
W = width of web pillar, m

Pillar Load Estimation

Load on pillars was estimated using Tributary area method, which reads as:

$$P = \frac{\gamma H (W + W_c)}{W} \quad (2)$$

Where,

P = the load on web pillar, MPa;
γ = the unit rock pressure (0.025 MPa/m) and
W_c = the web cut width, m

The design patterns provided by CSIR-CIMFR were reviewed thoroughly at the mine site to check the operational feasibility during field implementation (Figure 1). Figures 2 and 3 depict the roof stability of I seam extractions and stress-strain curve as well as plasticity states of a Model of OC-II, SCCL while Figures 4, 5 and 6 illustrate stress-strain curves and safety factor contours of Quarry SEB, Tata Steel Limited (TSL) obtained by numerical modelling.

Figure 1. Design review at the site of MOCP Medapalli OC Project

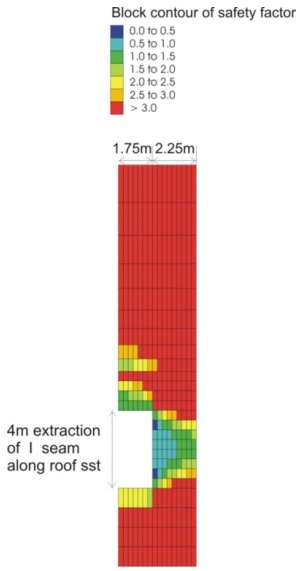

Figure 2. Roof stability of I seam extractions OC-II, SCCL

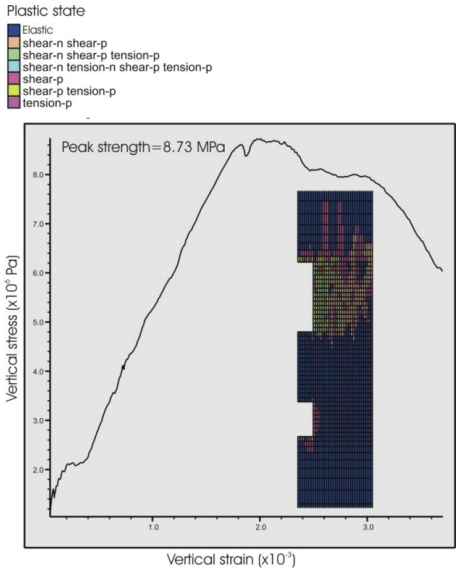

Figure 3. Stress-strain curve and plasticity states of a Model of OC-II, SCCL

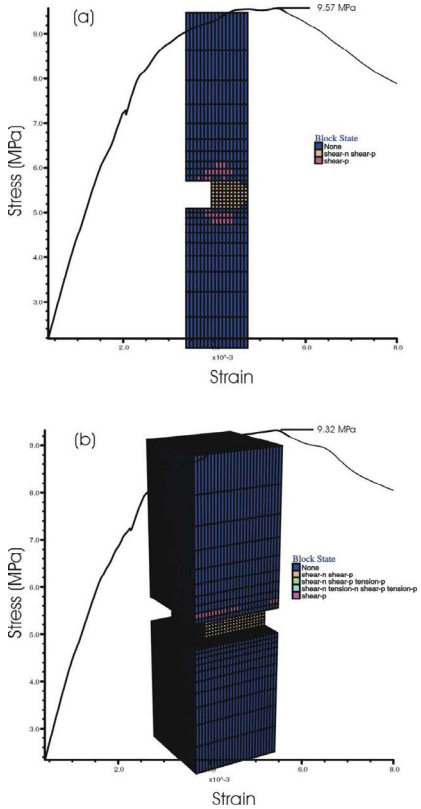

Figure 4. Stress-strain curves for width/height ratio of 2.5 in (a) long pillar

(b) equivalent square pillar of Quarry SEB, TSL

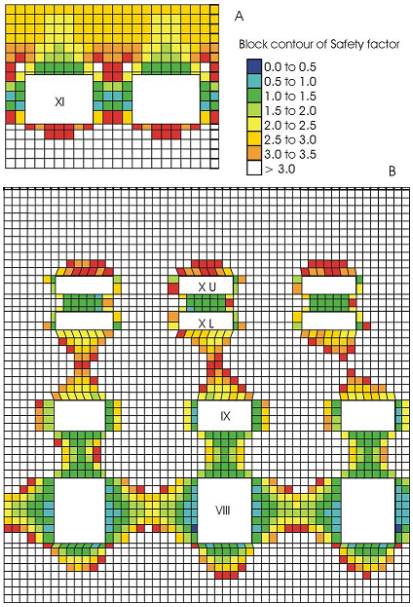

Figure 5. Closer view of safety factor contours in (A) Seam XI and (B) Seams XU, XL, IX and VIII of Quarry SEB of Tata Steel Limited (TSL) of the design of Highwall Mining carried out by CSIR-CIMFR for the first time in the country

Safety Factor

Safety factor (S.F.) of the pillars was calculated using the following equation:

$$S.F. = \frac{Strength\ of\ web\ pillar}{Load\ on\ web\ pillar} = \frac{S}{P} \quad (3)$$

The CSIR-CIMFR pillar strength equation had been developed over a couple of decades after analyzing a large number of pillar stability observations from a gamut of Indian mining scenarios. On the basis of past experiences from Indian coalfields it was observed that a pillar safety factor of more than 2.0 is long-term stable, i.e., for many decades. A safety factor between 1.5 and 2.0 may be taken as medium-term stable, stable for a few years. If the safety factor of the pillar is 1.0, it may be treated as short-term stable, with a standup time of a few weeks or a month.

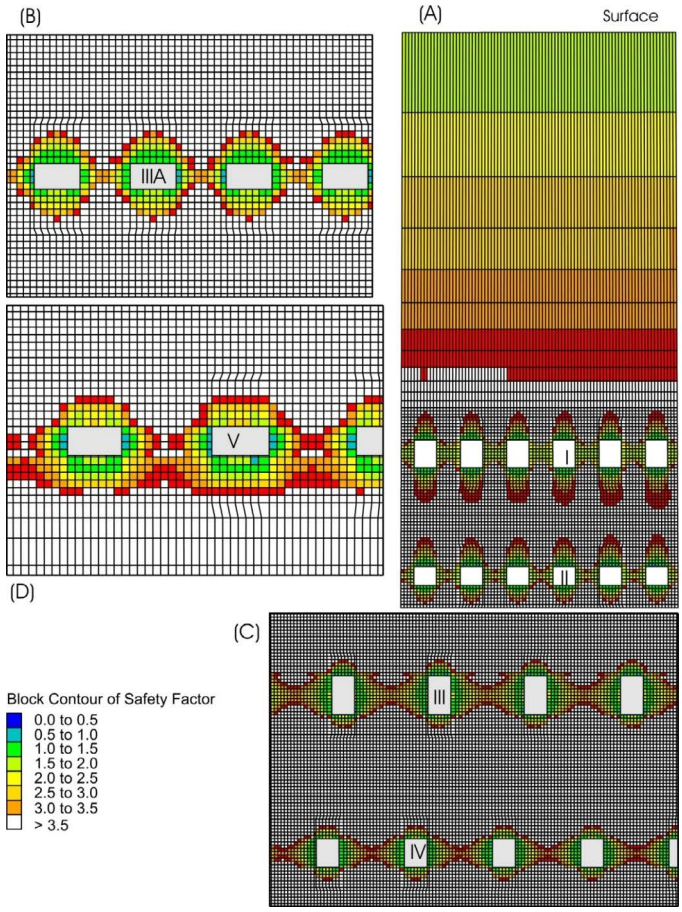

Figure 6. Closer view of safety factor contours in individual seams of Block A, MOCP

Pictorial views of highwall mining operations in India are shown in Figures 7, 8, 9 and 10.

Figure 7. Inauguration of 1st Highwall Mining System in India at OC-II, RG-III Area, on 10th December, 2010

Figure 8. View of ADDCAR-make Highwall Mining machine in operation at SCCL

Figure 9. View of Highwall Miner at Sharda Highwall Project of SECL

Figure 10. Production of coal from the first Highwall Mining in India at OC-II, RG-III Area of SCCL

MONITORING GROUND MOVEMENT AT SURFACE

In order to fulfill the statutory requirement, two panels/blocks were selected for highwall mining in OC-II at Ramagundam Area of M/s Singareni Collieries Company Limited. The highwall was inclined at an angle of 45° towards the dip of the seam (Panel–B) as well as along the seam strike (Panel–A). Initially, working was started in Panel–B of bottom seam No. 2. The height of the wall was 100 m vertically from the decoaled edge of seam No. 2. The dip of the seam was 1 in 4.5. No bench existed in the highwall within the study block. It was proposed to mine two seams namely, seam No. 2 and seam No. 1 (Prakash *et al.,* 2014).

The panels were designed for no ground movement. As the technique was adopted for the first time in India, DGMS proposed to evaluate the stability of the highwall during the course of extraction for the safety of men and machinery. Figure 11 shows the plan layout of monitoring stations over highwall panels at OC-II, SCCL.

Stability Study

The stability study was conducted continuously using Total Station having a linear least count of 1 mm with an accuracy of ±2 mm. A baseline (Figure 12) was established outside the influence zone of any ground movement due to highwall mining. The coordinates of baseline are given in Table 1. The reduced level was taken from Station No. 413 (Table 1). The lateral displacement of the ground as well as vertical movement of the surface was monitored to evaluate stability of the highwall during mining operation. Coordinate of each station was monitored from the base-line for lateral displacement and Missing Line Measurement (MLM) option was used for study of vertical displacement. Care was taken to keep the error of subsidence measurement minimum by maintaining the distance between instrument and the target within 100 m so as to accurately coincide centre of the target.

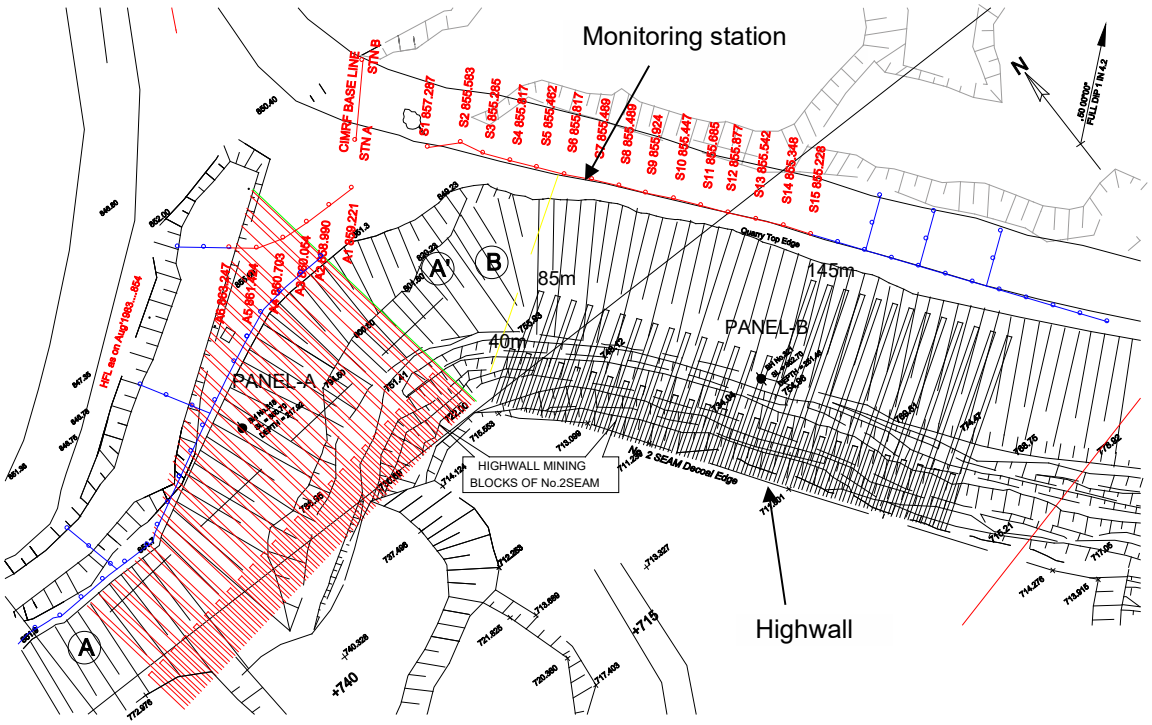

Figure 11. Plan showing layout of monitoring stations over highwall panels, OC-II, SCCL

Figure 12. Establishment of baseline for orienting highwall miner for parallel web cutting using Total Station

Table 1. Coordinates of baseline stations

Station	North (m)	East (m)	RL (m)
A	933704.305	3060397.341	
B	933745.895	3060436.186	
413	933681.369	3060412.522	860.400

Observations on Measured Values

Initially there was slight fluctuation in the measurement due to settlement of the monitoring stations over the dump. A few stations got disturbed during the course of road cleaning. There were variations in the coordinate measurements in few millimetres due to cumulative effect of parallax error and target levelling error. It was evident from data that there was no trend of lateral movement of the mine edge towards the open-pit during the mining operation. There was no vertical displacement of the surface ground i.e., subsidence, during the study period.

STABILITY OF THE HIGHWALL

Stability assessment of the highwall slopes was made based on the stability analysis using "Slope Stability Analysis Software" (GALENA version 4.02). The stability analysis was conducted considering circular and non-circular failure surfaces passing through the ultimate slope. Bishop's method of multiple analysis was used for circular failure conditions whereas Sarma's method was considered for non-circular failure conditions (Jhanwar *et al.,* 2014). At Medapalli OCP, the heights of ultimate slopes (Highwall) were considered at 105 m in the rise side/strike direction for Block A and at 152 m in the dip side for Block B of MOCP. The overall slope angle of Highwall/Ultimate slope was considered at 44^0 in both rise and dip side highwall (Figure-13).

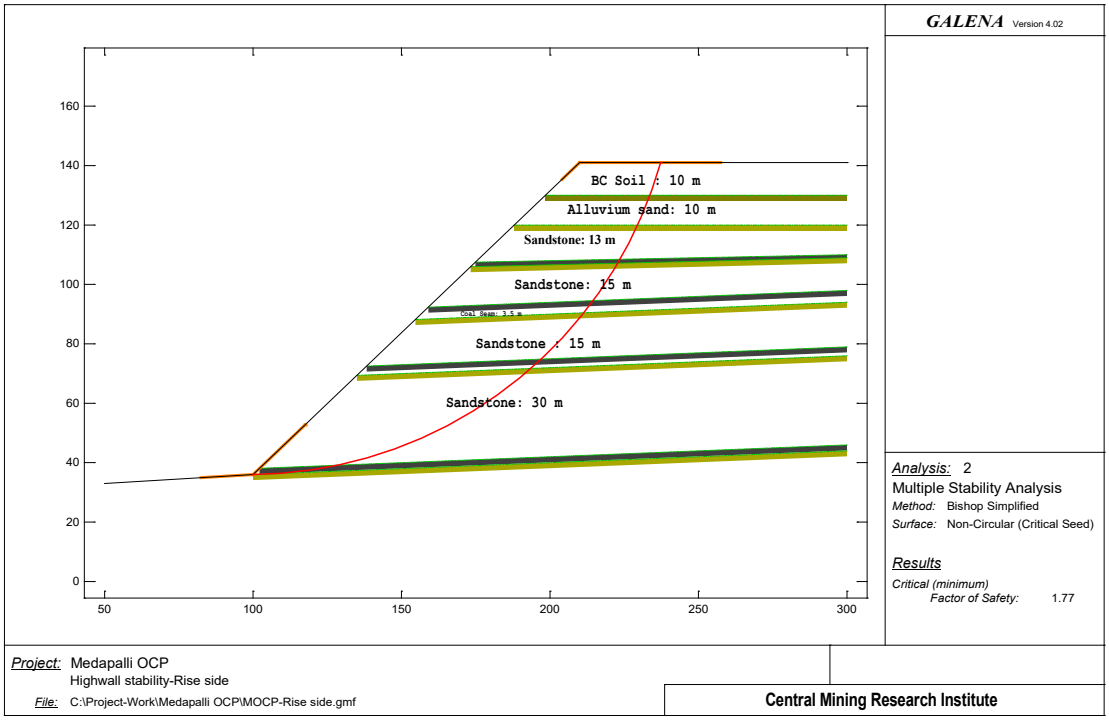

Figure 13. Stability analysis of the rise/strike side (Block A) highwall along Section C-C', MOCP

IMPACTS OF SURROUNDING BLASTING ON HIGHWALL MINING

Any blasting activity close to highwall mining may affect the stability of highwall mining entries, web pillars as well as highwall of the opencast from where the workings are to be executed. Ground vibrations generated by day-to-day blasting operations nearby the highwall mining entries can impose immature roof and side collapse, thereby, trapping the continuous miner (highwall hog or any other make, as the case may be) inside the mine entries. Flyrock generated from blasting nearby the highwall mining could also damage the equipment used for the mining like launch vehicle etc. and impose safety concern to the workers.

Blast-induced ground vibrations may also affect the stability of the highwall slope. Ground vibrations have two-fold actions on rock mass. On one hand, they affect the integrity of the rocks or their strength parameters while on the other, they can provoke wall or slope collapses when unstabilizing actions are introduced. During the process of blasting, the energy that is not used in fragmentation and displacement of rock, propagates through the rock-medium beyond the zone of disturbance and reduces the structural strength of the rock mass outside the theoretical radius of action of excavation. New fractures and planes of weaknesses are created and joint, declasses and bedding planes that initially behaved non-critical, when opened, result in an overall reduction of rock mass cohesion. This is manifested by overbreak, leaving fractured mass in a potential state of collapse. The following generalized criteria, as given in Table 2, for damage level of particle velocity on rock mass and slopes, were taken into account while designing the highwall mining operations (DGMS Technical Circular, 1997). As such there is a remote possibility of any damage on rock mass and slope due to nearby blasting operations beyond a distance of 500 m from the highwall face.

Table 2. Damage level of rock mass based on ground vibration

Particle velocity (mm/s)	Predictable damages
< 250	No danger in sound rock
250 – 600	Possible sliding due to tensile breakage
600 – 2500	Strong tensile and some radial cracking
> 2500	Complete break-up of rock masses

GENERAL SAFETY REQUIREMENTS

In addition to the specific requirements of a site, there are a few general requirements that must be fulfilled for safe highwall mining conditions as suggested by Porathur et al. (2017). These are given below-

a) No person shall be allowed to enter the web cuts.
b) Meticulous planning should be carried out to keep the highwall available so as to prevent the machine being idle.
c) Working platform of CHM formed by dump material should be thoroughly consolidated for safe positioning and operation of the equipment.
d) In no case should the bench width be less than the maximum dimension of the launch vehicle plus an additional 10 m for operational requirements, free movement of loaders, etc.
e) Pit floor should be kept free from water and, if required, a suitable pumping arrangement should also be made.
f) Effective drainage system should be implemented to divert surface run-off/rainwater entering into web cuts.
g) If highwall slope is steep and height is more than 50 m, catch benches should be provided on the highwall at regular intervals to arrest the fall of loose material, hence ensuring stability during mining.
h) Accurate and detailed up-to-date hole completion plan should be maintained for each and every seam targeted for highwall mining.
i) All electrical enclosures and operating sensors should be intrinsically safe or flameproof certified.
j) Preventive maintenance schedule should be planned and implemented for all equipment.
k) Every moving part of the machine should be adequately covered, fenced and guarded.
l) Operator should ensure proper functioning of all sensors and on-board cameras prior to the commencement of a web cut.
m) No unauthorised person should be allowed to enter into the mining area.
n) Adequate arrangements should be made for the training of personnel regarding drivages of web cuts and maintaining safe operating conditions near the highwall.

CONCLUSIONS

In India a huge potential for new coal mining technologies is envisioned to up the ante on much-needed coal demand for the energy sector. Seen as a proven technology in USA, Australia and some other parts of the world, it was not a difficult decision for Indian mining companies to try this technology though Indian coal geology is complex compared to some other parts of the world. The occurrence of thick and multiple seams, and some at close proximity, with frequently varying roof conditions etc., makes mining difficult and challenging. Available conventional design methods of highwall mining do not incorporate

multiple seam interaction, does not account for pillar slenderness ratio, safety factor variations due to hole deviations, end effect and combination of short and long holes. CSIR-CIMFR design methodology incorporates all the above complex geological concepts and is therefore more realistic and comprehensive from optimum coal recovery and safety point of view.

CSIR-CIMFR, being the sole developer of highwall mining design in the country, it is anticipated that huge amount of foreign currency can be saved (nearly US$ 0.21 million per Project). Coal recovery of even up to 60% had been designed by CSIR-CIMFR at the four said mining sites. In the process, novel approaches for pillar designing had also been formulated specifically for long and slender web pillars formed during highwall mining operations, which is unique in the world.

REFERENCES

CIMFR Technical Report. (2008). Highwall mining at Ramagundem Opencast Project –II (OC-II) of M/s Singareni Collieries Company Limited (SCCL). Project No. GC/MT/139/2007-2008 (Phase-I Study), February, 66 p.

CIMFR Technical Report. (2009). Feasibility study for highwall mining at Quarry SEB (and Quarry AB), West Bokaro Division of M/s Tata Steel Limited. Project No. GC/MT/174/2008-2009, March, 56 p.

CIMFR Technical Report. (2011). Highwall mining at Medapalli Opencast Project (MOCP) of M/s Singareni Collieries Company Limited (SCCL). Project No. CNP/2586/2010-2011, p. 57, March, 57 p.

CIMFR Technical Interim Report. (2015). Scientific study for improvement of blasting efficiency and pre-split blasting for the formation of highwall benches at Sharda Project, SECL. Project No. CNP/4012/2014-15, April, 40 p.

DGMS Technical Circular 7. (1997). Standards of safe level of blast induced ground vibration for safety of structures. Ministry of Labour, Government of India.

Loui, J. P., Karekal, S., & Pal Roy, P. (2013). Web pillar design approach for highwall mining extraction. *International Journal of Rock Mechanics and Mining Sciences*, *64*, 73-83.

Loui, J. P., Pal Roy, P., Verma, C. P., & Karekal, S. (2013). Extraction design for multiple seams highwall mining in India – A case example. Procs. 47th US Rock Mechanics Symposium, San Francisco, USA, 23-26 June, 3, 1656-1660.

Loui, J. P., Pal Roy, P., Prakash, A., Jhanwar, J. C. (2013). Extraction design of locked-up coal by highwall mining in India. 23rd World Mining Congress and Expo 2013, 11-15 August, Palais des congrèss de Montréal, Canada.

Loui, J. P., Verma, C. P., Pal Roy, P., & Sinha, A. (2013). Design and development norms for Highwall Mining in India. Procs. 25th National Convention of Mining Engineers & the National Seminar on Policies, Statutes & Legislation in Mines - Recent Reforms & their Impacts on Indian Mining Industry (POSTALE), India.

Loui, J. P., Verma, C. P., Pal Roy, P. (2014). Highwall Mining in India – Part 1: Design methodology and review of performance. *Journal of Mines, Metals and Fuels*, *IMME-2014 Special Issue (September-October)*, India, 245-253.

Loui, J. P., Pal Roy, P., Shen, B., Karekal, S. (2017). Highwall Mining: Applicability, Design and Safety. CRC Press, London, July, 324 p.

Prakash, A., Loui, J. P., & Pal Roy, P. (2014). Highwall Mining in India – Part 2: Subsidence management mechanism at mine-level. *Journal of Mines, Metals and Fuels*, *IMME-2014 Special Issue (September-October)*, India, 254-262.

Jhanwar, J. C., Loui, J. P., & Pal Roy, P. (2014). Highwall Mining in India – Part 3: Slope stability planning and management. *Journal of Mines, Metals and Fuels*, *IMME-2014 Special Issue (September-October)*, India, 263-266.

FARKLI TÜR ÇİMENTOLARIN ÖĞÜTME DAVRANIŞLARININ İNCE TANE BOYUTUNDA ARAŞTIRILMASI

INVESTIGATION OF THE GRINDING BEHAVIOR OF DIFFERENT TYPES OF CEMENT IN FINE SIEVE SIZE

Y. Umucu [1, *], V. Deniz [2], Y. H. Gürsoy [1], H. S. Gökçen [1], S. Oluklulu [1]

[1] Eskişehir Osmangazi Üniversitesi, Maden Mühendisliği Bölümü
*(*Sorumlu yazar: yakup.umucu@ogu.edu.tr)*
[2] Hitit Üniversitesi, Polimer Mühendisliği Bölümü

ÖZET

Bu çalışmada, katkılı çimento sınıfında yer alan CEM II ve CEM IV tür çimento örnekleri üzerinde, kesikli öğütme koşullarında kompozisyonu oluşturan malzemenin daha önce çalışılmayan ince tane boyutunun (-0.300+0.090 mm) kinetik model parametrelerine etkisi araştırılmıştır. Daha sonra laboratuar çaplı bilyalı değirmende (200×200 mm) tek bir malzeme doluluk ve bilya doluluk oranında farklı öğütme sürelerinde elde edilen boyut dağılımlarından özgül kırılma hızı ve kümülatif kırılma dağılımı fonksiyonları elde edilmiştir. Çalışmada, çimento üretim süreçlerinin tasarımı, modelleme ve simülasyon çalışmalarında daha doğru sonuçlar vermesi bakımından ince tane boyutları seçilmiştir. Çimento bileşenlerinden olan klinker miktarının azalması ile en üst boyutların bir alt boyuta daha hızlı kırıldığı ve orijinal parçanın daha çabuk alt boyuta indiği görülmüştür.

Anahtar Kelimeler: Çimento, öğütme, kırılma hızı

ABSTRACT

In this study, the effect of the fine particle size (-0.300 + 0.090 mm) of the material forming the composition, which was not studied before was investigated on the kinetic model parameters of CEM II and CEM IV cement samples, which are in the blended cement class. Then, specific breakage rate and cumulative breakage distribution functions were obtained from the size distributions was taken at different grinding times in a single material fill and ball fill ratio in a laboratory diameter ball mill (200×200 mm).

In the study, fine sieve sizes were chosen in order to give more accurate results in the design, modeling and simulation studies of cement production processes. It was observed that the upper sieve size was faster broken down to a lower sieve size and the original part was reduced to the lower sieve size more quickly with the decrease in the amount of clinker, one of the cement components.

Keywords: Cement, grinding, specific breakage rate

GİRİŞ

Türk çimento sanayisi 60 milyon tonun üzerindeki üretimi ile Avrupa'da birinci sırada, dünyada ise beşinci sırada yer almaktadır. Çimento üretimi, enerji kullanımının yoğun olduğu bir proses olup, bir ton çimentoyu üretmek için gerekli olan enerjinin yaklaşık üçte biri klinker ve katkı maddelerinin öğütülmesinde kullanılır.

Türkiye'de devam etmekte olan kentsel dönüşüm sebebiyle içinde bulunduğumuz 10 yıllık dönemde yaklaşık 300 milyon m^3 hazır beton gereksinimi ortaya çıkmaktadır. Ancak Türkiye enerji yönünden büyük ölçüde dışa bağımlı bir ülke olduğundan ve yüksek fiyatlara sahip enerji ithalatı nedeniyle, çimento üretim maliyeti de artmaktadır. Türkiye Çimento Müstahsilleri Birliği üye fabrikalarının 2014 yılı elektrik enerjisi tüketimi 6,2 milyar kWh olduğu belirlenmiştir ve bu veriye göre çimento üretim aşamaları için optimizasyon çalışmalarının önemi daha iyi anlaşılmaktadır. Çimento endüstrisi, dünya enerjisinin yaklaşık %3,5'unu kullanan en büyük endüstrilerden birisidir. Çimento endüstrilerinde, üretim prosesinde harcanan toplam enerjinin %40'ı öğütmede harcanmaktadır (Deniz, 2004; Hoşten vd., 1998; Umucu vd., 2015)

Çimento üretiminde öğütülebilirlik iki önemli faktörden dolayı önemlidir. Birincisi; çimentonun özellikleri kimyasal ve mineralojik bileşiminden başka çimentonun inceliğine ve tane boyutu dağılımına bağlıdır. İkincisi; çimentonun maliyetinde enerji harcamasının 1/3'ü öğütmede sarf edilmektedir. Sert klinkerin öğütülmesinde yumuşak klinkere göre %80 daha fazla enerji harcanabilir (Çimsa Çimento Araştırma ve Uygulama Merkezi, 2017; SGM, 2015).

SM (silikat modülü) arttıkça öğütülebilirliğin azaldığı, Al_2O_3 ve serbest CaO miktarının yükselmesiyle yine öğütülebilirliğin azaldığı gözlenmiştir. (C_3S / C_2S) oranı veya silikatların ara fazlara oranı, (C_3S + C_2S) / (C_3A + C_4AF), azaldığında öğünme zorlaşır ve enerji harcaması artar. Öğütülebilirliğe kimyasal ve mineralojik bileşenlerin yanında mikro yapının da etkisi vardır. Mikro yapının oluşumunda ısıtma ve soğutma hızları ve fırın tipide etkilidir. İnce kristalli yapı, özellikle küçük kalsiyum silikat kristalleri öğütmeyi iyileştirir. İri kristaller yalnız parçalanmayı zorlaştırmaz, aynı zamanda kırılma alanlarının sayısını artırır. Bu amaçla geliştirilen matris ve kinetik modeller ile öğütme esnasında malzemenin ton başına harcadığı enerjinin asgari düzeyde tutulması sağlanmaktadır (Çimsa Çimento Araştırma ve Uygulama Merkezi, 2017).

Bu çalışmada, çimento klinkeri ile katkı maddelerinin belirli oranlarda karıştırılması sonucu elde edilen ve katkılı çimentolar sınıfında yer alan CEM II ve CEM IV tür çimentoların ince tane boyutlarında (-0.300 + 0.090 mm) kinetik modele dayalı öğütme çalışmaları sonucu model parametreleri elde edilmiştir. Literatürde kırılma hızları için yapılan çalışmalar -1.00+0.100 mm arası tane boyutları arasında gerçekleştirilmiştir. Günümüzde çimento üretim süreçlerinde artık çimento değirmeni için beslenen malzeme tane boyut dağılımı -0.300 mm'dir. Özgül kırılma hızı ve dağılım fonksiyonu için bu boyut aralığında literatürde çalışmalar bulunmamaktadır. Çalışmada, çimento üretim süreçlerinin tasarımı, modelleme ve simülasyon çalışmalarında daha doğru sonuçlar vermesi bakımından ince tane boyutları seçilmiştir. Daha sonra çimento bileşenleri ile kinetik model parametreleri ile arasındaki ilişki mukayese edilmiştir.

Teori

Bilyalı değirmenler için özgül kırılma hızı ve kümülatif kırılma dağılımı kavramlarını içeren boyut küçültme yaklaşımı kullanılmaktadır. Özgül kırılma hızının bir matematikse formülü Austin vd. (1984) tarafından aşağıdaki gibi verilmiştir.

$$S_i = a_T X_i^{\alpha} \tag{1}$$

burada; X_i; i fraksiyonundaki üst boyutu (mm) ve a_T ise; öğütme şartlarına ve malzemenin özelliklerine bağlı olan model parametredir. Kırılan veya öğütülen malzemelerin hangi boyut fraksiyonlarına nasıl dağıldığı kümülatif kırılma dağılımı fonksiyonu olarak tanımlanmış ve aşağıda gösterilmiştir.

$$\sum_{i=n}^{j+1} b_{i,j} = 1 \quad (2)$$

Kısa öğütme süresi verilerinden elde edilen boyut dağılım eğrisini temsil eden bu fonksiyonda, söz konusu parametreler Austin vd. (1984) aşağıda verilen, BII yaklaşımından elde edilen $B_{i,j}$ değerlerine karşı nisbi boyut grafiği çizildiğinde bulunur (Şekil 1).

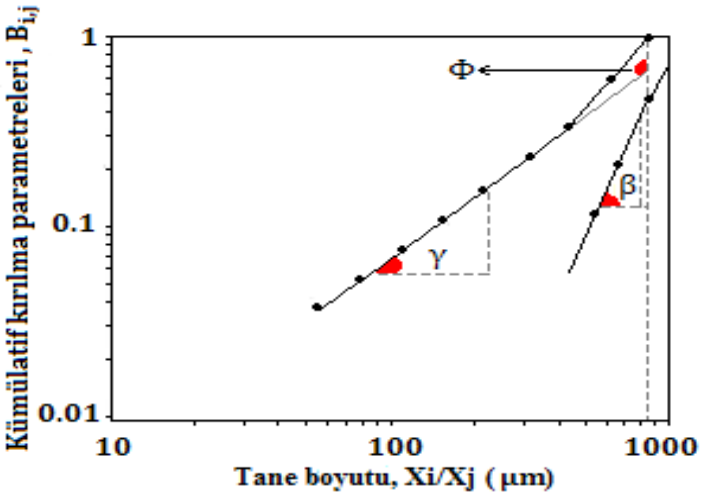

Şekil 1. Kırılma dağılım fonksiyonunun gösterimi

$$B_{i,j} = \phi_j \left(X_{i-1}/X_j\right)^{\gamma} + \left(1-\phi_j\right)\left(X_{i-1}/X_j\right)^{\beta} \quad (3)$$

burada; ϕ_j, γ ve β malzemelerin özelliklerine bağlı olan model parametrelerdir. Bu parametreler, farklı bilya oranları, değirmen çapları vb. için aynı olup, farklı malzeme özelliklerinde değişmektedir (Umucu vd., 2015).

MALZEME VE METOD

Malzeme

Deneysel çalışmalarda, Burdur Bucak'ta faaliyet gösteren As Çimento'nun üretmekte olduğu CEM II ve CEM IV tipi çimento kullanılmıştır. Bu örneklere ait reçeteler ve kimyasal analiz sonuçları sırasıyla Çizelge 1 ve 2'de verilmiştir.

Çizelge 1. CEM II ve CEM IV için reçeteler (ağırlıkça %)

	CEM II	CEM IV
Klinker	65	48
Tras	24	43
Kalker	7	5
Alçı taşı	4	4

Çizelge 2. CEM II ve CEM IV için kimyasal analiz sonuçları (ağırlıkça %)

	CEM II	CEM IV
SiO_2	27.57	33.78
Al_2O_3	8.69	10.84
Fe_2O_3	3.26	3.27
CaO	50.83	41.53
MgO	1.64	2.07
SO_3	2.35	2.47
Na_2O	0.77	1.32
K_2O	1.35	2.00

Çizelge 2'deki kimyasal analiz sonuçlarından, CEM II'ye göre CEM IV örneğinin SiO_2, Al_2O_3, alkali ve toprak alkali miktarının yüksek, CaO miktarının düşük olduğu görülmektedir. CEM IV'de klinker ve kalker miktarının düşük olması sebebiyle CaO miktarı düşmüştür. Ancak CEM II'ye göre daha fazla tras içerdiğinden dolayı da diğer oksitlerin miktarında artış görülmüştür. Çimento örneklerine ait X-ışını kırınımı analizi (XRD) sonuçları Şekil 2'de verilmiştir.

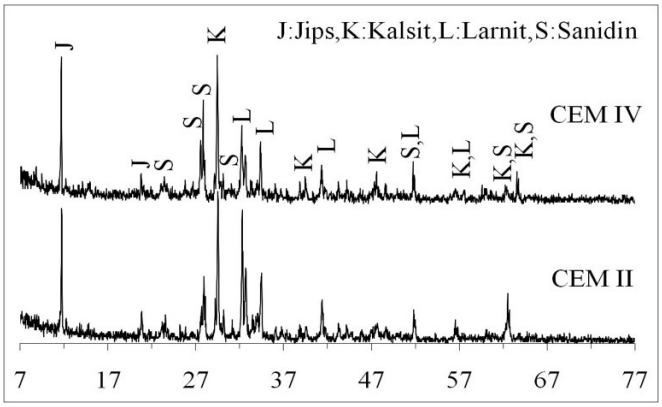

Şekil 2. CEM II ve CEM IV için X-ışını kırınımı diyagramı

Metot

Standart Bond değirmeninde kullanılmak üzere CEM II, CEM IV ve reçetelerde miktarları değişen Klinker ve Tras için -3.35 mm tane boyutuna sahip örnekler elde edilmiştir. Standart Bond değirmeninde yapılan deneyler sonucunda CEM II, CEM IV, Klinker ve Tras örnekleri için iş indeksleri sırasıyla 13.04, 12.68, 9.31 ve 9.24 kWh/ton olarak bulunmuştur.

Örneklerin özgül kırılma hızları ve kümülatif dağılım fonksiyonlarına bağlı kinetik model parametrelerinin belirlenmesi için √2 elek serisine göre 4 farklı dar tane boyut fraksiyonunda (-0.300+0.212, -0.212+0.150, -0.150+0.106, -0.106+0.090 mm) sınıflandırılmıştır. Her fraksiyon, f_c=0.072 malzeme doluluk oranında laboratuvar çaplı bilyeli değirmende kesikli olarak öğütülmüştür. Her bir öğütme periyodu sonrası tüm değirmen şarjı boşaltılarak kuru elek analizi yapılmıştır. Öğütme deneylerinde kullanılan bilyeli değirmen karakteristikleri ve deney koşulları Çizelge 3'te verilmiştir. Deneylerde bilyeli değirmenin dönüş hızı, değirmenin kritik hız değerinin %75'i alınmıştır.

Çizelge 3. Bilyalı değirmen karakteristikleri ve deney koşulları

Değirmen	İç çap, mm	200	
	İç uzunluk, mm	200	
	Hacim, cm^3	6283.2	
	Çalışma (N_c=%75), d/d	92	
Bilya	Malzeme	Döküm	
	Boyut, mm	50-40-30-25-20-17	
	Özgül ağırlık, g/cm^3	8.0	
	Hacim doluluğu, %*J*	30	
Malzeme	Örnek	CEM II	CEM IV
	Özgül ağırlık, g/cm^3	2.97	2.84
	Malzeme yükü, %f_c	0.072	
	f_c'ye göre boşluk doldurma oranı, %*U*	0.60	

BULGULAR VE TARTIŞMA

Özgül Kırılma Hız Fonksiyonlarının Belirlenmesi

Her bir tane boyut fraksiyonu için özgül kırılma hızları (S_i) birinci derece kırılma hız fonksiyonu grafiklerinden hesaplanmıştır. Değirmen çalışma koşullarından, f_c=0.072 malzeme doluluk oranında ve *J*=0.30 bilye doluluk oranında belirlenen S_i değerlerine karşı tane boyut fraksiyonu grafiği çizilmiştir (Şekil 3). Bu grafiğin doğrusal kısmından hesaplanan a_T değerleri Çizelge 4'te verilmiştir.

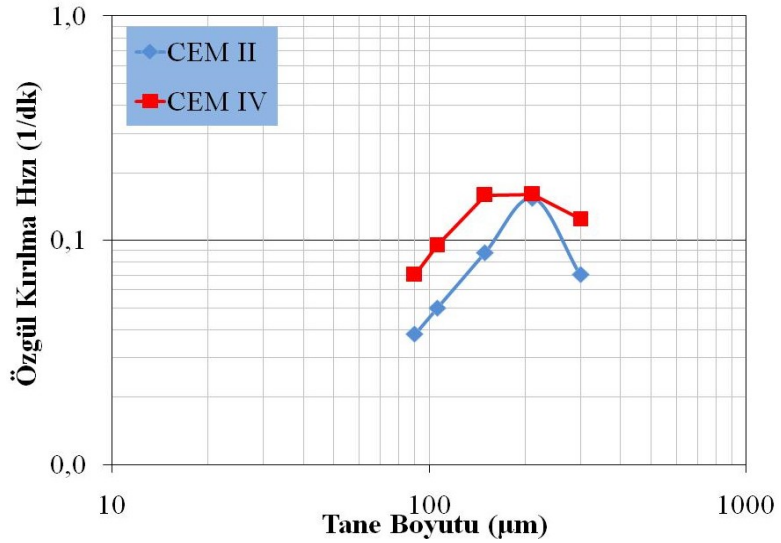

Şekil 3. CEM II ve CEM IV için özgül kırılma hızı eğrileri

CEM II ve CEM IV örneklerinin kırılma hızlarının belirli bir boyuta kadar arttığı ve azami bir değere ulaştıktan sonra azalmaya başladığı görülmektedir. Kuru ortamda gerçekleştirilen deneylerde, kırılma hızları sırasıyla yaklaşık olarak 0.212 ve 0.150 mm tane boyutlarından sonra azalmaya başlamıştır.

Genel olarak, öğütmenin başlangıcında kırılma hızı, tane boyutu ile artarken, belirli bir tane boyutundan sonra yavaşlamaya başlar. Bu tane boyutu her malzeme için farklılık gösterir. Yavaşlamanın nedeni, oluşan ince tanelerin yastıklama etkisi yaparak iri boyutların kırılmasını engellemesidir.

Ayrıca iki örnek aynı tane boyutuna göre değerlendirilirse, CEM IV'ün birincil kırılma hızının daha yüksek olduğu görülmüştür. Çizelge 1'e bakıldığında CEM IV örneğinin daha düşük Klinker ve daha yüksek Tras içerdiği görülmektedir. Örneklerin birincil kırılma hızı değerleri ile kompozisyonu oluşturan bileşenlerin iş indeksi değerleri arasında bir ilişki olduğu belirlenmiştir. Şekil 3'te, daha yüksek miktarda Klinker (%65) içeren CEM II örneğinin aynı tane boyutuna göre birincil kırılma hız değerlerinin daha düşük olduğu tespit edilmiştir.

Kümülatif Kırılma Fonksiyonlarının Belirlenmesi

Kümülatif kırılma fonksiyonu ($B_{i,j}$) değerleri, en kısa öğütme sürelerinden elde edilmiş ve verilerin normalize olduğu yani boyuttan bağımsız olduğu tespit edilmiştir. Elde edilen $B_{i,j}$ değerlerine karşılık nispi boyut (X_i/X_j) grafikleri Şekil 4'te verilmiştir. Bu grafiklerden hesaplanan ϕ, γ, β model parametre değerleri Çizelge 4'te verilmiştir.

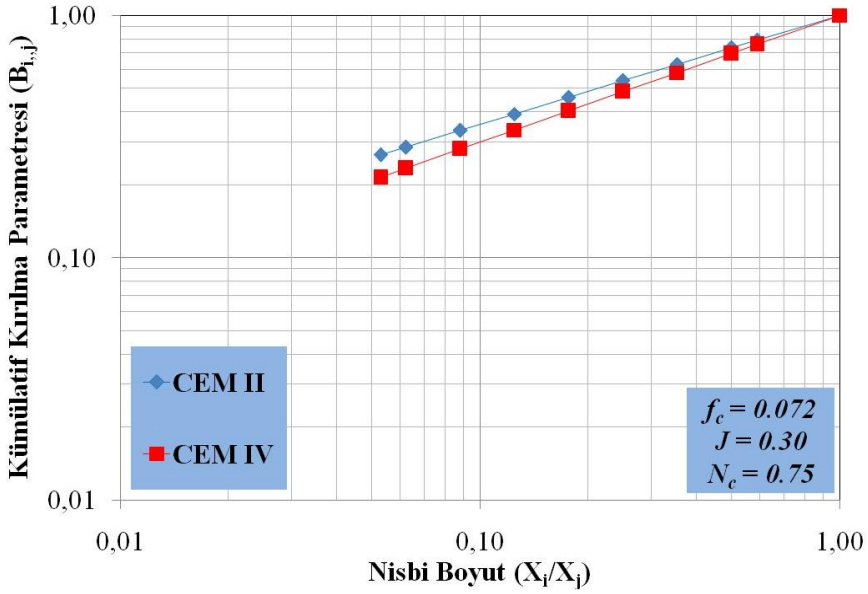

Şekil 4. CEM II ve CEM IV için kümülatif kırılma dağılım fonksiyonları

Çizelge 4. Bilyalı değirmen karakteristikleri ve deney koşulları

	α_T	φ_j	γ	β
CEM II	0.92	0.194	0.554	0.422
CEM IV	1.43	1.425	0.457	0.378

Çizelge 4 incelendiğinde, CEM II örneğinde α_T ve ϕ_j değerlerinin daha düşük olduğu görülmüştür. Bunun sebebi, CEM II'de Klinker oranının daha yüksek, Tras oranının daha düşük olmasıdır. CEM IV'de daha etkin bir kırılma gerçekleşmiştir ve dolayısıyla ince malzeme miktarında (düşük γ) artış gözlenmiştir.

SONUÇLAR

İki farklı kompozisyona sahip çimento örneklerinin kırılma hız fonksiyonlarının belirlenmesi için oluşturulan grafiklerde, S_i ya da α_T değerlerinin büyük olması, daha etkin bir kırılmanın olacağı ve orijinal

parçanın daha çabuk alt boyuta indirgeneceği anlamına gelmektedir. Çalışmalardan elde edilen deneysel verilerin a_T değerleri incelendiğinde, CEM IV örneğinin kuru öğütme deneylerinden elde edilen kırılma hızlarının, CEM II örneğine göre yüksek olduğu tespit edilmiştir. CEM IV örneğinin kırılma hızının yüksek olmasının sebebi, kompozisyonda daha az miktarda Klinker kullanılması ile bileşiminde XRD analizi (Şekil 2) sonucu gözlenen Larnit (Ca_2SiO_4) miktarının daha az olmasına bağlanabilir.

ϕ_j değerlerinin artması, en üst boyutların bir alt boyuta daha hızlı kırılacağını ifade etmektedir. CEM IV örneğinin ϕ_j değerinin, CEM II örneğine göre yüksek olduğu tespit edilmiştir. Klinker miktarının azaltılıp, Tras miktarının arttırılması ile ϕ_j değerinin arttığı görülmektedir.

γ değerinin büyük olması, ince malzeme miktarının az olduğunu gösterir. CEM II ve CEM IV örneklerinin, çalışmalardan elde edilen deneysel verilerin γ değerleri incelendiğinde, ince malzeme miktarı CEM IV örneğinde daha fazla bulunmaktadır. CEM II örneğinin kuru öğütülmesi esnasında, tane boyutunun küçülmesine bağlı olarak, katıyı bir arada tutan bağ kuvvetlerinin artması neticesinde, ayrıca içerisinde bulunan Larnitin yavaş öğütülmesi sonucunda γ değerleri CEM IV'e göre daha yüksek çıkmıştır.

Bu çalışma sonucunda, çimento bileşiminde bulunan Klinker içeriğinin, malzemenin ufalanmasını yavaşlattığı sonucuna varılmıştır.

KAYNAKLAR

Austin, L.G., Klimpel, R.R., Luckie, P.T., 1984. Process Engineering of Size Reduction: Ball Milling. AIME, New York, 561 s.

Deniz, V. The effect of mill speed on kinetic breakage parameters of clinker and limestone, Cement and Concrete Research, 2004. (SCI), 34(8), 1365-1371,

Hoşten, C., Avsar, C.,1998. Grindability of Mixtures of Cement Clinker and Trass. Cement and Concrete Research concrete research, 28(11), 1519-1524.

SGM 2015. Çimento Sektörü Raporu: Sektörel Raporlar ve Analizler Serisi. Sanayi Genel Müdürlüğü (2015/1):
http://sanayipolitikalari.sanayi.gov.tr/Public/SectorReports/7.

Umucu, Y., Haner, S., Tunay, T., 2015. The Investigation of Effect of Wet-Dry Grinding Condition and Ball Types on Kinetic Model Parameters for Kaolin. *Polish Mineral Engineering Society*, 35 (1), s.205-211.

Umucu, Y., Deniz, V., Saraç, M, F., Kuzgun, E. The relationship between cement quality and separation cut size, Inzynieria Mineralna-Journal of the Polish Mineral Engineering Society, 2015. (ESCI: Emerging Sources Citation Index), 16(36(2)), 189-194,

GAZ KROMATOGRAFI (HEADSPACE GC-FID) KULLANILARAK FENOL BAZLI DOLGU MALZEMELERİNİN İÇERİĞİNDEKİ FORMALDEHİT MİKTARLARININ TESPİT EDİLMESİ

DETERMINATION OF FORMALDEHYDE CONTENTS IN PHENOL BASED FILLING MATERIALS USING GAS CHROMATOGRAPH (HEADSPACE GC-FID)

M.Bilen [1,*], C. Tuz [1], A. Rasskazova [2], R. Kızılgedik [3], İ. Toroğlu [1], S. Yılmaz [1], A. Çakır [1], E. Kaymakçı [1]

[1] *Zonguldak Bülent Ecevit Üniversitesi Maden Mühendisliği Bölümü*
*(*Sorumlu yazar: mehmetubilen@yandex.com)*
[2] *Mining Institute of Far Eastern Branch of Russian Academy of Sciences*
[3] *RESlab Laboratuvar Cihazları ve Teknik Hizmetleri San. Ltd. Şti.*

ÖZET

Bu çalışmada gaz kromatografı kullanılarak fenol bazlı dolgu malzemelerinin içeriğindeki formaldehit miktarlarının tespiti için yararlanılacak yöntemler araştırılmıştır. Çalışma kapsamında bünyesinde FID (“Flame Ionization Detector”) detektörü bulunan bir GC HP 6890 cihazı ve bunun yanında “Headspace” olarak kullanılacak ikinci bir kromatografın da eşlik ettiği bir deney seti tasarlanmıştır. Headspace gaz kromatografisi dengeye getirilen bir sıvı veya katı içeren numuneden ayrılan gazın kromatograftaki kolonda (GC) ayrılması esasına dayanmaktadır. Bu teknik genellikle polimerlerin, yiyecek ve içeceklerin, kandaki alkol seviyelerinin, çevresel değişkenlerin, kozmetiklerin ve farmasötik bileşenlerin analizine uygulanmaktadır. Bu çalışma kapsamında Headspace gaz kromatografisinin fenol bazlı dolgu malzemelerindeki formaldehit içeriğinin tespiti amacıyla kullanılması planlanmaktadır. Headspace gaz kromatografisi ile biyolojik-kimyasal bozunma süreçlerinin gerçekleşip gerçekleşmediği, hangi oranda bozunmaların olduğu ve sonucunda oluşan bileşikler belirlenebilmektedir. Bu tayin yönteminde yalnızca en uçucu (en kolayca buharlaşan) maddeler kolona ulaşır. Bu şekilde fenol bazlı kimyasal dolgu malzemelerinin yapısında var olan formaldehitin de uçarak (buharlaşarak) kolonda ayrılması mümkün olacaktır.

Anahtar Sözcükler: Gaz kromatografı, fenol bazlı dolgu malzemeleri, formaldehit, headspace GC-FID.

ABSTRACT

In this study, the methods to be used to determine the amount of formaldehyde in the content of phenol-based fillers were investigated by using gas chromatography. Within the scope of the study, an experimental set was designed with the GC HP 6890 device available within the FID (“Flame Ionization Detector”) detector, as well as a second chromatograph to be used as a “Headspace”. Headspace gas chromatography is based on the separation of gas separated from a liquid or solid containing sample in the column (GC) in the chromatograph. This technique is generally applied to the analysis of polymers, food and beverages, blood alcohol levels, environmental variables, cosmetics and pharmaceutical ingredients. Within the scope of this study, it is planned to be used to determine the formaldehyde content in phenol-based filling materials. With headspace gas chromatography, it is possible to determine whether biological-chemical decomposition processes take place, at what rate there is decomposition, and the resulting compounds. In this determination method, only the most volatile (most readily available as vapor) substances reach the column. In this context, it will be possible to separate formaldehyde, which is present in the structure of phenol-based chemical filling materials, in the column by evaporation.

Keywords: Gas chromatograph, phenol-based filling materials, formaldehyde, headspace GC-FID.

INTRODUCTION

Phenol based filling materials are being extensively used in underground coal mining by means of prevention of spontaneous combustion of coal and gas discharge (Ni and Pereira 2000, Bichler and Simon 1996, Woodfin 1997, Hu et al. 2013, Gray et al. 2006, Hu et al. 2014). Phenol based filling materials are capable of blocking the air with their applicable properties of heat resistance, flame retardancy, low smoke, good sealing and construction convenience (Bichler and Simon 1996, Hu et al. 2014). Wang et al. (2014) have summarized the usage purposes of polymers & phenol-based filling materials in their graphical abstract (See Figure 1).

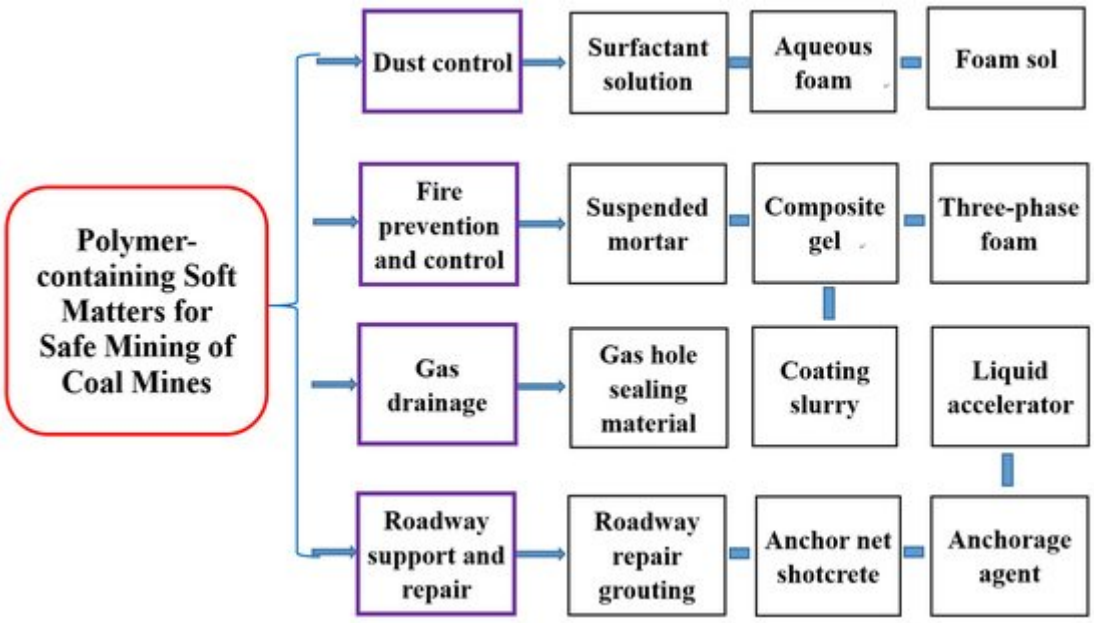

Figure 1. Graphical representation for usage purposes of polymers & phenol-based filling materials (Adapted from the study of Wang et al. 2014).

In addition to these abovementioned, although cost is primary concern for these filling materials, their toxicity & hazardous structure should be also well evaluated. According to Hu et al. 2014, very high amount of formaldehyde is being used and it was expressed as in the following statement: “currently 37% formaldehyde solution is commonly used as the raw material in the preparation of PF resin” (Grenier-Loustalot et al. 1996, Hu et al. 2014).

Free formaldehyde content of a material, either they are cosmetics (Engelhardt and Klinkner 1985) or polymers (Wang et al. 2019), or phenol-based filling materials used in mining, is significant in terms of the correct evaluation of safe working environment (AWES 2014). Engelhardt and Klinkner 1985 have tried to determine free formaldehyde in the presence of donators in cosmetics by HPLC and post-column derivation. Corresponding demonstration of the experimental set up conducted by Engelhardt and Klinkner 1985 is provided in Figure 2.

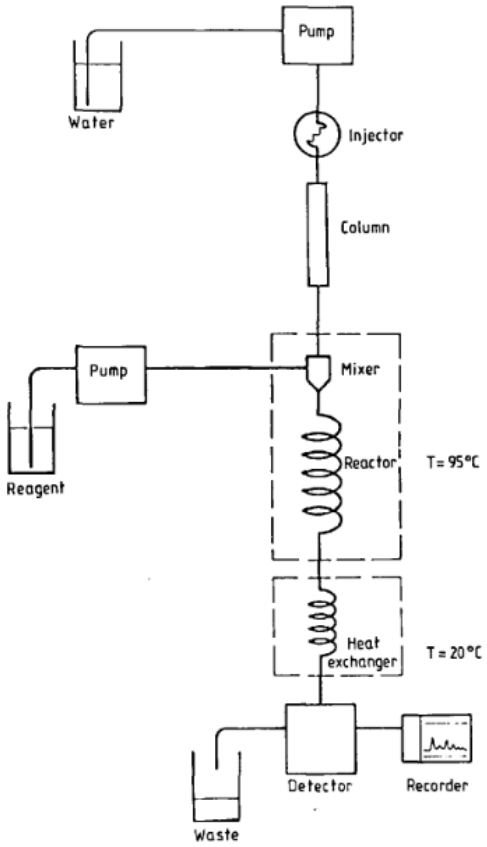

Figure 2. A schematic representation of the experimental method carried out by Engelhardt and Klinkner 1985

Determination of free formaldehyde content in cosmetics is rather interested by many researchers (Oliva-Teles et al. 2002, Benassi et al. 1991, Brandão et al. 2018), high performance liquid chromatography is mostly addressed in their methods presented. In the study of Yi et al. 2019, free formaldehyde content of leather chemicals was determined with an optimized method for leather chemicals based on ISO 27587. Del Barrio et al. ~~(~~2006~~)~~ have investigated simultaneous determination of formic acid and formaldehyde in pharmaceutical excipients using headspace GC/MS. Although Del Barrio et al. ~~(~~2006~~)~~ study was about pharmaceuticals, the procedure explained (See Section 2.2. *"Gas chromatography/mass spectrometry (GC/MS) conditions"* ~~in~~ of the same study) can be followed and optimized to determine the free formaldehyde content of mine polymers and phenol based filling materials. In addition, Daoud Agha Dit Daoudy et al. ~~(~~2018~~)~~ study can be also guided in the order of further understanding the headspace sampling parameters (See Section 2.3 of the same study), GC instrumental conditions (See Section 2.4 of the same study). Headspace GC-FID method presented in the body of abovementioned study (Daoud Agha Dit Daoudy et al. 2018) is still conducted to detect and quantify formaldehyde impurity in pharmaceutical excipients. In this context, a schematic representation of headspace GC-FID presented in the study of Boe et al. ~~(~~2007~~)~~ was provided (See Figure 3). Boe et al. ~~(~~2007~~)~~ has introduced this schematical representation as "diagram of the sampling system" in their study of "An Innovative Online VFA Monitoring System for the Anerobic Process, Based on Headspace Gas Chromatography".

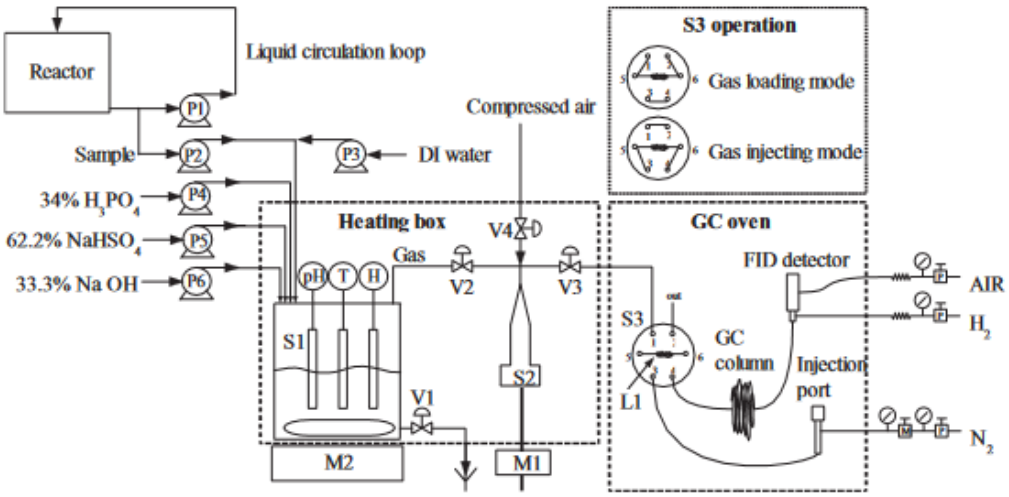

Figure 3. A schematic representation of headspace GC FID (Adapted from the study of Boe et al. 2007).

In addition, Derikvand et al. (2021) have employed a LP-HS-SPME device which was coupled to a gas chromatography-flame ionization detection (GC-FID) system for the direct analysis of polluted soil samples (See Figure 4). Although Derikvand et al. (2021) tried to determine polycyclic aromatic hydrocarbons (PAHs) which are classified as organic environmental contaminants in soil samples, the methodology can still be employed as a guide for the purpose of this study. In a similar manner, headspace gas chromatographic (HS-GC) method for the determination of the volatile organic compounds was employed by Lima et al. 2018 (See Figure 5). Based on the schematical representations provided by the literature researchers (Engelhardt and Klinkner 1985, Boe et al. 2007, Derikvand et al. 2021, Lima et al. 2018), a new method including headspace GC-FID to determine free formaldehyde in mine polymers & phenol-based filling materials can be investigated and optimized. Schematical representation partly adapted from the study of Derikvand et al. (2021) can be employed with its inclusion of syringes employment along with the evacuation, equilibration and extraction procedures application.

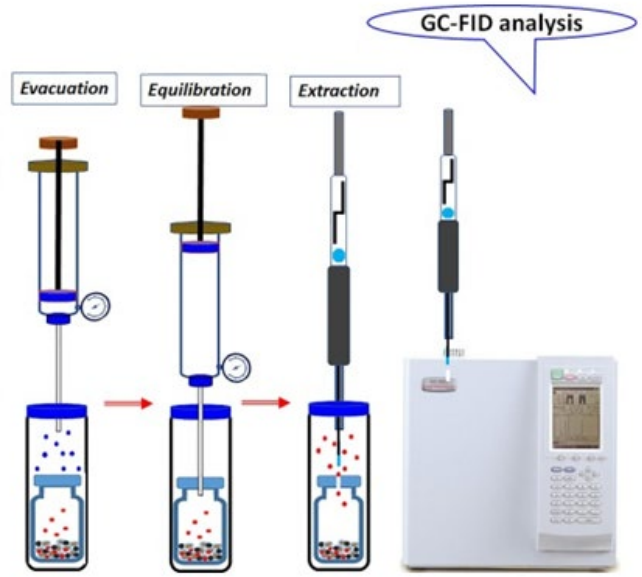

Figure 4. Schematical representation of the GC-FID analysis and corresponding steps carried by Derikvand et al. 2021. (Partly adapted from the study of Derikvand et al. 2021'study, modified accordingly to the context of this current study).

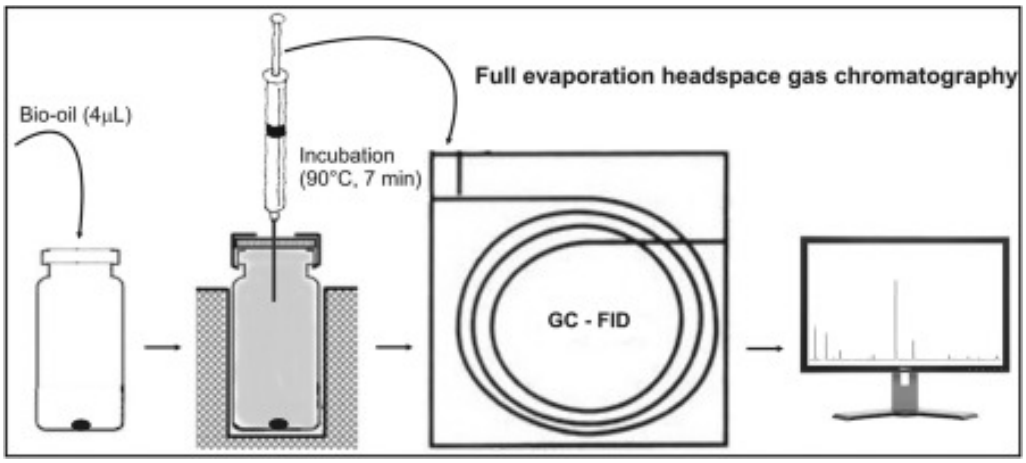

Figure 5. A schematical representation of headspace gas chromatographic (HS-GC) method for the determination of the volatile organic compounds employed by Lima et al. 2018 (adapted from graphical abstract of Lima et al. 2018).

Formaldehyde content of a material can be determined with a proper GC-FID orientation. However, determination of formaldehyde content in a liquid (resin in this case) or a solid (foam in this case) is somehow questionable. Based on the literature researches above provided and based on the testing procedure followed to determine the tendency of spontaneous combustion of coals by employing a GC-Oven in the study of Bilen et al. (2019), determination of formaldehyde content either in the free form or in the structure of the foam can be adapted. Corresponding GC-Oven in the study of Bilen et al. (2019) can be replaced by a Headspace and the gas injection would be sourced from this specific adjustable (isothermal, adiabatic) orientation. Bilen et al. (2019) study can be a guide in this context since the corresponding experimental set up they have built to determine the tendency of spontaneous combustion of coals includes a GC-Oven (Agilient 5890) and GC-FID (Agilient 6890) (See Figure 6).

Figure 6. Spontaneous combustion experiment set up, HP 5890 (employed only as an oven, left bottom) and HP 6890 (employed as GC-FID, left up) (Adapted from the study of Bilen et al. 2019).

In this context, an optimized method should be investigated to determine the free formaldehyde content in phenol-based filling materials used in mining industry. In this paper, a new method including headspace GC-FID was introduced and proposed in order to determine free/fixed formaldehyde content of phenol-based filling materials. In the context of this study, inspired by the employment of headspace GC-FID for the determination of specific materials/ingredients/impurities by various industry (cosmetics, pharmaceuticals, etc.), an optimized method for the determination of free formaldehyde content in phenol-based filling materials used in mining/coal mining industry was investigated. In this order, GC-FID (Agilient) was employed with a headspace (Perichrom GC), and a new experimental set-up was proposed and built.

EXPERIMENTAL METHOD

A representation of the new experimental set up for the determination of formaldehyde content of phenol-based filling materials is provided in Figure 7.

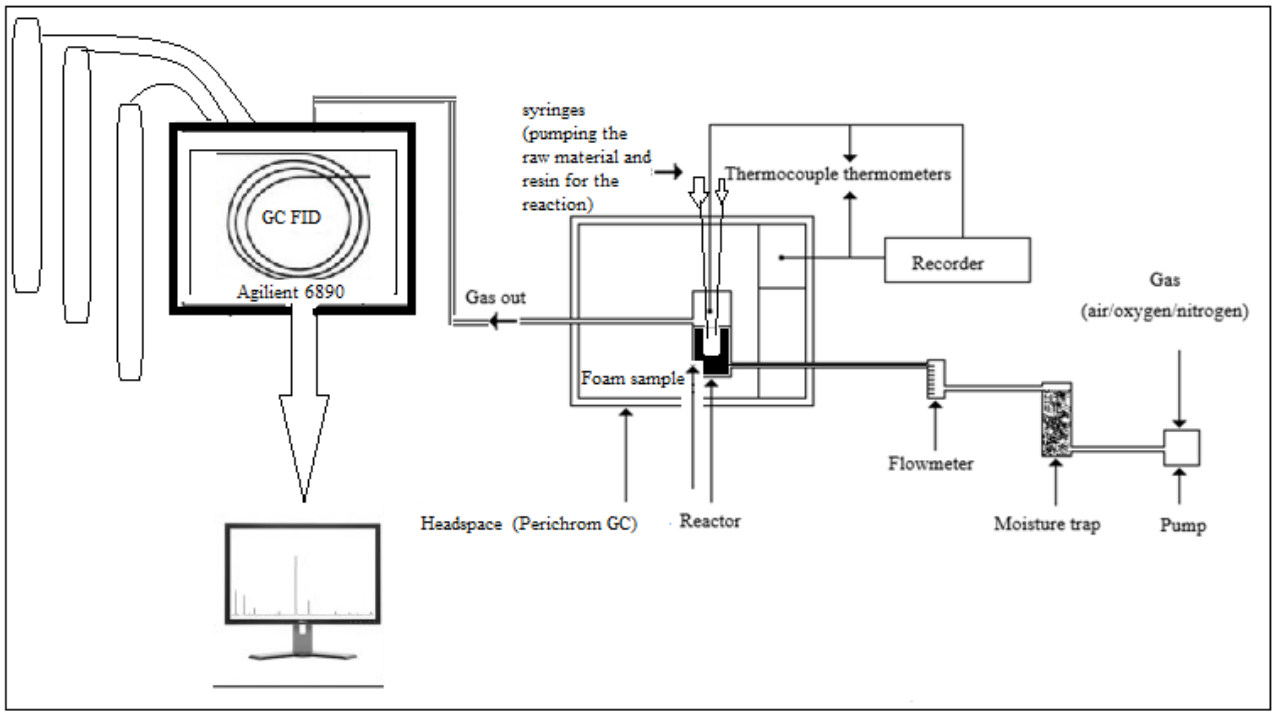

Figure 7. A schematical representation of the new experimental set up for the determination of formaldehyde content of phenol-based filling materials.

In this context, a photo is provided from the laboratory (See Figure 8) to better demonstrate corresponding new experimental set up for the determination of formaldehyde content of phenol-based filling materials. Perichrom GC is placed in addition to the laboratory equipments provided in Bilen et al. (2019). Perichrom GC is planned to employ as headspace and it will be worked as source of gas sampling from the foam and the reaction involving during the production of foam (phenol-based filling material). This abovementioned GC (Perichrom GC) would enable isothermal or adiabatic reaction environment, or any means of temperature ramps for the correct understanding the gas release during the chemical reaction between the composites of phenol-based filling materials. The reason of GC-Oven employment (Perichrom GC in this case) as a headspace is basically the adjustable temperature program availability and corresponding ease of control.

Figure 8. A photograph from the laboratory built for the determination of formaldehyde content of phenol-based filling materials (See Headspace Perichrom GC, right up) (See GC-FID left up).

Referring to Figure 8, it can be seen 3 separate GC, and only one is being employed as chromatographic purposes (GC-FID, Agilient 6890, left up). Previously served as a gas chromotograph, GC HP 5890 (left down), is being employed as GC-Oven, and this was explained in detail in the study of Bilen et al. {2019}. As it was stated earlier, Perichrom GC (right up) is also malfunctioning in terms of chromatographic purposes but it will be employed as a GC-Oven (Headspace) for the determination of formaldehyde content of phenol-based filling materials. Figure 9 is provided in order to correspond the inner presentation of headspace orientation for the experimental set up.

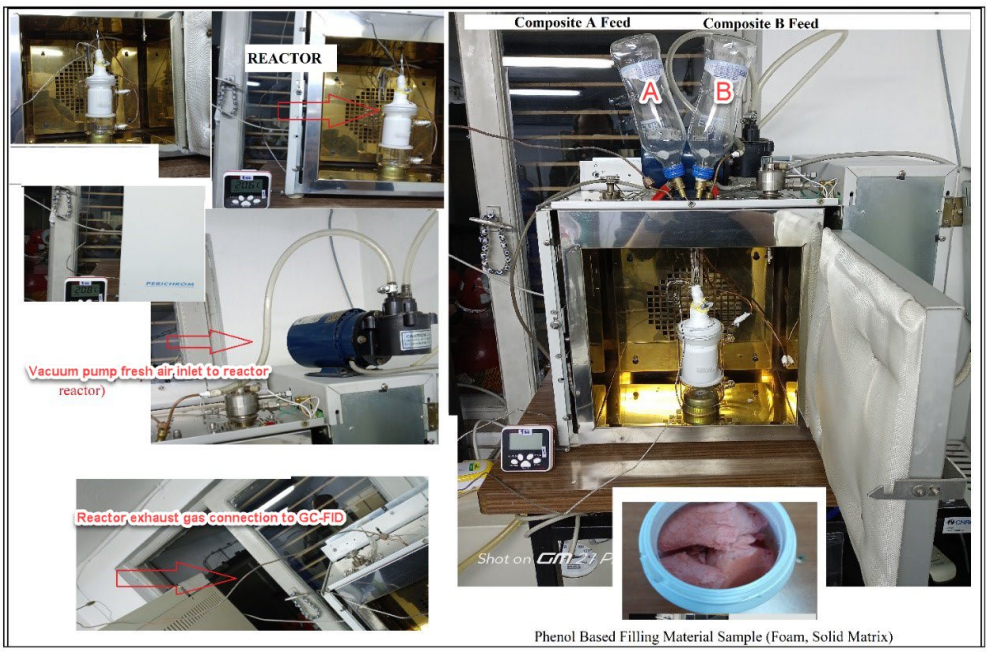

Figure 9. Inner presentation of the headspace orientation, reactor, and syringes in the body of the experimental set up.

There is a reactor (same as employed in spontaneous combustion liability tests) placed in the headspace (Perichrom GC). The reactor has one air inlet and one exhaust gas outlet. There is a thermocouple which has a joint to the sample chamber. Already reaction environment or the place of the sample is controlled by GC-Oven (Perichrom GC), the exothermic reaction and corresponding temperature rises are recorded with this thermocouple. Difference in spontaneous combustion liability test is the available syringe pumps (2 syringes) for the composites injection to the reaction chamber (reactor). Injection of each composites (composite A and composite B) is simultaneously realized and the following gas discharge is pumped with the air flow connected to GC-FID. This is the simulation of the reaction taking place for the production of phenol based filling materials. In terms of mining environment, there should be air ventilation which is actually provided air to the chamber of the reactor by the air inlet. Air inlet is controlled by a flowmeter like in the case for spontaneous combustion liability tests. This experimental procedure is readily available and initial tests are already completed. These initial tests were carried out to see any problems associated with the testing equipments and testing scheme. Initial tests were passed and it was understood that proposed experimental set up can be employed to determine the formaldehyde content in phenol based filling materials (either in free form or in the matrix of foam).

RESULTS AND DISCUSSION

In this study, initial test results of the formaldehyde determination analysis with headspace GC FID was provided. In this context, results include not only free formaldehyde content during the chemical reaction taking place between composite A and composite B (resin and raw material of phenol based filling material) but also the formaldehyde content of the foam itself (solid matrix of foam). Result of the analyses of free formaldehyde content during chemical reaction is tabulated in Table 1. Initial analyzes for the free formaldehyde content during chemical reaction were carried out for two different samples at different temperatures (18, 20, 22 and 24 °C). Corresponding temperatures are arranged as headspace oven orientation, which are considered as the representation for the underground coal mine temperature levels.

Table 1. Formaldehyde analysis result during chemical reaction between composite A and composite B (Analysis is carried out with headspace GC FID).

Analyzed Item	Analysis Description	Result (formaldehyde content) (%)
Sample No:1 (Reaction between composite A_1 and composite B_1)	Headspace GC-FID, headspace oven at 18 °C	0.005
	Headspace GC-FID, headspace oven at 20 °C	0.007
	Headspace GC-FID, headspace oven at 22 °C	0.008
	Headspace GC-FID, headspace oven at 24 °C	0.008
Sample No:2 (Reaction between composite A_2 and composite B_2)	Headspace GC-FID, headspace oven at 18 °C	0.172
	Headspace GC-FID, headspace oven at 20 °C	0.189
	Headspace GC-FID, headspace oven at 22 °C	0.194
	Headspace GC-FID, headspace oven at 24 °C	0.213

In addition to above mentioned analysis result for the formaldehyde determination (Table 1), gas composition analysis (Table 2) was also realized at different headspace oven temperature levels for two samples.

Table 2. Gas composition analysis result during the reaction between composite A and composite B (Analysis is carried out with headspace GC FID).

Sample	Headspace Oven Temperature (°C)	Composition of the Gas Out from the Reactor						
		CH_4	NO_x	H_2S	CO	CO_2	O_2	CH_2O
Sample No:1 (Reaction between composite A_1 and composite B_1)	30	n.d.	n.d.	n.d.	33 ppm	n.d.	22.60 %	0.009 ppm
	60	0.17 ppm	n.d.	n.d.	37 ppm	2276 ppm	23.10 %	0.009 ppm
	90	0.26 ppm	n.d.	n.d.	41 ppm	1919 ppm	23.70 %	0.010 ppm
	120	0.18 ppm	n.d.	n.d.	17 ppm	2006 ppm	24.00 %	0.011 ppm
	240	0.40 ppm	n.d.	n.d.	n.d.	4857 ppm	25.00 %	0.012 ppm
Sample No:2 (Reaction between composite A_2 and composite B_2)	30	0.48 ppm	n.d.	n.d.	59 ppm	1975 ppm	19.11 %	0.27 ppm
	60	0.55 ppm	n.d.	n.d.	52 ppm	2884 ppm	19.24 %	0.29 ppm
	90	0.57 ppm	n.d.	n.d.	65 ppm	3694 ppm	19.47 %	0.32 ppm
	120	0.41 ppm	n.d.	n.d.	46 ppm	4211 ppm	19.05 %	0.37 ppm
	240	0.62 ppm	n.d.	n.d.	39 ppm	5894 ppm	20.56 %	0.49 ppm

*n.d.: non-detected

Referring to Table 2, reaction gases at each temperature were investigated in term of their CH_4, NO_x, H_2S, CO, CO_2 and O_2 contents, respectively. In this context, it was obvious that H_2S was not detected for both of the samples. Since composites of each sample are organics to some extent, composition of the gas exhaust from reaction chamber (reaction between composite A and composite B) can be investigated at previously determined temperature levels. Corresponding temperatures are the headspace oven temperatures and reaction take place at this temperature levels.

As previously explained, in the context of this study, not only the reaction between composite A and composite B was investigated in terms of the formaldehyde (free) content but also the foam (solid matrix) was analyzed. Foam sample was placed into reactor as described in the Material and Method Section, and air (100ml/min) was fed with mini compressor. Air flow was a simulation of the ventilation in underground coal mines, and placing the solid foam sample (phenol-based filling material) inside the reactor is a way to monitor air quality shortcomings reasoned by the foam sample. In this context, result of the formaldehyde content of the gas exhaust was provided in Table 3.

Table 3. Formaldehyde analysis result for the foam sample (solid matrix of foam) (Analysis is carried out with headspace GC FID).

Analyzed Item	Analysis Description	Result (formaldehyde content) (%)
Sample No:1 (Foam Sample)	Headspace GC-FID, headspace oven at 18 °C, air fed to reactor is 100 ml/min	n.d.
	Headspace GC-FID, headspace oven at 20 °C, air fed to reactor is 100 ml/min	n.d.
	Headspace GC-FID, headspace oven at 22 °C, air fed to reactor is 100 ml/min	n.d.
	Headspace GC-FID, headspace oven at 24 °C, air fed to reactor is 100 ml/min	n.d.
Sample No:2 (Foam Sample)	Headspace GC-FID, headspace oven at 18 °C, air fed to reactor is 100 ml/min	n.d.
	Headspace GC-FID, headspace oven at 20 °C, air fed to reactor is 100 ml/min	n.d.
	Headspace GC-FID, headspace oven at 22 °C, air fed to reactor is 100 ml/min	n.d.
	Headspace GC-FID, headspace oven at 24 °C, air fed to reactor is 100 ml/min	n.d.

*n.d.: non-detected

Referring back and forth to the Table 3, formaldehyde content can only be observed during the chemical reaction between the composites, i.e. composite A and composite B. Once the solid matrix of the foam is formed, formaldehyde is linked to the matrix and it is not in the free form. Although formaldehyde is not detected from the exhaust gas of the reactor out (fresh air feed 100 ml/min, sample is solid foam), still depending on the air flowrate and depending on the time of the phenol-based filling material formation formaldehyde and other volatile organic carbons can readily be observed. This study summarizes the initial findings of the experimental set up (headspace GC-FID).

CONCLUSION

In this study, methods to determine the formaldehyde content of phenol-based filling materials were investigated. In this context, experimental set ups provided by literature researchers and the inclusion of headspace GC-FID orientation were considered. Being inspired by the alternative GC-Oven employment for spontaneous combustion liability tests conducted by Bilen et al. (2019), a new experimental set up was built with a malfunctioning GC (Perichrom GC, malfunctioning only for chromatographic purposes). Perichrom GC was employed in terms of headspace and the oven of this abovementioned equipment functions properly. Simulation of the foam production in underground coal mining environment/mining environment, reaction gases should be collected and analyzed. In a mining environment, ventilation takes place and corresponding simulation of this air ventilation in mining atmosphere was achieved with an air mini compressor to the reaction chamber of foam (phenol-based filling material) production. Air carries the gases discharged during the chemical reaction between composites of phenol-based filling materials, and this gas discharge is being analyzed with GC-FID (Agilient HP 6890). The experimental set up built in our laboratory is not only available for the analysis of free formaldehyde content released during the chemical reaction of the composites (composites of phenol-based filling materials, composite A and composite B) but also corresponding analysis of gases, formaldehyde, volatile organic carbons, etc. can be analyzed for the foam solid samples produced after the

chemical reaction. This study does not involve the corresponding test results since it is not the focus yet, but it presents the availability of testing procedure along with the description of the method.

REFERENCES

AWES (2014) Safe Work Australia The Australian Work Exposures Study (AWES): Formaldehyde, ISBN 978-1-74361-929-2 (pdf) 978-1-74361-902-5 (docx)

Benassi, C. A., Semenzato, A., & Bettero, A. (1991). High-performance liquid chromatographic determination of free formaldehyde in cosmetics. *Journal of Chromatography A*, *464*, 387-393.

Bichler, W. & Simon, L. Fuel Energy Abstr., 37, 251 (1996).

Bilen M., Kaymakçı E., Yilmaz S. & Çakır A. An alternative spontaneous combustion experiment set-up by employing an old version Gas Chromatograph, Proceedings of 7th International Congress of Mining Machinery and Technologies 24-25 October 2019, İzmir Turkey.

Boe, K., Batstone, D. J., & Angelidaki, I. (2007). An innovative online VFA monitoring system for the anerobic process, based on headspace gas chromatography. *Biotechnology and bioengineering*, *96*(4), 712-721.

Brandão, P. F., Ramos, R. M., & Rodrigues, J. A. (2018). GDME-based methodology for the determination of free formaldehyde in cosmetics and hygiene products containing formaldehyde releasers. Analytical and bioanalytical chemistry, 410(26), 6873-6880.

Daoud Agha Dit Daoudy, B., Al-Khayat, M. A., Karabet, F., & Al-Mardini, M. A. (2018). A robust static headspace GC-FID method to detect and quantify formaldehyde impurity in pharmaceutical excipients. *Journal of analytical methods in chemistry*, *2018*.

Del Barrio, M. A., Hu, J., Zhou, P., & Cauchon, N. (2006). Simultaneous determination of formic acid and formaldehyde in pharmaceutical excipients using headspace GC/MS. *Journal of pharmaceutical and biomedical analysis*, *41*(3), 738-743.

Derikvand, A., Ghiasvand, A., Dalvand, K., & Haddad, P. R. (2021). Fabrication and evaluation of a portable low-pressure headspace solid-phase microextraction device for on-site analysis. Microchemical Journal, 168, 106362.

Engelhardt, H., & Klinkner, R. (1985). Determination of free formaldehyde in the presence of donators in cosmetics by HPLC and post-column derivation. *Chromatographia*, *20*(9), 559-565.

Gray, T.A., Trevits, M.A., Crayne, L.M. & Glogowski, P. Trans. Soc. Mining Metallurgy Exploration,320, 31 (2006).

Grenier-Loustalot, M.F., Larroque, S., Grenier, P. & Bedel, D., Polymer, 37, 939 (1996)

Hu, X., Zhao, Y., Cheng, W., Wang, D., & Nie, W. (2014). Synthesis and characterization of phenol-urea-formaldehyde foaming resin used to block air leakage in mining. Polymer Composites, 35(10), 2056-2066.

Hu, X.M., Wang, D.M. & Wang, S.L., Int. J. Min. Sci.Technol.,23, 13 (2013).

Lima, N. K., Lopes, A. R., Guerrero Jr, P. G., Yamamoto, C. I., & Hansel, F. A. (2018). Determination of volatile organic compounds in eucalyptus fast pyrolysis bio-oil by full evaporation headspace gas chromatography. *Talanta*, *176*, 47-51.

Ni, X & Pereira, N.E. AIChE. J., 46, 37 (2000).

Oliva-Teles, M. T., Paıga, P., Delerue-Matos, C. M., & Alvim-Ferraz, M. D. C. M. (2002). Determination of free formaldehyde in foundry resins as its 2, 4-dinitrophenylhydrazone by liquid chromatography. *Analytica Chimica Acta*, *467*(1-2), 97-103.

Wang, H., Du, Y., Wang, D., & Qin, B. (2019). Recent Progress in Polymer-Containing Soft Matters for Safe Mining of Coal. *Polymers*, *11*(10), 1706.

Woodfin, R.L. "Rigid Polyurethane Foam (RPF) Technology for Countermine (Sea) Program-Phase 1," SandiaReport, SAND96–2841, Sandia National Laboratories, Albuquerque, NM, January (1997).

Yi, Y., Ding, W., Wang, Y. N., & Shi, B. (2019). Determination of free formaldehyde in leather chemicals. *Journal of the American Leather Chemists Association*, *114*(10), 382-390.

GÖRÜNTÜ İŞLEME TEKNİKLERİ İLE TENÖR KONTROLÜ; DEMİR EXPORT DİVRİĞİ DEMİR MADENİ

GRADE CONTROL WITH IMAGE PROCESSING; A CASE STUDY, DEMİR EXPORT DİVRİĞİ IRON ORE MINE

H.Çınar [1,*], B.Aksanı [1], P. Tekin [1], A.Yıldız [1]

[1] Demir Export A.Ş.
*(*Sorumlu yazar: haydarc@demirexport.com)*

ÖZET

Demir Export, 2016 yılında dijitalleşme sürecine başlamıştır. Bu kapsamda yapılan çalışmalardan biri de maden planlamada günümüz veri analiz trendlerini kullanmaktır. Bu amaçla, çeşitli özelliklerinden dolayı, Divriği Demir İşletmesi seçilmiştir. Divriği Demir Madeni İşletmesinde hematit ve ağırlıklı olarak manyetit minerallerini içeren cevher üretimi yapılmakta ve açık ocaktan üretilen cevher zenginleştirme işleminden sonra hem yurtiçi hem de yurtdışında pazar bulmaktadır. Üretilen demir konsantresi kalite açısından pelet kalitesinde olup, izabe tesisleri tarafından tercih edilen bir üründür.

İşletmede, tenör kontrol çalışmalarında uygulanan cevherden kesit alma (sondaj) ve üzerinden ölçümler yapma yöntemi yerine, görüntü ile elde edilen verilerin analizleri ile hızlı ve güvenilirliği yüksek alternatif bir yöntem geliştirilmiştir. Çalışmada başlangıç olarak, üretim kademeleri sıralı olarak fotoğraflanarak, alınan fotoğraflar üzerinde cevher ile pasa malzemesi arasında renk farklılığı oluşturulmuştur. Belirlenen bölgelerde, açık kaynak kodlu görüntü işleme yazılımlarıyla, cevher renginin pasa rengine oranı üzerinden hacimsel yüzde hesabı yapılarak, üretime ve planlamaya etki edecek şekilde hızlı ve düşük maliyetli bir yöntemle tenör kontrolü yapılabilmiştir. Daha geniş bir yüzey alanı taranarak sonuçların güvenilirliği artırılmıştır.

Anahtar Sözcükler: Görüntü işleme, dijital dönüşüm, veri analizi, tenör kontrolü

ABSTRACT

Demir Export started the digitalization process in 2016. One of the studies carried out in this context is to use today's data analysis trends in mine planning. For this purpose, Divriği Iron Mine Operation was chosen due to its various features. Divriği Iron Mine Operation produces ore containing hematite and predominantly magnetite minerals and the ore produced from open pit finds markets both in Turkey and abroad after the enrichment process. The iron concentrate produced is of pellet quality in terms of quality and is a product that is highly preferred by smelters.

A fast and reliable alternative method has been developed with the analysis of the data obtained from the images, instead of the ore sectioning (drilling) and related calculations. In the beginning of the study, the production stages were photographed sequentially, and color contrast was created between the ore and waste material on the photographs taken. By using the open-source image processing applications in the specified regions, the volumetric percentage calculation was made quickly over the ratio of ore to waste color. Using this method, grade control could be performed in a fast and cheap way that can positively affect production and planning stages. The reliability of the results is increased by scanning the larger surface area.

Keywords: Image processing, digital transformation, data analysis, grade control

GİRİŞ

Endüstri 4.0 devrimin başlamasıyla beraber savunma sanayi öncü olmak üzere hemen her sektörde dijitalleşme gerçekleşmeye başlamıştır. McKinsey&Company'nin yaptığı bir araştırmaya göre; Covid19 küresel salgını ile dijitalleşme şirketlerin hem organizasyon yapısını hem de iş yapış şekillerini değiştirmeyi bir seçenek olmaktan çıkarıp zorunluluk haline getirdiği gözler önüne serilmiştir (Laura LaBerge, 2020).

Her sektörde olduğu gibi madencilikte de dijitalleşme çalışmaları olanca hızıyla devam etmektedir. Günümüzde oldukça sık kullanılan görüntü İşleme teknikleri ile analizler, madencilikte de uzun yıllardır kullanılmaktadır. Öyle ki 2002 yılında yapılmış olan bir çalışma; büyük kaya parçalarının görüntü işleme yöntemleri ile tespit edilebileceğini göstermiştir. Bu çalışmada temel amaç kırıcı/elek gibi makineleri durduran büyük kaya parçalarını tespit etmektir. Bu amaçla alınan görüntüler çeşitli filtreleme ve düzeltme işlemlerinden geçirildikten sonra bir istatistiksel model yardımı ile görseldeki cisimlerin kaya olup olmadığının tespiti gerçekleştirilmiştir (Enrique Cabello, 2002).

Madencilikte görüntü işleme çalışmaları sadece ayırt edilmesi kolay olan cisimlerin tespit edilmesinden ibaret değildir, flotasyon gibi karmaşık süreçlere de dahil edilebilmektedir. Yapılan bir çalışmada süreç içerisinde flotasyon hücresindeki köpüğün görüntü işleme algoritmaları kullanılarak ayırt edilebildiği ve köpük özelliklerine bağlı olarak tesis performansının optimize edilebileceği belirlenmiştir (D.W. Moolman, 1994).

Planlama, diğer tüm sektörlerde olduğu gibi madencilik sektöründe de oldukça kritik öneme sahiptir. Madencilikte birçok kısa ve uzun vadeli planlar yapılmakta, şirketin nakit akışına bu planlar yön vermektedir. Bu planlar kısa ve uzun vadeli olup, yapılacak üretimin miktarı ve içeriğine bağlıdır. Planları daha doğru ve çevik bir şekilde geliştirmek için yeni dijital çözümler aranmaktadır. Türkiye'de madencilik sektöründe planlama sürecinde görüntü işleme ile ilgili çalışmalar bulmak oldukça zordur. Bu çalışmanın görüntü işleme teknolojilerinin üretim planlamasında kullanılması yönünden yenilikçi ve özgün değere sahip olduğu düşünülmektedir.

Çalışmanın yapıldığı Divriği Demir İşletmesi'nde cevherleşme hematit ve manyetit minerallerinin çeşitli tane boylarında ince ve killi yan kayaç içerisinde dağılımıyla oluşmuştur. Cevherleşme, üretim kademe yüzeylerinde renk farklılıkları sayesinde gözle de ayırt edilebilir bir durumdadır. Cevherleşmenin yapısal özellikleri nedeniyle numunelerin kimyasal analizi yerine görünen hematin ve manyetit minerallerinin kapladıkları alanlar temel alınarak hesaplanan hacimsel yüzde değerleri ile tenör tespiti yapılmaktadır. Hacimsel yüzde hesapları sondaj karotları üzerinden veya üretim yüzeylerinde ölçekli şeritler kullanarak yapılmaktadır.

GÖRÜNTÜ İŞLEME TEKNİKLERİ İLE TENÖR KONTROL ÇALIŞMALARI

Demir Export A.Ş. Sivas'ın Divriği ilçesinde yer alan Divriği Demir Madeni'nde çalışmalar gerçekleştirilmiştir. İşletmenin mevcut yıllık üretim kapasitesi 2014 yılı sonunda devreye alınan yeni zenginleştirme tesisi ile 500 bin ton/yıl kapasiteye çıkarılmıştır. (Demir Export A.Ş., 2020)

Divriği Madeni'ne ait sahada cevherleşme, hematit ve manyetit minerallerinin çeşitli tane boylarında ince ve killi yan kayaç içerisinde dağılımıyla oluşmuştur. Jeolojik birim içerisinde bulunan, hematit ve manyetit minerallerinden oluşan demir cevheri, tane boyu ve miktar anlamında yatay ve düşey yönde farklılıklar göstermektedir. Cevherdeki demir minerallerinin miktarının tespiti için cevhere özel yöntemler kullanılmaktadır.

Düzensiz dağılım gösteren demir içeren tanelerin, yapılan sondajlarla seviyeleri belirlenir ve hacimsel yüzde oranları hesaplanır. Hacimsel yüzde, cevherli seviyelerde kesilen ve uzun ekseni 5 cm'yi aşan manyetit çakıllarının toplam uzunluğunun, cevherli seviyelerin toplam uzunluğuna oranı ile hesaplanır (Şekil 1 ve 2). Hesaplamalar sonucunda çıkan oranlar demir içeren minerallerin tenör değerleri olarak varsayılırlar. Sondaj verilerinden elde edilen veriler kullanılarak sahanın jeolojik blok modeli oluşturulur, jeoistatistiksel yöntemler ile cevherli bloklara atama yapılarak kaynak model kestirimi yapılarak maden ömrü için üretim planları yapılırken, üretim aynalarından elde edilen bu veriler hem üretime yön vermek hem de haftalık, aylık ve yıllık üretim mutabakatları için kullanılırlar.

Şekil 1. Cevher Yapılaşması Örneği

Şekil 2. Sondaj Örneği

Cevherin yatay ve düşey düzlemdeki düzensiz dağılımı nedeniyle, cevher üretiminde zaman zaman sorunlar yaşanmakta, miktarlarda sık sık değişkenlik yaşanmaktadır. Düzensiz cevher dağılımı yüzünden, cevherden alınan kesit çoğu zaman bölgeyi düzgün temsil edememektedir. Üretime ve kısa vadeli planlara yön vermek amacıyla tenör kontrolü için hacimsel yüzde hesaplamaları, ölçekli şeritler kullanılarak, açık ocak kademelerinde üretim yüzeylerinde yapılmaktadır (Şekil 3). Maden yatağının büyüklüğü ile çalışma alanlarının dağınıklığı ve üretim hızı göz önüne alındığında, tenör kontrol çalışmalarının bu şekilde yapılması ve sonuçların sahada uygulanmasının daha hızlı olması ve elde edilen verilerin güvenilirliğinin artması gerekmektedir.

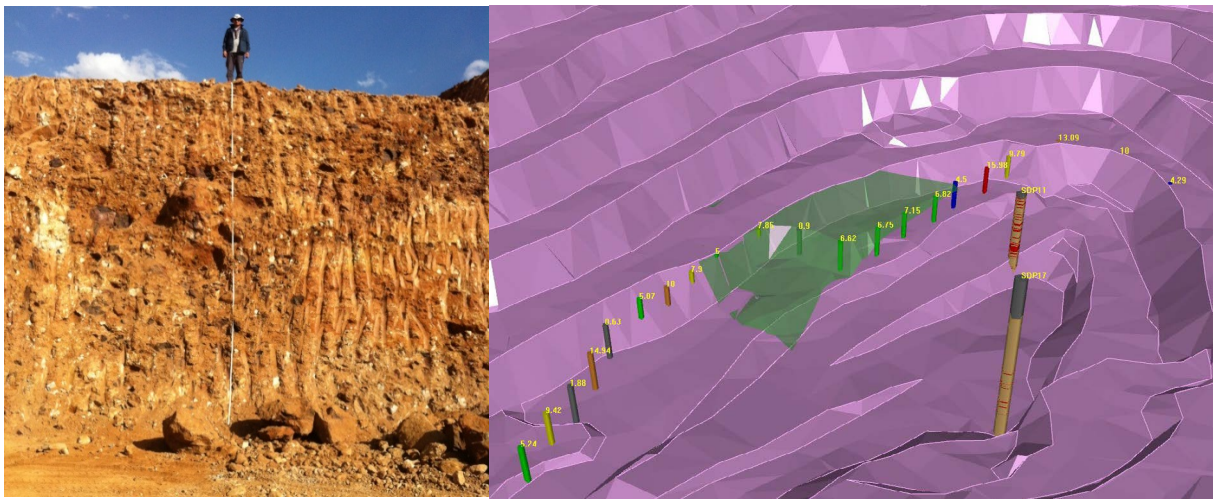

Şekil 3. Ölçekli Şerit Kullanımı ve Datamine Studio RM Uygulaması Çıktısı

Kullanılmakta olan yöntemlerden esinlenilerek günümüz teknolojilerini de kullanacak şekilde, daha hızlı ve az maliyetli çözüm üreten bir alternatif yöntem geliştirilmiştir. Bu yöntem üretim kademelerinin fotoğraflandırılması ve fotoğraflandırılan yüzey üzerinden hacimsel yüzdenin hesaplanmasıdır.

Daha hızlı ve güvenilir sonuçlar elde etmek amacıyla; aşağıdaki şekilde çalışma planı oluşturulmuştur (Şekil 4).

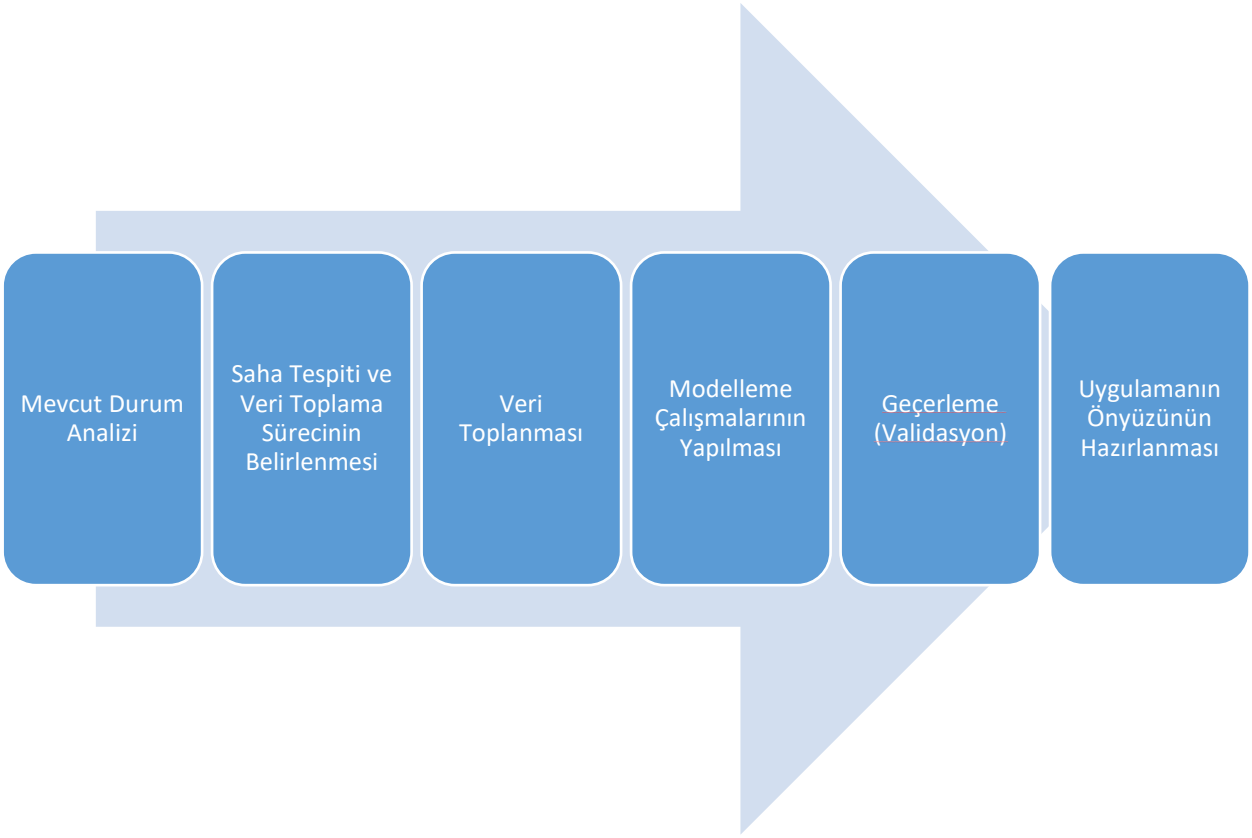

Şekil 4. Çalışmanın Aşamaları

Literatür taraması ve mevcut durumun analizinden sonra örneklem seçimi aşamasına geçilmiştir. İstatistiksel çalışmalar gerçekleştirebilmek için örneklem seçimi oldukça önem arz etmektedir. Örneklem kitleyi en iyi şekilde temsil eden bir alt gruptur. Bu çalışma için, örneklemi seçme amacı ile maden sahasındaki en uygun alanlar; maliyet ve zaman gibi kriterlere göre belirlenmiştir. Belirlenmiş olan kriterlere göre ilgili üretim kademeleri fotoğraflandırılmıştır (Şekil 5).

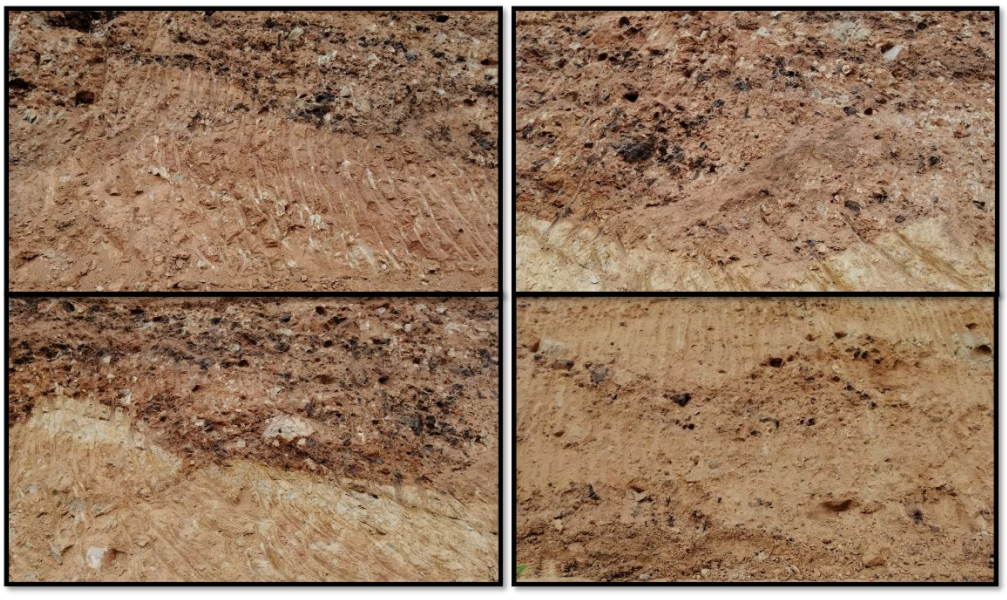

Şekil 5. Örnek Üretim Kademesi Görüntüleri

Toplanan görüntüler incelenmiş, uygun kalitede olan (istenilen özelliklere sahip) görüntüler seçilmiştir. Seçilen bu görüntüleri işleyebilmek ve doğru sonuçlar elde edebilmek amacıyla görüntüler düzenlenmiştir. Düzenlemede boyut küçültme, kırpma, renk tonu ayarlama gibi birtakım veri temizleme ve filtreleme işlemleri uygulanmıştır. Yapılan bu işlemlerden sonra görüntüler modelleme yapılmaya hazır hale getirilmiştir.

Fotoğraf seçim aşamasını ayrıntılandırmak için fotoğrafın ayırt edici bileşeni olan piksel bilgileri kullanılmıştır. Piksel, dijital göstergelerde görüntünün elde edilmesini sağlayan ve kontrol edilebilen en küçük birimdir (Wikimedia Foundation, 2020). Örneğin, 1024*768 çözünürlüğe sahip bir fotoğraf; yatay olarak 1024 piksel dikey olarak ise 768 piksel olmak üzere 768.432 adet pikselden oluşmaktadır. Fotoğrafta (uygulamada kullanılan) her bir piksel RGB olarak belirtilen bir sıralı üçlü ifade edilir (Şekil 6). Matematiksel tanım olarak $\{(r,g,b)\,|\,r,g,b \in [0,1]\}$ ile veya $\{(r,g,b)\,|\,r,g,b \in [0,255] \subset \mathbb{Z}\}$ ile ifade edilebilir. Buna göre 16.581.375 adet farklı renk elde edilebilir.

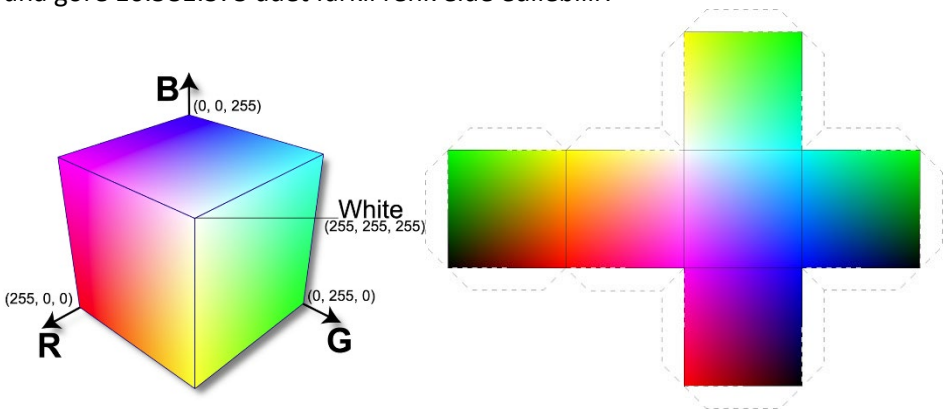

Şekil 6. RGB Renk Uzayı Gösterimi

Fotoğraflardaki RGB formatında bulunan renklerin üzerlerinde işlem yapmayı zaman ve donanım olarak kolaylaştırmak için gri tonlara (grey scale) döndürülmüştür (Şekil 7). RGB formatındaki renkler gri tona dönüştürülürken aşağıdaki eşitlik kullanılmıştır.

$r,g,b \in [0,255] \subset \mathbb{Z}, \quad x+y+z=1 \; ve \; x,y,z \in [0,1] \; olmak \; üzere;$

$GreyScale = \frac{x*r+y*g+z*b}{3}$ xyz->w1,w2,w3

Burada "x", "y"," z" değerleri renklerin ağırlıklarını temsil etmektedir. Fotoğrafın durumuna göre vurgulanması gereken renk bu tonlar sayesinde belirlenmektedir. Bu yönteme de Ağırlıklı Ortalama denmektedir. $x,y,z=1$ olması durumunda işlem basit bir şekilde aritmetik ortalama formülüne dönüşmektedir.

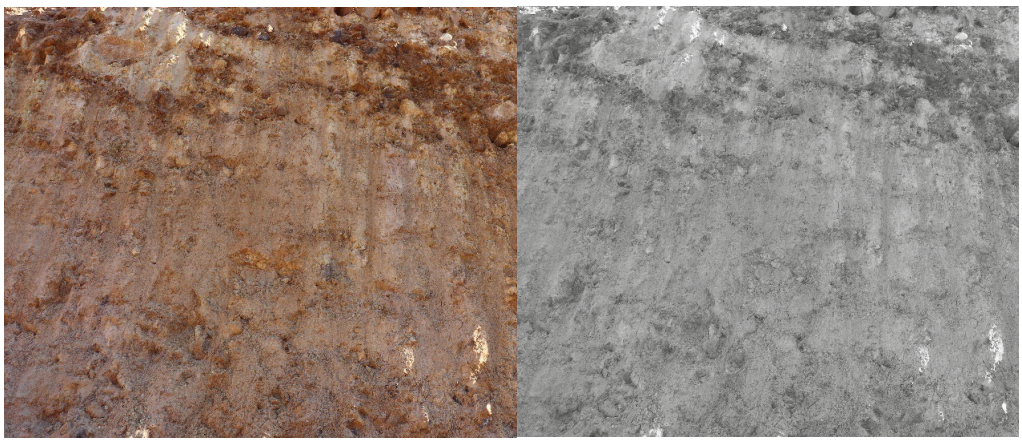

Şekil 7. Gri Ton Çevirme Örneği

Tenör kontrol çalışması geliştirilen ara yüz yardımıyla, orijinal resim üzerinden cevherli bölge seçimleri ile başlamaktadır. Uygulama belirlenen kriterlere ve toleransa göre; uzmanın seçmiş olduğu bölgeyle benzerlik gösteren diğer bölgeleri de tarayıp seçmektedir. Tolerans, seçim yapılan bölgeler ile benzerlik gösteren bölgelerin seçimindeki oranı belirtmektedir. Tolerans ne kadar düşük olursa seçim yapılan bölgelere en çok benzeyen bölgeler seçilmektedir. Tolerans değeri arttıkça ise seçim yapılan bölgeye belirtilen tolerans değeri oranında benzerlik yapan alanlar daha fazla seçilmektedir. Cevherli bölge seçimleri tamamlandıktan sonra uygulama hesaplamalara başlamaktadır. Hesaplamalar tamamlandıktan sonra sonuçları yüzde değeri olarak uygulama üzerinden görülebilmektedir.

Tüm hesaplamalar Python programlama dili kullanılarak gerçekleştirilmiştir. Bilimsel hesaplamalar için kullanılan Numpy kütüphanesi, temelleri Intel tarafından atılan gerçek zamanlı görüntü işleme kütüphanesi olan OpenCV gibi kütüphaneler kullanılmıştır (Python Software Foundation, 2020). Bu yaygın kullanımda olan kütüphane ve fonksiyonlarının yanı sıra piksel hesaplamaları, tolerans değerinin işlenmesi ve uygulamaya dahil edilmesi gibi; uygulamanın amacına yönelik özel fonksiyonlar ve algoritmalar da geliştirilmiştir.

Programın ön yüzü; fotoğrafların uygulamaya tanıtılması, tolerans değerinin girilmesi ve fotoğraf üzerinde bölgelerin seçiminin yapılması için yine bir Python kütüphanesi olan PyQt5 kütüphanesi kullanılmış ve bir ara yüz geliştirilmiştir (Şekil 8).

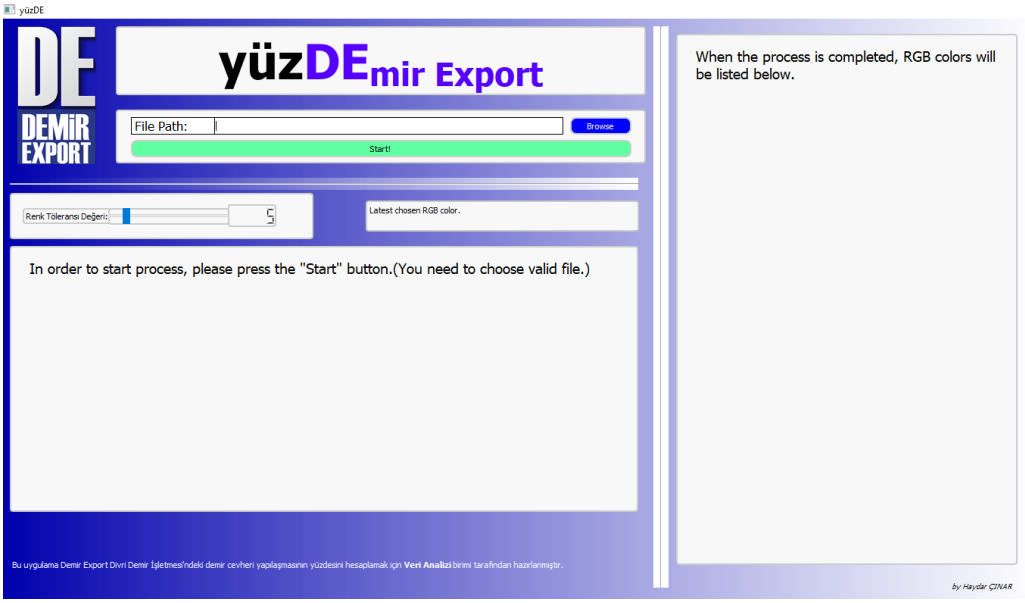

Şekil 8. Uygulama Örnek Görüntüsü

SONUÇLAR VE GELECEK ÇALIŞMALAR

Uygulamadan elde edilen sonuçlar geçerleme (validasyon) işlemine tabi tutulmuştur. Geçerleme için $n > 100$ olacak şekilde bir fotoğraf gurubu seçilmiş ve bu fotoğraflar üzerinde çalışma yapılmıştır. Yapılan çalışmadan sonra kaynak model ile hesaplanan değer kıyaslanmıştır. Kaynak modelin geometri olarak uyumluluğunun %95, tenör olarak uyumluluğunun ise %75 olduğu bilinmekte olup, kıyaslamalarda referans olarak kullanılmaktadır. Geçerleme işleminde uygulama, kaynak model ile kıyaslandığında ortalamada %3 hataya sahip sonuçlar üretmiştir. Sondaj işlemi gibi maliyetli 3 boyutlu analizlerin yanında bu çok düşük maliyetli bu yöntemin hızlı ve güvenilir sonuçlar verdiği söylenebilir (Şekil 9).

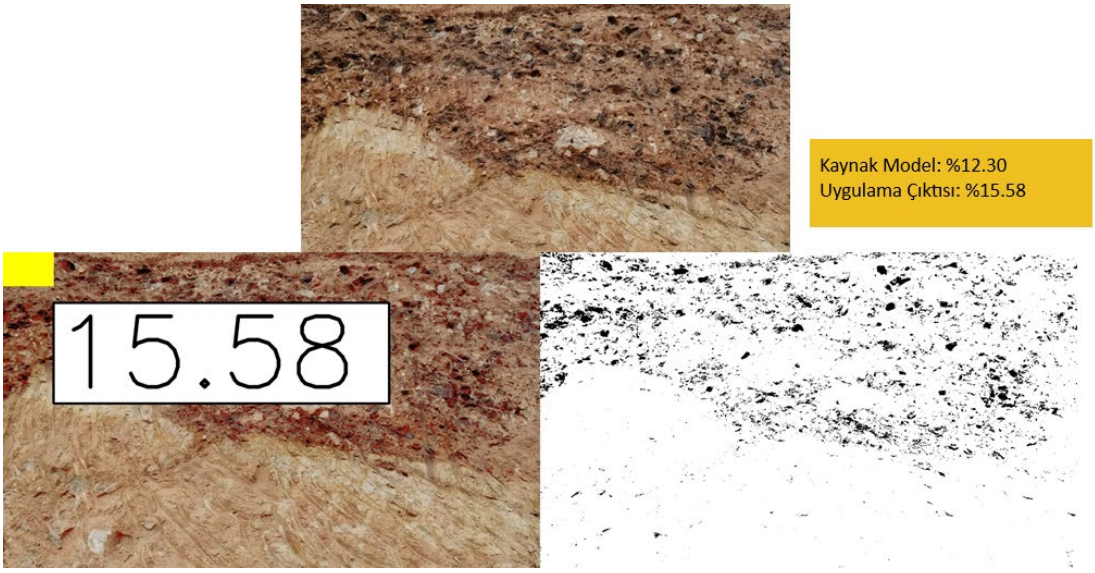

Şekil 9. Uygulama Çıktısı

Geçerleme sürecinde bazı örneklerde uygulamanın hesapladığı değerler ile Kaynak Model arasındaki fark ±%0.5'e kadar düştüğü görülmüştür.

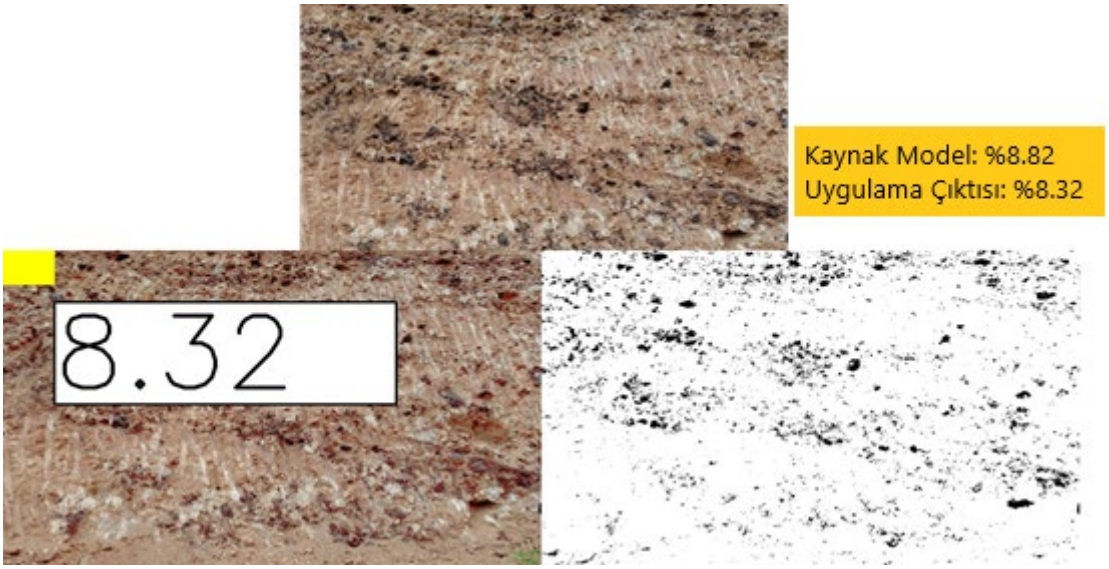

Şekil 10. Uygulama Çıktısı

Bu geçerleme çalışması ile beraber uygulamanın güçlü yönlerinin yanı sıra zayıf yönleri de ortaya çıkmıştır. Uygulama; fotoğrafın çekilme açısı, uzaklığı ve gün ışığı durumundan etkilenmektedir. Etkenler arasında en ön plana çıkan ise gün ışığıdır. Işık ile beraber fotoğrafta yüzeylerden kaynaklı gölgeler oluşmakta ve uygulama tarafından bu gölgeler cevherli bölge olarak seçebilmektedir (Şekil 11).

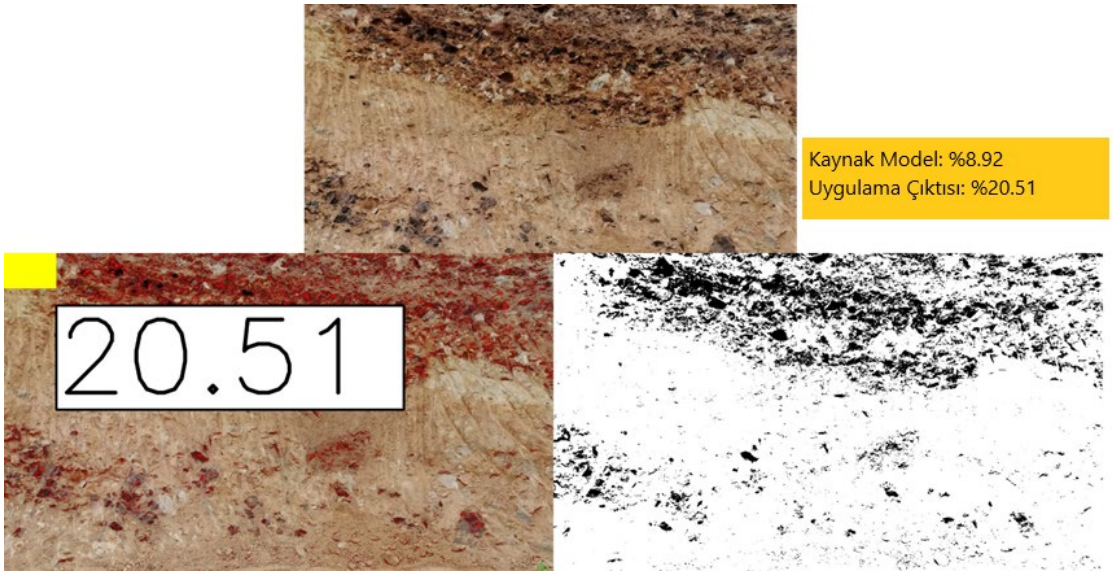

Şekil 11. Uygulama Çıktısı

Uygulama hızlı ve oldukça düşük maliyet ile sonuç üretebildiği için zayıf yönleri üzerine gidilmesi ve uygulamanın geliştirilmesi planlanmaktadır. Öyle ki sadece planlama sürecine değil, maden arama faaliyetleri ve üretim süreçlerine de insansız hava aracı kullanarak, ışığa duyarlı olmayan kameralar yardımıyla görüntü alarak ve o görüntüler üzerinden anlık sonuçlar elde ederek uygulamanın katkı sağlanması planlanmaktadır.

KAYNAKLAR

Cabello, E., Sanchez, M.A., and Delgado, J. (2002). A new approach to identify big rocks with applications to the mining industry. *Real-Time Imaging*, 8(1), 1-9.

Demir Export A.Ş. (2020). Retrieved from https://www.demirexport.com

LaBerge, L., O'Toole, C. (2020). McKinsey&Company. Retrieved from https://www.mckinsey.com/business-functions/strategy-and-corporate-finance/our-insights/how-covid-19-has-pushed-companies-over-the-technology-tipping-point-and-transformed-business-forever

Moolman, D.W., Aldrich, C. (1994). Digital image processing as a tool for on-line monitoring of froth in flotation plants. *Minerals Engineering*, 7(9), 1149-1164.

Python Software Foundation. (2020). Documentation. Retrieved from https://www.python.org

Wikimedia Foundation. (2020). Flotasyon. Retrieved from https://tr.wikipedia.org/wiki/Flotasyon

Wikimedia Foundation. (2020). Pixel. Retrieved from https://en.wikipedia.org/wiki/Pixel

HASANDAĞ VOLKANİKLERİNİN TEK EKSENLİ BASINÇ DAYANIM DEĞERLERİ İLE NOKTA YÜK İNDEKS DEĞERLERİ ARASINDAKİ İLİŞKİNİN İNCELENMESİ

INVESTIGATION OF THE RELATIONSHIP BETWEEN UNIAXIAL COMPRESSIVE STRENGTH VALUES AND POINT LOAD INDEX VALUES OF HASANDAĞ VOLCANICS

M.A. Demirçin [1,*], H. Tunçdemir [2]

[1] *M.T.A Genel Müdürlüğü, Sondaj Dairesi Başkanlığı*
*(*Sorumlu yazar: muratali.demircin@mta.gov.tr)*
[2] *İ.T.Ü. Maden Fakültesi, Maden Mühendisliği Bölümü*

ÖZET

Standart testler için örnek hazırlanamadığı durumlarda kayaçların "Tek Eksenli Basınç Dayanımı Değerleri" doğrudan elde edilemeyebilmektedir. Bu nedenle, detaylı örnek hazırlamayı gerektirmeyen ve taşınabilir donanımlarla hem arazide, hem de laboratuvarda kullanılabilen çeşitli yöntemler geliştirilmiştir. Bunlardan biri nokta yük testidir. Kayaçların basınç ve çekme dayanımı parametrelerinin, nokta yük indeks değerlerinden dolaylı olarak belirlenebilmesi için, literatürden derlenen deneysel çalışmalar incelendiğinde, tüm kayaçlar için standart bir "k" değerlerinin tanımlanmasının hatalı olduğu ve böylesi genellemeler yerine, kayaç veya saha bazlı korelâsyonların geliştirilmesinin daha doğru olacağı görülmektedir. Bu değerlendirme kapsamında; hem yerel yaygın bir formasyonun mekanik özelliklerinin tanımlanması, hem de düşük–orta dayanımlı ignimbirit ve tüf özelliğindeki volkanik kayaçlara dair dayanım parametrelerinin belirlenmesi için çalışmamızda, Nevşehir provensi volkanik istifi içerisinde yer alan Hasandağ Volkanikleri incelenmiştir. Burada boy çap oranı 1 ve 2.5 olan NX (54mm) çaplı karot örnekler kullanılarak, kuru ve suya doygun şartlarda, yönlenmelerde dikkate alınarak belirlenmiş olan tek eksenli basınç dayanım değerleri ile yine hem kuru, hem de suya doygun şartlarda yapılan nokta yük dayanım testlerinden, d_{50} eş değer karot çapı düzeltmesi sonrası bulunan sonuçların karşılaştırılması yapılarak yüksek korelasyonlu değerler elde edilmiştir.

Anahtar Sözcükler: Tek eksenli basınç dayanımı, nokta yük indeksi, dolaylı kayaç dayanım test yöntemleri, volkanik kayaçların dayanım değerleri

ABSTRACT

When suitable and standardized rock samples are not able to be prepared, then, the uniaxial compressive strength of that samples will not be obtained directly. In order to eliminate this kind of rock-related deficiencies, some techniques, which are used in both laboratory and field with some mobilized instruments, have been improved. One of them is the point load index test.In order to indirectly determine the compressive and tensile strength parameters of rocks from the point load index values, when the experimental studies compiled from the literature are examined, it is seen that the definition of a standard "k" value for all rocks is incorrect and it would be more accurate to develop rock- or site-based correlations instead of such generalizations. Within the scope of this evaluation; Hasandağ Volcanics, located in the Nevşehir province volcanic succession, were investigated in our study in order to define the mechanical properties of a locally widespread formation and to determine the strength parameters of low-medium strength ignimbrite and tuff volcanic rocks. Here, using NX (54 mm) diameter core samples with a length-to-diameter ratio of 1 and 2.5, uniaxial compressive strength valuesdetermined by considering orientations in dry and saturated conditions, and point load strength tests performed in both dry and water-saturated conditions, high correlation values were obtained by comparing the results found after d_{50} equivalent core diameter correction.

Keywords: Uniaxial compressive strength, point load index, indirect rock strength test methods, strength values of volcanic rocks

GİRİŞ

Kayaçların zayıflıkları ve buna bağlı standarda uygun örnek alma problemi nedeniyle, tek eksenli basınç dayanımı değerleri her zaman doğrudan elde edilemeyebilmektedir. Bu yüzden çok detaylı örnek hazırlamayı gerektirmeyen, taşınabilir donanımlar yardımı ile hem arazide hem de laboratuvarda uygulanabilen çeşitli yöntemler geliştirilmiştir. Nokta yük testi bu amaçla kullanılan mevcut testler arasında en güvenilir sonucu verenlerdendir (Brook, 1985).

Bu çalışmada Nevşehir provensi volkanik istifi içerisinde yer alan Hasandağ Volkaniklerini kapsayan bazı kayaç örnekleri üzerinde yapılan bir seri tek eksenli basınç dayanımı (TEBD) ve nokta yükleme dayanım test (NYD) sonuçları listelenecek ve aralarındaki ilişkiler irdelenecektir. Bugüne kadar araştırmacılar bu konuda çok sayıda çalışmalar yapmışlar, çeşitli arazi ve formasyonlar için NYD'den TEBD'nın tahmin edilebildiği, yüksek dereceli doğruluğu olan ilişki denklemleri ortaya koymuşlardır. Bu çalışmayı oluşturan veri tabanının özelliği ise boy/çap oranı 1 ve 2.5 olan karot örnekler üzerinde yapılan TEBD ile NYD testlerinin hem kuru ve hem de yaş, aynı zamanda da tabaka düzlemine dik ve paralel olarak da test edilmiş olması ve bu açıdan bu iki test sonuçlarının karşılaştırılması olarak ifade edilebilir.

TEBD ve NYD testlerinin değerlendirilmesi ile elde edilen sonuçlar kaya malzemelerinin dayanım sınıflaması için indeks değer olarak alındığı gibi, dolaylı olarak kayacın çekme dayanımının hesaplanmasında da kullanılmaktadır. Ayrıca, bu yöntemle kayanın zayıflık düzlemlerine dik ve paralel olarak ölçümler yapılarak, yöne göre en büyük ve en düşük değerleri veren, nokta yük dayanım değerleri belirlenebilmekte ve bu şekilde yönlenme dikkate alınarak bulunan değerlerin ortalamalarının oranı olarak tanımlanan, dayanım indeks anizotropisi (I_a) da tayin edilebilmektedir. Kayaç izotropik olduğunda I_a =1; anizotropik olduğunda ise I_a>1olmaktadır (ISRM, 1985; Broch et al., 1972; Topal, 2000).

YÖNTEM

Nokta yükleme deneyi; biri hidrolik yağla tahrik edilen pistondan oluşan iki sivri metal konik ucun arasına yerleştirilen standarda uygun örneklerin sıkıştırılması ve örneklerin kırıldığı anda dayandığı en yüksek yağ basıncının manometreden okunarak yük değerine çevrilmesi ve bu yük değerinin yükleme yönünde birim alana bölündüğünde elde edilen indeks bir gerilme değeridir. Bu değer kayaç özelliklerine göre belirlenen bir katsayı ile çarpıldığında kayacın dolaylı olarak TEBD değerine ulaşılabilmektedir.

Deney için gerekli düzenek, Şekil 1'de gösterildiği gibi yükleme sistemi, yük ölçüm sistemi ve yükleme sistemindeki platenlerin uç noktaları arasındaki uzaklığı belirleyen ölçüm sisteminden oluşmaktadır.

Şekil 1. Nokta yükleme deney düzeneği

Silindirik örneklerin aparata yerleştirme şekline göre eksenel ve çapsal olarak ifade edilen farklı deney uygulama yöntemleri bulunmaktadır. Tabakalanmaya dik doğrultuda yapılan eksenel deneyler (a) ile tabakaya paralel olarak yapılan çapsal deneyler (b), Şekil 2'de görülmektedir.

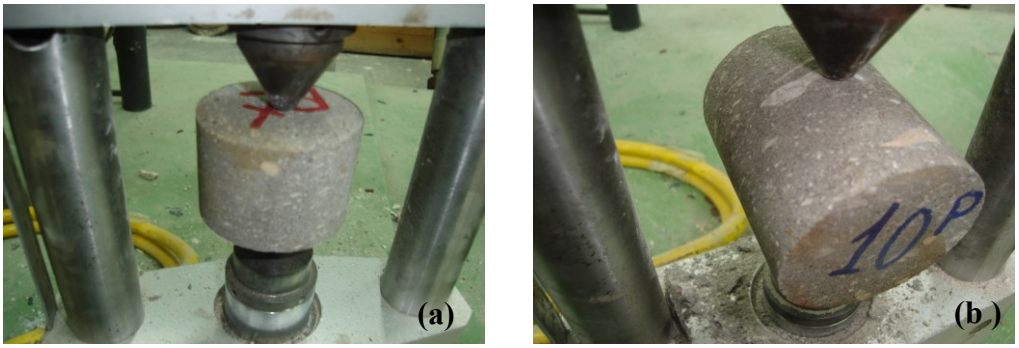

Şekil 2. Karot örneklerin aparata yerleştirme şekli (a) eksenel; (b) çapsal

Nokta yük testinde gözlenen kırılma şekli gerilme ile boyuna çatlamadır (Broch et al., 1972). Dayanım indeksi; boyut ile değişmekte, örneğin şeklinden de etkilenmektedir (Brook, 1977). Nokta yük dayanım indeksi karot örnekler için daha küçük olup, örnek boyutu arttıça azalmaktadır (Al-Jassar et al., 1979; Bieniawski, 1975). Broch ve Franklin 1972'de şekil ve boyut etkisinin; düzgün şekilli olmayan örnekler kullanılarak yapılan testlerde, düzenli bir geometriye sahip örneklerle yapılan testlere kıyasla çok daha şiddetli olduğunu, çapsal olarak yapılan testlerin şekil etkisinden daha az etkilendiğini, bu nedenle de dayanım sınıflaması açısından çok daha güvenilir olduğunu değerlendirmiş ve eksenel testlerin sadece dayanım indeks anizotropisi ölçüldüğünde kullanılmasını tavsiye etmişlerdir (Broch et al., 1972).

Düzgün şekilli olmayan örnekleri kırmak için gereken yük; minimum kesit alanının bir fonksiyonudur (ISRM, 1985). Bu nedenle; standart nokta yükleme indeks değerinin bulunabilmesi açısından bir boyut düzeltme faktörü kullanılması gerekmektedir. Deneyler 50 mm çaplı silindirik karotlar üzerinde yapıldığında, hiçbir düzeltmeye gerek bulunmadığı için, düzeltilmiş nokta yükleme değeri $Is_{(50)}$; 50 mm çaplı silindirik karot testleri ile çapsal olarak ölçülmüş Is değeri olarak tanımlanmış, diğer şekil ve boyutlu örnekler kullanılarak yapılan testler sırasında boyut düzletmenin gerekli olduğu vurgulanmıştır. NX 54 mm boyutundaki karot numuneler üzerinde yapılan çap deneylerinde de düzeltme prosedürünün uygulanması zorunlu görülmemekte (ISRM, 1985) ve hatta standart boyut olarak kullanılması önerilmektedir (Bieniawski, 1975).

Nokta yükleme indeks değeri; Eşitlik 1'de gösterildiği gibi hesaplanmaktadır.

$$Is = \frac{P}{De^2} \tag{1}$$

Is= Nokta yük indeksi (MPa) ya da (kg/cm^2)
P= Yük (kN) ya da (kgf)
De= Eşdeğer karot çapı (mm).

Nokta yükleme dayanımı; çapsal testler için Eşitlik 2'deki gibi D'nin fonksiyonu olarak, eksenel, blok ve düzensiz parça testlerinde ise Eşitlik 3'teki gibi De'nin fonksiyonu olarak değişmektedir.

$De^2 = D^2$ Çap deneyleri için (2)

$$De^2 = \frac{4A}{\pi};\quad A = W * D \text{ Eksenel deneyler için} \tag{3}$$

Burada;

A: Platen değme noktalarından geçen numune düzleminin en küçük kesit alanıdır.
D: Yükleme noktaları arasındaki mesafe (mm)
W: Yükleme noktaları arasındaki kesit alanı dik uzaklığıdır. Bu uzaklık şekilsiz bloklarda değişiyorsa ortalama değer alınarak hesaplamalar yapılmaktadır.

Numune büyüklüğüne göre boyut düzeltme üzerine çeşitli yöntemler geliştirilmiştir.

1) Bunlardan birisi D ve De'nin tüm oranlarında örnekleri test edip, P ve De^2 arasındaki ilişkiyi log-log grafik olarak değerlendirerek, bu grafikten De^2=2500 mm'ye karşılık gelen P_{50} değerinin interpolasyon yolu ile tayini yöntemidir (Şekil 3). Bu durumda düzeltilmiş nokta yükleme indeksini bulmak için eşitlik 4 kullanılır.

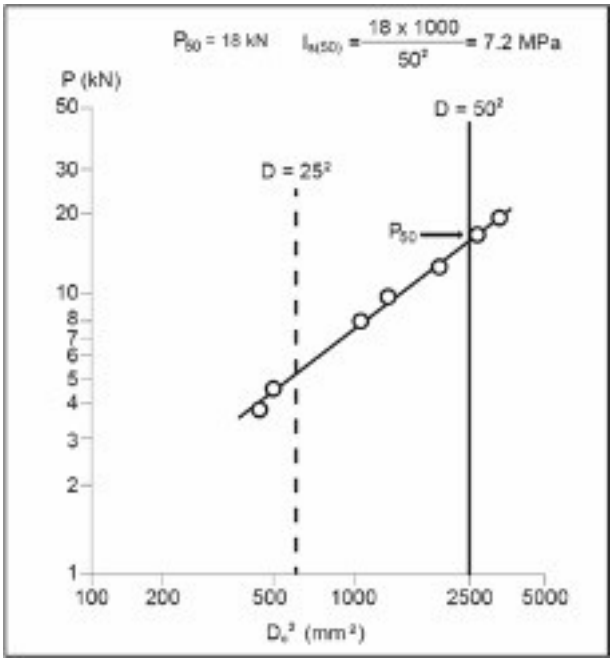

Şekil 3. $Is_{(50)}$ değerinin P ve De^2 arasındaki ilişki kullanılarak tayini (Brook, 1985)

$$Is_{(50)} = \frac{P_{50}}{50^2};\tag{4}$$

2) Test edilecek örneklerin; sınırlı sayıda 50 mm'den küçük parçalar biçiminde ya da 50 mm'den farklı çapta, ancak; sadece tek bir boyutta hazırlanabilmiş karotlar şeklinde olduğu bir test işleminde ise eşitlik 5'de tanımlanan düzeltme faktörünün kullanılması önerilmektedir (Brook, 1985).

$$F = (\frac{De}{50})^{0.45} \tag{5}$$

F: Boyut düzeltme faktörü (tüm kayaçlar için aynı olarak tanımlanmaktadır).

3) Eğer farklı karot çaplarında test yapılmış ise boyut düzeltme faktörü (F), Şekil 3'de gösterilen grafikten, ya da Şekil 4'de verilmiş olan logaritmik grafiğin eğiminden yararlanılarak, eşitlik 6'dan hesaplanabilir (Brook, N., 1985).

$$F = (\frac{De}{50})^m \quad ; \qquad m = 2(1-n) \tag{6}$$

n= log-log grafiğin eğimi

Bu durumda düzeltilmiş nokta yükleme dayanım indeksi; eşitlik 7'den hesaplanır.

$$Is(50) = FxIs \; ; \tag{7}$$

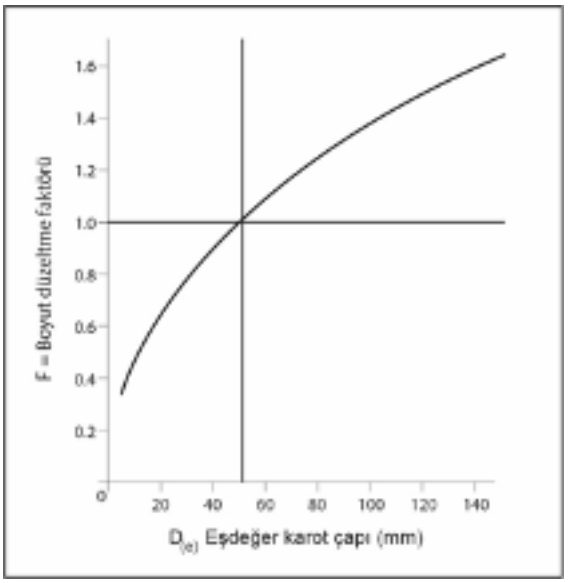

Şekil 4. Boyut düzeltme faktörünün grafik yardımı ile bulunması (Brook, 1985; ISRM, 1985)

İfade edilen düzeltme yöntemleri anizotropi derecesine ve yükleme doğrultusuna bağlı olmaksızın uygulanabildiği için, nokta yükleme deneylerinin kullanılabilirliği büyük ölçüde artmıştır.

NOKTA YÜK İNDEKS DENEYLERİ

Bu çalışmada yapılan deneylerde ELE Hemel Hempstead, Merts firmasına ait 14.426 cm^2 piston alanlı 700 bar azami yük kapasiteli deney aleti kullanılmıştır. Numuneler NX (54 mm) olarak hazırlanmış karot şekillidir. Boy çap oranları literatüre uygun olarak hazırlanan örnekler (Şekil 5) üzerinde çap deneyleri yapılmış, bu deney sonucu kırılan örneklerden yine literatürdeki boyutlara uygun olanların üzerinde (Şekil 2), eksenel deneyler gerçekleştirilmiştir. Örneklerin çoğunda gözle görülür yönlenme yoktur. Ancak, deneyler; farklı yönlerde dayanım parametrelerinde değişim olup olmadığının anlaşılması için, araziden çıkarılma yönlerine göre, tabakaya dik ve paralel olarak hazırlanan suya doygun ve oda şartlarında kurutulmuş örnekler üzerinde yapılmıştır.

Örnekler 54 mm çaplı oldukları için çap deneylerinde düzeltme yapılmamıştır. Ancak eksenel deneylerde standart bir Is_{50} değerinin bulunabilmesi için düzeltme yapılmıştır. Düzeltme yöntemi olarak yukarıda anlatılan iki yöntem de kullanılmış ve birbirine yakın sonuçlar elde edilmiştir. Bu çalışmada

eşitlik 5 kullanılarak elde edilen düzeltilmiş deney sonuçlarına yer verilmiştir.

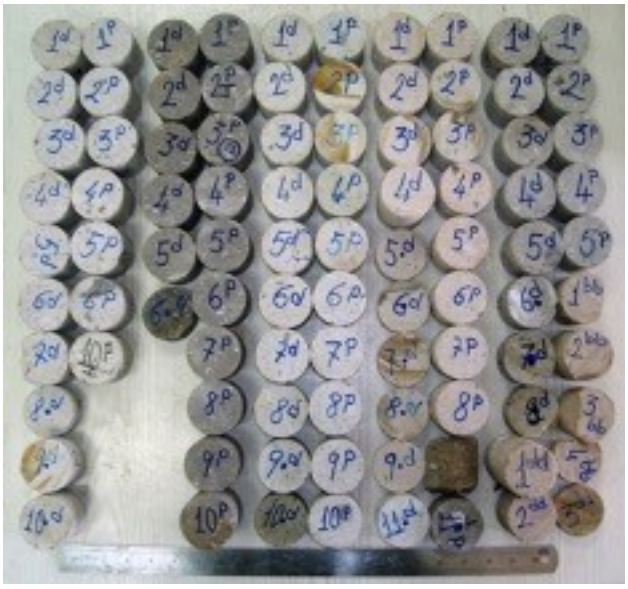

Şekil 5. Nokta yükleme deneyinde kullanılan örnekler.

Örnekler 54 mm çaplı oldukları için çap deneylerinde düzeltme yapılmamıştır. Ancak eksenel deneylerde standart bir Is_{50} değerinin bulunabilmesi için düzeltme yapılmıştır. Düzeltme yöntemi olarak yukarıda anlatılan iki yöntem de kullanılmış ve birbirine yakın sonuçlar elde edilmiştir. Bu çalışmada eşitlik 5 kullanılarak elde edilen düzeltilmiş deney sonuçlarına yer verilmiştir.

Deneyler sırasında her bir kayaç için, en az 10 adet geçerli deney yapılmış, en düşük ve en yüksek ikişer değer göz ardı edilip, geriye kalan değerlerin ortalaması alınarak, ortalama Is_{50} değeri bulunmuştur. Örnek sayısının 10'dan az olduğu Selime tüfünde ise, en yüksek ve en düşük değerler göz ardı edilmiş ve geriye kalan değerlerin ortalaması alınarak, ortalama Is_{50} değeri tespit edilmiştir. Bulunan Is(50) değerinden hareketle de, kayaçların tek eksenli basınç dayanımı değerlerinin ampirik olarak belirlenmesi hedeflenmiştir.

Bu amaçla yapılmış olan bazı çalışmalarda; ağırlıklı olarak tek eksenli basınç dayanımı ile nokta yükleme dayanım indeksi (NYDİ) oranı; "k" incelenmiş ve 22-24 arasında değişen bir oranın kullanılması yönünde eğilim oluşmuştur (Brook, 1985; ISRM, 1985; Quane et al., 2003). En çok kabul gören formül ise; k değerini 24 olarak alan eşitlik 6'da verilen bağıntıdır (Broch et al., 1972; Bieniawski, 1975; Aston et al., 1991).

$$\sigma_b = 24 x I_{s(50)}; \tag{8}$$

Chau ve Wong (1996) yaptıkları teorik çalışmalarında ise bu oranın 24'ten daha küçük bir değerde ve yaklaşık olarak 12,5 olması gerektiğini ileri sürmüşlerdir (Chau et al., 1996).

Söz konusu farklı değerlendirmeler dikkate alınıp, tek eksenli sıkışma dayanımı ile nokta yükleme dayanım indeksi oranı literatürdeki 50 kadar referans taranıp, incelenerek, Çizelge 1'de sunulmuştur.

Bu çizelge incelendiğinde elde edilen "k" değerinin; 3 - 82 gibi çok geniş bir aralıkta değiştiği (Tsidzi, 1991; Puech et al., 1988), ancak, genel kümelenmenin 6-30 arasında kaldığı, çok zayıf kayaçlarda; 2.8-6 (Chau et al., 1996), zayıf kayaçlarda; 6-20 (Topal, 2000) ve yüksek dayanımlı kayaçlarda ise 20-30

arasında olduğu gözlemlenmiştir (Quane et al., 2003; Liang et al., 2015).

Çizelge 1. Kayaçların nokta yük dayanım indeks değeri ile tek eksenli basınç dayanımı arasındaki bağıntılar

Referanslar	Önerilen Eşitlikler	Kayaç Tipi	K değeri	TESPİTLER
D'Andrea et al. (1964)	$\sigma_c = 15.3 * Is_{[50]} + 16.3$			
Broch ve Franklin (1972)	$\sigma_c = 24 * Is_{[50]}$	Kumtaşı, dolamit (sert kaya) (22-250 MPa); (1.25-9.5 NYD) NX karotlar tzerinde çapsal deneyler yapıldı.	24	Dayanımın saptanmasında, çeşitli boyuttaki karotların kullanılabilmesi için bir boyut düzeltme kartı hazırlandı. IS değerlerinin UCS değerlerine göre daha az saçılımlı olduğu gösterildi.
Bieniawski (1975)	$\sigma_c = 24 * Is_{[50]}$	Kumtaşı kuvarsit, norit (sert kaya) (57-312 MPa); (2.4-11.2 NYD)	24	Örrnek boyutu arttıça nokta yük dayanımının azaldığı, üç eksenli dayanımın amprik eşitlikler yardımıyla %10-20 hatayla bulunabileceği ifade edildi.
Wilson (1976)	$\sigma_c = 8 * Is$	Çok zayıf çamurtaşı	8	
Al- Jassar ve Hawkins(1979)	$\sigma_c = 17....30 * Is_{[50]}$	Kireçtaşı, dolomit ve kumtaşı Farklı çapta karot (30,50,70) ve farklı boyutta blok örnekler (30,50,70)	8-27 22	Örnek boyutu arttıça NYDİ azalmaktadır. NYDİ; karot örnekler için daha küçüktür. Karot ve blok örnekler için nokta yük ve basınç dayanımı arasındaki bağıntı farklıdır.
Read ve diğ.(1980)	$\sigma_c = 20 * Is_{[50]}$ bazalt $\sigma_c = 16 * Is_{[50]}$ sedimanter	Bazalt (30-132 MPa); (5-8 NYD) Kumtaşı, silttaşı (sedimanter kayaç) (27-180 MPa); (8.5-25 NYD)	8-24 10-45	Farklı kayaçlar için farklı alterasyon dercelerinin etkilerini inceledi. Tek eksenli basınç dayanımı ve nkta yük testi arasındaki ilişki kaya tipi ve alterasyon dercesine bağlıdır
Beake and Suttcliffe (1980)	$\sigma_c = 12.2 * Is_{[50]}$	Arap-Pers körfezi kalkerleri		
Forster(1983)	$\sigma_c = 14.5 * Is_{[50]}$	Dolerit, Kumtaşı (11-113 MPa); (1.52-10.32 NYD)	12-14 15-18	Eksenel nokta yük deneylerinde örnek boyut etkisini inceledi
Gunsallus and Kulhawy (1984)	$\sigma_c = 16.5 * Is_{[50]} + 51$	Doloston, kumtaşı, kireçtaşı (68-345 MPa) (0.69-10.8 NYD)		Sedimanter kayaçlar
Norbury(1986)		Kumtaşı Silttaşı Çamurtaşı Şeyl Magmatik ve metamorfik Kayaçlar Kristalize Kireçtaşı Taneli Kireçtaşı Tebeşir	8-30 15-35 18-35) 24 27 24-54 8 10-22	(Genellikle 20-25) (Genellikle. 20)
ISRM 1985	$\sigma_c = 20.....25 * Is_{[50]}$	Tüm kaya tipleri..	20-25	Ancak; özellikle anizotropikve çok farklı tipteki kayaçlar test edildiğnde "k" nın 15-50 arasında değiştine dikkat çekilmiş, nokta yük testinden tek eksenli dayanım değerlerinin tahmini için uygun eşitliklerin kullanılmasının önemi vurgulanmıştır..
Puech et al. (1988)	$\sigma_c = 3.11 * Is_{[50]}$	Arap-Pers körfezi kalkerleri		
Vallejo et al. (1989)	$\sigma_c = 8.6.....16 * Is_{[50]}$	Appalachian bölgesinde yüzey kömür madencilik sahalarına ait kayaçlar.	12.5 şeyl 17.7 kumtaşı	Şeyl ve kumtaşı örnekleri tzerinde UCS ve IS tetleri yapmıştır
Cargill ve Shakoor (1990)	$\sigma_c = 23 * Is_{[54]} + 13$	14 farklı kayaç (Kumtaşı, kireçtaşı, dolomit, mermer, siyanit ve gnays)	19-31) 17-30	(Genellikle 21-27)
Tsidzi (1991)	$\sigma_c = 14.....82 * Is_{[50]}$	Tabakalanmaların çok fazla değiştiği Gnays, Hornfels, fillit, şist, kayrak taşı gibi metamorfik kayaçlar [(65-250 MPa); (2-10.2 NYD)]	17-23	Anizotropinin etkisi incelendi . "k" değerinin; Zayıf tabakalanmalı kayaçlarda; 17, Orta dereceden daha fazla tabakalanmalı olanlarda 23 olduğu bulundu.
Ghosh and Srivastava (1991)	$\sigma_c = 16 * Is_{[50]}$	Batı Himalaya' ya ait granitler (25-119 MPa) (2.1-7.4 NYD)		
Grasso et al. (1992)	$\sigma_c = 25.67 * Is_{[50]}^{0.57}$ $\sigma_c = 9.30 * Is_{[50]} + 20.04$	Homojen kalkerli çamurtaşını inceledi.	.	UCS <70MPaolan yumuşak kayaçlar için Üstel eşitlikteki korelasyon katsayısı lineerdekine göre daha yüksek olduğunu göstredi.
Bell (1992)		Kumtaşı Kireçtaşı Tebeşir	12-19 (kuru), 20-30 (kuru), 68 (kuru),	7-12 (suya doygun) 14-24 (suya doygun) 31 (suya doygun)
SECRM (1995)	$\sigma_c = 22.82 * Is_{[50]}^{0.75}$	(Standard For Engineering Classification Of Rock Masses)(		GB50218-94)
Chau ve Wong (1996)	$\sigma_c = 12.5 * Is_{[50]}$	Hong Kong 'ait Granit ve tüfler (18-180 MPa)(0.2-10 NYD)	12.5	UCS/IS oranının; Gc/Gt , poisson oranına, örneğin çapına ve uzunluğuna bağlı olduğunu göstermiştir.
Anıl ve diğ.(1996)		Tortul ve magmatik kayaçlar	15-25 (kuru)	10-24 (suya doygun)
Smith (1997)	$\sigma_c = 14.3 * Is_{[50]}$	Kıyı alanlarında yataklanmış tipik zayıf kaya malzemeleri incelenmiştir.		Sert kayaçlarda 24 olan değer, buralarda 14.3'tür.
Hawkins,(1998)	$\sigma_c = 7.....68 * Is_{[50]}$	Sedimater ve vokanik kayaçlarda kuru ve suya doygun şartlarda testler yapmıştır. "	(7-68)	"k" oranının farklı litolojiler ve şartlar altında çok geniş aralıkta değiştiğini, suya doygun kayaçlar için bu oranın; kuru kayaçlar için olandan genellikle %50 daha düştük olduğunu göstermiştir.
Topal(2000)	$\sigma_c = 10.647 * Is_{[50]} + 2.47$	Tüf	10.65	
Kahraman (2001)	$\sigma_c = 23.621 * Is_{[50]} - 2.69$ $\sigma_c = 8.41 * Is_{[50]} + 9.51$	48 farklı kaya için 2 farklı eğilim bulmuştur.		Kömür yatağındaki kayaçlar için daha dik eğim. Diğer gruptaki 22 farklı kayaç için daha düştük eğim.
Quane and Russel (2003)	$\sigma_c = 24.4 * Is_{[50]}$ sert kaya $\sigma_c = 3.86 * Is^2_{[50]} + 5.65 * Is_{[50}$	Sert kayaçta lineer ilişki, Is<5 MPa); UCS=125MPa) Zayıf Kayaçta ise lineer olmayan ilişki elde edilmiştir.	.	İncelemeler sırasında; İgnimbiritlerin kaynaklanma derecesinin ölçümü için, kaya dayanımının kullanılabilirliği ve verimliliği araştırılmıştır. UCS değerleri 3.18-74.08 MPa, çoğunlukla >50 MPa olan kayaçlar incelenmiştir

Referanslar	Önerilen Eşitlikler	Kayaç Tipi	K değeri	TESPİTLER
Tsiambaos and Sabatakakis (2004)	$\sigma_c = 7.31 * Is_{[50]}^{1.71}$ $\sigma_c = 23 * Is_{[50]}$	Yunanistandaki elastik sedimanter kayaçlar (Kireçtaşı; marn; kumtaşı) kullanılmıştır. Kayaçlar <2MPa, 2-5 MPa, >5 MPa şeklinde sınıflandırılmışlardır	13 20 28	Lineer regreasyon modelinde kaya malzemesinin tüm dayanım sınırları için; tek bir dönüşüm faktörü nün uygulanabilir olmadığı vurgulanmıştır. Üç farklı nokta yük dayanım sınıfı için, orjinden geçen farklı dönüşüm faktörleri önerilmiştir
Palchik and Hatzor (2004)	$\sigma_c = 8.....18 * Is_{[50]}$ $\sigma_c = Is_{[50]} * k_1 * e^{-k_2 n}$	Gözenekli alçı taşında UCS/Is oranı ile çekme ve basma dayanımı üzerine porozitenin etkisini incelemiştir	8-18	Porozite %18'den %40'a çıktığında UCS/IS oranı18'den 8'e düşmektedir . UCS/Is oranının sabit olmadığını, poroziteye bağlı olarak 8-18 arasında değiştiğini bulmuşlardır. Burada ;"k_1 ve k_2"; amprik katsayılar "n"ise ;örneğin porozitesidir.
Kim et al. (2004)	$\sigma_c = 22 * Is_{[50]} + 49$	Tüfler (80.4-208 MPa)		
Kahraman et al. (2005)	$\sigma_c = 24.83 * Is_{[50]} - 39.64$ $\sigma_c = 10.22 * Is_{[50]} - 24.31$	38 farklı voklanik, sedimanter, metamorfik kayaçta nokta yük, dayanım ve porozite testleri yapıldı .		Porozitesine göre kayaçlar Porozite <%1 ve Porozite > %1 şeklinde ikiye sınıflandırıldığında daha sağlam korelasyonlar elde edilmiştir . Porizitesi %1< olan kayaçların regrasyon eğrisinin eğimi, yüksek poroziteli kayaçlara göre daha büyüktür.
Fener et al. (2005)	$\sigma_c = 9.08 * Is_{[50]} - 39.32$	Niğde kayaçları ; volkanik, metamorfik ve sedimanter 11 kayaç		
Santi (2006)	$\sigma_c = 12.25 * Is_{[50]}^{1.59}$	Lineer olmayan bir ilişki buldu.		Smith (1997) verilerini tekrar değerlendirdi
Kassim ve Mohammad (2007)	$\sigma_c = 12.23 * Is_{[50]} + 1.75$ $\sigma_c = 14.45 * Is_{[50]} + 0.096$	Zayıf altere kumtaşlarını inceledi	Kahraman'ın düzelttimi $\sigma_c = 8.66 * e^{0.45 I s_{[50]}}$	Is<1 MPa olan tamamen ve yüksek altere malzeme ile IS>1MPa olan zayıf ila orta altere malzeme için; bu ilişki, Kahraman'ca yeniden incelendi. Non lineer ilişki bulundu
Akram and Abu Bakar (2007)	$\sigma_c = 22.7921 * Is_{[50]} + 13.285$ $\sigma_c = 11.076 * Is_{[50]}$ yumuşak	Pakistan Punjab provensine ait Tuz sınırı alanına ait 9 farklı kayaç		Kayaçlar; sert ve yumuşak olarak iki gruba ayrılarak test edilmiştir. Yumuşaklar; Dandot kumtaşı, Sakkessa kumtaşı,marndır.
ASTM (2008)	$\sigma_c = 24 * Is_{[50]}$	Tüm kaya tipleri		
Binal (2009)	$\sigma_c = 9 * Is_{[50]}$	İgnimbirit	9	Orta derecede kaynaklanmış ve kaynaklanmamış
Diamantis et al. (2009)	$\sigma_c = 19.79 * Is_{[50]}$ $\sigma_c = 17.81 * Is_{[50]}^{1.06}$ $\sigma_c = 16.45 * e^{0.39 I s_{[50]}}$	Kumtaşı, çamurtaşı ve şeyl (23.1-173.9 MPa).		Orta Yunanistandaki serpantinitlerin fiziko mekanik özellikleri incelendi. Lineer ve lineer olmayan ilişkiler buldu. Üstel ilişkilerin dahi iyi korelasyonlar verdiği tespit edildi.
Kohno ve Meda (2011-2012)	$\sigma_c = 16.4 * Is_{[50]}$	Hidrotermal olarak altere olmuş çoğunluğu tüf ve UCS<25 MPa olan kayaçları inceledi.	Kahraman'ın düzeltimi $\sigma_c = 15.81 * Is^{0.95}$	Test sonuçlarının kuru ve yaş olarak önce ayrı ayrı, sonrasında tüm verinin birlikte değerlendirilmesi neticesinde lineer ilişki bulundu. Bu bağıntı; Kahramanca yeniden incelendi ve lineer olmayan bir ilişki elde edildi.
Kurtuluş ve diğer(2011)	$\sigma_c = 15.248 * Is_{[50]} - 2.2964$ $\sigma_c = 14.458 * Is_{[50]} + 0.3852$	Serpantinli ultrabazik kayaç örnekleri		Silindirik 20 örnek tabakaya dik ve 20 örnek tabakaya paralel olarak test edildi.
Singh et al. (2012)	$\sigma_c = 22.8 * Is_{[50]}$ $\sigma_c = 21.9 * Is_{[50]}$ $\sigma_c = 14.4 * Is_{[50]}$ $\sigma_c = 14.4 * Is_{[50]}$	Kuarsit (32.5-98.9 MPa Kumtaşı (17.6-56.4 MPa) Şeyl (9.9-18.8 MPa) Gabro (17.3-137 MPa) Kireçtaşı (86.9-129.8 MPa)	(14-24)	7 farklı staratigrafik birimden alınan 10 farklı kayaç tipi (volkanik, sedimanter, metamorfik) kullanıldı. "k" değerinin ; sert kayaçlar için (21-24) ve Yumuşak kayaçlar için (14-16) olarak alınması önerildi.
M. Heidari (2012)	$\sigma_c = 7.56 * Is_{[50]} - 23.68$ $\sigma_c = 11.96 * Is_{[50]} + 10.64$	150 adet jips örneği test edildi Jips (31.00 -33.69MPa kuru) Jips(17.44 - 29.84 MPa su doygun)		
Mısra and Basu (2013)	$\sigma_c = 10.9 * Is_{[50]} + 49.03$ $\sigma_c = 11.21 * Is_{[50]} + 40.01$ $\sigma_c = 12.95 * Is_{[50]} - 5.19$ $\sigma_c = 14.63 * Is_{[50]}$	Granit, şist, kumtaşı,		Lineer ilşki bulundu.
Li and Wong (2013)	$\sigma_c = (20-21) * Is_{[50]}$	Singapur meta kumtaşı ve meta siltaşı		
Kahraman (2014)	$\sigma_c = 2.68 * e^{0.93 I s_{[50]}}$ kuru $\sigma_c = 1.99 * e^{1.18 I s_{[50]}}$ suya doygun $\sigma_c = 2.27 * e^{1.04 I s_{[50]}}$ tüm veri	Kapodokya volkanik provensi içinde bulunan Yeşilhisar, Ürgüp formasyonu ve quaterner yataklardan alınan, dayanım sınırları 2.2-46.7 MPa arasında olan 32 farklı yumuşak pyroclastic kayaç incelenmiştir.	.	Testler; 38mm çaplı veboy çap oranı 1.2 olan örnekler üzerinde hem kuru (fırında kurutulmuş) hemde suya doygun olarak yapılmıştır
Salah et al. (2014)	$\sigma_c = 9.459 * Is_{[50]}^{0.75}$ $\sigma_c = 5.833^{0.57 * Is_{[50]}}$ $\sigma_c = 5.414 * e^{0.57 * Is_{[50]}}$ $\sigma_c = (11.08...11.24) * Is_{[50]}$ $\sigma_c = 6.05^{Is_{[50]}}$ $\sigma_c = 5.679^{Is_{[50]}}$	Tüm kaya tipleri Tüm kaya tipleri Çok zayıf kayaç Zayıf kayaç Tüm kristallin jipsler Tüm çamurtaşları Çok zayıf kumtaşı		

σ_c : Tek eksenli basınç dayanımı (MPa), k: Nokta yük dayanım indeksi ve basınç dayanımı arasındaki oran (Topal, 2000; Quane et al., 2003; Elhakim, 2015; Liang et al., 2015; Kahraman et al., 2009; Kahraman, 2014; Binal, 2009; Sheraz et al., 2014)

Bu durum; uygun bir eşitlik kullanılmaması halinde tek eksenli basınç dayanımının; sert kayaçlar için %50, zayıf kayaçlar için %250, tüm kayaçlar genellendiğinde ise %400 nispetinde hatalı tahmin edileceği anlamına gelmektedir. Bir de değerlendirmelere anizotropi, alterasyon, porozite ve su muhtevası gibi kayacın doğal konumuna ait özellikler de eklendiğinde, hata oranının; %2500'e kadar artabileceği görülebilmektedir.

Porozitenin; kayaçların çekme-basma dayanımı ve "UCS/Is= k" oranı üzerine etkisinin incelendiği bir çalışmada "UCS/Is" değerinin sabit olmadığı, gözenekli alçı için porozite'nin %18'den, %40'a çıkması halinde, "k" oranının; 18' den 8'e düştüğü bulunmuştur (Kahraman et al., 2009; Palchik et al., 2004). Yine suya doygun ve kuru olarak, hem sedimanter hem de vokanik kayaçlarda yapılan bir başka çalışmada ise suya doygun kayaçlar için bu oranın kuru kayaçlardakilerden, genellikle %50 daha düşük olduğu belirlenmiştir (Liang et al., 2015; Kahraman, 2014; Hawkins, 1998).

Görüldüğü üzere, nokta yük dayanım deneyinde; uygulamaların aynı standartta yapılamamasından gelen hata kaynakları söz konusudur. Bunlar; testler sırasında, 50 mm'den farklı çaptaki karot örnekler veya düzensiz şekilli örneklerin kullanılmasından, deneylerin; çapsal ya da eksensel yönde yük uygulanarak, kuru veya suya doyurulmuş, sert ya da yumuşak örnekler üzerinde, anizotropi dikkate alınıp ya da alınmadan yapılmasından ve nihai test sonuçlarının; d_{50} eş değer karot çapı düzeltmeli veya düzeltmesiz olarak sunulmasından kaynaklanabilmektedir. Konu ile ilgili formülasyonların oluşturulması sırasında bu ve buna benzer birçok parametre etken olduğu için, literatürden derlenen deneysel çalışmalara göre genellemeye gidilerek, kayaçların tümü için geçerli olabilecek standart tek bir "k" değerinin tanımlanması ve de kullanılması uygun görülmemektedir.

Bu nedenlerden dolayı; nokta yük indeksinin, bağımsız bir dayanım indeksi olarak kullanılması, kayaçların; basınç dayanımının belirlenmesi için kullanılmaması ya da çok zaruri durumlarda dikkatle ele alınıp değerlendirmesi (Greminger, 1982), özellikle konik ucun yumuşak kayaca batıp, çapsal hataya yol açmasından ötürü NYDİ<5 (Quane et al., 2003) ve tek eksenli basınç dayanımının <25 MPa olduğu zayıf kayaçlarda hiç kullanılmaması (Bieniawski, 1975); önerilmektedir. Oysa gerek tüfler ve gerekse anhidrit, alçı taşı ve kalkerli kumtaşı gibi formasyonlardan alınan örnekler üzerinde yapılan sonraki çalışmalardan elde edilen tutarlı sonuçlar, nokta yükleme deneyinin zayıf kayaçlar için de kullanılabilir olduğunu göstermektedir (Elhakim, 2015; Kahraman, 2014).

Tüflerin incelendiği ve "k" değerinin 20'nin altında bulunduğu bir çalışmada; elde edilen 13-14 değeri, literatürde zayıf kayaçlar için bulunan k-değeri (10-20) ile uyumluluk arz etmektedir (Topal, 2000; Singh et al., 2012). Bu bakımdan NYDİ ile zayıf kayaçların basınç dayanımlarının dolaylı olarak hesaplanması sırasında oluşan hata, aslında "k" değerinin; tüm kayaçlar için, 24 olarak sabit alınmasından kaynaklanmaktadır (Topal, 2000; ISRM, 1985). Bu değerin; anhidrit gibi son derece düşük dayanımlı kayaca böyle sabit bir lineer eşitlik ile uygulanması ise; gerçek "k" değeri 2-6 arasında olan bir kayacın basınç dayanımının gerçek değerinden %800 daha fazla tahmin edilmesi anlamına gelmektedir. Böylesi büyük hataların da mühendislik açıdan kabul edilebilirliği bulunmamaktadır (Elhakim, 2015).

Farklı kayaç tipleri ya da özel lokasyonlar için yapılan nokta yük testlerinin korelasyonu ile geliştirilmiş olan formülasyonlarda dikkat çeken diğer bir nokta ise, ifade edilen bağıntıların daima lineer özellik göstermemesidir. Kimi bağıntılarda katsayılı lineer (Kim et al., 2004; Quane et al., 2003), kimilerinde üstel (Tsiambaos et al., 2004) ve kimilerinde de explonensiyel fonksiyonlar, dönüşüm eşitlikleri olarak, kullanılmaktadır (Salah et al., 2014) (Çizelge 1). Bir genelleme yapıldığı takdirde, bu eşitliklerin; NYDİ>4 olan sert kayaçlarda lineer, NYDİ<5 olan zayıf kayaçlarda ise lineer olmayan karakterde olduğu görülmektedir (Quane et al., 2003; Kahraman, 2014).

Tüm bu değerlendirmeler ışığında; çalışmamızda incelenen örnekler, Nevşehir provensi volkanik istifi içersinde yer alan Hasandağ Volkaniklerini temsil edecek şekilde alınmıştır. Böylece hem yerel yaygın bir formasyonun mekanik özelliklerinin tanımlanması, hem de düşük–orta dayanımlı ignimbirit ve tüf özelliğindeki volkanik kayaçlara dair dayanım parametrelerinin belirlenmesine çalışılmıştır.

Burada boy çap oranı 1 ve 2.5 olan NX (54mm) çaplı karot örnekler kullanılarak, kuru ve suya doygun şartlarda, yönlenmelerde (tabakaya dik (⊥) ve paralel (//)) dikkate alınarak belirlenmiş olan tek eksenli basınç dayanım değerleri ile yine hem kuru hem de suya doygun şartlarda yapılan nokta yük

dayanım testlerinden, d_{50} eş değer karot çapı düzeltmesi de yapılarak bulunan sonuçların karşılaştırılması yapılmıştır.

Bu çalışmada nokta yük indeks değerinden yararlanılarak tek eksenli basınç dayanımı; eşitlik 8'den hesaplanmıştır. Bulunan sonuçlar, örneklerin tabakalanma ve suya doygunluk durumlarına göre nokta yük dayanım indeksi Çizelge 2'de gösterilmiştir.

Çizelge 2. Örneklerin nokta yük indeksi değerlerinden hesaplanan basınç dayanım parametreleri.

Kayaç Adı	Türü	Yükleme Yönü	Ortalama Is	Anizotrıpi Derecesi	Basınç Dayanımı (Mpa)
Kızılkaya Üst	Kuru	⊥	1.17 ± 0.20	1.16	25.67 ± 4.33
		//	1.00 ± 0.09		22.10 ± 2.09
	Yaş	⊥	0.96 ± 0.01	-	21.15 ± 0.29
Kızılkaya Orta	Kuru	⊥	1.50 ± 0.21	1.06	33.08 ± 4.72
		//	1.41 ± 0.16		31.13 ± 3.49
	Yaş	⊥	0.96 ± 0.06	-	21.11 ± 1.29
Kızılkaya Alt	Kuru	⊥	1.36 ± 0.07	1.08	29.93 ± 1.52
		//	1.26 ± 0.20		27.67 ± 4.37
	Yaş	⊥	1.09 ± 0.03	1.31	23.95 ± 0.74
		//	0.83 ± 0.17		18.23 ± 3.63
Gelveri	Kuru	⊥	1.62 ± 0.23	1.25	35.70 ± 4.96
		//	1.30 ± 0.03		28.52 ± 0.69
	Yaş	⊥	1.20 ± 0.06	1.36	26.39 ± 1.43
		//	0.88 ± 0.02		19.46 ± 0.48
Selime Alt	Kuru	⊥	0.15 ± 0.05	……..	3.41 ± 1.15
Selime Üst	Kuru	⊥	0.20 ± 0.09	……..	4.38 ± 1.91
Göstüg	Kuru	⊥	2.09 ± 0.03	2.94	46.05 ± 0.58
		//	0.71 ± 0.07		15.67 ± 1.46
	Yaş	⊥	1.93 ± 0.12	3.14	42.50 ± 2.65
		//	0.62 ± 0.09		13.54 ± 2.00

Kayaçların nokta yük dayanım indeksine göre sınıflandırılması ise Çizelge 3'te verilmiştir.

Çizelge 3. Kayaçların nokta yük dayanım indekslerine göre sınıflandırılması

Tanımlama	**UCS(MPa)** Bianewski (1974)	**NYDI(MPa)**
Çok düşük dayanım	<25	<1
Düşük dayanım	25-50	1-2
Orta dayanım	50-100	2-4
Yüksek dayanım	100-200	4-8
Çok yüksek dayanım	>200	>8

TEK EKSENLİ BASINÇ DAYANIMI DENEYLERİ

Maden makineleri ve kaya delme makinelerinin performanslarının tahmininde kayaçların dayanım özelliklerinin bilinmesi önemlidir. En genel olarak kullanılan ve dayanım ölçümünü tayin eden yöntem tek eksenli basınç dayanımıdır (Özdemir et al., 1992; Gehring, 1993; Thuro et al., 2011). Bu çalışmada dayanım deneyleri; 20 kN ve 300 kN basınç gövdeli, servo valf sistemi olan, hidrolik güç ünitesine sahip, bilgisayarlı veri toplama ve değerlendirme özellikli bir test makinesi ile yapılmıştır.

Tek eksenli basınç dayanım deneyleri için NX karot çaplı (54 mm), boy/çap oranı 1 ve 2.5 olan örnekler kullanılmıştır (Şekil 6).

Şekil 6. Tek eksenli basınç dayanımı için kullanılan örnekler.

Örnekler, test sırasında küresel merkezlendirici plakaya sahip test makinesine 55 mm çap, 60 mm yükseklik ve 1158 g ağırlığında küresel başlık kullanılarak yerleştirilmiştir. Bu örnekler, kayaç tipine göre önceden tespit edilen 0.10-0.15 kN/s yükleme hızlarında 5-10 dakikada yenilmeleri sağlanacak şekilde kırılmıştır. Tek eksenli basınç dayanımı (σ_c) değerleri eşitlik (9)'dan hesaplanmıştır.

$$\sigma_c = \frac{F}{A} \tag{9}$$

σ_c : Tek eksenli basınç dayanımı (MPa)
F : Yenilme anında kaydedilen yük (kN)
A : Silindirik numunenin kesit alanı (mm^2)

Bu çalışmada kuru ve suya doygun şartlarda, örnek boyutu ve yönlenmeler dikkate alınarak yapılan tek eksenli basınç dayanım deney sonuçları Çizelge 4'de verilmiştir.

Literatürde kayaçlar genellikle boy çap oranı en az 2 olan örneklerden elde edilen tek eksenli basınç dayanım değerlerine göre beş gruba ayrılarak, Çizelge 5'te olduğu gibi sınıflandırılmaktadır (Karaman et al., 2012; ISRM, 1981; Bieniawski, 1974; Kan, 2000; Deere et al., 1966).

Çizelge 4. Tek eksenli basınç dayanım deney sonuçları

Kayaç Adı	Basma Dayanımı (Mpa) boy/çap=1		Basma Dayanımı (MPa) boy/çap=2.5			
	Kuru		Kuru		Suya doygun	
	Tabakaya dik	Tabakaya paralel	Tabakaya dik	Tabakaya paralel	Tabakaya dik	Tabakaya paralel
Kızılkaya üst	21.303	21.511	16.652	15.542	10.542	11.579
Kızılkaya orta	33.288	33.229	21.863	20.887	15.234	13.886
Kızılkaya alt	27.72	26.205	22.277	18.576	14.956	14.483
Gelveri	24.168	24.247	17.214	15.782	14.525	11.692
Selime üst	5.921	----	4.996	----	2.3107	----
Selime alt	5.037	----	4.096	4.157	1.003	1.195
Karakaya	11.927	9.608	8.304	7.025	5.058	4.838
Göstüg	35.175	33.922	29.861	21.567	23.756	18.931
Acıgöl	8.465	----	5.443	----	2.436	----

Çizelge 5. Kayaçların tek eksenli basınç dayanımına göre sınıflandırılması

Tanımlama	UCS (MPa) ISRM(1981)	UCS (MPa) Bieniawski (1974)	UCS (MPa) Deere ve Miller (1966)	Sınıfı
Çok Yüksek Dayanımlı	>200	>200	>220	A
Yüksek Dayanımlı	60-200	100-200	110-220	B
Orta Dayanımlı	20-60	50-100	55-110	C
Düşük Dayanımlı	6-20	25-50	27.5-55	D
Çok Düşük Dayanımlı	<6	<25	<27.5	E

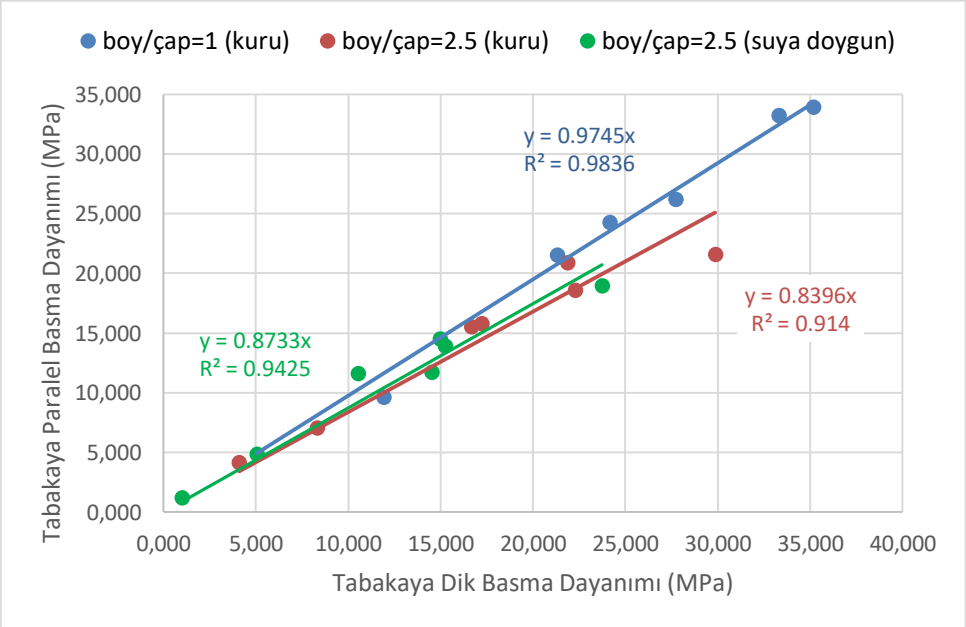

Şekil 5. Tabakalanmaya Dik ve Paralel Basma Dayanım Değerlerinin Karşılaştırması

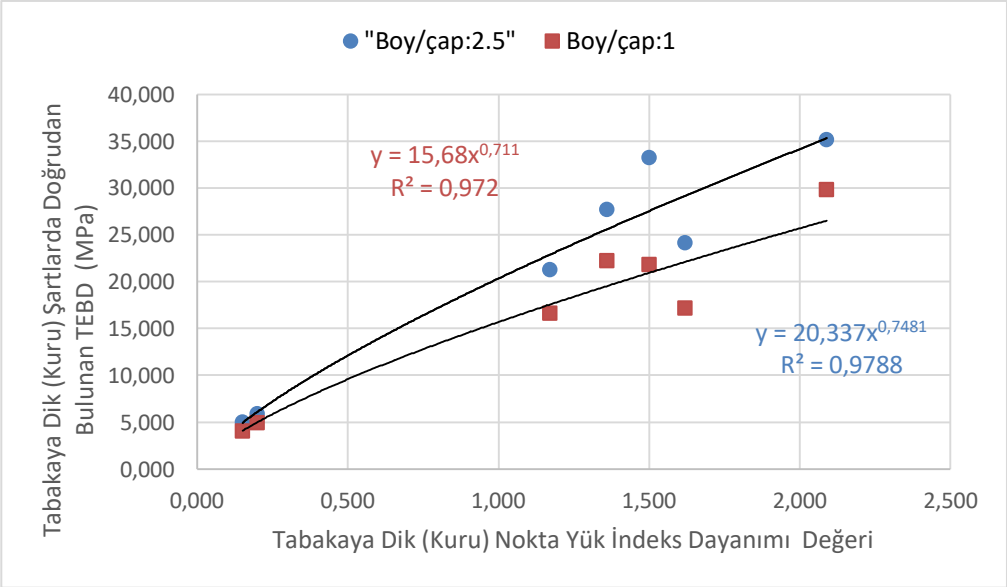

Şekil 6. Nokta Yük indeks değeri ile doğrudan bulunan TEBD arasındaki ilişki

Elde edilen veriler bir çok açıdan değerlendirilebilir ancak bu çalışmada tabakaya dik ve paralel basma dayanım değerleri arasındaki ilişki ve nokta yük indisinden dolaylı olarak ve doğrudan bulunan basma dayanımı arasındaki ilişkiden bahsedilecektir. Şekil 5'te görüldüğü gibi 1 ve 2.5 boy/çap oranına sahip kuru örneklerin tabakaya dik ve paralel basma dayanımı sonuçları arasında yüksek tahmin kapasitesine sahip sırasıyla %98,36 ve %91.40 ilişki katsayısı bulunmaktadır. Artık (intersept) sayılar çıkarıldığında 1 ve 2.5 boy/çap oranına sahip kuru örneklerin tabakaya dik basma dayanımının tabakaya paralel basma dayanımının sırasıyla yaklaşık %97,45'i ve %83.96'sı kadar olduğu görülmektedir. Aynı işlem 2.5 boy/çap oranına sahip suya doygun örnekler için de yapılmış ve aralarında yine yüksek tahmin kapasitesine sahip (r^2= 0.9425) ve tabakaya dik basma dayanımı değerlerinin %87.33ü kadar tabakaya paralel basma dayanımı değerleri ile karşılaşıldığı anlaşılmıştır.

Şekil 6 ise tabakaya dik nokta yük indeks değerleri ile doğrudan bulunan basma dayanımları arasında da yüksek tahmin yeteneğine sahip bir ilişki olduğunu göstermekte ve nokta yük değerlerinden, Şekil 6'da önerilen eşitlikle bulunacak basma dayanımı değerlerinin; tasarımda kullanılabileceğine işaret etmektedir.

SONUÇLAR

Çalışmada Nevşehir provensi volkanik istifi içerisinde yer alan Hasandağ Volkaniklerini kapsayan bazı kayaç örnekleri üzerinde yapılan bir seri tek eksenli basınç dayanımı (TEBD) ve nokta yükleme dayanım test (NYD) sonuçları irdelenmiştir.

1. Boy/çap oranı 1 ve 2,5 olan kuru ve suya doygun (yaş) örnekler üzerinde tabakalanmaya paralel ve dik olarak alınan örnekler üzerinde ayrı ayrı tek eksenli basma dayanımı deneyleri uygulanmıştır.
2. Çok düşük ve orta dayanımlı kaya grubuna giren bu istiften, tabakalanmaya paralel ve dik alınan örneklerin sıkıştırılmasıyla elde edilen sonuçlar arasında yüksek dereceli tahmin yeteneğine sahip ilişkiler bulunmuştur. Buna göre tabakaya dik suya doygun 2,5 boy/çap oranına sahip örneklerden tabakaya paralel basma dayanımı %94,23 doğruluk katsayısı (r^2) ile ; tabakaya dik kuru 2,5 boy/çap oranına sahip örneklerden tabakaya paralel basma dayanımı %91,40 doğruluk katsayısı (r^2) ile ; tabakaya dik kuru 1 boy/çap oranına sahip örneklerden tabakaya paralel basma dayanımı %98, 36 doğruluk katsayısı (r^2) ile

hesaplanabilmiştir.

3. Suya doygun örneklerin basınç dayanımının kuru örneklere kıyasla daha düşük olduğu ve boy/çap oranındaki artışla dayanım değerlerinin daha da düştüğü gözlemlenmiştir.
4. Ayrıca tabakaya dik nokta yük indeksi değerlerinden boy/çap oranı 1 ve 2.5 olan örnekler üzerinde tabakaya dik olarak yapılan tek eksenli basma dayanımı sonuçlarının da yüksek doğrulukta tahmin edilebileceği ortaya çıkmıştır. Bu eşitliklerin; NYDİ>4 olan sert kayaçlarda lineer, NYDİ<5 olan zayıf kayaçlarda ise lineer olmayan karakterde olduğu yönündeki görüşü doğrulayıcı nitelikte ve lineer olmayan karakterde olduğu belirlenmiştir.
5. Hasandağ volkanik istifinde yer alan Göstüg İgnimbiriti üzerinde yapılan deneylerde tabakaya paralel dayanım değerinin tabakaya dik dayanım değerinden belirgin olarak düşük olduğu tespit edilirken, bu durum nokta yük dayanım indeks değerinden bulunan anizotropi değeri ile de teyit edilmiştir (Göstüg kuru indeks anizotropisi (I_a):2,94; Göstüg yaş indeks anizotropisi (I_a): 3.14).
6. Tüm bu değerlerden çok değişkenli ilişki analizleri de yapılabilecek olup bu çalışma sınırları içerisinde değinilmemiştir.

TEŞEKKÜR

Bu çalışma MTA Genel Müdürlüğünce yürütülmüş bulunan, “Tehlikeli Atıkların Depolanması İçin Yer Seçimi Araştırmaları” Projesi kapsamında İnceleme sahasından, Bölgedeki Jeolojik istifi temsil edecek şekilde çıkartılan 100*100*50 cm ebatlı kayaç bloklarından alınan örnekler üzerinde, İTÜ Maden Fakültesi ve MTA Genel Müdürlüğü MAT Dairesi Başkanlığı laboratuvar imkanları kullanılarak yapılmıştır. Yazarlar; burada, MTA Genel Müdürlüğü’ne ve bu proje çalışanlarına teşekkürü bir borç bilmektedir.

KAYNAKLAR

Al-Jassar, S.H., and A.B. Hawkins. (1979). Geotechnical properties of the carboniferous limestone of the bristol area. The Influence of Petrography and Chemistry 4th ISRM Congress, Montreux, Switzerland, September.

Aston, T.R.C., MacIntyre, J.S., and Kazi, H.A. (1991). The effect of worn and chipped points on point load indices. *Mining Science and Technology*, vol. 13. pp. 69-74.

Bieniawski, Z.T. (1974). Estimating the strength of rock materials. *Journal of the South African Institute of Mining and Metallurgy*, vol. 74, March. pp. 312-320.

Bieniawski, Z.T. (1975). The point-load test in geotechnical practice. *Engineering Geology*, vol. 9, no.1. pp. 1-11.

Binal, A. (2009). Prediction of mechanical properties of non-welded and moderately welded ignimbrite using physical properties, ultrasonic pulse velocity, and point load index tests. *Quarterly Journal of Engineering Geology and Hydrogeology*. 42, 107-122.

Broch, E. and Franklin, J.A. (1972) The point-load strength test. *International Journal of Rock Mechanics and Mining Sciences*, 9, 669-697.

Brook, N. (1985). The equivalent core diameter method of size and shape correction in point load testing. *International Journal of Rock Mechanics & Mining Sciences and Geomechanical Abstract*. 22, 61-70.

Brook, N. (1977). The use of irregular specimens for rock strength test. *International Journal of Rock Mechanics & Mining Sciences and Geomechanical Abstract*, 14, 193-202.

Chau, K.T. and Wong, R.H.C. (1996). Uniaxial compressive strength and point load strength of rocks. International *Journal of Rock Mechanics & Mining Sciences and Geomechanical Abstract*. 33, V2, 183-188.

Deere D. and Miller R. (1966). Engineering classification and index properties for intact rock. Tech. Report No AFWL - TR-65-116, Air Force Weapons Lab., Kirtland Air Base, New Mexico.

Elhakim, A.F. (2015). The use of point load test for Dubai weak calcareous sandstones. *Journal of Rock Mechanics and Geotechnical Engineering.* 7 (4): 452–457.

Gehring, K.H. (1993) Evaluation of cutting performance of roadheaders. 12-14, BTV/Ge/ga/1408 Zeltveg, Austria.

Greminger, M. (1982). Tecnical note experimental studies of the influence of rock anisotropy on size and shape effects in point-load testing. *International Journal of Rock Mechanics, Mining Sciences & Geomechanical Abstract*. 19, 241-246.

Hawkins, A.B. (1998). Aspects of rock strength. *Bull. Eng. Geol. Environ*. 57, 17-30.

ISRM, (1985). Suggested method for determining point load strength. *International Journal of Rock Mechanics Mining Sciences & Geomechanical Abstract*. 22, 51-60.

ISRM, (1981). Basic technical description of rock masses. *International Journal of Rock Mechanics & Mining Sciences & Geomechanical Abstract.* 18, 85-110.

Kahraman, S. and Günaydın, O. (2009). The effect of rock classes on the relation between uniaxial compressive strength and point load index. *Bull Eng Geol Environ*. 68, 345-353.

Kahraman, S. (2014). The determination of uniaxial compressive strength from point load strength for pyroclastic rocks. *Engineering Geology*. 170, 33-42.

Kan, C.C. (2000) Index properties and a three-dimensional failure criterion of rocks. Hong Kong, The Degree of Master of Philosophy at The University of Hong Kong.

Karaman, K. ve Kesimal, A. (2012). Kayaçların tek eksenli basınç dayanımı tahmininde nokta yükü deney yöntemleri ve porozitenin değerlendirilmesi. *Madencilik*. 51, V4, 3-14.

Kim, H.G., Koh, Y.K. ve Oh, K.H. (2004). A study on the mechanical properties of the cretaceous tuffs in Goheung area, *The Journal of Engineering Geology*. 14, V3. 273-285.

Liang, W. (2015). Evaluation of uniaxial compressive strength by point load tests for irregular specimens of different rock types. *Engineering Journal of Geotechnical Engineering*. 20, 11265-11271.

Özdemir, L., Gertsch, L, Neil, D, and Friant, J. (1992). Performance predictions for mechanical excavators in Yucca Mountain tuffs; Yucca Mountain Site Characterization Project. United States.

Palchik, V. ve Hatzor, Y.H. (2004). The influence of porosity on tensile and compressive strength of porous chalk, *Rock Mech & Rock Eng.* 37, V4, 331-341.

Puech, A., Beunce, J.P. ve Colliat, J.L. (1988). Advances in the design of piles driven into non-cemented to weakly cemented carbonate formations. Proceedings Of The International Conference On Calcareous Sediments, Perth, Australia.

Quane, S.L. ve Russell, J.K. (2003). Rock strength as a metric of welding intensity in pyroclastic deposits. *Eur. J. Mineral.* 15, 855-864.

Salah, H., Omar, M. ve Shanableh, A. (2014) Estimating unconfined compressive strength ofsedimentary rocks in United Arab Emirates from point load strength index. Journal of Applied Mathematics and Physics, 2, 296-303.

Sheraz, A. M., Emad, M. Z., Shahzad, M., and Arshad, S. M. (2014). Relation between uniaxial compressive strength, point load index and sonicwave velocity for dolerite. Pakistan Journal of Science. 66, V1.

Singh, T.N., Kainthola, A. and Venkatesh, A. (2012). Correlation between point load index and uniaxial compressive strength for different rock types. Rock Mech Rock Eng. 45, 259-264.

Thuro, K., Plinninger R. J., Zah, S., and Schütz, S. (2011). Scale effects in rock strength properties, Part 1: Unconfined compressive test and brazilian test, ISRM Regional Symposium EUROCK 2001 Rock Mechanics a Challenge for Society, June 3-7, 2001, Espoo, Finland, pp. 169 - 174. -.

Topal, T. (2000). Nokta yükleme deneyi ile ilgili uygulamada karşılaşılan problemler. Jeoloji Mühendisliği. 24, Cilt I., 2.

Tsiambaos, G. ve Sabatakakis, N. (2004) Considerations on strength of intact sedimentary rocks. Engineering Geology. 72, V3-4, 261-273.

Tsidzi, K.E.N. (1991). Point load; uniaxial compressive strength correlation. Seventh international Congress on Rock Mechanics. Proceedings of the Congress of the International Society for Rock Mechanics, 1, 637-638.

HIG MILL PERFORMANCE AT COPPER FLOTATION CIRCUIT REGRIND APPLICATION

BAKIR FLOTASYON DEVRESİ REGRIND UYGULAMASINDA HIG DEĞİRMEN PERFORMANSI

O. Altun [1], Ö. Darılmaz [2, *], A. Hür [3], C.E. Karahan [2], Z. Göller [3], T. Sert [1], D. Altun [1], N.A. Toprak [1]

[1] *Hacettepe University, Mining Engineering Department*
[2] *Acacia Maden İşletmeleri A.Ş.*
*(*Corresponding author: ozgun.darilmaz@acacia.com.tr)*
[3] *Flotech Tesis Yönetimi Eğitim Danışmanlık*

ABSTRACT

HIG mill technology is one of the recent developments in the fine grinding area. It has a vertical orientation and is used for wet fine grinding application. This study argues HIG mill operation at copper regrind circuit. Initially, a survey was performed around the mill as well as the concentration circuit to evaluate the accuracy of the sensors and to provide a general knowledge. Then, series of tests were performed to investigate the effects of the operational conditions on the milling performance. In this context, solid content and rotor speed parameters were changed.

Keywords: Stirred mill, vertical stirred mill, regrind mill, fine grinding, comminution.

INTRODUCTION

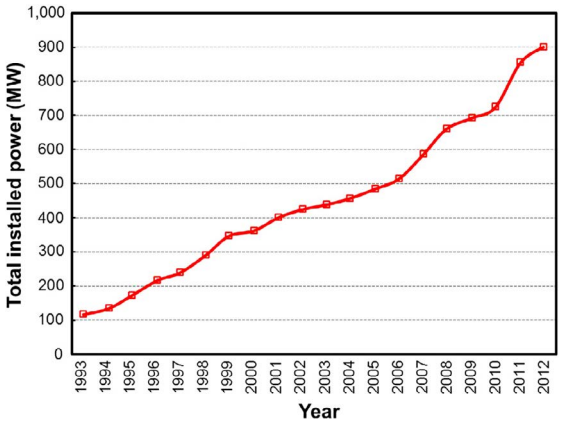

Figure 1. Installed power of fine grinding technologies till 2012 (Wills and Finch, 2016).

Until now, manufacturers have produced different types of stirred mills that are summarized by Giblett (2019). HIG mill is one of the recent developments operating in the size range between p_{80s} of 100 µm and sub 20 µm (Metso: Outotec, 2021). As it is a new technology it lacks industrial knowledge compared

to Isamill and ball mills. This study aimed at filling this gap by providing an industrial set of data on power consumption and milling performance.

MATERIALS & METHODS

Description of HIG Mill and the Operation

HIG mill at the mine (Figure 2) has the specifications given in Table 1.

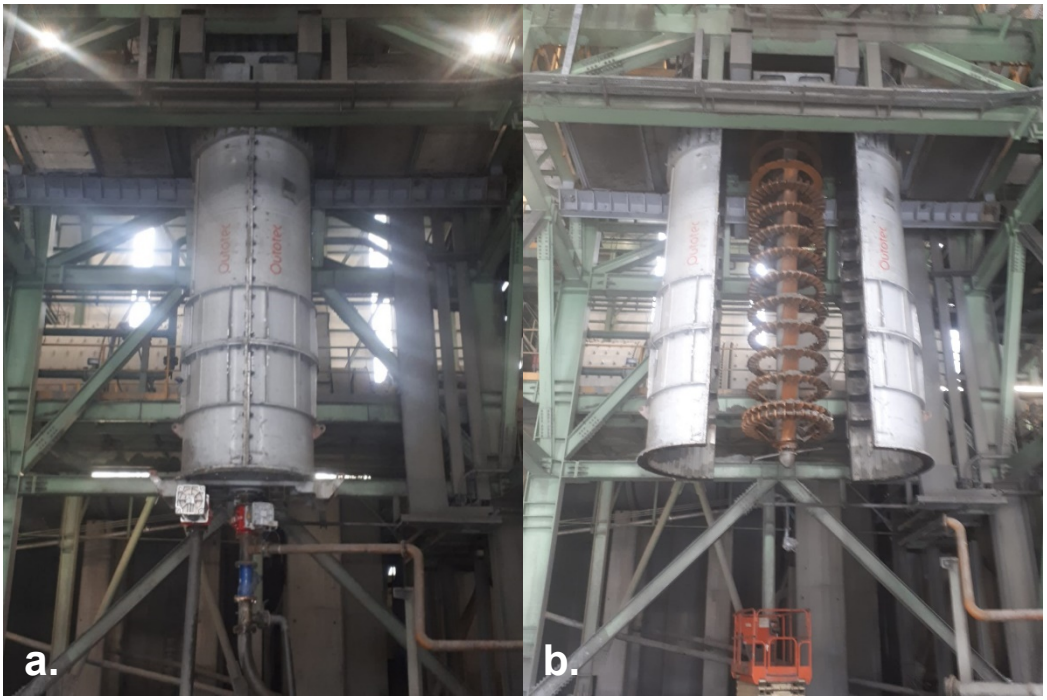

Figure 2. HIG mill at the copper mine.

Table 1. Mill specifications.

Inner height (m)	6.8
Inner diameter (m)	1.66
Dia. of agitator (m)	1.36
No. of agitator	16
Net volume (m^3)	13
Installed mill motor power (kW)	2650

Figure 2b illustrates the alignment of the agitators on shaft. The agitators are named as castellated and non-castellated as summarized by the manufacturer (HIG Mill manual, 2017). The first 11 from the bottom side are called as castellated and the rest 5 from the top is named as non-castellated.

HIG mill is utilized at regrind application. The flowsheet is depicted in Figure 3. Material to the HIG mill is pre-cycloned after the rougher circuit and the product is sent to the cleaner circuit.

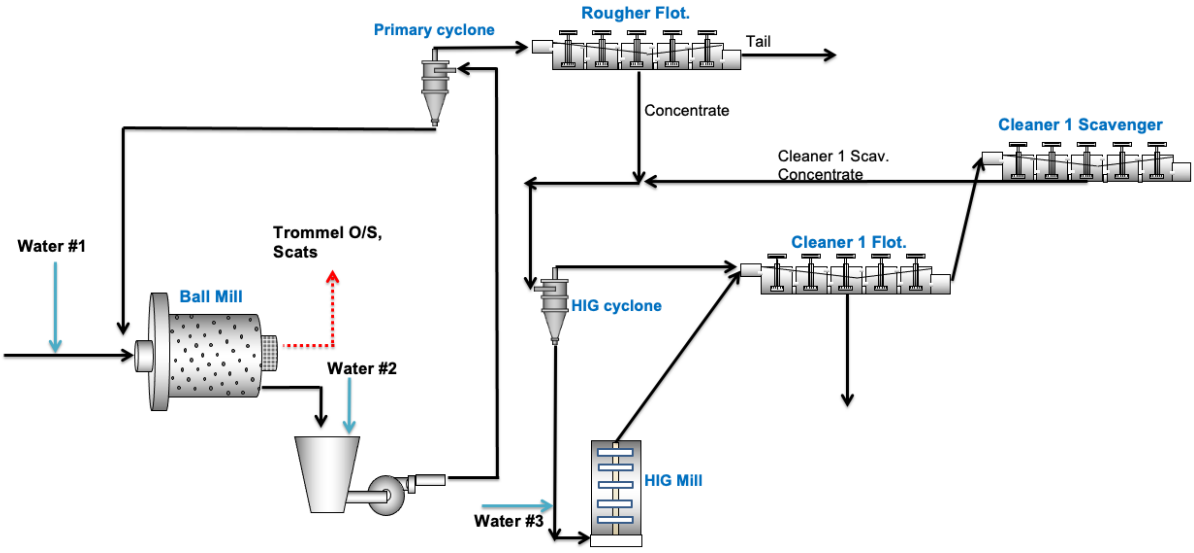

Figure 3. Flowsheet of milling & beneficiation circuit.

Sampling Campaigns

The whole study was conducted in 2 phases that comprised a full survey (general survey) to determine the flow rates for comparing the outputs with the measured ones via the instruments. The conditions are given in Table 2.

Table 2. Operating conditions of the general survey.

Mill power (kW)	1143
Speed of the mill (rpm)	800
Pressure of hydrocyclone (kPa)	112
No. of cyclone in operation	3
Speed of pump (%)	89

The second phase focused on investigating the effects of operating conditions on the performance of the milling. The test plan is given in Table 3 and Table 4.

Table 3. Scope of the sampling campaigns.

	Media Type #1
Agitator configuration (castellated + non-castellated)	11 + 5
Material of agitators	steel
Specific gravity of grinding media	3.8
Bead size (mm)	4
Bead filling (%)	64

Table 4. Conditions of the sampling campaigns.

	30% solid	40% solid	45% solid	50% solid
800 rpm (8.3 m/s)	✓	✓		✓
700 rpm (7.3 m/s)	✓	✓		✓
550 rpm (5.7 m/s)	✓	✓	✓	

Material Characterization

The collected samples were characterized regarding their particle size distribution and solid percentage. Particle size analyses were completed in two steps where the initial analyses included the sieves down to 38µm and below that wet centrifugal classification technique was utilized to have the distribution down 8 µm.

Mass Balancing

Mass balancing was completed via JK-SimMet mass balance module (Napier-Munn et al., 2016), which utilizes the algorithm of Quasi-Newton approach. Following the sample-taking and characterization studies, the data of size distributions, solid percent, and chemical assays were used to calculate the flows of streams and re-calculate the size analyses.

RESULTS AND DISCUSSIONS

Mass Balancing of the Circuit

The results of mass balancing are illustrated in Figure 4.

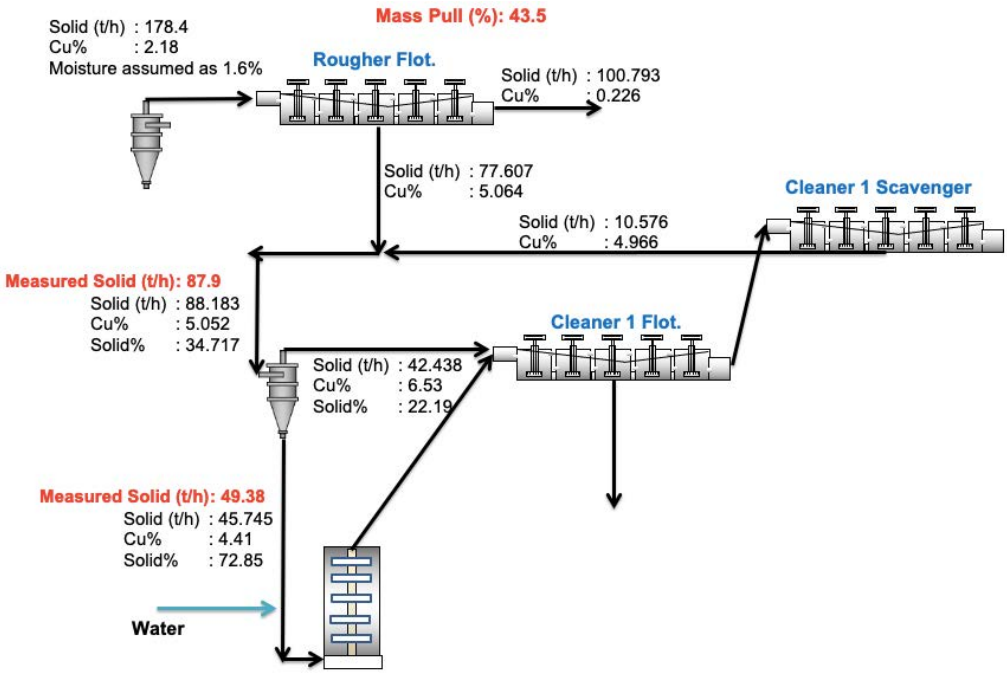

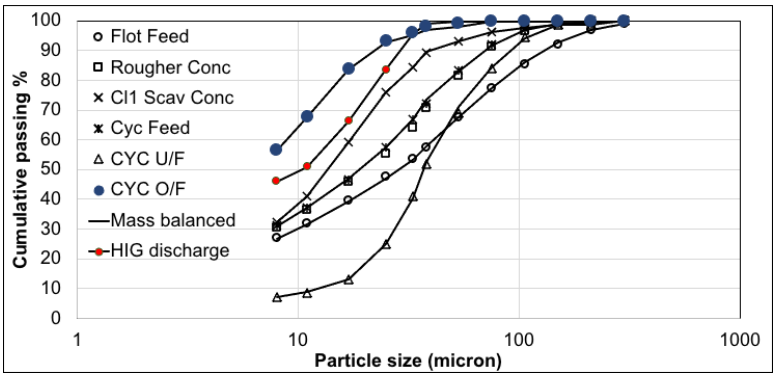

Figure 4. Mass balance of the beneficiation circuit.

Power Correlations of HIG Mill

Within the study, the power correlations were developed at different operating parameters, i.e., tip speed and solid concentration in the feed. Figure 5 illustrates the correlation between tip speed and power draw. The tip speed and power consumption parameters were found to be inter-dependent as expected.

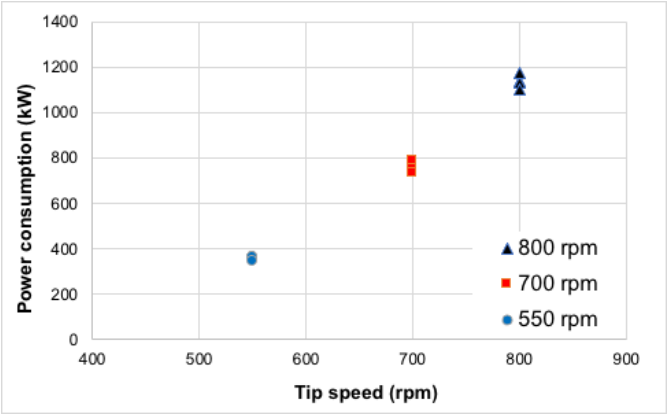

Figure 5. The variation of power draw with the tip speed.

In addition to tip speed, the solid percent also has an influence on the power consumption as it directly changes the load on the mill drive unit. For the operation with less solid content, the particles are easily transported to the discharge end of the mill. Consequently, the shaft rotates with less loading that allows higher number of collisions of beads and with the internal components. Such a phenomenon increases power consumption and vice versa. Within the literature, there exists no solid conclusion relating to the two parameters. Sepulveda (1981) showed that for some of the cases the two parameters were inversely/directly proportional to each other. It may be dependent on the mode of operation and the rheology.

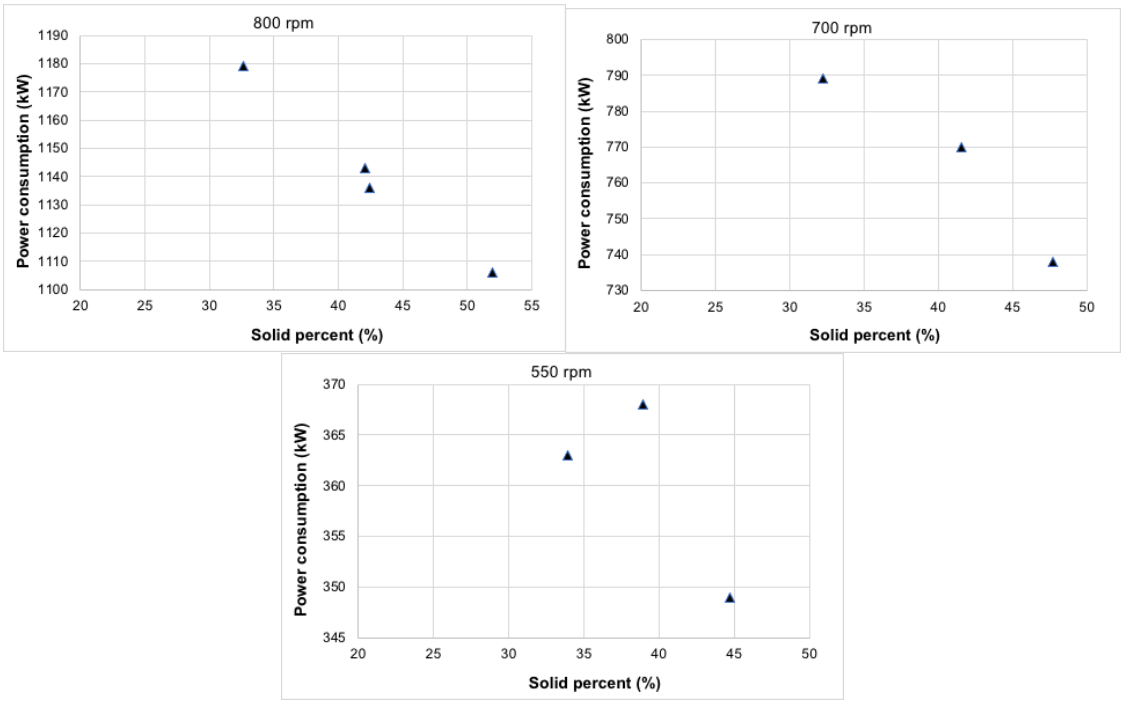

Figure 6. The variation of power draw with feed solid percent.

Comminution Performance of HIG Mill

The specific energy consumption is related to the product size. Figure 7 illustrates the variation of d_{80}s and d_{50}s with specific energy utilization.

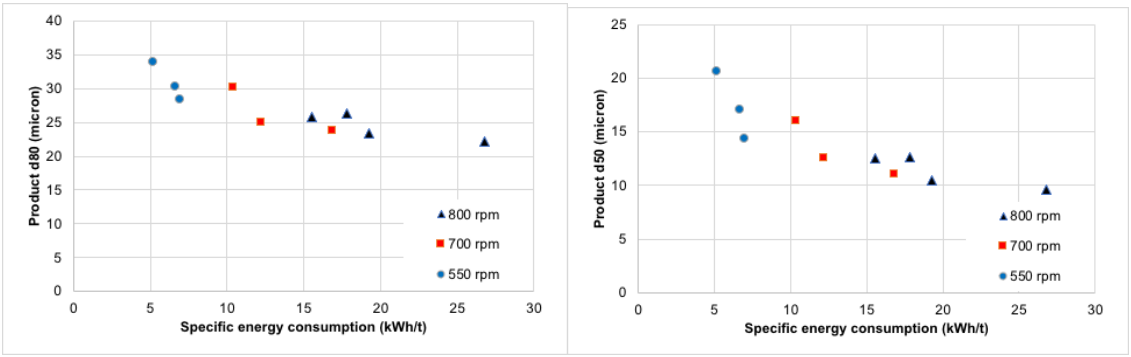

Figure 7. d_{80}s and d_{50}s with specific energy utilization.

The plots illustrated in Figure 8 are highly dependent on the variation in the feed size distributions. Therefore, it is wiser to consider the reduction ratio of the mill hence the effects of feed size are reflected accordingly.

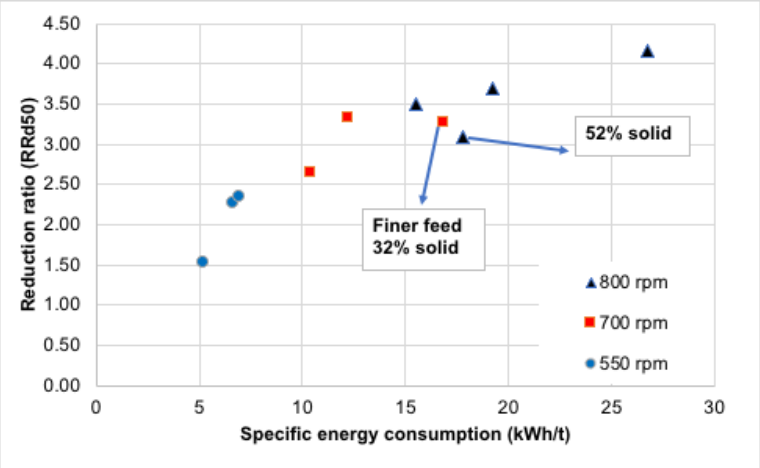

Figure 8. The correlation between reduction ratio and specific energy utilization (RR_{d50}: reduction ratio of d_{50s}).

The general trend indicates the two variables are in good agreement with each other. However, there are two points illustrated on the plot indicating some of the operating conditions tend to deteriorate the efficiency of the milling. These are;

Operation at high solid content: Rheology, a viscosity of a given pulp has effects on the dynamics of the grinding operation. Higher solid contents imply high viscosity hence the transportation of the material and power consumption of the mill change drastically. This is the case for the HIG mill as well. The solid content of 52% was found exceeding the limits of operation, and 40-45% range is reasonable.

Fine feeding with less solid content: There is a difference in the transportation characteristics of coarse and fine particles. Fines are more prone to be carried away by the up flow of slurry hence the probability of bypassing increases. The same phenomenon also applies to the less solid contents. If the two conditions overlap, then inefficiency occurs and this is the case that occurred for the HIG mill. The rest of the points are in good agreement and the energy-size reduction characteristics of the mill can be read from the plot.

CONCLUSIONS

The study aimed at providing information on HIG mill operation that is expected to be widely utilized by the minerals industry. Starting from the power correlations and then investigating the influences of the operating conditions may enable modeling of the mill that is useful for simulations studies. The study is at the preliminary stage hence the material characterization was not detailed, i.e., breakage function, work indice, etc. Completing the whole set of characterization will also be useful for an accurate simulation.

REFERENCES

Wills, B.A., Finch, F., (2016). Wills' Mineral Processing Technology 8th Edition, Elsevier, Butterworth-Heinemann

Giblett, A., (2019). Grinding Technologies, in: Dunne, R.C., Kawatra, K., Young, C.A. (Eds.) SME Mineral Processing & Extractive Metallurgy Handbook.

HIG Mill manual (2017). Description of equipment 900002

Metso: Outotech, (2021). HIG Mill – High Intensity Grinding Mill. Retrieved from https://www.mogroup.com/portfolio/higmill-high-intensity-grinding-mill/ (accessed 30.11.2021).

Napier-Munn, T.J., Morrell, S., Morrison, R.D., Kojovic, T. (1996). Mineral comminution circuits- Their operation and optimization, JKMRC monograph series in mining and mineral processing, Brisbane.

Sepulveda, J. L. (1981). A detailed study on stirred ball mill grinding. Ph. D dissertation, Department of Metallurgy and Metallurgical Engineering, The University of Utah, the USA

Wills, B.A., Finch, F., (2016). Wills' Mineral Processing Technology 8th Edition, Elsevier, Butterworth-Heinemann

IMPACT OF REGIONAL FAULTS ON COAL AND GAS OUTBURST; A CASE STUDY IN TABAS PARVADEH COAL MINE

Saman Karimpour [1], Jafar Khademi Hamidi [1,*], Jalal Karami [2], Ali Hosseini [3]

[1] *Tarbiat Modares University, Mining Engineering Department*
[2] *Tarbiat Modares University, Remote Sensing and GIS Department*
[3] *Tabas Parvadeh Coal Company (TPCCO)*

ABSTRACT

Coal and gas outburst as an extremely complex dynamic phenomenon in coal mine production process can endanger miners and damage equipment facilities. Various geological factors affect the coal and gas outburst. One of these important parameters is the impact of faults in the region. Due to the high cost of initial investment and time-consuming mine development, it is necessary to investigate the displacement of the coal seam by faults in the longwall mining method. Therefore, the purpose of this study is to investigate the effect of fault displacement in Tabas Mechanized Coal Mine No. 1 and to identify the faults that cause coal and gas outburst. To achieve this goal, Schulz classification and ArcGIS software were used. The faults were divided into three categories namely uniform, semi-uniform and non-uniform, on the basis of displacement index varying from 0 to more than 3. The data obtained from coal and gas outburst during the extraction of panel E3 and the geotechnical and geological delays related to mined out panel E2 showed that the occurrence probability of coal and gas outburst near the non-uniform faults is very high. Comparison of the final map and the results of the analyzes with the experiences obtained from the mined out areas and accident occurrence points in the mine showed that there is a very good agreement between the outburst forecast map and the number of events in the mine. The results of this study show the need for precautionary measures in the extraction of deeper panels.

Keywords: Geological information systems (GIS), outburst, fault displacement, longwall mining

INTRODUCTION

Coal plays an important role in the composition of the world's energy. With the depths of subsurface mining continuously increasing, coal mining accidents become more precarious causing thousands of fatalities in world every year. Globally, coal and gas outburst are recognized as one of the most catastrophic failures associated with the coal mining industry (Li et al., 2020). Studies have shown that most outburst incidents occur in strongly deformed zones along the axes of structures such as asymmetrical anticlines, the hinge zones of recumbent folds, and the intensely deformed zones of strike-slip, thrust, reverse, and normal faults (Cao et al., 2001; Mark, 2008; Shepherd et al., 1982). Tectonism has an important influence on coal pores (Jiang et al., 2020). During the coal mining process, faults are one of the major geological problems that have disrupted coal production (Lin et al., 2020). It has been investigated that the outburst of coal and gas is closely related to fault zones (Zai et al., 2016; Karacan et al. 2008). Fault zones are important since they disrupt the structure of coal and reduce its strength (Karacan et al, 2008). The presence of fault zones in coal basin is an important indicator and factor for predicting coal and gas outburst (Fisne and Esen, 2014).

In recent years, despite measures to prevent and control the coal and gas outburst, faults in the region have made the mining environment difficult, complex geological structure, increased pressure and stress, as a result, the risk of coal and gas outburst is still high.

Numerous studies have been conducted on the geological structures and the impact of regional faults on coal and gas outburst. Cao et al. (2001) checked out that coal seams in the footwalls of the reverse faults underwent greater tectonic deformation than those in the hanging walls and outbursts always occurred in tectonically deformed zones. Zhao et al. (2013) showed in their studies that tectonic soft coal is mainly formed on the fault top wall under the effect of the fault structure. Lin et al. (2020) checked out the influence of small faults on coal and gas outbursts in the working face, which has reference significance for the prediction and prevention of coal and gas outburst disaster in the working face. Their studies showed that the risk of small fault slip increases with the advancing working face. Jiang et al. (2020) checked out the mechanism of how faults affect coal pore structure and gas sorption characteristic. Gao et al. (2021) reported that fault zones increase the gas pressure and weaken the coal seam, which causes a sudden coal and gas outburst.

Experiences from the mined out panels in the Parvadeh Tabas mine show that as the mine deepens, the impact and increase in stresses complicate the geological structures of the coal. As a result, the impact of faults in the region increases the potential for gas and coal outburst in working face. The parameters affecting the formation of the outburst can be listed as the gas content of the coal seam, thickness, slope, depth, and distance to fault zones. In this study, an evaluation is made only by considering the distance to fault zones. Due to the importance of the issue and few similar studies on coal mines in the country, the impact of regional faults on the outburst of coal and gas in Tabas mechanized mine is investigated in this study. For this purpose, due to the high capability of Geographical Information System (GIS), ArcGIS software is used to prepare a map of the impact of faults on gas and coal outburst in the mine.

GEOLOGICAL SETTING AND OUTBURST OCCURRENCE

Parvadeh underground coal mine is located in Tabas coal basin with an area of about 1200 square kilometers in the eastern part of central Iran, 75 kilometers southeast of Tabas city (Fig. 1). Coal reserves are estimated to be 98 million tons. The Parvadeh coal basin is located between two major North–South trending fault systems, the Kalmard hidden fault to the West and the Nayband fault to the East. Second-order structures trending East–West between these faults are the Rostam fault and Parvadeh anticline. The Rostam fault forms the northern boundary to the mining area. It is a reverse fault with a displacement of up to 700 m, down throwing to the North. The mine lies on the central portion of the asymmetrical Parvadeh anticline. Stratigraphically, the coal bearing sequence is of Triassic age. The rocks are mostly mudstone with prominent coarsening up siltstone/sandstone sequences. Locally developed, thin marine limestone occurs. The main coal horizons in the mine are seams B1, B2, and C1 that occur within 50 m of strata. Other seams C2, D and possibly E will affect mining principally because of their methane content. Figure 2 shows the stratigraphic column of the area. The total extractable reserves in all three available seams in Tabas Mine No. 1 are summarized in Table 1.

Table 1. Total minable reserves of mine No. 1

Seam	Seam area (hectares)	Total extractable reserves (tons)
C1	629.91	15325000
B2	601.18	7342000
B	356.11	4940000

1

The understudy area consists of 11 panels, among which panels E0, E1, E2, E3, W1, W2 and W_3 have been mined out and Panel W_4 is currently under extraction. As the mine deepens, operations become more difficult and the occurrence potential of coal and gas outburst at the Tabas mine increases. With increasing depth in this mine, the effect of this phenomenon will increase. Figure 1 shows the frequency and distribution of outbursts occurred in Panel E_3.

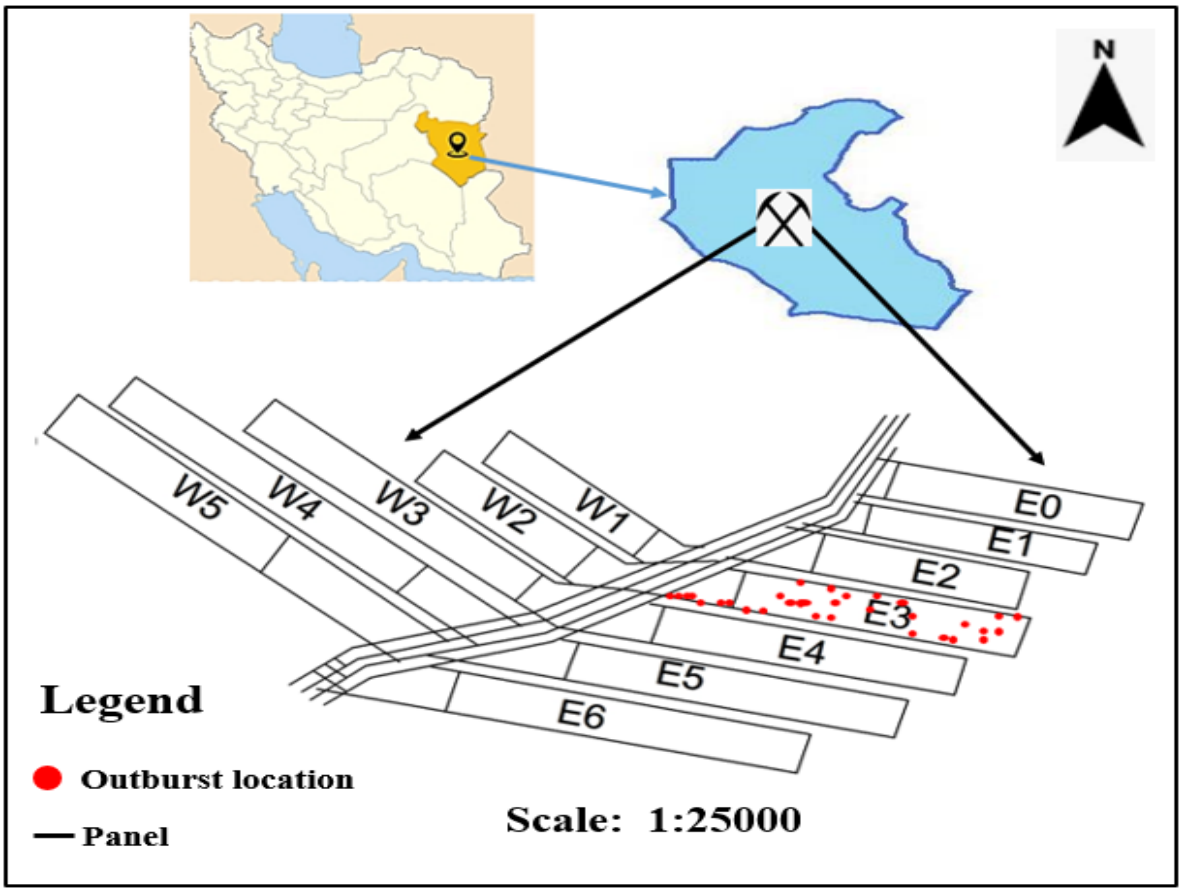

Figure 1. Location of the study area and distribution of outbursts occurred in Panel E3

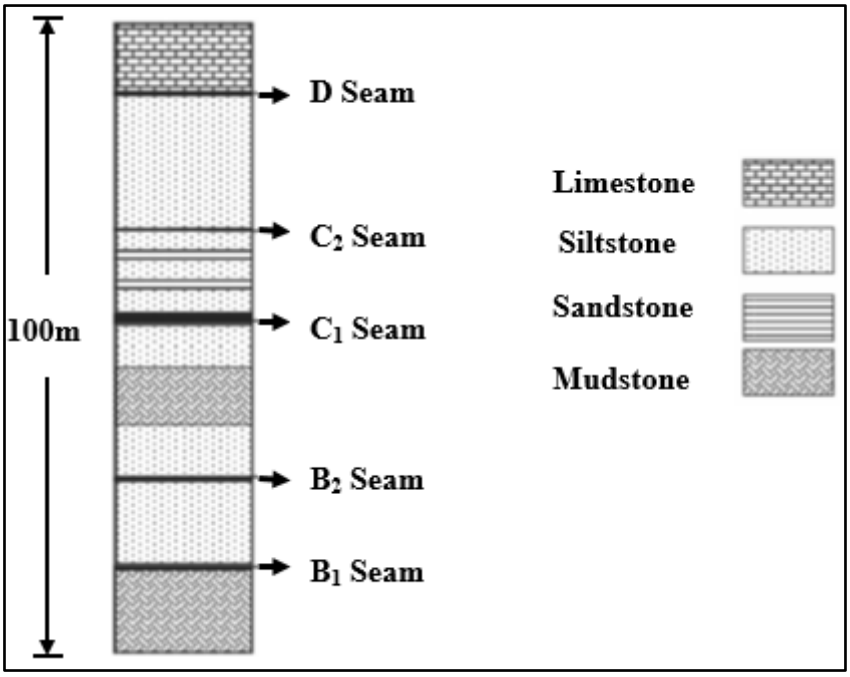

Figure 2. Stratigraphic column of Parvadeh Tabas coal field (Mohtasham Seyfi et al., 2018), (Sereshki et al., 2016)

METHODS

Fault Modeling in ArcGIS Environment

From the point of view of operational risk, the most suitable extraction Panel is a Panel that has low geological features and sufficient safety. In order to reduce risks and accidents, it is necessary to be aware of the ground conditions, especially faults. Due to the high cost of initial investment and time-consuming mine development, it is necessary to investigate the displacement of the coal seam by faults in the longwall mining method. Therefore, the purpose of this study is to investigate the effect of fault displacement in Tabas Mechanized Coal Mine No. 1 and to identify the faults that cause coal and gas outburst in this mine. To achieve this goal, Schulz classification and ArcGIS software have been used.

Schulz classification

After collecting the data, Schulz classification was used to determine the uniformity of the seam in the fault zones. In 1993, Schulz proposed a classification system in which the uniformity of the seam was determined by changes in the displacement index (V_x)(Ataei et al., 2009):

$$v_x=\frac{x}{m} \quad (1)$$

where, v_x is displacement index, *x* is the displacement of coal seam due to fault and *m* is the thickness of coal seam, both in meter. The degree of seam uniformity in this classification is assigned to the seam as a point according to the displacement index. The seam uniformity varies between 0 and 1. According to this theory, seams with a displacement index of 0 are perfectly uniform (uniformity rating equal to 1) and seams with a displacement index greater than 3 are non-uniform (uniformity score equal to 0). Table 2 shows the classification provided by Schulz.

Table 1. Classification of coal seam uniformity

Seam uniformity Condition	Fault displacement index
Uniform	0-0.5
Semi-uniform	0.5-1
	1-1.5
	1.5-2
Non-uniform	2-2.5
	2.5-3
	>3

Fault Displacement Map

Having used the Schulz classification to determine the changes in magnitude of coal seam displacement index in fault zones, layering was implemented in ArcGIS software. The faults of the mine were divided into three categories; faults with displacement index of 0 to 0.5 (uniform), faults with displacement index of 0.5 to 2 (semi-uniform) and faults with displacement index greater than 3 (non-uniform). As can be seen in Figure 3, the faults marked in red are non-uniform, and according to a survey of experts and engineers of this mine, shearer loader usually encounters problems when crossing these faults, and in these places coal and gas outburst are usually recorded. Three of the faults in panels W4, W5 and E2 are marked in red, and according to the results of this study, the possibility of coal and gas outburst and its intensity in panel W4, W5 will be very high. It is necessary to take precautionary measures during the extraction of these panels. Figure 4 shows the fault concentration map.

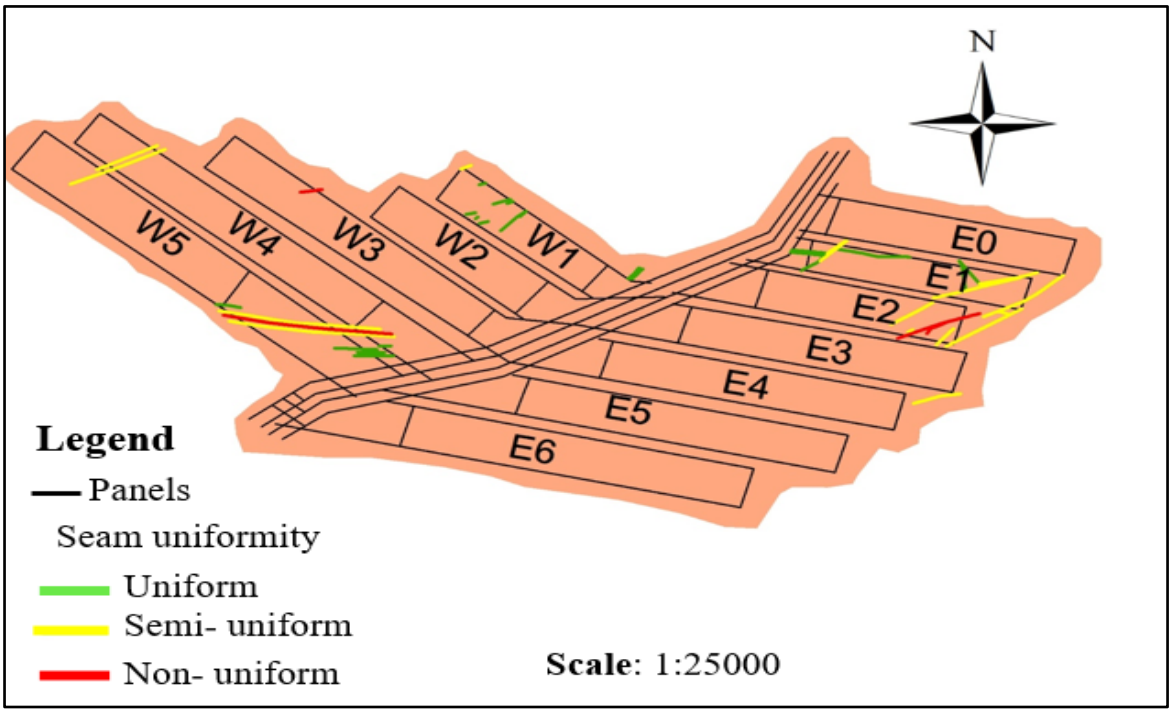

Figure 3. Classification map of fault displacement

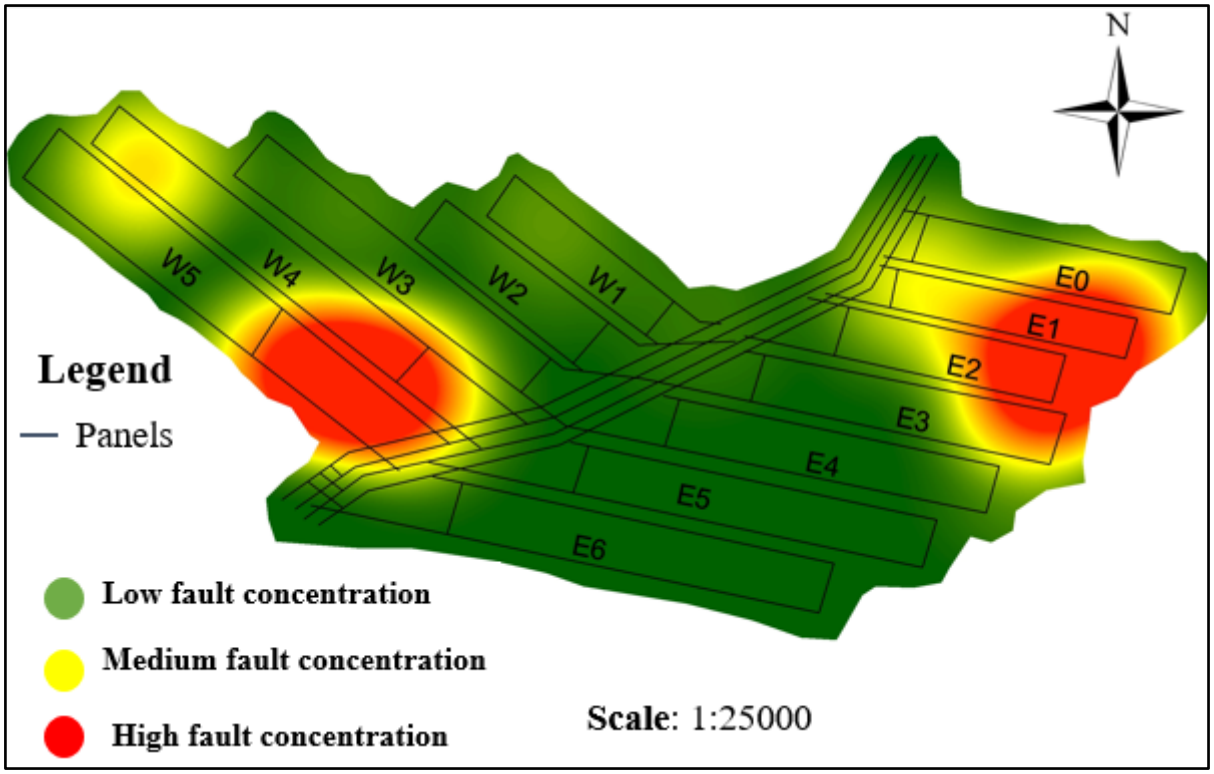

Figure 4. The final map of the intensity of coal and gas outburst due to the concentration of faults in the region

Underground coal mining has always been known as one of the most risky mining activities. Occurrence of potential accidents in underground coal mines and the resulting hazards create an unsafe work environment for workers and operational equipment.

Parvadeh Coal Mine is one of the important mines for supplying raw materials to steel mills in Iran. Many problems, including collapse of the roof, spontaneous ignition, instantaneous release of methane gas, groundwater influx, sudden collapse and subsidence, threaten the production and safety of the mine.

Verification of the performance of the final model and the emissions of gas and coal recorded during the extraction of panel E_3 shows the high reliability of this method. As shown in Figure 5, due to the impact of the faults, several outputs have occurred at the top of panel E_3.

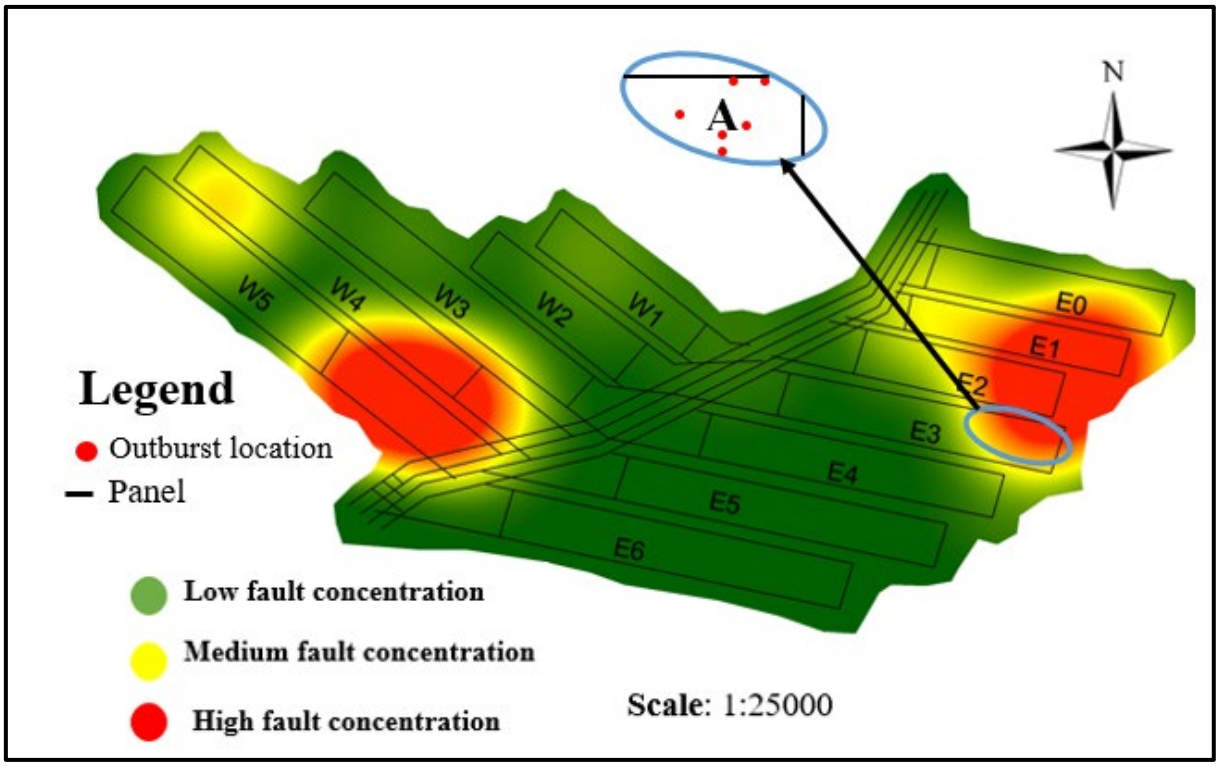

Figure 5. Fault focus map in panels

DISCUSSION AND CONCLUSION

In coal mining, geological structures such as faults in the region are important influencing factors affecting the coal and gas outburst. With the start of mining and disruption of regional stress, the impact of these factors intensifies as a result of the potential of the coal seam for this phenomenon increases. Schulz classification and GIS were used to identify high-risk areas in terms of outburst and to map faults in the area. The most important results of this study are:

(1) The combination of GIS technique and Schulz classification allows decision makers to identify the areas prone to high-risk coal and gas outburst.

(2) The results of the coal and gas forecast map show the high concentration of faults in Panels W4, W5. Preventive measures should be taken during the extraction of these Panels.

(3) Verification of the performance of the final model and the coal and gas outburst recorded during the extraction the top of the panels E3 show the reasonable reliability of this method and other events of Panel E3 are due to the effect of other parameters on gas and coal emissions.

REFERENCES

Ataei, M., Khalokakaei, R., and Hossieni, M. (2009). Determination of coal mine mechanization using fuzzy logic. *Mining Science and Technology*, 19(2), 149-154.

Fisne, A., Esen, O. (2014). Coal and gas outburst hazard in Zonguldak Coal Basin of Turkey, and association with geological parameters. *Natural Hazards*, 74(3), 1363–1390.

Gao, K., Huang, P., Liu, Z., Liu, J., Shu, C., and Qiao, G. (2021). Coal-rock damage characteristics caused by blasting within a reverse fault and its resultant effects on coal and gas outburst," *Sci. Rep.,* 1-13.

He, D., Cao, Y., and Glick, D.Y. (2001). Coal and gas outbursts in footwalls of reverse faults. *International Journal of Coal Geology,* 48(1-2), 47-63.

Li, Wei., Ren, T., Busch, A., den Hartog, S.A.M., Cheng, Y., Qiao, W., and Li, B. (2018). Architecture, stress state and permeability of a fault zone in Jiulishan coal mine, China: Implication for coal and gas outbursts. *International Journal of Coal Geology, 198, 1-13.*

Jiang, B., Zhao, Y., Lin, B., and Liu, T. (2020). Effect of faults on the pore structure of coal and its resultant change on gas emission. *Journal of Petroleum Science and Engineering*, 195.

Karacan, C.Ö., Ulery, J.P., and Goodman, G.V.R. (2008). A numerical evaluation on the effects of impermeable faults on degasification efficiency and methane emissions during underground coal mining. *International Journal of Coal Geology,* 75(4), 195–203.

Lin, J., Zuo**,** Y., Zhang, K., Sun, W., Jin, B., Li, T., and Chen, Q. (2020). Coal and gas outburst affected by law of small fault instability during working face advance. *Geofluids*, 2020.

Mark, C. (2018). Coal bursts that occur during development: A rock mechanics enigma. *International Journal of Mining Science and Technology*, 28(1), 35-42.

Sereshki, F., Vaezian, A., and Saffari, A. (2016). Evaluation of the effect of macerals on coal permeability in Tazareh and Parvadeh mines. *Journal of Stratigraphy and Sedimentology Researches*, 32(2), 23-34.

Seyfi, M.M., Hamidi, J.K., Monjezi, M., and Hosseini, A. (2018). Estimation of coal seams gas content for evaluating potential use of methane drainage system in Tabas coal mine. *Journal of Mining and Environment*, 9(3) , 667–677.

Shepherd, J., Rixon, L.K., and Griffiths, L. (1981). Outbursts and geological structures in coal mines: A review. *International Journal of Rock Mechanics and Mining Sciences & Geomechanics Abstracts*, 18(4), 267-283.

Vaziri, V., Hamidi, J.K., and Sayadi, A.R. (2018). An integrated GIS-based approach for geohazards risk assessment in coal mines. *Environmetal Earth Sciences*, 77(1), 29.

Zhai, C., Xiang, X., Xu, J., and Wu, S. (2016). The characteristics and main influencing factors affecting coal and gas outbursts in Chinese Pingdingshan mining region. *Natural Hazards*, 82(1), 507–530.

Zhao, W., Xiong, J., Zhang, J., and Ran, M. Y. (2013). Structure coal distribution law and affected to coal and gas outburst in Sichuan coal mining area. *Coal Science and Technology*, 41(2), 52–55.

INDUSTRIAL USE OF BACTERIAL IRON OXIDATION IN-SITU RECOVERY OF URANIUM

B. Shiderin [1,*], A. Altynbek [2], Y. Bektay [1], G. Turysbekova [1], E. Mukanov [1], A. Kalmukambetov [2], M. Bektayev [3], A. Duisenbay [4]

[1] *Satbayev University*
*(*Corresponding author: shbaur@mail.ru)*
[2] *Semizbay–U LTD*

ABSTRACT

The technology of bacterial iron oxidation during in-situ recovery (ISR) of uranium has been developed and proposed for industrial use. Results of pilot tests at a uranium mine in Kazakhstan for 24 months confirmed technology. Two bio-technological installations based on a new type of flow bioreactors with a volume of 20 m3 bioreactors installed in 40-foot containers. The capacity of the plants installed in the geo-technological field was more than 150,000 m3/year for leaching solution. The redox of the solution rose from 360 mV to 430-450 mV in the flow mode in bioreactors. The content of trivalent iron increased from 0.1 g/l to 1.5 g/l and higher. The bioprocess was carried out with temperature of solution 10-14^{0}C (the optimal is 25-35^{0}C). This eliminated energy consumption for heating the solution. The test results showed an increase in the uranium content in the productive solution by 10-20 % without adding additional sulfuric acid and 40 % with adding additional sulfuric acid. The economic costs of using the technology are 6-8 times lower than when it is used chemical oxidizers (hydrogen peroxide). This confirmed the potential of using this technology for underground borehole ISR of uranium.

Keywords: Uranium, in-situ recovery, bioleaching, bivalent iron, bacteria

INTRODUCTION

The use of underground in-situ uranium recovery technology (ISL) has developed significantly in the world in recent decades. Kazakhstan's success in uranium mining is based on this technology (over 20 thousand tons of uranium per year). Reducing the price of uranium requires the introduction of technologies aimed at reducing the cost of mining and processing of uranium and intensifying the process.

One approach is to use bacterial leaching with the use of iron-oxidizing bacteria *A. ferrooxidans* according to the main technological indicators corresponds to the modes that are used for underground borehole in-situ recovery of uranium. There have been repeated attempts to use bioleaching for uranium, but these methods have not been widely adopted. One-time supplies of bacterial solution did not give the necessary result, especially since during underground borehole in-situ recovery of uranium, the solution flows through the ore-bearing layer for 20-30 days. Conditions for the vital activity of bacteria in the ore-bearing layer did not allow them to multiply and show their activity.

The use of bio-geotechnology in mining practice differs significantly from the use of biotechnology in the production of specific medicines or food products. This is due to the significant heterogeneity of the composition, the presence of technological factors that significantly affect the process. It is necessary to take into account the complex nature of the ore body, as well as the fact that the material composition varies not only on different blocks, but also within the same block.

Bacteria capable of oxidizing iron (II) were first identified in the acidic waters of coal mines in the United States, and then – in the acidic waters of the Bindkham copper quarry (USA) (Colmer et al., 1950; Bryner et al., 1954). Similar bacteria were later discovered at the Rio Tinto mine in Spain, where copper has been leached for ~ 300 years. On the territory of Russia, such bacteria are present, for example, in the acidic mine waters of the sulfide deposits of the Urals, Altai and Kola Peninsula (Polkin, 1982). During microbiological leaching, bacteria oxidize sulfide minerals, which causes the formation of iron (III) and sulfuric acid ions in the aqueous phase – a set of reagents, due to redox reactions that oxidize U(IV) and form soluble U(VI). This transformation, due to the chemical activity of microorganisms, is the basis of a bio-metallurgical process that is economically justified in relation to poor, off-balance-sheet ores and dumps of uranium production (i.e., in cases where the standard process is not applicable) (Colmer et al., 1950; Bryner et al., 1954; Polkin et al., 1982).

There several studies in the possibility of commercializing bacterial leaching of uranium from poor raw materials were carried out in the early 1950s, and in 1952-1953 in Urgeirica (Portugal), industrial use of a heap version of this process began (iron-oxidizing bacteria *A.ferrooxidans* were used) (Brand, 2001; Harrison et al., 1966).Also at Elliot lake mine (Canada) using a solution of sulfuric acid and iron (III) sulfate as a bacterial medium (Hamidian et al., 2009; Guay et al., 1976; Tuovinen and Bhatti, 1999).

Several important factor is the nature of mineralization of uranium, since its oxide, phosphate, sulfate and carbonate minerals are easily opened, while silicate forms are difficult or not at all opened (Munoz et al., 1995; Rawlings, 2004). Also amount of nutrients (added artificially or extracted by minerals) sufficient for the growth of the bacterial culture (Rawlings, 2005). *A.ferrooxidans* is resistant to metal ions such as chromium, copper, zinc, nickel, thorium, uranium, and mercury. The presence of certain metals and organic compounds in the environment can block the process of pyrite oxidation by this type of bacteria (Brand, 2001; Munoz et al., 1995).

Temperature is a parameter that determines the diversity of microbiological populations (Kawatra and Natarajan, 2001). Moderately thermophyllite iron-and sulfur-oxidizing bacteria, initially isolated from mine waters and hot springs and operating at temperatures of 30-40^{0}C, proved to be the most suitable for research and industrial use (Rawlings, 2005; Brierley, 1978; Brierley et al., 1978; Holmes, 1988; Blais et al., 1994; Twardowska, 1986; Twardowska, 1987). In all leaching processes involving acidophilic bacteria, the degree of oxygen saturation of the solution or pulp is an important parameter. Under conditions of forced mixing, a drop in the oxygen concentration below 0.5-1.0 mg / dm3 causes the process to stop. It has been shown that the use of forced aeration (air consumption of 8t/t solid, oxygen utilization rate of 25 %) significantly reduces the leaching time during the heap bacterial leaching of ores from several Australian deposits (Brierley and Briggs, 2002). Lack of carbon dioxide stops the growth of autotrophic bacteria and can dramatically reduce the speed and completeness of their interaction with sulfide minerals (Pronk et al., 1992; Barrett et al., 1993). A number of studies have also established optimal process parameters (pH, temperature, and mixing time) (Polkin et al., 1982; Hamidian et al., 2009; Cerda et al., 1993; Schippers et al., 1995; Benedetto et al., 2005).

At the Canada enterprise Rio Elgom, the process of periodic irrigation of the walls of treatment faces with acidic mine water was tested; as a result, in 1964-1965, about 57 tons of uranium were additionally extracted. Currently, Rio Algom use of heap bacterial leaching of uranium. Since 1984, several variants of underground leaching of uranium using *A.ferrooxidans* bacteria have been tested (Rawlings, 2004; McCready and Gould, 1990). Other examples of industrial use of uranium bioleaching are factories using the heap option (Figueria in Brazil, Ranger in Australia, Stepnogorskaya in Kazakhstan and Saint Pierre in France) and the well option (Olympic Dam and Beverly in Australia) (Tuovinen and Bhatti, 1999; Munoz et al., 1995; Garcia, 1993; Dwivedy and Mathur, 1995). But the information on this project is presented in a compressed form in the sources, and currently the technology does not seem

to be used. There is evidence that bioleaching is used in China in relation to the extraction of uranium from tailings dumps (Jianguo et al, 2004; Campbell et al., 2015; Watling, 2015.

From this analysis, it follows that the use of bacterial iron oxidation and biotechnological methods for underground in-situ recovery of uranium is limited and there are no examples of effective organization for underground leaching “in-suti” (ISR).

Analysis data show main reaction taking place for uranium recovery using bialeching. Ion ferric iron resulting from oxidation of ferrous iron by bacteria is an oxidizing agent of tetravalent uranium:

$$UO_2 + Fe_2(SO_4)_3 \rightarrow UO_2SO_4 + 2\ FeSO_4 \quad (1)$$

Bacteria (A. Ferrooxidans) can oxidize ferrous iron:

$$2FeSO_4 + H_2SO_4 + 1/2O_2 \rightarrow Fe_2(SO_4)_3 + H_2O \quad (2)$$

Also exist possible direct oxidation of uranium by bacteria (direct mechanism):

$$2\ UO_2 + O_2 + 2\ H_2SO_4 \rightarrow 2\ UO_2SO_4 + 2\ H_2O \quad (3)$$

But in underground condition there is too small amount of O_2.

On another hand in such condition take place formation of iron hydroxides is one of the factors that can cause clogging in the ore-bearing layer.

$$Fe_2(SO_4)_3 + 6H_2O \Longleftrightarrow 2Fe(OH)_3 \downarrow + 3\ H_2SO_4 \quad (4)$$

The Methodology of the Tests

Uranium Deposit (Block for investigation)

For investigation bacterial leaching for uranium deposit was used uranium field in the north of Kazakhstan's is geologically complex, with a depth of about 120 m. The operation of the mine is characterized by a high consumption of sulfuric acid due to its complex material composition. Leaching dissolution of the this uranium Deposit have a relatively high content of divalent iron in leaching solutions up to 3 g/l and the salt content accumulated in the solution reaches 20-30 g/l.

Tests was done on one of the block (number 62) in this uranium deposit. Block consisted of several injection and pumping wells. Distance between wells 25 meters. an average thickness of the ore-bearing layer of about 10 m. The volumes of the leaching solution supplied are on average from 30 to 50 m3/h for a separate block of the Deposit. Pilot tests was done on an equipment with a solution flow of more than 20 m3 / hour, which in annual terms is more than 150 thousand m3 / year.

Leaching Solution and Productive Solution

The large-scale transition from laboratory research to pilot production and subsequent industrial application is associated with the presence of factors that are difficult to model in the laboratory. The Composition of leaching dissolutions differs from the model compositions used for growing bacteria, primarily a significant amount of salts (up to 25g/l). The content of Fe^{2+} of iron does not exceed 3 g/l, under simulated conditions up to 10 g/l. The relatively low content of divalent iron in the solution requires more fine-tuning of the technology and taking into account scale factors. The temperature of the dissolution (10-14^{0}C) are significantly different from optimum (25-35^{0}C). The heating costs are much higher than the potential effect of using solution with the volume of the leaching

dissolution flow (2000m^3/h). Trying to bring the temperature of the dissolution to the optimal temperature for the bacteria will require a cost comparable to the cost of the finished product. The operating Conditions of bioreactors in the flow mode differ from the model laboratory conditions, even if the solution compositions match. The Duration of leaching solutions passing (over 20 days) through the ore-bearing layer and the variety of physical and chemical processes taking place in the ore-bearing layer.

Equipment

Two units with a compressor station (up to 500 m3/h of air production each) and a pumping station with a capacity of up to 40 m3/h were used for testing. Flow bioreactors with a volume of 20 m3 provided a free solution flow with minimal removal of bacteria from the bioreactor due to design of equipment. A pumping station with a frequency Converter and a storage tank provided solution supply to the main network at a pressure of more than 8 bar. After the bioreactors, the activated leaching solution was fed into the injection wells. Measurements of the content of iron in the dissolution, sulfuric acid, pH, redox process, and the content of uranium in the productive solution were carried out by the mine laboratory in the current mode. Regulation of the dissolution supply to the bioreactors was regulated by cranes based on data from electromagnetic flow meters («Omega» type). Development of the installation project and its installation was carried out by the research laboratory "BioGeoTechnology of gold, uranium and polymetallic ores" (Satbayev University)". Mobile execution of bio-installations in containers allows to transfer equipment to problem blocks for solving local problems.

Biomass accumulation

Preliminary accumulation of biomass was carried out on the Sylvester-Langmuir medium. The accumulated biomass was fed to bioreactors on a one-time basis. During the month, biomass was accumulated in bioreactors in the cultivation mode. Biomass accumulation was carried out in the bubbling mode by air supply by a compressor. The dissolution was periodically updated as the divalent iron changed to the trivalent state. Measurements were made in the chemical laboratory of the mine on a daily basis.

Measurments and Calculations

Amount of U, Fe^{2+}, Fe^{3+} and H_2SO_4 was measured in labalatory of plant by titration methods. Redox , pH was measured by ionometr I-160MI, Amount of bacteria measured using microscope. For statistical analysis of data was used program SPSS statistics.

Testing

The first stage tests were carried out during 2018. The dissolution was supplied to two installations under the code name BOI-1 and BOI-2 (bacterial oxidation of iron) in the volume of 20 m3/hour. Since June 2019, only one BOI-1 installation has been operating in flow mode. Two weeks later, two installations were launched together. The total volume of the solution supplied to the unit was 30m3 / hour. No additional sulfuric acid was supplied. The volume of the activated leaching dissolution supplied was till 20m3 / hour, with the total supply of the solution to the injection wells up to 40m3/hour. Mixing the activated leaching solution and hydrous solution slightly reduced the redox parameter of the solution and the content of trivalent iron in the solution. Data on the content of the target metal in the production solution were determined in the normal mode directly by employees of the mine (Turysbekova, 2019).

The second stage tests were carried out during 2021. The leaching solution was supplied to installation under the code name BOI-2 (bacterial oxidation of iron) in the volume of 10 m3/hour with

adding sulfuric acid 2g/l. Testing took place Since 18 July 2021 till 18 October 2021. Only one BOI-2 installation has been operating in flow mode. The total volume of the solution supplied to the unit was 10m3 / hour. All leaching solution went through BOI-2.

RESULTS

Investigation Without Adding Additional Sulfuric Acid (1 stage)

On the first stage was done investigation without adding additional sulfuric acid. Usual leaching solution after uranium desorption was used. Part of leaching solution (50%) flow through bioreactors. After bioreactor solution redox increased from 360mV till 410-420 mV.

On the figure 1 is shown everyday data of the content of uranium in the production solution since the beginning of 1 January 2018. The arrows indicate the start time of the activated leach dissolution supply units. The content of sulfuric acid in the leaching dissolution was 3.5-4.5 g / l. The tests were performed without additional acid supply.

Figure 1 shows data on the content of uranium in the productive solution on the block since the beginning of the year. There is a clear tendency to reduce the content before the start of installations. After switching on the second unit and reaching the 30m3/h feed, there is a steady increase in the uranium content in the production solution, which allowed us to assume that the tests have reached their intended goal.

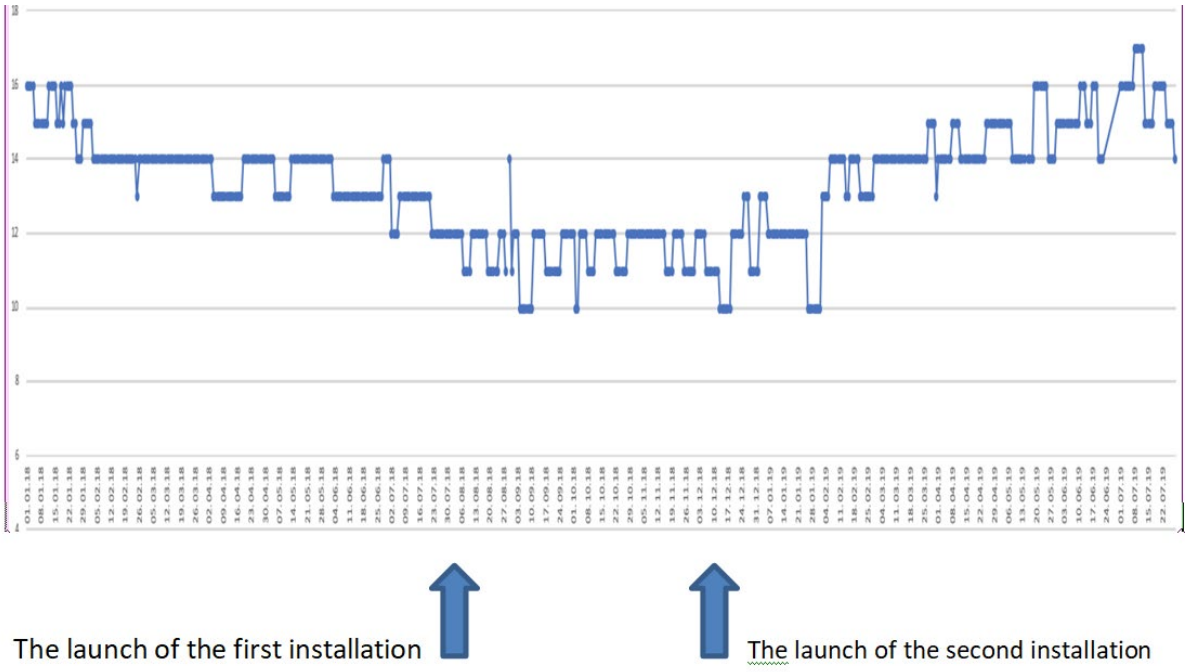

Figure 1. Dynamics of changes in the content of uranium in the production solution from January 2018 to 2019, indicating the time when bio-installations for the oxidation of divalent iron in the leaching dissolution were switched on. (U (g/l))

Taking into account that the reaction time of the system to the impact of the modified leaching dissolution is at least 20 days, it can be observed that the increase in the uranium content in the productive solution occurred after the launch of bio-installations. For individual wells on the block, the increase was more than 50 %. The average for the block was 10-20 %. The tests were performed without adding sulfuric acid.

Investigation With Adding Additional Sulfuric Acid (Stage 2)

For testing, sulfuric acid was supplied in the required amount of over 100 tons. The acid supply was adjusted by the acidification process unit (APU) through an electromagnetic flow meter. The acid supply was adjusted manually every hour. The acid supply was adjusted manually every hour. On average, the supply was carried out in the amount of 2 grams / liter, and after 20 days in the amount of 6-7 grams / liter.

The volume of the leaching solution was supplied in a volume of 10 m3/h through the installation Bacterial oxidation of Iron-2 (BOI-2). Samples were taken daily to analyze the parameters of the activated leaching solution (ALS): pH, Redox, Fe2+, Fe3+, H2SO4. Table 1 below presents data on the correlation of ATS indicators after leaving the BOI-2 facility. (Sample size 152)

Table 1. Correlation of indicators of the solution in the ALS (in the bioreactor)
**. The correlation is significant at the 0.01 level (two-tailed). ***RP- Redox potential

		pH	RP	Fe2	Fe3	H2SO4
pH	Pearson correlation	1	-,078	-,006	,016	-,880**
	N	152	152	152	152	152
RP***	Pearson correlation	-,078	1	-,888**	,906**	,050
	N	152	152	152	152	152
Fe2	Pearson correlation	-,006	-,888**	1	-,956**	-,027
	N	152	152	152	152	152
Fe3	Pearson correlation	,016	,906**	-,956**	1	,043
	N	152	152	152	152	152
H2SO4	Pearson correlation	-,880**	,050	-,027	,043	1
	N	152	152	152	152	152

Figure 3 presents data on the content of uranium in the PS (productive solution) since January 2021. As noted above, tests were carried out at the block with the use of BOI-2 from 2018, and there was an increase in the uranium content in the PS during the testing period (2018-2019) by 10-20% without supplying additional sulfuric acid.

New tests carried out with the addition of sulfuric acid showed that the content increased on the block by 40% (from 12 mg/l to 18 mg/l). Samples in the productive solution were analyzed daily (pH, U). Statistical analysis of the data on a sample of 225 data showed that the pH in the Productive Solution and the content of uranium are statistically significant and the correlation was 0.327. However, the mutual influence is not sharply expressed, which is connected with the indirect relationship of indicators. In contrast, for example, the relationship between the ORP of the solution and the content of ferric iron.

Table 2. Descriptive statistics for the block

	Mean	Standard deviation	N
H	2,1003	,05355	225
H	13,7018	1,38099	225

This table 2 is based on a statistical analysis of production fluid data during 2021

Table 3. Correlation (statisctics) of uranium content and pH values in the Productive Solution
**. The correlation is significant at the 0.01 level (two-tailed)

		pH	U
pH	Pearson correlation	1	0,327**
	N	225	225
U	Pearson correlation	,327**	1
	N	225	225

It follows from this analysis that there is a relationship between pH and U, but it is not very pronounced and the effect of pH on U is indirect

Table 4. Correlation of technological indicators of PS at block
*. The correlation is significant at the 0.05 level (two-tailed)

		pH	U	RP	Fe2+	Fe3+
PpH	Pearson correlation	1	,892*	-,591	,355	-,581
	N	5	5	5	5	5
U	Pearson correlation	,892*	1	-,704	,437	-,597
	N	5	5	5	5	5
RP	Pearson correlation	-,591	-,704	1	-,946*	,925*
	N	5	5	5	5	5
Fe2+	Pearson correlation	,355	,437	-,946*	1	-,899*
	N	5	5	5	5	5
Fe3+	Pearson correlation	-,581	-,597	,925*	-,899*	1
	N	5	5	5	5	5

Due to the small number of samples, the data are less statistically significant but give a general idea of the relationship between the parameters.

From these data, it should be noted a strong relationship between the uranium content and pH in the productive solution (correlation coefficient 0.892), as well as a strong relationship between the uranium content and RP (correlation coefficient 0.7) and a relatively high relationship with the content of ferric iron in the productive solution. As expected, there is a very high correlation between the content of ferric iron and the RP of the solution (correlation coefficient 0.925), which confirms the influence of a strong oxidizing agent (Fe3+) on the RP of the solution.

Figure 3 shows the data on changes in the metal content in the productive solution during 2021 during testing. The arrows mark the start of the acid supply and the end of the acid supply. It should be noted that a change in the composition of the leaching solution affects the composition of the productive solution with a delay of 20-30 days.

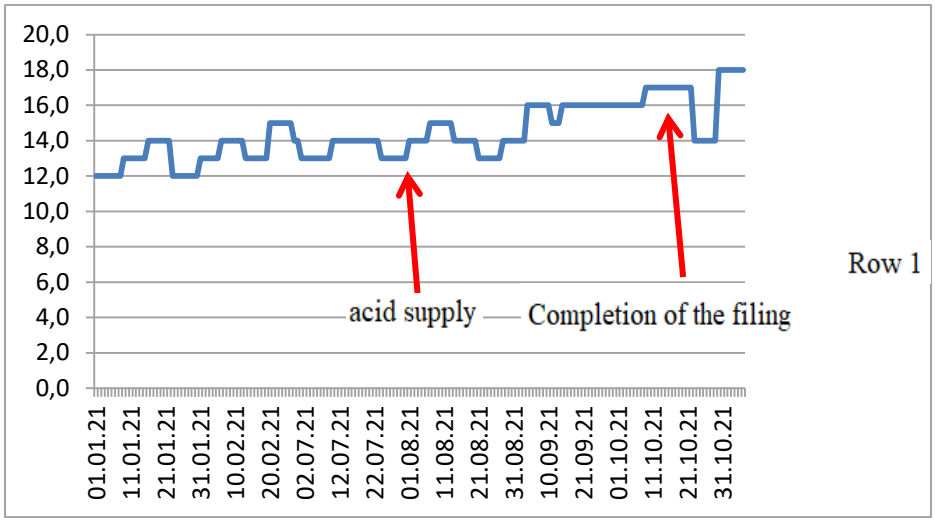

Figure 2. Change in the content of uranium in the Productive Solution at the block in the period from January to October 2021 (arrows indicate the period of supply of sulfuric acid - from 07/27/2021 to 10/15/2021)

Since the beginning of the year, the uranium content at block 62 has risen from 12 to 18 mg/l (40%)

DISCUSSION

The problem of increased production costs with a relatively high iron content required innovative approaches to reduce production costs. A chemical oxidizer (hydrogen peroxide) is successfully used, and its use is constrained by the high cost of chemicals. An alternative option is bacterial iron oxidation, where the final oxidizer is air oxygen, and bacteria act as a catalyst for the process. Laboratory studies have shown the applicability of bacterial iron oxidation to enhance the redox process of the solution and convert divalent iron to trivalent for existing mine leaching dissolutions. The problem remained open as to how bacterial iron oxidation would affect the uranium content in the productive solution.

The main problem in implementing a project on this scale is to establish a link between the operation of bacterial iron oxidation (BOI) plants and the increase in the content of uranium in the productive solution (Bektay et al. 2018). Modeling complex processes occurring in ore-bearing layer is complicated by the difference of material composition of ore-bearing layer and the composition changes as the flow of solution through the ore layer at 20-35 m at a depth of 120m (some another fields more than 700 m). Analysis of the results of using hydrogen peroxide (a chemical oxidizer) at the this mine allowed us to put forward a number of propositions that the activated leaching solution after bacterial oxidation of iron in bioreactors will affect the uranium content in the flushing liquid. In this situation, only direct tests on a separate unit allow us to understand and study the effect of bacterial iron oxidation on the uranium content in the production solution and determine the prospects for this technology.

The conditions under which bacterial iron oxidation occurs correspond to the conditions of underground in-situ recovery of uranium in terms of the content of sulfuric acid in the solution (from 3 g/l to 25 g/l), pH (1.5-2.5), redox process (360mv and higher), temperature and other technological conditions.

Studies were conducted on one of the blocks of a uranium deposit with industrial volumes of leaching dissolution flow. Studies have shown the effect of iron oxidation by *A. ferrooxidans* strains in flow bioreactors on the uranium content in the productive solution, despite the complex material composition of the ore body. Averaged indicators over the course of the year for the content of uranium in the productive solution for the block confirmed this effect. Tests were carried out in difficult natural conditions, the air temperature in winter reached minus 40^0C.

The Redox of the solution in bioreactors rose from 360 mV to 430-450 mV in the flow mode after passing the leaching solution through bioreactors. The content of trivalent iron increased from 0.1 g/l to 1.5 g/l and higher. The process of bacterial oxidation of iron in the solution took place at a solution temperature of 10-14^0C (the optimal is 25-35^0C), which eliminated the energy costs of heating the solution. The data obtained allowed us to determine several options for the industrial implementation of the technology at the mine. Operating costs when using flow bioreactors are 6-8 times lower than when using chemical oxidants (hydrogen peroxide).

Based on the conducted tests, it was done additional studies with the addition of "free" sulphuric acid, which improved the performance of bioreactors on leaching dissolutions and increased content of U in productive solution on 40 %. Influence of additional sulfuric acid can be explained by two reactions: (2) - acid need for this reaction and (4) – additional acid can dissolve iron hydroxides, which can block access to uranium minerals.

CONCLUSIONS

Increasing the Redox potential of leaching solutions up to 420-440 mV (with RP of leaching solution 360 mV), which ensured an increase in Productive Solution by 20% without adding of sulfur acid. The increase in the content of uranium in the Productive Solution at block was 40% with additional sulfuric acid 2 g/l. There was an increase in the content of ferric iron in leaching solutions due to bacterial oxidation of iron.

Industrial tests have confirmed the potential of this technology, as well as data obtained in the laboratory. As a result of studying the effect of BOI technology with the addition of sulfuric acid at one of the block (after-leaching stage) and control blocks, it was shown that the addition of sulfuric acid and the use of BOI technology increases the performance of productive solutions. The addition of sulfuric acid on other blocks did not show a significant increase in the uranium content in the productive solution.

Regression analysis of the data revealed statistically significant relationships between technological indicators in the Active Leaching Solution and in the Productive Solution, between RP and ferric iron content at a correlation level of 0.9.

Analysis of the data shows that the use of BOI technology can increase the depth of uranium extraction from the designed 85% to 95% and more. As a result of the work carried out, two patents for inventions and one patent for a utility model were obtained.

REFERENCES

Barrett J., Hughes M., Karavaiko G., Spencer P. Metal extraction by bacterial oxidation ofMineral. / Ellis Harwood. 1993. P. 127–134

Bektay E. K., Turysbekova G. S., Meretukov M. E., Bektayev M. E., '' Natural nanoparticles and nanostructures'', Almaty, KazNRTU, 2018, - 600 p.

Bektay E. K., Turysbekova G. S., Altunbek A.D., Shiderin B.N., '' Geochemistry of uran»'', Almaty, KazNRTU, 2020, - 243 p.

Benedetto J., de Almeida S., Gomes H., Vazoller R. Monitoring of sulfate-reducing bacteria inacid water from uranium mines. // Miner. Eng. 2005. V. 18. P. 1341–1343

Blais J., Tyagi R., Meunier N., Auclair J. The production of extracellular appendages duringbacterial colonization of elemental sulphur. // Proc. Biochem. 1994. V. 29. P. 475–482

Brand, H. (2001). Biotechnology. In. H.J. Rehm & G. Reed (Eds.), (pp 134- 152). Wiley.

Brierley J. Thermophilic iron-oxidizing bacteria found in copper leaching dumps. // Appl. Environ. Microbiol. 1978. V. 36. P. 523–525

Brierley J., Norris P., Kelly D., LeRoux N.Characteristics of a moderately thermophilic and acidophilic ironoxidizing *Thiobacillus*. // Eur. J. Appl. Microbiol. 1978. P. 291–299

Brierley C., Briggs A. Selection and sizing of biooxidation equipment and circuits. / Mineralprocessing plant design, practice and control. Ed. A. Mular, D. Halbe, D. Barret. / SME. 2002. P. 1540–1568

Bryner L., Beck J., Davis D., Wilson D. (1954). Microorganisms in leaching sulfide minerals. *Industrial Engineering and Chemistry,* 46, 2587–2592.

Campbell K., Gallegos T., Landa E. Biogeochemical aspects of uranium mineralization, mining,milling, and remediation. // Appl. Geochem. 2015. V. 57. P. 206–235

Cerda J. Gonzalez S., Rios J., Quintana T. Uranium concentrates bioproduction in Spain: a case study. // FEMS Microbiol. Rev. 1993. V. 11. P. 253–260

Colmer A., Temple K., and Hinkle M. (1950). An ironoxidizing bacterium from the acid drainage of some bituminous coal mines. *Journal of Bacteriology*, 59, 317–328.

Dwivedy K., Mathur A. Bioleaching – our experience. // Hydrometallurgy. 1995. V. 38. P. 99–109.

Garcia Junior O. Bacterial leaching of uranium ore from Figueira – PR, Brazil, at laboratory and pilot scale. // FEMS Microbiol. Rev. 1993. V. 11. P. 237–242.

Guay R., Silver M., Torma E. Microbiological leaching of a low-grade uranium ore by *Thiobacillus ferrooxidans*. // Appl. Microbiol. Biotechnol. 1976. V. 3. P. 157–167

Hamidian, H., Rezai, B., Milani S. et al. Microbial leaching of uranium ore. // Asian J. Chem. 2009.V. 21. P. 5808–5820

Harrison, V., Gow, W., Ivarson, K. (1966). Leaching of uranium from Elliot Lake ore in the presence of Bacteria. *Can. Miner*, 87, 64-67.

Holmes D. Biotechnology in the mining and metal processing Industries: challenges and opportunities. // Miner. Metall. Proc. 1988. V. 5. P. 49–56

Jianguo Z., Shaoqing C., Sun R., Jing Q. Analysis and evaluation of water coming from severaluranium processing areas, treatment of liquid effluent from uranium mines and mills. / Report ofa coordinated research project 1996–2000. // IAEA-1419. Vienna. 2004. P. 95–105

Kawatra S., Natarajan K. Mineral biotechnology: microbial aspects of mineral beneficiation, metal extraction and environmental control. / SME. 2001. P. 101–119

McCready R., Gould W. Bioleaching of uranium. / Microbial mineral recovery. Ed. H. Ehrlich,C. Brierley. / McGraw-Hill. N. Y. 1990. P. 107–126.

Munoz J., Gonzalez F., Blazquez M., Ballester A. A study of the bioleaching of a Spanish uranium ore. Part I: A review of the bacterial leaching in the treatment of uranium ores. // Hydrometallurgy. 1995. V. 38. P. 39–57

Polkin, S.I., Adamov, E.V., Panin, V.V. (1982). Technology of bacterial leaching of non-ferrous and rare metals*. M. Nedra, 288.*

Pronk J., de Bruyn J., Bos P., Kuenen J. Anaerobic growth of *Thiobacillus ferrooxidans*. // Appl.Environ. Microbiol. 1992. V. 58. P. 2227–2230

Rawlings D. Pure Appl. Chem. 2004. V. 76. P. 847–859

Rawlings D. Characteristics and adaptability of iron-and sulfur-oxidizing microorganismsusedfor the recovery of metals from minerals and their concentrates. // Microbial Cell Factories.2005.V. 4. 15 p.

Schippers A., Hallmann R., Wentzien S. Microbial diversity in uranium mine waste heaps. //Appl. Environ. Microbiol. 1995. V. 61. P. 2930–2935

Tuovinen O., Bhatti T. Microbiological leaching of uranium ores. // Miner. Metall. Proc. 1999.V. 16. P. 51–60

Turysbekova G.S. «BioGeotechnology methods for leaching “in situ”».UNECE - 10th Session of Expert Gorup in resource Management, Paldes Nations, Geneva. https://www.unece.org/fileadmin/DAM/energy/se/pp/unfc_egrm/egrm.10_apr2019/09b_Turysbekova_Gaukhar.pdf

Turysbekova G. S., Bektay E. K., Meretukov M. E., Bektayev M. E., ''Gidrometalurgy of uran'', Almaty, KazNRTU, 2020, - 243 p.

Twardowska I. The role of *Thiobacillus ferrooxidans* in pyrite oxidation in colliery spoil tips.I: Model investigations. // Acta Microbiol. Pol. 1986. V. 35. P. 291–304

Twardowska I. The role of *Thiobacillus ferrooxidans* in pyrite oxidation in colliery spoiltyps. II: Investigation of samples taken from spoil tips. // Acta Microbiol. Pol. 1987. V. 36. P.101–107

Watling H. Review of biohydrometallurgical metals extraction from polymetallic mineral resources. // Minerals. 2015. V. 5. N 1. P. 1–60

INTEGRATION OF RENEWABLE ENERGY IN THE PRODUCTION SCHEDULING PROBLEM USING GRAVITATIONAL SEARCH ALGORITHM

K. Tolouei [1], E. Moosavi [1, 2*]

[1] *Islamic Azad University, Department of Petroleum and Mining Engineering*
[2] *Islamic Azad University, Research Center for Modeling and Optimization in Science and Engineering*
([*] *Corresponding author: Se.Moosavi@yahoo.com*; *Se_Moosavi@azad.ac.ir)*

ABSTRACT

The mining industry has traditionally relied on conventional fossil-based fuel sources to meet its growing energy demand. The industry is now tasked with responding to the challenges of increasing fuel prices while commodity prices tighten, resulting in ever-narrowing operating margins and increased opposition from communities to new conventional energy sources. So far, research about such decision making on the use of renewable energy in production scheduling (PS) problem for open pit mining operation is underdeveloped. Due to the conflicting nature of economic and environmental objectives, the PS becomes a multi-objective problem. In this paper, a multi-objective gravitational search algorithm is used to provide Pareto optimal solutions which present the possible tradeoff between the cost and environmental objectives of PS problem. To solve the problem, weighted sum method is applied to convert multi-objective optimization to scalar optimization. The numerical results demonstrate the effectiveness of the proposed approach in solving multi-objective PS problem.

Keywords: Renewable energy, multi-objective, production scheduling, gravitational search algorithm.

INTRODUCTION

The mining industry has traditionally relied on conventional fossil-based fuel sources (diesel, oil, coal, and natural gas) to meet its growing energy demand. The industry is now tasked with responding to the challenges of increasing fuel prices while commodity prices tighten, resulting in ever-narrowing operating margins and increased opposition from communities to new conventional energy sources. The mining sector is expanding into new and often remote locations as a response to increasing demand from growing emerging markets. This often means having to deal with unreliable power supply from the grid and uncertain power prices. In most instances, grid-connected electricity needs to be supplemented with on-site generation, typically large-scale diesel generation, resulting in a dependency on diesel fuel. The more remote the mine, the more likely off-grid power solutions are required.

The sector is experiencing volatility in commodity prices and rising fossil fuel prices, placing margins under pressure. With global demand for energy set to increase 36% by 2035, the industry faces greater energy price increases and volatility. Managing costs sustainably is a priority for the sector. The mining sector is facing growing demand from governments, customers, communities and other key stakeholders to operate in a sustainable manner. Doing so has a growing influence on the mining industry's "social license" to operate (Judd, 2013).

Site-appropriate renewable energy solutions provide cost-competitive energy while delivering greater energy supply reliability and consistency. Reliable access to cost-efficient energy sources is a strategic imperative for mining companies. It is essential to their bottom lines and increasingly, their licenses to operate. In parallel, the sector is challenged with meeting the growing demand for mineral

resources often located in countries and sites where the supply of energy is not always available, reliable or, cost-effective.

Many of the world's largest mining companies are evaluating greater use of renewable energy plants (a trend set to intensify rapidly) as part of a broader strategy to lock in long-term fixed electricity prices and availability while minimizing exposure to regulatory changes, market pricing, and external fuels.

The main issue of this paper on the penetration of renewable energy into the production scheduling problem has been raised in different studies. This issue attracts attention from both scientific experts and industrial decision-makers. Mining and metal processing are very energy-intensive processes. Moreover, costs for traditional energy sources increase year by year; European mining companies are looking for new solutions for the substitution of fossil energy sources for renewables. The key point is that the costs of RE generation, grid connection and renewable energy integration system and software for implementation to the mining sector deployment are equivalent to those fossil energy sources. However, the implementation of renewable energy for mining needs still has many constraints in European countries.

Renewable Energy Investment in The Mining Industry

The European Union has increasing tendencies for development of renewable energy. It confirms by renewable energy development data and the National Action Plan until 2020 by 20%, 2040 by 40%, and 2050 by 80%. Taking in consideration Germany sample, the share of renewables in final energy consumption has risen steadily in the past decade to a current 12%. In the production of electricity of regenerative share of over 20% is already relatively high. Nevertheless, the electricity is still responsible for more than 40% of Germany's total CO2 emissions today. Therefore, decarbonizing the electricity sector for climate protection reasons has important significance. On the one hand, the mining industry is going to be less attractive in the modern society, who changes of the industrial priorities in favor of sustainable companies. Therefore, mining companies is searching of more sustainable way of production, and fulfill reorientation for renewable energy. In addition, the renewable energy becomes economically attractive year by year, thus motivating miners penetrate of renewable energy instead of fossil one (Judd, 2013).

The transformation of the mining sector is driven by a number of strong converging trends, including:

1. Energy security concerns,
2. A recent history in most countries of rising and volatile energy prices, coupled with a consensus that such trends will continue over the medium-to-long term,
3. The shift to a resource-efficient and low-carbon economy that will ensure community acceptance.

In response, the international mining sector is deploying innovative energy-saving strategies and making substantial industry-wide direct investments into renewable energy infrastructure. At the heart of recent innovations in corporate mining energy strategies lie the construction and acquisition of renewable energy-generating assets, on- and off-site, and the direct contracting for renewable energy through power purchase agreements. Renewable energy plants can be developed, funded, built and operated by third-party developers as captive plants, with the mine committing to purchase the generated electricity at a fixed price over a certain period (see Fig. 1).

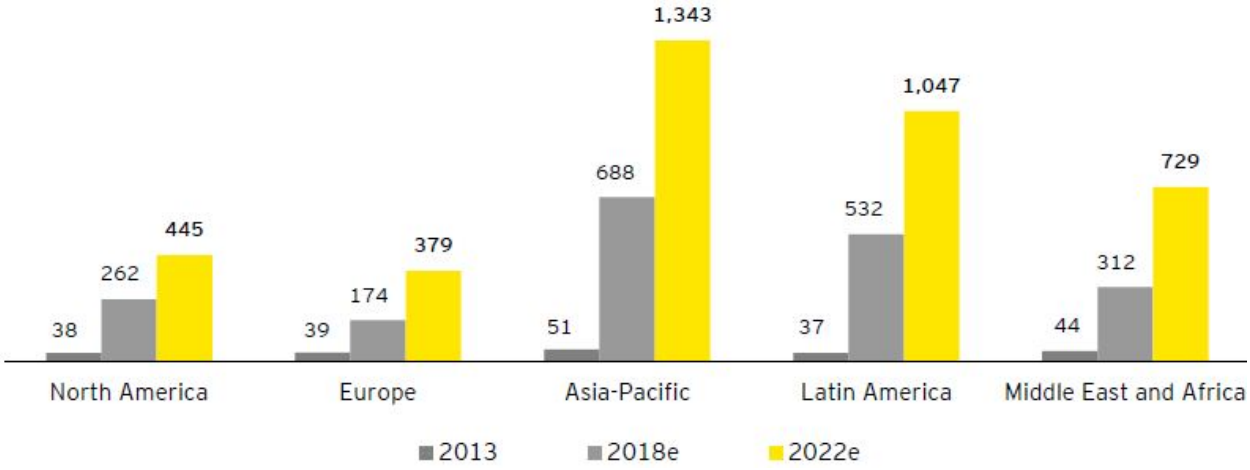

Figure 1. Renewable energy investment in the mining industry

The mining sector derives most of its energy from diesel (41%), natural gas (33%), and grid electricity (22%), with the remainder supplied by a mixture of other refined fuels, coal, LPG, renewables, and biofuels. The percentage contribution from diesel has fallen from 49% to 41% over the last decade and been largely replaced by natural gas and grid electricity, as infrastructure develops and oil prices continue to show volatility (Judd, 2013).

Mining energy intensity – the energy required per tonne of product – is a function of definitions, location, mining type, and processing type. Average energy intensity is estimated at 50.5 kWh/tonne for coal, 10.7 kWh/ tonne for minerals, and 54.5 kWh/tonne for metals, with the majority consumed in diesel equipment and comminution operations. The energy intensity in metals, however, ranges from 13 kWh/tonne for bauxite to 210 kWh/tonne for gold, due largely to differences in on-site beneficiation operations. Energy for metals with low on-site beneficiation, such as bauxite and iron ore, is predominately consumed as diesel for plant involved in extraction and transport. Energy for metals with high on-site site beneficiation, such as copper and gold, is predominantly consumed as electricity (see Fig. 2).

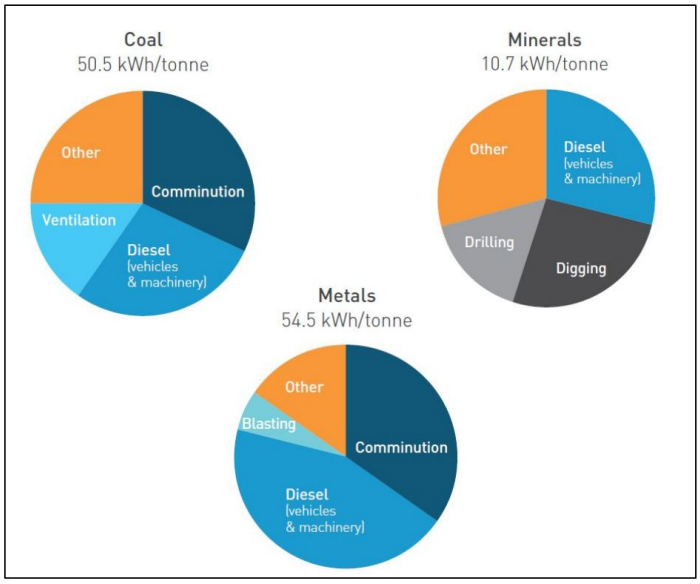

Figure 2. The estimated mining energy intensity and three most energy intensive operations for coal, metals, and minerals.

Integration of Renewable Energy in The Production Planning Problem

Major real-world problems utilize the optimization of several objectives, which are often conflicting in nature. A general, multi-objective optimization problem with *nm* decision variable, *mo* objectives and several equality and inequality constraints can be formulated as follows:

$$Min\ Z = (Z_1, Z_2, \dots, Z_{mo}) \tag{1}$$

Subject to:

$$g_j(x),\ \ j = 1, 2, 3, \dots, K \tag{2}$$

$$h_k(x),\ \ k = 1, 2, 3, \dots, L \tag{3}$$

Where, *K* and *L* are number of equality and inequality constraints respectively. $x = (x_1, x_2, \dots, x_{nm}) \in X$ is the decision vector and *X* is the parameter space; $y = (y_1, y_2, \dots, y_{mo}) \in Y$ is the objective vector and *Y* is the objective space. The set of all Pareto-optimal solutions in the decision variable space is called as Pareto optimal set (Abido 2003, 2006). The corresponding set of objective vector is called as Pareto-optimal front or optimal trade-off solution.

Gravitational Search Algorithm

The GSA, a new optimization algorithm based on the law of gravity, was introduced by Rashedi et al. (Roy 2013) in (2009). In the proposed algorithm, agents are considered as objects and their performance is measured by their masses. Masses of the agents are directly proportional to their fitness function. During each iteration, masses attract each other due to gravitational force of attraction acting on them and these forces causes a global movement of all agents toward the agents with heavier masses. A heavier mass means a more efficient agent. Suppose the system with *N* agents, the position of *i*th agent is defined as:

$$Y_i = (y_i^1, y_i^2, \dots, y_i^k, \dots y_i^\tau) \quad \forall i \in N \tag{4}$$

Where, y_i^k is the position of *i*th agent in the *k*th dimension, *τ* is the dimension of search space. The gravitational force acting on *i*th agent due to *j*th agent at *t*th iteration is given as:

$$F_{ij}^k(t) = G(t) \times \left(\frac{M_j(t) \times M_i(t)}{ED_{ij}(t) + \varepsilon}\right) \times (y_j^k(t) - y_i^k(t)) \tag{5}$$

Where, ε is a very small constant, $ED_{ij}(t)$ is the Euclidian distance between the *i*th agent and the *j*th agents which is defined as:

$$ED_{ij} = \left\| y_i(t), y_j(t) \right\|_2 \tag{6}$$

G(t) is the gravitational constant at time *t*, which is initialized at the beginning and reduces with time to control the search accuracy and is given by:

$$G(t) = G_o \times e^{-\alpha t / Iter_{\max}} \tag{7}$$

Where, G_o is initial value of gravitational constant, *α* is constant term and $Iter_{max}$ (=100) is the maximum number of iterations. The total force acting on the *i*th agent is given by:

$$F_i^k(t) = \sum_{\substack{j=1 \\ j \neq i}}^{Kbest} rand_j \times F_{ij}^k(t) \tag{8}$$

number in interval [0,1], *Kbest* is the set of *l* number of agents with heavier masses and best fitness value, and is evaluated in such a way that it decreases linearly with time and at last iteration, its value becomes 2 % of the initial number of agents. According to Newton's law of motion, the acceleration of the *i*th agent at the *t*th iteration in *k*th direction is given as:

$$A_i^k(t) = \frac{F_i^k(t)}{M_i(t)} \tag{9}$$

$$M_i(t) = \frac{m_i(t)}{\sum_{j=1}^{N} m_j(t)} \quad and \quad m_i(t) = \frac{fit_i(t) - worst(t)}{worst(t) - best(t)} \tag{10}$$

Where, $fit_i(t)$ is the fitness value of *i*th agent at the *t*th iteration. The iterative best (*t*) and worst (*t*) values are given as:

$$best(t) = \min(fit_i(t)) \quad and \quad worst(t) = \max(fit_i(t)) \ \forall i \in N \tag{11}$$

The updated velocity and position of each agent in the next iteration are calculated as:

$$v_{ik}(t+1) = rand_i \times v_{ik}(t) + A_{ik}(t) \tag{12}$$

$$y_{ik}(t+1) = y_{ik}(t) + v_{ik}(t). \tag{13}$$

CONCLUSIONS

In this paper, gravitational search algorithm (GSA) is used to provide Pareto optimal solutions. The Pareto-optimal solutions present the possible trade-off between the cost and emission. To solve the problem, weighted sum method is applied to convert multi-objective optimization to scalar optimization. The proposed GSA is combined with pseudo-code operators to create new set of individuals from higher potential individuals and further refines them to provide near optimal solution. The feasibility and performance of the proposed approach is demonstrated on a test system. The results obtained using the proposed approach are encouraging and it is found that by efficiently utilizing the production scheduling considering renewable energy sources, the total operating cost and emission of the system can be reduced significantly. The intermittency of solar and wind power generations is not considered in this paper, however, this can be considered as different of wind and solar power generations scenarios.

REFERENCES

Abido, M.A. (2003). Environmental/economic power dispatch using multiobjective evolutionary algorithm. IEEE Trans Power Syst 18(4):1529–1537.

Abido, M.A. (2006). Multiobjective evolutionary algorithms for power dispatch problem. IEEE Trans Evol Comput 10(3):315–329.

Judd, E. (2013). Building a wind farm in arctic conditions: Rio Tinto's Diavik mine, Canadian Clean Energy Conferences, Renewables and Mining.

Judd, E. (2013). Renewable Energy & Mining, Renewables and Mining, accessed via renewablesandmining.com/blog/, 15 January 2014).

Judd, E. (2013). Solar PV for Codelco and Collahausi, Canadian Clean Energy Conferences, Renewables and Mining.

Roy, P.K. (2013). Solution of unit commitment problem using gravitational search algorithm. J Electr Power Energy Syst 53:85–94.

World Energy Outlook. (2013). OECD/IEA Power sector cumulative investment by type and region in the New Policies Scenario, 2013-2035.

INVESTIGATION OF ENRICHMENT OPPORTUNUTIES OF ESKISEHIR BEYLIKAHIR REGION BARITE AND FLUORITE WITH PHYSICAL METHODS

ESKİŞEHİR BEYLİKAHIR BÖLGESİ BARİT VE FLORİT'İN FİZİKSEL YÖNTEMLER İLE ZENGİNLEŞTİRME OLANAKLARININ ARAŞTIRILMASI

E. Baştürkcü [1,*], C. Şavran [1], A. E. Yüce [1], H. Topal [1]

[1] *İTÜ, Maden Fakültesi, Cevher Hazırlama Mühendisliği Bölümü*
*(*Corresponding Author: tanisali@itu.edu.tr)*

ABSTRACT

As it is known, many studies have been carried out on the beneficiation of rare earth elements containing barite and fluorite in Eskişehir Beylikahır region. When the results of the previous studies are investigated, it is seen that although partially successful results have been obtained, a full enrichment has not been achieved yet. In this study, the main aim was the investigation of barite-fluorite enrichment by gravity separation techniques after the separation of high content rare earth products. Primarily, mechanical attrition on the original sample was applied based on literature information. 15 minutes with a 75% solids ratio was determined as the optimum conditions. According to the chemical analysis results, it was observed that the rare earth element content increased at -38 µm, 85-90% of REEs accumulated and total rare earth oxides (REOs) content increased up to 10%. By this information, +38 µm materials were ground to the different sizes for gravity experiments. As a result of the test at -150+38 µm size fraction, barite was obtained with 85.6% content and 88.3 % recovery. On the other hand, CaF2 pre-concentrate containing 62.9% was obtained with a recovery of 90.8%. Research continues within the scope of the project, and the findings obtained at this stage will be evaluated to obtain optimum conditions for both barite and fluorite.

Keywords: Barite, fluorite, rare earth elements, Beylikahır

INTRODUCTION

Barite ($BaSO_4$) is the most common mineral of the Barium element. Barite is the heaviest of the non-metallic minerals. High density (4.45 gr/cm^3), less abrasiveness (Mohs hardness 3-3.5), chemical stability under high heat and pressure, low solubility in water and acids, lack of magnetic properties and affordable cost of barite have enabled its increasingly widespread use in a variety of industries. More than 80% of barite is used in drilling fluids (Afolayan et al., 2021). Paint, glass, construction, automotive, paper, plastic, pesticides, chemistry, and ceramic industries are the other important sectors that barite is used.

Turkey has a large number of barite deposits; however, the most important ones are concentrated in four regions which are Alanya-Gazipaşa, Konya-Isparta, Muş, and Kahramanmaraş. Apart from these, Giresun, Kocaeli, and Kütahya districts have also significant barite deposits. According to a study conducted by the United States Geological Survey, all resources of barite found on Earth are about 2 million tons, but the proven reserves of barite are about 740 million tons. The graph containing reserve distributions by country is given in Figure 1.

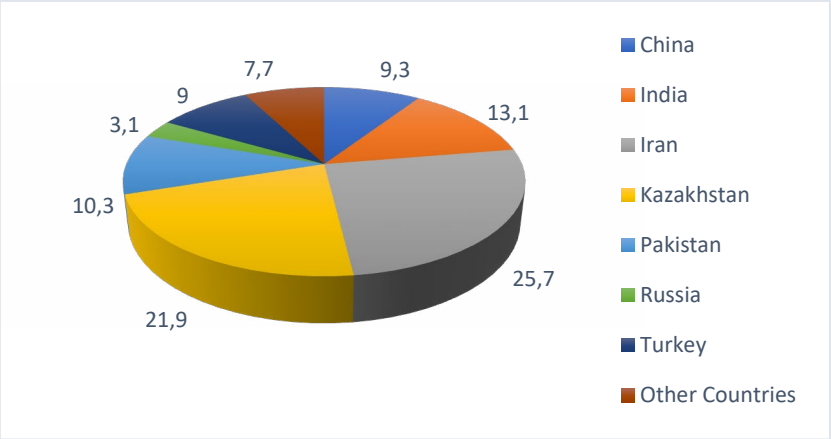

Figure 1. Distribution of Barite Reserves by Country in 2020, %

When annual production data by country is analyzed according to the same report, the annual production of the 11 countries with the largest global barite production in 2019 and 2020 is graphically shown in Figure 2.

China is at the top of the list, accounting for more than 30% of global barite production in 2019 and 2020, while Turkey is in 8th place with 2.82%. It is ranked 9th in 2020, with a production rate of 1.73% (USGS 2021).

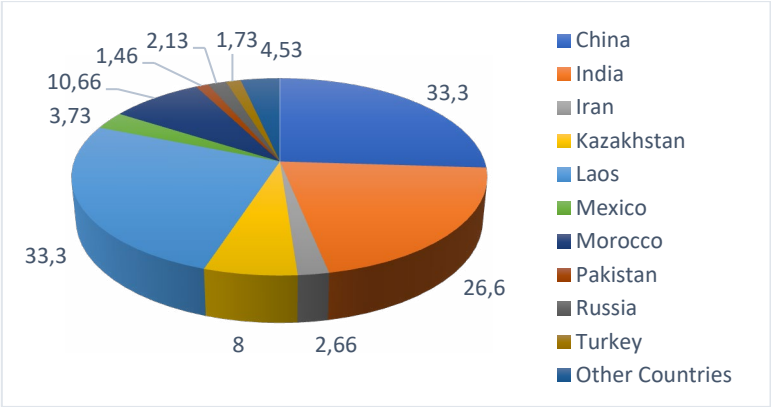

Figure 2. Distribution of World Barite Production by Country in 2020 (%)

Gravity and flotation are the most common processes for barite enrichment. The common gravity separation device is the jig for barite beneficiation if the particle liberation size is coarser (>2 mm). When the size becomes smaller, a shaking table and other gravity separators can be used.

Using Gravity enrichment methods such as jig, shaking table, and Multi Gravity Separator (MGS) have been investigated in the literature for barite concentration.

In the study conducted by Bhattacharyya and Singh (2011), the barite ore particle size was reduced below 74 µm. In the enrichment experiments carried out using MGS, the parameters such as pulp density, slope, washing water ratio and rotational speed of the feed were examined. According to the optimum data obtained as a result of the experiments, it was possible to concentrate $BASO_4$ with a recovery of about 53% and a content of more than 90%.

Fluorite (CaF2), is composed of 51.3 percent calcium and 48.7% fluorine when pure. It is a crystalline mineral with a Mohs hardness of 4, a specific gravity of 3.18 g/cm3, a melting point of 1330 oC, and a color range of purple, green, blue, yellow, white, pink, brown, bluish-black and it has transparent translucent. Fluorite has risen to the top of the world's strategic minerals list, and many countries are investigating its reserves and production. Fluorite is used in a variety of industries, including cement, glass, ceramics, metallurgy, refrigeration, aviation, medicinal, and chemical. Many countries regard fluorite to be a strategic resource due to the growing need for development in related industries (Gao, 2021). The primary areas of application are HF production, iron and steel, and aluminum. Fluorite content in these outputs is predicted to be between 85 and 95 percent. This ratio is expected to be at least 98% for technical quality HF production.

Considering the methods used in the enrichment of fluorite ore, physical enrichment methods are the first. Jigging, shaking tables and heavy media separators are the most preferred devices. The main reason for choosing jig and shaking table is that the density difference between fluorite and gangue minerals is too large. Yüce et al. (1992) employed a shaking table to conduct concentration experiments on fluorite and barite from the Beylikahır-Eskişehir complex ore, which included 34.7% CaF_2, 32.2% $BaSO_4$, 2.70% rare earth elements, and 0.11% ThO_2. For the -0.3 mm sample, shaking table tests were performed. A barite concentrate containing 85.5% $BaSO_4$ with a recovery of 55.8% and a fluorite pre-concentrate containing 63.2% CaF_2 with a recovery of 64.1% were obtained.

In addition, depending on the gangue mineral, methods such as calcination or flotation to liberate ore from calcite and getting fluorite concentrate are the alternatives (Güngör, 1967).

It is assumed that the fluorite resources found throughout the world are 5 billion tons (2021). It is also known that there are many fluorite deposits in Turkey. The main deposits are located at Eskişehir, Kırşehir, Sivas and Yozgat.

The production amounts of the 14 countries that ranked highest in the world fluorite production in 2019 and 2020 are shown in Table 1. China is the leading country in production, and Mexico is in second place.

In our country, the reserve studies are being carried out by MTA General Directorate in an area of 15 km^2 between Kızılcaören, Karkın and Okçu villages, 40 km northwest of Eskişehir province Sivrihisar district, with an average of 0.212% ThO_2, 37.44% CaF_2, 31.04% $BaSO_4$ and Beylikahır REE minerals reserve containing 3.14% rare earth oxide (MTA, 2017).

This deposit, which is the source of REE and Th in Eskişehir-Kızılcaören, has complex mineralization and contains fluorite, barite and bastnazite as valuable minerals. As a result of the reserve studies carried out between 1980-84, it was determined that 11.368.075 tons of Fluorite, 9.424.424 tons of Barite and 953.587 tons of REO (CeO_2, La_2O_3, Nd_2O_3) were found in Eskişehir Beylikahır region.

Table 1. Fluorite Production Data ($x10^3$ tons) for 2019-2020 by country

Countries	2019	2020
China	4300	4300
Mexico	1230	1200
Mongolia	718	720
South Africa	210	320
Vietnam	238	240
Spain	139	140
Pakistan	100	100

Canada	80	100
Morocco	88	88
Kazakhstan	88	77
Iran	55	55
Burma	53	53
Germany	50	50
Other Countries	107	110
Total	**7460**	**7600**

Pilot plant installation works have been started by ETI Maden for the concentrated production of Barite, Fluorite and REE minerals and R&D studies for increasing recovery are ongoing.

The possibilities of obtaining Fluorite and Barite minerals in high content in the Eskişehir-Beylikahir Region as saleable concentrates were investigated in this study, which would be carried out in light of data obtained from the literature.

MATERIAL & METHOD

The sample used in this study was taken from Eskişehir-Beylikova region. The ore contains barite, fluorite, rare earth minerals and also Th minerals basically.

For the sample preparation, after crushing & classification below 10 mm, as it is explained in literature, scrubbing was applied on sample. The scrubbing conditions were investigated. Time, and solids ratio were the parameters that affect the scrubbing efficiency. 60% and 75% solids ratios, 15 min-30 min scrubbing times were investigated and the recovery of scrubbing was controlled with particle size distribution.

In order to determine the beneficiation method for barite and fluorite by taking REE content into consideration, chemical analysis of the representative raw ore sample was performed on various particle size fractions. The analyses were carried out using the X-ray fluorescence method.

Table 2. Chemical composition of the run-of mine sample

CaF_2	$BaSO_4$	NTEO	Fe_2O_3	K_2O	MgO	MnO	SO3
36,1	32,4	6,2	3,1	0,4	0,7	0,8	6,3
Na_2O	P_2O_5	SiO_2	SrO	TiO_2	Al_2O_3	LOI	CaO
0,3	0,9	3,9	0,4	0,2	1,1	5,9	1,3

Regarding Table 2, the sample contained barite with a content of 32,4% and fluorite content was determined as 36.1%. The sample also contained 6,2 % rare earth oxides (REOs).

Separation of barite-fluorite was performed using Mozley table. Low REE containing fraction of +38 µm was subjected to these tests. In order to investigate the effect of particle size, sample was ground to -212, -150, -106 µm as a closed circuit controlling with 38 µm screen.

The experimental conditions of the gravitational tests using Mozley table are listed as follows:

- washing water : 2 L/min,
- amplitude : 8 mm,
- slope : 3^o
- particle size fraction : -212+38, -150+38, -106+38 µm.

The products obtained from the beneficiation tests were analyzed to evaluate the recovery. In order to explain the reason of losses for barite and fluorite, SEM (scanning electron microscope) visuals were discussed. These images were taken by MTA (General Directorate of Mineral Research and Exploration).

RESULTS & DISCUSSION

In this part of the study, scrubbing and gravity separation tests are presented. The performance of the scrubbing tests was evaluated regarding the particle size distributions of the products. Following the scrubbing application, Mozley table tests were performed on the particle size fractions of -212+38 µm, -150+38 µm, and -106+38 µm.

Scrubbing Tests

Application of scrubbing method provides not only a homogeneous particle size distribution (PSD) of the raw ore sample, but also it is a significant preparation/preconcentration stage for many types of ores. In our case, PSD of the raw ore sample was determined, while P_{80} was found as 1.8 mm. 16.8% of the material was accumulated in the -38 µm fraction (Figure 4).

When the sample was scrubbed for 15 min at a solids ratio of 75%, P_{80} size was decreased to 0.7 mm and the mass of -38 µm fraction increased to 35.2%. Although similar outcomes were obtained at 60% solids ratio for scrubbing times of 15 and 30 min, an application with higher solids ratio was found to be rational considering capacities at industrial scale.

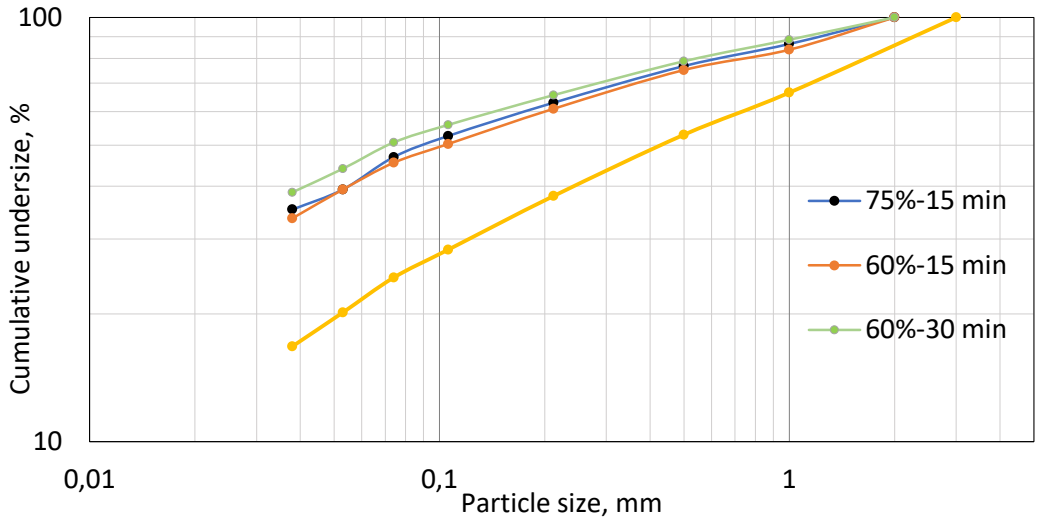

Figure 4. Particle size distribution of the raw ore sample and scrubbed products

Gravity Separation Tests

Following determination of the scrubbing conditions, gravitational separation was investigated on certain particle size fractions. The maximum sizes were arranged to -212, -150, and -106 µm. At these particle size fractions; many devices including shaking table and centrifugal separators may be utilized. However, Mozley table was used in the tests to make prediction, whether gravity separation worked. After removing the fine particle size fraction of -38 µm for each group, the Mozley table tests were carried out.

Regarding Table 3, 4, and 5, it was an attractive finding that 80-90% of the REEs were accumulated in the fine fraction. But nearly half of barite and fluorite were found in the coarser fractions. The results revealed that there can be a potential separation of barite and fluorite considering REEs.

- For the size fraction of -212+38 µm; it was determined that 80-85% of the REEs were accumulated in the fine fraction. The heavy product contained 80.3% $BaSO_4$ and 15.5% CaF_2. Also, the light product included 62.3% CaF_2.
- For the size fraction of -150+38 µm; 10-15% of the REEs were remained in the +38 µm fraction. A heavy product was obtained with 85.6% $BaSO_4$ and 9.7% CaF_2 grades.
- For the size fraction of -106+38 µm; quite similar results were achieved comparing with the results of -150+38 µm group.

As a result of gravity separation, it was concluded that -150+38 µm size fraction was determined as the optimum range for gravity separation for further studies. While 45.6% of barite was taken in the +38 µm fraction, 88.4% of it was obtained as heavy product. It was found out that 86% pure barite was achieved with fluorite impurity of 10%. It is known that 90-92% purity is required for potential usage in industries such as drilling mud, paint, and concrete aggregate. To reveal the reason of the insufficient enrichment, mineralogical analysis was performed.

Table 3. Metallurgical balance of the test conducted on -212+38 µm size fraction

-212+38 µm	Weight	Ce_2O_3		La_2O_3		Nd_2O_3		Pr_2O_3		$BaSO_4$		CaF_2	
Products	%	C, ppm	D, %	C, ppm	D, %	C, ppm	D, %	C, ppm	D, %	C, %	D, %	C, %	D, %
Heavy	20.8	12438	10.0	8594	7.6	1361.0	8.5	737.9	9.5	80.3	47.0	13.9	8.0
Light	26.9	7110	7.4	4797	5.5	852.3	6.9	430.0	7.1	8.2	6.2	56.1	41.8
-38 µm	52.2	40865	82.6	39175	86.9	5384.1	84.6	2584.8	83.4	31.9	46.8	34.6	50.1
Total	100.0	25853	100.0	23546	100.0	3325.5	100.0	1619.7	100.0	35.6	100.0	36.1	100.0

C: Content, D: Distribution

Table 4. Metallurgical balance of the test conducted on -150+38 µm size fraction

-150+38 µm	Weight	Ce_2O_3		La_2O_3		Nd_2O_3		Pr_2O_3		$BaSO_4$		CaF_2	
Products	%	C, ppm	D, %	C, ppm	D, %	C, ppm	D, %	C, ppm	D, %	C, %	D, %	C, %	D, %
Heavy	15.9	11364	6.8	8037	5.1	1271.2	5.9	695.1	6.7	85.6	40.3	8.7	3.8
Light	24.3	7665	7.0	5576	5.4	944.7	6.6	476.2	6.9	7.4	5.3	56.6	37.5
-38 µm	59.8	38441	86.2	37298	89.4	5065.8	87.5	2409.4	86.4	30.8	54.4	36.0	58.7
Total	100.0	26651	100.0	24930	100.0	3460.1	100.0	1666.6	100.0	33.9	100.0	36.7	100.0

Table 5. Metallurgical balance of the test conducted on -106+38 µm size fraction

-106+38 µm	Weight	Ce_2O_3		La_2O_3		Nd_2O_3		Pr_2O_3		$BaSO_4$		CaF_2	
Products	%	C, ppm	D, %	C, ppm	D, %	C, ppm	D, %	C, ppm	D, %	C, %	D, %	C, %	D, %
Heavy	15.5	10981	6.7	7820	5.1	1246.6	5.9	677.3	6.6	86.8	38.8	7.6	3.2
Light	22.3	7536	6.6	5471	5.1	1063.1	7.2	503.5	7.1	7.4	4.8	57.8	35.5
-38 µm	62.2	35376	86.7	34317	89.8	4602.2	86.9	2200.3	86.3	31.4	56.4	35.8	61.3

Total	100.0	25392	100.0	23783	100.0	3293.6	100.0	1586.2	100.0	34.6	100.0	36.3	100.0

Mineralogical Evaluation

A mineralogical investigation was done on the sample of -150+38 µm size fraction to observe particle liberation and possible mineral phase associations. In Figure 5, there are two images taken at a scale of 100 and 200 µm. It was found out that most of the barite and fluorite minerals were well liberated with relatively coarse grain sizes. However, associated particles were observed rarely.

Therefore, the reason for the insufficient enrichment of barite- fluorite could not attributed to only particle liberation, it could be necessary to apply additional gravitational forces. In this concept, the recovery and grades could be enhanced by application of centrifugal forces.

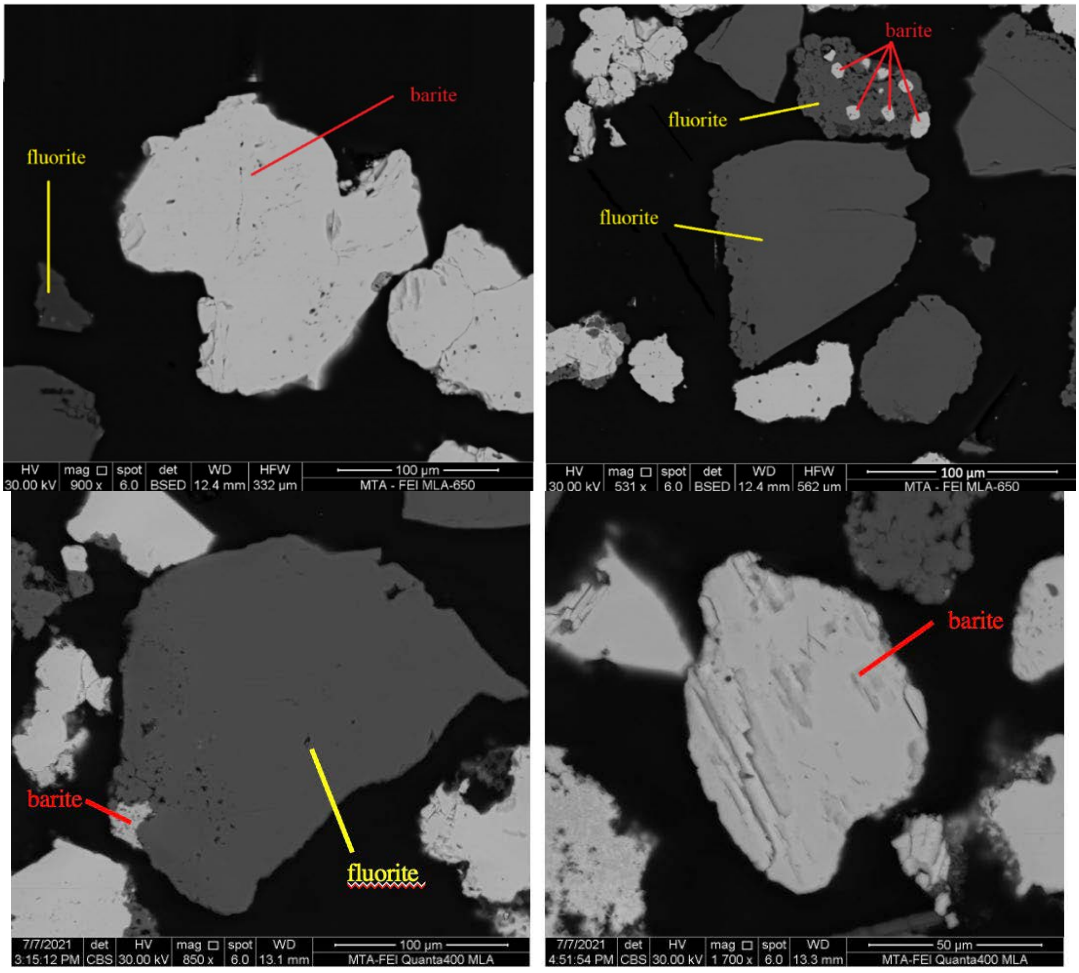

Figure 5. SEM-BSE images of -150+38 µm size fraction

CONCLUSION

Enrichment of fluorite and barite minerals of the Eskişehir-Beylikahir sample was aimed in this study. Due to the results of the preliminary experiments, general outcomes are listed as follows:

- The sample contained barite with a content of 32.4 % and fluorite content was determined as 36.1%. REE oxides were found as 6.2%.

- Following scrubbing the raw ore sample, P_{80} size was decreased from 1.8 mm to 0.7 mm. Also, the mass of -38 µm fraction increased from 16.8 to 35.2%.
- The optimum scrubbing conditions were determined as solids ratio of 75% and scrubbing time of 15 min.
- The scrubbed samples were divided into two fractions of -38 µm and +38 µm. While the finer fraction contained nearly 90% of the REEs, coarser fraction included 50-60% the barite and fluorite minerals.
- To predict the performance of gravity separation, Mozley table tests were carried out as a preliminary study. -150+38 µm size fraction was determined as the optimum.
- A heavy product was obtained with 85.6% $BaSO_4$ and 9.7% CaF_2 content.
- Since 90-92% purity is required for potential usage in drilling mud, paint, and concrete aggregate industries, improvement potential for the gravity separation was examined.
- Therefore, -150+38 µm size fraction was subjected to mineralogical analyses. According to the results, it was observed that most of the barite and fluorite particles were liberated enough.
- It is thought that gravitational force using conventional gravity units is not enough to separate barite and fluorite. Centrifugal separation would be suggested as a strong alternative and further tests are planned.

In conclusion, a preliminary flowsheet is established including a combination of scrubbing and gravity separation. While the particle size fraction of -38 µm is separated, +38 µm fraction was ground below 150 µm and classified as -150+38 µm. It is considered that when this group material is subjected to gravitational separation using centrifugal devices, it is strongly possible to separate barite and fluorite with high grade and recovery. The final evaluation using centrifugal gravitation techniques will be accomplished based on the ongoing project studies.

REFERENCES

Afolayan, D., Adetunji, A., Onwualu, A., Ogolo, Oghenerume Amankwah, R. (2021), Characterization of barite reserves in Nigeria for use as weighting agent in drilling fluid, Journal of Petroleum Exploration and Production, 11. 1-22. DOI: 10.1007/s13202-021-01164-8.

Bhattacharyya, P., Singh, R. (2011), Generation of Value Added Product by Beneficiation of Barite Waste, Conference Proceedings, *XII Internation Conference on Mineral Processing Technology MPT-2011*, India.

Gao, Z., Wang, C., Sun, W., Gao, Y., Kowalczuk, P. (2021), Froth flotation of fluorite: A review, Advances in Colloid and Interface Science, 290. 102382. DOI: 10.1016/j.cis.2021.102382.

Güngör, G. (1967), Düşük Tenörlü Fluorit Cevherinin Zenginleştirilmesi, *Bilimsel Madencilik Dergisi* , *6(2)*, 71-82, Retrieved from http://www.mining.org.tr/tr/pub/issue/32707/362858

MTA (2017). Dünya ve Türkiye'de Nadir Toprak Elementleri (NTE), Ankara.

U.S. Geological Survey, 2021, Mineral Commodity Summaries 2021, U.S., https://doi.org/10.3133/mcs2021.

Yüce, A.E., Doğan,M.Z., Önal,G., İpekoğlu,B.,(1992), The Beneficiation of Fluorite and Barite from Beylikahır-Eskişehir Complex Ore", *Aufbereitungs-Technik*, Nr:33, pp:274-281, 1992.

INVESTIGATION OF FRACTURE AND MECHANICAL PROPERTIES OF SEMI-CIRCULAR BENDING SHOTCRETE SPECIMENS USING 3D PRINTED MOLDS

C. Karataş Batan[1, *], M. Erkayaoğlu[1]

[1] *Middle East Technical University, Mining Engineering Department*
*(*Corresponding Author: cerenb@metu.edu.tr*)

ABSTRACT

Core samples can be considered as inherently available specimens for site investigation in rock engineering problems. The geometry of core samples is commonly beneficial for preparation of specimens for rock mechanics tests. However, the collection and preparation of rock samples also pose challenges for certain types of experiments, especially for fracture mechanics tests. The accuracy of fracture mechanics experiments is of great importance for the design of various applications. The preparation of these samples can be considered challenging due to the potential human errors during crack opening and flattening of the specimen surface. Available 3D printer technology can be useful in overcoming such difficulties. This study focuses on the preparation of Semi-Circular Bending (SCB) specimens for three-point bending in fracture tests. SCB sample molds were printed using 3D technology and samples were prepared by shotcrete mixture poured into the 3D printed molds. In this study, it is aimed to minimize sample preparation errors by using 3D printer technology. As a result, it was observed that the fracture and mechanical properties of the molded shotcrete by using 3D printer technology provided accurate results when compared to conventional sample preparation.

Keywords: Rock mechanics, 3D printer, fracture mechanics, molded shotcrete, Semi-Circular disc geometry

INTRODUCTION

Mining activities play a major role for developing countries according to primary energy generation and raw material supply. The increasing demand for energy resources of modern societies necessitate mining activities to be sustained. For these reasons, utilization of innovative technologies in the mining industry related to all stages of production including the engineering design studies performed prior to operation is essential.

Rock mechanics has an important role in tunneling activities and underground mining. Rock mass surrounding permanent or temporary structures in mining can be shafts, transportation galleries, production chambers, and other that might possess flaws and fractures. Improving the stability and maintaining the strength of surrounding rock is one of the main requirements of mining and construction projects. Support systems are designed and selected to meet this requirement where shotcrete is a major supporting unit for tunnel constructions, underground openings in mining applications and many other areas. The cracking of shotcrete is generally caused by a beam action. Furthermore, shrinkage of the shotcrete results in tensile loading that leads to the propagation of cracks. Cracks in the shotcrete pose a serious threat to the support system. Considering this phenomenon, the problem can be handled by performing valid fracture mechanics related experiments. Fracture mechanics experiments are of great importance in the realization of these activities. The accuracy of the fracture mechanics test results and the design criteria made according to these results ensure the continuity and reliability of mining and tunneling activities. The geometry of core samples is enabling rock sample preparation for fracture mechanics testing to be performed in laboratory

environment. However, the collection and preparation of rock samples also poses challenges for certain types of experiments. During the preparation of the samples required for these tests, both the creating flat surface stage and the errors caused by the person during the crack opening affect the test results. In this research, it is aimed to minimize these errors by using 3D printer technology in sample preparation and reduce time and costs related to sample preparation. The objective of this study is to investigate the fracture mechanism of shotcrete and to understand the crack behavior completely.

Available studies in the literature about this research field indicate that fracture properties, cracks and failure mechanisms of concrete have been investigated with different geometries by various researchers.

Griffith is one of the most important research in the field of fracture mechanics, as Kaplan (1961) discussed the Griffith crack theory of fracture strength. Tests on concrete beams were performed to determine the critical strain-energy-release rate. Fictitious crack analysis and crack growth in concrete (Hillerborg et al, 1976), expressing the fracture toughness of plain concrete through the specimen-size independent parameters (Nallathambi and Karihaloo, 1986), effective notch in three-point bend notched specimens used for the determination of the fracture toughness of plain concrete (Nallathambi and Karihaloo, 1988), the size effect on explaining cracks and failure mechanism in concrete and/or concrete structures (Bazant and Kazemi, 1990) and the peak load method for determining material fracture parameter (Tang, Ouyang and Shah, 1996) are some of the pioneering research studies focusing on fracture mechanism of concrete.

Jenq and Shah (1985) suggested a simple method to calculate size- independent fracture toughness parameter of concrete. The authors predicted the load crack mouth opening displacement on beam type concrete by using this constant K_{Ic} criterion.

Perdikaris et. al. (1986) studied four-point bending (SENB) method to investigate the effect of fatigue on fracture toughness of concrete. It was stated that the fracture toughness under fatigue shows an increasing trend with increasing crack length.

Wang et. al. (2010) developed a new test method for determining the fracture toughness of concrete materials. The method was defined as the spiral notch torsion test (SNTT) where the estimated K_{Ic} of the tested samples was found to be $MPa\sqrt{m}$.

Zhao et. al. (2020) examine the influence of the weight percentage of large aggregates with maximum size d_{max} on fracture toughness of concrete. Three-point bending specimens with different crack/depth ratios (0.1, 0.2, 0.3 and 0.4) were used in this study. The result of this study revealed that the peak load for the 3-p-b beams are affected by the amount of large aggregates with d_{max}.

This research aims to contribute to the current studies in rock mechanics literature by introducing the potential of 3D printing technology for sample preparation. In this context, it will also provide an opportunity to utilize available technology to improve the existing knowledge related to fracture mechanism of concrete.

NUMERICAL AND EXPERIMENTAL STUDY

Numerical and experimental work for three-point bending test specimens are covered within the scope of the methodology of this study. The numerical computation of stress intensity factor (SIF) in the models was performed in ABAQUS 2019. Semi-circular disk geometry (SCB) were modeled in three dimensional (3D) with ABAQUS. The numerical computation was completed in two-stages as before and after the experimental study. The first stage of the numerical computation was done to define loading configuration at the crack tip. To reach this aim, the unit load was applied to the model geometry. The

loading condition was defined for three different points whereas the second stage was completed after the experiments were performed. In this stage, fracture loads acquired from experimental work were applied to the numerical models that were created before. The mode I fracture toughness was computed for shotcrete specimens that were tested with the MTS 815 system that provides displacement-controlled loading.

The SCB specimen geometry modeled in 3D has a loading span length of S/R=0.50 The crack length was fixed as 10 mm resulting in a/R ratio of 0.20. The 100 mm diameter SCB geometry with 50 mm thicknesses (t/R=1) can be seen in Figure 1 illustrating the geometric details.

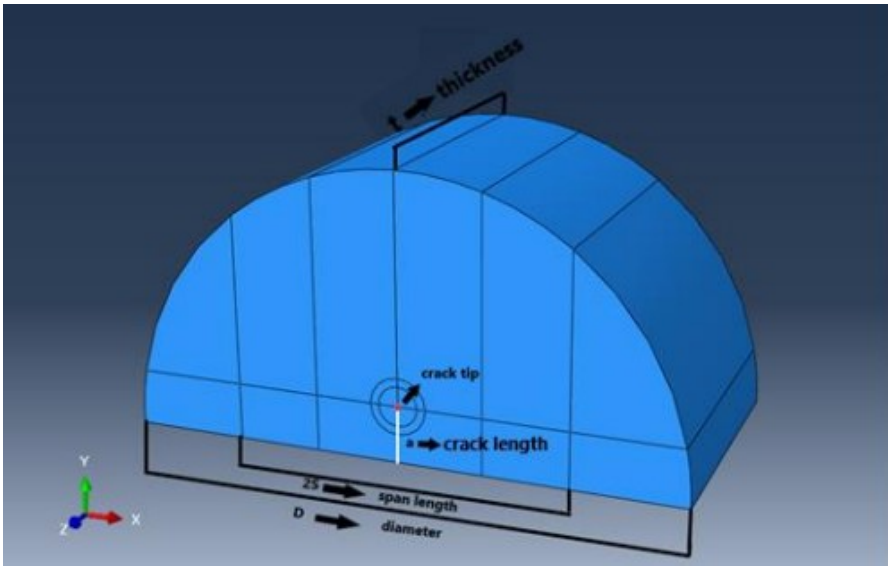

Figure 1. Undeformed and deformed shape of the SCB model geometry

The stress intensity factor (K_I) of SCB model geometry for mode I is calculated as 90.64 $Pa\sqrt{m}$. The dimensionless stress intensity factor (Y_I) of SCB model geometry for mode I is formulated by the following equations;

$$Y_I = \frac{K_I}{\sigma_0\sqrt{\pi a}} \quad (1)$$

$$\sigma_0 = \frac{P}{2Rt} \quad (2)$$

According to these formulas the dimensionless stress intensity factor (Y_I) of SCB is calculated as 2.56. The deformed shape and undeformed shape geometries are shown in Figure 2.

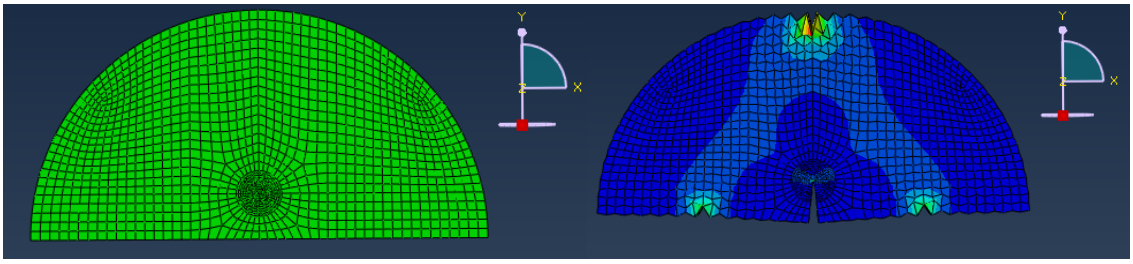

Figure 2. Undeformed and deformed shape of the SCB model geometry

Shotcrete molds were manufactured with a 3D printer to prepare samples in the desired size and geometry for experimental works. The ingredients of the mixture are 450 g cement, 225 g water, 4.5 g admixture (plasticizer) and 1664 g aggregates. The mixture of a 0.25 dm^3 volume was poured into the 3D molds after mixing with a Hobart N50 laboratory type mixer. Concrete sample was prepared as a shotcrete representation. The behavior of shotcrete is actually different due to the spray effect. The procedure to prepare the concrete samples can be summarized as follows; the aggregate and cement are mixed for 30 seconds at low speed which is followed by the addition of water and admixture into the mixer container. All materials are mixed first at low speed for 30 seconds and then at high speed for another 30 seconds. After the mixture was prepared, it was filled into the 3D molds and 7 days of time of was performed. Figure 3 shows a sample 3D mold of the SCB samples.

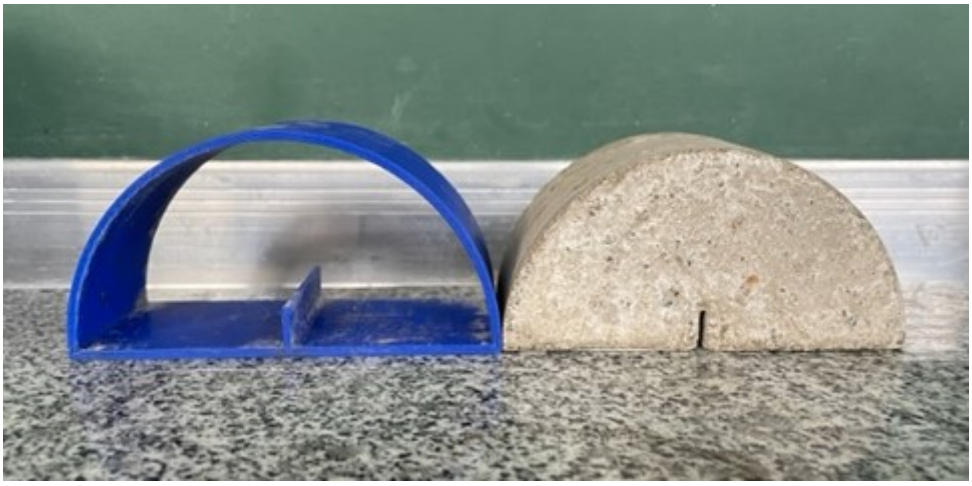

Figure 3. 3D mold of SCB and SCB sample

Static deformability tests were performed on shotcrete samples to predict and determine the mechanical behavior. The specimens were kept under load until failure to obtain the uniaxial compressive strengths (UCS), Elastic Modulus and Poisson's ratio values. The loading procedure was defined with a rate of 0.0005 mm/s. Figure 4 shows static deformability test configuration, samples before and after the test.

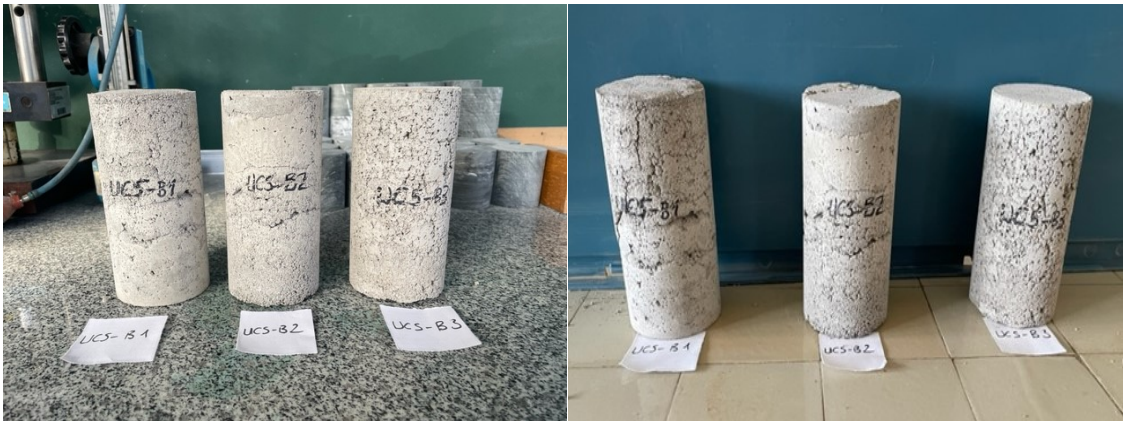

Figure 4. Static deformability test configuration, before and after test

The values of the uniaxial compressive strength, Elastic Modulus, and Poisson's ratio are listed in Table 1.

Table 1. Deformability test results

Specimen	Diameter (mm)	Length (mm)	Failure Load (kN)	Elastic Modulus (GPa)	Poisson's Ratio	Uniaxial Compressive Stress (MPa)
UCS-B1	72.16	154.82	21.23	3.16	0.24	5.21
UCS-B2	72.58	152.43	10.56	7.36	0.28	2.56
UCS-B3	72.43	152.18	22.22	2.96	0.25	5.51
Avg±Std. Dev.	72.39±0.21	153.14±1,46	18.07±6.47	4.49±2.48	0.26±0.02	4.43±1.63

Mode I fracture toughness tests were conducted on SCB test samples with 100 mm diameter and 50 mm span length. The ISRM suggested method states a range for SCB tests as 0.50 ≤S/R≤0.80 (ISRM, 2007). The thickness of the SCB samples was 50 mm and notch length were fixed at 10 mm. A two-stage loading procedure was defined to the test specimens with high rate at 0.0005 mm/s until the load limit detector is triggered. In the second loading stage, loading was applied with low rate as 0.0003 mm/s. The SCB specimens were tested with rollers that have 8 mm diameter under three-point bending condition to find the fracture toughness value for mode I. One of them was located at the upper surface of the specimen for loading purposes whereas the other two were located at the bottom surface of the specimen for supporting purposes. The specimens were coded in terms of the thickness, span length (S/R) and specimen number for SCB. The SCB specimen before, during, and after the fracture test can be seen in Figure 5.

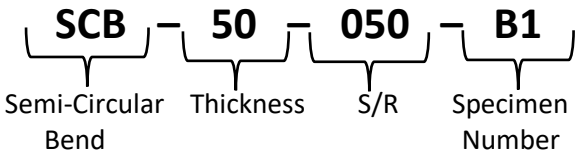

Figure 5. SCB sample before, during and after the test

The mode I fracture toughness (K_{Ic}) was calculated with Equation 3 and Equation 4. The critical load value was obtained from the load- displacement graph results of the fracture tests. Figure 6 shows load- displacement graph of the sample SCB-50-050-B1. According to the graph, load at fracture for sample 1 is 4.31 kN

$$\sigma_{cr} = P_{cr}/2Rt \quad (3)$$

$$K_{Ic} = Y_I \sigma_{cr} \sqrt{\pi a} \quad (4)$$

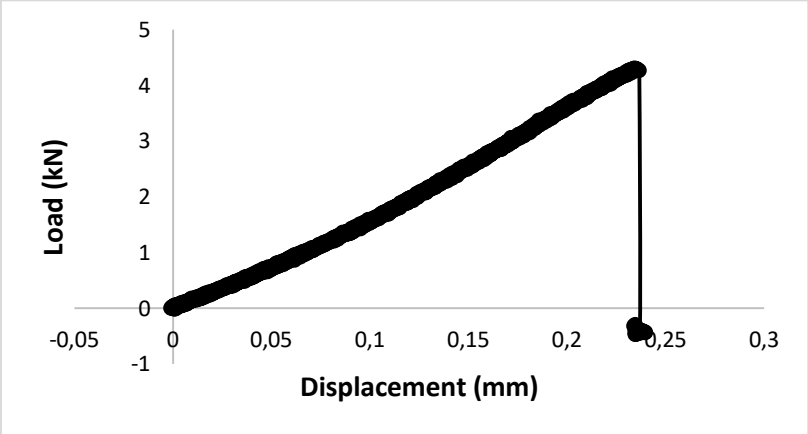

Figure 6. Load vs. displacement curve of SCB-50-050-B1

All fracture test results for SCB specimens with 50 mm thickness are summarized in Table 2.

Table 2. SCB fracture test results

Specimen Code	Fracture Load (kN)	Mode I Fracture Toughness (GPa)
SCB-50-050-B1	4.31	0.39
SCB-50-050-B2	6.76	0.61
SCB-50-050-B3	6.22	0.56
Avg±Std. Dev.	5.76±1.29	0.52±0.12

According to Table 2, mode I fracture toughness (K_{Ic}) of SCB specimen was found as 0.52±0.12 $MPa\sqrt{m}$.

In a study of Batan (2020), SCB tests were conducted on grey colored Ankara Gölbaşı andesite rock material to assign mode I fracture toughness (K_{Ic}). The fracture tests with SCB geometry that had 50 mm thickness were completed and the notch length was kept fixed as 10 mm for all SCB specimens. Numerical analyses were performed by ABAQUS finite element software to find mode I SIF. In the models, elastic properties of materials were taken as E= 12 GPa and υ = 0.15. The stress intensity factor (K_I) of SCB model geometry for mode I was calculated as 89.72 $Pa\sqrt{m}$. The dimensionless stress intensity factor (Y_I) of SCB model geometry for mode I was calculated as 2.53.

Table 3. SCB fracture test results for t=50 mm (Batan, 2020)

Specimen Code	Fracture Load (kN)	Mode I Fracture Toughness (GPa)
SCB-50-050-1	11.19	1.00
SCB-50-050-2	11.01	0.98
SCB-50-050-3	12.54	1.12
Avg±Std. Dev.	11.58±0.84	1.03±0.08

In this study, mode I fracture toughness (K_{Ic}) of SCB andesite specimen and SCB shotcrete sample were compared to determine internal structure and fracture behavior.

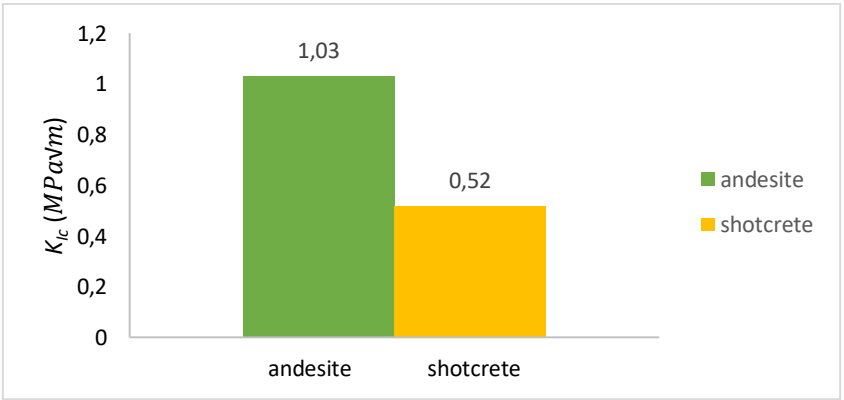

Figure 7. K_{Ic} values of SCB andesite sample and SCB shotcrete sample

As seen in Figure 7, the K_{Ic} measured by the SCB tests on shotcrete is about 50% lower than K_{Ic} measured by the SCB tests on andesite with 50 mm span length.

RESULTS AND DISCUSSION

In this study, the potential of using 3D printing technology was investigated to determine the fracture properties of concrete samples that were prepared by using molds. The shape and crack geometry of the shotcrete samples are achieved as nearly perfect with the help of the 3D printer technology. Therefore, more accurate test results were achieved with shorter preparation time than conventional sample preparation. Mode I fracture toughness (K_{Ic}) of SCB shotcrete specimen was found as 0.52±0.12 $MPa\sqrt{m}$. By comparing this value with the same diameter and span length andesite sample with K_{Ic} of 1.03±0.08 $MPa\sqrt{m}$, it can be concluded that the crack resistance under a specific loading condition of shotcrete specimen is lower than the andesite material. According to these results, rock samples and shotcrete samples have no similar internal structures as expected. As a conclusion, the mode I fracture toughness value (K_{Ic}) of SCB shotcrete specimen was assigned and further experimental studies will be performed to investigate the effects of the different notch angles and loading span on mode I fracture toughness of shotcrete with SCB method.

REFERENCES

Batan K., C. (2020). Effect of loading span on tensile mode fracture toughness for three-point bend specimen geometries. Unpublished thesis, Ankara.

Bazant, Z. P., & Kazemi, M. T. (1990). Determination of fracture energy, process zone longth and brittleness number from size effect, with application to rock and conerete. *International Journal of fracture*, *44*(2), 111-131.

Hillerborg, A., Modéer, M., & Petersson, P. E. (1976). Analysis of crack formation and crack growth in concrete by means of fracture mechanics and finite elements. *Cement and concrete research*, *6*(6), 773-781.

ISRM (2007) The complete ISRM suggested methods for rock characterization, testing and monitoring: 1974–2006. In: Ulusay R, Hudson JA (eds) Suggested methods prepared by the commission on testing methods. International Society for Rock Mechanics, Compilation Arranged by the ISRM Turkish National Group, Ankara, Turkey

Jenq, Y. S., & Shah, S. P. (1985). A fracture toughness criterion for concrete. *Engineering Fracture Mechanics*, *21*(5), 1055-1069.

Kaplan, M. F. (1961, November). Crack propagation and the fracture of concrete. In *Journal Proceedings* (Vol. 58, No. 11, pp. 591-610).

Karihaloo, B. L., & Nallathambi, P. (1989). An improved effective crack model for the determination of fracture toughness of concrete. *Cement and Concrete Research*, *19*(4), 603-610.

Kuruppu, M. D., & Chong, K. P. (2012). Fracture toughness testing of brittle materials using semi-circular bend (SCB) specimen. *Engineering Fracture Mechanics*, *91*, 133-150.

Nallathambi, P., & Karihaloo, B. L. (1986). Determination of specimen-size independent fracture toughness of plain concrete. *Magazine of Concrete Research*, *38*(135), 67-76.

Perdikaris, P. C., Calomino, A. M., & Chudnovsky, A. (1986). Effect of fatigue on fracture toughness of concrete. *Journal of engineering mechanics*, *112*(8), 776-791.

Tang, T., Ouyang, C., & Shah, S. P. (1996). Simple method for determining material fracture parameters from peak loads. *Materials Journal*, *93*(2), 147-157.

Yoncacı, S. (2019). Investıgatıon of fracture toughness on flattened brazilian disc type molded shotcrete specimens. PhD thesis, Ankara.

JEOSENTETİK MALZEMELERİN ÇEVREYE VE TOPLUMA SAĞLADIĞI KATKILAR

THE CONTRIBUTION OF GEOSYNTHETIC MATERIALS TO THE ENVIRONMENT AND SOCIETY

C. Ozan*

[1] *Yesti İnşaat ve Tic. Ltd. Şti.*
*(*celalettinozan@yestigroup.com)*

ÖZET

Yaşadığımız dünyada hammadde ve enerji ihtiyaçları günden güne artmaktadır. Enerji ve hammadde ihtiyaçlarının büyük bir kısmı doğal kaynaklardan sağlanmaktadır. Doğal kaynaklar, madencilik ile toplumun kullanımına sunulmaktadır. Madencilik faaliyetlerinde doğal topoğrafyada büyük değişikler olabilmektedir. Bu faaliyetlerin çevreye ve topluma etkisi kaçınılmazdır.

Madencilik faaliyetlerinin, çevre ve toplum üzerindeki etkisini teknik olarak korumak mümkündür. Modern yaklaşımlarla bu etkiler önlenebilir ya da en aza indirilebilir. Çevresel etkileri minimize etmek için günümüzde yaygın olarak jeosentetik malzemeler kullanılmaktadır.

Kullanım alanları oldukça geniş olan jeosentetik malzemeler, madencilik faaliyetlerin her aşamasında özellikle atık depolama tesisleri ve rehabilitasyon alanlarında kullanılmaktadır. Atıkların çevreye zarar vermeden bertarafını sağlamak üzere düzenli olarak depolanmasını, topoğrafyanın düzenlenmesini, farklı ürünler yetiştirilmesini, farklı ağaçlandırma yapılmasını sağlamaktadır. Bu ve buna benzer önlemler, madenciliğin çevre ve insan sağlığına olan negatif etkilerini azaltmakta yardımcı olmaktadır.

Bu bildiride, çevreye ve topluma minimum etkiyle madencilik faaliyetlerin yapılabilmesi konusunda bilgiler verilecektir.

Anahtar sözcükler: Madencilik, çevre, rehabilite, atık, jeosentetik, jeomembran

ABSTRACT

Raw materials and energy needs are increasing day by day in the world we live in. Most of the energy and raw material needs are sourced from natural sources. Natural resources are made available to the community through mining. There may be major changes in natural topography in mining activities. The environmental and society impact of these activities is inevitable.

It is technically possible to protect the impact of mining activities on the environment and society. With modern approaches, these effects can be prevented or minimized. Geosynthetic materials are widely used today to minimize environmental impacts.

Geosynthetic materials, which have a wide range of uses, are used especially in waste storage facilities and rehabilitation areas at every stage of mining activities. It ensures regular storage of wastes, arrangement of topography, cultivation of different products, different reforestation in order to ensure the disposal of wastes without harming the environment. These and similar measures helps reduce the negative effects of mining on the environment and human health.

In this statement, information will be given about the ability to carry out mining activities with minimal impact on the environment and society.

Keywords: Mining, environment, rehabilitation, waste, geosynthetics, geomembrane

GİRİŞ

Jeosentetikler, günümüzde daha çok inşaat sektöründe kullanılsa da, zamanla kullanım alanı çoğalmış ve son yıllarda özellikle madencilik sektöründe ilgi gören ürünler olmuştur.

1950'li yıllarda kullanılmaya başlanılan jeotekstiler ile toplumun ve çevrenin ihtiyaçlarını karşılamak amacıyla özellikle son 15 yılda farklı ürünler geliştirilmiştir. Jeotekstiller, jeogridler, jeomembranlar, jeonetler, jeokompozitler ve jeosentetik kil astarlar önde gelen jeosentetik malzemelerdir.

Jeosentetikler; zeminin birbirinden ayrılması, güçlendirme donatısı, drenaj sistemi, erozyon kontrolü, yalıtım uygulaması ve filtrasyon çözümü gibi farklı kullanım alanlarına sahiptir. Jeosentetik malzemeler tek tek ve/veya birlikte kullanılabilmesi ile şu avantajları sağlamaktadır; teknik üstünlük, yer kazanma, maliyetteki kazanımlar, inşaat süresini kısaltma, malzeme ve imalât kalite kontrolü, malzemede gelişim ve tedarik edilebilirlik ve özellikle çevresel duyarlılık…

Hazırlanan bildiri kapsamında geleneksel yöntemlere göre maliyetleri de düşürerek estetik çözümler sunabilen jeosentetiklerin çevreye ve topluma sağladığı avantajlar hakkında bilgiler aktarılacaktır.

JEOSENTETİK MALZEMELER

TS EN ISO (2015), jeosentetiği "*Geoteknik ve inşaat mühendisliği uygulamalarında toprak ve/veya diğer malzemelerle temasta olacak şekilde kullanılan levha, şerit ve üç boyutlu yapıda, bileşenlerinden en az bir tanesi sentetik veya doğal bir polimerden yapılmış mamulü tanımlayan genel terim."* olarak tanımlar (bk. Çizelge 1).

Çizelge 1. Jeosentetik türleri

TEMEL KİMYASAL	POLİMER	JEOSENTETİK TÜRLERİ
Etilen	Polietilen **(PE)**	**Jeotekstil, jeomembran, jeogrid, jeotüp, jeonet, jeokompozit**
Propan	Polipropilen **(PP)**	**Jeotekstil, jeomembran, jeogrid, jeokompozit**
VinilKlorürMonomer	PoliVinilKlorür **(PVC)**	**Jeomembran, jeokompozit, jeotüp**
Etilen (+terafitalik Asit)	Poliester/PolietilenTeraFtalat **(PET)**	**Jeotekstil, jeogrid**
Kaprolaktam (Benzen)	Poliamid **(PA)** *-(Nylon 6/6)*	**Jeotekstil, jeokompozit, jeogrid**
Stiren	Polistirenf **(PS)**	**Jeokompozit, jeoköpük**

Polimerik malzemelere örnek olarak jeotekstil, jeogrid, jeonet, jeomembran, jeosentetik kil örtü, jeokompozit, jeocell ve diğer jeo ürünler sayılabilir (bk. Şekil 1). Bu ürünler arasında kullanım alanları daha yaygın olan jeotekstil, jeomembran, jeokompozit ve jeosentetik kil örtü malzemeler hakkında bilgiler verilecektir.

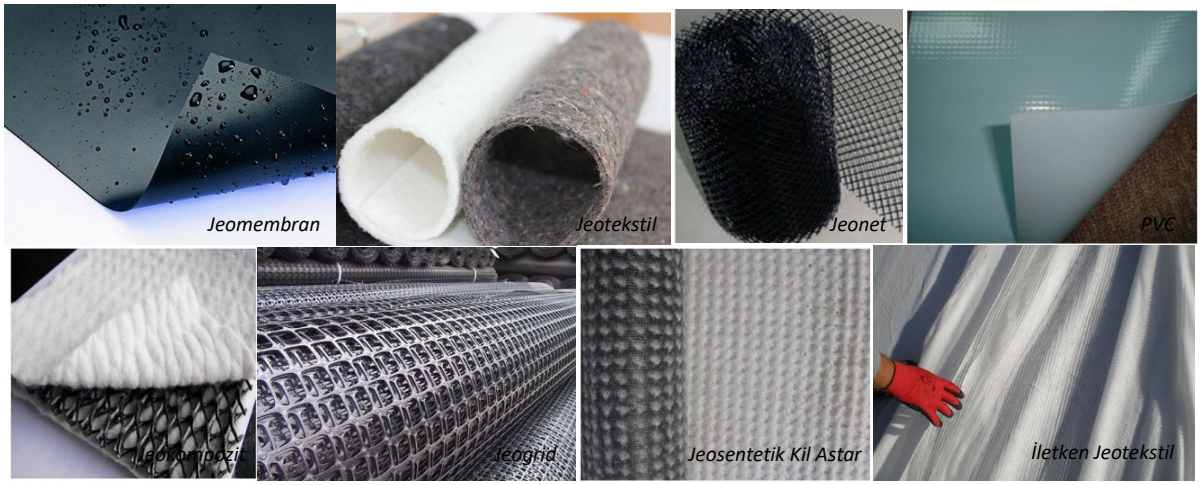

Şekil 1. Jeosentetik çeşitleri

Jeomembran

TS EN ISO (2015), jeomembranı *"Jeoteknik ve inşaat mühendisliği uygulamalarında yapı içerisine sıvı geçişini azaltmak veya önlemek amacıyla kullanılan düşük geçirimli jeosentetik malzeme"* olarak tanımlar.

Jeomembran kullanımında asıl amaç; yalıtım ve yüzey koruması sağlamaktır. Asfalt, polimer ve bunların karışımından üretilen pürüzlü veya pürüzsüz yüzeye sahip hazırlanan jeomembranlar kimyasal maddelere karşı oldukça yüksek bir dirence sahiptirler. Çekmeye karşı dayanımın yüksek olması, geçirgenliğinin düşük olması, delinmelere karşı dayanıklı bir yapıya olması vb. (bk. Çizelge 2) sebeplerden dolayı oldukça tercih edilen bir jeosentetik üründür.

Çizelge 2. Yüksek yoğunluklu polietilen (HDPE) jeomembranların kesme ve koparma dayanımları

Geomembrane Nominal Thickness	0.75 mm	1.0 mm	1.25 mm	1.5 mm	2.0 mm	2.5 mm	3.0 mm
Hot Wedge Seams[1]							
shear strength, N/25 mm	250	350	438	525	701	876	1050
shear elongation at break[2], %	50	50	50	50	50	50	50
peel strength, N/25 mm	197	263	333	398	530	661	793
peel separation, %	25	25	25	25	25	25	25
Extrusion Fillet Seams							
shear strength, N/25 mm	250	350	438	525	701	876	1050
shear elongation at break[2], %	50	50	50	50	50	50	50
peel strength, N/25 mm	170	225	285	340	455	570	680
peel separation, %	25	25	25	25	25	25	25

Günümüzde daha çok su yalıtım örtüsü olarak kullanılsa da, zamanla kullanım alanı çoğalmış ve özellikle yığın liçi sahaları, atık depolama sahaları, solüsyon (çözelti) havuzları, çöktürme havuzları ve atık su arıtma tesisleri gibi madenciliğinin birçok alanında kullanılmaktadır (bk. Şekil 2).

Şekil 2. Jeomembran kullanım alanları

Jeotekstil

TS EN ISO (2015), jeotekstili *"Geoteknik ve inşaat mühendisliği uygulamalarında toprak ve/veya diğer malzemeyle temasta olacak şekilde kullanılan, dokusuz, örülmüş veya dokulu olabilen ve düzlemsel, geçirimli, polimerik (sentetik veya doğal) tekstil malzemesi"* olarak tanımlar.

Üretim tekniği açısından örgülü ve örgüsüz olarak iki tip jeotekstil yapısı vardır. Jeotekstillerin 100'den fazla özel uygulama alanı bulunmaktadır; ama genelde ayırma, filtrasyon, drenaj, güçlendirme, koruma, yalıtım olarak altı fonksiyonu öne çıkmaktadır (bk. Çizelge 3).

Özellikle zemin mekaniği problemlerinde, ekonomik ve kalıcı çözümler sağladığı için son yıllarda kullanımı giderek artmıştır. Jeotekstiller, jeomembranlar gibi madenciliğinin birçok alanında kullanılmasının yanı sıra yığın liçi tesislerin atardamarları olan çözelti toplama borularını filtreleme ve korunması amacıyla bohçalama ve madencilik faaliyetleri sonrası rehabilitasyon işleri gibi önemli uygulama alanları mevcuttur (bk. Şekil 3).

Şekil 3. Jeotekstil kullanım alanları

Çizelge 3. Jeotekstillerin fonksiyonları

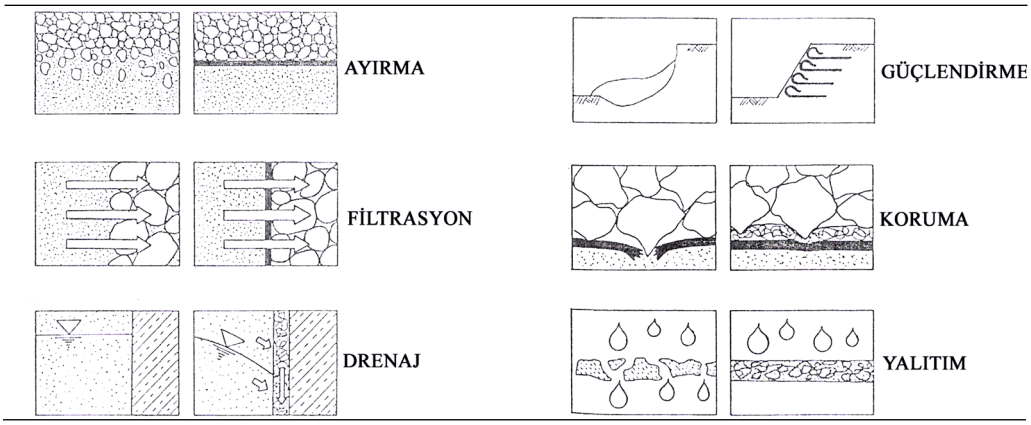

Jeosentetik Kil Astar (GCL)

TS EN ISO (2015), jeosentetik kil astarı *"Levha halindeki jeosentetik malzemelerin fabrikada birleştirilmesiyle elde edilen ve bariyer işlevinin esas olarak kil tarafından sağlandığı malzeme"* olarak tanımlar.

Jeotekstiller arasında bulunan bentonitin mineralojisi ile fiziksel ve kimyasal özellikleri geçirimsizliği önemli ölçüde etkilemektedir. İçindeki bentonit, toz veya granüler halde imal edilebilir. Literatürde, su ile süzdürüldüğü durumdaki hidrolik iletkenliğinin yaklaşık 2.0 x 10^{-9} cm/s olduğu rapor edilmektedir. Özdamarlar ve Ören'in (2018) yapmış olduğu çalışmada farklı alt zemin tabakaları, kür süreleri ve deney yöntemi ile hidrate edilen GCL'lerin hidrolik iletkenlik sonuçları Çizelge 4 'de yer almaktadır.

Düşük hidrolik iletkenlik özelliği ile katı atık depolama alanları, gölet tabanları, kanal yatakları ve çeşitli maden işletmelerinin rehabilitasyon ve atık havuzları dâhil pek çok alanda yaygın olarak kullanılmaktadır (bk. Şekil 4).

Şekil 4. Jeotekstil kil astar kullanım alanları

Çizelge 4. Jeosetetik kil örtülerin hidrolik iletkenlik sonuçları

Deney No	Alt Zemin Tabakası Tipi	Alt Zemin Örnek Boyu (cm)	Alt Zemin Görüntü Oranı	Deney Yöntemi	Hidrasyon Süresi (gün)	Hidrolik İletkenlik (cm/s)
1	Siltli Kum	11.6	1.14	KÖY	7	2.3×10^{-9}
2	Siltli Kum	17.4	1.14	TBÖY	7	1.7×10^{-9}
3	Siltli Kum	11.6	0.76	TBÖY	7	3.2×10^{-9}
4	Siltli Kum	11.6	1.14	KÖY	62	2.6×10^{-9}
5	Siltli Kum	17.4	1.14	TBÖY	62	1.7×10^{-9}
6	Zeolit	11.6	1.14	KÖY	17	1.8×10^{-9}
7	Zeolit	11.6	0.76	TBÖY	17	5.7×10^{-9}
8	Zeolit	11.6	1.14	KÖY	30	4.1×10^{-9}
9	Zeolit	11.6	0.76	TBÖY	30	2.5×10^{-9}

Jeokompozit

Genellikle suyun drenajı için tasarlanmış ve *levha halindeki iki ya da daha fazla jeosentetik malzemelerin fabrikada birleştirilmesiyle elde edilen* jeosentetik malzemedir.

Drenaj jeokompoziti, geogridin tek veya çift tarafının jeotekstille üst üste birleştirilmesi sonucu oluşturulur. Kullanılan geogrid malzemesi güçlendirme görevini üstlenirken, örgüsüz jeotekstil ise ayırma ve filtrasyon görevlerini üstlenmektedir. Jeokompozitler, su ve sıvı akışı için serbest bir iletim yolu sağlamaktadır.

Düşük eğimlerde ve basınç altında, yüksek akış kapasitesine sahip olan jeokompozitler, çevrenin korunmasında büyük rol oynamaktadırlar. Düzenli depolama sahalarında ve istinat yapılarında kullanımı yaygındır.

Şekil 5. Jeokompozit kullanım alanları

JEOSENTETİK MALZEMELERİN SAĞLADIĞI KATKILAR

Jeosentetikler, madencilik faaliyetlerinde barajlar, havuzlar, pasa stok alanları, yığın liçi sahaları gibi atık depolama alanlarının yanı sıra derivasyon kanalları, drenaj, istinat yapıları gibi donatılı jeoteknik projeleri, rehabilitasyon, peyzaj ve erozyon kontrol gibi çevre düzenlemeleri, tünel ve yer altı yapıları gibi galeri uygulamalarında katkılar sağlamaktadır (bk. Şekil 6 – Çizelge 5).

Şekil 6. Madencilik faaliyetlerinde jeosentetik malzemeler

Jeosentetik malzemelerinin sağladığı faydalar genel olarak şu şekildedir:

- Tehlikeli veya tehlikesiz atıkların insan sağlığı, bitki örtüsü ve çevreye karşı olumsuz etkilerini önlemektedir. Yer altı ve yerüstü sularının kirlenmesini engellemektedir.
- Katı ve sıvı gibi maddelere depolama alanı sağladığı için madencilik işlerinde önemli geri kazanımlar sağlamaktadır.
- Doğal malzemelerin sağladığı özellikler jeosentetiklerin bir çeşidi ile sağlanabilir. Örneğin, kil teminin mümkün olmadığı ya da temin mesafesinin fazla olduğu durumlarda kil yerine uygun bir jeosentetik malzeme kullanılması daha ekonomik bir çözüm olur.
- Doğal malzemelere göre nakliye ve taşınma kolaylığı sağladığı için taşıma maliyetleri daha düşüktür.
- Yerleştirilmesinin kolaylığı, stok ve istifleme imkânı sağladığı için zamandan ve maliyetten tasarruf sağlamaktadır.
- Jeosentetik malzemelerin filtrasyon özellikleri fabrika üretimi ve kontrollünde olduğundan doğal (mineral) malzemeler ile oluşturulan filtrelere nazaran kaliteleri daha uygun ve garantili olmaktadır. Kaliteden sapma olasılığı düşmektedir.
- Jeosentetik malzemelerin uygun derecelenmiş agrega ile kullanımı, toplayıcı borulara olan ihtiyacı azaltmaktadır. Maliyette önemli bir tasarruf söz konusudur.
- Uygulama kolaylığı sebebiyle jeosentetik malzemeler projelerde zaman ve maliyette önemli miktarda ekonomik kazanç sağlamaktadır.
- Jeosentetik malzemelerin sahip oldukları teknik özellikleri uygulamalarda oluşabilecek deformasyonlara uyum sağlar ve direnç sağladığı kabul edilmektedir.
- Elastisite ve sağlamlıkları ile sismik etkilere karşı kullanılabilir. Duvar arkalarında sismik etkileri sönümlemesi önemli bir avantaj olarak kabul edilebilir.
- Zemin iyileştirme ve güçlendirme ile uygun olmayan ve elverişsiz arazilerin kullanılabilmelerini mümkün kılan malzemelerdir.

- Yağmur suları, şiddetli rüzgâr gibi olumsuz hava şartlarında oluşan erozyonu azaltmak amacıyla kullanılmaktadır.
- Gereken kazı ve dolgu miktarının azaltılmasını ve daha uygun ve ekonomik malzemelerin kullanımını sağlamaktadır.
- Geliştirilen dayanım parametreleri ile şevlerin daha dik açılarla yapılabilmesi çok önemli yer kazanımları sağlamaktadır.
- Kayma ve göçmeye karşı dayanımı arttırmasının yanı sıra göçmüş yüzeylerin tamir edilebilmesini de sağlamaktadır.
- Donatılı zemin ve istinat duvarları uygulamalarında alternatif çözümler üretebilmektedir.
- Dayanım ve diğer teknik özellikleri net rakamlarla ifade edilebildiği için daha büyük, önemli ve spesifik projelerin hayata geçmesine imkân sağlar.
- Koruma örtüsü teşkil ederek, şev yüzeylerinin korunmasını ve parçalanmış kayaçları tutabilmesi ile can güvenliği sağlayabilmektedir.
- Yeşillendirilmiş yaşayan duvarlar ve rehabilite edilerek doğaya kazandırılan uygulamalar ile estetik görünüşlü güzel çevreler elde edilmektedir.

Jeosentetik malzemelerin sağladığı faydalardan; malzeme miktarı, imalat süresi ve maliyetlerin azalması ve çevresel duyarlılık doğrudan kazanım; sayılan diğer faydalar ise dolaylı kazanım olarak kabul edilebilir.

Çizelge 5. Madencilikte jeosentetik malzemelerin kullanım alanları

Kullanım alanı	Standard	Şematik gösterim	Kullanım alanları				
			Filtrasyon	Ayırma	Güçlendirme	Koruma	Drenaj
Rezervuarlarda ve barajlarda	EN 13254	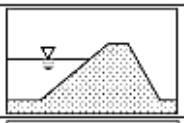	X	X	X	X	
Drenaj	EN 13252	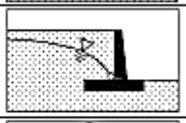	X	X			X
Erozyon kontrolü	EN 13253		X	X	X		
Toprak işleri	EN 13251	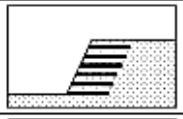	X	X	X		
Kanal	EN 13255	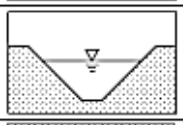	X	X	X	X	
Tüneller ve yer altı yapıları	EN 13256	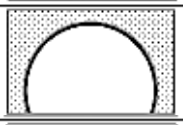				X	
Katı atık bertaraf	EN 13257		X	X	X	X	
Sıvı atık depolama	EN 13265	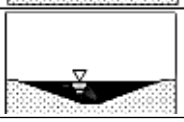	X	X	X	X	

SONUÇ

Jeosentetikler, mühendislik uygulamalarında sağladığı teknik ve ekonomik çözümler ile önem kazanmış ve kullanımları son 20-30 yılda giderek artmıştır. Geleneksel yöntemlerinin yerine çok çeşitli alanlarda kullanılabilen bu malzemeler; hayatımızı kolaylaştıran, çevreyi, doğal kaynaklarımızı ve yaşam alanlarımızı dizayn eden projelerde beşeri rol oynamaktadır.

Donatı, güçlendirme, ayırma, yalıtım, filtrasyon ve drenaj gibi fonksiyonlara sahip olabilen jeosentetikler, doğrudan ve dolaylı avantajlar sağlamakta ve muhtelif geri kazanımlara neden olmaktadır. Bu bildiri kapsamında bu malzemelerin sağladığı faydalardan bahsedilmiştir.

TEŞEKKÜRLER

“Jeosentetik Malzemelerin Topluma ve Çevreye Sağladığı Katkılar” başlıklı bildiriyi araştırma fırsatı sunan değerli YESTİ Group yöneticilerimizden başta Genel Müdür Cem PEKEL, Direktör Osman MARTİN ve Teknik ve İdari İşler Müdürü Murat TÜRKÖZÜ’ne teşekkür eder, bu konu üzerine araştırma yapmam için fikir veren değerli TÜPRAG Efemçukuru Açık Saha Yöneticisi Yavuz Selim İNCİ’ye şükranlarımı sunarım.

KAYNAKLAR

Akyıldız, M.H. (2019). Geosentetik Türlerinin İnşaat Mühendisliğindeki Uygulamaları ve Sağladığı Kolaylıklar. Dergi Park, Cilt 10, Sayı 2, 791 – 796.

Devlet Su İşleri Genel Müdürlüğü (2012). DSİ Genel Müdürlüğü Tarafından Yaptırılacak Depolamalarda (Rezervuarlarda) ve Barajlarda Kullanılacak Geosentetik Bariyerler İçin Teknik Şartname.

Devlet Su İşleri Genel Müdürlüğü (2014). DSİ Genel Müdürlüğü Tarafından Yaptırılacak Kanallarda, Rezervuarlarda ve Barajlarda Kullanılacak Geotekstiller ve Geotekstille İlgili Mamuller İçin Teknik Şartname.

Geosynthetic Institute (2021). GRI -GM19a Standard Specification, Seam Strenth and Related Propertis of Thermally Bonded Homogeneous Polyolefin Geomembranes/Barries, Rev. 10.

ISO 10318-1 (2015). Geosynthetics – Part 1: Terms and definitions.

Koçak, B. (2021). Mühendislik Uygulamalarında Geosentetik Ürün Kullanımı. URL -1= https://www.yeraltihaber.com/makale/muhendislik-uygulamalarinda-geosentetik-urun-kullanimi-7.

Özdamarlar Kul T. ve Ören A.H. (2018). Geosentetik Kil Örtü Hidrasyon Yönteminin Alt Zemin Koşullarına Bağlı Olarak Değerlendirilmesi. Teknik Dergi, Cilt 29, Sayı 3, 8385 – 8409.

Teknik Araştırma ve Kalite Kontrol Dairesi Başkanlığı (2021). Geosentetik Malzemeler ve DSİ’deki Uygulamaları. DSİ Genel Müdürlüğü.

TS EN ISO 10318-1 (2015). Jeotekstiller – Terimler ve tarifler: Bölüm-1.

URL -2= http://yestigroup.com/.

Zanbak, C. (2019). Madencilik Faaliyetlerinde Geosentetik Kullanım Alanları. Türkiye Madenciler Derneği, Madencilikte Atık Yönetim Uygulamaları Semineri.

KANADA MADENCİLİK DERNEĞİ- SÜRDÜRÜLEBİLİR MADENCİLİK- ATIK YÖNETİM PROTOKOLÜ VE TÜRKİYE'DEKİ UYGULAMASI

MINING ASSOCIATION OF CANADA- TOWARDS SUSTAINABLE MINING TAILINGS MANAGEMENT PROTOCOL AND APLICATION IN TURKEY

H. Ürkmez [1,*], C. Dumaresq [2], B. Chalmers [2], Y.S. İnci [1], G. Uzuncelebi, S. Ennis [3], E.R. Castro

[1] *TÜPRAG Efemçukuru Altın Madeni*
(Sorumlu Yazar: halil.urkmez@tuprag.com)*
[2] *The Mining Association of Canada (MAC)*
[3] *Stantec*

ÖZET

Hızla büyüyen madencilik, ülkeler için büyük ekonomik fırsatlar sağladığı gibi, insanlar ve çevre için zorluklar ve riskler de getiriyor. Hükümetler / ülkeler için zorluk, madenciliği sürdürülebilir kalkınma hedeflerine katkıda bulunacak ve insanları veya çevreyi tehlikeye atmayacak şekilde yönetmektir.

Bu bağlamda, Kanada Madencilik Derneği (MAC), hükümetlerin sürdürülebilir kalkınma hedefleriyle tutarlı, insanları ve çevreyi koruyan toplulukları ve madencilik endüstrisini birleştiren bir yapıda uluslararası ilkeleri, yaklaşımları ve standartları benimseyen bir Kanada endüstri derneğidir.

MAC, madencilik sektörünün çevresel ve sosyal performansını iyileştirmek için geliştirilmiş, uluslararası kabul görmüş bir kurumsal sürdürülebilirlik programı olan "Sürdürülebilir Madencilik" (TSM-SM) performans sistemini geliştirmiş ve uygulamaktadır. Sürdürülebilir Madencilik performans sisteminin amacı, madencilik şirketlerinin toplumun mineral, metal ve enerji ürünleri ihtiyaçlarını sosyal, ekonomik ve çevresel açıdan en sorumlu şekilde karşılamasını sağlamaktır. Sürdürülebilir Madencilik Protokolleri, belirli, ölçülebilir performans göstergelerini tanımlamaktadır.

TSM performans sisteminin protokollerinden biri olan "Atık Yönetim Protokolü", sahaya özel seviyede güvenli, sorumlu atık yönetimine odaklanır. BAP (Mevcut En İyi Uygulamalar) ve BAT'ın (Mevcut En İyi Teknikler) uygulanması dahil olmak üzere mühendislik uygulamalarını risk tabanlı bir yaklaşım içinde entegre eden atık yönetiminin sağlam kurumsal yönetimi için bir dizi yönetim sistemleri yaklaşımını tanımlar.

Anahtar Kelimeler: Kanada madencilik derneği, sürdürülebilir madencilik (SM), sürdürülebilir kalkınma hedefleri, atık yönetimi protokolü, işletme, bakım ve izleme kılavuzu, kademeli eylem planları, kayıt mühendisi (EOR), mevcut en iyi uygulamalar, mevcut en iyi teknikler

ABSTRACT

Rapidly growing mining provides great economic opportunities for countries as well as brings difficulties and risks for people and the environment. The challenge for governments / countries is to manage mining in a way that contributes to sustainable development goals and does not endanger people or the environment.

In this regard, The Mining Association of Canada (MAC) is a Canadian industry association that has adopted international principles, approaches, and standards in a structure that combines the mining

industry and communities that protect the people and the environment, consistent with the sustainable development goals of governments.

MAC has developed and implemented the Towards Sustainable Mining (TSM) performance system, an internationally recognized corporate sustainability program developed to improve environmental and social performance of the mining industry. The purpose of the TSM performance system is to enable mining companies to meet the needs of society for mineral, metal, and energy products in the most socially, economically, and environmentally responsible way. TSM Protocols describe specific, measurable performance indicators.

Tailings Management Protocol, one of the protocols of the TSM performance system, focuses safe, responsible tailings management at the site-specific level. It describes a management systems approach for sound corporate governance of tailings management that integrates engineering practice, including implementation of BAP (Best Available Practices) and BAT (Best Available Techniques), within a risk-based approach.

Keywords: The mining association of canada (MAC), towards sustainable mining (TSM), sustainable development goals, tailings management protocol, OMS manual, trigger action response plan (TARPs), engineer of record (EoR), best available practices (BAP), best available techniques (BAT)

GİRİŞ

Kanada Madencilik Derneği güçlü, sürdürülebilir ve uluslararası düzeyde rekabetçi bir Kanada madenciliği, mineral ve metal endüstrisinin geniş bir ulusal destekle oluşturulmasına ve sağlam bir kurumsal ve kamu politikasının geliştirilmesine katkıda bulunmak için 1935 yılında kurulmuştur. Kanada Madencilik Derneği'nin "Atık Tesislerinin Yönetimine Yönelik Bir Kılavuz"'unun (A Guide To The Management of Tailings Facilities) 1998'de yayınlanan ilk baskısı, 1990'larda meydana gelen bir dizi uluslararası atıkla ilgili olaya yanıt olarak geliştirilmiştir. MAC Atık Kılavuzu'ndaki yönetim sistemleri yaklaşımı, ISO 14001 Çevre Yönetim Sistemleri ile uyumlu, Kanada Baraj Birliği'nin Baraj Güvenliği Yönergeleri (2013) ve uluslararası yönergeler ve standartların uygulanmasıyla desteklenmektedir. 2003 yılında atık yönetim sisteminin ayrılmaz bir bileşeni olarak sahaya özel bir İşletme, Bakım ve İzleme (İŞBİK - OMS) kılavuzu yayınlamıştır. Atıkların güvenli ve çevreye duyarlı, etkili bir yönetim sistemi içinde ve tüm yaşam döngüsü boyunca sağlam mühendislik yeteneğinin tutarlı bir şekilde uygulanmasını sağlamak amaçıyla 2004 yılında MAC "Towards Sustainable Mining® (TSM®)" (MAC-Sürdürülebilir Madencilik - SM) girişimini başlatmıştır. 2015 yılı itibari ile MAC, üyeleri için Kanada'daki operasyonları için TSM'nin atık yönetimi bileşeni de dahil olmak üzere "Towards Sustainable Mining (TSM)" uygulamasını zorunlu hale getirdi.

"SÜRDÜRÜLEBİLİR MADENCİLİK" PROGRAMI NEDİR?

SM performans sistemi, Kanada Madencilik Birliği'nin sorumlu madencilik taahhüdüdür. Madencilik şirketlerinin çevresel ve sosyal sorumluluklarını değerlendirmelerine ve yönetmelerine yardımcı bir sistemdir (MAC 2021). SM uygulaması, tesis performansı artırmak ve temel madencilik risklerinin madencilik operasyonları tarafından etkin bir şekilde yönetilmesini sağlamak için bir dizi araç ve göstergelerden oluşur. Bu performans ölçüm araçları ve göstergeleri, aşağıda belirtilen SM Yol Gösterici İlkeleri ile uyumludur (MAC 2021):

"...eylemlerimiz (MAC üyeleri), ilgilendiğimiz toplulukların gelişen öncelikleriyle uyumlu sosyal, ekonomik ve çevresel performansa karşı sorumlu bir yaklaşım sergilemelidir. Eylemlerimiz, dürüstlük, şeffaflık ve bütünlük te dahil olmak üzere çalışanlarımız ve ilgilendiğimiz topluluklarla paylaştığımız geniş bir değer yelpazesini yansıtmalıdır. Ayrıca çalışanlarımızı, topluluklarımızı, müşterilerimizi ve doğal çevreyi korumak için devam eden çabalarımızın altını çizmeliler."

SM programının güçlü yönleri hesap verebilirlik, şeffaflık, güvenilirlik, etkin performansın desteklenmesi ve sürekli gelişimdir.

"SÜRDÜRÜLEBİLİR MADENCİLİK" PROGRAMI NASIL ÇALIŞIR?

SM programı, madencilik şirketlerinin çevresel ve sosyal taahhütlerini sahada eyleme dönüştürmesine olanak tanır. SM programı üç temel alana odaklanan (Topluluklar ve İnsanlar, Çevre Yönetimi ve Enerji Verimliliği) sekiz protokolden oluşmaktadır (Mayıs 2021'de yeni İklim Değişikliği protokolü TSM Protokollerine eklenmiştir). Her protokol, maden tesislerinin yönetim kalitesini ve performansını geliştirmesine, ölçmesine ve kamuya açık olarak raporlamasına yardımcı olan bir dizi performans göstergesini içermektedir (MAC 2021).

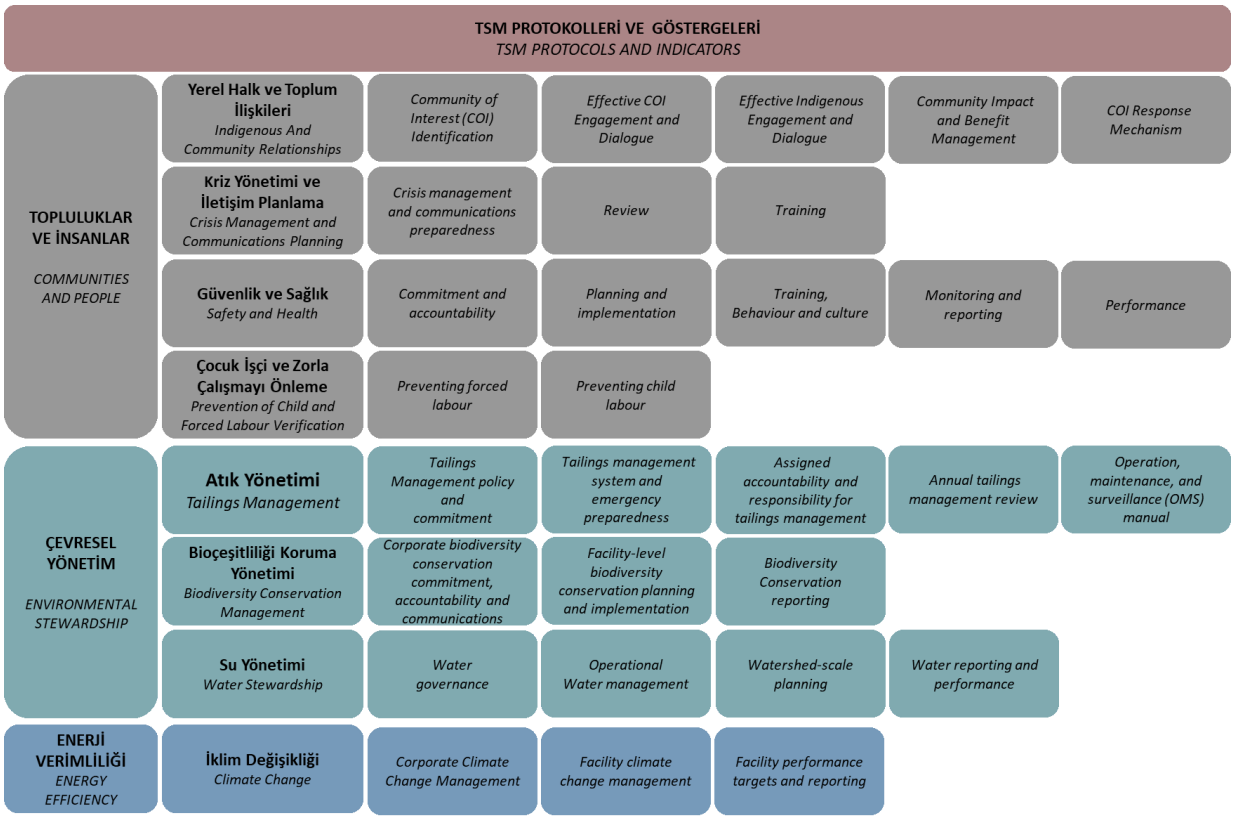

Şekil 1. SM (TSM) Protokolleri ve Göstergeleri (MAC 2021)

1. Yerel Halk ve Toplum İlişkileri
2. Kriz Yönetimi ve İletişim Planlaması
3. Güvenlik ve Sağlık
4. Çocuk İşçi ve Zorla Çalıştırmayı Önleme
5. Atık Yönetimi
6. Biyoçeşitliliği Koruma Yönetimi
7. Su Yönetimi
8. İklim Değişikliği

"SÜRDÜRÜLEBİLİR MADENCİLİK" PROGRAMI PERFORMANS DOĞRULAMASI

Maden şirketleri, SM protokollerinin her birindeki göstergelere göre operasyonel performanslarını yıllık olarak değerlendirir. SM programının en güçlü yönlerinden biri, madencilik şirketlerinin performanslarını tesis özelinde ve etkinlikleri düzeyinde ölçmesidir. Bu, performans değerlendirmesi SM sonuçlarının güvenilirliğini sağlamaya yardımcı olan SM doğrulama programı aracılığıyla daha da güçlendirilir. Bu doğrulama programı, Şekil 2.'de gösterildiği ve aşağıda ayrıntılı olarak açıklandığı gibi (MAC 2021) birkaç katmandan oluşur.

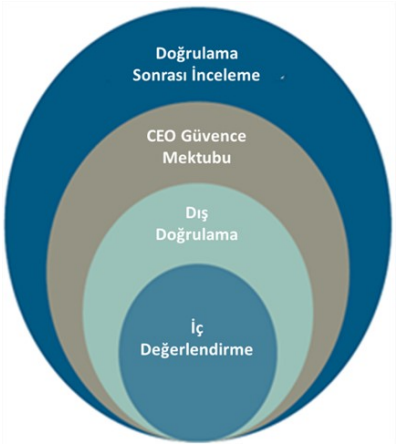

Şekil 2. Sürdürülebilir Madencilik (SM) Doğrulama Programı (MAC 2021)

SM Kriz Yönetimi ve İletişim Planlama Protokolü (Crisis Management and Communications Planning) "evet" veya "hayır" değerlendirme ölçeğine göre değerlendirilir; Çocuk İşçi ve Zorla Çalışmayı Önleme Protokolü'nde de (Preventing Child and Forced Labour), Sürdürülebilir Madencilik programı benzer bir "evet" veya "hayır" derecelendirme ölçeğine dayalı değerlendirme yapmaktadır. Diğer protokoller ise; Her gösterge için, "C" Düzeyinden, "AAA" Düzeyine kadar performanslarını yansıtan bir harf notu ile derecelendirilir.

İç Değerlendirme

Her yıl tüm tesisler, her bir protokol için ayrıntılı ve kapsamlı bir iç (öz) değerlendirme gerçekleştirir. Protokolde açıklanan kriterlere göre performansı yansıtmak için her göstergeye "C" ile "AAA" arasında değişen harf notları (bkz. Şekil 3) atanır. SM Kriz Yönetimi ve İletişim Planlama Protokolü ile Çocuk ve Zorla Çalıştırmanın Önlenmesi Protokolü'nde her bir göstergenin performansı harf notu vermek yerine "evet" veya "hayır" değerlendirme ölçeğine göre değerlendirilir.

Tablo 1. İç Değerlendirme Not Sistemi (MAC 2021)

AAA	Mükemmel liderlik.
AA	Yönetim kararlarına ve iş fonksiyonlarına entegrasyon.
A	Sistemler / süreçler geliştirilir ve uygulanır.
B	Prosedürler mevcuttur ancak tamamen tutarlı değildir veya belgelenmemiştir, Planlanan ve geliştirilmekte olan sistem süreçleri mevcuttur.
C	Yerinde sistem yoktur; faaliyetler reaktif olma eğilimindedir, Prosedürler olabilir ancak bunlar politikalara ve yönetim sistemlerine entegre değildir.

Dış Doğrulama

Her üç yılda bir, eğitimli bir Doğrulama Hizmet Sağlayıcısı (Verification Service Provider - VSP), tesis tarafından rapor edilen performans derecelendirmelerini belirlemek ve desteklemek için tesisin dahili (öz) değerlendirmelerini eleştirel bir şekilde gözden geçirir. Doğrulama Hizmet Sağlayıcıları, doğrulanan şirketten bağımsız ve SM tarafından akredite edilmiş deneyimli denetçilerdir.

CEO Güvence Mektubu

Harici doğrulama yılında, şirketin Kanada'daki CEO'su veya üst düzey yöneticisi, Kanada Madencilik Derneği'ne, Doğrulama Hizmet Sağlayıcısının Görev Tanımı'na uygun olarak harici bir doğrulamanın yapıldığını teyit eden bir mektup gönderir. CEO Güvence Mektupları, MAC web sitesinde kamuya açık halde yayınlanır.

Doğrulama Sonrası İnceleme

İlgili Danışman Topluluğu Heyeti, doğrulamada rol oynar ve SM'nin güvenilirliğini ve sürekli gelişimini sağlamaya yardımcı olur. Heyet, MAC tarafından kurulan ve yerli gruplar, topluluklar, çevresel ve sosyal sivil toplum kuruluşları, organize emek ve finans kuruluşlarının temsilcilerinden oluşan bağımsız, bir gruptur. Heyet, İlgili danışman toplulukları ve MAC üyeleri için ortak endişe konuları üzerinde tartışmak ve işbirliği yapmak için bir platform görevi görür. Heyet, SM geliştirme ve uygulamasını denetler ve madencilik sektörüyle ilgili ortaya çıkan sorunların veya endişelerin belirlenmesine yardımcı olur (MAC 2021a).

Heyet, her yıl, şirket sistemlerini ve uygulamalarını analiz etmek de dahil olmak üzere iki MAC üyesi şirketin SM sonuçlarının Doğrulama Sonrası İncelemesini gerçekleştirir. Bu gözden geçirmelerin bir parçası olarak şirketler, SM sonuçlarını ve destekleyici kanıtları tartışmak için heyet ile bir araya gelir ve heyet, performansı iyileştirmek için tavsiyelerde bulunabilir.

ATIK YÖNETİM PROTOKOLÜ

Atıklar, değerli maddelerin (örneğin altın) içinde oluştukları kayadan ayrıldığında ortaya çıkan madenciliğin bir ürünüdür. Sorumlu bir şekilde yönetilmezse, atıklar insan sağlığı ve güvenliği, çevre, altyapı ve madencilik şirketlerinin kendileri için potansiyel riskler oluşturabilir. Sorumlu atık yönetimi, bu riskleri en aza indirmek ve azaltmak için çok önemlidir.

MAC'in Bilim ve Çevre Yönetimi Başkan Yardımcısı Charles Dumaresq (2019), Vancouver, Kanada'daki "Tailings and Mining Waste 2019" kongresinde, " Overview of Governance Practices for Tailings Management" (Atık Yönetimine Ait Uygulamalara Genel Bakış) sunumunda sorumlu atık yönetiminin ilkelerini şu şekilde açıkladı: :

Hesap verebilirlik ve sorumluluk
Yönetim sistemleri yaklaşımı → Atık yönetim sistemi
Performansa dayalı, risk bilgisine dayalı yaklaşım
Etkili planlama ve tasarım
İşletme, Bakım ve İzleme Kılavuzu
Biyoçeşitliliği Koruma Yönetimi
Acil durum hazırlığı
Bağımsız inceleme dahil olmak üzere dış doğrulama

Dumaresq (2019), “bu ilkeleri izleyerek atık yönetimine yönelik sistematik bir yaklaşımın, belki de en büyük risk olabilecek şeyi azaltmaya yardımcı olduğunu belirtti: insan unsuru ve insan hatası potansiyeli. Kontroller ve dengeler içeren sistematik bir yaklaşım, insan hataları, deneyimler, önyargılar veya yerleşik cehaletlerin etkisiz atık yönetimine veya daha da kötüsü bir atık tesisinin arızalanmasına yol açma riskini azaltmaya yardımcı olur”. Dumaresq ayrıca, “bu ilkelerin uygulanmasının başarısızlıkların olmayacağını garanti etmeyeceğini, ancak bu ilkelerin etkin bir şekilde uygulanmasının başarısızlık olasılığını ve bir başarısızlık meydana gelirse olası sonuçları azaltmaya yardımcı olacağını vurguladı”.

2004 yılında tanıtılan Atık Yönetim Protokolü, SM programının önemli bir odak noktasıdır. Protokol bu ilkelerle uyumludur ve protokolün uygulanması, sorumlu atık yönetimi için bu ilkelerin uygulanması için paha biçilmez bir araçtır. Protokol, beş performans ölçüm göstergesini açıklar (MAC 2019d):

1. Bir kurumsal atık yönetimi politikası ve taahhüdü geliştirmek,
2. Sahaya özel bir atık yönetim sistemi geliştirmek ve uygulamak ve acil duruma hazırlık planları geliştirerek test etmek,
3. Atık yönetimi için hesap verebilirlik ve sorumluluk atama,
4. Sürekli iyileştirme için yıllık atık yönetimi incelemesi yapmak,
5. Sahaya özel bir İşletme, Bakım ve İzleme Kılavuzu’nun (İŞBİK) geliştirilmesi ve uygulanması.

Atık Yönetim Protokolü uygulanması, iki kılavuz belge ile desteklenmektedir:

İlk olarak 1998'de yayınlanan “A Guide To The Management of Tailings Facilities” (Atık Yönetimi Kılavuzu), atık yönetiminin kurumsal yönetimi ve sahaya özel atık yönetim sistemlerinin geliştirilmesi ve uygulanması hakkında rehberlik sağlar (MAC 2019).

İlk olarak 2003 yılında yayınlanan " Developing an Operation, Maintenance, and Surveillance Manual for Tailings and Water Management Facilities" (OMS- İŞBİK), yaşam döngüleri boyunca atık tesislerinin sahaya özel işletimi, bakımı ve izlenmesi hakkında rehberlik sağlar (MAC 2019).

2014 yılında British Columbia'daki Mount Polley Madeni atık tesisinde meydana gelen kazadan sonra MAC, TSM'nin Atık Yönetim Protokolü, İŞBİK ve Atık Yönetimi Kılavuzu’ndan oluşan atık yönetimi bileşeninin kapsamlı dış ve iç incelemelerini başlattı. Bu gözden geçirmeler, TSM'nin atık yönetimi bileşeninde herhangi bir iyileştirme ihtiyaçını belirleme amacıyla yapılmaktadır.

Dış inceleme, MAC Yönetim Kurulu'na sunulan ve 29 tavsiye içeren bir rapor (TSM Tailings Review Task Force, 2015) üretti. Bu tavsiyeler Protokolü ve her iki Rehberi ele almış ve Atık Rehberini güncellemek için tavsiyeleri içermiştir:

“*Atık Yönetimi Kılavuzu’nu, saha araştırması ve seçimi, tasarımı, inşaatı, işletimi, kapatılması ve atık tesislerinin kapatılması sonrasında bağımsız bir inceleme gerektirecek şekilde değiştirin.*

Mevcut En İyi Teknoloji (MET - BAT) ve Mevcut En İyi Uygulama (MEU - BAP) üzerine yorumları içeren Mount Polley'in Uzman Heyet İncelemesi ile ilgili olarak, MAC, hem BAT hem de BAP'nin Atık Yönetimi Kılavuzu’na en iyi şekilde nasıl dahil edeceğini değerlendirin ve Atık Yönetim Protokolünün 2. Göstergesinde bunlara atıfta bulunun.

Kayıt Mühendisi (Engineer Of Record - EoR) değişikliğini ve bir mülkiyet değişikliğini yönetmekle ilgili tanımları ve/veya rehberliği geliştirin ve Atık Yönetimi Kılavuzu’nun değişiklik yönetimi bölümünde dahil edin.

Uygunsuzluklar için riske dayalı bir sınıflandırma sistemi oluşturun ve ilgili sonuçları değerlendirin. Risk değerlendirme metodolojisine ilişkin rehberliği, Atık Yönetim Kılavuzu'na dahil edin.

Hedeflerin nasıl seçileceği ve tasarım kriterlerinin nasıl belirleneceği de dahil olmak üzere, saha seçimi ve tasarımı ile ilgili daha spesifik teknik rehberliği içerecek şekilde Atık Yönetimi Kılavuzu'nu gözden geçirin ve gerektiği şekilde değiştirin."

Dış ve iç değerlendirme sonuçlarına cevaben, MAC, Atık Yönetim Protokolü'nü (2017 ve 2019) ve OMS Kılavuzu'nu (2019) revize etti. Atık Yönetimi Kılavuzu'na ve OMS Kılavuzu'ndaki revizyonlar önceki sürümlerden temel kavramları güçlendirdi ve yeni kavramlar eklendi. Atık Yönetim Kılavuzu için, güçlendirilen ve eklenen kavramlar (MAC 2019):

Risk Esaslı Yaklaşım:

Atık yönetimini fiziksel ve kimyasal risklerle orantılı bir şekilde yönetmek.
Risk değerlendirmeleri yapmak ve yaşam döngüsü boyunca değerlendirmeleri güncellemek.
Riskleri yönetmek için mevcut en iyi uygulamaların (MEU - BAP) ve mevcut en iyi tekniklerin (MET - BAT) kullanımını ve entegrasyonu sağlamak.

Sonuçları yüksek olayları önlemek veya azaltmak için bir risk yönetimi aracı olan (özellikle, bir tür risk kontrolü) kritik kontrolleri sağlamak.

Atık Depolama Tesisi'nin sahibi adına teknik yönlendirme sağlayan Kayıt Mühendisi (Engİneer Of Record - EoR) belirlemek.

Yaşam döngüsü boyunca atık tesisleriyle ilişkili risklerin tanımlanmasına, anlaşılmasına ve yönetilmesine yardımcı olmak için, bağımsız incelemenin entegrasyonunu sağlayarak nesnel uzman yorumu ve tavsiyelerini almak.

Atık yönetimi teknolojisi ve tesis konumunun optimum kombinasyonunu belirlemek gibi konularında titiz ve şeffaf bir metodoloji ile atık yönetimi alternatiflerini değerlendirmek.

Atık taşıma ve depolama planları,
Su Yönetim Planları,
Kapatma Planları.

Atık Yönetim Protokolü, Atık Yönetimi Kılavuzu ve İŞBİK (OMS), atık yönetimi için uluslararası lider uygulama olarak kabul edilmiştir (Golder Associates, 2016, Morgenstern, 2018) ve atık tesislerinin katastrofik yıkım riskini minimize etmeyi amaçlayan, "The International Council On Mining And Metal (ICMM)" 2016 Atık Yönetimi Çerçevesi Durum Değerlendirmesi ile uyumlu ve onu tamamlayıcıdır.

2021'de, MAC, Birleşmiş Milletler'in ''Atık Yönetimine İlişkin Küresel Endüstri Standardı''nın (Global Tailings Review, 2020) yayınlanmasına yanıt olarak geliştirilen Atık Yönetimi Kılavuzu için bir güncelleme yayınladı. Güncelleme, kilit personellerin rolleri ve sorumlulukları hakkında daha fazla ayrıntı ve yaşam döngüsü boyunca belgelenecek bilgilere ilişkin yeni rehberliği içermektedir (örneğin, Atık tesislerinin tasarımının ve inşaatının dokümantasyonu). SM gereklilikleri ve rehberliği, BM Küresel Endüstri Standart'ındaki gereksinimlerin çoğunu karşılıyor ve hatta aşıyor olsa da, bu güncelleştirme (MAC 2021) ile BM Küresel Endüstri Standardı eşdeğerliliğinin iyileştirilmesi amaçlanmıştır.

Özellikle Kanada'daki madenler için, SM'nin atık yönetimi bileşeninin uygulanması, özellikle "Canadian Dam Association" (CDA) tarafından yayınlanan yönergelerle desteklenmektedir;

Canadian Dam Association Dam Safety Guidelines 2007 (2013 Edition)
Technical Bulletin: Implementation of Dam Safety Guidelines in Mining Dams (2014).

Ayrıca, bunların dışında aşağıdakiler gibi ilgili teknik rehberlik sağlayan çok çeşitli kuruluşlar ve programlar vardır;

International Commission on Large Dams (ICOLD)
Australian National Committee on Large Dams (ANCOLD)
International Organization for Standardization (ISO):

- ISO 9000 – Kalite Yönetimi (Quality Management)
- ISO 14000 – Çevre Yönetimi (Environmental Management)
- ISO 31000 – Risk Yönetimi (Risk Management)

International Code for Cyanide Management
Environment and Climate Change of Canada (ECCC)
Western Australia Department of Mines and Petroleum
Australian Government Leading Practice Sustainable Development Program for the Mining Industry
South African National Standards SANS 10286 1998
US Bureau of Reclamation
US Army Corps of Engineers
US Federal Emergency Management Agency
United Nations Environment Programme
European Union directive and Best Available Techniques (BAT) Reference Document for the Management.

MAC, sahaya özel atık yönetim sistemlerinin geliştirilmesini ve performanslarının iyileştirilmesi ve kurumsal politika ile ilgili yasal gereklilikleri ve yerel topluluk taahhütlerini karşılamak için, Atık Yönetimi Protokolü ve yönergelerinin uygulanmasını destekleyen bir araç olan "Tailings Guide implementation checklist" hazırlamıştır. Bu kontrol listesi doldurularak, atık yönetimi çerçevesinde uygulama durumunun bir anlık görüntüsü elde edilir (Şekil 4).

MAC ayrıca, Protokolde açıklanan göstergelere karşı performansı değerlendirmek için Atık Yönetimi Protokolü ile birlikte kullanılan bir Uygunluk Tablosu geliştirmiştir. “Tailings Guide implementation checklist” (Atık Kılavuzu Uygulama Kontrol Listesi) ve “Table of Conformance” (Uygunluk Tablosu) benzer olsalar da, bu araçlar farklı amaçlara hizmet etmektedir (Şekil 4 ve 5). “Table of Conformance”, Atık Yönetimi Protokolü’ndeki (MAC 2019) her bir gösterge için performans kriterlerini ve uygulanması gereken Atık Yönetim Kılavuzu ve İŞBİK unsurlarını tanımlar ve uygunluğunu denetler.

Gösterge 5: OMS Kılavuzu						
Kriterler	**Belge**	**Bölüm**	**Evet**	**Hayır**	**Yok**	**Yanıtı Destekleyecek Açıklama ve Kanıt**
Genel Gereksinimler						
OMS kılavuzu, uygulandığı atık tesisine özel olacak şekilde geliştirildi mi?	OMS Kılavuzu	2.1.2				
OMS kılavuzu, uygulama kapsamının sınırlarını açıklıyor mu?						
Kapsam, atık tesisinin performansını ve risk yönetimini etkileyebilecek operasyonel						

kontrolleri içeriyor mu?						
OMS kılavuzu, atık tesisinin mevcut koşullarını ve yaşam döngüsü aşamasını yansıtıyor mu?						
Diğer Sistemlerle Bağlantılar						
OMS kılavuzu, diğer ilgili maden sahası planları ve prosedürleri ile bağlantıları, bu diğer planlar ve prosedürlerin atık yönetimi ve OMS faaliyetleri ile nasıl ilişkili olduğunu açıklıyor mu?	OMS Kılavuzu	2.4.3				
Bağlantıların bu tanımı, çeşitli sorumlu kişiler veya gruplar arasında ilişkili roller, sorumluluklar, yetki seviyeleri ve iletişim prosedürlerini içeriyor mu?						
OMS kılavuzunun uygulanması						
OMS el kitabı, tanımlanmış sorumluluklara sahip her bir pozisyon için minimum bilgi ve yetkinlik gereksinimlerini tanımlıyor mu?	OMS Kılavuzu	2.5 ve 3.1.6				

Şekil 1. Uygunluk Tablosu "Table of Conformance" Kısmi Görüntüsü (MAC 2019).

Atık Kılavuzu Bölüm	Yönetim Eylemi	Sorumluluklar	Performans Ölçümü	Takvim	Referanslar
Kapsayıcı İlkeler					
Risk Değerlendirmesi ve Yönetimi					
2.2.1	Aşağıda Planlama başlığı altında ele alınmıştır.				
Atık Yönetimi için BAT ve BAP					
2.2.2	Belirli bir atık tesisi için atık yönetim teknolojisini seçerken aşağıdaki faktörleri göz önünde bulunduruyor musunuz:				
	• Bir atık tesisinin arızalanma olasılığı veya sonuçları azaltılıyor mu?				
	• Potansiyel bir jeokimyasal sorunu yönetmek için malzeme ayrımı gerekli mi?				
	• Taşıma ve yerleştirme sırasında atıklarda ne kadar su tutulacak?				
Bağımsız İnceleme					
2.2.3	Rutin olarak Bağımsız İnceleme yapmak için bir mekanizma oluşturulmuş mu?				
Kapatma için Dizayn ve Operasyon					
2.2.4	Atık tesisinin kavramsal planlamasında ve tasarımında uzun				

	vadeli kapatma hedefleri ve kapatma sonrası potansiyel arazi kullanımları dikkate alındı mı?				

Şekil 2. Atık Kılavuzu Uygulama Kontrol Listesi "Tailings Guide Implementation Checklist" Kısmi Görüntüsü (MAC 2019)

ATIK YÖNETİM PROTOKOLÜNÜN PERFORMANSININ DEĞERLENDİRİLMESİ

Yukarıda açıklandığı gibi, Atık Yönetimi Protokolündeki göstergelere karşı performans, "Table of Conformance" (Uygunluk Tablosu) kullanılarak değerlendirilir. Bu değerlendirmenin önemi uygun belgeler ve kanıtlar ile "Uygunluk Tablosu"'nda tanımlanan öğelerin uygun şekilde geliştirilip geliştirilmediğini, uygulanıp uygulanmadığını göstermektir. Atık Kılavuzu ve İŞBİK Kılavuzu, belgelenmesi gereken ve "Uygunluk Tablosu"'nun doldurulmasında başvurulabilecek çok çeşitli bilgileri tanımlar. Bu bilgilerin uygun şekilde değerlendirildiğinden ve bilgilerin atık tesisinin özellikleri ve yaşam döngüsü boyunça sahaya özel kozullar dikkate alınarak, Atık Yönetim Protokolü'ndeki göstergelere göre değerlendirilmesi şirket sorumluluğundadır.

Atık Yönetim Protokolü ve Kılavuzlar, şirketin/tesisin her Gösterge için Seviye A veya daha yüksek bir seviye elde etmek için hazırlanması, geliştirmesi ve uygulaması gereken bir dizi belgeden oluşmaktadır. Bu belgelerin nasıl düzenlendiği ve değerlendirmenin atık tesisinin özellikleri ve yaşam döngüsü aşaması dahil olmak üzere sahaya özgü koşulları dikkate alınarak yapılması şirketin sorumluluğundadır.

1. Kurumsal bir atık yönetim politikası ve taahhüdü geliştirmek.

Hedef; Şirketlerin, atık yönetimi ile ilgili niyet, taahhüt ve ilkeleri ifade eden bir politika ve / veya taahhüt oluşturduğunu ve etkili bir şekilde iletişimde olduğunu teyit etmek.

Şirketin atık yönetimine özel ayrı bir politika veya taahhüt geliştirmesine gerek yoktur. Bu göstergenin gereklilikleri, atık yönetimi taahhütlerini daha geniş olan şirket politikalarına veya taahhütlerine (örneğin, kurumsal sürdürülebilirlik politikası) dahil ederek karşılanabilir. Önemli kısım, kurumsal politika ve taahhütlerin güvenli, sorumlu atık yönetimi taahhütlerini içermesini veya bunlara atıfta bulunmasını sağlamak ve şirketin bu politika ve taahhütlere bağlı olduğunu göstermektir.

2. Sahaya özel bir atık yönetim sistemi geliştirmek/uygulamak ve Acil durum hazırlık planları geliştirerek test etmek.

Hedef;

Atık Yönetimi Kılavuzu'nda açıklanan atık yönetimi çerçevesine uygun olarak atık yönetimi sisteminin geliştirilmesi ve uygulanması.

Atık Tesislerinin Yönetimi Kılavuzu ile uyumlu Acil Durum Müdahale Planları ve Acil Durum Hazırlık Planları geliştirilmesi ve test edilmesi.

Şirketin, Atık Yönetimi Kılavuzu'nda açıklanan atık yönetimi çerçevesine uygun bir atık yönetim sisteminin uygulandığını dokümantasyon ve diğer kanıtlar yoluyla gösterebilmesi gerekir.

Benzer şekilde, atık depolama alanlarına ait Acil Durum Müdahale Planları ve Acil Durum Hazırlık Planları olması gerekli değildir. Acil Durum Müdahale Planları ve Acil Durum Hazırlık Planları atık yönetimi için ayrı olabileceği gibi genel sahanın tüm yönlerini kapsayan Acil Durum Müdahale Planları ve Acil Durum Hazırlık Planları'na dahil edilebilir ve çoğu durumda bu tercih edilir.

3. Atık yönetimi için hesap verilebilirlik ve sorumluluk atama

   Hedef; Atık yönetiminin hesap verilebilirliği için bir sorumlu yönetici (örneğin, CEO, COO veya Başkan Yardımcısı) atandığını ve şirkete atıkların sorumlu bir şekilde yönetildiğine dair güvence vermek için uygun bir yönetim yapısının ve kaynaklarının bulunduğunu onaylanması.

4. Sürekli iyileştirme için yıllık atık yönetimi incelemesi yapmak

   Hedef; Atık yönetimi üzerinde kurumsal yönetişimin sağlanması ve şirketin atık yönetimi organizasyonel yapılarının ve sistemlerinin etkin olduğundan ve atıkların güvenli, sorumlu yönetimine yönelik ihtiyaçları karşılamaya devam ettiğinden emin olmak için Sorumlu İcra Kurulu Üyesine raporlanan atık yönetiminin yıllık bir incelemesi olduğunu teyit edilmesi.

5. Sahaya özel İşletme ,Bakım ve İzleme Kılavuzu'nun geşiştirilmesi ve uygulanması

   Hedef; Şirketin, atık yönetim sisteminin uygulanmasını kolaylaştırmak amacıyla Sürdürülebilir Madencilik Atık Yönetimi Protokolü İşletme, Bakım ve İzleme Kılavuzu'na (İŞBİK - OMS) uygun olarak atık toplama tesisine özgü bir İşletme, Bakım Ve İzleme Kılavuzu (İŞBİK - OMS) geliştirip uyguladığının teyit edilmesi.

UYGULAMA ÖRNEĞİ – TÜPRAG EFEMÇUKURU ALTIN MADENİ

MAC, Sürdürülebilir Madencilik - Atık Yönetim Protokolü programı/sistemi Türkiye'de 2015 yılından bu yana TÜPRAG EFEMÇUKURU Altın Madeni'nde uygulanmaktadır. 2015 yılı içerisinde bir bağımsız değerlendirme raporu ve iç denetleme raporu hazırlanmıştır. 2017 yılı içerisinde bağımsız denetim kuruluşu tarafından hazırlanan MAC uyumluluk raporu sonrasında yol haritası belirlenerek çalışmalar başlanmıştır. Daha sonraki yıllarda diğer Sürdürülebilir Madencilik protokollerinin hazırlıkları tamamlanarak sisteme entegre edilmeye başlanmıştır.

TSM bileşenlerine 2015 yılından sonrada güncellemeler yapılmıştır. TÜPRAG EFEMÇUKURU Altın Madeni'nde Atık Yönetim Protokolü'nün ve Uygunluk Tablosu'nun 2019 versiyonu, Atık Kılavuzu ve OMS rehberinin 2021 versiyonları uygulanmaya başlanmıştır.

Mevcut operasyonel faaliyetlerde kullanılan sistemler/uygulamalar (Atık Yönetim Sistemi, Protokoller, İSG Uygulamaları ERP-EPP, prosedürler, BAT ve BAP'lar) TSM Atık Yönetim Protokolü uygulaması içerisine entegre edilmiştir.

Atık Yönetimi Politikası ve Taahhüdü

Atık yönetimine ilişkin taahhütler, şirketin politikalarına ve taahhütlerine dahil edilmiş ve Atık Kılavuzu ile tutarlıdır.

Atık Yönetim Sistemi ve Acil Durum Hazırlığı

Risk bazlı yaklaşım kapsamında atık depolama alanlarına özgü;

İş sağlığı ve güvenliği, çevre, mühendislik ve operasyonel, finansal, yasal ve yönetim süreçleri ile sosyal konuları kapsayan bir risk değerlendirmesi yapılmıştır.
Stabilite, temas suyu ve sızıntı, tozlanma, kapasite, izinler gibi konularda tehlikeler ve kritik kontroller belirlenmiştir.
Aşırı hava koşulları, atık nem içeriği, izleme verileri, deplasman gibi konuları kapsayan Kademeli Eylem Planları (KEP) hazırlanmıştır.

Risk değerlendirmesi ve kritik kontroller dikkate alınarak Acil Durum Müdahale Planı hazırlanmış ve KEP'lerle bağlanmıştır.

Mevcut saha Acil Durum Müdahale Planları'na ek olarak depolama alanları için özel Acil Durum Müdahale Planı oluşturulmuştur.

Depolama alanları için hazırlanan Acil Durum Müdahale Planları masabaşı ve genel saha tatbikatları yapılarak denetlenmiştir.

Atık Yönetimi Için Hesap Verilebilirlik Ve Sorumluluk

Atık Yönetimi Protokolü ve Atık Yönetim Kılavuzu uygulaması kapsamında sorumluluklar belirlenmiş ve Kayıt Mühendisi (EOR) atanmıştır.

Yıllık Atık Yönetimi İncelemesi

2017 yılından bu yana her sene Yıllık Gözden Geçirme Raporu hazırlanarak, yönetime sunulmaktadır. Ayrıca İç ve dış denetimler yapılarak raporlanmaktadır.

İşletme, Bakım ve İzleme Kılavuzu (İŞBİK)

Bir İŞBİK geliştirildi ve sahada uygulanmaktadır. Her yıl gözden geçirilerek uygun şekilde güncellenmektedir.

TÜPRAG EFEMÇUKURU Altın Madeni'nde 2021 Sürdürülebilir Madencilik Atık Yönetimi Protokolü performans değerlendirmesinde A seviyesine ulaşılmıştır. 2022 yılı 1. Çeyrekte yapılması planlanan Sürdürülebilir Madencilik Atık Yönetimi Protokolü performans değerlendirmesinin ardından (dış değerlendirme) AAA seviyesine ulaşılması hedeflenmektedir.

SONUÇLAR

Madencilik sektörünün ülkemizde ve dünyada hızla gelişmesi, sosyal ve çevresel etkilerindeki artışı da beraberinde getirmektedir. Bu durumu ülkeler yasal mevzuatlarında yaptıkları düzenlemeler ile yönetmektedir.

Sorumlu madencilik çercevesinde hem ülkelerin yasal mevzuatlarını, hemde madencilik faaliyetlerini mevcut en iyi teknikler ve mevcut en iyi uygulamalar ile destekleyecek bağımsız kuruluşların sürdürülebilir performans programlarına ihtiyaç artmıştır.

Kanada Madencilik Derneği, Sürdürülebilir Madencilik programı ve benzer performans programları, büyümekte ve gelişmekte olan sektöre mevcut en iyi teknikleri ve mevcut en iyi uygulamaları benimseterek sürekli gelişimi desteklemek ve yasal mevzuatlara uyumu sağlamak için bir rehber olmaktadır.

Bu tür programlar; madencilik sektörünün çevresel ve sosyal performansını iyileştirerek, işletmeye hesap verebilirlik, şeffaflık, ölçülebilirlik ve sürdürülebilirlik kazandırarak ülkemizdeki madencilik faaliyetlerinin mümkün olan en yüksek standartlarda yürütülmesine, yardımcı olacaktır.

KAYNAKLAR

Dumaresq, C. (2019). Overview of Governance Practices for Tailings Management. Presented at a short course entitled "Corporate Governance of Tailings Facilities – Challenges and Case Studies of Implementation. Short course was part of the "Tailings and Mine Waste 2019" congress. Vancouver, Canada.

Global Tailings Review (2020). Global Industry Standard on Tailings Management. https://globaltailingsreview.org/global-industry-standard/

Golder Associates (2016). Review of Tailings Management Guidelines and Recommendations for Improvement. Prepared for: International Council on Mining & Metals. https://www.icmm.com/en-gb/research/environmental-stewardship/tailings-report

International Council on Mining & Metals (2016, 2020). Tailings Governance Framework:

Position Statement. https://www.icmm.com/en-gb/about-us/member-requirements/position-statements/tailings-governance

Mining Association of Canada (2019a). A Guide to the Management of Tailings Facilities *Version 3.1*. https://mining.ca/our-focus/tailings-management/tailings-guide/

Mining Association of Canada (2019b). Developing an Operation, Maintenance, and Surveillance Manual for Tailings and Water Management Facilities *Second Edition. https://mining.ca/our-focus/tailings-management/oms-guide/*

Mining Association of Canada (2019c). Table of Conformance. https://mining.ca/documents/table-of conformance-2019/

Mining Association of Canada (2019d). Towards Sustainable Mining Tailings Management Protocol. https://mining.ca/towards-sustainable-mining/protocols-frameworks/tailings-management-protocol/

Mining Association of Canada (2021a). TSM 101: A Primer. https://mining.ca/documents/tsm-101-a-primer/

Mining Associaton of Canada (2021b). MAC Updates Tailings Management Guidance to Align with Global Standard. Press release issued in Ottawa, Canada, on 7 April, 2021. https://mining.ca/press-releases/mac-updates-tailings-management-guidance-to-align-with-global-standard/

Morgenstern, N.R. (2018). Geotechnical Risk, Regulation, and Public Policy. Sixth Victor de Mello Lecture. Presented in Salvador, Brazil, August, 2018.

https://victorfbdemello.com.br/en/de-mello-lectures-2__trashed/

TSM Tailings Review Task Force (2015). Report of the TSM Tailings Review Task Force. https://mining.ca/documents/report-tsm-tailings-review-task-force/

TSM Verification Guide (December 8, 2021). 2019 March Meeting Report_DRAFT_Apr_24_2019 BC an (mining.ca)

TSM Terms of Reference for Verifiers (Last Updated: November 19, 2021). 2021-TSM-Verifier-Terms-of-Reference.pdf (mining.ca)

Tailings Guide Implementation Checklist, Version 3.1 (2019). Tailings Guide Implementation Checklist, Version 3.1 (2019) - The Mining Association of Canada

Table of Conformance (March 20, 2019). Table of Conformance (2019) - The Mining Association of Canada

Kuru Atık Depolama Yöntemi - Dry Tailings Storage Method (IMCET - 16 April 2019 – Pages 1540-1530). Y.S. İnci, P. Kimball, G. Uzuncelebi, H. Ürkmez . ddcb03c09924b75_ek.pdf (maden.org.tr)

KARDEMİR A.Ş. KİREÇ FABRİKALARINDAKİ YANMIŞ KİREÇ TAŞI ELEME SİSTEMİNDE KULLANILAN ELEK PANELLERİNİN İYİLEŞTİRİLMESİ

IMPROVEMENT OF SIEVE PANELS USED IN BURNT LIMESTONE SCREENING SYSTEM AT KARDEMIR A.Ş. LIME PLANTS

E. Nakaş [1, *], C. Cantürk [2], F. Esin [2], O. Acur [2], M. Sevim [2], H. Gökkaya[3]

[1] *KARDEMİR A.Ş., İş Sağlığı ve Güvenliği Müdürlüğü*
*(*Sorumlu yazar: enakas@kardemir.com)*
[2] *KARDEMİR A.Ş., AR-GE Merkezi*
Karabük Üniversitesi, Mühendislik Fakültesi, Makine Mühendisliği

ÖZET

Günümüzde endüstriyel fabrikalar üretim maliyetlerini düşürebilmek ve rekabet etme gücünü arttırılabilmek için tesislerinde öneri ve iyileştirme çalışmalarına büyük önem vermektedirler. Dünyada her yıl yaklaşık olarak 1.9 milyar ton çelik üretimi yapılmakta ve bu miktarın % 60'ı yüksek fırınlardan elde edilmektedir. Kardemir A.Ş. entegre demir çelik fabrikasında çelik üretimi prosesi sırasında yanmış kireç taşı sıvı çelik içerisindeki empüritelerin giderilmesi için kullanılmaktadır. Yanmış kireçtaşlarının 50 mm'nin üzerindeki boyutta olması sıvı madende homojen bir şekilde çözünmesi için önem arz etmektedir. Yanmış kireç taşlarının boyutlandırılmasında kullanılan çelik esaslı elek panellerinde oluşan kopmalar yanmış kireç taşlarının sağlıklı boyutlandırılamamasına ve kopmalardan kaynaklı üretim duruşları, iş sağlığı ve güvenliği konularında olumsuzluklara neden olmaktadır. Bu çalışmada, çelik esaslı elek panelleri yerine aynı boyutlandırma alanına sahip olan kauçuk esaslı elek panelleri kullanılmıştır. Kauçuk esaslı elek panelleri kullanılarak yapılan iyileştirme ile birlikte, yanmış kireç taşlarının boyutlandırılması işlemi esnasında panellerde oluşan kopma ve kopmadan kaynaklı üretim duruşları, elek panellerinin değişimi esnasında yaşanan iş sağlığı ve güvenliği risklerinin önüne geçilmiştir.

Anahtar Sözcükler: Bazik oksijen fırını (BOF), yanmış kireç taşı, elek paneli, üretim duruşu, iş sağlığı ve güvenliği

ABSTRACT

Nowadays, industrial factories attach great importance to suggestions and improvement studies in their facilities in order to reduce production costs and increase their competitiveness. Approximately 1.9 billion tons of steel is produced every year in the world and 60% of this amount is obtained from blast furnaces. Burnt limestone is used to remove impurities in the liquid steel during the steel production process of KARDEMİR A.Ş. integrated iron and steel factory. The size of burnt limestone over 50 mm is important for homogeneous dissolution in liquid steel. The breaks in the steel-based sieve panels used in the sizing of the burnt limestone cause the burnt limestone not to be dimensioned properly and cause negativity on the production stops, occupational health and safety issues. In this study, instead of steel based sieve panels, rubber based sieve panels with the same sizing area are used. Along with the improvement made by using rubber-based sieve panels, the production stops caused by the break and break in the panels during the sizing process of burnt limestone, occupational health and safety risks experienced during the replacement of sieve panels were prevented.

Keywords: Basic oxygen furnace (BOF), burnt limestone, sieve panel, production stop, occupational health and safety

GİRİŞ

Çelik malzemeler yapı, otomotiv, sağlık sektörlerinde ve günlük kullandığımız araç gereç gibi pek çok alanda karşımıza çıkmaktadır. Dünyada her yıl yaklaşık olarak 1.9 milyar ton çelik üretimi yapılmakta olup bu miktarın % 60'ı yüksek fırınlarda demir içerikli ham maddelerin kok ve kireçtaşının ergitilmesiyle oluşturulmaktadır. Diğer %40'lık kısım ise ark ocaklarında hurda ergitme yöntemi ile yapılmaktadır. Çelik üretiminde yanmış kireç taşı vazgeçilmez bir parametredir. Yanmış kireç taşlarının boyutları da çok önemlidir. Belirli ebatlarda olması sıvı çelik yapısında daha optimum çözünüp çelik içerisinde istenmeyen kükürt silisyum gibi çeliğe zarar veren elementlerle bileşik oluşturarak çelik yapısında yüzeye çıkarılır ve yapıdan uzaklaştırılır. Kardemir A.Ş. çelik üretim prosesinde yanmış kireç taşlarının ebatlarının çelik üretim prosesi gereği 50 mm üzerinde olması istenmektedir.

Endüstriyel tesisler de eleme boyutlandırma işleminde genellikle çelik esaslı elek panelleri kullanılmaktadır. Çelik esaslı elek panellerinde deformasyonlara bağlı kısa sürelerde oluşan kopmalar, çelik esaslı elek panellerinin montaj ve demontaj işlemlerinin zorluğu gibi olumsuz özellikleri 7/24 çalışmaya devam eden endüstriyel şirketleri arayış içerisine sokmaktadır. Günümüz teknolojisinde çelik esaslı elek panellerinin yerini kauçuk esaslı elek panelleri almaktadır. Kauçuklar esneme kabiliyetlerinden ötürü üzerlerine uygulanan enerjiyi absorbe ederek yapısal hasara uğramayan malzemelerdir. Kauçuklar bu özellikleri ile mühendislik alanında pek çok uygulamada tercih edilirler.

Yapılan çalışma ile Kardemir A.Ş. çelik üretim müdürlüğüne bağlı kireç fabrikasında eleme boyutlandırma işlemi yapılan çelik esaslı elek panelleri yerine kauçuk esaslı elek paneli kullanımına geçilerek elek panellerinde oluşan kopmalara bağlı ünite duruşları, maliyet ve iş sağlığı güvenliği konularında iyileştirme gerçekleştirilmiştir.

Çelik Üretim Prosesi

Bazik Oksijen Fırını (BOF), ilk aşamada şarj bölümü yönünde eğilerek içerisine hurda şarj edilir. Hurda şarjını alan BOF, yine aynı pozisyonda pota kükürt giderme tesisinde işlenmiş şarja hazır haldeki sıvı maden potasını bekler ve belli bir zaman sonra içerisine sıvı maden şarj edilir. BOF, içerisine hurda malzeme ve sıvı maden alımından sonra ağzı dik konuma getirilir. BOF şarj ağzı dik konumda iken, içerisine flaks silolarından yanmış kireç taşı ve diğer malzemeler (dolomit mıcırı, pelet) şarj edilir. BOF içerisine yapılan şarj işlemlerinden sonra lans ile 15-20 dakika boyunca saf oksijen üfleme işlemi uygulanır. BOF içerisine daldırılan lans üfleme işlemi ile oksijen; karbon, kükürt, silisyum ve mangan ile kimyasal tepkimeye girer. Karbon, yapıdan karbon monoksit (CO) olarak uzaklaştırılır. Diğer elementler ise yanmış kireç taşı sayesinde yüzeyde cüruf olarak uzaklaştırılır. Lans vasıtasıyla gerçekleştirilen tepkimeler sonucunda çelik üretimi gerçekleştirilmiş olunur. İçerisinde çelik üretimi gerçekleştirilen BOF, boşaltma bölümü yönüne eğilerek içerisindeki çeliği transfer arabası üzerinde bekleyen çelik potası içerisine boşaltır. Yanmış kireç taşı sayesinde oluşan cüruf özkütle farkı nedeniyle BOF içerisinde kalır. BOF tekrar şarj bölümü yönünde eğilerek BOF içerisindeki cürufu, cüruf potasına boşaltır. Tüm bu işlemler tavan vinçleri ile yapılmaktadır.

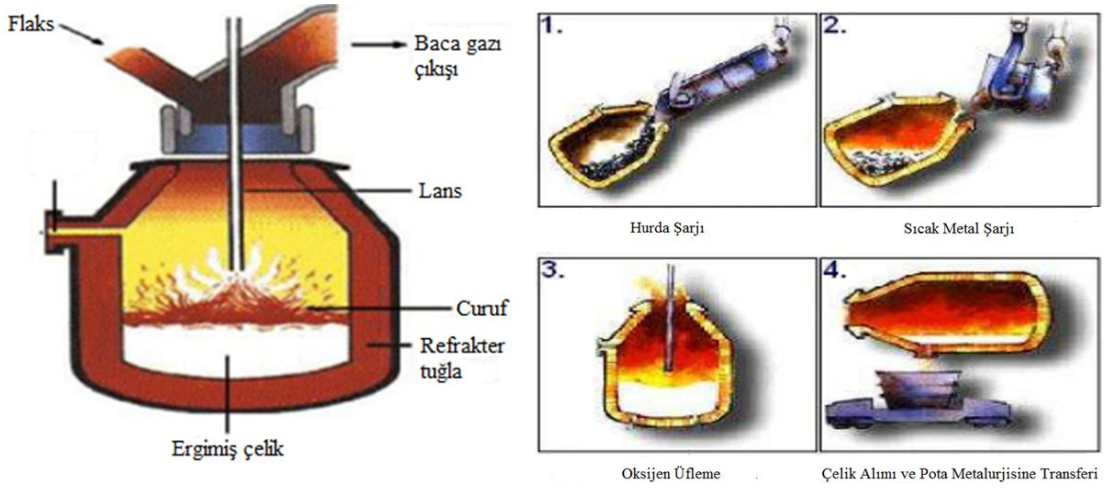

Şekil 1. BOF ile çelik üretim prosesi (2)

Bof'da Yanmış Kireç Taşı Kullanımı

BOF' larda üretilen çelik kalitesinin iyi olması için kullanılan yanmış kirecin de kaliteli olması istenilmektedir. Kaliteli yanmış kireç taşı; uygun büyüklüğe sahip, içerdiği kalsiyum oksit (CaO) oranı ve kükürt (S) , fosfor (P), silisyum (Si) gibi safsızlıklar ile tepkimeye girme reaktivitesi yüksek olan kireçtir. BOF ile çelik üretiminde kullanılan yanmış kireç taşı, BOF' un ısıl dengesini sağladığı ve safsızlıkların giderilmesini gerçekleştirdiği gibi oluşturduğu cüruf sayesinde BOF içerisindeki refrakter tuğla ömrünü de uzatmaktadır. BOF içerisindeki cüruflar refrakter tuğlalar üzerinde bir katman oluşturarak tuğlaların aşınmasını engellemektedir. Bu da, maliyeti çok yüksek olan refrakter tuğlaların uzun süre kullanımını arttırmaktadır.

<u>BOF'da Yanmış Kireç Taşı Boyutlarının Önemi</u>

BOF' larda kullanılan yanmış kirecin ebatları büyük önem arz etmektedir. BOF' da çelik üretimi esnasında oluşan karbon monoksit (CO), karbondioksit (CO2) gazları ve oluşan tozların ortama yayılmaması için lans ile oksijen üfleme esnasında 1200 d/dk dönen emiş gücü çok yüksek bir ID fan vasıtası ile çekilmektedir. Gaz ve tozdan oluşan karışım boru içerisinde ID fanın emiş yönüne doğru hareket etmektedir. Gaz ve toz karışımı hareket halindeyken su püskürten nozullarla toz çöktürme işlemi uygulanmaktadır. Tozdan arınan gaz karışımı değerlendirilmek üzere Kardemir A.Ş Enerji Tesislerine gönderilmektedir.

BOF' larda istenilen kalitede 92 ton çelik üretmek için 4-4.5 ton yanmış kireç taşı kullanılmaktadır. Yanmış kireç taşları istenilen boyutlardan küçük olması durumunda BOF içerisinde sıvı maden yapısına ulaşamadan fanın emiş gücü ile çekilmektedir. Küçük boyutlarda yanmış kireç taşı kullanılması durumunda BOF içerisine tekrar yanmış kireç taşı şarj etmek gerekmektedir. Bu durum, yanmış kireç taşı sarfiyatını artırmaktadır. Ayrıca BOF içerisine tekrar yanmış kireç taşı şarj alma ve lans ile yeniden oksijen üfleme sürelerinden dolayı üretimde kayıplara neden olmaktadır. Kardemir A.Ş. BOF'larında çelik üretim esnasında işletme standardınca yanmış kireç taşı boyutları 50 mm üzerinde kullanılmaktadır.

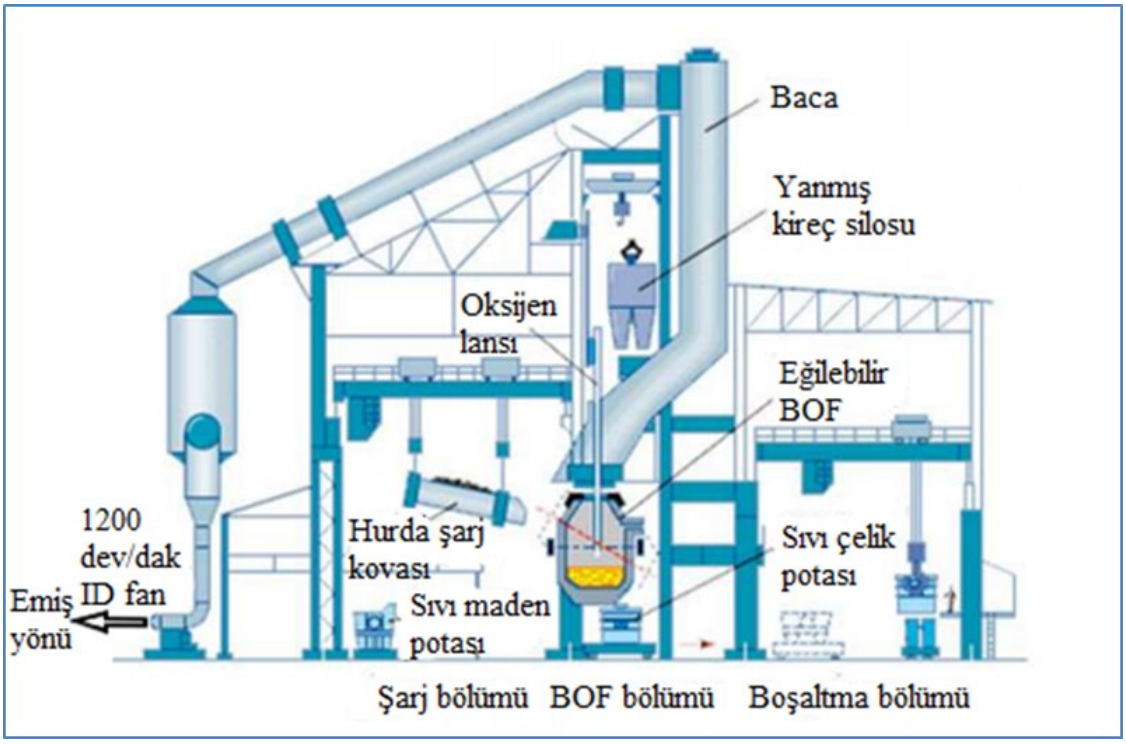

Şekil 2. BOF'un yardımcı bölümlerinin genel görünümü (2)

Kardemir A.Ş. Kireç Fabrikaları

Karabük ili, jeolojik açıdan zengin bir bölgededir. Kardemir A.Ş; kireç fabrikası hammadde kaynağı olan kireç taşını, Karabük ilinin Eskipazar ilçesinde bulunan kireç taşı ocaklarından temin etmektedir. Eskipazar'da çıkarılan kireç taşlarının kaliteli ve Kardemir A.Ş.' ye yakın oluşu lojistik açıdan avantaj kazandırmaktadır.

Kardemir A.Ş. çelik üretim ünitesindeki BOF' larda çelik üretimi için gerekli olan kireç taşları kamyonlarla Kardemir A.Ş. kireç fabrikası kireç taşı yer altı bunkerleri (150 Ton) sahasına getirilmektedir.

Şekil 3. Kardemir A.Ş. kireç fabrikasında bulunan kireç taşı yer altı bunkerleri genel görünümü

Kardemir A.Ş. bünyesinde bulunan kireç taşı fabrikasında 300 ton kapasiteli 2 adet kireç taşı silosu bulunmaktadır.

Şekil 4. Kireç taşı dolu skip arabasının eğik ray yolu üzerinde silo üstü bunkerine doğru hareketinin genel görünümü

Kireç taşları kireç fırınları içerisine şarj edildikten sonra 1000-1050 °C sıcaklıkta yakılarak kireç taşlarının kalsinasyonu gerçekleştirilerek metalürjik yanmış kireç taşı elde edilmektedir. Kireç fırınında her iki haznenin alt kısmında bulunan klapeler açılarak yanmış kireç taşları bant yollarına boşaltılır. Bant yolu üzerindeki yanmış kireç taşları kovalı elevatöre şarj edilir. Elevatör, içerisindeki kovalara doldurulan yanmış kireç taşlarını 50 m yüksekliğe çıkarır ve kovalardaki yanmış kireç taşlarını eleğe boşaltır. Yanmış kireç taşı eleğinde 50 mm üzerindeki yanmış kireç taşları 250 m uzunluğundaki bant yolu ile kireç fabrikasından çelikhaneye taşınırlar. Çelikhaneye gelen yanmış kireç taşları BOF'lar üzerindeki yanmış kireç silosuna şarj edilerek stoklanır.

Yanmış Kireç Taşı Boyutlandırmada Kullanılan Çelik Esaslı Elek Panelleri

BOF' larda çelik üretiminde BOF'un ısıl dengesinin sağlanması ve sıvı maden içerisindeki safsızlıkların giderilmesi için yanmış kireç taşına ihtiyaç bulunmaktadır. Yanmış kireç taşları 50 mm büyük boyutlarda olması yanmış kireç taşlarının BOF içerisindeki sıvı madende homojen bir şekilde çözünmesi için önem arz etmektedir. 50 mm üzerindeki boyutlarda yanmış kireç taşlarının elde edilmesi için Kardemir A.Ş. Kireç Fabrikaları kullanılmaktadır.

Şekil 5. Yanmış kireç taşı elemede kullanılan çelik esaslı elek paneli gösterimi

Kireç fabrikalarında genel olarak yanmış kireç taşını boyutlandırmada çelik esaslı elek panelleri kullanılmaktadır. Yanmış kireç taşı boyutlandırma ve nakil ünitesinde eleme görevi gören çelik esaslı elek panelleri, çelik profillerden imal edilmiş bir şase üzerinde çalışmaktadır. Çelik esaslı elek panelleri, her iki tarafında bulunan gergi plakalarına geçirilir ve yanmış kireç taşı eleğinin gövdesinin iç kısımlarına cıvatalar ile sabitlenir. Elek panellerinin çalışmalarında tahrik için elektrik motorları kullanılmaktadır. Elektrik motoru tahriki ile üretilen güç, kayış kasnak sistemi ile yanmış kireç taşı eleğinin ortasında bulunan uzun mile aktarılır. Dönen milin diğer ucunda bulunan eksantrik ağırlıkların oluşturduğu titreşim ile yanmış kireç taşlarının boyutlandırılma işlemi yapılmaktadır.

Çelik esaslı elek panelleri, titreşime bağlı olarak altında bulunan çelik profilden imal edilmiş şaseye çarpmalar meydana getirerek çalışmaktadır. Saatte 30 ton 55 ℃ sıcaklığında kireç taşı eleme kapasitesine sahip eleme ünitesi, titreşim ve çarpmaların etkisiyle üzerinde bulunan elek panellerinde kopmalar meydana gelmektedir. Çelik esaslı elek panellerinde oluşan kopmalar sonucunda 50 x 50 mm olması gereken göz aralığı, kopma durumuna göre farklılık göstererek daha büyük boyutlarda olabilmektedir. Bu durumda, yanmış kireç taşının boyutlandırılması sağlıklı olmamaktadır.

Şekil 6. Yanmış kireç taşı eleme esnasında çelik esaslı elek paneli üzerinde oluşan kopmaların gösterimi

Kauçuk Esaslı Elek Panelleri Tasarım ve Özellikleri

Yanmış kireç elek panellerinde oluşan kopmaların önüne geçmek için çelik esaslı elek panellerinin yerine kauçuk esaslı elek panellerinin kullanımı araştırılmıştır. Yapılan araştırmalar sonucunda kauçuk esaslı elek panellerinin sanayide kopma ve dağılma yaşanmadan uzun sürelerde kullanıldığı tespit edilmiştir. Kauçuk esaslı elek panelleri 65 ℃ sıcaklığındaki taşları boyutlandırabilme ve 60 shore sertlik değerine sahiptirler. Yanmış kireç taşının fırınlardan eleğe ulaştığındaki sıcaklığı 55 ℃'dir. Bu veriler göz önünde bulundurulduğunda kauçuk esaslı elek panellerinin Kardemir A.Ş. Kireç Fabrikaları yanmış kireç taşı eleğinde kullanılabileceği öngörülmüştür. Alman KÜPER firması ile yapılan görüşmeler sonucunda 1700 mm x 1600 mm ölçülerindeki 3 adet çelik esaslı elek panelleri yerine 839 mm x 300 mm ölçülerinde 30 adet kauçuk esaslı elek panellerinin kullanılması tasarlanmıştır. Yeni tasarımın, 10 adet kauçuk elek paneli 1 bölmeyi oluşturacak ve her bir bölme arasında 90 mm yükseklik farkı olacak şekilde toplamda 3 bölme olması kararlaştırılmıştır. Bu sayede elek panelindeki mesh alanını büyüterek olası bir kopmada sadece kopma olan kauçuk elek panelinin değiştirilip üretim duruşuna verilen ara çok kısa olacağı da düşünülmüştür.

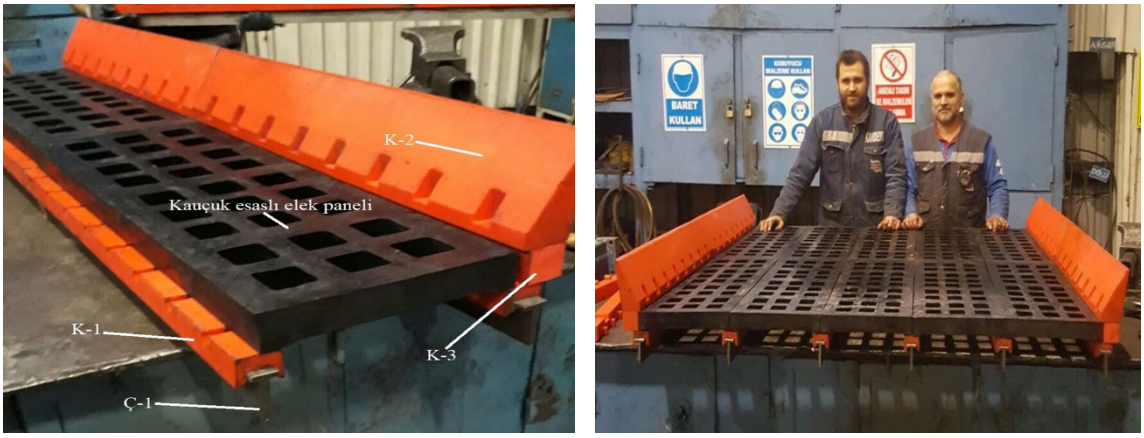

Şekil 7. Kauçuk esaslı elek paneli ve bağlantı elemanlarının gösterimi

Bu şase toplam 4 faklı pozdan oluşmaktadır. Ç-1 pozu çelik esaslı T profil ve K-1, K-2, K-3 pozları ile belirtilen kauçuk esaslı malzemeler kauçuk esaslı elek panelinin sağa ve sola kaymasını engellemektedir.

Çelik Esaslı Elek Panellerinin Demontaj İşlemi

Kauçuk esaslı elek panel şasesi çelik esaslı elek panel şasesinden farklıdır. İlk olarak eleğin üst kademesinde bulunan cıvata bağlantılı çelik esaslı elek panelleri taşıyıcı şaseden demontajı yapılmıştır. Üst kademedeki çelik esaslı elek panellerinin demontajından sonra elek içerisindeki çelik esaslı panel şasesi komple kesilerek alınmıştır. Yanmış kireç taşı eleği üst kademe şasesi kesilip alındıktan sonra elek iç yüzeyi kauçuk esaslı elek panellerinin şasesinin kaynağının yapılabilmesi için zımpara taşı ile taşlanarak elek iç yüzeyinde kalan parça ve çapakların temizliği yapılmıştır.

Şekil 8. Çelik esaslı elek panel şaselerinin kesilerek demontajı anı görünümü

Kauçuk Esaslı Elek Panellerinin Montaj İşlemi

Yanmış kireç taşı elek iç yüzeyinin temizlik işi bittikten sonra kauçuk esaslı elek şasesi olan 200 mm x 200 mm ebatlarındaki kutu profillerin kaynakları yapılmıştır. Montaj için daha önce atölyede hazır hale getirilmiş kauçuk esaslı elek panelleri yanmış kireç taşı eleği iç kısmında şase görevi gören kutu profillere M22 civata ile bağlanacak şekilde tasarlanmıştır. Elekteki titreşiminden dolayı cıvata somunları cıvatadan kurtulamayacak şekilde birbirine sıkı sıkıya kenetlenecek özellikteki fiberli somunlarla montajı yapılmıştır.

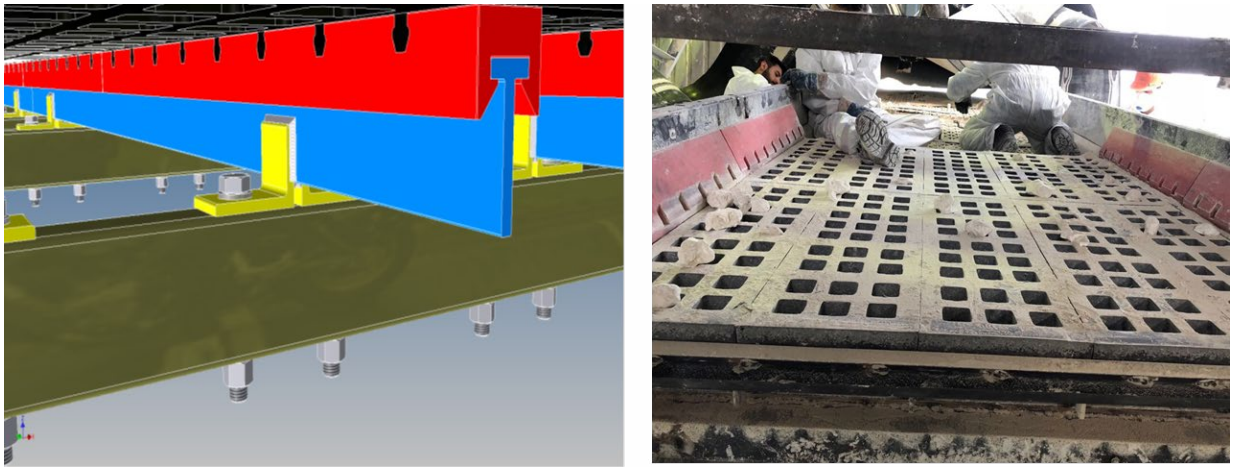

Şekil 9. Kauçuk esaslı elek panellerin montajının yapılması anı ve kauçuk esaslı panelinin bilgisayar ortamında oluşturulan şase görünümü

Çelik Esaslı Elek Panellerinde Oluşan Kopmalara Bağlı Olarak Kireç Fabrikası Üretim Duruşu

Kardemir A.Ş. kireç fabrikalarında yanmış kireç taşı eleme boyutlandırma işlemi çelik esaslı elek panelleri ile gerçekleştirilmektedir. Yanmış kireç taşını boyutlandırmada kullanılan elek 5034 mm x 1600 mm ölçülerinde dikdörtgen bir tarama-boyutlandırma alanına sahiptir. Bu tarama alanı 20 derece açı ile eğik bir şekilde olup 1678 mm x 2057 mm olmak üzere 3 eşit çelik esaslı elek paneli ile bölünmüştür. Yanmış kireç taşı eleğinde kullanılan çelik esaslı elek panellerinde oluşan kopmalar sonucunda sağlıklı boyutlandırma işlemi yapılabilmesi için deforme olan elek panelinin yenisi ile değiştirilmesi gerekmektedir.

Çizelge 1. Kireç Fabrikaları duruş süreleri ve üretim kaybı

Aylar	Çelik esaslı elek paneli (adet)	Ünite duruşu (saat)	Üretim kaybı (ton)
Ocak	2	8	240
Şubat	3	12	360
Mart	2	8	240
Nisan	3	12	360
Mayıs	1	4	120
Haziran	3	12	360
Temmuz	1	4	120
Ağustos	3	12	360
Eylül	1	4	120
Ekim	1	4	120
Kasım	3	12	360
Aralık	2	8	240

Kopmaların oluştuğu çelik esaslı elek paneli cıvata bağlantıları sökülerek demontajı yapılmaktadır. Cıvata bağlantıları sökülen çelik esaslı elek paneli 4 işçi ile elle taşınarak elek şasesinden alınmaktadır. Yeni elek paneli yine 4 işçi tarafından el gücü ile elek şasesi üzerine konularak cıvata bağlantıları tamamlanmaktadır. Bir adet çelik esaslı elek panelinin kopmadan kaynaklı demontajı ve yenisinin montajı işleminin yapılması ortalama 4 saat sürmektedir. Deforme olan her bir elek panelinin

değiştirilebilmesi için üretime 7/24 devam eden kireç fabrikaları duruşa geçmektedir. Çelik üretim müdürlüğü mekanik bakım faaliyet raporları incelendiğinde çelik esaslı elek panellerinin 2017 yılında toplamda 25 adet değiştirildiği tespit edilmiştir.

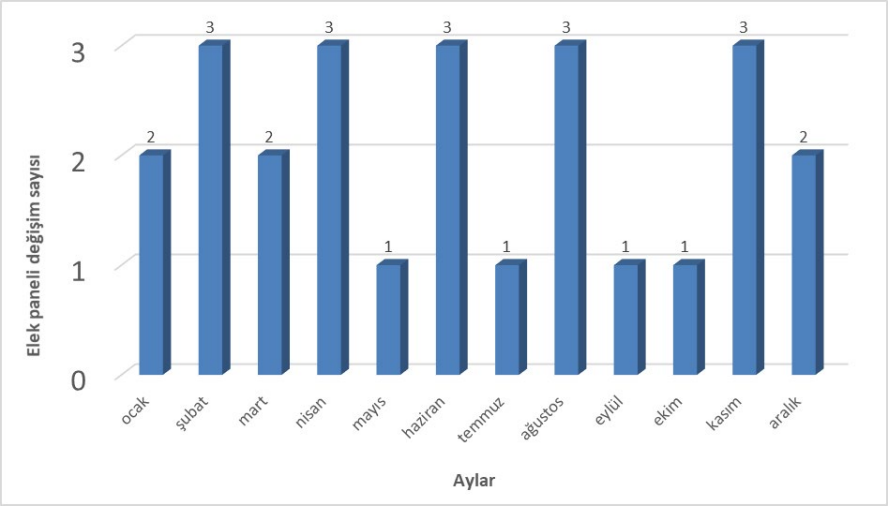

Şekil 10. Kardemir A.Ş. Çelik Üretim Müdürlüğü Mekanik Bakım faaliyet raporu verilerine göre çelik esaslı elek paneli değişim sayısı

Bir adet çelik esaslı elek panelinin değiştirilmesi 4 saat sürmektedir. Çelik esaslı elek paneli değişiminde ünite duruşu gerçekleşmektedir. 2017 yılında çelik esaslı elek panellerinin kopmasına bağlı olarak 100 saat ünite duruşu yaşanmıştır.

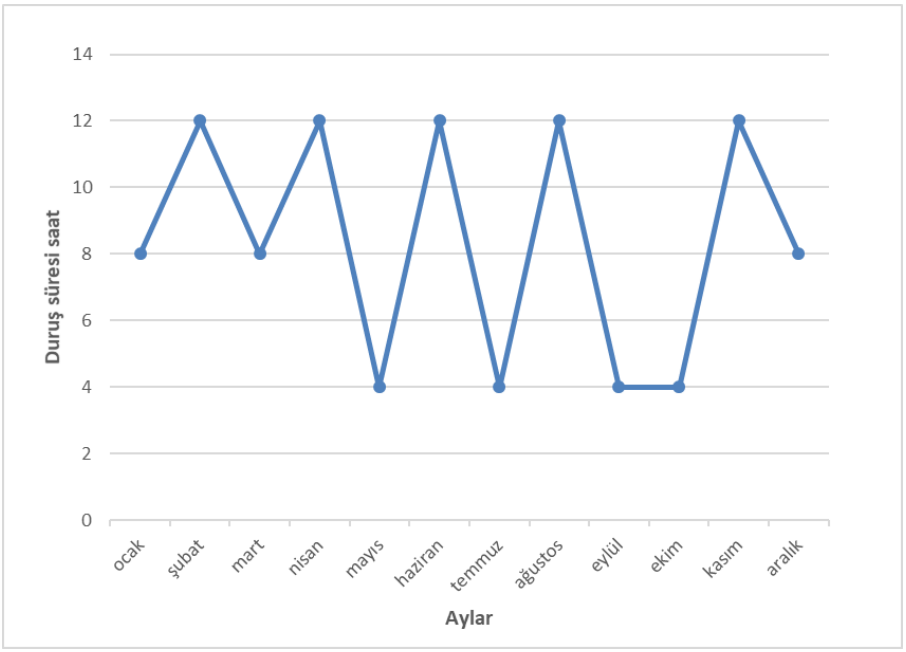

Şekil 11. Kardemir A.Ş. Kireç Fabrikaları çelik esaslı elek panelleri değişimi kaynaklı ünite duruş saatleri

Kardemir A.Ş. Kireç Fabrikalarında 30 ton/saat üretim yapılmaktadır. Çelik esaslı elek panellerinin değişiminden kaynaklı ünite duruşlarından dolayı 2017 yılında 3000 ton yanmış kireç taşı üretim kaybı yaşanmıştır. Kauçuk esaslı elek paneli kullanılarak yapılan iyileştirme sonucunda 1 yıl (Ocak 2018-Ocak 2019), zaman aralığında rutin duruşların dışında elek paneli kopmalarından kaynaklı kireç fabrikaları duruşu gerçekleşmemiştir. Bu durum; kireç fabrikalarının üretim verimliliğini arttırmıştır.

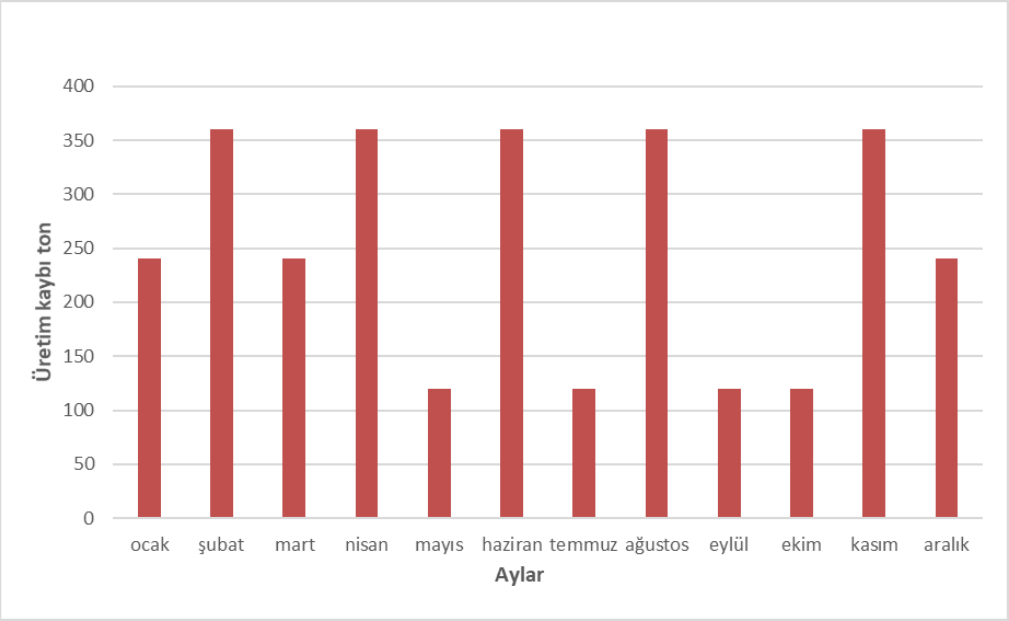

Şekil 12. Kardemir A.Ş. Kireç Fabrikaları çelik esaslı elek panelleri değişiminden kaynaklı yanmış kireç taşı üretim kayıpları

İş Sağlığı ve Güvenliği

Çelik esaslı elek panellerinin yenisi ile değiştirilmesi işlemi 4 kişi ile zor koşullar altında geçekleştirilmektedir. İSG uzmanı tarafından çelik esaslı elek panelleri ortalama haftada bir kez değiştirilmekte olduğundan olasılık değeri 5 olarak belirlenmiştir. Çelik esaslı elek panelleri el-kol sıkışması ayak burkulması, belde incinme, yaralanma gibi iş kazalarına sebep olduğu için İSG uzmanı tarafından şiddet değeri 3 olarak belirlenmiştir. L matrisine göre risk skor değeri olasılık ile şiddetin çarpımıdır. Çelik esaslı elek panelleri değişimi sırasındaki risk skoru Olasılık (5) x Şiddet (3) = 15 olarak tanımlanmıştır.

Kauçuk esaslı elek panellerinde kopmalar yaşanmamaktadır. Olasılık değeri İSG uzmanı tarafından 1 olarak belirlenmiştir. Kopma olup olası bir kauçuk esaslı elek paneli değişimi durumunda bir kişi herhangi bir el aleti kullanmadan kopan elek panelini değiştirebilmektedir. Kauçuk esaslı elek panelinin olası değiştirilme ihtimaline karşı İSG uzmanı tarafından şiddet değeri 3 olarak belirlenmiştir. Kauçuk esaslı elek panelleri değişimi sırasındaki risk skoru Olasılık (1) x Şiddet (3) = 3 olarak belirlenmiştir.

Kardemir A.Ş. kireç fabrikalarında kullanılan elek makinesi panellerinde gerçekleştirilen iyileştirme ile risk skor değeri 15'den 3'e düşürülerek, elek panelleri değişiminde oluşabilecek iş kazalarının önüne geçilmiştir.

RİSK DEĞERLENDİRME YÖNTEMİ

R = O x Ş
R = Risk
O = Olasılık
Ş = Şiddet (Zararın Derecesi)

Olasılık		Ortaya Çıkma Olasılığı
Çok küçük	(1)	Yılda bir veya daha az
Küçük	(2)	Altı ayda bir
Orta	(3)	Üç ayda bir
Yüksek	(4)	Ayda bir
Çok Yüksek	(5)	Haftada bir

Şiddet (Zararın Derecesi)		Derecelendirme
Çok Hafif	(1)	İş saati kaybı yok, ilkyardım gerektiren
Hafif	(2)	İş günü kaybı yok, ilkyardım gerektiren
Orta	(3)	Hafif yaralanma, tedavi gerektiriyor
Ciddi	(4)	Ağır yaralanma, uzuv kaybı
Çok ciddi	(5)	Ölüm, birden çok ölüm

RİSK MATRİSİ

Şiddet – Zarar / Olasılık-İhtimal	Çok Ciddi (5)	Ciddi (4)	Orta (3)	Hafif (2)	Çok Hafif (1)
Çok Yüksek (5)	25	20	15	10	5
Yüksek (4)	20	16	12	8	4
Orta (3)	15	12	9	6	3
Düşük (2)	10	8	6	4	2
Çok Düşük (1)	5	4	3	2	1

RİSK SKORU	EYLEM
25, 20, 16, 15	**KABUL EDİLEMEZ RİSK** Bu risk değeri ile ilgli mümkün olan en kısa sürede çalışma balşatılmalı, önlem alınmalı.
12, 10, 9, 8	**DİKKATE DEĞER RİSK** Risk seviyesini aşağıya düşürmek için önlem planlanmalı ve yakın - orta tarihte faaliyete geçirilmeli.
6, 5, 4, 3, 2, 1	**KABUL EDİLEBİLİR RİSK** Denetim ve kontroller ihmal edilmemeli. Eylem planı düşünülebilir.

Şekil 13. Kardemir A.Ş. Risk Skoru belirlemede kullanılan L tipi matrisin şiddet sayısal değerleri ve derecelendirme tanımları

SONUÇLAR

Kardemir A.Ş çelik üretim tesisi mekanik bakım onarım ekibi tarafından çelik esaslı elek panelleri, dinamik mühendislik uygulamaları için ideal olan esneyebilme özelliği sayesinde üzerine düşen enerjiyi absorbe edebilen kauçuk esaslı elek panelleri ile değiştirilerek 2018 yılı içerisinde elek panellerinde kopmalardan dolayı çelik üretim prosesinde gecikmeler yaşanmamıştır.

Kardemir A.Ş. kireç fabrikalarında kullanılan elek makinesi panellerinde gerçekleştirilen iyileştirme ile risk skor değeri 15'ten 3'e düşürülerek, elek panelleri değişiminde oluşabilecek iş kazalarının önüne geçilmiştir.

Yapılan iyileştirme çalışması ile küçük boyutlarda yanmış kireç taşı kullanılması durumunda BOF içerisine tekrar yanmış kireç taşı şarj edilmesi ortadan kaldırılarak yanmış kireç taşı sarfiyatında azalma sağlanmış, çelik esaslı elek panellerinde oluşan kopmalara bağlı olarak yenisi ile değişiminde harcanan zaman kireç fabrikalarında kestirimci bakım yapılarak değerlendirilmiştir.

KAYNAKLAR

Nakaş, E. (2019), "Kardemir A.Ş. Kireç Fabrikalarındaki Yanmış Kireç Taşı Eleme Sisteminde Kullanılan Elek Panellerinin İyileştirilmesi", Yüksek Lisans Tezi, Karabük Üniversitesi Fen Bilimleri Enstitüsü, Karabük.

Yıldız, K. (2013), "Demir Çelik Metalurjisi Ders Notları", Sakarya Üniversitesi Metalurji ve Malzeme Mühendisliği Bölümü, Sakarya.

KARDEMİR A.Ş'DE YERLİ VE İTHAL TOZ CEVHERLER İLE HAZIRLANAN HARMANLARDA ÜRÜN SİNTER KALİTESİNİN DEĞERLENDİRİLMESİ

EVALUATION OF PRODUCT SINTER QUALITY IN BLENDS PREPARED WITH DOMESTIC AND IMPORTED FINE ORES AT KARDEMIR A.Ş.

T. Timur [1], C. Cantürk [2], F. Esin [2,*], O. Acur [2], M. Sevim [2], Y. Sun[3]

[1] *KARDEMİR A.Ş., Kalite Güvence Metalurji ve Laboratuvarlar Müdürlüğü*
[2] *KARDEMİR A.Ş., AR-GE Merkezi*
*(*Sorumlu yazar: fesin@kardemir.com)*
[3]*Karabük Üniversitesi, Mühendislik Fakültesi, Metalürji ve Malzeme Mühendisliği*

ÖZET

Entegre Demir Çelik Tesislerinde yüksek fırınlara direkt olarak şarj edilemeyecek boyuttaki toz cevherler, ergime sıcaklığı altında yüzey ergitme işlemine tabi tutularak birleştirilmektedir. Sinterleşme neticesinde yüksek fırınlarda kullanılabilir boyuta gelmektedir. Sinter, yüksek fırınların en ekonomik demirli malzeme girdisidir. Yüksek fırınların üretim hızı, verimi, oluşan ürünün kalitesi ve ekonomikliği kullanılan hammaddelere bağlıdır. Bu çalışmada farklı oranlarda, yerli ve ithal toz demir cevherlerin harmanlanması sonucu elde edilen ürün sinterin kalitesinin değerlendirilmesi yapılmıştır. Harman sahasından her bir harmanı temsilen numune alınarak, harmanın fiziksel (elek analizi) ve kimyasal (XRF) özellikleri belirlenmiştir. Harmanlar yerli ve ithal toz cevher, kalibre cevher, pelet tozu ve diğer (birtakım işletme atık tozları) olarak kategorize edilmiş ve sinterleştirilmiştir. Elde edilen sinterlerin fiziksel (elek analizi, tambur testi), kimyasal (XRF) ve metalurjik analizleri (RUL, RDI) yapılmıştır. Tüm analiz sonuçları incelendiğinde yüksek fırınlarda kullanılan sinter için en uygun karışımın en az % 30 ithal cevher kullanılarak sağlanacağı sonucuna varılmıştır.

Anahtar Sözcükler: Harmanlama, toz cevher, sinter, sinter fabrikası, yüksek fırın

ABSTRACT

In Integrated Iron and Steel Plants, fine ores of a size that cannot be charged directly to the blast furnaces are combined by subjecting to surface melting under the melting temperature. As a result of sintering, it becomes usable in blast furnaces. Sinter is the most economical ferrous material input of blast furnaces. Blast furnaces production speed, efficiency, quality and economy of the product obtained depend on the raw materials used. In this study, the quality of the product sinter obtained by blending domestic and imported fine ores in different proportions was evaluated. Physical (sieve analysis) and chemical (XRF) properties of the blend were determined by taking samples from the blend area to represent each blend. Blends has been categorized and sintered as domestic and imported fine ore, calibrated ore, pellet dust and other (waste dusts of some plant). Physical (sieve analysis, drum test), chemical (XRF) and metallurgical analysis (RUL, RDI) of the obtained sinters were made. When all analysis results were examined, it was concluded that the most suitable mixture for sinter used in blast furnaces would be provided using at least 30% imported ore.

Keywords: Blending, fine ore, sinter, sinter plant, blast furnace

GİRİŞ

Ülkedeki diğer sanayi yatırımlarını desteklemek amacıyla, birçok fabrikanın kuruluşunda aktif bir biçimde rol alan "Fabrikalar Kuran Fabrika" unvanıyla bilinen KARDEMİR, Türkiye'de sanayileşme hamlesinin en önemli mihenk taşlarından biri olarak kurulmuş ilk entegre demir çelik fabrikasıdır. Temelleri 3 Nisan 1937 tarihinde atılan bu fabrika, 84 yıllık köklü bir geçmişe ve sanayi kültürüne sahiptir.

Sıvı çelik üretim kapasitesini 3.5 Milyon Ton/yıl seviyesine çıkarmayı hedefleyen yerli cevhere dayalı üretim yapan şirketimizin ana faaliyet konusunu her çeşit ham demir ve çelik mamullerinin, kok ve kok yan ürünlerinin üretimi ve satışı oluşturmaktadır. Bu doğrultuda, raylı sistemler, otomotiv, makine imalat, inşaat ve yapı sektörü, madencilik, savunma sanayi, mobilya ve bağlantı elemanları gibi geniş bir endüstriyel ekosisteme yüksek nitelikli ürünler ve hizmetler sunulmaktadır.

Kardemir'in ana cevher kaynağı yerli olmakla birlikte ithal kaynaklardan da cevher alımı yapılmaktadır. Bu süreçte cevherlerin kalite, maliyet ve harmanlama özellikleri değerlendirilmektedir.

Yerli cevherlerde genellikle tenör düşük, gang elemanları (SiO_2 + Al_2O_3) yüksektir. Ayrıca yüksek fırın prosesi ve sıvı metal kalitesi için zararlı olan K_2O, Zn, As, S gibi empüriteler bazı yerli cevherlerde oldukça yüksektir. Bu bakımdan yerli cevherlerin kendi içlerinde ve ithal cevherlerle optimum değerleri verecek şekilde harmanlanması gerekmektedir.

Bu çalışmada farklı oranlarda, yerli ve ithal toz demir cevherlerin harmanlanması sonucu elde edilen sinter kalitesinin değerlendirilmesi yapılmıştır.

Demir Cevherinin Harmanlanması ve Sinterleşmesi

Harmanlama; 0-10 mm boyutunda, demir tenörü ihtiva eden toz cevherlerin, yan ürün ve atık malzemelerin 16 adet yığın olacak şekilde harmanlama sahalarına serilmesi işlemidir. Toplam 420.000 ton cevher stoklama kapasitesine sahip 4 adet harman sahası bulunmaktadır. İki tanesi 140.000 ton, iki tanesi de 70.000 ton cevher kapasitelidir.

Harmanlama Tesisleri'nde, Yüksek Fırınlar'ın ihtiyacı olan parça cevher ve katkı malzemeleri ile Sinter Tesisi için gerekli olan demir cevherleri istenilen özellikte ve miktarda homojen olarak hazırlanır. Harmanlama işlemindeki asıl amaç, Sinter tesisine uygun fiziksel ve kimyasal özellikleri olan harman sahaları oluşturmaktır. Homojen bir harman sahası hazırlama işlemlerinde; şirkete gelen ithal ve yerli toz cevherleri ve stokları iyi yönetmek, gelen cevherleri ve atık malzemeleri harman sahası boyunca kesintisiz serebilmek önemlidir. Kardemir harmanlama sahası Şekil 1'de gösterilmektedir.

Şekil 1. Kardemir harman sahası

Sinter Fabrikaları, Yüksek Fırınlar'a direk olarak şarj edilemeyecek boyuttaki toz cevherlerin, ergime sıcaklığı altında yüzey ergitme işlemine tâbi tutularak birleştirilmesi sonucu yüksek fırınlara şarj edilebilecek boyuta getirilmesi sürecidir. Her birinin kapasitesi 1 250 000 ton/yıl olan 3 adet sinter fabrikası bulunmaktadır. Yüksek Fırınlar'ın ihtiyacı olan sinter malzemesi; demir cevheri tozu, kireçtaşı, kok tozu, sinter dönüş tozu ve katkı malzemeleri ile hazırlanıp belli oranlarda harmanlanır ve sinterlenir. Kardemir A.Ş. Sinter Fabrikası Şekil 2'de gösterilmektedir.

Şekil 2. Kardemir A.Ş.'de sinter fabrikası

Sinterlik malzeme harmanının % 55-75'ini harmanlanmış demir cevheri, % 10-30'unu sinter tozu, % 3-6'sını kok tozu oluşturur. Harmandaki demir cevheri ve kok tozu miktarı toplamının % 10-20'si oranında kireçtaşı tozu ve gerektiğinde % 1-5 oranında cüruf vb. katkı malzemeleri harmana ilave edilir.

Elde edilen sinterlik malzeme harmanı tutuşturma ocağında tutuşturularak hava emişi yardımıyla tüm malzeme külçeleştirilir.

DENEYSEL ÇALIŞMALAR

Sinter Harmanlarının Bileşim Oranları

Harman içeriği; yerli toz cevher, yerli kalibre ve pelet, ithal cevherler, şarj tozu, baca tozu, filtre tozu, tozsuzlaştırma tozu, atık çamur ve cüruf vb. demirli malzemelerden oluşmaktadır. Kardemir A.Ş. tarafından hazırlanan harmanların bileşimi çizelge 1'de verilmiştir.

Çizelge 1. Hazırlanan farklı harmanların bileşim oranları

Harman No	Yerli Toz Cevher (%)	Yerli Kalibre Cevher (%)	İthal Cevher (%)	Pelet Tozu (%)	Diğer (%)
1	30,32	2,52	41,36	1,28	24,52
2	53,36	1,89	18,32	1,04	25,39
3	54,22	1,36	28,7	0,49	15,23
4	48,11	1,65	24,06	0,49	25,69
5	50,4	0,25	28,5	4,39	16,46
6	48,61	3,72	23,57	4,18	19,92

Sinter Harmanın Kimyasal ve Fiziksel Analizleri

Her bir harmanın kimyasal ve fiziksel özelliklerini belirlemek için harmanların XRF ve elek analizleri yapılmıştır. Harmanların XRF analiz sonuçları çizelge 2'de ve harmanların elek analizleri çizelge 3'de verilmiştir.

Çizelge 2. Harmanların XRF analiz sonuçları

Harman No	Fe (%)	SiO_2 (%)	CaO (%)	Al_2O_3 (%)	MgO (%)	Mn (%)	S (%)	K_2O (%)	Na_2O (%)	Zn (%)	P (%)	Cu (%)	TiO_2 (%)	CaO/SiO_2
1	57,8	5,19	2,95	1,36	1,11	0,39	0,12	0,08	0,08	0,03	0,05	0,01	0,15	0,565
2	53,33	8,12	4,61	1,73	1,86	0,75	0,29	0,147	0,08	0,04	0,038	0,02	0,17	0,568
3	56,8	6,78	3,14	1,37	1,52	0,61	0,22	0,12	0,09	0,03	0,02	0,04	0,11	0,46
4	53,68	7,85	3,94	1,03	1,65	0,8	0,21	0,12	0,07	0,05	0,04	0,04	0,1	0,5
5	55,03	7,08	3,17	1,39	1,75	0,86	0,26	0,1	0,08	0,03	0,03	0,02	0,13	0,448
6	55,59	6,24	3,25	1,41	1,35	0,75	0,22	0,1	0,09	0,03	0,04	0,02	0,12	0,538

Sonuçlara baktığımızda demir cevheri oranı en yüksek olan harman 1 nolu, en düşük olan ise 2 nolu harmandır. Bazite değerini gösteren CaO/SiO_2 oranının 1'e yakın olması beklenir. Harmanların

hepsi asidik özellik göstermiştir. CaO/SiO_2 oranı en yüksek harman 2 nolu harmandır. P, Zn ve Cu yüzdeleri maksimum 0,1- 0,15 olması istenir. Tüm harmanlar bu yönde beklentiyi karşılamıştır.

Çizelge 3. Hazırlanan harmanların elek analizleri

Harman No	+10 mm	-10+6,30 mm	-6,30+3,15 mm	-3,15+1 mm	-1+0,5 mm	-0,5+0,21 mm	-0,21 mm
1	6,71	13,14	25,3	23,31	9,63	11,35	10,58
2	3,89	15,9	25,71	25,37	8,85	11,49	8,79
3	6,51	19,8	20,71	28,96	8,54	10,65	4,82
4	4,55	15,24	21,01	29,19	6,89	11,46	11,67
5	2,6	13,45	22,69	26,7	9,46	13,43	11,68
6	3,1	12,12	25,66	27,03	10,26	14,17	7,66

Toz cevherlerin tane boyutunun 10 mm'den küçük, 6,5 mm'den büyük olması istenmektedir. 12,5 mm'den büyük parçaları sinterlerken homojenliği sağlamada sıkıntı olur. Büyük parçalar sinterin geçirgenliğini artırsa bile iyi bir şekilde birleşmeyi engeller ve dağılmaya sebep olur. Tüm harmanların elek analizleri yaklaşık olarak birbirine yakındır ve sinter hazırlama harmanı için kabul edilebilir boyuttadır. Bu nedenle en iyi harman değerlendirmesi yaparken fiziksel analizinden ziyade kimyasal analizi göz önünde bulunduruldu.

Ürün Sinterin Kimyasal ve Fiziksel Analizleri

Her bir ürün sinterin kimyasal ve fiziksel özelliklerini belirlemek için harmanların XRF, elek analizi ve tambur testleri yapılmıştır.

Sinter XRF Analizi

Sinter için temel kriter azami demir içeriğine sahip olmasıdır. Ancak bu şekilde yüksek fırın için en makul ve indirgenebilir sinter oluşur. Sinter bileşimindeki demir dışındaki elementlerin belirli oranların dışında olması yüksek fırına veya üretilecek sıvı ham demire olumlu/olumsuz etkiler yaratabilir. Ürün sinterin XRF analiz sonuçları çizelge 4'te verilmiştir.

Çizelge 4. Ürün sinterin XRF analizleri

Harman No	Fe (%)	SiO_2 (%)	CaO (%)	Al_2O_3 (%)	MgO (%)	Mn (%)	S (%)	K_2O (%)	Na_2O (%)	ZnO (%)	TiO_2 (%)	P_2O_5 (%)	FeO (%)	CaO/SiO_2
1	56,86	6,43	6,11	1,49	1,19	0,4	0,01	0,1	0,04	0,03	0,25	0,18	8,8	0,95
2	54,18	8,18	8,02	2,09	2,01	0,74	0,01	0,11	0,06	0,01	0,22	0,13	10,44	0,98
3	56	7,18	7,38	1,76	1,39	0,56	0,01	0,12	0,05	0,01	0,17	0,18	10,61	1,03
4	54,96	8,45	7,94	1,27	1,4	0,86	0,01	0,11	0,05	0,02	0,14	0,07	11,44	0,94
5	56,14	7,31	6,31	1,66	1,9	0,9	0,01	0,11	0,05	0,03	0,17	0,1	10,44	0,86
6	56,81	6,68	6,42	1,62	1,67	0,79	0,01	0,14	0,05	0,04	0,19	0,13	10,68	0,96

Demir içeriği seçilen cevherlerle ilgilidir. Bu seçim neredeyse tamamen ekonomik nedenlerden dolayı yapılmaktadır. Sinter kimyasal analiz sonuçlarına göre 1 nolu harmanın %Fe oranı daha yüksektir. $\%SiO_2$, cüruf oluşumuna neden olduğundan yüksek olması istenmez. Bu silisi nötralize etmek için ilave edilen kireç taşı sıvı demir verimliliğini düşürür. Bu oranın en düşük olduğu harman 1 nolu harmandır.

Al_2O_3 değeri % 3'e kadar kabul edilebilir aralıktadır. Tüm sinterler bu şartı sağlamaktadır. Ancak 4 nolu harmandan üretilen sinterin Al_2O_3 değeri %1,27 çıkmıştır. Bu sonuç diğer sinterlere göre daha iyidir. Çünkü Al_2O_3 kok gazı kullanımını artırır.

Bazite değeri (CaO/SiO_2) oranı %1,03 ile en iyi 3 nolu harmanda olduğu gözlenmiştir. Şarjdaki TiO_2 miktarı % 2'nin altına inerse bunun % 50-60'ı cürufa geçer, kalan miktarı ise indirgenir ve demire geçer. Cüruftaki TiO_2'nin %1,5'i geçmesi cürufun viskozitesini artırır. Bu durum fırının çalışma şartlarında düzensizlik oluşturur. Tüm sinterler bu şartı sağlamaktadır.

Sinter Elek Analizi

Boyutu 5 mm'den küçük olan parçalar fırınlarda gaz geçirgenliğini azaltır. Çok tozlu olan sinter, fırına şarj edildiğinde fırın duvarlarına yapışarak kabuk halinde kalır ve ince tanelerin patlamaya sebep olacağı unutulmamalıdır. Ürün sinterin elek analizleri Çizelge 5'te verilmiştir.

Çizelge 5. Ürün sinterin elek analizleri

Harman No	40 mm	-40+25 mm	-25+10 mm	-10+5 mm	-5 mm
1	17,79	18	38,19	20,55	5,46
2	12,53	14,35	38,76	27,18	7,19
3	14,91	17,17	37,22	23,79	6,91
4	20,82	17,79	30,21	23,4	7,77
5	17,78	15,24	36,6	24,4	5,98
6	17,57	16,03	36,86	23,58	5,96

Harman 1'in %5,46'sı tozludur. 4 nolu harmanda ise bu değer %7,77'dir. Diğer harmanlara göre daha fazla tozlu parça içermektedir. Ayrıca 4 nolu harmanda 40 mm elek üstü yüzdesi yine diğer harmanlara göre daha yüksektir.

Sinter Tambur Testi

Tambur testi, sinterin aşınma ve ufalanmaya karşı direncini ölçmek için yapıldı. Sinter fabrikasında üretilen sinter, yüksek fırınlarda beslenene kadar birçok banttan transfer olur. Bu sebeple de darbelere maruz kalıp ufalanabilir. Sinterin tambur test sonuçları çizelge 6'da verilmiştir.

Çizelge 6. Sinter tambur test sonuçları

Harman No	Ufalanma İndeksi (%)	Aşınma İndeksi (%)
1	71,67	6,66
2	66,65	6,16
3	69,09	7,08
4	67,26	6,59
5	68,21	6,58
6	69,53	6,63

Küçük tane boyutu nedeni ile fırın iç basıncının artması, maksimum hava ve oksijen kullanımını kısıtlamaktadır. Bu sebeple aşınma indeksinin küçük olması gerekir. Sinterin mukavemeti artarsa, ince toz miktarı azalır ve yüksek fırın üretiminde demirin artışı sağlanır. Bu testte +6,3'ün (ufalanma indeksi)

minimum %65 olması istenir. Tambur test sonucu en iyi harman %71,67 ufalanma indeksine sahip olan 1 nolu harmandır.

Ürün Sinterin Mekanik Testleri

RUL Testi

Bu deney metodu, deney numunesi kısmı yatağı boyunca diferansiyel gaz basıncındaki değişimin (Dp) ve indirgeme süresince yük altında (50 kPa) bulunan yatağın yüksekliğindeki değişikliğin (Dh) ölçülmesi suretiyle, demir cevherlerinin fiziksel kararlılığının tayinine yönelik bir metodu kapsar.

Bu teste göre sinterin R40 değerinin en az 1 olması istenir. Sonuçlara baktığımızda 1 nolu harmanda bu değer 1,51 çıkmıştır. Basınç ve yükseklik farkına bakacak olursak; Dp (15 mmH_2O dan küçük) ve Dh (%10 dan küçük) değerleri hepsinde uygundur. Sinterin RUL testinin sonucu çizelge 7'de verilmiştir.

Çizelge 7. Sinterin RUL testinin sonuçları

Harman No	R40 (% O_2/min)	Dp (mm H_2O)	Dh (%)
1	1,51	1,02	2,67
2	1,01	1,02	0,82
3	0,83	1,02	1,25
4	0,96	1,02	0,54
5	0,98	1,02	1
6	1,44	1,02	1

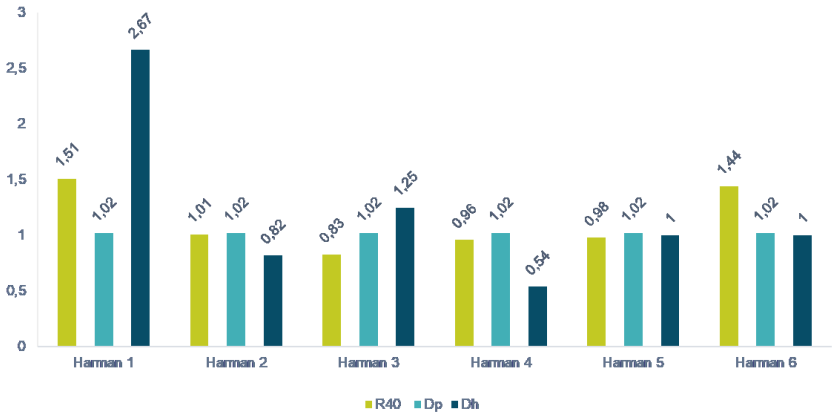

Şekil 3. Sinter RUL testi sonuçlarının grafiksel gösterimi

RDI Testi

500°C'lik sabit bir yatakta indirgenmiş (CO %20 + CO_2 % 20 + H_2 % 2 + N_2 % 58), 500 gram ağırlığındaki sinterin, oda sıcaklığında ufalanarak parçalanması değerlendirilir.

Çıkan sonuçlarda +6,3 mm en az %84 ve -0,5 mm en fazla % 3 olmalıdır. Bu testin yapılma amacı yüksek fırına beslenen malzemenin gövdede ilk değişim zonunu temsil ettiği içindir. Sinter RDI testinin analiz sonucu çizelge 8'de verilmiştir.

Çizelge 8. Sinter RDI testinin analiz sonuçları

Harman No	+6,3mm	+3,15-6,3mm	+0,5-3,15mm	-0,5 mm
1	33,10	33,31	27,18	6,41
2	27,06	36,45	31,07	5,42
3	46,23	27,42	21,13	5,22
4	48,17	28,74	18,77	4,33
5	35,72	31,52	27,04	5,71
6	33,25	32,60	26,95	7,20

Bu testte (-3,15 mm) değeri maksimum % 25 olmalıdır. 4 Nolu harman dışındaki tüm harmanlarda 3,15 mm'den küçük parça yüzdesinin 25'ten büyük olduğu görülmektedir. Beklenen kriteri sağlayan tek harman 4 nolu harmandır.

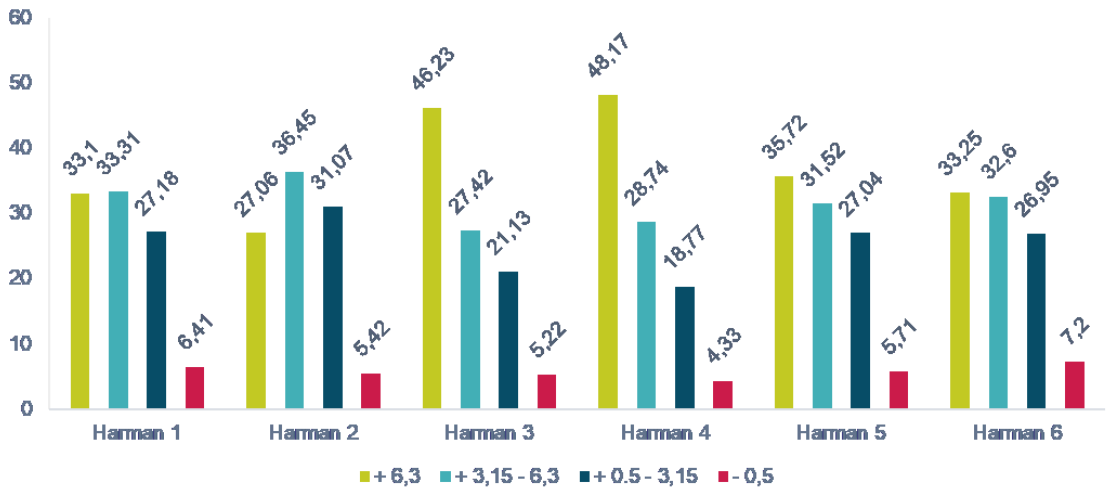

Şekil 4. Sinter RDI testi sonuçlarının grafiksel gösterimi

DEĞERLENDİRME

Hazırlanan 6 farklı harman ve bu harmanlardan üretilen sinterler için birçok test yapılmıştır. Tüm testlerin değerlendirilmesi fiziksel, kimyasal ve metalürjik olarak ayrı ayrı ele alınmıştır. Puanlama 1'den 6'ya kadar yapılmış olup en iyi özellik gösterene 6 puan verilmiştir. Puanlama yaparken dikkat edilecek kriterlere, önceki başlıklarda değinilmiştir. Tek başına sadece fiziksel veya kimyasal özeliklerinin iyi olması yeterli değildir. Tüm test sonuçları birlikte değerlendirilmiştir. Hazırlanan 6 farklı harman ve bu harmanlardan üretilen sinterler için birçok test yapılmıştır. Tüm testlerin değerlendirilmesi fiziksel, kimyasal ve metalürjik olarak ayrı ayrı ele alındı. 1'den 6'ya kadar puanlama yapılıp, en iyi özellik gösterene 6 puan verildi.

Harman Değerlendirilmesi

Harmanın kimyasal özelliklerinin karşılaştırılması Çizelge 9'da verilmiştir. Buna göre en iyi harman 1 nolu (6 puan), en kötü harman 5 nolu (1 puan) harmandır.

Çizelge 9. Harman özelliklerini değerlendirme

Harman No	Kimyasal Analiz Puanı
1	6
2	3
3	4
4	2
5	1
6	5

Sinter Değerlendirilmesi

Sinterin fiziksel ve kimyasal özelliklerinin karşılaştırılması Çizelge 10'da verilmiştir. Buna göre en iyi 1 nolu harmandan üretilen sinterdir. Harman 2 ve 4 ise beklenen fiziksel ve kimyasal özellikler bakımından puanlandığında diğerlerine göre daha az puan almıştır.

Çizelge 10. Sinter özelliklerinin değerlendirme

Harman No	Elek Analizi Puanı	Tambur Testi Puanı	Kimyasal Analiz Puanı	Toplam
1	6	6	6	18
2	2	1	1	4
3	3	4	4	11
4	1	2	2	5
5	4	3	3	10
6	5	5	5	15

Metalürjik Değerlendirme

Sinterin teknolojik test sonuçlarına göre değerlendirilmesi Çizelge 11'de verilmiştir. Sonuçlara göre metalürjik özelliği en iyi olan sinter 1 nolu harmandan üretilen sinter olup, 2 nolu harman sinteri en düşük puandadır.

Çizelge 11. Metalürjik özellikleri değerlendirme

Harman No	RUL Puanı	RDI Puanı	Toplam
1	6	3	9
2	4	1	5
3	1	5	6
4	2	6	8
5	3	4	7
6	5	2	7

SONUÇ VE ÖNERİLER

Yapılan çalışmalar sonucunda, Kardemir Sinter Fabrikası'nın sinter kalitesinde hedeflediği değerler göz önünde bulundurularak; 1 nolu harmanın en iyi, 2 nolu harmanın ise en kötü sonucu verdiği belirlenmiştir.

İthal cevher kullanım oranının en fazla olduğu harman 1 nolu (%41,36) harmandır. En düşük olduğu harman ise bu değerin yarısından az olduğu 2 nolu (%18,32) harmandır. 1 ve 2 nolu harmanlardan üretilen sinterlerden alınan sonuçlara göre yüksek oranlarda ithal cevher kullanıldığı zaman, aşınma ve ufalanma indeks sonucunun daha iyi olacağı görülmüştür.

İthal cevher kullanımının artmasıyla sinterin kimyasal analizi ve yüksek fırınlarda indirgenme davranışının iyileştiği görülmüştür.

Yerli cevher kullanım oranının en fazla olduğu harman 2 nolu (%53,36) ve 3 nolu (%54,22) harmandır. Harman kimyasal analizi sonuçlarında % S oranına bakıldığında en yüksek kükürt değerinin, ithal cevher kullanım oranının da en az olduğu 2 nolu harmanda olduğu görülmüştür.

Tambur sonuçlarının sinter bazitesiyle ilişkisine bakıldığında; ufalanma indeks değerinin her harmanda değişim gösterdiği, çalışılan harmanlardan üretilen sinterin bazite değerinin ise düşük (0,9 civarında) olduğu görülmüştür.

Atık tozlar %15-20 civarında olduğu takdirde sinter kalitesinde olumsuz bir etki yaratmadığı tespit edilmiştir.

Harman hazırlarken sahalardaki cevher stok miktarı, cevher satın alımındaki kriterler ve sinter kalite hedefleri dikkate alınarak yerli cevherlerle beraber yaklaşık %30 oranında ithal cevher kullanımının iyi olacağı sonucuna varılmıştır.

KAYNAKLAR

Kardemir A.Ş. sürdürülebilirlik 2019 raporu, https://www.kardemir.com/dosyalar/sayfalar/1338/22072020/2020072214385940_sayfalar_1309_22072020.pdf?v=c51fdc86_ccf9_1bf6_ddef_bec9c5307cc8.

Kardemir A.Ş. sürdürülebilirlik 2020 raporu, https://www.kardemir.com/dosyalar/sayfalar/1338/03082021/2021080311253005_sayfalar_1338_03082021.pdf?v=29c27cac_d919_8881_17d9_85684be786b4.

Timur, T. (2019), "Kardemir A.Ş'de Farklı Toz Cevherlerle Üretilen Sinterin Kalitesinin İncelenmesi", Yüksek Lisans Tezi, Karabük Üniversitesi Fen Bilimleri Enstitüsü, Karabük.

KİMYASAL DOLGU MALZEMELERİNİN KARAKTERİSTİKLERİ VE KÖMÜRÜN KENDİLİĞİNDEN YANMASI ÜZERİNE ETKİSİNİN İNCELENMESİ

INVESTIGATION OF THE CHARACTERISTICS OF CHEMICAL FILLING MATERIALS AND THE EFFECT ON SPONTANEOUS COMBUSTION OF COAL

C. Tuz[1,*], M. Bilen[1], E. Kaymakçı[1], İ. Toroğlu[1], Ö. Yılmaz[2], S. Yılmaz[1]

[1]*Bülent Ecevit Üniversitesi Maden Mühendisliği Bölümü, Zonguldak*
*(*Sorumlu yazar: canertuz@gmail.com*)
[2]*Bülent Ecevit Üniversitesi ZMYO, Madencilik ve Maden Çıkarma Bölümü, Zonguldak*

ÖZET

Enjeksiyon kimyasalları, kazı yapılacak ya da yapılmış kaya kütlesini iyileştirmek, su gelirini kesmek, tahkimat elemanları ile yan kayaç arasındaki boşlukları doldurmak, gibi çeşitli amaçlarla kullanılmaktadırlar. Yeraltı kömür madenciliğinde kimyasal dolgu malzemeleri olan köpük ürünleri kullanılmaktadır. Bu tip malzemelerin göçükte oluşan büyük çatlakların doldurulması ile göçük stabilizasyonu, havalandırma yönetimi için gerekli olan hava kapılarının yapılması ve sızdırmazlığın sağlanması ve yangınla mücadele uygulamalarında baraj yapımı gibi kullanım alanları da mevcuttur. Yeraltında kimyasal dolgu malzemesi olarak kullanılan köpük ürünleri kimyasal içeriklerine göre genellikle poliüretan ve fenol olmak üzere iki kategoride sınıflandırılmaktadır. Fenol bazlı dolgu köpüklerinin reçine bileşeni içeriğinde yer alan formaldehit maddesinin 1. Sınıf kanserojen madde kategorisinde yer almasından dolayı bu maddenin sınır değerine dikkat edilmesi gerekmektedir. Poliüretan bazlı kimyasal dolgu köpüklerin içeriğinde yer alan MDI toksik bir madde olduğundan dolayı tutuştuğunda sağlık açısında zararlı gaz salınımına sebep olmaktadır. Kimyasal dolgu köpükleri kömür madenlerinde yapılan uygulamalarda doğrudan kömür ile kontak halindedir. Poliüretan bazlı kimyasal dolgu malzemeleri yeraltı kömür madenlerinde yapılan uygulamalarda kendiliğinden yanmayı tetikleyici etkisinden ve yanıcı özelliğinden dolayı problem oluşturmaktadır. Diğer taraftan fenol bazlı kimyasal dolgu köpükleri özellikle yeraltı kömür madenlerinde yapılan uygulamalarda kömürün kendiliğinden yanmasına olan etkisi oldukça düşük seviyelerdedir. Bu çalışmada yeraltı kömür madenciliğinde kullanılmakta olan kimyasal dolgu malzemelerinin karakteristikleri ve kömürün kendiliğinden yanması üzerindeki etkiler incelenmiştir.

Anahtar Kelimeler: Yeraltı Kömür Madenciliği, Kimyasal Dolgu Malzemeleri, İSG (İş sağlığı ve güvenliği), Kendiliğinden Yanma, Fenol bazlı köpük, Formaldehit

ABSTRACT

Ground injections are used for various purposes such as improving the ground to be excavated or made, sealing the water inrush, filling the cavity between the support and the ground. Foam products, which are chemical filling materials, are used in underground coal mining. These types of products also have areas of use such as filling large cracks in goaf and stabilizing goaf, constructing air barriers, and sealing for ventilation requirements, and fighting underground fires by sealing off all entries connected to the fire area. Foam products used as underground cavity filling materials are generally classified into two categories, polyurethane, and phenol, according to their chemical content. Since formaldehyde, which is included in the resin component of phenol-based filling foams, is in the category 1st carcinogenic substance, attention should be paid to the limit value of this substance. Since MDI in the content of polyurethane-based chemical filling foams is a toxic substance, it causes harmful gas emissions in terms of health when ignited. In applications made in coal mines, filling foams form a large contact surface with coal. Polyurethane-based chemical filling materials cause problems in underground coal mines due to their

spontaneous combustion triggering effect and flammability. On the other hand, the effect of phenol-based chemical filling foams on spontaneous combustion of coal is very low especially filling operations in underground coal mines. In this study, the characteristics of chemical filling foams used in underground coal mining applications and their effects on spontaneous combustion of coal were investigated.

Keywords: Underground coal mining, chemical filling products, OHS (Occupational Health and Safety), Spontaneous combustion, Phenol based foam, Formaldehyde

GİRİŞ

Gelişen teknolojiyle birlikte geleneksel olarak bilinen çimento su enjeksiyon malzemesinin yerini kimyasal enjeksiyon ürünleri almaktadır. Yeraltı madenlerinde kazı yapılacak olan ya da yapılmış kaya kütlesinin yapısal olarak iyileştirilmesi, yeraltında çatlaklardan akan su gelirlerinin kesilmesi, tahkimat elemanları ile yan kayaç arasındaki boşlukların doldurulması gibi çeşitli uygulamalarda kimyasal enjeksiyon ürünleri büyük avantaj sağlamaktadır. Bu avantajlardan bazıları; kimyasal enjeksiyon malzemelerinin düşük viskozite değerlerinden dolayı ince çatlaklara kolaylıkla nüfuz etmesi, kolay ve basit uygulanabilirlikleri, reaksiyon hızlarının yüksek olmasından dolayı operasyonların bekleme sürelerinin düşük olması, kısa sürede yük taşıyıcı özellik göstermeleri, ıslak kayaçlara yapışabilmesiyle su geliri olan ortamlarda ve yapılarda kullanılabilir olması gibi birçok avantajı bilinmektedir (Aksoy O., 2017).

Yeraltında oluşan boşlukların doldurulması veya yangın gibi problemlere hızlı bir şekilde müdahale edebilmek için kimyasal dolgu malzemeleri olan köpük ürünleri kullanılmaktadır. Kimyasal köpük ürünleri uygulandıkları bölgede reaksiyona girerek yüksek kabarma faktörleri sayesinde az miktarda ürün ile büyük hacimlerin doldurulması sağlanabilmektedir. Genellikle kimyasal köpük ürünleri 20 ile 70 kat arasında değişen kabarma faktörüne sahiptirler.

Yeraltı Kömür Madenciliğinde Kimyasal Dolgu Malzemelerinin Kullanıldığı Uygulamalar

Kimyasal enjeksiyon ve köpük ürünleri yüksek maliyetleri olduğundan dolayı bazı özel operasyonlarda uygulanmaktadır. Genellikle alternatif yöntemler veya çözümlerin olmadığı durumlarda tercih edilmektedir. Yaygın olarak kullanılan yöntemlerin yetersiz kaldığı veya kısa sürede problemin çözülmesinin gerektiği durumlarda kimyasal uygulamalar gerçekleştirilmektedir. Yeraltı kömür madenciliğinde gerçekleştirilen başlıca kimyasal dolgu uygulamaları yeraltında oluşan boşlukların doldurulması, göçükte oluşan büyük çatlakların doldurulması ile göçük stabilizasyonu, havalandırma yönetimi için gerekli olan hava kapılarının yapılması ve sızdırmazlığın sağlanması ve yangınla mücadele uygulamalarında baraj yapımı olarak bilinmektedir.

Boşluk Doldurma

Yeraltında jeolojik koşullardan ve süreksizliklerden kaynaklı olarak geniş çaplı göçük ve boşluklar oluşmaktadır. Bu durum çoğu zaman üretimin durmasına veya üretim verimliliğinin düşmesi ile sonuçlanmaktadır. Aynı zamanda bu boşluklar ve göçük alanları madenciler için iş güvenliği problemleri oluşturmaktadır. Bu problemlerin bertaraf edilmemesi halinde risk artmaktadır. Daha büyük problemleri önlemek, emniyetli bir ortam oluşturmak ve üretim verimliğini arttırmak için bu göçük ve boşlukların güvenli bir şekilde doldurulması önem arz etmektedir. Bu tip dolgulama işlemlerinde hızlı reaksiyon ve yüksek kabarma faktörü ile genleşebilme özelliğine sahip kimyasal dolgu malzemelerinin kullanılması avantaj sağlamaktadır. Az miktarda malzeme kullanımıyla büyük boşlukların kolaylıkla ve kısa sürede doldurulması kimyasal dolgu malzemeleri ile mümkündür (Tuz ve ark., 2019; Yılmaz ve ark. 2022; Weber Madencilik, 2021).

Boşluk doldurma uygulamaları yeraltı kömür madenciliğinde zayıf kaya kütlesinden dolayı sıklıkla gerçekleştirilmektedir. Genellikle tam mekanize kömür üretiminde ayak ilerlemesi sırasında şilt tahkimatları ilerletilmesinde tavan kısmı geçici süreliği tahkimatsız bırakılır. Jeolik süreksizliklerden veya zayıf kömür yapılarından dolayı kısa süreli bu tavan açıklığında dökülmeler, boşalmalar hatta zaman zaman tavan göçmeleri yaşanmaktadır. Bu durumlardan kaynaklı olarak bu bölgelerin dolgulanması ve çalışma alanının emniyetli bir hale getirilmesi gerekmektedir. Bu işlem için kimyasal dolgu köpüklerinin kullanılarak kısa sürede problemin ortadan kaldırılması sağlanmaktadır (İbuk ve ark., 1996; Kahraman ve ark.,2011; Tuz ve ark, 2019). Bu işlem sayesinde ayak kolaylıkla ilerletilebilmekte ve oluşacak olan daha büyük problemlerin önüne geçilmektedir. (Şekil 1).

Şekil 1: Ayak içi yürüyen tahkimat üzeri boşlukların köpük ile doldurulması (Weber Kataloğu, 2019; Frith, 2006)

Yeraltında hazırlık galerilerinde ve kömür içerisinde sürülen taban yollarında jeolojik süreksizliklerden ve zayıf kaya kütlelerinden dolayı anlık boşalmalar yaşanmaktadır. Aynı şekilde bu boşlukların dolgulanması gerekmektedir. Aksi takdirde küçük olan bu boşluklar büyüyerek mevcut riski arttırmaktadır. Kimyasal dolgu köpükleri ile bu bölgelerin kolaylıkla dolgulanması sağlanmakta ve bozuk kaya kütleleri içerisine kimyasalın nüfuz etmesi sağlanarak çok zayıf ve aşırı çatlaklı yapılarda kaya kütlesinin dayanımının da arttırılması sağlanmaktadır. Böylece göçük olan bu bölge kontrol altına alınmış olup ortam emniyetli hale getirilerek risklerin ortadan kaldırılması sağlanmaktadır (Hu ve ark., 2014; Tuz ve ark., 2019).

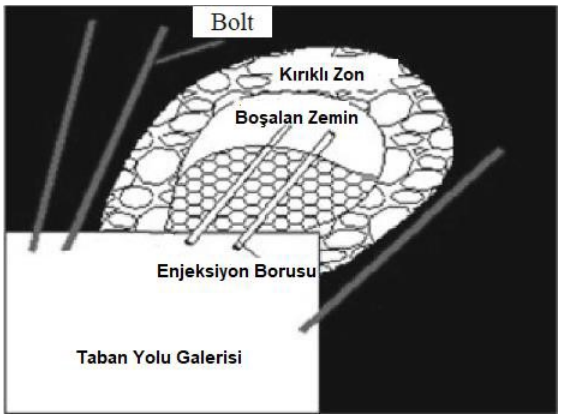

Şekil 2. Taban yolu oluşan galeri boşluğunun köpük ile doldurulması (Hu ve ark., 2014)

Boşluk doldurma uygulamalarında genellikle fenol bazlı köpük ürünleri aleve dayanıklı olduğundan kömür madenciliğinde tercih edilmektedir. Poliüretan bazlı dolgu köpükleri ise yanıcı özellikte olduğundan dolayı geçmişte kullanılmasına rağmen günümüzde kömür madenciliğinde kullanılmamaktadır.

Göçük Stabilizasyonu

Uzun ayak kömür üretimlerinde özellikle ayak sökümü esnasında şilt tahkimatların yerinden çıkarılması çok fazla problemin oluştuğu bir süreçtir. Ayak söküm işlemi için havalandırmanın düzenlenmesi ve göçük stabilizasyonu işlemleri yapılmaktadır. Çelik hasır ile şilt tahkimat arkasında göçüğün tutulması sağlanmaktadır. Fakat bu gibi geleneksel yöntemlerde şilt tahkimat ile göçüğün kontağı tam olarak kesilememektedir. Göçükten oluşan akmalar ile problem oluşmakta ve aynı zamanda söküm süresi uzamaktadır. Göçüğün stabilizasyonunun köpük uygulaması ile arttırılması sayesinde bu problem ortadan kaldırılabilmekte ve aynı zamana tahkimat ile göçüğün etkileşimini azaltmaktadır (Pile, 2013).

Şekil 3: Kimyasal köpük uygulamaları ile göçük stabilizasyonu (Pile, 2013)

Yapılan köpük enjeksiyonu sayesinde göçük geçici olarak statik bir yapı kazanmaktadır. Bu sayede şilt tahkimatların sökümü daha kolay ve rahat bir şekilde gerçekleştirilebilmektedir. Söküm sonrası stabilizasyon kazanan göçük şilt tahkimat ile ters açı oluşturacak bir eğime sahip olmakta ve bu durum göçük stabilizasyonunda kimyasal köpük uygulamalarının etkili bir şekilde çalıştığını göstermektedir (Şekil 3).

Havalandırma Yönetimi

Yeraltı madencilik uygulamalarında havalandırmanın yeterli olması gerekmektedir. Yeterli hava miktarının oluşturulması için verimli havalandırma yönetimi yapılması gerekmektedir. Havalandırma yönetiminde dikkat edilmesi gereken başlıca unsurlar:

1. Temiz hava kayıplarının engellenmesi, geri dönüş havasının neden olduğu çapraz kontaminasyonun düşürülmesi
2. Tavan boşluklarında hava akımının sağlanamamasından dolayı gaz birikmelerinin önlenmesi
3. Eski çalışma alanlarının yalıtılarak kirli hava akımının engellenmesi
4. Ayak içerisine göçükten kirli hava akımının engellenmesi
5. Temiz havanın göçüğe ilerlemesi
6.

gibi bunlara benzer durumlardan yer almaktadır (Weber Madencilik, 2019). Bu gibi durumlarda kimyasal dolgu köpükleri kullanılarak havalandırmanın verimliliği arttırılmaktadır.

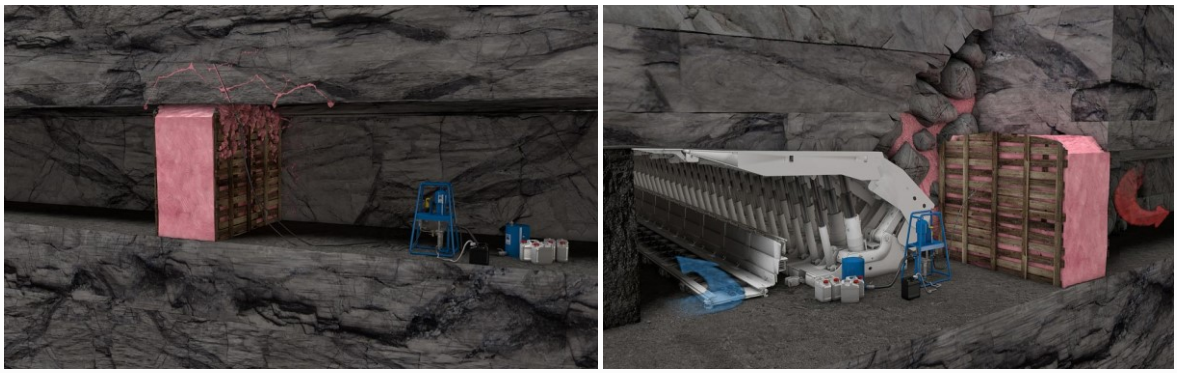

Şekil 4: Havalandırma yönetimi için kimyasal köpük ürünleri ile hava kapılarının yapılması (Weber Madencilik, 2019)

Kömür arını ile taban yolunun kesişme noktasında, alt galeriden gelen hava akımı doğrudan göçüğe ilerleme eğilimi gösterir. Bu durum metan salınımı ve arının üst ucunda birikme riskini doğurur. Bu nedenle göçük alanına giren hava akımını kontrol etmek ve arın hattının alt ucunda bir hava bariyeri inşa ederek akımı uzunayak arını boyunca yönlendirmek önemlidir. Bu sistem aynı zamanda göçük alanında kendiliğinden tutuşma riskini de azaltır (Arl, 2005).

Hasır paneller ve çuval bezi (gerekli olursa) kullanılarak hafif bir tahkimat oluşturulur. Bu hafif tahkimat, son arın tahkimatı ile taban yolunun karşı tarafındaki galeri duvarının arasına yerleştirilir. Ürün türüne ve ortam sıcaklığına bağlı olarak, uygulama yapılarak bu hafif tahkimatın iki "yüzünün" arasına köpük pompalanabilir veya doğrudan hasır panellere uygulama yapılabilir. Önerilen ürünlerin hızlı kürlenme süreleri ve yüksek genleşme oranları sayesinde bu bariyerler hızla ve kolaylıkla inşa edilebilir.

Yangınla Mücadele

Yeraltı kömür madenciliğinde yangın riski her zaman bulunmaktadır. Risklerin engellenememesi durumuna oluşan yeraltı yangınlarının sonucunda maden faaliyetleri ve kömür üretimi durmaktadır. Bu yangınlardan kaynaklı karbon monoksit ve karbondioksit başta olmak üzere tehlikeli gazlar yeraltı ortamında sınır değerlerinin üzerinde oluğunda insan sağlığı açısından problem oluşturmaktadır. Gazların konsantrasyon değerleri takip edilmeli ve yangınla mücadele için gerekli önlemlerin alınması gerekmektedir. Yangınla mücadele uygulamalarının en önemlilerinden biri kimyasal dolgu köpükleri ile yangın bariyerlerinin yapılmasıdır. Enjeksiyon pompası yardımı ile uygun kimyasal madde (izolasyon köpüğü) bu bölgelere uygulanarak yangın bölgesinin hava yalıtımı sağlanmakta (Şekil 5) ve bu sayede yangınlı bölgeye hava kaçması önlenmektedir. Aynı zamanda, yangının kontrol altında tutulması da sağlanmaktadır (Kahraman ve ark., 2012).

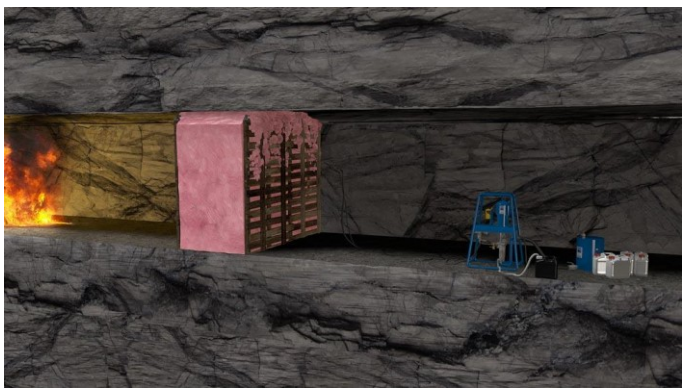

Şekil 5: Yangın bölgelerine köpük barajı yapılması (Weber Madencilik, 2019)

Yeraltı kömür madenlerinde oluşan yangınlar zaman zaman kontrolden çıkmakta ve bu durumlarda maden ocakları tahliye edilmek zorundadır. Bu gibi durumlarda yeraltındaki yangının sönmesi beklenmektedir. Bu gibi durumlarda iş güvenliği ve sağlığı açısından yeraltında çalışılabilir bir ortam söz konusu değildir. Havalandırma yönetiminin yapılması ve yangın olan bölgenin yalıtılması gerekmektedir (Trevits, 2008).

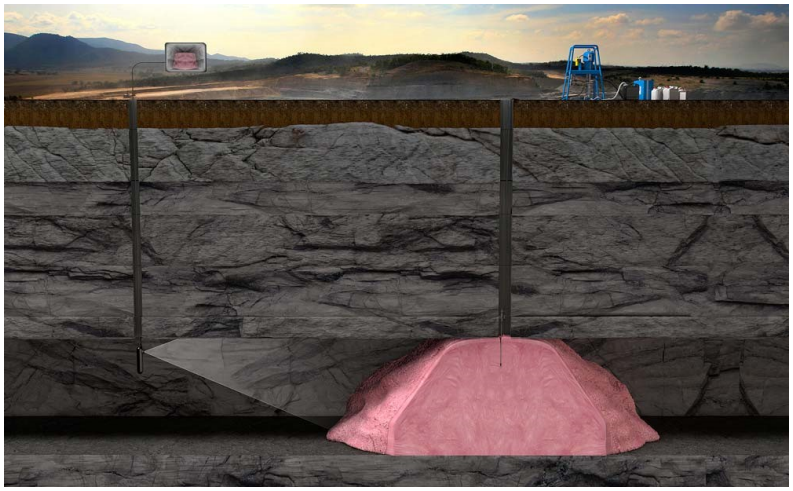

Şekil 6: Yerüstünden yeraltındaki galerilerin kimyasal köpük ürünleriyle dolgulanması (Weber Madencilik, 2019)

Kimyasal köpük ürünleri ile bu gibi durumlara yerüstünden müdahale edilebilmektedir. Bu sayede galerilerin yerüstünden dolgulanması sağlanmakta ve yangının olduğu pano yalıtılmaktadır. Panoların taban yollarına galeri eksenine gelecek şekilde yerüstünden sondajlar yapılmakta ve bu sondajlardan ekipmanların gönderilmesiyle taban yollarına köpük dolgusu gerçekleştirilmektedir. Tamamen dolgulanan taban yolları galerileri ile panonun yalıtımı sağlanmaktadır. (Trevits , 2008)

Şekil 7: Yerüstünden yeraltı galeri dolgusu sonrası görseller (Wilson Mining Service, 2019)

Şekil 8: Yerüstünden yeraltına yapılan kimyasal dolgu çalışması uygulama görseli (Wilson Mining Service, 2019)

Kimyasal Dolgu Malzemelerinin Karakteristik Özellikleri

Yeraltında kimyasal dolgu malzemesi olarak kullanılan köpük ürünleri kimyasal içeriklerine göre genellikle iki kategoride sınıflandırılmaktadır;

1. Fenol Bazlı Dolgu Köpükleri
2. Poliüretan Bazlı Dolgu Köpükleri

<u>Fenol Bazlı Kimyasal Dolgu Köpükleri</u>

Fenol bazlı kimyasal dolgu köpükleri Fenol-Formaldehit bakalitine anorganik şişirici ve sertleştirici maddeler eklenerek üretimi gerçekleştirilir (Arge-Yapı İzolasyon, 2021). Genellikle bu şişirici ve sertleştirici maddeler yoğunlaştırılmış asitlerden oluşmaktadır. Yeraltı madenciliğinde kullanılan fenol bazlı kimyasal dolgu köpükleri aynı prensiple iki bileşenden oluşmaktadır. Birinci bileşen fenol formaldehit bazlı reçine ürünleridir ve ikinci bileşen yoğunlaştırılmış asitlerden oluşmaktadır ve genellikle sülfirik asit içeriği yüksektir.

Bu iki bileşenin bir pompa yardımı ile uygulama bölgesine aktarılması sağlanmaktadır. Karıştırıcı bir tabanca ile karışımı sağlanmaktadır. İki bileşen genellikle hacimsel olarak 4:1 oranda karıştırılmaktadır. Fakat yapılan ürün içeriğine göre 3:2 oranda hacimsel karışımlarda olan fenol köpüklere mevcuttur.

Fenol bazlı dolgu köpükleri 30-70 kat arasında kabarma faktörüne sahiptir. Buda kimyasal köpük yoğunluğu olarak 17 kg/m^3 ile 40 kg/m^3 sınır değerlerine karşılık gelmektedir. Kimyasal üretici firmalar isteğe bağlı olarak farklı yoğunluklarda köpük üretimi gerçekleştirebilmektedir.

Foam weight : 24.3 g

Compression aproximatly 10% of deformation

Compression aproximatly 50% of deformation

MARIFLEX LS1 Resin	Batch n° 0282005
MARIFLEX LS1 Catalyst	Batch n° 1701905
Date of test	17/03/2020
Test temperature	20°C
Time of end reaction (sec)	23
Maximal temperature of reaction (°C)	91
Foam density (kg/m3)	24.3
Expansion ratio	51

Sample dimensions for compression test	100 x 100 x 100 mm
Conditions for the compression test	24 hours at 20°C
Strength at 10% of deformation (N)	403
Strength at 30% of deformation (N)	405
Strength at 50% of deformation (N)	460
Strength at 70% of deformation (N)	723
Compressiv strength at 10% of deformation (MPa)	0.040
Compressiv strength at 30% of deformation (MPa)	0.041
Compressiv strength at 50% of deformation (MPa)	0.046
Compressiv strength at 70% of deformation (MPa)	0.072

Şekil 9: Fenol bazlı dolgu köpükleri basma dayanımı testleri örneği (Weber Madencilik, 2020)

Ürün yoğunluğuna bağlı olarak ürünün basma mukavemeti değişmektedir. 50-70 kat kabarma faktörüne sahip bir ürün 10-45 kPa arasında %10 deformasyonda basma mukavemetine sahiptir. Diğer bir önemli parametre ise fenol bazlı dolgu köpüklerinin reaksiyon sıcaklıklarıdır. Genellikle maksimum ekzotermik reaksiyon sıcaklığı 90-100 °C arasında olmaktadır. Yeraltında kullanılan kimyasalların reaksiyon sıcaklıkları 150 °C aşmaması gerekmektedir (MDG3608, 2012). Ayrıca fenol bazlı dolgu köpükleri aleve dayanıklıdır. Aynı zamanda alev yürütmez özelliktedir. Yangınla mücadele gibi uygulamalarda kullanılması için bu parametre önem arz etmektedir.

Fenol bazlı dolgu köpüklerinin reçine bileşeni içeriğinde yer alan formaldehit maddesinin 1. Sınıf kanserojen madde kategorisinde yer almasından dolayı ürünün sınır değerine dikkat edilmesi gerekmektedir. CLP yönetmeliğinde belirtilen %0,1 sınır değerinin üzerinde formaldehit maddesi içeren ürünler 1. Sınıf kanserojen olduğundan H350 zararlılık ifadesi ile gösterilmeleri gerekmektedir (CLP, 2008).

Formaldehit içeriğinden dolayı tehlikeli olan fenol bazlı köpüklerin uygulamasında çalışan personel direk olarak ortamda maruz kalacağından ortamdaki formaldehit konsantrasyonunun ölçülmesi gerekmektedir. Formaldehit konsantrasyonunun zararlı seviyelere ulaştığı durumlarda uygulamanın durdurulması gerekmektedir.

Poliüretan Bazlı Kimyasal Dolgu Köpükleri

Yeraltı madenciliğinde kullanılan poliüretan bazlı kimyasal dolgu malzemeleri genellikle iki bileşenden oluşmaktadır. Poliüretan bazlı dolgu malzemelerinin basma dayanımları diğer kimyasal dolgu malzemelerine göre daha yüksektir. Mekanik özellik bakımından oldukça iyi değerler veren poliüretan dolgu malzemeleri boşlukların doldurulmasında tercih edilmektedir. Poliüretan dolgu malzemelerin basma dayanımı mukavemeti %10 deformasyonda 200 kPa kadar çıkmaktadır.

Poliüretan dolgu malzemeleri su ile karıştırıldığında reaksiyon sıcaklığı 170 °C kadar çıkmaktadır. Poliüretan bazlı köpük ürünlerinin 4:1 hacimsel olarak karıştırılması sonucunda reaksiyon sıcaklığı 198 °C ulaşmaktadır (Mining Monthly, 2007).

Poliüretan bazlı kimyasal dolgu malzemeleri yüksek reaksiyon sıcaklığına sahip olduğundan dolayı yeraltı kömür madenlerinde kullanılmamaktadır. Poliüretan bazlı dolgu köpükleri 60 °C üzerinde reaksiyon sıcaklığını 30-45 dakika arasında korumaktadır.

Şekil 10: Poliüretan köpük ürünlerinin uygulama görseli (Frontier, 2018)

Kimyasal Dolgu Köpüklerinin Kendiliğinden Yanma Üzerine Etkisi

Kömür normal şartlar altında hava ile temas ettiğinde okstilenme eğilimi göstermektedir. Oksijen moleküllerinin kömür yüzeyi ile temas etmesi sonucu adsorbe olur ve difüzyon ile gözeneklere ulaşır. Bu fiziksel olarak bağlanma işlemi sonrasında ortama ısı veren oksidasyon süreci başlar. Bu reaskiyon sürecinde ortama ısı verilir ve hava akımı ile bu ısı taşınır. Isı ortamdan uzaklaştırılmadığı takdirde ortam sıcaklığı artar. Kömürdeki su 100 ºC de buharlaşır. Isıya dayanıklı kömür-oksijen kompleksinin ortam sıcaklığı 130 ºC yi geçtiğinde oluştuğu gözlemlenmiştir. Bu oksidasyon sürecinde ortamdaki her 10 ºC sıcaklık artışı oksidasyon hızını 2,2 kat arttırmaktadır. Bu durum ortam sıcaklığının artışının kömürün kendiliğinden yanmasını etkilediğini göstermektedir (Yılmaz, 2016).

Kömürün kendiliğinden yanma süreci birçok farklı parametreye bağlıdır. Kömür türüne göre bu süreç değişkenlik göstermektedir. Kömür oksidasyon aşamaları yavaş, hızlanan ve hızlı olarak

sınıflandırılabilmektedir. Ortam sıcaklığı 70-100 °C aralığında yavaş oksidasyon aşaması, 140-150 °C aralığında hızlanan oksidasyon aşaması ve bu hızlanan oksidasyon aşamasını da hızlı oksidasyon aşaması takip etmektedir. Kömür türüne bağlı olarak 140-150 °C sonrasında kömür oksidasyon hızının arttığı görülmektedir (Wang ve ark., 2009; Li ve ark., 2016).

Kömürün kendiliğinden yanması üzerine yapılan testlerde fırın ve kömür numunesine ait sıcaklık değişim grafiği Şekil 11'de verildiği gibidir. Kömürün kesişme noktası 181 °C olarak görülmektedir (Bilen ve ark., 2019). Bu sıcaklık değeri kömürün kendiliğinden yanmasındaki kritik nokta olarak görülmektedir.

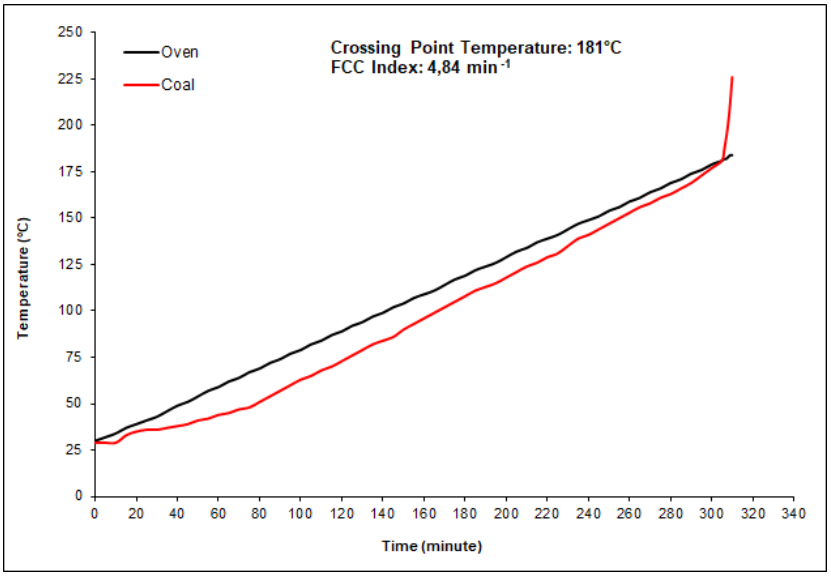

Şekil 11: Geleneksel deney düzeneğinde kömür numunesi ve fırının sıcaklık değişimi (Bilen ve ark., 2019)

Yukarıda yapılan deneyde bir fırın ile doğrusal olarak ortam sıcaklığının arttırılması sağlanmakta ve bu sayede ortam sıcaklığı-zaman ilişkisiyle kömür üzerindeki etkisi incelenmektedir. Deney sırasında fırın ve kömür örneğinin sıcaklıkları ayrı ayrı olarak gözlemlenmekte olup kömür sıcaklığının fırın sıcaklığına eşit olduğu nokta kesişme noktası olarak isimlendirilmektedir (Kaymakçı, 2000). Bundan dolayı yukarıda test düzeneğinde sıcaklık değişimi ile kömürün kendiliğinde yanması arasındaki etkileşim görülmektedir. Ortam sıcaklığının artması kömürün oksidasyonunu hızlandırmakta ve kendiliğinden yanmasını arttırmaktadır. Kesişme noktası da bu süreçte kritik aşama olarak görülmektedir.

Ancak genel olarak kömürlerin kendiliğinden yanma yatkınlığının belirlenmesinde kullanılan bu yöntem fenol köpük dolgu malzemesi için revize edilmiş ve fırın sıcaklığı üst limiti 250 °C olarak belirlenmiştir. Fırın alışılmış yöntemde 30 °C ile 220 °C arasında 0.5 °C/dak artarken köpük dolgu malzemesiyle yapılan deneyde 30 °C ile 250 °C arasında aynı sıcaklık artışıyla çalıştırılmış ve köpük dolgu malzemesinin bu süre zarfında sıcaklık artışı kaydedilmiştir. Bahsi geçen fenol bazlı köpük malzemesinin kendiliğinden yanma yatkınlığının belirlenmesi deneyi Şekil 12'de verilen deney düzeneğinde gerçekleştirilmiştir. Bu kapsamda ortalama sıcaklık artışı hesaplamaları yine 110 °C ile 220 °C arasında literatürdeki haliyle hesaplanmıştır. FCC (Feng, Chakravorty, Cochrane) indeksi hesaplanmış ve Çizelge-1'de verilmiştir. FCC indeksine göre fenol bazlı dolgu köpüklerinin kendiliğinde yanma eğilimlerinin (Şekil 13 ve Şekil 14) düşük olduğu görülmektedir.

Şekil 12. Numunenin kendiliğinden yanma fırınına ve reaktöre yerleştirilmesi ve gerekli hava bağlantılarının tamamlanmasına ait görsel.

Çizelge-1: Fenol bazlı dolgu köpük örneklerinin kendiliğinden yanma yatkınlık deneyi sonuçları.

Örnek Kodu	Kesişme Noktası Sıcaklığı (°C)	Ortalama Sıcaklık Artışı (110-220'C arası) (°C/dak)	FCC İndeksi (dak^{-1})	Kediliğinden Yanmaya Yatkınlık
Örnek 1	231	0.51	2.19	***Düşük***
Örnek 2	231	0.52	2.24	***Düşük***

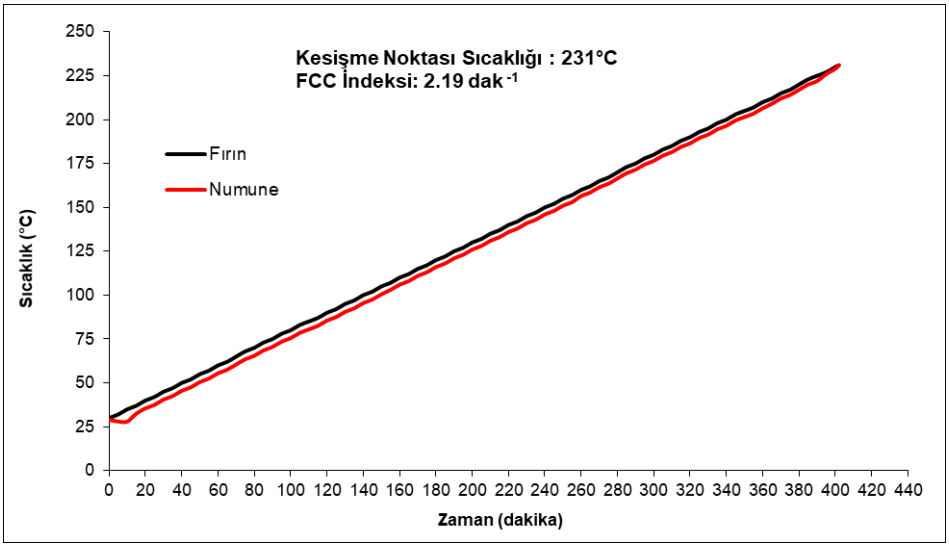

Şekil 13: Köpük dolgu malzemesi (Örnek 1) için elde edilen kendiliğinden yanma yatkınlığı deney grafiği.

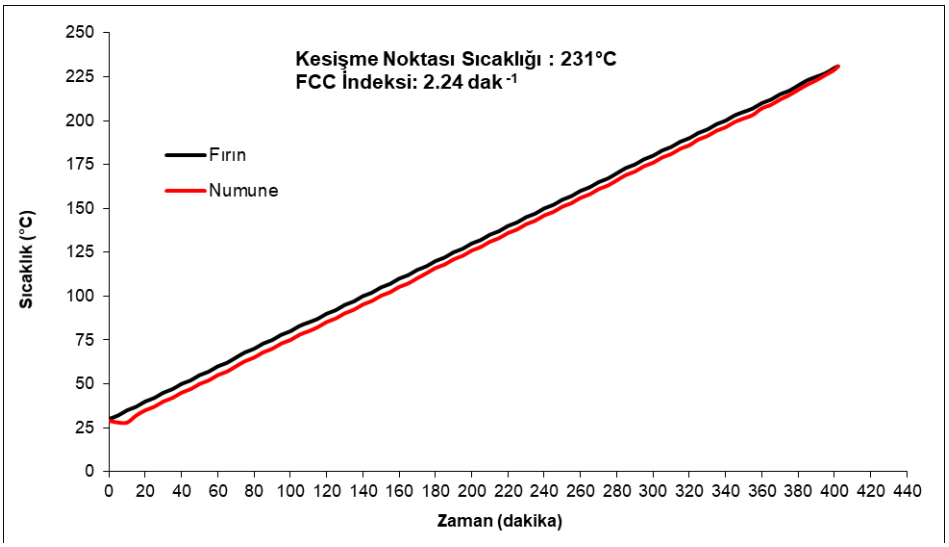

Şekil 14: Köpük dolgu malzemesi (Örnek 2) için elde edilen kendiliğinden yanma yatkınlığı deney grafiği.

Yukarıda belirtildiği üzere fenol köpük ürünü ortam sıcaklığının artması ile kendiliğinden yanma eğilimi olan bir ürün değildir.

Kimyasal dolgu köpükleri kömür madenlerinde yapılan uygulamalarda doğrudan kömür ile kontak halindedir. Uygulama esnasında ekzotermik reaksiyon sıcaklıkları ile ortamdaki sıcaklığa etki etmektedir. Fenol bazlı dolgu köpüklerinin reaksiyon sıcaklıkları 100 °C'nin altındadır (Şekil 15). Ekzotermik reaksiyon sıcaklık artış süresi 5 dakikanın altındadır. Fenol bazlı dolgu köpükleri ortalama 30 dakikada reaksiyonlarını tamamlamaktadır. Diğer bir deyişle ortam sıcaklığına olan etkileri 30 dakika sonunda tamamen ortadan kalkmaktadır.

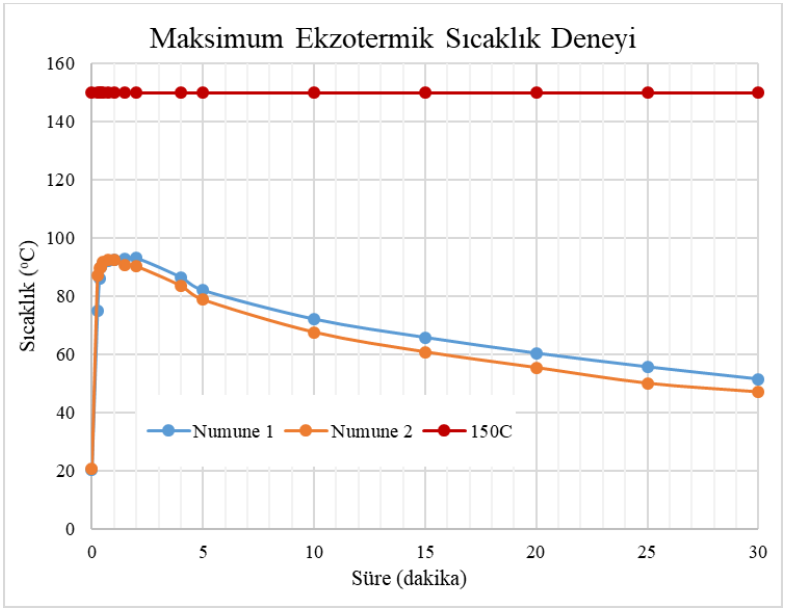

Şekil 15: Fenol bazlı dolgu köpüğü ekzotermik reaksiyon süresi (Erkayoğlu, 2020)

Poliüretan bazlı dolgu köpüklerinin reaksiyon sıcaklıkları 120-200 °C arasında değişmektedir (Şekil 16). Ekzotermik reaksiyon sıcaklık artış süresi 10 dakikanın altındadır. Poliüretan bazlı dolgu köpükleri ortalama 180 dakika da reaksiyonlarını tamamlamaktadır. Diğer bir deyişle ortam sıcaklığına olan etkileri 180 dakika sürmektedir.

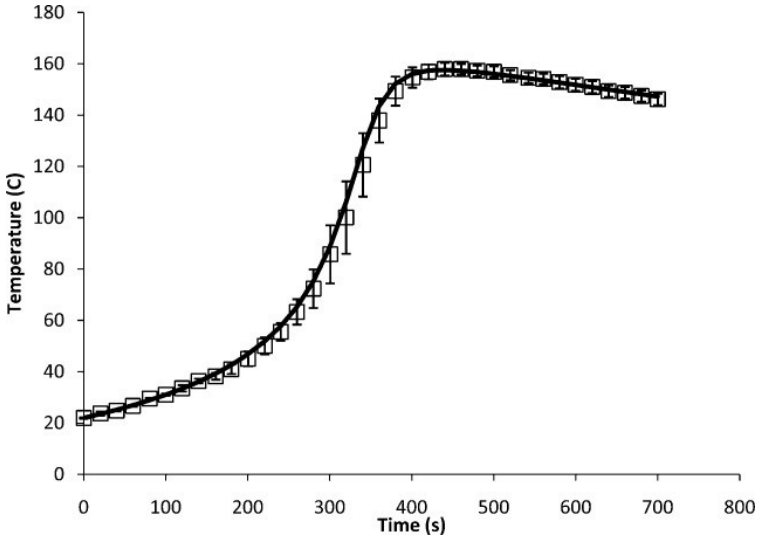

Şekil 16: Poliüretan bazlı dolgu köpüğü ekzotermik reaksiyon süresi (Zhao ve ark., 2013)

SONUÇ VE DEĞERLENDİRME

Yeraltı kömür madenlerinde kullanılan fenol bazlı dolgu köpüklerinin ekzotermik reaksiyon sıcaklığı ile ortam sıcaklığına olan etkisi oldukça düşük seviyelerdedir. Aynı zamanda reaksiyon süresi az olduğundan dolayı ortam sıcaklığına etki süreside düşüktür. Fenol bazlı dolgu köpükleri aleve dayanıklı olduğundan dolayı kömürde oluşabilecek kendiliğinden yanma durumlarında hava temasını keserek söndürücü eleman olarak kullanılabilmektedir.

Poliüretan bazlı dolgu malzemeleri yüksek reaksiyon sıcaklığı ve reaksiyon sürelerinden dolayı kendiliğinden yanmayı tetikleyici bir kimyasal köpük ürünüdür. Aynı zamanda yanıcı özellikte olan bu köpük ürünleri yangınla mücadele gibi uygulamalarda ve kömür kontağı olan bölgelere yapılacak olan uygulamalarda kullanıma uygun değildir. Olası yangın çıkması durumunda içerisinde yer alan MDI malzemesinden dolayı zehirli duman çıkışına sebep olmaktadır. Bu durum yeraltı kömür madenlerinde ciddi iş güveliği problemi oluşturmaktadır.

MDI (Metilen difenil diizosiyanat) ve TDI (Toluen diizosiyanat) içerikli kimyasalların Avustralya'nın kömür madenciliğinin en fazla yer aldığı Yeni Güney Galler eyaletinde yer alan yeraltı kömür madenlerinde kullanımı yasaklanmıştır (MDG 3608, 2012).

Poliüretan bazlı kimyasal dolgu malzemeleri yeraltı kömür madenlerinde yapılan uygulamalarda kendiliğinden yanmayı tetikleyici etkisinden ve yanıcı özelliğinden dolayı problem oluşturmaktadır. Diğer taraftan fenol bazlı kimyasal dolgu köpükleri özellikle yeraltı kömür madenlerinde yapılan uygulamalarda kömürün kendiliğinden yanmasına olan etkisi oldukça düşük seviyelerdedir.

KAYNAKLAR

Aksoy C. O., Kömürlü E., Yaman H. E., (2017), Temel Madencilik Bilgileri, Mayeb Yayıncılık p:108

Arge Yapı İzolasyon, (2021), Fenol Köpüğü Nedir?, www.argeyapiizolasyon.com

Bilen M., Kaymakçı E., Yılmaz S., Çakır A.,(2019), An Alternative Spontaneous Combustion Experiment Set-up by Employing an Old Version Gas Chromatograph, 7. Uluslararası Maden Makinaları ve Teknolojileri Kongresi Bildiriler Kitabı, sf:92

Erkayoğlu M, (2020), ODTÜ Kaya Mekaniği Laboratuvarı Deney Raporu Deney No: 20-03-05-502

Frith R., (2006), Recovering from Major Roof Cavities on the Longwall Face – A Current Perspective

Frontier Environmental Solutions, (2018), Gate Design for Abandoned Mines

Guideline MDG3608 Non-metallic Materials For Use in Underground Coal Mines, (2012), Mine Safety Operations Branch, www.resources.nsw.gow.au

Hu X., Cheng W., Wang D., (2014), Properties and Applications of Novel Composite Foam for Blocking Air Leakage in Coal Mine.

İbuk A., Özarslan A., Atlaş M., (1996), Orta Anadolu Linyitlerinde Ayaklarda Tavan Kontrol Sorunları ve Uygulanan Yöntemler, Türkiye 10. Kömür Kongresi, Zonguldak.

İvrin Y. A., (2016), Ocak Yangınlarında Kendiliğinden Yanmanın İş Sağlığı ve Güvenliği Yönünden Değerlendirilmesi

Kahraman E., Erdem H.H., Sığırcı C., (2011), Park Termik Çayırhan Linyit İşletmesi Kazı Tahkimat Söküm İşleri Eğitim Kitabı, Teknik Not, Ankara.

Kaymakçı E., Didari V., (2000), Kömür Özellikleri ile Kendiliğinden Yanma Parametreleri Arasındaki İlişkiler, Türkiye 12. Kömür Kongresi Bildiriler Kitabı, sf:149

Marc A., (2005), Application of Phenolic Foam in Longwall Mining, International Conference on Ground Control in Mining

Mining Monthly, (2007), Fatality prompts PUR warning, www.miningmonthly.com/markets/international-coal-news/1280655/fatality-prompts-pur-warning

Pile J.D., (2013), Longwall Shield Recovery, Using Phenolic Foam Injection for Gob Control As An Alternative to Recovery Mesh, International Conference on Ground Control in Mining

Trevits M.A., McCartney C., (2008), Use of Rocsil Foam to Remotely Construct Mine Seals

Tuz C, Çağlayan T, Erel A, Kahraman E, (2019), Yeraltı Kömür Madenciliğinde Enjeksiyon ve Köpük Pompasının Önemi, 7. Uluslararası Maden Makinaları ve Teknolojileri Kongresi Bildirileri Kitabı, Sf:102-110

Wilson Mining Service, (20199, WMS Bulk Chemical Handling System and Surface to Seam Technology

Weber Madencilik, (2019), Weber Madencilik Ürün Kataloğu, www.weber-mining.com

Weber Madencilik, (2020), MARIFLEX LS1 Laboratuvar Raporu

Yılmaz S., Bilen M., ve ark., (2022), Yeraltı Kömür Madenciliğinde Kullanılan Fenol Bazlı Dolgu Malzemelerinin Kanserojen Formaldehit İçeriği ve İSG Açısından Değerlendirilmesi

Zhao Y., Gordon M.J., Tekeei A., Hsieh F., Suppes G.J., (2013), Modeling Reaction Kinetics of Rigid Polyurethane Foaming Process, Journal of Applied Polymer Science

KOK BATARYALARI SULU SÖNDÜRME SİSTEMİ PARAMETRELERİNİN OPTİMİZE EDİLEREK SU TÜKETİMİNİN AZALTILMASI

REDUCING WATER CONSUMPTION BY OPTIMIZING COKE OVEN BATTERIES WET QUENCHING PARAMETERS

H. Zümrüt [1, *], Ö. Ece [1], S.C Güner [1]

[1]*İskenderun Demir ve Çelik A.Ş. Payas/HATAY*
*(*Sorumlu yazar: hzumrut@isdemir.com.tr)*

ÖZET

Geleneksel kok üretiminde üç tip söndürme yöntemi vardır. İskenderun Demir ve Çelik A.Ş. (İSDEMİR) kok fabrikasında kuru ve sulu söndürme yöntemleri kullanılmaktadır. Kuru söndürme tesislerinde sıfır nemde kok üretilmektedir. Sulu söndürme yönteminde ise söndürme sırasında kullanılan su miktarı ve süresi büyük ölçüde önem arz etmektedir. Buradan yola çıkarak, sulu söndürme sisteminde optimum su kullanım süresi ve miktarını belirlemek adına 32 deneylik tam faktöriyel bir deney tasarımı hazırlanmıştır. Bu çalışmalar sonucunda R-sq (adj) değeri %81,86, standart sapması 0,54 olan güçlü bir matematiksel model elde edilmiştir. Gerçekleştirilen deneyler sonucunda en düşük nem değerini elde etmemizi sağlayan faktör seviyeleri belirlenmiştir. Proje sonrası dönemde % nem ortalama ve değişkenliğinin proje öncesi döneme göre istatistiksel olarak daha düşük olduğu görülmüştür. Yüksek Fırınlar 'a daha az nem değişkenliğine sahip kok gönderilmesi ile birlikte, yüksek fırın prosesine katkı sağlayacaktır. Diğer taraftan 1 adet söndürme işlemi için kullanılan su miktarı proje öncesi yaklaşık 70 m^3 iken proje sonrası 56 m^3 ' e düşmesi ile 14 m^3 daha az su kullanarak aynı miktarda kızgın kok söndürülmesi sağlanmıştır. Bunun yanında söndürme sürelerinin optimize edilmesi ile proje öncesi söndürülen fırın başına 8,51 m^3 make up suyu kullanılırken, proje sonrasında bu miktar 6,53 m^3'e düşürülerek söndürülen fırın başına atmosfere salınan su buharı emisyonu yaklaşık 2 m^3 azalmıştır. Üretim kapasitesi göz önüne alındığında, sürdürülebilirlik açısından atmosfere su buharı emisyonu ve su tüketimlerinin azaltılması ile sürdürülebilir kalkınma için çevreye büyük ölçüde katkı sağlanmıştır.

Anahtar Kelimeler: Kok bataryaları, kuru söndürme, sulu söndürme, nem, sürdürülebilirlik, su buharı emisyonu

ABSTRACT

There are three types of quenching methods in coke production. The Iskenderun Iron and Steel Co. (ISDEMIR) use dry and wet quenching methods in coke plant. In wet quenching unit; amount and duration of water during quenching is very important. Full factorial experiment design with 32 experiments was prepared in order to determine optimum water usage time and amount, in system. Consequently, the value of R-sq is 81.86%; A strong mathematical model with a standard deviation of 0.54 was obtained. Also factor levels that enable us to obtain the lowest moisture value were determined. It was observed that average and variability of % moisture in post-project period was statistically lower than pre-project period. Moreover, amount of water used for per quenching process was approximately 70m^3 before project, but decreased to 56 m^3 after project, and same amount of hot coke was quenched by using 14m^3 less water. By optimizing quenching times, make-up water was used per-furnace was reduced from 8.51m^3 to 6.53m^3 and water vapor emission released into atmosphere per-furnace was reduced by approximately 2m^3. Considering production capacity, a significant contribution has been made to environment for sustainable development by reducing water vapor and water consumption in terms of sustainability.

Keywords: Coke oven batteries, dry quenching, wet quenching, moisture, sustainability, water vapor emission

GİRİŞ

Kok Fabrikalarının görevi; esas ürün olarak Yüksek Fırınların sıvı ham demir üretebilmesi için ihtiyacı olan metalürjik kokun üretilmesi ve bu esnada yan ürün olarak kok gazı, katran, benzol, amonyum sülfat, ceviz kok ve toz kokun üretilmesidir (Kural, 1998). Yükesk fırınlarda gerekli enerji kok kömürünün yakılması ve ısı veren kimyasal tepkimelrle elde edilmektedir (Yıldız, 2010). Kok fabrikası ürün akım şeması (Şekil 1) aşağıdaki gibidir;

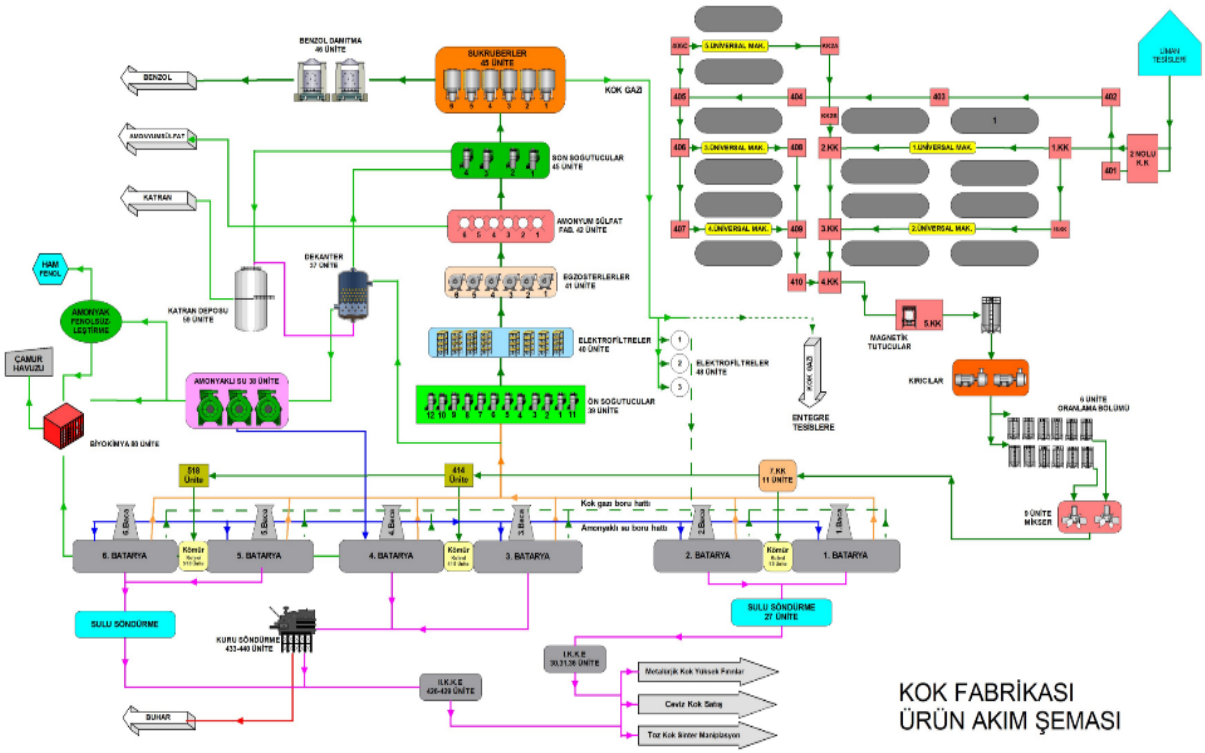

Şekil 1. Kok fabrikası ürün akım şeması

Bataryalarda koklaşma süresi tamamlanan kömür, koklaşma kamarasından itilerek söndürme arabalarına alınmaktadır. Söndürme arabasıyla söndürme tesislerine giden kok, yaş ya da kuru olmak üzere iki farklı yöntemle söndürülmektedir.

- Kuru söndürme sisteminde kok kamaralara alınmakta ve inert gaz (sirkülasyon gazı) ile söndürülmektedir. Sistemde kokun ısısı kullanılarak buhar üretimi gerçekleştirilmektedir. Kuru söndürme tesislerinde sıfır nemde kok üretilmektedir.
- Sulu söndürme sisteminde kömür koklaşmasını tamamladıktan sonra fırın itme arabası tarafından itilerek söndürme vagonuna alınır. (Şekil 2) Kızgın kok fırından çıktığında ortalama 1.050 ^{o}C sıcaklığa sahiptir. Söndürme işlemi, vagonun söndürme kulesi altına girmesi ile başlar. Söndürme işlemi kule içerisinde bulunan nozullar vasıtasıyla kızgın kok üzerine su boşaltarak gerçekleştirilir. Söndürme işlemi sonrasında kok sıcaklığı 70-80 ^{o}C civarına düşürülerek tamamlanır. Ardından söndürme rampasına boşaltılarak kullanıcı ünitelere manipülasyonu sağlanır.

ÇALIŞMANIN AŞAMALARI

Şekil 2. Kızgın kokun söndürme vagonuna aktarılması

Metalurjik kok üretiminde, fiziksel ve kimyasal kalite parametreleri yüksek fırın prosesinde büyük etkiye sahiptir (Lech vd., 2017; Loison vd., 1989). Sulu söndürme yönteminde söndürme sırasında kullanılan su miktarı ve süresi büyük ölçüde önem arz etmektedir. Buradan yola çıkarak, sulu söndürme sisteminde optimum su kullanım süresi ve miktarını belirlemek adına 32 deneylik tam faktöriyel bir deney tasarımı hazırlanmıştır. Bu çalışmalar sonucunda R-sq (adj) değeri %81,86; standart sapması 0,54 olan güçlü bir matematiksel model elde edilmiştir. (Çizelge 1)

Çizelge 1. Matematiksel model ve parametreler

Model Özeti

S	R-sq	R-sq(adj)	R-sq(pred)
0,539023	87,71%	81,86%	71,46%

Kodlanmış Katsayılar

Term	Effect	Coef	SE Coef	T-Value	P-Value	VIF
Constant		5,8719	0,0953	61,62	0,000	
1. Vana	0,3813	0,1906	0,0953	2,00	0,059	1,00
1. Sn	-0,2538	-0,1269	0,0953	-1,33	0,197	1,00
2. Vana	1,0612	0,5306	0,0953	5,57	0,000	1,00
2. Sn	1,1338	0,5669	0,0953	5,95	0,000	1,00
1. Vana*2. Sn	-0,7287	-0,3644	0,0953	-3,82	0,001	1,00
1. Sn*2. Vana	-0,4812	-0,2406	0,0953	-2,53	0,020	1,00
2. Vana*2. Sn	0,5588	0,2794	0,0953	2,93	0,008	1,00
1. Vana*1. Sn*2. Vana	1,0412	0,5206	0,0953	5,46	0,000	1,00
1. Vana*2. Vana*2. Sn	-0,6162	-0,3081	0,0953	-3,23	0,004	1,00
1. Vana*1. Sn*2. Vana*2. Sn	0,5312	0,2656	0,0953	2,79	0,011	1,00

Kodlanmış Birimlerde Regresyon Denklemi

Nem = 5,8719 + 0,1906 1. Vana - 0,1269 1. Sn + 0,5306 2. Vana + 0,5669 2. Sn
- 0,3644 1. Vana*2. Sn - 0,2406 1. Sn*2. Vana + 0,2794 2. Vana*2. Sn
+ 0,5206 1. Vana*1. Sn*2. Vana - 0,3081 1. Vana*2. Vana*2. Sn
+ 0,2656 1. Vana*1. Sn*2. Vana*2. Sn

Uncoded coefficients are not available with non-hierarchical model.

Şekil 3. Sulu söndürme işlemi

Gerçekleştirilen deneyler sonucunda en düşük nem değerini elde etmemizi sağlayan faktör seviyeleri belirlenmiştir. Sulu söndürme işlemi (Şekil 4) iki kademede gerçekleşmektedir.

1. Adım : Bu adım ön söndürme işlemidir. Amaç kızgın kokun vagon içinde yayılmasını sağlamaktır. Ön söndürme işlemi, 1. Adım vana açıklık yüzdesi ve 1. Adım söndürme süresinden oluşmaktadır.

2. Adım: Bu adım son söndürme işlemidir. Amaç kızgın kokun soğumasını sağlamaktır. Son söndürme işlemi, 2. Adım vana açıklık yüzdesi ve 2. Adım söndürme süresinden oluşmaktadır.

Sulu söndürme işlemi yapılırken bu iki adım için kullanılan vana açıklık ve söndürme süresi faktör seviyeleri olarak adlandırılmıştır (Şekil 5).

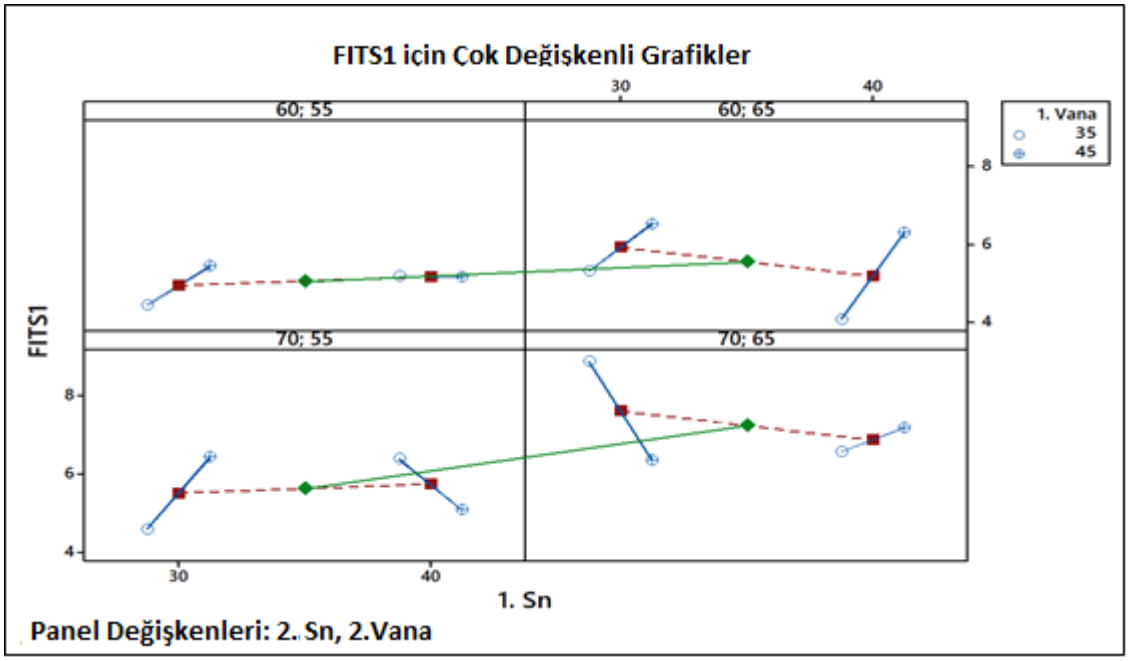

Şekil 4. Vana-süre

Çıkarılan matematiksel modele göre minitab programı çalıştırılarak en düşük neme ulaşmamız için kullanmamız gereken faktör seviyeleri tespit edilmiştir. Yüzdesel vana açıklıkları ve söndürme süreleri belirlenen parametreler de ayarlanmıştır.

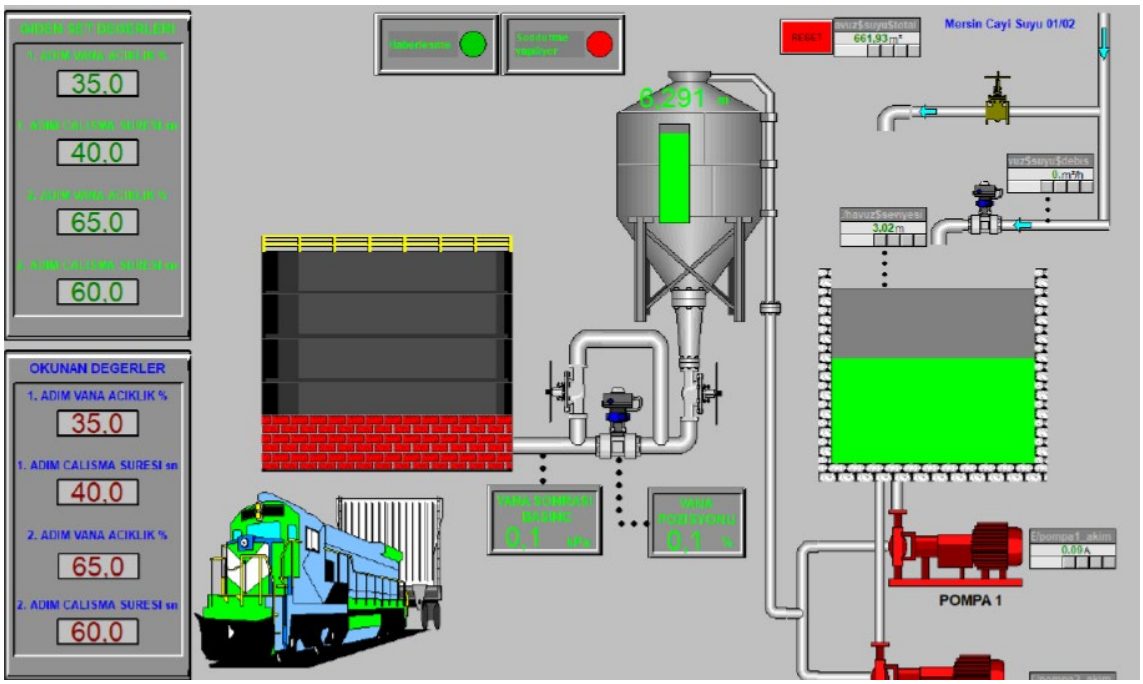

Şekil 5. Söndürme kulesi PLC ekranı

SONUÇLAR

5/6 Kok Bataryaları Sulu Söndürme Sistemi söndürme kulesi vana parametreleri optimize ederek su tüketiminin azaltılması hedeflenmiştir. Üretim kapasitesi göz önüne alındığında, sürdürülebilirlik açısından atmosfere su buharı emisyonu ve su tüketimlerinin azaltılması ile yıllık yapılan 56.575 adet sulu söndürme işleminde 85.428 m^3 su buharının atmosfere salınmasının önüne geçilmiştir.

Ayrıca bu çalışma ile sistem çalışma parametrelerinin standartlaştırılması sağlanarak, proses güvenliğine katkı sağlanmıştır.

Uygulama verileri analiz edildiğinde % nem ortalama ve değişkenliğinin proje öncesi döneme göre istatistiksel olarak daha düşük olduğu görülmüştür. Proje öncesi nem değerlerinin ortalaması %5,45, proje sonrası nem değerlerinin ortalaması ise %5,38 olarak gerçekleşmiştir. Bu sayede Yüksek Fırınlara daha az nem değişkenliğine sahip kok gönderilmesi ile birlikte, yüksek fırın prosesinin daha kolay yönetilmesine katkı sağlanmış olup ayrıca enerji ve yakıt tasarrufuna katkı sağlanmıştır. (Kok nemindeki %1 düşüş Yüksek Fırınların Sıvı Ham Demir üretim prosesinde ton başına 0,6 kg/TonSHD tasarruf sağlamaktadır.) Ayrıca kok nemindeki düşüş Yüksek Fırınlarda faydalı hacmin artışı ve üretim artışı da sağlamaktadır. İlgili çalışma endüstriyel tesiste kontrollü deneyler yapılarak hayata geçirlmiştir. Konuyla ilgili benzer literatür çalışmalarına rastlanılmamıştır.

TÜİK verilerine göre dört kişilik bir hanenin aylık su tüketimi 23 m^3 kabulüyle, yapılan çalışma 3.714 adet hanenin aylık su tüketimini karşılamaktadır. (14.857 kişinin aylık su tüketimine eş değerdir.)

KAYNAKLAR

Kural, O. (1998) Kömür Özellikleri, Teknolojisi ve Çevre İlişkileri. İstanbul

Yıldız, N. (2010) Demir Cevheri. Ankara

K. Lech, S. Jursova, P. Kobel, P. Pustejovska, JiriBilik, A. Figiel & L. Romański, (2017) The Relation Between

CRI, CSR Indexes, Chemical Composition and Physical Parameters of Commercial Metallurgical Cokes

Loison, R., Foch, P. and Boyer, A., 1989, Coke quality and production, Butterworth, London.

KOK BATARYALARINDA SÖNDÜRME PROSESİNİN OPTİMİZASYONU VE ÜRETİLEN KOKUN YÜKSEK FIRINLARDA ENERJİ VERİMLİLİĞİNE ETKİSİNİN İNCELENMESİ

OPTIMIZATION OF THE QUENCHING PROCESS IN COKE BATTERIES AND INVESTIGATION OF THE EFFECT OF PRODUCED COKE ON ENERGY EFFICIENCY IN BLAST FURNACES

H. Kalay [1, *], Z. Özer [1]

[1] *İskenderun Demir ve Çelik A.Ş.*
*(*Sorumlu yazar: hkalay@isdemir.com.tr)*

ÖZET

Koklaşma, belirli oranlarda harmanlanan kömürün, havasız bir ortamda, belirli bir sıcaklık ve basınçta uçucu maddeleri yok ederek sert ve gözenekli bir yapı oluşturmasıdır. Elde edilen bu gözenekli yapıya kok denir. Üretilen kok, sıvı ham demir üretimi için bantlarla yüksek fırınlara gönderilir. Demir üretimi için elde edilen bu kok, bazı önemli parametreleri sağlamalıdır. En önemli parametrelerden biri kokunun sahip olduğu nem miktarıdır. Kokun nem miktarı birçok parametreye bağlıdır, istenilen özelliklere sahip kok elde etmek için en önemli olan parametre su ile hızlı soğutma işlemidir. Bu işlem söndürme işlemi olarak tanımlanır. Sulu söndürme işleminde optimizasyon çalışmaları su verme süresi, vana açıklığı, su verme sonrası bekleme süresi ve kullanılan su miktarı için yapılır. Bu çalışmalar sonucunda elde edilen kok, yüksek fırınlarda kullanılan enerji miktarını etkilediğinden enerji verimliliğini doğrudan etkilemektedir. Bu çalışmada, İskenderun Demir Çelik A.Ş. (İSDEMİR) kok bataryalarında kok, koklaşma prosesi, nem içeriği optimizasyonu ve yüksek fırınların enerji verimliliğine etkisi incelenmiştir.

Anahtar Sözcükler: Kok, söndürme prosesi, optimizasyon, enerji verimliliği, yüksek fırın.

ABSTRACT

Coking is that coal, which is blended in certain proportions, creates a hard and porous structure by disappearing volatile substances at a certain temperature and pressure in an airless environment. This obtained porous structure is called coke. The produced coke is sent to blast furnaces with bands for the production of liquid raw iron. This coke obtained for iron production must provide some important parameters. One of the most important parameters is the amount of moisture the coke has. The amount of coke moisture depends on many parameters, the most effective one is the rapid cooling process with water to obtain the coke which has desired properties. This process is defined as quenching process. Optimization studies in the quenching process are carried out for the quenching time, valve opening, waiting time after the quenching and the amount of water used. Since the coke obtained as a result of these studies affects the amount of energy used in blast furnaces, it directly affects energy efficiency. In this study, the coke, coking process, optimization of moisture content and its effect on energy efficiency for blast furnaces in the Iskenderun Iron and Steel Co. (ISDEMIR) coke batteries were investigated.

Keywords: Coke, quenching process, optimization, energy efficiency, blast furnace.

GİRİŞ

Kömür, bitkisel kökenli organik ve inorganik bileşenlerden oluşan tortul bir kayadır. Bitki ve ağaç kalıntılarının bataklıklarda üst üste birikmesi sonucu oluşur. Milyonlarca yıl içinde gerçekleşen bu olayda fiziksel ve kimyasal etkileşimler ile karbonizasyon meydana gelir. Kömürün yapısında çoğunlukla C ve az miktarda H, O, S, N bulunur. Kömürlerin sınıflandırılması farklı şekillerde yapılabilir. Kömürler genel olarak turba, linyit, taşkömürü, antrasit ve grafit olarak sınıflandırılabilir.

Şekil 1'de başlıca kömür çeşitlerinin görselleri verilmiştir. Bataklık alanlarda bitki artıklarından oluşan turba, kömürün en ilkel şeklidir. Kahverengi kömür olarak da bilinen linyit, en düşük kaliteli kömür sınıfındadır. Linyit kömürünün sarı linyit ve kahverengi linyit gibi türleri vardır. Taşkömürü kalorifik değere bakıldığında en kaliteli kömür türlerinden birisidir. Antrasit %95 karbondan oluşur ve su içeriği çok düşüktür. Grafit saf karbondur.

Şekil 1. Kömür türleri

Kömürler çeşitli amaçlarla kullanılabildiği gibi yakıt hammaddesi olarak da kullanılabilmektedir. Genellikle elektrik üretimi, demir çelik ve çimento sanayi, buhar üretimi ve endüstriyel proseslerde ısıtma amaçlı kullanılmaktadır. Kullanım alanındaki en önemli sektörlerden biri de demir çelik sektörüdür. Kömür, yüksek kalorisi nedeniyle demir çelik endüstrisinde enerji kaynağı olarak sıklıkla kullanılmaktadır (Elif,2019; Selami,Ty).

Koklaşma Prosesi

Koklaştırma prosesi, demir çelik üretiminde sürecin ilk adımıdır. Koklaştırma prosesi kısaca şu şekilde özetlenebilir: yurt dışından ithal edilen kömürler bazı parametrelere göre ayrı ayrı harmanlanır. Harmanlanan kömürler istenilen boyuta ulaşmak için belirli kırıcılardan geçirilerek kullanıma hazır hale getirilir. Proseste kullanılacak kömürün %80'inin boyutu 3 mm'nin altında olmalıdır. Hazırlanan kömür karışımları, bantlar yardımıyla şarj edilmek üzere bataryalara gönderilir. Batarya, koklaştırma işleminin gerçekleştiği fırınlardan oluşur ve belirli kapasitelere göre dizayn edilir. Şekil 2, kok fabrikası bataryalarını göstermektedir. Fırınların yapısı, hacmi ve çalışma parametreleri değişiklik gösterebilir (Jacob vd., 2005; Erke, 2016).

Şekil 2. Bataryaların fırın yapısı

Bataryaya bantlar ile gelen kömürler fırınlara doldurulur, fırınlara şarj edilen kömürler belirli sıcaklık ve basınçlarda belirli bir süre tutularak koklaştırma işlemi başlatılır. İşlem havasız bir ortamda gerçekleşir ve işlem için gerekli olan ısı yan duvarlardaki ısı ile sağlanır. Bu işlemin tamamına koklaştırma, işlem sonucunda elde edilen ürüne ise kok denir. Koklaşma prosesi devam ederken belirli sıcaklık değerlerinde bazı reaksiyonlar ve değişimler meydana gelir. Şarj edilen kömür 200 °C'ye kadar nemini kaybeder ve CO_2 ve CH_4 gibi gazlar yapıdan uzaklaşmaya başlar. Kömürün yumuşaması ve erimesi 200-400 °C arasında gerçekleşir. Bu sırada kömürün hacmi küçülür. Isınma fırının merkezine doğru yan duvarların etkisiyle devam eder ve merkeze doğru ergiyerek dışta plastik bölge oluşur. 450 ile 550 °C arasında ham kok gazı oluşur. Oluşan ham kok gazı dışarı çıkmak ister ancak plastik bölgenin direnci sonucunda kömürde şişme olur ve böylece yarı koklaşma olayı meydana gelir. Sıcaklık 700-800 °C'ye ulaştığında H_2 ve CO gazları ortaya çıkmaya başlar. 800 °C'nin üzerinde grafitleşme meydana gelir ve 900 °C'nin üzerinde gözenekli kok oluşmaya başlar. Hidrojenin çoğu 1000 °C civarında yapıdan ayrılır. İşlemin tam olarak tamamlandığı sıcaklık değeri yaklaşık 1200-1300 °C'dir. Koklaşma işleminde plastik bölge oluşumu ve yapısı prosesin tamamlanmasında belirleyici rol oynar.

Şekil 3'te, plastik bölge ve kok fırınını itme anını içeren koklaştırma prosesinin şematik bir gösterimi verilmiştir. Plastik bölge, kömürün 350-500 °C arasında yumuşadığı, eridiği, hacminin küçüldüğü daha sonra hacminin tekrar arttırıldığı, partiküllerin birbirine yapışıp katılaştığı bölgedir. Proses için kullanılan enerji kaynağı kok gazıdır.

Şekil 3. Koklaşma prosesi ve plastik bölgenin oluşumu

Koklaştırma prosesinde oluşan kok gazı yan ürünler ünitesine gönderilir, yan ürünlerde birtakım işlemlerden geçtikten sonra borular yardımıyla bataryalarda kullanılmak üzere geri gönderilir. Koklaşma prosesinde kok gazının yanı sıra yüksek fırın gazı da kullanılmaktadır. Plastik bölge, iyi bir koklaştırma prosesinde en belirleyici faktördür. Koklaşma fırın duvarlarından içeriye doğru olduğu için plastik bölge tam ortada birleşmelidir. Koklaşma süresi birçok parametreye bağlıdır. En önemli parametreler fırın kapasitesi, kömür tipi, çalışma koşulları ve fırın tasarımıdır. Ortalama koklaşma süresi 18-22 saat arasında değişmektedir.

Söndürme Sistemi

Kok fabrikasında bataryalarda 2 farklı söndürme sistemi kullanılmaktadır. Fırınlarda koklaşma işlemi tamamlandıktan sonra fırın itme arabası ile itilir, itilen fırın batarya yapısına göre tasarlanmış söndürme sistemine göre söndürme işlemi yapılır ve bantlar yardımıyla yüksek fırınlara gönderilir. Söndürme sistemlerinden biri kuru söndürme sistemidir. 4. batarya kuru söndürme sistemi ile çalışır. Bu sistemle elde edilen kok içerisindeki nem miktarı %0'dır. Koklaşması tamamlanan ürünler nitrojen gazı ile soğutma işlemine tabi tutulur. Su ile teması olmadığı için nem oranı %0'dır. Diğer söndürme yöntemi olan sulu söndürmede ise koklaşma prosesi tamamlanan kok su ile söndürülerek yüksek fırınlara gönderilmektedir. Yüksek fırınlara gönderilen kokun nemi, söndürme sistemine bağlı olarak değişmektedir. Tüm bataryalarda işlem adımları aynıdır ancak kapasite, çalışma koşulları ve tasarıma göre söndürme işleminde bazı farklılıklar olabilir. Kullanılan su miktarı, su verme süresi, vana açıklığı, fırın kapasitesi, su verme nozulu tasarımı gibi parametreler su verme sistemini optimize etmek için kullanılan en önemli faktörlerdir. Söndürme süresi batarya yapısına göre değişir. Ortalama su verme süresi 100-140 saniye arasında değişmektedir. Bu süre içerisinde oluşan kok hala sönmemiş ise tekrar su verme işlemi yapılır. İkinci söndürme süresi yaklaşık 40 saniyedir. İkinci aşama söndürmenin nedeni kokun tamamen söndüğünden emin olmaktır. Sulu söndürme sisteminin şematik gösterimi Şekil 4'te verilmiştir. Söndürme yöntemleri ile söndürülemeyen kok bantlara zarar verir, prosesi olumsuz etkiler. İkinci önemli parametre valf açıklığıdır. Vana açıklığı, 1. kademe vana açıklığı ve 2. kademe vana açıklığı olmak üzere iki farklı durumda incelenir. Valf açıklığı proses koşullarına göre değişim gösterir.

Şekil 4. Sulu söndürme sistemi

Söndürülmemiş kok ve nem değerlerindeki artış gibi önemli parametreler vana açıklığında değişikliğe neden olur. 1. Bataryada söndürüldükten sonra söndürme arabası 4-5 dakika dinlendirilir, su iyice süzüldükten sonra kok rampasına boşaltılır. Buradaki amaç su ile teması engelleyerek nem değerlerindeki artışı önlemektir. Şekil 5'te söndürme işleminden sonra kömür süzme işlemi ve kok

rampasına ait görüntüler verilmektedir. Kok rampasına boşaltılan kok söndürülmezse, rampada yardımcı operatörler tarafından söndürmeye devam edilir. 26 ton koku söndürme işlemi için yaklaşık 90 ton su kullanılmaktadır. Kullanılan su miktarı fırın kapasitesine göre değişmektedir (Ivan, 2019; Anna, 2015).

Kısaca kok içerisindeki nemi etkileyen ana parametreler söndürme arabasına alınan kok miktarı ve porozite, söndürme arabasının kulenin altında ve kok rampasında kalma süresi, söndürme sistemindeki nozulların bakımı ve söndürme sisteminin ayarlanması gibi parametrelerdir.

Şekil 5. Kömürün süzülmesi ve kok rampası

Kok Nem Miktarının Yüksek Fırınlara Etkisi

Elde edilen kok ve koklaştırma prosesinde kullanılan kömürün nem içeriği, kokunun yüksek fırınlarda fiziksel, kimyasal ve termal fonksiyonlarını yerine getirebilmesi için dikkate alınması gereken çok önemli bir parametredir. Taş kömürünün içerdiği fazla nemi buharlaştırmak için daha fazla enerji gerekir. Kokun nem içeriğindeki %1'lik bir artış, üretilen 1 ton demir başına 5 kg kok tüketimi ve tüylerden üflenen havanın sıcaklığının 100 °C artması anlamına gelir.

Elde edilen kokunun nem içeriğinin sabit bir değerde olmaması, yakıt girdi dengesini ve fırının ısıl dengesini bozmaktadır. Kontrolsüz nem değişimleri yüksek fırınlarda çalışma sürecini etkiler, verimi düşürür ve kaliteli ürün üretimini engeller. Ayrıca yüksek fırınlarda kullanılan kok nemi yüksek ise kok fırın içinde parçalanır ve dayanım sağlanamaz. Nem analizi yapılacak kok numuneleri, yüksek fırın ile kok fabrikası arasındaki bant üzerinden alınmalı ve düzenli aralıklarla analiz edilmelidir. Düşük nemli bir kok (%0 nem) elde etmek için koklaştırma işleminin sonunda kuru söndürme tercih edilmelidir. Sistemde sulu söndürme varsa söndürme arabasına konulan kokun çok iyi yayılmasına, kullanılan suyun kokun her tarafına püskürtülmesine, suyun uygun zaman aralığında aralıklı olarak verilmesine ve rampada kokunun dinlendirilmesine dikkat edilmelidir (Umutcan, 2015).

DENEYSEL ÇALIŞMALAR

Üretilen kokun nem miktarının sabit bir değerde olması yüksek fırınlarda ısıl dengenin sağlanmasını ve kullanılan yakıt miktarının sabit bir değerde olmasını sağlar. Kokun nem miktarının plansız bir şekilde artması ya da azalması yüksek fırınların çalışma prosesini, elde edilen verimi ve kaliteli ürün üretimini etkiler. Bataryalarda elde edilen kokun ve kullanılan kömürün günlük olarak nem analizi yapılmaktadır ve bu değerler kontrol altında tutulmaktadır. Bu çalışmada da bataryalarda elde edilen ortalama nem miktarları, kullanılan kömür ve elde edilen kokun nem değerleri karşılaştırılacaktır. Yukarıda da bahsedildiği gibi 1. ve 5-6. Bataryada sulu söndürme, 4. Bataryada ise kuru söndürme yapılmaktadır. Alınan numunelerin nem analizleri İskenderun Demir Çelik Fabrikası (İSDEMİR) Kok Bataryaları Analiz Laboratuvarı'nda yapılmıştır. Nem tayini cihazı ile hem analitik hem toplam nem tayini analizleri yapılır. Taş kömüründe nem tayini analizi yapılırken bir miktar numune etüvde belirli bir süre kurutulur ve desikatörde soğutulur. Numunenin ilk tartım miktarı değeri ve kuruduktan sonraki tartım miktarı değerinden taş kömüründeki nem miktarı tayin edilir. Kok kömüründe nem tayini de taş kömüründe olduğu gibi yapılır. Burada numune koklaşma prosesi bittikten sonra üretilen tüm ürünü temsilen kok rampasından alınan numunedir.

Bu çalışmada sulu söndürme sisteminde su verme süresi, su miktarı ve söndürme arabasının rampada bekleme süresi optimize edilerek en düşük nem değeri elde edilmiştir. Optimizasyon çalışmaları 5-6.Bataryalar için yapılmıştır. Su verme süresi 60-70 sn, kullanılan su miktarı 85-97 ton, söndürme arabasının bekleme süresi 5-10 sn olarak ele alınmıştır. Optimizasyon çalışmaları kapsamında minimum nem değeri elde edilmeye çalışılırken elde edilen kokun tam sönmüş olması, proses koşullarına zarar verecek herhangi bir ateşlenmenin olmaması göz önünde bulundurulmuştur. Şekil 6, 7 ve 8'de yapılan optimizasyon çalışmalarının sonuçları gösterilmektedir. Optimizasyon çalışma sonuçlarına bakıldığında su verme süresi 60 sn, kullanılan su miktarı 90 ton ve bekleme süresi 5 sn olarak belirlenmiştir. 85 ton su kullanıldığında nem miktarının düşük olmasına rağmen elde edilen kok ateşli olup prosesi istenilen seviyede tamamlamadığı için bu su miktarı söndürme işlemi için yetersiz bulunmuştur.

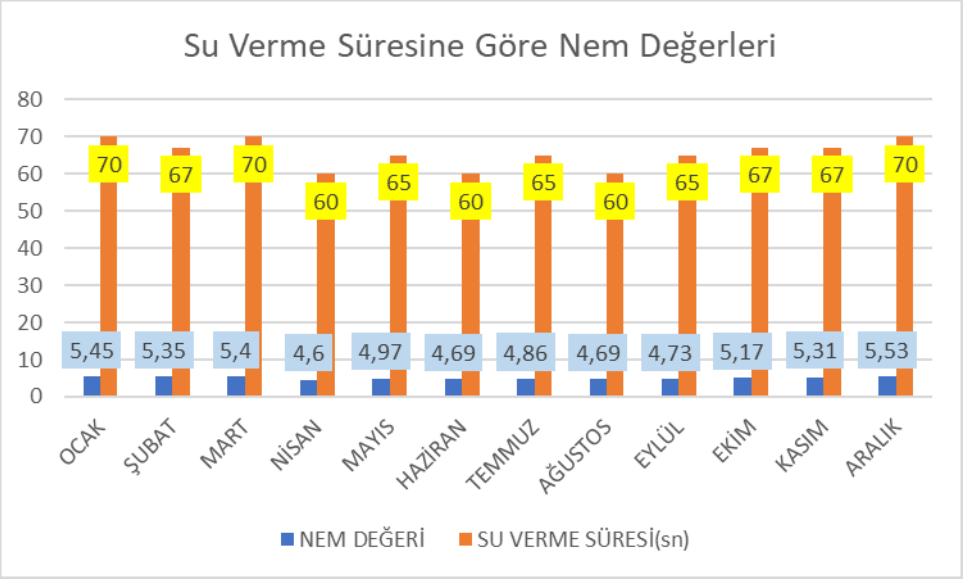

Şekil 6. Su Verme Süresine Göre Nem Değerleri

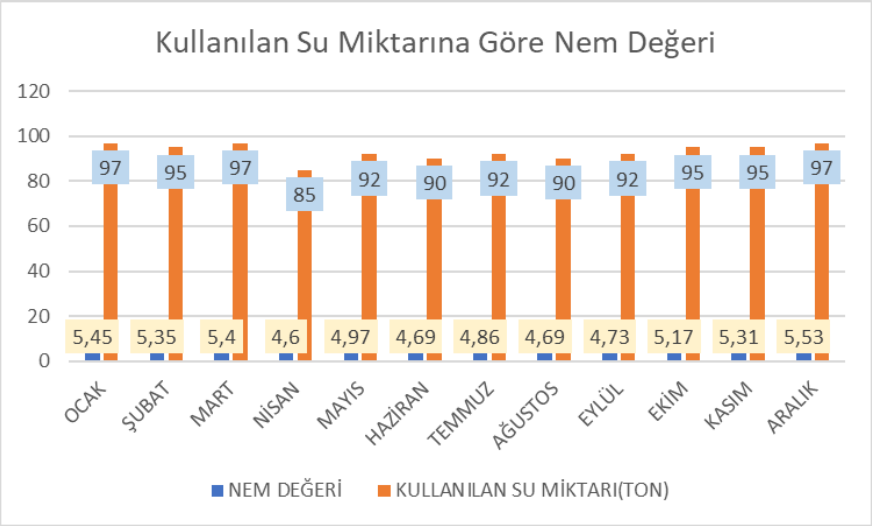

Şekil 7. Kullanılan Su Miktarına Göre Nem Değerleri

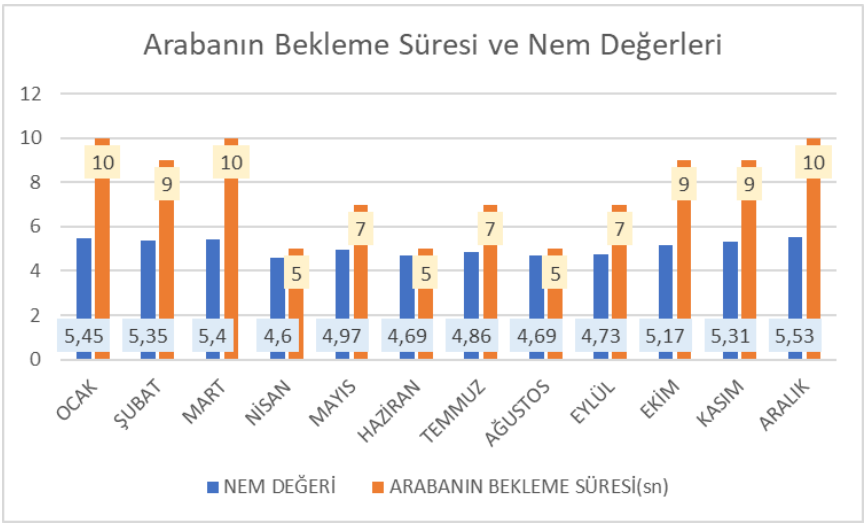

Şekil 8. Arabanın Bekleme Süresine Göre Nem Değerleri

Kok fabrikasında yer alan bataryalar için bu optimizasyon çalışmaları sonucunda su verme süresi 60 sn, kullanılan su miktarı 90 ton ve söndürme arabasının bekleme süresi 5 sn olarak belirlendiğinde elde edilen Ekim, Kasım ve Aralık aylarındaki nem değerlerinin ortalaması Şekil 9'da verilmiştir. Bu bataryalar için Aralık ayında kullanılan taş kömürü ve elde edilen koka ait ortalama nem değerleri ise Şekil 10'da verilmiştir. Hem taş kömürü hem kok için nem tayini hesabı yapılırken bir miktar numune etüvde belirli bir süre kurutulur ve desikatörde soğutulur. Numunenin ilk tartım miktarı değeri ve kuruduktan sonraki tartım miktarı değerinden taş kömürü ve kok kömüründeki nem miktarı tayin edilir.

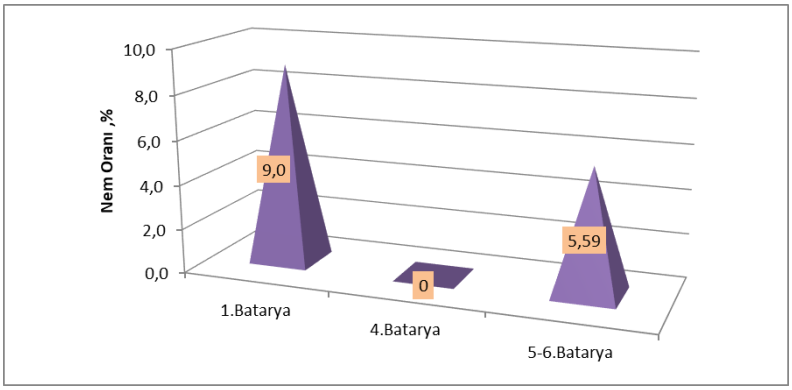

Şekil 9. Bataryaların ortalama nem değerleri

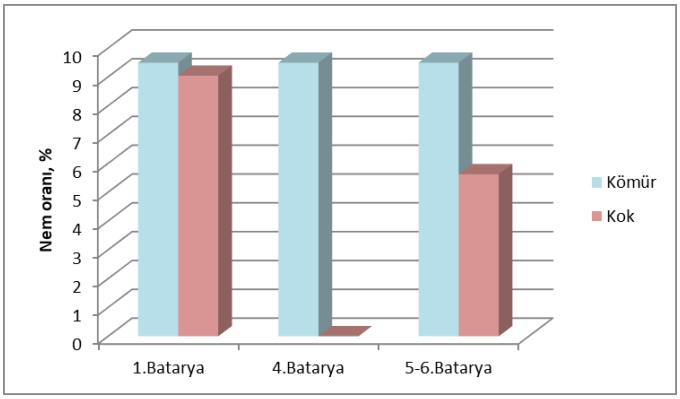

Şekil 10. Aralık ayında bataryalardaki taş kömürü ve kok için ortalama nem değerleri

TARTIŞMA VE YORUM

Kullanılan koklaşabilir taş kömürü ve elde edilen kok için nem tayini analizleri TSE standartlarına uygun olarak İSDEMİR analiz laboratuvarında yapılmıştır. Ekim, Kasım ve Aralık aylarında yapılan günlük nem tayini analiz sonuçları kaydedilmiştir ve ortalama değerleri hesaplanmıştır. Koklaşma prosesinde kullanılan taş kömüründe bulunan nemin buharlaştırılması için ısıya gereksinim vardır bu nedenle enerjinin çok fazla kullanımının önüne geçmek için bu nem değerinin belirli bir değerde olması gerekmektedir. Koktaki nem ise yüksek fırınlarda kokun parçalanmasına neden olur, ısıl denge sağlanamaz. Bu nedenle kokun içerdiği neminde belirli bir değerde olması gerekmektedir. Kokun nem miktarı koklaşma prosesinden sonra yapılan söndürme işlemi, işletme şartları ve kullanılan kömürün nem tutma kapasitesine göre değişmektedir. Kok fabrikasında bulunan bataryalarda su verme süresi, su miktarı ve söndürme arabası bekleme süresi için yapılan optimizasyon çalışmaları sonucunda elde edilen koka ait Ekim, Kasım ve Aralık aylarındaki nem değerlerinin ortalaması Şekil 6'da verilmiştir. 4. Bataryada kuru söndürme olduğu için koktaki nem miktarı sıfırdır ve bu özellik 4. Batarya'dan elde edilen kokun yüksek fırınlar tarafından en çok tercih edilme sebebidir. 1. Bataryada elde edilen kokun ortalama nem değeri %9,0 ve 5-6. Bataryada elde edilen kokun nem değeri %5,59'dur. Bu nem değerlerindeki kokta yüksek fırınlar için uygun bir kok çeşididir. Bataryalardan elde edilen bu koklar yüksek fırınlarda ya direk ya da harman yapılarak kullanılır. Şekil 7'de ise Aralık ayında bataryalarda hem taş kömürü hem kok için yapılan analiz sonuçlarının ortalaması verilmiştir. Bataryalarda kullanılan taş kömürünün ortalama değeri %9,49'dur. 4. Batarya için kuru söndürmeden dolayı nem miktarı sıfırdır, 1. Batarya ve 5-6. Batarya için ise nem değerleri sırasıyla %9,04 ve %5,62'dir. Her iki bataryada aynı şartlarda sulu söndürme yapılmasına ve aynı özellikte kömür kullanılmasına rağmen nem değerlerinin farklı olmasında işletme şartları ve bataryaların özellikleri etkili olmaktadır. Yüksek fırınlarda verimin ve çalışma koşullarının etkilenmemesi ve enerji verimliliğinin azalmaması için kullanılan kömürün ve elde edilen

kokun nem miktarının belirli nem değerleri aralığında olması gerekmektedir. Taş kömürünün içerdiği fazla nemi buharlaştırmak için daha fazla enerji gerekir. Kokun nem içeriğindeki %1'lik bir artış, üretilen 1 ton demir başına 5 kg kok tüketimi ve tüylerden üflenen havanın sıcaklığının 100 °C artması anlamına gelir.

SONUÇ

Kullanılan taş kömürünün nem miktarı ve suyu tutma özelliği, koklaşma prosesinde kullanılan söndürme prosesi ve işletme şartları yüksek fırınlarda kullanılacak olan kokun nem miktarını etkiler. Elde edilen kokun nem miktarı ise yüksek fırınlarda enerji verimliliğini, yüksek fırın verimliliğini ve kaliteli ürün üretmeyi doğrudan etkilemektedir. Yapılan bu çalışmada kok bataryalarındaki söndürme prosesi ve optimizasyonu, elde edilen kokun yüksek fırın enerji verimliliğine etkisi açıklanmıştır. Söndürme prosesi denilince akla ilk gelen özellik kokun ve kömürün içerdiği nem miktarıdır. Yüksek fırın enerji verimliliğinin ve ürün kalitesinin azalmaması için kokun neminin belirli değer aralığında olması gerekmektedir. Kuru söndürme ile çalışan bataryada ise elde edilen kok nem içermemektedir. Sulu söndürmede kızgın koka uygulanan söndürme işleminin belirli miktarda su ve belirli sürede daha önceden belirlenmiş vana açıklığı ile yapılması gerekmektedir. Ayrıca yapılan sulu söndürme prosesini etkileyen faktörlerin içerisinde söndürme arabasına alınan kok miktarı, kokun yüzey özellikleri, suyun püskürtülme özellikleri, söndürme sisteminde yer alan ekipmanların ayarlamalarının doğru yapılması, rampada kokun yayılma şekli de yer almaktadır. Literatürde yer alan daha öne yapılmış çalışmalara göre kokun nemindeki %3 artış, aynı miktarda ürün elde etmek için üflenen hava sıcaklığında 100°C' lik bir artışa neden olmaktadır (Gündüz, 1988; Eugene W.,1969). Bu nedenle yapılan enerji sarfiyatını arttırmamak için taş kömürü ve kokun nem değerlerinin günlük takip edilmesi ve uygun olmayan değerler var ise buna göre önlem alınması gerekmektedir. Yüksek fırınlarda elde edilen enerji verimliliği için direk yakıt kullanımını etkileyen kokun nem değerine dikkat edilmelidir, yapılan söndürme işlemi talimatlara uygun şekilde gerçekleştirilmelidir.

KAYNAKLAR

Ateşok, G. (1988). Koklaştırma, Kömür Kimyası ve Teknolojisi. *Mete Grafik*, 387-397.

Küçükkaya, E. (2019). Kömür Nedir? Çeşitleri Nelerdir?. https://www.enerjiportali.com/komur-nedir-cesitleri-nelerdir/ adresinden alınmıştır.

Kwiecinska, A. (2015). The Impact of Cooling Water Parameterson the WetQuenched Coke Quality. *Coke and Chemistry,* 57(11), 425-428.

Moulijn, J.A., Makkee, M., Van Diepen, A.(2005).Chemical Process Technology (2.Baskı). New York, John Wiley & Sons.

Mungan, E.(2016). Kömür Koklaşma Özelliği. https://slideplayer.biz.tr/slide/2996737/adresinden alınmıştır.

Nixon, E.W. (1969). Effect of Chemical and Physical Properties of Coke on Blast-Furnace Performance:Conference on Coke in Ironmaking. *The Iron and Steel Institute and the Institute of Fuel*, London.

Shulgaa, I. V. (2019). Moisture Content of Wet-Quenched Coke. *Coke and Chemistry*, 62(9), 402–407.

Toprak, S. (Ty). Kömür Nedir?. *MTA Genel Müdürlüğü Maden Analizleri ve Teknolojisi Dairesi*, Ankara.

Türk, U. (2015). Yüksek Fırınlarda Kok Etkileri. *Fırat Üniversitesi Mühendislik Fakültesi Malzeme ve Metalurji Bölümü.*

KONYA ILGIN KÖMÜR SAHASI KAYNAK MODELİ

KONYA ILGIN COAL MINE SITE RESOURCE MODEL

C.A. Öztürk[1,*], E. Nasuf [1], G. Eken [2], H. Ketizmen [2], R. Bozkurt [2]

[1] *İstanbul Teknik Üniversitesi, Maden Mühendisliği Bölümü*
*(*Sorumlu yazar: atilla.ozturk@itu.edu.tr)*
[2] *Konya Ilgın Elektrik Üretim ve Tic. AŞ*

ÖZET

Enerji ihtiyacı tüketimlere paralel olarak artmakta ve termik santrallerden üretilen enerjiye olan talep süreklilik arz etmektedir. Fosil yakıtları kullanan termik santrallere yakın bölgelerde bulunan kömür sahalarının, hammadde deposu olarak değerlendirilmesi ve termik santrallerin bu sahalardan beslenmesi, enerji üretimindeki optimizasyon için çok önemlidir. Bu sebepten dolayı, kömür kaynaklarının doğru olarak modellenmesi ve bu modellere dayanarak, kömür kaynaklarından üretilebilecek enerji miktarının tayin edilmesi önemli bir kestirim probleminin çözümüdür. Konya Ilgın kömür sahası, ülkemizin hemen ortasında bulunması ve bölgede tesis edilecek 500 MWe kapasiteli termik santrale hizmet edecek olmasından dolayı önem arz etmektedir. Bu çalışmada, Ilgın kömür sahasında bulunan kömürün jeoistatistiksel yöntemlerle değerlendirilmesi ve kaynak ve kalite ilişkisinin tayin edilmesi için yapılan çalışmalardan elde edilen sonuçlar paylaşılmıştır.

Anahtar Sözcükler: Enerji, jeoistatistik, kaynak modelleme, kömür.

ABSTRACT

Energy demand has been increasing due to the rise of consumption and the need of energy production from thermal power plants is continuous. The optimized use of coal mine sites close to the thermal power plants is vital as per raw material site. Resource modelling and the estimation of energy potential of a coal mine site is important stage and it is a part of estimation problem solution. Konya Ilgın coal mine site is an important site due to the location in which is in the middle of Turkey as well as serving to a 500 MWe capacity thermal power plant. Geostatistical evaluation of the coal mine site and the results of resource and quality investigations presented in this study.

Keywords: Coal, Energy, Geostatistics, Resource modelling.

GİRİŞ

Yerli kömürden enerji üretimi ülkemiz enerji politikaları açısından son yıllarda gittikçe önemi artan önemli hedeflerden biridir. Bu durum özellikle ülke ekonomisi ve gelişmişliği açısından kilit öneme sahip olan enerji üretiminin yerli kaynaklardan sağlanması ve dışa bağımlılığın azaltılması açısından son derece önemlidir. Denizli İli Tavas İlçesinde bulunan kömür sahası, bölgede tesis edilecek olan 1x150 MWe kapasiteli termik santrale hizmet vermeyi hedeflemektedir.

Bölgede kömür yapısı Sekköy ve Yenidere olarak isimlendirilen iki farklı kömür zonundan oluşmaktadır. Her iki kömür zonunda da kömür damarları ve damarların arasına yerleşmiş ara kesmeler bulunmaktadır. Kömürün mostra vermesi ve 150 m derinlere kadar ulaşmasından dolayı üretimin açık işletme faaliyetleri ile gerçekleştirilmesi planlanmaktadır. Bu durumda kömür üretim faaliyetleri sırasında dekapaj kazı miktarının yanında ara kesme miktarının da tayinine ihtiyaç duyulmaktadır. Ayrıca,

kömür damarlarının sahada yapılacak madencilik faaliyetleri sırasında kısa dönem faaliyetlerine uygun olarak modellenmesi ve ara kesmelerin seleftik madencilik esaslarına göre alınmasında yarar vardır. Bu sayede kömürün üretim kaynaklı kirlenmesinin en aza indirilmesi ve termik santrale beslenecek kömürün ideal olarak temini sağlanmış olacaktır.

Kaynağın modellenmesi amacıyla oluşturulan sondaj veri tabanında bölgede yapılmış olan 103 adet sondajın verisi kullanılmıştır. Bu sondajlardan 98'i kömür damarlarını kesmiştir. Sekköy ve Yenidere kömür zonlarına ait katı modeller oluşturulduktan sonra kaynak modelleme çalışmaları yapılmıştır. Yenidere kömür zonu kendi içerisinde 3 farklı yapıdan oluşmaktadır. Ancak katı modellerde Yenidere-2 ve Yenidere-3 kömür zonları da ortaya çıkartılmıştır. Bu iki kömür zonu açık işletme faaliyetleriyle yeryüzüne çıkartılamayacak derinlikte olması ve yeterli kaynak miktarına sahip bulunmamasından dolayı kaynak olarak değerlendirilmemiştir. Bildiriye konu olan çalışmaların temel amacı, kömür sahasındaki linyitin kömür zonları özelinde kaynak ve kalite değerlendirilmesinin yapılarak bölgede tesis edilecek termik santrali besleme potansiyelinin ortaya çıkartılmasıdır.

Bölgenin Tanıtımı ve Kısa Jeolojisi

Konya İlinin kuzeybatısında yer alan Ilgın İlçe merkezi ve İlçeye bağlı Çavuşcugöl köyü, Orhaniye, Gedikören, Çömlekçi, Yorazlar, Misafirli, Dereköy, Tekeler ve Gölyaka Köyleri ve içinde su bulundurmayan Kurugöl ile suyu bulunan Çavuşcugöl'ü de çevreleyen kısım yaklaşık 360 km^{2}'lik bir alanı kapsamaktadır. Bölgede ulaşım 300 No'lu Konya-Afyon Devlet Karayolundan ve demiryolundan tren ile sağlanmaktadır. Konya Ilgın arası karayolundan 90 km. uzaklıkta olup yaz-kış ulaşım rahat bir şekilde yapılabilmektedir. Alanın kuzeyinde yer alan kömür ve mıcır ocakları nedeniyle Çavuşcugöl'ün her iki yakasında asfalt yollar mevcuttur. Bölgeye ait yer buldu haritası ve hava fotoğrafı Şekil 1'de verilmiştir.

Bölgede tipik İç Anadolu iklimi hâkimdir. Yazlar sıcak ve kurak, kışlar soğuk ve yağışlı geçer. Bölge bitki örtüsü bakımından fakirdir ve çok az sayıda ağaç vardır. Ancak özellikle Çavuşcugöl'ün güneybatısında ağaçlandırma çalışması yapılarak önemli miktarda çam ağacı yetiştirilmiş ve bitki örtüsü zenginleştirilmiştir.

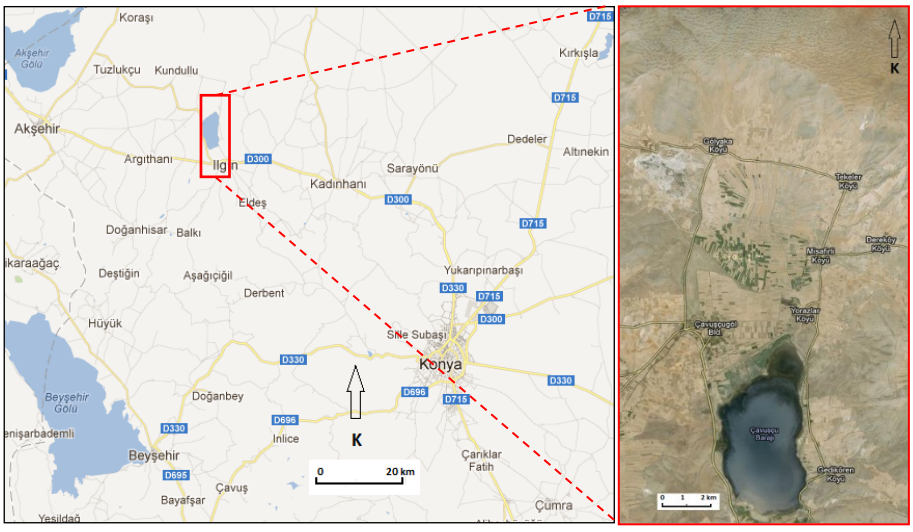

Şekil 1. Çalışma sahası lokasyonu

Konya ilinin kuzeybatısında bulunan Ilgın ilçe merkezinin yakınındaki Çavuşçugöl ve Kurugöl, anatolidler tektonik birliğine (Ketin, 1966) dahil olan Bolkardağı birliği içinde yer alır (Özgül, 1976). Menderes metamorfitlerinin kılıfını oluşturan yöre, Özcan vd. (1988)'ne göre "Kütahya Bolkardağı Kuşağı" içerisinde bulunmaktadır. Bu kuşak, Paleo-Tetis ve Neo-Tetis okyanuslarının evrimini gösteren kayaçları

kapsamakta ve neotektonik dönem içerisinde Orta Anadolu bölgesini karakterize eden değişik doğrultulu bloklu-faylı yapıları içermektedir.

Bölgedeki paleozoyik ve mesozoyik yaşlı birimler Alpin hareketlerine bağlı olarak çok evreli deformasyon geçirmişler, başkalaşıma uğramışlar ve yapraklanma kazanmışlardır. Bu deformasyonlar sonucunda Paleozoyik ve Mesozoyik yaşlı birimler en az üç evreli kıvrımlanma geçirmişlerdir (Hüseyinca ve Eren, 2007). Neo-tektonik dönemde ise inceleme alanında biri doğu-batı doğrultulu, diğeri ise kuzey-güney doğrultulu olmak üzere iki normal fay sistemi gelişmiştir. Bu sistemler arazide değişik doğrultulu horst-graben yapılarını oluşturmuşlardır. Kuzey-güney doğrultulu normal fay sistemi görünürde doğu-batı doğrultulu fay sistemini kesmektedir.

Bölgenin en yaşlı birimini, silüryen-alt karbonifer yaşlı Bozdağ Formasyonu'nun gri-beyaz yer yer siyah renkli mermer ve dolomit mermerleri oluşturur (Doğan, 1975). Bu birim yanal ve düşey olarak devoniyen-alt permiyen yaşlı Bağrıkurt formasyonuna geçiş gösterir (Üstündağ, 1987). Genelde metaçakıltaşı, metakumtaşı, fillit ve metaçört ardalanmasından oluşan Bağrıkurt formasyonu içinde birimin kırıntılıları ile uyumlu mermer arakatkıları (Ardıçlıtepe üyesi) ve ekzotik kökenli metakarbonat blokları (Bahçesaray olistolitleri) bulunmaktadır. Yörenin kimmeriyen temelini oluşturan bu kayaçlar üzerinde mesozoyik yaşlı metamorfitler açılı uyumsuz olarak yer alır (Eren vd. 2004). Birbirleriyle yanal ve düşey geçişler sunan mesozoyik yaşlı metamorfitler, alttan üste doğru; alt triyas yaşlı mor renkli metaçakıltaşı, metakumtaşı ve fillit ardalanmasından oluşan Bahcecik formasyonu (Üstündağ, 1987); alt triyas yaşlı metakumtaşı, fillit, mermer ve dolomit mermer şeklindeki Ertuğrul formasyonu (Doğan, 1975); üst triyas-alt jura yaşlı gri-koyu gri renkli yer yer breşik ve laminalı dolomit mermerlerden oluşan Kızılören formasyonu ve alt jura-kretase yaşlı genelde açık renkli mermer ve dolomit mermerlerden oluşan Lorasdağı formasyonu şeklinde sıralanmaktadır (Göğer ve Kıral, 1969).

Temeli oluşturan metamorfitler üzerine tersiyer yaşlı başkalaşım geçirmemiş örtü kayaçları uyumsuz olarak gelmektedir. Örtü kayaçlarının en alt birimi kömür ara tabakaları içeren kiltaşı, çamurtaşı, silttaşı ardalanmasından oluşan miyosen yaşlı Harmanyazı formasyonudur (Tüfekçi, 1987). Bu birim üstten uyumlu olarak üst miyosen-alt pliyosen yaşlı, gölsel kireçtaşı, marn, çamurtaşı ve çakıltaşından oluşan Ulumuhsine formasyonu tarafından üstlenir (Göğer ve Kıral, 1969). Ulumuhsine formasyonu da uyumlu olarak pliyosen yaşlı alacalı renkli çamurtaşı, kiltaşı ve yer yer çakıltaşından ibaret Sebiller formasyonu tarafından örtülür (Tüfekçi, 1987). Bu birim de üste doğru yanal ve düşey olarak alüvyal yelpaze çökellerinden yapılı üst pliyosen-kuvaterner yaşlı Tekeler formasyonuna geçiş gösterir (Tüfekçi, 1987). Yukarıda sözü edilen bütün birimlerin üzerinde yine açılı uyumsuzlukla çeşitli boyutlarda malzeme içeren güncel alüvyonlar bulunmaktadır.

Kaynak Modelleme ve Jeoistatistiksel Yöntemler

Kaynak ve rezerv sınıflamaları her ne kadar farklı ekoller tarafından tanımlanmış olsa da, günümüzde ve ülkemizde özellikle en çok rağbet göreni, Avusturalya'da kaleme alınan JORC kodudur (Jorc, 2012). Jorc kodunda maden kaynakları jeolojik bilgi ve güvenilirliğin artmasına bağlı olarak mümkün, muhtemel ve görünür olarak isimlendirilirler. Jeolojik bilgi ve güvenilirliğin artmasının en temel kaynağı ise sondajlar ve sondajlardan alınan numuneler üzerinde gerçekleştirilen testlerdir. Sondajlar arası mesafe bir başka ifadeyle sondajların etki mesafeleri kaynakların mümkün sınıfından görünür sınıfına doğru ilerlemesinde büyük rol oynamaktadır. Kaynakların kalitesinin ortaya çıkartılmasında çok önemli olan tenör ve/veya alt ısıl değer gibi değişkenlerin akredite laboratuvarlarda temin edilmiş ve raporlanmış olması da güvenilirliği ve bağlı olarak kaynak sınıfını artıran parametrelerdendir.

Jeoistatistik, bölgesel bağımlılık gösteren değişkenlerin, çalışılan uzay içerisinde dağılımlarının araştırılmasında kullanılan en güçlü istatistik araçlardan biridir. Jeoistatistiksel uygulamaların birincisi aşaması, sahada dağılımları araştırılan ve bölgesel değişken olarak tanımlanan değişkenlerin istatistiksel özelliklerinin araştırılmasıdır.

İstatistiksel olarak dağılım özellikleri belirlenen değişkenler, jeoistatistik araştırmalara hazır hale getirilir. Özellikle dağılımın normalden farklı olduğu durumlarda transformasyon çalışmaları ile verilerin mümkün mertebe normal dağılıma uygun hale getirilmesine çalışılır. Bu aşamadan sonra ise bölgeselleştirme çalışmaları her bir noktaya verilerin atanması işlemi ile gerçekleştirilir. Çalışılan uzayda bölgeselleştirilen değişkenler, bölgesel bağımlılıklarının ortaya konulduğu variogram fonksiyonların elde edilmesi ile jeoistatistik uygulamaların ikinci aşaması da tamamlanmış olunur. Semivariogram fonksiyonların elde edilmesinden sonra ise kriging tekniğinin çalıştırılması ile değeri bilinen noktalardan hareket ederek değeri bilinmeyen noktaların kestirimi işlemleri gerçekleştirilir. Özet olarak verilen bu çalışmaların yapılmasından sonra modellerden elde edilen kestirim haritalarının başarısı, çapraz doğrulama tekniği ile gerçek ve kestirim değerler arasındaki ilişkilerden elde edilir.

Kömür maden sahalarında alt ısıl değer, nem, kül ve kükürt gibi değişkenlerinin istatistik değerlendirmeleri ve dağılım haritaları çalışmanın ilk adımında elde edilir. Bunlara ek olarak, kömür damarlarının tavan, taban ve kalınlık izohipsleri ayrıca elde edilmelidir. Böylelikle, kömür madeni sahasında, kaç farklı damar ve bu damarların sahip olduğu alt damarlar çıkartılmış olur. Bunun yanında, incelenen tüm değişkenlerin istatistiksel özellikleri de tayin edilerek sahada dağılımı araştırılan bölgesel değişkenlere ait karakteristik özellikler tayin edilmiş olunur. Ortalama, standart hata, medyan, mod, standart sapma, varyans, basıklık, çarpıklık, aralık ve örnek sayısı istatistiksel olarak değerlendirme kullanılan parametreler olarak sıralanabilir.

Bu çalışma kapsamında, kömür kaynaklarının nitelik ve nicelik olarak değerlendirilmesi amacıyla yapılan uygulamalarda, kömürün niteliğinin kömür damarlarının farklı yüksekliklerindeki dağılımlarının da tespit edilmesi ve böylece kömür damarı bloklara ayrıldığında her bir bloğun kalite ve bağlı olarak enerji değerinin tespit edilmesi hedeflenmiştir. Örneğin, 10 m kalınlığında bir kömür damarının ilk beş metresinde 1000 kcal/kg ikinci beş metresinde ise 3000 kcal/kg değerlerin olması durumunda tüm damarda ortalama alt ısıl değeri 2000 kcal/kg olarak elde edilir. Oysa ilk beş metreden elde edilecek enerji miktarı, ikinci beş metreden elde edilecek enerji miktarının üçte biridir. Uygulamada bu çok ciddi sorunlara yol açmaktadır. Yapılan çalışmada kömürün niteliklerinin dağılımları sadece yatay değil aynı zamanda düşey yönde de araştırılarak modellenmiştir. Bu modelleme tekniği, üretim optimizasyonu için son derece faydalı çıkarımların yapılmasına imkân sağlamaktadır. Çalışmada uygulanan adımlar Şekil 2'de verilmiştir.

Yapılan çalışmalar sonucunda öncelikle kömür damarına ait katı model kesitler alınmak suretiyle elde edilmiştir. Daha sonra, kömür damarlarının nitelik ve nicelik olarak değerlendirilmesi jeoistatistiksel olarak gerçekleştirilmiştir. Bu aşamada yapılacak çalışmalar şu şekilde özetlenebilir.

Maden sahasının değerlendirilmesi sonucunda, maden sahaları içerisinde bulunan kömürün miktarı ve kalitesi matematiksel yöntemler ile uluslararası standartlara uygun olarak elde edilmiştir. Yapılan çalışmalar aşağıda iş algoritmasına uygun olarak gerçekleştirilmiştir. Bildiride örnek teşkil etmesi amacıyla alt ısıl değerin dağılımı ile ilgili sonuçlar paylaşılmıştır.

1. Kömür damarlarının katı modelleri.
2. Kömür damarlarının geometrik ve kalite değerlerinin istatistiksel değerlendirmeleri (kalınlık, kömüre giriş kotu, kömürden çıkış kotu, ara kesme kalınlığı, alt ısıl değeri, enerji, kükürt, nem, uçucu madde ve kül).
3. Jeoistatistiksel çalışmalar. Bu çalışmaların sonucunda, sondajlar arası mesafenin yeterliliği ve kömür kalite değerlerinin kömür sahası içerisinde her bir kömür damarı için ayrı ayrı değerlendirilmesi yapılacaktır.
4. Kömür damarlarına ait blok modeller.
5. Bloklara değer atanması ve kömür damarları için ayrı ayrı kalite ve rezerv değerlerinin tayini.
6. Kömür sahasında kömür damarlarının ayrı ayrı rezerv, kalınlık, kömüre giriş, kömürden çıkış, alt ısıl değeri, enerji, kükürt, nem, uçucu madde ve kül değişkenlerine ait haritaların elde edilmesi.

7. Rezerv kalite eğrisinin her bir damar için ayrı ayrı ve tüm saha için tek bir temsil gösterecek şekilde elde edilmesi.

Şekil 2. Ilgın kömür sahası kaynak modelinin tayininde uygulanan yöntemin akış şeması

Kaynak modellemesinde kullanılan jeoistatistiksel modellemeler, çalışma sahasındaki değişkenlerin bölgeselleştirilmesiyle gerçekleştirilir (Matheron, 1963). Jeoistatistiksel uygulamalar temel olarak iki aşamadan oluşmaktadır. Birinci aşamada, yeterli bir formda olayın yapısal özelliklerini vurgulamak için teorik bir zemin kurulması variogram fonksiyonunun elde edilmesi ile sağlanır. İkinci aşamada ise tahmin probleminde (kriging) çözümü sağlayacak olan fonksiyonların kullanıldığı bir modeli sağlamak ve rassal fonksiyonların olasılık teorilerini kullanarak ReV ile ilişkilendirmesi gerçekleştirilir (Öztürk, 2001).

ReV değerler z(x) ile gösterilir ve Z(x) olarak gösterilen rassal fonksiyonun anlaşılması için kullanılır. Rassal fonksiyon olarak tanımlanansa, uygulama sahası içerisinde incelenen doğal olaydır. Rassal fonksiyon, rassal değer Z(x)'in sonsuz bir toplamasıdır (Isaak ve Srivasta, 1989; Journel, 1974; Journel ve Huijbregts, 1978; Rendu, 1981).

Özetle söylemek gerekirse, jeoistatistiksel bir çalışmanın temel olarak iki basamağı bulunmaktadır. Bunların birincisi SV'ın elde edilişi, diğeri ise krigingin çalıştırılarak tahmin probleminin çözümüdür. Bu işlemlerin gerçekleştirilmesi ve jeostatistiksel olarak bir değişkenin bir uzay içerisinde nasıl dağıldığının araştırılabilmesi için, bu bölümde bahsedilen kabullere ihtiyaç vardır. Söz konusu bu kabuller 1. ve 2. sıra durağanlık hipotezleri ve sabitlik hipotezidir (Clark, 1979; Isaak ve Srivasta, 1989; Journel, 1974; Journel ve Huijbregts, 1978; Öztürk, 2001). Variogramın pratik uygulaması aşağıdaki formülle açıklanır.

$$\gamma(h) = \frac{1}{2N}\sum_{i=1}^{N}\left[Z(x+h)-Z(x)\right]^{2} \quad (1)$$

Farklı h değerleri için semivariogram değerleri bulunarak, (h) – h grafiğine çizilerek deneysel variogramlar elde edilir. Variogram uygulaması ile elde edilecek avantajlar şu şekilde özetlenmektedir (Isaaks ve Srivastava, 1989, Journel ve Huijbregts, 1978).

SV fonksiyonunun elde edilmesini müteakiben, ReV'in sahanın her noktasında hangi şiddetle dağıldığının araştırılabilmesi için kriging tekniği kullanılır. Genel olarak kullanılan blok kriging yönteminin avantajı, sadece kriging siteminin çözülmesi ile blok ortalamasının bir tahmininin yürütülebilmesidir. (Öztürk, 2001). Kriging matrisinin çözümü ile gerçekleştirilen bu teknik sonucunda, araştırma uzayında incelenen bölgesel değişkenin dağılımı elde edilmiş olunur.

$$Z(x_0) = \sum_{i=1}^{m} w_i Z(x_i) \qquad (2)$$

Ilgın Kömür Sahası Kaynak Modeli

Ilgın kömür sahasında kaynak modeli oluşturulurken 158'i kömür kesen, 218 adet sondaj verisinden faydalanılmıştır. Kömürün katı modeli kesit yöntemiyle çıkartılmış ve katı modelden elde edilen sonuçlara göre sahadaki kaynak miktarı 182,6 milyon tondur. Kömür kalınlığı için eşik değer 4 m, alt ısıl değer için ise 700 kcal/kg olarak tayin edilmiştir. Bu eşik değerlere ulaşılmayan noktalardaki kömürler zemin olarak kabul edilmiştir. Eşik değerler dikkate alınarak kaynak hesabı tekrarlandığında da sahadaki kaynak miktarı 175,3 milyon ton olarak hesaplanmıştır. Kaynağın görünür olup olmadığının tayin edilmesi içinse, sondaj etki mesafe 500 m olarak tayin edilmiştir. Bu değer semivariogram fonksiyonundan elde edilen etki mesafesi değerinin altındadır. Bu durum da yapılan kabulün başarısını temsil etmektedir. Sondajlarda kesilen kömür kalınlıklarına bağlı olarak oluşturulan kömür katı modelinin sondaj etki mesafeleriyle olan ilişkisi araştırılmış ve sonucu Şekil 3'te verilmiştir. Şekilden de görüleceği üzere kaynağın sınıfı yeter ve gerek sondaja sahip olunduğu ve sondajların kömür sınırları içerisinde tüm sahayı temsil ettiğinin anlaşılması üzerine görünür olarak tayin edilmiştir.

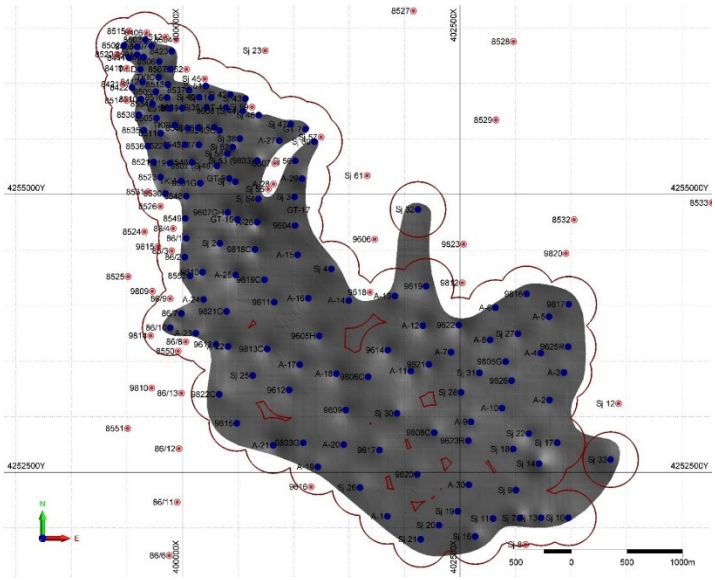

Şekil 3. Sondaj etki mesafeleri ve kömür sınırı plan görünümü

İstatistiksel Değerlendirmeler

Kömürün kalitesinin tayini için kaynağın miktarının modellenmesinin yanında kalitesinin belirlenmesi amacıyla da alt ısıl değerin dağılımı araştırılmıştır. Model çalışmalarının başarılı olması amacıyla kompozit yapı oluşturulmuş ve kömür damarının iki metrelik dilimler halinde kompozit bir

modele uyarlanarak her iki metre için kompozit değer ataması yapılmıştır. Bu bölümde alt ısıl değere ait istatistiksel büyüklükler ham veri ve kompozit veri için ayrı ayrı Çizelge 1'de verilmiştir. Bu sayede kompozit verinin ham veriyi temsil yeteneğine de tartışılabilmektedir.

Kaynak ve Kalite Modellemesi

Bölgesel Bağımlılık Fonksiyonu

Kaynak ve kalite arasındaki ilişki jeoistatistiksel yöntemlerle araştırılmıştır. Kalite değişkeni olarak bu çalışmada sadece alt ısıl değere ait sonuçlar paylaşılmıştır. Çalışmada öncelikle bölgesel bağımlılığın ortaya çıkartılması adına semivariogram (SV) fonksiyonu elde edilmiştir. Yapılan araştırma sonucunda elde edilen SV fonksiyonu ve variogram parametrelerine ait büyüklükler Şekil 4'da verilmiştir.

Çizelge 1. Alt ısıl değere ait istatistiksel büyüklükler

Tanımlama	Ham Veri	Kompozit Model
Ortalama (kcal/kg)	1955.65	1994.02
Standart Hata	19.42	10.82
Medyan (kcal/kg)	2087	2108.7
Mod (kcal/kg)	2233	2380
Standart Sapma	569.78	487.33
Basıklık	0.44	0.76
Çarpıklık	-0.86	-0.92
Aralık (kcal/kg)	3266	3155.36
Örnek Sayısı	861	2030

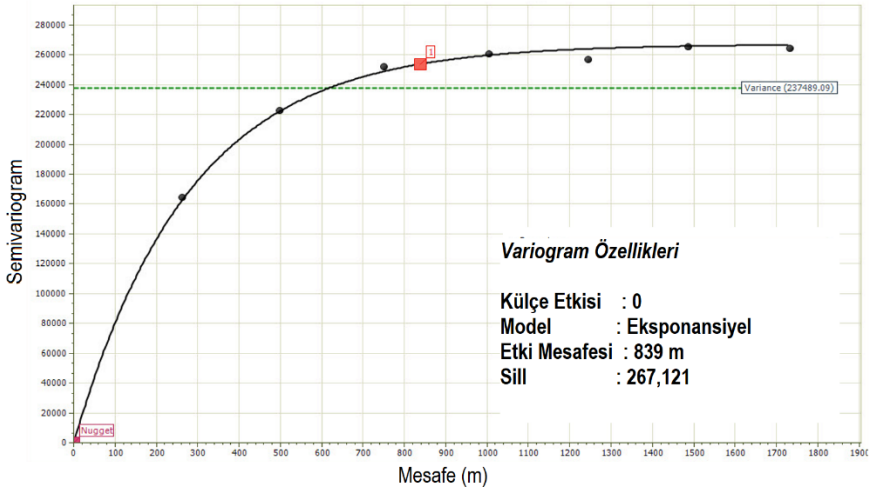

Şekil 4. Alt ısıl değere ait SV fonksiyonu

Arama Elipsoidinin Seçimi

Arama elipsoidinin seçimi için bir dizi iterasyon çalışması yapılmıştır. Yapılan bu çalışmada arama elipsoidinin farklı geometrilerinden hareket ederek, en düşük hatayı veren arama elipsoidinin geometrileri tayin edilmiştir. Yapılan çalışmada 50 farklı model oluşturulmuştur. Yapılan optimizasyon çalışması sonucunda, verinin kompozit, variogram fonksiyonunun eksponansiyel ve yönlü variogram olarak seçildiği, arama elipsoidinin 4 sektör, her bir sektörde 4 nokta olduğu ve elipsoidin boyutlarının 800 m, 400 m ve 80 m olduğu durumda yapılan modelin en düşük hata ile çalıştığı anlaşılmıştır. Modelin

başarısının karar vermede kullanılan çapraz doğrulama saçılma grafiğinde korelasyon katsayısı 0,93 olarak elde edilmiştir. Arama elipsoidinin özellikleri ve görünümüyle birlikte çapraz doğrulama grafiği Şekil 5'te verilmiştir.

Blok Modelleme ve Kestirim Probleminin Çözümü

Blok model ve kriging çalışmaları, katı modeli oluşturulan kömür damarlarının düzgün şekilli bloklara ayrılması ve daha sonra kriging tekniğinin çalıştırılması ile birlikte bloklara değer atanması aşamalarından oluşmaktadır. Arama elipsoidinin boyutunun ve geometrisinin tayin edilmesinden sonra ise 3 boyutlu olarak kestirim probleminin çözümü gerçekleştirilir. Blok boyutları seçilirken mümkün mertebe üretim geometrisine yardımcı olabilecek boyutlandırma yapılmasına özen gösterilmiştir. Alt bloklar ise özellikle kömür sınırlarında detaylı analizlerin yapılabilmesi için daha küçük boyutlu olarak tayin edilmiştir. Şekil 6'da blok modelin görünümü ve blok boyutları ve sayılarıyla ilgili bilgiler verilmiştir.

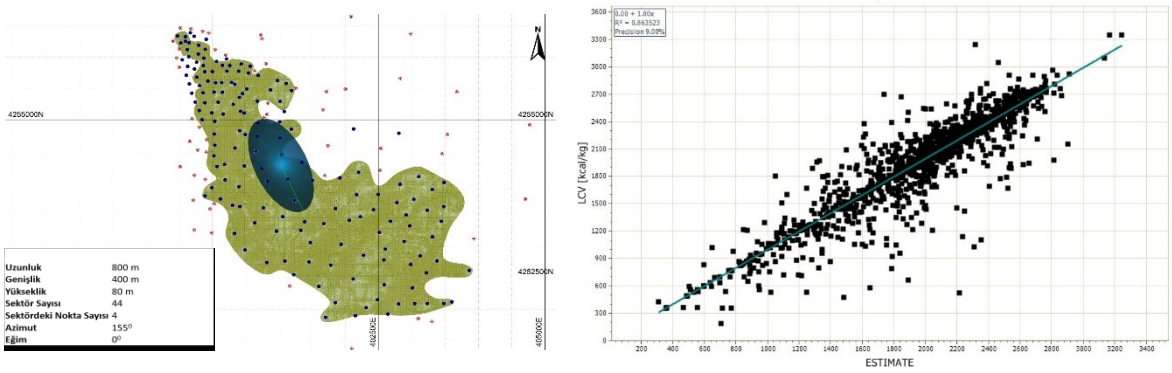

Şekil 5. Alt ısıl değerin kestiriminde kullanılan arama elipsoidi ve çapraz doğrulama grafiği

Bu çalışmadan sonra, her bir bloğa alt ısıl değerinin kestirimi gerçekleştirilerek, her bir bloğun miktarı ve kalitesine ait çıkarımlar elde edilmiştir. Şekil 7'de kriging tekniğinin çalıştırılmasından sonra bloklara değer atanması suretiyle elde edilen alt ısıl değerinin dağılım haritası görülmektedir. Plan görünümü üzerinden alınan kesitten de görüleceği üzere, yapılan çalışma sonucunda kömürün kalitesinin dağılımı kömürün tavanından tabanına farklılık arz edecek ve gerçek koşulları yansıtacak şekilde modellenmiştir.

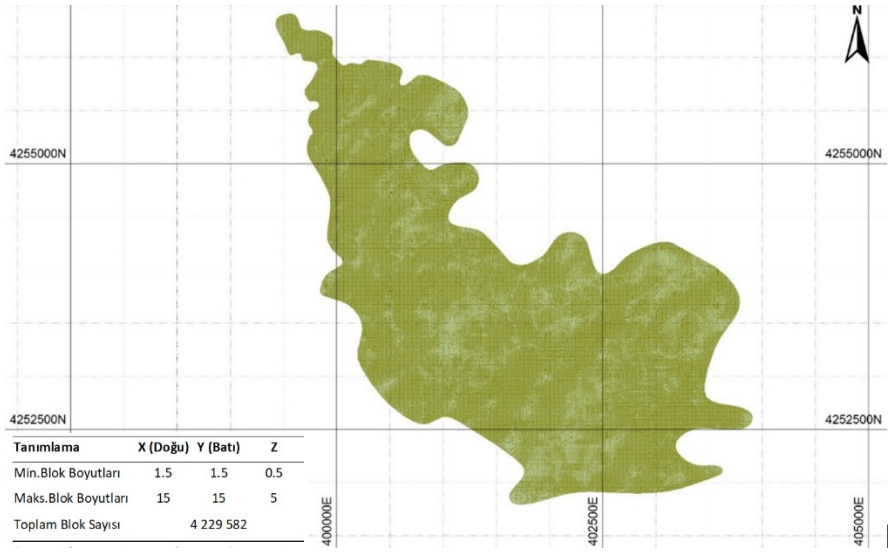

Şekil 6. Kömür sahasının bloklara ayrılması ve blok boyutları

Kaynak & Kalite Değerlendirilmesi

Yapılan çalışmalardan elde edilen sonuçlar, kaynağın alt ısıl değer değişkenine göre dağılımlarının araştırılmasında kullanılmıştır. Bu araştırma her bir bloktaki alt ısıl değerinin bloğun hacmi ve dolayısı ile tonajı ile ilişkilendirilmesi ile gerçekleştirilmiştir. Şekil 8'de kaynağın, alt ısıl değere göre değişimini gösteren kaynak kalite eğrisi verilmiştir.

Eğriden de görüleceği üzere sahadaki toplam kaynak 176 milyon ton mertebesinde olup, ortalama alt ısıl değeri 2069 kcal/kg olarak tayin edilmiştir.

Ortalama alt ısıl değerin 2069 kcal/kg olmasından dolayı, 500 MWe kapasiteli termik santrali besleyecek yıllık kömür miktarının 4 milyon ton olması gerektiği anlaşılmaktadır. Bu durumda, Ilgın kömür sahasında bulunan linyit rezervinin termik santrali 44 yıl boyunca güvenli bir şekilde besleyebilecek kapasiteye sahip olduğu anlaşılmaktadır.

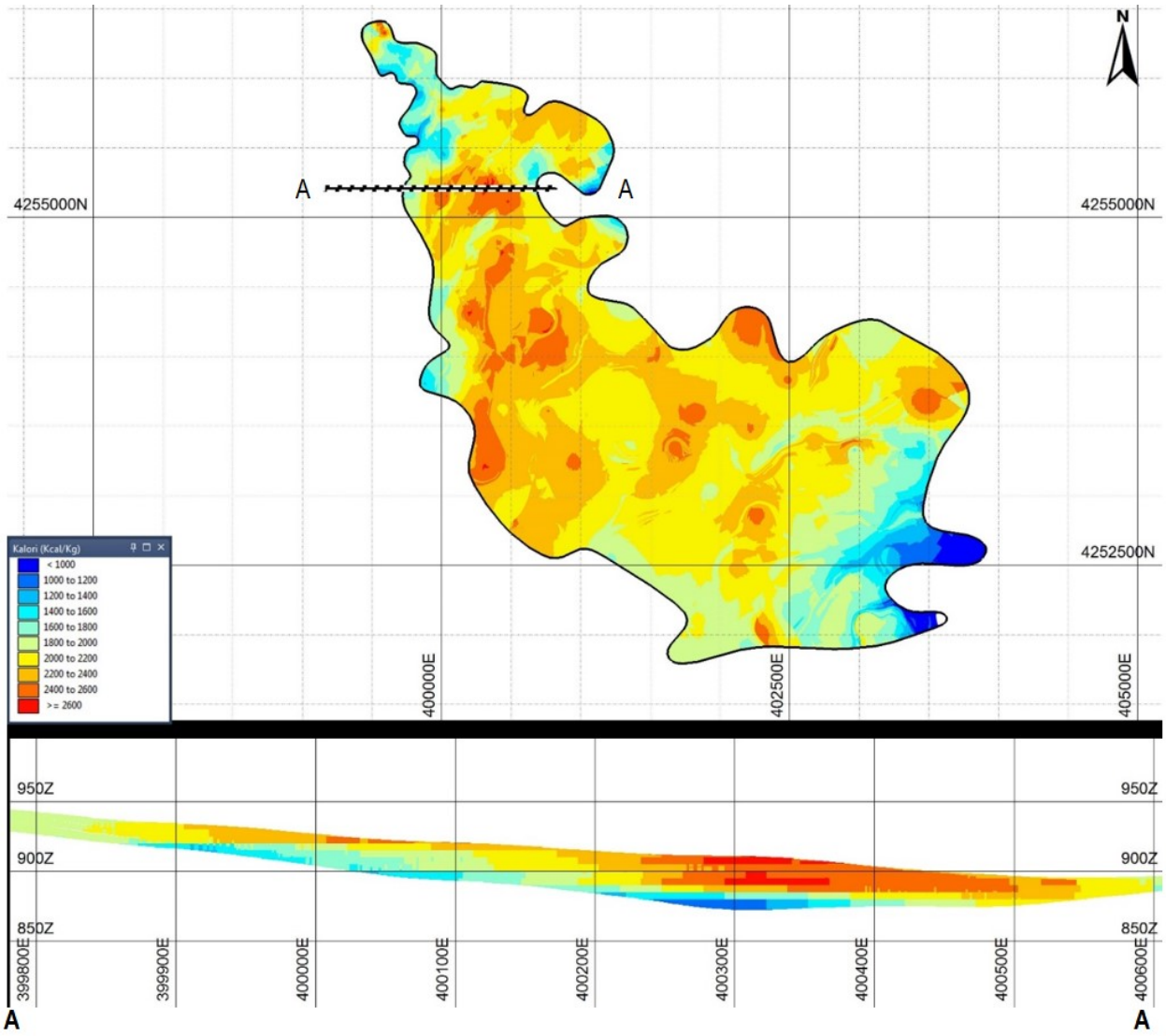

Şekil 7. Blok modelleme ve kömür sahasında alt ısıl değerin dağılımı

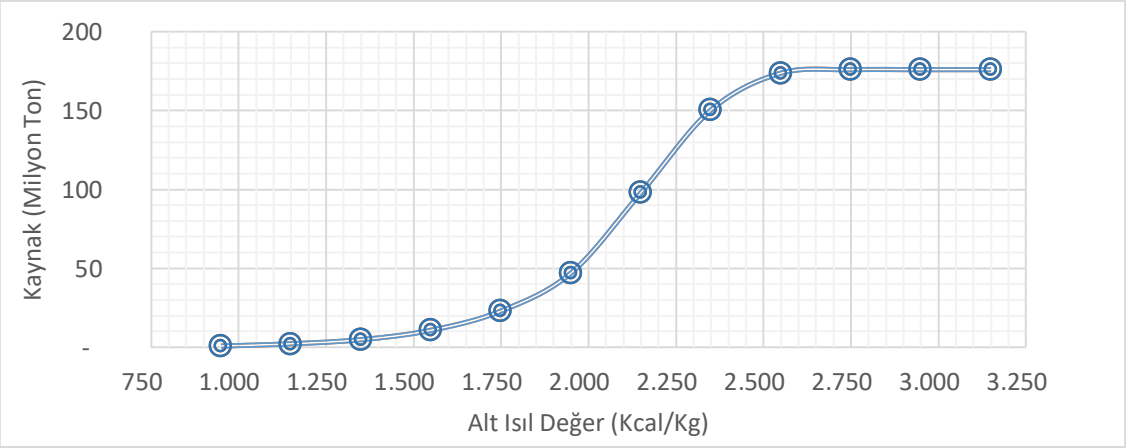

Şekil 8. Kaynak kalite eğrisi

SONUÇLAR

Bu çalışmada, Ilgın kömür sahasındaki linyitin kaynak modellemesi, jeoistatistiksel yöntemlerle üç boyutlu olarak gerçekleştirilmiş ve sonuçları temsil etmesi amacıyla alt ısıl değerin dağılımıyla ilgili çıktılar paylaşılmıştır. Çalışmaya öncelikle sondaj verilerinin değerlendirilmesi ve kömür katı modelinin oluşturulmasıyla başlanılmıştır. Katı model oluşturulduktan sonra, bölgesel bağımlılık semivariogram fonksiyonlarıyla araştırılmış ve kestirim probleminin çözümü için kriging tekniği kullanılmıştır. Blok modelleme yapılarak kömür damarları bloklarına ayrılmış ve böylece kaynağın kalitesi bloklar özelinde modellenmiştir. Yapılan modelleme çalışması sayesinde, sahadaki kömürün kalitesi üç boyutlu modellenmiş ve kaynağın bölgede tesis edilecek 500 MWe kapasiteli termik santrale 44 yıl hizmet etmeye yetecek potansiyele sahip olduğu ortaya çıkartılmıştır. Yapılan bu çalışmanın, benzer projelerde de tekrar edilmesi ve güvenilir sondaj veri tabanı ve jeoistatistiksel uygulamalarla proje fizibilitelerine olumlu katkılarda bulunulmasının önü açılmalıdır.

TEŞEKKÜR

Bildiri konusu faaliyetler, Konya Ilgın Elektrik Üretim ve Tic. A.Ş. tarafından EDA Enerji Dinamik Akustik San. ve Tic. Ltd. Şti.'ne yaptırılan "Arazi Kontrolü ile Şev Duraylılığının Araştırılması" isimli proje faaliyetlerinden elde edilen sonuçları içermektedir (2017). Yazarlar, proje faaliyetleri sırasında vermiş oldukları destekten dolayı, Konya Ilgın Elektrik Üretim ve Tic. A.Ş. yönetici ve mühendislerine teşekkür ederler.

KAYNAKLAR

Clark, I. (1979). Practical geostatistic. Applied Science Publisher LTD, London.

Doğan, A. (1975). Sızma-Ladik (Konya) civa sahasının jeolojisi ve maden yatakları sorunlarının incelenmesi. İ.Ü. Fen Fakültesi Min. Pet. Kürsüsü, Yük. Müh. Diploma Çalışması, İstanbul.

Eren, Y., Kurt H., Rosselet, F, Stampfli, G. (2004). Paleozoic deformation and magmatism in the northern area of the Anatolide block (Konya), witness of the palaeotethys active magrin. *Eclogae Geol. Helv., 97,* 293-306.

Göğer, E. ve Kıral, K. (1969). Kızılören dolayının jeolojisi. M.T.A Rapor No: 5204 (Yayınlanmamış).

Hüseyinca, M.Y. ve Eren, Y. (2007). Ilgın (Konya) kuzeyinin stratigrafisi ve tektonik evrimi. *S.Ü. Müh.-Mim. Fak. Derg., 22,* 1-2.

Isaaks, E. H. ve Srivastava, R. M. (1989). An introduction to applied geostatistics. Oxford University Press, New York.

Joint Ore Reserves Committee, (2012). The JORC code 2012 edition.

Journel, A. G. (1974). Geostatistic for conditional simulation of ore bodies. *Economic Geology, 68,* 673-687.

Journel, A. G. ve Huijbregts, C. J. (1978). Mining geostatistic. Academic Press, London.

Ketin, İ. (1966). Anadolu'nun tektonik birlikleri. *MTA Derg., 66,* 23-34.

Matheron, G. (1963). Principles of geostatistics. *Economic Geology, 58,* 1246–1266.

Özcan, A., Göncüoğlu, M.C., Turan, N., Uysal, Ş., Şentürk, K., Işık, A. (1988). Late Paleozoic Evolution of the Kütahya - Bolkardağ Belt. *METU Journal of Pure and Appl. Sci., 21 (1/3),* 211- 220.

Özgül, N. (1976). Torosların bazı temel jeoloji özellikleri. *Türkiye Jeoloji Kurumu Bülteni, 19,* 65-78.

Öztürk, C.A. (2001). Maden yataklarının değerlendirilmesinde PCSV ve kriging tekniklerinin karşılaştırılması. Yüksek Lisans Tezi, İTÜ Fen Bilimleri Enstitüsü.

Rendu, J. M., An introduction to geostatistical methods of mineral evaluation, South African İnstitute of mining and metallurgy monograph series, (1981).

Tüfekçi, K. (1987). Ilgın gölü ve dolayının jeomorfolojisi. Ankara Üniversitesi, Yük. Lis. Tezi Fen Bilimleri Enstitüsü, Ankara.

Üstündağ, A. (1987). Sızma-Kurşunlu-Meydan-Bağrıkurt köyleri arasında Karadağ çevresinin jeolojisi. S.Ü. Fen Bil. Enstitüsü, Yük. Lis. Tezi, Konya, 65s.

KÖMÜR FLOTASYONUNDA JAMESON FLOTASYON HÜCRESİ KİNETİĞİNİN MODELLENMESİ

MODELING OF JAMESON FLOTATION CELL'S KINETICS IN COAL FLOTATION

S. Karaca[1, *], O. Şahbaz[1], A. Uçar[1]

[1] *Kütahya Dumlupınar Üniversitesi, Maden Mühendisliği Bölümü*
*(*Sorumlu yazar: sevgi.karaca@dpu.edu.tr)*

ÖZET

Dünya genelindeki birçok kömür yıkama tesisinde 500 µm tane boyutuna kadar fiziksel zenginleştirme yöntemleriyle etkin bir zenginleştirme yapılabilmektedir. Buna karşın bu boyutun altındaki kömürler artık olarak atılmakta, bu durum çevresel problemlere ve ekonomik kayıplara neden olmaktadır. Son dönemde 500 mikrometre altı kömüre yönelik çalışmalar da bu çerçevede önem kazanmıştır. Fiziksel zenginleştirmenin etkin olmadığı bu boyutta en çok tercih edilen yöntemlerden birisi de flotasyondur. Bu çalışmada dünya genelinde 400'den fazla tesis boyutunda kullanımı olan fakat ülkemizde henüz uygulama alanı bulamayan Jameson flotasyon hücresi ile kömürlerin zenginleştirilebilirliği araştırılmıştır. 2^3 tam faktöriyel deney tasarım yöntemi kullanılarak yapılan flotasyon deneylerinde toplayıcı miktarı, bias hızı ve tane boyutunun Jameson hücresi kinetiğine etkisi belirlenmeye çalışılmıştır. Jameson hücresinde gerçekleştirilen deneylerden elde edilen veriler yardımıyla bu üç parametrenin hız sabitine olan etkileri ampirik olarak modellenmiştir. Modelde en etkin parametrenin tane boyutu olduğu belirlenmiştir.

Keywords: Jameson hücresi, kinetik, ince kömür

ABSTRACT

In many coal washery worldwide, an effective enrichment can be carried out with physical methods up to 500 µm grain size. However, coals below this size are now discharged, which causes environmental problems and economic losses. Therefore, studies on coal under 500 micrometres have also gained importance within this framework. Flotation is one of the most preferred methods in this dimension, where physical enrichment is not practical. In this study, the beneficiation of coals was investigated with Jameson flotation cell, which has more than 400 industrial-scale uses worldwide but has not yet found an application in our country. The effect of collector amount, bias velocity and grain size on Jameson cell's kinetics was determined in flotation experiments conducted using the 2^3 full factorial experimental design method. With the help of data obtained from experiments conducted in the Jameson cell, the effects of these three parameters on the kinetic constant were empirically modelled. It has been determined that the most effective parameter in the model is the particle size.

Keywords: Jameson cell, kinetic, fine coal

GİRİŞ

Düşük ranklı ince boyutlu kömürlerin zenginleştirilmesinde kullanılan en etkin yöntem flotasyondur. Türkiye'deki birçok kömür yıkama tesisinin, çevresel mevzuatlar ve ekonomik kaygılardan dolayı ince boyutlu kömürlerin kazanılmasında çok yakın bir gelecekte flotasyon yöntemini kullanacağı açıktır. Bu

nedenle, birçok araştırmacı kömür flotasyonu ile ilgili çalışmalar yapmıştır. Araştırmacılar en yüksek flotasyon performansına ulaşmak için Avustralya'dan, Amerika'ya, Avrupa'dan Türkiye'ye faklı bölgelerde kömür flotasyonu testleri uygulamışlardır (Aktaş ve Woodburn, 1995; Kowalczuk vd., 2011; Mohanty ve Honaker, 1999; Şahbaz, 2013; Şahbaz vd., 2013). Bu çalışmalara göre kömür flotasyonunda performans, kömür özellikleri; kimyasal ve alet parametrelerine bağlı olarak değişmektedir. Bu parametrelerin detaylıca incelenmesi ve modellenmesi, pilot/ endüstriyel çaptaki çalışmalar, onların simülasyonu ve tesis tasarımı için önem taşımaktadır (Chander and Polat, 1995).

Flotasyon prosesini en iyi tanımlayan modeller, kinetik modellerdir. Kinetik modeller, temel modeller olup herhangi bir kömür numunesinin zenginleştirilmesinin analizinde kullanılabilirler (Lynch et al., 1981). Birinci dereceden flotasyon kinetiği aşağıdaki gibidir (Tsai, 1985; Polat ve Chander, 2000):

$$R = R_{\alpha}[1 - e^{-(k.t)}] \quad (1)$$

burada, R yanabilir verim (%), k birinci dereceden hız sabiti (s^{-1}), t flotasyon süresi (s), and R_{α} sonsuz süredeki flotasyon verimidir.

Flotasyon kinetiğini tanımlamak için, Eşitlik 1'de verilen birinci dereceden flotasyon kinetiği modelinde görülen sonsuz süredeki flotasyon verimi ve birinci dereceden hız sabiti kullanılmaktdır. Her hangi bir cevher için elde edilen deneysel veriler modele yerleştirilerek, zaman-verim eğrisinden kolayca belirlenmektedir. Sonsuz süredeki flotasyon verimi toplayıcı miktarı gibi kimyasal değişkenlere bağlıyken, birinci dereceden flotasyon hız sabiti tane boyutu, hava akış hızı gibi fiziksel değişkenlere bağlıdır (Nguyen and Shulze, 2003).

Mekanik hücrenin kinetik özellikleri ile ilgili literatürde pek çok araştırma olmasına karşılık, Jameson hücresinin kinetik özelliklerinin belirlenmesi ile ilgili detaylı bir çalışma bulunmamaktadır. Bu çalışmada, çevresel kısıtlamalar nedeniyle 500 mikrometreden küçük ve konvansiyonel yöntemlerle verimli bir şekilde zenginleştirilemeyen düşük ranklı kömürlerin Jameson hücresiyle zenginleştirilebilirliği araştırılmıştır. Optimizasyon ve benzetim çalışmalarında, flotasyon aletlerinin kinetik özelliklerinin belirlenmesi önem taşımaktadır. Bu amaçla çalışmada, flotasyon kinetiklerine etki eden parametrelerin etkisi belirlenmeye çalışılacaktır. Ayrıca bu parametrelerin flotasyon hız sabitine etkisini tanımlayan modeller de oluşturulacaktır. Böylece performansı kötü yönde etkileyen parametre doğrudan değiştirilerek, flotasyon başarısında artış sağlanabilecektir.

MATERYAL VE YÖNTEM

Materyal

Deneylerde kullanılan kömür numunesi Tekirdağ ilindeki Akçelik Madencilik Firmasına ait Şahinköy linyit ocağından temin edilmiştir. Numune Kütahya Dumlupınar Üniversitesi Cevher Hazırlama Laboratuvarında önce çeneli kırıcı yardımıyla -20 mm boyuna getirildi daha sonra merdaneli kırıcı kapalı devre çalıştırılarak -500 µm boyutuna indirilmiştir. Bu malzeme 300, 212 ve 106 µm boyutlarındaki eleklerden elenerek -500+300, -300+212 ve -212+106 µm boyut aralıklarında sınıflandırılmıştır. Her bir boyut aralığındaki malzemeler homojen bir şekilde bölünüp flotasyon testlerinde kullanılmak amacıyla derin dondurucuda saklanmıştır. Kullanılan numunenin havada kuru olarak yapılan analiz değerlerine göre %47.1 kül ve %1.51 kükürt içerdiği belirlenmiştir.

Yöntem

Flotasyon Deneyleri

Flotasyon deneyleri Jameson hücresi kullanılarak yapılmıştır. Deneylerde aletin flotasyon kinetiği -500+300, -300+212 ve -212+106 µm boyut grupları kullanılarak belirlenmeye çalışılmıştır. Çizelge 1'de Jameson hücresi için deney şartları verilmiştir. Jameson hücresi deneylerinde, 1800 mm uzunluğunda ve 15 mm çapında düşey boruya sahip 200 mm ayırma tanklı Jameson hücresi kullanılmıştır. Alette deneyler için kullanılan nozul çapı ise 4 mm'dir.

Çizelge 1. Jameson flotasyonunda kullanılan deney şartları

Parametre	Değerler
Katı oranı (%)=	5
Toplayıcı (Kerosen) (g/t)=	10000, 20000, 30000
Köpürtücü (AF-65) (g/t)=	20
Bastırıcı (Sodyum silikat) (g/t)=	500
Hacimsel Besleme Akış Hızı (Q_b)=	6.00, 6.38, 6.55
Hacimsel Artık Akış Hızı (Q_a) (L/dk)=	5.08
Koşullandırma süresi (t) (dk)=	2+7 (Bastırıcı+Toplayıcı)
Köpük Alma Süresi (dk)=	0-1, 1-3, 3-5, 5-8
Ortalama Hold-up (%)=	39

Alet negatif biasta çalıştırıldığı için yıkama suyu kullanılmamıştır. Artık debisi sabit tutularak üç farklı bias hızı için besleme debisi değiştirilmiştir. Bias, artık debisi ile besleme debisi arasındaki fark olup, köpük zonunu oluşumundan sorumlu parametredir (pozitif bias değerinde köpük zonu vardır). İri taneli minerallerin flotasyonunda ise genellikle bias negatiftir (Montany ve Honaker, 1999; Oteyaka, 1993). Eşitlik 2 kullanılarak hücredeki bias hızını bulmak mümkündür.

$$J_b = \frac{Q_A - Q_B}{A_C} J_b = \frac{Q_A - Q_B}{A_C}$$

Burada;
J_b: bias hızı (m/s),
A_C: hücre kesit alanını (m^2) ifade etmektedir.

Artık ikinci bir peristaltik pompa kullanılarak besleme tankına geri beslenmiştir. Flotasyon hız sabitini belirlemek için farklı sürelerde konsantreler alınmıştır. Flotasyon aleti ve besleme tankı içinde kalan malzeme artık olarak alınmıştır.

Flotasyon işleminde toplayıcı olarak kerosen, köpürtücü olarak poliglikol türde olan Cytec firmasının ürettiği Aerofroth 65 (AF-65) kullanılmıştır. Ayrıca numune içinde bulunan kilin bastırılması için sodyum silikat kullanılmıştır. Tüm deneyler çeşme suyu kullanılarak gerçekleştirilmiştir.

Deney Tasarımı

Deneylerden elde edilen değerlerin istatistiksel olarak ANOVA yöntemi ile değerlendirilebilmesi için 2^3 tam faktöriyel deney tasarım yöntemi kullanılmıştır. Bağımsız değişken olan tane boyutu, bias hızı ve

toplayıcı miktarının düşük ve yüksek düzeylerinde 8 adet ve orta düzeyinde 4 adet olacak şekilde 12 adet deney yapılmıştır. 2^3 deney tasarımı için faktörler, seviyeleri ve değerler Çizelge2'de verilmiştir.

Çizelge 2. Değişkenler ve seviyeleri

Parametre	Birim	Düşük (-1)	Orta (0)	Yüksek (+1)
Toplayıcı Miktarı – Q_C	g/t	10000	20000	30000
Tane Boyutu - d	µm	-212+106	-300+212	-500+300
Bias Hızı – J_B	cm/s	0.10	0.13	0.16

Kinetiğin Saptanması

Kesikli deneylerle flotasyon kinetiğini bulmak için verim-zaman grafiği ile çizilebilir (Yuan, vd., 1996). Böylece, kesikli flotasyon deneyleri için hız denklemi aşağıdaki eşitlik ile ifade edilmektedir.

$$\frac{dC}{dt} = -k.C^n \frac{dC}{dt} = -k.C^n$$

burada, C yüzebilir tane konsantrasyonu, n denklemin derecesi, k flotasyon hız sabiti, t süredir. Eşitlik 3'ün integrali alınıp düzenlenirse, birinci dereceden flotasyon kinetiği elde edilir (Arbiter ve Harris, 1962). Yanabilir verim eşitlik 4 kullanılarak hesaplanmaktadır.

$$R = C \times (100 - c)/F \times (100 - f) \times 100 R = C \times (100 - c)/F \times (100 - f) \times 100$$

Burada, C yüzen malzeme miktarı (%), c yüzen malzemenin kül içeriği (%), F besleme miktarı (%), ve f beslemenin kül içeriğidir (%).

DENEYSEL ÇALIŞMALAR

Bu çalışmada, konvansiyonel zenginleştirme aletleriyle kazanılması güç olan 500 µm altı kömürlerin Jameson hücresi ile zenginleştirilebilirliği araştırılmıştır. Bu aletin Türkiye'deki kullanım potansiyeli nedeniyle kinetik modeli belirli parametreler (tane boyutu, toplayıcı miktarı ve bias hızı) için ilk defa ampirik olarak ortaya konulmaya çalışılmıştır. Böylece aletin endüstriyel boyutta potansiyel kullanımları değerlendirilmeye çalışılmıştır.

Jameson hücresi (Şekil 1) ile yapılan deneylerden elde edilen değerler yardımıyla, konsantre kazanma sürelerine bağlı olarak ln(1-R)'ye karşı çizilen grafiklerin eğimlerinden flotasyon hız sabitleri belirlenmiştir. Deneylerde genel olarak tane boyutunun azalmasıyla flotasyon hızı artmaktadır. Ayrıca flotasyon hızı bias hızının artmasıyla daha da artmaktadır. Bu durum, hava/besleme oranının artışıyla kabarcık miktarının artması ve tane boyutunun küçülmesi ile tane-kabarcık çarpışma olasılığının artması ile açıklanabilir. Şekil 1 incelendiğinde, Jameson hücresinden elde edilen flotasyon hız sabitlerinin, alette üretilen küçük kabarcıklar; hidrodinamik özellikler; düşey boru üst kısmında meydana gelen yüksek kesme kuvvetleri nedeniyle ortaya çıkan enerji ve aletteki düşük kalma süresi sayesinde yüksek olduğu görülür. Jameson hücresinde en yüksek hız sabiti değeri 0.9841 R^2 ile 0.0632 dk^{-1} olarak elde edilmiştir.

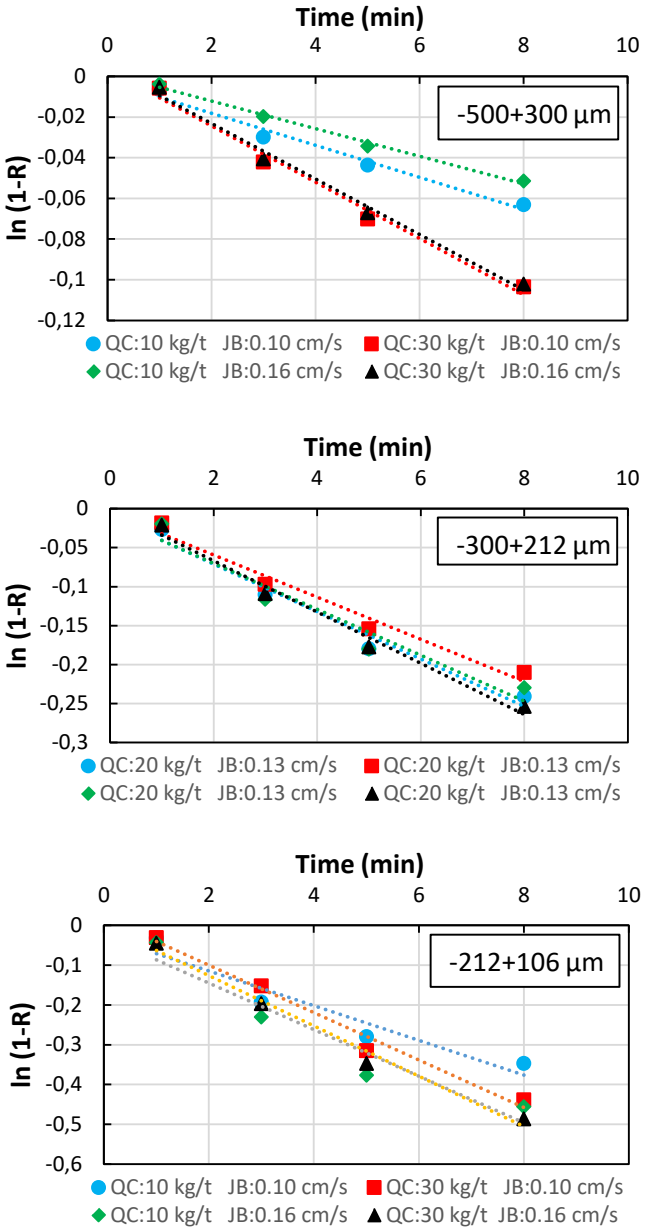

Şekil 1. Farklı tane boyutlarında Jameson hücresi ile yapılan flotasyonun birinci dereceden flotasyon kinetiği

Tane boyutu, toplayıcı miktarı ve bias hızı parametrelerinin Jameson hücresi ile yapılan deneylerin hız sabitine etkisi belirlenmiştir. Deneysel sonuçlardan elde edilen flotasyon hız sabiti değerleri Fisher Testi kullanılarak analiz edilmiştir (Çizelge 3). Böylece bağımsız değişkenler olan deney parametrelerinin flotasyon kinetiği (bağımlı değişken) üzerindeki etkileri %95 güven aralığında test edilmiştir. Deneylerden elde edilen ampirik model %95 güven aralığında anlamlı (significant) çıkmıştır. Çizelge 3, Fisher Testi F değerleriyle flotasyon kinetiği p değerlerini içermektedir. Jameson hücresi için bulunan model F değeri 51.89'dur ve anlamlıdır. Bu sonuç, deneylerden elde edilen kinetikle ilgili ampirik modelin (Eşitlik 5) sonuçları tahmin etmede kullanılabileceğini göstermektedir. Parametrelerin ana etkileri incelendiğinde, tane boyutunun anlamlı sonuçlar verdiği görülmektedir. Buna ek olarak, bias hızı değişiminin performans üzerindeki etkisinin

istatistiksel olarak anlamsız, toplayıcı miktarı için ise bunun anlamlı olduğu tespit edilmiştir. Ayrıca, ikili ve üçlü parametre etkileşimlerinin performans üzerindeki etkisi de anlamlıdır (Çizelge 3).

Çizelge 3. Jameson Hücresi flotasyon hız sabitine ait değişim analizi sonuçları

Factor	**F Value**	**p-Value Prob>F**
Model	51.89	0.0009
Q_C	11.35	0.0281
d	341.55	< 0.0001
J_B	3.06	0.1550
Q_C-d	0.64	0.4690
Q_C-J_B	1.09	0.3563
d-J_B	4.05	0.1144
Q_C-d-J_B	1.50	0.2881

Şekil 2'de görüldüğü gibi, toplayıcı miktarındaki artış ve tane boyutunun azalmasıyla ise flotasyon hız sabiti artmakta ve yüksek biasın kullanıldığı şartlarda 0.0632 dk^{-1} (Şekil 1 (f)) ile en yüksek değerini almaktadır. Bias hızındaki değişimin bir önemi olmaksızın, tane boyutu azaldıkça flotasyon hızının arttığı, toplayıcı miktarı-bias hızı arasındaki ikili etkinin ise istatistiksel olarak anlamsız olduğu görülmektedir. Toplayıcı miktarı, tane boyutu ve bias hızının, flotasyon hız sabiti üzerine etkilerini tanımlayan model Eşitlik 5'de verilmiştir.

$$k = 0.032225 + 4.16250E\text{-}003\ Q_C - 0.022838\ d + 2.16250E\text{-}003\ J_B - 9.87500E\text{-}004\ Q_C\ d - 1.28750E\text{-}003\ Q_C\ J_B - 2.48750E\text{-}003\ d\ J_B + 1.51250E\text{-}003\ Q_C\ d\ J_B \quad (5)$$

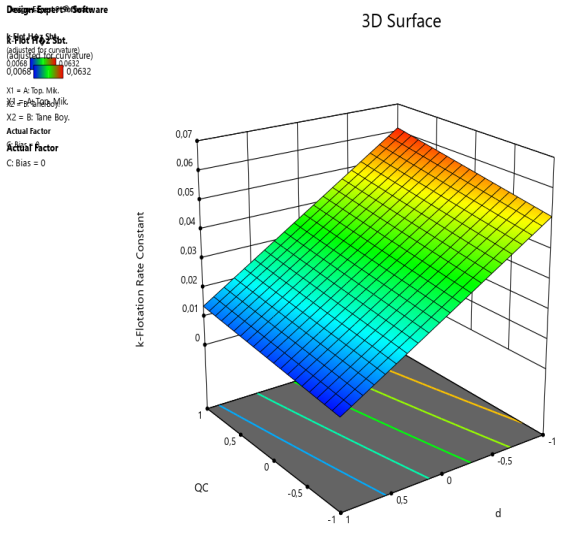

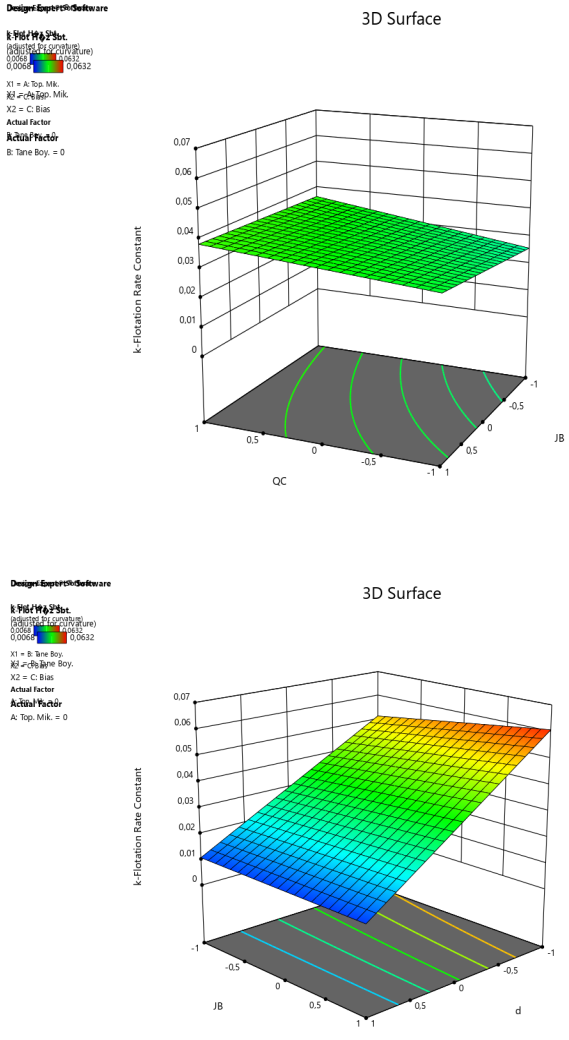

Şekil 2. Toplayıcı miktarı-Tane boyutu, Toplayıcı miktarı-Bias, Tane boyutu-Bias ikili etkilerinin flotasyon hız sabiti üzerine etkisi.

SONUÇLAR

Yüksek kil içerikli linyit kömürünün kullanıldığı bu çalışmada tane boyutu, toplayıcı miktarı ve bias hızının flotasyon hız sabitine etkisi Jameson hücresi için ampirik olarak modellenmiştir. Deneyler 2^3 tam faktöriyel deney tasarımı kullanılarak yürütülmüştür. Deney sonuçlarından elde edilen verilerden belirlenen flotasyon hız sabiti için parametrelerin ana ve çoklu etkilerini gösteren modeller oluşturulmuştur. Çalışmada oluşturulan modeller %95 güven aralığında istatistiksel açıdan anlamlı çıkmıştır.

Deneylerde genel olarak tane boyutunun azalmasıyla flotasyon hızı artmaktadır. Flotasyon hızındaki artış bias hızının yükselmesine bağlı olarak daha da fazla olmuştur. Jameson hücresinde en yüksek hız sabiti değeri 0.9841 R^2 ile 0.0632 dk^{-1} olarak elde edilmiştir.

KAYNAKLAR

Aktaş, Z., Woodburn, E.T. (1995). The effect of non-ionic reagent adsorption on the froth structure and flotation performance of two low rank British coals, Powder Technology, *83*, *2*, 149-158.

Arbiter, N., Harris, C.C. (1962). Flotation kinetics. Froth Flotat. 50th Anniv., New York, AIME.

Kowalczuk, P.B., Şahbaz, O., Drzmala, J. (2011). Maximum size of floating particles in different flotation cells, Minerals Engineering, *24*, *8*, 766-771.

Lynch, A.J., Johnson, N.W., Manlapig, E.V., Thorne, C.G. (1981). Mineral and Coal Flotation Circuits-Their Simulation and Control. D.W. Fuerstenau (Eds.) (pp. 291), Amsterdam, Elsevier.

Mohanty, M.K., Honaker, R.Q. (1999). Performance optimization of Jameson flotation technology for fine coal cleaning, Minerals Engineering, *12*, *4*, 367-381.

Nguyen, A., Shulze, H.J. (2003). Colloidal science of flotation, Boca Raton, CRC Press.

Oteyaka B. (1993). Modelisation D'une Colonne De Flottation Sans Zone D'ecume Pour La Separation Des Particules Grossieres. Universite Laval, PHD Thesis.

Polat, M., Chander, S. (1995). Coal flotation kinetics: Interactions between physical and chemical variables. In: Plenary Lecture, Proc. Int. Conf. on Mineral Proc.-Recent Advances and Future Trends, Kanpur-India, 615–631.

Polat, M., Chander, S. (2000). First-order flotation kinetics models and methods for estimation of the true distribution of flotation rate constants, International Journal of Mineral Processing, *58*, *1-4*, 145-166.

Şahbaz, O. (2013). Determining optimal conditions for lignite flotation by design of experiments and the halbich upgrading curve, Physicochemical Problems of Mineral Processing, *49*, *2*, 535-546.

Şahbaz, O., Uçar, A., Öteyaka, B. (2013). Velocity gradient and maximum floatable particle size in the Jameson cell, Minerals Engineering, *41*, 79-85.

Tsai, S.C. (1985). Effects of surface chemistry and particle size and density on froth flotation of fine coal, Colloids and Surfaces, *16*, 3-4, 323-336.

Yuan, X.M., Pålsson, B.I., Forssberg, K.S.E. (1996). Statistical interpretation of flotation kinetics for a complex sulphide ore, Minerals Engineering, *9*, 429-442.

KSANTAT ZİNCİR YAPISININ GALEN FLOTASYONUNA ETKİSİ

EFFECT OF CHAIN STRUCTURE OF XANTHATE ON GALENA FLOTATION

S. Özün [1,*], G. Ergen [1]

[1]*Süleyman Demirel Üniversitesi, Maden Mühendisliği Bölümü*
*(*Sorumlu yazar: savasozun@sdu.edu.tr)*

ÖZET

Sülfürlü minerallerin flotasyonla zenginleştirilmesinde yaygın olarak kullanılan ksantatların toplayıcılık kuvveti C-H zincir uzunlukları ve yapısına bağlı olarak değişmektedir. Toplayıcılık kuvvetleri artan zincir uzunluğu ile artarken, seçicilik özellikleri azalmaktadır. C-H zincir yapısı ise toplayıcının hedef mineral yüzeyine adsorplanma kabiliyetini etkilemektedir. Flotasyonla verimlerini etkileyen bir diğer önemli değişken de hidrofobik hedef mineral tanelerinin flotasyon hücresi dışına taşıyan hava kabarcıklarının boyutları ve kararlı yapılarıdır. Bu çalışma kapsamında farklı C-H zincir uzunluklarına ve yapılarına sahip ksantat türü toplayıcıların (PEX ve SIPX) galen flotasyon verimine olan etkileri toplayıcı derişimi ve pH'a bağlı olarak incelenmiştir. Çalışmada ayrıca her iki ksantat için de köpürtücü ilavesinin flotasyon verimine olan etkileri de belirlenmiştir. Sonuçlar; flotasyon verimlerinin pH'a bağlı olarak değişiklik gösterdiğini en yüksek flotasyon verimlerinin bazik pH koşullarında elde edildiğini göstermiştir. Köpürtücü ilavesi ile hava kabarcık boyutlarının küçüldüğü, böylece hava kabarcıkları ile mineral tanelerinin karşılaşma/çarpışma olasılıkları, dolayısıyla flotasyon verimleri de artmıştır. Sonuçlara göre artan toplayıcı miktarı ile flotasyon veriminin her iki ksantat için de arttığı ve düz C-H zincir yapılı PEX varlığında flotasyon verimlerinin daha yüksek olduğu belirlenmiştir. Ancak köpürtücü kullanımı ile dallanmış C-H zincir yapılı olan SIPX varlığında flotasyon verimlerinde elde edilen artış, düz C-H zincir yapılı PEX varlığında el edilen flotasyon verim artışından daha yüksek olmuştur.

Anahtar Sözcükler: Galen, flotasyon verimi, ksantat zincir uzunluğu/yapısı, toplayıcı miktarı, köpürtücü

ABSTRACT

Collecting strength of xanthates, which are widely used in flotation of sulfides, varies depending on C-H chain lengths and structures. While the collecting strength increase with increasing chain length, the selectivity decreases. C-H chain structure, on the other hand, affects the adsorption of a collector to a mineral surface. Another important variable affecting flotation recoveries is the sizes and stabilities of air bubbles that carry hydrophobic minerals out of the flotation cell. In this study, the effects of xanthates with different chain length and structure (PEX and SIPX) on galena flotation recovery were investigated depending on collector concentration and pH. The effect of frother addition on the flotation recovery was also determined for both xanthates. The results showed that the flotation recoveries varied depending on pH, and the highest flotation recoveries were obtained under alkaline pHs. With the addition of frother, the size of the air bubbles decreased, so the meeting/collision probability between air bubbles and minerals, and thus the flotation recoveries increased. According to the results, the flotation recoveries increased for both xanthates with increasing frother amount, and the flotation recovery was higher with PEX having straight chain structure. However, with the use of frother, the increase in flotation recoveries with SIPX having branched chain was higher than that of obtained with PEX.

Keywords: Galena, flotation recovery, chain length/structure of xanthate, collector concentration, frother

GİRİŞ

Goldschmids sınıflandırmasına göre yerkürenin manto kısmında yaygın olarak bulunan, kükürtle kolayca birleşme eğilimi gösteren, genellikle sülfürleri meydana getiren S, Zn, Pb, As, Sb vb. elementler kalkofil olarak tanımlanmaktadır. Bu sebeple nadiren serbest halde bulunan kurşun yaygın olarak başka minerallerle bileşik halinde bulunmaktadır (Goldschmidt, 1937).

En yüksek kurşun içeriğine sahip mineral olan galen (PbS) doğada çoğunlukla sfalerit (ZnS), kalkopirit ($CUFeS_2$), pirit (FeS_2) ve gümüş ile birlikte bulunmaktadır. Kurşun içeren cevherlerin doğrudan izabe edilmeleri ekonomik açıdan maliyetli olduğu için, izabe işlemleri öncesi uygulanacak zenginleştirme işlemleri ile yüksek tenörlü galen konsantre eldesi sağlanmaktadır.

Minerallerin serbestleşme tane boyutuna bağlı olarak tek başlarına veya kombinasyonları şeklinde uygulanabilen gravite yöntemlerinin (jig, ağır ortam ayırıcıları, spiral, sallantılı masalar vb.) birçok zenginleştirme yöntemine göre işletme/yatırım maliyetleri açısından oldukça ucuz olmalarına karşılık, metal kazanma verimlerinin düşüklüğü, kaçakların önlenememesi ve seçimli ayırmaya tam uyum sağlayamamaları nedeniyle yüksek tenörlü galen konsantresi elde edilebilmesi için zenginleştirme işlemleri çoğunlukla seçimli flotasyon uygulamaları ile yapılmaktadır (DPT, 2001; Craig ve Vaughan, 1994; del Villar vd., 2010).

Ksantatlar sülfürlü minerallerin flotasyonunda en yaygın kullanılan toplayıcı grubudur. İyonlaşan toplayıcılar arasında yer alan ksantatlar karmaşık yapılı moleküller olup asimetrik yapı özelliği gösterirler; apolar hidro-karbon (C-H) grup ve polar grup içerirler (Şekil 1). Apolar grup hidrofobik özelliğe sahipken, polar grup su ile reaksiyona girer (Bulut ve Göktepe, 2012).

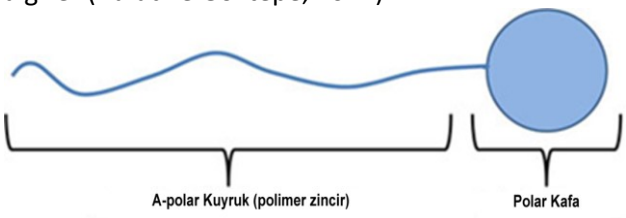

Şekil 1. Polar kafa ve a-polar kuyruk (polimer, hidrokarbon zinciri) (Ergen, 2016)

Ksantatların toplayıcılık kuvvetleri sahip oldukları apolar (C-H) zincir uzunluğu ve C-H zincir yapısına bağlı olarak değişiklik gösterir. Apolar zincir uzunluğunun artması ksantatın toplayıcılık kabiliyetini artırmaktadır. Buna bağlı olarak daha uzun C-H zincirleri olan ksantatlar kısa zincirli olanlara kıyasla yüzeye adsorbe olduklarında mineral yüzeyinin hidrofobiklik derecesini daha fazla artırmaktadırlar (Gaudin, 1957). Flotasyon başarısını ve seçimli ayrımı etkileyen bir diğer önemli değişken olan toplayıcı C-H zincir yapısı ise toplayıcının hedef mineral yüzeyine adsorplanma kabiliyetini etkilemektedir. Örnek olarak Wang, 2016 tarafından dallanmış zincir yapılı izo-ksantatların mineral yüzeyine adsorplanma kabiliyetlerinin düz zincirli ksantatlardan daha fazla olduğu belirtilmiştir (Wang, 2016).

Toplayıcı kullanımı ile yeterli hidrofobiklik sağlanan hedef mineral taneleri hava kabarcıkları yardımıyla öncelikle köpük bölgesine ve daha sonrasında ise flotasyon hücresi dışına taşınmaktadır. Bu aşamada birleşmeyen, kararlı ve küçük hava kabarcık oluşumu köpürtücü ilavesi ile sağlanmaktadır (Cho and Laskowski, 2002a; Cho and Laskowski, 2002b; Kurşun, 2005). Köpürtücü ilavesi ile hava kabarcık boyutlarının küçülmesi; birim zamanda flotasyon hücresine beslenen hava miktarında sayıca daha fazla hava kabarcığı elde edilmesine dolayısıyla toplam hava kabarcık yüzey alanının ve hava kabarcık-hedef mineral tane karşılaşma olasılığının artmasını neden olmaktadır.

Yukarıda belirtilen değişkenler dikkate alındığında, bu çalışma kapsamında; gerek farklı toplayıcı miktarları ve ortam pH'sında toplayıcı C-H zincir uzunluğu ve yapısının, gerekse her iki farklı toplayıcı (potasyum etil ksantat; potassium ethyl xanthate: PEX ve sodyum izobütil ksantat; sodium isobutyl xanthate; SIPX) varlığında belirlenen koşullarda köpürtücü (metil izobütil karbinol; metyl isobutyl carbinol; MIBC) ilavesinin galen flotasyon verimine olan etkilerinin belirlenmesi hedeflenmiştir.

MALZEME VE YÖNTEM

Deneysel çalışmalarda; Balıkesir Dursunbey'de faaliyet göstermekte olan bir zenginleştirme tesisinden temin galen konsantresi kullanılmıştır. X-ışını floresans spektrometresi (X-ray flourescence; XRF) (Çizelge 1) ve X-ışını difraksiyonu (X-ray diffraction; XRD) sonuçlarına göre numune yaklaşık olarak >%3 sfalerit (ZnS) ve pirit (FeS_2) mineralleri, >%1.5 kalkopirit ($CuFeS_2$) içermektedir. Deneysel çalışmalar öncesinde numune yaş eleme işlemi ile dar tane boyut aralıklarında sınıflandırılmış ve her bir boyut aralığındaki numune mineral tanelerinin yüzeylerinin temizlenmesi amacıyla sırasıyla seyreltik HCl çözeltisi ve distile su ile yıkanmıştır. Tane boyutunun flotasyon başarısına etkisinin giderilmesi amacıyla mikroflotasyon testlerinde -106+75 mikron boyutlu fraksiyon kullanılmıştır.

Mikroflotasyon testlerinde toplayıcı olarak kullanılan ksantat numuneleri (potasyum etil ksantat; PEX, sodyum izopropil ksantat; SIPX) (Şekil 2) ECS Kimya'dan temin edilmiştir. Analizler öncesinde her bir toplayıcının distile su'da çözünmesi ile hazırlanan 250 ppm stok çözeltiler, distile su ilavesi ile 1-50 ppm/lt'ye seyreltilmiş ve pH düzenlemeleri seyreltik HCl ve NaOH çözeltileri kullanılarak gerçekleştirilmiştir.

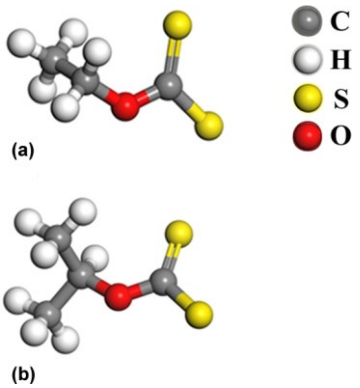

Şekil 2. (a) Potasyum etil ksantat ve (b) sodyum izopropil ksantat yapısı (Özün ve Ergen, 2019)

Zeta Potansiyel Ölçümleri ve Mikroflotasyon Testleri

Zeta potansiyel ölçümleri Malvern Zetasizer Nano-Z cihazı kullanılarak gerçekleştirilmiştir. Cihaz lazer doppler hızölçer ile 5 nm - 10 mikron boyutlarındaki tanelerin zeta potansiyellerini belirleyebilmektedir. Ölçümlerde -10 mikron tane boyutuna sahip temsili 10 mg galen numunesi 100 ml distile su içerisinde pH düzenlemelerinden sonra 5 dakika manyetik karıştırıcıda karıştırılmış, süre bitiminde 10 ml'lik şırınga yardımıyla Zetasizer numune hücresine aktarılarak zeta potansiyel ölçümüne tabi tutulmuştur. Ölçümler sonrasında 3 ölçümün aritmetik ortalaması zeta potansiyel değeri olarak kabul edilmiştir.

Şekil 3'de mikroflotasyon testlerinde kullanılan ve bu çalışma kapsamında kurulumu gerçekleştirilen Hallimond Tüp test düzeneği şematik görüntüsü verilmiştir. Hallimond Tüp ile gerçekleştirilen mikroflotasyon testleri öncesinde 1 gr galen numunesi 100 ml'lik beherde 5 dakika belirlenen pH ve flotasyon reaktifi koşullarında şartlandırılmıştır. Şartlandırma işlemleri sonrası mikroflotasyon test düzeneğine aktarılan pülp, önceden belirlenen karıştırma hızı, HAH ve köpük toplama süresinde mikroflotasyon işlemine tabi tutulmuştur. Flotasyon verimleri flote edilen ve pülpte kalan numunenin ayrı ayrı kurutulup tartılması ile hesaplanmıştır.

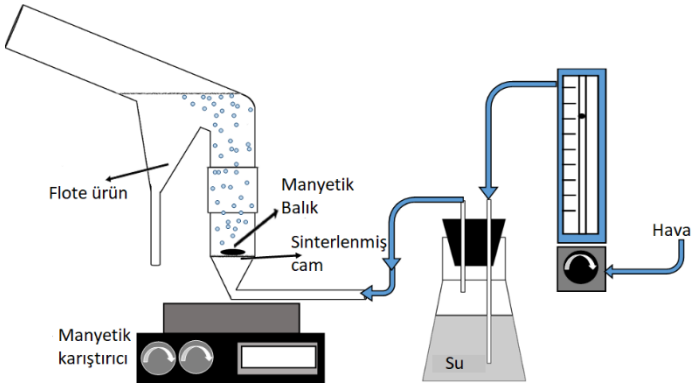

Şekil 3. Hallimond test ünitesinin şematik görüntüsü

DENEYSEL SONUÇLAR VE TARTIŞMA

Toplayıcı Derişiminin Flotasyon Verimine Etkisi

Flotasyonla zenginleştirme işlemlerinde kullanılanılan ksantatların apolar kuyruklarındaki karbon sayısının 1 ile 6 arasında değiştiği dikkate alındığında, toplayıcılık kabiliyetleri zayıftan güçlüye doğru; CH_3 (metil), C_2H_5 (etil), C_3H_7 (propil), C_4H_9 (bütil), C_5H_{11} (amil) ve C_6H_{13} (hekzil) ksantatlar şeklinde sıralanmaktadır. Uzun hidro-karbon (apolar) zincirleri olan ksantatlar kısa zincirli olanlara kıyasla yüzeye adsorbe olduklarında mineral yüzeyinin hidrofobiklik derecesini daha fazla arttırmaktadırlar (Gaudin, 1957). Birden fazla sülfürlü mineralin bir arada bulunduğunduğu karmaşık (kopleks) cevherlerde toplayıcılık kabiliyetleri yüksek olan ksantatlar çoğunlukla toplu (bulk) konsantre eldesi amaçlandığı durumlarda tercih edilirken, seçimli flotasyon uygulaması amaçlandığı durumlarda ise kısa C-H zincirli ksantatlar kullanılmaktadır. Ksantatların toplayıcılık özellikleri ayrıca ortam pH'ı, toplayıcı derişimi, C-H zincir yapısı, HAH, şartlandırma süresi vb. değişkenlere bağlı olarak da değişmektedir (Hamilton ve Woods, 1986; Wang, 2016).

Mikroflotasyon testleri öncesinde galenin deneysel çalışmalarda kullanılan ksantat örnekleri ile olan etkileşimlerinin belirlenebilmesi amacıyla zeta potansiyel çalışmaları yapılmış sonuçlar grafiksel olarak Şekil 4'de sunulmuştur. Elde edilen sonuçlara göre galen minerali pH 2.5-3 aralığında isoelektrik (pH_{iep}) noktaya sahipken belirtilen pH değerlerinden daha asidik koşullarda pozitif (+), daha bazik koşullarda ise negatif (-) yönde artan zeta potansiyel değişimleri göstermekte ve yaklaşık pH 10'da en düşük zeta potansiyel değerlerine (≈-30 mV) ulaşmaktadır.

Çizelge 1. Mikroflotasyon test koşulları

Tane boyutu	-106 +75 mikron	**pH**	2 – 11.5
Mineral miktarı	1 gr	**Hava akış hızı (HAH)**	4 lt/saat
Karıştırma hızı	1000 d/dk (şartlandırma) 400 d/dk (flotasyon)	**Flotasyon süresi**	2 dk
Şartlandırma süresi	5 dk	**Toplayıcı derişimi**	1 – 50 ppm

Çalışmanın bu aşamasında öncelikli olarak gerek karşılaştırma kolaylığının sağlanması, gerekse deneysel sonuçlara olan etkilerinin azaltılması amacıyla mineral miktarı, karıştırma hızı, HAH vb. (Çizelge 1) değişkenler sabit tutularak her iki ksantat için de toplayıcı miktarı ve ortam pH'ının galen flotasyon verimine olan etkileri 1-50 ppm toplayıcı derişimlerinde incelenmiştir. Ksantat varlığında gerçekleştirilen mikroflotasyon testleri öncesinde galenin distile su içerisinde toplayıcısız ortamda flotasyon davranışları

pH'a dayalı olarak belirlenmiş ve sonuçlar Şekil 5'de grafiksel olarak verilmiştir. Sonuçlara göre galenin toplayıcısız ortamda flotasyon verimi her bir pH değeri için %10'dan daha düşük olduğu belirlenmiştir.

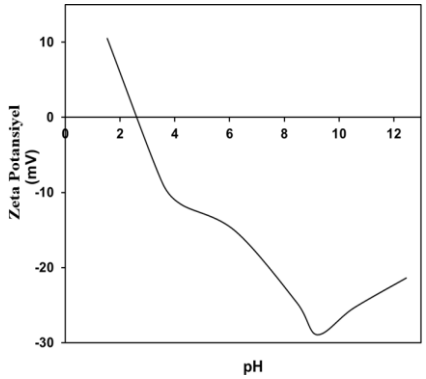

Şekil 4. Galen'in pH'a dayalı zeta potansiyel değişimi

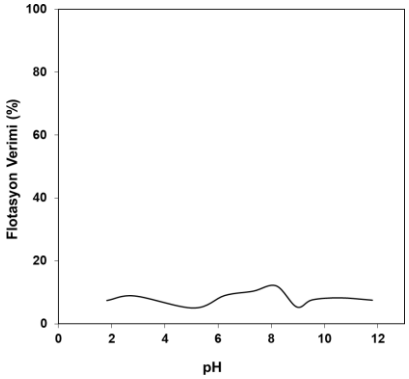

Şekil 5. Galen'in distile sudaki pH'a dayalı flotasyon verim değişimi

Şekil 6 (a-d)'da ise potasyum etil ksantat ve sodyum izopropil ksantat varlığında gerçekleştirilen mikroflotasyon test sonuçları 4 farklı pH aralığı için grafiksel olarak verilmiştir. Sonuçlara göre galen flotasyon verimi her iki farklı C-H zircir yapılı ksantat için de artan toplayıcı derişimi ile birlikte artmaktadır. Şekil 6 (a)'da pH 2-2.5 aralığında her iki toplayıcı için flotasyon verim değerleri dikkate alındığında; belirtilen pH aralığında galenin pozitif (+) zeta potansiyele sahip olduğu (Şekil 4) ve ksantatın negatif yüklü monomer (X^-) derişiminin artış gösterdiği (Şekil 7) görülmektedir. Bu durumda yüksek flotasyon verimlerinin için zıt yüklü Pb^{2+} ve ksantat monomerleri (X^-) arasında gerçekleşen elektrostatik etkileşim neticesinde elde edildiği sonucu çıkmaktadır (Özün ve Ergen, 2019). Şekil 6 (b)'de ise pH 6-6.5 aralığı için azalan Pb^{2+} derişimi ile her iki toplayıcı için de flotasyon verimlerinin bir miktar azaldığı görülmektedir.

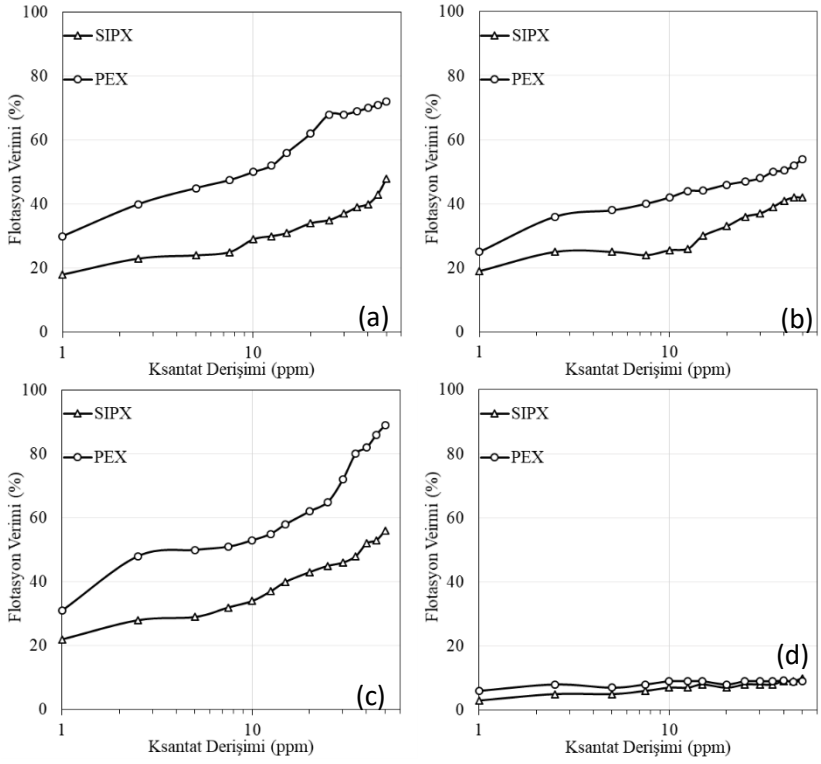

Şekil 6. Galen'in PEX ve SIPX varlığında (a) pH 2-2.5, (b) pH 6-6.5, (c) pH 9-9.5 ve (d) pH 11-11.5'de toplayıcı derişimine dayalı flotasyon verim değişimi

Artan ortam pH değeri ile birlikte ksantatın çözeltide çoğunlukla negatif yüklü monomer (X^-) olarak bulunduğu ve pH 9-9.5 için galenin ise yüksek negatif şiddetli zeta potansiyel değerlerine (≈-30 mV) sahip olduğu dikkate alındığında, elde edilen yüksek flotasyon verimlerinin negatif yüklü ksantat monomerlerinin (X^-) galen mineral yüzeyine ($Pb(OH)^+$) kimyasal olarak adsorplanması ile oluştuğu sonucunu ortaya çıkarmaktadır (Kartio vd., 1999; McFadzean vd., 2012). Belirtilen pH değerlerinde gerek düz C-H zincir yapılı PEX, gerekse dallanmış C-H zincir yapılı SIPX varlığında elde edilen en yüksek flotasyon verimleri elde edilmiştir. pH 11-11.5'de ise artan pH değerleri galen için bastırıcı görevi üstlenmekte ve sonuç olarak galenin her iki farklı C-H zincir yapılı ksantat varlığında da flotasyon verimi >%10' düşmektedir (Wark ve Cox, 1934; Sutherland ve Wark, 1955).

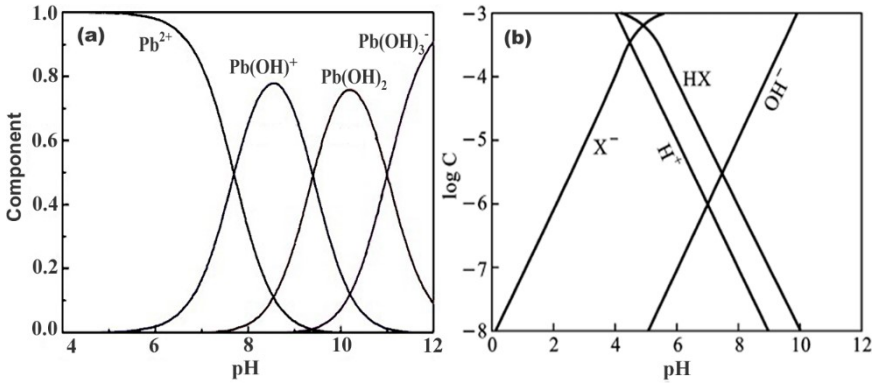

Şekil 7. (a) Pb^{2+} (Qin vd, 2015) ve (b) Ksantatın (Yongxin ve Changgen, 1983; Somasundaran ve Wang, 2006) pH'a dayalı tür değişim diyagramı

Köpürtücü İlavesinin Flotasyon Verimine Etkisi

Flotasyonla zenginleştirme işlemlerinde; canlandırıcı, toplayıcı vb. reaktiflerin kullanımı ile hedef minerallere yeterli hidrofobik yüzey özelliği sağlanması sonrası bu mineral tanelerini öncelikle köpük bölgesine, sonrasında da flotasyon hücresi dışına taşıma işlemi hava kabarcıkları ile gerçekleştirilmektedir. Bu süreçte flotasyon başarısı elde edilmesinde önemli bir rol üstlenen hava kabarcıklarının birleşmeyen küçük çaplı ve kararlı olmaları köpürtücü ilavesi ile sağlanmaktadır (Çilek, 2013). Çeşitli araştırmacılar tarafından gerçekleştirilmiş olan çalışmalarda köpürtücü miktarı ile hava kabarcık çapının birbiri ile ters orantılı olduğunu, artan köpürtücü miktarı ile hava kabarcık boyutlarının küçüldüğü belirlenmiştir (Goodal ve O'Conner, 1992; Tuteja vd.; 1995, Kurşun, 2005; Özün ve Ergen, 2019). Ayrıca benzer koşullar altında büyük hava kabarcıkları ile karşılaştırıldığında, küçük hava kabarcıkları ile mineral tanelerinin çarpışma/karşılaşma olasılığının daha yüksek olduğu ve hidrofobik mineral tanelerinin küçük hava kabarcıklarından kopma/ayrılma olasılığının daha düşük olduğu belirtilmiştir (Yoon and Luttrell, 1989; Sobhy and Tao, 2013). Bu bağlamda çalışmanın bu aşamasında her iki ksantat için de pH 9-9.5'da, 2.5 ppm toplayıcı derişiminde ve 4lt/dk hava hızında köpürtücü (0.8–4 ppm MIBC; metil izobütil karbinol) ilavesinin flotasyon verimine olan etkileri araştırılmıştır. MIBC varlığında her iki ksantat için elde edilen mikroflotasyon hücresi görüntüleri Şekil 8 ve Şekil 9'da, flotasyon verimi değişimleri ise Şekil 10'da verilmiştir.

Şekil 8-9'da verilen görüntüler incelendiğinde artan MIBC derişimi ile birlikte hava kabarcık boyutlarının küçüldüğü görülmektedir. Köpürtücü ilavesiz hava kabarcık boyutları Şekil 8 (a) ile karşılaştırıldığında her iki ksantat için de 0.8 ppm MIBC ilavesi ile hava kabarcık boyutlarının küçüldüğü (Şekil 8 (b-c)), MIBC ilavesinin 4 ppm'e çıkarılması ile ise çok daha küçük hava kabarcıklarının (Şekil 9 (a-b)) oluştuğu görülmektedir.

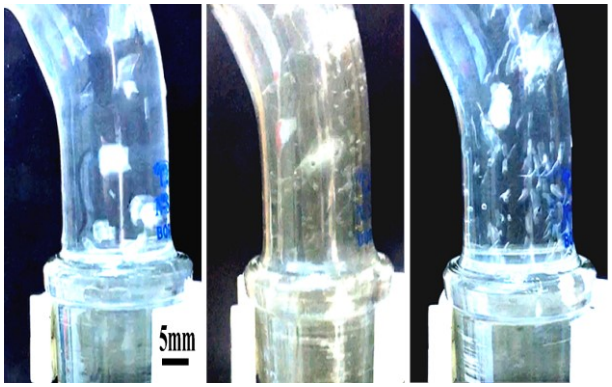

Şekil 8. (a) MIBC olmayan ve 0.8 ppm MIBC ilavesinde (b) PEX ve (c) SIPX varlığında Hallimond tüp test ünitesi görüntüsü

Şekil 9. 4 ppm MIBC ilavesinde (a) PEX ve (b) SIPX varlığında Hallimond tüp test ünitesi görüntüsü

MIBC varlığında elde edilen flotasyon verimleri (Şekil 10 (a-c)) incelendiğinde ise küçülen hava kabarcık boyutları ile birlikte mineral taneleri ile hava kabarcıklarının çarpışma/karşılaşma olasılıkları ve sonuç olarak flotasyon verimleri artmıştır. Daha uzun C-H zincir uzunluklu SIPX varlığında köpürtücüsüz ortamda beklenenin aksine PEX varlığında elde edilen flotasyon verimlerinden daha düşük flotasyon verimleri elde edilirken, MIBC ilavesi ile dallanmış C-H zincir yapılı SIPX ile şartlandırılmış galen tanelerinin hava kabarcıklarına daha kuvvetli tutunduğu sonucuna varılmıştır (Özün ve Ergen, 2019). Köpürtücüsüz ortamda elde edilen flotasyon verimleri ile karşılaştırıldığında 0.8 ppm MIBC ilavesi ile PEX varlığında flotasyon verimlerinin yaklaşık %50'den %60'ın üzerine çıktığı, SIPX varlığında ise yaklaşık %30'dan %60'a çıktığı belirlenmiştir. Hava kabarcık boyutlarının küçültülmesi ve daha kararlı hava kabarcıklarının elde edilmesi amacıyla MIBC ilavesi 4 ppm'e çıkarıldığında ise mineral taneleri ile hava kabarcıklarının karşılaşma/çarpışma olasılığı artmış ve dolayısıyla her iki ksantat için de flotasyon verimleri artmıştır. 4 ppm MIBC ilavesi ile PEX ve SIPX varlığında flotasyon verimleri sırasıyla >%90 ve >%80 olarak bulunmuştur.

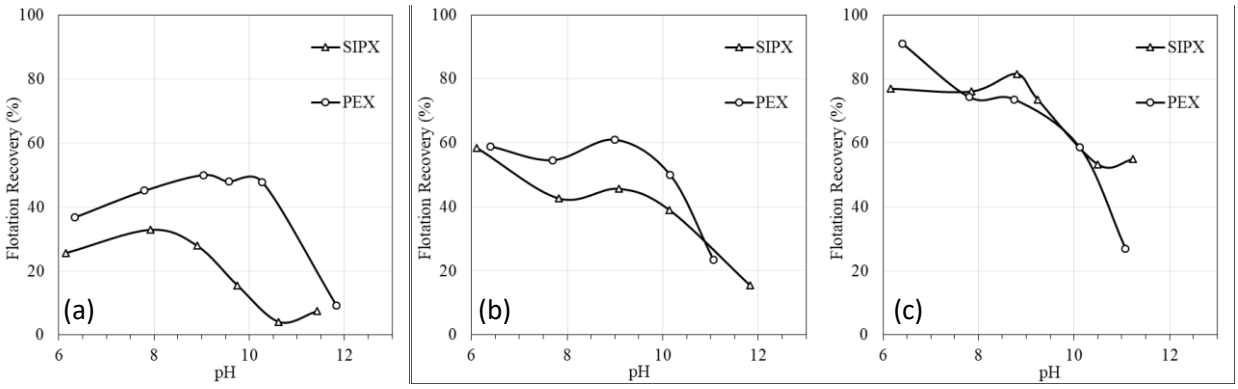

Şekil 10. (a) MIBC olmayan, (b) 0.8 ppm MIBC ve (c) 4.0 ppm MIBC ilavesinde pH'ya dayalı flotasyon verim değişimi

SONUÇLAR

Bu çalışma kapsamında gerçekleştirilen mikroflotasyon testleri ve elde edilen sonuçlar değerlendirildiğinde;

Her iki ksantat kullanımında da galenin flotasyon verimlerinin pH 8.5-9.5 aralığında yüksek olduğu belirlenmiş, toplayıcı derişiminin artması ile birlikte her iki ksantat için de flotasyon verimleri artmıştır.

Sonuçlara göre ksantat C-H zincir yapısının flotasyon verimini etkilediği, özellikle köpürtücüsüz ortamda daha kısa C-H zincir uzunluğuna sahip düz C-H zincir yapılı PEX varlığında daha yüksek flotasyon verimleri elde edilmiştir.

Köpürtücü (MIBC) ilavesinin her iki ksantat türü için de flotasyon verimine önemli etkilerinin olduğu, artan köpürtücü ilavesi ile birlikte hidrofobik galen taneleri ile hava kabarcıklarının çarpışma/karşılaşma olasılığının arttığı, sonuç olarak flotasyon verimlerinin arttığı görülmüştür.

Köpürtücü ilavesi ile birlikte dallanmış C-H zincir yapılı SIPX ile hava kabarcıkları arasında düz C-H zincir yapılı PEX ile elde edilen sonuçlara kıyasla daha kuvvetli bir etkileşimin olduğu, sonuç olarak SIPX varlığında flotasyon verimlerinin daha fazla arttığı belirlenmiştir.

TEŞEKKÜR

Çalışmanın #4713-YL1-16 No'lu proje kapsamında finansal olarak desteklenmesini sağlayan SDÜ BAP Koordinatörlüğü'ne, Zeta potansiyel ölçümlerinin gerçekleştirildiği ODTÜ Maden Mühendisliği Bölüm Başkanlığı'na ve galen numunesi teminini sağlayan AKSU Holding Balıkesir Flotasyonla Zenginleştirme Tesis Müdürlüğü'ne teşekkür ederiz.

KAYNAKÇA

Bulut, G., Göktepe, F. (2012). Madencilik ve Cevher Hazırlama İşlemlerinde Kullanılan Kimyasallar, Eskişehir Osmangazi Üniversitesi, Mühendislik Mimarlık Fakültesi Dergisi, 25, 37-56.

Cho Y. S., Laskowski J. S. (2002a). Effect of flotation frothers on bubble size and foam stability. Int. J. Miner. Process. 64, 69-80.

Cho Y. S., Laskowski J. S. (2002b). Bubble coalescence and its effect on dynamic foam stability. Can. J. Chem. Eng., 80, 299-305.

Çilek, E.C. (2013). Mineral Flotasyonu, Süleyman Demirel Üniversitesi Basımevi, 158s, Isparta.

Craig, J. R., Vaughan, D. J. (1994). Ore microscopy and ore petrography, 2nd ed.; A Wiley-Interscience Publication, John Wiley & Sons, Inc.: New York; pp. 259-326.

del Villar, R., Desbiens, A., Maldonado, M., Bouchard, J. (2010). Advanced control and supervision of mineral processing plants, Springer London Dordrecht Heidelberg: New York.

Devlet Planlama Teşkilatı (DPT) (2001). Metal Madenler (Bakır), 8. Beş Yıllık Kalkınma Planı. Madencilik Özel İhtisas Komisyonu Raporu, Metal Madenler Alt Komisyonu Diğer Metal Madenler Çalışma Grubu Raporu, DPT Rapor No: 2628-ÖİK 639, 163s.

Ergen, G. (2017). Farkli Hidro-Karbon Zincirli Ksantat Türü Toplayicilarin Galen Flotasyonuna Etkisi, Süleyman Demirel Üniversitesi, Fen Bilimleri Enstitüsü, Yüksek Lisans Tezi, 69s, Isparta.

Gaudin A.M. (1957). Flotation, 2nd edition, McGraw-Hill Book Company, 573p, New York.

Goldschmidt, V. M. The principles of distribution of chemical elements in minerals and rocks. J. Chem. Soc. 1937, 655-673.

Goodal, C.M., O'Connor, C.T. (1992). Residence Time Distribution Studies in a Flotation Column, Part 1-The Relationship Between Solids Residence Time Distribution and Metallurgical Performance, International Journal of Mineral Processing, 36, 219-228.

Kartio, I., Laajalehto, K., Suoninen, E. (1999). Characterization of the ethyl xanthate adsorption layer on galena by synchroton radiation excited photoelectron spectroscopy. Colloids Surf. A Physicochem. Eng. Asp., 154, 97–101.

Kurşun, H. (2005). The effect of air hold-up (εg), superficial air flow rate (Vh) and frother dosage in two-phase (air/water) and three-phase system (air/water/minerals) on the performance of column flotation, SDU J. Nat. Appl. Sci., 9(3), 1-8.

McFadzean, B., Castelyn, D. G., O'Connor, C. T. (2012). The effect of mixed thiol collectors on the flotation of galena. Miner. Eng., 36–38, 211–218.

Özün, S., Ergen, G. (2019). Determination of optimum parameters for flotation of galena: Effect of chain length and chain structure of xanthates on flotation recovery, ACS Omega, 4, 1516−1524.

Sobhy, A., Tao, D. (2013). Nanobubble column flotation of fine coal particles and associated fundamentals. Int. J. Miner. Process., 124, 109–116.

Sutherland, K.L., Wark, I.W. (1955). Principles of Flotation, The Australasian Institute of Mining and Metallurgy, 1, 237-263.

Tuteja, R.K., Spottiswood, D.J., Mishra, V.N. (1995). Recent Progress in the Understanding of Column Flotation-A Review, The Australasian Institute of Mining and Metallurgy, 2, 25-31.

Wang D. (2016). Flotation reagents: Applied surface chemistry on minerals flotation and energy resources beneficiation. Springer, Singapore.

Wark, I.W., Cox, A.B. (1934). Instıtute of Metals Division, Transactions of the American Institute of Mining and Metallurgical Engineers, Milling and Concentration, 389p, New York.

Yoon, R. H., Luttrell, G. H. (1989). The effect of bubble size on fine particle flotation. Miner. Process Extr. Metal. Rev., 5, 101-122.

LIFE CYCLE ASSESSMENT IN DEEP OPEN-PIT COPPER MINES

M. Heydari [1], M. Osanloo [1,*], A. Başçetin [2]

[1] *Amirkabir University of Technology, Mining Engineering Dept.*
*(*Corresponding author: morteza.osanloo@gmail.com)*
[2] *Istanbul University Cerrahpasa, Engineering Faculty, Mining Engineering Dept.*

ABSTRACT

While the consumption of copper is increasing worldwide, the depletion of near-surface deposits leads the future mining towards the exploitation of ore from greater depths. Although the transition from open-pit to underground method is an alternative, the last few years' experiences showed that the transition caused a reduction in production and income, an essential issue in low and medium-income countries. Deepening large open-pit mines is feasible due to the increasing price of copper and the growth of technology, leading to diverse environmental impacts. Limited studies surveyed the environmental impacts of deep open-pit copper mines. This study investigates these impacts to give an insight into the life cycle assessment of deep open-pit copper mines. Findings show that deepening the mine is accompanied by higher ground stress, rock strength, hydrology problems, temperature, stripping ratio, and lower grade. On the other hand, there is a higher production rate per employee, higher efficiency, higher recovery, and higher automation and mechanization possibility. Finally, deep open-pit mining will be expected shortly, and it is inevitable to increase knowledge about its environmental impacts in the path of green mining.

Keywords: Copper, deep open-pit, environmental impact assessment, life cycle assessment.

INTRODUCTION

Despite much attention to the problems of rock mechanics in deep mines, the definitions of "depth" and "deep mines" are disputed in the literature. The term "deep mining" is mainly used to refer to underground mines and is rarely referred to as open-pit mines. To date, open-pit mines with depths of more than 500 meters are considered deep open-pit mines (Rimmelin and Vallejos, 2020). Many large open-pit mines, especially metal porphyry mines, are expected to reach depths of more than 500m, and eventually, if the mine reserves are extended to depths near 1000m, open-pit mining operations may continue, or a decision may be made to move from the open-pit method to the underground. Transition experiences from open-pit to the underground have shown that production and income in these projects have decreased to one-third of the previous. In this study, a deep open-pit mine is referred to as expansion of the mineral continued to more than 1000m under the ground surface, while exploitation continues by the open-pit method (Heidari and Osanloo, 2021). Rimmelin and Vallejos (2020) estimated that in the future, more than 17% of existing open-pit mines would become deep open-pit mines with a depth of more than 1000 m, and insufficient knowledge of rock mass behavior at these depths is a significant challenge for the future of the mining industry.

Copper is the third most-produced metal globally after iron and aluminum (Torre and Espi, 2019) due to the high consumption of copper in various industries (Table 1). It has been observed that known copper reserves have increased about 25 times in the last century. Apart from successful explorations and price increases, the reasons for this tremendous growth can be traced to the natural mechanism for converting resources into reserves. Decreasing the average grade of copper mines over time, or the relationship between grade and tonnage, increases the number of extractable copper reserves. In addition, as technology has advanced, it has become possible to exploit these reserves at a much lower grade, at a lower cost, and with higher availability (Torre and Espi, 2019), which has a significant impact on energy consumption and global warming (Memary et al., 2012).

Table 1. Use of copper in Modern Industry in 2020

Usage of Copper in modern industry	Percentage
Electricity, electronics	21 %
Construction	43 %
Transportation equipment	19 %
Industrial machinery	7 %
Consumer and general products (coins, medicine)	10 %

Source: (https://www.statista.com/statistics/254870/use-of-copper-and-copper-alloys-in-the-us-by-purpose/) (2021)

In recent decades, the concept of responsible mining and green mining has risen to the world's knowledge and having an environmental impact assessment (EIA) as one of the first and essential steps for opening a mine has been confirmed. Among all the EIA models presented to date, the Life Cycle Assessment (LCA) model has been one of the most widely used models. As one of the methods of EIA after technical and economic assessment, LCA complements the third side of a sustainable assessment that helps to act environmental safety in addition to the technical and economic dimensions. The LCA makes it possible to estimate the cumulative environmental impacts of all project stages (Figure 1). The LCA process can help decision-makers choose the product or process with the most negligible environmental impact. Although EIA and LCA of mining projects have been quantified in various studies (Zhang et al., 2021a, Dong et al., 2020, Naseem et al., 2020, Saffari et al., 2019, Amirshenava and Osanloo, 2019, Heidari and Osanloo, 2018, Pahlevani and Osanloo, 2015) and some studies have examined specific aspects of the environmental impacts of mines, but a comprehensive study on the environmental effects of deep open-pit mines is missing. Since the depth of open-pit mines is expected to increase significantly in the coming decades, this paper examines and identifies the conditions of

deep open-pit mines and compares these conditions in the mining project's life cycle with those of shallow and medium depth open-pit mines.

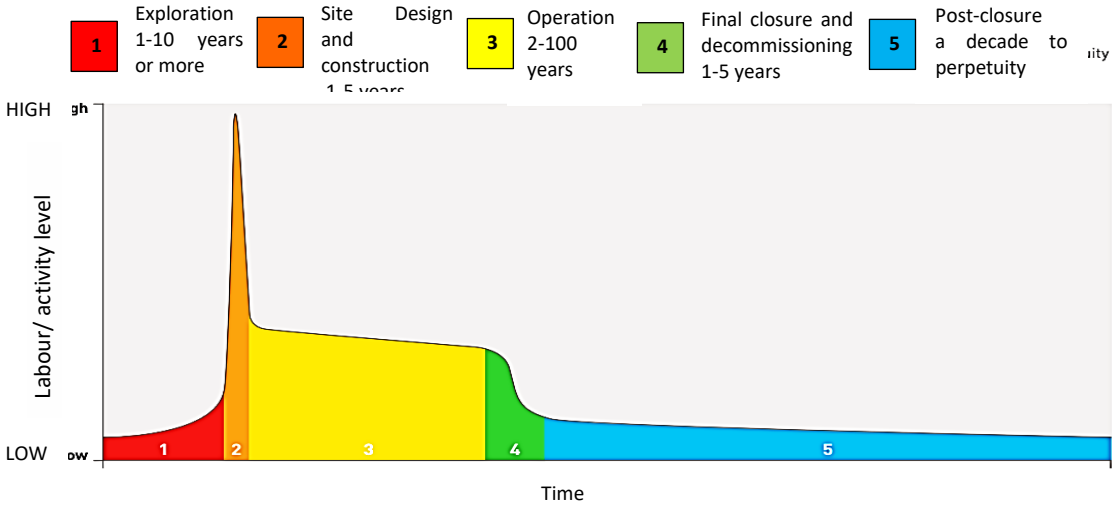

Figure 1. Life Cycle of a Mine Project (ICMM, 2012)

For this purpose, first, the existing studies on LCA of copper mines are reviewed. Next, the geological, geomechanical, and operational characteristics of deep open-pit mines are identified and categorized. The results of comparing the situation of deep open-pit copper mines by shallow and medium depth mines are discussed, and finally, the study's conclusions are highlighted.

LIFE CYCLE ASSESSMENT FACTORS OF A DEEP OPEN-PIT COPPER MINE

Various techniques are used to conduct EIA studies depending on the purpose of the project owners and the government, and the type of project. Each of these techniques has its advantages and disadvantage. LCA is one of the most accepted tools for EIA. In this method, the environmental impacts of a product or project will be measured by quantity. Therefore, many of the qualitative impacts are neglected. By investigating the LCA studies of copper mines from 2012 to 2021, 12 papers were available to the authors, 42% of which used the Recipe method, 33% the CML method, and 25% other LCA methods (Fig 2).

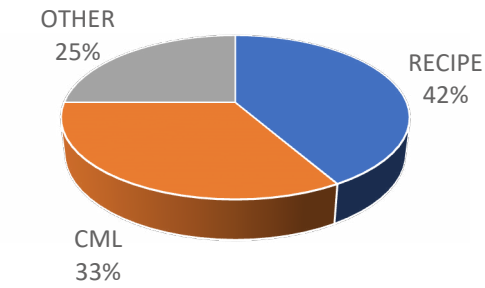

Figure 2. LCA methods used in copper EIA studies

The recipe method is the most completed and most used technique used in the mining industry LCA with 18 midpoint and three endpoint indicators, shown in fig 3. As seen in this figure, damage to human health, ecosystem and resource availability are the only aspects considered in this method. The pillars of a comprehensive sustainable development assessment are neglected: geological, geomechanical, operational, environmental, economic, and social. In addition, the conditions in deep open-pit mines are different from shallow and medium depth mines. If a standard EIA process is

developed, one of the first tasks is identifying the different sources of environmental impacts. In this study, the geological, geomechanical, and operational qualitative and quantitative factors, which should be considered in a comprehensive environmental impact assessment, were reviewed and determined.

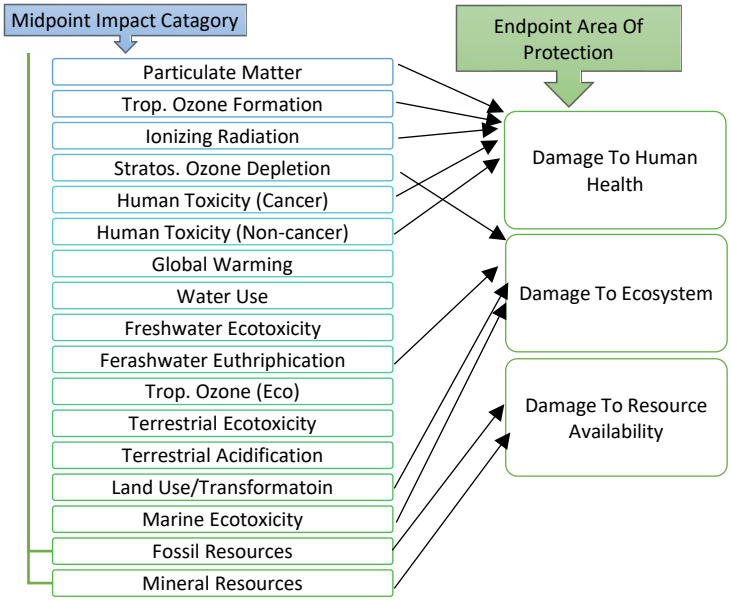

Figure 3. Outline of the impact categories covered in ReCiPe2 (Huijbregts et al., 2017).

Geomechanical and geological characteristics of deep open-pit copper mines

Figure 4 shows the geomechanical and geological factors that are significantly different in deep open-pit mines and shallow and medium depth mines, and some of the most important factors are explained in detail.

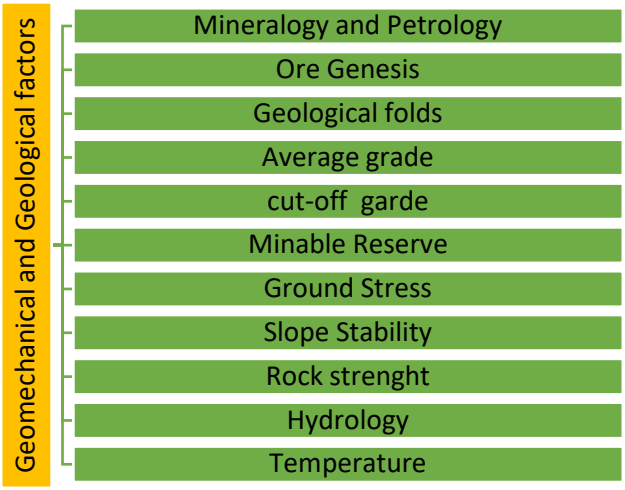

Figure 4. Differences of geomechanical and geological condition in deep open-pit mines with shallow and medium depth mines

Mineralogy and petrology

Copper porphyry deposits are large volumes (10 to 100 cubic kilometres) of modified hydrothermal rocks (Sillitoe, 2010). Mining and deep drilling in several large copper porphyry deposits

show that the mineral has a vertical depth of more than 2 km (Chuquicamata and Escondida in Chile and Grasberg in Indonesia). Mineralogy and petrology of a copper mineral deposit near the earth's surface differ from the depths and is highly dependent on the type of host rock and the characteristics of the magma. Host rocks to mineralization are invariably altered in varying degrees. Significant differences between mineralogy and petrology in different deposits relate primarily to significant differences in host-rock composition., carbonate rock skarns versus siliceous igneous and sedimentary rocks versus mafic igneous and sedimentary rocks. The degree of conversion of original rock to alteration ranges from the local and partial replacement of selected minerals to the complete conversion of all original minerals (Gustafson, 1978). Large sections of porphyry copper deposits in depth are mainly composed of potash alteration (Fig. 5) (Sillitoe, 2010).

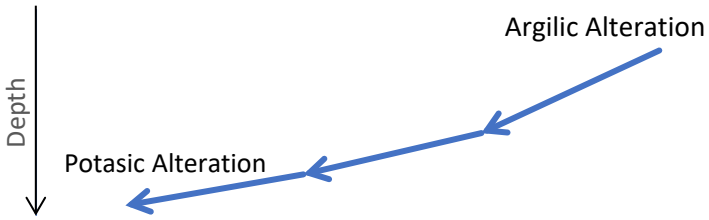

Figure 5 Porphyry copper deposit alteration with depth

Grade

The amount of copper in porphyry deposits is a function of the amount of magmatic liquids and the concentration of copper in these liquids (Chiaradia and Caricchi, 2017). Due to the increasing mining rate from copper mines in recent decades, copper's average and cut-off grade have decreased significantly (Dong et al., 2019). Many porphyry copper deposits form wide vertical dykes, and grades gradually decrease to the dyke boundaries and downward (Sillitoe, 2010). Therefore, increasing depth in open-pit mining will decrease the mineral grade, leading to more waste production, higher energy consumption in both mining and processing, and higher operational costs.

Ground Stress

Changes in the geomechanical characteristics of the rock mass at depth can be confirmed by considering the trend of the Geological Strength Index (GSI) and uniaxial compressive strength (UCS), and geological perception (Rimmelin and Vallejos, 2020). The Geological Strength Index (GSI) distribution for the Escondida copper open-pit mine shows an apparent variation of the GSI values between 625 and 650 m below the ground and estimates the sulfide boundary location. Deeper rock masses show higher GSI values and higher stress. There is a trend of GSI changes from higher potassic alteration values to lower argillic alteration values.

Rock Strength

The fracture mechanism defers as the depth increases. The fracture mechanism in deep mines is quasi-static, dynamic in shallow mines. He (2006) shows that rock strength generally increases with increasing depth. Intact rock strength is an indicator that can show the effects of changing the potash to argillic alteration to show the lowest strength in shallow mines and the highest strength in deeper mines. Rimmelin and Vallejos (2020) show that uniaxial compressive strength (UCS) for different rock types is directly related to the degree of alteration, which changes with depth.

Hydrology

Mining can be considered one of the most diverse industries interacting with water resources. Mining occurs in the full range of hydrological conditions: from the arid regions to the tropics and the polar regions. Climate and hydrology determine the infrastructure requirements of mining operations and profoundly affect the nature of risks related to mining water and adjacent communities, ecosystems, and industry (Northey et al., 2016). The effect of water on rock mass stability is significant due to geological disasters and hazards such as karst failure, water influx, landslides, and dam instability. Ali et al. (2021) state that the strength of rock decreases with increasing water content, leading to increased plasticity. In addition, the mechanical properties of the rocks are affected by the water content, which leads to a decrease in uniaxial compressive strength (UCS), elastic modulus and tensile strength. As the open-pit mine deepens, the bottom pit approaches the static level of water. Unexpected water flow in deep mines can lead to reduced production, delays in operations, environmental problems, and endanger the safety of the entire mine. The presence of water increases drilling and blasting costs and necessitates waterproof explosives. It also reduces the efficiency of machinery (due to the transport of wet ore and consequently high diesel fuel consumption and increased maintenance costs associated with tires and equipment), reduces the workforce's efficiency, and increases the number of accidents and electrical problems. Also, the water pressure behind the mine walls causes the instability of bench walls. On the other hand, wet mine conditions lead to wear and tear and early equipment depreciation (Bahrami et al., 2016).

Temperature

Table 2 shows that in terms of mineralization, copper can be formed from near the earth's surface to the depths of the earth's crust, and at great depths, the earth's temperature will change significantly.

Table 2. Sorting earth crust metals based on depth and temperature (Arndt et al., 2015)

Type	Metals	Temperature (^{o}C)	Depth
Telethermal	Pb, Zn,Cd,Ge	±100	Near Surface
Epithermal	Pb, Zn, Au, Ag, Hg, Sb, **Cu**, Se, Bi, U	50-200	Near Surface – 1.5 Km
Mesothermal	Au, Ag, **Cu**, As, Pb, Zn, Ni, Co, W, Mo, U, etc	200-300	1.5 km – 4.5 km
Hypothermal	Au, Sn, Mo, W, **Cu**, Pb, Zn, As	300-600	3 km - 15 km

Studies have shown that with a change in temperature of 1°C, rock stress changes from 0.4 to 0.5 MPa, and these stress changes significantly affect the mechanical behavior of rock mass (He, 2006). As a result, temperature changes will significantly affect rock stress, slope stability, drilling, and blasting operations in deep open pits. Most rocks are brittle at low temperatures and fracture sooner, in which most of the strain before fracture is reversible (elastic). As the temperature increases, the elastic part of the strain gradually decreases and the share of plastic strain increases. Most rocks are associated with decreased strength and increased ductility (Liu and Jin, 2014). Also, the studies show that the geothermal gradient is 40^{o}C in depth.

Operating characteristics of deep open-pit copper mines

Figure 6 shows the operational factors that are significantly different in deep open-pit mines and shallow and medium depth mines, and each of these factors is discussed in detail as follows.

Stripping ratio

The stripping ratio is the amount of overburden tonnage removed per ton of ore. High stripping ratios occur due to the higher depth of open-pit mines, intending to create space for access to the working benches (Sakantsev et al., 2014). the deeper the final pit limit, the more overburden must be extracted to mine a specific volume of ore. In other words: increasing the depth is associated with increasing the stripping ratio, and this amount in deep open-pit mines can reach tens of millions of cubic meters of overburden. This leads to higher stripping costs in deep open-pit mines. Therefore, this parameter is one of the most influential economic factors in choosing the final pit limit. The final open-pit limit is determined based on the break-even stripping ratio (BESR) (Eq. 1):

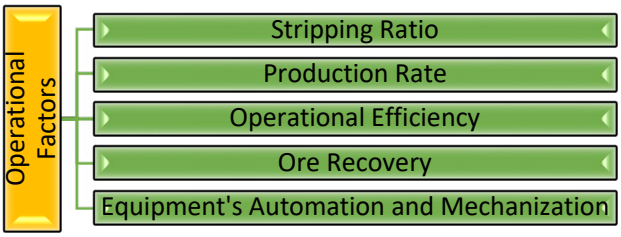

Figure 6. Differences of operational condition in deep open-pit mines with shallow and medium depth mines

$$\mathrm{BESR} = \frac{10\ \mathrm{R.g.y} - (\mathrm{b} + \mathrm{c})}{\mathrm{a}} \qquad (1)$$

Where
R is the price of the final product (per kilogram),
g is grade,
y is the amount of metal recovery in the concentration, smelting and refining stages,
a is the cost of stripping one ton of overburden,
b is mining cost of one ton of ore,
and c is the cost of processing, smelting, refining, and transporting the final product to the market.

In Equation (1), BESR has a direct relation to grade (which decrease by depth) and inverse relation with stripping costs (which increases by depth). Therefore, the price of copper must be higher in the future than these days for deep open-pit mines.

Production rate

Production rates are usually not fixed over the operation's life, and the decision to increase or decrease rates depends on many factors, including economic conditions and reserve tonnage. Most mining engineers use a single rate with a fixed commodity price. Production rate is inversely related to mine life. The higher the production rate, the shorter the life of the mine. A higher production rate produces a more significant annual net profit for a shorter period, and a lower production rate produces a lower annual net profit for a more extended time. The shallower the open-pit mine, the lower the production rate can be considered to maximize mine life. Taylor (1986) developed an equation for estimating mine life based on reserve tonnage, known as Taylor's law (Eq. 2&3) :

$$T = 0.2\ (M)^{0.25} \qquad (2)$$

$$Production\ Rate\ \left(\frac{mt}{day}\right) = \frac{M}{T \times Od} \qquad (3)$$

where T is the mine life, M is the total mineable reserve in metric tons, and Od is the number of working days in one year. However, Taylor's law has limitations on several factors such as transportation

capacity, mine depth and reserve geometry (Salama et al., 2017). With the open-pit mine final depth increase, mine life increases and by mine deepening and the use of high capacity machinery and advanced technology, a higher production rate can be considered for the mine. A higher production rate results in lower operating costs, while the shorter mine life maximizes the NPV of the operation. However, a higher production rate involves a superior capital cost as greater equipment and infrastructure is required.

Operation Efficiency

Operation efficiency mainly includes the efficiency of drilling, blasting, loading, and hauling. The performance of new mining machines has increased significantly due to better designs and experimental facilities, but the useful life and maintenance time has not changed much (Misita et al., 2021). The explosives effectiveness depends on many parameters, such as the holes diameter, the time between charging and blasting, the method of explosion starting, the rock mass temperature, and the conditions of the charging units (Mertuszka et al., 2020). the higher the efficiency of the operation, the lower the operating costs and environmental damage. The efficiency of deep open-pit mines using high-capacity technology and machinery is higher than that of shallow open-pit mines.

Mineral Recovery

Mineral recovery ratio can be expressed with the Eq. (4-6) as follows (Zhang et al., 2021b):

$$R_s = \frac{W_{out}}{W_{rcs}} \times 100\% \quad (4)$$

$$R_m = \frac{W_{out}}{W_{rcv}} \times 100\% \quad (5)$$

$$R_p = \frac{W_p}{W_{out}} \times 100\% \quad (6)$$

Where
R_s is the mineral recovery ratio in the resource,
W_{out} is the mineable deposit,
W_{rcs} is the remained deposit in the resource,
R_m is the mineral recovery percentage in the mining stage,
W_{rcv} is the remained deposit in the reserve,
R_p is the mineral recovery percentage at the processing stage,
and W_p is the production at the processing stage.

Resource recovery depends on many factors such as production planning, mining method, geological and geotechnical conditions, geological explorations, drilling and blasting plans, grade control, seismic events, rock bursting, and production, price, and management.

Equipment's Automation and Mechanization

Mining technologies have evolved and improved over time. Today, the mining sector faces technological and digital innovations. "Automation", "robotics", "Internet of Things", "big data", "real-time data", "machine learning", "artificial intelligence" and "3D printing" are key technologies for the mining industry. However, the use of technology and digital technologies largely depends on the production. Deeper mines appear to select and employ technologies tailored to their needs, while

operations with lower production rates do not implement existing digital tools and hardware technologies to the same extent (Barnewold and Lottermoser, 2020). Internationally the focus of mining automation and mechanization tools and technics has been in large-scale mines: large capital is deployed, and ensuring its effective use by increasing production scale is essential. However, these machines and tools have high capital and operating costs, and significant non-mining technical skills are needed to install and maintain them (Aguirre-Jofré et al., 2021).

RESULTS AND DISCUSSION

By comparing the factors assessed in this study (Figures 4 & 7) with the factors studied in LCA Recipe studies (Figure 3), it can be seen that many essential factors in the LCA studies are ignored. Table 4 shows the parameters set for a complete environmental assessment model in the columns and the LCA studies performed in the rows. According to this table, so far, no researcher has provided a complete assessment of the geological, geomechanical, and operational conditions of deep open-pit copper mines. Tables 5 and 6 show the results of comparing the situation in deep open-pit copper mines by shallow and medium depth mines.

Table 4. Parameters assessed in LCA studies of copper mines by different researchers (2012-2021)

Factor / Scientist	Mineralogy and Petrology	Ore Genesis	Geological folds	Average grade	cut-off grade	Minable Reserve	Ground Stress	Slope Stability	Rock Strength	Hydrology	Temperature	Stripping Ratio	Operational Efficiency	Ore Recovery	Mechanization Automation and Mechanization
(Zhang et al., 2021a)															
(Dong et al., 2020)															
(Islam et al., 2019)															
(Kuipers et al., 2018)															
(Hong et al., 2018)															
(Song et al., 2017)															
(Beylot and Villeneuve, 2017)															
(Kulczycka et al., 2016)															
(Wang et al., 2015)															
(Song et al., 2014)															
(Memary et al., 2012)															
(Vieira et al., 2012)															

CONCLUSION

In today's world, the use of minerals for the advancement and growth of life is inevitable. However, what matters is mining in line with sustainable development goals. To this end, mining companies should, in addition to technical and economic assessments, include environmental impact assessments from the initial stages of project design on their agenda. Mine planners have used many models for EIA of mines. The LCA method is one of the widely used EIA methods with limited application in the mining sector. The reason for this is the wide range of mining activities, the problems of collecting

the necessary data to perform life cycle assessment, and the inability of this method to take into account qualitative factors. This becomes especially important as the existing open-pit mines go deeper in the future. The lack of an environmental assessment model that examines the condition of deep open-pit mines will pose numerous challenges for engineers. For this purpose, the geological, geomechanical, and operational condition of deep open mines was evaluated in this study. Identifying these factors is the first step in designing a comprehensive environmental impact assessment model.

Table 5. Comparing geomechanical and geological conditions in deep open-pit mines with shallow and medium depth open-pit mines

	Impacting factor	**Details**	**Condition in shallow and medium depth open-pit mines**	**Condition in Deep open-pit mines**
Geomechanical and Geological Factors	Mineralogy and Petrology	The mineralogical composition of a copper mineral deposit near the surface is different from the depths.	The argillic alteration forms near the surface.	The potassic alteration occurs in depths.
	Ground stress	The deeper the mine, the greater the ground stress.	Lower	Higher
	Rock strength	The deeper the mine, the greater the Rock strength.	Lower	Higher
	Hydrology	As the depth of the mine increases, water problems become more acute due to the approach to the aquifer surface.	Lower	Higher
	Temperature	The geothermal gradient is 30^{o}C at low depths and 40^{o}C at about 1000 meters.	Lower	Higher
	Grade	Grade of porphyry copper decrease to the boundary and depth of the deposit	Higher	Lower

Table 6. Comparing operational conditions in deep open-pit mines with shallow and medium depth open-pit mines

	Impacting factor	**Details**	**Condition in shallow and medium depth open-pit mines**	**Condition in Deep open-pit mines**
Operational factors	Stripping Ratio	The depth of mining has a direct influence on the SR.	Lower	Higher
	Production rate	Production rate is inversely related to mine life and directly related to minable reserve tonnage.	Lower	Higher
	Operation efficiency	Operation efficiency mainly includes the efficiency of drilling, blasting, loading, and hauling.	Lower	Higher
	Ore recovery	The ore recovery in open-pit mines varies according to the deposit's geometry and slope stability.	Higher	Lower
	Equipment's Automation and Mechanization	The use of automation and digital technologies largely depends on production.	Lower	Higher

REFERENCES

Aguirre-Jofré, H., Eyre, M., Valerio, S., Vogt, D. (2021). Low-cost internet of things (IoT) for monitoring and optimising mining small-scale trucks and surface mining shovels. *Automation in Construction,* 131**,** 103918.

Ali, M., Wang, E., Li, Z., Jia, H., Li, D., Jiskani, I. M., Ullah, B. (2021). Study on Acoustic Emission Characteristics and Mechanical Behavior of Water-Saturated Coal. *Geofluids,* 2021.

Amirshenava, S., Osanloo, M. (2019). A hybrid semi-quantitative approach for impact assessment of mining activities on sustainable development indexes. *Journal of Cleaner Production,* 218**,** 823-834.

Arndt, N., Kesler, S., Ganino, C. (2015). *Metals and society: An introduction to economic geology*, Springer.

Bahrami, S., Ardejani, F. D., Baafi, E. (2016). Application of artificial neural network coupled with genetic algorithm and simulated annealing to solve groundwater inflow problem to an advancing open pit mine. *Journal of Hydrology,* 536**,** 471-484.

Barnewold, L., Lottermoser, B. G. (2020). Identification of digital technologies and digitalisation trends in the mining industry. *International Journal of Mining Science and Technology,* 30**,** 747-757.

Beylot, A., Villeneuve, J. (2017). Accounting for the environmental impacts of sulfidic tailings storage in the Life Cycle Assessment of copper production: A case study. *Journal of Cleaner Production,* 153**,** 139-145.

Chiaradia, M., Caricchi, L. (2017). Stochastic modelling of deep magmatic controls on porphyry copper deposit endowment. *Scientific reports,* 7**,** 1-11.

Dong, D., Van Oers, L., Tukker, A., Van Der Voet, E. (2020). Assessing the future environmental impacts of copper production in China: Implications of the energy transition. *Journal of Cleaner Production,* 274**,** 122825.

Dong, L., Tong, X., Li, X., Zhou, J., Wang, S., Liu, B. (2019). Some developments and new insights of environmental problems and deep mining strategy for cleaner production in mines. *Journal of Cleaner Production,* 210**,** 1562-1578.

Gustafson, L. (1978). Some major factors of porphyry copper genesis. *Economic Geology,* 73**,** 600-607.

He, M. 2006. Rock mechanics and hazard control in deep mining engineering in China. *Rock Mechanics In Underground Construction: (With CD-ROM).* World Scientific.

Heidari, M., Osanloo, M. Sustainability Assessment of Angouran Lead and Zinc Mining Complex. Proceedings of the 27th International Symposium on Mine Planning and Equipment Selection-MPES 2018, 2018 Santiago, Chile. Springer, Cham, 523-534.

Heidari, M., Osanloo, M. (2021). A review of environmental impact assessment (EIA) and life cycle assessment (LCA) methods in the mining project. *The second national conference on Data Mining in Earth sciences.* Arak, Iran.

Hong, J., Chen, Y., Liu, J., Ma, X., Qi, C., Ye, L. (2018). Life cycle assessment of copper production: a case study in China. *The International Journal of Life Cycle Assessment,* 23**,** 1814-1824.

Huijbregts, M. A., Steinmann, Z. J., Elshout, P. M., Stam, G., Verones, F., Vieira, M., Zijp, M., Hollander, A., Van Zelm, R. (2017). ReCiPe2016: a harmonised life cycle impact assessment method at midpoint and endpoint level. *The International Journal of Life Cycle Assessment,* 22**,** 138-147.

Icmm 2012. Role of mining in national economies. *Mining's contribution to sustainable development* International Council on Mining and Metals.

Islam, K., Vilaysouk, X., Murakami, S. (2019). Integrating remote sensing and life cycle assessment to quantify the environmental impacts of copper-silver-gold mining: A case study from Laos. *Resources Conservation and Recycling,* 154**,** 104630.

Kuipers, K. J., Van Oers, L. F., Verboon, M., Van Der Voet, E. (2018). Assessing environmental implications associated with global copper demand and supply scenarios from 2010 to 2050. *Global Environmental Change,* 49**,** 106-115.

Kulczycka, J., Lelek, Ł., Lewandowska, A., Wirth, H. & Bergesen, J. D. 2016. Environmental impacts of energy-efficient pyrometallurgical copper smelting technologies: The consequences of technological changes from 2010 to 2050. *Journal of Industrial Ecology,* 20**,** 304-316.

Liu, Z., Jin, D. Experimental research of rock strength and permeability characteristics under different confining and hydraulic pressure. 12th International Mine Water Association Congress (IMWA 2014): An Interdisciplinary Response to Mine Water Challenges, 2014. 183-186.

Memary, R., Giurco, D., Mudd, G. & Mason, L. 2012. Life cycle assessment: a time-series analysis of copper. *Journal of Cleaner Production,* 33**,** 97-108.

Mertuszka, P., Szumny, M., Fuławka, K. & Nikolov, S. 2020. Field evaluation of mine blasting efficiency. *SWS Journal of Earth and Planetary Sciences,* 2**,** 1-16.

Misita, M., Brkić, V. S., Brkić, A., Kirin, S., Rakonjac, I. & Damjanović, M. 2021. Impact of Downtime Pattern on Mining Machinery Efficiency. *Structural Integrity and Life,* 21**,** 29-35.

Naseem, S., Fu, G. L., Mohsin, M., Rehman, M. Z.-U. & Baig, S. A. 2020. Semi-Quantitative Environmental Impact Assessment of Khewra Salt Mine of Pakistan: an Application of Mathematical Approach of Environmental Sustainability. *Mining, Metallurgy & Exploration,* 37**,** 1185-1196.

Northey, S. A., Mudd, G. M., Saarivuori, E., Wessman-Jääskeläinen, H. & Haque, N. 2016. Water footprinting and mining: Where are the limitations and opportunities? *Journal of Cleaner Production,* 135**,** 1098-1116.

Pahlevani, D., Osanloo, M. 2015. Resumption of Deep Open-Pit Mining as a Future Challenge. *Application of Computers and Operations Research in the Mineral Industry (APCOM): Proceedings of the 37th International Symposium.* USA.

Rimmelin, R., Vallejos, J. 2020. *Rock mass behaviour of deep mining slopes: a conceptual model and implications*.

Saffari, A., Ataei, M., Sereshki, F., Naderi, M. 2019. Environmental impact assessment (EIA) by using the Fuzzy Delphi Folchi (FDF) method (case study: Shahrood cement plant, Iran). *Environment, Development and Sustainability,* 21**,** 817-860.

Sakantsev, G. G., Sakantsev, M. G., Cheskidov, V. I., Norri, V. K. 2014. Improvement of deep-level mining systems based on optimization of accessing and open pit mine parameters. *Journal of Mining Science,* 50**,** 714-718.

Salama, A., Nehring, M., Greberg, J. 2017. Financial analysis of the impact of increasing mining rate in underground mining, using simulation and mixed integer programming. *Journal of the Southern African Institute of Mining and Metallurgy,* 117**,** 365-372.

Sillitoe, R. H. 2010. Porphyry copper systems. *Economic geology,* 105**,** 3-41.

Song, X., Pettersen, J. B., Pedersen, K. B., Røberg, S. 2017. Comparative life cycle assessment of tailings management and energy scenarios for a copper ore mine: A case study in Northern Norway. *Journal of Cleaner Production,* 164**,** 892-904.

Song, X., Yang, J., Lu, B., Li, B., Zeng, G. 2014. Identification and assessment of environmental burdens of Chinese copper production from a life cycle perspective. *Frontiers of Environmental Science & Engineering,* 8**,** 580-588.

Torre, L. D. L., Espi, J. A. 2019. Making sense of the geology in the copper mining economy. *Boletin Geologico y Minero,* 130**,** 133-159.

Vieira, M. D. M., Goedkoop, M. J., Storm, P., Huijbregts, M. A. J. 2012. Ore Grade Decrease As Life Cycle Impact Indicator for Metal Scarcity: The Case of Copper. *Environmental Science & Technology,* 46**,** 12772-12778.

Wang, H. T., Liu, Y., Gong, X. Z., Wang, Z. H., Gao, F., Nie, Z. R. Life cycle assessment of metallic copper produced by the pyrometallurgical technology of China. Materials Science Forum, 2015. Trans Tech Publ, 559-563.

Zhang, W., Li, Z., Dong, S., Qian, P., Ye, S., Hu, S., Xia, B., Wang, C. 2021a. Analyzing the environmental impact of copper-based mixed waste recycling-a LCA case study in China. *Journal of Cleaner Production,* 284**,** 125256.

Zhang, Z.-X., Hou, D.-F., Aladejare, A., Ozoji, T., Qiao, Y. 2021b. World mineral loss and possibility to increase ore recovery ratio in mining production. *International Journal of Mining, Reclamation and Environment***,** 1-22.

LONG TERM PRODUCTION SCHEDULING OPTIMIZATION IN AN UNDERGROUND PB/ZN MINE

M. Shenavar[1], M. Ataee-pour[1], M. Rahmanpour[1]

[1]Department of Mining and Metallurgical Engineering, Amirkabir University of Technology, Tehran, Iran
*(*Corresponding author:m_shenavar@aut.ac.ir)*

ABSTRACT

Production scheduling optimization in mining activities has a significant effect on mining economics. In general, production scheduling in the mining process includes long-term, medium-term, and short-term scheduling. Long-term production scheduling is a strategic plan for mining operations. In contrast, the medium-term mine production schedule provides an operational scheme for mining while tracking the strategic plan, and it is also divided into short-term periods. In this paper, a mathematical optimization framework based on integer linear programming (IP) models is developed for long-term production scheduling in an underground Pb/Zn mine with the sublevel-caving method. Sublevel caving is one of the main underground mining methods for hard rock mining, and limited studies have been done about its long-term production scheduling. The objective of this mathematical model is the maximization of the net present value (NPV) of the mining process. The model contains acceptable technical and operational constraints of the sublevel caving method. The model was applied on an economic block model of the Gooshfil Pb/Zn mine, and the maximum NPV is determined. Comparing the results with the conventional scheduling method shows a 14% increase in NPV of the operation.

Keywords: Underground Mining, Production Scheduling, sublevel-caving method, NPV

INTRODUCTION

Optimization of production scheduling is a key aspect for both surface and underground mines that in the underground mines has received less attention than in the surface mines. This is due mainly to the diversity of underground mining methods and the complexity of underground mining parameters. The open-pit mining method has great importance among surface mining methods, and there are many studies to optimize this method that; over the past decades, there have been many gains in this regard. Today, optimization in the open-pit mines is an integral part of designing and planning. Optimization of the ultimate mine limit and production planning in other surface mining methods has not improved so much. Studies on optimization and planning in these methods are very limited and primitive (Shenavar et al., 2018). The algorithms of pit limit optimization are numerous and more than the algorithms available for underground methods. The true optimum solution is guaranteed for the pit limit optimization, and several computer packages are available to the industry. However, only a few algorithms have been developed to optimize ultimate stope boundaries in underground mines (Ataee-pour M., 2005).

Production scheduling defines the mining sequence and the tonnages and grades to be mined throughout the mine life. The scheduling problems are usually complex due to the nature and variety of the constraints (Pourrahimian Y., 2013). Long, medium and short-term are three-time horizons for production scheduling. The long-term mine production scheduling provides a strategic plan for the mining operations. In contrast, the medium-term mine production schedule provides an operational scheme for mining while tracking the strategic plan. Medium-term schedules include more detailed information that allows for a more accurate design of ore extraction from a special area of the mine or

information that would allow for necessary equipment substitution or the purchase of needed equipment and machinery. The medium-term schedule is also divided into short-term periods. A long-term production schedule contains fewer details than a short-term plan. However, a long-term plan includes clear definitions of mining reserves, production sequence, and production rate.

Various models have been developed to optimize the production planning in underground mining methods, and in general, none of these models have been commercialized. Most of them are short-term planning models with the objective of minimizing production deviations from the existing manual non-optimized long-term program (Williams et al., 1973; Gillenwater, 1988; Chanda, 1990; Jawed, M. 1993; Winkler, 1998; Topal, 2003; Rahal et al., 2003; Rubio and Diering, 2004; Kuchta et al., 2004; Sarin and Hansen, 2005; Newman and Kuchta, 2007). Some of these models are formulated for a specific mining operation, and they must be modified before applying to other cases (Carlyle and Eaves, 2001; McIsaac, 2005). Some models do not have real optimal solutions, which are some expert-oriented search-based methods (Fava et al., 2013; O'Sullivan and Newman, 2015; Magda, 1994; Whitchurch et al., 1996). In developing these underground mining production scheduling models, various objective functions are presented, such as profit maximization (Epstein et al., 2003) and project time minimization (Zimmermann, 2010). Recently some models have been developed with the objective function of NPV maximization for long-term production scheduling (Pourrahimian, Y., 2013; Shenavar et al., 2020).

Caving methods are favored among underground mining methods because of their low cost and high production rates. One of these methods is the sub-level caving method, which has gained popularity in hard rock mining methods due to its low operating cost and high productivity. There are limited studies about its long-term production schedule optimization. In this paper, a mathematical model is presented to sublevel caving production scheduling with the objective of NPV Maximization, and it is applied on a Pb/Zn mine of Iran.

MATERIAL AND METHODS

A new mathematical production scheduling model is developed for the sublevel caving method in this paper, and it is applied on the Gooshfil Pb/Zn mine of Iran. The floating stope optimizer is used to determine ultimate stope boundaries, and, in this section, the used material and methods are defined.

Floating Stope Optimizer

Floating Stope is a technique implemented in the DATAMINE package (Mineral Industries Computing Limited) to determine an ore reserve's optimal limits (boundaries), which may be economical to be extracted by underground mining methods. The general concept of the floating stope approach was outlined in 1995 as a search-based and heuristic approach, analogous to the Moving Cone method for pit limit optimization (Alford, C., 1995).

The term Floating Stope is derived from the technique of floating a minimum stope shape through the ore body and evaluating the grade of material inside the stope at any position. In that regard, two envelopes will be created. The maximum envelope is the union of all possible economic stope positions, while the minimum envelope is found by taking the union of all best grade stope positions for every ore block in the ore body. The envelopes provide a limit for the engineer to design final stope positions, with the recommendation that the minimum envelope should be used as the guide in the first instance.

Sublevel Caving Mining Method

Sublevel Caving is one of the most advanced mining methods. This method is usually undertaken when mining the ore body through an open pit is no longer economically viable. In Sublevel Caving,

mining starts at the top of the ore body and develops downwards. Ore is mined from sublevels spaced at regular intervals throughout the deposit (Figure 1). A series of ring patterns is drilled and blasted from each sublevel, and the broken ore is mucked out after each blast. Sublevel Caving can be used in ore bodies with very different properties, and it is an easy method to mechanize. This method is normally used in massive, steeply-dipping ore bodies with considerable strike length. In this method, dilution and ore loss are usually high.

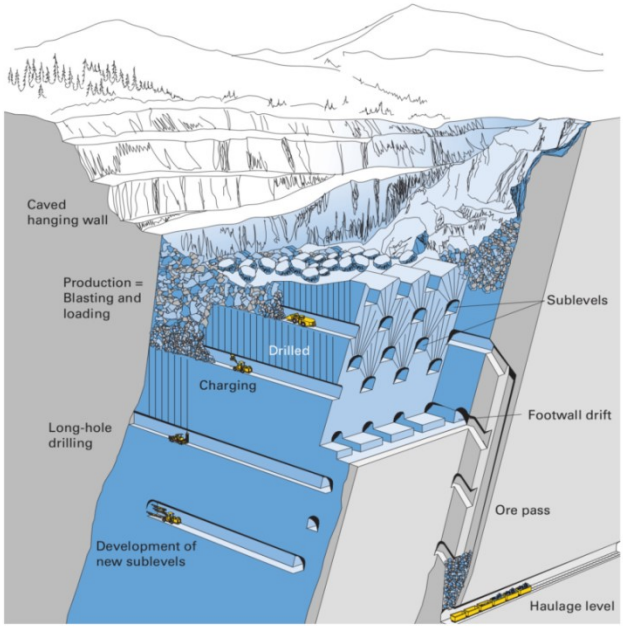

Figure 1 .Sublevel caving method

Gooshfil Pb/Zn Mine of Iran

Gooshfil Pb/Zn mine is located in the central part of Iran. It is an underground mine that operates with a sublevel caving method. Gooshfil mine was an open-pit mine until 2006. After that, because of the ore body depth, it changed to an underground mine with a sublevel caving method. This mine has an annual production capacity of 300,000 tons.

PROBLEM DEFINITION

The sublevel caving method is used in orebodies with very different properties, and it is easy to mechanize. Sublevel caving is used to mine large steeply dipping tabular or massive orebodies. In this method, the ore is extracted via sublevels which are developed in the orebody at regular vertical spacing. Each sublevel has a systematic layout of parallel drifts, along with or across the orebody. In this method, mining starts at the top of the ore body and develops downwards. Ore is mined from sublevels spaced at regular intervals throughout the deposit. A series of ring patterns is drilled and blasted from each sublevel, and the broken ore is mucked out after each blast. The mining cycle is illustrated in Fig. 2.

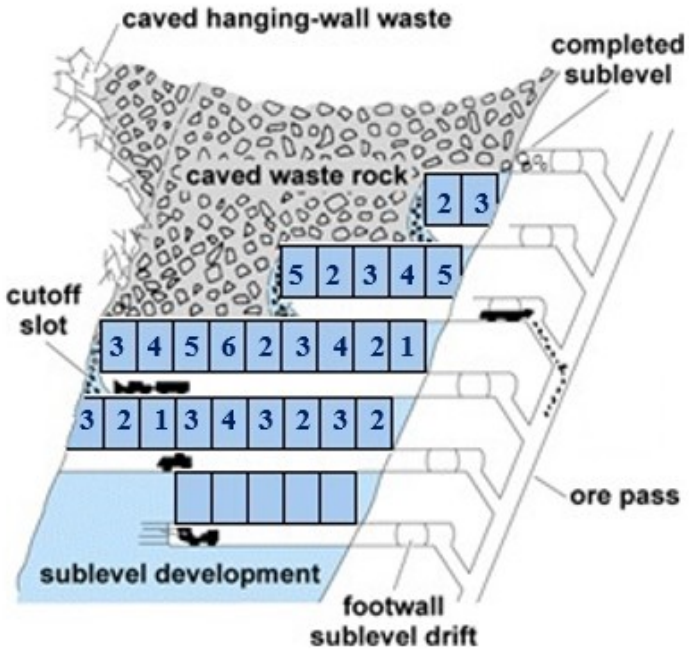

Figure 2 . Sublevel caving sequencing

As shown in Fig. 2, if the numbers inside each block represent the economic value of that block different NPVs are achievable for various mining sequences, so it shows that the production scheduling with the objective of maximizing NPV is applicable for the sublevel caving method. This shows the importance of production scheduling in reaching the objective of NPV maximization and satisfying the mining constraints.

In Fig. 3(a), the three-dimensional model of a cylindrical ore reserve near the surface part was mined by the open-pit method is shown schematically. As shown in Fig. 3 (b) and (c), sublevel openings can be excavated from different directions, and therefore, it is possible to extract this reserve in different directions. So, it is clear that development direction and production sequencing can make different NPVs for the mining operation. So, different NPVs are achievable for various mining sequences, and the production scheduling with the objective of NPV maximization is applicable for the sublevel caving method. In order to optimize the mining sequence, a new mathematical model is presented in this study that is suited for sublevel caving operations.

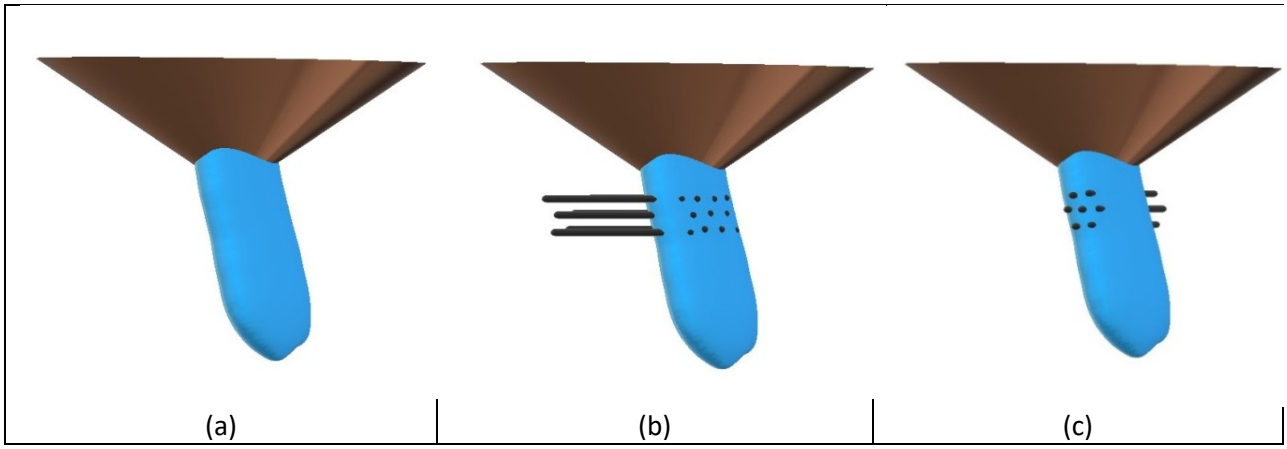

Figure 3. A hypothetical block model

MATHEMATICAL MODEL

The long-term production scheduling plan of the sublevel mining method with the objective of maximizing the NPV of the mining process is formulated within an integer linear programming framework. The schematic block model in three-dimensional space is shown in figure 4.

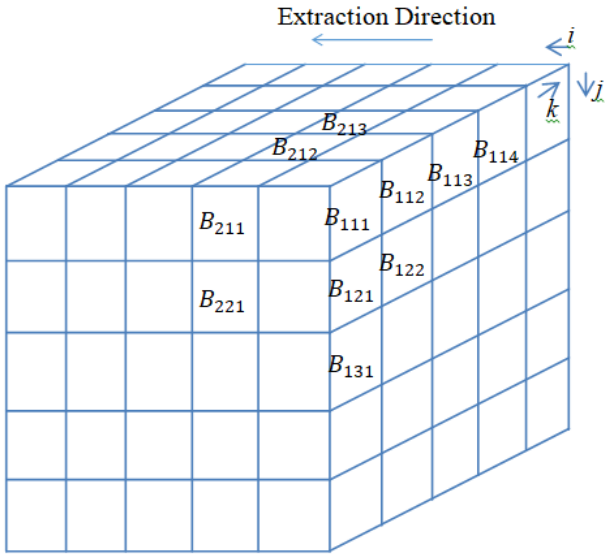

Figure 4. Schematic block model in three-dimensional space

Sets, Parameters and Decision Variable

- *I:* the number of blocks in x coordinate (Fig. 4),
- *J:* the number of blocks in z coordinate (Fig. 4),
- *K:* the number of blocks in y coordinate (Fig. 4),
- *T:* the number of scheduling periods,
- $B_{i,j,k}$: the block located in horizontal location *i* and vertical location *j*
- $P_{i,j,k}$: the amount of rock in block $B_{i,j,k}$
- $BEV_{i,j,k}$: the economic value of $B_{i,j,k}$,
- *d:* discount rate,
- *ppy (production per year):* the maximum annual production capacity.
- $x_{i,j,k,t} = \begin{cases} 1 & \text{If } B_{i,j,k} \text{ to be extracted in period } t \\ 0 & \text{Otherwise} \end{cases}$

Objective Function

The objective function of the model for maximizing mining operation NPV is given in Eq. 1.

$$\sum_{i=1}^{I}\sum_{j=1}^{J}\sum_{k=1}^{K}\sum_{t=1}^{T}\frac{BEV_{i,j,k}}{(1+d)^t}\times x_{i,j,k,t} \qquad (1)$$

Constrains

Two sets of constraints are taken into consideration. The first set is related to reserve and production capacity, and the second set deals with the sequence of blocks extraction in different coordinates. The constraints are given in Eq. 2-5.

$$\sum_{t=1}^{T} x_{i,j,k,t} \leq 1 \qquad \forall\ i=(1,\dots,I);\ j=(1,\dots,J);k=(1,\dots,K);\ t\in T \tag{2}$$

$$\sum_{i=1}^{I}\sum_{j=1}^{J}\sum_{k=1}^{K} P_{i,j,k}\, x_{i,j,k,t} = ppy \qquad \forall\ t \in T \tag{3}$$

$$x_{i+1,j,k,t'} \leq x_{i,j,k,t} \qquad \forall\ i=(1,\dots,I);\ j=(1,\dots,J);k=(1,\dots,K);\ t,t'\in T;\ t'\leq t \tag{4}$$

$$x_{i-2,j+1,k,t'} \leq x_{i,j,k,t} \qquad \forall\ i=(1,\dots,I);j=(1,\dots,J);k=(1,\dots,K);\ t,t' \in T;\ t' \leq t \tag{5}$$

In this model, Eq. 2 is the reserve constraint and ensures that each block to be mined ones. Eq. 3 controls production capacity, and it ensures that the number of blocks that must be mined each year does not exceed the predetermined capacity. Eqs. 4 and 5 are the most important technical and operational constraints in the sublevel caving method, and they are related to the sequence of blocks extraction. They are originated from the roof caveability. According to the principles of the sublevel caving method, extraction of some blocks involves the extraction of some other blocks, which is called precedence constraints (Eq. 4-5). For direction i, the constraint is given in constraint 4. According to this constraint for example extraction of block B_{212} involves the extraction of block no. B_{112}. For the direction k, extraction of block B_{122} involves the extraction of blocks B_{111},B_{112} and B_{113} which is given in Eq. 5. It should not be forgotten that the precedence of the extraction of blocks discussed in these constraints is affected by roof caveability and geomechanical parameters, which is unique in each mining operation and it must be determined for different mines.

APPLING THE MODEL

The presented MILP model (Eq. 1-5) is generated using the MATLAB programming platform. The model is applied on the Gooshfil mine block model. As mentioned before, Gooshfil is an underground Pb/Zn mine located in the central part of Iran. The annual production capacity of the mine is 300,000 tons, and the geometry of the sublevel mining method is shown in Figure 5.

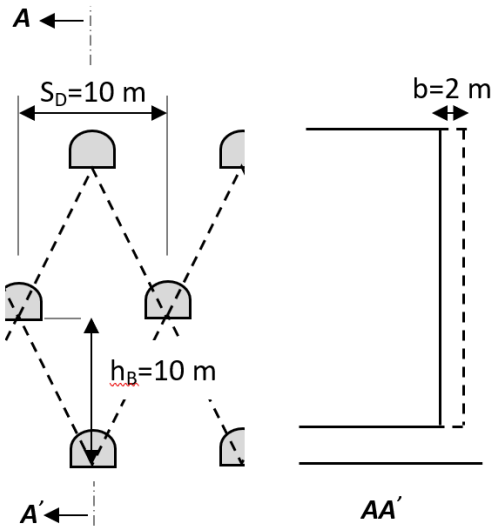

Figure 5. Geometry of the sublevel mining method in Gooshfil mine

As shown in fig.1, the horizontal distance between the sublevel drifts (S_D) is 10 meters, the vertical distance between the sublevels (h_B) is 10 meters, the height of the mining stopes is 20 meters and the depth of extraction sections (fired sections in each stage) is 2 meters. The block model of the Gooshfil mine is shown in figure 6.

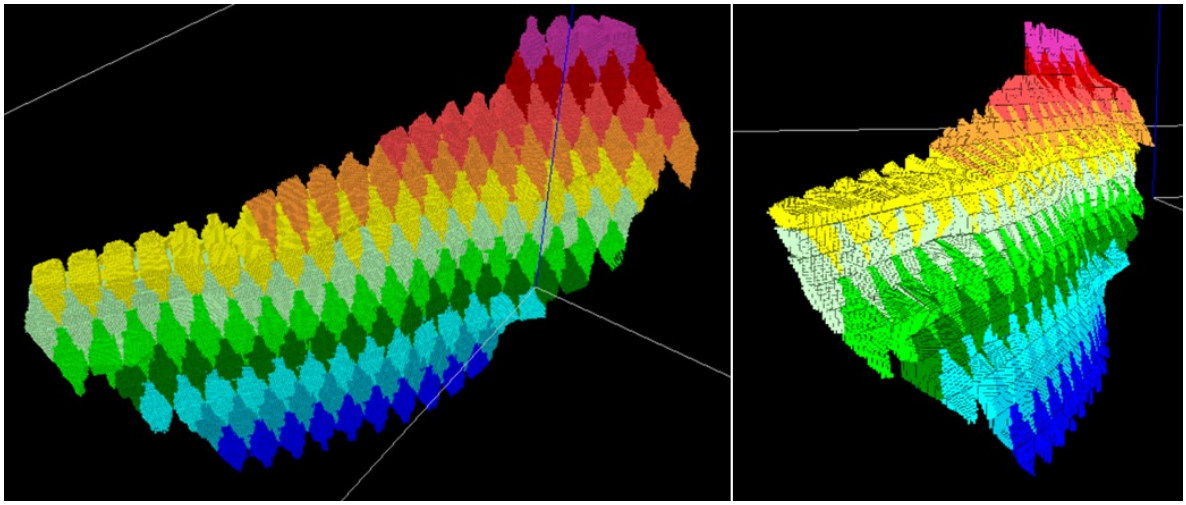

Figure 6. Block model of Gooshfil mine

After generating the block model, ultimate stope boundary is determined using the floating stope algorithm. Using this optimizer, in addition to optimizing the ultimate stope boundary, it removed about 20% of the blocks inside the model (less than 3% of reserve) that were not dimensionally suitable for the stope geometry. So, it results in a significant reduction in computation time. The model is applied on the Gooshfil block model presented in Fig. 6. This block model is formed with the shape of a rhombus cube (the real blocks in the sublevel caving method are rhombus-shaped) with dimensions of 5 * 10 * 20 cubic meters. In this block model, with the opinion of experts, geomechanical conditions and roof caveabilty, have been considered. The average grade of ore is 7.6% lead and zinc in this section. Other assumptions are as below:

- the number of scheduling periods is 5 years,
- discount rate is 10%,
- the minimum and maximum annual production rates are equal 280000 to 320000 tons per year,
- the minimum number of blocks that a sublevel must be in advance from its underlying sublevel is 3 blocks,
- the maximum number of active sublevels in each period is not considered in this mine.

The model optimizes the mining sequence such that the NPV is maximized. The maximum achievable NPV for the Gooshfil block model is M$34.7, and the optimum mining sequencing is shown in Fig. 7.

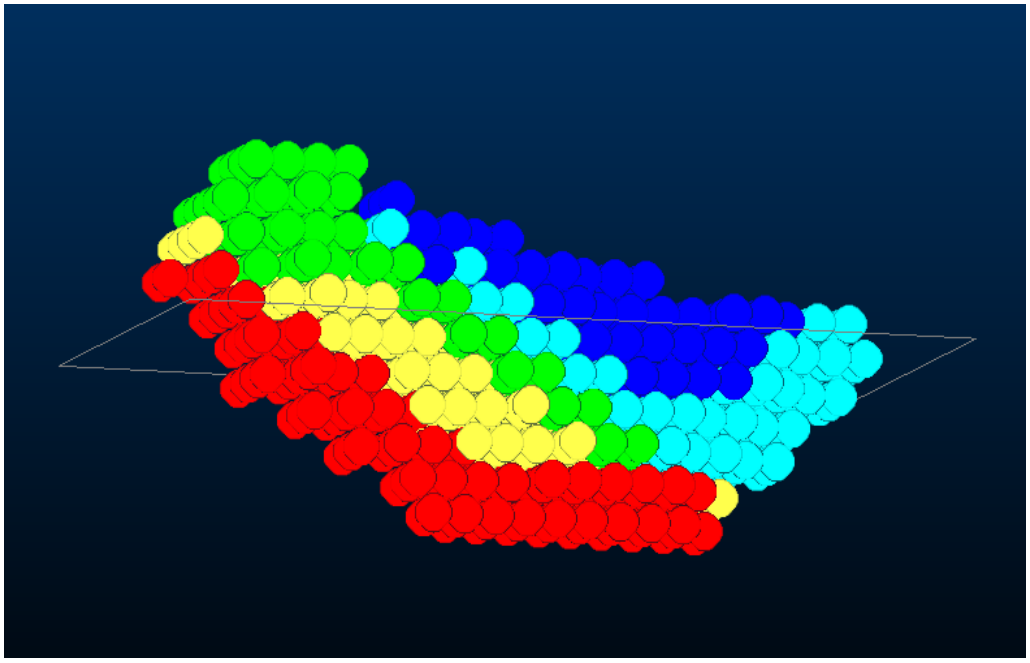

Figure 7. Production sequencing for achieving maximum NPV

The current production plan of the mine (the current development network is shown in figure 8), which was done manually, is such that the sublevels are mined in order. After the completion of one sublevel, it is possible to extract the next sublevel. According to this program, the net present value of the extraction of residual reserves by the manual method will be equal to M$ 30,4. Which the optimal production program resulting from solving the proposed mathematical model is 14% more than it.

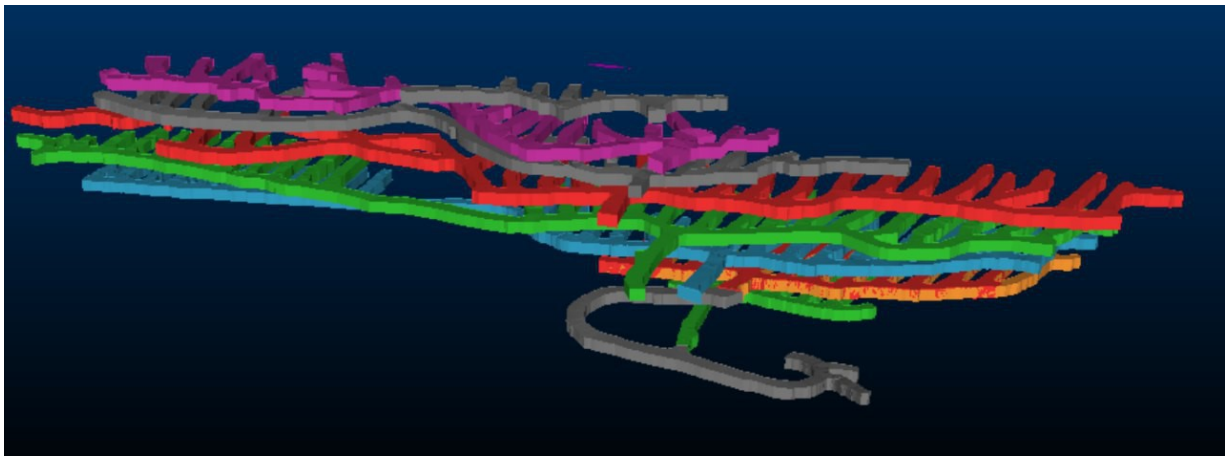

Figure 8. The current development network of the Gooshfil mine

Since the objective is to maximize NPV in production planning, high-grade reserves are extracted sooner. Figure 9 shows the average annual extraction grade of lead and zinc. As shown in figure 8, the extraction grade graph increases in the first year and decreases in the following years of the mine life.

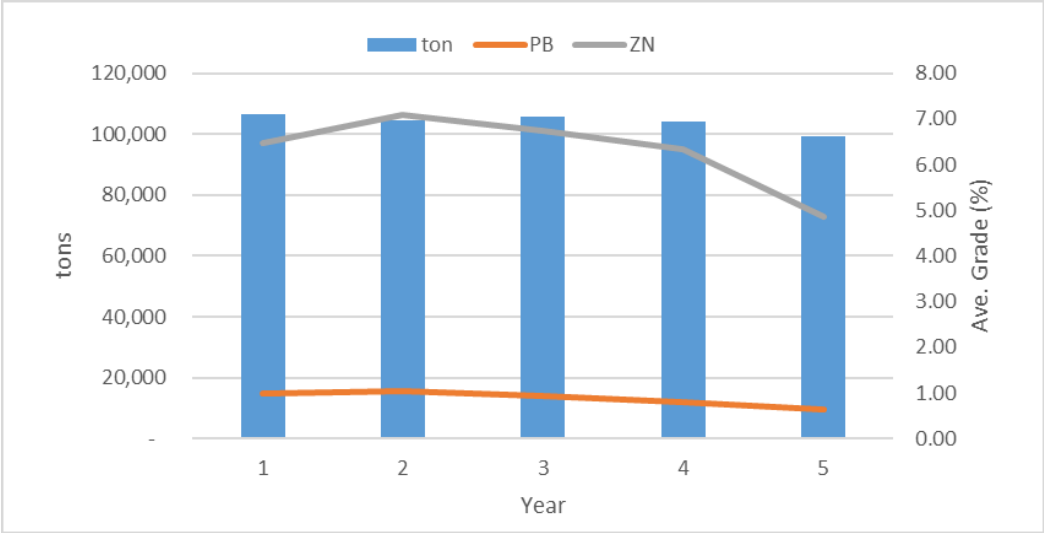

Figure 9. the average annual extraction grade of lead and zinc in Gooshfil mine

CONCLUSION

In this paper, a mathematical IP model is developed for optimization long-term production scheduling of sublevel caving mining method with the objective of net present value (NPV) maximization. This IP model is formulated for technical constraints that are present in sublevel mining methods. Considering these constraints will lead to a practical mining sequence that maximizes the NPV of the mining operation. The model is applied on a lead and zinc mine of Iran. In that regard, in order to determine the optimum stope boundary, a floating stope algorithm is used. Then, a minable stope envelope is determined prior to the application of the model. In that regard, the blocks that are not selected by the envelope are removed from the model. This will considerably reduce the number of blocks that improves the running time. Applying the production scheduling model optimizes the mining sequence in the Gooshfil mine and the maximum NPV that achieved equals M$34.7. Comparing the results with the conventional scheduling method shows a 14% increase in NPV of the operation.

REFERENCES

Alford, C., (1995), Optimization in underground mine design, APCOM 25, 213-218.

Ataee-pour, M., (2005), A critical survey of the existing stope layout optimization techniques. Journal of Mining Science, Vol. 41, No. 5, 447-466

Carlyle, W. M., Eaves. B. C. (2001), Underground planning at Stillwater Mining Company. Interfaces 31(4) 50–60

Chanda, E. K. C. (1990), An application of integer programming and simulation to production planning for a strati form ore body. Mining Sci. Tech. 11(2) 165–172

Edward Lee Gillenwater, (1988), An integrated model for production planning and scheduling in underground coal mining, Doctor of Business dissertation, University of Kentucky

Epstein, R., Gaete, S. Caro, F. Weintraub, A. Santibañez, P. Catalan. J. (2003), Optimizing long term planning for underground copper mines. Proc. Copper 2003-Cobre 2003, 5th Internat. Conf., Vol I, Santiago, Chile, CIM and the Chilean Institute of Mining, 265–279

Fava, L. Saavedra-Rosas, J. Tough V. and Haarala, P. (2013), Heuristic Optimization Of Scheduling Scenarios For Achieving Strategic Mine Planning Targets, the 23rd World Mining Congress, Montreal, Canada

Jawed, M. (1993), Optimal production planning in underground coal mines through goal programming: A case study from an Indian mine. J. Elbrond, X. Tang, eds. Proc. 24th Internat. Appl. Comput. Oper. Res. Mineral Indust. (APCOM) Sympos., CIM, Montréal, 44–50

Kuchta, M., Newman, A. Topal. E. (2004), Implementing a production schedule at LKAB's Kiruna Mine. Interfaces 34(2) 124–134

Magda, R. (1994), Mathematical model for estimating the economic effectiveness of production process in coal panels and an example of its practical application.Internat. J. Prod. Econom. 34(1) 47–55.

McIsaac, G., (2005), Long-term planning of an underground mine using mixed-integer linear programming, CIM Bulletin, Vol. 98, No.1089, 1–6

Newman, A., Kuchta. M. (2007), Using aggregation to optimize long-term production planning at an underground mine. Eur. J. Oper. Res. 176(2) 1205–1218

O'Sullivan, D. Newman, A. (2015), Optimization-based heuristics for underground mine scheduling, European Journal of Operational Research, Volume 241, Issue 1, Pages 248–259

Shenavar, M. Ataee-pour, M. Rahmanpour M.; (2018), Production Scheduling in Sublevel Caving Method with the Objective of NPV Maximization; 27th International Symposium on Mine Planning and Equipment Selection, Santiago, Chile

Shenavar, M. Ataee-pour, M. Rahmanpour M.; (2020), A New Mathematical Model for Production Scheduling in Sub-level Caving Mining Method; Journal of Mining and Environment (JME); Vol. 11, No. 3, 2020, 765-778. DOI: 10.22044/jme.2020.9139.1804

Subhash C. Sarin, Jan West-Hansen, (2005), The long-term mine production scheduling problem, JournalIIE Transactions, Volume 37, 2005 - Issue 2

Pourrahimian, Y., (2013), Mathematical programming for sequenceoptimization in block cave mining, Doctor of Philosophy Thesis, Department of Civil and Environmental Engineering, Edmonton, Alberta

Rahal, D., M. Smith, G. Van Hout, A. Von Johannides. (2003), The use of mixed integer linear programming for long-term scheduling in block caving mines. F. Camisani-Calzolari, ed. Proc 31st Internat. Appl. Comput. Oper. Res. Mineral Indust. (APCOM) Sympos., SAIMM, Cape Town, South Africa, 123–131

Rubio, E., Diering. E. (2004), Block cave production planning using operation research tools. A. Karzulovic, M. Alfaro, eds. Proc. MassMin 2004, Instituto de Ingenieros de Chile, Santiago, Chile, 141–149

Schulze, M. Zimmermann, J. (2010), Scheduling in the Context of Underground Mining, Operations Research Proceedings, DOI 10.1007/978-3-642-20009-0_96

TOPAL, E. (2003), Advanced underground mine scheduling using mixed integer programming. PhD thesis, Colorado School of Mines, Colorado.

Whitchurch, K. Cram, A.A. Ozawa, N. and Koizumf K. (1996), Underground and open-cut coal scheduling using expert systems; 26th apcom proceedings; 339-346

Williams JK, Smith L, Wells PM (1973), Planning of underground copper mining.10th Internat. Appl. Sympos. Appl. Comput. Mineral Indust. (APCOM), Johannesburg, South Africa, 251–254

Winkler, B. (1998), System for quality oriented mine production planning with MOLP. Proc. 27th Internat. Appl. Comput. Oper. Res. Mineral Indust. (APCOM) Sympos., Royal School of Mines, London, 53–59

MALİYET YAKLAŞIMI İLE ERKEN EVRE KÖMÜR SAHALARININ DEĞERLEMESİ

VALUATION OF EARLY-STAGE COAL FIELDS BY COST APPROACH

M. Aktan [1,] *, A.E. Tercan [2]

[1] *Türkiye Kömür İşletmeleri Kurumu Genel Müdürlüğü, Ankara*
*(*Sorumlu yazar: metin.aktan@gmail.com)*
[2] *Hacettepe Üniversitesi, Maden Mühendisliği Bölümü, Ankara*

ÖZET

Madencilik sektöründe üretilen halka açık raporlar; 1) Arama Sonuçları, Maden Kaynak / Maden Rezerv Kestirimi ve 2) Maden Değerleme raporları olmak üzere iki ana kategoriye ayrılabilir. Dünyada birinci kategoride raporlama yapan birçok uzman kişi varken, değerleme yapan kişi sayısı oldukça sınırlıdır. Bunun önemli bir nedeni Maden Değerlemenin yeni gelişen bir disiplin olmasıdır. Değerlemenin temel amacı, incelenen maden varlığının piyasa değerini belirlemektir. Ülkemizde maden sahalarının değerlemesi ile ilgili yeterli sistematik çalışma bulunmamaktadır. Değerleme yapılacak sahaların öncelikle uluslararası değerleme yaklaşımlarındaki kod esaslarına göre ve konusunda uzman değerlemeciler tarafından yapılması gerekmektedir. Bu çalışmada; Türkiye'de bulunan ve henüz işletilmemiş erken evre arama aşamasındaki iki adet kömür sahasının değerlemesi yapılmıştır. Sahaların özelliklerinden dolayı değerleme çalışmasında "Maliyet Yaklaşımı" kullanılmış olup, kömür sahalarındaki maden varlıkları ile ilgili bilgi düzeylerinin yanı sıra, kaynak miktarına ait parasal tutarlar ve yapılan harcamaların bugünkü değerleri hesaplanarak birbirileriyle kıyaslamaları yapılmıştır. Çalışmada, "Arama Harcamalarının Katları" ve "Kilburn Yerbilim Faktörü" gibi yöntemler kullanılarak değerleme tahminlerine ulaşılmıştır. Sonuçlar, maden varlıkları ile ilgili kaynak miktarı ve kalitesinin yanı sıra artan bilgi miktarının ve güvenilirliğinin saha değerini arttıran önemli bir unsur olduğunu göstermiştir.

Anahtar Kelimeler: Kömür değerleme, maden sahası değerleme, maliyet yaklaşımı, Kilburn Faktörü (KYY), Arama Harcamalarının Katları (AHK) Yöntemi.

ABSTRACT

The Public Reports issued in the mineral industry can be divided into two main categories: 1) Reports on Exploration, Mineral Resource / Mineral Reserve estimation and 2) Reports on Valuation of Mineral Assests. While there are many experts disclosing reports for the former in the world, the number of valuators are quite limited. An important reason for this situation is that mine valuation is an emerging discipline. The main purpose of valuation is to determine the market value of the mineral asset. There are not enough systematic studies on the valuation of Mineral Assests in our country. First of all, the Mineral Assests to be valuated must be studied by Practitioners according to the code principles based on international valuation approaches. In this study, two unexploited coal fields of Turkey in the early exploration stage were valuated. Due to the characteristics of the fields, the "Cost Approach" was used in the valuation study and the monetary amounts of the resource and the present values of the expenditures were calculated and compared with each other, as well as the knowledge level about the Mineral Assets in the coal fields. In the study, valuation estimates were obtained by using methods such as Multiples of Exploration Expenditures and Kilburn Factor. The results showed that the resource and quality of the

mineral assets, as well as the increased amount and reliability of information about the field, is an important factor that affects the valuation.

Keywords: Coal valuation, mining field valuation, Cost Approach, Kilburn Method, Multiples of Exploration Expenditures Method.

GİRİŞ

Maden varlığı; dar kapsamda maden potansiyelini, maden kaynağını, maden rezervini, üretim yapan bir madeni ya da maden stoğunu içerir. VALMIN (2015) kod maden sahalarını (1) arama sahaları, (2) ileri arama sahaları, (3) ön-hazırlık projeleri, (4) hazırlık projeleri ve (5) üretim yapan madenler şeklinde sınıflandırmıştır.

Değer, bir maden varlığının mülkiyetine sahip olmanın bir ölçüsüdür. Maden değerleme incelemelerinde kullanılan çeşitli değer türleri vardır (Gentry ve O'Neil, 1984). Bunlar: 1) Piyasa değeri, 2) Tam parasal değer, 3) Hurda değeri, 4) İkame değeri, 5) Defter değeri, 6) Takdir edilmiş değer, 7) Sigorta değeridir.

Burada önemli olan maden varlığının pazar ya da piyasa değeridir. Bir maden varlığının piyasa değeri *(market value),* değerleme tarihinde açık pazarda istekli bir satıcıya istekli bir alıcı tarafından maden varlığı için ödenen parasal tutardır. Bu süreçte her iki tarafın bir zorlama olmadan ve bilinçli bir şekilde hareket ettiği kabul edilir. Pazar değeri, satıcı ve alıcının isteklilik derecesi ve satışın koşulları ile değişir. Piyasa değeri uluslararası mahkemelerce '*bir sahanın bilinçli bir satıcı tarafından bilinçli bir alıcıya satıldığı nakdi değer*' olarak tanımlanmıştır. Pazar değeri, pazar koşulları ve beklentiler değiştikçe değişen dinamik bir özelliğe sahiptir. Maden ekonomistleri, değerleyiciler ve vergi görevlileri daha çok maden sahalarının kestirilen pazar değeri ile ilgilidirler. Çünkü belirli bir maden sahasına ilişkin pazar değeri, pazarda gerçekleştirilen gerçek bir satış işlemi ile belirlenebilir (Tercan, 2015).

Maden sahalarının pazar ya da piyasa değerinin sağlıklı bir şekilde belirlenebilmesi için maden değerleme uzmanlarının konularında son derece tecrübeli ve bilgi birikimli olmaları gerekmektedir. Ancak maden değerleme, dünyada yeni gelişen bir disiplin olup, ülkemizde ise henüz başlangıç aşamasında bulunmaktadır. Özellikle UMREK kodunun yürürlüğe girmesi ile birlikte madenlerin değerlemesi konusu da gündeme gelmiş olup, konuyla ilgili MAPEG'in koordinatörlüğünde çeşitli STK temsilcileri, akademisyenler ve sektör uzmanlarının katılımıyla çalışma grupları oluşturularak, ülkemize özgü değerleme kodu geliştirilmesi için çalışmalara başlanmıştır.

Dünya genelinde maden değerleme ile ilgili birçok çalışma bulunurken, ülkemizde akademik anlamda çalışma sayısı oldukça sınırlıdır. Özkan (2021), maden ruhsat sahaları değerleme yöntemleri ile ilgili bir kitap yayınlamıştır. Mevcut çalışmalar daha çok çeşitli banka ve danışmanlık şirketlerine ait ticari gizliliği olan raporlardır.

Bu bildiri, erken evre kömür sahası değerlemesi ile ilgili bir çalışmayı içermektedir. Çalışmanın birinci bölümünde öncelikle maden varlıklarının gelişim evreleri ve maden değerleme konusuna kısaca değinilmiş olup, erken evre arama sahaları için kullanılan Maliyet Yaklaşımı ve alt başlıklarından olan Takdir Edilmiş Değer (TED), Arama Harcamalarının Katları ve Kilburn Yerbilim Faktörü gibi yöntemler anlatılmıştır. Ardından ikinci bölümde Türkiye'de bulunan ve henüz işletilmemiş erken evre arama aşamasındaki iki adet kömür sahasının verileri değiştirilerek değerlemesi yapılmıştır. Sahaların özelliklerinden dolayı değerleme

çalışmasında "Maliyet Yaklaşımı" kullanılmıştır. Üçüncü ve son bölümde de elde edilen sonuçlar tartışılmıştır.

MADEN VARLIKLARININ GELİŞİM EVRELERİ VE MADEN DEĞERLEME

Değerleme yönteminin seçimi, maden varlığına ilişkin mevcut bilginin miktarı ve kalitesine dolayısıyla maden varlığının geliştirildiği evreye bağlıdır. Lawrance (2001), maden varlıklarını üç ana kategoriye ayırmaktadır: **(a)** arama sahaları, **(b)** maden geliştirme projeleri ve **(c)** işletilen madenler. *Arama sahalarında* cevherleşme tanımlanmış ya da tanımlanmamış olabilir ancak bir maden kaynağı henüz belirlenmemiştir. *Geliştirme projeleri*, üretime geçmek için bir kararın verildiği ancak henüz işletilmeyen maden varlıklarına ilişkin projelerdir. *İşletilen madenler*, üretime başlandığı ya da üretimin yapıldığı madenler ya da proses tesisleridir (VALMIN, 2015). Bununla birlikte bu üç kategori; temel arama bölgeleri, ileri arama sahaları, ön geliştirme projeleri, gelişmekte olan madenler ve işletilen madenler şeklinde beş kategoriye çıkarılabilir (Lawrance, 2001).

Bir maden yatağının tenörü ve tonajı bir maden varlığının en kritik parametreleridir. Bundan dolayı tenör ve tonaj kestirimleri detaylı bir doğrulama gerektirmektedir. Ayrıca maden haklarının durumu, satış sözleşmeleri, ekonomik parametreler, coğrafik kısıtlar, çevresel etkenler ve diğer sosyo-politik konular da tenör ve tonaj kestirimleri kadar önemlidir. Bahse konu maddelerin hepsi birden maden varlığını oluşturan bileşenlerdir.

Değerleme yaklaşımları temel olarak üç gruba ayrılmaktadır: (1) Maliyet yaklaşımı, (2) Pazar yaklaşımı ve (3) Gelir yaklaşımı.

Maliyet yaklaşımı, varlığı benzer başka bir varlıkla değiştirmek ya da yerine yenisini koymak için gerekli parasal tutarın hesaplanmasına dayanmaktadır. Bu yaklaşım, takdir edilmiş değer, arama harcamalarının katları ve yerbilim faktörü (Kilburn) gibi yöntemleri içermektedir. Daha çok erken evre arama sahalarının değerlemesi amacıyla kullanılmaktadır (Tercan, 2015).

Pazar yaklaşımı, benzer varlıkların piyasadaki alış-satışından üretilen fiyatlara ve ilgili diğer bilgiye dayanmaktadır. Bu yaklaşımın temel varsayımı, bir maden varlığına bir alıcının ödeyeceği tutarın, benzer özellikteki başka bir varlığa ödeyeceğinden daha fazla olmayacağıdır. Bu nedenle benzer varlıkların satışlarına ilişkin bilginin temini değerleme için oldukça önemlidir. *Pazar yaklaşımı*; benzer satışlar yöntemi, ölçüt (ton başına değer, alan başına değer gibi) yöntemi ve ortaklık yöntemi gibi yöntemleri içermektedir. Bu yaklaşım her türlü maden sahasına uygulanabilir (Tercan, 2015).

Gelir yaklaşımı, maden varlığının işletilmesinden elde edilecek net kazancın bugünkü değere indirgenmesine dayanmaktadır. Net bugünkü değer yöntemi, gerçek opsiyon yöntemi, Monte Carlo yöntemi gibi yöntemler gelir yaklaşımı içinde yer almaktadır. Maden varlığı kazanç elde etmek amacıyla işletileceği için gelir yöntemi, ileri evre maden sahalarına uygulanmaktadır (Tercan, 2015).

Bu üç yaklaşım, birbirleriyle bağlantılı yaklaşımlar olup, aynı veri kaynaklarını kullanırlar ancak verileri farklı yöntemlerle analiz ederler. Temel olarak üç yaklaşımın birbirlerinin bulgularını desteklemesi gerekmektedir. Şekil 1, maden varlıklarının değerlemesinde kullanılacak yöntemlerin maden projelerinin gelişim evreleri içindeki yerlerini grafiksel olarak göstermektedir (VenmyneDeloitte, 2013).

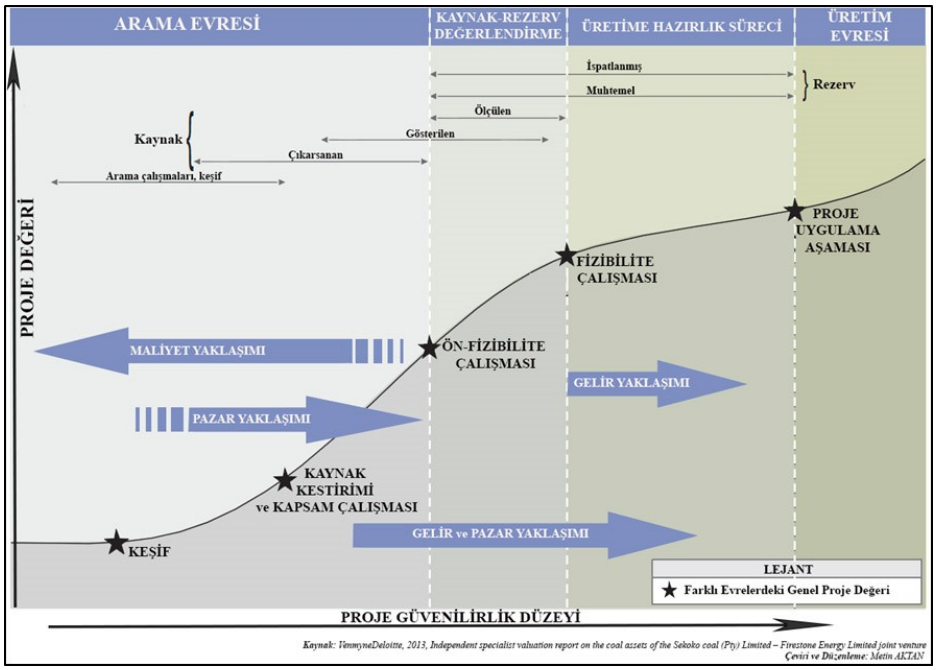

Şekil 1. Değerleme yaklaşımlarının proje gelişim evreleri içindeki yeri (VenmyneDeloitte (2013)'ten değiştirilerek).

Maliyet Yaklaşımı

Ellis (2001), maliyet yaklaşımını değere katkı ilkesine dayanan bir yaklaşım olarak tanımlamıştır. Bu yaklaşım, maden varlığının şimdiye kadar yapılan ve gelecekte garantili olarak yapılacak arama harcamalarının toplamı kadar değer içerdiği varsayımına dayanır. Saha üzerinde yapılan arama harcamalarının miktarı, sahanın değeri ile ilişkili olup burada yalnızca verimli olan harcamalar dikkate alınmaktadır. Verimli terimi, arama sonuçları ekonomik maden yatağının varlığı ve keşfine ilişkin bir potansiyeli ortaya koyup, ileri araştırmalar için yeterli bir teşvik ürettiği anlamına gelmektedir (Domingo ve Lopez-Dee, 2007). Aşağıda Maliyet Yaklaşımı ile ilgili temel yöntemler sırayla anlatılmaktadır.

<u>Takdir Edilmiş Değer (TED) Yöntemi</u>

Takdir edilmiş değer yöntemi, bir saha üzerinde yapılmış arama harcamalarının miktarının sahanın değeri ile ilişkili olduğu varsayımına dayanır (Roscoe, 2002). Yöntemin temel ilkesi, arama sahasının geçmişte yapılan arama harcamaları ve ayrıca gelecekte yapılması teminat altına alınmış harcamalar kadar değerli olduğudur. Yöntemin temel bir öğesi, yalnızca akılcı ve verimli olduğu düşünülen arama harcamalarının bir değer üreteceğidir. Gelecekte yapılması teminat altına alınmış arama harcamalarını, tanımlanmış bir potansiyeli test etmek amacıyla kullanılacak makul bir arama bütçesi oluşturur. Tanımlanmış potansiyel, jeofiziksel anomaliler, ya da daha önce tanımlanmış cevherleşme zonları ve ümit veren zuhurlar olabilir. Arama çalışması, potansiyelin derecesini düşürüyorsa çalışma verimli olmayıp maliyeti de bir değer olarak kaydedilmez ya da potansiyelin değeri düşer (Tercan, 2015). Geçmişte yapılan harcamalar genelde yıllık temelde analiz edilir. Geri kalan arama potansiyelinin tanımlanması amacıyla hangi harcamalarının alıkonacağı ve hangi harcamaların reddedileceğine teknik bir uzman karar verir. Enflasyonun yüksek olduğu zamanlarda geçmişte yapılan harcamaların günümüz koşullarına göre ayarlanması

ya da güncel birim maliyetlerin elde bulundurulan çalışmaya uygulanması gerekir. Bu tür çalışmalarda geçmiş beş yıla kadar olan arama harcamaları dikkate alınmalıdır (Tercan, 2015).

Takdir edilmiş değeri, geçmişte yapılan harcamalara teminat altına alınmış gelecekte yapılacak harcamaları ekleyerek belirlemek, bir saha üzerinde arama faaliyetinin maliyetini kestirmek amacıyla yapılan soyut bir uygulama gibi düşünülebilir. Gelecek harcama programının kimin tarafından karşılanacağının bir önemi yoktur. Ayrıca takdir edilmiş değeri, arama harcamalarının kaydedildiği ve zamanla ya da elde edilen gelirle silinecek olan bir muhasebe uygulaması şeklinde düşünmemek gerekir. Takdir edilmiş değerin en iyi uygulaması aktif bir şekilde aranan sahalar olabilir. Yöntemi, özellikle geçmişte önemli ölçüde harcamanın yapıldığı ancak bir süredir atıl duran sahalara uygulamak oldukça zordur. Aktif olmayan sahaların değerlemesindeki temel nokta, test edilmemiş hedefler, mevcut kaynağın tenör ve tonajını artırma potansiyeli ya da teknolojik ve ekonomik koşullardaki değişiklikle gelişme potansiyeli olan kalan arama potansiyelinin gerçekçi bir değerlendirmesidir.

Bölgesel piyasa koşulları belirgin bir şekilde baskı altında ya da yüksekse hesaplanan varlık değerini piyasa değerine göre ayarlamak gerekebilir. Bu işlem, hesaplanan varlık değerine prim ya da ceza şeklinde subjektif bir piyasa faktörü (%25'lik artışlarla) uygulayarak gerçekleştirilebilir. Örneğin işletilen bir madene yakınlık ve jeolojik benzerlik prim olarak göz önüne alınır (Tercan, 2015). TED yönteminin uygulaması, arama prosesinin, endüstri standartlarının, sondaj ve diğer arama tekniklerine ilişkin birim maliyetlerin iyi bilinmesini gerektirir. Değer biçen kişi, sahanın jeolojisi, aranacak hedef bölgeler, aramanın geçmişi ve sonuçları ve uygun arama teknikleri konusunda bilgili olmalıdır. TED yönteminin üstünlüğü, pek çok arama sahası için arama maliyet bilgisi ve teknik verilerin kolay bir şekilde erişilebilir olmasıdır. Ana kusuru ise verimli olduğu düşünülen geçmiş arama harcamalarını, sahanın değerine katkı koymayacak olan harcamalardan ayıracak ve gelecekte uygulanacak arama programı ve maliyetini değerlendirecek deneyimli bir kişinin olması gerektiğidir (Roscoe, 2002).

Arama Harcamalarının Katları (AHK) Yöntemi

TED yöntemi, geçmişte yapılmış ve gelecekte yapılacak arama harcamalarının nasıl değerlendirilmesi gerektiğine ilişkin bir çerçeve sunmaz. Lawrance (1994), bu eksikliği gidermek amacıyla arama harcamalarının katları yöntemini önermiştir. Yöntem, TED yöntemiyle belirlenen değeri, potansiyel artış katsayısı (PAK) (Prospectivity Enhancement Multiplier (PEM)) ile birlikte değerlendirir. AHK yönteminde geçmişte yapılmış ve gelecekte yapılacak olan arama harcamaları toplamı belirlendikten sonra bu toplam PAK ile çarpılır. Katsayı, harcamaların hedef varlığın potansiyel değerini artırıp artırmadığına göre belirlenir.

VenmynDeloitte (2013) ise kömür sahalarının değerlendirmesinde kullanmak üzere potansiyel artış katsayıları önermiş ve bu katsayılar Çizelge 1'de sunulmuştur.

Çizelge 1. Çeşitli arama evrelerine karşılık gelen potansiyel artış katsayıları $^{(*)}$

Arama evresi	PAK üst	PAK alt	Arama faaliyeti
Arama konsepti	0	0	Hiçbir şeyin bilinmediği ancak kuramsal olarak bir potansiyele sahip proje.
Masa üstü incelemesi	1	0	Önceki çalışmalar ve literatür incelemesi, sahadaki kömür bulgularının kayıtları ve kanıtları, tarihsel üretim verileri.
Keşif	1	1	Arazi uygunsa jeolojik haritalama. Temel topoğrafyası haritalaması. Geçmişte yapılan kömür kesmiş sondajlar,

Zemin çalışmaları	1	1	Ayrıntılı mostra haritalaması, kömür içeren tabakaların tanımlanması, kömür damarı mostra haritalaması, mostralardan örnek alma. Geçmişte yapılmış kömür
Zemin çalışmaları	2	1	Jeofizik, uzaktan algılama teknikleri, önceden yapılmış güvenilir ancak az sayıda sondajlar.
İlk evre sondaj	5	2	Karotlu sondajlar, ön kömür analizleri ile geniş aralıklı sondaj düzeni. İlk aşama tonaj kestirimleri. Mümkün
Kaynak sondaj çalışmaları ve laboratuvar testleri	11	5	Boşluk doldurma (in fill) sondajları, ayrıntılı kömür analizleri ve yıkama test çalışmaları. Kömür kalitesinin belirlenmesi, pazar potansiyeli, ayrıntılı kaynak tonaj kestirimi, yıkama eğrileri. İleri mümkün ve belirlenmiş
Tarihsel madencilik	20	11	Önceden yapılmış ticari üretim, güvenilir ve iyi hazırlanmış kalite tonaj eğrisi ve yıkanabilirlik. Ölçülmüş
Rezerv sınıflaması	>20	20	Tam fizibilite incelemesi, maden tasarımı ve para akış modeli. Kömür rezerv sınıflaması.

(*) Kaynak: VenmynDeloitte, 2013, Independent specialist valuation report on the coal assets of the Sekoko coal limited.

AHK yöntemi, sahanın algılanan değeri ile orantılı olarak arama harcaması yapılacağını varsayar. Bu varsayım, saha üzerinde yapılan harcamalar ile sahanın değeri arasındaki ilişkinin deneysel olarak test edilmesine olanak tanır. Böyle bir test günümüze kadar yapılmamıştır. Yöntemin çok sayıda sakıncalı tarafı bulunmaktadır (Sorentino, 2000). Örneğin geçmişte yapılan harcamalarla ilgili tüm bilgiler halka açıksa ve kolayca bulunabiliyorsa, geçmişteki arama maliyetlerinin bir önemi kalmaz. Burada önemli olan nokta, saha ile ilgili bilgiyi elde etmenin maliyeti değil, saha hakkında neyin bilindiğidir. Bu bilginin elde edilmesi çok yavaş olabilir, yanlış bir ipucunun peşinden gidilebilir, verimsiz olabilir ve bundan dolayı yalnızca konuyla ilgili bilginin kestirimde kullanılması son derece önemlidir. Bu bilgi mevcut olmadığında geçmişte yapılan harcamalar konu ile ilişkili olur. Aramayı değerli kılan bu bilgiler, geçmişteki değer algısının yerine geçer. Potansiyel artış katsayısının seçimi, kişiye bağlıdır ve değerleyiciler arasında oldukça farklılık gösterebilir hatta bazen aynı değerleyici aynı durumlarda farklı katsayılar kullanabilir. Arama harcamaları ile ilişkili birbirini izleyen çok sayıda kararı Bayes teoremi ile sentezleyerek yöntemin değeri test edilebilir (Tercan, 2015).

Kilburn Yerbilim Yöntemi (KYY)

KYY yöntemi, arama sahalarının fiziksel özelliklerini sistemli bir şekilde değerlendirmek amacıyla Kilburn (1990) tarafından geliştirilmiştir. Bu yöntem, bir sahanın jeolojik potansiyelini sayısal olarak ifade etmeye çalışır. Bunun için saha ile ilgili dört özelliği puanlar. Bunlar, (i) saha dışı faktörler (saha dışındaki olumlu jeolojik, jeokimyasal ve jeofizik anomaliler), (ii) saha içindeki faktörler (sahadaki cevherleşmenin tenörü, büyüklüğü), (iii) mevcut jeofiziksel ve jeokimyasal hedefler ve (iv) mevcut jeolojik yapılardır. Daha sonra değerlenecek saha ile ilişkili olarak her bir kategoriye bir puan verilir ve bunlar çarpılır. Bunu izleyerek sahanın birim alan başına edinme ve elde tutma maliyeti belirlenir. Bu maliyet başvuru harcını, yıllık kirayı ve bir yıl içinde yapılan yasal harcamaları toplayarak elde edilir. Sahanın değeri toplam alan, toplam puan ve birim maliyetin çarpımına eşittir.

Bu şekilde bulunan değer, uygun varsayımlar altında maden varlığının gelecekteki net ekonomik değerini yani teknik değerini verir. Piyasa değerini hesaplayabilmek için piyasaya ilişkin prim ve iskontolar,

stratejik ve diğer faktörleri gibi piyasa bileşenini de dikkate almak gerekir. Piyasa bileşeni zamana ve duruma göre pozitif, negatif ya da sıfır olabilir.

Değerleyicinin sahanın özünlü değerini azaltan ya da artıran çeşitli özelliklerini saptayıp sıralaması gerekir. Özünlü değer, sahanın temel edinme maliyeti (SEM) dir. SEM, arama sahasının birim alanına sahip olmak ve elde tutmak için gerekli ortalama maliyet şeklinde tanımlanabilir. Kilburn yöntemi, çoklu faktörleri belirlemek amacıyla sahanın dört temel değişkenini değerlendirir ve oranlar. Yöntemin başarıyla uygulanabilmesi için sahanın potansiyelini yansıtacak katsayıların uygun bir şekilde seçilmesi gerekir. Sonuçta bulunan değerin pazar değerini verdiği şeklinde bir beklenti vardır (Snowden, 2011). Yöntemin sakıncalı tarafları arasında en önemlisi gerçekte bir skorlama yöntemi olduğundan, farklı uzmanlar farklı bir şekilde skorlama yapabilirler ve bazı önemli görülen faktörler içerilmeyebilir. Ayrıca bu yöntem arama sahalarına ilişkin birim değerin seçimini gerektirir. Deneysel bir çalışma yapılmadan keyfi olarak verilen bu değer, çoğu zaman yanıltıcı sonuçlara götürür. Tüm bu nedenlerden dolayı Sorentino (2000), Kilburn yöntemi yerine Bayesyen yöntemler kullanılmasını önermektedir.

LİNYİT SAHALARININ DEĞERLEMELERİ

Sahaların Maliyet Yaklaşımına Göre Değerlemesi

Değerleme için Türkiye'de son yıllarda keşfedilen yeni linyit sahalarından ikisinin verileri ve yapılan harcamaları değiştirilerek kullanılmış ve değerlemeler bu değiştirilen verilere göre yapılmıştır. Bu çalışmada; A sahası: Hedef Saha, B sahası: Kaynak Saha olarak adlandırılmıştır. A sahasının değerlemesi, sahanın hemen güneyinde bulunan ve kaynak raporu ve ön fizibilite çalışmaları uluslararası standartlara göre yapılan B sahasının bilgilerinden faydalanılarak yapılmıştır. B sahasına ait özet bilgiler aşağıda verilmektedir.

Linyit projesi dâhilinde, Kasım 2018'den bu yana yaklaşık 2.5 senedir sondajlı arama ve geliştirme çalışmaları yürütülmüştür. Ruhsat alanında, bugüne kadar 41.600 m sondaj tamamlanmış olup, 1.200 adet linyit numunesi akredite bir laboratuvar tarafından analiz edilmiştir. Sahada sürdürülen tüm arama çalışmaları uluslararası bir firma danışmanlığında, uluslararası standartlara (JORC) uygun olarak yürütülmüştür. JORC (2012) koduna göre kömür kaynakları, jeolojik güvene bağlı olarak, ölçülmüş (measured), belirlenmiş (indicated) ve mümkün (Inferred) kaynaklar şeklinde üç kategoriye ayrılmaktadır. B sahası için JORC 2012 yönetmeliği dikkate alınarak kömür yatağına ilişkin jeolojik bir model geliştirilmiş ve daha sonra Maden Kaynak kestirimi yapılmıştır. Modellemede tüm sondaj verileri ve jeofizik loglama bilgileri kullanılmıştır. Kestirilen Kömür Kaynağı sondaj aralıklarının ortalama 200-500 m aralıklarda olması nedeniyle belirlenmiş kategoride sınıflandırılmış ve sonuçlar Çizelge 2'de gösterilmiştir.

Çizelge 2. B sahası kaynak kestirim sonuçları (Kaynak Saha)

Sınıf	Tonaj (Mt)	Kül % (hkb)	Uçucu madde % (hkb)	Isıl değer, kCal/kg (hkb)
Belirlenmiş	300	33,2	20,9	1.980

B sahasındaki kestirimi yapılan kömür kaynağının bilgilerinden faydalanılarak, kuzeydeki A sahasına ait sondaj verilerine göre 1,510 milyar tona yakın tonajın olduğu raporlanan hedef saha bulunmaktadır. A sahası, 8.328 ha'lık bir ruhsat alanında geniş bir havzada yayılmakta olup, büyük miktarda linyit kömürü içermektedir. Kalınlığı 0,2 m'den 15 m'ye değişen çoklu kömür damarları bulunmaktadır. Kömür kalite test çalışmaları linyit kömürünün ekonomik olarak B sahasının devamı niteliğinde ve daha yüksek kaliteye sahip olduğunu ortaya koymuştur. Bu arama çalışmaları JORC 2012 yönetmeliğine göre raporlanmamıştır. Ancak B

sahası ile olan benzerliği bilinmektedir. Sahasındaki linyit oluşumu, büyük bir gölsel çöküntü havzasında gelişmiş olup, A sahasına ait hedef saha bu havzanın ortasını ve kuzey kısmını, B sahası ise güney kısmını kapsamaktadır. A sahası ile ilgili JORC'a uygun raporlama çalışmalarına yeni başlanılmıştır. Hedef kömür sahasına ilişkin özet bilgi Çizelge 3'te sunulmuştur. Buna göre hedef saha, ortalama sondaj mesafeleri 500-700 m arası olduğundan Mümkün Kaynak kategorisine dâhil edilebilir.

Çizelge 3. A sahası sonuçları (Hedef Saha)

Sınıf	Tonaj (Mt)	Kül, % (hkb)	Uçucu madde, % (hkb)	Isıl değer, kCal/kg (hkb)
Mümkün	1.510	34,7	21,5	2.200

Her iki sahadaki mevcut kömür kalitesi ortalama 1.980-2.400 kcal/kg aralığında bulunduğu için, ısınma ya da sanayi amaçlı olarak kullanılması mümkün olmayıp ancak termik santralde değerlendirilebilir.

Arama Harcamalarının Katları (AHK) Yöntemine Göre Saha Değerlemeleri

Her iki saha da, erken evre arama linyit sahası olup Venmyn Deloitte (2013) yöntemi değerleme için uygundur. Geçmişte A sahasına ait hedef saha için yapılan harcamalar aşağıda verilmiştir:

A sahasının devri için MTA ile imzalanan tutanağın tarihi 2019'dur. A sahasının satış bedeli 245.500.000 TL'dir ve eşit taksitler halinde 10 yılda ödenecektir. JORC'a uygun etüt çalışmaları, kaynak raporu ve ön fizibilite raporu için yapılacak harcama miktarı da 73.000.000 TL'dir. Buna göre Eşitlik 1 kullanılabilir:

$$F = P\,(1+i)^N \qquad F = A\left[\frac{(1+i)^N - 1}{i}\right] \qquad P = A\left[\frac{(1+i)^N - 1}{(1+i)^N}\right] \tag{1}$$

Eşitlik 1'de F = Paranın gelecekteki değeri; A = Paranın dönem sonu nakit akışı; P = Paranın bugünkü değeri; i=Dönem başına faiz oranı; N = Dönem sayısını göstermektedir.

Dönem başına faiz oranı yapılan anlaşmaya göre yıllık i=%9 alınmıştır. Buna göre yapılan hesaplamalara ait dönemsel ödeme planı Şekil 2'de, sahanın ruhsat değerinin 10 eşit taksitte ve 10 yılda ödeneceği durumu ile ilgili NBD ve Gelecekteki değer ile ilgili Eşitlik (1)'deki formüller kullanılarak yapılan hesaplamalar Çizelge-4'te verilmektedir:

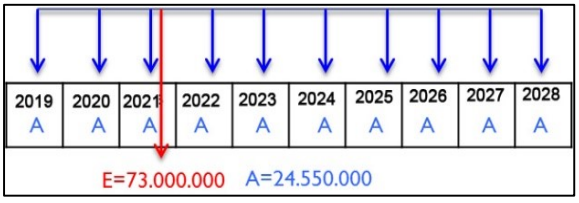

Şekil 2. A Sahası dönemsel ödeme planı

Çizelge 4. Hedef Saha (A Sahası) için NBD hesabı

Tarih	Yapılan/Yapılacak Ödeme Tutarı (TL)	21.11.2021 tarihine göre P veya F (TL)	Toplam (TL)
20.11.2019	24.550.000	1.421.316 TL	25.971.316 TL
20.11.2020	24.550.000	1.292.105 TL	25.842.105 TL
20.11.2021	24.550.000	0 TL	24.550.000 TL
20.11.2022	24.550.000	2.455.000 TL	22.095.000 TL
20.11.2023	24.550.000	5.130.950 TL	19.419.050 TL
20.11.2024	24.550.000	8.047.736 TL	16.502.265 TL
20.11.2025	24.550.000	11.227.032 TL	13.322.968 TL
20.11.2026	24.550.000	14.692.465 TL	9.857.535 TL
20.11.2027	24.550.000	18.469.786 TL	6.080.214 TL
20.11.2028	24.550.000	22.587.067 TL	1.962.933 TL
Toplam	**245.500.000**	**85.323.456**	**165.603.386**

Geçmişte A sahası için yapılan ve yapılacak harcamalara ait hesaplamalar Çizelge 5'te verilmiştir.

Çizelge 5. Hedef saha (A Sahası) için yapılan ve yapılacak harcamalara ait hesaplamalar

Harcama Kalemi	Tutar (TL)	Tarih	BD - Tutar (TL)	Tarih
Sahanın Devir Bedeli	245.500.000	20.11.2019	165.603.386	20.11.2021
Yapılan/Yapılacak Etüt Masrafları *(Jeofizik, Jeoteknik, Hidrojeolojik, Rezerv geliştirme, kendiliğinden yanma, kömür gaz içeriği, JORC/UMREK Kaynak Kestirimi, Maden üretim planlamasına yönelik tasarım ve ön fizibilite çalışmaları)*	73.000.000	20.11.2021	73.000.000	
		TOPLAM	**238.603.386 TL**	

A sahası ruhsat sahası bedelinin bugünkü değeri*:* 165.603.386 TL. Yapılan/yapılacak harcamalarla birlikte sahanın bugünkü değeri: 238.603.386 TL.

Çizelge 6. Kaynak saha (B Sahası) için yapılan ve yapılacak harcamalar

Harcama Kalemi	Tutar (TL)	Tarih	NBD - Tutar (TL)	Tarih
Sahanın Ruhsat Bedeli	50.000.000	20.11.2018	64.751.450	20.11.2021
Yapılan/Yapılacak Etüt Masrafları *(Jeofizik, Jeoteknik, Hidrojeolojik, Rezerv geliştirme, kendiliğinden yanma, kömür gaz içeriği, JORC/UMREK Kaynak Kestirimi, Maden üretim planlamasına yönelik tasarım ve ön fizibilite çalışmaları)*	9.000.000	20.11.2021	9.000.000	
		TOPLAM	**73.751.450 TL**	

Geçmişte B sahası için yapılan ve yapılacak harcamalar Çizelge-6'da verilmiştir. Buna göre B sahası ruhsat bedelinin bugünkü değeri*:* $F = P\ (1+i)^N$ = 50.000.000 $(1+0{,}09)^3$ = 64.751.450 TL. Yapılan/yapılacak harcamalarla birlikte sahanın bugünkü değeri: 73.751.450 TL'dir. **Hedef sahada** yapılan ve yapılacak harcama miktarı toplamı **238,6 M TL**; **kaynak sahada** da **73,8 M TL**'dir.

Hedef ve kaynak sahanın teknik değer aralığını arama harcamalarının katları yöntemi ile belirlemek için VenmynDeloitte (2013)'in çeşitli arama evrelerine karşılık gelen potansiyel artış katsayılarını gösteren Çizelge-1 kullanılmıştır. Yapılan değerlendirmeler aşağıda sunulmuştur:

Bu çizelgeye göre, kaynak saha olan B sahası için **"sondaj çalışmaları ve laboratuvar testleri"** çalışması olması, Kömür Kaynağının JORC 2012'ye göre gösterilen sınıfta raporlanması, ayrıntılı kömür analizleri ve yıkama test çalışmaları, kömür kalitesinin belirlenmesi, ayrıntılı tonaj kestirimine rağmen Pazar potansiyeli ile ilgili çalışma yapılmamış olması nedeniyle; PAK üst değerinin **8**, PAK alt değerinin de **5** olduğu değerlendirilmiştir.

Buna göre B sahası
Teknik alt değer $_{\text{Kaynak Saha (B)}}$: 73.751.450 TL x 5 = 368,8 M TL
Teknik üst değer $_{\text{Kaynak Saha (B)}}$: 73.751.450 TL x 8 = 590,0 M TL
Tercih edilen teknik değer $_{\text{Kaynak Saha (B)}}$: **479,4 M TL** hesaplanmıştır.

Aynı şekilde Çizelge-1'e göre, A sahası için **"İlk evre sondaj çalışması"** olması, karotlu sondajlar, ön kömür analizleri ile geniş aralıklı sondaj düzeni, ilk aşama tonaj kestirimleri, mümkün kömür kaynağı gibi verilerin olması fakat bu verilerin JORC'a uygun olarak raporlanmamış olması nedeniyle PAK üst değerinin **4**, PAK alt değerinin de **1,5** olduğu değerlendirilmiştir.

Buna göre A sahası
Teknik alt değer $_{\text{Hedef Saha (A)}}$: 238.603.386 TL x 1,5 = 357,9 M TL
Teknik üst değer $_{\text{Hedef Saha (A)}}$: 238.603.386 TL x 4 = 954,4 M TL
Tercih edilen teknik değer $_{\text{Hedef Saha (A)}}$: **656,2 M TL** olarak hesaplanmıştır.

Türkiye ve dünyada termik santral amaçlı linyit kömürünün Pazar durumunu araştırıp, kaynak saha ve hedef sahanın teknik değerine uygulanacak Pazar faktörünü (indirim ya da prim) belirlemek için Türkiye ve dünyada linyit kömürünün geleceği ile ilgili çeşitli kaynaklardan araştırmalar yapılmıştır. Dünyada ve Türkiye'de termik santral amaçlı kömür fiyatlarında pandemiden kaynaklı son dönemdeki ani fiyat yükselmelerini hariç tutarsak uzun vadede dalgalı seyirde bir düşüş olduğu görülmektedir. Kömür fiyatlarındaki düşüşün nedenleri arasında sadece iklim değişikliğinden kaynaklı karbon salınımı ile ilgili yaptırımlar ve Pazar payı azalması değil, gelişen teknoloji ile birlikte maliyetlerin düşmesi ve yenilenebilir enerjiye olan ilgi de gösterilebilir. Fiyatlardaki azalmaya rağmen, özellikle Avustralya'da ve Çin'de kömür üretimleri giderek artmaktadır. İncelemeye konu edilen sahalar linyit kökenli olduğu için, kıyas yapılması gereken ülkeler Almanya, Polonya ve Yunanistan'dır. Söz konusu ülkelerden Almanya, işçilik ve üretim maliyetlerinin yüksek olması ve iklim anlaşması hedefleri nedeniyle tüm kömür ocaklarını ve kömür santrallerini kademeli olarak kapatma kararı almıştır. Fakat Polonya ve Yunanistan termik santral amaçlı linyit üretimlerine devam etmektedirler. Avrupa ülkelerinde kömürün elektrik üretimi amaçlı oranları şu şekildedir: Polonya %84, Almanya % 45, İngiltere % 39, Romanya % 38 ve Danimarka % 34'tür (TKİ, 2020).

Türkiye enerji arz güvenliği için yerli linyitlerin elektrik üretimi amaçlı kullanımı son derece önemli olup, Hükümet programlarında, 10 Yıllık Kalkınma Planlarında ve ETKB ve ilgili kurumlara ait Stratejik Planlarda bu hususlara yer verilmektedir. Ancak İskoçya'nın Glasgow kentinde düzenlenen Birleşmiş

Milletler (BM) İklim Zirvesi 26. Taraflar Konferansı (COP26)'da 13 Kasım'da aralarında Türkiye'nin de bulunduğu taraflar Glasgow İklim Paktı üzerinde anlaşmaya vardılar. Bu anlaşmaya göre küresel sıcaklık artışının 1,5 dereceyle sınırlandırılması hedefine uyumlu olarak kömür kullanımının azaltılması ve fosil yakıtlara teşviklerin sonlandırılmasına yönelik kararlar, ilk defa resmi müzakere metinlerinde yer almıştır. COP26'ya göre emisyonların 2030'a kadar %45 azaltılması gerekmektedir. Çin, Hindistan ve Avustralya'nın kömüre yönelik temkinli yaklaşımlarına rağmen, azaltma yönünde irade gösterecekleri teyit edilmiştir. Çin, yurt dışındaki kömür projelerine finansman sağlamayacağını beyan etmiştir. Türkiye de yeşil enerji dönüşümüne destek verdiğini, bunun için de iklimle ilgili 2030 ve 2050 stratejilerini belirlemek üzere ivedilikle çalışmalara başlayacağını beyan etmiştir (AA, 2021).

COP26 sonrası yeni duruma bakıldığında, yerli linyitlerin elektrik üretimi amaçlı değerlendirilmesi ve ithal enerji kaynaklarının aşama aşama azaltılmasına yönelik tüm hedeflere rağmen, kömürün geleneksel kullanımı açısından geleceğinin Türkiye için belirsiz olduğu görülmektedir. Yerli kömürlerin temiz kömür teknolojileri kapsamında gazlaştırma/sıvılaştırma yoluyla çeşitli petrokimyasallar, yakıt, tarımsal amaçlı amonyak/üre gibi ürünlere dönüştürülmesi ile kullanılabileceği ve karbon azaltımının ve COP26 taahhütlerinin ancak bu şekilde sağlanabileceği anlaşılmaktadır. Fakat mevcut durumda söz konusu kaynak ve hedef sahanın kömür kalorilerinin düşük olması, gazlaştırma/sıvılaştırma ile ilgili herhangi bir çalışma yapılmamış olması, gazlaştırma/sıvılaştırma teknolojilerinin ilk yatırım maliyetlerinin son derece yüksek olması ve bu konuda henüz yerli teknoloji geliştirilememiş olması gibi nedenlerle bahse konu kaynak saha ve hedef sahanın teknik değerine uygulanacak Pazar faktörü, indirim şeklinde olacaktır. Bu nedenle sahalar ile ilgili bulunan teknik değerlere %25 indirim uygulanması makul bir yaklaşımdır.

Kömür Kaynağı ve Hedef Sahanın Pazar Değeri

Kaynak Saha ve Hedef Saha için tercih edilen teknik değerler dikkate alınarak Çizelge 7'de verilen hesaplamalar yapılmıştır. Hesaplama sonuçlarına göre Kaynak Saha (B Sahası) pazar değeri **359,5 M TL**; Hedef Saha (A Sahası) pazar değeri **492,1 M TL** hesaplanmıştır.

Çizelge 7. Pazar Değeri Hesaplamaları

Kaynak Saha Pazar Değeri Hesaplaması		**Hedef Saha Pazar Değeri Hesaplaması**	
Tercih edilen teknik değer	479,4 M TL	Tercih edilen teknik değer	656,2 M TL
Pazar değeri indirimi	119,8 M TL	Pazar değeri indirimi	164,0 M TL
Saha Pazar Değeri	**359,5 M TL**	**Saha Pazar Değeri**	**492,1 M TL**

SONUÇ

Sahalara ait değerlemelerin sonuç verileri Çizelge 8'de topluca sunulmaktadır.

Çizelge 8. Saha değerlemelerine ait sonuçlar

Sahalar	**Kaynak (Mt)**	**Ortalama AID (kcal/kg) (hkb)**	**Tercih Edilen Teknik Değer (Milyon TL)**	**Pazar Değeri (Milyon TL)**
B Sahası (Kaynak Saha)	300	1.980	479,4	359,5
A Sahası (Hedef Saha)	1.510	2.200	656,2	492,1

Maden Kaynak kestirim raporu uluslararası standartlara göre yapılan ve belirlenmiş kategoride maden varlığına sahip olan B Sahasının Maliyet Yaklaşımına göre tonajı daha az olmasına rağmen, Hedef Sahaya yakın bir değere yaklaştığı görülmüştür. Daha detaylı ve doğruluk payı yüksek saha çalışmaları ile sahaların tercih edilen teknik değeri artmaktadır.

Her iki sahaya ait pazar değerlerinin, kömürün gelecekte dünyadaki ve ülkemizdeki belirsizliğinden dolayı %25 indirimle değer kaybetmesi öngörülmüştür.

Özellikle "Hedef Sahanın" değerinin oldukça altında satın alındığı ve sahaya yönelik son derece az arama ve rezerv geliştirme harcamalarının yapıldığı söylenebilir. "Kaynak Sahanın" az olan tonajına rağmen, saha değeri ve yapılan harcamalar açısından yeterli olduğu değerlendirilmektedir.

Elde edilen sonuçlar, saha ile ilgili bilgi miktarı arttıkça saha değerlemesinin de arttığını, maden sahası değerlemesinin ülkemizde yeni gelişen son derece önemli bir disiplin olduğunu ve saha alım-satımlarında değerleme uzmanlarının muhakkak bulunması gerektiğini göstermektedir.

KAYNAKLAR

AA, (2021). COP26'da kömür kullanımının azaltılması ilk kez resmi metinde yer aldı: https://www.aa.com.tr/tr/cevre/cop26da-komur-kullaniminin-azaltilmasi-ilk-kez-resmi-metinde-yer-aldi/2421056 adresinden 12.12.2021 tarihinde alındı.

Domingo, E.V., ve Lopez-Dee, E.P. (2007). Valuation methods of mineral resources, 11th Meeting of the London Group on Environmental Accounting, 13 s.

Ellis, T.R. (2001). US Views on valuation methodology, Mineral Asset Valuation Issues 2001 (VALMIN 01), AusIMM, Carlton, Victoria, Australia 23 s.

Gentry, D.W. ve O'Neil, T.J. (1984). Mine Investment Analysis, New York, Society of Mining Engineers of AIMMPE, 502 s.

JORC, (2012). Avustralian code for reporting of exploration results, mineral resources and ore reserves, http://www.jorc.org

Kilburn, L. (1990). Valuation of mineral properties which do not contain exploitable reserves, CIM Bulletin, 83, 940, 90-93

Lawrance, M.J. (1994). An overview of valuation methods for exploration properties, in Mineral Valuation Methodologies 1994 (VALMIN 94), 202-223, (The Australian Institute of Mining and Metallurgy: Melbourne).

Lawrance, M.J. (2001). An outline of market-based approaches for mineral asset valuation best practice, Mineral Asset Valuation Issues 2001 (VALMIN 01), AusIMM, Carlton, Victoria, Australia 23 s.

Özkan, Y.Z. (2021). Maden Ruhsat Sahaları Değerleme Yöntemleri, İkinci Adam Yayınları, Ankara.

Roscoe, W.E. (2002). Valuation of mineral exploration properties using the cost approach, http://www.cim.org/mes/pdf/VALDAYBill_Roscoe.

Snowden, (2011). Independent valuation of the Eloise copper Project.

Sorentino, C. (2000). Valuation methodology for VALMIN, in MICA, The codes forum, Sydney, 37-55.

Tercan, A.E. (2015). Madenlerin Değerlemesi ve Değerlendirilmesi Ders Notları, Hacettepe Üniversitesi Maden Mühendisliği Bölümü.

TKİ, (2020). Kömür (Linyit) Sektör Raporu, https://webim.tki.gov.tr/file/edafdf77-e263-42c4-85bf-7ac9dfa6c090?download.

VALMIN, (2015). Code for the technical assessment and valuation of mineral and petroleum assets and securities for independent expert reports.

MEVZUAT DEĞİŞİKLİĞİ İLE BİRLİKTE YÜKSEK BASINÇLI HAVA PATLATMALI KAZI TEKNOLOJİSİNİN ZONGULDAK HAVZASI DİK KÖMÜR DAMARLARINDA YENİDEN UYGULANABİLMESİ

RE-APPLİCATION OF HIGH PRESSURE AIR BLAST EXCAVATION TECHNOLOGY IN VERTICAL COAL SEAMS OF THE ZONGULDAK BASIN WITH THE LEGISLATIVE CHANGE

C. Yamudi

Türkiye Taşkömürü Kurumu
(cyamudi@hotmail.com)

ÖZET

Bu çalışmada dünya madenciliğindeki başlangıcı 1930'lu yıllar olan ve zamanla teknolojik gelişimi ile beraber gelişerek 1990'lı yıllarda Türkiye kömür madenciliğinde uygulama alanı bulan ve 2015 yılında yasal mevzuat değişikliği ile birlikte rafa kaldırılan yüksek basınçlı hava patlatmalı kazı teknolojisi tanıtılacaktır. Zonguldak kömür havzasındaki dik damarlarda 1992-2015 yılları arasında uygulanan Sistemin avantaj ve dezavantajları incelenecektir. Yüksek basınçlı hava patlatmalı kazı sistemi ile üretimin devamı sürecinde karşılaşılan mevzuat sorunları ile birlikte üretim sistemi tamamen engellenmiştir. İşçi sağlığı ve iş güvenliği ön planda kalmak şartı ile ekonomiye katkıda bulunabilecek şekilde yönetmelik değişikliğinin tartışılması ve sistemin yeniden kullanıma sunulması amaçlanmıştır.

Anahtar Sözcükler: Delme patlama, dik damar, kömür, yüksek basınçlı hava

ABSTRACT

In this study, high pressure air blast excavation technology, which started in the 1930s in world mining and developed with its technological development over time, found an application area in Turkey's coal mining in the 1990s and was shelved in 2015 with the change in legal regulations will be introduced. The advantages and disadvantages of the System applied between 1992 and 2015 in vertical seams in the Zonguldak coal basin will be examined. With the high pressure air blast excavation system, the production system was completely blocked due to the legislative problems encountered during the continuation of production. It is aimed to discuss the regulation change and put the system back into use so that it can contribute to the economy, provided that occupational health and safety are at the forefront.

Keywords: Drilling and blasting, steep coal seems, coal, high pressure air.

GİRİŞ

Türkiye Taşkömürü Kurumu (TTK), Ülkemizin kamudaki tek taşkömürü üreticisi konumunda olup, havza geneli ile yurt içerisindeki diğer kömür havzaları ile kıyaslandığında yapısal Jeolojisi ve teknotik gelişimi İleri düzeyde olan kömür damarlarında çalışmalarını sürdürmektedir.

Havzanın iki kez tektonizma geçirmiş olması damarların faylarla bölünmesine, eğim ve kalınlıklarının sık sık değişmesine yol açmıştır. Bu damarlarda emek yoğun, yüksek maliyetli ve teknolojinin hâkim olduğu diğer kömür madenleriyle kıyaslandığında emniyet açısından riskli koşullarda üretim çalışmaları sürdürülmektedir.

1848'den bu yana üretim kültürü olan havzada bugüne kadar klasik yöntemlerle (uzun ayak, kısa ayak, dişli ayak ve karatumba) üretim yapılmıştır. Havzanın 1940 yılında devletleştirilmesinden sonra yapılan yatırımların büyük bir kısmı makine ve teçhizat alımı şeklinde olmuştur. Bu yatırımlarla ana kuyuların açılması, nakliyat ve havalandırma sistemlerinin iyileştirilmesi yoluna gidilmiştir (Yamudi, 2000).

Jeolojik koşulların uygun olmaması nedeniyle, üretim yöntemlerinin mekanize hale getirilmesi ve damar koşullarına uygun yeni yöntemlerin geliştirilmesi yönündeki çalışmalar dönemin şartlarıyla birlikte sınırlı kalmıştır.

1980'li yıllarda havzanın modernizasyonu ve yeniden yapılanması konusunda yapılan çalışmalarda bu konu daha geniş bir şekilde ele alınmıştır.

Ocakların giderek derinleşmesi ve genişlemesi dikkate alınarak "Havza Rehabilitasyon Projesi" gündeme getirilmiştir. Bu proje kapsamında ocakların alt yapılarının geliştirilmesi, üretim kapasitelerinin arttırılması ile işçi sağlığı ve iş güvenliği koşullarının iyileştirilmesi hedeflenmiştir. Temin edilecek makine ve teçhizatın finansmanında Dünya Bankası'ndan sağlanan 70 milyon dolarlık kredi kullanılmıştır. Bu proje kapsamında; elektro-hidrolik delici, elektro- hidrolik yükleyici, akülü lokomotif, çelik sarma, muhtelif uzunlukta hidrolik direk, monoray sistemi, telesiyej sistemi, toz ölçüm aletleri, ferdi CO maskeleri, gaz ölçüm aletleri, yer altı haberleşme ve izleme sistemleri, otomatik hava kapıları vb. alınmıştır. Bu bağlamda yapılan çalışmalar ve yatırımlar üretim yöntemlerini kolaylaştırmada direkt olmayıp dolaylı yolla iyileştirmeye yönelik olduğu görülmektedir.

Üretim yöntemlerinde kazı aracı seçimini belirleyen en önemli etkenler, kömür damarlarının jeoteknik ve jeolojik özellikleridir. Bunların yanı sıra, bir diğer önemli etken de, karar verici durumda olan işletmenin, içinde bulunduğu ekonomik şartlardır. Ekonomik şartlar ile birlikte, damarın jeolojik ve jeoteknik koşulları göz önüne alındığında işletmeci; işçi sağlığı ve iş güvenliğini de göz ardı etmemek kaydı ile yüksek randımanlı ve en düşük maliyetli üretim yöntemi ve kazı aracı tercih edecektir.

Damar eğimlerinin 45° 'den yüksek ve damar içi süreksizliklerinin yoğun olduğu Zonguldak Kömür Havzası'nda, 1990 öncesi dik damarların üretimi, oldukça güç ve maliyeti yüksek olan klasik üretim yöntemlerinden kara tumba veya dolgulu üretim yöntemleri (dişli ayak, uzun ayak) ile yapılmıştır.

Havzadaki kalın ve dik damarlarda uygulanan üretim yöntemlerinin olumsuzluklarını ortadan kaldırmak, daha güvenli ve daha ekonomik üretim yapmak için 1990'lı yıllarda yeni üretim yöntemlerinin arayışlarına başlanmıştır.

Havzanın yeniden yapılanması ve modernizasyonu kapsamında:

Yüksek basınçlı hava patlatmalı kazı sistemi

ANŞ dik damar mekanize kazı sistemi
CARDOX, sıvı karbondioksitle kömür kazısı sistemlerinin denenmesine karar verilmiştir (Akçın ve Kel, 1999)

Bahsi geçen bu sistemlerden Anş ve Cardox sistemlerinin başlangıç aşamasında ki kullanımlarında pratiklik açısından yaşanan olumsuzluklardan ötürü kabul görülmemiştir. Yüksek basınçlı hava patlatmalı kazı sistemi ise ilk olarak 1992 yılında, havzanın yeniden yapılanması çalışmaları çerçevesinde alınan, Yüksek Basınçlı Hava Patlatmalı Kazı Sistemi (YBHPKS), ilk olarak TTK Kozlu Taşkömürü İşletme Müessesesi, Sulu damarında pilot uygulaması gerçekleşmiştir.

Yüksek Basınçlı Hava Patlatmalı Kazı Sistemi 1990-2015 yılları arası TTK da birtakım panolarda uygulamalarına devam edilmiştir.

2015 yılından sonra ise mevzuat değişiklikleri sebebi ile sistem kullanım dışı kalmıştır.

YÜKSEK BASINÇLI HAVA PATLATMALI KAZI SİSTEMİNİN TARİHÇESİ

Yüksek basınçlı hava, ilk olarak kömür kırma işlemlerinde, delikler içine yerleştirilen özel patlatma üniteleri ile birlikte, 1934 yılında Amerika Birleşik Devletleri'nde kullanılmıştır. Sistemin Amerikan ocaklarında, oda topuk yönteminde ve uzun ayaklarda yaygın olarak kullanılması sonucunda, sistem 1953 yılında Fransız, 1955 yılında da İngiliz ocaklarında kullanılmaya başlanmıştır. 1960 yılı sonrasında sistemin dik damarlarda da kullanılabilmesi için Macaristan'ın Beta kömür ocağında çalışmalar başlatılmıştır. 1982 yılında geliştirilen ve daha önce 1,5 m uzunluğundaki kısa deliklerin yerine, 15-20 m uzunluğunda sondaj delikleri delinmiş, bunu takiben tijler çıkartılarak yerlerine patlatma üniteleri (shell) yerleştirilerek kömür üretimi yapılmıştır. Bu işlemlerin uzun süreler alması üzerine 1991 yılında sistem daha da geliştirilerek hem delik delen hem de patlatma işlemini kendi içinde gerçekleştiren özel patlatma üniteleri geliştirilmiştir (Kel, 1996)

Sistemin kurum içersindeki kronolojisi ise 1992 yılında Kozlu Müessesesi 1993 yılında Karadon Müessesesi 1994 ‘te ise Üzülmez Müessesesinde uygulanmaya başlanmış ve kullanımı panolarda giderek yaygınlaşmıştır.

TTK panolarında uygulama süreci boyunca bilimsel nitelikli çalışmalar da devam etmiştir. Şöyle ki 3 adet yüksek lisans tezi, 8 adet bilimsel makale ve 1 adet proje çalışmasında (DPT) konu irdelenmiştir.

Yüksek Basınçlı Hava Patlatmalı Kazı Sisteminin Kısaca Tanıtımı ve Çalışma Prensibi

Yüksek basınçlı hava patlatmalı kazı sistemi (YBHPKS), en kısa tarifiyle yüksek basınçtaki havanın deşarj sırasında hava partikülünün ani şok etkisi ile kömüre çarparak kömürde gevşetme esasına dayalı geliştirilmiş bir kazı sistemidir.

Yüksek basınçlı hava ile kömür kazısı, özellikle kalın ve dik damarlarda verimli ve güvenli olarak uygulanmış bir üretim yöntemidir.

Üretim yönteminin esası ise dik damarlarda ara katlı topuklardan üretim yöntemi olarak tarif edilmelidir. Yüksek basınç üretebilen kompresör, yüksek basınca dayanıklı boru şebekesi, delme-patlatma donanımı diye adlandırılan özel tijlerden oluşmaktadır. Kompresörden elde edilen 845 bar basınçtaki sıkıştırılmış hava panoya kadar oluşturulmuş yüksek dayanımlı boru şebekesi vasıtasıyla iletilir. Kömür damarı içinde sondaj makinası yardımıyla, tasarımı ve alaşımı özel olan patlatma tijleri ile açılan delikte hava deşarj yönlerinin istenen konumlandırma sağlandıktan sonra tij setinin yüksek basınç şebekesine yüksek basınca dayanıklı hortumlar yardımı ile güvenli bölgede olan şebeke valf kolunun bulunduğu kumanda tablasına bağlantısı yapıldıktan sonra çalışmaya hazır hale getirilir.

Bir sonraki aşama da ise kompresör çalıştırılarak sistem içersindeki basıncın yükselmesi beklenir. 800-840 bar'a ulaşan şebeke basıncı özel tijlerdeki hava kanallarının açılması ve tijdeki deşarj penceresinden sondaj deliği cıdarındaki kömüre ani şok etkisi ile kömürde kırma/ezme/itme şekilnde oluşan kazı şeklidir (Şekil 1).

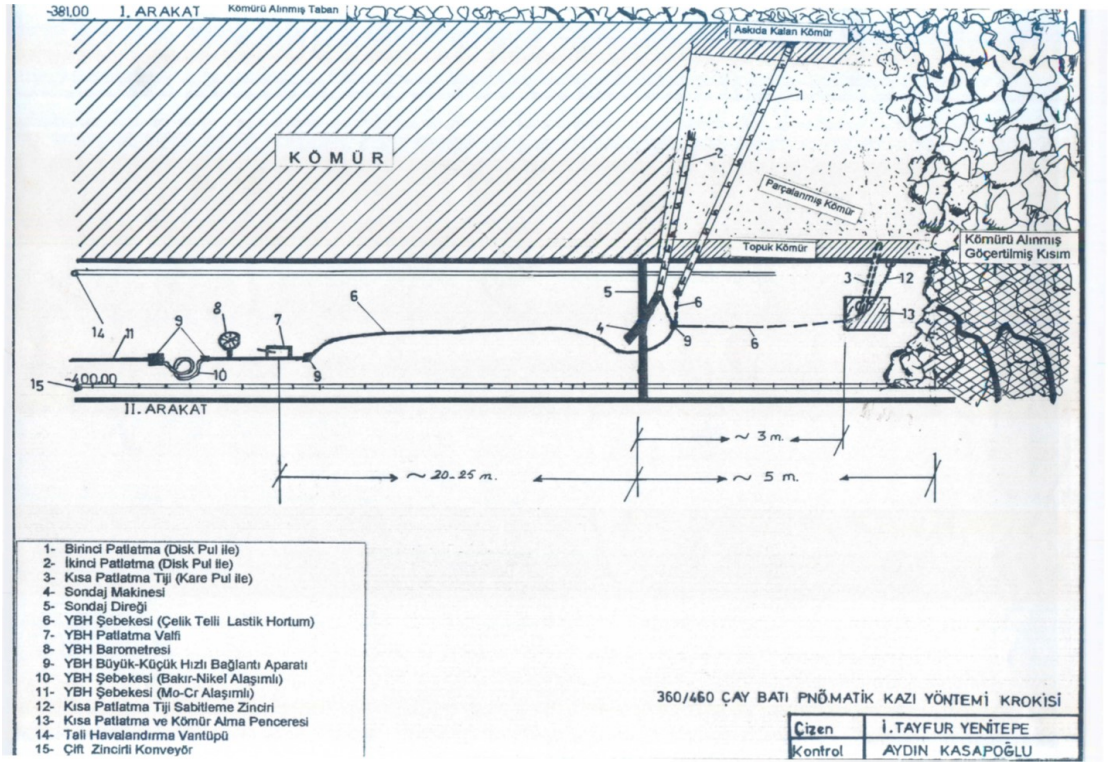

Şekil 1. Yüksek basınçlı hava patlatmalı kazı sistemi (YBHPKS) genel görünümü

Yapılan akademik çalışmalarda bahsi geçen şoktaki hava partikül hızının kömüre etkisi 20 ton olarak hesaplanmıştır. Bu şokun etkisiyle kömür damarında çatlaklar meydana gelerek kömürün parçalanması sağlanmaktadır.

YÜKSEK BASINÇLI HAVA PATLATMALI KAZI SİSTEMİNİN GÜNCEL DURUMU

Türkiye Taşkömürü Kurumunda 1992 – 2015 arasında nerdeyse çeyrek asra yakın bir zaman diliminde başarı ile uygulanmış bir sistem olarak kayıtlara geçmiştir. Hava patlatmalı kazı sistemi ile anılan dönemdeki tüvenan üretim miktarı; 4.500.000 ton dur.

Kasım 2013 Karadon Müessesesi, Kasım 2014 Kozlu Müessesesinde iş müfettişlerince havalandırma ile ilgili olarak tutulan raporlar nedeniyle kullanımı kısıtlanmıştır. Daha sonrasında ise Madenlerde İş Sağlığı ve Güvenliği Yönetmeliği'nde 10 Mart 2015 tarihinde tali havalandırma tarifinde yapılan değişiklikle yöntem tamamen yasaklanmıştır. Bu tarihten önce yönetmeliklerde ilgili çalışma alanına atfen bir tarif yoktur.

19 Eylül 2013 tarihinde 28770'nolu T.C. Resmî Gazete de yayınlan "Maden İşyerlerinde İş Sağlığı ve Güvenliği Yönetmeliği" ilgili madde de havalandırmanın tarifi şu şekilde tanımlanmıştır.

"10.7. Tali havalandırma sadece ana havalandırma akışı ile bağlantısı bulunan, ilerleme çalışmaları ve kurtarma çalışmalarının yapıldığı yerlerde uygulanır. Üretim yapılan yerlerde sadece çalışanların sağlık

ve güvenliği için yeterli ek tedbirler alınması şartıyla tali havalandırma yapılabilir. Tali havalandırmada kısa devreyi önleyecek tedbirler alınır."

Sistemin işleyişinde üretim bölgesindeki göçük sahada ortama deşarj olan metan gazının üst ara kat göçük bağlantısı ile pis hava istikametine geçişi olmaktadır. Üretim taban yolunda tali pervane yardımı ile yapılan güçlü bir havalandırma; göçük bölgesinden ani oturmalar dahil olmak üzere gelen yoğun metan gazı ile bir olumsuzluk yaşanmamıştır. İş güvenliği açısından oluşabilecek olumsuzluklar da dikkate alınarak yönetmelikteki ek tedbirler kapsamında geçmişte de uygulanmakta olan ilk patlatma anında tüm çalışanlar koruma amaçlı olarak temiz hava geliş istikametinde ki toplanma yerine toplanması talimatlandırılmıştır. Patlatma diye tabir edilen yüksek basınçlı havanın deşarj yapılması uygulaması yanı sıra çoklu sensör gurubu, yangın bekleme barajı, su barajı, her 20 metrede bir suni teneffüs istasyonu yapılandırılması gibi ilave ek tedbirler ile birlikte çalışmalara devam edilmiştir (Şekil 2).

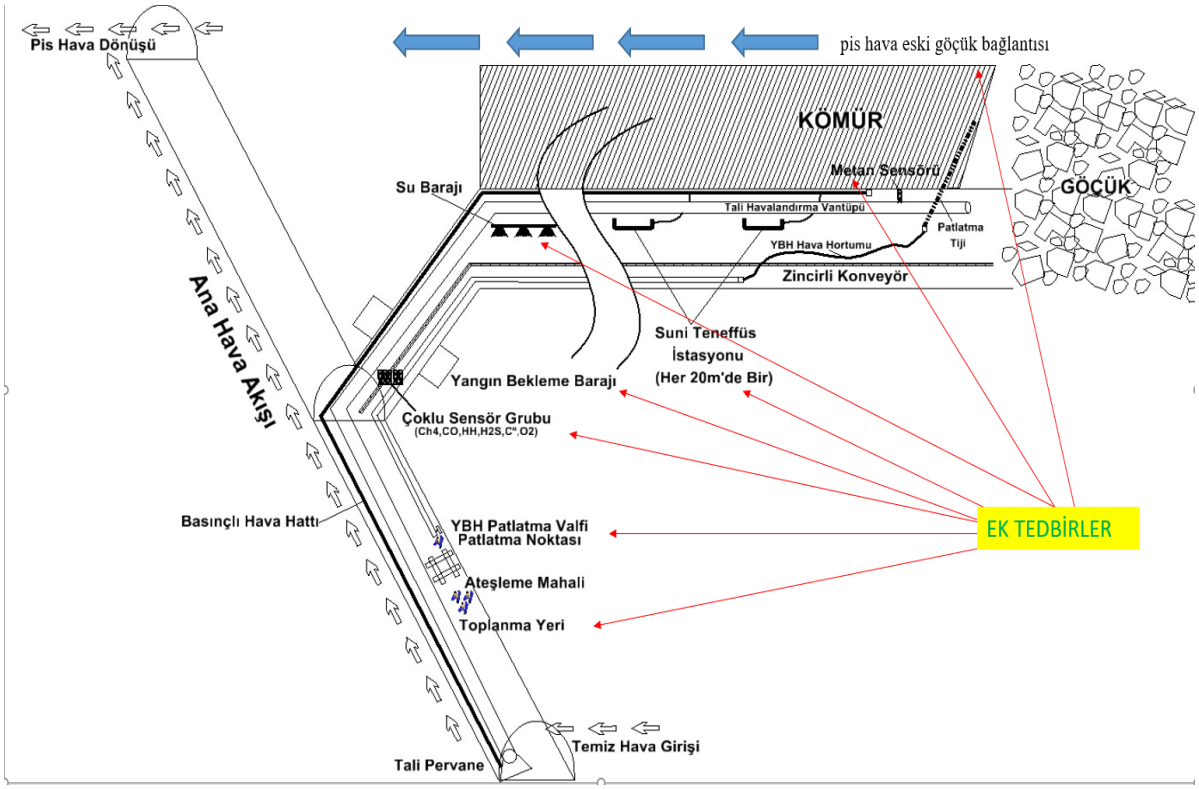

Şekil 2. Pnömatik kazı yapılan bölgenin ek tedbirler ile birlikte genel görünümü.

MEVZUAT İLE İLGİLİ HUKUKİ İKİ VAKANIN İNCELENMESİ

Vaka 1

Çalışanların sağlık ve güvenliği için yeterli ek tedbirler alınması şartıyla tali havalandırma ile üretim süreci devam ederken Kasım 2013'te Karadon Müessesesinde ÇSGB iş müfettişlerince alınan kapatma kararına ilişkin Kurumun itirazı olmuştur.

İtiraz sonucunda dosya bilirkişiye gitmiş ve bilirkişinin tespitleri ise şöyle olmuştur.

Yapılan keşif ve dosya içeriğinin incelemesi sonucu aşağıdaki bilgi ve bulgulara erişilmiştir.
1. Yüksek Basınçlı Delme Patlatma Sistemi (YBDPS) madencilik literatüründe yer bulmuş, dik ve yüksek eğimli damarlarda uygulanmaktadır. Belirtilen tipte damarlarda diğer yöntemlere göre iş güvenliği ve verimlilik açısından avantajları olduğu bilinmektedir. Yöntemde; tavan-taban taşı sağlam, birkaç metre kalınlıklı kömür damarı içinde bir ana başyukarı sürülmektedir. Bu başyukarının farklı kotlarından sağlı-sollu bacalar oluşturarak, ardından en üstteki bacadan başlamak üzere baca tavanından yukarı doğru sondaj yapılarak deliklerin açılmaktadır. Bu deliklere yerleştirilen tüplere ani şiddetli basınçlı hava vasıtasıyla kömürün parçalanmasının sağlanması ve eğimden faydalanarak gevşeyen kömürün alınması gerçekleştirilmektedir.
2. TTK'nın YBDP Sistemine yönelik detaylı bir araştırma sonucunda uluslararası uzman kuruluşlardan destek alarak 1990'lı yıllardan bu yana uygulamaya başlamış olduğu görülmüştür. Çalışmalar konuda uzmanlaşmış mühendis, teknik personel ve nezaretçiler tarafından yürütülmektedir. Arında az sayıda çalışan ile (5-6 çalışan) günde adam başı 15-20 ton gibi havza koşullarında oldukça yüksek sayılacak bir üretim değerine ulaşılabilmektedir.
3. Arının hemen gerisinde metan sensörü bulunmakta ve sensör değerinin 1,5'a erişmesi durumunda konveyör enerjisi otomatik olarak kesilmektedir.
4. Havalandırma sisteminde arıza olması durumunda işçiler temiz hava bölgesine çekilmektedir.
5. Patlatma güvenli bölgeye çekilmiş usta ve yardımcısı tarafından yapılmakta, bu esnada diğer işçiler temiz hava kesiminde beklemektedir.
6. Uygulanan YBDPS kömür kazısı yönteminin, Zonguldak Havzası'nda yaşanan iş kazaları göz önüne alındığında daha az riskli olduğu görülmüştür.

Sonuç ve kanaat:

Davaya konu olan Pnömatik diye adlandırılan ve basınçlı havalı patlatmalı kazı metodu ile üretim yapılan Tabanın" kapatılması kararı, üretim için kullanılan yöntemin güvenlik açısından sakınca yaratıp yaratmadığının tartışılmasından çok, yasal mevzuata uygunluk açısından ele alınması gerekir. Bu durumda Maden İşyerlerinde İş Sağlığı Ve Güvenliği Yönetmeliği'nin yukarıda belirtilen ilgili hükümleri gereğince; çalışma alanına iki farklı yoldan bağlantısı olmadığı ve tali havalandırma uygulandığı için işin durdurulması kararının yerinde olduğu görülmektedir. TTK'nın davaya konu olan kapatma kararına itirazı ancak ilgili yönetmelik hükümlerinde yapılacak değişikliklerle değerlendirilebilir. (Bilirkişi Raporu, 2013)

Bilirkişi heyetinin tespit ve keşif bulgularında, üretim yönteminin tarifinde özellikle iş güvenliği ve iş kazalarındaki düşük risk ve üretim verimliliği yüksek bir yöntem. Aynı zamanda uygulama deneyiminin de yeterli olan bir yapıdan bahsettiği dikkat çekmektedir. Yüksek üretim verimi ve düşük kaza risk oranı madencilik faaliyetlerinde istenen arzu edilen bir durumdur. Ancak yasal mevzuat bu şekilde bir çalışma şekline izin vermemektedir.
Başka bir deyişle bilirkişinin "sistem gerek işgüvenliği açısından gerek ekonomik ve kolaylık açısından gayet güzel ama siz Mevzuata takılıyorsunuz" demek istemiş olabilir mi sorusu akla gelmektedir.

Vaka 2

Kasım 2014 Kozlu Müessesesinde alınan kapatma kararına ilişkin Kurumun itirazı olmuştur. İtiraz sonucunda dosya bilirkişiye gitmiş ve bilirkişinin tespitleri ise şöyle olmuştur.

Durdurma kararının eleştirisi;
Durdurma kararına esas maddelerden ilki (Tüm yeraltı çalışmalarında, çalışanların kolayca ulaşabileceği, birbirinden bağımsız ve güvenli yapıda en az iki ayrı yoldan yerüstü bağlantısı bulunur. Bu yollar arasındaki topuk 30 metreden aşağı olmaz, bu yolların ağızları aynı çatı altında bulundurulmaz.) genel olarak bir yer altı ocağının altyapısı ile ilgili olup bir panoya indirgenmesi hatalıdır. Panonun havalandırma ve nakliyat alt yapısı uygundur. Dolayısıyla gerekçe geçersizdir.

Durdurma kararına esas ikinci madde ise (Tali havalandırma sadece ana havalandırma akışı ile bağlantısı bulunan, ilerleme çalışmaları ve kurtarma çalışmalarının yapıldığı yerlerde uygulanır. Üretim yapılan yerlerde sadece çalışanların sağlık ve güvenliği için yeterli ek tedbirler alınması şartıyla tali havalandırma yapılabilir. Tali havalandırmada kısa devreyi önleyecek tedbirler alınır.

-Hazırlık işleri veya grizu birikimlerini dağıtmak amacıyla yapılan işler dışında, bölmeyle veya borularla havalandırma yapılmaz."; işletme yönteminin gereği olarak pano içi bacalar tali havalandırma usülleri ile havalandırılmakta olduğundan geçersizdir. Pano içi bacalar üretim amaçlı değil, üretime alınacak topukları oluşturmak amaçlıdır. Topuklar göçertilirken (üretim yapılırken) tali havalandırma panodaki ana havalandırmaya yardımcı olmak üzere çalıştırılmaktadır. Tali vantilatörlü üfleyici havalandırma uygulanmaktadır. Dolayısıyla gerekçe geçersizdir.

SONUÇ:
Havzada, genel jeolojik koşullar ve tektonik hareketler itibarıyla, modern–mekanize kazı ve tahkimat donanımlarının uygulanmasına müsait üretim işyerlerinin oluşturulması mümkün değildir.
İş durdurulmasına konu olan pano, eğimi dolayısıyla (60-70^0) , "zor koşullarda madencilik" çalışmaları kapsamında olup bu tür bir panoda uygulanabilecek çeşitli işletme metotları vardır (diyagonal ayak, tavan ayak, taban ayak ve topuklu ayak). Kozlu Müessesesi uzun geçmişinde diyagonal ayak (dişli ayak) ve topuklu ayak (tumba bacaları, kılçık toplama, karatumba) yöntemlerini başarıyla uygulayagelmiş ve deneyim kazanmıştır. Bu yöntemlerin tümü iş sağlığı ve güvenliği açısından benzer tehlike ve risklere sahiptirler. Pano içinde kazı-tahkimat-havalandırma ve nakliyat çalışmaları özen ve dikkat gerektirir. Madencilik ilke ve kurallarından ödün verilmeden çalışılması koşuluyla Domuzcu panosunda üretim faaliyeti halen uygulanmakta olan "kılçık baca" yöntemiyle sürdürülebilir.
Sonuç olarak, ÇSGB İş Teftiş Kurulu Başkanlığı Ankara Grup Başkanlığı'nın Kozlu Müessesesi Domuzcu Panosunda "İşin Durdurulmasını" öngören Heyet Kararı'nın dayandırıldığı gerekçeler madencilik tekniği ve mevzuat açısından geçersiz olup TTK'nın itirazı yerindedir. İşin durdurulmasıyla ilgili heyet kararının kaldırılmasında yarar vardır. Saygılarımızla. 16.01.2015 (Bilirkişi Raporu, 2015)

Vaka 2'nin bilirkişi raporundan çok kısa bir süre sonra 10 Mart 2015 tarihli resmî gazetede Maden İşyerlerinde İş Sağlığı Ve Güvenliği Yönetmeliğinde Değişiklik Yapılması Hakkında Yönetmelik ile tali havalandırma tarifinde değişiklik yapılmıştır. Yeni madde şu şekildedir.

MADDE 18 – Aynı Yönetmeliğin Ek-3'ünün 10.7 nci bendi aşağıdaki şekilde değiştirilmiştir.
"10.7. Tali havalandırma sadece ana havalandırma akışı ile bağlantısı bulunan hazırlık ve kurtarma çalışmalarının yapıldığı yerlerde uygulanır. Tali havalandırmada kısa devreyi önleyecek tedbirler alınır. Tali havalandırmada kullanılan vantüpler antistatik ve alev yürütmez özellikte olur."

Görüldüğü üzere maddeden üretim sözcüğü çıkartılmıştır.

30 Mart 2013 tarihinde T.C. Resmi Gazete de yayınlanan "işyerlerinde işin durdurulmasına dair yönetmelik" yürürlükte iken hazırlanan 2. Vaka daki bilir kişi raporuna istinaden TTK açmış olduğu kapatma davasına itirazı kazanmıştır. Ancak 11 şubat 2016 ilgili yönetmeliğe ek olarak T.C. Resmi Gazete de yayınlanan (Ek: RG-11/2/2016-29621) İşin Acil Durdurulmasını Gerektiren Durumlar başlığı altında 2. Madde de

b) Yeraltı maden işyerlerinin hazırlık çalışmaları dışında en az iki yoldan yer üstü bağlantısı bulunmaması.

Şeklindeki ilave madde hem kara tumba yöntemini aynı zamanda delme patlatma yönteminin yasaklanmasında kesin hükümle tarifi yapılmıştır.

Bahsi geçen olayların kronolojik sıralanması şöyledir.

30 Mart 2013 işyerlerinde işin durdurulmasına dair yönetmelik
19 Eylül 2013 Maden İşyerlerinde İş Sağlığı Ve Güvenliği Yönetmeliği
Kasım 2013 Karadon Müessesesi kapatma kararı
13 Mayıs 2014 Soma Maden Kazası
28 Ekim 2014 Ermenek Maden Kazası
Kasım 2014 Kozlu Müessese durdurma kararı
16 Ocak 2015 Kozlu Müessese durdurma kararının kaldırılması (Vaka 2)
10 Mart 2015 Maden İş yerlerinde İş Sağlığı Ve Güvenliği Yönetmeliğinde Değişiklik Yapılması Hakkında Yönetmelik (tali havalandırmanın üretimde kullanılmaması)
11 Şubat 2016 iş yerlerinde işin durdurulmasına dair yönetmelikte değişiklik (en az iki yoldan yer üstü bağlantısı)

Bu kronolojik sıralamada dikkat çekilmek istenen; bilirkişilerin üretim yöntemi tarifinde güvenli diye tarif ettikleri Karadon Müessesesindeki delme patlatma panosunun kapatılma kararı ve daha sonra 2014 yılında ki iki büyük maden kazasının (Soma ve Ermenek) çok yakın bir zaman sonrasında ise daha kazaların paniği geçmeden Kozlu Müessesesindeki on yıllarca uygulanmış kara tumba yönteminin durdurma kararıdır. (Bu durdurma kararı iş mahkemesince daha sonra kaldırılmıştır.)

Durdurma kararının kaldırılmasından 2 ay gibi kısa süre sonra ise iş mahkemesinin durdurma kararının kaldırılmasında dayanağı olan bilirkişi atıflarının önüne geçebilecek şekilde ilgili maddeden üretim sözcüğü çıkartılarak yapılan yönetmelik değişikliği ise ilginç bir tesadüftür.

Yönetmelik Değişikliğinin Kurum ve Dik Damar Madenciliğindeki Etkileri

Zonguldak havzası taşkömürü toplam rezervi 1.513.731.677 (TTK 2020 faaliyet raporu tablo 15) ve bu rezervin %27' si eğim ve kalınlık olarak pnömatik üretim yöntemine uygun olarak gözükmektedir. Bu sayı yaklaşık 410 milyon tona tekabül etmektedir. Tabloda 2001-2012 yılları arasındaki kurum içerisindeki yüksek basınçlı hava patlatmalı kazı yöntemi ile yapılan üretim miktarlarını ve toplam üretimdeki payı verilmiştir. 1992-2015 yılları arasında hava patlatmalı kazı sistemi ile üretilen kömür miktarı 4.106.102 ton olarak kayıtlara geçmiştir. (Tablo 1)

Tablo 1. Yıllara göre pnömatik Kazı üretim miktarları.

YIL	Yüksek Basınçlı Hava Patlatmalı Kazı Yöntemi İle Üretim (ton)	Toplam üretimdeki payı (%)	TOPLAM (ton)
2001	363.449	10	3.492.104
2002	455.812	14	3.244.812
2003	471.863	16	2.954.333
2004	374.208	13	2.805.654
2005	353.853	14	2.621.263
2006	212.733	9	2.297.173
2007	351.482	14	2.423.719
2008	249.206	11	2.335.457
2009	280.743	10	2.833.243
2010	363.626	13	2.727.414
2011	317.643	12	2.607.182
2012	226.814	9	2.441.270

YÜKSEK BASINÇLI HAVA PATLATMALI KAZI SİSTEMİNİN İŞGÜVENLİĞİ AÇISINDAN DEĞERLENDİRİLMESİ

Örneklerle de gösterilen bilirkişi raporlarında delme patlatma üretim yönteminde özellikle iş kazalarının diğer klasik yöntemlere nazaran önemsenecek şekilde düşük olduğu vurgulanmıştır.

1992-2015 yılları arsında uygulanan bu sistemde uygulama boyunca havalandırma menşeili başta olmak üzere ve göçükten ötürü ölümlü iş kazası yaşanmamıştır. Oysa Klasik yöntem ve diğer yöntemlerde ki göçük menşeili ölümlü iş kazaları ise maalesef olmuştur.

Sistemin çalıştırma doğası gereği panoda çalışan sayısı diğer yöntemlere kıyasla çok çok düşük olduğundan genel kaza istatistikleri de düşüktür (el kol bacak yaralanmaları gibi). Hava ile patlatma sırasında ya da kömürü gevşetme sırasında arında kimse yoktur.

Hava patlatmalı kazı sisteminin uygulandığı hiçbir panoda kendiliğinden yanma olayı görülmemiştir.

Patlatma sonrası açığa çıkan metan gazının havadan hafif olması nedeniyle, metan; ayak arkası göçüğü takiben üst katlardaki eski imalatlara intikal etmektedir. Yapılan ölçümlerde metan oranının arakat üretim tabanlarında ve hava dönüş yollarında iş sağlığı ve güvenliği mevzuatındaki çalışma sınırlarının üzerine çıkmadığı tespit edilmiştir. Metan ve kömür tozu patlamalarına karşı güvenli olduğu da görülmektedir. Yüksek basınçta hava şoku sonrası zehirli gazlar ortaya çıkmadığı gibi, sıkıştırılmış yüksek basınçlı hava, deşarj sırasında sıcaklık düşüşü ile ortamı soğutarak ısıyı düşürücü etki yapmaktadır.

Hava patlatmalı kazı sisteminde üretim çalışmaları sırasında ateşli patlayıcı kullanılmamıştır.

SONUÇ VE ÖNERİLER

Türkiye Taşkömürü Kurumu'nda özellikle dik kömür damarlarında 1992-2014 yılları arasında başarı ile uygulanmış olan yüksek basınçlı hava patlatmalı kazı sistemiyle üretim yöntemi; iş sağlığı ve

güvenliğinin en üst düzeyde sağlandığı, diğer üretim yöntemlerine nazaran en düşük üretim kaybı ile en yüksek randımana ulaşılmasını sağlayan bir yöntem olarak görülmektedir.

Madenlerde İş Sağlığı ve Güvenliği Yönetmeliği'nde 10 Mart 2015 tarihinde tali havalandırma tarifinde yapılan değişiklikle, YBHP Kazı Sisteminin uygulama imkanı kalmamış, dik kömür damarlarında üretim faaliyeti sonlanmış bulunmaktadır. Yapılan tüm yatırımlar atıl kalmıştır. Zonguldak Taşkömürü Havzasında TTK'nın uhdesindeki rezervlerin yaklaşık %45'i dik damar kategorisinde olup havzada atıl duruma gelen dik kömür damarlarındaki rezervler 300 milyon ton olarak belirlenmiş bulunmaktadır.

Yerli ve milli kaynaklarımıza büyük ihtiyaç duyulan günümüzde Türkiye genelinde TTK dışında aynı durumda bulunan özel kömür ruhsatlarında da dik damarlardaki üretim durmuş ve kömür rezervleri üretilemez hale gelmiştir.

Devletin en önemli taşkömürü kuruluşu tarafından yıllarca başarıyla ve verimli bir şekilde uygulanan YBHP kazı sisteminin iş sağlığı ve güvenliği yönünden sakıncalı olmadığı mevcut uygulamalardan ve deneyimlerden görüldüğünden sistemin uygulanmasına imkan verilerek "dik kömür damarlarında" üretime olanak sağlanması ulusal çıkarlar açısından elzem olarak görülmektedir.

Mevcut yönetmelikler ile ara katlı pnömatik patlatmalı üretim yönteminin panosunun tüm hazırlıkları yapılabilmektedir. Bakir bir sahada gerek kat lağımı gerek arakat taban yollarının sürülmesinde ve hatta başyukarılarının sürülmesinde tali pervane kullanılabilmektedir. Çünkü hazırlık aşaması olarak değerlendirilir. Bu hazırlık aşaması aslında degaj, göçük ve akıntı anlamında en riskli dönemdir. Bağlantıları yapıldıktan sonra üretime hazır olan panonun degaj anlamında en risksiz devresi başlamıştır. Panonun rahatlamış olan bu döneminde üretim yapılamaz olması ise düşündürücüdür.

Öneri;

Tali havalandırmayı tanımlayan ve 19 Eylül 2013 tarih ve 28770 sayılı T.C. Resmi Gazete'de yayınlanarak yürürlüğe giren Maden İşyerlerinde İş Sağlığı ve Güvenliği Yönetmeliği'nin Yeraltı Maden İşletmelerinde İş sağlığı ve Güvenliği'ni düzenleyen ek-3'ün 10.7 maddesinin son değişiklik ten önceki hali ile devam edilmesi önerilmektedir.

"10.7. Tali havalandırma sadece ana havalandırma akışı ile bağlantısı bulunan, ilerleme çalışmaları ve kurtarma çalışmalarının yapıldığı yerlerde uygulanır. Üretim yapılan yerlerde sadece çalışanların sağlık ve güvenliği için yeterli ek tedbirler alınması şartıyla tali havalandırma yapılabilir. Tali havalandırmada kısa devreyi önleyecek tedbirler alınır" şeklinde.

Ya da mevcut yönetmelikte hava patlatmalı kazı sistemi ile üretim yönteminin kapsam dışına çıkarılması önerilir.

KAYNAKLAR

Akçın, N. A.KEL, K. (1999). Zonguldak Kömür Havzası'nda Klasik Üretim Yöntemlerine Alternatif Olarak Denenmekte Olan Yöntemler. Türkiye'de Kömür Politikaları ve Temiz Kömür Teknolojileri Sempozyumu Bildiriler Kitabı, TMMOB Kimya ve Maden Mühendisleri Odaları, Ankara

Bilirkişi Raporu 2013 1.iş mahkemesi dosya no: 2013/640

Bilirkişi Raporu 2015 2.iş mahkemesi dosya no: 2014/1144

Kasapoğlı, A (2019) Kişisel görüşme Maden Mühendisi Türkiye Taşkömürü Kurumu

Kayabalı, N (2020) Kişisel görüşme Maden Mühendisi Türkiye Taşkömürü Kurumu

Kel K. (1996) 10. Kömür kongresi, Yüksek basınçlı hava patlatmalı kazı teknolojisiin karadon ocaklarındaki uygulamaları

Yamudi, C. (2000) Cardox Kazı Sisteminin TTK Kozlu Ocaklarında Kullanımının Araştırılması Zonguldak Karaelmas Üniversitesi Fen Bilimleri Enstitüsü, Yüksek Lisans Tezi Zonguldak

MICRO GRINDING IN VERTICAL MILL OF ŞIRNAK ASPHALTITE SLIME, FLY ASH/ CHAR/ SOOT BY MICROWAVE RADIATION

Y.I. Tosun [1, *], F. Çiçek [2]

[1] *Şırnak University, Engineering Faculty, Mining Engineering Department*
*(*Sorumlu yazar: yildirimismailtosun@gmail.com)*
[2] *Azerbaijan National Science Academy, Radiation Institute*

ABSTRACT

Depending on advanced technological developments in energy production the low-quality coals needed the most economical technologies and even in order to make it possible to produce coal-derived products. Compliance with environmental norms of coal grinding or washing of various type of coals, feasible combustion systems and energy production facilities are needed in today's modern technology, also enable the production of liquid and gaseous coal fuels. However, raw materials and chemical nature of them requires a variety of adaptation methods. The chemical and cement industry need to work together to provide the basic information required in pilot scale grinding over many materials. This study examined the high sulfur and ash types of Kütahya Gediz lignite, Sirnak asphaltite and coal shale. The representative samples were taken from local areas of the lignite. Fundamentally, the conditions regarding better desulfurization way, easy grinding lignite and washing, high calorific value lignite yield, 24% high Hardgrove Grinding Index were determined at the chemical grinding of high fuel producing yield. For this purpose, chemical ground further washing for Kütayha Gediz lignite, Sirnak asphaltite and coal shale were discussed. The optimized use of microwave radiated vertical mill conditions is reported as 75 gr/l solid feed rate of char and fly ash received from combusted coal burning boilers in Şırnak, Turkey.

Keywords: Microwave grinding, coal grinding, coal breakage, hgi, micro grinding, vertical mill, şırnak asphaltite slime, fly ash, waste slag, char, microwave radiation

INTRODUCTION

For grinding raw materials in a grinding mill plant, the chemical treatment method is becoming much effective in energy consumption of mills. Power needs will decrease with chemically fractured material. In the standards, the tests of mainly Bond and Hardgrove Index are commonly used as an industrial standard providing distinct energy requirements in all industrial applications. A chemically activated grinding process can save energy in grinding of hard materials, such as cement clinker, granulated slag, limestone, and quartz. This process subjects to the aggregate materials to high internal fracturing weakness between the macro and micro fissures and crack faces. Although this comminution technique closely resembles natural alteration, the degree of alteration by chemical breakage in chemical activation achieved within the chemical pots is carried out, even after only a single pass. Howard & Datta determined that chemical comminution having many advantages, this method using ammonia, providing ash liberation in coal grinding with chemical breakage (Howard & Datta, 1977, Howard & Datta, 1976).

A Bond Work Index test is a standard test for determining the Ball Mill Work Index of a sample of ore. It was developed by Fred Bond in 1952 and modified in 1961 (Bond, 1952). In the design of

grinding circuits in a mineral processing plant, the Bond method is widely used for a particular material in dimensioning mills, determining power needs and in the evaluation of performance. Its use as an industrial standard is very common, providing satisfactory results in all industrial applications.

The Hardgrove work index can be used not only for determining the grinding power for coal and soft rocks but also to classify the difference in hardness of different coals and coal shale. Every coal material has a characteristic Hardgrove index at standard level. The power required to break the high ash coal fine is higher due to the high content of harder shale material (Refahi et al., 2007, Tavares& King, 2005).

The Hardgrove index is widely used to estimate the power required to grind microwave treated fractured coal materials. Because of the short determination of this index, fracturing intensity has investigated the effect of mechanical parameters on grinding, and the relationship between them (ASTM, 2008).

The strength values obtained by the micro-cracks, fractures, tensile stress cracks and pores created by microwave treatment are the common geological design parameters for the materials in concrete structures or rocks. The parameters regarding rocks give the failure values to the construction engineers. Thermal fracturing and following comminution on the purpose is to break rock to given sizes. It has improved the assessment of tests interrelated between the failure energy and the final size reduction and surface area.

It is significantly mentioned that alteration of cement raw materials, such as limestone, marl, tuff or shale rocks, interrelation between compressive strength and propagating fissures. Microwave alteration by improved thermal breakages changed the ground characteristics of coal (Unland & Szczelina, 2005, Toroman & Uçurum, 2012, Gökçen et al., 2012). The microwave heating improves the chemical technique. Microwave act and chemical treatment are especially useful for coal grinding in pulverized coal burning industries.

The uniaxial compressive failure load of the cement raw materials interrelated with the grinding so that the relationship can be defined among the Bond Work and Hardgrove Index values and compressive strength of chemically fractured coal characteristics will emphasize the great importance. The aim of this study is to investigate the behavior of coal and shale under different microwave conditioning methods using 0.1M sulfuric acid and waste acidic water to establish a relation among strength and HGI properties and Bond Grindability, Bond Work Index.

MATERIAL & METHODS

In this study, Point load index I_c and uniaxial strength were initially measured for the coal and shale samples. Standard Bond grindability tests were carried out and work indices (Wi) were calculated. The proximate analysis of coal samples is given in Table 1. The chemical composition of the shale sample is also presented in Table 1.

Table 1. Proximate Analysis of Coal and Chemical composition of shale samples used in experiments. FC: Fixed Carbon,DC:Dried Coal, ADC:Air dried Coal,OC: Original Coal

Samples	Fixed Carbon,%	Volatile Matter,%	Ash,% DC	Moisture,%ADC	Total S,%ADC	Calorific Value,
Kütahya Gediz Lignite	40.55	60.96	36.1	16	6.1	3207
Şırnak Asphaltite	40.28	62.5	39.4	0,2	6.6	4820
	CaO,%%	SiO_2,%	Na_2O,%	MgO,%	K_2O,%	LOI, ,%
Asphaltite Shale	5.42	54.8	2.1	4.1	2.1	2.15

The Standard Bond Grindability Test

The most widely known measure of grindability is Bond Work Index which was defined as the resistance of the material to grinding and quantified the specific work input (kWh/t) required to reduce the material from theoretically infinite size to 80% passing 0.106 mm[4]. The work index is subject to variations due to variations in the inherent properties of minerals and rocks, variations in the grinding environment and variations in the mechanism of energy transfer from the grinding equipment to its charge.

The standard Bond grindability test is a closed-cycle dry grinding and screening process, which is carried out until steady state condition is obtained. This test has been described as follows (Unland & Szczelina, 2005, Toroman & Uçurum, 2012, Gökçen et al., 2012).

In the design of grinding circuits in a mineral processing plant, the Bond method is widely used for a particular material in dimensioning mills, determining power needs and in the evaluation of performance. Its use as an industrial standard is very common, providing satisfactory results in all industrial applications. Despite having many advantages, this method has some drawbacks, such as being tedious and time consuming, and also requiring a special mill. Due to these difficulties, a number of easier and faster methods have been developed to determine the Bond work index (Toroman & Uçurum, 2012, Gökçen et al., 2012).

The general characteristic of all these methods is the need for either a Bond mill or a Standard laboratory mill. A different, non-standard method for determining the Bond work index was presented using an experimental relationship between the Bond work index and the mechanical and strength properties of the material (Li et al., 2005, Özbayoğlu et al.,2008).

The standard Bond grindability test is a closed-cycle dry grinding in a standard ball mill (30.5x30.5 cm) and screening process, which is carried out until steady state condition is obtained. This test was described as in the standard. The feed samples had the particle size distribution as illustrated in Figure 1 and 2. The microwave activated samples at 20 minutes time period were tested for HGI and Bond grindability.

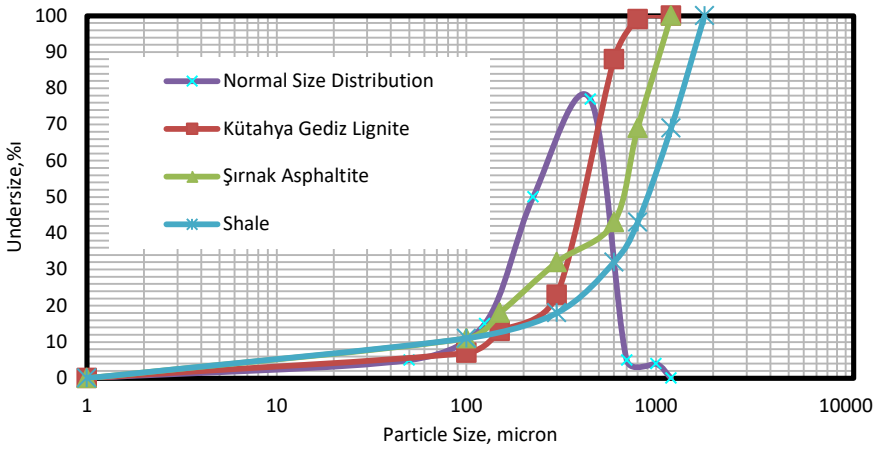

Figure 1. Particle Size Distribution and Normal Size Distribution of HGI Coal and Shale

Hardgrove Index Method

The HGI tests on parent coals and their binary and ternary blends were carried out using the standard Hardgrove method. For a comparative study, four standard reference coals were also used. The gross representative samples, weighing 1 kg, were collected by engineers for each coal seam with 10 increments taken following the ASTM D 409-08 procedure (ASTM, 2008). A representative sample was obtained using the coning and quartering technique.

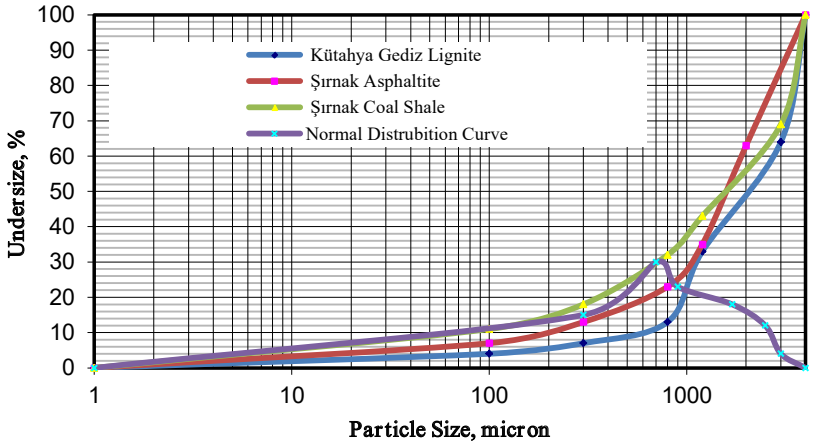

Figure 2. Particle Size Distribution and Normal Size Distribution of Bond Test Coal and Shale Samples.

For the determination of the HGI values, each gross sample was crushed to 4,75mm (4 mesh) in an impact crusher. The crushed sample was split into smaller lots of 250 g, using a standard method of sampling. Samples each weighing 250 g was dried in a microwave oven at 80^{o}C for 20 minutes until a constant heating observed. Each air-dried sample of 4.75mm in size was placed on a 1.18mm sieve nested with a 0,600 mm sieve. The 1.18mm fraction was ground in a laboratory grinding mill until the whole material passed through the 1.18mm sieve, followed by sieving through the 0,600 mm sieve. Sieving of each sample was performed by a mechanical sieving machine for five minutes. The fine sieving procedure was changed by the thermal grinding in the thermal tension method (Austin, 2005,

Bergstrom, 1985, Tavares and King, 1998). The below 75 μm fraction was weighed for determination by the standard Hardgrove Grindability Indice by an HGI machine.

RESULTS AND DISCUSSION

Bond Tests by Microwave Act

The material is packed to 700 cc volume using a vibrating table. This is the volumetric weight of the material to be used for grinding tests. For the first grinding cycle, the mill is started with an arbitrarily chosen number of mill revolutions. At the end of each grinding cycle, the entire product is discharged from the mill and is screened on a test sieve (P_i). Standard choice for P_i is 106 micron. The oversize fraction is returned to the mill for the second run together with fresh feed to make up the original weight corresponding to 700 cc. The weight of product per unit of mill revolution, called the ore grindability of the cycle, is then calculated and used to estimate the number of revolutions required for the second run to be equivalent to a circulating load of 250%. The process is continued until a constant value of the grindability achieved, which is the equilibrium condition. This equilibrium condition may be reached in 6 to 12 grinding cycles. After reaching equilibrium, the grindabilities for the last three cycles are being averaged. The average value was taken as the standard Bond grindability (G_{bg}).

The products of the total final three cycles are combined to form the equilibrium rest product. Sieve analysis is carried out on the material and the results are plotted in order to find the 80% passing size of the product (P_i). The samples are crushed in a laboratory scale jaw crusher, and then the standard Bond grindability test is performed. The Bond work index values (Wi) are calculated from the equation below.

$$W_i = 1.1 * \frac{44.5}{P_i^{0.23} * G_B^{0.82} * \left[\left(10/\sqrt{P_{80}}\right) - \left(10/\sqrt{F_{80}}\right)\right]} \quad (1)$$

where W_i is the work index (kwh/t); P_i, screen size at which the test is performed (106 μm); G_B, Bond standard ball mill grindability, net weight of ball mill product passing sieve size P_i produced per mill revolution (g/rev); P_{80}, sieve opening which 80% of the product passes (lm); F_{80}, sieve opening which 80% of the feed passes (μm).

The Grindability of samples was determined from HGI and Bond test and the average values with minimum and maximum values for each sample type are given in Table 2.

Table 2. Grindability properties of using rocks

Rock Name	G (g/rv)	Wi (Kwh/t)	HGI	Density
Asphaltite Shale	3.23	7.2	56	2.62
Claystone	3.73	7.6	52	2.61
Kütahya Gediz	2.52	6.7	72	1.71
Şırnak Asphaltite	3.39	7.7	57	1.81

In experimental studies, The Bond grindability of Şırnak coal shale is the most difficult than other samples. The biggest reasons of low Bond grindability, the porosity of sample was low is based on the solid rock texture.

The rocks of Şırnak asphaltite and shale were showing the similar mechanical quality. There were slight differences in comminution characteristics. The reason of this condition, their porosity has similar as the structure of coal.

Mechanical Quality of Şırnak Rocks

The strength of samples was determined from compressive load test and the average values with minimum and maximum values for each sample type are given in Table 3.

Table 3. Compressive strength of Coal and Shale Samples

	I_s Point load Strength, kg/cm^2	**σ,Uniaxial Compressive Strength, kg/ cm^2**
Asphaltite Shale	18.9-25.0	77.0
Claystone	19.8-26.0	86.0
Kütahya Gediz Lignite	24.0-44.0	52.0
Şırnak Asphaltite	27.0-44.0	60.0

HGI Tests by Microwave Act

The effect of period of microwave activation on grinding was tested. The graphs were observed as illustrated in Figure 3. Two days treatment was sufficient for developing grindability manner of the coal samples. HGI values increased at about 24 % at 20 minutes microwave radiation period. The relationship among Bond Grindability and HGI values were similar in microwave treated coal samples. The most important reason of the relationship was the same as in the breakage under chemical shattered samples and porous structure is more effective rather than solution in the grinding mill.

The microwave treated samples were ground in Bond and Hardgrove equipment and the results are illustrated in Figure 3 and 4. As seen in Figure 3 microwave treatment increased finer particle size fraction of minus 0,2 mm at about 13%. Bond breakage rate at 200 micron was higher for Şırnak asphaltite reaching 3%/min.

From the microwave activated test results, Hardgrove grinding Index are determined and the results were shown in Figure 4. Hardgrove index values increased to 85 values for Şırnak asphaltite. For Kütahya Gediz lignite reached to 105 values of HGI from 72.

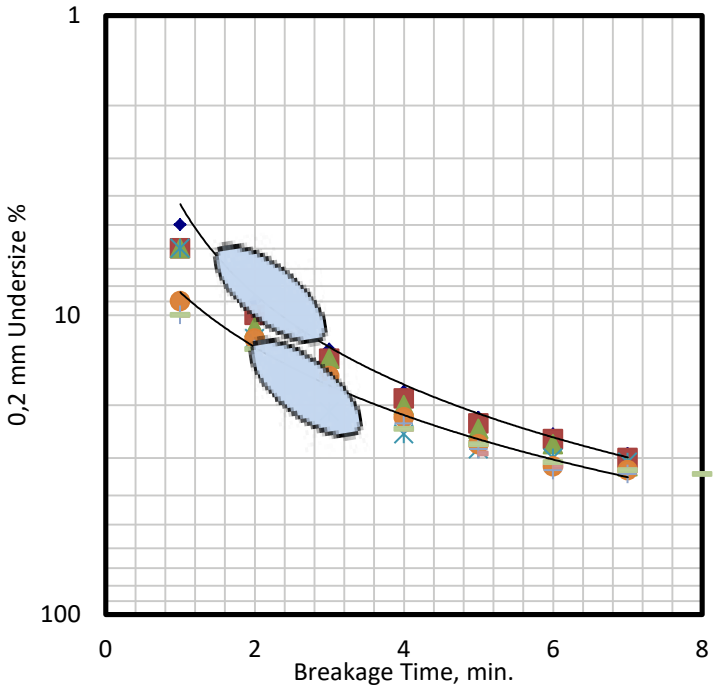

Figure 3. Bond breakage with microwave treated coal samples in 20 mins.

CONCLUSIONS

In this study, a method which reduces and eliminates inefficiency and problems during the determination of work index and Bond's grindability is described. The effect of physico- mechanical parameters of the materials on grindability and its relation with grindability are investigated. It is possible to determine physico-mechanical parameters. Statical methods contain difficult test procedures and problems as encountered at Bond's grindability process. However, tests are simple, easy and show minor problems in dynamic methods. A good correlation is obtained between Bond grindability and work index with the values determined from the Hardgrove Index method as a result of the tests done. The best correlation was found between Bond (grindability and work index) and HGI. Moreover, HGI give better results than static methods because coal grinding is also a compression process. The HGI method has many advantages, because of its ease of use and the relatively short time required compared to Bond methods. The depth of particle bed is a key variable in determining the fragmentation of coals and shale by high velocity impact. This may not be the case with static loading.

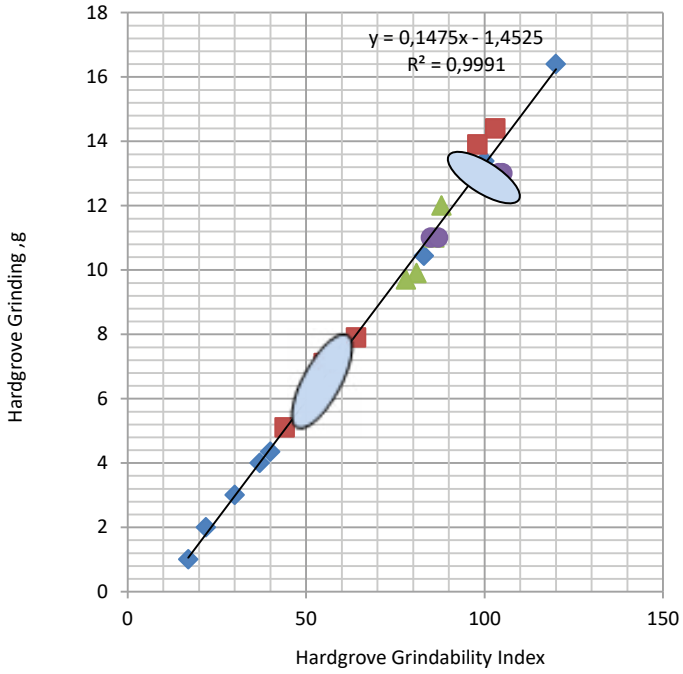

Figure 4. Bond breakage with microwave treated coal samples in 20mins.

Two different methods of characterizing breakage manner of coal are investigated for the purpose of predicting performance in the comminution. Bond method was performed as standard tests and assume that the common test best reflecting the dominant behavior of coals.

HGI method was important in the design of coal grinding plants and even mechanical properties of side rocks in coal.

The most important result of this study is managed by the correlation between Bond HGI and compressive strength for microwave activated grindability. In future studies, the other grinding mills should be clearly established by taking the porosity into consideration, and other lignite samples using alternative grinding media.

REFERENCES

ASTM D406-08, 2008, Hardgrove Grinding Index, ASTM Standards Inst.

Austin,L.G. (2004), A preliminary simulation model for fine grinding in high speed hammer mills, *Powder Technol., 143–144 (25*) ,pp. 240–252

Bergstrom,B.H. (1985). Crushability and grindability, N.L. Weiss (Ed.), *SME Mineral Processing Handbook, vol. 2* Littleton, pp. 30-65–30-68

Bond,F.C. (1952), The third theory of comminution, Trans. AIME, 193 (1952), pp. 484–494

G. Özbayoğlu, A.M. Özbayoğlu, M.E. Özbayoğlu, (2008). Estimation of Hardgrove Grindability Index of Turkish coals by neural networks*, Int J Miner Process, 85 (4)*, pp. 93–100

Gökçen HS., Çayırlı S, Ucbas Y.,Kayacı K, (2012). Dry Grinding of Sodium Feldspar in a Stirred Ball Mill, Proceedings of XIII International Mineral Processing Symposium, Bodrum, Turkey pp21-28Tavares, L.M., 2007, Breakage of Single Particles: Quasi-static, Salman,A.D.

Ghadiri,M. Hounslow M.J.(Eds.),2007, Handbook of Particle Breakage, vol. 12Elsevier (2007), pp. 3–69A.N. Sengupta,2002, An assessment of grindability index of coal,Fuel Process Technol, 76 (1) (2002), pp. 1–10

Howard, P.H. Datta, R.S., (1977). Chemical Cominution: A Process for Liberating the Mineral matter from Coal, Coal Desulfurization (Ed. T. Wheelock) Washington, *ACS Series 64*, pp.58-64.

Howard, P.H. Datta, R.S., Hanchett, A., (1976). Pre-combustion Coal Cleaning Using Chemical Cominution: NCA/BCR Coal Conference and Expo Coal: Energy for Independence, Lousville.

P. Li, Y. Xiong, D. Yu, X. Sun, (2005). Prediction of grindability with multivariable regression and neural network in Chinese coal,*Fuel, 84 (18)*, pp. 2384–2388

Refahi,A., Rezai,B., Mohandesi,J.A., (2007). Use of rock mechanical properties to predict the Bond crushing index, *Miner. Eng., 20*, pp. 662–669

Tavares,L.M., King,R.P., (1998). Single-particle fracture under impact loading, *Int. J. Miner. Process., 54*, pp. 1–28

Tavares,L.M., King,R.P., (2002). Modeling of particle breakage by repeated impacts using continuum damage mechanics, *Powder Technol., 123*, pp. 138–146

Tavares,L.M., King,R.P., (2005). Continuum damage modeling of particle fracture, *ZKG Int., 58*, pp. 49–58

Toroman Ö.Y., Uçurum, M., (2012). The effect of various operating parameters on fine grinding in a pilot scale Ball Mill, Proceedings of XIII International Mineral Processing Symposium, Bodrum, Turkey pp13-10

Unland G., Szczelina,P., (2005). Coarse crushing of brittle rocks by compression, Int. J. *Miner.Process., 74S*, pp. S209–S217

MİNİMUM EĞRİLİK ALGORİTMASI İLE YÖNLÜ SONDAJ VE KOMPOZİTLEME BİLGİSAYAR PROGRAMI

DRILLHOLE DATABASE APPLET: MINIMUM CURVATURE ALGORITHM AND DOWNHOLE COMPOSITE

G. Ertunç [1,*], A. İmer [2]

[1] *Hacettepe Üniversitesi, Maden Mühendisliği Bölümü*
*(*Sorumlu yazar: gertunc@hacettepe.edu.tr)*
[2] *Orta Doğu Teknik Üniversitesi, Jeoloji Mühendisliği Bölümü*

ÖZET

Çalışmada, yazarlar tarafından geliştirilen, grafik kullanıcı arayüzü (GUI) tabanlı sondaj veritabanı uygulaması sunulmuştur. İlk çalıştırılabilir uygulamanın içeriği, yönlü sondajlarda açı ölçüm noktaları arasında kalan lokasyonlarda iç kestirim yapılmasıdır. Kuyu derinliklerindeki konumların belirlenmesi için matematiksel model olarak Minimum Eğrilik Metodu (Minimum Curvature Method: MCM) kullanılmıştır. Ölçülen derinlik, eğim ve azimut değerleri girdi parametreleri olarak kullanılarak, koordinat bileşenleri çıktı olarak elde edilmektedir. Ayrıca, sondaja ilişkin grafik çıktısı da üretilebilmektedir.

İkinci uygulama, düşey yönde kompozit (eşit uzunluklu örneklem) üretmektedir. Bu uygulamanın ilk adımı 3B sondaj veritabanı dosyalarını okuma ve doğrulamadır. Ham öznitelik ve örnek uzunluk istatistikleri program tarafından detaylı olarak verilmektedir ve kullanıcılar istenilen uzunlukta ve en düşük kabul yüzdesine göre kompozitler oluşturabilmektedir. Koordinatlar ve kompozit değerleri ASCII veya MS Excel .csv formatlarında dışa aktarılabilir. Ayrıntılı istatistikler ayrıca rapor edilebilmektedir.

Anahtar Sözcükler: Sondaj veritabanı, kompozitleme, yönlü sondaj, minimum eğrilik metodu

ABSTRACT

In this study, two graphical user interface (GUI) based drillhole database applications, compiled by the authors, are introduced. The first executable applet is developed to automatically interpolate and calculate between survey stations in directional drillholes. In order to determine borehole position, Minimum Curvature Method (MCM) is assumed as the mathematical model. By employing measured depth, dip, and azimuth as input parameters, output parameters are obtained such as Dogleg Severity (DLS) and the 3D coordinates; northing, easting, and true vertical depth. Also, graphical output of the drillhole path is produced.

Second applet is the downhole compositing tool. This application starts with 3D drillhole database import and validation. Raw and sample length statistics are given in detail by the program and users are able to create composites with desired length and minimum sample coverage percentage. Composite coordinates and values can be exported in ASCII or MS Excel .csv formats. Detailed composite statistics can further be reported.

Keywords: Drillhole database, composite, directional drilling, minimum curvature method

GİRİŞ

Maden kaynak kestirim süreci, temel olarak veri tabanı oluşturma, jeolojik katı modelleme, blok modelleme ve kaynak modelleme adımlarını kapsar. Veri tabanı, cevher yatağı modelleme ve ocak tasarımına temel olan verileri (jeolojik haritalar, sondaj logları, numune analiz değerleri vs.) içermektedir ve cevher modellemesi için girdi parametrelerinin bütününü oluşturur.

Blok modelleme, büyük ölçüde, cevher kütlesinin geometrisinin gerçeğe yakın bir şekilde modellenmesine bağlıdır. Cevher kütlesinin geometrisi temel olarak litoloji, mineraloji, alterasyon, yapısal unsurlar gibi jeolojik değişkenler ile sondaj karotlarının analizinden elde edilen ve öznitelik olarak adlandırılan bu verilere bağlı olarak oluşturulur. Bu süreçte jeolojik değişkenlerle öznitelik dağılımı arasındaki ilişkilerin ortaya konması gerekmektedir. Başka bir deyişle, cevherleşme sınırları içerisinde jeolojik süreklilik ile öznitelik değer sürekliliğinin birbiriyle uyumlu olması beklenir. Yapısal jeoloji ve cevherleşmeyi kontrol eden diğer jeolojik unsurların bütünleşik ve karmaşık örüntülerinden oluşan cevher kütlesi, her saha için farklı karakter sergiler. Kaynak kestiriminde kullanılacak metodoloji de, öznitelik aynı olsa bile, farklı cevher geometrileri için farklı olacaktır. Jeolojik yapıya uymayan bir cevher modeli, standardın altında kestirimler elde edilmesine ve gerçekçi olmayan tenör-tonaj değerleri üretilmesine neden olacaktır.

Maden kaynak kestiriminden sonra; teknik, sosyal ve çevresel faktörlerin değerlendirilmesiyle ve buna ek olarak projenin ekonomik analizinin dahil edilmesiyle maden rezerv kestirimi yapılır. Bu analiz sonucunda projenin finanse edilip edilemeyeceği kararlaştırılır. Böylesine kritik bir karar ile sonuçlanan süreçte, saha jeolojisini doğru anlamak ve aynı zamanda elde edilen verilerin güvenilirliğinin sorgulanması/sağlanması maden kaynak kestirimi ve dolaysıyla maden rezerv kestiriminin temelini oluşturur. Verilerin doğrulanmasında ve/veya jeolojik model aşamasında yapılacak hatalı işlemlerin birikimli olarak hep bir sonraki aşamaya aktarılması kaçınılmazdır.

Maden kaynak kestirimi veri tabanı oluşturma ile başlar. Leapfrog Geo (2021), GEOVIA Surpac™ (2021), Datamine (2021), Micromine (2021), NETPROMine (2021) gibi madencilik yazılımlarında ilgili özniteliğe ilişkin koordinat bilgileri, litolojik tanımlar vb. veritabanında saklanır; istatistik ve jeoistatistiksel hesaplamalar bu veritabanına göre yapılır. Bu yazılımlar bünyesinde veritabanı girişi ve veri doğrulaması modüllerini içerirken Isatis (2021), mGStat (Hansen, 2021), S-GeMS (Remy, 2005) gibi yazılımlar veritabanı olmadan sadece istatistiksel araçlar ile kullanıcıya sunulmuştur.

Çalışmaya konu olan uygulamaların ilki yönlü sondajların açı ölçüm noktaları arasında kalan noktalarını iç kestirim ile belirlemeye yarayan uygulamadır. Kuyu derinliklerindeki konumların belirlenmesi için matematiksel model olarak Minimum Eğrilik Metodu (Minimum Curvature Method: MCM) kullanılarak; ölçülen derinlik, eğim ve azimut değerleri girdi parametreleri ile koordinat bileşenleri çıktı olarak elde edilmektedir. İkinci uygulama ise, 3B sondaj veritabanı dosyalarını okuma ve doğrulama süreçlerini kapsayan ve düşey yönde kompozit (eşit uzunluklu örneklem) üretilmektedir.

"Yöntem" başlığı altında sırasıyla Minimum Eğrilik Metodu ve kompozitleme yöntemlerinin detaylı açıklaması ve yer almaktadır. "Kullanıcı Grafik Arayüzleri" başlığında ise MATLAB Compiler ile oluşturulan exe uygulamasının akım şemaları ile birlikte uygulama örnekleri verilmiştir. Sonuçlar ve Öneriler kısmında ise gelecek dönemlerde yapılacak çalışmalar yer almaktadır.

YÖNTEM

Yönlü sondajlar, Minimum Eğrilik Algoritması'na (MEA) (Minimum Curve Algorithm (MCA)) göre örneklem lokasyonlarını hesaplar (Sawaryn ve Thorogood, 2005). Algoritma, açı dosyasındaki derinlik, eğim ve azimut alanlarını kullanır ve öznitelik değerlerinin 3 yöndeki (sağa, yukarı, derinlik) koordinat bileşenlerini hesaplar. Başka bir deyişle, EKEA, veritabanlarında analiz dosyasındaki "Başlangıç - Bitiş" aralıklarına karşılık gelen sondaj derinliğine, eğimine ve azimutuna göre kartezyen koordinat sistemine dönüşüm yapar. Şekil 1'de, EKEA hesabında kullanılan açı değerleri ve hesaplanan sondajın temsili kavisi (kesikli kırmızı çizgi) gösterilmektedir.

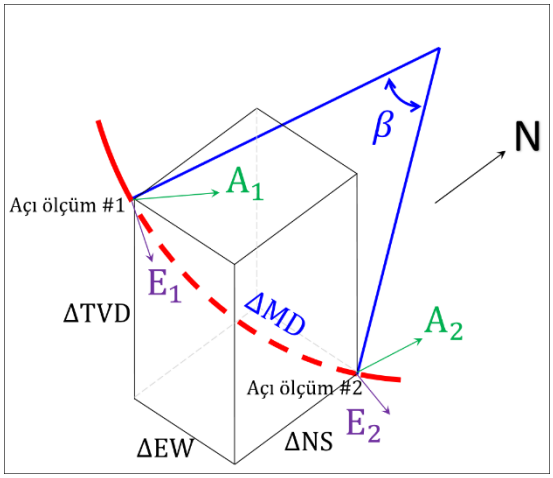

Şekil 1. MEA hesabında kullanılan açı değerleri ve hesaplanan sondajın temsili kavisi (kesikli kırmızı çizgi)

MEA algoritmasında hesaplamaların ilk adımı kavis tepe açısı (dogleg angle) β'nın hesaplanmasıdır. Kavis tepe açısının formülü Eşitlik 1'de verilmektedir.

$$\beta = \cos^{-1}(\cos(E_2 - E_1) - \sin(E_1) \times \sin(E_2) \times (1 - \cos(A_2 - A_1)) \quad (1)$$

Eşitlik 1'de E1,2 ve A1,2 açı dosyasında ardışık gelen iki açı ölçüm noktalarının sırasıyla eğimlerini (dip) ve azimut değerlerini (azimuth) ifade etmektedir.

Kavis tepe açısı hesaplandıktan sonra oran çarpanı (ratio factor) RF hesabı Eşitlik 2'teki formül ile hesaplanır.

$$RF = \frac{2 \times \tan\left(\beta/2\right)}{\beta} \quad (2)$$

Son aşamada, açı ölçüm noktaları arasındaki noktaların koordinat bileşenlerinin değişim miktarları (ΔNS: Yukarı, ΔEW: Sağa ve ΔTVD: Yükseklik) Eşitlik 3'teki gibi hesaplanır.

$$\Delta NS = \frac{\Delta MD}{2} \times (\sin(E_1) \times \cos(A_1) + \sin(E_2) \times \cos(A_2)) \times RF$$
$$\Delta EW = \frac{\Delta MD}{2} \times (\sin(E_1) \times \cos(A_1) + \sin(E_2) \times \sin(A_2)) \times RF \quad (3)$$
$$\Delta TVD = \frac{\Delta MD}{2} \times \left(\cos(E_1) - \cos(E_2)\right) \times RF$$

Burada ΔMD iki açı ölçüm noktası arasındaki mesafeyi ifade etmektedir (Şekil 1).

Kompozitleme

Kompozitleme, veritabanındaki ham örneklemlerin belli uzunluklara göre ağırlıklandırlarak ortalama hesaplanması prosedürüdür (Şekil 2). Kompozitleme kaynak kestirimi için bir kesinlik derecesinde gereklilik değildir; ancak verinin türetildiği ölçeğin homojenleştirilmesi veya eksik örneklenmiş aralıklar için düzeltme durumudur. Çoğu kaynak kestirimi yazılımı, verilerin tümünün aynı kaynaktan türediğini (constant support) varsayar.

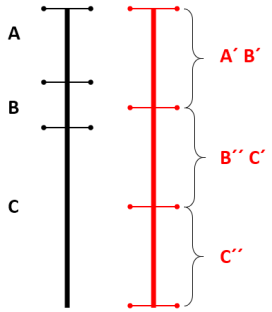

Şekil 2. Kompozitleme, eş uzunluklu örneklem oluşturma.

Bu işlem aynı zamanda kestirim veya jeositatistiksel benzetimden önce ham verilere belirli bir miktarda seyrelmeyi (dilution) de dahil eder. Madencilikte ham örneklem ölçeğinden daha büyük belirli bir seçicilik (selectivity) düzeyinde çalışılır. Açık ocaklarda düşey boyuttaki seçicilik genellikle basamak yüksekliği ile kontrol edilmektedir. Yeraltı madenlerinde ise seçicilik, madencilik yönteminin bir fonksiyonudur. Kes ve doldur veya benzer bir yöntemde dilimin yüksekliği düşey yönde seçiciliği belirler. Kompozit uzunluğu, verileri maden seçiciliği ile aynı düşey boyuta göre veya ham örneklemin uzunluk istatistiğine bağlı olarak belirlenebilir.

Kompozit tipik olarak uzunluk ağırlıklı bir ortalama ile hesaplanır ve ayrıca birim hacim hacim ağırlık veya geri kazanımı (recovery) ile de ağırlıklandırılabilir. Bu çalşıma kapsamında düşey yönlü kompozitler oluşturulmaktadır.

Şekil 3'te, temsili bir düşey kompozit oluşturma işlemi verilmiştir. Pratikte böyle bir kompozitleme işlemi uygun değildir ancak kavramsal olarak kompozitleme işleminin detaylı olarak anlatılması amacıyla bu durum bir kurgu mantığı ile sunulmuştur.

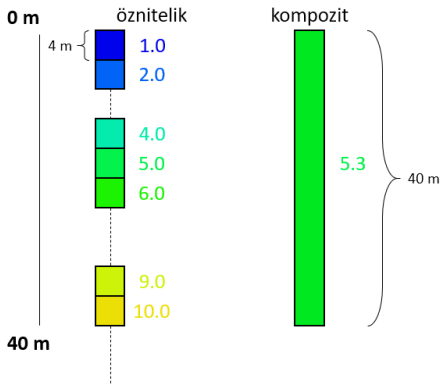

Şekil 3. Kompozitleme, eş uzunluklu örneklem oluşturma. (https://www.seequent.com'dan değiştirilerek)

Bu örnekte her biri 4 m'lik ham örneklem noktalarından 40 m'lik bir kompozit oluşturulmuştur. Bu sondajda 7 geçerli analiz bulunur. Her birinin uzunluğu 4 m olan ve değerleri 1, 2, 4, 5, 6, 9 ve 10 olan özniteliklerin ağırlıklı ortalaması 5.3 olarak hesaplanır. Şekil 3'te görüldüğü gibi, 12 – 16 m ve 28 – 32 m aralığında ham örneklem yokken kompozit değeri oluşturulduğunda 0 – 40 m aralığında tek değer 5.3 olarak belirlenmiştir.

GRAFİK KULLANICI ARAYÜZÜ (GUI)

Bu bölümde minimum eğrilik algoritması ile açı ölçüm noktalarına göre sondaj kuyusunu görselleştiren uygulama ile veri tabanı girişi ve doğrulaması yapan ve düşey yönde kompozit oluşturan uygulama grafik kullanıcı arayüzlerinin detaylı açıklamaları yer almaktadır.

Yönlü Sondaj

Bu uygulama kullanıcının çalışma klasörü, sondaja ait kuyu koordinat bilgileri ve açı ölçüm noktalarının girdiği bir arayüzden oluşur (Şekil 4).

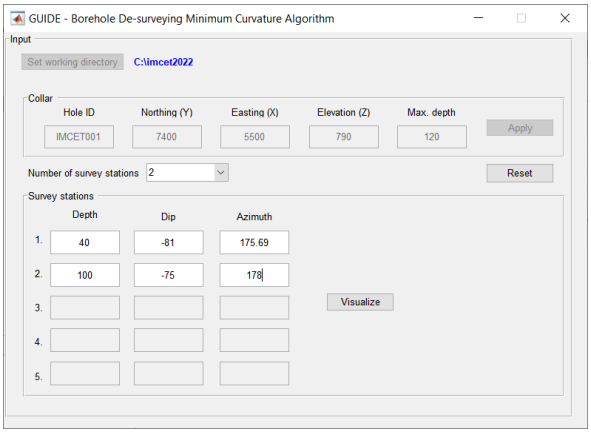

Şekil 4. Yönlü sondaj kullanıcı arayüzü.

Bu arayüzde girilmesi gereken veriler Çizelge 1'de detaylı olarak açıklanmaktadır.

Çizelge 1. Yönlü sondaj kullanıcı arayüzü alanları

Alan Adı	***Açıklama***
Collar	Kuyu koordinat bilgileri
Hole ID	Kuyu adı
Northing (Y)	Yukarı (Y)
Easting (X)	Sağa (X)
Elevation (Z)	Yükseklik
Max. depth	Kuyu derinliği
Survey Stations	Açı ölçüm noktaları
Depth	Derinlik
Dip	Eğim (-90° = düşey yön)
Azimuth	Azimut (0° = Kuzey)

İlgili alanların tamamı doldurulduğunda "Visualize" tuşu ile bir sonraki pencere açılmaktadır. Bu pencere (Şekil 5) görselleştirme penceresidir.

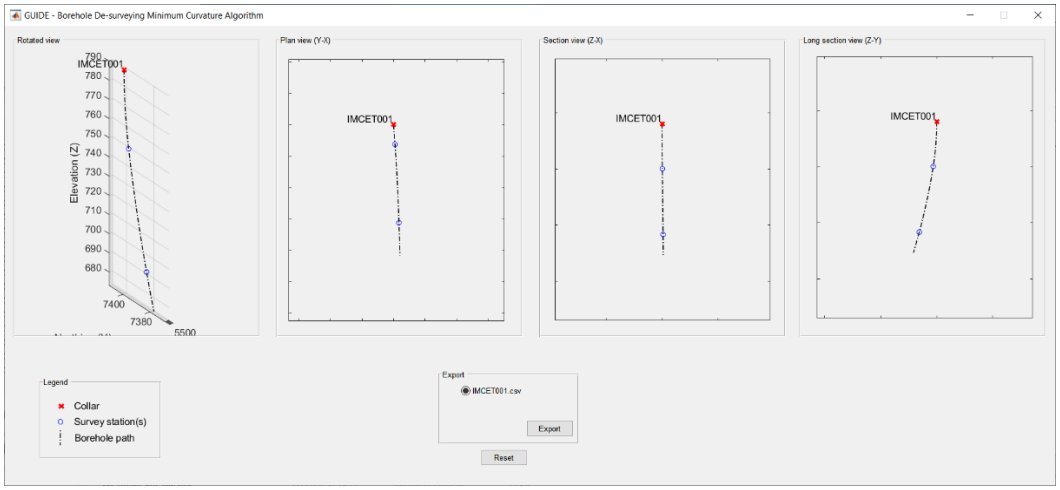

Şekil 5. Görselleştirme ekranı

Bu ekranda, girilen sondaj bilgilerine göre sondaj izinin üstten, kesit ve uzun kesit görüntüsü kullanıcıya gösterilir. Ayrıca kullanıcı fare hareketi ile sondajı istediği açıdan inceleyebilir. Kuyu başlangıcından sonuna kadar belli aralıklardaki sondaj koordinat bileşenleri dışa MS Excel "sondaj adı.csv" olarak aktarılabilir. Şekil 5'teki örnek için IMCET001.csv dosyasının ilk ve son satırları Şekil 6'da verilmektedir.

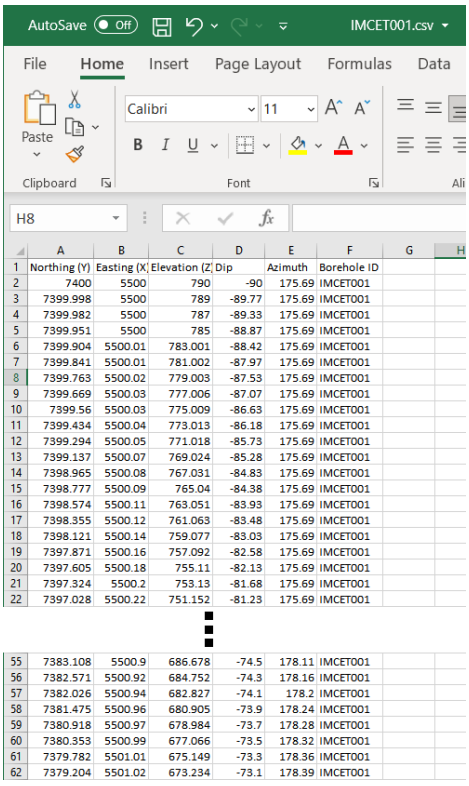

AutoSave Off — IMCET001.csv

File Home Insert Page Layout Formulas Data

Clipboard Font

H8

	A	B	C	D	E	F
1	Northing (Y)	Easting (X	Elevation (Z	Dip	Azimuth	Borehole ID
2	7400	5500	790	-90	175.69	IMCET001
3	7399.998	5500	789	-89.77	175.69	IMCET001
4	7399.982	5500	787	-89.33	175.69	IMCET001
5	7399.951	5500	785	-88.87	175.69	IMCET001
6	7399.904	5500.01	783.001	-88.42	175.69	IMCET001
7	7399.841	5500.01	781.002	-87.97	175.69	IMCET001
8	7399.763	5500.02	779.003	-87.53	175.69	IMCET001
9	7399.669	5500.03	777.006	-87.07	175.69	IMCET001
10	7399.56	5500.03	775.009	-86.63	175.69	IMCET001
11	7399.434	5500.04	773.013	-86.18	175.69	IMCET001
12	7399.294	5500.05	771.018	-85.73	175.69	IMCET001
13	7399.137	5500.07	769.024	-85.28	175.69	IMCET001
14	7398.965	5500.08	767.031	-84.83	175.69	IMCET001
15	7398.777	5500.09	765.04	-84.38	175.69	IMCET001
16	7398.574	5500.11	763.051	-83.93	175.69	IMCET001
17	7398.355	5500.12	761.063	-83.48	175.69	IMCET001
18	7398.121	5500.14	759.077	-83.03	175.69	IMCET001
19	7397.871	5500.16	757.092	-82.58	175.69	IMCET001
20	7397.605	5500.18	755.11	-82.13	175.69	IMCET001
21	7397.324	5500.2	753.13	-81.68	175.69	IMCET001
22	7397.028	5500.22	751.152	-81.23	175.69	IMCET001
55	7383.108	5500.9	686.678	-74.5	178.11	IMCET001
56	7382.571	5500.92	684.752	-74.3	178.16	IMCET001
57	7382.026	5500.94	682.827	-74.1	178.2	IMCET001
58	7381.475	5500.96	680.905	-73.9	178.24	IMCET001
59	7380.918	5500.97	678.984	-73.7	178.28	IMCET001
60	7380.353	5500.99	677.066	-73.5	178.32	IMCET001
61	7379.782	5501.01	675.149	-73.3	178.36	IMCET001
62	7379.204	5501.02	673.234	-73.1	178.39	IMCET001

Şekil 6. Dışa aktarılan sondaj izi koordinat bileşenleri

Kompozitleme

Üç boyutlu sondaj kompozit oluşturma bu çalışma kapsamında "proje" olarak anılır. Kullanıcı, programa projeyle ilgili tüm dosyaları içeren klasör olan "Çalışma klasörü"nü seçtiğinde başlar. Bu modül, oluşturulan veritabanında ham örneklem lokasyonları ve özniteliğin tematik harita ile görselleştirilmesi ve takip eden menüde ise kompozitleme işlemi ile sonlanır. Uygulamaya ilişkin akış şeması Şekil 7'de verilmiştir.

Veritabanına aktarılması zorunlu ilk dosya, temel olarak sondaj koordinat bilgilerini içeren kuyu bilgisi (collar) dosyasıdır. Bu dosyada (MS Excel (*.xlsx, *.csv)) bulunması zorunlu alanlar Çizelge 2'de verilmiştir.

Çizelge 2. Kuyu bilgisi dosyası zorunlu alanlar

Alan Adı	***Açıklama***
Sondaj Adı	Her bir sondajın adı.
Y	Yukarı (Y)
X	Sağa (X)
Z	Yükseklik
En büyük derinlik	Kuyu derinliği

Veritabanı kuyu koordinat dosyası aktarıldıktan sonra tüm alanlarda hata kontrolü yapılır ve hata varsa *.txt uzantılı bir metin dosyası ile kullanıcıya bilgi verilir. Bu dosyadaki sondaj adı dışındaki tüm alanların sayısal olması gerektiğinden, doğrulama algoritması yalnızca koordinat değerlerinin ve en büyük derinliğin sayısal olup olmadığını bildirir. Sondaj adı alanında, aynı şekilde adlandırılmış sondajlar rapor edilir. Ayrıca, boş girişler hata olarak kabul edilir. Tüm alanlar doğrulandığında, analiz dosyasının veritabanına girişini sağlayan buton aktif hale gelir.

Analiz dosyasındaki zorunlu alanlar Çizelge 3'te verilmiştir.

Çizelge 3. Analiz dosyası zorunlu alanlar

Alan Adı	***Açıklama***
Sondaj Adı	Analiz dosyasının kuyu koordinat dosyasındaki sondaj adları ile bağlantısı, bu alanda seçilen sondaj adı sütunu eşleştirilerek sağlanır.
Başlangıç	Analiz edilen örneğin başlangıç derinliği.
Bitiş	Analiz edilen örneğin bitiş derinliği. (Bu durumda fark ham örneklem uzunluğudur.)
Öznitelik	Değişkenin analiz değeri

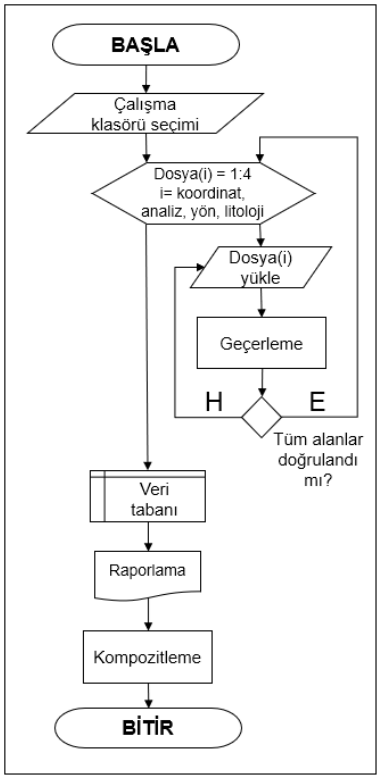

Şekil 7. Kompozitleme uygulaması akış şeması

Analiz dosyasının doğrulama, doğrulama ve hata raporu oluşturma süreci, kuyu koordinat dosyasına kıyasla karmaşık ve daha çeşitlidir. Her zorunlu alan için olası hatalar ve doğrulama rutinleri Çizelge 4'te açıklanmıştır.

Çizelge 4. Analiz dosyası hataları ve doğrulama rutinleri

Alan Adı	***Açıklama***
Sondaj Adı	Analiz dosyasında bulunan ancak kuyu koordinat dosyasında olmayan sondajlar. Aynı durum, tersi için de geçerlidir. Ayrıca analiz dosyasındaki boş değerler de kontrol edilmelidir.
Başlangıç	Sayısal olmayan veya boş girişler. Sondaj deliğinin "En büyük derinlik" i aşan değerler. "Bitiş" değerlerinden daha küçük "Başlangıç" değerleri. Aynı sondaj boyunca yinelenen "Başlangıç" değerleri.
Bitiş	Sayısal olmayan veya boş girişler. Sondaj deliğinin "En büyük derinlik"i aşan değerler. "Başlangıç" değerlerinden daha büyük "Bitiş" değerleri. Sondaj boyunca üstüste çakışan Başlangıç – Bitiş aralıkları. Aynı sondaj boyunca yinelenen "Bitiş" değerleri.
Öznitelik	Sayısal olmayan girişler. Boş girişler uyarı olarak listelenir, hata olarak kabul edilmez.

Sonraki adım, açı dosyasını veritabanına aktarmakdır. Çalışmaya konu olan uygulamada veritabanına sadece dik sondajlar değil, yönlü sondajlar da girilebilir. Algoritma, açı dosyasındaki derinlik, eğim ve azimut alanlarını kullanır ve analiz dosyasındaki öznitelik değerlerinin 3 yöndeki (sağa, yukarı,

derinlik) koordinat bileşenlerini hesaplar. Şekil 8'de, veritabanı dosyalarının programa girişinde kullanılan ekranlar verilmiştir.

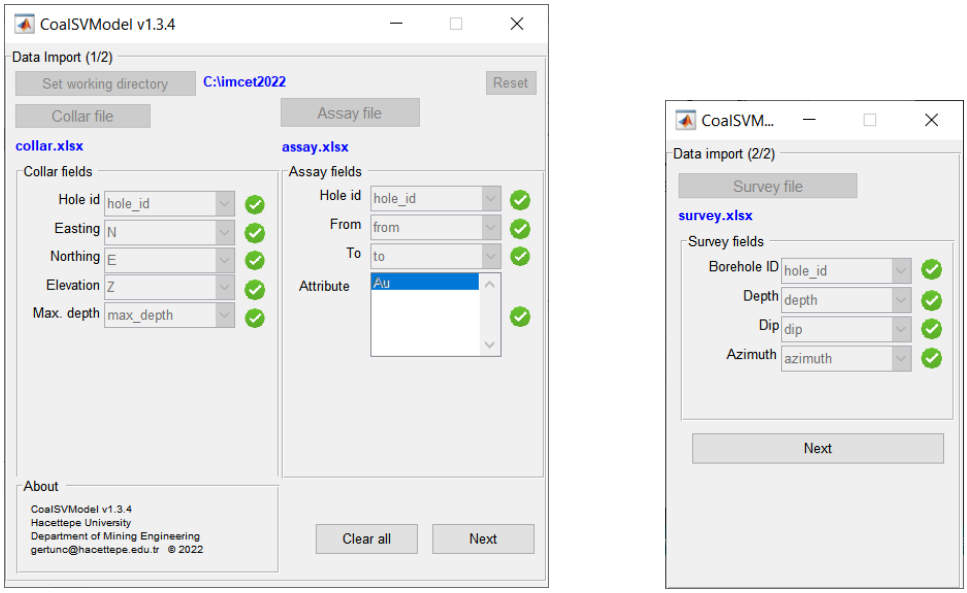

a) b)

Şekil 8. Veritabanı dosya giriş ekranları: a) Kuyu koordinat ve analiz, b) Sondaj açı dosya giriş

Veritabanına giriş için kullanılan tüm alanlar geçerliği olduğunda, "Next" tuşu ile sondajlar ve seçilen özniteliğin tematik harita ekranı (Şekil 9) kullanıcıya gösterilir.

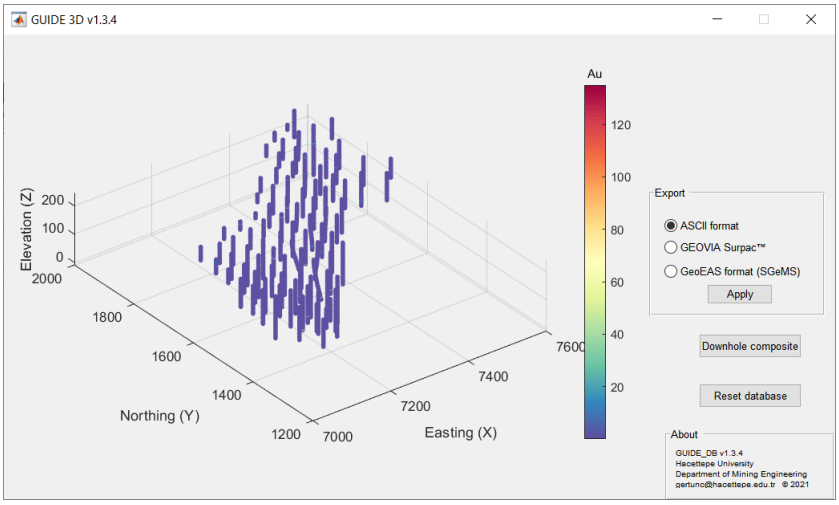

Şekil 9. Sondaj lokasyonları ile öznitelik tematik haritası

Kompozit oluştururken dikkat edilmesi gereken göstergelerden başlıcası ham örneklem uzunluklarının tanımlayıcı istatistikleridir. Kompozitleme uygulama ekranında hem özniteliklerin, hem de ham örneklem uzunluklarının tanımlayıcı istatistikleri kullanıcıya gösterilmektedir. Kullanıcı kompozit oluştururken hem kompozit uzunluğunu *(composite length)* hem de en düşük kabul yüzdesi *(minimum*

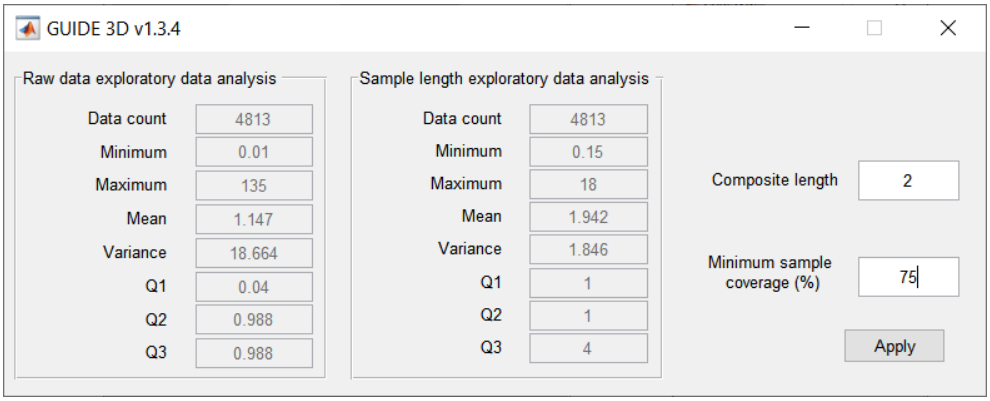

Şekil 10. Düşey yönde kompozit oluşturma uygulama ekranı

Şekil 10'a göre ham örneklemlerin uzunluklarının ortalaması ile varyans değeri sırasıyla 1.942 ve 1.846 olarak belirlenmiştir. Kompozit uzunluğu ise bu iki değer göz önüne alınarak 2 m olarak belirlenmiştir.

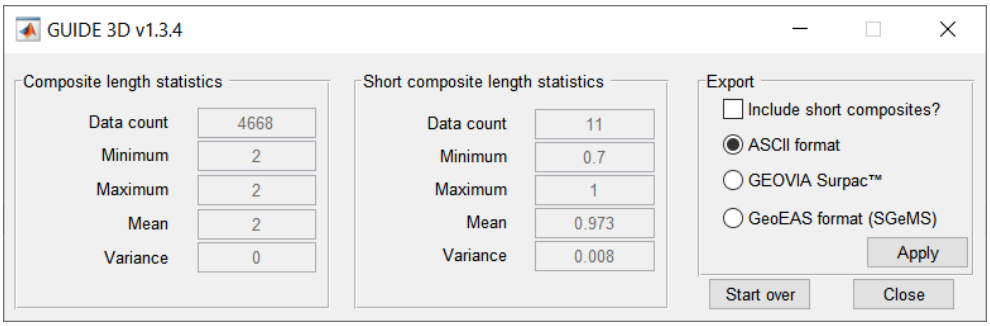

Şekil 11. Kompozit işlemi çıktı ekranı

SONUÇLAR

Çalışmada sunulan sondaj veritabanı ile ilgili iki uygulama da ilerleyen çalışmalarda maden kaynak kestirimi için kullanılacak bir dizi uygulama için temel oluşturma amacıyla oluşturulmuştur.

Veri tabanı, cevher yatağı modelleme ve ocak tasarımına temel olan verileri (jeolojik haritalar, sondaj logları, numune analiz değerleri vs.) içermektedir ve cevher modellemesi için girdi parametrelerinin bütününü oluşturur. Veri tabanı hatasız ve eksiksiz olmalıdır. Bu aşamalardaki hata, zincirleme şekilde ilerleyen süreç gereği birikimli olarak diğer aşamalara taşınabilir ve sonuçlar üzerinde olumsuz şekilde doğrudan etkisi olduğu için son derece önemlidir.

Bu çalışma kapsamında yalnızca düşey yönde kompozitleme seçeneği sunulmuştur. Ancak kompozitleme yalnızca sürekli değişken niteliğindeki öznitelikler için değil, litoloji gibi kategorik

değişkenlere de uygulanabilir. Dolayısıyla ilerleyen aşamalarda çalıştırılabilir uygulamanın yeni versiyonlarında bu yönde geliştirme yapılması yerinde olacaktır.

Geliştirmeye uygun başka bir konu ise tanımlayıcı istatistik uygulamalarıdır. Seçilen özniteliğe ilişkin aykırı değer analizi ile değişken ortalamasının yöne bağlı değişkenliğini ortaya koyan yönelim *(swathplot)* bir sonraki version güncellemesinde dahil edilmesi söz konusudur.

Ayrıca, uzaklığa bağlı değişkenlik ölçütü olan variogram analizi ile çok değişkenli yapıdaki veritabanları için programın uygun hale getirilmesi önerilebilir.

KAYNAKLAR

Hansen, T.H., GitHub, https://github.com/cultpenguin/mGstat/releases/tag/1.0 Son erişim tarihi: 15 Aralık 2021.

https://www.3ds.com/products-services/geovia/products/surpac/ Son erişim tarihi: 15 Aralık 2021.

https://www.dataminesoftware.com Son erişim tarihi: 15 Aralık 2021.

https://www.geovariances.com/en/software/isatis-geostatistics-software/ Son erişim tarihi: 15 Aralık 2021.

https://www.micromine.com/ Son erişim tarihi: 15 Aralık 2021.

https://www.netcad.com/tr/urunler/netpromine Son erişim tarihi: 15 Aralık 2021.

https://www.seequent.com/products-solutions/leapfrog-geo/ Son erişim tarihi: 15 Aralık 2021.

Remy, N. (2005) "S-GeMS: The Stanford Geostatistical Modeling Software: A Tool for New Algorithms Development." In: Leuangthong O., Deutsch C.V. (eds) Geostatistics Banff 2004. *Quantitative Geology and Geostatistics, vol 14.* Springer, Dordrecht. https://doi.org/10.1007/978-1-4020-3610-1_89

Sawaryn, S.J., Thorogood, J.L. (2005). "A Compendium of Directional Calculations Based on the Minimum Curvature Method", *SPE Drill & Compl, 20 (01)*, 24–36.

MODELLING OF COPPER ELECTROREFINING IN IONIC DIFFUSION CONTROL CONDITION BY COMSOL MULTIPHYSICS

M.D. Inalou [1], A.M. Beygian [1], E.K. Alamdari [1, *]

[1] *Amirkabir University of Technology, Department of Materials and Metallurgical Engineering*
*(*Corresponding author: alamdari@aut.ac.ir)*

ABSTRACT

Electrorefining of copper is one of the most used processes to obtain high quality copper by electricity. The copper dissolves from an anode electrode and deposits on a cathode electrode. The main parameters that affect the process are temperature, anodic and cathodic current density, copper and sulfuric acid concentration, impurities, and suspended particles. For simplicity, the effect of temperature and impurities are not considered. Experimental design to consider the effect of three other variable parameters by the central composite design (CCD) for twenty runs is done, which current density varies from 50 to 550 A/m^2, copper concentration varies from 10 to 90 g/L and sulfuric acid vary from 20 to 340 g/L. The copper electrorefining process is modeled by COMSOL Multiphysics software in which condition that only the diffusion affects the movement of ions. The current density and concentration of acid and copper in the batch process are predicted by considering the hydrogen evolution reaction in the process current efficiency and energy consumption are optimized. In the end, to validate the results, the available experimental tests are used.

Keywords: Copper electrorefining, simulation, optimization, energy consumption, cathodic efficiency, anodic efficiency

INTRODUCTION

Electrorefining of copper is one of the most used processes to obtain high quality copper by Electricity. The copper dissolves in the anode electrode and deposits at the cathode electrode. The main parameters that affect the process are temperature, anodic and cathodic current density, copper and sulfuric acid concentration, impurities, and suspended particles. Due to the importance of the electric electrorefining process, it is of special importance to study this process and the factors affecting it, and find a way to increase its efficiency (Mark E. Schlesinger et al., 2011), (Zeng et al., 2016). One of the methods to study the process of electrorefining is to perform simulations, by using equations of mass balance, energy balance, and momentum balance, via commercial software. The absence of laboratory errors, cost reduction, and time savings are the advantages of using simulation methods in examining processes. It is very difficult and expensive to study some mechanisms of the electric purification process in the laboratory and it requires advanced and expensive devices. However, by using relatively accurate equations of mass and energy balance, laboratory results can be obtained with reasonable accuracy at a low cost and at the right time. The optimization of the process is the most important thing of the process because of energy consumption and the current efficiency. This has not considered until today. Zeng et al. (2015) modeled the electrorefining process and considered the impurity particles behavior in this process (Zeng et al., 2015).

In this study, the optimization of the process and the effect of diffusion were considered. By using COMSOL Multiphysics, an electrochemical cell simulation was utilized. Concentration, the weight of deposited copper, and electrical potential were generated as results of the model. There are three mechanisms in the movement of ions: diffusion (based on Fick's law), convection (due to mechanical

movement of fluid), and migration (due to potential gradient). In this model, the movement of fluid due to density gradient was not considered. The model results show the three model variables' effect (effect of concentration of copper and hydrogen ions, and applied current density), which can be used to find an optimum condition of the system.

MODELING FRAMEWORK

Comsol Multiphysics uses the finite element method to compute model solutions. In this model, an electrodeposition module is used to simulate the electrochemical cell. To model the electrodeposition process, the Tertiary Nernst-Plank current distribution model is utilized to solve for the cell variables. A set of governing equations is used and solved.

Model Geometry

The geometry of the model is presented in Figure 1. In a three-dimensional coordinate system, the size of the cell is 0.1m×0.1557m×0.09m and two anodes with 0.08×0.006×0.8 and the cathode with 0.08×0.003×0.08 size. Only the front side faces of anodes and cathode contribute to electrode reactions.

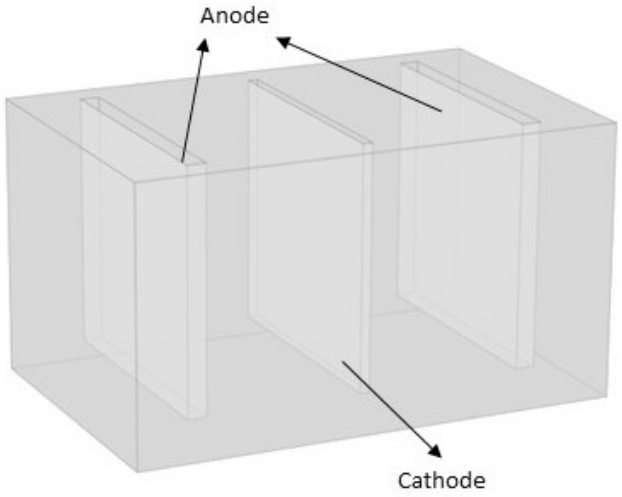

Figure 1. The geometry of the model with two anodes and a cathode in the center of the cell

Governing Equation

In the electrolyte, the mass transfer is controlled by the Nernst-Plank equation:

$$\mathbf{N_i} = -z_i u_i F c_i \nabla \Phi_l - D_i \nabla c_i + c_i \mathbf{v} \quad (1)$$

Where $\mathbf{N_i}$, z_i, u_i, F, c_i, D_i, $\nabla\Phi_l$, ∇c_i, $\mathbf{v}$ are flux density, charge, mobility, Faraday's constant, the concentration, diffusivity of species i, an electrical field, a concentration gradient, and velocity vector, respectively. No homogeneous reaction in the electrolyte in electrorefining cell is assumed, so the material balance equation is given as below:

$$\frac{\partial c_i}{\partial t} + \nabla \cdot \mathbf{N_i} = 0 \quad (2)$$

As in the electrolyte $\boldsymbol{i}_l = F \sum_i z_i . \boldsymbol{N_i}$, so the current density is given by:

$$\mathbf{i}_l = -F^2 \nabla \Phi_l \sum_i z_i^2 u_i c_i - F \sum_i z_i D_i \nabla c_i + F\mathbf{v} \sum_i z_i c_i \quad (3)$$

Where $\mathbf{i}_l$ is the current density in the electrolyte. Also due to the electroneutrality of the electrolyte solution, the third term in Equation 3 ($\sum_i z_i c_i = 0$) removes from this equation. Therefore:

$$i_l = -F^2 \nabla \Phi_l \sum_i z_i^2 u_i c_i - F \sum_i z_i D_i \nabla c_i \quad (4)$$

The kinetic of electrode reaction is given by concentration dependant Butler-Volmer equation:

$$i_{loc} = i_0 \left[\frac{C_{R,S}}{C_{R,B}} \exp\left(\frac{\alpha_a z F}{RT} \eta \right) - \frac{C_{O,S}}{C_{O,B}} \exp\left(-\frac{\alpha_c z F}{RT} \eta \right) \right] \quad (5)$$

Where i_{loc}, i_0, α_a, α_c, η, $C_{R,S}$, $C_{R,B}$ are the localized current density in the interface of electrode and electrolyte due to overpotential, the equilibrium exchange current density, the anodic symmetry factor, the cathodic symmetry factor, the overpotential, the concentration of reductant species in the surface of the electrode, the concentration of the reductant species in the bulk of electrolyte respectively. For the hydrogen evolution, the kinetic equation obeys from Tafel equation that is given below:

$$i_{loc,H} = -i_{0,H} 10^{-\eta_H / A_c} \quad (6)$$

Hydrogen reaction doesn't contribute to the rate of copper deposition, but it contributes to the local current density on the cathode surface:

$$\mathbf{n} \cdot \mathbf{i}_l = i_{loc,Cu} + i_{loc,H} \quad (7)$$

Equation 7 shows the balance of the current density, which means an equal amount of current that left at the anode also enters at the cathode (Comsol Multiphysics Users Guides V 5.5, 2019), (Pryor, Roger W, 2009), (Zeng et al., 2016):

$$\int_{\text{anode surf.}} \mathbf{i_l} \cdot \mathbf{n} dS = \int_{\text{cathode surf.}} \mathbf{i_l} \cdot \mathbf{n} dS = i_{\text{ave.}} \int_{\text{anode surf.}} dS \quad (8)$$

Electrode reactions

Two Cathodic reactions are assumed in this model:

$$Cu^{2+}_{(aq)} + 2e^- \rightarrow Cu(s) \quad (9)$$

$$H^+ + e^- \Leftrightarrow \frac{1}{2} H_2 \quad (10)$$

For simplicity, only one anode dissolve of copper is assumed between all anodic reactions:

$$Cu(s) \rightarrow Cu^{2+}_{(aq)} + 2e^- \quad (11)$$

All the other surfaces except anode and cathode are insulated:

$$-n \cdot i = 0 \quad (12)$$

Experimental Design

To design the experiment and extract results, there are four input variables which are copper and acid concentration, applied density, and time. Table 1 represents variables. This method helps to extract responses and at the end will consider the effect of each parameter on each other and also on responses.

Table 1. Variale parameters in experimental design

Name	Units	Minimum	Maximum	Coded Low	Coded High	Std. Dev.
Cu2+	Gr/L	10.00	90.00	-1 ↔ 30.00	+1 ↔ 70.00	18.19
H2SO4	Gr/L	20.00	340.00	-1 ↔ 100.00	+1 ↔ 260.00	72.78
Current Density	Amp/m^2	50.00	550.00	-1 ↔ 175.00	+1 ↔ 425.00	113.71
Time	Sec	5000	45000	-1 ↔ 15000	+1 ↔ 35000	9097.18

Input Variables and Simulation

Some initial inputs are constant in all runs that are given in Table 1 (Situmorang et al., 2020), (Zeng et al., 2015). By using the central composite method twenty runs with three different variables are utilized. Table 2 shows each simulation input variables.

Table 2. Initial values for the model

Parameter	Value	unit e
Anodic symmetry factor	1.5	-
Cathodic symmetry factor	0.5	-
Equilibrium exchange current density of copper	0.2	A/m^2
Equilibrium exchange current density of hydrogen	0.01	A/m^2
Cathodic potential	-0.337	V
Anodic potential	0.337	V
Temperature	323	K
Hydrogen diffusion coefficent	$9.31 \cdot 10^{-9}$	m^2/s
Hydrogen diffusion sulfate	$1.07 \cdot 10^{-9}$	m^2/s
Hydrogen diffusion copper	$7.33 \cdot 10^{-10}$	m^2/s
Cathodic Tafel slope of hydrogen	-0.118	V

RESULTS

Different simulations are being used to show why this type of meshing is used for the modeling procedure. Four types of meshes are considered here: Extra coarse mesh, Coarser mesh, Coarse mesh, and normal mesh. Different types of meshes are available in the software. The chosen mesh was

Coarser. Figure 2 shows the difference between the chosen type of meshing and three others for simulation 1. The chosen meshing depends on the accuracy and the time that takes each simulation.

Table 3 shows the errors between the Coarser meshing run and the others and the time that is needed for each run. Therefore, it is acceptable to use the coarser meshing. Table 4 shows the ANOVA for current efficiency. Two responses are extracted from model results: Current efficiency and energy consumption. The optimized value for results by considering the maximum value for current efficiency is shown in Table 5.

As this model only considers the diffusion of ions and the fluid flow isn't considered, the current efficiency of the model in the whole simulation is below. The results of the numerical optimization are presented in Table 5. It should be noted that these values are obtained according to this specific model. Table 6 compare predicted points from software and obtained values for each simulation.

According to Faraday's law, an increase in applied current density increases cathodic reactions. Therefore, if the copper ions are available, they can deposit at the cathode. But when copper

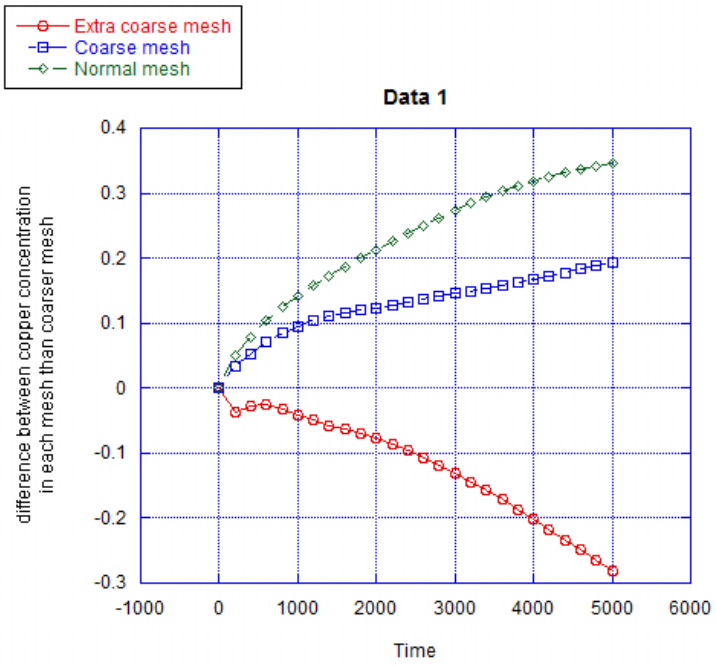

Figure 2. The difference between the concentration of copper by each mesh

Table 3. Variable parameters for each run (Copper and acid concentration, applied current density)

Simulation No.	Cu(g/L)	H_2SO_4(g/L)	I(A/m^2)
1	30	260	425
2	50	340	300
3	70	100	425
4	70	260	425
5	54	176	304
6	50	20	300
7	30	100	175
8	51	179	301
9	50	180	50
10	70	260	175
11	51	178	299
12	49	182	298
13	30	100	425
14	10	180	300
15	90	180	300
16	46	184	296
17	50	180	300
18	70	100	175
19	50	180	550
20	30	260	175

Ions aren't available, since the hydrogen diffusion coefficient is bigger than the copper diffusion coefficient (copper ions are bigger and heavier than hydrogen ions) the increase in applied density can decrease the current efficiency.

Table 4. The effect of mesh sizes on simulation time and precision of the concentration of copper

	Extra Coarse	Coarser*	Coarse	Normal
Required time for each simulation	29 mins	52 mins	1 h 50 mins	2 h 58 mins
errors after 50000 seconds	1.28%	-	0.55%	1.33%

Table 5. Analysis of variance (ANOVA) for current efficiency- response surface

Source	Coefficient Estimate	Sum of squares	df	Mean square	F-value	p-value	
Model	***44.73***	***6621.7***	***14***	***473***	***19.67***	***3.85E-07***	***significant***
A-Cu2+	10.53	2661.3	1	2661	110.7	2.55E-08	
B-H2SO4	-4.67	524.52	1	524.5	21.82	0.000301	
C-Current Density	-9.79	2300	1	2300	95.67	6.68E-08	
D-Time	-4.23	429.01	1	429	17.85	0.000736	
AB	-0.7447	8.8721	1	8.872	0.369	0.552606	
AC	-2.4	91.796	1	91.8	3.818	0.069597	
AD	-0.8409	11.314	1	11.31	0.471	0.503156	
BC	-0.227	0.8243	1	0.824	0.034	0.855573	
BD	-0.1551	0.3849	1	0.385	0.016	0.900989	
CD	0.9801	15.37	1	15.37	0.639	0.436432	
$A^{2\bar{1}}$	-0.8215	18.51	1	18.51	0.77	0.394065	
$B^{2\bar{1}}$	2.63	189.82	1	189.8	7.896	0.013191	
$C^{2\bar{1}}$	3.71	377.09	1	377.1	15.69	0.001256	
$D^{2\bar{1}}$	0.964	25.49	1	25.49	1.06	0.319465	
Residual		360.6	15	24.04			
Lack of Fit		322.74	10	32.27	4.262	0.061575	not significant
Pure Error		37.862	5	7.572			
Cor Total		6982.3	29				
Std. Dev.	4.9		R^2	0.948			
Mean	49.92		Adjusted R^2	0.9			
C.V. %	9.82		Predicted R^2	0.726			
			Adeq Precision	18.64			

Table 5. Optimized values for the variables of the model

	Cu^{2+} g/L	H_2SO_4 g/L	Current Density Amp/m^2	Time Sec	Current Efficiency %	Energy Consumption KWh/Kg
maximize current efficiency (A)	68.7	105.2	190.8	5506	89.16	0.367
minimize energy consumption (B)	67.8	100	175	5000	92.28	0.295
maimaize current efficiency and minimiaze energy consumption (C)	70	103	175	5000	93.3	0.291

Table 6. Predicted values and obtained values for three simulations mentioned above simulation

	predicted points			obtained values		
	A	B	C	A	B	C
curren efficiency	89.16	92.28	93.42	85.1	87	89
energ consumptin	0.367	0.295	0.29	0.5	0.48	0.45

When copper ions concentration increases in the bulk electrolyte (initial electrolyte) the current efficiency increases by the increase in applied current density, because of that copper ions are available near of cathode to deposit on it. This effect can be seen in Figure 3. As seen from Figure 3 that the maximum current efficiency is obtained when the concentration of copper ions is high and applied density is minimum. This is because hydrogen ions can evaluate better than copper ions in higher applied current density.

Figure 4 shows the interaction between acid concentration and applied current density on energy consumption. As can be seen from Figure 4 that when the acid concentration increases, because of the high mobility of hydrogen ions, the conductivity of electrolyte increases and voltage

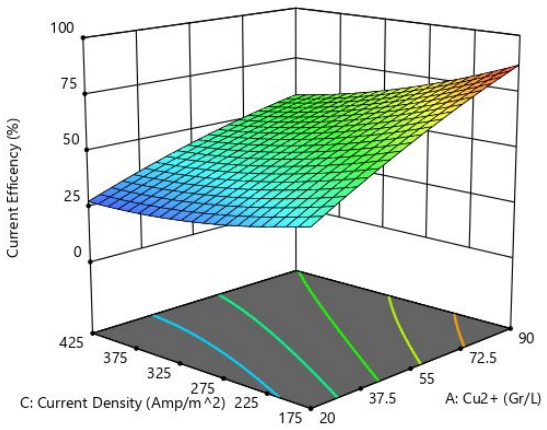

Figure 3. Surface graph of the effect of Copper ions and applied current density on current efficiency (after 20000 sec and acid concentration is 180 g/L)

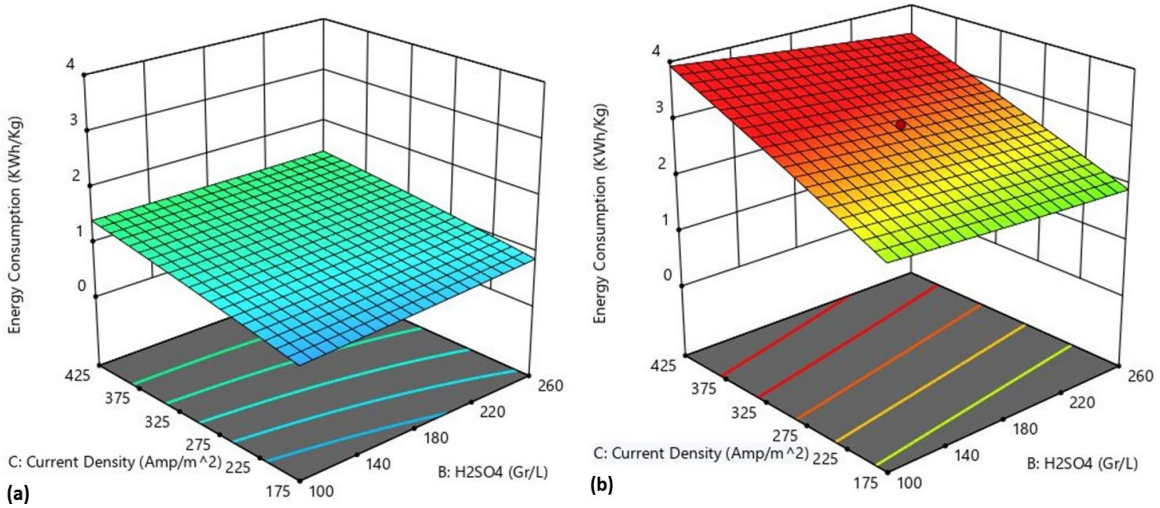

Figure 4. Surface graph of the effect of Acid concentration and applied current density on energy consumption after 25000 sec a) copper concentration is 10 g/Land b) copper concentration is 90 g/L

drop decreases, so energy consumption decreases. But in low current density and high copper concentration copper ions. Due to the small diffusion coefficient of copper ions, it prevents the diffusion of hydrogen ions and by increasing the concentration of acid, a negative effect on energy consumption is seen (Figure 4 (b)), but in higher applied current density diffusion of hydrogen ions in high copper concentration must happen due to applied density, so the energy consumption can e constant (Figure 4 (b)).

But there is a negative effect: When the concentration of hydrogen ions increases too much, in low concentration of copper ions, because of hydrogen evolution, recovery decreases. As you see in Figure 5 this effect in a lower concentration of copper in more. This is because of the higher mobility of hydrogen ions in a lower concentration of copper ions.

Figure 6-a shows copper concentration between anode and cathode when the initial copper concentration is different but the other parameters are the same. As seen in Figure 6 when copper concentration increases the amount of copper ions in the solution increase, and it can be seen that the boundary layer is constant due to the same applied current density and acid concentration. Figure 6-b shows the effect of applied current density on the copper concentration ions in the electrolyte. It can be seen that when applied current density increases the amount of copper that there is in the electrolyte increases (integral of each curve shows this effect). Figure 6-c shows the effect of acid concentration on copper concentration in the electrolyte. It can be seen from Figure 6-c that when acid concentration increases, due to an increase in electrolyte conductivity, the amount of copper that moves into electrolyte increases. It is noteworthy to say that Figures 6 are plotted for the concentration of copper from a line of the center of the cell.

CONCLUSION

After obtaining the optimum condition for the model that is 70 g/L copper concentration 103 g/L acid concentration and 175 A/m^2 applied current density, the interaction between three variables is considered. Each variable affects two others. Higher applied density needs higher ionic conductivity and on the other hand, higher conductivity in a higher concentration of hydrogen is available and consequently more evolution of hydrogen ions, this decreases the current efficiency. In higher copper ionic concentration, the higher concentration of hydrogen could have. Higher copper

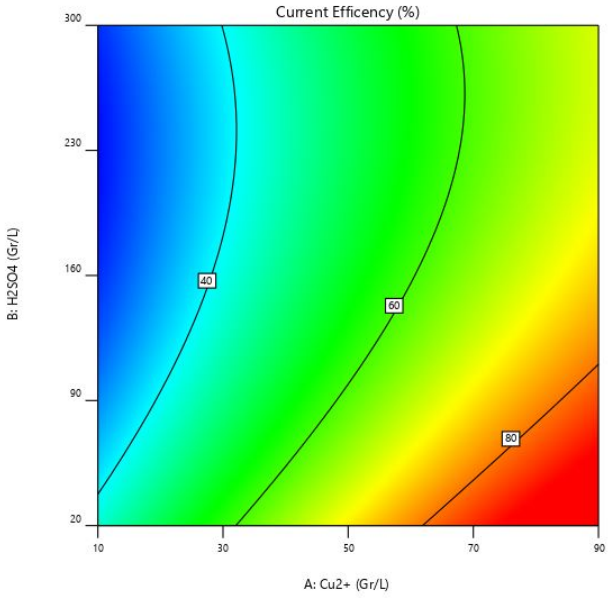

Figure 5. Effect of copper concentration and acid concentration on current efficiency (after 40000 sec and applied current density is 175 A/m^2)

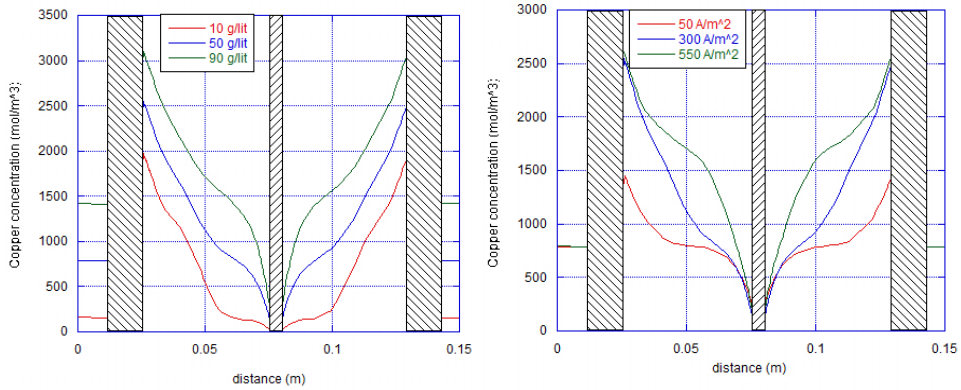

(a) (b)

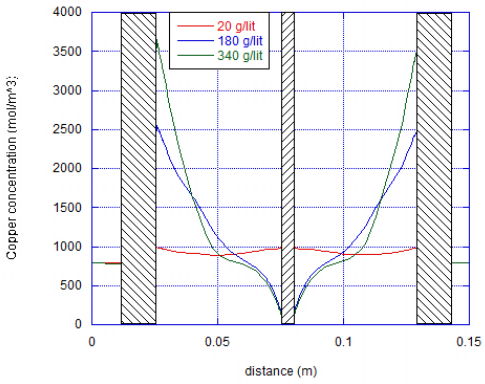

(C)

Figure 6. Copper concentration between anode and cathode in different copper concentration simulations a) copper concentration, b) applied current density are constant are same, c) acid concentration

Concentrations can have a higher applied current density. But after a while, that process proceeds, hydrogen higher mobility, decreases current efficiency. Therefore, it needs a below current density to have maximum current efficiency and minimum energy consumption in this model.

REFERENCES

Comsol Multiphysics Users Guides V 5.5. (2019). US.

Mark E. Schlesinger Matthew J. King Kathryn C. Sole William G.I. Davenport. (2011). *Extractive Metallurgy of Copper, Fifth Edition.* Elsevier.

Pryor, Roger W. (2009). *Multiphysics modeling using COMSOL: a first principles approach.* Jones \& Bartlett Publishers.

Situmorang, Riky Stepanus and Seri, Osami and Kawai, Hideki. (2020). Estimation of exchange current density for hydrogen evolution reaction of copper electrode by using the differentiating polarization method. *Applied Surface Science, 505*(Elsevier), 144300.

Zeng, Weizhi and Free, Michael L and Werner, Joshua and Wang, Shijie. (2015). Simulation and validation studies of impurity particle behavior in copper electrorefining. *Journal of The Electrochemical Society, 162*(IOP Publishing), E338

Zeng, Weizhi and Free, Michael L and Wang, Shijie. (2016). Simulation study of electrolyte flow and slime particle transport in a newly designed copper electrorefining cell. *ECS Transactions, 72*(IOP Publishing), 23..

MODELLING OF ROCK COMMINUTION USING STATISTICAL AND SOFT COMPUTING ANALYSES – A CASE STUDY ON A LABORATORY-SCALE JAW CRUSHER

E. Köken

Abdullah Gul University, Nanotechnology Engineering Department
(ekin.koken@agu.edu.tr)

ABSTRACT

The present study encompasses a quantitative investigation on rock comminution using statistical and soft computing analyses. For this purpose, physical and mechanical rock aggregate properties were determined for nine different rock types (R1–R9) in Turkey. Then, crushability tests were performed to determine the size reduction ratio (SRR) using a laboratory-scale jaw crusher. Based on statistical and soft computing analyses, five different predictive models (M1 to M5) were established to estimate the SRR in this study. Consequently, the SRR values are associated with water absorption by weight (w_a), dry unit weight (γ_d), and aggregate impact value (AIV) of the investigated rocks. However, the individual use of these independent variables results in undulating SRR estimations. Therefore, among the established predictive models, the empirical formulation based on artificial neural networks (ANN) (M5) was found to be the most reliable model with a correlation of determination value (R2) of 0.88. However, the predictive models stated in this study should be implemented to several portable jaw crushers to observe the similarities or difficulties in quantifying SRR as a function of rock properties in future studies.

Keywords: Rock crushability, crushed stone, size reduction ratio, jaw crusher, soft computing.

INTRODUCTION

Rock comminution is the first mechanical step in aggregate manufacturing. Different types of crushing equipment have been used in various combinations to produce rock aggregates. For instance, jaw and gyratory type crushers are mainly used to break down huge rock blocks in crushing – screening plants and, therefore, they are declared primary crushers. However, in secondary and tertiary crushing processes, cone, horizontal, and vertical shaft impact crushers are preferred to obtain rock aggregates with specific size fractions (Nikolov 2004; Johansson et al., 2017). In addition to such industrial crushers, portable crushing machines endowed with jaw or cone crushers are mainly operated in-pit crushing and conveying systems (Liu and Pourrahimian 2021).

It is essential to note that the settings of the crusher and the physicomechanical properties of rocks become prominent to achieve the maximum output from the crushing equipment. In this sense, the rock-crusher interaction is of prime importance, and several studies have documented the effective parameters on the degree of rock crushability (DRC). More deeply, the particle size distribution of the product is associated with the setting of the crusher and the nature of the material fed (King 2012). It has long been experienced that the greater the strength of the rock, the more energy is required to break down the rocks. At the same time, lower size reduction ratios and higher wear rates in the crushing equipment are expected under the dominance of high-strength rock properties. Since rock strength and abrasion properties, such as Los Angeles abrasion value (LAAV), are clear indicators of rock aggregate quality, they have gained popularity to evaluate the rock comminution (Metso 2018). However, operational characteristics or crusher settings are by far the most critical variable in rock

quarrying. In this regard, the crusher discharge settings (i.e., open-side setting (OSS) and closed-side setting (CSS)) have been mainly considered to control general size reduction for compressive crushers (Evertsson 2000; Lee and Evertsson 2011; Fladvad and Onnela 2020).

The particle size distribution (PSD) of the feed material and the CSS of the compressive crushers also play an essential role in product flakiness, which is another critical parameter for quantifying the quality of rock aggregates (Eloranta, 1995). Recently, Itävuo and Vilkko (2021) modeled the control of size reduction in cone crushing by adopting variables such as CSS, eccentric speed, and feed rate. As a result of their analyses, the researchers estimated the throughput and PSD of the product with high precision. Furthermore, Köken and Lawal (2021) also investigated the effects of feeding properties (i.e., feed quantity and feed size) on the DRC parameters such as size reduction ratio (SRR), specific energy consumption (E_{cs}), and product flakiness (FI_p). Their laboratory test results demonstrated that the characterized feed size (F_{80}) dominates the general size reduction, whereas the variations in the feed quantity (m_f) are associated with crushing energy consumption and product flakiness.

When it comes to the rock strength parameters in terms of DRC, Bearman et al. (1997) concluded that the tensile strength of rocks has a remarkable effect on the performance of cone crushers. Donovan (2003) found that fracture toughness affects the specific energy consumption of jaw crushers. Szczelina and Raaz (2002) and Tavares and da Silveira (2008) investigated the potential use of mechanical aggregate properties (LAAV, Axb breakage index, and Bond Work index) for their use in the selection and optimization of crushers for the mining industry. More recently, Korman (2015), Kahraman et al. (2018), and Köken and Özarslan (2018) concluded that the uniaxial compressive strength (UCS) of rocks determines the DRC for jaw crushers. On the other hand, the Brazilian tensile strength (BTS) of rocks is closely related to the energy consumption of cone crushers (Köken 2020a; Köken 2020b).

The studies mentioned above provide quantitative information on using some rock strength properties to evaluate the DRC for several crushers. However, there is a lack of information on how to model the quantitative DRC parameters (e.g., SRR) as a function of the physicomechanical properties of rocks, which are easy to handle and based on highly repeatable testing methods.

Such empirical models based on physicomechanical properties of rocks, which reveal the comminution rate for several crushers, would be beneficial in estimating the power draw and establishing a solid basis for quantifying the size reduction rate. These empirical models would also enable one to stress the performance of crushers with a view to physicomechanical properties. Modeling some DRC parameters for compressive crushers could also give one a chance to understand the weathering degree of feed material. All these potential benefits, which are based on quantifying some of the DRC parameters, constitute a solid basis for the performance of crushers and allow for understanding rock-crusher interactions in a detailed manner.

In this study, detailed laboratory studies were carried out to reveal the comminution rate of nine different rock types from Turkey. For this purpose, the physical and mechanical aggregate properties, which are easy to handle in the laboratory, were determined for each rock type. The crushability tests were then performed using a laboratory-scale jaw crusher. Adopting sieve analyses, the SRR values of the investigated rocks were determined. Several predictive models were established to estimate the SRR using statistical and soft computing analyses. The performance of the proposed predictive models was compared with one another, and it was concluded that the artificial neural network (ANN) based predictive model (M5) outperformed the other predictive models established in the present study. In the present study, explicit mathematical formulations of the established models were also introduced to estimate the SRR, indicating how to model the SRR as a function of the physicomechanical properties of the rocks.

MATERIALS AND METHODS

Representative rock blocks were obtained from several parts of Turkey, and nine different rock types were considered in this study (Table 1). First, the initial size of the rock blocks obtained was reduced using a sledgehammer. Subsequently, rock aggregates with a particle size range of 11.2 to 16 mm were prepared. Next, the physical and mechanical properties of the rock aggregates were determined for each rock type. In the last stage, crushability tests were performed using a laboratory-scale jaw crusher, whose technical properties are listed in Table 2. Eliminating the flakiness effect on the rock crushability was based on the use of an 8 mm bar sieve. More profoundly, flaky particles were removed or minimized from the feeding material using an 8 mm bar sieve before crushability tests were performed.

Table 1. Sampling locations and descriptive codes of the investigated rocks.

Rock-type	Code	Location	Number of rock blocks obtained
Basalt	R_1	Erkilet / Kayseri	6
Basaltic andesite	R_2	Mimarsinan / Kayseri	8
Basalt	R_3	Işıkkara / Kütahya	4
Granodiorite	R_4	Havran / Balıkesir	8
Andesite	R_5	Çaycuma / Zonguldak	7
Dacite	R_6	Yenice / Karabük	8
Sandstone	R_7	Üzülmez / Zonguldak	6
Gabbro	R_8	Yenice / Karabük	5
Limestone	R_9	Yahyalı / Kayseri	6

For each crushability test, the weight of the feeding material (W0) was 1000 ± 5 g, and the total amount of the feeding material was manually fed to the crusher in a single charge. The CSS and the throw (Δx) of the crusher were 8mm and 4 mm, respectively. In other words, the jaw crusher operated in the range of 8 to 12 mm during crushability tests. After every five crushability tests, the CSS of the crusher was controlled and calibrated, if necessary.

Table 2. Technical properties of the laboratory-scale crusher used in crushability tests.

Laboratory-scale jaw crusher	
Nominal voltage (V)	220
Nominal current (A)	≤ 14
Frequency (Hz)	50
Cos(ϕ)	0.94
Power (kW)	2.20
Feeding gape (mm)	100
Capacity (t/h)	≤0.20
CSS adjustment (mm)	≤ 40
Plate type	Convex with stiffeners
Plate length (mm)	340
Jaw speed (rpm)	285 – 290

Laboratory studies

The physical and mechanical properties of rock aggregates determined in this study were water absorption by weight (w_a, %), dry unit weight (γ_d, kN/m^3), and aggregate impact value (AIV, %). The w_a and γ_d of the rock aggregates were determined according to TS EN 1097-6 (2013), while the AIV values were obtained following BS 812-112 (1990). The tests mentioned above were repeated three times for each rock block, and the average values were transformed into a comprehensive database for statistical and soft computing analyses.

Crushability tests provide quantitative data on the production yield and comminution rate of several crushers (Köken 2020b). In the context of the crushability tests, the material with a particle size range of 11.2 – 16.0 mm and weighing 1000 ± 5 g was fed to the laboratory-scale jaw crusher in a single crusher by hand. After the crushing action had been completed, the crushed particles were sieved to quantify the size reduction ratio (SRR), which was determined by Eq. 1 as follows:

$$SRR = \frac{F_{80}}{P_{80}} \quad (1)$$

where F_{80} and P_{80} denote the theoretical square mesh aperture sizes (mm) corresponding to 80% of the cumulative undersize of the feed and product particle size distributions, respectively.

Some of the laboratory studies are illustrated in Figure 1. Laboratory studies were carried out under oven-dried conditions. The physical and mechanical properties of the rock aggregates are listed in Table 3. Accordingly, the w_a, γ_d, and AIV values of the investigated rocks were found to be between 0.211 and 3.661%, 24.980 and 27.885 kN/m^{3,} and 8.682 and 23.586%, respectively. On the other hand, the crushability test results are given in Figure 2. From Figure 2, it can be observed that the values of F_{80}, $P_{80,}$ and SRR ranged between 13.737 and 15.537 mm, 5.114 and 7.827 mm, and 1.878 and 2.950, respectively.

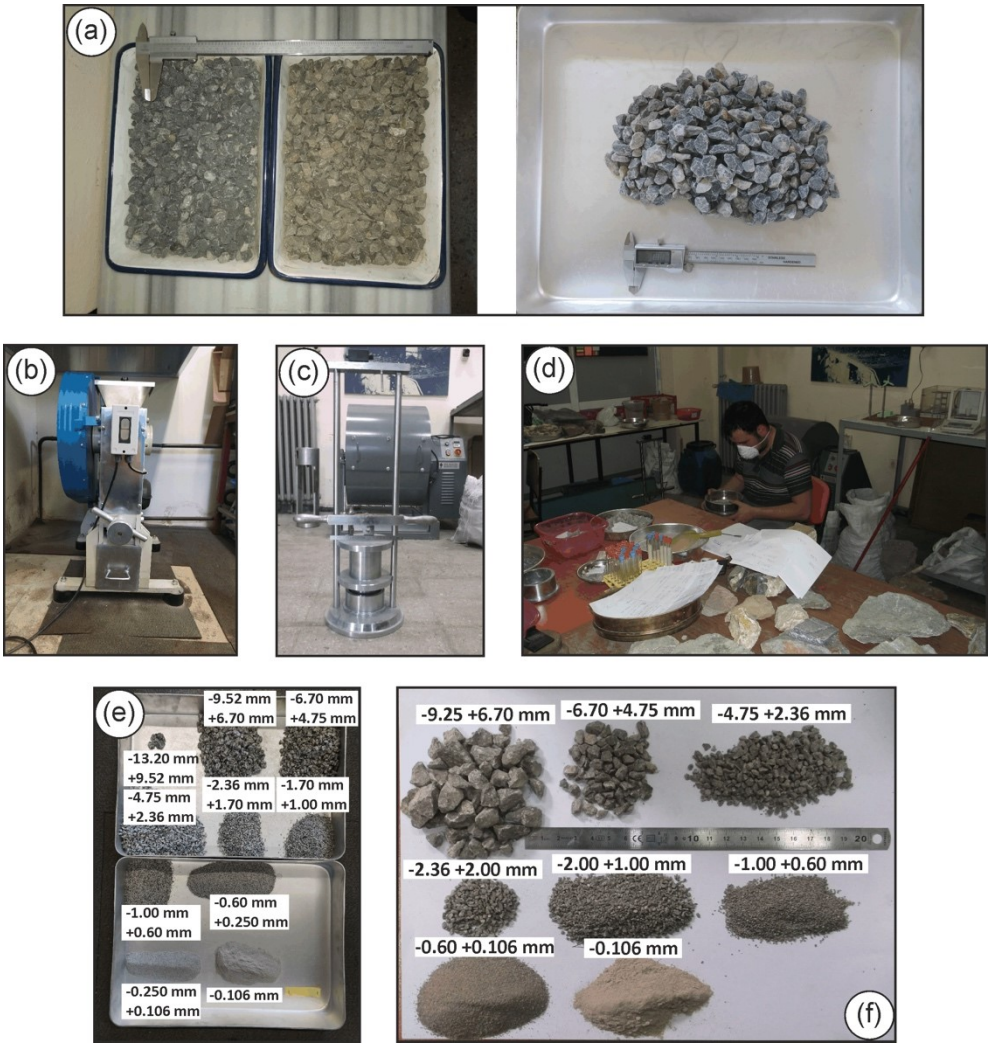

Figure 1 Laboratory studies a) Some of the feeding materials (11.2–16 mm) for crushability tests b) Laboratory-scale jaw crusher c) Aggregate impact value apparatus d) Sieving procedure e) Typically crushed particles obtained from a single crushability test f) Typically crushed particles obtained from a single AIV test.

Table 3. Laboratory test results.

Rock type	w_a (%)	γ_d (kN/m^3)	AIV (%)
R1	1.80[(1)] ± 0.10[(2)] (18)[(3)]	26.55 ± 0.17 (18)	17.76 ± 0.43 (18)
R2	2.53 ± 0.29 (24)	26.53 ± 0.27 (24)	17.90 ± 1.24 (24)
R3	0.27 ± 0.06 (12)	27.26 ± 0.32 (12)	9.89 ± 1.13 (12)
R4	1.04 ± 0.06 (24)	26.99 ± 0.37 (24)	11.97 ± 1.48 (24)
R5	3.23 ± 0.28 (21)	25.42 ± 0.31 (21)	19.52 ± 2.67 (21)
R6	1.42 ± 0.12 (24)	26.14 ± 0.26 (24)	15.74 ± 1.22 (24)
R7	2.42 ± 0.24 (18)	25.67 ± 0.25 (18)	19.96 ± 0.99 (18)
R8	0.79 ± 0.25 (15)	27.60 ± 0.29 (15)	14.11 ± 1.51 (15)
R9	1.40 ± 0.15 (18)	25.45 ± 0.11 (18)	15.85 ± 1.74 (18)

[(1)]Mean [(2)]Standard deviation [(3)]number of samples

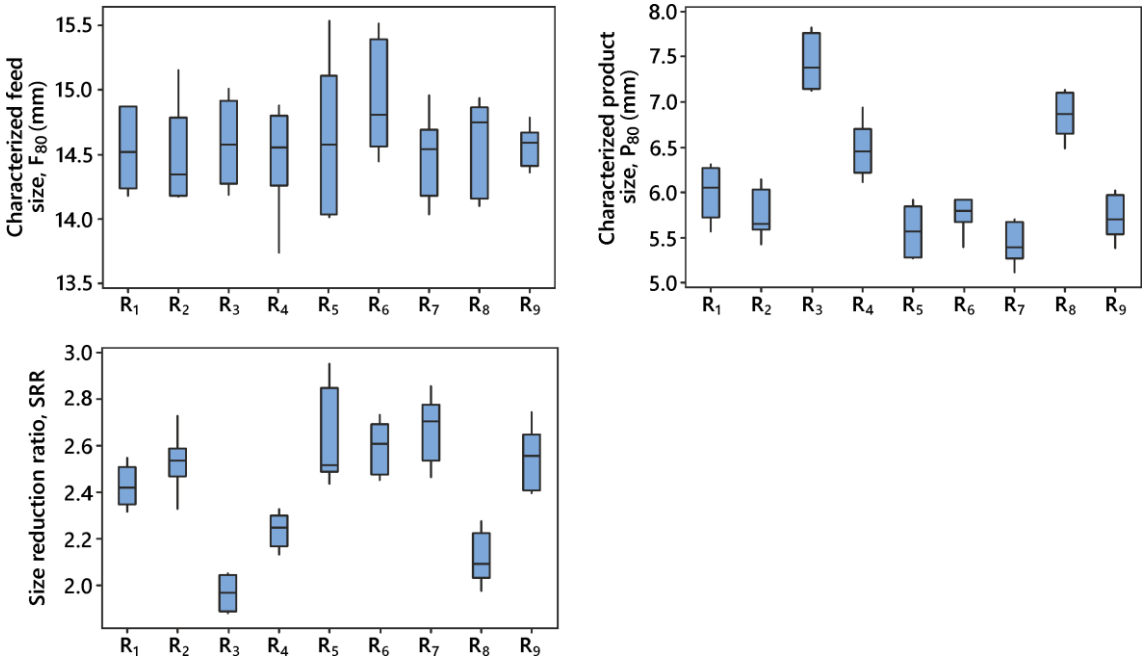

Figure 2. Box plots of the crushability test results

Statistical and Soft Computing Analyses

In this section, statistical and soft computing analyses were introduced to evaluate the SRR. Based on the single and multiple regression analyses, several correlations were obtained. The regression-based models (M1–M4) yielded a correlation of determination (R^2) ranging from 0.47 to 0.71, only stating some correlative parameters to evaluate SRR. Additional soft computing analyses were also performed to obtain other empirical formulations to estimate the SRR with higher accuracy. Soft computing analyses adopted in this study were based on artificial neural networks (ANN). ANN analyses were performed in a MATLAB environment. For this purpose, a neural network toolbox (nntool) was utilized to establish several neural networks. The database was randomly divided into training (70/100) and testing/validating (30/100) parts. Various possible network architectures with variable hidden layers and neurons were attempted to determine the most reliable structural combination. To estimate the SRR values, the most convenient ANN architecture was found to be 3–6–1. Before performing the ANN analyses, the database was normalized between –1 and 1 using the following equation (Singh et al., 2012; Lawal and Idris, 2020).

$$V_N = 2\left(\frac{X_i - X_{\min}}{X_{\max} - X_{\min}}\right) - 1 \quad (2)$$

where V_N is the normalized value, x_i is the relevant parameter to be normalized, x_{min}, and x_{max} are the minimum and maximum values in the relevant dataset.

Based on the ANN analyses, the SRR values can be estimated by model 5 (M5), which is given in Table 4. The subequation systems for M5 are also listed in Table 5. When comparing the R^2 values of the developed models, M5 provided the highest R^2 value (R^2 = 0.88), which shows the most reliable model for estimating the SRR in this study.

Table 4. Proposed empirical models for the evaluation of SRR in this study.

Model No	Empirical formula	R^2
M1	$SRR = 2.1131 + 0.1883 w_a$	0.47
M2	$SRR = 8.654 - 0.2357 \gamma_d$	0.55
M3	$SRR = 1.5426 + 0.05703 AIV$	0.63
M4	$SRR = 5.158 - 0.1261 \gamma_d + 0.03861 AIV$	0.71
M5	$SRR = 0.5357 \tanh\left(\sum_{i=1}^{6} A_i - 1.593 \right)$	0.88

The developed empirical models (M1–M5) provide a piece of practical knowledge on how to model the size reduction process that occurred in a laboratory-scale jaw crusher. In other words, the SRR values increase with increasing w_a and AIV of the rocks, while they decrease when increasing the γ_d values. Furthermore, empirical formulations (M1-M5) can be used to evaluate rock aggregate quality in a rock quarry. In other words, considering fixed operational features in crushing equipment, higher SRR values obtained from crushability tests can indicate lower rock aggregate quality or the presence of weathered rock types. Nevertheless, the variations in SRR values can also indicate the heterogeneity of the host rock.

In this context, such empirical relationships to evaluate the DRC parameters can save time and provide practical information on the quality of feed material. Furthermore, the anomalies in the SRR values can also show undulating energy consumption values, which were not considered in this study. However, further studies are required to obtain relationships between the SRR values and their correspondence with the energy consumption.

Table 5. Sub-equation systems for the developed ANN model (M5).

$A_1 = -2.2047 \tanh\left(4.6846^n w_a - 2.4569^n AIV - 6.4191^n \gamma_d - 6.0146\right)$
$A_2 = 3.0404 \tanh\left(2.2891^n w_a - 0.02924^n AIV - 1.9587^n \gamma_d - 3.1045\right)$
$A_3 = -0.54611 \tanh\left(2.651^n w_a - 3.658^n AIV - 0.72175^n \gamma_d + 0.57849\right)$
$A_4 = -2.2676 \tanh\left(1.1376^n w_a - 2.8478^n AIV + 0.08619^n \gamma_d + 0.95445\right)$
$A_5 = -1.3759 \tanh\left(1.8914^n w_a + 3.7618^n AIV + 1.111^n \gamma_d + 1.4537\right)$
$A_6 = 2.3332 \tanh\left(5.1893^n w_a + 0.2412^n AIV + 2.3619^n \gamma_d + 4.5938\right)$
Normalization Functions
$^n w_a = 0.5798 w_a - 1.1229$
$^n AIV = 0.1342 AIV - 2.1651$
$^n \gamma_d = 0.6956 \gamma_d - 18.375$

RESULTS AND DISCUSSION

Statistical analyses indicated that the w_a, γ_d, and AIV of rocks have some influence on the SRR that occurred in a laboratory-scale jaw crusher. However, the regression-based models (M1-M4) are not high enough for precise estimations on the SRR. By implementing such ANN analyses, M5 was developed, which provides the highest R^2 value (R^2 = 0.88) among the models developed (Table 4).

The predicted and measured SRR values obtained from the M5 model are plotted in Figure 3. Accordingly, it can be claimed that the predicted SRR values are in good agreement with the measured ones. In summary, the comparison of all the developed models is given in Figure 4. It can be seen from Figure 4 that a single use of physical and mechanical rock aggregate properties would not allow one to assess size reduction processes by jaw crushers with a higher prediction capability. This phenomenon can be interpreted as the size reduction process in jaw crushers is a complex issue; therefore, the complexities arising from the nature of the rock can be overcome by multiple-choice of rock properties. In this manner, the ANN-based model (M5) can be an example of quantifying or modeling the size reduction process in a jaw crusher. However, the practical information stated in this study should be tried with a portable jaw crusher to observe similarities or difficulties in quantifying SRR values as a function of different rock properties.

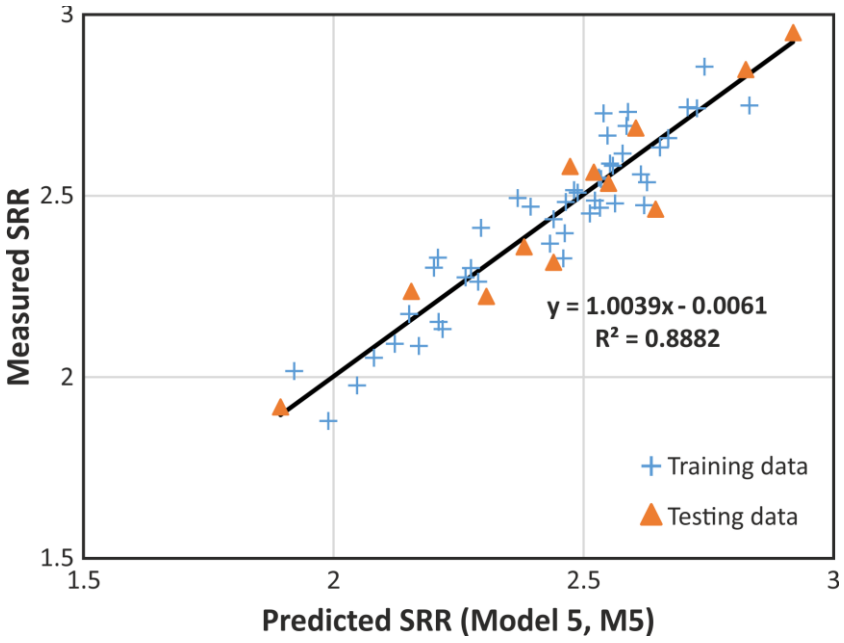

Figure 3. Predicted and measured SRR values based on the M5 model.

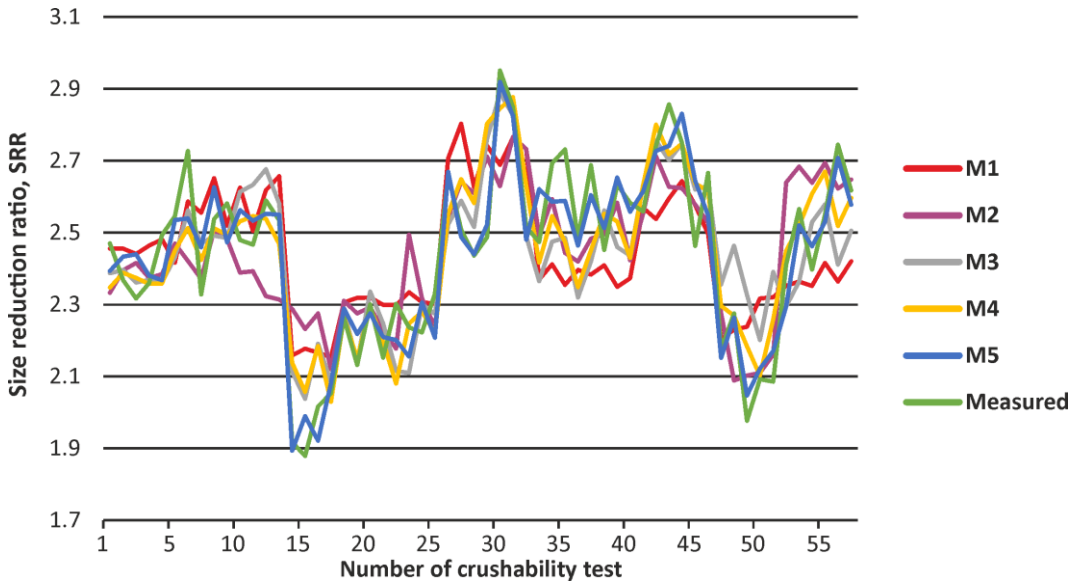

Figure 4. Comparison of all predictive models to estimate SRR.

CONCLUSIONS

In this study, the size reduction processes that occurred in a laboratory-scale jaw crusher were investigated using nine different rock types from Turkey (Table 1). The physical (w_a, γ_d) and mechanical (AIV) aggregate properties were determined for each rock type (Table 3). Then, detailed crushability tests were carried out (Fig 2). The SRR values were obtained from the sieve analyses of the crushed particles. The laboratory test results were transformed into a comprehensive database for statistical and soft computing analyses. The statistical and soft computing analysis results emphasize the importance of the selected rock properties for evaluating the SRR. However, it can be claimed that the ANN-based model (M5) provides the highest R^2 value (Table 4), showing that soft computing analyses can be reliably implemented for the size reduction process that occurred in jaw crushers. However, more studies are required to observe similarities or difficulties in quantifying SRR values in portable jaw crushers for the industry.

Conflict of Interest

The author declares that he has no known competing financial interests or personal relationships that could have influenced the work reported in this document.

REFERENCES

Bearman RA, Briggs CA, Kojovic T (1997) The application of rock mechanics parameters to the prediction of comminution behavior. Miner Eng 10(3):255–264.

BS 812-112 (1990) Testing aggregates - Method for determination of aggregate impact value (AIV), British Standards Institution.

Donovan J. G. (2003) Fracture toughness based models for the prediction of power consumption, product size, and capacity of jaw crushers, Dissertation, Virginia Polytechnic Institute, and State University.

Eloranta, J. (1995). Influence of crushing process variables on the product quality of crushed rock. Dissertation, Tampere University of Technology

Evertsson C.M. (2000) Cone crusher performance, Dissertation, Chalmers University of Technology, Götebord, Sweden.

Fladvad M. and Onnela T. (2020) Influence of jaw crusher parameters on the quality of primary crushed aggregates, Min. Eng. 151: 106338.

Johansson M., Bengtsson M., Evertsson M., Hulthén E. (2017) A fundamental model of an industrial-scale jaw crusher, Min. Eng. 105: 69 – 78.

Kahraman S, Toraman OY, Cayirli S (2018) Predicting the strength and brittleness of rocks from a crushability index. Bull Eng Geol Environ 77(4):1639–1645.

King, R.P. (2012) Modeling and Simulation of Mineral Processing Systems; 2nd edition, C.L. Schneider and E.A. Kind (eds), Elsevier: Amsterdam, 457 pp, The Netherlands

Köken E, Özarslan A (2018) New testing methodology for the quantification of rock crushability: compressive crushing value (CCV). Int J. Miner Metall Mater 25(11):1227–1236.

Köken E. (2020a) Evaluation of size reduction process for rock aggregates in cone crusher, Bull. Eng. Geol Environ. 79: 4933 – 4946.

Köken E. (2020b) Size Reduction Characterization of Underground Mine Tailings: A Case Study on Sandstones, Natur. Res. Res. 30: 867 – 887.

Köken E. and Lawal A.I. (2021) Investigating the effects of feeding properties on rock breakage by jaw crusher using response surface method and gene expression programming, Adv. Powder. Tech. 32(5): 1521 – 1531.

Korman T, Bedekovic G, Kujundzic T, Kuhinek D (2015) Impact of physical and mechanical properties of rocks on energy consumption of jaw crusher. Physicochem Probl Miner Process 51(2):461–475.

Lawal A.I., and Idris M.A., An artificial neural network-based mathematical model for the prediction of blast-induced ground vibrations. Int. J. Environ. Stud., 77(2): 318 – 334, (2020), DOI:10.1080/00207233.2019.1662186.

Lee, E. and Evertsson C. M. (2011). A comparative study between cone crushers and theoretically optimal crushing sequences, Min. Eng., 24(3–4), 188–194.

Liu D. and Pourrahimian Y. (2021) A Framework for Open-Pit Mine Production Scheduling under Semi-Mobile In-Pit Crushing and Conveying Systems with the High-Angle Conveyor, Mining, 1(1): 59 – 79.

Metso. (2018). Basics in mineral processing handbook. Metso Corporation.

Nikolov S. (2004) Modelling and simulation of particle breakage in impact crushers, Int. J. Min Process., 74: 219 – 225.

Singh R., Kainthola A., and Singh T.N., Estimation of elastic constant of rocks using an ANFIS approach, Appl. Soft Comput. J. 12: 40–45, (2012), DOI: 10.1016/j.asoc.2011.09.010.

Szczelina, P., Raaz, V., (2002) Development of hard rock jaw crushers at Krupp Fördertechnik - quantitative characterization of rock properties, Aufbereit.-Tech., 43 (2), 28-31.

Tavares L.M., Da Silverira M.A.C.W. (2008) Comparison of measures of rock crushability, In: Fine Particle Technology and Characterization, Meftuni Yekeler (Ed). ISBN: : 978-81-308-0241-1

TS EN 1097-6 (2013) Tests for mechanical and physical properties of aggregates - Part 6: Determination of particle density and water absorption, Turkish Standards Institution, Ankara

NADİR TOPRAK ELEMENTLERİNİN KAZANIMI İÇİN POTANSİYEL BİR KAYNAK: KÖMÜR YIKAMA TESİSİ ATIKLARI

A POTENTIAL SOURCE FOR RECOVERY OF RARE EARTH ELEMENTS: COAL WASHERY WASTE

N.İ. Dinç [1,*], F. Burat [1]

[1] *İstanbul Teknik Üniversitesi, Maden Fakültesi, Cevher Hazırlama Mühendisliği Bölümü*
*(*Corresponding author: dincnaz@itu.edu.tr)*

ÖZET

Nadir toprak elementleri (NTE) üretimi ve rezervi konusunda lider ülke konumunda bulunan Çin'in ihracatta uyguladığı sınırlamalar ile yüksek teknoloji üreten ülkeler açısından kaynak ihtiyacı doğmaktadır. Bu sebeple artan NTE ihtiyacını karşılamak için ikincil kaynaklara olan yönelim son yıllarda giderek artmaktadır. Bu kaynakları kömür yakıtlı termik santrallerin atıkları olan taban ve baca külleri, kömür yıkama atıkları, cevher zenginleştirme tesislerinin atıkları, fosfat üretimi yapılan maden sahalarının yan ürünleri ve elektronik atıklar oluşturmaktadır. Dünyada gelişen endüstriye paralel olarak, hızla gelişen ve büyüyen ülkemizin de sanayide kullanmış olduğu maden çeşitliğini arttırması, yer altı kaynaklarımızın daha etkin bir şekilde belirlenmesi ve ortaya çıkarılmasını zorunlu hale getirmektedir. Ülkemiz için vazgeçilmez, güvenilir ve ucuz bir enerji kaynağı olan kömür ve kömür yan ürünlerinden kömürün ve NTE'nin, çevresel ve endüstriyel etkileri göz önünde bulundurularak, seçimli olarak eldesini sağlayacak teknolojilerin, metodların ve proseslerin oluşturulması oldukça önemlidir. Bu çalışma kapsamında küresel pazarda yüksek teknoloji üreten ülkeler için ikincil kaynaklardan NTE üretiminin avantajları, kömür ve yan ürünlerinden NTE geri kazanımının önemi ve elde edilmesinde uygulanan yöntemler ile ilgili bilgiler sunulmaktadır.

Anahtar Sözcükler: Nadir toprak elementleri, geri kazanım, kömür atıkları

ABSTRACT

China is the leading country in rare earth elements (REE) production and reserves; therefore, the other countries need resources in terms of high technology raw materials for possible restrictions. For this reason, the tendency of high technology producing REE supply has been increasing in recent years and they are directed to secondary resources to meet this demand. These resources consist of the wastes of coal-fired thermal power plants, tailings of ore enrichment facilities, by-products of mine sites where phosphate production is made, and electronic wastes. Parallel to the developing industry in the world, our rapidly developing and the growing country also increases the variety of minerals used in the industry, making it necessary to determine and reveal our underground resources more effectively. Coal reserves are an indispensable, reliable, and cheap energy source for our country and it is very important to create technologies that will enable the selective recovery of coal and REE from coal by-products by considering its environmental and industrial effects. Studies in the literature show that coal and coal by-products have a significant REE content. Within the scope of this study, information about the advantages of REE production from secondary sources, the importance of REE recovery from coal and its by-products, and the applied methods are presented for high technology-producing countries in the global market.

Keywords: Rare earth elements, recovery, coal waste

GİRİŞ

Yerkabuğunda kimyasal özellikleri çok benzer olan, atom numaraları 57 (lantan) ile 71 (lütesyum) arasında 15 lantanit ile itriyum ve skandiyumdan oluşan 17 metalik element grubuna Nadir Toprak Elementler (NTE) denilmektedir. Atomik ağırlıklarına göre ağır ve hafif nadir toprak elementler olmak üzere iki gruba ayrılır. NTE grubu elementler atomik ağırlıklarına göre 2 alt gruba ayrılmaktadır; lantanyum'dan (La) europiyum (Eu) elementine kadar olan ve atom numaraları 57 ile 63 arasında değişen elementler hafif nadir toprak elementler, atom sayıları 64 ile 71 arasında değişen ve gadolinyum (Gd) ile lutesyum (Lu) arasındaki elementler ise ağır nadir toprak elementler olarak ayrılmaktadır. Yttrium ve skandiyum elementleri, atom numaraları sırasıyla 39 ve 21 olmasına rağmen, ağır nadir toprak elementlerine benzer kimyasal ve fiziksel özellikler sunmaları nedeniyle bu grup elementlere dahil edilmektedir. (Gupta ve Krishnamurthy, 1992). Nadir toprak elementleri, adında söylendiği gibi "nadir" değildir. Bu elementlere "nadir" denmesinin nedeni, nadir olarak görülen mineraller içinde oksit bileşenleri olarak 18. ve 19. yüzyıllarda tespit edilmiş olmalarıdır (Url-1).

Tüm NTE'leri (Pm hariç) yer kabuğunda miktar bakımından gümüş ve civa elementlerinden daha fazla bulunurlar (Taylor ve McLennan, 1985). En bol nadir toprak elementleri seryum, itriyum, lantan ve neodimyumdur (Gupta and Krishnamurthy, 1992). Nadir toprak element cevherleşmeleri esas olarak, alkalin kayaçlar ve karbonatitler olarak adlandırılan özel magmatik kayaçlar ile ilişkilidir. Bunun dışında, plaser yataklarda da NTE içeren mineral konsantrasyonlarına ekonomik olarak rastlanılmaktadır. Ayrıca, magmatik kayaçların derinlerde bozunmasıyla oluşan artık yataklarda, pegmatitlerde, Fe-oksit Cu-Au yataklarında ve denizel fosfatlarda da NTE cevherleşmelerine rastlanılmaktadır. Volkanizmalarla ilişkili yataklar çoğunlukla suların etkisiyle bozuşmuşlardır. Bu yataklara ince dağılmış olarak ya da çatlak dolguları şeklinde rastlanmaktadır. Volkanik kayaçlar genellikle tüf, riyolit ve trakit olup, örtü tabakaları da kumtaşlarından oluşmuştur. Yataklarda flüorit, bastnazit, bertrandit az miktar da baritle birlikte düşük oranda Rb, U, Th, Ta, Nb, Y, Be, Cs ve Re elementlerini içeren mineraller bulunmaktadır. Karbonatitler ile ilişkili NTE cevherleşmeleri rezerv bakımından en büyük yataklardır. Dünyadaki NTE'lerin en önemli üretim kaynağı bastnazit (Ce, La, Nd, Pr) $F(CO_3)$ mineralidir. Bunların yanı sıra NTE'ler ksenotim içeriğinde, plaser yataklarda, uranyum ve bozuşmuş killerle birlikte ve karbonatitlerde de bulunmaktadır. NTE'ler yer kabuğunda değişik oranlarda çok geniş bir alana yayılmış olarak yaklaşık 160'dan fazla mineralin içeriğinde bulunmaktadır.

NTE'leri kullanılan ürünlerin kararlı, yüksek sıcaklığa, aşınmaya, korozyona karşı dirençli, savunma sektöründe değişik amaçlı ileri teknoloji ürün üretiminde kullanılmaları nedeniyle NTE'ler yüzyılın stratejik ve vazgeçilmez elementleridir. Cep telefonu, diz üstü bilgisayar, modern tıp cihazları, araçlarda katalitik çeviriciler, uçak motorları, seramik, petrol rafineri, televizyon üretimi gibi teknolojik ürünlerde NTE'ler kullanılmaktadır. NTE'ler oksit, metal ve değişik kimyasal bileşikler olarak pazarlanıp kullanıldığı gibi yüksek sıcaklıkta duraylı olmaları nedeniyle kaliteli metal alaşım üretiminde de kullanılmaktadır. Katkı maddesi olarak NTE'leri içeren malzemeler kararlı, yüksek sıcak ve korozyona dayanıklı hafif malzemelerdir. Bu özellikleriyle NTE'leri bilgisayar, hibrid araçlar, yüklenebilir piller, cep telefonları, düz televizyon ekranları, dizüstü bilgisayarları, rüzgar türbinleri, tıbbi görüntüleme cihazları, radar sistemleri, katalitik çeviriciler, korozyona daha dayanıklı metal alaşımları, uçak motorları, tıp, seramik, cam üretiminde, petrol arıtmada kullanılmaktadır. NTE'ler değişik malzeme üretiminde değişik oranlarda kullanılmaktadır. Fotoğraf makinesi, gözlük camları ve televizyon ekranlarının parlatılmasında seryum oksit kullanılmaktadır (Yıldız, 2016). Bazı NTE'ler flüoresan ve LED aydınlatmada kullanılır. Yttrium, europium ve terbiyum fosforları, birçok ampul, panel ve televizyonda kullanılan kırmızı-yeşil-mavi fosforlardır. Cam endüstrisi NTE hammaddelerinin en büyük tüketicisidir ve bunları cam parlatma için ve renk ve özel optik özellikler sağlayan katkı maddeleri olarak kullanmaktadır. Lantan, cep telefonu kameraları da dahil olmak üzere dijital kamera lenslerinin yüzde 50'sinde kullanılmaktadır. Ayrıca lantan bazlı katalizörler, petrolü rafine etmek için kullanılmaktadır. Seryum bazlı katalizörler otomotiv katalitik konvertörlerinde kullanılmaktadır. NTE'leri kullanan mıknatısların uygulamaları günümüzde hızla

artmaktadır. Neodimyum-demir-bor mıknatıslar bilinen en güçlü mıknatıslardır. Nadir mıknatıslar bilgisayar sabit disklerinde ve CD – ROM ve DVD disk sürücülerinde kullanılırlar. Bir disk sürücüsünün mili, bir nadir toprak mıknatısı tarafından çalıştırıldığında dönme hareketinde yüksek stabilite elde eder. Bu mıknatıslar ayrıca hidrolik direksiyon, elektrikli camlar, elektrikli koltuklar ve hoparlörler gibi çeşitli geleneksel otomotiv alt sistemlerinde de kullanılmaktadır. Nikel metal hidrit piller, anot olarak lantan bazlı alaşımlardan yapılmıştır. Bu pil türleri, hibrit elektrikli otomobillerde kullanıldığında, elektrikli araç başına 10 ila 15-kilogram gerektiren önemli miktarda lantan içerir. Seryum, lantan, neodimyum ve praseodmiyum, genellikle miskmetal olarak bilinen karışık oksit formunda, çelik yapımında safsızlıkları gidermek için ve özel alaşımların üretiminde kullanılmaktadır (Url-2). NTE'lerin genel kullanım alanları ve yüzdesel dağılımları Şekil 1'de gösterildiği gibidir. Saf neodimiyum oksit cama mor renk vermektedir. Praseodimiyum ve neodimiyum karışımı, televizyon ekranlarında parlamayı önlemektedir. NTE kullanılarak alüminyum, magnezyum, vanadyum gibi çok değişik özel metal alaşımları üretilebilmektedir. NTE'li alaşımlar demir-krom ve çelik alaşımlarında korozyona karşı direnci arttırmaktadır (Yıldız, 2016; Lin vd., 2017). ABD Jeoloji Araştırmaları Kurumu 2021 verilerine göre nadir toprakların son kullanıma göre tahmini dağılımı şu şekildedir: katalizörlerde %75, metalurjik uygulamalar ve alaşımlarda %4, seramik ve camda %6, parlatmada %5 ve diğerleri olarak %10'dur. Ayrıca Amerika Birleşik Devletleri tarafından 2020'de ithal edilen nadir toprak bileşiklerinin ve metallerinin tahmini değeri, 2019'daki 160 milyon dolardan ciddi bir düşüş ile 110 milyon dolar olmuştur (Url-3).

20-30 yıl öncesine kadar elektronik sistemlerde 11 değişik malzeme kullanılırken günümüzde daha işlevsel bilgisayar ve akıllı telefonlarda 60'dan daha çok sayıda değişik malzeme kullanılmaktadır. Gereksinimlerin karşılanması için geleceğe yönelik çalışmalar; ArGe çalışmaları ile NTE'ler yerine kullanılabilecek malzemelere, geri dönüşüm ve yeni NTE kaynaklarının bulunmasına yönelik olacaktır. 2025 yılında NTE talebinin $220x10^3$ ton/yıl, 2035 yılında $350x10^3$ ton/yıl olacağı öngörülmektedir. Yeni kaynaklar ya da ArGe çalışmalarından sonuç alınamaması durumunda bu yıllardan sonra bazı NTE'lerde arz sıkıntısı yaşanacağı, rezervlerin, haliyle arzın talebi karşılanamayacağı riski vardır.

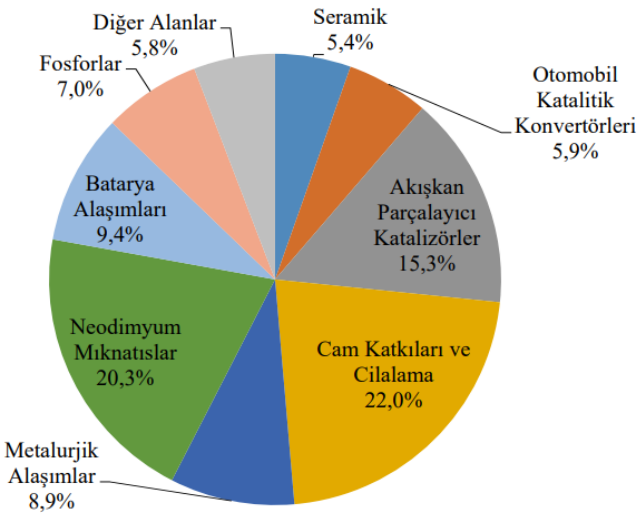

Şekil 1. NTE'lerin genel kullanım alanları ve yüzdesel dağılımları.

Dünyada NTE rezervleri 8 ülkede yoğunlaşmış olup $140x10^6$ ton civarındadır. Çin NTE rezervi bakımından $55x10^6$ ton ile dünyada ilk sırada yer almaktadır. Kaynaklardaki NTE ile ilgili bilgiler incelendiğinde çok farklı rakamlarla karşılaşılmaktadır. Bunun nedeni ülkelerin stratejik olarak gerçek rakamlarını diğer ülkelerle paylaşmadıklarından, kaynaklanmaktadır. Bu gerçeğe dayalı olarak dünyada gerçek rezervin bundan çok daha yüksek olduğu tahmin edilmektedir. Bayan Oba nadir toprak element oksit rezervi $44x10^6$ ton görünür rezerv olarak dünyanın en büyük rezervine sahiptir. Bu rezerv 1957

yılından bu yana işletilmekte olup Çin'in %70 hafif nadir toprak elementi bu işletmeden sağlanmaktadır. Bayan Oba madeninin yanı sıra Shandong, Sichuan da Çin'in önemli NTE yataklarıdır. Çin'de Bayan Obo demir madeninden yan ürün olarak yıllık yaklaşık 50.000 ton NTE oksit üretilmektedir. Sichuan ve Mianning'teki bastnasit içeren karbonatit yataklarından 30.000 ton ve güneydeki kil yataklarından da yılda yaklaşık 10.000 ton NTE oksit üretimi gerçekleştirilmektedir. ABD 4.000 ton/yıl ile dünya nadir toprak element üretiminin %3,5'ini gerçekleştirmektedir. 10.000 ton/yıl civarında tüketim ile Çin ve Japonya'dan sonra 3.sırada yer almaktadır. NTE'lerin birçok önemli kullanımı nedeniyle, Japonya, Amerika Birleşik Devletleri ve Avrupa Birliği üyeleri gibi yeni teknolojilere bağımlı olan ülkeler, Çin'in NTE ihracatını azaltma niyetinden dolayı, NTE'lerin ekonomik yataklarını keşfetmeye ve bunları üretime kazandırmaya yönelik arama faaliyetlerini arttırmıştır (Yıldız, 2016).

Ülkemizde NTE'ler, alkalin-ultramafik ve karbonatit komplekslerine ek olarak yaygın bir şekilde peralkalin ve peraliminyumlu volkanikler, granitler ve granitik pegmatitler içinde de cevherleşmişlerdir. Ticari yönden en önemli yataklar çoğunlukla pegmatit ve karbonatlarla ilişkilidir. Birincil nadir metal yataklarının ayrışması sonucu oluşan ikincil yataklar, esas olarak denizel ya da alüvyal plaserler şeklinde birikmişlerdir (Gültekin vd., 2003). MTA Genel Müdürlüğü 1959 yılında, Eskişehir ili Sivrihisar ilçesinin 40 km kuzeybatısındaki Kızılcaören, Karkın ve Okçu köyleri arasındaki 15 km^2'lik bir alanda yaptığı çalışmalar sonrası ortalama %0.212 ThO_2 , %37.44 CaF_2, %31.04 $BaSO_4$ ve % 3.14 nadir toprak oksit içeren Beylikahır NTE rezervini belirlemiştir. NTE ve toryum kaynağı olan bu yatak karmaşık mineralleşmeye sahip olup değerli mineraller olarak florit, barit ve bastnazit içermektedir. Nadir toprak elementlerin çoğu bastnazit içeriğinde yer almıştır (Yıldız, 2016).

Kömür ve Kömür Yan Ürünlerinde Nadir Toprak Elementleri

Dünya enerji talebinin, nüfus artışı ve teknolojik gelişmelere bağlı olarak artması sonucu enerji kaynakları olan kömür, petrol gibi yakıtların kullanımı günümüzde de önemini korumaktadır. Yenilenebilir enerji kaynaklarına olan ilginin giderek artmasına rağmen kömürün küresel enerji üretimindeki payı artmaya devam etmektedir (Bertani, 2010). Kömür tüketiminin, gelişmekte olan ülkelerde gelişmiş ülkelere göre daha fazla artmakta oluşunun nedenleri arasında yüksek ekonomik büyüme oranları ve artan elektrik ihtiyacı nedeniyle gelişmekte olan ülkelerin daha kolay ve daha ucuz ulaşabilecekleri kömürü tercih etmesidir. Başta Avrupa Birliği olmak üzere gelişmiş ülkeler özellikle çevresel duyarlılıklar nedeniyle elektrik üretiminde giderek daha fazla doğal gaz ve yenilenebilir kaynakları tercih etmektedir. Özellikle kömür; petrol rezervlerinin dünyada belirli yerlerde olması ve bu yüzden de bazı politik pazarlıklara ve bazı krizlere yol açması yüzünden, daha da önem kazanmıştır. Dünyadaki birçok ülkede özellikle de gelişmekte olan ülkeler daha güvenilir olan öz kaynakları durumundaki kömüre yönelmiş olup, bu ilginin ilerleyen yıllarda da devam edeceği öngörülmektedir.

Bilinen dünya petrol rezervlerinin 40 yıl, doğalgaz rezervlerinin 60 yıl ve kömür rezervlerinin ise 200 yılda tükeneceği tahmin edilmektedir. Fosil enerji kaynaklarından olan kömür sahip olduğu bazı özelliklerden dolayı vazgeçilmez bir enerji kaynağıdır. Bu özellikler şu şekildedir; dünya üzerinde daha homojen bir dağılıma sahip olması, üretilmesi ve görünür kömür rezervlerinin uzun ömürlü olması, fiyat istikrarı, taşıma kolaylığı, depolama imkanlarının rahatlığı ve kullanım kolaylığıdır. Ülkemizde, doğal gaz ve petrol rezervleri oldukça sınırlı olmasına karşın, 506 milyon tonu görünür olmak üzere, yaklaşık 1,3 milyar ton taşkömürü ve 13,9 milyar tonu görünür rezerv niteliğinde toplam 14,2 milyar ton linyit rezervi bulunmaktadır (TKİ 2015; TTK 2015).

Ocaklardan çıkarılan kömürler, çeşitli boyutlarda kömür tanelerinin yanı sıra, çeşitli cins ve miktarlarda kömür dışı inorganik maddeler de içermektedir. Tüvanan kömürde bulunan kömür dışı maddeler, kömür damarı içerisinde bulunan ve jeolojik yapıdan kaynaklanan mineral maddeler (kuvars, kil mineralleri, karbonat mineralleri, sülfür mineralleri vb) olabileceği gibi kömürün kazılması sırasında dışarıdan kömüre karışan yabancı maddeler de olabilmektedir. Gerek endüstrinin istediği özelliklerde, gerekse hava kirliliği yaratmayan düşük kül ve kükürt içerikli kömür üretimi için kömür içerisinde yer alan

bu safsızlıkların giderilmesi gerekmektedir. Bu amaç için kömür hazırlama tesislerinde, belirli boyuta indirilen kömürler yıkanarak mevcut tane boyutundaki serbestleşmiş mineral maddeler kömürlerden uzaklaştırılmaktadır. Kömür kullanımına paralel olarak da açığa çıkan artık da artmaktadır. Kömür yıkama ve hazırlama sırasında oluşan atıklar farklı karakterlere sahiptirler (Ural vd., 2002). Kömür işletmelerinde iri taneli atıklar genellikle açıkta yığınlar halinde depolanırken, daha sulu ve ince taneli çamur şeklindeki atıklar, atık barajlarına sevkedilmekte veya filtrelenmektedir. Genel olarak kömürün işlem görmesinden çıkan tüm atıklar kömür atığı veya şist olarak adlandırılmaktadır. Bu atıkların tipi, karakteri, deşarj limitleri başarılı bir atık yönetimi açısından oldukça önemlidir. Ayrıca, Sıfır Atık proses hedefine yönelik bu katı sıvı ve gaz atıkları bertaraf etmek için geliştirilmiş yöntemler önem arzetmektedir. Bu atık malzemelerin içerisindeki kömürün geri kazanımı atık stoklama problemleri ve maliyetini azaltacaktır. Sonuçta atık içerisindeki kömür bir enerji kaynağıdır. Kömür periyodik cetveldeki elementlerin birçoğunu içermektedir. Farklı kimyasal özelliklere sahip olan nadir toprak elementleri, kömür küllerinde yoğun olarak bulunmaktadır.

Germanyum'un halihazırda bir yan ürün olarak elde edildiği yüksek Ge (240-850 g/t) içeren kömür yataklarından yılda yaklaşık 150-170 ton Ge elde edilmektedir. Nispeten daha düşük Ge içeriğine (yaklaşık 10 g/t) sahip bazı kömürler, koklaştırma ya da gazlaştırma için kullanıldıklarında Ge geri kazanımı için potansiyel bir kaynak olabilmektedir (Ivanov vd., 1984; Shpirt vd., 1990; Yudovich ve Ketris, 2006). Bu nedenle, Ge taşıyan kömürler şu anda dünya endüstrisi için ve yakın gelecekte (Seredin, 2006) Ge için ana kaynak olarak düşünülebilir. Dünya'daki kömürlerin ortalama Galyum içeriği 5,8 g/t ve kömür külünde ise 33 g/t'dir (Ketris ve Yudovich, 2005). Bununla birlikte, daha yüksek Ga içeriğine sahip birçok kömür yatağı vardır. Kömürde 20-40 g/t'a kadar ve külde ise 100-600 g/t'a kadar çıkabilmektedir (Seredin, 2004; Seredin, 2006; Yudovich ve Ketris, 2006). Güney Çin'de bazı kömür havzalarının taban ve ana kayaçlarında, 50-300 g/t Ga içeren kil tabakaları bulunmuştur. Bazı kömürlerin endüstriyel olarak yakılmasından elde edilen uçucu küller, % 0.1-0.5 kadar Ga içerebilir (Kler ve diğ., 1987). Selenyum, dünya'daki kömürde ortalama 1.3 g/t, küllerde ise 8.8 g/t gibi düşük bir içerikte bulunur. Bununla birlikte, bu rakamlar yerkabuğunda bulunan Se konsantrasyonundan (0.09 g/t) çok daha yüksektir. Bazı kömürler ve bazı kömür yan kayaçları, birkaç kg/t Se içerebilmektedir. Bu kadar yüksek Se konsantrasyonları sadece U içeren kömür yataklarında bildirilmiştir (Kislyakov ve Shchetochkin, 2000). Ek olarak, sülfür minerallerince zengin bazı kömürlerde 10-100 g/t arasında Se içeriği bildirilmiştir (Dai vd., 2008). Se'nin yüksek uçuculuğu ve gaz fazında iken kül parçacıkları üzerinde adsorplanması nedeniyle, uçucu küldeki konsantrasyonu, tüvenan kömürden 20-100 kat daha yüksek olabilir.

Tang ve Huang (2002), kömür örneklerini ve buna bağlı uçucu maddeleri analiz etmek için modern analitik yöntemleri kullanarak kömürde 74 iz elementi tespit etmişlerdir. Kömür ve kömür yan ürünleri gibi alternatif kaynaklardan NTE'nin geri kazanımı, ileri teknoloji malzemelerinin güvenilir bir şekilde tedarik edilmesini sağlarken, kömür madenciliğinin ekonomik olarak uygulanabilirliğini sürdürebilir hale getirme potansiyeli taşımaktadır. Dünya genelinde ortalama toplam NTE konsantrasyonları kömürde 68.5 g/t'dir (Seredin et al., 2012; Ketris ve Yudovich, 2009; Zhang vd., 2015). Rusya'daki Far East kömür ocaklarında 300 ila 1000 g/t içerikli, Doğu Kentucky'de Fire Clay kömür yatağında 500 g/t civarında, Kanada'nın Nova Scotia kentinde bulunan Sydney Havzasında 72-483 g/t arasında yüksek miktarda NTE içeriğine sahip olan kömür yatakları bulunmaktadır. Türk kömürlerinin NTE içerikleri 116 g/t olarak verilmiş ve dünya kömür ortalamasının neredeyse iki katıdır (Birk ve White, 1991; Seredin, 1996; Hower vd., 1999; Blissett vd., 2014). Kömür ve kömür yan ürünlerindeki NTE'lerin oluşumu üç tipe ayrılabilir: (1) monazit ve ksenotim gibi nadir toprak mineralleri, (2) killere iyonik olarak adsorbe olan NTE ve (3) organik matrislerle eşlik eden NTE.

Seredin (1996) nadir toprak elementleri ile zenginleşmiş kömürlerde NTE'lerinin çoğunlukla çapları 0,5-5 mikron olan otojenik taneli ve organik malzemeye veya kil minerallerine adsorbe olarak oluştuğunu öne sürmüştür. Hower vd. (1999), doğu Kentucky kömür havzalarından aldıkları numunelerdeki NTE'lerinin NTE açısından zengin fosfat formunda olduğunu, kil ve hücrelerdeki çatlakları dolduran monazit'in çok küçük (<2 mikron) düzensiz şekilli tanelerden oluştuğunu belirtmektedirler.

Çin'deki Jungar kömür yatağında bulunan NTE'ler ağırlıklı olarak kaolinit, goyazit, goreksiksit ve boehmit ile eşlik etmektedir. Ağır NTE'lerinin hafif NTE'lerine göre daha fazla organik madde içerisinde bulunma yatkınlığı vardır. NTE'lerinin kömür içerisindeki organik malzeme ile bağlanma mekanizması hümik ve fulvik asite koagüle olarak soğurulması olarak açıklanabilir. NTE'nin organik madde ile ne derece bağlı oldukları konusunda çelişkili görüşler vardır. En genel görüş, organik madde ile ilişkili NTE'nin toplam NTE'e göre çok düşük oranda olduğudur. Dai vd. (2012) kömürdeki NTE'ni beş forma ayırmıştır: suda çözünür, değiştirilebilir, karbonat bileşikli, organik ve alüminyum silikatle birleşmiş. Sıralı kimyasal ekstraksiyon deneyleri aynı ekip tarafından Shitan madencilik bölgesi kömürleri için gerçekleştirilmiştir. Alüminyum silikat bileşiminde olan NTE'nin oranı toplamın yaklaşık % 90'ını oluşturduğu, organik NTE'lerinin yalnızca %10 civarında bulunduğu belirtilmiştir. Dünya'daki kömür oluşumlarına bakıldığında hafif NTE miktarlarının ağır NTE'ne göre daha fazla olduğunu, hafif NTE'nin daha yüksek inorganik yatkınlığa sahip olduğu görülmektedir.

Bilindik nadir toprak minerallerinin (bastnaesit, monazit, vb.) ve iyonik olarak adsorbe olan minerallerin asgari ölçekteki nadir toprak oksit (NTO) içerikleri endüstriyel olarak sırasıyla yaklaşık % 1,5-2.0 ve % 0,06-0,15'dir. Bu konsantrasyonlardan daha azını ihtiva eden nadir toprak mineral yatakları, rezerv ne kadar büyük olursa olsun ekonomik olarak işlenememektedir. Kömürün yanmasından sonra oluşan külde 800-900 g/t aralığında nadir bir toprak oksit (NTO) konsantrasyonu, 5 m'den büyük damar kalınlığına sahip kömürlerden metallerin faydalı bir şekilde geri kazanılması için en düşük işletebilme tenörü olarak kabul edilmiştir (Seredin, 2012; Dai, 2012; Seredin, 2004). İşletilebilir NTE içeriklerinin 677-762 g/t olduğu tahmin edilmektedir. Ketris ve Yudovich tarafından kömür içerisindeki NTE'nin bulunma oranı kömür külüne göre yaklaşık olarak 0.17 olarak hesaplanmıştır. Bu nedenle, kömürdeki NTE'lerin ekonomik olarak kazanılabilmesi için gerekli en düşük içerik (cut-off grade) 115-130 g/t'dir. Dolayısıyla, birçok kömür yatağının NTE geri kazanımı için uygun olduğu düşünülmektedir.

Genel olarak kömür, NTE'nin geri kazanımı için umut verici bir hammaddedir ve bu alanda bir dizi çalışma başlatılmıştır (Ren, 2000; Seredin, 2012; Hu, 2006; Karayigit, 2000; Malikov, 2013; Sarı vd., 2015). Bununla birlikte, bu araştırmaların çoğu basitçe, NTE'lerin karakterize edilmesine odaklanmakta, NTE'nin kazanımı ile ilgili proseslere yer vermemektedir. Hu vd. (2006), Karayiğit vd. (2000) ve Eskenazy (1987) çalışmalarında NTE içeriklerinin kömürün kül içeriği arttığında yükseldiğini belirtmişlerdir. Kömürün diğer birçok eser metale ek olarak nadir toprak elementlerini (NTE) içerdiği ve bu elementlerin çoğunluğunun kömürdeki inorganik minerallerle birlikte bulunduğu bilinmektedir. NTE üretimi için hammadde olarak kömür ve kömür yan ürünlerini kullanmanın avantajları şunlardır; 1) büyük ve güvenilir kaynaklar, (2) zaten madenciliği yapılan malzemeler, (yeni maden ruhsatına gerek yok), (3) yeni çıkarılan bir maden olmadıklarından potansiyel çevre ve sağlık faydası sağlaması, ve (4) potansiyel atık maddelerin kullanılması (Dai et al., 2012).

Kömür ve kömür yan ürünlerindeki NTE'lerin oluşumu üç türe ayrılabilir:

Monazit ve ksenotim gibi nadir toprak mineralleri,
Killere iyonik olarak adsorbe olan NTE ve
Organik matrislerle eşlik eden NTE'dir.

Kömür ve kömür yan ürünlerindeki NTE'ler, parçacık boyutunda çok küçük olup genellikle mikrometre ve / veya nanometre boyutlarındadır (Zhang vd., 2017). Karayiğit ve arkadaşları tarafından (2000) yapılan çalışmada Türkiyedeki on farklı kömür termik santrallerine beslenen kömürlerin içindeki ana ve iz elementler çok detaylı bir şekilde incelenmiştir. Kömürler yüksek nem içeriğine (%14-47), yüksek kül verimine (%23-64), geniş bir toplam kükürt içeriği aralığına (%0,4-4,8) ve değişken brüt kalorifik değerlere (1368-4977 kcal/kg) sahip oldukları saptanmıştır. İncelenen kömürlerde genel olarak kil mineralleri (simektir, illit, kaolinit/klorit), kuvars feldspat, kalsit, dolomit, pirit ve jips bulunmaktadır. Al, K ve Ti konsantrasyonlarının kül verimleri ile pozitif korelasyonda olduğunu tespit etmişlerdir ve bu değerlerden bazıları Tablo 1'de gösterilmektedir. Besleme kömürlerinde bulunan (Ba, Bi, Ga, Nb, Pb, Rb, Sc, Ta, La, Ce, Pr, Nd, Sm, Eu ve Gd) iz elementlerinden bazıları, inorganik bir benzerliğe işaret eden kül

verimleri ile pozitif korelasyon göstermektedir. Tüm kömür iz element verileri incelendiğinde ve çoğu dünya kömürü aralığıyla karşılaştırıldığında, zenginleşebildikleri ortaya çıkmıştır. Yapılan çalışmada, nadir toprak elementlerinin kömürün inorganik kısımlarında kaldığı, bu yüzden de kömür külllerinde kalma eğiliminde oldukları belirlenmiştir.

Tablo 1. Türkiye'deki bazı termik santrallerden alınan kömürlerin analiz sonuçları.

İçerik / Bölge	Nem, %	Kül, %	Toplam S, %	Brüt Kalorifik Değer, kcal/kg	Al, %	K, %	Ti, %	∑NTE g/t (kül)
Çatalağzı	14	56	0,4	4141	6	1,6	0,3	190,2
Elbistan	47	35	3,2	2670	1,6	0,2	0,1	40,1
Kangal	33	37	4,8	3503	2,6	0,4	0,1	52,1
Soma B5-6	21	64	0,8	1368	8,4	0,8	0,3	251,9
Tunçbilek A3	23	23	2,4	4977	2,4	0,4	0,2	71,3

İ.T.Ü. Cevher Hazırlama Mühendisliği Bölümünde beş farklı kömür yıkama tesisi artığının NTE içerikleri araştırılmıştır. Ömerler'den A ve B kodlu iki farklı numune temin edilmiştir. B numunesinin girene göre toplam NTE içeriğinin, A numunesinin toplam NTE içeriğinin yaklaşık olarak iki katı olduğu görülmüştür (123-244 g/t). Toplam küle göre NTE içerikleri incelendiğinde; Ömerler A 265 g/t, Ömerler B 281 g/t, İmbat 250 g/t, Dereköy 227 g/t ve Uysal 186 g/t olarak bulunmuştur. Elde edilen sonuçlara göre %87 kül içeriğine sahip Ömerler B numunesinin en yüksek NTE içeriğine ulaştığı tespit edilmiştir. Ömerler A numunesinin kül içeriği ise %46,3 olarak bulunmuştur. Farklı kül içeriğine sahip ürünlerin değişen analizleri sonucunda NTE'nin inorganik kısım ile hareket ettiği saptanmıştır. Beş farklı yıkama atığının NTE içeriklerinin yanısıra yüksek nadir metal içerikleri de göze çarpmaktadır. En yüksek Sr içeriği 379 g/t ile Dereköy numunesinde bulunmuştur. İmbat ve Dereköy kömürlerindeki Ga içerikleri dünya ortalamasının üzerindedir ve V içerikleri ise oldukça dikkat çekmektedir (Ga: 43-42 g/t, V: 126-112 g/t). Kısacası, kömür üretiminin her aşamasında (çıkarma, yıkama ve yakma) ortaya çıkan ve atık olarak depolanan bu ürünler NE/NTE açısından zengin bir kaynak niteliğindedir.

NTE Üretim ve Zenginleştirme Yöntemleri

Geleneksel fiziksel ayırma yöntemleri nadir toprak minerallerinin zenginleştirilmesi için nadir toprak cevher yataklarında kullanılmaktadır. Bu yöntemler ise; tane boyut ayrımı, manyetik ayırma, yoğunluk farkına göre (veya gravite, yüzdürme-batırma) ayırma, elektrostatik ayırma ve flotasyondur. Son çalışmalarda sınırlı olsa da NTE'nin geri kazanımında bu yöntemlerin kömür ve kömür yan ürünleri üzerlerinde de uygulandığı belirtilmiştir (Hower vd., 2013; Blissett vd., 2014; Lin vd., 2017). Literatürdeki çalışmalar incelendiğinde kömür ve yan ürünlerindeki nadir toprak elementlerinin kazanımı için uygulanan boyutlandırma, gravite ve manyetik ayırma gibi fiziksel yöntemlerden en başarılı sonuç gravite yöntemi ile elde edilmiştir (Lin vd., 2017). Ayrıca nadir toprak elementlerinin güçlü bir şekilde Al/Si oluşumlarına bağlı olduğu bu çalışmada ortaya konulmuştur.

Honaker ve arkadaşları (2016), Fire Clay, Fire Clay Rider ve Eagle kömür damarlarından alınan üç farklı kömür hazırlama tesisinin kaba kömür atığı (+150 mikron) ve tikiner alt akımının temsili örnekleri üzerinde zenginleştirme işlemleri yapmıştır. İri kömür atığının boyutu (+150 mikron) -6,25 mm olacak şekilde kırılmış olup sırasıyla +0,6 mm, -0,6+0,15 ve -0,15 mm olacak şekilde üç farklı boyut grubuna ayrılmıştır. Bu boyut gruplarına uygulanan zenginleştirme işlemleri Tablo 2'de verilmiştir.

Tablo 2. Farklı boyut gruplarına uygulanan zenginleştirme işlemleri.

Boyut, mm	Uygulanan Test
-6,25+0,6	Yüzdürme-Batırma Testi
-0,6+0,15	Yüzdürme-Batırma Testi
-0,6+0,15	Sarsıntılı Masa
-0,6+0,15	Yüksek Alan Şiddetli Yaş Manyetik Ayırma
-0,15	Yüksek Alan Şiddetli Yaş Manyetik Ayırma
Tikiner alt akım	Flotasyon

Tablo 2'de uygulanan zenginleştirme işlemlerinin sonuçlarına göre; en umut verici sonuçlar flotasyon yöntemi ile elde edilmiştir. Yapılan çalışmada 1 litrelik laboratuvar tipi Denver flotasyon hücresi ve 1200 rpm dönüş hızı kullanılarak tikiner alt akım numuneleri üzerinde nadir toprak minerallerinin (Monazit) flotasyon testleri yapılmıştır. Öncelikle dekarbonizasyon işlemi için dizel ve MIBC kullanılmıştır ve çok yüksek kül içeriğine (>%93) sahip karbonsuz malzeme elde edilmiştir. İnce atıklardaki nadir toprak minerallerini yüzdürmek için Talon 9400, sodyum oleat ve oleik asit olmak üzere üç farklı toplayıcı kullanılmış ve pH, monazite flotasyonu için gerekli olan 9,5'te sabit tutulmuştur. Fire Clay, Fire Clay Rider ve Eagle damarlarından gelen karbonsuzlaştırılmış tikiner alt akımının NTE içerikleri sırasıyla 247 g/t, 245 g/t ve 189 g/t'dur. Talon 9400 veya sodyum oleat kullanılarak daha yüksek geri kazanım değerleri elde edilirken, konsantrelerin NTE içerikleri daha düşük elde edilmiştir. Bu üç farklı malzeme için toplayıcı olarak oleik asit kullanılarak yaklaşık 380 g/t NTE içerikli konsantreler %20 verim ile elde edilmiştir. Kaba-temizleme ve tekrar temizleme devrelerinin kombinasyonu ile tüm kömür bazında 1182 g/t içerikli nadir toprak konsantresi elde edilmiştir.

Lin vd. kömür ve kömür yan ürünlerinde yaptıkları fiziksel ayırma deneylerinin (boyuta göre ayırma, manyetik ayırma ve yoğunluk farkına göre ayırma) sonuçları incelendiğinde; daha ince tane boyutuna geçildikçe NTE içeriğinin arttığı gözlemlenmiştir. Manyetik ayırma deneylerinde kül numuneleri için NTE'lerin manyetik olmayan fraksiyonlarda zenginleştiğini gözlemlemiş ve bunun nedeninin demir içermeyen minerallerden kaynaklı olabileceğini düşünmüşlerdir. Elde ettikleri sonuç, Dai ve arkadaşları (2010) tarafından uçucu kül numunelerinin ayrılması hakkında yapmış oldukları çalışma ile uyuşmaktadır. Ancak Honaker ve arkadaşlarının (2014) kömür ve kömür yan ürünlerinin manyetik fraksiyonlarında daha yüksek NTE konsantrasyonu bulunduğu ile ilgili yapmış oldukları çalışma ile uyuşmamaktadır. Bu durumun açıklamalarından biri, Honaker ve arkadaşlarının önyakma malzemeleri kullanarak monazitin serbestleşmesini sağlaması ve yüksek alan şiddetli yaş manyetik ayırıcı ile ayrılarak manyetik fraksiyonda daha yüksek NTE konsantrasyonu sağlamasıdır. Bir diğer açıklama ise çalışmalarda kullanılan manyetik alan şiddetinin farklı olması ve bu nedenle elde edilen manyetik ve manyetik olmayan fraksiyonların farklı manyetik duyarlılıkta olmasıdır.

Üç yaygın nadir toprak minerali olan monazit, bastnasit ve ksenotim'in yoğunlukları 3.9-5.5 g/cm^3 aralığındadır. Bu nedenle, yoğunlukları deneyde kullanılan ağır sıvınınkinden daha büyük olduğu için nadir toprak minerallerinin en ağır fraksiyonda (>2,95 g/cm^3) konsantre olacağı öngörülmektedir.

Temiz kömür ağırlıkça %7,8 kuru kül içermektedir ve beklendiği gibi yoğunluğu kömür külü, kil ve şeyl örneklerinden çok daha düşük olmaktadır. Yoğunluk >1.45 g/cm^3'ten 1.34-1.30 g/cm^3'e düştüğünde, kül verimi %49'dan %4'e önemli ölçüde düşmektedir ve kuru kül bazlı NTE konsantrasyonu 1143 g/t'dan 2056 g/t'a önemli ölçüde yükselmektedir. Yoğunluk daha da düştükçe kül verimi %3-5'te sabit kalmakta ve NTE konsantrasyonu bazı dalgalanmalarla biraz azalmaktadır. En yüksek NTE konsantrasyonu (kuru kül bazında), 2056 g/t, kömürün %30'unu oluşturan 1.34-1.30 g/cm^3 fraksiyonundan elde edilmiştir. Kuru kül bazlı NTE konsantrasyonu genellikle kül verimi arttıkça azalmaktadır, bu da nadir toprak olmayan

minerallerin seyreltme etkisiyle açıklanabilmektedir. Bununla birlikte, tüm kömür bazlı NTE konsantrasyonu, kül verimi arttıkça artmaktadır (2017).

Kömür ve kömür yan ürünleri üzerinde gerçekleştirilen fiziksel ayırma yöntemlerinin düşük verim ve yüksek üretim maliyetleri ile sonuçlanmasından dolayı bir çok araştırmacı kimyasal zenginleştirme yöntemleri üzerine yoğunlaşmıştır. NTE'lerin kimyasal zenginleştirilmesi üzerine yapılan çalışmada asit liçinin verimini arttırmak için alkali ve termal ön işlemleri uygulanmıştır.

Yang ve arkadaşları (2019), asit liçinden önce iki saat boyunca 75°C'de karbondan arındırılmış ince atıkları 8 M NaOH solüsyonu ile muamele etmişlerdir. Hafif NTE'lerin özütlenebilirliği üzerindeki olumlu etki nedeniyle NTE'lerin geri kazanımının %22'den %75'e önemli ölçüde arttığı bulunmuştur. Aynı deneysel koşullar altında, ANTE'ler için iyileşmede küçük bir kademeli artış elde edilmiştir (%38 ila %48). Kuppusamy ve ark. (2019), ince kömür atık malzemesinin alkali asit liçi ile temiz kömür ve NTE'lerin eşzamanlı üretimi üzerine bir çalışma yürütmüştür. Malzemenin kül içeriği, 190°C'de 30 dakika boyunca bir NaOH çözeltisi (ağırlıkça %30) ve ardından 50°C'de 30 dakika süreyle bir HCl çözeltisi (ağırlıkça %7.5) ile muamele edildikten sonra %46.21'den %14.17'ye düşürülmüştür. Eş zamanlı olarak malzemede meydana gelen hafif NTE'lerin %97'si ve ağır NTE'lerin %76'sı ekstrakte edilmiştir. Kömür ve kömür yan ürünlerinden NTE'lerin alkali-asit liç işlemleri ile kazanımının genel akım şeması Şekil 2'de verilmektedir.

Alkali liç aşamasının olumsuz bir yönü, NTE'ler ile birlikte çözelti içinde çözünen önemli miktarda kirletici maddedir. Diğer bir olumsuz yön, kömür bazlı hammaddelerde nispeten düşük NTE içeriği göz önüne alındığında harcanacak kimyasal maliyetinin yüksek olmasıdır. Seyreltilmiş alkali çözeltiler ve/veya zayıf alkaliler kullanılarak NTE özütlenebilirliğini seçici olarak artırma olasılığını araştırmak için ek çalışmaların yapılması gerekmektedir (Zhang vd., 2020).

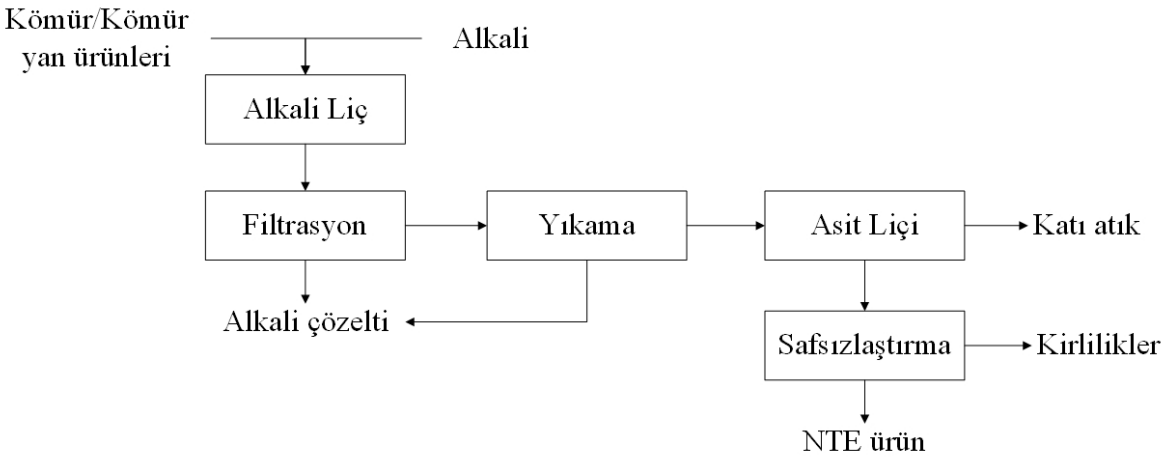

Şekil 2. Kömür ve kömür yan ürünlerinden NTE'lerin alkali-asit liç işlemleri ile kazanımının genel akım şeması

SONUÇLAR

Nadir toprak elementleri, sahip oldukları çeşitli özellikler sayesinde temiz enerji üretimi, sağlık hizmetleri, elektronik ve savunma sanayiinde kullanılmaktadır ve stratejik bir öneme sahiptirler. NTE üretimi ve tüketiminde Çin'in lider konumda olması ve ihracatta getirdiği sınırlamalar ile bir çok ülke kaynak arayışına girmiştir. Nadir toprak elementlerinin yüksek maliyetleri ve sınırlı rezervleri nedeniyle, günümüzde bulunan rezervlerin yanısıra ikincil kaynaklardan, yan ürün ve atıklardan elde edilmesi oldukça önemlidir. Yapılan çalışmalar incelendiğinde nadir toprak elementlerinin kömürdeki inorganik kısım ile hareket ettiği görülmektedir. Kömür yıkama tesislerinden elde edilen atıkları cevher hazırlama ve zenginleştirme işlemleri ile değerlendirebilmemiz mümkündür. Atık kapsamındaki bu ikincil

kaynaklarımızın NTE içerikleri dünya ortalamasından oldukça fazladır. Günümüzde artan petrol ve doğalgaz ücretleri gözönüne alındığında gelişmekte olan ülkeler kömür kullanmaya devam edeceklerdir ve daha fazla kaynak ihtiyacı arayışına gireceklerdir. Ayrıca atık olarak nitelendirilen bu ürünlerin geri kazanımı ile ince boyutlu kömürler de geri kazanılabilmekte olup ülke ekonomisine katkı sağlayabilecektir. Kömür ve kömür atıklarındaki NTE'lerin kazanım olanaklarının araştırılması ve yüksek metal içerikli ön konsantre eldesi çalışmaların yapılması ülke ekonomisi için oldukça önem arz etmektedir.

KAYNAKLAR

Ateşok, G. (2017). Kömür Hazırlama ve Teknolojisi (3üncü bas.) İstanbul.

Bertani R (2010) Geothermal power generation in the world 2005–2010 update report. In: Proceedings of the world geothermal congress, Bali (Indonesia), April 25–29, 2010.

Birk, D., and White, J.C., 1991, "Rare earth elements in bituminous coals and underclays of the Sydney Basin, Nova Scotia: Element sites, distribution, mineralogy," International Journal of Coal Geology, Vol. 19, pp. 219-251.

Blissett, R.S., Smalley, N., and Rowson. N.A., 2014, "An investigation into six coal fly ashes from United Kingdom and Poland to evaluate rare earth element content," Fuel, Vol. 119, pp. 236-239.

Blissett, R.S., Smalley, N., and Rowson. N.A., 2014, "An investigation into six coal fly ashes from United Kingdom and Poland to evaluate rare earth element content," Fuel, Vol. 119, pp. 236-239.

Dai S, Yan X, Ward CR, Hower JC, Zhao L, Wang X, et al. Valuable elements in Chinese coals: a review. Int Geol Rev 2016:1–31. http://dx.doi.org/10.1080/ 00206814.

Dai S, Zhao L, Peng S, Chou C-L, Wang X, Zhang Y, et al. Abundances and distribution of minerals and elements in high-alumina coal fly ash from the Jungar Power Plant, Inner Mongolia, China. Int J Coal Geol 2010; 81:320–32.

Dai, S., Ren, D., Zhou, Y., Chou, C.-L., Wang, X., Zhao, L., Zhu, X., 2008. Mineralogy and geochemistry of a superhigh-organic-sulfur coal, Yanshan coalfield, Yunnan, China: evidence for a volcanic ash component and influence by submarine exhalation. Chem. Geol. 255, 182–194.

Dai, S., Y. Jiang, C. R. Ward, L. Gu, V. V. Seredin, H. Liu, D. Zhou, X. Wang, Y. Sun, J. Zou, and D. Ren. 2012. "Mineralogical and geochemical compositions of the coal in the Guanbanwusu Mine, Inner Mongolia, China: Further evidence for the existence of an Al (Ga and REE) ore deposit in the Jungar Coalfield", International Journal of Coal Geology, 98, 10–40.

Eterigho-Ikelegbe, O., Harrar, H., & Bada, S. (2021). Rare earth elements from coal and coal discard–A review. *Minerals Engineering*, *173*, 107187.

Honaker R, Hower J, Eble C, Weisenfluh J, Groppo J, Rezaee M, Bhagavatula A, Luttrell GH, Bratton RC, Kiser M, Yoon R-H. Laboratory and bench-scale testing for rare earth elements. December 30, 2014. Available at: <https://edx.netl.doe.gov/ree/?page_id=1587>; 2014 [accessed 2016.04.21].

Honaker, R., Groppo, J., Bhagavatula, A., Rezaee, M., & Zhang, W. (2016, April). Recovery of rare earth minerals and elements from coal and coal byproducts. In *International Coal Preparation Conference* (pp. 25-27).

Hower JC, Groppo JG, Joshi P, Dai S, Moecher DP, Johnston MN. Location of cerium in coal-combustion fly ashes: implications for recovery of lanthanides. Coal Combust Gasificat Prod 2013;5: 73–8.

Hower, J.C., Ruppert, L.F., and Eble C.F., 1999, "Lithanide, yttrium, and zirconium anomalies in the Fire Clay Coal Bed, Eastern Kentucky," International Journal of Coal Geology, Vol. 39, pp. 141-153.

https://pubs.usgs.gov/fs/2014/3078/pdf/fs2014-3078.pdf, erişim tarihi Ocak 2022.

https://pubs.usgs.gov/periodicals/mcs2020/mcs2020-rare-earths.pdf , erişim tarihi Ekim 2021.

https://pubs.usgs.gov/sir/2010/5220/, erişim tarihi Ocak 2022.

Ivanov, V.V., Katz, A.Ya., Kostin, Yu.P., Meitov, E.S., Solov'ev, E.B., 1984. Economic Types of Natural Germanium Concentrations. Nedra, Moscow.

Karayiğit, A. I., R. A. Gayer, X. Querol, and T. Onacak. 2000. Contents of major and trace elements in feed coals from Turkish coal-fired power plants. International Journal of Coal Geology 44: 169–184.

Ketris, M. P., and Y. E. Yudovich. 2009. Estimations of Clarkes for carbonaceous biolithes: World average for trace element content in black shales and coals. International Journal of Coal Geology, 78: 135–148.

Kislyakov, Ya.M., Shchetochkin, V.N., 2000. "Hydrogenic Ore Formation. Geoinformmark, Moscow.

Kler, V.R., Volkova, G.A., Gurevich, E.M., Dvornikov, A.G., Zharov, Yu.N., Kler, D.V., Nenakhova, V.F., Saprykin, F.Ya., Shpirt, M.Ya., 1987. Metallogeny and Geochemistry of Coal-bearing and Pyroschist-bearing Sequences. Geochemistry of Elements. Nauka, Moscow.

Kuppusamy, V.K.; Kumar, A.; Holuszko, M. Simultaneous extraction of clean coal and rare earth elements from coal tailings using alkali-acid leaching process. *J. Energy Resour. Technol. Trans. ASME* 2019, *141*, 1–7.

Lin, R., Howard, B. H., Roth, E. A., Bank, T. L., Granite, E. J., & Soong, Y. (2017). Enrichment of rare earth elements from coal and coal by-products by physical separations. *Fuel*, *200*, 506-520.

Lin, R., Howard, B. H., Roth, E. A., Bank, T. L., Granite, E. J., & Soong, Y. (2017). Enrichment of rare earth elements from coal and coal by-products by physical separations. *Fuel*, *200*, 506-520.

Maden Tetkik Ve Arama Genel Müdürlüğü. (2017*). Dünyada Ve Türkiye'de Nadir Toprak Elementleri,* Fizibilite Etütleri Daire Başkanlığı. Erişim adresi https://www.mta.gov.tr/v3.0/sayfalar/bilgi-merkezi/maden-serisi/dunyada_ve_turkiyede_nadir_toprak_elementleri.pdf

Seredin, V. V. 2004. The Au-PGE mineralization at the Pavlovsk brown coal deposit, Primorye. Geology of Ore Deposits 46: 36–63.

Seredin, V. V., and S. Dai. 2012. Coal deposits as potential alternative source of lanthanides and yttrium. International Journal of Coal Geology 94: 67–93.

Seredin, V. V., Dai, S., Sun, Y., & Chekryzhov, I. Y. (2013). Coal deposits as promising sources of rare metals for alternative power and energy-efficient technologies. *Applied Geochemistry*, *31*, 1-11.

Seredin, V.V., 1996, "Rare earth element-bearing coals from the Russian Far East deposits," International Journal of Coal Geology, Vol. 30, pp. 101-129.

Seredin, V.V., 2006. Germanium deposits. In: Laverov, N.P., Rundkvist, D.V. (Eds.), Large and Superlarge Ore Deposits, vol. 3. IGEM RAS, Moscow, pp. 707–736.

Tang, X., and W. Huang. 2002. Trace elements in coal and significance of the research. Coal Geology of China, 14 (Suppl.): 1–4.

Ural, S., Yıldırım, M., Anıl, M. (2002). Kömürün mineral madde içeriğinin toz kömür yakma sistemindeki rolü. *Türkiye 13. Kömür Kongresi Bildiriler Kitabı*, 151-160.

Yang, X.; Werner, J.; Honaker, R.Q. Leaching of rare earth elements from an Illinois basin coal source. *J. Rare Earths* 2019, *37*, 312–321.

Yıldız, Necati. (2016). Rare Earth Elements Nadir Toprak Elementleri. 10.13140/RG.2.2.27743.87206.

Yudovich, Ya.E., Ketris, M.P., 2005. Toxic Trace Elements in Coal. UrB RAS, Ekaterinburg.

Yudovich, Ya.E., Ketris, M.P., 2006. Valuable Trace Elements in Coal. UrB RAS, Ekaterinburg.

Zhang, W., Honaker, R., Groppo J., 2017, Concentration of rare earth minerals from coal by froth flotation, Minerals & Metallurgical Processing, 2017, Vol. 34, No. 3, pp. 132-137.

Zhang, W., Noble, A., Yang, X., & Honaker, R. (2020). A comprehensive review of rare earth elements recovery from coal-related materials. *Minerals*, *10*(5), 451.

Zhang, W., Rezaee, M., Bhagavatula, A., Li, Y., Groppo, J., and Honaker, R., 2015, "A review of the occurrence and promising recovery methods of rare earth elements from coal and coal by-products," International Journal of Coal Preparation and Utilization, Vol. 35, No. 6, pp. 295-330.

NARROW, TABULAR STOPE 3D SCANNING IN DEEP-LEVEL GOLD MINES USING AN IPAD PRO LIDAR

C. Birch [1,*], A. Olivier[1]

[1] *The University of the Witwatersrand, School of Mining Engineering*
*(*Corresponding author: clinton.birch@wits.ac.za)*

ABSTRACT

Excessive hangingwall or footwall dilution in narrow, tabular gold mines affects the payability of the mine. 3D scanning of the stope faces is seen as an option to quickly create maps that can be incorporated into the mine's digital map. The mine's current 3D scanner is bulky, expensive and only used in the mine's haulages. From March 2020, the iPad Pro models incorporate a LiDAR scanner. The scanner has a limited range of five metres. A 3D printed iPad holder was created, which also holds a compact yet powerful LED light, and an iPad Pro was tested in the mine mock-up at the University of the Witwatersrand. It was found to create excellent scans of both the tunnels and stopes. Underground testing then occurred in the ultra-deep stopes of Mponeng Gold Mine. It was found to be effective in capturing the contacts of the ore body, and the scans can be geo-referenced into the mine's existing digital models. However, the iPad Pro is not waterproof, and the large screen makes it susceptible to being damaged. The mine is now testing LiDAR-equipped iPhone Pro as a more robust, compact option.

Keywords: iPad Pro, LiDAR, 3D scanning

INTRODUCTION

This research project was initiated to identify orebody dilution on an ultra-deep South African gold mine. Mponeng Mine is southwest of Johannesburg (Figure 1) and mines the Ventersdorp Contact Reef (VCR). The narrow, tabular stopes are currently over 3,500m below the surface. The VCR is highly variable as it forms an unconformity with the underlying sediments of the Witwatersrand Supergroup. The orebody is typically 120 cm thick and dips approximately 18 degrees towards the south.

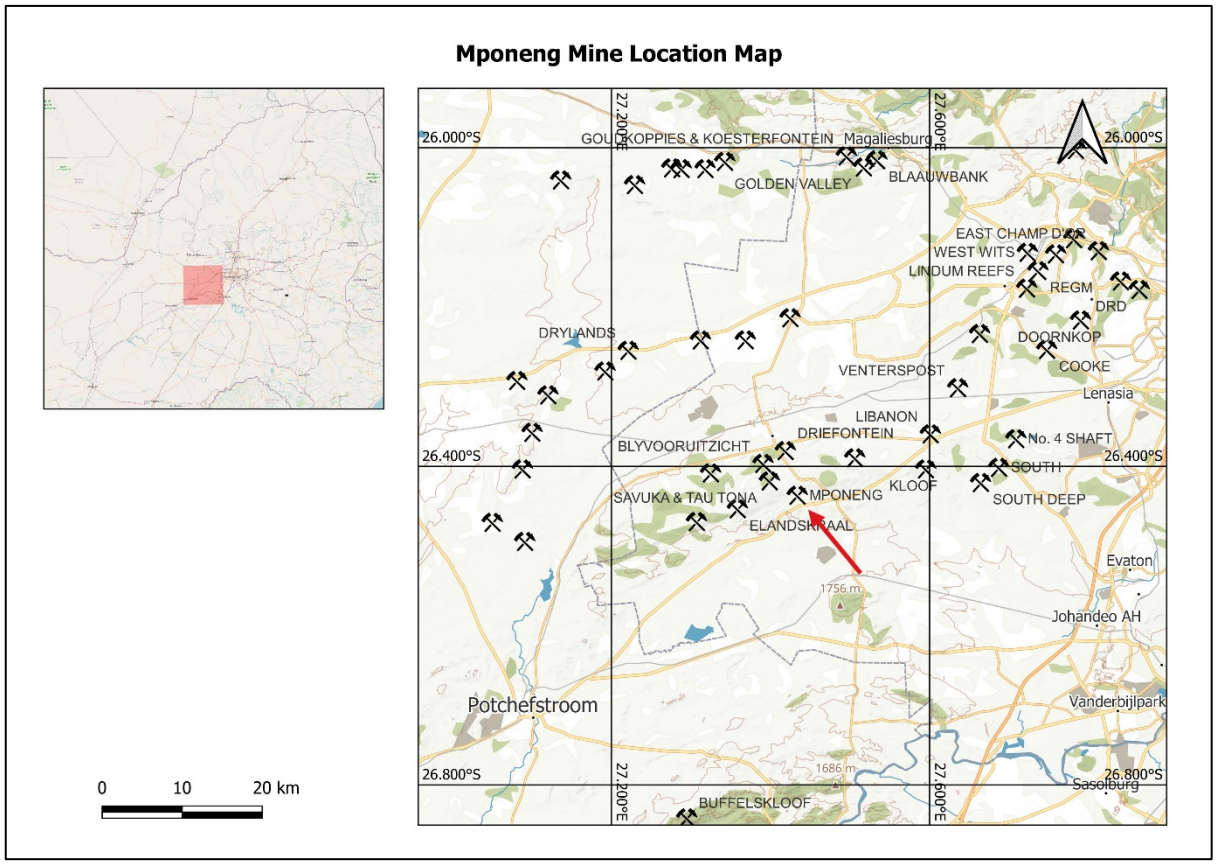

Figure 1. Location of Mponeng Mine, South Africa.

Mine planning requires three-dimensional (3D) spatial measurements of the orebody. Currently, on Mponeng Mine, the geological and valuation departments gather this information on a regular grid. However, this information is not in a form that can easily be incorporated into the mines' 3D model. The purpose of the study is to investigate how to best supply dynamic 3D information to the underground mine planning department and highlight any excessive dilution. Light detection and ranging (LiDAR) has been identified as a technology that will assist with gathering and disseminating 3D information of the orebody.

Sishen mine is a large open-pit mining operation in South Africa that requires reliable geotechnical data to design and evaluate pit wall stability. Currently, the primary data sources to achieve this are "geotechnical borehole data, face mapping data, geotechnical laboratory testing data and implicit structural models" (Russell and Stacey, 2019, p. 11). Face mapping has traditionally been done via direct contact with the mapping face through techniques such as line mapping or window mapping (Russell and Stacey, 2019). Digital mapping of faces to capture geological discontinuity and structural orientation has become more prevalent. In 2013, Sishen mine acquired a terrestrial laser scanner with the resolution, photographic capabilities and software capable of carrying out geotechnical face mapping (Russell and Stacey, 2019).

Although digital mapping is more practical than the traditional method of face mapping, digital photogrammetry does have drawbacks. This is because a surveyed reference point needs to be positioned on the face, and two camera tripod positions need to be accurately surveyed (Russell and Stacey, 2019). This is important if the scanned image needs to be geo-referenced to feed into a larger geological model. Sishen mine realised the following advantages from laser scanning:

1. The laser scanner provided faster and more accessible data collection.
2. The laser scanner provided faster data processing and was less demanding on software systems.
3. More accurate discontinuity orientation measurements were obtained using the laser scanner (up to 15° difference in dip measurements between the two techniques was observed); and
4. Planes oblique to the exposed face were more readily observable with the laser scanner (Russell and Stacey, 2019).

Once a stope face has advanced, it is impossible to capture the geological mapping of that stope face as it is lost. If stope faces are mapped regularly, a complete picture of the ore body's behaviour is possible. The greater the distance between mapping, the greater the interpretation of geology required. In complex ore bodies, the grade may fluctuate over short distances, and for this reason, it is vital to map geology regularly. The data needed to estimate local grade and undertake stope design is provided by the mapping and sampling these exposures (Dominy and Platten 2012). The geological mapping information assists the geologist when he recommends the maximum stope width of a stope panel to ensure minimum grade dilution.

Studies have shown that electronic mapping is less time-consuming than the traditional manual mapping method of using field books, tapes and clinometers (Dominy and Platten, 2012). Time at a particular face is limited and seldom exceeds 30 minutes. Therefore, the geologist must capture as much accurate information about the stope as possible. Once the stope face is blasted, this mapping information is lost. The mining process can be more efficient and cost-effective when a well-designed grade control programme, including geological knowledge, is applied. Such measures are also favourably received by stakeholders (Dominy and Platten, 2012).

Identifying ways of identifying and reducing excessive dilution at Mponeng Mine forms part of an MSc research project conducted by one of the authors. This MSc is being done through the University of the Witwatersrand (Wits) School of Mining Engineering.

Justification for the Research

The mine has a LiDAR scanner available for use by the survey department on Mponeng Mine. This instrument is bulky and unsuitable for use in the narrow stopes prevalent on the mine. Simple, low-cost solutions are explored in this paper that will allow for 3D scanning to be undertaken by geologists, valuation officers and production personnel to provide further coverage of the mine.

Research Background

The focus of this paper is primarily on the qualitative research where the Structure Sensor (Mark 2) and iPad Pro was initially evaluated at the Wits School of Mining Engineering research tunnel and stope in the basement of the Chamber of Mines Building. Further testing was conducted at the University of Johannesburg in a simulated mine tunnel and stope environment available for educational purposes. The final portion of the research covered by this paper is the initial underground testing of the iPad Pro on Mponeng Gold Mine.

INITIAL INVESTIGATIONS

The research methodology aimed to investigate using a cost-effective 3D LiDAR scanner for underground use. The primary purpose of this scanner will be to capture underground information without interrupting the production in any way. The data captured underground should then be

distributed among relevant stakeholders daily as soon as an employee comes to the surface. Finding a fast and easy way was essential without losing any data.

The research was done using both quantitative data and qualitative data. During the quantitative phase of the study, various scanners were considered for use as part of the study. The short-listed scanners were tested in a controlled environment during the qualitative research phase before further testing continued underground at Mponeng Mine. This was done to test the durability and practicality of the scanner. With free software (CloudCompare), the scans were geo-referenced and pulled into Deswik CAD for further use.

The following criteria were followed to choose the final scanner considering the underground conditions of narrow tabular mining:

1. Ease of use. The scanner must be used daily to share information productively. It was essential to consider the buy-in and willingness of underground users to use the device optimally.
2. Accuracy and quality of scanners. It is vital to build the 3D block model from accurate information; and
3. Cost of 3D scanners and software. This included the software required for capturing the scans and geo-referencing and viewing scans.

Cost played an essential role since the project was in the test phase. Therefore, it was essential to keep all the costs as low as possible to ensure the possible implementation of the 3D LiDAR scanner for underground use.

The aim is that Geology should use geo-referenced scans to digitise the underground stope mapping directly onto Deswik CAD. This mapping will then inform the 3D geological block model. This may help proactive action to control stoping width and grade dilution better.

This portion of the study is focused on the following two options:

1. Structure Sensor Pro and (Mark II) by Occipital; and
2. The non-cellular Apple iPad Pro 11-inch.

The Structure Sensor (Mark II)

The Occipital Structure Sensor (Mark II) is a scanner that fits onto an iPad or iPhone mobile device (Figure 2). It has been indicated that the scanner ranges up to 10m and has an inbuilt infrared light source (Occipital 2019).

Figure 2. Occipital Structure Sensor (Mark II)

The biggest problem with the Structure Sensor Mark II was finding a suitable application to scan large, open-ended volumes. The available applications are aimed predominantly at scanning objects or closed rooms.

Since the Occipital Structure Sensor (Mark II) is attached to the iPad, it is more difficult to protect in underground use. This increases the risk of damaging the scanner. The Structure Sensor (Mark II) is not considered suitable for the expected underground applications, and no further testing was conducted.

Apple iPad Pro 11 inch

The iPad Pro 11 inch was released in March 2020 (GSMArena 2020). This iPad Pro is now possible to do 3D LiDAR scanning. This functionality is also available on the iPhone 12 Pro and iPhone 12 Pro Max. This scanning range is up to five metres.

The Apple iPad Pro 11-inch was tested in the DigiMine of the University of the Witwatersrand in May 2021. The DigiMine represents an underground stope panel of a narrow tabular mining method. It also has a crosscut tunnel that displays geological features. Scans were created from the Apple iPad Pro 11-inch with the following software:

1. Scaniverse;
2. 3D Scanner App;
3. Polycam; and
4. Sitescape.

The 3D Scanner App appears to be the most suitable of the applications tested, and the fully functional version is available for no charge. Polycam and Scaniverse are very similar in capabilities to 3D Scanner App but require subscriptions to allow the full suite of file formats to be available. Sitescape has limited points it can capture in a single scan. This is adequate for smaller spaces, but not mine stopes.

The Apple iPad Pro 11 inch may seem a bit bulky for underground use because of its size. Unfortunately, the Apple iPad Pro 11 inch has not proven dust-proof or water-resistant (GSMArena 2020). The initial scanning exercise in the School of Mining Engineering highlighted the need for additional lighting and protection for the iPad Pro. A mobile LED video light was attached to the iPad during testing scans. A 3D printed holder was designed (Figure 3) and printed (Figure 4) to protect the iPad Pro in the underground environment. The light bracket was incorporated into the print.

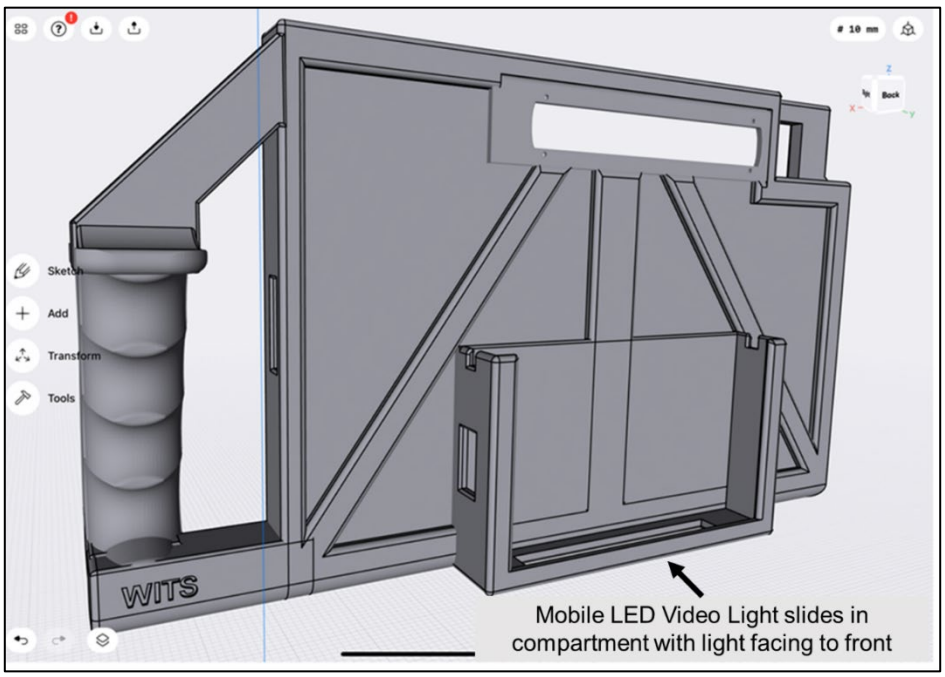

Figure 3. iPad and light holder designed using Shapr 3D.

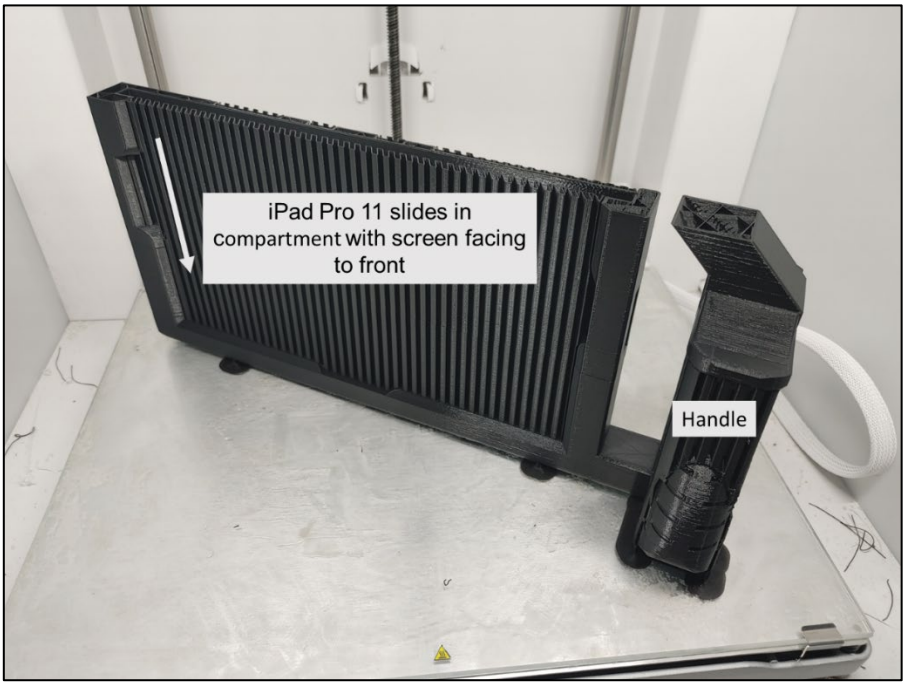

Figure 4. 3D printing the iPad holder using an Ultimaker 5 printer.

SURFACE AND UNDERGROUND TESTING

The initial testing conducted in the DigiMine stope and tunnel at the University of the Witwatersrand exposed that the lack of lighting was an issue that needed to be addressed. The scans were clear once the light was added, and the geology was clearly visible (Figure 5 and 6). The geo-referenced points could be identified. The geo-referenced scans could be imported into other software like Cloudcompare.

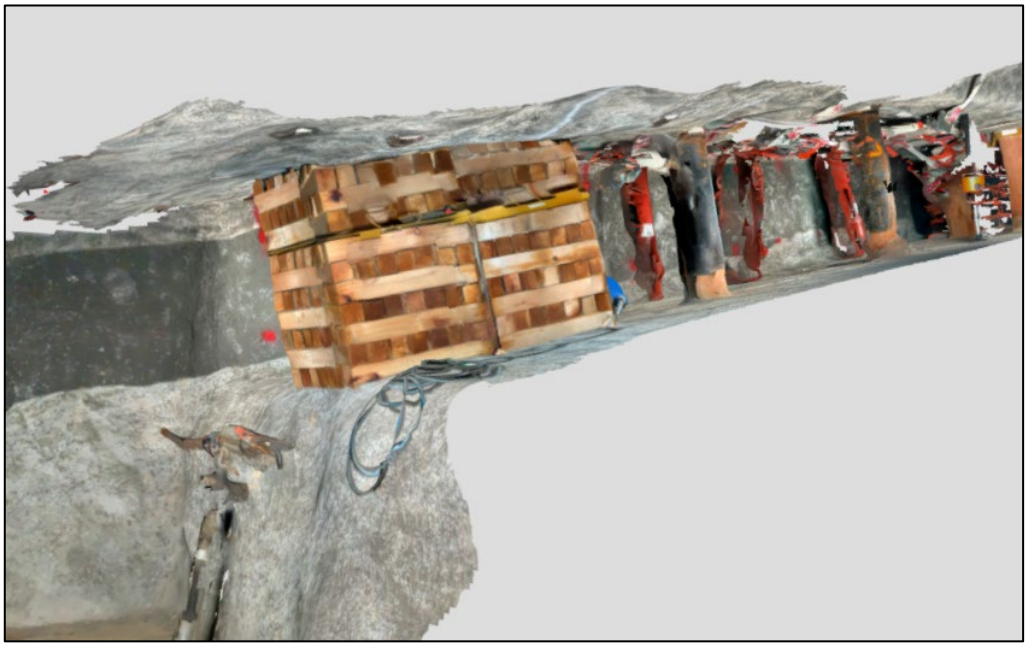

Figure 5. The University of the Witwatersrand Digimine stope.

Figure 6. The University of the Witwatersrand Digimine tunnel.

Similar results were obtained in the University of Johannesburg's tunnel and stope. Once the technique for scanning was determined, underground testing at Mponeng Mine was undertaken. Two stopes on 113 Level (11,300 feet below the surface) were scanned (Figures 7 and 8).

Figure 7. 113-68 East 2 Panel

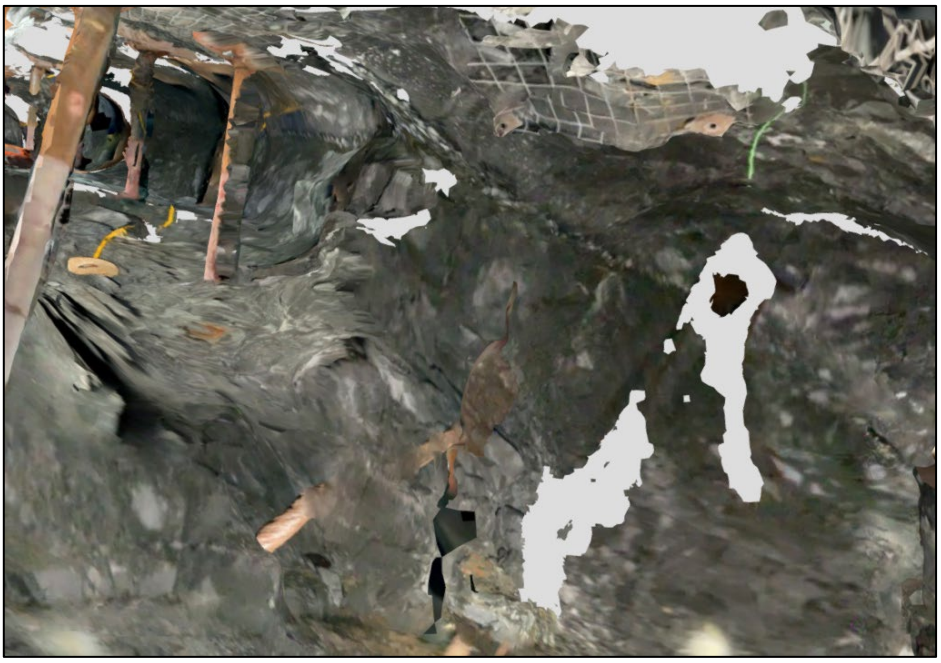

Figure 8. 113-68 East 2 Panel.

The results of the underground testing were considered very successful. The target geological formation (VCR Reef) could clearly be identified in the scans (Figure 9). Even though the iPad Pro's LiDAR scanner only has a range of 5 m, this is more than adequate. The scans can be paused, and the operator can move to the next position down the stope face to resume the scan. There must be sufficient overlap for the software to link the new position with the previous one, and the scan appears to be continuous.

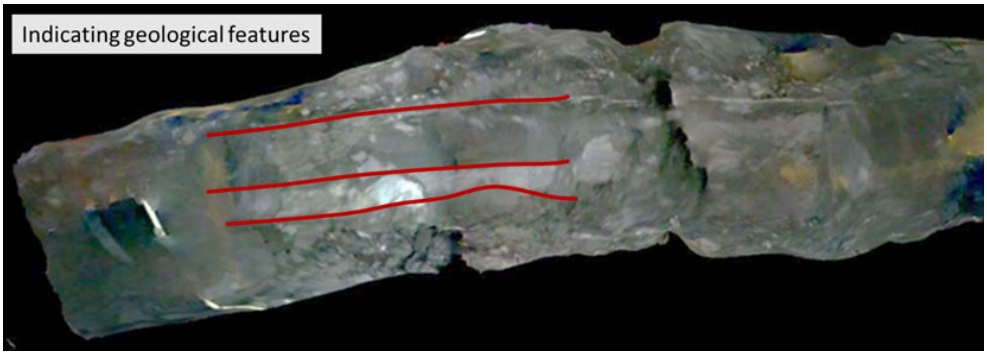

Figure 9. Visible differences in ground formation in the 113-68-East 5 stope panel

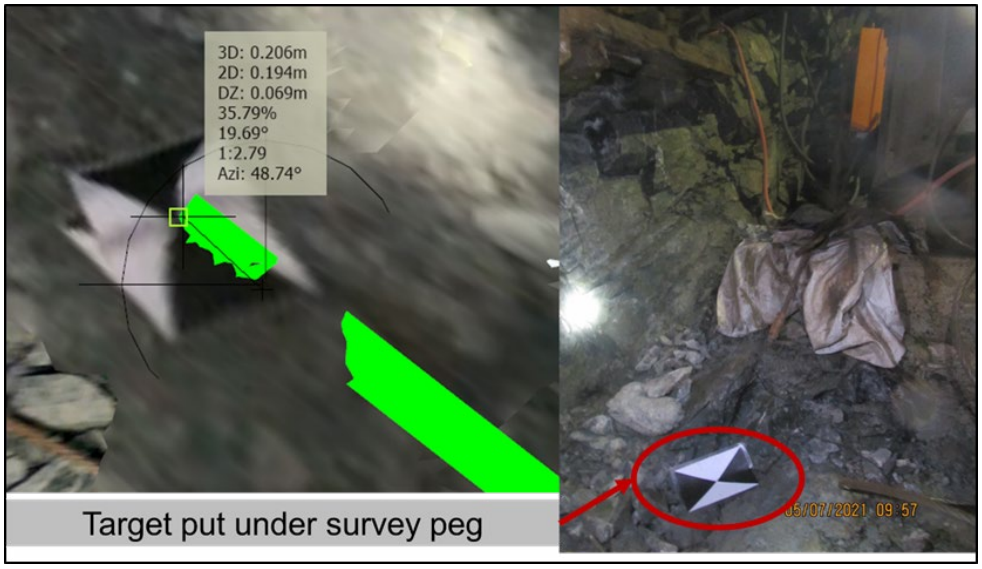

Figure 10. Geo-referencing the underground scans using markers under the survey pegs.

The geo-referenced scans could be imported into the mine's 3D modelling software (Deswik). An accuracy test was conducted comparing the scanned face position with the one obtained using the traditional method of measuring (tapes). This is shown in Figure 11.

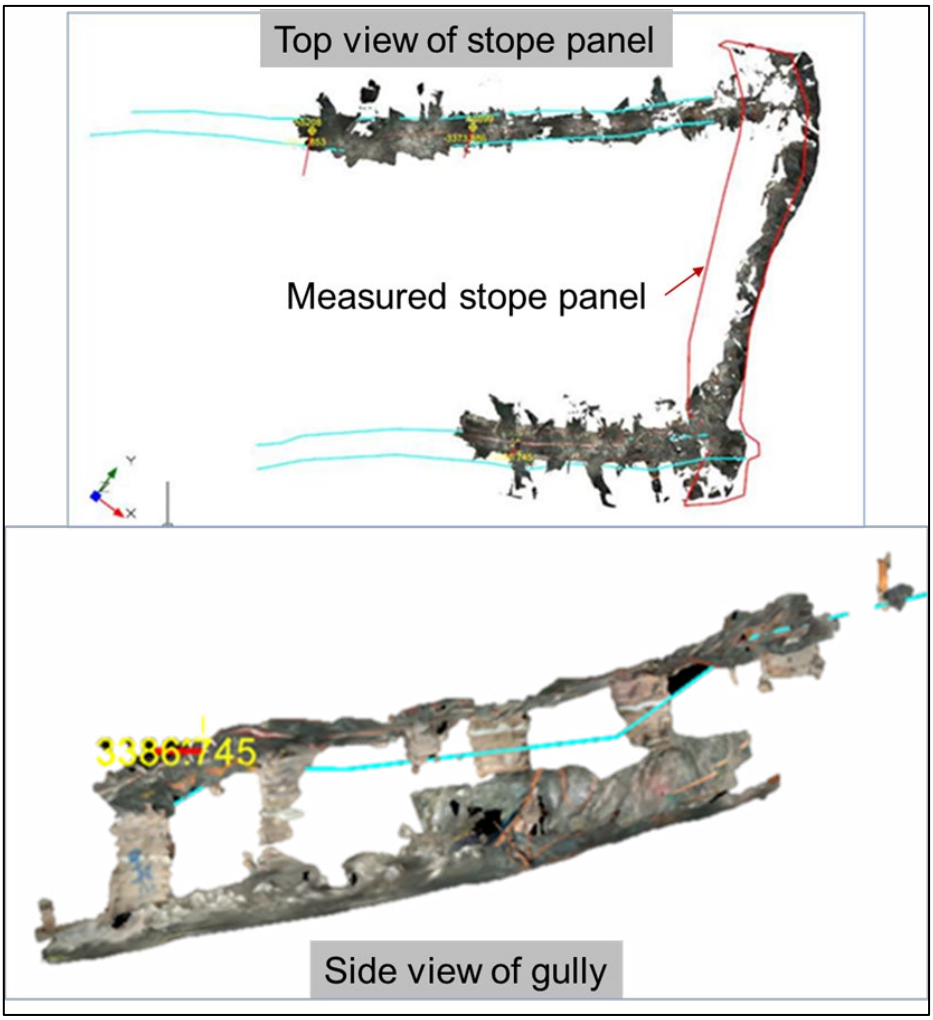

Figure 11. Accuracy test of the position of the scan.

Besides the geology, the stope support could also clearly be seen in the scans. The temporary supports could be clearly measured for the correct spacing distances in the two panels tested, and the permanent support (backfill) distance from the face could be determined. This shows that production departments can use the scans for mining quality and safety purposes. The accuracy of the scans is considered adequate for its purposes, replacing simple measurements made by tapes and clino-rules. Further testing is being conducted to establish the accuracy of the scans. However, it is unlikely that the scans will replace the month-end measurements being carried out by the Survey Department (using tapes and total stations).

Table 1 shows measurements compared at 5m intervals from the 113-68-East 5 stope panel of the VCR from three different sources, namely:

1. Measurements underground on 5 July 2021;
2. Measurements from Deswik CAD; and
3. Measurements conducted by the sampling team on 6 July 2021. There was no advance on the face after the measurements from 5 July 2021.

Table 1. Measurement comparisons in 113-68-East 5 stope

Method	iPad Pro, 3D Scanner App and Deswik Software		Surveyor Measurements		Sampler Measurements	
Date	5 July 2021		5 July 2021		6 July 2021	
	Range of measure.	Average of stope	Range of measure.	Average of stope	Range of measure.	Average of stope
Stope width (cm)	103-161	138	119-139	130	88-136	120
Hangingwall (cm)	7-41	23	0-75	21	0-32	12
Footwall (cm)	47-74	65	58-85	69	55-108	84
Channel Width (cm)	5-46	23	4-41	20	0-50	24

Note: Measurements are taken at 5m intervals.

Table 2 shows the stope volume determined from the iPad Pro scanner measurements using the Deswik software compared to the volumes calculated using the traditional measuring methods on the mine.

Table 2. Volume comparisons in 113-68-East 5 stope.

Method	iPad Pro, 3D Scanner App and Deswik Software	Surveyor Measurements	Sampler Measurements
Stope width (m)	1.38	1.30	1.20
Face length (m)	33.60	33.60	33.60
Advance (m)	4.70	4.70	4.70
Volume (m^3)	217.93	205.30	189.50

It can be observed from Tables 1 and 2, showing the initial accuracy tests, that the area measured using the iPad Pro scanner are very similar to those obtained using the traditional measuring systems. The differences in the volume come from differences in the stoping width measurements. It should be noted that these results are from the first test. As the mine geologists become more comfortable with the scanning process, the accuracy will improve.

ACKNOWLEDGEMENTS

The authors wish to thank the University of the Witwatersrand Mining Institute for access to the DigiMine and the University of Johannesburg for the initial testing. The School of Mining Engineering at the University of the Witwatersrand funded the purchase of the iPad Pro and the Occipital Structure Sensor (Mark II). Furthermore, Mponeng Mine Geology Department for assisting with the underground testing and the follow-on work they are carrying out using the iPhone 12 Pro.

CONCLUSIONS

The Occipetal Structure Scanner (Mark II) was found to be unsuitable for the underground scanning of mine stopes. The iPad Pro created excellent scans of both the tunnels and stopes at the University of Witwatersrand DigiMine and the University of Johannesburg. Underground testing then commenced in the ultra-deep stopes of Mponeng Gold Mine.

The scanner was found to be effective in capturing the contacts of the VCR ore body, and the scans can be geo-referenced into the mine's existing digital models. However, the iPad Pro is not waterproof, and the large screen makes it susceptible to being damaged. The mine is now testing LiDAR-equipped iPhone 12 Pro as a more robust, compact option. Further testing is also taking place at the Maseve Platinum Mine to compare the accuracy of the iPad Pro and iPhone 12 Pro scans to the survey quality laser scans. This research is being conducted in conjunction with the University of Johannesburg and the Mandela Mining Precinct.

REFERENCES

Dominy, S C, and I M Platten. (2012). "Grade Control Geological Mapping In Underground Gold Vein Operations." *Applied Earth Science (Transactions of the Institute of Mining and Metallurgy)* (Maney on behalf of the Institute and The AusIMM) 121 (2): 97-103. Accessed August 9, 2021. doi:10.1179/1743275812Y.0000000019.

GSMArena. (2020). *Apple iPad Pro 2020.* Accessed May 2021. https://www.gsmarena.com/apple_ipad_pro_11_(2020)-10137.php.

Location of Mponeng Mine [Map, 21 November]. Scale unknown. Data layers: Open Streetmap. National Geo-spatial Information (NGI) CDNGI_2mil_Mosaic.; Maptiler Topo. Using: QGIS for Desktop [GIS].

Occipital. (2019). *Structure Sensor Mark II.* Accessed March 2021. https://structure.io/structure-sensor-markii/specs.

Russell, T M, and T R Stacey. (2019). "Using laser scanner face mapping to improve geotechnical data confidence at Sishen mine." *Journal of the Southern African Institute of Mining and Metallurgy* 119 (1): 11-20. Accessed September 9, 2021. doi:http://dx.doi.org/10.17159/2411-9717/2019/v119n1a2 .

NEW AND ECOLOGICAL METHOD FOR THE PRODUCTION OF CR_2O_3 FROM CHROMITE ORE

YENİ VE EKOLOJİK YÖNTEMLE KROMİT CEVHERİNDEN Cr_2O_3 ÜRETİMİ

H. Şahan [1, *], H. Xu [2]

[1] *Northeastern University, Department of Chemistry and Chemical Biology, Center for Renewable Energy Technology*

[2] *National Engineering Laboratory for Hydrometallurgical Cleaner Production Technology, Institue of Process Engineering, Chinese Academy of Sciences*

ÖZET

Önemli kimyasal maddelerden biri olan krom (III) oksit (Cr_2O_3), metalürjik malzemelerde, yeşil pigmentlerde, yapı malzemelerinde, refrakter malzemelerde, yüzey kaplama işlemlerinde ve katalizör olarak birçok alanda kullanılabilme potansiyeline sahiptir. Günümüzde Cr_2O_3 endüstriyel olarak başlıca iki yöntemle üretilmektedir. Bunlardan birinde sodyum dikromat amonyum sülfat ile indirgenirken, diğerinde kromik anhidritin (CrO_3) termal bozunması ile üretim yapılmaktadır. Her iki yöntemde de 6^+ yükseltgenme basamağındaki krom başlangıç kimyasalı olarak kullanılmaktadır. Bu tür zehirli kimyasalların endüstriyel boyutta başlangıç maddesi olarak kullanımı ciddi çevre problemlerine ve kaynakların verimsiz kullanımına sebep olmaktadır.

Bu çalışmada Kayseri, Pınarbaşı bölgesinden çıkarılan konsantre kromit cevherinden yeni ve ekolojik yöntemle Cr_2O_3 sentezlenmiştir. Kromit cevheri belli oranda NaOH ile 1000 ^{0}C de açık havada 2 saat süre ile ısıtılmıştır. Bu işlem sonrası su leach işlemi yapılarak çözünen krom sulu çözeltiye alınmıştır. Su leachi sonrası başlıca demir, mağnezyum, silisyum ve bir miktar alüminyumdan oluşan katı kısım ise süzülerek ayrılmıştır. Çözeltiye geçen bir miktar alüminyum iyonları uygun pH değerinde $Al(OH)_3$ şeklinde çöktürülerek geri kazanılmıştır. Çözeltide başlıca kalan Cr^{6+} iyonları oksalik asit kullanılarak uygun pH da Cr^{3+} iyonlarına indirgenmiştir. Son aşamada Cr_2O_3 bileşiği saf olarak elde edilebilmiştir. Bu çalışma krom oksit sentez verimini etkilen parametreler araştırılmış, çalışmanın endüstriyel olarak uygulanabilmesi için temel bilgi birikimi oluşturmuştur.

Anahtar Sözcükler: Kromit cevheri, Cr_2O_3, alkali kavurma, Cr^{6+} iyonlarının indirgenmesi.

ABSTRACT

Chromic oxide is an important basic chemical and finds many applications including metallurgical materials, green pigments, construction materials, refractory materials and catalysts. Presently, the industrial production of chromic oxide generally employs two processes : one is the reduction of sodium dichromate with ammonia sulfate; the other is the thermal decomposition of chromic anhydride. Both of the processes employ hexavalent chromium as the raw materials. However, the industrial production of hexavalent chromium compounds, including sodium dichromate and chromic anhydride, leads to serious environmental problems and low resource utilization.

Cr_2O_3 is synthesized from chromite ore which is extracted in the Pınarbaşı region in Kayseri via a new and ecological method. Chromite ore is mixed with the determined amount NaOH and roasted 1000 ^{o}C in the air atmosphere. After that step, we carried out a water leach process for the extraction of chromium ions. After the water leach step, the solid waste which contains mainly iron, magnesium, silicon and a part of aluminum could be separated from the solution via filtration. Residual aluminum cations in the solution were precipitated as an $Al(OH)_3$ in the certain pH. All Cr^{6+} ions in the solution were reduced by a certain amount of oxalic acid in the specific pH. The Cr_2O_3 compound could be

successfully synthesized in the final step. The effects of parameters on the preparation yields of Cr_2O_3 were systematically investigated in this study. Those research datas can be used in the industrial production of Cr_2O_3.

Keywords: Chromite ore, Cr_2O_3, alkali roasting, reduction of Cr^{6+} ions.

INTRODUCTION

Chromium is an important metallic element, known for high and low temperature corrosion and oxidation-resistance properties, which the element imparts to the stainless steel and superalloys (Stringer et al, 1972). Other usages of chromium are in the production of chemicals [2,3] (SC, T and L. F, 1984) for manufacturing dyes and pigments, tanning of leather, chrome plating and catalysts (Wang, 2000). Since the year 2000, chromite ore production has been steadily on the rise, increasing from 15 million tons to 40 million tons in 2020 (Statista.com).

While many minerals contain chromium, chromite ($FeCrO_4$) is the only commercial ore mineral of chromium. The general formula of chromite ore can be described as $(Mg_xFe_{1-x})O(Al_yCr_{1-y})_2O_3$, since silicon is mixed as gangue in chromite ores.

The traditional route for manufacturing chromium products is based on the extraction of chromium oxide as sodium chromate via the oxidative alkali roasting of chromite ores, in air or oxygen. The generic chemical reaction for chromite to sodium chromate may be explained by considering the oxidation of iron chromite ($FeCr_2O_4$), as shown below in reactions. In this reaction, the iron chromite ($FeCr_2O_4$) is the main Cr^{3+}-ion bearing spinel in a quaternary solid-solution of three other spinels in natural chromite (Antony et al., 2001).

$$(Fe,Mg)[Cr,Al,Fe]_2O_4 + 2Na_2CO_3 + 3O_2 \rightarrow 2Na_2CrO_4 + (Fe,Mg)[Al,Fe]_2O_4 + 2CO_2 \quad (1)$$

Conventionally, industrial production of Na_2CrO_4 can be via either pyrometallurgical or hydrometallurgical processes for treating chromite ore. Soda-ash alkaline roasting is a commonly used pyrometallurgical processing method (Tathavadkar, 2001). However, kiln-ringing is always a bottleneck for consecutive pelletizing processes and normal operation of the soda-ash alkaline roasting process (Ji et al., 2010). Consequently, both lime-based and lime-free processes were developed to avoid the kiln-ringing problem. In the lime-based roasting process, approximately 2.5 to 3.0 tons of chromite ore processing residues (COPR) is discharged per ton of sodium dichromate ($Na_2Cr_2O_7{\cdot}2H_2O$) product. Furthermore, in the discharged COPRs, the content of carcinogenic calcium chromate ($CaCrO_4$) is as high as 1.0 wt.% counted as $Na_2Cr_2O_7{\cdot}2H_2O$ (Ji et al, 2010). Therefore, extensive research work was widely carried out on the utilization and treatment of the chromium ore processing residues (Walawska and Kowalski, 2000; Kowalski and Wzorek, 2002). In this study, chromium (III) oxide was prepared via the reaction of the Turkish chromite ore and alkali (NaOH) at 1000 °C in air. Cr^{6+} ions in the leaching solution were reduced and complexed via oxalic acid. Oxalic acid was used as both reducing and complexing agent for the first time in this study

EXPERIMENTAL

Ore and Reagents

In this work, a chromite concentrate was obtained from an ore dressing plant in Pınarbaşı/Kayseri, Turkey. The X-ray fluorescence spectrum of the as-received chromite ore is shown in Figure 1. In addition, XRF analysis of the chromite ore is presented in Table 1. Physico-chemical characterisation of the ore is discussed in further detail in the results and discussion section. All of the

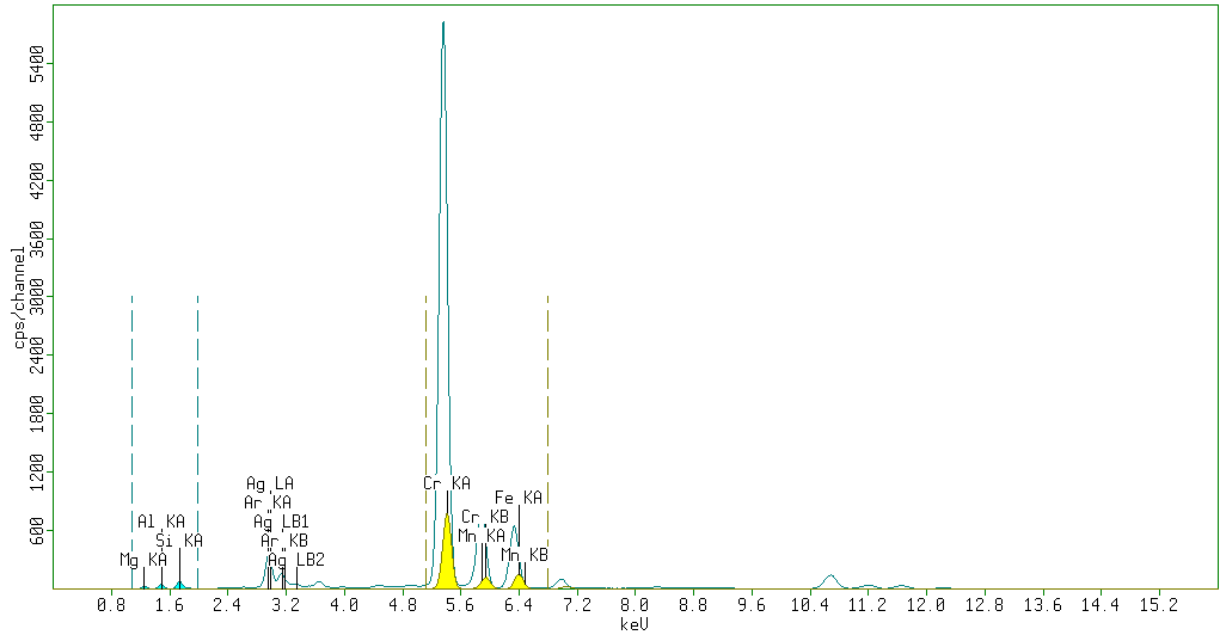

Figure 1. The X-ray fluorescence spectrum of the chromite ore

Table 1. Chemical composition of the chromite ore

Component	Cr_2O_3	Al_2O_3	SiO_2	Fe_2O_3	MgO	Na_2O	CaO	NiO	TiO_2
Wt.%	56.52	10.81	3.67	14.57	14.01	-	0.137	0.187	0.128

Experimental Setup and Procedure

All roasting experiments were performed in an electrically heated tube furnace where the temperature was controlled by a programmable temperature-controlling device. The molar ratios of Cr_2O_3:MOH were determined as 1:7.8, 1:12 and 1:15, respectively. For every experiment, chromite mineral and NaOH were mixed in agate mortar and then pressed at 6 tons/cm^2. Solid patterns were placed in a cylindrical alumina crucible. All samples were roasted for 2 hours with excess NaOH at 1000^{o}C in the air atmosphere. Roasted samples were water leached for 2 hours at 60 ^{o}C. These samples were water leached and the remaining residues were analyzed via titrimetric method.

After the fusing and subsequent leaching with water, the pH of highly basic impure chromate solution was adjusted as a 7.5 via 1:1 sulfuric acid solution. After all Al^{3+} cations in the solution were precipitated as a $Al(OH)_3$, precipitate was filtered and washed. After the vacuum filtration, the yellow solution was acidified with 1:1 sulfuric acid and heated at 70 ^{o}C. Oxalic acid was added in the orange solution to ensure that all chromium (VI) ions were reduced to chromium (III). The solution was heated and mixed until excess water evaporated in order to obtain $Na_3[Cr(C_2O_4)_3]$ complex material. Dried complex was heated at 500 ^{o}C in the air. Subsequently, the decomposed complex was suspended in the pure water and chromium hydroxide precipitation was performed using an ammonia solution (% 25 v/v) around pH = 9. After the chromium hydroxide was completely precipitated, all precipitate was washed with pure water several times. The gely $Cr(OH)_3$ precipitate was dried at 115 ^{o}C for overnight. In order to obtain chromium oxide, dried solid was calculated to 700 °C for 5 h in the air atmosphere. The flow chart of the production process is given in Figure 2.

Characterization techniques

After roasting and leaching, the powder samples were analyzed using a Philips X'Pert X-ray, APD-10X diffractometer. Samples were analyzed over an angle 2θ with a maximum range of 10 to 90°, using Cu-Kα radiation. X'Pert HighScore Plus database software was used for phase identification of the XRPD patterns obtained. Scanning electron microscope (SEM, Zeiss EVO) was used to observe the morphology of the powders by equipping energy dispersive spectroscopy (EDS) to perform element composition of the powders. X-ray fluorescence spectroscopy (XRF, Malvern Panalytical, Epsilon 1) was employed for analyzing the chemical composition of solid samples. The particle size distribution analysis was carried out via Malvern Zetasizer. Thermal analysis of the precursor sample ($Cr(OH)_3$) was carried out using a Pekin Elmer (Diamond) TG/DTA thermal analyser at a heating rate of 10°C min^{-1} under air atmosphere to specify the optimum temperature for phase formation of Cr_2O_3.

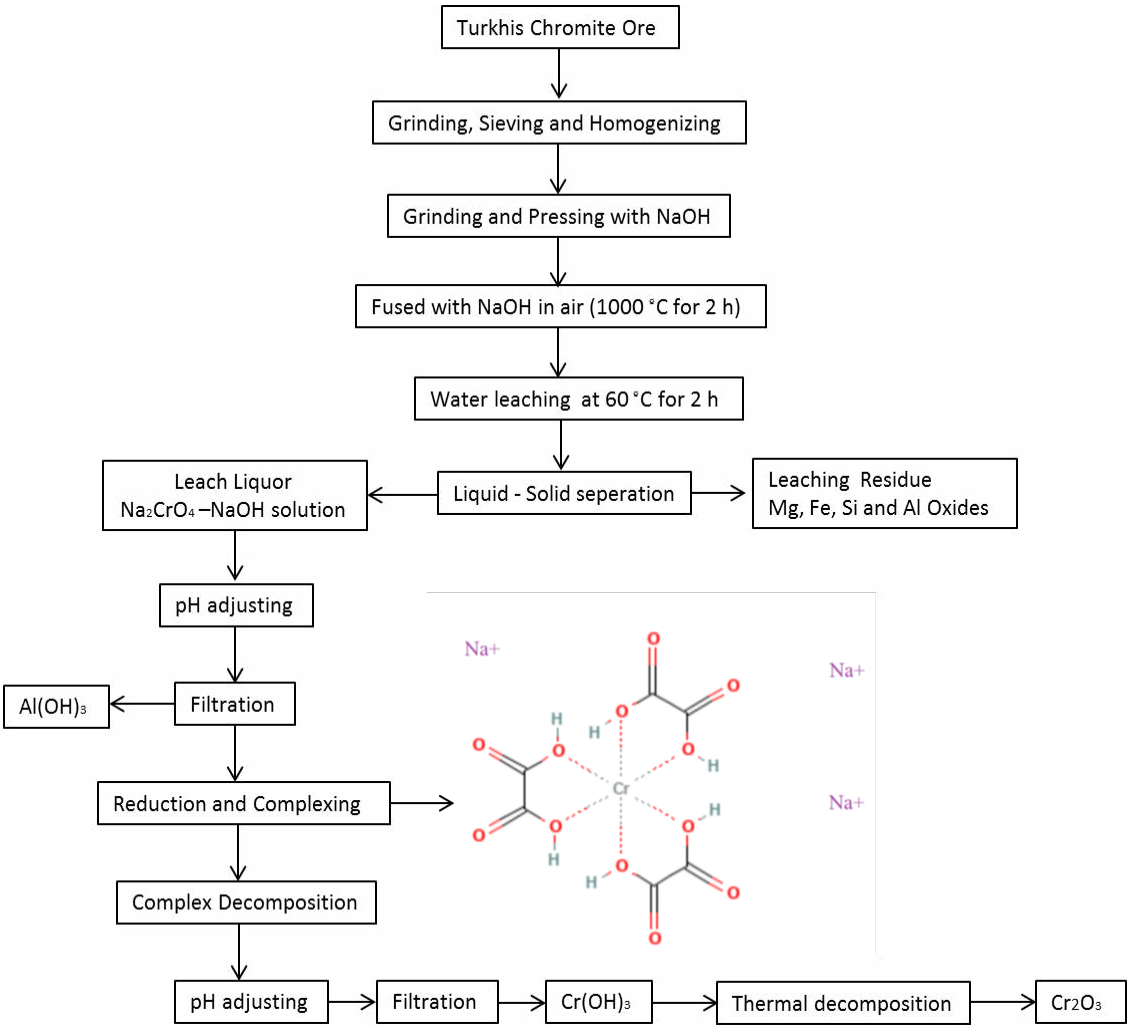

Figure 2. The flow sheet of the Cr_2O_3 production process

RESULTS AND DISCUSSION

Characterization of the chromite ore

According to the X-ray diffraction (XRD) pattern as illustrated in Figure 3, the major crystallized phase of the chromite ore was (Mg, Fe) $(Cr, Al)_2O_4$, with minor phase of $(Mg, Fe, Al)_6(Si, Cr,)_4O_{10}(OH)_8$. The morphology and distribution of elements of the chromite ore were characterized by the scanning

electron microscopy (SEM). Based on the secondary electron image in Figure 4(a), the particle of the chromite ore was compact with a rough surface. In Figure 3(b)-(g), the mapping of elements from the energy dispersive X-ray spectrometer (EDX) indicated that the distribution of Cr, Mg, Fe and Al was uniform in the chromite ore.

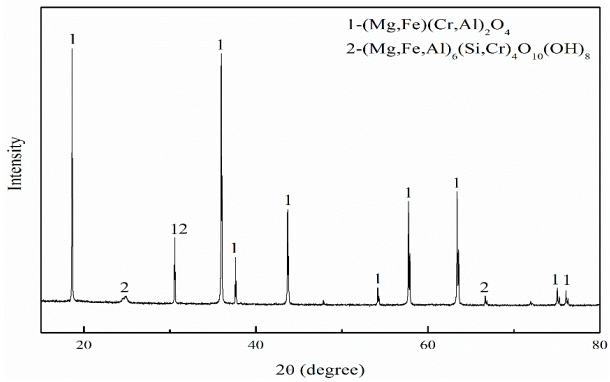

Figure 3. XRD pattern of the chromite ore

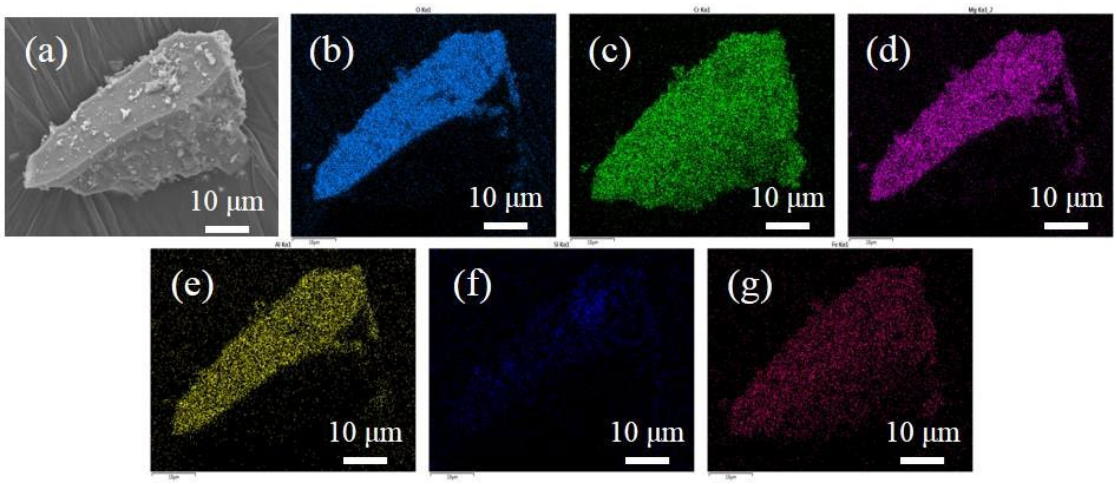

Figure 4. Secondary electron image (a) and the mapping of elements (b: O, c: Cr, d: Mg; e: Al; f: Si; g: Fe) of chromite ore

Since some coarse particles are present in the chromite ore, the ore was ball-milled further and then sieved to a particle size smaller than 48 µm to obtain the ground sample used for the hydrometallurgical process. The particle size distributions (PSDs) of the received chromite ore and the ground sample were shown in Figure 5. Furthermore, the values of D(0.1), D(0.5) and D(0.9) were listed in Table 2.

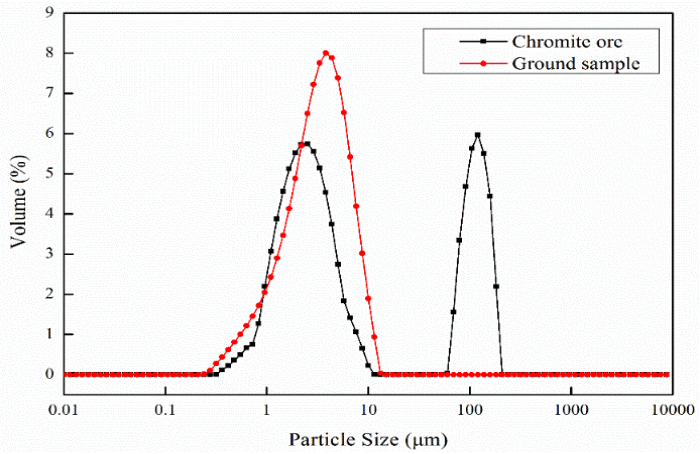

Figure 5. PSDs of the chromite ore and the ground sample

Table 2. The values of D(0.1), D(0.5) and D(0.9) of the chromite ore, ground sample and COPR

	D (0.1)	D (0.5)	D (0.9)
Chromite ore	1.30	3.76	145.20
Ground Sample	7.39	12.65	21.18

The chemical composition of the chromite ore was shown in Table 1. The chromium content (calculated as Cr_2O_3) was 56.52 wt.%. According to the X-ray diffraction (XRD) pattern as illustrated in Figure 2, the major crystallized phase of the chromite ore was (Mg, Fe) $(Cr, Al)_2O_4$, with minor phase of $(Mg, Fe, Al)_6(Si, Cr,)_4O_{10}(OH)_8$. The morphology and distribution of elements of the chromite ore were characterized by the scanning electron microscopy (SEM). Based on the secondary electron image in Figure 3(a), the particle of the chromite ore was compact with a rough surface. In Figure 3(b)-(g), the mapping of elements from the energy dispersive X-ray spectrometer (EDX) indicated that the distribution of Cr, Mg, Fe and Al was uniform in the chromite ore.

Characterization of the leaching residue

The effect of the NaOH content on the dissolution process was investigated via determining the Cr content in both leaching solution and leaching residue. For that purpose, a titrimetric method is carried out for all reaction mixtures. The Cr_2O_3 wt.% in the leaching residue were calculated as 33.3, 24.2 and 32.3 for the 1:7.8, 1:12 and 1:15 samples, respectively. In addition, the Cr_2O_3 wt.% in the leaching solution were calculated as 65.5, 73.2 and 61.3 for the 1:7.8, 1:12 and 1:15 samples, respectively. From the Cr analysis results, it can be said that the optimum molar ratio of NaOH for the fusion reaction was 1: 12 (Cr_2O_3: NaOH). Because of the excessive amount of NaOH in the fusion reaction, the viscosity of the reaction mixture may be increased and the oxygen diffusion which is the important factor for the ore decomposition can be limited during the decomposition reaction.

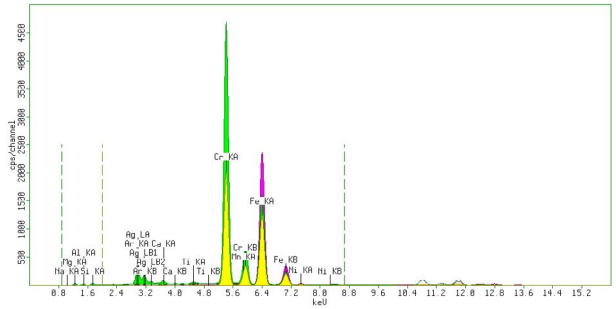

Figure 6. X-ray fluorescence spectrum of leaching residue (1:12 / Cr_2O_3: NaOH)

Table 3. Chemical composition of leaching residue (1:12 / Cr_2O_3: NaOH)

Component	Cr_2O_3	Al_2O_3	SiO_2	Fe_2O_3	MgO	Na_2O	CaO	NiO	TiO_2
Wt.%	27.14	4.09	2.69	22.78	32.54	10.13	0.22	0.285	0.198
Component	MnO								
Wt.%	0.50								

After the oxidative leaching, the spinel phases were decomposed and more than 73% of chromium was leached. The XRF spectra and chemical composition of the leaching residue are shown in Figure 6 and table 3, respectively. As shown in Figure 6 and table 3, leaching residue still contains chromium oxide because the fusion reaction may not effectively occur during the dissolution process. It can be seen in the Table 3, titrimetric analysis result for the Cr_2O_3 in the leaching residue is similar to XRF analysis result.

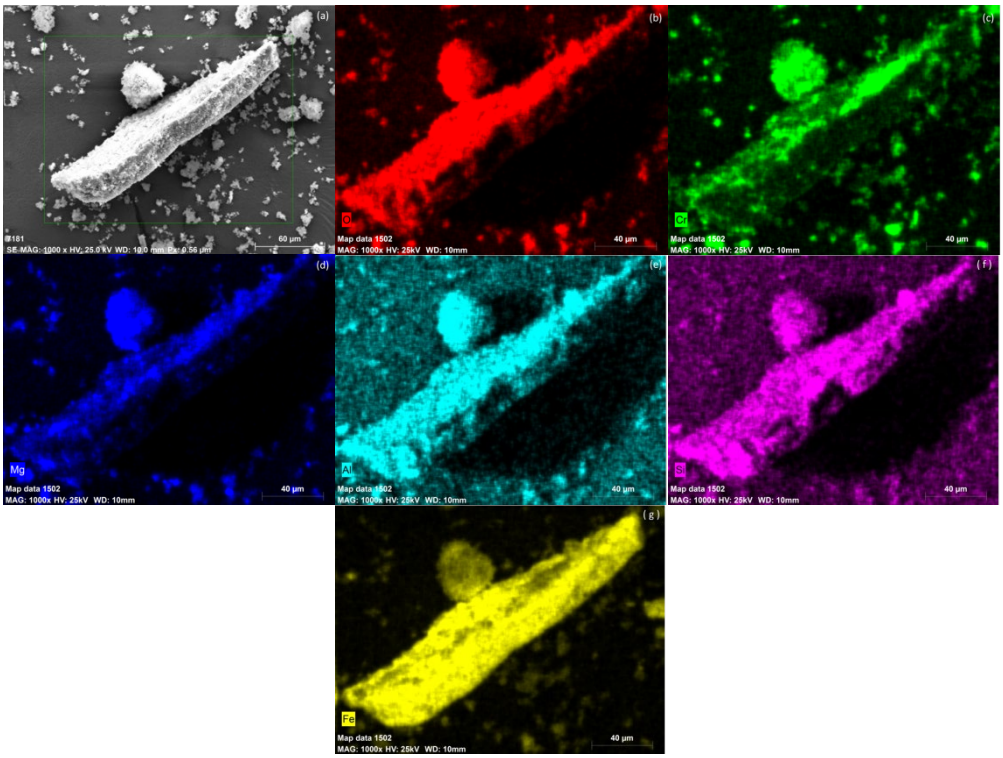

Figure 7. SEM image (a) and the mapping of elements (b: O, c: Cr, d: Mg; e: Al; f: Si; g: Fe) of leaching residue

In Figure 3(b)-(g), the mapping of elements from the energy dispersive X-ray spectrometer (EDX-SEM) indicated that O, Cr, Mg, Al, Si and Fe elements can be detected after the water leaching process. However, the Cr element signals much lower than that of the Fe element signals. The EDX mapping analysis is in good agreement with both XRF and titrimetric analysis results.

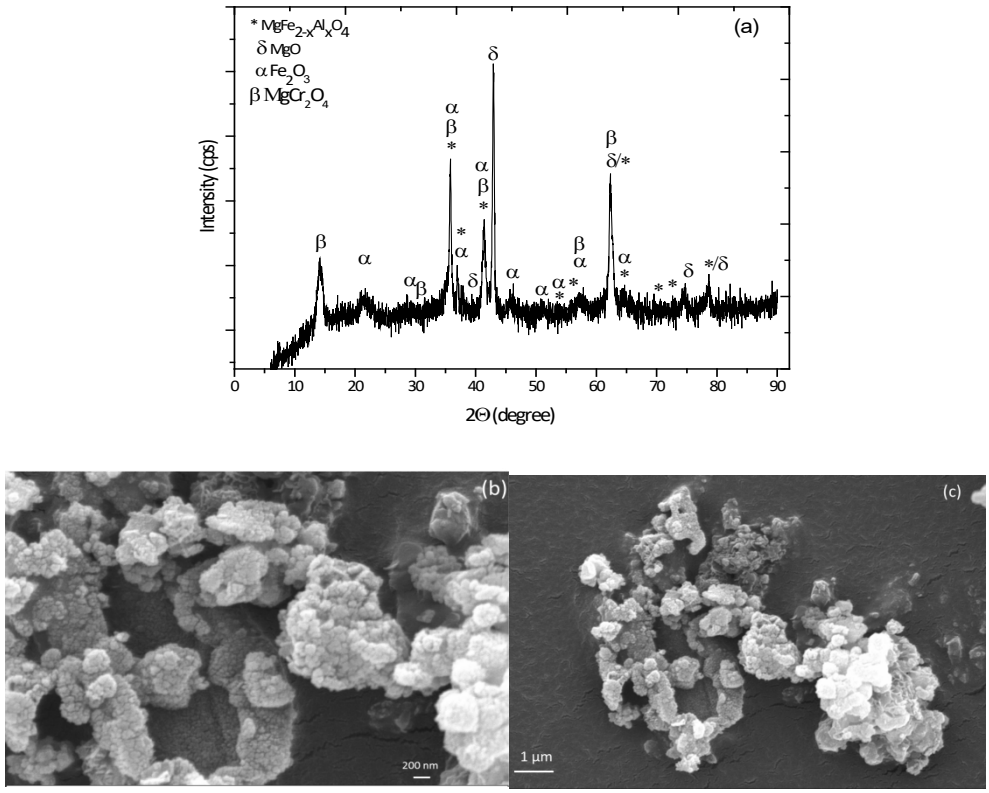

Figure 8. a) XRD diffraction pattern b, c) High and low magnified SEM micrograph of the leaching residue (1:12 / Cr_2O_3: NaOH)

The XRD pattern of the leaching residue is given in Figure 8a. It can be clearly seen in the XRD pattern, the leaching residue contains different phases because of decomposition of the chromite ore. Those phases are $MgFe_{2-x}Al_xO_4$, MgO, Fe_2O_3 and $MgCr_2O_4$, respectively. The XRD phase analysis datas coincide with XRF datas. Furthermore, the SEM micrograph shows that the particles are mutually connected and the particle sizes are smaller than 200 nm. Heterogeneous phases can be seen in the SEM micrograph (Figure 8c).

Characterization of the Cr_2O_3 product

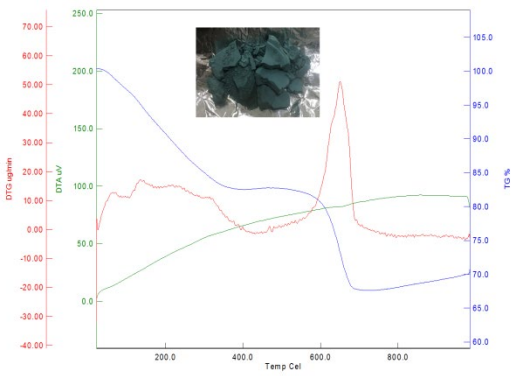

Figure 8. Thermal analysis of the $Cr(OH)_3$ precipitate

The TG/DTA curve of Cr_2O_3 precursor [$Cr(OH)_3$] is described in Fig. 8. In order to better find out the decomposition reactions occurring in the synthesis, TG analysis was fulfilled on the precursor sample at a ramp rate of 10 °C min^{-1}. The TGA shown in Fig. 8 is in good agreement with the one reported by Music et al. (1999). The TG curve clearly displays several-step weight loss regions. The first mass loss is assigned to loosely bound molecular water, while the second loss, observed between 120 and 200 °C, is

attributed to the loss of adsorbed water. The third, and steeper,mass loss to a partial condensation reaction, by which some –OH groups react to transform $Cr(OH)_3$ into $CrO(OH)x$.

$$Cr(OH)_3 \rightarrow CrO(OH)\,H_2 \quad (1)$$

$$2CrO(OH) \rightarrow Cr_2O_3 + H_2O \quad (2)$$

The TG/DTA curve presents a well defined exothermic peak at 680 ˚C suggesting the formation of Cr_2O_3. The DTG curve advocates no further thermal reactions beyond 800 ˚C.

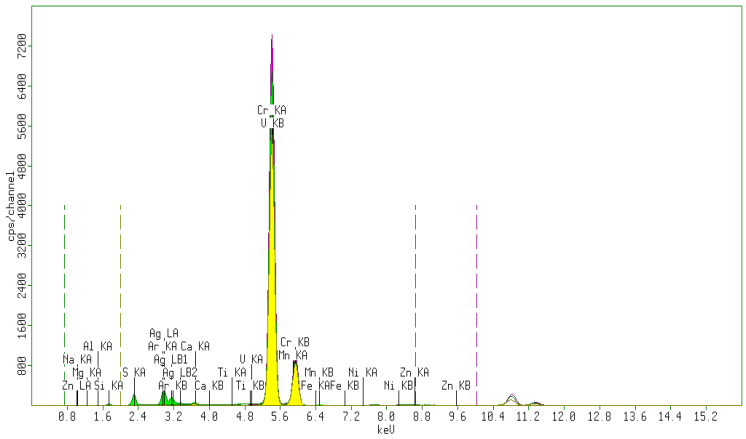

Figure 9. X-ray fluorescence spectrum of Cr_2O_3 (1:12 / Cr_2O_3: NaOH)

Table 4. Chemical composition of the Cr_2O_3

Component	Cr_2O_3	Al_2O_3	SiO_2	Fe_2O_3	MgO	Na_2O	CaO	NiO	TiO_2
Wt.% or ppm	95.5	-	-	-	-	0.56	485 ppm	165 ppm	116 ppm
Component	MnO	SO_3	V_2O_5	ZnO					
Wt.% or ppm	-	3.89	413 ppm	79.7 ppm					

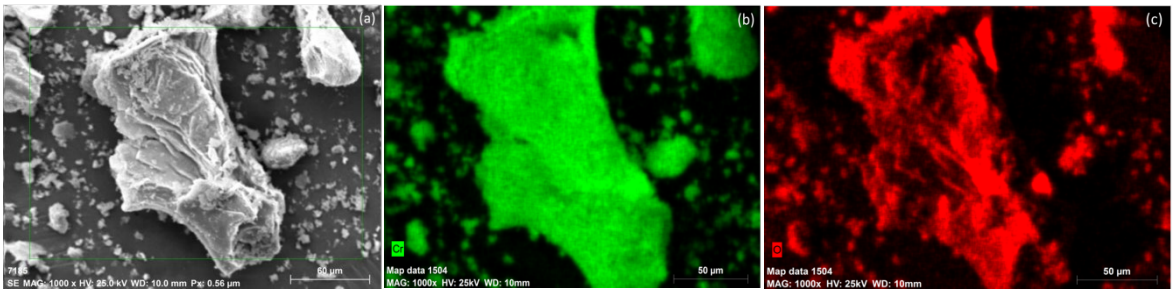

Figure 10. SEM image (a) and the mapping of elements (b): Cr ,(c):O of Cr_2O_3

Fig. 10b and c shows EDS analysis and elemental mapping of final product Cr_2O_3. As seen in Figure 10b and c, Cr and O is homogeneously distributed onto Cr_2O_3. The EDS spectrum of the sample exhibits the characteristic peaks of Cr and O Cr_2O_3 phase purity in the synthesized particles. No other element was detected in EDS analysis with SEM. Furthermore, to verify the chemical composition of the synthesized particles, the XRF analysis of Cr_2O_3 was conducted. The XRF spectrum of the sample exhibits the characteristic peaks of Cr. From the XRF spectrum, the Cr_2O_3 content in the sample was calculated as 95.5 wt.%. SO_3 and Na_2O content in the sample were calculated as 3.89 wt.%. and 0.56 wt.%.,

respectively. Those impurities are related to NaOH and H_2SO_4 which is used during the synthesis procedure and reduction process, respectively.

The crystalline nature and composition of Cr_2O_3 was examined by XRD. The XRD patterns of as-synthesized Cr_2O_3, is shown in Fig 11.a. Fig. 11 shows the XRD patterns of the final product, which is in agreement with Cr_2O_3 (JCPDS card No. 038-1479). All of the diffraction peaks in this pattern are in good agreement with the standard crystallographic data for the rhombohedral α-Cr_2O_3. In addition to the major phase of Cr_2O_3, small amounts of Na_2SO_4 peak is found as impurity phase.

The SEM images depicting the morphologies and microstructures of the materials are shown in Fig 11b and c. It can be seen clearly from Figs 11b and 11c the particle distribution of Cr_2O_3 material is homogenous. As seen in SEM micrographs, the particles agglomerate and the particle size of Cr_2O_3 is smaller than 200 nm.

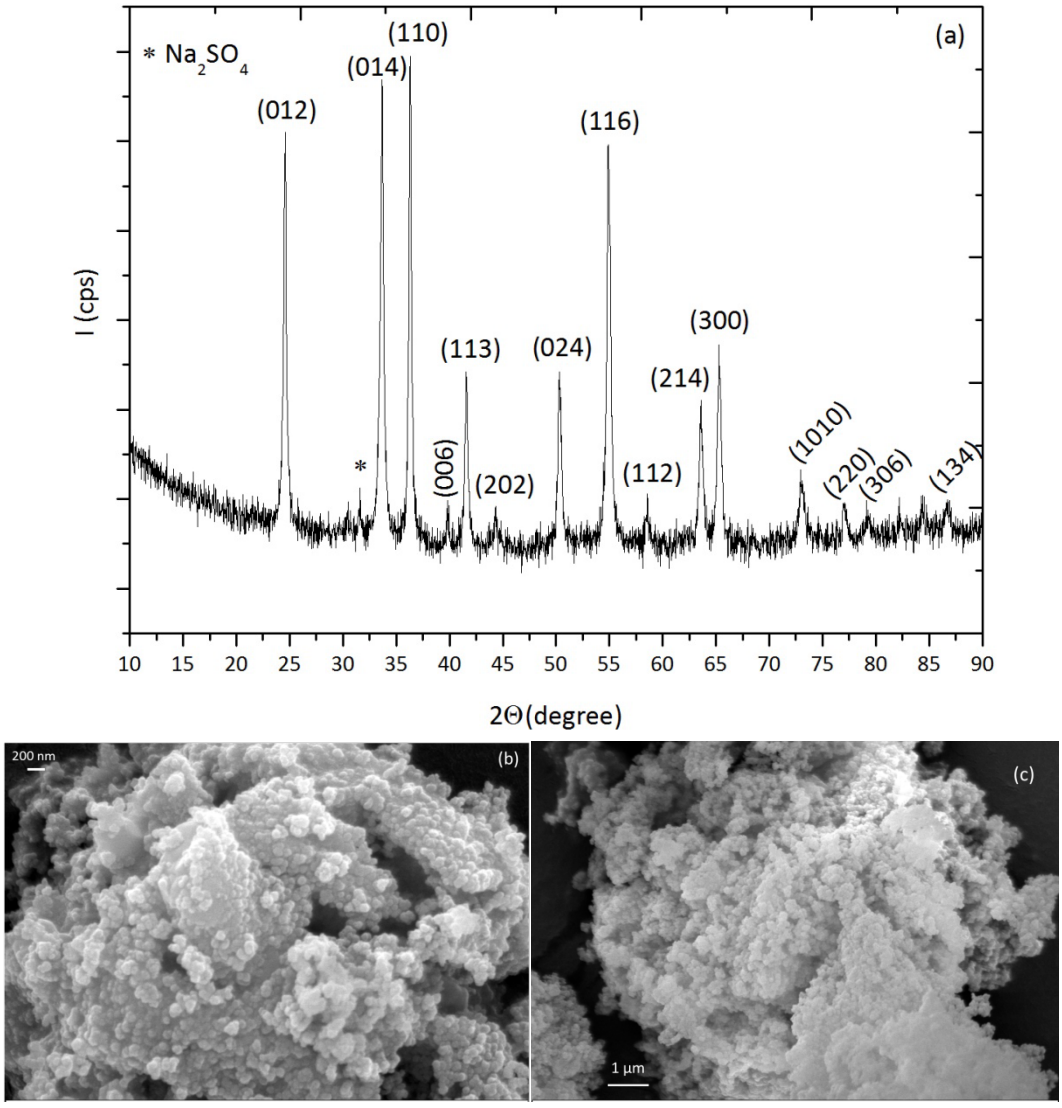

Figure 11. a) XRD diffraction pattern b, c) High and low magnified SEM micrograph of Cr_2O_3(1:12 / Cr_2O_3: NaOH)

Figure 12. Photo of the Cr_2O_3

In Figure 12, the Cr_2O_3 product exhibited the typical color for chromium oxide green pigment of a yellowish-green color (GB/T 20785-2006).

CONCLUSIONS

Characterization of as-received samples showed that the Turkish chromite ore used in this study is constituted by a solid solution of $FeCr_2O_4$, $MgCr_2O_4$, $FeAl_2O_4$ and $MgAl_2O_4$. The main phase identified by XRD was (Mg, Fe)(Cr, $Al)_2O_4$, with calcium and aluminum silicates and free silica also present as gangue. Optimum molar ratio of Cr_2O_3:MOH was determined as 1:12 in the alkali fusion reaction. Experimental results showed that the chromium yield is greater than 92% in the 1:12 molar ratio of Cr_2O_3:MOH. Also, the extraction of $Al(OH)_3$ reduces the amount of waste and recovery of the Al in the leaching solution can help the industrial process economy. A novel process with zero emission of hazardous chromium-containing residue has been proposed. Cr^{6+} ions in the leaching solution can be successfully converted Cr^{3+} via oxalic acid. In addition, excess oxalic acid ih the solution can be recovered as ammonium or sodium oxalate crystals during the process. The green-novel strategy is simple and low cost and promising for mass production of the Cr_2O_3. We demonstrated that a novel and ecological method can be used to produce for Cr_2O_3.

ACKNOWLEDGMENTS

The authors gratefully acknowledge Elmaci Mining Company for financial support. The authors gratefully acknowledge the helpful suggestions from İlhan Mollamustafaoğlu and Alper Tuna Elmacı.

REFERENCES

Antony, M.P., Tathavadkar, V.D., Calvert, C.C., Jha, A., 2001. The soda-ash roasting of chromite ore processing residue for the reclamation of chromium. Metall. Mater.Trans. B 32 (6), 987–995.

Chrome oxide green pigments, GB/T 20785-2006.

https://www.statista.com/statistics/598320/mine-production-of-chromium-worldwide/

Ji, Z., Liu, H.J., Lu, B.Q., Zeng, Y.B., 2010. Engineering Practical Technology of ChromiumResidue. Chemical Industry Press, Beijing, China Ji et al., 2010.

Kowalski, Z., Wzorek, Z., 2002. Utilization of chromic waste in the sodium chromate (VI) production process. Journal of Loss Prevention in the Process Industries 15, 169–178.

Music, S., Maljkovic, M., Popovic, S., Trojko, R.,1999, Croat. Chem. Acta, 72, 789.

SC, T, L. F, 1984. Chromite Ore for the Production of Chromium Chemicals in Proceedings of Australian Institute of Mining & Metallurgy.

Stringer, J., Wilcox, B.A., Jaffee, R.I., 1972. The high-temperature oxidation of nickel-20 wt. % chromium alloys containing dispersed oxide phases. Oxid. Met. 5 (1), 11–47.

Tathavadkar, V.D., Antony, M.P. and Jha, A., 2001, The soda-ash roasting of chromite minerals: Kinetics considerations, Metallurgical and Materials Transactions B, 32B, p. 593.

Vardar, E., Eric, R.H., Letowski, F.K., 1994. Acid leaching of chromite. Miner. Eng. 7 (5), 605–617.

Walawska, B., Kowalski, Z., 2000. Model of technological alternatives of production of sodium chromate (VI) with the use of chromic wastes. Waste Management 20, 711–723.

Wang, S., et al., 2000. Dehydrogenation of ethane with carbon dioxide over supported chromium oxide catalysts. Appl. Catal. A Gen. 196 (1), 1–8. Wang et al., 2000

NEW ERA OF AUTOMATION IN LEAK DETECTION INDUSTRY

T. Gregor

ELIS Technologies Limited

ABSTRACT

An innovative solution for integrity monitoring of a fully submerged geomembrane with a new automatic floating robotic device technology and its positive impact on the mining industry is presented in this article. Advances in technology in line with the developments in IT, robotics and GPS technologies, together with extensive experience in geomembrane leak detection, have enabled us to develop the new eLagoon robotic device. A comparison of the traditional methods and the new geomembrane monitoring technology in the mining industry is also presented.

Keywords: Leak detection, monitoring, geomembrane, lagoon, floating drone, IT technology, mining industry, tailings ponds, tailings management

INTRODUCTION

The future of mining in the current push for a circular economy is unthinkable without innovation in green technologies as well. The mining industry, particularly the extraction of various ores, uses materials that could contaminate the surrounding environment. To prevent possible contamination, high-quality waterproofing geomembranes (mainly PEHD or LDPE) are used. These liners have high chemical resistance but significantly lower mechanical resistance. Mechanical damage to geomembranes may thus result in the release of contaminants into the environment, especially when toxic liquids leak from the lagoons.

It is therefore important to ensure that the monitoring of the integrity of waterproofing membranes is performed regularly in order to secure the best prevention against possible contamination during the processes involved in mining and ore extraction. The leak-detection inspection must identify problem with the integrity of geomembrane early and accurately so that contaminants are not released, and any damage can be repaired as soon as possible before the surrounding environment is negatively affected. Leachate spills not only damage the environment, but also result in the loss of the raw material being extracted. Therefore, the resources invested in the geomembrane monitoring process are returned many times over.

Proper and timely leak-detection monitoring practices have the power to improve the public perception of mining activities, particularly in communities living in the vicinity of the mining facilities. In fact, proper practices also help investors to protect their investments, which are not small, because if contamination of groundwater happens, the entire mining project may be delayed and/or severely disrupted by regulators.

Currently, there are several methods for leak-detection monitoring on waterproofing membranes, but these cannot be used on already filled lagoons and tanks. It is for this reason that we have developed a new type of innovative floating drone that is capable of leak detection on submerged geomembranes.

DESCRIPTION OF THE DEVICE

There are several ways in which monitoring of integrity of geomembranes is performed around the world. The most well-known and the most effective method of leakage monitoring in the world is the method of electrical leak localization in geomembranes.

The first reference to electric leak location systems (ELLS) appeared in the USA. The initial work, carried out by the Southwest Research Institut (SRI) on behalf of the US Environmental Protection Agency, showed that the electrical resistivity technique was able to assess the integrity of geomembranes used in fluid impoundments and landfills (Shultz et.al. 1984).

Subsequently, the method (ELLS) began to be developed and used not only in America, but also in Europe and later in Asia.

The method was described in detail and in a comprehensive manner in 2000 at a prestigious international conference in Bologna, Italy (Second European Geosynthetics Conference „Nosko, V., Gregor, T., Ganier. F. : The boundary conditions of the electrical monitoring systems in practice“), as well as in the article by the authors Nosko V., Bishop I., Konishi. Y., 2002: Study of the use of electrical leak/damage detection and location systems around the word.

The (ELLS) method has gradually made its way into technical standards in various countries around the world, such as ASTM D6747 in the U.S. *“ Standard Guide for Selection of Techniques for Electrical Leak Location of Leaks in Geomembranes “*.

All the described methods and technical standards are used in the work of technical personnel moving in lagoons and tanks (Figure 1).

Figure 1. Technician measuring the tightness of the geomembrane insulation

The device we have designed and constructed is fundamentally different from all the solutions described so far. First of all, it is a fully autonomous drone on which the measuring device is placed (Fig.1).

Figure 2. Innovative monitoring drone eLagoon

This device is fully programmable, it can move independently and take measurements at the same time. It then sends the measured data to the evaluation centre. At the same time, it is able to use a GPS device to pinpoint its position and thus pinpoint the location of the measured data. Since it is an autonomous floating drone, it has many advantages over technicians performing monitoring.
First of all, the measurement is fully automated, digitised and therefore much more efficient. It can measure the monitored area in a significantly shorter time. On the top of everything, the measurement performed is many times more accurate. In addition to more precise data, the accuracy of the measurement also relates to a more precise localisation of the measurement location. A unique advantage of the eLagoon is that it can take measurements even when the reservoir is filled (Fig.3) and there is no need to drain the reservoir due to technicians needing access.

Figure 3. Measurement with a floating drone in a filled lagoon

eLagoon can also perform leak-detection in reservoirs with highly toxic waste, where any movement of technicians would be severely restricted or even impossible.
Another advantage of this autonomous floating monitoring device is that it can be equipped with other measuring devices, such as sonar or GPR. This allows us not only to monitor the integrity of the insulation but also to provide the reservoir operator with a 3D accurate image of the reservoir bottom, and possibly with accurate sediment depth information.
The advantage of the autonomous floating drone is its size, which allows relatively easy transport by a regular passenger car.

CONCLUSION

The autonomous floating leak monitoring drone eLagoon used to track contaminant leaks is a highly efficient device that allows us to perform quality leak-detection measurements quickly and accurately in tanks and lagoons used by the mining industry. Unlike other technologies on the current market eLagoon can perform leak detection on a fully submerged geomembrane, without the need for

tailings pond drainage. Measured data cannot be tampered with and modified because the measuring device uses blockchain technology. The floating drone is an innovative solution that improves the processes employed by the mining industry players.

REFERENCES

ASTM D6747: Standard Guide for Selection of Techniques for Electrical Leak Location of Leaks in Geomembranes.

Nosko V., Bishop I., Konishi. Y., 2002: Study of the use of electrical leak/damage detection and location systems around the word. Geosysnthetics – 7thNice, France, 769-774

Nosko, V., Gregor, T., Ganier. F.,2000: The boundary conditions of the electrical monitoring systems in practise. Proceedings of the Second European Geosynthetics Conference Eurogeo 2. Bologna, Italy,15-18

Schultz, et al., 1984. Electrical resistivity technique to assess the integrity of geomembranes liners: Final technical report. US Environmental Protection Agency, Contract No. 68-03-03-0331, Southwest ResearchInstitute Project 14-6289.

NÜMERİK MODELLEME İLE KAYA TASARIMINDA DEFORMASYON MODÜLÜNÜN ÖNEMİ

THE IMPORTANCE OF DEFORMATION MODULUS ON DESIGN OF ROCKS WITH NUMERICAL MODELING

C.O. Aksoy [1,*], G.G. Uyar Aksoy [2], H.E. Yaman [3]

[1] Dokuz Eylül Üniversitesi, Mühendislik Fakültesi, Maden Mühendisliği Bölümü
*(*Sorumlu yazar: okay.aksoy@deu.edu.tr)*
[2] Hacettepe Üniversitesi, Mühendislik Fakültesi, Maden Mühendisliği Bölümü
[3] Dokuz Eylül Üniversitesi, Torbalı Meslek Yüksek Okulu, Maden Teknolojileri Bölümü

ÖZET

Nümerik modelleme, kaya yapılarının tasarımında yaygın olarak kullanılır. Bu araçlarda tasarımın en önemli parametrelerinden biri Deformasyon Modülüdür (E_m). E_m değerleri derinlik, yön, gerilme, kaya kütle parametreleri gibi parametrelere bağlı olarak değişebilir. Bu sebeple, sabit bir E_m değeri kullanmaktansa, derinlik, yön ve/veya gerilmelere bağlı olarak değişen bir E_m değeri kullanmak çok daha hassas sonuçlar verir. Bu sonuçlarla elde edilen güvenlik katsayıları ile tasarımı sonuçlandırmak daha doğru olacaktır.

Anahtar Kelimeler: Kaya kütlesi, bozulmamış kaya, deformasyon modülü, deformasyon karakteri, kaya yapısı

ABSTRACT

Numerical modeling methods are widely used in the design of rock structures. One of the most important parameters of the design in these tools is the Deformation Modulus (E_m). E_m varies depending on parameters such as depth, direction, stress, rock mass properties. Therefore, instead of using a fixed E_m value in designs, using E_m values that vary depending on depth, direction and/or stress will give more accurate results. It will be more correct to conclude the design with the safety factors obtained with these results.

Keywords: Rock mass, intact rock, deformation modulus, deformation characteristic, rock structure

GİRİŞ

Kaya Mühendisliğinde tasarım parametrelerinin doğru belirlenmesi, inşa edilen kaya yapısının (yeraltı ve yüzey) hem güvenli bir inşaat sürecine sahip olmasını, hem de uzun süre kullanıma uygun olmasını sağlar. İnşa edilen kaya yapılarının kaya kütle deformasyon davranışları süreksizlikler, süreksizlik özellikleri yeraltı sularının durumları ve kaya malzemesinin özellikleri gibi değişkenlere bağlıdır. Deformasyon modülü (E_m) gerilime bağlı bir değer olduğu için, deformasyonun davranışı da gerilim düzeyine bağlı olarak etkilenir (Kulhawy, 1975; Fattahi ve Moradi, 2017; Torbica ve Lapcevic, 2019). Bunun yanında, E_m en önemli tasarım parametrelerinden birisidir. Genellikle E_m nin belirlenmesi için üç farklı yöntem kullanılır. (Bieniawski, 1978; Blankenship vd.,1983; Palmström ve Singh, 2001). Bunlardan ilki, formül ve

labaratuvar deneyleri sonucunda oluşturulan bir model kullanmaktır. İkincisi yerinde yapılan deneyler ve üçüncüsü ise kaya kütle sınıflama sistemlerindeki görgül formülleri kullanmaktır.

Elastik Modül (E_i), birim gerilim ve birim gerinim arasındaki orandır, ve gerilime bağlı olarak değişir. Kulhawy (1975), yanal gerilmenin E_i üzerinde etkili olduğunu belirtmiş ve yanal gerilme nedeniyle E_i değerini değiştiren bir formül önermiştir. Verman ve ark. (1997), Kulhawy'nin (1975) önerdiği bu formülü, farklı tünellerde yaptığı ancak yanal gerilmeyi derinliğe bağladığı ölçümlerle doğrulamıştır. Fattahi ve Moradi (2017), derinlik, RQD, tek eksenli başınç dayanımı, süreksizlik yoğunluğu, süreksizliklerin durumu, yeraltı suyu durumu ve süreksizliklerin oryantasyonu için ayarlama parametrelerini kullanan bir model önermiştir. Bu parametreler kaya kütlesi sınıflandırma sistemlerinin içeriğinde bulunur ve kaya kütlesinin durumunu temsil eder. Torbica ve Lapcevic (2019), belirli bir derinlikte sınırlı bir model önermiştir. Bu derinlik, artan derinlikle birlikte kaya süreksizliklerinde meydana gelen normal gerilmeler nedeniyle E_m'nin E_i'ye çok yaklaştığı derinliktir. Zhao (2014), kaya kütlesinin dayanımı kaya malzemesine yakın olduğunda, kaya malzemesinin deformasyon özelliklerinin kaya kütlesini temsil edebileceğini belirtmiştir.

Kaya yapıları inşa edildikleri andan itibaren farklı gerilmelere maruz kalırlar. Bu gerilmeler ilk aşamada birincil gerilmelerden başlayarak farklı değerlere ulaşır ve bir değerde sabit hale gelir. Her inşaat aşamasında gerilimler bozulur ve yeni duruma göre yeni bir denge oluşturulur. Yeni denge koşulları kaya kütlesinin dayanımını aşmazsa, sistem dengede kalır ve bu yeni denge koşulları altında gerilmeler kaya kütlesini etkilemeye devam eder. Bu süre zarfında kaya kütleleri bir süre deforme olur ve sonra durur. Aksi takdirde yenilme meydana gelir. Bu süreçte kaya kütlesinin maruz kaldığı gerilmeler, kazı derinliğine, şekil ve geometrisine göre değişirken, süreksizliklere, süreksizlik özelliklerine (yoğunluk, süreklilik, pürüzlülük vb.), kaya malzemesinin cinsine ve kaya karakterizasyonuna (kayalar kaya kütlesinin en küçük birimidir) bağlı olarak kaya kütlesinin deformasyon davranışı da değişmektedir. (Lo Pesti vd., 1995; Fahimifar, 2015; C.-K. Chung vd. 2013; Aksoy vd., 2018a; Aksoy vd., 2018b; Aksoy vd., 2019; Aksoy vd., 2020).

Yerinde testler E_m'nin belirlenmesi için kullanılan bir diğer yöntemdir. 1960'larda silindirik hidrolik kuyu basınç hücreleri (CPC'ler) ve düz hidrolik kuyu basınç hücreleri (BPC'ler) geliştirildi (Panek, vd., 1964). Hustrulid (1975), membran kullanan ve kalibrasyonu basitleştiren başka bir sistem geliştirmiştir. Ljunggren ve Stephansson (1986) bu sistemi daha da geliştirmiştir. Blankenship vd. (1983), E_m ve Poisson oranının gerilmeye bağlı olduğu için çekirdek kaldırma test modelini önerdi. E_m'i belirlemek için kullanılan diğer bir test prosedürü, flatjack yöntemidir (Loureico-Pinto, 1986). Bu test, plaka taşıma testi ve radyal kriko testidir (Coulson, 1979). Bu yöntemlerin üçündede E_m'nin gerilmeye bağlı olduğu ihmal edilmiştir. Palmström ve Singh (2001), E_m'i belirlemek için 3 yerinde test yönteminden türetilen E_m değerlerini, kaya kütlesi sınıflandırma sistemlerinden türetilen ampirik formüller ile hesaplanmış olan E_m değerleriyle karşılaştırmıştır. Bu araştırmada, yerinde testler sırasında patlatma kaynaklı kaya hasarı, test yöntemleri ve test prosedürlerinden kaynaklanan belirsizlikler nedeniyle görgül formüllerin kullanılmasının daha uygun olacağı ifade edilmiştir. E_m'nin hesaplanması sırasında kullanılan bazı Görgül formüller Çizelge 1'de verilmiştir.

E_m hesaplanmasında kullanılan yöntemlerin hem avantajları hem de dezavantajları bulunur. Bunun yanında, hepsi kaya kütle özelliklerinin temsil eder. Bu araştırmada, gerilme (birçok faktöre bağlı olarak derinlikle değişebilen), kaya kütlesi özellikleri, kayanın deformasyon karakteri, zaman ve dayanım gibi parametreleri içeren bir model geliştirilmiştir.

Çizelge 1. Deformasyon Modülünü Tahmin Etmek Için Denklemler

Araştırmacılar	**Eşitlikler**	**Notlar**
Bieniawski (1978)	$E_{mass} = 2\,RMR - 100 \quad (GPa)$	RMR>50 için
Serafim ve Pereira (1983)	$E_{mass} = 10^{(RMR-10)/40} \quad (GPa)$	RMR<50 için
Nicholson ve Bieniawski (1990)	$E_{mass} = \frac{E_i}{100}\left[0.0028\,RMR^2 + 0.9\exp\left(\frac{RMR}{22.82}\right)\right]$	
Mitri vd. (1994)	$E_{mass} = E_i\left[0.5\left\{1-\cos\left(\pi\frac{RMR}{100}\right)\right\}\right]$	
Palmstrom (1996)	$E_{mass} = 5.6\,RMi^{0.375} \quad (GPa)$	1>RMi>0.1, orta derece girintili kaya kütlesi için
Palmstrom ve Sing (2001)	$E_{mass} = 7\,RMi^{0.4} \quad (GPa)$	1<RMi<30, orta derece girintili kaya kütlesi için
Hoek ve Brown (1997)	$E_{mass} = \sqrt{\frac{\sigma_{ci}}{100}}\,10^{\left(\frac{GSI-10}{40}\right)} \quad (GPa)$	σ_{ci} <100Mpa için
Read vd. (1999)	$E_{mass} = 0.1\left(\frac{RMR}{10}\right)^3 (GPa)$	
Barton (2002)	$E_{mass} = 10\,Q_c^{\frac{1}{3}} \quad Q_c = Q\,\sigma_{ci}/100$	
Kayabasi vd (2003)	$E_{mass} = 0.135\left[\frac{E_i(1+RQD/100)}{WD}\right]^{1.1811}$	
Gokceoglu vd. (2003)	$E_{mass} = 0.001\left[\frac{(E_i/\sigma_{ci})(1+RQD/100)}{WD}\right]^{1.5528}$	
Sonmez vd. (2004)	$E_{mass} = E_i\left(s^a\right)^{0.4} \quad s = \exp[(RMR-100)/9]$ $a = 0.5 + 1/6\left[\exp(-GSI/15) - \exp(-20/3)\right]$	
Sonmez vd. (2006)	$E_{mass} = E_i\,10^{[((RMR-100)(100-RMR)/4000\ \exp(-RMR/100))]}$	
Hoek ve Diederichs (2006)	$E_{mass} = E_i\left(0.02 + \frac{1-D/2}{1+e^{(60+15D-GSI)/11}}\right)$	Eğer bozulmamış kayada deformasyon ölçülmemiş ise: $E_i = MR\cdot\sigma_{ci}$

RQD : Kaya kalitesi tanımı
RMR : Kaya kütlesi değerlendirmesi
RMi : Kaya kütle indeksi
Q : Kaya kütle kalite değerlendirmesi
E_i : Bozulmamış kayanın deformasyon modülü
E_{mass} : Kaya kütlesinin deformasyon modülü
MR : Modül oranı

GSI	: Jeolojik dayanım indeksi	WD	: Aşınma derecesi
σ_{ci}	: Tek eksenli basınç dayanımı	D	: Bozulma faktörü
		s, a	: Hoek-Brown kaya kütle sabiti

DAYANIM, GERİLİM, ZAMAN VE DEFORMASYON DAVRANIŞLARININ E_m ÜZERİNE ETKİSİ

Süreksizlikler, süreksizliklerin özellikleri (pürüzlülük, bozuşma, alterasyon, mesafe, derinlik vb.), yeraltı suyu koşulları ve akışı, kaya malzemesi gibi parametreler E_m'i etkiler. Bunlar doğrudan parametreler olarak adlandırılabilirler. Öte yandan mühendislik yapılarında dikkate alınması gereken dolaylı parametreler de vardır. Dolaylı parametreler arasında yük, yük yönü, maruz kalma süresi, kazı destek sistemleri gibi parametreler sayılabilir. Şekil 1'de kaya malzemesindeki E_i 'nin gerilmeye bağlı olarak nasıl değiştiği ve buna göre E_m'nin nasıl değişebileceğine ilişkin ölçeksiz bir model verilmiştir.

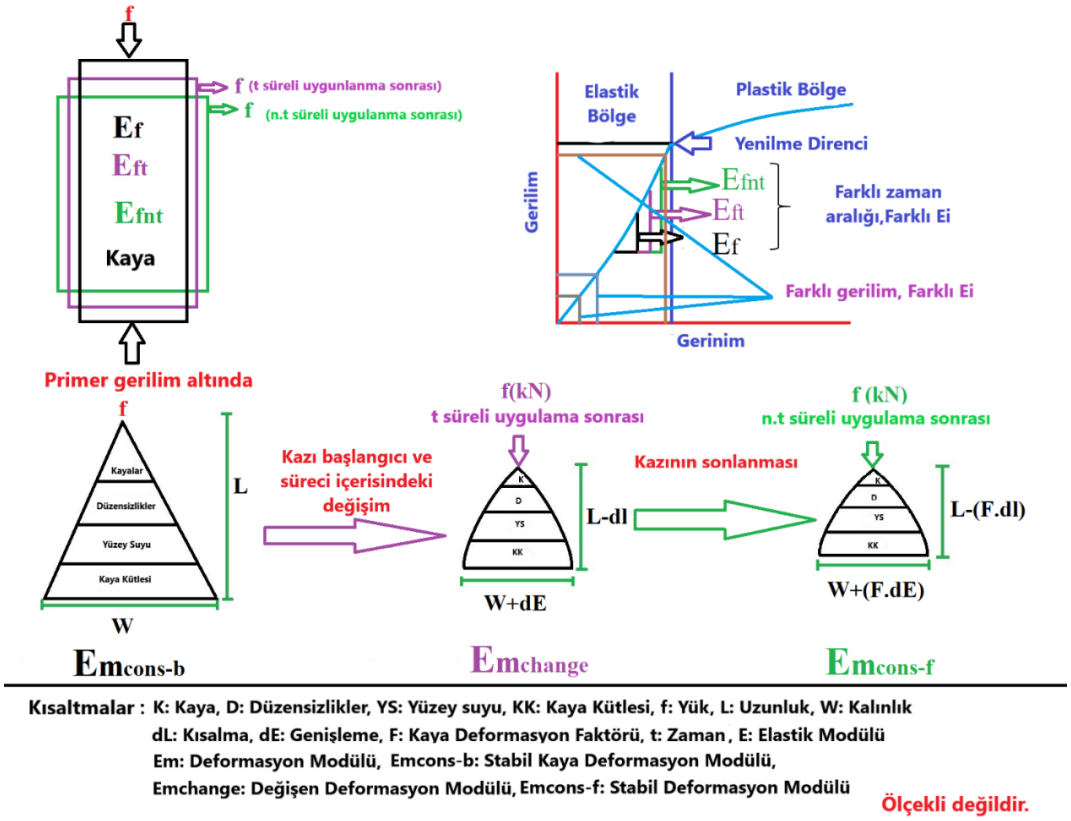

Şekil 1. Değişen kaya malzemesi, süreksizlikler ve yeraltı suyu ile deformasyon modülü modeli

Doğada birincil gerilmeler altında olan kaya kütlesi, kaya malzemesi, süreksizlikler ve süreksizlik özellikleri, yeraltı suyu gibi kendine has özelliklere sahiptir ve dengededir. Bu kararlı kaya kütlesine farklı bir yük etki ettiğinde deformasyon başlar. Bu deformasyon, kısalma-uzama ve genişleme-daralma şeklinde gelişir. Bu andan itibaren kaya kütlesinin deformasyonu kaya malzemesine, süreksizliklere, yeraltı suyu koşullarına ve özelliklerine bağlı olarak başlar, gelişir ve yeniden denge haline gelir. Bu yük ile süreksizliklerde bir miktar kapanma veya açılma olur. Yeraltı suyu da yeni konumlara ve süreksizliklere göre

hareket eder. Kayaların yük altındaki geçirgenlik değişimi de yeraltı suyunun davranışında etkili olacaktır. Karşılaşılan deformasyon miktarı maruz kalınan gerilime göre değişecektir. Ayrıca gerilme süresi doğrudan parametreleri (yukarıda bahsedilen) etkileyecek ve deformasyon miktarı değişecektir (Funte vd., 2019; Ghabezloo vd., 2008b; Barla vd., 2012; Brantut vd., 2013; Damjanac ve Fairhurst, 2010; Li ve Xia, 2000; Tsai vd., 2008; Yang vd., 2014). Şekil 1'deki kaya kütlesi zayıf kayalardan oluşuyorsa, piramidin uzunluğu daha kısa ve genişliği daha kalın olacaktır (dl ve dE daha büyüktür). Kaya kütlesi sert kayadan oluşuyorsa, piramit daha az kısalır ve daha fazla genişler (dl ve dE, yumuşak kayadakinden nispeten daha küçüktür). Bu açıdan kaya malzemesinin dayanımı ve deforme olabilirliği, kaya kütlesinin deformasyonunu doğrudan etkileyecektir. Zayıf kayalardan oluşan kaya kütlelerinde süreksizliklerin daha hızlı kapandığı (dolgu tipi ve miktarı gibi değişkenlere bağlı olarak süreksizlik aralığı değişmektedir) ve yeraltı suyunun kapalı süreksizliklerden geçiş bulamadığı bilinen bir sonuçtur. Bu durumda, yeraltı suyu kaya üzerinde bir gerilme etkisi görür. Sert kayalarda aynı ancak daha küçük etki beklenir. Elbette burada belirtmek gerekir ki kazı boyutu, yöntemi, geometrisi de E_m'de değişikliğe neden olan gerilmelerde etkilidir. (Singh ve Rajvansi, 1996; Tomanovic, 2005; Tomanovic, 2012).

Bu modele göre E_m belirlenirken, kaya malzemesinin özellikleri, süreksizlikler ve süreksizlik özellikleri, yeraltı suyu durumu, aktif yük (sadece derinlik değil hem yatay hem de düşey yükler), yükün süresi ve deformasyon miktarıda bu etki süresi içinde dikkate alınmalıdır.

YENİ MODEL YAKLAŞIMININ TEMELLERİ

Kaya kütle sınıflama sistemleri, kaya yapılarının tasarımında kullanılan en önemli ve en çok kullanılan ön tasarım araçlarıdır (Ulusay ve Sönmez; 2007). Bu sistemler, kaya kütlelerini tanımlarken süreksizlikleri, süreksizlik özelliklerini, kaya malzemesi özelliklerini ve yeraltı suyu koşullarını dikkate alır. Diğer bir deyişle kaya kütlesinin tüm özelliklerini bünyesinde barındıran ve tamamı kullanıcı dostu sistemlerdir. Bu sistemler, kaya kütlesinin özelliklerine göre puanlama yapmaktadır. Kaya kütlesi puanı, kaya yapısının üzerine inşa edileceği kaya kütlesini tanımlar. Bu bildiride önerilen yeni model için kaya kütlesi sınıflama sisteminden elde edilen puan önemlidir. Bu puan, dolaylı olarak gerilmeye bağlı E_m tahmininde kullanılacaktır.

E_m'nin kaya kütlesi sınıflama sistemlerine dayalı olarak tahmini, en pratik ve güvenli yöntemlerden biridir (Bieniawski, 1978; Clerici, 1993; Sharma vd., 1989; Singh, vd., 1996). Kaya kütlesi sınıflama sistemlerini kullanan görgül formüller E_m tahmini için oldukça faydalıdır. Bu formüllerden bazıları Çizelge 1'de verilmiştir. Bu formüllerin zaman içindeki gelişimi incelendiğinde, son 20 yılda geliştirilen formüllerde kaya malzemesinin E_i değerinin önemli bir parametre haline geldiği görülmektedir. E_i değeri, laboratuvarda yapılan deformasyon testi sonucunda elde edilen ve gerilme-deformasyon eğrisinin %50'sine tekabül eden noktadaki değerdir. Ancak, kayaların farklı gerilmelere karşı gösterdiği deformasyon farklıdır. Laboratuvarda yapılan deformasyon testinden elde edilen grafiğin %50 ve %80'inden elde edilen E_i değerleri farklıdır. E_i değeri gerilme-deformasyon eğrisinden elde edildiğinden ve gerilme miktarı değiştiğinde deformasyon miktarı da değişeceğinden E_i değeri de değişecektir. Ayrıca, E_i değerini etkileyen faktörler de vardır. Feldmann (1972) bu konuyu detaylı olarak incelemiştir. Öte yandan, gerilmeye bağlı olarak E_m'nin değiştiği kabul edildiğinden, gerilmeye bağlı olarak E_i değerinin de değişeceğini kabul etmek doğru bir yaklaşım olacaktır. Ayrıca, kazı aşamaları sonrasında duraylı hale gelen sistemin, sabit bir yük altında bekleyeceği ve kayadaki deformasyonun belirli bir süre devam edeceği bilinmektedir. Bu durumda, zamanla yük altındaki E_i değeri de değişecektir. Yukarıda "Deformabilite, uygulanan yük ile gerinim arasındaki ilişkinin karakterizasyonudur" denilmişti (Palmström ve Singh, 2001). Bu durumda uygulanan yük karşısında yükün süresi, gerilme ve kaya dayanımının karakterizasyonu E_m'i sabit bir değer olmaktan çıkararak, değişen yüke,

kaya dayanımına, yük etki süresi ve maruz kalan deformasyona göre farklı değerler almasını sağlayacaktır. Bu durumda, yük altında kalan E_i değeride zamanla değişecektir.

Labaratuvar Araştırmaları

E_m 'i sabit bir değer olmaktan çıkarmak ve zamana, dayanıma, yüke ve deformasyona bağlı bir fonksiyon haline getirmek için laboratuvar ortamında uzun ve yoğun çalışmalar yapılmıştır. Bu çalışmada, farklı çalışma alanlarından farklı projelerden (maden, tünel, demiryolu inşaatı, baraj inşaatı vb.) kaya örnekleri alınmış alınmıştır. Bu kayaçlara ilişkin jeolojik-jeoteknik bilgiler ve kayaların alındığı projeler Çizelge 2'de verilmiştir.

Çizelge 2. Farklı projelerden toplanan kaya örnekleri

Proje	Kaya	E_i (MPa)	σ_{ci} (MPa)	RMR	GSI	Q
Ankara-Afyon Yüksek Hızlı Demiryolu Tünel Yapım Çalışması-1	Konglomera	1180	9.99	33	30	0.46
Ankara-Afyon Yüksek Hızlı Demiryolu Tünel Yapım Çalışması -2	Konglomera	2050	13.07	42	40	0.80
Soma-Eynez Yeraltı Kömür Madeni	Kireçli Toprak (Marl)	1910	24.29	54	50	3.04
Tavşanlı-Ömerler Yeraltı Kömür Madeni	Kiltaşı	3210	28.40	49	45	2.18
Soma-Işıklar Yeraltı Kömür Madeni	Kiltaşı	1560	29.42	59	55	5.29
Soma-Işıklar Yeraltı Kömür Madeni	Kireçtaşı	8360	12.39	48	40	1.56
Soma-Işıklar Yeraltı Kömür Madeni	Konglomera	4900	20.74	56	50	3.79
Soma-Işıklar Yeraltı Kömür Madeni	Kireçli Toprak (Marl)	4420	52.07	63	60	8.26
Ordu-Mesudiye Demiryolu Tünel İnşaatı	Kireçli Toprak	1740	62.07	71	65	22.45
Soma-Kınık Yeraltı Kömür Madeni Galeri Kazısı	Şist	2090	20.16	53	45	2.72
Tokat-Topçam Demiryolu Tünel İnşaatı	Bazaltik Tüf	4440	52.26	68	65	14.39
Tokat-Topçam Demiryolu Tünel İnşaatı	Kumtaşı	12020	80.63	80	75	68.19

Bu kayalar üzerinde üç aşamalı deneyler planlanmıştır. İlk aşamada, kayaçların tek eksenli basınç dayanımı değerleri, ikinci aşamada deformasyon deneyleri yapılarak E_i değerleri ve üçüncü aşamada, farklı sabit yükler altında E_i değerlerinin zamana bağlı değişimi belirlenmiştir. Bu deneyler servo-kontrollü bir pres ile gerçekleştirilmiştir (Şekil 2). Bu deneyler sırasında kayaçlara dayanımlarının %50, %60, %70 ve %80 kadar yükler uygulanmıştır. E_i değerlerinin zamana ve uygulanan yüke göre değişimi Şekil 3'de verilmektedir. Bir numunedeki deformasyon miktarı sabitlendikten iki gün sonra testler sonlandırılmıştır. Testler ortalama 15 günlük bir süre almıştır. Şekil 3'te görüldüğü üzere, tüm kayalar için E_i değerleri zamanla azalmıştır. Ayrıca, her bir kaya için elde edilen 4 adet E_i eğrisi incelendiğinde, bunlardan üçü genel olarak birbirine yakın eğriler

oluşturmaktadır. Bir E_i eğrisi ise diğerlerinden oldukça farklı bir eğri oluşturur. Bu, kayanın dayanımı, kohezyonu ve gözenekliliği ile ilgilidir. Dolayısıyla bu deneylerde kayaların mekanik ve fiziksel özelliklerinin E_i değerine etkisi olduğu doğrulanmıştır.

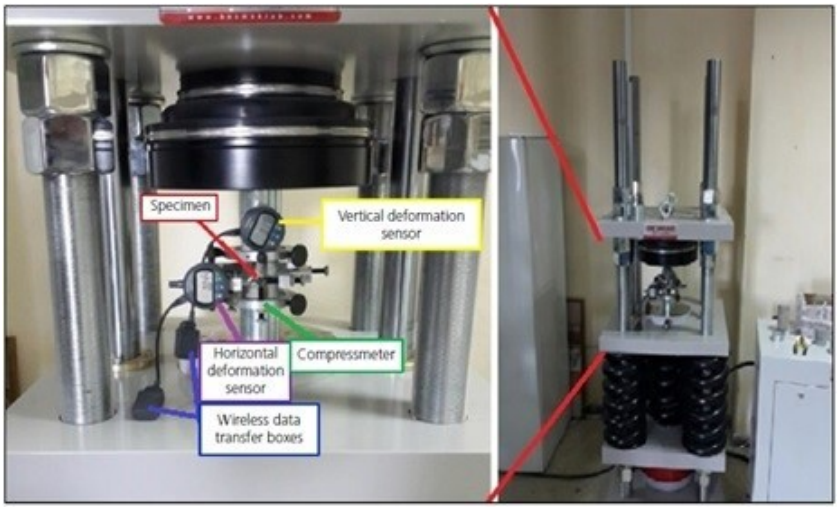

Şekil 2. Laboratuvar araştırmalarında kullanılan Servo Kontrollü pres

Laboratuvarda yapılan çalışmalarda ölçülen E_i değerlerinin zamana ve yüke bağlı maksimum, minimum ve ortalama değerleri Çizelge 3'de verilmiştir. Çizelgeden dea görüleceği üzere kayanın maruz kaldığı yük gerilmesi miktarı arttıkça E_i değerlerinde artış olmaktadır. Ankara-Afyon Yüksek Hızlı Demiryolu Tünel İnşaatı Konglomera-1 kayasında E_i değerlerinde %11,03'lük artış olmuştur. Öte yandan Soma-Işıklar Yeraltı Kömür Madeni Konglomera kayasında %104,91 artış olduğu belirlenmiştir. Farklı E_i değerleri, kaya kütlesi sınıflandırma sistemlerinden elde edilen ampirik formüllerden hesaplanan E_m değerlerini de değiştirecektir. Sabit E_m değerleri ve değişken E_m değerleri, kaya mühendisleri tarafından yaygın olarak kullanılan ve kaya kütlesi sınıflandırma sistemleri oranı (RMR, GSI ve Q ile) ve E_i değerlerini içeren 3 ampirik formül kullanılarak hesaplanmıştır. Hesaplamalar sonucunda elde edilen E_m değerleri toplu olarak Çizelge 4'de verilmiştir.

NUMERİK MODELLEME İLE E_M DEĞİŞİMİNİN İNCELENMESİ

Birçok araştırmacı, Em değerinin strese bağlı olduğu konusunda hemfikirdir. E_m ayrıca, E_i ve kaya kütlesi özelliklerinin çeşitliliği nedeniyle zamana ve dayanıma bağlı olarak değişir. Çalışmada ortaya çıkan bilgiler, E_m değerinin farklı stresler altında ve zamanla değiştiğini göstermiştir. Bu parametre değeri, kaya kütlesi özelliklerine, gerilmeye, geometriye, derinliğe vb. özelliklere bağlı olarak belirli bir süre sonra sabit hale gelir. Bu bilgiler kaya mühendisliği tasarımlarına önemli katkı sağlar. Nümerik modelleme analizi için 1000m x 1000m x 500 m (uzunluk, genişlik ve derinlik) boyutlarında bir katı seçilmiştir. Bu modelde toplam gerilmeler incelenmiş ve toplam gerilme bölgeleri oluşturulmuştur (Şekil 4a). Konvansiyonel olarak yapılan analizlerde E_m sabit tutulmuş ve tek bir kaya birimi tanımlanmıştır. (Şekil 4b). Daha önce kullanılan formüllerden elde edilen sabit E_m değerleri ile Nümerik modelleme analizleri yapılmıştır. E_m değişkeni için yapılan analizlerde oluşan gerilme değerlerine bağlı olarak her 125 m derinlik için E_m değerleri atanmıştır. Bu

E_m değerleri, araştırma içeriği olarak geliştirilen zaman-gerilme-dayanım-deformasyon bağımlı fonksiyonda görgül formüllerdeki değişken Ei değerleri kullanılarak hesaplanmıştır. Nümerik modellerde, ilk olarak yerçekimi yükü hesaplanarak başlangıç koşulları oluşturulmuştur. Açık ocak analizinde, her 10 m'lik adımda bir kazı yapılacak fazlar tanımlanmıştır. Tünel kazısında ise her 1 m'de bir kazı ve destekleme aşamaları tanımlanmıştır. E_m değerleri dışındaki tüm veriler sabit tutuldu (Şekil 4c). Eğimli kaya yapısı (derin açık ocak madeni) ve tünelde yapılan analizler sonucunda elde edilen toplam deformasyonlar, yatay deformasyonlar, dikey deformasyonlar ve güvenlik faktörü incelenmiştir. Derin bir açık işletmeyi temsil eden nümerik modelleme analizine göre, 5 m genişliğinde, 10 m yüksekliğinde ve 60 derece eğim açısında basamaklar kullanılmış ve daha sonra modele entegre edilerek 30 basamak planlanmıştır (Şekil 4d). Tünel modeli de Şekil 4'de verilmiştir. Tüm analizlerde aynı başlangıç ve sınır koşulları kullanılmıştır. Belirtilen derinlikler için ortamdaki birincil gerilmeler incelendiğinde Ankara-Afyon Yüksek Hızlı Tren Tüneli İnşaatı Konglomera-2 numunesi alınmıştır.

Kaya kütlelerinde kullanılan sabit E_m parametresi, görgül formüllerin bir sonucu olarak elde edilir. Tablo 4'te görgül formüllerden geleneksel yöntemle elde edilen E_m değerleri verilmiştir. Aynı tabloda Ankara-Afyon Yüksek Hızlı Demiryolu Tünel İnşaatı Konglomera-2 için farklı yükler altında hesaplanan E_m değerleri de verilmiştir. Bu veriler kullanılarak regresyon eğrileri çizilmiş ve bu eğrilerin formülleri belirlenmiştir (Şekil 5). Bu formüllerden hareketle nümerik modellerde kullanılan değişken E_m değerleri hesaplanmıştır. Tablo 5'te modelde kullanılan değişen E_m değerleri gösterilmiştir.

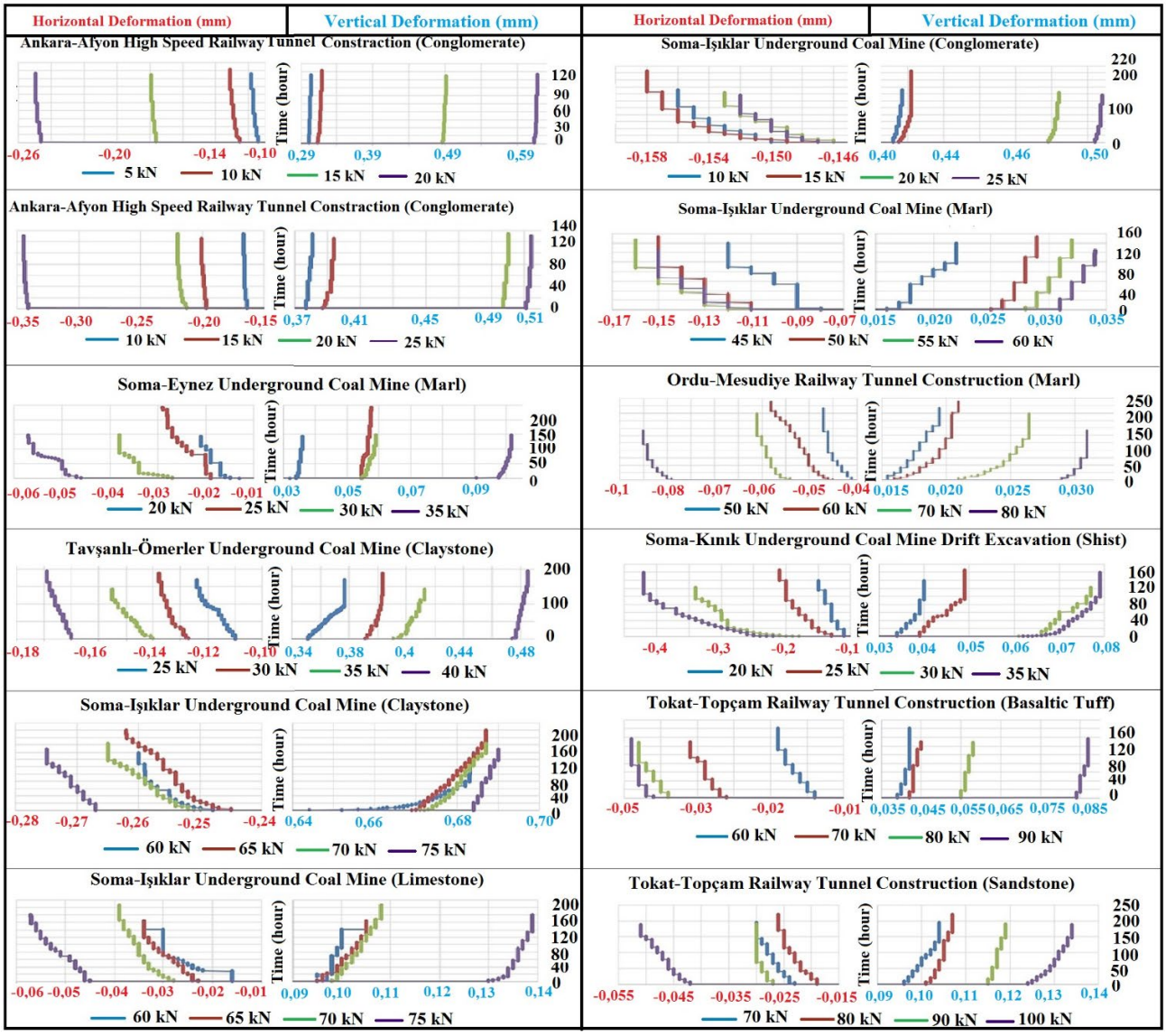

Şekil 3. E_i değerlerinin zamana bağlı ve yüke bağlı değişimi

Çizelge 3. Zaman-Yüke Bağlı Testlerden Ei'nin Varyasyonu

Zamana Bağlı Testlerden Ei'nin Varyasyonu									
Ei'nin Maksimum, Minimum ve Ortalama Değeri (MPa)	**Numune**	**Ankara-Afyon Yüksek Hızlı Demiryolu Tüneli İnşaatı Konglomera-1**				**Ankara-Afyon Yüksek Hızlı Demiryolu Tüneli İnşaatı Konglomera -2**			
	Yük(kN)	5	10	15	20	10	15	20	25
	Max.	1570	1580	1620	1710	1400	2030	2100	2560
	Ort.	1550	1570	1610	1700	1390	2000	2090	2550
	Min.	1540	1560	1590	1690	1380	1990	2080	2540
	Numune	**Soma-Eynez Yeraltı Kömür Madeni Marl**				**Tavşanlı-Ömerler Yeraltı Kömür Madeni Kiltaşı**			
	Yük (kN)	20	25	30	35	25	30	35	40
	Max.	1610	1590	1660	1800	3720	4010	4200	4240
	Ort.	1530	1550	1580	1690	3570	3960	4130	4190
	Min.	1450	1500	1490	1630	3480	3900	4040	4160
	Numune	**Soma-Işıklar Yeraltı Kömür Madeni Marl**				**Soma-Işıklar Yeraltı Kömür Madeni Konglomera**			
	Yük (kN)	50	55	60		10	15	20	25
	Max.	1050	1030	1020	-	1280	1900	2120	2500
	Ort.	960	960	970	-	1250	1890	2100	2480
	Min.	900	900	920	-	1220	1880	2080	2460
	Numune	**Soma-Işıklar Yeraltı Kömür Madeni Kiltaşı**				**Soma-Işıklar Yeraltı Kömür Madeni Kireçtaşı**			
	Yük (kN)	35	40	45	50	60	65	70	75
	Max.	2840	3140	3500	3390	3600	3600	3760	3920
	Ort.	2740	3100	3460	3180	3380	3380	3580	3800
	Min.	2680	3060	3420	2980	3240	3240	3400	3680
	Numune	**Ordu-Mesudiye Demiryolu Tünel İnşaatı Marl**				**Soma-Kınık Yeraltı Kömür Madeni Galeri Kazısı Şist**			
	Yük (kN)	50	60	70	80	20	25	30	35
	Max.	3120	3330	3540	3780	1800	1960	2030	2330
	Ort.	2990	3170	3360	3720	1670	1760	1820	2080
	Min.	2850	3010	3180	3650	1530	1550	1600	1830
	Numune	**Tokat-Topçam Demiryolu Tünel İnşaatı Bazaltik Tüf**				**Tokat-Topçam Demiryolu Tünel İnşaatı Kumtaşı**			
	Yük (kN)	70	80	90	100	60	70	80	90
	Max.	4780	5200	5130	5280	8100	8800	9200	10900
	Ort.	4600	5100	5050	5090	7800	8500	8900	10700
	Min.	4410	4900	4960	4890	7500	8200	8700	10500

Çizelge 4. Sabit Ei ile yaygın olarak kullanılan 3 formülden hesaplanan ve aynı formülden değişen E_i ile hesaplanan E_m değerleri

		*Hoek ve Diederichs (2006)				**Nicholson ve Bieniawski (1990)				***Ramamurthy (2004)			
Numune		**Ankara-Afyon Yüksek Hızlı Demiryolu Tüneli İnşaatı Konglomera-1**											
Formülden bulunan static Em değeri (MPa)		54				81				450			
Yük (kN)		5	10	15	20	5	10	15	20	5	10	15	20
E_m (MPa)	Max	72	73	74	79	108	109	111	117	599	603	618	652
	Ort.	71	72	74	78	107	108	111	117	591	599	614	649
	Min	71	72	73	78	106	107	109	116	588	595	607	645
Numune		**Ankara-Afyon Yüksek Hızlı Demiryolu Tüneli İnşaatı Konglomera -2**											
Formülden bulunan static Em değeri (MPa)		169				217				833			
Yük (kN)		10	15	20	25	10	15	20	25	10	15	20	25
E_m (MPa)	Max	116	168	174	212	149	215	223	272	569	825	853	1040
	Ort.	115	166	173	211	147	212	222	271	565	813	849	1036
	Min	114	165	172	210	146	211	221	269	561	809	845	1032
Numune		**Soma-Eynez Yeraltı Kömür Madeni Marl**											
Formülden bulunan static Em değeri (MPa)		318				339				903			
Yük (kN)		20	25	30	35	20	25	30	35	20	25	30	35
E_m (MPa)	Max	268	265	276	300	286	282	295	320	762	752	786	852
	Ort.	255	258	263	281	272	275	281	300	724	733	748	800
	Min	241	250	248	271	257	266	265	289	686	710	705	771

Numune		**Tavşanlı-Ömerler Yeraltı Kömür Madeni Kiltaşı**											
Formülden bulunan static Em değeri (MPa)		373				463				1462			
Yük (kN)		25	30	35	40	25	30	35	40	25	30	35	40
E_m (MPa)	Max	433	467	489	494	537	579	606	612	1695	1827	1913	1932
	Ort.	416	461	481	488	515	571	596	605	1626	1804	1882	1909
	Min	405	454	471	485	502	563	583	600	1585	1777	1841	1895

	*Hoek ve Diederichs (2006)				**Nicholson ve Bieniawski (1990)				***Ramamurthy (2004)				
Numune	**Soma-Işıklar Yeraltı Kömür Madeni Marl**												
Formülden bulunan static Em değeri (MPa)	1489				1120				2343				
Yük (kN)	50	55	60		50	55	60		50	55	60		
E_m (MPa) Max	354	347	344		266	261	259		557	546	541		
Ort.	324	324	327		243	243	246		509	509	514		
Min	303	303	310		228	228	233		477	477	488		
Numune	**Soma-Işıklar Yeraltı Kömür Madeni Konglomera**												
Formülden bulunan static Em değeri (MPa)	816				943				2377				
Yük (kN)	10	15	20	25	10	15	20	25	10	15	20	25	
Max	213	316	353	416	246	366	408	481	621	922	1029	1213	
Ort.	208	315	350	413	241	364	404	477	607	917	1019	1203	

E_m (MPa)	Min	203	313	346	410	235	362	400	474	592	912	1009	1194
Numune		**Soma-Işıklar Yeraltı Kömür Madeni Kiltaşı**											
Formülden bulunan static Em değeri (MPa)		371				338				786			
Yük (kN)		35	40	45	50	35	40	45	50	35	40	45	50
E_m (MPa)	Max	677	748	834	808	616	681	759	735	1431	1583	1764	1709
	Ort.	653	739	825	758	594	672	750	690	1381	1563	1744	1603
	Min	639	729	815	710	581	664	742	646	1351	1542	1724	1502
Numune		**Soma-Işıklar Yeraltı Kömür Madeni Kireçtaşı**											
Formülden bulunan static Em değeri (MPa)		691				1155				3666			
Yük (kN)		60	65	70	75	60	65	70	75	60	65	70	75
E_m (MPa)	Max	298	298	311	324	498	498	520	542	1579	1579	1649	1719
	Ort.	280	280	296	314	467	467	495	525	1482	1482	1570	1666
	Min	268	268	281	305	448	448	470	509	1421	1421	1491	1614

		*Hoek and Diederichs (2006)				**Nicholson and Bieniawski (1990)				***Ramamurthy (2004)			
Numune		**Ordu-Mesudiye Demiryolu Tünel İnşaatı Marl**											
Formülden bulunan static Em değeri (MPa)		808				597				1034			
Yük (kN)		50	60	70	80	50	60	70	80	50	60	70	80
E_m (MPa)	Max	1449	1547	1644	1756	1071	1143	1215	1297	1854	1979	2104	2247
	Ort.	1389	1472	1561	1728	1026	1088	1153	1277	1777	1884	1997	2211
	Min	1324	1398	1477	1695	978	1033	1091	1253	1694	1789	1890	2169
Numune		**Soma-Kınık Yeraltı Kömür Madeni Galeri Kazısı Şist**											
Formülden bulunan static Em değeri (MPa)		243				356				976			
Yük (kN)		20	25	30	35	20	25	30	35	20	25	30	35
E_m (MPa)	Max	210	228	237	271	307	334	346	397	841	916	948	1089
	Ort.	195	205	212	242	285	300	310	355	780	822	850	972
	Min	178	181	186	213	261	264	273	312	715	724	748	855
Numune		**Tokat-Topçam Demiryolu Tünel İnşaatı Bazaltik Tüf**											
Formülden bulunan static Em değeri (MPa)		2062				1361				2508			
Yük (kN)		70	80	90	100	70	80	90	100	70	80	90	100
E_m (MPa)	Max	2220	2415	2383	2452	1466	1594	1573	1619	2700	2938	2898	2983
	Ort.	2137	2369	2346	2364	1411	1564	1549	1561	2599	2881	2853	2876
	Min	2048	2276	2304	2271	1352	1503	1521	1499	2491	2768	2802	2763
Numune		**Tokat-Topçam Demiryolu Tünel İnşaatı Kumtaşı**											

Formülden bulunan static Em değeri (MPa)		9407				5756				8108			
Yük (kN)		60	70	80	90	60	70	80	90	60	70	80	90
E_m (MPa)	Max	6339	6887	7200	8531	3879	4215	4406	5220	5464	5936	6206	7353
	Ort.	6105	6652	6965	8374	3736	4071	4263	5125	5262	5734	6004	7218
	Min	5870	6418	6809	8218	3592	3927	4167	5029	5059	5532	5869	7083

***Hoek ve Diederichs (2006):** $E_{mass} = E_i\ (0.02 + \frac{1+D/2}{1+e^{(60+15D-GSI)/11}})$

****Nicholson ve Bieniawski (1990):** $E_{mass} = \frac{E_i}{100}(0.0028RMR^2 + 0{,}9\exp(\frac{RMR}{22{,}82})$

*****Ramamurthy (2004):** $E_{mass} = E_i e^{-0.0035\ [250\ (1-0.3\log Q)]}$

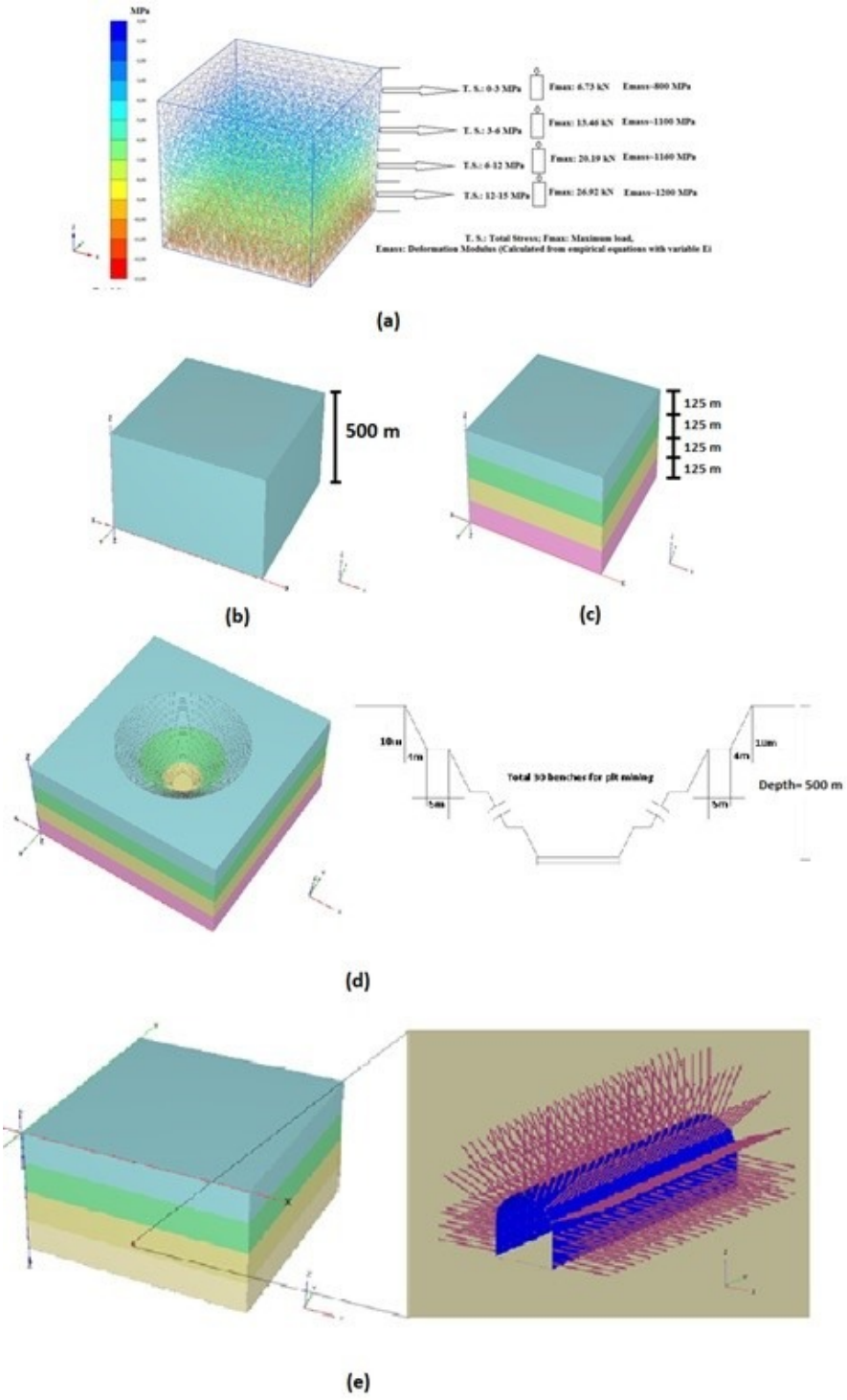

Şekil 4. Nümerik Modelleme Analizinin Detayları

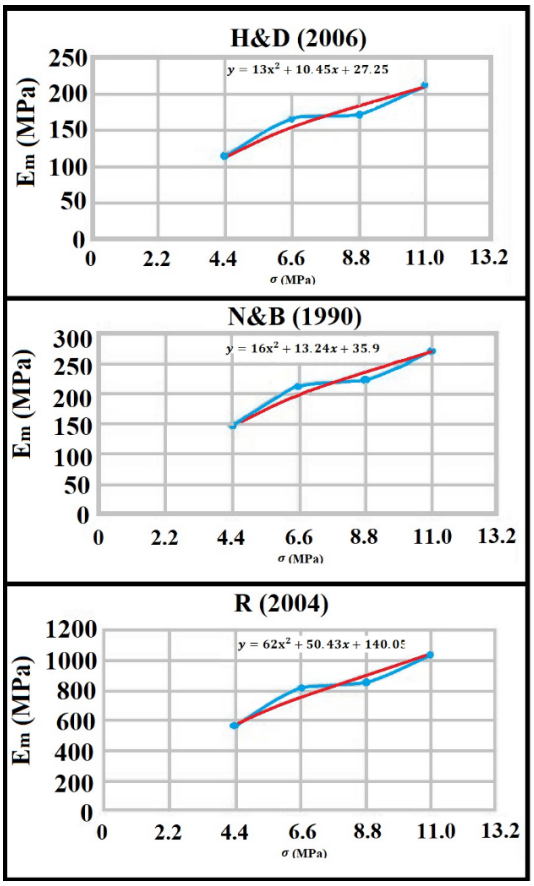

Şekil 5. Ankara-Afyon Yüksek Hızlı Demiryolu Tünel İnşaatı Konglomera-2'den Elde Edilen Regresyon Eğrileri ve Formüller

Çizelge 5. Modelde Kullanılan Değişken Em Değerleri

Hoek ve Diederichs (2006)		Nicholson ve Bieniawski (1990)		Ramamurthy (2004)	
σ (MPa)	E_m (MPa)	σ (MPa)	E_m (MPa)	σ (MPa)	E_m (MPa)
2.94	91.69042	2.94	117.1583	2.94	451.9422
5.88	144.3547	5.88	184.5229	5.88	707.7771
8.82	185.2428	8.82	237.3938	8.82	908.3547
11.76	214.3548	11.76	275.771	11.76	1053.675

Model normal yüklenme koşulları altında yüklenmiştir. Bu koşullar altında, birincil gerilmelerin değişimi incelenmiştir. Şekil 4a incelendiğinde birincil gerilmelerin 15 MPa seviyelerine kadar çıktığı görülmektedir. Yeni model için 125 metre derinlikte toplam gerilme bölgeleri oluşturulmuştur. Bu bölgelerde birim kayaç malzemesinin maruz kalacağı gerilmeler belirlenmiştir. Bu gerilmelere göre laboratuvar deneylerinde kullanılan Ankara-Afyon Hızlı Tren Tünel İnşaatı Konglomera-2'nin iyi bir örnek

olduğu düşünülmektedir. Her gerilme seviyesi için model, bu örnekten elde edilen E_m değerleri ile bölgelendirilmiştir. Daha sonra yeni model ile açık ocak için çözümler yapılmıştır. Aynı model çözümleri, halihazırda kullanımda olan görgül formüller kullanılarak hesaplanan sabit E_m değeri ile çözülmüştür. (Hoek ve Diederichs, 2006; Nicholson ve Bieniawski, 1990; Ramamurthy, 2004). Hoek ve Diederichs'a (2006) bağlı sabit E_m değerleri ile gerçekleştirilen nümerik modelleme analizinde model 12. basamak kazısında yenilirken, diğer iki görgül formül ile yapılan analizlerde modelin 17. basamak kazısında yenildiği görünmektedir. Aynı 3 görgül formül kullanılarak hesaplanan ve bu çalışmanın temelini oluşturan değişen E_m değerleri içeren tüm modellerde 18. basamak kazısında modeller başarısız olmuştur. Farkı belirtmek için, güvenlik faktörü belirleme prosedürü, tüm modellerde yenilme aşamasından önceki aşama olarak tanımlanmıştır. Güvenlik faktörünün hesaplanmasında c-ϕ indirgeme yöntemi kullanılmıştır. Ayrıca toplam deformasyon, dikey deformasyonlar ve yatay deformasyonlar da incelenmiştir. Şekil 6a'da sabit E_m analizlerinin sonuçları gösterilirken, Şekil 6b'de değişen E_m analizlerinin sonuçları verilmiştir.

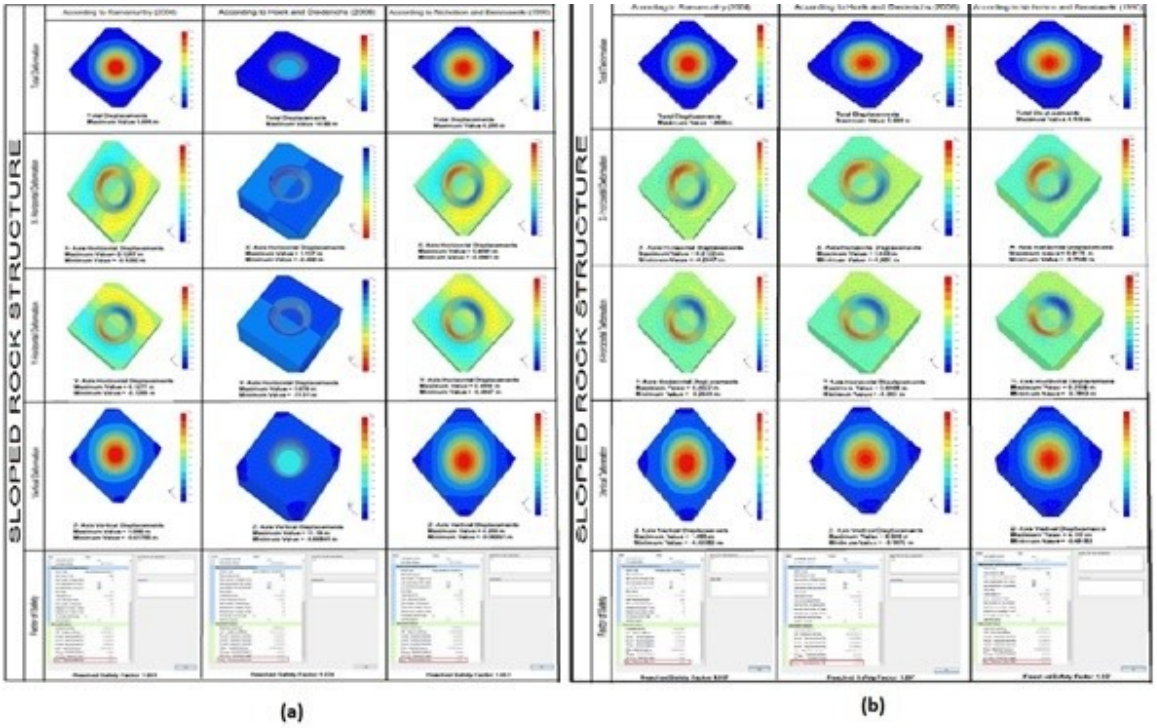

Şekil 6. Eğimli Kaya Kütlesine İlişkin Sabit Em ve Değişen Em Değerleri İçin Yapılan Nümerik Modelleme Çalışmalarının Sonuçları; (a) Sabit Em, (b) Değişen Em

Bir derin açık ocak madeni için sabit E_m değerleri ve değişen E_m değerleri için yapılan analizlerin sonuçları sırasıyla Çizelge 6 ve 7'de verilmiştir.

Çizelge 6. Derin Açık Ocak Madeni için Sabit Em ile Yapılan Nümerik Analiz Sonuçları

Araştırmacı	Yenilme (Derinlik-m)	E_m (MPa)	Toplam Def. (m)	Yatay X-Def. (m)	Yatay Y-Def. (m)	Dikey Z-Def. (m)	Güvenlik Faktörü
H&D	120	169	14.9	6.5	11.9	11.2	1.034
N&B	170	217	4.2	0.5	0.5	4.2	1.051
R	170	833	1.1	0.2	0.2	1.1	1.051

Çizelge 7. Derin Açık Ocak Madeni İçin Değişken Em İle Yapılan Nümerik Analiz Sonuçları

Araştırmacı	Yenilme (Derinlik-m)	E_m (MPa)				Top Def (m)	X-Eksen Yatay. Def. (m)	Y-Eksen Yatay. Def (m)	Z-Eksen Dikey. Def (m)	Güvenlik Faktörü
		T.S. 0-3	T.S. 3-6	T.S. 6-12	T.S. 12-15					
H&D	180	91.9	144.3	185.2	214.4	5.4	1.1	1.1	5.4	1.037
N&B	180	117.1	184.5	237.4	275.8	4.2	0.8	0.8	4.2	1.037
R	180	451.9	707.7	908.3	1053.7	1.1	0.2	0.2	1.1	1.037

TARTIŞMA VE SONUÇ

Hem E_i hem de E_m değerleri gerilmeye bağlı değerlerdir. Bu araştırmada, kaya kütleleri içerisinde daha ekonomik ve güvenli yapıların sağlanması için çalışmalar yeni bir model üzerinde yoğunlaşmıştır. Çizelge 2'de bu çalışmada kullanılan kaya malzemelerine ilişkin E_i değerleri verilmiştir. Şekil 3'de, aynı kaya malzemesinin çeşitli yükleme koşulları altında E_i değerlerinin gösterilmesi için grafikler verilmiştir. Şekil 3'de çeşitli gerilme koşulları altında E_i değerlerinde önemli değişiklikler görülmektedir. E_i değerinin E_m hesaplarında kullanıldığı düşünüldüğünde, bu farkın tasarımlara da yansıtılması gerekmektedir. Çizelge 3'de, uzun bir süre boyunca çeşitli yükleme koşulları altında E_i test sonuçları görülmektedir. Bu sonuçlara göre kaya yenilme yükünün %50'sine maruz kaldığında E_i değeri 1540 MPa iken, aynı kaya, yenilme yükünün %80'ine maruz kaldığında E_i değeri 1710 MPa olabilmektedir. Bu durumda Ankara-Afyon Hızlı Tren Tünel İnşaatı Konglomera-1 kayası için aynı kayanın farklı yükler altındaki E_i değerleri arasındaki fark %11,03 kadar iken Soma-Işıklar Yeraltı Kömür Madeni Konglomera kayasında bu değişim %104.91 olarak belirlenmiştir (Çizelge 3).

E_m hesaplamasında 3 farklı görgül formül esas alındığında, bu formülün farklı yükler altında farklı E_m sonuçları vereceği ortaya çıkmaktadır.

Çizelge 4'de, farklı Ei değerleri kullanılarak elde edilen Em değerleri ile laboratuvarda yapılan klasik deformasyon testi sonucunda elde edilen E_i değerleri kullanılarak elde edilen Em değerleri karşılaştırılmıştır.

Yapılan bu karşılaştırmaya göre farklı Ei (gerilmeye bağlı) değerleri kullanıldığında çok farklı Em değerleri ortaya çıkmaktadır. Örneğin, oldukça sert olan Tokat-Topçam Demiryolu Tüneli İnşaatı Kumtaşı örneğinin E_i değeri laboratuvarda 12020 MPa olarak bulunmuştur. Bu kaya malzemesi sırasıyla 60, 70, 80 ve 90 kN'luk yüklere maruz kaldığında maksimum E_i değerleri sırasıyla 8100, 8800, 9200 ve 10900 MPa olmaktadır. Her iki yöntemin sonuçları incelendiğinde, geleneksel yöntemden elde edilen sonuçların diğerine göre %9,32 daha düşük olduğu görülmüştür. Öte yandan, geleneksel yöntemle elde edilen E_i değerlerinden hareketle, Hoek ve Diederichs (2006), Nicholson ve Bieniawski (1990), Ramamurthy (2004) tarafından önerilen görgül formüllerle hesaplanan E_m değerleri sırasıyla 9407 ,5756 ve 8108 Mpa olmaktadır. Yeni modele göre kaya kütlesinin maruz kalacağı gerilme miktarına bağlı olarak hesaplanan E_m değeri, Hoek ve Diederichs (2006) tarafından önerilen formüle göre 5870-8531 MPa arasında değişmektedir; Nicholson ve Bieniawski (1990) tarafından önerilen görgül formüle göre 3592-5220 MPa ve Ramamurthy (2004) tarafından önerilen formüle göre 5059-7353 MPa arasındadır.

Bu çalışma kapsamında; Ankara-Afyon Yüksek Hızlı Demiryolu Tünel İnşaatı Konglomera-2'ye ait kaya malzemesinin Ei değeri 2050 MPa iken, yeni modele göre bu değer 1380 ile 2560 MPa arasında değişmektedir. Bu değerlerle hesaplanan E_m değerleri sırasıyla 114-212 MPa, 146-272 MPa ve 561-1040 MPa değerleri arasında iken sırasıyla 169, 217 ve 833 MPa değerlerine dönüşmüştür. Bu araştırma sonucunda Hoek ve Diederichs (2006) tarafından geliştirilen ampirik formül kullanılarak iki farklı nümerik modelleme yöntemi izlenmiştir. Yeni modele göre hesaplanan E_m değeri (değişken derinlik, değişken Em değeri) ile gerçekleştirilen nümerik modelleme analiz sonuçları ile elde edilen E_m değeri ile aynı formül kullanılarak yapılan klasik nümerik modelleme analiz sonuçları arasında anlamlı bir farklılık olduğu gözlemlenmiştir. Yeni modele göre üretilen E_m değeri ile yapılan analiz sonucunda güvenlik katsayısı 1,124 olarak bulunurken, diğer analizler sonucunda bulunan güvenlik katsayısı daha yüksek çıkmaktadır.

Bunun temel nedeni, yeni modelin artan derinliğe bağlı olarak kaya kütlesinin maruz kalacağı gerilme miktarını hesaba katmasıdır. Derinlik arttıkça kaya kütlesine uygulanan yük miktarı artacak ve bu da E_i'nin artmasına ve dolayısıyla E_m değerinin de artmasına neden olacaktır. Bu durumda derinlik arttıkça güvenlik faktörleri yeni model yönünde olumlu yönde değişecektir. Çünkü yeni modelde daha yüksek gerilme seviyelerinde daha yüksek E_i değerleri elde edilmekte, bu da daha yüksek E_m değerleri anlamına gelmektedir.

SONUÇLAR

Bilim adamları uzun zamandır E_i ve E_m değerlerinin gerilmeye bağlı olduğunu vurguladılar. Bu noktadan hareketle, kaya yapılarının tasarımına katkı sağlamak amacıyla yeni bir model üzerinde çalışılmıştır. Bu model, Em tahminine yeni bir bakış açısı getirmeyi amaçlamaktadır. Kaya yapıları, doğal olarak çeşitli yüklenme koşullarında ve çeşitli derinliklerde inşa edilirler. Yapım aşamasında gerilmeler değişir ancak bir süre sonra duraylı hale gelir ve denge durumuna ulaşır. Her kazı operasyonunda aynı kural geçerlidir, ancak sonunda gerilme koşulları dengelenir. Kaya kütlesinin en küçük birimi olan kaya malzemesi, değişen derinliğe bağlı olarak çeşitli gerilmelere maruz kalır ve bu nedenle farklı Ei değerleri gösterir. Ei, laboratuvar ortamında elde edilen bir değerdir. Bu değer görgül formüllerde kullanılarak Em değeri hesaplanır. Bu, tasarımcının işini kolaylaştıran ve çok yaygın bir yöntemdir. Kaya malzemesinin çeşitli derinliklerde çeşitli gerilme koşullarına maruz kalması durumunda, bu malzemenin farklı Em değerleri içermesi de kaçınılmazdır. Bu durum, kaya yapılarının tasarım aşamasında mutlaka dikkate alınmalıdır. Bu

çalışmada, kaya kütlelerinin gerilmeye bağlı davranışlarını yapıların tasarımına yansıtmak için yeni bir model geliştirilmiştir. Bu çalışmanın sonuçları dikkatlice tartışıldığında, geleneksel yöntemde olduğu gibi sabit bir E_i değeri kullanmak yerine derinliğe dolayısıyla gerilmeye bağlı farklı E_i değerlerinin kullanılmasının, kaya mühendisliği yapılarının daha ekonomik ve güvenli bir şekilde tasarlanmasına önemli katkılar sağlayacağı açıkça görülmektedir.

TEŞEKKÜR

Bu araştırma TÜBİTAK tarafından desteklenmiştir. Proje numarası 114M566'dır. Yazarlar TÜBİTAK'a (TÜRKİYE BİLİMSEL VE TEKNOLOJİK ARAŞTIRMALAR KURUMU) finansal destekleri için teşekkür eder.

KAYNAKLAR

Aksoy, C.O., Uyar Aksoy, G.G., Guney, A., Özacar, V., Yaman, H.E. (2020). Influence of time-dependency on elastic rock properties under constant load and its effect on tunnel stability. *Geomechanics and Engineering*, 20(1), 1-7.

Aksoy, C.O., Uyar, G.G., Utku, S., Safak, S., Ozacar, V. (2019). A new integrated method to design of rock structures. *Geomechanics and Engineering*, 18(4), 339-352.

Aksoy, C.O., Şafak, S., Uyar Aksoy, G.G., Özacar, V. (2018). A new mathematical approach for representing the deformation mechanism of rocks under constant load. *Geotechnique Letters,* 8, 80-90.

Aksoy, C.O., Uyar, G.G., Şafak, S. (2018). A new approach to time-load-deformation-stress hypersurface of rocks to stability analysis of underground openings. *Arabian Journal of Geoscience,* 11, 101.

Barla, G., Debernardi, D., Sterpi, D. (2012). Time-dependent modeling of tunnels in squeezing conditions. *International Journal of Geomechanics*, 12(6), 697-710.

Barton, N. (2002). Some new Q value correlations to assist in site characterization and tunnel design. *International Journal of Rock Mechanics and Mining Sciences*, 39, 185–216.

Bieniawski, Z.T. (1978). Determining rock mass deformability: Experience from case histories. *Int. J. Rock Mechanics Mineral Science & Geomechanics Abstract*, 15, 237 – 247.

Blankenship, D.A., Amadei, B., Stickney, G. (1983). Potential Applications of the Corejacking Test to Characterize the Mechanical Behavior of Rock Masses, Proc. 24th U.S. Symp. on Rock Mech., Texas A&M University (pp. 335-342).

Brantut, N., Heap, M.J., Meredith, P.G., Baud, P. (2013). Time-dependent cracking and brittle creep in crustal rocks: A review. *Journal of Structural Geology,* 52, 17-43.

Chung, C.K., Jang, E.R., Baek, S.H., Jung, Y.H. How contact stiffness and density determine stress-dependent elastic moduli: a micromechanics approach, Granular Matter, DOI 10.1007/s10035-013-0456-2.

Clerici, A. (1993). Indirect determination of the modulus of deformation of rock masses - Case histories. Proc. Conf. Eurock '93 (pp. 509-517).

Coulson, J. (1979). Suggested methods for determining in situ deformability of rock. *International Journal of Rock Mechanics and Mining Science,* 16(3), 195-214.

Damjanac, B., Fairhurst, C. (2010). Evidence for a long-term strength threshold in crystalline rock. *Rock Mechanics and Rock Engineering*, 43 (5), 513-531.

Fahimifar, A., Karami, M. (2015). Modifications to an elasto-visco-plastic constitutive model for prediction of creep deformation of rock samples. *Soils and Foundations*, 55(6), 1364-1371.

Fattahi, H., Moradi, A. (2018). A new approach for estimation of the rock mass deformation modulus: A rock engineering systems-based model. *Bulletin of Engineering Geology and the Environment,* 77, 363–374.

PARAMETRIC STUDY OF HIGH-LEVEL NUCLEAR WASTE STORAGE IN UNDERGROUND HARD ROCK CAVERNS

T.E. Altıntaş [1], A.A.A. Abduljabar [1], A.G. Yardımcı [1, *]

[1]*Middle East Technical University, Department of Mining Engineering*
*(*Corresponding author: ygunes@gmetu.edu.tr)*

ABSTRACT

Rising global energy demand has set nuclear energy as a trending power generation method due to its production cost and efficiency advantages. Remnants of the reactive process create large amounts of radioactive waste that pose environmental risks in case of improper management. High-level wastes are widely isolated by burying into deep geological voids or man-made excavations due to continuous heat emission for hundreds of years. Although design and excavating large underground caverns is a part of ordinary Rock Engineering practice, high temperature leads to challenging mechanical problems due to changing rock mass properties. Unexpected fracture propagation is risky in terms of seepage of polluted groundwater. Hence, the thermal effect on rock mass geomechanical properties must be considered for a proper cavern design. This study presents an experimental and numerical work to assess nuclear waste storage in hard rock caverns. The thermal effect on geomechanical properties of andesite samples was explored. Parametric studies were performed on Finite Element simulations to investigate alternative cavern designs. Thermal damage on rock mass has proven to be an effective mechanism for stability of storage caverns.

Keywords: Nuclear waste storage, thermal damage, finite element analysis

INTRODUCTION

Industrial revolution was a milestone for fossil fuels to dominate the global energy supply. Today, due to rapidly depleting non-renewable resources, the world is on the verge of an energy crisis. The common sense in favor of cost-effective and carbon-free energy policies has made nuclear a popular alternative. Besides the advantages, nuclear end products, especially the high-level wastes, pose an environmental threat as radioactivity remains long. Waste burial into deep geological voids or man-made excavations assures maximum safety by isolating radioactive material (Plúa et al., 2021). Storage room stability is of utmost importance as groundwater seepage from wall, roof or floor fractures may allow transportation of polluted materials. Conventional means of empirical and numerical methods can handle the design tasks for large underground openings. However, the heat produced from nuclear wastes elevates rock mass temperature around the storage opening, and the thermal damage disturbs rock mass geomechanical properties. In other words, mechanical and thermal stresses work together and pose a multiphysics condition. Long-term exposure to high temperatures have the potential to trigger instability issues within the rock mass governed by the altered rock strength parameters (Heap, et al. 2013). Previous studies of different authors have shown that elastic (modulus of elasticity, Poisson's ratio), plastic (cohesion, internal friction angle) and strength parameters (uniaxial compressive strength) change by temperature (Brotóns et al., 2013; Ranjith et al., 2012). Therefore, characterization of temperature-dependent mechanical properties of rock in laboratory and field-scale is an essential step of a stable and reliable waste storage opening (Kim et al., 2011; Sygała et al. 2013). Rock mechanics testing at extreme temperatures is tricky as it requires a complicated electromechanical loading frame, special measurement instrumentation, and precise thermocouple units. Alternatively, rock specimens exposed to high temperatures for a certain time are tested to

measure the thermal damage and used as an estimator for the actual mechanical properties working under high temperature.

A review of the literature points out that temperature increase leads to a decreasing trend in overall for elastic modulus and uniaxial compressive strength of granite up to 1000℃; however, the trend is opposite only between 100℃ and 200℃ (Fang et al., 2016; Shao et al., 2015). The authors describe the anomalous behavior by evaporation of bounded water molecules at 100℃ (Zhang et al., 2016). Another study mentions an increase in axial and radial borehole deformations due to temperature buildup induced by the radioactive wastes filling inside the borehole (Zhao et al., 2015). They claim that the hard rock elastoplastic properties deteriorate around 200℃. Observations on the stress-strain path of granite indicated an almost linear increase in stresses with increasing strain, creating a concave-up stress-strain graph (Jin et al., 2019). Even though this trend is constant among the observed temperature levels, the stress/strain ratios decrease with increasing temperature. The literature provides some useful experimental observations, however most of them are laboratory-scale studies, and they lack representation of the mass behavior (Zhao and Feng, 2019).

This paper aims to present a parametric study that investigates the stability of underground hard rock waste storage caverns under different temperature, rock mass quality, and opening geometry conditions. Experimental works constitute a base for the prediction of rock mass properties. Andesite specimen were tested to represent hard rocks. The elastoplastic parameters of pre-heated core samples were observed under uniaxial and triaxial loading conditions. The mass parameters were calculated for a range of rock mass quality, and finite element simulations were used to investigate the stability of man-made storage excavations. Ideal storage opening geometry and rock mass conditions were determined from numerical model interpretations.

METHODOLOGY

Core samples taken from hard rock blocks were prepared according to the suggested methods by the International Society of Rock Mechanics (ISRM) and flattened on the top and bottom ends using a rock surface grinder. Static deformability test, triaxial compression test, and indirect tensile strength tests were performed on samples. Experimental values for unit weight, modulus of elasticity, Poisson's ratio, uniaxial compressive strength, tensile strength, cohesion, and internal friction angle were calculated. Later, intact rock parameters were upscaled to the rock mass. Elastoplastic numerical models were simulated using Rocscience RS2 software and finite element method to investigate different excavation geometries, rock mass qualities, and temperature-dependent behavior. Staged analyses were done to observe the progress of stress and deformations within the rock mass by changing temperature.

EXPERIMENTAL WORK

Ankara Andesite was used to represent hard rocks. Intact cylindrical core samples with 54 mm diameter and 2.5:1 length/diameter ratio were taken from andesite blocks according to ISRM suggested methods. Core samples were exposed to different temperature levels (25 to 1000°C) for a period of fourteen days. In total, 55 specimens were heated up to 25, 100, 200, 400, 600, 800, and 1000°C. The specimens to be heated higher than 200°C were only exposed to the exact temperature level in the last four hours but were conditioned at 200°C in the first thirteen days. The specimens were cooled down to room temperature before testing. For each level, three static deformability tests and three indirect tensile strength tests were conducted. Some visuals from the test specimen and the set up can be seen in Figure 1. A servo-hydraulic stiff testing frame was used to conduct mechanical tests on core samples. Axial and lateral deformations were measured on static deformability and triaxial compression tests using extensometers and strain gauges. Induced loads are measured by means of an electronic load cell component. The rock samples were loaded on a displacement-controlled manner using an MTS 815

Figure 1. Experimental set up and test specimen

Figure 2 plots the fitted curves for uniaxial compressive strength and modulus of elasticity of andesite samples that are thermally conditioned for fourteen days. Both strength and elastic properties peak at 200°C and fall below the unconditioned state as soon as the temperature exceeds 800°C. A similar experimental outcome has been obtained with the literature that was presented in the previous sections. In other words, hard rock strength and elastic properties improve up to 200°C. However, the mechanical properties show a remarkable decrease around the temperature levels that are expected to be effective for high-level radioactive wastes (around 900°C).

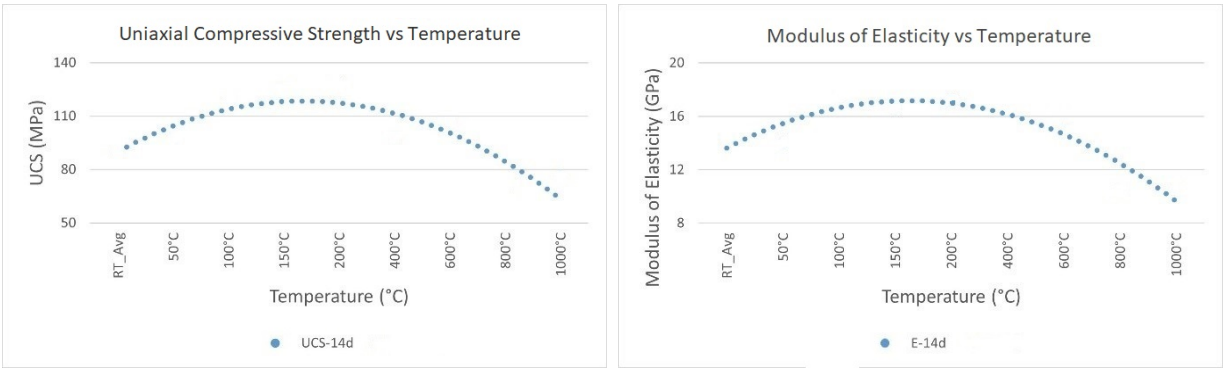

Figure 2. Experimental results for temperature-dependent UCS and Modulus of Elasticity of Ankara andesite

ROCK MASS GEOMECHANICAL PARAMETERS

Generalized Hoek & Brown failure criterion was used to calculate rock mass parameters from lab test results obtained from intact rock samples (Hoek and Brown, 1980, 2004). The numerical model input parameters were calculated based on the Geological Strength Index (GSI) and the empirical equation given in (1).

$$\sigma_1 = \sigma_3 + \left(m\frac{\sigma_3}{\sigma_c} + s\right)^a \quad (1)$$

Here σ_c indicates the uniaxial compressive strength of intact rock, σ_1 refers to the major principal stress, and σ_3 is the minor principal stress, the constants m, s, and a are characteristic parameters for Hoek&Brown criterion and they are a function of GSI as shown in equations (2)-(4)

$$\frac{m}{m_i} = \exp\left(\frac{GSI-100}{28-14D}\right)^a \quad (2)$$

$$s = \exp\left(\frac{GSI-100}{9-3D}\right) \quad (3)$$

$$a = \frac{1}{2} + \frac{1}{6}\left(e^{-\frac{GSI}{15}} - e^{-\frac{20}{3}}\right) \quad (4)$$

Using RocData software, the numerical input parameters were calculated for a GSI range of 30 to 80. Figure 3 shows the calculated values for the internal friction angle, modulus of elasticity, cohesion, and tensile strength of rock mass. It is evident that experimentally observed relation between mechanical parameters and temperature increase remains on the mass scale, as also observed in previous studies (Peng et al., 2016). Besides, natural density of the rock was determined to be 2.3 g/cm^3. Due to the insignificant change in Poisson's ratio, the average value of 0.2 was implemented for all levels.

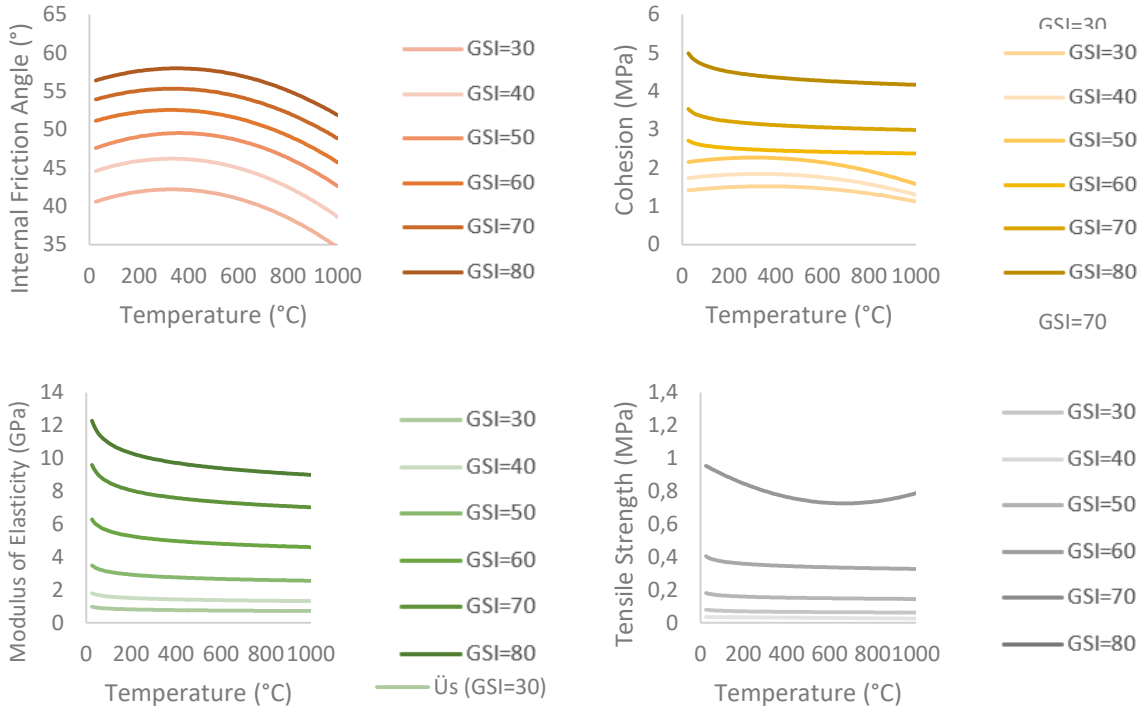

Figure 3. Rock mass parameters for different GSI and temperature levels

NUMERICAL ANALYSIS

Temperature-dependent geomechanical properties shown in Figure 3 were used to simulate the thermal damage effect of radioactive wastes on a two-dimensional finite element code. A hypothetical

deep and large, underground cavity with dimensions of 30 m in width and 50 m in height was modeled 1000 m below the ground. Assuming plane strain condition, two alternative cross-sections, each with three different width/height ratio (0.6,1.0 and 1.6) governed by Mohr-Coulomb material model and hard rock mass elastoplastic properties were analyzed. A horse-shoe-shaped profile with vertical walls and a half-circle roof (30 m for width/height=0.6 and 1.0, and 50 m for width/height=1.6 in diameter) was compared to a rectangular opening with rounded corners on the roof (10 m in diameter). Pre-excavation field stresses were implemented by a horizontal-vertical stress ratio of 1, and the vertical stress was calculated based on depth and gravity. Knowing heat dissipates radially, a circular temperature transition zone around the storage opening with an assumed effective radius of 150 m was created and the related material properties were assigned. Coupled numerical codes are capable of computing thermally developed stresses in charge of extra computational cost. This study follows an alternative modeling scheme, which is a modification of the conventional method. Thermal damage was induced in multiple model stages by individual material properties for each temperature level. Stress concentrations and deformations around openings were analyzed. A common application to preserve long-term stability in any underground opening is to have sophisticated support configurations. As our research focuses on mechanical effects of high temperature on rock mass in a progressive manner, unsupported openings were modeled and investigated.

RESULTS AND DISCUSSION

Total displacements on critical excavation points with different width/height ratios were extracted from FEM simulations and plotted for different opening geometry, rock mass temperature, and rock mass quality. Because we analyzed the unsupported state of openings focusing only on the mechanical behavior of rock mass with thermal damage, the models with low GSI computed extremely large displacements and therefore excluded from the plots. Only GSI 50 – 80 range is covered in the rest of the text.

Figure 4 presents the case where opening width/height ratio is 0.6. Independent of the excavation profile, a clear negative association was observed between the rock mass quality and the roof&wall deformations. Total displacements nonlinearly increase with decreasing rock mass quality. Larger wall displacements are related to the opening width/height ratio. While roof deformations are more sensitive to the opening geometry at low rock mass quality, the effect of geometry considerably decreases with increasing rock mass quality.

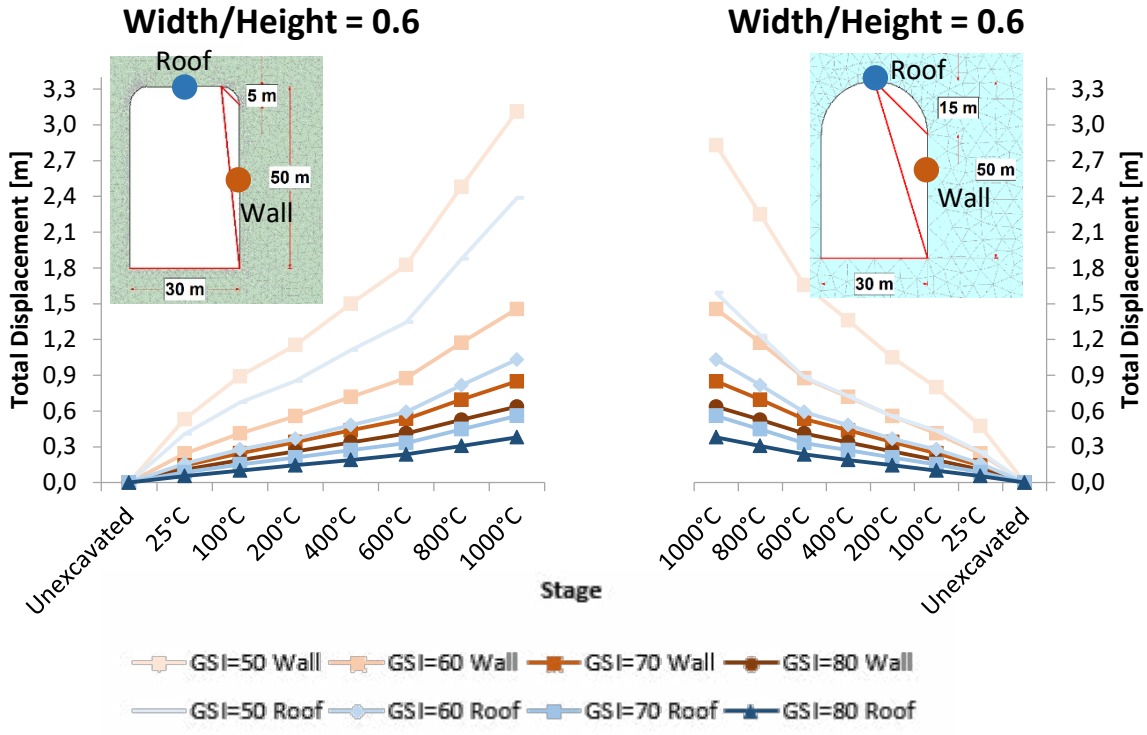

Figure 4. Total displacements on roof and wall at different temperatures when width/height ratio is 0.6

Figure 5 shows the total displacements on roof and wall of two different opening profiles when width/height ratio is 1.0. Unlike the tall profile in the previous case, roof and wall displacements are close to each other in rectangular cross-section with rounded edges. However, wall displacements are larger on the horse shoe, similar to the previous case. Overall, displacements both on roof and wall significantly decrease in horse-shoe shaped profile. Deformations significantly increase with decreasing rock mass quality.

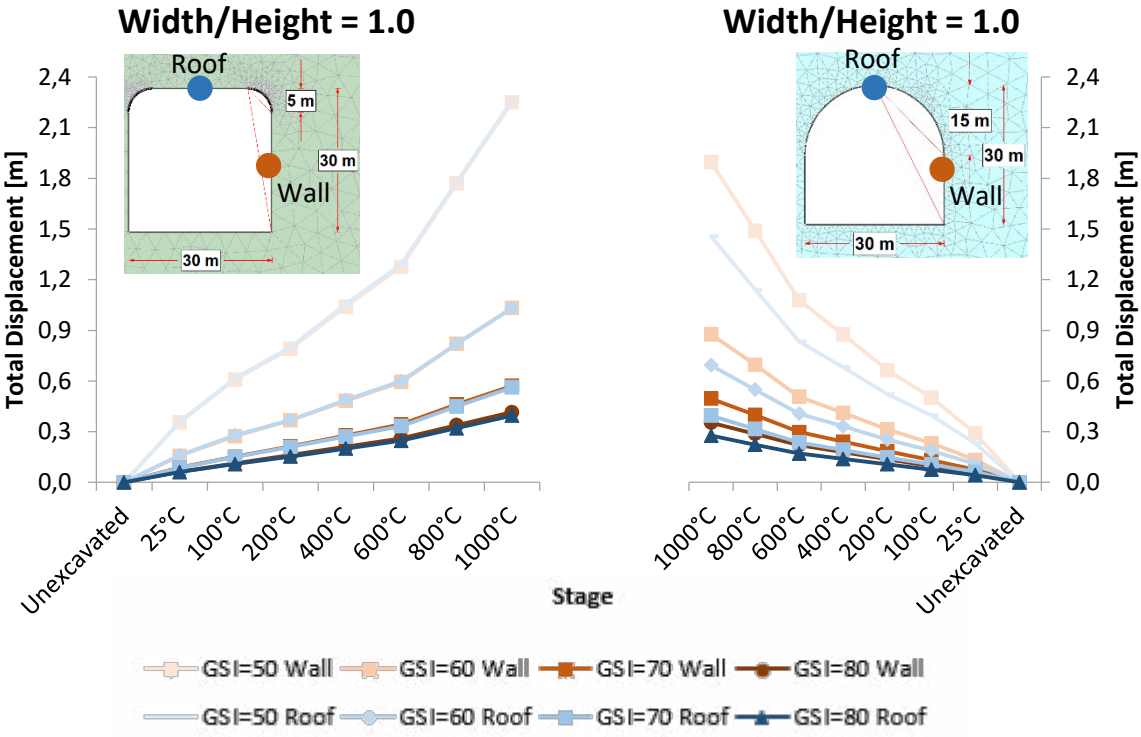

Figure 5. Total displacements on roof and wall at different temperatures when width/height ratio is 1.0

Figure 6 shows a wide opening profile where the width/height ratio is 1.6. Unlike the previous cases, roof displacements are larger compared to the wall in the investigated rock mass quality range. The nonlinear increase of total displacements with decreasing rock mass quality is also valid for this case. Compared to the rectangular opening with rounded edges on the roof, the horseshoe induces less displacement on roof and walls and the difference is observed more clearly at low rock mass qualities.

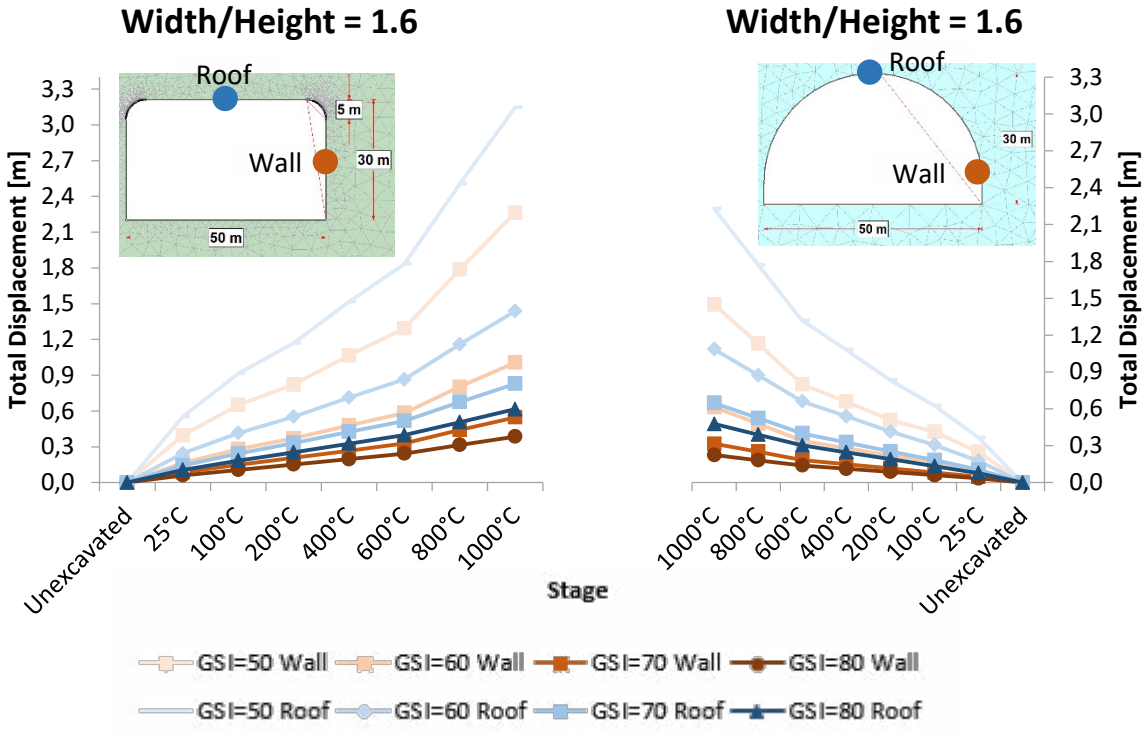

Figure 6. Total displacements on roof and wall at different temperatures when width/height ratio is 1.6

At elevated temperatures independent of the rock mass quality, opening geometry, and width/height ratio, there appears to be a positive association with roof and wall displacements. Comparing the model stages at extreme temperatures, thermal damage leads to an increase in total displacements up to six times. Rock mass quality does not control the trend but the magnitudes of displacements are larger at low GSI values. Figure 7 showing the major principal stress contours for different opening geometry proves that stress concentrates more around the sharp edges. The yielded elements densify on the shoulders and the crown. The horseshoe shape apparently can be expected to mechanically perform better and be more reliable in long-term.

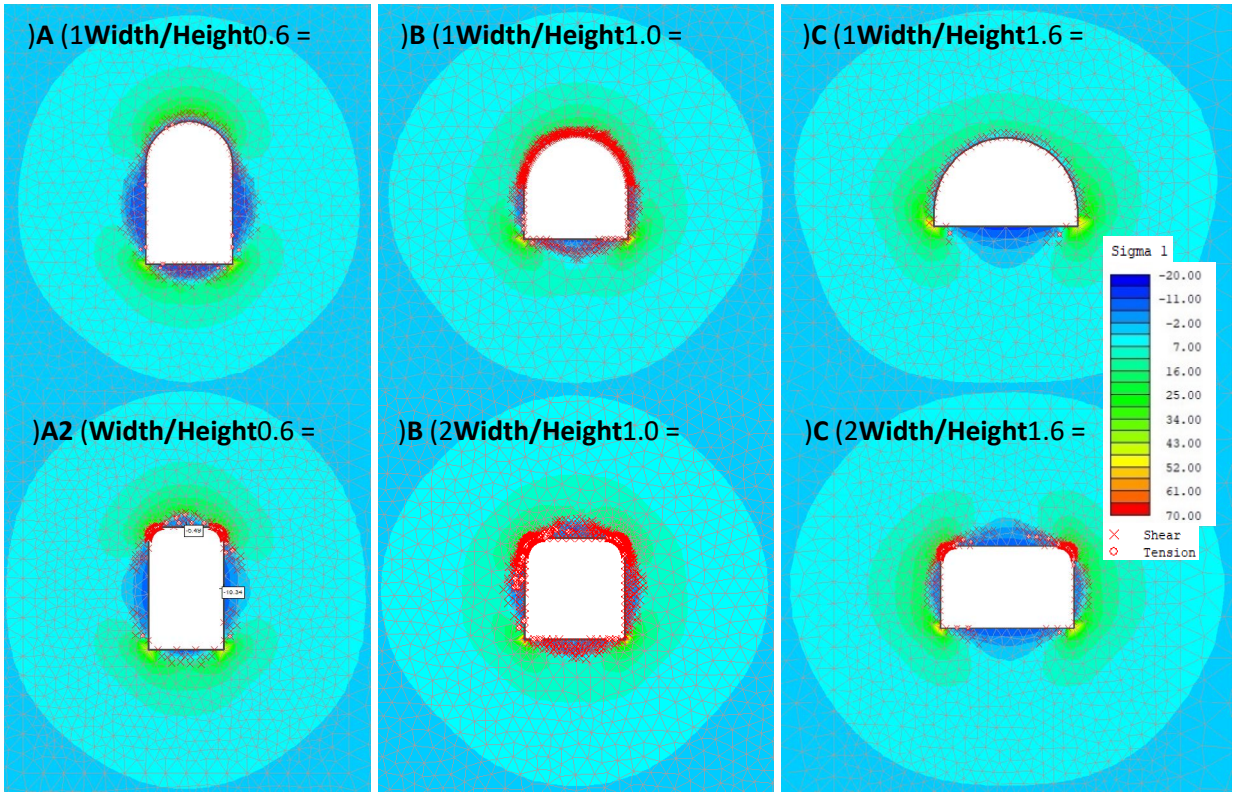

Figure 7. Major principal stress contours around openings with different geometry and width/height ratio at GSI = 70

Figure 8 shows the propagation of plastic region and total displacements around the excavation by changing the temperature. Considerable deformations are observed on a larger region around the excavation with the influence of thermal damage. This implies the conventional support design will be incapable of providing a sufficient configuration, and thermally degraded rock mass properties should be taken into consideration.

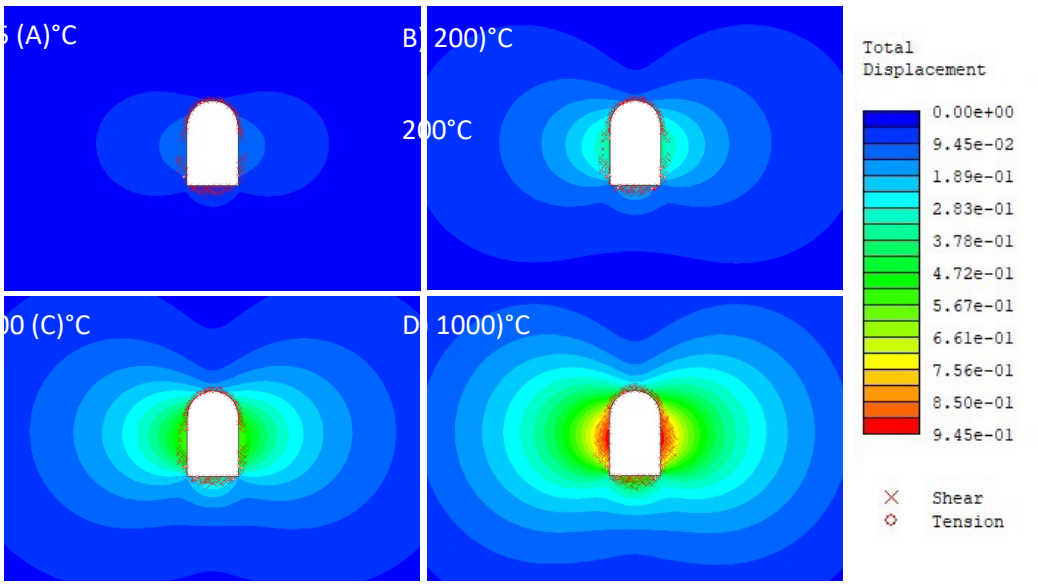

Figure 8. Total displacement contours and yielded elements around a storage opening under different temperatures when width/height ratio is 0.6

CONCLUSION

As an emerging problem related to the growing demand, the energy crisis enforces quick actions to match the required power supply. Recently, the nuclear alternative has been popular due to being the largest carbon-free source. The end-products of the reactive process pose a serious environmental risk. However, systematic and sustainable waste management policies established by governments and multinational organizations do not progress as fast as the new plants on order or under construction. The current waste disposal strategy is to bury the wastes away from the human interaction, in the deep ocean or geological voids. Low and medium-level wastes create no technical difficulty as they can be preserved in protected containers even at shallow depth storage caverns. On the other hand, high-level wastes produce heat from radioactive decay, and the thermal damage mechanically influences the rock mass covering the underground storage. Fracture growth and propagation around the storage cavern has potential for groundwater seepage and transportation of radioactive material. Considering the expected life of a storage cavern is limited by the half time of the waste, which may be up to thousands of years, the long-term stability must be satisfied.

This research investigates the influence of thermal damage on hard rock storage openings by experimental and numerical methods. Rock mechanics laboratory tests were applied on andesite core samples to characterize the overall mechanical properties of hard rocks. Test specimen were exposed to different temperature levels for a period of fourteen days. Mechanical tests were conducted on cool samples. An alternative numerical modeling approach was used by implementing thermal damage with reduced model input parameters. Finite element simulations for a single storage opening have shown that opening geometry influences the stability more dramatically at high temperatures and low-quality rock mass, and the geometry becomes less influential by increasing rock mass quality. Another research outcome is the positive association of deformations with the temperature increase. Although rock mass quality controls the displacement magnitudes, the deformation trend for the incremental temperature is similar irrespective of the rock mass quality. The plastic region around the excavation significantly expands around 800°C and classical support design systems lack of sustaining opening stability.

Finally, it is worth mentioning about shape distortion that was experimentally observed for conditioning at extreme temperatures (around 1000°C). It implies the post-failure behavior of the rock tends to have a transition from brittle to ductile. Although numerical simulations with reduced mechanical properties successfully represented the thermal damage at low temperatures, the rock material should be expected to behave significantly different at high temperatures compared to the cooled-down state.

REFERENCES

Brotóns, V., Tomás, R., Ivorra, S., Alarcón, J.C., (2013). Temperature influence on the physical and mechanical properties of a porous rock: San Julian's calcarenite. Eng. Geol. 167, 117–127.

E. Hoek and E T. Brown. (1980). Underground Excavation in Rock, London, U.K.:, Institute Mining Metallurgy.

E. A. Hoek. (2004). Brief History of the Development of the Hoek-Brown Failure Criterion. [Online]. Available: http: //www.rocscience.com

Fang, X., Xu, J., Lui, S., & Wang, P. (2016). Research on splitting-tensile tests and thermal damage of granite under post-high temperature. *Chinese Journal of Rock Mechanics and Engineering*, *35*, 2687–2694. https://doi.org/10.13722/j.cnki.jrme.2014.1631

Heap, M. J., Mollo, S., Vinciguerra, S., Lavallée, Y., Hess, K.-U., Dingwell, D. B., Baud, P., & Iezzi, G. (2013). Thermal weakening of the carbonate basement under Mt. Etna Volcano (italy): Implications for volcano instability. *Journal of Volcanology and Geothermal Research*, *250*, 42–60. https://doi.org/10.1016/j.jvolgeores.2012.10.004

Jin, P., Hu, Y., Shao, J., Zhao, G., Zhu, X., & Li, C. (2019). Influence of different thermal cycling treatments on the physical, mechanical and transport properties of granite. *Geothermics*, *78*, 118–128. https://doi.org/10.1016/j.geothermics.2018.12.008

Kim, JS., Kwon, SK., Sanchez, M. et al. (2011). Geological storage of high level nuclear waste. KSCE J Civ Eng 15, 721–737 (2011). https://doi.org/10.1007/s12205-011-0012-8

Peng, J., Rong, G., Cai, M., Yao, M., Zhou, C.. (2016). Comparison of mechanical properties of undamaged and thermal-damaged coarse marbles under triaxial compression. Int. J. Rock Mech. Min. Sci. 83, 135–139.

Plúa, C., Vu, M.-N., Seyedi, D. M., & Armand, G. (2021). Effects of inherent spatial variability of rock properties on the Thermo-hydro-mechanical responses of a high-level radioactive waste repository. *International Journal of Rock Mechanics and Mining Sciences*, *145*, 104682. https://doi.org/10.1016/j.ijrmms.2021.104682

Ranjith, P.G., Viete, D.R., Chen, B., & Perera, M.S. (2012). Transformation plasticity and the effect of temperature on the mechanical behaviour of Hawkesbury sandstone at atmospheric pressure. Engineering Geology, 151, 120-127.

Shao, S., Ranjith, P. G., Wasantha, P. L. P., & Chen, B. K. (2015). Experimental and numerical studies on the mechanical behaviour of Australian strathbogie granite at high temperatures: An application to geothermal energy. *Geothermics*, *54*, 96–108. https://doi.org/10.1016/j.geothermics.2014.11.005

Sygała, A., Bukowska, M., & Janoszek, T. (2013). High Temperature Versus Geomechanical Parameters of Selected Rocks – The Present State of Research. Journal of Sustainable Mining, 12, 45-51.

Zhang, W., Sun, Q., Hao, S., Geng, J., & Lv, C. (2016). Experimental study on the variation of physical and mechanical properties of rock after high temperature treatment. *Applied Thermal Engineering*, *98*, 1297–1304.https://doi.org/10.1016/j.applthermaleng.2016.01.010

Zhao, Y., Feng, Z., Xi, B., Wan, Z., Yang, D., & Liang, W. (2015). Deformation and instability failure of borehole at high temperature and high pressure in hot dry rock exploitation. *Renewable Energy*, *77*, 159–165. https://doi.org/10.1016/j.renene.2014.11.086

Zhao, P., & Feng, Z. (2019). Thermal Deformation of Granite under Different Temperature and Pressure Pathways. Advances in Materials Science and Engineering.

PATLATMA KAYNAKLI TİTREŞİMLERİN 3 BOYUTLU NÜMERİK MODELLEME İLE TAHMİN EDİLMESİ

PREDICTION OF BLAST INDUCED VIBRATION WITH 3D DYNAMIC NUMERICAL MODELING

C.O. Aksoy [1, *], G.G.U. Aksoy [2], H. E. Yaman[3]

[1] *Dokuz Eylül Üniversitesi Maden Mühendisliği Bölümü*
*(*Sorumlu yazar: okay.aksoy@deu.edu.tr)*
[2] *Hacettepe Üniversitesi, Maden Mühendisliği Bölümü*
[3]*Dokuz Eylül Üniversitesi Torbalı Meslek Yüksek Okulu*

ÖZET

İnşaat ve madencilik sektöründe en çok kullanılan kazı yöntemi patlatmadır. Mühendislik projeleri kapsamında patlatmanın neden olduğu sismik dalgalar, çevredeki yapılara zarar verebileceği gibi stabilite sorunlarına da neden olabilir. Bu olumsuzlukların önüne geçebilmek için ölçekli mesafe teorisi kullanılarak patlama paternleri oluşturulur ve patlatma yapılır. Bununla birlikte, ölçekli mesafe kuramı ile güvenilir bir model oluşturmak için 20-30 ayrı patlatma verisine ihtiyaç vardır. Bu maliyetli, zaman alıcı olabilir ve olumsuzluğa neden olabilir. Bu çalışmada, daha önce patenti alınmış bir model ile tek bir pilot delikten elde edilen verilerden üretilen patlama modeli verileri kullanılarak grup patlama sinyalleri simüle edilmiş ve bu veriler 3D dinamik sayısal modelleme yöntemi ile analiz edilmiştir. Sonuçlar, tek bir pilot delikten elde edilen sismik sinyallerin, grup patlatmanın sahadaki etkilerini tahmin edebileceğini göstermektedir.

Anahtar Sözcükler: Nümerik modelleme, patlatma, sismik sinyal, pilot delik, kaynak

ABSTRACT

The most used excavation method in the construction and mining industry is blasting. Seismic waves caused by blasting within the scope of engineering projects can cause damage to structures in the vicinity and also cause stability problems. In order to prevent these negativities, blast patterns are created by using the scaled distance theory. Blasting is done with these patterns. However, in order to create a reliable pattern with the scaled distance concept, 20-30 separate blasting data is needed. This can be costly, time consuming and cause negativity. In this study, group blast signals were simulated using blast pattern data generated from data from a single pilot hole with a previously patented model and these data were analyzed by 3D dynamic numerical modeling method. The results show that the seismic signals obtained from a single pilot hole can predict the effects of group blasting on the field.

Keywords: Numerical modeling, blasting, seismic signal, pilot hole, source

GİRİŞ

Madenlerde üretim ve dekapaj faaliyetleri için patlatma birçok yönden çok önemlidir. Doğru ve verimli bir patlatma, maden işletmesine hem ekonomik olarak hem de patlatma sonrası madende yapılacak işler açısından rahatlık sağlar. Kaya kütlesinde bir patlatmanın neden olduğu titreşimleri etkileyen ana parametreler, hedef bölge ile patlatma grubu arasındaki mesafe, patlatma süresi, her bir delikteki patlayıcı miktarı, delikler ve sıralar arasındaki gecikmeler, patlatma kaynaklı oluşan dalgaların frekansları, bölgenin jeolojisi ve jeolojik oluşumdaki değişikliklerdir (Aksoy ve Aksoy, 2020; Blair, 2020).

Delik başına düşen patlayıcı miktarı optimum düzeyde değilse etkin parçalanma sağlanamayacaktır. Delikler arasındaki ve sıralar arasındaki gecikmeler doğru seçilmezse delikler birlikte patlayacak ve dolayısıyla titreşimler artacak ve en önemlisi bölgenin jeolojisi doğru belirlenmezse yanlış patlatma paterni uygulanması kaçınılmaz olacaktır.

Literatüre baktığımızda, kırıklı, eklemli kayalarda ve süreksizliklerde patlatma ölçümlerine ve modellemelerine nadiren tanık oluyoruz. Bu nadir çalışmalardan biri Singh ve Narendra'nın (2004) çalışmasıdır. Bu çalışma, özellikle 10, 20, 30, 45, 60 ve 90 derece eklemli yapılarda oluşan patlatma kaynaklı en yüksek parçacık hızlarının karşılaştırılması üzerinedir. Mesafe aynı kalmak koşulu ile, 10 derece eklemli yapıda yapılan patlatmadan kaynaklı parçacık hızı 228.5 mm/s iken, 45 derece eklemde parçacık hızı 111,3 mm/s olarak ölçülmüş, 90 derece eklem için hızın 272,9 mm/s'ye yükseldiği gözlemlenmiştir. Ayrıca Simangunsong ve Whayudi (2015) değişken oryantasyonlu ve değişken aralıklarla süreksizliklerdeki titreşimi ölçmüştür. Simangunsong ve Whayudi (2015) çalışmalarında süreksizlik sayısındaki artışın genel olarak titreşimin azalmasına neden olduğunu ortaya koymuştur. Bu durum Zou ve Gong (2017) tarafından tabakalanma düzlemi ve foliasyonlarla, kaya kütlelerinde ve kaya kütlelerinde titreşim ölçümleri yapan modelleme tahminleri ile örtüşmektedir.

Blair yaptığı çalışmada, anizotropik kaya kütlelerinde patlatma sonrası oluşan titreşimlerin yayılımını araştırmış; sismik dalga ve titreşimlerin davranışını sayısal modelleme ile tahmin etmeye çalışmıştır. Bu tahminde, patlama grubundaki her bir delikten üreyen sismik dalgaların tüm yönlere eşit olarak yayıldığı varsayımı kabul edilmiştir (Blair, 2008-2018). Oysa ki, doğada böyle bir şey söz konusu değildir. Çünkü jeoloji her yönde farklılık arz etmektedir.

Bu çalışma, patlatma yapılacak sahada yapılan bir pilot delik patlatmasından alınan sismik dalgaları veri olarak kullanmaktadır. Böylelikle, doğayı baz alan bir çalışma olarak, en doğru bilgiyi içermektedir. Bu sebeple, önerilen bu çalışma kapsamında patlatma yapılacak bölgedeki süreksizliklerin belirlenmesi için ayrıca bir çalışma yapmaya gerek bulunmamaktadır. Çünkü, ölçülen sismik dalgalar bahsi geçen süreksizliklerden geçerek ve onların etkileri ile form alarak sismograflara ulaşmaktadır. Bu nedenle, patlatma yapılacak sahada bulunan süreksizlik sayısı, eğimi, eğim yönü gibi parametreler ile ayrıca uğraşmaya gerek kalmamaktadır. Tek yapılması gereken kaynak ile hedef arasına birkaç jeofon yerleştirilmesi ve patlatma sonucu veri kaydı alınmasıdır. Bu mevcut çalışma iki aşamadan oluşmaktadır. Bir pilot delik patlatması ve bu patlatmanın neden olduğu sismik dalgalar sismograflar yardımıyla kayıt altına alınır ve elde edilen veriler bilgisayar ortamına aktarılır. İkinci aşama ise sayısal modelleme aşamasıdır. Bu aşamada kullanılan bilgisayar programında çalışma alanında yapılan işlemler tek tek yazılıma aktarılır ve elde edilen sonuçlar gerçek sonuçlarla karşılaştırılır.

Bu bildiride, patlatmaların etkilerinin tahmini için önerilen yeni metodun kullanılabilirliğini anlatmak amacıyla bir metal madeninde yapılmış uygulama verilmiştir.

Saha Çalışması

Saha çalışması bir metalik madende gerçekleştirilmiştir. Bu uygulama için 200 delikli bir grup patlatması ve grup içerisindeki her bir deliği simgeleyen bir tek delik pilot patlatması yapılmıştır. Şekil 1’de kayıt için kullanılan ekipman ve Şekil 2’de Grup ve Pilot patlatma yerleri ile sismograf lokasyonları verilmiştir.

Çalışma alanı volkanik kayaçlardan oluşmaktadır. Sayısal modelde kullanılan kaya parametreleri tarafımızca belirlenmiş olup bu parametreler Çizelge 1'de verilmiştir.

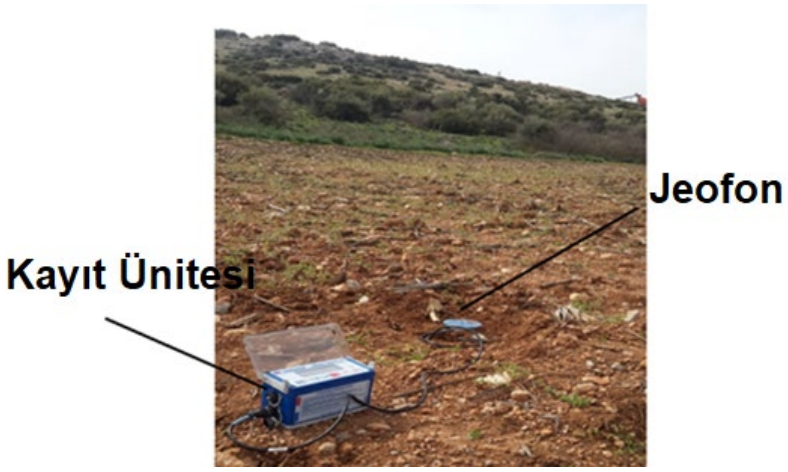

Şekil 1. Patlatma ölçümlerinin alındığı sismograf

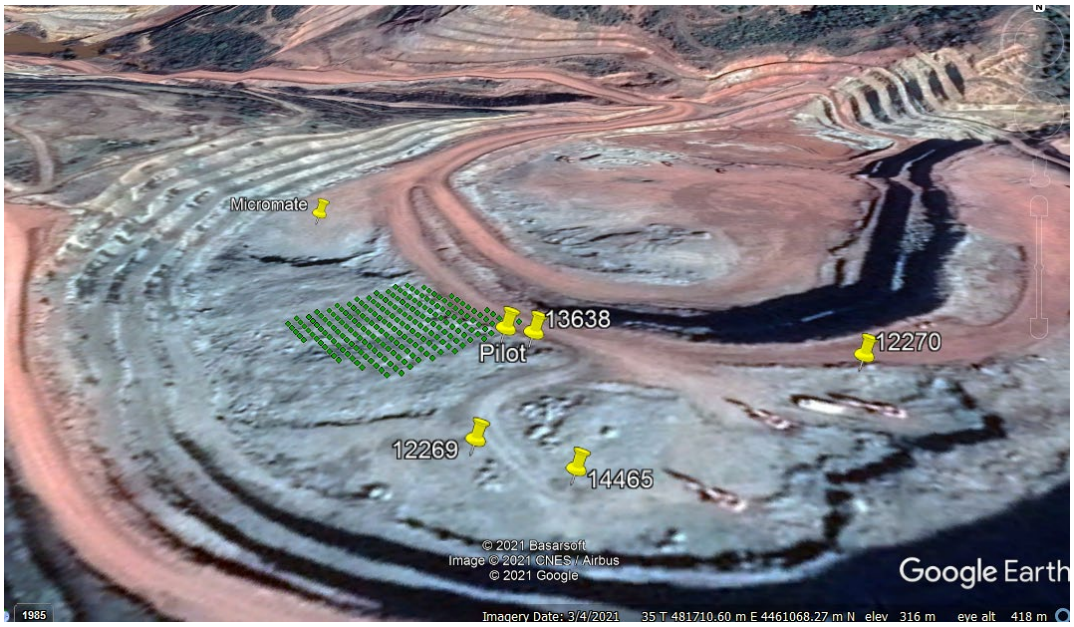

Şekil 2. Patlatma grubunun, pilot patlatma deliğinin ve sismografların (12269, 14465, 13638, 12270, micromate) lokasyonu

Çizelge 1. Kaya kütle parametreleri

Birim	ɣ (kN/m^2)	σc (MPa)	Ø (º)	v	C (kPa)	E (MPa)
VOLKANİK KAYA	23,61	18,53	22,62	0,22	667	553.20

Grup ve pilot patlatma deliklerinin patlatma geometrisine ait bilgiler Çizelge 2'de yer almaktadır.

Grup patlatması ve pilot patlatmasından kaynaklı sismik dalgalar, 5 adet sismografla kaydedilmiştir. Böylece patlatmalardan ortaya çıkan sismik dalgaların analizi, incelenmesi mümkün olabilmiştir. Sismograflar Şekil 2'de de görüleceği üzere patlatmalara çok yakın mesafelere yerleştirilmişlerdir. Buradaki amaç şudur; patlatmanın kaynağında, yani sıfır noktasında oluşan enerjinin tahmini edilmesidir. Bu yöntem kullanılarak sayısal modelleme ile kaynaktan istenilen mesafe uzaklıkta

oluşacak sismik dalga kaynaklı titreşimlerin belirlenmesi gerçekleştirilebilmektedir. Bu yöntem 114M566 no'lu Tübitak projemizde (Aksoy vd., 2017) Deformasyona izin vermeyen tahkimat sisteminin oluşturulması amacı için geliştirilmiş olup nümerik modelleme ile patlatma kaynaklı titreşimlerin tahmininde kullanılmaya başlanması, bahsi geçen projenin doğurduğu yeni Ar-Ge faaliyetlerinden biridir ve bu bildiri ile tanıtılmak istenmektedir.

Çizelge 2. Kaya kütle parametreleri

Patlatma Lokasyonu	**Delik çapı, (mm)**	**Ortalama Delik Boyu, (m)**	**Patlatma geometrisi**	**Patlayıcı miktarı, (kg)**	**Ateşleme Elemanı**	**Delik sayısı**
SV-2 Grup	102	5.92	Yük mesafesi: 2.5m Delikler arası mesafe: 3 m	Anfo: 18kg 0.5kg yemleme	Elektronik kapsül	200
SV-2 Pilot	102	5.3		Anfo: 18kg 0.5kg yemleme	Nonel kapsül	1

Gerçekleştirilen grup patlatması sonrasında elde edilen sismik dalga formu Şekil 3'te verilmektedir.

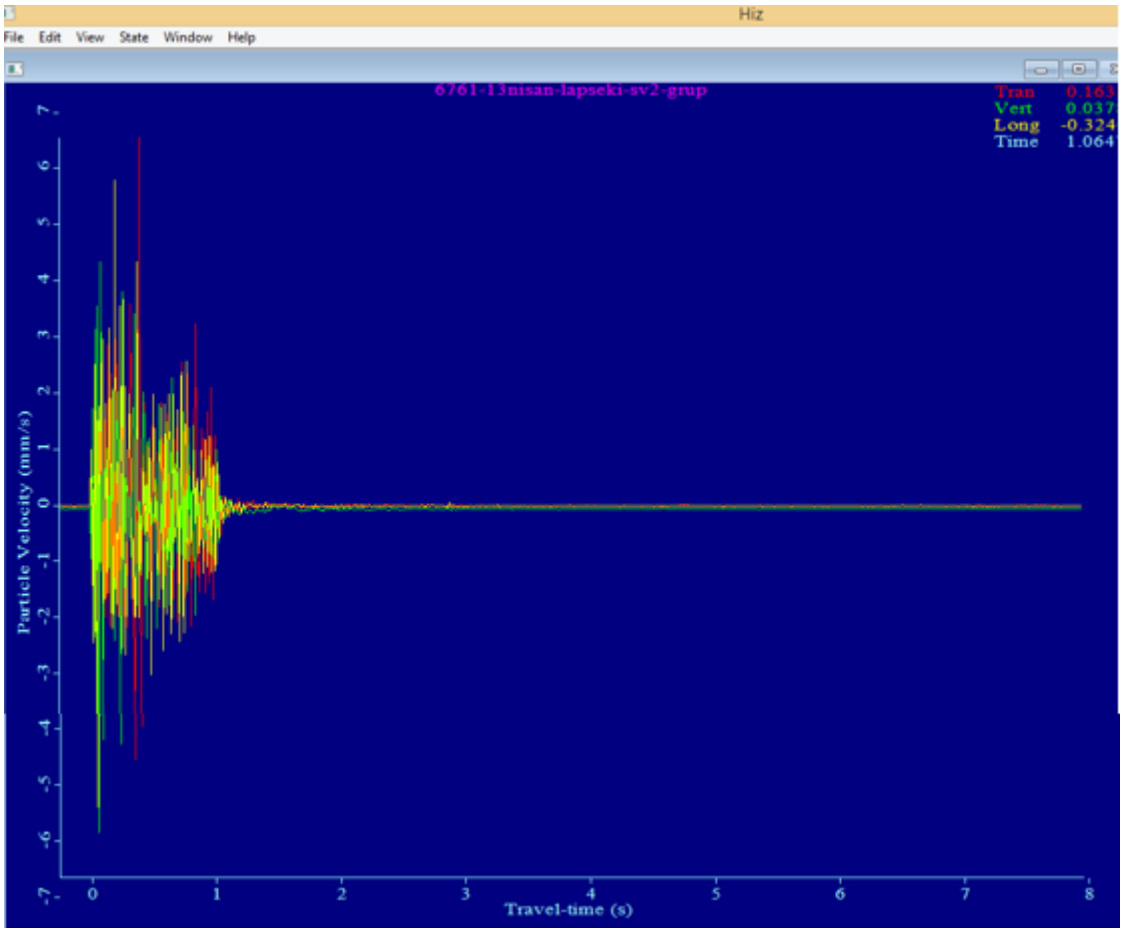

Şekil 3. Grup patlatması sonrasında kaynakta (patlatma noktasında) hesaplanan parçacık hızı-zaman eğrisi

Sayısal Modelleme

Sayısal modelde, açık ocağın yüzeyi 1:1 ölçeğinde kullanılır. Modele, gerçek patlatma grubunun konumu temsil etmesi için topoğrafyanın beş metre altına bir yüzey eklenmiş olup, bu yüzeyin alanı eş alan hesaplamalarından ortaya konmuştur. Eklenen yüzeyin topografyanın beş metre altında tanımlanmasının nedeni, patlatma deliklerinin beş metre uzunluğunda olduğu ve dolayısıyla ana patlama kaynağının topografyanın beş metre altında olacağı varsayımından kaynaklanmaktadır. Grup patlatma sonucunda zamana karşı üç bileşende (yanal, dikey, boyuna) veriler elde edilmiş ve bu veriler Elastik-Plastik Enerji Dağılımı kuramına göre değerlendirildikten sonra sayısal modele eklenen patlatma yüzeyine kaynak verisi olarak tanımlanmıştır. Yani sayısal modelde, sanal patlatma senaryosu gerçekleştirilmiştir. Buradaki amaç, gerçek bir patlamadan elde edilen verileri sayısal modelde kullanmaktır. Çalışma alanının genel model görünümü ve modelde tanımlanan kaya parametresi Şekil 4'te verilmiştir.

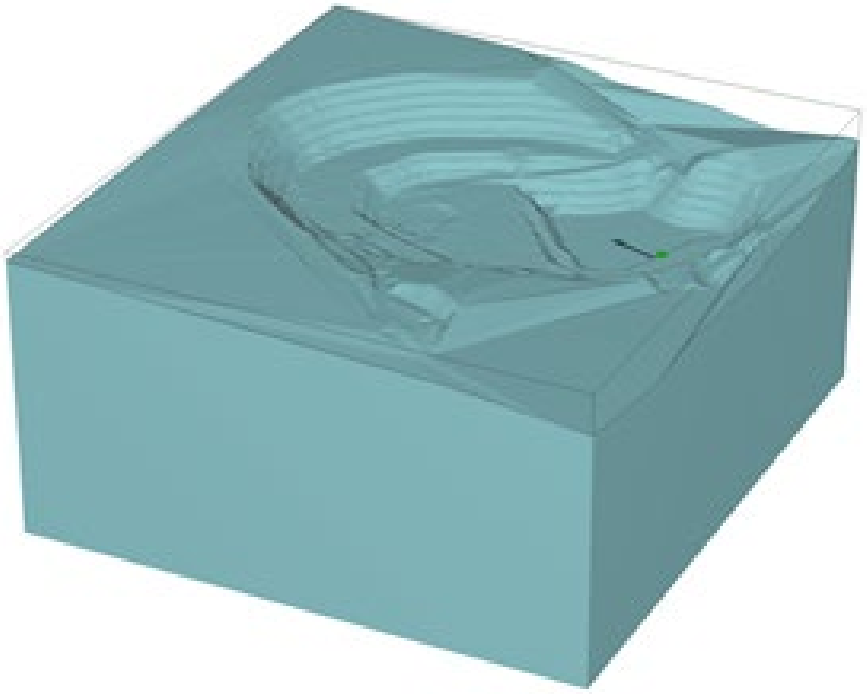

Şekil 4. Oluşturulan sayısal modelin görünümü

Sayısal modelleme iki aşamadan oluşmaktadır. İlk aşamada, modelin yükleme koşulları oluşturulmuştur. Bu aşamada, modele gravite yüklemesi yapılmıştır. İkinci aşama, patlatma verilerinin modelde çalıştırıldığı ve dinamik analiz bölümünün yapıldığı aşamadır. Bu veriler, modelde patlatma için belirlenen yüzey üzerinde tanımlanmıştır. Çalışma alanındaki patlatma sonucunda üç bileşende elde edilen ve sayısal modelde eklenen yüzey üzerinde tanımlanan verilerin sinüsoidal grafikleri Şekil 5'de verilmiştir.

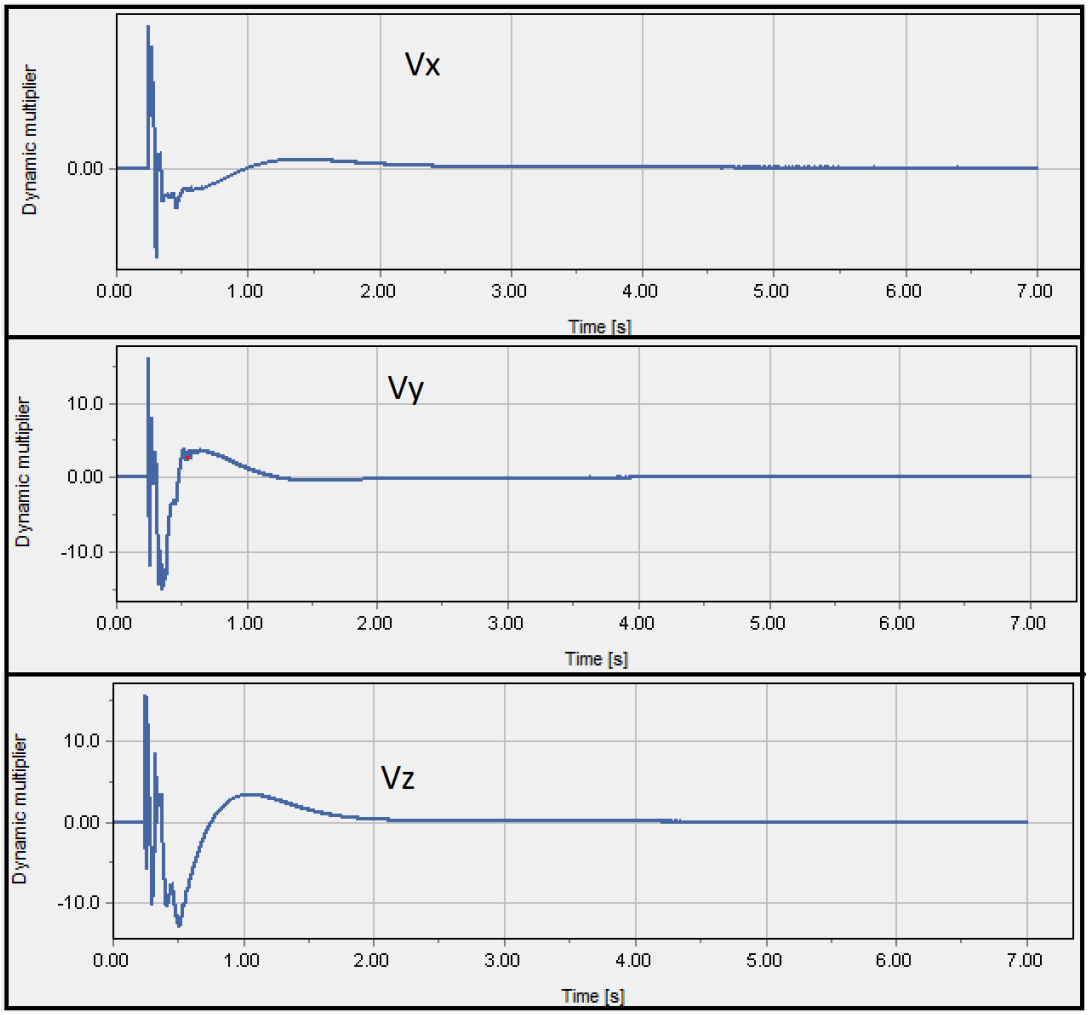

Şekil 5. Enine, düşey ve boyuna bileşenlerin sinüzoidal eğrileri

Tüm bu tanımlamalar tamamlandıktan sonra, çalışma alanına yerleştirilen sismografların konumları, gerçek konumlarıyla birebir örtüşecek şekilde sayısal modele entegre edilmiştir. Patlatma öncesinde, patlatma etkilerini yakın mesafede görebilmek adına patlatma bölgesinin yakınlarına sismograflar yerleştirilmiştir. Bu sismograflardan 13368 no'lu sismograf patlatma lokasyonuna 10 m ve Micro adı verilen sismograf ise 75 m uzaklıkta konumlandırılmıştır. Modelde ise Micro adlı sismografın tam lokasyonunda bir nokta bulunmadığı için patlatma bölgesine yaklaşık 80 m mesafede bir nokta seçilebilmiştir. Şekil 6 ve 7'de bu iki sismograf lokasyonlarında elde edilen model sonuçları V_x ve V_y olarak verilmektedir. Sonuçlar incelendiğinde, model ile sahada yerleştirilen sismograf verilerinin çok yakın olduğu görülmektedir. Şekil 6'da 13368 no'lu sismografın bulunduğu ve patlatmaya 10 m mesafede V_x değerinin 86 mm/sn ve V_y değerinin ise 56 mm/sn olduğu görülmektedir. Bu değerlerin sahada gerçek ölçülmüş değerleri sırasıyla 81 mm/sn ve 44 mm/sn'dir. Diğer taraftan, Micro adlı sismografı temsil eden model noktasında tahmin edilen V_x değeri 4,6 mm/sn iken V_y değeri 5,1 mm/sn olarak belirtlenmiştir (Şekil 7). Bu değerlerin gerçek patlatma sonucu ölçülen değerleri sırasıyla 7,015 mm/sn ve 7,15 mm/sn'dir. Buradaki temel amaç, patlatma sonucu ortaya çıkan gerçek veriler ile sayısal model sonucunda üretilen verilerin ne kadar örtüştüğünü belirlemektir.

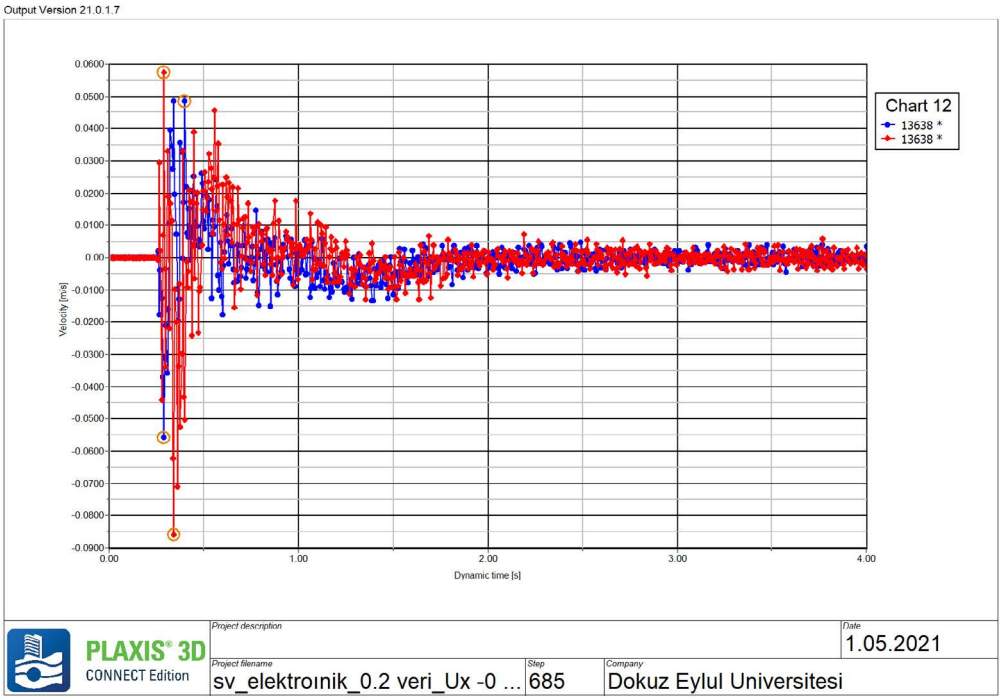

Şekil 6. Sayısal modelde patlatma lokasyonuna 10 m mesafedeki 13368 no'lu sismografın Partikül hızı-zaman grafiği (Kırmızı: V_x, Mavi: V_y)

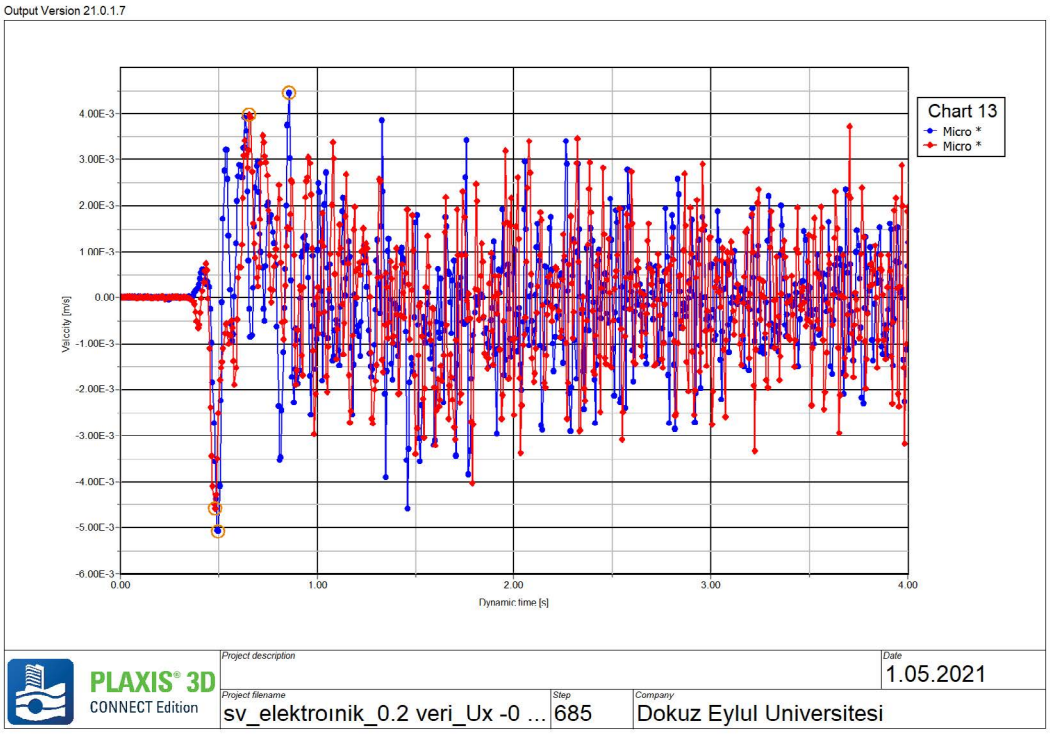

Şekil 7. Sayısal modelde patlatma lokasyonuna 80 m mesafedeki Micro adlı sismografın Partikül Hızı-Zaman grafiği (Kırmızı: V_x, Mavi: V_y)

SONUÇLAR

Günümüzde patlatmaların etkilerini önceden tahmin etmek ya da patlatma etkilerini minimize etmek için "Ölçekli Mesafe Kuramı"na dayalı çalışmalar yapılmaktadır. Ancak, bu çalışmalar tam doğru cevap verememenin ötesinde çok yoğun saha çalışması gerektirmektedir. Parçacık hızı-ölçeklli mesafe ilişkisinin yüksek doğrulukta çıkabilmesi için, en az 30 patlatma verisi gerekmektedir. Ayrıca, bu çalışmalarda patlatma yönü değiştiğinde saha çalışmalarının yenilenmesi gerekmektedir.

Tarafımızca önerilen yeni yöntemde ise sahada yapılacak bir pilot delik patlatmasından elde edilen sismik dalgaların sayısal model yazılımına entegrasyonu ile patlatma etkileri oldukça kolay şekilde tahmin edilebilmekte ve grup patlatması yapılmadan yeni tasarımların kontrolü kolaylıkla sağlanabilmektedir. Ek olarak, bu yöntem ile patlatmaların şev duraylılığına etkileri de incelenebilmektedir.

Bir metal madeninde yapılan çalışmaların sadece bir tanesinin sunulduğu bu makalede, öncelikle bir pilot delik patlatma verisi alınmıştır. Bu veriler ile patlatmanın kaynağındaki enerji hesaplanmış ve Elastik-Plastik Enerji Paylaşımı Kuramı ile kaynaktaki patlatmanın kaya parçalamaya harcanan bölümü hesaplanmıştır. Bu enerji sayısal modele kaynak enerjisi olarak tanımlanmış ve değişik mesafelerde maksimum parçacık hızı tahminlerinde bulunulmuştur.

Yapılan çalışma sonucunda gerek patlatma noktasına 10 m kadar yakında ve gerekse 80 m kadar uzaktaki veriler karşılaştırılmıştır. Elde edilen sonuçlar, yeni önerilen yöntemin oldukça sağlıklı şekilde çalıştığını göstermektedir.

KAYNAKLAR

Aksoy, G.G.U., Aksoy C.O., (2020), Patlatma kaynaklı titreşimlerin tahmininde sismik kalite faktörü kullanımı, MT Bilimsel, Sayı:18, sayfa 133-146.

Aksoy, C.O., Aksoy G.G.U., (2014) "Deformasyona İzin Vermeyen Tahkimat Sisteminin Geliştirilmesi", TübitakProje No:114M566, 2014-2017.

Blair, D.P., (2020), Approximate models of blast vibration in non-isotropic rock masses, *International Journal of Rock Mechanics and Mining Sciences, 128*

Blair, D.P., (2018), Vibration modelling and mechanisms for wall control blasting. In: Twelfth Int.Symp. Rock Fragmentation by Blasting, Lulea., 269–280, 11-13.

Blair, D.P., (2008), Non-linear superposition models of blast vibration. Int J Rock Mech Min Sci.,45:235–247.

Simangunsong, G.M., Wahyudi S., (2015), Effect of bedding plane on prediction blast-induced ground vibration in open pit coal mines. *Int J Rock Mech Min Sci., 79*,1–8.

Singh, S.P., Narendrula R., (2004), Assessment and prediction of rock mass damage by blast vibrations. In: Proc. 13th Int. Symp. Mine Planning and Equipment Selection, Wroclaw., 317–322, 1-3. 2

POST-MINING LAND-USE PLANNING: AN INTEGRATION OF MINED LAND SUITABILITY ASSESSMENT AND SWOT ANALYSIS IN CHADORMALU IRON ORE MINE OF IRAN

S. Amirshenava [1], M. Osanloo [1, *]

[1] *Amirkabir University of Technology, Mining Engineering Dept*
*(*Corresponding author: morteza.osanloo@gmail.com)*

ABSTRACT

Post-Mining Land-Use (PMLU) planning is one of the crucial stages of mine comprehensive plan to obtain sustainable mining operations. However, the suitable PMLU selection is a challenging task for mine reclamation planner. According to the mine reclamation objectives, the selected PMLU option should be sustainable. To this end, the suitability and vulnerability of the PMLU should be maximum and minimum, respectively. Therefore, Mined Land Suitability Assessment (MLSA) is essential for evaluating the mined land's suitability for PMLU options. In addition to MLSA, it is required the PMLU option's vulnerability aspects are identified, and appropriate solutions are provided to reduce them, relying on the PMLU option's strengths and existing opportunities. The SWOT (Strengths, Weaknesses, Opportunities, and Threats) analysis method is one of the best tools for solving this problem. The aim of this study is to develop a new hybrid general PMLU planning approach based on the MLSA and SWOT analysis. This new approach will facilitate choosing the sustainable PMLU with high accuracy due to the assurance of mined land's suitability and providing appropriate strategies for ensuring mine reclamation plan success. This approach is verified in the Chadormalu iron ore mine of Iran and the results' reliability is confirmed by considering this mine's characteristics.

Keywords: Post-mining land-use, mine reclamation, mined land suitability assessment, SWOT analysis, sustainable mining

INTRODUCTION

Mining plays a vital role in economic growth and human development. However, these benefits have come with a cost to the environment and society that threaten Sustainable Development (SD) goals. Hence, one of the challenges of modern mining is to keep mining on an SD path (Amirshenava and Osanloo, 2019; Alves et al., 2020). Mine reclamation is an accepted stage in the Modern Mining Life Cycle (MMLC) to keep mining in an SD path by performing the responsible mining (Amirshenava and Osanloo, 2018). Post-Mining Land-Use (PMLU) is the most important element of the mine reclamation plan, and it should be raised and discussed in the primary stage of the mining study. PMLU profoundly affects all mine reclamation activities and their associated costs. PMLU is not necessarily similar to pre-mining land-use, and other land-uses may be introduced according to the regional potentials and the community needs (Mborah et al., 2015; Amirshenava and Osanloo, 2018). Several studies have been conducted to present a classification of possible post-mining land uses regarding the importance of the type of PMLU in the mine reclamation planning and operation (Rowe, 1977; Dogan and Kahriman, 2008; Soltanmohammadi et al., 2008; Bielecka and Król-Korczak, 2010; Kaźmierczak et al., 2017; Amirshenava and Osanloo, 2018, 2021). By reviewing the literature, the latest and most comprehensive classification of general and specific PMLU alternatives has been presented by Amirshenava and Osanloo (2021) (Fig. 1). This clasification's main superiority is identifying and classifying all possible PMLU alternatives into

general and specific groups based on mine reclamation objectives and hierarchy, with minimal overlapping between groups. This classification covers all three environmental, social, and economic indexes of SD entirely.

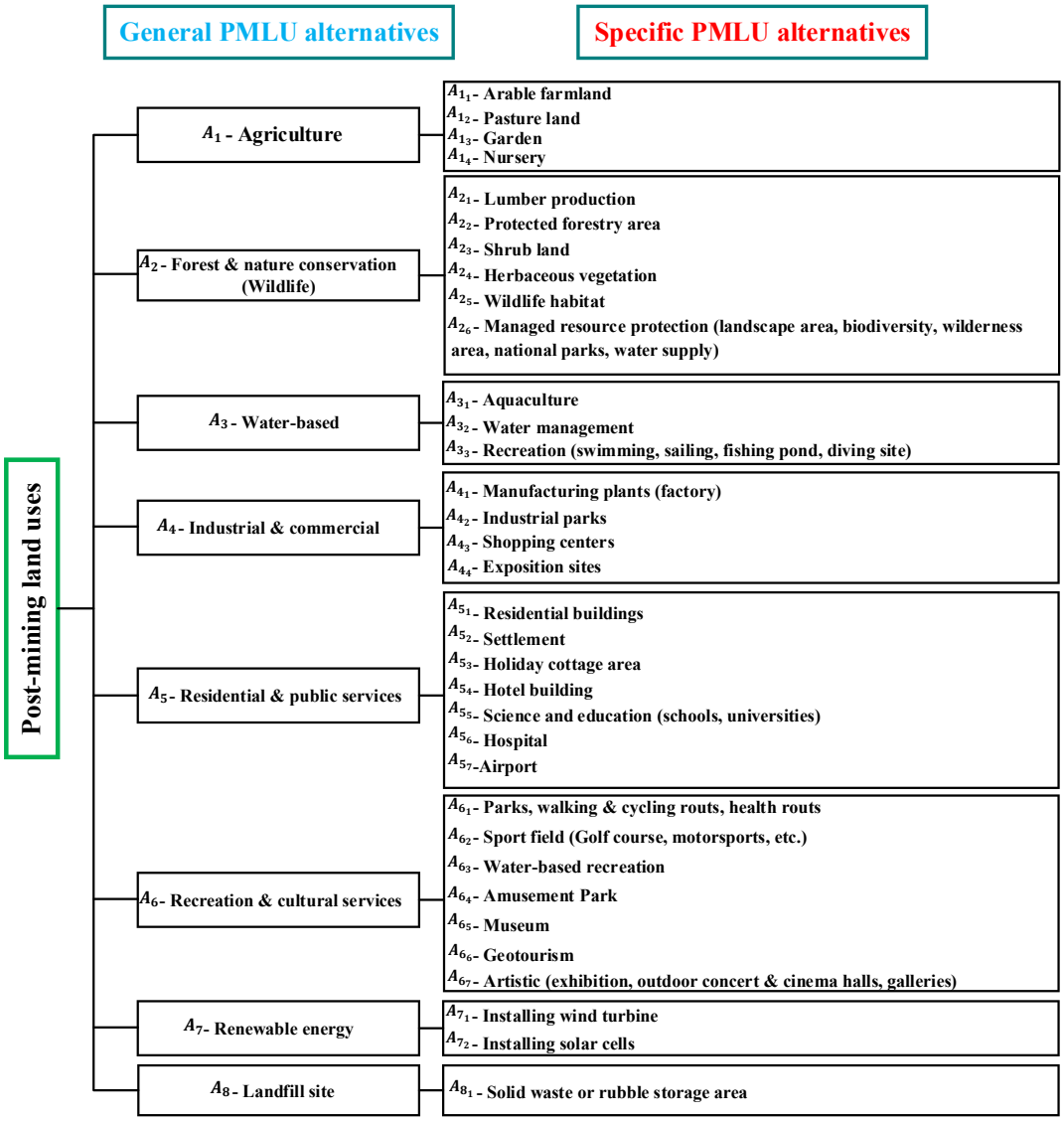

Figure 1. The comprehensive classification of PMLU alternatives (Amirshenava and Osanloo, 2021b)

The suitable PMLU selection is the fundamental step in the mine reclamation plan so that a correct choice can guarantee the success of the reclamation project (Soltanmohammadi et al., 2010). According to mine reclamation objectives, PMLU as a permanent use for mined land should be sustainable (McHaina, 2001; Christoffersen *et al.*, 2019). To this end, the suitability and vulnerability of land-use should be maximum and minimum, respectively (Prakash, 2003). As the primary condition for the PMLU sustainability and to determine the applicable PMLU options, Mined Land Suitability Assessment (MLSA) has been investigated by many researchers, and several models have been developed in this field (Rowe, 1977; Sharma et al., 1996; Soltanmohammadi et al., 2008; Wang and Yang, 2011; Wang et al., 2011; Hao et al., 2015; Asmarhansyah et al., 2017; Cheng and Sun, 2019; Sukarman and Gani, 2020; Amirshenava and Osanloo, 2021). The MLSA process is responsible for evaluating the mined land's appropriateness for any PMLU and determining the applicable PMLU options (Ramani et al., 1990).

Although the mined land suitability is necessary for the PMLU option's sustainability, it alone is not enough. According to Amirshenava and Osanloo (2021), in addition to MLSA, the mine reclamation planner should also evaluate the vulnerability aspects of the chosen suitable PMLU option and provide the appropriate solutions to reduce them relying on the PMLU option's strengths and existing opportunities. The SWOT analysis technique is the best tool for identifying the internal strengths and weaknesses of the PMLU option and the opportunities and threats that exist from the external environment for that option. Hence, to minimize the PMLU option's vulnerability and ensure the option's implementation successfully, the appropriate strategies can be provided based on this method (Smyth and Krebs, 2019; Mhlongo et al., 2020).

The SWOT analysis technique is a strategic planning tool that was originated in the 1960s by Albert Humphrey in the Stanford Research Institute. The SWOT word is created by putting together the first letters of the four words Strengths, Weaknesses, Opportunities, and Threats. As a robust strategic planning and environmental analysis tool, this qualitative strategic technique is used to identify the key internal (strengths and weaknesses) and external (opportunities and threats) strategic factors that an organization (group, person, etc.) faces and affect its objectives. Based on this technique's results, appropriate strategies can be developed to maximize strengths, eliminate weaknesses, exploit opportunities, and counter threats. Despite the importance of SWOT analysis and the role that strategic planning can play in ensuring the PMLU option's sustainability, very few studies (Dias et al., 2008; Carrión-Mero et al., 2020; Kurniawan et al., 2020; Mhlongo et al., 2020) have addressed the SWOT analysis of PMLU options to the best of our knowledge. Based on the literature review, there is no universal and perfect study for strategic planning of all possible PMLU options while focuses on evaluating the strategic position of PMLU options quantitatively and determining the appropriate strategies to ensure the sustainable deployment of PMLU.

The aim of this study is to develop a new hybrid general PMLU planning approach based on the MLSA and SWOT analysis. In this regard, applying the MLSA model will determine the applicable PMLU options among all the possible general options. By identifying the possible strengths, weaknesses, opportunities, and threats of all the possible general PMLU options, the SWOT matrices are created for each PMLU alternative. Then, the External Factor Evaluation (EFE) and Internal Factor Evaluation (IFE) methods are applied to quantify the SWOT matrices. Based on the identified position in the Internal-External (IE) matrix, the best strategies for each PMLU option are proposed, leading to the sustainability of PMLU options. Finally, this approach is applied in the Chadormalu Iron Ore Mine as the case study, and the results are reported and discussed.

METHODOLOGY

The research framework of this study is shown in Figure 3. As shown in Figure 3, the first stage of PMLU planning is applying the MLSA model to identify the applicable PMLU options. After identifying the viable options, the strategic planning process of the PMLU options is performed based on the approach developed in this study.

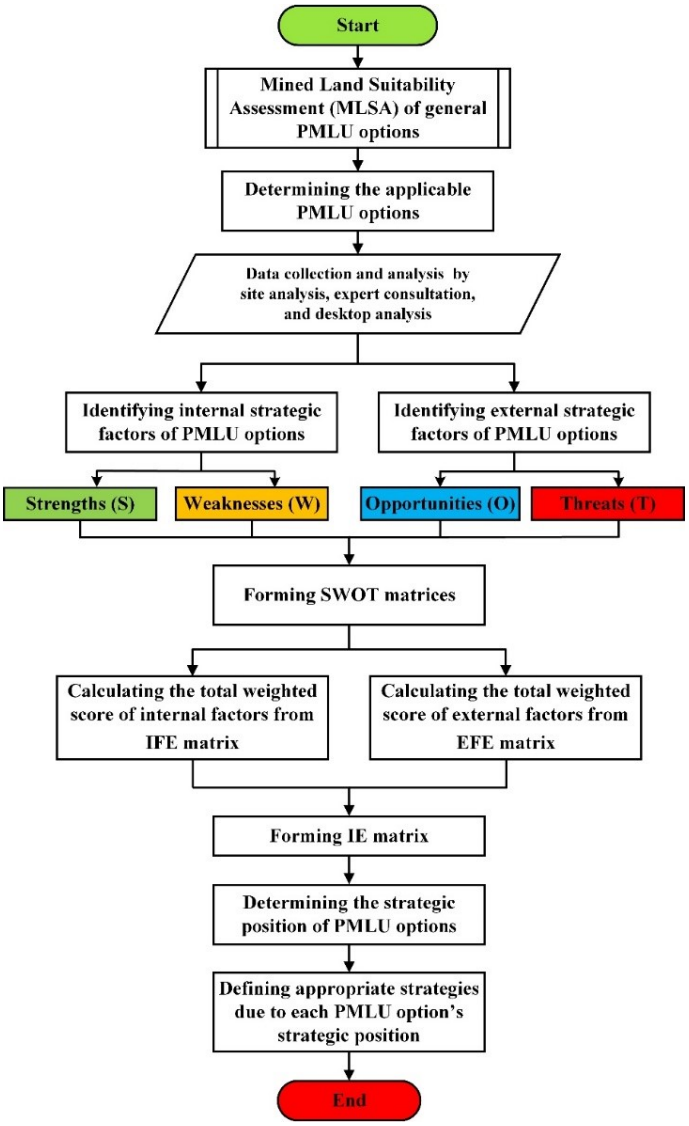

Figure 2. Research framework of the study

Mined Land Suitability Assessment (Mlsa)

The first stage of the proposed PMLU planning approach is applying the MLSA model to identify the applicable general PMLU options. Indeed, the applicable PMLU options with an acceptable mined land suitability class, enter into the PMLU strategic planning approach. According to the literature review, Among the MLSA models presented by various researchers, the Amirshenava and Osanloo (2019) model, due to considering all possible general PMLU options, calculating the suitability score, determining the suitability level qualitatively, and classifying the suitability classes, is the most appropriate model. As a result, in this study, in order to MLSA of the general PMLU options, this model is applied as the newest and most efficient model in this field.

SWOT Analysis of PMLU Options

According to the comprehensive classification of post-mining land uses proposed by Amirshenava and Osanloo (2021) (Figure 1), each general PMLU alternative has several potential specific

PMLU options. This classification is so that the characteristics of the specific options in each group correspond to the general option's characteristics of the same group. Nevertheless, the strategic analysis of general PMLU alternatives can broadly cover the strategic factors related to their subgroup's specific options. Therefore, only general PMLU alternatives are evaluated in the PMLU planning approach. In order to determine the strategic factors of PMLU options, the following questions are raised:

Question 1. What *strengths* and advantages does this PMLU option have?
Question 2. What are the *weaknesses* of this PMLU option?
Question 3. What are the good *opportunities* for this PMLU option?
Question 4. What are the *threats* of this PMLU option?

The SWOT matrices are formed after identifying the internal and external strategic factors. This matrix consists of 4 parts, 2 of which are related to internal factors, and the other sections are dedicated to external factors. Based on the results of this matrix, appropriate strategies can be proposed with the aims of maximum use of the strengths, minimizing and stopping the weaknesses, making the most of the opportunities, and preventing and treating potential threats. To achieve these objectives, the appropriate strategies are defined based on the identifies strategic factors in four general types (Table 1).

Table 1. The classification of strategies (David and David, 2017; Shahba et al., 2017)

ID	Type of strategy	Strategy title	Description
SO	Strategies based on Strengths - Opportunities	Aggressive	Using strengths to take advantage of opportunities
ST	Strategies based on Strengths - Threats	Competitive	Using strengths to avoid the negative impacts of threats and even trying to eliminate the threats
WO	Strategies based on Weaknesses - Opportunities	Conservative	Reducing weaknesses by taking advantages of opportunities
WT	Strategies based on Weaknesses - Threats	Defensive	Preventing to be damaged due to weaknesses against threats from external environment

Establishment of IFE Matrix

The IFE matrix is a strategic tool for quantitative analysis of internal strategic factors. In this method, firstly, the relative weights of internal strategic factors are determined. In this regard, the experts were asked to determine the importance of each factor with numbers from 1 (low importance) to 5 (high importance). Then, the mean value of each factor's score is calculated, and these values are normalized based on Eq. (1) to determine the relative weight of each internal factor (Tahernejad et al., 2013).

$$W_{IF_i} = \frac{MVIF_i}{\sum_{i=1}^{n}\left(MVIF_i\right)} \quad (1)$$

Where $MVIF_i$ is mean value of importance of internal factor i and W_{IF_i} is the weight of internal factor i. Each factor's weight indicates its relative importance compared to other factors, and the sum of these weights is equal to 1. Then, experts give each factor a score from 1 to 4 (1 and 2 for weaknesses

and 3 and 4 for strengths). The weighted score of each internal factors is calculated based on Eq. (2). Then, the total weighted score of internal factors is calculated according to Eq. (3).

$$WS_{IF_i} = W_{IF_i} \times S_{IF_i} \quad (2)$$

$$TWS_{IF} = \sum_{i=1}^{n} (W_{IF_i} \times S_{IF_i}) \quad (3)$$

where WS_{IF_i} is the weighted score of internal factors i, S_{IF_i} is the score of internal factor i, and TWS_{IF} is the total weighted score of internal factors. The minimum and maximum value of TWS_{IF} is 1 and 4, respectively. Therefore, the mean value of TWS_{IF} is 2.5. The TWS_{IF} below 2.5 represents the superiority of weaknesses over strengths, and TWS_{IF} equal to or above 2.5 indicates a strong internal position (David and David, 2017).

Establishment of EFE Matrix

The EFE matrix examines the external strategic factors quantitatively. Calculation of the EFE is similar to IFE, with the difference is that external factors (opportunities and threats) are examined in this method.

$$W_{EF_j} = \frac{MVEF_j}{\sum_{j=1}^{m} (MVEF_j)} \quad (4)$$

Where $MVEF_j$ is mean value of importance of external factor j and EF_j is external factor j and W_{EF_j} is the weight of external factor j. Then, experts give each external factor a score from 1 to 4 (1 and 2 for threats and 3 and 4 for opportunities). The weighted score of each external factor is calculated based on the Eq. (5). Then, the total weighted score of external factors is calculated according to Eq. (6).

$$WS_{EF_j} = W_{EF_j} \times S_{EF_j} \quad (5)$$

$$TWS_{EF} = \sum_{j=1}^{m} (W_{EF_j} \times S_{EF_j}) \quad (6)$$

where WS_{EF_j} is the weighted score of external factor j, S_{EF_j} is the score of external factor j, and TWS_{EF} is the total weighted score of external factors. The minimum and maximum value of TWS_{EF} is 1 and 4, respectively. Therefore, the mean value of TWS_{EF} is 2.5. The TWS_{EF} below 2.5 represents the superiority of threats over opportunities (weak external position), and also TWS_{EF} equal to or above 2.5 indicates a strong external position (David and David, 2017)

Establishment of IE Matrix

In order to determine each PMLU option's strategic position, the IE matrix method is applied (Figure 3). The IE matrix examines the internal and external factors simultaneously. The horizontal and vertical axis of the IE matrix is dedicated to the TWS_{IF} and TWS_{EF}, respectively. As shown in Fig. 3, this matrix consists of 4 sections (blocks) that show the strategic position. (Ardeshir, Safaei and Abtahi, 2016). Based on the strategic position determined by connecting TWS_{IF} and TWS_{EF} in the axes, the most appropriate strategies are defined to ensure PMLU deployment success.

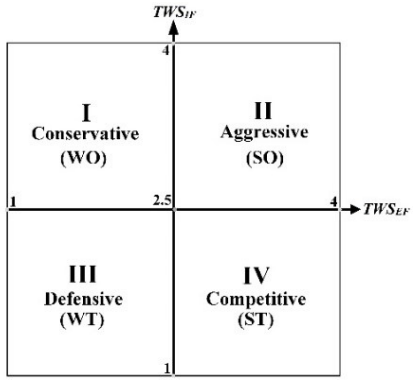

Figure 3. The IE matrix – Adopted from Ardeshir et al. (2016)

VERIFYING THE PROPOSED APPROACH

The proposed PMLU planning approach is implemented in the Chadormalu iron ore mine of Iran. Chadormalu iron ore mine is located in the central desert of Iran, 180 km northeast of Yazd, and 833 km from Tehran, capital of Iran (Figure 4). The total mineable reserve of the mine is 295 Mt with an average grade of Fe 55.2%, a total stripping ratio of 2:1, and an average annual production of 15.1 Mt. Chadormalu has a dry and cold climate in winter and hot in summer due to its geographical location in the desert. The annual average temperature of the region is 20.8 ◦c. The annual average wind speed is 52 Km/h, and the average yearly precipitation is 107mm in the area. The area's vegetation is low, and only in some places, plants resistant to drought, heat, and salinity can grow (About company, 2021).
Based on Amirshenava and Osanloo (2021), the applicable PMLU options in the Chadormalu mine are given in Table 4. Therefore, strategic planning is performed for these five PMLU options (Table 2) with an acceptable mined land suitability class.

Figure 4. Location and a view of the Chadormalu iron ore mine of Iran

Table 2. The applicable PMLU options in the Chadormalu mine (Amirshenava and Osanloo, 2021)

No.	The applicable PMLU option	No.	The applicable PMLU option
1	A_2- Forestry & nature conservation	4	A_7- Renewable energy
2	A_4- Industrial & commercial	5	A_8- Landfill sites
3	A_6 - Recreation & cultural services		

For generating the SWOT matrices, by considering the characteristics of Chadormalu iron ore mine, the internal and external strategic factors are identified according to site analysis, experts' opinions, and literature review. In this study, the expert team includes 10 persons selected with great care to provide a good and accurate view of PMLU options' strategic factors (Table 3). The SWOT matrices of PMLU options for five applicable PMLU options are given in Tables 4 to 8.

Table 3. The experts' team characteristics

Skill	Education	Number of persons
Academic persons	PhD	2
Public sector's stakeholders	MSc	1
	PhD	2
Private sector's stakeholders	MSc	2
Mining engineers	MSc	1
	PhD	1
Non-governmental organizations	MSc	1

Table 4. SWOT matrix for the forestry and nature conservation PMLU alternative

Internal factors	External factors
Strengths (S):	**Opportunities (O):**
(S_1A_2) - Improvement of the aesthetic appearance of the mined land	(O_1A_2) - Creating job opportunities
(S_2A_2) - Reverse the loss of biodiversity and wildlife populations	(O_2A_2) - Opportunity to create added value by planting rare medicinal herbs
(S_3A_2) - Shelter and food supply for wildlife	(O_3A_2) - Potential high demand in the timber market
(S_4A_2) - Wood production	(O_4A_2) - Opportunity to use native and drought-friendly species
(S_5A_2) - Soil protection and improvement	(O_5A_2) - The potential of phytoremediation
(S_6A_2) - Improving per capita income of residents	(O_6A_2) - Persian Gulf water transfer project to the central plateau of Iran
(S_7A_2) - Improving the morale of mine workers and indigenous people (increasing life expectancy)	
Weakness (W):	**Threats (T):**
(W_1A_2) - Requires intense earthwork and large volumes of topsoil	(T_1A_2) - Environmental threats (e.g., drought, bushfire, etc.)
(W_2A_2) - Difficulties of preparing and maintaining	(T_2A_2) - Key threats for wildlife habitat (i.e., illegal

native plant species compatible with arid and semi-arid regions	hunting, etc.)
(W_3A_2) - Vulnerability to climate changes	(T_3A_2) - Climatic condition of Chadormalu iron ore mine
(W_4A_2) - Ecological and environmental vulnerability	(T_4A_2) - Lack of legal requirement to implement the progressive reclamation plan by the mining company
	(T_5A_2) - Soil erosion and salinity

Table 5. SWOT matrix for the industrial and commercial PMLU alternative

Internal factors	**External factors**
Strengths (S):	**Opportunities (O):**
(S_1A_4) - Ensure continued economic activities in the region	(O_1A_4) - Creating job opportunities
(S_2A_4) - High return on investment	(O_2A_4) - New investment opportunities
(S_3A_4) - Improving per capita income of residents	(O_3A_4) - Reusing potential of mine infrastructures
(S_4A_4) - GDP improvement and wealth creation	(O_4A_4) - Persian Gulf water transfer project to the central plateau of Iran
(S_5A_4) - Availability of market and trading places for residents	(O_5A_4) - Development of local business opportunities
	(O_6A_4) - The potential of establishing the mining industries factory
Weakness (W):	**Threats (T):**
(W_1A_4) - Industrial pollution	(T_1A_4) - The potential of intensification of mine closure environmental risks
(W_2A_4) - High dependence on the existence of infrastructures	(T_2A_4) - Limited water resources
(W_3A_4) - lack of improvement of the aesthetic appearance of the mined land	(T_3A_4) - Investment risk due to unstable political and economic conditions
(W_4A_4) - Does not address the environmental risks of mine closure	(T_4A_4) - Legal restrictions (e.g., environmental permits, etc.)
(W_5A_4) - High maintenance and monitoring requirements	(T_5A_4) - Hostility of natives
	(T_6A_4) - Lack of legal requirement to implement the progressive reclamation plan by the mining company
	(T_7A_4) - Lack of proper monitoring and maintenance

Table 6. SWOT matrix for the recreation & cultural services PMLU alternative

Internal factors	**External factors**
Strengths (S):	**Opportunities (O):**
(S_1A_6) - Support of local and regional recreational and entertainment needs	(O_1A_6) - Creating job opportunities
(S_2A_6) - Improve the livelihood quality and longer life expectancy	(O_2A_6) - New investment opportunities
(S_3A_6) - Improving per capita income of residents (increase tourism incomes)	(O_3A_6) - Reusing potential of mine infrastructures, welfare facilities, and the legacy of mining activities
(S_4A_6) - Improvement of the aesthetic appearance of the mined land	(O_4A_6) - Proximity to areas with tourism and cultural heritage potentials

(S_5A_6) - Preservation of mining heritage and unique geological phenomena	(O_5A_6) - Existence of higher education centers with mining and earth sciences fields in the region
	(O_6A_2) - The potential of desert ecotourism
Weakness (W):	**Threats (T):**
(W_1A_6) - Environmental pollution and destruction by tourists	(T_1A_6) - Climatic condition of Chadormalu iron ore mines
(W_2A_6) - High population density in the area and increase in traffic	(T_2A_6) - Investment risk due to unstable political and economic conditions
(W_3A_6) - High dependence on the existence of infrastructures and welfare facilities in the region	(T_3A_6) - Health and safety risks left by mine closure
(W_4A_6) - Strong dependence on climatic, geographical, anthropological, and cultural characteristics	(T_4A_6) - Hostility of natives
	(T_5A_6) - Lack of legal requirement to implement the progressive reclamation plan by the mining company
	(T_6A_6) - Lack of proper monitoring and management

Table 7. SWOT matrix for the renewable energy services PMLU alternative

Internal factors	External factors
Strengths (S):	**Opportunities (O):**
(S_1A_7) - Reducing ecological costs (reducing carbon footprints)	(O_1A_7) - High demand to generate electricity in the country
(S_2A_7) - Lower cost and sustainable energy supply	(O_2A_7) - Creating sustainable job opportunities
(S_3A_7) - Improving the real estate value	(O_3A_7) - High efficiency of solar energy in central desert of Iran
(S_4A_7) - Reduced earthwork requirements	(O_5A_7) - Existence of energy-intensive industries in the surrounding areas
(S_5A_7) - High revenue from electricity generation	(O_6A_7) - Possibility of reusing existing infrastructure
(S_6A_7) - Improving living standards	(O_7A_7) - Government support policies
Weakness (W):	**Threats (T):**
(W_1A_7) - Relatively high initial investment required	(T_1A_7) - Technological weakness
(W_2A_7) - Strongly depends on climatic and geographical conditions	(T_2A_7) - Low energy prices in Iran and lack of sufficient incentives to invest in renewable energy sources
(W_3A_7) - The advanced and complex nature of renewable technologies (requiring of specialized personnel)	(T_3A_7) - Unpredictable weather events that disrupt these technologies
(W_4A_7) - High maintenance and monitoring requirements	(T_4A_7) - Lack of proper maintenance and monitoring
	(T_5A_7) - Lack of founds
	(T_6A_7) - Lack of legal requirement to implement the progressive reclamation plan by the mining company

Table 8. SWOT matrix for the landfill site PMLU alternative

Internal factors	External factors
Strengths (S):	**Opportunities (O):**
(S_1A_8) - Low investment requirements	(O_1A_8) - Existence of need for a place to dispose of industrial and domestic waste
(S_2A_8) - Low corrective measures requirements	(O_2A_8) - Climatic condition of Iran's iron ore mine
(S_3A_8) - Eliminating safety risks of the mine pit (e.g., pit slope failure, etc.)	(O_3A_8) - The potential of using the completed landfill site for other land uses in the future
	(O_4A_8) - Creating job opportunities
Weakness (W):	**Threats (T):**
(W_1A_8) - Low efficiency of land-use	(T_1A_8) - Legal restrictions (e.g., environmental permits, etc.)
(W_2A_8) - Environmental impacts of landfill sites	(T_2A_8) - Hostility of natives
(W_3A_8) - Negative impacts on aesthetic values	(T_3A_8) - Lack of studies on the chemical composition of wastes and intensity of their risks
(W_4A_8) - Does not address the environmental and socio-economic risks of mine closure	(T_4A_8) - The potential of intensification of mine closure health and environmental risks
(W_5A_8) - Human and animals health problems	(T_5A_8) - Lack of legal requirement to implement the progressive reclamation plan by the mining company
(W_6A_8) - High maintenance and monitoring requirements	

After forming the SWOT matrices for all of the possible general PMLU options, the TWS_{IF} and TWS_{EF} are calculated based on the expert opinions, according to Eqs. (1) to (6). The total weighted scores of strategic factors and the strategic position of the PMLU alternatives in the IE matrix are shown in Table 9. The appropriate strategies for each of the PMLU options regarding their strategic position are defined in Table 10.

Table 9. The final scores of strategic factors and the strategic position of the PMLU alternatives

PMLU alternative	TWS_{IF}	TWS_{EF}	Strategic position in IE matrix	The type of strategy
A_2- Forestry & nature conservation	2.778	2.604	II	Aggressive (SO)
A_4- Industrial & commercial	2.744	2.554	II	Aggressive (SO)
A_6 - Recreation & cultural services	2.528	2.478	IV	Competitive (ST)
A_7- Renewable energy	2.957	2.808	II	Aggressive (SO)
A_8- Landfill sites	2	2.333	III	Defensive (WT)

Table 10. The strategic position of PMLU alternatives in the IE matrix

PMLU alternative	Proposed strategies based on the PMLU alternatives' strategic position in the IE matrix	The effective strategic factors
A_2	- Soil stabilization and improvement by planting the native and drought-friendly species and also using the potential of phytoremediation	S_5A_2, O_4A_2, O_5A_2
	- Creating a beautiful and eye-catching landscape by planting the native species and homogeneous with surrounding lands	S_1A_2, S_7A_2, O_4A_2
	- Creating shelter and food supply for wildlife by planting the native species	S_2A_2, S_3A_2, O_4A_2
	- Creating sustainable job opportunities and income by planting high value-added rare medicinal herbs	S_6A_2, O_1A_2, O_2A_2
	- Utilizing the benefits of the Persian Gulf water transfer project to increase the efficiency of wood production for economic purposes	S_1A_2, S_4A_2, S_6A_2, O_1A_2, O_3A_2, O_6A_2
A_4	- Creating job opportunities by continuing intensive economic activities in the region through new investment opportunities	S_1A_4, S_2A_4, S_3A_4, S_4A_4, O_1A_4, O_2A_4, O_3A_4
	- Development of the mining industries factory through the potentials of re-using of mine infrastructures and utilizing the Persian Gulf water transfer project	S_1A_4, S_2A_4, S_3A_4, S_4A_4, O_1A_4, O_3A_4, O_4A_4, O_6A_4
	- Improving per capita income of residents by development of local business regarding the market and trading	S_3A_4, S_5A_4, O_1A_4, O_5A_4
A_6	- Create a sustainable income for residents by employing local people in jobs related to tourism guidance and monitoring and maintenance	S_2A_6, S_3A_6, T_4A_6, T_6A_6
	- Development of desert ecotourism due to the climatic conditions of Chadormalu mine	S_1A_6, S_4A_6, S_5A_6, T_1A_6, T_2A_6
	- Implementing the progressive reclamation activities to develop mine geotourism with the aim of preserving the mining heritage and reducing investment risks	S_4A_6, S_5A_6, T_2A_6, T_3A_6, T_5A_6
A_7	- Development of solar cells farm considering the high efficiency of solar energy in central desert of Iran	S_2A_7, S_3A_7, S_5A_7, S_6A_7, O_1A_7, O_2A_7, O_3A_7, O_6A_7
	- Generation and transfer of electricity to the power grid using infrastructure in the mine in order to make income and benefit from government support policies	S_2A_7, S_3A_7, S_4A_7, S_5A_7, S_6A_7, O_1A_7, O_2A_7, O_3A_7, O_5A_7, O_6A_7
	- Lower cost and sustainable energy supply for energy-intensive industries in the surrounding areas	S_1A_7, S_2A_7, S_5A_7, O_1A_7, O_2A_7, O_3A_7, O_4A_7, O_5A_7
A_8	- Establishing effective periodic monitoring to assess and control the environmental impacts and health problems of the landfill site	W_2A_8, W_5A_8, W_6A_8,T_1A_8, T_2A_8, T_3A_8, T_4A_8
	- Implementation of this option as a last resort in areas where the mined land is not suitable for other PMLU options	W_1A_8, W_3A_8, W_4A_8,T_1A_8, T_2A_8

- Establishing waste management system	W_2A_8, W_5A_8, W_6A_8, T_1A_8, T_3A_8, T_4A_8
- Implementing progressive reclamation activities regarding the landfill site earthworks	W_3A_8, W_6A_8, T_5A_8

DISCUSSION

The PMLU planning approach presented in this study is a new approach that makes it possible to achieve a sustainable PMLU option. This approach effectively evaluates the mined land suitability as the most important condition for the sustainability of the chosen PMLU. Besides, to ensure the sustainability of PMLU, using the PMLU strategic planning model, the best strategies are provided to reduce the selected alternative's vulnerability. Due to the interdisciplinary nature of mine reclamation science, strategic planning helps the mine reclamation planner create a competitive advantage for the mine reclamation project and manage and even overcome fluctuations and uncertainties. Indeed, strategic planning can ensure the successful deployment of the PMLU by reducing the vulnerability of the PMLU option through defining and implementing appropriate strategies.
A novel strategic planning approach was developed for all the possible general post-mining land uses based on the SWOT analysis method. This approach's main superiority is defining internal and external strategic factors in the SWOT matrices for all the possible general PMLU alternatives that fully cover mine reclamation objectives and three indexes of SD. Besides, determining the strategic position of PMLU options in the IE matrix through the IFE and EFE matrices' outputs and defining the appropriate strategies corresponding to the PMLU options' strategic position are some of the other innovative aspects of this study.

In this study, to form SWOT matrices for 5 applicable general PMLU options in the Chadormalu iron ore mine, in total, 26, 23, 28, and 29 items of strengths, weaknesses, opportunities, and threats were identified, respectively. According to the obtained results of IFE and EFE matrices given in Table 9, except for PMLU options A_8, TWS_{IF} for other PMLU alternatives is greater than 2.5. It indicates the superiority of strengths over weaknesses of these PMLU options. Given the positive role of mine reclamation activities in improving environmental and social conditions, ongoing economic activities in the region, generating GDP, and increasing the life expectancy of local people, these results are consistent with the actual situation. The PMLU option A_8 has the lowest value of TWS_{IF} among all options (TWS_{IF} = 2). Given that this option is a lower value land-use that is considered the last resort for mine reclamation, its weaknesses are more prominent than its strengths, and the results of this study confirm this point. The maximum value of TWS_{EF} is related to PMLU option A_7 (TWS_{EF} = 2.808), which means the superiority of opportunities over the threats of this option. The reason is the high potential of Chadormalu iron ore mines for the development of solar cells farm due to its climatic conditions.

Given the SWOT matrices and TWS_{EF} scores, many of the opportunities available for PMLU options are related to the positive aspects of mining activities, especially in developing infrastructures and facilities. These results confirm that the positive aspects of mining activities are not limited to the operating life of the mine. After the mine closure, these positive aspects can be considered as opportunities to implement the desired PMLU options, and local people will still be able to take advantage of these benefits. For example, the Persian Gulf Water Transfer Project to the central and east plateau of Iran is a megaproject. Large Iranian mining companies have the most significant contribution to this investment. In addition to supplying the water needed by these mines and their related industries during their lifetime of operation, this project creates tremendous opportunities to provide the water required for agricultural, drinking water, industrial, and other economic activities.

The proposed approach is a practical tool for decision-making in choosing the most appropriate PMLU option. So far, various models based on the decision theory approach have been proposed to

select the suitable PMLU option. In these models, the PMLU option with the highest rank is selected as the suitable option. However, the option with the highest rank will not necessarily be the most appropriate. In choosing the suitable PMLU option based on the decision theory approach, there is a shortcoming in the lack of considering the strengths, weaknesses, opportunities, and threats of the PMLU options. Therefore, it is necessary to analyze the SWOT of the options that have earned the highest ranking (first to third place) and updating the ranking by considering the TWS_{IF} and TWS_{EF}. The proposed strategic planning approach in this study is a good solution for this problem. Therefore, the most appropriate option is the option that, in addition to gaining the most points in terms of decision criteria, the most important of which is the mined land suitability score, also has the most appropriate strategic position. Indeed, its strengths and opportunities are superior to its weaknesses and threats, respectively. In this case, due to considering the MLSA and SWOT analysis processes in the Multi-Criteria Decision-Making (MCDM) problem to select the suitable PMLU option, the mine reclamation planner can ensure the sustainability of the chosen option. Besides, by defining appropriate strategies according to the strategic position of the PMLU option, the probability of successfully deploying the selected PMLU option will increase.

CONCLUSION

This study focuses on developing a new hybrid general PMLU planning approach based on the MLSA and SWOT analysis. This new approach ensures the achievement of a sustainable PMLU due to the assurance of mined land's suitability and providing appropriate strategies for ensuring mine reclamation plan success. The advantage of the proposed PMLU strategic planning approach is defining internal and external strategic factors for all the possible general PMLU options based on the mine reclamation objectives and consequently developing SWOT matrices. This general strategic planning approach is responsible for determining the strategic position of PMLU options in the IE matrix based on IFE and EFE matrices, which are applied to quantify the SWOT matrices. Defining appropriate strategies corresponding to the strategic position of PMLU options is another innovative aspect of the proposed approach that will lead to ensure the mine reclamation project's success. This PMLU planning approach paves the way for decision-making to choose the sustainable PMLU option and provide a general vision for the success of the mine reclamation project. The proposed approach was implemented in the Chadormalu iron ore mine. To form SWOT matrices for 5 applicable general PMLU options in this mine, in total, 26, 23, 28, and 29 items of strengths, weaknesses, opportunities, and threats were identified, respectively. It is worth noting that this number of strategic factors has not been identified and evaluated in similar studies. Based on the results of IFE and EFE matrices, the A_7- renewable energy, A_2- forest & nature conservation, and A_4- Industrial & commercial alternatives are ranked first to third in TWS_{IF} and TWS_{EF}. The A7 option earned the best strategic position in the IE matrix. The obtained result is verified due to the climatic conditions of the Chadormalu iron ore mine. Based on the strategic position of PMLU options, a total of 18 strategies were defined. These strategies are defined so that each of them covers several strategic factors related to the type of strategy to overcome the overlap of strategies.

REFERENCES

About company. http://chadormalu.com/en-us/AboutCompany (accessed Apr. 21, 2021).

Alves, W., Ferreira, P. and Araújo, M. (2020) 'Challenges and pathways for Brazilian mining sustainability', *Resources Policy*, (February), p. 101648. doi: 10.1016/j.resourpol.2020.101648.

Amirshenava, S. and Osanloo, M. (2018) 'Mine closure risk management: An integration of 3D risk model and MCDM techniques', *Journal of Cleaner Production*, 184, pp. 389–401. doi: 10.1016/j.jclepro.2018.01.186.

Amirshenava, S. and Osanloo, M. (2019) 'A hybrid semi-quantitative approach for impact assessment of mining activities on sustainable development indexes', *Journal of Cleaner Production*, 218, pp. 823–

834. doi: 10.1016/j.jclepro.2019.02.026.

Amirshenava, S. and Osanloo, M. (2021) 'Mined Land Suitability Assessment: A Semi-Quantitative Approach based on a New Classification of Post-Mining Land Uses', *International Journal of Mining, Reclamation and Environment*, (Published Online). doi: https://doi.org/10.1080/17480930.2021.1949864.

Ardeshir, A., Safaei, A. and Abtahi, S. (2016) 'Providing an Example of Scheduling Model for Marine Transportation Companies', *American Journal of Civil Engineering and Architecture*, 4(5), pp. 165–170. doi: 10.12691/ajcea-4-5-3.

Asmarhansyah, A. *et al.* (2017) 'Land suitability evaluation of abandoned tin-mining areas for agricultural development in Bangka Island, Indonesia', *Journal of Degraded and Mining Lands Management*, 04(04), pp. 907–918. doi: 10.15243/jdmlm.2017.044.907.

Bielecka, M. and Król-Korczak, J. (2010) 'Hybrid expert system aiding design of post-mining regions restoration', *Ecological Engineering*, 36(10), pp. 1232–1241. doi: 10.1016/j.ecoleng.2010.04.023.

Carrión-Mero, P. *et al.* (2020) 'Quantitative and Qualitative Assessment of the "El Sexmo" Tourist Gold Mine (Zaruma, Ecuador) as A Geosite and Mining Site', *Resources*, 9(3), p. 28. doi: 10.3390/resources9030028.

Cheng, L. and Sun, H. (2019) 'Reclamation suitability evaluation of damaged mined land based on the integrated index method and the difference-product method', *Environmental Science and Pollution Research*, 26(14), pp. 13691–13701. doi: 10.1007/s11356-018-2020-4.

Christoffersen, L. *et al.* (2019) 'Innovative community engagement for the quantitative risk assessment for a mine closure and reclamation plan', *Proceedings of the 13th International Conference on Mine Closure*, pp. 355–368. doi: 10.36487/acg_rep/1915_29_christoffersen.

David, F. R. and David, F. R. (2017) *Strategic Management: A Competitive Advantage Approach, Concepts and Cases*. 16th Ed. Pearson education, inc., ISBN: 0134167848.

Dias, S., Panagopoulos, T. and Loures, L. (2008) 'Post-mining Landscape Reclamation : A Comparison between Portugal and Estonia', *4th IASME/WSEAS International Conference on ENERGY, ENVIRONMENT, ECOSYSTEMS and SUSTAINABLE DEVELOPMENT*, pp. 440–445.

Dogan, T. and Kahriman, A. (2008) 'Reclamation planning for coal mine in Istanbul, Agacli Region', *Environmental Geology*, 56(1), pp. 109–117. doi: 10.1007/s00254-007-1144-5.

Dong Wang and MuZhuang Yang (2011) 'Mining land reclamation and ecological restoration-a case study of Limestone Mine of GaoYao', in *2011 International Symposium on Water Resource and Environmental Protection*. IEEE, pp. 1790–1794. doi: 10.1109/ISWREP.2011.5893597.

Hao, G. *et al.* (2015) 'Soil diagnosis and land suitability assessment for vegetation restoration on coal waste piles in Liupanshui, Guizhou, China', *International Journal of Mining, Reclamation and Environment*, 30(3), pp. 209–216. doi: 10.1080/17480930.2015.1036519.

Kaźmierczak, U., Lorenc, M. W. and Strzałkowski, P. (2017) 'The analysis of the existing terminology related to a post-mining land use: a proposal for new classification', *Environmental Earth Sciences*, 76(20). doi: 10.1007/s12665-017-6997-7.

Kurniawan, A., Susanti, F. and Yunianti, S. R. (2020) 'Strategy to develop tourism objects at Ijobalit, a former pumice mine in East Lombok', *IOP Conference Series: Earth and Environmental Science*, 413(1). doi: 10.1088/1755-1315/413/1/012028.

Mborah, C., Bansah, K. J. and Boateng, M. K. (2015) 'Evaluating Alternate Post-Mining Land-Uses: A Review', *Environment and Pollution*, 5(1), p. 14. doi: 10.5539/ep.v5n1p14.

McHaina, D. M. (2001) 'Environmental planning considerations for the decommissioning, closure and reclamation of a mine site', *International Journal of Surface Mining, Reclamation and Environment*, 15(3), pp. 163–176. doi: 10.1076/ijsm.15.3.163.3412.

Mhlongo, S. E., Amponsah-Dacosta, F. and Kadyamatimba, A. (2020) 'Appraisal of strategies for dealing with the physical hazards of abandoned surface mine excavations: A case study of frankie and nyala mines in South Africa', *Minerals*, 10(2). doi: 10.3390/min10020145.

Prakash, T. N. (2003) *Land Suitability Analysis for Agricultural Crops: A Fuzzy Multicriteria Decision Making Approach*. Master of Science Thesis, International Institue for Geo-information Sience and

Earth Observation.

Ramani, R. V., Sweigard, R. J. and Clar, M. L. (1990) 'Surface mining', in Kennedy, B. A. (ed.) *Surface mining*. 2nd edn. Inc, Littleton: Society for mining, metallurgy, and Exploration, pp. 750–769.

Rowe, J. E. (1977) 'A suitability matrix for selecting land use alternatives for reclaimed strip mined areas', *Landscape Planning*, 4, pp. 257–271. doi: 10.1016/0304-3924(77)90028-4.

Shahba, S. *et al.* (2017) 'Application of multi-attribute decision-making methods in SWOT analysis of mine waste management (case study: Sirjan's Golgohar iron mine, Iran)', *Resources Policy*, 51, pp. 67–76. doi: 10.1016/j.resourpol.2016.11.002.

Sharma, D. K., Saharan, M. R. and Parihar, S. K. (1996) 'Evaluation of land use potential for quarrying area around Ramganjmandi (Kota, Rajasthan), India', *International Journal of Surface Mining, Reclamation and Environment*, 10(1), pp. 13–16. doi: 10.1080/09208119608964789.

Smyth, C. R. and Krebs, V. (2019) 'Application of SWOT-C analysis and state-and-transition modeling to the design of reclamation plans for abandoned or operating mines in British Columbia', *[Online]. Available: https://open.library.ubc.ca/cIRcle/collections/59367/items/1.0391912. [Accessed: 13-May-2021].*

Soltanmohammadi, H. *et al.* (2008) 'Achieving to some outranking relationships between post mining land uses through mined land suitability analysis', *International Journal of Environmental Science and Technology*, 5(4), pp. 535–546. doi: 10.1007/BF03326051.

Soltanmohammadi, H., Osanloo, M. and Aghajani Bazzazi, A. (2010) 'An analytical approach with a reliable logic and a ranking policy for post-mining land-use determination', *Land Use Policy*, 27(2), pp. 364–372. doi: 10.1016/j.landusepol.2009.05.001.

Sukarman and Gani, R. A. (2020) 'Ex-coal mine lands and their land suitability for agricultural commodities in South Kalimantan', *Journal of Degraded and Mining Lands Management*, 7(3), pp. 2171–2183. doi: 10.15243/jdmlm.2020.073.2171.

Tahernejad, M. M., Ataei, M. and Khalokakaei, R. (2013) 'A Strategic Analysis of Iran's Dimensional Stone Mines Using SWOT Method', *Arabian Journal for Science and Engineering*, 38(1), pp. 149–154. doi: 10.1007/s13369-012-0422-z.

Wang, S. D., Liu, C. H. and Zhang, H. B. (2011) 'Suitability evaluation for land reclamation in mining area: A case study of Gaoqiao bauxite mine', *Transactions of Nonferrous Metals Society of China (English Edition)*, 21(SUPPL. 3), pp. s506–s515. doi: 10.1016/S1003-6326(12)61633-1.

POTAŞ CEVHERİNİN AMİN TİPİ TOPLAYICI İLE FLOTASYONUNDA ŞLAM UZAKLAŞTIRMASININ ETKİSİ

EFFECT OF SLIME REMOVAL IN THE FLOTATION OF POTASH ORE WITH AMINE TYPE COLLECTOR

A. Hamrayev [1], M. Terzi [1], C. Gungoren [1], I. Kursun Unver [1], O. Ozdemir [1,] *

[1] *İstanbul Üniversitesi-Cerrahpaşa, Mühendislik Fakültesi, Maden Mühendisliği Bölümü*
*(*Sorumlu yazar: orhanozdemir@iuc.edu.tr)*

ÖZET

Başlıca tarım sektöründe gübre olarak kullanılan potaştan cam, sabun, plastik ve ilaç yapımında da yararlanılmaktadır. Potaş cevherlerinin zenginleştirilmesi genellikle flotasyon yöntemiyle yapılmakta ve amin tipi toplayıcılar sıklıkla tercih edilmektedir. Potaş cevherleri başta silvin (KCl) ve halit (NaCl) olmak üzere suda yüksek çözünürlüğe sahip tuz tipi minerallerin yanı sıra kil ve karbonat mineralleri gibi suda çözünmeyen kısımlar da içermektedir. Silvin ve halitin sudaki yüksek çözünürlüğü sebebiyle flotasyon işlemi doygun potaş çözeltisi içerisinde yapılmaktadır. 6-7 mol/L'yi geçen bu konsantrasyonlar deniz suyu konsantrasyonundan yaklaşık 10 kat daha yüksektir. Çok yüksek konsantrasyonlardaki bu iyon varlığına ek olarak ortamda şlam bulunması arayüzeylerde gerçekleşen mineral/reaktif/hava kabarcığı etkileşimlerini de ciddi oranda etkilemekte ve flotasyon işlemini zorlaştırmaktadır. Bu çalışmada Türkmenistan'ın Karlyuk potasyum tuz yatağından temin edilen potaş cevher numunesi üzerinde amin tipi toplayıcı (dodesilamin hidroklorür-DAH) kullanılarak mikro-flotasyon deneyleri ve kabarcık-tane yapışma verimi ölçümleri gerçekleştirilmiştir. Deneyler sonucunda şlam varlığında yüksek flotasyon verimlerine ulaşılamadığı görülmüştür. Flotasyon verimini arttırmak amacıyla dağıtma ve filtrasyon işlemleri ile şlam uzaklaştırması yapılmış ve şlamsız cevherin mikro-flotasyonu gerçekleştirilmiştir. Sonuç olarak şlam uzaklaştırma işleminin silvin flotasyon verimini 5×10^{-4} mol/L toplayıcı konsantrasyonunda %41'den %83 seviyesine arttırdığı saptanmıştır.

Anahtar Sözcükler: Potaş, flotasyon, silvin, şlam uzaklaştırma, amin

ABSTRACT

Potash, which is mainly used as a fertilizer in the agriculture industry, is also used in the production of glass, soap, plastic, and pharmaceuticals. The beneficiation of potash ores is carried out by flotation method and amine type collectors are widely preferred. Potash ores contain salt-type minerals with high solubility in water, especially sylvite (KCl) and halite (NaCl), as well as insoluble parts such as clay and carbonate minerals. Due to the high solubility of sylvite and halite in water, the flotation process is carried out in a saturated potash solution. These concentrations exceeding 6-7 mol/L are approximately 10 times higher than the concentration of seawater. In addition to the presence of ions in very high concentrations, the presence of slime in the medium significantly affects the mineral/reagent/air bubble interactions at the interfaces, and hence hinders the flotation. In this study, the micro-flotation experiments and bubble-particle attachment measurements were carried out using potash ore sample obtained from the Karlyuk potassium salt deposit of Turkmenistan using an amine type collector (dodecylamine hydrochloride-DAH). As a result of the experiments, it was observed that high flotation recoveries could not be achieved in the presence of slime. In order to increase the flotation recovery, slime removal was carried out by dispersion and filtration processes, and micro-flotation of the de-slimed ore was carried out. As a result, it was determined that the slime removal process substantially increased the sylvite flotation recovery from 41% to 83% at 5×10^{-4} mol/L collector concentration.

Keywords: Potash, flotation, sylvite, slime removal, amines

GİRİŞ

Potasyum hem insanlara hem de hayvanlara besin kaynağı olan bitkiler için vazgeçilmez elementlerden biridir. Dünyada üretilen potasyum cevherinin ortalama %95'i gübre, geri kalan %5'i ise ilaç, boya ve kimyasal olarak kullanılmaktadır (Laskowski, 2008). Potaş, jeolojik ve hidrolojik süreçler sonucunda oluşan ve suda kolayca çözünmeye maruz kalan potasyum tuzları içeren bir kayaç türüdür. Potaş cevherlerinin içerisinde, silvit (KCl) ve karnalit [$KCl.MgCl_2{\cdot}6(H_2O)$] yeterli miktar bulunduklarında ekonomik açıdan uygun cevher haline gelir (Warren, 2006; Barker ve Gundiler, 2008). Silvit mineralojik olarak, karnallit ve halit (NaCl) gibi flor, klor, brom ve/veya iyot içeren mineraller grubu olan halojenler grubuna ait bir mineraldir (Yager, 2016). Dünyanın en büyük potasyum ve sofra tuzu havzalarından birisi Asya kıtasında yer alan Türkmenistan'ın Gaurdak-Köytendağ bölgesinde bulunmaktadır. Bölgedeki potasyum tuz yatakları aktif olarak Karlyuk kasabasında özel bir şirket tarafından üretilmektedir.

Potaş cevherlerinin zenginleştirilmesi flotasyon ve kimyasal (halürjik) olmak üzere iki ana yöntemle gerçekleştirilir. Halürjik yöntem, 19. yüzyılın ikinci yarısında potaş endüstrisinin başlangıcından beri kullanılmaktadır. Bu yöntemle tarımda ve kimya endüstrisinde kullanılan %98'lik yararlı bileşen içeriğine sahip kimyasal olarak saf potasyum klorür elde etmek mümkündür (Pokrovsky, 2001).

Potasyum klorürün flotasyonu cevher suda çözündüğünden doygun çözelti içerisinde yapılmaktadır. Silvit cevherinin flotasyon yöntemi ile zenginleştirilmesi için potasyum klorürü hidrofobik hale getirmek gereklidir. Bunun için, yüksek hidrokarbon zincirine sahip aminler (C12-22) kullanılır (Laskowski, 1994; Ozdemir vd., 2011).

Şlam kaplama, flotasyonda yaygın olarak karşılaşılan bir sorundur ve potaş gibi tuz mineralleri de dahil olmak üzere birçok mineralin flotasyonunda meydana gelebilmektedir (Qian vd., 2019; Yu vd., 2017). Çok düşük kil içerikleri (%0,4-0,6) varlığında bile, potasyum klorür yüzeyindeki amin adsorpsiyonu keskin bir şekilde azalmakta ve dolayısıyla silvit mineralinin flotasyonu olumsuz olarak etkilenmektedir. Kil/karbonat yapılı şlam varlığının tuz tipi minerallerin katyonik flotasyonu üzerindeki bu olumsuz etkisinin önüne geçilebilmesi için, bu gibi minerallerin zenginleştirme proses akım şemalarında bir şlam uzaklaştırma kademesinin de bulunması gerekmektedir (Tiktov, 2004; Filippov vd., 2021).

Bu çalışmada Türkmenistan'ın Karlyuk potasyum tuz yatağından temin edilen potaş cevher numunesinin amin tipi toplayıcı (dodesilamin hidroklorür (DAH)) ile flotasyonunda şlam uzaklaştırma işleminin etkileri; mikro-flotasyon deneyleri ve kabarcık-tane yapışma verimi ölçümleri kullanılarak araştırılmıştır.

MALZEME VE YÖNTEM

Malzeme

Deneylerde kullanılan potaş cevheri, Türkmenistan'ın Lebap İli, Köytendağ Kasabası, Karlyuk Köyü bölgesinde silvinit cevherinin üretimini ve zenginleştirilmesini yapan özel şirketten temin edilmiştir. Cevherin mineralojik bileşiminin belirlenmesi amacıyla gerçekleştirilen X-Işını Kırınımı (XRD) analizi sonucunda numunedeki baskın mineral fazının silvit ve halit olduğu belirlenmiştir. Bu mineraller haricinde bişofit de ikincil mineral fazı olarak tespit edilmiştir. Bu mineraller haricinde numunede bulunan kil mineralleri ve diğer safsızlıklar, XRD yönteminin dedeksiyon limitleri altında kaldığı için doğal cevherin XRD analizinde tespit edilememiş olup, bu minerallerin varlığı çözünmeyen faz (~%4) üzerinde yapılan XRD analizlerinde ortaya konulmuştur. Bu analizler sonucunda cevherde dolomit, montmorillonit, kuvars ve manyezit gibi çözünmeyen minerallerin pikleri gözlenmiştir.

Ocaktan gelen cevher maksimum tane boyutunun ~2,5 cm olması nedeni ile deneysel çalışmalar öncesinde kırma ve öğütme işlemlerine tabi tutulmuştur. Bu kapsamda cevher numunesi merdaneli kırıcı ile kırma işleminden sonra elek açıklığı 1 mm olan elekle elenmiştir. Kapalı devre olarak gerçekleştirilen kırma-eleme işlemleri sonucunda boyutu kırma ile küçültülemeyen elek üstü malzeme bilyalı değirmende yine kapalı devre olarak 5 dk süre ile öğütülerek malzemenin tamamı -1 mm tane boyutuna indirilmiştir. Boyut küçültme işlemleri sonrasında malzemenin d_{80} ve d_{50} boyutları sırasıyla 0,78 mm ve 0,45 mm olarak belirlenmiştir. Ufalanan cevher doygun çözelti hazırlama işlemlerinde ve sınıflandırma sonrasında mikroflotasyon deneylerinde kullanılmıştır.

Potaş cevherlerinin ana bileşenleri olan silvit (KCl) ve halit (NaCl) suda çözünür tuzlar olduğundan, ticari potaş cevheri flotasyonu doygun çözelti içinde gerçekleştirilmektedir (Laskowski, 2013; Cahuas, 2015). Bu kapsamda doygun çözelti hazırlamak amacıyla, cevherin kendisi kullanılmıştır. -1 mm boyutundaki cevher ve saf su karışımının (800 mL) manyetik karıştırıcıda 500 dev/dk hızda 360 dk karıştırılması suretiyle yapılan çözünme analizleri sonucunda, cevherin kendisinden hazırlanan doygun çözeltinin doyma noktasının 325 gr cevher/L olduğu belirlenmiştir. Deneysel çalışmaların tamamında belirlenen doygunluk derecesindeki çözelti, çözünen tuzların çökmesinin önüne geçilmesi amacıyla taze olarak hazırlanarak kullanılmıştır.

Flotasyon deneylerinde ve kabarcık-tane yapışma verimi ölçümlerinde toplayıcı reaktif olarak Sigma-Aldrich firmasından elde edilmiş dodesil amin hidroklorür (DAH, %99 saflıkta, CMC: $1{,}5\times10^{-2}$ mol/L) kullanılmıştır. Deneylerde kullanılan farklı konsantrasyonlardaki DAH çözeltileri 1×10^{-2} mol/L'lik stok çözeltiden gerekli miktarlarda kullanılarak hazırlanmıştır.

Yöntem

Mikro-flotasyon Deneyleri

Flotasyon deneylerinde 155 mL hacme sahip cam mikro-flotasyon hücresi kullanılmıştır. Deneylerde kullanılan süspansiyonlar, 2 gr potaş cevheri üzerine 155 mL'ye tamamlanacak şekilde doygun çözelti eklenerek hazırlanmış olup, kondisyonlama ve adsorbsiyon süresi ise toplam 5 dk olarak uygulanmıştır. Bu kapsamında hazırlanan süspansiyonlar 2 dk boyunca karıştırılarak kondisyonlanmış, daha sonra reaktif eklemesi yapılarak mineral yüzeyine reaktif adsorbsiyonun gerçekleşmesi 3 dk daha karıştırmaya tabi tutulmuştur. Kondisyonlama ve adsorbsiyon sürecine tabi tutulan pülp, mikro-flotasyon düzeneğine beslenmiş ve 2 dk karıştırma sürecinden sonra sisteme 1 dk boyunca 50 mL/dk debi ile azot gazı verilerek flotasyon işlemi gerçekleştirilmiştir.

Zenginleştirme işlemine tabi tutulan cevherden elde edilen yüzen ürün konsantre, batan ürün ise artık olarak alınmış, ardından yüzen ve batan ürünler 4 µm açıklığa sahip filtre kağıdı ile vakum filtre kullanılarak, hızlı bir şekilde susuzlandırılmıştır. Ardından filtre edilen ürünler 80°C sıcaklıktaki etüvde kurutulmuştur. Kurutulan ürünler tartılmış ve flotasyon deneyleri sonucunda elde edilen verim değerleri gravimetrik olarak hesaplanmıştır.

Kabarcık-Tane Yapışma Verimi Ölçümleri

Flotasyon deneylerinde elde edilen sonuçların mikro ölçekte incelenmesi amacıyla kabarcık-tane yapışma verimi ölçümü deneyleri gerçekleştirilmiştir. Deneylerde temas süresi 100 ms olarak uygulanmış; doğal cevherin ve şlamdan arındırılmış cevherin 5×10^{-4} mol/L DAH varlığında ve yokluğundaki kabarcık-tane yapışma verimleri belirlenmiştir. Deneylerde kabarcık-tane yapışma süresi tayini cihazı (Bratton Engineering, ABD) kullanılmıştır (Şekil 1).

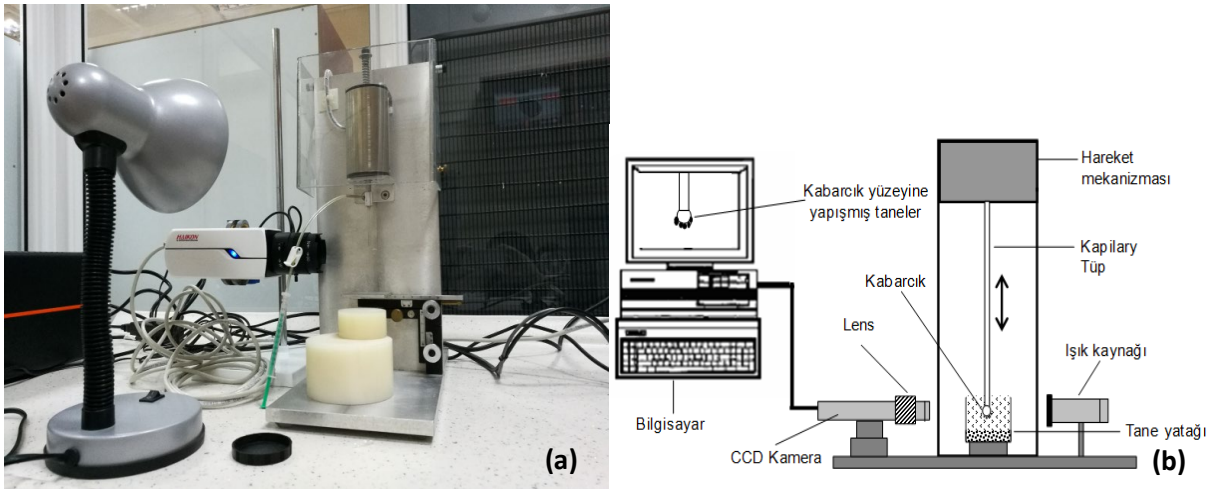

Şekil 1. Kabarcık-tane yapışma verimi ölçümlerinde kullanılan deney düzeneği (a) ve yöntemin şematik görünümü (b)

Şlam Uzaklaştırma İşlemleri

Cevherde varlığı XRD analizleri ile belirlenmiş olan kil minerallerinin uzaklaştırılması amacıyla şlam uzaklaştırma işlemleri gerçekleştirilmiştir. Bu kapsamda flotasyon deneylerinde kullanılacak 212×150 µm boyutlu cevher numunesi; cam beher içerisinde (250 mL), %10 katı oranında (cevher/doygun çözelti) olacak şekilde ve 10 dk'lık periyotlar ile cevher bünyesinde bulunan kil mineralleri serbest hale gelene kadar manyetik karıştırıcı kullanılarak karıştırılmıştır. Her bir karıştırma periyodu sonrasında iri boyutlu tanelerin çökmesi için 3 dk beklenmiş ve süspansiyonun üst kısmı dekantasyon yöntemi ile uzaklaştırılmıştır. Bu işlem süspansiyonun sıvı fazı çökme sonrasında berrak hale gelinceye kadar 4 kez tekrarlanmıştır. Doğal ve şlamı uzaklaştırılmış cevherin görünümü Şekil 2'de verilmiştir.

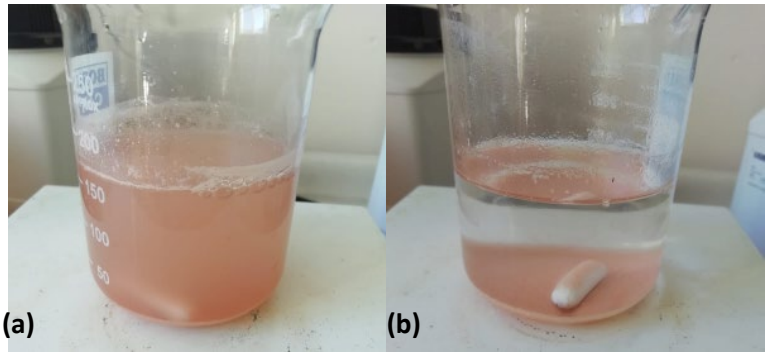

Şekil 2. Doğal (a) ve şlamı uzaklaştırılmış (b) cevherin görünümü

BULGULAR

Flotasyon Deneyleri

Doğal ve şlamı uzaklaştırılmış cevher üzerinde gerçekleştirilen flotasyon deneylerinin sonuçları Şekil 3'te karşılaştırmalı olarak verilmiştir.

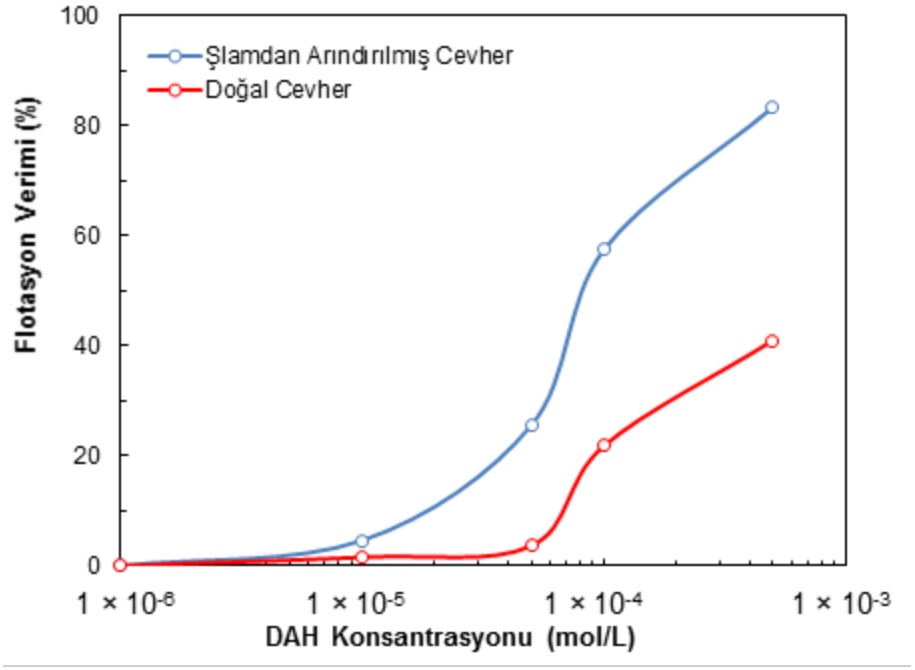

Şekil 3. Doğal ve şlamı uzaklaştırılmış cevherin DAH konsantrasyonuna bağlı flotasyon sonuçları

Şekil 3'ten görüldüğü gibi 1×10^{-5} mol/L DAH varlığı her iki durumda da etkili bir flotasyonun gerçekleşmesi için yeterli olmamıştır. Bununla beraber, 5×10^{-5} mol/L DAH varlığından itibaren elde edilen verim oranları arasındaki fark açılmaya başlamıştır. Bu konsantrasyonda doğal cevherde elde edilmiş yaklaşık %4 olan flotasyon verimi, şlam uzaklaştırma işlemi sonrasında yine aynı konsantrasyonda 8 kattan fazla artış göstererek yaklaşık %26 seviyesine ulaşmıştır.

5×10^{-4} mol/L DAH varlığında elde edilen verimde de önemli derecede artış gözlenmiş olup, flotasyon verimi %100'den fazla bir oranda artış göstererek %41 seviyesinden %83 seviyesine yükselmiştir.

Doğal (şlamlı) ve şlamdan arındırılmış cevherin flotasyon davranışı karşılaştırıldığında, doğal cevher flotasyonu sırasında süspansiyonda bulunan kil minerallerinin cevher yüzeyini kapladığı, bu durumun toplayıcı reaktifin mineral yüzeyine etkili bir şekilde adsorblanmasını engellediği düşünülmektedir.

Sonuç olarak şlam varlığının silvit minerallerinin flotasyon verimini olumsuz yönde etkilediği belirlenmiştir. Şlam uzaklaştırma işlemi sonucunda ise bu durumun önüne geçilerek şlamı uzaklaştırılmış cevher tanelerinin yüzeyine DAH'ın etkin bir şekilde adsorbe olabilmesi sağlanmıştır.

Kabarcık-Tane Yapışma Verimi Ölçüm

Doğal ve şlamı uzaklaştırılmış cevher üzerinde gerçekleştirilen kabarcık-tane yapışma verimi ölçümü sonuçları Çizelge 1'de verilmiştir.

Çizelge 1. Kabarcık-tane yapışma verimi ölçümü sonuçları

	Kabarcık-Tane Yapışma Verimi (%)	
Malzeme	**Reaktifsiz**	**5×10^{-4} mol/L DAH**
Doğal	4,6	18,6
Şlamsız	30,0	90,0

Kabarcık-tane yapışma deneyinde, doğal cevher yüzeyinde kil mineralleri olduğundan kabarcığa tane yapışmamıştır. Doğal cevhere reaktif eklendiğinde ise cevher yüzeyi aynı şekilde kil mineralleri ile kaplı olduğundan toplayıcı reaktif cevher yüzeyine yeteri kadar adsorbe olamamakta ve kabarcık-tane yapışması düşük bir verimde gerçekleşmektedir.

Şlamdan arındırılmış cevhere reaktif eklemeden yapılan kabarcık-tane yapışma deneyinde cevher yüzeyi kil minerallerinden arındırıldığından dolayı cevherin kabarcığa kısıtlı bir verim ile yapışabildiği belirlenmiştir. Şlamdan arındırılmış cevhere 5×10^{-4} M DAH eklenerek yapılan deneyde ise, eklenen reaktif cevher yüzeyine etkin bir şekilde adsorbe olabilmiş, bunun sonucunda da cevher taneciklerinin kabarcığa yüksek bir verimde (%90) yapışması sağlanmıştır. Kabarcık-tane yapışma verimi ölçüm görüntü örnekleri Şekil 4'te verilmiştir.

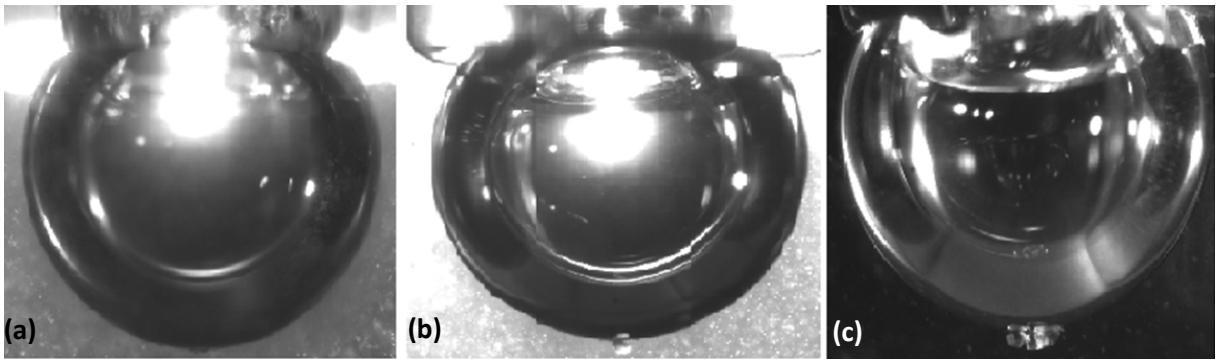

Şekil 4. 5×10^{-4} mol/L DAH varlığında doğal cevher (a), şlamsız cevher (DAH'sız) (b), 5×10^{-4} DAH varlığında şlamsız cevher (c)

5×10^{-4} mol/L DAH varlığında doğal cevher ile tane arasında çok zayıf bir etkileşim tespit edilirken (Şekil 4.a), şlam uzaklaştıma işlemi sonrasında reaktif kullanılmaması durumunda bile 100 ms temas süresinde kabarcık yüzeyine tutunabilen tane miktarında artış gözlenmiştir (Şekil 4.b) Şlam uzaklaştırma işlemi sonrasında 5×10^{-4} mol/L DAH varlığında ise hem kabarcığa yapışan tane miktarının kayda değer oranda arttığı, hem de tanelerin hava kabarcığına daha stabil bir şekilde tutunabildikleri gözlenmiştir (Şekil 4.c).

TARTIŞMA VE SONUÇ

Bu çalışmada, Türkmenistan'ın Karlyuk potasyum tuz yatağından temin edilen potaş cevher numunesinin amin tipi bir toplayıcı (dodesilamin hidroklorür-DAH) ile flotasyonunda şlam uzaklaştırma işleminin etkilerinin mikro-flotasyon deneyleri ve kabarcık-tane yapışma verimi ölçümleri kullanılarak araştırılmıştır. Elde edilen sonuçlar, flotasyon ile zenginleştirme yönteminin Türkmenistan'ın Karlyuk yatağındaki potasyum tuz cevherlerinin zenginleştirilmesi için şlam uzaklaştırma prosesi sonrasında başarıyla uygulanabileceği ortaya konulmuştur.

KAYNAKLAR

Barker, J., and Gundiler, I. (2008). New Mexico Potash–Past, Present, and Future. New Mexico Earth Matters, 8(2).

Cahuas, L. B. (2015). Phase inversion and wettability in testing the extender oil for the flotation of coarse potash ore fractions (Doktora Tezi, University of British Columbia).

Filippov, L. O., Filippova, I. V., Barres, O., Lyubimova, T. P., & Fattalov, O. O. (2021). Intensification of the flotation separation of potash ore using ultrasound treatment. *Minerals Engineering*, 171, 107092.

Gündüz, M., & Doğan, R. (1997). Türkmenistan'ın maden kaynakları envanteri. İstanbul, TİKA yayın evi.

Laskowski, J. S. (1994). Flotation of potash ores. Reagents for better metallurgy, Society for Mining, Metallurgy, and Exploration, 225-243.

Laskowski, J. S. (2013). From amine molecules adsorption to amine precipitate transport by bubbles: A potash ore flotation mechanism. *Minerals Engineering*, 45, 170-179.

Laskowski, J. S., Yuan, X. M., & Alonso, E. A. (2008). Potash Ore Flotation–How does it work? In W. D. Duo, S. C. Yao (Eds.) Proceedings of the XXIV International Mineral Processing Congress (pp. 1270-1276). Science Press.

Ozdemir, O., Du, H., Karakashev, S. I., Nguyen, A. V., Celik, M. S., and Miller, J. D. (2011). Understanding the role of ion interactions in soluble salt flotation with alkylammonium and alkylsulfate collectors. *Advances in Colloid and Interface Science*, 163(1), 1-22.

Pokrovsky, P. (2001). Silvinitten potasyum klorür elde etmek için yüzdürme yöntemi. (Rusça) https://www.bestreferat.ru/referat-61505.html

Qian, Y., Qin, X., and Peng, Y. (2019). Mitigating the coating of fine quartz in fluorite flotation using a triblock copolymer. *Minerals Engineering*, 136, 81-88.

Titkov, S. (2004). Flotation of water-soluble mineral resources. *International Journal of Mineral Processing*, 74(1-4), 107-113.

Warren, J. K. (2006). Evaporites: sediments, resources and hydrocarbons. Springer Science & Business Media.

Yager, D. B. (2016). Potash—A vital agricultural nutrient sourced from geologic deposits (No. 2016-1167). US Geological Survey.

Yu, Y., Ma, L., Cao, M., and Liu, Q. (2017). Slime coatings in froth flotation: A review. *Minerals Engineering,* 114, 26-36.

POTENTIAL DIFFERENCE BETWEEN PRE-PASSIVE AND NON-PASSIVE ANODES IN COPPER ELECTROWINNING PROCESS IN THE PRESENCE OF IRON IONS

H. L. Shahsavar [1], A. M. Beygian [1], E. K. Alamdari [1, *]

[1]*Department of Material Science and Engineering, Amirkabir University of Technology*
*(*Corresponding Author: alamdari@aut.ac.ir)*

ABSTRACT

In copper electrowinning processes, the oxygen evaluation on the anode surface has a very oxidizing effect on the reactions performed. The amount of produced H^+ ions around the anode reduces by the oxidation of Fe^{2+} to Fe^{3+} or Mn^{2+} to Mn^{4+} reactions, causing a decreasing effect on the anode materials corrosion. To investigate this process, two types of lead anodes, pre-passive and fresh (non-passive) anodes, were placed around the cathode with the same conditions. The potential difference between the anodes and the cathode was measured, and finally, the voltage difference between the two was calculated. Factors affecting the amount of potential include the concentration of acid, copper ions, iron ions, and the amount of forward and backward current flow through the circuit. Experiments at five different levels for these variables were performed by experimental design software based on the central composite method (CCM). Based on the obtained data, it was concluded that at concentrations of 10g/l copper, 22.44g/l acid, fixed 200g/l iron, 200A/m^2 forward current flow, and 700A/m^2 backward current flow, the potential difference is minimized. In this circumstance, the anode oxidation is expected to be minimal, resulting in reduced energy consumption.

Keywords: Copper electrowinning, lead anode, energy consumption, overpotential of OER

INTRODUCTION

Copper electrowinning (EW) is an electrolytic reduction of copper ions from an acidic solution to produce high purity copper material. The main anodic reaction in this process is the oxygen evolution reaction (OER)(Parada T and Asselin 2009, Tunnicliffe, Mohammadi et al. 2012). The overpotential for this reaction determines the anodic protection and influences the total cell potential of the process. The OER overpotential depends on the electro catalytical capacity of the anode material (Rüetschi and Cahan 1957, Matsumoto and Sato 1986). However, some other reactions occur on the surface of the anode that effects anodic protection and overall cell potential.

$$2H_2O \rightarrow O_2 + 4H^+ + 4e^- \quad E^+ = 1.23\ V_{SHE} \tag{1}$$

$$Cl_2 \rightarrow 2Cl^- + 2e^- \quad E^+ = 1.35\ V_{SHE} \tag{2}$$

$$Fe^{3+} \rightarrow Fe^{2+} + e^- \quad E^+ = 0.77\ V_{SHE} \tag{3}$$

Although a wide variety of anode materials has been used in the electrowinning of copper, the characteristic features of lead, such as high corrosion resistance and electrical conductivity, as well as the reasonable economical price, make it the best choice as the anode material. Lead and lead alloys can form a continuous protective layer of PbO_2 which is highly conductive for the circuit and prohibits the corrosion

attack of the anode (Elrefaey, Gu et al. 2020). The fundamental efficacy of lead anodes depends on the properties of PbO_2 (Prengaman and McDonald 1980). Lead anodes are used predominantly in sulfate-based electrolyte systems because of the protective ability of PbO_2. In particular, the protective adherent α-phase, which is the brown PbO_2 layer closest to the anode surface, isolates the lead from the corrosive electrolyte. It is composed of large, rhombic, closely packed crystals. The formation of PbO marks the β-phase, $Pb(OH)_2$, $PbSO_4$, and other complex sulfates as reaction intermediates (Mirza, Burr et al. 2016). The first stage in lead oxidation is the presence of oxygen in the formation of lead monoxide (PbO) and lead sulfate ($PbSO_4$). As the anode potential increases, the surface layer of $PbO/PbSO_4$ transforms to $Pb(OH)_2$, followed by conversion to the insulating tetragonal PbO, and then finally by diffusion of oxygen through β-PbO_2 and react with the lead surface the protective and adherent α-PbO_2 layer is formed between beta layer and lead itself at higher potentials (figure 1). According to (Burbank 1956), it is necessary to maintain an anode potential above 1.77V to maintain the protective α-PbO_2. Unless the anode potential is consistently maintained above this value, the protective, adherent α-PbO_2 converts to the loosely adherent β-PbO_2 that flakes off and causes cathode contamination. This electrochemical layering effect explains the commercial success of lead-based anodes in sulfate media electrowinning in the last few decades.

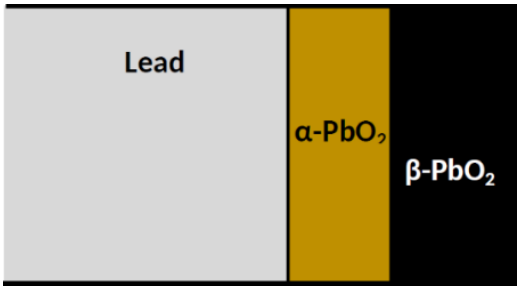

Figure 1. lead anode corrosion layers in sulfuric acid (Prengaman and Siegmund 1999)

Invariably copper-bearing ores are associated with iron. During hydrometallurgical extraction of copper from these ores, the leach liquors often contain a substantial amount of iron. Recovery of copper from these solutions is generally achieved through cementation or electrolysis. Since low purity copper is produced by cementation, the electrolytic method is widely practiced. Copper is either directly electrowon from these solutions when iron contamination is relatively low, or won after purification from iron. Solvent extraction is usually adopted to separate copper from these solutions. The pregnant electrolyte thus generated often contains a substantial amount of Fe^{3+}. When the electrowinning step is coupled with solvent extraction, and a closed circuit is formed, Fe^{3+} contamination builds up during copper electrowinning. The presence of Fe^{3+} in the electrolyte causes a loss in current efficiency and often produces poor quality, cathode copper.

The present paper uses reverse (backward) current on an electrowinning circuit to achieve pure Cu from electrolyte that includes a high amount of Fe ions. In addition, the voltage difference between anodes was calculated by ADAMVIEW BUILDER software. This software gives voltage differences between each anode and cathode every second to investigate the effect of various factors such as copper and iron concentrations. Furthermore, the effect of forward and backward current on the potential difference between the pre-passive lead anode and fresh (newly used) lead anode was studied. So, the optimum amount of concentrations and current are carried out.

MATERIALS AND METHODS

Cell And Placement of Electrodes

The experimental work was carried out in a laboratory-sized cell (100×100×100mm) with a total electrolyte volume of 700cc, using stainless steel 716 as a cathode, with a total surface area of 0.025m^2 a pure rolled lead (7×5) as an anode. To prevent the formation of copper on top of the cathode, some nun conductive liquid was used to isolate it from the electrolyte. Electrodes (each anode and cathode) are first washed with a 1M caustic soda solution to clean their surface and then cleaned with distilled water and placed in the cell. Two types of anodes were used around the cathode, pre-passivate and fresh lead anode, to realize the voltage difference between anodes. The pre-passive anode was always used in the cell and had a passive layer before the experiment. The electrowinning cell used for this work is continuous, so it has two canals for solution input with the same rate of flow and one output canal. The construction of the cell is shown in figure 2. The duration of each experiment is 5 hours with a total of 4L (liter) solution.

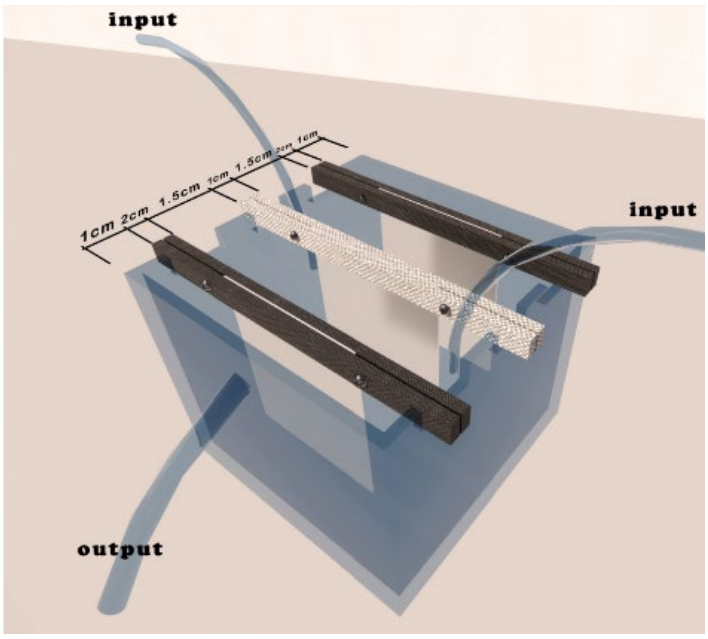

Figure 2. Electrowinning cell configuration

Solution Preparation

All chemicals were reagent grade and were used without further purification. Sulfate-based electrolytes were prepared using $CuSO_4$;($7H_2O$), $FeSO_4$;($7H_2O$), and 98% pure H_2SO_4. All reagents were mixed with distilled water to produce 4L of electrolyte for copper electrowinning experiments. All electrolyte concentrations are listed in Table 1, and all experiments were performed at room temperature.

X-Ray Diffraction (XRD) Analysis and Voltage Difference Measurements

Using X-ray diffraction (XRD) analysis, information about the composition of the surface layer on the Pb anode was obtained. At the 5 hours of anodic polarization at different voltages listed in Table 1, the sample

was rinsed, dried, and analyzed as a powder of corroded lead, which separated quickly from the surface of the anode.

Table 1. Electrolyte concentrations and current at 38 experimental 5-hour run

Runs	Cu (g/l)	H_2SO_4 (g/l)	Fe (g/l)	Forward current (amp/m^2)	Backward current (amp/m^2)
1	5.00	20.00	20	300.00	500.00
2	20.00	30.00	20	400.00	700.00
3	15.00	0.00	20	300.00	500.00
4	20.00	10.00	20	400.00	700.00
5	15.00	20.00	20	300.00	500.00
6	10.00	10.00	20	400.00	700.00
7	20.00	30.00	20	200.00	700.00
8	15.00	20.00	20	500.00	500.00
9	15.00	20.00	20	300.00	500.00
10	25.00	20.00	20	300.00	500.00
11	10.00	10.00	20	200.00	700.00
12	15.00	20.00	20	300.00	500.00
13	15.00	20.00	20	300.00	100.00
14	10.00	10.00	20	200.00	300.00
15	15.00	20.00	20	300.00	500.00
16	20.00	30.00	20	400.00	300.00
17	20.00	10.00	20	400.00	300.00
18	5.00	20.00	20	300.00	500.00
19	15.00	20.00	20	100.00	500.00
20	15.00	20.00	20	300.00	900.00
21	25.00	20.00	20	300.00	500.00
22	10.00	30.00	20	400.00	300.00
23	15.00	20.00	20	500.00	500.00
24	20.00	30.00	20	200.00	300.00
25	20.00	10.00	20	200.00	300.00
26	15.00	0.00	20	300.00	500.00
27	15.00	20.00	20	300.00	100.00
28	10.00	10.00	20	400.00	300.00
29	15.00	20.00	20	300.00	500.00
30	10.00	30.00	20	200.00	300.00
31	15.00	40.00	20	300.00	500.00
32	15.00	20.00	20	300.00	500.00
33	15.00	40.00	20	300.00	500.00
34	10.00	30.00	20	200.00	700.00
35	15.00	20.00	20	300.00	900.00
36	20.00	10.00	20	200.00	700.00
37	10.00	30.00	20	400.00	700.00
38	15.00	20.00	20	100.00	500.00

The power supply used is a pulse generator made in International Silicon Power Conversion (IPC) in Iran, which switches the direction of DC (direct current) in the ratio of 40/1 Sec. The voltage difference between two types of anodes was measured every second using ADAM-4017-PLUS and ADAM-4561 manufactured by Advantech company also shunt used for accessible voltage measurements. The measured voltage differences data are recorded with the ADAMVIEW-BUILDER software. After five hours of electrowinning (18472 sec), approximately 18476 digits of voltage differences were claimed in every 38 runs; thus, the average voltage differences as a final data used for every run claimed by following the example formula. All data was analyzed and optimized by experimental design software based on the central composite method (CCM).

$$\frac{\int_0^{18476} \mathrm{Vdt}}{\mathrm{t}_{18476}-\mathrm{t}_0} = \overline{\mathrm{V}} \tag{4}$$

RESULTS AND DISCUSSIONS

XRD Analysis

As shown in figure 3, XRD detection was carried out on the anodic layers, which are claimed as a powder after five hours of the electrowinning process. The results indicated that these anodic layers are mainly composed of $PbSO_4$ and β-PbO_2. Furthermore, as shown in figure 3 intensity of PbO_2 is higher than $PbSO_4$; it shows that more lead oxide components are formed than the lead sulfate. As (Zhang and Guo 2017) reported, because the α-PbO_2 is adherent to the surface, there is no α-phase, but on the other hand, there is too much β-phase that is visible in figure 3.

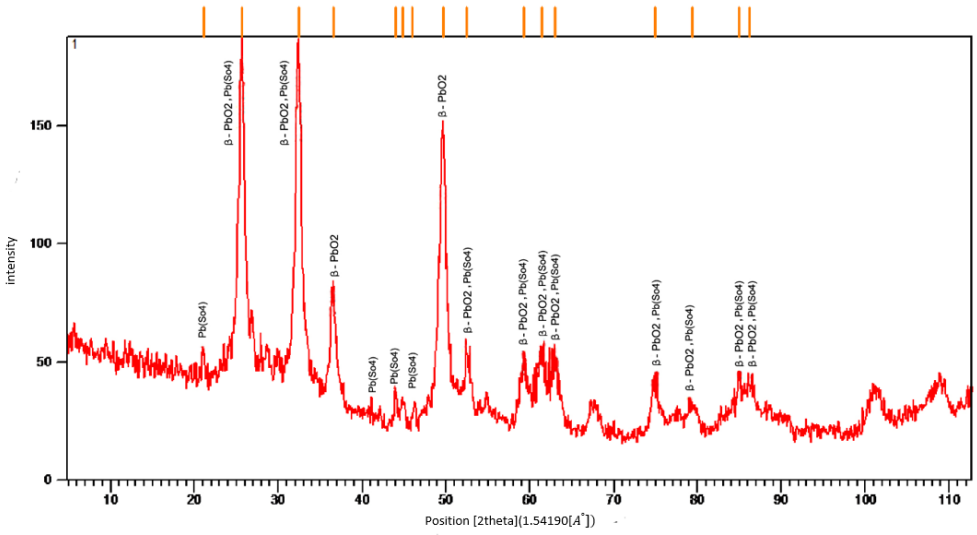

Figure 3. XRD of Pb after 5 hours of electrowinning process

Average Voltage Differences Analysis and Reasons for It

Design Expert Software Analysis

After all the experiments were performed, the results were analyzed at design expert software. The suggested model was linear with a reasonable R^2—the sequential model sum of squares listed in Table 2. The

fit summary and analysis of variance (ANOVA) are visible in Table 3. The F-value and p-value are calculated at 31.79 and <0.0500, respectively. These facts release that this model is significant for these experimental data.

Table 2. The sequential model sum of squares

Source	Sum of squares	Degree of Freedom	Mean square	F-value	P-value	Suggestions
Mean vs total	0.4528	1	0.4528	-	-	-
Linear vs Mean	***0.0452***	***4***	***0.0113***	***31.79***	***<0.0001***	***Suggested***
2FI vs Linear	0.0018	6	0.0003	0.7922	0.5841	-
Quadratic vs 2FI	0.0003	4	0.0001	0.1938	0.9391	-
Cubic vs Quadratic	0.0047	8	0.0006	1.81	0.1522	Aliased
Residual	0.0049	15	0.0003	-	-	-
Total	0.5097	38	0.0134	-	-	-

Table 3. The fit summary and analysis of variance (ANOVA) for the linear model

Source	Sum of Squares	Degree of Freedom	Mean Square	F-value	P-value	Description
Model	***0.0452***	***4***	***0.0113***	***31.79***	***<0.0001***	***Significant***
A-Cu(g/l)	0.0001	1	0.0001	0.2563	0.6161	-
B-H_2SO_4(g/l)	0.001	1	0.001	2.88	0.0992	-
C-I-F (amp/m^2)	0.0393	1	0.0393	110.55	<0.0001	-
D-I-R (amp/m^2)	0.0048	1	0.0048	13.49	0.0008	-
Residual	0.0117	33	0.0004	-	-	-
Lack of fit	0.0080	20	0.0004	1.39	0.2753	Not significant
Pure Error	0.0037	13	0.0003	-	-	-
Total	0.0569	37	-	-	-	-
R^2	0.7940	-	-	-	-	-
Adjusted R^2	0.7690	-	-	-	-	-
Predicted R^2	0.7256	-	-	-	-	-
Precision	20.4957	-	-	-	-	-

The Predicted R^2 of 0.7256 is in reasonable agreement with the Adjusted R^2 of 0.7690; i.e., the difference is less than 0.2. Precision measures the signal/noise ratio, and a ratio greater than four is desirable. The ratio of 20.496 indicates an adequate signal. This model can be used to navigate the design space. After 38 runs that some of them were repeated, some validation runs were carried out to confirm models results. These validation runs are reported in table 4.

Table 4. Validation runs values

Runs	A-Cu (g/l)	B-H2SO4 (g/)	C-I-F (amp/m^2)	D-I-R (amp/m^2)	Actual voltage difference (V)	Predicted voltage difference (V)	Standard deviation	Repeat
1	20	40	100	100	0.07243	0.0766	0.0189	3
2	20	20	200	500	0.08962	0.0758	0.0189	2

As shown in Table 4, the actual voltage difference and predicted one are close to each other according to standard deviation; additionally, the runs were repeated three or two times to confirm the voltage difference. As a result, the given model is acceptable. The maximum and minimum voltage difference between the two pre-passive and the fresh anode is calculated with DESIGN EXPERT software shown in Table 5.

Table 5. Extremum of the voltage difference between two anodes

extremum	A-Cu (g/l)	B-H2SO4 (g/)	C-I-F (amp/m^2)	D-I-R (amp/m^2)	voltage difference (V)
Minimum	10	22.44	200	700	0.053
Maximum	10	30	400	300	0.177

The design expert software was used to investigate the effect of parameters on the average voltage difference. Results indicated a linear relationship between X and Y. The linear equation for these parameters is as follows.

$$\text{Average Voltage Difference} = 0.1092 + 0.0017(\text{copper concentration}) + 0.0057\ (\text{sulfuric acid concentration}) + 0.0350\ (\text{forward current voltage}) - 0.0122\ (\text{backward current voltage}) \quad (5)$$

Effect Of Sulfuric Acid Concentration on Corrosion of Lead and Voltage Difference

As shown in figure 4, the results indicate that increasing sulfuric acid from 0 to 30 (g/l) or even more cause more lead corrosion. Additionally, as shown in figure 4 average voltage difference between two anodes is slightly increased by increasing sulfuric acid; because the fresh anode consumes more power than the pre-passive anode to form a passive layer. As (Cifuentes, Astete et al. 2005) reported, as the standard equilibrium potential for lead is more negative than the standard equilibrium potential for hydrogen, so metallic lead oxidation can couple spontaneously with hydrogen ion reduction. At the same time, increasing hydrogen ion concentration caused the exchange current density for the hydrogen reduction reaction to increase, thus increasing the corrosion current density for the lead/hydrogen couple.

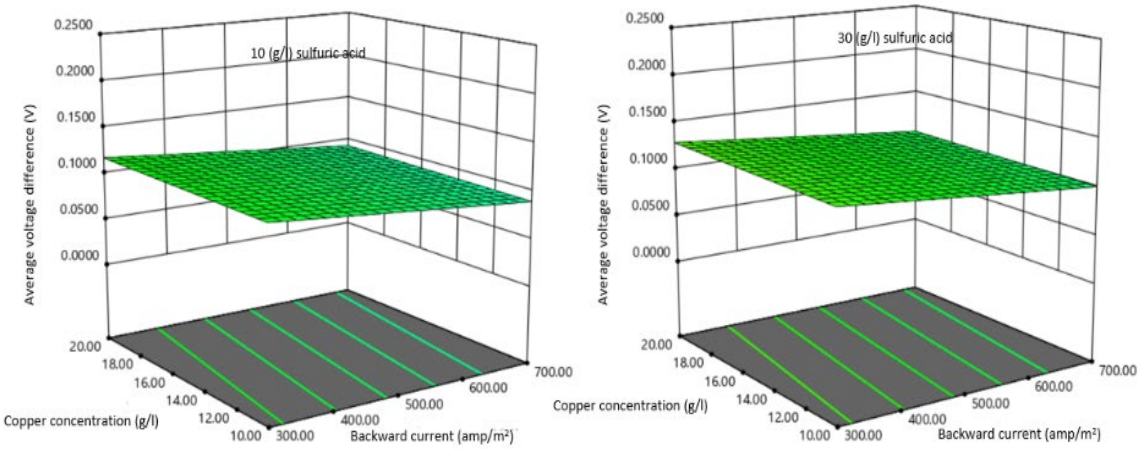

Figure 4. Effect of sulfuric acid concentration on voltage differences between two anodes

Effect Of Copper Concentration on Corrosion of Lead and Voltage Difference

The results (figure 5) indicate that increasing copper concentration from 10 to 20 (g/l) will accelerate lead corrosion slightly. This result shows that, as backward current is applied, copper in solution allows spontaneous copper deposition on the lead anode. This phenomenon provides an added cathodic reaction to couple with anodic lead dissolution; it leads to accelerated lead anode corrosion. Copper deposition on the lead anode during backward current has been observed in laboratory tests and industrial plants. As lead anode corrosion increases, the average voltage differences also slightly increase because copper concentration does not play a significant role in forming the passive layer on the anode; this is more dependent on OER (oxygen evaluation reaction) and lead oxide formation on the anode surface.

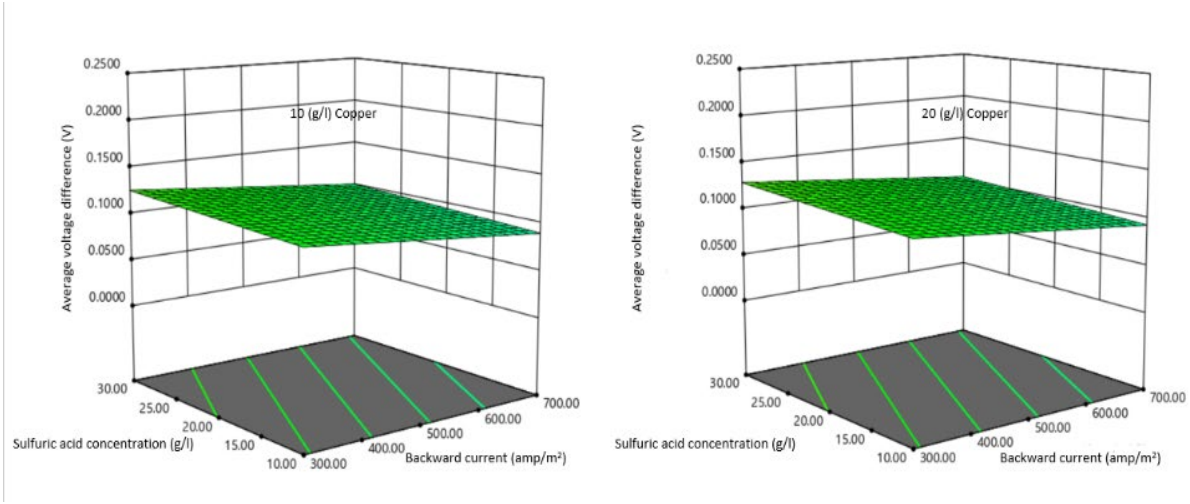

Figure 5. Effect of copper concentration on voltage differences between two anodes

Effect Of Current Direction on Corrosion of Lead and Voltage Difference

The voltage difference of the two anodes is shown in figure 5 (A) effect of forward current and figure 5 (B) effect of backward current. It can be seen (figure 5 A), the voltage differences between the two pre-passive and the fresh anode are increased by increasing forward current density from 200 to 400 (amp/m^2). The corrosion rate of the new anode at the beginning of the reaction is higher than the pre-passive anode because it consumes more power to form the passive layer. It means on the surface of the fresh anode, both main OER (oxygen evaluation reaction) and leads oxidizing reaction and other reactions like Fe^{2+} oxidizing and Cl^- reduction are happening simultaneously. On the other hand, only the OER is happening on the surface of the pre-passive anode. The oxidizing of lead plays a significant role in average voltage differences between two anodes. Figure 5 (A) shows that the average voltage differences and corrosion of 2 anodes increase each time the current density increases.

Figure 5(B) shows that average voltage differences between two anodes decrease with increasing backward current from 300 to 700 (amp/m^2). The main reason for this could be the dissolving of the passive layer as lead oxide or even lead sulfide in the electrolyte. Also, because one of the anodes is pre-passivated, the passive layer of this anode will dissolve more than the fresh anode. As a result, the average voltage difference is decreases. It also seems that while backward current is applied, the placement of anode and

cathode changes, which means the oxidation reactions occur on cathode and reduction reactions appear on the anode; hence, Fe^{3+} reduces to Fe^{2+}. As (Cifuentes, Astete et al. 2005) investigate, while the concentration of Fe^{2+} is more than Fe^{3+}, corrosion of lead decreases, it causes a decrease in average voltage differences. Furthermore, iron ions (Fe^{2+}) and lead components dissolved in electrolytes do not affect copper purity.

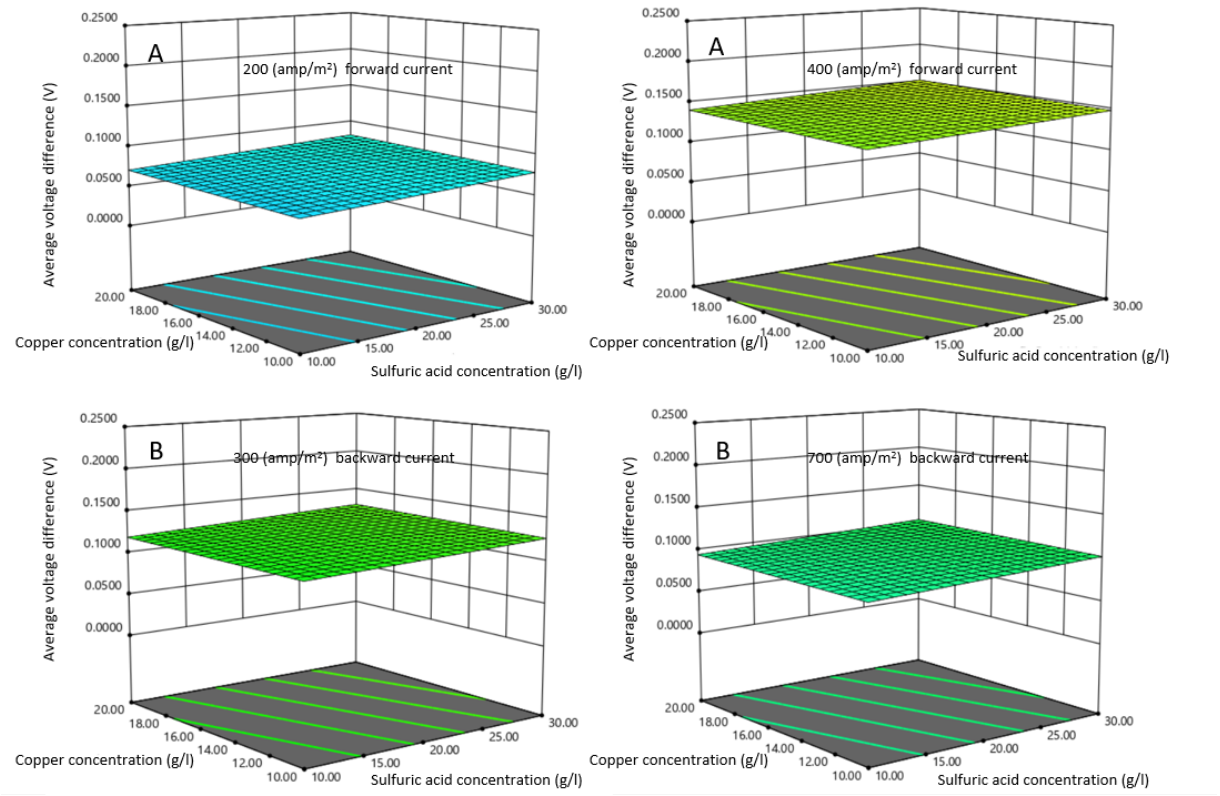

Figure 5. Effect of current direction on voltage differences between two anodes

Effect Of Iron on Corrosion of Lead And Voltage Difference

Although during the forward current applies for 40 seconds, Fe^{2+} oxidize to Fe^{3+} on the anode surface, during one second of backward current, Fe^{3+} reduced to Fe^{2+}, as (Dew and Phillips 1985) researched, electrowinning and extraction of copper with a high concentration of ferric ion cause higher energy consumption and non-adhesive copper on the cathode. As a result, backward current, even for one second, will help to lower the energy consumption for electrowinning. Additionally, it helps to reduce the corrosion of anodes and average voltage differences.

CONCLUSION

This investigation highlights the effect of some essential elements and operating parameters found in copper electrowinning electrolytes on corrosion of the lead anodes and the average voltage differences between two different anodes that one of them was pre-passive and another one was fresh anode. The XRD analysis of powder that separated from the surface of the anode indicates that it is mainly PbO_2 formed on the surface of the anode, and it is more than $PbSO_4$.

The results analyzed by the design expert software indicated that the linear model significantly fits with experiments. Additionally, validation runs were carried out that show the results match with the model concerning standard deviation. The final linear equation is gained after the model is accepted. The equation below shows the effect of parameters on average voltage difference ideally. The equation indicates that the forward current has the most impact on the average voltage differences, and the backward (reverse) current has a contrariwise effect. The effect of sulfuric acid and copper in the electrolyte is not as impressive as the current, but they positively impact lead corrosion.

$$\text{Average Voltage Difference} = 0.1092 + 0.0017(\text{copper concentration}) + 0.0057\ (\text{sulfuric acid concentration}) + 0.0350\ (\text{forward current voltage}) - 0.0122\ (\text{backward current voltage}) \quad (5)$$

Finally, the optimum average voltage differences were obtained through this equation, which shows how much the single reaction on the lead anode surface (lead oxidizing) can help toward energy consumption and corrosion resistance.

REFERENCES

Burbank, J. (1956). "Anodization of lead in sulfuric acid." Journal of the Electrochemical Society 103(2): 87.

Cifuentes, L., E. Astete, G. Crisóstomo, J. Simpson, G. Cifuentes and M. Pilleux (2005). "Corrosion and protection of lead anodes in acidic copper sulphate solutions." Corrosion engineering, science and technology 40(4): 321-327.

Elrefaey, A., Y. Gu, J. James, C. Kneen, I. Crabbe and J. Sienz (2020). "An investigation of the failure mechanisms of lead anodes in copper electrowinning cells." Engineering Failure Analysis 108: 104273.

Matsumoto, Y. and E. Sato (1986). "Electrocatalytic properties of transition metal oxides for oxygen evolution reaction." Materials chemistry and physics 14(5): 397-426.

Mirza, A., M. Burr, T. Ellis, D. Evans, D. Kakengela, L. Webb, J. Gagnon, F. Leclercq and A. Johnston (2016). "Corrosion of lead anodes in base metals electrowinning." Journal of the Southern African Institute of Mining and Metallurgy 116(6): 533-538.

Parada T, F. and E. Asselin (2009). "Reducing power consumption in zinc electrowinning." JOM 61(10): 54-58.

Prengaman, R. and A. Siegmund (1999). Improved copper electrowinning operations using wrought Pb-Ca-Sn anodes, Copper 99-Cobre 99 International Symposium (Phoenix, Arizona), October.

Prengaman, R. D. and H. B. McDonald (1980). Stable lead dioxide anode and method for production, Google Patents.

Rüetschi, P. and B. D. Cahan (1957). "Anodic corrosion and hydrogen and oxygen overvoltage on lead and lead antimony alloys." Journal of the Electrochemical Society 104(7): 406.

Tunnicliffe, M., F. Mohammadi and A. Alfantazi (2012). "Polarization behavior of lead-silver anodes in zinc electrowinning electrolytes." Journal of the Electrochemical Society 159(4): C170.

Zhang, Y. and Z. Guo (2017). "Anodic behavior and microstructure of Pb-Ca-0.6% Sn, Pb-Co3O4 and Pb-WC composite anodes during Cu electrowinning." Journal of Alloys and Compounds 724: 103-111.

PREDICTIVE MAINTENANCE: A VIABLE MAINTENANCE OPTION FOR MACHINES/EQUIPMENT/PLANTS IN MINING AND MINERAL PROCESSING

O. Dayo-Olupona [1], B. Genc [1, *], S. Bada [2], T. Celik [3]

University of the Witwatersrand, School of Mining Engineering
*(*Corresponding author: bekir.genc@wits.ac.za)*
[2] *University of the Witwatersrand, School of Chemical Engineering*
[3] *University of the Witwatersrand, School of Electrical Engineering*

ABSTRACT

Mining equipment requires significant capital investment; therefore, equipment failures and associated downtimes lead to significant increases in operating, production and maintenance costs and, in some instances, loss of revenue. Conservatively, the average mining equipment maintenance cost ranges from 20-40% of the mine's operating cost, and it is increasing gradually. Hence, the need for reliable maintenance initiatives designed to enhance equipment availability, reduce unscheduled downtime and minimize maintenance costs.

This study aims to give an up-to-date overview of equipment maintenance procedures in the mining industry as a prerequisite to establishing operational integration of artificial intelligence (AI) and machine learning technology for predictive equipment maintenance inside existing mining operations. Journal articles, reports and other publications were systematically reviewed and analysed to understand the historical development and evolution of equipment used in mining. In addition, machine maintenance, understanding of the reactive, preventive, and predictive maintenance environment in the industry were also examined. Other factors attributed to predictive maintenance, understanding the type of equipment failure and identifying critical data-worthy variables that are used to build a predictive AI model have been extensively analysed. The outcome of the review will provide decision-makers with some guidance in considering predictive maintenance as a viable maintenance option within their operations.

Keywords: Mining Equipment, Maintenance, Predictive Maintenance, Artificial Intelligence

INTRODUCTION

Breakdowns are typical of mechanical equipment and minimizing them over the useful lifespan of the equipment requires regular maintenance. For most organizations, the maintenance service helps reduce production losses and minimizes maintenance labour and material costs. A key determinant of a successful maintenance program is the healthy balance between too little and too much maintenance. The risk of breakdown is increased with the formal while the latter lead to a high operating cost. Another success factor is the willingness and commitment of the management. This usually comes down to how the interaction between the maintenance unit and the company's production unit is co-ordinated (Chan and Kuruppu, 2006).

A major difficulty in quantifying the benefits of servicing mining equipment is that equipment wears, and degradation occurs over a long period of time. These degradations are compounded by the complex processes and a large number of variables usually interacting with each other within and outside the machine (Jalili et al., 2015). Some of them are controlled by the operator, independently controlled, based on the properties of the ore and even variables based on the results.

As a precursor to developing the operational integration of Artificial Intelligence (AI) and machine learning technology for predictive equipment maintenance in existing mining operations. this study seeks to provide an up-to-date review of maintenance practices for equipment used in the mining industry. Journal articles, reports and other literature were reviewed and analysed to understand the historical development and evolution of equipment and machine maintenance. Predictive maintenance is further explored to understand the type of equipment failure and the identification of critical data-worthy variables/factors to be monitored and used to build a predictive AI model.

Equipment and Maintenance Cost

Mining equipment require significant capital investment; therefore, equipment failures and their associated downtime mean significant increase in operating, production, and maintenance costs, and in some cases revenue losses. Conservatively, the average mining equipment maintenance cost ranges from 20 - 40% of the mine's operating cost and it is increasing gradually (Dhillon, 2008). Hence, the need for reliable maintenance initiatives designed to enhance equipment availability, reduce unscheduled downtime, and minimize maintenance costs.

Factors Contributing to Equipment Maintenance Cost in Mines

Due to the increasing complexity of machines used in mining and mineral processing, several factors influence maintenance costs. Though not exhaustive, Dhillon (2008) points to eight factors that contribute significantly to the cost of maintenance. They are further categorized into 3 broad areas.

1. The machine/equipment;
2. The working environment; and
3. The labour involved.

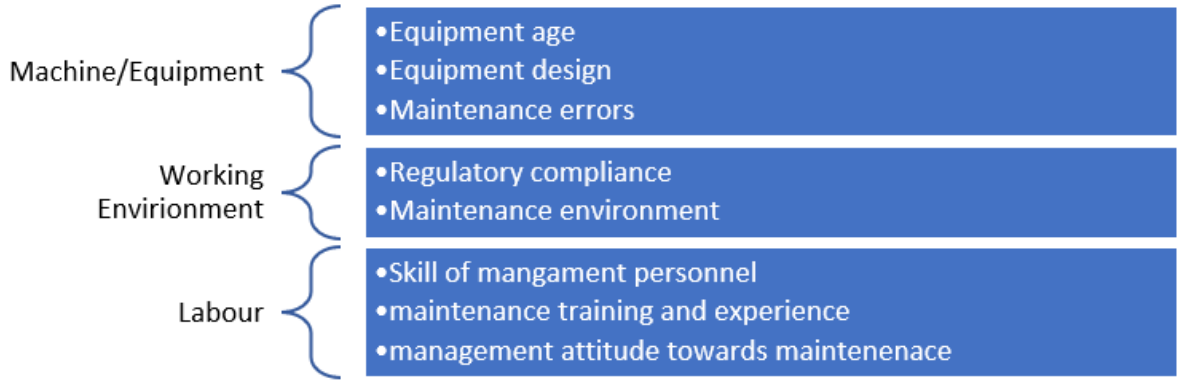

Figure 1. Factors affecting mining equipment maintenance cost.

Similarly, Caterpillar claims that the cost of mining equipment repair and maintenance is typically influenced by the equipment's application, operating circumstances, ownership time, maintenance procedures, and age (Lashgari & Sayadi, 2013).

The realization from the above listed variables is that multiples factors are usually responsible for the equipment cost. The factors directly related to machine/equipment are usually subjected to wear and tears and can be effectively managed if prioritized. The working environment factors are the set of factors that are not usually directly controlled by the organization and it effects are usually quite significant. For example, decarbonization is forcing mining companies to adopt and significantly modernize the technologies used on majority of their equipment. This naturally increases maintenance

related cost. Labour related factor in most cases can be controlled and managed by the host organizations.

Mining Equipment Downtimes and Maintenance Strategies

Downtime of equipment is not desirable, especially as mining equipment becomes larger, costly, and difficult to tow. Therefore, it is very important to maintain this equipment, as breakdown will cause significant production and revenue losses. Although these outages and downtime are not completely avoidable, a good maintenance program can help minimize them, thereby increasing the availability of the machine (Safiuddin, 1967). According to (Faitakis et al., 2004), maintenance has evolved through three major ages;

- **The first generation (1940 - 1950):** The approach to maintenance at that time was "fix when it broke" and that is because automation was minimal in the industry.

- **The second generation (1950 - 1980):** Here, due to the increased mechanization and automation of the industry, a fixed-time maintenance practice was adopted. However, maintenance costs have gone up significantly.

- **The third generation (1980 - present):** A computerized maintenance approach has been gradually introduced because of the complexity of mining. In addition, there is a better understanding of the malfunction modes of the equipment.

One of the most notable features of the first generation was the lack of mechanization. Mine production was typically small-scale, and the consequences of breakdowns were less severe than they are now. However, rising globalization and the associated exponential mineral demand caused mining enterprises to boost production in the second generation. Following it, there was an increase in mechanization. The time-based maintenance strategy used here was more effective than the first generation, but the scale at which it was implemented quickly resulted in an exponential increase in associated operational expenses. In addition, the fact that not all of the components and parts being replaced are nearing their end-of-life indicated that the technique was ineffective. The computing age spread significantly in the third generation. In the third generation, the computing technology became widely adopted across several industry. Its combined use with mechanization allowed for a greater understanding of the various critical component and the operations of the equipment to which it was applied. This in-depth knowledge generated makes scalability easy. It also aids the management of the more complex future mining operations.

Similar to the once outline above, Carvalho et al. (2019) outlined three maintenance strategies:

- The Run-to-failure or Corrective
- Preventive; and
- Predictive maintenance.
-

All have gained ground over the three generations listed above, respectively.

Computerised maintenance has also evolved rapidly and remained relevant and profitable, as organizations are now dependent on the ability to adopt and adapt these emerging technologies to their existing and new operations. Over the past two decades, condition-based monitoring (CBM) has been on the rise in the mining industry (Faitakis et al., 2004). It is a subfield of the computerized maintenance approach, whose goal was to improve the predictability of failure and spur proactive maintenance

nature. In these situations, the maintenance team will be given sufficient time to implement corrective actions prior to equipment failures.

Despite the fact that CBM is a proactive approach to asset management, its underutilization, limited unitary conditioning monitoring capability, and restricted ability to analyze several datapoints or variables at the same time limit its maximum effectiveness (Faitakis et al., 2004; Kerr, 2021). As a result, decision-makers are forced to revert to corrective maintenance systems where maintenance is only carried out after a breakdown notification alarm (Emiling & Stan, 2001; Faitakis et al., 2004).

Although schedule/time-based maintenance or preventive maintenance, as recommended by original equipment manufacturers, is generally effective in avoiding failure, and increase in operating costs is unavoidable. In general, this involves corrections and replacements required for non-worn components. This necessitates predictive maintenance.

Human-Centred Maintenance

Even though predictive maintenance can be used to detect a number of failures and breakdowns in advance, its complementary use with the human-centred maintenance program makes it a success. Dhillon (2008) describes three basic human-centred maintenance processes that may be carried out on mining equipment. This involves a visual inspection, a physical inspection and routine work.

In visual inspection, checks are done on visible components such as fasteners, labels, windows, operational pushbuttons, and handles. These checks are conducted to detect cracks and imperfections and to ensure that the equipment is generally serviceable and free from dust.

In physical inspections, the aim is to ensure that there is no physical damage and that the general state of operation of the equipment is good. This includes checking wiring and electrical connections, making sure they are tight and not arching or overheating. Others include flame path verification, operational status of protective equipment, blank plugs/covers, etc.

Some routine work involves tasks such as lubrication and cleaning of threaded holes, fasteners, and flame paths to impede rust and oxidation; ensuring indicators instruments are operational; ensuring protection and control relays are functional.

Even though these inspections might seem simple, Jalili et al. (2015). highlighted their effectiveness in identifying wear in mechanical and electrical components of plants and other mining equipment provided the site maintenance program allows for it to be done frequently.

PREDICTIVE MAINTENANCE, ARTIFICIAL INTELLIGENCE, AND DATA.

Predictive maintenance uses predictive tools to determine when maintenance actions are necessary (Carvalho et al., 2019). It generally uses historical data which is obtained by continuous machine monitoring. This method makes it possible to detect faults quickly and in advance.

The use of artificial intelligence (AI) techniques has been a major component of the prediction tools used recently (over the past five years) (Ong & Gupta, 2019). This increase in global adoption reflects the efficiency of technology to surpass humans in a few specialized tasks, including prediction. This success has been attributed to the combined effect of the following:

- Ease of access to a large amount of data;
- Exponential improvement in computing power; and

- Incremental improvement in data-driven machine learning (ML) algorithms (McCoy & Auret, 2019; Ong & Gupta, 2019).

The operational data to be used to build AI predictive algorithmic model can be collected from the existing equipment sensors and log files from the Computerized Maintenance Management System (CMMS) software. These will serve as input data used by data engineers for the AI/ML solution design. In addition, the AI/ML solution design process includes collecting, cleaning, and labelling operational data, constructing, and training the algorithmic ML model, and testing the model for accuracies and biases. Subsequently, they can be deployed in a coal or other mineral project.

Data Collection and Failure Patterns

Modelling the operating characteristics and failure patterns of a machine is important because it gives a blueprint of its operating conditions. In addition, it helps to design a suitable solution to minimize the recurrence of failures. However, before this can be done, Veganas et al. (1997) emphasised the need for a machine to be classified into systems and sub-systems. Data generated from each system or subsystem can be used and analysed independently or in an integrated format to generate useful insight about the machine. An example of system and sub-system classification for a load-haul-dump machine (LHD) provided by Veganas et al. (1997) is presented in Table 1.

Table 1. A mining LHD system & sub-system classification

No	Systems/Sub-system	Equipment components
1	Drive train	Drivelines, Torque Convertor, Transmission
2	Structural	Frame, Canopy, and Seat
3	Hydraulic system	Cylinders, Hoses, Pumps
4	Engine	Exhaust and Intakes Included
5	Electrical System	Charging, Wiring, Gauges, Starter
6	Bucket	-
7	Braking system	-
8	Tires	-
9	Fire suppression	-

Like the LHD, other mining machines and equipment can be classified into systems from which data can be systematically collected and analysed to understand the failure pattern and provide data-centric solutions.

Equipment Maintenance Data Analysis

The processing of data and the acquisition of meaningful information from this equipment data has been carried out in the past using several methods. Vegenas et al. (1997) highlighted two predominantly used processes, namely, basic graphical maintenance analysis and reliability maintenance analysis. Over time the condition-based maintenance analytic method has also evolved.

In the basic graphic maintenance analytical method, only static measurements of equipment behaviour are generated. This static measurement is then used to evaluate equipment variables such as system availability, repair frequency, total repair time, total number of repairs and hours of operation.

In reliability-based maintenance, a combined probabilistic and statistical approach is primarily employed. It is subsequently used to fit a probability distribution to the failure data. This result is used to evaluate the failure behaviour of the system or machine to be evaluated.

In condition-based monitoring, the emphasis is on integrating the equipment data from various data islands within the mining operation. It is usually real-time information capture and its integration with an alarm system make notification easy. Statistical and probabilistic approaches are also applied to select data from the pool of the integrated equipment data.

Possible Equipment Data Points

Safiuddin (1967) identified the following as the major contributors to wear on various components of electrical mining equipment:

- Excessive ambient temperature variation
- Dirty and contaminated air
- Mechanical shocks and vibrations
- Humidity and rainwater
- Momentary electrical grounds
- Electrical noise pickup
- Line voltage variations
- Operating conditions and operator abuse

All of these potential data sources that can be tracked serve as input data to the algorithms in order to predict potential wear and tear in advance. Çınar et al. (2020) further provided examples of how data were collect from this sources and used in the manufacturing industry. In accordance with the above list, Emiling & Stan (2001) and Çınar et al. (2020) described in more detail the data-dependent analyses that have been implemented in some operations to identify equipment degradation. The analyses are:

- Oil analysis/tribology: lubricants are examined for impurities such as the wear of the internal components.
- Thermography: heat variation in the different regions of a machine is measured and transformed into visible signals. They are useful for temperature measurement in rotating devices such as roller chocks or motor armatures. It is also used to monitor electrical devices such as switchgear, transformer bushings, transmission lines, reactor, DC Rectifiers, etc.
- Vibration monitoring: vibration signals and information generated over time are collected for processing. These are typically performed by hard wired sensors positioned to pick up data from a uniform location.

CONCLUSION

This paper provides an overview of the implications of equipment maintenance in the mining industry. The cost associated with mining equipment and the factors influencing this cost was highlighted. Maintenance strategies, their evolution over the last six decades and their transition to the current era of computerisation and digitisation were highlighted. Predictive maintenance was also studied to illustrate the categorization of equipment components into sub-systems. This has resulted in the systematic identification of critical data points from which an AI-infused predictive model can be built. The maintenance cost saving potential for adopting this predictive technology would be significant for any adopting mining operation. In addition, the increased knowledge of the operating condition of the machines and its various components used in the operations would provide a significant foundation on which more advance technology would be layered upon.

ACKNOWLEDGEMENTS

The work presented in this paper is part of a PhD research study in the School of Mining Engineering at the University of the Witwatersrand, Johannesburg, South Africa.

REFERENCES

Carvalho, T. P., Soares, F. A. A. M. N., Vita, R., Francisco, R. da P., Basto, J. P. & Alcalá, S. G. S. (2019) A Systematic Literature Review of Machine Learning Methods Applied to Predictive Maintenance. *Computers & Industrial Engineering*, 137 November, p. 106024.

Çınar, Z. M., Abdussalam Nuhu, A., Zeeshan, Q., Korhan, O., Asmael, M. & Safaei, B. (2020) Machine Learning in Predictive Maintenance towards Sustainable Smart Manufacturing in Industry 4.0. *Sustainability*, 12 (19), p. 8211.

Dhillon, B. S. (2008) Mining Equipment Maintenance [Online]. In: *Mining equipment reliability, maintainability, and safety*. Berlin ; London: Springer. Available from: <https://link.springer.com/content/pdf/10.1007%2F978-1-84800-288-3_8.pdf> [Accessed 14 November 2021].

Emiling, W. H. & Stan, W. S. (2001) Integrated Condition Monitoring: The Future Direction of Predictive Maintenance Strategies. Canadian Institute of Mining, Metallurgy and Petroleum.

Faitakis, Y., Mackenzie, C. & Powley, G. J. (2004) Reducing Maintenance Costs through Predictive Fault Detection. *CIM Bulletin*, 97 (1076).

Jalili, A., Murphy, B. & Tolvanen, P. (2015) Unlocking Value through Flotation Equipmemt Maintenance. Ottawa, Ontario,: Canadian Institute of Mining, Metallurgy and Petroleum.

Kerr, A. (2021) Predictive Maintenance for Productive Mining. *Chege Publishing | Mining* [Online blog]. Available from: <http://chegepublishing.net/predictive-maintenance-for-productive-mining/> [Accessed 17 August 2021].

Lashgari, A. & Sayadi, A. R. (2013) Statistical Approach to Determination of Overhaul and Maintenance Cost of Loading Equipment in Surface Mining. *International Journal of Mining Science and Technology*, 23 (3) May, pp. 441–446.

McCoy, J. T. & Auret, L. (2019) Machine Learning Applications in Minerals Processing: A Review. *Minerals Engineering*, 132 March, pp. 95–109.

Ong, Y.-S. & Gupta, A. (2019) AIR5: Five Pillars of Artificial Intelligence Research. *IEEE Transactions on Emerging Topics in Computational Intelligence*, 3 (5) October, pp. 411–415.

Vagenas, N., Runciman, N. & Clément, S. (1997) A Methodology for Maintenance Analysis of Mining Equipment. *International Journal of Surface Mining, Reclamation and Environment*, 11 (1) January, pp. 33–40.

PREMATURE MINE CLOSURE, RISK ASSESSMENT AND POST-MINING LAND-USE OF GALALI OPEN-PIT IRON MINE OF IRAN

M. Zangeneh [1], M. Osanloo [1,*], S. Amirshenava [1]

[1]*Amirkabir University of Technology, Department of Mining Engineering*
(*[*] Corresponding author: morteza.osanloo@gmail.com*)

ABSTRACT

Premature closure of mine before fully extraction of mineable reserve cause deviation from the durability of life cycle and leads to a significant impact on the economy, social and the investment sector. This paper analyzes factors associated with the risks of premature closure for the Galali iron mine located in Kurdistan province of Iran. To this end, after determining the most significant risks involved in the closure of this mine, the optimal Post Mining Land Use (PMLU) selection is regarded as a risk management measure. To determine the causes, twenty-one factors, including economic, technical, social, environmental, safety, and health are identified. Based on the ten experts ' opinions, these factors were evaluated using the Technique of Order Preference Similarity to the Ideal Solution (TOPSIS). Two items had high safety and health risks in the two-dimensional risk matrix. Six alternatives based on 17 criteria were proposed to select the optimal PMLU. According to the experts' team opinions, using Analytic Hierarchy Process (AHP) and the TOPSIS as two of the Multi-Criteria Decision Making (MCDM) methods, the most suitable options for PMLU in the Galali mine were determined. Garden, agriculture, and pasture have the priority in this mine.

Keywords: Mine closure, mine reclamation, risk management, multi-criteria decision making.

INTRODUCTION

Earlier mine closure, which is often referred to as “premature mine closure (PMC)”, may occur due to depletion of mineral reserves or environmental, social, and economic factors. Due to PMC occur in the unplanned form may lead to adverse impacts such as health and safety problems, job loss, loss of community services and facilities, water, air, and soil pollution on-site or off-site (Laurence, 2001; Unger et al., 2015; Venkateswarlu, 2016). These negative impacts can be considered a risk to PMC, threatening sustainable development goals. Therefore, PMC factors in the risk management process must be managed to reduce the negative impacts (Eggart, 2015; Espinoza and Morris, 2017; Laurence, 2006). One of the best methods for assessing the risks associated with mine closures is the 2D risk matrix (Gheisari et al., 2014; Laurence, 2001, 2006; Taveira and Sánchez, 2016). Mine reclamation is essential to keep mining activities sustainable development and protect future generations’ rights. Choosing the appropriate Post Mining Land Use (PMLU) is the foremost step of the mine reclamation plan.

Since mine reclamation has a multidisciplinary nature, in this project, various fields of science and engineering such as soil mechanics and slope stability, soil fertilization, hydrology for quantitative and qualitative control of groundwater, agriculture for growing plants and trees, ecology as the basis of basic studies and sociology are used. In general, reclamation is not a separate operation from planning and mine design operations. Indeed, it is a part of the mining operation that begins in the exploration stage and continues until the decommissioning of the mineral processing plant. Due to the importance of mine reclamation, many researchers have worked on this issue, and many of them have considered

Multi-Criteria Decision-Making (MCDM) methods to select the most suitable PMLU (Dimitrijevic et al., 2014; Narrei and Osanloo, 2011; Shenavar and Osanloo, 2016; Yavuz and Altay, 2015). Ruiz et al. (2020) proposed the construction of technosols from human and animal waste as a low-cost strategy for waste management and reclamation of mined lands, because these technosols create a favorable environment in mined areas for plant growth. Broda et al. (2020) offered a new method for reclamating abandoned open-pit mines using geotextiles. In the post-closure opencast lignite mine Zechau in Germany, they also used this method to create suitable housing areas for agricultural, forestry, and nature conservation.

In the present study, an attempt has been made to determine the factors of premature closure of the Galali iron mine by using Technique of Order Preference Similarity to the Ideal Solution (TOPSIS) method. Then, the PMC risks are evaluated with a 2D risk matrix, and finally, the optimal PMLU for the mined areas is offered by application AHP and TOPSIS method.

METHODOLOGY

This study consists of three main parts. The first part probes the causes of the PMC, the second step investigates the risk of PMC, and finally the third step suggests the optimal PMLU. In the following section, each of these steps is described in detail (Figure 1).

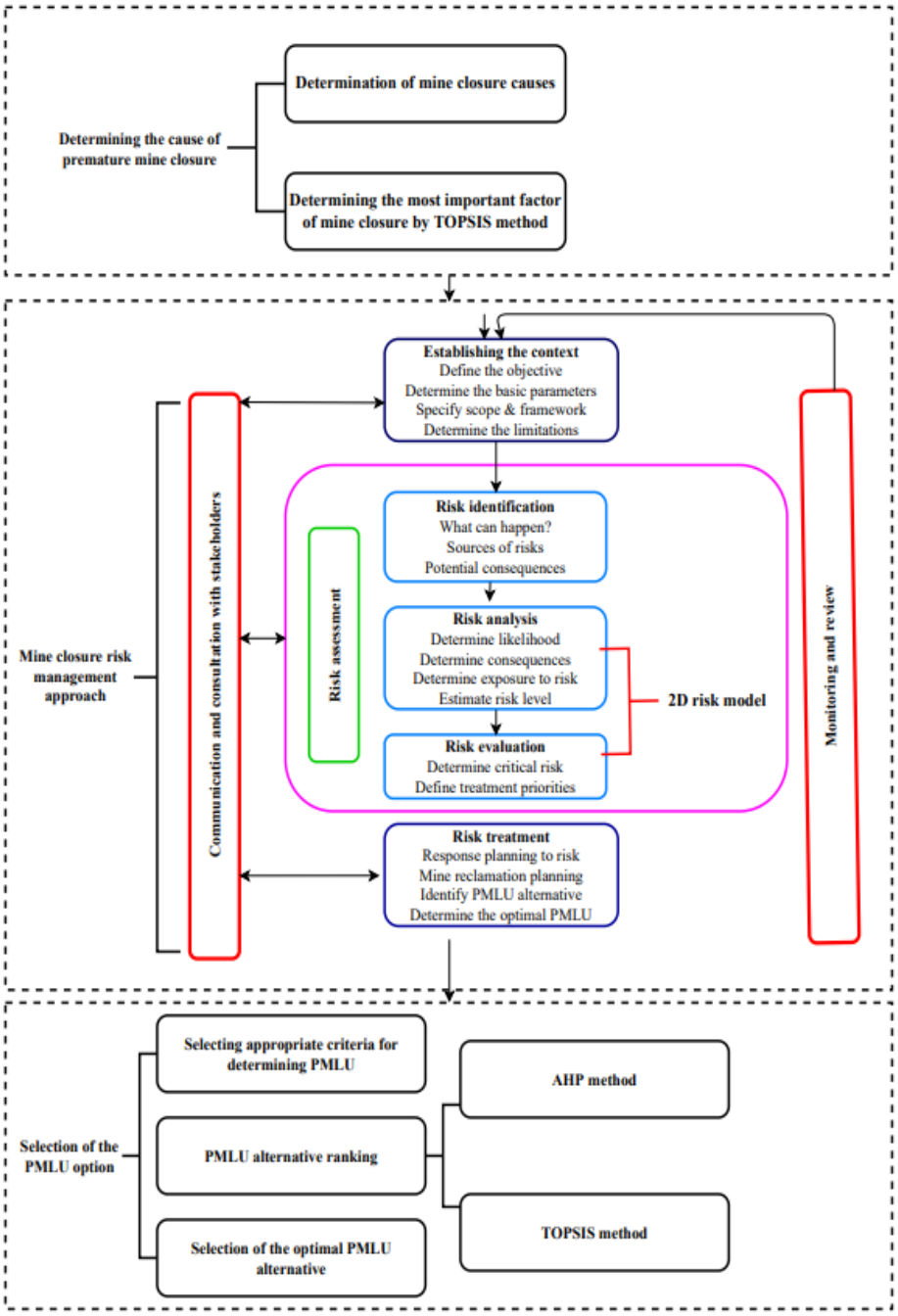

Figure 1. Flowchart of research method

PMC Causes Determination

PMC is associated with negative environmental and social impacts that needs to be managed to achieve sustainable mining. Therefore, it is notable to ascertain the causes of PMC to reduce these negative consequences. As displayed in Table 1, PMC causes are categorized into five groups, and each is divided into sub-categories. A questionnaire was created that asks experts to allocate the importance of each item by a number from 1 to 5. Number 1 means less likelihood of occurrence, while number 5 indicates high likelihood. Mean, and standard deviation of scores determined by experts are the criteria

for decision-making of TOPSIS method. Then, based on the results of questionnaires and the TOPSIS method, PMC causes are ranked from the most important to the least important.

Table 1. Causes for PMC

Issue	Causes for PMC
Economic	Low prices More appropriate use Production difficulties Loss of markets High costs Downturn Financial problems of the mine owner in the development phase of the mine
Technical	Geology or geotechnical problems Open cut resource depleted (but remaining underground resource) destruction of equipment lake of exploration Poor grade estimation Equipment/technical difficulties Lack of mining planning
Social	Regulatory or government intervention Change of ownership The hostility of natives with mine owners and mine activities
Environment	Environmental issues Weather Conditions
Health Safety	Safety and health issues

Risk Assessment by 2D Risk Matrix

The level of risk was characterized based on the questionnaire results. The questionnaire was provided to the experts team for this intention (Table2). Tables 3 and 4, are showing the probability and consequences of occurrence risk. The risk level of each declared case was calculated and determined using scores assigned by experts for each case, the 2D risk matrix in figure 2 and Equation 1.

Table 2. Classification of PMC risks

Risk type	Specific event	Explanation
Environmental	Acid mine drainage	Contamination of water caused by seepage of acid mine drainage
	Decreasing the water level	The decline in groundwater level caused by unconventional harvesting of water resources for mining purposes (extraction, processing, etc.)
	Greenhouse gases	Air pollution and climate change due to greenhouse gases emission
	Dust	Particulate material suspended by the wind causes air pollution

	Aesthetic values	Dissatisfaction with the unpleasant landscape caused by mining activities
	Waste dump reshaping	Problems arising from the final shaping of the waste dump (e.g., slope stability problems, drainage problems, topographic problems)
	Soil contamination	Destruction of soil fertility due to pollution from heavy metals
	Overflowing of tailings dam	Overflowing of tailings dam caused by intense precipitation and/or flood (occurrence of environmental pollutions)
Community	The hostility of natives with mine owners	Natives dissatisfied due to lack of fair distribution of wealth in the community (sometimes natives think that the mine owners have plundered the resources without creating any infrastructure and development in the region)
	Damage to the business of residents around the mine	Decline business boom (that types of business which are directly or indirectly related to mining operation)
	Impact on residential property value	Reduce the value of residential property
	Impact on lifestyle	Adverse effects on lifestyle mainly because of unemployment
Law and Financial	The financial risk of employees	Problems caused by employee's financial issues (e.g., unpaid wages, etc.)
	The financial risk of contractors	Problems caused by the financial debts to the contractors (failure to pay the cost of the completed projects)
	The financial risk of government	Problems due to unpaid taxes and royalties
	Financial provision for mine reclamation	Failure to finance the reclamation activities during mining operations or inaccurately estimation of reclamation cost
Technical	Mine closure plan	Failure to prepare a mine closure plan from the beginning of the mine's life
	Lack of a professional team for mine closure	Closure activities entail a group of highly knowledgeable persons in mining, environment, sociology, and economics. In some cases, the lack of such persons may impose risks to the project.
Health and Safety	Falling into the pit	Injuries due to falling of equipment, person, or animal into the pit
	Unexploded blast hole	The possibility of unexpected blasting of previously charged blast hole
	Pit slope failure	Safety problems caused by pit slope failure
	Tailings dam failure	Slope failure caused by hydric erosion or an earthquake creates problems for residents around the mine (e.g., damage to homes and agricultural lands, etc.)
	Toxic gases	Respiratory diseases due to toxic gases emission

	Toxic elements	Diseases caused by releasing toxic elements to the surrounding water resources

Table3. Probability of occurrence

Probability of occurrence	Score
Very High	5
High	4
Moderate	3
Low	2
Very Low	1

Table4. Consequences of the occurrence

Consequences of the occurrence	Score
Catastrophic	5
Major	4
Moderate	3
Minor	2
Insignificant	1

$$RS \qquad (1)$$

Where RS indicates the risk score, L is regarded as the likelihood of occurrence, and C displays the potential of occurrence

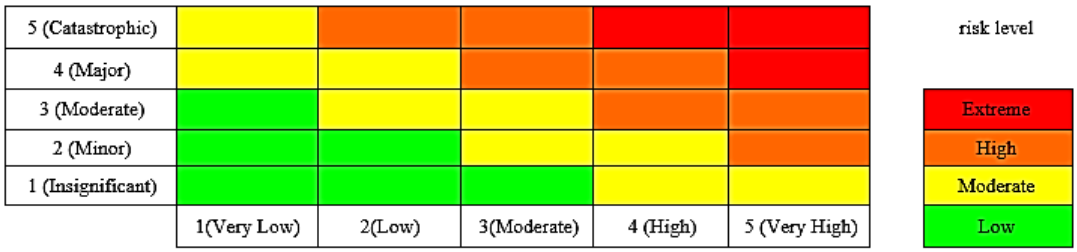

Figure 2. A schematic plan of 2D risk model

Reclamation and Post Mining Land Use (PMLU)

Selecting Appropriate Criteria for Determining PMLU

To determine the optimal PMLU for extracted lands, criteria are first specified to select alternatives based on them. These criteria include 17 items (Table 5).

Table 5. Decision-making criteria in PMLU selection

Type of group	Criteria
Economic factor	Capital cost Operating cost Increasing local community income the potential of Capital attraction
Social factors	Employment opportunities due to implementation of PMLU Reducing immigration from the mining area Consistency with concerns and needs of locals
Technical factor	Shape and size of the mined land Distance to nearest water supply Current land use in the surrounding area of the mine Ability to implement the reclamation plan
Mine site factors	Properties of soil Land slope Precipitation
Landscape & environmental factors	Impact on the desertification stop Environmental acceptability of the PMLU option Landscape quality caused by the implementation of the PMLU

Impact Matrix

The impact matrix illustrates the importance of each criterion to each alternative. The experts have assigned a number between 1 to 9 for each matrix element. Then, the weight of each criterion was determined by the AHP method. Finally, the proposed alternatives for PMLU were ranked using the TOPSIS method.

VERIFICATION OF PROPOSED METHOD

Galali open-pit iron ore mine is located in the west of Iran at 62 km from the center of Sanandaj Province. The approximate distance from the capital of Iran, Tehran, is 489 km (Figure 3). Its climate is cold and humid. Galali mine is located 1 km away from residential areas. The village's economy is based on agriculture, livestock, and gardening.

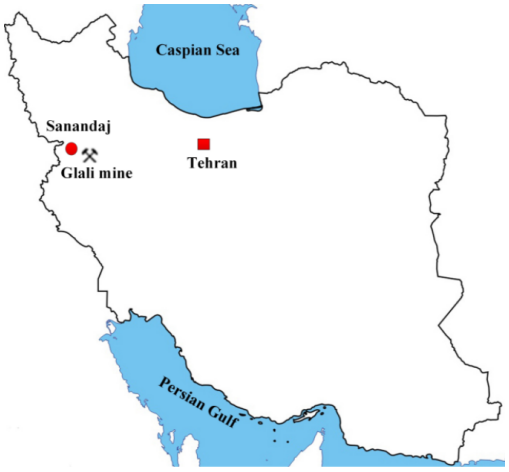

Figure 3. Location of the Galali iron ore mine of Iran.

To determine the most important causes for the PMC of the Galali iron mine, the questionnaire form was sent to experts (Table 7). They were asked to assign a number from 1 to 5 for 21 factors mentioned in the survey form. Fewer numbers mean that the option is less likely to occur. These numbers' mean and standard deviation were calculated, and the normalized and weighted matrix was formed. The positive and negative ideal solutions and distances from those were calculated in the next step. Finally, the similarity index was calculated, and causes for PMC were ranked (Table 8).

Table 7. Experts' qualification

Participant's job position	education	
	No. MSc	No. BSc
Engineering team	5	1
Management team	3	0
HSE team	1	0

Table 8. Similarity index and ranking

Causes for PMC	Similarity index
Environmental issues	0.7203
Downturn	0.6684
Low prices	0.6627
The hostility of natives with mine owners and mine activities	0.6029
High costs	0.5412
Loss of markets	0.5172
More appropriate use	0.4721
Regulatory or government intervention	0.469
Lake of exploration	0.4626
Production difficulties	0.4413
Weather Conditions	0.4072
Geology or geotechnical problems	0.3992

Poor grade estimation	0.3533
Equipment/technical difficulties	0.3533
Destruction of equipment	0.3266
Safety and health issues	0.3174
Change of ownership	0.2984
Open cut resource depleted (but remaining underground resource)	0.2576
Lack of mining planning	0.2234
Financial problems of the mine owner in the development phase of the mine	0.1918

As exhibited in Table 8, at Galali mine, environmental issues are the most important causes for the PMC. Therefore, it is required to investigate these issues and provide appropriate solutions to prevent premature closure of the Galali iron mine. The most critical environmental issues that cause the mine to close prematurely and the solutions presented to address them are as follows (Table 9):

Table 9. environmental issues and solutions

environmental issues that cause PMC	proposed solution
Dust	- Water spraying the traffic route by trucks and machines in summer - Reduced dust caused by the explosion by modifying the pattern and methods of explosion - Purchasing the surrounding agricultural lands and turning the lands into gardening and planting trees. - Improving and renovating the local roads
Vibration and noise	- Modifying explosion pattern - Recording earthquakes continuously at the time of the explosion, by using a seismograph
Acid Mine Drainage (AMD)	- Analysis water quality in the mine regularly - Starting studies about AMD prevention methods

Determination the Most Important Mine Closure Risks in the Galali Iron Mine

After a survey from the Galali iron mine expert team, based on what was described in Section Risk Assessment by 2D Risk Matrix, obtained the mine risk matrix in Table 8. Then low, medium, and high risks were determined (Table 10). There are some ways to prevent and control them.

To stem the unexploded blast hole, it should make them discharge from the blast hole, which to do this, compressors can be used. Of course, some solutions such as operating skillful experts, carefully charging the explosion holes, and checking the expiration date of explosive material can be offered to prevent this from occurring.

Table 10. Risk analysis results

Row	Risk type	Specific event	likelihood value	consequence value	risk	risk level
1	Environmental	Acid mine drainage	2	3	6	Moderate
2		Decreasing the water level	1	4	4	Moderate
3		Greenhouse gases	1	1	1	Low
4		Dust	3	3	9	Moderate
5		Aesthetic values	3	3	9	Moderate
6		Waste dump reshaping	2	2	4	Low
7		Soil contamination	2	1	2	Low
8		Overflowing of tailings dam	2	1	2	Low
9	Community	Hostility of natives with mine owners	1	4	4	Moderate
10		Damage to the business of residents around the mine	3	2	6	Moderate
11		Impact on residential property value	1	2	2	Low
12		Impact on life style	1	2	2	Low
13	Law and Financial	Financial risk of employees	1	2	2	Low
14		Financial risk of contractors	1	3	3	Low
15		Financial risk of government	2	3	6	Moderate
16		Financial provision for mine reclamation	1	3	3	Low
17	Technical	Mine closure plan	1	2	2	Low
18		Lack of a professional team for mine closure	2	3	6	Moderate
19	Health and Safety	Falling in to the pit	2	3	6	Moderate
20		Unexploded blast hole	3	4	12	High
21		Pit slope failure	2	5	10	High
22		Tailings dam failure	2	3	6	Moderate
23		Toxic gases	1	3	3	Low
24		Toxic elements	1	3	3	Low

In order to decrease the risk of pit slope failure, the following measures are proposed, some of them are being used in the Galali iron mine:

1. Geotechnical measures include control of cracks on benches in the form of visual observation and use the compass
2. Detailed rock mechanics studies to correct the final pit slope

The pit slope should be adjusted after PMC. For this purpose, the edges of the benches are exploded, and the stones resulting from the explosion are accumulated at the toe of the benches; therefore, the pit shape has a proper appearance. Then, suitable soil can be provided to create vegetation by utilizing technosols. These technosols can be fertilizers, domestic refuse, and sewage sludge related to Galali village, which is adjacent to the mine. As the Garden choice is determined as the most suitable PMLU, walnut and almond trees can be cultivated in these fields after providing an appropriate environment for growing trees. These trees are the most suitable species for this region.

Selecting the Optimal PMLU

According to the criteria noted in Table 5 and conditions of the region, the proposed alternatives for PMLU, including six items, were presented in Table 11(Narrei and Osanloo, 2011; Wei et al., 2011; Vickers et al., 2012).

Table 11. Proposed alternatives for PMLU and Reasons

PMLU alternatives	Reasons
Agricultural lands	Earning income Reducing rehabilitating costs Previous use of these lands
Garden	Adequate and sufficient rainfall Favorable results from planting walnut and almond trees by mine owners
Pasture Pasture	The location of the mine is suitable for Pasture use because it is located around the village (Reduce health and environmental risks) Help create jobs Existence of a suitable market for the supply of agricultural and livestock products
Park	Creating favorable conditions for recreation and favorable weather for residents Reduced opposition of the region natives
Residential	Attracting the population and village development
Industrial and Commercial uses	Reduce migration Create employment and income

Determination of the Most Suitable Option

The six offered alternatives for PMLU of Galali mine mentioned in Choosing the optimal PMLU Section were ranked using the AHP and TOPSIS methods. In the next step, calculate the positive and negative ideal solutions, and the distances from them were also calculated. Finally, the similarity index was calculated and ranked the proposed alternatives regarding the PMLU. Based on the results, the

order of optimal PMLU priority is shown in table 12:

Table 12. Ranking of proposed alternatives for PMLU

PMLU alternatives	Rank of alternative
Garden	1
Agricultural Lands	2
Pasture	3
Industrial and Commercial Uses	4
Park	5
Residential	6

Accordingly, the garden is the best alternative for PMLU and considering that this mine is located near the Galali village. In this village, most people are farmers and ranchers, and of course, the amount of rainfall is appropriate in this region, so creating a garden can be one of the best options for PMLU. In this regard, mine owners have planted some trees (walnuts and almonds) in this area, which had favorable results. Of course, because of the existence of suitable pastures and the previous land use of mine, which was agriculture, pasture and agriculture are suitable options for PMLU in this mine.

DISCUSSION

This paper aims to provide causes for closing and determine the most important risks due to PMC and the selection of optimal PMLU for the Galali iron mine in Iran. In this regard, environmental factors were identified as the most important causes for PMC by using the TOPSIS method and survey of experts team of this mine, including mine manager, Head of the technical office, HSE expert, and mining exploration manager, and six other experts. These environmental factors mainly include dust, ground vibration, and noise pollution from explosions and AMD. To prevent pollution and dust problems which were caused by explosions and machine traffic, proposed some solutions such as water spraying in mine roads, modifying the blasting pattern, purchasing surrounding lands of the mine, and changing their usage to the garden. In addition, using seismometers and sound level meters and correcting the explosion pattern suggested preventing the problem of ground vibration and noise pollution caused by extraction. High rainfall in the area and available springs periphery of Galali mine make the formation of AMD possible. Since these mine waters are used to irrigate agricultural lands, the quality of these waters is checked periodically. Although there are no worrying situations reported from water analysis yet, starting AMD studies were proposed because AMD studies are needed for warning situations to prevent contacting water with minerals.

In the next part of this study, among 24 possible risks due to the closure of this mine, the risks related to the safety and health sector, including pit slope failure and unexploded blast hole, were identified as a high level of risk in the 2D risk matrix. To prevent unexploded blast holes, some solutions such as ensuring the discharge of holes by compressors, using skillful experts, being careful in charging the explosion holes, and checking the expiration date of explosive material were suggested. To prevent the risk of pit slope failure, should adjust the pit slope after closing the mine. For this objective, the stones resulting from the explosion of benches should be accumulated at the toe of the benchs so that the pit's shape has a proper appearance. Then, using technosols makes it possible to create a suitable environment for vegetation creation.

In the final step of this study, to select the optimal PMLU, at first, 17 criteria affecting PMLU selection were determined. The mining experts' surveys and AHP, determined the weight of these criteria. Then, 6 PMLU alternatives were ranked by using the TOPSIS methods. Based on the results, optimal PMLU for extracted lands of the Galali iron mine were determined garden, agriculture, and pasture.

CONCLUSION

Economic, social, technical, environmental, health and safety factors cause PMC. PMC before the reserve exhaustion will significantly affect production planning and create environmental, social, and economic risks. Therefore, it is necessary to minimize the risks of PMC during the mine project life cycle. This paper will present a clear vision of premature closure on the Galali iron mine in Sanandaj province, west of Iran. To this end, after determining the most significant risks involved in the premature closure of this mine, the optimal PMLU selection is regarded as a risk management measure. To determine the causes for the PMC, twenty-one factors, including economic, technical, social, environmental, safety, and health issues, were identified. Based on the ten experts ' opinions, these factors were evaluated using the Technique of Order Preference Similarity to the Ideal Solution (TOPSIS) method. The environmental issues are identified as the PMC causes in this mine. Also, between twenty-four possible risks due to the PMC, only two items had a high level of safety and health risks (8.3 percentage) in the two-dimensional (2D) risk matrix. Six alternatives were proposed to select the optimal PMLU based on 17 criteria; four economic, three social, four technical, three mine site factors, and three landscape and environmental factors. Finally, according to the experts' team opinions, using the Analytic Hierarchy Process (AHP) and the TOPSIS as two of the MCDM methods, the most suitable options for PMLU in the Galali iron mine were determined. Garden, farmland, and pasture scored 0.84, 0.82, and 0.76, respectively, prioritize Galali Iron ore mine.

REFERENCES

Al-Harbi, K.M.A.-S., (2001). Application of the AHP in Project Management. *International Journal of Project Management, 19(1*), pp.19–27. Available at: http://dx.doi.org/10.1016/s0263-7863(99)00038-1.

Amirshenava, S. & Osanloo, M., (2018). Mine closure risk management: An integration of 3D risk model and MCDM techniques. *Journal of Cleaner Production, 184,* pp.389–401. Available at: http://dx.doi.org/10.1016/j.jclepro.2018.01.186.

Betrie, G.D. et al., (2013). Selection of Remedial Alternatives for Mine Sites: A multicriteria decision analysis approach. *Journal of Environmental Management, 119*, pp.36–46. Available at: http://dx.doi.org/10.1016/j.jenvman.2013.01.024.

Broda, J. et al., (2020). Reclamation of Abandoned Open Mines with Innovative Meandrically Arranged Geotextiles. *Geotextiles and Geomembranes, 48(3)*, pp.236–242. Available at: http://dx.doi.org/10.1016/j.geotexmem.2019.11.003.

Delgado-Martin, J. et al., (2013). Four Years of Continuous Monitoring of the Meirama End-Pit Lake and Its Impact in the Definition of Future Uses. *Environmental Science and Pollution Research, 20(11),* pp.7520–7533. Available at: http://dx.doi.org/10.1007/s11356-013-1618-9.

Dimitrijevic, B. et al., (2014). Multi-criterion Analysis of Land Reclamation Methods at Klenovnik Open Pit Mine, Kostolac Coal Basin. *Journal of Mining Science, 50(2)*, pp.319–325. Available at: http://dx.doi.org/10.1134/s106273911402015x.

Espinoza, R.D. & Morris, J.W.F., (2017). Towards Sustainable Mining (Part II): Accounting for Mine Reclamation and Post Reclamation Care Liabilities. *Resources Policy, 52*, pp.29–38. Available at: http://dx.doi.org/10.1016/j.resourpol.2017.01.010.

Gheisari, N. et al., (2014). Closure Risk Assessment in Atashkooh Stone Quarry Using Risk Matrix. *Mine Planning and Equipment Selection*, pp.791–802. Available at: http://dx.doi.org/10.1007/978-3-319-02678-7_77.

Hwang, C.-L. & Yoon, K., (1981). Methods for Multiple Attribute Decision Making. *Lecture Notes in Economics and Mathematical Systems*, pp.58–191. Available at: http://dx.doi.org/10.1007/978-3-642-48318-9_3.

Jarvie-Eggart, M.E. ed., (2015). Responsible Mining: Case Studies in Managing Social & Environmental Risks in the Developed World. SME.

Laurence, D., (2001). Classification of Risk Factors Associated with Mine Closure. *Mineral Resources Engineering, 10(03*), pp.315–331. Available at: http://dx.doi.org/10.1142/s0950609801000683.

Laurence, D., (2006). Optimisation of the Mine Closure Process. *Journal of Cleaner Production, 14(3-4*), pp.285–298. Available at: http://dx.doi.org/10.1016/j.jclepro.2004.04.011.

Narrei, S. and Osanloo, M., (2011). Post-Mining Land-Use Methods Optimum Ranking, Using Multi Attribute Decision Techniques with Regard to Sustainable Resources Management, *OIDA International Journal of Sustainable Development, 2(11),* pp.65-76.

Ruiz, F. et al., (2020). Revealing Tropical Technosols as an Alternative for Mine Reclamation and Waste Management*. Minerals, 10(2),* p.110. Available at: http://dx.doi.org/10.3390/min10020110.

Shenavar, M. and Osanloo, M., (2016). Land Use Selection and Reclamation Layout Planning by MCDM–Case Study: Sangan Placer Iron Ore Mine Of Iran. In 16th International Symposium on Environmental Issues and Waste Management in Energy and Mineral Production (SWEMP) (pp. 5-7).

Taveira, A.L.S., Sánchez, L.E., (2016). A Risk-Based Framework for Managing Mine Closure. In: 24th World Mining Congress. Mining in a World of Innovation, Rio de Janeiro, Brazil, 18-21 October.

Unger, C.J. et al., (2015). A Jurisdictional Maturity Model for Risk Management, Accountability And Continual Improvement of Abandoned Mine Remediation Programs. *Resources Policy, 43,* pp.1–10. Available at: http://dx.doi.org/10.1016/j.resourpol.2014.10.008.

Venkateswarlu, K. et al., (2016). Abandoned Metalliferous Mines: Ecological Impacts And Potential Approaches For Reclamation. *Reviews in Environmental Science and Bio/Technology, 15(2),* pp.327–354. Available at: http://dx.doi.org/10.1007/s11157-016-9398-6.

Yavuz, M. & Altay, B.L., (2014). Reclamation Project Selection Using Fuzzy Decision-Making Methods. *Environmental Earth Sciences, 73(10*), pp.6167–6179. Available at: http://dx.doi.org/10.1007/s12665-014-3842-0.

PROPOSITION OF A NEW SCALED DİSTANCE EQUATION IN OPEN PIT BLASTING

AÇIK OCAK PATLATMALARINDA YENİ BİR ÖLÇEKLİ MESAFE DENKLEMİ ÖNERME

A. Tosun [1, *], S. Ercins [2], V.O. Tenorio [3]

[1] *Dokuz Eylul University, Buca-Bergama-Izmir, Turkey*
*(*Corresponding author: abdurrahman.tosun@deu.edu.tr)*
[2] *Cumhuriyet University, Sivas, Turkey*
[3] *University of Arizona Department of Mining and Metallurgy Engineering, Tucson, Arizona, U.S.*

ABSTRACT

Scaled distance equations used for estimating peak particle velocity have been investigated by some researchers. The most widely used equation among these is one formulated by Duvall and Fogelson. In this study, peak particle velocity values were measured by a number of blast tests that were conducted in a limestone quarry by using a vibration meter. Scaled distance values for each blast test were calculated according to the equation proposed by Duvall and Fogelson. Subsequently, a new equation that calculates the scaled distance was proposed. The proposed equation gave more realistic values than the equation proposed by Duvall and Fogelson.

Keywords: Blasting, peak particle velocity, scaled distance.

ÖZET

Açık ocak patlatmalarında en yüksek parçacık hız tahmininde kullanılan ölçekli mesafe denklemleri, bazı araştırmacılar tarafından araştırılmaktadır. Bunlar arasında en yaygın olarak kullanılan denklem Duvall ve Fogelson tarafından geliştirilen denklemdir. Bu çalışmada, bir kireçtaşı ocağında bir titreşim ölçer kullanılarak gerçekleştirilen bir dizi patlatma testi ile en yüksek parçacık hız değerleri ölçülmüştür. Her bir patlatma testi için ölçekli mesafe değerleri, Duvall ve Fogelson tarafından önerilen denkleme göre hesaplanmıştır. Ardından, ölçekli mesafeyi hesaplayan yeni bir denklem önerilmiştir. Önerilen denklemin, Duvall ve Fogelson tarafından önerilen denklemden daha gerçekçi değerlerin verdiği tespit edilmiştir.

Anahtar Sözcükler: Patlatma, en yüksek parçacık hızı, ölçekli mesafe

INTRODUCTION

The research method and idea in this study were taken from the research conducted by A. Tosun in 2020. This paper supports this research with data from a different field test.

As it is known from the literature, there are three controllable parameters that affect the peak particle velocity as a result of blasting operations. The first of these is the maximum amount of explosives used per delay. The second is the distance between the point of measured peak particle velocity and the blast point. The last of the controllable variables is the delay time. It is ensured that all blast holes do not explode at the same time with the delayed system used in blasting operations. Among the controllable parameters, the maximum amount of explosives blasted at once and the distance between the point of measured the peak particle velocity and blast point affect the peak particle velocities. Many researchers have carried out relations that predict peak particle velocity. (Duvall and

Fogelson, 1962; Ambraseys and Hendron, 1968; Langefors and Kihlstorm, 1978; Ghosh and Daemen, 1984; Pal Roy, 1991; Singh et al., 2002). However, the most widely used of these is the relation developed by Duvall and Fogelson. In this relation, firstly, the relationship between the maximum amount of explosives blasted at once and the distance to the blast point is determined. This relationship is called scaled distance.

In this equation, the scaled distance is calculated as follows: (Duvall and Fogelson 1962).

$$SD=R/(\sqrt{Q}) \quad (1)$$

SD: Scaled distance
R: The distance between the point of measured PPV and the blast point (m.)
Q: The maximum amount of explosives blasted at once (kg.)

According to Equation 1, the relation between the calculated scaled distances and the peak particle velocities caused by vibration is calculated by the equation 2 given below. (Duvall and Fogelson 1962).

$$V=K*(R/(\sqrt{Q}))^{-ß} \quad (2)$$

V: The peak particle velocity (mm/s)
K and ß: The coefficients the uncontrollable parameters in the blast field

Here, the coefficients K and ß represent the uncontrollable parameters in the blast area. These coefficients can have different values for each field. In order for the K and ß coefficients not to have different values in the same area, the peak particle velocity measurements as a result of blasting must always be made in the same direction. With the Equation 2, the peak particle velocity is estimated according to the explosives and distance for subsequent detonations in the same area. The distance between the point of measured PPV and the blast point affects the peak particle velocity. As seen in Figure 1, this distance has two components, v and h distances. While v distance expresses the vertical distance reached by the blast energy; the h distance represents the horizontal distance reached by the blast energy.

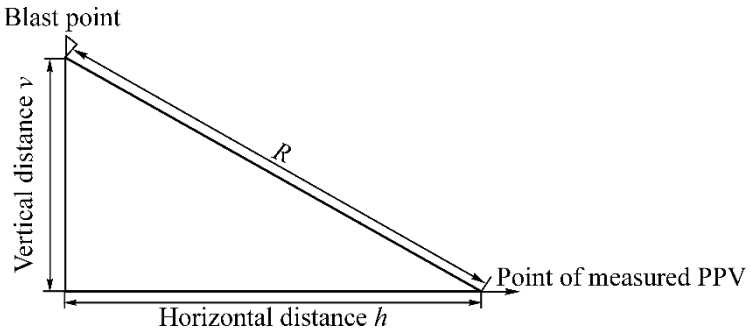

Figure 1. The distance components between the point of the peak particle velocity measured and blast point.

The distances *v* and *h* can be calculated as follows:

$$v = y_1 - y_2 \quad (3)$$

$$h = x_1 - x_2 \quad (4)$$

x_1, y_1 are the coordinates of blast point, x_2, y_2 are the coordinates of the point of measured peak particle velocity.

Vertical (v) and horizontal (h) distances can vary considerably in blasting operations. In some blasts, the vertical distance is very small and the horizontal distance is very high; In some explosions, the opposite situation may occur. For this reason, it is very important how much the R distance used in the equations estimating the peak particle velocity represents the vertical and horizontal distances. In this study, seven blast tests were conducted in a Turkish limestone quarry. For all blast tests, peak particle velocity values were first measured by using a vibration meter in the same direction. After that the distances *R*, *v* and *h*, the maximum amount of explosives blasted at once were determined. Scaled distances were calculated according to Equation 1, and correlation analyses were established between the peak particle velocities and scaled distances. Finally, the ratios h / v were determined for each blast test. These ratios were divided into groups with values of 0-0.7; 0.70–2.25; 2.25–3.00; 3.0–7.0; and over 7.0. A scaled distance equation was proposed by using these ratios, and new scaled distance values were determined for all blast tests. Correlation analyses were conducted between the peak particle velocities and new scaled distances again. The correlation analyses established according to the proposed scaled distance equation increased considerably according to the scaled distance equation developed by Duvall and Fogelson.

FIELD STUDIES

Seven blast tests were conducted to measure the peak particle velocities in a limestone quarry. Peak particle velocity measurements were performed in the same direction. Two geophones were used for the first blast test, and one geophone were used for the other blast tests to measure peak particle velocities. In the scope of the field studies, the coordinates of the blast points and the points of peak particle velocity measured were sensitively determined by using a GPS device. Subsequently, the distances between the point of measured peak particle velocity and the blast point were calculated by the following formula:

$$R = [(x_1 - x_2)^2 + (y_1 - y_2)^2]^{0.5}. \quad (5)$$

The obtained distances *R* are presented in Tables 1 and 2. Maximum amounts of explosives blasted at once were determined through observations in a sensitive manner for each blast test. Nitroglycerine based dynamite was used as the igniter and ANFO type explosive was used to provide the disintegration in all the performed blast tests. Afterwards, scaled distance values were calculated for all blast tests by using the equation proposed by Duvall and Fogelson.

EVALUATION

The value of h / v ratios were determined for each blast test. In general, PPV can be expressed as $V = K(R/\sqrt{Q})^{-\beta}$ Coefficient *k* was introduced to define the result more exactly, then the PPV expression takes the form:

$$V = K\left(k\frac{R}{\sqrt{Q}}\right)^{-\beta}. \quad (6)$$

The values of coefficients *K*, *k* and β were determined by the experimental data. Then, the most suitable coefficients giving the PPV values measured realistically belonging to the first study site were determined by means of a computer program, by using these defined coefficients ranges. During the

determination of these coefficients, it was determined by creating a mathematical code with a software called Force 2.0. The main point here, h/v ratio values only allowed to be connected to coefficient *k*. A new equation used to calculate scaled distance is proposed by using the limitations belonging to the parameters in Table2. Coefficients *k* of the proposed equation are determined as 0.9; 0.7; 1.3; 0.4 and 1.6 in a fixed manner for performed blast tests belonging to the first study site. Depending on h/v value, the coefficient *k* was chosen. The same coefficients *k* corresponding to h/v values were applied for other study sites when processing the data of experimental blasts. Maximum amounts of explosives blasted at once in delay interval and scaled distances are given in Table 2. The PPV values are also given in that Table. Using the data obtained, the correlation analysis was made between scaled distance values calculated by both methods and PPV values (Fig. 2). In the study area, using the proposed equation, the coefficient of determination R^2 increased from 0.2550 to 0.6446 compared to formula (1),

Table 1. Intervals of change in h/v parameter and proposed equations to calculate scaled distance (Tosun, 2020)

Limits for h/v	0	$0.7 < h/v < 2.25$	$2.25 < h/v < 3.00$	$3.00 < h/v < 7.00$	$h/v > 7.00$
Proposed equations to calculate scaled distance $k(R/\sqrt{Q})$	0.	$0.7\frac{R}{\sqrt{Q}}$	$1.3\frac{R}{\sqrt{Q}}$	$0.4\frac{R}{\sqrt{Q}}$	$1.6\frac{R}{\sqrt{Q}}$

Table 2. The data for study field

Blast no.	Geophone no.	Maximum amount of explosives blasted at once, kg	Distance between blast point and geophone point, m	Scaled distance (equation (1)), m	PPV, mm/s	Scaled distance (according to proposed equation), m	*h*, m	*v*, m	h/v
1	1	16	287.09	71.77	2.519	28.71	284	42	6.762
	2	16	314.72	78.68	1.67	55.08	268	165	1.624
2	1	45	227.00	33.84	2.034	43.99	355	142	2.500
3	1	35	241.00	40.74	2.453	36.66	366	565	0.648
4	1	32	288.00	50.91	3.841	35.64	455	302	1.507
5	1	55	241.00	32.50	3.795	22.75	625	288	2.170
6	1	61	227.00	29.06	4.339	26.16	485	755	0.642
7	1	45	202.00	30.11	4.043	27.10	356	854	0.417

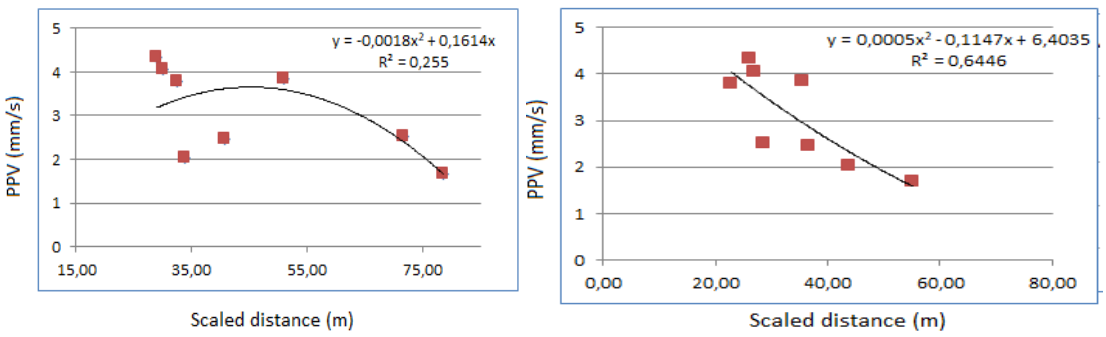

(a) (b)

Figure 2. Relationship between the measured PPV and scaled distance calculated for study sites (a) according to formula (1), (b) according to Table 2.

It can be seen that PPV was estimated with a higher accuracy using the expression (6). Therefore, using this expression, it is possible to control the parameters of explosives and scaled distances effectively, for blast designing with a lesser effect on the environment. The limitation values of h/v parameters must be determined more sensitively by performing several blast tests in different sites.

RESULTS

In this study, the relation between peak particle velocity values caused by the blast and the scaled distance were examined by performing blast tests in four different sites with different rock mass characteristics. The distance *R* in the calculation was divided into two components—vertical *v* and horizontal *h* distances, which are required to calculate scaled distance. In this calculation, the h/v. ratio is an important parameter, and these ratios were determined separately for each study site. They were divided into groups with values of 0–0.7; 0.7–2.25; 2.25–3.0; 3.0–7.0; and over 7, and fixed coefficients *k* were developed by using the remaining h/v ratio. A new relationship developed by using fixed coefficients increased the correlation between the PPV and scaled distance (Fig. 2).

The research method and idea in this study were taken from the research conducted by A. Tosun in 2020. This paper supports this research with data from a different field study.

FUNDING

The authors wish to thank the management of Scientific Research Projects of Dokuz Eylul University (BAP) for providing funding for this research project whose number is 2019 K.B. FEN 046.

REFERENCES

Ambraseys, N.R. and Hendron, A.J. (1968). Dynamic behavior of rock masses. *Rock Mech.*, In: Stagg and Zeinkiewicz (eds.), Eng. Practice, John Wiley and Sons Inc., London.

Dowding, C.H. (1985). *Blast Vibration Monitoring and Control*, Prentice-Hall.

Duvall, W.I. and Fogelson, D.E. (1962). *Review of Criteria for Estimating Damage to Residences from Blasting Vibrations*, U.S. Bureau of Mines, RI 5868.

Ghosh, A.K. and Samaddar, A.B. (1984). Design of surface mine blast. *Min. Eng. J. Inst. Eng.*, , (I), pp. 52–57.

Hajihassani, M., Armaghani, D.J., Marto, A., and Mohamad, E.T. (2014). Ground vibration prediction in quarry blasting through an artificial neural network optimized by imperialist competitive algorithm. *Bul. of Eng. Geol. and Env.*, Sept., 4 online first articles.

Langefors, U. and Khilström, B. (1978). *The Modern Technique of Blasting,* 3rd Ed, Halsted Press, Sweden.

Roy, P. (1991). Prediction and control of ground vibrations due to blasting. *Colliery Guardian*, 239(7), pp. 210–215.

Singh, T.N., Amit, P., Saurabh, P., and Singh, P.K. (2002). Prediction of explosive charge for efficient mining operation. *Rock Eng. Problems and Approaches in Underground Construction*, South Korea, pp. 777–785.

Tosun, A. (2020). Modified scaled distance equation used for estimation of peak particle velocity. *Journal of Mining Science*, 56 (3), pp. 67-74

PULSE TIME RATIO OPTIMIZATION IN A PRC COPPER ELECTROWINNING SYSTEM

H. Zerafat[1], A. M. Beygian[1,*], E. K. Alamdari[1]

[1]*Department of Materials and Metallurgical Engineering, Amirkabir University of Technology*
([*]Corresponding Author: ashkanmb@aut.ac.ir)

ABSTRACT

Iron removal is one of the necessities of extracting copper via electrowinning process. This substance causes a severe decrease in current efficiency in different stages of electrowinning. For this purpose, pulse reverse current (PRC) is applied with the aim of increased surface quality, increased current efficiency, optimal energy consumption and elimination of solvent extraction stage before electrowinning for small production workshops and rich electrolytes. The process of pulsed reverse current electrowinning was designed and performed in continuous cells. Copper, iron and sulfuric acid concentrations as well as forward (positive) and reverse (negative) current densities are fixed design parameters. The ratio of forward to reverse current time is the acquired variable and the experiments were performed at room temperature. The optimal state with 30 gpl copper, 5 gpl sulfuric acid and 10 gpl iron concentrations with a forward current density of 200 amps/m^2 and a reverse current density of 600 amps/m^2 was achieved through a pulse ratio of 40 to 1 seconds. Optimal current efficiency of 76.71% And energy consumption of 2.84 kwh per kg of produced copper were attained and also the cathode quality is acceptable.

Keywords: Copper electrowinning, iron removal, pulse reverse current, pulse time ratio

INTRODUCTION

Copper has high electrical and thermal conductivity as well as excellent machinability and formability, and for this reason it is considered to be a base metal in today's industry (Neikov, Naboychenko, and Murashova 2019). Hydrometallurgy is a common method of copper production. The electrowinning process is generally applied for the purpose of reduction and recovery of copper from an aqueous solution (Das and Krishna 1996). Electrowinning electrolyte is a highly acidic solution with a high concentration of copper. In this electrolyte, in addition to copper, there are amounts of elements such as sulfur, lead, manganese and iron (Najminoori et al. 2019). The presence of iron in this process reduces efficiency and increases costs in such a way that iron turns from Ferro to Ferric on anode surface and vice versa on cathode again stablishing a detrimental loop of current consumption (Subbaiah and Das 1994).

Most electrowinning cells have 316L reusable stainless-steel cathodes. these are almost identical to the electrical cathodes of the refining section. Older reservoirs use copper plate cathodes (Anderson 2016). Starter sheets are obtained from an electrical factory or made from electrowinning itself (Anderson 2016). Electrowinning anodes almost always consist of cold rolled Pb alloy (Mirza et al. 2016). In conventional electrowinning processes, electrolyte mixing and electrolyte flow through the electrochemical cell is produced by water decomposition reaction at the anode, producing oxygen bubbles on the anode surface (States 2003) which causes the electrolyte to mix and the oxygen bubbles reach the cell surface (Elrefaey et al. 2020). However, since the Ferro/Ferric iron anode reaction does not release any oxygen bubbles in the

anode, electrolyte circulation is the main source of mixing in the electrochemical cell (Cifuentes, Glasner, and Casas 2004).

In an industrial electrowinning process, reactions other than the reduction of copper play a role in the consumption of electric current, which reduce the cathode efficiency. Possible electrode reactions involved during copper electrowinning are as follows (Davenport et al. 2002).

On cathode surface (Cifuentes et al. 2007; Hannula et al. 2019):

$$Cu^{2+} + 2e \rightarrow Cu \quad (main\ reaction) \quad (E = 0.34V) \tag{1}$$
$$Fe^{3+} + e^{-} \rightarrow Fe^{2+} \quad (secondary\ reaction) \quad (E = 0.773V) \tag{2}$$
$$2H^{+} + 2e^{-} \rightarrow H_2 \quad (secondary\ reaction) \quad (E = 0.00V) \tag{3}$$

On anode surface (Cifuentes et al. 2007):

$$Fe^{2+} \rightarrow Fe^{3+} + e^{-} \quad (main\ reaction) \quad (E = -0.773V) \tag{4}$$
$$H_2O \rightarrow 0.5O_2 + 2H^{+} + 2e^{-} \quad (secondary\ reaction) \quad (E = 1.23V) \tag{5}$$

The duration of forward and reverse pulse may be from 20-200 seconds forward and 1-5 seconds reverse (States 2003). The aim of this study is to achieve the best ratio of forward and reverse pulse time. obtaining this ratio will result in the highest current efficiency and the lowest energy consumption combined with the best quality and surface adhesion of the cathode.

EXPERIMENTAL PROCEDURE

The electrolyte used in the electrowinning tests consists of copper sulfate heptahydrate and industrial iron sulfate heptahydrate with 98% assay sulfuric acid. In this study, a constant concentration of electrolyte contents was applied, which are 20gpl of iron, 30gpl of copper and 5gpl of sulfuric acid. In this experiment, a continuous solution injection system was used in a way that the electrolyte flows from a main reservoir to a chamber with a pump, which has 2 nozzles with specific output flows and the cell is filled with these nozzles. The cell has dimensions of 10 * 10 * 10 cm. The volume of the electrolyte solution in the cell is 700 ml, an electrolyte sink is provided to keep the volume constant throughout the experiment. The source of electric current is a pulse generator and shunts were applied to convert high current to suitable voltages. A copper cathode and 2 lead anodes were used as working electrodes. The electrodes were held by a brass clamp and placed in the electrolyte solution with specified dimensions of 5 x 5 cm. seven experiments were designed according to the existing conditions (table 1). The variable parameters are the forward-to-reverse pulse ratio and the frequency of each pulse, and the fixed parameters are 200 Amp/m^2 and 600 Amp/m^2 current densities, forward and reverse respectively; the test duration is 5 hours. A computer was used to record instantaneous data. Using Faraday's law, the amount of copper deposition was theoretically obtained when electrowinning was undergone for 5 hours, and the current efficiency was calculated by dividing the actual weight of the sediment by the theoretical amount of sediment. In addition, the amount of consumed energy was obtained through integration of the available data. $m_{theoretical}$ is the theoretical weight of copper that is supposed to deposit on the cathode when applying a current I during a period of time t. It was calculated from Faraday's law:

$$m_{theoretical} = \frac{M \times i.dt}{n \times f} \tag{6}$$
$$C.E.(\%) = \frac{m_{measured}}{m_{theoretical}} \times 100 \tag{7}$$

Table1. Designed Experiment conditions

Test number	Forward to reverse time ratio	Forward time (s)	Reverse time (s)	Current condition
Test 1	40 to 2	40	2	PRC
Test 2	40 to 0	40	0	DC
Test 3	40 to 1	4	0.1	PRC
Test 4	40 to 1	40	1	PRC
Test 5	49 to 1	49	1	PRC
Test 6	40 to 1	400	10	PRC

RESULTS AND DISCUSSION

DC and PRC Current Comparison

In this section, a comparison was made between Test 2 and Test 4. Current efficiency and energy consumption were calculated for both experiments. As shown in Figure 1, in DC mode the current efficiency was 89% and in PRC mode this value reached 77%. Converting DC current to PRC is associated with reduced efficiency because in PRC mode part of the current dissolves the reduced cathode at return. Power consumption was acceptable for both cases and its value is equal to 2.50 kWh in DC mode and 2.84 kWh in PRC mode. In DC mode, according to Figure 2 the cathode does not have good adhesion and separates as a powder, and it is difficult to collect the powder from the solution. Due to the surface quality of the cathode and its better adhesion in PRC mode, it was selected as the optimal mode despite lower current efficiency.

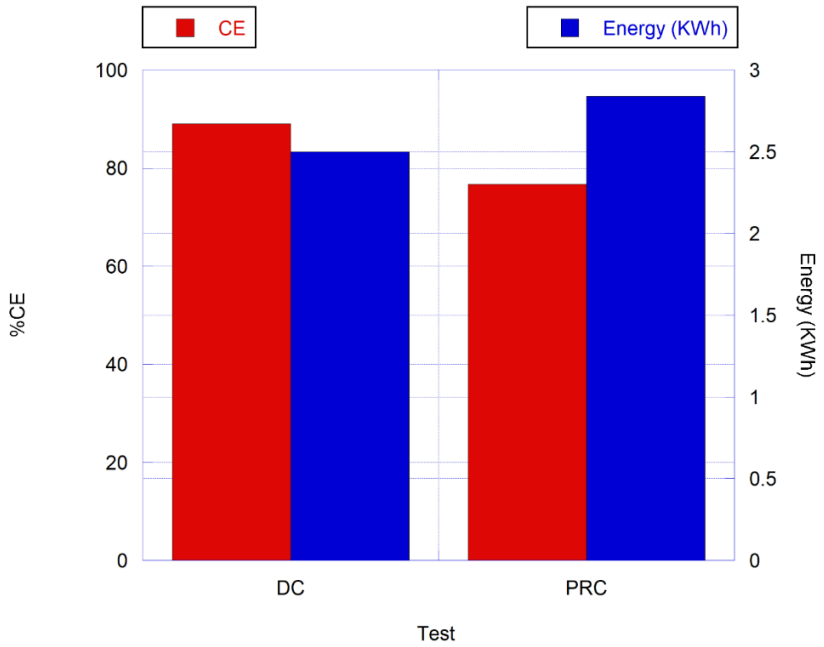

Figure 1. Current efficiency and energy consumption comparison.

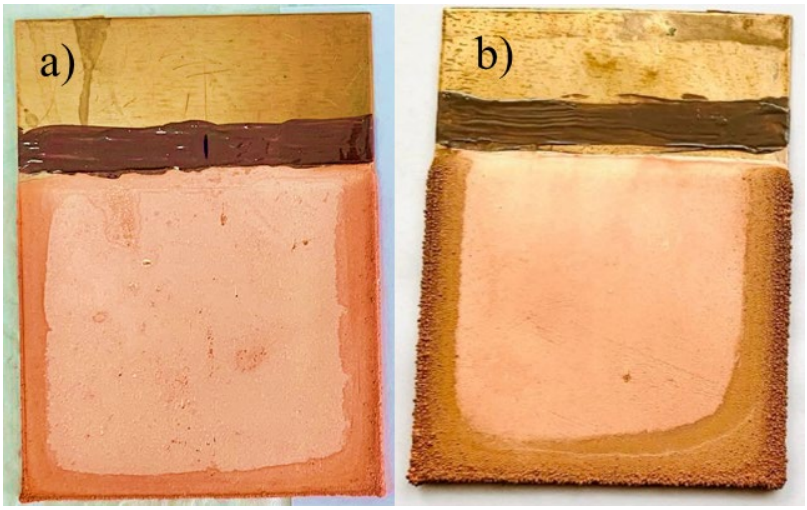

Figure 2. Cathode surface quality in a) PRC mode and b) DC mode.

Forward-to-Reverse Time Ratio Comparison

In this section, experiments were performed in 3 different ratios. The forward to reverse current time ratios of 40:2, 40:1, and 49:1 was evaluated. According to the results presented in table 2, the current efficiencies and energy consumptions were calculated for each experiment.

Table2. Current efficiency and power consumption results

Test Number	C.E. %	Energy (KWh/kgCu)
Test 1 (40:2)	67.56	3.03
Test 4 (40:1)	76.71	2.84
Test 5 (49:1)	74.34	2.85

From this comparison (Figure 3) it was concluded that the highest current efficiency is in the ratio of 40 seconds forward and 1 second reverse in Test 4 and also the lowest amount of energy consumption is in this ratio. In addition, the surface quality of the cathode and the degree of adhesion comply with Test 4 as shown in Figure 4, hence the ratio of 40 to 1 is selected as optimal condition.

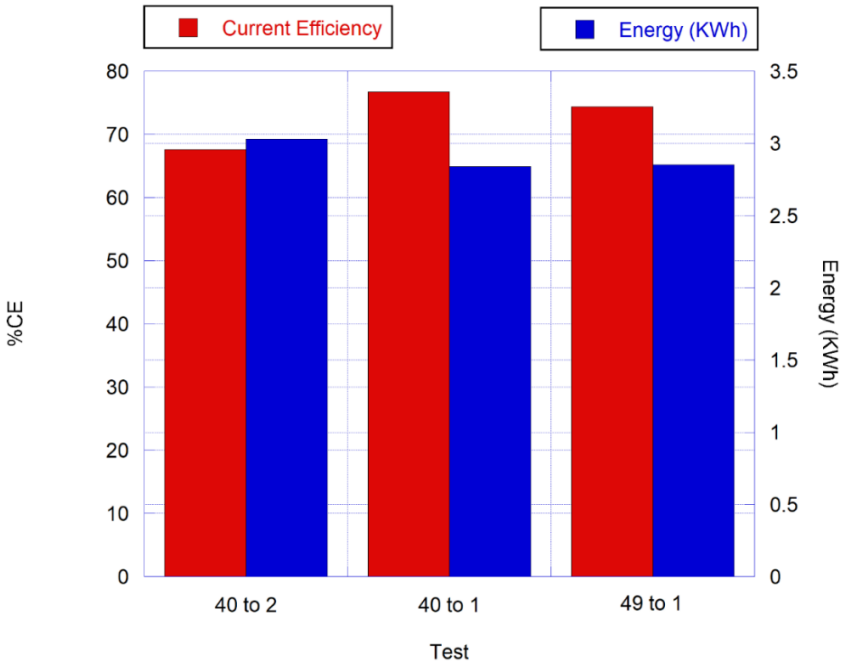

Figure 3. Current efficiency and energy consumption comparison in different forward-to-reverse time ratios.

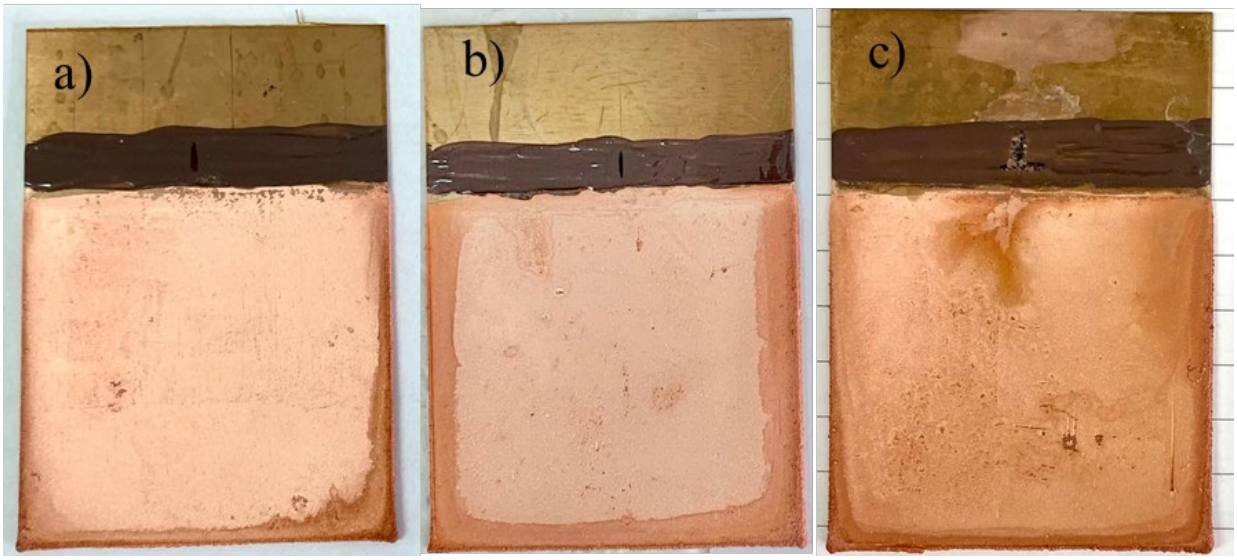

Figure 4. PRC Cathode surface quality in a) Test 1 (40:2), b) Test 4 (40:1) and c) Test 5 (49:1).

Duration Comparison

According to the abovementioned results, experiments were performed in 3 different periods with a ratio of 40 to 1. These times include 0.1 of a second, 1 second and 10 seconds. This time means that by converting 1 second to 0.1 second, this coefficient is multiplied by a ratio of 40 to 1, and in fact there will be a forward current of 4 seconds and a reverse current of 100 milliseconds, and the same thing is done for 10 seconds which means there will be a forward current of 400 seconds and a reverse current of 10 seconds and in these 10 second repetitions, a long time is expected to reach steady state. Table 3 provides the results of these performed experiments.

Table 3. Current efficiency and power consumption results in different duration

Test Number	%CE	Energy (KWh/kgCu)
Test 3 (0.1 sec)	60.02	3.28
Test 4 (1 sec)	76.71	2.84
Test 6 (10 sec)	79.52	2.81

Figure 5-a shows cathode surface is not of good quality and copper does not adhere well to the cathode surface. Figure 5-c also shows that the surface is powdery and not suitable, but Figure 5-b has both good surface adhesion and good cathode quality and separates as a sheet.

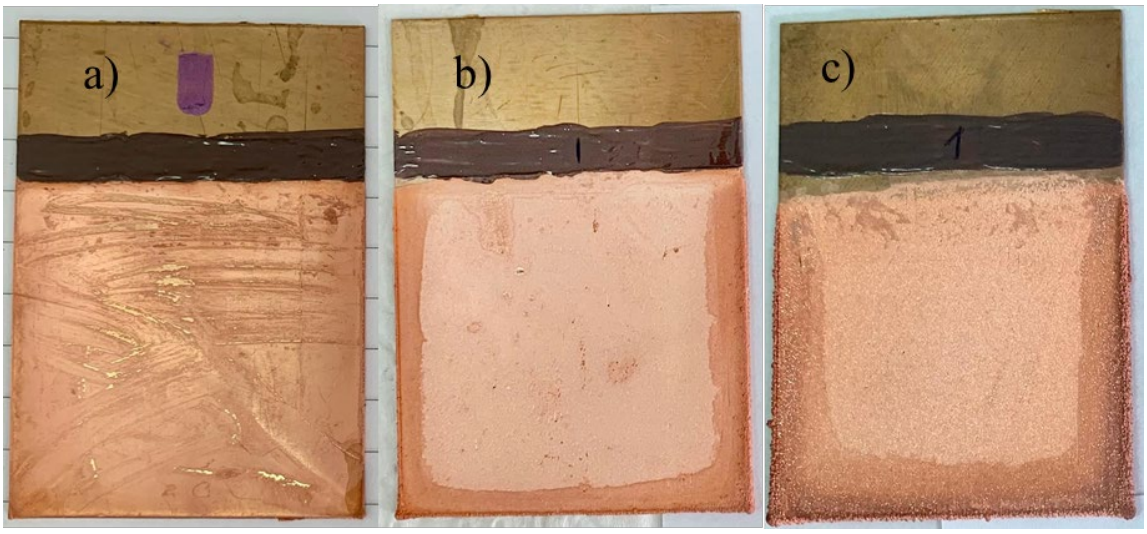

Figure 5. PRC Cathode surface quality in a) Test 3 (0.1 sec), b) Test 4 (1 sec) and c) Test 6 (10 sec).

According to the Figure 6 below and by comparing these 3 values, it should be concluded that duration 10 seconds have the highest current efficiency, but by comparing the quality of the cathodes and its adhesion, which is more important, duration 1 second is the best possible case.

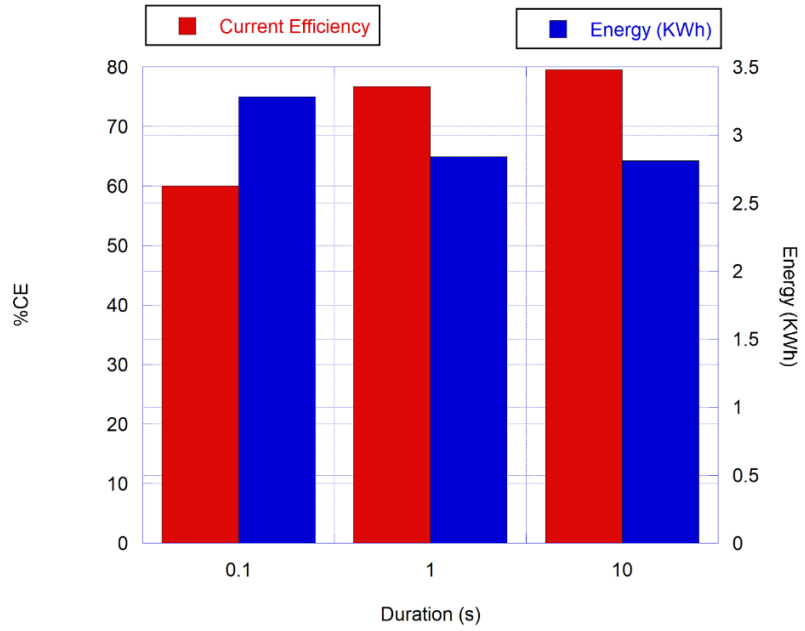

Figure 6. Current efficiency and energy consumption comparison in different duration.

CONCLUSION

This study on the use of pulse reverse current on the surface of cathodes used for copper electrowinning has shown interesting and practical results:

1) Using reverse current, the quality of the cathode is much better than the direct current mode, and copper sits on the cathode in the form of a sheet.
2) In the ratio of 40 to 1, the highest current efficiency and the lowest energy consumption and the best cathode quality were observed.
3) The coefficient of 1 second, despite the lower efficiency than the duration of 10 seconds, has a much better cathode quality.

As a result, the optimal mode in this study is 40 to 1 with a duration of 1 second in the PRC mode.

REFERENCES

Anderson, Corby G., (2016). Optimization of Industrial Copper Electrowinning Solutions. ,*IMPC 2016 - 28th International Mineral Processing Congress* 2016 (October). https://doi.org/10.4172/2090-4568.1000156.

Cifuentes, L., J. M. Castro, G. Crisóstomo, J. M. Casas, and J. Simpson., (2007). Modelling a Copper Electrowinning Cell Based on Reactive Electrodialysis., *Applied Mathematical Modelling* 31 (7): 1308–20. https://doi.org/10.1016/j.apm.2006.02.016.

Cifuentes, L., R. Glasner, and J. M. Casas., (2004). Aspects of the Development of a Copper Electrowinning Cell Based on Reactive Electrodialysis. *Chemical Engineering Science* 59 (5): 1087–1101. https://doi.org/10.1016/j.ces.2003.12.013.

Das, S. C., and P. Gopala Krishna., (1996). Effect of Fe(III) during Copper Electrowinning at Higher Current

Density. *International Journal of Mineral Processing* 46 (1–2), 91–105. https://doi.org/10.1016/0301-7516(95)00056-9.

Davenport, W.G., M. King, M. Schlesinger, and A.K. Biswas., (2002). Electrowinning. *Extractive Metallurgy of Copper*, 327–39. https://doi.org/10.1016/b978-008044029-3/50022-8.

Elrefaey, A., Y. Gu, J. D. James, C. Kneen, I. Crabbe, and J. Sienz., (2020). An Investigation of the Failure Mechanisms of Lead Anodes in Copper Electrowinning Cells. *Engineering Failure Analysis* 108. https://doi.org/10.1016/j.engfailanal.2019.104273.

Hannula, Pyry Mikko, Muhammad Kamran Khalid, Dawid Janas, Kirsi Yliniemi, and Mari Lundström., (2019). Energy Efficient Copper Electrowinning and Direct Deposition on Carbon Nanotube Film from Industrial Wastewaters. *Journal of Cleaner Production* 207, 1033–39. https://doi.org/10.1016/j.jclepro.2018.10.097.

Mirza, A., M. Burr, T. Ellis, D. Evans, D. Kakengela, L. Webb, J. Gagnon, F. Leclercq, and A. Johnston., (2016). Corrosion of Lead Anodes in Base Metals Electrowinning. *Journal of the Southern African Institute of Mining and Metallurgy* 116 (6): 533–38. https://doi.org/10.17159/2411-9717/2016/v116n6a7.

Najminoori, Mahjabin, Ali Mohebbi, Kambiz Afrooz, and Babak Ghadami Arabi., (2019). The Effect of Magnetic Field and Operating Parameters on Cathodic Copper Winning in Electrowinning Process. *Chemical Engineering Science* 199, 1–19. https://doi.org/10.1016/j.ces.2018.12.061.

Neikov, Oleg D., Stanislav S. Naboychenko, and Irina B. Murashova., (2019). *Production of Copper and Copper Alloy Powders*. *Handbook of Non-Ferrous Metal Powders*. 2nd ed. Elsevier Ltd. https://doi.org/10.1016/b978-0-08-100543-9.00019-1.

States, United., (2003). (12) Patent Application Publication (10) Pub . No .: US 2003 / 0124222 A1 Patent Application Publication. *Optics Express* 1 (19), 1–4.

Subbaiah, T., and S. C. Das., (1994). Effect of Some Common Impurities on Mass Transfer Coefficient and Deposit Quality during Copper Electrowinning. *Hydrometallurgy* 36 (3), 271–83. https://doi.org/10.1016/0304-386X(94)90026-4.

REMOVAL OF ORGANIC MATTER FROM BLACK PHOSPHATES BY CALCINATIONS; CASE OFF DJEBEL ONK PHOSPHATE; ALGERIA

D. Nettour [1, *], S. Grairia [2], S. Bensehamdi [1], M. Chettibi [1]

[1] *Ecole Nationale Supérieure des Mines Et Métallurgie ENSMM Amar Laskri Annaba*
*(*Corresponding author : djamel.nettour@ensmm-annaba.dz)*
[2] *Faculté des sciences de la terre Université Badji Mokhtar Annaba*

ABSTRACT

The phosphates of Djebel Onk in the extreme east of Algeria constitute a part of a vast set of phosphate deposits formed during the Cretaceous period on the southern and south-eastern shores of the Mediterranean. These concentrations of economic interest are exploited near the town of Bir El Ater (Wilaya of Tébessa) by the national company SOMIPHOS, a subsidiary of the MENAL group. This work concerns the beneficiation of black phosphate ore of Kef Es Sennoun by wet process. The appropriate treatment of the latter is settling; after removing the clay from the concentrate phosphate, the product undergoes heat treatment. The objective of this work is to study the variation of the temperature of heat treatment (Calcination) of black phosphate settled out of the wet process of Kef Es Sennoun. In order to see the influence of the temperature on the organic matter (Moukannaa and al 2020), therefore the effect the optimization of this treatment on the chemical, physical and mineralogical characteristics of the various major elements (MgO, P_2O_5, CO_2).

Keywords: Calcinations, djebel onk, phosphate ore, heat treatment, physico-chemical analyses.

INTRODUCTION

Despite of the Algerian underground conceals high potential of useful materials, namely the phosphate ores; in Djebel Onk deposits only, the proven reserves are about 2.2 billion tons, the production achieved remains relatively low, (about 1.5 million tons per year). (Nettour and al 2018). To respond to both increasing local and international demands for fertilizers, producing companies are expected to rise their production capacities and create strategies for the development and modernization of their production tools (Nettour et. al. 2018). To adopt an adequate technique to achieve this goal, a detailed identification and characterization of the ore in question is required.

This paper presents the calcinations method of Djebel Onk black phosphate; first the study is based on the particle size analysis of phosphate ore which has shown that the particle size range (00+63) µm represents the major part of the total mass of the sample, because of the friability of region phosphate ore, followed by a mineralogical analysis to determine the different mineralogical phases (carbonate apatite, carbonate hydroxyapatite, fluorapatite, and carbonate fluorapatite etc, as phosphate elements. The gangue is consisted of dolomite, silica, calcite, deerite, quartz, and ankerite). Thus, a chemical analysis was done to highlight the different elements that make up the phosphate ore of Djbel Onk and results in that the P_2O_5 contents vary from 27.932 to 34.249% with an average = 30.156 %. The contents of MgO vary from 0.508 to 3.214 %, hence the average content = 1.934 %) (Nettour D. and al 2019).

To lead to the rise of the fertilizers' production, this work targets the elimination of the organic matter of the product beneficiated by the wet way and to see the loss on ignition at different temperature degree of calcinations.

MATERIALS AND METHODS

A sample of black phosphate ore was taken from Bled Elhadba deposits; Djebel Onk - Tébessa; Algeria, was used in this study. The fragments of the raw ore samples were reduced by crushing to a particle size of -2 mm.

Then, the broken product was homogenized, divided into 100 g bags and stored for later use in grinding and granular analysis, and chemical analysis. After the crushing operation, the resulted phosphate ore samples were dried ground in a ceramic mortar mill (Figure 1). The granular analysis was carried out in narrow particle size intervals, the product crushed for 3 min, collected for sieving in an assortment of sieves classified as follows: 4000 m, 2000 m, 1000 m, 125 m, 63 and 45 m.

Figure 1. Ceramic mortar mill

Particle Size Analysis of Jebel Onk Ore

To identify the particle size composition of the ore, after the different stages of fragmentation, the sieving analysis is carried out by particle size analysis, to determine the respective size and weight percentage of the different families of grains called particle size fractions constituting the samples. Kechiched R. (2017). These fractions consist of particles whose size covers a relatively small range and decreases from one fraction to another. There are several methods of particle size analysis. Among them, the sieving method possibly used in our study, covers almost all ranges of particle sizes targeted. In addition, they allow the recovery of separate samples depending on the particle size. (Alain, 1994).

The collected sample is sent to the mechanical ore preparation laboratory, divided by the quartering (in two rifles), for the next chemical analysis as well as for the reserve. The sample is divided into four equal parts of which only half is retained by joining two opposite quarters. This selection is homogenized and a new quartering is carried out, the operation is repeated three or four times until 1.5 to 2 kg is obtained, Figure 2. The sample used is the black phosphate concentrate recovered by the wet process.

Figure 2. Quartering operation

A high precision balance and moisture meter were used to measure the humidity of our sample, Figure 3. After the weighing operation, samples of 10 g are treated at different temperatures, 6 degrees of temperature ranging from 600 to 900 ° C, for different times 5mn, 10mn 15mn, 20mn.

Figure 3. Moisture instruments measurements

The process begins by introducing four samples of phosphate into the oven, such that each sample weighs 10g at 400C °, after using a timer, we put a sample in the air for 5 minutes, and therefore the same is done for the rest of the temperatures up to 900C ° to obtain samples as follows. Figure 4.

Figure 4. Muffle furnace used in the test

The ore is heated to below its melting point either in the absence of air or in limited quantities. This method is commonly used to convert carbonates and hydroxides to their respective oxides.

RESULTS AND DISCUSSION

To determine the nature of our ore and highlight the physico-mechanical properties, a particle size analysis is recommended, the results of this analysis are presented in the table 1.

The main mode represented by the mesh [-500 + 200] µm, equals to 43.52% in weight; the weight yield of the second mode of mesh equals to -200 + 125 microns is about 16%; the third mode represents the coarse particle size range of a mesh of [-2000 + 1000] µm with a yield of 6.6%; and finally the thin slice [- 45 +0] µm presented the fourth mode with a weight yield of about 4%. Furthermore, the cumulative yields of passers-by are increasing as a function of sieve mesh. But the cumulative yields of the holdings are decreasing according to the openings of the sieves Figure 5.

Table 1. Granular analysis results of black phosphate ore

Size fractions (µm)	Cumulative yield (%).	
	+ γ (%)	– γ (%)
+ 4000	3,16	100
- 4000 + 2000	9,76	96,84
- 2000 + 1000	13,92	90,24
- 1000 + 500	27,56	86,08
- 500 + 200	71,08	72,44
- 200 + 125	87,15	28,92
- 125 + 063	94,35	12,85
- 63 + 45	96,40	5,65
- 45	100	3,60
sum		

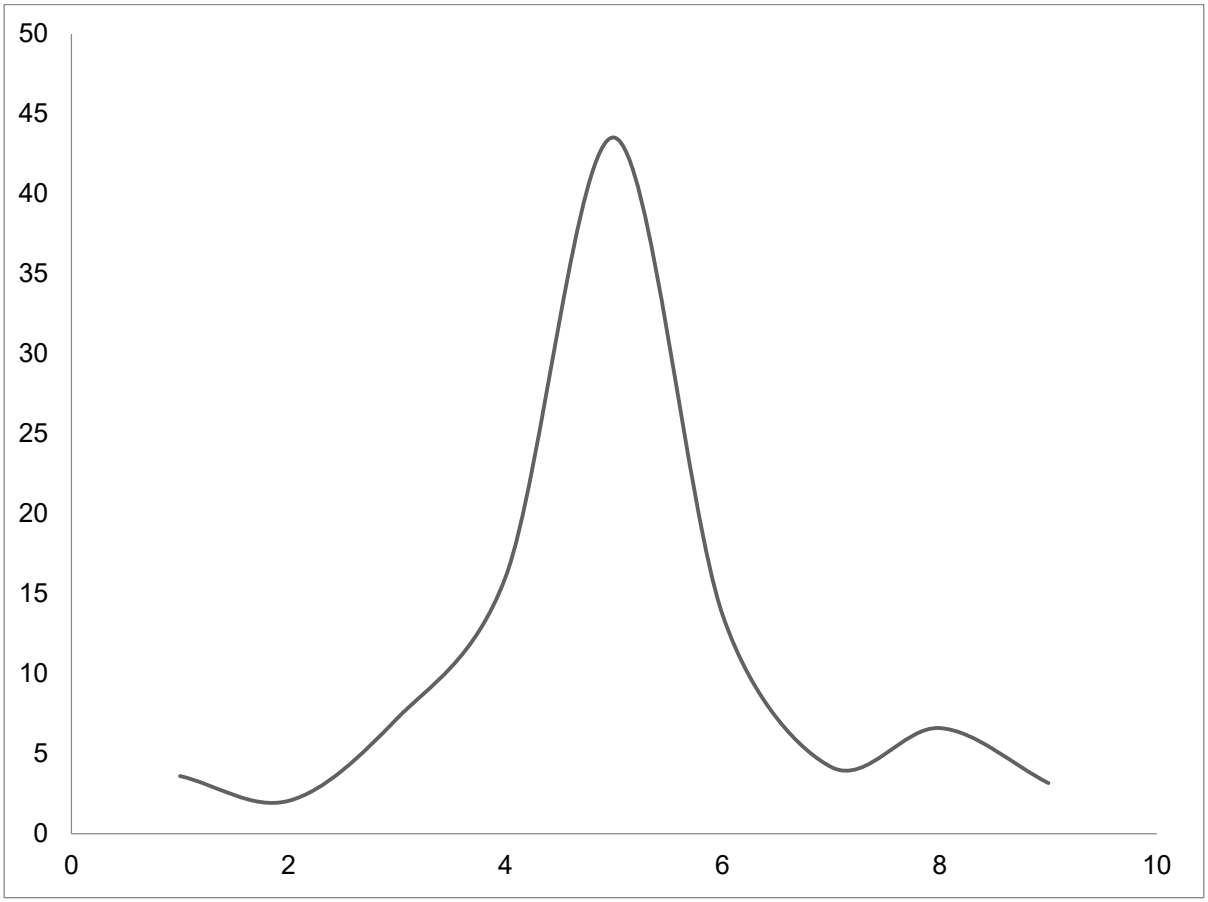

Figure 5. Variation of weighted fractions

Physico-Chemical Analyses

The purpose of the physico-chemical analyses is to determine the chemical composition of the various elements or combinations that go into the composition of the sample studied. To determine the content of P_2O_5 by the automatic spectrophotometer method (Auto analyzer), this technique of Auto Analyzer System is the latest in a comprehensive line of instruments for automatic liquid phase chemical analysis (Wissem et. al. 2016). But the determination of the magnesium oxide (MgO) is by atomic absorption (Atomic absorption spectrometry) to determine magnesium content in a test solution by

atomic adsorption spectrometry in the presence of lanthanum oxide, or lanthanum chloride. The absorbed photons being characteristic of absorbent elements, and their quantity being proportional to the number of atoms absorbent element, absorption makes it possible to measure the concentrations of the elements which one has decided to assay.

To determine the dioxide carbon, a calcimeter measures the volume of CO_2 released by the action of hydrochloric acid (HCl) on calcium carbonate ($CaCO_3$) in a soil or rock sample. The value of the ore is expressed by its tricalcic phosphate content of (% TPL) or P_2O_5 Such as: TPL = % P_2O_5 equal 2.185 see table 2.

Table 2. The results of the fire loss at 400 C°

Temperature	Duration in minutes	% loss on ignition	% CO_2	TPL MgO	TPLP_2O_5
400° C	5 min	2.42 %	7.12	1.17	67.49
	10 min	3.39 %	7.12	1.27	67.73
	15 min	3.73 %	7.04	1.27	67.93
	20 min	4.61 %	6.96	1.14	68.23

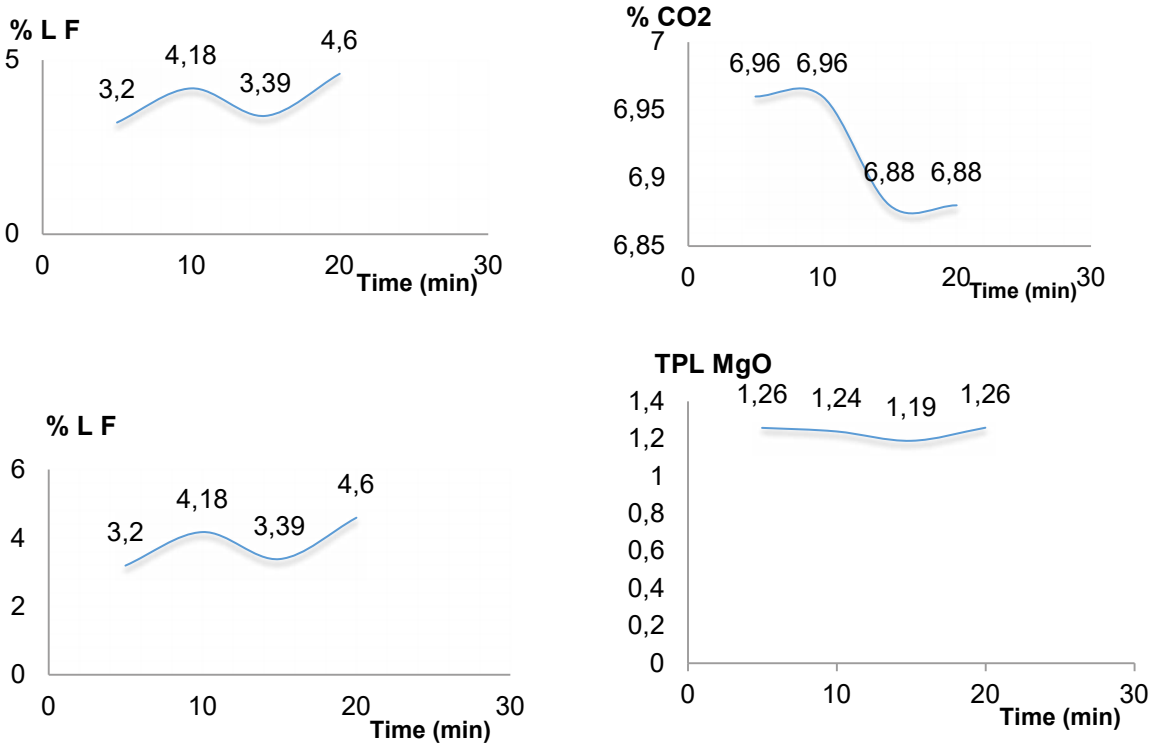

Figure 6. Variation of major elements contents after calcination at 400 °C

Table 3. The results of the fire loss at 500 C°

Temperature	Duration in minutes	% Loss on ignition	% CO_2	TPL MgO	TPLP_2O_5
500°C	5 min	3.2 %	6.96	1.26	68.23
	10 min	4.18 %	6.96	1.24	69.04
	15 min	3.39 %	6.88	1.19	69.17
	20 min	4.6 %	6.88	1.26	69.28

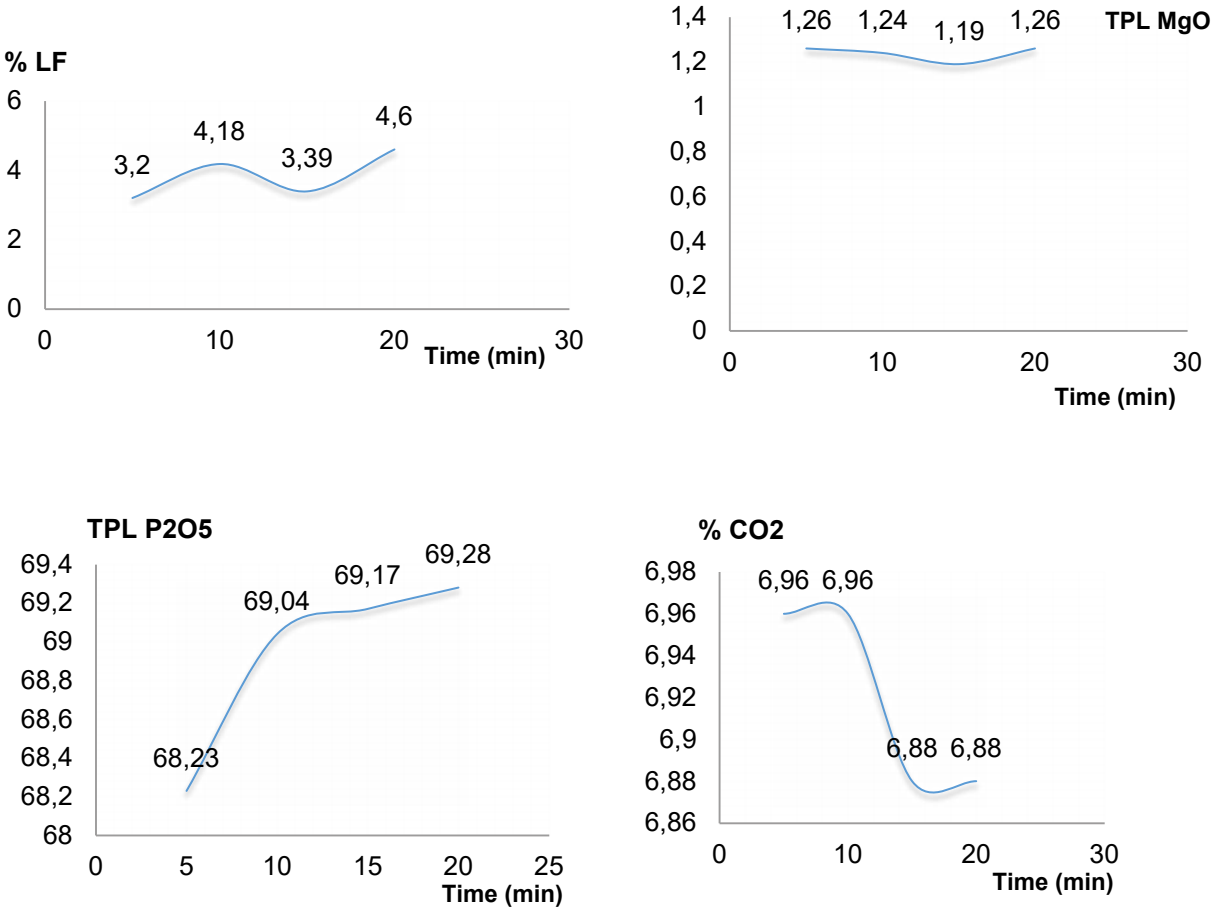

Figure 7. Variation of major elements contents after calcinations at 500 °C

Table 4. The results of the fire loss at 700 C°

Temperature	Duration in minutes	% Loss on ignition	% CO_2	TPL MgO	TPLP_2O_5
700°C	5 min	6.47 %	6.23	1.21	68.47
	10 min	6.97%	5.81	1.12	68.91
	15 min	8.07 %	5.48	1.24	69.15
	20 min	10.42%	5.40	1.60	69.72

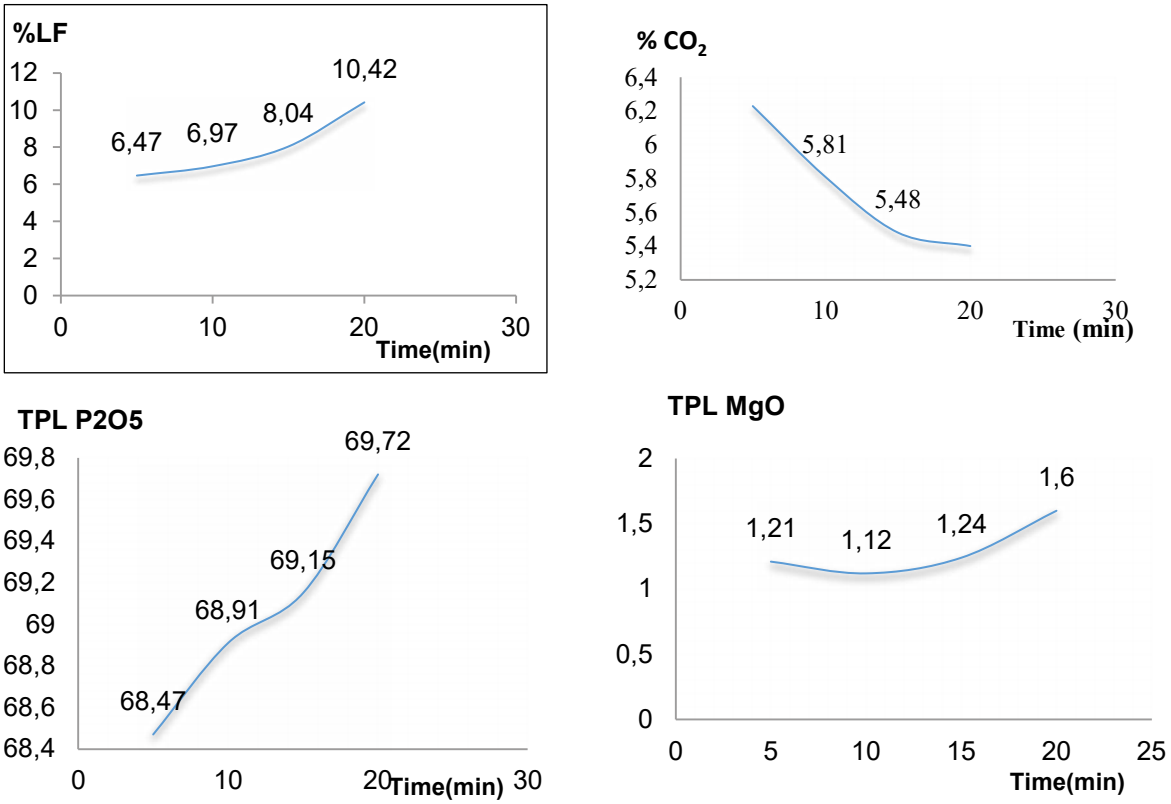

Figure 7. Variation of major elements contents after calcinations at 700 °C

Table 4. The results of the fire loss at 800 C°

Temperature	Duration in minutes	% Loss on ignition	% CO_2	TPL MgO	TPLP_2O_5
800°C	5 min	10.04 %	3.77	1.27	70.07
	10 min	11.41%	3.03	1.24	71.34
	15 min	13.84 %	2.7	1.26	71.36
	20 min	13.93 %	2.37	1.29	70.94

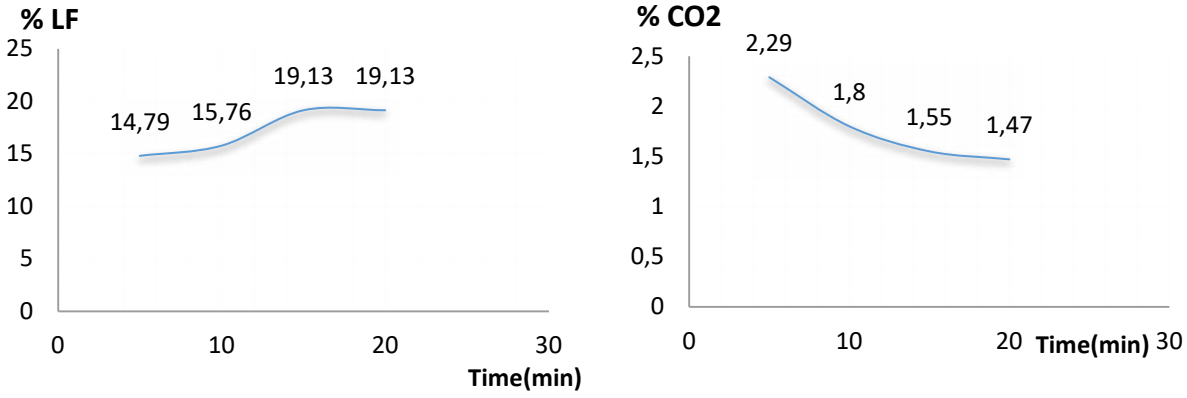

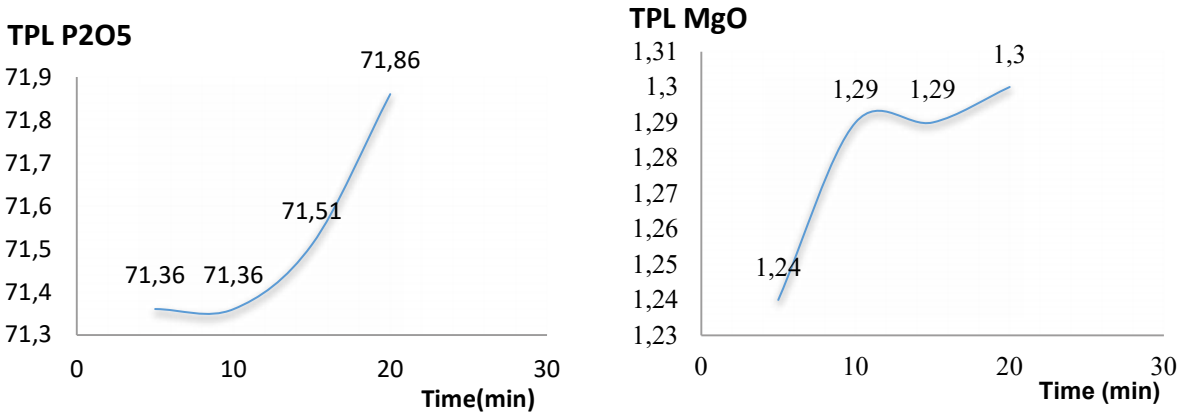

Figure 10. Variation of major elements contents after calcinations at 900° C

CONCLUSIONS

This work was done on the black phosphate of Djebel Onk deposits it shows the evolution of the elimination of the organic matter at different temperature degrees. The results obtained and presented in figure 3-9 made it possible to conclude the following:

1 / From 400 to 650 ° C: elimination of surface water.
2 / From 650 to 750 ° C: elimination of organic matter and constitutional water.
3 / From 750 to 900 ° C: decomposition of carbonates.

Through the graphs, the magnesium element (MgO) was hardly affected by the heat treatment, and its content remained almost the same. Besides, from 400 to 650 ° C, the surface water was eliminated.

The optimal conditions of the calcinations in time and temperature, makes the product meets the market profiles and the requirements of use. At 900 ° C and in a time of about 20 minutes, the organic carbon decreases to 79.35% and TPL increases to 6.08% in the phosphate. Noting that the use of techniques for characterization and monitoring of mineral concentration and enrichment technologies is efficient and the mastery of these techniques can help to improve the quality of final and intermediate products used in the mineral industry, mentioning that in the research field, there is a wide application of these techniques.

ACKNOWLEDGEMENTS

I would like to thank our colleagues at SOMIPHOS research Center in Djebel Onk phosphate complex, for their assistance to complete the analysis tests.

REFERENCES

Alain Lamotte (1997). L'échantillonnage du prélèvement à l'analyse Journées Laboratoires du 25 au 27 octobre 1994 Éditions de l'ORSTOM, Paris, 1997

Gulsum. A and al (2020) Production, characterization, and cytotoxicity of calcium phosphate ceramics derived from the bone of meagre fish, Argyrosomus regius. Journal of the Australian Ceramic Society volume 57, pages37–46 (2021). Inorganic chemistry frontiers issue 18. 2021
https://doi.org/10.1016/j.matchemphys.2020.123678
https://doi.org/10.33271/mining13.04.084

Kechiched (2017). Les phosphates du nord de Tébessa (dyr et elkouif): étude sédimentologique, gîtologique et géochimique. Doctoral thesis from Badji Mokhtar University - Annaba.

Merabet et al (2003). Etude comparative des minerais de phosphate : noir (djemi-djema) et beige de Kef Es Ennoun)- djebel, Algerie. Technique de l'industrie minérale, N° 19 ISSN 1296-2981, 2003

Moukannaa S.Bagheri A. Benzaazoua M. (2020) Elaboration of alkali activated materials using a non-calcined red clay from phosphate mines amended with fly ash or slag : A structural study. Materials Chemistry and Physics V 256, 12; 2020, 123678.

Nettour D. and al (2018) Determination of physicochemical parameters of Djebel Onk phosphate flotation (Algeria), Solid State Physics, Mineral Processing DOI: 10.29202/nvngu/2018-4/8.

Nettour D. Chettibi M., Bulut G., (2019) Beneficiation of Phosphate sludge rejected from Djebel Onk plant (Algeria), Solid State Physics, Mineral Processing DOI: 10.29202/nvngu/2018-4/8.

Wissem et al (2016), Beneficiation of Phosphate Solid Coarse Waste from Redayef (Gafsa Mining Basin) by Grinding and Flotation Techniques Procedia Engineering 138) 85 – 94

Xiaowen G. YuxiaXu Y. Yongcai Z. Huan P. (2019) Amorphous cobalt phosphate porous nanosheets derived from two-dimensional cobalt phosphonate organic frameworks for high performance of oxygen evolution reaction. *Applied Materials Today* Volume 18, March 2020, 100517; https://doi.org/10.1016/j.apmt.2019.100517

RİSK ESASLI MADEN ATIK YÖNETİMİ

RISK BASED TAILINGS MANAGEMENT

H. Ürkmez [1,*], Y.S. İnci [1], S. Ennis [2], E.R. Castro, G. Uzunçelebi

[1] *TÜPRAG Efemçukuru Altın Madeni*
(Sorumlu Yazar: halil.urkmez@tuprag.com)*
[2] *Stantec, CANADA*

ÖZET

Madencilik endüstrisinin son yıllardaki büyüme ve gelişmesi, sektöre yeni teknolojileri ve yöntemleri kazandırdığı gibi beraberinde yeni sosyal ve çevresel riskleri de getirmiştir.

Kanada Madenciler Birliği Sürdürülebilir Madencilik - Atık Yönetim Protokolü'nün risk esaslı atık yönetimi/yaklaşımı, atık depolama tesisinin yaşam döngüsü boyunca (planlama, inşaat, işletme, kapatma ve kapatma sonrası) oluşabilecek sağlık, güvenlik, çevresel, sosyal, ekonomik ve yasal risklerin önceden tanımlanarak kapsamlı bir şekilde değerlendirilmesini içermektedir. Bu değerlendirme ile risklerin ortadan kaldırılması veya etkilerinin en aza indirilmesi hedeflenmiştir. Risk esaslı yönetim/yaklaşım ile atık tesislerinin performansı arttırılmakta ve temel madencilik risklerinin etkin bir şekilde yönetilmesi sağlanmakta ve sürekli iyileştirme sürecinde uygulanabilir en iyi teknoloji ve uygulamalar ile sorumlu madencilik gereklilikleri yerine getirilmektedir.

Atık depolama tesislerinin riskleri, maden sahası genel risk değerlendirmesinden ayrı olarak ele alınmalıdır. Her atık depolama alanının/tesisinin çevresel ve fiziksel özelliklerinin farklı olması tesise özgü bir performans ve risk yönetimini ortaya çıkarır.

Risk esaslı yönetimde/yaklaşımda sahaya özgü risk değerlendirmesi, sonuçları yüksek potansiyelli olaylar, kritik kontroller, Kademeli Eylem planı, acil durum müdahale ve hazırlık planları, performans değerlendirmesi ve sürekli iyileştirme için yönetim değerlendirmesi önemli yer tutmaktadır. Çevre yönetim sistemi ISO14001 gibi sistemler ile tutarlı olarak, atık yönetimi çerçevesi Planla - Uygula - Kontrol Et - Önlem Al döngüsünü izler ve kontrol ve sürekli iyileştirme için bir yönetim modeli oluşturulmasını sağlar.

Anahtar Sözcükler: Risk esaslı atık yönetimi/yaklaşımı, sonuçları yüksek potansiyelli olaylar, kritik kontroller, kademeli eylem planları (KEP), acil durum müdahale planları, acil durum hazırlık planları, mevcut en iyi uygulamalar (MEU – BAP), mevcut en iyi teknikler (MET- BAT)

ABSTRACT

The growth and development of the mining industry in recent years has brought new technologies and methods to the industry, as well as bringing new social and environmental risks.

The risk-based management/approach of the MAC-TSM Tailings Management Protocol includes pre-defined and comprehensive assessment of health, safety, environmental, social, economic and legal risks that may occur in tailings storage facilities throughout their lifecycle/life. With this evaluation, it is aimed to eliminate the risks or to minimize their effects. With a risk-based management/approach, the

performance of waste facilities is increased and risks are managed effectively, and the responsible mining goal is fulfilled with the BAT and BAP in the continuous improvement process.

The risks of tailings storage facilities should be considered separately from the mine site overall risk assessment. The Different environmental and physical characteristics of each tailings storage facilities reveals a facility-specific performance and risk management.

In risk-based management/approach, site-specific risk assessment, potential high-consequence events, critical controls, TARPs, ERP, EPP, performance assessment and management assessment improvement have an important place. Consistent with systems such as the environmental management system ISO14001, the tailings management framework follows the Plan-Do-Check-Take Action cycle and ensures that a management model is established for control and continuous improvement.

Keywords: Risk-based tailings management/approach, risk assessment, potential high-consequence events, critical controls, tarp's, ERP, EPP, best available practices (BAP), best available techniques (BAT)

GİRİŞ

Maden endüstrisinin sürdürülebilir ve çevreye duyarlı (sorumlu) madencilik faaliyetleri için atık yönetim çerçevesini belirlemeleri önemlidir. Madencilik faaliyetleri sırasında ve özellikle Atık Depolama Tesisleri'nin oluşturabileceği fiziksel ve kimyasal riskler için riske dayalı bir yaklaşımla yönetim sistemleri oluşturulmalıdır.

Gelişmekte olan madencilik endüstrisinin değerlendirilmesi ve yönetilmesine katkı sağlaması için faaliyet gösteren kurum ve kuruluşların hazırladığı yardımcı sistemler mevcuttur. Kanada Madenciler Derneği (MAC), Sürdürülebilir Madencilik (Towards Sustainable Mining - TSM) Atık Yönetim Protokolü'nde (Tailings Management Protocol) özellikle Atık Depolama Tesisleri'nin risk esaslı yönetim çerçevesinde yönetilmelerini desteklemektedir. MAC Atık Depolama Tesisleri için hazırladığı Atık Yönetim Kılavuzu (Tailings Management Guide) ve İşletme, Bakım ve İzleme Kılavuzu (İŞBİK - Operation, Maintenance, and Surveillance Manual - OMS) Birleşmiş Milletler'in ''Atık Yönetimine İlişkin Küresel Endüstri Standardı (Global Industry Standard on Tailings Management, 2020) İle çalışmalarını eş değer hale getirmiştir.

Maden işletmeleri risk esaslı yönetim sistemi kapsamında, tesis yaşam döngüsü boyunca (planlama, inşaat, işletme, kapatma ve kapatma sonrası) oluşabilecek riskleri tanımlayarak değerlendirmeli ve şirket taahhüt ve politikalarına eklenerek, uygulamalıdır. Risk esaslı yönetim sisteminde, Atık Depolama Tesisleri'nin yaşam döngüsü boyunca uygulanan risk stratejilerini sürekli ve düzenli olarak gözden geçirmeli ve iyileştirmelidir.

Atık Depolama Tesislerinde uygulanan risk stratejileri (uygulamaları) ve bu stratejilerin iyileştirmeleri için iç ve dış denetlemeler kritik önem taşımaktadır. Ayrıca tesis yönetiminin bağımsız gözden geçirilmesi ve performansının değerlendirilmesi, yönetimin ve tesisin iyileştirilmesini ve sürdürülebilir olmasını sağlayacaktır.

Bu iç, dış ve bağımsız denetlemeler sorumlu ve şeffaf tesisler oluşturmak için en iyi uygulamalardır. Atık yönetim çerçevesinde risk esaslı yaklaşım ve uygulamalarında Planla – Uygula – Kontrol Et – Önlem Al döngüsü takip edilerek sürekli iyileştirme ve geliştirme sağlanmaktadır.

Risk esaslı yönetim sistemi temelde aşağıdakileri içermelidir;

- Sahaya özel potansiyel riskleri belirlemek ve güncellemek ve düzenli olarak performansını değerlendirmek (İç-dış ve bağımsız denetimler)
- Sahaya özel riskleri yönetmek için Mevcut En İyi Teknolojilerin (MET) kullanılması
- Sahaya özel riskleri yönetmek ve performans hedeflerine ulaşmak için Mevcut En İyi Uygulamaların (MEU) kullanılması

RİSK ESASLI ATIK YÖNETİM ÇERÇEVESİ

Risk esaslı yönetim çerçevesi, hesap verilebilirlik ve sorumlulukları, hazırlanması gereken dokümanları, risklerin değerlendirilmesi ve eylem planlarının oluşturulması ve performansın değerlendirilerek denetlenmesi gibi temel konuları kapsamaktadır.

Hesap Verilebilirlik ve Sorumluluklar

Atık Depolama Tesisleri'nde rollerin ve rollere göre hesap verilebilirliğin, sorumlulukların ve yetkinin açıkça tanımlanması önemlidir. Her işletmenin ve Atık Depolama Tesisi'nin yönetim ve organizasyon yapısı farklılık gösterebilir. Bu nedenle rol tanımlamaları tesisin ihtiyacına ve yapısına göre şekillendirilmelidir.

Bu yapı içerisinde en azından Atık Depolama Tesisleri'nde aşağıdaki roller için hesap verilebilirlik, sorumluluklar ve yetkiler açıkça tanımlanmalıdır.

Yönetim Kurulu veya Üst Yönetim

Şirket büyüklüğüne bağlı olarak yönetimin en üst kademesidir. Şirket politika ve taahhütlerinin onay mekanizmasıdır.

Sorumlu Yönetici

Sorumlu Kişi(ler) ve Kayıtlı Mühendisinin tavsiyesi ile atık yönetimi için gerekli sistemlerin oluşturulması ve geliştirilmesi süreçlerinden sorumlu kişidir.

Sorumlu Kişi(ler)

Atık Depolama Tesisi'nin yaşam döngüsü boyunca (planlama, inşaat, işletme, kapatma ve kapatma sonrası) atık yönetim sisteminin uygulanması, geliştirilmesi ve performansının değerlendirilmesinden sorumlu kişidir.

Kayıt Mühendisi (KM) (Engineer Of Record – EoR)

İşletme için tesis yaşam döngüsü boyunca tesis güvenliğinden emin olmak, teknik yönlendirme sağlamak, atık yönetim sistemlerinin uygulanmasından, geliştirilmesinden ve performansının değerlendirilerek raporlanmasından sorumlu kişidir.

Yönetim ve Acil Durum Hazırlığı

<u>İşletme Bakım ve İzleme Kılavuzu (İŞBİK)</u>

İŞBİK, atık depolama tesisleri yönetimi için çevre ve güvenlik kriterlerini içeren bir atık yönetim sistemi çerçevesi sağlamak ve atık depolama tesislerinde yönetim ilkelerinin uygulanmasını ve tutarlılığını özetleyen ve rehberlik sağlayan, sahaya özel bir dokümandır ve referans materyalleri içeren modüllerden oluşur.

İŞBİK, risk yönetimi ve atık tesis performansının iyileştirilmesini, tasarım amacına ulaşılmasını ve yasal gerekliliklerin, kurumsal politikanın ve taahhütlerin yerine getirilmesini kolaylaştırmayı amaçlamaktadır. İŞBİK kapsamı, atık depolama tesisinin özellikleri ve yaşam döngüsü aşaması ve diğer

ilgili planlar ve prosedürlerle olan bağlantılar dikkate alınarak sahaya özel olarak tanımlanır ve aşağıdaki konuları da içermelidir.

İŞBİK Kapsam ve Amaç / Faaliyet Takibi
- Kalite Yönetimi
- Kaynaklar ve Planlama
- Raporlama

Roller, Sorumluluklar ve Yetki
- Eğitim ve Yeterlilik

İş Sağlığı ve Güvenliği
Atık Depolama Tesisi Tanımı
İşletme
- Performans Hedefleri
- İşletme Prosedürleri
- Atık Taşıma ve Yerleştirme
- Devam Eden Atık Tesisi İnşaatı
- Atık Depolama Tesislerinin sınıflandırılması
- Su Yönetimi
- Kapatma
- Site Erişimi

Bakım
- Bakım Faaliyetlerinin Tanımı
- Bakımla İlişkili Belgeler

İzleme
- Bir İzleme Programı için Tasarım Hususları
- İzleme Faaliyetleri
- Saha İzlemeleri ve Denetimleri
- İzleme Ekipmanları
- İzleme Sonuçlarının Analizi, İletişimler ve Karar Verme

Acil Müdahale Planları
- Kritik Kontroller ve Kademeli Eylem Planları

Performansın Değerlendirilmesi
- Yönetimin Gözden Geçirilmesi
- İç ve Dış Denetleme
- Bağımsız İnceleme

İŞBİK, risk kontrollerinin ve kritik kontrollerin etkin yönetimi için önemli bir kılavuzdur. İŞBİK dokümanı tüm personeller için kolay ulaşılır olmalıdır. İŞBİK amaç, kapsam ve uygulama eğitimleri kurum içi kaynaklar kullanılarak Kayıt Mühendisi desteği ile geliştirilmelidir. İŞBİK gözden geçirme sıklığı, tesisin risk profiline ve yaşam döngüsüne bağlı olarak düzenli olarak belirlenmelidir.

Risklerin Değerlendirilmesi

Risklerin değerlendirilmesi ve yönetimi hem işletmenin hem de Atık Depolama Tesisleri'nin etkin yönetilmesi konusunda önemli bir husustur. Riskler, maden yaşam döngüsü boyunca Atık Depolama Tesisleri'ne özel olarak, İş güvenliği ve sağlığı, çevre, mühendislik ve operasyonel, finansal, yasal, yönetimsel ve sosyal çerçevelerde değerlendirilmeli ve düzenli olarak güncellenmelidir.

Riskler, Hata Türü ve Etkileri Analizi (Failure Mode Effect Analysis – FMEA) modelli bir olasılık-sonuç matrisi veya benzer matrisler kullanılarak değerlendirilmelidir. Bu tür bir değerlendirmede riskler, aşırı yüksek, yüksek, orta ve düşük olarak tanımlanabilir.

Risk değerlendirmesi ile tehlikeler tanımlanarak risklerin potansiyel sonuçları, şiddeti ve olasılığı belirlenir. Böylece tehlikelerin ya da risk olasılığı ve şiddetinin, atık yönetiminde uygulanacak en iyi teknolojiler ve en iyi uygulamalar ile azaltılması veya ortadan kaldırılması sağlanacaktır.

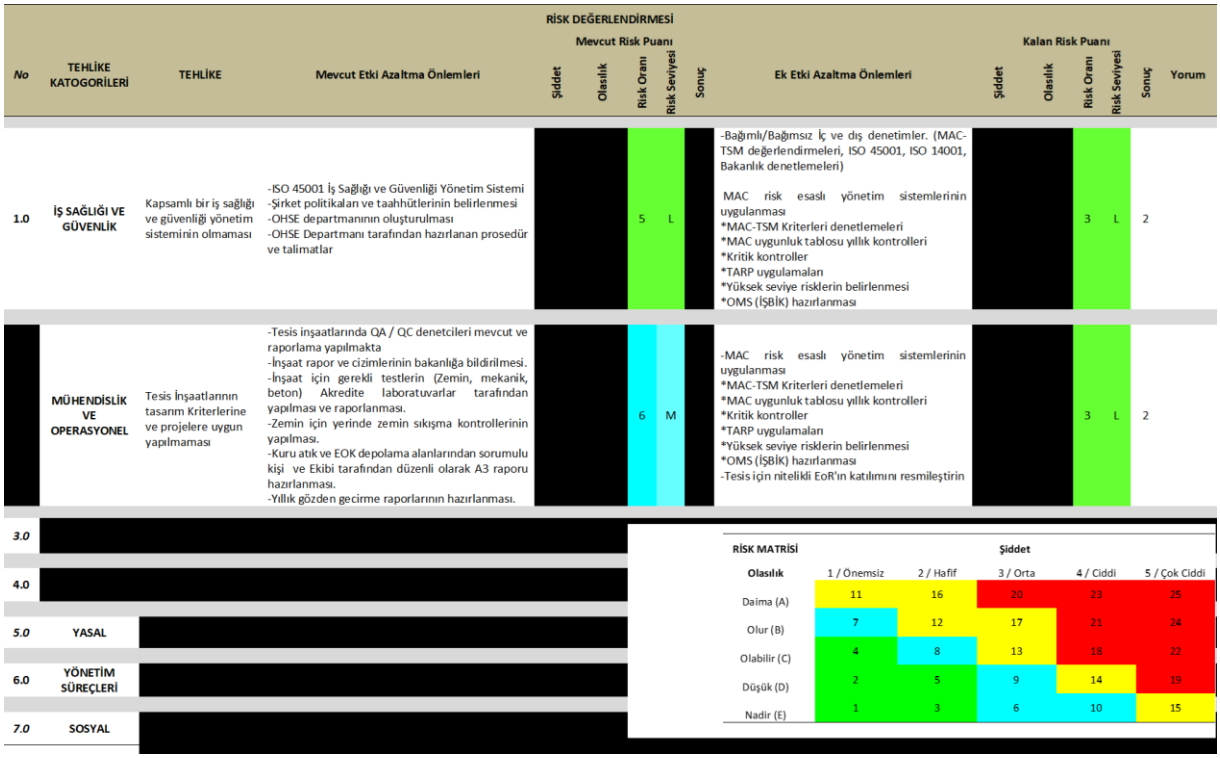

No	TEHLİKE KATOGORİLERİ	TEHLİKE	Mevcut Etki Azaltma Önlemleri	RİSK DEĞERLENDİRMESİ – Mevcut Risk Puanı: Şiddet	Olasılık	Risk Oranı	Risk Seviyesi	Sonuç	Ek Etki Azaltma Önlemleri	Kalan Risk Puanı: Şiddet	Olasılık	Risk Oranı	Risk Seviyesi	Sonuç	Yorum
1.0	İŞ SAĞLIĞI VE GÜVENLİK	Kapsamlı bir iş sağlığı ve güvenliği yönetim sisteminin olmaması	-ISO 45001 İş Sağlığı ve Güvenliği Yönetim Sistemi -Şirket politikaları ve taahhütlerinin belirlenmesi -OHSE departmanının oluşturulması -OHSE Departmanı tarafından hazırlanan prosedür ve talimatlar			5	L		-Bağımlı/Bağımsız İç ve dış denetimler. (MAC-TSM değerlendirmeleri, ISO 45001, ISO 14001, Bakanlık denetlemeleri) MAC risk esaslı yönetim sistemlerinin uygulanması *MAC-TSM Kriterleri denetlemeleri *MAC uygunluk tablosu yıllık kontrolleri *Kritik kontroller *TARP uygulamaları *Yüksek seviye risklerin belirlenmesi *OMS (İŞBİK) hazırlanması			3	L	2	
	MÜHENDİSLİK VE OPERASYONEL	Tesis İnşaatlarının tasarım Kriterlerine ve projelere uygun yapılmaması	-Tesis inşaatlarında QA / QC denetcileri mevcut ve raporlama yapılmakta -İnşaat rapor ve cizimlerinin bakanlığa bildirilmesi. -İnşaat için gerekli testlerin (Zemin, mekanik, beton) Akredite laboratuvarlar tarafından yapılması ve raporlanması. -Zemin için yerinde zemin sıkışma kontrollerinin yapılması. -Kuru atık ve EOK depolama alanlarından sorumulu kişi ve Ekibi tarafından düzenli olarak A3 raporu hazırlanması. -Yıllık gözden gecirme raporlarının hazırlanması.			6	M		-MAC risk esaslı yönetim sistemlerinin uygulanması *MAC-TSM Kriterleri denetlemeleri *MAC uygunluk tablosu yıllık kontrolleri *Kritik kontroller *TARP uygulamaları *Yüksek seviye risklerin belirlenmesi *OMS (İŞBİK) hazırlanması -Tesis için nitelikli EoR'ın katılımını resmileştirin			3	L	2	
3.0															
4.0															
5.0	YASAL														
6.0	YÖNETİM SÜREÇLERİ														
7.0	SOSYAL														

RİSK MATRİSİ

Olasılık	Şiddet: 1 / Önemsiz	2 / Hafif	3 / Orta	4 / Ciddi	5 / Çok Ciddi
Daima (A)	11	16	20	23	25
Olur (B)	7	12	17	21	24
Olabilir (C)	4	8	13	18	22
Düşük (D)	2	5	9	14	19
Nadir (E)	1	3	6	10	15

Şekil 1. Atık Depolama Tesisleri İçin Risk Değerlendirme Tablosu Örneği Kısmi Görüntüsü

Kritik Kontroller

Kritik kontroller operasyonel, teknik veya yönetimsel kaynaklı sonuçları yüksek olayları önlemek veya olayın sonuçlarını hafifletmek için yapılan kontrollerdir. Kritik kontrollerin geliştirilmesi ve uygulanması katastrofik olayların olasılığını ve şiddetini önemli ölçüde azaltacaktır. Bu kontroller dolaylı yoldan birçok riski önleyerek olasılığını ve şiddetini azaltacaktır.

Potansiyel İstenmeyen Durum	İstenmeyen Durum Etkenleri	Performans Göstergeleri	Kritik Kontroller	Performans Değerlendirme Kriterleri
Depolama Tesislerinin Stabilitesinin Bozulması	Şev Duraysızlığı Sıvılaşma Oturma Göçme	* VWP Piezometreleri ve Dikey Boru Su Seviyesi Kontrolleri * Atık Depolama Kriterleri * Şev Hareketi İzlemeleri * Deformasyon Ölçümleri	* Kaya Drenajları * Sıkışma Kriterleri ve QA/QC Denetimleri * Nitelikli Personel ve Kayıt Müh. Tarafından Düzenli Denetim * Bağımsız Değerlendirme	* Tasarım Kriterleri Sınır Değerleri * İŞBİK Kılavuzunda Belirtilen Operasyonel Sınırlar Değerler (KEP) * QA/QC denetimiyle İnşaat Programı Ve Şartnamelerine Uyumluluk

Şekil 2. Kritik Kontrol Tablosu Örneği Kısmi Görüntüsü

Acil Durum Eylem Planı (ADEP)

Tüm maden işletmeleri maden genelini kapsayan Acil Durum Eylem Planı ve Acil Durum Hareket Plan'ları geliştirmektedir. Ayrıca Atık Depolama Tesisleri'ne özel (özgü), tesis risk profili ile bağlantılı olarak Acil Durum Eylem Planı hazırlanarak, maden genelini kapsayan Acil Durum Eylem Planı içerisine entegre edilmelidir.

Atık Depolama Tesisleri Acil Durum Eylem Plan'ları, maden genelinde acil durum ilan edilmesine neden olacak, Atık Depolama Tesisi performansından veya operasyonel faaliyetlerden kaynaklı acil durumlara müdahaleyi hızlandırarak risk şiddetini azaltacaktır. Böylece maden genelinde acil durum ilan edilmesine gerek kalmadan, Atık Depolama Tesisi performansını ve operasyonel faaliyetlerini etkileyen acil durumlar Atık Depolama Tesisi Sorumlu Kişi ve ekibi tarafından yönetilebilecektir.

Atık Depolama Tesisi Sorumlu Kişi ve ekibi tarafından yönetilemeyen veya yönetilemeyecek acil durumlarda, maden geneli Acil Durum Eylem Planı uygulanmasına hızlı bir şekilde geçiş sağlayacaktır.

Kademeli Eylem Planları (KEP)

Kademeli Eylem Planları, kritik kontroller ve sonuçları yüksek olaylar dahil olmak üzere Atık Depolama Tesisi risk kontrollerini yönetmek için kullanılan bir araçtır. Kademeli Eylem Planları, Atık Depolama Tesisleri'nin performans hedeflerine ve risk profiline bağlı olarak geliştirilen performans kriterleri için önceden tanımlanan Kademe (başlangıç) seviyelerini göstermektedir.

Her performans kriteri için ve her seviye için risk yönetim eylemleri tanımlanmalıdır. Her kademe seviyesi için belirlenen eylemler kademe seviyeleri aşıldığında (performans normal aralığın dışında olduğunda) uygulanmaya başlanmalıdır. Böylece, acil durum ilan edilmesi gereken kademe seviyesine gelinmeden önceki seviyelerde gerekli müdahaleler yapılmış olacaktır. Genel olarak dört kademe seviyeli (1. Seviye Yeşil, 2. Seviye Sarı, 3. Seviye Turuncu, 4. Seviye Kırmızı) Kademeli Eylem Planları hazırlanmaktadır.

KEP – Aşırı Meteorolojik Koşullar (Aşırı Yağış) KEP NO: 02		
KEP Seviyeleri	Kademe Seviyesi	Eylemler
Kademe 1 **Normal Risk**	Yağış miktarı; 1-5 mm 12 Saat	Depolama çalışmalarına devam edilebilir. İzlemelere devam edilmelidir. Su yönetim sistemleri kontrol edilmelidir.
Kademe 2 **Orta Risk**	Yağış miktarı; 6-20 mm 12 Saat	Filtre atık nakliyesi kontrollü bir şekilde sürdürülebilir. Yayma ve sıkıştırma çalışmaları yapılamaz. Malzeme alanda stoklanabilir. İzlemelere devam edilmelidir. Personel hava durumunu takip etmelidir. Su yönetim sistemi kontrol edilmelidir.
Kademe 3 **Orta Risk**	Yağış miktarı; 20-100 mm 12 Saat	Filtre atık nakliyesi ve Yayma ve sıkıştırma çalışmaları durdurulmalıdır. Malzeme filtre tesisinde depolanır veya tesis durdurulur. Su yönetim sistemi gözden geçirilmelidir. İzlemelere devam edilmelidir. Personel hava durumunu takip etmelidir.
Kademe 4 **Yüksek Risk**	Yağış miktarı; > 100 mm 12 Saat	Malzeme filtre tesisinde depolanır veya tesis durdurulur. Su yönetim sistemi gözden geçirilmelidir. KEP'in Bağlı olduğu ADEP başlatılmalıdır. Tasarım Sınırı aşılırsa; İş Güvenliği yöneticisini bilgilendirin ve Site genelinde Acil Durum başlatın.

Şekil 3. Kademeli Eylem Planı Örneği

Kademeli Eylem Planları için Acil Durum Eylem Planı

Atık Depolama Tesisleri performans kriterleri kapsamında belirlenen Kademeli Eylem Planları tetik seviyelerinde, kritik kademe seviyesine gelindiğinde uygulanacak eylemler için senaryolar hazırlanmalıdır. bu seviyeler genel olarak Kademeli Eylem Planları'nda 3. Seviye turuncu ve 4. Seviye ise kırmızı renk ile gösterilmektedir.

Bu acil durum eylem planları maden genelinde acil durum ilan edilmesinden önce acil durum için yapılması gereken bilgi ve görselleri içeren (acil durum senaryosunu anlatan) ve sahada bulunan personele yol gösterici bir doküman niteliğindedir.

Atık yönetim çerçevesinde geliştirilen ve uygulanan risk değerlendirmeleri, kritik kontroller, acil durum eylem planları, Kademeli Eylem planları ve Kademeli Eylem planları için hazırlanan acil durum eylem planları düzenli olarak gözden geçirilmeli ve güncellenmelidir. Ayrıca periyodik olarak masabaşı ve genel saha tatbikatları planlanarak performansları denetlenmeli ve değerlendirilmelidir.

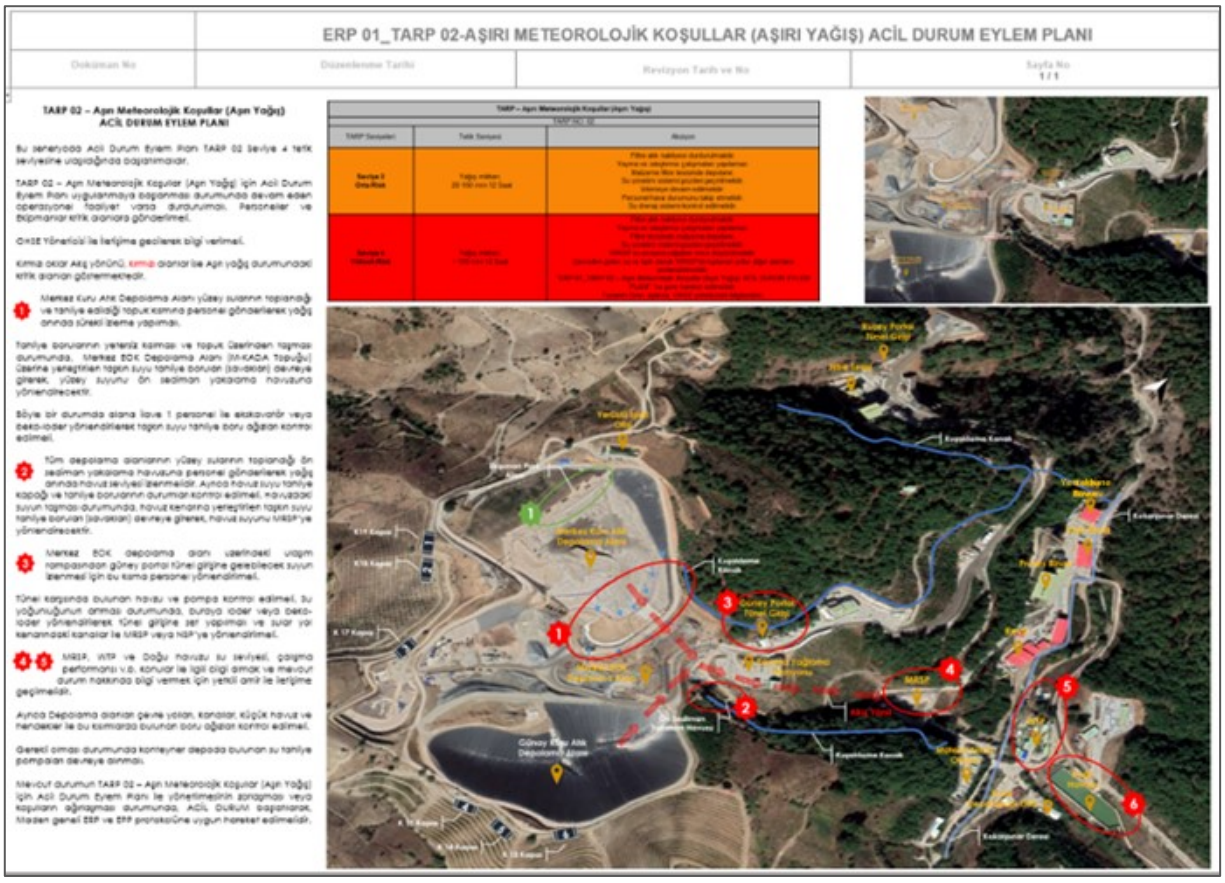

Şekil 4. Kademeli Eylem Planı İçin Acil Durum Eylem Planı Örneği

Performansın Değerlendirilmesi

Etkili risk yönetimi kararlarını destekleyen atık yönetim sistemleri, atık tesislerinin kullanım ömürleri boyunca stabilitesini korumak ve artırmak için kritik öneme sahiptir. Bunun için tesisin ve sistemlerin performansının periyodik olarak denetlenmesi ve değerlendirilmesi gerekmektedir.

Yıllık Gözden Geçirme Toplantısı

Atık Yönetiminin ve Atık Depolama Tesislerinin yıllık performansının değerlendirilmesi için Atık Depolama Tesisi performansını ve operasyonel faaliyetleri kapsayan bir rapor, ilgili ve sorumlu yöneticiler ve Kayıt Mühendisi'nin katılım sağladığı bir toplantıda sunulmalıdır. Rapor ve toplantı konularının aşağıdaki veya benzer konuları kapsaması faydalı olacaktır.

Operasyonel Faaliyetler – (Statik, su yönetimi, depolama kapasitesi, personel, ekipman, izlemeler, bakım, dokümantasyon, diğer faaliyetler)
Çevre
Finansal
İş sağlığı ve güvenliği
Sosyal
Yasal gereklilikler
Yönetimsel değerlendirme
Yeni projeler – (gelecek planları)

<u>İç ve Dış Denetlemeler</u>

Yönetim ve Atık Depolama Tesisi performansı sorumlu kişi tarafından (iç) ve Kayıt Mühendisi tarafından (dış) denetlemeye tabi tutulmalıdır. Kanada Madencilik Derneği, Sürdürülebilir Madencilik performans programları ve benzer sistemlerin uygulanması, madencilik faaliyetlerine hesap verilebilirliği, ölçülebilirliği ve sürdürülebilirliği sağlayarak, faaliyetlerin yüksek standartlarda yürütülmesine yardımcı olacaktır.

MAC, TSM programı Atık Yönetim Protokolü ile işletmenin Sürdürülebilir Madencilik - Atık Yönetim Protokolü uygulamaları ve tesis ve yönetim performansları değerlendirilir. Bu değerlendirmeler aşağıdaki dokümanlar ile gerçekleştirilir.

Atık Yönetim Protokolü dokümanı ile protokolün her bir göstergesi ayrıntılı ve kapsamlı olarak not sistemiyle değerlendirilir.
Atık Kılavuzu Uygulama Kontrol Listesi (Tailings Guide implementation checklist) ile
Uygunluk Tablosu (Table of Conformance) ile Atık Yönetim Protokolü'nün her bir göstergesi için performans kriterleri ve uygulanması değerlendirilir.

OMS Manual: *Assessment Criteria*

C	The company has not met all Level B criteria.
B	An OMS manual has been developed for the tailings facility but it is not in conformance with the OMS Guide. The company has developed an action plan to meet all requirements for a Level A.
A	An internal audit has been conducted and determined that an OMS manual has been developed and implemented for the tailings facility that is in conformance with the OMS Guide.
AA	An external audit has been conducted and determined that an OMS manual has been developed and implemented for the tailings facility that is in conformance with the OMS Guide.
AAA	The external audit for Level AA included an evaluation of the effectiveness of the development and implementation of the OMS manual.

OMS Manual: *Frequently Asked Questions*

#	FAQ	PAGE
5	What is an audit?	
6	What is an evaluation of effectiveness?	
8	How long are audits valid?	

Şekil 5. "TSM- Tailings Management Protocol" Kısmi Görüntüsü (MAC 2019a)

Section in Tailings Guide	Management Action	Responsibility	Performance Measure	Schedule	References
Overarching Principles					
Risk Assessment and Management					
2.2.1	Addressed below under Planning				
BAT and BAP for Tailings Management					
2.2.2	Have the following factors been considering in selecting the tailings management technology for a specific tailings facility: Are the likelihood or consequences of a failure of a tailings facility reduced? Is material separation required to manage a potential geochemical concern? How much water will be retained in the tailings during their transport and placement? Is there potential to place any tailings in mined-out areas? Is the post-mining land use best served by a given technology?				
Independent Review					
2.2.3	Has a mechanism been established for conducting Independent Review on a routine basis? Is Independent Review being implemented according to the established mechanism?				
Designing and Operating for Closure					
2.2.4	Have long-term closure objectives and potential post-closure land uses been considered in the conceptual planning and design of the tailings facility? Has the tailings facility been designed to remain physically and chemically stable for the long-term?				

Şekil 6. "Atık Kılavuzu Uygulama Kontrol Listesi (Tailings Guide Implementation Checklist)" Kısmi Görüntüsü (MAC 2019a)

Indicator 1: Tailings Management Policy and Commitment						
Criteria	Document	Section	Yes	No	N/A	Description and Evidence to Support Response
Does the Owner have a demonstrated commitment to: protection of public health and safety; responsible management of tailings with the objective of minimizing harm; allocation of appropriate resources to support tailings management activities; implementing a tailings management system through the actions of its employees, contractors and consultants?	Tailings Guide	3				

Şekil 7. "Uygunluk Tablosu (Table of Conformance)" Kısmi Görüntüsü (MAC 2019c).

Bu değerlendirmeler (Atık Yönetim Protokolü dokümanı, Uygunluk Tablosu) Sorumlu Kişi tarafından yapılarak bir iç denetleme sağlanır ve yıllık gözden geçirme toplantısında yönetime ve kayıt mühendisine sunulur. Değerlendirmelerin (Atık Yönetim Protokolü dokümanı, Uygunluk Tablosu) Kayıt Mühendisi tarafından yapılması ile bir dış denetleme sağlanır. Kayıt Mühendisi tarafından performans değerlendirmesini içiren bir rapor hazırlanarak yıllık gözden geçirme toplantısında yönetime sunulur.

Bağımsız İnceleme

Bağımsız inceleme; işletmelerin özellikle atık depolama tesislerinin yönetiminin ve risklerinin tanımlanmasını ve anlaşılmasını sağlamak ve sürdürülebilirliği ve sürekli gelişimi desteklemek için işletmeden bağımsız üçüncü taraf uzman kişi(ler) veya kuruluş tarafından yapılan denetleme ve bir dizi tavsiyelerden oluşur. Bağımsız incelemenin sıklığı, Atık Depolama Tesisi risk profiline ve yaşam döngüsüne bağlı ve tesise özel olarak, bağımsız inceleme temsilcisi, işletme yönetimi ve kayıt mühendisi ile birlikte belirlenmelidir.

Bağımsız incelemeyi gerçekleştiren üçüncü taraf uzman kişi(ler) veya kuruluş hazırladığı raporla sürekli iyileştirmeyi teşvik eden tavsiyelerde bulunur. Bu tavsiyeler sonrasında karar alma, uygulama ve sorumluluk işletmeye aittir.

Bağımsız inceleme programı genel olarak, aşağıdaki konuları da kapsayacak şekilde geniş bir çerçevede odaklanır;

Risk değerlendirmesi ve risk yönetim planları,
Tasarım ve inşaat bilgileri de dahil olmak üzere tesisin tanımı,
Kilit personel ve İşletme, Bakım ve İzleme Kılavuzu (İŞBİK)
İç ve dış denetlemeler ile performans değerlendirmeleri ve yönetimi gözden geçirme incelemelerinin sonuçlarına,
Önceki Bağımsız inceleme sonuç ve tavsiyelerine ve uygulanma durumuna,
Tesisin orta ve uzun vadeli planlarına,
Mevcut en iyi uygulamaların ve Mevcut en iyi teknolojilerin uygulanmasına,
Atık Depolama Tesisi'nin mevcut en iyi uygulama ve mevcut en iyi teknolojilere dayalı olarak yönetilip yönetilmediği,
Atık Depolama Tesisi'nin tasarım kriterlerine, yasal gerekliliklere, risk profiline uygun metodolojiler ile tutarlı olup olmadığı.

SONUÇ

Son yıllarda Madencilik sektöründe küresel çapta yaşanan, atık depolama tesislerinin performansından kaynaklı, Brezilya'nın Brumadinho kentinde meydana gelen atık barajı çökmesi (2019) gibi kazalar meydana gelmiştir. Madencilik sektörü bu kazalar sonrasında sistemlerini risk temelli/esaslı olarak hazırlamaya başlamışlardır.

Risk Esaslı Maden Atık Yönetim Sistemi, işletmedeki mevcut uygulanan yönetim sistemine entegre edilebilir. Bu sistemler, amacı çevre ve sosyal performansı iyileştirmek olan uluslararası sürdürülebilir performans programları ile desteklenebilir.

Böylece oluşturulan risk esaslı yönetim sistemleri, mevcut en iyi uygulama ve mevcut en iyi teknolojiler ile birlikte Atık Depolama Tesisileri'nin performanslarının arttırılmasını sağlayacaktır. Bu sonuç, sürdürülebilir madencilik sürecine ilişkin yapılan çalışmaların temelini oluşturacaktır.

KAYNAKLAR

Dr. Franco Oboni, Prof. Cesar Oboni (2020). Tailings Dam Management for the Twenty-First Century. What Mining Companies Need to Know and Do to Thrive in Our Complex World.

Environmental and Social Responsibility - Risk Assessment For Tailings Management (23 Mar 2021 - Pages 9-24). K. M. Chovan, M. R. Julien, É.-P. Ingabire, E. Masengo, T. Lépine, M. James, P. Lavoie - CIM Journal, DOI: https://doi.org/10.1080/19236026.2020.1866336

Global Tailings Review (2020). Global Industry Standard on Tailings Management. https://globaltailingsreview.org/global-industry-standard/

Kuru Atık Depolama Yöntemi - Dry Tailings Storage Method (IMCET - 16 April 2019 – Pages 1540-1530). Y.S. İnci, P. Kimball, G. Uzuncelebi, H. Ürkmez . ddcb03c09924b75_ek.pdf (maden.org.tr)

Members And Associate Members Of The Mining Association Of Canada. *Firms İmplementing The MAC Risk-Based Management System* - Our Members - The Mining Association of Canada

Mining Association of Canada (2019a). A Guide to the Management of Tailings Facilities *Version 3.1*. https://mining.ca/our-focus/tailings-management/tailings-guide/

Mining Association of Canada (2019b). Developing an Operation, Maintenance, and Surveillance Manual for Tailings and Water Management Facilities *Second Edition. https://mining.ca/our-focus/tailings-management/oms-guide/*

Mining Association of Canada (2019c). Table of Conformance. https://mining.ca/documents/table-of-conformance-2019/

Mining Association of Canada (2019d). Towards Sustainable Mining Tailings Management Protocol. https://mining.ca/towards-sustainable-mining/protocols-frameworks/tailings-management-protocol/

Mining Association of Canada (2021a). TSM 101: A Primer. https://mining.ca/documents/tsm-101-a-primer/

Mining Associaton of Canada (2021b). MAC Updates Tailings Management Guidance to Align with Global Standard. Press release issued in Ottawa, Canada, on 7 April, 2021. https://mining.ca/press-releases/mac-updates-tailings-management-guidance-to-align-with-global-standard/

Wikipedia. Tailings Dam – List Of Largest Tailings Dams. Tailings dam - Wikipedia

RMQR SİSTEMİNİN HONAZ TÜNELİ İÇİN UYGULANABİLİRLİĞİNİN DEĞERLENDİRİLMESİ

EVALUATION OF THE APPLICABILITY OF THE RMQR SYSTEM FOR HONAZ TUNNEL

E. Karakaplan [1,*], D. Alkaya [2], H. Başarır [3]

[1] *Pamukkale Üniversitesi, Madencilik ve Maden Çıkarma Bölümü*
*(*Sorumlu yazar: ekarakaplan@pau.edu.tr)*
[2] *Pamukkale Üniversitesi, İnşaat Mühendisliği Bölümü*
[3] *Norwegian University of Science and Technology, Department of Geoscience and Petroleum*

ÖZET

Tünellerin projelendirmesinde hâlihazırda birçok yöntem mevcutken teknoloji ve tecrübeler ile bu yöntemler geliştirilmekte veya literatüre yenileri eklenmektedir. Bu çalışmada; zayıf kaya kütlesinde açılan Honaz tünelinde, Kaya Kütle Kalitesi Puanlaması (RMQR) ile değerlendirme yapılarak sistem tarafından önerilen destekleme sistemi tasarımı sonlu elemanlar yöntemiyle analiz edilmiştir. Bu amaçla; Honaz dağında açılan 2540 m kazı uzunluğuna sahip tünel bölgesine ait jeolojik veriler elde edilmiştir. Söz konusu bölgeden elde edilen veriler ışığında RMQR değerleri hesaplanarak, sistem tarafından belirtilen desteklemeler sayısal modellemeye girilip deformasyon sonuçları elde edilmiştir. Elde edilen sonuçlar, tünelin kazısı ve desteklenmesinde kullanılan Yeni Avusturya Tünelcilik Metodu (NATM) ve sahada ölçülen deformasyon değerleri ile karşılaştırılmıştır. Kaya kütle özelliklerinin tahmininde kullanılan eşitliklerin çok zayıf kaya kütlelerinde gerçekten uzak sonuçlar vermesi bu eşitliklerin gözden geçirilmesi gerektiğini göstermektedir. RMQR sisteminin destekleme elemanı önerileri kullanılabilir olmakla beraber bu ve benzer çalışmalarla geliştirilmeye devam edilmelidir.

Anahtar Sözcükler: Tünelcilik, RMQR, NATM, destek tasarımı, sayısal modelleme

ABSTRACT

While there are already many methods for the design of tunnels, these methods are being improved with technology and experience or new ones are added to the literature. In this study; The quality of rock masses were assessed using Rock Mass Quality Rating (RMQR) along 2540 m long Honaz tunnel excavated in weak rock masses. Support systems were designed considering recommendations from RMQR system and analyzed by finite element method. The obtained results were compared with the New Austrian Tunneling Method (NATM) used in the excavation and support of the tunnel and the deformation values measured in the field. The fact that the equations used in the estimation of rock mass properties give results far from those measured in very weak rock masses indicates that these equations should be reviewed. Although the support element suggestions of the RMQR system can be used, they should continue to be developed with this and similar studies.

Keywords: Tunneling, RMQR, NATM, support design, numerical modeling

GİRİŞ

Ülkemizdeki araç sayısı her geçen gün daha da artmaktadır. Bu artış beraberinde geniş ve yüksek standartlı yolların yapımını getirmektedir. Ülkemiz coğrafyası düşünüldüğünde birçok doğal engelin mühendislik çözümleri ile aşılması gerekmektedir. Bu çözümlerden biri de karayolu tünelidir. Tüneller içinden geçilen kaya kütlesinin yapısı ve üzerine gelen yüklerin çeşitliliği açısından çok karmaşık yapılardır. Bu sebeple tünel kazı ve destekleme işleminin en az maliyet ve en uygun destek elemanı

kullanılarak projelendirilmesi önemlidir. Tünelcilik ve madencilik amaçlı birçok araştırmacı (Terzaghi, 1946; Lauffer, 1958; Deere vd., 1967; Wickham vd., 1972; Bieniawski, 1974; Barton vd., 1974; Pacher vd., 1974; Palstörm, 1985; Rabcewicz, 1964) tarafından kaya kütlesi ile ilgili sınıflama sistemleri geliştirilmiştir. Geliştirilen bu sistemler analitik (Aydan vd., 1993; Hoek vd., 1995; Carranza-Torres vd., 2000) ve sayısal (Sonlu elemanlar, sonlu farklar, ayrık elemanlar vb.) yöntemler ile birlikte kullanılarak, mühendislik projelerinin hesaplamalarında gerçeğe çok yakın sonuçlar vermektedir.

Bu çalışmada, kazı ve destekleme işlemi tamamlanan Honaz Tüneli araştırılmıştır. Tünel, Honaz dağında bulunmakta ve Denizli çevre yolunun önemli bir parçasını oluşturmaktadır. Şekil 1'de çalışma alanını içeren yer bulduru haritası verilmiştir.

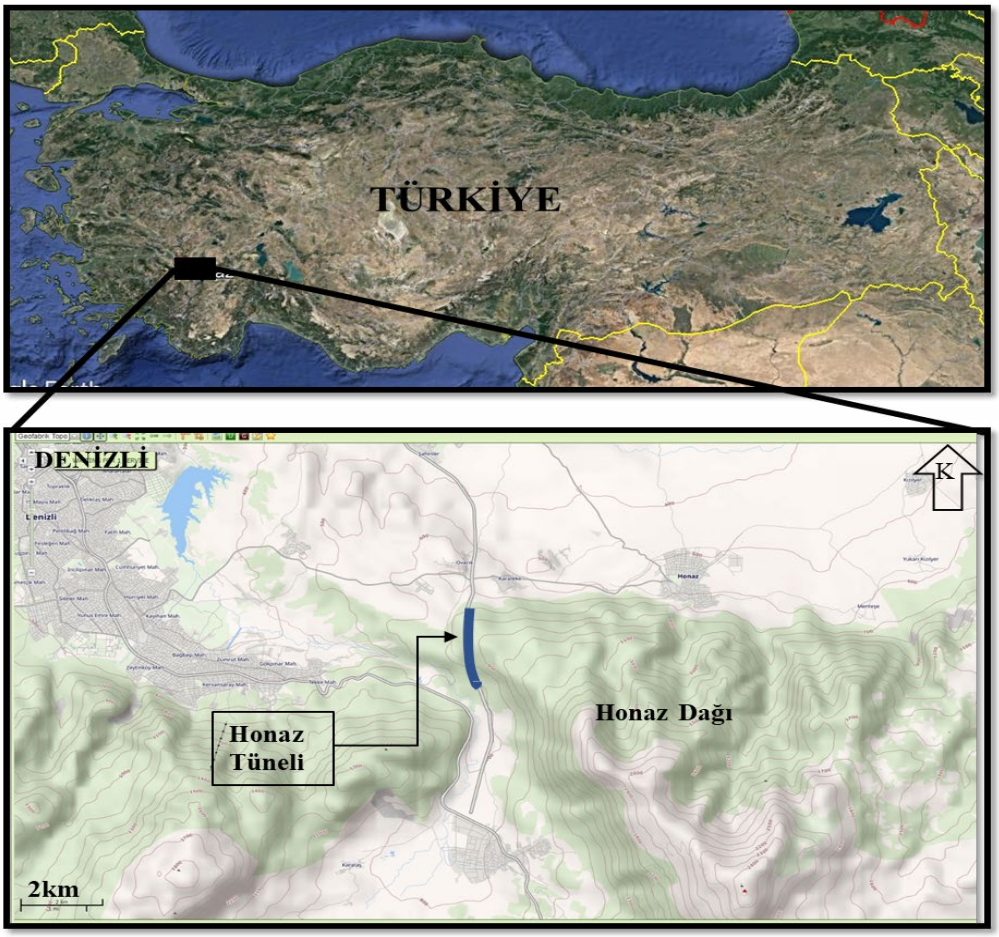

Şekil 1. Honaz Tüneli yer bulduru haritası

Denizli şehir merkezinden geçen İzmir – Antalya karayolu, Ege ve Akdeniz bölgelerini birbirine bağlayan en önemli karayollarından biridir. Mevcut karayolu şehir merkezi trafiğini yoğunlaştırmakta ve trafik güvenliğini azaltmaktadır. Bu sorunu ortadan kaldırmak için 2007 yılında yapımına başlanan Denizli çevreyolu inşasının 2. kısmında Honaz tüneli yer almaktadır. Honaz dağında açılan 2540 m çift tüp uzunluklarına sahip bu tünelin kazı genişliği 12,5 m kazı yüksekliği 10 m'dir. İki tüp merkezi arası mesafe 28 m ve tüpler arası 5 adet bağlantı tüneli mevcuttur. Tünel boyunca dokuz farklı kaya birimi ile karşılaşılmaktadır.

Tünelin projelendirilme aşamasında kaya sınıflarının belirlenmesinde, Jeomekanik Sınıflandırma Sistemi (Q) ve Kaya Kütle Puanlama (RMR) Sistemlerinden yararlanılmış ve NATM sistemine göre kazı-destekleme uygulanması yapılmıştır (Karayolu Teknik Şartnamesi, 2013). Tünelde NATM (ÖNORM

B2203) sınıflama sistemine göre 3 sınıftan geçilmektedir (B3i, C2, C3). Bu sınıflarda farklı türde destekleme sistemi uygulanması yapılmaktadır. Bu bölümlere ek olarak tünel giriş-çıkış portları, çeşitli istasyonlar ve bağlantı tünellerinin boyutlandırılması ile destekleme sistemi uygulanması NATM sisteminin önerilerine göre yapılmaktadır. Bu çalışmada RMQR sistemi kullanılarak kaya kütle puanlamaları yapılmıştır. NATM ve RMQR sistemlerinin önerdiği destekleme elemanları kullanılarak farklı koşullar için sayısal analizler yapılmıştır.

MATERYAL VE METOT

Bölgenin Jeolojisi

Denizli'nin Honaz ilçesi ve çevresi Menderes masifinin güney bölümünde yer almaktadır. Masifin temelinde Paleozoyik yaşlı, her seviyede metamorfizmaya uğramış kayaç toplulukları içeren gnayslarla, migmatitlerden oluşan bir çekirdek kısmı ile, şist, kuvarsit ve mermerden oluşan, bu çekirdeği çevreleyen örtü zonları görülmektedir. Bölgede, Neojen birimler gölsel ortamda çökelmişlerdir. Bu birimler Menderes masifinin kuzeyinde ve güneyinde, kristalin temelli kayaçlar üzerine uyumsuz olarak gelmişlerdir ve kalınlıkları yer yer yüzlerce metreye kadar çıkmaktadır. Neojen yaşlı birimler çeşitli irilikte kum ve çakıllardan, konglomera, kumtaşı, kil, marn-kil ardalanmasından oluşmuştur. Bölgede kuru ve sulu dere ağızlarında ve dik yamaçlı topoğrafyanın ovaya girişte bıraktığı kesimlerde yamaç molozları, alüvyonlar ve alüvyon yelpazeleri izlenmektedir. Bu birimler, temeldeki birimler üzerine uyumsuz olarak çökelmişlerdir. Bölgede ayrıca Pliyokuvaterner yaşlı birimler ya da karbonatlı suların bıraktığı travertenler de görülmektedir. Bu birimler Menderes masifinin her iki yanında da çökelmişlerdir (Okay, 1989).

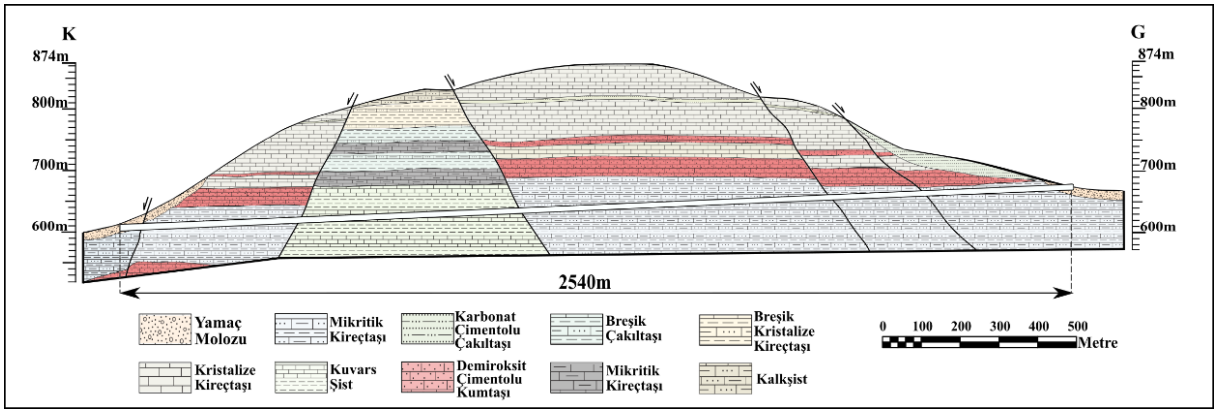

Şekil 2. Honaz Tünel güzergahının jeolojik kesiti

Kaya Kütle Kalitesi Puanlama (RMQR) Sistemi

Kaya Kütle Kalitesi Puanlama (RMQR) Sistemi, nicel ve güncel kaya kütlesi sınıflama sistemlerinde kullanılan önemli parametreler de dikkate alınarak ve parametre tekrarından kaçınılarak, kaya kütlelerinin fiziksel durumunun daha iyi tanımlanması amacıyla Aydan vd. (2014) tarafından geliştirilmiştir. Bu sınıflama sistemi Çizelge 1'de verilen, beş ana girdi parametresi ile bunlardan

bazılarına ait alt parametrelerden oluşmaktadır. Ölçülen veya tanımlanan bu parametrelerle Çizelge 1'de verilen puanların toplamından kaya kütlesine ait RMQR değeri hesaplanmaktadır.

Çizelge 1. RMQR sistemi girdi parametreleri

Bozunma Derecesi (BD)	Taze	Lekeli Yüzey	Az Bozunmuş	Orta Derecede Bozunmuş	İleri Derecede Bozunmuş	Tamamen Bozunmuş
Puan	15	12	9	6	3	1-0
Süreksizlik Takım Sayısı (STS)	Yok (sağlam veya masif)	Tek Takım + Rasgele	İki Takım + Rasgele	Üç Takım + Rasgele	Dört Takım + Rasgele	Ezilmiş veya Paramparça
Puan	20	16	12	8	4	1-0
Süreksizlik Aralığı (SA) veya RQD	Yok veya SA ≥24m	24m> SA ≥6m	6m> SA ≥1.2m	1.2m> SA ≥0.3m	0.3m> SA ≥0.07m	0.07m> SA
	100			100> RQD ≥75	75> RQD ≥35	35> RQD
Puan	20	16	12	8	4	1-0
Süreksizliklerin Durumu (SD)	Yok	İyileşmiş veya Aralıklı	Pürüzlü	Nispeten Pürüzsüz ve Sıkı	İnce Dolgulu veya Ayrık Kaygan Yüzey (t<5mm)	Kalın Dolgulu veya Ayrık (t>10mm)
Puan	30	26	22	15	7	1

veya alternatif olarak, "Yok" ve "İyileşmiş veya Aralıklı" sınıf yüzeyleri hariç

Süreksizlik Durumu (SD) $R_{SD} = R_{SDA} + R_{SDD} + R_{SDP}$											
	Açıklık		Yok veya Çok Sıkı <0.1mm		0.1-0.25mm	0.25-0.5mm		0.5-2.5mm	2.5-10mm		> 10mm
	Puan (R_{SDA})		6		5	4		3	2		1
	Dolgu		Yok		Sadece Yüzey Sıvaması	İnce Kaplama <1mm		İnce Dolgu 1mm< t <10mm	Kalın Dolgu 10mm< t <60mm		Çok Kalın Dolgu veya Makaslama Zonu
	Puan (R_{SDD})		6		5	4		3	2		1-0
	Pürüzlülük	Tanımlayıcı	Çok Pürüzlü		Pürüzlü	Düz - Dalgalı		Düz - Düzlemsel	Kaygan		Makaslama Zonu
		ISRM (2007)'deki profil numarası	10	9	8 7	6		5 4	3	2	1-0
	Puan (R_{SDP})		10	9	8 7	6		5 4	3	2	1-0

Yeraltı Suyu Sızma Durumu (YSSD)	Kuru	Nemli	Islak	Damlama	Sürekli Akış	Fışkırarak Akış
Puan	9	7	5	3	1	0
Yeraltı Suyu Emme Durumu (YSED)	Emici Olmayan	Kılcal veya Elektriksel Su Emen	Çok Az Su Emen	Orta Derecede Su Emen	Çok Su Emen	Aşırı Su Emen

Puan	6	5	4	3	2	1-0

Çizelge 1'deki girdi parametrelerinden biri olan yeraltı suyu sızma koşulu ve su emme durumunu daha iyi hesaplayabilmek için araştırmacılar tarafından sunulan ek çizelgeler de kullanılmaktadır. RMQR değerine göre tüneller için önerilen destekleme miktarı ve türü Çizelge 2'de (Aydan vd. 2015) verilmiştir. Destek elemanlarının uzunluk, aralık ve kalınlıklarının hesaplanması için kullanılan formüller ilgili çalışmada yer almaktadır.

Çizelge 2. Tüneller için RMQR sistemi destekleme önerisi (10m açıklık)

RMQR Aralığı	Kaya Bulonu		Püskürtme Beton	Çelik Kafes		Çelik Hasır	Beton Astar	Taban Kemeri	
	L_b	e_b	t_s	Tip	e_r		(mm)	Astar	Bulon L
100≥RMQR>95	-	-	-	-	-	-	-	-	-
95≥RMQR>80	2-3	2.5	50	-	-	-	-	-	-
80≥RMQR>60	3-4	2.0	100	Hafif	1.5	Evet	200	-	-
60≥RMQR>40	4-5	1.5	150	Orta	1.2	Evet	300	300	-
40≥RMQR>20	5-6	1.0	200	Ağır	1.0	Evet	500	500	5-6
20≥RMQR	6-7	0.5	250	Çok Ağır	0.8	Evet	800	800	6-7

L: uzunluk (m) e: aralık (m) t_s: kalınlık (mm)

Kaya Kütle Özellikleri

Bu çalışmada laboratuvar deneyleri sonucu elde edilen kaya malzemesi özellikleri ve saha gözlemlerine dayalı kütle özellikleri kullanılarak; RMR (Bienawski, 1989), Q (Barton vd., 1974), NATM (Rabcewicz, 1964), RQD (Deere, 1963), GSI (Hoek, 1994), RMQR (Aydan vd. 2014) kaya kütle sınıflama sistemlerinde dokuz kaya birimi için puan hesaplaması yapılmıştır. Bu sistemler kaya kütlesini karakterize eder ve kaya kütle dayanım parametrelerinin tahmininde kullanılan eşitliklerin girdisini oluştururlar. Jašarević ve Kovačević (1996), Aydan vd. (1997), Hoek ve Brown (1998), Hoek ve Diederichs (2006) gibi araştırmacılar tarafından önerilen eşitlikler kullanılarak; kaya kütlesi deformasyon (elastisite) modülü gibi tasarım parametreleri hesaplanmıştır. Tünel güzergahı boyunca geçilen jeolojik birimleri temsil eden kaya kütlesi türleri ve sınıflama sistemlerine göre hesaplanan puanlar Çizelge 3'te verilmiştir.

Çizelge 3. Kaya kütle sınıflama sistemlerinin puanları

No	Kaya Birimi	RMQR	NATM	NATM*	GSI	RQD	RMR	Q
1	Mikritik Kireçtaşı	42	B2	B3i	35	10	40	1.32
2	Mikritik Kireçtaşı	32	B3	B3i	30	12	35	0.528
3	Kristalize Kireçtaşı	49	B2	B3i	39	18	44	4.752
4	Breşik Kristalize Kireçtaşı	35	B3	B3i	25	10	30	0.176
5	Kalk – Kuvars Şist	22	C2	C2	23	6	24	0.010417
6	Demir Oksit Çimentolu Kumtaşı	25	C2	C2	22	5	27	0.020833
7	Karbonat Çimentolu Çakıltaşı	17	C3	C3	16	3	17	0.007333
8	Yamaç Molozu	10	C4	C3	8	1	10	0.0022
9	Fay Breşi	14	C4	C3	11	1	13	0.0055

*: Tünel projesinde kullanılan puanlama

Destek Tasarımı

RMQR ve NATM sistemleri tarafından, kaya kütlesi puanına göre önerilen destekleme elemanı türü ve miktarları Çizelge 4 ve Çizelge 5'te verilmiştir.

Çizelge 4. RMQR puanına göre sistem tarafından önerilen destekleme elemanı türü ve miktarları

No	RMQR Puanı	Kaya Birimi	Kaya Bulonu L_b (m)	Kaya Bulonu e_b (m)	Püskürtme Beton (mm)	Çelik Kafes Tipi	Çelik Kafes e_r(m)	Çelik Hasır	Beton Astar (mm)	Taban Astar (mm)	Taban Bulon (m)
1	42	Mikritik Kireçtaşı	5	1.5	150	Orta	1.2	Evet	300	300	Yok
2	32	Mikritik Kireçtaşı	6	1	200	Ağır	1	Evet	500	500	6
3	49	Kristalize Kireçtaşı	5	1.5	150	Orta	1.2	Evet	300	300	Yok
4	35	Breşik Kristalize Kireçtaşı	6	1	200	Ağır	1	Evet	500	500	6
5	22	Kalk – Kuvars Şist	6	1	200	Ağır	1	Evet	500	500	6
6	25	Demir Oksit Çimentolu Kumtaşı	6	1	200	Ağır	1	Evet	500	500	6
7	17	Karbonat Çimentolu Çakıltaşı	7	0.5	250	Çok ağır	0.8	Evet	800	800	7
8	10	Yamaç Molozu	7	0.5	250	Çok ağır	0.8	Evet	800	800	7
9	14	Fay Breşi	7	0.5	250	Çok ağır	0.8	Evet	800	800	7

Çizelge 5. NATM sınıfına göre sistem tarafından önerilen destekleme elemanı türü ve miktarları

No	NATM Sınıfı	Kaya Birimi	Çelik Kafes	Kaya Bulonu (m)	Kaya Bulonu (adet)	Süren (m)	Çelik Hasır	Püskürtme Beton (mm)
1	B2	Mikritik Kireçtaşı	Hafif	4	17-18	6	2 kat	250
2	B3	Mikritik Kireçtaşı	Hafif	4-6	17-18	6	2 kat	250
3	B2	Kristalize Kireçtaşı	Hafif	4	17-18	6	2 kat	250
4	B3	Breşik Kristalize Kireçtaşı	Hafif	4-6	17-18	6	2 kat	250
5	C2	Kalk – Kuvars Şist	Orta	6-8	22-23	6	2 kat	300
6	C2	Demir Oksit Çimentolu Kumtaşı	Orta	6-8	22-23	6	2 kat	300
7	C3	Karbonat Çimentolu Çakıltaşı	Ağır	8-12	24-25	6	2 kat	350
8	C4	Yamaç Molozu	Ağır	8-12	24-25	6	2 kat	350
9	C4	Fay Breşi	Ağır	8-12	24-25	6	2 kat	350

Sayısal Modelleme

Hazırlanan saha verilerinin 2 boyutlu çözüm yapan RS2 (Rocscience 2021) yazılımına girişinde Kulhawy (1974) dikkate alınarak, dış sınırlar tünel çapının 5 katı olacak şekilde oluşturulup, sonrasında alan sonlu elemanlar örgüsüne (mesh) ayrılmıştır. Çizelge 6'da verilen formüller kullanılarak deformasyon modülü değerleri hesaplanmış ve bu değerlerin ortalaması alınmıştır. Kaya malzemesi ve kaya kütlesine ait Çizelge 7'de yer alan (tek eksenli basınç dayanımı, kohezyon, içsel sürtünme açısı, endirekt çekme dayanımı, poisson oranı, arazi yükü gibi) özellikler yazılıma aktarılmıştır. Mohr-Coloumb yenilme modeli ve plastik malzeme türü seçilmiştir. Açıklıklara NATM ve RMQR sistemlerinin önerdiği destek elemanları (kaya bulonu, püskürtme beton, çelik hasır, çelik kafes türünden) uygulanmış iki sistem için hesaplama sonuçları elde edilmiştir.

Çizelge 6. Çeşitli araştırmacılar tarafından önerilen kaya kütlesine ait deformasyon modülü eşitlikleri

Deformasyon Modülü (E_m) Eşitlikleri	Birim	Öneren	Yıl	No
$E_m = e^{(4.407+0.081*RMR)}$	MPa	Jašarević ve Kovačević	1996	(1)
$E_m = 0.0097 * RMR^{3.54}$	MPa	Aydan vd.	1997	(2)
$E_m = 10^{\left(\frac{RMR-10}{40}\right)}$	GPa	Serafim and Pereira	1983	(3)
$E_m = \left(1-\frac{D}{2}\right) * \sqrt{\frac{\sigma_{ci}}{100}} * 10^{\left(\frac{GSI-10}{40}\right)}$ ($\sigma_{ci<100MPa}$ için)	MPa	Hoek vd.	2002	(4)
$E_m = 100\frac{(1-0.5D)}{1+e^{\left(\frac{75+25D-GSI}{11}\right)}}$	GPa	Hoek ve Diederichs	2006	(5)
$E_m = 0.135\left[\frac{E_i\left(1+\frac{RQD}{100}\right)}{WD}\right]^{1.1811}$	MPa	Kayabaşı vd.	2003	(6)
$E_m = 5{,}6 * RMi^{0,3}$ (RMi>0,1 için)	GPa	Palmström	1996	(7)
$E_m = 5\sqrt{Q'}$	GPa	Diederichs ve Kaiser	1999	(8)
$E_m = 0.876 * RMR + 1.056(RMR-50) + 0.015(RMR-50)^2$	GPa	Galera vd.	2005	(9)
$E_m = 10\ Q^{\frac{1}{3}}$	GPa	Barton	1995	(10)
$E_m = 10\ \left(Q\frac{\sigma_{ci}}{100}\right)^{\frac{1}{3}}$	GPa	Barton	2002	(11)
$\frac{E_m}{E_i} = \frac{RMR}{RMR+\beta(100-RMR)}$		Aydan ve Kawamoto	2000	(12)
$\frac{E_m}{E_i} = \frac{RMQR}{RMQR+6*(100-RMQR)}$		Aydan vd.	2014	(13)
$\frac{E_m}{E_i} = 0.009e^{RMR/22.82} + 0.000028 * RMR^2$		Nicholson ve Bieniawski	1990	(14)
$\frac{E_m}{E_i} = \frac{(1-0.5D)}{1+e^{((60+15D-GSI)11)}}$		Hoek ve Diederichs	2006	(15)

Çizelge 7. Sayısal modellemede kullanılan kaya malzemesi ve kaya kütlesine ait veriler

Kaya Birimi Numarası	1	2	3	4	5	6	7	8	9
Tek eksenli basınç – σ_{ci} (MPa)	48.81	24.71	39.40	41.49	11.67	22.17	2.05	0.25	0.25
Kohezyon – C (MPa)	9.29	5.47	7.80	8.12	3.49	5.06	0.28	0.10	0.10
İçsel sürtünme açısı – ϕ	38	44	40	39	27	28	25	22	24
Endirekt çekme – σ_t (MPa)	0.27	0.48	0.41	0.42	1.13	0.30	0.15	0.00	0.00
Poisson oranı – v	0.31	0.27	0.29	0.30	0.38	0.37	0.39	0.41	0.40
Doğal yoğunluk – ρ (kg/m^3)	2.68	2.65	2.65	2.60	2.42	2.72	2.30	1.90	2.00
Deformasyon modülü – E_i (MPa)	4757	3082	4028	3436	1128	2366	-	-	-
Deformasyon modülü – E_m (MPa)	3134	2139	3984	1747	978	1141	675	418	505
Derinlik (m)	150	150	200	150	150	150	25	10	25

Sayısal analiz sonuçlarının elde edilmesini gösteren yazılıma ait ekran görüntüsü Şekil 3'te verilmiştir. Sahadan ölçülen tünel ekseni, sağ omuz ve sol omuzdaki deformasyon değerleri ile NATM ve RMQR sistemlerinin analiz sonuçları Şekil 4'te verilmiştir.

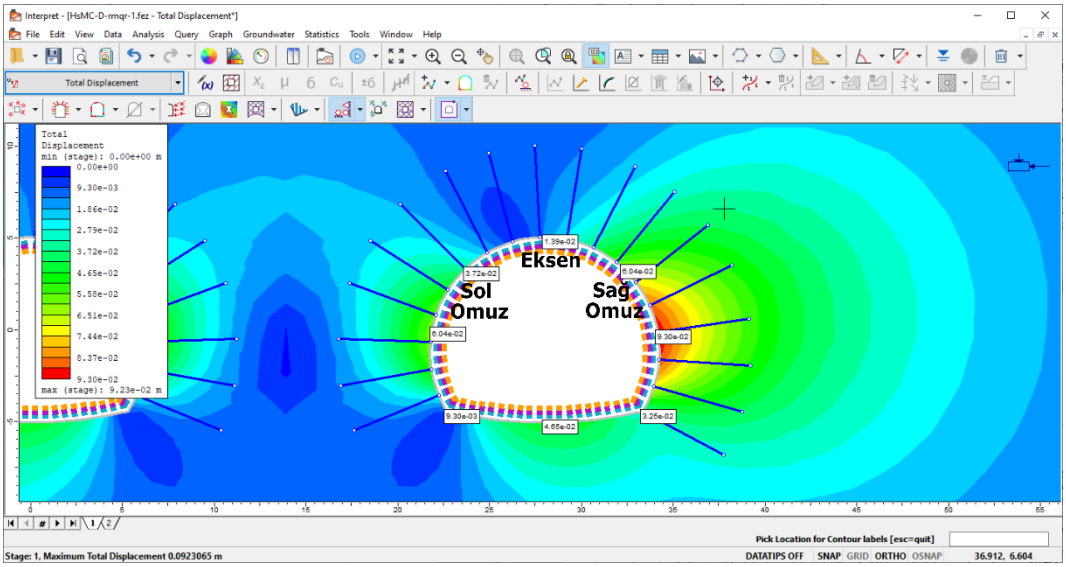

Şekil 3. RS2 yazılımında oluşturulan tünel kesiti ve analiz sonucu

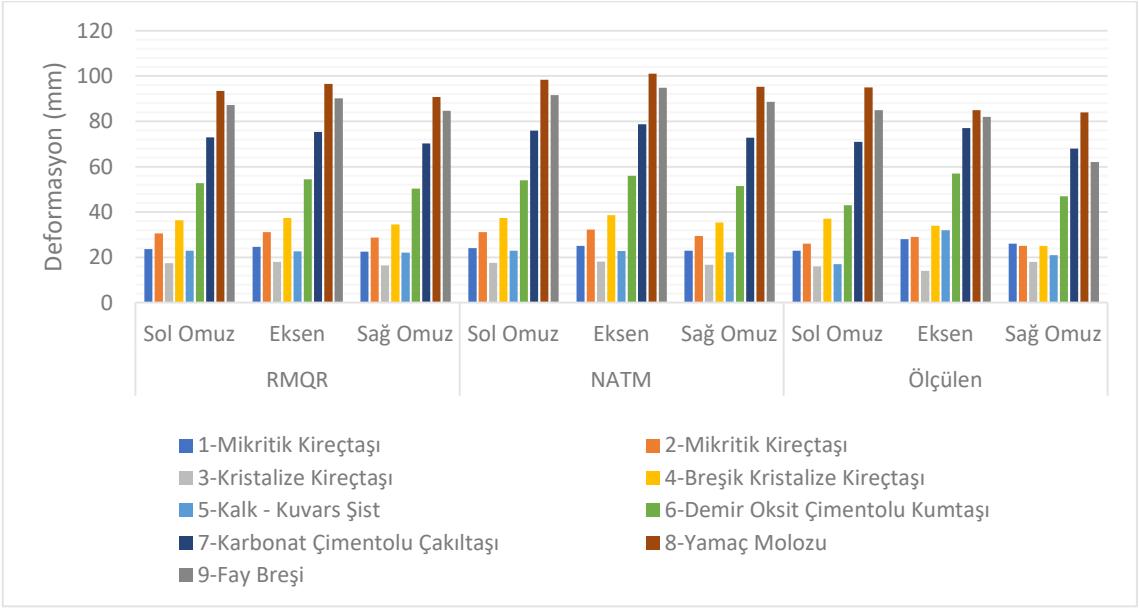

Şekil 4. Kaya kütlesi türüne göre tünel eksen ve omuzlardaki deformasyon değerleri

Tünel eksen ve omuzlarında meydana gelen düşey yönlü deformasyon miktarlarının ortalamasının RMQR, NATM ve sahada ölçülen değerler ile karşılaştırmasını içeren grafik Şekil 5'te verilmiştir.

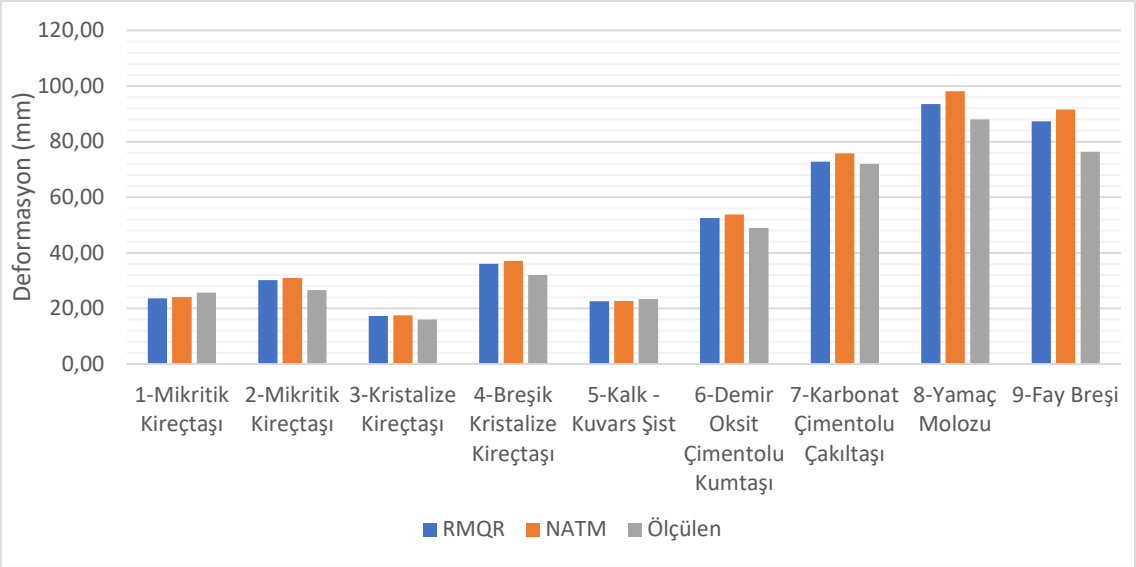

Şekil 5. Kaya kütlesi türlerine göre ortalama deformasyon değerleri

SONUÇLAR VE TARTIŞMA

Bu çalışmada, sahadan ve laboratuvardan elde edilen bilgiler ile kaya kütlelerini karakterize etmek için RMR, Q, RQD, GSI, NATM ve RMQR sınıflama sistemlerinden yararlanıldı. Hesaplanan deformasyon modülü, tek eksenli basınç dayanımı, içsel sürtünme açısı, poisson oranı parametreleri ile destekleme önerileri sayısal analizler için girdi olarak kullanıldı.

NATM sistemine göre projelendirilip yapılan Honaz Tünelinin jeolojik birimleri için kaya kütle kalite puanlaması (RMQR) sistemine göre puanlama yapıldı. Bu iki sistem tarafından önerilen destekleme elemanlarının duraylılıkları sayısal modelleme ile analiz edildi. Elde edilen sonuçlar saha ölçüm değerleri ile karşılaştırıldığında tam olarak örtüşmese bile tutarlı sonuçlar elde edildi. RMQR tasarımlı sayısal modellerde NATM sistemine göre benzer sonuçlar gözlendi. Sahada ölçülen deformasyon değerleri ile karşılaştırma yapıldığında, çok zayıf kaya kütlesi olan karbonat çimentolu çakıltaşı, yamaç molozu ve fay breşi olan bölgelerde gerçek değerlere yakın sonuç elde edilse de diğer birimlere göre benzerlik açısından uzak kalmıştır. Deformasyon modülü ve diğer kaya kütle özelliklerinin tahmininde kullanılan eşitliklerin çok zayıf kaya kütlelerinde gerçekten uzak sonuçlar vermesi bu eşitliklerin gözden geçirilmesi gerektiği göstermektedir.

Kaya özelliklerinin tahmini, kesin bir sonuç vermediğinden hem sayısal modellemeler hem de tünel yapımı sırasında elde edilen gözlemler bu sonuçların gerçeğe daha yakın olmasını sağlamaktadır. Bu çalışmada yapıldığı üzere tünel davranışının analizi, sadece kaya kütle özelliklerinin belirlenmesinde kullanılan empirik eşitliklerin geliştirilmesine katkıda bulunmakta kalmayıp aynı zamanda RMQR sistemi destek önerilerinin gelişmesinde de katkıda bulunabilir.

TEŞEKKÜRLER

Bu çalışma Pamukkale Üniversitesi Bilimsel Araştırma Projeleri Koordinatörlüğü'nce 2019FEBE053 numaralı proje kapsamında desteklenmiştir.

KAYNAKLAR

Aydan, Ö., Akagi, T., Kawamoto, T. (1993). Squeezing potential of rocks around tunnels; theory and prediction. Rock Mechanics and Rock Engineering, *26*, 137-163.

Aydan, O., Ulusay, R. and Kawamoto, T. (1997). Assessment of rock mass strength for underground excavations. International Journal of Rock Mechanics and Mining Science *34 (3/4)*, 777-786.

Aydan, Ö, Kawamoto, T. (2000). Assessing mechanical properties of rock masses through RMR rock classification system. In: Proceedings of the GeoEng 2000 symposium, Sydney, Australia, November 2000. Paper no. OA0926 (on CD).

Aydan, Ö., Ulusay, R. and Tokashiki, N. (2014). A new Rock Mass Quality Rating System: Rock Mass Quality Rating (RMQR) and its application to the estimation of geomechanical characteristics of rock masses, Rock Mech. and Rock Eng., 47:1255-1276.

Aydan, Ö., Tokashiki, N. and Ulusay, R. (2015). Rock Mass Quality Rating (RMQR) for Rock Engineering, International Journal of the Japanese Committee for Rock Mechanics, 11:17-20.

Barton N., Lien R., Lunde J. (1974). Engineering classification of rock masses for the design of tunnel support. NGI Publication No. 106, Oslo, 48.

Barton N. (1995). The influence of joint properties in modelling jointed rock masses. In: Proceedings of the 8th international congress on rock mechanics, Tokyo, Japan, September 1995, pp 1023–1032.

Barton, N. (2002). Some new Q-value correlations to assist in site characterization and tunnel design. Int. J. Rock Mech. Min. Sci. *39 (1),* 185- 216.

Bieniawski, Z.T. (1974). Geomechanics classification of rock masses and its application in tunneling. Proceedings of the third international congress on rock mechanics, s. 27-32. Denver: International Society of Rock Mechanics.

Carranza-Torres, C., & Fairhurst, C. (2000). Application of the convergence confinement method of tunnel design to rock masses that satisfy the Hoek-Brown failure criterion. Tunneling and Underground Space Technology, *15(2),* 187-213.

Deere, D.U. (1963). Technical Description of Rock Cores for Engineering Purpose. Rock Mechanics and Engineering Geology, Vol. 1, No. 1, pp. 16-22.

Deere, D.U., Hendron, A.J., Patton, F.D., Cording, E.J. (1967). Design of surface and near-surface construction in rock. In: Fairhurst, C. (Ed.), Proceedings of the US Rock Mechanics Symposium, Failure and Breakage of Rock. Society of Mining Engineers of AIME, New York, pp. 237–302.

Diederichs, M.S., Kaiser, P.K. (1999). Tensile strength and abutment relaxation as failure control mechanisms in underground excavations. Int J Rock Mech Min Sci 36:69-96.

Galera, J.M., Alvarez, M., Bieniawski, Z.T. (2005). Evaluation of the deformation modulus of rock masses: comparison of pressuremeter and dilatometer tests with RMR prediction. In: Proceedings of the ISP5-PRESSIO 2005 international symposium, Madrid, Spain, August 2005, pp 1-25.

Grimstad, E., Barton, N. (1993). Updating the Q-system for NMT. In: Proceedings of the international symposium on sprayed concrete modern use of wet mix sprayed concrete for underground support, Fagernes, Norway, October 1993. Norwegian Concrete Association, Oslo, pp 25–32.

Hoek, E. (1994). Strength of Rock and Rock Masses. ISRM News Journal, *2*, 4-16.

Hoek, E., & Brown, E. (1980). Underground excavations in rock. London: Instn Min. Metall.

Hoek, E., Kaiser, P., & WF, B. (1995). Support of underground excavations in hard rock. Rotterdam: AA Balkema.

Hoek, E., & Brown, E. (1997). Practical estimates of rock mass strength. Int. J. Rock Mech. Min. Sci., 1165-1186.

Hoek, E. (2000). Big tunnels in bad rock. ASCE journal of geotechnical and geoenvironmental engineering, 726-740.

Hoek, E., Carranza-Torres, C. and Corkum, B. (2002). Hoek-Brown Failure Criterion - 2002 Edition, Proceedings of the 5th North American Rock Mechanics Symposium, Toronto, Canada, Vol. 1, p. 267 – 273.

Hoek E, Diederichs MS (2006) Empirical estimation of rock mass modulus. Int J Rock Mech Min Sci *43(2),*203–215.

Jašarević I., Kovačević M.S. (1996). Analyzing applicability of existing classification for hard carbonate rock in Mediterranean area. In: Proceedings of EUROCK'96, Turin, Italy, September 1996, pp 811–818

Karayolu Teknik Şartnamesi (2013). Yol Altyapısı, Sanat Yapıları, Köprü ve Tüneller, Üstyapı ve Çeşitli İşler, T.C. Ulaştırma Denizcilik ve Haberleşme Bakanlığı Karayolları Genel Müdürlüğü, Ankara.

Kayabaşı A., Gökçeoğlu C., Ercanoğlu M (2003). Estimating the deformation modulus of rock masses: a comparative study. Int J Rock Mech Min Sci *40(1),* 55-63.

Kulhawy, F.H. (1974). Finite Element Modelling Criteria for Underground Openings in Rock, Int. J. Rock mech. Min. Sci. Geomech. Abstr., Vol. 11, No. 12, New York, p. 465 – 472.

Nicholson, G.A., Bieniawski, Z.T. (1990). A nonlinear deformation modulus based on rock mass classification. Int J Min Geol Eng *8,*181–202.

Okay A.İ. (1989). Geology of the Menderes Massif and The Lycian Nappes South of Denizli, Western Taurides, Mineral Res. Expl. Bull., *109*, 37-51.

Pacher, F., Rabcewicz, L. V., Golser, J. (1974). Zum derzeitigen stand der gebirgsklassifizierung im stollen- und tunnelbau. *Straßenforschung*, (18).

Palmström, A. (1985). Application of the volumetric joint count as a measure of rock mass jointing. International Symposium on Fundamentals of Rock Joints, September, Sweden, Proceedings book: 103-110.

Palmström, A. (1996). RMi—a system for characterizing rock mass strength for use in rock engineering. J Rock Mech Tunn Technol 1(2):69–108.

Rabcewicz, L. (1964). The New Austrian Tunneling Method. Water Power, 453-457.

Rocscience RS2. (2021). Finite element analysis of excavations and slopes. Toronto: Rocscience Inc. https://www.rocscience.com/help/rs2 (Mayıs 2021).

Terzaghi K. (1946). Rock defects and loads on tunnel support. Introduction to rock tunneling with steel supports. Eds, R.V., Proctor and White, T.L., Commercial Sheering & Stamping Co., Youngstown, Ohio, U.S.A., 271.

SCALE INHIBITION IN HIGH SOLIDS SLURRY – FINANCIAL AND PRODUCTION IMPACT IN A GOLD MINE OPERATION

K. Bakeev [1], O. Toprak [2, *], V. Lugo-Gonzalez [2], F. Espinosa [2], F. Ramirez [2], L. Danks [2], A. Zhang [3], E. Martinez [4], W. Vargas [4]

[1] Global Technology, IWT, Solenis
[2] Commercial, IWT, Solenis
*(*Corresponding author: otoprak@solenis.com)*
[3] Equipment Design and Development Team, Solenis, USA
[4] Operations, Metal Extractions Circuits, Barrick PVDC, Dominican Republic

ABSTRACT

Gypsum saturation in lime-neutralized, high-density, sulphide ore slurries combined with high temperature triggered scale deposition at the Barrick (PVDC) slurry cooling towers' (SCT) discharge pipelines to the carbon-in-leach (CIL) plant contributed to inflow restrictions and throughput constraints. Mechanical cleaning to restore pipeline flow was implemented but it was expensive and labour intensive, it required a cleaning frequency of approximately every 2.5 months and subjected operators to safety hazards. PVDC approached Solenis to help solve this problem. Solenis mimicked the process conditions, developed an antiscalant product, and proposed it for field validation. Following its implementation, the time between cleanings of the discharge pipelines increased from 2.5 to 21 months, resulting in cost savings of $6,5 million per year, and ore throughput increased by 28,380 tons per year. The prior antiscalant dosing setup was a manually adjusted pump that targeted a fixed dosage. Solenis implemented an OnGuard™i Controller system that used a dosing algorithm. The automation eliminated excess consumption of the antiscalant. No environmental impact was noted on effluent containing the antiscalant, and the antiscalant did not inhibit the gold or silver recovery process.

Keywords: Antiscalant, cost saving, high temperature, high density slurry

INTRODUCTION

The Pueblo Viejo gold mine (PVDC), located in the Dominican Republic, is the second largest Gold mine in the Americas and the fourth largest in the world with ownership shared between Barrick Gold Corporation and Newmont Corporation. The PVDC mine started production in 2012 and reached plant processing capacity of 29,000 tons of ore per day in 2021. The projected life of the mine is 20–25 years with ore grades of 2.5 g/t gold, 17.4 g/t silver and 0.1% copper dating back to 2017. Current gold reserves are 6.2 MM oz, (Barrick, 2020).

An important unit of operation for the PVDC is its slurry cooling towers (SCT) circuit, which is composed of five cooling towers, processing 2,400 m^3/h slurry at 40% approximately solids with temperature reduction from 95 °C to 45 °C. The lime boil tank (LBT), located upstream of the SCT circuit, is where hot acidic slurry gets neutralized with lime as part of the silver recovery process. The SCT circuit is a high efficiency operation, critical to overall mine production. However, significant and progressive scaling of the SCT circuit, mainly of the discharge piping from the SCT to the CIL circuit, required the operation to be disrupted every 2–3 months to swap the pipes and conduct descaling to correct inflow restrictions and throughput constraints. This paper addresses the innovative technical solutions that improved the SCT circuit operation, improved throughput to achieve higher production targets and reduced cleaning costs.

EXPERIMENTAL

Scale formation within the SCT circuit is the result of lime neutralization of acidic, sulphate containing, slurry occurring in the LBT. Gypsum, Calcium Sulphate Dihydrate, scale readily forms in highly saturated slurry streams, creating bottlenecks in the piping and pumps of the SCT as the slurry discharges to the CIL, as shown in Figure 1, with ~40wt% slurry and temperature is 90 °C.

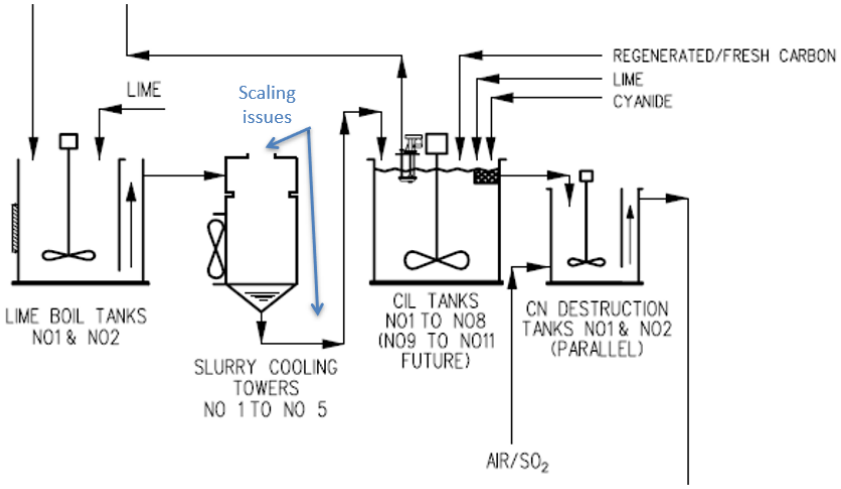

Figure 1. Process flow chart for SCT and adjacent circuits

Solenis and Barrick PVDC partnered together to validate and launch a novel antiscalant Zalta™ MA11-556 product, which had been designed for high slurry, medium to high pH and high temperature process conditions with gypsum as the pre-dominant scale. The original goal was to extend up to 12 months continuous operation of treated with antiscalant SCT circuit without negative impact on gold and silver recovery. The analysis conducted by the Solenis and Barrick PVDC laboratories confirmed the scale type and addressed the dry slurry and process water compositions. For this analysis, we employed well-established industry protocols and used the methods of XRF/XRD for dry samples analysis and ICP (Inductively Coupled Plasma) spectroscopy (Blue, manufactured by Spectro) for process water analysis. Additionally, we used the Brookhaven 90Plus zeta analyser to measure Z-potential and the Horiba LA-950 laser diffraction particle size analyser to determine dry slurry particle size (P80).

Scale type analysis indicated mainly, up to 90 percent, gypsum with minor impurities of pyrophyllite, kaolinite and quartz. Dried slurry analysis indicated quartz as main component with Fe, Al and Ca oxides as well as Al-silicates present in smaller quantities. Particle size (P80) of dried solids was 150 microns. Slurry had Z-potential of -31 mV and pH=7-8. Process water analysis revealed Ionized calcium concentration of 850 ppm average and sulphate ion concertation of 2100 ppm average. Ionized calcium concentrations varied in the field between (580-1100) ppm, as measured two times per day. Figures 2 represents pipe with scale deposited.

Figure 2. Scale deposited in pipe section

The initial analysis of scale formation and inhibition using the novel Zalta™ MA11-556 antiscalant in the laboratory while mimicking the field conditions was conducted using a proprietary scale deposition test. A set of metal alloy jars were placed on an airtight shaker platform, shown in Figure 3, and a shaking motion was subsequently applied at fixed rotations per minute (rpm) under a constant temperature.

Figure 3. Jar scaling test

Threshold inhibition for soluble Ionized calcium measurements by ICP was used for scale formation/inhibition tests using Solenis-designed 316 stainless steel jars. To screen for multiple conditions, shaker tests were conducted at temperatures ranging from 60 to 80 °C, for 16 hours per test at 200 rpm. Testing of gypsum scale formation and inhibition was conducted with process water from LBT. Slurry content in the laboratory tests was limited to 20wt% to ensure good mixing conditions. The impact of the process water pH, wt% slurry and the Zalta™ MA11-556 antiscalant ppm on scale inhibition was measured using this setup. Percent of threshold scale inhibition (by Ionized calcium ICP) was calculated as follows.

$$\frac{Conc.\ of\ Ca\ in\ treated\ Jars\ (ppm) - \ Conc.\ of\ Ca\ in\ Blank\ (ppm)}{Total\ amount\ of\ Ca\ used\ (control\ run\ every\ test)\ (ppm) - \ Conc.\ of\ Ca\ in\ Blank\ (ppm)} X\ 100$$

The Zalta™ MA11-556 antiscalant was developed by Solenis using a three-phase approach: a scale deposition test without slurry, a high temperature shock test followed by a deposition test and a scale inhibition test of the impact of the slurry composition. The results of the laboratory tests and the results of the trial are discussed in the next section.

RESULTS AND DISCUSSION

Scale inhibition tests were conducted in the Solenis laboratory for the LBT slurry at various pH values and temperatures. The results are presented in Figures 4–6.

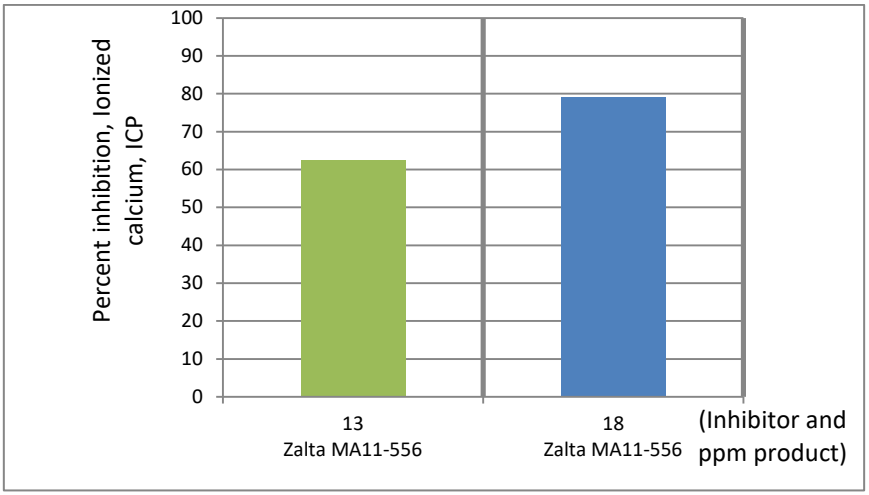

Figure 4. Scale inhibition for LBT tank 20% slurry, pH=11

In this test, the mimic water contained 840 ppm Ionized calcium total and 6000 ppm added SO_4-ion with 20% dried LBT tank slurry per 200 ml total mimic water. These test results support product efficacy at the 13 and 18 ppm doses with the 18-ppm dosage showing improved scale inhibition.

Test results with lower pH are shown in Figure 5. In this case, mimic water contained 900 ppm Ionized calcium total and the same other components amounts, as in Figure 4, except for slurry pH was adjusted with HCl down to 7–8. Product efficacy was retained at ~18 ppm dose level but reduced significantly at 13 ppm versus high pH test.

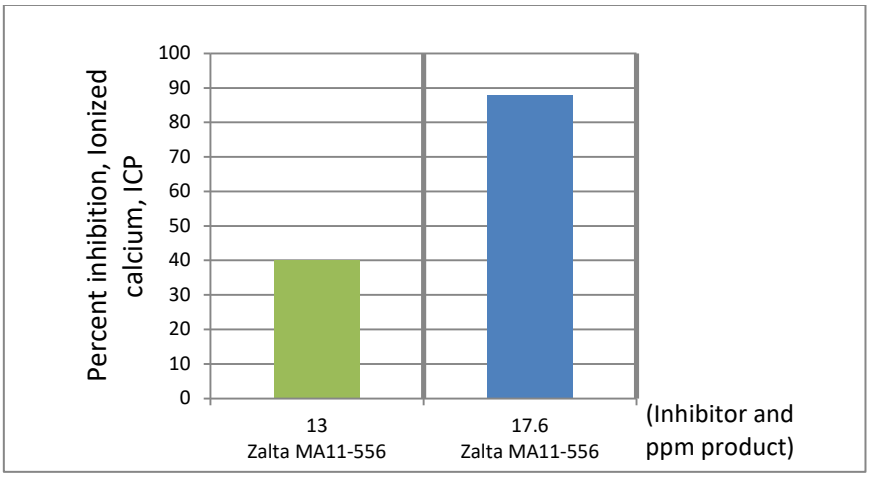

Figure 5. Scale inhibition for LBT tank 20% slurry, pH is 7–8

Scale inhibition results for 18 ppm and different temperatures are shown in Figure 6 with the same other conditions as for Figure 4. Product efficacy is retained at 60 and 80 °C although higher temperature reduces scale inhibition.

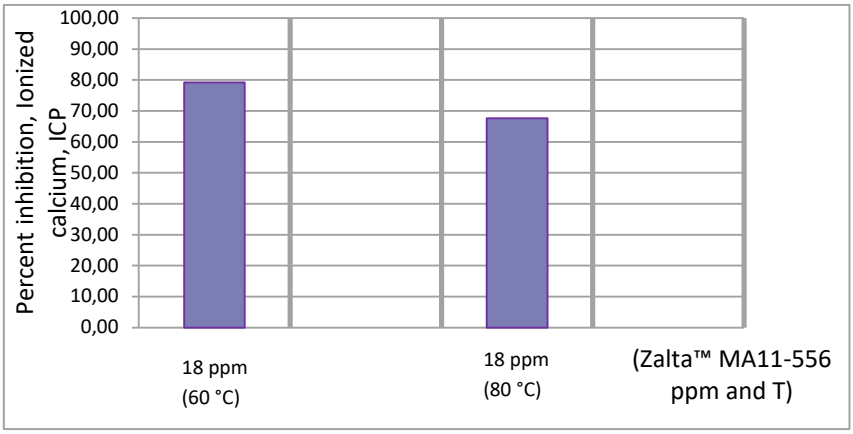

Figure 6. Scale inhibition for LBT tank 20% slurry, pH is 11, T – impact

For the impact of the LBT tank slurry concentration on scale inhibition, we measured adsorption of the scale inhibitor onto the slurry. The results are summarized in Figure 7.

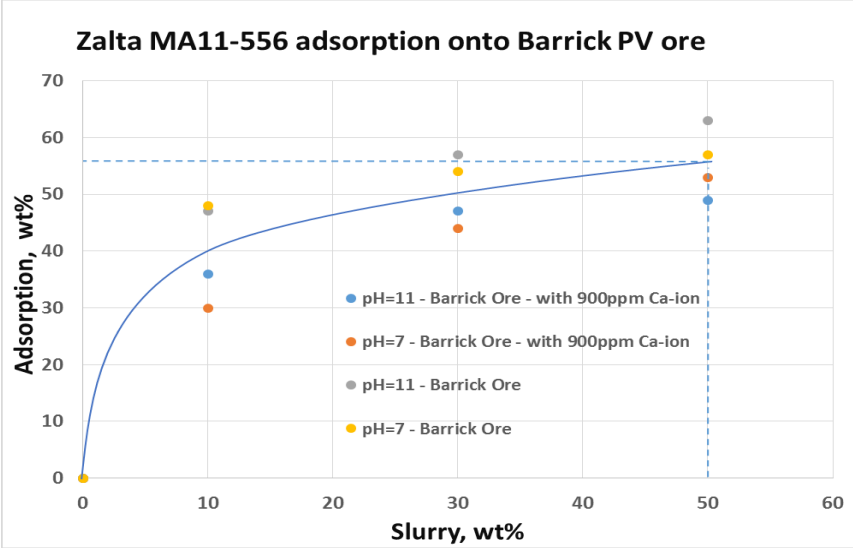

Figure 7. Scale inhibitor adsorption onto gold ore slurry, pH and Ionized calcium impacts

In the adsorption test, 500 ppm of the Zalta™ MA11-556 antiscalant was added to the gold ore slurry in high density propylene jars and placed on the shaker at 60 °C for 16 hours. Ore was then filtered out and the product concentration in the aqueous phase was analysed by size exclusion chromatography. The percentage of the antiscalant retained on the ore surface compared with the original amount added to the slurry (500 ppm) was then calculated. Product adsorption onto the ore varied with Ionized calcium and the pH level. However, only a minimum change in precent adsorption occurred after reaching the 20 wt% slurry level.

To verify that the antiscalant product would not inhibit gold and silver recovery, tests were conducted at the PVDC metallurgical laboratory using mixtures of LBT tank slurry and the antiscalant, simulating the lime boil and leaching processes. The results are summarized in Table 1.

Table 1. Gold and silver recovery data and the impact of Zalta™ MA11-556

Conditions/Essay repeat	Essay 1		Essay 2			Essay 3		
Amount of Slurry (g)	1200		1200			1200		
Solid WT%	50		44			44.4*		
grams of Ca(OH)2 added (35 kg/Ton)	21		18.48			18.65		
mL of water added to get to 40%WT	300		120			132		
Dose of Zalta MA11-556	0 ppm	30 ppm	0 ppm	15 ppm	30 ppm	0 ppm	15 ppm	30 ppm
average pH of Blend before Lime Boil simulation	13.04	13.02	12.46	12.46	12.46	12.32	0.32	12.42
Temp at the beginning of Lime Boil simulation	95	95	91	91	91	88.1	88.1	88.1
Average pH of Blend after Lime Boil simulation	12.78	10.75	11.48	11.74	11.79	12.08	12.25	12.24
Average Make-up water due to evaporation losses	n.a.	n.a.	40	47	105	0.0	44.0	36.0
Au recovery	77.6%	77.7%	**88.6%**	**89.4%**	**89.5%**	**76.7%**	**77.5%**	**78.2%**
Ag recovery	89.8%	85.5%	**76.9%**	**87.7%**	**87.7%**	**89.5%**	**87.7%**	**88.6%**

Table 1 data refer to laboratory tests conducted to simulate LBT conditions of gold ore pre-treatment as is and with added variable amounts of the antiscalant. Subsequently, gold and silver recovery tests were completed. The results achieved indicate that, for the range of dose applied, 0–30 ppm, and within the test's margin of error, the antiscalant did not inhibit gold and silver recovery.

The successful results achieved in the laboratory using the antiscalant for scale inhibition efficacy and gold and silver recovery encouraged us to pursue field trials with the antiscalant. Initially, two trial campaigns were conducted with product doses in the range of 13–18 ppm, dose adjusted manually per slurry flow rate while and collecting Ionized calcium data over the same period, however, inconsistently. The trials lasted 8 and 7 months, well above 2-3 months Blank operation, but each resulted in abrupt scaling of the SCT pipelines. Scale monitoring was challenging because the coupons installed in the SCT circuit did not result in any scale deposit that was due to the abrasive properties of the slurry. The only remaining option was a visual inspection of the pipes, as shown in Figure 7, during a brief period, typically, prior to shut down.

Figure 7. Scaling severity assessed in SCT discharge pipelines during brief shutdown

Based on our research, we concluded that to improve the continuous run time of the SCT circuit using the antiscalant, while continuing to provide cost savings, we would need to implement a dosing algorithm. Consequently, several changes to protocols were made, including more systematic collection of Ionized calcium data, generating product dose ppm versus Ionized calcium ppm trend based on laboratory scale inhibition data and extrapolation method. Additionally, the team introduced the OnGuard™ i Controller dosing system as part of the dosing skid, with additional sensors, to automate dosing of the antiscalant based on distributed control system (DCS) data for Ionized calcium and the defined product parts per million trend.

The automated dosing equipment and the Ionized calcium data that was or were collected are shown in Figures 8 and 9, respectively.

Figure 8. The Solenis OnGuard™ i Controller installed at the SCT circuit, PVDC

Programmed algorithm for product dose level with systematic DCS input of Ionized calcium data, slurry flow rate, was automatically managed by OnGuard™ i Controller as well as providing alarms with various sensors indicating level of the product left in a tote, Temperature, pH, etc.

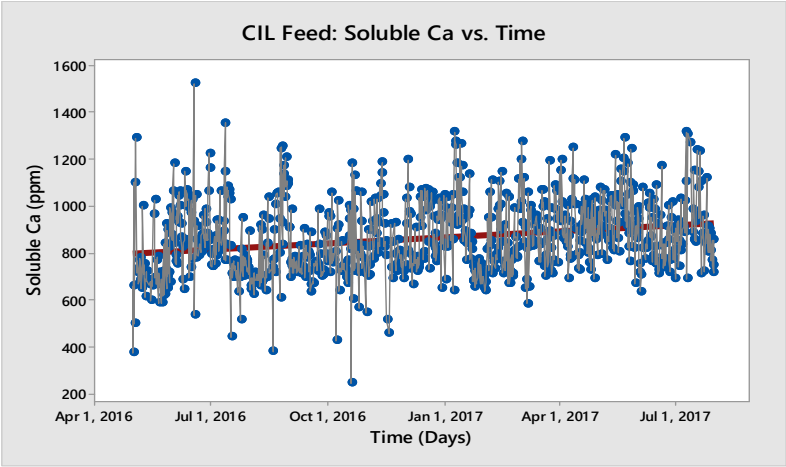

Figure 9. Soluble Ionized calcium data measured and fed to OnGuard™ i Controller

Measurements of soluble Ionized calcium were conducted by the PVDC mine two times per day and logged into the DCS. Algorithm design was based on tying in Ionized calcium data to Zalta™ MA11-556 dose level for minimum 90% level of inhibition. Initial performance data were generated using laboratory testing. Table 2 shows the test results.

Table 2. Scale inhibition for Zalta™ MA11-556, 20 wt% LBT tank slurry, pH=11 - effect of dose level, Temperature.

Temp.°C	Ionized calcium/ppm	-556/ppm	% Inhibition
60	900	13	62.5
60	900	18	79.2
80	900	18	67.7

The results in the table were further extrapolated to T=(80–90)°C and 35wt% slurry concentration noted as average in the field.

The following assumptions were made to complete the extrapolation.

(1) Linear relationships existed between the % Inhibition and the

- Product dosage per parts per million
- Ionized calcium per parts per million
- Scale(s) saturation indices

(2) Targeting minimum 90% inhibition results for laboratory data to ensure required field performance.

(3) “Active” product in solution = {total product} - {product adsorbed onto ore} in the slurry.

As the results of it, extrapolated data were generated, Table 3.

Table 3. Dosage for Zalta™ MA11-556 versus Ionized calcium ppm for 90% inhibition, (20 wt% LBT tank slurry, pH=11, 35wt% LBT tank slurry, T=80–90 °C).

Ionized calcium/ppm	580	650	700	750	800	850	**900**	1100
Zalta™ MA11-556/ppm	17	19	21	22	24	25	**27**	33

Figure 10 shows the Ionized calcium content plotted over time and further assigned dosing levels of Zalta™ MA11-556.

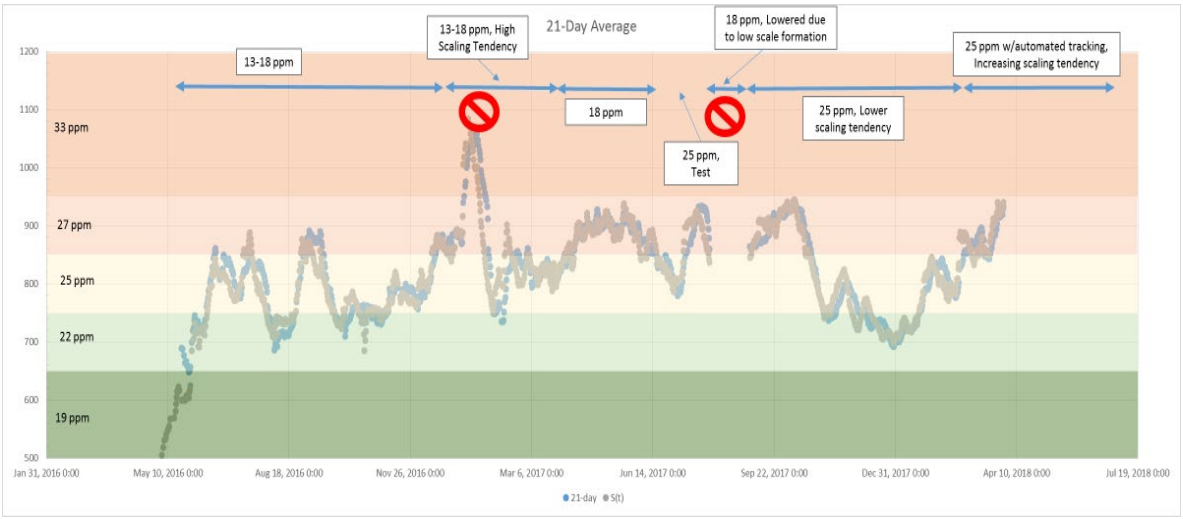

Figure 10. Ionized calcium data plotted as 21-day averages over a few years period with assigned Zalta™ MA11-556 dosages

The blue points in Figure 10 are a rolling 21-day averages for Ionized calcium, not immediately available on OnGuard™ i Controller; the grey points are exponential smoothing with α = 0.05 for Ionized calcium, available on OnGuard™ i Controller:

$$S_t = (1- \alpha)S_{t-1} + \alpha X_t \text{ where } S_0 = X_0$$

Color changes from green to red indicate enhanced scaling trends associated with higher Ionized calcium content in the slurry, with average dose levels of Zalta™ MA11-556 assigned to five ranges/bands of Ionized calcium. At the top of the plot are comments associated with scaling tendencies in the field based on visual observations and two original events when there were shutdowns prior to implementing dosing algorithm.

The result of dosing algorithm implementation can be seen in Figure 11.

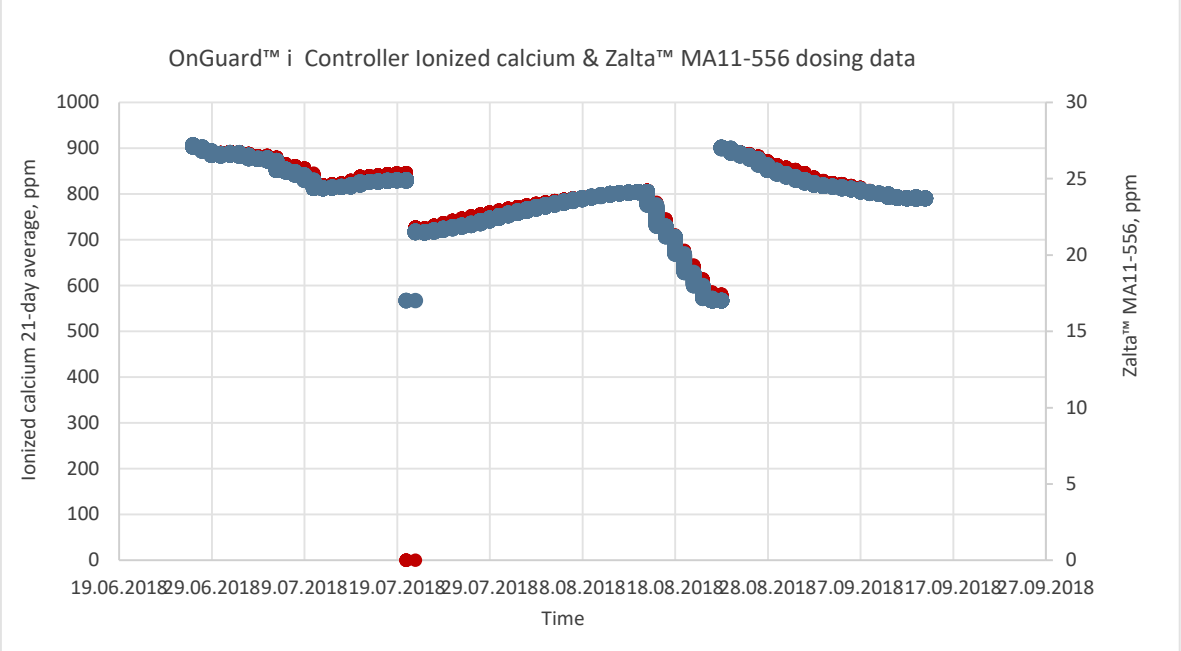

Figure 11. Overlay for Ionized calcium data (red) and Zalta™ MA11-556 dosing (blue) over time

As shown in Figure 11, after we implemented the dosing algorithm, we were able to achieve a very robust match between the 21-day average of the Ionized calcium data and the Zalta™ MA11-556 antiscalant dosed with the OnGuard™ i Controller programmer dosing for Zalta™ MA11-556. More importantly, that step was crucial to make substantial progress towards further extension of continuous operation for SCT circuit without scaling events.

As the result of combined benefits for novel Zalta™ MA11-556 scale/deposit inhibitor with implemented dosing algorithm powered by OnGuard™ i Controller, the time between cleanings of the SCT discharge pipes increased significantly, from an average of 2.5 to 21 months, resulting in cost savings of $6,5 million per year, and ore throughput increased by 28,380 tons per year.

This positive outcome is also manifested in significantly reduced scaling rates in the field, as shown in Figure 12.

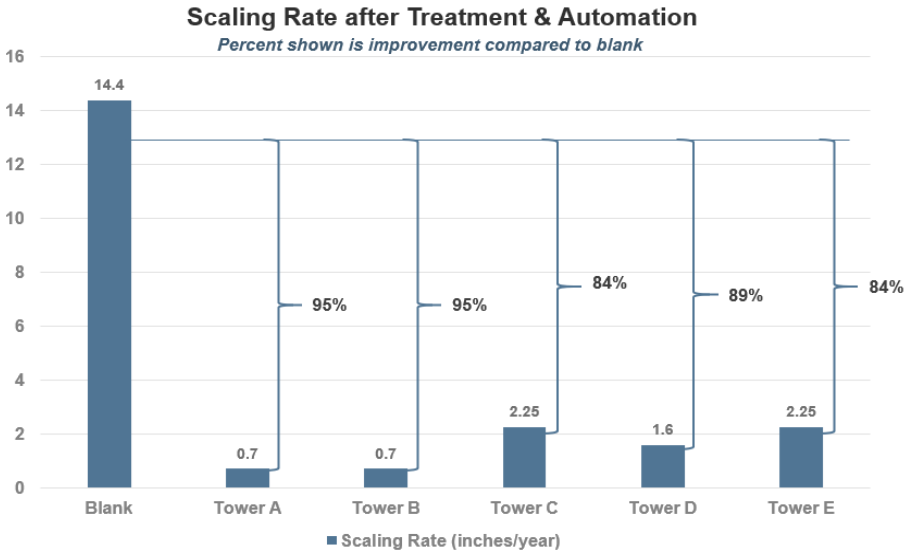

Figure 12. Scaling rates for SCT five tours with Zalta™ MA11-556 and implemented dosing algorithm with automation

CONCLUSIONS

In summary, the use of a novel antiscalant product combined with a systematic approach to validation and algorithm-controlled product dosing have proven critical to the success of large scale mining operations.

The cooperation between Solenis and Barrick PVDC allowed us to meet and exceed the original targeted return on investment to the PVDC plant while maintaining safe operations with a reduced frequency of shutdowns and pipe cleaning, which typically had required two separate teams to be scheduled and present at the same time. The time between cleanings of the discharge pipelines increased from 2.5 to 21 months, resulting in cost savings of $6,5 million per year, and ore throughput increased by 28,380 tons per year.

The antiscalant approach is further helping mines with water management issues by reducing cleaning frequency for SCT pipes, thereby improving sustainability of operations.

ACKNOWLEDGMENTS

The authors acknowledge Markus Broecher and Erin Dougherty, Solenis Global Technology, and Michael Hagarty, Solenis Commercial, for their support and key input at various stages, which ensured technical success of the project. Andrew DiMaio's, Solenis Global Technology, contribution was invaluable in conducting laboratory testing. Martin Zalite's, Solenis Equipment Group, installation of OnGuard™ i Controller and sensors was critical to overall project success. Carmen DeLeon, PVDC Metallurgy Group, was instrumental in coordinating the project at PVDC.

REFERENCES

Barrick PVDC Annual Report, 2020.

SİNTER TESİSİNDE SO_2 EMİSYON AZALTICI ÜRE UYGULAMASI

SO_2 EMISSION REDUCTION UREA APPLICATION IN SINTER PLANT

B.E. Kesemen [1, *], V. Kızılay [1], S. Balaban [1]

[1] İSDEMİR A.Ş.
*(*Sorumlu yazar: ekesemen@isdemir.com.tr)*

ÖZET

Günümüzde, SO2'nin büyük bir endüstriyel emisyon kaynağı olduğu kabul edilmiş bir gerçektir. Demir cevherinin sinterlenmesi, demir çelik endüstrisindeki ana SO_2 emisyon işlemidir. Çin'de, ülke çapındaki toplam endüstriyel emisyonların %10,3' ünü temsil eden yıllık olarak yaklaşık 2x106 ton SO2, demir ve çelik endüstrisi tarafından işletilen tesislerden ve bu 2x106 ton SO_2' nin %70' inden fazlası da demir cevheri sinterleme işleminden deşarj edilmektedir. Demir cevheri sinterlemesindeki baca gazları, yüksek yatırım ve işletme maliyetine neden olan kükürt giderme ekipmanlarıyla temizlenmeye çalışılmaktadır. Baca gazı kükürt giderme (FGD) işlemleri, dünyadaki sinter tesislerinde yaygın olarak kullanılmaktadır. FGD işlemleri yaş, yarı ve kuru işlemler olarak ayrılabilir. Bu işlemlerin üçü de büyük yatırım gereksinimleri ve yüksek işletme maliyetleri olarak nitelendirilmektedir. Demir cevheri sinterleme işleminde SO_2 emisyonlarını düşük maliyetle azaltmak için yeni teknolojilerin geliştirilmesi ihtiyacının karşılanmasına yönelik çalışmalar devam etmektedir. Bu çalışmada, demir cevheri sinterleme işlemi sırasında baca gazı emisyonunun azaltılmasına yönelik yeni bir teknoloji "üre eklenmesi" incelenmiştir, üre ilavesiyle kükürt gidermenin uygulanabilirliği amacıyla bir sinter işletmesinde çalışmalar yapılmış ve kullanıma geçilmiştir. Sonuçlar, baca gazı içindeki SO_2 emisyon konsantrasyonunun, üre eklenerek önemli ölçüde azaldığını göstermektedir. Endüstriyel uygulama sonuçları değerlendirilmiş olup sinterleme indeksleri ve nihai sinter kalitesi üzerinde olumsuz bir etkisi görülmemiştir.

Anahtar Sözcükler: Sinter fabrikası, demir cevheri sinterlemesi, sinter, üre, çevre, sürdürülebilirlik, SO_2 emisyonu, değişkenlik

ABSTRACT

It is an accepted fact that SO_2 is a major source of industrial emissions today. Sintering of iron ore is the main SO2 emission process in the iron and steel industry. In China, approximately 2x106 tons SO2, which represents 10.3 wt% of the total industrial nationwide emissions, are discharged annually from facilities operated by the iron and steel industry, and over 70% of this 2x106 tons SO2 is discharged from the iron ore sintering process. Flue gases in iron ore sintering are tried to be cleaned with desulfurization equipment, which causes high investment and operating costs. Flue gas desulfurization (FGD) processes are widely used in sinter plants around the world. FGD processes can be divided into wet, semi and dry processes. All three of these transactions qualify as large investment requirements and high operating costs. In order to reduce SO2 emissions at low cost, efforts are continuing to meet the need to develop new technologies to reduce SO2 emissions in the iron ore sintering process. In this study, a new technology "urea addition" for reducing flue gas emissions during iron ore sintering process was investigated, studies were carried out in a sinter plant for the applicability of desulfurization with the addition of urea and it was put into use. The results show that the emission concentration of SO2 in the flue gas is significantly reduced by adding urea. Industrial application results have been evaluated and no adverse effect on sintering indexes and final sinter quality has been observed.

Keywords: Sinter plant, iron ore sintering, sinter, urea, environment, sustainability, SO2 emission, variability

GİRİŞ

Demir cevherinin sinterlenmesi; kireç taşı, kok tozu, geri dönüş tozları ve diğer flaks yapıcılarla 1100-1200°C'de toz formundaki malzemelerin aglomerasyonu şeklinde daha büyük tanelere boyutlandırılmasıdır. Sinter üretiminde amaç, toz cevherin yüksek fırında kullanımının sağlanmasıdır. Diğer demirli malzemelerin yerine yüksek fırında sinter kullanımı maliyet avantajı sağlayabilmektedir.
Yüksek fırınlara şarj edilen demirli malzemeler içinde sinter malzemesi, diğer demirli malzemelere göre üretim maliyeti en düşük olandır. Bir aglomerasyon işlemi olan demir cevherinin sinterlenmesinde, toz formunda sinterlik harman, kok tozu/antrasit, kireç taşı, dünit/dolamit, geri dönüş sinter tozu, yanmış kireç, silobas tozları ana girdileri oluşturur. Değişen cevher cinsi, kok tozu/antrasit vb. kükürt girdisi olan hammaddeler ve proses parametrelerinin optimizasyon yetersizliği baca gazında kükürt dioksit değerlerinin yüksek seviyede gerçekleşmesine sebep olabilmektedir. Bunun için üretim verimini ve çevresel sorumlulukları esas alan bir işletmenin sürdürülebilir çözümleri uygulama zorunluluğu bulunmaktadır.

Sinter tesisleri, Şekil 1'de gösterildiği gibi stok-harman sahaları, kırma-eleme üniteleri, dozajlama sistemleri ve sinter makineleri gibi kısımlardan oluşur. Cevher, kok ve ilave malzemeler karıştırılıp nemlendirilerek sinter makinesine aktarılır. Sinter makinalarında ilk tutuşturma sinter fırınlarında gerçekleşir. Burada üst yüzey kok gazı ve hava yardımı ile tutuşturulur. Üst bölgede başlayan bölge fan emişi sayesinde makinanın alt bölgelerine doğru ilerler ve sinterleme reaksiyonları gerçekleşir. Emiş yapılan hava elektrostatik çöktürücü ünitesine girer ve burada akımı geçen hava içerisinden tozlar tutulur. Sinterleşme esnasında açığa çıkan gazlardan biri de kükürt dioksit gazıdır.

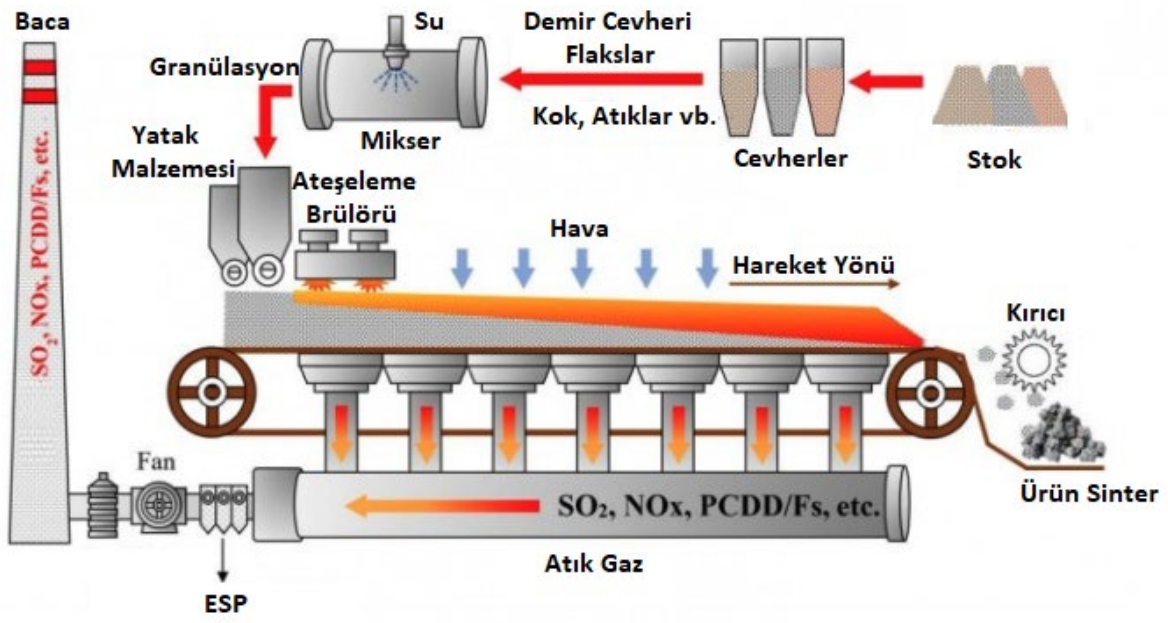

Şekil 1. Demir cevheri sinterleme işleminin şematik diyagramı (Wang et al., 2020).

Sinter prosesi entegre demir çelik üretimi yapılan tesisler için önemli bir işletmedir. SO_2 ve NO_2 sinter prosesi sonucu oluşmaktadır ve baca gazı emisyonlarına neden olmaktadır.
Günümüzde sinter prosesinde ortaya çıkan emisyonlarının azaltılabilmesi adına yüksek verimli fluttering teknolojisi, fiziksel absorblama teknolojisi ve katalitik dekompozisyon teknolojileri dünyada yapılan

çalışmalarda genişçe yer alan metotlardır. Bu metotlar bir şekilde efektif olsa da; komplike teknoloji nedeniyle bir takım sorunlar ortaya çıkmakta, sürecin akışı, sürekliliği ve büyük yatırım maliyetleri uygulamaları kısıtlamaktadır.
Sinter prosesinde, baca gazındaki SO_2 emisyonlarını azaltmak için sinterlemede üre ekleyen yeni bir teknoloji önerilmektedir.
Sinter prosesi esnasında sıcaklığın yükselmesiyle birlikte ürenin aşağıda belirtilen reaksiyon mekanizmalarını takip ederek parçalandığı ve SO_2'yi amonyum sülfata dönüştürdüğünü söylemek mümkündür.

$$(NH_2)2CO + H_2O = NH_4COONH_2 \quad (1)$$

$$NH_4COONH_2 = 2NH_3 + CO_2 \quad (2)$$

$$SO_2 + 2NH_3 + H_2O + 0{,}5O_2 = (NH_4)2SO_4 \quad (3)$$

Üre (Latince Urea Pura), organik bir bileşiktir. Formülü H_2N-CO-NH_2'dir. Karbonik asidin diamidi olan üre aynı zamanda karbamik asidin de amidi olduğundan karbamid adı ile de bilinir. En çok gübre ve hayvan yemi olarak kullanılan üreden ilaç ve plastik yapımında da faydalanılır.
Sinter tesislerinin SO2 emisyonunun önemli bir kaynağı olmasından dolayı konuyla ilgili önemli araştırmalar yapılmıştır. H. Long ve arkadaşları yaptıkları çalışmada, üre eklenmeden yapılan baz testte, sinterleme hammaddelerinden elde edilen toplam kükürtün %59,93' ünün sintere girdiğini ve geri kalanının sinterleme baca gazına girdiğini göstermiştir. Üre ilave edilen kükürt giderme testinde, toplam kükürtün %53,62' si sintere girmiş, %36,22'si amonyum sülfat ($NHSO_4$) 'a dönüştürülmüş ve sadece %4,77'si sinter baca gazına girmiştir (Long et al., 2016). Diğer bir çalışmada H. Long ve arkadaşları, ticari bir sinter tesisinde pilot ölçekli bir deney yapılmıştır. Sonuçlar, üre ilavesiz baca gazı içindeki SO_2 konsantrasyonuyla karşılaştırıldığında, SO_2 konsantrasyonunun ağırlıkça %0,10 üre eklendiğinde önemli ölçüde 694.2'den 108 mg/m^3'e düştüğünü göstermiştir. Üre ile ayrıştırılan NH_3, (NH_4) $2S0_4$ üretmek üzere $S0_2$ ile reaksiyona sokulmuş ve baca gazı içindeki $S0_2$ konsantrasyonunu düşürmüştür (Long et al., 2016). T. Chun ve arkadaşlarının çalışmasında, baca gazı içindeki SO_2 emisyon konsantrasyonunun, yatağa üre eklenerek önemli ölçüde azaldığını göstermektedir. Yatakta %0,05 üre yatak tabanından 70-150 mm yükseklikten eklendiğinde, kükürt giderme oranı %85'ten daha yüksek elde edilmiştir (Chun et al., 2017). H. M. Long ve arkadaşlarınan yaptığı çalışmada, sinterleme deneylerinden çıkan atık gazın analizinde, %0,05, 0,1 ve %0,5 oranında üre eklendiğinde, dioksin emisyonlarının sıfır üre ile karşılaştırıldığında %63,1, 66,8 ve %72,1 oranında azaldığını göstermektedir (Long et al., 2011). H.Long ve arkadaşları başka bir çalışmada İnhibitör olarak üre ilavesiyle demir cevheri sinterlemesinden çıkan egzoz gazı dioksinin emisyon azaltma deneyleri gerçekleştirilmiştir ve sonuçlar % 0,05, % 0,1 ve % 0,5 (w) üre eklendiğinde, dioksinin emisyon konsantrasyonlarının 0,187 0.258 ve 0.217 ng-TEQ/m^3 olduğunu, dioksin emisyon oranı üre içermeyen 0.777 ng-TEQ/m^3 ile karşılaştırıldığında önemli ölçüde azaldığı tespit edilmiştir (Long et al., 2010). Chin-Lu Mo' nun çalışmasında deneysel sonuçlar sinter karışımına ağırlıkça %1 şeker ilavesinin sinterleme süresini 23'50" ila 19'16" arasında kısalttığını göstermiştir. Azot fragmanlarının azot oksitlere dönüşüm oranı önemli ölçüde azaltılmış, emisyon kütlesi 533.8'den 283.3 g/t.sinter'e düşürülmüş ve emisyon konsantrasyonu 223'ten 160 ppm'e (%15 0_2 baz) düşmüştür (Mo, 1997).

Ayrıca Britishsteel uygulamasının; harmanda %0,0125 oranında, ortalama 90 kg/saat granül formda mikser öncesi vibromotorlu bir bunkerden beslendiği bilgisi edinilmiştir.

DENEYSEL ÇALIŞMA

Sinter tesisinde SO_2 emisyon azaltıcı üre uygulaması, İsdemir A.Ş. Sinter ve Hammadde Maniplasyon işletme tesisleri' nde yapılmıştır. Entegre demir-çelik tesisi olan İsdemir A.Ş.' de, ana ham maddeler olan demir cevheri ve kömür deniz yolu ve demir yolu vasıtası ile gelir. Ham maddenin tesislere getirilmesiyle birlikte üretim süreci başlamış olur. Kömür, koklaştırma süreci için kok

fabrikalarına; toz cevher ise yüksek fırınlarda kullanılabilmesi için sinterleştirmek amacı ile sinter fabrikasına iletilir. Kok fabrikası silosuna konveyör bant sistemi ile taşınan kömür, fırınlara şarj edilerek yüksek sıcaklıkta ve oksijensiz ortamda koka dönüştürülür, böylelikle yüksek fırınların ihtiyacı olan kok üretilir. Toz cevher, demirli baca tozları ve tufal, sinter fabrikasında yüksek fırınların kullanılabileceği ebata getirilerek sinter üretilir ve konveyör bant sistemi ile yüksek fırınlara gönderilir. Yüksek fırınlar sıvı ham demir üretir. Sıvı ham demir üretimi için demir cevheri, sinter, pelet ve kok girdi olarak kullanılır. Üretilen sıvı ham demir cüruftan arındırılarak torpidolara alınır. Torpidolardaki sıvı ham demir kükürt giderme tesislerinde kükürdü giderildikten sonra üretime girmek üzere çelikhaneye nakledilir. Çelikhanede; sıvı ham demir, hurda ve istenilen kaliteye göre farklılık gösteren çeşitli alaşım elementleri kullanılarak saf oksijen üfleme yöntemi ile sıvı ham demirdeki karbon oranı düşürülür, böylelikle sıvı ham demir, sıvı çeliğe dönüştürülür. Üretilen sıvı çelik sürekli döküm tesislerinde kalıplara kesintisiz olarak dökülüp, istenilen ebatlarda katılaştırılarak yarı mamuller olan slab veya kütük haline getirilir. Şekillendirilen çelik, slab ise sıcak haddehanelere; kütük ise kangal haddehanesine gönderilir. Slabtan yassı sıcak ürünler olan bobin ve levha, kütükten ise uzun ürün olan kangal üretilir. Tesisler üretilen ürünler deniz yolu, demir yolu ve kara yolu ile müşterilere ulaşır (İsdemir).

Sanayi Kaynaklı Hava Kirliliğinin Kontrolü Yönetmeliği 03.07.2009 Resmî Gazete'de yayımlanmıştır. Sanayi Kaynaklı Hava Kirliliğinin Kontrolü Yönetmeliği Ek1' deki Kirletici Vasfı Yüksek Tesisler İçin Özel Emisyon Sınırları Ek-5' teki Beşinci Grup Tesisler kapsamına giren Demir Sinterleme Tesisleri için Tesisten kaynaklanan kükürt dioksit emisyonu %16 hacimsel oksijen oranına göre 500 mg/Nm^3 değerini aşmamalıdır şeklinde tanımlama mevcuttur (T.C. Çevre ve Şehircilik Bakanlığı).

Kullanılan cevhere göre harman analizlerinde dönemsel farklılıklar yaşanabilmektedir. Seviye 1-2-3 gibi otomasyon, yazılım sistemleri ve laboratuvar sonuçlarıyla proses değişkenlikleri izlenmektedir ve proses parametreleriyle ilgili değişkenlikler kontrol altında tutulmaktadır.
Yüksek fırın girdisi olan sürün sintere ait tipik analiz değerini gösterir tipik ürün sinter değerleri Çizelge 1.' de verilmiştir.

Çizelge 1. Tipik ürün sinter değerleri

Ürün Sinter	Değer
ISO Tumbler Index (+6.3 mm)	~81 %
Sinter Boyut Aralığı	5-150 mm
-5mm Oranı	Max. 5 %
+50mm Oranı	Max. 8 %
Sinter Deşarj Sıcaklığı	Max. 100 ℃
Fe total	~56,40 %
CaO	~10,35 %
SiO2	~5,75 %
MgO	~1,32 %
Al2O3	~1,73 %
P	~0,069 %
S	~0,018 %
CaO/SiO2	~1,8

Tesiste üre beslemesi amacıyla, vibromotoru bulunan seyyar bir bunker tesisin besleme noktasına montajı yapılmıştır.

Beslenen üre malzemesi; 1-2 mm arası granül tane iriliğinde, minimum %46 azot, maksimum %0,7 nem içeriğine sahiptir. Karışımda toprağa, bitkilere ve canlılara zararlı madde bulunmamaktadır.

Şekil 1. Beslenen üre malzemesi

Tesiste deneysel çalışmalar kapsamında farklı zamanlarda 20 adet deneme yapılmış olup 1 adet deneme sonucu aşağıda grafiklerle paylaşılmıştır.

Deneme

Farklı denemeler yapılarak harmanın yaklaşık %0,88' i kadar üre beslemesinin optimum oran olduğu değerlendirilmiştir. Üre Beslemesi yapılan 16:20 ile 23:30 arasında en düşük 20,82 mg/Nm^3 en yüksek 424,11 mg/Nm^3 ortalama 126,03 mg/Nm^3 olarak SO_2 ölçümü gerçekleşmiştir. Üre beslemesi yapılmayan zaman dilimlerinde en düşük 193,795 mg/Nm^3 en yüksek 482,198 mg/Nm^3 ortalama 369,95 mg/Nm^3 olarak SO_2 ölçümü gerçekleşmiştir.

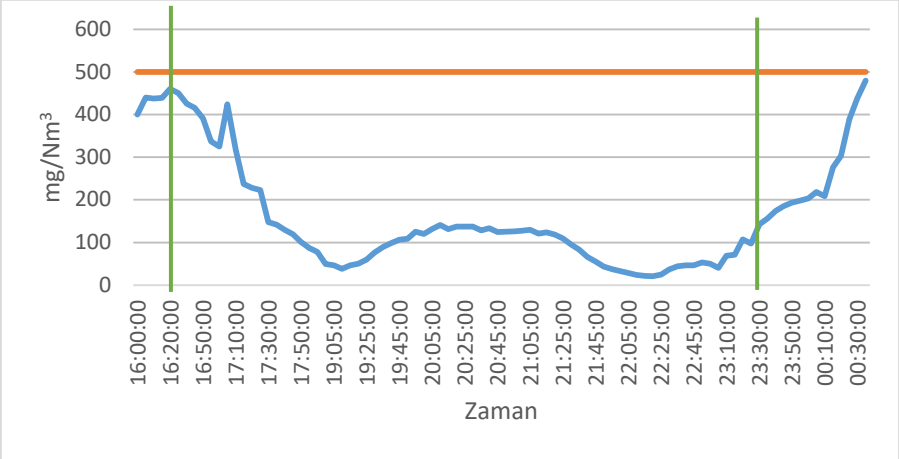

Şekil 2. Deneme çalışmasının sonuçları

Diğer 8 deneme çalışmasına ait değerler Çizelge 2.' de verilmiştir.

Çizelge 2. Diğer sekiz deneme çalışmasının sonuçları

Denemeler		En Düşük SO_2 mg/Nm^3	Ortalama SO_2 mg/Nm^3	Beslenen Süre
1. Deneme	Üre Beslenen	97,031	262,391	03:12
	Normal	123,906	446,652	
2. Deneme	Üre Beslenen	118,564	420,351	07:56
	Normal	116,154	Emisyon Sınırına Yakın Değer	
3. Deneme	Üre Beslenen	172,637	401,196	25:00
	Normal	239,183	Emisyon Sınırına Yakın Değer	
4. Deneme	Üre Beslenen	176,304	387,087	10:24
	Normal	117,943	Emisyon Sınırına Yakın Değer	
5. Deneme	Üre Beslenen	154,481	298,472	14:34
	Normal	240,954	Emisyon Sınırına Yakın Değer	
6. Deneme	Üre Beslenen	156,172	397,553	24:19
	Normal	222,596	Emisyon Sınırına Yakın Değer	
7. Deneme	Üre Beslenen	310,471	443,755	21:12
	Normal	253,768	Emisyon Sınırına Yakın Değer	
8. Deneme	Üre Beslenen	270,34	459,26	6:25
	Normal	169,636	Emisyon Sınırına Yakın Değer	

Çizelge 2.’ de görüleceği üzere 3 saatten 25 saate kadar farklı sürelerde ve farklı zamanlarda üre beslemesi yapılmıştır, böylece işletme şartlarındaki değişkenlikler ile deneysel çalışmasının kararlılığı gözlenebilmiştir.

SONUÇLAR VE TARTIŞMA

Demir cevherinin sinterlemesinde baca gazı emisyonunun azaltılmasına yönelik yeni bir teknoloji olan “üre eklenmesi” deneme çalışmaları endüstriyel bir işletmede yapılmış ve sinter tesisinden salınan kükürt dioksit emisyon değerleri istenen sınırlar içinde tutulmuştur. Bu sayede birçok atık malzeme ve düşük kalite hammaddelerin harman içinde kullanılması ile üretim maliyetinin düşürülmesi sağlanırken çevreye duyarlı üretim anlayışında da devamlılık sağlanmıştır. Yapılan 20 adet deneme çalışması sonucunda, beslenen harmanın yaklaşık %0,8 ’i kadar üre beslemesi yapılmıştır ve SO_2 emisyon değerinde %25 iyileşme tespit edilmiştir. Deneme çalışması yapılan tesiste SO_2 emisyonundaki sınır değer aşımı riski göründüğünde saatlik yaklaşık 6,1 ton üre kullanımı gerçekleşmiş olup kabul edilebilir seviyelerde üre beslenmemiştir.

Çalışma öncesi ve sonrası dönem performansını karşılaştırmak amacıyla analizler yapılmıştır. Analizler yapılırken, Sanayi Kaynaklı Hava Kirliliğinin Kontrolü Yönetmeliği Ek1’ deki Kirletici Vasfı Yüksek Tesisler İçin Özel Emisyon Sınırları Ek-5’ teki Beşinci Grup Tesisler kapsamına giren Demir Sinterleme Tesisleri için mevcut bulunan yönetmelik dikkate alınmıştır. Çalışma öncesi ve sonrası dönemde yönetmelikte belirtilen hususlar için süreç yeterlilik analizleri yapılmıştır, yönetmelikte belirtilen sınır değerlere tam uyum sağlandığı görülmüştür. Çalışma öncesi-sonrası dönem sonuçları karşılaştırıldığında kükürt dioksit emisyonlarının proseste %25 oranında azaltılmıştır. Yapılan teknolojik testlerde üre beslemesinin ürün sinterde olumsuz sonuçları tespit edilmemiştir. Sinter proses şartlarına ve proses değerlerine de olumsuz yönde etkisi olmamıştır. Bu sayede daha fazla atık malzeme ve düşük kalite

hammaddeler değerlendirilerek maliyet avantajı sağlanabilir. Sonuçta yönetmeliklere tam uyum sağlanarak çevre dostu tesis anlayışında da devamlılık sağlanmıştır.

Ayrıca, yüksek fırın prosesinde yapılan gözlemlerle, üre beslemesinin olumsuz sonuçlarına rastlanılmamıştır.

Bu çalışmada İsdemir A.Ş. Sinter ve Hammadde Maniplasyon işletme tesislerinden salınan SO_2 emisyonunun yeni bir yaklaşım olan üre beslenmesi işletme uygulamaları hayata geçirilebilir. Bu çalışmalar ile SO_2 emisyonundaki sınır değer aşım risklerindeki kararsızlıkların önüne geçilebilir. Bu sayede hem ilgili yönetmeliğe tam uyum sağlanarak çevre dostu üretim anlayışı devam ettirilmiş olup hem de maliyet avantajı elde edilebilir.

KAYNAKLAR

H. Long, X. Chen, T. Chun, Q. Meng, P. Wang, Sulfur Balance Calculation of New Desulfurization Technology in The Iron Ore Sintering Process, Metallurgical Research Technology, Volume 113, Number 1, 2016

H. Long, X. Wu, T. Chun, Z. Di, P. Wang, Q. Meng A Pilot-Scale Study of Selective Desulfurization Via Urea Addition in Iron Ore Sintering, International Journal of Minerals, Metallurgy and Materials 23, 1239-1243, 2016

H. M. Long, J. X. Li, P. Wang, G. Gao, G. W. Tang, Emission Reduction of Dioxin in Iron Ore Sintering by Adding Urea as Inhibitör, Ironmaking & Steelmaking, Processes, Products and Applications, Volume 38, 2011 - Issue 4

H.Long, J. Li, P. Wang, G. Gao, J. Zhang, Reaction Mechanism of Emission Reduction of Dioxin by Addition of Urea in Iron Ore Sintering Process, The Chinese Journal of Process Engineering, Volume 10, Issue 5, 944-949, 2010

https://www.isdemir.com.tr/kurumsal/celigin-hikayesi/

Mo, C. L., A study of in-plant de-NOx and de-SOx in the iron ore sintering process, 1997

T. Chun, H. Long, Z. Di, X. Zhang, X. Wu, L. Qian, Novel Technology of Reducing SO2 Emission in the Iron Ore Sintering, Process Safety and Environmental Protection, Volume 105, 297-302, 2017.

Türkiye Cumhuriyeti, Çevre ve Şehircilik Bakanlığı, Yönetmelikler, Sanayi Kaynaklı Hava Kirliliğinin Kontrolü Yönetmeliği, RG:03.07.2009-27277

Y. Wang , L. Qian , Z.Yu, T. Chun, H. Long, X. Wu, J. Li Inhibition Behavior of PCDD/Fs Congeners by Addition of N-containing Compound in the Iron Ore Sintering, Wang et al., Aerosol and Air Quality Research, 20: 2568–2579, 2020

STATE OF THE ART BULK DOZING IN MINING

MADENCİLİKTE DOZERLE YIĞIN ÖTELEME İŞİNDEKİ EN SON TEKNOLOJİLER

M. Doktan [1,*], Y.S. İnci [2]

[1] *Mining Engineer, Brisbane*
*(*Corresponding author: m.doktan@gmail.com)*
[2]*TÜPRAG, Efemçukuru Altın Madeni*

ABSTRACT

Dozers are playing an increasing role in strip mining in Australian Opencut mining. Not only they are supporting draglines, shovels, diggers and do rehab work but also, they are widely used in bulk overburden removal reducing mining costs and Carbon Emission.

A typical strip mine in Australia starts with a cast blast followed by bulk dozing and finally dragline or digger stripping to uncover the coal. “Cast to Final” volume typically varies from 10 – 20% of the Insitu prime depending on drill and blast design and rock mass characteristics and possibly the cheapest waste removal. Dozer horizon level and dozer waste volume on the other hand depends on many other factors, including strip width, depth, cast profile, fragmentation and fluffiness of the muck pile, traction, dozer size and type and equivalent digger or dragline unit cost for the waste in question and may be 10-30% of the total waste volume. The cut off level for dozing is defined by conducting iterative slicing analysis using either 2D modelling (Vulcan, Deswik) or 3D simulation tools such as 3Ddig.

This paper sums up the current “State of the Art” developments in bulk dozing and planning in open cut mining in Australia for improved efficiency, reduced cost and hence reduced carbon emissions.

Keywords: Strip Mining, cast blast, dozer horizon level, iterative slicing analyse, cut of level, bulk dozing

ÖZET

Dozerler Avustralya Madenciliğinde yüzey sıyırma işlerinde artmakta olan bir role sahiptir. Dozerler sadece dragline, yükleyici, kazıcıları desteklemekte kalmamakta rehabilitasyon, ayrıca hafriyatın uzaklaştırılması işlerinde madencilik maliyetini ve karbon salınımını düşürerek, yaygın olarak kullanılmaktadır.

Avustralya’ da yüzey sıyırma işi tipik olarak öteleme-dökme patlatması ile başlar ardındanda dozerler ile sıyırma, dragline ile kazı sıyırması ile kömür yüzeyi açığa çıkarılır. Nihai duruma ötelenen-dökülen malzemenin hacmi, delme-patlatma dizaynı ve kaya kütlesinin karekteristiklerine bağlı oarak, yerindeki hacmin %10-20’ si oranındadır ve işin bu kısmı pasa uzaklaştırma işinin en ucuza mal olan kısmıdır. Diğer yandan dozerle yapılan sıyırma işine ait yüzey ve hacim miktarı, dilim genişliği, derinliği, döküm profili, yığın malzemesinin kırılganlığı, kabarması, dozer gücü ve boyutu ve muadili bir kazıcı veya dragline’ ın birim maliyetine bağlı olarak, toplam pasa hacminin %10-30’ u dur. Dozer ile yapılacak işin durdurulacağı seviye 2D modelleme (Vulcan, Deswik) veya 3DDig gibi 3D simülasyonları kullanılarak belirlenir.

Bu bildiri, Avutralya Açık Ocak Madenciliğinde kullanılan ve maliyet ile karbon salınımında düşüş sağlayarak verimliliği artıran dozerler ile yüzey sıyırma işi ve planlanmasına ait en son teknolojik gelişmeleri anlatmaktadır.

Anahtar Sözcükler: Dilimli madencilik, öteleme-dökme patlatması, dozer basma seviyesi, ardışık dilimleme analizi, duruş seviyesi, dozerle yığın öteleme

INTRODUCTION

Bulk dozing is a significant component of strip mining in Australia and many parts of the world. Properly designed and implemented, it would have significant cost benefits compared to other stripping methods (Figure 1).

Figure 1. Typical Bulk Dozing in an Opencut mine

A typical strip mine takes advantage of cast blasting techniques to move 10-20% of the Insitu material to its final position. The resulting profile then is either generally dozed to either fully up to coal roof or to a predetermined level. Then the rest of the waste can be taken as postrip by a digger fleet uncovering coal. Prestrip, Doze, Postrip proportions of the cast waste need to be defined precisely by the dozer engineer to minimize the waste removal cost. If draglines are used as the last pass, then the cut off levels need to be defined for draglines working range. The method is collectively called “Cast, Doze and Excavate” or CDX (shown in Figure 2 and 3).

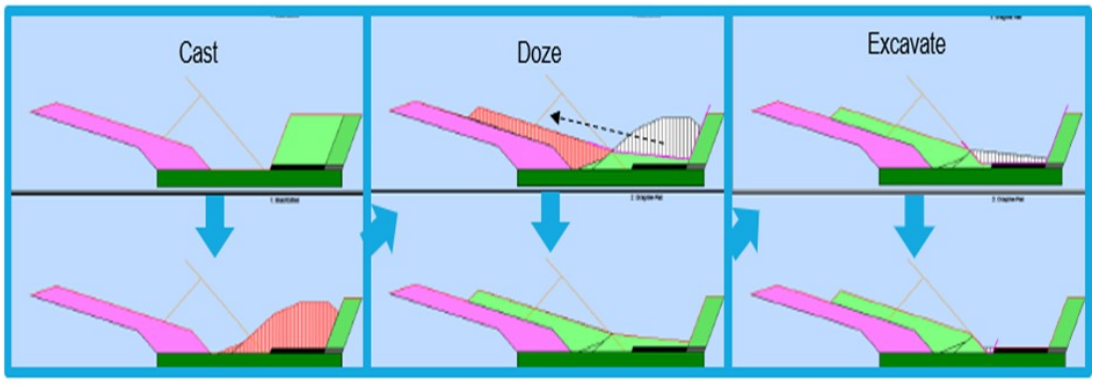

Figure 2. “CDX” or “Cast-Doze-Excavate” Process

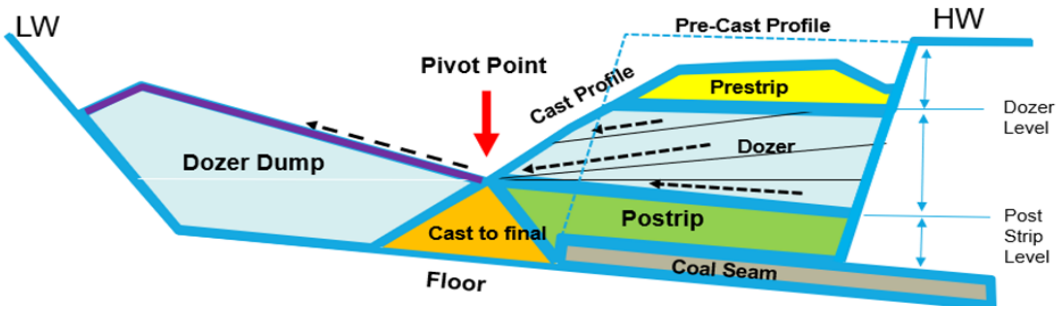

Figure 3. Prestrip, Doze and Postrip Levels and Typical Mining Sequence

Doktan (1998) has conducted an industry wide research on the status of bulk dozing in Australia and the world as part of an ACARP project. He has identified further opportunities for bulk dozing in coal mines, developing a calculator to estimate dozer push and rip productivity based on first principals. In an open cut mine, generically speaking, dozers can benefit from the unit cost gap between the cast and dig & haul processes (Figure 4).

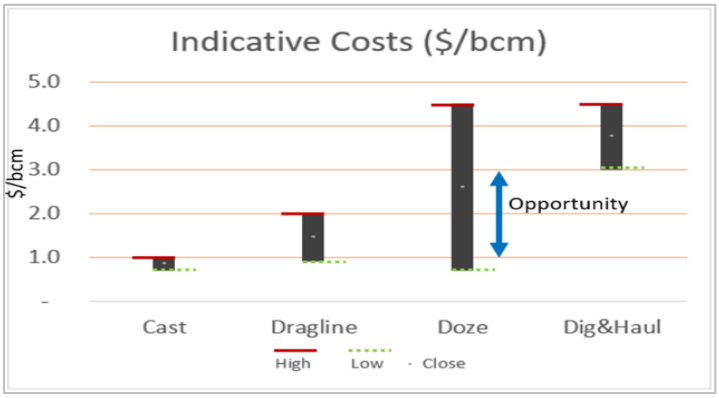

Figure 4. Example typical stripping unit costs at a strip mine with the cost gap opportunity for dozing

Sinclair (2019) has conducted a comprehensive study and proved the cost effectiveness of an excavator side casting on the highwall in a dozer operation compared to dozer side cutting.

Remote dozing technology that allows a single operator to control multiple machines from a remote operator station is already in use at several sites across Australia. The system has been delivering consistent results and high productivity. Fortescue Metals Group in Western Australia has also been trialling remote dozing technology since October 2019 and has now successfully implemented in their operations. They claim to have achieved 15% or more increases in utilisation and productivity.

While remote dozers are successfully operating, significance of fully autonomous dozers are rapidly increasing due to increased demand for mining products and Net Zero Emission commitments in mining.

Kulkaev, 2021 developed a novel mathematical framework called the two-level hierarchical search algorithm. It was found that constraints on bulldozer operations is often non-linear and finding an approach to address them can be crucial to developing a computationally feasible planner. Additionally, the search space would grow exponentially with the number of terrain discretisation (i.e. the accuracy at which the terrain is being represented in the model), and how far ahead the

model is planning. An accurate estimation of the volumetric capacity is also a crucial parameter as a small deviation can drastically alter the optimal solution.

The University of Queensland (McAree, 2021) and a prominent dozer manufacturer are now trialling fully automated STAM dozer technology at a QLD coal mine site. Remote or fully autonomous dozers are soon to be part of regular operations in Australia and mining companies are looking at reducing their costs and increase dozer utilizations through fully autonomous operation.

Various path planning algorithms and methodologies with minimal operating time have been developed for fully Autonomous dozers (Hirayama et all,2019).

COST DRIVERS in BULK DOZING

Cost effectiveness of bulk dozing is dependent on several factors. These can be broadly classified into design, material and work conditions and may include but not limited to hourly operating costs, push and reverse distances, grades, dozer rehandle, soft or hard wall conditions, highwall cutting methodology, dozer tactics, pivot point location, dozer/blade size and capacity, traction, fragmentation, fluffiness, elevation, and operator experience. Out of all these and assuming similar work conditions, the push tactics is the most important and can be optimized to suit the geometry and mining conditions at site for the maximized return of investment. To that end, most companies in Australia have developed a “Dozer Management Plan” which covers site specific dozer design and operational practices and “How to Guides”.

Dozer hourly operating costs can be built from first principals and forms an important component of an optimization study. This would normally incorporate cost items such as and similar to the digger& haulage fleet hourly cost, operator costs, fuel, amortisation, GET, other consumables and maintenance costs.

While dozer hourly operating cost may be fixed, the dozing unit cost ($/bcm “Dozed to Final” -DtF) varies based on rehandle, push and reverse speeds and grades. Dozer prime productivity drops asymtothically with longer and steeper pushes. The design therefore should try to minimize rehandles, push distances and grades through smarter design tactics.

DOZER TACTICS (PUSH DESIGN AND PLANNING)

A typical dozer push design involves several steps and usually an iterative and evolving process. Figure 5 below demonstrates the process at high level and in workflow diagram format.

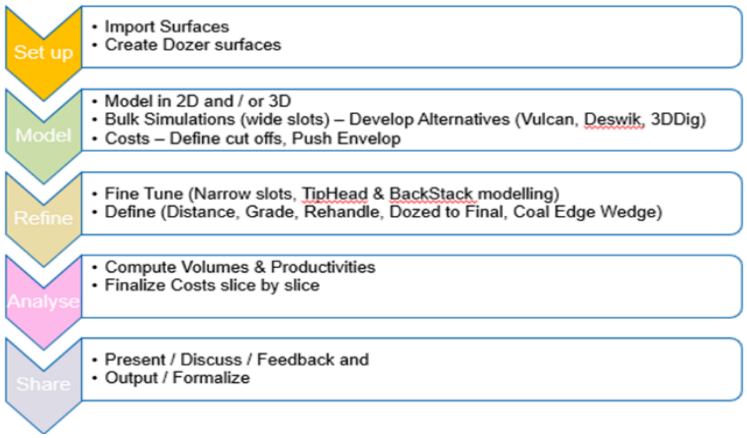

Figure 5. Typical Workflow in Dozer Planning

Dozer engineer builds a project data folder including the following items: Pre-cast and Post-cast surfaces, Roof & Floor surfaces (including mid burdens), mine design data (New Highwall, Lowwall and Endwall, Ramps, Roads, Accesses and Bridges, Strip and Block lines, Structural data). A number of equally spaced sections are cut using Vulcan, Deswik or 3DDig and are then studied for physical dozing limits such as rehabilitated areas, Endwalls, lease limits, offsets and any risk areas, or structural challenges such as intrusions, faults, and structures. At this stage, a decision is made and agreed on whether to use a 3D or 2D modelling tool. If the geology or mining geometry is complicated and/or if it is a short-term design then 3D modelling should be used.

Once potential dozing limits are established, and mining & geological conditions are understood, equivalent dig & haul costs are estimated using strings constructed from "dig point to dump location" and site's cost matrix. The "Rise and Run" (R&R) unit costs for the proposed dozing location should be estimated, if possible, in 5m height increments. These costs provides a roof line for dozing costs may go up to (Figure 6). Then several sections are created perpendicular to the strip lines an at regular intervals for volume balance and to establish push limits and potential split between prestrip, dozer and postrip. Each section is then divided into several slices, slice lines passing through the Pivot Point" and in a fanning manner.

The maximum slope of the steepest slice should not exceed 26% (or a site specific defined & tested grade) downhill (or uphill). It is important to keep push slices downhill as much as practical to utilise gravity for the dirt in front of blade roll down. Then using centroid to dump point push distances and grades, dozer productivities for each slice are estimated. Productivity and rehandles, dozer hourly costs are then used to calculate dozer unit cost for "Dozed to Final" volumes (DtF) and compared with the equivalent digger fleet R&R costs.

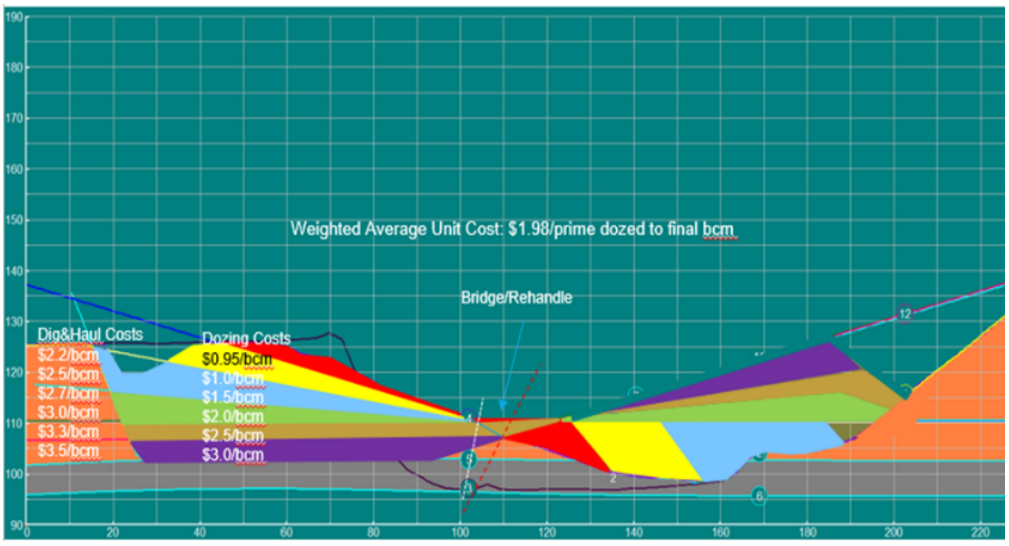

Figure 6. Rise&Run (R&R) costs for digger fleet and Calculated Dozing Costs (DtF)

Based on these numbers, a decision is made to define the cut off level for dozing for each slide and finally a combined surface is created from all sections.

Tipheading

Tip heading refers to pushing waste downhill and tipping ahead of dozer creating a flat surface as seen in Figure 7 below. The maximum downhill grade is a site and muckpile dependent parameter and needs to be defined by a site trial program but usually less than 26%. The idea of

maximizing tipheading in any dozer operation comes from the fact that the gravity helps to reduce drawpull force required to push the same dirt on a flat surface and speed ups the dozer. It is in some cases ideal to raise the pivot point to maximize tiphead volume while incurring a slight increase in rehandle.

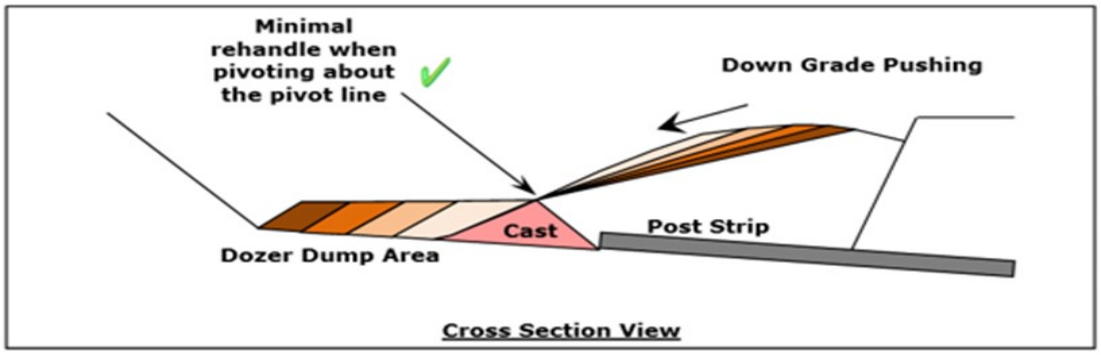

Figure 7. Simplified Tipheading

Backstacking

Backstacking is on the other hand involves dozing the lower section of HW in slices and stacking the dirt in inclined surfaces in the lowwall side past the Pivot Point (Figure 8) . Gravity is working against the push, hence Backstacking is naturally lower in productivity and needs to be minimized as much as possible. Backstacking is done in successive cuts and dumps moving away from the pivot point towards HW.

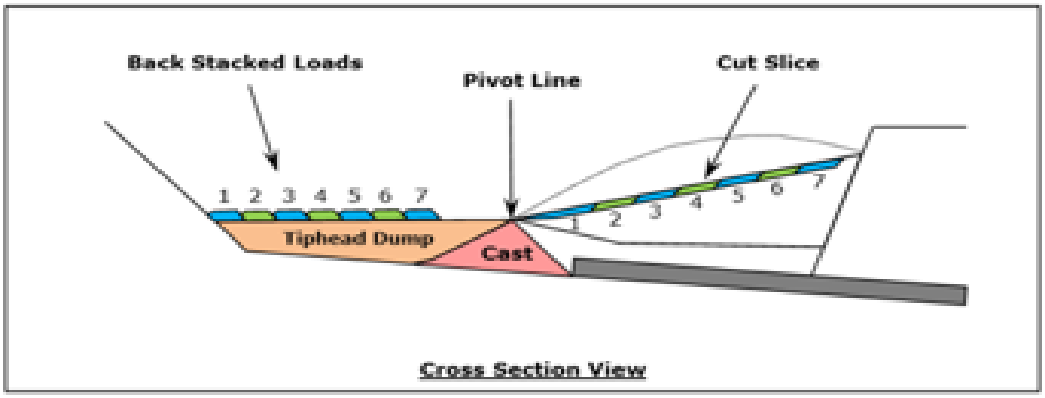

Figure 8. Typical Backstacking

Slot Dozing

Slot dozing has been proved to be 10-15 % more productive compared to surface dozing. Slot walls prevent material spilling from the side of the blade and hence keeping full blade along the push. Slot walls are usually as high as blade and removed at the end of completion of each slot as rehandle.

Defining Dozer Push Limits/Envelop

The cost effectiveness of CDX mining (or dozer push alone) is related to the waste allocation and hence defining splits precisely. Then question is asked when to stop dozing? The answer lies in another question which is:

"What should be the dozer productivity to achieve a cost breakeven point with the digger fleet?"

When you reach to that point (digger unit cost = dozer unit cost), dozing is no longer cost beneficial and hence postrip (dig&haul) needs to be considered.

To this end, a process (Figure 9) and unique "Dozer Push Limit Calculator" has been developed as part of this study. The process of defining dozer limits involves dividing dozer area (cast) into a number sub regions represented by a section and each section into a reasonable number of slices. Then productivity and cost can be estimated for each slice until equivalent digger cost is reached. These can be done using Vulcan or 3DDig (Figure 10).

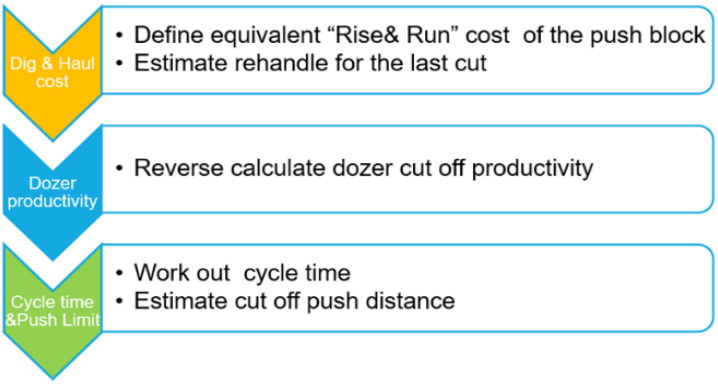

Figure 9. High Level Process to Define Dozer Push Limits or Envelop

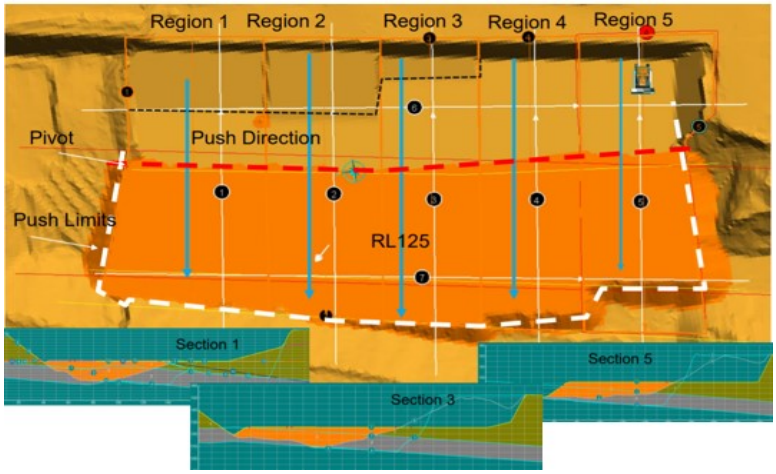

Figure 10. Defining Dozer Push Envelope

Slicing Analysis

When the mining conditions allow 2D slicing method using software such as Vulcan or Deswik can be used to assess the viability of dozing and define the cut off limits. This is particularly suitable for Long term and Midterm planning purposes. The method involves creating several section

lines along the pit and then each section is divided appropriate number of slices (Figure 11 and 12) and volume balance for each slice is obtained. The push parameters such as distance and grade are recorded and used for productivity estimate using a spreadsheet model. This method is quite manual and may requires a set of iteration to reach the goal.

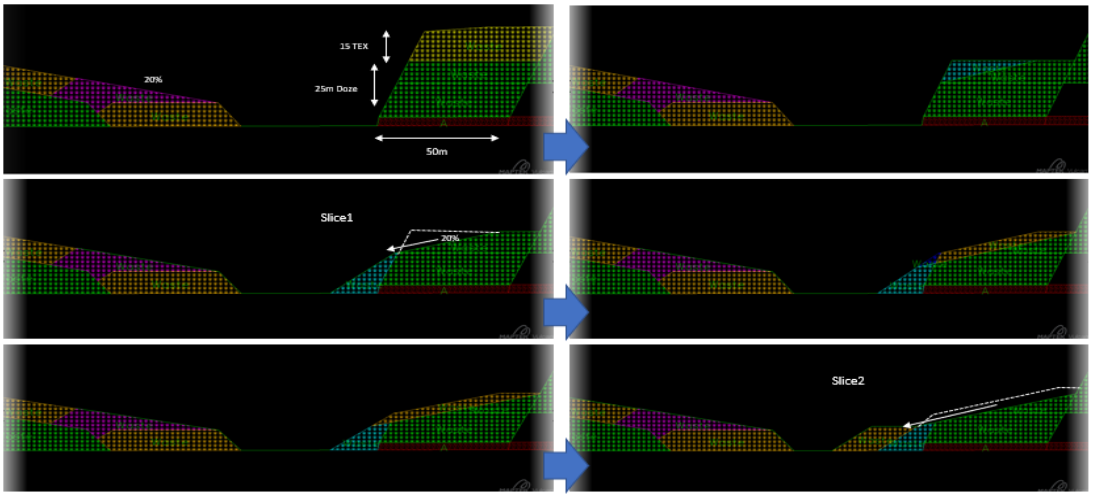

Figure 11. Slicing Method – 1

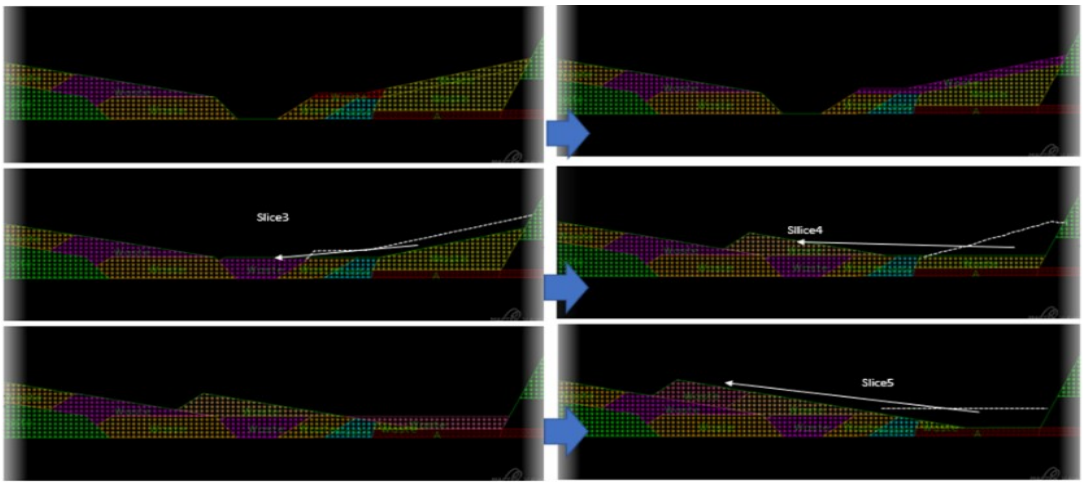

Figure 12. Slicing Method – 2

Pivot Point and Importance

Pivot point or Pivot Line is a conceptual point (or line) along push profile (usually at around midway more towards LW side) which separates dig or cut area from dump area and where push grade break point occurs. It is often accepted or defined as intersection of cast profile with a line draw from coal toe at the appropriate undercut angle (low pivots are at 45°or raised ones are at or up to 90° measured from LW floor). These are usually accepted as standard at each site and commonly not modified or optimized according to the muckpile profile for each cast. This may however result in higher rehandle, reduced dump space or reduced tiphead volumes. It is hence important to optimize pivot point at each section according to cast profile and volumetric balance for each cast.

Rehandle in Bulk Dozing

The primary objective in bulk dozing is to move prime material to its final location in a safe and cost-effective manner. But doing that as with other mining equipment, some rehandle inevitable occur. The rehandle in dozing can be classified into two categories:

Operational

- Establishing pads
- Establishing slots
- Removal of slot walls
- Cutting Highwall
- Dirt Spilling side of blade

Sectional

- Building bridge
- Tipping ahead to ride on

Operational rehandle in dozing cannot be physically measured by surveys and only discernible to the dozer engineer or to the dozer operator. On the other hand, still not measured by surveys, the sectional rehandle (Figure 13) can be easily estimated by the dozer engineer.

If rehandle is not considered and productivities are estimated based on pre and post dozing surveys, a much lower dozer (total) productivity estimate is obtained. Experience indicates up to 30% dozer rehandle may incur if the design is not detailed enough and not due attention paid to minimizing it.

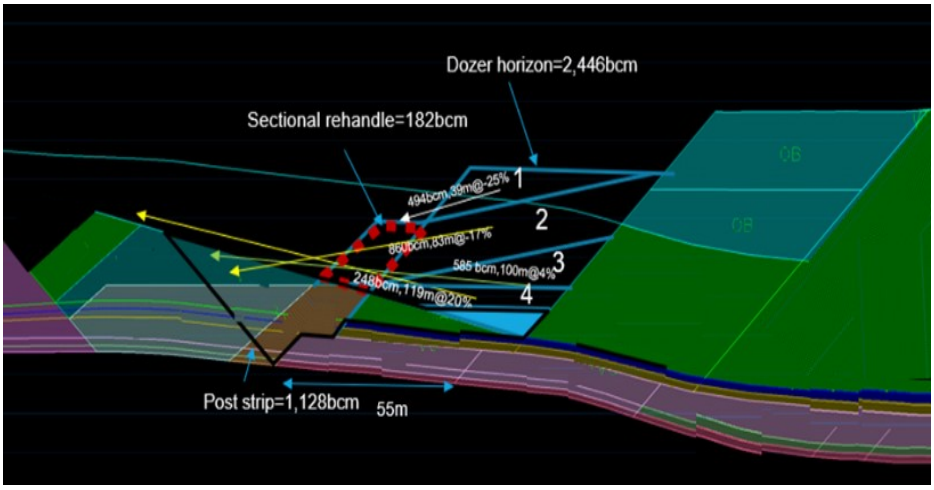

Figure 13. Sectional Rehandle

Cast Profile

Cast blast is the cheapest way of moving dirt and often operations try to maximize it. However, it must be noted that if the cast profile is lowered below certain level to maximize cast, the

dozing may become costly as the tip head component of the push is significantly reduced and the benefits from the additional cast can be cancelled out by the increase in dozing cost.

3DDIG MODELLING TOOL & SIMULATIONS

It is important to identify the differences in 2D and 3D planning. In long term or midterm schedules, 2D approach may possible be appropriate provided there is no significant anomaly exists in the existing mining conditions or geology. For short term planning and implementation, a 3D dimensional approach needs to be adapted. A typical pit may have some significant complications due to intrusions, faults, seam rolls, buffer requirements, bridges, ramps (LW and HW) and access logic. Hence relying on sectional models will not suffice on its own and these need to be supported and verified by 3D models.

The Earth Technology's Dozer Simulation Module of 3DDig offers a set of modelling tools where a bench can be cast blasted, swelled to appropriate swell factors, and dozed in a way the user defines. The riling of material and volume balance are simulated close to reality. It also offers manual or automatic slot generation facilities (Figure 14).

Figure 14. Modelling Dozing in 3DDig (Post-Doze surface)

MONITORING AND RECONCILIATION

In order to reconcile and improve dozer design and planning, dozer engineers need to be able to monitor and measure how dozers are performing at least 1/3 and 2/3 of the implementation if not all the time. While this can be done through conventional surveying or drone scanning, surface surveys do not provide sufficient data on its own to assess the ongoing performance. The current instrumentation and data capture systems (IControl, IVolve or Blueview) (Figure 20) on the other hand, although they provide some indication, do not provide KPI data that are necessary to assess and improve the performance of the dozing either. These KPIs include dozer push direction, push grades, push distance, cycle time (forward and return) and dozing speed in both ways.

A unique automated data acquisition and reporting system has been developed by the primary author of this paper and data science engineers. The reporting system generates all these KPIs automatically in a standardized format and on a shift basis (Figure 15,16 and 17).

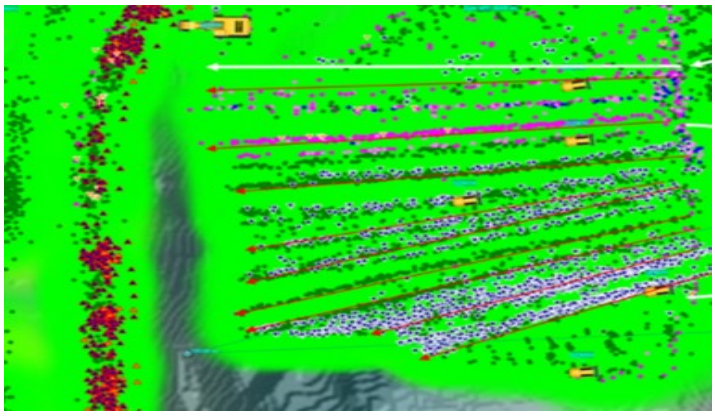

Figure 15. Example of Spatial data of Operating Dozers (GPS Locations)

The following KPIs are reported for each dozer and summarized automatically as a shift report.

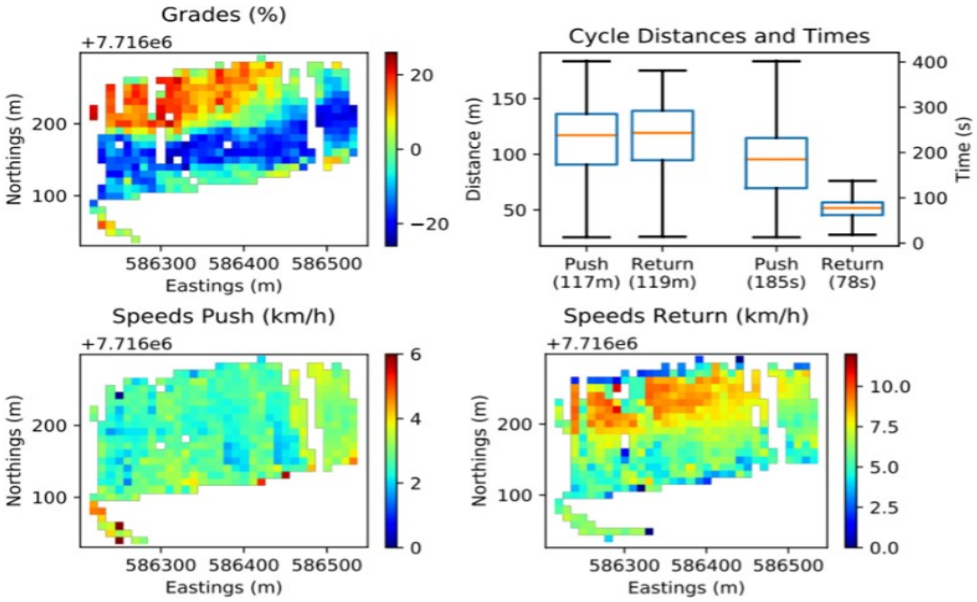

Figure 16. Automatic Reporting of Dozer KPIs-1

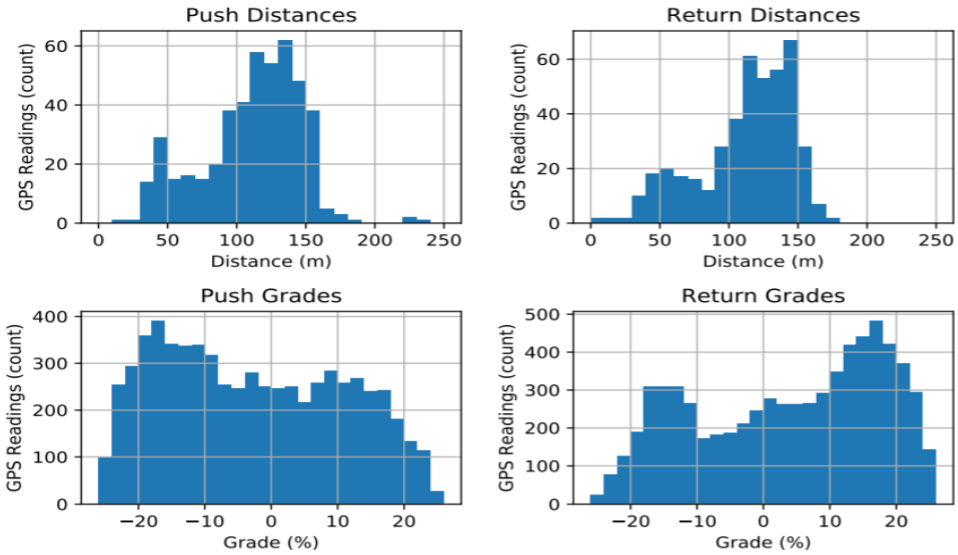

Figure 17. Automatic Reporting of Dozer KPIs-2

DOZER MANAGEMENT PLAN

The scope of a site specific "Dozer Management Plan" should ideally include but not limited to the following documents and processes:

- Detailed list of site specific cost drivers in dozing & how to manage them
- Guidelines to define maximum push distances and grades for each waste horizon and
- How to create cost efficient dozing envelops
- Site specific documenttaion where to use 2D and 3D modelling tools
- Step by step process how to define dozer and digger fleet cut off
- Ways to maximize dozer waste while still staying economic
- Guidelines to optimize Pivot point location and how to vary its position
- Identifying the sources of rehandle in dozing and ways to reduce them
- Step by step "How to Guides" for design and planning
- Criteria for wall cutting with a small digger
- Demonstrating the impact of Cast profile and fragmentation on dozer productivity
- Discussing available tools to measure dozer performance real time (or near real time)
- Providing examples of the use of a calculator for dozer operators to define dozing limits (cycle time calculator)
- Dozer operator training manuals & schedule
- Dozer related TARPs and safety manuals

A recent successful installation and implementation of a "Dozer Management Plan" at a mine site resulted 20% increase in productivity and cost reduction in dozer stripping.

Every site with a dozer fleet needs to develop site specific "Dozer Management Plan" to help engineers and operations people to maximize the benefit from dozing.

CONCLUSIONS

Dozers are being increasing used in open cut mining due to their flexibility, low capital cost and low operating costs. They also help reduce "Carbon Emissions" in mines simply by reducing Truck

Excavator Fleet (TEX) requirements at a given operation. A set of novel methodologies, processes, and tools (calculators) have been developed and presented here to help dozer engineers plan, design, and implement a cost-effective and low emission dozer operation at their respective operations.

REFERENCES

Doktan, M. 1998. Optimization of Dozer Operations in Open Cut Coal Mines, ACARP Project Report. Brisbane.

Doktan, M. 2020-21, Various Dozer Projects Unpublished. Brisbane.

Hirayama, M., Whitty, J., Katupitiya, J., Guivant,J., 2018. An Optimized Approach for Automatic Material Distribution Operations of Bulldozers. International Journal of Advanced Robotic Systems 15 (2).

https://im-mining.com/2018/06/30/mining-contractor-wolff-first-australia-see-benefits-cat-command-dozing/

https://im-mining.com/2021/06/21/australian-first-demonstration-remote-dozing-fmg-display-resources-technology-showcase/

Kulkaew, P. 2021. Optimisation of bulldozer earthmoving plans. PhD Thesis, School of Mechanical and Mining Engineering, The University of Queensland.

McAree,R. 2019. Personal Correspondence, School of Mechanical and Mining Engineering, The University of Queensland.

Sinclair, N. 2016. A Cost Benefit Analysis of comparing Dozer Side Cutting and Excavator Side Casting Techniques on The Highwall in a dozer bulk Push Operation, The UQ Honours Thesis. Brisbane.

SURFACE CHEMISTRY OF THE LOCKED PARTICLES FOR SULPHIDE MINERALS

SÜLFÜRLÜ MİNERALLERDE BAĞLI TANELERİN YÜZEY KİMYASI

D. İzerdem

Hacettepe Universitesi, Maden Muhendisligi Bolumu
(damlagucbilmez@hacettepe.edu.tr)

ABSTRACT

The electrochemical methods have been used in flotation of sulphide minerals by utilizing the semiconductor properties of the minerals. Electrochemistry is one of the tools that can be preferred to identify problems in flotation systems faster and to achieve more effective flotation results. In this study, some of the electrochemical methods such as open circuit potential (OCP), cyclic voltammetry (CV), and electrochemical impedance spectroscopy (EIS) were used to determine the galvanic interactions between locked and liberated sulphide particles. As it was assumed that the surface area of the sulphide minerals effects the flotation characteristics, some mineral electrodes were prepared to simulate this phenomenon. For this purpose, a three-electrode system was set up to investigate the electrochemical responses of galena-pyrite (0.52 cm^2), pure galena (0.20 cm^2) and pure pyrite (0.18 cm^2) minerals. The tests were carried out in a buffer solution at pH 9.2. The changes of the surface chemistry of the minerals, with (10^{-4} M NaEX) and without collector, were also examined. During the process, charge transitions between the minerals were occurred due to the galvanic interactions regardless of the surface area and changed the flotation behavior of these minerals by reducing and oxidizing each other.

Keywords: Electrochemistry, sulphide minerals, surface chemistry

ÖZET

Flotasyonda elektrokimyasal yöntemler, sülfürlü minerallerin yarı iletken özelliklerinden yararlanılarak kullanılmaktadır. Elektrokimya, flotasyon sistemlerindeki problemleri daha hızlı tespit edebilmek ve daha etkili flotasyon sonuçlarına ulaşabilmek için tercih edilebilecek araçlardan biridir. Bu çalışmada, bağlı ve serbest sülfürlü taneler arasındaki galvanik etkileşimleri belirleyebilmek için, açık devre potansiyeli (OCP), voltametrik (CV) ve empedans (EIS) ölçümleri gibi bazı elektrokimyasal yöntemler kullanılmıştır. Kazanılmak istenilen sülfür minerallerinin yüzey alanının, flotasyon özelliklerini etkilediği düşünüldüğünden, hazırlanan mineral elektrotlarıyla çeşitli deneysel çalışmalar yapılmıştır. Bu amaçla, galen-pirit (0.52 cm^2), saf galen (0.20 c cm^2) ve saf pirit (0.18 cm^2) minerallerinin elektrokimyasal tepkilerini araştırmak için üç elektrotlu bir sistem kurulmuştur. Testler, pH 9.2'de bir tampon çözelti içinde gerçekleştirilmiştir. Minerallerin yüzey kimyasındaki değişimler, toplayıcılı (10^{-4} M NaEX) ve toplayıcısız olarak da incelenmiştir. Uygulama sırasında, yüzey alanından bağımsız olarak, galvanik etkileşimler nedeniyle mineraller arasında yük geçişlerinin meydana geldiği ve bu minerallerin birbirlerini indirgeyerek veya yükseltgeyerek flotasyon davranımlarını değiştirdiği gözlenmiştir.

Anahtar Sözcükler: Elektrokimya, sülfürlü mineraller, yüzey kimyası

INTRODUCTION

Most of the sulphide minerals have semi-conductive properties. Thus, surface changes and reagent adsorptions occur mainly through electrochemical mechanisms (Ekmekçi, 2008). Electrochemical properties of these minerals enable them to be used as electrodes (Peters, 1977) so electrochemical techniques can easily be applied to these minerals.

Electrochemical methods are faster to evaluate surface responses and low cost compared to the other techniques. Some of the most common electrochemical techniques used in the sulphide minerals are open circuit potential (OCP), cyclic voltammetry (CV), electrochemical impedance spectroscopy (EIS).

Open circuit potential is a method that is often used to find the resting potential of a system. In sulphide mineral flotation, OCP measurements are useful for monitoring changes either in the liquid phase or at the mineral/solution interface.

Cyclic voltammetry is one of the most common electrochemical methods used to determine the reactions on the surface of sulphide minerals. In this technique, the potential of the mineral electrode is varied linearly at a desired rate using a potentiostat. When a current peak is observed during potential scanning, it can be used to identify the undergoing reaction.

Electrochemical impedance spectroscopy (EIS) is based on measurement of conductance and resistance at of the electrode surface to the electrical current flow and it can be used to determine the species formed on mineral surfaces regardless of the reaction type (Zhao, Guo, Peng, & Mai, 2017). This method is used for characterization of solid/liquid interfaces. As the formation of non-conductive layer of oxides, hydroxides, elemental sulphur or collector reagents cause increase in resistance, the EIS method can be combined with the floatability of sulphide minerals.

Since the mineral-collector interaction is electrochemical in nature, a sulphide mineral can be measured by the above-mentioned electrochemical techniques. The electrochemical methods can only be used successfully if there is measurable electron transfer due to adsorption of collector molecules at mineral electrode surface. EIS can successfully be used to measure adsorption of different types of collectors on mineral electrode surface.

The effects of the locked particles on flotation are thought to depend on the surface area of the mineral to be recovered (Vianna, Franzidis, Manlapig, Silvester, & Ping-hao, 2003). However, galvanic interactions between minerals are observed in the locked particles, regardless of the area (Liu, Li, & Zhou, 2009). Due to the galvanic interactions, charge transitions between minerals are observed. So that, they reduce and oxidize each other which results the change in the flotation behavior (Urbano, Meléndez, Reyes, Veloz, & González, 2007). Investigating the galvanic interactions of the sulphide minerals by electrochemical techniques have been studied by many researchers (Mielczarski & Mielczarski, 2003; Moslemi, Shamsi, & Alimohammady, 2012; Rao & Finch, 1988).

In this study, open circuit potential (OCP), cyclic voltammetry (CV) and electrochemical impedance spectroscopy (EIS) techniques were performed in an alkaline solution (pH 9.2), where the galena and pyrite electrodes were used to simulated free particles. Galvanic interactions occurring between the minerals and their effects on the surface chemistries were investigated by simulating the locked particle behavior. For this purpose, mineral pieces of galena and pyrite were paired to be in contact with each other and prepared

binary-bounded mineral electrodes. Effects of the addition of collector (NaEX) to possible surface reactions were also studied.

MATERIALS AND METHODS

Sulphide ores are adequate to get some reasonable electrochemical responses according to their natural semi-conductor properties. For better electrochemical responses, it is known that the sulfide content of a mineral sample should be high. For this purpose, mineral electrodes composed of high purity sulphide ore samples (pure galena and pure pyrite) were tested to investigate the surface characteristics, in this study.

Mineral electrodes (working electrodes) were prepared by cutting a rectangular cross section of the minerals (0.18-0.80 cm^2 surface area) from a massive mineral specimen, mounting the mineral piece into an electrochemically inert epoxy resin and placing it in a glass tube. The mineral electrode was connected to a potentiostat by a copper wire.

Two sulphide minerals were also adhered to one another to simulate the locked particle behavior, besides single use of mineral piece in a mineral electrode. For this purpose, galena-pyrite mineral electrode was prepared. The mineral percentages of the mineral electrodes are given in Table 1.

Table 1. Mineral contents and the surface areas of the mineral electrodes

Electrodes	Galena (%)	Pyrite (%)	Surface Areas (cm^2)
Galena El.	100	-	0.20
Pyrite El.	-	100	0.18
Galena + Pyrite El.	50	50	0.52

After each experiment, the surfaces of the mineral electrodes were polished by alumina paste to remove any kind of contaminants for the next electrochemical process. The electrode was rinsed with distilled water and immediately transferred to the cell after polishing the surface.

Gamry Reference 600 model potentiostat was preferred to perform electrochemical techniques in this work. To isolate the system form the outer noises, the potentiostat was placed in a Faraday cage. A conventional three-electrode electrochemical cell was used throughout the tests. A saturated calomel electrode as reference electrode, a platinum plate electrode with 1 cm^2 area as counter electrode and mineral electrodes (galena, pyrite and galena + pyrite) were used in the electrochemical cell.

All electrochemical experiments were performed in a buffer solution of pH 9.2 (0.05 M $Na_2B_4O_7 \cdot 10H_2O$) and at room temperature (~25 °C). Buffer solution was used to keep the pH value at the same level during the measurements and to prevent possible pH changes as a result of the reactions between the minerals and the solution. Prior to each run for 15 minutes, high purity nitrogen gas was introduced to the cell for intensive bubbling through the buffer solution to eliminate the fluctuations during measurements due to oxygen presence in the system. During the electrochemical measurements, nitrogen flow was ended and the cell was completely sealed to prevent the diffusion of any atmospheric oxygen into the system.

The electrochemical methods were studied in the absence and presence of 1×10^{-4} M sodium ethyl xanthate (NaEX) to investigate the possible electrochemical reactions upon adsorption of the collectors on the minerals.

In this study, the electrochemical techniques such as Open Circuit Potential (OCP), Cyclic Voltammetry (CV) and Electrochemical Impedance Spectroscopy (EIS) were tested to investigate the changes in the surface characteristics of locked and liberated particles.

RESULTS AND DISCUSSION

The electrochemical responses of the mineral electrodes (galena and pyrite) were studied in the absence of collector by three methods; open circuit potential, cyclic voltammetry and electrochemical impedance spectroscopy tests. To observe oxidation/reduction reactions between the locked particles and their possible galvanic interactions, two mineral pieces (galena + pyrite) were glued together so that one more mineral electrode was produced. Adsorption of 1×10^{-4} M sodium ethyl xanthate (NaEX) collector was also investigated in all the above-mentioned mineral electrodes by using the same techniques.

The OCP Method Results

Open circuit potential measurements of the samples were performed to compare their electrochemical reactivity in the presence and absence of the collector. The OCP values were recorded continuously for 20 minutes (Figure 1).

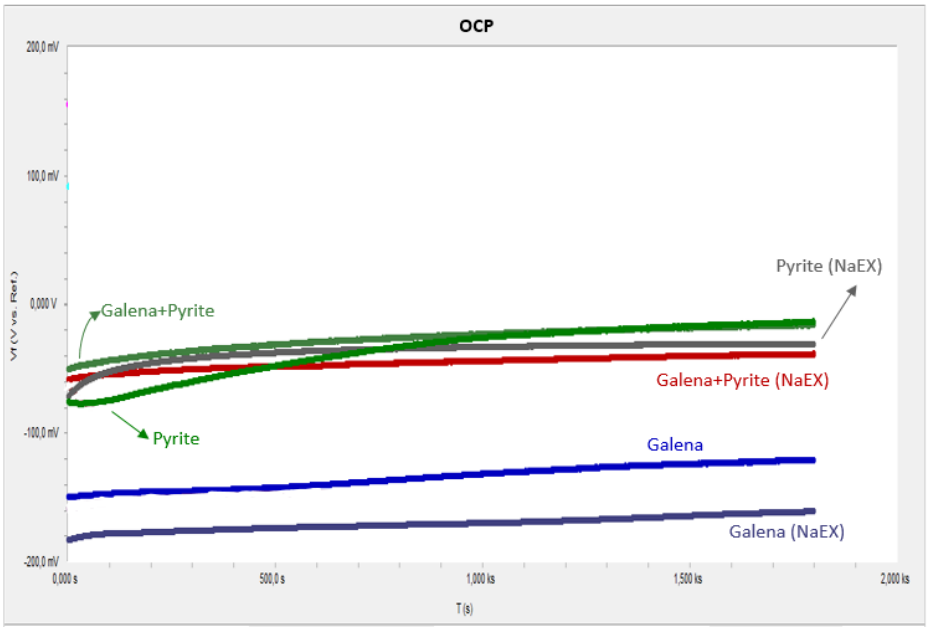

Figure 1. Open Circuit Potential measurements

According to the OCP results, galena mineral itself has lower potential values than being associated with pyrite mineral. However, pure pyrite mineral showed similar potential values as galena + pyrite locked particle after a while during the potential measurements. This indicates that different minerals have varying electrochemically reactive surfaces under significant conditions.

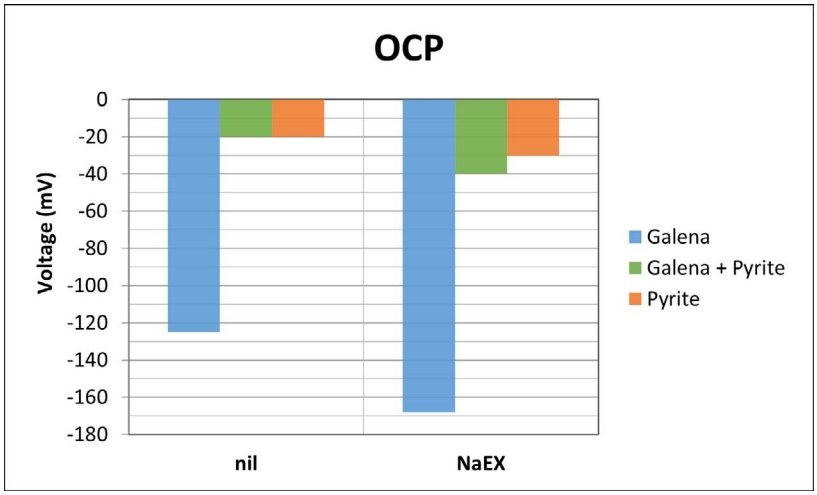

Figure 2. A schematic view of the OCP comparisons of all the studied minerals in the presence and absence of the collector (nil: absence of collector, NaEX: collector)

In Figure 2, the OCP changes of the minerals in all conditions are presented. According to this, the voltage values decreased regardless of the mineral type when there was collector in the system. To reveal the surface characteristics of the mineral electrodes, further tests such as CV and EIS were conducted.

The CV Results

Comparative voltametric studies were performed to identify galvanic interactions. Figure 3 and Figure 4 show voltammograms of the mineral electrodes in the absence of collector and in the presence of 1×10^{-4} M NAEX. In the voltammogram obtained from the collectorless condition, galena had very narrow response interval in terms of current density throughout the studied potential range (-0.80 V to +0.40 V). When the scan potential was initiated in positive direction in the presence of collector, an oxidation process was observed with one small peak that begins near 0.20 V value. This indicates the oxidation of galena to form PbX.

In the voltammograms of the pyrite electrode, as the scan potential becomes negative, a reduction peak was observed at nearly -0.450 V both in the presence and the absence of collector. More apparent peak in the oxidation phase was observed at -0.365 V with collector.

In order to identify different processes in the locked particles, involving the oxidation of galena, voltametric studies were carried out using galena + pyrite mineral electrode. Typical voltammograms of the positive scans on these electrodes were shown in Figure 4.

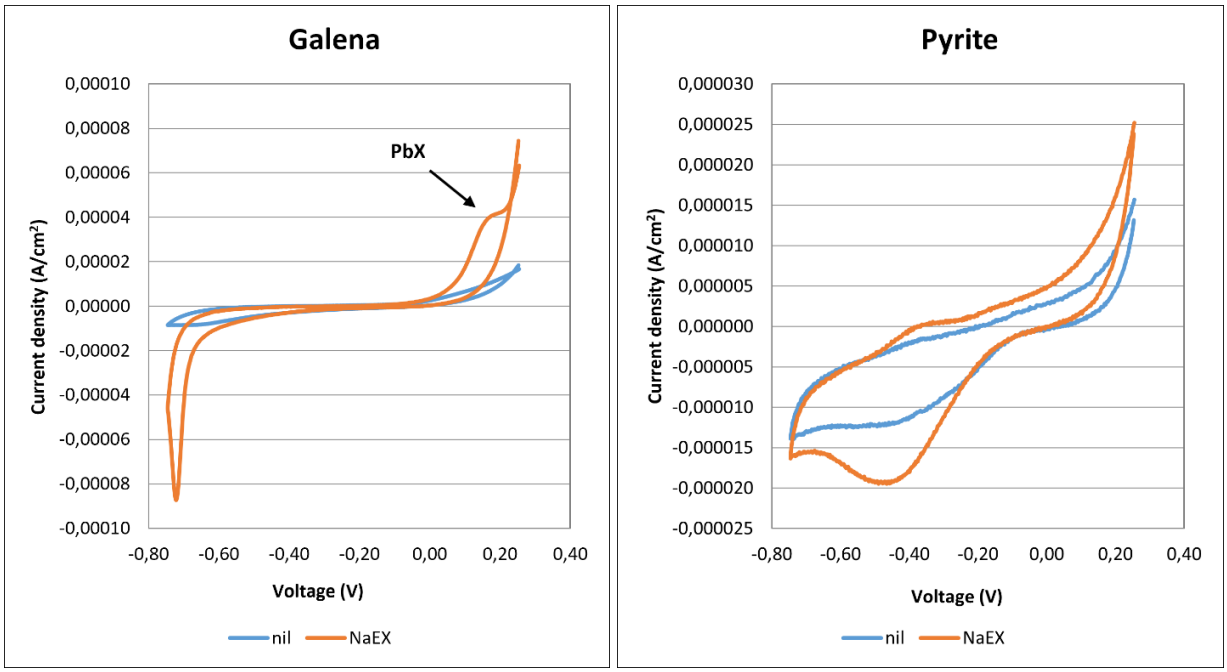

Figure 3. Cyclic voltammograms of galena (left) and pyrite (right) minerals in the presence and absence of the collector

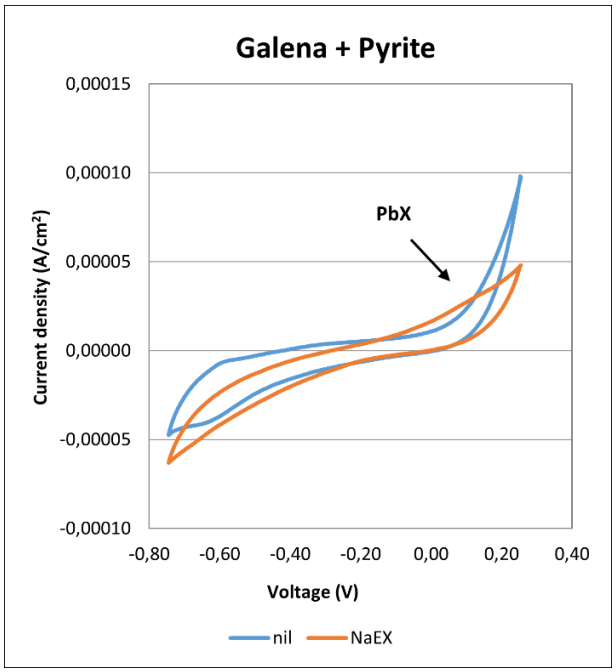

Figure 4. Cyclic voltammograms of galena + pyrite mineral electrode in the presence and absence of the collector

The peak in the galena + pyrite electrode is related to the formation of PbX on the electrode surface by anodic oxidation of galena with the collector. The analysis of the voltammograms obtained in those

conditions showed that the galena oxidation was associated to peaks at 0.20 V and 1.20 V in the mineral electrodes of galena and galena + pyrite electrodes, respectively.

The EIS Results

Differences between the surface characteristics of the studied mineral electrodes were also demonstrated by EIS measurements. The EIS experiment results of different mineral samples are given as Bode diagrams in the form of Phase Angle and Magnitude plots in Figure 5 and Figure 6, respectively.

When the Bode diagrams are evaluated at the lowest frequency (0.01 Hz), it was observed that the galena electrode have higher rates than pyrite electrode. However, when galena + pyrite electrode was used as a locked particle representative, the phase angle or Zmod values were determined in between each of the individual mineral electrodes.

There were significant differences when the collector was absent or present in the system, especially in galena electrode. The results also help interpreting the collector adsorption mechanisms. For instance, at low frequencies high phase angle values imply that the adsorption rates are low and diffusion controlled (Ertekin, Pekmez, & Ekmekçi, 2016).

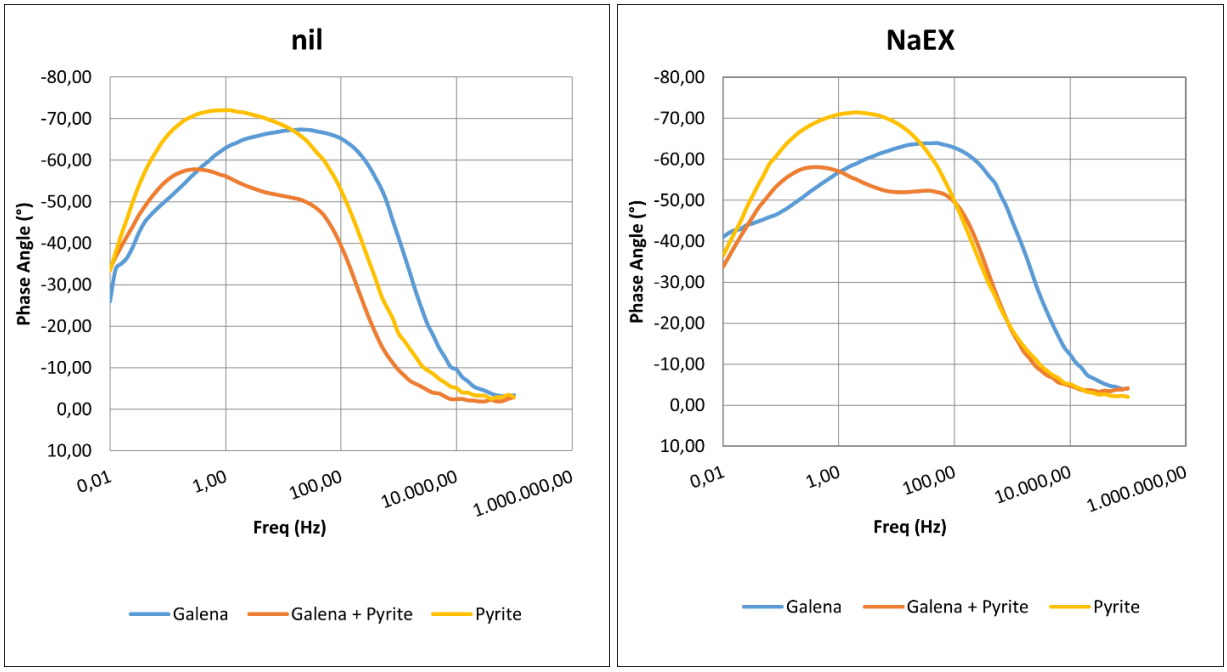

Figure 5. EIS results (Phase Angle) of all the studied minerals in the absence (left) and presence (right) of collector NaEX

In Figure 6, at higher frequencies, Zmod values were typically low and mostly constant, reflecting the solution resistance. At medium frequencies, the relationships between Zmod and the frequencies are linear. That explains as capacitive behavior caused by the electrical double layer at the mineral/solution interface and the adsorption of NaEX (Ekmekci, Becker, Tekes, & Bradshaw, 2010).

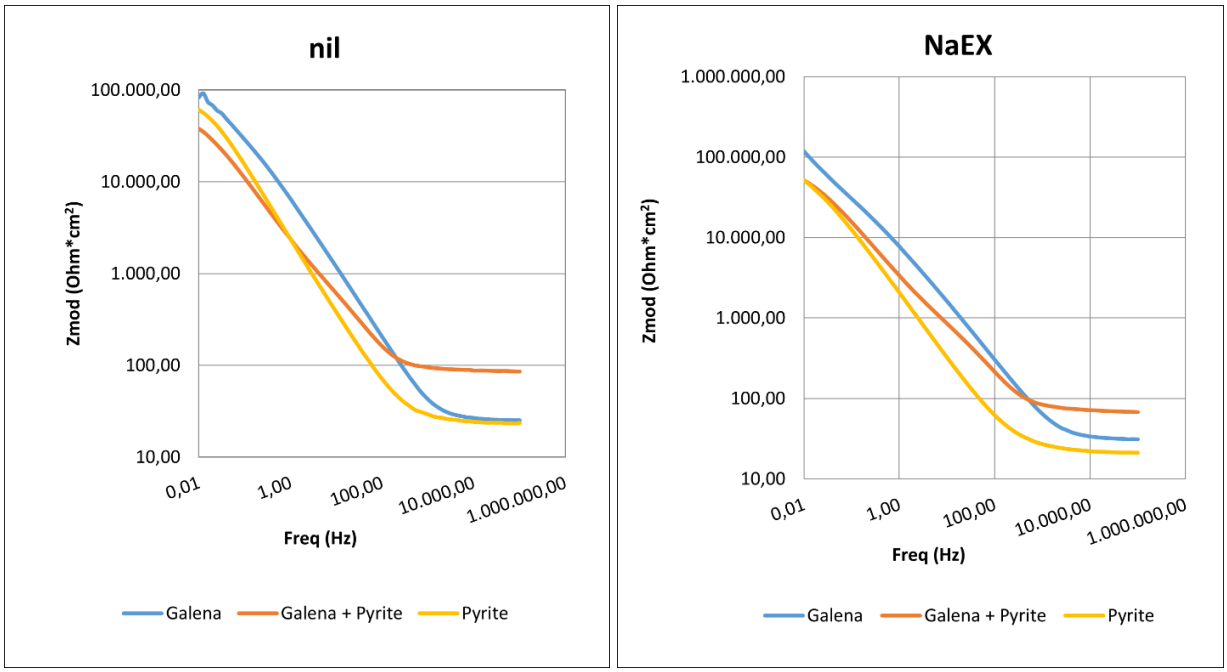

Figure 6. The EIS results (Magnitude) of all the studied minerals in the absence (left) and presence (right) of collector NaEX

CONCLUSIONS

The surface changes of the pure mineral electrodes (galena and pyrite) and the locked-particle electrode (galena + pyrite) were observed by open circuit potential (OCP), cyclic voltammetry (CV) and electrochemical impedance spectroscopy (EIS) methods.

The galvanic interaction plays a major role in the locked-particle electrode surface and it completely changes the surface properties. When two sulphide minerals interacted with each other in the bulk solution as locked-particle electrode, it was observed from the measured electrochemical techniques that their responses changed compared to liberated pure mineral electrode responses.

Collector (NaEX) adsorptions to the electrode surfaces were also clearly observed from the electrochemical responses of the measured techniques. Although NaEX adsorption on the galena electrode was obvious in the CV results, the collector adsorption on the galena + pyrite electrode was not clear enough. This was attributed to the galvanic effect. The presence of pyrite together with galena caused a decrease in galena reactivity and avoid its free oxidation.

REFERENCES

Ekmekçi, Z. (2008). Electrochemistry in sulphide mineral research. In *"Surface Chemistry and Flotation" lecture notes* (Vol. Chapter 2, pp. 8–26). Ankara.

Ekmekci, Z., Becker, M., Tekes, E. B., & Bradshaw, D. (2010). An impedance study of the adsorption of CuSO4 and SIBX on pyrrhotite samples of different provenances. *Minerals Engineering*, *23*(11–13), 903–907. https://doi.org/10.1016/j.mineng.2010.02.007.

Ertekin, Z., Pekmez, K., & Ekmekçi, Z. (2016). Evaluation of collector adsorption by electrochemical impedance spectroscopy. *International Journal of Mineral Processing*, *154*, 16–23.

https://doi.org/10.1016/j.minpro.2016.06.012.

Liu, Q., Li, H., & Zhou, L. (2009). Experimental study of pyrite-galena mixed potential in a flowing system and its applied implications. *Hydrometallurgy*, *96*(1–2), 132–139. https://doi.org/10.1016/j.hydromet.2008.09.002.

Mielczarski, E., & Mielczarski, J. A. (2003). Influence of galvanic effect on adsorption of Xanthate on pyrite , galena and chalcopyrite. In *XXII International Mineral Processing Congress* (pp. 866–873).

Moslemi, H., Shamsi, P., & Alimohammady, M. (2012). Electrochemical properties of pyrite, pyrrhotite, and steel: Effects on grinding and flotation processes. *Journal of the Southern African Institute of Mining and Metallurgy*, *112*(10), 883–890.

Peters, E., (1977). The Electrochemistry of Sulphide Minerals. In *Trends in Electrochemistry* (pp. 267–290). Boston, MA: Springer US. https://doi.org/10.1007/978-1-4613-4136-9_16

Rao, S. R., & Finch, J. A. (1988). Galvanic interaction studies on sulphide minerals. *Canadian Metallurgical Quarterly*, *27*(4), 253–259. https://doi.org/10.1179/cmq.1988.27.4.253.

Urbano, G., Meléndez, A. M., Reyes, V. E., Veloz, M. A., & González, I. (2007). Galvanic interactions between galena-sphalerite and their reactivity. *International Journal of Mineral Processing*, *82*(3), 148–155. https://doi.org/10.1016/j.minpro.2006.09.004.

Vianna, S. M., Franzidis, J., Manlapig, E. V, Silvester, E., & Ping-hao, F. (2003). The influence of particle size and collector coverage on the floatability of galena particles in a natural ore. In *XXII International Mineral Processing Congress* (pp. 816–826).

Zhao, S., Guo, B., Peng, Y., & Mai, Y. (2017). An impedance spectroscopy study on the mitigation of clay slime coatings on chalcocite by electrolytes. *Minerals Engineering*, *101*, 40–46. https://doi.org/10.1016/j.mineng.2016.09.027.

ŞLAM KÖMÜRDEN ORGANİK REAKTİFLERLE SÜPER TEMİZ KÖMÜR ÜRETİMİ

SUPER CLEAN COAL PRODUCTION WITH ORGANIC REAGENTS FROM SLIME COAL

A. Akın [1,], H. Hacıfazlıoğlu[1]*

[1]İstanbul Üniversitesi-Cerrahpaşa, Mühendislik Fak. Maden Müh. Böl. ISTANBUL
(Sorumlu yazar: aydadikici@gmail.com)

ÖZET

Bu çalışmada, %29.67 küllü Zonguldak şlam kömüründen tamamen organik bir prosesle süper temiz kömür üretimi hedeflenmiştir. Bu amaç doğrultusunda, şlam kömür önce flotasyonla zenginleştirilmiş, daha sonra organik asitlerle liç yapılarak süper temiz kömür üretilmiştir. Laboratuvar ölçeğinde yapılan çalışmalarda sadece organik sarf malzemeleri kullanılmıştır. Bu sayede, çevreye zararlı herhangi bir kimyasal kullanılmadan tamamen yenilenebilir kaynaklarla süper temiz kömür (kül <%3) üretilmiştir. Proseste kullanılan yenilenebilir kaynaklar sırasıyla ayçiçek yağı (kollektör), okaliptüs yağı (köpürtücü) ve liç reaktifi olarak çeşitli organik asitlerdir. 2 kademeli zenginleştirme sonucunda kül %29.67'den %2.92'ye kadar düşürülmüştür.

Anahtar Sözcükler: Süper temiz kömür, şlam kömür, flotasyon, liç

ABSTRACT

In this study, it was aimed to produce super clean coal from Zonguldak slime coal with 29.67% ash with a completely organic process. For this purpose, slime coal was first enriched by flotation, and then super clean coal was produced by leaching with organic acids. Only organic consumables were used in laboratory-scale studies. In this way, super clean coal (ash <3%) was produced with completely renewable resources without using any chemicals harmful to the environment. Renewable resources used in the process are sunflower oil (collector), eucalyptus oil (frother) and various organic acids as leaching reagents, respectively. As a result of the 2-stage enrichment, the ash of the coal was reduced from 29.67% to 2.92%.

Keywords: Super Clean Coal, Slime Coal, Flotation, Leaching

GİRİŞ

Kül içeriği %3'ün altında olan kömürlere süper temiz kömür denir. Süper temiz kömürler, yüksek karbon içerikleri ve düşük mineral madde içerikleri ile yüksek teknolojinin ihtiyacı olan hammaddedir. Süper temiz kömürler; aktif karbon, karbon elektrot, karbon nanotüp ve aromşlam kimyasalların üretiminde kullanılmaktadır. Ayrıca, gıda, kozmetik ve askeri amaçlar için de kullanılabilmektedir. Yapılan çalışmalar göstermiştir ki, ham kömürden süper temiz kömür üretmek fiziksel zenginleştirme yöntemleri ile mümkün değildir. Çoğu çalışmada, ham kömür kimyasallarla muamele edilerek süper temiz kömüre (kül <%3) ya da ultra temiz kömüre (kül <%1) dönüştürülmektedir. Yüksek korozif etkilere sahip olan HF, HCL, HNO_3, H_2SO_4 gibi kimyasallarla yapılan liç işlemi sonucunda ham kömürden süper temiz kömür üretilebilmektedir. Ancak, literatürde daha zayıf, çevre dostu ve yenilenebilir olan organik asitlerle süper temiz kömür üretimine yönelik herhangi bir çalışma yapılmamıştır (Bolat, vd., 1998; Steel vd.,2003; Gülen vd.,2013; Hacıfazlıoğlu, vd. 2016, Hacıfazlıoğlu ve Dikici, 2019).

Zonguldak havzasında yer altı madenciliği ile üretilen ham kömürler, üretim yöntemine ve kömürün kırılganlığına bağlı olarak, farklı boyutlarda (0-300 mm) ve farklı kül içeriklerinde (%20-%60) olabilmektedir. Tüvenan kömür, bir yıkama tesisine girmeden önce, 100 mm açıklıklı bir elekten elenmekte ve elek üstü genellikle elle ayıklama (triyaj) yöntemi ile zenginleştirilmektedir. 100 mm'nin altındaki kömür ise ağır ortam esaslı yıkama makinesine girmektedir. 1-18 mm boyut grubu ağır ortam siklonu ile zenginleştirilirken, 18-100 mm boyut grubu ağır ortam tamburu veya Drewboy teknesi ile zenginleştirilir. 1 mm'nin altındaki kömür ise önce hidrosiklona beslenmekte, hidrosiklon üst akımı şlam (~30 µm'lik çok ince boyutlu killi şlam kömür) uzaklaştırılmakta, alt akım ise spiral bataryasına gönderilmektedir. Spiralden elde edilen temiz kömürler metalurjik kömür (kül ~%10) olarak isimlendirilmekte ve demir çelik sektörüne verilmektedir. Hidrosiklon üst akımı çok ince boyutlu killi şlam kömürler ise suyun geri kazanımı amacıyla tikinere ve ordan da ya şlam havuzuna ya da filtrelere basılmaktadır. Her iki durumda da kömür içerikli çamurlar (şlamlar) oluşmaktadır. Bu şlamlar içersinden kömürün kazanılmasına yönelik çeşitli çalışmalar yürütülmektedir. Dünya genelinde şlam kömürlerin zenginleştirilmesi için kullanılan yegane yöntem flotasyon yöntemidir. Özellikle, bir jet flotasyonu tekniği olan Jameson hücresi bu alanda başı çeken flotasyon makinesidir. Çok ince boyutlu şlamların zenginleştirilmesi için pek çok araştırmacı jet flotasyonu ve kolon flotasyonu tekniklerini önermektedir. Şlamların klasik flotasyon hücreleri ile zenginleştirildiği uygulamalarda mevcuttur. Kömür flotasyonunda genellikle gazyağı ve dizel gibi petrol türevi ürünler kullanılmaktadır. Bu ürünler toplayıcı olarak kullanılır. Köpürtücü olarak MIBC ve Octanol en yaygın kullanılan reaktiflerdir. Bu reaktifler, fosil yakıtlardan üretildiği için bir gün tükenecektir. Bu bakımdan araştırmacılar yeni reaktif arayışına girmiş ve yenilenebilir kaynaklardan üretilen reaktifleri kullanmaya başlamışlardır. Özellikle yemeklik bitkisel yağların ve pişirme işlemleri sonucunda ortaya çıkan atık bitkisel yağların kömür flotasyonunda etkili bir şekilde kullanılabileceği pek çok araştırmacı tarafından belirtilmektedir (Alonso vd., 2000; Vasumati vd., 2013; Lang, 2017; Hacifazlioglu ve Senol-Aslan, 2017).

Bu çalışmada, Zonguldak şlam kömürden süper temiz kömür üretimi için flotasyon ve liç yöntemlerinden faydalanılmıştır. Hem flotasyonda hem de liç yönteminde sadece organik yenilenebilir sarf maddeleri kullanılmıştır. Flotasyonda, köpürtücü olarak okaliptüs yağı, toplayıcı olarak ayçiçek yağı kullanılmış, liç deneylerinde ise sitrik (limon asidi), formik (karınca asidi), asetik (sirke asidi) ve oksalik asit (bitki asidi) gibi organik asitler tercih edilmiştir.

MALZEME VE YÖNTEM

Şlam Kömür Numunesi Hakkında Bilgi

Şlam kömür numuneleri, Zonguldak-Çatalağzı beldesinde faaliyet gösteren bir kömür yıkama tesisinin artık havuzundan 3 hafta boyunca biriktirilerek alınmıştır (Şekil 1). Alınan numuneler laboratuar ortamında büyük bir kova içerisine dökülmüş, bir mikser yardımıyla karıştırılmış ve homojenleştirilmiştir. Homojenleştirme çalışmalarından sonra, numuneler kurutulmuş ve deneysel çalışmalarda kullanılmıştır. Numuneye öncelikle kuru bazda ASTM standartlarına göre kısa kimyasal analiz yapılmıştır. Daha sonra yaş eleme yöntemi ile boyutu belirlenmiştir. Şlam kömürün kül, kükürt ve uçucu madde içeriği sırasıyla %29.67, %0.70 ve %30.10 bulunmuştur. Ortalama tane boyutu (d_{50}) 30 mikron civarındadır.

Şekil 1. Kömür yıkama tesisi (Zonguldak) artık havuzu ve şlamların görüntüsü

Deneylerde İzlenen Yöntem

Süper temiz kömür üretme çalışmaları tamamen organik yenilenebilir reaktiflerle yürütülmüştür. Süper temiz kömür üretimi için 2 kademeli zenginleştirme işlemi uygulanmıştır. Şekil 2'den de görülebileceği gibi, önce flotasyon yöntemi ile kül belli ölçüde azaltılacak ve ardından daha maliyetli bir işlem olan organik asitlerle liç yapılacaktır. Bu sayede, flotasyon ile önce serbest kül giderilecek ve ardından liç yöntemi ile bünye külü giderilmeye çalışılacaktır. Ön zenginleştirme işlemi olarak flotasyon yönteminin tercih edilmesinin nedeni, şlam kömürünün çok ince boyutlu ve oldukça hidrofobik özellikte olmasıdır. Denver hücresindeki flotasyon işleminde 10 kg/t ayçiçek yağı toplayıcı olarak ve 0.1 kg/t okaliptüs yağı köpürtücü olarak kullanılmıştır. 2 kademe temizleme işlemi uygulanmış ve bir konsantre ile 3 artık elde edilmiştir. Kaba flotasyon işleminde 10 dakika kıvamlanma süresi sonrasında 600 sn köpük alma işlemi yapılmış ardından alınan temiz kömür testin devamı için ayrılmış, çıkan artık ise ürün 1 olarak isimlendirilmiştir. Testin ilk kısmından alınan temiz kömür aynı şartlarda temizleme flotasyonuna tabii tutulmuş ve alınan temiz kömür devam edecek temizleme flotasyonu için ayrılmış, alınan artık-batan ise ürün 2 olarak isimlendirilmiştir. Testin son kısmında temiz kömürün ikinci temizleme flotasyonuna tabi tutulmuş ve buradan bir nihai konsantre alınmıştır.

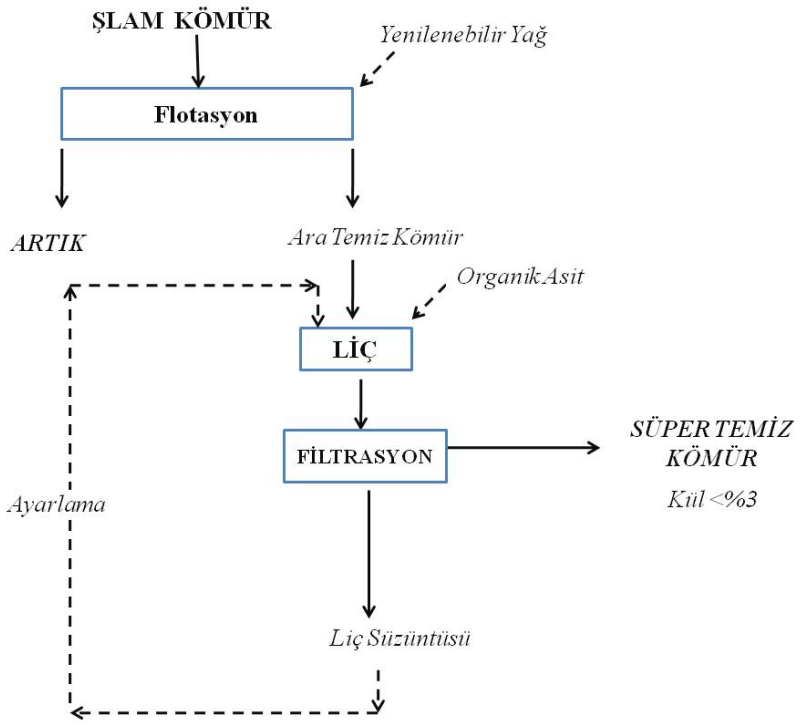

Şekil 2. Şlam kömürden süper temiz kömür üretimi için izlenen yöntemin akım şeması

Liç deneyleri, manyetik karıştırıcılı hot-plate üzerine yerleştirilen 500 ml'lik kapaklı beher içerisinde farklı asit tipleri ve farklı asit miktarlarında yapılmıştır. Ayrıca, sıcaklık ve liç süresinin etkisi araştırılmıştır. Liç deneylerinde ayrı ayrı sitrik asit, formik asit, asetik asit ve organik asit kullanılmıştır. Test edilen asit miktarları; 25, 50, 100, 150 ve 200 kg/t'dur. Her deneyde kullanılan kömür miktarı 20 gr, su miktarı ise 200 ml'dir. Asit ilavesi de dikkate alındığında katı oranı yaklaşık %8.5 civarındadır. Manyetik balığın dönüş hızı ise 200 rpm'dir. Liç deneyleri ekonomik olması bakımından önce ortam sıcaklığında (25 ^{o}C) ve kısa süreli (30 dk) olarak gerçekleştirilmiştir. Daha sonra liç süresi arttırılmış ve 180 dk'ya çekilmiştir. Son aşamada, en maliyetli yöntem olan pülpü ısıtma işlemi uygulanmış ve 65 ^{0}C'de deneyler yürütülmüştür. Liç parametresi değişikliği süper temiz kömür elde edinceye kadar devam etmiştir. Elde edilen liç çözeltileri, liç işlemi sonrasında 3 mikronluk filtre kağıtlarından süzülmüş (Şekil 3) ve asidinden tam ayırma için birkaç defa sıcak suyla yıkanmıştır. Filtre kağıdı üzerinde kalan süper temiz kömür önce 105 ^{0}C'lik etüvde kurutulmuş ve daha sonra kül analizine tabi tutulmuştur. Deneysel çalışmaların sonuçların değerlendirilmesi için "yanabilir verim" ve "kül giderim" değerlerinden faydalanılmıştır.

Şekil 3. Liç ve flotasyon işlemi sonrasında ürünlerin filtrasyonun görüntüsü

BULGULAR

Flotasyon Deney Sonuçları

Flotasyon test sonuçları Tablo 1'de verilmiştir. Buna göre, şlam kömüre toplamda 3 kademe flotasyon zenginleştirmesi uygulandığı zaman elde edilen nihai konsantrenin kül içeriği %6.10'a kadar düşebilmektedir. %6.10 küllü ürünün alınması durumunda ağırlıkça verim %13.60 olmaktadır. Yanabilir verim ise %18.16'dır. Ayçiçek ve okaliptüs yağı ile yapılan flotasyon deneylerinin bir görüntüsü Şekil 4'de verilmiştir. Bu fotoğraflardan görüldüğü gibi söz konusu ikili ile oldukça temiz bir artık atmak mümkün olmaktadır.

Tablo 1. Flotasyon test sonuçları (ayçiçek yağı+okaliptüs yağı ikilisi ile)

Ürünler	Ağırlıkça Verim (%)	Kül (%) --	Yanabilir Verim (%)	Toplamlı Miktar (%)	Toplamlı Kül (%)	Toplamlı Yanabilir Verim(%)
Konsantre	13.60	**6.10**	18.16	13.60	6.10	18.16
Ürün 3	29.90	9.50	38.48	43.50	8.44	56.63
Ürün 2	34.50	28.75	34.95	78.00	17.42	91.59
Ürün 1	22.00	73.10	8.41	100	29.67	100
Toplam	100	29.67	100	-	-	-

Şekil 4. Ayçiçek ve okaliptüs yağı ile flotasyonun başlangıcı ve bitiş anı görüntüleri

Liç Deney Sonuçları

Ayçiçek yağı ile yapılan flotasyon çalışmaları sonucunda elde edilen %6.10 küllü temiz kömürler biriktirilerek liç deneylerinde kullanılmıştır. Organik reaktiflerden, sitrik asit, formik asit, asetik asit ve oksalik asit ile ayrı ayrı deneyler yapılmış ve kül giderimi için en uygun asit tipi belirlenmiştir. İnorganik asitlerin kül gideriminde oldukça başarılı olduğu, süper temiz kömür hatta HF ile ultra temiz kömürün (kül<%1) bile üretilebileceği pek çok çalışmada belirtilmiştir (Steel vd., 2001; Steel vd., 2003; Yılmaz, 2004; Hacıfazlıoğlu, 2016; Hacıfazlıoğlu ve Dikici, 2019). Bu bakımdan, bu çalışmada süper temiz kömür üretimi için yalnızca yenilenebilir organik asitler kullanılmıştır.

Liç deneylerinin ekonomik olması bakımından, öncelikle ortam sıcaklığında (25 ^{0}C) ve kısa süreli (30 dk) liç yapılmıştır. Bu deneylerin sonuçları Tablo 2'de verilmiştir. Bu deneylerde organik asitlerle pülpün pH değeri 2.60'a kadar düşmüştür. Tablo 2 incelendiği zaman, hiçbir organik asit ile temiz kömür külü %3'ün altına düşürülememiştir. En yüksek kül giderim değerleri sitrik ve formik asitle elde edilmiştir. 200 kg/t asit miktarında, sitrik asitle liç sonucu elde edilen kömürün kül içeriği %3.70, formik asit ile %3.80 bulunmuştur. Asetik ve okzalik asit kömürün kül içeriğini %4'ün altına indirememiştir. Diğer koşullar sabit tutulmak koşuluyla liç süresinin 30 dk'dan 180 dk'ya çıkarılması durumunda (Tablo 3), sitrik asit kömürün kül içeriğini %6.10'dan %3.50'ye düşürebilmiştir. Liç süresinin 6 kat arttırılması durumunda kül giderim değeri %39.34'den %42.62'ye yükselmiş, kül içeriği ise %3.70'den 3.50'ye kadar düşürülebilmiştir. Ancak, ortam sıcaklığında liç süresinin arttırılması da süper temiz kömür üretimini sağlayamamıştır. Formik, asetik ve oksalik asitler ile de kül içeriği %3.5'in altına düşürülememiştir. Bu bakımdan, ortam sıcaklığı arttırılarak deneylere devam edilmiştir. 65^{0}C'lik ortam sıcaklığında yapılan deneylerin sonuçları Tablo 4'de verilmiştir.

Tablo 2. Farklı asitlerin ürün kül içeriğine ve kül giderimine etkisi (25^{0}C - 30dk)

ASİT MİKTARI (kg/t)	SİTRİK ASİT		FORMİK ASİT		ASETİK ASETİK		OKSALİK ASİT	
	Kül (%)	Kül Gid. (%)	Kül (%)	Kül Gid. (%)	Kül (%)	Kül Gid. (%)	Kül (%)	Kül Gid. (%)
0	6.10	0.00	6.10	0.00	6.10	0.00	6.10	0.00
25	5.30	13.11	5.50	9.84	5.90	3.28	5.90	3.28
50	4.90	19.67	5.30	13.11	5.50	9.84	5.90	3.28
100	4.60	24.59	4.90	19.67	5.15	15.57	4.80	21.31
150	4.20	31.15	4.50	26.23	4.80	21.31	4.30	29.51
200	3.70	39.34	3.80	37.70	4.80	21.31	4.25	30.33

Tablo 3. Farklı asitlerin ürün kül içeriğine ve kül giderimine etkisi (25^0C - 180dk)

ASİT MİKTARI (kg/t)	SİTRİK ASİT		FORMİK ASİT		ASETİK ASETİK		OKSALİK ASİT	
	Kül (%)	Kül Gid. (%)	Kül (%)	Kül Gid. (%)	Kül (%)	Kül Gid. (%)	Kül (%)	Kül Gid. (%)
0	6.10	0.00	6.10	0.00	6.10	0.00	6.10	0.00
25	5.20	14.75	5.50	9.84	5.80	4.92	5.70	6.56
50	4.90	19.67	5.00	18.03	5.30	13.11	5.20	14.75
100	4.45	27.05	4.60	24.59	4.80	21.31	4.50	26.23
150	4.00	34.43	4.10	32.79	4.50	26.23	4.00	34.43
200	3.50	42.62	3.60	40.98	4.00	34.43	3.90	36.07

Tablo 4. Farklı asitlerin ürün kül içeriğine ve kül giderimine etkisi (65^0C - 180dk)

ASİT MİKTARI (kg/t)	SİTRİK ASİT		FORMİK ASİT		ASETİK ASETİK		OKSALİK ASİT	
	Kül (%)	Kül Gid. (%)	Kül (%)	Kül Gid. (%)	Kül (%)	Kül Gid. (%)	Kül (%)	Kül Gid. (%)
0	6.10	0.00	6.10	0.00	6.10	0.00	6.10	0.00
25	4.20	31.15	4.50	26.23	4.80	21.31	4.70	22.95
50	3.90	36.07	4.00	34.43	4.30	29.51	4.30	29.51
100	3.45	43.44	3.65	40.16	3.70	37.70	3.70	39.34
150	3.02	50.49	3.10	49.18	3.20	47.54	3.20	47.54
200	**2.92**	52.13	2.98	51.15	3.10	47.54	3.10	49.18

Tablo 4 verilerine göre, 65^0C'lik bir liç sıcaklığında 180 dk liç süresinde sitrik asit ile yapılan deneyler sonucunda elde edilen temiz kömürün kül içeriği %2.92 bulunmuştur. Benzer koşullarda formik asitte süper temiz kömür üretmiş olup, elde edilen kömürün kül içeriği %2.98'dir. Organik asitlerle süper temiz kömür üretiminde, liç süresinden ziyade liç sıcaklığı daha etkin bir parametre olup, kül gideriminde önemli etkilere sahiptir. 65^0C'lik liç sıcaklığında ve 180 dk liç süresinde sitrik, formik asetik ve oksalik asidin 200 kg/t miktarlarında kül giderim değerleri sırasıyla %52.13, %51.15, %47.54 ve %49.18 bulunmuştur. Yukarıdaki sonuçlar ışığında, tamamen organik reaktiflerle şlam kömüründen süper temiz kömür üretilebileceği görülmüştür. Şlam kömürden süper temiz kömür üretim prosesenin akım şeması Şekil 5'de gösterilmiştir. Buna göre, %8-10 katı oranlı şlam kömür önce kıvam tankına alınıp, 5 dk süresince ayçiçek yağı (10 kg/t) ve okaliptüs yağı (0.2 kg/t) ilavesi ile kıvamlandırılır. Daha sonra, 10 dk flotasyon uygulanır. Elde edilen şlam sistemden uzaklaştırılır. Elde edilen konsantreye 2 kademe daha temizleme uygulanır. Sonuçta %6.10 küllü bir temiz kömür elde edilir. Bu temiz kömür alınarak 65 ^{0}C'de 180 dk boyunca ve 200 kg/t sitrik asit ilavesiyle liç yapılır. Liç işleminden sonucunda elde edilen bulamaç filtrelere gönderilir ve filtrasyon işlemi sonucunda %2.92 küllü süper temiz kömür elde edilmiş olur. Filtrasyon çözeltisi ayarlanarak tekrar tekrar liç işleminde kullanılır.

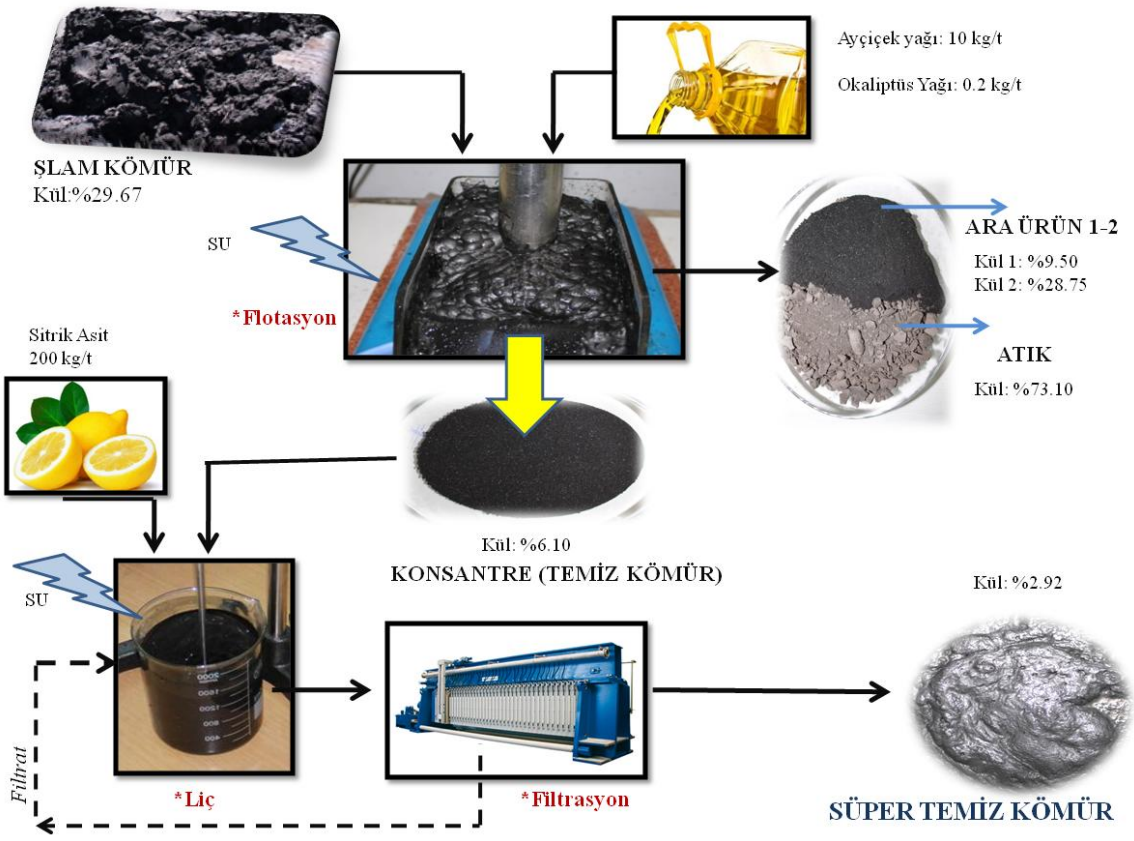

Şekil 5. Şlam kömürden organik bir prosesle süper temiz kömür üretiminin akım şeması

SONUÇLAR

Bu çalışmada tamamen organik reaktifler ile Zonguldak kömür şlamlarından süper temiz kömür üretilmiştir. Üretim prosesinde kömürün çok ince boyutlu olması nedeni ile öğütmeye ihtiyaç duyulmamıştır. Proseste öğütmenin olmaması enerji tasarrufu için önemli bir avantajdır. Süper temiz kömür üretimi 2 kademeli zenginleştirme işlemi ile yapılmıştır. İlk aşamada flotasyon, ikinci aşamada liç işlemi uygulanmıştır. Kullanılan reaktifler sırasıyla ayçiçek yağı, okaliptüs yağı ve sitrik asittir. Burada sitrik asite alternatif olarak formik asitte kullanılabilir. Üretim prosesinde en önemli maliyet unsuru reaktiflerin yüksek dozajlarda kullanılmış olmasıdır. Ancak, tamamen organik reaktiflerle süper temiz kömür üretilebiliyor olması, sürdürülebilirlik ve çevrenin korunması açısından büyük önem arz etmektedir.

Laboratuvar ölçeğinde ayçiçek yağı (10 kg/t) ve okaliptüs yağı (0.2 kg/t) ile yapılan flotasyon çalışmaları sonucunda %29.67 küllü kömürden %6.10 küllü bir temiz kömür üretilmiştir. Bu ürün için, 1 kaba, 2 temizleme flotasyonu yapılmıştır. Elde edilen temiz kömürün 200 kg/t sitrik asitle 65^0C'lik bir sıcaklıkta 3 saat liç edilmesi sonucunda, kül %6.10'dan %2.92'ye kadar düşmüştür. Aynı liç işleminin formik asitle yapılması durumunda, kül %2.98 bulunmuştur. Asetik ve oksalik asit ile süper temiz kömür üretilememiştir.

KAYNAKLAR

Alonso, M.I. Castano, C. and Garcia, A.B. (2000). Performance of vegetable oils as flotation collectors for the recovery of coal from coal fines wastes, *Coal Preparation 21-4*: 411-420.

Bolat, E. Sağlam, S. Pişkin, S. (1998). Chemical demineralization of a Turkish high ash bituminous coal, *Fuel Processing Technology 57*: 93–99

Drake, S. S., O'Carroll, D. M., Gerhard, J. I. (2013). Wettability contrasts between fresh and weathered diesel fuels*. Journal of Contaminant Hydrology, 144(1),* 46-57.

Gulen, J., Doymaz, I., Piskin, S., and Ongen, S. (2013). The effects of temperature and mineral acids on the demineralization degree of nallihan lignite, *Energy Sources, Part A: Recovery, Utilization, and Environmental Effects 35*: 202–208.

Hacifazlioğlu H. ve Dikici A. (2019). "Zonguldak-Karadon Kömüründen Liç Yöntemi ile Ultra Temiz Kömür Üretimi*", Yer Altı Kaynakları Dergisi*, ss.35-41.

Hacifazlioğlu H. ve Dikici A. (2019). "Kömür Flotasyonu için Yeşil Kollektör: Şlam Bitkisel Yağ", *Türkiye 26. Uluslararası Madencilik Kongresi Bildiriler Kitabı*, pp.1169-1176

Hacıfazlıoğlu, H. (2011). ‘’*Jameson Hücresinden Bitümlü Şlam Kömürden Flotasyon İçin En Uygun Köpürtücü ve Toplayıcı Tipinin Araştırılması’’*, Dicle *Üniversitesi Mühendislik Dergisi,* s.33-34

Hacifazlioglu, H. (2016). The production of ultra-clean coal from Zonguldak bituminous coal by chemical leaching, *Energy Sources, Part A: Recovery, Utilization, and Environmental Effects, 38* (24): 3586-3592.

Hacifazlioglu, H. and Senol-Arslan, D. (2017). Sunflower oil as green collector in bituminous coal flotation, Energy Sources, *Part A: Recovery, Utilization, and Environmental Effects, 39:15*, 1602-1609.

Lang, X. (2017). Application of cyclonic microbubble flotation column in Xiezhuang coal preparation plant: From laboratory to industrial scale. *Int. J. of Coal Preparation and Utilization*. https://doi.org/10.1080/19392699.2017.1365065

Sönmez, İ. ve Cebeci, Y. (2006). Performance of classic oils and lubricating oils in froth flotation of Ukraine coal, Fuel, 85, 1866-1870.

Steel, K. M., and Patrick, J. W. (2003). The production of ultra clean coal by sequential leaching with HF followed by HNO_3, *Fuel 82*:1917–1920.

Steel, K.M., Besida, J., O’Donnell,T., Wood,D.G. (2001). Production of Ultra Clean Coal Part I—Dissolution behaviour of mineral matter in black coal toward hydrochloric and hydrofluoric acids, *Fuel Processing Technology*, *70*, 171–192.

Vasumathi, N. Vijaya Kumar, T.V., Subba Rao, S. Prabhakar, S. Bhaskar Raju, G. Shiva Kumar S. and Raman, U. (2013). Eco Friendly and Cost-Effective Reagent for Coal Flotation, *International Journal of Engineering Research 2-7*: 418-423.

Yılmaz, S. Katı fosil Yakıtlarda Mineral Giderme Üzerine Etkisi, Karaelmas University, Msc Thesis (2004). Zonguldak, Turkey.

Zhou, G., Xu, C., Cheng, W., Zhang, Q., Nie, W. (2015). Effects of oxygen element and oxygen-containing functional groups on surface wettability of coal dust with various metamorphic degrees based on XPS experiment. *Journal of analytical methods in chemistry*, 1-8.

TEMEL SÜRTÜNME AÇISI TESTİNDE DENEY ÖRNEĞİ ŞEKLİNİN ETKİSİ

EFFECT OF EXPERIMENT SAMPLE SHAPE ON BASIC FRICTION ANGLE TEST

M. Özdemir [1, *], S. Beyhan [1], A. Özgür [1]

[1] *Kütahya Dumlupınar Üniversitesi, Maden Mühendisliği Bölümü*
*(*Sorumlu yazar: mehmet.ozdemir@dpu.edu.tr)*

ÖZET

Kaya şev stabilitesinin değerlendirilmesinde jeolojik süreksizlikler önemli bir parametredir. Doğal süreksizlik yüzeyleri genellikle pürüzlüdür ve kayma mukavemetleri üzerinde önemli bir etkiye sahiptir. Doğal, dolgusuz ve pürüzlü süreksizliklerin kesme mukavemeti, doğrusal olmayan bir yenilme kriteri ile tahmin edilebilmektedir. Bu kriterin ana girdilerinden biri, tilt testi sonucu elde edilen veya doğrudan kesme testi ile belirlenen temel sürtünme açısıdır. Bu çalışmada; düzlemsel, dairesel ve kama modelde hazırlanmış 5 farklı bölgeye ait mermer örnekleri üzerinde tilt cihazı ile eğim testleri gerçekleştirilmiştir. Böylece, farklı kayma modellerinin temel sürtünme açısına etkisi ile aşınmanın yüzeyler üzerindeki etkisi araştırılmıştır. Düzlemsel ve dairesel tip modellerin kama modele oranla temel sürtünme açısı değerlerinin daha düşük çıktığı belirlenmiştir. Ayrıca, aynı yüzeyler üzerinde yapılan test tekrarında ve artan her test sayısında, sürtünme açısının azalma eğiliminde olduğu tespit edilmiştir.

Anahtar Sözcükler: Temel sürtünme açısı, tilt test, numune şekli, aşınma

ABSTRACT

Geological discontinuities are an important parameter in the evaluation of rock slope stability. Natural discontinuity surfaces are generally rough and have a significant effect on their shear strength. The shear strength of natural, unfilled and rough discontinuities can be estimated using a nonlinear failure criterion. One of the main inputs to this criterion is the basic friction angle, which is obtained as a result of the tilt test or determined by the direct shear test. In this study; tilt tests were carried out on marble samples belonging to 5 different regions prepared in planar, circular and wedge models. Thus, the effect of different sliding models on the basic friction angle and the effect of wear on the surfaces were investigated. It was determined that the basic friction angle values of the planar and circular type models were lower than the wedge model. In addition, it was concluded that the friction angle tended to decrease in the repetition of the test on the same surfaces and with each increasing number of tests.

Keywords: Basic friction angle, tilt test, shape of sample, weathering

INTRODUCTION

Discontinuities have significant effects on engineering properties of rocks. Especially, discontinuities must be taken into consideration in slope stability studies. These discontinuities could be geological structures such as joint, fault, crack and fissure. These types of discontinuities cause different types of slope shear failures in engineering studies. Planar, circular, wedge and toppling types of failures could be seen in open pit mines, highway and railway access slopes. It is of great importance to determine the properties of the discontinuities that cause these failure types (Alejano et al., 2012).Within this scope, Equation 1 proposed by Barton and Bandis (1982) is used to determine the residual internal friction angle of discontinuities.

$$\tau = \sigma_n tan\left[\varphi_r + JRC\ log\left(\frac{JCS}{\sigma_n}\right)\right] \quad (1)$$

where τ shear strength of the joint, σ_n normal stress to the joint, φ_r residual friction angle, JRC the joint roughness coefficient, JCS the compressive strength of the joint surface. The residual friction angle, φ_r is estimated according to Barton and Choubey (1977) and as follows (Equation 2) :

$$\varphi_r = (\varphi_b - 20°) + 20\frac{r}{R} \quad (2)$$

where ϕb is the basic friction angle, r is the Schmidt hammer rebound number for a weathered and wet discontinuity, R is the Schmidt hammer rebound number for the unweathering surfaces of the same rock.

In this study, experiments have been carried out by considering the ISRM standards proposed by Alejano et al. (2018), to determine the basic friction angle which is one of the nonlinear failure criterion input. Unlike other studies, 5 different marble samples with dimensions of 150x100 mm were prepared as planar, circular and wedge type, similar to some slope slide types and subjected to the test. Besides, three core and two core surface contact tests were carried out in accordance with the standards. Tilt device was used to determine the basic friction angle. As a result, the effect of the sample shape (according to the slope slide type) and the number of tests on basic friction angle were specified.

MATERIAL AND METHOD

In this study, metamorphic marbles named Afyon White (AW), Afyon Grey (AG), Marmara (M), Muğla White (MW) and Kemalpaşa White (KW) belonging to the marble fields from different regions of Turkey were used. Experimental studies were carried out in Kütahya Dumlupınar University Rock Mechanics Laboratory. In the study; samples with dimensions of 150x100 mm which were prepared similarly to slope slide types such as planar, circular and wedge types were used. These samples were prepared with dimensions of 55x60 mm for planar slide model, diameter of 55 mm for circular slide model and 55 mm length and 60 mm height for wedge type (Figure 1).

Basic internal friction angles can be measured by tilt device or portable shear box (Alejano et al., 2012; Hencher and Richards, 2015; Jang et al., 2018; Muralha et al., 2014; Ulusay and Karakul, 2016; Zhang et al., 2018). In this study, basic internal friction angle of samples were measured by specially designed tilt device (Beyhan and Özdemir, 2021). The device is driven by an electric motor system. The measurement is conducted on an inclined plate with dimensions of 30 × 40 cm on the device. Apparatuses are placed around the plate to fix the samples. The measuring incline rate can be adjusted between 5.2°/min and 21°/min. The sensor on the device, deactivates test device automatically when the test sample slides >16 mm. Additionally, a mobile digital inclinometer with ±0.1° precision is used to measure the tilt angle (Figure 2).

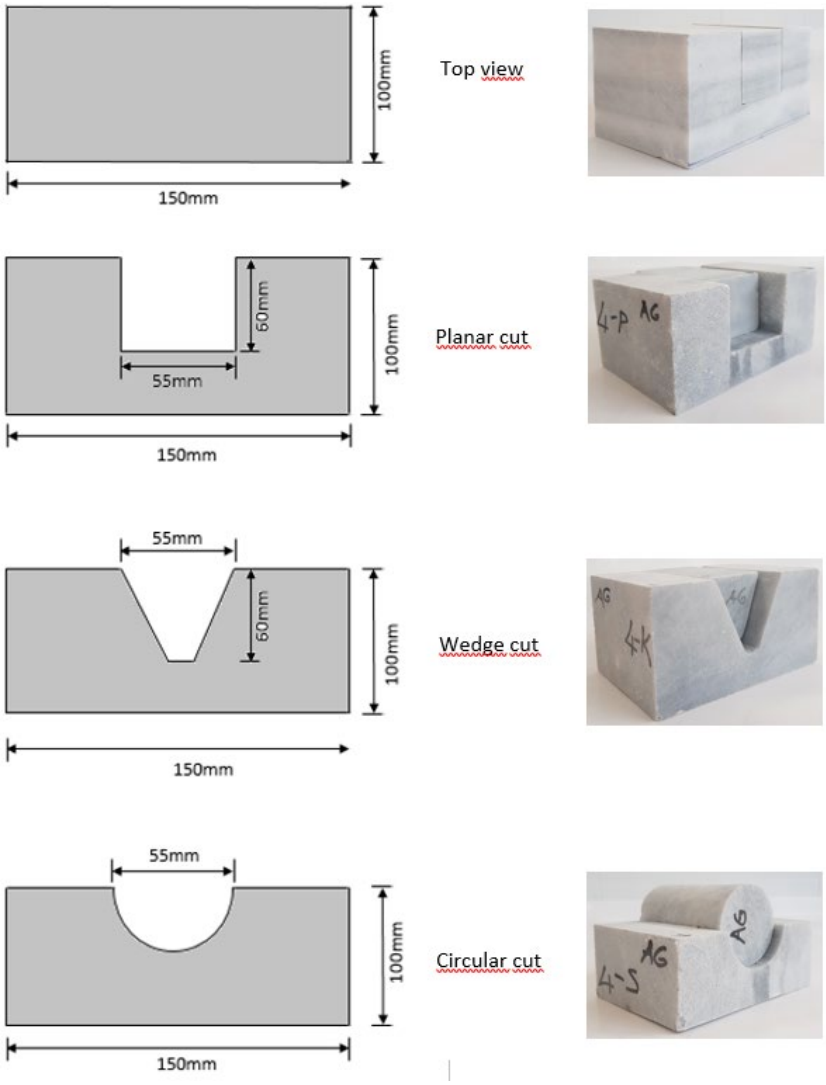

Figure 1. Dimensions of sample models prepared for tilt test

Figure 2. Tilt device used in experimental studies

According to ISRM standards (Alejano et al., 2018), 5 measurements were made for each sample and their medians were taken (Equation 3). The contact surfaces of samples were cleaned after every measurement. In this way, the negative effect of dust or particles accumulating on the surfaces on the

experiment is prevented (Figure 3). The incline speed is set to be between 5°/min-20°/min. When the test samples slid up to 10% of their 100 mm length, the sensor deactivated the device and measurement was performed with inclinometer.

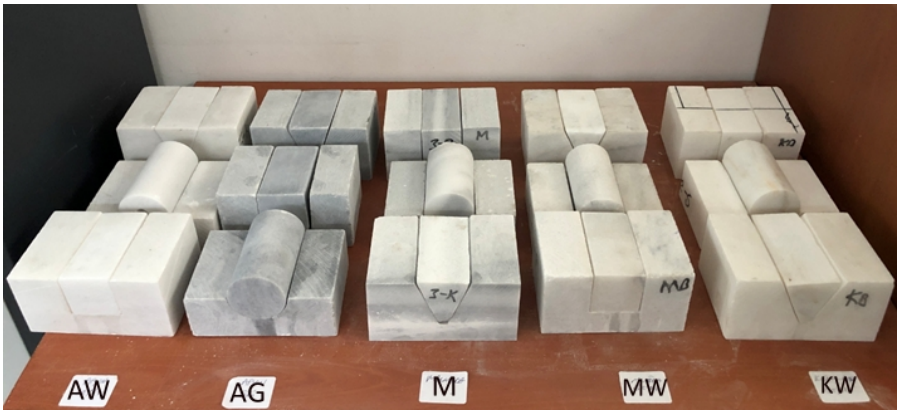

Figure 3. Samples used in the experimental study

To determine the basic internal friction angle, according to the ISRM standards proposed by Alejano et al. (2018); rectangular plate cut in half, rock core samples cut in half lengthwise, three core system and two core surface contact (Figure 4a) test methods are used (Alejano et al., 2012; Kim et al., 2016; Ruiz and Li, 2014). In this study, in addition to the sample types recommended in the standards, planar, circular and wedge type slide models, the dimensions of which are given in Figure 1, were designed and the basic internal friction angles of the geometric structures in these models were evaluated (Figure 4b). The samples were tested after drying at 105 °C for 24 hours and cooling for 30 minutes in a desiccator by preventing moisture from the air. Three core and two core surface contact tests were also carried out under the same conditions (Figure 5).

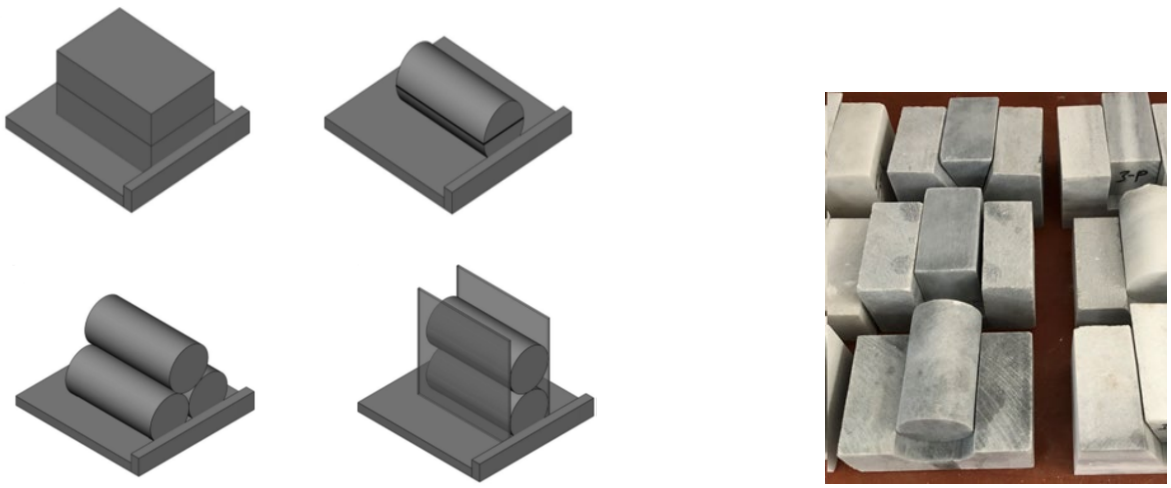

(a) (b)

Figure 4. a) Cutting methods recommended by ISRM (Alejano vd., 2018), b) planar, circular and wedge cutting methods applied in this study

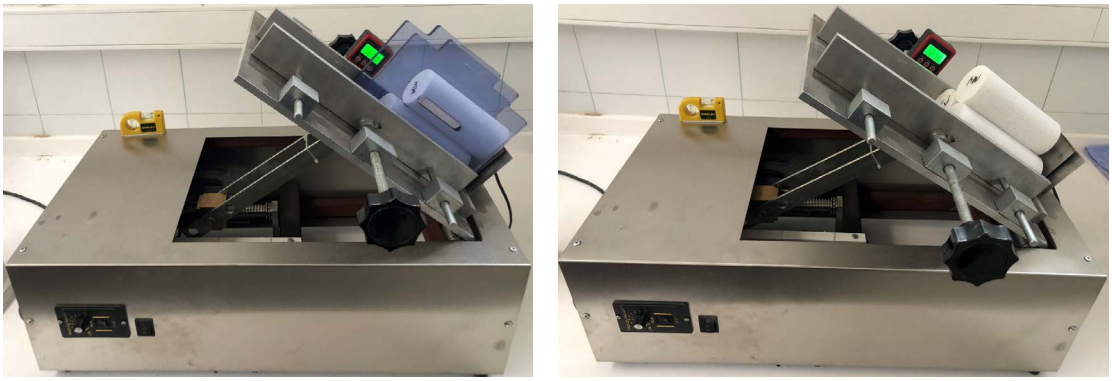

(a) (b)

Figure 5. a) Two-cores set up b) Three-cores set up

EXPERIMENTAL RESULTS

Experimental studies were carried out to determine the physical properties of each marble sample used in this study, such as unit weight, apparent porosity and water absorption. Experimental study results are given in Table 1. Accordingly; it was determined that the water absorption and apparent porosity values of AG and KW samples were lower than the other samples. The unit weights of the samples vary between approximately 25-27 kN/m^3 (Table 1).

The basic internal friction angle values can vary between 25°–30° for sedimentary rocks and 30–35° for igneous and metamorphic rocks (Alejano et al., 2012). In this study, the results of the basic internal friction angle values of the samples obtained by applying different cutting models are given in Figure 6 and 7. According to these results, as the basic friction angle varies between 20°-33° for planar and circular forms of all samples (Figure 6a ve 6b), approximate values between 31°-41° were obtained for wedge type slide model (Figure 6c).

Table 1. Physical properties of test specimens

Test Name	Rock Type				
	AW	M	MW	AG	KW
Unit weight (kN/m^3)	26,24	25,89	25,57	25,80	26,06
Apparent porosity (%)	0,25	0,20	0,23	0,12	0,12
Water absorption (%)	0,09	0,08	0,09	0,05	0,05

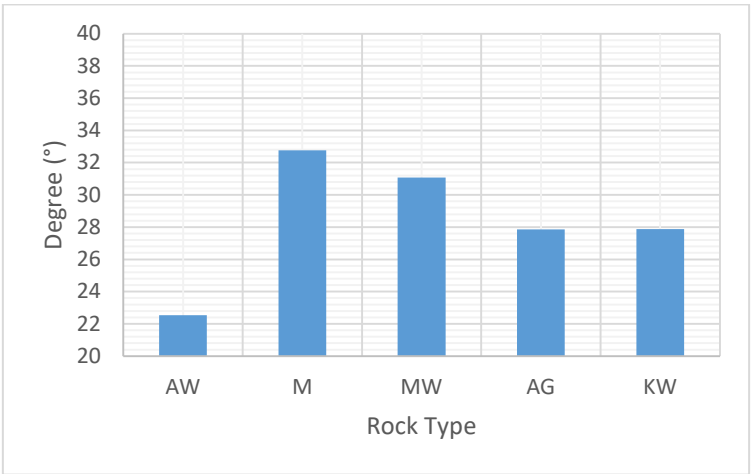

(a)

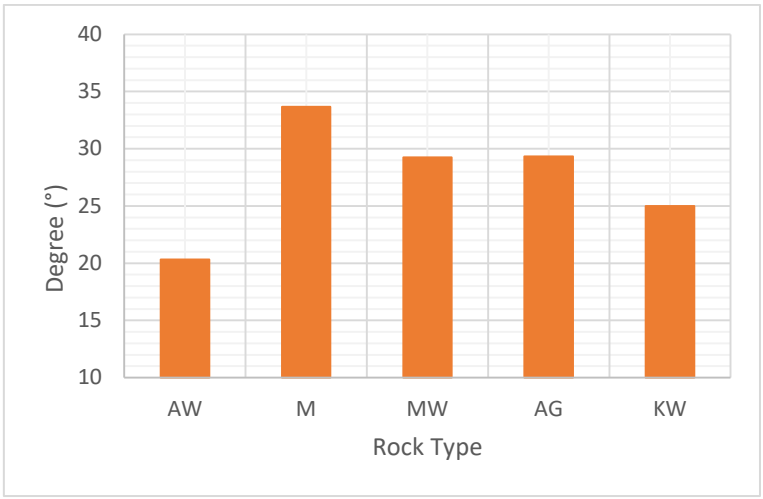

(b)

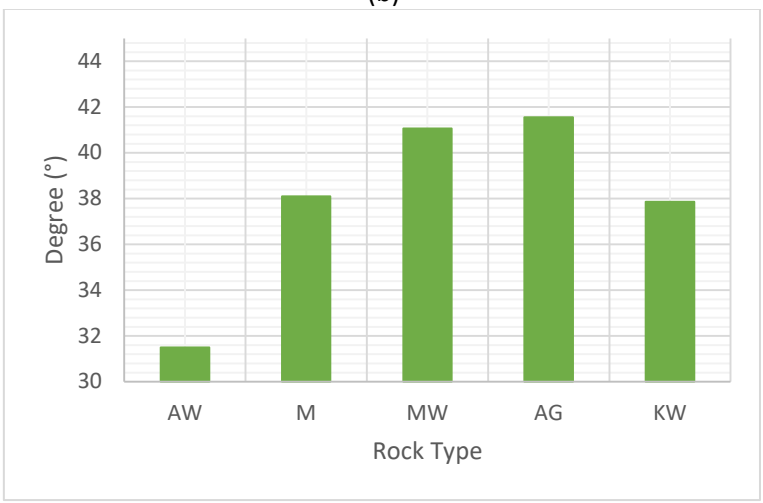

(c)

Figure 6. a) Results of planar sliding model b) Results of circular sliding model c) Results of wedge type sliding model

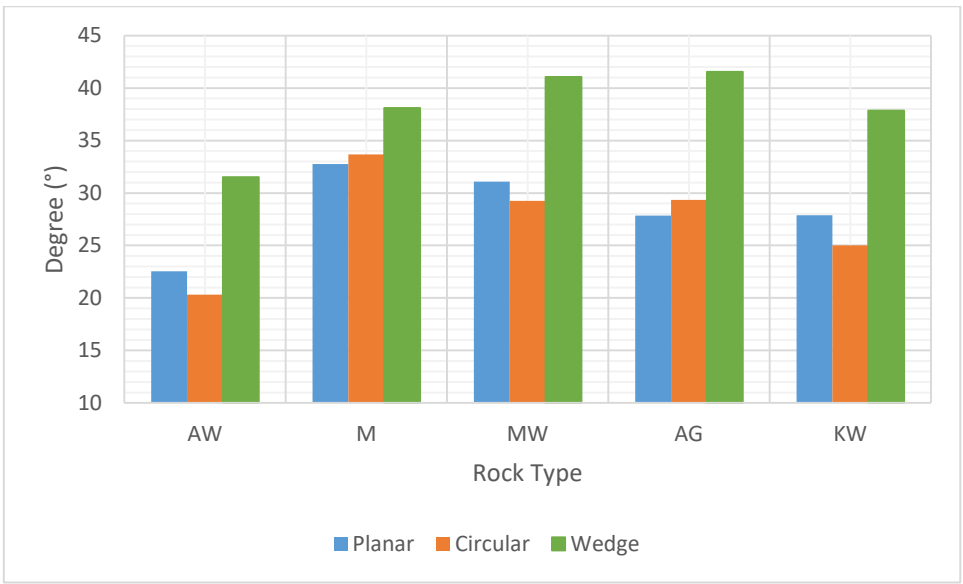

Figure 7. Tilt test results of all models

Experimental studies were also carried out in order to compare the planar, circular and wedge type samples with two and three surface contact test results specified in standards. According to the study conducted in compliance with ISRM standards (Alejano vd., 2018), higher values were obtained from the two cores set up than the three cores set up. The greatest results were obtained from MW sample in all experiments (Figure 8).

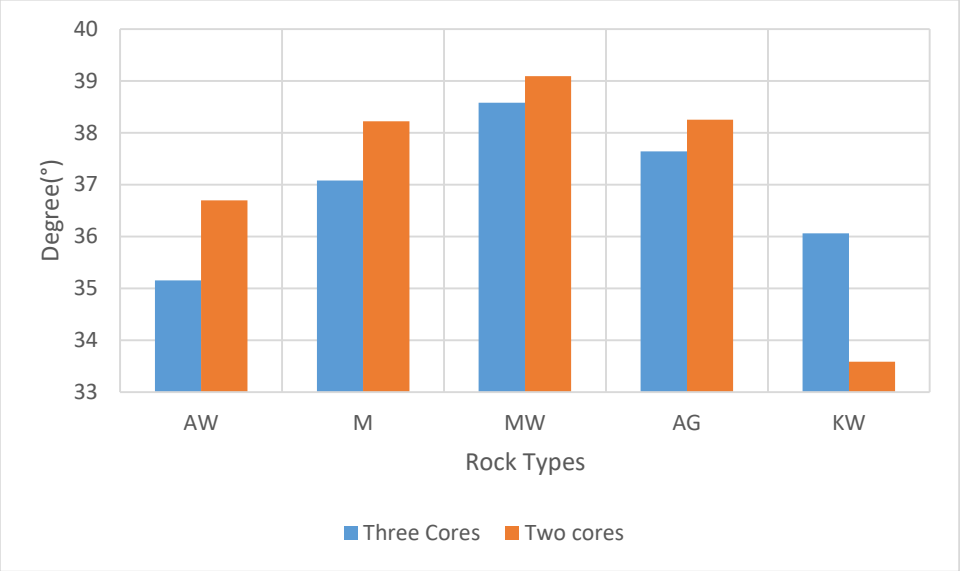

Figure 8. Two-three cores experiment set-up results

CONCLUSION

The basic internal friction angle is one of the important input parameters in the transition to the residual internal friction angle in rocks. In this study, the basic internal friction angles were determined by applying the tilt test to marble samples, which were cut similar to some slope slide types (planar, circular and wedge). Thus, the effect of different cutting patterns on the basic friction angle was investigated.

In the experiments with planar and circular type slide models, values in the range of 20-33° were obtained. In the wedge type slide model, values in the range of 31-41° were determined. It was observed that the results obtained using the wedge type slide model and the two-three cores set-up in accordance with ISRM standards were close to each other.

In planar and circular cut types, minimum results were obtained from Afyon White marble samples (AW) and maximum results were obtained from Marmara marble (M) samples. After the tests, wear on the sliding surfaces or surface roughness may decrease. For this reason, as the number of experiments increased, there was a decrease in the basic internal friction angle values.

Five different types of marble have different crystal structures. It is thought that these crystal structures cause the basic friction angles to be of different values. Therefore, it is considered that it is important to research the crystal structures in marbles in future studies.

In basic internal friction angle tests, it would be more appropriate to use samples of different shapes and sizes as well as standard samples. Especially, the use of sample shapes similar to slope slide models will provide the conditions in the field environment. As seen in the results obtained from this study; the different shapes and sizes of the test sample caused the test results to be different. Specially

for rock types with different lithology, it would be more appropriate to use samples similar to the slope slide types as suggested in this study, in order to obtain more optimal basic internal friction angle values. It is thought that this will be useful for comparing the basic internal friction angle values for different types of sample models.

ACKNOWLEDGEMENTS

The tilt device used in experimental studies was financed by Kütahya Dumlupınar University BAP project no: 2019-05.

REFERENCES

Alejano, L. R., González, J. ve Muralha, J. (2012). Comparison of different techniques of tilt testing and basic friction angle variability assessment. *Rock Mechanics and Rock Engineering*, *45*(6), 1023–1035. doi:10.1007/s00603-012-0265-7.

Alejano, L. R., Muralha, J., Ulusay, R., Li, C. C., Pérez-Rey, I., Karakul, H., … Aydan, Ö. (2018). ISRM Suggested Method for Determining the Basic Friction Angle of Planar Rock Surfaces by Means of Tilt Tests. *Rock Mechanics and Rock Engineering*, *51*(12), 3853–3859. doi:10.1007/s00603-018-1627-6.

Barton, N. R. ve Bandis, S. (1982). Effects of block size on the shear behavior of jointed rock. *The 23rd U.S Symposium on Rock Mechanics (USRMS)* içinde (ss. 739–760). California. doi:10.1016/0148-9062(83)91360-8.

Barton, N. R. ve Choubey, V. (1977). The shear strength of rock joints in theory and practice. *Rock Mechanics*, *10*, 1–54. doi:10.1016/j.ijfatigue.2014.08.012.

Beyhan, S. ve Özdemir, M. (2021). Evaluation of the basic friction angle in dry and conditioned fluids by tilt tests. *IOP Conference Series: Earth and Environmental Science* içinde (C. 833). doi:10.1088/1755-1315/833/1/012028.

Hencher, S. R. ve Richards, L. R. (2015). Assessing the Shear Strength of Rock Discontinuities at Laboratory and Field Scales. *Rock Mechanics and Rock Engineering*, *48*(3), 883–905. doi:10.1007/s00603-014-0633-6.

Jang, H. S., Zhang, Q. Z., Kang, S. S. ve Jang, B. A. (2018). Determination of the Basic Friction Angle of Rock Surfaces by Tilt Tests. *Rock Mechanics and Rock Engineering*, *51*(4), 989–1004. doi:10.1007/s00603-017-1388-7.

Kim, D. H., Gratchev, I., Hein, M. ve Balasubramaniam, A. (2016). The Application of Normal Stress Reduction Function in Tilt Tests for Different Block Shapes. *Rock Mechanics and Rock Engineering*, *49*(8), 3041–3054. doi:10.1007/s00603-016-0989-x.

Muralha, J., Grasselli, G., Tatone, B., Blümel, M., Chryssanthakis, P. ve Yujing, J. (2014). ISRM suggested method for laboratory determination of the shear strength of rock joints: Revised version. *Rock Mechanics and Rock Engineering*, *47*(1), 291–302. doi:10.1007/s00603-013-0519-z.

Ruiz, J. ve Li, C. (2014). Measurement of the basic friction Angle of rock by three different tilt test methods. *ISRM Regional Symposium - EUROCK 2014* içinde (ss. 260–266). Vigo, Spain: ISRM.

Ulusay, R. ve Karakul, H. (2016). Assessment of basic friction angles of various rock types from Turkey under dry, wet and submerged conditions and some considerations on tilt testing. *Bulletin of Engineering Geology and the Environment*, *75*(4), 1683–1699. doi:10.1007/s10064-015-0828-4.

Zhang, N., Li, C. C., Lu, A., Chen, X., Liu, D. ve Zhu, E. (2018). Experimental studies on the basic friction angle of planar rock surfaces by tilt test. *Journal of Testing and Evaluation*, *47*(1), 256–283. doi:10.1520/JTE20170308.

THE ARCHAEOLOGICAL USE OF MINING AND ROCK MECHANICS KNOWLEDGE

G.G.U. Aksoy [1,*], C.O. Aksoy[2]

[1] *Hacettepe University Mining Engineering Department, Ankara, Turkey*
*(*Corresponding author: gulsevaksoy@hacettepe.edu.tr)*
[2] *Dokuz Eylül University Mining Engineering Department, İzmir, Turkey*

ABSTRACT

Geological and Geotechnical Investigation and Reinforcement of the Ancient City Hasankeyf in Turkey, is carried out by a private company under the control of General Directorate of State Hydraulic Works (DSI). In the related site on the cliffs there are huge rock blocks which might cause a serious damage to the environment and historic fabric around. Prior to the reinforcement and protecting studies of stronghold the controlled dropping of the blocks mentioned must be performed. Knowledge and prediction of the seismic effects will be caused by dropping of the blocks to the historic fabrics called" Orta Kapı" and "Küçük Saray" and keeping induced effects below the thresholds existing in the literature are crucially important in means of reducing the blocks sizes before dropping. During the dropping of blocks previously specified which are of numbers 2, 3, 6 and 24 respectively, probable induced accelerations at "Orta Kapı" and "Küçük Saray" are determined and then the verification of the acceleration values whether they remain below or above the thresholds limiting maximum allowable accelarations to prevent any damage might be caused, is done. When the acceleration values originate at the locations where the blocks are dropped are previously calculated, small samples of rocks are dropped, acceleration for unit mass is determined and used as a scale factor in subsequent calculations. Effective absorption factor on the route between the points where the blocks are dropped and the target, is evaluated by performing in-situ tests and induced amplitudes are calculated after the absorption is applied to the equations.

Keywords: Acceleration, hasankeyf, seismic effects.

INTRODUCTION

The study was conducted at Batman/Hasankeyf historical places at Turkey. Hasankeyf location map of Batman Province is given in Figure 1.

Figure 1. Location map of Batman/Hasankeyf region

Within the scope of the work of "Investigation and Strengthening of the Hasankeyf Ancient City in terms of Geological and Geotechnical Ways" undertaken by the contractor company, there are activities to reduce the hazardous rocks in the region. In case the large block stones on the cliffs in the region are dropped, it is determined that the historical texture in the area and especially in the protection works of the company; serious damages can occur in historical buildings called ancient “Orta Kapı-Middle Gate” and “Kucuk Saray-Small Palace”. In order to know the seismic effects that may occur in these structures in advance and to prevent the threshold values permitted in the literature to be exceeded, the blocks should be reduced and reduced in a controlled manner. At this stage, to determine the vibrations that will be created during the dropping of the blocks, to make modeling studies with physical and geophysical approaches; it is the main purpose of the study to predict how important the structures will be affected by the acceleration value during the block drops by determining the important historical buildings as targets. Thus, the rocks in the literature that have the risk of exceeding the threshold-values in the acceleration / damage charts used in the earthquake-structure interaction will be determined and these rocks, which have been reduced in size by splitting into smaller pieces, can be lowered over the hill. The blocks to be dropped are named blocks numbered 2, 3, 6 and 24, respectively. The volume and ground heights of the blocks are given in Table-1, respectively.

Table 1. Volumes and height of blocks to be dropped

Rock no	Volume (kg/m^3)	Height (m)
2	60	69
3	80	69
6	6000	53
24	500	72

As rocks 2, 3, 6, and 24 fall to the ground, the acceleration value that occurs on the ground when the falling mass hits the ground and absorbed acceleration have been calculated.

According to the literature, the maximum acceleration value that can be allowed to occur at the target points is 0.025 g, the results related to the reduction of the specified rocks into one or more parts have been obtained in order not to exceed this acceleration value.

MATERIAL AND METHOD

The method applied in the study was carried out in two stages. A formulation study was carried out using the data from the experiments carried out in these two stages. At this point, the aim is to predict the acceleration values that will occur when the blocks are lowered and to reduce the blocks to the required dimensions so as not to exceed the maximum acceleration value determined at the target points as 0.025 g.

The stages of the method:

1. Reducing small size stones from the inn of the rocks numbered 2, 3, 6 and 24, which are planned to be dropped in a controlled manner; It is the calculation of the acceleration per unit mass by measuring the accelerations they create at the target point and where they fall.
2. To calculate the absorption between the place where the rocks fall and the target points (Orta Kapı-Middle Gate, Kucuk Saray-Small Palace), artificial accelerations are created with an external effect.

CASE STUDY

The coordinates of the blocks (2-3-6-24 Nolu Kaya) where the impact effect will be predicted when they are dropped and the target points (Orta Kapı and Küçük Saray), which are the aim of the experiment, are given in Figure 2.

Figure 2. Coordinates of target places and the rocks (2 Nolu Kaya, 3 Nolu Kaya, 6 Nolu Kaya, 24 Nolu Kaya) planned to be dropped.

First Stage of The Field Study

In the first stage, accelerations formed on the ground as a result of dropping only sample rocks were calculated (particle velocities were measured, converted to accelerations). Thus, particle-acceleration, k (scale coefficient) per unit mass and unit height could be calculated in the calculations section. The damping along the road could not be calculated at this stage, since the geophones on the foot of the door and on the door could not record. For this reason, the second stage was planned, and the experiment was carried out.

Second Stage of the Field Study

At this stage, in order to calculate the absorption in the route between the location where the rocks will be dropped and the target points (the route between the rocks to be dropped and the target (Middle Gate / Small Palace), the JCB backhoe loader has been hit on the ground at certain intervals with the bucket of the machine; 3 seismographs were also on the same line. The vibrations created by measuring at intervals were measured. These measurements were completed in 7 stages between the source and the target, since the vibrations caused by hitting the bucket to the ground were damped at short distances. The absorption factor between average and source-target was found. The positions of the devices along the line and 7 stages are shown in Figure 3 in different colors. Vibrations obtained from JCB measurements done at 7 stages are given in Table 2.

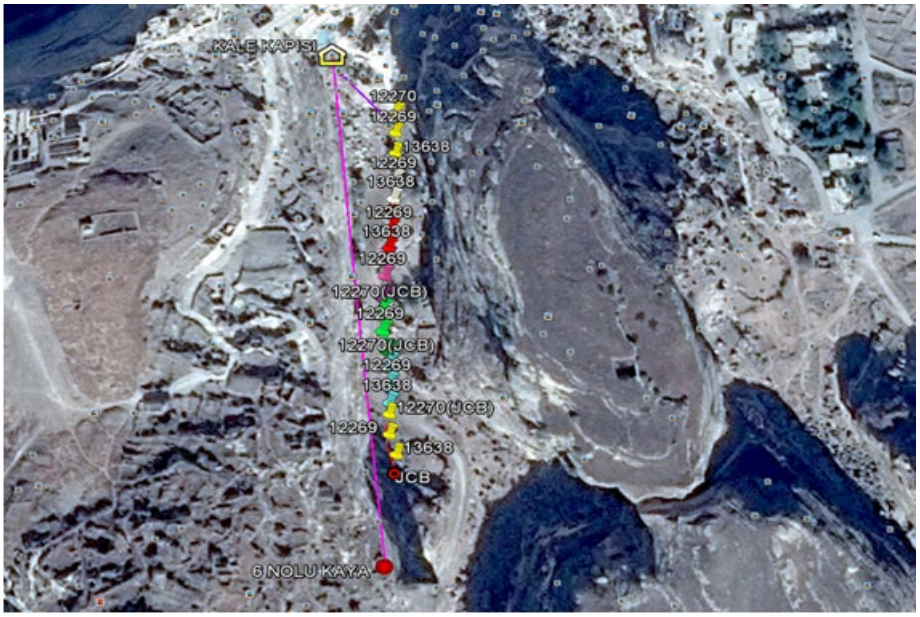

Figure 3. Geophone positions along the line

Table 2. Vibration records

Stages	Instrument	Particle Velocity, Vector-Sum, mm/s
1	13638	2.117
	12269	1.078
2	13638	3.378
	12269	1.000
	12270	0.554
3	13638	2.685
	12269	0.751
4	13638	2.896
	12269	1.198
	12270	0.751
5	13638	1.856
	12269	0.696
	12270	1.171
6	13638	3.219
	12269	0.730
	12270	0.539
7	13638	2.789

CALCULATIONS

In the calculation phase, Linear-System Theory assumption is valid. The α absorption coefficient, which is effective between the near station A and the remote station B (two seismograph with a certain distance between them on the same line on the route where JCB hits when performing the absorption test), is defined in Formula (1). The absorption coefficient is calculated from the formula (2) (Mares et al., 1984).

$$B=Ae^{-\alpha\,\Delta x} \quad (1)$$

$$\alpha = \frac{ln\frac{A}{B}}{\Delta x} \quad (2)$$

$$\alpha_e = \frac{\sum_{i=1}^{n} \alpha_i \, \Delta x_i}{\sum_{i=1}^{n} \Delta x_i} \quad (3)$$

A : Acceleration from Near-Station (g)
B : Acceleration from Far-Station (g)

Δx : Distance between two stations (m)
α : Absorption coefficient (m^{-1})
α_e : Affective absorption coefficient (m^{-1})
n, i : Number of measurements

Formula (4) gives the relationship between sample particle-acceleration A_0 and potential energy. k scale coefficients are calculated from Formula (5). The effective scale coefficient is calculated from the weighted-average of particle-accelerations with the help of Formula (6).

$$A^2{}_0 = k m_0 G h_0 \quad (4)$$

$$k = \frac{A^2{}_0}{m_0 G h_0} = \frac{A^2{}_0}{V_0 d_0 G h_0} \quad (5)$$

A_0 : Sample particle acceleration (g)
k : Scale coefficient (g kg^{-1} m^{-1})
m_0 : Sample mass (kg)
G : Gravity acceleration (= 1 g)
h_0 : Sample height (m)
V_0 : Sample volume (m^3)
d_0 : Sample density (kg/m^3)

$$k_e = \frac{\sum_{i=1}^{l} k_i \, A_{0,i}}{\sum_{i=1}^{l} A_{0,i}} \quad (6)$$

k_e : Affective scale coefficient (g kg^{-1} m^{-1})
l, i : Number of measurements

Particle accelerations of A_{kaya} ar calculated by Formula 7. Particle accelerations at target B_{hedef} are calculated by Formula 8. The target corresponds to Orta Kapı (Middle Gate) and Küçük Saray (Small Palace).

$$A_{kaya} = \sqrt{k_e V d G h} \quad (7)$$

$$B_{hedef} = A_{kaya} e^{-\alpha_e x} \quad (8)$$

A_{kaya} : Particle accelerations at the rock (g)
B_{hedef} : Particle accelerations at the target (g)
V : Volume of rock (m^3)
d : Density of rock (kg/m^3)
h : Height of rock (m)
x : Distance between the rock and the target (m)

$$R_{limit} = \frac{ln\frac{A_{kaya}}{B_{limit}}}{\alpha_e} \quad (9)$$

R_{limit} : Limit radius (m)
B_{limit} : Limit particle acceleration (= 0.025 g)

The target particle accelerations in Table 3 and Table 4 were calculated from Formula 8 and 9.

Table 3. Particle Acceleration calculated at Orta Kapı-Middle Gate (Bhedef)

Rock no	Volume (kg/m^3)	Density Kg/m^3	Height (m)	X(m)	A_{kaya} (g)	B_{hedef} (g)
2	60	2000	69	166	6.9235	0.000410463
3	80	2000	69	217	7.9946	0.000023827
6	6000	2000	53	290	60.6795	0.000002503
24	500	2000	72	48	20.4164	1.223766000

Table 4. Particle Acceleration calculated at Küçük saray-Small Palace (Bhedef)

Rock no	Volume (kg/m^3)	Density Kg/m^3	Height (m)	X(m)	A_{kaya} (g)	B_{hedef} (g)
2	60	2000	69	256	6.9235	0.000002097
3	80	2000	69	306	7.9946	0.000000129
6	6000	2000	53	397	60.6795	0.000000005
24	500	2000	72	135	20.4164	0.007452716

EVALUATIONS AND CONCLUSIONS

When Table-3 and Table-4 are examined, the accelerations are below 0.025g, which is determined as the limit value on the Middle Gate and Small Palace, except that the rocks number 24. For this reason, it is suggested that only rock numbered 24 should be divided into small pieces. Particle accelerations (g) at the place where rocks 2, 3,6 and 24 are dropped (o point) and at distances ranging from 0-150m are given in Figure 4. Threshold value of 0.025 g was chosen.

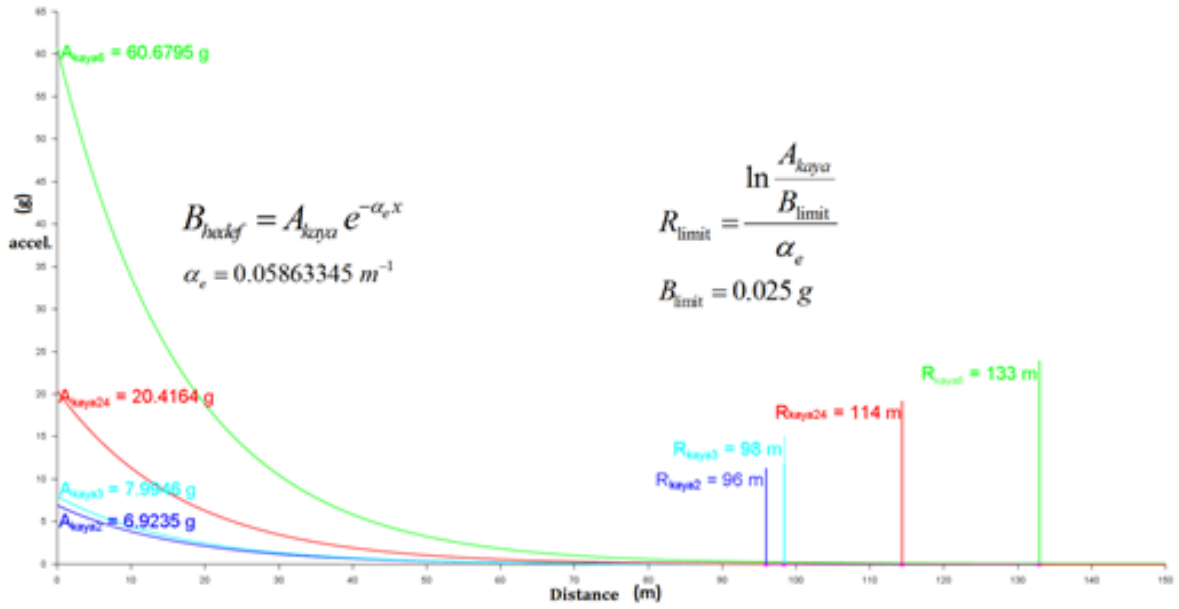

Figure 4. Particle accelerations vs distance

According to these calculations:

- Accelerations induced from dropping of rock-2 falls below 0.02g at a distance of 96 m from the source,
- Accelerations induced from dropping of rock-3 falls below 0.02g at a distance of 98 m from the source,
- Accelerations induced from dropping of rock-6 falls below 0.02g at a distance of 133 m from the source,
- Accelerations induced from dropping of rock-24 falls below 0.02g at a distance of 114 m from the source.

ACKNOWLEDGEMENTS

The authors would thank to Prof. Dr. Berkan Ecevitoğlu for his theoretical approaches used in the study and Ozan Gungor for helping in field studies.

REFERENCES

Mares S., “Introduction to applied geophysics”, Publisher: Dordrecht, holland; Boston: D. Reidel Pub. Hingham, MA, Sold and distributed in the U.S.A. and Canada by Kluwer Academic Publishers group, 1984

THE DETERMINATION OF SYNERGIC EFFECTS OF DIFFERENT TYPES OF FROTHERS IN FLOTATION

G. Güven [1], B. Tunç [1], Ş.B. Aydın [1,*], G. Bulut [1]

[1] *Istanbul Technical University, Mineral Processing Engineering Department*
*(*Corresponding author: beste.aydin@itu.edu.tr)*

ABSTRACT

Frothers that are surfactants are used in flotation to reduce bubble size and produce stable froth. The term critical coalescence concentration (CCC) is described the minimum concentration giving the minimum bubble size. The aim of this study is to examine the effect of single and dual-use of different types of frothers on bubble coalescence and bubble size. The bubble size was stated as Sauter mean bubble size (d_{32}) which is expressed as the ratio of bubble volume to the area is measured by ImageJ program. Aliphatic alcohol type frother (MIBC) and polyglycol type frother (Dow Froth 250) were used in this study. Depending on the increase of the frother concentrations, critical coalescence concentration (CCC), froth height, surface tension measurements were performed for single and dual-use of the frothers. According to the results, it was determined that MIBC reached the CCC value at a higher concentration compared to Dow Froth 250. Besides, smaller size froth was produced with the Dow Froth 250. However, better results were obtained in terms of bubble size when using frother blend.

Keywords: Frothers, critical coalescence concentration, froth height, surface tension

INTRODUCTION

Froth flotation method patented in 1905 has been widely used for separating minerals based on the difference in surface properties of hydrophobic and hydrophilic minerals. In its application, the air or gas bubbles are introduced into suspension and the collision of air bubbles and mineral particles is performed. The bubbles attached to hydrophobic particles carry these particles to the froth phase (Wills and Finch, 2016; Ata 2012).

Frothers in flotation are used to facilitate air dispersion into fine bubbles by preventing bubble coalescence in the pulp phase, and stabilization of flotation froths (Gupta et al., 2007). They are mainly heteropolar organic reagents that provide strength to the air bubbles to transport the collected hydrophobic particles as the froth products. It is known that the surface tension of the solution decreases because of the heteropolar nature of the reagent when the frothers are added to water. As the surface tension of solution lowers, more stable froths are generated and bubble coalescence is prevented in pulp phase (Klimpel and Hansen, 1988). Froth structure and froth stability have a significant role to determine mineral grade and recovery. The type and amount of frother, particle hydrophobicity, particle size, quality of process water, gas dispersion and particle contact angle influence froth stability (Farrokhpay, 2011; Schwarz and Grano, 2005).

Frothers can be classified into three groups. The first group is alcohols which contain aromatic alcohol such as α-creasol and 2, 3-xylenol and aliphatic alcohols such as 2-ethylhexanol, diacetone and methyl isobutyl carbinol (MIBC). A second group is the alkoxy types such as triethoxy butane (TEB). Finally,

the third group is synthetic frothers consisting of PEO (polyethylene oxide), PPO (polypropylene oxide) and PBO (polybutylene oxide) types have been formed (Gupta et al, 2007; Gelinas and Finch, 2005).

Critical coalescence concentration (CCC) is the most useful parameter used to evaluate frothers. Cho and Laskowski introduced this parameter in 2002. CCC is defined as a particular concentration at which the bubble size decreased with increasing frother concentration and then became stable. Critical coalescence concentration is the minimum frother concentration that effectively prevents air bubbles from joining during flotation (Szyszka, 2018).

The aim of this study is to determine the effect of frothers and their blends on flotation. Therefore, first of all, the influence of frothers and their blends were examined in two phases systems. Sauter mean bubble diameter and the critic coalescence concentration of the bubbles were obtained in the usage single and blend of frothers. In addition, froth height and surface tension measurement were undertaken.

MATERIALS AND METHODS

The tests were carried out in a two-phase system (water- nitrogen gas) using microflotation cell in order to specify their characteristics and differences depending on the concentration of frothers used as single or blend. Methyl isobutyl carbinol (MIBC) and Dow Froth-250 were used as frothers. The tests were performed with distilled water. After the images of the bubble formed in the froth zone in the microflotation cell were taken by a camera, the bubble diameter was determined with image analysis program (Image J). The experimental procedure for the measurements of bubble size has been described in Figure 1. Sauter mean diameter was calculated with the bubble diameter values. In addition, surface tension measurements were done for usage single and the blend of frothers. The froth height was measured with a scale placed at the edge of the microflotation cell.

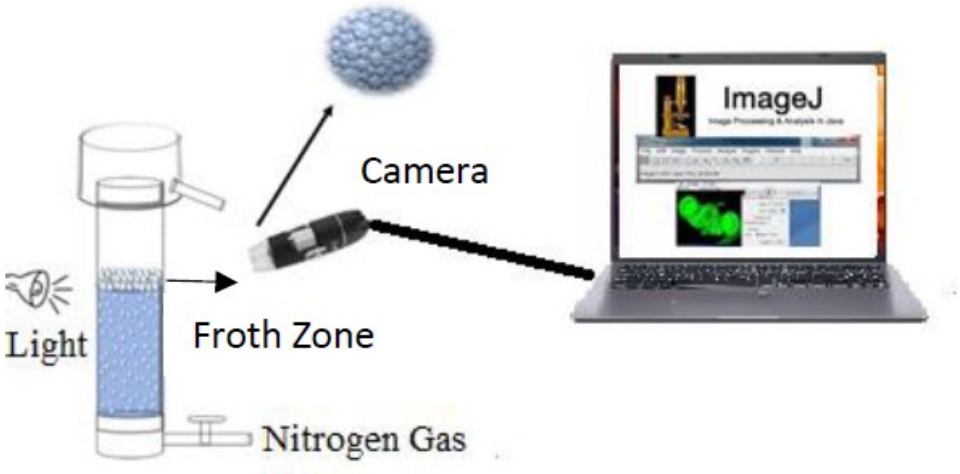

Figure 1. The experimental setup for the measurements of bubble size

Microflotation

The microflotation tests were conducted in the modified Hallimond tube. 100 ml nitrogen gas per minute at a constant pressure of 1 bar was supplied to the microflotation cell with a volume of 170 ml through frit of 15 µm pore diameter located at the bottom of the cell. Frothers and their blend were added at 1, 3, 5, 8, 10, 15, 20, 25, 30, 40, 50 ppm concentrations and volume of 100 ml into microflotation cell. The frother blend was prepared adding at a ratio of 50:50 from both of the frothers.

Bubble Size Measurement

In the test technique, after the rising bubbles through the microflotation cell were collected on the froth zone, the Digital USB microscope with 1000X zoom (Bushman CMOS 8 Led Microscope) connecting to the computer was used for taking photos from the froth zone. The diameters of all the bubbles taken in each image were measured with Image J software (version 1.8.0) to figure the Feret diameter. Sauter mean diameter formula was used for the transformation Feret diameter of the bubble.

Sauter mean diameter is one of the main indications to define bubble size of frothers. Equation (1) was utilized to calculate Sauter mean diameter, which is given below;

$$d_{32} = 6\frac{Vp}{Ap} \quad (1)$$

A_p and V_p are the surface area and volume of the bubbles, respectively.

Surface Tension Measurement

A Du Nouy Ring Tensiometer (Krüss®) was used to measure the surface tension of frothers at varying concentrations. Surface tension was measured to determine the effect of concentration on their surface activity. For each frother, stock solution (2000 ppm) was prepared with distilled water and then diluted for desired concentration. Surface tension measurements were carried out for MIBC, Dow Froth 250, and their blend in the range of concentration of 0-300 ppm. The blend was prepared by mixing the frothers in half the proportions.

RESULTS AND DISCUSSION

Bubble Size

The tests were performed in the microflotation cell based on concentration of MIBC, Dowfroth 250 and their blend. After the bubble size diameters were determined on the froth zone using Image-J programme at the end of the tests, they were calculated into Sauter mean diameters. In Figure 2, the sample images of MIBC, Dowfroth 250, and their blend at 50 ppm concentration are given. Figure 3 shows the effect of frother concentration on the Sauter mean diameter (d_{32}) for the frothers and their blend. The results indicated that the bubble size decreased with increasing frother concentration. When the frother concentration reached critical coalescence concentration (CCC) the bubble coalescence was prevented and concentration above the CCC value did not have any effect on the size of air bubbles. The CCC value for MIBC was found to be the highest as 11.0, while that for the blend was the lowest as 6.0. The CCC value for Dowfroth 250 was between that for MIBC and blend. The minimum bubble sizes obtained using these frothers were correlated with their CCC values. The results indicate that MIBC- Dow Froth 250 blend is the most effective in terms of bubble size reduction and the least effective one is MIBC. The Sauter mean diameter values for MIBC, Dow Froth 250, and blend were obtained as about 3.55, 2.70, and 1.30 mm, respectively.

Figure 2. The images of MIBC, Dowfroth 250 and their blend at 50 ppm concentration

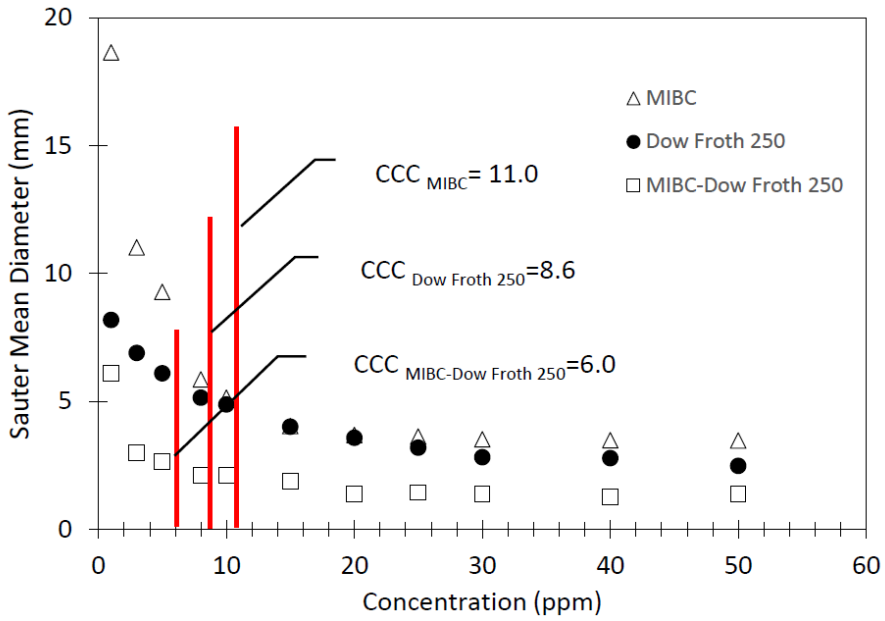

Figure 3. CCC values determined depending on Sauter mean diameters and concentration of frothers

Froth Height

In general, frothers reach the highest froth height between 30 - 40 ppm concentrations. Afterward, the froth heights mostly remain constant or there are small increases. Concentrations of less than 10 ppm are typically used to measure froth height in flotation applications (Cappucitti and Finch, 2008). Figure 4 shows the froth heights based on frother concentration. While MIBC has the lowest froth height, Dow Froth 250 and the blend have the highest height at 10 ppm concentration. However, the froth height of the blend at concentrations higher than 10 ppm increased more than Dow Froth 250. As a result, it can be said that the polyglycol type frother (Dow Froth 250) has a higher froth height than the alcohol type frother (MIBC)

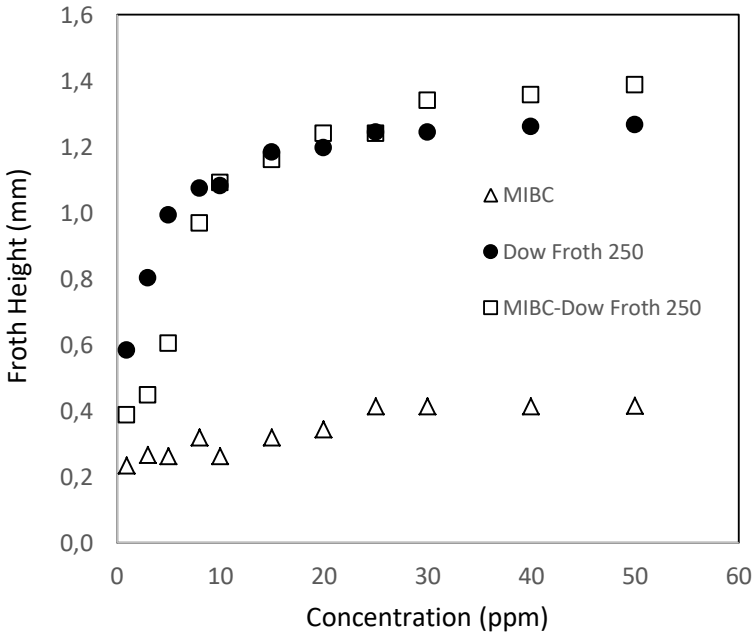

Figure 4. The effect of MIBC, Dow Froth 250 and their blend on froth height

Surface Tension

Surface tensions for MIBC, Dow Froth 250 and blend used in this study were measured and the results are shown in Figure 5. It is known that the frother molecules disrupt the hydrogen bonding between water molecules which lowered surface tension (Gelinas and Finch, 2005, An et al., 2018). According to the results, it can be seen that the surface tension decreased with increasing frother concentrations. It was found that the decrease in surface tension for Dow Froth 250 was more than MIBC, indicating that Dow Froth 250 is more surface-active. Surface tension for the blend was between that for MIBC and Dow Froth 250. The surface tension of the frother from the highest to the lowest is as given below.
Dow Froth 250 < Blend (MIBC-Dow Froth 250) < MIBC

CONCLUSION

Flotation of fine particles has become particularly important in recent years. One of the significant reasons for the decrease in flotation recoveries is stated as the inability of fine particles (<10 μm) to adhere to the bubble. It is necessary to produce small sized bubbles in order to increase of particle–bubble interaction. In this study, the synergic effect of the mixtures of frothers on the formation of small bubbles was investigated. The behaviour of industrial frothers such as MIBC and Dow Froth 250 and their blend in terms of critical coalescence concentration (CCC), surface tension and froth height were determined. The frothers showed the same characteristic with increasing concentration changes in all bubble diameter measurement tests. The bubble diameters first decreased rapidly and were almost fixed when they reached a certain concentration (CCC) and from this value, they were not affected by the frother concentration. While Dow Froth 250 was the frother with the lowest CCC value, the frother with the highest CCC value was MIBC in single use of frothers. However, the blend prepared with the mixture of both frothers has the lowest CCC value. In the froth heights tests, it was determined that polyglycol type frother (Dow Froth 250) has a higher froth height than the alcohol type frother. In addition, the tests related to surface tension of

frothers indicated that Dow Froth 250 was more surface-active due to its low surface tension. These data, which are measured in a binary system (liquid and gas), should also be examined with systems including ore or solid. Thus, the effects of frothers and their mixtures will be presented in a more realistic way for practice.

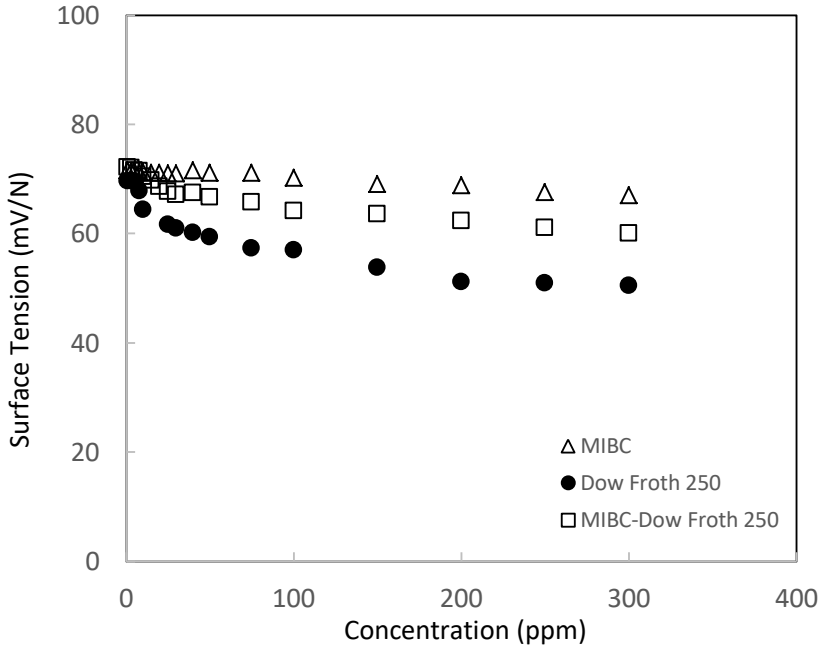

Figure 5. Surface tension measurements of MIBC, Dow Froth 250 and their blend

ACKNOWLEDGMENTS

This study was financially supported by the Istanbul Technical University, BAP (Scientific Research Project) Department with the project ID 42787.

REFERENCES

An, M., Liao, Y., Zhao, Y., Li, X., Lai, Q., Liu, Z., He, Y., (2018). Effect of frothers on removal of unburned carbon from coal-fired power plant fly ash by froth flotation. Separation Science and Technology, 53(3), 535-543.

Ata S., (2012). Phenomena in the froth phase of flotation-A review. International Journal of Mineral Processing, Vol. 102–103, 1-12.

Cappuccitti, F., Finch, J. (2008). Development of new frothers through hydrodynamic characterization. Mineral Engineering, vol. 21, 944-945.

Farrokhpay S., (2011). The significance of froth stability in mineral flotation — A review. Advances in Colloid and Interface Science, 166, 1-7.

Gelinas, S., Finch, J.A., (2005). Colorimetric determination of common industrial frothers. Mineral Engineering, 18, 263–266.

Gupta, A.K., Banerjee, P.K., Mishra, A., Satish, Pradip, P., (2007). Effect of alcohol and polyglycol ether frothers on foam stability, bubble size and coal flotation. International Journal of Mineral Processing, 82, 126–137.

Klimpel, R.R., Hansen, R.D., (1988). Frothers. In: Somasundaran, P., Moudgil, B.M. (Eds.), Reagents in Mineral Technology. Marcel Dekker, New York, 385–409.

Schwarz, S., Grano, S., (2005). Effect of particle hydrophobicity on particle and water transport across a flotation froth, Colloids and Surfaces A, 256, 157-164.

Szyszka, D., (2018). Critical Coalescence Concentration (CCC) for surfactants in aqueous solutions. Minerals, 8, 431.

Wills, B., Finch J., (2016). Wills' Mineral Processing Technology, chapter 12th, Elsevier, 265-380.

THE EFFECT OF FINE GRINDING ON CYANIDE LEACHING OF GOLD MINE TAILINGS

B. Bıyıklı [1, *], S. Sevgül [1], H. Dündar [2]

[1] *Koza Altın Co.*
*(*Corresponding Author: beril.bykli@gmail.com)*
[2] *Hacettepe University, Mining Engineering Department*

ABSTRACT

Ultra-fine grinding has been employed mainly to extract gold from refractory ores in which the gold particles are encapsulated. The liberation of gold particles, as well as the increased surface area achieved by ultra-fine grinding enhance the cyanide leaching performance. In contrast to refractory gold ores, oxidized ores are processed at relatively coarser sizes obtained by conventional grinding. This study is focused on the recovery of gold from oxide ore residue by utilizing fine grinding. The ore residue from a plant processing by agitated tank leaching was used in this study. The particle size (d_{80}) of the residue is approximately 75 micrometers (μm) and according to the chemical analysis results, it contains 0.52 ppm (g/tonne) Au. It is aimed to increase the gold dissolution efficiency by decreasing the particle size by fine/ultrafine grinding, allowing the gold to be liberated. After the grindings carried out at different times, the particle sizes of leaching were determined as 75, 38, 31, 20, 12 and 6 (μm) (d_{80}), respectively. For each particle size, leaching (bottle roll) tests were carried out in the laboratory under predetermined test conditions, and recovery of gold dissolution found as 15,62% and 36.37%, 40.12%, 57.65%, 63.99%, 91.48%, respectively. These results showed that, as expected, fine grinding had a positive effect on the dissolution of not only refractory but also oxidized gold ore.

Key words: Oxide gold ore, gold tailings, fine grinding, ultrafine grinding, cyanide leaching

INTRODUCTION

Cyanide has been widely used in metal extraction worldwide since 1887, especially in gold extraction. There are a few chemical reagents that dissolve gold in water, cyanide is readily available and economical compared to others. Extremely dilute solutions of sodium cyanide, typically in the range of 0.01% to 0.05% cyanide (100 to 500 parts per million) is used in gold mining operations (Logsdon, *et al.*, 1999). One of the main factors affecting the gold dissolution rate in cyanide leaching is the surface area of the particle. Particle size and shape are the main factors affecting the surface area of a mineral particle. The exposed surface area is directly related to the grain size, distribution and release properties of the feed material and is affected by the efficiency of the pre-leaching milling processes. Efficiency generally increases with decreasing grain size due to an increase in gold liberation and/or surface area of gold particles (Marsden & House, 2006). Because of both the capital and maintenance costs of the equipment and the energy consumption, grinding cost can reach up to 70% of the operating costs of a mining facility. This plays an important role like the decision of the required process method for the ore extraction. In order to determine the ideal grain size of the ore by fine or ultrafine grinding, the mill efficiency and cost comparison should be made optimally (Gao & Holmes, 2008).

Today, while free milling high-grade ore deposits are decreasing, the economic value of low grade ore deposits has increased with fine liberalization grain size. As a result, demand for fine and ultra-fine grain size in industrial minerals and the need for reprocessing of mine tailings has increased therefore the importance of Fine and Ultra Fine Grinding has also increased (Wills & Napier–Munn, 2006). In 1990, accepted technology for economically regrinding to ultrafine sizes in the processing of metallic minerals was almost negligible. According to the 1990 and 1991 test studies, high-speed horizontal mills can efficiently grind to 80% of product passing 7 microns at laboratory scale, consequently metallurgical performance increase significantly (Harbort, Hourn & Murphy, 1998). Pretreatment processes are required for the extraction of refractory gold ores before direct cyanide leaching. There are certain conditions for a gold ore to be classified as refractory. Some of these are;

- Presence of gold grains in physical inclusions, sulfide, oxide mineral and/or silicate structures (Afenya 1991; Brooy ve diğ, 1994).
- Presence of gold grains in sulfide structures (mostly arsenopyrite) in sub-microscopic sizes as “invisible gold” or “solid solution” (Brooy ve diğ, 1994; Chen ve diğ, 2002; Komnitsas ve Pooley, 1989).

Ultrafine grinding (<10µm) can be used as an alternative to other pretreatments, especially for sulfide gold ores, because, it is a more environmentally and economically advantageous method (Corrans & Angove, 1991). Processes of fine and ultrafine grinding are carried out by mechanisms consisting of mechanical activation, effect of liberation and removal of the passivating film layer that will form on the grains (Balaz, 2003).

In this study, the effects of fine grinding on the dissolution efficiency of gold in the tailings of an agitated tank leach plant were investigated. Firstly, the sample was ground at different times to obtain different particle sizes, after that, cyanide leaching was performed for each particle size. Finally, gold dissolution rates were calculated for each different particle sizes.

MATERIAL AND METHODS

In this study, the gold mine tailings from an agitated tank leach plant was used. The tailings obtained as pulp from the Detox unit and it was washed with water to purify the chemicals, and then solid-liquid separation was carried out using laboratory-scale pressure press filters. The chemical composition of the sample (Table 1.) was determined by wet chemical analysis method using ICP-OES, LECO and AAS after hot digestion in aqua regia for Au-Ag analysis.

Table 1. Chemical Composition of the Gold Mine Tailings

Elements	Au	Ag	Cu	Ni	As	Sb	Fe	S	C
Units	ppm	ppm	ppm	ppm	ppm	ppm	ppm	%	%
Equipments	AAS	AAS	ICP-OES	ICP-OES	ICP-OES	ICP-OES	AAS	LECO	LECO
Gold Mine Tailings	0,52	2,11	71,76	1462,00	2687,00	49,32	64403	1,09	0,48

In order to determine the composition of the minerals, backscatter mapping and linear and point spectrum analysis were performed on sample's surface. The texture, shape and content properties of ore minerals and gangue minerals were tried to be determined using SEM-EDX.

The sulfide minerals observed in the sample by the optical mineralogy method are mainly pyrite, and the goethite mineral representing the oxidation zone (Figure1 and Figure 2). The pyrites, which are observed in places as free, have a porous structure. The porous structure of pyrites develops due to high temperature. It shows anisotropy in bluish tones, but its anisotropy is partially masked by its internal reflection in red, orange or yellowish colors. Pyrite crystals are very fine-grained, usually completely transformed into secondary goethite, and rarely partially replaced by goethite and manifest as residual pyrites.

Barite ($BaSO_4$) mineral, approximately 5 micron in size, was observed in the study sample in the analyzes made by SEM-EDS method. When the samples are examined in general, the density of Fe, O and S elements draws attention. Pyrite, Arsenopyrite, associations were determined. Accordingly, it was determined that the ore mineral determined as a result of mineralogy and petrographic analysis and the minerals observed in SEM-EDX support each other. No Au can be found in the samples in optical and electron microscopy examinations.

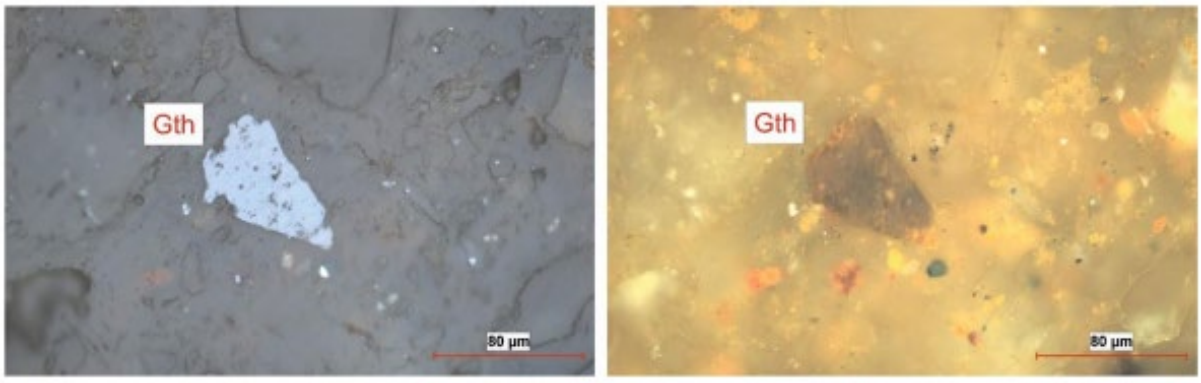

Figure 1. Goethite Mineral within the Fe-Ox Group

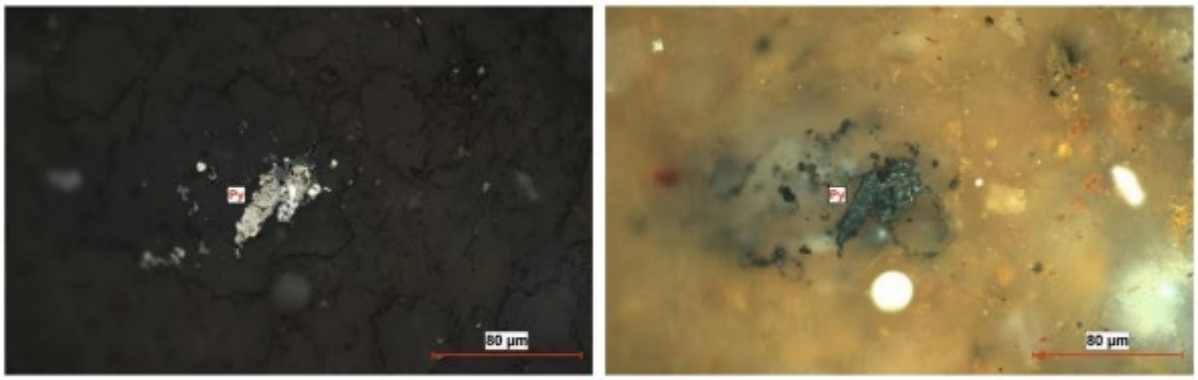

Figure 2. General View of the Pyrites

First of all, the samples are divided homogeneously for the tests to be performed. The particle size distribution analysis of the feed sample was determined using Malvern Master Sizer 2000 and the particle size distribution graph is shown Figure 3.

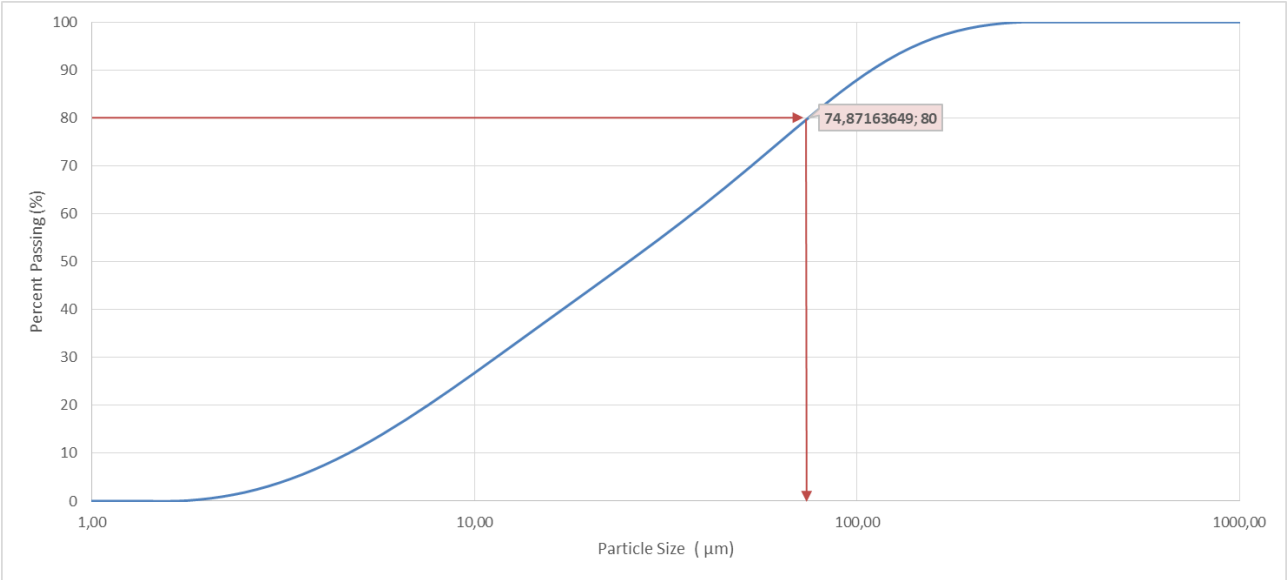

Figure 3. Particle Size Distribution Graph of Feed

According to the particle size distribution plot, d_{20}, d_{50} and d_{80} sizes of the sample were determined as 7.55 µm, 25.35 µm and 74.87 µm, respectively.

In order to determine the amount of Au in the particle size fractions for the gold mine tailings, a sieve analysis was carried out using the Retzsch AS200 Basic wet sieving device and the distribution of Au in different size groups is given in Table 2.

Table 2. Au in the Different Particle Size Fractions

Particle Size Ranges (mm)	Amount (%)	Au Amount (ppm)	Au Amount (%)
+0,106	9,11	0,54	10,22
-0,106,+0,075	5,81	0,55	6,65
-0,075+0,053	17,22	0,55	19,68
-0,053+0,038	9,60	0,53	10,57
-0,038+0,020	12,26	0,50	12,74
-0,020	46,00	0,42	40,15
Total	100,00		

NETZSCH vertical batch mill and zirconia balls as grinding media, shown in Figure 4, were used for laboratory scale fine/ultrafine grinding. Zircon balls used as grinding media were selected in 2 different sizes, 1.5 mm and 3.5 mm. It was decided that the ball charge would be 35%, and 80% of this was composed of 1.5 mm and 20% 3.5 mm balls. The grinding was carried out as wet grinding and the pulp solid ratio was determined as 30%.

Figure 4. Vertical Batch Mill and Zirconia Balls

For each sample, five grindings were carried out separately, with different durations. After that, d_{80} sizes of the samples 37.66 µm, 30.68 µm, 21.31 µm, 12.74 µm and 6.14 µm were reached. It can be seen from the Figure 5. that as the milling time increases, greater size reduction is achieved and more milling energy is required to obtain finer particle sizes.

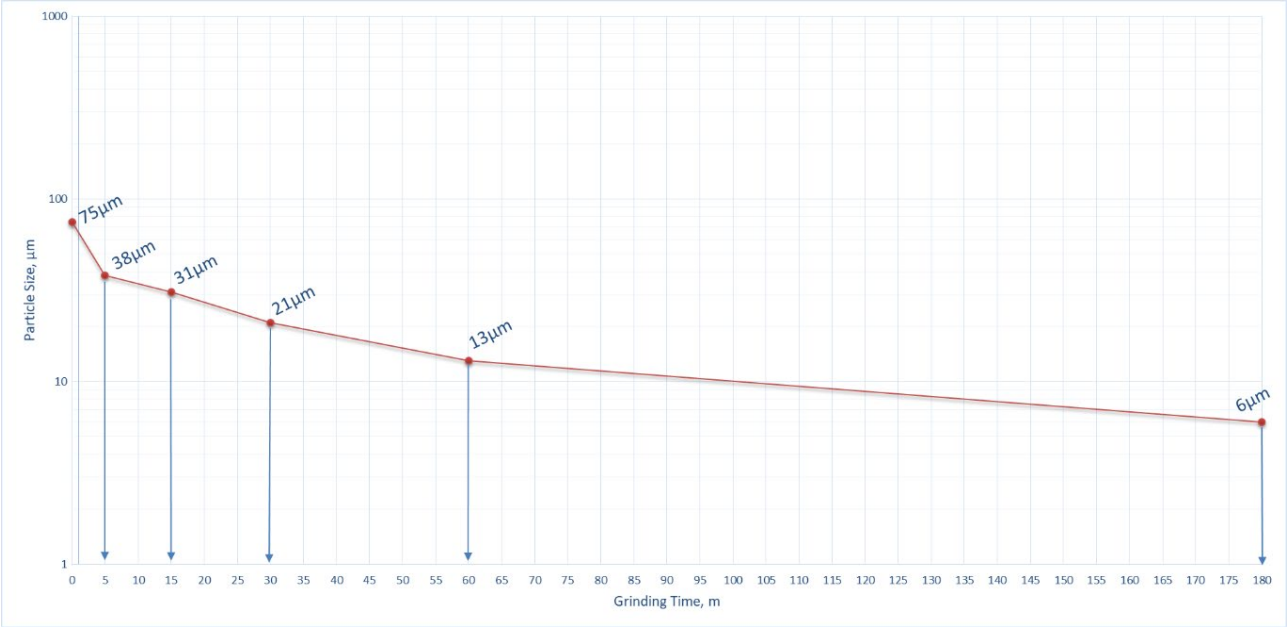

Figure 5. Particle Size vs Grinding Time Graph

Particle size distributions of these ground samples and the feed sample are shown Figure 6.

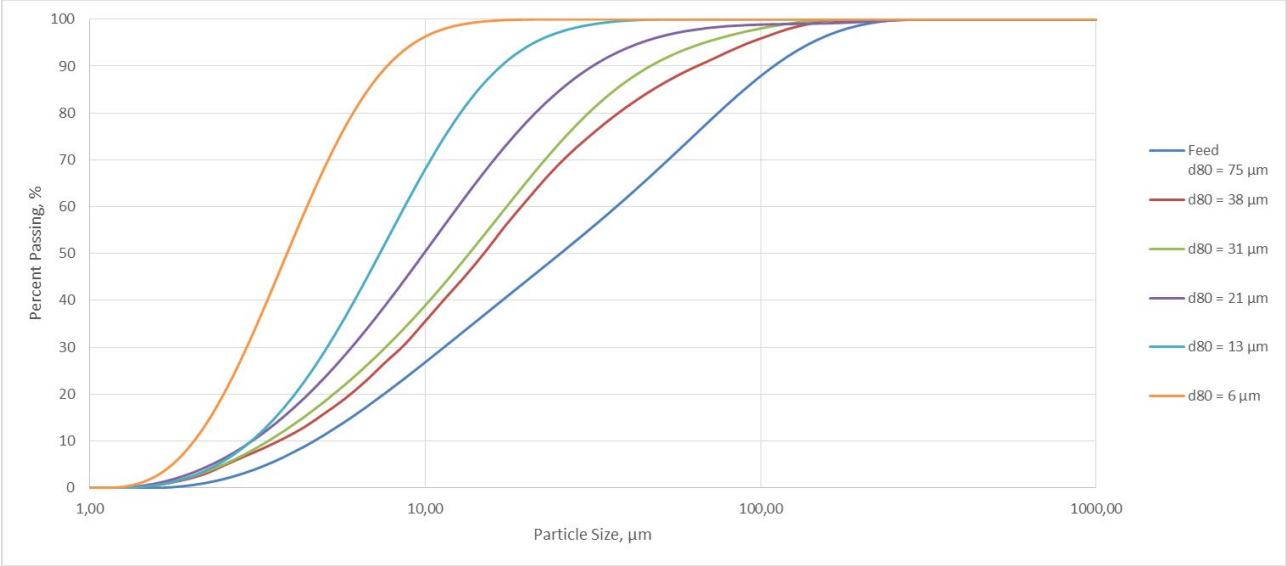

Figure 6. Particle Size Distribution of Ground Samples

The ore was used in this study, is the gold mine tailings from an agitated tank leach plant therefore, for determining the leaching behavior of the ores lab scale bottle roll tests were used. The conditions for this study are shown in the Table 3.

Table 3. Cyanide Leach Conditions

Pulp Density (%)	30
NaCN (g/L)	2
Dissolved Oxygen (ppm)	15-25
Residence Time (h)	48
pH (Controlled with $Ca(OH)_2$)	10,5-11

Cyanide leaching tests were carried out in a 3 L glass bottle, agitated at 1000 rpm under these conditions. After the tests were completed, solid-liquid separation of the pulp was carried out using press filters and the residues dried for chemical analysis. Silver nitrate titration (0.02mol/L $AgNO_3$) using p-dimethylamino-benzal-rhodanine (0.02%w/w in acetone) as the indicator was used for to determine the concentration of NaCN in final solution. The consumption of NaCN and $Ca(OH)_2$ was recorded.

RESULT AND DISCUSSION

In this study, six different particle sizes were studied: d80 = 75 µm, 38 µm, 31 µm, 21 µm, 13µm and 6 µm, including the feed particle size.

The gold recovery of the ground samples after cyanide leaching is shown in the Figure 7. According to the figure, the initial gold dissolution rate is faster up to the first 4 hours and reaching almost its maximum value after 24 hours. Although the amount of gold dissolution between 24 and 48 hours is slightly difference compared to the first 24 hours, it is seen that these differences are more significant especially in fine grain sizes.

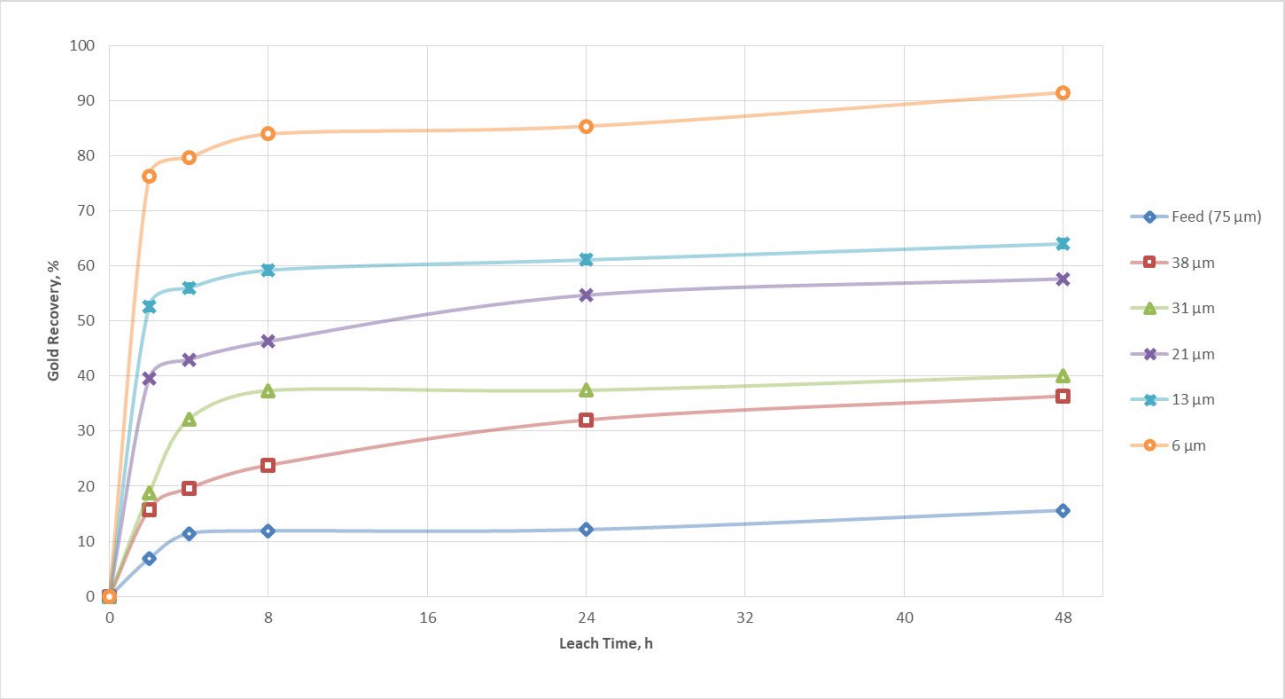

Figure 7. Gold Recovery of the Ground Samples

The Figure 8. presents the gold recovery and cyanide consumption for each grain size. Reduction in particle size means increasing the surface area, therefore it is clear from the Figure 8. that while the gold dissolution increases as the particle size decreases, the cyanide consumption also increases at the same proportion. One of the reasons for this is the dissolution of not only gold but also other metals due to the increased surface area.

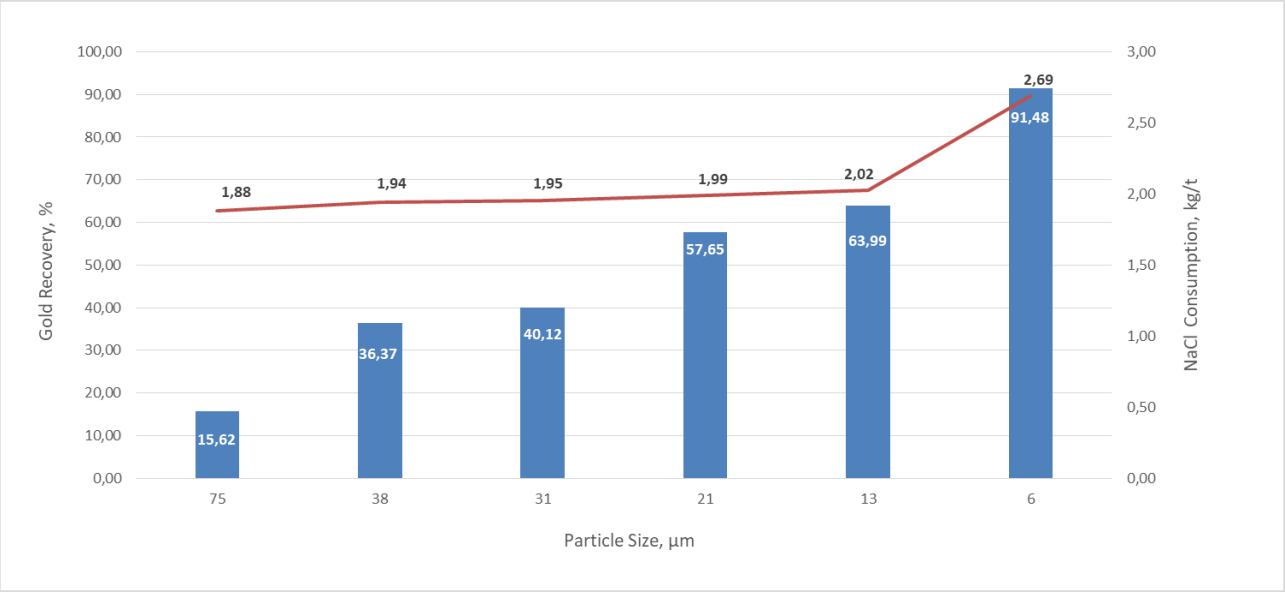

Figure 8. Au Recovery vs NaCl Consumption

CONCLUSION

Considering the absence of Au in the samples in both optical and electron microscopy examinations and the results of the sieve analysis performed to determine the amount of Au in the particle size fractions, it can be interpreted that the gold in the studied sample is highly fine-grained.

The gold mine tailings studied (initially at a feed size of 75 µm) contained 0.52 g/t Au. Only 15.6% of the gold from this tailing could be obtained directly by cyanide leaching. The gold recovery rate reached 95% when the ore was ground to 6 µm, confirming the expectation that the recovery would increase as the particle size decreased. Also, it was observed that the minerals liberated with the decreasing grain size caused an increase in NaCl consumption during the leaching stage. For the same reason, it can be said that an increase is also expected in the consumption of chemicals such as CaOH used for pH adjustment and flocculant used in most mineral processes where there is a need for sedimentation, filtration or centrifugation.

An IsaMill Cost-Benefit Study was conducted for this gold mine in 2013. The energy consumption of the ball mill is about 20 kW/m3 whereas IsaMill operates at a high energy levels (up to 350 kW/m3). According to the report of this study, it has been observed that the recovery of this ore, which is produced with a particle size of 70 µm and an average gold recovery of 88.2%, increases up to 94% by grinding below 10 µm. However, it is necessary to use approximately 96 kW/m3 of power to reach 9 µm. In general, it was observed that the recovery increased significantly when the grain size decreased below 20 µm.

While the samples used in this study and the study conducted in 2013 were different, a similar trend was observed in recovery increase depending on particle size. Therefore, similar results are expected in parameters such as grinding and chemical consumption costs.

Although grinding is an expensive process, according to different studies, there are much more efficient mills today (Harbort et al., 1998; Ellis, 2003; Ellis and Gao, 2003; Jankovic, 2003; Deschenes et al., 2005). The economic balance of energy and other consumptions required for ultrafine grinding is not considered within the scope of this study.

REFERENCES

Afenya, P. M. (1991). Treatment of carbonaceous refractory gold ores. Minerals Engineering, 4(7–11), 1043–1055.

Baláž, P. (2003). Mechanical activation in hydrometallurgy. *International journal of mineral processing*, *72*(1-4), 341-354.

Brooy, S. R. La, Linge, H. G. I., & Walker, G. S. (1994). Review of gold extraction from ores. Minerals Engineering, 7(10), 1213–1241. https://doi.org/10.1016/0892-6875(94)90114-7

Chen, T. T., Cabri, L. J., & Dutrizac, J. E. (2002). Characterizing gold in refractory sulfide gold ores and residues. Jom, 54(12), 20–22.

Corrans, I. J., and J. E. Angove. "Ultra-fine milling for the recovery of refractory gold." Minerals Engineering 4.7-11 (1991): 763-776. (91)

Deschenes, G., McMullen, J., Ellis, S., Fulton, M., & Atkin, A. (2005). Investigation on the cyanide leaching optimization for the treatment of KCGM gold flotation concentrate—phase 1. *Minerals Engineering*, *18*(8), 832-838.

Dikmen, S., & Ergün, Ş. L. (2004). KARIŞTIRMALI BİLYALI DEĞİRMENLER. *Bilimsel Madencilik Dergisi*, *43*(4), 3-15. (54)

Ellis, S., & Gao, M. (2003). Development of ultrafine grinding at kalgoorlie consolidated gold mines. *Mining, Metallurgy & Exploration*, *20*(4), 171-177.

Ellis, S., Mines, K. C. G., & Kalgoorlie, W. A. (2003). Ultra fine grinding-a practical alternative to oxidative treatment of refractory gold ores. In *Eighth Mill Operators Conference* (pp. 11-17). Townsville QLD, Australia.

Gao, M., & Holmes, R. (2008). Developments in fine and ultrafine grinding technologies for the minerals Industry. *The Institute of Materials and Mining (IOM3) Mining, Feature, March*, *1*, 20078.

Harbort, G., M. Hourn, and A. Murphy. "IsaMill ultrafine grinding for a sulphide leach process." AJM (1998): 1-6.

Jankovic, A. (2003). Variables affecting the fine grinding of minerals using stirred mills. *Minerals Engineering*, *16*(4), 337-345.

Komnitsas, C., & Pooley, F. D. (1989). Mineralogical characteristics and treatment of refractory gold ores. Minerals Engineering, 2(4), 449–457

Logsdon, M. J., Hagelstein, K., & Mudder, T. (1999). *The management of cyanide in gold extraction* (p. 10). Ottawa: International Council on Metals and the Environment.

Marsden, J., & House, I. (2006). *The chemistry of gold extraction*. SME.

Wills, B. A., & Napier–Munn, T. J. (2006). Mineral Processing Technology*: an introduction to the practical aspects of ore treatment and mineral recovery*, Elsevier Science & Technology Books.

THE EFFECT OF STATIC ELECTRIC ON SETTLING BEHAVOUR OF AN INDUSTRIAL BLAST FURNACE WASTE WATER

E. Gülcan

Hacettepe University, Mining Engineering Department
(ergingulcan@hacettepe.edu.tr)

ABSTRACT

Dewatering process has critical importance in terms of waste and process water treatment, reduction of harmful environmental effects of waste water, and reusability of scarcing water resources. Domestic and industrial (especially ore beneficiation) processes produce large volumes of wastewater contaminated with fine particles. The most common method used in dewatering is the conditioning and precipitation of pollutants with special chemical agents. The equipment commonly used for this purpose in mining industry is called thickener.

The aim of this study is to examine the effect of static electricity on the sedimentation behavior, in addition to the methods used for dewatering industrial wastes. In this context, the flocculation and coagulation behavior of the sludge obtained from a blast furnace used in the iron and steel industry was investigated. Following the determination of the optimum flocculant and coagulant dosage, precipitation tests were performed using natural (without chemicals) and triboelectric implementation. Two commonly used methods (Talmage-Fitch and Coe-Clevenger) were used and compared for the determination of settling rates.

Results of this preliminary study under certain conditions showed that triboelectricity yields higher rate of precipitation results compared to tests performed without chemicals and with the use of coagulants. However, they are quite low compared to the settling times obtained with the use of flocculants.

Keywords: Dewatering, static electric, settling rate

INTRODUCTION: BASICS of STATIC ELECTRICITY and DEWATERING

Triboelectricity is based on the principle of changing the natural surface charges of the grains by the effect of static electric. Chemical bonds are formed at the molecular level between the particles touching/rubbing each other, and electron exchange takes place between the molecules with the breaking of these bonds (Bittnera et al., 2014; Iuga et al., 2001). Triboelectric series, on the other hand, is the name given to the material scale that provides a very general information about the amount and direction of the charges that will be formed by the touching/rubbing of different materials. Polymer structures, metals, minerals, many materials that we use in our daily life are located in different levels in the triboelectric series. When a material on the positive side of the triboelectric series is rubbed/touched with any material on the negative side, one of them is positively charged and the other negatively charged. The farther these materials are from each other on the triboelectric series, the higher the charge density (Diaza and Felix-Navarrob, 2004; Park et al., 2008; Wu et al., 2013; Panat et al., 2014).

Micronized solid particles are widely used as intermediate or final product in many industries, especially in mining. These charged particles tend to suspend in the air and in the liquid which can cause

serious problems in the processes and in overall environment. For example, charged particles that encounter electrostatic forces on conveyor belts cause adhesions and thickening on equipment walls, reducing equipment performance. In another example, uncontrolled static electricity causes explosions with serious discharges in the air (Nifuku et al., 1989; Guardiola et al.; Yao et al., 2004; Ohsawa, 2003). On the other hand, many useful applications have been developed by utilizing the movements of static electrically charged particles in the electric field. Some of these are electrostatic separators (Dizdar et al., 2019), electrostatic dust collectors (Kleber and Makin, 1998) and dry electrostatic precipitators (Lawless, 1999).

Although static electricity has been studied by many researchers for many years, this subject still contains many unknowns and conflicting results have been published. The reasons for this are briefly listed in the study compiled by Matsusaka (et al., 2010). There are many factors affecting the static electric based processes such as chemical, physical and electrical properties of materials and environmental conditions, uncertainties in the distribution of the amount of charge on the grains, and the difficulty of estimating and controlling the electrostatic charge. In this context, it is important to measure the electrostatic charge and evaluate the electrostatic properties in order to analyze and control the loading of the particles. However, it is also important to explore new areas of industrial applicability of static electric. Dewatering process has a critical importance in terms of purification of water from solid particles and recycling, reduction of harmful environmental effects and reusability of water. The aim of this study is to examine the effect of static electricity on the sedimentation behavior broadly in combination to the methods used for dewatering industrial wastes. In this context, the flocculation and coagulation behavior of the sludge sample obtained from a blast furnace used in the iron and steel industry was investigated. Experimental studies covered the determination of the optimum flocculant and coagulant dosages, precipitation tests with static electricity and comparing common methods used for the determination of settling times.

Coagulation, Flocculation and Settling Time

Coagulation and flocculation process are the unit physicochemical methods used for wastewater management (AWWA, 1999; Gregory, 2006). The purpose of this process is to 'flocculate' the particles in the water into larger particles using chemicals (Davis, 2010). Flocculants are small molecules or polymers that can be inorganic or organic (Tian et al., 2007). Polymeric flocculants can be classified as anionic, nonionic and cationic.

Blast furnace sludge wastes are generally treated with polyacrylamides and FeCl3 (ferric chloride) for efficient dewatering. Polyacrylamides are a type of high molecular weight nonionic flocculants well known in mineral processing applications (Owen et al., 2002). FeCl3, which is a coagulant agent, is used in water treatment to precipitate sulfide and in wastewater treatment plants to precipitate phosphate, but it is very ineffective as a flocculant (Abbasi and Taheri, 2013). With the effect of static electric, there is a change in the natural surface charges of the grains. When the grains touch each other, they form a molecular level chemical bond (Dizdar et al., 2018). A flocculant and/or coagulant, which has an electric charge opposite to the electric charge of the particle, has to be used in order to reduce the zeta-potential and to accelerate the sedimentation/dewatering. For this reason, within the scope of this study, it is aimed to compare the precipitation times calculated using polyacrylamide, FeCl3 and static electricity.

Industrial dewatering is primarily performed with thickeners in mineral processing operations, followed by industrial filters. Coe - Clevenger and Talmage - Fitch approaches are the most commonly used methods to determine the area and settling time of the thickener equipment (Parsapouret al., 2014). In these methods, the settling time is calculated by measuring the change with time (**Figure 1**). The equations used to calculate the thickener areas with Coe-Clevenger and Talmage-Fitch approaches

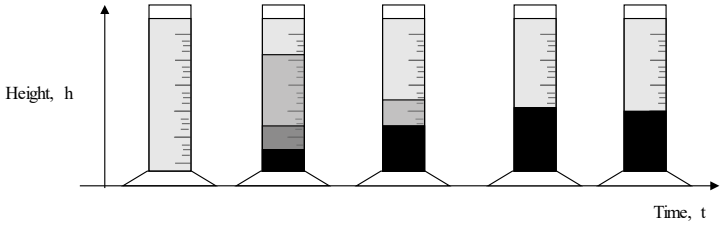

Figure 1. Experimental method used to calculate the thickener area is schematized

$$A = 1.25\ x\ W\ x\ \frac{tu}{Co\ x\ Ho} \quad (1)$$

$$A = \frac{W(1/C - 1/Cu)}{(H - Hu)/tu} \quad (2)$$

Where;
A= thickener area (m^2)
W= tph dry solids fed to the thickener
F= liquid to solids ratio by weight at any region within the thickener
D= liquid to solids ratio of the thickener discharge
S= specific gravity of liquid (kg/lt)
C= pulp concentrations (kg/lt)

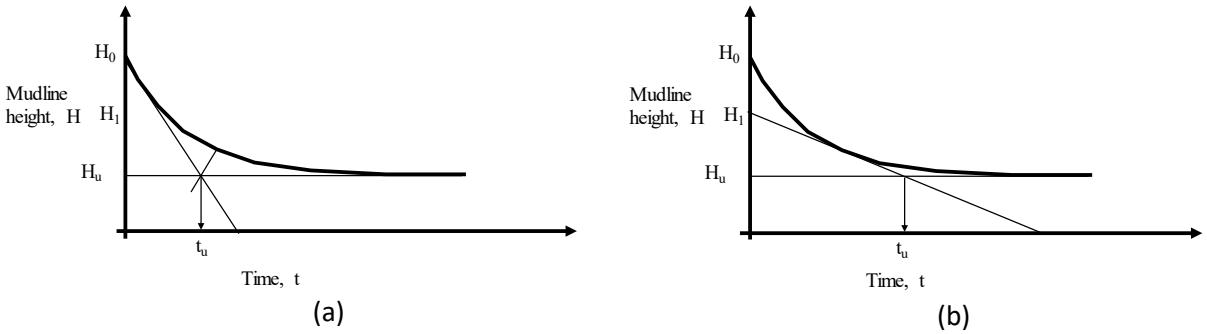

Figure 2. Exemplary batch settling curves and t_u determination with Talmage-Fitch (a) and Coe-Clevenger (b) methods.

MATERIALS AND METHODS

Sample Preparation and Characterization

Slag samples obtained from a blast furnace used in the iron and steel industry was used in experimental studies. This reaction by-product material was obtained from the existing thickener downstream located in the industrial plant. The analyzes of this material, whose contents and solid ratios radically change with time, were evaluated over average values. The sample was delivered to the laboratory having approximately 34% solids. The particle size distributions of the sample taken from different points (A, B, C, D and E) and the average contents of the feed sample are given in Figure 3 and Table 1, respectively.

Approx. 150 ml samples from master sludge batch with 34% solids were obtained via a pulp sampler after strongly shaking the container. Solid amount of each 150 ml was also measured after completing sedimentation tests. Required calculations were performed according to measured weights.

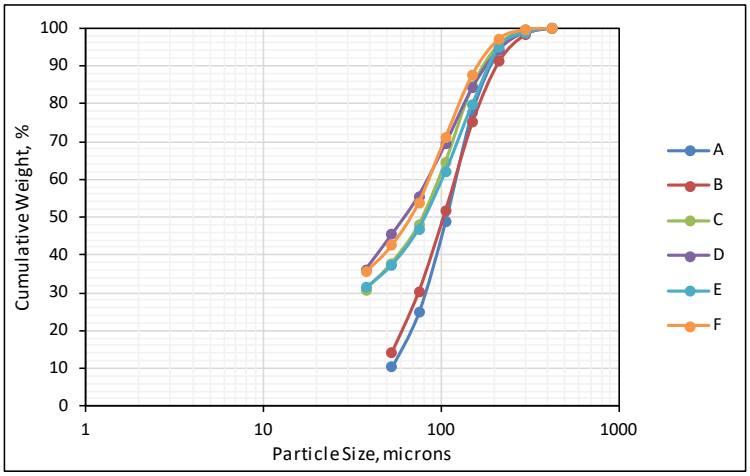

Figure 3. Particle size analyzes of samples taken from different parts of the thickener (top and bottom) at different times

Table 1. Average chemical contents of the sample

Content	%, W
Total Fe	34.377
SiO_2	7.591
CaO	2.97955
MgO	0.86625
Al2O3	2.45
Na2O	0.0755
K2O	0.178
TiO2	0.157
S	0.636
Loss of Ignition	3 4.555

Experimental Studies

Flocculation tests were initially carried out with approx. 150 ml of sludge samples (50 gr solids) with Polyacrylamide solutions (concentration=0.1%). Applied flocculant dosages were 10, 20, 30, 40, 50, 60, 70, 80, 90 and 100 g/t for 50 grams of solids at each test. Following, coagulation tests were performed out with also 150 ml of sludges at dosages of 500, 1000 and 1500 g/t by using a $FeCl_3$ solution (concentration=10%).

In order to provide static-electricity, a laboratory scale static electricity generator unit was designed and used. In this setup, "rolls" and "bands" were produced from the materials at opposite ends of the triboelectric series in order to produce static electricity. Copper brushes were used to collect the generated electrical charges. By connecting the copper brushes to an electrode, the generated charge could be able to measured. The schematic and general views of the static electric generation unit are given in Figure 4. In the previous studies, it was determined that static electricity generation performance could reach a max of 35 kV when positively charged woven nylon-kestamide is used. When woven nylon-teflon and woven wool-delrin (Polyoxymethylene) are used, generated charges were measured as 28 kV and 28.6 kV, respectively. Experimental studies were carried out using a positively charged woven nylon-kestamide/teflon pair tape and roller at highest possible static charge. Settling tests with static electric was performed at the highest static charge possible.

Natural settling times with no chemical addition were also tested. In both flocculation and coagulation tests, actual solid amounts were determined by drying the precipitate after the tests, and the applied dosages were recalculated according to actual weights. Each settling test was performed in 3 repetitions and the average values were used in the calculations. Settling time determination with static electric application was performed at highest generated charge possible with 3 repetitions. Results of the settling times obtained with flocculant and coagulant were used to compare settling times calculated with Talmage-Fitch and Coe-Clevenger methods, along with the optimum dosage determination. Finally, results with optimum settling times obtained with flocculant, coagulant, static electric and natural conditions were compared.

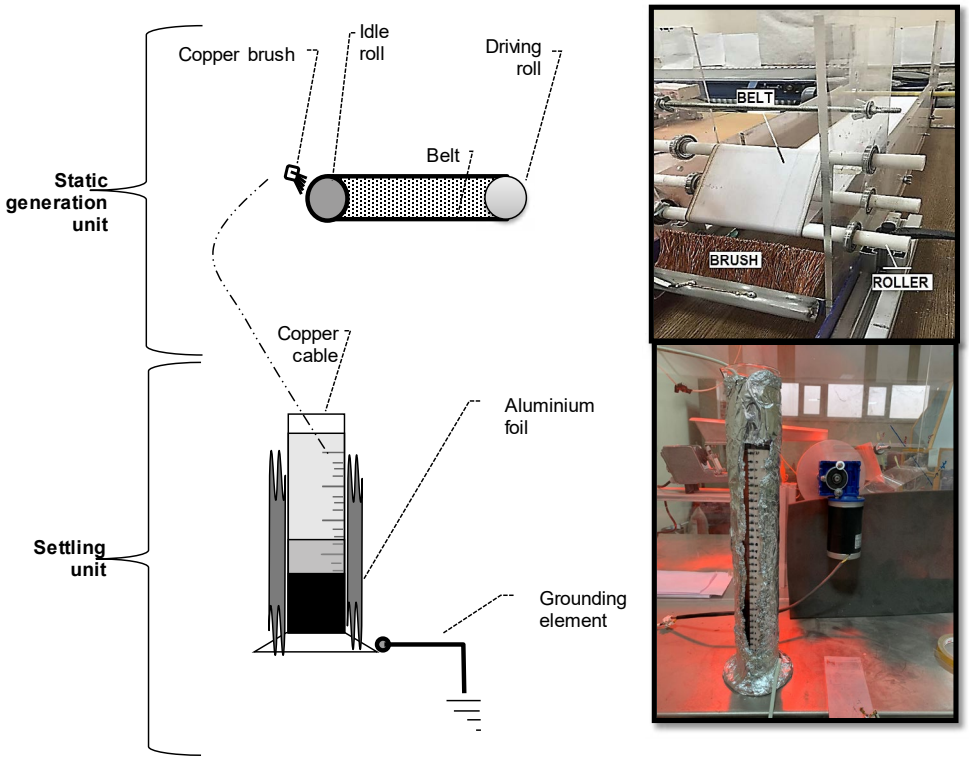

Figure 4. Generation and transfer of static electric to settling unit with schematical and actual images

RESULTS AND DISCUSSIONS

Collection and Evaluation of Settling Data

The raw data obtained within experimental studies are given in Figure 5, collectively. Settling heights were noted for 24 hours of periods for each test. Afterwards, the settling time (t_u) was calculated for test series using the Talmage-Fitch and Coe-Clevenger methods.

Repeated tests were used to measure the error values in the settling rate calculations. The effect of polyacrylamide dosage on the settling rate calculated by Talmage-Fitch and Coe-Clevenger methods is given comparatively in Figure 6. It is seen that the optimum settling rate is around 50-60 g/t. Similarly, the effect of $FeCl_3$ dosage on the precipitation rate calculated by Talmage-Fitch and Coe-Clevenger methods separately and given comparatively in Figure 7. Here, it is observed that the optimum settling rate has been achieved around 1000 g/t $FeCl_3$ dosages. As stated in previous studies, Talmage-Fitch method has been found to give relatively lower rates (Parsapour et al., 2014). Since, Talmage-Fitch method is considered to be relatively more reliable.

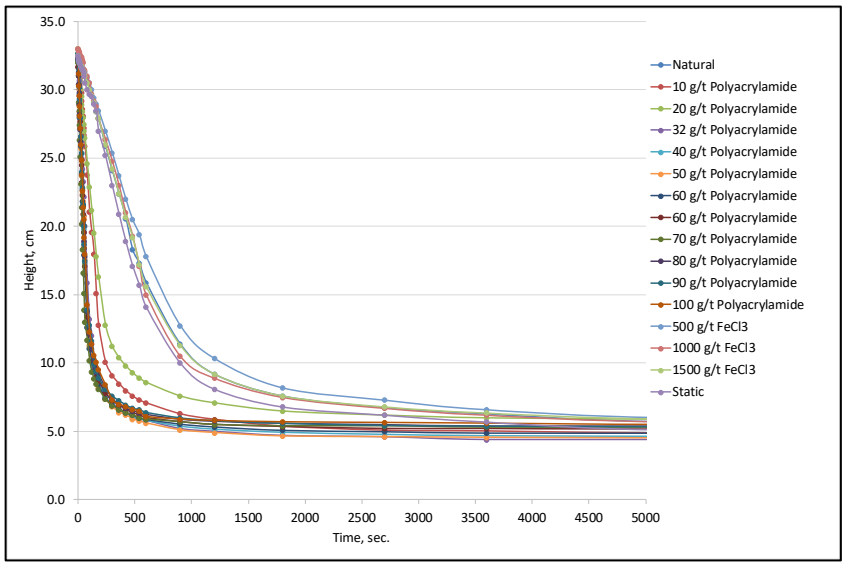

Figure 5. Average settling curves obtained from each experiment

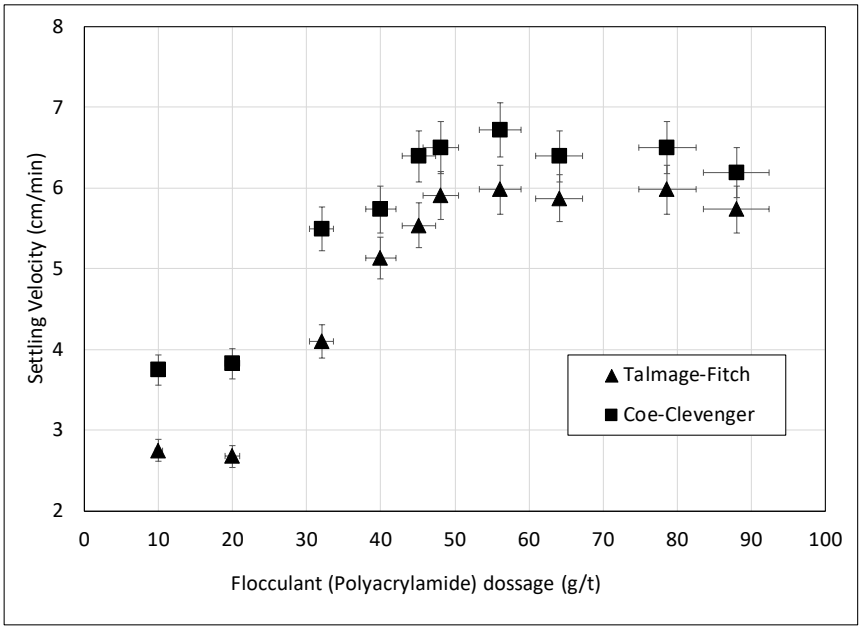

Figure 6. Comparative analysis of the effect of polyacrylamide dosage on settling rate with Talmage-Fitch and Coe-Clevenger methods

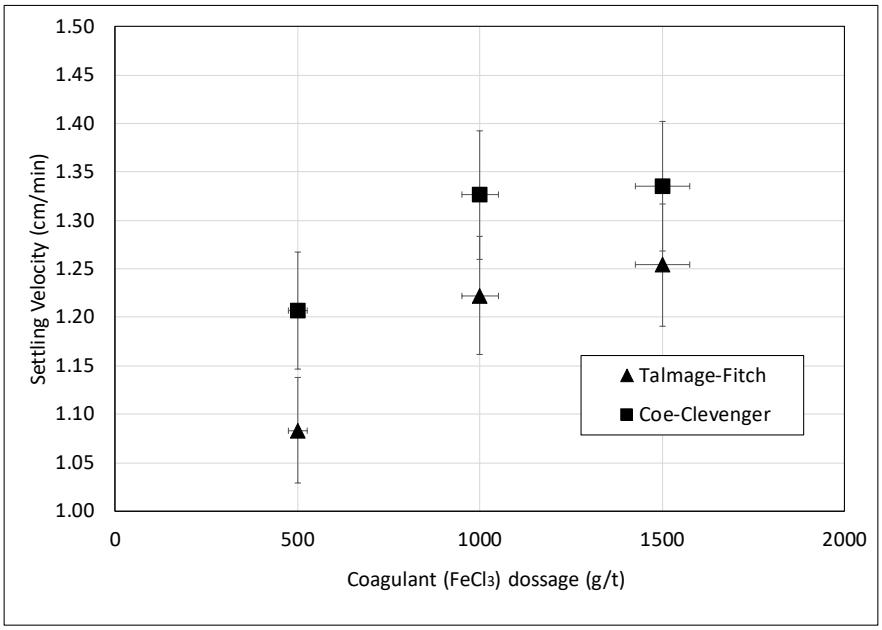

Figure 7. Comparative analysis of the effect of FeCl3 dosage on settling rate with Talmage-Fitch and Coe-Clevenger methods

In Figure 8, the comparison of the settling test results performed with 60 g/t Polyacrylamide and 1000 g/t FeCl3, which are measured as optimum conditions, along with natural and static electric applications is given. Figure 9 also visualizes the comparison of optimum flocculant and coagulant dosages with chemical-free and static electric conditions. The highest precipitation rates were achieved with polyacrylamide, which is a widely used and powerful flocculant. However, in Figure 10, in which FeCl3, natural and triboelectric settling rates are compared, it is seen that static electric application provides better results in comparison with both chemical-free (natural) and FeCl3 conditions.

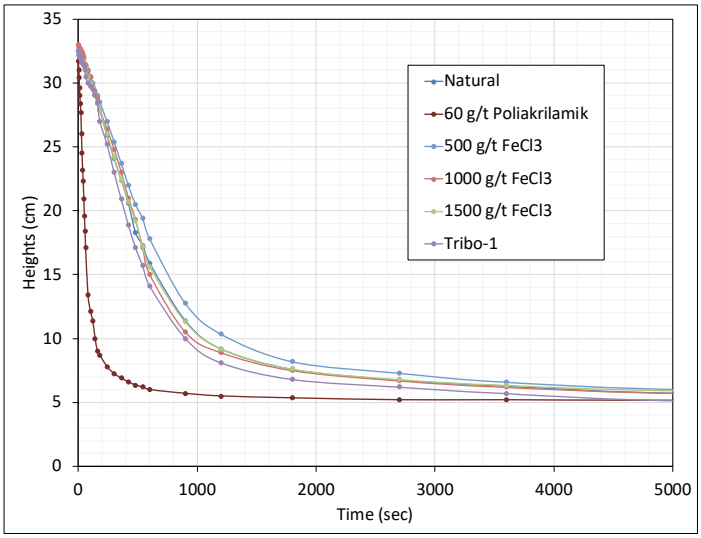

Figure 8. Comparison of polyacrylamide, FeCl3, natural and static electric raw settling curves

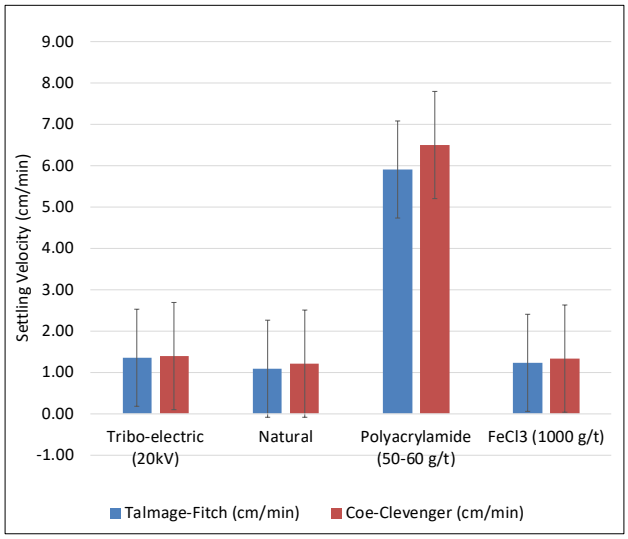

Figure 9. Comparison of setting rates with polyacrylamide, FeCl3, natural and static electric conditions

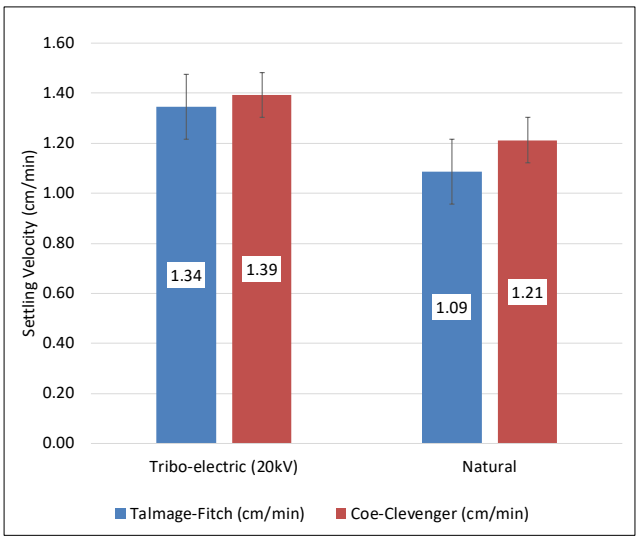

Figure 10. Comparison of settling rates with FeCl3, natural and static electric conditions

CONCLUSIONS

The results and recommendations can be listed as follows:

1. Preliminary tests showed that static electricity (triboelectric) phenomena can be benefited for improved setting rates when generated and applied correctly.
2. It is observed that static electricity has a positive effect on settling in comparison with natural and with coagulant conditions. However, it is far from catching the settling rate observed with the flocculant within given experimental route.
3. In prospective studies, static electricity is planned to be tested with different flocculant and coagulant dosages. Also, experimental studies on testing the effect of different flocculants species (A110, A130, Magnefloc, Rheomax, etc.) and coagulant ($Al_2(SO_4)_3$) types are also planned.

REFERENCES

Abbasi, M., Taheri, A. (2013). Effect of Coagulant Agents on Oily Wastewater Treatment Performance Using Mullite Ceramic MF Membranes: Experimental and Modeling Studies, Chinese Journal of Chemical Engineering, Volume 21, Issue 11, Pages 1251-1259.

AWWA (American Water Works Association), Water Quality and Treatment—A Handbook of Community Water Supplies, McGraw-Hill, New York, NY, USA, 5th edition, 1999.

Bittnera, J.D., Hracha, F.J., Gasiorowskia, S.A., Canellopoulusb, L.A., Guicherd, H. (2014). Triboelectric Belt Separator For Beneficiation Of Fine Minerals, 2nd International Symposium on Innovation and Technology in the Phosphate Industry Procedia Engineering 83, 122 – 129.

Davis, M. L. (2010). Water and Wastewater Engineering. Design Principles and Practice, McGraw-Hill.

Diaza, A.F., Felix-Navarrob, R.M. (2004). A Semi-Quantitative Tribo-Electric Series for Polymeric Materials: The İnfluence of Chemical Structure and Properties, Journal of Electrostatics, 62, 277–290.

Dizdar, T.O., Kocausta, G., Gülcan, E., Gülsoy, Ö.Y. (2018). A new method to produce high voltage static electric load for electrostatic separation – Triboelectric charging. Powder Technology 327, 89–95.

Gregory, J. (2006). Particles in Water Properties and Processes, Taylor & Francis.

Guardiola, J., Rojo, V., Ramos, G. (1996). Influence of particle size, fluidization velocity and relative humidity on fluidized bed electrostatics, Journal of Electrostatics, 37, pp. 1-20.

Iuga, A., Cuglesan, I., Samuila, A., Blajan, M., Vadan, D., Ascalescu, L. (2001). Electrostatic Separation of Muscovite Mica from Feldspathic Pegmatites, 0-7803-7116-X/01 (C) IEEE, 2249- 2255.

Kleber, W., Makin, B. (1998). Triboelectric powder coating: a practical approach for industrial use, Particulate Science and Technology, 16, pp. 43-53.

Lawless, P.A. (1999). Electrostatic precipitators, J. Webster (Ed.), Wiley Encyclopedia of Electrical and Electronics Engineering, vol. 7, John Wiley & Sons, Inc., pp. 1-15.

Matsusaka, S., Maruyama, H., Matsuyama, T., Ghadiri, M., (2010). Triboelectric charging of powders: A review, Chemical Engineering Science, Volume 65, Issue 22, Pages 5781-5807.

Nifuku, M., Ishikawa, T., Sasaki, T. (1989). Static electrification phenomena in pneumatic transportation of coal, Journal of Electrostatics, 23, pp. 45-54

Ohsawa, A. (2003). Computer simulation for assessment of electrostatic hazards in filling operations with powder, Powder Technology, 135/136, pp. 216-222.

Owen, A.T, Fawell, P.D., Swift, J.D., Farrow, J.B. (2002). The impact of polyacrylamide flocculant solution age on flocculation performance,International Journal of Mineral Processing, Volume 67, Issues 1–4, Pages 123-144.

Panat, R., Wang, J, Parks E. (2014). Effects of Triboelectrostatic Charging Between Polymer Surfaces in Manufacturing and Test of Integrated Circuit Packages, IEEE Transactions on Components, Packaging And Manufacturing Technology, VOL. 4, NO. 5, 943-946.

Park, C.H., Park, J.K., Jeon, H.S., Chul Chun, B. (2008). Triboelectric Series and Charging Properties of Plastics Using The Designed Vertical-Reciprocation Charger, Journal of Electrostatics 66, 578–583.

Parsapour, Gh.A., Hossininasab, M., Yahyaei, M., Banisi, S. (2014). Effect of settling test procedure on sizing thickeners, Separation and Purification Technology, Volume 122, Pages 87-95.

Tian, B., Ge, X., Pan, G., Luan, Z. (2007). Effect of nitrate or sulfate on flocculation properties of cationic polymer flocculants, Desalination, vol. 208, no. 1–3, pp. 134–145.

Wu, G., Li, J., Xu, Z. (2013). Triboelectrostatic Separation for Granular Plastic Waste Recycling: A Review, Waste Management 33, 585–597.

Yao, J., Zhang, Y., Wang, C.-H., Matsusaka, S., Masuda, H. (2004). Electrostatics of the granular flow in a pneumatic conveying system, Industrial & Engineering Chemistry Research, 43, pp. 7181-7199.

THE IMPACT OF MAIN HAUL ROAD IN SELECTION OF WASTE DUMP IN OPEN-PIT MINES REGARDING ENVIRONMENTAL CONSIDERATION

A. Hajarian [1], M. Osanloo [1, *]

[1] *Amirkabir University of Technology, Dept. of Mining Engineering*
*(*Corresponding author: morteza.osanloo@gmail.com)*

ABSTRACT

The location of the mine facilities, type of mine fleets, road, and its geometric factors form a dynamic process. Besides, a growing volume of waste dump during the mine life unquestionably yields exponential higher levels of environmental crisis. In this regard, wrong site selection of haul road and dumpsite may damage the environment, wildlife, and even the ecosystem. Since the hauling system is the most influential factor in the hauling costs, there is a need for a plan to avoid waste of high capital expenditures associated with the appropriate locations. Allocating the waste dump is a challenging stage with many stochastic variables and related costs. This research provides a simulation framework to determine waste dump location and relocating time with an alternative, considering random factors and ecologically sensitive areas. The validation of the method was launched in an actual open pit mine. The synergistic effect of curvature and slope in each section, distance changing, parking, and repair shop location, with particular attention to reducing the road's negative impact on locating the dumpsite, were considered. The result leads to several modifications in the current case study.

Keywords: Open-pit mine, waste dump, haul road, simulation, ecological constraints

INTRODUCTION

During recent decades, regarding the deepening of the open-pit mines, waste production crisis has plagued mine surroundings in case of environmental and economic issues. Since this problem contrasts to mining operations, it requires a long-term view to prevent a repeat of the unacceptable events such as wrong-site location seen over the waste displacing period before starting any operation. It is important to start with a consensus on objective factors with today's aim-oriented waste dump site determining. Most researchers agreed on distance and proximity to the road's exit point from the pit, crusher location, construction cost, mine fleet strategies, geological, environmental, and geotechnical properties (Osanloo and Ataei, 2003, Hajarian and Osanloo, 2020, Hekmat et al., 2008, Fu et al., 2015, Choi et al., 2009, Ramezanalizadeh et al., 2020, Puell Ortiz, 2017, Li et al., 2014, Li et al., 2016, Sari and Kumral, 2018, Kumral and Dimitrakoponlos, 2008, Li et al., 2013). Mainly, if several options for storation are available, looking for a common detonator is necessary. In order to assess the preferred choices, criteria for assessment must be chosen. The foundation ideal for selecting these criteria resides in the described factors as well as environmental policies. Mining operation mostly transportation affects surrounding wildlife populations (Davey et al., 2017). Also, the risk of closing mines by regulators and communities could happen if social and environmental constraints break(Cruz and Wakolbinger, 2008, Prno and Scott Slocombe, 2012). The damaging impression on wildlife on public roads is growing. In the United States, between 15 and 20% of terrains are affected by roads, leading to ecological events (Forman and Alexander, 1998). In the discussion of facility location in the mining realm, both in the waste dump and plant section, the main factors considered by researchers are as follows: 1-Economical Factors, 2- Technical Aspects, 3-Geomechanics, 4-Site Characteristics, 5-Environmental Subject, 6-

Geological Factors, 7-Legal Factors; The diagrams in Figures 1 and 2 show a closer look at the statistics of these factors.

Figure 1. Statistics of factors investigated in the discussion of waste dump location in open-pit mines

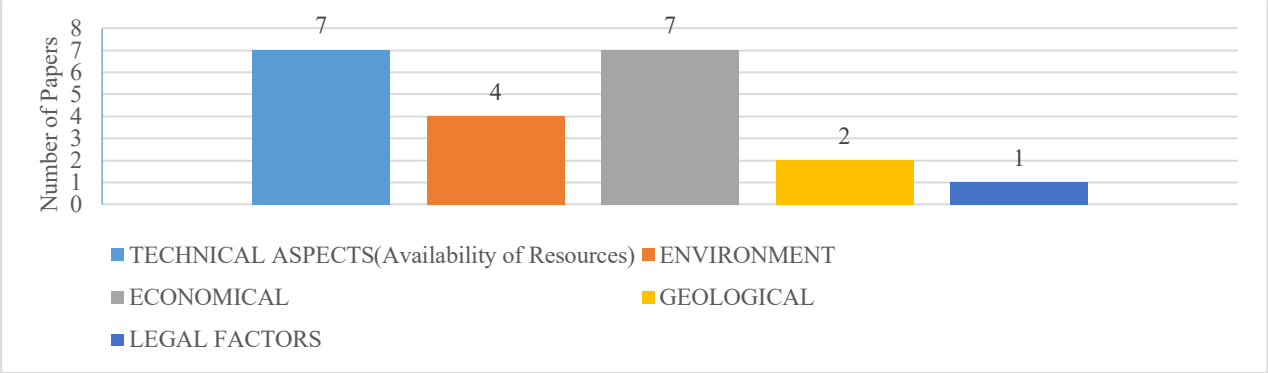

Figure 2. Statistics of factors investigated in the discussion of plant location in open-pit mines

Given the environmental factor's weight and importance, it is imperative to judge ecological effects, set threshold indexes, and incorporate the ecological model within waste dump allocation. Ensuring complete conformity with the main principles enshrined in the framework of environmental regulations and engineering principles, the stages of planning waste dump location in open-pit mines must be as follows:

1- Maintain the sustainability of ecological terms.
2- Ensure sufficient capacity for disposal place is available
3- Safekeeping of natural features in the area of disposal and appropriate observation treatment
4-Waste disposal planning from its origin through the haulage phase up to the final place and monitor the environmental and technical sector's concerns.

Meanwhile, the following particulars about these objectives are noteworthy: First, these objectives play an instrumental role in reaching the dump site selection criteria but not as goals. Second, because objectives are in struggle, and the long-term goal is to reduce the cost of waste displacement, a simulation-oriented approach is necessary. Many studies with the general approaches, characteristics, and limitations focused on simulation models in open-pit mines. In the field of mine fleet simulation, the main goals are to analyze and increase equipment utilization, select type and combination of hauling trucks, dispatching systems, and maintenance plan (apos et al., 1968, Krause and Musingwini, 2007, Zhang, 2019, Muniappen and Genc, 2020, Roberts, 2002, Camargo et al., 2018, Lashgari and Sayadi, 2013, Ogbonlowo and Wang, 1987, Dindarloo et al., 2015, Dindarloo and Osanloo, 2015).

Simulation is also well established in other fields like economic and investment factors such as cost, NPV, related items, grade estimation, blasting, Ex-Pit and In-Pit crusher location, selection optimum mining method, and mine planning (Franco-Sepulveda et al., 2017, Lisboa et al., 2019, Tahmasebi and Hezarkhani, 2012, Paricheh and Osanloo, 2018, Ataei et al., 2013, Paricheh and Osanloo, 2017, Ding et al., 2019, Abbaspour et al., 2018, Leng et al., 2020, Sari et al., 2014, Koushavand et al., 2014). Nip and tuck to disquisitions, intelligent object-based simulation software handles the problem using the power of computers. They allow building a simulation model that fully captures both the details constraints and variation within the system, producing a feasible solution.

SIMULATION APPROACH FRAMEWORK

Qualitative factor analysis is the first step in modeling a dumpsite location, illustrated in Figure 3/first ring. The first ring is well considered in contents, but sub-criteria's superposition in the second ring changes the condition. Hajarian and Osanloo(Hajarian and Osanloo, 2020), while considering the main criterion in the first ring, highlighted the role of distance and planning of construction cost on waste dump site location but haulage distance, stochastic road condition variables, and stochastic distribution haulage system, increasing of mine deep and developing direction derivates of topography and technical aspects, respectively is neglected. Other researchers less see the second ring's superposition effect in the case of stochastic haulage conditions.

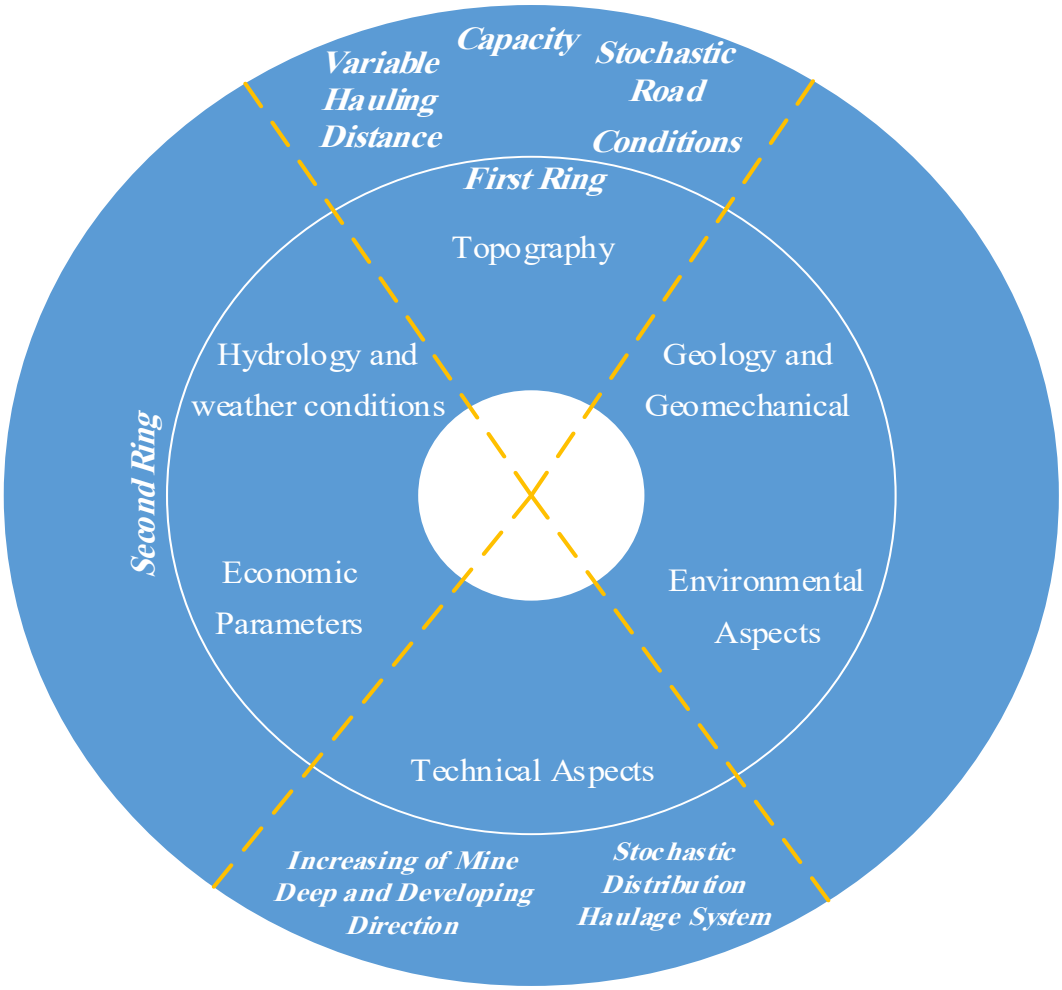

Figure 3. Qualitative factors and derivatives

Performance Measure Metrics

To operate the simulation cycle, affecting parameters and related sets of data must be supplied as follows:

1- Distance
2- Road gradient
3-Environmental and safety parameters/restrictions
4-Truck Speed
5-Stochastical depending time (Load/Unload/Maintenance).

The statistical result can be derived and analyzed to measure performance metrics based on such data. The performance metrics from the view of the time study data are briefly described in Table 1.

Table 1. Performance metrics

Performance Metric	Description
Production	Number of entities* exited the system in the simulation time (Number of loads hauled by truck)
Flowtime/Cycle Time	Average time of entities in a system
Non-Value-Added Time	Waiting in queues
Number Waiting on In Queue	The average number of entities expected to be seen in a waiting line
Utilization	Percentage time of busy server** when servicing entities

*Any object like a truck. ** Any intersection point in space

Since the state of objects in the open pit only changes at defined event time, the open-pit mine simulation atmosphere is a discrete-event simulation. To compute the performance statistics at the first step, we need to facilitate simulation to track events using an event calendar (which contains records of what will happen arranged by time). Input modeling and simulation output analysis need matching observed processing time to a standard statistical distribution in the second step.
Figure 4 shows the travel range, pit exit, and waste dump unloading points that need to be observed due to the scattering of time when the trucks arrive. The algorithm follows the steps in Table 2.

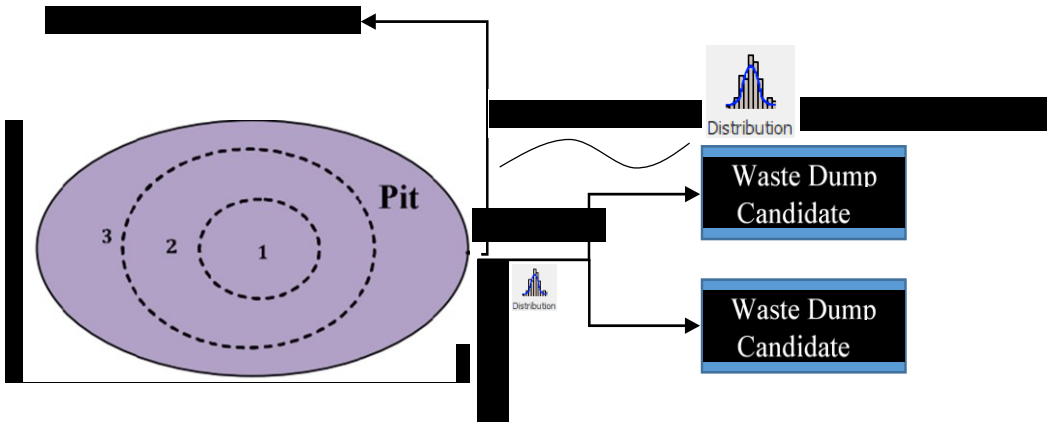

Figure 4. A schematic plan view of sensitive points during waste dumping

Table 2. Algorithm steps

1:	Compute Procedure Utilization of Trucks
2:	Create Table of Events based on Arrival Time, Interarrival Time, Processing Time)/Event Calendar.
3:	Setup the simulation (Determine the number of trucks, Initial Network Path, Distances, Associated times in loading and unloading points, Initial Speed, Initial capacity, Initial Sequence, Routing Logic).
4:	Remove the next event from the calendar and update the time.
5:	Execute the processes such as adding additional events and collecting statistics (Arrival and Departure Event Process, End Event).
6:	Repeat Algorithm Step 4-6

Tools preparing

Before getting started, setting up the correct variables that can consider the scope of the work is necessary. Objects of the simulation environment are shown in the hierarchy ranked in Figure 5. Table 3 represents the description of the ambiguous items in Figure 5. To establish the approach, we must logically relate to each other, so it needs programming and defining complementary objects. For example, since we need to observe the waste dump and truck capacity, a TANK object can model a weight or volume capacity-constrained location for holding entities representing mass quantities. It includes initial content, refill, and empty mode states. Since processing and interarrival times are random variables, we can match a statistical model using observed data. Depending on the nature of the data, try to pick out a statistical distribution, to match the model.

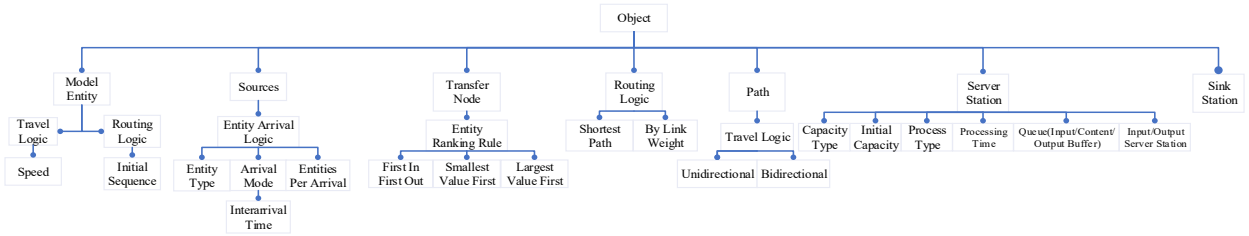

Figure 5. Object designation for simulation

Table 3. Description of items in figure 5

Item	Description
Initial sequence	Specifying an entity to follow the desired sequence toward the station.
Entity type	The type (Name) of the entity that arrives on the source (s).
Arrival mode	The method used by the source object to generate a stream of entity arrivals.
Entities per arrival	The number of entities that will be arriving at the source.
Interarrival time	An expression that evaluates whenever an arrival occurs. Indicate the time until the next arrival. It can be derived from a distribution.
Entity ranking rule	The rule is used to rank entry into nodes among competing entities.
By Link Weight	The probability of choosing a particular path.
Unidirectional/ Bidirectional	only allows movement in one direction / Only allows entities to move in both directions
Capacity type	Fixed/Work Schedule.
Process type	The method used to model the processing of an entity.
Processing time	The time required to process an entity
Input/Output of server station	A node that supports connection to paths and selecting a destination, path.

CASE STUDY

Once the target and content of the proposed model are appropriately established, we run it for current and alternative waste dump locations. For this, we chose the SARVIAN iron ore mine environment located in the central part of IRAN. By Using the photogrammetry method, the mine area's digital terrain model (DTM) was obtained (Figure 6). Over two weeks, other required data were collected from direct observation in the loading, dumping, switchback, curvature, and grade breakpoint. The source of other data is listed in Table 4. The alternative location was selected according to environmental constraints and hosting capacity. Using the following objective function equation presented in the article by Hajarian and Osanloo, the alternative hauling road was designed (Hajarian and Osanloo, 2020). Details have been omitted to shorten the text.

$$Min: \sum_{t\in T}\sum_{b\in(B^{-}\cup \mathfrak{B})}\sum_{b'\in(B^{+}\cup \mathfrak{W})}\left\{(D_{b,b'}\times T^{t}_{b,b'})\times a_{b,b'}\right\}/(1+r)^{t} \quad (1)$$

Where:

$D_{b,b'}$: Flat distance between the middle point of two blocks b: Block model index

$T^{t}_{b,b'}$: Volume to be cut from block b and moved to block b' during period t

$a_{b,b'}$: (binary variable): 1 if block b is adjacent to block b' and have directed path, 0 otherwise

r: Discount rate B^{-}: Set of cut blocks $\mathfrak{B}$: Set of pit blocks

B^{+}: Set of fill blocks $\mathfrak{W}$: Set of waste dump blocks T: Set of the time period

Figure 6. A limited plan view of SARVIAN iron ore mine environment

Having determined the road path, we follow the steps in Table 4 to determine the optimal location of the waste dump location. The current established fleet system has the properties according to table 5.

Table 4. Comparison Steps

1:	Start
2:	Initialize Value
3:	Compute Performance Index (Cycle Time, Transferred Tonnage Volume)
4:	Update and Store Model ⟵ Alternative Model
5:	Compare Both Model
6:	Return Best Waste Dump Location

Table 5: Properties of the current fleet system

Item	Metric
Number of excavators	2 Kumatsu PC 400/ 1 Kumatsu PC 250
Number of trucks	14 (25 Ton)
Working schedule	Mine policy
Maintenance schedule	Not considered
Hauling distance	Derived from DTM
Road gradient (Each Segment)/Forbidden Area	Derived from DTM
Waste tonnage	Engineering reports
Truck travel speed	Statistical data
Truck capacity	Statistical data (Mean)
Loading/Unloading time	Statistical data
Waste dump capacity	Derived from DTM

The following points are noteworthy:

- In the eastern part of the mine, animals such as foxes and turtles were observed whose lives were affected by the transportation system.
- There was no hauling dispatching system in the mine
- Due to the proximity of the crushing line and waste dump location, the bottleneck formed the entry point.

Distribution fitting software was used for data analysis and fitting distribution charts (Table 6). The processing times at the working bench, dump location, and different haul road segments vary with the type of entities.

Table 6. Type of processing times for truck entity, Source, and sink objects

Entity type	Load/Unload time (minutes)	Interarrival time (minutes)	Speed at curvature/ Switchback (Km/h)
Mine truck	Random/Uniform	-	Random/Pert
Source (Working Bench)	-	Random/Pert	-

The model entity object has a container element that will hold up to each truck capacity. The truck entity arrives at a node and mass transfers from the first tank (Waste mass) into the container on the entity. Mass flow is transferred until the entity's container is full. At this point, the transfer of mass flow is stopped, and the entity travels to the next node. At this point, mass is transferred from the entity's container into the second tank (Waste dump).
When the entity's container is empty, the entity leaves the node and travels to the sink. Figure 7 shows the logical processes of the proposed assumption in four steps. Having and analyzing collected data, the model coded in SIMIO (student version). The case study block diagram is shown in Figure 8.

RESULTS AND DISCUSSION

Truck productivity has a key measure which is a function of the total operating time of the equipment. Implicit factors such as turns, road quality, and road grade (Figure 9) are also highly influential. However, the most important factor is distance. With the physical progress of the operation and increasing the hauling distance, their impact is multiplied. Figure 10 is a simulation of truck cycles considering travel distance with progressive operation vs. wavering it.

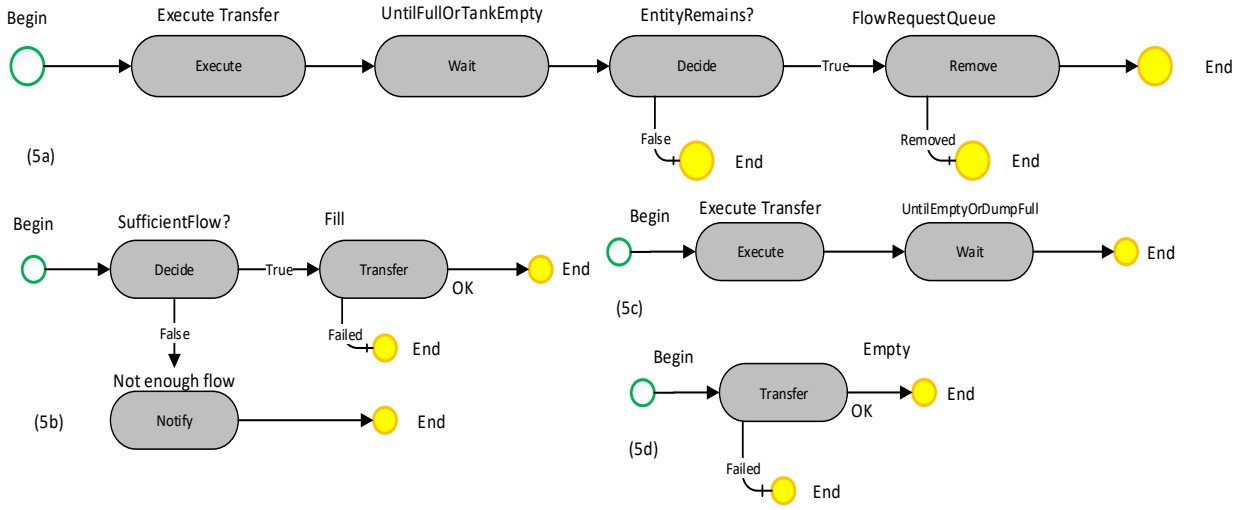

Figure 7. The logical process of transferring waste to a truck (7a), Fill truck (7b), Transfer from truck to dump (7c), and Empty truck (7d).

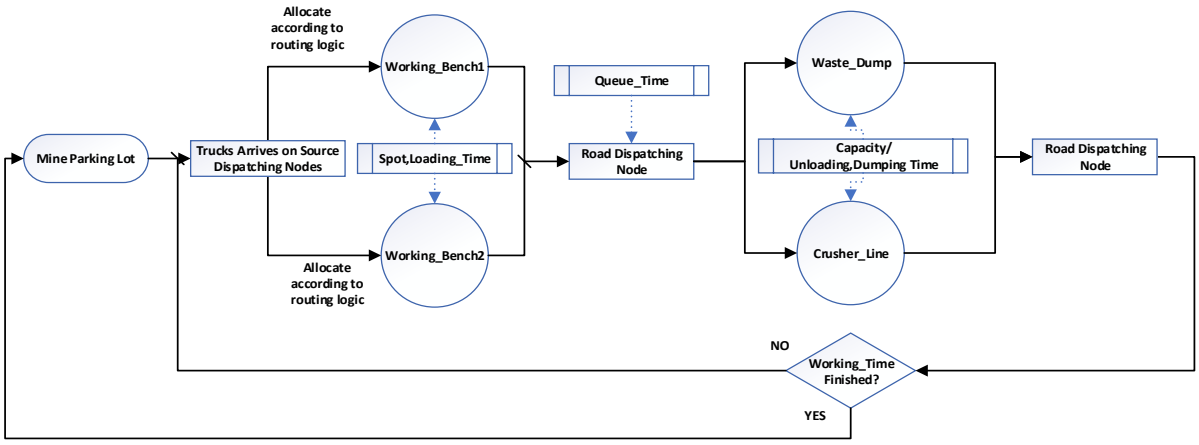

Figure 8. Waste dumping cycle diagram

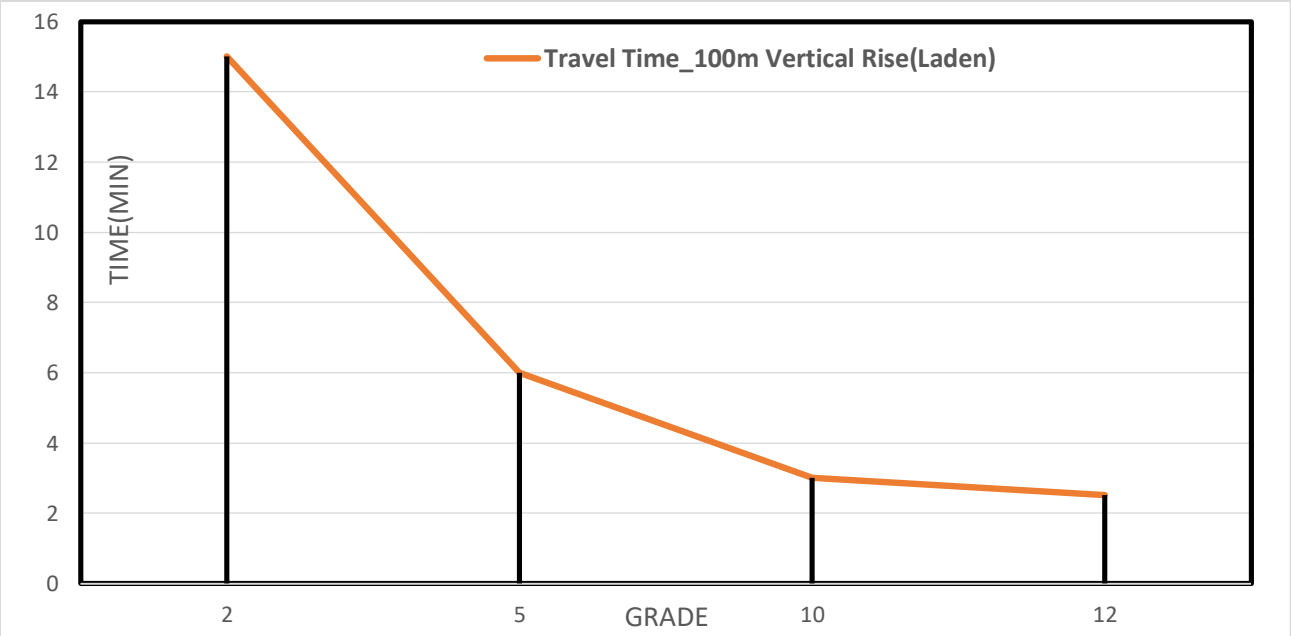

Figure 9. Average travel time for 100m Vertical Rise (Laden) considering turns and road conditio

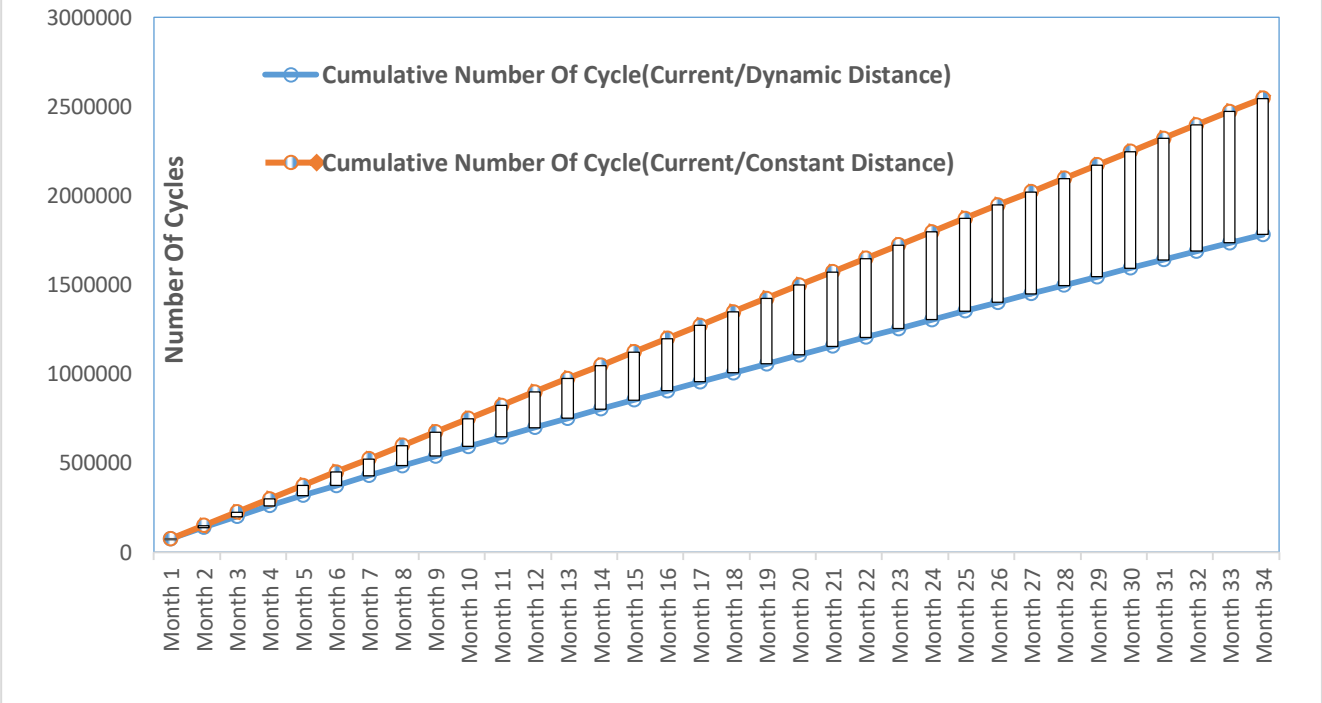

Figure 10. Simulation of truck cycles in both constant and dynamic distance for the current study

It can be deduced that the intensity of the effects increases over time and is not a constant value. For a better mindset, the difference in results is shown in Table 7. This amount of cycle differences can have economic benefits in many ways. After defining the waste dump location, the tangible result is that it is necessary to study the results in detail. In the current study, the results of these nonlinear changes can be seen in the waste tonnage displacement diagram for 34 months in Figure 11.

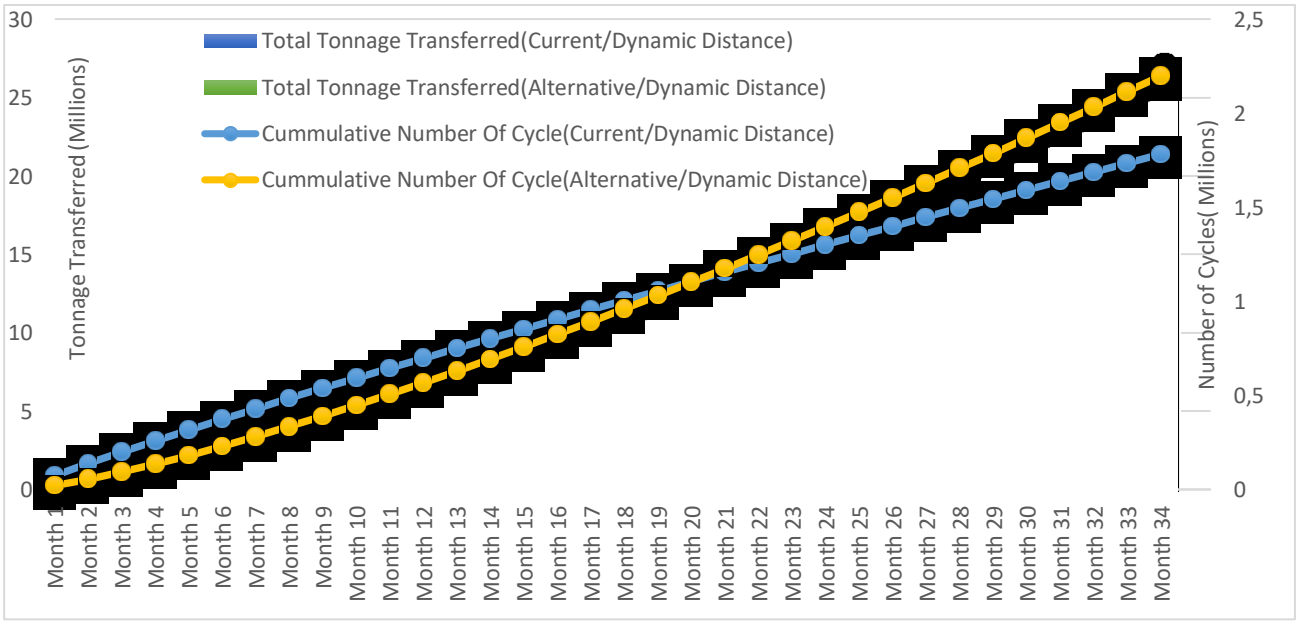

Figure 11. Simulation of waste tonnage displacement for current and alternative

Table7.Constant distance simulation vs. dynamic distance for 14 trucks and 34 months

	Constant Distance	Dynamic Distance
Cumulative Cycles	2880514	2017393
Difference: 762725		

The location of the alternative dump is such that the distance manifests its impact on operation progress. In the meantime, the existing turns and grades are also effective in intensifying this factor. In this chart, the 20th month is a turning point. Simultaneously with the increase of the truck cycle in the alternative case, the amount of cumulative waste tonnage exceeds the first case. From another point of view, the waste dump location can be replaced by an alternative at the turning point. In this case, the investment costs for the preparation should be considered.

CONCLUSION

This article aims to investigate the effect of the main road on the site of waste dumps in open-pit mines. Activities of other researchers are categorized in both Figures 1 and 2. The influential factors were shown synergistically in Figure 3. Based on this Figure, a framework was designed to focus and analyze factors that participate in waste dump location that originates from the main haul road. Unlike previous multi-objective models that only relied on ranking and screening methods for finding a waste dump location, the current methodology tries to find alternative ones using scenario-based simulation. The nature of this method is based on the reality that can be measured over time. Using the equations in Hajarian and Osanloo's (Equation 1) article, we designed the path leading to the dumpsite. Then, by collecting data simulate the factors affecting the dumpsite location. The returned results show that the capacity, type of turn, road grade, distance, and road quality effectively affect the waste dump location. In the design process, restriction areas such as wildlife, woodland area to consider an environmental restriction considered in the model. Another tangible result is the turning point in the relocation of the waste dump, which occurs when the cumulative hauling tonnage is balanced in two modes. The role of processing plan and stockpile location also need to be involved in the calculation for future work.

REFERENCES

Abbaspour, H., Drebenstedt, C., Badroddin, M., Maghaminik, A. (2018). Optimized design of drilling and blasting operations in open pit mines under technical and economic uncertainties by system dynamic modelling. *International Journal of Mining Science and Technology,* 28**,** 839-848.

Apos, Neil, T. J., Manula, C. B. (1968). Operations Research - Computer Simulation of Materials Handling in Open Pit Mining. The American Institute of Mining, Metallurgical, and Petroleum Engineers.

Ataei, M., Shahsavany, H., Mikaeil, R. (2013). Monte Carlo Analytic Hierarchy Process (MAHP) approach to selection of optimum mining method. *International Journal of Mining Science and Technology,* 23**,** 573-578.

Camargo, L. F. R., Rodrigues, L. H., Lacerda, D. P., Piran, F. S. (2018). A method for integrated process simulation in the mining industry. *European Journal of Operational Research,* 264**,** 1116-1129.

Choi, Y., Park, H. D., Sunwoo, C., Clarke, K. C. (2009). Multi-criteria evaluation and least-cost path analysis for optimal haulage routing of dump trucks in large scale open-pit mines. *International Journal of Geographical Information Science,* 23**,** 1541-1567.

Cruz, J. M.,& Wakolbinger, T. (2008). Multiperiod effects of corporate social responsibility on supply chain networks, transaction costs, emissions, and risk. *International Journal of Production Economics,* 116**,** 61-74.

Davey, N., Dunstall, S., Halgamuge, S. (2017). Optimal road design through ecologically sensitive areas considering animal migration dynamics. *Transportation Research Part C: Emerging Technologies,* 77**,** 478-494.

Dindarloo, S., Osanloo, M. (2015). *Results of discrete event simulation in a large open pit mine*.

Dindarloo, S. R., Osanloo, M., Frimpong, S. (2015). A stochastic simulation framework for truck and shovel selection and sizing in open pit mines. *Journal of the Southern African Institute of Mining and Metallurgy,* 115**,** 209-219.

Ding, X., Lu, X., Zhou, W., Shi, X., Luan, B., Li, M. (2019). Blasting Impact Simulation Test and Fragmentation Distribution Characteristics in an Open-Pit Mine. *Shock and Vibration,* 2019**,** 4080274.

Forman, R. T. T., Alexander, L. E. (1998). ROADS AND THEIR MAJOR ECOLOGICAL EFFECTS. *Annual Review of Ecology and Systematics,* 29**,** 207-231.

Franco-Sepulveda, G., Campuzano, C., Pineda, C. (2017). NPV risk simulation of an open pit gold mine project under the O'Hara cost model by using GAs. *International Journal of Mining Science and Technology,* 27**,** 557-565.

Fu, Z., Li, Y., Topal, E., Williams, D. (2015). A New Tool for Optimisation of Mine Waste Management in Potential Acid Forming Conditions. *Tailings and Mine Waste Management for the 21st Century.* Sydney, Australia.

Hajarian, A., Osanloo, M. (2020). A new developed model to determine waste dump site selection in open pit mines: An approach to minimize haul road construction cost. *International Journal of Engineering,* 33.

Hekmat, A., Osanloo, M., Shirazi, A. M. (2008). New approach for selection of waste dump sites in open pit mines. *Mining Technology,* 117**,** 24-31.

Koushavand, B., Askari-Nasab, H., Deutsch, C. V. (2014). A linear programming model for long-term mine planning in the presence of grade uncertainty and a stockpile. *International Journal of Mining Science and Technology,* 24**,** 451-459.

Krause, A., Musingwini, C. (2007). Modelling open pit shovel-truck systems using the Machine Repair Model. *Journal of The South African Institute of Mining and Metallurgy,* 107**,** 469-476.

Kumral, M., Dimitrakoponlos, R. (2008). Selection of waste dump sites using a tabu search algorithm. *Journal of the Southern African Institute of Mining and Metallurgy,* 108**,** 9-13.

Lashgari, A., Sayadi, A. R. (2013). Statistical approach to determination of overhaul and maintenance cost of loading equipment in surface mining. *International Journal of Mining Science and Technology,* 23**,** 441-446.

Leng, Z., Fan, Y., Gao, Q., Hu, Y. (2020). Evaluation and optimization of blasting approaches to reducing oversize boulders and toes in open-pit mine. *International Journal of Mining Science and Technology,* 30**,** 373-380.

Li, Y., Topal, E., Ramazan, S. (2016). Optimising the long-term mine waste management and truck schedule in a large-scale open pit mine. *Mining Technology,* 125**,** 35-46.

Li, Y., Topal, E., Williams, D. (2013). Waste rock dumping optimisation using mixed integer programming (MIP). *International Journal of Mining, Reclamation and Environment,* 27**,** 425-436.

Li, Y., Topal, E., Williams, D. J. (2014). Optimisation of waste rock placement using mixed integer programming. *Mining Technology,* 123**,** 220-229.

Lisboa, A. C., Souza, F. H. B. D., Ribeiro, C. M., Maia, C. A., Saldanha, R. R., Castro, F. L. B., Vieira, D. A. G. (2019). On Modelling and Simulating Open Pit Mine Through Stochastic Timed Petri Nets. *IEEE Access,* 7**,** 112821-112835.

Muniappen, K., Genc, B. (2020). Dynamic simulation of an opencast coal mine: a case study. *International Journal of Coal Science & Technology,* 7**,** 164-181.

Ogbonlowo, D. B. & Wang, Y. J. (1987). A case study in surface mining simulation with special reference to the problem of model evaluation. *International Journal of Mining and Geological Engineering,* 5**,** 109-119.

Osanloo, M., Ataei, M. (2003). Factors Affecting the Selection of Site for Arrangement of Pit Rock-Dumps. *Journal of Mining Science,* 39**,** 148-153.

Paricheh, M., Osanloo, M. (2017). A simulation-based framework for estimating probable open-pit mine closure time and cost. *Journal of Cleaner Production,* 167**,** 337-345.

Paricheh, M., Osanloo, M. (2018). A simulation-based risk management approach to locating facilities in open-pit mines under price and grade uncertainties. *Simulation Modelling Practice and Theory,* 89**,** 119-134.

Prno, J., Scott Slocombe, D. (2012). Exploring the origins of 'social license to operate' in the mining sector: Perspectives from governance and sustainability theories. *Resources Policy,* 37**,** 346-357.

Puell Ortiz, J. (2017). Methodology for a dump design optimization in large-scale open pit mines. *Cogent Engineering,* 4**,** 1387955.

Ramezanalizadeh, T., Monjezi, M., Sayadi, A. R., Mousavinogholi, A. (2020). Development of An Integrated Mathematical Model to Optimize Waste Rock dumping Satisfying Environmental Aspects. *Journal of Mining and Environment,* 11**,** 577-586.

Roberts, B. H. (2002). Computer simulation of underground truck haulage operations. *Mining Technology,* 111**,** 123-128.

Sari, M., Ghasemi, E., Ataei, M. (2014). Stochastic Modeling Approach for the Evaluation of Backbreak due to Blasting Operations in Open Pit Mines. *Rock Mechanics and Rock Engineering,* 47**,** 771-783.

Sari, Y. A., Kumral, M. (2018). A landfill based approach to surface mine design. *Journal of Central South University,* 25**,** 159-168.

Tahmasebi, P., Hezarkhani, A. (2012). A hybrid neural networks-fuzzy logic-genetic algorithm for grade estimation. *Computers & Geosciences,* 42**,** 18-27.

Zhang, C. (2019). Integrating machine learning, optimization and simulation to increase equipment utilization: Use case study on open pit mines. Available from: https://www.hitachi.com/rd/sc/aiblog/009/index.html.

TUNÇBİLEK ŞLAM GÖLETİNDEN KAZANILAN KÖMÜRÜN BİRİKETLENMESİNDE BASINÇ DAYANIMI TAHMİNİ

PREDICTION OF COMPRESSIVE STRENGTH IN BRIQUETTING COAL RECOVERED FROM TUNÇBILEK SLIME POND

S. Karaca[1,*], O. Şahbaz[1], A. Uçar[1]

[1] *Kütahya Dumlupınar Üniversitesi, Maden Mühendisliği Bölümü*
*(*Sorumlu yazar: sevgi.karaca@dpu.edu.tr)*

ÖZET

Bu çalışmada, kömür briketlemede en önemli parametrelerden olan basınç dayanımı parametresinin tahmini, bulanık mantık kullanılarak araştırılmıştır. Garp Linyitleri İşletmesi (GLİ)'ne ait şlam göletinden alınan numune -500+212 µm ve -212+38 µm olarak boyutlandırılmış ve humprey spirali ile zenginleştirilmiştir. Zenginleştirme sonucu elde edilen numuneler biriketleme işleminde kullanılmıştır. Briketler üç farklı çap (20, 30, 40 mm), basınç (7,5, 10, 12,5 MPa) ve melas oranında (%10, %15, %20) hazırlanmıştır. Tahmin çalışmalarında giriş değişkeni olarak pres basıncı, briket çapı ve melas oranı, çıkış değişkeni olarak ise basınç dayanımı kullanılmıştır. Bulanık mantık tahmin sonuçları gerçek değerlerle karşılaştırılmış ve elde edilen sonuçlar doğrultusunda bulanık mantık sisteminin biriketleme işleminde başarıyla kullanılabileceği ortaya konmuştur.

Anahtar Sözcükler: Briket, basınç dayanımı, bulanık mantık.

ABSTRACT

This study investigated the compressive strength parameter, which is one of the most critical parameters in coal briquetting, using the fuzzy logic method. The coal sample was obtained from the slime pond belonging to the Garp Lignite Enterprise (GLI). The sample was sized into two groups (-500+212 and -212+38 µm) and enriched using the Humprey spiral. The enriched materials were used in the briquette preparation. Briquettes have been prepared at three different diameters (20, 30 and 40 mm), pressure (7.5, 10, 12.5 MPa) and molasses ratio (%10, %15 and 20%). The prediction studies used press pressure, briquette diameter and molasses ratio as the input variables, and compressive strength was used as the output variable. The fuzzy logic prediction results were compared with the actual values. It was revealed that the fuzzy logic system could be successfully used in the briquetting process according to the results obtained.

Keywords: Briquetting, compressive strength, fuzzy logic.

GİRİŞ

Kömür ülkemizde en yaygın kullanılan yakıt türlerinden biridir. Organik tortul kayaç olan kömür, çoğunlukla minerallerden oluşan inorganik maddeleri ve maseral yapıdaki yanıcı organik maddeleri içermektedir. Kömür hazırlama işlemleri ile ham kömürden safsızlıkların (inorganik madde) içeriğini azaltarak değerini yükseltilmektedir. Proses kalitesinin en yaygın kriteri, yıkama işlemleri sırasında kül yapıcı maddeler kömürden tamamen uzaklaştırılamaz, ancak daha düşük inorganik madde içeriğine sahip partiküller, daha

yüksek inorganik madde içeriğine sahip olanlardan ayrılır (Meyers, vd., 2001). Kömürlerde bulunan gang mineralleri, kil ve marnlardan arındırılması için kurulan kömür yıkama tesislerinden çıkan atıklar ise düşük kalorili kömür içermektedir. Yüksek nem içeriğine sahip bu ince boyutlu artık kömürlerin kurutularak tekrar yakıt olarak kazanılması hem çevresel etki hem de ekonomik açıdan önem kazanmaktadır.

Briketleme, kompakt, dayanıklı ve kararlı bir form elde etmek için malzemeleri sıkıştırma işlemidir (Altun vd., 2003). Yüksek nem içerikli şlam kömürün kurutulduktan sonra sıkıştırılarak yoğunluğunun arttırılması ile elde edilen briketler, lavvar artıklarından kazanılan kömürlerin değerlendirilmesi için kullanılabilmektedir. Briketleme işlemleri bağlayıcılı ve bağlayıcısız olarak yapılabilmektedir. Briketleme işlemlerinde kullanılan bağlayıcılar genellikle melas, pirina yağı gibi maddelerden oluşmaktadır. Bağlayıcı oranı arttıkça dayanıklılığın arttığı yapılan çalışmalarda görülmektedir. Xu vd. (2002), kömürün briketlenmesinde bağlayıcı oranının artmasıyla briket performansının arttığını belirlemiştir. Gürbüz Beker (1997) ise biyolojik kökenli başlayıcıları kullandığı düşük kalorili kömürle yaptğı briket çalışmasında, bağlayıcı miktarı arttıkça basınç dayanımı ve darbe direncinin arttığını bulmuştur. Briketleme işlemleri basınç altında gerçekleştiği için, bir diğer önemli briketleme parametresi ise uygulanan pres basıncıdır. Oluşturulan briketlerin yapısının bozulmaması, atmosfer koşullarına uygun olması için dayanıklı bir yapıda olması beklenmektedir. Briketlerin kalitesini gösteren mukavemet (basınç dayanımı, suya karşı direnç ve darbe direnci) ve dayanıklılık (aşınma direnci) parametreleri açısından test edilmesi gerekmektedir. Basınç dayanımı bir briketin çatlamadan veya kırılmadan önce dayanabileceği maksimum kırma yüküdür. Briketin basınç dayanımı, tek bir briketin, briketin alanından daha büyük bir alana sahip iki düz, paralel plaka arasına yerleştirildiği ve briket çatlayana kadar sabit bir oranda artan bir yükün uygulandığı bir test ile belirlenir. Kırılmadaki yük, kuvvet veya stres olarak belirlenir (Kaliyan ve Morey, 2009).

Zarringhalam-Moghaddam vd. (2011) yaptıkları çalışmada, bağlayıcı olarak kullandıkları melas, talaş ve katranın farklı miktarlarında basınç dayanımı ve suya dayanıklılığın değişimini incelemişlerdir. 4 farklı kömür yatağından alınan numune ile yapılan deneylerde, melas kullanımının hem basınç dayanımını hem de suya dayanıklılığı arttırdığını belirlemişlerdir. Manyuchi vd. (2018), talaş ve melas oranının briketin kalori değeri, sabit karbon, basınç dayanımı ve kırılma indeksi üzerine etkisini araştırmışlardır. Melas ve talaş miktarı arttıkça basınç dayanımının %50 oranında arttığını belirlemişlerdir. Janewicz vd. (2019), bağlayıcı olarak selüloz lifi ve yulafı kullanmış ve farklı pres basınçlarında briket oluşturmuşlardır. Çalışmanın sonuçlarına göre yanabilir seviyede oluşturulan briketlerin mekanik dayanımının yüksek olduğu ancak suya dayanıklılığının yeterli olmadığı görülmüştür. Guo vd. (2020) briketleme işleminde etkin olan dört parametrenin etkilerinin tek tek görmenin yanı sıra birbirleri ile etkisini ortaya koymak için Design Expert programını kullanarak cevap yüzey grafiğini oluşturmuşlardır. Elde ettikleri modelin tahmin değeri ise %98.72 olarak belirlenmiştir.

Bulanık mantık bilgisayarlara karar verme yeteneği kazandırma yöntemlerinden birisidir. Bulanık mantıkta giriş verileri, klasik mantıkta olduğu gibi 0 ve 1 olmak üzere iki aşamalı değil 0-1 aralığında birçok seviye ile ifade edilmektedir. Kural tablosu oluşturularak bilgisayarın karar verme kriterleri belirlenir. Çıkış biriminde ise bulanık çıktı değerleri tekrar durulanarak sayısallaştırılmaktadır (İnan vd., 2008). Bulanık mantık ile modelleme çalışmaları madencilik alanında da kullanılmaktadır. Güleç vd. (2015), yaptıkları çalışmada lintyit kömürü alt ısı değerinin bulanık mantık ile tahmin edilmesi konusunda çalışma yapmışlardır. Geliştirilen bulanık mantık modelin alt ısıl değerleri ile kömürün gerçek alt ısıl değeri arasında istatistiksel olarak önemli bir korelasyon olduğunu bulmuşlardır (R^2=0.75, c=0.864 ve p>0.05). Abkhoshk vd. (2010), bulanık mantık kullanarak flotasyon kinetiğine tane boyutunun etkisini belirledikleri bir çalışma yapmışlardır. Önerilen bulanık modelin R^2 değerleri 37.5 µm, 112.5 µm, 225 µm, 400 µm ve 625 µm tane boyutları için sırasıyla 0.986, 0.993, 0.983, 0.977 ve 0.972 olarak belirlenmiştir.

Briket kalitesinin tahmini için elde edilen veriler kullanılarak, klasik mantık yaklaşımı ile belli bir noktaya kadar parametreler kontrol edilebilmektedir. Bunun yerine bulanık mantık yöntemi kullanılarak farklı parametrelerde oluşturulacak briketler için bir sonuç değeri elde etmek daha hızlı ve kesin sonuç vermektedir. Bunun bir sonucu olarak bu çalışmada, kömür briketlemede basınç dayanımının değişimini melas oranı, briket çapı ve pres basıncının bir fonksiyonu olarak, bulanık mantık yardımıyla tahmin edilmesi amaçlanmıştır.

MATERYAL VE YÖNTEM

Materyal

Deneysel çalışmalarda kullanılan numune, GLİ İşletmesine ait 4 No'lu şlam göletinden alınmıştır. Numuneye ait kimyasal analiz Şekil 1'de görülmektedir. Kütahya Dumlupınar Üniversitesi Cevher Hazırlama Laboratuvarı'nda -500+212 µm ve -212+38 µm boyutlarında sınıflandırılan numune, humprey spirali kullanılarak zenginleştirilmiştir. Zenginleştirme sonucu elde edilen her iki boyuttaki numuneler kül değeri %20 olacak şekilde karıştırılmış ve briketleme işlemlerinde kullanılmıştır.

Briketlerin hazırlanmasında, yanma esnasında kükürdü tutması için %7 oranında kireç kullanılmıştır. Bağlayıcı olarak, şeker pancarından şeker çıkarma işlemi esnasında yan ürün olarak alınan melas kullanılmıştır. Briketler %10, %15 ve %20 melas oranlarında hazırlanmıştır.

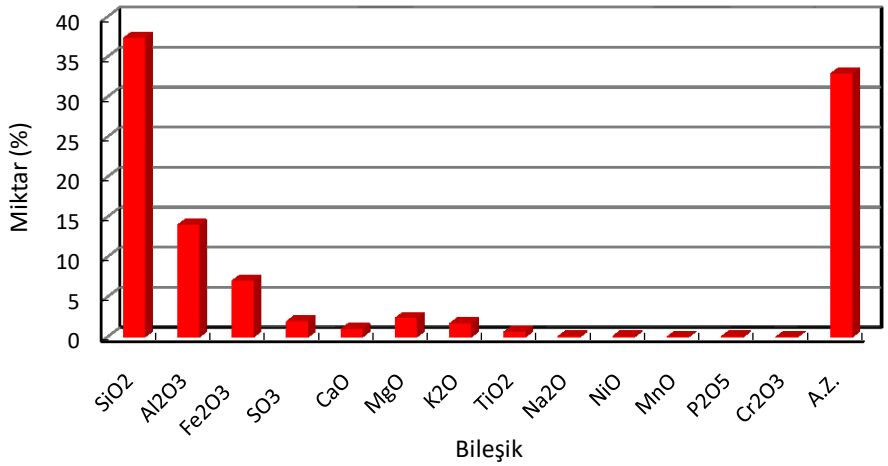

Şekil 1. 4 Nolu şlam numunesine ait kimyasal analiz

Yöntem

Çalışmanın ilk kısmında bağlayıcı miktarı ve briketleme basıncının etkisini belirlemek için bir dizi deney yapılmıştır. Briketleme işlemi Carver firmasına ait briketleme presi ve özel olarak üretilen, iç çapı 20, 30 ve 40 mm olan briketleme kalıplarında yapılmıştır (Şekil 2). Laboratuvar ölçekli bu hidrolik pres ile 7,5, 10 ve 12,5 MPa altında silindir şekilli briketler elde edilmiştir. Çalışmanın ikinci kısmında ise briketleme kalitesini belirlemek için, basınç dayanımını ölçümleri gerçekleştirilmiştir. Basınç dayanımı ölçümleri UTEST markasına ait laboratuvar ölçekli cihazda yürütülmüştür. Birbirine paralel iki düz plaka arasına yerleştirilen brikete, artan bir şekilde basınç uygulanmıştır. Briketin kırılmasına kadar sabit hızda yüklenen bu kuvvet, kırılma esnasındaki basınç dayanımı olarak kaydedilmiştir. Tüm ölçümler TS 12055'e göre yapılmıştır.

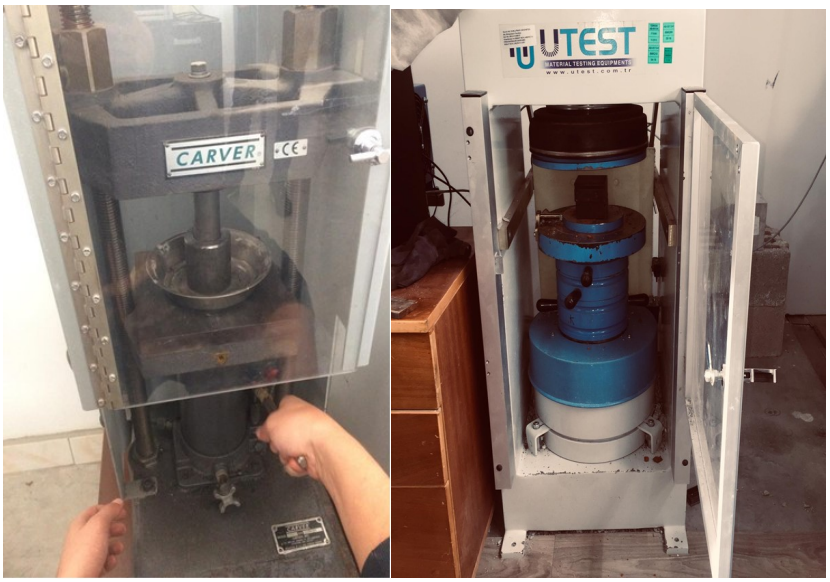

Şekil 2. (a) Briketleme cihazı, (b) Basınç dayanımı cihazı

Çalışmanın son kısmında ise, kömür briketlemede işlemindeki kalite parametresi olarak görülen basınç dayanımının tahmini bulanık mantık kullanılarak belirlenmiştir. MATLAB programının bulanık mantık modülü kullanılarak yapılan bu çalışmada, Mamdani yöntemi kullanılmıştır. Modelleme işlemlerinde giriş (bağımsız) değişkeni olarak pres basıncı, melas oranı ve briket çapı alınmıştır. Çıkış (bağımlı) değişken ise tahminini yaptığımız basınç dayanımı parametresidir. Şekil 3'te modelde kullanılan giriş ve çıkış değişkenleri görülmektedir.

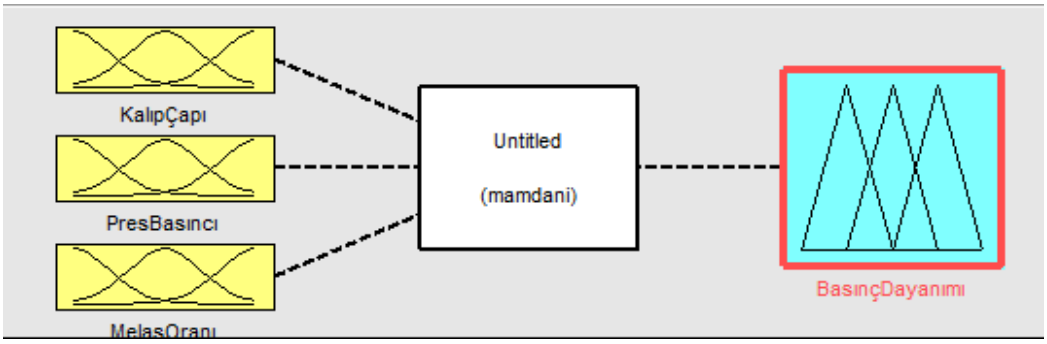

Şekil 3. Giriş ve çıkış değişkenleri

Bulanık kümeler üyelik fonksiyonları ile tanımlanmaktadır. Bu çalışmada, en iyi sonuçları verdiği için giriş ve çıkış değişkenleri için üçgen fonksiyonu kullanılmıştır. Üyelik dereceleri, üyelik kümesinin şekline göre Eşitlik 1 kullanılarak hesaplanmıştır. Parametrelerin üyelik fonksiyon isimleri dar, orta, geniş; zayıf, normal, güçlü; düşük, normal, yüksek olarak verilmiştir (Şekil 4).

$$\mu_a(x) = \begin{cases} 0, & x<a_1 \\ \frac{x-a_1}{a_2-a_1}, & a_1 \le x \le a_2 \\ \frac{a_3-x}{a_3-a_2}, & a_2 \le x \le a_3 \\ 0, & x>a_3 \end{cases} \mu_a(x) = \begin{cases} 0, & x<a_1 \\ \frac{x-a_1}{a_2-a_1}, & a_1 \le x \le a_2 \\ \frac{a_3-x}{a_3-a_2}, & a_2 \le x \le a_3 \\ 0, & x>a_3 \end{cases} \quad (1)$$

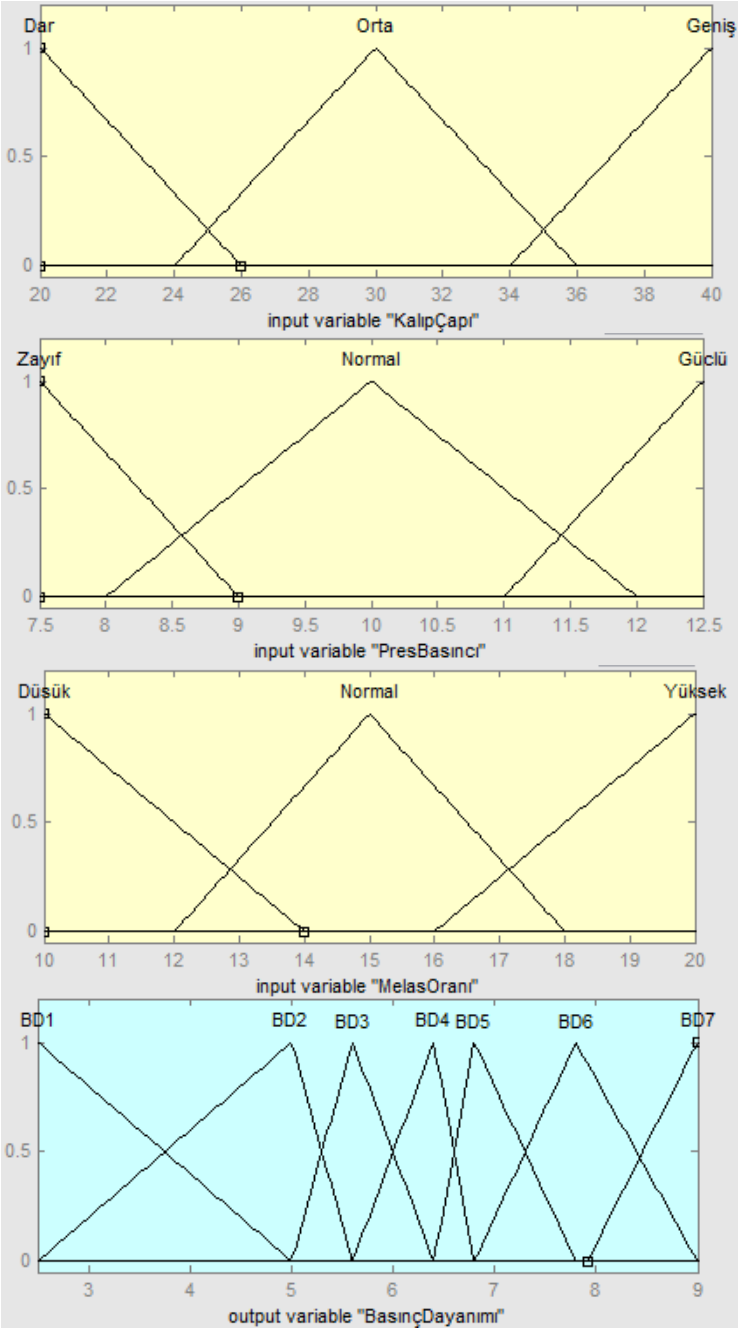

Şekil 4. Parametrelere ait üyelik fonksiyonları

Giriş değişkenleri ile çıkış değişkenleri arasındaki dilsel ilişkilerin tanımlanması kural tablosu ile yapılmaktadır. Kural tablosundaki giriş değişkenleri arasındaki tüm ilişkiler “ve” bağlacı ile oluşturulmuştur.

Buradaki “ve” bağlacı ilişkiler ortaya konulurken çıkış kümesinin üyelik derecesinin atanmasında giriş üyelik derecelerinin en küçük değerinin atanmasını göstermektedir. Üç adet giriş değişkenine ait her bir fonksiyonun sayısını çarparak kural sayısı belirlenmektedir. Bu çalışmada üç adet giriş değişkeninin üç kümesi arasında 27 adet ilişki kuralı oluşturulmuştur (Şekil 5).

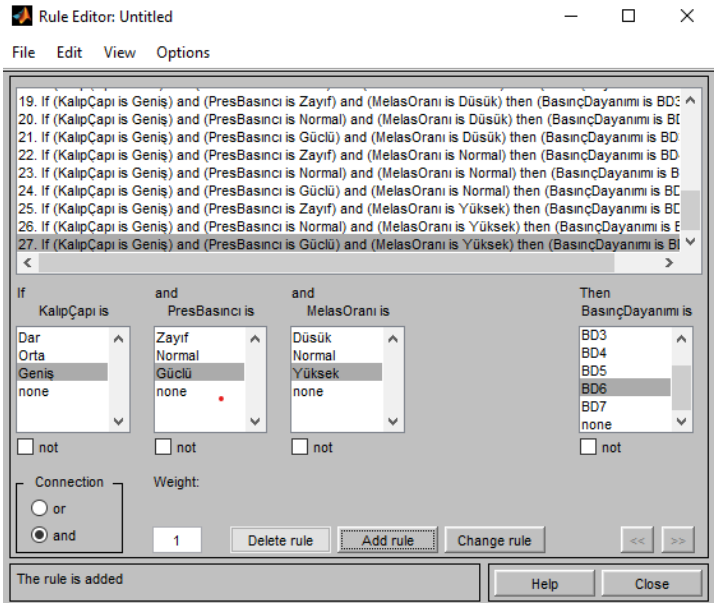

Şekil 5. Modele ait kurallar

Çıkarım işlemi “min-max” çıkarım kuralına göre oluşturulmuştur. Çalışmada durulama işlemi için yaygın olarak kullanılan ağırlık ortalaması (centroid of gravity, COG) yöntemi kullanılmıştır. Ağırlık ortalaması yöntemi en yaygın kullanılan durulaştırma yöntemlerinden birisidir (Lee, 1990). Ağırlık ortalamasını hesaplamak için;

$$WI = \sum_{i=1}^{n} \frac{\mu_i . u_i}{\mu_i} \tag{2}$$

bağıntısı kullanılmıştır. Burada μ_i üyelik derecesini, μ_i üyelik kümesinin bulanık olmayan değerini ve “WI” ise durulanmış çıkış değerini göstermektedir.

DENEYSEL ÇALIŞMALAR

Basınç dayanımının bulanık mantık ile tahmininin amaçlandığı bu çalışmada geliştirilen Mamdani modeli ile hem giriş hem de çıkış değişkenlerine ait üyelik fonksiyonlarının şekil ve sayısı ile oluşturulan kural tablosu tamamen elde edilecek sonuçların gerçeğe yakınlığına göre belirlenmiştir. Buna bağlı oluşturulan modele verilerin girilmesi ile belirli bir seviyede basınç dayanımı tahmini sağlanabilmektedir.

Üyelik fonksiyonları arasındaki ilişki kurallara bağlı olarak oluşturulduktan sonra, her bir giriş değişkeni için yeni veriler girilirse, farklı üyelik fonksiyonları ve bunlarla ilişkili kurallar etkinleştirilmiş olur. Buna bağlı olarak etkinleşen çıkış kümesi sayesinde çıkış değişenine ait yeni bir değerin elde edilmesini sağlayacaktır. Şekil 6’da giriş değişkeni olan kalıp çapı 22 mm, pres basıncı 8 MPa ve melas oranı %18 olarak

girildiği görülmektedir. Bu verilere bağlı olarak sonuç göstergesinde basınç dayanımı ise 7,03 MPa olarak belirlenmiştir. Çıkış parametresinin giriş parametrelerine bağlı olarak değişimi 3 boyutlu olarak Şekil 7'de görülmektedir.

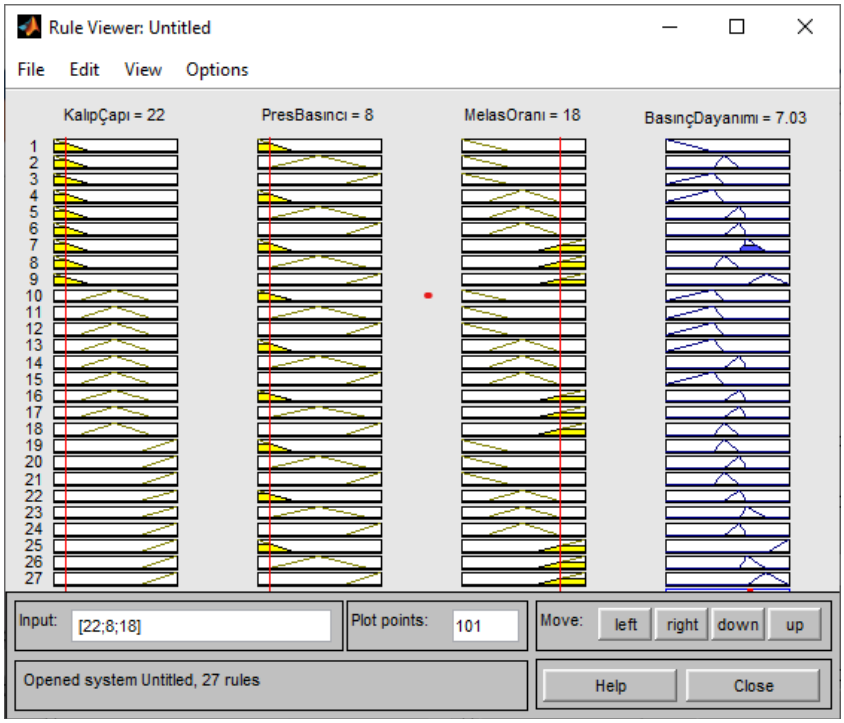

Şekil 6. Basınç dayanımına ait bulanık model için kurallara bağlı sonuç göstergesi

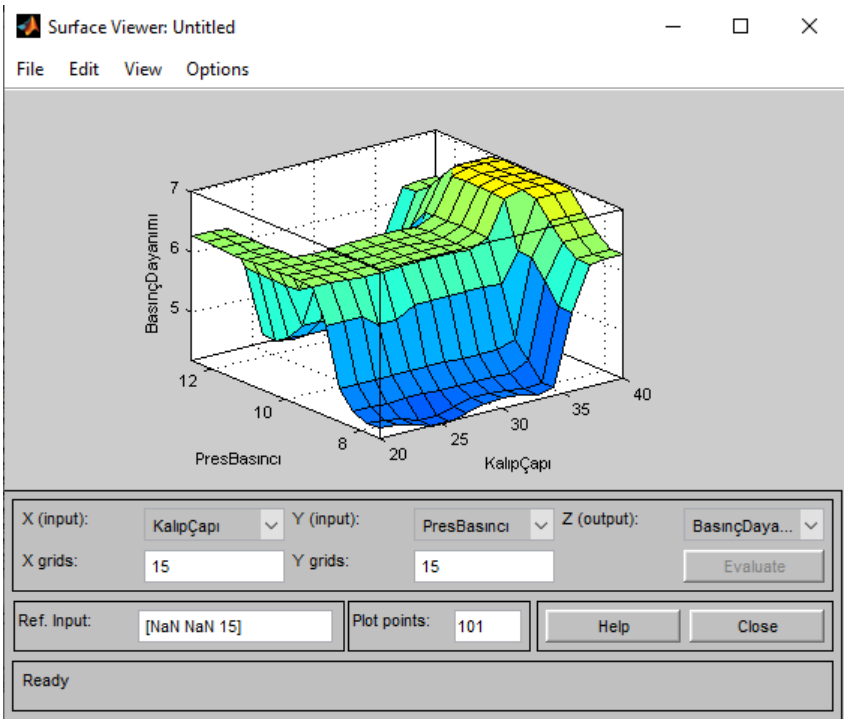

Şekil 7. Basınç dayanımına ait giriş değişkenleri değişiminin 3 boyutlu sonuç göstergesi

Model ile bulunan basınç dayanımı sonuçları ve laboratuvarda yapılan gerçek deneysel sonuçlar modeli doğrulamak için karşılaştırılmıştır (Şekil 8). Grafiğe göre R^2 değeri 0.9054 olarak elde edilmiştir. Bu, modelden elde edilen değerler ile gerçek değerlerin birbirine benzer sonuçlar verdiğini göstermektedir.

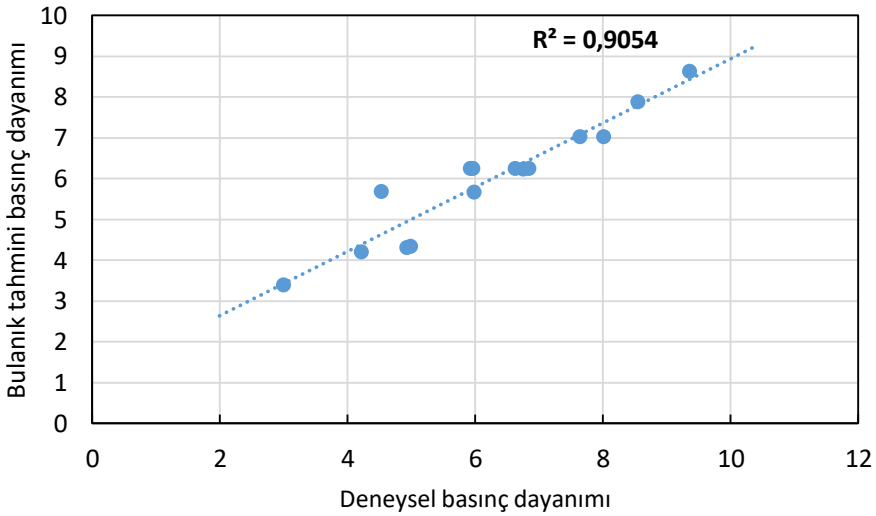

Şekil 8. Denesel sonuçlar ile bulanık sonuçların dağılımı

SONUÇLAR

Bulanık mantık kullanılarak briketlerin basınç dayanım değerlerinin değişimini incelediğimiz çalışmada, Mamdani yöntemi kullanılmıştır. Melas oranı, pres basıncı ve briket çapının giriş değişkeni olarak girildiğinde basınç dayanımı tahmini yapılmıştır. Model ile bulunan basınç dayanımı sonuçları ile deneysel olarak elde ettiğimiz sonuçlar kıyaslandığı zaman, grafikten R^2 değeri 0.9054 olarak elde edilmiştir. Bu değer, modelin gerçek basınç değerine benzer sonuçlar üreteceğini göstermektedir. Böylece kömür briketleme için kullanımının işçilik maliyeti ve zaman bakımından kazanç sağlayacaktır. Bu çalışmada kullanılan parametreler çeşitlendirilerek ve ek olarak farklı bölgelerden alınan kömürlerden elde edilen veriler modele dahil edilerek, modelin gücü ve uygulanabilirliği arttırılabilir.

KAYNAKLAR

Abkhoshk, E., Kor, M., Rezai, B. (2010). A study on the effect of particle size on coal flotation kinetics using fuzzy logic, Expert Systems with Applications, *37, 7*, 5201-5207.

Altun, N.E., Hicyilmaz, C., Bagc,i, A.S. (2003). Combustion Characteristics of Coal Briquettes. 1. Thermal Features, Energy & Fuels, *17*, 1266-1276.

Guo, Z., Wu, J., Zhang, Y., Cao, K., FengJie, Y., Liu, J., Li, J. (2013). Briquetting optimisation method for the lignite powder using response surface analysis, Fuel, *44*, 1078-1085.

Güleç, M., Uçar, A., Gülbandılar, E. (2015). Linyit Kömürünün Alt Isı Değerinin Bulanık Mantık Kullanılarak Tahmin Edilmesi, Akademik Bileşim, Eskişehir.

Güler, İ., Tunca, A., Gülbandılar, E. (2008). Detection of traumatic brain injuries using a fuzzy logic algorithm, Expert Systems with Applications, *34, 2*, 1312-1317.

Gürbüz Beker, Ü. (1997). Briquetting of Af$n-Elbistan lignite of Turkey using different waste materials, Fuel Processing Technology, *51*, I37- 144.

Janewicz, A., Kosturkiewicz, B., Magdziarz, A. (2019). Briquetting Lignite-Biomass Blends to Obtain Composite Solid Fuels for Combustion Purposes, IOP Conf. Ser. Earth Environ. Sci., 214.

Kaliyen, N., Morey, R.V. (2009). Factors affecting strength and durability of densified biomass products, Biomass and Bioenergy, *33,* 337-359.

Lee, K.H. (1990). Fuzzy logic in control systems: fuzzy logic controller, Part II, IEEE Transactions on Systems, Man and Cybernetics, *20, 2*, 419-435.

Manyuchi, M.M., Mbohwa, C., Muzenda, E. (2018). Value-adding coal fines and sawdust to briquettes using molasses as a binder, S Afr J Chem Eng, *26*, 70–73.

Meyers, R. A., Laskowski, J. S., Walters, A. D. (2001). Coal Preparation. in: EInyclopedia of physical science and technology. R. A. Meyers (Eds.) (pp. 277), California: Academic Press.

Xu, K. (2002). Briquetting method for biomass coal and its influencing factors, Fuel and Energy Abstracts, *43*, *4*, 239.

Zarringhalam-Moghaddam, A., Gholipour-Zanjani, N., Dorosti, S., Vaez, M. (2011). Physical properties of solid fuel briquettes from bituminous coal waste and biomass, J Coal Sci Eng China, *17*, 434–438.

TÜRKİYE YERALTI KÖMÜR MADENLERİNDE DELME PATLATMA PROBLEMLERİ VE ÇÖZÜM ÖNERİLERİ

DRILLING BLASTING PROBLEMS AT THE UNDERGROUND COAL MINES IN TURKEY AND SUGGESTIONS FOR ITS SOLUTION

M. Erdil

Maden Mühendisi
(mufit.erdil@gmail.com)

ÖZET

Yeraltı kömür madenciliği delme patlatma uygulamalarına, ortamın metan ve kömür tozu içermesi, bunlara bağlı olarak grizu ve kömür tozu patlama tehlikesi nedeniyle özel önem verilmesi gerekir. Bu yüzden tüm dünyada bu konuda çok sıkı yasal kurallar uygulanır. Ancak Türkiye'de geçerli tüzük ve yönetmeliklerde, kömür madenciliğine yönelik, delme ve patlatma hükümleri maalesef çok azdır. Gelişmiş ülkelerin yasal yönetmeliklerine bakıldığında, bizim yönetmeliklerimizde olmayan çok sayıda kısıtlayıcı tedbirlerin olduğu görülmektedir. Günümüzdeki gelişmiş delici makineler ve patlayıcı maddeler göz önüne alındığında, işletmelerdeki mühendislerin bilimsel gerçekler ve olmayan yasal kurallar arasında sıkıştığı gözlenmektedir. Örneğin, verimli ilerlemeler için gecikmeli kapsül kullanımında gecikmenin belirlenmesi, deliklere konulacak patlayıcı miktarı, güvenli delik düzeni gibi konular, yol gösterici yönetmelikler olmaması nedeniyle mühendislerin karar vermesini zorlaştırmaktadır. Bu bildiride olması gereken kısıtlayıcı tedbirler ele alınacak ve uygulanabilir çözüm önerileri sunulacaktır.

Anahtar Sözcükler: Yeraltı, kömür, grizu, patlayıcı maddeler, çözüm

ABSTRACT

Particular attention should be paid to drilling and blasting applications in underground coal mining due to the mine atmosphere contains gaseous, primarily methane and associated fire damp and coal dust. Therefore, very strict legal regulations are applied in this regard all over the world. Unfortunately, there are few rules for drilling and blasting specific to coal mining in the current regulations in Turkey. When we look at the legal regulations of developed countries, it is seen that there are many restrictive rules that are not in our regulations. Considering today's advanced drilling machines and explosive materials, it is observed that engineers working at mine sites are stuck between scientific facts and non-existent legal rules. For example, issues such as the how long delay time in the use of delayed detonators, the amount of explosive to be charged in the holes, the safe drilling pattern for efficient advances make it difficult for engineers to make decisions due to the lack of guiding regulations. In this paper, the necessary restrictive rules will be discussed and applicable solution suggestions will be presented.

Keywords: Underground, coal, firedamp, explosives, solution

GİRİŞ

Yerüstü madenciliğine göre koşulları daha ağır olan yeraltı madenciliğinde, çıkarılan cevher kömür olunca koşullar daha da ağırlaşmaktadır. Gazlı ortam, metan salınımı ve buna bağlı grizu tehlikesi ile kömür tozu patlamasına yol açabilecek ortam, yapılacak çalışmalarda iş güvenliği önlemlerinin üst düzeyde alınmasını gerektirmektedir. Tüm dünyada yaşanan acı tecrübeler sonucu, yeraltı kömür madenciliği ile ilgili zorunlu yasal düzenlemeler özel bir yer tutmaktadır. Yasal düzenlemelerin en önemli

konusunu ise, kullanılacak patlayıcı maddeler, ateşleme sistemleri ile bunlara bağlı yapılacak delik düzeni, doldurma ve ateşleme yöntemleri oluşturmaktadır.

Grizu patlamalarıyla ağır bedeller ödediğimiz Türkiye yeraltı kömür madenciliğinde, delme ve patlatma uygulamaları için yasal düzenlemeler maalesef yok denecek kadar azdır. Bu durum işletmelerdeki mühendisleri üretimi arttırırken, olmayan kurallar ile alınması bilimsel gereklilik olan iş güvenliği önlemlerinin arasına sıkıştırmaktadır. Bu bildiride, iş güvenliği tüzük veya yönetmeliklerinde olmayan kurallar, gelişmiş ülkelerin yasal düzenlemelerinde aranmış ve işletmecilere yol gösterici çözüm önerileri olarak sunulmuştur.

YASAL MEVZUAT ve SORUNLAR

Türkiye yeraltı kömür madenciliğinde, delme ve patlatma uygulamalarını düzenleyen kurallar;

1. 87/12028 sayılı Tekel Dışı Bırakılan Patlayıcı Maddelerle İlgili, Av Malzemesi ve Benzerlerinin Usul ve Esaslarına İlişkin Tüzük,
2. 2013/28770 sayılı Maden İşyerlerinde İş sağlığı ve Güvenliği Yönetmeliğinde yer almaktadır.

Bu kurallar da, sadece "2013/28770 sayılı Maden İşyerlerinde İş sağlığı ve Güvenliği Yönetmelik" te yer almaktadır. 87/12028 sayılı tüzük, sadece grizu güvenli patlayıcıların ithalinde, galeri denemelerinin yapıldığının belgelenmesini şart koşmuştur.

2013/28770 sayılı Maden İşyerlerinde İş sağlığı ve Güvenliği Yönetmeliğinde yer alan maddeler özetle aşağıdaki gibidir;

Grizulu maden ocaklarında yalnız bu tür ocaklar için uygun olan patlayıcı maddeler ve ateşleyiciler kullanılacağı (Madde 10.16-), patlayıcı maddenin boyunun, delik derinliğinin yarısını geçemeyeceği ve kalan boşluğun sıkılama maddesiyle doldurulacağı (Madde 6.7), patlayıcı madde kullanım kısıtlamalarını (Madde 9), grizulu yerlerin tanımı ve %1 den fazla metan varlığı halinde deliklerin doldurulup ateşlenemeyeceğini (Madde 10, 10.1, 10.17, 10.18), toz patlaması tehlikesi karşısında patlayıcı yasağı (Madde 11.2) ve fitille ateşleme yapılamayacağını (Madde 6.8) belirleyen kurallardır.

Maalesef bu yasal düzenlemeler günümüzde işletmecilerin önünü açmamaktadır. Birçok madenimizde mekanizasyona geçilmiş, delikler Jumbo adı verilen delici makinelerle delinmekte, uzun ve çok delik ihtiyacı, bunların verimli olabilmesi için ateşlemede bol gecikme verilmesi istenmektedir. Burada önümüze çıkan başlıca sorunlar şunlardır;

1. Ne kadar uzun delikler delmeliyiz ve bunlara doldurulacak patlayıcı miktarı ne olmalıdır? Yürürlükte olan yasal kurallarımız, delik boyuna ve deliğe doldurulacak patlayıcı miktarı delik boyunun yarısını geçmediği sürece miktara karışmamaktadır (2013/28770 nolu yönetmelik madde 6.7). Gelişmiş ülkelerin yasal düzenlemelerine baktığımızda ise, örneğin Amerika Birleşik Devletleri MSHA (Mine Safety & Health Administration), taşta hariç, kömürde yapılan patlatmalarda bir deliğe koyulan patlayıcı madde miktarını 3 pound (1.36 Kg) olarak sınırlamış ve 6 feet den (1.8 mt) kısa deliklerde toplam patlayıcı miktarını, azalan her foot (30 cm) başına ½ pound (450 gr) azaltılmasını şart koşmuştur. Buradaki amaç, infilakı ocak atmosferinden uzak tutmaktır (Pantovic R. 2008). ABD de, infilakı ocak atmosferinden uzak tutmak için, kömürde 60 cm, taşta 50 cm delik yük uzaklık şartı getirilmiştir (USA Code of Federal Regulations).
2. Bir seferde toplam kaç delik patlatılmalıdır? Bu konuda Türkiye'de yasal bir kısıtlama yoktur. ABD de 20 den fazla deliğin birlikte patlatılması MSHA' nın iznine bağlanmıştır (Verakis H.C.).
3. Gecikmeli kapsül kullanabilir miyiz? Gecikme süreleri ne olmalıdır? İşletmedeki mühendisleri en çok meşgul eden ancak yasal mevzuatımızda herhangi bir kısıtlama öngörülmeyen gecikme konusu, gelişmiş ülkelerde çok sıkı kurallara bağlanmıştır. Örnek olarak, ABD de Bir atımdaki toplam gecikme süresi 1000 ms, delikler arası gecikme en az 50 ile en fazla 100 ms olarak

sınırlandırılmıştır. İngiltere'de bu süreler, kömür içermeyen kuyu ve taşta sürülen galerilerde 5 sn, aynasında 30 cm kömür olan taş galerilerde 750 ms, aynasında 30 cm'den fazla kömür içeren galerilerde 300 ms, kömürde çalışılan yerlerde 100 ms olarak detaylı şekilde belirlenmiştir (ICI Nobel Explosives Booklet ve UK Explosives at Coal Regulation 1993).

4. Ülkemizde ve dünyada yeraltı kömür madenlerinde kullanılacak patlayıcılar grizu güvenli olmak zorundadır. Türkiye'de maalesef grizu güvenli olmayan patlayıcılar bazı madenlerde kullanılmaktadır. Ayrıca üreticilerin grizu güvenli olarak piyasaya sürdükleri patlayıcıların bağımsız bir yetkili kurumdan galeri testlerini yaptırma ve sertifikalandırma zorunluluğu bulunmamaktadır. ABD de yeraltı kömür madenlerinde sadece galeri testleri yapılmış, MSHA onaylı grizu güvenli (permitted) patlayıcılar kullanılabilir.

ÇÖZÜM ÖNERİLERİ

Yukarda belirtildiği üzere, Türkiye'de yeraltı kömür madenciliğinde delme ve patlatma açısından, yasal mevzuat oldukça yetersizdir. Bu durum işletmecileri hem yasal açıdan hem de bilimsel olarak iş güvenliğini sağlama ve aynı zamanda günümüz teknolojilerini kullanarak üretimi arttırmak için nasıl davranacakları konusunda tedirgin etmektedir. Bu amaçla temel sorunlara çözüm aşağıda önerilmektedir.

1. Delik boyu ve delik başına doldurulacak patlayıcı miktarı: Bu konuda öncelikle iş güvenliği amacımızın ne olduğu açık bir şekilde anlaşılmalıdır. Hedeflenen iş güvenliği, delik içerisinde infilak eden patlayıcı maddenin, aynanın gerisinden gelebilecek metan gazının maden atmosferindeki oksijen ile buluşması ve ortaya çıkacak kömür tozunun da patlayabilirliği göz önüne alınarak, infilakın çok kısa sürede tamamlanması olmalıdır.
2. Bilindiği üzere Grizu patlamasının olabilmesi için üç etkenin bir araya gelmesi gerekir. Bunlar; metan gazı, oksijen ve karışımın patlamasına yol açacak bir ısı kaynağıdır (Güyagüler 2002). Grizu patlamaları, havada %5-15 arası metan bulunduğunda, en şiddetlisi ise, bu oranın %9-9.5 civarında olması halinde meydana gelmektedir. Şekil 1 grizu patlayabilirlik grafiğinde (Coward üçgeni) kırmızı bölge patlayabilir oksijen-metan karışım oranını vermektedir. Metanın ateşlenme ısısı 650-750°C dir. Ancak özelliği itibarıyla, hemen değil, ısı kaynağının belirli bir süre uygulanması sonucunda ateşlenebilir.

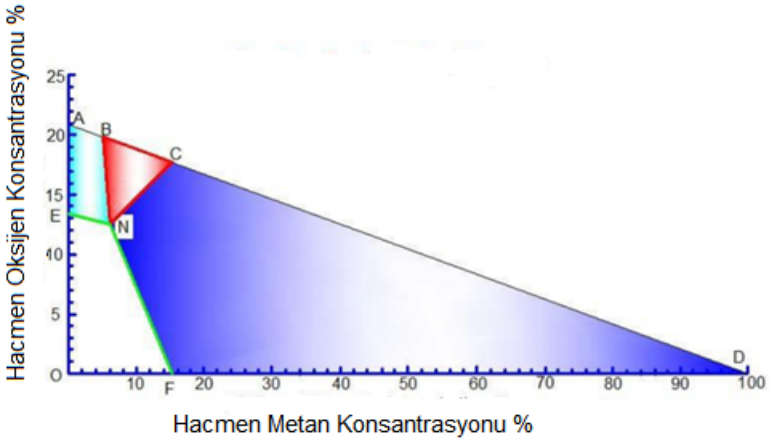

Şekil 1. Grizu patlayabilirlik grafiği Coward Üçgeni (Cheng J.2017)

O halde atım öncesi %1 in altında olan metan konsantrasyonu, deliklerin infilakı sırasında geriden gelecek metan ile yükselerek, ocak havasındaki oksijen ile patlayabilir bir karışım olan grizuya sebep olabilecektir. Delik içerisindeki patlayıcı da gerekli ısıyı sağladığında, ortamda oluşan kömür tozu ile istenmeyen patlama gerçekleşebilecektir (Şekil 2). Kömür tozu, grizu kadar tehlikeli bir ortam

yaratmaktadır. Bu nedenle patlayıcı infilakı, grizuyu ateşleyebilecek ısı ve sürenin altında tutulmalı ve ocak havasına yakın olmamalıdır.

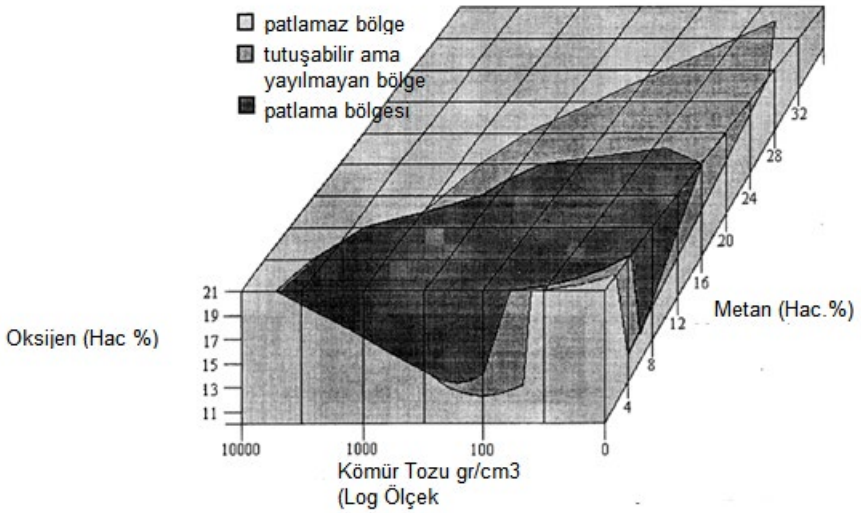

Şekil 2. Metan-Oksijen-Kömür tozu patlayabilirlik grafiği (Bartknecht 1996)

3. Grizu güvenli patlayıcılar bünyesinde bulunan tuzun etkisi ile diğer patlayıcılara göre daha düşük ısı ortaya çıkartır. Örnek olarak, 4000 m/s infilak hızına sahip, infilak sıcaklığı yaklaşık 2300°C olan ve 250gr ağırlık, Ø32x260mm kartuş boyutundaki grizu güvenli bir patlayıcıyı, delik içerisinde 1 metre boyunca doldurursak, infilak süresi 1ms'nin ¼ ü kadar olacaktır. Grizunun ateşlenmesi ile ilgili yapılan çalışmalarda, 1000°C lik bir ısı kaynağı ile 1 saniye, 1200°C ısıda ise, 20ms süre içerisinde grizunun ateşlendiği görülmüştür. (Skochinsky ve Komarov 1969). Bu dikkate alındığında, kömürde yapılan patlatmalarda, delik başına en fazla bir kilogram ateşlenmesi yerinde olacaktır. Ancak delik boyu ve sıkılama uzunluğu dikkate alınmalıdır. Patlayıcı şarj uzunluğu delik boyunun yarısını geçmemeli, sıkılama boyu 60 cm'den az olmamalıdır.
4. Bir atımda azami delik sayısı: Türkiye'deki yasal bir kısıtlama olmamasına rağmen, ABD de 20 delik ile sınırlama getirilmiş, daha fazlası için bu konuda yetkili otorite (MSHA) den özel izin alınması zorunluluğu getirilmiştir. Bu konuda elimizde mühendisçe yorum yapabileceğimiz veri bulunmamaktadır. Bu yüzden, kömürde en fazla 20 delik, taşta sürülen galerilerde, metan varlığı veya uzaklığına bağlı her işletmeye göre bir komisyon kararıyla sayı belirlenebilir. Sınırlanan delik sayısı, anayol hazırlık galerileri gibi büyük aynalarda yeterli gelmediğinde, ayna iki aşamalı olarak patlatılmalıdır.
5. Gecikmeli kapsül kullanımı ve gecikme süreleri: Gecikmeli kapsül kullanımında, ABD ve İngiltere'de uygulanan kısıtlamalar göz önüne alınmalı, kömürde yapılan atımlarda, birinci delik ile son delik arasındaki toplam gecikme 100ms'yi aşmamalıdır. Bu durumda 25ms'lik gecikmeli bakır kapsüller ile 50ms atlamalı iki gecikme verilmesi uygundur. Taşta sürülen galeri veya kuyularda, kömüre yakın yerlerde 750-1000ms, kömürden çok uzak ise 5000ms ye toplam gecikme süresi verilebilir.
6. Kullanılacak patlayıcı cinsi: Yeraltı kömür madenlerinde mutlaka grizu güvenli patlayıcı maddeler kullanılmalıdır. Kullanılacak patlayıcı maddelerin grizu testleri kesinlikle bağımsız (notified body) bir enstitü tarafından yapılmış ve sertifikalandırılmış olmalıdır.
7. Galerileri atımlarında delik düzeni: Mekanize Jumbo delicilerle veya el tabancaları ile yapılan delik paterni için sadece V kesme uygulanmalıdır. Paralel delik düzeninde, ortada açılacak boş delik ocak atmosferini temsil edeceği ve kesme bölgesi deliklerinin, bu boş deliğe 10-15 cm'lik yük uzaklığında olması riskli olup, yeraltı kömür madenciliğine uygun değildir. Delik başına

patlayıcı kısıtlamaları ve V kesme açıları nedeniyle, uzun delik hedeflenmemeli, buna bağlı olarak uzun kızaklı delici yatırımlarından kaçınılmalıdır. Kömürde açılan deliklerin yük mesafesi 60 cm den, taşta sürülen galerilerdeki ise 50 cm den az olmamalıdır.

SONUÇLAR

Yeraltı kömür işletmelerimiz, yetersiz tüzük ve yönetmeliklere rağmen, hem ülkemizde geçerli olan tüzük ve yönetmeliklere uygun, hem de gelişmiş ülkelerde uygulanan kuralları temel alarak, kendi işletme şartlarına göre, işyeri yönetmeliklerini yapabilir. Bunun için işletme bünyesinde oluşturulacak bir iş güvenliği komisyonu, kendi ocak şartlarını bölge bazında tanımlayarak hazırlayacakları işyeri yönetmelikleri ile yukarda önerilen kuralları hayata geçirebilir. Burada temel alınması gereken, koyulan kuralın nedeni tüm işletme çalışanlarınca bilinmesi ve özümsenmesi olmalıdır.

KAYNAKLAR

Cheng J., Ziming, B., and Apurna, G. (2017). Explosion Risk Assessment Model for Underground Mine Atmosphere, *Journal of Fire Sciences*, 35 (1), 21-35.

Erdil, M. (2011). Türkiye Yeraltı Kömür Madenlerinde Kullanılan Patlayıcı Maddeler ve Yaşanan Grizu Kazalarındaki Olası Etkileri. Türkiye 22. Uluslararası Madencilik Kongresi (syf 181-187). Ankara

Gillies. A.D.S., and Jackson, S. (1998). Some Investigations into the Explosibility of Mine Dust Laden Atmospheres, COAL98 Conference WoUongong 18- 20 February

Güyagüler, T, (2002). Türkiye'de Meydana Gelen Grizu Patlamalarının İrdelenmesi ve Önlem Önerileri, Türkiye 13. Kömür Kongresi Bildiriler Kitabı.

ICI Nobel's Explosives Company Limited, Explosives in Coal Mining, Booklet, printed by Armac Scotland, NDP 409/6 Ed/33/1172/R577

Pantovic. R., Zikic. M., and Stojkovic. Zoran. (2008) Blasting Development at Drifting in Underground Coal Mines, *Journal of Mining and Metallurgy*, 44 A (1), 9 - 16

Skochinsky, A., & Komarov V. (1969). Mine Ventilation, Mir Publishers, Moskow, 580

UK, Explosives at coal and other safety-lamp mines (explosives) regulations 1993, HCS (Health&Safety Commission)

USA The Code of Federal Regulations (CFR) MSHA,30 Annual Edition, Subpart N-Explosives and Blasting (syf 626-633)

Verakis, H.C. (1988). MSHA's New Regulations for Explosives Used in Coal Mines (pp 780-785),

TÜRKİYE'DE PÜLPTE KARBON ALTIN İŞLEME YÖNTEMİNİN SU AYAK İZİ DEĞERLENDİRMESİ

WATER FOOTPRINT ASSESSMENT OF CARBON IN PULP GOLD PROCESSING IN TURKEY

*E. Güney [1, *], N. Demirel [1]*

[1] Orta Doğu Teknik Üniversitesi (Ankara/Türkiye), Maden Mühendisliği Bölümü
*(*Sorumlu Yazar: emre.guney@metu.edu.tr)*

ÖZET

Bu çalışmanın ana hedefleri, pülpte karbon (CIP) altın işleme tesisindeki proseslerin gri ve mavi su ayak izlerini belirlemek ve su ayak izi özelinde kritik noktaları bulmaktır. Sonuçlar, altının çıkarılması ve işlenmesi dahil olmak üzere toplam mavi su ayak izinin 452,40 m^3/kg Au ve toplam gri su ayak izinin 2300,69 m^3/kg Au olduğunu ortaya koymuştur. Doğrudan mavi su ayak izi tarafında, 260,61 m^3/kg Au değeriyle en büyük pay kayıp dönüş akışına aittir ve bu akışın tek kaynağı atık havuzudur. Dolaylı tarafta ise liç işlemi için kullanılan oksijen tüketiminin 37,38 m^3/kg ile en yüksek değere sahip olduğu görülmektedir. Gri su ayak izi için kritik bileşen, 1777 m^3/kg Au değeriyle maden atıklarındaki dokuz kirletici arasında açık ara farkla arseniktir. Sonuçlar, madencilik faaliyetlerinde su tüketimini azaltmak için önerilerde bulunmak ve çevre için sürdürülebilir tasarımlar geliştirmek için kullanılacaktır. Çalışma, Türkiye'de altın madenciliğinde su ayak izi değerlendirmesinin ilk uygulaması olan öncü bir çalışma olarak değerlendirilmektedir.

Anahtar Sözcükler: Sürdürülebilirlik, su ayakizi analizi, altın işleme, sürdürülebilir su kullanımı, Türkiye

ABSTRACT

The main objectives of this study are determining grey and blue water footprints and identifying the hotspots of the carbon in pulp (CIP) gold processing using water footprint assessment (WFA). Results revealed that the total blue water footprint, including the extraction and processing of the gold, was found 452.40 m^3/kg Au, and the grey WF 2300.69 m^3/kg Au. On the direct blue WF side the lost return flow has the largest contribution, with a value of 260.61 m^3/kg Au, and the only source of the lost return flow is the tailing pond. On the indirect side, it is seen that the oxygen consumption used for the leaching process has the highest value, with 37.38 m^3/kg. For the grey water footprint, the critical component is by far arsenic among the nine contaminants in the mine tailings, with a value of 1777 m^3/kg Au. The results will be used to make recommendations for reducing water consumption in mining operations and to develop sustainable design for environment. The study is a pioneering study, being the first implementation of water footprint assessment in gold mining in Turkey.

Keywords: Sustainability, water footprint assessment, gold processing, sustainable water use, Turkey

GİRİŞ

Sürdürülebilir üretim yöntemlerinin giderek öneminin arttığı günümüzde, dünya için en önemli sektörlerden biri olan madencilik sektörünün de bu alandaki gelişmelere ayak uydurması zorunlu hale gelmiştir. Bu anlamda en önemli endüstriyel girdilerinden biri su olan bu sektör üretimin devamı ve büyümesini sürdürmek için daha iyi su yönetimi stratejileri benimsemesi gerekmektedir çünkü bu konu hakkında dünya çapında yapılan araştırmalar göstermektedir ki en büyük küresel madencilik şirketlerinin madencilik faaliyetlerinin yaklaşık yüzde 70'inin su sıkıntısı çeken ülkelerde bulunmaktadır. Uygulanacak

stratejiler ise daha az su tüketimi ve kirleticilerin azaltılması özelinde geliştirilmelidir (Martin vd., 2020; Fashola vd. 2016).

Bu konu Türkiye özelinde madencilik sektörü açısından incelendiğinde, Türkiye'nin dünya ile aynı kaderi paylaştığı bir gerçektir. Türkiye İstatistik Kurumu (TÜİK), 2010 yılından itibaren 2 yılda bir OECD/EUROSTAT'ın tanımı, kapsamı, sınıflandırmaları ve uluslararası düzenlemeler dikkate alınarak madencilik, su, atık su ve atık istatistiklerine göre veriler üretmektedir. Hazırlanan rapora göre madencilik operasyonları 2010 yılında kuyulardan, denizden, maden ocaklarından, nehirlerden, göllerden ve diğer kaynaklardan toplam 55 milyon m^3 su çekmiştir. Bu sayı 2012 yılında 116 milyon m^3, 2014 yılında 220 milyon m^3, 2016 yılında 241 milyon m^3 ve 2018 yılında 219 milyon m^3 olarak bulunmuştur (TÜİK, 2010, 2012, 2014, 2016, 2018). Üretimdeki büyüme ve yaklaşan su kıtlığı krizi nedeniyle artan su talebi göz önüne alındığında, madenlerin etkin su yönetimi stratejilerini uyarlayarak su ayak izlerini ölçmeleri ve değerlendirmeleri gerektiği kaçınılmaz bir gerçektir.

Son yirmi yılda, su yönetimi sorununun baskısı, bölgelerin, ürünlerin ve süreçlerin su tüketimini ve su kirliliğini ölçmeye yönelik yaklaşımların geliştirilmesine yol açmıştır. Yeni yaklaşımlardan biri su ayak izi değerlendirmesi (SAD) kavramıdır. Bu kavram bir sürecin, bir ürünün, bir tüketicinin, bir tüketici grubunun, coğrafi olarak belirlenmiş bir alanın, bir ulusun, bir işletmenin, bir belediyenin veya bir devlet kurumunun, bir havzanın veya bir nehir havzası, hesaplanan su ayak izinin (SA) çevresel, sosyal ve ekonomik sürdürülebilirliğini değerlendirmek, hesaplanan SA değerini düşürmek ve daha sürdürülebilir bir süreç elde etmek için bir çözüm üretmek temeline dayanan bir metodolojidir (Zhang vd., 2013).

Bu alandaki gelişmelere rağmen, bu metodolojinin küresel anlamda bu sektöre uygulanması sınırlı kalmıştır. Bu yöndeki çalışmalar Güney Amerika ve Güney Afrika'da yoğunlaşmıştır ve Türkiye'de bu konuda daha önce yapılmış bir çalışma bulunmamaktadır. Ayrıca çalışmaların çoğu bakır ve platin madenciliği üzerine olup, literatürde CIP işleme yöntemi ile üretim yapan bir proses tesisinde detaylı bir çalışma bulunmamaktadır.

METOD

SAD dört farklı aşamadan oluşur: hedef ve kapsam belirleme, su ayak izi hesaplama, su ayak izi sürdürülebilirlik değerlendirmesi ve su ayak izi etki değerlendirmesi. İlk aşamada, SAD sürecinin amacı ve kapsamı belirlenir. Bu çalışmanın temel amacı, madenin doğrudan ve dolaylı SA değerini belirlemektir. Bu bilgi ile kritik noktalar tespit edilecek ve SA değerini azaltmak için alınabilecek aksiyonlar belirlenecektir (Aldaya, vd., 2012).

Bu çalışmanın kapsamı, altın cevherinin hem çıkarılması hem de işlenmesi için çalışılan madenin mavi ve gri SA' sını hesaplamaktır. Çalışmada doğrudan ve dolaylı SA incelenmiştir. Dolaylı SA değerine altını üretmek için kullanılan elektrik, yakıt ve kimyasallar dahildir. Ayrıca sahada çalışanların günlük ihtiyaçlarını karşılamak için kullandıkları su da bu kapsamdadır. Hesaplamalar Ocak-Aralık arası on iki aylık bir periyod için yapılmıştır ve fonksiyonel birim olarak 1 kg altın üretmek için kullanılan su miktarı belirlenmiştir.

SAD'de üç tür SA değeri vardır. Mavi SA, yeraltı ve yüzey kaynaklarından (mavi SA kaynakları) ne kadar su tüketildiğini gösteren bir göstergedir. Yeşil SA, yağmur suyundan (yeşil SA kaynağı) ne kadar su tüketildiğini gösterir. Ancak burada dikkat edilmesi gereken kritik nokta, bu kaynağın hiçbir şekilde yer üstü veya yer altı suları ile karıştırılmaması gerektiğidir. Gri SA, kirlenmiş suyu doğal konsantrasyonuna ve mevcut su kalitesi standardına getirmek için harcanan su miktarıdır (Aldaya, vd., 2012).

Mavi SA, tüketilen su kullanımının bir göstergesidir. Tüketimli su kullanımı ise 3 durumu temsil eder ve mavi SA bu 3 durumun toplamıdır. Bu durumlar, Denklem (1)'de görüldüğü gibi, açık yüzeylerden buharlaşan su (Buharlaşan Mavi Su), sanal su içeriği veya gömülü su olarak bilinen ürüne dahil edilen su

(Ürüne Dahil Edilen Mavi Su) ve kullanıldıktan sonra aynı havzaya veya aynı periyotta geri dönmeyen suyu (Kayıp Dönüş Akışı) kapsamaktadır (Aldaya, vd., 2012).

SA_{mavi} =Buharlaşan Mavi Su + Ürüne Dahil Edilen Mavi Su + Kayıp Dönüş Akışı (1)

Denklem (2), tesisteki tanklardan ve atık havuzundan kaynaklanan buharlaşmayı hesaplamak için kullanılmıştır. Denklemde V_{Buhar} (ML) buharlaşma kayıplarını, S_{Buhar} hesaplama döneminde suyun kapladığı ortalama yüzey alanını (ha) temsil eder, Pan_{Buhar} raporlama döneminde ölçülen buharlaşma oranlarının (mm) değeridir ve f ise düzeltme faktörüdür. A Sınıfı bir pan ile ölçülen pan buharlaşma oranları için düzeltme faktörü genellikle 0,75 civarındadır (*Water Accounting Framework*, 2014).

$$V_{Buhar} = 0.01 \times S_{Buhar} \times Pan_{Buhar} \times f \quad (2)$$

Alanda toplanan yağmur suyunun hesaplanmasında Denklem (3) kullanılmıştır. Denklemde $V_{Yağış}$ (ML) yağış hacmi, R (mm) hesaplama periyodu sırasında ölçülen yağış miktarı ve $SA_{R,M}$ (ha) açık yüzey alanıdır(*Water Accounting Framework*, 2014).

$$V_{Yağış} = 0.01 \times R \times SAR,M \quad (3)$$

Ürüne dahil edilen su, V_{ent} (ML) de cevherdeki mavi su olarak kabul edilir. Su miktarını bulmak için, Denklem (4) kullanılır; burada P, raporlama döneminde (Mt) işlenen gelen cevherin miktarıdır ve m, bir kesir olarak nem içeriğidir (*Water Accounting Framework*, 2014).

$$V_{ent} = 1000 \times P \times m \quad (4)$$

Yıllık dolaylı su ayak izi ($SA_{Dolaylı}$) hesaplanırken, bu kaynakları üretirken tüketilen su miktarı ile (W_i) 1 kg altın üretmek için bu kaynaklardan gerekli miktar (W_i) ile yıllık üretim miktarına (P) bölünerek 1 yıl içindeki bu kaynaklardan gelen su tüketim miktarı bulunur (Aldaya, vd., 2012):

$$SA_{Dolaylı} = \sum_{i=1}^{n} \frac{R_i W_i}{P} \quad (5)$$

Denklem (6), bir proses adımında gri su ayak izini hesaplamak için kullanılır (Aldaya, vd., 2012):

$$SA_{Gri} = \frac{L}{Cmax - Cnat} \quad (6)$$

(6) numaralı denklemde, SA_{Gri} (hacim/zaman) bir ürünün toplam gri su ayak izini gösterir, burada L (kütle/zaman) kirletici yükü, C_{max} (kütle/hacim) kirleticinin kabul edilebilir maksimum konsantrasyonudur ve C_{nat} (kütle/hacim) alıcı su kütlesindeki doğal konsantrasyonu gösterir.

Veri

Altın işlemenin SAD uygulanması için Türkiye'de faaliyet gösteren ve CIP yöntemini kullanarak altın cevheri işleyen madenler referans alınmıştır. Bu madenler için teknik raporlar, sürdürülebilirlik çalışmaları ve literatür taraması detaylı olarak incelenmiştir.

Tasarlanan tesiste su tüketiminin bulunabilmesi için proseslerde kullanılan katıların kütlece oranı (pülp oranı), tankların yüzey alanları, tikiner ve atık havuzu da gerçekçi verilere dayalı olarak belirlenmiştir (Önal, 2013; Köksal vd. 2003; Yüce, 2001; *SRK Danışmanlık ve Mühendislik*, 2014; Akçıl, 2002; Sarıkaya ve Orhan, 2018). Evsel atık su deşarjı 30 m^3/gündür. Madendeki ocak susuzlaştırma değeri için Northey vd. (2014) tarafından sağlanan 0.15 m^3/ton değer kullanılmıştır. Kırıcı ünitesindeki toz bastırma işlemi için kullanılan su miktarı hesaplanırken her kırıcı için temsili olarak bir su spreyi olduğu düşünülmüş ve bu spreyler için su tüketim değeri 10 litre/dakika olarak belirlenmiştir (*Guidance*

for Controlling Silica Dust from Stone Crushing with Water Spray Technology, 2008). Öğütme devresi ise kütlece %75 katı madde içeren bir çubuklu değirmen ve kütlece %72 katı madde içeren bir bilyalı değirmenden oluşmaktadır (Sarıkaya, 2018; Gupta ve Yan, 2006).

Bu çalışma için yapılan araştırma sonucunda Mavi SA'yı hesaplamak için pan buharlaşma verileri Ovacık Altın Madeni Üçüncü Atık Depolama Tesisi ÇED Başvuru Dosyasından elde edilmiştir. Bu raporun verileri Türkiye Cumhuriyeti Meteoroloji Genel Müdürlüğü Bergama İstasyonu'ndan alınmıştır. 1960-2012 yılları arasında toplanan verilerin ortalaması alınarak buharlaşma verileri oluşturulmuştur. Buharlaşma durumunda olduğu gibi, Ovacık Altın Madeni Üçüncü Atık Depolama Tesisi Projesi ÇED Uygulama Dosyasından metrekareye düşen yağış miktarı da alınmıştır (SRK Danışmanlık ve Mühendislik, 2014).

Ayrıca madende üretim aşamalarında kullanılan dizel miktarı, madende kullanılan elektrik miktarı, kullanılan kimyasallar için hesaplanan gömülü sanal mavi SA değerinin hesaplanması için literatüre dayalı bir veri analizi yapılmıştır ve sonuçlar Tablo 1'de gösterilmektedir (Northey vd. (2014); Ecoinvent, 2009; Gu vd. 2018).

Tablo 1. Madende kullanılan malzemelerin birim SA değerleri

Kaynak	Birim Başına SA	Birim
Sodyum Siyanür	0.1956	m^3/kg
Kireç	0.02	m^3/kg
Hidroklorik Asit	0.0254	m^3/kg
Patlayıcılar	0.0338	m^3/kg
Elektrik	0.021	m^3/kWh
Oksijen	0.0042	m^3/kg
Aktif Karbon	0.012	m^3/kg
Dizel	0.0013	m^3/kg

Gri SA'yı hesaplamak için, kirletici yükü Ovacık Altın Madeni'nin 9 kirletici için haftalık atık havuzu metal analizinden elde edilmiştir ve değerler Tablo 2' de paylaşılmıştır.

Tablo 2. Gri SA'ya neden olan kirleticilerin değerleri

Kirletici	C_{max} (mg/L)	C_{nat} (mg/L)	L (mg/L)
Arsenik (As)	0.1	0.02	0.1
Kadmiyum (Cd)	0.1	0.002	0.01
Krom (Cr)	0.5	0.02	0.01
Bakır (Cu)	0.5	0.02	0.44
Demir (Fe)	3.0	0.3	0.047
Kurşun (Pb)	0.1	0.01	0.05
Cıva (Hg)	0.01	0.0001	0.00121
Nikel (Ni)	0.5	0.02	0.05
Çinko (Zn)	2.0	0.2	0.00687

Bu veri setindeki tüm kirleticiler için 83 haftalık verilerin ortalaması alınarak değerler hesaplanmıştır. Kabul edilebilir maksimum konsantrasyon değeri, Su Kirliliği Kontrolü Yönetmeliği (Tablo 7.1) ve eski IFC Genel Çevre Yönergeleri (1998'de yayınlanmıştır) göre belirlenmiştir. Suyun boşaltıldığı derenin su kütlesindeki doğal konsantrasyon değerleri ise Su Kalite Sınıflandırması (II) değerleri olarak kabul edilmiştir.

SONUÇ

Çalışma, Türkiye'de CIP yöntemiyle altın üreten bir altın madeninin proses tesisinde mavi ve gri SA'sını bulmak için yapılmıştır. Tüm hesaplamalarda fonksiyonel birim olarak 1 kg altın alınmıştır. Çalışma sonunda madene ait mavi SA 452,40 m^3/kg Au ve gri SA 2300,69 m^3/kg Au olarak bulunmuştur. Sonuçlar, çalışmaya konu olan madenin toplam su ayak izinin %84'ünün gri SA, %16'sının ise mavi SA olduğunu göstermektedir.

Doğrudan ve Dolaylı Mavi SA ve Gri SA

Çalışma sonucunda mavi SA için hem doğrudan hem de dolaylı SA hesaplamaları yapılmıştır. Gri SA dokuz kirletici için hesaplanmıştır. Tesiste gri SA'ya neden olan tek yer atık havuzudur. Madenin doğrudan ve dolaylı mavi SA ve gri SA değerlerine katkıda bulunan tüm etkenlere ait ayrıntılı bilgi Tablo 3'te sunulmaktadır.

Tablo 3. Doğrudan ve Dolaylı Mavi WF

SA Kategorisi	Alt Kategori	Etken	Değer (m^3/kg Au)
Mavi SA	Doğrudan SA	Ocak Susuzlaştırma	39.09
		Kayıp Dönüş Akışı	260.61
		Günlük Kullanım	3.28
		Nem Miktarı	12.93
		Toz Bastırma	3.72
		Yağmur	3.38
		Buharlaşma	7.95
	Dolaylı SA	Sodyum Siyanür	25.49
		Kireç	0.02
		Hidroklorik Asit	0.81
		Patlayıcılar	22.24
		Elektrik	32.55
		Oksijen	37.38
		Aktif Karbon	0.11
		Dizel	2.73
Toplam Mavi SA			452.40
Gri SA		Atık Havuzu	2300.69

Bu tablo, çalışmada elde edilen sonuçların bir özeti olarak değerlendirilebilir. Belirtildiği gibi, madenin mavi SA değerine doğrudan neden olan yedi etken varken, dolaylı bir mavi SA' ne neden olan sekiz etken vardır. Tüm değerler arasında kayıp dönüş akış değeri en yüksek mavi SA değerine sahipken, kireç kullanımına bağlı mavi SA değeri en düşük değere sahiptir. Dolaylı tarafta ise liç işlemi için kullanılan oksijen tüketiminin en yüksek değere sahip olduğu görülmektedir. Tablo 1'deki birim SA değerleri dikkate alınarak bir değerlendirme yapıldığında, oksijenin ikinci en düşük değere sahip olduğu görülmektedir. Öte yandan, en büyük dolaylı SA değerine sahiptir. Bunun nedeni, madende oksijen tüketiminin diğer dolaylı katkı sağlayanlara göre çok daha fazla kullanılmasıdır. Gri SA değerinin sadece atık havuzundan kaynaklandığı da tabloda görülmektedir. Tablo 4' te madende gri SA' ne neden olan dokuz kimyasalın katkısını göstermektedir.

Tablo 4. Gri SA Değerleri

Kirletici	Gri SA Değeri (m^3/kg Au)
Arsenik (As)	1777

Kadmiyum (Cd)	29
Krom (Cr)	6
Bakır (Cu)	261
Demir (Fe)	5
Kurşun (Pb)	158
Cıva (Hg)	35
Nikel (Ni)	30
Çinko (Zn)	1

Dokuz kirletici arasında gri SA değeri en yüksek olan açık ara ile arseniktir. Arsenik, 1777 m^3/kg Au değeri ile toplam gri SA'nın %77,23'ünü oluşturur. Burada su kirliliği hakkında genel bir yorum yapmak ve bir gösterge bulmak için arsenik kaynaklı gri su SA değerine odaklanmak yeterli olacaktır. Ancak, diğer kirleticiler için de gri SA değerine azaltmaya yönelik olarak formül bulmak elbette çok önemlidir.

Öneriler

Sürdürülebilir su yönetimi için bir başlangıç noktası olarak, atık barajından operasyonlarda kullanılmak üzere daha fazla suyun geri dönüştürülmesi, kaybedilen geri dönüş akışını azaltabilir. Kaybedilen dönüş akış değeri, atık tesisinden alıcı ortama verilen deşarj suyu olduğundan, daha fazla geri dönüşüm ile deşarj değeri azalacaktır. Bu sayede proses tesisi için gerekli suyu elde etmek için kuyulardan daha az su çekilecektir. Aynı zamanda atıkların atık barajına gönderilmeden önce son bir filtrasyon işlemi de kayıp geri dönüş akış değerini azaltacaktır (Gunson vd., 2012). Bölgesel olarak özellikle atık barajının en geniş yüzey alanına sahip olduğu yaz aylarında buharlaşmayı önleyecek çözümler alınmalıdır.

Arsenik oldukça toksik ve birikim yapan bir elementtir. Dünya Sağlık Örgütü, arseniği sulu atık akışlarındaki ana kirleticilerden biri olarak ilan etmiştir. Bu nedenle, arsenik konsantrasyonunun atık su ile doğal bir sisteme verilmeden önce azaltılması önemlidir. Arsenik içeriği en çok gri SA'ne neden olduğundan, atık su çevreye salınmadan önce sudaki arsenik konsantrasyonu yeni yöntemler kullanılarak daha da azaltılmalıdır. Bu önlemler, arsenik giderimi için yeni teknolojilerin kullanılmasıyla alınabilir. Langsch vd. (2012), arsenik konsantrasyonun düşürmek amacı ile 14 yönteminin avantaj ve dezavantajları çalışmışlardır. Bu yöntemlerin değerlendirilmesi ve maden atıklarına uygun olanın uygulanması ile arsenik konsantrasyonu azaltılabilir.

KAYNAKLAR

Akçıl, A. (2002). Cyanide control in tailings pond: Ovacık gold mine. In Proceedings of the Symposium on Environmental Issues and Waste Management in Energy and Mineral Production (SWEMP Conference). Kaynak adresi: https://www.researchgate.net/publication/256445900_Cyanide_control_in_tailings_pond_Ovacik_gold_mine

Aldaya, M.M., Chapagain, A.K., Hoekstra, A.Y., Mekonnen, M.M (2012). *The Water Footprint Assessment Manual*; Earthscan; Kaynak adresi:

Ecoinvent (2009). *Ecoinvent Database v3.7.1*; Ecoinvent Center: Dubendorf, Switzerland.

Fashola, M.O., Ngole-Jeme, V.M., Babalola, O.O (2016). Heavy metal pollution from gold mines: Environmental effects and bacterial strategies for resistance. *Int. J. Environ. Res. Public Health*, *13*, 1047.

Gu, H., Bergman, R., Anderson, N., Alanya-Rosenbaum, S. (2018). Life cycle assessment of activated carbon from woody biomass. *Wood Fiber Sci.*, *50*, 229–243.

Guidance for Controlling Silica Dust from Stone Crushing with Water Spray Technology. (2008). Kaynak adresi:

http://www.okinternational.org/docs/Guidance%20for%20Controlling%20Silica%20Dust%20from%20Stone%20Crushing% 20with%20Water%20Spray%20Technology%20-%20for%20Employers.pdf

Gunson, A.J., Klein, B., Veiga, M., Dunbar, S. (2012). Reducing mine water requirements. *J. Clean. Prod. 21*, 71–82.

Gupta, A., Yan, D. (2006). M*ineral. Processing Design and Operation an Introduction*, 1st ed.; Elsevier: Amsterdam, The Netherlands, 2006.

https://waterfootprint.org/media/downloads/TheWaterFootprintAssessmentManual_2.pdf

Köksal, E., Ormanoğlu, G., Devuyst, E.A. (2003) Cyanide destruction: Full-scale operation at Ovacık gold mine. *Eur. J. Miner. Process. Environ. Prot., 3*, 270–280.

Langsch, J.E., Costa, M., Moore, L., Morais, P., Bellezza, A., Falcão, S. (2012) New technology for arsenic removal from mining effluents. *J. Mater. Res. Technol.*, *1*, 178–181.

Maden İşletmeleri Su, Atıksu ve Atık İstatistikleri. 2010. Kaynak adresi https://data.tuik.gov.tr/Bulten/Index?p=Maden-Isletmeleri-Su,-Atiksu-ve-Atik-Istatistikleri-2010-10799

Maden İşletmeleri Su, Atıksu ve Atık İstatistikleri. 2012. Kaynak adresi https://data.tuik.gov.tr/Bulten/Index?p=Maden-Isletmeleri-Su,-Atiksu-ve-Atik-Istatistikleri-2012-16173

Maden İşletmeleri Su, Atıksu ve Atık İstatistikleri. 2014. Kaynak adresi https://data.tuik.gov.tr/Bulten/Index?p=Maden-Isletmeleri-Su,-Atiksu-ve-Atik-Istatistikleri-2014-21625

Maden İşletmeleri Su, Atıksu ve Atık İstatistikleri. 2016. Kaynak adresi https://data.tuik.gov.tr/Bulten/Index?p=Maden-Isletmeleri-Su,-Atiksu-ve-Atik-Istatistikleri-2016-24879

Maden İşletmeleri Su, Atıksu ve Atık İstatistikleri. 2018. Kaynak adresi https://data.tuik.gov.tr/Bulten/Index?p=Maden-Isletmeleri-Su,-Atiksu-ve-Atik-Istatistikleri-2018-30670

Martín, A., Arias, J., López, J., Santos, L., Venegas, C., Duarte, M.; Ortíz-Ardila, A., de Parra, N., Campos, C., Zambrano, C.C., (2020). Evaluation of the effect of gold mining on the water quality in Monterrey, Bolívar (Colombia). *Water*, *12*, 2523.

MCA, (2014);. *Water Accounting Framework for the Minerals Industry*; Sustainable Minerals Institute: St Lucia, Australia, Volume 1.3, Kaynak adresi: https://www.minerals.org.au/sites/default/files/WAF_UserGuide_v1.3_(Jan_2014).pdf

Northey, S.A., Haque, N., Lovel, R., Cooksey, M.A. (2014). Evaluating the application of water footprint methods to primary metal production systems. *Miner. Eng.*, *69*, 65–80

Önal,G. BAT Practice at Ovacık Gold Mine. (2013). Available online: https://docplayer.net/24286042-Bat-practice-at-ovacikgold-mine-g-onal.html

Sarıkaya, S. (2018). *Investigations on the Effects of Main Operating Parameters on the Leaching Recovery for a Gold Ore*, Msc. Thesis, Hacettepe University: Ankara, Turkey, 2018.

SRK Danışmanlık ve Mühendislik, A.Ş, (2014). Ovacık Altın Madeni Üçüncü Atık Depolama Tesisi Projesi ÇED Başvuru Dosyası. Kaynak adresi: http://eced.csb.gov.tr/ced/ jsp/dosya/dosyaGoster.htm?id=26456

Yüce, A., Köksal, E., Önal, G. (2001). Gold Mining and Tailings Dam in Ovacık, Turkey. VI SHMMT I XVIII ENTMME., pp. 527–530. Kaynak adresi: http://artigos.entmme.org/download/2001/environmental_issues/1006%20-%20A.%20Ekrem%20Y%C3%BCce_Erkan%20Koksal_G%C3%BCven%20Onal%20%20GOLD%20MINING%20AND%20TAILINGS%20DAM%20IN%20 OVACIK,%20TURKEY.pdf

Zhang, G.P., Hoekstra, A.Y., Mathews, R.E. (2013). Water Footprint Assessment (WFA) for better water governance and sustainable development. *Water Resour. Ind.*, *1–2*, 1–6.

ULTRASONİK ÖN İŞLEMİN FLOTASYON YÖNTEMİ İLE KÖMÜRDEN KÜL VE KÜKÜRT UZAKLAŞTIRMAYA ETKİSİNİN ARAŞTIRILMASI

INVESTIGATION OF THE EFFECT OF ULTRASONIC PRETREATMENT ON COAL DEMINERALIZATION AND DESULFURIZATION BY FROTH FLOTATION METHOD

U. Demir [1, *], A. Aydın[1]

Dumlupınar Üniversitesi, Mühendislik Fakültesi Maden Mühendisliği Bölümü
*(*Sorumlu yazar: ugur.demir@dpu.edu.tr)*

ÖZET

Dünyadaki enerji üretimin ¾'ü fosil kökenli kaynaklardan elde edilirken elektirik enerjisi üretiminin ise yaklaşık %25'i kömürden üretilmektedir. Dünyada olduğu gibi ülkemizde de kömür önemini koruyan bir enerji hammaddesidir. Enerji üretiminde kömürün kullanımı hava kirliliği, sera etkisi, asit yağmurları gibi ciddi çevresel problemlere neden olduğu bilinmektedir. Bu problemin önemli bir bölümünü ise kömürün içeriği kükürtten kaynaklanmaktadır. Kömürden kükürt uzaklaştırma, kömürde bulunan kükürdün yapısı ve serbestleşme tane boyutuna bağlı olarak fiziksel yöntemler ile uzaklaştırılabilmekte, fakat bu uzaklaştırma çok sınırlı seviyelerde kalmaktadır. Yüzey özellik farklılığından yararlanılan flotasyon yöntemi ile kömürden inorganik kükürt ve mineral madde önemli oranlarda uzaklaştırılabilmektedir. Bu çalışmada ön işlem olarak uygulanan ultrasonik ses dalgalarının kömür flotasyonuna olan etkileri incelenmiştir. İnorganik kükürt ve mineral madde uzaklaştırmak için en uygun çalışma parametreleri (tane boyutu, katı oranı, bastırıcı miktarı, köpürtücü miktarı ve pH) belirlenmiş, ultrasonik ön işlemden sonra belirlenen bu parametreler uygulanarak elde edilen sonuçlar değerlendirilmiştir. Ultrasonik ön işlem laboratuvar tipi 35 kHz frekans ve 350 W güce sahip ultrasonik banyo farklı sürelerde (1-15 dak) kullanılarak uygulanmıştır. 5 dakikalık ultrasonik ön işlem sonrasında yapılan flotasyon işlemi sonucu %54,90 mineral madde uzaklaştırma ve %14,46 kükürt uzaklaştırma oranları elde edilmiştir. %25,99 kül ve %7,06 toplam kükürt içeren Gediz yöresi kömürlerinden ultrasonik ön işlem sonrasında yapılan flotasyon ile %11,72 kül ve %6,04 toplam kükürt içeren temiz kömür elde edilmiştir.

Anahtar kelimeler: Ultrasonik, kömür, kükürt uzaklaştırma, kül uzaklaştırma, flotasyon

ABSTRACT

Three-quarters of the energy production in the world is produced from fossil origin sources and approximately 25% of the electricity production is from coal. As in the world, coal is an important energy raw material in our country. The use of coal in energy production causes serious environmental problems such as air pollution, greenhouse effect, acid rains. An important part of this problem arises from the sulfur content of coal. Sulfur removal from coal can be removed by physical methods depending on the structure of sulfur in the coal and liberalization grain size, but this removal rate remains very limited. Inorganic sulfur and mineral material can be removed from coal with the flotation method, which utilizes the surface feature difference. In this study, the effects of ultrasonic sound waves as a pretreatment on coal flotation were investigated. The most suitable working parameters for removing inorganic sulfur and mineral substances were determined and the results obtained after applying ultrasonic pretreatment were evaluated. Ultrasonic pretreatment laboratory type 35 kHz frequency and 350 W power ultrasonic bath was applied using different times (1-15 minutes). As a result of the flotation process performed after 5 minutes of ultrasonic pretreatment, 54.90% mineral material removal and 14.46% sulfur removal rates were obtained. After the ultrasonic pretreatment, clean coal

containing 11.72% ash and 6.04% total sulfur was obtained from the coals of Gediz region containing 25.99% ash and 7.06% total sulfur.

Keywords: Ultrasonic, coal, desulfurization, demineralization, froth flotation

GİRİŞ

Flotasyon yöntemi, minerallerin yüzey özellik farklılıklarını kullanarak ince boyutta serbestleşen mineraller ve toz kömürlerin zenginleştirilmesinde kullanılan etkili bir yöntemdir (Xia ve Xie 2017, Yang vd. 2019a, Li vd. 2019a, Mao vd. 2019a, 2019b, 2020). Maalesef, bu yöntemin etkinliği düşük kaliteli ve oksitlenmiş kömürlerin zenginleştirilmesinde sınırlı seviyelerde kalmaktadır. Bunun nedeni olarak da düşük kaliteli ve oksitlenmiş kömürlerin yüzeylerindeki hidrofilik fonksiyonel gruplar (C-O, C=O ve O-C=O) ve gözenekli yapısı gösterilmektedir. Bu durum kömür yüzeyinde stabil su film tabakasının oluşmasına ve kabarcık-tanecik yapışma olasılığının düşmesine neden olmaktadır (Mao vd. 2019a, 2020, Xia vd. 2013, Peng vd. 2018, Yang vd. 2019b, Chen vd. 2020). Kömür yüzeyindeki hidrofilik grupların ve oluşan su filminin çeşitli ön işlem uygulanarak deforme edilmesi flotasyon kabiliyeti düşük kömürün flotasyon yöntemi ile zenginleştirilmesine (kül ve kükürt uzaklaştırma) imkân tanımaktadır. Belirtilen ön işlemlere örnek olarak mekanik dağıtma, daha ince boyutlara ufalama, ısıl işlem, mikrodalga enerji ve ultrasonik ses dalgaları (Özkan ve Kuyumcu 2006, Kang vd. 2008, 2009, Altun vd. 2009, Özkan 2012, Xia vd. 2019) ile muamele sayılabilir.

Ultrasonik ses dalgaları, insan kulağının algılayabileceği frekanstan daha yüksek frekanstaki (> 20 kHz) ses olarak tanımlanmaktadır. Ultrasonik ses de normal sese benzer bir salınım hareketidir. Salınım hareketi olarak meydana gelir, yayılır ve salınım hareketi olarak algılanır. Bu nedenle ultrasonik ses bir mekanik enerjidir. X ışınları, ışık ve radyo dalgaları ile birçok ortak özelliğe sahiptir. Elektriksel olarak meydana getirilmesi, bir noktaya yoğunlaştırılabilmesinin mümkün olması ortak özelliklerden bazılarıdır. En büyük farklılık ise boşlukta ilerleyemiyor olması, ilerleyebilmesi için bir ortamım (hava, sıvı, katı, doku gibi) gerekli olmasıdır (Pesic 1996, Alp 1998, Önal vd. 2003).

Ultrasonik ses dalgaları bir sıvı ortam içerisinde kavitasyon olarak bilinen bir mekanik etki meydana getirir. Ses salınımları herhangi bir ortam içerisinde basınç ve gevşeme aşamalarından oluşan bir dalga olarak hareket etmektedir. Ultrasonik ses dalga kaynağını sıvı içerisine batırılmış oldukça hızlı ileri-geri hareket eden bir pistona benzetmek mümkündür. Bu benzerlikten basınç dalgalarının, sıvı içerisindeki molekülsel etkileşimler aracılığıyla iletilen ileriye doğru vuruş şeklinde anlatılabilir (Alp 1998). Belirtilen bu hareket 10 mikro saniyeden daha kısa bir sürede meydana gelmektedir (Kyllönen vd. 2004).

Dalganın gevşeme aşamasını oluşturan pistonun geri çekme hareketidir. Bu piston saniyede 20000 ileri geri hareket ile çalıştığı zaman ortamda ultrasonik ses oluşmaktadır. Eğer gevşeme aşaması gerektiği kadar güçlüyse, sıvıyı bağlayan moleküller arası kuvvetleri kıracak büyüklükte negatif bir basınç oluşur. Bu işlem aşamasında moleküller ortam boyunca küçük mikro kabarcıklar oluşturarak birbirlerinden ayrılır. Ultrasonik kavitasyon için gevşeme evresini takip eden bir sıkıştırma evresi mevcuttur. Bu mikro kabarcıklar daha sonra büyük bir miktarda enerji açığa çıkararak ani olarak patlamaktadırlar (Şekil 1). 25 ^{o}C'lik sıcaklıktaki bir suda güçlü ultrasonik ses dalgaları tarafından oluşturulan kavitayon etkisi ile kabarcıkların çökelmesi yoluyla 5000 ^{o}K sıcaklık ve 1000 atmosfer basıncına yakın basınçların oluşturulduğu, ısınma hızının 109K/s'den daha hızlı olduğu tahmin edilmektedir (Pesic 1996, Alp 1998, Suslick ve Price 1999, Farmer vd. 2000a, 2000b, Önal vd. 2003, Kyllönen vd. 2004, Teipel vd. 2004, Küncek ve Sener 2010, Bang ve Suslick 2010, Seidi ve Yamini 2012).

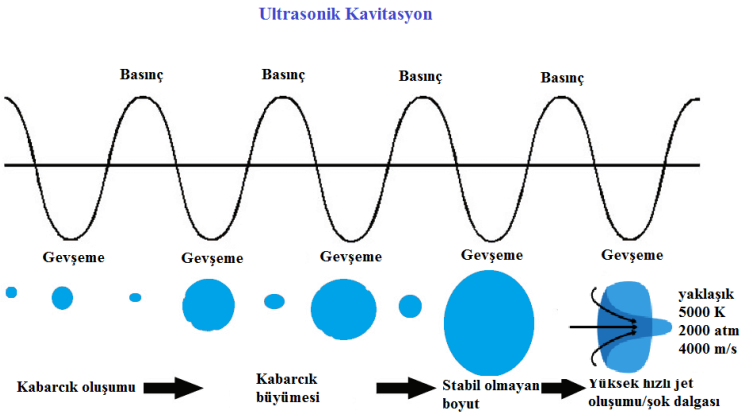

Şekil 1. Ultrasonik ses dalgalarının oluşturduğu kavitasyon etkisi (Leonelli ve Mason 2010, Turan 2007)

Ultrasonik ses dalgalarının cevher ve kömür hazırlama/zenginleştirme işlemlerinde kullanımı son 10-15 yılda belirgin bir şekilde artmış, birçok araştırmacı tarafından kullanılmıştır (Mao vd. 2000, Özkan ve Kuyumcu 2006, Özkan 2012, Özkan 2017, Mao vd. 2019b, Demir 2019).

Ultrasonik ses dalgalarının neden olduğu kavitasyon etkisi, sıvı ortam içerisinde yüksek hızlı şok dalgaları ve mikrojetlerin oluşmasını sağlamaktadır. Bu etki mineral veya kömür yüzeylerinin temizlenmesi sağlamakta, oluşacak kırık ve çatlakla neticesinde ufalanma ve taze yüzeylerin oluşması gibi fiziksel etkilere neden olmaktadır (Özkan 2017), oksidasyon gibi kimyasal etkiler ve mikro kabarcıkların oluşması ultrasonik kavitasyonun pozitif etkilerini oluşturmaktadır. Uygulanan ultrasonik ön işlemin flotasyon yöntemi ile daha yüksek kül ve kükürt uzaklaştırma oranlarının elde edildiği çeşitli araştırmacılar tarafından belirtilmiştir (Mao vd. 2019b, 2000).

Ultrasonik ses dalgaları tarafından oluşturulan kavitasyon kabarcıkları, katı yüzeyde veya yüzeye yakın bir bölgede patlamaları sonucu oluşan mikro jetler, kömür taneciklerinin yüzeyinde bulunan ince kil tabakasını uzaklaştırmakta, yüzeyde kırık ve çatlaklar oluşturarak tane boyutunda bir miktar küçülmeye neden olmakta bununla beraber oksitlenmiş yüzeylerin tahrip edilmesini sağlamaktadır. Bunun sonucu olarak ta taze/hidrofobik yüzeylerin oluşmasına neden olmaktadır (Cao vd. 2017). Taze/oksitlenmemiş yüzeyler kömür flotasyonunun verimini arttırmakta, konsantrenin kül ve kükürt oranının düşmesine neden olmaktadır.

Özkan ve Kuyumcu (2006) ultrasonik ses dalgalarını flotasyon işlemi sırasında kullanmak amacıyla flotasyon hücresini modifiye etmiş, normal hücre ile modifiye hücre sonuçlarını karşılaştırmıştır. Ulrtasonik ses dalgalrının yardımı ile daha yüksek yanabilir verim ve daha düşük kül içeren temiz kömür elde ettiğini belirtmiştir. Kang vd. (2007) ultrasonik işlem öncesi ve sonrasında kömür numunelerinin yüzeylerinde meydana gelen değişimleri incelemişler, kömür yüzeyinin hidrofobisitesinin artığını, kükürt ve mineral maddelerin de hidrofilisitelerinin arttığını ifade etmişlerdir. Kang vd. (2008) ultrasonik ses dalgalarının kömür yüzeyinde meydana getirdiği değişimleri çeşitli teknikler ile incelemişler, ultrasonik öncesi ve sonrası değişimlerin flotasyon performansına olan etkilerini belirlemişlerdir. Elde edilen sonuçlardan ultrasonik ön işlemin kömürde bulunan kül ve kükürdün uzaklaştırılmasında iyileşmelere neden olduğu belirtilirken, aynı yazarlar başka bir çalışmada (2009) ultrasonik ses dalgalarının kömür flotasyonunda pülpün özelliklerinde meydana getirdiği değişimleri incelemişler, pülpün oksijen miktarı, pH ve sıcaklığında meydana gelen değişimler belirlenmiş ve kömürden mineral madde ve kükürt uzaklaştırmada olumlu etkilerinin olduğunu ifade etmişlerdir. Altun vd. (2009) iki farklı oil shale'in flotasyon ile mineral maddesinin uzaklaştırılmasında ultrasonik ses dalgalarının ön işlem olarak kullanıldığı çalışmada, farklı güç ve sürelerde uygulanan ultrasonik ses dalgalarının flotasyon performansına pozitif yönde etkilerinin olduğu belirtilmektedirler. Özkan (2012) bir başka çalışmasında

taş kömürü şlamlarına uyguladığı flotasyon işleminde yine ultrasonik ses dalgalarından yararlanmış, ulrtasonik ses dalgaları ile oluşan temiz yüzeyler sayesinde daha yüksek yanabilir verim ve daha düşük kül içeriğine sahip ürün elde edebildiğini belirtmiştir. Şahinoğlu ve Uslu (2013a, 2013b) ultrasonik ses dalgalarının kömür yüzeyinde meydana getirdiği değişikliklerin yağ aglomerasyonuna olan etkileri incelenmiş ve artan güç ve süreye bağlı olarak elde edilen ürünlerin kül ve kükürt uzaklaştırmada etkisinin pozitif yönde oluğunu belirtmişlerdir. Chandaliya vd. (2018) ultrasonik ses dalgaları ve mikrodalga enerjiyi kimyasal işlem öncesinde kullanmışlar ve kömürden ultra temiz kömür elde edilmesi üzerine çalışmışlardır. Farklı kimyasal-kömür karışımı, ön işlem gücü ve süresinin etkileri araştırılmış, ön işlemlerin kömürden kül uzaklaştırmada pozitif etkilerinin olduğunu belirtmişlerdir. Dehbani ve Rahimi (2018) ultrasonik ses dalgalarını kullanarak tabaka halinde akan akışkan ortamda yüzey özellik farkından yararlanarak bitümün kömür kül içeriğinin düşürülmesine çalışılmış, farklı işlem parametrelerinin etkilerini araştırmışlarıdır. Mao vd. (2019a) ultrasonik ses dalgalarını flotasyonda ön işlem ve flotasyon sırasında kullanılması durumunda flotasyon performansına etkisi incelenmiş, flotasyon sırasında uygulanan ultrasonik işlemin flotasyon performansına daha yüksek oranda etki ettiğini ifade etmişlerdir. Zhang vd. (2020) toz kömür flotasyonunda ultrasonik ses dalgaları yardımı ile dizel yağı içerisinde oluşturulan dodecyl trimethylammonium bromide (DTAB) mikroemilsiyonların flotasyon performansına etkilerini araştırmışlar, mikroemilsiyonların kömür hidrofobisitesini ve temas açısının önemli oranda arttırdığını ifade etmişlerdir.

Bu çalışmada Gediz yöresi kömürlerinde kül ve kükürt uzaklaştırmada, flotasyon yöntemi öncesi ön işlem olarak ultrasonik ses dalgalarının etkileri araştırılmıştır. Optimum flotasyon şartları belirlendikten sonra (katı oranı, tane boyutu, toplayıcı miktarı, köpürtücü miktarı vs.) farklı sürelerde uygulanan ultrasonik ön işlemin etkileri incelenmiştir. Ultrasonik ön işlemin kömürden mineral madde ve inorganik kükürt uzaklaştırmada belirgin etkilerinin olduğu tespit edilmiş, bu etkilerin neden kaynaklandığı çalışmada açıklanmaya çalışılmıştır.

MALZEME VE YÖNTEM

Malzeme

Deneysel çalışmalarda kullanılan kömür numuneleri, Kütahya-Gediz'de faaliyet gösteren özel bir şirket tarafından çalıştırılan kömür ocağından temin edilmiştir. Numune alma kurallarına dikkat edilerek alınan kömür numuneleri deneysel çalışmalarda kullanılmak üzere ufalanmış (-4 mm), uygun yöntemler ile azaltılmış ve özelliklerinin değişmemesi amacıyla kilitli poşetlerde saklanmıştır.

Temsili kömür numunlerinin %25,99 kül, %3,3 nem, %32,81 uçucu madde, 5607 kcal/kg ısıl değere sahip olduğu belirlenmiş, ayrıca %7,06 toplam kükürt içerdiği, önemli bir bölümünün (%2,89) ise organik kökenli olduğu tespit edilmiştir. Yüksek oranda kükürt içermesi bu kömürlerin herhangi bir iyileştirme (mineral madde ve kükürt uzaklaştırma) işlemi uygulanmadan ev ve sanayi yakıtı olarak kullanımının önemli çevresel sorunlara neden olacağı aşikardır. Gediz yöresi kömürleri taramalı elektron mikroskop (SEM) ile incelendiğinde, kömür numuneleri çok ince boyutta pirit tanecikleri (5-20 mikrometre boyutta) ve kil mineralleri içermektedir. Numunenin pirit içeriği kömür parçaları içinde kenetli halde (melnikovit), az miktarda kükürdün serbest taneler halinde bulunduğu tespit edilmiştir (Demir ve Elbinsoy 2019). Ayrıca mineralojik analiz (Rigaku MiniFlex marka XRD cihazı) sonucunda ikincil olarak kaolin, illit, dolomit, jibs ve markasit bulunurken, az miktarda da karışık kil mineralleri, feldispat ve opal varlığına rastlanmaktadır.

Deneysel çalışmalarda kullanılan kömürlerinin kimyasal analizi Spectro marka X Lab 2000 model XRF cihazı ile gerçekleştirilmiştir. Kömür bünyesinde önemli miktarda silikat mineralleri (%4,15) ve demirin varlığı (%3,75) tespit edilmiştir.

Deneysel çalışmalarda kullanılan temsili kömür numuneleri laboratuvara getirildikten sonra çeneli kırıcıda iki kademe olarak kırılmış ve farklı boyut gruplarına ayrılmıştır. Kömür numunelerinin tane boyutuna bağlı olarak kül ve kükürt içeriğinde meydana gelen değişim Çizelge 1'de verilmiştir. Çizelgeden de görüldüğü gibi tane boyutuna bağlı olarak kül içeriğinde belirgin bir artış gözlemlenirken, kükürt içeriğinde çok belirgin bir değişim görülmemektedir. Bu durum kömür numunesi bünyesinde bulunan killi yapılar dağılarak daha ince boyutta birikmesi ve yapılan mikroskobik incelemeler sonucu piritik kükürdün oldukça ince boyutta olmasından kaynaklanmaktadır.

Çizelge 1. Ocaktan alınan temsili kömür numunesinin tane boyut dağılımı ve boyuta bağlı olarak kül, kükürt ve ısıl değer analizleri

Tane Boyutu (mm)	Kül (%)	Toplam Kükürt (%)	Alt Isıl Değer (Kcal/kg)
+63	19.51	6.90	6237
-63+31.5	25.21	7.42	5683
-31.5+16	25.20	6.93	5685
-16+12.5	24.48	7.08	5754
-12.5+4	23.97	7.35	5803
-4+2	26.80	6.62	5529
-2+1	35.50	6.68	4684
-1	46.85	6.42	3582
Toplam	25.99	7.06	5607

Yöntem

İnce boyuttaki kömürden mineral madde ve piritik kükürt uzaklaştırmada yaygın olarak kullanılan flotasyon yöntemi, bu çalışmada da kullanılmıştır. Deneysel çalışmalarda mekanik flotasyon makinesi ve 1 litre hacimli flotasyon hücresi kullanılmıştır. Flotasyon yönteminin çeşitli çalışma parametrelerinin (tane boyutu, katı oranı, pH, toplayıcı miktarı, köpürtücü miktarı) mineral madde ve kükürt uzaklaştırmaya etkileri incelenmiştir. Çalışmanın diğer bir aşaması olan ultrasonik ses dalgalarının etkilerinin belirlenmesi amacıyla Bandalin Sonorex marka 35 kHz frekans ve 320 W güce sahip ultrasonik banyodan yararlanılmıştır.

1 litre hacimli hücrenin kullanıldığı deneylerde önceden belirlenen katı oranının (%15) elde edilmesi amacıyla belli bir tane boyutuna indirilmiş kömür numunesi ve çeşme suyu kullanılmıştır. Kömür numunesinin bütünüyle ıslanması ve homojen bir karışım elde edilmesi için 10 dakika süre ile 1250 rpm karıştırma hızında muamele edilmiştir. Akabinde 5 dakika 500 g/t bastırıcı ($Fe(SO_4)_3$) ile 5 dakika 600 g/t toplayıcı (gaz yağı) ile kondisyonlama yapıldıktan sonra 400 g/t köpürtücü (Aerofroth 65) ilave edilmiş, flotasyon makinesinin rotor devri 1050 rpm seviyesine indirildikten sonra hava açılarak 2 dakika boyunca köpük alınmıştır. Alınan köpük ve hücrede kalan kömür numuneler önce vakum filtre kullanılarak susuzlaştırılmış, ardından standart kül ve kükürt analizlerinin yapılabilmesi için kurutulmuştur. Kül analizi Nüve marka kül fırınında, kükürt analizleri ise Leco marka SC144 DR model kükürt karbon cihazında yapılmıştır. Elde edilen analiz sonuçlarından mineral madde ve kükürt uzaklaştırma oranları (%) hesaplanmıştır. Yüksek oranda mineral madde ve kükürt uzaklaştırma oranlarının tespit edildiği en uygun çalışma şartları belirlenmiştir. Daha sonra ön işlem olarak uygulanan ultrasonik ses dalgalarının etkisinin belirlenmesi amacıyla farklı sürelerde bir seri deney yapılmıştır. Ultrasonik ses dalgalarının oluşturdukları kavitasyon kabacıkları kömür yüzeyleri veya yüzeye yakın bölgelerde oluşan şok dalgaları ve mikrojetler sayesinde hem mekanik hem de kimyasal etkilere maruz kalmaktadır. Bu etkiler kömür yüzeyinde bulunan ince kil tabakasının dağılması, yeni kırık ve çatlakları oluşması, taze yüzeylerin meydana gelmesi, yüzeydeki oksitli yapıların tahrip edilmesi gibi çeşitli etkilere

neden olmaktadır. Bu amaçla ultrasonik banyoda farklı sürelerde (1-15 dakika) işleme tabi tutulan kömür numunesi, belirlenen optimum şartlarda flotasyon işlemine alınmıştır.

BULGULAR VE TARTIŞMA

Bu çalışma iki bölümden oluşmakta, birinci bölümde Gediz kömürlerinden mineral madde ve kükürt uzaklaştırmak için yapılan flotasyon deneylerinin optimizasyon çalışmaları (tane boyutu, katı oranı, pH, toplayıcı miktarı, köpürtücü miktarı), ikinci bölümde ise ultrasonik ön işlemin (işlem süresi) belirlenen optimum şartlarda uygulanan flotasyon çalışmalarında meydana getirdiği mineral madde ve kükürt uzaklaştırmadaki etkileri verilmektedir.

İlk parametre olan tane boyutunun mineral madde ve kükürt uzaklaştırmaya olan etkilerinin belirlenmesi amacıyla laboratuvar tipi çubuklu değirmen kullanılarak farklı sürelerde (15-60 dak) öğütme yapılış ve d80 boyutları belirlenmiştir. 15, 20, 30, 45 ve 60 dakikalık öğütme sürelerinde sırasıyla 500, 350, 212, 125 ve 75 mikrometre d80 boyutuna sahip numuneler elde edilmiştir. Öğütme işlemini tamamlandıktan sonra kömür numunelerinin oksitlenmesinin önüne geçmek amacıyla hızlı bir şekilde flotasyon hücresine numune aktarılmış, yöntem kısmında belirtilen flotasyon şartları (%15 PKO, 600 g/t toplayıcı, 500 g/t bastırıcı, 400 g/t köpürtücü, pH 8,5-9) uygulanarak flotasyon deneyleri gerçekleştirilmiştir.

Farklı tane boyutlarındaki kömür numuneleri ile yapılan flotasyon deneylerinden elde edilen mineral madde ve kükürt uzaklaştırma oranları Şekil 2'de verilmiştir. Şekil 2 incelendiğinde tane boyutunda meydana gelen değişimle birlikte uzaklaştırılan mineral madde miktarında belirgin bir değişim meydana gelirken (%10,54-19,58), uzaklaştırılan kükürt miktarında birbirine yakın düşük oranlar (%2,83-4,82) elde edilmiştir. Tane boyutu 500 mikrometreden 350 mikrometreye indirildiğinde mineral madde uzaklaştırma oranında belirgin bir miktar artış olurken, tane boyutundaki küçülme devam ettiğinde hem mineral madde hem de kükürt uzaklaştırma oranında belirgin azalmaların olduğu görülmektedir. Bu durum tane boyutu küçüldükçe artan serbestleşme ile birlikte kömür taneciklerinin hava kabarcıklarına yapışarak yüzme olasılığını arttırmakta, ilave olarak ince boyutlu kil içerikli mineral maddelerin hava kabarcıkları ile mekanik taşınma ile yüzdükleri, böylece temiz kömürün mineral madde ve kükürt içeriklerinin artmasına neden olmaktadır. Gediz kömürleri malzeme bölümünde belirtildiği gibi kül oranı oldukça yüksek (%25,99) ve önemli oranda killi yapılar barındırmaktadır. Ayrıca kükürtlü yapılar hemen hemen yarı yarıya organik ve piritik kükürt içermekteler, piritik kükürdün serbestleşme tane boyutu ise oldukça küçüktür (5-20 µm). Bu nedenle elde edilen sonuçlardan da görüldüğü gibi uzaklaştırılan kükürt miktarı oldukça düşük seviyelerde (%4) kalmıştır. Bu durum dikkate alınarak en yüksek mineral madde uzaklaştırma oranının elde edildiği 350 mikrometre tane boyutu en uygun boyut olarak belirlenmiştir.

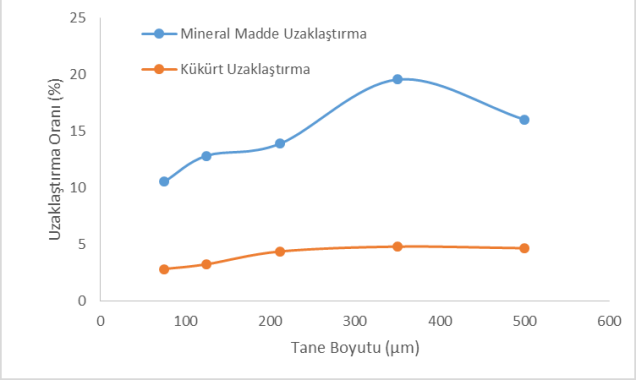

Şekil 2. Tane boyutunun mineral madde ve kükürt uzaklaştırmaya etkisi (%15 PKO, 600 g/t toplayıcı, 500 g/t bastırıcı, 400 g/t köpürtücü, pH 8,5-9)

Farklı katı oranının (%5-30) mineral madde ve kükürt uzaklaştırmaya etkisinin belirlenmesi amacıyla yapılan flotasyon deney sonuçları Şekil 3'de verilmiştir. Şekil 3 incelendiğinde yüksek katı oranlarında yapılan flotaston deneylerinde hem mineral madde hem de kükürt uzaklaştırma oranlarında istenilen oranlar elde edilememiştir. Yüksek katı oranı kömür flotasyonunda tanecik-kabarcık karşılaşma olasılığını yükselttiği, böylece hem kabarcığa yapışan taneciklerin miktarını arttırmakta hem de yanabilir verimin yükselmesine neden olduğu bilinmektedir. Bu durum hem kömür hem de ince boyutlu özellikle killi minerallerin kabarcıkların peşinde sürüklenerek yüzmesine maalesef selektivitenin de azalmasına yani temiz kömürün kül oranının artmasına neden olmaktadır. Daha düşük katı oranlarında daha temiz yüzen ürün elde edilmekte, fakat proses kapasitesinin düşmesine neden olduğu bilinmektedir. Artan katı oranı yüzen ürünün mineral madde ve kükürt içeriğinin artmasına neden olurken, yanabilir verimde belirgin artışların elde edilmesine neden olmuştur. En yüksek mineral madde uzaklaştırma oranı olan %22,43 değerine %10 katı oranında ulaşıldığı için bu oran devam eden deneylerde kullanılmak üzere belirlenmiştir.

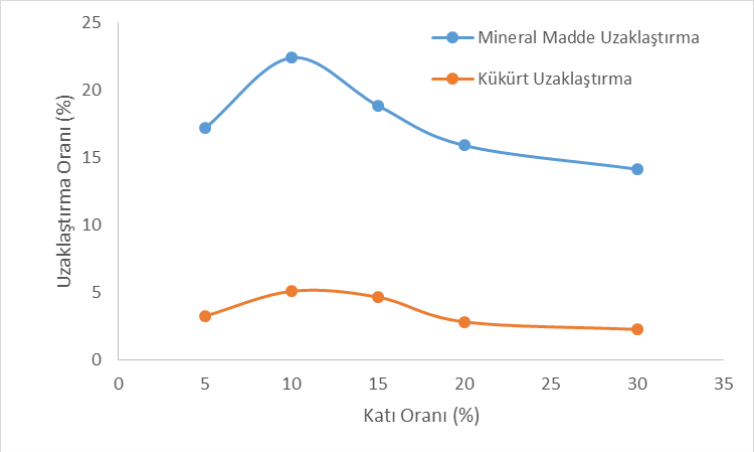

Şekil 3. Katı oranının mineral madde ve kükürt uzaklaştırmaya etkisi (350 µm tane boyutu, 600 g/t toplayıcı, 500 g/t bastırıcı, 400 g/t köpürtücü, pH8,5-9)

Gediz yöresi kömürleri üzerinde yapılan flotasyon deneylerinde, yöre kömürlerinin flotasyon kabiliyetinin yüksek olduğu, bünyede bulunan piritik kükürdün hem ince boyutlarda olması hem de oksitlenme nedeniyle hava kabarcıklarına yapışarak yüzme eğiliminde olması elde edilen yüzen ürünün kükürt içeriğinde belirli oranda artışların olmasına neden olmaktadır. Bu durumun önüne geçmek amacıyla piritik kükürdün bastırılarak hücrede kalması için bastırıcı olarak demir sülfat (Fe(SO4)3) farklı miktarlarda (200-2000 gr/t) kullanılmıştır. Gerçekleştirilen flotasyon deney sonuçları Şekil 4'de verilmiştir. Şekil 4 İncelendiğinde artan bastırıcı miktarı 1000 g/t'a kadar hem mineral madde hem de kükürt uzaklaştırma oranında belirgin artışların meydana gelmesine neden olurken, daha yüksek bastırıcı miktarı uzaklaştırma oranlarında belirgin azalmalara neden olduğu görülmektedir. Uzaklaştırılan kükürt miktarında çok belirgin fark gözlemlenirken, mineral madde miktarı daha ılımlı seviyelerde kaldığı tespit edilmiştir. Elde edilen sonuçlar değerlendirildiğinde 1000 g/t bastırıcı miktarı en uygun miktar olarak belirlenmiştir.

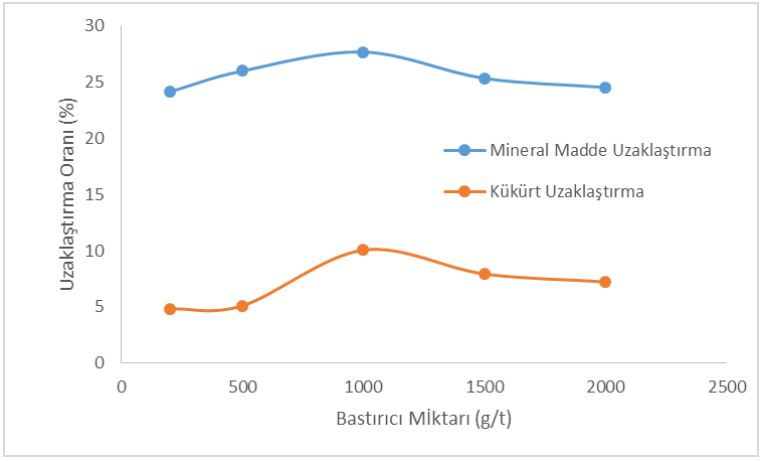

Şekil 4. Bastırıcı miktarının mineral madde ve kükürt uzaklaştırmaya etkisi (350 µm tane boyutu, %10 PKO, 600 g/t toplayıcı, 400 g/t köpürtücü, pH8,5-9)

Piritik kükürdün kömürden uzaklaştırılmasının amaçlandığı bu çalışmada, daha fazla piritik kükürt uzaklaştırmak için NaOH çözeltisi kullanılarak farklı ortam pH'larında (8-10) deneyler gerçekleştirilmiştir. Artan pH değeri piritik kükürdün yüzeylerinin daha fazla hidrofilik özellik kazandığı dikkate alınarak deneyler gerçekleştirilmiş ve elde edilen sonuçlar değerlendirildiğinde %12,89 oranında kükürt uzaklaştırma pH 9,5'da elde edilmiştir. Bu oran piritik kükürdün bir miktar daha fazla bastırılabildiğini göstermektedir. Bilindiği gibi ortam pH değeri flotasyon şartlarının önemli oranda değişmesine neden olmakta, bu durumda flotasyon veriminin önemli ölçüde değişmesini sağlamaktadır.

Daha sonra sırası ile farklı toplayıcı ve köpürtücü miktarlarının mineral madde ve kükürt uzaklaştırma oranlarına etkileri incelenmiştir. Toplayıcı olarak kolay temin edilen ve ucuz olan gaz yağı kullanılırken, kömür flotasyonunda önemli sonuçların elde edildiği Aerofroth 65 köpürtücü kullanılmıştır. Zaten flotasyon kabiliyeti yüksek olan Gediz kömürlerinin yüzdürülmesinde en düşük toplayıcı ve köpürtücü miktarı olan 200 g/t değerleri uygulanmıştır. Daha önce belirlenen en yüksek mineral madde ve kükürt uzaklaştırma oranları olan sırasıyla %41,67 ve %11,61 değerleri, 350 mikron tane boyutu, %10 katı oranı, 1000 g/t bastırıcı miktarı ve pH 9,5'de gerçekleştirilen flotasyon deneylerinde elde edilmiştir.

İkinci aşama olan, en uygun flotasyon şartları (350 mikron tane boyutu, %10 katı oranı, 1000 gr/t bastırıcı miktarı, pH 9,5, 200 g/t toplayıcı miktarı, 200 gr/t köpürtücü miktarı) belirlendikten sonra ultrasonik ses dalgalarının ön işlem olarak uygulanmasına ve mineral madde ve kükürt uzaklaştırmaya olan etkileri incelenmiştir. Bilindiği gibi ultrasonik ses dalgaları yüksek frekanslarda (>20 kHz) elde edilen ve insan kulağı tarafından algılanamayan ses dalgalarıdır. Bu dalgalar sıvı ortam içerisinde oluşturulduğunda kavitasyon kabarcıkları olarak tanımlanan mekanik ve kimyasal etkilere neden olmaktadır. Bu kavitaston kabarcıkları çok kısa sürelerde oluşmakta ve patlamakta, oluşan mekanik etki, kömür yüzeyinde bulunan ince kil tabakasının dağıtılmasına, yeni kırık ve çatlakların oluşmasına, taze yüzeylerin meydana gelmesine, okside olmuş tabakaların tahrip olmasına neden olduğu birçok araştırmacı tarafından ifade edilmektedir (Mao vd. 2019a, 2019b).

Çubuklu değirmen ile d80 boyutu 350 mikrometre boyut altına indirilen kömür numunesi, %10 katı konsantrasyonu olacak şekilde su ile karıştırılıp ultrasonik banyo içerisinde farklı sürelerde (1, 5 ve 15 dakika) ön işleme tabi tutulduktan sonra, belirlenen flotasyon şartlarında deneylere tabi tutulmuştur. Ultrasonik ses dalgalarının mineral madde ve kükürt uzaklaştırma üzerine etkileri Şekil 5'de verilmiştir. Şekil 5'den de görüldüğü gibi ultrasonik ön işlem süresinin artışı ilk 5 dakikalık süre boyunca hem mineral madde hem de kükürt uzaklaştırmada olumlu etkiler gösterirken, artan ultrasonik ön işlem süresi, oranların belirgin bir şekilde değişmesine neden olduğu görülmektedir.

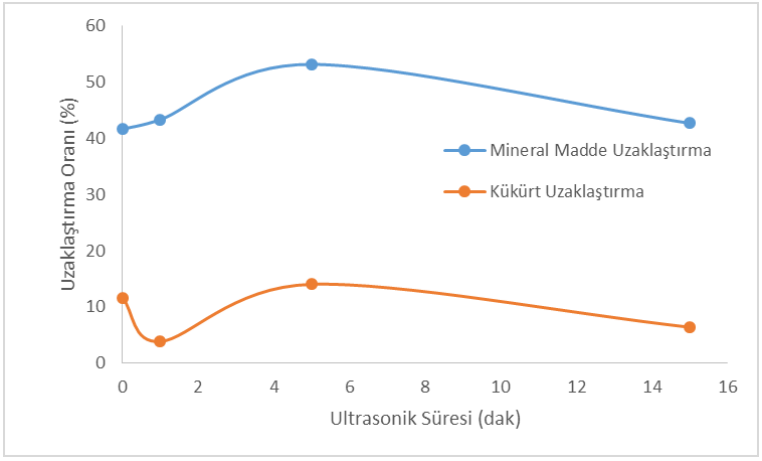

Şekil 5. Ultrasonik ses dalgalarının mineral madde ve kükürt uzaklaştırmaya etkisi (350 mikron tane boyutu, %10 katı oranı, 1000 gr/t bastırıcı miktarı, pH 9,5, 200 g/t toplayıcı miktarı, 200 gr/t köpürtücü miktarı)

Ultrasonik ön işlem yukarıda bahsedilen çeşitli etkiler nedeni ile kömür yüzeyinin ince kil minerallerinden temizlenmesi ve taze hidrofobik yüzeylerin oluşmasına neden olurken, pirit taneciklerinin ise yüzeylerinin hidrofilik olmasına neden olmakta böylece, uzaklaştırılan mineral madde ve kükürt oranında belirgin artışlara neden olmaktadır. Şekil 5'den de görüldüğü üzere artan ultrasonik işlem süresi, durumu tersine çevirmeye başlamaktadır. Uzun ultrasonik işlem köpük-tanecik agregasının bozulmasına, kömür yüzeylerinin yeniden oksitlenmesine neden olduğu ve çeşitli negatif etkilerin görüldüğü birçok araştırmacı tarafından belirtilmektedir (Altun vd. 2009, Feng ve Aldrich 2004). Optimum flotasyon şartlarında (350 mikron tane boyutu, %10 katı oranı, 1000 gr/t bastırıcı miktarı, pH 9,5, 200 g/t toplayıcı miktarı, 200 gr/t köpürtücü miktarı) %41,67 mineral madde uzaklaştırma ve %11,61 kükürt uzaklaştırma oranları elde edilirken, 5 dakikalık ultrasonik ön işlem sonrasında yapılan flotasyon işlemi sonucu %54,90 mineral madde uzaklaştırma ve %14,46 kükürt uzaklaştırma oranları elde edilmiştir. Ultrasonik ön işlem ile mineral madde uzaklaştırmada yaklaşık 13, kükürt uzaklaştırmada yaklaşık 3 puanlık bir artışın olduğu görülmektedir. Böylece %25,99 kül ve %7,06 toplam kükürt içeren Gediz yöresi kömürlerinden %11,72 kül ve %6,04 toplam kükürt içeren temiz kömür elde edilebilmiştir. Sonuçlar ultrasonik ön işlemin Gediz yöresi kömürlerinden mineral madde ve kükürt uzaklaştırmada etkili olduğunu göstermektedir.

Daha yüksek mineral madde ve kükürt uzaklaştırma oranlarının elde edilmesinin sağlanması için ultrasonik ön işlemin farklı frekans ve sürelerde prob tipi ultrasonik ses üreteçleri ile uygulanabileceği gibi, flotasyon işlemi sırasında/eş zamanlı olarak ultrasonik ses dalgalarının uygulanması ile elde edilebileceği düşünülmekte ve bu konu ile ilgili çalışmalar devam etmektedir.

SONUÇ VE ÖNERİLER

Ultrasonik ön işlemin kömür flotasyonunda mineral madde ve kükürt uzaklaştırmaya etkisinin araştırıldığı bu çalışmada aşağıdaki değerlendirmeler yapılabilir.

Kömür flotasyonu, kömürün kalitesi ve flotasyon kabiliyeti ile doğrudan alakalıdır. Kütahya-Gediz yöresi kömürleri yapı itibariyle flotasyon kabiliyeti yüksek olan bir kömürdür.

Flotasyon kabiliyeti yüksek olan bu kömür, yüksek oranda kül ve kükürt içermekte, flotasyon işlemi sırasında ince boyuttaki kil mineralleri ve çok ince boyutta kömür içinde dağılmış vaziyette bulunan piritik kükürtte hava kabarcıklarına yapışarak temiz kömürün kül ve kükürt oranının yüksek olmasına neden olmaktadır.

Flotasyon öncesinde farklı sürelerde uygulanan ultrasonik ön işlem, bünyede bulunan ince kil minerallerinin kömür yüzeyinden temizlenmesine, yeni kırık ve çatlakların oluşmasına ve taze hidrofobik yüzeylerin oluşarak daha düşük kül içeriğine sahip temiz kömürün elde edilmesine neden olmaktadır.

Ultrasonik ön işlem sırasında meydana gelen kırık ve çatlaklar, kömür içerisinde çok ince boyutta dağılmış olan pirit taneciklerinin cüzzi miktarda da olsa yerlerinde ayrılmasına neden olarak temiz kömürde düşük seviyelerde de olsa kükürt oranında bir azalmaya neden olmuştur.

Optimum flotasyon şartlarında (350 mikron tane boyutu, %10 katı oranı, 1000 gr/t bastırıcı miktarı, pH 9,5, 200 g/t toplayıcı miktarı, 200 gr/t köpürtücü miktarı) %41,67 mineral madde uzaklaştırma ve %11,61 kükürt uzaklaştırma oranları elde edilirken, 5 dakikalık ultrasonik ön işlem sonrasında yapılan flotasyon işlemi sonucu %54,90 mineral madde uzaklaştırma ve %14,46 kükürt uzaklaştırma oranları elde edilmiştir.

Ultrasonik ön işlem ile mineral madde uzaklaştırmada yaklaşık 13, kükürt uzaklaştırmada yaklaşık 3 puanlık bir artışın olduğu görülmektedir. Böylece %25,99 kül ve %7,06 toplam kükürt içeren Gediz yöresi kömürlerinden %11,72 kül ve %6,04 toplam kükürt içeren temiz kömür elde edilebilmiştir.

Ultrasonik ses dalgalarının flotasyon öncesinde bir ön işlem olarak kullanılmasının yanında, flotasyon işlemi sırasında hem pülp tabakasına hem de köpük tabakasına uygulanmasının daha temiz yüzen ürün elde edilmesine yardımcı olabileceği, bunun yanında kullanılacak reaktif miktarının da önemli oranda azalabileceği ön görülmektedir.

KAYNAKLAR

Alp İ. (1998). Yüksek frekanslı ses dalgalarının cevher zenginleştirmede kullanabilirliliğinin araştırılması. Doktora tezi, Osmangazi Üniversitesi Fen Bilimleri Enstitüsü, Eskişehir.

Altun N. E., Hwang J.Y., Hicyilmaz C. (2009). Enhancement of flotation performance of oil shale cleaning by ultrasonic treatment. *Int. J. Miner. Process. , 91*, 1–13.

Bang J. H., Suslick K. S. (2010). Applications of Ultrasound to the Synthesis of Nanostructured Materials. *Adv. Mater. , 22*, 1039–1059.

Cao Q., Cheng J., Feng Q., Wen S., Luo B. (2017). Surface cleaning and oxidative effects of ultrasonication on the flotation of oxidized pyrite. *Powder Technology, 311*, 390–397.

Chandaliya V.K., Biswas P.P., Dash P.S., Sharma D.K. (2018). Producing low-ash coal by microwave and ultrasonication pretreatment followed by solvent extraction of coal. *Fuel, 212*, 422–430.

Chen Y., Truong Vu N.T., Bu X., Xie G. (2020). A review of effects and applications of ultrasound in mineral flotation. *Ultrasonics Sonochemistry, 60*, 104739.

Dehbani M., Rahimi M. (2018). Ash removal from bitumen using ultrasonic falling film contactor. Fuel *Processing Technology, 173*, 30–39.

Demir U. (2019). Ultrasonik ses dalgalarının gümüş liçi performansına etkisinin araştırılması. DPU Bilimsel Araştırma Projeleri Birimi, Proje No: 2016-60, Proje Sonuç Raporu.

Demir U., Elbinsoy S. (2019). Aktif Karbon Üretiminde Yüksek Kükürtlü Kömürlerin Kullanılabilirliğinin Araştırılması. *Academic Platform Journal of Engineering and Science, 7-1*, 45-51.

Farmer A.D., Collings A.F., Jameson G.J. (2000a). Effect of ultrasound on surface cleaning of silica particles. *Internation Journal of Mineral Processing, vol:60*,101-113.

Farmer A.D., Collings A.F., Jameson G.J. (2000b). The application of power ultrasound to the surface cleaning of silica and heavy mineral sands. *Ultrasonics Sonochemistry, 7,* 243–247.

Feng D., Aldrich C. (2004). Effect of particle size on the flotation performance of complex sulphide ores. *Miner. Eng., 12 (7)*, 721–731.

Kang W., Xun H., Chen J. (2007). Study of Enhanced Fine Coal De-sulphurization and De-ashing by Ultrasonic Flotation. *Journal of China University of Mining & Technology, 17(3)*, 0358–0362.

Kang W., Xun H., Hu J. (2008). Study of the effect of ultrasonic treatment on the surface composition and the flotation performance of high-sulfur coal. *Fuel Processing Technology, 89*, 1337-1344.

Kang W., Xun H., Kong X., Li M. (2009). Effects from changes in pulp nature after ultrasonic conditioning on high-sulfur coal flotation. *Mining Science and Technology, 19*, 0498–0502.

Kang W., Xun H., Kong X., Li M. (2009). Effects from changes in pulp nature after ultrasonic conditioning on high-sulfur coal flotation. *Mining Science and Technology, 19*, 0498–0502.

Küncek İ., Sener S. (2010). Adsorption of methylene blue onto sonicated sepiolite from aqueous solutions. *Ultrasonics Sonochemistry, 17,* 250–257.

Kyllönen H., Pirkonen P., Hintikka V., Parvinen P., Grönroos A., Sekki H. (2004). Ultrasonically aided mineral processing technique for remediation of soil contaminated by heavy metals. *Ultrasonics Sonochemistry, 11*, 211–216.

Leonelli C., Mason T.J. (2010). Microwave and ultrasonic processing: Now a realistic option for industry. *Chemical Engineering and Processing, 49*, 885–900.

Li B., Liu S., Guo J., Zhang L., Sun X. (2019a). Increase in wettability difference between organic and mineral matter to promote low-rank coal flotation by using ultrasonic treatment. *Applied Surface Science, 481*, 454–459.

Li M., XiaY., Zhang Y., Ding S., Rong G., Cao Y., Xing Y., Gui X. (2019b). Mechanism of shale oil as an effective collector for oxidized coal flotation: From bubble–particle attachment and detachment point of view. *Fuel, 255*, 115885.

Mao Y., Bu X., Peng Y., Tian F., Xie G. (2020). Effects of simultaneous ultrasonic treatment on the separation selectivity and flotation kinetics of high-ash lignite. *Fuel, 259*, 116270.

Mao Y., Chen Y., Bu X., Xie G. (2019a). Effects of 20 kHz ultrasound on coal flotation: The roles of cavitation and acoustic radiation force. *Fuel, 256*, 115938.

Mao Y., Xia W., Peng Y., Xie G. (2019b). Ultrasonic-assisted flotation of fine coal: A review. *Fuel Processing Technology, 195*, 106150.

Önal G., Özer M., Arslan F. (2003). Sedimentation of clay in ultrasonic medium. *Minerals Engineering, vol:16*, 129-134.

Özkan S. G. (2012). Effects of simultaneous ultrasonic treatment on flotation of hard coal slimes, *Fuel, Volume 93*, Pages 576-580.

Özkan S.G. (2017). Further Investigations on Simultaneous Ultrasonic Coal Flotation. *Minerals, Vol:7*, 177. DOI:10.3390/min7100177.

Özkan S. G., Kuyumcu H. Z. (2006). Investigation of mechanism of ultrasound on coal flotation. *International Journal of Mineral Processing, Volume 81, Issue 3*, Pages 201-203.

Peng Y., Mao Y., Xia W., Li Y. (2018). Ultrasonic flotation cleaning of high-ash lignite and its mechanism. *Fuel, 220*, 558–566.

Pesic B. (1996). Application of ultrasound in solvent extraction of nickel and gallium. Idaho National Engineering Laboratory, Idaho Falls, Idaho.

Seidi S., Yamini Y. (2012). Analytical sonochemistry; developments, applications, and hyphenations of ultrasound in sample preparation and analytical techniques. *Cent. Eur. J. Chem. 10(4*), 938-976.

Suslick K. S., Price G. J. (1999). Application of ultrasound to materials chemistry. *Annual Reviews Materials Scinece, vol:29*, 295-326.

Şahinoğlu E., Uslu T. (2013a). Increasing coal quality by oil agglomeration after ultrasonic treatment. *Fuel Processing Technology, 116*, 332–338.

Şahinoğlu E., Uslu T. (2013b). Use of ultrasonic emulsification in oil agglomeration for coal cleaning. *Fuel, 113*, 719–725.

Teipel U., Leisinger K., Mikonsaari I. (2004). Comminution of crystalline material by ultrasonics. Int. J. *Miner. Process. 74*, 183–190.

Turan Ö. (2007). Boraks çözeltilerinden probertit çökmesine ultrases dalgalarının etkisinin incelenmesi. Yüksek Lisans Tezi, İTÜ Fen Bilimleri Enstitüsü, İstanbul.

Xia W., Xie G. (2017). A technological review of developments in chemical-related desulfurization of coal in the past decade. *International Journal of Mineral Processing, 161,* 65–71.

Xia W., Yang J., Liang C. (2013). A short review of improvement in flotation of low rank/oxidized coals by pretreatments. *Powder Technology, 237*, 1–8.

Xia Y., Wang L., Zhang R., Yang Z., Xing Y., Gui X., Cao Y., Sun W. (2019). Enhancement of flotation response of fine low-rank coal using positively charged microbubbles. *Fuel, 245*, 505–513.

Yang L., Li X., Li W., Yan X., Zhang H. (2019a). Intensification of interfacial adsorption of dodecylamine onto quartz by ultrasonic method. *Separation and Purification Technology, 227*, 115701.

Yang Z., Xia Y., Li M., Ma Z., Xing Y., Gui X. (2019b). Effects of pore compression pretreatment on the flotation of low-rank coal. *Fuel, 239*, 63–69.

Zhang R., Xia Y., Guo F., Sun W., Cheng H., Xing Y., Gui X. (2020). Effect of microemulsion on low-rank coal flotation by mixing DTAB and diesel oil. *Fuel, 260*, 116321.

UTILISATION OF BY-PRODUCTS AND ALTERNATIVE CONSTRUCTION MATERIALS IN MINE CONSTRUCTION

M. Koivulahti [1, *], H. Jyrävä [1], P. Potila [1], A. Virtanen [2], A. Nissinen [3]

[1] *Ramboll Finland Oy, Environmental Geotechnics R&D*
*(*Corresponding author: marjo.koivulahti@ramboll.fi)*
[2] *Fortum Waste Solutions Oy*
[3] *Skarta Finland Oy*

ABSTRACT

UPACMIC (Utilisation of by-products and alternative construction materials in new mine construction LIFE12 ENV/FI/000592) is project aiming to utilize alternative construction materials in mining facilities. Alternative construction materials are industrial by-products such as fibre clay. Initial problem targeted by this project is that mine closure consumes high volumes of aggregates. Alternative construction materials can replace non-renewable natural materials such as gravel and moraines and commercial sealing products like bentonite mats and geosynthetic geomembranes. UPACMIC project pilot's alternative material mixtures for cover layers, bottom sealing layers and reactive barriers. Best practices learned in the project are available at a guideline. Cover structures have been tested first in field tests in Pyhäsalmi Mine and Hitura Mine which is being closed. Fibre clay was used for the first time in the mining environment in Finland in cover structures. The sealing bottom piloting includes Sorsasalo and Hitura mine water treatment industrial by-product utilization in vertical sealing barrier construction. The piloting of the reactive barrier was carried out in Hitura Mine. The aim of the pilot is to test two passively operating water treatment structures. The impact of the project actions will be monitored by evaluation of the results from environmental and technical monitoring.

Keywords: Alternative materials, industrial by-products, cover structures, bottom structures, reactive barrier

INTRODUCTION

Rapid growth in Finnish mining industry has been a trend in recent years as of the mined ore and number of companies with mining operations in Finland. Profitability is dependent on metal and industrial minerals price development and simultaneously the global mining sector has suffered from a longer period of lower commodity prices. This means that mines have pressures to reduce costs and improve productivity. Especially in Finland, the public debate is focused on environmental and social impacts of the mines and ministry-level action plan for making Finland a leader in the sustainable extractive industry gives pressure for the mining companies to develop best practices for environmental, ecological and social considerations. Continuous improvement actions are related especially to resource efficiency, new technologies for water purification and waste management. (Ruokonen, E. and Temmes, A. 2018). For these issues UPACMIC project tries to find new solutions.

COVER LAYERS FIELD TESTS IN PYHÄSALMI

Field tests were done in Pyhäsalmi Mine, located in Pyhäjärvi in Finland. The mine has produced copper, zinc and pyrite and in 2019 the mine is gradually closing its operations. Lysimeters were implemented in 2016 as 10 m3 lysimeter structures. Total number of lysimeters were 10. The objective of the field tests was to study materials in real circumstances. Tested materials were earlier tested in the laboratory. Focus in the lysimeter tests was to complement laboratory studies (water permeability and leaching characteristics) with the seeping water results. When the lysimeters were built, notice was taken especially on the material handling, mixing and compacting. The materials chosen for the lysimeters were the most interesting and potential ones which could be later used in larger scale pilot cover structures.

Lysimeter Pilot Materials and Methods

Fine and coarse enrichment sand used in the test was sands hails from the enrichment sand basin D of the Pyhäsalmi mine, from the depth of 0...2,5 m. The enrichment sand segregates to finer and coarser material when it is deposited to the basin as very watery material with the help of outlet pipe. The coarser enrichment sand was more homogenous than the finer sand, so the need of homogenisation was lesser with the coarser material. Based on previous studies, the enrichment sand mainly consists of sulfidic minerals (76%) which occurs mainly as pyrite (iron sulphide) and baryte (barium sulphate). Enrichment sand also contains smaller amount (<5%) of pyrrhotite and small quantity (<5%) silicate minerals e.g. plagioclase, quartz and olivine. Enrichment sands contains also some amount of burnt lime, which is added after the enrichment process to prevent the acid generation caused by sulphide minerals. (Räisänen&Bäcknäs, 2016) Materials used in the test and material information are presented in Table 1.

Table 1. Total concentrations and material properties of the used construction materials.

Material	Al (mg/kg)	Cu (mg/kg)	Fe (mg/kg)	Mn (mg/kg)	Zn (mg/kg)	Ca (mg/kg)	S (mg/kg)	pH (-)	ρ_d (kg/m^3)
Enrichment sand (fine)	7180	680	297000	590	1680	25400	294000	7,0	1870
Enrichment sand (coarse)	6910	720	315000	430	2180	20700	310000	6,7	2380
Ash	52400	120	142000	2430	240	72100	12800	9,5	830
Gypsum	340	13	400	21	20	277000	215000	2,8	1290
Moraine	12800	55	17500	240	63	5040	350	4,8	2300
Inert material	11000	20	20800	190	33	6570	210	7,5	-

Moraine used in the tests was local moraine from the southern part of the mining area. Grains over d60mm were sieved off. Based on the preliminary leaching tests, the moraine might have acid generating properties while the leachate pH was relatively low (4,4 in L/S = 8). However, based on the acid-base accounting (ABA) test results the moraine is non-acid producing. Gypsum used in the test was waste gypsum from Yara fertilizer plant located in Siilinjärvi. Gypsum was stored on top of tarpaulin and covered with tarpaulin. Ash was moistened fresh fly ash from Oulu Energia energy plant. Ash was

moistened in the plant three days before construction to 15,5 % water content when the ash was unloaded from the silo. During the construction the ash was stored in piles on top of the tarpaulin and it was also covered with the tarpaulin. In the lysimeter the ash functioned as a reactive layer, which objective was to change water seeping through the structures. Lawn topsoil was used as a soil layer in the lysimeter. Soil was built to all test lysimeters despite structures numbers 5 and 8. Grass was planted on top of the soil. Inert material refers to the bottom layer made of gravel and functioning as a filtration layer directing the water through the material. Inert material used is equal to sandy gravel.

Lysimeter Structures

The used vessels are 10 m^3 volume cylindric containers, with inner diameter 2.4 m and height 2.2 m. Every vessel is equipped with three drainage pipes (surface runoff, lysimeter, bottom of the vessel). The waters are steered to collecting wells. The waters for analyses are steered to lysimeter wells, from where the water is collected for amount and quality checks. (Karjalainen, N., Autiola, M. and Jyrävä, H. 2016.)

The material layer structure and thickness in each lysimeters are presented in Figure 2. Layer composition was selected based on the preliminary laboratory tests (Karjalainen, N. 2016). 5 different top structures were tested for both coarse and fine enrichment sands including reference structures without top structures (lysimeters 5 and 8). Lysimeter 4 represents traditionally used top structure, moraine and soil cover, used in closure of enrichment sand basins in Pyhäsalmi mine.

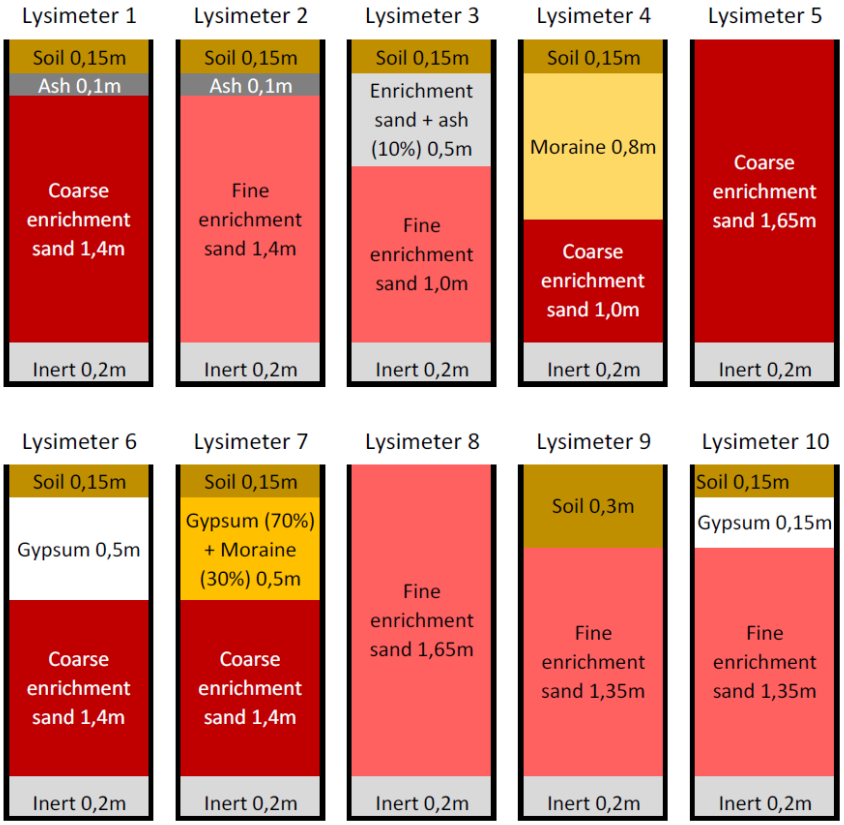

Figure 1. The layer structure of the tested lysimeters in Pyhäsalmi Mine.

Sampling from the Lysimeters and Analytics

The bottom wells and lysimeter wells were emptied 2-5 times in month and the seepage water amount was measured. The quality of the seepage water was monitored after 42, 134, 165, 233, 345,

375, 453/459 days. The samples were collected during one-week period from the lysimeter well between emptying. The seepage water amounts varied during the test due to weather conditions.

Lysimeter water samples were analysed for Al, As, Ba, Cd, Cr, Cu, Fe, Hg, Mn, Mo, Ni, Pb, Sb, Se, V, Zn, Ca, K, Mg, Na and S (µg/l) and also for sulphate, fluoride, chloride and DOC (mg/l). The focus in this study was the leachability of the main components in the enrichment sand Cu, Fe, Zn, S, Ca and sulfate. In addition, pH and conductivity were measured weekly, on average, at the same time when the lysimeter wells were emptied. The main objective was to compare different top structures for fine and coarse enrichment sands and find the most suitable cover structures for future large-scale piloting.

Seepage Water Quality and Amount

The seepage water quality was monitored from each lysimeter wells 6-7 times during the follow-up period 23/05/2016-24/08/2017. The amount of seepage water was determined almost every week. The measured average concentrations of selected parameters (SO_4^{2-}, Al, Cu, Fe, Mn, Zn, Ca), pH and cumulative seepage water amount and calculated L/S ratio based on cumulative water amount and dry solid amount, including enrichment sand, moraine and by-products in lysimeters, during follow-up period are shown in Table 2. The average concentrations were calculated mg/kg dry matter based on the cumulative seepage water amount and dry solids.

The comparison of main metal leachate concentrations Cu, Zn and Fe calculated per dry solids are shown in Figure 2 for different coarse and fine enrichment sand top structures. The comparison of S, Ca and sulphate calculated per dry solids are shown in Figure 3 for different coarse and fine enrichment sand top structures.

Table 2. Average concentrations of seepage water and calculated L/S ratios during the test. 6-7 measurements were conducted from each lysimeters during 459-day follow-up. Dry solids used in calculations includes enrichment sand, moraine and industrial by-products. Inert material and soil are excluded. * Lysimeter 6 well had leaked during the tests. **Calcium was determined only from 3 samples during the monitoring period.

Lysimeter no.	SO_4^{2-} (mg/l)	Al (µg/l)	Cu (µg/l)	Fe (µg/l)	Mn (µg/l)	Zn (µg/l)	Ca** (mg/l)	pH	Cumulative seepage water (l)	Dry solids (kg)	L/S ratio
1	4986	17,1	2,6	10,5	3573	237,1	456	7,7	995	14153	0,07
2	3229	710,8	2,5	30,0	2827	37,9	513	5,8	780	12733	0,06
3	2786	33,8	12,0	25,6	7740	21,0	603	6,0	1120	14065	0,08
4 (traditional)	3103	42,1	2,0	75,3	146	193,3	404	7,5	1047	14090	0,07
5 (no cover)	4914	72,8	4,6	24,3	2464	75,9	547	6,5	1169	15370	0,08
6*	4692	15,9	5,1	11,9	1065	502,6	357	7,3	739	10930	0,06
7	4104	22,0	5,5	11,8	1377	666,7	570	7,4	1043	14430	0,09
8 (no cover)	3443	2753	6,7	48,3	8717	203,4	447	5,2	1273	15345	0,09
9	2214	1337	5,4	41,7	8509	123,6	501	4,9	985	11900	0,10
10	1600	2632	15,6	175	11835	206,0	587	4,5	248	13760	0,01

Coarse enrichment sand
Fine enrichment sand

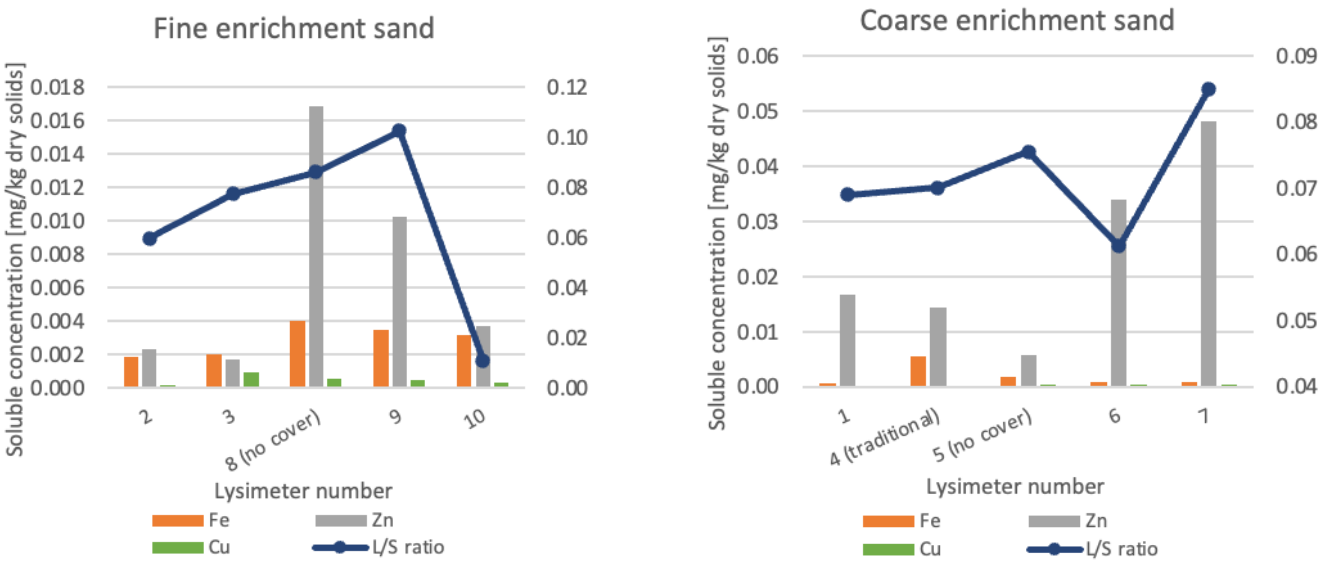

Figure 2. Average soluble Fe, Zn and Cu concentrations from different top structures in comparison with dry solids content (mg/kg dry).

Values are calculated by using average metal concentrations, dry solids content and amount of seepage water shown in Table 2.

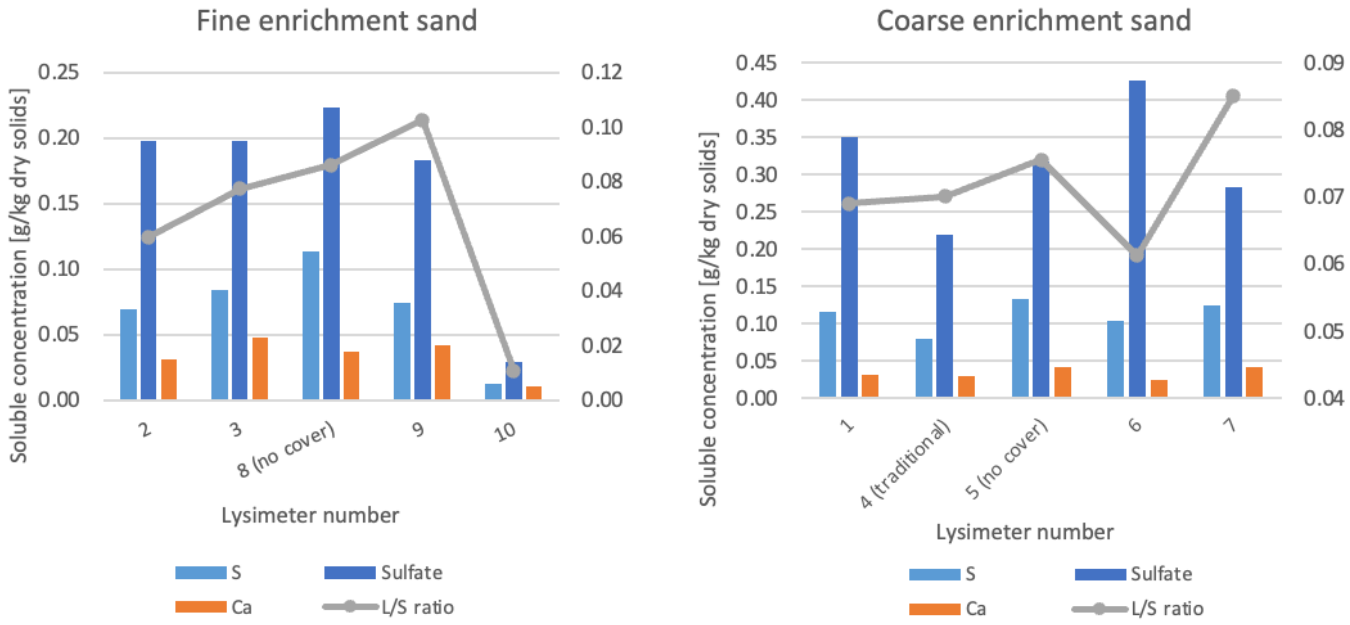

Figure 3. Average soluble concentrations of sulphur, sulphate and calcium from different top structures in comparison with dry solids content (g/kg dry).

Values are calculated by using average metal concentrations, dry solids content and amount of seepage water shown in table 2.

The variations in seepage water amounts between different top structures showed remarkable variations during the test. Especially lysimeters 2, 6 and 10 had lower seepage water amount (248-780 l) compared to rest of the lysimeters (985-1273 l). Lysimeter 6 emptying valve had leaked during the test.

L/S ratios of lysimeters varied at the end of the test between 0,01-0,1. The average pH of lysimeters varied between 4,5-7,7 during the test.

The average metal concentrations (Table 2) measured from fine enrichment sand lysimeters 2, 3 and 9 were mainly lower in covered structures compared to uncovered enrichment lysimeter 8. Lysimeter 10 had higher Mn, Zn, Cu and Fe concentrations compared to uncovered structures. The Fe, Cu, Zn, S, Ca and sulphate concentrations were calculated to mg/kg dry (Figures 2 and 3) for comparison leachability from the dry solids. The comparison showed that ash cover in lysimeters 2 and 3 seems to be effective to reduce leachability of most metals as well as sulphur and sulphate compared to uncovered structure. The calculated metal and sulphur compound amounts were relatively lower from lysimeter 10 due to almost 10 times lower seepage water amount. Therefore, the calculated concentrations showed in the Figures 3 and 4 are not directly comparable.

The average metal concentrations (Table 2) measured from covered coarse enrichment sand lysimeters 1, 4, 6 and 7 had more variations compared to uncovered enrichment lysimeter 8. Leachability of Al, Fe and S were lower with covered structures. However, the leachability of Zn was remarkably lower with uncovered structure which seemed to be illogical. Comparison of metal leachability form covered coarse enrichment sand structures (Figure 2) the Cu leachability was low for all tested structures; Zn leachability was lowest for ash cover structure (lysimeter 1) and traditional structure (lysimeter 4).
Based on the results, the coarser enrichment sand seems to have different leaching properties compared to fine enrichment sand. The weathering of the coarse and fine sands might have effect on the leaching properties.

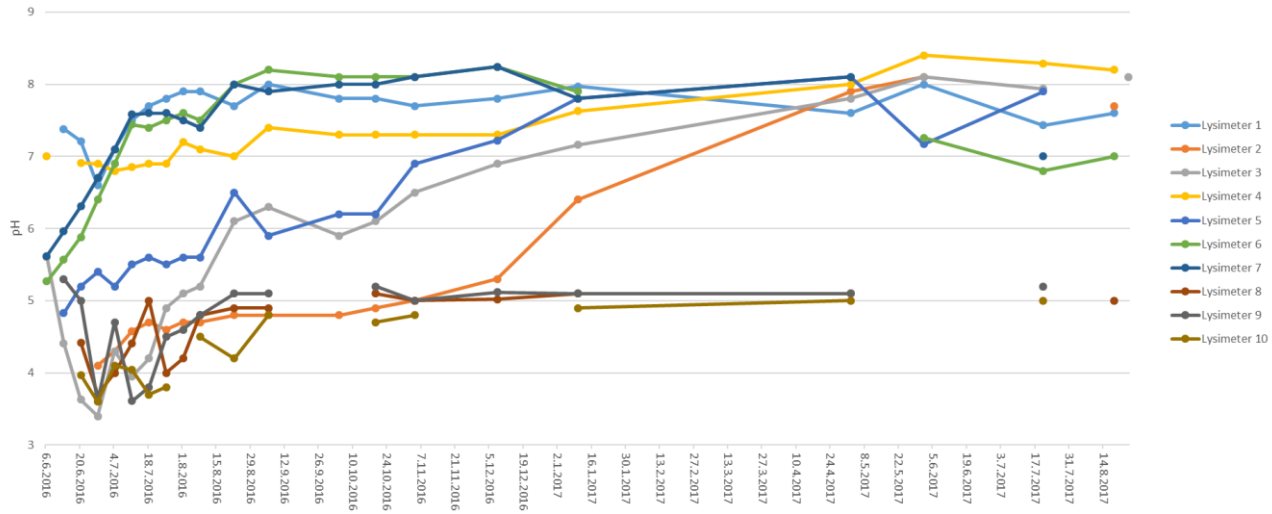

Figure 4. pH of the seepage waters from different lysimeters during 6.6.2016-24.8.2017.

The pH monitoring results (figure 4) show, that lysimeters 1, 4, 5, 6 and 7 with coarse enrichment sand have averagely higher pH than lysimeters 2,3,8,9 and 10 with finer enrichment sand. Even the coarse enrichment sand with no cover (lysimeter 5) has increasing pH during the test. Finer enrichment sand with no cover, only soil cover or with soil and gypsum cover (lysimeters 8, 9 and 10) had lower pH during the test. The finer enrichment sand with ash cover (lysimeters 2 and 3) had increasing pH during the test. The ash addition with both enrichment sands seemed to have positive effect on pH.

However, the use of industrial waste materials in cover layers of different type of mine tailings or enrichment sands needs to be verified case by case. The industrial waste (e.g. fly ash) quality as well

as the mine waste composition may variate a lot and the compatibility of different materials needs to be verified. (Niemelin, 2019)

FIBRE CLAY SEAL LAYER TEST STRUCTURES IN HITURA

Initial situation in Hitura mine is that the enrichment sand deposited in the basins has grain size distribution varying from silt to fine sand. The finest materials are in the middle of the basins and more coarser materials are in the sides. Enrichment sand contains sulphide minerals 1,4-5,9 % and sulphur 0,6-2,5 % but it is not characterized as acid producing waste. The nickel and copper contents exceed the threshold value of the national Decree 214/2007 (Government Decree on the Assessment of Soil Contamination and Remediation Needs) and zinc, cobalt and chromium contents are below of the Decree threshold values. In addition, the sand contains small amounts of benzene, carbon bisulphite, diethyl sulphate and terpenes. (Niemelin, 2019)

The constructing licenses demanded water permeability value of sealing layer is $k < 1{,}0x10^{-8}$ and minimum sealing layer thickness for moraine is 200 mm and fibre clay 250 mm. The cover/growth layers on top of sealing layer minimum thickness is 100 mm in both cases. (Niemelin, 2019)

Sealing layer materials

Fibre clay is produced as a residual material in paper recycling process in Paper industry. Fibre clay is easy to modify, and it is a light material with good resistance for deformations. It is a weatherproof material, so it can be transported and stored already in winter at its construction site. Fibre clay (Mänttä, Finncao) has water permeability between $k= 1 \times 10^{-9}$ m/s - $k=1 \times 10^{-8}$ m/s. The environmental eligibility has been analysed and despite of the process materials, all the generated fibre clay fills earth construction and land fill requirements. Fibre clay has been used several decades in landfill liners as cover and bottom structures. In addition, references can be found in shaping of ski slopes, bicycle and pedestrian lane structures, 10 exercise path structures and encapsulating contaminated soils. Most recent applications are golf course structures and field structures and different types of embankments and barriers.

Fibre clays from Äänekoski, Mänttä and from Oulu were tested for compactibility, water permeability and environmental properties and the conclusion was that all of those are suitable to use for sealing the enrichment sand basins. (Niemelin, 2019)

In order to ensure the usability of fibre clay, a test field was constructed on 14th September 2017 by utilizing fibre clay from Metsä Tissue Mänttä. The size of the test field was approximately 10 m x 20 m and the bottom of the field was equivalent for the actual structure. The seal course was constructed as one layer, and the compacted thickness was 250 mm. The fibre clay was spread by using 20-30 t crawler excavator. When driving over the seal course (fibre clay) the amount of overdriving was varied in order to determine the needed compaction work for the target dry unit weight (445 kg/m^3). The compaction of the structure was followed with Troxler measurement and the achieved water permeability value $k < 1{,}0x10^{-8}$ m/s is conformed using laboratory samples which are prepared afterwards from field samples from field troxler points. The results are showed in Table 3. Other two fibre clay were similar properties wise. All three of them were used in sealing layer construction. (Niemelin, 2019)

Table 3. Measurement of test structure characteristics and laboratory samples Mänttä fibre clay (Niemelin, 2019).

Troxler points	Over driving times (back and forth)	Layer thickness (mm)	Dry density (kg/m^3)	Wet density (kg/m^3)	Water content (%)	k (*10^{-9} m/s)
1-5	1	320	441	1200	173	
6-10	2	290	475	1222	162	
11-14	3	280	542	1248	131	
TRX 1			447	1201		7,3
TRX 8			445	1199		5,5
TRX 14			447	1203		5,8
TRX 1			449	1208		9
TRX 6			453	1207		7,5
TRX 6 (2)			454	1210		7,6
TRX 8			446	1201		4,5
TRX 11			467	1213		7,6
TRX 14			447	1204		5,6

Altogether, fibre clay materials were utilized in 148 850m^2 Hitura I stage construction. The whole compaction layer area in enrichment sand basin 2 was 265 092 m^2, which lead to: 56 % of the sealing layer area in enrichment sand basin 2 was constructed with fibre clay. During the construction, the densities of the used fibre clays were tested. Density targets were achieved with all used fibre clays (and moraine). Construction with fibre clay did not need any special equipment. The material was levelled and compacted with crawler excavators (Niemelin, 2019).

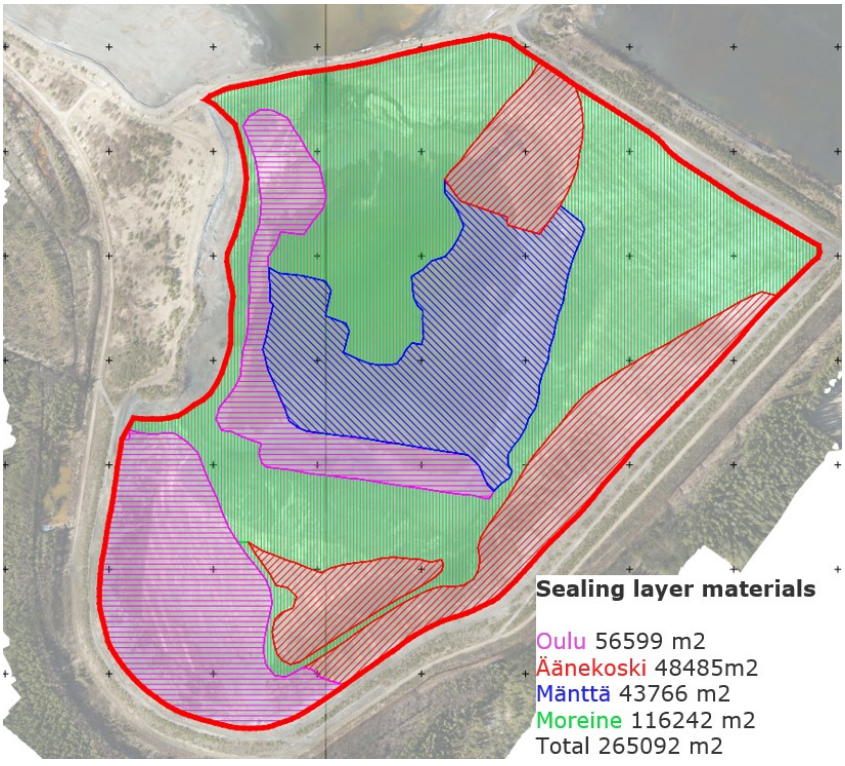

Figure 5. Map of different fibre clay and moraine areas in Hitura's enrichment sand basin 2. (Niemelin, 2019)

VERTICAL SEALING BARRIER PILOT

In Sorsasalo near Kuopio, vertical sealing barrier structure is piloted and construction is continued. Idea behind barrier is that it utilizes waste and surplus materials which will be already dumped to the landfilling site. That's reduce virgin material usage and shorter transport distances. Before it there is done pilot structure which conform the barriers feasibility. It is constructed by utilization of waste materials. Objective of vertical sealing barrier is to prevent hazardous leaching water to seep from hazardous waste material dumbing sites to ordinary landfilling area. These two areas are side by side. (Fortum, 2020)

The constructing license says that minimum thickness of barrier is 1000 mm and its water permeability value k must be under $1*10^{-9}$ m/s. Barrier can be build any soil material that can achieve that water permeability value. On both side of the barrier needs to be 500 mm wide drainage layer. (Fortum, 2020)

The core of the barrier is made of surplus clay. It is compacted by mould which is about 1 m wide, 3m long and 1 m high. The clay is compacted with crawler excavator by thin layer at a time. On the bottom of barrier is on each side drainage pipes which collect seeping water and transport it to water treatment. The drainage layer on both side of barrier is constructed by using coarse sieved bottom ash from Riikinvoima Oy. After drainage layer on each side is about 4-6 m wide support layer. On hazardous side it is constructed using Hitura mine's water treatment sediment and Mondi Powerflute Oy's fly ash. And common waste side with same fly ash mixed to contaminated soil which is dumbed on the landfill site. These horizontal layers will be constructed on top of each other's as the landfill sites rise on same level. (Fortum, 2020)

Vertical Sealing Barrier's Feasibility Tests

Pilot structure is 1 m high 3m long and 1 m wide block of barrier layer, which was constructed using surplus clay. Clay barriers density was measured in 50 mm intervals layer by layer. When pilot structure was ready one sample was taken from the top of barrier and after that it were cut in half horizontally and from middle has taken another sample for laboratory analysis. In laboratory from both samples has prepared samples with same density and water permeability of samples was tested. Results were from between $1{,}5*10^{-10}$ – $5*10^{-10}$ m/s. That fulfil the threshold value $1*10^{-9}$ m/s and clay fit perfectly to usage case. Barrier' fulfil parameters what are demanded from it, so construction was continued. (Fortum, 2020)

REACTIVE BARRIERS

In Hitura mine is waste rock pile where seeping low metal concentrations water to the ditch. The idea of the pilot is to test passive (gravity driven and low maintenance) water treatment systems for mine seepage waters with low metal concentrations. The location was selected based on preliminary water analysis and available free space for piloting. Reactive barrier piloting is carried out in Hitura mine area. In reactive barrier pilot has tested by two different type structure. First is Industrial by-product-based reactive barrier structure and second is commercial material-based bottom structure. Water is taken from the ditch by submerged dam to elevate water level. From forming pond, water is taken as a side stream and divide to the two constructed test structures. Preliminary construction works were done in summer 2020 and pilot construction during summer 2021.

Industrial by-product-based structure contains two water treatment steps: 1) pH adjustment with limestone barrier and metal precipitation and 2) metal adsorption with by-product based geopolymer adsorbent. Limestone fraction used in the pilot is 5-20mm and it is surplus material from limestone

producer SMA Minerals Oy. Geopolymer adsorbent for the pilot is provided by KAIVASU-project and it is produced in Oulu University. The principle of by-product-based reactive barrier pilot is shown in figure 6.

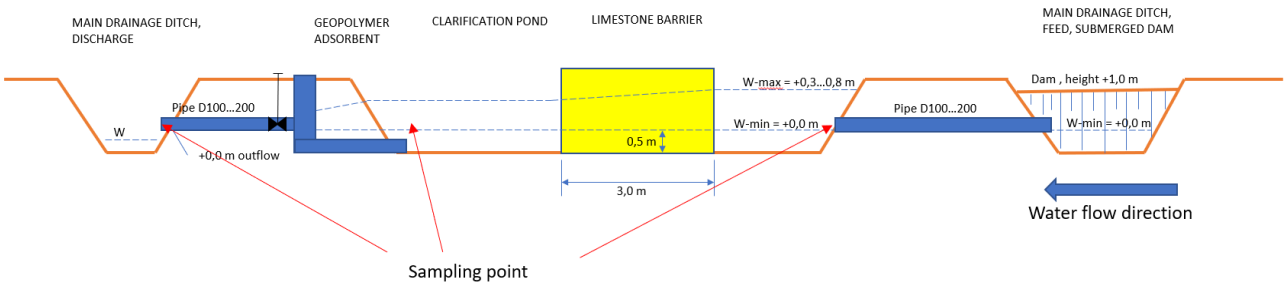

Figure 6. Reactive barrier pilot structure.

Main working mechanism is in first step that limestone increse pH value from acidic to alkalic. In alkaline condition ionic metals precisipate as metalsalts and form with calcium low solubility sediment. After this first step the second is residual metal adsorption with geopolymer. Geopolymer is packed to bag which water can penetrate easily. Bag is fitted into the well after precipitation pond section (figure 6). Idea is that most of the reduction occured in barrier presipitation pond and residual metals is adsorbed by adsorbent. Monitoring is still ongoing so geopolymer adsorpton results is not yet fully combined and evalueted.

Table 4. Average values of inflow water of reactive barrier pond.

pH	EC mS/m	SO_4^{2-} (mg/l)	Al (mg/l)	Co (mg/l)	Cu (mg/l)	Fe (mg/l)	Mn (mg/l)	Ni (mg/l)	Zn (mg/l)
5,48	278	2083	3,082	0,188	0,435	0,391	1,426	6,013	0,601

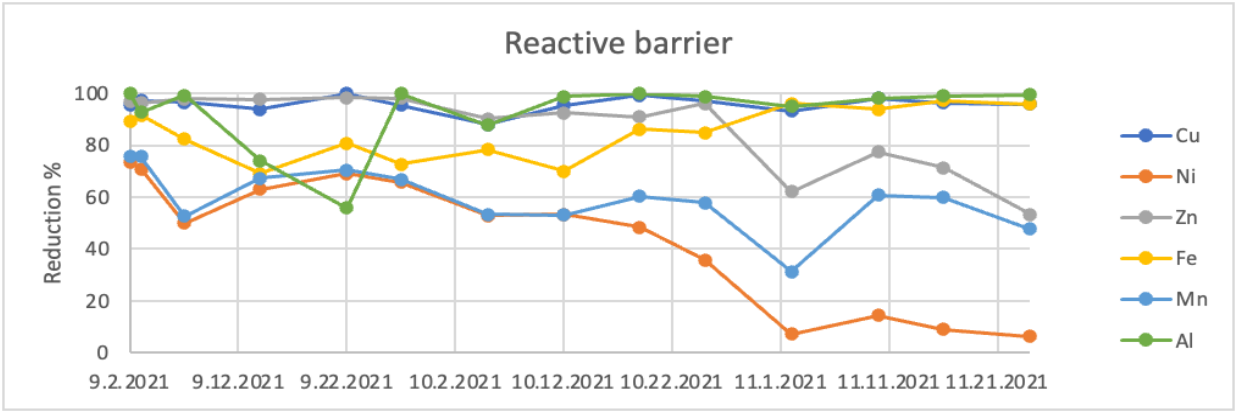

Figure 7. Reactive barrier performance monitoring.

As can see from figure 7 the reactive barrier removes effectively metals and heavymetals from water. Al, Fe, Cu during whole monitoring period. Zn removing efficiense is over 90% during first 2 months but removal efficiensy decrease after that. Nickel removal efficiensy is in first 2 month quite good but after that it about 10 %. Nikkel initial concentration is much higher (t. e. 10 time higher than zinc) than other metals, so lover reduction prosentage is resonable.

Commercial material-based structure contains two water treatment ponds with similar structure. The idea is, that water flows through active geocomposites in each pond. The geocomposite is Tektoseal Active HM 4000 which is manufactured by HUESKER Sythetic Gmbh. Geocomposite keeps inside cationic adsorbent which adsorb metals from water. The system is gravity driven (passive). The water flow is adjusted so that the water level in each pond is approximately 10-20cm. The planned flow rate is 4 m3/day but – with regard to lab test results - the material can handle flow rate up to 12 m3/day. The principle of horizontal reactive barrier pilot is shown in figure 8.

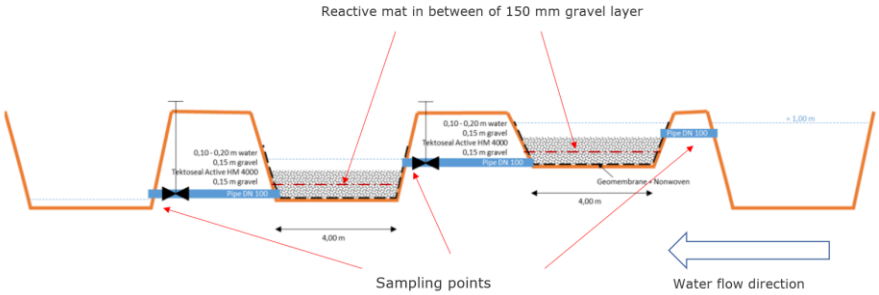

Figure 8. Reactive mat's pilot structure.

Table 5. Mat system waters average initial values.

pH	EC mS/m	SO_4^{2-} (mg/l)	Al (mg/l)	Co (mg/l)	Cu (mg/l)	Ni (mg/l)	Zn (mg/l)
5,63	290,00	2241,43	2,56	0,17	0,37	6,19	0,57

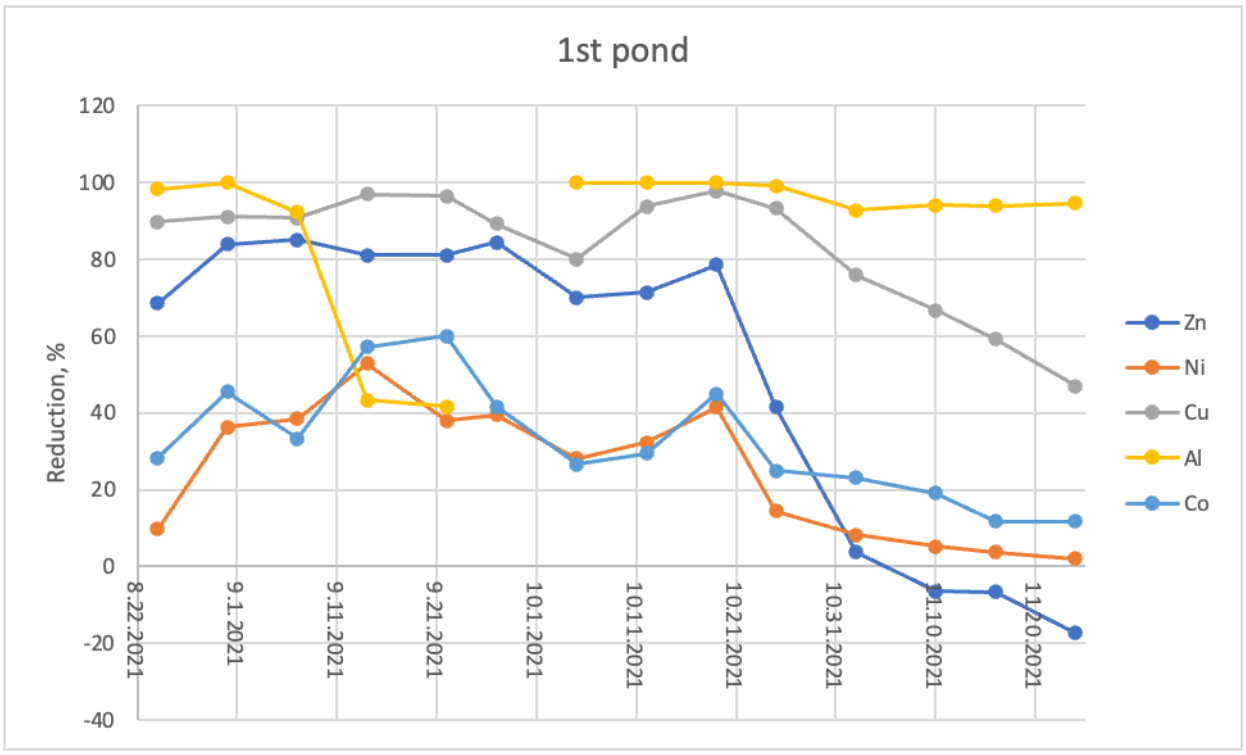

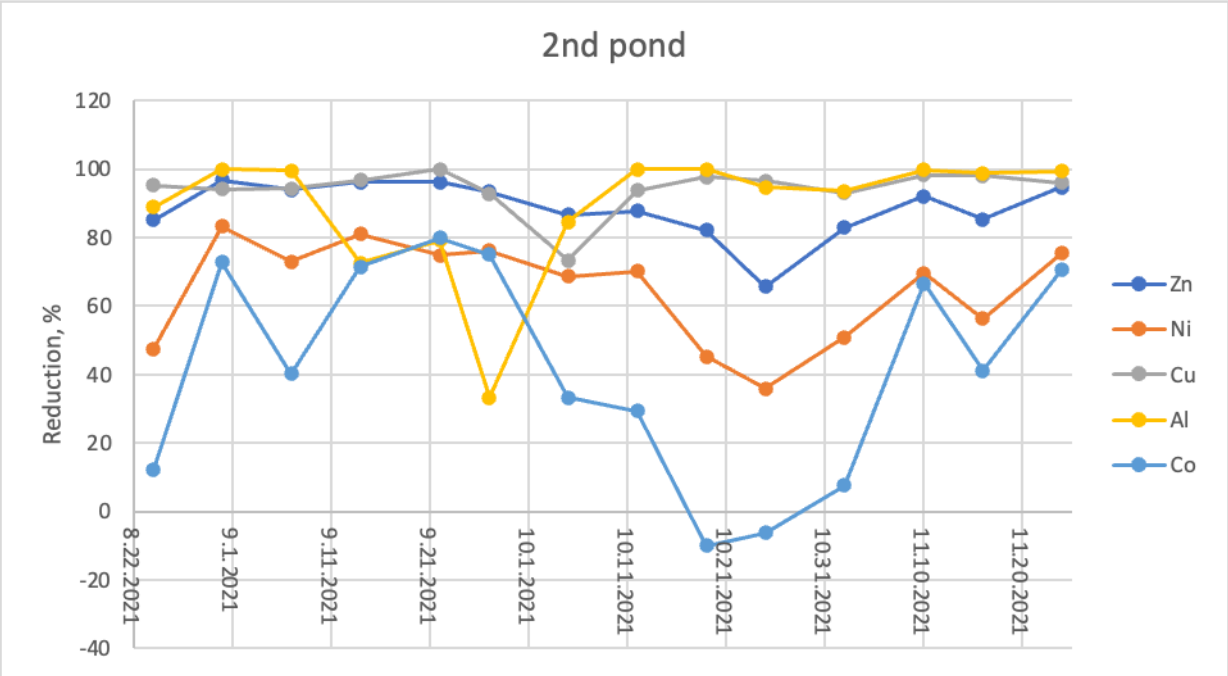

Figure 9. Mat structures 1st and 2nd ponds metal reductions compared to initial concentration.

In figure 9 is shown the reduction of metals and heavy metals in reactive mat pilot structure during monitoring period. As can see the first mats removal efficiency is weakened during monitoring period dramatically. The breakthrough is occurred with zinc and almost nickel. Metals compete about space on the adsorbent surface. In the end of monitoring period the zinc atoms start to give their spots to other metals and reduction is negative. After the second mat removal efficiency is still in good level during whole monitoring period.

CONCLUSIONS

The lysimeter testing carried out in Pyhäsalmi showed some promising results for utilization of industrial wastes in mine cover structures. Especially use of fly ash in cover structures of acid generating enrichment sand seemed to lower the leachability of metals and hold the pH level of leachates near neutral with both tested enrichment sand grades. Compared to the traditional moraine cover structure the use of fly ash has potential in material savings in. In this testing 0,1m thick fly ash cover layer gave similar or even better leachability results with coarser enrichment sand compared to 0,8m thick moraine layer. UPACMIC project continues with large scale construction in Hitura Mine, which is located in Nivala, Finland. Fortum Waste Solutions has used fibre clay in the cover structure of enrichment sand basins. In addition, reactive dam has been constructed as a reference structure for mobile water treatment plant for the comparison of these two different water treatment methods. Alternative materials are tested in Hitura Mine, in bottom structure and in reactive dam structure, which is meant to filtrate harmful substances from the mining area waters.

In the cover structure construction, fibre clay materials were utilized in 148 850m^2 which is 56 % from the sealing layer area of enrichment sand basin 2. The vertical sealing barrier pilot was success and it work as intended. The required water permeability value is reached, and construction will be continued layer by layer when more height is needed. At the first 2 month of the monitoring period both pilot structures for passive water treatment perform quite well. Heavy metals such as nickel, copper, and zinc concentrations has reduced 60-95 % and almost all aluminium has been removed from water. The limits of structures are also almost reached which helps designing larger structures in the future.

AKNOWLEDGEMENTS

The authors thank EU LIFE funding (LIFE12 ENV/FI/000592) for the project funding and Ministry of the Environment and Yara Finland for co-funding.

REFERENCES

Fortum. (2020). KOEKENTTÄRAPORTTI, MÄKELÄ ALUE 2 SAVI KUOPIONKÄSITTELYKESKUS, PYSTYERISTYSSEINÄ TAV/VJ-KP VÄLI. (non-public). Research report.

Niemelin, T. and Suikkanen, t. (2019). Technical report, piloting cover structure. (action B1) UPACMIC LIFE12 ENV/FI/000592. Available: https://projektit.ramboll.fi/life/upacmic/matsku/deliverables/Reports/B1%20Technical%20report,%20piloting%20cover%20structure%20with%20PR4.pdf.

Räisänen, M-L. Bäcknäs, S. (2014). Pyhäsalmen kaivoksen kaivannaisjätteiden geokemialliset ominaisuudet, hapontuotto- ja metallien liukenemispotentiaali (non-public). Research report. Geological survey of Finland.

Ruokonen, E. and Temmes, A. (2018). The approaches of strategic environmental management used by mining companies in Finland. Journal of Cleaner Production 210 (2019) 466-476.

ÜNYE (ORDU) BÖLGESİNE AİT KALSİYUM TİP BENTONİTİN UV-VIS ABSORPSİYON SPEKTROSKOPİSİ İLE KARAKTERİZASYONU

CHARACTERIZATION OF CALCIUM TYPE BENTONITE FROM UNYE (ORDU) REGION BY UV-VIS ABSORPTION SPECTROSCOPY

Y. Erdoğan [1], O.E. Kök [2, *]

[1]*T.C. Enerji ve Tabii Kaynaklar Bakanlığı, Ankara, Türkiye*
[2]*İskenderun Teknik Üniversitesi, Petrol ve Doğalgaz Mühendisliği Bölümü, Hatay, Türkiye*
*(*Sorumlu yazar: oeserkok@iste.edu.tr)*

ÖZET

Bentonit, alüminyum ve magnezyum bakımından zengin volkanik kül, lav ve tüflerin bozunması ve ayrışması sonucunda oluşan kristal yapılı, poroz ve yumuşak kil olarak tanımlanmaktadır. Bileşiminde yoğun olarak (>%75) montmorillonit olmasından dolayı smektit grubu kil minerallerine dahil olan bentonit, yumuşak yapıda kolloidal özellikli alüminyum hidrosilikatlar arasında yer almaktadır. Bentonitlerin adlandırılması ise kimyasal bileşiminde bulundurduğu baskın element (genellikle sodyum ve kalsiyum) türüne göre değişim göstermektedir. Bileşiminde birçok element bulunmasına rağmen temelde Sodyum Bentonit (Na-Ben), Ara Tip Bentonit (Na/Ca-Ben) ve Kalsiyum Bentonit (Ca-Ben) olmak üzere üç farklı türü bulunmaktadır. Bentonit, rezervlerinin dünyada geniş coğrafyada yer alması ve birçok sektörde doğrudan kullanılabilmesinden dolayı önemli endüstriyel hammaddeler arasında yer almaktadır. Kullanım alanları ise bentonit türüne göre değişim göstermektedir. Dolayısıyla hem mevcut kullanım alanlarının daha iyi belirlenebilmesi hem de yeni sektörlerde yer alabilmesi amacıyla fiziksel ve kimyasal karakteristiklerinin detaylı olarak belirlenebilmesi gerekmektedir. Yapılan çalışmada, ülkemizin yüksek kaliteli Ca-Ben türü olan Ünye (Ordu) bentonitinin UV-Vis absorpsiyon spektroskopisi yöntemi ile karakteristik özellikleri belirlenmiştir. Çalışma kapsamında 200-1100 nm dalga boyu arasında optik ölçüm yapılmış olup; elde edilen sonuçlar literatürde yer alan fiziksel ve kimyasal analizler ile ilişkilendirilerek mevcut ve potansiyel kullanım alanları arasında değerlendirmeler yapılmıştır.

Anahtar Sözcükler: Bentonit, uv-vis absorpsiyon spektroskopisi, ca-ben

ABSTRACT

Bentonite is defined as a crystalline, porous and soft rock formed as a result of the weathering of volcanic ash, lava and tuffs rich in aluminum and magnesium. Bentonite, which is included in the smectite group clay minerals due to the fact that the dominant mineral (>75%) in its composition is montmorillonite, is among the soft colloidal aluminum hydrosilicates. The named and types of bentonites varies according to the dominant element/mineral type in their chemical composition. Although there are many minerals in its composition, there are basically three different types: Sodium Bentonite (Na-Ben), Mix-Type Bentonite (Na/Ca-Ben) and Calcium Bentonite (Ca-Ben). Bentonite is among the important raw materials because its reserves are located in a wide geography in the world and can be used directly in many sectors. The usage areas vary according to the bentonite types. Therefore, it is necessary to determine the physical and chemical characteristics in detail in order to better determine the existing usage areas and to take place in new sectors. In this study, the characteristic properties of Ünye (Ordu) bentonite, which is the high-quality Ca-Ben type of our country, were determined by UV-Vis absorption spectroscopy method. Within the scope of the study, optical measurements were made between 200-1100 nm wavelength; the results obtained were associated

with the physical and chemical analyses in the literature, and evaluations were made between the current and potential usage areas.
Keywords: Bentonite, uv-vis absorption spectroscopy, ca-ben

GİRİŞ

Kil mineralleri, kristal yapılı, ince taneli ve sulu süspansiyonlarında plastik özelliğe sahip hidratlaşmış alüminyum silikatlı doğal bir endüstriyel hammadde olarak tanımlanabilmektedir. Alüminyum silikatlı yapı bazı durumlarda magnezyum veya demir silikatlı yapılarda da bulunabilmektedir. Kil mineralleri doğal ortamda saf olmayan bir yapıda bulunmaktadırlar. Bu yapı, ağırlıklı olarak kuvars, kalsit, feldspat ve pirit gibi safsızlık meydana getiren kil dışı mineraller tarafından sağlanmaktadır. Ancak safsızlıklar bulundurmasına rağmen geneli incelendiğinde baskın olarak kil mineralleri yer almaktadır (Erdem, 2004; Kayıkçı, 1989).

Kil mineralleri, doğal ortamda yapı ve kimyasal bileşimlerine bağlı olarak farklı türlerde yer almaktadır. Kaolin, smektit, illit-mika ve klorit olmak üzere başlıca dört türde kil minerali bulunmaktadır. Endüstriyel kullanım amacına bağlı olarak bu dört grupta yer alan kil mineralleri kullanılmasına rağmen hem rezerv miktarı hem de geniş kullanım alanı dikkate alındığında smektit grubu kil mineralleri öne çıkmaktadır (Hancıoğlu, 2015).

Smektit grubu kil mineralleri $2Al_2O_3.8SiO_2.2H_2O.nH_2O$ genel formülüne sahip olup; genel molekül formülünde bulunan nH_2O, kil tabakaları arasında yer alan su moleküllerini temsil etmektedir. Bu kil tabakaları, smektit grubu kil mineralleri için iki tetrahedral ve bir oktahedral yapıdan (2:1) oluşmaktadır. Bu tabakalar arasında ise zayıf bir bağ türü olan Van der Waals bağları bulunmakta ve tabakalar arasında yaklaşık olarak 0,96 nm bazal mesafe bulunmaktadır (Holtz ve Kovacs, 2010).

Smektit grubuna ait kil mineralleri, doğada farklı oluşum mekanizmalarına bağlı olarak çeşitli türlerde yer almaktadır. Ancak en yaygın tür olarak 'Montmorillonit' minerali öne çıkmaktadır. Ancak katyon değişimlerine bağlı olarak nontronit, hektorit, saponit gibi türlerde de bulunabilmektedir (Hancoıoğlu, 2015).

Smektit grubu kil mineralleri detaylı olarak incelendiğinde ise 'Bentonit' ön planda yer almaktadır. Bentonit, en az %75 oranında montmorillonit minerali içeren ve yumuşak formlu, sulu süspansiyonları plastik özellik gösteren alüminyum hidrosilikat olarak tanımlanmaktadır. Bileşiminde yüksek oranda bulundurduğu montmorillonit mineralinden dolayı bentonit, bazı endüstriyel uygulamalarda doğrudan 'montmorillonit' olarak da adlandırılabilmektedir. Volkanik kül ve tüflerin kimyasal alterasyonu neticesinde meydana gelen bentonit, sulu süspansiyonlarda kolloidal özellik göstermektedir ve katı formunda poroz bir fiziksel yapıya sahiptir (El-Nagar ve Sary, 2021).

Bentonit, ülkemizde ve dünyada kullanılan önemli endsüstriyel hammaddeler arasında yer almaktadır. Fiziksel ve kimyasal özelliklerine bağlı olarak sondaj, döküm, inşaat, boya, gıda, besicilik, ilaç, arıtma ve kozmetik gibi sektörlerde kullanılmaktadır. Dolayısıyla geniş kullanım alanlarından dolayı rezerv miktarlarının belirlenmesi ve mevcut rezervlerin endüstriye uygun şekilde yüksek verimde kullanılabilmesi açısından çok sayıda bilimsel araştırma yapılmaktadır. Dünya rezervleri incelendiğinde rezerv hacmi ve kalitesi bakımından en önemli bentonit yatakları Wyoming (ABD), Ponza ve Sardunya (İtalya), Milos (Yunanistan), Bavyera (Almanya) ve Almeria (İspanya) bölgelerinde bulunmaktadır. Görünür ve muhtemel rezerv miktarı ise yaklaşık olarak 1820 milyon ton olarak tespit edilmiştir (MTA, 2018). Ülkemiz ise yaklaşık 242 milyon ton görünür ve muhtemel rezerv miktarı ile en önemli yataklarını Ordu, Çankırı, Tokat, Kütahya ve Ankara illerinde bulundurmaktadır (Şekil 1). Bu rezerv miktarı ile toplam dünya rezervlerinin yaklaşık %13'lük kısmını oluşturmaktadır (Kök, 2017; Bakır vd., 2012).

Şekil 1. Türkiye bentonit yatakları (Kök, 2017; MTA, 2018)

Bentonitler, bileşimlerinde bulundurduğu Na ve Ca miktarına bağlı olarak adlandırılmaktadır. Bileşimlerinde farklı kil ve kil dışı mineraller yer almasına rağmen ağırlıklı olarak Sodyum Bentonit (NB), Kalsiyum Bentonit (CB) ve Ara Tip Bentonit (NCB) olmak üzere üç tip bentonit bulunmaktadır. Bu adlandırma yapılırken kimyasal analiz sonuçlarına bağlı olarak Eşitlik 1'de verilen hesaplama yöntemi kullanılmaktadır. Bu oran 1 ve daha büyük bir değerde ise NB; 1/3-1 aralığında ise NCB ve 1/3 değerinden küçük ise CB olarak adlandırma yapılmaktadır (Çinku, 2008; Akbulut, 1996). Ülkemiz rezervleri bu bağlamda değerlendirildiğinde ağırlıklı olarak NCB tipi bentonitlerden oluştuğu görülmektedir. NB ve CB tipi bentonitler ise nispeten daha az miktarda bulunmaktadır. NB tip bentonitler ağırlıklı olarak Çankırı ve

Tokat bölgelerinde yer alırken CB tip bentonitler ise Ordu bölgesi civarında bulunmaktadır.

$$\frac{Na_2O + K_2O}{CaO + MgO} \quad (1)$$

Yapılan çalışmada, Ordu bölgesine ait CB tipi bentonitin mevcut karakterizasyon yöntemlerine ilave olarak UV-Vis absorpsiyon spektroskopi incelemesi yapılmıştır. Bu sayede hem farklı bir tanımlama metodu hem de endüstriyel kullanım alanları açısından farklı bir değerlendirme yönteminin kullanılması sağlanacaktır. Ayrıca çeşitli kullanım alanları için de hammadde potansiyeli oluşturulabilecektir.

KARAKTERİZASYON ÇALIŞMALARI

Ülkemizin bentonit rezevleri incelendiğinde, Ordu ili bulundurduğu CB tip bentonitler ile ön plana çıkmaktadır. Ağırlıklı olarak Ünye ve Fatsa ilçelerinde yer alan maden ocakları ve endüstriyel fabrikalar ile hem yurtiçi hem de yurtdışı bentonit ticaretinde önemli bir konumdadır.

Yapılan bilimsel çalışmalar neticesinde Ünye bölgesine ait bentonitlerin sulu süspansiyonlarda plastisite, tiksotropi, jelleşme ve akış reolojisi bakımından diğer bentonit tiplerine göre daha düşük seviyelerde olduğu belirlenmiştir. Bu sebeple başta sondaj sektörü olmak üzere şişme özelliğinin önemli olduğu alanlarda kullanım imkanı bulunmamaktadır. Ancak, özel amaçlı boya üretiminde bağlayıcı materyal, kimya endüstrisinde absorban malzemesi, gıda ürünlerinin berraklaştırılmasında ve

ağartılmasında katkı malzemesi ve kedi kumu gibi farklı alanlarda yüksek kalitede CB kullanılabilmektedir.

Çalışma kapsamında kullanılan bentonit numuneleri, Ordu ili Ünye ilçesi sınırlarında yer alan özel amaçlı ticari bir maden sahasından temin edilmiştir. Temin edilen bölgeye ait yer bulduru haritası Şekil 2'de belirtilmiştir.

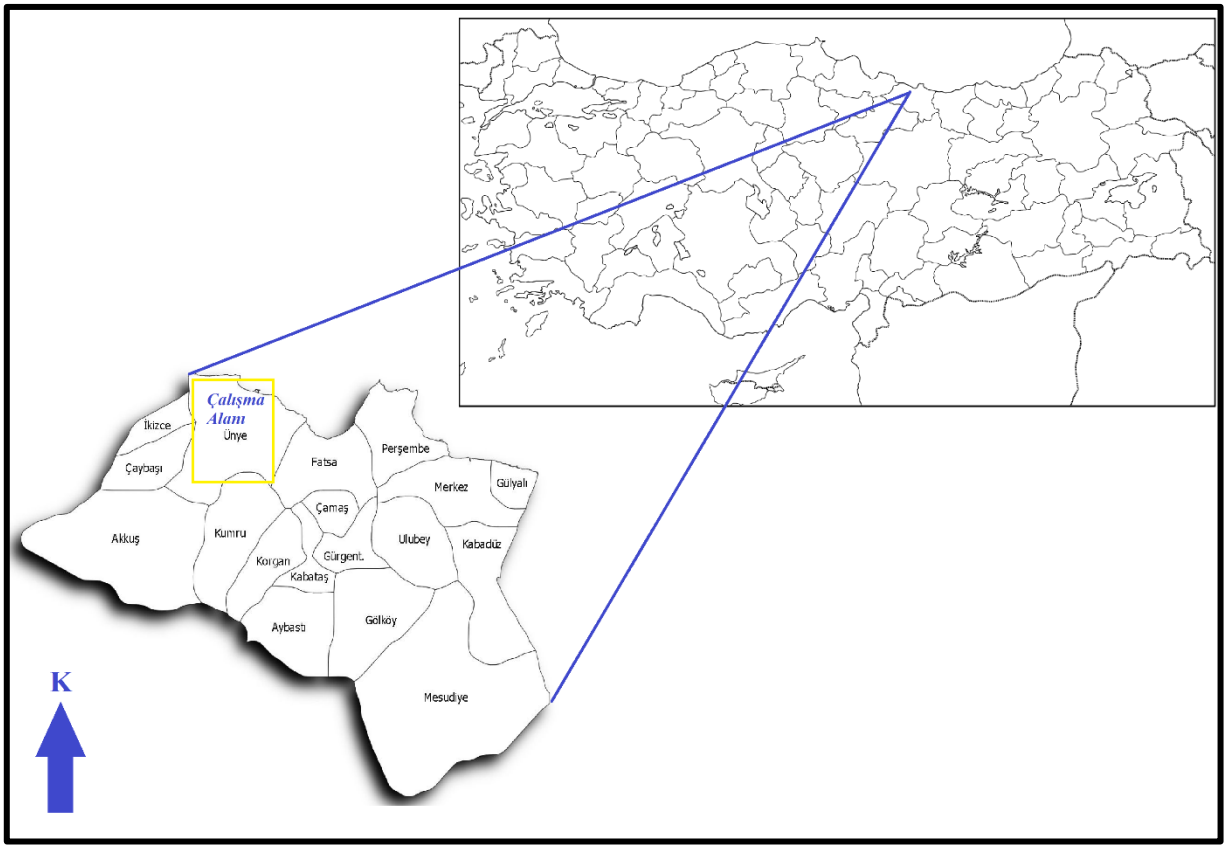

Şekil 2. Temin edilen numunelere ait ölçeksiz yer bulduru haritası

Çalışma kapsamında temin edilen bentonit numunelerinin karakterizasyon tanımlamaları amacıyla X-ışını floresans spektrometresi (XRF) (Rigaku marka ZSX Primus II model), X-ışını difraksiyon spektrometresi (XRD) (PANalytical marka Empyrean model), taramalı elektron mikroskobu (SEM) (FEI marka Quanta 650 model) ve Brunauer-Emmett-Teller yüzey alan analizi (BET) (COSTECH marka Sorptometer 1042 model) ile kimyasal ve morfolojik incelemeleri yapılmıştır. Bu analizler neticesinde ise XRF analiz sonuçları Çizelge 1'de verilmektedir. Ayrıca XRD kırınım deseni ve SEM görüntüleri sırasıyla Şekil 3 ve Şekil 4'te verilmiştir.

Çizelge 1. Temin edilen numunenin XRF analizi

	SiO_2	Al_2O_3	Na_2O	CaO	K_2O	MgO	Fe_2O_3	TiO_2	CuO	ZnO	ZrO_2	K.K.
%	65,94	20,14	0,87	4,97	0,45	0,44	2,89	0,22	0,032	0,008	0,03	4,01

Bentonit tiplerinin belirlenmesi için verilen denklem Eşitlik 1'de verilmiştir. Bu denkleme göre çalışma kapsamında kullanılan numunenin oranı ~0,24 olarak hesaplanmıştır. Dolayısıyla 1/3 değerinden küçük olduğu için CB tip bentonit olarak tanımlanmaktadır.

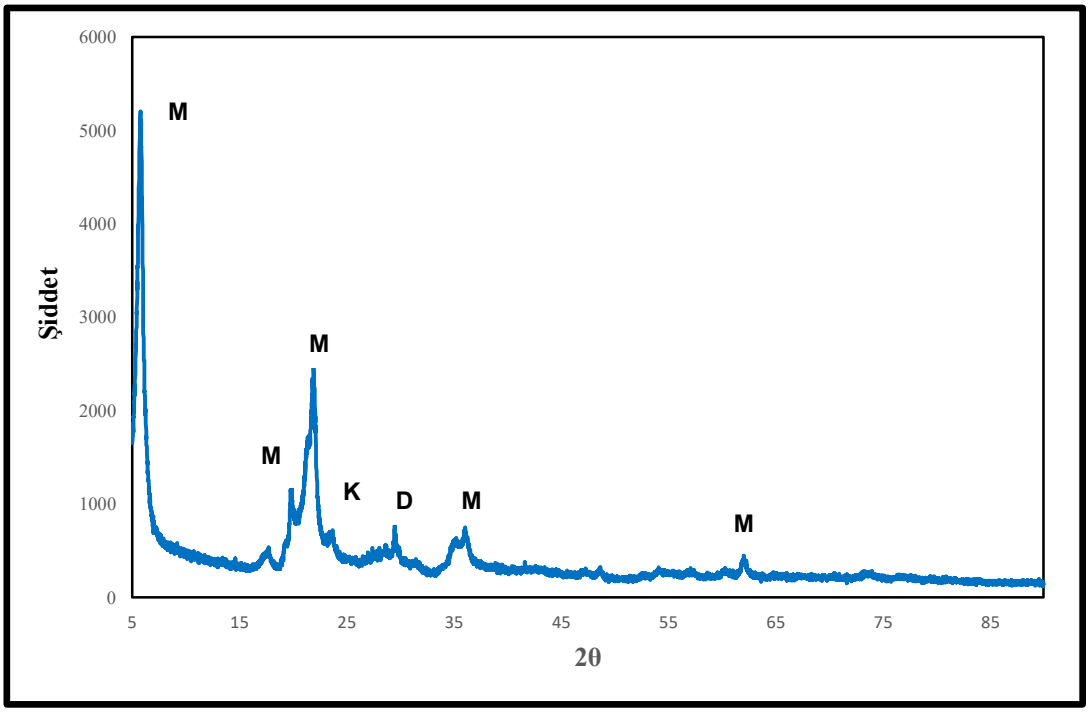

Şekil 3. Temin edilen numunenin XRD kırınım deseni

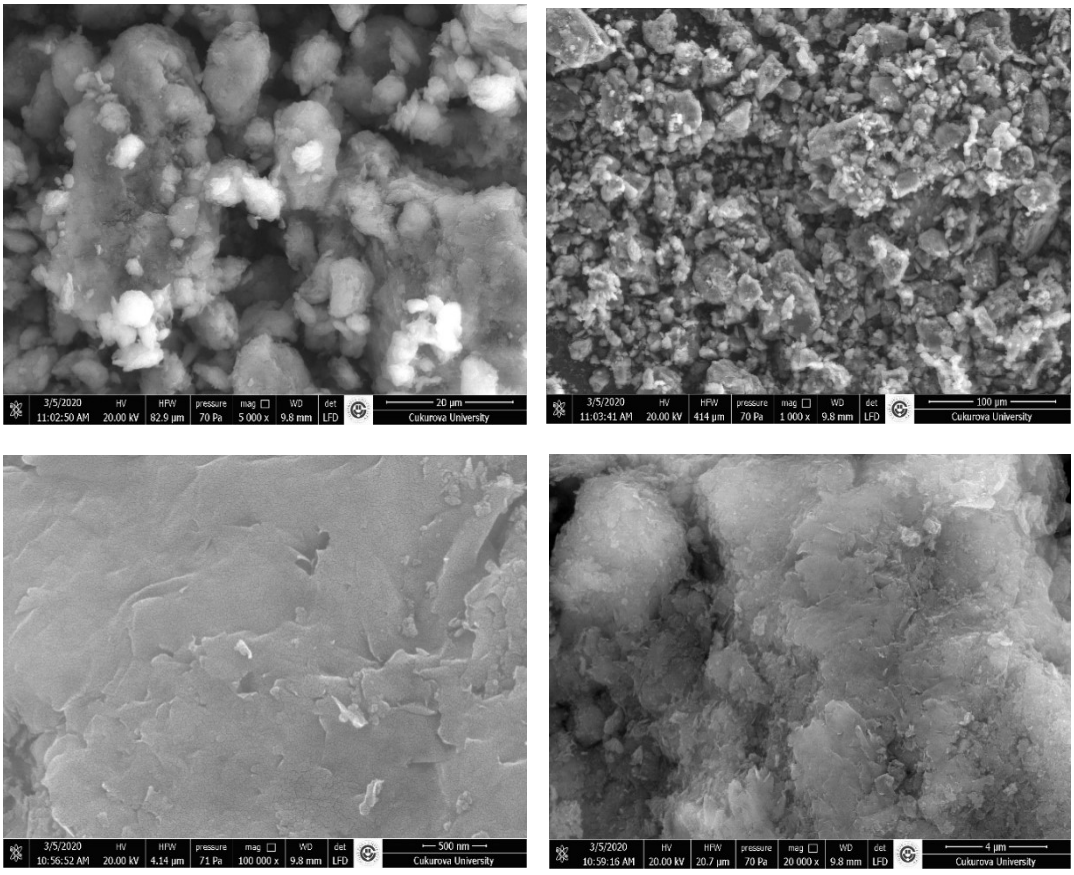

Şekil 4. Temin edilen Numunelerin SEM görüntüleri

Yapılan karakterizasyon çalışmaları değerlendirildiğinde, XRD kırınım deseninin montmorillonit mineralini temsil ettiği görülmektedir. Kırınım deseninde ise yüksek oranda montmorillonit minerali bulunmakla birlikte düşük oranda kuvars ve dolomit gibi kil dışı minerallerin de yer aldığı görülmektedir. SEM görüntülerinde ise tabakalı yapı ve bentonit uyumlu morfolojisi görülmektedir. Bu sonuçlar değerlendirildiğinde, çalışma kapsamında kullanılan numunenin yüksek oranda montmorillonit içeren bentonit olduğu ve kimysal analiz sonucu yapılan hesaplama ile CB tip olduğu belirlenmiştir.

UV-VIS ABSORPSİYON SPEKTROSKOPİSİ

Temin edilen CB tip bentonitler için 200-1100 nm dalga boyu arasında optik ölçüm yapılmış olup; ölçümler sonucu elde edilen UV-Vis absorpsiyon spektroskopisi Şekil 5'te verilmiştir.

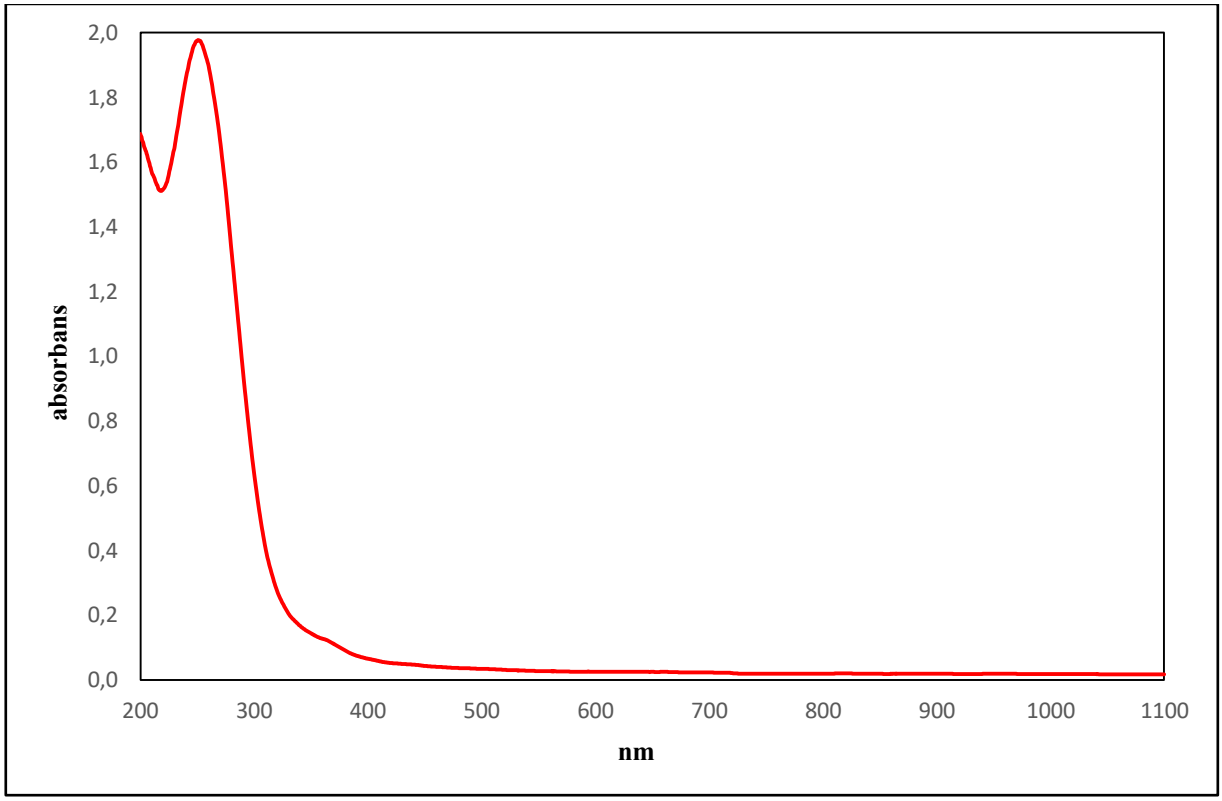

Şekil 5. Ünye (Ordu) bölgesine ait kalsiyum tip bentonitlerin UV-Vis absorpsiyon spektrumu

Şekil 5'te verilen spektrum incelendiğinde farklı dalga boyu aralıklarında safsızlık oluşumuna sebep olan kil dışı minerallerden kaynaklı çeşitli absorbans değerlerinin olduğu görülmektedir. Tetrahedral ve oktahedral yapılarda yer alan Fe^{+3} iyonlarına bağlı olarak da yüksek absorbans değerleri meydana gelmektedir. Ancak bu değerlerin genel olarak 200-400 nm aralığında değişim gösterdiği; 400-1100nm aralığında ise sabit bir dağılım olduğu görülmektedir. Detaylı olarak incelendiğinde ise 200 nm dalga boyunda yaklaşık olarak 1,6 absorbans değerinde olmasına rağmen 230-235 nm dalga boyu aralığına ulaşana kadar azalma meydana geldiği görülmektedir. Devamında 275 nm dalga boyuna kadar absorbans değeri artış göstermektedir. Son olarak ise 400-420 nm aralığına kadar bir düşüş meydana gelmekte ve 1100 nm dalga boyu değerine kadar önemli değişimler olmamaktadır.

Literatürde yer alan bilimsel çalışmalar incelendiğinde Şekil 5'te verilen grafiğin dünyanın önemli bentonit yataklarına (özellikle CB tip) ait absorpsiyon spektroskopileri ile yüksek oranda benzerlik gösterdiği anlaşılmaktadır. Dolayısıyla CB tip bentonitler için genelleştirilmiş yaklaşımlarda bulunulmasına imkan sağlamaktadır.

SONUÇLAR

UV-Vis absorpsiyon spektroskopisi başta fizik ve kimya olmak üzere birçok bilimsel alanda yaygın olarak kullanılmaktadır. Analizi yapılacak olan malzemenin molekül veya inorganik iyonları ve bileşiklerin tayini yapılabilmektedir. Ayrıca çözelti veya süspansiyon halindeki fonksiyonel grupların tespiti, organik ve inorganik bileşiklerin nicel tayini, sıcaklığa bağlı reaksiyon mekanizmaları, denge sabitlerinin bulunması, bileşenlerin saflık oranlarının tayini ve türbidimetrik çalışmalarda kullanılabilmektedir.

Bu kapsamda, Ünye (Ordu) bölgesine ait CB tip bentonitlerin kullanım alanlarında yaygın olarak kullanılan karakterizasyon yöntemlerine ilave bir analiz yöntemi olabileceği düşünülmektedir. Bu durum bentonitin ilaç, kozmetik, ağartıcı, gıda ve boya sektörleri başta olmak üzere farklı alanlarda da kullanılabilirliği için bir karakterizasyon metodu olabilmektedir.

KAYNAKLAR

Akbulut, A. (1996). Bentonit. MTA eğitim serisi no: 32, Ankara.

Bakır, S., Akbulut, A., Kapkaç, F., Karahan, D.S., Çetin, C. (2012). Türkiye Bentonit Envanteri. MTA Envanter Serisi No: 204, Ankara.

Çinku, K. (2008). Aktivasyon yöntemleri ile bentonitten su bazlı kıvamlaştırıcı üretiminin araştırılması. Doktora Tezi. İstanbul Üniversitesi Fen Bilimleri Enstitüsü. İstanbul.

El-Nagar, D. A., Sary, D. H. (2021). Synthesis and characterization of nano bentonite and its effect on some properties of sandy soils. *Soil and Tillage Research*, *208*, 104872.

Erdem B. (2004). Na-Bentonit ve organo-bentonit üzerine boya adsorpsiyonunun incelenmesi. Yüksek Lisans Tezi. Anadolu Üniv. Fen Bilimleri Enstitüsü. Eskişehir.

Hancıoğlu Ç. (2015). Kaolin ve bentonit türü killerde bulunan silikaların belirlenmesi. Yüksek Lisans Tezi. Ankara Üniversitesi Fen Bilimleri Enstitüsü. Ankara.

Holtz, R., Kovacs, W. (2010). Geoteknik Mühendisliğine Giriş. Ankara, Gazi Kitapevi.

Kayıkçı N. 1989. Eskişehir yöresi bentonitlerinin yağ ağartma kapasitelerinin belirlenmesi ve boyarmadde adsorpsiyonlarının incelenmesi. Doktora Tezi. Anadolu Üniv. Fen Bilimleri Enstitüsü. Eskişehir.

Kök, O. E., (2017). Nanobentonit Eldesi ve Karakterizasyonu. Yüksek Lisans Tezi. İskenderun Teknik Üniversitesi Mühendislik ve Fen Bilimleri Enstitüsü. Hatay.

Yücel, B., Gül Ö. (2018). Dünyada ve Türkiye'de bentonit. MTA Genel Müdürlüğü Fizibilite Raporları Daire Başkanlığı. Ankara.

YAŞ ÖĞÜTME VE MEKANİK DAĞITMANIN KIZILDAM HALLOYSİT CEVHERİNİN SİNTERLEME ÖZELLİKLERİNE ETKİSİ

EFFECT OF WET GRINDING AND MECHANICAL DISPERSION ON THE SINTERING PROPERTIES OF KIZILDAM HALLOYSITE ORE

E. Durgut [1], M. Terzi [2], I. Kursun Unver [2], M. Cinar [3], O. Ozdemir [2,*]

[1] *Canakkale Onsekiz Mart University, Can Vocational School*
[2] *İstanbul Üniversitesi-Cerrahpaşa, Mühendislik Fakültesi, Maden Mühendisliği Bölümü*
*(*Sorumlu yazar: orhanozdemir@iuc.edu.tr)*
[3] *Canakkale Onsekiz Mart University, Department of Mining Engineering, Faculty of Engineering*

ÖZET

Kaolin grubu kil cevherleri genellikle seramik endüstrisinde değirmenlerde öğütülerek bünye kompozisyonuna katılmaktadır. Öğütme esnasında iri boyutlu ve sert karakterli empürite olarak sayılan mineraller ince boyuta geçerek bünye kompozisyonuna girmekte ve kalite kaybına neden olan hatalara yol açmaktadırlar. Bu çalışmada Kızıldam halloysit cevherinin sodyum hegzametafosfat varlığında mekanik işlemle dağıtıldıktan sonra 212 µm'luk elek ile sınıflandırılarak, demir içerikli sert minerallerin göreceli olarak daha yumuşak kaolin grubu kil minerallerinden ayrılması sağlanmıştır. Mekanik dağıtma sonucu elde edilen -212 µm tane boyutuna sahip malzeme ve tüvenan cevher ayrı koşullarda hazırlandıktan sonra duvar karosu (1145°C, 49 dk.) ve granit (1205°C, 63 dk.) şartlarında sinterlenerek % küçülme, su emme ve renk değerleri açısından karşılaştırılmıştır. Tüvenan cevherin yaş öğütülmesiyle elde edilen hammadde pişmesinde L (beyazlık) değeri sırasıyla duvar karosu ve granit pişirim şartlarında 64,55 ve 58,14 olarak elde edilirken, mekanik dağıtma ve sınıflandırma sonucunda elde edilen malzeme için ise 73,07 ve 70,76 olarak bulunmuştur. Mekanik dağıtma ile empürite uzaklaştırma işleminin sinterlenmiş ürünlerin beyazlık (L) değerini arttırıldığı görülmüştür.

Anahtar Sözcükler: Kil mineralleri, halloysit, mekanik dağıtma, sinterleme, seramik.

ABSTRACT

Kaolin type clay ores are generally ground in mills in the ceramic industry and are included in the body composition. During grinding, hard, coarse-sized impurities are ground into finer size, got involved the body composition and increased defects that cause loss of quality. In this study, the Kızıldam halloyite ore was dispersed by mechanical mixing in the presence of sodium hegzametaphosphate, than it was eliminated from the 212 µm sieve, allowing the separation of hard minerals containing iron-bearing minerals from the relatively soft kaolin group clay minerals. -212 µm sized material that was gained from mechanical mixing and raw halloysite that was ground in the wet media were sintered in the wall tile (1145°C, 49 min.) and porcelain body (1205°C, 63 min.) sintering conditions, then the sintered materials were compared in terms of shrinkage, water absorption and color values. The L (whiteness) values of the materials that were gained with wet grinding were obtained as 64.55 and 58.14 in wall tile and porcelain sintering conditions respectively, while 73.07 and 70.76 were found for mechanical distribution. It was observed that the empurity removal from the halloysite ore by mechanical mixing increased the whiteness (L) value of the sintered product.

Keywords: Clay minerals, halloysite, mechanical mixing, sintering, ceramics.

GİRİŞ

Kil mineralleri kendine has kimyasal ve fiziksel özelliklerinden dolayı çok eski dönemlerden beri insanlar tarafından kullanılan, doğada yaygın olarak bulunan önemli bir endüstriyel hammadde grubudur. Killer malzeme tanımı olarak yeterince su ilave edildiğinde plastikleşerek kullanıldığı bünyeye şekil vermeye yarayan, kuruyunca ve pişirildiğinde mukavemet kazanan hammaddeleri ifade etmektedir. Bu özelliklerinden dolayı killerin kullanımıyla ilgili birçok araştırma yapılmış ve günümüzde de yapılmaya da devam etmektedir (Ferrari ve Gualtieri, 2006; Kahraman, 2006; Tarhan ve Tarhan, 2019). Doğal kil mineralleri seramik endüstrisi için önemli hammaddelerdir. Kil mineralleri öncelikle seramik üretimi olmak üzere bunun yanında kâğıt, boya, plastik ve diğer sanayi kollarında da kullanılmaktadır (Murray, 2000). Kilin seramik endüstrisine katkı sağlayan özellikleri kimyasal bileşim, pişme öncesi ve sonrası mukavemet, termal özellikler, sinterleme sırasında oluşturduğu fazlar ve refrakterliktir (Ngun vd., 2011). Bu özelliklerin kil minerallerinin seramik endüstrisinde optimize edilerek kullanılması büyük bir öneme sahiptir.

Kil mineralleri literatürde, oluştukları tabaka sayılarına göre sınıflandırılmaktadır (Bergaya ve Lagali, 2006). Kaolin grubu kil mineralleri bir oktahedral tabakayla bir tetrahedral tabakanın birleşmesiyle oluşmuştur. Grubun en yaygın bulunan kil minerali kaolinit olmakla beraber dikit, nakrit ve halloysit mineralleri de bu grupta yer almaktadır. Kaolin grubu kil mineralleri seramik endüstrisinde sinterleme sonrası sergilediği beyaz pişme rengi, hidrofobisite, düşük görünür porozite, ürüne kattığı optik ve elektriksel özellikleri nedeniyle tercih edilmektedir (Chandrasekhar ve Ramaswamy, 2002). Kaolin grubu minerallerinin termal davranışı 100°C'ye kadar nem içeriğinin uzaklaşması şeklindedir. Sıcaklık 400-500°C'ye ulaştığında minerale bağlı kimyasal su yapıdan giderilmekte ve metakaolen adı verilen puzolanik malzeme oluşmaktadır. Sıcaklık 900°C'ye ulaştığında birincil mullit kristalleri oluşmaktadır, 1000–1100°C'de ise birincil mullit kristalleri uzayarak ikincil ve üçüncül mullit kristalleri oluşmaktadır (Castelein vd., 2001).

Kil mineralleri feldspatik kayaçların bozunumu ve başkalaşımı sonucunda oluşmaktadır. Birincil kil yatakları yerinde oluşmuş cevherler olup düşük miktarda safsızlık içermektedirler. İkincil kil yatakları taşınmayla birlikte ana kayaçtan uzakta oluşurlar ve bu esnada yapılarına kuvars, mika, demirli ve titanyumlu mineralleri safsızlık olarak alabilmektedirler. Bu safsızlıkların seramik bünye üzerinde olumsuz etkileri bulunmaktadır (Mahmoudi vd., 2017). Özellikle titanyumlu ve demirli mineraller pişirim esnasında ürünün renginin koyulaşmasına neden olarak özellikle sırlı ürünlerde istenilen dekoratif uygulamaların elde edilmesini zorlaştırmaktadır. Diğer yandan kuvars minerali sinterleme esnasında cam oluşumu sağlayıp bünyeye olumlu etkileri olan mullit kristal oranını azaltmaktadır. Mika mineralleri ise pişirim esnasında ürün üzerinde deliklenmeye neden olarak ürün kalitesini azaltmaktadır.

Türkiye'deki bilinen halloysit kaynakları Biga Yarımadası'nda bulunmaktadır. Biga Yarımadası, Çanakkale/Yenice bölgesindeki Alt Triyas yaşlı Karakaya Karmaşığı'yla ilişkili mostra halindeki temel kayaçlardan oluşmaktadır. Temel kayaçlar üzerinde ise andezitik piroklastik/lavlardan oluşan Alt Miyosen yaşlı volkanojenik yığın bulunmaktadır. Volkanojenik yığın içinde kireçtaşlarıyla alakalı oluşmuş Kuzey-Güney doğrultusunda eni yaklaşık 45-50 m, uzunluğu 125-130 m ve derinliği yaklaşık 12-15 m halloysit zuhuru vardır. Zuhur içerisinde farklı boyutlarda kireçtaşı blokları da haizdir. Bölgede bulunan halloysit mineralleri genellikle 10 Å yapısında olup bunun yanında kaolinit, smektit, illit, alünit, jakopsit, pirokroit, hematit, götit ve birnessit gibi mineraller de bulunmaktadır (Ece vd., 2008). Halloysitleşmenin meteorik ve/veya magmatik kökenli hidrotermal çözeltilerin faylar boyunca yükselerek andezitik piroklastikleri etkilemesi sonucu gerçekleştiği sanılmaktadır. Bölgedeki halloysit oluşumuna en önemli etkenlerden birisinin ortamın pH'sını düzenleyen kireçtaşlarının olduğu düşünülmektedir (Laçin ve Yeniyol, 2006; Aydın vd., 2019).

Bu çalışmada halloysit cevherine uygulanan mekanik dağıtma işleminin yaş öğütmeye kıyasla hammadde sinterleme özelliklerine ve elde edilen malzemelerin karakterizasyonuna etkilerinin incelenmesi amaçlanmıştır.

MALZEME VE YÖNTEM

Malzeme

Deneysel çalışmalar için Çanakkale ili Yenice ilçesi Kızıldam köyündeki halloysit kaynağından alınan numune öncelikle çeneli kırıcı ile kırılarak -10 mm tane boyutuna getirilmiştir. Sonrasında konileme-dörtleme yöntemiyle temsili olarak azaltılan örnek üzerinde XRF yöntemi ile kimyasal analizler gerçekleştirilmiştir. Numunenin 105°C'deki etüvde 4 saat boyunca kurutularak ölçülen rutubet içeriği %9,4 olarak tespit edilmiştir. Çizelge 1'de -10 mm boyutuna getirilmiş tüvenan halloysit numunesinin kimyasal analizi görülmektedir.

Çizelge 1. Tüvenan halloysit numunesinin kimyasal analizi

*K.K.	SiO_2	Al_2O_3	TiO_2	Fe_2O_3	CaO	MgO	Na_2O	K_2O
12,0	50,9	29,7	0,7	3,9	0,2	0,4	0,2	1,1

*K.K: Kızdırma kaybı

Çizelge 1'den görüldüğü üzere, numunede halloysit mineralinin kimyasal içeriğinde bulunmayan TiO_2, Fe_2O_3, CaO, MgO, Na_2O ve K_2O de tespit edilmiştir. Ayrıca numunenin kalitatif mineralojik analizinde (XRD) ise kuvars, kaolinit, halloysit, gibsit ve götit minerallerinin varlığı tespit edilmiştir. (Şekil 2).

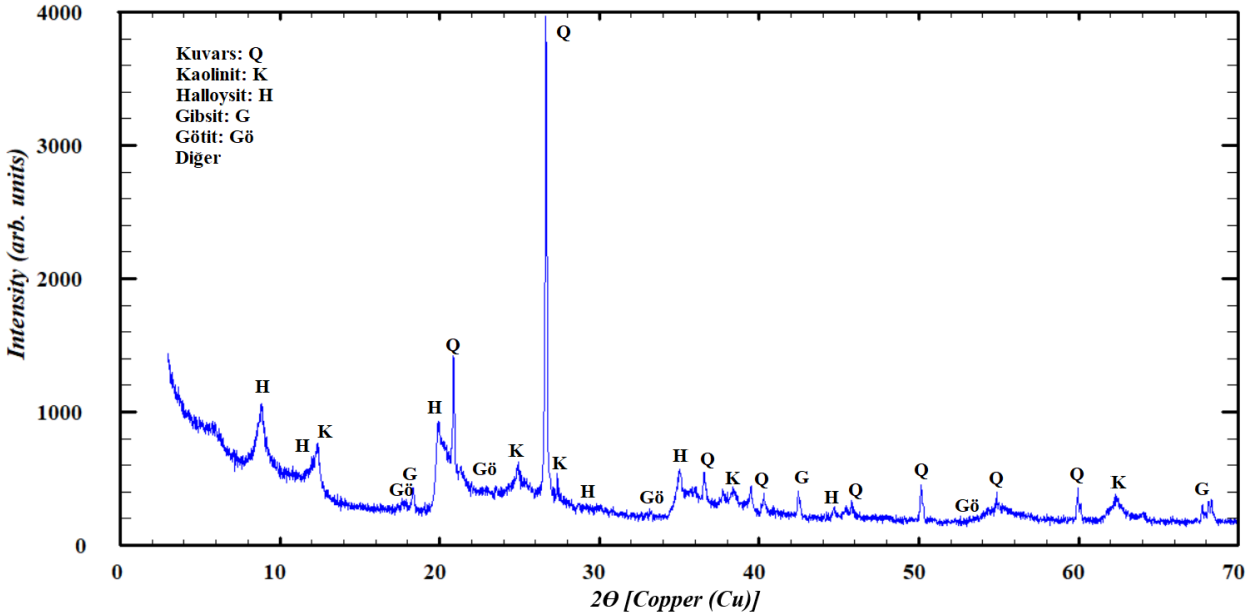

Şekil 2. Tüvenan halloysit numunesinin mineralojik analizi

Yöntem

Seramik bünyeler hazırlanırken sinterleme işlemine fayda sağlamak için yüzey alanının oldukça yüksek olması istenir. Bu nedenle bünyeyi oluşturan hammaddeler tane boyut küçültme işlemlerine tabi tutulmaktadırlar. Seramik bünye hazırlama işlemlerinde kaolin grubu kil mineralleri değirmenlerde öğütülerek tane boyutları küçültülmektedir.

Kızıldam halloysit cevherine uygulanan öğütme ve mekanik dağıtma işlemlerinin sinterleme özelliklerine etkisinin incelenmesi kapsamında yaş öğütme işleminde laboratuvar tipi jet değirmen ve mekanik dağıtma işleminde ise pilot çaplı mekanik dağıtıcı kullanılmıştır.

Yaş öğütme işleminde -10 mm boyutuna kırılmış halloysit cevheri kuru hammadde miktarına oranla dispersant olarak %0,75 sodyum hegzametafosfat ve saf su ile pülpte katı oranı %35 olacak şekilde laboratuvar tipi jet değirmende öğütülmüştür. Pişirme işlemi yapılacak hammaddelerin boyut kontrolü olarak elek üzerindeki kuru madde bakiyesi baz alınmıştır. Bu değerler duvar karosu pişirim şartları için +63 µm ve granit pişirim şartları için +45 µm için %2 olacak şekilde çalışılmıştır.

Mekanik dağıtma işleminde ise -10 mm boyutuna kırılmış halloysit cevheri yine kuru hammadde miktarına oranla dispersant olarak %0,75 sodyum hegzametafosfat ve saf su ile pülpte katı oranı %35 olacak şekilde mekanik dağıtıcıda 500 devir/dk hızında 4 saat süresince karıştırılmış ve eleme ile -212 µm boyutuna sınıflandırılmıştır.

Hazırlanan pülpler 150 µm'lik elek ile sınıflandırılıp etüvde 105^{o}C'de 4 saat süresince kurutulmuştur. Kurutulan pülp agat öğütücü kullanılarak öğütülmüş, %6 rutubetlendirilerek granüle edilmiştir. Elde edilen granüller duvar karosu şartları için 325 kg/cm^2 ve granit şartları için 400 kg/cm^2 sıkıştırma basıncında 5x5 cm'lik dairesel şekilli olacak şekilde el presinde şekillendirilmiştir. Hazırlanan 5x5 cm'lik tabletler yine etüvde 105^{o}C'de 4 saat süresince kurutulduktan sonra duvar ve granit şartlarında pişirilmiştir. Şekil 2'de hammadde hazırlama ve sinterleme işlemlerinin akım şeması halinde gösterimi bulunmaktadır.

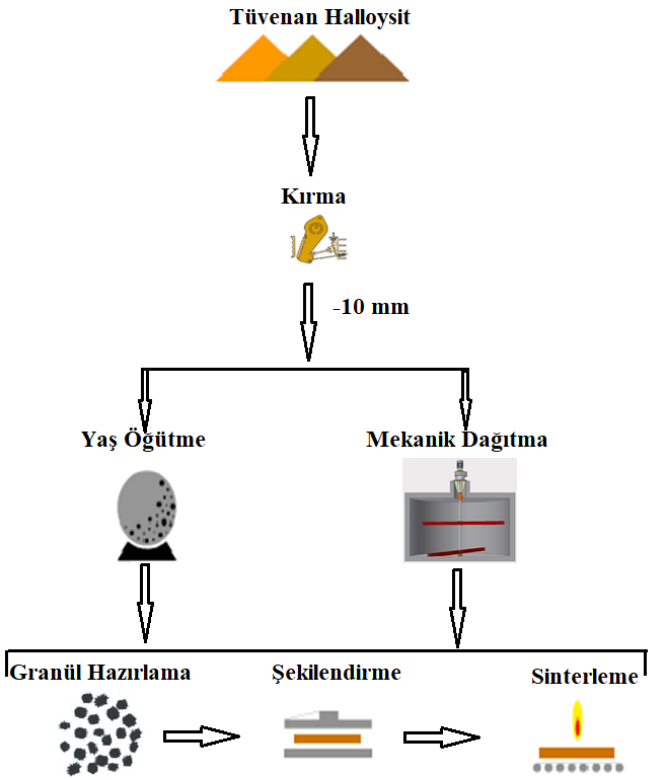

Şekil 2. Hammadde hazırlama ve sinterleme işlemleri akım şeması

Pişme sonrası tabletler küçülme, su emme ve renk değerleri olacak şekilde sinterleme özellikleri açısından incelenmiştir. Küçülme ölçümü tabletlerin pişme öncesi ve sonrası kumpasla ölçülerek, ilk ölçüme göre elde edilen % fark şeklinde belirlenmiştir. Küçülme değeri TSE EN 10545-2 standardına, su

emme testi TSE EN 10545-3 standardına ve renk ölçümleri ise TSE EN 10545-16 standardına uygun olarak gerçekleştirilmiştir.

BULGULAR

-10 mm Boyutuna Kırılmış Halloysit Cevherinin Tane Boyut Dağılımı Analizi

Halloysit cevherinin boyut fraksiyonlarına göre kimyasal içeriğinin değişiminin incelenmesi amacıyla -10 mm boyutuna kırılmış cevher kuru elemeyle -10+5, -5+2, -2+1, -1+0,5 ve -0,5 mm boyut gruplarına ayrılarak her boyut grubu kimyasal analize tabi tutulmuştur (Çizelge 2).

Çizelge 2. -10 mm boyutuna kırılmış halloysit numunesinin boyut gruplarına göre kimyasal analizi

Tane boyut, mm	K.K.	SiO_2	Al_2O_3	TiO_2	Fe_2O_3	CaO	MgO	Na_2O	K_2O
-10+5	10,4	51,6	27,7	0,7	8,0	0,0	0,3	0,0	1,3
-5+2	12,5	50,1	31,0	0,6	4,7	0,0	0,2	0,0	1,0
-2+1	11,9	51,9	30,4	0,6	3,6	0,0	0,2	0,0	1,3
-1+0,5	11,8	52,7	30,2	0,7	3,1	0,0	0,3	0,0	1,2
-0,5	12,5	53,0	29,5	0,7	2,7	0,0	0,3	0,0	1,3

Çizelge 2'den görüldüğü üzere tane boyut artıkça demir içeriğinin arttığı görülmektedir. -0,5 mm boyutundaki Fe_2O_3 içeriği %2,7 iken -10+5 mm boyut grubu için bu değerin %8,0'a çıktığı görülmektedir. Kaolin grubu kil mineralleri kimyasal açıdan Al_2O_3, SiO_2 ve kızdırma kaybı olarak ifade edilen H_2O'dan oluşmaktadır. Buna göre kil minerallerinin Al_2O_3 değerinin en yüksek olduğu (%31,0) -5+2 mm boyut grubunda yoğunlaştığı düşünülmektedir. Diğer yandan kuvars mineralini işaret eden SiO_2 içeriğinin (%53,0) ince boyut grubunda (-0,5 mm) yoğunlaştığı görülmüştür.

-10 mm Boyutuna Kırılmış Halloysit Cevherinin Mekanik Dağıtma Sonuçları

Halloysit cevherinin mekanik dağıtmayla dağıtıldıktan sonra 212 µm'luk açıklığa sahip elekten elenerek iki boyut fraksiyonuna ayrılmıştır. Çizelge 2'de mekanik dağıtma sonrası +212 µm ve -212 µm boyut grubuna ayrılmış fraksiyonların kimyasal analiz sonuçları görülmektedir.

Çizelge 3. Mekanik dağıtma uygulanmış halloysit cevherinin boyuta göre kimyasal analizi

Boyut	Miktar %	K.K.	SiO_2	Al_2O_3	TiO_2	Fe_2O_3	CaO	MgO	Na_2O	K_2O
+212 µm	17,5	11,9	50,2	26,4	0,6	9,6	0,1	0,2	0,1	1,0
-212 µm	82,5	12,2	50,9	31,3	0,7	3,2	0,1	0,3	0,2	1,2

Mekanik dağıtma işlemi sonucunda yaş elemeyle +212 µm boyut grubunda %17,5 ve -212 µm boyut grubunda ise %82,5 oranında malzeme olduğu görülmüştür. Diğer yandan yapılan kimyasal analizler sonucunda Al_2O_3, SiO_2 ve Fe_2O_3 içerikleri +212 µm boyutu için sırasıyla %26,4, %50,2 ve %9,6 iken -212 µm boyutu sırasıyla %31,3, %50,9 ve %3,2 olarak tespit edilmiştir.

Yaş Öğütme ve Mekanik Dağıtma Uygulanmış Halloysit Cevherinin Sinterleme Davranışı

Yapılan öğütme ve mekanik dağıtma çalışmalarından elde edilen malzemelerin seramik özelliklerindeki değişimi incelemek amacıyla sinterleme testleri yapılmıştır. Sinterleme çalışmaları duvar karosu için 1145°C maksimum sıcaklık ve 49 dk sinterleme süresi ve granit için 1205°C maksimum sıcaklık ve 63 dk sinterleme süresi koşullarında gerçekleştirilmiş olup uygulama şartları ve elde edilen sonuçlar Çizelge 4'te verilmiştir.

Çizelge 4. Yaş öğütme ve mekanik dağıtma uygulanmış malzemelerin sinterleme özellikleri

ÇALIŞILAN KRİTERLER			**Birim**	**Yaş Öğütme**	**Mekanik Karıştırma**
Granül/Toz Rutubeti			**%**	6	
Sıkıştırma Basıncı			**kg/cm^2**	325	
DUVAR KAROSU PİŞME ÖZELLİKLERİ	Maksimum Pişirim Sıcaklığı		**°C**	1145	1145
	Pişirim Süresi		**dk.**	49	49
	Pişme Küçülmesi		**%**	9,12	4,90
	Su Emme		**%**	10,51	17,01
	RENK	L		64,55	73,07
		a		10,36	7,12
		b		13,06	10,01
Granül/Toz Rutubeti			**%**	6	
Sıkıştırma Basıncı			**kg/cm^2**	400	
GRANİT PİŞME ÖZELLİKLERİ	Maksimum Pişirim Sıcaklığı		**°C**	1205	1205
	Pişirim Süresi		**dk.**	63	63
	Pişme Küçülmesi		**%**	9,72	6,22
	Su Emme		**%**	7,95	12,72
	RENK	L		58,14	70,76
		a		9,24	6,31
		b		11,52	9,48

Çizelge 4'ten görüldüğü üzere yaş öğütme uygulanmış halloysit cevherinin küçülme/su emme değerleri duvar karosu ve granit pişirim şartlarında sırasıyla %9,12/%10,51 ve %9,72/%7,95 olarak ölçülürken; mekanik dağıtma uygulanmış halloysit cevherinin küçülme/su emme değerleri duvar karosu ve granit pişirim şartlarında sırasıyla %4,90/%17,01 ve %6,22/%12,72 olarak tespit edilmiştir. Mekanik karıştırmayla iri boyutta kalan demir içerikli minerallerin önemli derecede uzaklaştırıldığı görülmüştür. Yaş öğütmede ise demirli mineraller öğünerek bünye içerisine dâhil olmaktadır. Demir mineralleri 900°C'den itibaren indirgenerek FeO'ya dönüşmektedir. Seramik bünyede bulunan FeO ve serbest silika bir araya geldiğinde ötektik oluşturarak camsı faz oluşumu için gerekli sıcaklığın düşürmekte bu da bünyede camsı faz oluşumunu desteklemektedir (Pekdemir, 2008). Yaş öğütmeyle hazırlanan bünyenin mekanik dağıtmayla hazırlanan bünyeye göre su emme değerlerinin düşük ve küçülme değerlerinin yüksek olması demir içeriğinin yüksek olmasıyla açıklanmaktadır. Diğer yandan L (beyazlık) değerleri duvar karosu ve granit pişirim şartlarında sırasıyla yaş öğütmeyle hazırlanan malzeme için 64,55 ve 58,14 olarak elde edilirken, mekanik dağıtma için ise 73,07 ve 70,76 olarak bulunmuştur. Ferro (+2 değerlikli) demir mineralleri seramik endüstrisinde önemli renk problemleri yaratabilmektedir. Çünkü sinterleme aşamasında ferrik (+3 değerlikli) demire dönüşerek, ürünlere turuncu bir renk vermektedir (Marabini vd., 1993). Mekanik dağıtma uygulanmış halloysit cevherinin yaş öğütmeyle hazırlanan malzemeye göre L (beyazlık) değerinin artmasının nedeni yapısındaki demirli minerallerin uzaklaştırılmasıyla ilgilidir.

TARTIŞMA VE SONUÇ

Kızıldam halloysit cevherinin mineralojik analizinde halloysit, kaolinit, kuvars, gibsit ve götit minerallerinden oluştuğu görülmüştür. Cevherin yapılan kuru elek analizinde özellikle demir içerikli minerallerin iri boyutta kaldığı gözlenmiş, mekanik dağıtmayla da demir içeriğinin iri boyutta arttığı analiz edilmiştir. Buradan cevher içerisindeki demirli empüritelerin göreceli olarak diğer minerallere göre

daha yüksek sertliğe ve iri tane boyutuna sahip olduğu anlaşılmıştır. Yaş öğütmeyle birlikte bu demirli mineraller öğünerek ince boyuta geçmektedir. Bu durum seramik bünyelerde sinterleme aşamasında ürünün beyazlığını düşürerek özellikle beyaz renk istenilen ürün üretiminde ve sırlı ürünlerde yüzeyde istenilen rengin sağlanmasında zorluklar çıkarmaktadır. Bu çalışmada mekanik dağıtma uygulanarak yaş öğütmeye göre Kızıldam halloysit cevherinin kil mineral içeriğinin arttırıldığı ve seramik bünye çalışmalarında pişme sonrası renginin iyileştirildiği görülmüştür. Mekanik dağıtma sonrası manyetik ayırma ve liç çalışmalarıyla ürünün bu özelliklerinin daha da iyileştirilebilceği öngörülmektedir.

KAYNAKLAR

Aydın, Ü., Şen, P., Özmen, Ö., Şen, E., (2019). Biga Yarımadası'ndaki granitoyitlerin (KB Anadolu, Türkiye) petrolojik ve jeokimyasal özellikleri, MTA Dergisi (2019) 160: 81-116.

Bergaya, F., Lagaly, G. (2006). *Chapter 1 General Introduction: Clays, Clay Minerals, and Clay Science*. Developments in Clay Science, 1, 1-18.

Castelein, O., Soulestin, B., Bonnet, J.P., Blanchart, P., (2001). The influence of heating rate on the thermal behavior and mullite formation from a kaolin raw material, *Ceramics International*, 27 (5), 517–522.

Chandrasekhar, S., Ramaswamy, S., (2002). Influence of mineral impurities on the properties of kaolin and its thermally treated products, *Applied clay science, 21*, 133–142.

Ece, O.I., Schroeder, P.A., Smilley, M.J., Wampler, J.M., (2008). Acid-sulphate hydrothermal alteration of andesitic tuffs and genesis of halloysite and alunite deposits in the Biga Peninsula, Turkey. *Clay minerals*, *43 (2),* 281-315.

Ferrari, S., Gualtieri, A.F. (2006). The use of illitic clays in the production of stoneware tile ceramics. *Applied clay science*, *32 (1-2),* 73-81.

Laçin, D., Yeniyol, M., 2006, Andezitik piroklastikler ile ilişkili oluşmuş halloysit yataklarına bir örnek: Soğucak halloysit yatağı (Yenice-Çanakkale). *İstanbul üniversitesi müh. fak. yerbilimleri dergisi*, *19 (1),* 27-41.

Kahraman, S. (2006). Yapı tuğlalarında renk oluşumu. *KSÜ, Fen ve Mühendislik Dergisi*, 9 (1), 125-128.

Mahmoudi, S., Srasra, E., Zargouni, F., (2017). Preparation, qualities and defects of ceramic materials from Tunisian clay minerals. *Surface engineering and applied electrochemistry*, *53 (3)*,295-301.

Marabini, A. M., Falbo, A., Passariello, B., Esposito, M. A., Barbaro, M., (1993). Chemical leaching of iron industrial minerals. XVIll international mineral processing congress, Sydney, p. 23-28.

Murray, H.H., (2000). Traditional and new applications for kaolin, smectite, and palygorskite: A general overview, *Applied clay science*, *17*, 207–221.

Ngun, B.K., Mohamad, H. Sulaiman, S.K., Okada, K., Ahmad, Z.A., (2011). Some ceramic properties of clays from central Cambodia, *Applied clay science*, *53*, 33–41.

Pekdemir A.D., (2008). *Kaolinitik bir kilin sinterleşme özelliklerinin incelenmesi*. Yüksek Lisans Tezi. Ankara Üniversitesi, Türkiye.

Pruett, R.J., Pickering S.M., (2006). Kaolin. Pp. 383-399 in: Industrial minerals and rocks: commodities, markets and uses (J.E. Kogel, N.C. Trivedi, J.M. Barker and S.T. Krukowski, editors) 7th edt. SME. Colorado.

Tarhan, M., Tarhan, B., (2019). Investigation of the usage of Afyon clay in porcelain tile bodies. *Uluslararası Muhendislik Arastirma ve Geliştirme Dergisi*, *11(1)*, 275-281.

YERALTI İŞLETME OPTİMİZASYONU VE İŞLEVSEL PLANLAMA

A TUTORIAL on STOPE OPTIMISATION and OPERATIONAL SCHEDULING

A. Eşiyok [1, *], B. Kahraman [2]

[1] Micromine Pty Ltd, Türkiye temsilcisi
*(*Sorumlu yazar: gesiyok@micromine.com)*
[2] Dokuz Eylül Üniversitesi, Maden Mühendisliği Bölümü

ÖZET

Yeraltı maden işletmesinde üretim miktarını arttırmak ve planlanan periyodik cevher üretim ton-tenör hedeflerini tutturmak amacıyla ekonomik ve tasarım parametreleri kullanılarak yeraltı maden üretim blokları biçimlendirmesi yapabilen madenciliğe özel bilgisayar desteli tasarım yazılımları geliştirilmiştir. Söz konusu yazılımların yeraltı optimizasyonu modülleriyle kaynak blok model veya cevher katı modeli temel alınarak hedeflenen cevher miktar-tenör değerinde yeraltı maden üretim blokları verimli bir şekilde oluşturulabilmektedir. Bu yaklaşım ile maden üretim sürecinde hedeflenen tüvenan cevher üretimini gerçekleştirebilecek işlevsel maden işletme planı oluşturulabilmektedir. Ayrıca belirlenmiş kaynağın ekonomik olarak işletilebilir parçası rezerv olarak belirlenebilmektedir.

Ayrıca üretim kapasitesini arttırmak için verimli (uygun) bir patlatma tasarımına ihtiyaç vardır. Söz konusu yazılımlar patlatma tasarımlarının verimli bir şekilde yapılır hale gelmesini sağlamaktadır. Yeraltı maden işletmelerinde, patlatma deliklerinin cevher sınırları ve maden blokları ile uyumlu olarak tasarlanması, patlayıcı ve sarf malzemelerinin hesaplanması, atım sonrası serbestleşecek pasa ve cevher miktar-tenör hesaplanması alternatifli olarak hızlı bir şekilde oluşturulabilmektedir.

Bu bildiride örnek bir yeraltı maden işletmesinde sektörde kabul görmüş bilgisayar destekli tasarım yazılımı olan Micromine 2022 ile verimli bir yeraltı kazı arını/üretim yeri (stope) planı ve patlatma tasarımı sistemi oluşturmanın metodolojisi ele alınmıştır.

ABSTRACT

Stope optimisation is developed to define a minable portion of ore deposit in an underground mine operation by considering cost and revenue items satisfying the targeted values of projected ore tonnage and grade. Stopes are designed, grade-tonnage is calculated, and extraction order is optimized by getting the solid ore model and resource block model as input. Stopes are transferred to a Gantt Chart to optimise monthly or yearly operation plans by the strategic scheduling. Finally, operational scheduling could be conducted to create a short-term mining plan following the extraction order of stopes defined by the strategic scheduling. Minable reserve could be determined based on the output obtained through stope optimisation and strategic scheduling optimisation.

Ring design in a stope is important to reduce the dilution and to increase the ore production. Rings could be designed to accommodate the exact edge of a vein, especially for thin veins.

A computer application on above mentioned issues are explained in detail by using Micromine 2022 exploration and mining software.

GİRİŞ

Bu çalışmada öncelikle işletme gelir-gider kalemleri dikkate alınarak Micromine Stope (kazı arını-üretim yeri) Optimisation modülü ile kaynağın yeraltı maden işletme yöntemiyle üretilebilecek kısmı rezerv olarak belirlenecektir. Kazı arını (stope) optimizasyonu ile ayrıca optimum ve nihai (ultimate) rezerv, sadece cevher üretim ton ve tenör dikkate alınarak değil, ek olarak net bugünkü değerdeki periyodik değişim dikkate alınarak da belirlenecektir. Stope optimizasyonu sonucu, üretimi ekonomik olduğu belirlenen kazı arını (stope) blokları Micromine Scheduling (planlama) modülü kullanılarak Gantt diyagramına aktarılacak ve Strategic Scheduling Optimisation ile maden ömrü boyunca periyodik üretim hedeflerine uygun olarak kazı arını (stope) bloklarının üretime alma sırası belirlenecektir.

Son olarak ince damarlarda kazı arını (stope) ring (üretim delikleri) tasarımı Micromine Ring Design modülü kullanılarak hazırlanacaktır. Özellikle seyrelmeyi minimize etmek ve yeraltından üretilen cevher kazanım oranını yükseltmek için ring tasarımının önemi vurgulanacaktır.

YERALTI İŞLETME (STOPE) OPTİMİZASYONU VE ÜRETİLEBİLECEK KAYNAK BELİRLEME

Kazı arını (stope) optimizasyonuna başlamak için kaynak blok model, cevher katı model ve topoğrafya modeline gerek duyulur. Kaynak blok model genel olarak cevher katı modelin içindeki tenör dağılımını verir. Şekil 1'de cevher katı model ve topoğrafya, Şekil 2'de kaynak blok model ve topoğrafya gösterilmiştir.

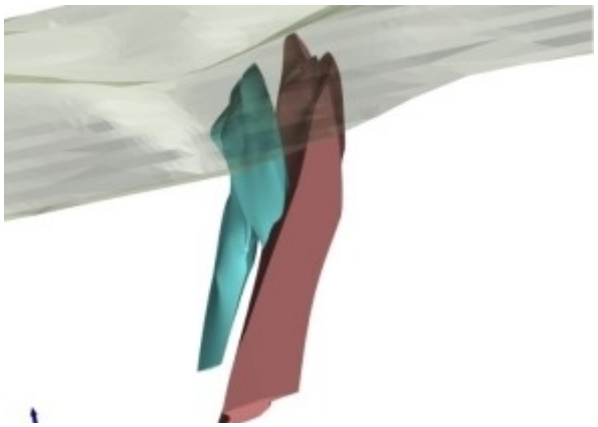

Şekil 1. Cevher katı model ve topoğrafya

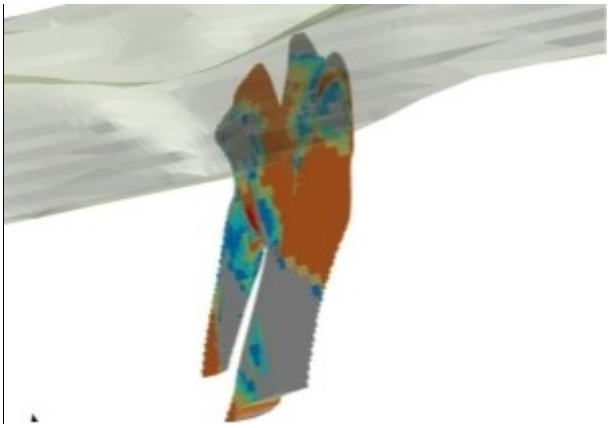

Şekil 2. Kaynak blok model ve topoğrafya

Kazı arını (stope) optimizasyonunda yukardaki temel verilerin yanında aşağıdaki verilerinde girilmesi gerekir. Optimizasyon verilerini girmek için Micromine da Mining / Stope Optimiser ikonları seçilir. Öncelikle temel element seçilir, varsa sınır (cut-off) tenörü belirtilir, sınırlanacak alanlar varsa koordinatlar, poligonlar veya katı modeller ile tanımlanır. Cevher seyrelme ve cevher kazanım oranları belirtilir. Yeraltı cevher üretim ve pasa kazı maliyeti girilir, dolgu yapılıyorsa dolgu maliyeti cevher üretim maliyetine eklenir. Optimum ve nihai (Ultimate) üretim zonları kazı arını (stope) kenarları ile belirleneceğinden kazı arını (stope) boyutları tanımlanır. Kazı arını (stope) yönlendirmesi cevher katı modeli, üretim katı galeri merkez hatları veya yüzey üçgenlemeleri ile yapılabilir. Micromine da Staging (evreleme-hazırlama) diye adlandırılan zonların oluşturulması için Stage (aşama-evre/safha) faktör 0 ile 1 arasında tanımlanır ve zon sayısını belirlemek üzere artış miktarı, örneğin 0.02 olursa, 0.2 – 1 aşama (stage) faktörü alındığında 40 zon demektir.

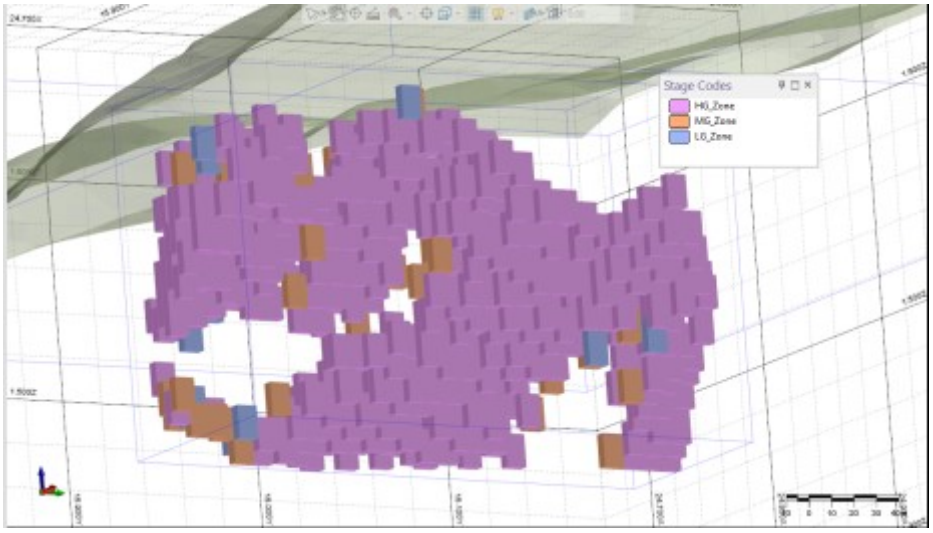

Şekil 3. Üretilebilecek zonlar (Yüksek, orta ve düşük tenörlü stope blokları)

Gerek Micromine tarafından ücretsiz sağlanan Solver (çözücü) ile optimizasyon çalıştırılır. Optimizasyon sonucunda Stage noktaları bir dosyaya kaydedilir. Aşamaların (stage) katı modelleri oluşturularak kaydedilir. Kaynak blok modele ise zonların sınıfları (Ore, inaccessible Ore, Waste vs.), optimum değerleri, Stage Code ve Stage parametreleri kaydedilir. İşte blok modele kaydedilen bu bilgilerle filtreler oluşturularak kaynak blok modelin üretilebilecek parçası tespit edilir. İlave olarak proses maliyeti, yönetim ve idari işler maliyeti, satış geliri ve maliyet bilgileri girilir. Optimizasyon sonrası işletilebilecek stoplar yüksek tenörlü, orta tenörlü ve düşük tenörlü zonları belirler. Şekil 3'de kazı arını (stope) blok kenarları ile sınırlanan bu zonlar farklı renkler ile gösterilmektedir.

Ancak daha önce belirtildiği gibi optimum ve nihai (Ultimate) üretim zonlarını belirlemek için stage analizleri grafiksel olarak yapılabilir. Şekil 4'de stage ton – Net bugünkü değer (NBD-NPV:Net present value) değerleri grafiksel olarak verilmiştir. Şekil 5'de stage ton – altın ppm tenör değerleri grafiksel olarak verilmiştir. Karar verici NPV eğrisinin artık artmadığı, düzleştiği aşama (stage) sonrasını üretim zonu olarak kabul etmeyebilir. Benzer şekilde tenör eğitişinin arzu edilmeyen bir değerden daha aşağı düştüğü bir aşama (stage) sonrası üretim zonu olarak kabul edilmeyebilir.

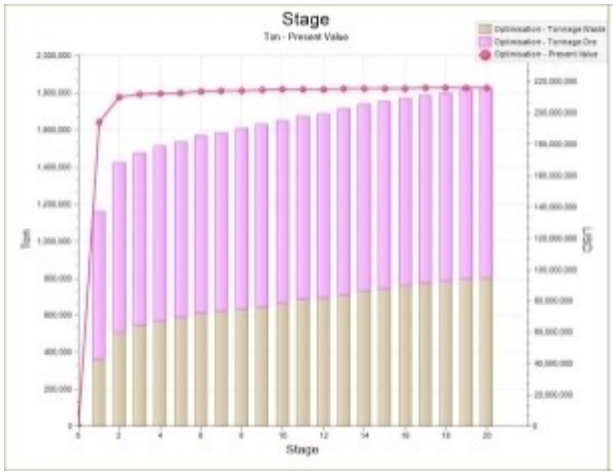

Şekil 4. Stages Ton – NPV

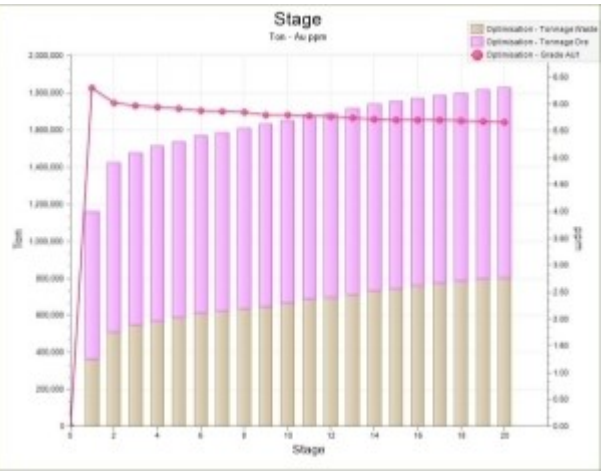

Şekil 5. Stages Tn - Auppm

Aşama (stage) analizlerine benzer şekilde periyod analizleri yapılır. Periyodlar toplam madencilik kazısı ile belirlenir, cevher ve pasa kazısı birlikte ele alınır. Şekil 6'da Periyot ton – İndirgenmiş nakit akışı

(discounted cashflow) değerleri grafiksel olarak verilmiştir. Şekil 7'de Periyod ton – altın ppm tenör değerleri grafiksel olarak verilmiştir. Karar verici indirgenmiş nakit akış eğrisinin artık artmadığı, düzleştiği periyod sonrası üretiml durdurabilir. Benzer şekilde tenör eğrisinin arzu edilmeyen bir değerden daha aşağı düştüğü bir periyod sonrası üretim yapılmayabilir.

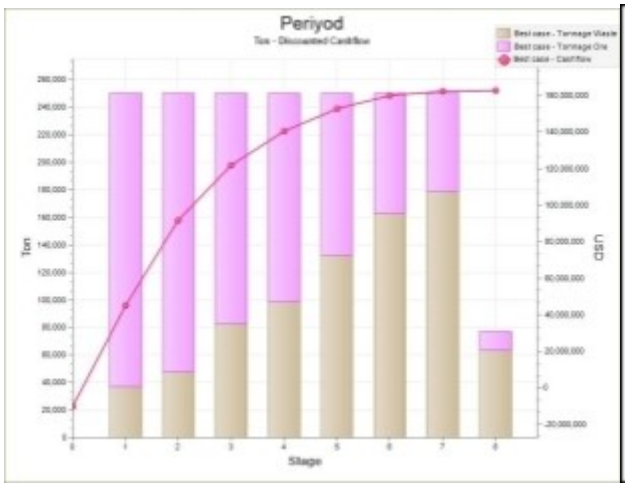

Şekil 6. Periyod Ton – Discounted Cashflow

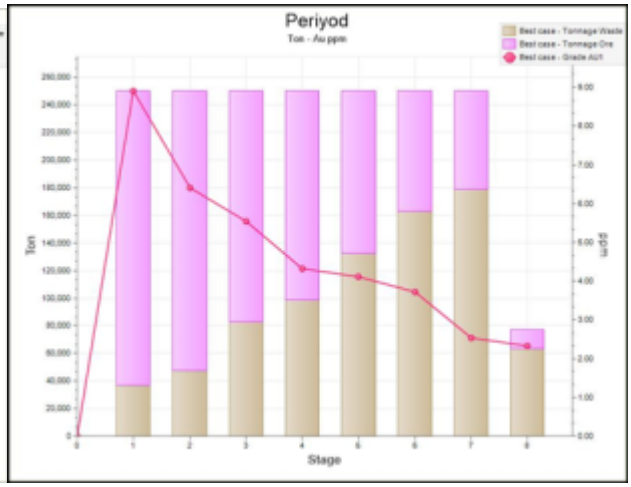

Şekil 7. Periyod ton – Au ppm

Kazı arını (stope) optimizasyonu sonucu elde edilen periyod, stage, stage kod, optimizasyon değeri ve extraction no gibi çıktılar blok modele işlenir (Şekil 8). Bu bilgileri kullanarak rezerv blok model oluşturulabilir. İstenirse Class alanındaki Ore yazılı kayıtlar filtre edilerek veya Periyot alanında istenen periyodları içeren kayıtları seçilerek veya Stage Code alnında yazılı Stage lerden istenen aşamalar (stage) seçilerek Rezerv blok model elde edilir. Karşılaştırma amacıyla Şekil 9'da kaynak blok model ve Şekil 10'da Class alanında Ore içeren kayıtlar seçilerek oluşturulan rezerv blok model verilmektedir.

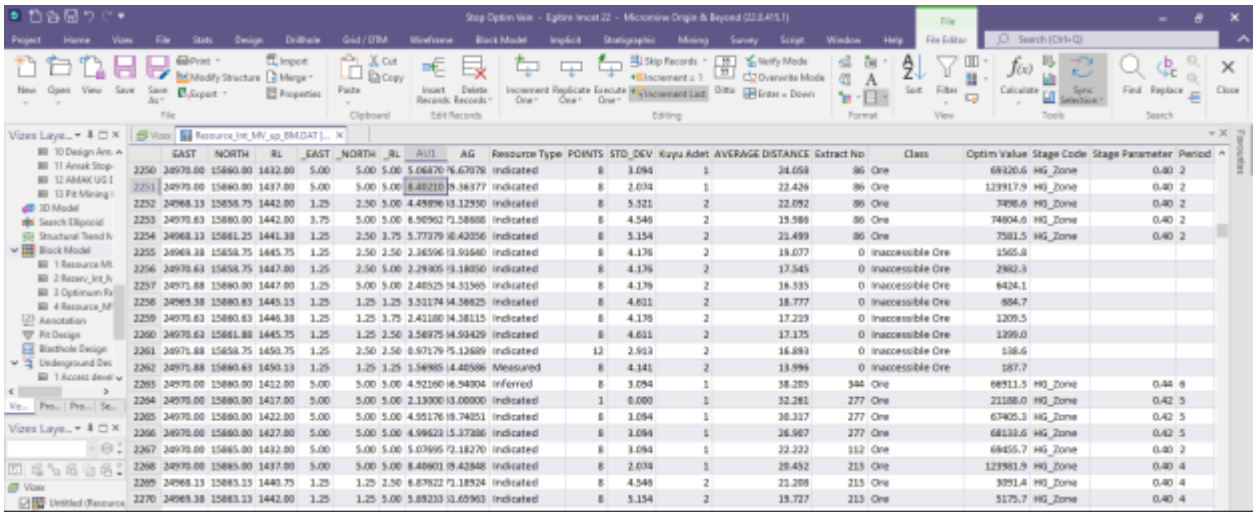

Şekil 8. Kaynak (Resource) blok modele işlenen veriler

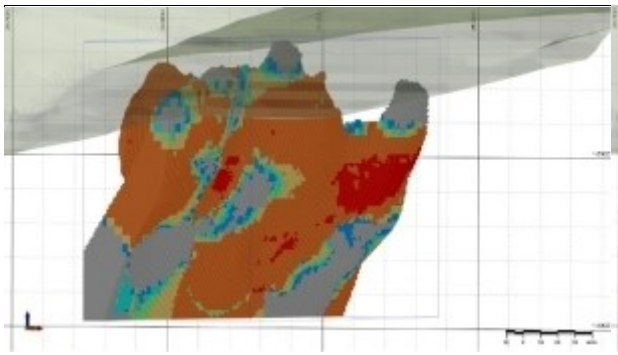

Şekil 9. Kaynak blok model

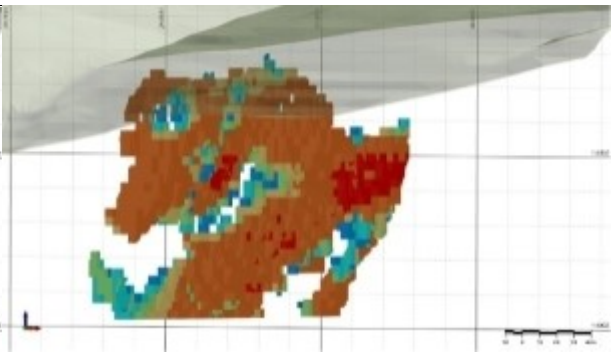

Şekil 10. Rezerv blok model

Kazı arını (Stope) optimizasyon sonuçları analiz edildikten, çıktılardan rezerv blok model oluşturulduktan sonra işletme sahibi isterse işlevsel maden planını, operasyonel veya kısa vadeli planlama (short term scheduling) ile yapabilir. Micromine Scheduling modülü veya diğer yazılımlar ve hatta bir yazılıma ihtiyaç duymadan Excel de sonuçları değerlendirerek oluşturur. Kat planlarına kazı arınları, rezerv blok modeli alarak tasarımları güncelleyebilir (Şekil 11). Bu sunumun takip eden bölümlerinde stratejik, uzun dönem, maden ömrü boyunca maden işletme planı ele alınacaktır (Strategic Scheduling).

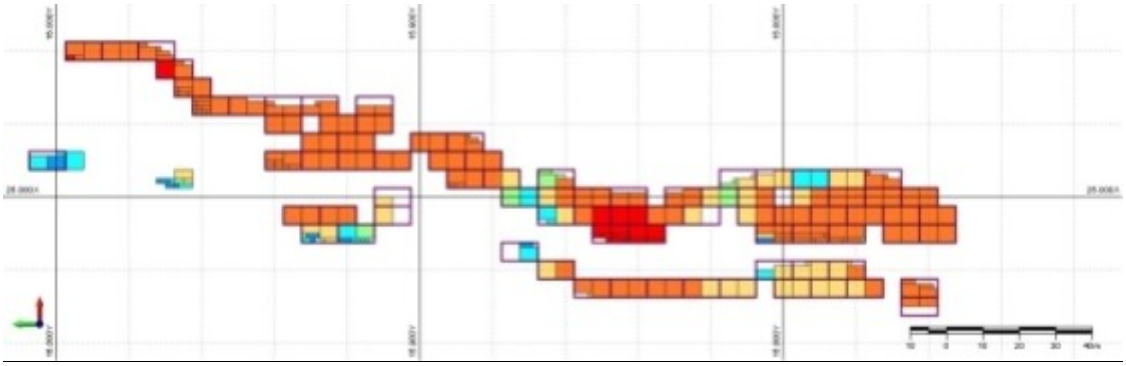

Şekil 11. Operasyonel işletme tasarımı için bir kat planı, yüksek tenörlü evreler (stage) içinde bulunan kazı arınları (stope) ve cevher rezerv sınıfı (ore class reserve) blokları

UZUN DÖNEM MADEN İŞLETME PLANI (STRATEGİC SCHEDULİNG)

Stratejik işletme planı, indirgeme oranı değerleri dikkate alınarak başka bir değişle doğrudan gelir değil de indirgeme oranına göre düzeltilmiş geliri gözeterek (NBD-Net Bugünkü Değer) aylık veya yıllık dönemlerde hedeflenen toplam kazı, cevher ton veya tenörü verebilecek işletme planı hazırlamak için gereklidir. Kazı arını (stope) optimizasyon yapmadan stratejik maden planına başlanırsa yeraltı işletme maliyetleri ve gelire göre belirlenen zonlar dikkate alınmadan bir işletme planı yapılmış olur. Başka bir deyişle, stratejik işletme planı rezerv blok modele göre değil kaynak blok modele göre hazırlanmış olacaktır. Sonuçta sağlıklı bir stratejik işletme planı hazırlamak için kazı arını (stope) optimizasyonunda elde edilen sonuçlar ile entegrasyon oluşturulmalı (Hybrid). Takip edilen bölümlerde, 20 – 30 metreden daha az kalınlıkta ince damar tipi maden yataklarında entegrasyonun nasıl oluşturulduğu ele alınacaktır.

Eğer damar eğimli ise ve birkaç yüz metre derinliğe devam ediyorsa üretim kademelerinin belirlenmesi istenebilir. Bu durumda damar iki veya daha fazla üretim dilime ayrılarak kademeler belirlenir. Üretime önce yukardaki kademeden ve daha sonra aşağıdaki kademeden devam edilmesi istenebilir. Yukardaki kademenin bitmesine yakın alt kademede de üretime başlanabilecektir. Micromine

yazılımında dilim oluşturmaya Wireframe / Slice Wireframe komutları ile başlanır. Örnek işletmemizde ilk üretim kademesi 1470 kotu üstünde ve ikinci üretim kademesi 1470 kotu altında oluşturulacaktır. Kademe için oluşturulan dilimler Şekil 12'de verilmiştir.

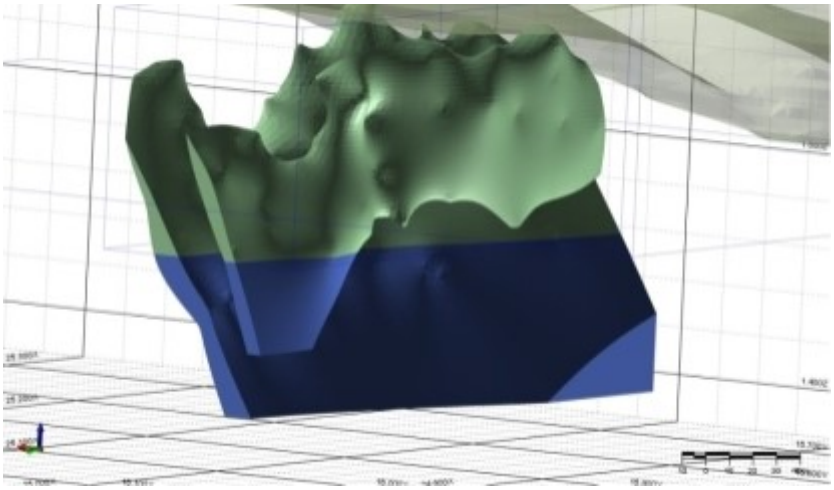

Şekil 12. Üretim kademesi belirlemek için oluşturulan cevher katı model dilimleri

İnce damarlarda diğer bir sorun kazı arını (stope) kesitinin damar kenarları ile uyumlu olması zorunluluğudur. Ek olarak seyrelmenin az olması ve cevher kazanım oranın yüksek olması için patlatma (ring) tasarımının da damar kenarları ile uyumlu olması zorunluluğu vardır. Bunu sağlamak üzere kazı arını (stope) kenarlarını otomatik olarak damar kenarlarına yaslayarak kazı arınları (stope) oluşturulur (Şekil 13).

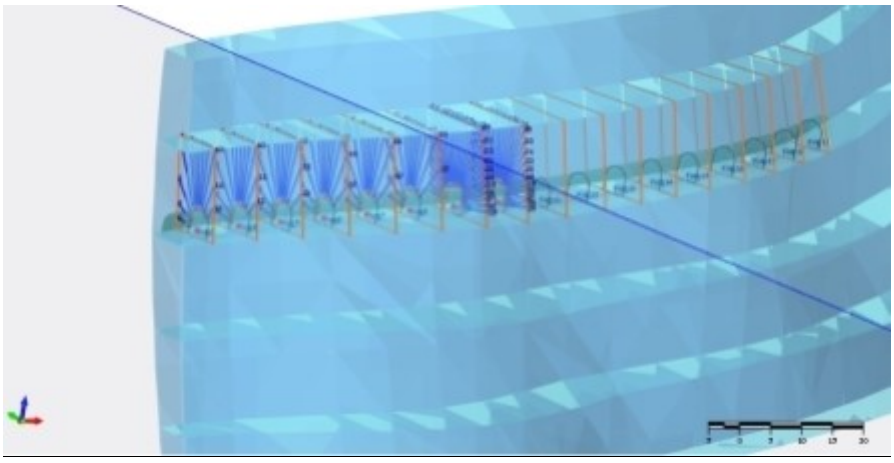

Şekil 13. İnce damar kenarları ile uyumlu oluşturulan kazı arını (stope) kesitleri ve üretim delikleri (ring) tasarımı

Damar kenarlarını dikkate alarak kazı arını (stope) oluşturmak için Micromine yazılımında Mining / Mining Blocks ikonları seçilir. Kazı arını (stope) kenarlarını belirleyecek damarlar Şekil 12'de gösterildiği gibi kademeli olarak çağrılır, kazı arını (stope) boyutları ve yükseklikleri tanımlanarak kazı arını (stope) blokları oluşturulur. Üretime üst kademeden başlanacaksa ilk sırada yer alır. İkinci sıraya alt kademe alınır. Planlama (scheduling) işleminde kullanılmak üzere blok indeks, üretim katı, üretim katı adı, kademe, kademe ve üretim katı gibi öznitelikler oluşturulur ve her bir kazı arını (stope) bloğuna kaydedilir.

Kazı arını (stope) blokları oluşturulduktan sonra Micromine yazılımında Mining / Material Bins ikonları seçilerek içerdikleri cevher ton ve tenörleri ile pasa ton değeri hesaplanır. Kazı arını (stope) blokunda bulunan pasa ve cevher birlikte alınarak seyrelmiş cevher tenör hesaplanır. Hesaplanan cevher ton, cevher tenör, seyrelmiş cevher tenör, pasa yoğunluk, cevher yoğunluk, pasa ton gibi öznitelikler kazı arını (stope) bloklarına kaydedilir. Sonuç olarak bir maden işletme planında gerekli olan ve yukarıda bazıları belirtilen bilgiler kazı arını (stope) bloklarına işlenir.

Kazı arını (stope) optimizasyon ve stratejik planlama (strategic scheduling) entegrasyonu için öncelikle oluşturulan kazı arını (stope) adlarının kaynak blok modele ve rezerv blok modele atanması gerekir. Micromine yazılımında Wireframe / Point (Assign) ikonları seçilir. Sonrasında Micromine yazılımı Wireframe / Attribute Assign (Advanced) (Assign) ikonları kullanılarak kaynak blok modele stope optimizasyon çıktıları olarak kaydedilmiş olan Stage Code, Stage Parameter, Class, Optimum Value gibi öznitelikler kazı arını (stope) bloklarına atanabilir.

Damar kenarlarına ile uyumlu olarak oluşturulan kazı arını (stope) blokları Şekil 14'de verilmiştir. Ancak schedule işlemine bu blokların tamamı alınmayacaktır. Kazı arını (stope) optimizasyonu ile belirlenen Class, Stage Code, Optimum Value gibi öznitelikler kullanılarak seçilecek kazı arını (stope) blokları planlama (schedule) işlemine alınacaktır. Hangi özniteliklerin seçileceği tek tek tüm öznitelikler denerek bulunabilir veya öznitelikler kombinasyonu kullanılabilir. Bu çalışmada Stage Code öznitelik değerleri kullanılmıştır. Stage Code HG_Zone ile kodlanan yüksek tenörlü zon ile Stage Code MG_Zone ile kodlanan orta tenörlü zonda bulunan kazı arını (stope) blokları planlama (Schedule) işlemine alınacaktır. Planlama (Schedule) işlemine alınacak bloklar Şekil 15'de gösterilmiştir.

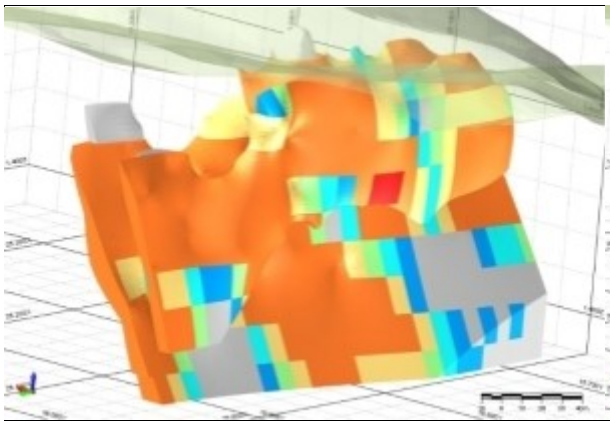

Şekil 14. Stope blokları

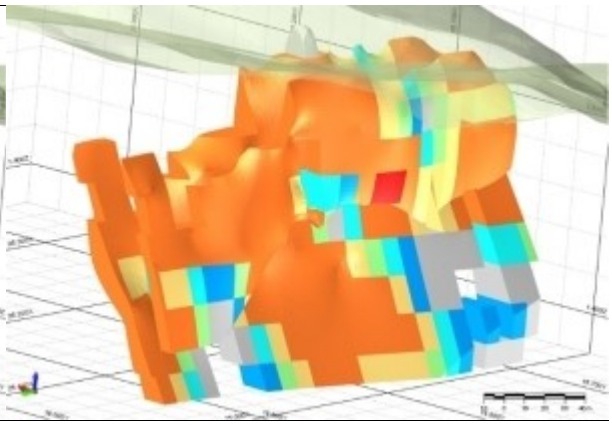

Şekil 15. Schedule işlemine alınacak stope blokları

Planlama (schedule) işlemine alınacak kazı arını (stope) blokları belirlendikten sonra Micromine Scheduling modülü ile stratejik maden işletme planı oluşturulmuştur. Schedule işleminde kazı arını (stope) blokları görev (Task) olarak tanımlanır. Kazı arını (stope) bloklarında oluşturulan cevher ton, cevher tenör, cevher metal, cevher yoğunluk, pasa ton, pasa yoğunluk, üretim katı, üretim katı adı, stage code, optimum value gibi öznitelikler planlama (schedule) görevlerine atanır ve planlama (schedule) optimizasyonunda girdi veri olarak kullanılır.

Planlama (schedule) görevleri öznitelikleri oluşturulduktan sonra görevler Gantt çizelgeye alınır. Görevler arasında yatay ve dikey bağımlılıklar oluşturularak görev alım sıralaması oluşturulur. Özellikle ince damarlarda kazı arını (stope) blokları ardışık geldiğinden ve biri üretildikten sonra takip eden kazı arını (stope) bloğunda üretime devam edileceğinden yatay bağımlılıkların oluşturulması önem kazanır. Hatırlatalım ki bu çalışmada operasyon önceliği iki dilim ile belirlenmişti. İlk cevher üretimi 1470 kotu üzerindeki stoplarda yapılacak ve daha sonra 1470 kotu altında üretime devam edilecekti. Üretim dilimlerini stratejik maden işletme planına yansıtmak için Micromine Scheduling modülünde dikey

sıralamada Build Interstage Dependency seçilmeli ve Stage öznitelik seçilmeli. Dilimler birbiri ardına sırayla üretime alınacaksa Lag değeri 1 olarak belirtilmeli. Yatay ve dikey görev bağımlılıkları oluşturulduktan sonra Gantt çizelgede görevler Şekil 16'da sergilendiği gibi gösterilir.

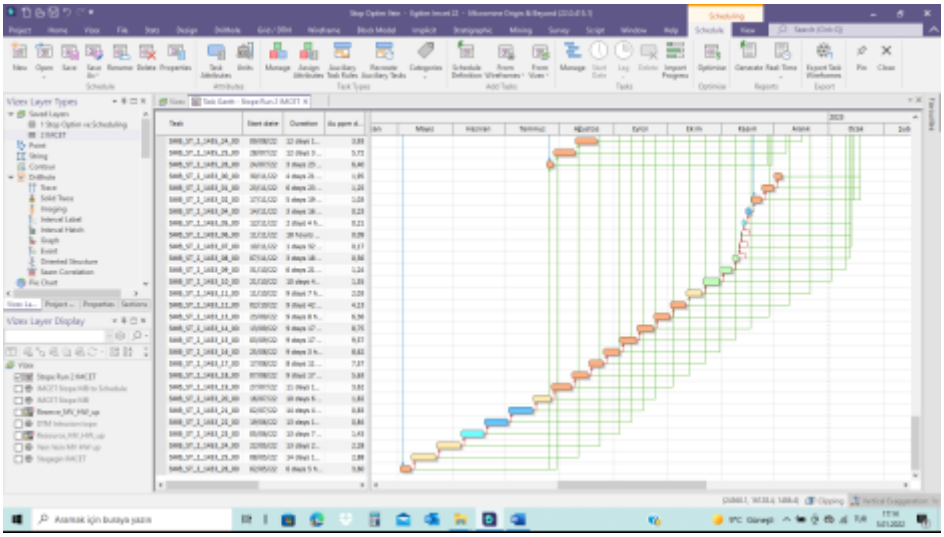

Şekil 16. Gantt Çizelge, schedule görevleri ve yatay ve dikey bağımlılıkları

Görev bağımlılıkları kurulduktan sonra maden ömrü boyunca stratejik maden planını hazırlamak için planlama (Schedule) optimizasyon işlemine başlanır. İlk olarak periyod seçilir. Maden ömrü boyunca yapılacak toplam kazı ve üretilecek cevher tonajı bir periyodda yapılacak toplam kazı ve cevher üretimine bölünürse periyod adedi ortaya çıkar. Projenin ilk yıllarında düşük tonaj üretim yapılacaksa ilk bir ya da birkaç periyod ayrıca belirlenir. Net bugünkü değer (NBD) hesaplaması için objektif olarak metal miktarı veya metalin parasal değeri seçilebilir. İndirgeme oranı seçilir. Periyodik toplam kazı, cevher ton ve tenör hedef değerleri girilir. Hedeflerle uyumlu bir işletme planı oluşturulana kadar hedef kalemleri kombinasyonları değiştirilerek işlem sürdürülür. Kazı arını (stope) optimizasyon sonuç çıktısı Excel kopyası Şekil 17'de gösterilmektedir.

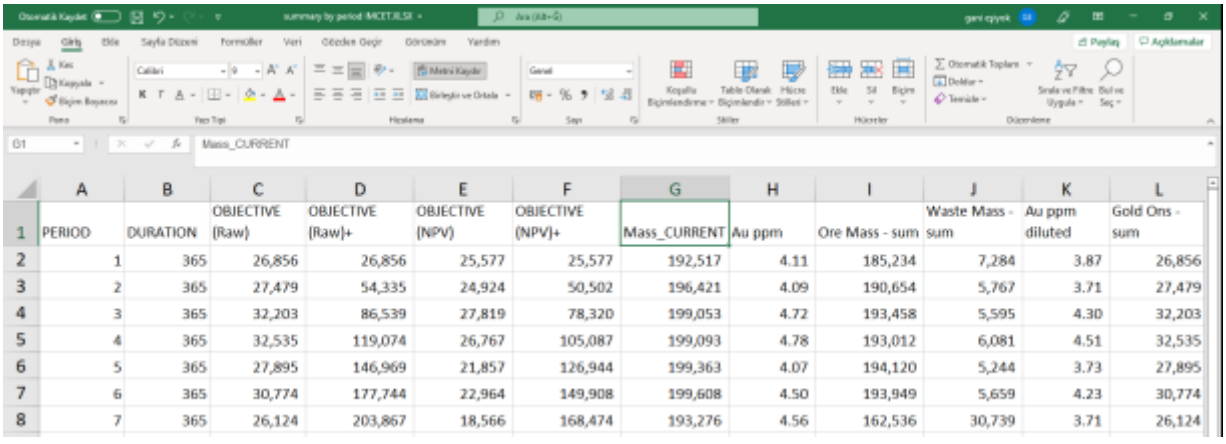

	A	B	C	D	E	F	G	H	I	J	K	L
1	PERIOD	DURATION	OBJECTIVE (Raw)	OBJECTIVE (Raw)+	OBJECTIVE (NPV)	OBJECTIVE (NPV)+	Mass_CURRENT	Au ppm	Ore Mass - sum	Waste Mass - sum	Au ppm diluted	Gold Ons - sum
2	1	365	26,856	26,856	25,577	25,577	192,517	4.11	185,234	7,284	3.87	26,856
3	2	365	27,479	54,335	24,924	50,502	196,421	4.09	190,654	5,767	3.71	27,479
4	3	365	32,203	86,539	27,819	78,320	199,053	4.72	193,458	5,595	4.30	32,203
5	4	365	32,535	119,074	26,767	105,087	199,093	4.78	193,012	6,081	4.51	32,535
6	5	365	27,895	146,969	21,857	126,944	199,363	4.07	194,120	5,244	3.73	27,895
7	6	365	30,774	177,744	22,964	149,908	199,608	4.50	193,949	5,659	4.23	30,774
8	7	365	26,124	203,867	18,566	168,474	193,276	4.56	162,536	30,739	3.71	26,124

Şekil 17. Schedule optimizasyon sonuç çıktısı Excel kopyası.

Kazı arını (stope) optimizasyon sonucunda hedefleri tutturan bir işletme planı çözümü bulunduğunda simülasyon ile stopların üretime alım sırası görsel olarak kontrol edilebilir. Önceden belirtildiği gibi üretim 1470 kotu üzerindeki ilk dilimde başlayacak ve devam edecek. Üretime 1470 kotu altında başlamak için ilk dilimdeki üretimin sona yaklaşması gerekir. Maden işletme planı simülasyonunda bu durumun temin edildiği görülmelidir. Bu çalışmada takip ettiğimiz örnek projenin

maden işletme planı simülasyon ile kontrol edilmiş ve sonuçlar Şekil 18 ve Şekil 19'da gösterilmiştir. Şekil 18'de gösterildiği gibi üretime 1470 kotu üzerindeki ilk dilimden başlanıyor ve ilk dilimde üretimin bitmesine yakın üretime 1470 kotu altındaki ikinci dilimde devam edilmektedir (Şekil 19).

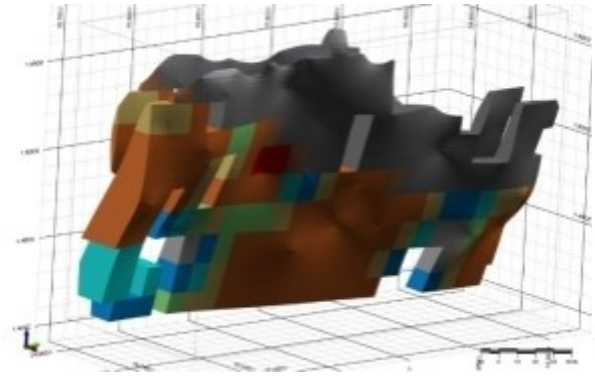

Şekil 18. 1470 kotu üstü ilk üretim dilimi

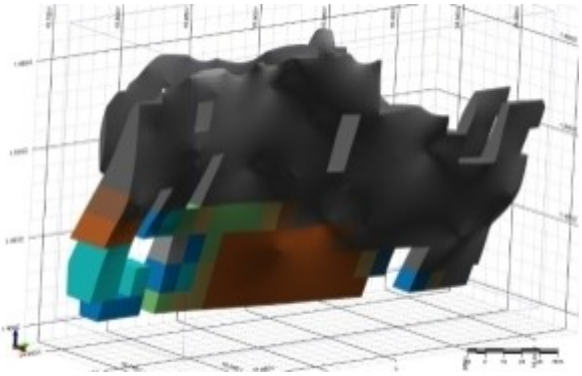

Şekil 19. 1470 kotu altı ikinci üretim dilimi

Stratejik planın üretim hedeflerine ulaşılabilirliği grafiksel olarak da değerlendirilebilir. Örnek projede yapılan stratejik plan ile her periyodda 200 bin ton cevher üretilebileceği ve cevher tenörünün de 3,6 ppm Au ile 4,2 ppm Au arasında değişebileceği Şekil 20'de görülebilir. Örnek projede net bugünkü değerin (NPV) periyodik değerlendirmesi Şekil 21'de verilmiştir. Görüleceği gibi net bugünkü değer her periyodda artış göstermektedir. Maden ömrü boyunca maden işletme planının her açıdan incelendiğinde tutarlı sonuçlar verdiği izlenmiştir.

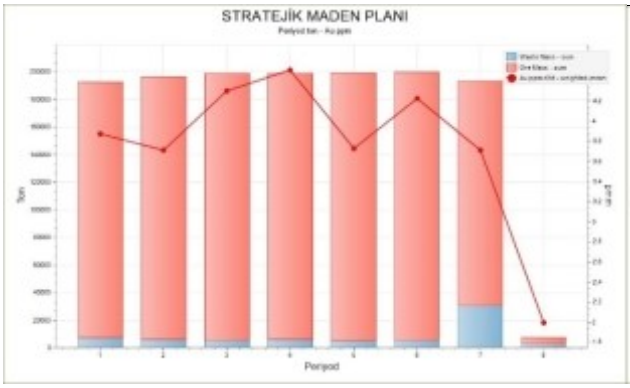

Şekil 20. Periyodik cevher ton ve Au ppm

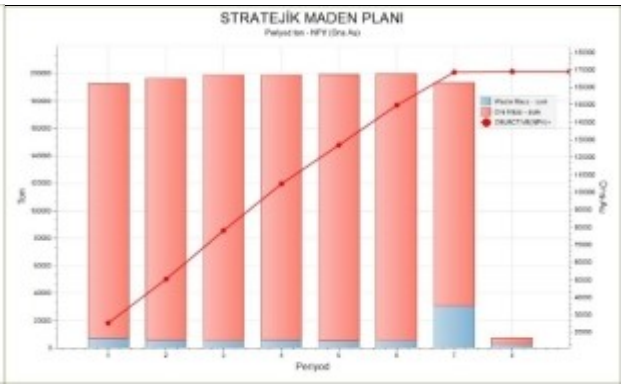

Şekil 21. Periyodik cevher ton ve NPV (Ons Au)

SONUÇLAR

Bu bildiride maden ömrü boyunca yeraltı işletme yöntemi ile üretilebilecek kaynağın belirlenmesinde son birkaç yıldır kullanımına başlanan Stope Optimizasyonu ince damarlar konu edilerek ele alınmıştır. Elbette maden yatak tiplerine göre farklı uygulamalar söz konusu olacaktır. Söz konusu yazılımın geliştirdiği modüller ile bu durumların çözümlenmesi mümkün olmaktadır.

Stratejik maden planlamasında kazı arını (stope) optimizasyonu ile entegrasyon daha efektif ve verimliliği yüksek maden işletme planı hazırlanabilir. Proje bazında entegrasyon imkanları araştırılmasında fayda vardır.

KAYNAKLAR

Micromine Stope Optimization kurs notları, (2021)
Micromine Scheduling kurs notları, (2021)

YERALTI KÖMÜR İŞLETMELERİNE YAPILAN DESTEK ÖDEMELERİ VE ÖNEMİ

SUPPORT PAYMENTS AND IMPORTANCE OF UNDERGROUND COAL BUSINESS

B. Kocaman [1,*], C. Doğruöz [2], R. Kocaman [3], C. Acar [4]

[1] *Maden ve Petrol İşleri Genel Müdürlüğü, Kömür Koordinatörlüğü, Maden Mühendisi*
*(*Sorumlu yazar: birsen.kocaman@mapeg.gov.tr)*
[2] *Çankırı Karatekin Üniversitesi, Mühendislik Fakültesi, İnşaat Mühendisliği Bölümü*
[3] *Maden ve Petrol İşleri Genel Müdürlüğü, İSG Koordinatörlüğü, Maden Mühendisi*
[4] *Yılmaden Holding Inc, Mineral Processing Director*

ÖZET

Yaşadığımız dünyada hammaddeye ve enerjiye olan ihtiyaç her geçen gün artarak devam etmektedir. Enerji ve hammaddeye olan ihtiyacın büyük kısmı madenlerden çıkartılarak elde edilmektedir. Bugün Çin, ABD, Hindistan, Endonezya, Avustralya, Rusya ve Güney Afrika gibi ülkeler kömür üretiminde ön sıralarda bulunmaktadır. Ülkemiz açısından yerli enerji kaynaklarının kullanılması ise ayrı bir önem taşımaktadır. Söz konusu yerli kaynaklarımızdan birisi de kömür rezervlerimizdir. Kömür üretimi için fizibilite çalışmaları, arama dönemi, işletmeye açılması ve üretimin devam ettirilmesi için yatırım yapılması gerekmektedir. Günümüzde firmaların uzun süreli ayakta kalabilmeleri için teşvik ve destek gelirlerine de ihtiyaçları vardır. Yeraltı kömür işletmelerine yapılan destekler ise ekonomik açıdan girdi sağlamaktadır. Destek ödemesinden yararlanabilmek için; "Linyit" ve "Taşkömürü" ruhsat sahasında yeraltı işletme yöntemi ile üretim ve/veya hazırlık yapılıyor olması, özel hukuk tüzel kişisi ile kamu kurum ve kuruluşlarının iştiraklerinin işlettirdikleri yeraltı maden işletmelerinde çalışan işletmeciler olunması gerekmektedir. Linyit ve Taşkömürü üretiminde bulunan firmalara yeraltı maden işletmelerinde meydana gelen maliyet artışlarının karşılanması amacıyla yapılan destek ödemeleri çerçevesindeki düzenlemelerin, sektör açısından çok önemli olumlu sonuçlar verdiği, üretim miktarlarının artışını, işsizliğin azalmasını sağladığı, kazaların da önlenmesinde önemli bir etken olduğu düşünülmektedir. Bu makalede destek ödemeleri ile ilgili bilgiler verilerek sektörel açıdan önemi vurgulanmaktadır.

Anahtar Sözcükler: Yeraltı, kömür, destek, üretim.

ABSTRACT

In the world we live in, the need for raw materials and energy is constantly increasing. Most of the energy raw material needs are obtained by extracting them from mines. It is at the forefront of coal production in China, the USA, India, Indonesia, Australia, Russia, South Africa. One of our domestic resources is coal reserves. In coal production, investments are required for feasibility studies, exploration period, commissioning, and continuation of production. Nowadays, companies also need incentives and support income. The support provided to underground coal enterprises provides economic input. To benefit from the support payment, it is necessary to be operators working in underground mining enterprises operated by a private legal entity and subsidiaries of public institutions and organizations to have production or preparation done by underground operation method at the Lignite and Coal license pit. Arrangements within the framework of support payments made to companies engaged in the production of lignite and coal to cover cost increases in underground mining operations provide positive results for the sector. This article gives information about support payments, and their importance from a sectoral point of view is emphasized.

Keywords: Underground, coal, support, production.

GİRİŞ

Dünya nüfusu her geçen gün artarak devam etmektedir. Nüfus artışı ve sanayinin gelişmesine paralel olarak enerjiye olan gereksinim de artmaktadır. Elektrik enerjisine olan ihtiyaç günümüzde vazgeçilmez bir hal almıştır (T.C. Enerji ve Tabii Kaynaklar Bakanlığı). Ülkelerin ekonomik kalkınmalarında zorunlu olan temel girdilerin başında, enerji kaynakları yer almaktadır. Sürdürülebilir enerji politikaları, arz güvenliğinin sağlanması ve temin kaynaklarının çeşitlendirilmesinin yanı sıra, kullanılmak istenen enerji türünün düşük maliyetli, talep edilen miktar ve kalitede topluma arz edilmesini hedeflemektedir (Kocaman, 2017). Bunları yanında yenilenebilir enerji kaynakları da değerlendirilmektedir. Kömürün önemi ise Sanayi Devrimi'nin yakıtını sağlamakla başlamıştır. 20.yy.'da elektrik (enerji) üretiminde kullanılması nedeniyle kömür stratejik bir yakıt hammaddesi haline gelmektedir ve enerji yatırımları bu yönde de değerlendirilmektedir. Kömürün önemi ise Sanayi Devrimi'nin yakıtını sağlamakla başlamıştır. 20.yy.'da elektrik (enerji) üretiminde kullanılması ile zirve yapmıştır. Günümüzde elektrik enerjisinin %37'lik kısmı kömürden üretilmektedir. Aynı zamanda dünya demir-çelik endüstrisi de kömüre bağlıdır ve metal sanayisinin ana girdilerinden biridir. Dünya kömür rezervleri 80'den fazla ülkede bulunmakta ve 2015 yılı toplam kömür üretimi dikkate alındığında, küresel kömür rezervlerinin yaklaşık 134 yıl ömrü bulunduğu hesaplanmaktadır. Diğer enerji kaynaklarına göre Kömür durağan olduğu için taşınması, depolanması ve kullanılması en kolay fosil yakıttır. Kömür rezervleri birçok ülkede dağınık olduğu için tekelleşme ve bunun sonucu olarak alıcıların zor durumda kalması olasıdır. Alıcılar hemen başka kaynaklara yönelebilmektedir. Günümüzde gelişen teknoloji kullanılarak çevreye zarar vermeden kömür yakılabilir konuma gelmiştir. Kömür, dünya çapında hayati derecede önemli olan elektrik enerjisini sağlamada rekabet yaratmaktadır. Bütün dünyada elektrik enerjisinin ana kaynaklarından biri olduğu belirtilmiştir. Yaşadığımız dünyada enerji talebi özellikle güçlü bir şekilde ve devamlı olarak büyümeye devam etmektedir; özellikle gelişmekte olan ülkelerde enerji ekonomik büyüme ve yoksulluğun azalması için gerekli olmaktadır. Bütün enerji kaynakları talebi dengeli ve çeşitli olarak karşılayacak şekilde olması beklenir. Dünyada birincil enerji kaynaklarının en önemlisi ve en ucuzu kömür olarak görülmektedir. Tüm gelişmiş ve gelişmekte olan ülkeler öncelikle arz güvenliği yüksek olan kendi öz kaynaklarını kullanmaktadırlar. Kömür dünya çapında enerji güvenliği için hayati öneme sahiptir ve bol miktarda, zararsız bir şekilde elde edilebilmekte, güvenli, kolay ve güvenli bir şekilde taşınabilmektedir. Dünya enerji rezervinin büyük kısmını kömürün oluşturduğu bilinmektedir. Enerji açığı bulunan dünyada kömürün diğer fosil yakıtlara karşı üstünlüğünü sağlamlaştırmak için zararlı gaz ve diğer emisyonlar azaltılmalıdır. Gelişen teknoloji kömürü çevreye uyumlu enerji kaynağı haline getirmektedir. Aynı zamanda büyük ekonomik ve sosyal gelişme ile enerji güvenliğine sağladığı katkıyı da devam ettirmelidir (Kimyasal Teknoloji Enstitüsü).

Ülkemiz enerji konusunda dışa bağımlı durumdadır. Bu nedenle enerjinin üretilmesi konusunda çok ciddi adımların atılması ve dışa bağımlılığın azaltılmasına yönelik çalışmaların yapılması gerekmektedir. Petrol ve doğal gaz kaynakları bakımından dışa bağımlı olunması nedeniyle kömür stratejik bir madde haline gelmektedir ve enerji yatırımları bu yönde de değerlendirilmelidir.

KÖMÜR OLUŞUMU

Kömür yanabilen sedimanter organik bir kayadır. Kömür başlıca karbon, hidrojen ve oksijen gibi elementlerin bileşiminden oluşmuş olup, diğer kaya tabakalarının arasında damar haline uzunca bir süre (milyonlarca yıl) ısı, basınç ve mikrobiyolojik etkilerin sonucunda meydana gelmiştir. Kömür, nebatların bataklık alanlarda birikmesi sonucu oluşan tabakaların değişime uğraması neticesi meydana gelmiştir. Bu tabakalar üzerine çeşitli çökeltilerin birikmesi ve arz'ın hareketleri sonucu derinliklere gömülmüştür. Gömülmüş olan bu nebatlar; artan ısı ve basınca maruz kaldıklarında bünyelerinde fiziksel ve kimyasal değişikliğe uğrayarak kömüre dönüşürler. Bu süreç milyonlarca yıl içinde gerçekleşerek kömürler

organik olgunluklarına göre Linyit, Alt bitümlü, Kömür, Bitümlü kömür ve Antrasit tiplerine ayrılırlar. Linyit ve kısmen Alt Bitümlü kömürler genellikle yumuşak, kırılgan ve mat görünüştedirler. Bu tip kömürlerin ana özelliği göreceli olarak yüksek nem içerirler ve karbon içerikleri düşüktür. Antrasit ve Bitümlü kömürler ise genellikle sert ve parlak görünüştedirler. Göreceli olarak nem içerikleri düşük olup, karbon oranları yüksektir. Jeolojik olarak kömürlerin yaşları 400 milyon yıl ile 15 milyon yıl arasında değiştiği ve genellikle yaşlı kömürler daha kaliteli olduğu belirtilmiştir (Kocaman vd., 2017). Kömürün sınıflandırılması Şekil 1'de gösterilmiştir.

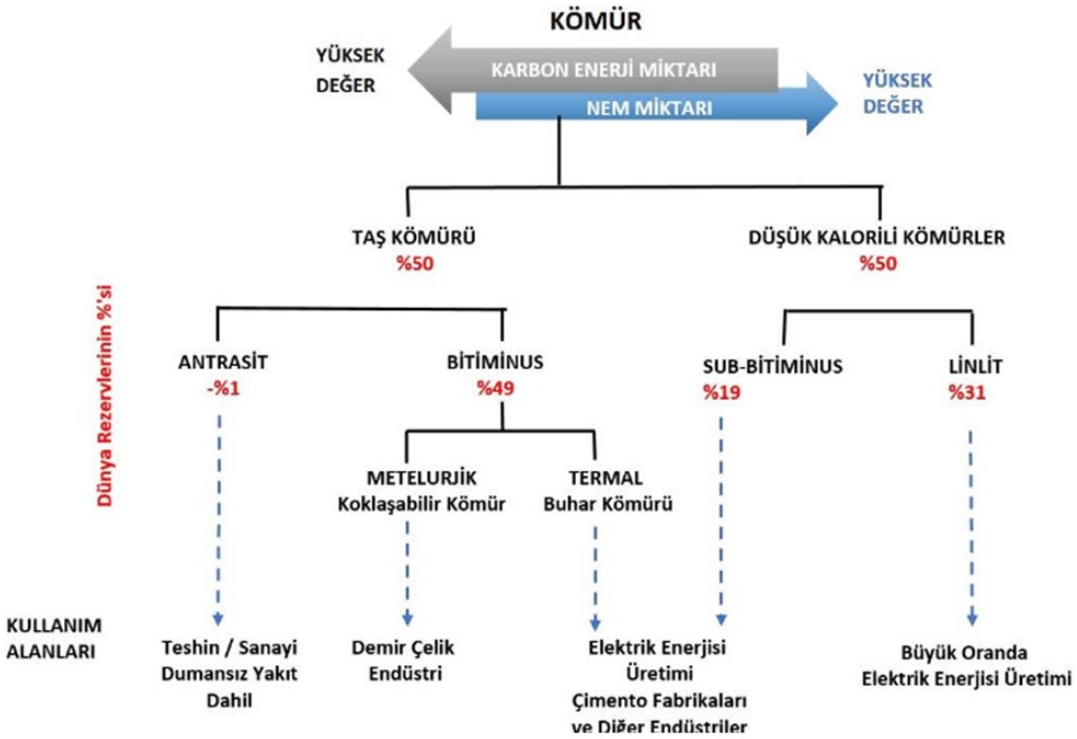

Şekil 1.Kömürün sınıflandırılması (T.C. Enerji ve Tabii Kaynaklar Bakanlığı)

Kömür dünyada en yaşlı bir şekilde bulunan, güvenilir aynı zamanda düşük maliyetlerle elde edilebilen temiz bir fosil yakıttır. Kömür Dünya'da 50'den fazla ülkede üretilmektedir. Kömür rezervleri diğer fosil yakıtlar gibi (petrol ve doğalgaz) Dünya'nın belli bir bölümünde değil fakat tüm dünyada yaygın bir şekilde bulunmaktadır. Kömür kullanımı, depolaması ve nakliyesi açısından en emniyetli fosil yakıttır. Endüstriyel ve diğer alanlarda elektrik enerjisinin rekabetçi fiyatlarla ve güvenilir olarak temini açısından, kömürün Dünyada yaygın bir şekilde bulunuşu ve birçok ülke tarafından üretiliyor oluşu tedarikte güvenirliliği sağlamakta olduğu belirtilmiştir. Elektrik Enerjisi Üretiminde ucuz ve rekabetçi bir yakıt olması nedeniyle Dünya elektrik üretiminin yaklaşık %40' ı kömürden karşılanmaktadır. Kömür homojen olmayan, kompakt, çoğunlukla lignoselülozik bitki parçalarından meydana gelen, tabakalaşma gösteren, içerisinde çoğunlukla C, az miktarda H-O-S ve N elementlerinin bulunduğu ama inorganik (kil, silt elementleri gibi) maddelerinde olabildiği, bataklıklarda oluşan, kahverengi ve siyah renk tonlarında olan, yanabilen, katı fosil organik kütlelerdir. Kömürler yakıt hammaddesi oldukları gibi, değişik amaçlarda (kok yapımı, kimyasal madde üretimi gibi alanlarda) da kullanılırlar (T.C. Enerji ve Tabii Kaynaklar Bakanlığı). Ülkemizde Petrol ve doğal gaz kaynakları bakımından dışa bağımlı olunması nedeniyle kömür stratejik bir madde haline gelmektedir ve enerji yatırımları bu yönde de değerlendirilmelidir. Şekil 2'de sülo içindeki üretilen kömürden bir görünüm bulunmaktadır.

Şekil 2. Sülo içindeki üretilen kömürden görünüm (Kocaman, 2018)

Ülkemiz rezerv ve üretim miktarları açısından linyitte dünya ölçeğinde orta düzeyde, taşkömüründe ise alt düzeyde değerlendirilebilir. Toplam dünya linyit/alt bitümlü kömür rezervinin yaklaşık %3,2'si ülkemizde bulunmaktadır. Bununla birlikte linyitlerimizin büyük kısmının ısıl değeri düşük olduğundan termik santrallerde kullanımı ön plana çıkmıştır. Ülkemiz linyit rezervinin yaklaşık %46'sı Afşin-Elbistan havzasında bulunmaktadır. Ülkemizin en önemli taşkömürü rezervleri ise Zonguldak ve civarındadır. Zonguldak Havzası'ndaki toplam taşkömürü rezervi 1,30 milyar ton, buna karşılık görünür rezerv ise 506 milyon ton düzeyinde bulunmaktadır. Kurumlara ait linyit rezervleri Çizelge 1'de gösterilmiştir.

Çizelge 1. Kurumlara ait linyit rezervleri (bin ton 2019 yılı sonu) (Türkiye Kömür İşletmeleri)

Kurumlar	Görünür	Muhtemel	Mümkün	Toplam
EÜAŞ	v.y.	v.y.	v.y.	11.800.000
TKİ	1.979.368	489.441	1.560	2.470.369
MTA	515.000	-	-	515.000
Özel Sektör	v.y.	v.y.	v.y.	4.538.809
TOPLAM	-	-	-	19.324.178

EÜAŞ ve TKİ sahalarında 1.658 milyar ton, MTA sahalarında ise,8.982 milyar ton olmak üzere, ülkemiz linyit rezervleri toplam 10,82 milyar ton artırılmış ve özel sektör rezervleri (200 milyon ton) ile birlikte 19.32 milyar tona ulaşmıştır. 8,3 milyar ton olan ülkemiz rezervi ise %130 arttırılmıştır (MTA Genel Müdürlüğü). Çizelge 2'de kömür üretim miktarları gösterilmektedir.

Çizelge 2. Kömür üretim Miktarları (Maden ve Petrol İşleri Genel Müdürlüğü)

Yıllar	Kömür Üretim Miktarları
2015	61.929.916 ton
2016	81.717.017 ton
2017	87.866.620 ton
2018	100.831.833 ton
2019	97.371.718 ton
2020	88.410.405 ton

Şekil 3. Ayak içinde kömür üretiminden görünüm (Kocaman, 2018)

Kömürün Kullanım Alanları

Ülkemizde kömürler yüksek oranda kül, kükürt, nem ve alkali bileşikler içermektedir. Şekil 3'te ayak içinde kömür üretiminden bir görünüm bulunmaktadır. Kül, kükürt ve nem değerleri azaltılmış, kömürlerin sanayi ve ısıtma sektörlerinde daha fazla kullanılması mümkün olabilecektir. Bu kapsamda Kül miktarını azaltmaya yönelik teknolojilerin geliştirilmesi, Nem miktarını azaltmaya yönelik teknolojilerin geliştirilmesi, Briketleme /pelletleme teknolojilerinin geliştirilmesi, gibi çalışmalar MAM Kimyasal Teknolojiler Enstitüsünde yapıldığı, Isıl değeri düşük kömürlerin (Linyit, Turba ve Leonardit gibi) yakıt haricinde farklı alanlarda kullanılmasına yönelik birçok uygulama mevcuttur. Ekstraksiyon yöntemi ile kömürden hümik asit ve montan vaksı gibi değerli ürünler üretilmekte olduğu belirtilmiştir. Linyit kömürleri ve/veya atık toz kömürlerin (şlamlardan kazanılan kömürler) doğrudan veya farklı kömürlerle veya çeşitli zirai artıklarla (biyo-kütle) briketleneceği belirtilmiştir. Kömürden Hümik Asit Üretim Çalışmaları ise; Doğal organik polimer olarak adlandırılan hümik asit, linyit, turba ve leonardit gibi kömürlerde bulunmaktadır (Kimyasal Teknoloji Enstitüsü). Termik santrallarda yakıt olarak kullanılan tozlaştırılmış kömür atık olarak değişik karakterde kül ve cüruflardan uçucu küllerin katkılı çimento, yüksek dayanımlı beton, portland çimentosu, hafif agrega, duvar elemanları üretiminde, jeoteknik uygulamalarda ve yol yapımında kullanılmaktadır (Kızgut vd., 2001).

KÖMÜRÜN SEKTÖREL BAZDA KULLANIMI

Kömürün Enerji Sektöründe Kullanımı

Türkiye'de bulunan 41 Kömür ve linyit yakıtlı termik santrallerinin toplam kurulu gücü 19.557,00 MWe'dır. 2017 yılında Kömür ve Linyit Yakıtlı Termik Santrallerile 101.952 GWh elektrik üretimi yapılmıştır. 2016 yılı sonu itibariyle 136,2 Milyon Ton Eşdeğer Petrol (MTEP) olan ülkemizin toplam birincil enerji tüketiminde kömürün payı %28'dir. Ülkemizin 2018 ilk yarısı itibariyle kömüre dayalı santral kurulu gücü 18.666 MW olup toplam kurulu gücün %21, 4'üne karşılık gelmektedir. Yerli kömüre dayalı kurulu güç 10.570 MW (%12,1) ve ithal kömüre dayalı kurulu güç ise 8.794 MW (%10,1) şeklindedir. 2018 yılı ilk yarısında kömüre dayalı santrallerden toplam 53,9 TWh elektrik üretilmiş olup toplam elektrik üretimi içerisindeki payı %33,0 düzeyindedir. Kömür ve Linyit Yakıtla Termik Santraller Profili Aktif santral sayılı3 9 adet Kurulu Güç 17.510 MWeKurulu Güce Oranı 22,08%Yıllık Elektrik Üretimi~ 101.952 GWh Üretimin Tüketime Oranı 39,21 olarak belirtilmiştir (Enerji Atlası).

Kömürün Gazlaştırmada Kullanımı

Kömürden gaz üretimi 2 yolla mümkün olmaktadır; Kok üretimi esnasında uçucu maddenin parçalanması sonucu oluşan gaz. Gazlaştırma reaksiyonları sonucu elde edilen gaz. Koklaştırma esnasında yan ürün olarak önemli miktarda gaz çıkmaktadır. Kömür cinsine göre, 1 ton kömürden, 320-410m3gaz elde edilmekte olduğu, bu gaz 3800-4000 kcal/m3ısı değerine sahip olduğu belirtilmiştir. Koklaştırma esnasında elde edilen gazın ısı değeri yüksek olduğundan, şehir gazı olarak kullanılabilirliği düşünülmüştür.

Koklaştırmada elde edilen gaz türlerigazlaştırma yolu ile kömürden gaz üretimi, kömürün belirli bir sıcaklıkta, oksijen veya hava, su buharı, hidrojen ve karbondioksit gibi gazlaştırıcılarla, reaksiyona sokulması sonucu elde edilmektedir. Kömürün hava, oksijen ve hidrojenle reaksiyonu, ekzotermik bir reaksiyondur. Su buharı ve karbondioksitle reaksiyonu endotermiktir. Gazlaştırma reaksiyonları yüksek sıcaklıkta meydana gelmektedir. Gazlaştırma işlemi yüksek sıcaklık prosesi olduğu belirtilmiştir.

Metanizasyon yöntemi ile gazlaştırma. Metan gazı üretimini mümkün kılan 2 reaksiyonda ekzotermik reaksiyonlardır ve bu nedenle de ısı kayıpları biraz yüksekolduğu belirtilmiştir. Metan gazı elde edilen iki reaksiyonun sonunda, gaz hacmi küçülmekte olduğu, gazlaştırmanın basınç altında yapılması, metan oluşumunu arttırmakta olduğu belirtilmiştir. Gazlaştırma reaktöründe, gazlaştırma sıcaklığı, gazlaştırma basıncı ve reaksiyona giren kok ve gazlaştırıcıların oranları, gaz bileşimini tayin etmekte olduğu belirtilmiştir (Resmi Gazteze, 2016).

Humik Asit Yapımı

<u>Leonarditten Elde Edilen Humik Asit Leonardit</u>

Oluşumunu milyonlarca yılda bitki ve hayvansal atıkların hava alarak çürümesi sonucu oluşmuş tarım ve endüstriyel alanlarda hammadde olarak kullanılan değerli bir madendir. En kaliteli humik asitte leonarditten elde edilir. Leonardit kullanılarak üretilen hümik ve fulvik asit içeren doğal organik toprak düzenleyicisi bir üründür. TKİ HÜMAS'ı diğer toprak düzenleyicilerden ayıran temel özellik leonarditten üretilmesi, hümik ve fulvik asit oranlarının yüksek düzeyde olması, devletin güven duyulan bir kurumu olan Türkiye Kömür İşletmeleri Kurumu tarafından üretilmektedir (T.C. Enerji ve Tabii Kaynaklar Bakanlığı). Büyük çapta hümik asit üretimi, söz konusu maddelerden alkali ekstraksiyon yöntemi ile üretilmektedir.Modifiye humik asit türevlerinin pilot tesislerinde pilot ölçekte 50 kg'lık miktarlarda üretilmiş ve aşağıda belirtilen alanlarda kullanılabilirliği gösterilmiştir.•Atık ve / veya içme suyu ile saflaştırılması•Boya•Seramik•Çimento, sondaj sıvıları•Değerli elementlerin geri kazanımıKömürden Organomineral Gübre Üretim Çalışmaları ise: Organik tarımda önemli bir yeri olan organomineral

gübreler, bir veya birden fazla organik ürünün bir veya birden fazla basit veya kompoze kimyevi gübre ile reaksiyonu veya karışımı ile elde edilmektedir.Ticari olarak üretilmekte olan organik toprak düzenleyicileri ve organomineral gübrelerin elde edilmesinde hammadde olarak genellikle hümik asit içerikli kömür (linyit, leonardit, turbo) kullanılmaktadır. Bu kapsamda ülkemizin önemli bir doğal kaynağı olan linyit veya leornardit esaslı kömürden laboratuar ve pilot ölçekte değişik oranlarda azot (N), fosfor (P), potasyum (K) ve kükürt (S) içeriğine sahip organomineral gübre üretimi gerçekleştirilmiş ve üretim prosesi ortaya çıkarıldığı belirtilmiştir (Kimyasal Teknoloji Enstitüsü).

YERALTI KÖMÜR İŞLETMELERİNE YAPILAN DESTEK ÖDEMELERİ

Kömür üretimi yapan yeraltı işletmelerinde asgari ücretin iki katı ödenmesi, çalışma sürelerinin kısalması ve yıllık izin gün sayısının artması sonucu oluşan maliyet artışlarından dolayı destek verilmesine karar verilmiştir. Kömür işletmelerinde işçi maliyetlerine destek Linyit ve taşkömürü çıkaran ve özel hukuk tüzel kişilerinin ruhsat sahibi olarak işlettikleri yer altı maden işletmelerinde meydana gelen maliyet artışlarının karşılanması amacıyla bu işletmelere destek verilmesine ilişkin usul ve esaslar belirlenmiştir. Yeraltı Kömür İşletmelerinde İşçi Maliyetlerine Uygulanacak Desteğe İlişkin Tebliğ, Resmi Gazete'de yayımlanarak yürürlüğe girmiş, buna göre, söz konusu işletmelere verilecek destek; asgari ücretin iki katı ödenmesi, bir işçi için çalışma saatinin azalması, bir işçi için verilen yıllık izin gün sayısının artması sonucu oluşan maliyetleri kapsayacak şekilde düzenlenmiştir. Üretim ve hazırlık yapılan yer altı kömür işletmesinde aylık üretimin, o ayda işletmede çalışan toplam işçi sayısına bölünmesi ile bulunan işçi başına düşen kömür miktarı olarak randıman (ton/yevmiye sayısı) değerine göre destek katsayısı hesaplanarak bulunmaktadır. Ruhsat sahiplerinin verilen destekten yararlanabilmesi için ruhsat sahasında yeraltı işletme yöntemi ile üretim veya hazırlık yapması, özel hukuk tüzel kişisi olması ve ruhsat sahasında üretim faaliyetinin ruhsat sahibi şirketçe yapılması gerekecek. Destekten yararlanacaklardan ruhsat sahipleri, bu Tebliğ kapsamında istenen bilgileri kendilerine verilecek şifre ile elektronik sistemde Maden ve Petrol İşleri Genel Müdürlüğü kayıtlarına girecek. Sistemden alınan çıktılar ruhsat sahibi tarafından imzalanacak ve bu belgelerle Genel Müdürlüğe başvuru yapılacak. 1 Ocak 2016'tan itibaren geçerli Ruhsat sahibince destek için hazırlanan başvuru dosyasında destek talebinde bulunulan aya ait SGK'ya bildirilen işçilerin yer altı ve yer üstü olarak isim listesi, aylık işçi bazında yevmiye sayıları, tahakkuk eden ücreti içeren bordro listesi, işçilere yapılan ödemelere ait banka onaylı ödeme dökümü, maden çalışanları zorunlu ferdi kaza sigorta poliçe bilgilerinin yer alması gerekecek. Söz konusu tebliğe göre hesaplanacak destek ödemeleri, 1 Ocak 2016 tarihinden itibaren başlamış olup, 5 yıl süreyle hesaplanarak ödenerek devam edeceği belirtilmişti.

Destek Verilebilecek Durumlar

İlk işletme izni düzenlenmiş ruhsat sahalarında ya da ruhsat sahasında ilk defa yer altı işletmesi açılması durumunda, işletme projesinde madene ulaşmak, ocak alt yapısı, nakliyat ve havalandırma amaçlı galeri, kuyu, desandre ve kömür içerisinde taban yolları ve baş yukarı sürülmesi ve üretim panosu oluşturma gibi hazırlık faaliyetlerinin verilen hazırlık termin projesine uygun olarak sürdürüldüğünün mahallinde tetkik ile tespitinin yapılması durumunda bu hazırlık faaliyetlerine projede sunulan hazırlık termin süresi sonuna kadar destek ödemesi yapılabilir (Resmi Gazete, 2016).

Aynı ruhsat sahasında, aynı işyeri sicil numarası ile birbirinden bağımsız birden fazla yeraltı kömür ocağı işletmesi bulunması durumunda, işletme güvenliği açısından üretim faaliyetleri durdurulan ocak/ocakların Maden Kanunu'nun 32'nci maddesine uygun şekilde terk edildiğinin Genel Müdürlükçe kabul edildiği yönündeki yazının ruhsat sahibine tebliğ edilmesini müteakip işletme güvenliği sağlanmış bir şekilde üretim faaliyetleri devam eden ocak/ocaklar için destek ödemesi yapılabilir.

Aynı ruhsat sahasında farklı işyeri sicil numarasına sahip birbirinden bağımsız üretim faaliyeti durdurulmayan işletmeler için destek ödemesi yapılabilir. İşletme ruhsat sahalarında işletme güvenliği

sağlanmış yeraltı ocağında üretim faaliyetleri devam ederken aynı işyeri numarası ile mevcut ocaktan bağımsız yeni bir yeraltı kömür ocağı hazırlanması durumunda destek ödemesi yapılabilir.

Destek Verilmeyecek Durumlar

Aile, Çalışma ve Sosyal Hizmetler Bakanlığınca 6331 sayılı İş Sağlığı ve Güvenliği Kanunu kapsamında, işin durdurulmasına karar verilen işyerlerinde, işin durdurulması kararının uygulanması ile bu kararın kaldırılmasına ilişkin İş Mahkemeleri veya Çalışma ve Sosyal Güvenlik Bakanlığı tarafından alınmış kararların uygulanması arasında geçen sürede destek ödemesi yapılmaz.

Enerji ve Tabii Kaynaklar Bakanlığınca 3213 sayılı Maden Kanunu kapsamında işletme güvenliği açısından (Kanunun 31 inci maddesi ve 29 uncu maddesinin birinci ve ikinci fıkrası gereğince) üretim faaliyetleri durdurulan işletmelerde, üretim faaliyetlerinin durdurulması ile üretim faaliyetlerine müsaade edildiği tarihe kadar geçen sürede destek ödemesi yapılmaz (Resmî Gazete, 2016).

Ayrıca işletme güvenliği açısından tehlikeli durumlar bulunması nedeniyle üretim faaliyetleri durdurulan dönemde yapılan hazırlık faaliyetleri için de destek ödemesi yapılmaz.

- Çalışanların ücreti ödenmeden destek ödemesi yapılmaz.
- Yeraltı işletme yöntemi ile faaliyette bulunulan linyit ve taşkömürü işletme izinli ruhsat sahalarında; Maden Kanunu'nun 31 inci maddesine istinaden teknik/daimî nezaretçi ataması olmayan dönemdeki günlerde destek ödemesi yapılmaz.
- Zorunlu ferdi kaza sigorta poliçesi, destek ödenmesi için başvuruda bulunan ruhsat sahibi özel hukuk tüzel kişisi adına yaptırılmayan yeraltı çalışanları için ödeme yapılmaz.
- Aynı ruhsat sahasında, aynı işyeri sicil numarası ile birbirinden bağımsız birden fazla yeraltı kömür ocağı işletmesi bulunması durumunda, ocaklardan herhangi birisinde üretim faaliyetlerinin/işin durdurulması halinde destek ödemesi yapılmaz.
- Hazırlık termin süresi sonunda işletme güvenliği sağlanmış bir şekilde üretim faaliyetlerine geçilmemesi durumunda sonraki aylar için destek ödemesi yapılmaz (Resmî Gazete, 2016).

Destekten Yararlananlardan İstenilen Bilgi ve Belgeler

İlk defa destek ödemesinden yararlanmak isteyen ruhsat sahipleri başvuruları için, Ek Form-1 de ve Tebliğ kapsamında istenen bilgileri kendilerine verilecek şifre ile elektronik sistemde Genel Müdürlük kayıtlarına girmek zorundadır. Sistemden alınan çıktılar ruhsat sahibi tarafından imzalanır. Ruhsat sahibince imzalanmış bilgi ve belgeler ile Genel Müdürlüğümüze başvuru yapılması gerekir. Destek talebinde bulunulan aya ait; Aylık üretim miktarı, Üretim panosunun adı ve kotlarına ilişkin bilgiler, çalışanların ücretlerinin ödenip ödenmediğine dair bilgi, işçi başına brüt ve net ücret, Zorunlu ferdi kaza sigortası poliçe no, Bölgesel teşvikten yararlanıp yararlanamadığına dair bilgi, Yatırım teşvikten yararlanıp yararlanılmadığına dair bilgi, varsa faaliyet durdurma ve başlama zamanına ait bilgilerin, Genel Müdürlüğümüzün internet sayfası üzerinden girişleri yapılır. Destek ödemesinden yararlanabilmek için kömür üretimi de yapılması erekir. Şekil 4'te kömür üretimi yapan ayakta çalışanlardan bir görünüm vardır. Şekil 5'de Kömür şehri Zonguldak da Taş kömürü anıtı ile kömürün önemi vurulanmaya çalışılmıştır.

Şekil 4. Ayak içinde kömür üretiminde çalışanlardan görünüm (Kocaman, 2018)

Destek Hesaplamasında Dikkate Alınan Hususlar

- Tüzel kişiliğe haiz ruhsat sahibi tarafından yeraltı kömür ocağından/ocaklarından yapılan aylık tüvenan kömür (ton) üretim miktarı ve SGK'dan alınan; faaliyette bulunan işletmeyle ilgili tüm çalışanların (yeraltı + yerüstü) aylık yevmiye sayısı üzerinden randıman hesabı yapılır.
- SGK'dan bildirilen faaliyette bulunulan yeraltı işletmesindeki yeraltı olarak verilen yevmiye sayısına aylık bazda destek ödenir.
- Açık ve yeraltı işletme faaliyetleri ortak olarak yürütülen ruhsatta, her iki faaliyete ortak hizmet sunan işçiler açık ve yeraltı işletmesinde çalışan işçi sayısına oranlanarak randıman hesabında kullanılır. Randıman hesabında açık işletmeden yapılan üretim ve açık işletmedeki işçi sayısı dikkate alınmaz.
- Ödeme tutarlarında; randımana bağlı kişi başı aylık ödenecek destek tutarı ay gün sayısına bölünerek elde edilen rakam; 5 inci maddede düzenlenen destek verilmeyecek hükümler
- Kapsamındaki hususlar çıkarıldıktan sonra kalan yevmiye sayısı ile çarpılarak ruhsat sahibine o ay için ödenecek toplam tutar belirlenir ve bu miktar üzerinden ödeme yapılır.
- Destekten yararlanan ruhsat sahibinin Genel Müdürlüğe bildirmiş olduğu KEP adresine yapılacak olan durdurma veya başlatma bildiriminin yapıldığı tarih tebliğ tarihi olarak kabul edilir ve bu bildirim tarihleri arasında destek ödemesi yapılmaz.
- 6331 sayılı İş Sağlığı ve Güvenliği Kanunu kapsamında, mülki idare amirlikleri tarafından gerçekleştirilen işin durdurulması ve durdurma kararının kaldırılmasına ilişkin işlemler, Çalışma ve İş Kurumu İl Müdürlükleri tarafından, işleme ilişkin tutanağın kendilerine ulaşmasını takiben iki iş günü içerisinde Genel Müdürlüğe bildirilir.
- İşverene verilecek işçi desteğinin hesabında; esas alınacak asgari ücret, işverenin çalıştırdığı sigortalılardan dolayı yararlandığı teşvik ve destek tutarları düşülmek suretiyle hesaplanır.
- Destek ödemesine konu işlemlerde ruhsat sahibinin beyanı ile SGK verilerinin uyuşmaması halinde SGK verileri esas alınır.

- 1/9/2014 tarihinden sonra faaliyete geçen işletmeler için, 2014 yılının ilk sekiz ayında faaliyette bulunan işletmeler için hesaplanan (lo) değeri kullanılır.
- Destek ödemeleri; Genel Müdürlük kayıtları, Tebliğ ekinde yer alan başvuru formundaki bilgiler, SGK verileri ve SBM (Sigorta Bilgi Merkezi) verileri de dikkate alınarak Genel Müdürlükçe yapılacak kontrol ve hesaplamalar sonrasında ruhsat sahibi tarafından bildirilen Banka hesabına yatırılır.
- Genel Müdürlük gerekli gördüğü hallerde, Tebliğ kapsamında her türlü bilgi ve belgeyi isteyebilir ve bunların doğruluğunu denetleyebilir.
- Destek ödemesi ile ilgili olarak ruhsat sahiplerinin tereddüte düştüğü durumlarda Genel Müdürlüğün kararı doğrultusunda işlem yürütülür.

Destek ile İlgili Cezai Hükümler

Açık ve yer altı üretim yöntemi ile faaliyette bulunulan sahalarda, açık işletmelerden üretilen kömürün yer altı üretimi olarak beyan edilmesinin ve/veya dışarıdan kömür alındığının tespiti halinde, fazla ödenen destek tutarının 10 (on) katı tutarında ceza tahsilatı yapılır. Fazladan ödenen destek tutarının 10 (on) katı tutarındaki ceza, varsa işverene ödenecek müteakip destek tutarlarından mahsup edilir. Bu durumda karşılanamayan ceza tutarı genel hükümlere göre takip ve tahsil edilir (Resmî Gazete, 2016).

Destek Ödemeleri ile İlgili İstatiksel Veriler

1/1/2016 tarihinden itibaren; 2016 -2021 yıllarında faydalanılan destek miktarları tablo halinde aşağıdaki şekildedir.

Kömür Desteği: 25/3/2020 tarihli ve 31079 sayılı Resmi Gazete'de yayımlanan 24/3/2020 tarihli ve 2282 sayılı Cumhurbaşkanlığı Kararı ve “Yer Altı Kömür İşletmelerinde İşçi Maliyetlerine Uygulanacak Desteğe İlişkin Tebliğ” hazırlanarak 3/6/2020 tarih ve 31144 sayılı Resmi Gazete’de yayımlanmıştır. Ayrıca, kömür destek ödemeleri için 2021 yılında 299.517.000₺ ödenek ayrılmıştır.

Bu kapsamda yıllara sâri olmak üzere yapılan kömür destek ödemeleri Çizelge 3’te gösterilmiştir.

Çizelge 3. Yıllar itibari ile destek ödemeleri (Maden ve Petrol İşleri Genel Müdürlüğü)

2016	2017	2018	2019	2020	2021	Genel Toplam
12.650.858	10.264.010	57.447.082	37.661.779	251.073.535	209.486.845	578.584.110

Destek ödemeleri beş yıllık ödeme yapıldıktan sonra 2021 yılındada Cumhurbaşkanlığı kararı ile bir yıl daha uzatılmıştır. Önümüzdeki yılllarda da destek ödemelerinin devam etmesi yönünde beklentiler oluşmuştur.

Şekil 5. Taş kömürü anıtı, Zonguldak (Kocaman, 2018)

SONUÇLAR

Son yıllarda maliyet artışları nedeniyle çalışanların üçretlerini ödemede sıkıntı çeken firmaların ayakta kalabilmeleri için teşvik ve destek gelirlerine de ihtiyaç duymaya başlamışlardır. Yeraltı kömür işletmelerine yapılan desteğin de ekonomik açıdan firmalara girdi sağlamıştır. Linyit ve Taşkömürü üretiminde bulunan firmalara yeraltı maden işletmelerinde meydana gelen maliyet artışlarının karşılanması amacıyla yapılan destek ödemeleri çerçevesindeki düzenlemelerin; sektör açısından çok önemli olumlu sonuçlar verdiği aşikar olduğu, üretim miktarlarının artışını, mevcut çalışanların isdihdamını koruduğu, işsizliğin azalmasını sağladığı, yeni çalışanlara isdihdam sağladığı, çalışan sayılarındaki artışa parallel olarak üretim mikterında da artış sağladığı, üretim faaliyetlerinin durdurulmasının önlendiği, madenlerde zorunlu ferdi kaza siğortasını yaptırmalarını sağladığı, daimi nezaretci olmadan çalışılmamasını sağladığı, üretimlerin kontrol edilerek denetimlerin artmasının sağladığı, ocaklara yatıtım yapılmasına katkısının olduğu, uygulanabilir üretim planlamalarının yapıldığı, kazaların da önlenmesinde azalmasında önemli bir etken olduğu düşünülmektedir. Bir avuç kömür için canını verenlerin anısına saygılarımızla.

KAYNAKLAR

Dünya ve Türkiye Kömür Kaynak ve Rezerv Durumu. Türkiye Kömür İşletmeleri. (n.d.). Erişim tarihi: 21 Şubat 2022, erişim adresi: https://www.tki.gov.tr/istatistikler

Elektrik. Elektrik - T.C. Enerji ve Tabii Kaynaklar Bakanlığı. (n.d.). Erişim tarihi: 21 Şubat 2022, erişim adresi: https://enerji.gov.tr/bilgi-merkezi-enerji-elektrik

Kızgut, S., Çuhadaroğlu, D., & Çolak, K. (2001). Çatalağzı Termik Santralı Uçucu Küllerinden Tuğla Üretim Olanaklarının Araştırılması. Uluslararası Madencilik Kongresi ve Sergisi-TUMAKS.

Kocaman, R. ve Kocaman, B. (2017, Ocak). Kömürden Enerji Elde Edilmesi. 8. Enerji Verimliliği Forumu ve Fuarı Bildiriler Kitabı.

Kocaman, R., Ateş, S., Toprak, H., & Kocaman, B. (2017, September). Kömür Atıklarının Farklı Değerlendirilmesi. In 5th International Symposium on Innovative Technologies in Engineering and Science 29-30 September 2017 (ISITES2017 Baku-Azerbaijan).

Kocaman, R. (2018). Fotoğraf Albümü.

Kömür Arama Araştırmaları. MTA Genel Müdürlüğü. (n.d.). Erişim tarihi: 21 Şubat 2022, erişim adresi: https://www.mta.gov.tr/v3.0/arastirmalar/komur-arama-arastirmalari

Kömür Esaslı Alternatif ürünlerin üretimi. Kömür Esaslı Alternatif Ürünlerin Üretimi | Kimyasal Teknoloji Enstitüsü. (n.d.). Retrieved February 21, 2022, from https://kte.mam.tubitak.gov.tr/tr/arastirma-alanlari/komur-esasli-alternatif-urunlerin-uretimi

Kömür ve linyit Yakıtlı termik santraller. Enerji Atlası. (n.d.). Erişim tarihi: 21 Şubat 2022, erişim adresi: https://www.enerjiatlasi.com/komur/

Maden İstatistikleri. Maden Petrol İşleri Genel Müdürlüğü. (n.d.). Erişim tarihi: 21 Şubat 2022, erişim adresi: https://www.mapeg.gov.tr/Custom/Madenistatistik

Yeralti Kömür İşletmelerinde İşçi Maliyetlerine Uygulanacak Desteğe İlişkin Tebliğ. (2016, 26, Haziran). *Resmi Gazete*. (Sayı: 29754). Erişim adresi: https://www.resmigazete.gov.tr/eskiler/2016/06/20160626-14.htm

YERALTI KÖMÜR MADENCİLİĞİNDE HALAT SAPLAMA OPERASYONUNUN MEKANİZE DELGİ VE ENJEKSİYON SİSTEMLERİ İLE GELİŞTİRİLMESİ: YATAĞAN ÖRNEK ÇALIŞMASI

DEVELOPMENT OF CABLE BOLT OPERATION IN UNDERGROUND COAL MINING WITH MECHANIZED DRILLING AND INJECTION SYSTEMS: YATAGAN CASE STUDY

A. Erel [1, *], C. Tuz [2]

[1] *Entek Elektrik İnşaat A.Ş.*
*(*Sorumlu yazar: ahmet.erel@entekinsaat.com.tr)*
[2] *Weber Madencilik San. ve Tic. LTD. ŞTİ.*

ÖZET

Halat saplama uygulamaları son yıllarda yeraltı kömür madenciliğinde yaygın olarak kullanılmaktadır. Özellikle zayıf kaya kütlesi koşullarında halat saplama uygulamaları önemli avantajlar sağlamaktadır. Geleneksel yöntemde uygulama elle tutulan ve yönetilen delici makinalar ile gerçekleştirilmekte ve gerdirme işlemlerinde taşınabilir germe krikolu pompalar kullanılmaktadır. Montaj işleminde kimyasal kartuşlar kullanılarak halat saplamalar stabilize edilmektedir. Bu geleneksel yöntemlerden kaynaklı uygulamasal zorluklar oluşmakta, iş gücü artmakta ve iş güvenliği açısından problem oluşturabilecek durumlar meydana gelmektedir. Bu çalışma kapsamında halat saplama uygulamalarında delgi işleminin galeri açma makinası ile uyumlu mekanize sistemlere dönüştürülmesi için göz önünde bulundurulması gereken teknik parametreler belirtilmiştir. Aynı zamanda halat saplamaların stabilizasyonunda pompalanabilir kaya saplama reçinelerinin kullanımının sağladığı avantajlar ve teknik değerlendirmeleri yer almaktadır. Oluşturulan bütünleşmiş halat saplama uygulaması sisteminin iş güvenliği açısından değerlendirmeleri yapılmıştır.

Anahtar Sözcükler: Halat Saplama Uygulaması, Mekanize Delici, Pompalanabilir Kaya Saplama Reçinesi, Kimyasal Enjeksiyon Sistemleri

ABSTRACT

Cable bolt operations have been widely used in underground coal mining in recent years. Especially in weak ground conditions, cable bolts provide important advantages. In the traditional method of cable bolt, the application is carried out with hand-held drilling machines, and portable tensioning jack with pumps are used in the tensioning process. In the assembly process, the cable bolts are stabilized by using chemical cartridges. Due to these traditional methods, operational difficulties arise, the labor force increases, and situations that may create occupational safety problems are encountered. Within the scope of this study, the technical parameters to be considered in order to transform the manual drilling process into mechanized drilling systems compatible with the roadheader machine in cable bolt operations are specified. At the same time, there are advantages and technical evaluations of the use of pumpable resins in the stabilization of cable bolts. Evaluations of the integrated cable bolt application system were made in terms of occupational safety.

Keywords: Cable bolt operation, mechanized drilling, pumpable rock bolt resin, chemical injection systems

GİRİŞ

Destek sistemleri kullanılarak yeraltında galeri ilerlemelerindeki açıklıkların tahkimatlandırılması çalışma ortamının güvenli hale getirilmesi ve çalışanların iş güvenliğinin sağlanması için gereklidir. Zayıf kaya kütlesi yapılarında farklı tahkimat tipleri kullanılmaktadır. Zayıf kaya kütlelerindeki açıklıkların tahkim edilmesi için kaya saplamalar başta olmak üzere çelik tahkimat, püskürtme beton vb. birçok tahkimat tipi kullanılmaktadır (Kahraman, 2019).

Yaygın olarak kullanılan kaya saplamaları kaya kütlesi yapısına bağlı olarak çeşitlilik göstermektedir. Kaya saplamalar; montajlanma şekillerine (kaya kütlesi ile kaya saplama arasındaki stabilizasyon sağlanmasına) ve kaya saplamalarının çeşitlerine göre sınıflandırılmaktadır. Montaj şekline göre mekanik ankrajlı sürtünme kuvvetinden faydalanan ve enjeksiyonlu yapışma kuvvetinden faydalanan sistemler örnek verile bilinir. Mekanik ankraj olarak split set ve swellex bilinen kaya saplaması tipleridir. Reçine kartuşlu, çimento enjeksiyonlu ve kimyasal enjeksiyonlu olmak üzere enjeksiyonlu kaya saplama türlerini gruplandırmak mümkündür. Kaya saplaması çeşitine göre ise nervürlü inşaat demiri (rebar), ibo bulon (ortasi delik çubuk), çelik halat, fiberglas vb. örnek olarak verile bilinir (Hoek, 2007; Öge, 2019).

Zayıf kaya kütlelerinde ve zemin özelliği gösteren yapılarda mekanik ankrajlı kaya saplamalarını kullanmak verimli olmadığından tercih edilmemektedir. Zayıf yapılarda sürtmeden faydalanmak olası değildir. Kaya saplaması yüke girdiği anda kaya kütlesinin yenilmesinden dolayı kaya saplamalarının verimliliği ciddi oranda düşmektedir. Zayıf kaya kütlesi yapılarında ve zemin özelliği gösteren matrisi çok zayıf olan kaya kütlelerinde genellikle enjeksiyonlu sistemler tercih edilmektedir (Hoek, 2007).

Kaya saplamalar diğer tahkimat türlerine göre ekonomik açıdan daha avantajlıdır. Kömür madenlerinde son dönemlerde kaya saplamaları yaygın olarak kullanılmakta ve tercih edilmektedir. Yüksek performansları ve mekanik özelliklerinin iyi olmasından dolayı tercih edilmektedir. Özellikle ön germeli halat saplamaların ve tam reçine dolgulu kaya saplamaların kullanımı her geçen gün yaygınlaşmaktadır. Kaya saplamalarında uygulama sonrasında sahada yapılan testler önem arz etmektedir. Bu sayede duraylılık analizleri yapılabilmekte ve nümerik analizler ile karşılaştırma olanağı oluşmaktadır. Bu analizler neticesinde kaya saplamaların zayıf kaya kütlelerinde büyük avantajlar oluşturduğu görülmektedir (Kang, 2014; Tuz vd., 2021).

Bu gibi avantajlar göz önünde bulundurulduğuna halat saplama uygulamalarının kömür madenciliğinde her geçen gün önemi artmaktadır. Halat saplama uygulama yöntemlerine göre geleneksel yöntem ve teknolojik olarak geliştirilmiş modernize sistemlere sahip yöntemler olmak üzere iki ana başlık altında gruplandırılmaktadır.

Geleneksel Halat Saplama Uygulama Yöntemi ve Operasyonel Zorluklar

Geleneksel halat saplama uygulaması yöntemi üç aşamadan oluşmaktadır. İlk aşamada iş gücüne dayanan pnömatik yüksek rotasyonlu delgi makineleri kullanılarak delik delinmektedir. İkinci reçine kartuş delik içerisine yerleştirmek ve çelik halatın stabilizasyonunu sağlamaktaır. Son aşamada da kriko yardımı ile gerdirme işleminin yapılmasıdır. Pnömatik yüksek rotasyonlu delici makinalar tavan delici (roof bolter), radyal delici (radial drill rig) ve kolonlu deliciler (column drill) olarak bilinmektedir (Kahraman, 2019).

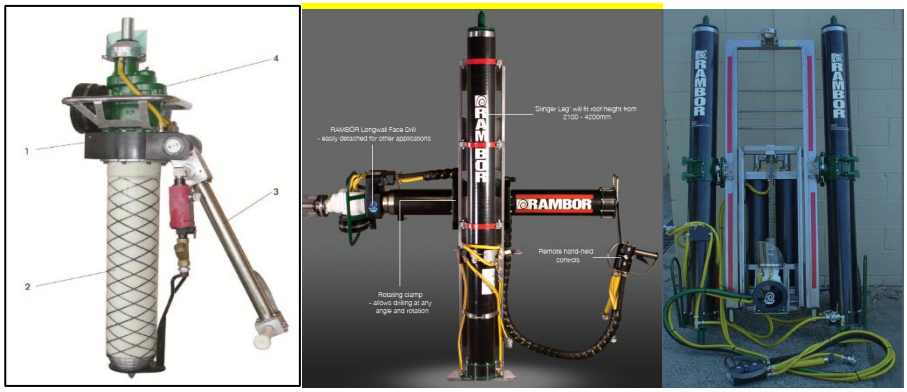

Şekil 1. Yüksek Rotasyonlu Delici Makinalar: tavan delici, radyal delici ve kolonlu delici-soldan sağa (Rambor, 2018; Jiangyin Jinniu Technology, 2008).

Delme işlemi için pnömatik delici makinalara ilave olarak yardımcı ekipmanlara ihtiyaç duyulmaktadır. Bu yardımcı ekipmanlar, eklemeli rod (hexagonal veya burgu tip), delici kafa (drill bit) ve bağlantı manşonlarıdır. Delgi boyu eklemeli rodlar sayesinde uzatılabilmektedir.

Geleneksel halat saplama uygulamasında delgi işlemi sonrasında delik içerisine reçine kartuş sokulmaktadır. Çift bileşenden oluşan bu reçine kartuşları, çelik halat yardımı ile delik içerisine ötelenir ve pnömatik delici makine ile çelik halat döndürülerek reçine kartuşun çift bileşeninin karışması sağlanmaktadır. Yapılan işlem sonrasında çelik halatın kaya kütlesine tutunması sağlanmaktadır.

Kaya kütlesine sabitlenen çelik halat, sıktırma takozu (wedge and barrel) ve ortası delik kare plaka kullanılarak montajı tamamlanır. Montajı tamamlanan halat saplamalar, halat üzerinde hareket edebilen hidrolik ünite (pnömatik yağ pompası) yardımı ile çalışan germe krikoları (tension jack) sayesinde ön germesi yapılmaktadır.

Geleneksel halat saplama uygulamasında tüm yapılan işler insan gücüne dayanmaktadır. Özellikle delik delme işlemi genellikle tahkimatsız veya yüksek riskli bölgelerde gerçekleştirilmektedir. Yeraltı madencilik faaliyetleri arasında özellikle zayıf tavan kaya kütlesi koşullarında en tehlikeli operasyonlardan biridir. Halat saplama operatörleri tahkimatsız bölgelerde çalışmak zorunda kalmanın yanı sıra çok fazla sayıda ekipmanla (pnömatik delici, eklemeli rodlar ve bit, reçine kartuş, ankraj plakası, çelik halatlar, vb.) çalışmak zorundalardır. Bu gibi durumlar iş güvenliği açısından yüksek riskler oluşturmakta ve bundan dolayı operasyonun nitelikli personel gereksinimini arttırmaktadır. Bahsedilen uygulama zorluklarından ve nitelikli personel gereksiniminden dolayı halat saplama uygulaması sürekli madencilik uygulamaları arasında yavaş ve hantal uygulama olarak görülmektedir. (Schmidt, 2014)

Günümüzde yeraltında tavan açıklıklarının olduğu bölgelerde çalışan hemen hemen her makine sistemi üzerinde geçici hidrolik bir tahkimat ünitesi yer almaktadır. Bu durum sayesinde jeolojik koşullardan kaynaklanan tavandan kaya düşmeleri ve ufak kayaların dökülmesinden kaynaklanacak iş kazalarının önüne geçmektir. Özellikle kendini tutma süresi sınırlı olan zayıf kaya kütlesi koşullarında tavandan düşen kaya parçalarından kaynaklı kaza oranı ne yazık ki çok yüksektir. Yer altı kömür madenciliğinde bu duruma en uzun süre maruz kalan ve risk düzeyi en yüksek grup tavan saplama uygulaması ekibidir. Geleneksel yöntemler ile yapılan delgi uygulamalarında tavandan oluşabilecek olan dökülmelere yönelik geçici bir hidrolik tahkimat sistemi ile koruma sağlanması mümkün değildir. Bundan dolayı madencilerin riskli bölgede dikkatli bir şekilde çalışması ve sürekli olası duraysızlık sorunlarını gözlemlemeleri gerekmektedir (Fiscor, 2002).

Halat saplama operatörleri hantal ve ağır ekipmanları zor pozisyonlarda kaldırması gerektiğinden dolayı halat saplama uygulaması zor ve ergonomi problemlerin yer aldığı bir uygulamadır. Çalışma

koşullarının ve ortamlarının değişmesinden dolayı operatörler kendi çalışma standartlarının dışında kaldıkları (ergonomik olmayan durumlar) için iş güvenliği problemleri oluşabilmektedir. Yüksek yeraltı açıklıklarında küçük ekipmanlar ile çalışmak zorunda kalmak bu gibi durumlara örnek verilebilir. Bu durumun tersi olan alçak yeraltı açıklıklarında ergonomik olmayan büyük ekipmanlar ile çalışmak da problem oluşturmaktadır (Fiscor, 2012).

Operasyonel zorluklardan kaynaklı olarak iş güvenliği ve ergonomi problemleri oluşmaktadır. Bu problemlerin yanı sıra operasyonel zorluklardan kaynaklı iş verimliliğini düşüren problemlerde oluşmaktadır. Bu problemlerin başında reçine kartuştan kaynaklanan problemler gelmektedir.

Reçine kartuşların priz alma sürelerine göre tasarlanması önemli parametrelerden biridir. Halat saplamalarının sıkılama işlemi ile delik içerisine ötelenmesi işlemi göz önünde bulundurularak reçine kartuşların sertleşme sürelerine göre delik içerisinde sıralanması önemlidir. Yapılacak olan priz alma süresine bağlı kartuşun delik içerisinde sıralanması yani kartuş tasarımı montajlama işlemi için önem arz etmektedir. Kısa reaksiyon süresine sahip reçine kartuşlar genellikle delik içerisine en son yerleştirilmektedir. Tasarıma dikkat edilmemesi durumunda halat saplamanın tam delik içerisine ilerletilememesi gibi montaj problemleri yaşanmaktadır. Ayrıca sık olarak görülen tasarımdan kaynaklı bir diğer problem yapılan çekme testlerine göre halat saplamanın mekanik özelliklerinin düşmesidir (Öge, 2019).

Halat saplama uygulamalarında reçine kartuştan kaynaklı yaşanan en bilindik problem kaya yüzeyi (delik iç yüzeyi) ile kartuş arasında bağlantının sağlanamamasıdır (Glove finger effect). Reçine kartuşlar plastik kapsül filmler içerisinde bulunmaktadır. Bu plastik kapsüller zemin ile reçine kartuş arasında kalarak bariyer oluşturmaktadır. Eldivenli parmak etkisi olarak bilinen bu durumdan dolayı kaya kütlesi ile reçine kartuş bütünleşememektedir. Bu durumun reçine kartuşla yapılan uygulamalarda tamamen engellenebilmesi mümkün değildir. Montajlama sırasında bazı teknik parametrelere dikkat edilmesi bu durumun oluşmasını azaltmaktadır. Delik çapının olabildiğince küçük tutulması yüksek oranda fayda sağlamaktadır. Çelik halatın delik içine ötelenmesinde rotasyon hızının yüksek tutulması gerekmektedir. Yüksek rotasyonla yapılan montajlamalarda reçine kartuşlar daha iyi karışmakta ve yapılan test sonuçlarında daha başarılı sonuçlar elde edilmektedir (Pettibone, 1987; Öge, 2019; Craig, 2012). Reçine kartuşların kullanımından kaynaklı oluşan eldivenli parmak etkisinden dolayı halat saplama uygulamalarında iş verimliliği düşmektedir.

Reçine kartuşların kaya saplama operasyonlarında oluşturduğu bir diğer problem reçine kayıplarıdır. Çatlaklı ve zayıf kaya kütlesi koşullarında reçine kartuşlar ile yapılan kaya saplamalarda teorik (hesaplanan) kolon kaplama (kapsülleme) mesafesi ile gerçek (görülen) kapsülleme mesafeleri arasında fark araştırılmıştır. Araştırma sonucunda zemin yapısından kaynaklı olduğu düşünülen delik çapının 27 mm olması durumunda %28 reçine kaybı oluşmaktadır. Delik çapının 28 mm olarak ayarlandığı testlerde ise reçine kaybı oluşmamaktadır. Reçine kartuşlar ile tam kolonlama (tam delik dolgulu) yapılması durumunda da reçine kaybı oluşmamaktadır (Craig, 2012). Yapılan testlerden ve gözlemlerden edinilen bilgiler doğrultusunda delik çapının reçine kartuşlu kaya saplama uygulamalarında yüksek hassasiyet içerdiği görülmektedir. Aynı zamanda kapsülleme mesafesinin de önemli olduğu görülmektedir. Geleneksel halat saplama uygulamalarında reçine kartuş kullanımı ile tam kolonlu halat saplama yapılması operasyonel olarak mümkün değildir. Çelik halatın esnek yapısı ve delik uzunluklarının yüksek olmasından dolayı kolon kaplama mesafesinin arttırılması operasyonu zorlaştırmaktadır. Diğer bir değişle reçine kartuşla yapılan halat saplamalarda reçine kolon kaplama mesafesinin düşük tutulması reçine kayıplarına sebep olurken reçine kolon mesafesinin arttırılması operasyonu zorlaştırmaktadır.

Operasyonel olarak karşılaşılan bir diğer zorluk taşınabilir ekipmanların (pnömatik delici, yağ pompası ve germe krikosu) çok sık arızalanmasıdır. Özellikle yağ pompası ve delici ekipman darbelere karşı dayanaksız makinelerdir. Arızaların temel sebebi ekipmanların taşınabilir olmasından dolayı yüksek oranda darbeye maruz kalmasıdır. Aynı zamanda pnömatik ekipmanların motor içi arızalarının hava

girişinden motor içerisine giren partiküllü yapılardan olduğu görülmektedir. Hava girişinden partiküllü yapıların girişi genellikle taşıma sırasında gerçekleşmektedir. Taşımadan kaynaklanan bu gibi arızalardan dolayı iş akışında aksamalar yaşanmakta ve bu aksamalardan dolayı iş verimliliği düşmektedir.

Halat Saplama Uygulaması Teknolojik Gelişmeler ve Yatağan Örnek Çalışması

Abdullah Erhan Tercan ve Bahtiyar Ünver tarafından hazırlanan Yatağan Sektör A yeraltı maden sahası raporunda kaya kütlesinin zayıf bir yapıda olduğu belirtilmiştir. *"Sahada gözlenen kaya yapısının genel anlamda diyajenezi tamamlanmamış olduğu görülmektedir. Bu nedenle sahada gözlenen neredeyse tüm kaya yapısının zemin niteliğinde olduğunu söylemek doğru olacaktır. Ocak derinliği arttıkça örtü yüklerine bağlı olarak basınçların artması beklenmelidir. Yüksek basınç ortamında zayıf kaya/zemin içerisinde açılacak yer altı galerilerinin duraylı tutulmasının problemli olacağı ön görülmektedir. Buna ilave olarak ortama su geliri olması durumunda sorunun daha da büyüyeceği aşikardır."* Bu tür zayıf kaya kütlelerinde halat saplama uygulaması yaygın bir şekilde kullanılmaktadır.

Soma bölgesinde Polyak Eynez yeraltı kömür madeninde elde edilen deformasyon verilerine göre halat saplama uygulamasının zayıf kaya kütlesinde duraylılık açısından fayda sağladığı görülmektedir (Tuz vd., 2021).

Halat saplama ve kaya saplama uygulamalarının yeraltı madenciliğinde önemli yere sahip olmasından dolayı ve bu uygulamalarda yaşanan operasyonel zorlukların iş güvenliği ve iş verimliliğine olumsuz etkilerinin azaltılması amaçlı bu alanda teknolojik gelişmeler yer almaktadır.

Bu teknolojik gelişmelerin başında halat saplama uygulamasının açıklık tavanı bölgesinde en yüksek risk ihtiva eden operasyonu olan delik delme işlemi gelmektedir. Geleneksel yöntemlerde kullanılan pnömatik tavan delici ekipmanların yerine modern sistemlerde mekanize deliciler kullanılmaktadır.

Yeraltı kömür madenciliğinde de mekanize deliciler hazırlık operasyonlarında yaygın olarak kullanılmaktadır. Galeri açma makineleri (roadheader, continuos miner) üzerine montajlanan delici ataçmanlar delgi operasyonlarını kolaylaştırmaktadır. Aynı zamanda sabit olan bu üniteler taşınabilir ekipmanlara göre daha yüksek performans sağlamaktadır. Bu durumlar sayesinde delgi operasyonundan kaynaklanan zorluklar azalmaktadır.

Yatağan projesinde galeri açma makinasına montajlanacak olan delici ataçman seçiminde göz önünde bulundurulan önemli teknik parametreler;

1. Ataçman galeri ilerlemesi sırasında pasif pozisyonda operasyonlara (kazı, çelik bağ montajı vb.) engel teşkil etmemelidir. Delici ataçmanın çalışmadığı pasif pozisyonda operasyonel olarak aktif olan ön bölgenin gerisine konumlanması gerekmektedir. Aktif pozisyona ise galeri açma makinasının kolunun önünde 180° delgi işlemi gerçekleştirecek şekilde konumlanabilmesi gerekmektedir. Hareket mekanizmasını sağlayan kızakların boylarının bu durumlar göz önünde bulundurularak ayarlanması gerekmektedir. (Şekil 2)
2. Maksimum çalışma yüksekliği ve genişliği galeri boyutlarına uygun olarak tasarlanmalıdır.
3. Operasyon verimliliğinin arttırılması için delici ataçman iki teleskobik delici üniteye sahip olmalıdır. Aynı anda iki delgi işleminin gerçekleştirilebilmesi olanağı operasyon hızını arttıracaktır.
4. Tavan ve taban destek pistonları ile tavanda ve tabanda kontak destek oluşturularak delici ataçmanın stabilizasyonu sağlanmaktadır. Bu sayede delgi işleminde titreşim ve sarsıntı probleminin önüne geçilmektedir.

5. Tavan destek sistemi tahkimatsız olan bölgede geçici tahkimat sağlamaktadır bu sayede bu bölgede çalışacak olan halat saplama operatörünün emniyetli bir bölgede çalışması sağlanmaktadır.
6. Delgi işlemi sırasında gevşek ve özellikle killi kaya yapısı koşullarında delik içindeki pasanın atılamamasından dolayı delgide sıkışmalar ve problemler oluşmaktadır. Aynı problem tabana yapılan uygulamalarda da görülmektedir. Bu gibi problemlerin yaşandığı bölgelerde burgu tipi rod kullanılması operasyonel olarak avantaj sağlamaktadır. Sert ve çatlaklı yapılarda hexagonal rod kullanımı operasyon verimliliğini arttırmaktadır. Delici ekipmanın bu durumlar göz önünde bulundurulduğunda burgu tipi rod ve hexagonal rod ile adaptasyonunun sağlanabilmesi gerekmektedir.
7. Yapılacak olan delgi işleminde halat saplama uygulamalarında önemli olan delik çapı parametresine dikkat edilmesi gerekmektedir. Rod çapları ve delici kafa çaplarının küçük tutulması önem arz etmektedir.

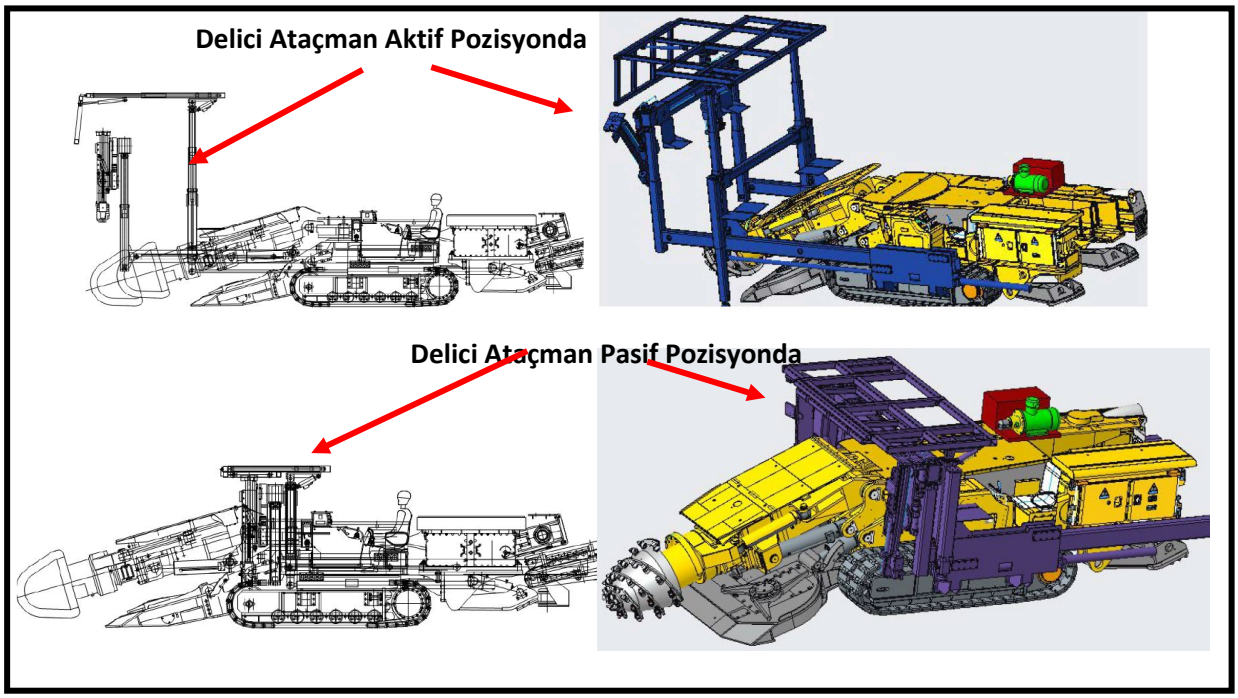

Şekil 2. Galeri açma makinası delici ataçmanı kapalı ve açık pozisyonlarda (NHG, 2021).

Halat saplama operasyonu için diğer önemli gelişme halat saplamanın kaya kütlesi stabilizasyonu için pompalanabilir kaya saplama reçinelerinin kullanımıdır. Geleneksel halat saplama yönteminde bu işlem için kimyasal kartuşlar kullanılmaktadır. Kartuş kullanımında yaşanan birçok problemin ortadan kaldırılmasının yanı sıra pompalanabilir kaya saplama reçinelerinin kullanımı ile operasyonel verimliliğin ve operasyon hızının artması sağlanmaktadır.

Pompalanabilir kaya saplama reçinelerinin uygulamasında enjeksiyon sistemlerine ihtiyaç vardır. Enjeksiyon sistemleri pompa ünitesi, besleme tankları, iletim hatları ve karıştırıcı tabanca ekipmanlarından oluşmaktadır.

Yatağan projesinde pompalanabilir kaya saplama reçineleri için tasarlanan enjeksiyon sistemlerinde göz önünde bulundurulan önemli teknik parametreler;

1. Operasyonel olarak aktif olan bölgede enjeksiyon sistemleri problem oluşturacağından dolayı bu sistemlerin arın ilerlemesinin gerisinde kurulması gerekmektedir. Bu sistemlerin galeri ilerlemesine bağlı olarak taşınmasının minimize edilmesi gerekmektedir. Bundan dolayı sistem içerisine yer alan pompanın basma mesafesinin yüksek tutulması gerekmektedir.

2. Pompa ile uygulama bölgesi arasında mesafe olmasından dolayı pompanın uygulama bölgesinden yönetilebilmesi gerekmektedir. Enjeksiyon sistemleri basit hidrolik sistemler oluğundan dolayı bu işlem için basınç şalteri gerekmektedir. Basınç şalteri ile elektrikli pompa basıncın yükselmesine bağlı olarak devre dışı kalmaktadır. Uygulama sırasında karıştırıcı tabanca üzerinde yer alan vanaların kapatılması ile basınç yükselmekte ve elektrik motoru pompalamayı durdurmaktadır.
3. İletim hatlarının pompanın basma mesafesini en yüksek seviyede tutacak şekilde tasarlanması gerekmektedir.
4. Kimyasal ürünlerin yeraltına naklinin nakliyata problem oluşturmaması ve operasyon sürekliliğinin sağlanması için IBC (Intermediate bulk container) tipi tanklarda olması gerekmektedir. Pompanın beslemesi yüksek hacimde IBC tanklar ile yapılmalıdır. Halat başı kimyasal tüketimi düşük miktarlarda olduğundan dolayı operasyonel süreklilik sağlanmış olacaktır.

Şekil 3. Pompalanabilir kaya saplama reçinesi için kullanılan enjeksiyon sistemleri örneği (Weber Madencilik, 2020).

SONUÇ VE DEĞERLENDİRME

Yatağan projesinde halat saplama operasyonu mekanize delgi ve enjeksiyon sistemleri ile geliştirilebilmesi için proje çalışması yapılmış ve bu proje çalışmasında göz önünde bulundurulan önemli teknik parametrelerden yukarıda bahsedilmiştir.

Yapılan bu geliştirme projesi ile ön görülen iyileştirmeler aşağıda yer almaktadır;

Geleneksel yöntemlerde tahkimatsız bölgelerde veya tavan açıklıklarına yakın olan bölgelerde yapılan uygulamalarda oluşan iş güvenliği probleminin ortadan kaldırılması geçici tavan tahkimatı ile sağlanmaktadır.

Ekipman taşınması ve ekipmanın kullanımı sırasında oluşan ergonomik problemler ekipmanların sabit olması ve ekipmanların hidrolik sistemler ile kumanda edilmesiyle engellenmektedir.

Ekipmanların sabit olması ile taşınabilir ekipmanlara göre oluşan arızaların azalması sağlanacaktır.

Delgi sisteminin mekanize olması ve enjeksiyon sisteminin pompalanabilir ve uzaktan kontrol edilebilir olması ile insan gücüne dayalı iş gücünün azaltılması sağlanmaktadır.

Çift delgi ünitesi sayesinde delgi operasyonu hızının artması sağlanmaktadır.

Pompalanabilir kaya saplaması reçinesi ile geleneksel yöntemlerde oluşan eldivenli parmak problemi tamamen ortadan kaldırılmaktadır. Montajdan kaynaklı oluşan halat saplamanın mekanik özelliklerinin düşmesi problemi engellenecektir. Bu sayede halat saplama tahkimatının verimliliği artmaktadır.

Pompalanabilir kaya saplama reçineleri tam reçine kolonlu kaya saplama uygulamasına olanak sağlamaktadır. Bu sayede halat saplamalarda oluşacak olan korozyon problemi engellenmiş olacaktır. Bu durum halat saplamanın mekanik özelliklerini de arttırmaktadır.
Pompalanabilir kaya saplama reçinesi çatlak yapılara nüfuz edeceğinden dolayı çatlaklı ve zayıf kaya kütlesi yapılarında enjeksiyon olarak da kullanılabilmektedir. Zayıf yapılarda konsolidasyon olanağı ve kaya kütlesi kalitesinde kısmi iyileşme sağlamaktadır.

Ayrıca geleneksel halat saplama uygulamasında karşılaşılan riskler ve tehlikeler aşağıdaki Çizelge 1' de yer almaktadır. Bu tehlike ve riskler yapılan geliştirmeler ile modernize sistemlerde ortadan kaldırılmaktadır ve iş güvenliği açısından avantajlar sağlanmaktadır.

Çizelge 1. Geleneksel yöntemde oluşan tehlikeler ve riskleri ortadan kaldırmaya yönelik modernize sistemlerdeki geliştirmeler

Geleneksel Yöntemde Tehlike/Riskler	Modernize Sistemlerdeki Geliştirmeler
Halat saplama makinesi operatör tarafından GAM platformu üzerinde yüksekte kullanılacaktır. Bu durumda ağır malzeme tehlikesi, devrilme tehlikesi ve düşme tehlikesi oluşmaktadır.	Delgi işlemi mekanize sistemler ile gerçekleştirileceğinden halat saplama operatörü uzaktan kumanda ettiği sabit sistem ile çalışacaktır.
Dar bölgede çok sayıda kişinin çalışmasından dolayı iş kazası riskinin yüksek olmaktadır	Delgi sistemi mekanize olduğundan kalabalık çalışma ortamı oluşmamaktadır.
Halat saplama ekipmanı ile ergonomik olmayan durumlarda çalışmaktan dolayı düşme riski ve vücut iskelet yapısında oluşacak bozukluklardan dolayı sakatlanma riski	Delici ekipmanın sabit ve mekanize olmasından dolayı ergonomik problemler ortadan kaldırılmış olacaktır.
Eğimli yerde halat saplama yaparken makine pistonunun kayması, çalışana çarpma riski,	Delici ekipman platform üzerinde mekanizmalı sistem ile hareket ettiğinden dolayı kayma ve çarpma riskleri ortadan kalkmaktadır.
Tavan akması, delik delinmesi sırasında taş düşme tehlikesi,	Tavanda yer alan geçici tahkimat sistemi ile tavan akması ve taş düşmesi problemi engellenmektedir.
Reçinenin delik içine montajı sırasında çalışanın eline taş ve parça düşme tehlikesi,	Enjeksiyon sistemine yer alan çubuk yardımı ile emniyetli bölgeden delik içerisine şarj yapılabilmektedir.

KAYNAKLAR

Craig, P. (2012) Addressing Resin Loss and Gloving İssues at a Mine with Coal Roof, Proceedings of the 2012 Coal Operators' Conference, Mining Engineering, University of Wollongong, 18-20 February 2019

Fiscor, S. (2002) New Approches Offer Better Ergonomics and Quality for Roof Bolters

Fiscor, S. (2012) Roof Bolting Technology, Coal Age Cilt 117 Sayı: 5

Hoek, E. (2007) Practical Rock Engineering, Rock Bolts and Cables, Rocscience Inc.

Jiangyin Jinniu Technology, 2008, MQT 120/2.7 Product Catalog

Kahraman, E., Tuz, C. ve Erel, A. (2019) Yeraltı Kömür Madenciliğinde Halat Saplama Makinalarının Güvenli Kullanımı, 7. Uluslararası Maden Makinaları ve Teknolojileri Kongresi

Kang, H. (2014) Support Technologies for Deep and Complex Roadways in Underground Coal Mines: a Review, International Journal of Coal Science and Technology

NHG (2021) Bolter with roadheader – Yatağan Project

Öge, İ., Tuz, C., Erel, A. ve Kahraman, E. (2019) Sedimanter Zayıf Kaya Kütlesinde Reçineli Halat Saplamaların Uygulama Parametrelerinin Çekme Dayanımına Etkisi, Türkiye 26.Uluslararası Madencilik Kongresi, Antalya

Pettibone, C., H. (1987) Avoiding Anchorage Problems With Resin-Grouted Roof Bolts

Rambor (2018) Bolter Equipment [Brochure] Retrieved from www.rambor.com.au

Schmidt, D. (2014) Roof Bolting Tools, Coal Age Cilt 119 Sayı:4

Tuz, C., Yılmaz, Ö., Bilen, M. ve Yılmaz, S. (2021) Soma Bölgesi Yeraltı Kömür Madenlerinde Hazırlık Galerilerinde Uygulanan Kaya Saplaması Çeşitleri ve Deformasyon Üzerindeki Etkileri, 8. Uluslararası Maden Makinaları ve Teknolojileri Kongresi

Weber Madencilik (2020) Pompa ve Ekipman Kataloğu [Broşür]

YERALTI KÖMÜR MADENLERİNDE KULLANILAN FENOL BAZLI DOLGU MALZEMELERİNİN KANSEROJEN FORMALDEHİD İÇERİĞİ ve İSG AÇISINDAN DEĞERLENDİRİLMESİ

EVALUATION OF PHENOL BASED FILLING MATERIALS IN TERMS OF CARCINOGENIC FORMALDEHYD CONTENT AND OHS (OCCUPATIONAL HEALTH AND SAFETY)

S. Yılmaz [1, *], M. Bilen [1], E. Kaymakçı [1], C. Tuz [1], E. Bahadır [2], İ. Toroğlu [1], H. Hacıfazlıoğlu [3], M. Şahin [4], Ö. Yılmaz [5]

[1] *Bülent Ecevit Üniversitesi Maden Mühendisliği Bölümü*
*(*Sorumlu yazar: s.yilmaz67@gmail.com)*
[2] *Maden Yüksek Mühendisi ve İş Güvenliği Uzmanı(A)*
[3] *İstanbul Üniversitesi Cerrahpaşa Maden Mühendisliği Bölümü*
[4] *İstanbul Üniversitesi, Fen Fakültesi, Kimya Bölümü*
[5] *Bülent Ecevit Üniversitesi ZMYO, Madencilik ve Maden Çıkarma Bölümü*

ÖZET

Bu çalışma kapsamında, formaldehit maddesi ve formaldehit içerikli kimyasal karışımların zararları ve oluşturduğu risk grupları üzerinde durulmuştur. Bu kanserojen ve mutajen maddelerin çalışma ortamlarında oluşturduğu tehlikeler ve kullanımı esnasında alınması gereken güvenlik önlemleri vurgulanmıştır. Gelişen teknolojiyle birlikte yer altı kömür madenciliğinde, gerek tam mekanize yöntemle sürekli üretim yapılması ve gerekse konvansiyonel madencilik çalışmalarında, yurtdışı yeraltı kömür madenciliğinde de başarı ile kullanılan ve istenmeyen açıklıkların kısa süre içerisinde kapatılabilmesi için köpük kullanılmasının madencilik gündemine girdiğinden söz edilmiştir. Yeraltı kömür madenciliği gibi yüksek riskli iş gruplarında tehlikeli madde kullanımında dikkatli olunması gereken hususlar üzerinde durulmuştur. Zorlu iş koşullarında formaldehit içerikli kimyasalların kullanımından ortaya çıkacak sonuçlar ve bu gibi durumların engellenmesi için alınması gereken önlemlerden bahsedilmiştir.

Anahtar Sözcükler: Formaldehit, kanserojen ve mutajen maddeler, yeraltı kömür madenciliği, kimyasal dolgu malzemeleri, İSG (iş sağlığı ve güvenliği)

ABSTRACT

In this study, the harms of formaldehyde substance and formaldehyde-containing chemical mixtures and the risk groups they create are emphasized. The dangers of these carcinogenic and mutagenic substances in the working environment and the safety precautions that should be taken during their utilization/application are emphasized. It has been mentioned that with the developing technology, continuous production with fully mechanized method and the use of foam in order to close the unwanted openings in a short time, which is used successfully in both conventional mining and underground coal mining, has entered the mining agenda with the developing technology. The issues should be raised for the use of hazardous materials in high-risk business groups such as underground coal mining are emphasized. The results of the use of chemicals containing formaldehyde in difficult work conditions and the precautions to be taken to prevent such situations are mentioned.

Keywords: Formaldehyde, carcinogenic and mutagen substances, underground coal mining, chemical filling materials, ohs (occupational health and safety)

GİRİŞ

Formaldehit FAA (CH_2O – Formalin-Aceto-Alcohol) metanolün oksidasyonu sonucu oluşan bir sıvı maddedir. Elektrofilik özelliğinden dolayı bulundukları ortamda reaksiyona girme eğilimindedir. Aynı zamanda kolaylıkla gaz formuna kavuşabilen özellikleri vardır ve yanıcıdır. Formaldehit sulu ortamlarda yüksek çözünürlüğü sahiptir. Fiziksel olarak renksiz özellikte bir maddedir. Aynı zamanda formaldehit keskin kokulu olduğundan özellikle kapalı ortamlarda hemen fark edilebilmektedir. Ayrıca irrite edici özelliğe sahip olduğundan dolayı ürün deri üzerinde hassasiyet oluşturmaktadır. Formaldehit toksik etkilere sahip zehirli bir gaz olarak sınıflandırılmıştır. (Smith, 1992; Shahem ve ark.,1996; Ünsaldı ve ark., 2009). Formaldehit aynı zamanda Metanol, Metil aldehit, Metilen oksit olarak da bilinir.

Çalışma kapsamında, formaldehitin kullanım alanları, formaldehitin zararları, formaldehit gibi kanserojenik veya mutajenik maddelerin gerek ABD'de gerek Avrupa Birliği'nde ve gerekse ülkemizdeki yasal düzenlemelerdeki yerleri ve bu alanlarda güvenli kullanımında alınması gereken önlemler incelenmiştir. Ayrıca spesifik olarak kömür madenciliğinde dolgu malzemesi olarak kullanılan formaldehit içerikli fenol bazlı köpük ürünlerinin üzerinde durulmuştur.

FORMALDEHİT İÇERİKLİ KİMYASALLARIN KULLANIM ALANLARI

Formaldehit kimya endüstrisinde düşük maliyet ve renksiz oluşu gibi avantajlarından dolayı yaygın olarak kullanılmaktadır. Formaldehit maddesi genel olarak üre formaldehit ve fenol reçinelerin üretiminde kullanılmaktadır. Bu reçinelerin yaygın kullanım alanları; Mobilya sektöründe ağırlıklı olarak MDF ve sunta yapımı, dekoratif duvar kaplamaları, kontraplaklar ve köpük yalıtıcılar olarak görülmektedir. (Aksakal ve ark.,2005) Ayrıca boya sektöründe, plastik malzemelerin yapımında, tekstil sektörü ve ev temizliği ürünlerinde de yaygın olarak kullanılmaktadır. İnşaat sektöründe özellikle son dönemlerde kaplama ve yalıtımda da kullanımı yapılmaktadır. (Blair ve ark., 1990; Smith, 1992; Usanmaz ve ark, 2002; Ünsaldı ve ark., 2009)

Bunların yanı sıra; madencilikte, özellikle son yıllarda önemli miktarda kullanımında artış görülen, yeraltı kömür madenciliğinde boşluk doldurmak amaçlı olarak reçine ile katalizör katılımı sonucunda oluşan köpük imalatında da reçine hazırlanması sürecinde formaldehit kullanılmaktadır.

FORMALDEHİTİN ZARARLARI

Yapılan deneysel araştırmalar sonucunda edinilen bulgalara göre formaldehit maddesi kanserojenik ve toksik olarak sınıflandırılmaktadır. Solunum, sindirim ve sinir sistemlerine toksik olarak etkilediği daha önce yapılan deneyler sonucu görülmektedir. (Smith, 1992; Usanmaz ve ark., 2002; Zararsız ve ark., 2006; Ünsaldı ve ark., 2009, IARC, 2012).

Çalışanlar üzerinde gerçekleştirilen çalışmalar sonucunda formaldehitin nazofarinks kanseri ve kan kanserine sebep olduğuna yönelik güçlü ve yeterli bulgular elde edilmiştir. Aynı zamanda formaldehite maruz kalma ile ağız boşluğu, sinüs, oro- ve hipofarenks, gırtlak, akciğer, beyin ve pankreas bölgeleri ile kanser arasında istatistiksel olarak anlamlı pozitif ilişkiler belirlenmiştir (IARC, 2012). Formaldehite maruz kalan işçilerin maruz kalmayan insanlara göre yapılan istatiksel araştırmalar sonucunda daha yüksek oranda kan kanseri, beyin kanseri ve kolon kanserinden öldükleri görülmektedir (Shahem ve ark., 1996; Schlink ve ark. 1999; Ünsaldı ve ark., 2009). Mesleki olarak formaldehite maruziyeti olan işçiler arasında yapılan diğer araştırmalarda ise akciğer kanseri nedeniyle ölüm oranının %30 daha yüksek olduğu bilgisi elde edilmiştir. (Halperin ve ark. 1983; Hayes ve ark. 1986, Ünsaldı ve ark., 2009).

Formaldehitin en önemli toksik etki gösterdiği sistemlerden biri de üreme sistemidir. Üreme sistemi üzerinde ciddi toksik etkileri olan formaldehit maddesinin fertilite (kısırlık) problemlerine yol

açtığı bilinmektedir. Aynı zamanda sperm sayısını azalttığı ve testosteron hormonu serum değerlerini azalttığı bilinmektedir (Chowdhury ve ark., 1992; Thrasher ve ark., 2001; Özen ve ark., 2005; Ünsaldı ve ark., 2009). Diğer bir deyişle üreme sistemlerine vermiş olduğu kalıcı hasarlardan dolayı kısırlık gibi ciddi problemlere yol açmaktadır. Formaldehit kaynaklı üreme sistemleri etkilenmelerinde halsizlik ve güç ve iktidar kaybı gibi belirtilerin de oluşabileceği bilinmektedir. Üreme sürecinde formaldehite maruz bırakılan gebe fareler üzerinde yapılan araştırmalarda embriyo ölümleri gerçekleştiği ve fetüse ait anomalilerin arttığı görülmüştür (Chowdhury ve ark., 1992; Trasher ve ark., 2001; Ünsaldı ve ark., 2005). Embriyo ve fetüs üzerinde çoklu bozukluklara sebep olmaktadır.

Solunum yolu ile maruz kalma sonucunda formaldehit irite edici ve toksik olduğundan dolayı burun ve boğazda yanma hissi oluşturmaktadır. Aynı zamanda yaygın olarak görülen semptomlar öksürük, nefes darlığı ve hırıltılı solunum olduğu bilinmektedir. Maruz kalınan ortamda konsantrasyonun yüksek olması durumunda akciğer ödemi, yangı ve zatürre geliştiği gözlemlenmiştir (Balir ve ark., 1990; Smith, 1992; Heck ve ark., 1999; Kriebel ve ark, 2001; Ünsaldı ve ark., 2009).

Formaldehit maruziyeti soluma, cilde temas, göze temas ve yutma olarak sınıflandırılmaktadır. Formaldehit kolaylıkla gaz haline dönüşebildiğinden dolayı ortamdaki konsantrasyonu kısa sürede kritik seviyelere ulaşabilmekte ve yüksek konsantrasyonda solunması zehirlenmelere neden olabilmektedir. Toksik formaldehit maddesinin sıvı halinin cilt ve göz ile temas ettirilmemesi gerekmektedir. Göz, cilt ve solunum yolları için iritant diğer bir değiş ile tahriş edici madde özelliğindedir. Kuş ve arkadaşlarının (2007) yapmış olduğu çalışmaya göre akut olarak (solumayla) formaldehite maruz kalan kişilerde *"baş ağrısı, baş dönmesi, keyifsizlik, uykusuzluk ve iştahsızlık gibi semptomlar ortaya çıkarken, uzun süreli maruz kalmalarda; davranış bozuklukları ve epilepsi gibi kalıcı nörotoksisite belirtileri ortaya çıkmaktadır"* (Kuş ve ark. 2007).

Formaldehit ve Formaldehit İçeren Kimyasallar ile İlgili Yasal Düzenlemeler

2013 yılında çıkan 28848 sayılı "*Maddelerin ve Karışımların Sınıflandırılması, Etiketlenmesi ve Ambalajlanması Hakkında Yönetmelik*" gereğince karışım olan kimyasalların etiketlerinde H zararlılık ifadelerinin yer alması gerekmektedir. Ürünlerin ve karışımların içeriğinde %0,1 oranında ve daha fazla formaldehit bulunması durumunda ürün 2. sınıf kansorejen madde grubunda yer alır. Bu grupta yer alan ürünlerin H351 zararlılık ifade kodu ile gösterilmesi gerekmektedir. (Avrupa Parlementosu ve Avrupa Konseyi 1272/2008 sayılı tüzüğü) Yönetmelik eki tablo 3.6.3.'de H350 zararlılık ifadesi *"Kansere yol açma şüphesi var*" olarak tanımlanmaktadır ("*Maddelerin ve Karışımların Sınıflandırılması, Etiketlenmesi ve Ambalajlanması Yönetmeliği"*, 2013).

5 Haziran 2014 tarihinde 605/2014 sayılı Avrupa Birliği Komisyonu tarafından yapılan yasal düzenleme ile formaldehit maddesinin kanserojen kategorisi değiştirilmiştir. Yapılan bu değişiklikle ürün veya karışım içeriğinde %0,1 oranında ve daha fazla formaldehit bulunması durumunda ürün 1. Sınıf kansorejen madde kategorisinde yer almaktadır. Bu grupta yer alan ürünlerin H350 zararlılık ifade kodu ile gösterilmesi gerekmektedir. Yönetmelik eki tablo 3.6.3.'de H350 zararlılık ifadesi *"Kansere yol açabilir"* olarak tanımlanmaktadır ("*Maddelerin ve Karışımların Sınıflandırılması, Etiketlenmesi ve Ambalajlanması Yönetmeliği*", 2013). Ürün içeriğinde %0,1 oranından daha az formaldehit bulunması durumunda sınır değerlerinin altında olduğundan dolayı ürün güvenlik bilgi formunda içerik yüzdesinin gösterilmesine gerek yoktur.

Yönetmelik ("*Maddelerin ve Karışımların Sınıflandırılması, Etiketlenmesi ve Ambalajlanması Yönetmeliği (2013)*) Madde 3b uyarınca *"31/12/2008" tarihli "Avrupa Birliği Resmî Gazetesi'nde yayımlanan 1272/2008 sayılı "Madde ve Karışımların Sınıflandırılması, Etiketlenmesi ve Ambalajlanması" Hakkındaki Avrupa Parlamentosu ve Avrupa Konseyi Tüzük hükümleri temel alınarak paralel hazırlanmıştır"* Diğer bir ifade ile SEA (Sınıflanırma Etiketleme ve Ambalajlama) yönetmeliği CLP

(Clasification Labeling and Packaging) yönetmeliğine dayanmaktadır. Bundan dolayı SEA yönetmeliğinde yer almamasına rağmen CLP yönetmeliğinde yapılan değişiklik SEA yönetmeliğini bağlayıcı niteliktedir.

Sonuç olarak karışımların içerisinde %0,1 oranından daha yüksek formaldehit olması durumunda ürün 1. Sınıf kanserojen olarak sınıflandırılmakta olup etiketinde ve güvenlik bilgi formunda H350 zararlılık ifadesi ile gösterilmesi gerekmektedir.

Formaldehit ve formaldehit içerikli kimyasalların araştırılması bazı uzman kuruluşlar tarafından ele alınmıştır. Bu uzman kuruluşların formaldehit hakkında yapmış oldukları düzenlemeler ve kararlar aşağıda belirtilmiştir.

Ulusal Toksikoloji Programı (NTP-National Toxicology Program)

NTP (2021) formaldehit “insan kanserojen olarak bilinir” olarak listeler. Kanserojenler Raporu, NTP'nin HHS Sekreteri için hazırladığı, konvansiyonel olarak zorunlu, bilime dayalı bir halk sağlığı belgesidir. Bu kümülatif rapor şu anda insanlarda kansere neden olduğu bilinen veya makul olarak tahmin edilen 256 ajan, madde, karışım ve maruz kalma koşullarının bir listesini içermektedir.
Bu rapor dahilinde;
Formaldehit CAS No. 50-00-0 İnsan kanserojen olduğu bilinmektedir.

Uluslararası Kanser Araştırmaları Ajansı (IARC- International Agency for Research on Cancer)

Dünya Sağlık Örgütü (World Health Organization, WHO) bir parçasıdır. Başlıca amacı, kanser nedenlerini tespit etmektir. IARC, formaldehitin, nazofarenks kanseri ve lösemi riskleri nedeniyle "insanlara kanserojen" olduğu sonucuna varmıştır. 2006 yılında Kasım ayında IARC nihai raporunu yayınlamış, formaldehitin insan için karsinojenik olduğuna dair yeterli kanıtın bulunduğunu belirterek formaldehiti "insanlar için kanserojenik" (Grup 1) sınıfına dahil etmiştir. (IARC, 2014)

Çevre Koruma Ajansı (EPA- Enviromental Protection Agency)

Entegre Risk Bilgi Sistemi (IRIS), çevrede çeşitli maddelere maruz kalmaktan dolayı insan sağlığına etkileri hakkında bilgi içerir elektronik bir veritabanı oluşturur. EPA formaldehit "olası insan kanserojen" olarak sınıflandırmıştır. Benzer şekilde; 2010 yılında Amerika'da EPA (ABD Çevre Koruma Ajansı) " formaldehit ile ilgili sınıflandırmasını "muhtemel kanserojen (B1) olarak güncellemiştir.

Ulusal Kanser Enstitüsü (NCI-National Cancer Institute)

Ulusal Kanser Enstitüsü araştırmacıları, insanlardaki çalışmalardan ve laboratuvar araştırmalarından elde edilen verilere dayanarak formaldehit maruziyetinin insanlarda lösemiye, özellikle miyeloid lösemiye neden olabileceği sonucuna varmışlardır. (NIH, 2022)

Toksik Maddeler Ve Hastalık Kayıt Ajansı (ATSDR-Agency for Toxic Substances and Disease Registry)

Bu sitede de genel bilgiler verilmektedir;

Formaldehit CAS Kimlik No: 50-00-0

Etkilenen Organ Sistemleri: Dermal (Deri), Gastrointestinal (Sindirim), İmmünolojik (İmmün Sistem), Solunum (Burundan Akciğerlere) Kanser Sınıflandırması: EPA: İnsanlarda sınırlı delillere dayanan ve insanlarda yeterli kanıtlar bulunan muhtemel insan kanserozu IARC: İnsanlara kanserojendir. NTP: Oldukça insan kanserojen olduğu tahmin ediliyor. (ATSDR, 2016)

Kömür Madenciliğinde Formaldehit İçerikli Kimyasal Ürünlerin Kullanımı ve Alınması Gereken Önlemler

Kömür madenciliğinde gelişen teknolojiyle birlikte üretimin verimliliğin arttırılması, yangınla mücadele ve gaz izolasyonu gibi birçok alanda fenol bazlı köpük ürünleri kullanılmaktadır. Bu uygulamalar arasında en yaygın olarak bilineni boşluk doldurma ve gaz izolasyonudur.

Yeraltında jeolojik koşullardan ve süreksizliklerden kaynaklı olarak geniş çaplı göçükler oluşabilir bu durum üretimin durmasına ve üretim verimliliğinin düşmesine yol açmaktadır. Bu boşluklar her maden çalışanı için risk oluşturmaktadır. Kontrol altına alınmaması durumunda bu boşluklar büyüyerek mevcut riski arttırabilir. Daha ciddi sorunları önlemek, üretimi aksatmamak ve iş yeri güvenliğini sağlamak için bu boşlukların hızlı bir şekilde doldurulması gerekir. Bu gibi durumlarda hızla genleşebilen az miktarda malzeme kullanımıyla büyük boşlukların rahatlıkla doldurulması fenol bazlı köpük ürünleri ile mümkündür. (Tuz vd., 2019)

Fenol bazlı köpük ürünlerinin reçine bileşeni fenol-formaldehit ham reçinesine katkılar konularak oluşturulmaktadır. Fenol formaldehit ham reçine içerisinde formaldehit yer almaktadır.

Yeraltı uygulamalarında kullanılan formaldehit içerikli kimyasal ürünlerin kullanımında gerekli önlemlerin alınması gerekmektedir. Kapalı ortamlarda uygulanan kimyasallar anlık olarak havadaki konsantrasyon artışına sebep olmaktadır.

Yeraltında zaman zaman havalandırmanın az olduğu zorlu alanlarda çalışma yapılması durumları oluşabilmektedir. Bu bölgelerde yapılan operasyonlarda formaldehit içerikli kimyasalların kullanımına dikkat etmek gereklidir. Formaldehit konsantrasyonu yüksek olan kimyasallar ile yapılan köpük uygulamalarında zehirlenmeler ve oksijen yetersizliğinden kaynaklı bilinç kayıpları gibi durumlar oluşabilmektedir.

Formaldehit, ilk maruziyette bağışıklık sisteminin tepkisine neden olabilen hassaslaştırıcı bir maddedir. Aynı zamanda bir kanser tehlikesidir. Akut maruz kalma gözler, burun ve boğaz için oldukça tahriş edicidir ve herkesi öksürük ve hırıltıya maruz bırakabilir. Daha sonraki maruz kalma cilt, gözler ve solunum yollarında ciddi alerjik reaksiyonlara neden olabilir. Formaldehit yutulması ölümcül olabilir ve havada düşük seviyelere uzun süre maruz kalmak astım gibi birçok solunum problemine sebep olmaktadır. Cilt yolu ile düşük dozajda maruz kalma durumunda ise cilt hassasiyeti ve kaşıntı gibi cilt tahrişine neden olabilir. 100 ppm konsantrasyonları yaşam ve sağlık için çok tehlikelidir. IDLH (The Immediately dangerous to life or healt) yaşam veya sağlık için ivedilikle tehlikelidir ibaresi ile kimyasal ürünler hakkında belli değerlerin üzerindeki kullanılmaması gereken konsantrasyon değerleri ifade edilir. Ulusal Mesleki Güvenlik ve Sağlık Enstitüsü (NIOSH) ve Uluslarası Kanser Araştırma Ajansı (IARC) 20 ppm formaldehitin IDLH olduğunu belirtmektedir. (IARC, 1982; CDC, 2014) Ortam havasındaki 0.1 ppm üzerindeki formaldehit konsantrasyonları solunum yollarının tahriş olmasına neden olabilir. Tahrişin ciddiyeti, konsantrasyonlar arttıkça yoğunlaşır.

Ülkemiz yeraltı kömür madenciliğinde 2016 yılında kullanılmaya başlanan ve her geçen yıl kullanımı artan fenol formaldehit köpüklerin 2019 ve 2020 yılında yaklaşık kullanım miktarları Tablo 1'de yer almaktadır. 2023 yılında beklenen kullanım miktarının 2020 yılına kıyasla iki katına çıkması ve 6.100.000 kg olarak gerçekleşmesi ön görülmektedir. Bu durum Tablo 1'de gösterilmektedir.

Çizelge 1. Ülkemiz yeraltı kömür madenciliğinde fenol formaldehit köpük kullanımı.

HAVZA	2019 yılı kullanım miktarı (Ton)	2020 yılı kullanım miktarı (Ton)	2021 yılı kullanım miktarı (Ton)
SOMA	1650	2880	2900
ANKARA	300	400	650
ZONGULDAK	160	210	170
DİĞER	30	45	65
TOPLAM	2140	3535	3785

Çizelge 1'den de anlaşılacağı üzere fenol formaldehit köpük kullanımı ülkemizde yeraltında giderek kullanımı artmaktadır. Kullanımın artması yüksek maruziyetler oluşturacağı düşünüldüğünden işverenin durum ile ilgili hükümlülükleri de artmaktadır. İşverene düşen hükümlülükler;

OSHA (Occupational Safety and Health Administration) standardının hükümleri, işverenlerin aşağıdakileri yapmasını gerektirir:

Formaldehit normal kullanım sırasında 0,5 ppm üzerindeki seviyelerde serbest bırakılabilen tüm malzemeler için, etiket "potansiyel kanser tehlikesi" kelimelerini içermelidir.

Yüzde 0,1'den büyük formaldehit ve formaldehitin 0,1 ppm'e ulaşan veya bu konsantrasyonun üstündeki konsantrasyonlarda serbest kalmasını sağlayabilen malzemelerden oluşan tüm karışımları veya çözeltilerde iş veren aşağıda belirtilen durumları yapmak zorundadır.

İlk işe atanma zamanında ve çalışma alanına yeni bir formaldehit maruz kaldığında, 0.1 ppm veya daha yüksek formaldehit konsantrasyonlarına maruz kalan tüm çalışanların eğitilmesi ve bu eğitimin her yıl tekrarlanması gereklidir.

30 yıl boyunca maruz kalma kayıtları saklanmalı.

İstihdam sona erdikten sonra tıbbi kayıtları 30 yıl boyunca arşivde tutması gerekmektedir (OSHA, 2013).

28733 Sayılı (2013) Kimyasal Maddeler ile çalışmalarda Sağlık ve Güvenlik Hakkındaki Yönetmelik kapsamında işverenin yükümlülükleri:

(*Madde 8)* *"Tehlikeli kimyasal maddelerle yapılan çalışmalarda aşağıda belirtilen özel önlemler" (Madde 8; a, b) alınır:*

a) *"İşveren çalışanların sağlık ve güvenlik yönünden tehlikeli kimyasal maddelerden kaynaklanan risklerin ortadan kaldırılması veya en az düzeye indirilmesi için her türlü önlemi alır".*
b) *Bu maddenin (a) bendinin uygulanmasında;*

"Öncelikle ikame yöntemi uygulanarak, tehlikeli kimyasal madde yerine çalışanların sağlık ve güvenliği yönünden tehlikesiz veya daha az tehlikeli olan kimyasal madde veya işlem kullanılır".

(Madde 10) *"Tehlikeli kimyasal maddelerle çalışanların eğitimi ve bilgilendirilmesi ile ilgili esaslar":*

a) *"İşveren, çalışanlara veya temsilcilerine, 6331 sayılı İş Sağlığı ve Güvenliği Kanununun 16 ve 17'nci maddesinde belirtilen hususlara ve çalışanların iş sağlığı ve güvenliği eğitimlerinin usul ve esasları" ile ilgili yönetmelikte belirtilen hususlarla birlikte özellikle;*
   1) *"Risk değerlendirmesi sonucunda elde edilen bilgiler ve çalışma koşullarında önemli bir değişiklik olması halinde gerekli yeni bilgiler",*
   2) *"İşyerinde bulunan veya ortaya çıkabilecek tehlikeli kimyasal maddelerle ilgili, bu maddelerin tanınması, sağlık ve güvenlik riskleri, mesleki maruziyet sınır değerleri ve diğer yasal düzenlemeler",*
   3) *"Çalışanların kendilerini ve diğer çalışanları korumaları için alınması gerekli önlemler ve yapılması gerekli işler",*
   4) *"Tehlikeli kimyasal maddeler için tedarikçiden sağlanan malzeme bilgi formları, hakkında bilgi sağlamak ve eğitim vermekle"* yükümlüdür.

28730 Sayılı (2013) "Kanserojen veya Mutajen Maddeler ile Çalışmalarda Sağlık ve Güvenlik Önlemleri Hakkında" yönetmelik kapsamında işverenin yükümlülükleri:
(Madde 6) *"İşverenler çalışanların sağlık ve güvenliğini korumak amacıyla teknik olarak mümkün olduğu hallerde, tehlikesiz veya daha az tehlikeli madde, müstahzar veya işlem kullanarak işyerinde ki kanserojen veya mutajen maddelerin kullanımını azaltır".*

Çevre, Şehircilik ve İklim Değişikliği Bakanlığı'nın bu konudaki görüşü de şu şekilde olmuştur:
"formaldehit maddesi veya formaldehit reçinesine ilişkin hâlihazırda herhangi bir kısıtlama veya yasaklama bulunmadığı, Bununla birlikte ilgili Yönetmeliğin, Avrupa Birliğindeki 1907/2006 sayılı REACH Tüzüğünü uyumlaştıran mevzuat olduğundan ve REACH Tüzüğüne göre AB'de formaldehit maddesinin veya bu maddeyi içeren karışımların halka satışı yasaklandığından, Kimyasalların Kaydı, Değerlendirilmesi, İzni ve Kısıtlanması Hakkında Yönetmeliğini güncellemek amacıyla yapılacak çalışmalar kapsamında söz konusu yasaklama hükümlerinin Ülkemiz mevzuatına aktarılması öngörülmektedir" denilmiştir.

SONUÇ ve DEĞERLENDİRME

Bu çalışma kapsamında formaldehit ve formaldehit içerikli kimyasal maddelerin veya karışımların zararları, bu zararlara yönelik yasal ve uzman kurumlar tarafından yayınlanan bildiriler ve bu tehlikeli kimyasalları ihtiva eden ürünlerin kullanım alanları hakkında bilgiler verilmiştir. Son olarak son dönemde gelişmekte olan teknoloji ile yeraltı kömür madeni sektöründe yaygın olarak kullanılan formaldehit içerikli fenol bazlı kimyasal köpük ürünleri üzerinde durulmuştur. Günümüzde riskli işler gurubunda ilk sıralarda yer alan yeraltı kömür madenciliğinde zorlu koşullarda verimliliği ve iş güvenliğini sağlamak amaçlı kullanılan bu ürünlerin bilinçsiz kullanımından kaynaklanacak olumsuz durumlar irdelenmiş, bu olumsuz durumların oluşmaması için işverene düşen yükümlülüklerden bahsedilmiştir.

Formaldehit maddesinin ve formaldehit içerikli kimyasalların sağlık açısından oldukça tehlikeli ürünler olduğu bilinmektedir. Formaldehitin kansere ve üreme sistemlerinde bozukluklara sebep olduğu yapılan testler sonucunda ortaya konulmuştur. Yüksek dozajda formaldehite maruz kalan çalışanlarda akciğer kanseri ve kısırlık gibi problemlerin görülme olasılığının daha yüksek olduğu bilinmektedir.

Kanserojen maddelerin kullanımında dikkatli olunması ve bilinçli kullanımın veya üretimin yapılması gerekmektedir. Formaldehit gibi kanserojen madde içerikli ürünlerin bilinçsiz bir şekilde kullanımı normal şartlarda risk ihtiva eden madencilik gibi sektörlerin daha problemli ortamlar oluşturmasına sebep olmaktadır. Bundan kaynaklı yasaların ve uzman kuruluşların düzenlemeleri ve bildirileri göz önünde bulundurularak kanserojen sınıfına giren kimyasal karışımların yeraltı gibi kapalı ortamlarda kullanılmaması veya tehlikesiz ya da daha az tehlikeli kimyasal ürünlerin kullanımı opsiyonunun değerlendirilmesi gerekmektedir.

Tehlikeli kimyasal madde veya karışım kullanımına alternatif olarak tehlikesiz veya potansiyel olarak daha az tehlikeli kimyasal madde kullanımının yapılması gerekmektedir. Formaldehit maddesinin kimyasal karışımlardaki konsantrasyonunun %0,1 değerinin altında olması maddenin kullanımında ortamdaki konsantrasyonunun zararsız seviyelerde olmasını ve aynı zamanda maruziyet etkisinin düşük olmasını sağlayacaktır. Almanya gibi Avrupa ülkelerinin bazılarında yapılan yasal düzenlemeler sonrasında %0,1 oranından fazla formaldehit ihtiva eden kimyasal karışımların madenlerde ve kapalı alanlarda kullanımı yasaklanmıştır. (Umwelt Bundesamt, 2015).

Kömürün özellikle kendiliğinden yanma konusunda etkisini diğer köpüklere nazaran en aza indiren fenol bazlı köpüklerin görülen o ki kullanımı giderek artacaktır. Burada düşünülmesi gereken başlıca olay, köpüğü oluşturan reçine ve katalizör içerisinde bulunan serbest formaldehitin Avrupa normları neticesinde %0,1'in altında olmasıdır. Ülkemizde fenol bazlı köpükler kullanılırken insan sağlığı açısından zaten var olan kanun ve yönetmeliklerin uygulamaya konulması ve bu durumun ciddiyetle üzerine gidilmesi kaçınılmaz bir durumdur.

KAYNAKLAR

Aksakal N, Vaizoğlu SA, Güler Ç, (2005) Formaldehit ve Sağlık Etkileri, Türk Tabipler Birliği Mesleki Sağlık ve Güvenlik Dergisi, sf 40-44

ATSDR, 2016, Formaldehyde and Your Health, Agency for Toxic Substance and Disease Registry, www.atsdr.cdc.gov/

CDC, 2014, Table of IDLH Values, NIOSH Publication and Products, Center for Disease Control and Prevention, www.cdc.gov/niosh/idlh

Chowdhury AR, Gautam AK, Patel KG, Trivedi HS (1992). Steroidogenic inhibition in testicular tissue of formaldehyde exposed rats, Indian J Physiol Pharmacol, 36, 162-168.

COMMISSION REGULATION (EU) No 605/2014 of 5 June 2014

EPA, 2021, Facts About Formaldehyde, www.epa.gov/formaldehyde/facts-about-formaldehyde

Halperin WE, Goodman M, Stayner L, Elliot LJ, Keenlyside RA, Landrigan PJ (1983). Nasal cancer in a worker exposed to formaldehyde, JAMA, 249, 510- 512.

Hayes RB, Raatgever JW, de Bruyn A, Gerin M (1986). Cancer of the nasal cavity and paranasal sinuses and formaldehyde exposure, Ind J Cancer, 37, 487-492.

IARC, 1982, IARC monographs on the evaluation of the carcinogenic risk of chemicals to humans. Vol. 29. Some industrial chemicals and dyestuffs. Lyon, France: International Agency for Research on Cancer, pp. 345-389.

IARC, 2012, Chemical Agents and Related Occupations Volume 100 F A Review of Human Carcinogens, sf: 401-435

IARC, 2014, World Cancer Report, https://www.iarc.fr/cards_page/iarc-publications/

Kanat KÇ, 2019, Formaldehit ve Formaldehit Maruziyeti, Haliç Çevre Laboratuvarı, www.haliccevre.com/blog

Kanserojen ve Mutajen Maddelerle Çalışmalarda Sağlık ve Güvenlik Önlemleri Hakkında Yönetmelik, 6 Ağustos 2013, Resmî Gazete Sayı: 28730

Kimyasal Maddelerle Çalışmalarda Sağlık ve Güvenlik Önlemleri Hakkında Yönetmelik, 12 Ağustos 2013, Resmî Gazete Sayı: 28733

Kuş İ, Zararsız İ, Ögetürk M, Yılmaz HR, Formaldehit Nörotoksisitesine Bağlı Hipokampusta Gelişen Oksidatif Hasar ve Melatonin Hormonunun Koruyucu Etkisi: Deneysel Bir Çalışma, Fırat Tıp Dergisi, Sayı 4, Sf: 256-260

Maddelerin ve Karışımların Sınıflandırılması, Etiketlenmesi ve Ambalajlanması Hakkında Yönetmelik, 11 Aralık 2013, Resmî Gazete Sayı: 28848 (Mükerrer)

Maddelerin ve Karışımların Sınıflandırılması, Etiketlenmesi ve Ambalajlanması Hakkında Yönetmelik Ekleri 11 Aralık 2013, Resmî Gazete Sayı: 28848 (Mükerrer)

ZİNCİRLİ KOLLU KESİCİ MAKİNALARDA TEKNOLOJİK GELİŞMELER VE KESME TAKIMINDA KIRILMA NEDENLERİ

TECHNOLOGICAL DEVELOPMENTS ON CHAIN SAW MACHINES AND REASONS OF BROKEN CHAIN SAW PARTS

S. Kulaksız

Hacettepe Üniversitesi, Maden Mühendisliği Bölümü
(seyfi@hacettepe.edu.tr)

ÖZET

Kömür madenciliğinde kullanılan ilk kollu kesiciler Korfmann (1946) tarafından geliştirilerek traverten ve mermerlerde kullanılmaya başlanmıştır. 1998 yılından itibaren klasik raylı (kızaklı) tiplerin yürüyüş takımı paletli, lastik tekerli ve paletli sabit raylı şeklini almıştır. Kesici uçlarda ise elmas uçlar geliştirilmiş ve keski geometrisi ve dizilimlerde farklılıklar başlamış bunun sonucu kesim verimliliğinde artışlar sağlanmıştır. Zincirli kollu kesicilerde (ZKK) en önemli kısım kesme işini yapan zincir takım topluluğudur. ZKK makinasının en fazla çalışan ve en fazla yıpranan elemanları zincir takımındaki kesici uçlar, kesici uç tutucular ve zincir baklalarıdır. Saha gözlemleri ve bazı araştırıcı maliyet hesaplamalarında bunlarla ilgili rakamlar verilmekle beraber nedenlerine değinilmemiştir. Temel sorun, kesici ucun takımdaki dizilimi ve zincir üstündeki düzenlenme yetersizliğidir. Doğal taş ve ocak koşulları dikkate alınmadan zincirli kollu kesici makinalar aşağı yukarı fabrika tasarımı ve genel işletme kavramları ile çalıştırılmaktadır. Bu bildiride doğal taş ocaklarında kullanılan zincirli kollu kesici makinaların verimliliklerinin artırılması hakkında bilgiler sunulacak, sorunlar açıklanarak tartışılacak ve olası çözümler verilecektir.

Anahtar Sözcükler: Doğal taş, zincirli kollu kesici makinalar, kesici uç, zincir topluluğu, kesici uç dizilimi, kesme kuvveti.

ABSTRACT

Chain saw cutting machines were used first in coal mine. Later they were developed by Korfmann (1946) and started to be used in travertine and marble. Since 1998, the undercarriage of the classical rail (sliding) types has taken the form of tracked, rubber wheeled and tracked fixed rail. Diamond tips have been developed in the cutters, and differences have started in the chisel geometry and arrangement, resulting in an increase of cutting efficiency. In chain saw cutters (CSC), the most important part is the chain tool assembly that does the cutting work. The hardest working and most wearing elements of the CSC machine are the cutters in the chain set, the insert holders and the chain links. In field observations and some researcher cost calculations, the related subjects and figures are given, but the reasons are not mentioned. The main problem is the alignment of the insert in the tool and the lack of arrangement on the chain. Chain saw machines are operated with more or less factory design and general operating concepts, regardless of natural stone and quarry conditions. In this paper, information about increasing the efficiency of chain arm cutters used in natural stone quarries will be presented, problems will be explained and discussed and possible solutions will be given.

Keywords: Natural stone, chain saw cutting machines, cutting pick, chain, cutting pick array, cutting force.

GİRİŞ

İlk olarak kömür madenciliğinde kullanılan kollu kesiciler daha sonra kesici kol yapısı ve kesme düzeneği yeniden düzenlenerek doğal taş işletmeciliğinde de kullanılmaya başlanmıştır (Şekil 1). Bugün makinalar doğal taş işletmelerinde ana kayadan blok kesimi, blok sayalama, galeri ve tünel ağız açılmasında sivil yapılaşma için yıkım ve kazı işlerinde kullanılmaktadır. Doğal taş madenciliğinde üretimi artırmak maliyetleri düşürmek kesme verimliliği ile birlikte zaman kazanım tasarrufu için kullanılmaya başlanılmıştır. İlk makinalarda kesici uç olarak tungsten karbür kullanılırken 1977'den sonra elmas kesici uçlu makinalarla blok üretilmeye başlanmıştır.

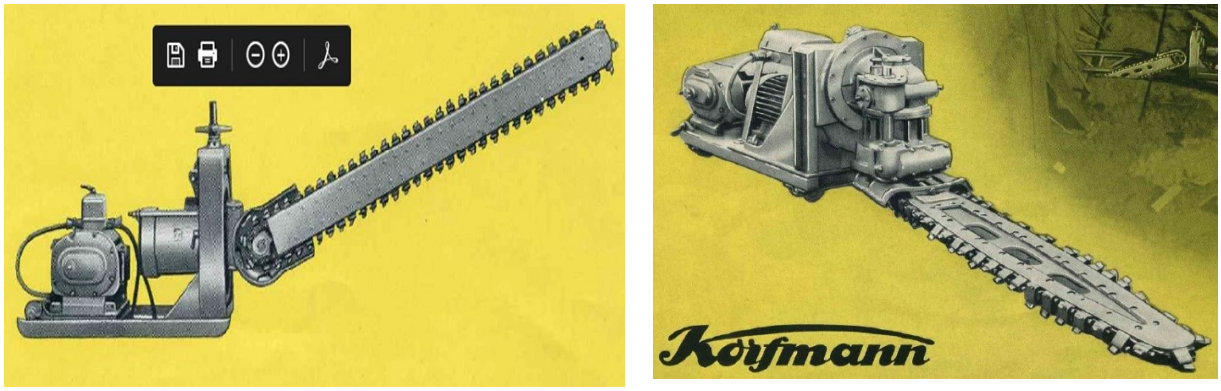

Şekil 1. Kömür ve mermerde kullanılan ilk kollu kesiciler (Korfmann, 1946)

Günümüzde zincirli kollu kesiciler (ZKK) kireçtaşı hakiki mermer, traverten ve geniş bir çerçeve içine giren orta aşındırıcılıkta silisli malzemelerin (kumtaşı, bazı volkanik kayaçlar,) blok üretiminde kullanılmaktadır. Hem birincil kesimlerde (dağ kesimlerinde), hem de ebatlamada kullanılabilir. En iyi sonuçları çatlak yapısı bol, düşük homojenlikteki kayaçları keserken elde edilmektedir. Klasik zincirli kollu kesme makinalarında kesime hazırlanması biraz zaman almakla birlikte, paletli ve traktöre montajlı sistemli olanlarda zaman kaybı olmamakta, uzun süreli kesimler için tercih edilmekte, ocakta düz bir hat boyunca sürekli olarak metrelerce kesim yapabilmektedir.

ZİNCİRLİ KOLLU BLOK DOĞAL TAŞ KESME MAKİNALARI ANA PARÇALARI

Kollu zincirli kesme makinesi genel olarak bir motor ünitesi ve dişli bir zincir taşıyan hareketli bir kol ile kumanda panosu raylardan oluşur (Şekil 2). Zincirli kollu kesici makinalar, çeşitli firmalarca çok değişik tip ve kapasitelerde imal edilmektedir. Bu makinaların toplam ağırlığı yaklaşık 2-20 ton arasındadır. Zincirli kollu kesicilerde kesme kolu hidrolik güç kaynağı ile kolayca yatay ve düşey kesme pozisyonlarına getirilebilir. Böylece aynı makina ile hem yatay hem de düşey kesim yapılabilir. Kesme kolu uzunluğu 10 metreye kadar çıkabilmektedir.

Makinanın kesici kol takımı iki kısımdan oluşur; kesme kolu gövdesi, zincir takımı.

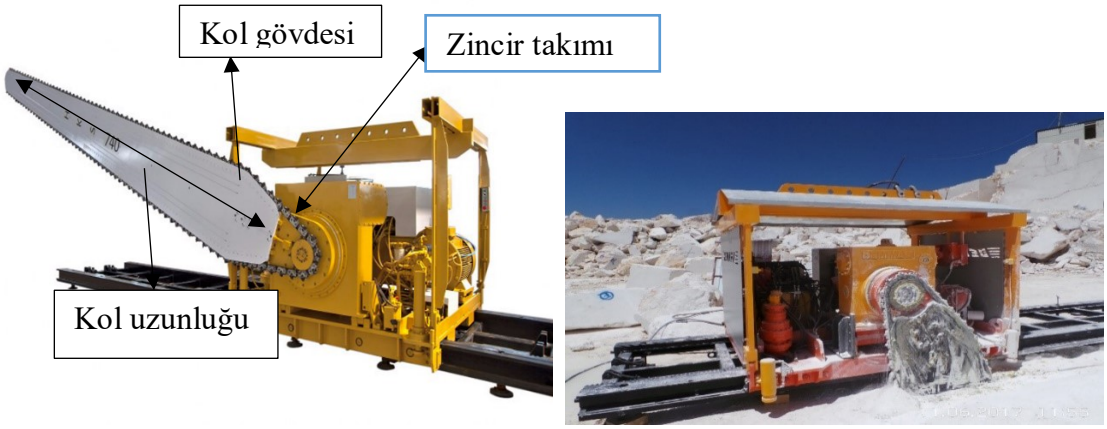

Şekil 2. Kesme kol gövdesi ve zincir takımı, makine çalışmada konumu

Kesme Kol Gövdesi

Özel olarak çelikten imal edilmiş olup, kolaylıkla sökülüp takılabilmektedir. Kolun etrafında dönen zincir üzerinde özel alaşımlı kesici uçlar bulunur . Kol takımını hareket ettiren redüktör sistemi (Şekil 3) hidrolik silindir vasıtasıyla kolu 360 derece döndürmekle yatay ve düşey kesim yapmaktadır. Kol takımı sökülerek değişik boyutlarda kol gövdesi takılabilmektedir. Kol uzunluğuna bağlı olarak 2.0-9.0 m arasında derinliklerde kesim yapabilmektedir. Tüm tahrik sistemi hidrolik olup, bazı makinelerde kesici kolun dönme hareketi galeri açma makinelerinde olduğu gibi bir dişli kutusu üzerinden doğrudan elektrik motorlarıyla gerçekleştirilmektedir.

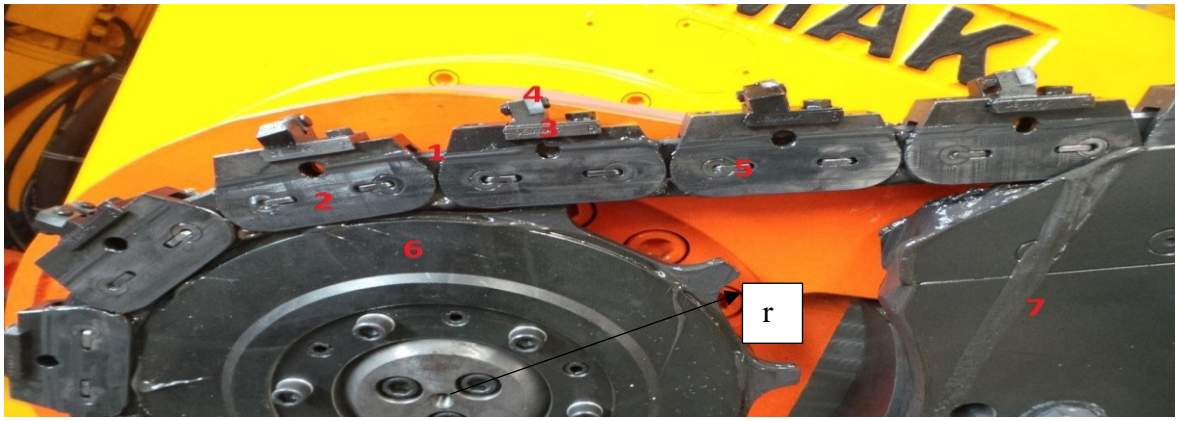

Şekil 3. Redüktör tahrik kasnak sistemi (6) ve zincir takımı parçaları (r yarı çap) Kollu zincirli kesme makinesinin zincir takımı elemanları (1-Zincir gövdesi-iç bakla, 2-İç bakla, 3-Kesici uç tutucusu, 4-Kesici uç, 5- Rulman, 6-Kasnak, 7-Kol gövdesi)

Zincir Takımı

Kesme işlemini yapan zincir düzeneği Şekil 3'de verilen elemanlardan oluşmaktadır. Doğal taş blok kesimlerinde ise dört ve sekiz köşeli keskiler kullanılmaktadır. Kollu kesicilerde kesme kalınlığı 32-42 mm arasında olmaktadır. Kollu zincirli kesme makinesinin en fazla çalışan ve en fazla yıpranan parçası kol ve kol üzerindeki kesicilerdir. Keski tutucuları taşıyan iç–dış baklalar keskilerden sonra ikinci çok aşınan elemanlardır. Şekil 4'de değişik boyutlu keski ucu ve keski tutucusu taşıyan dış baklalar gösterilmiştir.

Şekil 4. Kollu zincirli kesme makinesinin değişik dış-iç bakla ve keski uçları.

Mermer ve doğal taşların kesiminde kullanılan zincirli kollu kesme (ZKK) makinelerinde normal kesme koşullarında tungsten karbür tipli kesici uçlar, aşındırıcı ve zor kesme koşullarında ise PCD türü elmaslı uçlar kullanılması önerilmektedir. Kare-dikdörtgen keskilerinin bir köşesi aşındığında konumları değiştirilerek yeni bir köşeyle kesme yapabilmektedir. Böylece bir kesici ucun toplam sekiz köşesinin ayrı olarak kullanılabilme olanağı bulunmaktadır.

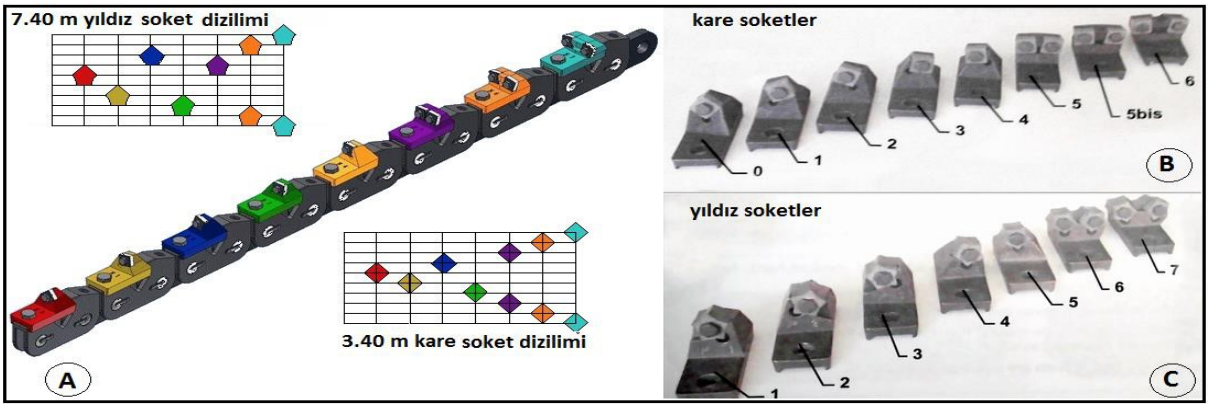

Şekil 5. Kare ve yıldız kesici uç dizilim geometrisi (A) ve uç şekilleri (B Kare, C Yıldız) (Demirel, 2008)

Uygulamada birçok kesici uç dizilimleri bulunmakta olup bunlardan bazıları Şekil 5 ve 6'da verilmiştir. Görüldüğü gibi kesici uçların profil görünüşleri dikkate alındığında, yalnızca ilk keski genel olarak dik konumdadır. Bunu izleyen iki ya da dört adet keski düşük açılı eğime sahip iken köşeye doğru gidildikçe eğim artmaktadır. Dizilim sonuna doğru gidildikçe bir keski tutucusu üzerinde çift keski kullanımı egemen olmaktadır. Zincirli kollu kesme makinelerinde kesici uçlar belli bir sıralama düzeni içinde (dizilim) sonsuz zincir üzerine yerleştirilirler. Her bir dizilim belli sayıda kesici uç içerir.

Yürüyüş Sistemine Göre Zincirli Kollu Kesici Makina Sınıflandırması

2000'li yılların teknolojisine göre ZKK da yürüyüş sistemleri üç grupta sınıflandırılabilir: Klasik raylı sistemler, Paletli sistemler ve paletli raylı sistemler, Lastik tekerlekli traktörlü sistemler.

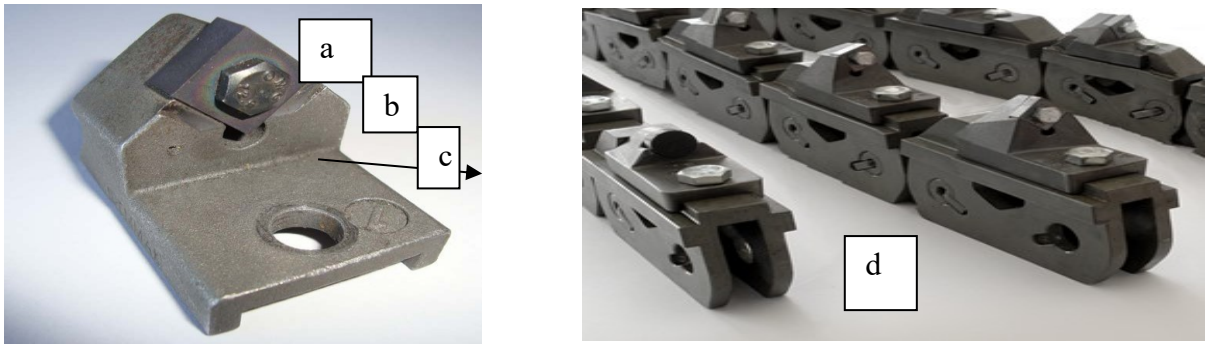

Şekil 6. Kesici uç (a), kesici uç tutucusu (b), keski sabitleme cıvatası (c), PCD ve kare keskiler (d)

Klasik Raylı Sistemler

Makinanın ileri-geri yürüyüşünü sağlayan ray düzeneği olup üstünde araba-vagon, hareket mekanizmasını taşır. Raylar sökülüp uç uca eklenebilir olması nedeniyle fazlaca uzun değillerdir. Kesim biten taraftan sökülen parça, ilerleme yönünde monte edilir. Bir ocak için iki tane 3 metrelik, bir tane 2-3 metrelik ve bir tane 1 metrelik olmak üzere toplam 9 metre ray yeterli olmaktadır (Şekil 5-7). Yeni teknolojik gelişmeler sonucu hidrolik sabitleyiciler ve/veya kendiliğinden hareketli raylar kullanılmaktadır.

Paletli Sistemler

Paletli sistemler, kesici kolun ray veya kule taşıyıcı sistemine göre iki gruba ayrılır. Yeni nesil kollu kesici makinaların, paletli yürüyüş takımlı olanlarda, makine ray sistemi hidrolik ayaklar (teleskopik) üstüne alındıktan sonra palet takımı ile birlikte ileri-geri hareket edebilmektedir. Paletli raylı sisteme sahip makinalarda ray düzeneği yekpare olup, şase üstünde taşınmaktadır. Sökme-kurma işlemine gerek yoktur. Burada makinanın sadece kesme konumu alması yeterlidir. Kasaya bağlı hidrolik ayaklarla sabitleme ve dengeleme işlemi gereklidir (Şekil 7). Dizel motor da bu sehpa üzerinde olduğundan elektriğe ihtiyaç yoktur. Her mevsim çalışabilir. Makinanın uzaktan kumandalı olarak çalışmakta olup emniyetli bir mesafede idare edilebilmektedir. Makina 14º eğimde bile hidrolik sabitleme ayakları ile yatay konumlanabilmektedir.

Şekil 7. Paletli sabit raylı ve kule tipli paletli kollu zincirli kesici makinaları

Paletli kule tipli zincirli kollu kesiciler ayaklar üzerindeki kulede bulunan dişli sistemi ile aşağı-yukarı kademeli olarak kesim yapılabilmektedir Şaryo sistemi ile en az iki düşey kesim yapılabildiği gibi, kesici kol döngü sistemi ile yatay kesimde yapılabilmektedir. Kesme takımını taşıyan kuleye bağlı şaryo sistemi kendi ekseni etrafında 180 derece döndürülebilmektedir (Şekil 7).

Lastik Tekerlekli Traktörlü Sistemler

Traktör monteli kollu zincirli blok kesme makinası, traktörün kuyruk miline monte edilen kesme düzeneği ve kesme kolundan oluşmaktadır.

Şekil 8.Traktör montajlı kollu kesici ve kesim yönleri(x-y) (Demmak)

Kol uzunluğu 3-4 metre, arasında yatayda (iki kesim arası) 0-2 metre sağa-sola hareket edebilme sahip olup, kule yapısına bağlı olarak yerden yüksekliği 3 metreye(Şekil 8) ulaşabilmektedir. Traktör üstüne monte edilmiş olmasından dolayı hızlı ve kolay bir şekilde nakledip kurulabilmektedir.

Kesim Takımındaki Elemanlarda Kırılma ve Aşınma

Kesim takımındaki elemanlardan iç ve dış baklalar, rulmanlar, kesici uç tutucusu ve kesici uçta (soket-keski) kırılma, aşınmalar ile ilgili araştırma nedeni baklaların parasal değerinin kesici uçlara göre 20-30 misli fazla olmasıdır. Bazı durumlarda koldaki toplam kesici uç bedeli bir çift iç-dış bakla bedeline denk gelmektedir. Gözlemlerim sonucu saptanan, resimlenen İÇ-DIŞ HALKA kırılma ve aşınmalar Şekil 9'da verilmiştir.

Şekil 9. Değişik marka makina ve ocaklarda iç-dış halka aşınma ve kırılma örnek resimleri

Yukarıda bahsedilen kırılma ve aşınmaların olası kaynakları ise: a-Doğal taşın petrografik ve sedimantolojik yapısından kaynaklanan nedenler; b-Kesici uç ,güç kaynağı ve malzeme yapısı; c-Operatör yetkinliği ve bakımdır.

Her karbonatlı doğal taş yatağının oluşum ve ortamı aynı değildir. Özellikle sedimanter kökenli karbonatlı kayaçların oluşum ortam koşulları doğrudan kesilebilirliği etkiler. Doğal taşın petrografik yapı ve dokusu, mineral bileşenleri birincil neden olmakla beraber kayaç oluşum esnasında sedimantolojik ortam koşulları ve ortama gelen sediman malzemesinin bileşenlerinin değişmesi etken olmaktadır. Örneğin ortama gelen silisli malzeme, dolomit lensler veya seviyeler.

Operatör ve Makine Bakımı

Zincirli kollu kesici makine kullanımında operatörlerin eğitim ve yetkinliği makine kullanımı kesme verimini doğrudan etkilemektedir. Makinanın çalışma programlanmasının dışı koşulları oluşması veya zorlanması durumda uyarı sinyalleri vermesi durması yeterli olmamaktadır. Aynı marka makine ve ortam kayaçta çalışan iki operatörden bir tanesinde kırılmalar olmaz iken diğerinde parça kırılması kayıtları görülmemiştir.

Kesici Uçların Dizilimi ve Geometrisi

Genelde doğal taş blok kesiminde üç tip kesici uç kullanılmaktadır (Kare /dik dörtgen uçlar; Yıldız uçlar; Silindirik uçlar). Bazı üretici firmalar bu kesici uçlarla değişik dizilimler sunmaktadır. Aşağıda bir takımdaki keski uçların dizilim sıralaması verilmiştir (keski tutucu sayısı 5-17 arasında). Keski ucuna etkiye gerilme kuvvetleri Şekil 10'da sunulmuştur. Burada kesme kuvvetlerinin dengeli sağlanması gerekir.

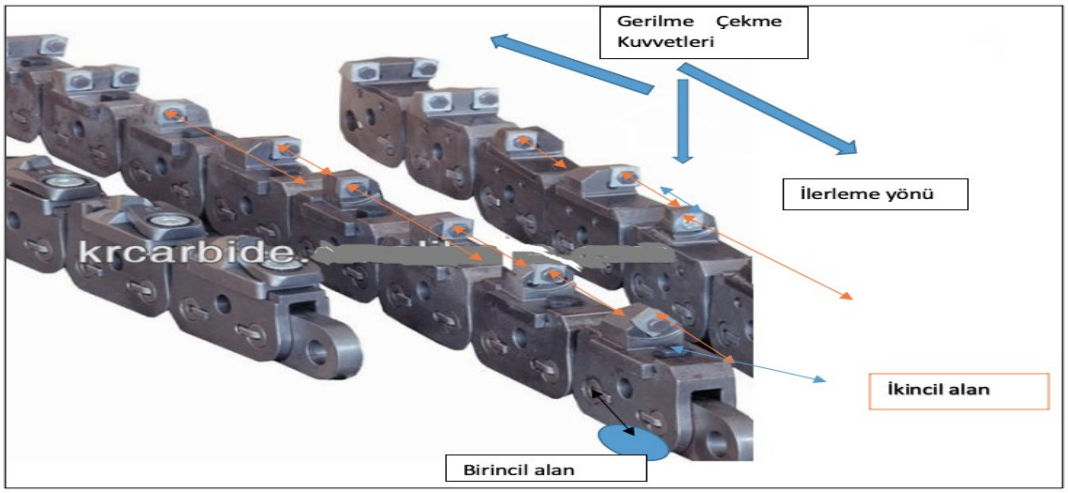

Şekil 10. Dış-İç halka, rulman, keski uçlarına gerilme kuvvetleri alanları

Saha incelemeleri ve literatür verilerine göre değerlendirmeler oldukça girift olmasına rağmen üretici firma paket dizilimlerin kesme verimliliği açısından yetersiz olduğu belirtilmektedir (Çopur, 2006; Çopur vd., 2010; Sarıışık, 2010; Hekimoğlu, 2014; 2015; Çalışkan, 2018; Çelik vd., Dagrain, 2011; 2012). Kesici uçların tipi, cinsi keski uç tutucularında diziliminin ortam kayaç için uygun olup olmadığı saptanmadan makine üreticisi firma abağına göre çalıştırılması sorunun başka boyutu olarak ortaya çıkmaktadır. Araştırmada incelemeye alınan zincirli kollu makinalar özellikleri, kesici uçların bir takımdaki dizilimleri Çizelge 1'de verilmiştir. Bu araştırma-incelemede dört çeşit doğal taş seçilmiş olup, bunlar traverten, limra, kireçtaşı (bej mermer) ve hakiki mermerdir. Bölgeler ise Afyon, Burdur, Antalya, Isparta'dır. Dayanımlar açısından sıralama yapılırsa traverten – limra - kireçtaşı – mermer---bej kireçtaşı

şeklinde sıralama yapılabilir. Çizelge 1'de özetlenerek sunulan veriler incelendiğinde komşu ocakta, aynı marka eşit güç ve kol uzunluklarında farklı kesme verimliliği bulunması nedenleri şöyle sıralanabilir:

1. Makine üreticisi firmanın hidrolik pompa düzeneğinde yaptığı yenilikler,
2. Makinanın yıllara göre yıpranması,
3. Kesici uç geometrisi, dizilimi,
4. Farklı kompleks dizilimler ve malzeme yapısı,
5. Makina markasına göre yapı değişikleri ve teknik özellikleri, kol uzunlukları,
6. Bakım ve yağlama, erken uyarıda müdahalede gecikmeler,
7. Kayaçta yapı, doku ve bileşenlerin değişmesi.

Kırılma Yerlerinin Görsel ve Nümerik Analizi

Zincirli kollu kesicilerin zincir elemanlarında kırılmalar daha çok gerilmelerin yoğun olduğu parçaların birbirleri ile bağlantı yerlerinde yer almaktadır. Bu yerler iç ve dış halka bağlantı yerleri rulman bölgesi ve rulmanlar, keski tutucusu yuvaları, vidalama yerleri keski tutucusu dış halka bağlantılarıdır. Her bir parçada baskı ve gerilmelerin özellikle iç-dış halkada dengesiz dağılımı bu kuvvetlerin burkulma veya eğilme hareketlerinin ritmik olarak tekrarı kırılmanın(üretim hatası, kayaç parametreleri ve kullanım hatası hariç) ana nedenidir. Kullanımda özellikle yetersiz yağlama da sürtünmeyi artırarak aşınma sonucu metal zayıflamasına neden olmaktadır. Yukarıdaki nedenlere bağlı sorunlar farklı üretici firmalarca farklı farklı ölçülerde halka üretmeleri veya keski uç tipi ve dizilim yapmakla beraber sorunlar kısmen devam etmektedir. Şekil 11'de üç farklı keski ucunun bir takımdaki dizilimi görülmektedir. Buradaki alt yazılar üretici firmanın keski tipi, sağ-sola eksen eğimlerini, dizilim sıralamasını göstermektedir.

Şekil 11. Farklı keski uçlarının bir takımdaki dizilimi

Aynı doğal taşta uzun süre kesimde kullanılacak keski uçları ve uçların dizilim şekli, geometrisi önemli olup daha önce belirlenmelidir. Bu konuda yapılan bazı çalışmalarda (Mancini vd., 1994, Çopur, 2006, Çopur vd., 2010, Sarıışık vd., 2009; 2010; Yeşilkaya vd., 2009, Hekimoğlu, 2014; 2015) keski uç dizilim tasarımı, kazı verimliliği, net kazı alanı ve özgül enerji değerlerine bağlı modeller geliştirmişlerdir.

Çizelge 1. Araştırma yapılan zincirli kollu makinalar doğal taş ocakları keski uç dizilimi kesim hızları(L-literatür verileri, Seyfi Kulaksız-kişisel verileri)

Kullanıldığı Ocak	Markası	Modeli	İmal Yılı	Seri No	Bıçak Uzunluğu (m)	Kesici uç Dizilimi	Kesim Hızı (m^2/sa)	Öneri	Kaynak
Traverten	XF	Star Sup 13	2005	5593	6,2	pcd 0/#0/*2/*3/*3A/*3B/#0/*4/*5/*6D/*6S/*6A Çiftli/#6	4,45		AKSOY SEY
	XF	ön 2014	2014	6214	3,4	pcd0/*1/*2/*3/*4/*5/*6 Çiftli/*7 Çiftli	11,82		AKSOY
Burdur Bej	XF	Star Sup 13	2008	5777	7,2	pcd 0/#0/*2/*3/*3A/*3B/#0/*4/*5/*6D/*6S/*6A Çiftli/#6	3,17		AKSOY
	XF	Sup H	2018	6581	7,4	pcd 0/#0/*2/*3/*3A/*3B/#0/*4/*5/*6D/*6S/*6A Çiftli/#6	4,23		SEY
Limra	XF	Sup H	2011	5995	7,4	*#0/#1/#2/#3/#4/#5/#5 bis/#6*	7,65		SEY
	XF	Sup H	2008	5781	3,4	*#0/#1/#2/#3/#4/#5/#5 bis/#6*	5,42		AKSOY
	XF	ön 2015	2016	6374	3	pcd0/*1/*2/*3/*4/*5/*6 Çiftli/*7 Çiftli	12,3		SEY
	XF	ön 2016	2016	6410	3,4	pcd0/*1/*2/*3/*4/*5/*6 Çiftli/*7 Çiftli	12,2		SEY
Bucak Bej	XF	Star Sup 13	2011	5986	3,4	pcd 0/#0/*2/*3/*3A/*3B/#0/*4/*5/*6D/*6S/*6A Çiftli/#6	3,15		SEY
	XF		2012		7,4	0 #########Çift ##	5,2		SEY
Şuhut Bej K	XF		2014		7,4	0# **** ##**** Çift *	7,2		SEY
Şuhut Bej AYY	XF		2O14		7,4	0	7,3		SEY
AFY Gri	B		2021		7,4	### Ç####### ÇİFTLİ####	9,3		SEY
Limra	ZG	MRCH	2007		5,4	######### Çiftli #	6- 6,5	6,5-7,0	ÇA-YA L
TravertenANT	YD				4,3	####### Çiftli ###	6,8-7,0	7,0	YA L
Ant Bej	XF		2012		4,9	pcd 0 16 adet	2,8-4,3	5,0-5,5	YA L
Ant Bej	XF		2014		7,2	0 # XXXX # XXXX ÇiftliXX Çiftli#	7,0-8,0	8,0-9,0	YA L
Senir Bej	XF		2017		7,4	##### Çiftli##	8,5		ÇE L
Senir Bej	XF				3,4	* * * * * Çiftli * *	6,29		ÇE L
kak TRAV	YD		2013		6,8	####### ÇİFT ###	11,5	18,5	ALSA L
AFY BE	YD		2013		6,8	# # # # # # # Çift ##	9.0	12,0	ALSA L
BEJ	YD		2013		6,8	#########Çift#	4,5	9,0	ALSA± L
Bej süt	B		2015		7,2	Ô 1 2 3 4 o 1 2 5R 5L 6Çİ 7 7BİS 8	9.o		SEY
Bej süt	HB		2O14		7,2	0 1 2 3 4 5 6 7 8 9 10 11 11.5 12KARE	5-7.0		SEY
Bej süt	XF		2012		7,2	o* * * * * # **** Çift* Çify#	10.5		SEY

Simscale programında statik sonlu eleman analizi yapılmıştır. Özellikle **zincir rulman tutucu bölgelerinde** baskı dağılım alanları gözlemlenmiştir (Şekil 15).

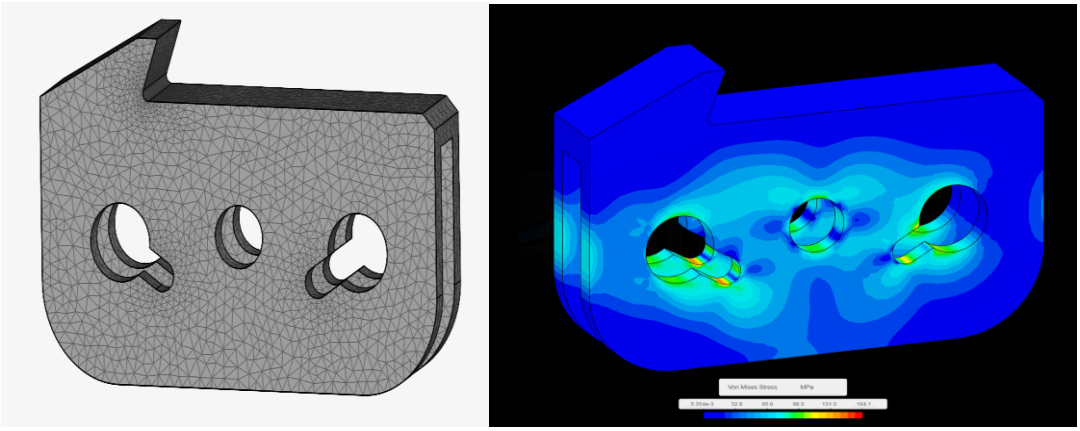

Şekil 15. Kesici uç taşıyıcısı dış halka parçasına Simscale FEA programında yapılan ağ ve baskı dağılımları

SONUÇ

Her ne kadar çalışma şartları sırasında, zincirde oluşan gerilme kuvvetleri zamana bağlı değişimleri ve değerleri kesin olarak bilinmese de, yapılan sonlu eleman analizi sonuçlarında elde edilen stres birikim noktaları, bizim elimizdeki hasarlı parçaların (Şekil 1) kırılma noktaları ile ciddi paralellik taşımaktadır. Bu bölgelerde, kullanım sırasında zamanla oluşacak aşınmalar ve çatlaklardan, malzemenin bütünlüğünü bozacak hasarların geliştiği rahatlıkla söylenebilir. Bundan sonraki çalışmada atılacak adımlar şu şekilde sıralanabilir:

Zincirdeki gerilme kuvvetinin zamana bağlı değişimlerinin ölçülmesi,
Statik FEA analizlerin en yüksek kuvvetlere göre yapılması,
Wöhler S-N eğrisi veya benzer yöntemler kullanarak malzeme ömürlerinin çıkarılıp, gerçek şartlardaki yüklemelerdeki malzeme ömürleriyle karşılaştırılması, elde edilen bilgilerle, gerekli tasarımsal düzenlemelerin yapılıp, malzeme ömürlerinin arttırılması.

YORUM ve ÖNERİLER

Çalışma sonucunda aşağıdaki yorum ve öneriler yapılabilir:

Kayaç fiziko –mekanik özelliklerine uygun keski ucu seçilmeli.
Uygun keski uçlarının dengeli kuvvetler dağılımına göre dizilim yapılmalı,
Uzun hat boyunca kesimlerde her 9-10 metrede zincir takımlarının bakımı yapılmalı,
Özellikle iç-dış halka bağlantı yeri rulmanların bakımı,
Denenmiş dizilimler ve keski uçları ile(aynı kayaç da) sunulan ve önerilenler mutlaka karşılaştırmalı gerilme kuvvetlerinin keski uçlarındaki dağılımı otomatik izleme yapılarak ideal keski uç dizilimi sağlanmalıdır. Bu konuda üç boyutlu modellemeler ve yazılımlar karar destek sistemine yarar sağlayacaktır.

TEŞEKKÜR

Araştırmanın değişik aşamalarında yardımları bulunan Doç. Dr. Erkan Özkan, Doç. Dr. Fatih Bayram, Dr. Öğr. Üyesi Emre Yılmazkaya, Dr. Öğr. Üyesi Fırat Atalay, maden mühendisleri Bektaş Cavlak, Mustafa Olcay, Kemal Aksoy, makina mühendisi Emrah Erden'e çok teşekkür ederim.

KAYNAKLAR

Çalışkan, M. A. (2018). Mermer Ocaklarında Kullanılan Zincirli Kesme Makinelerinin Performanslarının Belirlenmesi. Süleyman Demirel Üniversitesi, Fen Bilimleri Enstitüsü, Yüksek Lisans Tezi, 119s, Isparta.

Çopur, H. (2010). Linear stone cutting tests with chisel tools for identification of cutting principles and predicting performance of chain saw machines. Int J Rock Mech Min Sci. 2010; 47: 104–120.

Çopur, H., Balcı, C., Bilgin, N., Tumac, D., Feridunoğlu, C., Dincer, T. (2006). Cutting Performance Of Chain Saws In Quarries And Laboratory. Proceeding of the 15th International Symposium on Mine Planning and Equipment Selection. Torino, Italy, 1-6.

Dagrain F, Marchandise P, Brux P. (2012). Monitoring of chain saw machines to follow their performances in quarries. Diam Appl Tecnol. 69:43–49.

Dagrain F. (2011). Understanding stone cutting mechanisms for the design of new cutting tools sequences and the cutting optimization of chain saw machines in Belgian Blue Stone quarries. Diamante Applicazioni & Tecnologia; 66, 54-67.

Hekimoğlu, O.Z. (2014). Studies on increasing the performance of chain saw machines for mechanical excavation of marbles and natural Stones". Int J Rock Mech Min Sci. 72: 230–241.

Hekimoğlu, O.Z. (2015). Zincirli Kollu Mermer ve Doğal Taş Kesme Makinalarının Bazı Dinamik , Kinematik ve Tasarım Özellikleri 5. Uluslararası Maden Makinaları Sempozyum ve Sergisi Maden Müh.Odası Bildiriler Kitabı

https://www.cliftonsteel.com/knowledge-center/tensile-and-yield-strength

https://www.fracturemechanics.org/hole.html

https://www.simscale.com

Mancini, R., Linares, M., Cardu, M., Fornaro, M., Bobbio, M. (1994). Simulation of the operation of a rock chain cutter on statistical models of inhomogenous rocks. Proc. Mine Planning and Equipment Selection, 461-468.

Sarıışık, A., Sarıışık, G. (2010). Efficiency Analysis Of Armed-Chained Cutting Machines In Block Production In Travertine Quarries. Journal Papers, 110, 473-480.

Tiryaki, B. (1998). Tamburlu Kesicilerde Keski Dizilim Parametrelerinin Optimizasyonu, Doktora Tezi, H.Ü. Fen Bilimleri Enst. 264 s.

Yeşilkaya, L., Ersoy, M., Çelik, M., Çatalpınar, A. (2009). Kaklık-Denizli Traverten Ocağında Zincirli Kollu Kesicinin Kullanımının Araştırılması. Madencilik Dergisi, Eylül. 48(3), 33.

BAKIR CEVHERİ İÇİN FARKLI PARÇACIK BOYUTU GRUPLARINA AİT KIRILMA PARAMETRELERİNİN TEK DARBELİ KIRILMA İLE BELİRLENMESİ

DETERMINATION OF BREAKAGE PARAMETERS FOR SEVERAL SIZE CLASSES OF COPPER ORE BY SINGLE IMPACT BREAKAGE TEST

İ.C. Duman [1,*], B. Ozlu [1], M. İtik [2]

1 Çolakoğlu Mühendislik Mak. San. ve Tic. Ltd. Şti.
*(*Sorumlu yazar: can@colakoglumakina.com)*
2 İzmir Demokrasi Üniversitesi, Makina Mühendisliği Bölümü

ÖZET

Maden endüstrisinde, üretim süreci boyunca cevherler maden ekipmanları ile etkileşimde bulunduklarından kırılmaya maruz kalmaktadırlar. Tesisin iş akış süreci boyunca aktarım olukları, kırıcılar, değirmenler vb. ekipmanlar, geniş aralıklarda değişen farklı boyut dağılımlarına sahip parçacıkların kırılması sebebiyle ciddi deformasyonlara uğramaktadırlar. Özellikle öğütücü değirmenler ve kırıcılarda parçacıkların teması sonucu ortaya çıkan darbe etkisi oldukça yüksektir. Bu nedenle parçacık kırılmasının tesis ekipmanları üzerindeki yarattığı etkinin anlaşılması, ilgili ekipmanların tasarımında ve ömür tayininde, hatta tesis üzerindeki maliyet iyileştirmelerinde önemli rol oynamaktadır. Bu çalışmada, boyut dağılımlarına göre gruplara ayrılmış olan bakır cevherleri, ağırlık düşürme test düzeneği kullanılarak ve tek darbeli kırılma yaklaşımı esas alınarak kırılmıştır. Her bir parçacık için, parçacığın üzerine düşen ağırlığa ait yüksekliğe bağlı olarak özgül ufalama enerjisi değeri belirlenmiştir. Ardından bu yükseklik, tekrarlanan deneyler boyunca arttırılmıştır ve çeşitli boyutlarda alt parçacıklara ayrılan cevherler, ilgili parçacığın başlangıçtaki boyutunun 1/10'u kadar açıklığa sahip elekten geçirilmiştir. Darbe enerjisine ve elde edilen elek altı kütlenin başlangıç kütlesine oranına bağlı olan tek darbeli kırılma yaklaşımı formülleri kullanılarak kırılma parametreleri belirlenmiştir.

Anahtar Sözcükler: Kırılma, bakır cevheri, tek darbeli kırılma, ağırlık düşürme testi

ABSTRACT

In mining industry, particles are exposed to breakage in the interaction with mining equipments throughtout the whole process. Equipments like transfer chutes, crushers, mills etc. suffer remarkable deformations due to the particle breakage which varies in a wide range of particle sizes. The impact effect which arises at the contact areas of mills and crushers is particularly enormous. Therefore, it is important to understand the effect of breakage above facility equipments for their design, to predict equipments life spans and moreover the cost enhancements about the facility. In this study, copper ores in various size classes have been broken based on the single impact breakage event via using drop weight test set up. For every particle, specific crumbling energy value which is related to the height of the drop weight is determined. Then, this height has been increased with repeated experiments and the ores which are divided into various fragments have been sieved by the screen of the 1/10th of the initial particle size. At last, as using the formula which is related to the impact energy and the proportion of under screen weight of broken particle to the initial weight, breakage parameters have been determined.

Keywords: Breakage, copper ore, single impact breakage, drop weight test

GİRİŞ

Maden endüstrisine parçacık kırılmasının karakterizasyonu üzerine yapılan araştırmalar uzun yıllardır devam etmektedir. Özellikle bir parçacığın kırıcılar ve değirmenler içerisinde nasıl kırıldığının doğru bir şekilde tahmin edilebilmesi önemlidir (Napier-Munn vd., 1996). Ayrıca cevherler çıkartıldıkları bölgeye göre farklılık gösterdiklerinden her farklı tesis ve her bir cevher türü için, ilgili cevherin kırılma davranışının bilinmesi ve tesis ekipmanlarının bu doğrultuda dizayn edilmesi önem teşkil etmektedir

.

Parçacık kırılması üzerine çeşitli test düzenekleri mevcuttur. Tavares (2007) tarafından yapılan çalışmada bu test düzeneklerinin çalışma prensiplerinden detaylıca bahsedilmiştir. Şekil 1'de gösterilen ve bu çalışma içerisinde kullanılan düzenek olan ağırlık düşürme test düzeneği, tek parçacık için kırılma parametrelerinin belirlenmesi amacıyla yaygın olarak kullanılmaktadır.

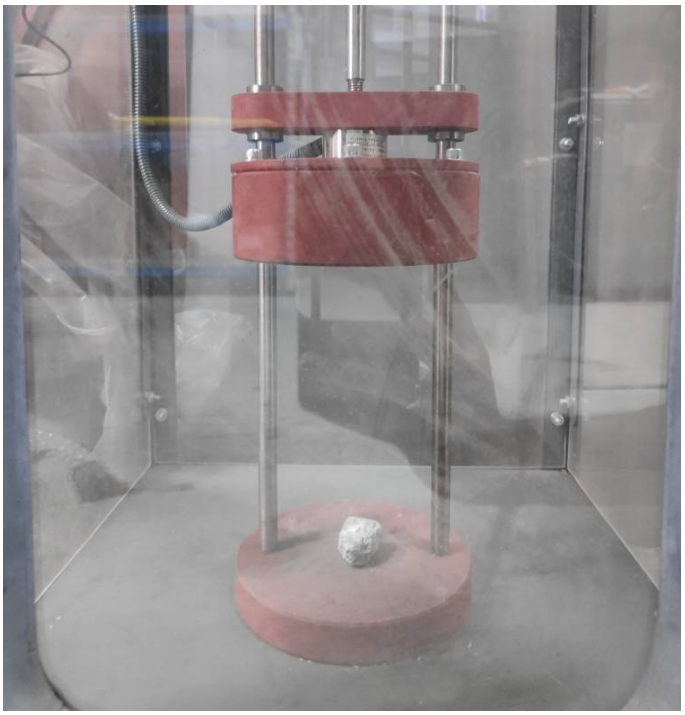

Şekil 1. Ağırlık düşürme test düzeneği

Bu çalışmada, Giresun yöresinden alınan bakır cevheri numuneleri için cevher kırılma parametreleri belirlenmiştir. Cevherler için ön boyutlandırma işlemi uygulanarak farklı boyut dağılımlarına göre gruplandırma yapılmıştır. Her boyut aralığı için, parçacığın kırılmaya başladığı ağırlık düşürme yükseklikleri ve buna bağlı olarak özgül ufalama enerji değerleri belirlenmiştir. Tekrarlanan deneyler sonucunda her bir gruba ait kırılan cevherler, ortalama tane boyutunun 1/10'una tekabül eden elek açıklığına sahip test eleklerinden geçirilmiştir. Eleme işlemi sonrasında, kırılan cevherlerin kütle kaybı oranı ölçülmüş ve buna bağlı olarak elde edilen cevher kırılma parametreleri (*A* ve *b*) belirlenmiştir.

Tek Darbeli Kırılma Yaklaşımı

Narayanan ve Whiten (1988) tarafından geliştirilen ve darbe altında parçacığın kırılma olasılığı ile ilişkili olan t_{10} parametresi, ağırlık düşürme testinin parçacıkların kırılma ihtimalinin anlaşılmasında ve alt

boyut dağılımının belirlenmesindeki etkinliğini vermektedir (Napier-Munn vd., 1996). Farklı türden parçacıklar, malzeme karakteristiklerinin yanısıra sahip oldukları boyutlara göre kırılma davranışı sergilemek için farklı enerji seviyelerine ihtiyaç duymaktadırlar.

Parçacıklar, kırılma oluşumu için belirli bir minimum enerjiye ihtiyaç duymaktadırlar. Tek darbeli kırılma yaklaşımı; boyut, şekil vb. özellikleri sebebiyle her parçacık türüne için farklılık gösteren parçacık çatlama enerjisine göre karakterize edilmektedir. Parçacık üzerindeki stres veya çarpışma enerjisi çatlama enerjisinden yüksek olduğunda parçacık kırılmaya uğrayıp alt fragmanlara ayrılmaktadır. Stres veya çarpışma enerjisi ne kadar yüksek olursa, alt fragmanların boyut dağılımı o kadar ince ve düzgün olmaktadır (Barrios vd., 2011). Boyut dağılım aralığı bilinen bir parçacık sınıfı için *E* enerji seviyesindeki bir darbe sonucu oluşan kırılmada alt parçacık oluşumu, t_{10} boyut dağılım formülü ile ele alınmaktadır.

$$t_{10} = A\,[\,1 - exp(-b.E_{cs})] \tag{1}$$

Burada t_{10}, parçacığın kırılma sonrası 1/10'undan geçen kütlenin başlangıç kütlesine oranı olarak tanımlanmaktadır. Ayrıca, t_{10} değerini sınırlayan ve farklı enerji seviyelerinde kırılan parçacığa ait en yüksek t_{10} değeri *A* olarak belirtilirken, *b* ise özgül ufalama enerjisi E_{cs} değerine karşı boyutta olan bir kırılma parametresidir (de Magalhães & Tavares, 2014). Özgül ufalama enerjisi E_{cs} değeri, parçacığın maruz kaldığı darbe enerjisine ve parçacık kütlesine bağlıdır. Buna göre parçacığın kütlesine bağlı olarak elde edilen kırılma enerjisi, veya özgül ufalama enerjisi, değeri aşağıdaki gibidir.

$$E_{cs} = \frac{E_i}{m_p} \tag{2}$$

Burada E_i, çarpışma veya darbe enerjisi değeri ve m_p, kırılan parçacığın kütlesi olarak tanımlanmaktadır (Genç, 2017). Bu enerji değeri esas alınarak parçacıkların kırılma davranışının modellendiği ve Napier-Munn vd. (1996) tarafından öne sürülen tek parçacık darbeli kırılma yaklaşımı denklem (1'de verilmiştir. Düşen ağırlığın sahip olduğu potansiyel enerjiden kaynaklanan ve parçacığın maruz kaldığı darbe enerjisi aşağıdaki gibi tanımlanmaktadır.

$$E_i = m_d g(h_i - h_f) \tag{3}$$

Burada yerçekimi ivmesi *g*, düşen ağırlığın kütlesi m_d , düşen ağırlığın parçacığın durduğu örs yüzeyine göre sahip olduğu başlangıç yüksekliği h_i ve düşürülen ağırlığın çarpışma sonrası örs yüzeyine göre sahip olduğu son yükseklik h_f olarak tanımlanmaktadır.

A ve *b* cevher sertlik parametreleri, parçacığın alt parçacıklara dağılımın davranışını karakterize etmektedirler. *A*b* değeri, E_{cs} - t_{10} grafiğinde oluşturulan eğrinin başlangıç eğimi olarak tanımlanmaktadır ve ilgili malzeme için bir sertlik göstergesi olarak kabul edilmektedir. *A*b* değeri, yüksek darbe direncine sahip malzemeler için 10 kadar düşük olabilecek iken; zayıf darbe direncine sahip malzemeler için 250 civarlarına kadar çıkabilmektedir (Tavares, 2007).

DENEYSEL ÇALIŞMALAR

Ağırlık Düşürme Testi

Şekil 1'de gösterilen test düzeneği kullanılarak, farklı boyut aralıklarında tanımlanmış bakır cevheri için çeşitli testler gerçekleştirilmiştir. Testlerde kullanılan numuneler ve parçacıkların özellikleri

Tablo 1.'de verilmiştir. Söz konusu testte kırılmak üzere ön boyutlandırma işlemi yapılan bakır cevheri numuneleri Şekil 2'de gösterilmiştir.

Şekil 2. Ön boyutlandırma işlemine tâbi tutulan bakır cevheri numuneleri

Kırılacak olan bakır cevheri, boyut ve ağırlık ölçümlerinin ardından Şekil 1'de gösterilen ağırlık düşürme test düzeneğinin alt kısmında sabitlenmiş konumdaki örs üzerine yerleştirilmiştir. Kırma işlemini gerçekleştirecek olan ağırlık, bir mıknatıs yardımıyla başlangıç yüksekliğinde tutulmaktadır. Söz konusu ağırlık, mıknatıs bağlantısı kesildiğinde cevherin üzerine serbest düşüş hareketi yaparak cevheri kırmaktadır. Eğer cevher kırılmamış ise ağırlığa ait bu yükseklik cevher kırılana kadar arttırılmaya devam ekmektedir.

Ağırlığın düşürülmesinin ardından, çarpışma sonrasında ağırlık ile örs arasında kalan yükseklik, denklem (3'de h_f değeri yerine yazılmak üzere ölçülmektedir. Aynı potansiyel enerji seviyelerinde tekrarlanan deneyler sonrasında ağırlığa ait yükseklik, aynı cevher grubu için belirli bir seviyede arttırılmış ve deneyler tekrarlanmıştır. Bu yükseklik arttırmaları sonrasında parçacığın kırılmaya maruz kaldığı ilk yükseklik, kırılma parametrelerinin elde edilmesi için kullanılan Denklem (1'deki özgül ufalama enerjisi E_{cs} değerine karşılık gelmektedir.

Kırılan bakır cevherleri, kırılma eylemi sonucu alt parçacıklara ayrılmaktadır. Tüm bu alt parçacıklar, cevherin başlangıç boyutunun 1/10'u kadar açıklığa sahip bir elekten geçirilmiştir. Elek altı kütlesinin, cevherin kırılma öncesi sahip olduğu kütlesine oranı; kırılma parametrelerinin belirlenmesi için kullanılan formülde yer alan başka bir parametre olan t_{10} değerine karşılık gelmektedir.

Cevher parçacığının yer aldığı grup içerisindeki diğer cevher parçacıkları ile, cevhere ait ilk kırılmanın gerçekleştiği E_{cs} değerinden daha yüksek bir enerji seviyesine çıkılarak testler tekrarlanmaktadır ve Denklem (1 için t_{10} değerleri belirlenmektedir. Her bir cevher grubu için gerçekleştirilen test sayıları ve enerji seviyesi aralıkları Tablo 1'de belirtilmiştir.

Tablo 1. Testlerde kullanılan bakır cevherinin özellikleri

Grup No	Elek Boyutu [mm]	Cevher Boyut Aralığı [mm]	E_{cs} [kWh/t]	Enerji Seviyesi Aralığı [kWh/t]	Test Sayısı
1	0.5	5 (-0.8 + 0.9)	0.965	0.965 - 6.452	19
2	1.0	10 (-0.7 + 1.0)	0.278	0.278 - 1.826	16
3	1.4	14 (-1.0 + 1.3)	0.199	0.199 - 1.172	24
4	2.0	20 (-1.5 + 2.0)	0.235	0.235 - 0.635	16
5	2.5	25 (-2.0 + 1.9)	0.138	0.138 - 0.431	22

Tüm bu testlerin ardından, her bir cevher grubu için elde edilen en yüksek t_{10} değerleri, *A* cevher kırılma parametresi değerine karşılık gelmektedir. Deneyler sonucu elde edilen değerler, her bir cevher grubu için denklem (1'de yerine konularak gruplara ait *b* kırılma parametreleri belirlenmiştir.

Bulgular

Testler sonucunda elde edilen değerler Tablo 2'de verilmiştir. Bu değerler kullanılarak, her bir cevher grubu için özgül ufalama enerjisi – t_{10} ilişkisi ve sonuçlara bağlı olarak oluşturulan uyum eğrileri Şekil 3-7 aralığında verilmiştir.

Tablo 2. Deneysel çalışmalar sonucu elde edilen kırılma parametreleri

Grup No	*A*	*b*	*A* x *b*
1	33.7	1.10	37.07
2	20.00	2.81	56.20
3	7.059	1.784	12.59
4	10.204	3.017	30.79
5	5.45	3.09	16.84

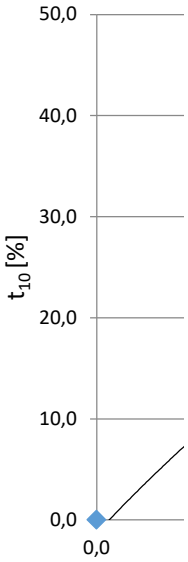

Şekil 3. Bakır cevherine ait 1 numaralı grup için özgül ufalama enerjisi – t_{10} ilişkisi

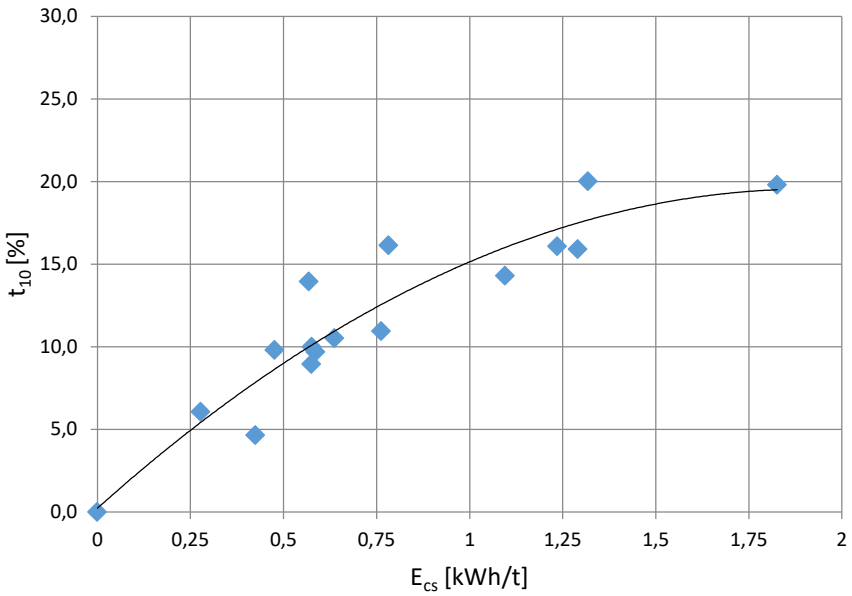

Şekil 4. Bakır cevherine ait 2 numaralı grup için özgül ufalama enerjisi – t_{10} ilişkisi

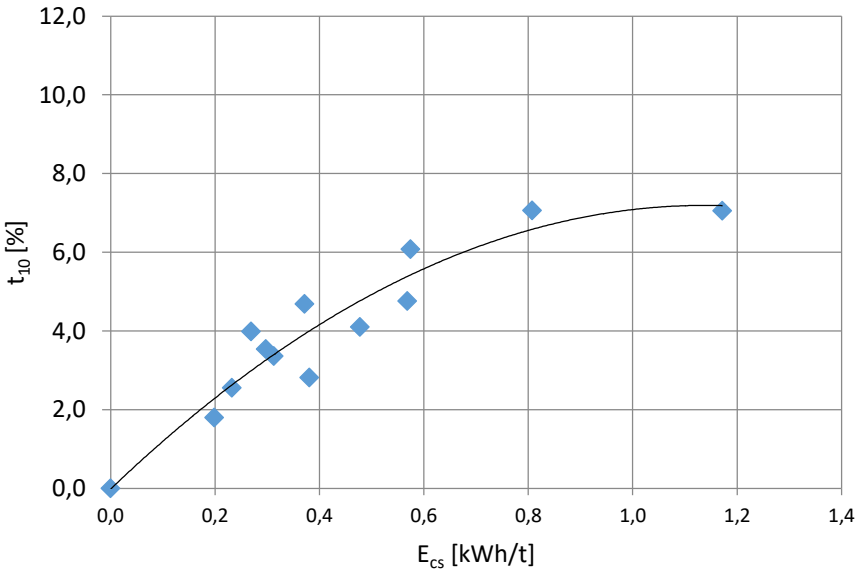

Şekil 5. Bakır cevherine ait 3 numaralı grup için özgül ufalama enerjisi – t_{10} ilişkisi

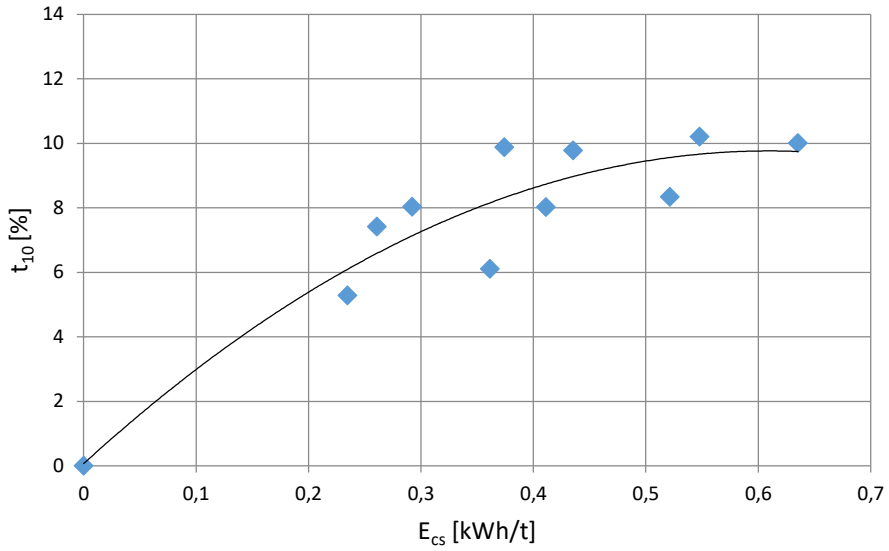

Şekil 6. Bakır cevherine ait 4 numaralı grup için özgül ufalama enerjisi – t_{10} ilişkisi

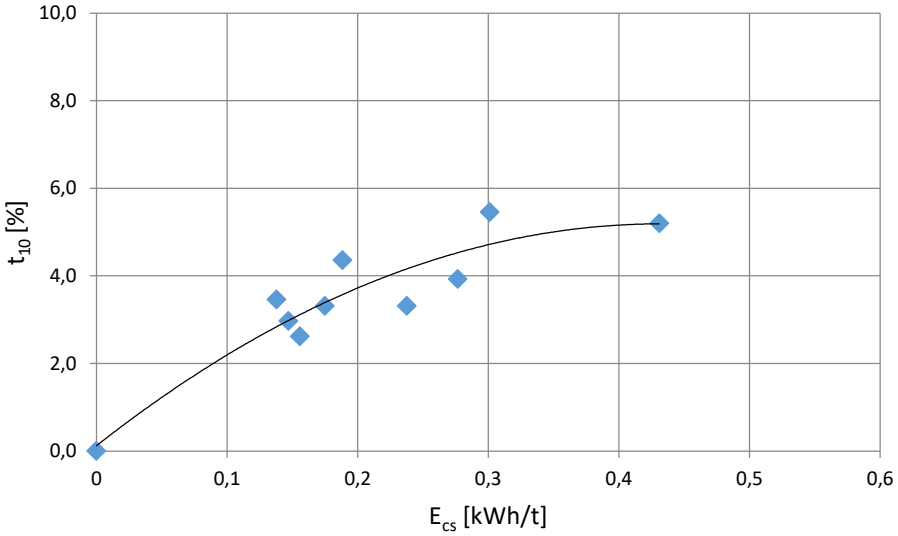

Şekil 7. Bakır cevherine ait 5 numaralı grup için özgül ufalama enerjisi – t_{10} ilişkisi

SONUÇLAR

Bu çalışmada Giresun yöresinden çıkartılan bakır cevheri için cevher kırılma parametreleri elde edilmiştir. Kullanılan bakır cevheri için, Tavares (2007) tarafından belirtilen cevher sertlik değeri aralığı baz alındığında ortalama 30.69 *A*b* değeri ile sert bir yapıya sahip olduğu belirlenmiştir. Gerçekleştirilen testler sonucunda ulaşılan E_{cs} ve t_{10} değerleri için doğrusal olmayan regresyon ile oluşturulan uyum eğrileri ortalama 0.85 çoklu R değerine sahiptir. Bu değerin uyum eğrisi için yüksek bir değer olmasına karşın, buna bağlı olan R^2 determinasyon katsayısı değeri düşük gelmektedir. Bu sebepten ötürü, Tablo 1'de verilen gerçekleştirilmiş test sayılarının arttırılması ile daha yüksek doğruluk elde edilmesi mümkün olacaktır.

Bu çalışma, Türkiye Bilimsel ve Teknolojik Araştırma Kurumu (TÜBİTAK, Proje no:3181181) tarafından 1501 – TÜBİTAK Sanayi Ar-Ge Projeleri Destekleme Programı kapsamında desteklenmiştir. TÜBİTAK'a destekleri için teşekkür ederiz.

KAYNAKLAR

Barrios, G. K. P., de Carvalho, R. M., & Tavares, L. M. (2011). Modeling breakage of monodispersed particles in unconfined beds. *Minerals Engineering*, *24*(3-4), 308-318.

de Magalhães, F. N., & Tavares, L. M. (2014). Rapid ore breakage parameter estimation from a laboratory crushing test. *International Journal of Mineral Processing*, *126*, 49-54.

Genç, Ö. (2017). ALTIN CEVHERİNİN TEK TANE DARBE KIRILMA FONKSİYONLARININ AĞIRLIK DÜŞÜRME TEKNİĞİ İLE İNCELENMESİ. *Maden Tetkik ve Arama Dergisi*, 154.

Napier-Munn, T. J., Morrell, S., Morrison, R. D., & Kojovic, T. (1996). Mineral Comminution Circuits, Their Operation and Optimisation. *Julius Kruttschnitt Mineral Research Centre*.

Narayanan, S. S., & Whiten, W. (1988). Determination of comminution characteristics from single-particle breakage tests and its application to ball-mill scale-up. *Trans.* C115-C124.

Tavares, L. M. (2007). Chapter 1 Breakage of Single Particles: Quasi-Static. *Handbook of Powder Technology* (C. 12, ss. 3-68).